

Abbildung: Dr. Werner Zischner, Magdeburg

# Proceedings

## Sixth Meeting of the German Neuroscience Society

30<sup>th</sup> GÖTTINGEN  
NEUROBIOLOGY CONFERENCE  
February 17-20, 2005



Proceedings of the 6th Meeting of the German Neuroscience Society /  
30th Göttingen Neurobiology Conference 2005

Prof. Dr. Herbert Zimmermann  
Biozentrum - Zoologisches Institut  
AK Neurochemie  
Marie-Curie-Str. 9  
D-60439 Frankfurt am Main  
Germany

Prof. Dr. Kerstin Krieglstein  
Abt. Anatomie / Neuroanatomie  
Bereich Humanmedizin / Universität Göttingen  
Kreuzberggring 36  
D-37075 Göttingen  
Germany

Cover picture: Dr. Werner Zuschratter, Magdeburg  
Cover design: Eta Friedrich, Berlin

This CD is a Supplement to  
Neuroforum 2005, February; 1  
ISSN 0947-0875  
<http://www.spektrum-verlag.com/>

For advanced search of the abstracts use the Itinerary Planer on  
<http://www.neuro.uni-goettingen.de/>

Copyright is held by the authors of the abstracts.

Some of the product names, patents and registered designs referred to are in fact registered trademarks or proprietary names even though specific reference to this fact is not always made in the text. Therefore, the appearance of a name without designation as proprietary is not to be construed as a representation by the publisher that it is in the public domain.



# **Index**

**[Plenary Lectures](#)**

**[Symposia](#)**

**[Satelite Symposia](#)**

**[Poster Subject Areas](#)**

**[Index of Authors](#)**

## Plenary Lectures

- #P1 B. Dickson, Wien (A)  
*Axon guidance at the Drosophila midline*
- [#P2](#) LG. Cohen, Bethesda (USA)  
*Mechanisms of cortical reorganization underlying recovery of motor function after stroke*
- [#P3](#) MAL. Nicolelis, Durham (USA)  
*Computing with Neural Ensembles*
- [#P4](#) C. Miller, Waltham (USA)  
*Proteins that move ions across membranes: our evolving picture*
- [#P5](#) ME. Schwab, Zurich (CH)  
*Axonal repair in the adult mammalian central nervous system.*
- [#P6](#) WT. Newsome, Stanford (USA)  
*Reward, Value and Decisions*
- [#P7](#) M. Theis, New York (USA)  
*Conditional gene replacement: the benefits of a direct link between loss of gene expression and reporter activation*
- [#P8](#) D. Schmitz, Berlin  
*Comparison of different forms of synaptic plasticity in the hippocampus*
- [#P9](#) H. Monyer, Heidelberg  
*GABAergic interneurons at the cellular and network level*

Mechanisms of cortical reorganization underlying recovery of motor function after stroke  
Leonardo G Cohen  
Human Cortical Physiology Section, NINDS

Stroke is the leading cause of long-term disability worldwide and a condition for which there is no universally accepted treatment. The development of new effective therapeutic strategies relies on a better understanding of the mechanisms underlying recovery of function. Non-invasive techniques to study brain function including fMRI, PET, TMS, EEG and MEG led to recent studies that identified some of these operating mechanisms resulting in the formulation of novel approaches to motor rehabilitation based on principles of neuroplasticity.

Recent neuroimaging studies documented the involvement of multiple primary and nonprimary motor regions of both cerebral hemispheres in the process of recovery of motor function following stroke. In general, patients with no residual impairment show activation patterns close to those exhibited by normal individuals while those with more profound impairment activated multiple regions in both cerebral hemispheres. TMS studies have shown that both primary and nonprimary motor regions contribute to functional recovery after stroke. Evidence is mounting for the involvement of interhemispheric interactions as influential factors in the process of motor recovery.

It is clear that functionally relevant adaptive changes take place in the human brain after focal injury. But can we modulate them? Basic science studies showed that manipulation of environmental, behavioural, and pharmacological factors can influence cerebral reorganization. From our knowledge of how the brain responds to focal injury and how this relates to recovery we can now generate hypothesis-driven approaches to neurorehabilitation. Recent studies addressed the effects of reduction of somatosensory input from the intact hand, increase in somatosensory input from the paretic hand, anaesthesia of a body part proximal to the paretic hand, enhancement of plasticity within the affected motor cortex, down regulation of activity within the intact motor cortex and pharmacological interventions on motor performance of a paretic hand. Results from these studies started to provide valuable data for the development of new strategies in neurorehabilitation.

## **Computing with Neural Ensembles**

**Miguel A. L. Nicolelis, MD, PhD**  
**Depts. of Neurobiology, Biomedical Engineering,**  
**and Psychological and Brain Sciences**  
**Co-Director, Duke Center for Neuroengineering**

In this talk, I will review a series of recent experiments demonstrating the possibility of using real-time computational models to investigate how ensembles of neurons encode motor information. These experiments have revealed that brain-machine interfaces can be used not only to study fundamental aspects of neural ensemble physiology, but they can also serve as an experimental paradigm aimed at testing the design of modern neuroprosthetic devices. I will also describe evidence indicating that continuous operation of a closed-loop brain machine interface, which utilizes a robotic arm as its main actuator, can induce significant changes in the physiological properties of neurons located in multiple motor and sensory cortical areas. This raises the hypothesis of whether the properties of a robot arm, or any other tool, can be assimilated by neuronal representations as if they were simple extensions of the subject's own body.

## Proteins that move ions across membranes: our evolving picture

Christopher Miller  
HHMI, Brandeis University  
Waltham, Mass, USA

We do not yet understand how we think, but we do know that movement of ions across nerve membranes form the physical basis of all mental activity. The physical devices that move these ions – integral membrane proteins of the channel, pump, and secondary transporter, families -- have now for the first time become visible by x-ray crystallography. In some cases, such as the  $K^+$  channels, many of the features of these proteins had been anticipated from close electrophysiological analysis of their functional properties, of the sort that Roger Eckert would have found familiar. Others, such as the CLC  $Cl^-$  channels, have produced completely unanticipated surprises. This lecture will touch upon a few early examples of what crystal structures have taught us about the basic molecular hardware underlying the generation of electrical signals in the nervous system.

**AXONAL REPAIR IN THE ADULT MAMMALIAN CENTRAL NERVOUS SYSTEM.**  
**Schwab, Martin E., Chair of Neurosciences, Brain Research Institute, University of Zurich and Department of Biology, ETH Zurich, Winterthurerstr. 190, 8057 Zurich, Switzerland.**

Spinal cord injuries with very extensive destruction of ascending and descending fiber tracts lead to paralysis without or with only minimal functional recovery (ASIA A,B). In contrast, smaller lesions which spare parts of the white matter can be followed by substantial functional recovery. Extensive rehabilitative training is required to reach an optimal, well adapted level of function. The neuroanatomical basis for this recovery process is not known. Animal experiments show that injured fiber tracts in spinal cord or brain show a spontaneous but small regeneration response. In the case of the pyramidal tract of the adult rat, transected hindlimb fibers sprout into the cervical spinal cord and form new contacts with spared propriospinal axons running from the cervical to the lumbar cord. In this way a new, indirect circuit is formed which allows to transmit information from the motor cortex to the hindlimbs through a cervical relay pathway. This spontaneous nerve fiber growth is limited in distance to about 1 mm, however.

Specific proteins were discovered in the adult spinal cord and brain that inhibit nerve fiber growth in the adult organism. A major factor is found in the myelin sheath of the fiber tracts and is called Nogo-A. The growth-inhibitory effect of Nogo-A can be neutralized by specific antibodies in vitro and in vivo. Infusion of Nogo neutralizing antibodies into the CSF of adult spinal cord injured rats or macaque monkeys leads to a massive enhancement of regenerative fiber growth. Extensive tests of locomotor behavior (rats) and skilled hand movements (monkeys) show a high degree of restoration of function. These findings indicate that adult spinal cord fibers can be stimulated in their regenerative ability, and that these growing fibers are able to form new circuits that mediate functional recovery in the absence of malfunctions. These results in animals form the basis for the development of a new therapeutic approach in spinal cord injured patients.

## **Reward, Value and Decisions**

*William T. Newsome*

*Howard Hughes Medical Institute and Department of Neurobiology  
Stanford University School of Medicine*

### **Abstract**

In the study of decision-making, psychophysicists and sensory physiologists traditionally emphasize the effects of sensory stimuli on the outcome of the decision process. Psychologists and economists, however, have long known that decision-making is influenced not only by the sensory stimulus, but also by an organism's prior experience or beliefs concerning the "value" of the alternative choices, expressed in terms of likely positive or aversive consequences. Brain circuitry that mediates decision-making must presumably reflect both influences, and we have recently been able to demonstrate both effects at the behavioral and neurophysiological levels. To measure "experienced value" objectively, we have developed a probability matching paradigm for rhesus monkeys in which the animal's valuation is revealed through the proportion of choices allocated to alternative behaviors. In neurophysiological recordings, we have found that neurons in the lateral intraparietal area (LIP) code experienced value, although LIP is unlikely to be the site where experienced value is originally computed. Our results to date suggest that signals from multiple sources within the brain, including representations of sensory stimuli as well as internal valuation converge in areas such as LIP to render simple behavioral decisions.

**Conditional gene replacement: the benefits of a direct link between loss of gene expression and reporter activation**

Martin Theis

Center for Neurobiology and Behavior, Columbia University, New York, U.S.A., mt2050@columbia.edu

Cre recombinase activity for cell-type restricted deletion of floxed target genes (i.e. flanked by Cre recognition sites) is often measured by a separate recombination-activated reporter gene. However, recent reports on locus-dependent differences in the susceptibility to recombination of floxed DNA question the usefulness of Cre-excision reporter mice to monitor deletion of the actual target gene. Here we demonstrate the benefits of a direct link between reporter gene expression and target gene deletion.

By gene targeting, we generated a floxed connexin43 (Cx43) mouse line, in which a lacZ reporter gene was activated upon Cre-mediated recombination. Cell-type restricted Cx43 deletions were obtained by interbreeding with Cre transgenic mice. Cre activity leading to loss of Cx43 expression was monitored by gain of lacZ expression, encoding beta galactosidase, whose activity was determined by X-gal staining.

Mice with Cx43 deletion in all cells showed a lacZ expression pattern which matched the endogenous Cx43 expression pattern. In mice with hGFAP-cre mediated deletion of Cx43, the floxed allele was recombined in neurons besides astrocytes, yet lacZ expression indicative of loss of Cx43 expression occurred only in astrocytes and not in neurons. Thus, the lacZ gene indicated phenotypically relevant recombination leading to loss of Cx43 expression at the cellular level.

The conditional replacement of Cx43 by a reporter gene indicated loss of target gene expression as a positive signal, i.e. by gain of lacZ expression. This feature was very helpful in delineating subsets of cells with Cre-mediated loss of Cx43 expression which were surrounded by other cell types still expressing Cx43 at high levels, such as putative neural crest cells targeted by an Insulin promoter Cre transgene during development.

The lacZ reporter gene embedded in the floxed Cx43 allele is so far the best functional reporter for astrocytes: Our lacZ reporter strongly indicated Cre-mediated recombination in astrocytes, whereas conventional Cre-excision reporter mice did not properly indicate gene deletion in this cell type.

It is assumed that cell-type specific Cre-mediated recombination is reliable and invariant between different individual animals. However, X-gal staining of a large number of mice (>30 for each line) with different restricted Cx43 deletions indicated that spontaneous ectopic Cre activity is a common phenomenon among most Cre lines tested, raising concerns about the reproducibility of Cre action. Individual mice with non cell-type specific recombination had to be identified and discarded, a task which was strongly facilitated by the embedded lacZ gene.

**Conclusions:** The conditional replacement of a floxed gene by a reporter gene 1) focuses on phenotypically relevant deletion, 2) highlights targeted cells with gene inactivation which are surrounded by other cell types still expressing the target gene at high levels, 3) guarantees functionality of the Cre-excision reporter in the cell type of interest and 4) allows a rigid control for proper Cre-mediated gene inactivation at the cellular level after phenotypical assessment of individual mice.

**Support:**

Martin Theis received a fellowship of the Graduiertenkolleg "Pathogenese von Krankheiten des Nervensystems".

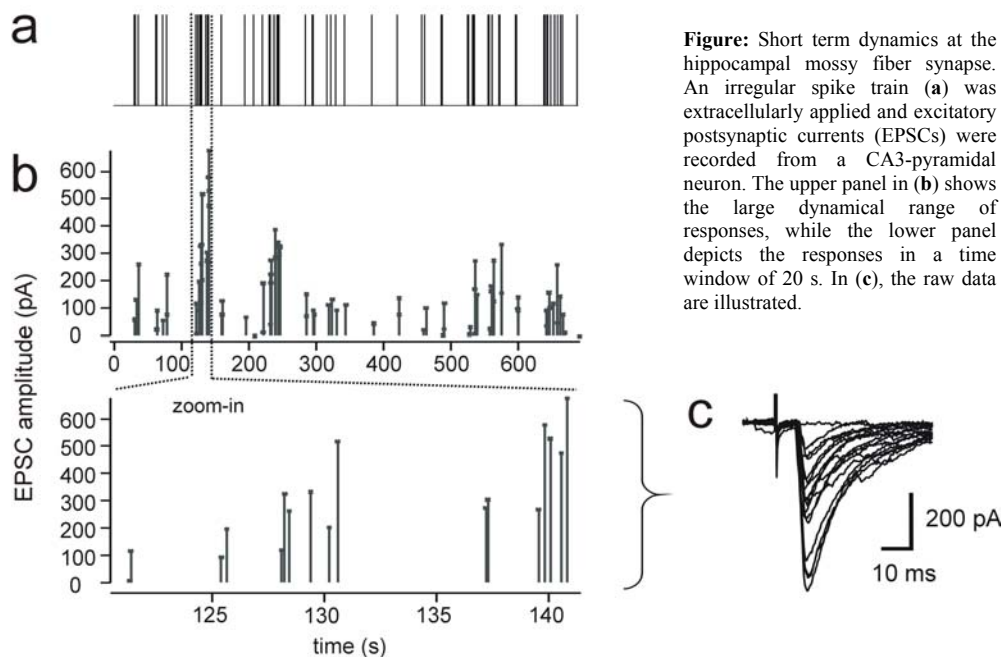


## Comparison of Different Forms of Synaptic Plasticity in the Hippocampus

Dietmar Schmitz

Neuroscience Research Center, Charité, Universitätsmedizin Berlin, Schumannstr. 20/21, 10117 Berlin

How does our central nervous system encode information on environmental changes and experience into short- and long-term memories? It is now generally accepted that activity-dependent changes in synaptic efficacy are critically involved in certain forms of learning and memory, with long term potentiation (LTP) as well as long term depression (LTD) as bidirectional examples of these changes. In this context, NMDA-receptor dependent LTP in area CA1 of the hippocampus represents the most widely studied form of synaptic plasticity. On the other hand, hippocampal mossy fiber synapses also show a form of LTP, however, this form of plasticity is NMDA-receptor independent and presynaptically expressed. Furthermore, mossy fiber synapses exhibit pronounced short term dynamics, in which the size of synaptic currents depends critically on the specific history of presynaptic spike activity. This phenomenon results in a huge variability in the postsynaptic responses (see Figure). The talk will compare the different forms of synaptic plasticity within the hippocampus, present some of the underlying molecular mechanisms.



Supported by the DFG Schm 1383/3-3 and the SFB 618 'Theoretical Biology'.

# GABAergic interneurons at the cellular and network level

Hannah Monyer

Department of Clinical Neurobiology, Univ. Heidelberg, INF 364, 69120 Heidelberg, Germany.

Analysis of single identified neurones in acute brain slices with respect to their electrophysiological and molecular characteristics revealed cell-specific use of different genetic mechanisms in the generation of functionally different glutamate receptors. The question as to the functional significance of different AMPA receptors on interneurons at the system level will be discussed. We have approached this problem by generating transgenic mice with altered AMPA receptors in interneurons. Thus, mice lacking the GluR-D subunit showed altered LTP, perturbed synchronous network activity and changed behaviour in hippocampus-dependent tasks.

In addition, gap junction-forming proteins and their differential expression in the central nervous system appears to be a key determinant for synchronous oscillatory network activity. Expression and functional data will be presented and the functional significance of gap junctions at the cellular and system level will be discussed. Furthermore, we have GFP-tagged different neuronal gap junction proteins to investigate their localization in different neuronal compartments.

Furthermore, using transgenic approaches we have generated mice in which the in vivo marker EGFP is expressed in specific interneurone subpopulations. The easy identification of neuronal subpopulation in the acute slice preparation will help in the functional characterization of native receptors in neurones that are critical in controlling network behaviour. These mice will also help in establishing the participation of specific neuronal cell types for the generation of synchronous oscillatory activity at specific frequencies. Furthermore, in these mice it is easy to identify intercellular communication via electrical synapses and establish their contribution for rhythmic oscillatory network activity.

## Symposia

- [#S1](#) Threshold currents: modulators of neuronal excitability  
JR. Schwarz, Hamburg
- [#S2](#) Amyloid and Neurodegeneration  
K. Fassbender, Göttingen
- [#S3](#) Ion channels and transporters in the cochlea: from current to molecule to pathology  
J. Engel and M. Knipper, Tübingen
- [#S4](#) Pushing toward the limits of what insects can know: Case studies for comparative cognition  
M. Giurfa and B. Smith, Toulouse and Columbus
- [#S5](#) Signals in early neural development  
T. Pieler and E. Pera, Göttingen
- [#S6](#) Brain plasticity and cognition: cellular mechanisms and clinical perspectives  
E. Fuchs and G. Kempermann, Göttingen and Berlin
- [#S7](#) Extracellular matrix molecules in regeneration and synaptic plasticity  
CG. Becker, A. Dityatev, T. Becker, Hamburg
- [#S8](#) Efference Copies and Corollary Discharge Mechanisms in Sensory and Mental Processing  
B. Hedwig and JFA. Poulet, Cambridge
- [#S9](#) Real time processing vs. variability of neural responses  
RM. Hennig and B. Ronacher, Berlin
- [#S10](#) Plasticity and Task-Dependence of Auditory Processing  
FW. Ohl and H. Schulze, Magdeburg
- [#S11](#) The integrated role of glial cells in the CNS: new methodological approaches  
P. Bezzi and C. Schipke, Lausanne and Berlin
- [#S12](#) Cellular and molecular control of vertebrate neurogenesis  
A. von Holst, Bochum
- [#S13](#) Use of two-photon fluorescence microscopy to study neuronal calcium signalling in brain slices and in the intact brain  
R. Kurtz and J. Waters, Bielefeld and Heidelberg
- [#S14](#) Neuronal injury and infection  
R. Nau and W. Brück, Göttingen

- [#S15](#) Nitric oxide / cyclic nucleotide signaling as regulator of developmental processes and cell motility in the nervous system  
G. Bicker and V. Rehder, Hannover and Atlanta
- [#S16](#) New vistas on insect vision  
R. Strauss and R. Wolf, Würzburg
- [#S17](#) Genomic and Proteomic Expression Profiling in Neural Repair  
J. Verhaagen and HW. Müller, Amsterdam and Düsseldorf
- [#S18](#) Brain-Computer-Interfaces (BCI): neuroprostheses for the paralyzed  
U. Strehl, Tübingen
- [#S19](#) Neural mechanisms of visual perception and learning in man and monkey  
G. Rainer, Tübingen
- [#S20](#) Amyotrophic Lateral Sclerosis (ALS) and Motoneuron Disease: From basic molecular and cellular mechanisms to novel clinical applications  
BU. Keller, J. Weishaupt, M. Bähr, Göttingen
- [#S21](#) What the nose tells the brain - News and views in olfactory coding  
I. Manzini and F. Zufall, Göttingen and Baltimore
- [#S22](#) Function of the glial cell line derived neurotrophic factor family in development and disease  
H.Peterziel, KH. Schäfer, K. Unsicker, Heidelberg
- [#S23](#) Possible mechanisms contributing to memory consolidation during sleep  
S. Gais and J. Born, Lübeck
- [#S24](#) Comparative insights into genetic and activity-dependent mechanisms of CNS development  
C. Lohr and C. Duch, Kaiserslautern and Berlin

**Symposium #S1:**  
**Threshold currents: modulators of neuronal excitability**  
**JR. Schwarz, Hamburg**

**Introduction**

[#S1](#) JR. Schwarz, Hamburg  
*Threshold currents: modulators of neuronal excitability*

**Slide**

[#S1-1](#) D. Isbrandt, HC. Peters, H. Hu, JF. Storm and O. Pongs, Hamburg and Oslo (N)  
*Transgenic mouse models for the study of M-channels*

[#S1-2](#) DA. Brown, London (UK)  
*KCNQ/M-currents*

[#S1-3](#) CK. Bauer, W. Hirdes, M. Schweizer, KS. Schuricht, SS. Guddat, I. Wulfsen and JR. Schwarz, Hamburg  
*Neuronal  $erg K^+$  currents*

[#S1-4](#) JF. Storm, H. Hu, K. Vervaeke and N. Gu, Oslo (N)  
*Threshold currents in hippocampal neurons*

[#S1-5](#) H-C. Pape, T. Kanyshkova, L. Caputi, R. Staak, C. Abrahamczyk, T. Munsch and T. Budde, Magdeburg  
*I<sub>h</sub>: pacemaker current for rhythmic activities in the thalamus during sleep and epilepsy*

[#S1-6](#) J. Röper, Marburg  
*Molecular determinants and function of A-type currents in dopaminergic midbrain neurons*

**Poster**

[#1A](#) T. Geisel, B. Naundorf and F. Wolf, Göttingen  
*Dynamic Response Properties of Type-I Excitable Membranes*

## **Introductory Remarks to Symposium 1**

### **Threshold currents: modulators of neuronal excitability**

**Jürgen R. Schwarz, Hamburg**

Information processing within the brain involves the generation of action potentials which are responsible for fast communication between nerve cells. Action potentials have a short duration and are generated by a transient influx of  $\text{Na}^+$  and a subsequent outflow of  $\text{K}^+$  through voltage-gated ion channels. In addition to these canonical channels, nerve cells are equipped with a large number of voltage-gated and  $\text{Ca}^{2+}$ -gated ion channels which are able to modulate the action potential parameters. These "threshold currents" do not only influence the threshold potential, they can also change the action potential duration, induce various forms of afterhyperpolarizations and set the interspike interval. By modulating the shape of action potentials and spiking patterns they are able to change information processing in neurons, thus contributing to neuronal plasticity.

$I_h$  and M-current belong to the most important threshold currents.  $I_h$  is a pacemaker current, mediated by hyperpolarization-activated cyclic-nucleotide-gated cation channels (HCN). The M-current is mediated by members of the family of voltage-gated KCNQ channels. One important function of M-currents is the induction of frequency adaptation. The current mediated by ether-à-go-go-related gene  $\text{K}^+$  channels (erg) takes part in repolarizing the heart action potential. Erg channels have recently been shown to also modulate neuronal electrical activity. The symposium includes the A-type current mediated by voltage-gated  $\text{K}^+$  channels of the Kv4 family, and  $\text{Ca}^{2+}$ -gated SK channels. Both types of current are involved in the modulation of the frequency of action potential firing.

The symposium will start with an overview of the transgenic animal models which are used to study the properties of e.g. KCNQ, ERG and HCN channels. The following talks will cover the molecular and biophysical properties of each of the channels and provide insight into the study of their complex subunit composition and mechanisms of regulation underlying their physiology. The chosen speakers have expert knowledge about the molecular properties and physiology of the ion channels mediating the different types of threshold currents.

## **Transgenic mouse models for the study of M-channels**

Dirk Isbrandt<sup>1</sup>, H. Christian Peters<sup>1#</sup>, Hua Hu<sup>2#</sup>, Johan F. Storm<sup>2</sup>, Olaf Pongs<sup>1</sup>

<sup>1</sup> Institut für Neurale Signalverarbeitung, Zentrum für Molekulare Neurobiologie Hamburg, Martinistrasse 52, 20246 Hamburg, Germany

<sup>2</sup> Department of Physiology, Institute of Basal Medical Sciences, and Centre for Molecular Biology and Neuroscience, University of Oslo, PB 1103, Blindern, N-0317 Oslo, Norway

The presentation will give an overview on mouse models presently available for the study of M-channels and primarily focus on our own work. M-channels have been implicated in inherited human epilepsy linked to mutations in KCNQ2 or KCNQ3. We generated transgenic mice with a conditional functional M-channel knockout in brain. M-current-deficient mice developed spontaneous seizures, marked morphological alterations in hippocampus and conspicuous behavioral hyperactivity. Hippocampal CA1 neurons of these mice exhibited markedly increased excitability, reduced spike frequency adaptation, attenuated medium afterhyperpolarization amplitudes, and altered intrinsic resonance properties. Restriction of transgene expression to defined developmental periods revealed that attenuation of M-current in the first weeks of life was correlated with the development of morphological alterations. In contrast, mice that had functional M-channels during this period developed normal hippocampi albeit their CA1 neurons showed similar changes in their biophysical properties. As adults, these mice showed only a mild hyperactivity, but also signs of abnormally increased neuronal excitability and cognitive deficits. Our results strongly support the notion that M-channels are critical determinants of cellular and neuronal network excitability; their attenuation has far-reaching consequences for brain morphology, behavior and cognitive performance.

## KCNQ/ M - currents

David A. Brown.

*Department of Pharmacology, University College London  
Gower Street, London, WC1E 6BT, UK*

M-current was originally identified as a voltage-gated K-current with a threshold of around -60 mV, which activated relatively slowly (in tens of msec) with membrane depolarization, and which served to dampen repetitive spike discharges rather than to repolarize individual action potentials (Adams & Brown, 1980; Brown et al., 1982; Brown, 1988). A key property was its inhibition following stimulation of muscarinic acetylcholine receptors (hence the "M"), with consequent facilitation or induction of spike trains. More recently, it has been established that the subunits of the channels responsible for this current are composed of members of the KCNQ (Kv7) gene family – most notably KCNQ2 and 3 (Wang et al., 1998) - though all members of this family (KCNQ1-5) can generate M-like currents (Jentsch, 2000; Selyanko et al., 2000). KCNQ1 is confined to the heart, epithelial and smooth muscle, and KCNQ4 primarily to the auditory system, but KCNQ2,3 and 5 are widely distributed in the central and peripheral nervous system. Minor mutations in human KCNQ2 and 3 genes cause a form of juvenile epilepsy (Benign Familial Neonatal Convulsions, BFNC), while mutations in KCNQ4 generate a form of progressive deafness. In mice, deletion of the KCNQ2 gene is postnatally lethal in homozygotes, while heterozygotes show enhanced sensitivity to epileptogenic agents (Watanabe et al., 2000).

Some outstanding questions with respect to their role in neuronal function are as follows:

- (1). Most native M-channels appear to be formed by heteromeric assembly of KCNQ3 with KCNQ2 and/or KCNQ5 (e.g., Shah et al., 2002; Hadley et al., 2003). To what extent does subunit composition affect kinetics and function? Likewise, KCNQ2 and 3 show multiple splice variants, some of which affect current kinetics (Pan et al., 2001): how important is this?
- (3). Why are the effects of spontaneous mutations in human KCNQ2 transient? Is it because of secondary neuronal adaptation (Okada et al., 2003) or is there developmental substitution by other subunits? Recent experiments on KCNQ2 'knock-out' mice will be described in this context.
- (4). Some evidence suggests that KCNQ channels are involved in pain regulation (Passmore et al., 2003): what other specific neuronal functions are they important for?

## References.

- Adams, P.R. et al. (1982). *J. Physiol.* 330, 537-572  
 Brown, D.A. & Adams, P.R. (1980). *Nature*, 283, 673-676.  
 Brown, D.A. (1988). *Ion Channels*, ed. T.Narahashi, 1, 55-99  
 Hadley, J.K. et al. (2003). *J. Neurosci.*, 22, 5012-5019  
 Jentsch, T.J. (2000). *Nat. Revs. Neurosci.*, 1, 21-30.  
 Okada, M. et al. (2003). *Epilepsy Res.*, 53, 83-94  
 Pan, Z. et al. (2001). *J. Physiol.* 531, 347-358.  
 Passmore, G.M. et al. (2003). *J. Neurosci.*, 23, 7227-7236  
 Selyanko, A.A. et al. (2000). *J. Physiol.*, 522, 349-355.  
 Shah, M.M. et al. (2002). *J. Physiol.* 544, 29-37.  
 Wang, H-S. et al. (1998). *Science*, 282, 1890-1893.  
 Watanabe, H. et al (2000). *J. Neurochem.*, 75, 28-33.



## Neuronal erg K<sup>+</sup> currents

Christiane K. Bauer<sup>1</sup>, Wiebke Hirdes<sup>1</sup>, Michaela Schweizer<sup>2</sup>, Kristina S. Schuricht<sup>1</sup>, Saskia S. Guddat<sup>1</sup>, Iris Wulfsen<sup>1</sup>, Jürgen R. Schwarz<sup>1</sup>

Institute of Applied Physiology<sup>1</sup> and Center for Molecular Neurobiology, ZMNH<sup>2</sup>, University Hospital Hamburg-Eppendorf, University of Hamburg, Martinistr. 52, D-20246 Hamburg.

Erg (eag-related gene) K<sup>+</sup> channels form one subfamily of the voltage-gated EAG (ether-à-go-go gene) K<sup>+</sup> channels and consist of three members, erg1-3. The best known function of an erg current is its contribution to the repolarization of the heart action potential. Inherited or acquired malfunction of erg channels induce one form of long QT syndrome (LQT-2) which may lead to heart arrhythmia and sudden death. In the heart, only isoforms of erg1 are expressed, whereas erg2 and erg3 subunit expression has been described to be nervous system-specific (Shi et al., 1997). Erg-mediated currents have also been recorded in various other types of excitable cells, e.g. in neuroblastoma cells, smooth muscle fibres and neuroendocrine cells. In these cell types erg currents serve the function of threshold currents, which modulate cell excitability, e.g. by changing the resting membrane potential (reviewed by Bauer and Schwarz, 2001). Since erg channels exhibit an inverse gating behaviour with inactivation being faster than activation, and recovery from inactivation being faster than deactivation, they are functional inward rectifier channels.

In rat brain, the three erg-channels are differentially expressed (Saganich et al., 2001). Erg1 is present predominantly in several brainstem nuclei and in the cerebellum, erg2 in olfactory bulb mitral cells and erg3 in neurons of the cerebral cortex and hippocampus. A recent study by Papa et al. (2003) confirmed these results, but also demonstrated a more generalized expression of the three erg channels in the rat brain. Up to now, little information is available concerning the biophysical properties of neuronal erg currents and their possible function. There is only one report about erg currents in mice Purkinje cells (Sacco et al., 2003).

We have now characterized a fast erg current in neurons dissected from the median part of rat embryonic rhombencephala (E15-16) in primary culture. A relatively uniform erg-like current was regularly found in large multipolar serotonergic neurons, and occurred also in other neurons less well characterized. This current was sensitive to the antiarrhythmic substance E-4031 confirming that it was carried by erg channels. Single-cell RT-PCR revealed the expression of erg1a, erg1b, erg2 and erg3 mRNA in different combinations in large multipolar neurons exhibiting erg current. These cells regularly contained neuronal tryptophan hydroxylase, a key enzyme for serotonin production. A comparison of the neuronal erg current with erg1a, erg1b, erg2 and erg3 currents in CHO cells showed that the voltage- and time-dependence of activation and deactivation of the native current was within the range determined for the heterologously expressed erg currents. Our data suggest that the erg channels in rat embryonic rhombencephalon neurons may be heteromultimers formed by different erg channel subunits.

Bauer CK & Schwarz JR (2001). *J Membr Biol* **182**, 1-15.

Papa M, Boscia F, Canitano A, Castaldo P, Sellitti S, Annunziato L et al. (2003). *J Comp Neurol* **466**, 119-135.

Sacco T, Bruno A, Wanke E & Tempia F (2003). *J Neurophysiol* **90**, 1817-1828.

Saganich MJ, Machado E & Rudy B (2001). *J Neurosci* **21**, 4609-4624.

Shi W, Wymore RS, Wang HS, Pan Z, Cohen IS, McKinnon D et al. (1997). *J Neurosci* **17**, 9423-9432.

Supported by the Deutsche Forschungsgemeinschaft

## Threshold currents in hippocampal neurons

Johan F. Storm, Hua Hu, Koen Vervaeke and Ning Gu

*Institute of Physiology, IMB and Centre for Molecular Biology and Neuroscience,  
University of Oslo, 0317 Oslo, Norway.*

In addition to the fast and large ionic currents underlying the action potentials, neurons are equipped with a range of ion channel types that primarily operate in the sub-threshold voltage range, i.e. at membrane potentials negative to the action potential threshold. Although the sub-threshold currents mediated by these channels are relatively small, they can play pivotal roles in determining the spike timing, frequency and pattern in response to stimuli, thus shaping the information processing of the neuron.

Accordingly, neuronal ion channels may be crudely divided into three functional classes: (1) Those activated in the sub-threshold voltage range, i.e. even prior to occurrence of an action potential, thus being able to influence the initial spike timing and patterning, and to some extent spike threshold, amplitude and duration. (2) Those that rapidly activate and deactivate during the action potential, primarily serving to generate the spike itself. (3) Channels that activate during the spike, but remain open for longer, thus causing afterpotentials and feedback regulation of excitability and subsequent spiking. The latter class include several calcium-activated channels that cause after-hyperpolarizations (AHPs), after-depolarizations (ADPs), and related spike frequency adaptation and bursting.

In this presentation I will focus on ion channels that primarily operate in the sub-threshold voltage range in CA1 hippocampal pyramidal cells – an intensively studied cell type of special interest in relation to certain forms of learning and memory, as well as to brain disorders like epilepsy, brain ischemia, and dementia.

First, I will discuss channels that regulate excitability and spike timing in response to excitatory stimuli, including temporal integration, postsynaptic modulation of excitatory synaptic input, and modulation of the threshold for long-term synaptic plasticity. Further, mechanisms of sub-threshold resonance that provide a basis for coherent network oscillations will be discussed. Such oscillations are correlated with behavioural states. In particular, CA1 pyramidal neurons show resonance at theta ( $\theta$ ) frequencies (2-7 Hz) and participate in  $\theta$  network oscillations during exploration, spatial learning and REM sleep. We combined whole-cell recordings from CA1 pyramidal cells and computational modelling to study the mechanisms underlying  $\theta$ -resonance. Oscillating current injections revealed clear  $\theta$  resonance with peak impedance at 2-7 Hz, while the three underlying sub-threshold currents were measured by voltage clamp: (1) M-current ( $I_M$ ) and (2) persistent  $\text{Na}^+$  current ( $I_{\text{NaP}}$ ) both activated positive to  $-65\text{mV}$ , and (2) h-current ( $I_h$ ) activated negative to  $-65\text{mV}$ . Current clamp recordings and computer simulations showed that these cells have two forms of  $\theta$  resonance: *M-resonance* generated by the M-current and persistent  $\text{Na}^+$  current in depolarized cells, and *H-resonance* generated by the h-current in hyperpolarized cells. Our subsequent studies of transgenic mice lacking M-current, showed that these animals lacked *M-resonance* and were impaired in hippocampus-dependent learning (Peters et al., *submitted*). These results suggest a novel function for M-/KCNQ-channels in the brain: to facilitate neuronal resonance and network oscillations in cortical neurons, thus providing a basis for an oscillation-based neural code.

Next, I will discuss mechanisms of spike repolarization and modulation of action potential duration, and finally mechanisms and functions of after-potentials and feedback regulation of excitability in CA1 hippocampal pyramidal cells. The focus will be on the roles of several types of voltage- and Ca-activated channels (A, D, M, h, BK, SK, sAHP, NaP channels), in causing and regulating AHPs, ADPs, spike frequency adaptation and bursting, including the mechanisms underlying the sequence of three AHPs: the fast (fAHP), the medium (mAHP), and the slow AHP. In particular, a novel role of the persistent Na current in feed-back regulation of excitability, spike frequency and dynamic range will be discussed. The presentation is based on previous and recent results from intracellular, somatic and dendritic whole-cell recordings from CA1 pyramidal cells, using current- and voltage clamp, as well as dynamic clamp and detailed computational modelling of the electrical activity in this cell type.

1. Ramakers, G.M.J., and Storm, J.F. (2002). *Proc Nat Acad Sci USA* 99: 10144-10149.
2. Storm, J.F. (1988) *Nature* 336: 379-381
3. Hu, H., Vervaeke, K., and Storm, J.F. (2002). *J. Physiology* 545: 783-805.
4. Storm, J.F. (1987) *J Physiol* 385: 733-759
5. Shao, L.-R. et al. *J Physiol* 521: 135-146.
6. Hu, H. et al. *J Neurosci* 21: 9585-9597.
7. Storm, J.F. (1989) *J Physiol* 409: 171-190
8. Pedarzani, P. and Storm, J.F. (1995). *Proc Nat Acad Sci USA* 92:11716-20.
9. Pedarzani, P. and Storm, J.F. (1993). *Neuron* 11: 1023-1035.
10. Sailer, C.A., et al. (2002) *J Neurosci* 22:9698-707
11. Vervaeke K, Hu H, Storm JF. (2004) *FENS Abstr.* Vol 3
12. Gu, N, Hu H, Vervaeke, K and Storm JF (2004) *FENS Abstr.* Vol 3
13. Peters H.C., Hua H., Pongs O., Storm J.F., Isbrandt, D. (submitted)

## $I_h$ : pacemaker current for rhythmic activities in the thalamus during sleep and epilepsy

*Hans-Christian Pape, Tatyana Kanyshkova, Luigi Caputi, Rainer Staak, Christian Abrahamczyk, Thomas Munsch, and Thomas Budde*

Institut für Physiologie, Medizinische Fakultät, Otto-von-Guericke-Universität,  
39120 Magdeburg

The neurons and synaptic networks of the thalamo-cortical system that maintain rhythmic electroencephalographic activities during sleep are considered important elements also for the generation of spike-and-wave discharges characterizing absence seizure during petit-mal epilepsies. Rhythmogenesis in this system largely depends on intrinsic pacemaker properties of thalamic neurons and their synaptic interrelations. Through the use of established genetic rat models of absence epilepsy, the Wistar Albino Glaxo Rats from Rijswijk (WAG-Rij) and the Genetic Absence Epilepsy Rats from Strasbourg (GAERS), dysfunctions could be identified on the molecular, cellular and systems level that are critically involved in seizure generation. One focus is on the hyperpolarization-activated cyclic-nucleotide (HCN) gated channels and the respective current ( $I_h$ ), which function as important pacemakers for rhythmic neuronal activity during sleep. Our present results indicate that the expression pattern and properties of the channel proteins are altered in the thalamus from epileptic compared with non-epileptic animals, in a period of time prior to seizure occurrence. In vivo, pharmacological blockade of HCN channels resulted in a prolongation of burst discharges in thalamo-cortical relay neurons related to spike-and-waves on the electroencephalogram during spontaneous absence seizures. In vitro analyses in thalamo-cortical neurons revealed a hyperpolarizing shift in the voltage dependence of  $I_h$  in epileptic compared with non-epileptic control animals, due to an impaired regulation by intracellular cyclic AMP that was associated with an increased expression of HCN1 subunits possessing low cyclic AMP sensitivity. Functionally, this dysfunction of  $I_h$  prevented the shift from burst to tonic firing in thalamo-cortical neurons, thereby facilitating the generation of spike-wave discharges during absence seizures.

In summary, these results indicate that HCN channels control rhythmic activities in thalamic synaptic networks during spike-and-wave discharges and that in imbalance in the expression pattern of HCN subunits results in an impaired regulation by intracellular cyclic nucleotide that, in turn, makes an important contribution to absence seizure generation and epileptogenesis.

*Supported by grants from the Deutsche Forschungsgemeinschaft*

## **Molecular determinants and function of A-type currents in dopaminergic midbrain neurons**

Jochen Röper

Institute of Physiology, Philipps-University Marburg, Germany

Fast inactivating voltage-gated potassium (A-type K) channels are present in many central and peripheral neurons where they control integration of synaptic inputs and spontaneous discharge. Somatodendritic A-type channels are oligomeric protein complexes, which contain pore-forming  $\alpha$ -subunits of the Kv4-family as well as auxiliary beta-subunits of the KChip- and DPPX-family. We used qualitative and quantitative single-cell mRNA expression profiling to address the functional and molecular diversity of  $\alpha$ - $\beta$  combination in identified dopaminergic (DA) midbrain neurons. DA neurons in the substantia nigra (SN) expressed Kv4.3 and Kchip3 mRNAs and fast-inactivating A-type K channels. The number of functional A-type K channels in single DA SN neurons was linearly correlated with the number of Kv4.3 and KChip3 cDNA molecules detected by single-cell real-time RT-PCR indicating a tight transcriptional control of the functional pool of A-type K channels in individual neurons. In addition, the number of functional A-type K channels determined the spontaneous firing rate of SN DA neurons. DA neurons in the ventral tegmental area (VTA) possessed slowly inactivating A-type K currents and expressed additional KChip subunit mRNAs. Quantitative single-cell RT PCR experiments revealed a correlation between the ratio of KChip4/KChip1 cDNA and the inactivation kinetics of A-type K currents. Immunocytochemical experiments revealed that KChip4 protein is preferentially expressed in DA neurons projecting to prefrontal cortical areas in contrast to subcortical areas like dorsal striatum and nucleus accumbens. We currently carry out experiments to understand the functional role of slowly inactivating KChip4-containing A-type K channels in meso-prefrontal DA neurons.

# Dynamic Response Properties of Type-I Excitable Membranes

Theo Geisel, Björn Naundorf, Fred Wolf

*Dept. of Nonlinear Dynamics, Max-Planck Institut für Strömungsforschung, Göttingen, Germany*

We study the dynamic response properties of Type-I neuronal oscillators in the presence of either a temporally correlated or an uncorrelated noise in a generalization of the  $\theta$ -neuron [1,2] with an adjustable action potential onset speed. We calculate the transmission functions for small sinusoidal modulations in the mean input current and in the noise amplitude.

Surprisingly the decay of the transmission function in the high frequency limit is completely independent of the action potential onset dynamics and however strongly depends on the phase  $\theta_s$  of the oscillator at which a spike is emitted: If at  $\theta_s$  the dynamics is insensitive to external inputs, the transmission function decays as (i)  $\omega^{-3}$  for the case of a modulation of a white noise input and as (ii)  $\omega^{-2}$  for a modulation of the mean input current in the presence of a correlated and uncorrelated noise as well as (iii) in the case of a modulated amplitude of a correlated noise input. If the insensitivity condition is lifted, the transmission function always decays as  $\omega^{-1}$ , as in conductance based neuron models and in contrast to integrate-and-fire models, which predict a non-decaying transmission function in the high frequency limit.

Using a novel sparse matrix representation of the Fokker-Planck operator we compute the full transmission function for arbitrary frequencies and both types of input stimulation. We show that frequencies up to the stationary rate of the neuron are in general transmitted unattenuated. In the classical  $\theta$ -neuron, the transmission function decays rapidly to zero for larger frequencies. When the action potential onset speed is increased this decay can be shifted to very large frequencies up to 1kHz, where the transmission amplitude for modulations in the noise amplitude is typically much larger for high frequencies than for a modulation in the mean input current.

Our results identify the generalized  $\theta$ -neuron as a simple phase neuron model, which, while still being tractable analytically, accurately reproduces the dynamic response properties of real neurons. They corroborates and extend recent reports [3,4], indicating that integrate-and-fire models are incapable of mimicking the dynamical response properties of conductance based model neurons. In addition our new method provides efficient computational tools for the analysis of dynamical neuronal responses.

[1] Ermentrout GB, Kopell N (1986). Parabolic bursting in an excitable system coupled with a slow oscillation. *SIAM-J. Appl.-Math.*, **2**

[2] Gutkin BS, Ermentrout GB. (1998). Dynamics of membrane excitability determine interspike interval variability: a link between spike generation mechanisms and cortical spike train statistics. *Neural Comput.*, **10**

[3] Naundorf B, Geisel T, Wolf F. (2003). The Intrinsic Time Scale of Transient Neuronal Responses. [xxx.lanl.gov, physics/0307135](http://xxx.lanl.gov/physics/0307135), e-print

[4] Fourcaud-Trocm  , Hansel D, van Vreeswijk C, Brunel N. (2003). How spike generation mechanisms determine the neuronal response to fluctuating inputs. *J Neurosci.*, **23**

This work was supported by the Max-Planck Society.

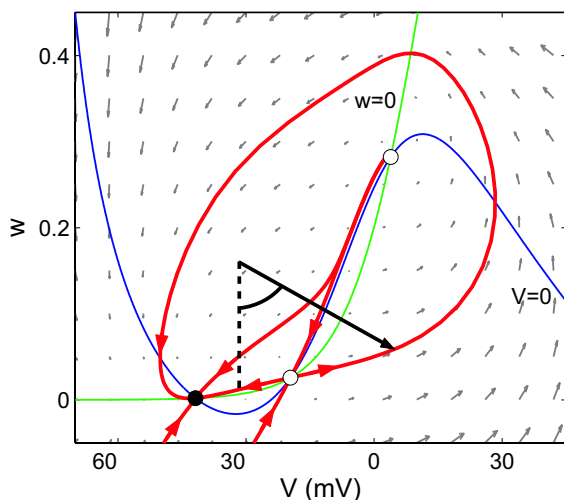


FIGURE 1: Sketch of the phase reduction of the Morris-Lecar conductance based neuron model leading to the  $\theta$ -neuron. The complex 2-dimensional dynamics of the conductance based model is reduced to the dynamics on the invariant manifolds depicted in red. The remaining dynamical parameter is the phase  $\theta$ . The null-clines are denoted by  $V = 0$  and  $w = 0$ .

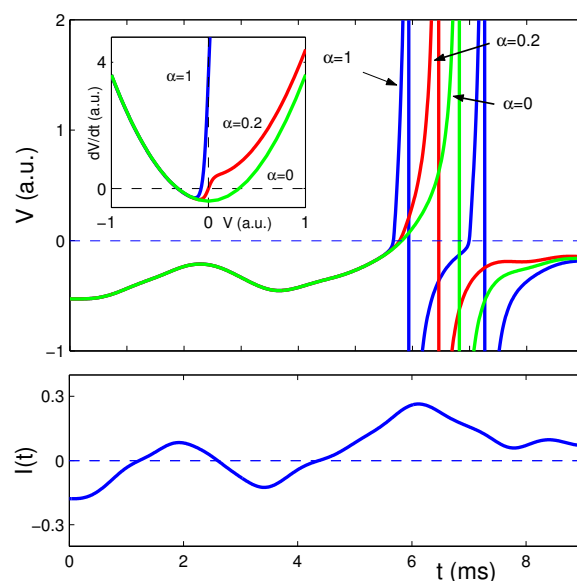


FIGURE 2: Example trajectories of the generalized  $\theta$ -neuron with increasing values of the action potential onset speed (top: green  $\rightarrow$  blue) subject to the same fluctuating input current  $I(t)$  (bottom). Once the unstable fixed point, denoted by the dashed line, is crossed, an action potential is initiated.

**Symposium #S2:  
Amyloid and Neurodegeneration  
K. Fassbender, Göttingen**

**Introduction**

[#S2](#) K. Fassbender, Göttingen  
*Amyloid and Neurodegeneration*

**Slide**

[#S2-1](#) M. Jucker, M. Herzig, M. Meyer-Lühmann, J. Coomaraswamy, R. Radde, T. Bolmont and S. Käser, Tübingen  
*Transgenic Mouse Models of Cerebral Amyloidosis*

[#S2-2](#) M. Heikenwälder and A. Aguzzi, Zürich (CH)  
*Immunobiology of peripheral prion pathogenesis*

[#S2-3](#) S. Walter, Y. Liu, M. Letiembre and K. Fassbender, Göttingen  
*Innate immunity and neurodegeneration*

[#S2-4](#) TA. Bayer, O. Wirths, C. Schmitz, C. Casas, P. Benoit, G. Tremp, V. Blanchard, G. Multhaup and L. Pradier, Homburg/Saar, Maastricht (NL), Paris (F) and Berlin  
*Intraneuronal A $\beta$  as a major risk factor for neurodegeneration in Alzheimer's disease*

[#S2-5](#) K. Beyreuther, Heidelberg  
*Amyloid and axonal transport*

**Poster**

[#2A](#) C. Touma, O. Ambrée, N. Görtz, K. Keyvani, R. Palme, W. Paulus and N. Sachser, Munich, Muenster and Vienna (A)  
*Behavioural and Endocrine Alterations in a Transgenic Mouse Model of Alzheimer's Disease: Early Indicators of Neuropathological Changes?*

[#3A](#) P. Gorlovoi, M. Stagi, I. Bartoszek and H. Neumann, Göttingen  
*Dimerization of the microtubulin associated protein tau induced by inflammatory mediators.*

[#4A](#) S. Klopffleisch, M. Schmitz, S. Klöppner and HH. Althaus, Göttingen  
*Simvastatin Affects Oligodendroglial Process Formation*

[#5A](#)

GJ. Burbach, R. Hellweg, CA. Haas, D. Del Turco, U. Deicke, D. Abramowski, M. Jucker, M. Staufenbiel and T. Deller, Frankfurt, Berlin, Freiburg, Basel (CH) and Tübingen

*Induction of brain-derived neurotrophic factor (BDNF) in plaque-associated glial cells of aged APP23 transgenic mice*

## **Introductory Remarks to Symposium 2**

### **Amyloid and Neurodegeneration**

**Klaus Fassbender, Göttingen**

Since most neurodegenerative diseases share the key feature of a deposition of pathologically folded amyloidogenic proteins, e.g., Alzheimer's disease (amyloid peptide), Parkinson's disease ( $\alpha$ -synuclein), amyotrophic lateral sclerosis (SOD), Huntington's disease (huntingtin), certain forms of ataxia (ataxin) and even prion diseases (prion-protein), common mechanisms could contribute to neuronal injury in these different disorders. Therefore, this symposium targets on such rather universal mechanisms how excessive formation and deposition of these different peptides may ultimately injure brain tissue.

M. Jucker will report key tools for investigation of neurodegenerative diseases, i.e., animal models of cerebral amyloidoses. Prion diseases, although representing a very specific group of diseases, possess striking similarities with Alzheimer's disease, e.g., the progressive accumulation of pathologically folded proteins. The molecular biology of these diseases will be covered by A. Aguzzi. Neuroinflammation is a histopathological feature of nearly all of these neurodegenerative diseases. The role of innate immunity receptors in Alzheimer's disease, prion diseases and further neurodegenerative diseases will be discussed (K. Fassbender). T. Bayer will address the potential importance of the intraneuronal accumulation of amyloid peptide in mediation of neurodegeneration in Alzheimer's disease. Finally K. Beyreuther will discuss general principles of neuronal damage by amyloid, focusing on the crucial relationship between amyloid and axonal transport in Alzheimer's disease, the prototype of brain amyloidoses.



## Transgenic Mouse Models of Cerebral Amyloidosis

Mathias Jucker, Martin Herzig, Melanie Meyer-Lühmann, Janaky Coomaraswamy, Rebecca Radde, Tristan Bolmont, Stephan Käser

Department of Cellular Neurology, Hertie-Institute for Clinical Brain Research, University of Tübingen, D-72076 Tübingen, Germany

Cerebral proteopathy is a unifying term for cerebral neurodegenerative diseases in which aggregated proteins are abnormally deposited in the brain. The hallmark proteopathy is Alzheimer's disease (AD) in which fibrillar amyloid- $\beta$  (A $\beta$ ) peptide is deposited extracellularly in the form of parenchymal plaques, as well as in the vasculature resulting in cerebral amyloid angiopathy (CAA). To understand how abnormal protein processing and aggregation leads to cerebral amyloidosis, cellular dysfunction, and dementia, several amyloid precursor protein (APP) transgenic mouse models have been generated that develop, to varying degrees, the age-related deposition of parenchymal vs. vascular amyloid. Results reveal that shifting the ratio of neuronally-produced A $\beta$ 40:42 towards A $\beta$ 42 favors the production of parenchymal amyloid plaques, while shifting the ratio towards A $\beta$ 40 favors A $\beta$  deposition in the form of cerebral amyloid angiopathy. Cerebral amyloidosis can be initiated and accelerated in a time- and concentration-dependent manner by the intracerebral injection of AD brain extracts into young transgenic mice. However, injections of various synthetic amyloid preparations do not induce amyloidosis, suggesting that additional factors such as chaperones, or different A $\beta$  conformations, are necessary for the initiation of cerebral amyloidosis *in vivo*. The further understanding of the mechanism of cerebral amyloidosis and its relationship to neuronal dysfunction is crucial for current developments in anti-A $\beta$  therapeutic strategies.

## **Immunobiology of peripheral prion pathogenesis**

Mathias Heikenwälder and Adriano Aguzzi.

Institute of Neuropathology, Universitätsspital Zürich. Schmelzbergstrasse 12, CH-8091 Zürich, Switzerland.

### **Abstract**

For more than two decades it has been contended that prion infection does not elicit immune responses: transmissible spongiform encephalopathies do not go along with conspicuous inflammatory infiltrates, and antibodies to the prion protein are typically undetectable. Why is it, then, that prions accumulate in lymphoid organs, and that various states of temporal or genetically modified immune deficiency prevent peripheral prion infection and replication? There is current evidence of the involvement of the immune system in prion diseases, while attempting to trace the elaborate mechanisms by which peripherally administered prions invade the brain and ultimately provoke damage. The investigation of these questions leads to unexpected detours, including the neurophysiology and microarchitecture of secondary lymphoid organs as well as migration of lymphocytes induced by pro-inflammatory cytokines or homeostatic chemokines.

**Innate immunity and neurodegeneration**

Silke Walter, Yang Liu, Maryse Letiembre, K. Fassbender

Department of Neurology, University of Goettingen  
Robert Koch Str. 40, 37075 Göttingen  
Tel: 0551-39-6715, Fax: 0551-39-8014

Neuroinflammation is a histopathological feature of many neurodegenerative diseases that are associated with deposition of pathologically folded amyloidogenic proteins, e.g., Alzheimer's disease. Recent observations link the innate immunity with Alzheimer's disease and possibly related diseases associated with deposits of aggregated proteins. The key innate immunity receptor, the LPS receptor (CD14) was shown to interact with fibrils of amyloid peptide and to mediate microglial activation and release of neurotoxic inflammatory products after stimulation with this peptide. Further studies revealed presence of the LPS receptor in brains of patients with Alzheimer's disease. Together, this data suggests that the LPS receptor, CD14 may contribute to the overall neuroinflammatory response to amyloid peptide, highlighting the possibility that the progress currently being made in the field of innate immunity could be extended to research on neurodegenerative diseases.

## **Intraneuronal A $\beta$ as a major risk factor for neurodegeneration in Alzheimer's disease**

Thomas A. Bayer<sup>1</sup>, Oliver Wirths<sup>1</sup>, Christoph Schmitz<sup>2</sup>, Caty Casas<sup>3</sup>, Patrick Benoit<sup>3</sup>, Günter Tremp<sup>3</sup>, Veronique Blanchard<sup>3</sup>, Gerd Multhaup<sup>4</sup>, and Laurent Pradier<sup>3</sup>

- 1 Department of Psychiatry, Division of Neurobiology, University of Saarland, Medical Faculty, Homburg/Saar, Germany
- 2 Department of Psychiatry and Neuropsychology, Division of Cellular Neuroscience, University of Maastricht, Maastricht, The Netherlands
- 3 Aventis Pharma S.A., CNS/Alzheimer Group and Functional Genomics, Centre de Recherche de Paris, Vitry sur Seine, France
- 4 Institute for Biochemistry, Free University of Berlin, Germany

**Background:** According to the 'amyloid hypothesis of Alzheimer's disease',  $\beta$ -amyloid is the primary driving force in Alzheimer's disease pathogenesis. Despite the development of many transgenic mouse lines developing abundant  $\beta$ -amyloid-containing plaques in the brains, the actual link between amyloid plaques and neuron loss has not clearly been established yet as reports on neuron loss in these models have remained controversial. **Objective(s):** We investigated double-transgenic mice expressing human mutant amyloid precursor protein APP751 (KM670/671NL and V717I) and human mutant presenilin-1 (PS1 M146L) named APP751/PS1, or with the M233T/L235P early onset FAD mutations knocked-in in the presenilin-1 gene named APP751/PS1KI. **Methods:** We used molecular-neuropathological methods and unbiased stereologic image analyses. **Results:** We identified substantial age-related neuron loss in the hippocampal pyramidal cell layer of APP751/PS1 double-transgenic mice at 16 months of age. The loss of neurons was observed at sites of A $\beta$  aggregation and surrounding astrocytes but, most importantly, was also clearly observed in areas of the parenchyma distant from plaques. Moreover, the APP751/PS1KI mice produce abundant A $\beta$ 42 with an advanced onset of plaque formation, which correlated to the PS-1 knock-in gene dosage. At the age of six months the mice hemizygous for APP751 and homozygous for PS1KI revealed a dramatic hippocampal neuron loss predominantly in CA1. Before plaque formation, we identified Thioflavin-S positive intraneuronal aggregates, which were also positive for A $\beta$  immunoreactivity in cortical and hippocampal neurons. Predominantly CA1 and subicular pyramidal neurons were affected, however, many other neurons in the cortex were also positive depending on the number of PS1KI alleles. The same held true for the amount of neuron loss in an age related manner. **Conclusions:** Both models elicit abundant neuron loss in the hippocampus. The APP751/PS1KI mouse model shows major neuropathological hallmarks with abundant neuron loss that is clearly independent from extracellular amyloid deposition and identifies intraneuronal A $\beta$  as a major neurotoxic risk factor.

## **Behavioural and Endocrine Alterations in a Transgenic Mouse Model of Alzheimer's Disease: Early Indicators of Neuropathological Changes?**

Chadi Touma<sup>1</sup>, Oliver Ambrée<sup>2</sup>, Nicole Görtz<sup>2</sup>, Kathy Keyvani<sup>3</sup>, Rupert Palme<sup>4</sup>, Werner Paulus<sup>3</sup>, Norbert Sachser<sup>2</sup>

<sup>1</sup>Department of Behavioural Neuroendocrinology, MPI of Psychiatry, Munich, Germany

<sup>2</sup>Department of Behavioural Biology, University of Muenster, Germany

<sup>3</sup>Institute of Neuropathology, University of Muenster, Germany

<sup>4</sup>Institute of Biochemistry, University of Veterinary Medicine Vienna, Austria

Alzheimer's disease (AD) is the most prevalent neurodegenerative disorder worldwide. In recent years, genetically modified mice are increasingly used as animal models to unravel the underlying mechanisms and possible treatments of the disease.

We investigated behavioural, endocrine and neuropathological alterations during the course of the disease in the TgCRND8 mouse line, a transgenic mouse model of AD.

Our results show that transgenic (Tg) and wild-type (Wt) mice did not differ in their general health status, exploratory and anxiety related behaviour as well as in the activity of their sympathetic-adrenomedullary system. Significant differences, however, were found regarding body weight, amyloid plaque formation, and the activity of the hypothalamic-pituitary-adrenocortical (HPA) axis. Continuous monitoring of glucocorticoid (GC) concentrations, utilizing faecal hormone metabolite analysis, revealed that Tg animals of both sexes showed adrenocortical hyperactivity. It is hypothesized that these changes in the activity of the HPA axis are linked to amyloid- $\beta$  associated pathological alterations in the hippocampus, causing degenerations in the negative feedback regulation of the HPA axis leading to hypersecretion of GC. Furthermore, distinct alterations in the spontaneous behaviour were observed well before amyloid deposits in the brain are described. Compared to Wt animals, Tg mice showed higher general home cage activity and displayed significantly higher frequencies of stereotypic behaviours, which were paralleled by increased GC concentrations.

Thus, the development of adrenocortical hyperactivity as well as stereotypic behaviours might represent early indicators of neuropathological changes in the brain and could promote our understanding of AD.

## **Dimerization of the microtubulin associated protein tau induced by inflammatory mediators.**

**Philippe Gorvoloi, Massimiliano Stagi, Ilonka Bartoszek and Harald Neumann**

**Neuroimmunology Unit, European Neuroscience Institute Goettingen,  
Germany**

Intracellular tau aggregation in neurites is the major component of neurofibrillary tangles in Alzheimer's disease and other neurodegenerative tauopathies. The exact molecular mechanism of tau aggregation is not known. Genetic mutations of tau and extracellular deposits of amyloid- $\beta$  peptide oligomers have been shown to facilitate aggregation of tau and to be diseases-causative.

To analyze whether inflammatory cytokines such as tumor necrosis factor- $\alpha$  (TNF- $\alpha$ ) have any effects on dimerization/polymerization of tau in neurons, we performed fluorescence lifetime-based fluorescence resonance energy transfer (FRET) analyses of cultured primary neurons transfected with 441 amino acids human normal tau tagged to green fluorescent protein (GFP) and its variants (YFP and Cerulean).

The transfected tau tagged to GFP interacted with tubulin as demonstrated by FRET between GFP-tau and beta-tubulin, labeled with monoclonal antibodies conjugated with Cy3. Treatment of neurons with nitric oxide or TNF- $\alpha$  for 1 hour resulted in dimerization/polymerization of tau, which demonstrated by FRET showed shifting in the lifetime of the Cerulean in cells, cotransfected with Cerulean-tau and YFP-tau. Dimerization occurred preferentially in neurites compare to the cell body.

The data demonstrate that inflammatory mediators are prevalent in degenerative brain diseases, induce dimerization/ polymerization of tau and might be involved in the first steps of neurofibrillary tangle formation.

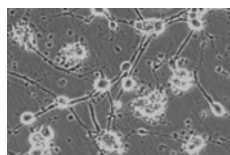
## Simvastatin Affects Oligodendroglial Process Formation

Klopfleisch S., Schmitz M., Klöppner S., Althaus HH

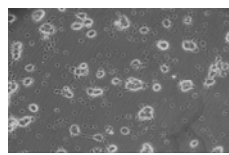
MPI exp Medicine, AG 8600, H-Reinstr.3, 37075 Göttingen

E-mail: klopfleisch@em.mpg.de

Statins are therapeutically used for reducing an elevated cholesterol level. Recently, several studies have reported about immunomodulatory effects of statins. Based on these findings, statins were subsequently discussed as therapeutics for multiple sclerosis (MS) (1). Concerning remyelination, another challenge of MS treatment, statins could, however, interfere with oligodendroglial process formation and myelin production. To address this question, we exposed cultured pig oligodendrocytes (OL) to Simvastatin (Sst), which is used in ongoing MS studies. Our first results showed that Sst reduced the cholesterol content in OL. Oligodendroglial process formation was retarded (+/-NGF); already formed



processes were  
mevalonate but not  
reversed this effect



retracted. Addition of  
PEG-cholesterol  
indicating that

intermediates such as farnesylpyrophosphate and geranylpyrophosphate were no longer provided due to an inhibition of HMG-CoA-reductase via Simvastatin. Indeed, MAPK activity of OL exposed to Sst was reduced compared to controls as evidenced by an in-gel-kinase assay. A possible effect on p21Ras is presently under investigation.

Supported by the Hertie Foundation

1. Wekerle H (2002): Tackling multiple sclerosis. Nature 420: 39-40

**Induction of brain-derived neurotrophic factor (BDNF) in plaque-associated glial cells of aged APP23 transgenic mice.**

Guido J. Burbach<sup>1</sup>, Rainer Hellweg<sup>2</sup>, Carola A. Haas<sup>3</sup>, Domenico Del Turco<sup>1</sup>, Uwe Deicke<sup>2</sup>, Dorothee Abramowski<sup>4</sup>, Mathias Jucker<sup>5</sup>, Matthias Staufenbiel<sup>4</sup>, and Thomas Deller<sup>1</sup>

<sup>1</sup>Institute of Clinical Neuroanatomy, J. W. Goethe University, Frankfurt, Germany; <sup>2</sup>Department of Psychiatry and Psychotherapy, Charité (CBF), 14050 Berlin, Germany; <sup>3</sup>Institute of Anatomy and Cell Biology, University of Freiburg, Freiburg, Germany; <sup>4</sup>Novartis Institutes of BioMedical Research Basel, Basel, Switzerland; <sup>5</sup>Hertie-Institute for Clinical Brain Research, University of Tübingen, Tübingen, Germany

Brain-derived neurotrophic factor (BDNF) is a versatile neurotrophic factor that has been implicated in cell survival, cell differentiation, axonal growth, and activity-dependent synaptic plasticity. Changes in BDNF expression have also been reported during the course of several neurological disorders, including Alzheimer's disease (AD). The role of BDNF in AD, however, has remained elusive. To learn more about this neurotrophic factor, we investigated BDNF expression in brain of amyloid precursor protein overexpressing mice (APP23 transgenic mice). *In situ* hybridization revealed BDNF mRNA signals associated with amyloid plaques. Laser microdissection in combination with quantitative RT-PCR demonstrated a six-fold increase of BDNF mRNA in the immediate plaque-vicinity, a three-fold increase in a tissue ring surrounding the plaque, and control levels in inter-plaque areas comparable to those measured in age-matched non-transgenic mice. Double-immunofluorescence localized BDNF to microglial cells and astrocytes surrounding the plaque. Cortical BDNF protein levels were quantified by ELISA demonstrating a more than ten-fold increase compared to age-matched controls. This upregulation of BDNF protein significantly correlated with the  $\beta$ -amyloid load in the transgenic animals. Taken together, our data demonstrate a plaque-associated upregulation of BDNF in APP23 transgenic mice, and implicate this neurotrophin in the regulation of inflammatory and axonal growth processes in the plaque-vicinity.



**Symposium #S3:**

**Ion channels and transporters in the cochlea: from current to molecule to pathology**

**J. Engel and M. Knipper, Tübingen**

**Introduction**

- [#S3](#) J. Engel and M. Knipper, Tübingen  
*Ion channels and transporters in the cochlea: from current to molecule to pathology*

**Slide**

- #S3-1 M. Knipper, Tübingen  
*Short introduction to the function of the cochlea*
- [#S3-2](#) CJ. Kros, SL. Johnson and W. Marcotti, Brighton (UK)  
*From action potential to receptor potential: developmental changes in inner hair cell signalling.*
- [#S3-3](#) T. Moser and A. Brandt, Göttingen  
*Coupling of Ca<sup>2+</sup> channels and exocytosis at hair cell ribbon synapses*
- [#S3-4](#) J. Engel, M. Knirsch, M. Michna, N. Waka, S. Münkner, C. Braig and M. Knipper, Tübingen  
*Development, characteristics and function of inner and outer hair cell calcium channels*
- [#S3-5](#) D. Oliver, Freiburg  
*Prestin, an anion transporter modified to generate ultrafast cellular motility in auditory outer hair cells*
- [#S3-6](#) H. Winter, C. Braig, U. Zimmermann, J. Cimerman and M. Knipper, Tübingen  
*Transcriptional control of ion channels prior to hearing function*
- [#S3-7](#) TJ. Jentsch, Hamburg  
*Pathology of cochlear ion transport: insights from deaf mice and humans*

**Poster**

- [#6A](#) C. Braig, H. Winter, M. Knirsch, U. Zimmermann, K. Rohbock, I. Köpschall, J. Engel and M. Knipper, Tuebingen  
*SK2 IN THE COCHLEA*

- [#7A](#) C. Harasztosi, B. Müller, T. Kaneko and AW. Gummer, Tuebingen  
*Ca<sup>2+</sup> SIGNALS IN THE STEREOCILIA OF OUTER HAIR CELLS*
- [#8A](#) K. Löffler, S. Fink, F. Grauvogel, A. Koitschev and M. Langer, Ulm and Tübingen  
*Stiffness changes of cochlear hair bundles induced by ATP*
- [#9A](#) J. Cimerman, H-S. Geissler, U. Zimmermann, C. Braig, H. Winter and M. Knipper, Tuebingen  
*PRESTIN - YEAST-BASED SCREENING FOR PUTATIVE INTERACTION PARTNERS*
- [#10A](#) L. Rüttiger, SB. Kilian and M. Knipper, Tübingen  
*Alteration of behavior and responses of auditory neurons after application of Salicylate in an animal model for Tinnitus*

### **Introductory Remarks to Symposium 3**

#### **Ion channels and transporters in the cochlea: from current to molecule to pathology**

**Jutta Engel and Marlies Knipper, Tübingen**

Hearing impairment is one of the most common sensory disorders and the second most common chronic disease. 15 million people are affected in Germany and 350 million people worldwide. Regarding the socio-economic and epidemiological relevance of hearing deficits and the still very limited therapeutic strategies to treat hearing impairments/deafness, a deeper understanding of hearing function is required. In particular, the molecular components and the cellular mechanisms of cochlear inner and outer hair cell function need to be identified. Using physiological studies and transgenic mouse techniques, multiple ion channels and transporters with cochlea-specific characteristics have been identified and characterised. The special demands of the highly sensitive hearing organ seem to be met by the expression of specialised ion channels and transporters, which appear in the critical developmental period of final cochlear differentiation prior to the onset of hearing. The functional analysis and phenotyping of mouse mutants will help to unravel and understand corresponding sensorineural hearing loss in humans.

Prior to the onset of hearing, a subset of ion channels with a distinct expression develops in hair cells (Speaker: Corne Kros), a process which is paralleled by the maturation of exocytosis in the inner hair cell (Speaker: Tobias Moser). Specialised isoforms of distinct cochlear channels such as calcium channels (Speaker: Jutta Engel), the transporter-like membrane motor prestin (Speaker: Dominik Oliver) and the potassium channels KCNQ4, BK, and SK2 are precisely regulated during the critical period of final differentiation that precedes the onset of hearing (Speaker: Harald Winter/Marlies Knipper). These distinct channels as well as other cochlear ion channels and transporters have been defined as novel deafness genes (Speaker: Thomas Jentsch).

### From action potential to receptor potential: developmental changes in inner hair cell signalling

Corné J. Kros, Stuart L. Johnson and Walter Marcotti

*School of Life Sciences, University of Sussex, Falmer, Brighton BN1 9QG, UK*

Inner hair cells (IHCs) are the primary sensory receptors in the mammalian cochlea. The cells respond to sound with fast, graded receptor potentials. However, before the onset of hearing at postnatal day 12 (P12), mouse inner hair cells (IHCs) fire spontaneous and evoked action potentials (Kros et al., 1998). These action potentials are likely to induce release of neurotransmitter onto afferent nerve endings (Beutner & Moser, 2001). We are investigating developmental changes in the expression of ion channels that underlie this switch in the function of IHCs.

IHCs can first be recognized just after terminal mitosis at embryonic day 14 (E14). At this early stage small and slowly activating delayed-rectifier  $K^+$  currents can be recorded and these currents gradually increase in size during further embryonic and postnatal development (Marcotti et al., 2003a). From E16.5 onwards IHCs express a  $Ca_v1.3$   $Ca^{2+}$  current (Platzer et al., 2000) and a TTX-sensitive ( $K_D$  4.8 nM)  $Na^+$  current (Marcotti et al., 2003b). This mix of currents enables the IHCs to fire spontaneous action potentials between E17.5 and P6 (the day of birth, P0, being equivalent to E19.5 in CD-1 mice). The  $Ca^{2+}$  current is necessary for the action potentials whereas the  $Na^+$  current shortens the inter-spike interval.

From just after birth until the onset of hearing, IHCs are transiently innervated by efferent nerve fibres en route to the outer hair cells. During this time the cells hyperpolarize in response to ACh application (Glowatzki & Fuchs, 2000), due to secondary activation of an SK current by  $Ca^{2+}$  flowing in through  $\alpha 9\alpha 10$  nicotinic ACh receptors (Marcotti et al., 2004b). Efferent activity would thus lead to inhibition of spontaneous action potentials. Surprisingly, the SK current is also important for sustaining repetitive action potentials, in the absence of ACh. This is because the SK current can also be activated by  $Ca^{2+}$  influx through  $Ca_v1.3$   $Ca^{2+}$  channels (Marcotti et al., 2004b).

In the second postnatal week IHCs can still fire action potentials in response to current injection, but no longer spontaneously. An inward rectifier,  $I_{K1}$ , that increases in size during this period is mainly responsible by hyperpolarizing the resting potential (Marcotti et al., 1999), together with a hyperpolarizing shift in activation and an increase in size of the delayed rectifier currents (Marcotti et al., 2003a).

The transition to a functionally mature sensory receptor comes about at the onset of hearing by the expression of a large BK current,  $I_{K,f}$ , with extremely fast activation kinetics. This current is unusual in that it appears insensitive to extracellular  $Ca^{2+}$  but is activated by  $Ca^{2+}$  released from intracellular stores (Marcotti et al., 2004a). At the same time an additional delayed-rectifier  $K^+$  current,  $I_{K,n}$ , that activates at very hyperpolarized potentials is expressed. This current takes over the role of  $I_{K1}$ , which is downregulated at the onset of hearing, in setting the resting potential of mature IHCs (Marcotti et al., 2003a; Oliver et al., 2003).

### Supported by the MRC and the Wellcome Trust

Beutner D, Moser T (2001) *J Neurosci* 21:4593-4599

Glowatzki E, Fuchs PA (2000) *Science* 288:2366-2368

Kros CJ, Ruppersberg JP, Rüsch A (1998) *Nature* 394:281-284

Marcotti W, Géléoc GSG, Lennan GWT, Kros CJ (1999) *Pflügers Arch* 439:113-122

Marcotti W, Johnson SL, Holley MC, Kros CJ (2003a) *J Physiol* 548:383-400

Marcotti W, Johnson SL, Rüsch A, Kros CJ (2003b) *J Physiol* 552:743-761

Marcotti W, Johnson SL, Kros CJ (2004a) *J Physiol* 557:613-633

Marcotti W, Johnson SL, Kros CJ (2004b) *J Physiol* in press

Oliver D, Knipper M, Derst C, Fakler B (2003) *J Neurosci* 23:2141-2149

Platzer J et al (2000) *Cell* 102:89-97

### **Coupling of $\text{Ca}^{2+}$ channels and exocytosis at hair cell ribbon synapses**

Tobias Moser & Andreas Brandt, Department of Otolaryngology and Center for Molecular Physiology of the Brain, University of Goettingen

Hearing relies on the synchronous synaptic transfer between hair cells and auditory nerve. We have investigated stimulus-secretion coupling in cochlear inner hair cells (IHCs) from normal mice and mouse mutants lacking the  $\text{Ca}_v1.3$  L-type  $\text{Ca}^{2+}$  channel. Normal IHCs from the low-frequency part of the cochlea hold about 1.800  $\text{Ca}^{2+}$  channels and about 10 ribbon synapses. The IHC  $\text{Ca}^{2+}$  current is reduced by ~ 90 % when  $\text{Ca}_v1.3$  channels are genetically deleted and this results in a ~ 90 % block of exocytosis. Pharmacological inhibition of the  $\text{Ca}_v1.3$  channels by dihydropyridines causes a linear reduction of exocytosis arriving at a maximal reduction of  $\text{Ca}^{2+}$  current and exocytosis of ~90 %. We interpret the dihydropyridine effect as shifting channels to the mode zero, hence reducing the number of available channels. Modulating the number of channels by changes in membrane potential also resulted in a linear modulation of release until the peak  $\text{Ca}^{2+}$  current potential was reached. When passing beyond we obtained more exocytosis for the same  $\text{Ca}^{2+}$  current when compared to potentials in the rising limb of the current voltage relationship. On the contrary, we observed a supralinear dependence of exocytosis on the  $\text{Ca}^{2+}$  current when we modulated the single channel current by changes in extracellular  $\text{Ca}^{2+}$  or by the fast flickering blocker  $\text{Zn}^{2+}$ . Our data suggest that readily releasable vesicles of the hair cell ribbon synapse are under the control of a few channels per vesicle, imposing their nanodomain  $\text{Ca}^{2+}$  onto the release site.

## Development, characteristics and function of inner and outer hair cell calcium channels

Jutta Engel, Martina Knirsch, Marcus Michna, Nobuhiko Waka, Stefan Münkner, Claudia Braig<sup>1</sup>, Marlies Knipper<sup>1</sup>

Institute of Physiology Dept. II and Dept. of Otolaryngology, Tübingen Hearing Research Centre THRC, University of Tübingen, Germany; <sup>1</sup>Department of Otolaryngology, Tübingen Hearing Research Centre THRC, University of Tübingen, Germany  
Email: jutta.engel@uni-tuebingen.de

Mammals have two types of cochlear hair cells (HC), inner hair cells (IHCs) and outer hair cells (OHCs). IHCs transmit sound-evoked deflections of their stereocilia into graded receptor potentials which open voltage-activated  $\text{Ca}^{2+}$  channels that in turn trigger exocytosis. In contrast, OHCs act as cochlear amplifiers and guarantee the unique sensitivity and frequency selectivity of the mammalian inner ear.

IHCs and OHCs express L-type  $\text{Ca}^{2+}$  channels before and after the onset of hearing. Neonatal IHC currents serve the generation of  $\text{Ca}^{2+}$  action potentials [1-3], (immature) synaptic transmission [2-4], and gene expression. Whole-cell  $\text{Ca}^{2+}$  channel currents in mouse IHCs were rapidly activating, showed 11.1 % inactivation of the peak current with 10 mM  $\text{Ba}^{2+}$  (OHCs: 3.6 %) and 21.1 % with 10 mM  $\text{Ca}^{2+}$  (OHCs: 50.7 %) after 300 ms and activated at very negative potentials (-65 mV) with physiological extracellular (1.3 mM)  $\text{Ca}^{2+}$ . They were of L-type because  $I_{\text{Ba}}$  increased to 292 % (OHCs: 178 %) by 5  $\mu\text{M}$  Bay K 8644 and were partially inhibited by 44 - 90 % by the DHP antagonists nifedipine, nimodipine and isradipine (3 - 10  $\mu\text{M}$ ).  $I_{\text{Ba}}$  densities of  $\text{Ca}_v1.3^{-/-}$  IHCs and OHCs were reduced by >90 % indicating that the vast majority of IHC and OHC presynaptic  $\text{Ca}^{2+}$  channels are of class D L-type [5,6]. Apart from the difference in  $\text{Ca}^{2+}$ -dependent inactivation and Bay K 8644-sensitivity, neonatal OHCs showed only 38 % of the  $I_{\text{Ba}}$  density compared to IHCs.

Upon the onset of hearing, IHCs  $\text{Ca}^{2+}$  channel currents decline [2,3] which is probably due to maturation and increased efficiency of the IHC presynapse. Current decline was more pronounced in OHCs in which 10-15 pA  $I_{\text{Ba}}$  remained at P19.  $\text{Ca}_v1.3$ -specific transcripts could still be amplified at P30 in OHCs (and IHCs) by RT-PCR suggesting that afferent signalling to type II fibres nevertheless might work in mature OHCs. The effect of  $\text{Ca}_v1.3$  gene disruption for phenotypic maturation of IHCs and OHCs will be discussed.

Supported by DFG grants En 294/2,1-4

### Literature cited:

- [1] Kros, C.J. et al. 1998. Nature 394, 281-284.
- [2] Beutner, D. and T. Moser. 2001. J. Neurosci. 21, 4593-4599.
- [3] Marcotti, W., et al. 2003. J. Physiol. 552, 743-761.
- [4] Glowatzki E, Fuchs PA. 2002. Nat. Neurosci. 5, 147-154.
- [5] Platzner, J., et al. 2000. Cell 102, 89-97
- [6] Michna, M., et al. 2003. J. Physiol. 553, 747-758

## **Prestin, an anion transporter modified to generate ultrafast cellular motility in auditory outer hair cells**

Dominik Oliver

Physiologisches Institut II, Universität Freiburg, Hermann-Herder-Str. 7, 79104 Freiburg, Germany

Outer hair cells (OHC) of the mammalian cochlea actively change their cell length in response to changes in membrane potential. This type of cellular movement – termed electromotility – occurs at acoustic frequencies up to at least tens of Kilohertz and is assumed to produce the amplification of vibrations in the cochlea that enables the high sensitivity and frequency selectivity of the mammalian hearing organ.

Electromotility results from a membrane protein of the OHC that is highly enriched in the basolateral membrane. This protein is voltage sensitive, changing its conformation in response to de- or hyperpolarisation. Coupling of protein conformation to transmembrane voltage is mediated by a charged 'voltage sensor' within the protein that can move through the membrane's electrical field. Consequently, cell contraction or elongation always goes along with an electrical charge transfer across the membrane. This charge can be measured either as a transient current (similar to the gating current of ion channels) or as a voltage dependent 'non-linear' capacitance (NLC). Since all properties of NLC reflect electromotility itself and NLC can be measured conveniently using patch-clamp techniques, NLC has usually been used to characterize the behaviour of the motor protein.

Dallos and coworkers cloned the motor protein from an OHC cDNA library and named it prestin. Upon heterologous expression, prestin reproduces all hallmarks of the OHC electromotility. In particular, (i) it generates mechanical force upon electrical stimulation with constant amplitude and phase up to a frequency of at least 20 kHz, (ii) it generates a voltage driven charge movement, equivalent to the NLC of OHCs. In fact, in prestin knock-out mice electromotility is lost and cochlear sensitivity is greatly reduced. Sequence homology classifies prestin as the fifth member of a larger superfamily of anion transporters, termed SLC26. It is a hydrophobic membrane protein of 744 amino acids with hydrophilic N- and C-termini, both located in the cytoplasm.

We are interested in the mechanism by which voltage controls protein conformation in prestin.

To address this question, we used neutralization of charged residues in the core region of prestin by site-directed mutagenesis to map out the voltage sensor of prestin. However, this did not abolish NLC. In contrast, it turned out that removal of monovalent anions from the cytoplasmic side but not the extracellular side completely removed NLC as well as electromotility. Moreover, the characteristics of NLC and electromotility were directly dependent on the species and concentration of monovalent anions at the cytoplasmic side of the membrane.

The model that arises suggests that prestin binds monovalent anions at the cytoplasmic face. The anion itself then confers at least part of the voltage sensitivity to prestin. After binding to a site with millimolar affinity, the anion is translocated across the membrane by the transmembrane voltage: towards the extracellular surface upon hyperpolarization, towards the cytoplasmic side in response to depolarization. As a consequence, this translocation triggers conformational changes of the protein that finally change its dimensions in the plane of the plasma membrane. The area occupied by prestin decreases when the anion is near the cytoplasmic face of the membrane (short state, equivalent to cell contraction), it increases when the ion has crossed the membrane to the outer surface (long state equivalent to cell elongation). Thus, prestin works as an 'incomplete transporter' that shuttles anions across the membrane without allowing them to dissociate at the extracellular surface of the cell.

Future research will be directed towards the identification of protein domains involved in anion binding, translocation and coupling to conformational changes.

**Transcriptional control of ion channels prior to hearing function**

Winter Harald, Braig Claudia, Zimmermann Ulrike, Cimerman Jelka, Knipper Marlies

University of Tuebingen, Molecular Neurobiology, THRC Tuebingen Hearing Research Center, Elfriede-Aulhorn-Str. 5, 72076 Tuebingen, Germany.

During analysis of the expression profile of different ion channels upregulated prior to the onset of hearing (Kv, Kir4.1, KCNQ4, BK, SK2, Prestin) we learned that ion channels can be subdivided in two groups which are under differential transcriptional control of thyroid hormone (TH). Both mechanisms are even realized within a single outer hair cell, presented by prestin the OHC motor protein and KCNQ4, the potassium channel protein responsible for the major OHC K<sup>+</sup> conductance. The distribution of these proteins overlap extensively, occupying the entire OHC membrane from P6 onwards. Towards P12, in conjunction with the onset of hearing, the cellular distribution of both proteins is simultaneously converted to neighboring subcellular areas, the basal pole in the case of KCNQ4 and the lateral wall for prestin, a process differentially controlled by thyroid hormone (TH). While TH enhances expression of the prestin gene, it has a permissive effect on the KCNQ4 gene through derepression of the TRalpha1 aporeceptor, shown as a direct negative suppressive effect of a TH response element (TRE-KCNQ4) on KCNQ4 promoter activity. TRbeta, in contrast, appears to be involved in the timing of prestin's redistribution, but not that of KCNQ4. Data indicate that TH target genes can differ in their sensitivity to TH receptors even within single cells. Most interestingly, it appears that hair cell ion channels upregulated during the earlier postnatal time period of the cochlea are regulated like prestin, while those upregulated during the most final differentiation process of hair cells appear to be negatively controlled by TRalpha1. The results are discussed in the context of a novel role for TRalpha1 for final OHC differentiation and a possible function of TH to influence neuronal activity of fibers and fiber reorganisation processes through the control of hair cell ion channels.

This work was supported by the Deutsche Forschungsgemeinschaft DFG RU 403, SFB

430/Kni-B3, DFG Kn 316 4-1



**Pathology of cochlear ion transport: insights from deaf mice and humans**

Thomas J. Jentsch

Zentrum für Molekulare Neurobiologie, ZMNH,  
Universität Hamburg

Ion homeostasis is essential for the hearing process. Depolarizing K influx into sensory hair cells through apical mechanosensitive channels requires a high K concentration (150 mM) in the scala media. It is generated by the epithelium of the stria vascularis which needs basolateral Cl channels for the recycling of Cl taken up by NaK2Cl cotransport. These channels are ClC-K/barttin heteromers. Mutations in barttin lead to Bartter syndrome IV, which combines severe renal salt loss with congenital deafness.

K leaves outer hair cells (OHCs) through KCNQ4 K channels. KCNQ4 mutations lead to slowly progressive hearing loss in humans. After exiting OHCs, K must be removed by supporting Deiter's cells which express the K-Cl cotransporters KCC3 and KCC4. Knock-out of either cotransporter leads to deafness in mice, with KCC3 disruption resulting in a slowly progressing hearing loss that is associated with hair cell degeneration. In addition, KCC4 KO leads to renal tubular acidosis, while the mice lacking KCC3 display severe neurodegeneration similar to patients with Anderman syndrome who also lack KCC3.

## SK2 IN THE COCHLEA

Braig, Claudia<sup>1</sup>, Winter, Harald<sup>1</sup>, Knirsch, Martina<sup>2</sup>, Zimmermann Ulrike<sup>1</sup>, Rohbock, Karin<sup>1</sup>, Köpschall, Iris<sup>1</sup>, Engel, Jutta<sup>2</sup>, Knipper, Marlies<sup>1</sup>.

<sup>1</sup> University of Tuebingen, Molecular Neurobiology, Tuebingen Hearing Research Center THRC, Elfriede-Aulhorn-Str.5, 72076 Tuebingen, Germany

<sup>2</sup> University of Tuebingen, Institute of Physiology Dept. II and Dept. of Otolaryngology, Tuebingen Hearing Research Centre THRC, Elfriede-Aulhorn-Str.5, 72076 Tuebingen, Germany

Hair cells are the targets of olivocochlear fibers that carry efferent inhibitory feedback from the brain. In particular, IHCs initially are contacted by olivocochlear efferent fibers that make contacts with IHCs before targeting OHCs (Simmons et al., 1996). In the adult system IHCs are innervated mainly by afferent fibers, having few if any remaining efferent contacts (Liberman et al., 1990). In contrast, adult OHCs are the principal targets of cholinergic olivocochlear efferents (Guinan, 1996). The efferent feedback to IHCs and OHCs is predominantly provided by the release of acetylcholine (ACh), that acts on AChR  $\alpha 9/\alpha 10$  subunits. In OHCs and IHCs calcium influx through the receptor complex is presumed to activate nearby calcium-dependent SK2 channels, leading to inhibitory postsynaptic currents (Oliver et al., 2000; Elgoyhen et al., 1994, 2001; Glowatzki et al., 2000). Accordingly, we note the localization of SK2 channel protein during the early (IHC), respectively late (OHC) postnatal period.

Aiming to identify transcriptional regulators for SK2 we could identify thyroid hormone (TH) as one of the presumptive modulators. While under hypothyroid conditions the SK2 protein in OHCs is completely absent most interestingly SK2 expression persists in IHCs.

Using *in situ* hybridisation, immunohistochemistry, reporter gene study, RT-PCR and EMSA we start to elucidate the obvious differential regulatory role of TH on SK2 ion channels in IHCs and OHCs.

Supported by a grant from the Deutsche Forschungsgemeinschaft DFG 316/3-1; DFG316/4-1 and SFB430/KniB3.

## **Ca<sup>2+</sup> SIGNALS IN THE STEREOCILIA OF OUTER HAIR CELLS**

Csaba Harasztosi, Barbara Müller, Toshihiko Kaneko, Anthony W. Gummer

Eberhard Karls University Tübingen, Department of Otolaryngology, Tübingen Hearing

Research Centre, Section of Physiological Acoustics and Communication, Germany

(e-mail: csaba.harasztosi@uni-tuebingen.de)

Ca<sup>2+</sup> ions play important roles in the function of outer hair cells (OHCs). In general, elevated intracellular Ca<sup>2+</sup> levels in hair cells can initiate transmitter release, activate K(Ca<sup>2+</sup>) channels, and modulate receptor current through mechanosensitive channels in their stereocilia. Although information about the regulation of the intracellular Ca<sup>2+</sup> level in the stereocilia of lower vertebrates is available, there is no information about mammalian systems.

The goal of the present experiments was to investigate the origin of Ca<sup>2+</sup> signals in the hair bundle of freshly isolated OHCs from an adult mammalian hearing organ, the guinea-pig cochlea. Ca<sup>2+</sup> transients were evoked by deflection of the stereocilia using a fluid-jet stimulator, which contained Ca<sup>2+</sup>-rich (4 mM) Hanks' balanced salt solution. The stimulus was a single 5 s pulse, which deflected the stereocilia in the depolarizing direction. Intracellular Ca<sup>2+</sup> changes were monitored using the acetoxymethyl ester form of the fluo-3 dye. The fluorescence signal was detected by a confocal laser scanning microscope, in framescan (1 s/frame) and linescan (2 ms/line) modes. The time course of the onset of the intracellular Ca<sup>2+</sup> transient of 6 cells was exponential; the average time constant ( $\tau$ ) was  $0.26 \pm 0.19$  s. Application of the transduction channel blocker dihydropyridine (DHP, 100  $\mu$ M) caused the speed of the Ca<sup>2+</sup> elevation to become significantly slower,  $\tau = 2.14 \pm 1.36$  s; this change was partially reversible ( $\tau = 0.75 \pm 0.24$  s) after washout. Application of DHP did not influence the steady-state amplitude of the Ca<sup>2+</sup> transients. The decay of the intracellular Ca<sup>2+</sup> signal after removal of the fluid-jet stimulus was also exponential; the time constant was  $3.15 \pm 1.31$  s. Linescan images indicated that Ca<sup>2+</sup> ions enter the stereocilia at the basal third of the hair bundle and diffuse to the tip with a speed of approximately 0.1 mm/s.

In conclusion, the observation that DHP reduces the rate of Ca<sup>2+</sup> entry, but not the steady-state Ca<sup>2+</sup> concentration, suggests that Ca<sup>2+</sup> entry into the stereocilia of these cells is not restricted to the transduction channels.

## Stiffness changes of cochlear hair bundles induced by ATP

<sup>1</sup>Karsten Löffler, <sup>1</sup>Stefan Fink, <sup>1</sup>Francois Grauvogel, <sup>2</sup>Assen Koitschev, <sup>1</sup>Matthias G. Langer

<sup>1</sup> Department of Applied Physiology, University of Ulm, Germany

<sup>2</sup> Tübingen Hearing Research Center (THRC), University of Tübingen, Germany

The cochlea is the organ of hearing in mammals and embeds the organ of Corti with the mechanosensitive cells - the hair cells. The rod-like stereocilia located on top of these sensory cells are graded in height and transduce mechanical stimuli into electrical signals by the so-called mechanoelectrical transduction channel. Displacement of stereocilia by incoming sound increases tension of so-called tip links, pulling directly at the transduction channel. Thus, stiffness of stereocilia is critical for sensitivity of the transducer channel to applied forces. Since it is known that ATP-sensitive P2X-receptors are located in the hair bundle the effect of extracellular ATP-concentrations on stereocilia stiffness for different ATP-concentrations was investigated. Elasticity measurements were performed approaching an AFM tip to the top of cochlear hair bundles from the rat under light microscopic control. Individual stereocilia were displaced in excitatory and inhibitory direction scanning the AFM tip across the entire hair bundle. Experiments were performed using a new experiment control and automation software called ScanClamp. It supports arbitrary definition of measurement protocols and some 2D/3D visualization modes. Thereby not only precise control of the AFM setup but also of electrophysiology equipment like patch clamp amplifiers can be achieved in the same software environment.

For further information:

Sensory Biophysics Group: [http://physiologie.uni-ulm.de/pages/langer\\_team.html](http://physiologie.uni-ulm.de/pages/langer_team.html)

ScanClamp: <http://scanclamp.thrc.de>

## **PRESTIN - YEAST-BASED SCREENING FOR PUTATIVE INTERACTION PARTNERS**

Cimerman, Jelka, Hyun-Soon, Geissler, Zimmermann, Ulrike, Braig, Claudia, Winter, Harald, Knipper, Marlies.

University of Tuebingen, Molecular Neurobiology, Tuebingen Hearing Research Center THRC, Elfriede-Aulhorn-Str. 5, 72076 Tuebingen, Germany.

Membrane-based electromotility, the phenomenon of rapid length change produced by electrical stimulation of an outer hair cell (OHC), is mediated by a voltage-dependent motor protein prestin. Prestin, identified as a member of the SLC26 superfamily of anion-bicarbonate transporters (Zheng et al., 2000) is expressed in the cochlear OHCs and emerging evidence points to prestin as an eligible candidate/ regulator responsible for the cochlear amplifier (Oliver et al. 2001, Dallos et al. 2002). It is now established, that prestin is redistributed towards the lateral membrane prior to the onset of hearing (Weber et al., 2002). Recent studies in our laboratory show that the failing of the redistribution during hypothyroidism leads to hair cells which are able to generate motility but no force (Zimmermann, Knipper et al., in preparation). It is unknown whether the prestin redistribution and generation of force can be mediated by prestin alone or by other cytoskeleton anchor proteins. To address this issue, the identification and isolation of putative novel prestin anchor proteins based on protein-protein interaction remains one imperative method. Using the motor protein as a bait in a yeast two-hybrid interaction screen, based on rat cochlear cDNA expression library, the first putative results will be rejudged.

Supported by a grant from the Interdisciplinary Center of Clinical Research Tübingen (IZKF), and Deutsche Forschungsgemeinschaft (Kni 316/3-2).

**Alteration of behavior and responses of auditory neurons after application of Salicylate  
in an animal model for Tinnitus**

Lukas Rüttiger, Susanne B. Kilian, Marlies Knipper

University of Tübingen, Department of Otorhinolaryngology, Molecular Neurobiology,  
THRC Tübingen Hearing Research Center, Elfriede-Aulhorn-Straße 5, D-72076 Tübingen,  
Germany

Behavioral conditioning studies on rats have been proven to be a valid animal model for the evaluation of acute and chronic phantom auditory experience (Tinnitus). We recently developed an animal model for short-term acute induced phantom auditory sensations in rats on the basis of systemic and local application of salicylate (Rüttiger et al., 2003). The expression of activity dependent genes in cochlear spiral ganglion neurons and auditory cortical tissues after application of salicylate - systemically and also locally to the round window of the cochlea - has been shown to be highly specific for excitability changes in the auditory system (Tan et al., 2004; Hadjab et al., 2004). The question arises whether the response of auditory neurons can be correlated to the expression changes of activity dependent genes and the performance of rats in the behavioral animal model. Single cell recordings are presented and discussed in the context of salicylate induced phantom auditory experiences and neuronal excitability as indicated by the expression of activity dependent genes.

Supported by the Deutsche Forschungsgemeinschaft DFG 316/3-1, DFG 316/4-1 and Fortune 816-0-0.

**Symposium #S4:**  
**Pushing toward the limits of what insects can know: Case studies for**  
**comparative cognition**  
**M. Giurfa and B. Smith, Toulouse and Columbus**

**Introduction**

- [#S4](#) M. Giurfa and B. Smith, Toulouse and Columbus  
*Pushing toward the limits of what insects can know: Case studies for comparative cognition*

**Slide**

- [#S4-1](#) TS. Collett and PR. Graham, Brighton (UK)  
*Are visual patterns in hymenopterans stored elementally or configurally?*
- [#S4-2](#) R. Menzel, A. Smith and U. Greggers, Berlin and Harpenden Herts (UK)  
*Navigation of Honeybees: evidence for map-like organization of spatial memory*
- [#S4-3](#) RJ. Greenspan and B. van Swinderen, San Diego, CA (USA)  
*Arousal and "Selective Attention" in Drosophila*
- [#S4-4](#) S. Shafir, Jerusalem (IL)  
*Risk-sensitivity and comparative evaluations in honey bees*
- [#S4-5](#) M. Giurfa and B. Smith, Toulouse (F) and Columbus (USA)  
*#S4: GENERAL DISCUSSION - Neural mechanisms of cognitive performances in insects*

**Poster**

- [#11A](#) H. Wolf and R. Wehner, Ulm and Zurich (CH)  
*Olfactory orientation in desert ants: Strategies and use in foraging navigation*
- [#12A](#) H. Wolf, CHG. Müller and S. Harzsch, Ulm and Rostock  
*Cellular characteristics of the nervous system, and a new view on arthropod evolution*
- [#13A](#) M. Wittlinger, H. Wolf and R. Wehner, Ulm and Zurich (CH)  
*Possible roles of head and gaster in 3-dimensional path integration in the desert ant*
- [#14A](#) J. Benard, A. Avargues, G. Portelli and M. Giurfa, Toulouse (F)  
*A study on color categorization in honeybees*

- [#15A](#) M. Schubert, J.C. Sandoz and M. Giurfa, Toulouse (F)  
*Stimulus interactions in single and multi trial conditioning of binary odour mixtures in honeybees, Apis mellifera*
- [#16A](#) M. Giurfa and S. Stach, Toulouse (F) and Berlin  
*The influence of training length on visual categorization in honeybees*
- [#17A](#) V. Vergoz, J.C. Sandoz and M. Giurfa, Toulouse (F)  
*A new aversive conditioning paradigm in honeybees: different contributions of D1 and D2 dopaminergic receptors to olfactory conditioning of the sting extension reflex*
- [#18A](#) I. Massou, C. Leclerc, M. Moreau, M. Giurfa and J-C. Sandoz, Toulouse (F)  
*Optical imaging of odour-evoked Nitric Oxide signals in the antennal lobe of the honey bee, Apis mellifera.*
- [#19A](#) N. Deisig, J-C. Sandoz and M. Giurfa, Toulouse (F)  
*Olfactory mixture processing in the honey bee: an optical imaging study*



## **Introductory Remarks to Symposium 4**

### **Pushing toward the limits of what insects can know: Case studies for comparative cognition**

**Martin Giurfa and Brian Smith, Toulouse(F) and Columbus (USA)**

Insects have traditionally been considered simple and small reflex machines. This perspective has been fruitful, as insects have served as inspiration for numerous works on robotics and machine building. However, this particular view of insect behavior overlooks the fact that insects, like most living organisms, process information flexibly in order to rapidly adapt to their environment. Behavioral processes that range from gathering sensory information through perception and decision-making to the resulting appropriate actions allowing the animal to cope with a changing environment can be identified and studied in insects. Since cognition can be defined in a broad sense as the sum of such processes, we are confronted with the necessity of considering insect behavior from a cognitive perspective.

Research on invertebrate learning and memory has focused mainly on elemental associations linking two specific stimuli or a specific behavior with a specific reinforcer. But insects exhibit behavioral complexity that is far richer than previously thought. In this symposium we will ask to what extent learning performance in insects involves more complex forms of learning, such as attention, inhibition, risk sensitivity or configural (non-elemental) associations, which may or may not be accounted for by elemental processes. We will focus on studies of behavioral performance as well as on the neural substrates underlying these forms of learning in insects in an attempt to unravel the mechanistic basis of complex learning.

**Are visual patterns in hymenopterans stored elementally or configurally?**

Tom Collett and Paul Graham  
Sussex Centre for Neuroscience  
University of Sussex  
Brighton BN1 9QG  
UK

Evidence from landmark navigation suggests that visual patterns are often learnt as views taken at defined locations. Are these views stored as picture elements or are the elements bound together? We will review recent behavioural results, which taken together, suggest that elemental storage cannot explain an insect's behaviour.

## **Navigation of Honeybees: evidence for map-like organization of spatial memory**

Randolf Menzel<sup>1</sup>, Alan Smith<sup>2</sup> and Uwe Greggers<sup>1</sup>

(1) Institut für Biologie, Neurobiologie, Freie Universität Berlin

(2) Plant and Invertebrate Ecology, Rothamsted Research, Harpenden Herts AL5 JQ, U.K.

Using harmonic radar, we report the complete flight paths of displaced bees. Test bees forage at a feeder, or are recruited by a waggle dance indicating the feeder, and are recorded after they are released at an unexpected release site. A sequence of behavioral routines become apparent: (1) initial straight flights in which they fly the course they were on when captured (foraging bees) or which they learned during dance communication (recruited bees), (2) slow search flights with frequent changes of direction, in which they attempt to "get their bearings", and (3) straight and rapid flights directed either to the hive or first to the feeding station and then to the hive. These straight homing flights start at locations all around the hive and at distances far out of the visual catchment area around the hive or the feeding station. Two essential criteria of a map-like spatial memory are met by these results, bees can set course at any arbitrary location in their familiar area, and they can choose at least between two goals. This suggests a rich, map-like organization of spatial memory in navigating honeybees.

**Arousal and "Selective Attention" in *Drosophila*.**

Ralph J. Greenspan and Bruno van Swinderen  
The Neurosciences Institute  
San Diego, CA

Attention constitutes a state of heightened arousal in the nervous system and is considered to be an essential component of consciousness in higher organisms. Experimental demonstrations of the mechanisms of attention have been nearly as difficult to pin down as have those for consciousness itself. In animals that are unlikely to possess full-blown consciousness, the ability to exhibit graded states of arousal, to restrict behavioral responses to one among many stimuli, and to recognize particular percepts as salient are nonetheless important as an aspect of their ability to function adaptively in the world. Examination of neural correlates of attention-like and heightened arousal states in the fruit fly brain, and genetic manipulation of these responses, reveal similarities to perceptual phenomena typically studied in higher vertebrates.

## **Risk-sensitivity and comparative evaluations in honey bees**

Sharoni Shafir

B. Triwaks Bee Research Center, Department Of Entomology, Hebrew University of Jerusalem, Rehovot 76100, Israel. E-mail: [shafir@agri.huji.ac.il](mailto:shafir@agri.huji.ac.il)

In classic economics, and similarly in the study of animal behavior, during a choice process humans and animals, respectively, were hypothesized to evaluate alternatives in an absolute manner, such that each alternative receives some subjective value, or utility. Under such an evaluation scheme, choice behavior is context-independent, that is, the presence or absence of alternatives in the choice set does not affect the subjective value that the decision maker assigns to each alternative. Such an evaluation mechanism leads to two basic axioms of rationality theory: 1) transitivity, that if A is preferred to B, and B is preferred to C, then A is preferred to C, and 2) regularity, that the addition of an alternative to a choice set cannot increase the preference to any of the preexisting alternatives in the set. An alternative to absolute evaluations is comparative evaluations, in which alternatives are evaluated across their various dimensions. Such an evaluation mechanism may be context-dependent and lead to violations of both transitivity and regularity. Humans have been shown to violate both transitivity and regularity, in support of comparative evaluations. In conceptually similar choice experiments to those with humans, honey bees foraging on artificial flowers also demonstrate context-dependent choice, consistent with comparative evaluations.

Another central theme in both human and animal decision-making is the sensitivity to variability of reward, or risk-sensitivity. Honey bees, like other animals, tend to be risk-averse to variability in amount of reward, preferring the sure-thing over the variable option. However, perception of variability seems to be influenced by the coefficient of variation, which is a relative measure of variability (standard deviation/ mean), rather than by the variance. Recent choice experiments with humans, inspired by the honey bee findings, revealed that the coefficient of variation is a strong predictor of risk-aversion, especially when the alternatives are experienced (as is always the case with animals) rather than described.

The similarities in choice phenomena between honey bees, other animals, and humans, in such cognitive domains such as context-dependent evaluations and risk-sensitivity raise the question of whether similar processes account for them, or do they arise via different mechanisms. In particular, is risk-sensitivity, for example, a meta-phenomenon of associative learning processes, or is there an independent evaluation process for variability? Successful attempts of using associative learning theory to predict risk-sensitive choice with free-flying bees support the former. However, in support of the latter, experiments with harnessed honey bees employing the proboscis-extension response conditioning paradigm modified for a choice procedure found no correlation between individual performance in risk-sensitivity and in either a latent inhibition or a reversal-learning task.

## Olfactory orientation in desert ants: Strategies and use in foraging navigation

Harald Wolf<sup>1</sup> and Rüdiger Wehner<sup>2</sup>

<sup>1</sup>Abteilung Neurobiologie, Universität Ulm, D-89069 Ulm; [harald.wolf@biologie.uni-ulm.de](mailto:harald.wolf@biologie.uni-ulm.de)

<sup>2</sup>Institute of Zoology, University of Zurich, CH-8057 Zurich, Switzerland

Desert ants, *Cataglyphis fortis*, do not only rely on their well-studied path integration system during foraging trips. They also use olfactory cues when approaching a familiar food source (Wolf H, Wehner R, 2000, J Exp Biol 203, 857), particularly when a constant wind is blowing (which is characteristic of their desert habitat). Rather than approaching the feeder directly, the ants steer some distance downwind of the food source on fairly straight outbound trajectories. Here, they pick up odour filaments emanating from the food and follow the odour trail upwind. This strategy allows quick and reliable location of even small food sources, which might otherwise be missed due to inaccuracies of the path integration system.

This approach behaviour was examined in more detail to identify the underlying orientation strategy. First, the bases of the ants' antennae – scape and pedicel joints - were immobilised to deprive the animals of wind perception. Operated animals initially maintained their downwind approach and started searching after they had passed the food source. This held even under changed wind conditions, including the rare occurrence of calms! Only during the following trips some animals gradually adopted a direct approach of the feeder (ibid).

These observations suggest that the ants combine different strategies: They use (i) their path integration system to approach a learned downwind area where to pick up the food odour, and (ii) (zigzagging) upwind orientation is elicited and guided by the odour stimulus.

Second, the strategy underlying the margin of downwind orientation was studied.

1. Either the ants may use a **“goal expansion strategy”**, using odour spread as a spatially limited indicator for the presence of food. In that case, the distance steered downwind of the feeder should be determined by the range of the odour plume (and e.g. wind speed and turbulence). It should be independent of the distance between nest and feeder.

2. Or the ants may apply an **“error compensation strategy”**, using the odour as a guide line towards the food source. Steering downwind by a margin just exceeding their maximum navigation error will lead the ants safely across the odour guide. In that case, the distance steered downwind of the feeder should increase almost linearly with nest-feeder distance.

Our results unambiguously support the second strategy. When feeders were established at distances of 5 to 60m from the nest, the distances steered downwind of the food increased from about 0.75m to 3.25m in a linear fashion, and independent of wind speed. This translates into an ant's estimate of its navigation error of 3-8°.

Supported by Volkswagenstiftung (I/78 580) and Schweizerischer Nationalfonds.



# Cellular characteristics of the nervous system, and a new view on arthropod evolution

Harald Wolf<sup>1</sup>, Carsten H.G. Müller<sup>2</sup> and Steffen Harzsch<sup>1,3</sup>

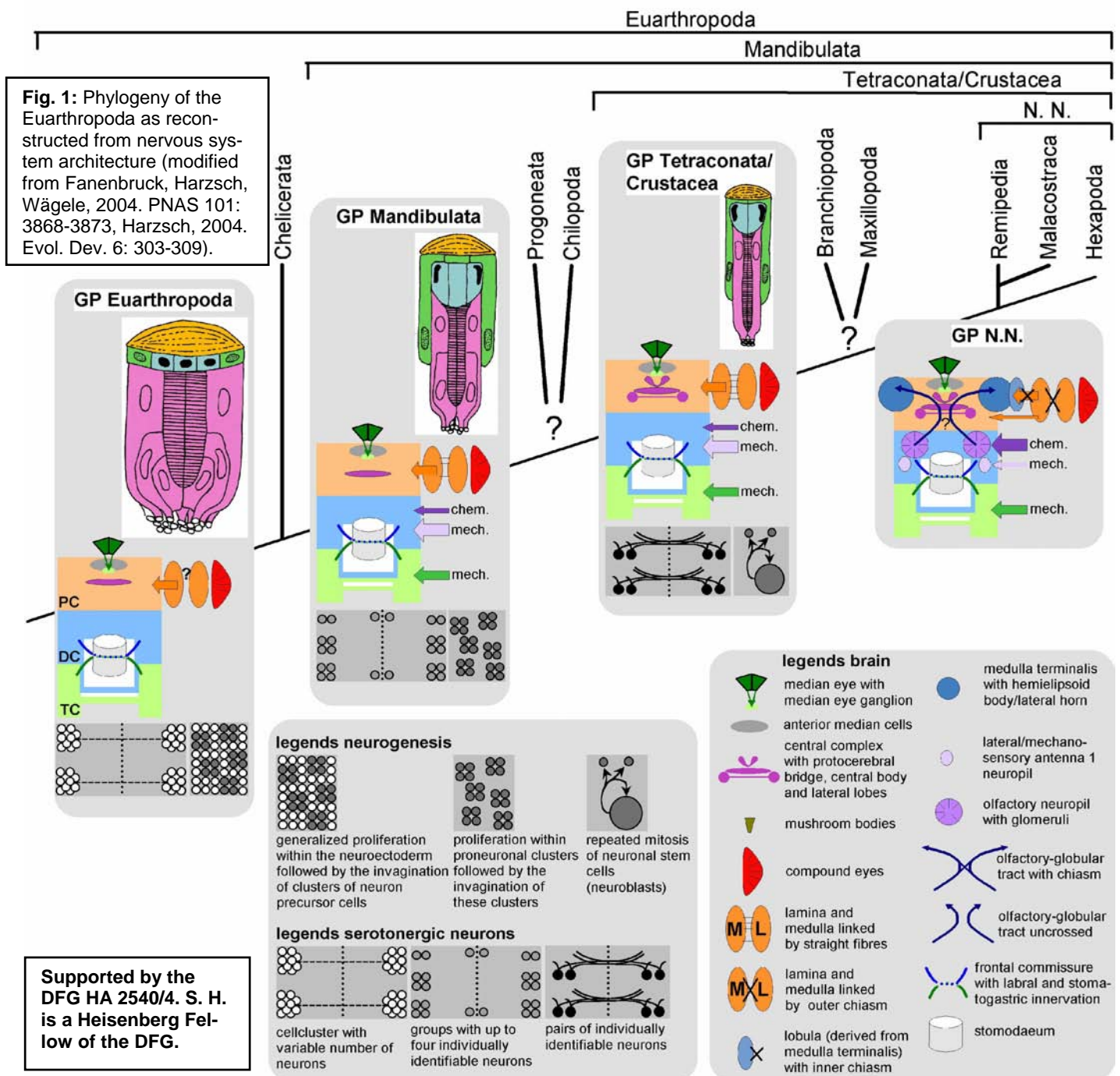
<sup>1</sup> Abt. Neurobiologie und <sup>3</sup> Sektion Biosystemat. Dokumentation, Universität Ulm, D-89069 Ulm. <sup>2</sup> Inst. f. Biodiversität, Allg. und Systemat. Zoologie, Universität Rostock, D-18051 Rostock. harald.wolf@biologie.uni-ulm.de, steffen.harzsch@biologie.uni-ulm.de

In the new debate on arthropod phylogeny, structure and development of the nervous system provide important arguments. The architecture of the brains of Hexapoda, Crustacea, and Chelicerata has been thoroughly compared with an evolutionary background in recent years (e. g. Breidbach, 1995. „The nervous system of invertebrates: an evolutionary and comparative approach“ Breidbach, Kutsch eds., Birkhäuser, Basel: 383-406). On the cellular level, however, comparative aspects of the nervous systems have been examined in only few studies.

Here we collate and review existing cellular data and analyse them with respect to the concept of individually identifiable neurons. In particular, (i) the mechanisms of neurogenesis, (ii) the morphologies of serotonergic interneurons, (iii) the numbers of leg motoneurons, and (iv) cellular features and development of

the lateral eyes are discussed. We conclude that in comparison to the Mandibulata, the Chelicerata possess variable and much higher numbers of neurons in the different cell classes examined. Cell numbers in Mandibulata are lower and neurons are individually identifiable, at least in Hexapoda and Crustacea.

The characters explored in this contribution are mapped onto an existing phylogram as derived from brain architecture (Fig. 1). Hexapoda are an in-group of the Crustacea according to this phylogram, and the current data are in no conflict with such a phylogenetic position. However, these characters clearly argue against a sister-group relationship of “Myriapoda” and Chelicerata, as has recently been suggested by molecular studies (e. g. Hwang et al., 2001. Nature 413: 154-157). Instead, they provide strong evidence in favour of the Mandibulata concept.





## Possible roles of head and gaster in 3-dimensional path integration in the desert ant

Matthias Wittlinger<sup>1</sup>, Harald Wolf<sup>1</sup> and Rüdiger Wehner<sup>2</sup>

<sup>1</sup>Abteilung Neurobiologie, Universität Ulm, D-89069 Ulm; [harald.wolf@biologie.uni-ulm.de](mailto:harald.wolf@biologie.uni-ulm.de)

<sup>2</sup>Institute of Zoology, University of Zurich, CH-8057 Zurich, Switzerland

Foraging desert ants, *Cataglyphis fortis*, monitor their position relative to the nest by path integration. This enables them to return on a direct path, rather than retracing the tortuous outbound journey performed when searching for food. This path integration is also applied in the 3<sup>rd</sup> dimension, for instance, when the ants travel across hilly terrain. That is, animals that have travelled across a series of artificial hills (Fig.1), covering a walking distance of 10m, correctly gauge the return distance on level ground to be just 6m (Wohlgemuth S, Ronacher B, Wehner R, 2001, Nature 411, 795).

We examined possible mechanisms the ants may use to measure the slope of uneven terrain in the context of 3-dimensional path integration. Two body parts that could conceivably be employed to determine the body's attitude with regard to gravity, and hence terrain slope, are head and gaster (Markl H, 1962, Z Vergl Physiol 45, 475). We therefore manipulated sensory input from the hair fields which signal the relative positions of head and thorax, located in the neck region, and thorax and gaster, located on the petiolus.

Ants were trained to forage at a feeder they could reach via a series of artificial hills, requiring a walking distance of 10m (Fig.1; above). During tests, the return path was on

level ground, and intact ants correctly started to search for the nest entrance after 6m home journey in the test channel (corresponding to the base length of the training set-up). To manipulate graviception, the fields of hair sensillae in the neck region, or on the petiolus, were shaved with a razor splinter. The animals were caught and operated at the feeding site, and placed into the test channel as soon as they had picked up their food item again. Further tests were performed in operated ants after they had returned to the nest, re-emerged, and performed another journey to the feeder.

If an operation had incapacitated the ant's graviception, one would expect it to disregard the slopes in the outbound travel. The home run should in that case extend over about 10m.

Unexpectedly, manipulation of hair fields in neither neck nor petiolus regions affected the distances of home runs. If anything, the ants slightly underestimated, rather than overestimated, the distance to the nest. These results indicate that operated animals were still able to perform (almost) correct 3-dimensional path integration. This may be due either to a lack of input from neck and petiolus hair fields to the path integrator, and / or to pronounced redundancy of graviception (Markl *ibid*).



Fig.1

Supported by Volkswagenstiftung and Schweizerischer Nationalfonds.



## A study on color categorization in honeybees

BENARD Julie, AVARGUES Aurore, PORTELLI Geoffrey and GIURFA Martin

Centre de Recherches sur la Cognition Animale  
CNRS - Université Paul Sabatier - Toulouse III - UMR 5169 - 118 Route de Narbonne  
31062 Toulouse cedex 4 - France  
E-mail: benard@cict.fr

Categorization is a fundamental cognitive ability that allows treating similar stimuli as equivalents, and thus responding to them in the same manner [1]. It promotes cognitive economy, since it allows adaptive responses to novel objects in the environment. Spectral stimuli form a physical continuum, which humans divide verbally into discrete color categories. Whether or not animals possess comparable categories, and thus group different but similar color stimuli within a specific color category, is a subject of debate. Here we asked whether the honeybee *Apis mellifera* categorize color stimuli such that they discriminate between color classes and generalize within color classes.

We trained marked free-flying bees to collect sugar solution on a parallel-arm maze. Individual bees were trained and tested in dual-choice situations such that only one color at the entrance of one of the arms led to the sugar solution. The other color led to a blocked arm. We defined two color categories, based on the color opponent coding space defined for honeybee color vision [2]. Within this color space, we chose short-wavelength stimuli (bluish to the human eye) vs. long wavelength stimuli (yellowish to the human eye). Each category was composed by 5 different stimuli. One group was rewarded on the short-wavelength stimuli and not on the long-wavelength stimuli; another group got the inverse training schedule. During the training, each bee was trained with 4 of the 5 stimuli of each category in all possible combinations presented randomly (16 different stimuli pairs). After extensive training, the bee was tested with the remaining members of the two categories that it had never experienced before.

Bees learned very well to differentiate between short- and long-wavelength stimuli. Moreover, they generalized successfully their choice to the new colors which belonged to the rewarded category and avoided the colors which belonged to the non-rewarded category. Control experiments were performed to ensure that within a color class, bees were indeed capable of discriminating between the five stimuli proposed, as defined by the honeybee color space [2]. Bees could discriminate between each member of the same category. Our results thus show that the prerequisites for color categorization (i.e. discrimination between two color categories, generalization between distinguishable stimuli within a color category) are fulfilled in the case of the honeybee.

[1]: Herrnstein R.J. (1990). Levels of stimulus control: a functional approach. *Cognition* 37, 133-166.

[2]: Backhaus W. (1991). Color opponent coding in the visual system of the honeybee. *Vision Res.* 31, 1381-1397.

## Stimulus interactions in single and multi trial conditioning of binary odour mixtures in honeybees, *Apis mellifera*

M. Schubert\*, J.C. Sandoz and M. Giurfa

Centre de Recherches sur la Cognition Animale, CNRS-Université Paul Sabatier – UMR 5169, 118 route de Narbonne, 31062 Toulouse, France. \*E-mail: schubert@cict.fr

Honey bees *Apis mellifera* foraging on flowers learn to associate complex odour blends with nectar or pollen reward. In this context, they may discriminate or generalise from single odours to olfactory compounds and vice versa. We investigated stimulus interactions in binary odour mixtures by conditioning honeybees to different odours and odour compounds. We used the olfactory conditioning of the proboscis extension reflex in which odours (the conditioned stimuli or CS) are paired with a reward of sucrose solution (the unconditioned stimulus or US). We performed overshadowing (OVS) experiments in which a compound of two odours A and B was rewarded (AB+). After compound conditioning, bees were tested with the single odours and the compound (A, B, AB). Two control groups (Ctrl A and Ctrl B) were trained, each with one of the single odours (A+ or B+, respectively), and then subjected to the same tests as the OVS group. Six different odours were used as A and B in all possible combinations. Tests were performed after a single conditioning trial or after three conditioning trials.

Results of the OVS groups showed that overshadowing occurred depending on the odour combination and on the amount of conditioning trials (1 or 3 trials) such that it was not a consistent phenomenon. The response of the OVS group to the single odorants A and B could be explained, not on the basis of interactions between odorants within the mixture but rather on the learning and cross-generalisation levels of the single odours when trained alone. For instance, the response to A in the OVS group corresponded to that of Ctrl A to A (learning) plus that of Ctrl B to A (generalisation). Thus, OVS in the olfactory modality in honeybees is a phenomenon that seems to rely more on elemental properties of the odour in the compound than on configural properties of the binary odour compound.

## The influence of training length on visual categorization in honeybees

MARTIN GIURFA (1\*) & SILKE STACH (1, 2)

(1): Centre de Recherches sur la Cognition Animale, CNRS-Université Paul Sabatier, 118 route de Narbonne, 31062 Toulouse, France.

(2) : AG Neurobiologie, Freie Universitaet Berlin, Koenigin-Luise Str. 28/30, 14195 Berlin, Germany

\*: E-mail: [giurfa@cict.fr](mailto:giurfa@cict.fr)

Generalisation and categorisation are fundamental abilities that allow treating similar stimuli as equivalents, and thus responding to them in the same manner. Typically, a categorisation experiment involves a discrimination in which reward is not signalled by a single stimulus, but rather by a variety of stimuli that share a common feature. Recently, we showed that honeybees can categorize visual patterns on the basis of a common configuration of orientations [1]. Bees trained with randomly changing patterns sharing only a common layout made up of four edge orientations extracted all four orientations and integrated them into a global representation, which allowed them to respond to novel stimuli that preserved the trained layout. Contrarily to this kind of training, training with a single, constant pair of patterns does not impose explicitly the extraction of specific features as any available cue could be used to discriminate between patterns. Here we show that after training free-flying bees with a single, constant pair of patterns, categorisation of novel stimuli can also occur based on the extraction of four different edge orientations arranged in a specific spatial layout. We demonstrate that different levels of experience with the single pair of training stimuli determine important changes in the discrimination strategies employed by the bees. Higher levels of generalisation were attained with increasing training length. Controlling precisely the level of experience of individuals is therefore crucial in experiments on visual recognition.

[1] Stach S, Benard J, Giurfa M (2004) Local-feature assembling in visual pattern recognition and generalization in honeybees. *Nature* 429:758-761

**A new aversive conditioning paradigm in honeybees: different contributions of D1 and D2 dopaminergic receptors to olfactory conditioning of the sting extension reflex**

**Vanina Vergoz, Jean-Christophe Sandoz and Martin Giurfa**

Centre de Recherches sur la Cognition Animale, CNRS - Université Paul Sabatier – UMR 5169,  
118 route de Narbonne, 31062 Toulouse, France.

The aim of this work was to establish a new aversive conditioning paradigm in individually harnessed honeybees. We conditioned the sting extension reflex by presenting odours in temporal association with an electric shock. Bees were able to build odour –shock associations and extended their stings to the mere presentation of the odour reinforced with the shock. This conditioning process was clearly associative since bees could differentiate between different odorants in differential conditioning experiments, thus responding to the odour associated with the electric shock but not to another odour presented without shock.

Using pharmacological blocking of octopamine (blockers: miansérine and epinastine) and dopamine (blocker: fluphénazine and flupenthixol) receptors at different doses, we showed that dopamine, but not octopamine, is crucial for supporting aversive conditioning of the sting extension reflex. As dopamine may be the neurotransmitter related to the electric shock, we studied the specific contribution of D1 and D2 dopaminergic receptors. We show that D1 and D2 receptor antagonists, SCH23390 and spiperone, respectively, have different effects on retention tests such that D2 receptors seem to be more relevant for maintaining the aversive olfactory memory over time.

**Optical imaging of odour-evoked Nitric Oxide signals in the antennal lobe of the honey bee, *Apis mellifera*.**

Isabelle MASSOU<sup>1</sup>, Catherine LECLERC<sup>2</sup>, Marc MOREAU<sup>2</sup>, Martin GIURFA<sup>1</sup> and Jean-Christophe SANDOZ<sup>1</sup>

<sup>1</sup> Centre de Recherches sur la Cognition Animale, UMR 5169, Bât IVR3, 118, route de Narbonne, F - 31062 Toulouse cedex 4, FRANCE

<sup>2</sup> Centre de Biologie du Développement, UMR 5547, Bât IVR3, 118, route de Narbonne, F - 31062 Toulouse cedex 4, FRANCE

Nitric oxide (NO) is a gaseous neuronal messenger involved in intercellular processes like synapse plasticity during LTP in vertebrates. In the honey bee, NO was shown to be involved in the establishment of olfactory memories and to be important for behavioural odour discrimination. Moreover, histochemical stainings have shown the presence of Nitric Oxide Synthase, the enzyme responsible for NO production in the antennal lobe. This structure is the first relay of the olfactory pathway (equivalent to the olfactory bulb of vertebrates), where olfactory sensory neurons connect onto local interneurons and projections neurons, which in turn relay the olfactory information to higher brain centres. Since the antennal lobe is a primary centre for the establishment of the olfactory memory, we have carried out optical imaging experiments after bath application of the NO-sensitive dye DAF-FM, to reveal NO activity in the antennal lobe of honey bees. Our recordings show that odours evoke biphasic signals in the glomeruli of the antennal lobe. Different odours induced different arrangements of active glomeruli within each individual, and odour-evoked NO-activity patterns were similar in different individuals. Overall, NO-signals were found to be very similar, both spatially and temporally, to calcium-signals recorded in similar conditions in the honey bee antennal lobe. In order to understand the relationship between the two signals, we use a range of pharmacological treatments with both NOS blockers and calcium-chelators in NO- and calcium-imaging experiments. Our goal will be to study the cellular origin of NO signals, as well as its involvement during olfactory memory formation.

**Olfactory mixture processing in the honey bee: an optical imaging study****Nina Deisig, Jean-Christophe Sandoz, Martin Giurfa**

Centre de Recherches sur la Cognition Animale, Université Paul Sabatier - Toulouse III, 118 Route de Narbonne, 31062 Toulouse cedex 4, France ; email : deisig@cict.fr

Odour stimuli in the natural environment consist of many components, thus raising the question of how the olfactory system processes such complex olfactory mixtures. Our previous work on honeybee olfactory learning and processing showed that honeybees can treat binary mixtures in a non-linear way. We showed that bees trained to solved non-linear olfactory discriminations tasks like negative patterning, in which they must learn to respond to the single odours A and B reinforced, but not to their binary mixture AB non-reinforced, treat the mixture in a non-linear way. The mixture is treated as the sum of the individual odour representations plus a “unique cue”, i.e. an additional internal stimulus representation, which is specific to the olfactory mixture AB. In the present work, we search for the neural basis of such a unique cue and study the neural basis of differentiation between the representation of mixtures and the simple sum of their single component representations.

To investigate mixture processing at the physiological level, we used *in vivo* calcium imaging in the antennal lobe (AL), the first relay of the olfactory pathway in the insect brain. Receptor neurons on the antennae detect odorants and convey the olfactory information to the glomeruli of the antennal lobe. There they connect with inhibitory local interneuron networks and with projection neurons which in turn convey processed information to higher brain centres, like the mushroom bodies. Calcium imaging studies have showed that odours elicit combinatorial activity patterns in the glomeruli of the antennal lobe, according to a highly conserved code (Galizia et al. 1999). After incubating the bee brain with a calcium sensitive dye (Calcium Green 2 AM), we presented bees with 4 different odorants (previously used in our behavioural experiments) and with all possible binary, ternary, quaternary mixtures of these odorants. After calcium measurements, the brain was incubated with a protease and a dye (RH 795) in order to stain the glomerular layout, so that we could identify the glomeruli individually. We found that all odours induced calcium signals in the antennal lobe in a different combination of glomeruli. Overall, the number of activated glomeruli increased with the number of mixture elements, but reached a saturation with ternary mixtures. Moreover, the response patterns broadened with the number of mixture components. Generally, less-active glomeruli increased their number for rich mixtures. When comparing the representation of mixtures with that of their elements, we found that the glomerular patterns obtained for the mixtures differ from the simple sum of the patterns recorded for the single odours. This suggests that the information necessary for the extraction of a “unique cue”, and the successful differentiation between elements and compound in non-elemental learning tasks, may already be found at the level of the antennal lobe.

**Symposium #S5:**  
**Signals in early neural development**  
**T. Pieler and E. Pera, Göttingen**

**Introduction**

[#S5](#) T. Pieler and E. Pera, Göttingen  
*Signals in early neural development*

**Slide**

[#S5-1](#) T. Edlund, Umea (S)  
*Induction and Early Patterning of the Vertebrate Central Nervous system*

[#S5-2](#) S. Hou and E. Pera, Göttingen  
*The secreted serine protease HtrA1 acts as a posteriorizing factor by stimulating FGF signaling in Xenopus embryos*

[#S5-3](#) S. Scholpp and M. Brand, Dresden  
*Endocytosis controls spreading and effective signaling range of Fgf8 protein during early neural development of the zebrafish*

[#S5-4](#) T. Müller, H. Wildner, D. Zechner, M. Treier and C. Birchmeier, Berlin and Heidelberg  
*Creating neuronal diversity in the dorsal spinal cord*

[#S5-5](#) G. Edenfeld, T. Stork, S. Bogdan, M. Zhu and C. Klämbt, Münster  
*Analysis of neuron-glia interaction in Drosophila*

[#S5-6](#) E. Knust, Duesseldorf  
*Drosophila crumbs - From epithelial polarity to retinal degeneration*

**Poster**

[#20A](#) S. Golz and J. Mey, Aachen  
*Retinoic acid-dependent regulation of BMP4 and Tbx5 in chick retinal development*

[#21A](#) TJ. Klisch, K. Jürgens, J. Souopgui, T. Pieler and KA. Henningfeld, Göttingen  
*The role of Xmx1 in primary neurogenesis in Xenopus laevis*

[#22A](#) B. Rust, T. Pieler and K. Henningfeld, Göttingen  
*Isolation and Characterization of Xenopus Sox1*

[#23A](#)

T. Ruediger, D. Bagnard and J. Bolz, Jena and Strasbourg (F)

*Response of cortical axons to semaphorin gradients*



## **Introductory Remarks to Symposium 5**

### **Signals in early neural development**

**Tomas Pieler and Edgar Pera, Göttingen**

How does a single cell, the fertilized egg, give rise to many thousands of differentiated cell types and form organs as complex as the human brain? In recent years, significant progress has been made in elucidating the signals involved in this process. Work in different model systems, from the fly embryo to the mammalian nervous system, has uncovered a small set of cell-cell signaling pathways that are integrated during development and lead to the differentiation of a vast variety of cell types. The mechanisms that determine cell fate in CNS development are re-used in other aspects of development, and basic principles of signal integration are conserved across species. The idea for the symposium on "Signals in early neural development" is to highlight recent advances in our understanding of the molecular network that leads to the formation of the CNS. The proposed speakers form a representative cross-section of relevant topics, ranging from the induction and patterning of the neural plate to differentiation of individual cell types in the CNS. Emphasis is given to a broad spectrum of experimental model organisms to provoke new insights into CNS development in both vertebrates and invertebrates. We expect that the talks covering different aspects of neural development provide important stimuli for future research in this exciting field of neurobiology.

**Induction and Early Patterning of the Vertebrate Central Nervous system**

Thomas Edlund

Umeå Center for Molecular Medicine, Umeå University

901 87 Umeå, Sweden

One central problem of neurodevelopment is how distinct neural progenitor cells are generated from a uniform population of stem or precursor cells. The early development of the CNS depends on three major inductive events i) neural induction whereby embryonic ectodermal cells are induced to generate neural stem or precursor cells, ii) induction of rostrocaudal neural identity resulting in a precise regional variation in neural cell identity along the rostrocaudal neuroaxis and iii) induction of dorsoventral identity in cells located at different rostrocaudal positions of the neural tube. In vertebrates, most celltypes and organs develop by a series of inductive events which control both multicellular pattern and differentiation of individual cells and during the last decade it has become evident, that the early development of most tissues and organs is regulated by interactive signalling by the same or similar, and surprisingly limited number of extra-cellular signalling molecules. Each family of signals and receptors consists, however, of multiple members that interact with different specificity. The concerted actions of signals like HH, BMP/TGF $\beta$ , FGF, Wnt and Notch appear to control many of the processes that lead to the formation of most organs. Thus, the challenge now is not so much to identify novel signals, but to understand the mechanisms by which a limited number of signalling pathways interact to control the development of cells and organs. One needs to understand how at different developmental stages signals can act in either a convergent, opponent or hierarchial manner, and how cells in different organs change with time, their competence to respond to these signals. Genetic studies can provide information on the requirement of these signals and on epigenetic interactions, but is less suitable to dissect mechanisms of integrative signalling. Thus, to understand the development of the CNS, there is great need to develop in vitro systems that can be used to study interactive mechanisms. We have defined assay systems in chick, that permits a clean dissection of individual tissues that can be used to perform gain and loss of function studies and to define and interactive mechanisms, which in turn can dissect in fine detail the steps of early CNS development. These assays have generated novel and seminal information that is not available from other vertebrate organisms that traditionally have not been used for the type of in vitro studies. Results on the mechanisms of neural induction and of rostrocaudal and dorsoventral patterning of neural progenitor cells will be presented.

**The secreted serine protease HtrA1 acts as a posteriorizing factor  
by stimulating FGF signaling in *Xenopus* embryos**

Shirui Hou and Edgar Pera

Georg-August-Universität Göttingen, Institut für Biochemie und Molekulare  
Zellbiologie, Abt. Entwicklungsbiochemie,  
Justus-von-Liebig-Weg 11, 37077 Göttingen, E-mail: epera@gwdg.de

The induction and pattern formation of the central nervous system are fundamental events in vertebrate development. Studies in *Xenopus* have identified many signals that induce anterior neural fate, including Insulin-like growth factors (IGFs) and extracellular growth factor antagonists that inhibit BMP and Wnt signaling (Pera et al., 2001; 2003). Other signals such as Fibroblast growth factors (FGFs) are known to posteriorize neural tissue. In a direct screen for secreted proteins we isolated the *Xenopus* homolog of the serine protease HtrA1. HtrA1 contains a secretory signal sequence, an IGF binding domain, and a serine protease domain. Microinjection of *HtrA1* mRNA into *Xenopus* embryos resulted in loss of head structures, induction of ectopic tails and expansion of mesoderm. *HtrA1* also enlarged the neural plate at the expense of neural crest and epidermal tissue and induced ectopic neurons. A mutant *HtrA1* construct, in which the catalytic serine residue was replaced by alanine, failed to induce anencephaly and ectopic tails, indicating a crucial role of the proteolytic domain for the activity of *HtrA1*. In loss-of-function experiments, an antisense morpholino oligonucleotide that blocks HtrA1 protein synthesis (*HtrA1*-MO) enlarged head structures and reduced tail development. HtrA1 cooperated with FGF signals to induce mesoderm in ectodermal explants. In whole embryos, a dominant-negative FGF receptor (XFD) blocked the ability of HtrA1 to inhibit head development, to induce secondary tails and to stimulate mesoderm formation. Moreover, a dominant-negative FGFR4a (dnFGFR4a) impaired ectopic neuronal differentiation by HtrA1, suggesting that HtrA1 relies on an intact FGF signaling pathway to exert its activities. Thus, *Xenopus* HtrA1 promotes posterior development in an FGF-dependent manner. (This work was supported by the DFG grant PE 728/3 and the DFG Research Center Molecular Physiology of the Brain.)

**References**

- Pera E.M., Wessely O., Li S.Y., and De Robertis E.M. (2001). Neural and head induction by insulin-like growth factor signals. *Dev. Cell* 1, 655-665.
- Pera E.M., Ikeda A., Eivers E., and De Robertis E.M. (2003b). Integration of IGF, FGF, and anti-BMP signals via Smad1 phosphorylation in neural induction. *Genes Dev.* 17, 3023-3028.

## Endocytosis controls spreading and effective signaling range of Fgf8 protein during early neural development of the zebrafish

Steffen Scholpp<sup>1,2</sup> and Michael Brand<sup>1</sup>

1: Max-Planck Institute of Molecular Cell Biology and Genetics, and Dept. of Genetics, University of Technology, Dresden; email: [brand@mpi-cbg.de](mailto:brand@mpi-cbg.de); 2: Present address: MRC Centre for Developmental Neurobiology, London SE1 1UL, UK

Secreted signalling molecules are of great importance during development, and elicit induction, proliferation, differentiation, and patterning events in target cells. Fgf8 is a member of the fibroblast growth factor family, with key inductive and patterning functions during vertebrate development, e.g. of the forebrain, midbrain, cerebellum, heart, inner ear and mesoderm. In spite of the importance of this signalling molecule, the mechanisms that control spreading of Fgf8 through vertebrate tissues are largely unknown. We studied Fgf8 as a potential morphogen in the nascent neuroectoderm of living zebrafish embryos. By fluorescently labelling recombinantly manufactured zebrafish Fgf8 protein *in vitro* with Cy3 chromophore we monitored spreading of Fgf8 protein from a focal source. We find that spreading of tagged Fgf8 through target tissue is carefully controlled via endocytosis and subsequent degradation in lysosomes, or '*restrictive clearance*' from extracellular space. If internalisation is inhibited, Fgf8 protein accumulates between cells, spreads further, and activates target gene expression over a greater distance. Conversely, enhanced internalisation increases Fgf8 uptake and shortens its effective signalling range. Target cells can therefore influence the availability of Fgf8 ligand to other target cells in an active way.

This work was supported through the Max-Planck-Society and a grant by the European Union (QLG3-CT-2001-02310).

**Creating neuronal diversity in the dorsal spinal cord**

Thomas Müller<sup>1</sup>, Hendrik Wildner<sup>1</sup>, Dietmar Zechner<sup>1</sup>, Mathias Treier<sup>2</sup>, and Carmen Birchmeier<sup>1</sup>

<sup>1</sup>Max-Delbrück-Center for Molecular Medicine, Berlin, Germany; <sup>2</sup>EMBL, Heidelberg, Germany

Neurons of the dorsal spinal cord receive sensory information from the periphery, process this information and relay it to higher brain centres and to motor neurons in the ventral spinal cord. The complex circuitry in which these sensory interneurons participate is established during development, and depends on a spatially and temporally ordered appearance of neuron types. We showed that two classes of dorsal spinal cord interneurons (class A and B) can be distinguished during development. The bHLH gene *Olig3* is expressed in progenitor cells that generate class A neurons and that *Olig3* is an important factor in the development of these neuron types. In *Olig3* mutant mice, class A neurons are not correctly specified and assume the identity of class B neurons. Conversely, *Olig3* represses the emergence of class B neurons and a combinatorial code of *Olig3* and other bHLH factors specifies the fate of class A neuronal subtypes. Canonical Wnt-signals are important for the specification of class A neurons. Gain-of-function mutation of  $\beta$ -catenin cause pronounced ventral shifts in the expression of patterning genes like *Olig3*, and result in the specification of supernumerary class A neurons. In contrast, loss-of-function mutation of  $\beta$ -catenin interferes with the expression of *Olig3* in dorsal progenitors. The homeobox factor *Lbx1* is expressed in all class B neuronal subtypes and is required for their differentiation. *Olig3* and *Lbx1* are therefore important determinants in the development of class A and B dorsal spinal cord neurons.

Analysis of neuron-glia interaction in *Drosophila*

G. Edenfeld, T. Stork, S. Bogdan, M. Zhu and C. Klämbt

*Institute of Neurobiology, University of Münster, Badestrasse 9, 48149 Münster, Germany.*

There is no doubt that neurons provide the mechanics of neural computing but it is interesting to note that as more complex a nervous system gets and as more efficient it functions as more glial cells are integrated into the neural network. In insects and other more primitive organisms only few % of all neural cells are of glial nature, whereas in humans, glial cells outnumber neurons by a factor of 10. However, despite this difference in relative cell numbers, glial cells perform quite similar tasks in all organisms analyzed. At first, neuron-glia interaction is important during the development of the embryonic nervous system. In *Drosophila*, the migration of midline glial cells is essential for the establishment of the commissural axon pattern and the longitudinal glial cells are needed to establish the longitudinal connectives. Both glial cell types must migrate along neuronal substrates to perform their tasks. The most extensive migration is displayed by the peripheral glial cells. They are born in the CNS cortex and during formation of the peripheral nerves, they migrate out along the nerve root to stereotyped positions in the periphery.

In order to identify genes that specifically play a role in glial migration, we have conducted several mutagenesis experiments and screened for mutations affecting the migration of the different glial cell types. We have identified about 50 genes that cause defects in glial cell migration. The molecular analyses of 4 of these genes will be presented.

***Drosophila crumbs* – from epithelial cell polarity to retinal degeneration**

Elisabeth Knust

Institut fuer Genetik, Heinrich-Heine-Universitaet Duesseldorf, Universitaetsstr. 1,  
40225 Duesseldorf, Germany. e-mail: knust@uni-duesseldorf.de

Cell polarity is manifested by the shape of the cell, the orientation of the cytoskeleton and the uneven distribution of organelles and molecules. There is accumulating evidence that multiprotein complexes built from transmembrane and cytoplasmic proteins into larger protein scaffolds are instrumental to compartmentalise the cell membrane and the underlying cytocortex, thereby providing both structural and signalling functions.

*crumbs* and *stardust* are essential for the maintenance of polarity and tissue integrity of many ectodermally derived epithelia of the *Drosophila* embryo. The transmembrane protein Crumbs organises a protein complex in the subapical region, apical to the zonula adherens. Its four C-terminal amino acids ERLI directly interact with the PDZ-domain of one of the isoforms encoded by Stardust, a scaffolding protein of the MAGUK (membrane associated guanylatekinase) protein family. Stardust itself recruits the four PDZ-domain protein DPATJ and the single PDZ-domain protein DLin-7 by interactions with its two L27-domains into the complex. A further interaction between Crumbs and DmPar-6, a member of the Bazooka/aPKC complex, suggests a connection between the two complexes.

In addition to their role in epithelial polarity, *crumbs* and *stardust* are required later in the photoreceptor cells. In these highly polarised cells, a similar protein complex, composed of Crumbs, Stardust, DPATJ and DLin-7 is localised at the stalk membrane, which topologically corresponds to the subapical region of epithelia cells. Loss of either gene results in defective morphogenesis and in light dependent retinal degeneration of the photoreceptor cells. Degeneration can be prevented by several means, such as inhibition of apoptosis, reduction in rhodopsin levels or prevention of endocytosis. This makes *Drosophila* an ideal model to study the genetic and molecular basis of RP12 and LCA, two severe forms of retinal degeneration in humans, some of which are associated with mutations in *CRB1*, which is homologous to *Drosophila crumbs*.

## Retinoic acid–dependent regulation of BMP4 and Tbx5 in chick retinal development

Sarah Golz and Jörg Mey

Institut für Biologie II, RWTH Aachen, Kopernikusstr. 16, 52074 Aachen, Germany  
e-mail: golz@bio2.rwth-aachen.de

The transcriptional activator retinoic acid (RA) has a morphogenic role in the embryonic development of vertebrates, especially in the polarization of body axis. RA has been proposed to be a determining factor in setting up the dorsoventral polarity of the eye axes, thereby organizing the later developing retinotopic visual projection [1]. The pathfinding of retinofugal axons along the dorsoventral axis of the visual system is controlled by the family of ephrinB ligands and EphB tyrosine kinase receptors. Their action is in turn controlled by signals with spatially restricted expression domains in the dorsal (Tbx5, BMP4) or ventral eye cup (ventroptin, cVax, Pax2) [2]. The consequence of changing RA levels on regional patterning within the retina and on projecting retinal axons has not been tested so far. To this end we manipulated the RA distribution in the early chick eye anlage at E2 and subsequently monitored the expression of spatial signals with quantitative RT-PCR at E3.5. We found that injections of all-trans RA suppressed the expression of dorsal molecules Tbx5 and BMP4, while EphrinB1 was reduced, but not significantly. In good accord with these data, the injection of Citral, an inhibitor of RA-synthesis, enhanced the expression of BMP4 and Tbx5. Thus, retinoic acid may prevent BMP4 and Tbx5 from influencing the ventral retina. EphrinB1 was regulated to a lesser extent, indicating, that it is affected by RA only indirectly, possibly via the regulation of Tbx5. In contrast to these dorsal factors, the ventral transcription factor Pax2 was not affected by a changes in retinoic acid signalling. This observation was corroborated on the protein level by immunohistochemical analysis of retina sections. Therefore, RA appears not to be upstream of Pax2. To analyze the effect of exogenous RA on the retinotectal projection, anterograde tracing was performed between E16 and E18 by Dil injections into the dorsalmost point of the retina. Irrespective of the RA treatment, all labeled primary axons projected to the expected position in the lateral tectum, where they formed a condensed termination zone. Contrary to our expectation, that a lowered ephrin-B1 expression in the retina would lead to a ventralized retinotectal projection, these tracing experiments revealed no alteration of the innervation pattern in the tectum.

*Supported by the Deutsche Forschungsgemeinschaft, ME1261-5.*

[1] Mey et al., *Dev. Brain Res.* 127 (2001): 135-148. [2] Schulte et al., *Neuron* 24 (1999): 541-553.



**The role of Xmx1 in primary neurogenesis in *Xenopus laevis*.**

Tiemo J. Klisch, Kathrin Jürgens, Jacob Souopgui, Tomas Pieler and Kristine A. Henningfeld. Developmental Biochemistry, University of Goettingen, Justus-von-Liebig Weg 11, 37077

[tklisch1@gwdg.de](mailto:tklisch1@gwdg.de)

Members of the Myc-Max-Mad network are essential regulators of cellular growth, proliferation and differentiation. Proteins of this family are characterized by a conserved basic-helix-loop-helix-leucine zipper (bHLHZ) domain that facilitates DNA binding and protein dimerization. In general, Myc positively regulates cell growth and proliferation and requires the association with Max to bind to DNA regulatory sequences. The Mads can antagonize the activity of Myc by sequestering Max, and by binding and repressing a subset of Myc-Max target genes. We have isolated and characterized *Xenopus* Mxi1, a member of the Mad family. Xmx1 transcripts are found by whole mount in situ hybridization to be broadly expressed throughout the open neural plate, earlier and in broader domains as compared to neurogenin (X-ngnr-1). As development proceeds, Xmx1 transcripts are detected in the CNS including the eye, olfactory placodes, midbrain, hindbrain and spinal cord, where it is located in the proliferating cells of the ventricular zone. Consistent with an early role in primary neurogenesis, Xmx1 is regulated positively by BMP inhibition and negatively by lateral inhibition. Overexpression of Xmx1 or Xmx1 fused to the engrailed repressor domain in *Xenopus* embryos inhibited the neuronal differentiation marker N-tubulin but did not alter the expression of early determination and differentiation markers such as X-ngnr-1 and MyT1. Both constructs also ectopically activated XSox3, an early pan-neural marker of proliferating neural precursor cells. Consistently, as shown by BrdU incorporation, overexpression of Xmx1 increased proliferation as well down-regulated the expression of cell cycle control genes XPak3 and XGadd45. Moreover, the described *in vivo* activities of Xmx1 were shown to require a functional DNA binding domain. These results demonstrate a role for Xmx1 in the maintenance of neural precursor cells in a proliferative state prior to terminal differentiation.

**Isolation and Characterization of *Xenopus* Sox1** Barbara Rust, Tomas Pieler and Kristine Henningfeld. Department of Developmental Biochemistry, University of Goettingen, Justus-von-Liebig Weg 11, 37077  
email: hrust@gwdg.de

The Sox family of transcription factors plays an essential role in cell fate decisions during embryogenesis. Members of the Sox-B1 subgroup (Sox1-3) are expressed in the early developing vertebrate nervous system. Despite the high protein homology within the HMG-box, members of this group do not exhibit redundant functions. In mammalian cells, Sox2 and Sox3 are thought to maintain neural precursor identity, while Sox1 drives neuronal differentiation. To gain insight into the function of Sox1 during *Xenopus* neurogenesis we have overexpressed mSox1 in *Xenopus* embryos. Consistent with previous results in higher vertebrates, Sox1 down-regulated the expression of Sox3 and induced ectopic neurons. To further evaluate the function of Sox1, we have isolated the *Xenopus* Sox1 gene. XSox1 exhibits 70% overall amino acid identity with mSox1 and a higher degree of homology within the HMG box (100%). The expression of XSox1 was evaluated by whole mount in situ hybridization. In contrast to XSox2 and XSox3, which are expressed maternally and broadly throughout the neural ectoderm, the expression of XSox1 is more limited and can first be detected in the anterior region of the open neural plate. Later expression is observed in the central nervous system, including the forebrain, midbrain, hindbrain, floorplate and a subset of differentiated neurons. The isolation of Sox1 together with the previously isolated XSox2 and XSox3 will aid in the elucidation of the function of Sox-B1 subgroup in the molecular events of vertebrate neurogenesis.

### **Response of cortical axons to semaphorin gradients**

Tina Ruediger<sup>1</sup>, Dominique Bagnard<sup>2</sup> and Juergen Bolz<sup>1</sup>

<sup>1</sup> Friedrich-Schiller Universitaet Jena, Institut für Allgemeine Zoologie und Tierphysiologie, Erbertstrasse 1, 07743 Jena, Germany; <sup>2</sup> INSERM U575 Physiopathologie du Système Nerveux, Centre de Neurochimie, 5 rue Blaise Pascal, 67084 Strasbourg, France

Different members of the secreted class III semaphorin protein family have been implicated in mediating axonal guidance during development of the nervous system. Previous in vitro-studies with the stripe assay demonstrated that Sema 3C acts as an attractive and Sema 3A as a repulsive guidance cue for cortical axons (Bagnard et al., Development 125, 5043, 1998). In the present study we examined the behaviour of cortical axons exposed to semaphorin gradients. For this we dissociated cortical neurons from E14 mouse brains and plated them on membrane gradients prepared from Sema3C- and Sema3A transfected HEK 293 cells. On Sema3C gradients, most axons extending from the cortical neurons were oriented toward the side of higher membrane concentration (uphill the gradient). In contrast, on Sema3A gradients the majority of the axons grew toward the side of lower membrane concentration (downhill the gradient). A chemorepulsive effect of Sema3A, the reduction of axonal length, was only observed when axons were growing towards increasing concentrations of this molecule. Cortical axons growing towards decreasing Sema3A concentrations were as long as axons growing on control substrates. For Sema3C we observed no difference in length of axons growing uphill or downhill the gradient. Finally, when cortical neurons were cultured on homogeneous Sema3A or Sema3C membrane carpets, they showed no orientation preference for axon outgrowth and axonal length was also not affected by the presence of these semaphorins. These data indicate that cortical axons are very sensitive to changing concentrations of semaphorins, whereas they appear to adapt semaphorins when the concentration is constant. As a first step to characterize possible signalling mechanisms that allow cortical neurons to read semaphorin gradients we used inhibitors of kinases and guanylate cyclases. Application of ODQ, a specific inhibitor of soluble guanylate cyclase, strongly reduced the orientation of cortical fibers within Sema3C gradients. PD98059, a selective MAPK kinase inhibitor, abolished the "uphill preference" for Sema3C and the "downhill preference" for Sema3A, suggesting that this kinase is required for the orientation of cortical axons within semaphorin gradients.

#### References:

D. Bagnard et al., Semaphorins act as attractive and repulsive guidance signals during the development of cortical projections. Development, 125, 5043-5053, 1998.

**Symposium #S6:**  
**Brain plasticity and cognition: cellular mechanisms and clinical perspectives**  
**E. Fuchs and G. Kempermann, Göttingen and Berlin**

**Introduction**

[#S6](#) E. Fuchs and G. Kempermann, Göttingen and Berlin  
*Brain plasticity and cognition: cellular mechanisms and clinical perspectives*

**Slide**

[#S6-1](#) E. Fuchs, Göttingen  
*Introduction to Symposium 6*

[#S6-2](#) G. Kempermann, Berlin  
*Stem cells in the adult brain: new players in concepts of plasticity*

[#S6-3](#) FA. Henn, Mannheim  
*Clinical Implications of Neuroplasticity*

[#S6-4](#) PJ. Lucassen, VM. Heine, B. Czeh, E. Fuchs and M. Joels, Amsterdam (NL) and Göttingen  
*Live and let die: changes in cell birth and cell death in the stressed brain.*

[#S6-5](#) T. Shors, Piscataway, NJ (USA)  
*Neurogenesis and the Makings of Memories*

[#S6-6](#) TD. Palmer, Palo Alto, CA (USA)  
*Interplay between the immune system and brain plasticity*

**Poster**

[#24A](#) K. Boekhoorn, R. Lasrado, P. Borghgraef, D. Terwel, O. Wiegert, M. Joels, H. Krugers, F. Van Leuven and PJ. Lucassen, Amsterdam (NL) and Leuven (B)  
*NEUROGENESIS AND LONG-TERM POTENTIATION IN THE HIPPOCAMPUS OF TWO TAU TRANSGENIC MOUSE MODEL ARE NOT RELATED*

## **Introductory Remarks to Symposium 6**

### **Brain plasticity and cognition: cellular mechanisms and clinical perspectives**

**E. Fuchs and G. Kempermann, Göttingen and Berlin**

Over the last decades the concept of plasticity has fundamentally changed our view on brain function in health and disease. Plasticity describes the interaction between function and form. However, it remains a sometimes vague and problematic term. In the proposed symposium we would like to address some of the most exciting new aspects of brain plasticity. The discovery of stem cells in the adult brain and of adult neurogenesis has added a new dimension to plasticity research. New theories have linked neuropsychiatric disorders such as depression, dementia and temporal lobe epilepsy to a failure of adult neurogenesis.

We will gather a panel of some of the leading experts in this field and aim at providing a comprehensive session on a topic that has not yet been covered in comparable depth at an international conference attracting researchers from all areas of neurobiology. We believe that this symposium would be timely and well received by the audience. We have chosen an interdisciplinary approach and will discuss aspects from basic research to the clinic.

**Stem cells in the adult brain: new players in concepts of plasticity**

Gerd Kempermann, Max-Delbrück-Center for Molecular Medicine (MDC) Berlin-Buch, and VolkswagenStiftung Research Group at the Dept. of Experimental Neurology, Charité University Medicine Berlin, Robert-Rössle-Str. 10, 13125 Berlin  
E-mail: gerd.kempermann@mdc-berlin.de

The adult mammalian brain contains precursor cells that contribute to cell genesis throughout life. Except for the development of few new oligodendrocytes it was long assumed that this cell generation mainly consisted of astrocytic proliferation in cases of damage. However, two lines of evidence have changed this view. First, adult neurogenesis can be found in the hippocampus and olfactory system. Second, cells with precursor cell properties proliferate throughout the brain even under physiologic conditions and generate new astrocytes and oligodendrocytes. This cell genesis is regulated dependent on activity. It even includes an activation of microglia, which is not of neuroectodermal lineage. The exact function and the relevance of this cellular plasticity for cognition are not yet known, but research on adult hippocampal neurogenesis leads the way in demonstrating how new cells can be involved in plasticity that is linked to concrete function. Precursor cell populations in the adult brain are heterogeneous and do not respond uniformly to identical stimuli. This suggests that the functional relevance of precursor cell activity in the adult brain might not be homogenous either.

One intriguing aspect of activity-dependent regulation of adult hippocampal neurogenesis is the reciprocal link between cognitive or other brain “activity” and neuronal development. Neuronal maturation is influenced by cognitive stimuli: “learning” appears to recruit immature neurons into function, which otherwise would die. One can interpret such finding in a Hebbian way and hypothesize that the new neurons have particular functions in hippocampal plasticity that is directly linked to learning. There are first network theories that incorporate neurogenesis and call for growing networks. Function of new neurons might have distinct short-term and long-term benefits.

The role of new glia in this context is even less clear than the contributions of precursor cell-based neurogenesis. Given the fact, however, that astrocytes, for example, participate in network function by the modulation of synaptic transmission, there is room for expanding the theory of a contribution of precursor cells to brain plasticity beyond neurogenesis.

## **Clinical Implications of Neuroplasticity**

Fritz A. Henn

Central Institute of Mental Health, Heidelberg University, J5, 68159 Mannheim, Germany  
<http://www.zi-mannheim.de>

**Depression, a re-occurring disease, appears to result in changes in information processing which lead to a negative valuation of events, resulting in low mood, helplessness, hopelessness, decreased energy and reduced concentration. These changes may relate to alterations in hippocampal function, in the recording of memories, which results in changes in a wide-spread circuit modulating affect. Within the hippocampus it is clear that a variety of inputs can affect mood. These include nor-epinephrine (NE), serotonin (5HT), and cortisol, all factors activated by stress. These are thought to act through activation of CREB and neurotrophins such as BDNF and have been postulated to lead to changes in either neurogenesis or synaptogenesis. Stress has been shown to decrease neurogenesis, and most antidepressants have been shown to increase hippocampal neurogenesis leading to the hypothesis that changes in the rate of new neuron formation may underlie depressive illnesses. This hypothesis is critically reviewed. Evidence that synaptogenesis plays a critical role in regulating affect will be reviewed. Methods to measure this in patients directly in the CNS will be presented.**

## Live and let die: changes in cell birth and cell death in the stressed brain

Paul J. Lucassen<sup>1</sup>, Vivi M. Heine<sup>1</sup>, Boldizsar Czéh<sup>2</sup>, Eberhard Fuchs<sup>2,3</sup> & Marian Joels<sup>1</sup>

1) Section Neurobiology, Swammerdam Institute of life Sciences, University of Amsterdam, Kruislaan 320, 1098 SM Amsterdam, T: + 31 20 525 7631, F: +31 20 525 7709, [lucassen@science.uva.nl](mailto:lucassen@science.uva.nl)

2) Clinical Neurobiology Laboratory, German Primate Center, Göttingen, Germany

3) Department of Neurology, Medical School, University of Göttingen, Göttingen, Germany

Although earlier hypotheses on the pathophysiology of major depression generally focused on aberrant neurotransmitter concentrations, recent neuroimaging studies have demonstrated selective structural alterations in brains of depressed patients, supporting the idea that depression involves impairments of structural plasticity.

Stressful life events are major predisposing risk factors for the development of depression in genetically predisposed individuals. Indeed, an hypothalamic-pituitary-adrenal (HPA) hyperdrive, glucocorticoid resistance and hippocampal volume reductions are commonly observed in depressed patients. To address whether stress could be instrumental in this, we studied structural dynamic alterations, i.e. cell birth, neurogenesis, apoptosis, hippocampal cell number and volume, in 2 stress-related animal models for aspects of depression, i.e. rats and tree shrews, and relate this to observations in postmortem hippocampal tissue from depressed patients (Lucassen et al., 2001; Muller et al., 2001).

In tree shrews, 1 month of psychosocial stress decreased dentate proliferation rate and reduced hippocampal volume. Even though long-lasting social conflict does not lead to a loss of principal cells, a lower incidence of apoptosis and alterations in intrinsic and synaptic excitability of pyramidal neurons were measured. Notably, these suppressive effects of stress on hippocampal function and structure could be counteracted by treatment with the antidepressant tianeptine, that also had an anti-apoptotic effect, both in hippocampal subregions as well as the temporal cortex (Lucassen et al., 2004).

In rats, both chronic unpredictable, but also acute, stress decreased the numbers of adult-generated cells. The reduced proliferation after acute stress, however, normalized again already within 24 hrs, whereas most of the structural dynamic changes after *chronic* stress required minimal 3 weeks before recovery became apparent. Apoptosis on the other hand, increased after acute, but was decreased after chronic stress (Heine et al., 2004). Further data on treatment with the glucocorticoid receptor (GR) antagonist RU486, that e.g. reduced symptoms in patients with (psychotic) depression (Belanoff et al., 2002), will be presented.

The present data indicate that not only neurogenesis but also apoptosis continues to be present in the adult hippocampus, which is notably affected by stress and antidepressant treatment in an adaptive, non-lasting manner (Heine et al., 2004). These findings have important consequences for our understanding of (the reversibility of) stress-related (hippocampal volume) changes in depression. Although at least some antidepressants thus correct aberrant levels of neurogenesis as well as apoptosis, thereby suggesting a causal link between neurogenesis and depression, reduced neurogenesis on its own, however, is not sufficient to induce depressive symptoms in rodents (Hen & Vollmayr, 2004), indicating that also other parameters must be involved.

PJL is supported by the HersenStichting Nederland and the Volkswagen Stiftung.

### References;

- Belanoff JK, et al., Biol Psychiatry. 2002 Sep 1;52(5):386-92.
- Henn FA, Vollmayr B. Neurogenesis and depression: etiology or epiphenomenon? Biol Psychiatry. 2004; 56(3):146-50.
- PJ Lucassen, M Müller et al.: Am. J. Pathol., 158: 453-468, 2001.
- M Müller, PJ Lucassen, et al.: Eur. J. Neurosci., 14 : 1603-1612, 2001.
- PJ Lucassen, E Fuchs and B Czéh: Biol. Psychiatry 55: 789-796, 2004.
- VM Heine, S Maslam, J Zareno, M Joels, PJ Lucassen. Eur. J. Neurosci., 19; 131-144, 2004.
- E Fuchs, B Czéh, T Michaelis, MHP Kole and PJ Lucassen. Alterations in Neuroplasticity in Depression: the Hippocampus and Beyond. Eur. J. Neuropsychopharmacol., in press, 2004.



## Neurogenesis and the Makings of Memories

Tracey J. Shors, Ph.D.

Rutgers University

The number of new neurons produced each day in the adult brain is in the thousands if not tens of thousands (Gould et al., 1999, Cameron and McKay, 2001). The vast majority of these new neurons are produced in the hippocampus, a brain region known to be critical for certain types of learning. Most of these new cells die within weeks of their birth. Given that so many cells are born in the hippocampus, we have proposed that they may be involved in the formation of new memories and have accumulated considerable evidence that they are. First, we found that learning affects their survival. More specifically, animals that are trained on a learning task that requires the hippocampus maintain many more of these new neurons after training than animals not exposed to the learning task or trained on a task that does not require the hippocampus (Gould et al., 1999). Thus, acquisition of new information can rescue these new neurons from death. Moreover, once rescued from death by learning, they survive for months (Leuner et al., 2004). Finally, we have found that the new neurons may be involved in memory formation of very specific types – those in which animals must associate events over time (Shors et al., 2001, 2002, 2004). Together, our data suggest that these new neurons are affected by new learning and may be involved in the formation of memories themselves.

[supported by NIH(MH59740)]

## Interplay between the immune system and brain plasticity

Theo Palmer

Department of Neurosurgery, Stanford University  
Palo Alto, CA, USA

With very few exceptions, the adult brain learns and adapts by altering the strength and number of existing connections while maintaining a fixed number of neurons. However, the hippocampal dentate gyrus is one area where plasticity includes the loss and addition of neurons. Within the dentate granule cell layer, neural progenitor cells continually produce new neurons and this insertion of elements within the preexisting circuitry correlates with hippocampal-mediated learning and memory as well as mood/depression. In recent work we have noted that a variety of insults can lead to a persistent neuroinflammatory response and that neurogenesis and hippocampal function are attenuated. In cancer patients and in animals treated with cranial irradiation, the combined impact of cell killing from radiation and the subsequent long-lived neuroinflammatory response lead to progressive cognitive deficits with prominent impairment in hippocampal learning and memory. We have noted that treatment of irradiated animals with non-steroidal anti-inflammatory drugs (NSAIDs) can partially reverse the inflammation-induced deficit in neurogenesis and are currently studying the mechanisms by which inflammation and NSAID treatment alter local neural progenitor cell signaling. Ultimately, the modulation of neuroinflammatory responses may provide an effective clinical strategy for enhancing the restorative capacity of neural progenitor/stem cells within the adult brain.

# NEUROGENESIS AND LONG-TERM POTENTIATION IN THE HIPPOCAMPUS OF TWO TAU TRANSGENIC MOUSE MODEL ARE NOT RELATED

K. Boekhoorn<sup>1</sup>, R. Lasrado<sup>2</sup>, P. Borghgraef<sup>2</sup>, D. Terwel<sup>2</sup>, O. Wiegert<sup>1</sup>, M. Joels<sup>1</sup>, H. Krugers<sup>1</sup>, F. Van Leuven<sup>2</sup>, and P.J. Lucassen<sup>1</sup>.

<sup>1</sup> Section Neurobiology, SILS, University of Amsterdam, the Netherlands

<sup>2</sup> The Experimental Genetics Group, Centre for Human Genetics, Katholieke Universiteit Leuven, Belgium.

The hippocampus, an important area in learning and memory, is one of the few brain areas where adult neurogenesis occurs. Amongst many factors, damage is known to stimulate neurogenesis. In line with this, in Alzheimer's disease (AD), expression of cell cycle markers and mitotic phosphoepitopes is increased in the hippocampus. This area is one of the first locations where the two major pathological features of AD, plaques and tangles, are found. Here we focus on the tangles, since these intracellular occlusions of hyperphosphorylated tau correlate well with cognitive decline. Also alterations in tau isoform expression are known to cause dementia. Here, we investigate whether alterations in tau isoform expression and/or tau phosphorylation affect neurogenesis, and in parallel hippocampal functioning, by measuring long-term potentiation (LTP) in two novel tau transgenic mouse models.

We show that in the first transgene (the tau "knock-in knock-out" mouse), which has alterations in tau isoform expression and hyperphosphorylation, neurogenesis (BRDU + Doublecortin counts) is indeed increased, correlating with decreased apoptosis and increased hippocampal size. In the other model, (the P301L mutation) which only displays hyperphosphorylation of tau, we found increased LTP in the dentate gyrus, corresponding with decreased paired pulse depression. Thus, LTP and neurogenesis did not correlate in either of the two models. We are currently studying the effect of these tau alterations on behaviour.

Supported by the Internationale Stichting Alzheimer Onderzoek (ISAO).

Karin Boekhoorn

e-mail: boekhoorn@science.uva.nl

**Symposium #S7:**  
**Extracellular matrix molecules in regeneration and synaptic plasticity**  
**CG. Becker, A. Dityatev, T. Becker, Hamburg**

**Introduction**

- [#S7](#) CG. Becker, A. Dityatev, T. Becker, Hamburg  
*Extracellular matrix molecules in regeneration and synaptic plasticity*

**Slide**

- [#S7-1](#) CG. Becker, J. Schweitzer, M. Schachner and T. Becker, Hamburg  
*ECM molecules as guidance factors during development and regeneration in the central nervous system of adult zebrafish*
- [#S7-2](#) JW. Fawcett, Cambridge (UK)  
*Manipulation of ECM in axon regeneration and plasticity*
- [#S7-3](#) G. Brückner, Leipzig  
*Perineuronal nets - a basic principle of extracellular matrix organization in the central nervous system*
- [#S7-4](#) H. Rauvala, Helsinki (FIN)  
*Functions of N-syndecan (syndecan-3) in developing and adult brain*
- [#S7-5](#) O. Bukalo, O. Nikonenko, M. Schachner and A. Dityatev, Hamburg  
*Extracellular matrix glycoprotein tenascin-R and hippocampal meta-plasticity*

**Poster**

- [#25A](#) J. Kern, T. Kuenzel, PD. Dalton, H. Luksch and J. Mey, Aachen  
*Interactions of retinal ganglion cell axons with oriented electrospun fibres in vitro*
- [#26A](#) AU. Bräuer, R. Nitsch and NE. Savaskan, Berlin and Amsterdam (NL)  
*Identification and classification of a novel gene family in humans and other vertebrates homologous to PRG-1*
- [#27A](#) SW. Schwarzacher, M. Vuksic, CA. Haas, G. Burbach, RS. Sloviter and T. Deller, Frankfurt, Zagreb (HR), Freiburg and Tucson (USA)  
*The regulation of the extracellular matrix molecule neurocan in the rat hippocampus is activity-dependent*

- [#28A](#) N. John, K-H. Smalla, MR. Kreutz, ED. Gundelfinger and CI. Seidenbecher, Magdeburg  
*Brevican-Containing Perineuronal Nets of Extracellular Matrix Develop in Dissociated Hippocampal Primary Cultures.*
- [#29A](#) D. Malin, A. Dityatev, G. Dityateva, A. Aszódi, R. Wagener and D. Riethmacher,  
Hamburg, Martinsried and Cologne  
*Distribution and functions of extracellular matrix protein matrilin-2 in the nervous system of mice*

## Introductory Remarks to Symposium 7

### Extracellular matrix molecules in regeneration and synaptic plasticity

**Catherina G. Becker, Alexander Dityatev, Thomas Becker, Hamburg**

This symposium will be a forum to present and discuss recent exciting developments in the field of extracellular matrix (ECM) molecules. Traditionally viewed as important morphogenic components regulating proliferation, migration, and differentiation of cells during development, ECM molecules also appear as important players in neuroplasticity in adults. Contributions of glycoproteins of the tenascin family and chondroitin sulfate proteoglycans (CSPGs) to axon regeneration and synaptic plasticity will be in the focus of the presentations.

Many ECM molecules are inhibitors for axonal re-growth in the adult mammalian CNS. Homologs of the mammalian ECM molecules are expressed in the CNS of adult zebrafish, which show successful axonal regeneration of axon tracts, for example in the spinal cord and the visual system. **Dr. Catherina G. Becker** will outline how ECM molecules, such as CSPGs or tenascin-R are used as repellent guidance factors in the regenerating adult CNS and during development of the zebrafish nervous system.

**Dr. James W. Fawcett** will focus on the dual roles of CSPGs in the adult mammalian CNS. The enzymatic removal of the sugar side chains by chondroitinase ABC facilitates axonal re-growth after injury in the spinal cord. Chondroitinase treatment also enhances synaptic plasticity in areas that under normal conditions cannot remodel.

Conspicuous structures that are enriched in ECM molecules in the central nervous system are the so-called perineuronal nets, which surround cell bodies and proximal dendrites in a mesh-like structure that interdigitates with synaptic contacts. **Dr. Gert Brückner** will present data on development and composition of perineuronal nets in vivo and in vitro and will discuss their putative functions.

**Dr. Heikki Rauvala** will discuss the properties of HB-GAM (heparin-binding growth-associated molecule). Mutant mouse approaches and in vitro studies implicate HB-GAM and its receptor Syndecan-3 (N-syndecan) in the regulation of migratory responses of neurons and in synaptic plasticity.

Electrophysiological and ultrastructural analysis of mice deficient in tenascin-R revealed severe deficits in perisomatic inhibitory currents and synapses in the hippocampus. **Dr. Olena Bukalo** will present data supporting a view that disinhibition in tenascin-R deficient mice elevates basal excitatory transmission and number of perforated synapses in Schaffer collateral synapses, and increases the threshold for induction of LTP.

## **ECM molecules as guidance factors during development and regeneration in the central nervous system of adult zebrafish**

Catherina G. Becker, Jörn Schweitzer, Melitta Schachner, Thomas Becker

Zentrum für Molekulare Neurobiologie, D-20246 Hamburg, Germany.

Adult zebrafish, in contrast to mammals, are capable of regenerating tracts of the central nervous system, including the optic projection. In zebrafish, new retinal ganglion cells are continuously added to the periphery of the retina during development and in adult animals. Thus, regenerating optic axons may rely on the same guidance cues as newly growing axons in unlesioned developing and adult animals to find their way to different targets in the brain. Components of the extracellular matrix (ECM), such as tenascin-R and chondroitin sulfate (CS) proteoglycans repel neurites when presented as a substrate border in vitro. Tenascin-R borders on the optic tract caudally in 3-day-old zebrafish. When protein expression is reduced by injection of anti-sense morpholino oligonucleotides, optic axons invade the diencephalon caudal to the optic tract. This suggests a repellent guidance function for tenascin-R during development. In adult animals, boundary-like expression is also found, e.g. next to intraretinal fascicles of newly growing optic axons, the optic tract and in non-retinorecipient pretectal brain nuclei. These patterns undergo little change after a lesion of the optic nerve and adult regenerating optic axons are still repelled by a substrate border of tenascin-R in vitro. This suggests that tenascin-R is a repellent guidance molecule during development and regeneration. CSs are co-expressed with tenascin-R in non-retinorecipient pretectal brain nuclei in unlesioned and lesioned adult animals. Enzymatic removal of CSs in vivo leads to erroneous regeneration of optic axons into non-retinorecipient nuclei, suggesting a repellent guidance function during regeneration also for CSs. We speculate that correct pathfinding of regenerating optic axons in adult zebrafish after a lesion of the optic nerve may be attributable to multiple developmental guidance cues that are retained in the adult to guide newly growing optic axons in unlesioned animals.

Supported by the Deutsche Forschungsgemeinschaft and the University Hospital Eppendorf Special Fund for Promotion of Women in Science.

**Manipulation of ECM in axon regeneration and plasticity****James Fawcett**

Cambridge University Centre for Brain Repair, Robinson Way, Cambridge CB2 2PY

Chondroitin sulphate proteoglycans (CSPGs) are upregulated in glial scar tissue and inhibit axon regeneration. Not only are the protein cores upregulated, but also there is more glycosaminoglycan (GAG) attached to them. The final stage of GAG synthesis is sulfation, which can occur in three positions. Both 6 sulfated GAG and the sulfotransferase that sulfates n-acetyl galactosamine in the 6 position is specifically upregulated in glial scar tissue, in inhibitory glial cells, and in astrocytes treated with TGF alpha and beta. Removal of GAG chains by digestion with chondroitinase or inhibition of GAG synthesis with chlorate or beta-d-xylosides removes much of the inhibition from CSPGs in vitro. We therefore tested to see whether GAG digestion by chondroitinase would promote axon regeneration in vivo. We first treated mechanical lesions of the nigrostriatal tract, and saw regeneration of about 4% of axons back to their target. Next dorsal column lesions of the spinal cord at C4 were treated. Both sensory and corticospinal axons regenerated in treated cords, and there was rapid return of function in beam and grid walking tests. The return of function was so rapid that we hypothesised that some of it might be due to enhanced plasticity. Many neuronal cell bodies and dendrites are coated in thick perineuronal nets of inhibitory CSPGs and tenascin-R which would certainly be expected to prevent the formation of new synapses. We therefore tested the effects of chondroitinase treatment in a plasticity model, ocular dominance shift in the visual cortex following monocular deprivation. Monocular deprivation in adult animals normally produces no ocular dominance shift. However in adult animals in which the cortex was treated with chondroitinase there was a large shift in response to monocular deprivation. The structures that block plasticity are probably the perineuronal nets, which are layers of CSPG, tenascin and hyaluronan that surround many neurones and their dendrites, and which appear at the same time as critical periods terminate. We have investigated the composition of these structures, and determined which cells make the various components.



## Perineuronal nets – a basic principle of extracellular matrix organization in the central nervous system

Gert Brückner

Paul Flechsig Institute for Brain Research, University of Leipzig, Jahnalle 59, D-04109 Leipzig, Germany

The extracellular matrix in the CNS, for long time considered as space-filling ground substance, has been shown to express region- and cell type-dependent patterns (Fig.1). This heterogeneity provides a spatial and chemical organization of the intercellular space required to maintain specific structural and physiological properties of neurons and glial cells. The most conspicuous examples of extracellular matrix specialization are the perinodal gap substance around nodes of Ranvier and perineuronal nets (PNs)<sup>1</sup>. PNs can be defined as accumulations of aggregating chondroitin sulfate proteoglycans, hyaluronan and tenascin-R<sup>2</sup>, forming lattice-like structures around the soma, proximal parts of dendrites and the axon initial segment. Within these highly hydrated, polyanionic macromolecular complexes especially the proteoglycans (aggrecan, neurocan, brevican) contribute to the chemical heterogeneity of PNs by coexistence in different proportions and by large variations in the glycosylation of the major component aggrecan<sup>3</sup>. In addition to the chemical heterogeneity, the quantity and arrangement of matrix components form different structural types of PN, such as robust lattice-like PNs around parvalbumin-positive interneurons, faint pyramidal PNs and diffuse PNs in the rat cerebral cortex<sup>4</sup>. PNs have been shown to appear postnatally during the period of synaptic refinement and myelination, in parallel with the commencement of mature physiological properties of neurons. The matrix patterns formed persist in the adult as intrinsic part of the cortical maps and the region-specific architecture of subcortical nuclei. The partial destruction of PNs by intracerebral injection of chondroitinase ABC and the long-lasting in-vivo labelling with lectins revealed a slow reorganization of their matrix components in adult animals.

Possible common functions of PNs and the relevance of the various cell type-specific phenotypes remain to be elucidated. The temporal course of activity-dependent PN formation led to the hypothesis that PNs are involved in the stabilization of synaptic contacts<sup>5</sup> and may thus play a role in the regulation of synaptic plasticity. The frequent association of PNs with particular physiological types of neuron, such as the fast-spiking cortical interneurons, and their absence around slow modulatory cholinergic and aminergic neurons, suggest a role in the maintenance of the high electrophysiological activity of net-associated neurons. Moreover, PNs may potentially contribute to neuroprotection. To investigate such functional aspects, as well as the dynamics of the development and reconstitution of PNs, organotypic slice cultures<sup>6</sup> and dissociated cell cultures are promising models, in which the cell type-specific formation of PNs is retained.

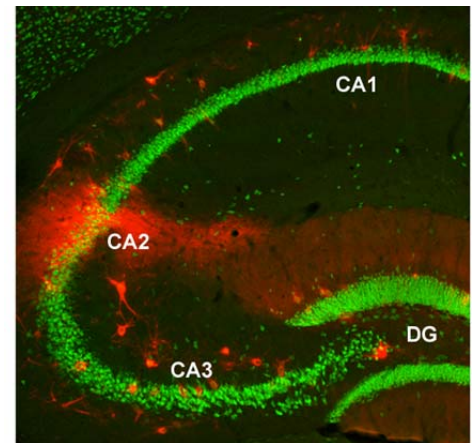


**Fig. 1.** Aggrecan immunofluorescence (red) in the mouse dorsal hippocampus (CA1-3) and dentate gyrus (DG). Intensely labelled perineuronal nets are associated with interneurons. Predominant neuropil staining indicates the CA2 region.

<sup>1</sup> Brückner, G., Brauer, K., Härtig, W., Wolff, J.R., Rickmann, M.J., Derouiche, A., Delpech, B., Girard, N., Oertel, W.H., Reichenbach, A., 1993. *Glia* 8, 183-200.

<sup>2</sup> Brückner, G., Grosche, J., Schmidt, S., Härtig, W., Margolis, R.U., Delpech, B., Seidenbecher, C.I., Czaniera, R., Schachner, M., 2000. *J. Comp. Neurol.* 428, 616-629.

<sup>3</sup> Matthews, R.T., Kelly, G.M., Zerillo, C.A., Gray, G., Tiemeyer, M., Hockfield, S., 2002. *J. Neurosci.* 22, 7536-7547.

<sup>4</sup> Wegner, F., Härtig, W., Bringmann, A., Grosche, J., Wohlfarth, K., Zuschratter, W., Brückner, G., 2003. *Exp. Neurol.* 184, 705-714.

<sup>5</sup> Hockfield, S., Kalb, R.G., Zaremba, S., Fryer, H., 1990. *Cold Spring Harbor Symp. Quant. Biol.* 55, 505-514.

<sup>6</sup> Brückner, G., Grosche, J., 2001. *Exp. Brain Res.* 137, 83-93.

(Supported by the Deutsche Forschungsgemeinschaft)

**Functions of N-syndecan (syndecan-3) in developing and adult brain**

Heikki Rauvala

Neuroscience Center, University of Helsinki, Finland

N-syndecan is the major transmembrane heparan sulfate proteoglycan of the nervous system. The carbohydrate chains of N-syndecan provide binding sites to several growth and matrix factors, like FGFs, GDNF-family members and HB-GAM (pleiotrophin). Ligation of N-syndecan triggers a cytosolic signaling pathway through src-kinase-cortactin that mediate regulation of the cytoskeleton.

We have produced N-syndecan knockout mice to analyze the roles in brain development and plasticity. Embryonic neurons from the -/- mice are defective in haptotactic migration to HB-GAM and in radial migration in brain slices. Migration is defective even when the neuroblasts are stimulated by EGF that is known to function as a scatter factor for the type of neurons used in the assays. We suggest that N-syndecan participates in activation of the EGF receptor by sensitizing the receptor through the src-kinase. Histological analysis of the N-syndecan null mice is compatible with the migration defect observed in vitro. In the adult mice, HB-GAM/N-syndecan was found to form a unique ligand/receptor pair that is induced by high-frequency stimulation in the hippocampus but suppresses LTP. In addition, a role in the hypothalamus regulating feeding behaviour was found. We suggest that N-syndecan is an essential component in the migration machinery in neuroblasts and an activity-induced gene regulating behaviour in the adult brain.

**Extracellular matrix glycoprotein tenascin-R and hippocampal meta-plasticity**

Olena Bukalo, Olexander Nikonenko, Melitta Schachner and Alexander Dityatev

Zentrum für Molekulare Neurobiologie, Universität Hamburg,

Martinistr. 52, D-20246 Hamburg, Germany

The extracellular matrix glycoprotein tenascin-R (TN-R) is highly expressed in the pyramidal layer of the CA1 region of the hippocampus, being one of the major components of perineuronal nets surrounding parvalbumin-positive interneurons. In previous investigations of TN-R deficient (TN-R<sup>-/-</sup>) mice, long-term potentiation (LTP) induced by the theta-burst stimulation of Schaffer collaterals in the CA1 region was found to be impaired. Here, we report that pairing of low-frequency presynaptic stimulation with a depolarization of postsynaptic CA1 pyramidal cells to 0 mV induced normal LTP of approximately 190% in TN-R<sup>-/-</sup> mice. However, pairing of presynaptic stimulation with a weaker depolarization to -10 mV produced LTP of approximately 150% in wild-type mice, but not in TN-R<sup>-/-</sup> mice. These differences between genotypes appeared between second and third weeks of postnatal development. The increased threshold for induction of LTP correlated with an increased level of excitatory transmission and an elevated number of perforated asymmetric axospinous synapses in the *stratum radiatum* of TN-R<sup>-/-</sup> mice. Since excitatory transmission and perisomatic GABAergic inhibition are abnormal in TN-R<sup>-/-</sup> mice, we further examined whether a rescue of these processes could lead to a recovery of LTP. Lowering levels of excitatory transmission by induction of LTD did not increase LTP in TN-R mutants. However, pre-treatment of hippocampal slices with GABA<sub>A</sub> receptor agonists, muscimol and zolpidem, recovered LTP in TN-R<sup>-/-</sup> mice. Furthermore, injection of TN-R<sup>-/-</sup> mice with muscimol completely restored both LTP and levels of excitatory synaptic transmission. These observations provide the first evidence that reduced levels of inhibition in TN-R<sup>-/-</sup> mice cause elevation of excitatory transmission and adaptive changes in LTP.

## Interactions of retinal ganglion cell axons with oriented electrospun fibres *in vitro*

Johanna Kern<sup>1</sup>, Thomas Kuenzel<sup>1</sup>, Paul D. Dalton<sup>2</sup>, Harald Luksch<sup>1</sup> and Jörg Mey<sup>1</sup>

<sup>1</sup> Institut für Biologie II, RWTH Aachen, Kopernikusstr. 16, 52074 Aachen, Germany

<sup>2</sup> Deutsches Wollforschungsinstitut, Veltmanplatz 8, 52062 Aachen, Germany

e-mail: mey@bio2.rwth-aachen.de

The most successful strategy for the surgical repair of nerve lesions consists in transplantation of autologous peripheral nerves. However, this approach reaches its limits with the availability of tissue after larger lesions and causes sensory deficits at the donor site. Since xenografts entail other disadvantages, including the need for immunosuppression, our long term goal is a completely artificial nerve bridge to induce and guide axonal regeneration *in vivo*. A promising tool for this are electrospun polyester fibers, which are biodegradable, have a high surface area to mass ratio and can be used as delivery devices for specific growth promoting peptides. Current electrospinning collection techniques typically result in random mats of material, while for neural tissue engineering, orientated fibers are needed as guidance scaffolds.

In the present study, we produced 1 – 10 µm thin, oriented fibers made of poly-ε-caprolactone (PCL). After electrospinning they were deposited on glass cover slips, which were then sputter-coated with gold and additional bioactive peptides. The peptides IKVAV and RGD, representing integrin-activating epitopes from the extracellular matrix were tested as well as poly(L)lysine and other substrates. Fibre splitting was controlled by voltage, with 15 kV producing single fibres with lengths of 8 cm and diameters of  $1.26 \pm 0.19$  µm, and 30 kV resulted in web-like structures due to extreme fibre splitting. The ability of different mechanical and biochemical properties to guide axonal growth was investigated with two cell culture systems: (1) telencephalic neurons, isolated from E6/7 chick embryos cultured for 8 days in serum-free media, and (2) organ explants of chick E10 retinas which were cultivated for 48 hrs. In both cases axonal growth was elicited and the behavior of neurites in contact with PCL fibers was monitored. As would be expected on gold surfaces, cell adhesion was poor; however cultures were successfully established with polylysine, IKVAV, RGD or combinations of these substrates. Neurites that extended from telencephalic neurons or retinal ganglion cells were influenced by the shape of the electrospun fibres and were guided along their lengths for some distances. While we did not observe a significant effect of fiber diameter, their biochemical properties exerted an orienting impulse on growing neurites. With retina explants, uncoated PCL fibers on polylysine only rarely deflected axonal growth (in 8.7% of encounters), while IKVAV coating caused an oriented growth of axons in 65% of the cases when neurites touched electrospun fibers. To develop suitable scaffolds for axonal guidance *in vivo*, different chemical compositions of fibers combined with different substrates are now being tested.

*Supported by the Helmholtz Gesellschaft (Virtuelles Institut Bioelektrische Hybridschaltkreise) and the Alexander von Humboldt Stiftung (grant to P.D.).*

## **Identification and classification of a novel gene family in humans and other vertebrates homologous to PRG-1**

*Anja U. Bräuer, Robert Nitsch & Nicolai E. Savaskan*

<sup>1</sup>Institute of Cell Biology & Neurobiology, Center for Anatomy, Charité University Medical School Berlin, Germany,

<sup>2</sup>Division of Cellular Biochemistry, Netherlands Cancer Institute, 1066 CX Amsterdam, The Netherlands

Axon outgrowth in the central nervous system is governed by specific molecular cues. Molecules detected so far act as ligands that bind to specific receptors. We have recently uncovered a novel molecule, PRG-1, which facilitates axon growth during development and regenerative sprouting. Here, we report on the identification and cloning of other members of this hitherto unknown family of putative integral membrane proteins we named plasticity-related genes (PRGs) from several vertebrate species including human, mouse and rat. The six vertebrate genes identified seem to belong to an unknown gene family. Phylogenetic analysis indicates these mRNAs comprise two distinct groups within this gene family. Structural analysis of the translated cDNAs indicate these genes encode membrane proteins with six transmembrane domains. The messenger RNAs of rodent PRGs varied from 2.5 kb to 5.2 kb and showed distinct distributions in neuronal and reproductive tissues. Immunocytochemical analysis further revealed that at least three members of the PRG family are expressed in neurons. Expression of these genes in neurons further induce spontaneous axonal outgrowth and filopodia formation. These results suggest this is a new family of neuron-specific membrane proteins involved in axonal growth and regenerative sprouting. Our Group is sponsored by the German Research Council(SFB 515/A5)

The regulation of the extracellular matrix molecule neurocan in the rat hippocampus is activity-dependent

Schwarzacher SW<sup>1</sup>, Vuksic M<sup>1,2</sup>, Haas CA<sup>3</sup>, Burbach GJ<sup>1</sup>, Sloviter RS<sup>4</sup> and Deller T<sup>1</sup>

<sup>1</sup>Institute of Clinical Neuroanatomy, University of Frankfurt, Germany, <sup>2</sup>Croatian Institute for Brain Research, University of Zagreb, Croatia, <sup>3</sup>Institute for Anatomy and Cell Biology, Freiburg, Germany, <sup>4</sup>Department of Pharmacology Tucson, Arizona. E-mail: Schwarzacher@em.uni-frankfurt.de

A candidate molecule that could be involved in the regulation of physiological and pathological neuronal activity is the chondroitin sulphate proteoglycan neurocan. Like several other extracellular matrix molecules it is involved in important cell functions such as proliferation, migration, morphological differentiation and synaptic plasticity. In order to test whether neuronal activity can regulate neurocan expression in the adult brain, we have used a well established animal model of hippocampal excitotoxicity (Sloviter RS, 1987, Science 235:73-76). In this model, 24h high frequency stimulation of the perforant path, the main afferent input to the hippocampus, was performed in adult rats. In situ hybridization revealed upregulation of neurocan mRNA in astrocytes within the ipsi- and contralateral hippocampus 0-1 days after 24 hours of high frequency stimulation. mRNA upregulation was confirmed by laser-microdissection of selected hippocampal regions and subsequent quantitative RT-PCR. Neurocan-immunoreactivity exhibited a more defined localization to the dentate gyrus with strongest immunostaining in the hilar area and ipsilateral outer molecular layer. The expression of neurocan was dependent on the intensity and duration of perforant path stimulation. Under conditions of low frequency paired pulse stimulation, neurocan mRNA upregulation and immunoreactivity was restricted to the ipsilateral outer molecular layer, i.e. the termination site of the stimulated afferent fibers. Our results demonstrate that neurocan is strongly expressed in the dentate gyrus of adult rats following high frequency stimulation of the perforant path as well as under conditions of forced afferent stimulation. This suggests an activity-dependent regulation of neurocan in the adult nervous system. (Supported by DFG)

## **Brevican-Containing Perineuronal Nets of Extracellular Matrix Develop in Dissociated Hippocampal Primary Cultures**

Nora John, Karl-Heinz Smalla, Michael R. Kreutz, Eckart D. Gundelfinger and Constanze I.

Seidenbecher

Department for Neurochemistry/Molecular Biology, Leibniz Institute for Neurobiology Magdeburg, Germany

Brevican is one of the most prominent constituents of mature rodent brain extracellular matrix (ECM), which is strongly up-regulated during postnatal development. The C-terminal lectin domain of brevican has been shown to interact specifically with the extracellular glycoprotein tenascin R and with sulfated glycolipids at the cell surface. The central region contains matrix metalloprotease cleavage sites. Specific proteolytic cleavage leads to the separation of the N-terminal HA-binding region from the C-terminal cell surface- and protein-interacting part of the molecule and may have implications for the integrity and biophysical features of brain ECM.

Brevican was shown to be a structural constituent of perineuronal nets (PNN), a specialization of the ECM in the mature brain, which surrounds and insulates synaptic contact sites. PNN in brains of brevican-deficient mice display a less structured and more diffuse appearance. Brevican staining is generally widely distributed in the rodent brain but shows perisynaptic deposits of immunoreactivity at the ultrastructural level. Several independent approaches revealed brevican to be a true constituent of subcellular postsynaptic density protein fractions and electrophysiological studies on brevican knock-out mice revealed a phenotype of clearly reduced synaptic plasticity. The mode of synaptic action of extracellular proteoglycans, however, is still enigmatic. Furthermore, it is not completely understood, how single components are integrated into these networks, how PNN are anchored at neuronal surfaces and how these relatively stable structures relate to plastic brain properties.

During the last decade much insight into molecular components affecting synaptogenesis, synaptic structure and function was obtained employing the model of cultured hippocampal primary neurons. Brevican is detected in these cultures decorating the surface of neurons, and the immunoreactivity is diminished after hyaluronidase or chondroitinase ABC treatment, indicating that these carbohydrates play a role in the binding of brevican to neuronal surfaces. Proteoglycan-containing PNN structures, thus far thought to be a hallmark of intact mature neural tissue, can be formed in dissociated neural cultures. In mixed neuron-glia co-cultures astroglia turned out to be the cellular source of brevican, which is made under *in vitro* conditions after approx. one week in culture. The brevican-containing PNN are not restricted to GABAergic neurons and have intimate contact with both excitatory and inhibitory synapses.

## Distribution and functions of extracellular matrix protein matrilin-2 in the nervous system of mice

D. Malin<sup>1</sup>, A. Dityatev<sup>1,2</sup>, G. Dityateva<sup>1</sup>, A. Aszódi<sup>3</sup>, R. Wagener<sup>4</sup> and D. Riethmacher<sup>1</sup>

*Centre for Molecular Neurobiology<sup>1</sup> and Institute for Neurophysiology and Pathophysiology<sup>2</sup>, University of Hamburg, D-20246 Hamburg, Department for Molecular Medicine, Max Planck Institute for Biochemistry, D-82152 Martinsried<sup>3</sup>*

*Center for Biochemistry, Medical Faculty, University of Cologne, D-50931 Cologne<sup>4</sup>*

Matrilins are putative adaptor proteins of the extracellular matrix, which can form collagen-dependent and collagen-independent filamentous networks. Matrilin-2 is expressed in a variety of tissues, including the peripheral nervous system. Here we provide first evidence that matrilin-2 is expressed by premyelinating Schwann cells in developing peripheral nerves and also by the immortalized S16 Schwann cell line. Additionally, we show - by in situ hybridisation and immunohistochemical analysis - expression of matrilin-2 in several regions of the mouse brain such as the hippocampus and olfactory bulb. Expression pattern of matrilin-2 suggests potential roles of this protein, as an ECM component, in these regions. To investigate functions of matrilin-2 in the nervous system, we used several in vitro approaches. We found that purified matrilin-2 promotes migration of Schwann cells and fibroblasts from dorsal root ganglia (DRG) explants and increases neurite outgrowth of DRG sensory neurons. Furthermore, axonal length and the number of migrating cells are decreased in DRG cultures prepared from matrilin-2 deficient mice compared to cultures from wild-type mice. Matrilin-2 also strongly stimulates migration of S16 Schwann cells, as well as adhesion of these cells, as revealed by agarose drop migration assay. Matrilin-2 also promotes neurite outgrowth of cultured hippocampal neurons. Interestingly, when matrilin-2 and laminin were coated together as a substrate, we observed a higher number of neurites compared to laminin alone, suggesting that matrilin-2 and laminin can act synergistically. In summary, our findings suggest that matrilin-2 may influence different processes in both the developing peripheral and central nervous system.



**Symposium #S8:**  
**Efference Copies and Corollary Discharge Mechanisms in Sensory and**  
**Mental Processing**  
**B. Hedwig and JFA. Poulet, Cambridge**

**Introduction**

[#S8](#) B. Hedwig and JFA. Poulet, Cambridge  
*Efference Copies and Corollary Discharge Mechanisms in Sensory and Mental Processing*

**Slide**

[#S8-1](#) B. Hedwig, Cambridge (UK)  
*#S8: Introduction*

[#S8-2](#) J. Poulet and B. Hedwig, Cambridge (UK)  
*A corollary discharge modulates auditory processing in crickets*

[#S8-3](#) A. Roberts, W-C. Li and SR. Soffe, Bristol (UK)  
*Efference copies in the nervous system of hatchling frog tadpoles during locomotion*

[#S8-4](#) CC. Bell, Beaverton, OR (USA)  
*Plastic and Non-Plastic Corollary Discharge Effects In An Electric Fish.*

[#S8-5](#) MA. Sommer, Pittsburgh (USA)  
*Corollary discharge of eye movements in primates*

[#S8-6](#) DH. Mathalon, West Haven, CT (USA)  
*Evidence of Corollary Dysfunction in the Auditory System of Patients with Schizophrenia*

**Poster**

[#30A](#) JP. Engelmann, Y. Sugawara, E. van den Burg, J. Bacelo and K. Grant, GIF SUR  
YVETTE (F) and Tokyo (J)  
*Analysis of Interneurons in the ELL of Gnathonemus peterii using Neuropharmacology,  
Immunohistochemistry and Modelling*

[#31A](#) JFA. Poulet, Cambridge (UK)  
*Presynaptic inhibition of cricket auditory afferent neurons*

## Introductory Remarks to Symposium 8

### Efference Copies and Corollary Discharge Mechanisms in Sensory and Mental Processing

**B. Hedwig, JFA Poulet, Cambridge(UK)**

A fundamental challenge for all nervous systems is the differentiation between self-generated and external sensory inputs, e.g. how do animals distinguish between movements of objects in their visual field, as compared to retinal stimulation imposed by movements of their eyes. In 1950 two similar neurobiological concepts were developed that dealt with this question: Sperry proposed that a *corollary discharge* of motor patterns into sensory systems might play an important role to adjust sensory perception. At the same time v. Holst and Mittelstaedt more specifically proposed that during voluntary movements the central nervous system generates a copy of its motor commands (*efference copy*) that cancels any self-generated sensory feedback (*reafference*). Since the self-generated afference is cancelled any externally caused afference is available for central processing. In more general terms these concepts may be regarded as *feed-forward* mechanisms in sensory processing.

Since the formulation of these concepts advances in neurobiological recording techniques have allowed considerable progress in analysing the neuronal pathways and mechanisms underlying sensory information processing at the systems and cellular level. Our symposium aims to present the best-analysed model systems, in which the neuronal pathways of corollary discharge mechanisms/efference copies have been identified. The symposium brings together invertebrate models (auditory processing in crickets) as well as vertebrate models (locomotion in tadpoles and communication in electric fish). It finally deals with work on primate eye movements and the possible role of corollary discharge mechanisms in human mental processing. The comparison of different animals and sensory systems will emphasize the fundamental importance of these concepts for sensory processing.

**A corollary discharge modulates auditory processing in crickets**

J.F.A. Poulet and B. Hedwig

Department of Zoology, University of Cambridge, UK

How do animals discriminate between self-generated and environmental sensory stimuli, and, how do they prevent desensitisation of their own sensory pathway during behaviour? To solve these fundamental problems of sensory processing it has been proposed that responses to self-generated stimuli could be reduced or cancelled out from the responses to environmental stimuli (Grüsser, 1986). Singing crickets generate very intense sensory information. During sound production, the terminals of auditory afferents receive presynaptic inhibition and auditory interneurons are inhibited postsynaptically. The inhibition is independent from the strength of auditory feedback and persists in an isolated, fictively singing cricket nervous system. It is therefore the result of a *corollary discharge*, a feed forward signal from the singing motor network, rather than a sensory feedback. The corollary discharge is mediated by an intersegmental interneuron, with its soma in the mesothoracic ganglion - the Corollary Discharge neuron. In this way, singing crickets reduce auditory responses to self-generated songs and are able to hear rival males and predators in the environment. Grüsser, O.-J., (1986) Acta Psychologica 63, 3-21. Supported by the BBSRC.

*Efference copies in the nervous system of hatchling frog tadpoles during locomotion***Alan Roberts, Wen-Chang Li and Steve R Soffe**, School of Biological Sciences,

University of Bristol, Bristol, BS8 1UG, UK

Most animals have withdrawal responses to touch stimulation when they are at rest that would be inappropriate once they start to move themselves. There are therefore a range of inhibitory mechanisms to gate sensory pathways during locomotion. The inhibition produced can be thought of as an efference copy since it has a time-course which represents the time course of the motor action. One of the best known examples is Primary Afferent Depolarization (PAD) seen in the terminals of tactile sensory neurons in animals as different as the crayfish and the cat. The neurons producing this inhibition during escape swimming were first found in the crayfish (1). We have examined the inhibition that coordinates the responses of frog tadpoles to touch.

In immobilized frog tadpoles inhibition gates spinal cord skin touch sensory pathways during fictive swimming. The phasic inhibition of spinal sensory interneurons during the first half of each swimming cycle gates reflex responses to skin stimulation (2) and in this way coordinates responses during swimming. Using a new preparation of the hatchling *Xenopus* tadpole where neuron cell bodies can be seen using a water immersion lens on an upright microscope, we made whole-cell patch clamp recordings from pairs of spinal neurons. We found neurons that were active during swimming and produced glycinergic gating inhibition of sensory interneurons (3). Neurobiotin filling showed that these efference copy neurons had an ascending axon which branched reliably to form a second descending axon. These axons were located in a wide range of positions, some dorsal to contact sensory interneurons but others more ventral where they could contact motoneurons. By recording from further pairs of neurons we showed that the same interneurons also produced phasic inhibition of neurons that were rhythmically active during swimming and therefore components of the central pattern generating circuit (4). Neurons with remarkably similar anatomy and function are present in zebrafish larvae where they express the transcription factor engrailed (5) that also defines some spinal interneurons in the mouse spinal cord.

Our observations suggest that efference copy neurons are a fundamental, feature of the vertebrate nervous system from the earliest stages of their functional development. What is surprising is that recurrent inhibition within each side of the spinal cord is produced by a single class of interneuron that inhibits both sensory pathways and the motor circuits.

(1) Kirk MD, Wine JJ (1984) *Science* **225**: 854-856

(2) Sillar KT, Roberts A (1988) *Nature* **331**, 262-5.

(3) Li WC, Soffe SR, Roberts A (2002) *J Neurosci* **22**, 10924-34.

(4) Li WC, et al., (2004) *J Neurosci* **24**, 5840-8.

(5) Higashijima S, et al., (2004) *J Neurosci* **24**, 5827-39

**Plastic And Non-Plastic Corollary Discharge Effects In An Electric Fish.**

Curtis C. Bell, Neurological Sciences Institute, Oregon Health and Sciences University.

Corollary discharge effects are a prominent feature of the electrosensory system of mormyrid electric fish. The effects are associated with the motor command that elicits the electric organ discharge (EOD) of the fish. These electric organ corollary discharge (EOCD) effects prepare the electrosensory system for the reafferent input from electroreceptors that is evoked by the EOD. EOCD effects are present at all levels of the electrosensory system but have been studied most intensively in the electrosensory lobe, the very first central stage in the processing of afferent input from electroreceptors.

The EOCD input to the electrosensory lobe serves the functions of gating, latency measurement, and removal of predictable features from the sensory input. The gating and latency measurement functions are relatively invariant and non-plastic, whereas the removal of predictable features relies on a plastic, memory-like process. With regard to gating, the EOCD enhances the self-induced, EOD-evoked, reafferent input from the electroreceptors involved in measuring nearby conductances (active electrolocation), but blocks such input from the electroreceptors involved in detecting other electric fish (electrocommunication). In latency measurement, a precisely timed EOCD signal is used to decode latency as a measure of stimulus intensity in the reafferent input from electroreceptors involved in active electrolocation. In removal of predictable features from the sensory input, the EOCD elicits a memory-like negative image of the sensory input that has followed the EOD in the recent past. Addition of this negative image to the actual input, removes the predictable components of the response.

## Corollary Discharge of Eye Movements in Primates

Marc A. Sommer

Department of Neuroscience and the Center for the Neural Basis of Cognition, University of Pittsburgh, Pittsburgh, Pennsylvania 15213, USA

How do we see objects in the world and decide where to look next? Neurophysiologists have progressed a long way toward answering this question through careful analysis of the visuomotor transformations occurring from retina to brain to muscle. Yet anatomical studies indicate that this is only half of the story. Running against the normal flow of visuomotor transformation are myriad ascending pathways from subcortical regions up to cortex. The functions of most of these feedback paths remain a mystery. One compelling hypothesis is that many of them convey corollary discharge signals, i.e. copies of outbound movement commands. Instead of causing a movement such as a saccade, a corollary discharge would inform the rest of the brain about the upcoming movement. Primates are thought to use corollary discharge of saccades for two main purposes, to execute quick patterns of complex movements and to ignore the sudden shifts of the visual field caused by quick ocular rotations.

In collaboration with Robert Wurtz, I examined one likely conduit of corollary discharge in the primate brain, a pathway that ascends from a brainstem region, the superior colliculus (SC), to a cortical area called the frontal eye field (FEF). This pathway is relayed via the mediodorsal thalamus (MD; see Figure). Our first goal was to

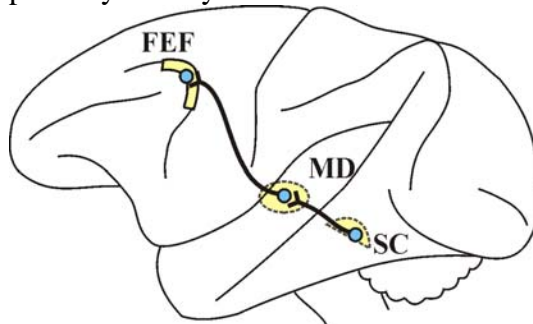


Figure: Lateral view of the rhesus monkey brain (anterior to left). The ascending pathway that we studied is indicated: blue circles represent neurons and thick black lines depict projections. Subcortical structures are drawn with dashed lines.

characterize the signals carried by neurons along the pathway in behaving rhesus monkeys. A major technical barrier was that we could not simply record from any neuron encountered in the SC, MD, or FEF; neurons in these areas may belong to many different circuits, yet we were interested only in those neurons belonging to our pathway. Thus we recorded only from neurons identified as part of the pathway according to the results of anti- and/or orthodromic stimulation. We found that the major signal carried from SC up to the FEF was a sudden burst of neuronal activity preceding specific vectors of saccades. Via this pathway, therefore, the brainstem gives the cerebral cortex advanced warning about where an eye movement will go and when it will begin – clearly a promising candidate for a corollary discharge. To test this possibility we then inactivated the pathway by injecting muscimol amongst the MD relay neurons. This had no effect on the ability to make saccades but impaired the ability to internally monitor them, supporting the corollary discharge hypothesis. Most recently we have been silencing the pathway to assess how this influences the activity of FEF neurons. In sum, to our knowledge these results represent the most explicit description yet of a corollary discharge pathway in the primate brain. Supported by the National Eye Institute.

## Evidence of Corollary Dysfunction in the Auditory System of Patients with Schizophrenia

DH Mathalon

Yale University

Failure of corollary discharge, a mechanism for distinguishing self-generated from externally-generated percepts, has been posited to underlie certain positive symptoms of schizophrenia, including auditory hallucinations. Although originally described in the visual system, corollary discharge may exist in the auditory system, whereby signals from motor speech commands prepare auditory cortex for self-generated speech. While associated with sensorimotor systems, it might also apply to inner speech or thought, regarded as our most complex motor act. The goals of our studies are 1) to demonstrate the corollary discharge phenomenon during talking and inner speech in human volunteers using event-related brain potentials (ERPs); 2) to demonstrate that the corollary discharge is abnormal in patients with schizophrenia using ERPs; 3) to identify the specific regions of lateral and medial frontal and temporal lobes that are communicating during talking using fMRI; and 5) to relate the dysfunction of the corollary discharge in schizophrenia to auditory hallucinations. Using EEG, ERP and fMRI measures, we addressed each goal in patients with schizophrenia and healthy control subjects. The N1 component of the ERP reflects dampening of auditory cortex responsivity during talking and inner speech in control subjects but not in patients. EEG measures of coherence indicated inter-dependence of activity in the frontal speech production and temporal speech reception areas during talking in control subjects, but not in patients, especially those who hallucinated. FMRI data showed that in healthy controls, activity in superior temporal gyrus was more negatively correlated with activity in Broca's area during talking than during listening. This was not observed in patients. These data suggest that a corollary discharge from frontal areas where thoughts are generated fails to alert auditory cortex that they are self-generated, perhaps leading to the misattribution of inner speech to external sources and producing the experience of auditory hallucinations.

## Analysis of Interneurones in the ELL of *Gnathonemus petersii* using Neuropharmacology, Immunohistochemistry and Modelling

Engelmann J<sup>1)</sup>, Sugawara Y<sup>2)</sup>, van den Burg E<sup>1)</sup>, Bacelo J and K<sup>1)</sup>. Grant<sup>1)</sup>

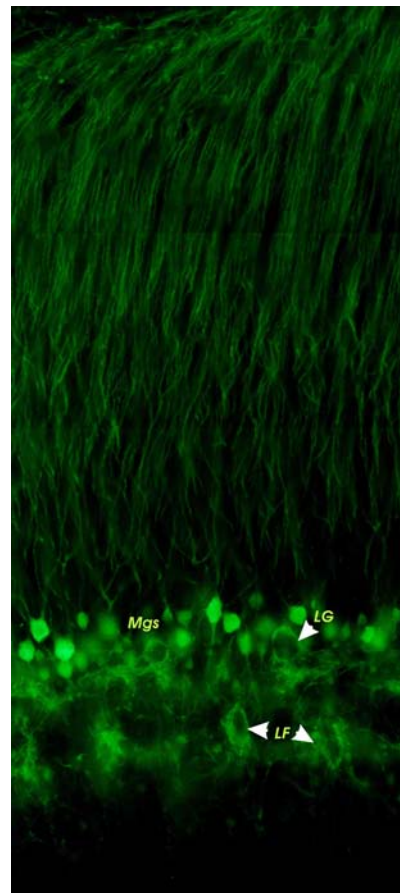
<sup>1)</sup>Unité de Neurosciences Intégratives et Computationnelles, C.N.R.S., 1. Avenue de la Terrasse, 91198 GIF SUR YVETTE, France

<sup>2)</sup>Dept. of Physiol., Teikyo University, Kaga 2-11-1, Itabashi-ku, TOKYO, Japan

The electrosensory lobe (ELL) of *Gnathonemus petersii*, a mormyrid electric fish, is a cerebellum-like sensory structure that removes predictable features of electrosensory input following anti-Hebbian rules. Plasticity is mediated by associative depression at synapses between parallel fibres and Purkinje-like interneurons (MG-cells) and requires NMDA receptor activation, changes in postsynaptic calcium and especially the occurrence of a backpropagating postsynaptic dendritic broad spike within a few milliseconds following EPSP onset.

Here we present theoretical and experimental work which reveal (1) where in the cell the broad spike is initiated, (2) the distribution of voltage gated sodium (VGS) channels underlying the backpropagation, (3) the role of K-currents in its propagation and (4) the distribution of Kv3.3 potassium channels.

*In vitro* sharp and perforated patch recordings, while locally applying TTX, and a conductance-based model of MG-cells all indicate that broad spikes are actively generated in the proximal segments of the apical dendrites, whereas spikelets are initiated in the axon hillock and invade the soma incompletely. While dendritic recordings of MG-cells currently are not feasible, the distribution of VGS channels (see figure) supports previous data that speculated on an active back-propagation of the broad spikes over the total apical dendritic arbour. In contrast to the ELL of *Apteronotus*, where a Kv3.3 channel was shown to be involved in switching the firing mode of ELL cells from tonic to bursting, the ELL of *Gnathonemus* shows only weak Kv3.3 expression. Further electrophysiological data indicate that a variety of 4AP and TEA-sensitive K-channels are expressed in the ELL of *Gnathonemus*, but that their expression is predominantly restricted to efferent cells for which backpropagation has not been described yet. We conclude that the apparent low density of K-channels in dendrites of MG cells accounts for the long duration of broad spikes, which allows a strong interaction between the synaptically evoked EPSP and the actively backpropagating signal. This may be at the basis of plasticity of MG cells to electrosensory stimuli, which underlies updating of the electrosensory system.



Supported by Marie-Curie Fellowship (QLK6-CT-2002-5172) and the Japanese PICS



**Presynaptic inhibition of cricket auditory afferent neurons.**

J.F.A. Poulet

Department of Zoology, University of Cambridge, UK.

The first stage of sensory information processing in the CNS is at the afferent to interneuron or motor neuron synapse. A common strategy to control the inflow of sensory information is presynaptic inhibition of the afferent axon terminals, mediated by primary afferent depolarisations (PADs). In this study, I made intracellular recordings close to auditory afferent terminals in the prothoracic ganglion of the cricket. I found that: (1) At sound levels below spiking threshold, PADs were evoked to acoustic stimuli both at the neuron's best and non-best frequency. This could indicate a gain control function to prevent saturation; or lateral inhibitory effects to enhance frequency selectivity. (2) PADs were present after removing either the ipsi- or contra-lateral ear and therefore might play a role in directional hearing. (3) The amplitude of the PADs depended on the temporal structure of the acoustic stimulus. Short duration stimuli elicited smaller PADs than longer duration stimuli. (4) Acoustically evoked spikes that coincided with PADs were reduced in amplitude, which strongly suggests an inhibitory function for the PADs. Presynaptic inhibition of the afferent axon therefore may fine tune and contribute to acoustic processing in the auditory pathway. Supported by the BBSRC.

**Symposium #S9:**  
**Real time processing vs. variability of neural responses**  
**RM. Hennig and B. Ronacher, Berlin**

**Introduction**

[#S9](#) RM. Hennig and B. Ronacher, Berlin  
*Real time processing vs. variability of neural responses*

**Slide**

[#S9-1](#) R. Krahe, Montreal (CDN)  
*Reliability of neuronal coding in the electrosensory system of weakly electric fish*

[#S9-2](#) R. Hahnloser, Zurich (CH)  
*In search of online learning mechanisms for birdsong*

[#S9-3](#) A. Vogel, B. Ronacher and RM. Hennig, Berlin  
*Acoustic pattern recognition in insects: real time processing vs. variability of neural responses*

[#S9-4](#) A-K. Warzecha, Bielefeld/Münster  
*Getting on the track of noise: Constraints on the reliable computation of visual motion information by fly motion sensitive neurons*

[#S9-5](#) A. Delorme, La Jolla, CA (USA)  
*Human brain dynamics leading to fast responses*

[#S9-6](#) G. Curio, Berlin  
*High-frequency (600 Hz) bursts of cortical population spikes in non-invasive human EEG and MEG recordings*

**Poster**

[#32A](#) S. Schreiber, I. Samengo and AVM. Herz, Berlin and San Carlos de Bariloche Rio Negro (RA)  
*Frequency dependence of spike timing reliability: lessons from conductance-based modeling*

[#33A](#) GG. de Polavieja, A. Harsch, I. Kleppe, R. Robinson and M. Juusola, Madrid (E) and Cambridge (UK)  
*Do action potential waveforms convey information about the stimulus?*

- [#34A](#) G. Wenning, T. Hoch, P. Kallerhoff and K. Obermayer, Berlin  
*Pulse-detection in single neurons and neural populations in a colored noise setting*
- [#35A](#) S. Rotter, Freiburg  
*Statistical properties of non-stationary spike trains*

## **Introductory Remarks to Symposium 9**

### **Real time processing vs. variability of neural responses**

**RM. Hennig and B. Ronacher, Berlin**

Sensory systems of animals perform under two ubiquitous and serious constraints: (i) the necessity to respond quickly to single events and (ii) the variability of neural responses due to the stochastic nature of the neuronal integration processes. In order to achieve high precision in real-time, nervous systems had to evolve mechanisms to extract information about relevant object properties despite a rather high variability of neural responses observed in many examples. Besides parallel processing, there are two basic strategies to reduce variability. First, to integrate over time and second, to average across several processing elements. The first strategy is constrained by its possible interference with temporal resolution. The benefits of averaging across neurons, on the other hand, depend on uncorrelated responses, a factor that may be crucial for the performance and evolution of nervous systems.

In this symposium insights from different sensory modalities (acoustic, visual, electrosensory) as well as theoretical approaches will be presented. In doing so we will compare large (vertebrate) and small (insect) nervous systems as in the latter, due to size limitations, we expect to find solutions for specific tasks that are stripped to the computational basics. Special emphasis is given to model systems in which both the neuronal variability as well as the system's output were determined, i.e. systems in which real-time processing capacity can be directly compared to behavioural precision.

## Reliability of neuronal coding in the electrosensory system of weakly electric fish

Rüdiger Krahe

Department of Biology, McGill University  
Montreal, Quebec H3A 1B1, Canada

Most biologically relevant stimuli are not static. Behavioral responses are usually elicited by stimulus transients, such as they occur in communication signals or when environmental conditions change. In order to understand the reliability of sensory processing under natural conditions, we therefore need to investigate neuronal coding with realistic, time-varying stimuli. We studied the reliability of neuronal information transmission at the first two stages of electrosensory processing in South American weakly electric fish.

Weakly electric fish sense perturbations of their self-generated electric field and use this information for orienting in their habitat. The perturbations can be of two major origins. 1) They can be caused by nearby objects, such as prey, with electric impedance different from the surrounding water. These perturbations typically are local, they only affect a limited area of the fish skin. 2) Perturbations can also be caused by overlapping of the fish's own field with the field of a nearby conspecific resulting in "global" changes, i.e. changes that affect most of the surface of the fish. Electroreceptors distributed over the entire skin monitor global and local changes in the electric field. P-type primary afferents relay the information on changes in stimulus amplitude to the electrosensory lateral line lobe (ELL) of the hindbrain where topographically arranged pyramidal cells perform spatial and temporal filtering on the primary afferent input. Whereas the primary afferents encode local amplitude changes in their instantaneous firing rate, the responses of pyramidal cells are more complex. They are determined by their receptive field properties, by feedback from higher centers of processing, and by their intrinsic burst properties (Bastian et al. 2002; Krahe and Gabbiani 2004).

We used several measures to quantify the variability of P-receptor afferent spike trains in response to repeated time-varying stimuli (Kreiman et al. 2000). The mean spike count and its variance measured in short time windows turned out to be poorly correlated with the trial-to-trial variability of P-receptor afferent spike trains. We then quantified spike timing jitter using the notion of spike train distances and found that the trial-to-trial jitter in spike timing is on the order of a few milliseconds. When we artificially introduced spike timing jitter in recorded spike trains, information transmission as quantified by stimulus estimation techniques was only degraded for amounts of jitter significantly larger than the ones observed experimentally. This suggests that the intrinsic variability of the primary afferents lies outside of the range where it might compromise information transmission. Yet, it may still allow for improvement in stimulus encoding by averaging across multiple afferent fibers.

At the level of the ELL, many P-receptor afferents converge onto any given pyramidal cell. However, when the encoding of spatially global, randomly time-varying stimuli is quantified using stimulus estimation, pyramidal cells perform significantly worse than primary afferents (Gabbiani et al. 1996). Even when stimuli are estimated from pairs of simultaneously recorded pyramidal cell spike trains, coding fractions are still lower than for single P-receptor afferents (Krahe et al. 2002). It appears that most pyramidal cells of the ELL do not encode the detailed stimulus time course. Instead, they appear to indicate the occurrence of behaviorally relevant stimulus features by firing brief bursts of spikes. In an analysis of feature extraction, spike bursts of pyramidal cells performed significantly better than isolated spikes at detecting upstrokes and downstrokes in stimulus amplitude. And spike bursts of single pyramidal cells were again outperformed by spikes fired by two simultaneously recorded pyramidal cells within a time window of a few milliseconds. Thus, our results suggest that the reliable encoding of the stimulus time course by primary afferents is transformed into extraction of behaviorally relevant stimulus features at the level of the hindbrain. Spike bursts appear to play a central role in this process. Beyond the level of individual pyramidal cells, feature extraction can be further improved by evaluation of stimulus-induced coincident activity of pyramidal cells.

Recent evidence suggests that the response properties of pyramidal cells are dynamically regulated by the spatial extent of stimulation and by feedback from higher electrosensory processing centers in the brain (Chacron et al. 2003; Doiron et al. 2003). Feedback also appears to be shaped by the spatial characteristics of electrosensory stimuli, that is it affects pyramidal cell responses differently depending on whether modulations of stimulus amplitude occur on a small spatial scale (as caused by prey-like objects) or whether they occur on a global scale (as caused by the electric field of a nearby conspecific or when a fish approaches a non-conducting boundary like the water surface).

Thus, weakly electric fish are a promising model system in which to study the processing of naturalistic, time-varying stimuli and its control by feedback, which dynamically adjusts lower-level processing to the current behavioral conditions.

Funded by NSF.

Bastian J, Chacron MJ, Maler L (2002) Receptive field organization determines pyramidal cell stimulus-encoding capability and spatial stimulus selectivity. *J Neurosci* 22:4577-4590.

Chacron MJ, Doiron B, Maler L, Longtin A, Bastian J (2003) Non-classical receptive field mediates switch in a sensory neuron's frequency tuning. *Nature* 423:77-81.

Doiron B, Chacron MJ, Maler L, Longtin A, Bastian J (2003) Inhibitory feedback required for network oscillatory responses to communication but not prey stimuli. *Nature* 421:539-543.

Gabbiani F, Metzner W, Wessel R, Koch C (1996) From stimulus encoding to feature extraction in weakly electric fish. *Nature* 384:564-567.

Krahe R, Gabbiani F (2004) Burst firing in sensory systems. *Nat Rev Neurosci* 5:13-23.

Krahe R, Kreiman G, Gabbiani F, Koch C, Metzner W (2002) Stimulus encoding and feature extraction by multiple sensory neurons. *J Neurosci* 22:2374-2382.

Kreiman G, Krahe R, Metzner W, Koch C, Gabbiani F (2000) Robustness and variability of neuronal coding by amplitude-sensitive afferents in the weakly electric fish *Eigenmannia*. *J Neurophysiol* 84:189-204.

In search of online learning mechanisms for birdsong

Richard Hahnloser  
Institute for Neuroinformatics UNIZH / ETHZ  
Winterthurerstrasse 190  
8057 Zurich  
Switzerland

Birdsong is a learned behavior depending on auditory feedback. There exist a group of brain areas in the avian anterior forebrain that are homologous to the basal ganglia in mammals and that are specifically involved in song learning. Bilateral lesions in these areas produce a profound impairment of song learning in juveniles but have little effect on vocal production in adults.

The songs of many birds such as the zebra and the bengalese finch are very complex and evolve on a timescale of just a few milliseconds. The desire to understand the neural mechanisms of song learning in a singing finch creates the need for technology capable of providing song-triggered feedback on the timescale of just a few milliseconds. We have developed a song recognition program able to detect specific notes of a song in real time. The underlying support vector machine needs to be trained on just 1-2 song bouts.

Using our real-time song recognizer we can provide distorted auditory feedback or electrically stimulate the brain of a singing bird at a particular note of choice whilst recording from neurons in the anterior forebrain pathway. We test whether the neural activity signals a mismatch between the distorted auditory feedback and the stored song template, a critical computation during the sensory-motor phase of song learning that is believed to be performed in anterior forebrain areas.

## Acoustic pattern recognition in insects: real time processing vs. variability of neural responses

Astrid Vogel, Bernhard Ronacher, R. Matthias Hennig

Institute of Biology, Humboldt-University Berlin, e-mail: [vogel.astrid@web.de](mailto:vogel.astrid@web.de).

Acoustic signals are characterized by their carrier frequency spectra and their pattern of amplitude modulations (AM), their envelope. Signal recognition is known to depend in many cases on envelope cues, and hearing systems are highly specialized to detect and resolve fast changes in sound amplitudes. Hearing systems, however, have to cope with the inherent variability of spike trains, which results from stochastic processes during signal transduction, during spike generation, and synaptic transmission. The intrinsic variability of spike responses is a general problem for neural information processing, but is especially serious if sensory systems deal with changes on fast time scales, as is the case in the acoustic domain.

The impact of variability can be relieved by averaging across several processing elements, or by temporal integration. The first strategy, averaging across units, depends on the number of available elements and on possible correlations between the responses of these elements. Temporal integration, on the other hand, has to comply with two constraints: (i) to preserve temporal resolution to a sufficient degree, and (ii) not to interfere with the need for fast decisions.

We investigated the consequences of neural variability on temporal resolution and explored the size of temporal integration windows in the auditory pathway of orthopteran insects (crickets and grasshoppers). For mate finding these animals use acoustic signals, in which specific information is conveyed by a characteristic AM pattern. The relevant AM frequencies may amount to several 100 Hz, and small changes in a pattern may already destroy the effectiveness of a signal. In a grasshopper species, the receivers (males) are able to extract the relevant information already from a single presentation of a shortened signal segment as short as ~200 ms (Ronacher & Krahe 1998; *J Comp Physiol A* 183: 729). Similarly, there are indications that the evaluation time windows of females of two cricket species are in a similar range (Hennig 2003, *J Comp Physiol A* 189: 589).

With these constraints in mind, we investigated the responses of auditory neurons at the first three stages of processing (sensory, local and ascending neurons) in the auditory pathway of locusts. By simultaneous intracellular recordings response variabilities and correlated spiking activities were quantified. Response variability increased from sensory to local neurons, and was highest at the level of ascending neurons. The relatively high response variability of ascending neurons seemed to be caused by filter processes in which inhibitions played an important role. Spike time correlations mainly occurred between elements of successive processing levels. Higher correlations values between elements within the same level were only observed among ascending neurons, but not for sensory and local neurons. Hence, at the level of local neurons reliability could be enhanced by averaging across several sensory cells, while for ascending neurons the higher average correlations as well as the smaller number of similarly reacting elements probably prevent such a strategy by higher order neurons. While sensory neurons show a pronounced locking of spikes to the signal's envelope, several ascending neurons revealed a reduction of phase locking and seemed to extract characteristic features of the signal. This specialization was often reflected in a strong dependency of the mean spike rate on the stimulus' modulation frequency. These results suggest that a transformation of encoding occurs between sensory cells and ascending interneurons. Consequently, neural responses of ascending neurons might be less susceptible to inherent stochastic variability.

## Getting on the track of noise: Constraints on the reliable computation of visual motion information by fly motion sensitive neurons

Anne-Kathrin Warzecha,

Lehrstuhl für Neurobiologie, Universität Bielefeld, Postfach 100131, 33501 Bielefeld  
and Institut für Psychologie II, Westfälische Wilhelms-Universität Münster,

Fliegenderstr.21, 48149 Münster

e-mail: [warzecha@psy.uni-muenster.de](mailto:warzecha@psy.uni-muenster.de)

When flying around flies experience retinal luminance changes with spatial and temporal characteristics that are determined by the flies' movements as well as by the spatial layout of their environment. Neuronal circuits evaluating the motion information obtained during flight manoeuvres are thought to play an important role in visually guided behaviour. In the focus of my talk will be the neuronal mechanisms that underlie visual motion computation and that constrain the reliability and precision by which the information is extracted. I use the fly as a model system of visual motion computation because here it is possible to investigate individually identifiable neurons and small neuronal networks *in vivo* using a broad range of methods that otherwise can only be applied to much reduced preparations. The following topics concerning the reliability of the computations taking place in the flies' visual motion pathway will be discussed in the talk.

- To what extent does photon noise limit the reliability of the fly visual motion pathway?
- How does environmental noise as may occur when leaves wiggle in the wind influence the reliability with which motion information is represented?
- How does the variability of synaptic transmission influence the reliability of fly motion sensitive neurons?
- What is the impact on neuronal reliability of the nonlinear integration of local motion information by the large motion-sensitive neurons?
- How do the dynamical properties of the stimuli influence the precision with which motion information is represented?
- How do variable neuronal responses relate to the behavioural output?

Supported by Deutsche Forschungsgemeinschaft  
and VolkswagenStiftung



## Human brain dynamics leading to fast responses

Arnaud Delorme

Swartz Center for Computational Neuroscience, INC, University of San Diego  
California, CA9209-0961, La Jolla, USA; arno@ucsd.edu

Sudden responses to world events are often crucial for survival, so understanding the neural origins of fast behavioral responses from a neuroscientific perspective may be key to understanding the global organization and dynamics of neural systems. Despite the large number of studies on reaction times, few have addressed the correlation between behavioral responses and brain activity preceding responses in specific brain regions. Hemodynamic studies cannot address this issue because of the poor time resolution of BOLD signal changes and for the first time, we attempt to tackle specifically this problem using ERP/EEG analysis. In target trials of a spatial attention task in which 15 subjects, recorded using a 32-channel EEG montage, responded to infrequent stimuli presentation at a cued location. Subjects responded faster when activity at a far frontal right periocular electrode was larger in a 3-cycle 4.5-Hz (theta) window centered 100 ms before button press (figure 1). Both across and within subjects reaction times were negatively correlated with theta power in this time window. Detailed analysis indicates that this effect is uniformly distributed across all data trial as the distribution of power values shift with reaction time (figure 1B). Independent component analysis identified a cluster of far frontal processes (previously termed P3f or P2a), common to most subjects, whose behavior was similar to the right periocular frontal electrode signal. In an additional 256-channel recording session, this component was best modeled using 2 bilateral equivalent dipoles that localized to the region of inferior frontal cortex (residual variance <0.01%). We conclude that increased activity in this area, possibly involving inhibition of cognitive planning in frontal inferior areas, precedes fast selective response times.

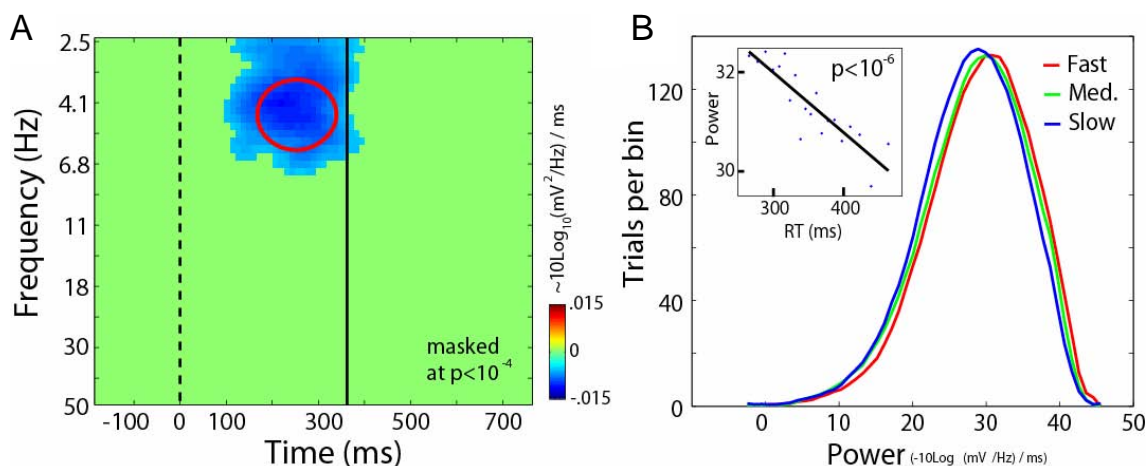


Figure 1: Correlations between response-locked non-artifact activity at the right periocular electrode and actual reaction times for all subjects. A. Correlation image showing correlations between reaction time and single-trial EEG power averaged over all trials and subjects (subject median reaction time had been subtracted from the collection of subjects' reaction time before computing correlations to remove the subject effect). In blue (negative) regions, more EEG power was associated with faster reaction times. Median reaction is 352 ms (vertical line). The negative correlation circled at low frequency prior to reaction time indicates that larger single-trial activity in this frequency band precedes fast responses. B. power histogram for the center of the circled region in A for 3 groups of data trials (of equal size) for fast, medium and slow reaction times. Distribution of power across trials is shifted uniformly with reaction time, irrespective of absolute power. It also shows that variations of power due to reaction time are small relative to the global distribution of power values. The inset panel show that the relation between spectral power and reaction time is close to linear in 20 quantile groups of increasing reaction time ( $R=.87$ ;  $P<10^{-6}$ ).

Acknowledgement: this report was supported by The Swartz Foundation and the National Institutes of Health (NIMH MH36840).

## High-frequency (600 Hz) bursts of cortical population spikes in non-invasive human EEG and MEG recordings

*Gabriel Curio*

Neurophysics Group, Dept. of Neurology, Campus Benjamin Franklin,  
Charité - University Medicine Berlin, Germany  
*curio@charite.de*

Human somatosensory evoked potentials (SEP) and magnetic fields (SEF) elicited by electrical median nerve stimulation comprise a brief (10-15 ms) burst of high-frequency (approximately 600 Hz) wavelets, overlapping in time with both, the thalamic 'P15' component and the primary cortical response 'N20'.

This high-frequency wavelet burst can be functionally differentiated from lower-frequency (< 400 Hz) EEG and magnetoencephalography (MEG) signals, which predominantly reflect synchronized mass excitatory and, partially, inhibitory postsynaptic potentials. Thus, these 'classical' macroscopically summed responses at frequencies < 400 Hz can contain modulations of the membrane potential below the spike threshold, which are not transmitted into the cortical network.

It is in this context that the 600 Hz SEP/SEF components, referred to as  $\sigma$ -bursts given their "spikelike" wavelet appearance, provide an opportunity to monitor non-invasively spike-related activity in the human cerebral somatosensory system: Converging evidence from recent recordings in rats, piglets, awake monkeys [1] and humans [2] shows that these macroscopic  $\sigma$ -bursts reflect the timing of highly synchronized and rapidly repeating population spikes which are generated by cuneothalamic and thalamocortical relay cells, cortical bursting pyramidal cells and, possibly, fast-spiking inhibitory interneurons. The human EEG  $\sigma$ -burst comprises multiple components with differential sensitivity to stimulus rate, vigilance, intensity, tactile interference, subject age, drugs, and certain movement disorders. Theoretical analyses suggest that cellular burst coding relays information with high efficiency; moreover, intraburst frequency can index graded sensory stimulus attributes.

As these 600 Hz EEG activities can be assessed using routine SEP equipment,  $\sigma$ -burst recordings open a unique and easy approach for non-invasive studies of human cerebral population spike responses.

### References:

- [1] Baker SN, Curio G, Lemon RN: EEG oscillations at 600 Hz are macroscopic markers for cortical spike bursts. *J Physiol.*, 550: 529-34 (2003).
- [2] Curio G: Ultrafast EEG activities. In: *ELECTROENCEPHALOGRAPHY*, 5th Edition. Niedermeyer E, Lopes da Silva F (Eds.); Lippincott, Williams & Wilkins, Baltimore, in press (2004).

*Acknowledgements: This work was supported by DFG SFB 618, TP B4.*

## Frequency dependence of spike timing reliability: lessons from conductance-based modeling

Susanne Schreiber<sup>1</sup>, Inés Samengo<sup>2</sup> & Andreas V.M. Herz<sup>1</sup>

<sup>1</sup> Humboldt-Universität zu Berlin, FachInstitut Theoretische Biologie, 10115 Berlin, Germany

<sup>2</sup> Centro Atómico Bariloche, 8400 San Carlos de Bariloche Río Negro, Argentina

The reliability of spike timing, estimated from the reproducibility of spiking responses to repeated presentation of a stimulus, can be reduced in the presence of neuronal noise. “Symptoms” of impaired reliability are a decreased probability of the occurrence of spikes and temporal jitter. Previous experimental and theoretical studies have provided evidence that spike timing reliability depends on the frequency content of the stimulus. Two mechanisms have been associated with this frequency dependence: on the one hand the occurrence of subthreshold oscillations in a particular frequency band and on the other hand a resonance of the stimulus frequency with the DC firing rate (Fellous *et al.*, 2001; Hunter *et al.*, 1998).

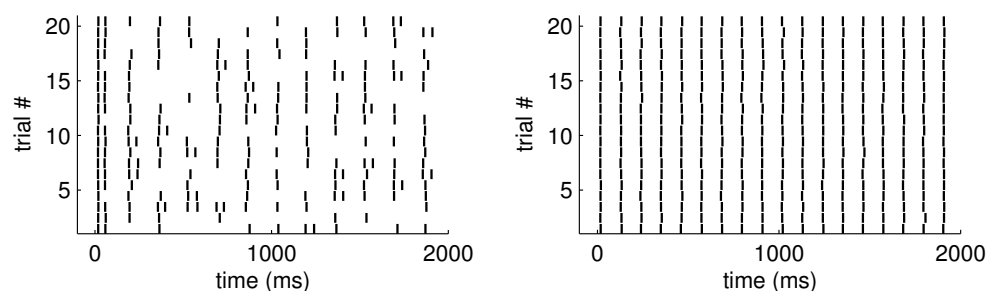


Figure 1: Spike rastergrams of 20 responses of a conductance-based model neuron to the presentation of a 6-Hz and a 9-Hz sine stimulus (left and right panels, respectively). Both stimuli are of equal variance and amplitude. Nevertheless, spike timing reliability of this cell is significantly higher for responses to the 9-Hz stimulus.

Employing conductance-based model neurons, we investigate the frequency selectivity of spike timing reliability and review the mechanisms in a systematic way. We demonstrate that two stimulus regimes have to be distinguished, depending on whether the stimulus mean is above or below threshold. For stimuli with a mean above threshold the neuronal firing rate in response to the DC stimulus component determines the most reliable frequency. For stimuli whose mean is below threshold, the frequency-dependent membrane impedance, as characterized by the subthreshold resonance profile, sets the most reliable frequency. While for stimuli with subthreshold mean reliability is strongly impaired by a reduced probability of spike occurrence, reliability of responses to stimuli with suprathreshold mean mainly suffers from noise-induced temporal jitter.

Because the subthreshold resonance frequency and the DC firing rate change with the DC level, spike timing reliability varies with the mean current. Our analysis demonstrates that the dependence of the frequency selectivity on the DC is shaped by the intrinsic currents and is related to the dynamical properties and the activation ranges of individual ionic conductances. For stimuli with a mean below threshold, in particular, an H conductance in addition to a slow potassium conductance can serve to create a preferred frequency of spike timing reliability that is relatively independent of the DC, as it is for example observed in stellate cells of the entorhinal cortex. Our results also provide evidence that nonlinearities are responsible for deviations from the frequency estimates for larger stimulus amplitudes. This is of particular interest for stimuli with a mean far below threshold, where large stimulus amplitudes are required to elicit spikes. In these cases large-amplitude sine waves of frequencies increasing with time (so-called ZAP stimuli) can be used to obtain a better estimate of frequency preference. Finally, we investigate how spike timing reliability evolves around threshold, where both stimulus regimes coincide.

### References:

- Fellous, J. M., Houweling, A. R., Modi, R. H., Rao, R. P., Tiesinga, P. H., and Sejnowski, T. J. (2001). Frequency dependence of spike timing reliability in cortical pyramidal cells and interneurons. *J Neurophysiol.*, 85(4):1782–7.
- Hunter, J. D., Milton, J. G., Thomas, P. J., and Cowan, J. D. (1998). Resonance effect for neural spike time reliability. *J. Neurophysiol.*, 80:1427–1438.

Supported by: Studienstiftung des Deutschen Volkes, DFG (SFB 515), and Alexander von Humboldt Foundation.

## **Do action potential waveforms convey extra information about the stimulus?**

Gonzalo G. de Polavieja<sup>†§\*</sup>, Annette Harsch<sup>‡</sup>, Ingo Kleppe<sup>‡</sup>, Hugh P. C. Robinson<sup>‡</sup> & Mikko Juusola<sup>‡\*</sup>

<sup>‡</sup>*Physiological Laboratory, University of Cambridge, Cambridge CB2 3EG, UK*

<sup>§</sup>*Neural Processing Laboratory, Department of Theoretical Physics, Universidad Autónoma de Madrid, Madrid 28049, Spain.*

**We test whether significant information is carried in the spike waveforms of cortical neurons. We find that when pyramidal neurons in rat visual cortex are driven by a conductance stimulus that resembles natural synaptic input, somatic action potential waveforms show a large variability that reliably signal the history of the input for up to 50 ms before the spike. This waveform code has a low noise and a much larger correlation to stimulus variations than the instantaneous spike rate, resulting in information rates four times larger.**

# Pulse-detection in single neurons and neural populations in a colored noise setting

G. Wenning, T. Hoch, P. Kallerhoff and K. Obermayer

Neuronale Informationsverarbeitung, Fakultät IV, Technische Universität Berlin,  
Germany

Cortical neurons in the visual system are exposed to an enormous synaptic activity, which determines fundamental properties of the cell (high conductance state) and hence the way the cell processes information [1]. For example the statistical properties of the membrane voltage depends critically on the actual synaptic input, which can change on a short time scale, and the question arises how a neuron or a population of neurons can react rapidly, reliably and temporally precise to transient, unexpected stimuli. The detection of transient changes in the input statistic can be considered as a basic neural computation and is important for coincidence detection as well as for the detection of synchronous spiking events in neural systems.

Using a leaky integrate-and-fire (LIF) neuron as well as a biologically more realistic Hodgkin-Huxley (HH) type point neuron we investigate how noise enhances the detection of sub-threshold input signals. First we consider a single neuron which receives a regular train of sub-threshold pulses and additional colored noise as inputs. The time interval is large compared to the membrane time constant, such that the preceding pulse has no significant influence on the following one. In order to quantify the neuron's response to the pulse train the total error is considered, which is proportional to the number of the false positive events and the number of pulses that are not detected, i.e. that are not immediately followed by an output spike. We find that pulse detection becomes more robust if the noise is colored, because the number of false positive events decreases with increasing the temporal correlation while the number of correctly detected events is almost unaffected. The optimal variance of the noise also changes with the degree of temporal correlations of the background activity. We provide numerical results for the LIF and HH framework and an approximate analytical description based on [2].

For a single neuron only half of the pulses can be detected at best. This is a consequence of the zero mean noise. Because of this fact one can question the biological relevance of the described pulse detection scenario in single neurons. Therefore we made additional numerical simulations with populations of neurons, where each neuron received mutually independent colored noise. We find that the pulse detection performance improves dramatically and that even small transient excitations can be detected by the population. Furthermore we show how the quality of detection (measured by ROC like curves) is influenced by the correlation time of the noise, the pulse height, the membrane potential variance and the population size.

*Supported by the DFG (SFB 618).*

- [1] A. Destexhe, M. Rudolph and D. Paré, *The high conductance state of neocortical neurons in Vivo*, Nat. Rev. Neurosci., **4**, 739-751, 2003.
- [2] N. Brunel and S. Sergi, *Firing frequency of leaky integrate-and-fire neurons with synaptic currents dynamics* J. Theor. Biol., **195**, 87-95, 1998.

# Statistical properties of non-stationary spike trains

Stefan Rotter

*Theory & Data Analysis, Institute for Frontier Areas of Psychology  
and Mental Health, Freiburg, Germany*

*Neurobiology & Biophysics, Institute of Biology III,  
Albert-Ludwigs-University, Freiburg, Germany*

Neuronal activity *in vivo* is highly dynamic (or variable, depending on the point of view) on multiple time scales, due to the joint action of several sources of 'input' impinging upon each neuron (presynaptic neuronal populations) and additional mechanisms internal to the neuron (e.g. ion channel noise). Can one dissect and separately characterize these different sources of variability from recordings of single neurons?

In its general form, this is obviously an ill-posed question. Only on the basis of suitable mathematical models can its analysis be attempted. Stochastic point processes and, in particular, renewal processes [1] have been frequently employed in this context, because they can be arranged to match any type of inter-spike interval distribution. Beyond that, the resulting models often turn out to be mathematically tractable. Within the neurosciences, a prime example for a renewal process is the integrate-and-fire neuron subject to stationary Poissonian inputs. It produces output spike trains by means of a cascade involving a linear filter in combination with a threshold/reset mechanism for spike generation [2].

The analysis of spike trains recorded *in vivo*, however, typically reveals distinct non-renewal aspects of neuronal firing, especially at larger time scales [3]. Technically, violations of the stationarity assumption, which is implicit in the definition of a renewal process, will lead to a rejection of the renewal hypothesis. Therefore, a more detailed analysis of the situation and a restatement of the results is necessary. In the present model study we consider in particular the second-order statistics (variance) of certain counting variables and inter-event intervals for a generalized renewal process model, where the non-stationarities are specified in terms of spectral properties of the underlying rate function.

Related to the above is a question of great practical importance: What happens if statistical tools developed for strictly stationary processes are applied to observations that were obtained under non-stationary conditions? Indeed, mathematical tools to deal with non-stationary data sets are not abundant. Here, we present explicit models for non-stationary behavior, along with their analysis. It is shown that the answer to the question posed above depends strongly on the *time scale* of the non-stationarities. We study essentially two extreme cases: the time scale of the fluctuations is faster than the typical inter-spike interval, and the fluctuations are slower than the duration of each observation/trial. The case of broadband fluctuations is also briefly considered.

[1] Cox DR, Isham V (1980) Point Processes. Chapman & Hall

[2] Tuckwell HC (1988) Introduction to Theoretical Neurobiology. Cambridge University Press. Vols. 1 & 2

[3] Nawrot MP, Riehle A, Aertsen A, Rotter S (2000) Spike Count Variability in Motor Cortical Neurons. EJM 12, Suppl. 11: 506

**Symposium #S10:**  
**Plasticity and Task-Dependence of Auditory Processing**  
**FW. Ohl and H. Schulze, Magdeburg**

**Introduction**

[#S10](#) FW. Ohl and H. Schulze, Magdeburg  
*Plasticity and Task-Dependence of Auditory Processing*

**Slide**

- [#S10-1](#) J-M. Edeline, Orsay (F)  
*Dynamic modulation of rate and temporal coding in the thalamo-cortical auditory system of awake guinea-pigs*
- [#S10-2](#) G. Ehret, J. Yan and P. Grün, Ulm and Calgary (CDN)  
*Corticofugal modulation of auditory processing in the mouse*
- [#S10-3](#) FW. Ohl, Magdeburg  
*Cognitive aspects of animal auditory learning*
- [#S10-4](#) B. Grothe, A. Seidl, I. Kollmar, P. Tripathi and H. Schnürch, Martinsried  
*Developmental and adult plasticity in the mammalian sound localization system*
- [#S10-5](#) JB. Fritz, M. Elhilali and S. Shamma, College Park (USA)  
*Rapid task-related plasticity of spectrotemporal receptive fields in the auditory cortex*
- [#S10-6](#) G. Klump, Oldenburg  
*Bottom-up and top-down processing in auditory scene analysis*
- [#S10-7](#) H. Schulze, Magdeburg  
*Correlates of AM discrimination learning in auditory cortex of the gerbil*

**Poster**

- [#36A](#) R. Schaette and R. Kempter, Berlin  
*A Computational Model of the Development of Tinnitus-Related Hyperactivity in the Early Auditory Pathway*
- [#37A](#) A. Boonman, Tübingen  
*The key to accurate timing resides in the signal design used by echolocating bats*

[#38A](#)

P. Eichhammer, B. Langguth, J. Marienhagen, T. Kleinjung and G. Hajak, Regensburg  
*Neuronavigated Repetitive Transcranial Magnetic Stimulation in Patients with Tinnitus*



## Introductory Remarks to Symposium 10

### Plasticity and Task-Dependence of Auditory Processing

Frank W. Ohl and Holger Schulze, Magdeburg

Traditionally, most of our knowledge on stimulus processing in the auditory system (as well as in other sensory systems) has been gained from the study of neuronal response changes associated with parametric variation of physical stimulus features. Recently, an increasing number of researchers focus on the complementary situation, i.e. changes of neuronal responses with physical stimulus parameters held constant. In this situation the sources of response variation are internal to the organism.

One such source of internal response variation is the history of the subject's previous experiences giving rise to what here is termed plasticity of neuronal responses. This type of influence can be studied by experimentally interfering with developmental processes (*developmental plasticity*) or by exposing the subject to learning situations (*learning-induced plasticity*). A related, but separable, source of internal response variation can be studied when a subject processes identical stimuli in the context of variable tasks to be performed (*task dependence*). As a common denominator between both aspects of internal response variation the concept of *top-down modulation of bottom-up processes* is discussed.

The symposium aims at characterizing how our understanding of auditory processing is complemented by taking the phenomenon and the underlying mechanisms of internal sources of response variation into consideration. Current achievements from various experimental and theoretical approaches (represented by the speakers' main research traditions) will be reviewed and future research strategies will be suggested.

## Dynamic modulation of rate and temporal coding in the thalamo-cortical auditory system of awake guinea-pigs.

Jean-Marc Edeline

NAMC, UMR-CNRS 8620, Université Paris-Sud 91405 Orsay, France

Over the last 15 years, an important concept has been validated by many laboratories: adult sensory systems can exhibit plastic changes under various circumstances ranging from peripheral lesions to behavioral training. Initially, several experiments showed that when a particular sound frequency is associated with an unconditioned stimulus (US) selective Receptive Field (RF) reorganizations can emerge after a few tens of training trials (review in Edeline 2003, Weinberger 2004). Recent findings also indicate that rapid changes in spectrotemporal RF can occur when the animal attention is focused around a particular frequency during instrumental training (Fritz et al., 2003). Other experiments indicated that months of training in a discrimination task led to important reorganizations of the cortical tonotopic map (Recanzone et al., 1993; Rutkowski et al., 2002; but see Brown et al., 2004). On the other hand, an impressive amount of studies has described the effects induced by pairing protocols between a sensory stimulus and a neuromodulatory system. These studies showed that a neuromodulator, in particular acetylcholine, can promote RF and map plasticity as extensive than those typically observed after behavioral training (Bakin & Weinberger, 1996; Kilgard & Merzenich 1998). These studies have provided useful “rate coding” descriptions of adult sensory plasticity, but we should consider that the firing rate is only one way (among others) to encode information in the central nervous system. After presenting key findings of “rate coding” descriptions in learning-induced sensory plasticity, we will present a few examples where the temporal organization of neuronal discharges is affected during the induction or expression of sensory plasticity. It will be suggested that future investigations should combine “rate coding” and “temporal coding” descriptions of sensory plasticity to unravel the richness and complexity of the neural code, and to elucidate how sensory experience can modify this code.

### References

- Bakin, J. S., & Weinberger, N. M. (1996) Induction of a physiological memory in the cerebral cortex by stimulation of the nucleus basalis. *Proc. Natl. Acad. Sci. USA*, 93, 11219-11224.
- Brown M, Irvine DR, Park VN.. Perceptual learning on an auditory frequency discrimination task by cats: association with changes in primary auditory cortex. *Cereb Cortex*. 2004 Sep;14(9):952-65.
- Edeline J-M. (2003) The thalamo-cortical auditory receptive fields: Regulation by the states of vigilance, learning and the neuromodulatory systems. *Exp Brain Res*. 153 (4), 554-572.
- Fritz, J., Shamma, S., Elhilali, M. & Klein, D. (2003) Rapid task-related plasticity of spectrotemporal receptive fields in primary auditory cortex. *Nature neurosci*. 11, 1216-1223.
- Kilgard, M.P., & Merzenich, M.M. (1998) Cortical map reorganization enabled by nucleus basalis activity. *Science*, 279, 1714-8.
- Recanzone, G. H., Schreiner, C. E. & Merzenich, M. M. (1993) Plasticity in the frequency representation of primary auditory cortex following discrimination training in adult owl monkeys. *J. Neurosci.*, 13, 87-103.
- Rutkowski, R., Than, K., & Weinberger, N.M. (2002) Evidence for area of frequency representation encoding acquired stimulus importance in rat primary auditory cortex. *Society for Neuroscience Abstract*, 24, 80.3.
- Weinberger NM. (2004) Specific long-term memory traces in primary auditory cortex. *Nat Rev Neurosci*;5(4):279-90.

## **Corticofugal modulation of auditory processing in the mouse**

Günter Ehret<sup>1</sup>, Jun Yan<sup>2</sup>, Philipp Grün<sup>3</sup>

<sup>1</sup>Dept. of Neurobiology, <sup>3</sup>HNO-Dept. and Clinic, University of Ulm, D-89069 Ulm, Germany

<sup>2</sup>Dept. of Physiology and Biophysics, Faculty of Medicine, University of Calgary, Calgary, Canada

The auditory cortex (AC) can influence, via corticofugal projections, neural response properties to sounds in lower centers of the ascending auditory pathway (e.g. Suga et al., 2000). Thus, cortical plasticity induced by learning or state of vigilance may feed back to the ascending auditory system. In order to quantify effects of corticofugal modulation by local activation in the AC under controlled conditions, one can simulate a learning situation by applying an electrical stimulus (unconditioned stimulus) in combination with a tone stimulus (conditioned stimulus), for example at the characteristic frequency (CF) of the stimulated neurons and, thus, to a defined position of the primary AC tonotopy and measure changes in the tonotopy and in neural response characteristics in lower centers due to the conditioning in the AC .

In a series of studies of corticofugal effects on sound processing in the mouse auditory system, we conditioned for 7 min by electrical pulses at the end of CF tones the primary AC in anesthetized mice at a position corresponding to a certain CF of the local neurons. The long-lasting (more than 8 hours) effects of this conditioning were measured in response properties of neurons in the central nucleus of the inferior colliculus (auditory midbrain) and the in auditory evoked responses (AERs). We found an increase of the CF representation over about one critical bandwidth (perceptual measure of spectral resolution) for the conditioned frequency (Yan and Ehret, 2001), an average increase in sensitivity of neurons tuned to the conditioned frequency, and a loss of sensitivity and a change in the shape of tuning curves and rate-level functions and of the dynamic ranges in neurons not tuned to the conditioned frequency (Yan and Ehret, 2002; Yan et al. to be published). Further, amplitudes of AERs (first 7 waves) significantly increased and latencies (waves 1-3 and V) and thresholds significantly decreased in response to the conditioned tone.

The data indicate that the primary auditory cortex can selectively enhance the processing of tones of learned significance in lower auditory centers both collectively and on the single neuron level. At the same time, the processing of tones about one critical bandwidth away from the tone of interest is somewhat suppressed. This shows that corticofugal modulation due to a local stimulation in the AC is organized in a center (excitatory) - surround (inhibitory) way in the auditory midbrain.

Supported by the Deutsche Forschungsgemeinschaft, Eh 53/17, 18, and the Campbell McLaurin Chair for Hearing Deficiencies, University of Calgary.

Suga N, Gao E, Zhang Y, Ma X, Olsen JF (2000) Proc Natl Acad Sci **97**: 11807-11814

Yan J, Ehret G (2001) NeuroReport 12: 3313-3316

Yan J, Ehret G (2002) Eur J Neurosci 16 : 119-128

## Cognitive aspects of animal auditory learning

Frank W. Ohl

*Leibniz-Institut für Neurobiologie, Magdeburg*

The talk will review the physiology of learning-induced plasticity in auditory cortex and then focus on novel results on the physiological basis of category learning (concept formation) as a fundamental element of cognition. During category learning equivalence classes of meaning (categories) are established over stimuli that enable an organism to adequately respond even to novel, previously unfamiliar, stimuli when they are encountered.

Using a recently developed experimental paradigm Mongolian gerbils (*Meriones unguiculatus*) were trained to discriminate linearly frequency-modulated (FM) tones with respect to their modulation direction (i.e. 'rising' vs. 'falling'). The training can be conducted such that the animals form the respective categories of 'rising' and 'falling' modulations, and transfer the concept of modulation direction to novel, previously unheard, FM tone stimuli (Wetzel et al. 1998, *Behav. Brain Res.* **91**, 29-39) after a behavioral state transition.

Since FM tone discrimination learning has been demonstrated to be dependent on auditory cortex (Ohl et al. 1999, *Learn. & Memory* **6**, 347-362) the potential neural correlates of this behavioral state transition were studied using multichannel recordings of epidural electrocorticograms. State space analysis of spatio-temporal activity patterns revealed that the initial response components to FM tones were predominantly determined by physical stimulus features and anatomical connectivity patterns (Ohl et al. 2000, *J. Neurophysiol.* **83**, 3123-3132). Later response components showed transient epochs (several 10s of ms) of clustering into particular subregions of the state space after discrimination learning. Moreover, after the transition to categorization behavior the state space representation of these clusters reflected the perceptual scaling exhibited by the animals in their behavioral category selection (Ohl et al. 2001, *Nature*, **412**, 733-736). These data suggest the coexistence of separate coding principles for information relevant for stimulus identification using physical features and for information subjectively relevant for an individual's categorization of stimuli (Ohl et al. 2003, *Biol. Cybern.*, **88**, 374-379; Ohl et al. 2003, *Reviews Neurosci.*, **14**, 35-42).

**Developmental and adult plasticity in the mammalian sound localization system**

Benedikt Grothe<sup>1,2</sup>, Armin Seidl<sup>2</sup>, Ida Kollmar<sup>1,2</sup>, Pratibha Tripathi<sup>1,2</sup>, and Harald Schnürc<sup>2</sup>

Department Biology II, Biocenter, Munich University, Martinsried, Germany  
Max-Planck-Institute of Neurobiology, Martinsried, Germany

Interaural time differences (ITD) are the most important physical cue to localize low frequency sounds. In mammals, they are initially processed in the medial superior olive (MSO) via a complex interaction of binaural excitatory and inhibitory inputs that is yet not fully understood. Most likely, ITD sensitivity of single MSO cells is basically set up by a coincidence detection of the binaural excitatory inputs. The fine-tuning of ITD sensitivity in MSO neurons to the animal's behaviourally relevant range, however, seems to depend on glycinergic inhibition (Brand et al., Nature 417:543). Anatomical data show that the normal arrangement of the inhibitory inputs is achieved only after hearing onset and that this development can be partially suppressed by mild exposure to omnidirectional noise surpassing most spatial cues (Kapfer et al., Nature Neurosci 5:247).

Our recent studies in Mongolian gerbils show that, in fact, normal ITD tuning at the level of single auditory brainstem neurons is significantly and permanently altered by exposure to omnidirectional noise during a critical period after hearing onset. This change could be explained by a lack of maturation of the glycinergic MSO inputs.

In contrast, during adulthood exposure to identical noise and for the same duration does not cause a permanent alteration of ITD tuning of auditory brainstem neurons. However, it causes a short-term (up to several days) shift of ITD sensitivity in the direction ITD functions of single MSO cells are shifted due to the mature glycinergic inhibition. The simplest explanation for such a shift of ITD sensitivity would be that noise exposure causes a temporary increase of glycine induced inhibitory current. We therefore used quantitative PCR to test whether the expression of glycine receptors (Gly $\alpha$ 1) is increased during or shortly after exposure to omnidirectional noise. Our preliminary results indicate such a temporarily dramatic increase of Gly $\alpha$ 1 mRNA in the MSO but, interestingly, not in the neighbouring nucleus, the lateral superior olive (LSO), although LSO receives the same glycinergic input. Such a differential change even in the same individual is surprising but strongly suggests that glycinergic inhibition is involved in adult plasticity of the mammalian sound localization system.

Taken together, our results from electrophysiological, anatomical and molecular studies indicate that glycinergic inhibition is crucial for the tuning of auditory brainstem neurons to the physiological range of ITDs as well as for adjusting the adult system according to changes in the acoustic environment.

*Supported by DFG GR 1205/12-1*

## Rapid task-related plasticity of spectrotemporal receptive fields in the auditory cortex

Jonathan Fritz\*, Mounya Elhilali, Shihab Shamma  
Center for Auditory and Acoustic Research, Institute for Systems Research,  
University of Maryland, College Park, Maryland, USA, 20742  
\*ripple@isr.umd.edu

During active listening, the auditory system attends to salient, task-related acoustic cues. Cortical neuronal response properties can change dynamically so as to selectively enhance responses to these acoustic features of interest. We studied changes in cortical spectrotemporal receptive fields (STRFs) that occurred when animals were engaged in: (1) spectral tasks, such as tone detection or discrimination, (2) temporal tasks such as gap detection or tone duration discrimination. We measured STRFs of single neurons in A1 in the ferret using standard reverse-correlation techniques and quantitatively analyzed changes in STRF shape which resulted during task performance. We trained ten ferrets, using avoidance conditioning, to detect variable tonal targets against a background of rippled noise. They quickly learned a variety of other tasks, all of which were variations on a basic behavioral paradigm (AA...B), in which the animal discriminated between a set of similar reference stimuli (variable length sequence) and distinct target stimuli. Performance on each task required attention to a different salient acoustic cue. In our initial study of neural plasticity arising during a tone detection task, we found (*Nature Neuroscience* (2003) **11**, 1216-1223) that more than 60% of neuronal STRFs changed within minutes of task onset in a consistent pattern. At both the single unit and at the population level, responses were enhanced to frequencies near the tonal target with a precision of about 0.25 octave. Our subsequent studies of neural plasticity during tone discrimination indicate that an opposite effect can occur, as a population analysis of neural responses indicates that STRF responses are specifically suppressed to the reference tone. Our working hypothesis is that these differing task-dependent STRF changes serve to adaptively enhance task performance. These results may provide insight into the adaptive neural mechanisms which underlie auditory attention during active listening.

Supported by NIH (NIDCD) R0-1 & R0-3 grants to SAS and JBF

## **Bottom-up and top-down processing in auditory scene analysis**

**Georg M. Klump**

Zoophysiology and Behavior Group, Oldenburg University  
Carl-von-Ossietzky Str. 9-11, 26129 Oldenburg, Germany

In analysing the acoustic environment, the auditory system has the task to segregate the sounds that originate from multiple sources. At the same time, the auditory analysis requires the grouping of the sound components originating from one source that, for example, differ in spectral frequency. Both the processes of source segregation and grouping are combined in the analysis of acoustic scenes. The presentation will provide a brief review of the approaches to the study of auditory scene analysis in animal experiments and evaluate the evidence. The available results from animal experiments suggests, that many of the mechanisms involved in the processing of acoustic scenes are bottom-up mechanisms that do not require attending to the stimulus. Examples are the segregation of signals from a simultaneously presented acoustic background on the basis of common modulation, or the segregation of consecutive tones in a sequence into separately processed auditory streams that is dependent on the frequency separation between the tones. In humans, under some conditions the auditory stream segregation of sequential tones is dependent on the instruction and top-down mechanisms of auditory processing appear to be involved. However, conclusive evidence from animal experiments for the action of top-down mechanisms in the context of auditory streaming is lacking. Top-down effects on the processing of the sensory input can be suspected on the basis of results indicating that auditory memory has an effect on the analysis of complex acoustic stimuli. However, the differences in sensory perception that result from differences in auditory memory can be the consequence of long-term adaptation and plasticity of the auditory processing mechanisms which would again indicate a dominance of bottom-up over top-down processing in the animal experiments. More conclusive evidence for top-down processing in auditory scene analysis may be provided by studies that apply short term shifts of attention as a tool.

Supported by the Deutsche Forschungsgemeinschaft (SFB 517, FOR 306)

## Correlates of AM discrimination learning in auditory cortex of the gerbil

Holger Schulze

Leibniz Institute for Neurobiology, Brenneckestr. 6, 39118 Magdeburg, Germany

The perceptual quality associated with periodic, 100% sinusoidally amplitude modulated (AM) tones varies as a function of modulation frequency ( $f_m$ ): AM tones of low  $f_m$  (up to about 100 Hz) evoke percepts of rhythm and roughness whereas those of higher  $f_m$  evoke percepts of periodicity pitch. Recent studies provided evidence that these different perceptual qualities are paralleled by differences in neuronal responses: AM tones of low  $f_m$  are represented by a temporal, non-topographical (synchrony) code in primary auditory cortex (AI) [1] and AM tones of high  $f_m$  are represented by a spatial (rate-place) code (periodotopic map, [1,2]). Furthermore, learning performance also differs for low and high  $f_m$  in an AM tone discrimination task in gerbils: Learning proceeds faster and discrimination performance is slightly better for low than for high  $f_m$  [3]. Based on these latter results we follow the hypothesis that different learning mechanisms might be involved in discrimination learning of AM with different low or high  $f_m$ , that is, the synchrony or rate-place representation might be altered by different learning mechanisms. Whereas learning induced alterations of stimulus representations in sensory maps are well described (e.g. [4]), only little is known about the plasticity of temporal stimulus representations like the synchrony code.

By mapping of the AI before and after AM tone discrimination learning in individual animals we were able to demonstrate that the number of neurons that code for the training stimuli increases with learning [5]. Furthermore, by recording from implanted electrodes, responses from individual neurons or small clusters of neurons could be obtained before and after the training, revealing plastic changes of temporal and spectral response properties in AI neurons. In particular, some neurons shifted their best frequencies towards the carrier frequency of the AM tone, and increased the temporal precision of their phase-locked responses to AM tone envelopes [5]. In any case, the observed plastic changes of neuronal response properties were highly specific with respect to both the spectrum and the time structure of the training stimuli. The data suggest a neural mechanism of differential alteration of the timing of excitatory and inhibitory afferent input to auditory cortical neurons due to AM tone discrimination learning.

[1] Schulze H, Langner G, 1997, J. Comp. Physiol. A 181: 651-663

[2] Schulze H et al., 2002, Europ. J. Neurosci., 15: 1077-1084

[3] Schulze H, Scheich H, 1999, Neurosci. Lett. 261: 13-16

[4] Recanzone GH et al., 1993, J. Neurosci. 13: 87-103

[5] Schulze H et al., 2002, Acta Acustica united with Acustica, 88: 399-407



# **A Computational Model of the Development of Tinnitus-Related Hyperactivity in the Early Auditory Pathway**

**Roland Schaette and Richard Kempter**

Institute for Theoretical Biology, Biology Department, Humboldt University Berlin  
Invalidenstr. 43, 10115 Berlin, Germany

Tinnitus is the perception of a sound in the absence of acoustic stimulation. In many cases, tinnitus is associated with hearing loss in the high-frequency range. The pitch of the tinnitus sensation is correlated to the extent and range of the hearing impairment (Henry et al., ITS Proceedings 1999). The question of how hearing loss leads to the development of tinnitus, however, still remains unanswered.

In animals, hearing loss induced by acoustic trauma leads to signs of tinnitus (Heffner et al., *Hear. Res.* 2002). A manifestation of tinnitus-related changes in the auditory pathway is found in the dorsal part of the cochlear nucleus, which is the first neuronal processing stage in the auditory pathway. In the dorsal cochlear nucleus (DCN) of animals with behavioral evidence of tinnitus, the spontaneous neuronal activity is significantly increased (Kaltenbach et al., *Neurosci. Lett.* 2004). These experimental results present a paradox situation: hearing loss leads to an overall decrease of auditory nerve activity, but there is increased spontaneous activity, or ‘hyperactivity’ in the DCN.

We address the question of tinnitus development from a theoretical perspective, following the hypothesis that the auditory pathway can be modified by sensory experience. Plasticity mechanisms like activity-dependent changes in synaptic weight or neuronal excitability are to ensure proper information processing. Hearing loss, however, causes drastic changes in the input received by the auditory system, and this imbalance might lead to the development of pathological hyperactivity in the brain stem.

In order to explore this hypothesis, we set up a computational model of the auditory nerve (AN) and the DCN. The model captures how the population firing rate of AN fibers depends on the intensity of acoustic stimuli and the integrity of inner and outer hair cells of the cochlea. Changes in the activity of the auditory nerve are assumed to drive a homeostatic compensation mechanism in output neurons of the DCN. Therefore, synapses from the AN to DCN neurons obey rules of homeostatic plasticity to maintain a pre-set target value of mean activity of the postsynaptic neuron. After hearing loss, our model develops hyperactivity in those parts of the DCN that are innervated by the damaged parts of the cochlea. The amount of hyperactivity depends on the amount of cochlear hair cell loss. The observed hyperactivity patterns are similar to those seen in animals.

Supported by the DFG, Ke 788/1-2,3

## **The key to accurate timing resides in the signal design used by echolocating bats**

Arjan Boonman

*University of Tübingen, Animal Physiology, Auf der Morgenstelle 28  
72076 Tübingen, Germany*

Bats use echolocation to navigate and find food in the dark. It is still unknown how returning sets of echoes are transformed into a spatial representation, but the timing of individual echoes seems to play an important role in this process. Due to sound propagation losses bats need to emit relatively long pulses, up to 40 times longer than the integration time of their hearing system. Using a model simulating a bat's typical cochlear functions I found the frequency-time course of echolocation pulses to be optimized for separating returning echoes. Signal design therefore appears to be an adaptation to optimize temporal resolution. Further simulations revealed that bats use a far broader bandwidth in their echolocation than needed to reduce statistical uncertainty in the estimation of distance (echo timing). I show that this excess bandwidth can be used to resolve returning echoes occurring within the bat's integration time. This ability is meaningful to navigate near vegetation and is supported by psychophysical experiments on bats.

## **Neuronavigated Repetitive Transcranial Magnetic Stimulation in Patients with Tinnitus**

Peter Eichhammer, Berthold Langguth, Jörg Marienhagen\*,

Tobias Kleinjung\*\*, Göran Hajak

Department of Psychiatry and Psychotherapy, University of Regensburg,

93053 Regensburg, Universitaetsstrasse 84, Germany

\* Department of Nuclear Medicine, University of Regensburg,

93053 Regensburg, Franz-Josef-Strauss Allee, Germany

\*\* Department of Otorhinolaryngology and Audiology, University of Regensburg,

93053 Regensburg, Franz-Josef-Strauss Allee, Germany

### **Introduction:**

Clinical as well as neurophysiological and neuroimaging data suggest that chronic tinnitus resembles neuropsychiatric syndromes characterized by focal brain activation. Low frequency repetitive transcranial magnetic stimulation (rTMS) has been proposed as an efficient method in treating brain hyperexcitability disorders by reducing cortical excitability.

### **Methods:**

In ten patients suffering from chronic tinnitus, the effect of magnetic-resonance-imaging and positron-emission-tomography guided neuronavigated 1 Hz rTMS on auditory cortex activity was evaluated.

### **Results:**

Neuronavigated rTMS led to a considerable improvement in tinnitus complaints which was accompanied by changes in cortical excitability as measured by paired-pulse TMS as well as changes of structural neuroplasticity as measured by voxel-based morphometry.

### **Conclusions:**

Neurophysiological as well as imaging data suggest that neuronavigated rTMS may offer a new option for treating auditory phantom perceptions like chronic tinnitus.

**Symposium #S11:**  
**The integrated role of glial cells in the CNS: new methodological approaches**  
**P. Bezzi and C. Schipke, Lausanne and Berlin**

**Introduction**

- [#S11](#) P. Bezzi and C. Schipke, Lausanne and Berlin  
*The integrated role of glial cells in the CNS: new methodological approaches*

**Slide**

- [#S11-1](#) CR. Rose, Munich  
*Imaging of glial calcium transients*
- [#S11-2](#) G. Carmignoto, Padova  
*Neuronal synchrony in the hippocampus mediated by glutamate released from astrocytes*
- [#S11-3](#) P. Bezzi, E. Pilati, V. Gundersen, H. Stubbe and A. Volterra, Lausanne (CH), Oslo (N) and Milan (I)  
*Dynamic Imaging of glutamate exocytosis from astrocytes*
- [#S11-4](#) CG. Schipke, B. Haas, G. Söhl, K. Willecke and H. Kettenmann, Berlin and Bonn  
*Imaging of activity dependent transmitter release from astrocytes*
- [#S11-5](#) V. Gundersen, P. Bezzi and A. Volterra, Oslo (N) and Lausanne (CH)  
*IMMUNOGOLD DETECTION OF VGLUTs IN HIPPOCAMPAL ASTROCYTES*
- [#S11-6](#) T. Lang, Göttingen  
*MOLECULAR INSIGHTS INTO THE EXOCYTOTIC MACHINERY USING UNROOFED CELLS*

**Poster**

- [#39A](#) A. Wallraff, R. Köhling, G. Söhl, K. Willecke and C. Steinhäuser, Bonn  
*Functional consequences of loss of Connexin43 and Connexin30 in astrocytes*
- [#40A](#) Y. Wang, W. Luo, R. Stricker and G. Reiser, Magdeburg  
*The mechanism of IL-8-like chemokine (GRO/CINC-1) release from rat astrocytes mediated by protease-activated receptor-1*

- [#41A](#) K. Nieweg, C. Göritz and FW. Pfrieder, Strasbourg (F)  
*Cholesterol homeostasis in neurons and glial cells*
- [#42A](#) CC. Steinmetz, I. Buard, T. Claudepierre, K. Naegler and FW. Pfrieder, Strasbourg (F)  
*GLIAL INFLUENCE ON SYNAPSE DEVELOPMENT IN DIFFERENT BRAIN REGIONS*
- [#43A](#) J. Hirrlinger, C. Braun, PG. Pawlowski, S. Hülsmann and F. Kirchhoff, Göttingen  
*Morphological analysis of neuron-glia interaction in transgenic mice with cell-type specific expression of fluorescent proteins*
- [#44A](#) PG. Pawlowski, A. Schuchardt, C. Braun, J. Hirrlinger and F. Kirchhoff, Göttingen  
*Transgenic expression of fluorescent proteins derived from jellyfish or reef corals in the mouse nervous system – a comparative analysis*
- [#45A](#) A. Schuchardt, PG. Pawlowski and F. Kirchhoff, Göttingen  
*Characterization of transgenic mice with expression of the red fluorescent protein mRFP under the human GFAP promoter*

## **Introductory Remarks to Symposium 11**

### **The integrated role of glial cells in the CNS: new methodological approaches**

**Paola Bezzi and Carola Schipke, Lausanne (CH) and Berlin**

The integrated role of glial cells, especially the role of astrocytes in synaptic transmission, is the central topic of this symposium.

It is a very recent acquisition that glial cells generate signalling loops which are integral to the brain circuitry and participate interactively with neuronal networks in the processing of information. While neuronal signalling, based on electrical excitability, has been successfully studied with electrophysiological approaches, glial cell signalling was not revealed by these approaches and remained unknown until a few years ago. It was only the use of optical recording techniques and dyes sensitive to changes in the intracellular calcium concentration ( $[Ca^{2+}]_i$ ) that allowed the chemical excitability of glial cells to become apparent. Studies using these new techniques have shown for the first time that glial cells are activated by surrounding synaptic activity and translate neuronal signals into their own calcium code.  $[Ca^{2+}]_i$  elevations in glial cells have been shown to underlie spatial transfer of information in the glial network, accompanied by release of chemical transmitters such as glutamate and back-signalling to neurons. As a consequence optical imaging techniques applied to cell cultures or intact tissue have become a state-of-the-art technology for studying glial cell signalling. As the morphological basis and the molecular mechanisms leading to release of "gliotransmitters" from glia is still under debate, only cell biology and electron microscopic work of glial cells within the neuronal network in combination with dynamic imaging elucidates the morphology, subcellular organization and possible release machinery in glia. The speakers in this symposium will address these questions in their talks . from (subcellular) morphology to the integrated role of astrocytes in neuronal circuits.

## IMAGING OF GLIAL CALCIUM TRANSIENTS

Christine R. Rose

Physiological Institute, University of Munich, Munich, Germany

Glial cells possess a wealth of transmitter receptors and typically respond to synaptic release of transmitters with intracellular calcium transients. Such calcium transients represent an important cellular signal which in turn results in the release of neuroactive substances by the glial cells. Calcium-induced release of glutamate by astrocytes has been demonstrated to induce the activation of ionotropic glutamate receptors of neighboring neurons and to modulate the properties of synaptic transmission as determined at neuronal cell bodies. Up to now, however, the influence of glial calcium transients on the electrical and chemical information processing at single synapses is not known.

In this symposium, I will discuss different techniques for the measurement of calcium transients in glial cells. Emphasis will be given on high-resolution imaging in the intact tissue using two-photon-laser scanning microscopy. A particular property of two-photon microscopy is that excitation and thus the generated fluorescence are confined to the focal plane, making the use of a detector pinhole unnecessary. This allows more efficient signal detection than in confocal microscopy. Imaging deep in the intact, scattering tissue such as in living brain slices, and even *in vivo* is significantly improved. Another advantage of two-photon microscopy is that photobleaching and photodamage are minimal. Thus, two-photon-imaging enables the measurement of local calcium transients in fine cellular processes of glial cells close to neuronal synapses (cf. Figure 1) and is a promising tool to investigate the role of these transients in the information processing in the brain.

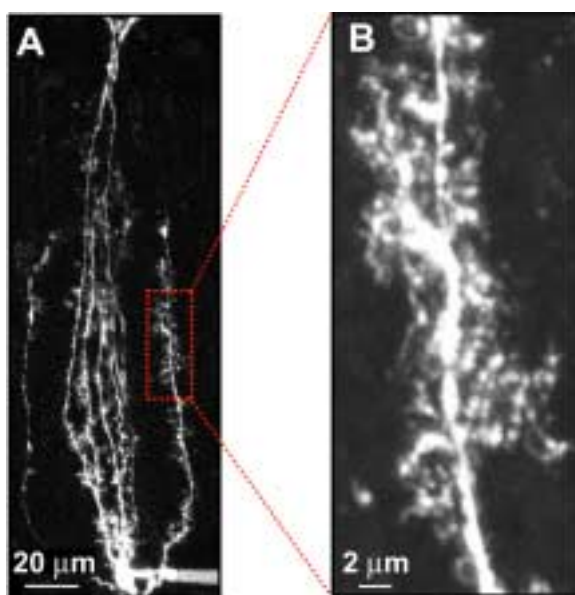


**Fig. 1: Two-photon imaging of a Bergmann glial cell.** **A:** Montage of a stack of 30 optical sections taken at 5 µm intervals through a Bergmann glial cell filled with 200 µM Fura-2 in a cerebellar slice of a 12-days-old mouse. The red box indicates the area enlarged in B. **B:** Fine process from the same cell as in A taken at higher resolution.

## Neuronal synchrony in the hippocampus mediated by glutamate released from astrocytes

Giorgio Carmignoto

Istituto CNR di Neuroscienze and Dipartimento di Scienze Biomediche Sperimentali, Università di Padova, viale G. Colombo 3, 35121 Padova, Italy.

Synchronization of activity of anatomically distributed groups of neurons represents a fundamental event in the processing of information. While this phenomenon is believed to result from dynamic interactions within the neuronal circuitry, how exactly populations of neurons become synchronized remains largely to be clarified. We propose that astrocytes are directly involved in the generation of neuronal synchrony in the hippocampus. By using a combination of experimental approaches in hippocampal slice preparations, including patch-clamp, pair recordings and confocal microscopy calcium imaging, we studied the effect on CA1 pyramidal neurons of glutamate released from astrocytes upon various stimuli that trigger  $\text{Ca}^{2+}$  elevations in these glial cells, including Schaffer collateral stimulation. We found that astrocytic glutamate evokes synchronous, slow inwards currents and  $\text{Ca}^{2+}$  elevations in multiple CA1 pyramidal neurons by acting preferentially, if not exclusively, on extrasynaptic NMDA receptors.

Our results reveal a functional link between astrocytic glutamate and extrasynaptic NMDA receptors that contributes to the overall dynamics of neuronal synchrony. Our observations also raise a series of questions on the possible role of this astrocyte-to-neuron signaling in pathological changes in the hippocampus such as excitotoxic neuronal damage or the generation of epileptiform activity.



## DYNAMIC IMAGING OF GLUTAMATE EXOCYTOSIS FROM ASTROCYTES

P. Bezzi<sup>1</sup>; E. Pilati<sup>1</sup>; V. Gundersen<sup>3</sup>; H. Stubbe<sup>1</sup>; A. Volterra<sup>1,2</sup>

1. IBCM, Univ Lausanne, Lausanne, Switzerland 2. CEND, Univ Milan, Milan, Italy 3. Anat Inst and Center for Mol Biol and Neurosci, Univ Oslo, Norway

We have recently shown that astrocytes possess synaptic-like microvesicles expressing vesicular glutamate transporters and the v-SNARE, cellubrevin. Such vesicles release glutamate via a  $\text{Ca}^{2+}$ -dependent exocytosis process in response to physiological stimuli (Bezzi et al., Nat. Neurosci., 2004). Total internal reflection fluorescence (TIRF) imaging of vesicles tagged with VGLUT-EGFP and filled with Aridine Orange enabled us to monitor individual vesicle fusion events in living astrocytes and to collect information on the kinetic properties of the secretory process evoked by activation of metabotropic glutamate receptors (mGLURs). Application of the group I mGLUR agonist (DHPG 100  $\mu\text{M}$ , 2 sec pulse) induced in the TIRFM field a single burst of  $\text{Ca}^{2+}$ -dependent exocytosis, which reached the maximal fusion rate within 100-200 ms and lasted for about 600 ms. Prostaglandins (PGs), cyclooxygenase (COX) metabolites of arachidonic acid, are known to be produced in response to mGluR stimulation and to participate in the  $\text{Ca}^{2+}$ -dependent process of glutamate release from astrocytes, both in cultured cells and in hippocampal slices (Bezzi et al., Nature, 1998; Bezzi et al., Nat. Neurosci., 2001; Pasti et al., J. Neurosci., 2001; Zonta et al., J. Physiol., 2003). However, it remains undefined whether PGs regulate specifically the glutamate exocytosis process and, if so, by which mechanism. To clarify these issues, here we use TIRF microscopy and study the consequences of suppressing PGs formation with a broad-spectrum COX inhibitor, indomethacin (INDO 5  $\mu\text{M}$ ), on the exocytosis process evoked by mGluR stimulation. In the presence of INDO, astrocytes respond to DHPG stimulation (as above) with: (a) a drastic reduction in the total number of fusion events; (b) a significant change in the time distribution of the residual fusions

Email corresponding author: Paola.Bezzi@ibcm.unil.ch

## IMAGING OF ACTIVITY DEPENDENT TRANSMITTER RELEASE FROM ASTROCYTES

**Carola G. Schipke, Brigitte Haas, Goran Söhl\*, Klaus Willecke\*, Helmut Kettenmann**

Max-Delbrück-Centrum for Molecular Medicine, Cellular Neuroscience, Robert Rössle Str. 10,  
13092 Berlin, Germany

\* Institut of Genetics, Div. of Molecular Genetics, University of Bonn, 53117 Bonn, Germany  
for correspondence: [schipke@mdc-berlin.de](mailto:schipke@mdc-berlin.de)

Astrocyte activity is propagated in form of  $\text{Ca}^{2+}$  signals. Astrocyte  $\text{Ca}^{2+}$  waves spread within the astrocytic population with a speed of 10 – 20  $\mu\text{m/s}$  and thus orders of magnitude slower than neuronal signal propagation. Two different mechanisms have been described to explain how the  $\text{Ca}^{2+}$  wave propagates within an astrocytic network in culture: 1) the intra- and intercellular diffusion of second messengers via gap junctions between highly coupled astrocytes with subsequent  $\text{Ca}^{2+}$  release from intracellular stores, and 2) the release of ATP from astrocytes into the extracellular space followed by purinergic receptor activation on neighboring cells, which, in turn, leads to elevation of  $[\text{Ca}^{2+}]_i$ . So far there are only few reports on astrocytic  $\text{Ca}^{2+}$  waves in tissue. In situ studies support the hypothesis that in the intact tissue the astrocyte wave propagates via the purinergic mechanism and does not depend on gap junctions. To visualize ATP release during wave propagation in the intact tissue, we used a novel assay to detect the release of ATP from slices, the “sniffer cells”. The glioma cell line GL 261 expresses highly sensitive purinergic receptors and these cells were seeded onto the surface of acute neocortical slices during staining with Fluo-4-AM. ATP-release was recorded as a calcium signal from the “sniffer cells”.

In this preparation, we elicited astrocytic  $\text{Ca}^{2+}$  waves in the neocortex by electrical stimulation. The astrocytic  $\text{Ca}^{2+}$  wave was accompanied by  $\text{Ca}^{2+}$  signals in the “sniffer cell” population. Astrocytes express connexin43 as the major gap junction protein. In mice deficient for astrocytic expression of connexin43, the  $\text{Ca}^{2+}$  wave did not propagate within the neocortex. Nevertheless, in the cortex of connexin43-deficient mice we recorded wave-like spreading  $\text{Ca}^{2+}$  signals in the “sniffer cells” population without an underlying astrocytic  $\text{Ca}^{2+}$  wave. Our findings indicate that after focal electrical stimulation, ATP release can propagate within the neocortex independent from  $\text{Ca}^{2+}$  waves but with the same speed.

Supported by: DFG, SFB 515

**IMMUNOGOLD DETECTION OF VGLUTs IN HIPPOCAMPAL ASTROCYTES**

VIDAR GUNDERSEN<sup>1,2</sup>, PAOLA BEZZI<sup>1</sup> AND ANDREA VOLTERRA<sup>1</sup>, IBCM,  
University of Lausanne, Switzerland<sup>1</sup> and Dept. of Anatomy, University of Oslo, Norway<sup>2</sup>  
E-mail: vidar.gundersen@basalmed.uio.no

Glutamate release from cultured astrocytes has been shown to be Ca<sup>2+</sup> and a clostridium toxin sensitive. However, no evidence for a vesicular compartment capable of glutamate release has been detected in astrocytes in the intact brain. Here we show, by use of electron microscopic immunogold techniques, that astrocytes (identified by labelling for the astrocytic glutamate transporters GLT and GLAST or by filaments) in the dentate gyrus contain synaptic-like vesicles resembling synaptic vesicles, inasmuch as they are small (about 30 nm in diameter), round and clear. In addition, like synaptic vesicles, the astrocytic vesicles express the vesicle-associated membrane protein cellubrevin together with VGLUT1 and VGLUT2. We also found that VGLUT positive astrocytic vesicles were located close to neuronal membranes, of which some carry NMDA receptors. Our findings strongly suggest that astrocytes in the intact hippocampus contain a vesicular compartment competent of glutamate exocytosis and that the VGLUT-containing vesicles in the astrocytes could form sites for point-to-point transmission between astrocytes and neurons.

## Litterature cited:

Bezzi, P., *et al.* Prostaglandins stimulate calcium-dependent glutamate release in astrocytes. *Nature* **391**, 281–285 (1998).

Bezzi, P. *et al.* CXCR4-activated astrocyte glutamate release via TNF $\alpha$ : amplification by microglia triggers neurotoxicity. *Nat. Neurosci.* **4**, 702–710 (2001).

Chilcote, T.J. *et al.* Cellubrevin and synaptobrevins: similar subcellular localization and biochemical properties in PC12 cells. *J. Cell. Biol.* **129**, 219–231 (1995).

Freneau, R.T. Jr. *et al.* The expression of vesicular glutamate transporters defines two classes of excitatory synapse. *Neuron* **31**, 247–260 (2001).

Parpura, V. *et al.* Glutamate-mediated astrocyte-neuron signalling. *Nature* **369**, 744–747 (1994).

Volterra, A. & Bezzi, P. Release of transmitters from glial cells. in *The Tripartite Synapse: Glia in Synaptic Transmission* (eds. Volterra, A., Magistretti, P.J. & Haydon, P.G.) 164–182 (Oxford Univ. Press, Oxford, UK, 2002).

## Functional consequences of loss of Connexin43 and Connexin30 in astrocytes

Anke Wallraff<sup>a,\*</sup>, Rüdiger Köhling<sup>b</sup>, Goran Söhl<sup>c</sup>, Klaus Willecke<sup>c</sup> and Christian Steinhäuser<sup>a</sup>

<sup>a</sup>Experimentelle Neurobiologie, Neurochirurgie, Universität Bonn, 53105 Bonn, Germany

<sup>b</sup>Klinik für Epileptologie, Universität Bonn, 53105 Bonn, Germany

<sup>c</sup>Institut für Genetik, Abteilung Molekulargenetik, Universität Bonn, 53117 Bonn, Germany

\*Corresponding author. E-mail address: anke.wallraff@ukb.uni-bonn.de

Astrocytes have been shown to be most extensively coupled by gap junctions, which serve as intercellular conduits for direct transfer of small molecules (up to 1 kDa molecular mass) including ions involved in cellular excitability, metabolites, and second messengers.

Different connexins, i.e. the protein subunits of gap junction channels, can be expressed within the same cell type. Hippocampal astrocytes, for instance, show prominent dye-coupling even in absence of the Connexin43 (Cx43) gene, coding for their major connexin [Cx43(fl/fl);hGFAP-cre] mice (Theis et al., 2003). To determine which connexins mediate residual coupling in these mice, we performed tracer coupling experiments in hippocampal slices of mice which additionally lack Cx30 [Cx30(-/-)/Cx43(fl/fl);hGFAP-cre mice], another connexin expressed in wild type astrocytes. Injecting biocytin via the patch pipette revealed that gap junctional coupling was totally abolished in hippocampal astrocytes of these mice. Connexin26, suggested to be additionally expressed, at least in spinal cord astrocytes (Altevogt et al., 2004, but compare Filippov et al., 2003), does not appear to contribute to tracer spreading between hippocampal astrocytes. Cx30 alone mediates residual coupling in [Cx43(fl/fl);hGFAP-cre] mice. In heterozygous [Cx30(+/-)/Cx43(fl/fl);hGFAP-cre] mice, the contribution of a single Cx30 allele to gap junctional coupling was assessed: Coupling was reduced to about 40 % of [Cx30(+/+)/Cx43(fl/fl);hGFAP-cre] controls.

Astrocytic gap junctions have been claimed to contribute to the dispersion of K<sup>+</sup>, taken up by astrocytes after neuronal activity. Changes in ion concentrations of the extracellular space are probably involved in the pathology of CNS diseases such as epilepsy. However, the role of astrocytic gap junctions in epilepsy is still ambiguous: Do they have a neuroprotective role or do they add to the spread of neuronal activity?

We therefore studied epileptiform activity in acute hippocampal slices of [Cx30(-/-)/Cx43(fl/fl);hGFAP-cre] mice with extracellular field recordings. Using the zero Mg<sup>2+</sup> model, a significantly reduced latency in the appearance of epileptiform activity along with an enhanced frequency of epileptiform events were recorded in slices of these mice, compared to slices of age-matched mice with coupled astrocytes. In addition, only slices of [Cx30(-/-)/Cx43(fl/fl);hGFAP-cre] mice showed brief episodes of spontaneous and stimulus-evoked synchronized activity under normal Mg<sup>2+</sup> conditions. Obviously, shut-down of astrocytic coupling enhances neuronal activity. These results support the notion of “spatial buffering”, i.e. that astrocytic gap junctions counteract the accumulation of ions or neurotransmitters.

Altogether, our data demonstrate that mice with genetic inactivation of astrocytic gap junction genes are valuable tools for studying the impact of astrocytic gap junctional coupling without the use of possibly unspecific gap junction blockers.

Supported by DFG (SFB/TR3, JA 942/4, SFB 400)

Literature: Altevogt et al. J. Neurosci. 24 (2004) 4313-4323

Filippov et al. Eur. J. Neurosci. 18 (2003) 3183-3192

Theis et al. J. Neurosci. 23 (2003) 766-776

## **The mechanism of IL-8-like chemokine (GRO/CINC-1) release from rat astrocytes mediated by protease-activated receptor-1**

Yingfei Wang, Weibo Luo, Rolf Stricker and Georg Reiser

Institut für Neurobiochemie, Medizinische Fakultät, Otto-von-Guericke-Universität  
Magdeburg, Leipziger Straße 44, 39120 Magdeburg, Germany.  
Yingfei.Wang@Medizin.Uni-Magdeburg.DE

Protease-activated receptors (PARs), a unique class of G protein-coupled receptors, are widely expressed in the central nervous system (CNS), such as neurons, microglial cells, astrocytes and oligodendrocytes. Now, it is clear that PARs are involved in multiple physiological processes, such as platelet aggregation, inflammation, apoptosis, cell proliferation, immune response, pain, morphological changes and calcium mobilization. The inflammatory roles of PARs are well understood in some systems, but not in the CNS. Till now, only very limited direct evidence has shown that PARs play a role in inflammation in the CNS. But the inflammatory mechanisms of PARs remain largely unknown. Rat chemokine growth-regulated oncogene/cytokine-induced neutrophil chemoattractant-1 (GRO/CINC-1), a counterpart of the human growth-regulated oncogene product (GRO), has been suggested to play critical roles as a mediator of inflammatory reactions with neutrophil infiltration in rats. In the present study, we investigated by RT-PCR and ELISA whether PAR-1 activation could increase chemokine GRO/CINC-1 in rat astrocytes. We found that thrombin and TRag time- and concentration-dependently upregulates GRO/CINC-1 at both mRNA level and protein level. Then we further investigated the mechanism of PAR-1-mediated GRO/CINC-1 production by rat astrocytes in vitro. ELISA results suggested that inhibitors of protein kinase C (PKC), mitogen-activated protein kinase kinase 1/2 (MEK1/2), phosphatidylinositol 3-kinase (PI3K), p38 MAPK, c-Jun N-terminal kinase (JNK), nuclear transcription factor-kappa B (NF- $\kappa$ B) and Janus kinase 2 (JAK2) significantly reduced PAR-1-induced GRO/CINC-1 production. Signaling cascades of GRO/CINC-1 production were further studied by western blot. Our observations for the first time indicate that JNK is very sensitive to thrombin and TRag stimulations in rat astrocytes. Both thrombin and TRag can time- and concentration-dependently phosphorylate JNK, but not p38 MAPK. JNK activation was mediated by PKC, PI3K and MEK1/2. In addition, three interesting nuclear transcription factors, which are supposed to play important roles in regulating GRO/CINC-1 release, were also studied. Our observations indicate that phosphorylation and activation of c-Jun was involved in upregulation of GRO/CINC-1 and c-Jun gene expression. NF- $\kappa$ B, which could be activated by thrombin independent of PAR-1 activation, maybe have indirect effects on GRO/CINC-1 release. However, signal transducer and activator of transcription (STAT)3 functions as a negative regulator of GRO/CINC-1 release.

## **Cholesterol homeostasis in neurons and glial cells**

K. Nieweg, Christian Göritz, F.W. Pfrieger

Max-Planck/CNRS Group, UPR 2356; Centre de Neurochimie; F-67084 Strasbourg Cedex,  
France.

It is well established that the metabolism of cholesterol in the brain is separated from the rest of the body, but surprisingly little is known of how neurons of the central nervous system regulate their cholesterol content. Previously, we showed that the ability of cultured neurons to form and maintain synapses depends on an external source of cholesterol (Mauch et al., 2001, Göritz et al., submitted). We therefore hypothesized that postnatal neurons synthesize only little cholesterol and rather depend on the delivery by astrocytes via lipoproteins (Pfrieger, 2003). Furthermore, we postulate an active export of excess cholesterol, which is then taken up by astrocytes to mediate its elimination from the brain.

Currently, the only model to study cholesterol metabolism in postnatal CNS neurons are cultures of retinal ganglion cells which can be purified from postnatal rats and cultured under defined conditions in the absence of glia. We studied cholesterol synthesis in these neurons in the absence and presence of glia-conditioned medium using radioactive labeling in combination with high resolution thin-layer chromatography. For comparison, we also analysed sterol synthesis in cultured glial cells from rat optic nerve.

Our results show that neurons from postnatal brain produce cholesterol when cultured without glia. In the presence of glia-conditioned medium cholesterol synthesis was reduced by  $83 \pm 6\%$  ( $n=3$ ). Separation of cholesterol precursors allowed dissection of the biosynthesis pathway: Whereas the precursor pattern differed slightly in neurons and glia, a common feature was the accumulation of lanosterol indicating that conversion of lanosterol is rate-limiting. To analyse this further, we performed pulse-chase experiments and found that all of the accumulated lanosterol was finally converted to cholesterol. In optic nerve cultures, but not in neurons intermediates in the two pathways of cholesterol synthesis, namely desmosterol and 7-dehydrocholesterol, were synthesized.

To study cholesterol release we analysed labeled sterols in neuron- and glia-conditioned media. No release could be detected from neurons that were cultured in the absence of glia. Addition of lipoprotein-containing GCM, which acts as donor and acceptor of cholesterol, induced cholesterol release from these cells. Glial cells released cholesterol as well as the precursors lanosterol and 7-dehydrocholesterol. Treatment with neuron-conditioned medium had no influence on glial release of sterols.

Taken together, our study, which is the first on cholesterol synthesis in postnatal CNS neurons, confirmed that neurons are able to form the sterol *de novo* and revealed interesting differences with glial cells. These results form the basis for further investigations on cholesterol homeostasis in the brain.

Supported by DFG (SPP 1085), Ara Parseghian Medical Research Foundation, Region Alsace.

## GLIAL INFLUENCE ON SYNAPSE DEVELOPMENT IN DIFFERENT BRAIN REGIONS

C.C. Steinmetz, I.Buard, T.Claudepierre, K.Nagler, F.W. Pfrieger

Max-Planck/CNRS Group, UPR 2356, Centre de Neurochimie, F-67084 Strasbourg, France

Survival and differentiation of neurons depend on signals from glial cells. Recently, new forms of glia-synapse interactions have been revealed by studies of retinal ganglion cells (RGCs), which can be highly purified from postnatal rats by sequential immunopanning (Pfrieger & Barres, 1997; Mauch et al., 2001). So far, however, studies of glia-neuron interactions in other types of postnatal neurons have been hampered by the lack of appropriate isolation procedures. We report here the establishment of new procedures for the immunoisolation of hippocampal (HIP) and cerebellar (CER) neurons and of RGCs from postnatal mice. The procedure yields, respectively, about 27000  $\pm$  11600 (n = 13; HIP), 850000  $\pm$  546000 (n = 19; CER) and 23000  $\pm$  12000 (n = 34; RGCs) cells/P7 mouse. Immunostaining with cell type-specific markers reveals >99.5% purity. To assess the survival and growth requirements, we cultured purified cells under defined conditions. Depending on the brain region, the survival rates average between 9 to 15% after 3 days in vitro (DIV). Addition of growth factors and an increase in the cAMP level enhanced survival rates (17 to 40%) as reported for rat RGCs (Meyer-Franke et al., 1995). Treatment with glia-conditioned medium (GCM) did not affect survival. To determine the presence of functional synapses in the different preparations, we performed whole-cell recordings of spontaneous and evoked synaptic currents at 7 DIV. Hippocampal and cerebellar neurons showed spontaneous excitatory postsynaptic currents (EPSC) and asynchronous currents under glia-free conditions. GCM and cholesterol enhanced asynchronous release in hippocampal neurons. Spontaneous inhibitory postsynaptic currents (IPSC) occurred in hippocampal and cerebellar neurons under glia-free condition with hippocampal cultures showing a higher frequency of IPSCs than cerebellar neurons. Experiments on isolated mouse RGCs are currently under way. Taken together our results suggest that not all synapses are created equal and that there are region- and possibly neuronal cell type-specific differences in the requirement for glial signals. Our goal is now to identify the molecular mechanisms that underly these differences. The new preparations of isolated neurons will allow to study the relevance of glial signals for development and function of postnatal neurons in an unprecedented manner.

Supported by the DFG (SPP 1085), Ara Parseghian Medical Research Foundation, Fondation Electricite de France, Fondation pour la Recherche Medical and Ministere de l'Education et de la Recherche.

## MORPHOLOGICAL ANALYSIS OF NEURON-GLIA INTERACTION IN TRANSGENIC MICE WITH CELL-TYPE SPECIFIC EXPRESSION OF FLUORESCENT PROTEINS

J. Hirrlinger<sup>1,3</sup>, C. Braun<sup>1</sup>, P.G. Pawlowski<sup>1</sup>, S. Hülsmann<sup>2,3</sup>, F. Kirchhoff<sup>1,3</sup>

*(1) Neurogenetics, Max Planck Institute of Experimental Medicine, Göttingen, Germany*

*(2) Sensory and Neurophysiology, Georg August University, Göttingen, Germany*

*(3) DFG Research Center Molecular Physiology of the Brain, Göttingen, Germany*

The highly complex organization of mammalian brains is mirrored by a functional heterogeneity of cell types. To investigate this cellular diversity and structural interactions within the nervous system, we generated a series of transgenic mouse lines with cytoplasmic expression of various fluorescent proteins. In mice expressing the red reef coral fluorescent protein HcRed1 under the control of the neuron-specific Thy1.2-promotor principal projection neurons in cortical layers 4-6 (fewer also in layer 2) and neurons of deeper brain nuclei (e.g. red nucleus) were fluorescently labelled. In the CA1 and CA2 regions as well as in the dentate gyrus hippocampal pyramidal neurons expressed HcRed1 as well. Interestingly, in none of the lines transgenic expression could be detected in CA3 neurons. To visualize structural neuron-glia interaction, these TgN(Thy1.2-HcRed)-mice were crossbred with TgN(hGFAP-EGFP) mice expressing the green fluorescent protein EGFP under the control of the human GFAP-promotor. In these double transgenic mice the enormous process branching of astrocytes around synaptic structures of HcRed1-positive neurons could be visualized by confocal microscopy in acutely isolated brain slices. Similarly, structural details of astroglial endfeet at brain capillaries could be resolved. Fine astroglial processes were also found between densely packed cell bodies of hippocampal neurons. In the dentate gyrus processes of single astrocytes spanned the entire length from the molecular through the granular layer up to the polymorphic layer. These astroglial structures could contribute to the signaling, i.e. the information transfer between different layers of the dentate gyrus. In conclusion, this double-transgenic mouse line represents an excellent tool to study both the structure as well as the functional dynamics of neuron-glia interaction.

For correspondence: [kirchhoff@em.mpg.de](mailto:kirchhoff@em.mpg.de)

Support: DFG research center Molecular Physiology of the Brain (CMPB)



TRANSGENIC EXPRESSION OF FLUORESCENT PROTEINS DERIVED FROM  
JELLYFISH OR REEF CORALS IN THE MOUSE NERVOUS SYSTEM –  
A COMPARATIVE ANALYSIS

P.G. Pawlowski<sup>1</sup>, A. Schuchardt<sup>1</sup>, C. Braun<sup>1</sup>, J. Hirrlinger<sup>1,2</sup>, F. Kirchhoff<sup>1,2</sup>

(1) *Neurogenetics, Max-Planck-Institute of Experimental Medicine, Göttingen, Germany*

(2) *DFG Research Center for Molecular Physiology of the Brain, Göttingen, Germany*

Several variants of the green fluorescent protein (GFP) of the jellyfish *Aequorea victoria* are commonly used as reporters in transgenic mice (ECFP, EGFP and EYFP). Recently, chromoproteins from various reef coral anthozoa have been identified as a novel family of fluorescent proteins. Their emission maxima range from 470 to 630 nm. Therefore, reef coral fluorescent proteins (RCFPs) should be ideal tools to generate transgenic mice in which different cell populations can be labelled with spectrally different FP using appropriate promoters. Focussing on the central nervous system, we used the RCFPs AmCyan1, AsRed2, DsRed1, mRFP1 and HcRed1 to selectively label astrocytes, oligodendrocytes and neurons. Transgenic mice were generated with cytoplasmic FP expression driven by the human GFAP, the mouse PLP and Thy1.2 promoters and investigated by laser-scanning microscopy.

Similar to transgenic mice with variants of GFP, RCFP transgenic mice developed normally, were fertile and got older than a year. In addition, the three promoters induced correct cell-type specific expression of the various RCFPs. In contrast to transgenic mice expressing the GFP variants, however, RCFPs displayed various degrees of protein aggregation. The highest level was observed with AsRed2. Almost all astrocytes contained fluorescent particles of about 1 µm in size. Aggregation of DsRed1 in oligodendrocytes was more variable, in the young brain (less than 2 weeks) almost no fluorescent particles were visible, while in the aged brain (older than 1 year) oligodendroglial somata contained numerous DsRed1 clusters. HcRed1 clustering was also cell-type dependent: strong in Purkinje cells and less pronounced in pyramidal cells. We observed aggregated RCFPs (including the monomeric DsRed variant mRFP1) in all RCFP transgenic mouse lines. In all lines, protein precipitates increased with age. In contrast, mice expressing variants of the jellyfish protein EGFP did never show formation of aggregates. Interestingly, we have not yet detected obvious pathological alterations of the brain. Conclusion: Although RCFPs have ideal spectral properties to be used for cell-labeling in transgenic mice, the degree of protein precipitates of RCFPs limits their use for morphological brain analysis.

For correspondence: [kirchhoff@em.mpg.de](mailto:kirchhoff@em.mpg.de)

Support: DFG research center Molecular Physiology of the Brain (CMPB)

## CHARACTERIZATION OF TRANSGENIC MICE WITH EXPRESSION OF THE RED FLUORESCENT PROTEIN mRFP UNDER THE HUMAN GFAP PROMOTER

A. Schuchardt, P.G. Pawlowski and F. Kirchhoff

*Neurogenetics, Max Planck Institute of Experimental Medicine, Göttingen, Germany*

Several recent studies analyzing the function of astrocytes in situ took advantage of transgenic mice with human GFAP promoter-driven expression of the green fluorescent protein EGFP. Here we describe new transgenic mouse lines in which astrocytes express mRFP (monomeric red fluorescent protein). This variant of the reef coral protein DsRED has been generated by substitution of several amino acids to reduce intrinsic protein aggregation. Transgenic labelling of a cell with a red fluorescent protein offers the unique opportunity to use green fluorescent calcium indicators simultaneously to study signaling in identified cell populations in situ.

Expression of mRFP in astrocytes of the two transgenic mouse lines was characterized by confocal laser scanning microscopy. Common to both lines was the specific labelling of astrocytes in all regions of the brain such as cortex, hippocampus, striatum, brainstem and cerebellum. Red fluorescent astrocytes were not only found in the gray matter as protoplasmic type of astrocytes with contacts to blood vessels, but also in white matter tracts or as radial glia (Bergmann glia of the cerebellum). In contrast, however, to expression of mRFP in transiently transfected cell lines we do not observe a uniform expression throughout the astroglial cytoplasm, but we rather see numerous mRFP precipitates. These precipitates accumulate with age and show regional variations. Interestingly, we could not yet correlate aggregate formation with the appearance of pathological alterations.

The two lines differ significantly in the number of labelled cells. This is particularly evident in the cerebellum, where almost all the Bergmann glia cells express mRFP in one line, and less than a quarter in the other.

To study astroglial network activity we loaded astrocytes in acutely isolated brain slices obtained from early postnatal mice with the green calcium indicators Fluo4 or Fluo4-AM, respectively. After both approaches, bulk loading with the membrane permeable acetoxymethylester or dialysis via the patch pipette during whole-cell patch-clamp recordings, clear calcium signals could be recorded from astrocytes labelled and identified by their transgenic mRFP expression. Ongoing studies are performed to establish the TgN(GFAP-mRFP) mice as a model system for the analysis of calcium signaling as a major pathway in neuron-glia interaction.

For correspondence: [kirchhoff@em.mpg.de](mailto:kirchhoff@em.mpg.de)

**Symposium #S12:**  
**Cellular and molecular control of vertebrate neurogenesis**  
**A. von Holst, Bochum**

**Introduction**

- [#S12](#) A. von Holst, Bochum  
*Cellular and molecular control of vertebrate neurogenesis*

**Slide**

- [#S12-1](#) WB. Huttner, A. Attardo, F. Calegari, V. Dubreuil, L. Farkas, J. Fish, A. Grzyb, C. Haffner, Y. Kosodo, K. Langenfeld, A-M. Marzesco and D. De Pietri Tonelli, Dresden  
*The cell biology of neurogenesis*
- [#S12-2](#) M. Götz, M. Hack, B. Berninger and T. Mori, Neuherberg/Munich  
*Glial cells generate neurons: Pax6 as neurogenic master regulator of neural stem cells*
- [#S12-3](#) RR. Waclaw, SM. Bell, WJ. Scott, SS. Potter and K. Campbell, Cincinnati, OH (USA)  
*Molecular mechanisms of embryonic and postnatal neurogenesis in the mouse telencephalon*
- [#S12-4](#) E. Arenas, Stockholm (S)  
*Role of region specific glia in the induction of midbrain dopaminergic neurons*
- [#S12-5](#) L. Campos, E. Garcion, A. Halilagic, DP. Leone, J. Bettencourt Relvas, C. Brakebusch, R. Fässler, U. Suter, A. von Holst, A. Faissner and C. ffrench-Constant, Cambridge (UK), Zürich (CH), Martinsried and Bochum  
*Regulation of neural stem cells by extracellular matrix*
- [#S12-6](#) A. von Holst, S. Sirko and A. Faissner, Bochum  
*Cellular and Functional Characterisation of Chondroitinsulfates During Neurogenesis*

**Poster**

- [#46A](#) FG. Wulczyn, L. Smirnova, A. Graefe and R. Nitsch, Berlin  
*Regulation and function of miRNA in neural cell specification*
- [#47A](#) MA. Laplante, AZ. Komisarczuk, H. Kikuta, J. Ghislain, S. Ellingsen, P. Mourrain, B. Adolf, G. Pezeron, A. Lesslauer and TS. Becker, Bergen (N), Paris (F), Neuherberg and Zuerich (CH)  
*A large-scale enhancer detection screen for genes involved in vertebrate retinal development.*

- [#48A](#) EG. Ponimaskin, L. Kvachnina, G. Liu, A. Dityatev, M. Schachner, DW. Richter and T. Voino-Yasenetskaya, Göttingen, Chicago (USA) and Hamburg  
*The 5-HT receptors are involved in regulation of gene transcription and neuronal morphology by activating the new signaling pathways*
- [#49A](#) KV. Allebrandt and PG. Layer, Darmstadt  
*Cholinesterases and development of the avian pineal gland*
- [#50A](#) O. Britanova, S. Akopov, S. Lukyanov, P. Gruss and V. Tarabykin, Göttingen and Moscow (RUS)  
*ROLE OF NOVEL TRANSCRIPTION FACTOR STIX IN THE DEVELOPMENT OF CEREBRAL CORTEX*
- [#51A](#) P. Heine, KM. Bumsted o'Brien and D. Schulte, Frankfurt/Main  
*The role of the homeodomain transcription factors Meis1 and Meis2 during early development of the vertebrate retina*

## **Introductory Remarks to Symposium 12**

### **Cellular and molecular control of vertebrate neurogenesis**

**Alexander von Holst, Bochum**

During mammalian CNS development neurons and glial cells are generated from precursors and/or neural stem cells. Neurons are born first in a highly orchestrated process called neurogenesis. Over the last two or three years we have seen an exciting increase in the understanding of the cell types that can give rise to neurons, identifying them as neuroepithelial cells, radial glial cells and even astrocytes. It became apparent that cells of the glial lineage are much more plastic than previously thought, contributing considerably to the final neuron numbers. On the molecular level several transcription factors that control neurogenesis and reflect regional specification have been identified. Much less well understood are how regional differences and signalling events that control the birth of neurons and the subtypes that they will ultimately give rise to, are integrated on a cellular level. Also, the molecules defining the local neurogenic environment - the stem cell niche -and their functions are only in the beginning of being elucidated.

The symposium intends to give a state of the art overview of the cellular processes leading to the birth of neurons in the brain, and provide a framework for discussion how intrinsic determinants and extracellular cues are integrated by neural stem cells. Wieland Huttner will discuss symmetric and asymmetric modes of neuroepithelial cell division and how they are linked to the birth of neurons. He will talk about the cell cycle control gene TIS21 that has allowed to label and monitor neuronal precursors in their last round of cell division leading to the birth of postmitotic neurons. Magdalena Götz will talk about her findings that radial glia cells contribute to telencephalic neurogenesis. In addition to fate mapping of radial glia progeny she will present data on the function of Pax6 and transcription factors of the bHLH-family and how they might determine radial glia cell fate. Kenneth Campbell will discuss neurogenesis in the context of axial patterning. He will introduce the nuclear orphan receptor Tlx and report the consequences of Tlx-deficiency that lead to patterning defects, reduced proliferation and altered neuronal development in the ventral telencephalon. He will also speak about the genetic interaction of Tlx with other transcription factors, for example Pax6. The region specific expression of transcription factors (patterning) correlates with the region specific differentiation of defined neuronal cell types. Ernest Arenas will talk about the selective induction of dopaminergic neurons by astroglial cells of midbrain origin. He will discuss candidate molecules secreted by astrocytes and the role of Wnt-family members in the development of ventral midbrain dopaminergic neurons. Charles French-Constant will address the role of the extracellular matrix in neural stem cells. In particular he will discuss the functional consequences of Tenascin-C deficiency and the importance of integrins in neural stem cells. Alexander von Holst will present findings on the cellular specificity of defined chondroitinsulfate proteoglycans identifying them as radial glia associated and, how interference with them alters neural stem cell differentiation.

As many of the molecular and cellular players continue to be present in the neurogenic regions of the adult brain, the topic of the symposium will be of considerable interest not only to developmental neuroscientists but also to other researchers in the field of neuroscience.

### **The cell biology of neurogenesis**

Wieland B. Huttner, Alessio Attardo, Federico Calegari, Veronique Dubreuil, Lilla Farkas, Jennifer Fish, Anna Grzyb, Christiane Haffner, Yoichi Kosodo, Katja Langenfeld, Anne-Marie Marzesco, Davide De Pietri Tonelli.  
Max Planck Institute of Molecular Cell Biology and Genetics, Dresden, Germany

Our group studies the cell biological mechanisms underlying the switch of neuroepithelial (NE) cells from proliferation to neurogenesis in the mouse embryo (1,2). Prior to, during, and as a consequence of, neurogenesis, NE cells down-regulate a number of epithelial features (3,4). Expression of the anti-proliferative gene TIS21 can be used as a tool to distinguish between proliferating and neuron-generating NE cells (5). Time-lapse microscopy of neuron-generating divisions of NE cells using transgenic mouse embryos expressing GFP under the control of the TIS21 promoter reveals the existence of a novel neuronal progenitor dividing at the basal side of the neuroepithelium (6). We also investigate the role of cell cycle length in determining the onset of neurogenesis (7). To study the distribution, during mitosis, of cellular components in the context of the apico-basal axis of NE cells, we focus on prominin-1, a pentaspan membrane protein sorted to the apical surface of NE cells and specifically retained in plasma membrane protrusions (8-10). Prominin-1 is associated with a novel, cholesterol-based lipid raft which is involved in prominin's retention in microvilli (9). Using prominin-1 to define the apical surface of NE cells, we investigate the symmetric vs. asymmetric distribution of the apical plasma membrane during proliferating vs. neuron-generating divisions of NE cells (11). Finally, we have developed a method to knock-down gene expression in NE cells using RNA interference in the developing mouse embryo (12).

1. Huttner and Brand (1997) *Curr. Opin. Neurobiol.* 7, 29-39.
2. Wodarz and Huttner (2003) *Mech. Dev.* 120, 1297-1309.
3. Aaku-Saraste et al (1996) *Dev. Biol.* 180, 664-679.
4. Aaku-Saraste et al (1997) *Mech. Dev.* 69, 71-81.
5. Iacopetti et al (1999) *Proc. Natl. Acad. Sci. USA* 96, 4639-4644.
6. Haubensak et al (2004) *Proc Natl. Acad. Sci. USA* 101, 3196-3201.
7. Calegari and Huttner (2003) *J. Cell Sci.* 116, 4947-4955.
8. Weigmann et al (1997) *Proc. Natl. Acad. Sci. USA* 94, 12425-12430.
9. Röper et al (2000) *Nature Cell Biol.* 2, 582-592.
10. Corbeil et al (2001) *Traffic* 2, 82-91.
11. Kosodo et al (2004) *EMBO J.* 23, 2314-2324.
12. Calegari et al (2002) *Proc. Natl. Acad. Sci. USA* 99, 14236-14240.

## Glial cells generate neurons: Pax6 as neurogenic master regulator of neural stem cells

M. Götz, M. Hack, Benedikt Berninger and T. Mori, GSF, National Research Center for Environment and Health, Institute for Stem Cell Research, Ingolstädterstr. 1, D-85764 Neuherberg/Munich, Germany

During development and in adulthood, neurons arise from multipotent precursors by hierarchical fate restriction. Thus multipotent precursors generate precursors restricted to the generation of a single cell type, e.g. neurons. The molecular cues regulating this transition, however, are not well understood. To elucidate these fate determinants we have separated neurogenic versus non-neurogenic radial glial cells by FACS and performed microarray analysis. This revealed a notable enrichment of Pax6 in neurogenic and Olig2 in non-neurogenic radial glia. Retroviral vectors were then used to overexpress these candidate genes or block their respective function as a transactivator by fusion to a repressor domain (Pax6-engrailed) or as a repressor by fusion to an activator domain. These functional experiments were performed in expanded neural stem cell cultures and astrocytes derived from non-neurogenic regions in vitro, as well as in astrocytes of neurogenic and non-neurogenic regions in the adult brain in vivo. In all of these systems, Pax6 was found to be a potent activator of neurogenesis, and proved to be even sufficient to instruct astrocytes of the postnatal cortex in vivo towards the generation of neurons. We also found Pax6 to be essential for adult neurogenesis of olfactory bulb interneurons in vivo, and gain-of-function experiments revealed that Pax6 governs specifically the generation of dopaminergic neurons in the periglomerular layer of the olfactory bulb. We could therefore identify Pax6 as the first fate determinant for adult neurogenesis of dopaminergic neurons in the adult mammalian brain in vivo. In contrast, Olig2 performs a converse role driving adult neural stem cells towards the generation of oligodendrocytes and GABAergic granule cells. Taken together, these experiments identified crucial fate determinants that allow us to direct adult astroglial cells towards specific neuronal phenotypes in vivo.

Heins, N., P. Malatesta, F. Cecconi, M. Nakafuku, K. L. Tucker, M. A. Hack, P. Chapouton, Y. Barde and M. Götz (2002) Generation of neurons from glial cells: the role of the transcription factor Pax6. *Nature Neuroscience* 5, 308-315.

Malatesta, P., E. Hartfuss, M.A. Hack, W. Klinkert, F. Kirchhoff, H. Kettenmann and M. Götz (2003). Neuronal or glial progeny: regional differences in radial glial fate. *Neuron* 37: 751-764.

**Molecular mechanisms of embryonic and postnatal neurogenesis  
in the mouse telencephalon**

R.R. Waclaw, S. M. Bell, W.J. Scott, S.S. Potter and K. Campbell.

Division of Developmental Biology, Children's Hospital Research Foundation,  
Cincinnati, OH 45229, USA

The lateral ganglionic eminence (LGE) is a known source of striatal projection neurons and olfactory bulb interneurons. Recent studies have suggested the dorsal region of the LGE (i.e. dLGE) gives rise to olfactory bulb (OB) interneurons at embryonic stages. We have identified a novel marker of the dLGE during embryogenesis called *Sp8*. This gene is also found in the subventricular zone (SVZ), rostral migratory stream and OB interneurons at postnatal stages. Previous studies have shown that the dLGE is reduced in *Gsh2* mutants and expands dorsally in *Pax6* mutants. In line with this, *Sp8* expression is reduced in the *Gsh2* mutant LGE and ectopically expressed in the ventral pallidum of the *Pax6* mutant. Consistent with the reduced size of the dLGE in the *Gsh2* mutant, the number of *Sp8*-expressing interneurons in the *Gsh2* mutant OB is severely reduced. *Sp8* encodes for a zinc finger transcription factor that has been shown to be required for normal limb outgrowth and neural tube closure. Germline *Sp8* mutants exhibit exencephaly and therefore, it is not possible to study its requirement for OB interneuron generation from the dLGE and SVZ of these mutants. To address this issue, we have made a conditional knockout of *Sp8* restricted to the ventral telencephalon by mating *Dlx5/6-cre-IRES-EGFP* mice with floxed *Sp8* mice. These conditional mutants, have closed heads and form a grossly normal looking telencephalon with noticeably smaller OBs. Preliminary studies show a severe reduction in the numbers of olfactory bulb interneurons at perinatal stages. Interestingly, the number of OB projection neurons (i.e. mitral and tufted cells) appears rather similar to the control brains. These findings point to an important role for *Sp8* in the generation of OB interneurons from embryonic dLGE and postnatal SVZ cells.



## Role of region specific glia in the induction of midbrain dopaminergic neurons

Ernest Arenas.

Laboratory of Molecular Neurobiology, Department of Medical Biochemistry and Biophysics, Karolinska Institute, Stockholm 17177, Sweden. (ernest.arenas@mbb.ki.se).

The development of mouse dopaminergic neurons (DNs) depends on the establishment of adequate patterns of gene expression and on the acquisition of regional and cell type specific identity by neural cells. Analysis of mutant mice have allowed to identify several genes required for the development of the midbrain-hindbrain region and for the development of midbrain DNs. The first category includes two genes in a common genetic pathway, *wnt1* and its receptor *LRP-6*. The second group includes genes expressed in dopaminergic (DA) precursors and neurons, such as the orphan nuclear receptor, *Nurr1*, and the homeobox genes, *Lmx1b* and *Pitx3*. Since *Nurr1* was found to be required for DN development we examined whether *Nurr1* was also sufficient to induce a DA phenotype in neural progenitor/stem cells. Interestingly we found that *Nurr1* was not sufficient to induce a DA phenotype in neural stem cells (NSCs) and therefore examined whether VM cells expressed a putative *Nurr1* ligand. Despite none of the signals derived from VM cells regulated *Nurr1* mediated transactivation in reporter assays, we found that signals derived from embryonic and neonatal ventral midbrain (VM) glia, including radial glia and astrocytes, were required for the DA differentiation of *Nurr1*-expressing NSCs. Interestingly cells from other stages or brain regions did not mimic that effect, and in the absence of *Nurr1*, the VM glial-derived signals did not induce the DA differentiation of NSCs. These results suggested that the signals derived from the VM glia do not include a *Nurr1* ligand and that these signals are required but not sufficient to induce the DA differentiation of NSCs. We are currently working to identify the VM glial derived signals. Following a candidate approach we examined the Wnt family of lipid-modified glycoproteins. We found that some Wnts are developmentally regulated in the VM and highly expressed by VM glial cells. We also found that DNs express Wnt receptors and key signaling components. Moreover, administration of pure Wnts or activation of Wnt signaling was found to regulate different aspects of DN development, including the proliferation of DA precursors and their differentiation into DNs. We are currently analyzing mice with mutations in different Wnts and Wnt signaling components to determine their relative contribution to DN development in vivo. We are also performing gene chip experiments and analyzing the proteome of pure glial cultures from VM and cerebral cortex, to identify genes and proteins specifically expressed by VM cells during the induction of DNs. The results obtained so far suggest a model in which the induction of midbrain DNs requires the convergence of cell-autonomous signals, including the expression of the nuclear orphan receptor *Nurr1*, and non cell-autonomous signals, including Wnts and additional glial-derived factors. We think that the identification of such signals will contribute to understand the role of glia in DA neurogenesis and to develop stem cell replacement strategies for Parkinson's disease.

*Regulation of neural stem cells by extracellular matrix*

Lia Campos<sup>1</sup>, Emmanuel Garcion<sup>1</sup>, Aida Halilagic<sup>1</sup>, Dino P Leone<sup>2</sup>, Joao Bettencourt Relvas<sup>2</sup>, Cord Brakebusch<sup>3</sup>, Reinhard Fässler<sup>3</sup>, Ueli Suter<sup>2</sup>, Alexander von Holst<sup>4</sup>, Andreas Faissner<sup>4</sup> and Charles ffrench-Constant<sup>1</sup>.

<sup>1</sup>Depts of Pathology and Medical Genetics, University of Cambridge, Tennis Court Road, Cambridge, CB2 1QP, UK. <sup>2</sup>Institute of Cell Biology, Department of Biology, Swiss Federal Institute of Technology, ETH Hönggerberg, CH-8093 Zürich, Switzerland. <sup>3</sup>Department of Molecular Medicine, Max-Planck-Institut für Biochemie, Am Klopferspitz 18a, D-82152 Martinsried, Germany. <sup>4</sup>Ruhr-University Dept of Cell Morphology and Molecular Neurobiology, Bochum, Germany.

We and others have shown that extracellular matrix (ECM) molecules, acting through integrin cell surface receptors, provide temporal and spatial control of growth factor signalling to committed precursor cells in the developing CNS [1]. Here we explore the hypothesis that these integrin/growth factor interactions regulate neural stem cell behaviour. In the embryonic CNS, these stem cells were found within a microenvironment that contains the ECM molecule laminin alpha2 (a component of laminin trimers 2, 4 and 12) [2]. In the adult CNS, laminin is also present in the stem cell microenvironment as a result of basal lamina-like extensions from blood vessels termed “fractones” [3, 4]. We have shown that neural stem cells express high levels of the alpha6beta1 integrin, a laminin receptor, and that integrin signalling contributes to neural stem cell maintenance, at least in part through the MAPK signalling pathway [2]. The neural stem cell microenvironment (or “niche”) also contains high levels of another ECM protein, tenascin-C. In contrast to laminin, this appears to promote neural stem cell development as transgenic mice lacking tenascin-C show a delay in the acquisition of the EGF receptor associated with the phase of gliogenesis in late embryonic and postnatal development [5]. Together these results suggest that the ECM within the neural stem cell niche provides significant and distinct instructive cues for stem cell maintenance and differentiation.

This study was supported by the 5<sup>th</sup> framework EC grant number QLG3-CT-2000-30911, the Wellcome Trust, DFG SPP-1109, the National Competence Center in Research “Neural Plasticity and Repair” and the Swiss National Science Foundation.

1. ffrench-Constant, C. and H. Colognato, *Integrins: versatile integrators of extracellular cues*. Trends in Cell Biology, 2004. **in press**.
2. Campos, L.S., et al., *Beta1 integrins activate a MAPK signalling pathway in neural stem cells that contributes to their maintenance*. Development, 2004. **131**(14): p. 3433-44.
3. Mercier, F., J.T. Kitasako, and G.I. Hatton, *Anatomy of the brain neurogenic zones revisited: fractones and the fibroblast/macrophage network*. J Comp Neurol, 2002. **451**(2): p. 170-88.
4. Alvarez-Buylla, A. and D.A. Lim, *For the long run: maintaining germinal niches in the adult brain*. Neuron, 2004. **41**(5): p. 683-6.
5. Garcion, E., et al., *Generation of an environmental niche for neural stem cell development by the extracellular matrix molecule tenascin C*. Development, 2004. **131**(14): p. 3423-32.

## CELLULAR AND FUNCTIONAL CHARACTERISATION OF CHONDROITINSULFATES DURING NEUROGENESIS

ALEXANDER VON HOLST, SWETLANA SIRKO &amp; ANDREAS FAISSNER

Chair for Cell Morphology &amp; Molecular Neurobiology, Ruhr-University Bochum

Correspondence: [alexander.vonholst@rub.de](mailto:alexander.vonholst@rub.de); [andreas.faissner@rub.de](mailto:andreas.faissner@rub.de)

Stem cells are present in many organs throughout the lifetime of an organism, where they are required for the maintenance and homeostasis of most tissues. They are often slowly dividing cells that are at the base of a lineage tree. Upon division the daughter cells either remain stem cells or undergo lineage commitment, leading to terminally differentiated cell types. This raises the fundamental question how stem cell residency is achieved, which signals are required to control their proliferation and which signals lead to self-renewing vs. differentiating stem cell divisions. It has become clear that stem cells reside in a specialized environment generally referred to as stem cell niche, which consists of several different cell types and contains a specialized microenvironment composed of soluble factors, membrane bound molecules and extracellular matrix (ECM) components. One ECM component present in the adult neural stem cell (NSC) niche, is the DSD-1 epitope recognized by the monoclonal antibody 473HD. It detects a complex mixture of cell surface-associated chondroitinsulfate-glycosaminoglycan (CS-GAG) motifs that are present on the proteoglycan gene products of the receptor protein tyrosine phosphatase (RPTP)-beta gene. The DSD-1 epitope is also found in the ventricular and subventricular zones of the brain, the developmental NSC niche. When we isolated 473HD-positive cells by immunopanning and cultivated them under neurosphere forming conditions, we observed an increase in the number of neurospheres compared to the non-selected cell population at all stages examined. Under adherent conditions the 473HD-positive cells formed largely neurons. This suggest that the DSD-1 epitope is associated with a subpopulation of NSCs or presursors. Indeed, the 473HD-positive cells express markers of radial glia cells, which are thought to act as NSCs during development. (see also poster abstract by Sirko et al.)

To address the functional importance of CS-GAGs we are using GAG-lyases to remove the CS-GAGs from the cell surface. We are currently investigating the functional consequences of CS-GAG removal on neural stem cell behaviour in several cell biological assays.

Supported by the DFG SPP 1109

## Regulation and function of miRNA in neural cell specification

F. Gregory Wulczyn, Lena Smirnova, Anja Graefe and Robert Nitsch

Center for Anatomy, Institute for Cell and Neurobiology, Charité University Hospital,  
Schumannstraße 20-21, 10098 Berlin Germany

We are investigating the role of miRNA in neural differentiation and CNS development. We describe the temporal regulation of a set of major neural miRNA, including let-7, during mouse brain development and in vitro differentiation of embryonic stem (ES) cells. Many of the miRNA in our study displayed coordinate regulation, specified by differential regulation of miRNA precursor processing. An in vitro processing assay revealed increased activity after neural differentiation of ES cells and in primary neurons compared to astrocytes. Maturation of a transfected miRNA transcript was also enhanced after neural differentiation of P19 cells. Processing activity correlated with Fragile X Mental Retardation Protein (FMRP) levels. The presence of FMRP in a neuron-specific miRNA binding complex could be demonstrated in an antibody super-shift experiment. Consistent with lineage specificity in miRNA maturation, we found strong differences in the miRNA expression repertoire between primary neurons and astrocytes. Using reporter constructs designed for several neural miRNA, we demonstrate cell specificity in miRNA-mediated mRNA suppression in primary cultures and during neural differentiation of ES cells. We present a novel strategy for the investigation of miRNA function: monitoring the effect of ectopic target site overexpression on ES cell differentiation. Interference with either let-7 or mir-125 disrupted the quantitative specification of astrocyte progenitors, implicating miRNA in neuronal lineage commitment.

**A large-scale enhancer detection screen for genes involved in vertebrate retinal development.**

Mary A Laplante, Anna Zofia Komisarczuk, Hiroshi Kikuta, Julien Ghislain, Staale Ellingsen, Philippe Mourrain, Birgit Adolf, Guillaume Pezeron, Annegret Lesslauer and Thomas S. Becker

Sars International Centre for Marine Biology, HIB, Thormoehlgate 55, 5008 Bergen, Norway.

Biologie Moléculaire du Développement INSERM U368 Ecole Normale Supérieure 46 rue d'Ulm, 75230 Paris cedex 05, France.

GSF-Research Center for Environment and Health Institute of Developmental Genetics Ingolstaedter Landstrasse 1 D.85764 Neuherberg Germany.

ETH Zürich Institut fuer Hirnforschung Winterthurerstr. 190 CH-8057 Zuerich, Switzerland

In order to gain better understanding of the hierarchy of genes involved in early cell specification during retinal development in the zebrafish, we have generated a YFP enhancer detection bank in zebrafish. F1 embryos carrying random insertions of a recombinant mouse retrovirus containing a minimal promoter/YFP construct were scored for expression initially in the CNS and neural retina using a standard fluorescent microscope and subsequently by immunohistochemistry using an antibody to YFP. This approach allowed us to identify transgenic lines of fish expressing the reporter in various retinal populations, including: i) early cycling retinal precursors ii) identified neurons and iii) radial glia and possibly astrocytes. Sequencing of genomic DNA flanking the viral integration sites in these stable lines followed by Blast search of the Sanger Institute zebrafish genome assembly has been performed revealing candidate genes. A detailed analysis of the YFP expression profile of these lines will be presented along with an in situ analysis of the candidate genes. Overall, our results highlight the potential of the enhancer detection approach to study retinal cell development and function.

**The 5-HT receptors are involved in regulation of gene transcription and neuronal morphology by activating the new signaling pathways**

**E. Ponimaskin**<sup>1</sup>, L. Kvachnina<sup>1</sup>, G. Liu<sup>2</sup>, A. Dityatev<sup>3</sup>, M. Schachner<sup>3</sup>, D.W. Richter<sup>1</sup> and T. Voynoyasenetskaya<sup>2</sup>

**1** Abteilung Neuro- und Sinnesphysiologie, Physiologisches Institut, Universität Göttingen, Humboldtallee 23, D-37073 Göttingen, Germany. E-mail: evgeni@ukps.gwdg.de

**2** Department of Pharmacology, University of Illinois, Illinois 60612, Chicago, USA

**3** Zentrum für Molekulare Neurobiologie, University of Hamburg, Martinistr. 52, D-20246 Hamburg, Germany

Serotonin (5-hydroxytryptamine or 5-HT) is an important neurotransmitter involved in a wide range of central and peripheral physiological functions. A number of different G-protein coupled 5-HT receptors are known to sensitively modify different neuronal networks by their specific action on synaptic transmission and postsynaptic excitability. Here we show for the first time that the 5-HT<sub>4</sub> receptor is coupled not only to the heterotrimeric Gs, but also to G13 protein. Activation of this signaling pathway results in RhoA-mediated modulation of gene transcription and in reorganization of the actin cytoskeleton. We also demonstrated that serotonin receptor 5-HT<sub>7</sub> can activate heterotrimeric G12 protein, leading to the selective activation of small GTPases RhoA and Cdc42. Agonist-dependent activation of the 5-HT<sub>7</sub> receptor induced pronounced filopodia formation via a Cdc42-mediated pathway paralleled by RhoA-dependent cell rounding. Analysis of mouse hippocampal neurons demonstrated that activation of the endogenous 5-HT<sub>7</sub> receptors significantly increased neurite length, whereas stimulation of the endogenous 5-HT<sub>4</sub> receptors lead to a pronounced decrease in the length and number of neurites. These data demonstrate distinct roles for the 5-HT<sub>7</sub>R/G12 and 5-HT<sub>4</sub>R/G13 signaling pathways in the neurite outgrowth and retraction, and also suggest that serotonin plays a prominent role in regulating the neuronal cyto-architecture in addition to its classical role as neurotransmitter. From a more general cell biological point of view our study demonstrates that functional co-existence of 5-HT<sub>7</sub>R/G12 and 5-HT<sub>4</sub>R/G13 signaling pathways in neurons may provide a molecular link between the serotonin, which operates as an extracellular guidance factor, and the Rho GTPases machinery, controlling neuronal morphology and motility.

## **Cholinesterases and development of the avian pineal gland**

**Karla Viviani Allebrandt** and Paul G Layer

Institute of Zoology, Darmstadt University of Technology

**e-mail: allebrandt@bio.tu-darmstadt.de**

The avian pineal consists of pinealocytes, supportive cells and nerve cells. It is a photosensory/endocrine organ and its structure resembles the retina of the eye. The pineal organ is responsible for the control of physiological functions that follow a circadian rhythm, like sleep and awake cycles. The circadian organisation is modulated by the pineal's melatonin production, affected by the stimulus of light perceived by the retina. Though structurally similar, retina and pineal differ in relation to acetylcholinesterase (AChE) activity; distributed on amacrine and ganglion cells of the retina and on the inner segments of the photoreceptors on the pineal (1). The cholinesterases (ChEs) are not restricted to cholinergic innervated tissues. Their structure similarity to other proteins, including precursors of hormones and cell adhesion factors, suggest they may have non-cholinergic or non-enzymatic functions. To investigate the physiological role of cholinesterases in the pineal organ we first localised histochemically their expression during development of the chicken embryo.

BChE expression precedes AChE in specific structures of the pineal during development. The pineal gland appears outlined on the roof of the third ventricle by E3 and grows intensively till E12, when a differentiation between structural zones can be seen. It is also the time point when BChE activity diminishes and AChE starts to increase drastically, till E21. The intensive and clear pattern of cholinesterases activities is co-localised to the photoreceptors position in the adult pineal. The early onset of BChE is suggested to be related to cell proliferation and the appearance of AChE to cell differentiation. Mitotic and cell differentiation markers are being used to address the critical shift of BChE to AChE expression. Initial results showed that the distribution of the proliferating cell nuclear antigen PCNA-immunoreactive cells correlate with BChE activity. In addition, BrdU has been also used as a proliferation marker. The differentiation of photoreceptors and its relation to AChE expression has been investigated. Eventually, the association of AChE with morphogenetic processes in the pineal will be elucidated.

- 1) Wake K, Ueck M, Oksche A. Cell. Tissue Res. 1974;154(4):423-42.

## ROLE OF NOVEL TRANSCRIPTION FACTOR *STIX* IN THE DEVELOPMENT OF CEREBRAL CORTEX

Olga Britanova<sup>1</sup>, Sergey Akopov<sup>2</sup>, Sergey Lukyanov<sup>2</sup>, Peter Gruss<sup>3</sup> and Victor Tarabykin<sup>1\*</sup>.

Department of Molecular Biology of Neuronal Signals, Max-Planck Institute for Experimental Medicine, 37075 Goettingen, Germany <sup>1</sup>

Shemiakin and Ovchinnikov Institute of Bioorganic Chemistry RAS, Miklukho-Maklaya 16/10, 117871 Moscow, Russia <sup>2</sup>

Department of Molecular Cell Biology, Max-Planck Institute for Biophysical Chemistry, 37077 Goettingen, Germany <sup>3</sup>

\*Corresponding author: vtaraby@gwdg.de

### ABSTRACT

SATB1 is a first cell type-specific transcription factor of a novel type that functions as a regulator of the transcription of large chromatin domains. We identified a close homologue of *SATB1*, *Stix* in a cDNA subtraction screening in a search for genes controlling development of cerebral cortex. It showed 61% of homology to SATB1 at aminoacid level. *Satb2* and *Stix* expression was detected in different cell subpopulations of developing mouse CNS in a mutually exclusive manner. In the electrophoretic mobility shift assay we demonstrate that nuclear extracts from the E18.5 mouse developing neocortex, in contrast to basal ganglia, contain a protein complex interacting with matrix attachment region DNA elements (MARs) with high affinity. Endogenous *Stix* protein is a part of this complex.

In order to investigate the role of *Stix* in the development of cerebral cortex we have produced mouse mutants where expression of the gene was altered. For this task two genetic approaches: “loss-of-function” and “gain-of-function” have been employed. For the first approach a mouse line with the targeted deletion of *Stix* gene has been generated. For the second approach, several transgenic lines expressing *Stix* gene ectopically have been produced. Both “loss-of-function” and “gain-of-function” animals demonstrate morphological abnormalities in the developing cortex.

Our data suggest that *Stix* may regulate differentiation of subsets of cortical neurons at the level of higher order chromatin structure via binding to matrix attachment region DNA elements (MARs).



**The role of the Homeodomain transcriptions factors Meis1 and Meis2 during early development of the vertebrate retina.**

Peer Heine, Keely Bumsted o'Brien<sup>1</sup> and Dorothea Schulte\*

*Max Planck Institut für Hirnforschung  
Deutschordenstr. 46, 60528 Frankfurt am Main*

<sup>1</sup>present address: *Department of Optometry and Vision Science, University of Auckland,  
Private bag 92019, Auckland, New Zealand*

\*corresponding author: phone: ++49-69-96769-335  
fax: ++49-69-96769-206  
email: schulte@mpih-frankfurt.mpg.de

During embryogenesis, ectodermally derived stem cells give rise to all neurons of the vertebrate central nervous system. As development proceeds, proliferation of these cells needs to be tightly controlled and balanced with differentiation. Proliferation has to be terminated and differentiation has to begin at the correct times and locations in the central nervous system to ensure that all cell types are generated at the right time, in the right relative ratios and at their proper location in the nervous system. Studies of cell fate determination in the neural retina have uncovered several mechanisms and a multitude of molecules that act together to achieve this task.

Here we describe the expression of two members of the TALE-class of Homeodomain transcription factors, Meis1 and Meis2, during vertebrate eye development. Both proteins are related to *homothorax (hth)* of *Drosophila melanogaster*, which plays an important role during the development of the fly compound eye. In the fly eye imaginal disc, *hth* is restricted to uncommitted, 'stem cell like' progenitor cells anterior to the morphogenetic furrow, where it promotes cell proliferation and blocks expression of later acting factors in the eye development cascade acting together with the Pax6 homolog *eyeless (ey)* and the zinc-finger transcription factor *teashirt (tsh)* (1).

As we show here, expression of the *hth* related proteins Meis1 and Meis2 is also restricted to retinal progenitor cells during early eye development. Like *hth* during invertebrate eye development, expression of both proteins begins to decline as soon as the first retinal neurons are born. Moreover, by retroviral misexpression of Meis2 or a dominant negative form, we found similarities in the function and regulation of Meis2 and *hth* in vertebrate and invertebrate eye development respectively.

## Symposium #S13:

### Use of two-photon fluorescence microscopy to study neuronal calcium signalling in brain slices and in the intact brain

R. Kurtz and J. Waters, Bielefeld and Heidelberg

#### Introduction

- [#S13](#) R. Kurtz and J. Waters, Bielefeld and Heidelberg  
*Use of two-photon fluorescence microscopy to study neuronal calcium signalling in brain slices and in the intact brain*

#### Slide

- [#S13-1](#) O. Garaschuk, H. Adelsberger and A. Konnerth, München  
*In vivo calcium imaging of endogenous brain rhythms*
- [#S13-2](#) Y-P. Zahng and TG. Oertner, Basel (CH)  
*Activity-dependent changes in protein concentration in dendritic spines*
- [#S13-3](#) F. Helmchen, Heidelberg  
*TWO-PHOTON MICROSCOPY: STANDARD AND FIBER-OPTIC APPROACHES*
- [#S13-4](#) J. Waters, Heidelberg  
*Imaging action potential back propagation in anaesthetized and in awake rats*
- [#S13-5](#) R. Kurtz, Bielefeld  
*In vivo multiline two-photon microscopy of calcium dynamics in the visual system of the fly*

## **Introductory Remarks to Symposium 13**

### **Use of two-photon fluorescence microscopy to study neuronal calcium signalling in brain slices and in the intact brain**

**Rafael Kurtz and Jack Waters, Bielefeld and Heidelberg**

Less than 15 years after its inception, two-photon laser scanning fluorescence microscopy has become established as an invaluable tool in neuroscience. The aim of this symposium is to present and critically discuss advantages and limitations of two-photon techniques in the study of neuronal calcium dynamics. One major focus of this symposium is on *in vivo* applications, since two-photon techniques have revolutionized studies in the intact brain, allowing deep imaging over extended periods of time.

The symposium will be opened by Fritjof Helmchen, who will introduce the fundamental principles of two-photon microscopy and discuss some recent technical developments. These include fiberoptic-based miniaturized microscopes, mounted on the head of freely moving rodents. In the second talk Jack Waters will demonstrate the use of two-photon calcium imaging in the cortex of anaesthetized rats to elucidate how ongoing synaptic activity in pyramidal neurons shapes intracellular signal propagation. He will show that action potential backpropagation and the resulting calcium influx, major computational features of pyramidal cells in slice preparations, are also present during states of high synaptic input in *in vivo*. Rafael Kurtz will then illustrate the use of multi-line two-photon microscopy to study calcium dynamics in the fly visual system. This technique utilizes a beam splitter to allow simultaneous imaging in multiple locations. Thomas Oertner will focus on the role of synaptic plasticity-related proteins in dendritic spines. By measuring protein concentration and postsynaptic calcium transients, he will address the question of cooperativity between neighboring synapses. The symposium will be closed by Olga Garaschuk, who will present a method for *in vivo* functional imaging of neuronal networks. She will discuss approaches to monitor calcium levels in non-anaesthetized animals and illustrate the applicability of these techniques by showing that large-scale spontaneous calcium waves can be monitored in behaving newborn mice.

*In vivo* calcium imaging of endogenous brain rhythms

O. Garaschuk, H. Adelsberger and A. Konnerth  
Institut für Physiologie, Universität München

Endogenous rhythms are present in the mammalian brain throughout the entire life, but their roles and mechanisms of their generation remain unclear. To characterize endogenous brain rhythms in the mouse cortex we developed an approach for direct monitoring of network activity *in vivo*. Large populations of neurons and glial cells were stained with the membrane-permeant acetoxymethyl (AM)-ester form of a  $\text{Ca}^{2+}$  indicator dye, which was delivered locally from a micropipette. Good staining was obtained with the large spectrum of indicators, including Calcium Green-1 AM, Fura-2 AM, Fluo-4 AM, Indo-1 AM thus allowing hundreds of individual cells (located up to 300  $\mu\text{m}$  below the cortical surface) to be visualized by means of two-photon microscopy. We applied the technique in newborn mice to monitor early network oscillations (ENOs), a kind of large-scale spontaneous  $\text{Ca}^{2+}$  waves initially found by our group in rat cortical slices. *In vivo*, however, ENOs were entirely blocked by anesthetics like isoflurane and urethane. For recordings in non-anaesthetized animals, an optical fiber was implanted into the stained area of the cortex. The fiber was used both for the excitation of the dye and for the collection of emitted light. In behaving mice ENOs occurred at a frequency of 3-10 per minute and were strikingly similar to their counterparts found in *in vitro* cortical slices. A combined *in vivo/in vitro* analysis performed in the same brains showed that ENOs involve 95% of cortical neurons, depend on glutamatergic synaptic transmission, require action potential firing and spread with a mean speed of 7 mm/s. A motion analysis showed that ENOs occur mainly during the periodically recurring resting states that are characteristic for early stages of postnatal development. Thus, our results suggest that in newborns,  $\text{Ca}^{2+}$  dependent cortical maturation takes place predominantly during the intermittent sleep-like resting periods. Further, they provide versatile techniques for monitoring activity of neuronal ensembles *in vivo*, in anaesthetized as well as behaving animals.

## Activity-dependent changes in protein concentration in dendritic spines

Yan-Ping Zhang & Thomas G. Oertner

Friedrich Miescher Institute of the Novartis Research Foundation,  
Basel, Switzerland

Long-term potentiation (LTP) in the CA1 region of the hippocampus is dependent on NMDA receptor activation. Downstream of NMDA receptor signaling, the activation of  $\alpha$ -calcium-calmodulin-dependent protein kinase II ( $\alpha$ CaMKII) is both necessary and sufficient for the induction of this form of LTP. Dynamic translocation of  $\alpha$ CaMKII following the activation of NMDA receptors has been demonstrated in dissociated hippocampal cultures and in intact zebrafish. It is not clear, however, how threshold, time course and specificity of  $\alpha$ CaMKII translocation are related to the induction of plasticity at individual synapses.

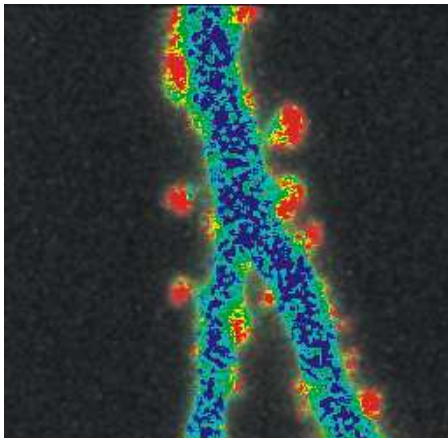


**Figure 1: Detail of a CA1 pyramidal cell dendrite. Color-coded ratio of green/red fluorescence reveals elevated CaMKII concentration in spine heads.**

To investigate activity-dependent  $\alpha$ CaMKII translocation, we co-transfected pyramidal cells in hippocampal slice cultures with  $\alpha$ CaMKII-GFP and RFP by particle-mediated gene transfer. Using two-photon laser scanning microscopy ( $\lambda_{\text{ex}} = 980 \text{ nm}$ ), we could quantify the fluorescence in individual spines over extended periods of time ( $>2 \text{ h}$ ) without significant bleaching. At each time point, we acquired 3D datasets at high resolution to exclude measurement errors due to spine motility or focal drift. The ratio of  $\alpha$ CaMKII-GFP to RFP fluorescence intensity (G/R) was used as a volume-independent measure of  $\alpha$ CaMKII concentration (Fig.1).

The concentration of  $\alpha$ CaMKII in spines and dendrites was stable over time under baseline conditions ( $34^\circ\text{C}$ ), but highly variable between different spines. Electrophysiological recordings of neighboring neurons were used in parallel to the optical measurements to assess changes in synaptic strength induced by different stimulation protocols. Bath application of L-glutamate or high  $\text{K}^+$  (30s) led to rapid translocation of  $\alpha$ CaMKII-GFP to the spine heads. Presently, we are comparing  $\alpha$ CaMKII concentration changes in spines during potentiation and depotentiation protocols using local electrical stimulation.

**TWO-PHOTON MICROSCOPY: STANDARD AND FIBER-OPTIC APPROACHES**

Fritjof Helmchen

Abteilung Zellphysiologie, Max-Planck-Institut für medizinische Forschung,  
Jahnstr. 29, 69120 Heidelberg, Germany

Two-photon laser scanning microscopy [1] is exceptionally well suited for fluorescence imaging several hundred microns deep inside intact biological tissue, enabling for example functional imaging of neuronal activity in the living brain. In this talk I will give an introduction to the fundamental principles of two-photon microscopy and present an overview of the current status in the field. The various technological approaches to implement laser scanning in standard microscopes will be summarized and the current limitations in terms of scanning speed and depth penetration will be discussed. These issues will be illustrated by examples from *in vivo* two-photon imaging in the neocortex of anesthetized rodents.

To extend high-resolution optical imaging to awake, freely behaving animals, small and flexible microscopes are required [2]. Microscope miniaturization necessitates efficient two-photon excitation through an optical fiber, which will be discussed in the second part of the talk. A major problem of this approach has been the temporal broadening of femtosecond laser pulses due to material dispersion and non-linearities in the glass fiber, which markedly reduces the efficacy of two-photon fluorescence excitation. A solution to this problem is offered by a new type of optical fiber, so-called photonic crystal fibers (PCFs), which can be designed to propagate light in a hollow air core [3]. This greatly reduces the impact of the bulk material properties and permits distortion-free delivery of femtosecond pulses through PCF fibers [4]. The hollow core fiber thus is excellently suited for fiber-optic two-photon-excited fluorescence microscopy. We have incorporated it in a miniaturized microscope and demonstrate *in vivo* cellular imaging in the intact neocortex of adult rats.

Finally, I will discuss a different approach to miniaturize two-photon microscopes, which makes use of thin optical fiber bundles in combination with gradient-index (GRIN) lenses that can be endoscopically inserted in deep brain regions [5]. In this case, a standard microscope is used for laser scanning. First fluorescence images taken in the intact rat brain using a two-photon fiber-bundle microscope will be presented [6].

**References**

- [1] W. Denk, J. H. Strickler, and W. W. Webb, "Two-photon laser scanning fluorescence microscopy," *Science* **248**, 73-76 (1990).
- [2] F. Helmchen, M. S. Fee, D. W. Tank, and W. Denk, "A miniature head-mounted two-photon microscope: high-resolution brain imaging in freely moving animals," *Neuron* **31**, 903 (2001).
- [3] R. F. Cregan, B. J. Mangan, J. C. Knight, T. A. Birks, P. S. J. Russell, P. J. Roberts, and D. C. Allan, "Single-mode photonic band gap guidance of light in air," *Science* **285**, 1537 (1999).
- [4] W. Göbel, A. Nimmerjahn, and F. Helmchen, "Distortion-free delivery of nanojoule femtosecond pulses from a Ti:sapphire laser through a hollow-core photonic crystal fiber", *Opt. Lett.* **29**, 1285 (2004).
- [5] J. C. Jung and M. J. Schnitzer, "Multiphoton endoscopy", *Opt Lett.* **28**, 902 (2003).
- [6] W. Göbel, J. N. D. Kerr, A. Nimmerjahn, and F. Helmchen, "Miniaturized two-photon microscope based on a flexible coherent fiber bundle and a gradient-index lens objective", *Opt. Lett.* in press (2004).

## Imaging action potential back propagation in anaesthetized and in awake rats

Jack Waters

Abteilung Zellphysiologie, MPI Heidelberg

and

Department of Physiology, The Feinberg School of Medicine  
Northwestern University, Chicago

In many neurones, action potentials initiate in the axon initial segment and propagate both forwards along the axon and backwards into the dendritic tree. The back propagating action potential provides a retrograde signal to the sites of synaptic input, distributing information about the recent firing activity of the neuron. In the dendrites, back propagating action potentials (and other active dendritic phenomena such as dendritic spike initiation) activate voltage-gated channels, including calcium channels. Dendritic calcium imaging is therefore useful for studying action potential back propagation, particularly where direct dendritic recordings are not feasible, such as in anaesthetized and awake rats.

To date, active dendritic properties have been studied almost exclusively in slice preparations, where background synaptic activity is minimal. In contrast, in the intact brain (in both anaesthetized and awake animals) neurons are subjected to substantial spontaneous and evoked synaptic activity, which necessarily activate and/or inactivates dendritic channels. As action potential back propagation is supported by dendritic channels, back propagation cannot occur if channels are unavailable. Synaptic activity can therefore modulate and could potentially eliminate back propagation *in vivo*.

Do action potentials back propagate *in vivo*? To answer this question, I have been studying action potential initiation and back propagation in the dendrites of layer 2/3 neocortical pyramidal neurons *in vivo* using calcium imaging techniques. 2-photon imaging is essential for these experiments, allowing the experimenter to monitor back propagation far deeper (up to ~500  $\mu\text{m}$ ) into the brain than with conventional imaging techniques.

I will show that back propagation occurs in the anaesthetized rat, much as it does in slice preparations. Under urethane anaesthesia, cortical neurons periodically receive bursts of synaptic activity which drive the membrane potential into a depolarized 'up' state. During up states, action potential back propagation is slightly enhanced. Hence rather than inhibiting back propagation, spontaneous synaptic activity slightly enhances it, favouring the spread of action potentials further into the dendritic tree.

I will also show that back propagation occurs in the awake rat, where both spontaneous and evoked calcium transients are visible throughout much of the dendritic tree. Hence active dendritic properties, such as action potential back propagation, persist in the awake animal, where they almost certainly play important roles in the integration of synaptic input.

## *In vivo* multiline two-photon microscopy of calcium dynamics in the visual system of the fly

Rafael Kurtz

Neurobiologie, Fakultät Biologie, Universität Bielefeld, Postfach 100131, D-33501 Bielefeld, Germany  
e-mail: [rafael.kurtz@uni-bielefeld.de](mailto:rafael.kurtz@uni-bielefeld.de)

The investigation of dynamic processes in single nerve cells and in neuronal circuits often requires imaging of neural activity and its correlates with high temporal and spatial resolution. In conventional wide-field fluorescence microscopy of intact tissue spatial resolution is affected considerably by light scattering. Temporal resolution is limited by the time needed to acquire two-dimensional images. Laser-scanning fluorescence techniques, in particular two-photon laser scanning microscopy (TPLSM), can provide a better spatial resolution than conventional imaging and allows three-dimensional reconstructions based on series images at different focal planes. Imaging speed can be raised to the kHz-level with laser microscopy, but only in line scans, i.e. when the laser is scanned repeatedly along a single axis. In contrast, scanning entire images or even image stacks in the z-plane is as time-consuming as conventional imaging. This bears considerable problems, because it is often required to compare functional signals from several neuronal structures, which cannot be covered entirely by a single scan line.

In TPLSM, an elegant solution to this problem is to split the single excitation laser beam into multiple beams, in order to illuminate several points in the sample simultaneously. Laser scanning can then be performed along several lines in the focal plane at the same speed as single-line scanning. Numerous cellular structures, which are far apart from each other, can thus be imaged simultaneously at a high rate. By means of a mirror-based beamsplitter a matrix of up to 64 unitary beams is generated and directed to the sample via the scan mirrors and the optics of the microscope<sup>1</sup>. Through the use of a highly sensitive electron-multiplying CCD camera as a detector, descanning and isolation of the fluorescence emitted from individual laser foci is not required, as would be the case when using an array of conventional photomultiplier tubes or avalanche photodiodes<sup>2</sup>.

One drawback of our detection scheme is, however, that spatial resolution may be compromised by the pixel size of the CCD and by scattering of emitted fluorescence light on its way from the laser foci inside the sample to the detector. In this talk, the new multiline laser-scanning principle will therefore be critically evaluated with respect to *in vivo* imaging of calcium concentration changes in single visual motion-sensitive neurons of the fly (*Calliphora vicina*)<sup>3</sup>. Some of these neurons receive motion information from a large part of the fly's visual surroundings. Their dendrites are retinotopically organized and local visual stimulation leads to calcium accumulation, which remains spatially restricted to the corresponding dendritic subarea. Hence, high-resolution imaging of dendritic calcium signals sheds light on the receptive field characteristics and the integration properties of these neurons. Moreover, the study of presynaptic calcium signalling may benefit from the new technique's ability to perform fast imaging over extended areas<sup>4</sup>.

### References:

- 1 Nielsen T, Fricke M, Hellweg D, Andresen P. J Microsc, 201 (2001) 368-376.
- 2 Kalb J, Nielsen T, Fricke M, Egelhaaf M, Kurtz R. Biochem Biophys Res Commun, 316 (2004) 341-347.
- 3 Borst A, Egelhaaf M. Proc Natl Acad Sci USA, 89 (1992) 4139-4143.
- 4 Kurtz R, Warzecha AK, Egelhaaf M. J Neurosci, 21 (2001) 6957-6966.



**Symposium #S14:**  
**Neuronal injury and infection**  
**R. Nau and W. Brück, Göttingen**

**Introduction**

[#S14](#) R. Nau and W. Brück, Göttingen  
*Neuronal injury and infection*

**Slide**

- [#S14-1](#) TJ. Mitchell, Glasgow (UK)  
*The action of pneumolysin and other bacterial haemolysins on immune cells and neurons*
- [#S14-2](#) JR. Weber, Berlin  
*Innate sensors for Gram-positive and Gram-negative bacteria*
- [#S14-3](#) M. Stagi, N. Frank, P. Gorlovoi and H. Neumann, Göttingen  
*Cytotoxic effects of microglia on neurons*
- [#S14-4](#) G. Stuchbury, J. Webster, A. Huber, K. Berbaum and G. Münch, Townsville (AUS)  
*Neuro-inflammatory processes in Alzheimers disease*
- [#S14-5](#) VH. Perry, Southampton (UK)  
*The impact of systemic inflammation on the progression of neurodegenerative disease.*
- [#S14-6](#) R. Nau, Göttingen  
*Strategies aiming at minimizing the liberation of proinflammatory and toxic products from pathogens during the treatment of infections*

**Poster**

- [#1B](#) S. Müller-Röver, K. Warnke, F. Siebenhaar, S. Sallach, G. Goelz, C. Brandt, M. Maurer and R. Nitsch, Berlin  
*MAST CELL INFLUENCE ON AXONAL OUTGROWTH AND NEURONAL INJURY*
- [#2B](#) A-S. Michal, G. Orit, R. Ram and T. Oren, Jerusalem (IL)  
*Inhibition of MnSOD Expression as a mechanism for glutamate-induced death in HT4 neuronal cells*
- [#3B](#) U-K. Hanisch and T. Möller, Berlin and Göttingen  
*THE MICROGLIA-ACTIVATING POTENTIAL OF THROMBIN*

- [#4B](#) D. Stojkov, I. Lavrnja, S. Pekovic, S. Subasic, S. Jovanovic, M. Mostarica-Stojkovic, S. Stosic-Grujicic, N. Nedeljkovic, Lj. Rakic and M. Stojiljkovic, Belgrade (YU)  
*Attenuation of Experimental Autoimmune Encephalomyelitis clinical signs by combined therapy of ribavirin and tiazofurin*
- [#5B](#) M. Hosseini, C. Koester-Patzlaff, J. Chowdhury, S. Grebenshchikova and B. Reuss, Göttingen  
*Expression profiling for regulators of adult neurogenesis in dentate gyrus and cerebellum of Borna disease virus infected rats*
- [#6B](#) E. Koutsilieri, S. Czub, C. Scheller, S. Sopper, E. Grünblatt, G. Gosztonyi, V. ter Meulen and P. Riederer, Würzburg and Berlin  
*Dopamine accelerates progression of HIV-dementia*
- [#7B](#) S. Michalak, Poznan (PL)  
*The effect of tumor necrosis factor, interleukin-1 and interleukin-6 on the expression of heat shock protein 70 in the central nervous system.*
- [#8B](#) A. Spreer, J. Gerber, M. Hanssen, P. Lange, H. Eiffert and R. Nau, Göttingen  
*Adjuvant therapy with dexamethasone increases neuronal apoptotic cell death in the dentate gyrus in experimental Escherichia-coli-meningitis*
- [#9B](#) L. Dreesmann, M. Lietz, S. Oberhoffner, A. Ullrich, M. Dauner and B. Schlosshauer, Reutlingen and Denkendorf  
*MICRO TISSUE ENGINEERING: NEURON-, GLIA-, AND FIBROBLAST CELL INTERACTIONS IN POLYMER-BASED NERVE GUIDES*
- [#10B](#) J. Sellner, DN. Meli, D. Grandgirard, B. Storch-Hagenlocher, U. Meyding-Lamade and SL. Leib, Berne (CH) and Heidelberg  
*Hydroxyproline as a marker for collagenolytic activity in neuroinflammatory disorders*
- [#11B](#) J. Sellner, F. Dvorak, Y. Zhou, S. Strand, PR. Galle and U. Meyding-Lamade, Berne (CH), Heidelberg and Mainz  
*Involvement of FasL(CD95L) and Perforin mediated apoptosis in the pathogenesis of Herpes-simplex Virus Encephalitis*

## **Introductory Remarks to Symposium 14**

### **Neuronal injury and infection**

**Roland Nau and Wolfgang Brück, Göttingen**

In central nervous system infections, death and long-term neurologic sequelae can be caused by 1.) the host's systemic inflammatory response leading to leukocyte extravasation, vasculitis, brain edema and secondary ischemia, 2.) stimulation of resident microglia within the central nervous system by bacterial compounds and 3.) direct toxicity of bacterial compounds on neurons. Autoimmune diseases of the central nervous system can be induced or aggravated by extracerebral infections. Moreover, the progression of neurodegenerative diseases appears to be accelerated by extracerebral infections.

The symposium will cover the different mechanisms, how infectious agents can affect the central nervous system either directly or by stimulating the host's immune reaction. Particular emphasis will be placed upon the innate immunity. Approaches to counteract pathogen-mediated neuronal injury will be discussed.

## The action of pneumolysin and other bacterial haemolysins on immune cells and neurons

Tim J. Mitchell

Division of Infection and Immunity, Joseph Black Building, Institute of biomedical and Life Sciences, University of Glasgow, Glasgow, G12 8QQ, United Kingdom.  
[T.Mitchell@bio.gla.ac.uk](mailto:T.Mitchell@bio.gla.ac.uk)

Pneumolysin (PLY) is a member of the family of cholesterol-dependent pore forming cytotoxins produced by several genera of Gram-positive bacteria. This family of toxins have several activities on eukaryotic cells. At high concentrations they cause cell lysis of all eukaryotic cells which contain cholesterol in their membranes. At lower concentrations the toxin can have other effects and has been shown to affect the production of pro-inflammatory mediators such as TNF, IL-1 and IL-6. The toxin can stimulate nitric oxide production from macrophages as well as increased transcription of the genes for COX-2. Pneumolysin may act as a general activator of macrophages possibly through activation of NF- $\kappa$ B. Interaction of the toxin with neutrophils causes increased production of superoxide, increased production of elastase, increased expression of beta-2 integrins and increased production of prostaglandin E<sub>2</sub> and leukotriene B<sub>4</sub>. Cell recruitment may also be affected by the toxin as it can promote IL-8 secretion from neutrophils. The effects of pneumolysin on macrophages may also involve an interaction with Toll-like receptor 4 (TLR4) as the stimulation of macrophages to produce TNF and IL-6 is dependent on the cytoplasmic TLR-adaptor molecule, myeloid differentiation factor 88 (MyD88), and macrophages from mice with the targeted deletion of MyD88 did not respond to PLY.

The contribution of pneumolysin to apoptosis has also been investigated in a range of cell types. The toxin induces mainly necrosis in neutrophils. Use of a pneumolysin-negative mutant of *Streptococcus pneumoniae* has shown that PLY contributes to macrophage apoptosis induced by whole bacteria. Using cells of cerebral origin as a model of blood-brain barrier has shown that much of the damage induced in these cells by the pneumococcus is due to PLY. The damage induced by the toxin was dependent on protein synthesis, tyrosine phosphorylation and caspase activity.

The most detailed studies of the role of PLY in apoptosis have been done in neuronal tissues. PLY can induce an apoptosis-inducing factor (AIF)-dependent form of apoptosis. PLY induces the increase of intracellular calcium levels and release of AIF from mitochondria in primary rat neurons. The apoptotic effect could be blocked by chelation of calcium. An effect of PLY on calcium levels has also been demonstrated in neuroblastoma cells, in which purified PLY was shown to induce apoptosis in a calcium-dependent manner. The apoptotic effect in these cells involved mitogen-activated protein kinase p38.

The details of these effects of PLY activity on cells will be discussed and compared with other bacterial haemolysins.

**Innate sensors for Gram-positive and Gram-negative bacteria**

Joerg R. Weber, Department of Neurology, Charité – Universitaetsmedizin Berlin

Invasive bacterial infections of the CNS generate some of the most powerful inflammatory responses known in medicine. Although the components of bacterial cell surface are now chemically defined in exquisite detail and the interaction with the toll-like receptor pathway has been discovered, it is only very recently that definitive studies combining these advanced biochemical and cell biological tools have been done.

The blood brain barrier separates the brain very effectively from the systemic circulation and bacteria have to invade over this protective barrier. Before receptor mediated signaling events come into play soluble general recognition molecules such as CD14 or LPS binding protein may sense and augment the effect of bacterial cell wall components and direct them towards intra- and extracellular receptors. The inflammatory activation caused by these events is the prerequisite for further bacterial invasion. These steps happen well before any bacterial components interact with the powerful immune cells of the brain e.g. microglia and astrocytes.

This presentation will cover recent sentinel studies that go a long way toward settling the controversies that surround the process by which Gram positive and Gram negative bacterial surfaces and metabolites trigger the immune system of the brain.

**Cytotoxic effects of microglia on neurons****Massimiliano Stagi, Nadja Frank, Philippe Gorlovoi, Harald Neumann****Neuroimmunology Unit, European Neuroscience Institute Goettingen,  
Germany**

Neuronal and axonal injury are early signs of inflammatory brain diseases, but the exact molecular mechanism is unclear. Activated microglial cells releasing inflammatory mediators and cytokines are observed in close proximity to dystrophic neurites. Confocal microscopy was performed to study the interaction between microglia and neurons. Particularly, axonal transport of vesicle precursors, mitochondria and changes of axonal cytoskeleton associated proteins were studied in transfected cultured hippocampal neurons.

Microglia, pre-stimulated by inflammatory cytokines to produce nitric oxide (NO) and tumor necrosis factor-alpha (TNF-alpha), focally suppressed the axonal motility of synaptophysin-EGFP at the contact point. Direct application of TNF-alpha or a short-term NO donor to cultured hippocampal neurons inhibited axonal motility of synaptophysin-EGFP within 10 minutes. Inhibition of axonal transport by this inflammatory mediator significantly increased the immobile fraction of synaptophysin-EGFP and was dependent on phosphorylation of c-jun NH(2)-terminal kinase (JNK). TNF-alpha stimulated phosphorylation of JNK in axons and blockade of synaptophysin-EGFP transport by TNF-alpha treatment was reverted by the JNK inhibitor SP600125.

Production and release of inflammatory mediators by activated microglial cells inhibit axonal transport of synaptic vesicle precursor via phosphorylation of JNK. Prolonged inhibition of axonal transport by inflammatory mediators may cause axonal dysfunction and injury in neuroinflammatory diseases.

*Neuro-inflammatory processes in Alzheimer's disease*

**Grant Stuchbury, Julie Webster, Anke Huber, Katrin Berbaum, Gerald Münch**  
Dept of Biochemistry & Molecular Biology, James Cook University, Townsville 4811  
Australia, Email: Gerald.Muench@jcu.edu.au

One of the many possible causes of AD is a chronic inflammatory response, which is most pronounced in the vicinity of amyloid plaques. Involvement of the immune system in the pathogenesis of AD is evident both by the presence of complement proteins in diseased tissue and by the activation of micro- and astroglia, as well as the release of pro-inflammatory cytokines. These cytokines are important modulators of brain inflammation and accumulated evidence suggests that many occur at abnormal levels in brain regions affected by disease or injury.

It is widely accepted that the amyloid plaque is the center of glial activation and chronic inflammation in AD. Since the major proteinaceous component of the amyloid deposits is  $\beta$ -amyloid peptide ( $A\beta$ ), it has been proposed to be the major inducer of glial activation. However, mice overexpressing beta-amyloid peptide do not present the full set of inflammatory markers as human Alzheimer's patients indicating that human plaques contain a further inflammatory stimulus.

These "extra" age-related proinflammatory stimuli are 'Advanced Glycation Endproducts (AGEs)', which form by the reaction of lysine and arginine with oxidation products of sugars. The effect of AGEs as pro-inflammatory ligands was first discovered in hemodialysis-associated amyloidosis.  $\beta$ 2-microglobulin ( $\beta$ 2M), the major protein in these deposits, is modified with AGEs. In this case, AGE-modified, but not the unmodified  $\beta$ 2M, was shown to induce IL-6 from human macrophages. AGE-modified proteins can cause increased expression of extracellular matrix proteins, vascular adhesion molecules, cytokines and growth factors associated with diabetic complications.

A synergistic action of  $A\beta$  with other pro-inflammatory stimuli (LPS, AGEs or interferon- $\gamma$ ) increases its proinflammatory potential. AGEs and  $A\beta$  bind to a cell surface binding site comprised of a integral membrane protein (receptor for AGE = RAGE) and a lactoferrin-like polypeptide (LF-L). RAGE has been shown to mediate the induction of oxidant stress and the activation of microglia. AGEs induce nitric oxide (NO), TNF and IL-6 production, and RAGE and the transcription factor NF- $\kappa$ B are both involved in pathways mediating the expression of these cytokines. Furthermore, the combination of  $A\beta$  and AGEs synergistically enhances the expression of the pro-inflammatory cytokines TNF, IL-6 and M-CSF.

If these findings are put into a clinical context, treatment of Alzheimer's disease patients with anti-inflammatory drugs is likely to attenuate inflammation and will most likely result in a slower progression of their dementia and a longer period of high quality life.

The impact of systemic inflammation on the progression of neurodegenerative disease.  
V. Hugh Perry, CNS Inflammation Group, School of Biological Sciences, University of Southampton, Southampton SO16 7PX, UK

Systemic infection or indeed other insults that provoke a systemic inflammatory response may lead to a relapse in multiple sclerosis (MS) or an acute delirium in the patient with Alzheimer's disease (AD), or aged person. The mechanisms underlying these acute neurological states are not fully understood but the evidence suggests that enhanced cytokine synthesis in the brain is driven by systemically generated cytokines signalling across the intact blood-brain barrier. Recent evidence suggests that interactions between brain inflammation and low grade systemic infection can contribute to cognitive disturbances over several months duration (Holmes et al, 2003).

To investigate the role of inflammation in chronic neurodegeneration we have studied an animal model of chronic neurodegenerative disease, murine prion disease. In this disease the microglia are morphologically activated but have an atypical cytokine profile (Perry et al, 2002). This atypical cytokine profile is similar to that detected in macrophages which have phagocytosed cells undergoing apoptosis. At the early stage of the disease when the first behavioural symptoms can be detected this is associated with microglia activation, increased levels of transforming growth factor-beta (TGF) and also increased CO-2 expression but there is no neuronal loss only loss of synapses (Cunningham et al, 2003). However, following peripheral challenge with endotoxin to mimic components of a systemic infection we have found enhanced synthesis of pro-inflammatory cytokines and this enhanced cytokine synthesis is associated with exaggerated behavioural symptoms when compared to normal animals challenged with endotoxin (Combrink et al, 2002). By analogy with the relapses in MS, many of which may be precipitated by a systemic infection, we suggest that the activated microglia in persons with AD are "primed" by the pathology, and respond more vigorously than normal when the cytokines generated by the systemic infection impact on the brain. The increased synthesis of cytokines and other inflammatory molecules within the brain may contribute to disease progression.



## **Strategies aiming at minimizing the liberation of proinflammatory and toxic products from pathogens during the treatment of infections**

Roland Nau, Dept. of Neurology, University Hospital, Robert-Koch-Str. 40, D-37075

Göttingen, E-mail: rnau@gwdg.de

Several bacterial products (endotoxin, teichoic and lipoteichoic acids, peptidoglycan, DNA, pneumolysin, and others) and viral components can induce inflammation via stimulation of Toll-like receptors or may be directly toxic in eukariotic cells. Endogenous and microbial ligands of Toll-like receptors may have an additive or synergistic effect. This probably is the molecular basis of the frequently observed aggravation of neurodegenerative diseases by infections.

In the case of bacteria, any effective antibiotic treatment reduces the release of proinflammatory products in comparison with uninhibited growth. Bactericidal antibiotics which inhibit bacterial protein synthesis release smaller quantities of proinflammatory/toxic bacterial compounds compared to  $\beta$ -lactams and other cell-wall active drugs. High antibiotic concentrations induce the release of less bacterial proinflammatory/toxic compounds than concentrations close to the minimal inhibitory concentrations. In several in-vitro and in-vivo systems, bacteria treated with bacterial protein synthesis inhibitors induce less inflammation than bacteria treated with  $\beta$ -lactam antibiotics. In animal models of *Escherichia coli* and *Staphylococcus aureus* sepsis and of *Streptococcus pneumoniae* meningitis, a lower antibiotic-induced release of proinflammatory bacterial compounds was associated with a reduced mortality (sepsis, meningitis) and glutamate release, free radical formation and neuronal injury (meningitis).

In conclusion, sufficient evidence for the validity of the concept of modulating the release of proinflammatory bacterial compounds by antibacterials has been accumulated in vitro and in animal experiments to justify clinical trials in humans. A properly conducted study addressing the potential benefit of bacterial protein synthesis inhibitors versus  $\beta$ -lactam antibiotics will require both a strict selection and inclusion of a high number of patients. The benefit of this approach should be greatest in patients with a high bacterial load.

## MAST CELL INFLUENCE ON AXONAL OUTGROWTH AND NEURONAL INJURY

Sven Müller-Röver<sup>1\*</sup>, Katharina Warnke<sup>1</sup>, Frank Siebenhaar<sup>2</sup>, Stephanie Sallach<sup>1</sup>, Greta Goelz<sup>1</sup>, Christine Brandt<sup>1</sup>, Marcus Maurer<sup>2</sup>, Robert Nitsch<sup>1</sup>

<sup>1</sup>Center for Anatomy, Institute of Cell Biology and Neurobiology, Charité, University Medicine, Berlin, Germany

<sup>2</sup>Dept. of Dermatology and Allergy, Charité, University Medicine, Berlin, Germany,

\*corresponding author: sven.mueller-roever@charite.de

Mast cells (MCs) have been demonstrated to play a key role in allergy and to be important effectors in the development and severity of multiple sclerosis and its animal model, experimental autoimmune encephalomyelitis. Here we have investigated the effects MCs exert after a mechanical injury to the brain. To show the presence of MCs in our region of interest, the hippocampus (HC) and entorhinal cortex (EC), we used the following labelling methods on sections of paraffin-embedded murine brains: GIEMSA, toluidine blue, FITC-Avidin and c-kit immunoreactivity. MCs were present perivascularly or within the parenchyma, both in the HC and EC. The average number of mast cells in the HC and EC was 2-4 mast cells/microscopic field. Using an axonal outgrowth assay, we studied the influence of mast cells on axonal outgrowth *in vitro*. In the outgrowth assay, MCs induced a significantly higher axonal density and an increased length of neurites in EC explants in a dose-dependent manner. Furthermore, we compared mast cell-deficient W/W<sup>v</sup>-mice and wildtype controls after an entorhinal cortex lesion (ECL), applying immunohistochemical markers such as glial fibrillary acidic protein (GFAP), neurofilament 200, and IB-4. Expression of GFAP around the lesion was two times higher in mast cell-deficient mice compared to controls, while neurofilament 200 expression at the lesion site was substantially reduced in W/W<sup>v</sup> mice. Finally, mast cell-deficient mice showed a significantly lower number of activated IB-4-positive cells in the lesion area compared to controls. These data suggest that MCs stimulate axonal outgrowth, activate microglia, and modulate the development of astrogliosis.

## **Inhibition of MnSOD Expression as a Mechanism for Glutamate-Induced Death in HT4 Neuronal Cells**

Aharoni-Simon Michal, Golan Orit, Reifen Ram, Tirosh Oren

Elevated levels of extracellular glutamate are responsible for neuronal damage and degeneration in brain disorders, including stroke, epilepsy, and Parkinson's disease. In this study we found a direct link between Manganese Superoxide Dismuthase (MnSOD) expression to the signaling cascade of glutamate-induced cell death. Mouse hippocampal-derived HT4 cell line was treated with Glutamate (10 mM) for 6 h. Such treatment induced accumulation of intracellular ROS and depletion in intracellular GSH, followed by cell death after 12 h. 100  $\mu$ M tempol (superoxide dismutase mimetic compound) added simultaneously with glutamate for 12 h, protected the cells from death, which indicates that superoxide plays a role in the death cascade. Analysis of mitochondrial MnSOD showed depletion in the protein and mRNA levels, generated by 6 h treatment with glutamate. Transient transfection with si-RNA to MnSOD increased glutamate toxicity, while overexpression of MnSOD attenuated glutamate toxicity in cells treated with glutamate for 12 h. The decline in the expression of MnSOD is not a result of mitochondrial degradation, as there was no reduction in the level of cytochrome c, or any damage to the mitochondrial DNA following glutamate treatment. Preincubation of the cells with the antioxidant selenium (0.5  $\mu$ M, 10  $\mu$ M) for 24 h before glutamate treatment prevented MnSOD depletion and ROS generation, and rescued the cells from glutamate-induced cell death.

The results of this study demonstrate that depletion of mitochondrial MnSOD expression is a key event in glutamate-induced neuronal cell death. Hence, regulating MnSOD expression is a significant process which can assist in preventing neuronal damage and brain degeneration.

## THE MICROGLIA-ACTIVATING POTENTIAL OF THROMBIN

**Uwe-Karsten Hanisch and Thomas Möller**

<sup>1</sup>Department of Cellular Neurosciences, Max Delbrück Center for Molecular Medicine, D-13092 Berlin, Germany

<sup>2</sup>Institute for Neuropathology, University of Göttingen, D-37075 Germany

<sup>3</sup>Department of Neurology, School of Medicine, University of Washington, Seattle, WA, 98195-6465, USA

The serine protease thrombin is known as a blood coagulation factor. Through limited cleavage of proteinase-activated receptors (PAR) it can also control growth and functions in various cell types, including neurons, astrocytes and microglia (brain macrophages). A number of previous studies indicated that thrombin induces the release of proinflammatory cytokines and chemokines from microglial cells, suggesting an additional role for the protease beyond hemostasis. In the present study, we provide evidence that this effect is not mediated by thrombin proper, but by a high molecular weight (HMW) fraction in thrombin preparations. We found that (1) only long exposure (hours) of microglia to thrombin preparations triggered cyto/chemokine release, which is incompatible with rapid PAR signalling. (2) Agonists directly activating PARs did not trigger release. (3) Inhibitors preventing the interactions of thrombin with endogenous (receptor) substrates, including hirudin and heparin, did not block the release response. (4) Thrombin-specific active site inhibitors blocked the proteolytic activity but did not affect the cytokine release. In contrast, we identified a minor fraction of associated proteins which is solely responsible for the release induction. HMW material can be isolated in trace amounts even from apparently homogenous  $\alpha$ - and  $\gamma$ -thrombin preparations. It contains thrombin-derived peptides as revealed by mass spectrometry but is devoid of thrombin-like enzymatic activity. Our findings may force a revision of the notion that intact thrombin itself is a direct proinflammatory release signal for microglia. In addition, they could be relevant for the study of other cellular activities and their assignment to this protease.

## ATTENUATION OF EXPERIMENTAL AUTOIMMUNE ENCEPHALOMYELITIS CLINICAL SIGNS BY COMBINED THERAPY OF RIBAVIRIN AND TIAZOFURIN

Stojkov D.<sup>a</sup>, Lavrnja I.<sup>a</sup>, Pekovic S.<sup>a</sup>, Subasic S.<sup>b</sup>, Jovanovic S.<sup>a</sup>, Mostarica-Stojkovic M.<sup>c</sup>,  
Stosic-Grujicic S.<sup>a</sup>, Nedeljkovic N.<sup>b</sup>, Rakic Lj.<sup>a</sup>, Stojiljkovic M.<sup>a</sup>

<sup>a</sup>Dept. Neurobiol. & Immunol. "Sinisa Stankovic" Inst. Biol. Res., Belgrade, 11000, Serbia and Montenegro

<sup>b</sup>Faculty of Biology, Belgrade, 11000, Serbia and Montenegro

<sup>c</sup>Inst. Microbiol. & Immunol., School of Medicine, Belgrade, 11000, Serbia and Montenegro

Experimental Autoimmune Encephalomyelitis (EAE), an animal model of human demyelinating disease multiple sclerosis (MS), is commonly used for evaluation of potential therapies for MS. Clinical signs of this neurological disorder are consequences of an autoaggressive T-cell response against myelin. The aim in this study was to investigate how combined drug administration (ribavirin – R + tiazofurin – T) from the onset of the first EAE signs or from more difficult symptom (paresis) will affect further development of EAE. Ribavirin is synthetic guanosine analogue, originally designed by Robins and co-workers as an antiviral agent. Tiazofurin is synthetic C-nucleoside that exhibits significant antitumor activity. In sensitive cells, like activated lymphocytes, they act through their active metabolites which inhibit enzyme Inosine Monophosphate Dehydrogenase (IMPDH), binding on its different sites. Result of such inhibition is reduction in guanine nucleotide levels, which then cause interruption of cell metabolism. The disease was induced in male Dark Agouti (DA) rats with rat spinal cord homogenate and it had a self limited acute monophasic course. For one group of animals treatment started when first clinical sign of EAE appeared (9th day after EAE induction). They received i.p ribavirin at a daily dosage of 30mg/kg and tiazofurin at a dosage of 10mg/kg every other day for 15 days. The other group of animals was also treated with R and T in same dosages and in same way but treatment started after appearance of more severe EAE symptom – paresis (13<sup>th</sup> day after EAE induction). Control group of animals was immunized and treated only with saline. Amelioration of clinical signs and faster recovery was obtained in both group treated with combination of R and T in compare to control group of animals. Immunohistochemical analysis of the lumbosacral spinal cord tissue isolated after 15 days of combined therapy revealed decrease in number of T-cells and macrophages/microglia, which were pronounced in control group. Also, in group of animals treated with combination of R and T diminution in presence of demyelination areas was showed. Results gained in this study revealed that R and T have EAE protective effects and recommended them for future therapy of multiple sclerosis.

**Keywords:** EAE, MS, ribavirin, tiazofurin, demyelination

(This work was supported from Ministry of Science and Environmental Protection, Republic of Serbia, Serbia and Montenegro, Grants 1647, 1664, 2020)

## Expression profiling for regulators of adult neurogenesis in dentate gyrus and cerebellum of Borna disease virus infected rats

Hosseini M.<sup>1</sup>, Koester-Patzlaff C.<sup>1</sup>, Chowdhury K.<sup>2</sup>, Grebenshchikova S.<sup>2</sup> and Reuss B.<sup>1</sup>

<sup>1</sup> Georg-August-University Goettingen, Center for Anatomy/Neuroanatomy, Neurovirology group

<sup>2</sup> Max Plank Institut of Biophysical Chemistry, Goettingen

**Introduction:** Borna disease virus (BDV) is a neurotropic, noncytolytic, nonsegmented negative stranded RNA virus and the prototype of the family of Bornaviridae, within the order of Mononegavirales. Borna virus has a broad host range in warm-blooded animals, probably including humans. A characteristic feature of rats with a latent BDV infection is degeneration of the dentate gyrus. The dentate gyrus is also known to be a brain area where adult neurogenesis takes place. This suggested to us that disturbed proliferation and /or differentiation of neuronal stem cells could play a role for BDV dependent dentate gyrus degeneration. To understand the interrelation between dentate gyrus degeneration and disturbed neurogenesis we investigated markers for adult neurogenesis in BDV infected rats as compared to control treated animals by indirect immunohistochemistry. In addition we analysed changes of gene expression levels in BDV infected rats by DNA microarray analysis.

**Methods:** Newborn Lewis rats were injected with 30 µl of a 10% w/v brain homogenate in PBS from BDV infected or control animals. Rats were killed 4 or 8 weeks after infection and processed for further experiments. First, BDV infection was verified by immunohistochemistry and RT-PCR analysis. We then analysed adult neurogenesis, with the hippocampus of infected and control treated rats being explored for expression of the neuronal stem cell marker Nestin, and the proliferation marker Ki67, as well as for the integration of the proliferation marker BrdU by RT-PCR and indirect immunohistochemistry. Finally expression profiling was performed by hybridising labeled cRNA, derived from pools of the total hippocampal and cerebellar RNA from six animals, to the Affymetrix Rat 230 DNA microarray.

**Results:** As we could show by immunohistochemistry, expression of Nestin, as well as numbers of cells positive for BrdU and Ki67 are distinctly increased four weeks post infection. In contrast, eight weeks post infection numbers of cells with immunoreactivity for Nestin, BrdU and Ki67 showed a clear decrease. By DNA microarray analysis we could identify 1027 genes to be up-, and 281 genes to be downregulated in the hippocampus at a factor of >1,5. Likewise in the cerebellum at a cutoff level of >1,5 944 genes were up-, and 387 genes were downregulated. With respect to gene classes regulated during BDV infection, a large part is formed by genes related to the immune response, like antibodies, Interferons, and Interleukins. In addition, intracellular signalling molecules (i.e. for calcium homeostasis), cytoskeletal proteins (microtubule and actin associated proteins), extracellular matrix molecules (lectins, integrins, collagen), as well as growth factors, transcription factors, and genes involved in protein degradation were changed. With respect to neurons and neuronal stem cells, markers and regulatory factors like noggin, notch1, notch2, CD44, Nedd4a as well as of BMP related genes turned out to be changed in their expression. In addition to this, a general BDV dependent upregulation of apoptosis related genes, and differential changes in several cell cycle regulators could be observed. In the meantime we have analysed a selected subset of these genes in more detail by real time RT-PCR of individual samples and by in situ hybridization.

**Conclusions:** Our results show for the first time that Nestin mRNA and protein as well as the proliferation markers Ki67 and BrdU are differentially regulated in the hippocampal formation of BDV infected rats. They demonstrate a distinct upregulation of Nestin expression and cell proliferation at 4 weeks p.i. and a marked decrease in Nestin positive cells and cell proliferation at 8 weeks p.i.. In addition we could demonstrate up- and downregulation of a wide variety of other genes by DNA microarray analysis including regulators of proliferation and differentiation of neuronal stem cells. Together these results suggest an important role of postnatal hippocampal neurogenesis for the onset of BDV dependent morphological deficits in the dentate gyrus.

**Dopamine accelerates progression of HIV-dementia**

E Koutsilieri<sup>1,3</sup>, S Czub<sup>2</sup>, C Scheller<sup>3</sup>, S Sopper<sup>3</sup>, E Grünblatt<sup>1</sup>, G Gosztonyi<sup>4</sup>, V ter Meulen<sup>3</sup>, P Riederer<sup>1</sup>

Institutes of Clinical Neurochemistry-Dept. Psychiatry<sup>1</sup>, <sup>2</sup> Pathology and Virology <sup>3</sup>, University of Würzburg, Germany, Institute of Neuropathology, Berlin, Germany

HIV and drugs of abuse act synergistically and result in enhanced damage in the CNS. Elevated extracellular dopamine is thought to be the primary mediator for reinforcing as well as for toxic effects of addictive substances. To investigate the potential involvement of increased dopamine availability in the pathogenesis of immunodeficiency dementia, SIV-infected rhesus monkeys were treated with drugs increasing dopamine availability, such as L-DOPA and selegiline. Both of these substances are administered to HIV-patients to counteract parkinsonian symptoms and cognitive impairment, respectively. We found that both dopaminergic substances increased dopamine concentrations which were reduced by SIV infection. However, a spongiform polioencephalopathy accompanied by an accelerated SIV-encephalitis and enhanced intracerebral SIV expression were observed. Detected enhanced TNF-alpha expression in the brains of the infected monkeys may indicate a microglia activation through dopaminergic substances in combination with virus and suggest a potentiation of immunodeficiency dementia.

## The effect of tumor necrosis factor, interleukin-1 and interleukin-6 on the expression of heat shock protein 70 in the central nervous system.

Slawomir Michalak

Department of Clinical Neurochemistry, Chair of Neurology, University of Medical Sciences, Poznan, Poland

**Introduction.** Heat shock protein 70 kDa (Hsp 70) is involved in the degradation pathway of cellular proteins during stress condition, assists new synthesized proteins in their correct folding and is also directly involved in the translocation of proteins across membranes into different cellular compartments. It may also induce both humoral and cellular responses. This effect is known for experimental vaccines against tumors. Up-regulation of heat shock protein lead to the presentation of tumor antigens which may be either masked or inaccessible to antigen – presenting cells preventing in such way lack of tumor cell immunogenicity. Vaccination of mice with Hsps isolated from tumor cells indicate that the induced heat shock proteins may have promising applications for antitumor, T-cell immunotherapy. Our previous studies have been shown the increased Hsp 70 expression in the central nervous system (c.n.s) in the course of experimental neoplastic disease. Cytokines are factors involved in number of the reactions between host and the tumor.

The **aim** of this study is to examine the effect of selected cytokines on the expression of Hsp 70 in central nervous system.

**Material and methods.** Cytokines were injected intraperitoneally to male Buffalo rats, 3½ - months of age in following doses: 4 µg/kg for tumor necrosis factor (TNF), 2 µg / kg for interleukin – 1 (IL –1) and 4 µg / kg for interleukin-6 (IL –6). The same volume of physiological salt was injected intraperitoneally in the control animals. After 24 hours the animals were sacrificed under halotane anaesthesia. The brain was dissected macroscopically in the white and grey matter, brain stem, cerebellum and basal ganglia. The expression of heat shock protein 70 kDa was analyzed after 12% polyacrylamide gel electrophoresis (SDS-PAGE) according to Laemmli (1970) and subsequent Western blotting (Towbin et al., 1979). The Hsp 70 was identified with monoclonal mouse anti – rat antibodies (SIGMA), as the second antibody goat anti-mouse conjugated with horseradish peroxidase (SIGMA) was used. The semiquantitative analysis was performed using densitometer GS-710 (Bio-Rad) and the software „Quantity One”. The density of bands corresponding to Hp 70 was normalized to the actin band.

**Results (Table 1):** Interleukin –1 and interleukin – 6 caused significant ( $p < 0.05$ ) increase in expression of Hsp 70 in grey matter.

Table 1. The effect of TNF $\alpha$ , IL -1 and IL-6 on the expression of Hsp70 in the central nervous system. The values represents optical density (OD).

	Grey matter	White matter	Cerebellum	Brain stem	Basal ganglia
Control	0,695 ± 0,065	0,860 ± 0,044	0,893 ± 0,084	0,938 ± 0,166	0,805 ± 0,080
TNF $\alpha$	0,965 ± 0,244	0,892 ± 0,222	0,806 ± 0,057	0,890 ± 0,188	0,875 ± 0,089
IL – 1	<b>0,882</b> ± <b>0,043 *</b>	0,893 ± 0,056	0,881 ± 0,048	0,865 ± 0,038	0,860 ± 0,044
IL –6	<b>0,855</b> ± <b>0,056 *</b>	0,856 ± 0,057	0,834 ± 0,034	0,865 ± 0,018	0,984 ± 0,192

\* -  $p < 0.05$  – statistically significant difference. The results are presented as mean ± SD. Number of animals in each group = 6.

In **conclusion**, we may state that we have been able to demonstrate that the short-term effect of the interleukins on the expression of heat shock protein 70 appears in the grey matter. The significance of this mechanism for the development of paraneoplastic syndromes needs further elucidation.



## Adjuvant therapy with dexamethasone increases neuronal apoptotic cell death in the dentate gyrus in experimental *Escherichia-coli*-meningitis

Annette Spreer<sup>1</sup>, Joachim Gerber<sup>1</sup>, Mareike Hanssen<sup>1</sup>, Peter Lange<sup>1</sup>, Helmut Eiffert<sup>2</sup>, Roland Nau<sup>1</sup>

Departments of Neurology<sup>1</sup> and Bacteriology<sup>2</sup>, Georg-August-University of Göttingen

Mortality and morbidity rates are high among patients with acute bacterial meningitis. Neurological sequelae include paralysis, mental retardation and learning disorder. Standard therapy of bacterial meningitis is based on bacteriolytic  $\beta$ -lactam antibiotics, which result in increased release of proinflammatory compounds. Anti-inflammatory treatment with dexamethasone has recently been shown to improve the outcome in therapy of pneumococcal meningitis under treatment conditions of developed countries (1). In animal models of pneumococcal meningitis, dexamethasone has been shown to aggravate the apoptotic neuronal damage, and hippocampal neuronal apoptosis also occurs in patients during bacterial meningitis (2). It remains to await follow-up studies to evaluate the effect of dexamethasone on cognitive functions in pneumococcal meningitis.

At present, the effect of dexamethasone on the hippocampal formation is unknown in non-pneumococcal forms of meningitis. Therefore we evaluated the effect of adjunctive dexamethasone treatment in a rabbit meningitis model of Gram-negative *E. coli* meningitis on parameters of neuronal damage (rate of apoptotic neurons in the hippocampal granular layer, neuron-specific enolase (NSE) in the cerebrospinal fluid (CSF) and ischaemic areas), neurochemical parameters (cells, proteins, lactate in CSF) and arterial oxygen saturation and pH.

**Methods:** 34 NZW rabbits were intracisternally infected with a clinical isolate of *E. coli*. 12 h post infection all animals were treated with ceftriaxone (125 mg/kg body weight). 17 animals received dexamethasone as adjunctive therapy (1 mg/kg body weight) 15 min before onset of antibiotic treatment and 6 h later. CSF and arterial blood were drawn repeatedly during course of infection. The experiment was terminated 24 h post infection. Apoptotic neurons in the hippocampal dentate gyrus were histologically detected by in-situ labelling of DNA strand breaks in 4 coronal sections from the rabbits left hemisphere and related to the respective area of the dentate gyrus. The extent of ischaemic damage was estimated by calculation of the ratio between ischaemic area and surface area of 4 coronal sections stained with HE. The other parameters evaluated were quantified according to standard methods.

**Results:** All animals surviving until the end of the experiment were included in the data analysis (control group n = 14, dexamethasone group n = 15). No significant difference was found between the two groups concerning CSF inflammatory parameters of meningitis (pleocytosis, protein, lactate), NSE in CSF as a global marker of neuronal damage, the estimation of ischaemic damage or arterial oxygen saturation and pH. However, a significant increase was found in the rate of apoptotic neurons in the granular layer of the hippocampal dentate gyrus after adjunctive treatment with dexamethasone ( $p = 0.0013$ ).

**Conclusion:** Adjuvant treatment of bacterial meningitis with dexamethasone increases neuronal apoptotic cell death in the dentate gyrus independent of the meningitis-causing bacterial agent. In bacterial meningitis in adults, nevertheless, adjunctive therapy with dexamethasone should be added to antibiotic treatment, since it is the best option presently available. Yet, dexamethasone probably is not the ideal adjunctive treatment and may not be effective in all forms of bacterial meningitis, such as neonatal meningitis, bacillary Gram-negative meningitis and iatrogen forms of meningitis (e.g. following neurosurgery).

1. de Gans J et al. (2002): Dexamethasone in adults with bacterial meningitis. *N Engl J Med*; 347(20):1549-56.
2. Nau R, Soto A, Bruck W (1999): Apoptosis of neurons in the dentate gyrus in humans suffering from bacterial meningitis. *J Neuropathol Exp Neurol*; 58(3):265-74

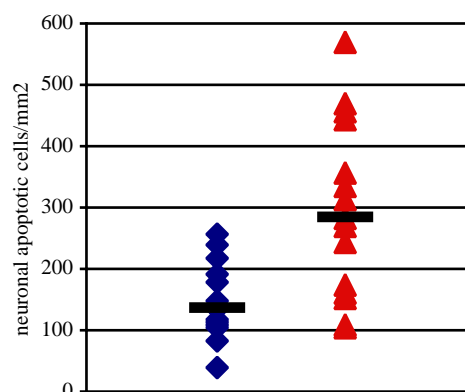
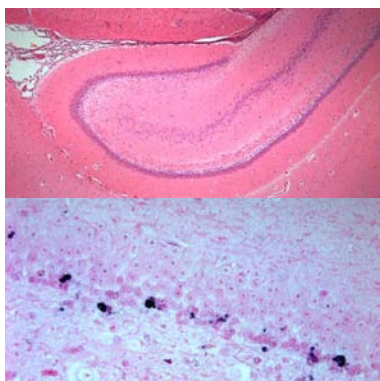


**Figure 1:** Rate of neuronal apoptotic cell death in the dentate gyrus is increased by adjuvant treatment with dexamethasone (red triangles) in comparison to control animals (blue diamonds).

## MICRO TISSUE ENGINEERING: NEURON-, GLIA-, AND FIBROBLAST CELL INTERACTIONS IN POLYMER-BASED NERVE GUIDES

*Lars Dreesmann<sup>1</sup>, Martin Lietz<sup>1</sup>, Sven Oberhoffner<sup>2</sup>, Andreas Ullrich<sup>2</sup>, Martin Dauner<sup>2</sup>,  
Burkhard Schlosshauer<sup>1</sup>*

- (1) NMI Naturwissenschaftliches und Medizinisches Institut an der Universität Tübingen,  
Markwiesenstraße 55, 72770 Reutlingen, Germany  
(2) Deutsches Zentrum für Biomaterialien und Organersatz, Denkendorf, Germany

We have developed resorbable nerve guide tubes (diameter: 1 mm) made of trimethylene-carbonate/caprolacton-copolymer to bridge nerve lesions. The 100 µm thick, semipermeable walls of the nerve guides allowed free passage of 2.000 kD dextran but prevented transmigration of fibroblasts in vitro. Encapsulation of Schwann cells (SC) inside the tube demonstrated cell survival in vitro even when fibroblasts coated the conduit surface. Co-cultivation of dorsal root ganglia (DRG) with Schwann cells resulted in pronounced axonal outgrowth inside the nerve guide. In order to accelerate regeneration, meandering of axons inside nerve guides will be abrogated by the insertion of Schwann cell-seeded microstructured polymer filaments into the nerve guide in an attempt to imitate glial bands of Büngner in vivo. To render the surface of polymer filaments biocompatible, we tested 14 different extracellular matrix (ECM) components. Type IV collagen, heparan sulphate proteoglycan and laminin enhanced cell attachment and proliferation. In vitro experiments indicated that Schwann cells oriented along ECM coated microgrooves. Furthermore, in co-cultures, outgrowing axons of DRG were perfectly guided by longitudinally oriented Schwann cells on polymer filaments with microgrooves. We also investigated the guiding performance of microgrooves by time lapse video recording. Microgrooves decreased the migration velocity of Schwann cells considerably. Surprisingly, fibroblast-derived factors stimulated Schwann cell mobility on microgrooves fivefold. However, fibroblasts did not affect the alignment of Schwann cells on microgrooves, and they tended to displace glial cells and hamper neurite extension. Though minor numbers of fibroblasts neither inhibit Schwann cell orientation on polymer filaments nor neurite growth, massive invasion of repulsive fibroblasts into nerve guides could displace Schwann cells also in vivo and reduce neural regeneration. Consequently, Schwann cells are best integrated into nerve guides before implantation. Thus, nerve guides composed of semipermeable, resorbable tubes with internal Schwann cell-seeded microstructured polymer filaments promise to enhance nerve regeneration.

Schlosshauer et al. (2003). Brain Res. **963**, 321-326.

Schlosshauer, B., Lietz, M. (2004) Nerve guides. In Encyclopedia of Biomaterials and Biomedical Engineering (Ed. Wnek and Bowlin, Marcel Dekker, Inc., New York). 1043-1055.

Funded by BMBF

## Hydroxyproline as a marker for collagenolytic activity in neuroinflammatory disorders

Johann Sellner, Damian N. Meli, Denis Grandgirard, Brigitte Storch-Hagenlocher\*, Uta Meyding-Lamade\*, Stephen L. Leib

Department of Infectious Diseases, University of Berne; \*Department of Neurology, Ruprecht-Karls-University Heidelberg; email: johann.sellner@ifik.unibe.ch

**Objectives:** Pathophysiologic mechanisms that contribute to brain injury in neuroinflammatory disorders include breakdown of the blood-brain-barrier, extravasation of leukocytes, cerebral hypoperfusion and vasculitis. Matrix-Metalloproteinases (MMPs) including the collagenases MMP-2 and -9 are crucially involved in all these steps. In this study we aimed to assess the extent of in-vivo collagenolytic activity in cerebrospinal fluid (CSF) by determination of the amino acid hydroxyproline, a major and exclusive degradation product of collagen.

**Methods:** Paired serum and CSF samples from patients with bacterial meningitis (n=11), aseptic meningitis/encephalitis (n=17), multiple sclerosis (n=13), and normal CSF (n=12) were assessed. Degraded collagen was hydrolysed to dissolve its major component hydroxyproline, which subsequently was determined spectrophotometrically. CSF levels of MMP-2 and -9 were studied by gel zymography. In a rat model of pneumococcal meningitis localization of collagenolytic activity was performed by in-situ zymography with intramolecularly quenched gelatin

**Results:** Hydroxyproline in CSF from patients with bacterial meningitis was significantly increased compared to all studied groups ( $P < 0.001$ ) while serum hydroxyproline did not differ significantly between the groups. The amount of hydroxyproline in CSF correlated significantly with the amount of MMP-9 ( $r = 0.8$ ;  $p < 0.001$ ). In the rat model in-situ zymography gelatinolytic activity was localized to the subarachnoidal and ventricular space inflammation and in association to cortical lesion.

**Summary & Conclusions:** The study documents a significant increase of the collagen degradation product hydroxyproline in CSF of patients with bacterial meningitis. The close correlation of hydroxyproline and MMP-9 in the CSF validates the assessment of hydroxyproline as an index for CSF collagenolytic activity in neuroinflammatory diseases and supports a role for collagenase in the pathogenesis of bacterial meningitis.

## Involvement of FasL(CD95L) and Perforin mediated apoptosis in the pathogenesis of Herpes-simplex Virus Encephalitis

Johann Sellner<sup>\*#</sup>, Florian Dvorak<sup>#</sup>, Yilin Zhou<sup>#</sup>, Susanne Strand<sup>%</sup>, Peter R. Galle<sup>%</sup>, Uta Meyding-Lamade<sup>#</sup>

\*Department of Infectious Diseases, University of Berne; #Department of Neurology, University of Heidelberg; Ruprecht-Karls-University Heidelberg; %Department of Internal Medicine, University of Mainz; email: johann.sellner@ifik.unibe.ch

**Objectives:** Herpes-simplex Virus encephalitis (HSVE) is a devastating disease which still possesses unacceptably high morbidity and mortality. However, apoptosis might play a key role in the pathogenesis of HSVE and also account for neuronal injury. In the present study we report the detection of apoptosis in a mouse model of HSVE by TUNEL staining and the expression pattern of the apoptosis inducing signals perforin and FasL(CD95L) using a semiquantitative real-time RT-PCR.

**Methods:** Focal HSVE was induced by intranasal inoculation with HSV-1 Strain F, sham infected mice received sterile saline. Animals were assigned to three treatment groups: i) saline ii) acyclovir and iii) acyclovir plus adjuvant methylprednisolone. Therapy was conducted through the intraperitoneal route from day 1 to 14 post inoculation (d.p.i). Furthermore, clinical scoring was performed daily and viral load was determined exemplarily in whole brain tissue.

**Results:** Clinical alteration started at 2-3 d.p.i and peaked at 7-10 d.p.i. At 21 d.p.i the clinical score returned to baseline. TUNEL-positive cells were found during the entire acute course of experimental HSVE in different regions of the brain. Perforin mRNA expression increased in close correlation to clinical impairment, and was upregulated at 3 d.p.i ( $P<0.05$ ) and maximal expression was found at 7 d.p.i ( $P<0.001$ ). FasL mRNA transcripts were significantly upregulated at 7 d.p.i ( $P<0.05$ ) and peaked at 10 d.p.i ( $P<0.05$ ). No changes in mRNA expression were found at 60 d.p.i. Acyclovir ( $P<0.05$ ) as well as adjunctive cortisone ( $P<0.001$ ) treatment lead to a significant downregulation of perforin transcripts while FasL expression was not affected.

**Discussion & Conclusion:** We report the sequential mRNA regulation of two mediators of apoptotic cell death in the acute course of HSVE and were able to detect apoptosis by immunohistochemistry in different brain regions. Our study provides evidence for the involvement of Fas/FasL and perforin mediated pathways of cytotoxicity in the pathogenesis of HSVE. Further studies are mandatory to define the exact role of different apoptotic signals in HSVE and could lead to the development of improved strategies for the treatment of this highly disabling disease.

## **Symposium #S15:**

### **Nitric oxide / cyclic nucleotide signaling as regulator of developmental processes and cell motility in the nervous system**

**G. Bicker and V. Rehder, Hannover and Atlanta**

#### **Introduction**

- [#S15](#) G. Bicker and V. Rehder, Hannover and Atlanta  
*Nitric oxide / cyclic nucleotide signaling as regulator of developmental processes and cell motility in the nervous system*

#### **Slide**

- [#S15-1](#) S. Arnhold and K. Addicks, Köln  
*The expression of different NO-synthase isoforms during murine nervous system development*
- [#S15-2](#) G. Bicker and A. Haase, Hannover  
*Stop and Go with NO: Nitric oxide regulates cell motility in embryonic insect neurons*
- [#S15-3](#) H. Schmidt, S. Schäffer, M. Werner, PA. Heppenstall, M. Henning, MI. Moré, S. Kühbandner, GR. Lewin, F. Hofmann, R. Feil and FG. Rathjen, Berlin and München  
*cGMP signalling and pathfinding of sensory axons within the spinal cord*
- [#S15-4](#) V. Rehder, Atlanta, GA (USA)  
*The Nitric Oxide/Soluble Guanylyl Cyclase Signaling Pathway In Neurons Regulates Growth Cone Behavior Through Calcium.*
- [#S15-5](#) D. Blottner, Berlin  
*NOS / NO Assembly in Neuromuscular Junction Formation*
- [#S15-6](#) J. Schachtner, Marburg  
*Regulation and role of the NO/cGMP signaling pathway during antennal lobe development of the sphinx moth Manduca sexta.*

#### **Poster**

- [#12B](#) SE. Kammann, M. Hamann and A. Richter, Berlin  
*Examinations on the functional relevance of deficient NOS-reactive interneurons in the striatum of the dt(sz) mutant*
- [#13B](#) S. Schäffer, H. Schmidt and FG. Rathjen, Berlin  
*cGMP-mediated signalling in sensory axon pathfinding*

[#14B](#)

PA. Stevenson, J. Rillich, K. Schoch and K. Schildberger, Leipzig

*Suppression of aggression by nitric-oxide in the cricket *Gryllus bimaculatus**

## **Introductory Remarks to Symposium 15**

### **Nitric oxide / cyclic nucleotide signaling as regulator of developmental processes and cell motility in the nervous system**

**Gerd Bicker and Vincent Rehder, Hannover and Atlanta (USA)**

Nitric oxide (NO) is a membrane-permeable signaling molecule that activates soluble guanylyl cyclase (sGC) and leads to the formation of cGMP in target cells. Our symposium will explore the contribution of NO signaling via cGMP and other transduction pathways to the developmental processes of neurogenesis, postmitotic neuron migration, growth cone behavior, and synaptogenesis.

The talk of Stefan Arnhold will shed light on the time dependent expression of different NOSynthase (NOS) isoforms in various nervous compartments during neurogenesis of the mouse. The functional role of NO is investigated in embryonic stem cell derived neuronal differentiation as well as in neural precursor cells of different brain compartments. Gerd Bicker introduces an accessible insect model in which NO/cGMP signaling is essential for cell migration of enteric neurons and axonogenesis of pioneer fibers. Fritz Rathjen analyzes the trajectories of axons within the spinal cord showing a longitudinal guidance defect of sensory axons within the developing dorsal root entry zone in the absence of cGMPdependentprotein kinase I (cGKI). These axon guidance defects in cGKI-deficient mice are leading also to a substantial impairment in nociceptive flexion reflexes. The work by Vincent Rehder describes that NO orchestrates two aspects of growth cone behavior in identified snail neurons, namely neurite outgrowth and filopodial dynamics. The findings support the hypothesis that NO can function as a potent slow/stop signal for developing neurites. The lecture of Dieter Blottner deals with recent molecular assembling models for NOS as part of the postsynaptic apparatus in the developing neuromuscular junction. In addition, NO signaling actions will be discussed for development, maintenance and plasticity of the neuromuscular system. Finally, Joachim Schachtner addresses the contribution of NO to synaptogenesis in an insect brain. Pharmacological interference with the NO/cGMP signaling pathway results in reduction of the ubiquitous synaptic vesicle protein synaptotagmin, suggesting that NO enhances the rate of synaptogenesis during development of olfactory glomeruli via cGMP.

## **The expression of different NO-synthase isoforms during murine nervous system development**

Stefan Arnhold and Klaus Addicks

Department of Anatomy I, University of Cologne, Josef-Stelzmann Str. 9, 50931 Köln, Germany

Nitric oxide (NO), a cell derived highly diffusible and unstable gas is regarded to be involved in inter- and intra-cellular communication in the nervous system. Furthermore, NO has been reported to regulate neuronal differentiation, mediating a switch from proliferation to differentiation. In order to elucidate a further role of NO during neuronal differentiation processes, we investigated the expression of the three NOS-isoforms in various nervous compartments during neurogenesis of the mouse. Out of the three NOS-isoforms exclusively the inducible NO-synthase isoform is found to be expressed during development of early mouse olfactory as well as vestibulocochlear receptor neurons. In order to prove a general role for this isoform in the process of neuronal differentiation, using immunohistochemical techniques, we also looked for the expression of the NOS-isoforms in early postmitotic neurons of the developing mouse cortex, retina as well as in the enteric nervous system. Confirming the findings of olfactory and vestibulocochlear development also in these compartments during early neurogenesis there is an exclusive expression of the NOS-II isoform detectable. In later developmental stages NOS-II immunoreactivity vanishes in favour of the constitutive isoforms. In a pharmacological approach using cultures of the mouse cortex as well as embryonic stem cell derived neural precursor cells, we investigated the functional role of NO on initial neuronal differentiation. Effects of NOS inhibitors and NO donors on the morphological differentiation were correlated with developmentally regulated calcium current densities, focusing on the effects of the specific NO-synthase-II inhibitor GW 274150. Furthermore, involvement of the guanylate cyclase/cGMP signalling cascade was pharmacologically investigated. Our data indicate that while a specific block of NO-synthase-II provokes a clear inhibition of neurite outgrowth formation as well as a decrease of calcium current densities, the inverse is true for exogenous NO donation. In line with lacking immunoreactivity for the soluble guanylate cyclase and cGMP there are only minor effects of compounds manipulating the guanylate cyclase/cGMP pathway, suggesting the downstream guanylate cyclase/cGMP pathway not to be essential in these early differentiation steps.

In conclusion our in vivo and in vitro results suggest that in early developmental stages NO not only mediates a switch from proliferation to differentiation but may have important roles during both synaptogenesis and neurite outgrowth formation. These effects can be ascribed to mainly NOS-II derived NO, before in later developmental stages the important NO-synthesis is taken over by the constitutive isoforms.



**Stop and Go with NO: Nitric oxide regulates cell motility in embryonic insect neurons****Gerd Bicker and Annely Haase**

School of Veterinary Medicine Hannover, Cell Biology, Bischofsholer Damm 15,  
D-30173 Hannover, Germany, gerd.bicker@tiho-hannover.de

Nitric oxide (NO) is a membrane-permeable signaling molecule that activates soluble guanylyl cyclase (sGC) and leads to the formation of cyclic GMP in target cells. The dynamic regulation of nitric oxide synthase (NOS) activity and cyclic GMP levels suggests a functional role in the development of both vertebrate and invertebrate nervous systems (1). Here, we summarize evidence for a key role of the NO/cGMP signalling cascade on migration of postmitotic neurons in the enteric nervous system of the embryonic grasshopper. During development, a population of enteric neurons migrates on the surface of the midgut. These midgut (MG) neurons exhibit nitric oxide-induced cGMP-immunoreactivity coinciding with the migratory phase. Using a histochemical marker for NOS, we identified potential sources of NO in subsets of the midgut cells below the migrating MG neurons. Inhibition of endogenous NOS, sGC, and protein kinase G (PKG) activity in whole embryo culture results in a significant retardation of MG neuron migration. This inhibition can be rescued by supplementing with protoporphyrin IX free acid an activator of sGC, and membrane-permeant cGMP, indicating that NO/cGMP signalling is crucial for MG neuron migration (2). Conversely, the stimulation of the cAMP/protein kinase A signalling cascade results in an inhibition of cell migration. Activation of either the cGMP or the cAMP cascade influences the cellular distribution of F-actin in neuronal somata in a complementary fashion. The cytochemical stainings and experimental manipulations of cyclic nucleotide levels provide clear evidence that NO/cGMP/PKG signalling is permissive for MG neuron migration whereas the cAMP/PKA cascade may be a negative regulator. Since NO/cGMP signaling is also involved in axonal extension of pioneer neurons (3), these investigations reveal an accessible insect model in which the role of the NO/cGMP/PKG signalling cascade on neuronal cell motility can be analyzed in a natural setting.

Supported by grants of the DFG

Literature cited:

- (1) Bicker (1998) Trends Neurosci 21:349-355
- (2) Haase and Bicker (2003) Development 130 : 3977-3987
- (3) Seidel and Bicker (2000) Development 127: 4541-4549

## **cGMP signalling and pathfinding of sensory axons within the spinal cord**

Hannes Schmidt<sup>1</sup>, Susanne Schäffer<sup>1</sup>, Matthias Werner<sup>2</sup>, Paul A. Heppenstall<sup>3</sup>, Mechthild Henning<sup>1</sup>, Margret I. More<sup>1</sup>, Susanne Kühbandner<sup>2</sup>, Gary R. Lewin<sup>3</sup>, Franz Hofmann<sup>2</sup>, Robert Feil<sup>2</sup>, and Fritz G. Rathjen<sup>1</sup>

- 1) Developmental Neurobiology Group, Max-Delbrück-Centrum für Molekulare Medizin, Robert-Rössle-Str. 10, D-13092 Berlin, Germany
- 2) Institut für Pharmakologie und Toxikologie, TU München, Biedersteiner Str. 29, D-80802 München, Germany
- 3) Growth Factors and Regeneration Group, Max-Delbrück-Centrum für Molekulare Medizin, Robert-Rössle-Str. 10, D-13092 Berlin, Germany

During embryonic and early postnatal development axons are steered by environmental guidance cues to their target regions where they establish synaptic contacts. These molecular cues activate specific guidance receptors on the surface of growth cones. While many axonal guidance receptors have been identified in past years our understanding of the intracellular signal transduction cascades initiated by them is limited. Previous in vitro studies by Poo and associates using a growth cone turning assay revealed that signalling systems activated by guidance receptors could be modulated by cyclic nucleotides. For example, increasing levels of cGMP converted a repulsion of spinal cord neuronal growth cones induced by semaphorin 3A into an attractive extension. However, the molecular target(s) of cGMP within the growth cones remained unknown. cGMP is a widely used second messenger that acts on several signalling components including activation of cGMP-dependent protein kinases I and II (cGKI and II), regulation of cAMP levels through the activation or inhibition of cAMP-dependent phosphodiesterases (PDEs), and opening of cyclic-nucleotide-gated cation channels (CNGs).

Our studies on cGMP targets indicated that cGKI is required for sensory axons to find their way within the dorsal root entry zone (DREZ) of the spinal cord. Once sensory axons arrive at the DREZ of the spinal cord, each axon bifurcates into a rostral and caudal branch extending over several segments. After a waiting period, collaterals grow out from these longitudinal stem axons and form lamina-specific projections within the gray matter. In the absence of cGKI we observed by DiI tracing and antibody staining that many sensory axons fail to bifurcate correctly at the DREZ and instead grow directly to the central canal. These axon guidance defects in cGKI-deficient mice result in a substantial reduction of the amplitude of the nociceptive flexion reflex. Alternative splicing produces two isoforms of cGKI that differ in their N-termini. Biochemical investigations revealed that the alpha isoform of cGKI is expressed in sensory axons. In summary, our studies therefore showed that cGMP signalling via cGKI is important for directing axonal growth of sensory axons.

These findings encouraged us to further unravel the cGMP signalling pathway upstream and downstream of cGKI to understand aspects of signalling within growth cones. Recent findings on the enzymes which generate cGMP, the soluble and particulate guanylyl cyclases, as well as putative downstream targets which are phosphorylated by cGKI are discussed.

The Nitric Oxide/Soluble Guanylyl Cyclase Signaling Pathway In Neurons Regulates Growth Cone Behavior Through Calcium. V. Rehder, Biology Department, Georgia State University, Atlanta, GA 30302

Nitric Oxide (NO) has been demonstrated to act as a signaling molecule during neuronal development in both vertebrates and invertebrates, but its precise function is unclear. Because many of the effects of NO occur during the time when nerve cells extend their axons and dendrites, and because targeting errors occur when the NO system is perturbed, we are interested in the roles by which NO may function as a signaling molecule at the tip of advancing processes, the neuronal growth cone. Employing the well established *in vitro* model system of identified neurons from the buccal ganglion of the gastropod snail *Helisoma trivolvis*, we demonstrate that NO serves a dual function as modulator of growth cone morphology and of neuronal outgrowth. B5 neurons show a rapid and transient increase in filopodial length in response to NO, and this effect is mediated by soluble guanylyl cyclase (sGC). Filopodial elongation increases the sensory span of an advancing growth cone and, *in vivo*, this is often coupled with a decrease in the rate of neurite outgrowth. We demonstrate that NO could function as a combined “slow-down and search signal” for growth cones by decreasing neurite outgrowth. In the presence of the NO donor NOC-7, neurites of B5 neurons show a concentration dependent effect on neurite outgrowth, ranging from slowing at low, stopping at intermediate, and collapsing at high concentrations. The effects of the NO donor are mimicked by directly activating sGC with YC-1, or by increasing its product with 8-bromo-cGMP. In addition, blocking sGC in the presence of NO with NS2028 blocks NO’s effect, suggesting that NO affects outgrowth via sGC.  $\text{Ca}^{2+}$  imaging of growth cones with Fura-2 indicates that the intracellular calcium concentration ( $[\text{Ca}^{2+}]_i$ ) increases transiently in the presence of NOC-7. To investigate if a spatial and temporal correlation exists between the  $[\text{Ca}^{2+}]_i$  and one aspect of growth cone behavior, namely the regulation of filopodia length,  $\text{Ca}^{2+}$  was released from the caged compound NP-EGTA (o-nitrophenyl EGTA tetrapotassium salt) via UV laser on a confocal microscope to simulate a signaling event in the form of a transient increase in  $[\text{Ca}^{2+}]_i$ .  $\text{Ca}^{2+}$  was released either globally (within an entire growth cone), or locally (within a single filopodium). We find that global photolysis of NP-EGTA causes an increase in  $[\text{Ca}^{2+}]_i$  throughout the growth cone lasting several seconds and results in filopodial elongation which is restricted to the stimulated growth cone. The effects of uncaging calcium on growth cone morphology are inhibited upon pharmacological blockage either of calmodulin or the  $\text{Ca}^{2+}$ -dependent phosphatase, calcineurin, suggesting that these enzymes act downstream of calcium. Local elevation of  $[\text{Ca}^{2+}]_i$  within individual filopodia leads to the selective elongation of stimulated filopodia, which may represent a first step towards directed filopodial steering events seen during pathfinding *in vivo*. Taken together, our findings suggest that NO can act as a potent intercellular signaling molecule that affects growth cone behavior in *Helisoma* neurons through an elevation of  $[\text{Ca}^{2+}]_i$ . The results support the hypothesis that NO can function as a potent slow/stop signal for developing neurites. When coupled with transient filopodia elongation, this phenomenon emulates growth cone searching behavior.

## **NOS / NO Assembly in Neuromuscular Junction Formation**

**Dieter Blottner**

**Charité University Medicine Berlin, Campus Benjamin Franklin, Anatomy and Neuromuscular Group, 14195-Berlin, Germany; [dieter.blottner@charite.de](mailto:dieter.blottner@charite.de)**

Neuromuscular junction formation is characterized by multiple cellular actions including axonal outgrowth and neuron-target cell contact, induction of postsynaptic markers at the site of the putative synaptic region (e.g. acetylcholine-receptor, AChR) and, subsequently, addition of anchoring or modulatory molecules, peptides and channel proteins, that build up the molecular complexity of a functional synaptic contact between motoneurons and their target skeletal muscle cells (1). More than 50 synaptic proteins have been characterized at present, however, spatiotemporal assembly of the complex molecular architecture as well as the fine tuning of protein functions are far from being understood. We recently showed that nitric oxide synthase (NOS) that generates the diffusible messenger NO is part of postsynaptically AChR clusters on the myotube membrane induced by the motoneuron factor agrin, and that motoneurons induce *de novo* formation of NO in their target myotubes in nerve-muscle cocultures by e.g. agrin-independent mechanisms (ms. submitted) suggesting a functional role for NO as e.g. retrograde signal or postsynaptic organizer/mediator in synapse formation and function (2). In early development, neuronal NOS 1 proteins are expressed in the myoblast and myotube cytosol. Postnatally, NOS is found at sarcolemmal compartments suggesting unique intracellular NOS targeting actions that need further investigations (3). This lecture discusses recent aspects of NO signaling mechanisms in skeletal myocytes and myotubes covering neuromuscular synaptogenesis, assembly of postsynaptic proteins, NO-signaling cascades, and the significance of NO signals in normal neuromuscular system actions.

*Supported by DFG project BI-259/3-1,2,3*

*Literature cited:* (1) SJ Burden (1998) Genes Dev 12:133-148; JR Sanes and JW Lichtman (2001) Nature Rev Neurosci 2:791-805. (2) G Lück et al., (2000) Mol Cell Neurosci 16:269-281. Blottner et al., ms. submitted. (3) D. Blottner and G. Lück (1998) Cell Tissue Res 292:293-302.

## **Regulation and role of the NO/cGMP signaling pathway during antennal lobe development of the sphinx moth *Manduca sexta*.**

**Joachim Schachtner**, Dept. Biology, Animal Physiology, Philipps-University, 35032 Marburg, Germany, email [schachtj@staff.uni-marburg.de](mailto:schachtj@staff.uni-marburg.de)

The antennal lobe is the primary integration unit for odor information in the insect brain and compares to the olfactory bulb of vertebrates (Eisthen, 2002, *Brain Behav Biol* 59:273). Antennal lobe and olfactory bulb not only share their principal morphological organization into so called olfactory glomeruli, but also a number of basic physiological properties with respect to information processing (Hildebrand and Shepherd, 1997, *Annu Rev Neurosci* 20:595). Olfactory glomeruli represent the basic functional units for odor processing and contain thousands of synapses between olfactory receptor neurons and neurons of the antennal lobe or the olfactory bulb.

The aim of our studies is to reveal mechanisms underlying the formation of the neuronal network in the olfactory glomeruli during development. The system we are using to study this task is the particularly well established antennal lobe of the sphinx moth *M. sexta*.

Formation of the antennal lobe of *M. sexta* occurs during the defined period of metamorphosis (Tolbert et al., 2004, *Prog Neurobiol* 73:73). During the phase of glomerular formation cGMP-levels are specifically elevated in a set of local interneurons of the antennal lobe (Schachtner et al., 1998, *J Neurobiol* 396:238). These elevations of cGMP concentrations are mediated by NO- (nitric oxide) sensitive soluble guanylyl cyclase (sGC) but also by NO-insensitive guanylyl cyclase(s). The NO-dependent elevation of cGMP seems to be mediated by activity of the olfactory receptor neurons releasing NO and can be enhanced by biogenic amines (Schachtner et al., 1999, *J Comp Neurol* 41:359; Gibson and Nighorn, 2000, *J Comp Neurol* 422:191). As shown by immunocytochemistry, members of at least two neuropeptide families (A-type allatostatins, Manse-allatotropin) colocalize during the phase of glomerular formation with NO-induced cGMP immunostaining in local antennal lobe neurons. This opens the possibility that increases of cGMP concentrations lead to the release of neuropeptides, as shown for other cells in *M. sexta* during ecdysis (Gammie and Truman, 1997, *J Comp Physiol* 180:329; Kingan et al., 1997, *J Exp Biol* 200:3245).

Artificially shifting the pupal 20-hydroxyecdysone (20E) peak to an earlier developmental time point resulted in the precocious appearance of glomeruli, neuropeptide immunoreactivity, and the ability of antennal lobe cells to elevate cGMP-levels (Schachtner et al., 1999, *J Comp Neurol* 41:359; Schachtner et al., 2004, *J Exp Biol* 207:2389). These results support the hypothesis that the pupal rise in 20E plays a key role in controlling glomerular development. Immunostaining with a specific antiserum against the  $\alpha$ -subunit of the sGC (sGC $\alpha$ 1) revealed that this subunit is present shortly before formation of the glomeruli starts. This suggests that a functional sGC might be one of the regulatory mechanisms in NO/cGMP signaling pathway regulation during antennal lobe development. It still has to be tested, whether sGC $\alpha$ 1-expression is also under the control of 20E.

An antibody against the ubiquitous synaptic vesicle protein synaptotagmin was used to study glomerular development in *M. sexta* on a light microscopical basis (Dubuque et al., 2001, *J Comp Neurol* 441:277). Pharmacologically interfering with the NO/cGMP signaling pathway during the phase of glomeruli formation resulted in reduction of synaptotagmin immunoreactivity as revealed by optical density measurements in Vibratom sections over all glomeruli. This result suggests that NO enhances the rate of synaptogenesis during glomerular development via cGMP. Currently we are going a step further in analyzing the effect of inhibitors of the NO/cGMP signaling pathway on the level of single identified standard glomeruli.

Supported by DFG grant SCHA 678/3-3

## **Examinations on the functional relevance of deficient NOS-reactive interneurons in the striatum of the $dt^{sz}$ mutant**

**Svenja E. Kammann, Melanie Hamann, Angelika Richter**

Department of Pharmacology and Toxicology, School of Veterinary Medicine,  
FU Berlin, Berlin, Germany, email: richtera@zedat.fu-berlin.de

The  $dt^{sz}$  mutant hamster represents a model of idiopathic paroxysmal dystonia in which dystonic episodes can be induced by stress. Paroxysmal dystonia is age-dependent in the  $dt^{sz}$  mutant with maximum expression at an age of 30-40 days and complete remission of dystonia at an age of about 10 weeks. Recent immunohistochemical studies revealed a deficit of striatal nitric oxide synthase (NOS)-positive interneurons in mutant hamsters at an age of 31 days (-21%) compared to age-matched non-dystonic control hamsters. In order to examine the relevance of these changes, the density was examined in older animals after disappearance of dystonic symptoms. Furthermore, the effects of intrastriatal injections of inhibitors of the neuronal NOS and of L-arginine, the precursor of the NO synthesis, on the severity of dystonia were examined in dystonic hamsters at an age of 31 days. Spontaneous remission of paroxysmal dystonia (age >90 days) was accompanied by a normalization of the density of NOS-reactive interneurons within the whole striatum of  $dt^{sz}$  hamsters. However, there remained a reduced density in distinct striatal subregions (anterior and dorsolateral) in mutant hamsters in comparison with age-matched controls. Intrastriatal microinjections of L-arginine and of the NOS inhibitors 7-nitroindazole and *N*-propyl-L-arginine failed to exert any effects on severity of stress-induced dystonic episodes, suggesting that a striatal decrease of NO is not critically involved in the pathophysiology of paroxysmal dystonia. As shown by previous immunohistochemical and pharmacological studies, an age-dependent deficit of GABAergic parvalbumin-reactive interneurons which provide the main inhibitory source within the striatum is obviously more important for the pathophysiology of paroxysmal dystonia. Possibly, the migration of striatal parvalbumin- and NOS-reactive interneurons is retarded in  $dt^{sz}$  mutant hamsters. (Supported by: DFG Ri 845).

## **cGMP-mediated signalling in sensory axon pathfinding**

**Susanne Schäffer, Hannes Schmidt and Fritz G. Rathjen**

Max-Delbrück-Centrum für Molekulare Medizin, Robert-Rössle-Str. 10, 13125 Berlin

Cyclic GMP (cGMP) – a widely distributed second messenger – is synthesized by soluble and particulate guanylyl cyclases and degraded by the specific phosphodiesterase V. Known mediators of cGMP include cGMP regulated phosphodiesterases, cyclic nucleotide gated cation channels and cGMP dependent kinases. The serine/threonine kinases cGKI and II are composed of an NH<sub>2</sub> –terminal domain, a regulatory segment, and a catalytic domain. In mammals, two alternatively spliced isoforms of cGKI, termed  $\alpha$  and  $\beta$ , with differing NH<sub>2</sub>-terminal domains are expressed.

Our previous studies on the pathfinding of sensory axons indicated that the  $\alpha$ -isoform of cGKI is required for sensory axons to find their way within the dorsal root entry zone (DREZ) of the spinal cord. In the absence of cGKI we observed by DiI tracing and antibody staining that many sensory axons fail to bifurcate correctly at the DREZ and instead grow directly to the central canal.

To broaden our knowledge about the role of cGKI $\alpha$  in sensory neurons we analysed the expression of this kinase in the developing mouse nervous system. Expression of cGKI $\alpha$  could be detected at E 9,5 in the notochord and in subsets of cranial nerves. At developmental stage E11 a strong expression in the dorsal root ganglia, cranial nerves, notochord and peripheral nerves was observed. Sagittal brain sections of postnatal mice showed the strongest cGKI $\alpha$  expression in Purkinje cells of the cerebellum. Other immunopositive structures include the hippocampus, fimbria hippocampus, corpus callosum, fibers in the striatum and the mitral cells in the bulbus olfactorius. Wholemout stainings for neurofilament in wildtype and cGKI-deficient embryos at E10-E12 are currently analysed for pathfinding errors in the structures mentioned above.

To further our understanding about cGKI $\alpha$ 's function in the nervous system we aim to establish downstream targets of cGKI $\alpha$  in sensory neurons. One approach is the search for substrates of cGKI $\alpha$  making use of the 2D-Electrophoresis method. By comparison of wildtype and cGKI-deficient tissues stimulated with cGMP-analogs we are looking for an altered phosphorylation of putative targets.

## Suppression of aggression by nitric-oxide in the cricket *Gryllus bimaculatus*

*Paul A. Stevenson, Jan Rillich, Korinna Schoch and Klaus Schildberger  
Universität Leipzig, Institut für Biologie II, Liebigstr. 18, 04103 Leipzig*

Our studies have shown that the aggressiveness of male crickets is considerably enhanced by various behavioural experiences, such as flying, and that the effect of these experiences may be mediated by the natural release of the biogenic amine octopamine (Stevenson et al., J. Neurobiol 43:107-120, 2000, and submitted). We now present evidence suggesting that the expression of aggression in crickets is suppressed by the endogenous release of the gaseous neuromodulator nitric-oxide. Firstly, brain neuropiles presumed to be involved in controlling aggression in crickets, such as the mushroom bodies and mechanosensory-antennal neuropil, exhibited strong labelling with an antibody directed against universal nitric-oxide-synthetase. Secondly, male crickets treated with a nitric-oxide donor (SNP) subsequently showed significantly reduced levels of aggressive behaviour towards conspecific males. Thirdly, although crickets normally retreat from an approaching opponent for some hours after a defeat, crickets pretreated with a nitric oxide synthesis inhibitor (L-NAME) regained their aggressiveness some 15 minutes after losing. We speculate that activation of the nitridergic system during fighting may be important for timing the decision to flee.



**Symposium #S16:**  
**New vistas on insect vision**  
**R. Strauss and R. Wolf, Würzburg**

**Introduction**

[#S16](#) R. Strauss and R. Wolf, Würzburg  
*New vistas on insect vision*

**Slide**

[#S16-1](#) J. Rister, I. Sinakevitch, K. Ito, M. Heisenberg and NJ. Strausfeld, Würzburg, Tucson, AZ (USA) and Tokyo (J)  
*Neurogenetic analysis of the functional role of the T1 basket cell, a prominent interneuron of the fly's visual system*

[#S16-2](#) J. Haag and A. Borst, Martinsried  
*Network interactions underlying complex receptive field properties of fly visual interneurons*

[#S16-3](#) HG. Krapp and SJ. Huston, Cambridge (UK)  
*Encoding self-motion: From visual receptive fields to motor neuron response maps*

[#S16-4](#) M. Mronz and R. Strauss, Würzburg  
*A simple model for visual object orientation in the walking fruit fly*

[#S16-5](#) U. Homberg and K. Pfeiffer, Marburg  
*Polarization vision and sky compass in the desert locust*

[#S16-6](#) R. Wolf and M. Heisenberg, Würzburg  
*Pattern recognition in *Drosophila* requires selective visual attention*

**Poster**

[#15B](#) C. Trischler, N. Boeddeker, R. Kern and M. Egelhaaf, Bielefeld  
*Functional properties of visual neurons in male blowflies presumably involved in chasing behaviour*

[#16B](#) K. Hartmann, S. Schillo, G. Belusic, R. Paulsen and A. Huber, Karlsruhe and Ljubljana (SLO)  
*Posttranslational modification of the *Drosophila* visual Ggamma subunit: protein farnesylation facilitates membrane attachment of the betagamma complex in vivo*

- [#17B](#) J. Heitwerth and M. Egelhaaf, Bielefeld  
*A new role of motion adaptation in the visual motion pathway of the blowfly*
- [#18B](#) H. Weiss, JP. Lindemann and M. Egelhaaf, Bielefeld  
*Closed loop simulation of the visually guided course control of a fly*
- [#19B](#) R. Kern, L. Dittmar, G. Schwerdtfeger, N. Böddeker and M. Egelhaaf, Bielefeld  
*Blowflies exhibit saccadic flight style under various free flight conditions*
- [#20B](#) R. Kern, G. Schwerdtfeger, M. Egelhaaf and JH. van Hateren, Bielefeld and Groningen (NL)  
*Response of the blowfly H1-neuron to natural optic flow*
- [#21B](#) K. Pfeiffer, M. Kinoshita and U. Homberg, Marburg and Yokohama (J)  
*Integration of celestial orientation cues in an identified neuron in the brain of the desert locust *Schistocerca gregaria**
- [#22B](#) N. Boeddeker, JP. Lindemann, M. Egelhaaf and J. Zeil, Bielefeld and Canberra (AUS)  
*Analysis of neuronal responses in the blowfly visual system to optic flow under natural outdoors conditions.*
- [#23B](#) K. Karmeier, HG. Krapp and M. Egelhaaf, Bielefeld and Cambridge (UK)  
*Population coding of self-motion in the blowfly visual system*
- [#24B](#) J. Grewe, N. Matos, M. Egelhaaf and A-K. Warzecha, Bielefeld  
*Non-linear Dendritic Integration of Visual Motion Stimuli in Fly Motion-Sensitive Neurons*

## **Introductory Remarks to Symposium 16**

### **New vistas on insect vision**

**Roland Strauss and Reinhard Wolf, Würzburg**

Sensory information is processed through multiple stages in the nervous system before an appropriate motor output is produced. Recent research in insects has considerably furthered our understanding of the underlying processes and neural substrates. Rister, Heisenberg, Sinakevitch and Strausfeld disentangle the often parallel pathways of peripheral visual processing in *Drosophila* using latest neurogenetic techniques. Haag and Borst can explain complex receptive field properties of visual interneurons in the blowfly in terms of network interactions. By studying the visual receptive fields of motor neurons in the fly Krapp and Huston follow up and analyze in depth distinct pathways from the sensory input to the motor output. In their analysis of landmark orientation behavior in *Drosophila* Mronz and Strauss found new evidence for weighted integration of motion to be the basis. Their simple model derived from the biological original does produce fly-like autonomous orientation behavior of a camera-equipped robot. Traveling further into the center of the insect brain, Homberg and Pfeiffer will describe the processing of polarized light information in the brain of the desert locust, and how this information is converted into a sky compass. Last not least Wolf and Heisenberg show that visual pattern recognition in *Drosophila* is invariant for the retinal position. Moreover, they provide compelling evidence for the usage of selective visual attention in this process.

## Neurogenetic analysis of the functional role of the T1 basket cell, a prominent interneuron of the fly's visual system

**Jens Rister<sup>1</sup>, Irina Sinakevitch<sup>2</sup>, Kei Ito<sup>3</sup>, Martin Heisenberg<sup>1</sup> and Nicholas James Strausfeld<sup>2</sup>**

<sup>1</sup>Lehrstuhl für Genetik und Neurobiologie, Universität Würzburg, Am Hubland, 97074 Würzburg, Germany

<sup>2</sup>Division of Neurobiology, University of Arizona, 611 Gould-Simpson, Tucson, AZ 85721, USA

<sup>3</sup>Institute of Molecular and Cellular Biosciences, University of Tokyo, Yayoi 1-1-1, Bunkyo-ku, Tokyo 113-0032, Japan

In flies, each visual sampling unit (VSU) comprises six photoreceptors (R1-R6) that look at the same point in space. Beneath the retina, VSU are organized as functional units, called lamina cartridges, in which six photoreceptor endings are associated with 12 types of neurons. One of these is the T1 basket centripetal neuron that receives indirect input from surrounding cartridges via the alpha components of the type 1 lamina amacrine cell (Campos-Ortega and Strausfeld, 1973). Recent functional and immunocytological studies (Douglass and Strausfeld, 2003; Sinakevitch and Strausfeld, 2004) propose that the first step of motion detection is non-directional and is achieved through interaction between the basket-like dendrites of T1, with its participating presynaptic network of amacrine processes, and the L2 monopolar cell that accompanies T1 to the medulla. We are currently testing this model in *Drosophila melanogaster* by means of the GAL4/UAS system (Brand and Perrimon, 1993), where the transcription factor GAL4 is used to drive cell- and tissue-specific expression of desired transgenes. In a screen of a GAL4-line image database, we have identified a GAL4 line which selectively labels the T1 basket cells. This should allow us to block the output of T1's chemical synapses by GAL4-directed expression of tetanus neurotoxin light chain (TNT; Keller et al., 2002), which specifically cleaves neuronal synaptobrevin and therefore prevents evoked synaptic vesicle release (Sweeney et al., 1995).

The behavioural consequences of targeted TNT expression in T1 cells were studied in classical optomotor experiments for testing walking but not flying flies. TNT expression in T1 was confirmed by detection of the neurotoxin with an anti-TNT antibody. When stimulated with a striped drum moving around the animal at a constant velocity (contrast frequency: 1.2 Hz), freely walking flies with GAL4-driven TNT expression in T1 neurons show wild-type optomotor turning responses and compensate for the large field stimulus with changes in body angles not significantly different from control flies. Next, the GAL4/TNT flies were tested under different light intensities at a constant contrast frequency (1Hz; 45°) while walking on a locomotion recorder (Buchner, 1976). The direction-sensitive (open loop) optomotor turning response of flies expressing TNT in T1 is also not different from control flies, even in the vicinity of the low intensity threshold. Finally, head roll responses of tethered flies elicited by large field motion were measured and also turned out to be unaffected by TNT expression in the basket cells. One interpretation of the current results is that T1 has an exclusive role in flight optomotor behaviour. Another is that the level of neurotoxin expression was not sufficient to fully block the output of all T1 cells or, thirdly, that their synapses are characterized by a molecular machinery which is not affected by TNT expression. We are currently investigating all three hypotheses.

### References:

- Brand, A. and Perrimon, N.: "Targeted gene expression as a means of altering cell fates and generating dominant phenotypes", *Development* 118:401-415 (1993)
- Buchner, E.: "Elementary movement detectors in an insect visual system", *Biol Cybern* 24:85-101 (1976)
- Campos-Ortega, J.A. and Strausfeld, N.J.: "Synaptic connections of intrinsic cells and basket arborizations in the external plexiform layer of the fly's eye", *Brain Res* 59:119-136 (1973)
- Douglass, J. and Strausfeld, N.J.: "Anatomical organization of retinotopic motion-sensitive pathways in the optic lobe of flies" *Microsc Res Tech* 62:132-150 (2003)
- Keller, A.; Sweeney, S.T.; Zars, T.; O'Kane, C.J. and Heisenberg, M.: "Targeted expression of tetanus neurotoxin interferes with behavioral responses to sensory input in *Drosophila*", *J Neurobiol* 50:221-33 (2002)
- Sinakevitch, I. and Strausfeld, N.J.: "Chemical neuroanatomy of the fly's movement detection pathway", *J Comp Neurol* 468:6-23 (2004)
- Sweeney, S.T.; Broadie, K.; Keane, J.; Niemann, H. and O'Kane, C.J.: "Targeted expression of Tetanus Toxin Light Chain in *Drosophila* specifically eliminates synaptic transmission and causes behavioural defects", *Neuron* 14:341-351 (1995)

## Network interactions underlying complex receptive field properties of fly visual interneurons

Juergen Haag and Alexander Borst

Max-Planck-Institute of Neurobiology  
Department of Systems and Computational Neurobiology  
Am Klopferspitz 18a  
D-82152 Martinsried, Germany

Neurons responding to visual motion found at higher processing stages in many species are often specifically tuned to particular flow-fields. However, the neural circuitry leading to this selectivity is not yet understood. We studied this problem in the so-called VS-cells (*Vertical System*) of the lobula-plate in the fly. Within each brain hemisphere, the lobula plate contains only 10 VS-cells that can be individually identified (Hengstenberg et al., 1982). These neurons possess distinctive local preferred directions in different parts of their receptive field (Krapp et al., 1998). Investigating the connectivity between different VS-cells by means of dual recordings, we found that they are electrically coupled with each other. The coupling strength thereby depended on the anatomical distance of the VS-cell dendrites within the lobula plate. The analysis of the responses to current injection revealed that each VS-cell is not directly connected to all other VS-cells, but only indirectly via its immediate neighbors. This coupling is responsible for the elongated horizontal extent of the receptive fields of VS-cells. For VS-cells with a lateral receptive field we found in addition connections to the horizontal system, tuning these cells to rotational rather than to translational flow fields.

Hengstenberg R., Hausen K. and Hengstenberg B. The number and structure of giant vertical cells (VS) in the lobula plate of the blowfly *Calliphora erythrocephala*. *J.Comp.Physiol.A* **149**, 163-177 (1982).

Krapp H. G., Hengstenberg B. and Hengstenberg R. Dendritic structure and receptive-field organization of optic flow processing interneurons in the fly. *J.Neurophysiol.* **79**, 1902-1917 (1998).

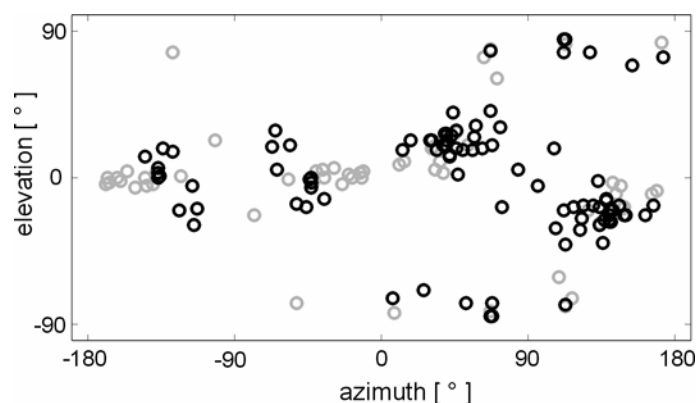
## Encoding self-motion: From visual receptive fields to motor neuron response maps

Holger G. Krapp and Stephen J. Huston

Department of Zoology, University of Cambridge, Downing Street, Cambridge CB2 3EJ, UK

Sensory systems sample information about the environment using arrays of local receptors. Behaviourally relevant features are then extracted from these receptor arrays by integrating local receptor responses. At some stage sensory information has to be transformed into a pattern of motor-activity that mediates and controls adequate behaviour. One of the most fundamental questions in Neuroscience is how, and at which stage such sensory-motor transformations take place in the nervous system.

In the fly visual system identified visual interneurons, tangential neurons (TNs), selectively integrate local motion information. The receptive field organisation of individual TNs is highly reminiscent of optic flow fields resulting from particular aspects of the animal's self-motion in space (Krapp & Hengstenberg 1996). Ten Vertical System TNs (VS neurons) integrate local motion information that matches the structure of optic flow fields generated during rotations around horizontal body axes while three Horizontal System TNs (HS neurons) may be involved in indicating rotations around the vertical body axis and horizontal translations. We used the receptive field organization of these TNs to quantitatively estimate each neuron's preferred axis of rotation.



VS and HS tangential neurons provide direct and, via descending neurons, indirect visual input to neck motor neurons (NMNs). NMNs control gaze stabilizing head movements. We apply extracellular recording techniques to locally determine the visual response properties of several NMNs. The resulting NMN response maps allowed us to run the same analysis as used on the TNs. As a result we obtain the distribution of preferred rotation axes of NMNs. In the figure each

circle indicates the orientation of a preferred rotation axis defined by angles of elevation and azimuth, where azimuth = elevation = 0° corresponds to the fly's longitudinal body axis. The distribution of NMN rotation axes (black circles) is plotted on top of the distribution of TN rotation axes (grey circles). The good correspondence between the two distributions suggests that TNs and NMNs use a common coordinate system to encode self-motion and control head movements, respectively.

Where does the sensory motor transformation in the gaze stabilization system take place? Local motion information is analysed along ommatidial rows in the fly's hexagonal eye lattice. Thus sensory information on directional motion is encoded in local retinal coordinates. The transformation to motor coordinates is achieved at the TNs by selectively integrating local motion information. Embedding self-motion information into motor coordinates at such early stage facilitates visual gaze stabilization.

## A simple model for visual object orientation in the walking fruit fly

Markus Mronz <sup>1,2</sup> and Roland Strauss <sup>1</sup>

<sup>1</sup> LS Genetik und Neurobiologie, Biozentrum der Universität Würzburg, Am Hubland,  
97074 Würzburg, Germany

<sup>2</sup> Current address: Neurobiologie, Universität Ulm, Albert-Einstein-Allee 11, 89081 Ulm, Germany

*Drosophila* is known to choose, with a high probability, the nearest of several similar objects first. The flies use self-induced parallax motion of the object images on the eye to evaluate their distances (Schuster et al. 2002, Curr Biol 12:1591-4). The amplitude of the parallax motion depends not only on the distance but also on the angular position of an object image on the eye of the fly. The closer the object the larger is the shift. The shift increases from frontal to lateral image positions and it is greatest at 90°.

The present study asked whether the distance estimation system is selective for parallax motion created by the fly's self-motion or whether motion of objects can increase their attractiveness because they appear to be closer to the fly. A computer-controlled cylindrical panorama made of light-emitting diodes has been used to create a virtual world for the fly (Strauss et al. 1997, J exp Biol 200:1281-96). Using virtual-reality techniques, objects were simulated at different distances and angular positions. In some experiments the fly's self-motion was taken into account and used to keep objects stationary on the retina of the freely moving fly (virtual open loop). The data show that flies prefer objects the more, the larger the shift of the object image becomes on the retina. Attractiveness is independent of the source of the retinal shift, object motion or self-motion of the fly. However, front-to-back motion (the natural direction created by a forward-moving fly) is preferred over back-to-front motion. Surprisingly, the preference for near objects disappeared when a near object was presented together with several distant objects on one eye and within a viewing angle of less than 90°. This observation led to the assumption that parallax motion is spatially integrated over larger areas of the eye and not perceived by the fly as an entity of the single object. The extent of parallax motion caused by a stationary object on the retina of a walking fly depends not only on the distance but also on the angle under which it is seen. The closer the object, the larger becomes the parallax motion. But by physics the retinal shift of the object reaches also a minimum during a head-on approach and a maximum when the fly passes the object under 90°. Although *Drosophila* prefers the larger amount of visual motion at a given presentation angle, it clearly prefers frontal over lateral objects. In order to account for the preference for frontal objects an amplification of the frontal and caudal eye regions is postulated which would otherwise receive less parallax motion than the lateral regions. It turned out that walking flies responded only delayed to the presentation of a novel single object. This delay is consistent with the idea of temporal integration of parallax motion for distance estimation. Astonishingly, the subsequent course change depended on the viewing angle of the object. If an attractive object was shown in the fronto-lateral eye region the flies turned towards it. If it appeared in the caudo-lateral part of the retina the flies preferentially turned away from it. Based on these findings a minimal model for object orientation has been proposed. This model neither comprises object identification nor any form of object representation. Visual input is restricted to visual flow only. This visual motion is integrated in four compartments, a fronto-lateral and a caudo-lateral compartment per eye. Depending on which compartment reaches a chosen threshold first, a turning response will be elicited either towards (fronto-lateral compartment) or away from the target object (caudo-lateral compartment). To compensate for the small amount of parallax motion in the frontal and caudal eye regions a weighting function has been introduced. Additionally and in accord with fly data, also front-to-back motion has been weighted stronger in the model than back-to-front motion. The algorithm was finally implemented on a mobile robot equipped with a video camera with fish-eye lens allowing for panoramic vision. The performance of the robot was measured and quantitatively compared to the orientation behaviour of walking fruit flies in up scaled, otherwise identical surroundings. The robot indeed reproduced successfully many aspects of the fruit fly's object orientation behaviour and showed fly-like autonomous orientation behaviour in the presence of various object arrangements. (Supported by a BMBF-BioFuture grant to R.S., FKZ: 0311855)

E-mail address for correspondence: markus.mronz@biologie.uni-ulm.de

## Polarization vision and sky compass in the desert locust

Uwe Homberg and Keram Pfeiffer

Department of Biology, Animal Physiology, University of Marburg, 35032 Marburg, Germany, [homberg@staff.uni-marburg.de](mailto:homberg@staff.uni-marburg.de)

Similar to many vertebrate species, insects rely on a sun compass for spatial orientation. In addition to the perception of direct sunlight, they can also detect the polarization pattern of the blue sky and use it to estimate navigational directions (Wehner 1992, in F. Papi, ed. Animal homing. Chapman, London, pp 45-144). Photoreceptors adapted for the detection of the sky polarization pattern are concentrated in a small dorsal rim area of the compound eye (Labhart and Meyer 1999, Microsc Res Tech 47:368-379). To understand the neural mechanisms involved in sky compass orientation, we have analyzed the polarization vision system in a favorable insect, the desert locust *Schistocerca gregaria*.

The locust compound eye has a prominent dorsal rim area that shows ultrastructural features typical for polarization analyzers and has photoreceptors with high polarization sensitivity (Eggers and Gewecke 1993, in Wiese K et al., eds. Sensory systems of arthropods. Birkhäuser, Basel pp 101-109). Stationary flying locusts show polarotactic yaw-torque responses when illuminated through a rotating polarizer from above (Mappes and Homberg 2004, J Comp Physiol A 190:61-68). This response is abolished when the dorsal rim areas are painted black. Photoreceptors from the dorsal rim areas project to distinct dorsal rim areas in the lamina and medulla. Tracer injections revealed central processing stages of the polarization vision system, including the anterior lobe of the lobula, the anterior optic tubercle, the lateral accessory lobe, and the central complex in the locust median protocerebrum.

Physiological analysis of polarization-sensitive (POL) neurons has focussed on the anterior optic tubercle and the central complex. Most POL neurons show polarization opponency, i.e. they receive maximal tonic excitation at a particular e-vector ( $\Phi_{\max}$ ) and are maximally inhibited at an e-vector perpendicular to  $\Phi_{\max}$ . In addition to dorsally presented polarized light, most neurons in both areas are also sensitive to unpolarized light. Three pairs of commissural POL neurons of the anterior optic tubercle have been studied most extensively. The neurons have characteristic  $\Phi_{\max}$ -orientations, which are symmetric in the bilateral pairs of neurons. Their response to unpolarized light is highly dependent on stimulus azimuth, and is maximal at an azimuth roughly perpendicular to their preferred e-vector orientation ( $\Phi_{\max}$ ). The response to unpolarized light is not mediated by photoreceptors of the dorsal rim area. These properties suggest that information on solar azimuth and sky polarization pattern is combined in a meaningful way by these neurons to increase the robustness of the navigation system against various clouding and daylight conditions.

Many POL neurons of the central complex receive polarization input from both compound eyes. The neurons have large visual fields of more than 90° and show highly similar  $\Phi_{\max}$ -orientations throughout their field of view. Visual fields for polarization sensitivity are zenith-centered which allows for coding of solar azimuth independent of solar elevation. These neurons are, therefore, suited to encode head direction of the locust under various sky conditions. Analysis of the polarization vision system in the locust brain suggests that visual signals from the sky are processed in several distinct steps. Together with still unknown mechanisms for time compensation, this might, finally, enable neurons of the central complex to provide a robust compass signal for the control of flight and walking directions.

Supported by DFG grants HO 950-13 and HO 950-14



## Pattern recognition in *Drosophila* requires selective visual attention

Reinhard Wolf and Martin Heisenberg

Lehrstuhl für Genetik und Neurobiologie, Universität Würzburg  
Biozentrum, Am Hubland, 97074 Würzburg, Germany

In the flight simulator, *Drosophila* is flying stationarily (fixed to a torque meter) in the centre of a cylindrical panorama. The angular velocity of the panorama is made negatively proportional to the fly's yaw torque. In this way, the fly can visually control its flight direction with respect to visual patterns<sup>1</sup>.

In a learning paradigm (flight simulator learning), two pairs of visual patterns are displayed in alternating order spaced by 90°. The fly quickly learns to avoid flying towards one of the two patterns, if this is associated with dangerous heat, applied by a beam of infrared light. In the standard experiment, the fly can discriminate the two patterns only by the height of their centers of gravity (COG)<sup>2</sup>.

In a different learning paradigm (yaw torque learning) in which the fly receives no motion feedback from the panorama, two different patterns are simultaneously presented at fixed lateral positions of +45° and - 45°. The spontaneously generated yaw torque of the fly is used to switch the heat beam on or off, depending on the fly's *intended* turns either to the right or to the left side (training). During the memory test, the fly's yaw torque is measured while heat is permanently switched off. Between training and memory test, the patterns can be shifted to new positions (transfer test). Surprisingly, if the two patterns at the +/-45° positions are just switched, the fly also switches its yaw torque bias and preferentially tries to fly towards the very side that was dangerous and therefore avoided during training(!). Thus, the fly had associated heat (and/or no-heat) with the visual patterns<sup>3</sup>.

In both learning paradigms the fly has to associate the two patterns differentially with heat (and/or no-heat) during acquisition. Yet, the two features are simultaneously visible, irrespective of whether heat is on or off. It follows, that the fly must be able to confine the formation of associations to visual patterns *in special positions*. In flight simulator learning the fly might, for instance, limit the acquisition process to the frontal part of the visual field. (If the occurrence of a certain pattern in the frontal visual field would coincide with heat, it would be labeled 'dangerous to approach'.) In yaw torque learning the fly also attaches different 'values' to the two patterns if turning towards one of them during training causes being heated. In this experiment the position at which the association is formed can be as far lateral as +/-80° (and perhaps even further). Pattern positions can be freely chosen by the experimenter. Hence, the fly must have considerable flexibility in choosing the critical part of the visual field. Assuming that in the two learning paradigms the fly uses the same translation-invariance mechanism, one also needs a common mechanism of position selectivity in the two paradigms. Considering that 'selection of visual half-fields' does not work in flight simulator learning and 'fixed frontal positions' does not work in yaw torque learning, we have to assume a temporally and spatially variable gating process, which we call 'window of attention'. Evidence for selective visual attention in *Drosophila* has been found earlier<sup>1,4-6</sup>.

<sup>1</sup> Heisenberg M, Wolf R (1984): Vision in *Drosophila*: *Genetics of Microbehavior*. Braitenberg V, Ed. (Studies of Brain Function, vol 12, Springer Verlag, Berlin)

<sup>2</sup> Wolf R, Heisenberg M (1991): *J. Comp. Physiol. A* **169**: 699-705

<sup>3</sup> Tang S, Wolf R, Xu S, Heisenberg M (2004): *Science* **205**: 1020-1022

<sup>4</sup> Wolf R, Heisenberg M (1980): *J. Comp. Physiol. A* **140**: 69-180

<sup>5</sup> Schuster S (1996): Doctoral Thesis, University of Tübingen

<sup>6</sup> van Swinderen B, Greenspan RJ (2003): *Nature Neurosci.* **6**:579-586

Functional properties of visual neurons in male blowflies presumably involved in chasing behaviour

Christine Trischler, Norbert Boeddeker, Roland Kern and Martin Egelhaaf

Neurobiology, University of Bielefeld; P.O. Box 100131, 33501 Bielefeld, Germany  
christine.trischler@uni-bielefeld.de

Male blowflies chase females in the context of mating behaviour in fast acrobatic flights. Chasing-behaviour has been concluded to be guided by information about the direction and the size of the target as seen by the chasing fly (Boeddeker et al., 2003, *Proc R Soc Lond B.*, 270: 393-399). This visual information is thought to be processed in male-specific visual interneurons that reside in the blowfly's third visual neuropile (Strausfeld, 1991, *J Comp Physiol. A*, 169: 379-393).

These neurons are investigated by intracellular recordings during presentation of two classes of visual stimuli. On the one hand, properties of the neurons are determined by presentation of simple visual stimuli. On the other hand, a novel approach is applied to unravel the role of male-specific neurons as potential control mechanism of chasing behaviour: Blowflies chasing either dummy targets or other blowflies are filmed with a pair of digital highspeed-cameras with an image acquisition rate of 500 Hz. On the basis of these data the blowfly's and the target's position and orientation during the chase are reconstructed and thus, the size and the position of the target as seen by the pursuer is calculated. These stimuli are replayed on a monitor, thus presenting complex, dynamic stimuli as they occur in natural behavioural situations.

Simple visual stimulation allows us to classify the neurons on the basis of their response characteristics, such as selectivity for small-field motion and sensitivity for motion in different directions. The response amplitudes are large for movement directions which dominate during a chase. All investigated neurons spread their receptive field over the dorsofrontal area of the retina, covering the 'acute zone', a region where the image of a pursued target is stabilised. The predominantly large receptive fields are in some neurons extended far into the contralateral visual field.

Currently, it is being analysed with complex visual stimuli which visual cues can be extracted by the neurons from natural retinal input. These cues will be related to predictions based on a phenomenological model of the control system mediating chasing behaviour (see Boeddeker and Egelhaaf, 2003a, *Proc R Soc Lond B.*, 270: 1971-1978) to assess to which extent information processing by the male-specific neuronal system is adapted to behaviourally relevant conditions.

Supported by the DFG via the Graduate and Postdoctoral Program 'Strategies and Optimisation of Behaviour'

## Posttranslational modification of the *Drosophila* visual G $\gamma$ subunit: protein farnesylation facilitates membrane attachment of the betagamma complex in vivo

Kristina Hartmann<sup>1</sup>, Simone Schillo<sup>1</sup>, Gregor Belusic<sup>2</sup>, Reinhard Paulsen<sup>1</sup>, and Armin Huber<sup>1</sup>

From the <sup>1</sup>Institut für Zoologie, Universität Karlsruhe, Germany and <sup>2</sup>Department of Biology, Biotechnical Facility, University of Ljubljana, Slovenia

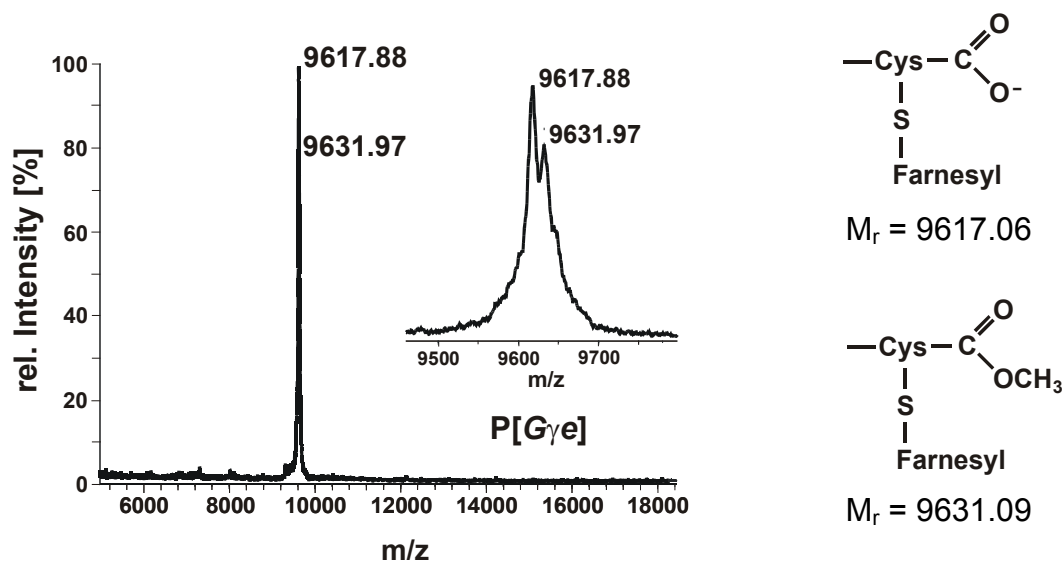


**Fig.1** Maldi-ToF spectrum of overexpressed non-mutated *Drosophila* G $\gamma$ e. The determined molecular masses correspond to  $\gamma$ -subunits which have been modified by acetylation, farnesylation and cleavage of last three amino acids. A methylated (9631.97) and a non-methylated (9617.88) form of G $\gamma$ e have been detected.

Activation of phototransduction in the compound eye of *Drosophila* is mediated by a heterotrimeric G protein which couples to the effector enzyme phospholipase C $\beta$ . The  $\gamma$ -subunit of this G protein (G $\gamma$ e), as well as  $\gamma$ -subunits of vertebrate transducins contain a carboxy-terminal CAAX-motif with a consensus sequence for protein farnesylation. After farnesylation of the cysteine residue the last three amino acids of the CAAX-motif are cleaved off and the terminal cysteine usually becomes methylated. To study farnesylation of *Drosophila* G $\gamma$ e, we mutated the farnesylation site and overexpressed the mutated G $\gamma$ e as well as non-mutated G $\gamma$ e in *Drosophila* photoreceptor cells. Mass spectrometry of overexpressed G $\gamma$ e subunits revealed that non-mutated G $\gamma$ e is modified by farnesylation and acetylation (Fig. 1), whereas the mutated G $\gamma$ e is not farnesylated. Native G $\gamma$ e is also modified by acetylation and farnesylation. In the transgenic flies, mutated G $\gamma$ e forms a dimeric complex with G $\beta$ e, and the fraction of membrane bound G $\beta\gamma$  is decreased. Thus, farnesylation of G $\gamma$ e facilitates the membrane attachment of the G $\beta\gamma$  complex. Electoretinogram recordings revealed a significant loss of light-sensitivity in eyes of transgenic flies which express mutated G $\gamma$ e. This loss in light-sensitivity reveals that post-translational farnesylation is a critical step for the formation of membrane-associated G $\alpha\beta\gamma$  required for transmitting light-activation from rhodopsin to phospholipase C $\beta$ .

## A new role of motion adaptation in the visual motion pathway of the blowfly

J. Heitwerth & M. Egelhaaf

Department of neurobiology, Bielefeld University

email: Jochen.Heitwerth@Uni-Bielefeld.de

The properties of motion sensitive neurons of blowflies have been shown in previous studies (e.g. Maddess & Laughlin 1985, de Ruyter van Steveninck et al 1986, Borst A. & Egelhaaf 1987, Kurtz et al 2000, Fairhall et al 2001, Harris & O'Carroll 2002 ) with various stimulus paradigms to depend on stimulus history. These changes in responses properties are usually termed 'motion adaptation', although their adaptive value is not always evident. In all these studies artificial stimuli, such as constant velocity motion, motion steps or white-noise velocity fluctuations were employed. Since under behavioural conditions, the motion stimuli encountered by blowflies have characteristic dynamical properties, we investigated the potential functional significance of motion adaptation with natural optic flow. As a consequence of the saccadic flight and gaze strategy of blowflies, the major rotations of the animal occur during saccades; between saccades the translatory optic flow component dominates in the low frequency range. We investigated the motion adaptation with a natural optic flow sequence that was generated by a blowfly flying virtually a loop. 15 repetitions of this loop were used as our stimulus to assess changes in the neuronal response.

The performance of the spiking H1 neuron was investigated by various measures. As in previous studies, the mean spike count of the responses decreased considerably during maintained stimulation. However, the spike count variability as related to the mean spike count (i.e. Fano factor) did not improve with prolonged stimulation. The timing precision did not change consistently as well. And the latency of the first spike after the onset of a saccade even increased slightly with prolonged stimulation. Hence, the reliability of the neuronal responses did not increase as a consequence of prolonged motion stimulation. Although the spike count decreased by approximately 45% during maintained motion stimulation, the amount of information conveyed by the neuronal responses only slightly decreased (15%). Thus the cell needs fewer spikes for transmitting almost the same amount of information. The information per spike thus increased accordingly (Fig. 1). Since the generation of spike has relatively high energy costs, our finding suggests that parsimonious coding is realised by adaptation.

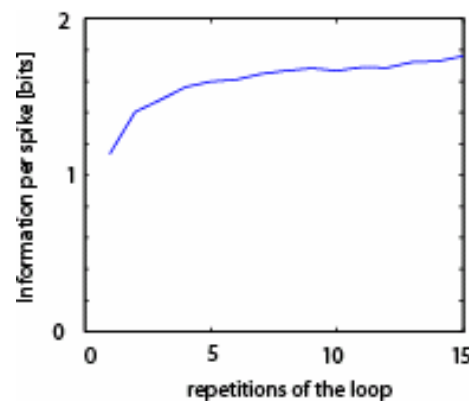


Figure 1: Information per spike increases with prolonged stimulation. One loop lasts about 0.7 seconds.

### References:

- Maddess T, Laughlin SB. Adaptation of the motion-sensitive neuron H1 is generated locally and governed by contrast frequency. *Proceedings of the Royal Society London B*. 225: 251-275, 1985
- de Ruyter van Steveninck RR, Zaagman WH, Mastebroek HAK.: Adaptation of transient responses of a movement-sensitive neuron in the visual system of the blowfly *Calliphora erythrocephala*. *Biological Cybernetics*, 54: 223-236, 1986
- Borst A, Egelhaaf M: Temporal modulation of luminance adapts time constant of movement detectors. *Biological Cybernetics*, 56:209-215, 1987
- Kurtz R, Durr V, Egelhaaf M. Dendritic calcium accumulation associated with direction-selective adaptation in visual motion-sensitive neurons in vivo. *J Neurophysiol*. 2000 Oct;84(4):1914-23.
- Fairhall AL, Lewen GD, Bialek W, de Ruyter Van Steveninck RR. Efficiency and ambiguity in an adaptive neural code. *Nature*. 2001 Aug 23;412(6849):787-92.
- Harris RA, O'Carroll DC. Afterimages in fly motion vision. *Vision Res*. 2002 Jun;42(14):1701-14.

## Closed loop simulation of the visually guided course control of a fly

Holger Weiss, Jens Peter Lindemann\*, Martin Egelhaaf

Neurobiology, Bielefeld University, P. O. Box 10 01 31  
D-33501 Bielefeld, Germany

Flies traverse their environment mostly driven by their visual input. As a precondition, a large part of the fly's brain processes visual information. The question that arises is, what does the fly do with all the information? It has been shown, that many neurons encode the optic flow a fly observes when moving through its environment. This optic flow information is most certainly involved in the steering process. For the horizontal plane we have modelled visually guided behaviour with a pair of cells, the so-called HSE-cells, that encode information about the horizontal optic flow and are suggested to be involved in flight control.

The model consists of four major modules: First the renderer that generates the artificial world of the virtual fly. Second the visual input system is a realistic model of the two HSE-cells. The third module generates translational and rotational forces to steer the fly. The fourth module moves the fly according to the generated forces, friction and inertia. The new coordinates and the orientation of the virtual fly are then passed again to the renderer closing the loop.

The virtual fly was confronted with tasks that have been tested in behavioural experiments, including obstacle avoidance, flying straight in a tunnel and the optomotor following response. Using a continuous feedback control system the fly was not able to navigate through the tunnel but always crashed into one of the walls due to the fact that it was not able to distinguish between the rotation it just initiated and the translation.

Turning into another direction lets fast flying insects drift sideways because of inertial forces. This drifting makes a continuous steering far more complicated as the drift needs to be taken into account when analysing the optic flow. This is particularly challenging because motion detectors in flies encode velocity in a nonlinear way.

Saccade-like turns, i.e fast changes in body orientation, as they are observed during normal flight of flies, represent a means by which the mechanism that analyses the optic flow may separate rotational and translational flow. Shortly after a saccade the sideward drift is at a maximum and during the intersaccade it decreases until the next saccade is generated.

Using this saccadic flight mode, the virtual fly was able to navigate safely through tunnels of different widths and with diverse patterns on their walls.

---

\*Jens.Lindemann@Uni-Bielefeld.DE

## Blowflies exhibit saccadic flight style under various free flight conditions

R. Kern, L. Dittmar, G. Schwerdtfeger, N. Böddeker, M. Egelhaaf

Dept. of Neurobiology, Faculty for Biology, Bielefeld University, D-33501 Bielefeld, Germany.

Blowflies change their direction of flight by saccadic turns of the body, at least when flying in relatively small cubic flight arenas (Schilstra, C. & van Hateren, J.H. Stabilizing gaze in flying blowflies. *Nature* 395, 654 (1998). Between saccades body and head orientation is kept rather stable. This saccadic flight and gaze strategy can be interpreted as a means to largely separate the rotational and translational components of optic flow. As a consequence, optic flow on the eyes of the fly in the intersaccadic intervals can be used to obtain information about the 3D layout of the present environment (Kern et al., submitted).

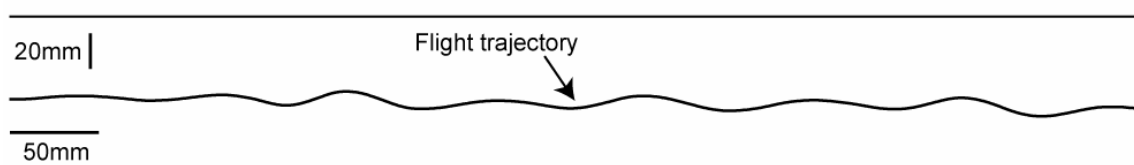
Here, we systematically investigated whether the saccadic flight style of blowflies persists under various environmental conditions, c.f. when flying in elongated boxes with and without obstacles or with and without much textural coating. Flies flying spontaneously in the flight box (length 2.3 m, height 20 cm) of variable width (9, 18, 36, and 40 cm) were recorded with high speed cameras (500 frames/sec). Evaluation of the high-speed videos provided us with the position of the fly in space and the orientation of the body long axis over time.

Blowflies exhibit a saccadic flight strategy not only when flying around obstacles, but also when flying along an elongated flight arena without obstacles where, in principle, no turns were needed (see figure). As a result their trajectory meanders, though the overall course is rather straight (see figure). The frequency of saccades and their peak velocities depend on the width of the flight box. For instance, flies make more and faster saccades per second in the wide tunnel than in the medium one. The translation velocity depends on tunnel width, i.e. flies move faster in the wide than the narrow flight box.

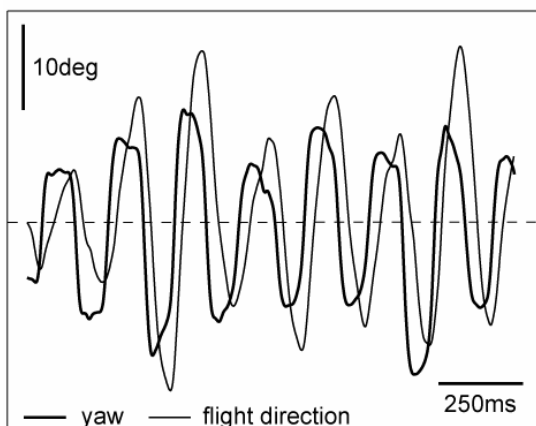
Due to the frequent body (head) turns of the flies and the consequences of inertia the fly is subject to sideward motion (drift) for a remarkably large portion of the total flight time. During these time intervals gaze direction and flight direction do not coincide (see figure).

In experiments performed with unilaterally blinded flies we challenge our hypotheses on the mechanisms of saccade initiation.

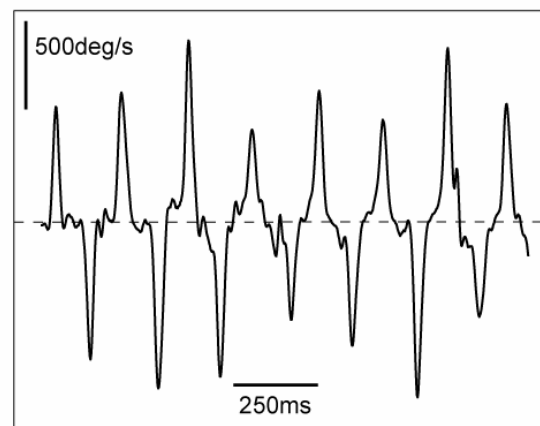
Flight tunnel



Body yaw and flight direction



Body yaw velocity



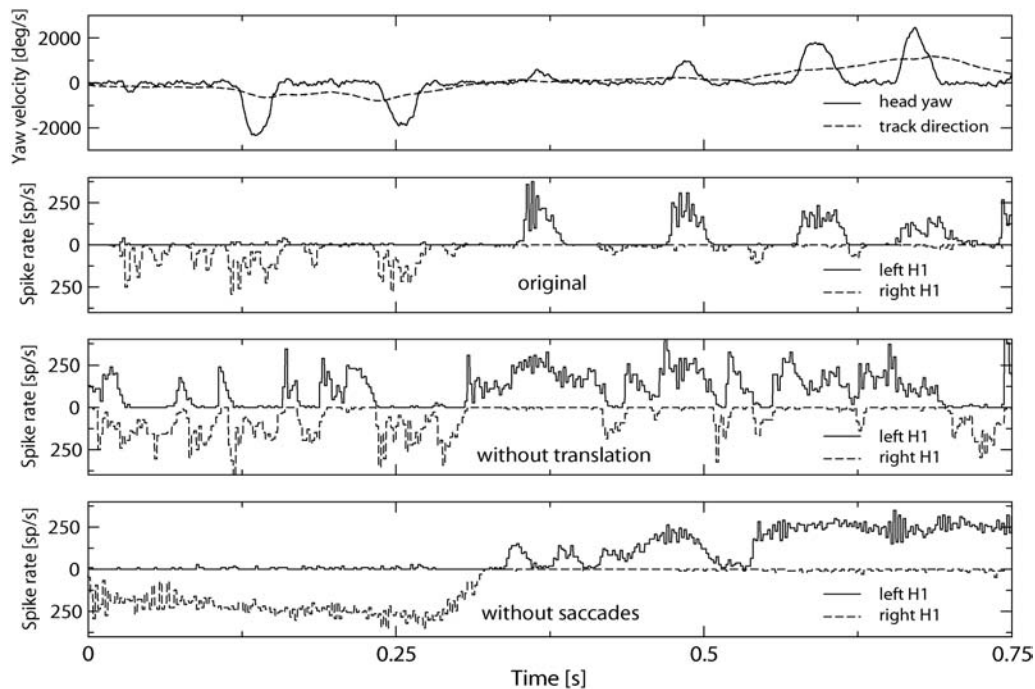
## Response of the blowfly H1-neuron to natural optic flow

R. Kern\*, G. Schwerdtfeger\*, M. Egelhaaf\*, J.H. van Hateren#

\* Dept. of Neurobiology, Faculty for Biology, Bielefeld University, D-33501 Bielefeld, Germany.

# Dept. of Neurobiophysics, University of Groningen, 9747 AG Groningen, The Netherlands.

We investigated the processing of natural optic flow by the H1-neuron, a wide-field motion sensitive neuron in the blowfly visual system. Natural optic flow was obtained by first measuring the flight paths and head movements of flies flying in a cage (J. Exp. Biol. 202:1491-1500, 1999), and subsequently reconstructing the visual stimulus as viewed by the head during these flights. We replayed the resulting movies on a fast, panoramic stimulus device (Vision Res. 43:779-791, 2003), whilst recording from the H1-neuron. The optic flow in the movies consists of contributions from translation and rotation. Furthermore, blowfly flight is characterized by fast, saccadic turns of the thorax, with a more stable orientation in the periods between the saccades. Compensating head movements further enhance the stability of gaze between the saccades. Because earlier studies of H1 using naturalistic optic flow have ignored both the flow due to translation and the existence of saccades, we constructed two control stimuli for investigating the consequences of neglecting either of these. The control stimulus “without translation” was made by constructing movies with the normal rotational movements of the fly, but with its (virtual) position fixed in the centre of the cage. The control stimulus “without saccades” was constructed by assuming that the (virtual) fly would be looking into the local direction of its flight path. Although the flight path contains turns, these are much smoother and occurring less frequently than the saccades.



The figure shows the resulting spike rates for the H1-cells from the left and right eye (upward and downward going histograms, respectively; the response of the right H1-cell was approximated by recording the response of the left cell to a properly mirrored movie). The upper panel shows the yaw velocity (rotation about a vertical axis) for the original movie (continuous trace, with the peaks showing saccades) and for the movie without saccades (broken line, marked “track direction”). During normal optic flow (panel marked “original”), the H1-cell mainly responds to the saccades. This is because H1 is sensitive to back-to-front motion, and is therefore normally suppressed during forward flight (i.e., front-to-back motion). Only a saccade producing strong back-to-front motion pulls the cell out of suppression. The panel marked “without translation” shows that H1 is indeed active for a much larger proportion of the time when the suppression due to translation lacks. Finally, the response is again dramatically changed when the saccades are neglected (but with the translational flow still there).

We conclude that, in normal flight, H1 is mainly responding to saccades. Since H1 gives input to a number of tangential cells being part of different neuronal networks in the fly lobula plate, its functional role in various behavioural contexts – for example in Figure-Ground discrimination - will be discussed.

## **Integration of celestial orientation cues in an identified neuron in the brain of the desert locust *Schistocerca gregaria***

Keram Pfeiffer<sup>1</sup>, Michiyo Kinoshita<sup>2</sup>, and Uwe Homberg<sup>1</sup>

<sup>1</sup>University of Marburg, Animal Physiology, 35032 Marburg, Germany, <sup>2</sup>Yokohama City University, 22-2 Seto, Kanazawa-ku, 236-0027 Yokohama, Japan, corresponding author: Pfeiffer@staff.uni-marburg.de

Long-distance traveling requires a reliable compass system for accurate navigation. The inhomogeneity of celestial light provides a number of directional information sources, such as spatial differences in light intensity, wavelength, e-vector orientation and degree of polarization that can be exploited to build a neuronal sky-compass. Many insects, amongst them the desert locust, are known to use the celestial polarization pattern for compass orientation (reviewed by Homberg 2004, *Naturwissenschaften* 91:199).

A specialized dorsal rim area of the compound eye consisting of highly adapted ommatidia allows the perception of the plane of polarized light. The e-vector information is processed by polarization-sensitive interneurons (POL-neurons). Recent morphological findings (Homberg et al. 2003, *J Comp Neurol* 462:415) suggested that POL-neurons of the anterior optic tubercle of the desert locust do not only receive input from the dorsal rim area, but also from lateral and ventral regions of the compound eye that are not polarization-sensitive.

With intracellular recordings combined with tracer injections, we investigated whether an identified POL-neuron from the anterior optic tubercle also processes celestial cues other than the e-vector pattern to estimate solar azimuth directions. In addition to dorsally presented linearly polarized light with rotating e-vector, we stimulated with a "white" LED moving on a circular path around the center of the locust head at an elevation of 45° and with laterally presented, isoquantal, monochromatic light between 330 nm and 600 nm.

The lobula-tubercle neuron (LoTu1) shows a sinusoidal all-activation e-vector-response curve to dorsally presented linearly polarized light. A small white light spot (LED) activates the cell, but only when presented at a particular azimuth. The preferred e-vector orientation differs approximately 90° from the preferred azimuth of the LED, reflecting the angular relationship between e-vector orientation and solar azimuth in the natural sky. In addition, LoTu1 shows color opponency for ipsilaterally presented unpolarized light. While UV (350 nm) leads to inhibition, green light (530 nm) activates the cell. This response characteristic might reflect spectral gradients in the sky, but the azimuthal dependency of this response remains to be tested. The results suggest that LoTu1 neurons signal the angular relationship between the locust's head and the solar azimuth by integrating at least three sources of information: (1) e-vector angle, (2) position of the sun, and (3) chromatic gradients in the sky.

This work was supported by DFG grant Ho-950/13



**Analysis of neuronal responses in the blowfly visual system to optic flow under natural outdoors conditions.****Boeddeker N<sup>1,2</sup>, Lindemann JP<sup>1</sup>, Egelhaaf M<sup>1</sup>, and J. Zeil<sup>2</sup>**<sup>1</sup>Lehrstuhl Neurobiologie, Universität Bielefeld, Postfach 10 01 31, D-33501 Bielefeld<sup>2</sup>RSBS Australian National University PO Box 475, Canberra, ACT 2601 Australia

e-mail: norbert.boeddeker@uni-bielefeld.de

Visual information is important for biological and artificial visual systems to control and guide locomotion. The optic flow at the eyes of a moving observer contains information on both the observer's own movement and on the three-dimensional structure of the environment. The goal of this project is to characterise the optic flow under natural conditions and to understand how an insect's nervous system extracts useful information from it to guide behaviour.

Flight paths of blowflies were recorded outdoors with two orthogonally oriented digital high-speed cameras and reconstructed in 3D, including yaw orientation, using custom-made software (FlyTrace: Lindemann JP, Bödder N & Egelhaaf M; Göttingen Neurobiology Conference, p.1065, 2003). The next day around the same time, we moved a panoramic imaging device (Zeil et al. J Opt Soc Am A 20: 450-469, 2003) along exactly the same flight paths to reconstruct the optic flow experienced by the fly during these flight manoeuvres. Panoramic image sequences were transformed and processed by 3D rendering software to generate the data format required by our flight simulator (FliMax: Lindemann et al. Vision Research 43: 779-791, 2003) and to feed the image sequences into a computational model of the fly's visual system. The image sequences were replayed in the flight stimulator while recording from visual interneurons (HS-cells) in the blowfly's visual motion pathway. HS-cells are thought to play a role in extracting optic flow information from the retinal input for the control of visually guided behaviour. With FliMax it is possible to stimulate large parts of the blowfly's almost panoramic visual field at sufficiently high frame rates (370 Hz) for fast insect vision.

We created different types of optic flow, which allow us to compare the original motion signals to signals originating from modified trajectories. We find that rotational velocity dominates the neuronal responses under all conditions tested and that it is represented in a highly nonlinear way. However, responses to the optic flow generated by the original trajectories diverge from the pure rotation condition, for instance when a leaf on which the fly will eventually land appears in the receptive field of the three different HS-Cells.

We conclude that under "real life conditions", HS-Cells code information about self-motion and about the spatial layout of the environment. In future behavioural and electrophysiological studies we will assess the dependence of neuronal information processing on the animal's self-motion and on the specific properties of the surroundings.

Supported by Deutsche Forschungsgemeinschaft and Centre for Visual Sciences, ANU

## Population coding of self-motion in the blowfly visual system

Katja Karmeier<sup>1</sup>, Holger G. Krapp<sup>2</sup>, Martin Egelhaaf<sup>1</sup>

<sup>1</sup>Bielefeld University, Department of Neurobiology, PO Box 10 01 31, 33501 Bielefeld, Germany

<sup>2</sup>University of Cambridge, Department of Zoology, Downing Street, Cambridge CB2 3EJ, UK

Sensory information is usually represented by the joint activities of populations of neurons where each single neuron is tuned to a slightly different aspect of the stimulus. In the fly visual system a subgroup of 10 individually identifiable motion-sensitive interneurons in each half of the brain offers a well described biological system to investigate population coding. The sophisticated receptive field organization of these so-called VS-cells (vertical system) indicates that each cell senses an optic flow pattern induced when the animal rotates around a particular horizontal body axis (Krapp and Hengstenberg 1996).

In a systems analysis approach we demonstrate how the accuracy of the VS-population depends on integration time. VS-cell activity was recorded intracellularly in a panoramic high-speed virtual reality optic flow stimulator (Lindemann et al. 2003). We stimulated the fly with randomly textured patterns simulating rotations around different horizontal body-axes. Based on the recorded activities we modeled the neurons' responses to the panoramic optic flow stimuli to facilitate the further analysis. Applying a Bayesian estimator on the modeled data, we could show that the population of VS-cells can estimate the rotation axis within 10 ms after response onset with an accuracy of better than 7°. This integration time matches the time scale relevant for real self-motions of the fly. The most prominent feature of blowfly flight, fast head- and/or body saccades as well as the intersaccadic intervals, take place on a time scale of some tenths of milliseconds. (Hateren and Schilstra 1999). Hence the reliability of the population of VS-cells appears to be appropriate to extract behaviorally relevant information from the neuronal response under natural conditions.

In a replay approach, developed to play back visual stimuli generated by the flies own behavior (Kern et al. submitted), we investigate whether it is possible to reconstruct the actual horizontal rotations of the fly from the population response as suggested by our systems analysis approach.

Hateren JH, Schilstra C. Blowfly flight and optic flow. II. Head movements during flight. *J Exp Biol* (1999) 202: 1491-500.

Kern R, van Hateren J, Michaelis C, Lindemann J, Egelhaaf M. Eye movements during natural flight shape the function of a blowfly motion sensitive neuron. *Nature* (submitted).

Krapp HG, Hengstenberg R. Estimation of self-motion by optic flow processing in single visual interneurons. *Nature* (1996) 384: 463-466.

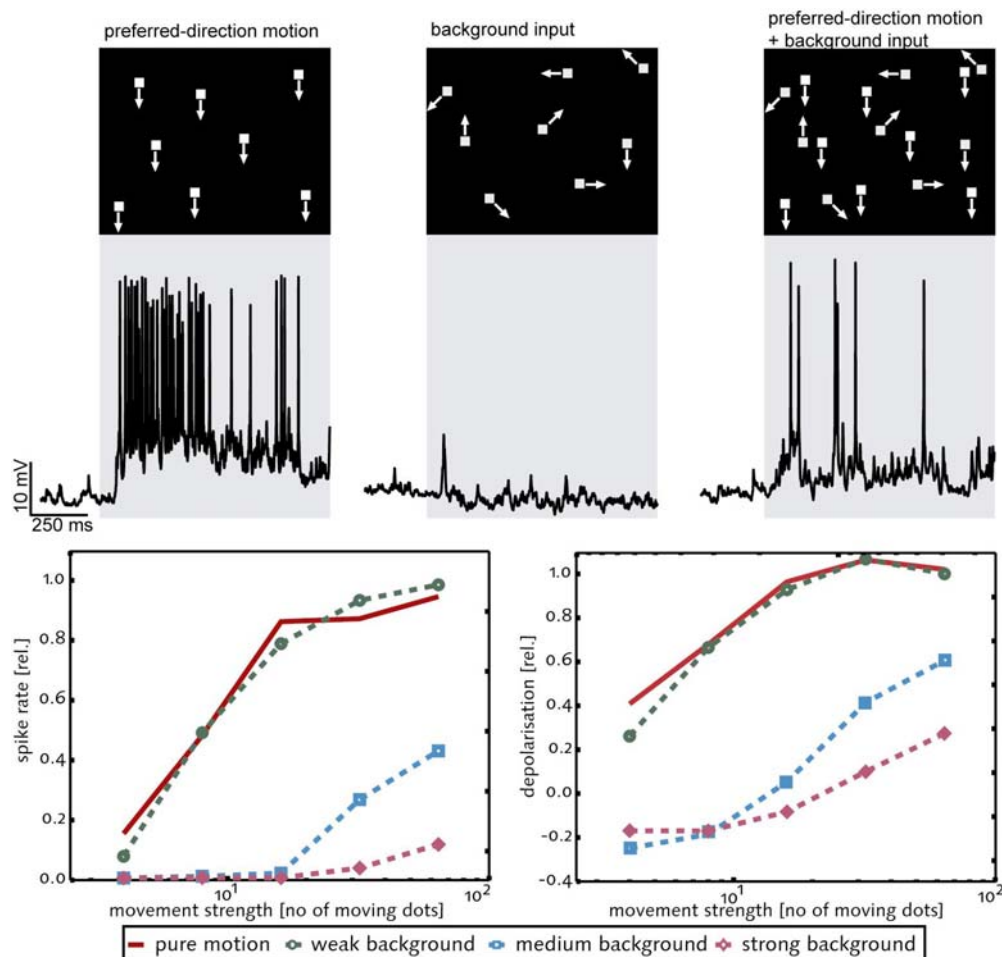
Lindemann JP, Kern R, Michaelis C, Meyer P, van Hateren JH, Egelhaaf M. FliMax, a novel stimulus device for panoramic and highspeed presentation of behaviourally generated optic flow. *Vision Res* (2003) 43: 779-91.

# Non-linear Dendritic Integration of Visual Motion Stimuli in Fly Motion-Sensitive Neurons

Jan Grewe, Nélia Matos, Martin Egelhaaf and Anne-Kathrin Warzecha  
 Department of Neurobiology, Bielefeld University, Bielefeld, Germany  
[jan.grewe@uni-bielefeld.de](mailto:jan.grewe@uni-bielefeld.de)

One of a neuron's central tasks is to integrate input signals on its dendrites and in this way extract the information needed for further processing. In the fly we can investigate how visual motion information is integrated on the dendrites of the tangential cells (TCs). The TCs receive excitatory and inhibitory input from a large number of retinotopically arranged local motion-sensitive elements. Both excitatory as well as inhibitory inputs are activated by a motion stimulus. However during preferred direction motion excitation dominates over inhibition whereas this ratio inverts during null direction motion. Motion orthogonal to the preferred direction induces an approximately equal activation of both inputs. Thus, the response amplitude of the TCs depends on the particular motion stimulus. So far, the TCs were mainly characterised by the use of stimuli that moved either in preferred or anti-preferred direction. In the freely behaving animal this is a rather unlikely situation. We therefore tested how background motion containing motion in any direction influences the representation of preferred direction motion.

We use visual stimuli that contain a group of dots moving in the cell's preferred direction combined with another group of dots that perform a random walk. This so called background input is balanced in a way that on its own it does not drive the cell. Nevertheless, we show that the background input considerably modulates the gain (see figure) but does not much deteriorate properties like direction tuning and the representation of pattern velocity. It is currently tested how the background input affects the integrating properties of the dendrite and thereby alters the way preferred direction motion is processed. This approach will be complemented by an analysis of the contribution of single moving dots.



**Symposium #S17:**  
**Genomic and Proteomic Expression Profiling in Neural Repair**  
**J. Verhaagen and HW. Müller, Amsterdam and Düsseldorf**

**Introduction**

- [#S17](#) J. Verhaagen and HW. Müller, Amsterdam and Düsseldorf  
*Genomic and Proteomic Expression Profiling in Neural Repair*

**Slide**

- [#S17-1](#) FJ. Stam, CR. Jimenez, N. Armstrong, Y. Zhang, AB. Smit and J. Verhaagen, Amsterdam (NL) and London (UK)  
*Large scale screening for regeneration-associated proteins and genes*
- [#S17-2](#) P. Küry, F. Kruse, N. Klapka, D. Abankwa, F. Bosse and HW. Müller, Düsseldorf  
*Comparison of Axotomy-Induced Neuronal Gene Expression in PNS and CNS*
- [#S17-3](#) F. Bradke, Martinsried  
*Molecular Mechanisms of Axonal Regeneration*
- [#S17-4](#) L. Dimou, FM. Bareyre, L. Montani and ME. Schwab, Zurich (CH)  
*Gene expression changes induced by blocking or ablation of Nogo-A in spinal cord and brain*

**Poster**

- [#25B](#) SP. Niclou, N. Klapka, HW. Müller, RC. van der Schors, KW. Li, AB. Smit and J. Verhaagen, Amsterdam (NL) and Düsseldorf  
*CHARACTERIZATION OF NEURITE GROWTH-INHIBITORY MOLECULES IN THE SPINAL CORD SCAR*
- [#26B](#) L. Dimou, L. Schnell, M. Gullo, M. Simonen, T. Liebscher, R. Schneider and ME. Schwab, Zurich (CH) and Basle (CH)  
*Different regeneration abilities of Nogo-A knockout animals after spinal cord injury depending on the mouse strain*
- [#27B](#) MJ. Rossner, C. Boehm, D. Newrzella, H. Hiemisch, G. Eisenhardt, C. Stuenkel, O. von Ahsen and K-A. Nave, Goettingen and Heidelberg  
*Combining GFP labelling, laser mediated microdissection and microarray analysis to snapshot the gene expression profiles of defined neuronal cell types in adult mice*

[#28B](#)

AM. Jacob, T. Ziemssen, F. Weber and CW. Turck, Munich and Dresden  
*Identification of biomarkers for Multiple Sclerosis*

## **Introductory Remarks to Symposium 17**

### **Genomic and Proteomic Expression Profiling in Neural Repair**

**Joost Verhaagen and Hans W. Müller, Amsterdam (NL) and Düsseldorf**

The study of changes in gene and protein expression at a comprehensive or (near) genome wide scale can be used to help elucidate the molecular mechanisms underlying key neurobiological events. In this symposium we will highlight the application of genomics and proteomics approaches to study the molecular response of neurons and glial cells to traumatic injury of the peripheral and central nervous system. So far, studies on the molecular biology of neuroregeneration have dealt with only single or small sets of molecules. In this symposium we will discuss key developments that allow for the first time the simultaneous study of thousands of genes and proteins in the injured nervous system.

Injury to the central nervous system (CNS) will usually result in abortive nerve sprouting and the formation of an inhibitory scar at the site of the injury. In contrast, peripheral nerve injury results in successful regeneration of injured axons over long distances, synapse formation and consequently functional recovery. The molecular changes that govern successful regeneration of the peripheral nervous system and that prevent regeneration in the CNS are very complex.

This symposium will cover the first genomics and proteomics studies that are performed to understand the molecular differences between the injured CNS and PNS. These studies have revealed differences in specific expression patterns in the innate neuronal response to CNS and PNS injury. Moreover, genomics and proteomics studies on the glia cell environment are beginning to reveal why Schwann cells or CNS glia do have a profound decisive influence on the regenerative capacity of injured axons.

## LARGE SCALE SCREENING FOR REGENERATION-ASSOCIATED PROTEINS AND GENES

Floor J. Stam<sup>1,2,5</sup>, C.R. Jiménez<sup>1</sup>, N. Armstrong<sup>3</sup>, Y. Zhang<sup>4</sup>, A.B. Smit<sup>1</sup> and J. Verhaagen<sup>1,2</sup>

<sup>1</sup>Dept. of Molecular and Cellular Neurobiology, Vrije Universiteit Amsterdam, The Netherlands.

<sup>2</sup>Workgroup Neuroregeneration, Netherlands Institute for Brain Research, Amsterdam, The Netherlands. <sup>3</sup>Dept. of Mathematics, Vrije Universiteit Amsterdam, The Netherlands. <sup>4</sup>Academic Department of Neurosurgery, Queen Mary University of London, London, UK. <sup>5</sup>Corresponding author: [fjstam@bio.vu.nl](mailto:fjstam@bio.vu.nl)

In the central nervous system, regeneration after injury is abortive, resulting in permanent damage and paralysis. In contrast, nerve injury in the peripheral nervous system leads to successful regeneration. In this study, we set out to identify factors that are specifically involved in successful regeneration.

Using a proteomics approach, we identified 82 proteins, which are differentially regulated in the growth promoting nervous tissue surrounding regenerating axons of the dorsal root ganglion (DRG) neurons at three time-points after sciatic nerve crush. Classification and cluster analysis of the expression profiles highlight the simultaneous processes of Wallerian degeneration, dedifferentiation and activation of Schwann cells and altered lipid metabolism in the nerve tissue.

Not only the environment, but also intrinsic properties of the neuron can determine the success of regeneration. For instance, DRG neurons exhibit a strong regenerative response after crush of the peripheral neurite and a slower, reduced regenerative response after injury of the central neurite. A Genomic approach was taken to compare the time-courses of transcriptional activity during unsuccessful and successful regenerative responses. Our results indicate that the cellular processes which are initiated after damage of the central or peripheral neurite are divergent already from 6hrs post-lesion onwards and that regeneration-associated genes are indeed causally related to nerve growth. These studies highlight genes that are specific to successful outgrowth and therefore might comprise important targets for genetic intervention.

## **Comparison of Axotomy-Induced Neuronal Gene Expression in PNS and CNS**

Patrick Küry, Fabian Kruse, Nicole Klapka, Daniel Abankwa, Frank Bosse and Hans Werner Müller

Molecular Neurobiology Laboratory, Department of Neurology, Heinrich-Heine-University, Düsseldorf, Germany; Corresponding author: [kuery@uni-duesseldorf.de](mailto:kuery@uni-duesseldorf.de)

In contrast to the peripheral nervous system (PNS) nerve fiber tracts of the adult central nervous system (CNS) cannot spontaneously regenerate in response to lesions. As a result injured individuals suffer from chronically impaired neuronal connections leading to major motor-, sensory- and cognitive deficits. It is generally assumed that combinatorial effects account for this regeneration failure including a growth non-permissive environment within CNS lesion zones as well as incomplete activation of axonal growth programmes. In order to investigate a) whether and how injured central nervous system neurons react to remote axonal lesions and b) such responses include regeneration-associated or growth-related genes we have applied gene expression array technology on a variety of different lesion paradigms. Early and late transcriptional responses of two central neuronal populations, the subiculum and cortex, were investigated following postcommissural fornix- and cortical spinal tract transection, respectively. These gene expression patterns were then compared to changes observed in dorsal root ganglia following sciatic nerve crush and transection in order to reveal beneficial and harmful gene activities. In addition, we have analysed changes in gene expression occurring within central nervous system lesion zones. This identified a number of so far undetected factors which relate to chronic axonal growth arrest and represent therefore promising candidates for lesion induced axonal growth inhibitors. This work was supported by grants of the German Research Council (DFG).



*Molecular Mechanisms of Axonal Regeneration*

Frank Bradke

Max-Planck-Institute of Neurobiology, Am Klopferspitz 18, 82152 Martinsried (Munich), Fax.: + 49-89-856 1121, Tel.: + 49-89-8578 3641

We used gene microarray technology to identify genes whose expression in spinal sensory neurons from adult rats is modified following procedures that can induce robust axonal growth both *in vitro* and *in vivo*. We used two different manipulations to induce axonal growth of lesioned spinal sensory neurons, (i) lesioning the peripheral branch of primary sensory axons and (ii) injecting membrane-permeable cAMP analogues. Genes that change their expression after both of these manipulations are candidate effectors of axonal growth. We tested their function by expressing these genes in dissociated primary neurons.

## **Gene expression changes induced by blocking or ablation of Nogo-A in spinal cord and brain**

Leda Dimou, Florence M. Bareyre, Laura Montani and Martin E. Schwab

Brain Research Institute, University of Zurich, and Dept. Biology, Swiss Federal Institute of Technology (ETH), Zurich, Switzerland

Regeneration of the adult central nervous system (CNS) of mammals after injury is very limited. Myelin-associated proteins like Nogo-A, the best characterized neurite outgrowth inhibitory molecule, seem to play a main role in the restricted regeneration properties of the CNS. Nogo-A neutralization by antibodies, e.g. the IN-1 antibody, or its gene ablation enhance regenerative axon growth, compensatory sprouting and functional recovery in the injured adult spinal cord and brain. In order to understand better the way of function of Nogo-A, we performed GeneChip microarray experiments with naive or lesioned rats treated with the anti-Nogo-A antibody IN-1. In the naive spinal cord, IN-1 antibody treatment was associated with upregulation of growth factors, growth related, cytoskeletal proteins and transcription factors. Unilateral lesion of the corticospinal tract (CST; pyramidotomy) and treatment with IN-1 antibody triggered compensatory reorganization of sprouts across the midline, suggesting lesion-induced CST sprouting and rewiring. On the transcription level, pyramidotomy and IN-1 led to enhanced expression of guidance molecules and neurotrophic factors/receptors. The results imply two mechanisms for compensatory sprouting after injury; first the more general growth promoting effects caused by the IN-1 antibody (blocking of Nogo-A) and secondly the modulation of guidance molecules and growth factors due to the lesion.

In order to understand the long-lasting role and function of Nogo-A, we are currently performing genomics and proteomics studies of mice lacking Nogo-A. These studies will reveal differences in specific expression patterns of neural tissues between Nogo-A knockout and wild type mice and between knockouts of different backgrounds.

# CHARACTERIZATION OF NEURITE GROWTH-INHIBITORY MOLECULES IN THE SPINAL CORD SCAR

**S.P. Niclou, N. Klapka\*, H.W. Müller\*, R.C. van der Schors<sup>+</sup>, K.W. Li<sup>+</sup>, A.B. Smit<sup>+</sup> and J. Verhaagen.** Netherlands Institute for Brain Research, Neuroregeneration Group, Amsterdam. \* Heinrich-Heine University, Department of Neurology, Düsseldorf, Germany. <sup>+</sup> Vrije Universiteit, Department of Molecular and Cellular Neurobiology, Amsterdam.

Email: s.niclou@nih.knaw.nl

Injury to the human central nervous system (CNS) leads to lasting functional deficits which is in striking contrast to the immature CNS or the peripheral nervous system (PNS) where spontaneous fiber growth and functional recovery take place. Neurons in the adult CNS are unable to regenerate, as a result of both an inhibitory environment and insufficiencies in their inherent ability to regrow. Several neurite growth inhibitory proteins have been found associated with the damaged myelin sheath and with the glial-fibroblastic scar that forms at the lesion site (Schwab, 2004; Silver and Miller, 2004). Despite evidence that glial scarring is a major culprit of regeneration failure in the CNS, there is surprisingly little knowledge on the molecules expressed in the neural scar that inhibit axonal growth. This work focuses on the identification and characterization of neurite growth inhibitory molecules expressed in the glial-fibroblastic scar of the injured spinal cord.

Using a proteomics approach based on isotope-coded affinity tag labeling (ICAT) (Gygi et al., 1999), we aim at determining the full protein composition of the glial-fibrotic scar. In a first step the protein profile of normal spinal cord scar formed after transection of the dorsal corticospinal tract will be compared with collagen-depleted scar. Collagen-depleted scar is obtained by application of cAMP together with the iron chelator 2,2-bipyridine (BPY) which results in a strong reduction of basement membrane deposition and an increase in regenerating axons through the scar area (Stichel et al., 1999; Hermanns et al., 2001). This direct comparison between a non-permissive scar and a permissive scar will allow to identify inhibitory proteins associated with the extracellular matrix of the non-permissive scar. In a second step scar tissue from adult rats will be compared to the scar of immature rats, which is morphologically very different and supports axonal regeneration. This comparison will allow to identify inhibitory molecules associated with the adult scar and growth supportive molecules that may be differentially expressed in the scar of young rats. Scar material is isolated using laser microdissection and catapulting technology in order to enrich the sample for scar material. Protein samples will be labeled with ICAT reagent (Applied Biosystems), followed by trypsin digest and separation of cysteine-containing peptides by liquid chromatography and tandem mass spectrometry (LC-MS/MS) (Li et al., 2004). This powerful technology allows sensitive protein detection and does not discriminate against proteins of high molecular weight or high hydrophobicity, which are abundant in extracellular matrix material. The molecular profile of neural scar tissue should lead to the identification of novel neurite growth inhibitory proteins and provide new targets for experimental manipulation.

1. Schwab ME. *Curr Opin Neurobiol.* 2004 Feb;14(1):118-24. Review.
2. Silver J, Miller JH. *Nat Rev Neurosci.* 2004 Feb;5(2):146-56. Review.
3. Gygi SP, Rist B, Gerber SA, Turecek F, Gelb MH, Aebersold R. *Nat Biotechnol.* 1999 Oct;17(10):994-9.
4. Stichel CC, Hermanns S, Luhmann HJ, Lausberg F, Niermann H, D'Urso D, Servos G, Hartwig HG, Müller HW. *Eur J Neurosci.* 1999; 11(2):632-46.
5. Hermanns S, Klapka N, Müller HW. *Restor Neurol Neurosci.* 2001; 19(1-2):139-48.
6. Li KW, Hornshaw MP, Van Der Schors RC, Watson R, Tate S, Casetta B, Jimenez CR, Gouwenberg Y, Gundelfinger ED, Smalla KH, Smit AB. *J Biol Chem.* 2004; 279(2):987-1002.

## **Different regeneration abilities of Nogo-A knockout animals after spinal cord injury depending on the mouse strain**

Leda Dimou<sup>1</sup>, Lisa Schnell<sup>1</sup>, Miriam Gullo<sup>1</sup>, Marjo Simonen<sup>2</sup>, Thomas Liebscher<sup>1</sup>, Regula Schneider<sup>1</sup> and Martin E. Schwab<sup>1</sup>

<sup>1</sup> Brain Research Institute, University of Zurich, and Dept. Biology, Swiss Federal Institute of Technology (ETH), Zurich, Switzerland

<sup>2</sup> Novartis Institutes for Biomedical Research, Novartis Pharma, 4000 Basle, Switzerland

Corresponding author: dimou@hifo.unizh.ch

Growth inhibition in the adult central nervous system (CNS) is a major barrier to axon regeneration. Many evidences support the crucial role of myelin-associated neurite outgrowth inhibitors in preventing CNS regeneration. Nogo-A is the best characterized neurite outgrowth inhibitory molecule found in CNS myelin; its neutralization by antibodies or its gene ablation enhance regenerative axon growth, compensatory sprouting and functional recovery. Lesion experiments with Nogo-deficient mice of three independent laboratories came to different results in terms of regeneration properties of the Nogo knockout animals. In these studies embryonic stem cells of the 129Sv strain were implanted into C57Bl/6 blastocytes resulting in mice with a mixed genetic background. To study the implication of Nogo-A in inhibition of regeneration under more defined conditions and to further understand the variation in results, we backcrossed Nogo-A knockout mice into pure 129X1/SvJ and pure C57Bl/6 backgrounds. After lesion of the corticospinal tract (CST) we observed a strong enhancement in regeneration of the Nogo-A deficient mice compared to wild type animals. The scatter among the individual animals within each group, although still high as it is known for partial spinal cord lesion models, is lower and the data therefore much more consistent than in the previous studies. Interestingly, Nogo-A deficient mice of the 129 strain showed a much higher number of fibers resulting from regeneration and arborisation of the CST than knockout Bl/6 mice. Both strains showed improved recovery of locomotion in the absence of NogoA. We believe that the contradictory results obtained in the earlier Nogo knockout studies are due to specific properties of the background mixture of the mouse lines used. The present results obtained with a Nogo-A specific knockout in two pure strains of mice demonstrate the importance of Nogo-A as an *in vivo* inhibitor of neurite growth and regeneration in the spinal cord, as well as mouse strain determinant of axonal growth.

**Combining GFP labelling, laser mediated microdissection and microarray analysis to snapshot the gene expression profiles of defined neuronal cell types in adult mice**

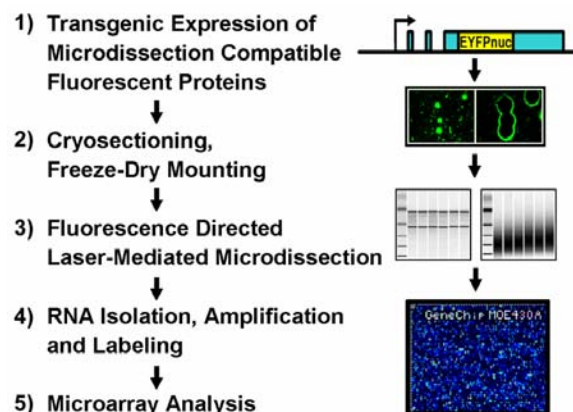
M. J. Rossner<sup>1,2\*</sup>, C. Boehm<sup>2</sup>, D. Newrzella<sup>2</sup>, H. Hiemisch<sup>2</sup>, G. Eisenhardt<sup>2</sup>, C. Stuenkel<sup>1</sup>, O. von Ahsen<sup>2</sup>, K.-A. Nave<sup>1</sup>

<sup>1</sup> MPI for Experimental Medicine, Goettingen, Germany; <sup>2</sup>Axaron Bioscience AG, Heidelberg, Germany

[rossner@em.mpg.de](mailto:rossner@em.mpg.de)

Adaptive gene expression changes play an important role in the cellular processes thought to provide the basis for learning and memory. Powerful tools for gene expression profiling at a global scale have recently been developed, which allow the simultaneous monitoring of relative mRNA abundances of thousands of genes. However, the enormous cellular complexity complicates global gene expression profiling in the brain. Physiologically or pathologically relevant gene expression changes originating from minor cell populations are unlikely to be detected, even when the tissue samples were obtained from histological defined regions. Particularly challenging is the determination of the gene expression changes correlating with adult nervous system plasticity phenomena such as learning and memory as: (I) the physiologically relevant gene expression changes in neurons are comparably low in their amplitude, (II) different neuronal and glial cell types respond highly variable to selective stimuli and (III) only a proportion of cells within a particular brain structure will respond to a specific physiological event. Dissecting gene expression changes in the brain on a global scale is even more complicated because the networks formed between neurons -the actual information storing units- are flexible assemblies.

In a first attempt to overcome some of the problems neurobiologists are faced with when trying to perform meaningful global gene expression profiling experiments, we developed a technical procedure combining the genetic labelling of neuronal cells with laser directed microdissection and microarray analysis. The experimental strategy is as follows:



This labelling strategy is fully compatible with the tissue specimen requirements for both fluorescence directed laser microdissection as well as for the isolation of intact RNA, a prerequisite for performing global transcriptome analysis with high fidelity. Comparing layer V projection neurons isolated from either motor or somato-sensory cortex, we find changes in gene expression between these two 'identical' neuronal cell types that are not detectable when analyzing the respective cortical subfields. Strikingly, in primary cortical motor neurons, besides others, clusters of ribosomal and mitochondrial genes are upregulated compared to somato-sensory neurons. This coordinated change in gene expression probably reflects the higher metabolic demand of motor neurons. We believe that our experimental approach is a first step towards the goal to map patterns of behaviourally induced electrical activity onto patterns of gene expression within neuronal assemblies in vivo.

## Identification of biomarkers for Multiple Sclerosis

A M. Jacob<sup>1</sup>, T. Ziemssen<sup>2</sup>, F. Weber<sup>1</sup>, C W. Turck<sup>1</sup>

<sup>1</sup>Max Planck Institute of Psychiatry, Munich, <sup>2</sup>Neurological University Clinic, Dresden

Proteomics, the comprehensive analysis of the protein complement of the genome of an organism, can be used to gain a better understanding of the pathology and to search for targets of disease. The main focus of this project is the characterization on the protein level of the different types and phases of *Multiple sclerosis* (MS), an autoimmune disorder of the central nervous system. *Experimental autoimmune encephalomyelitis* (EAE) is a well established animal model showing many features that resemble human MS. EAE can be induced in mice by active or passive immunization with myelin antigens. We have examined the proteome of the mouse brain and spinal cord for both passive and active models of EAE and appropriate controls, and have found several proteins specifically expressed or up or down regulated in EAE animals. In addition, we have analyzed the phosphoproteome of the two models of EAE and have identified proteins differentially regulated with regard to their phosphorylation state. Furthermore, we have extended our screening efforts to human MS brain lesions and have identified differentially expressed proteins. Interestingly, some of these proteins overlap with the proteins detected in the mouse study. In future studies we plan to analyze different disease stages in the progression of EAE in mice in order to determine protein markers that are characteristic for specific phases of the disease. Subsequently we will look for these tissue markers in the CSF of MS patients in order to define new diagnostic and therapeutic targets for MS.

**Symposium #S18:**  
**Brain-Computer-Interfaces (BCI): neuroprostheses for the paralyzed**  
**U. Strehl, Tübingen**

**Introduction**

- [#S18](#) U. Strehl, Tübingen  
*Brain-Computer-Interfaces (BCI): neuroprostheses for the paralyzed*

**Slide**

- [#S18-1](#) K-R. Müller, B. Blankertz and G. Curio, Berlin  
*Algorithms for on-line differentiation of neuroelectric activities*
- [#S18-2](#) JR. Wolpaw, Albany, NY (USA)  
*Invasive and non-invasive brain-computer interfaces using fast brain oscillations*
- [#S18-3](#) G. Pfurtscheller, Graz (A)  
*Thought-based navigation in virtual reality and control of functional electrical stimulation in tetraplegic patients*
- [#S18-4](#) N. Birbaumer, G. Widmann, C. Elger, M. Schröder, T. Hinterberger, TN. Lal, B. Schoelkopf, M. Tatagiba and D. Freudenstein, Tübingen and Bonn  
*Invasive and Non-Invasive Brain-Computer-Interfaces for Communication in Locked-in Syndrome*

**Poster**

- [#29B](#) C. Mehring, T. Ball, MP. Nawrot, A. Aertsen and A. Schulze-Bonhage, Freiburg  
*Human brain-machine interfacing based on epicortical field potentials: I. Inference of arm movement direction*
- [#30B](#) T. Ball, C. Mehring, MP. Nawrot, A. Schulze-Bonhage and A. Aertsen, Freiburg  
*Human brain-machine interfacing based on epicortical field potentials: II. Topography of directional information in frontal cortex*
- [#31B](#) MP. Nawrot, C. Mehring, A. Schulze-Bonhage, A. Aertsen and T. Ball, Freiburg  
*Human brain-machine interfacing based on epicortical field potentials: III. Spatial resolution of directional information gain and implications for the design of intracranial electrode arrays*
- [#32B](#) MP. Nawrot, C. Boucsein, Y. Seamari, C. Mehring, A. Aertsen and S. Rotter, Freiburg  
*Serial spiking statistics of cortical neurons in vivo and in vitro.*

[#33B](#)

S-W. Chen and H-C. Chen, Taoyuan (RC)

*Damped Exponential Modeling for Feature Extraction of Self-controlled Brain Waves*



## **Introductory Remarks to Symposium 18**

### **Brain-Computer-Interfaces (BCI): neuroprostheses for the paralyzed**

**Ute Strehl, Tübingen**

Recent advances in invasive and non-invasive self-control of neuroelectric activities using EEG and ECoG and in animals cellular recordings lead to the development of different types of BCIs for communication in locked-in-patients and first steps in the application of BCIs for motor paralysis after spinal cord lesions. Patients learn to produce differential brain responses to select letters, words or motor activities from a computer menu. Slow cortical potentials, mu-rhythm of the EEG, high-frequency beta and gamma-oscillations and extracellular field potentials in animals are classified on-line with fast algorithm differentiating the neuroelectric activities in such a way to allow flexible production of one or several brain signals.

The symposium presents the most recent advances in the BCI-field for application in human neurological disorders and provides the audience with an overview of the possibilities of thought-translation and neuronal learning mechanisms underlying direct brain control.

## Algorithms for on-line Differentiation of Neuroelectric Activities

Klaus-Robert Müller<sup>1,2</sup>, Benjamin Blankertz<sup>1</sup> and Gabriel Curio<sup>3</sup>

<sup>1</sup>Fraunhofer FIRST.IDA, Kekuléstr. 7, 12 489 Berlin, Germany

<sup>2</sup>University of Potsdam, August-Bebel-Str. 89, 14 482 Potsdam, Germany  
Dept. of Neurology, Campus Benjamin Franklin, Charité University Medicine Berlin,  
Hindenburgdamm 30, 12 203 Berlin, Germany  
{klaus,blankertz}@first.fhg.de, curio@zedat.fu-berlin.de

Brain Computer Interfacing (BCI) aims at making use of brain signals for e.g. the control of objects, spelling, gaming and so on. This talk will first provide a very brief overview of Brain Computer Interfacing from a machine learning and signal processing perspective. In particular it shows the wealth, the complexity and the difficulties of the data available, a truly enormous challenge: In real-time a multi-variate very strongly noise contaminated data stream is to be processed and neuroelectric activities are to be accurately differentiated.

Finally, we report in more details about the Berlin Brain Computer (BBCI) Interface that is based on EEG signals and take the audience all the way from the measured signal, the preprocessing and filtering, the classification to the respective application (e.g. gaming).

1. Müller, K.-R., Kohlmorgen, J., Ziehe, A., Blankertz, B., Decomposition Algorithms for Analyzing Brain Signals, *IEEE Symposium 2000 on adaptive Systems for Signal Processing, Communications and Control*, (eds.) S. Haykin and J. Principe, IEEE Publishing, Piscataway, NJ, 105-110 (2000)
2. Müller, K.-R., Mika, S., Rätsch, G., Tsuda, K., Schölkopf, B., An Introduction to Kernel-Based Learning Algorithms, *IEEE Transactions on Neural Networks*, 2 (2), 181-201 (2001)
3. Blankertz, B., Curio, G., Müller, K.-R. (2002), Classifying Single Trial EEG: Towards Brain Computer Interfacing, *Advances in Neural Information Processing Systems 14*, eds. T.G. Dietterich, S. Becker and Z. Ghahramani, MIT Press: Cambridge, MA, 157-164.
4. Blankertz, B., Dornhege, G., Schäfer, C., Krepki, R., Kohlmorgen, J., Müller, K.-R., Kunzmann, V., Losch, F., Curio, G., BCI bit rates and error detection for fast-pace motor commands based on single-trial EEG analysis, *IEEE Transactions on Neural Systems and Rehabilitation Engineering*, June, 11(2), 127-131 (2003)
5. Dornhege, G., Blankertz, B., Curio, G., Müller, K.-R., Boosting Bit Rates in Noninvasive EEG Single-Trial Classifications by Feature Combination and Multi-class Paradigms, *IEEE Transactions on Biomedical Engineering*, 51, 6, 993-1002 (2004)
6. Müller, K.-R., Krauledat, M., Dornhege, G., Curio, G., Blankertz, B., Machine Learning Techniques for Brain-Computer Interfaces, *Biomedizinische Technik – Biomedical Engineering* (invited paper), to appear (2004)

The studies were partly supported by the *Bundesministerium fr Bildung und Forschung* (BMBF), FKZ 01IBB02A and FKZ 01IBB02B, by the *Deutsche Forschungsgemeinschaft* (DFG), FOR 375/B1 and the PASCAL Network of Excellence, EU # 506778.

**Invasive and non-invasive brain- computer interfaces using fast brain oscillations**

*Jonathan R. Wolpaw*

Laboratory of Nervous System Disorders, Wadsworth Center, New York State Department of Health and State University of New York, Albany, New York, USA

Recent advances in invasive and non-invasive self-control of neuroelectric activities using EEG and ECoG and in animals cellular recordings lead to the development of different types of BCIs for communication in locked-in-patients and first steps in the application of BCIs for motor paralysis after spinal cord lesions. Patients learn to produce differential brain responses to select letters, words or motor activities from a computer menu. Slow cortical potentials, mu-rhythm of the EEG, high-frequency beta and gamma-oscillations and extracellular field potentials in animals are classified on-line with fast algorithm differentiating the neuroelectric activities in such a way to allow flexible production of one or several brain signals.

The symposium presents the most recent advances in the BCI-field for application in human neurological disorders and provides the audience with an overview of the possibilities of thought-translation and neuronal learning mechanisms underlying direct brain control.

**Thought-based navigation in virtual reality and control of functional electrical stimulation in tetraplegic patients**

**G. Pfurtscheller**  
**Institute of Human-Computer Interfaces**  
**Graz University of Technology**  
**e-mail: [pfurtscheller@tugraz.at](mailto:pfurtscheller@tugraz.at)**

**For design and realization of a Brain-Computer Interface (BCI) the following components are of importance: Type of signal recording (invasive or non-invasive), type of brain signal (ERP or ERD/ERS), mode of operation (cued or uncued), type of mental strategy (operation conditioning, focused attention, motor imagery), presentation of feedback (1-D, 2-D, 3-D) and last but not least signal processing including feature extraction and classification.**

**We report on two BCI applications. First, the asynchronous (uncued) control of the functional electrical stimulation with the goal to restore hand grasp in 2 tetraplegic patients and second the synchronous (cue-based) control of “walking” in the virtual environment (VE). In both cases motor imagery was used as mental strategy and 2 (3) EEG channels were online analyzed. In both applications the feedback was given by viewing a moving object (hand grasp, avatar in the VE). One question is whether this visual feedback by observation of moving objects has an impact on sensorimotor rhythms. We will demonstrate that the viewing of a moving object can modify brain oscillations dependent on the type of moving object.**

## **Invasive and Non-Invasive Brain-Computer-Interfaces for Communication in Locked-in Syndrome**

Niels Birbaumer<sup>1,2</sup>, Guido Widmann<sup>3</sup>, Christian Elger<sup>3</sup>, Michael Schröder<sup>4</sup>, Thilo Hinterberger<sup>1</sup>, Thomas Navin Lal<sup>5</sup>, Bernhard Schoelkopf<sup>5</sup>, Marcos Tatagiba<sup>6</sup>, Dirk Freudenstein<sup>6</sup>

<sup>1</sup> Institute of Medical Psychology and Behavioral Neurobiology, University of Tübingen, Germany

<sup>2</sup> Center for Cognitive Neuroscience, University of Trento, Italy

<sup>3</sup> Epilepsy Clinic, University of Bonn, Germany

<sup>4</sup> Department Technische Informatik at the Wilhelm Schickard Institute of the University of Tübingen, Germany

<sup>5</sup> Max-Planck-Institute of Biological Cybernetics, Tübingen, Germany

<sup>6</sup> Clinic of Neurosurgery, University of Tübingen, Germany

A brain-computer-interface (BCI) based on voluntary regulation of slow cortical potentials (SCP) or mu-rhythm was developed and tested on 12 patients with advanced amyotrophic lateral sclerosis (ALS) and three patients with a complete locked-in-syndrome. All patients with advanced ALS were able to learn to regulate their neuroelectric brain activity and use the regulation-skill to select letters, words or commands from a computer menu with their own brain response. None of the 3 patients who started training with a complete locked-in syndrome learned to spell words with their brain response. Only unreliable affirmative signals were possible. Therefore an invasive BCI was tested with 4 epilepsy patients with presurgically implanted electrode grids over centro-frontal brain areas. The invasive implanted BCI is based on support vector machine (SVM) automatic classification of electrocorticographic (ECoG) activity ranging from 1-100 Hz during motor imagery of hand and tongue movements. After successful classification (>80% correct) patients copied words by selecting letters with their ECoG-activity from a computer menu using the pretrained imagery. Spelling was possible within one to two hours training after SVM-classification. In an ALS patient with complete locked-in syndrome who was trained unsuccessfully with the noninvasive BCI the same 64 electrode-grid was implanted over left centrofrontal areas. After a short training period with the SVM based BCI communication was achieved with a special auditory spelling device.

These data suggest that direct brain communication is possible in paralyzed patients. Completely locked-in patients may, however, need an invasive BCI based on ECoG. For the first time, communication with all types of locked-in patients seems possible.

Supported by the Deutsche Forschungsgemeinschaft (DFG) and the Max-Planck-Institute of Biological Cybernetics.

## ***Human brain-machine interfacing based on epicortical field potentials: I. Inference of arm movement direction***

C. Mehring<sup>1</sup>, T. Ball<sup>2</sup>, M.P. Nawrot<sup>3</sup>, A. Aertsen<sup>3</sup>, A. Schulze-Bonhage<sup>2</sup>

<sup>1</sup>Institute for Biology I, Albert-Ludwigs-University Freiburg, Germany

<sup>2</sup>Epilepsy Center, University Clinics, Albert-Ludwigs-University Freiburg, Germany

<sup>3</sup>Institute for Biology III, Albert-Ludwigs-University Freiburg, Germany

Currently, great efforts are being made towards implantable brain-machine interfaces (BMIs) recording and decoding neuronal activity directly from the human brain. Here and in two companion posters (Ball et al., Nawrot et al., this Volume) we address currently still open questions that need to be resolved when developing such BMIs for clinical use in humans. To this end, we recorded epicortical field potentials (EFP) with dense electrode arrays (up to 112 electrode contacts, 7mm spacing) while subjects performed center-out arm reaching movements in four directions. Movement related EFPs and power spectra of EFPs were off-line decoded on a single-trial basis. Here we show: (1) The direction of arm reaching movements can be accurately inferred from neuronal population activity of the human frontal lobe. (2) Single-trial movement inference can be achieved by decoding activity from electrodes placed directly on the brain surface, presenting an alternative approach to previous animal models of BMIs using electrodes penetrating, and thus disrupting, intact brain tissue.

Taken together, our results indicate that epicortical field potentials from human frontal cortex may provide a control signal for neuronal motor prostheses with a minimal risk of lesioning brain tissue.

Supported by the Heidelberg Academy of Science and Humanities and BMBF-DIP

## ***Human brain-machine interfacing based on epicortical field potentials: II. Topography of directional information in frontal cortex***

T. Ball<sup>1</sup>, C. Mehring<sup>2</sup>, M.P. Nawrot<sup>3</sup>, A. Schulze-Bonhage<sup>1</sup>, A. Aertsen<sup>3</sup>

<sup>1</sup>Epilepsy Center, University Clinics, Albert-Ludwigs-University Freiburg, Germany

<sup>2</sup>Institute for Biology I, Albert-Ludwigs-University Freiburg, Germany

<sup>3</sup>Institute for Biology III, Albert-Ludwigs-University Freiburg, Germany

Recordings of epicortical field potentials (EFPs) using implanted electrodes for brain-machine interface applications offer an attractive alternative to intracortical electrodes (see also companion posters by Mehring et al., Nawrot et al., this Volume). We used densely spaced electrode grids of up to 112 electrodes covering an area of approx 7 cm x 7 cm to record EFPs from subjects performing center out arm movements in four directions and index finger flexion movements. We decoded movement related potentials on a single-trial basis.

We found a gradient of directional information from primary motor cortex (M1) over premotor cortex (PM) to the prefrontal cortex (PF), constituting a new aspect of the generally assumed functional gradient of motor functions in human frontal cortex, with M1 most closely related to encoding of kinematic movement parameters, and PM and PF preferentially involved in higher-order motor functions and more cognitive aspects of motor control, respectively. Further, we investigated the detailed spatial distribution of directional information and of information about finger movements. These maps revealed a fine-grained structure: for center-out movements highest information was found in the region of cortex showing hand and arm motor responses upon direct electrical stimulation through the implanted electrodes. Likewise, for finger flexion maximal information about movement was located at the electrodes eliciting index finger movements.

In summary, our results show that M1 is best suited for decoding information about arm and finger movements, but also PM and PF carry significant information about voluntary movements. This suggests that PM and PF may be useful as an alternative to M1 in case of pathological alterations of M1.

Supported by the Heidelberg Academy of Science and Humanities and BMBF-DIP

***Human brain-machine interfacing based on epicortical field potentials: III. Spatial resolution of directional information gain and implications for the design of intracranial electrode arrays***

M.P. Nawrot<sup>1</sup>, C. Mehring<sup>2</sup>, A. Schulze-Bonhage<sup>3</sup>, A. Aertsen<sup>2</sup>, T. Ball<sup>3</sup>

<sup>1</sup>Institute for Biology III, Albert-Ludwigs-University Freiburg, Germany

<sup>2</sup>Institute for Biology I, Albert-Ludwigs-University Freiburg, Germany

<sup>3</sup>Epilepsy Center, University Clinics, Albert-Ludwigs-University Freiburg, Germany

Epicortical field potentials (EFPs) are an attractive candidate signal for interfacing the human cerebral cortex with external devices (see also companion posters by Mehring et al., Ball et al., this Volume). Here, we address the issue of optimal electrode array layout to record EFPs for brain-machine interfaces (BMI). We recorded EFPs from human frontal cortex during a center-out reaching movement paradigm. Signal relations and directional information were analyzed to probe at which spatial scale the information content of EFPs becomes highly redundant.

We found a statistically significant and substantial gain of decoded information for simultaneously recorded EFPs from densely spaced electrodes above motor cortex, even for the smallest used inter-electrode distance of about 7 mm. Our results show that very dense spatial sampling of cortical field potentials is an effective means to increase decodable information. Development of densely spaced subdural electrode arrays optimized for BMI purposes therefore presents an important future direction to fully appreciate the potential of BMI solutions based on EFP recordings made directly from the human brain surface.

Supported by the Heidelberg Academy of Science and Humanities and BMBF-DIP



# Serial spiking statistics of cortical neurons *in vivo* and *in vitro*.

Martin P. Nawrot<sup>1</sup>, Clemens Boucsein<sup>1</sup>, Yamina Seamari<sup>1</sup>,  
Carsten Mehring<sup>2</sup>, Ad Aertsen<sup>1</sup>, Stefan Rotter<sup>1,3</sup>

<sup>1</sup> Neurobiology & Biophysics, Biology III, Albert-Ludwigs-University, Freiburg, Germany

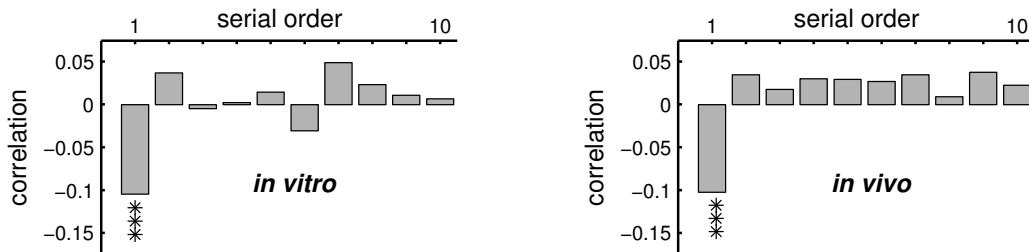
<sup>2</sup> Neurobiology & Animal Physiology, Biology I, Albert-Ludwigs-University, Freiburg, Germany

<sup>3</sup> Theory & Data Analysis, Institute for Frontier Areas of Psychology and Mental Health, Freiburg, Germany

In the intact brain, neocortical neurons exhibit a spiking behaviour that is often best described as a stochastic point process. In particular, renewal processes are commonly used as mathematical models for neuronal spiking in neocortex. There, intervals between successive events (action potentials) are independently and identically distributed (i.i.d.) according to a fixed interval distribution that completely defines the stochastic properties of the process. The most fundamental renewal process is the Poisson process with an exponential interval distribution. Further prominent examples are the gamma-type renewal process and the integrate-and-fire neuron with stationary Poisson inputs [1]. Extension to the rate-modulated renewal process, as e.g. in the inhomogenous Poisson model, allows to account for temporal modulations of the neuronal firing rate [2,3].

Here, we first tested to which extent cortical neurons satisfy the renewal assumption by measuring the serial correlation in experimental spike trains *in vitro* and *in vivo*. Second, we estimated the dependency of the instantaneous spiking probability on the previous spiking history. In extension to the rate-modulated renewal process, we propose a new class of models which allow to parameterize serial interval dependencies. The *in vitro* data were collected in intracellular whole-cell patch clamp recordings from pyramidal cells in acute slices of rat somatosensory cortex. Neurons were stimulated for up to 20 minutes by injecting dynamic current traces mimicking balanced excitatory and inhibitory synaptic input. *In vivo* intracellular recordings were made in the prefrontal cortex of anesthetized rats.

We found that a large portion of the investigated neurons, both *in vitro* and *in vivo*, exhibited a small but significant negative first-order serial correlation of successive inter-spike intervals (c.f. Figure), marking a clear deviation from the renewal model. Higher-order correlations did not significantly deviate from 0.



Typical examples with significant ( $P < 10^{-3}$ ) negative serial rank-order correlation of order 1 (neighbouring ISIs).

To further characterize the dependence of the instantaneous spike probability on the process history we studied the following more general model [2,3], with the overall process intensity (spike rate)

$$f(t, t_0, t_{-1}) = \lambda(t) \cdot f_0(t - t_0) \cdot f_{-1}(t - t_{-1}) \quad (1)$$

composed of three independent deterministic intensities:  $\lambda(t)$  describes the explicit rate function which modulates the firing probability independently of process history,  $f_0(t, t_0)$  describes the dependence of firing probability on the time elapsed since the previous spike at  $t_0$ , and  $f_{-1}(t, t_{-1})$  denotes the dependence on the time since the penultimate spike at  $t_{-1}$ . For a renewal process,  $\lambda = 1$  and  $f_{-1} = 1$ , and  $f_0$  is called the hazard function. We performed a non-parametric fit of the model (1) to our data. Based on the resulting probability function  $f(t, t_0, t_1)$  we propose a new parametric model family that incorporates the process history up to the penultimate spike.

Supported in parts by the Heidelberg Academy of Science and Humanities and GIF

[1] Tuckwell (1988) Introduction to Theoretical Neurobiology, Vol. 2, Cambridge University Press

[2] Kaas and Ventura (2001) A Spike-Probability Model. Neural Computation 13: 1713-1720

[3] Brown et al. (2001) The time-rescaling theorem and its application to neural spike train data analysis. Neural Computation 14: 325-346

# Damped Exponential Modeling for Feature Extraction of Self-controlled Brain Waves

Szi-Wen Chen and Hsiao-Chen Chen

Department of Electronic Engineering, Chang Gung University, Taiwan

## I. INTRODUCTION

The development of *electroencephalogram* (EEG) has made physicians and neuroscientists be able to understand more about brain functions and neuroscience-related areas. In addition, in the past few decades researchers also found that it is achievable for paralyzed patients to direct/indirect control the amplitudes of their own EEG rhythms if appropriate training is given. This serves as the basis of *brain computer interface* (BCI), a completely new communication modality that does not depend on neuromuscular pathways. In fact, BCI development is a complex problem and depends on close interdisciplinary cooperation. This abstract stresses on the issue in signal processing based feature extraction; a *damped exponential* (DE) modeling algorithm is proposed for extracting features from self-controlled brain waves in a cursor movement experiment. The advantage of the algorithm is that it gives higher frequency resolution than conventional FFT or *autoregressive* (AR) methods. This improved resolution capability may yield more accurate frequency mode estimates as well as subject-specific spectral patterns to account for the brain states when a subject intends to move a cursor. The proposed algorithm was evaluated against the data set IIa provided by the BCI competition 2003.

## II. METHODOLOGY

Given a set of  $N$ -point EEG sequences  $\{s_i(n)\}_{n=0}^{N-1}$  a “multi-snapshot” DE modeling over these sequences is expressed as

$$s_i(n) = \sum_{k=1}^p A_{i,k} \lambda_k^n + e_i(n), \quad n = 0, \dots, N-1, \quad i = 1, \dots, 5, \quad (1)$$

where  $\{\lambda_k\}_{k=1}^p$  and  $\{A_{i,k}\}_{k=1}^p$  represent the DE *poles* and *amplitudes*, respectively;  $\{e_i(n)\}_{n=0}^{N-1}$  is the residual error, which is assumed *uncorrelated* with the modeled component.  $s_1(n), s_2(n), s_3(n), s_4(n), s_5(n)$  represent a set of digitized EEG recordings measured from the five electrode designations just above the sensorimotor cortex: C<sub>3</sub>, CP<sub>5</sub>, CP<sub>3</sub>, CP<sub>1</sub>, and P<sub>3</sub>, respectively. From (1) we may see that all the five EEG signals (or snapshots) are modeled simultaneously using *common poles but different amplitudes*. Basically, this application lies in an assumption that a particular brain state, *e.g.*, intent of cursor movement, can be approximately represented by a subspace spanned by all or part of the common poles. The common poles can be alternatively referred to as the common spectral patterns. Therefore, intents such as making cursor go up or down may be reflected simply by magnitudes of the complex amplitudes associated with these poles. The feature extraction algorithm is performed in the following manners. During the training phase, the modeling parameters in (1) are first estimated by a *total least squares* (TLS) technique. For each subject a number of common poles corresponding to the  $\mu$  wave (8-12 Hz) and/or  $\beta$  wave (18-24 Hz) bands are found at this stage. Secondly, the most significant *four* DE poles are then selected to form a set of the common spectral patterns used for representing the brain state for the subject. Thirdly, the amplitudes  $A_{i,k}$  can be then estimated by projecting the original EEG signals onto the spectral patterns obtained after training phase simply using the standard least squares algorithm. An average of the absolute values of the estimated amplitudes corresponding to the five

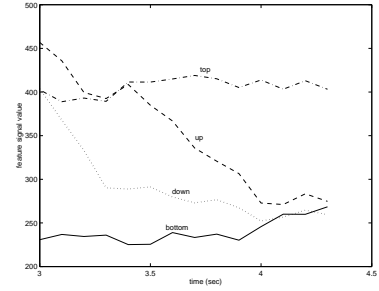


Fig. 1. Continuous feature signal monitoring during feedback for the four targets. Note each curve was generated by taking an average over 48 trials.

designated channels can be then used to define a feature signal for the cursor movement control.

## III. PERFORMANCE EVALUATION AND CONCLUSION

The EEG used in this research is provided by BCI competition 2003. EEG was recorded from 64 scalp electrodes (Sharbrough *et al.* 1991) at sampling rate of 160 Hz during an experiment of the following trail design. After staying blank for 1 s, a target appears on the right side of the screen in one of the four possible position: *top*, *up*, *down*, or *bottom*, at the following second. Later, a cursor shows on the left side of the screen and moves continuously from left to right. The aim of the subject is to steer the cursor such that the result target coincides with the target indicated at the beginning of the trail. Note that in our study the spectral patterns were built only using the training classes *top* and *bottom*. A training session consists of 192 trials and each target position was randomly assigned into 48 trials in a session. Table I gives the four predominant DE poles obtained after training on the EEG data recorded from subject A in session 3 (AA003.mat). From the table we may see that the predominant frequency components for subject A undergoing the cursor movement experiment mostly fell into the  $\mu$  wave band. Further, to evaluate the capability of continuous feedback classification a simulation task was performed as follows. Each one of the five EEG channels in the time interval [2,4.3] s during feedback was divided into 14 overlapping short segments (length = 1 s, overlap = 0.1 s). Next, all segments on the same time interval from the five channels were modeled by the common DE poles as given by Table I. Then, the feature signal corresponding to each 1 s interval was generated simply by taking an average of the absolute values of the estimated amplitudes over the five segments. Fig. 1 provides a demonstrative plot for target classification. In conclusion, according to the preliminary results we may speculate that the DE modeling might possess good potentials in developing innovative features for BCI systems.

TABLE I  
THE PREDOMINANT DE POLES OBTAINED AFTER TRAINING.

DE poles $\lambda_k$	frequency (Hz)
$\lambda_{1,2} = 0.8941 \mp j0.4553$	$\mp 11.9951$
$\lambda_{3,4} = 0.8890 \mp j0.4696$	$\mp 12.3757$

**Symposium #S19:**  
**Neural mechanisms of visual perception and learning in man and monkey**  
**G. Rainer, Tübingen**

**Introduction**

- [#S19](#) G. Rainer, Tübingen  
*Neural mechanisms of visual perception and learning in man and monkey*

**Slide**

- [#S19-1](#) MW. Greenlee, Regensburg  
*Neural correlates of visual exploration: Event-related fMRI analysis of eye movements during visual search*
- [#S19-2](#) A. Ishai, Zurich (CH)  
*fMRI studies of face perception and memory*
- [#S19-3](#) B. Röder, L. Demuth, C. Spence and F. Rösler, Hamburg, Oxford (UK) and Marburg  
*Functional recovery after visual deprivation in early childhood*
- [#S19-4](#) R. Vogels, Leuven (B)  
*Stimulus selectivities and effects of perceptual learning in macaque inferior temporal cortex*
- [#S19-5](#) L. Chelazzi, Verona (I)  
*From perception to action in the activity of macaque V4 and 7a neurons*
- [#S19-6](#) G. Rainer, Tuebingen  
*Neural Correlates of Learning in Primate Visual and Prefrontal Cortex*

**Poster**

- [#34B](#) S. Ohlendorf, O. Speck, S. Haller and H. Kimmig, Freiburg, Basel (CH) and Luebeck  
*Smooth pursuit eye movements: FMRI studies on sensory and motor components of their cortical control, covert shifts of attention and their influences on cortical activations*
- [#35B](#) K. Boelmans, H-J. Heinze, S.J. Luck and J-M. Hopf, Magdeburg and Iowa City, IA (USA)  
*Does feature-based attention operate at ignored locations?*

- [#36B](#) A. Maye, M. Werning, P. König and AK. Engel, Berlin, Düsseldorf, Osnabrück and Hamburg  
*Advancing Dynamic Binding Theory: Implementation of Complex Concepts*
- [#37B](#) A. Alfaro-Sáez, R. Climent, H. Vilanova, L. Concepción, M. Bongard and E. Fernández, Alicante (E)  
*VISUAL PERCEPTIONS IN BLIND: FROM SENSORY DEPRIVATION TO VISUAL ACTIVITY.*
- [#38B](#) F. Michler and R. Eckhorn, Marburg  
*Sequence learning as a base for object invariance coding in a network of spiking neurons*
- [#39B](#) T. Zwickel and R. Eckhorn, Marburg  
*A recurrent neural network encoding border ownership of visual objects*

## **Introductory Remarks to Symposium 19**

### **Neural mechanisms of visual perception and learning in man and monkey**

**Gregor Rainer, Tuebingen**

Vision is an active process, during which behaviourally relevant information is extracted from the visual environment and made available to guide actions. Understanding the neural underpinnings of visually based behaviour remains a key subject of investigation in systems neuroscience. One area of recent progress has been the documentation that the visual system does not remain static during adult life, but is instead subject to continuous experience dependent modification and optimization involving neural plasticity at different levels of the visual system, as well as recurrent feedback among areas. The particular past experience of each individual thus shapes how incoming sensory signals are processed and analyzed. It has also become apparent that a comprehensive understanding of visual processing must include investigations of how visual areas interact with other brain regions such as parietal and frontal areas involved in controlling information flow through sensory areas and in generating plans or actions based on visual information.

In this symposium, we present a multidisciplinary view of recent advances in our understanding of how visual signals are analyzed and used to guide behaviour. We will begin by focusing on neural mechanisms at the level of brain networks using functional imaging in human subjects, and on studies in humans of recovery of function after deprivation. Mark Greenlee will use fMRI to explore visual and eye-movement related signals during visual search focusing on effects on parietal and frontal brain areas. Alomit Ishai will examine the nature of object representation in human visual cortex using fMRI, and also the interaction between visual and fronto-parietal brain regions during imagery. Brigitte Roeder will explore how plasticity in the visual system can aid recovery of visual functions after sensory deprivation. The remaining presentations will focus on neural mechanisms at the level of single neurons using extracellular electrophysiological recording in awake behaving monkeys. Rufin Vogels describe how learning changes the responses of neurons to visual stimuli in the monkey inferior temporal cortex, and relate these changes to behavioral improvements in processing these learned patterns. Leonardo Chelazzi then will then discuss recent results on the relationship between visual and parietal cortex as sensory signals are transformed to actions, and finally Gregor Rainer will examine learning-related changes in distinct regions of prefrontal and visual cortex, showing that neural activity is modified in a qualitatively different manner in these two regions.

Neural correlates of visual exploration: Event-related fMRI analysis of eye movements during visual search  
Mark W. Greenlee

Visual exploration is an active process involving sensory and motor control components. Using functional MRI we have studied the neural correlates of saccadic eye movements in various visual search tasks. By comparing the BOLD responses evoked during steady fixation to that found for conditions requiring the subjects to saccade to visual targets, we assessed the role of oculomotor and associational cortical areas in different tasks. In these tasks subjects followed a visual cue to execute or inhibit a saccade (Go-NoGo), or they followed an internal rule to move their eyes or their attention to specific locations in space. We also compare these visually guided tasks to memory- or self-guided tasks, in which the subject saccades to remembered locations in the dark. Comparison of the resulting patterns of activation indicate that areas in and beyond eloquent “oculomotor” cortex underlie our ability to direct attention, and our eyes, to locations of interest within the visual field.

## fMRI Studies of Face Perception and Memory

Alumit Ishai, Ph.D.

Institute of Neuroradiology, University of Zurich

The functional architecture of the human ventral visual pathway is a matter of ongoing debate (e.g., are faces and objects represented and processed in a modular or distributed fashion?) In this talk I will discuss fMRI studies suggesting that the representation of faces and other objects is not restricted to small, highly selective patches of cortex but, instead, is distributed across a broad expanse of cortex. (Ishai et al., 1999, PNAS; Ishai et al., 2000, Journal of Cognitive Neuroscience). Moreover, I will show that visual imagery of faces and objects stored in long-term memory is mediated by content-specific activation in extrastriate cortex, and controlled by a “top-down” network of parietal and frontal regions (Ishai et al., 2000, Neuron; Ishai et al., 2002, NeuroImage, Mechelli et al., 2004, Cerebral Cortex). Finally, I will show that within a network of face-responsive regions, emotional faces, as compared with neutral faces, are processed faster and their cortical representations are enhanced (Ishai et al., 2004, PNAS).

### Functional recovery after visual deprivation in early childhood

Brigitte Röder 1, Lisa Demuth 1, Charles Spence 2, Frank Rösler 3.

University of Hamburg (Germany), Biological Psychology and Neuropsychology

2 University of Oxford (U.K.), Experimental Psychology

3 University of Marburg (Germany), Experimental and Biological Psychology

There are two main views how multisensory functions emerge: (1) the different senses develop independently and the links between modalities and integration across senses gradually emerge after the single senses have differentiated; (2) the different senses are initially linked and a separation between modality processing streams emerges later. The visual deprivation model provides a unique opportunity to study the role of sensory experience for both visual and multisensory functions. We have investigated congenitally and late blind people and demonstrated that the lack of vision does not only lead to a compensatory improvement within the intact senses but also to changes in the interaction between the latter. Moreover, people born with bilateral dense cataracts were investigated to study the consequences of congenital, temporally limited visual deprivation in humans. When the visual deprivation lasted longer than six months we found that higher visual functions as the perception of illusory contours were impaired. While elementary multisensory processes as the redundancy reaction time gains from visual-auditory and visual-tactile stimulation were similar in cataract patients and controls more complex multisensory processes as audio-visual speech perception were reduced. These results are in accordance with the view that sensory experience shapes not only perception within single modalities but also the interaction between different senses. It may therefore be concluded that the development of the different senses is not completely independent and that the emergence of specific multisensory functions requires adequate experience during development.



**Stimulus selectivities and effects of perceptual learning in macaque inferior temporal cortex**

Rufin Vogels

Laboratory for Neuro- and Psychophysiology  
Catholic University Leuven,  
Herestraat 49,  
B-3000 Leuven, Belgium

Previous studies have shown that extensive experience with complex objects changes the selectivity of neurons in macaque inferior temporal (IT) cortex. We used a backward masking paradigm to investigate the relation between these neurophysiological effects and behavioural improvements. Training to recognize backward masked objects was associated with an object-specific increase in object selectivity of IT neurons, at least if the behavioural effect of training was partly object-specific. Furthermore, training lead to a strong reduction of responses to the mask patterns, an effect that might underlie the substantial object-aspecific part of the behavioural training effect. These two neurophysiological effects of training, increased object selectivity and reduced mask responses, seemed to be associated with behavioural effects, while a third effect of training, lower responses to trained than to untrained objects, was not. We conclude that training resulted in neurophysiological changes that represent the specific constraints posed by rendering objects hardly visible by backward masking.

## **From perception to action in the activity of macaque V4 and 7a neurons**

Leonardo Chelazzi

Department of Neurological and Vision Sciences, Section of Physiology  
University of Verona, Strada Le Grazie 8, 37134 Verona, ITALY

Goal-oriented behaviour requires that task-relevant sensory information is selected for further processing, while irrelevant and potentially distracting information is filtered out – the realm of visual selective attention. Visual selective attention is known to modulate activity in primate visual cortex under a variety of conditions. For example, attention directed to spatial locations and to target objects enhances responses to attended compared to ignored visual input. In a series of experiments we investigated whether activity in primate area V4 and 7a can also be modulated by selective attention to the component features of a multidimensional visual object when advantageous to the current task. Animals were trained to discriminate either the colour or the orientation of a coloured oriented bar, and we measured responses of single V4 and 7a neurons to stimuli presented inside their receptive field (RF) when one vs. the other feature of the stimulus was task relevant. One prediction was that selectivity of V4 neurons for a given stimulus feature might be enhanced when that feature was to be discriminated vs. when the same feature was task irrelevant. Contrary to this prediction, only a few V4 cells changed their pattern of selectivity as a function of the required discrimination. Instead, activity shortly after onset of the RF stimulus reflected whichever feature was capable of driving the neuron's response, regardless of task. However, for many V4 cells, activity in a later phase of the trial developed to encode which of two alternative behavioural responses was required by the relevant stimulus feature. A second prediction was that 7a neurons might display selectivity for a given stimulus feature only when such feature was relevant for task performance. In keeping with this prediction, many 7a neurons were selective for a specific feature of the stimulus, but only when it was relevant in a given trial. Moreover, similar to V4 neurons, many 7a neurons encoded the behavioural response required by the relevant stimulus feature in a late portion of the trial. Thus, it appears that feature-selective attention can exert profound effects on neural activity in both the ventral and dorsal streams of cortical visual processing, allowing flexible and selective perception-to-action coupling.

## Neural Correlates of Learning in Primate Visual and Prefrontal Cortex

Gregor Rainer

Max Planck Institute for biological cybernetics, Tuebingen, Germany

### Abstract:

To study how learning affects the mechanisms of visual perception, we trained monkeys to identify visual stimuli that were parametrically degraded by interpolation with noise patterns. Whereas monkeys had great difficulty in identifying degraded stimuli before learning, they were able to reliably identify such stimuli after several days of practice. We recorded the activity of single neurons in the prefrontal (PF) cortex, a brain region that has been implicated in many high-level cognitive functions, and in extrastriate visual cortex (V4), a brain region that is involved in intermediate-level analysis of visual form. We found that learning systematically affected neural activity in both of these regions, in qualitatively different ways: Learning led to invariance of neural activity across degradation in prefrontal cortex, so that neurons tended to respond in an identical fashion to undegraded and moderately degraded stimuli after, but not before learning. By contrast, we found that many V4 neurons exhibited an enhancement in neural activity specifically for degraded stimuli after learning. Thus, V4 neurons are recruited during recurrent processing that takes place as the visual system attempts to find an interpretation of the visual stimulus, whereas PF neurons tend to represent hypotheses about the incoming visual information. These findings suggest that modification of recurrent interactions between prefrontal and visual cortex play a key role in learning.

## **Smooth pursuit eye movements: FMRI studies on sensory and motor components of their cortical control, covert shifts of attention and their influences on cortical activations**

Sabine Ohlendorf<sup>1</sup>, Oliver Speck<sup>2</sup>, Sven Haller<sup>3</sup> and Hubert Kimmig<sup>1,4</sup>

<sup>1</sup> Neurologische Universitätsklinik, Breisacher Str. 64, 79106 Freiburg, Germany

<sup>2</sup> Abteilung Röntgendiagnostik, Medizin Physik, Hugstetter Str. 55, Universitätsklinikum Freiburg, 79106 Freiburg, Germany

<sup>3</sup> Abteilung für Neuroradiologie, Petersgraben 4, Kantonsspital Basel, 4031 Basel, Switzerland

<sup>4</sup> Klinik für Neurologie, Ratzeburger Allee 160, Universitätsklinikum Schleswig Holstein, Campus Lübeck, 23538 Luebeck, Germany

Smooth pursuit eye movements (SP) serve to keep a moving object in our fovea, the place of highest visual acuity. For this purpose, the SP system must detect an object moving across our retina (sensory input), process its velocity, and prepare a motor command signal being sent to the eye muscles (motor output), which enables the eyes to follow the object. The purpose of the first experimental study was to identify which cortical regions process the sensory input information which process the motor output signals and which are related to both processes (possibly sensorimotor transformation sites). In the second experiment we investigated the influence of attention on cortical activation during smooth pursuit eye movements and visual stimulation.

Eye movements were measured with an infrared light technique (MR-Eyetracker), cortical activations were measured via functional Magnetic Resonance Imaging (fMRI) (in the first experiment with a 3T Siemens Trio and in the second experiment with a 1.5T Siemens Avanto scanner). Twelve healthy subjects participated in the study. A central fixation dot and a second dot, 4° below the centre dot, were presented in complete darkness. Subjects always directed their gaze to the centre dot. Moving the lower dot sinusoidally in the horizontal plane yielded a visual (sensory) stimulation. Moving both dots while subjects pursued the upper dot yielded oculomotor (but almost no sensory) stimulation. Moving only the upper dot while subjects tracked this dot yielded oculomotor plus sensory stimulation. In the first experiment subjects were instructed to pay attention always to the centre dot. In the second experiment subjects had to separate the direction of attention from the direction of gaze. A colour change of the stationary dots during the rest condition indicated to which of the two dots attention had to be shifted. We tested four different tasks: (a) pure visual (sensory) stimulation when attention and gaze direction were located on the stationary centre dot with the lower dot moving, (b) pure visual stimulation with gaze located on the centre dot, but attention directed to the moving lower dot, (c) mixed oculomotor and sensory stimulation with subjects pursuing and paying attention to the upper moving dot, the lower dot being stationary, (d) mixed oculomotor/sensory stimulation with pursuit of the moving upper dot, but paying attention to the stationary lower dot.

We could show that visual stimulation activated mainly occipito-parietal regions V5/V5A and the intraparietal sulcus, while oculomotor stimulation activated predominantly the frontal regions FEF and SEF, precuneus and the cingulate gyrus. This was confirmed by the combined visuo-oculomotor stimulation which activated all these regions. Parts of V5/V5A and the intraparietal sulcus seem to be involved in both sensory and motor processing. These are possible sites for sensorimotor transformation. Shifts of attention led to differential effects in the pursuit related cortical network.

## **Does feature-based attention operate at ignored locations?**

Kai Boelmans<sup>1</sup>, Hans-Jochen Heinze<sup>1</sup>, Steven J. Luck<sup>3</sup>, Jens-Max Hopf<sup>1,2</sup>

<sup>1</sup> Dept. of Neurology II, Otto-von-Guericke-University, D-39120 Magdeburg, Germany

<sup>2</sup> Leibniz-Institute for Neurobiology, D-39120 Magdeburg, Germany

<sup>3</sup> Dept. of Psychology, University of Iowa, Iowa City, IA, 52242-1407, USA

This study addresses an important issue about the role of feature and location-based attention in visual search using the ERP technique. In a previous study (Hopf et al., 2004) we have shown that when searching for a conjunctively defined target (color, orientation), the presence of relevant features (e.g. orientation) at non-target locations (items with irrelevant color) is reflected by a modulation of an negative-going voltage deflection between 140 and 300 ms over the occipital cortex. The topography of this modulation reflected the spatial distribution of relevant features independent of the actual location of the target item. Here, we investigated the time-course of this location-independent modulation with respect to the timing of location-based attention effects in the ERP response.

Our findings clearly show that we can (1) replicate earlier effects of feature-specific but location-independent mechanisms. (2) feature-based attention operates at ignored locations, with the constraint that under conditions of short target presentations feature-based attention is not sufficient to highlight any potential target location containing relevant features. To summarize, our results show that feature-based attention operates independently from location-based attention. But location-based attentional mechanisms are faster than a feature-specific analysis in a visual search.

# Advancing Dynamic Binding Theory: Implementation of Complex Concepts

A. Maye<sup>1</sup>, M. Werning<sup>2</sup>, P. König<sup>3</sup>, and A.K. Engel<sup>4</sup>

<sup>1</sup> Zuse Institute Berlin, <sup>2</sup> University of Düsseldorf, <sup>3</sup> University of Osnabrück,

<sup>4</sup> University Hospital Hamburg-Eppendorf

Different features of a visual stimulus are processed by spatially disparate neuronal populations [2]. In order to generate a holistic perception of an object in the visual field, responses of neurons activated by this object have to be associated with one another. Synchronization of single spikes or oscillatory modulated neuronal activity is considered a primary candidate mechanism for this purpose. Many experiments (reviewed by [3]) show that neurons tend to synchronize their activity if stimulated by the same object. They do much less so if they receive the same stimulation, but from different objects.

On a more general account we can say that the perception of an object (e.g., a vertical red bar) is composed from the activation of more primitive concepts (e.g., ‘redness’, ‘verticality’) and call it a complex concept. A fundamental property of concepts is that they are compositional and decomposable. Compositionality, especially with respect to perception, has not, to a sufficient extent, been taken into regard in the context of dynamic binding, yet.

Our modeling study suggests that dynamic binding can account for the compositionality of visual perception. The model network (introduced in [1]) reflects the recurrent interactions between excitatory and inhibitory neurons in layer 2 and 3 of the primary visual cortex. We analyzed the dynamics of the network by computing the principal modes and the time course of the associated order parameters. While principal modes are constant over time, order parameters are the weight of each mode in the network state for each point in time. This can be seen as complete separation of spatial information, contained in the principal modes, from temporal information in the the order parameters.

In [1] we found that principal modes hold different interpretations of a stimulus, and hence represent different epistemic possibilities (see figure 1b). Here we concentrate on the order parameters. Figure 1c shows that the oscillation of the order parameter with the highest eigenvalue (blue curve) constitutes an envelope for the oscillation of the one with the second largest (green). We regard this as a mechanism for the representation of part-whole relations, which is a fundamental requirement of many complex concepts. At the same time it is the key to hierarchical binding. We hypothesize, therefore, that neural synchronization is not only a mechanism for binding representations of attributes of one and the same object together to form the representation of the object with its attributes. Beyond that it is general enough to also bind together the representations of the parts of an object to form the representation of the object with its parts.

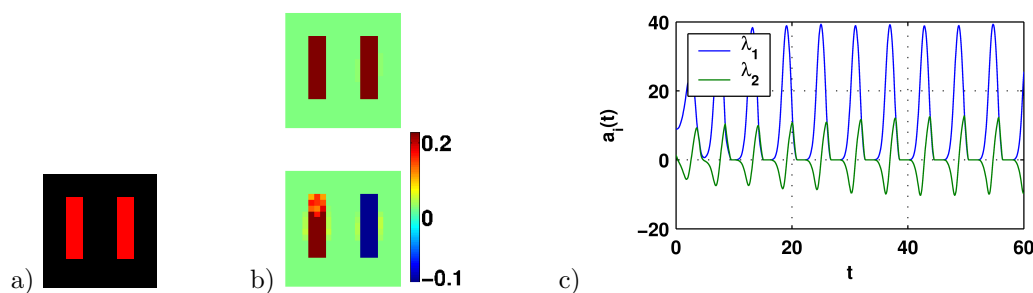


Figure 1: **a)** A stimulus consisting of two vertical bars. **b)** Principal modes with two largest eigenvalues (top to bottom). The vectors were reshaped and color-coded to facilitate visual inspection of the contribution of each principal mode to the overall network activity. The first principal mode (top panel) shows that the oscillators activated by the two bars make the same positive contribution to the activity. It accounts for the synchronization of the two regions and can be interpreted as a mode in which the two bars are seen as a single object. In the second mode (lower panel), the contributions in the two regions have opposite signs. This accounts for a residual phase difference between the oscillations in the two regions which can be interpreted as representing two separate objects. **c)** Time course of the order parameters:  $a_1(t)$  is an envelope of  $\pm a_2(t)$ .

- [1] A. Maye and M. Werning. Temporal binding of non-uniform objects. *Neurocomputing*, 58–60:941–948, 2004.
- [2] D. J. Felleman and D. C. van Essen. Distributed hierarchical processing in the primate cerebral cortex. *Cerebral Cortex*, 1:1–47, 1991.
- [3] W. Singer. Neuronal synchrony: A versatile code for the definition of relations? *Neuron*, 24:49–65, September 1999.

**VISUAL PERCEPTIONS IN BLIND: FROM SENSORY DEPRIVATION TO VISUAL ACTIVITY.**

Alfaro A<sup>1,2</sup>, Climent R<sup>2</sup>, Vilanova H<sup>2</sup>, Concepción L<sup>3</sup>, Bongard M<sup>2</sup>, Fernández E<sup>2</sup>.

<sup>1</sup>Neurology Department. University General Hospital, Alicante, Spain. <sup>2</sup>Bioengineering Institute, Miguel Hernández University, Alicante, Spain. <sup>3</sup>Magnetic Resonance Imaging Department. INNSCANER. University General Hospital, Alicante, Spain.

Any attempt to restore visual functions in blind subjects with pregeniculate lesions provokes the question of the extent to which deafferented visual cortex is still able to generate conscious visual experience. Short-lasting light deprivation in sighted humans enhances rapid increased excitability of the visual cortex, expressed as decreased phosphene threshold to transcranial magnetic stimulation of occipital regions and enhanced activation in response to incoming visual input, as measured by functional magnetic resonance imaging. Nevertheless, visual cortex excitability is reduced in subjects with a high degree of visual deafferentation, especially in those without previous visual experience which suggest that visual deprivation leads to reduced function and excitability of the occipital cortex. However, cerebral areas normally used for vision retain their macroanatomy in spite of visual deprivation, which contradict any suggestion that visually deafferented cortex has undergone degeneration. These areas display levels of glucose metabolism that are higher than or similar to that of the visual cortex of sighted individuals with their eyes covered or closed. What is more, techniques of magnetic stimulation (TMS), cortical surface or intracortical microstimulation of the visual cortex have managed to elicit small circumscribed subjective sensations of light (phosphenes) in blind subjects.

We report an early blind patient who described elementary and complex visual hallucinations in his right visual field following a focal non epileptic lesion (an arteriovenous malformation) located in his left calcarine cortex. Other conditions causing hallucinatory experience were excluded. These findings further strengthen the notion that deafferented visual pathway remains active and could be recruited to subserve the visual information processing among blind subjects despite the lack of visual input.

Starting for these dates, we decide to design a research protocol using TMS in order to create 'virtual lesions' in the occipital cortex of blind volunteers, for evoking visual experiences. TMS was applied with a figure of eight coil to 28 positions arranged in a 2x2 cm grid over the occipital area in a group of 17 blind volunteers and 21 sighted ones. A digitizing tablet connected to a PC computer running customized software, and audio and video recording were used for detailed and accurate data collection and analysis of evoked phosphenes. A frameless image-guided neuronavigational device was used to describe the position of the actual sites of the stimulation coils relative to the cortical surface. Our results show that TMS is able to elicit phosphenes in almost all sighted subjects and in a proportion of blind subjects. Evoked phosphenes were topographically organized. Despite minor inter-individual variations, the mapping results were reproducible and show good congruence among different subjects. This procedure has potential to improve our understanding of physiologic organization and plastic changes in the human visual system and to establish the degree of remaining functional visual cortex in blind subjects. Such information could be useful to evaluate the success of sensory implants in humans and provided insight into the mechanisms of plasticity associated with deafferentation.

*Supported by EU Grant CORTIVIS (QLK6-CT-2001-00279).*

## Sequence learning as a base for object invariance coding in a network of spiking neurons

Frank Michler, Reinhard Eckhorn

Philipps-University, Physics Department, NeuroPhysics Group, 35032 Marburg, Germany

**Introduction and Goal.** Our visual system is able to recognize familiar objects independent of its actual view. This capability of invariant object recognition requires that different retinal input patterns activate the (probably invariant) neural representation of the same object. During natural vision sequences of scenes are spatio-temporally highly correlated because the view of an object changes slowly. Földiák (1991) [1] and others have shown that invariant representations can be learned from temporally correlated input sequences of object views. Their networks learned object representations and were based on feed forward convergence: outputs of neurons driven by the different features and views of an object converge to the same cardinal neuron or group of (*grandmother*) neurons. With our model we want to learn invariant object representations in which the different component features and views of a visual object are systematically related so that sequences of views and their corresponding feature relations can be activated according to the learned natural sequences (see concepts of *aspect graph* and *visual potential* [2]).

**Methods.** Our network consists of recurrently connected excitatory and inhibitory spiking neurons. The excitatory connections partly have short and long delays (similar to [3,4]). Initially each neuron is connected to a random set of inhibitory and excitatory neurons. Additionally, all excitatory neurons drive one common inhibitory interneuron feeding back with short latency to all excitatory neurons, and thus supports oscillations in the gamma frequency range. Excitatory connections are strengthened using a Hebbian synaptic learning rule (STDP, [5]), for inhibitory connections an anti-Hebbian rule is used. The learning rule is implemented using exponentially decreasing learning potentials which are increased with every presynaptic spike. The learning input sequences are constructed as follows: Each object to be learned consists of a set of input patterns according to different views. With high probability consecutive input patterns belong to the same object, as with visual objects in natural viewing conditions during self-motion of the observer. With low probability the input switches to a pattern belonging to a different object.

**Results.** After learning there are strong connections with short delay between neurons representing the same view (auto-associative connections) and long delay connections between neurons representing different views of the same object (hetero-associative connections). Common inhibition, often cycling at gamma frequency, thus can separate representations of different views (neurons activated during the same gamma cycle represent the same view). In a test simulation the network is activated with single views (patterns). Because of the learned recurrent connections, the neurons representing neighboring views of the same object are activated successively.

**Discussion and Conclusions.** Although correlated sequences of object views have already been used for learning invariant object representations [1,6], they used learning algorithms leading to cardinal neurons for all views of an object. We demonstrate learning of distributed object representations in which consecutively appearing views are systematically mapped so that one view can activate the neighboring ones, depending on the succession of the learned sequence. This is not possible with cardinal cell representations.

[1] Földiák P (1991) Neural Computation 3:194-200

[2] Koenderink, van Doorn (1979) Biol Cybernetics 32:211-216

[3] Kleinfeld (1986) Proc Natl Acad Sci. USA 83:9469-9473

[4] Schott U, Eckhorn R, Reitboeck HJ (1997) Proc. of the 25th Göttingen Neurobiol Conf:1025

[5] Bi, Poo (1998) J Neurosci 18:10464-10472

[6] Wallis (1996) Neural Networks 9:1513-1519

Supported by Deutsche Forschungsgemeinschaft (FOR 254) to R.E.



## A recurrent neural network encoding border ownership of visual objects

Timm Zwickel, Reinhard Eckhorn

Philipps-University, Physics Department, NeuroPhysics Group, 35032 Marburg, Germany

**Introduction and Goal.** Visual cortical areas V1, V2 and V4 in awake monkeys were shown to be involved in encoding global information of visual objects. A large percentage of their neurons can encode *border ownership* (BO) properties of visual objects [1]. These neurons respond specifically to edges and parts of contours belonging to a visual object, i.e., they are activated by features lying at the contour's inner (surface) side of an object. The BO-coding is present already during the first post stimulus activation phase and it is largely independent of object size, reaching far beyond the diameters of classical receptive fields (cRF) in these cortical areas. We are interested in the neural mechanisms of BO-coding, and more generally, in mechanisms of figure-ground segregation in the visual cortex. **Methods.** We modelled BO-coding in a simplified neural network of the visual cortex, consisting of 3 hierarchically organized 2-dimensional topographic layers of graded response neurons. The lowest layer consists of mutually inhibiting pairs of BO-neurons with orientation specific simple-cell properties having the same unsymmetric luminance sensitivity profile differing only in their feedback from higher areas. One of a pair is disinhibited by feedback when the contrast edge it encodes belongs to an object stretching out to one side of the edge. Conversely, the other neuron is disinhibited when the object stretches to the other side. Lateral medium-range linking connections facilitate neighboring neurons with curvilinear arranged cRFs. Neurons inhibit each other locally via inhibitory interneurons. Excitatory feedforward connectivity is structured to increase invariances for object properties with each successive layer by convergence of neurons with similar cRF-properties (as in striate cortex from simple- to complex-cells). Intermediate layer neurons of appropriate orientation and spatial relation, encoding the Gestalt property of convexity, converge on the highest layer neurons, such that the neurons are activated if an object is present. The crucial information of object presence is then passed back to the lower areas via disinhibition. The network's performance is tested with input image sequences of varying noisy objects and non-objects at different sizes. **Results.** The activity of a BO-neuron is raised when it is part of an object and lowered if its antagonistic BO-neuron is activated. There is no change in activity of BO-neurons through feedback, when encoding an edge not belonging to any object (resembling the monkey data [1]). In addition, figure-ground segregation is markedly improved by these properties. **Discussion.** With a biologically plausible model we show how a network with fast inter-areal feedback (according to measurements [2]) can support global object-information in lower visual areas, i.e., the detection of a visual object, independent of its identity. This model can explain the BO-properties found in monkey visual cortex [1]. It resembles biologically plausible mechanisms: The increase of invariance throughout cortical areas in the dorsal visual pathway, with layers first encoding simple Gestalt properties (e.g. common fate) and then location of entire objects. With our model we are able to explain the fast responses of BO-neurons in early visual areas independent of stimulus size - impossible to account for by intra-areal connections having lateral delays dependent on object size [2]. Our model further demonstrates that fast feedback connections can play a crucial role in figure-ground segregation, improving the signal-to-noise ratio (SNR) of visual object representations in early visual areas. Through the disinhibition of BO-neurons these are able to prevail against less active neurons not belonging to the encoded object's contour in their surround through inhibition.

[1] Zhou, Friedman, von der Heydt (2000) J. of Neuroscience 20:6594-6611

[2] Bullier (2001) Brain Research Reviews 36:96-107

Supported by Evangelisches Studienwerk Villigst to TZ and Deutsche Forschungsgemeinschaft grant EC53/10-1 to RE.

## **Symposium #S20:**

### **Amyotrophic Lateral Sclerosis (ALS) and Motoneuron Disease: From basic molecular and cellular mechanisms to novel clinical applications**

**BU. Keller, J. Weishaupt, M. Bähr, Göttingen**

#### **Introduction**

- [#S20](#) BU. Keller, J. Weishaupt, M. Bähr, Göttingen  
*Amyotrophic Lateral Sclerosis (ALS) and Motoneuron Disease: From basic molecular and cellular mechanisms to novel clinical applications*

#### **Slide**

- [#S20-1](#) M. Sendtner, Wuerzburg  
*Signals for survival and axon growth in motoneurons*
- [#S20-2](#) A. Clement, Mainz  
*The neuron-glia connection: Glial cell involvement in SOD1-mediated motor neuron disease.*
- [#S20-3](#) BU. Keller, Göttingen  
*Mitochondria and calcium signalling in motoneurons: implications for selective motoneuron vulnerability*
- [#S20-4](#) J. Weishaupt, G. Rohde, K. Meuer and M. Bähr, Göttingen  
*Cyclin-dependent kinase 5 (CDK5) and neuronal cell death in motoneuron disease*
- [#S20-5](#) JD. Rothstein, Baltimore, MD (USA)  
*Non-Neuronal cells in ALS Neurodegeneration: Mechanisms and Therapies*
- [#S20-6](#) AC. Ludolph and T. Meyer, Ulm and Berlin  
*Novel insights into the aetiology and pathogenesis of ALS: implications for clinical therapeutic strategies*
- [#S20-7](#) R. Dengler, Hannover  
*Clinical and therapeutic aspects of amyotrophic lateral sclerosis: current and future developments*

#### **Poster**

- [#40B](#) B. Spielbauer, J. Landgrebe and BU. Keller, Göttingen  
*Molecular characterisation of the hSOD1(G93A) transgenic mouse model of human familial amyotrophic lateral sclerosis (fALS) using gene expression profiling*

[#41B](#)

MK. Jaiswal, S. Balakrishnan and BU. Keller, Göttingen

*Rapid CCD fluorescence imaging reveals functional impairment of mitochondria in the adult SOD1 G93A mouse model of human amyotrophic lateral sclerosis (ALS)*

[#42B](#)

H. Steffens, BU. Keller and ED. Schomburg, Göttingen

*In vivo investigations on the monosynaptic reflex of the adult SOD1 G93A mouse model of human amyotrophic lateral sclerosis (ALS)*

[#43B](#)

B. Schütz, MT. Heneka, GE. Landreth and A. Zimmer, Bonn and Cleveland, OH (USA)

*Protective effect of the peroxisome proliferator-activated receptor gamma (PPARgamma) agonist pioglitazone in a mouse model of amyotrophic lateral sclerosis*

## **Introductory Remarks to Symposium 20**

### **Amyotrophic Lateral Sclerosis (ALS) and Motoneuron Disease: From basic molecular and cellular mechanisms to novel clinical applications**

**BU. Keller, J. Weishaupt and M. Bähr, Göttingen**

Amyotrophic Lateral Sclerosis (ALS) is a fatal neurodegenerative disease characterized by the selective loss of motoneurons in the cortex, brain stem and spinal cord. While many questions about the underlying aetiology and pathogenesis are still unresolved, novel basic and clinical research activities have provided valuable insights into the molecular and cellular basis of this important neurodegenerative disorder.

The focus of the symposium is to highlight recent insights into motoneuron function and disease and to evaluate the significance of these findings for future clinical developments. At first, Michael Sendtner will present evidence for the critical role of axonal transport for motoneuron survival, axon growth and cell death. This presentation will be followed by an illustration of the important interaction between motoneurons and glial cells in a mouse model of motoneuron disease presented by Albrecht Clement. Consequently, talks by Bernhard Keller and Jochen Weishaupt will highlight the central role of mitochondria- and apoptosis related mechanisms for motoneuron function and disease, in particular for the regulation of  $[Ca]_i$  dependent processes. Subsequently, Jeffrey Rothstein will present evidence for disrupted glutamate transport and regulation in ALS, and will address the question how insights into the molecular basis of glial glutamate transporters might be utilized for novel clinical approaches. Finally, Albert Ludolph and Reinhard Dengler will present novel insights from clinic-related studies and will evaluate the potential of future therapeutic developments. Triggered and supported by activities within the novel DFG - Center of Molecular Physiology of the Brain (CMPB). in Göttingen, the symposium will thus provide a challenging link between novel basic and clinical research initiatives.

## Signals for survival and axon growth in motoneurons

Michael Sendtner

*Institute for Clinical Neurobiology, University of Wuerzburg, Josef-Schneider-Str. 11,  
97080 Wuerzburg, Germany*

In higher vertebrates, a significant proportion of newly generated motoneurons undergo cell death during development. This so-called “physiological cell death” is regulated by neurotrophic factors (NTF) which are produced by skeletal muscle and glial cells. So far, a variety of these factors which are members of various gene families have been identified. They support motoneuron survival in cell culture, and gene inactivation by homologous recombination revealed that they play together in supporting survival of developing and postnatal motoneurons. The upregulation of proteins of the IAP family plays a crucial role for neuronal survival and seems as an essential part of the signaling pathways which mediate the survival effects. In order to investigate the signaling pathways for upregulation of IAP proteins, we have focussed on the role of Raf-kinases. These serin/threonin-kinases coordinate various signaling pathways in response to NTFs including the MAPK pathway, the PI-3K/AKT pathway and others. The Raf-kinase family in mammals includes 3 members, A-Raf, B-Raf and C-Raf-1. Mice in which B-Raf or C-Raf is deleted die during embryonic development between day 12 and 15 due to various organ defects. Therefore, we have isolated motoneurons from E12 C-Raf- and B-Raf-deficient mice and investigated responsiveness to NTFs *in vitro*. Motoneurons lacking C-Raf can survive in the presence of neurotrophic factors. In contrast, B-Raf-deficient neurons have lost their response to neurotrophic factors. This appears interesting, as the B-Raf-kinase, in contrast to C-Raf, is activated by extracellular signals which lead to elevated cAMP. Thus, B-Raf could be an important integrator of neurotrophic factors and neural activity through neurotransmitter receptors.

Interestingly, gene defects for such regulatory proteins for neuronal survival have not been identified in human motoneuron disease (MND). Evidence increases that other mechanisms such as defects in axonal transport or axonal maintenance play a major role in the pathophysiology of MND. This is based on the finding that mutations in tubulin specific chaperone E cause MND in the pmn mouse model, and that mutations in the dynactin gene are associated with MND in patients. Classical spinal muscular atrophy (SMA), a common autosomal recessive form of motoneuron disease in infants and young adults is caused by mutations in the *SMN1* gene. The corresponding gene product is part of a multiprotein complex for assembly of spliceosomal snRNP complexes. It is still not understood why reduced levels of the ubiquitously expressed SMN protein cause specific motoneuron degeneration without affecting other cell types. A yeast 2 hybrid screen revealed hnRNP R as specific interaction partner for Smn in motor axons. Isolated motoneurons from *Smn*<sup>-/-</sup> *SMN2* tg mice, a mouse model of SMA exhibit normal survival in the presence of survival factors but their axon growth is disturbed. In differentiating PC12 cells, overexpression of Smn or its binding partner hnRNP R enhance NGF mediated neurite growth, indicating that a complex of Smn and hnRNP R is involved in the regulation of axon growth and maintenance. Reduced axon growth in Smn deficient motoneurons correlates with reduced  $\beta$ -actin staining in distal axons and growth cones. Subsequent molecular analyses revealed that hnRNP R specifically binds to the 3'UTR of  $\beta$ -actin mRNA *in vitro*. This interaction depends on the presence of Smn protein. Taken together, these findings indicate that spinal muscular atrophy is caused by defects in axonal transport of  $\beta$ -actin mRNA which results in disturbed local  $\beta$ -actin synthesis in growth cones and presynaptic structures of the motor endplate.

## References:

1. Wiese et al., *Nature Neurosci.* **2**, 978-983, 1999.
2. Wiese et al., *Nature Neurosci.* **4**, 137-142, 2001.
3. Thoenen and Sendtner, *Nat. Neurosci.* **5**, Suppl1, 1046-1050, 2002.
4. Boemmel et al., *J. Cell Biol.* **159**, 563-569, 2002
5. Rossoll et al., *J. Cell Biol.* **163**, 801-812, 2003.

**The neuron-glia connection: Glial cell involvement in SOD1-mediated motor neuron disease.**

Albrecht Clement

Institute for Physiological Chemistry and Pathobiochemistry, University of Mainz,  
Duesbergweg 6, 55128 Mainz

Amyotrophic lateral sclerosis (ALS) is a devastating late onset neurodegenerative disorder characterized by the progressive loss of primarily upper and lower motor neurons in the spinal cord and the brain stem. Most of the familial cases are caused by dominant mutations in the ubiquitously expressed cytosolic Cu-Zn superoxide dismutase (SOD1) by the acquisition of as yet unidentified toxic properties. Although SOD1-linked familial cases represent only a small proportion of all ALS-patients, pathological hallmarks are indistinguishable from sporadic cases. Mice transgenic for several human SOD1 mutations develop a motor neuron disorder with many features of human pathology including ubiquitinated, neurofilamentous and hyaline inclusions, astrogliosis and the activation of microglia cells.

A central question for understanding disease mechanisms and development of possible therapies is, whether toxicity of mutant SOD1 arises solely within motor neurons or whether motor neuron surrounding cells are damaged and thus mediating motor neuron degeneration. We have generated a panel of chimeric mice that comprise of a mixture of normal and mutant SOD1 expressing cells. These reveal that toxicity of mutant SOD1 leading to motor neuron degeneration does not exclusively arise inside motor neurons. Normal motor neurons surrounded by mutant SOD1 expressing cells develop some pathological signs. On the other hand and more importantly for therapeutic interventions, motor neurons that express mutant SOD1 in a level sufficient to provoke motor neuron degeneration in mice when expressed systemically, live much longer when surrounded by wild type non-neuronal cells. Some chimeric mice even with low contributions of wild type cells, do not develop disease after two times the live span of animals transgenic for mutant SOD1.

This indicates that stem cell therapy might be an effective ALS-treatment even if “just” non-neuronal cells are replaced by wild type cells.

**Mitochondria and calcium signalling in motoneurons:  
implications for selective motoneuron vulnerability**

Bernhard U. Keller

Zentrum Physiologie, Humboldtallee 23, Universität Göttingen, 37073 Göttingen, Germany

Motoneurons (MNs) are selectively vulnerable both in human forms of amyotrophic lateral sclerosis (ALS) and corresponding mouse models of this fatal neurodegenerative disorder. While most motoneuron populations in the brain stem and spinal cord are selectively impaired, oculomotor and dorsal vagal motoneurons are essentially resistant to ALS-related damage. Interestingly, selective motoneuron vulnerability has been closely linked to disruptions of cytosolic calcium signalling and associated disturbances of mitochondrial metabolism. To elucidate underlying events, we utilized pharmacological inhibitors of the mitochondrial respiratory chain and investigated cellular responses in vulnerable (hypoglossal, facial) and resistant (oculomotor, vagal) MN types. In vulnerable hypoglossal MNs, bath application of the mitochondrial “uncoupler” CCCP collapsed the electrochemical potential across the inner mitochondrial membrane, which was associated with substantial Ca release from intracellular stores (ampl. > 200nM) and a significant retardation of cytosolic Ca clearance rates (> 2-fold). Similar results were obtained after bath application of CN, an inhibitor of complex IV of the mitochondrial respiratory chain. Inhibition of complex IV also activated Na<sup>+</sup> conductances in vulnerable MNs and increased their action potential activity by a reactive oxygen species (ROS) dependent mechanism. Taken together, our comparative studies on selectively vulnerable and resistant neurons support a model where selective MN vulnerability results from a synergistic accumulation of risk factors, including low cytosolic Ca<sup>2+</sup> buffering, strong mitochondrial impact on [Ca<sup>2+</sup>]<sub>i</sub>, and a mitochondria-controlled increase in electrical excitability during metabolic disruptions.

References:

- Vanselow & Keller (2000), J. Physiol. 525, 433 - 445  
Ladewig et al. (2003), J. Physiol. 547, 775 – 787  
Bergman & Keller (2004), J. Physiol. 555, 49 - 59

## **Cyclin-dependent kinase 5 (CDK5) and neuronal cell death in motoneuron disease**

Jochen H. Weishaupt, Gundula Rohde, Katrin Meuer and Mathias Bähr

University of Göttingen, Department of Neurology, 37075 Göttingen, Germany

Mitochondrial dysfunction and deregulated calcium signalling has been implicated in death and selective vulnerability of motoneurons in amyotrophic lateral sclerosis. In this talk, candidate molecular mechanisms linking disturbed calcium homeostasis, mitochondrial dysfunction and finally motoneuronal cell death will be presented.

Cyclin-dependent kinase 5 (CDK5) belongs to the family of CDKs and has also been termed neuronal CDK1-like kinase, but is not involved in cell cycle control. Subcellular redistribution and over-activation of CDK5 in one mutant SOD-transgenic mouse model for amyotrophic lateral sclerosis (ALS) supports a role of this kinase in the pathogenesis of motoneuron disease. In some models for neurodegenerative diseases, over-activation of CDK5 was caused by proteolytic conversion of the CDK5 activator p35 to p25 by calpain, a calcium activated protease, and inhibition of CDK5 was neuroprotective. We will present and discuss the possible involvement of CDK5 in motoneuronal cell death. It could be shown that deregulation of CDK5 precedes mitochondrial dysfunction during neuronal apoptosis, and inhibition of CDK5 prevents decline of mitochondrial function. However, the link between CDK5 deregulation and mitochondrial dysfunction has not been elucidated yet. Recently, fragmentation of mitochondria has been shown during apoptosis of mammalian cells, and inhibition of mitochondrial fission, which can also be induced by treatment with calcium ionophores, by a dominant negative mutant of Drp1 prevented cytochrome c release and apoptosis. Therefore, we investigated whether inhibition of cyclin-dependent CDK5 reduces mitochondrial fragmentation as a possible downstream event mediating detrimental effects of CDK5 deregulation on mitochondria.

As a result of mitochondrial decline, increased free radical formation is among the major mechanisms discussed in ALS. Nevertheless, several compounds with antioxidative properties failed to ameliorate disease symptoms in in vivo models for ALS or in clinical trials. Melatonin has a unique broad spectrum of effects including scavenging of hydroxyl carbonide, alkoxyl, peroxy, and aryl cation radicals, stimulation of glutathion peroxidase and other protective enzymes as well as suppression of NO synthase. This combination of properties is not provided by any classical antioxidant, and might address the antioxidative requirements for treatment of ALS. Thus, we have been exploring the neuroprotective potential of melatonin in a transgenic model for ALS.



**Non-Neuronal cells in ALS Neurodegeneration: Mechanisms and Therapies**

Jeffrey D. Rothstein MD, PhD,  
Johns Hopkins University, Dept of Neurology, Baltimore, MD 21287

Amyotrophic lateral sclerosis is an adult onset neurodegenerative disease characterized clinically by muscle wasting and weakness. Traditionally the disease is characterized by loss of cortical and spinal motor neurons. However, recent studies have strongly suggested that disease progression and death of motor neurons depends upon participation of non-neuronal cells including focal inflammatory responses and dysfunction of astroglia. Chimeric animal studies and multiple transgenic mouse studies provide evidence for the critical participation of non-neuronal cells in the ultimate degeneration of spinal motor neurons. In addition, human and animal model studies demonstrate multiple abnormalities in astroglial function in ALS. These abnormalities are detectable even in astroglia and neuronal stem cells derived from transgenic models. Using this data, attempts at therapies include the use of neuronal and astroglial stem cells and successful engraftment of motor neuron stem cells as well as astroglial stem cells have been achieved. Finally- pharmacological means to modulate CNS inflammation (e.g. COX2 inhibition) and astroglial dysfunction (e.g. glutamate transporter enhancement) will be presented in both animal models and human clinical trials.

Novel insights into the aetiology and pathogenesis of ALS: implications for clinical therapeutic strategies

A.C. Ludolph, T. Meyer\*

Department of Neurology, University of Ulm and (\*) Humboldt University Berlin

Since Charcot, amyotrophic lateral sclerosis (ALS) is a clinically defined entity with a largely undefined aetiology. However, access to clinical therapeutics may derive from pathogenetic aspects alone which govern the characteristic pattern of vulnerability.

We are currently investigating chromosomal instability (Th. Meyer), the role of the AMPA receptor subunit GluR2, the dopaminergic system, motor proteins, the apoptotic cascade, and microglial activation and immunomodulation both in vitro and in vivo.

The results show that

- experimental changes in the dopaminergic system in vivo may be relevant for symptomatic therapies in humans
- changes in the glutamatergic system are likely to be relevant for neuroprotective approaches in humans
- immunomodulation, motor proteins and axonal transport, and the apoptotic cascade are possible targets for neuroprotection in humans and
- in contrast, currently chromosomal instability is a relevant etiological factor only.

In conclusion, investigations of aetiology and pathogenesis of ALS are not only relevant for a better understanding of the multiple etiologies of the disease, they also lead to therapeutic targets in a field which urgently waits for practical therapeutic progress.

Clinical and therapeutic aspects of amyotrophic lateral sclerosis: current and future developments.

Reinhard Dengler, Department of Neurology, Medical School Hannover, Germany; dengler.reinhard@mh-hannover.de

Clinical diagnosis of ALS and its formal classification according to the El Escorial Criteria (EEC) requires both signs of upper and lower motor neuron involvement, i.e. muscle weakness and atrophy in combination with spasticity. The newest version of the EEC includes molecular genetics (SOD-1 mutations) and EMG abnormalities proving disseminated muscle denervation beyond clinically affected muscles to allow earlier diagnosis. The clinical demonstration of upper motor neuron involvement (UMNI), however, can be difficult. Two approaches aim to improve detection of UMNI: (i) the novel MRI techniques „diffusion tensor imaging“ and „magnetization transfer“ appear to be able to detect very early signs of degeneration of the pyramidal tract even if there are not yet clinical signs, (ii) improved techniques of transcranial magnetic stimulation (TMS), especially the so called triple stimulation, may also be capable of demonstrating pyramidal tract dysfunction in very early stages.

Concerning pharmacological treatment, so far only the glutamate-antagonist riluzole has shown significant efficacy prolonging life by several months while various nerve growth factors failed, at least using subcutaneous and intrathecal application. Large trials testing drugs with anti-inflammatory, anti-apoptotic a.o. effects are on the way. In parallel, symptomatic treatment has been considerably improved during the last decade. Dysphagia and aspiration are now routinely treated by percutaneous endoscopic or radiologically controlled gastrostomy (PEG, RIG). Non-invasive ventilation to compensate for incipient respiratory insufficiency is widely used. Symptoms such as sialorrhea, pathological laughing and weeping, depression, spasticity and cramps, pain and others can be considerably alleviated. Additionally, there is now a broad consensus among experts on palliative measures and terminal care. The future hopes in ALS-research currently rest on neurogenetics, molecular pathology/pathophysiology and cellular therapies.

## **Molecular characterisation of the hSOD1(G93A) transgenic mouse model of human familial amyotrophic lateral sclerosis (fALS) using gene expression profiling**

Bettina Spielbauer<sup>1</sup>, Jobst Landgrebe<sup>2</sup> and Bernhard U. Keller<sup>1</sup>

<sup>1</sup>*Abteilung Neuro- und Sinnesphysiologie, Georg-August-Universität Göttingen, Humboldtallee 23, D-37073 Göttingen*

<sup>2</sup>*Abteilung Biochemie II, Georg-August-Universität Göttingen, Heinrich-Düker-Weg 12, D-37073 Göttingen*

Amyotrophic lateral sclerosis (ALS) is one of the most common adult-onset neuro-degenerative diseases. Since its description by Charcot in 1869, the molecular mechanisms underlying the selective loss of motor neurons in brain and spinal cord, leading to muscle weakness, atrophy and spasticity, remain still unresolved. To elucidate the potential role of mitochondrial processes in the pathogenesis of ALS, we systematically investigated the disease-specific gene expression pattern by using high-density DNA microarray technology.

Of the approximately 22,000 genes studied in spinal cords obtained from transgenic mice expressing the human SOD1 gene with a G93A mutation [1] as well as from non-transgenic littermates as controls, 211 genes showed a statistically significant differential expression [2]. Of the 211 regulated genes found, 120 were annotated with known or inferred biological function, 124 (59%) were upregulated and 87 (41%) downregulated.

The classification of these differentially regulated genes into functional groups (enzymes: 9%; transcription: 8%; protein synthesis and turnover, unfolded protein response (UPR), apoptosis: 7%; immune response: 7%; cell surface, cytoskeleton: 7%; transporters, channels: 3%; calcium ion binding: 2%; growth factors: 2%; signal transduction: 2%; lipoprotein metabolism: 1%; miscellaneous, function inferred: 8%, unknown function: 43%) indicates a synergistic involvement of abnormal protein aggregation and folding, oxidative stress, axonal transport and cytoskeletal dysfunction in the pathogenesis of familial ALS.

Both up- and downregulated gene candidates could be associated with mitochondria-related mechanisms, where oxidative stress responses and disrupted protein processing appeared as dominant hallmarks of SOD1(G93A)-mediated pathological cascades.

### Literature

[1] Gurney ME, Pu H, Chiu AY, Dal Canto MC, Polchow CY, Alexander DD, Caliendo J, Hentati A, Kwon YW, Deng HX, et al.

Motor neuron degeneration in mice that express a human Cu,Zn superoxide dismutase mutation. *Science*. 1994 Jun 17;264(5166):1772-5.

[2] Spielbauer B, Landgrebe J, Jaiswal MK, Keller BU. High-density Microarray Technology: Efficient Interaction of Experimental Design, Array Production and Data Analysis. *Statusseminar Chiptechnologien* 2005, submitted.

**Rapid CCD fluorescence imaging reveals functional impairment of mitochondria in the adult SOD1 G93A mouse model of human amyotrophic lateral sclerosis (ALS)**

Manoj Kumar Jaiswal, Saju Balakrishnan and Bernhard.U. Keller

*Center of Physiology, Humboldtallee 23, 37073 Göttingen, Germany*

Amyotrophic lateral sclerosis (ALS) is a fatal neurodegenerative disorder characterized by the selective loss of defined motoneuron populations in the brain stem and spinal cord. While low cytosolic calcium buffering and a strong interaction between metabolic mechanisms and  $[Ca]_i$  have been associated with selective motoneuron vulnerability, the underlying cellular mechanisms are only little understood. In this report, we utilized rapid CCD imaging to evaluate Ca signaling and metabolic signatures in brain stem slice preparations from mouse containing selectively vulnerable hypoglossal motoneurons. More specifically, we investigated cytosolic pathways in the SOD1 G93A mouse model of human ALS at the beginning of serious ALS-like symptoms (14 – 15 weeks) and compared the results to corresponding wild-type littermates.

Intrinsic NADH fluorescence in motoneurons and glial cells has been shown to serve as a valuable tool to characterize the metabolic signature of intrinsic energy profiles. Accordingly, evaluation of intrinsic NADH fluorescence after inhibition of mitochondrial complex IV with azide indicated that the mitochondrial respiratory chain was significantly disturbed in SOD1 G93A animals. Furthermore, measurement of the mitochondrial membrane potential (Rhod 123) indicated substantial mitochondrial disruption in SOD1 G93A motoneurons. A third series of experiments investigated the impact of impaired mitochondrial mechanisms on cytosolic Ca regulation by using the membrane-permeable indicator Fura-AM. Taken together, our investigations indicate that mitochondrial disruptions are critical elements of the pathology of SOD1 G93A-mediated motoneuron degeneration, and that stabilisation of mitochondria-related signal cascades might represent a useful strategy for clinical neuroprotection in ALS.

## ***In vivo* investigations on the monosynaptic reflex of the adult SOD1 G93A mouse model of human amyotrophic lateral sclerosis (ALS)**

*H. Steffens, B.U. Keller and E.D. Schomburg*

Physiological Institute of the University of Göttingen, 37073 Göttingen, Humboldtallee 23

Transgenic mouse models for neurological diseases have gained a lot of scientific attention in the last decade. These mice have preferentially been used for *in vitro* investigations (slice preparations and nerve cell cultures) or pathophysiological observations of the behaving animal. Indeed, previous studies on the transgenic SOD1 G93A mouse model of human amyotrophic lateral sclerosis (ALS) have provided valuable insights into the molecular and cellular disruptions underlying familial ALS. However, little is known about the significance of previous *in vitro* observations for the *in vivo* situation of the intact animal. To elucidate underlying mechanisms, we developed a set-up for electrophysiological *in vivo* experiments including laminectomy. In a first study, we investigated the sensorimotor network of the lumbar spinal cord in SOD1 G93A mice and compared the results to those from wild type (WT) littermates.

Adult WT (older than 90 days) mice of the strain B6SJL and transgenic SOD1 G93A mice (around 90 days old) were initially anaesthetized with pentobarbital sodium i.p., a jugular vein was cannulated for continuation of the anaesthesia with infusion of methohexital sodium, and a tracheotomy was performed for artificial ventilation. Body core temperature, ECG, breathing volume and rate, and depth of anaesthesia were controlled throughout the experiment. SOD1 G93A mice either showed no evident sign of motor disease, or started to show motor dysfunction before being operated. After the tracheotomy a laminectomy was performed at the level of L1 to L5. Several nerves of the left hind, such as posterior biceps, common peroneal, tibial, and sural nerve were exposed, cut distally, and mounted on platinum wire electrodes for recording of monosynaptic reflex responses. The left side dorsal root L4 that covers the main input from the left hind leg, was cut near the dorsal root ganglion and mounted on platinum wire electrodes for stimulation of the proximal part. Stimulation was repetitively performed with rectangle pulses of 0.1 ms duration, 2-10 times electrical threshold of the dorsal root. The recurrence interval of the stimulus started with 1.84 s, and was then reduced in steps down to 50 ms. The reduction of the amplitude of the monosynaptic reflex with increasing stimulus frequency and the duration required for the recovery of the reflex after repetitive stimulation were determined.

WT mice showed a stable reflex amplitude with 1.84 s stimulus interval, and a decreasing reflex amplitude during higher stimulus frequencies. In all animals, recovery of reflexes was complete within a few minutes. SOD1 G93A mice with *light* behavioural motor deficits showed a distinct reduction of the monosynaptic reflex amplitude during repetitive stimulation, even with long stimulus intervals. In mice with *severe* behavioural motor deficits, a monosynaptic response could hardly be elicited. In general, recovery of monosynaptic reflexes after repetitive stimulation required a longer time in SOD1 G93A mice and was mostly incomplete. In SOD1 G93A mice *without* obvious behavioural motor deficits, the monosynaptic reflex amplitude was normal with 1.84 s stimulus interval. Although recovery times were longer compared to WT, recovery was in most cases complete.

In summary, our experiments demonstrate a clear deficit in the monosynaptic reflex of SOD1 G93A mice, where reflex profiles correlated with apparent motor deficits. Our results on reflex recoveries i) are in good agreement with previous models suggesting that impairment of cellular energy supply contributes to the pathogenesis of ALS and ii) provide a valuable basis to directly investigate the capacity of novel neuroprotective compounds on spinal neuronal networks in this *in vivo* model of ALS.

Supported by DFG Schwerpunktprogramm „Funktionsanalyse von definierten Mutanten“ to B.U.K.

## **Protective effect of the peroxisome proliferator-activated receptor gamma (PPAR $\gamma$ ) agonist pioglitazone in a mouse model of amyotrophic lateral sclerosis**

Burkhard Schütz<sup>1</sup>, Michael T. Heneka<sup>2</sup>, Gary E. Landreth<sup>3</sup>, Andreas Zimmer<sup>1</sup>

<sup>1</sup>Laboratory of Molecular Neurobiology, Clinic for Psychiatry and Psychotherapy, University of Bonn, Germany, <sup>2</sup>Laboratory of Neuroinflammation, Department of Neurology, University of Bonn, Germany; <sup>3</sup>Alzheimer Research Laboratory, Department of Neuroscience, Case Western Reserve University, Cleveland, Ohio, USA.

*Correspondence to:* bschuetz@uni-bonn.de

### **Introduction**

Amyotrophic lateral sclerosis (ALS) is a fatal neurodegenerative disease that is characterized by a progressive loss of motor neurons in cortex, brainstem, and spinal cord. While clinically observable symptoms include loss of bodyweight, muscle wasting and lessened motor performance, the histopathological features include a pronounced astrogliosis and microgliosis, suggesting that inflammation may contribute to ALS pathogenesis. Recently, PPAR $\gamma$  agonists have been shown to exert potent anti-inflammatory properties and were found to be neuroprotective in mouse models of multiple sclerosis and Parkinson's disease. The aim of our study was therefore to assess the effect of the PPAR $\gamma$  agonist pioglitazone on SOD1-G93A transgenic mice, a well-characterized mouse model for ALS.

### **Methods**

Male SOD1-G93A transgenic mice and non-transgenic littermates were fed with Pioglitazone-containing rodent chow (240 ppm/day Pioglitazone), starting at day 57 of life. Non-treated animals of both genotypes served as controls. On a weekly basis, all mice were weighed and their motor performance evaluated using the paw grip endurance test. In addition, the survival times of the transgenic mice were monitored.

### **Results**

While SOD1-G93A mice showed a mean life span of  $123 \pm 7$  days, Pioglitazone treatment extended the mean survival by 10 days to  $133 \pm 6$  days ( $p = 0.019$ ). Pioglitazone-treated SOD1-G93A mice also showed a significantly higher body weight compared to non-treated transgenic mice ( $p < 0.05$ ) that lasted from 77 days of life until the end of the study. Importantly, loss of motor performance was delayed in Pioglitazone-treated SOD1-G93A mice compared to non-treated transgenic mice by 14 days ( $p < 0.001$ ).

### **Conclusions**

Our study unveiled a protective effect of a PPAR $\gamma$  agonist in ALS mice that includes an extension of life span and a prolonged preservation of muscular function and bodyweight. This suggests that inflammation plays a role in the pathogenesis of ALS and that blockade of inflammatory mediators is protective, at least in this mouse model. A histopathological and molecular biological analysis now aims in elucidating the cellular and molecular basis of this protection.

**Symposium #S21:**  
**What the nose tells the brain - News and views in olfactory coding**  
**I. Manzini and F. Zufall, Göttingen and Baltimore**

**Introduction**

- [#S21](#) I. Manzini and F. Zufall, Göttingen and Baltimore  
*What the nose tells the brain - News and views in olfactory coding*

**Slide**

- [#S21-1](#) P. Feinstein and P. Mombaerts, New York, NY (USA)  
*A CONTEXTUAL MODEL FOR SELF-SORTING OF AXONS INTO GLOMERULI IN THE MOUSE OLFACTORY SYSTEM*
- [#S21-2](#) J. Strotmann, O. Levai, S. Conzelmann, K. Schwarzenbacher, J. Fleischer and H. Breer, Stuttgart  
*Olfactory receptors: spatial expression and topographic projection*
- [#S21-3](#) CG. Galizia, AF. Silbering and D. Pelz, Riverside, CA (USA) and Berlin  
*Processing of olfactory information in the fruit fly *Drosophila melanogaster**
- [#S21-4](#) I. Manzini and D. Schild, Göttingen  
*Responses of olfactory receptor neurons in *Xenopus laevis* tadpoles and their projection onto olfactory bulb neurons*
- [#S21-5](#) F. Zufall, Baltimore, MD (USA)  
*Molecular Mechanisms of Pheromone Detection in Mice*
- [#S21-6](#) CH. Wetzel and H. Hatt, Bochum  
*Modulation of odorant signalling pathways*

**Poster**

- [#44B](#) W. Zhang, A. Mashukova, J. Barbour, H. Hatt and EM. Neuhaus, Bochum  
*A specific heat shock protein as expression enhancer of mammalian olfactory receptor proteins*
- [#45B](#) KA. Jellinger and J. Attems, Vienna (A)  
*Tau pathology in the olfactory system correlates with Alzheimer pathology*



- [#46B](#) LP. Nezlin and D. Schild, Göttingen  
*Individual olfactory sensory neurons project into more than one glomerulus in *Xenopus laevis* tadpole olfactory bulb*
- [#47B](#) P. Knüsel, MA. Carlsson, BS. Hansson and PFMJ. Verschure, Zürich (CH) and Alnarp (S)  
*Spatiotemporal response properties of optically recorded moth projection neurons*
- [#48B](#) M. Schmuker and G. Schneider, Frankfurt/Main  
*Towards Predicting Olfactory Receptor Responses*

## **Introductory Remarks to Symposium 21**

### **What the nose tells the brain - News and views in olfactory coding**

**Ivan Manzini and Frank Zufall, Göttingen and Baltimore (USA)**

The sensing of molecules in the environment is critical to the success of every organism. As an indication for the importance of this task, most animals have developed highly sophisticated olfactory systems and large portions of the genome are devoted to encode chemosensory receptors and other molecules necessary for a normal sense of smell. It is therefore hardly surprising that the past years have seen an explosion in studies aimed at understanding the functioning of the olfactory system. These studies span all levels of analysis - from genes to behavior. Efforts to determine the cellular, molecular and genetic basis underlying the detection and transduction of an almost unlimited number of odour molecules have laid the foundation of this field. Other important current efforts focus on the question of how the information contained in these molecules is encoded and mapped onto neural space. Particularly interesting in this respect is the relationship between neural activity in the peripheral sensory neurons and neural circuits in higher olfactory centres such as the olfactory bulb. Especially challenging has been the quest to decipher the signalling codes that underlie odour-dependent mammalian social behaviours, but even these complex questions - which require an understanding of the mechanisms for the detection of genetic individuality - are now within reach.

This symposium brings together several researchers that will discuss new results with respect to these topics. Because of the strikingly conserved functional organization of peripheral olfactory pathways across many species throughout the animal kingdom, an important aspect of this symposium will be to highlight similarities but also differences in olfactory coding mechanisms in various animal models, from flies to amphibians to mice.

## **A CONTEXTUAL MODEL FOR SELF-SORTING OF AXONS INTO GLOMERULI IN THE MOUSE OLFACTORY SYSTEM**

**Paul Feinstein and Peter Mombaerts**  
**The Rockefeller University, 1230 York Avenue,**  
**New York, NY 10021, USA**

No models fully account for how odorant receptors (ORs) function in the guidance of axons of olfactory sensory neurons (OSNs) to glomeruli in the olfactory bulb. Here, we use gene targeting in mice to demonstrate that the OR amino acid sequence imparts OSN axons with an identity that allows them to coalesce into glomeruli. Replacements between the coding regions of the *M71* and *M72* OR genes reroute axons to their respective glomeruli. A series of *M71*-*M72* hybrid ORs uncover a spectrum of glomerular phenotypes, leading to the concept that the identity of OSN axons is revealed depending on what other axons are present. Naturally occurring amino acid polymorphisms in other ORs also produce distinct axonal identities. These critical amino acid residues are distributed throughout the protein and reside predominantly within transmembrane domains. We propose a contextual model for axon guidance in which ORs mediate homotypic interactions between like axons. Consistent with this model, we find that the OR protein is present in cilia, axons, and glomeruli. A functional OR appears necessary for odorant reception, neuronal survival, axon outgrowth, and axonal identity, and perhaps for regulation of OR gene choice. The  $\beta 2$  adrenergic receptor can substitute for an OR in this context. Such functions of 7TM receptors may be more general in the nervous system.

**Olfactory receptors: spatial expression and topographic projection**

Jörg Strotmann, Olga Levai, Sidonie Conzelmann, Karin Schwarzenbacher, Jörg Fleischer and Heinz Breer

University of Hohenheim, Institute of Physiology, Garbenstrasse 30, 70599 Stuttgart, Germany

Olfactory information is conveyed from the nasal neuroepithelium to the main olfactory bulb, the first relay station in the brain, via axons of the olfactory sensory neurons. Each neuron extends a single axon to the bulb where it synapses onto second order neurons in a spherical region of neuropil, called glomerulus. A glomerulus represents the site of convergence for neurons expressing the same olfactory receptor. The glomeruli from neurons expressing the highly homologous receptors of the mOR37 subfamily are located in immediate vicinity, nevertheless each glomerulus receives input with very high precision from only one, receptor-subtype specific population of neurons. To monitor the unfolding of this precise olfactory map during development, the onset of receptor expression, outgrowth of axons as well as glomerulus formation for two neuron populations expressing different mOR37 subtypes was investigated on transgenic mouse lines. The data indicate a synchronous onset of receptor expression at about embryonic day 10 (E10). From E15, axons of both populations terminate in a common, small area of the presumptive olfactory bulb. During a short postnatal phase, the two axon populations segregate into distinct, protoglomerular structures.

Between E11 and 16, populations of cells expressing distinct olfactory receptor types are located in the cribriform mesenchyme, between the prospective olfactory epithelium and the developing telencephalon. Molecular phenotyping demonstrated that these 'extraepithelial' cells co-express key elements characteristic for neurons in the nasal epithelium. Studies on transgenic mice showed that they are positioned along the axon tracts, and each population expressing a given receptor gene is specifically associated with the axons of those olfactory sensory neurons with the same receptor type. The data suggest that they either might be guide posts for the outgrowing axons or migrate along the axons into the brain.

This work was supported by the Deutsche Forschungsgemeinschaft.

**Processing of olfactory information in the fruit fly *Drosophila melanogaster***

C.G. Galizia<sup>1</sup>, A.F. Silbering<sup>2</sup>, D. Pelz<sup>2</sup>

<sup>1</sup> University of California, Riverside, Department of Entomology, Riverside 92521 CA, USA

<sup>2</sup> Freie Universität Berlin, Institut für Biologie – Neurobiologie, 14195 Berlin, Germany.

Odors elicit combinatorial patterns of activity across olfactory sensory neurons. The axons of the latter converge onto olfactory glomeruli in the insect antennal lobe (AL), the analog of the vertebrate olfactory bulb. Each glomerulus receives input from but one (or very few) families of cells that all express the same (or the same few) olfactory receptor genes. Therefore, the combinatorial activity pattern across receptors is transformed into a combinatorial activity pattern across olfactory glomeruli, which contains all the olfactory information available to the animal. Within the AL, a network of local neurons processes this information, and a reshaped version of it is transferred to higher order brain centers via the projection neurons. In *Drosophila* there are at least two distinct networks of local neurons that can be labeled separately with genetic markers. The logic of olfactory reshaping in the AL, however, remains to be elucidated: proposals during the last few years have included the narrowing of olfactory response profiles, no change in the profile, and a broadening of the profile. We are investigating this question in the *Drosophila* AL using genetically expressed calcium indicators in order to measure odor-evoked activity patterns. This approach allows us to analyze the representation of odors at the level of the sensory neurons, at the level of several distinct populations of local neurons and at the output level of the AL. In order to quantitatively analyze the logic of olfactory reshaping (if any) we measure the response to a representative panel of odors across concentrations, and compare these for the different cell populations involved.

## Responses of olfactory receptor neurons in *Xenopus laevis* tadpoles and their projection onto olfactory bulb neurons

*Ivan Manzini and Detlev Schild*

*Department of Molecular Neurophysiology, University of Göttingen,  
Humboldtallee 23, 37073 Göttingen, Germany  
email: [ivan@ukmn.gwdg.de](mailto:ivan@ukmn.gwdg.de)*

We recorded responses of olfactory receptor neurons (ORNs) upon application of amino acids and pharmacological agents activating the cAMP transduction pathway using a slice preparation of the olfactory epithelium of *Xenopus laevis* tadpoles. Responses were measured using the patch-clamp technique and calcium imaging. Both amino acids and the cAMP pathway activators proved to be potent stimuli. Interestingly, a substantial number of ORNs that responded to amino acids did not respond to the pharmacological agents activating the cAMP pathway. This suggests that sensory transduction of a number of amino acids is cAMP-independent. The differential processing of cAMP-mediated stimuli on one hand and amino acid stimuli on the other was further elucidated by calcium imaging of olfactory bulb neurons using a nose-olfactory bulb preparation of *Xenopus laevis* tadpoles. Olfactory bulb neurons activated by amino acids were located laterally compared to those activated by cAMP pathway activators, and only a small proportion responded to both groups of stimuli.

Regarding the responses to amino acids, we were able to determine the response profiles of 283 ORNs to 19 amino acids, where one profile comprises the responses of one ORN to 19 amino acids. Surprisingly, 204 out of the 283 response profiles differed from each other. Adopting the view that each ORN is member of a class of ORNs that respond identically to a number of stimuli leads to the surprising conclusion that there are 204 receptor classes for the detection of the 19 amino acids. Furthermore, our recordings show that the sensitivity spectra of ORNs become more selective over ontogenetic stages, i.e., ORNs of later developmental stages responded to less amino acids than ORNs of earlier stages. These observations are rather unexpected and difficult to reconcile with the prevailing view of olfactory coding. We set out to elucidate the above observations carrying out a theoretical analysis of the 283 response profiles.

## **Molecular Mechanisms of Pheromone Detection in Mice**

**Frank Zufall**

Department of Anatomy and Neurobiology and Program in Neuroscience  
University of Maryland School of Medicine,  
20 Penn Street, Baltimore, MD 21201 USA

Current work in this laboratory is focused on the question how the brain processes information that is necessary for social recognition. In most non-primate mammals, a predominant source of this type of information is encoded by olfactory or pheromonal signals. Aggression, sexual behavior, kin and individual recognition, pair-bond formation, selective pregnancy termination, territoriality and dominance hierarchies all depend on the recognition and processing of specific chemosensory cues. We use a systems-oriented approach involving several levels of analyses, from genes to cells to behavior, to elucidate the molecular and cellular basis underlying social recognition by the mouse olfactory system. During the past few years, we have identified several key components necessary for aggression and sexual behavior, including a novel second messenger-operated ion channel that is gated by the lipid messenger diacylglycerol. Null-mutants lacking these signaling components show no aggressive behaviors and are defective in identifying appropriate mating partners. Our most recent work has identified a novel family of pheromone-like molecules that provides a unique molecular signature to each individual, thus conveying information about the genotype of an individual mouse. Detection of these molecules seems to be essential for avoiding inbreeding during reproduction and, therefore, ultimately serves the survival of the species.

Supported in part by grants from the National Institute on Deafness and Other Communication Disorders (NIH/NIDCD).

## Modulation of odorant signalling pathways

*Christian H. Wetzel, Hanns Hatt*

*Lehrstuhl für Zellphysiologie, Ruhr-Universität Bochum,  
Universitätsstrasse 150, D-44780 Bochum, Germany*

[Christian.H.Wetzel@RUB.DE](mailto:Christian.H.Wetzel@RUB.DE)

The sense of smell has the exquisite capacity to recognize and discriminate among an immense variety of volatile chemical compounds that are present in the environment. In mammals, olfactory cues are detected by sensory neurons belonging to three different sensory modalities harboured in the nasal cavity. Olfactory and vomeronasal primary sensory neurons (OSNs and VSNs, respectively) detect odorants and pheromones, whereas free nerve endings of the V cranial nerve (*N. trigeminus*) constitute the common chemical sense and convey pain, touch, temperature, and chemosensory information. Our interest is to understand the molecular and cellular mechanisms of chemosensation and the various aspects of signal modulation in the diverse subsystems. A first common step in signal transduction is the specific binding of odorant molecules to receptor proteins located in specialized membrane protrusions, the cilia, microvilli or free nerve endings innervating the nasal mucosa. Olfactory receptor and pheromone receptor proteins of OSNs and VSNs, respectively, are identified and functionally characterized to some extent. The intracellular mechanisms that transduce the initial chemical information into an electrical signal in OSNs involve the adenylate cyclase – cyclic nucleotide-gated channel pathway in addition to a recently identified phosphoinositides pathway. In contrast, a phospholipase C – diacylglycerol – transient receptor potential (TRP) channel pathway seems to play the major role in VSNs. The molecular mechanisms used by trigeminal neurons to detect odorant molecules are largely unknown. The beginning characterization of thermosensitive TRP channels among other receptors and ion channels expressed in trigeminal sensory neurons revealed their role in detection of chemical compounds and chemosensory signalling in these cells. Recently, we could show that in the olfactory subsystem, the modulation of the odorant signalling pathway by phosphoinositides plays an important role, although the molecular mechanism in detail is still not known. It will be of specific interest to identify similar modulatory processes in the other sensory modalities.



## **A specific heat shock protein as expression enhancer of mammalian olfactory receptor proteins**

Weiye Zhang, Anastasia Mashukova, Jon Barbour, Hanns Hatt and Eva M. Neuhaus

Multiple trials failed to express significant amounts of olfactory receptors in heterologous cells, as they are typically retained in the endoplasmic reticulum. Evidence is accumulating that cell-type-specific accessory proteins regulate the folding of olfactory receptors, their exit from the endoplasmic reticulum, and the trafficking to the plasma membrane of the olfactory cilia where the receptors gain access to odorants. The folding and membrane trafficking requirements of olfactory receptors appear to be available only in olfactory sensory neurons and other specialized cell types where odorant receptors are expressed on the membrane, e.g. mature spermatozoa.

To identify proteins that are specific for olfactory sensory neurons, we started to analyse the protein expression in the mouse olfactory epithelium with a proteomics approach performing MudPit. In one of our screens we identified Hsc70t in the protein preparations, a protein belonging to the Hsp70 family of heat shock proteins. Hsp70 proteins constitute the central part of an ubiquitous chaperone system that is present in eukaryotic cells, eubacteria and many archaea. In mammals, two principle isoforms exist in the cytoplasm, a 73kD form that is constitutively expressed (Hsc70), and a 72 kD, stress inducible form (Hsp70). The importance of Hsp70 proteins is highlighted by the fact, that in addition to the general assistance of protein folding, they are involved in important processes like transport of proteins across membranes, the disassembly of clathrin coated vesicles, and regulation of the heat shock response. Hsc70t is a testis specific variant of the Hsp70 family and is specifically expressed in post-meiotic germ cells. It appears in the cytoplasm of spermatids as they progress to the final step of spermatogenesis. Moreover, the Hsc70t gene is located in the major histocompatibility complex (MHC) region in mice and human, where a class of odorant receptors are located nearby. We verified the expression of Hsc70t in olfactory epithelium by RT-PCR analysis and found RNA in human and mouse olfactory epithelium, as well as testis. Due to the fact that Hsc70t is specifically expressed in mature sperm and in olfactory epithelium, two cell types where odorant receptor proteins are present, we assumed that it might be involved in the folding or trafficking of these receptors. To test this hypothesis, we cotransfected HEK293 cells with Hsc70t and different GFP-tagged odorant receptors from mouse and man. We found that coexpression of Hsc70t significantly enhanced odorant receptor expression in these cells. To test whether the enhanced expression level also changed the amount of receptors present at the cell surface we performed calcium imaging measurements in the heterologous HEK293 system. When cells were co-transfected with Hsc70t the number of cells responding to odorants significantly increased.

Molecular chaperones are a functionally defined set of proteins which assist the structure formation of proteins in vivo. Hsc70t is a specialized chaperone molecule that it is only expressed in very few cell types. Our results demonstrate that it helps expression of odorant receptors in heterologous cell systems. Overexpression of Hsc70t could also enhance or facilitate odorant receptor expression in the olfactory epithelium. Increasing its expression level by treatment of olfactory epithelium with recombinant adenoviruses could therefore potentially be used to treat smell dysfunctions which result from lowered olfactory receptor expression levels.

## **Tau pathology in the olfactory system correlates with Alzheimer pathology**

K.A. Jellinger (1), J. Attems (2)

(1) Institute of Clinical Neurobiology, Vienna, Austria

e-mail kurt.jellinger@univie.ac.at

(2) Institute of Pathology, Otto Wagner Hospital, Vienna, Austria

*Background:* Olfactory dysfunction is a common feature in Alzheimer's disease (AD), Parkinson disease (PD) and other neurodegenerative disorders. Recent autopsy studies of the olfactory bulb revealed positive tau pathology (neurofibrillary tangles /NFTs/ and neuropil threads /NTs/) in 84-100% of definite AD, in most cases of dementia with Lewy bodies (DLB), and in 10.5% of cases with mild cognitive impairment (MCI) (1,2). *Objective:* To report the results of an ongoing autopsy study of the olfactory system (OS) in aged humans.

*Material and methods:* 90 consecutive autopsy cases (61 females, 29 males, aged 61-98 /mean 84.4±6.4/ years) were examined. All brains underwent a standardized histopathological assessment including the olfactory bulb and nerve using routine stains, modified

Bielschowsky silver method and immunohistochemistry for tau and amyloid- $\beta$  protein.

Diagnosis of AD followed established criteria including Braak staging (3). Apolipoprotein

(Apo)E genotyping is in progress. *Results:* All cases of definite AD (Braak stages 5 and 6 - n=26) showed considerable numbers of both NTs and NFTs in the OS with amyloid deposits

in only 8/22 (36%). Braak stages 4 and 3 were associated with positive tau pathology of varying intensity in the OS in 86 and 52%, respectively. For both types of limbic AD, the total incidence of tau pathology in the OS was 59%, while amyloid plaques were seen in only 7% and neuritic plaques in none. Braak stage 2 showed olfactory tau lesions in 30%, while

Braak stages 1 and 0 were all negative. Two cases of PD and DLB without considerable AD-pathology showed no tau lesions in the OS. *Conclusions:* Both this and other recent studies

demonstrate a strong correlation between tau pathology in the OS with increasing severity of AD pathology, suggesting that the involvement of both the olfactory and hippocampal systems, that are functionally connected is associated with a high risk of cognitive decline.

Together with clinical data about the relationship between olfaction and dementing disorders, these and future studies should validate the diagnostic sensitivity and sensibility of olfactory dysfunction or olfactory mucosa biopsies in the early diagnosis of AD and other neurodegenerative disorders.

### **References:**

(1) Christen-Zach S et al. Can J Neurol Sci 30;2003:20-5

(2) Tsuboi Y et al. Neuropathol Appl Neurobiol 29;2003:503-10

(3) Braak H, Braak E. Acta Neuropathol 82;1991:239-59.

Individual olfactory sensory neurons project into more than one glomerulus in *Xenopus laevis* tadpole olfactory bulb

Leonid P. Nezlin and Detlev Schild

Department of Molecular Neurophysiology, University of Göttingen D37073, Göttingen, Germany

An essential step in the coding of odorants is the way olfactory sensory neurons (OSNs) convey their information to the olfactory bulb. This projection determines how the specificities of OSNs are mapped onto the spatial activity patterns of the olfactory bulb (OB). Despite the fact that virtually nothing is known about how individual OSN axons project to glomeruli, it is generally believed that OSNs always project to one glomerulus each. Our recent findings in tadpoles of *Xenopus laevis* challenge this view. By injection of a tracer into individual OSNs we show for the first time that axons typically project into more than one glomerulus and that they do so in a characteristic way. Upon entering the olfactory bulb, an axon bifurcates to give two primary branches. Each of these branches bifurcates again to give two subbranches, thus resulting in four subbranches per OSN. The two subbranches of each primary branch project into two different glomeruli. Variations of this characteristic innervation pattern include the innervation of three and, occasionally, one glomerulus. In any case, and independent of the number of glomeruli innervated by an OSN, each glomerulus receives at least two axonal branches of the same OSN.

## Spatiotemporal response properties of optically recorded moth projection neurons

Philipp Knüsel<sup>1</sup>, Mikael A. Carlsson<sup>2</sup>, Bill S. Hansson<sup>2</sup>, Paul F.M.J. Verschure<sup>1</sup>

Email: [pknuesel@ini.phys.ethz.ch](mailto:pknuesel@ini.phys.ethz.ch)

Address: <sup>1</sup>Institute of Neuroinformatics, University/ETH Zürich  
Winterthurerstr. 190, CH-8057 Zürich, Switzerland

<sup>2</sup>Neurobiology Research Group, Chemical Ecology,  
Dept. of Crop Science, Swedish University of Agricultural Sciences,  
Box 44, S-230 53 Alnarp, Sweden

Optical imaging of insects antennal lobe (AL) in response to odors is usually analyzed with respect to glomerular response amplitudes, suggesting a spatial encoding. Here we investigate the hypothesis that both response amplitude and duration are uncorrelated and independently modulated by odors, suggesting two independent encoding dimensions. Non-linear functions are fitted to the glomerular responses recorded from male moth *Spodoptera littoralis* using a dye (FURA-dextran) that is injected into the projection neurons (PN), the AL output neurons. Four odors at two different concentrations are used and their effects on the resulting fitting parameters, response amplitude and duration, are investigated. No correlation between amplitude and duration is found in most of the glomeruli (23 out of 33), excluding the trivial result of the duration depending linearly on the amplitude. Pooled for all animals (n=3) and glomeruli, odor and concentration significantly modulate response duration and amplitude. In individual glomeruli, duration and amplitude can be modulated simultaneously. The effect size (eta squared) onto duration is 55% and 29% for odor and concentration respectively, which is comparable to the effect size of odor and concentration onto amplitude (49% and 33% respectively). Thus, since both the PN response duration and amplitude are modulated by stimuli, this suggests that PNs can use them as two independent encoding dimensions.

This project is supported through the EU Future and Emerging Technologies Programme (IST-2001-33066 (AMOTH))

<http://www.amoth.org>

# Towards Predicting Olfactory Receptor Responses

Michael Schmuker\*, Gisbert Schneider

Johann Wolfgang Goethe-Universität, Beilstein Endowed Chair for Cheminformatics

Institut für Organische Chemie und Chemische Biologie

Marie-Curie-Str. 11, 60439 Frankfurt/Main, Germany

\*corresponding author. Email: michael.schmuker@chemie.uni-frankfurt.de

Results from vertebrate receptor assays as well as from *in vivo* studies on insects indicate that most olfactory receptors (ORs) are activated by a range of molecules sharing similar properties. Also, many odor molecules seem to activate several ORs. Except for a handful of ORs, it is still unclear which features of an odor molecule determine the activity profile it evokes in the panel of ORs. Due to limited data on molecular stimuli and their OR activity profile, there are currently no tools available to predict OR responses to a given substance.

De Bruyne *et al.* (2001) examined responses from *Drosophila* olfactory receptor neurons (ORNs) to selected molecules. Based on this data, we performed a cluster analysis with a self-organizing map (SOM) using various molecular representations. Our results indicate that substructure fingerprints might be suited for modeling OR response patterns and predict ORN responses in *Drosophila*. Unsupervised SOM-based clustering of the substances according to their substructure representation resulted in a pattern of clusters that correlates with the experimentally observed ORN activation pattern (Figure 1). The SOM can be used to predict new compounds that might bind to a defined set of ORs. Although our model is still in a preliminary stage it can be applied to designing screening experiments by suggesting candidate molecules. These results can in turn be used to refine the model.

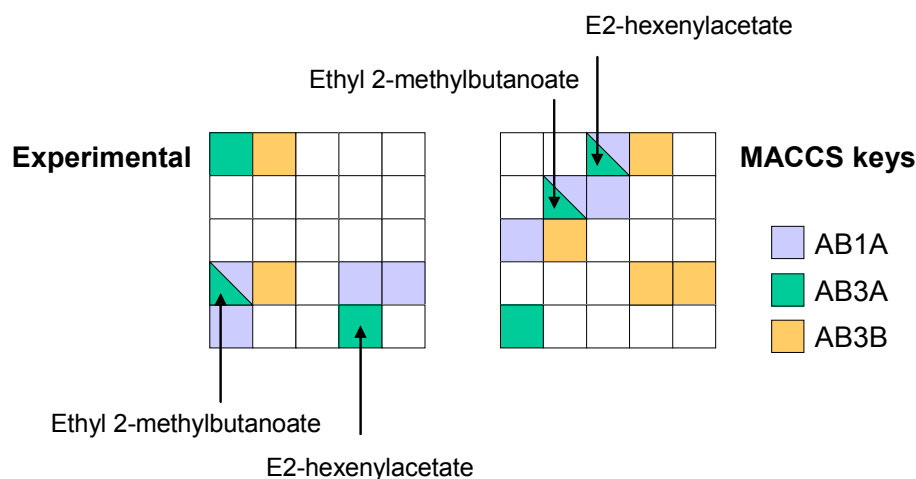


**Figure 1.** Location of substances on SOMs that were trained with experimentally observed OR response patterns (left), and MACCS substructure fingerprints (right). Colors indicate clusters of molecules which activate selected *Drosophila* OR subtypes. The locations of two selected substances with activity at both the AB1A and AB3A receptor are highlighted. Both compounds are inactive at the AB3B receptor. Note that the maps form a torus.

## Reference

De Bruyne M, Foster K, Carlson JR (2001) Odor coding in the *Drosophila* antenna. *Neuron* **30**, 537-552.

**Symposium #S22:**  
**Function of the glial cell line derived neurotrophic factor family in  
development and disease**  
**H.Peterziel, KH. Schäfer, K. Unsicker, Heidelberg**

**Introduction**

- [#S22](#) H.Peterziel, KH. Schäfer, K. Unsicker, Heidelberg  
*Function of the glial cell line derived neurotrophic factor family in development and disease*

**Slide**

- [#S22-1](#) J. Thomas-Crusells, T. Sigl, B. Leiner, Q. Yan, AA. Welcher, P. Mestres, W. Tetzlaff, M. Saarma, K. Kaila, M. Meyer, C. Rivera and KM. Giehl, Homburg/Saar, Thousand Oaks (USA), Vancouver (CDN), München, Helsinki (FIN) and Dallas (USA)  
*Neurotrophins and GDNF-family ligands: mechanisms of trophic support and lesion-induced switches*
- [#S22-2](#) V. Pachnis, London (UK)  
*The co-ordinate role of Glial cell line-derived neurotrophic factor (GDNF) and Endothelin-3 (ET-3) in the development of the mammalian enteric nervous system*
- [#S22-3](#) H. Peterziel, Heidelberg  
*Signalling crosstalk in GFL-mediated neuron survival*
- [#S22-4](#) M. Saarma, Helsinki (FIN)  
*Structure of GFRalpha1 receptor and its implications to GDNF and RET binding*
- [#S22-5](#) K-H. Schäfer, Zweibrücken  
*Influences of the GDNF-family upon postnatal development of the enteric nervous system*

**Poster**

- [#49B](#) GPH. Dietz, PC. Valbuena, K. Meuer, JH. Weishaupt and M. Bähr, Göttingen  
*Application of a Blood-Brain-Barrier-Penetrating Form of GDNF in an in vivo Model for Parkinsons Disease*
- [#50B](#) A. Ducray, M. Meyer, B. Teisner, CH. Jensen and H. Widmer, Berne (CH) and Odense (DK)  
*Fetal antigen-1 expressing cells in rat ventral mesencephalic cultures: Neural phenotype identification and effects of GDNF family ligands.*

## **Introductory Remarks to Symposium 22**

### **Function of the glial cell line derived neurotrophic factor family in development and disease**

**H. Peterziel, KH. Schäfer and K. Unsicker, Heidelberg und Kaiserslautern**

Members of the glial cell line-derived neurotrophic factor (GDNF) family serve important functions in development and maintenance of distinct sets of central and peripheral neurons. All four GDNF-family ligands (GFL), GDNF, neurturin (NRTN), artemin (ARTN) and, persephin (PSPN), interact with a multi-subunit receptor complex formed by the c-Ret tyrosine kinase, RET, and a cystine-rich glycosyl phosphatidylinositol-anchored binding receptor (GDNF receptor alpha. 1-4). Since their discovery, GFL have received particular attention because of their therapeutic potential in numerous neurological diseases, such as Parkinson's disease, motor neuron diseases, or sensory regeneration and neuropathic pain. Targeted mutagenesis in transgenic mice has shown that Ret, and GFL are required for multiple developmental events including development of the enteric nervous system (ENS) affected in Hirschsprung's disease. The symposium focuses on the molecular mechanisms of the initiation and the contextual dependence of signal transduction by GDNF family ligands, their neuroprotective and neuroregenerative potential and their involvement in developmental processes.

## Neurotrophins and GDNF-family ligands: mechanisms of trophic support and lesion-induced switches

J. Thomas-Crusells<sup>1,2,+</sup>, T. Sigl<sup>1,+</sup>, B. Leiner<sup>1</sup>, Q. Yan<sup>4</sup>, A.A. Welcher<sup>4</sup>, P. Mestres<sup>1</sup>, W. Tetzlaff<sup>5</sup>, M. Saarma<sup>2</sup>, K. Kaila<sup>3</sup>, M. Meyer<sup>6</sup>, C. Rivera<sup>2,3</sup>, and K.M. Giehl<sup>1,7</sup>

<sup>1</sup> Universität des Saarlandes, Institut für Anatomie und Zellbiologie, 66421 Homburg/Saar, Germany;

<sup>2</sup> Program of Molecular Neurobiology, Institute of Biotechnology, University of Helsinki, Helsinki, Finland

<sup>3</sup> Division of Animal Physiology, Viikki Biocenter, FIN-00014 University of Helsinki, Helsinki, Finland

<sup>4</sup> Amgen Inc., Thousand Oaks, USA

<sup>5</sup> University of British Columbia, Department of Zoology and ICORD, Vancouver, Canada

<sup>6</sup> Ludwigs-Maximilians Universität München, Physiologisches Institut, 80336 München, Germany

<sup>7</sup> The University of Texas Southwestern Medical Center, Department of Cell Biology, 5323 Harry Hines Blvd., Dallas, Texas 75390-9039, USA

<sup>+</sup> equal contribution

Neurotrophins and GDNF-family ligands play an important role for the regulation of neuronal survival. We show in the corticospinal system that injury to the adult brain switches growth factor-mediated survival regulation of the affected neurons:

- (1) During cortical development, the neurotrophin NT3 acts as a differentiation factor promoting progenitors to adopt a neuronal phenotype that depends on the neurotrophin BDNF for survival (1),(2). BDNF-dependency is lost during postnatal development (3) and for intact adult corticospinal neurons (CSN). Also NT3 does not affect the survival regulation of intact adult CSN. However, both NT3 and BDNF regain a function for survival regulation after axotomy. NT3, via its receptor TrkC, initiates BDNF-dependent survival of lesioned adult CSN by inducing their expression of the common neurotrophin receptor p75. After the lesion, those CSN that are not sufficiently supplied with BDNF are eliminated by the neurotrophin precursor proNGF through p75. Similar to the roles of NT3 and BDNF after the lesion, also the role of p75 is reminiscent to the embryonic situation since p75 is expressed at high levels during development and downregulated postnatally (4). The data indicate that NT3/TrkC is important to install the lesion-specific survival regulation of CSN, and that adult CSN establish an embryonic mode of survival regulation after damage.
- (2) Internal capsule lesion of adult CSN switches their BDNF-mediated KCC2-regulation to an embryonic mode. KCC2 is a neuronal cation-chloride cotransporter that is responsible for the switch of GABAergic transmission from being depolarizing in immature to being hyperpolarizing in mature neurons (5). BDNF upregulates KCC2 in embryonic neurons while it has an opposite effect on adult neurons (6),(7). This situation is reiterated in adult CSN after lesion as BDNF downregulates KCC2 in intact CSN while it upregulates KCC2 in lesioned CSN. In this context, KCC2 might be involved in GABA's neurotrophic function during development: Downmodulating KCC2 in intact adult CSN to levels seen during development induces BDNF-dependent survival of these cells.
- (3) Survival of lesioned CSN is supported not only by BDNF but also by GDNF. The GDNF effects, however, completely depend on the presence of BDNF suggesting that the two growth factor families interact for the survival regulation of lesioned neurons. Expression analyses of the BDNF and GDNF receptors and the effects of BDNF and GDNF on KCC2 regulation in lesioned CSN further suggest that BDNF and GDNF act in sequence after lesion.

Taken together, our data suggest that NT3/TrkC and KCC2 are important factors for lesion-induced switches of trophic dependencies of adult CSN, that the lesion induces an embryonic program encompassing survival regulation, and that neurotrophins and GDNF-family members interact in this context.

1. A. Ghosh, J. Carnahan, M. E. Greenberg, *Science* **263**, 1618 (Mar 18, 1994).

2. A. Ghosh, M. E. Greenberg, *Neuron* **15**, 89 (Jul, 1995).

3. H. Junger, S. Varon, *Brain Research* **762**, 56 (Jul 11, 1997).

4. G. Dechant, Y. A. Barde, *Nature Neuroscience* **5**, 1131 (Nov, 2002).

5. J. A. Payne, C. Rivera, J. Voipio, K. Kaila, *Trends in Neurosciences* **26**, 199 (Apr, 2003).

6. C. Rivera *et al.*, *Journal of Cell Biology* **159**, 747 (Dec 9, 2002).

7. F. Aguado *et al.*, *Development* **130**, 1267 (Apr, 2003).



**The co-ordinate role of Glial cell line-derived neurotrophic factor (GDNF) and Endothelin-3 (ET-3) in the development of the mammalian enteric nervous system.**

Vassilis Pachnis, Division of Molecular Neurobiology, MRC National Institute for Medical Research, Mill Hill, The Ridgeway, London NW7 1AA, UK

The enteric nervous system (ENS) in vertebrates is derived mainly from vagal neural crest cells which enter the foregut and colonise the wall of the gastrointestinal tract in an orderly anterior to posterior direction. Failure of complete colonisation of the gut by neural crest cells results in the absence of enteric ganglia (aganglionosis) leading to peristaltic misregulation, intestinal obstruction and megacolon (Hirschsprung's disease). Two signalling molecules, GDNF and ET-3 (and their corresponding receptors RET and EDNRB), and the transcriptional regulator SOX10 have been identified independently as critical players in enteric neurogenesis in mammals. To study the interaction between the GDNF/RET and ET-3/EDNRB signalling pathways and SOX10, we have analysed the effects of various combinations of mutant alleles at the *Ret*, *Et-3/Ednrb* and *Sox10* loci on enteric ganglia formation. Our experiments highlight strong genetic interactions between these loci and indicate that normal development of the ENS requires the co-ordinate spatial and temporal regulation of their activities.

**Signalling crosstalk in GFL-mediated neuron survival**

**Heike Peterziel, Institute for Neuroanatomy and Interdisciplinary Center for Neurosciences, University of Heidelberg, Heidelberg, Germany**

E-mail address: heike.peterziel@urz.uni-heidelberg.de

The glial cell line-derived neurotrophic factor (GDNF) family comprise a subclass of cystine-knot superfamily ligands that interact with a multi-subunit receptor complex formed by the c-Ret tyrosine kinase and a cysteine-rich glycosyl phosphatidylinositol-anchored binding subunit called GDNF family receptor alpha (GFR $\alpha$ ). All four GDNF family ligands (GFL), GDNF, neurturin (NRTN), persephin (PSPN) and artemin (ARTN), utilize c-Ret as a common signalling receptor, whereas specificity is conferred by differential binding to four distinct GFR $\alpha$  homologues (GFR $\alpha$ 1-4). The consequences of GFL binding and subsequent activation of downstream signalling pathways are dependent on the cellular context. Integration of different signal transduction pathways may thus be an important general cellular strategy to tightly regulate GFL-mediated effects.

Both GDNF and NRTN constitute target-derived factors in the development and maintenance of different parasympathetic neuron populations including ciliary ganglion (CG) neurons. Results from our group indicate, that the presence of transforming growth factor- $\beta$  (TGF $\beta$ ) is mandatory for GDNF-mediated survival of CG neurons and various other neuronal populations of the central and peripheral nervous system in vitro and in vivo. In CG neurons, TGF $\beta$  induces responsiveness to GDNF by recruiting GFR $\alpha$ 1 to its active site at the cell surface by a mechanism involving TGF $\beta$  signalling via its specific receptor complex. Interestingly, in contrast to GDNF, NRTN is not dependent on cooperation with TGF $\beta$  but efficiently promotes neuronal survival and intracellular signalling in the absence of TGF $\beta$ . Consistently, cell surface localization of the specific NRTN receptor GFR $\alpha$ 2 does not require TGF $\beta$  signalling. These observations indicate that context-dependent interactions between GFL and other signalling pathways may be important for fine-tuning the response to these neurotrophic factors in vivo. The differences in TGF $\beta$ -dependence of GDNF and NRTN signalling might be important for the regulation of essential developmental processes like ontogenetic cell death or differentiation.

The low number of cells and the general difficulty to transfect CG neurons has prompted us to investigate the molecular mechanism of the GDNF/TGF $\beta$  interaction in an alternative in vitro model system. We have engineered a mouse neuroblastoma cell line responsive for both GDNF and TGF $\beta$  by transfecting the appropriate receptors. GDNF treatment of the parental cell line results in activation of the phosphatidylinositol-3-kinase (PI3K) pathway and phosphorylation of mitogen-activated protein kinase ERK1/2. The effect on ERK1/2 is biphasic as there is a fast increase in phosphorylation within minutes which declines after 1 hour and a second sustained increase after 12 hours. In the transfected cells, TGF $\beta$  treatment results in an increased rapid activation of GDNF downstream signalling molecules via the PI3K pathway. Interestingly, the effect of TGF $\beta$  on GDNF-mediated ERK-phosphorylation differs depending on the time of activation. While fast ERK-phosphorylation is increased in the presence of TGF $\beta$ , the late GDNF-mediated ERK-phosphorylation is completely abolished. Whether the regulation of GDNF-mediated intracellular signalling by TGF $\beta$  results in functional changes, including proliferation or differentiation of the cells, is under current investigation. Taken together, we conclude that the neuroblastoma cell line modified in our laboratory provides a useful tool to investigate the molecular mechanisms triggered by the interaction of GDNF and TGF $\beta$ .

## Structure of GFR $\alpha$ 1 receptor and its implications to GDNF and RET binding

Mart Saarma

Institute of Biotechnology, Biocenter 1, University of Helsinki, FIN-00014, Finland

Glial cell line-derived neurotrophic factor (GDNF) and related ligands neurturin (NRTN), artemin (ARTN) and persephin (PSPN) form a subgroup in TGF- $\beta$  superfamily. Responses to GDNF family ligands (GFL) are mediated by a receptor complex composed of the transmembrane tyrosine kinase c-Ret and one of the glycosyl-phosphatidyl inositol (GPI-) anchored GDNF family  $\alpha$ -receptors (GFR $\alpha$ 1 – GFR $\alpha$  4). GFR $\alpha$ 1 is the principal co-receptor for GDNF, GFR $\alpha$ 2 for NRTN, GFR $\alpha$ 3 for ARTN and GFR $\alpha$ 4 for PSPN<sup>1</sup>. Recent data demonstrate that GDNF family ligands can also signal via neural cell adhesion molecule NCAM.

Binding studies suggest that homodimeric GDNF serves mainly to dimerize the co-receptor, GFR $\alpha$ 1, and brings together the ternary complex with RET. The general principles of GFL signalling utilizing multi-subunit receptor complexes is beginning to be understood, but many questions related to GDNF-receptor interaction remain open. Therefore, structural studies on the GFR $\alpha$ 1 were initiated to address these questions at the molecular level. The crystal structure of GDNF has already been solved at 1.9 Å resolution<sup>2</sup>.

GFR $\alpha$ 1 has a signal peptide for secretion at the amino terminus, a glycosylphosphatidylinositol (GPI) -anchor signal at the C-terminus and three potential N-glycosylation sites. Conserved cysteine patterning in all GFR $\alpha$  receptors suggests a putative domain structure with three homologous cysteine-rich domains for GFR $\alpha$ 1-3 and with two cysteine-rich domains for GFR $\alpha$ 4. In GFR $\alpha$ 1 each domain is about 100 residues long, bound together with hinge regions, where domains 2 and 3 make up a central domain responsible for GDNF binding. We solved the 1.8 Å crystal structure of GFR $\alpha$ 1 domain 3 showing a new protein fold. It is an all-alpha five-helix bundle with five disulfide bridges. The structure was used to model the homologous domain 2, the other half of the GDNF-binding fragment, and to construct the first structural model of the GDNF-GFR $\alpha$ 1 interaction<sup>3</sup>. Using site-directed mutagenesis, we identified closely spaced residues, Phe213, Arg224, Arg225 and Ile229, comprising a putative GDNF binding surface. Mutating each one of them had slightly different effects on GDNF binding and RET phosphorylation. In addition, the R217E mutant bound GDNF equally well in the presence and absence of RET. Arg217 may thus be involved in the allosteric properties of GFR $\alpha$ 1 or in binding RET.

<sup>1</sup> Airaksinen, M. S. & Saarma, M. (2002) *Nature Rev. Neurosci.*, 3: 383-394.

<sup>2</sup> Eigenbrot, C. & Gerber, N. (1997). *Nat. Struct. Biol.*, 4: 435-438.

<sup>3</sup> Leppänen *et al.* (2004) *EMBO J.* 23:1452-1462.

## Influences of the GDNF-family upon postnatal development of the enteric nervous system

Karl-Herbert Schäfer, University of Applied Sciences Kaiserslautern, Zweibrücken, Germany

Developmental failures in the enteric nervous system (ENS) might lead to severe disturbances of the gastro-intestinal function. So a lack of GDNF support as seen in GDNF knock-out mice results in complete absence of the ENS from the stomach to the colon. The modeling of known diseases such as Hirschsprung's disease, is much more complicate. Nevertheless it could be demonstrated that a combination of ret-tyrosinkinase and endothelin-B-receptor knockout delivers a Hirschsprung-like morphology. So far there is only a surgical therapy for this kind of disease. Isolation and transplantation of neuronal precursors is a promising alternative. The influence of neurotrophic factors upon the development and differentiation of postnatal neurons, but also presumptive postnatal precursor cells is crucial, although decreasing neuronal numbers in older animals and humans give evidence for a changing trophic support or dependency.

We therefore investigated the influence of GDNF, Neurturin, Artemin and Persephin upon postnatal enteric neuronal growth in two- and threedimensional cultures. Myenteric plexus of postnatal rats at various ages were isolated, dissociated and kept in vitro. Culture medium was supplemented with either one of the trophic factors or used with no additional supplement in the controls. It could be shown, that GDNF and Neurturin do enhance neuronal survival and neurite outgrowth depending on the age of the animal and the localization of the isolated plexus. The GDNF effect generally decreased with age, while Neurturin seems to be still effecting neurite outgrowth in older animals. Artemin and Persephin do not influence significantly neurite outgrowth, while there might be a more intense stimulation of the glia. To study growth patterns in a three-dimensional surrounding, dissociated myenteric plexus was resuspended in an extracellular matrix gel. There it formed a secondary network, where the size of the ganglia and the density of the neurite network depended on the growth factor provided. In GDNF and Neurturin supplemented cultures the ganglia appeared larger and the neurite network denser, where Neurturin even provoked a more intricate network.

To investigate the natural target organ for the future transplantations, tissue from patients with Hirschsprung's disease were homogenized and ELISA analysis of GDNF content were performed. Muscle from aganglionic and ganglionic regions were compared in the same patient. Generally also in the aganglionic bowel there was a substantial GDNF content, although it was usually lower as that of the ganglionic muscle. We therefore consider the microenvironment in Hirschsprung's disease as permissive for transplantation.

The experiments performed so far underline the influence of GDNF or relatives also in postnatal development. If enteric progenitor cells will be transplanted to the aganglionic bowel, a priming with an appropriate GDNF-family-cocktail might be useful.

## **Application of a Blood-Brain-Barrier-Penetrating Form of GDNF in an *in vivo* Model for Parkinson's Disease**

Gunnar P.H. Dietz, Paola C. Valbuena, Katrin Meuer, Jochen H. Weishaupt, and Mathias Bähr

The first two authors contributed equally.

Neurologische Universitätsklinik, Waldweg 33, D-37073 Göttingen, Germany

E-mail: [gdietz@gwdg.de](mailto:gdietz@gwdg.de)

Homepage: <http://www.mi.med.uni-goettingen.de/baehr-lab/>

### **ABSTRACT**

Glial cell line-derived neurotrophic factor (GDNF) promotes mesencephalic dopaminergic neuronal survival in several *in vitro* and *in vivo* models. As the demise of dopaminergic neurons is responsible for clinical symptoms in Parkinson's Disease, GDNF is a promising therapeutic agent for its treatment. However, this neurotrophin is unable to cross the blood-brain-barrier, which has prevented its clinical use. Therefore, ways to deliver this protein into the central nervous system in an effective manner are needed. The TAT protein transduction domain (PTD) provides a means to get fusion proteins into the brain.

In this study, we have generated a fusion protein between the 11 amino acid-PTD of TAT and the rat GDNF mature protein, to deliver bioactive GDNF across the blood-brain barrier. We have tested its effect in a subchronic scheme of 1-methyl-4-phenyl-1,2,3,6-tetrahydropyridine (MPTP) application into the mouse as a model for Parkinson's disease, in order to evaluate the effect of TAT-GDNF fusion protein in dopaminergic neuron survival.

The data presented here suggest that *in vivo* application of TAT-GDNF provides neuroprotection of dopaminergic neurons, as revealed by immunohistochemistry and counting of the number of tyrosine hydroxylase immunoreactive (TH-IR) neurons in the substantia nigra pars compacta. There was also a mild effect to alleviate the loss of TH-IR fibers in the striatum.

**Keywords:** animal models for diseases, blood-brain barrier, neuroprotection

Fetal antigen-1 expressing cells in rat ventral mesencephalic cultures: Neural phenotype identification and effects of GDNF family ligands.

A. DUCRAY, M. MEYER#, B. TEISNER##, C.H. JENSEN## and H.R. WIDMER.

Dept. Neurosurgery, Univ. of Berne, CH-3010 Berne, Switzerland.

#Dept. Anatomy & Neurobiology and ##Dept. Immunology & Microbiology, Institute of Medical Biology, Univ. of Southern Denmark, DK-5000 Odense C, Denmark.

The Fetal antigen-1 (FA1/dlk) protein, encoded by the gene DLK1, is a part of a transmembrane protein belonging to the epidermal growth factor superfamily. FA1/dlk is found in the adult rat midbrain and it has been suggested as a potential alternative marker for immature dopaminergic neurons. The glial cell line-derived neurotrophic factor (GDNF) family of ligands (GFLs) consisting of GDNF, Neurturin (NRTN), Artemin (ARTN) and Persephin (PSPN) have been demonstrated to promote survival and morphological differentiation of dopaminergic (TH) neurons. The present study aimed at characterizing the phenotype of FA1/dlk-ir cells and investigating the effects of GFLs on densities of FA1/dlk-immunoreactive(FA1/dlk-ir) neurons in rat (E14) ventral mesencephalic (VM) primary cultures grown for 5 days. Interestingly, FA1/dlk expression was not observed in nestin-ir and vimentin-ir precursor cells. All FA1/dlk-ir cells, however, were found to express b-III-tubuline and  $60.0 \pm 3.3\%$  also NeuN. No colocalization was seen with the astroglial marker GFAP. Furthermore,  $30.5 \pm 5.6\%$  colocalized with TH and  $18.6 \pm 3.1\%$  with 5-HT. Preliminary data demonstrated that  $12.7 \pm 4.8\%$  of FA1/dlk-ir neurons expressed GABA. GDNF, NRTN or ARTN [10ng/ml] exposure significantly increased densities of FA1/dlk-ir neurons (by 1.5 fold) as compared to controls. In contrast, PSPN failed to show an effect. Based on our previous observations that GFLs also promoted densities of cultured non-dopaminergic neurons (Ducray et al., FENS abstract, 2004) we performed a more detailed analysis. We observed that GDNF and NRTN significantly increased TH-negative/FA1-positive cell densities, while ARTN had no effect. Hence the increase of FA1-ir cell densities observed after ARTN exposure may reflect an effect on dopaminergic neurons. In conclusion, we identified FA1/dlk expression in different neuronal subpopulations. The demonstration that GDNF, NRTN and ARTN but not PSPN influenced FA1/dlk-ir cell densities points to a heterogeneous role of the GFLs during midbrain development. Given that FA1/dlk has been suggested to be involved in proliferation and differentiation processes it is tempting to speculate that GFLs may mediate their effects on neural differentiation via FA1/dlk.

## Symposium #S23:

### Possible mechanisms contributing to memory consolidation during sleep

S. Gais and J. Born, Lübeck

#### Introduction

[#S23](#)

S. Gais and J. Born, Lübeck

*Possible mechanisms contributing to memory consolidation during sleep*

#### Slide

[#S23-1](#)

P. Anderer, B. Saletu, W. Klimesch and J. Zeitlhofer, Vienna (A) and Salzburg (A)

*Significance of electrophysiological neuroimaging in studying memory formation during sleep*

[#S23-2](#)

J. Fell, C. Helmstaedter, CE. Elger and G. Fernández, Bonn and Nijmegen (NL)

*Neural correlates of impaired memory encoding during sleep in humans*

[#S23-3](#)

P. Peigneux, Liège (B)

*Cerebral correlates of memory consolidation through the sleep-wake cycle: contributions from functional neuroimaging.*

[#S23-4](#)

SJ. Sara, O. Yeshenko and J. Lelong, Paris (F)

*Locus Coeruleus activity in the rat during task acquisition, task performance and during sleep episodes following new learning or memory reactivation*

[#S23-5](#)

T. Schiffelholz and JB. Aldenhoff, Kiel

*Novel object presentation enhances theta and spindle activity within the sleep EEG of the rat*

[#S23-6](#)

MA. Wilson, Cambridge, MA (USA)

*Hippocampal activity, plasticity and sleep*

[#S23-7](#)

S. Gais, B. Rasch and J. Born, Lübeck

*Changes in brain cholinergic activity during sleep and wakefulness in humans affect memory consolidation*

#### Poster

[#51B](#)

Z. Clemens, D. Fabó and P. Halász, Budapest (H)

*Overnight verbal but not visual memory retention correlates with the number of sleep spindles*

[#52B](#)

R. Ramseger, M. Annies, S. Wöll, J. Löschinger and S. Kröger, Mainz and Tübingen  
*The Transmembrane Form of Agrin Reorganizes the Cytoskeleton in Neurons and Non-Neuronal Cells*

[#53B](#)

OP. Hornung, F. Regen, H. Danker-Hopfe, M. Schredl and I. Heuser, Berlin and Mannheim  
*Procedural Motor Skill Learning is Associated with REM-Sleep in Healthy Older Adults*

[#54B](#)

O. Yesenko and SJ. Sara, Paris (F)  
*Sleep spindle activity after different learning experiences in rats*



## **Introductory Remarks to Symposium 23**

### **Possible mechanisms contributing to memory consolidation during sleep**

**Steffen Gais and Jan Born, Lübeck**

Many recent studies show that sleep contributes to the consolidation of new memories. This symposium will discuss research on mechanisms thought to underlie the memory enhancing effect of sleep primarily from two directions: On the one hand, a reactivation of neuronal ensembles or brain areas has been found during sleep in neurons that have been active during a preceding learning episode, indicating a processing of newly learned information during sleep. On the other hand, sleep provides a particular pattern of neurotransmitter and neuroendocrine activity which facilitates occurrence of consolidation processes. Here, we will present recent rat and human research that tries to understand these mechanisms

A technique that allows recording simultaneously the activity of ensembles of hundreds of single neurons in freely behaving animals made possible to monitor specific memory patterns in the rat hippocampus and neocortex. Matthew Wilson will provide evidence that the neocortex may be creating memories that attempt to generalize across experience, while the hippocampus stores the experiences themselves, and he will explain what this has to do with the dreaming life of rats.

Functional brain imaging experiments have demonstrated the re-expression and modulation of learning-related cerebral activity in the sleeping brain. Emphasizing human PET studies Philippe Peigneux will trace the cerebral correlates of the journey of a new memory, from its initial acquisition and maintenance during wakefulness to its re-expression and consolidation during post-training sleep.

Low-resolution brain electromagnetic tomography (LORETA) is another new method that offers the possibility of investigating under undisturbed sleeping conditions when (in which sleep stages) and where (in which cortical brain regions) experience-dependent reactivation occurs during sleep. Peter Anderer will present recent results from studies using EEG and LORETA in human subjects.

It is possible to record directly the human hippocampal EEG in rare epileptic patients who have electrodes implanted for diagnostic purposes. Jürgen Fell will show that during sleep rhinal-hippocampal EEG coherence of gamma activity, induced by declarative memory encoding, is reduced compared to the waking state, which may explain the deficiency of memory encoding during sleep.

Spatial learning tasks have been shown to increase the amount of REM sleep with its typical theta rhythm (6-8 Hz) and spindle activity (12-15 Hz) within the EEG of non-REM sleep. Thomas Schiffelholz will show recent data indicating that these learning dependent changes within the EEG also occur following non-spatial learning tasks in rats.

Norepinephrine from the locus coeruleus plays an important role in the modulation of long-term memory consolidation. Its participation in the regulation of sleep makes it a possible candidate for mediating sleep's influence on memory. Susan Sara will present research done in rats that links noradrenergic locus coeruleus activity to sleep spindles and to memory consolidation.

Acetylcholine (ACh) is another neurotransmitter involved in sleep regulation and memory. While memory encoding needs high levels of ACh, the low concentration of ACh during SWS is important for memory consolidation. Jan Born and Steffen Gais will show data from several experiments in humans using post-learning cholinergic agonists and antagonists.

## Significance of electrophysiological neuroimaging in studying memory formation during sleep

Peter Anderer<sup>1</sup>, Bernd Saletu<sup>1</sup>, Wolfgang Klimesch<sup>2</sup> und Josef Zeitlhofer<sup>3</sup><sup>1</sup>Department of Psychiatry, Medical University of Vienna, Austria<sup>2</sup>Department of Physiological Psychology, University of Salzburg, Austria<sup>3</sup>Department of Neurology, Medical University of Vienna, Austria

Experience-dependent cortical plasticity observed during posttraining sleep has been hypothesized to be part of the global process of memory consolidation. Low-resolution brain electromagnetic tomography (LORETA) offers the possibility of investigating under normal (undisturbed) sleeping conditions when (in which sleep stages) and where (in which cortical brain regions) experience-dependent reactivation occurs. Recent studies suggest a connection between explicit memory tasks and the activity of sleep spindles in the night following learning.

Twenty four healthy volunteers between 20 and 29 years spent 3 nights in the sleep-lab. The first night served for adaptation purposes, while the second and third nights were randomly assigned either to a control condition without intentional learning or to an experimental condition in which subjects had to perform a declarative memory task (paired-associate word list) approximately 2.5 hours before sleep. A set of 160 word pairs was presented twice in randomized order. Subjects performed a cued recall task after the encoding session in the evening and after sleep in the morning. Spindles were detected automatically in channel C3-A1 using a recently developed two-step procedure with bandpass filtering and subsequent linear discriminant analysis. Spindle density (number / minute S2) and intensity (sum of discriminant scores / minute S2) were determined for all spindle events as well as for fast and slow spindles for the entire night and for five 1.5-hours parts of the night.

Subjects correctly retrieved 62.6% of all word-pairs in the evening and 63.7% in the morning after the experimental night. This slight improvement between evening and morning recall was not significant. Moreover, there were no significant differences regarding sleep efficiency and sleep architecture as well as spindle density and spindle intensity between experimental and control night. However, there was a significant correlation between changes in spindle density and intensity (experimental minus control night) and overnight changes in memory performance ( $r=.44$ ,  $p<.05$  and  $r=.52$ ,  $p<.01$  for density and intensity, respectively). These correlations were most prominent in the first three 1.5-hours parts of the night. Interestingly, changes in memory performance correlated significantly only with fast but not with slow spindle measures.

In summary, we found a relationship between changes in the density and intensity of fast spindles during S2 sleep (experimental minus control night) and changes in declarative memory performance (morning minus evening recall). LORETA sources for fast spindles have been found to be generated predominantly in parietal lobe (precuneus, BA 7) a brain region involved in language comprehension and complex sensory appreciation. Moreover, significant correlations were observed in the first parts of the night, which is in line with the hypothesis that sleep in the first part of the night is critical for consolidation of declarative memory. The differential effect on fast and slow spindles provide further evidence for differential functional significances of slow (frontally generated) and fast (parietally generated) spindles. Thus, the present study directly proves the involvement of sleep spindle activity in the consolidation of explicit memory.

**Acknowledgment:** Research supported by Austrian Industrial Research Promotion Fund (Project 806765). The Austrian Research Institute for Artificial Intelligence is supported by the Austrian Federal Ministry of Education, Science and Culture and the Austrian Federal Ministry of Transport, Innovation and Technology.

## Neural correlates of impaired memory encoding during sleep in humans

Juergen Fell<sup>1</sup>, Christoph Helmstaedter<sup>1</sup>, Christian E. Elger<sup>1</sup>, Guillén Fernández<sup>1,2</sup>

<sup>1</sup>Dept. of Epileptology, University of Bonn, Sigmund-Freud Str. 25, D-53105 Bonn, Germany

<sup>2</sup>F.C. Donders Center for Cognitive Neuroimaging, P.O. Box 9101, 6500 HB Nijmegen, The Netherlands

Human declarative memory formation crucially depends on processes within the medial temporal lobe (MTL). These processes can be monitored in real-time by recordings from depth electrodes implanted in the MTL of epilepsy patients, which undergo presurgical evaluation. In our studies, patients performed a word memorization task during depth EEG recording. Afterwards, the difference between event-related potentials corresponding to subsequently remembered versus forgotten words was analyzed. These kind of studies revealed that successful memory encoding is characterized by an early process generated by the rhinal cortex within 300 ms following stimulus onset preceding a hippocampal process, which starts about 200 ms later.

Direct evidence for a memory related cooperation between both structures has been found in a study analyzing induced gamma activity around 40 Hz. Here, successful as opposed to unsuccessful memory formation was accompanied by an initial enhancement of rhinal-hippocampal phase synchronization, which was followed by a later desynchronization. Present knowledge about the function of synchronized gamma activity suggests that this phase coupling and decoupling initiates and later terminates communication between both MTL structures. Furthermore, the memory related changes of gamma synchronization were found to be correlated with increases of rhinal-hippocampal coherence in the theta range. This correlation may suggest an interaction of both mechanisms during memory formation.

During sleep (at least during REM sleep) memory encoding seems to be impaired compared to the waking state, as indicated by the facts that dreamed experiences are rarely recalled, that scene shifts typically are not recognized by the dreamer and that the duration of dreams is usually tremendously misestimated. We observed a general reduction of rhinal-hippocampal EEG coherence during sleep compared to waking state, which was most pronounced within the gamma band. In the context of our prior findings this decrease of rhinal-hippocampal EEG coherence may yield an electrophysiological explanation for the sleep related deficiency of declarative memory. When comparing patients, who remember their dreams quite well, with patients who rather do not remember their dreams, we detected that rhinal-hippocampal coherence during sleep is about twice as large across all frequency bands in those patients with superior dream recall. This result corroborates the hypothesis that rhinal-hippocampal connectivity plays an essential role in declarative memory formation.

Supported by the German Research Council (grant DFG-El-122-8)

Fell J, Städtgen M, Burr W, Kockelmann E, Helmstaedter C, Schaller C, Elger CE, Fernández G. Rhinal-hippocampal EEG coherence is reduced during sleep. *Eur J Neurosci* 2003; 18:1711-1716.

Fell J, Klaver P, Elfarid H, Schaller C, Elger CE, Fernández G. Rhinal-hippocampal theta coherence during declarative memory formation: interaction with gamma synchronization? *Eur J Neurosci* 2003; 17:1082-1088.

Fell J, Klaver P, Elger CE, Fernández G. The interaction of rhinal cortex and hippocampus in human declarative memory formation. *Rev Neurosci* 2002; 13:299-312.

Fell J, Klaver P, Lehnertz K, Grunwald T, Schaller C, Elger CE, Fernández G. Human memory formation is accompanied by rhinal-hippocampal coupling and decoupling. *Nat Neurosci* 2001; 4:1259-1264.

Fernández G, Effern A, Grunwald T, Pezer N, Lehnertz K, Dümpelmann M, Van Roost D, Elger CE. Real-time tracking of memory formation in the human rhinal cortex and hippocampus. *Science* 1999; 285:1582-1585.

## **Cerebral correlates of memory consolidation through the sleep-wake cycle: contributions from functional neuroimaging.**

Philippe PEIGNEUX

Cyclotron Research Centre, University of Liège,

Bât. B30 Sart Tilman, B-4000 Liège, Belgium

Tel +32 4 366 2335 Fax +32 4 366 2946

Email : [Philippe.Peigneux@ulg.ac.be](mailto:Philippe.Peigneux@ulg.ac.be)

Web : <http://www.ulg.ac.be/crc>

Sleep is hypothesized to be useful for a series of functions including, e.g., energy conservation, brain thermoregulation, and brain detoxification. Beyond physiological processes however, scientific evidence suggests that the mind remains active in the sleeper, including processing of external stimulations, dreams and consolidation of memories.

During the last decade, functional brain imaging techniques have demonstrated the re-expression and modulation of learning-related cerebral activity during post-training sleep in man. Using positron emission tomography (PET) then functional magnetic resonance imaging (fMRI), we have shown that regional patterns of cerebral activity measured during sequence learning in a procedural memory task (i.e., the serial reaction time [SRT] task), or during a topographical memory task in a 3D virtual town, are re-expressed during subsequent sleep. Moreover, experience-dependent modifications of regional cerebral activity were found to occur during distinctive sleep stages (REM versus slow wave sleep, respectively) according to specific memory types (procedural versus spatial/episodic, respectively). Such modifications are not restricted to isolated brain areas, but rather involve the cooperative activity of cortical and subcortical networks that participate in the reactivation of recent memory traces during sleep. It is hypothesized that such processes participate to the sleep-dependent optimisation of neuronal circuits subtending memory performance on the next day.

Noteworthy, modifications of brain activity during post-training sleep are not merely the consequence of extended pre-sleep practice, but are crucially contingent upon the underlying cognitive content of the task. This emphasizes the importance of pre-sleep information processing during, and after, the acquisition episode. Recent data obtained in our laboratory evidence the off-line persistence of learning-related cerebral activity during post-training periods of wakefulness, which may provide a mechanism to support information maintenance prior to the first night of sleep.

Finally, we have evidenced functional relationships between cerebral activity during post-training sleep and memory consolidation. On the one hand, the level of acquisition of sequential rules attained in the SRT practice is correlated to the increase in regional cerebral blood flow during subsequent REM sleep, suggesting that post-training cerebral reactivation is modulated by the strength of the memory traces developed during the learning episode. On the other hand, and most importantly, the amount of hippocampal activity re-expressed during slow wave sleep has been shown to predict the overnight improvement of performance in route retrieval, strongly suggesting a functional connection between reactivations during sleep and memory consolidation.

As a whole, these data represent a preliminary attempt to delineate the cerebral correlates of the journey of a new memory, from its initial acquisition and maintenance during wakefulness to its re-expression and consolidation during post-training sleep, which eventually leads to the plastic changes underlying the subsequent improvement in performance.

Supported by : FNRS; IAP – Belgian Science Policy; FMRE; ULg Special Funds

**Locus Coeruleus activity in the rat during task acquisition, task performance and during sleep episodes following new learning or memory reactivation**

S. J. Sara, O. Yeshenko, J. Lelong

*Neuromodulation and Memory Processes, CNRS, UMR 7102, University Pierre and Marie Curie, Paris, France*

Extensive research from our laboratory has implicated the noradrenergic nucleus Locus Coeruleus (LC) in learning and subsequent off-line memory consolidation. Neurons of the LC discharge phasically to novel stimuli, to stimuli that predict reward, or to primary reward in the absence of a conditioned stimulus. These LC neuronal responses show striking plasticity as a function of changing stimulus-reinforcement contingencies, i.e. during extinction, reversal learning or intra-dimensional shift. This plasticity is observed very early in the learning process, before any behavioral expression of learning (Sara and Segal, 1991; Bouret and Sara, 2004). Changes in firing patterns of LC neurons also precede adaptation of forebrain responses during learning (Bouret and Sara, 2004), corroborating evidence from many studies that have suggested that the noradrenergic system plays an important role in promoting experience dependent plasticity.

In addition to its role in short term information processing and learning established by the electrophysiological studies, we have provided evidence for a role of the noradrenergic system in a late stage of memory consolidation, 90-120 minutes after initial learning. Injections of a beta-adrenergic antagonist intracerebroventricularly 2h after training on a three-way odor discrimination task or after reactivation of a radial arm maze or passive avoidance task produced enduring amnesia, while injections made immediately after or 5h after the training or reactivation did not (Przybylski et al, 1999; Sara et al., 1999). A similarly restricted time window of efficacy of beta blockade in inducing amnesia was observed when the injections were made into the prelimbic region of the prefrontal cortex. Moreover, a significant increase in release of noradrenaline (NA) into this same frontal region after training on the odor discrimination task was observed in a narrow time window 2 h after learning (Tronel et al., 2004). No such increase was observed in rats subjected to a backwards conditioning procedure.

In order to further evaluate this late activation of the noradrenergic system during memory processing, we recorded activity of LC neurons for several hours before and after memory reactivation, extinction or relearning using a modified version of the three-way odor discrimination task. Hippocampal and cortical EEG recorded simultaneously with LC units provided information concerning wakefulness and sleep phases. The firing rate of LC units (n=8) was strikingly elevated in a time window around 1.5-2.5 hours after the behavioral manipulation. On average, LC activity was twice as high during this time window than during comparable periods during the baseline recordings. LC cells during this period of elevated spike rate tended to fire in short bursts of 3-6 action potentials at about 6 Hz. This type of activity occurred during slow wave sleep (SWS). In addition, an increase in spindle density during SWS was observed immediately after each type of learning situation and lasted up to 3 hours (see poster abstract for details).

The bursting activity in LC, within the precise time window where injection of beta antagonists induces amnesia and NA release is increased, shows that this late involvement of the noradrenergic system in memory consolidation is mediated directly through the LC and not by local control of NE release. Thus LC neurons are engaged not only during the early stages of learning, but re-engaged off-line during SWS. This sporadic increase in bursting at a critical time window provides optimal release of NA thereby facilitating the intracellular signaling for new protein synthesis known to be necessary for long-term memory formation.

*Supported by Volkswagenstiftung grant to S.J. Sara and J. Born*

## **Novel object presentation enhances theta and spindle activity within the sleep EEG of the rat**

Thomas Schiffelholz & Josef B. Aldenhoff

ZiP gGmbH, Klinik für Psychiatrie & Psychotherapie, Kiel, Germany

Several learning tasks have been shown to increase the percentage of rapid eye movement sleep (REMS) in rodents, which is electroencephalographically characterized by high theta activity (6 - 8 Hz) [2, 6, 7]. This theta activity within the EEG of additional REMS following learning tasks is suggested to serve as a background for the highly synchronous reactivation of the related neuronal pathways and the activation of neurotransmitter systems, which seem to play a crucial role in memory consolidation [5]. But, there also is increasing evidence, that nonREMS might be related to memory performance, as well. Recently, a highly synchronous reactivation has been shown for those neuronal networks during nonREMS and REMS, that were activated during a preceding spatial learning task [3, 4, 10]. Additionally, Louie et al. presented a profound increase in theta and sigma activity within the EEG power spectra of REMS and nonREMS, respectively [4]. Siapas and Wilson described a high temporal correlation between spindle oscillations within nonREMS and high frequency network oscillations in the hippocampus in rats [9]. A third sleep stage in animals is the intermediate stage, usually appearing at the transition from nonREMS to REMS. The EEG power spectrum is characterized by spindles (12-15 Hz), that are much longer and have a higher amplitude than those during nonREMS [1, 6]. As in our previous work, this stage is called preREMS [8].

In the present study we explored the effects of novel object presentation at lights on different sleep parameters of the subsequent sleep-wake behavior in freely moving rats. This presentation enhanced the amount of preREMS, an intermediate sleep stage with high spindle activity, within the first 2 hours of the subsequent sleeping phase. 4 hours later, the amount of REMS was increased as well. However, there were no changes in the EEG power spectra of nonREMS, preREMS and REMS. As in spatial information processing we hypothesize, that the increase of preREMS and REMS amounts and the related spindle and theta activity stands for the processing and storage of new informations about the presented novel objects.

- [1] Gottesmann, C., The transition from slow-wave sleep to paradoxical sleep: Evolving facts and concepts of the neurophysiological processes underlying the intermediate stage of sleep, *Neurosci. Biobehav. Rev.*, 20 (1996) 367-387.
- [2] Graves, L., Pack, A., and Abel, T., Sleep and memory: a molecular perspective, *TiNS*, 24 (2001) 237-243.
- [3] Kudrimoti, H.S., Barnes, C.A., and McNaughton, B.L., Reactivation of hippocampal cell assemblies: Effects of behavioral state, experience, and EEG dynamics, *J. Neurosci.*, 19 (1999) 4090-4101.
- [4] Louie, K., and Wilson, M.A., Temporally structured replay of awake hippocampal ensemble activity during rapid eye movement sleep, *Neuron*, 29 (2001) 145-156.
- [5] Maquet, P., The role of sleep in learning and memory, *Science*, 294 (2001) 1048-1052.
- [6] Neckelmann, D., and Ursin, R., Sleep stages and EEG power spectrum in relation to acoustical stimulus arousal thresholds in the rat, *Sleep*, 16 (1993) 467-477.
- [7] Sara, S.J., Retrieval and Reconsolidation: Toward a neurobiology of remembering, *Learn. Mem.*, 7 (2000) 73-84.
- [8] Schiffelholz, T., and Lancel, M., Sleep changes induced by lipopolysaccharide in the rat are influenced by age, *Am. J. Physiol.*, 280 (2001) R398-R403.
- [9] Siapas, A.G., and Wilson, M.A., Corrdinated interactions between hippocampal ripples and cortical spindles during slow-wave sleep, *Neuron*, 21 (1998) 1123-1128.
- [10] Wilson, M.A., and McNaughton, B.L., Reactivation of hippocampal ensemble memories during sleep, *Science*, 265 (1994) 676-679.

# Hippocampal-Neocortical interactions in the memory of time and space

Matthew Wilson, Cambridge, USA

The spiking patterns of hippocampal neurons in the rodent are strongly influenced by two dominant factors - place and behavioral state. Spatial receptive fields or "place fields" undergo rapid experience-dependent changes that are paralleled by changes in the timing of spike discharge with respect to the macroscopic theta rhythm during active behavior. These effects may directly relate to mechanisms that support the encoding and retrieval of temporal event memory expressed at the level of neuronal ensembles. I will discuss the properties of temporal reactivation as it is expressed at different timescales during distinct phases of sleep, as well as the coordination of hippocampal and neocortical single unit activity with respect to macroscopic rhythms that may reflect the communication of information between the hippocampus and neocortex in the formation and processing of memory

## **Changes in brain cholinergic activity during sleep and wakefulness in humans affect memory consolidation**

Steffen Gais, Björn Rasch and Jan Born

*Dept. of Neuroendocrinology, University of Lübeck, Ratzeburger Allee 160, Hs. 23a, 23538 Lübeck, Germany*

Central nervous cholinergic systems modulate memory and are involved in the control of the structure of the sleep-wake cycle. Recent data point to a possible interaction of these two functions of acetylcholine (ACh). Because brain cholinergic nuclei (mainly the N. basalis Meynert and the pontine tegmentum) have long axons that spread across most of the cortex, a change of activity in these areas modulates the activity of large parts of the brain. The levels of ACh availability in the brain varies between sleep stages: During wakefulness and rapid eye-movement (REM) sleep, ACh levels are high; during slow-wave sleep (SWS), they drop to a minimum. During wakefulness, ACh is commonly found to be important for proper encoding of new information into hippocampal storage. This is regarded as a cause for memory loss in Alzheimer's dementia. Less is known about the effect of ACh on memory processing during sleep. Hasselmo (1999) proposed that ACh modulates the direction of the information flow between neocortex and hippocampus. In his model, high levels of ACh allow transfer of information into the hippocampus, whereas low levels permit a transfer from hippocampus to neocortex required for systemic consolidation of memories.

One prediction derived from this model of memory consolidation is that increasing the level of cholinergic activity during SWS should lead to a deterioration of memory consolidation. In fact, we could show this in a recent study where we infused healthy human subjects with a low dose (0.75 mg) of the cholinesterase inhibitor physostigmine during the SWS-rich first 3 hrs of sleep. Memory for declarative material learned before sleep was significantly less well remembered after sleep than under placebo conditions. Procedural memory, which does not depend on the hippocampus, was not affected by physostigmine.

A second prediction derived from this model is, that decreasing cholinergic activity during post-learning wakefulness should improve memory consolidation. We tested this in a group of 16 healthy subjects. We blocked muscarinic and nicotinic cholinergic neurotransmission during wakefulness after subjects had acquired declarative and procedural knowledge. Subjects learned paired-associate word lists and a procedural finger tapping task in the morning. Directly after learning, placebo or a combination of the muscarinic antagonist scopolamine (4 µg/kgBW i.v. over 20 min) and the nicotinic antagonist mecamylamine (5 mg p.o.) were given according to a randomized cross-over design. Memory retention was tested nine hours later. When cholinergic neurotransmission was blocked after learning, subjects remembered significantly more word pairs compared to the placebo condition. Recall of words learned some days earlier and the consolidation of procedural memories were not affected by this treatment. Additional experiments showed that neither scopolamine nor mecamylamine alone produced the enhancing effect on declarative memory consolidation.

Together, these studies show that the common view of ACh as a neurotransmitter that enhances memory function is too simple. It has to be taken into consideration that ACh is also a modulator of the brain state that sets different dynamics of information processing during sleep and wakefulness.

*Supported by Deutsche Forschungsgemeinschaft*



## OVERNIGHT VERBAL BUT NOT VISUAL MEMORY RETENTION CORRELATES WITH THE NUMBER OF SLEEP SPINDLES

Zsófia Clemens, Dániel Fabó, Péter Halász

National Institute of Psychiatry and Neurology, Department of Neurology, Budapest, Hungary

### *Objectives*

Considerable evidence supports a role for sleep in memory consolidation. However the issue of relative contribution of different stages of sleep has remained controversial for a number of memory domains. Based on electrophysiological studies in rats, synchronous sleep oscillations have been long proposed as possible origins of sleep-related memory improvement. Nevertheless, no studies to date have directly investigated sleep oscillations with regard to overnight memory retention in humans. The present study was carried out to examine whether overnight retention of verbal and visual memory contents correlates with the number of sleep spindles during the same night.

### *Methods*

Nineteen right-handed males spent two consecutive nights in the sleep laboratory. Testing was carried out before and after the second night. A face-name association test was used to assess visual and verbal memory. Sleep spindles were detected by an automatic algorithm for the whole sleep period and for 21 scalp electrodes. Time spent in different stages of sleep was also determined. Sleep and memory retention measures were correlated by means of Pearson Product Moment Correlation test.

### *Results*

Overnight verbal memory retention (defined as the difference between evening and morning performance) significantly correlated with the number of spindles at F3, C3, Fz and Cz recording sites but not with time spent in either stages of sleep. On the contrary, visual retention correlated with NREM sleep time but not with spindle numbers.

### *Conclusions*

Our data strongly support theories suggesting a link between sleep spindle activity and verbal memory consolidation while visual consolidation seems to depend on NREM sleep mechanisms other than sleep spindles.

## **The Transmembrane Form of Agrin Reorganizes the Cytoskeleton in Neurons and Non-Neuronal Cells**

Rene Ramseger<sup>§</sup>, Maik Annies<sup>§</sup>, Stefan Wöll<sup>§</sup>, Jürgen Löschinger<sup>#</sup> and Stephan Kröger<sup>§</sup>

<sup>§</sup> Dept. of Physiological Chemistry, University of Mainz, Duesbergweg 6, D – 55099 Mainz  
email: skroeger@mail.uni-mainz.de;

<sup>#</sup> Max-Planck-Institute for Developmental Biology, Spemannstr. 35, D – 72076 Tübingen

Agrin is a heparansulfate proteoglycan which is widely expressed in the central and peripheral nervous system as well as in non-neuronal tissues. Agrin's function is best understood in skeletal muscle where it plays a key role during formation, maintenance and regeneration of the neuromuscular junction. Usage of alternative first exons generates two agrin isoforms: a soluble, secreted basement membrane-bound form responsible for synapse formation at the neuromuscular junction, and a type II transmembrane protein with a single membrane-spanning region. The transmembrane form of agrin is primarily expressed in the CNS on growing axons, and it was suggested that it might be a receptor with signal transducing activity. Since downstream signaling pathways of transmembrane receptors can be activated ligand-independently by antibody-mediated oligomerization, we clustered the transmembrane form of agrin using polyclonal anti-agrin antibodies. Clustering of TM-agrin induced the formation of numerous filopodia-like processes on growing axons from the CNS and PNS. The processes contained a complex cytoskeleton, required calcium and could be inhibited by cytochalasine D. Likewise, heterologous expression of TM-agrin in different cell lines induced the formation of numerous long, actin-containing processes extending from the transfected cells, indicating that TM-agrin alone is sufficient for reorganizing the cytoskeleton and that this activity of TM-agrin is not limited to neurons. While the intracellular and the transmembrane domains could be deleted without loss of the process-forming activity, the heparansulfate chains, and their close association with the plasma membrane were necessary and sufficient for the process inducing activity. These results are consistent with TM-agrin being a receptor or co-receptor involved in axonal growth of CNS neurons.

## Procedural Motor Skill Learning is Associated with REM-Sleep in Healthy Older Adults

Hornung, O. P. <sup>1</sup>, Regen, F. <sup>1</sup>, Danker-Hopfe, H. <sup>1</sup>, Schredl, M. <sup>2</sup>, Heuser, I. <sup>1</sup>

<sup>1</sup> Department of Psychiatry and Psychotherapy, Charité-University Medicine Berlin, Campus Benjamin Franklin

<sup>2</sup> Sleep Laboratory, Central Institute of Mental Health Mannheim

e-mail: orla.hornung@charite.de

Sleep and memory are both affected by aging processes. Some of the most characteristic age-related changes in REM-sleep are the reduction of REM-sleep percentage, the shortening of REM-latency and the changes in organizational aspects of rapid eye movement activity. With regard to procedural motor skill learning, age-related decrements have been found in task acquisition and performance. Furthermore, strong decreases in declarative episodic memory performance have been reported as a function of age. In light of recent findings, which underline the importance of REM-sleep for memory consolidation in young adults, the investigation of the memory promoting effects of REM-sleep in older adults is of particular interest.

120 participants (60–85 years old, 49% male and 51% female) spent one adaptation night in the sleep laboratory before taking part in the subsequent study. They were randomly assigned to five groups with  $n = 24$  per group. Based on the information of the adaptation night, 13 participants had to be excluded from the final analyses due to not fulfilling the inclusion criteria. The research question was approached from two different angles, i.e. REM-sleep deprivation and REM-sleep augmentation. Within the REM-sleep deprivation paradigm, a first group was deprived of REM-sleep by being woken whenever REM-sleep set in, while a second group was matched with group one in terms of frequency of awakenings, but in contrast was woken during stage 2 NREM-sleep (deprivation group:  $n = 24$ ; control group:  $n = 20$ ). REM-sleep augmentation was achieved either physiologically through REM-rebound after a night of REM-sleep deprivation or pharmacologically by the application of an AchE inhibitor in a placebo-controlled, double-blind design (rebound group:  $n = 21$ ; medication group:  $n = 22$ ; placebo group:  $n = 20$ ). Performance in a procedural motor skill task (mirror tracing) and declarative episodic learning task (word pair associates) was investigated before and after the study night.

Statistical analyses, controlling for age and sex, showed a significant decrease in duration of total REM-sleep as well as phasic, i.e. eye movement related, REM-sleep in the REM-sleep deprivation group compared to the control group woken during stage 2 NREM-sleep ( $p < .001$ ). The two REM-sleep augmentation paradigms, in contrast, did not lead to any significant increase in duration of total REM-sleep, however, a significant increase regarding duration of phasic REM-sleep was achieved for both the rebound group ( $p = .014$ ) as well as the medication group ( $p = .037$ ) compared to the placebo group. In line with previous research, a significant association between REM-sleep and *morning* mirror tracing performance was found for duration of total REM-sleep as well as phasic REM-sleep across all five groups (correlation of total / phasic REM-sleep duration with number of errors:  $r_{SP} = -.126$ ,  $p = .002$  /  $r_{SP} = -.138$ ,  $p = .001$ ; correlation of total / phasic REM-sleep duration with percentage of error time:  $r_{SP} = -.090$ ,  $p = .024$  /  $r_{SP} = -.111$ ,  $p = .005$ ). Furthermore, a significant association between *evening* mirror tracing performance and REM-sleep was observed in the placebo group, which was most pronounced between percentage of error time and duration of phasic REM-sleep ( $r_{SP} = .406$ ,  $p < .001$ ). No comparable significant associations were found for the declarative learning task.

In accordance with previous findings in young adults, REM-sleep seems to be more closely associated with procedural learning than with declarative learning in older adults. The association between REM-sleep and *morning* mirror tracing performance found in the present study is, however, weaker than that reported in previous studies with younger adults, which may indicate that memory consolidation during REM-sleep is less pronounced in older adults. The comparatively high association between *evening* mirror tracing performance and duration of phasic REM-sleep supports previous findings in young adults, which found an enhancement of REM-sleep after a period of intensive training. To conclude, the results of the present study suggest that, while an intensive training period before bedtime may still enhance REM-activity in old age, the beneficial effects of REM-sleep with regard to memory consolidation may be less pronounced in this age group.

Supported by the German Research Foundation (DFG)

**Sleep spindle activity after different learning experiences in rats**

O. Yeshenko, S. J. Sara

*Neuromodulation and Memory Processes, CNRS, UMR 7102, University Pierre and Marie Curie, Paris, France*

The occurrence of off-line information processing has been reported in humans and animals using various recording and imaging techniques and behavioral tasks. An increase in spindle activity during slow wave sleep (SWS) was shown in humans after intensive training on a declarative task (Gais et al., 2002). Such learning-induced activation of cortico-thalamic circuitries was proposed to contribute to a memory consolidation during sleep. A recent study in rats showed an increase in total amount of sleep episodes rich in spindles (preREM sleep stage) following a novel object presentation. However, there was no novelty-induced change in EEG during SWS reported in this study (Schiffelholz and Aldenhoff, 2002).

The present study measured spindle activity during SWS episodes in rats after variety of learning situations differing in sensory modality and cognitive demand. Male Sprague-Dawley rats were implanted with cortical EEG and neck EMG electrodes. After recovery rats underwent a sequence of behavioral testing. Each rat was first exposed and habituated to a novel environment for 10 min. Next day the rat was trained in the same box on an olfactory discrimination task. Three cups were placed in the corners of the box. Each cup contained a sponge impregnated with almond, mint, or lemon odor. There was a food reward (chocolate rice cereal) hidden in a hole in the sponge with the target odor. Placement of the cups varied randomly over the five massed trials in which the rat learned the odor-reward association. On the third day, rat was exposed to an elevated 8-arm radial maze. Chocolate rice cereal grains were evenly dispersed throughout the maze. The rat moved freely in the maze collecting the food. EEG activity was monitored for three hours before and after each behavioral session. Power spectrums of delta (0-4 Hz), theta (5-10 Hz), and sigma (12-15 Hz) frequency bands were calculated over 10 sec intervals. Sleep episodes were scored manually. Custom-made software was used for detecting spindles.

All rats showed a high level of exploratory activity during the habituation session in the square training box and in the radial maze. Olfactory discrimination learning was completed by most of rats in the five trials. An increase in spindle density during SWS episodes was observed after all types of behavioral episodes compared to the spindle activity before testing. Although the amplitude of the increase varied from rat to rat, the mean increase of 22% was statistically significant. The effect was present from the first SWS episode and was still present up to 3-hours after the behavioral testing. Increase in spindle density was not associated with an increase in power of the spindle frequency band or a general change of sleep EEG. The power spectrum of the delta frequency band and theta/delta ratio did not differ significantly before and after behavioral testing. Post-hoc analysis revealed a significant effect of complexity of a novel environment ( $9.6 \pm 1.7$  spindles/min after habituation to a square box compared to  $10.9 \pm 3.1$  spindles/min after exploring the radial maze).

The phenomenon described here is strikingly similar to changes in spindle density observed in humans after declarative learning sessions. Although the present experiments did not reveal significant differences in spindle density after different types of learning, the overall increase in spindle density indicates that rats show experience-dependent activation of cortico-thalamic circuits. This encourages further studies aimed at refinement of behavioral protocols for declarative learning in the rat. Development of such models will permit pharmacological and electrophysiological investigation of the role of neuromodulatory systems in off-line memory consolidation occurring during sleep.

*Supported by Volkswagenstiftung grant to S.J. Sara and J. Born*

**Symposium #S24:**  
**Comparative insights into genetic and activity-dependent mechanisms of**  
**CNS development**  
**C. Lohr and C. Duch, Kaiserslautern and Berlin**

**Introduction**

[#S24](#) C. Lohr and C. Duch, Kaiserslautern and Berlin  
*Comparative insights into genetic and activity-dependent mechanisms of CNS development*

**Slide**

[#S24-1](#) RA. Baines, CJ. Mee, ECG. Pym and KG. Moffat, Coventry (UK)  
*Regulation of neuronal excitability through Pumilio-dependent control of a sodium channel gene*

[#S24-2](#) A. Prokop, W. Bottenberg, U. Haessler, B. Kueppers-Munther, R. Loehr and N. Sanchez-Soriano, Mainz and Manchester (UK)  
*Compartmentalization of central neurons in Drosophila studied by a new transplantation-based mosaic analysis strategy*

[#S24-3](#) C. Lohmann, Martinsried  
*Role of calcium signaling in dendrite development during synaptogenesis*

[#S24-4](#) JF. Evers and C. Duch, Berlin  
*The role of activity for postembryonic synapse acquisition and dendritic growth during Manduca metamorphosis*

[#S24-5](#) S. Löhrke, V. Balakrishnan, I. Ehrlich, G. Srinivasan and E. Friauf, Kaiserslautern  
*Mechanisms of the development of inhibition in the auditory brainstem*

[#S24-6](#) C. Lohr, Kaiserslautern  
*Two-photon microscopy reveals requirement of calcium signalling for glial cell migration during the development of the Manduca olfactory system*

**Poster**

[#55B](#) JF. Evers, A. Maye, S. Schönknecht, M. Sibila and C. Duch, Berlin  
*Are changing behaviorual demands supported by postembryonic remodelling of neuronal structure?*

## Introductory Remarks to Symposium 24

### Comparative insights into genetic and activity-dependent mechanisms of CNS development

**Christian Lohr and Carsten Duch, Kaiserslautern and Berlin**

Following up the phylogenetic tree of the animal kingdom, we find an increasing number of neurons in the central nervous system, from a few hundreds in lower invertebrates up to several billions in the mammalian brain establishing trillions of synapses. The precise wiring of this large number of neurons is one of the most challenging and fascinating processes during brain development. Many aspects of CNS development and remodelling such as cell migration, dendritic growth, synaptogenesis and alterations in excitability are controlled by electrical activity and intracellular calcium signalling, which lead to structural and physiological modifications and ultimately result in long-lasting changes in gene expression. During the last few years novel molecular and imaging techniques have enabled exciting new insights into the mechanisms underlying neural circuit maturation and refinement.

In this symposium, each speaker emphasizes particular aspects of the development of central synapses and circuits, from the molecular level to the system level, employing up-to-date techniques. The contributions not only highlight different steps of circuit development, like synaptogenesis, cell migration and differentiation, but also compare mechanisms found in different taxa, i.e. in invertebrates, as well as in mammals. A comparative approach is inevitable towards our understanding of neural circuit maturation, as the roles of activity and genetic programs appear to be weighted differentially in different types of neurons, in different brain areas, and especially in different species. On the other hand, intrinsic and extrinsic signalling pathways involve molecules with highly conserved structure, which is paralleled by conserved roles in CNS development. Hence, the discovery of clear organizational roles for specific factors in different species might shed light on the evolution and the principles of neural circuit development.

Richard Baines applies patch clamp recordings from identified neurons in the CNS of genetically modified *Drosophila* embryos to reveal the roles of activity and PKA for the development of motoneuron shape and excitability. Staying in the *Drosophila* embryo but moving down to the level of synapses, Andreas Prokop visualizes the three-dimensional synaptic compartmentalization of interneurons by combining targeted gene expression and transplantation of single cell clones. Jumping the taxa, Christian Lohmann employs two-photon microscopy to investigate the role calcium signalling in developing hippocampal neurons, labelled by either ballistic calcium indicator application or single-cell electroporation, during synaptogenesis. Jan Felix Evers and Carsten Duch also investigate the roles of activity and calcium for dendritic growth and synaptogenesis, but not during embryonic development but in the context of postembryonic neural circuit remodelling during the metamorphosis of the sphinx moth *Manduca sexta*. Here, morphological changes of dendrites and dendritic filopodia are quantified by semi-automated three-dimensional image analysis of high resolution confocal data. The last two talks move from the single neuron to the circuit level. Stefan Löhrke and Eckhard Friauf investigate the switch from depolarizing to hyperpolarizing responses during the development of inhibitory synapses in rat auditory brainstem nuclei using perforated patch clamp analysis and voltage-sensitive dye-based multi-diode array recordings. Christian Lohr uses two-photon calcium imaging as well as surgical and pharmacological in-vivo manipulation to reveal physiological mechanisms underlying glial cell migration, and the role of glial cell migration for the construction of synaptic neuropil in the antennal lobe of *Manduca sexta*.

## Regulation of neuronal excitability through Pumilio-dependent control of a sodium channel gene

Richard A. Baines, Christopher J. Mee, Edward C.G. Pym and Kevin G. Moffat.  
Neuroscience Group, Department of Biological Sciences, University of Warwick,  
Coventry, CV4 7AL, UK.

The mechanism by which neuronal excitability is regulated in response to changes in synaptic excitation has been termed homeostatic compensation. This regulation has been observed principally when neurons are developing during embryogenesis and when neurons undergo synaptic remodelling during learning. Regulation and adaptation to synaptic excitation is important, as neurons must guard against becoming saturated or from falling silent as synaptic excitation changes. Though these regulatory mechanisms have been well documented, the molecular and physiological mechanisms involved are poorly understood.

Our current study focuses on the *Drosophila* voltage-gated sodium channel *paralytic* (*para*) and its role in the regulation of membrane excitability. Previous studies have shown that in the absence of cholinergic excitation, sodium currents ( $I_{Na}$ ) in identified motoneurons are significantly elevated, while increased excitation results in a significant reduction in  $I_{Na}$ . This present study examines changes in *para* mRNA levels, measured using real time RT-PCR, in activity mutants. We show that *para* mRNA is significantly increased in the absence of synaptic vesicle release. By comparison, *para* mRNA is significantly reduced in genetic backgrounds that increase synaptic excitation.

These changes in mRNA are likely due to activity-dependent translational repression. We show that the known translational repressor *pumilio* (*pum*) is both necessary and sufficient for the activity-dependent changes in *para* mRNA. Bioinformatic analysis of the *para* transcript shows it to contain sequence specific binding motifs, or Nanos Response Elements (NRE), in the 5'-UTR. These motifs have been shown necessary for Pum protein binding to *hunchback* (*hb*) RNA. Binding of Pum to *hb* leads to translational repression. The presence of these motifs in *para* indicates a possible direct interaction between the Pum protein and *para* mRNA, resulting in suppression of the *para* transcript.

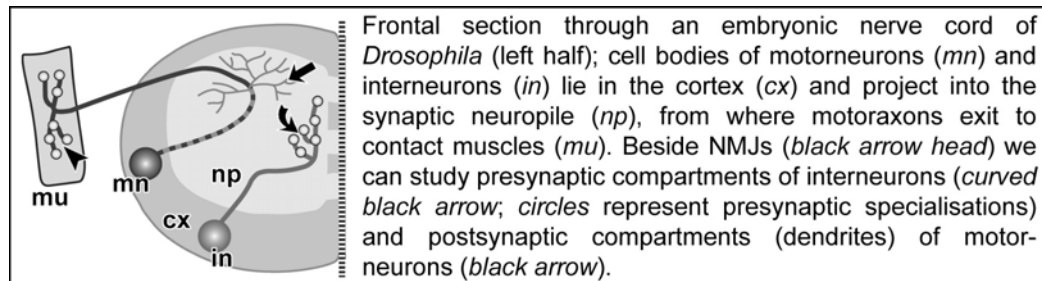
## Compartmentalization of central neurons in *Drosophila* studied by a new transplantation-based mosaic analysis strategy

Andreas Prokop<sup>1</sup>, Wolfgang Bottenberg<sup>1</sup>, Ulrike Haessler<sup>2</sup>, Barbara Küppers-Munther<sup>2</sup>, Robert Löhr<sup>2</sup>, and Natalia Sánchez-Soriano<sup>1</sup>.

1) School of Biol. Sci., Univ. Manchester, UK; 2) Inst. of Genet., Univ. Mainz, Germany

Unravelling how and where synaptic contacts form and differentiate in developing nervous systems is crucial, if we want to understand how functional neuronal circuits are established *de novo*. We study mechanisms underlying *de novo* formation of synaptic neuritic compartments in the model organism *Drosophila*, capitalising on its powerful genetics and using its reproducibly identifiable neurons as precise phenotypic readouts. So far such work in *Drosophila* has been focussed mainly on glutamatergic neuromuscular junctions, although only central synapses allow investigation of neuronal postsynaptic mechanisms and display a greater variety of structural and functional features. Therefore, we have begun to expand studies to the embryonic *Drosophila* CNS.

To this end, we designed strategies which allow three-dimensional mapping of neurites in the synaptic neuropile (Landgraf M *et al.*, 2003, *Dev. Biol.* 260, pp.207ff.). To define and visualise synaptic compartments within these identified neurites, we established and used mosaic strategies based on heterogenetic transplantations or targeted gene expression (Gal4/Uas; Löhr R *et al.*, 2002, *J. Neurosci.* 22, pp.10357ff.). These studies clearly demonstrated that, like motorneurons, also the primary neurites of interneurons represent axon-like processes in which presynaptic compartments are restricted to reproducible locations, mostly towards the neurite tip. *Vice versa*, we could show that motorneuronal side branches in the CNS represent true dendrites. Like vertebrate dendrites they lack presynaptic proteins, harbour postsynaptic transmitter receptors, display calcium elevation upon excitation, and have cytoskeletal features distinct from axons (no Tau).



Like most arthropod neurons, *Drosophila* motorneurons are unipolar, and dendrites are localised on their primary neurites, rather than their cell bodies. Using primary cell culture (Küppers-Munther B *et al.*, 2004, *Dev. Biol.* 269, pp.459ff.) and experimental shift of cell bodies in the CNS, we could show that this positioning of dendrites is not determined intrinsically, but through external signals residing most likely in the dorsal neuropile. Our findings indicate that dendrites of vertebrates and *Drosophila* motorneurons are homologous. We deduce hypotheses explaining how the distinct shapes of vertebrate and arthropod neurons have evolved from a common urbilaterian ancestor.

Supported by the Deutsche Forschungsgemeinschaft (DFG; PR605/1 and 2), the European Commission (QLG3-CT-2001-01181, Synaptogenet) and Volkswagen-Stiftung (I/75 471 and I/78 743).





# Role of calcium signaling in dendrite development during synaptogenesis



Christian Lohmann

MPI für Neurobiologie, Am Klopferspitz 18, 82152 Martinsried-  
München, Germany, lohmann@neuro.mpg.de

The development of neuronal networks is a dynamic process: axons and dendrites establish contacts, some of which mature and become synapses whereas others are eliminated. We addressed the question of how the structural dynamics of neurons - in particular those of dendrites - are regulated. Since neuronal activity is known to play a major role in dendritic plasticity, we monitored the structural plasticity of dendrites and their activity levels simultaneously. To do so, we labeled single neurons and their entire dendritic arborizations in neuronal tissue with fluorescent calcium indicators employing the gene gun ("calistics") or a single cell electroporation technique.

Optical recordings from labeled neurons revealed that developing neurons spontaneously generated not only global, but also local dendritic calcium transients (Fig. 1). These local calcium transients lasted for several seconds and spread within dendritic stretches of about 10  $\mu\text{m}$ . They required release of calcium from internal stores and occurred in neurons as diverse as chick retinal ganglion cells as well as rat hippocampal pyramidal and interneurons during the period when synapses form. While neurotransmission was necessary for a proportion of these transients, others seemed to be triggered by different factors.

We investigated the role of local calcium transients in two types of dendritic plasticity: stabilization of entire dendritic branches and the spontaneous motility of dendritic filopodia.

1. In retinal ganglion cells from embryonic chicks, blocking acetylcholine triggered local calcium signaling induced the retraction of dendritic branches. Dendritic retraction could be prevented by uncaging of calcium in single dendrites. These results demonstrated that entire dendritic branches can be stabilized by transmitter induced local calcium signaling.

2. In hippocampal slices the spontaneous motility of dendritic filopodia and local calcium signaling were tightly correlated. Analysis of this correlation suggested that local calcium transients may inhibit filopodial outgrowth and stop ongoing growth in filopodia that have already started to grow. This presumption was supported by the observation that the rapid blockade of local calcium signaling caused immediate growth of filopodia.

Together, our data show that calcium signaling has diverse roles in directing the structural plasticity of dendrites during the formation of synapses. Specifically, local calcium transients may determine (1) the outgrowth of filopodia to search for synaptogenic contacts, (2) the retraction of filopodia and dendritic branches to break inappropriate contacts, and (3) the stabilization of entire dendritic branches to maintain suitable inputs. Such processes can help neurons to interconnect and form functional networks.

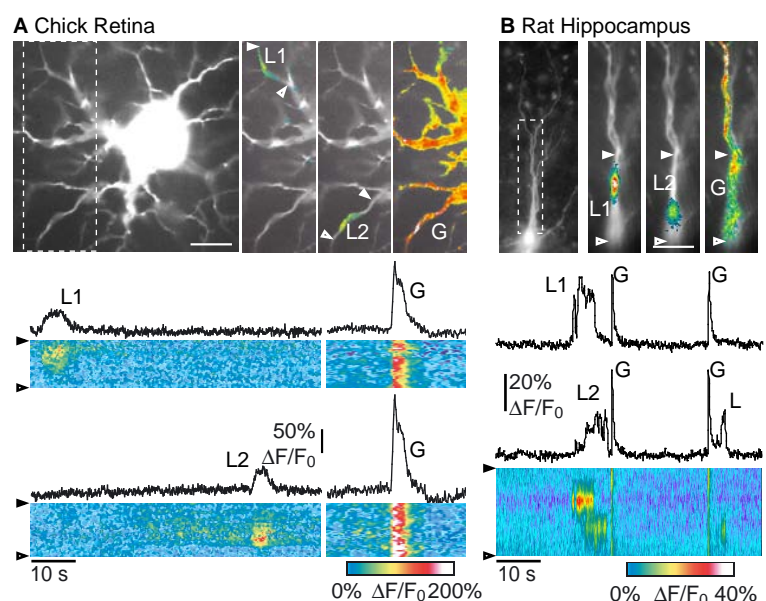


Fig. 1: Developing chick retinal ganglion cells and rat hippocampal neurons spontaneously generate local (L) and global (G) calcium transients.

## **The role of activity for postembryonic synapse acquisition and dendritic growth during *Manduca* metamorphosis**

Evers JF, Duch C

Free University of Berlin, Institute of Neurobiology, 14195 Berlin

Dendritic morphology is crucial for neural signal integration and the proper wiring of neuronal circuits. During dendritic development growth-cones play a key role in path finding and synaptogenesis. Their morphogenesis may be regulated by innate genetic factors, neuronal activity and external molecular cues. We use the individually identified flight motoneuron, MN5, of the moth *Manduca sexta* as a model system to quantify growth-cone morphology *in situ*, and to conduct manipulation experiments *in vivo* during normal development.

During metamorphosis MN5 undergoes dramatic changes in its function and its dendritic structure. Severe dendritic regression during the dismantling of larval crawling motor circuits is followed by two distinct phases of dendritic growth during the integration into the newly formed flight motor network: An initial growth-cone-dependent phase of dendritic growth and branching and a subsequent growth-cone-independent phase with new branch formation restricted to high order dendrites. Changes in growth-cone morphology are analyzed by novel 3D-reconstructions of high resolution confocal images.

During the initial phase of dendritic growth and branching filopodia are found to be mostly localized at the tips of the dendrites at growth-cones. In contrast, after dendritic branching has progressed, filopodia are also formed at internodal segments. Growth-cone filopodia and internodal filopodia differ significantly in their morphology. During new dendrite formation and elongation both filopodia number and filopodia length are decreased significantly ( $p < 0.001$ ) until they disappear. Moreover, growth-cone and filopodia morphology differ systematically among different compartments of the dendritic tree. Filopodia number and growth-cone complexity are enhanced by steroid hormone signals *in vitro*. However, reducing calcium inward current *in vivo* during pupal development alters normal growth-cone and filopodia morphogenesis, and in turn, the architecture of the dendritic field. Older and less complex growth-cones receive more putative input synapses as compared to younger and more complex growth-cones as demonstrated by mapping the staining density of labeled synapse proteins onto highly exact 3-reconstructions of dendritic growth-cones. These data suggest that dendritic growth-cones are informed independently from each other about the status of synaptogenesis by local activity-dependent calcium influx.

*Supported by the Deutsche Forschungsgemeinschaft, SFB 515, A7*

## Mechanisms of the development of inhibition in the auditory brainstem

Stefan Löhcke, Veeramuthu Balakrishnan, Ingrid Ehrlich, Geetha Srinivasan, and Eckhard Friauf

Animal Physiology Group, Department of Biology, University of Kaiserslautern, POB 3049, D-67653 Kaiserslautern, Germany

Within the mammalian auditory brainstem, inhibitory signals are mainly mediated by the amino acids glycine and GABA. Like in other CNS regions, the glycine/GABA action on auditory brainstem neurons is depolarizing early in development, shifting to a hyperpolarization during the period of synaptic maturation. The early depolarizations of inhibitory pathways increase the intracellular  $\text{Ca}^{2+}$  concentration and thus influence the development and stabilization of inhibitory synapses. The shift from depolarizing to hyperpolarizing action of glycine and GABA is due to a decrease in the intracellular  $\text{Cl}^-$  concentration ( $[\text{Cl}^-]_i$ ). Therefore, the developmental change in  $\text{Cl}^-$  homeostasis, which is based on an active  $\text{Cl}^-$  regulation, is essential for the maturation of inhibitory synapses.

In the first part of this talk, we describe the mechanisms responsible for the developmental shift in  $[\text{Cl}^-]_i$  in neurons of the rat and mouse lateral superior olive (LSO), a nucleus of the superior olivary complex (SOC) in the auditory brainstem. In the second part, we illustrate the shift in glycine action in additional SOC nuclei, namely the medial superior olive (MSO), the superior paraolivary nucleus (SPN), and the medial nucleus of the trapezoid body (MNTB). In the last part, we present evidence for the participation of activity-dependent mechanisms in the development of inhibitory pathways in the SOC.

Recently, we showed that the K-Cl cotransporter KCC2 is accountable for the low  $[\text{Cl}^-]_i$  by extruding  $\text{Cl}^-$  in older LSO neurons (postnatal day (P) 12; Balakrishnan et al., 2003, J Neurosci 23:4134-4145). The low  $[\text{Cl}^-]_i$  is the prerequisite for inhibition, i.e., for hyperpolarizing responses. Regarding the high  $[\text{Cl}^-]_i$  in young LSO neurons (P3/4) and the underlying  $\text{Cl}^-$  accumulation, we tested the presence of several  $\text{Cl}^-$  transporters. Gramicidin perforated-patch recordings from wild type and knock-out animals revealed that the Na-K-Cl cotransporter NKCC1 is not involved in  $\text{Cl}^-$  inward transport. Surprisingly, we found that the glycine transporter GlyT2 and the GABA transporter GAT1, both known for an inward transport of  $\text{Cl}^-$ , play a role in  $\text{Cl}^-$  buildup.

Voltage-sensitive dye recordings with high spatio-temporal resolution were performed to determine the presence and time of the shift in glycine action in MSO, SPN, and MNTB. We found that a shift from depolarization to hyperpolarization appears at P5 in the MSO and between embryonic days 18-20 in the SPN. In contrast, no shift was observed in the MNTB during the age range tested (P3-10). In addition, we reinvestigated the time of the shift in glycine action in the LSO, and found that it appeared in a chronological and regional order, i.e., from P4 in the dorsomedial part to P6 in the ventrolateral part.

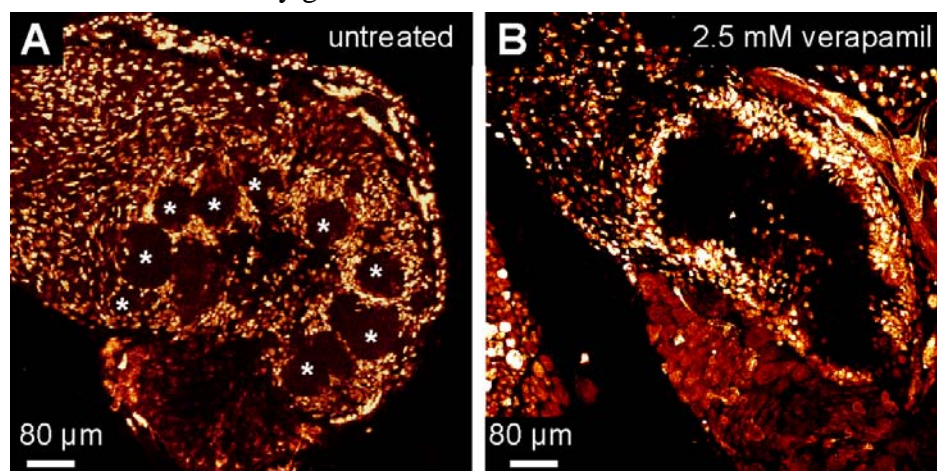
By means of perforated-patch and whole-cell recordings, spontaneous activity was measured in LSO neurons from acute brainstem slices. Spontaneous inputs were always subthreshold, i.e., spiking activity was not observed. Consistent with the developmental shift in  $[\text{Cl}^-]_i$ , the number of hyperpolarizing responses increased with age. Acute axotomy of the MNTB-LSO projection did not alter the properties of sPSCs, indicating that in SOC slices, spontaneous synaptic activity is presumably mediated by action potential-independent, spontaneous transmitter release.

In summary, we have revealed some mechanisms involved in the developmental  $\text{Cl}^-$  regulation in LSO neurons. Our results demonstrate a differential timing of the development of glycinergic inhibition within functionally related nuclei in the auditory brainstem.

## Two-photon microscopy reveals requirement of calcium signalling for glial cell migration during the development of the *Manduca* olfactory system

Christian Lohr, Abt. Allg. Zoologie, TU Kaiserslautern  
clohr@rhrk.uni-kl.de

The olfactory systems of vertebrates and invertebrates has been used to study bidirectional neuron-glia interactions during development. Anatomical studies of the organization of both the primary olfactory system of mammals, the olfactory bulb, and of arthropods, the antennal lobe, have revealed striking similarities between disparate taxa. In the olfactory bulb and the antennal lobe, a specialized class of glial cells which originate from the central nervous system is associated with olfactory glomeruli, aiding the construction of protoglomeruli during synaptogenesis and enveloping the neuropil of mature glomeruli. The glial cells separate one glomerulus from each other and thus enable odor discrimination. Migration of these glomeruli-associated glial cells is an essential step in the development of the antennal lobe to establish the borders between olfactory glomeruli. Here we used two-photon microscopy to visualize calcium signalling in developing antennal lobe glial cells of the sphinx moth *Manduca sexta*. We found a correlation between the upregulation of functional voltage-gated calcium channels and the onset of glial cell migration. In addition, glial cells migrating into the centre of the antennal lobe express larger voltage-gated calcium transients than glial cells that remain at the periphery. Migration behaviour and calcium signalling of glial cells in vivo were manipulated either by deafferentation, by injection of the calcium channel blockers diltiazem, verapamil and flunarizine, or by injection of the calcium chelators BAPTA-AM and Fluo-4-AM. In deafferented antennal lobes, glial cells failed to express functional voltage-gated calcium channels and did not migrate. Calcium channel blockage or reducing glial calcium signals by calcium chelators prevented glial cell migration and resulted in antennal lobes lacking glial borders around glomeruli, indicating that voltage-gated calcium signalling is required for the migration of antennal lobe glial cells and the development of mature olfactory glomeruli.



Propidium iodide staining of glial nuclei in antennal lobes (AL) that developed in an untreated animal (**A**) and in an animal treated with the the calcium channel blocker verapamil (**B**). In untreated ALs, glial cells migrate to surround glomeruli (asterisks), while in the presence of verapamil glial cells failed to migrate.

## Are changing behavioural demands supported by postembryonic remodelling of neuronal structure ?

**Jan Felix Evers, Alexander Maye†, Susanne Schönknecht\*,  
Michael Sibila\*, Carsten Duch**

Free University of Berlin, Institute of Neurobiology, 14195 Berlin

\* Technical University of Berlin, Institute for Theoretical Computer Science, 10587 Berlin

† Zuse Institute Berlin, Division Scientific Computing, 14195 Berlin

Although neuronal morphology and function are strongly linked (Mainen and Sejnowski, 1996; Krichmar et al., 2002), up to data, it is only poorly understood how neuronal morphology is optimized to support behavioral output (van Pelt, 2001). This question can be addressed by relating electrophysiological and behavioral data to the shape of corresponding neurons. We have chosen the individually identifiable Motoneuron 5 (MN5) of the holometabolous insect *Manduca sexta* as a model. In larvae, MN5 is a slow motoneuron innervating a slowly contracting crawling muscle. This behavioural function requires only low demands on temporal single spike precision, low spiking threshold and bursting activity. During metamorphosis, neuronal structure and network connectivity of MN5 are heavily altered while it is remodelled into a fast adult flight motoneuron (Duch and Levine, 2000). Consequently, the adult function of MN5 requires a high temporal single spike precision, no bursting activity and a high spiking threshold. In this study we ask whether developmental alterations in dendritic shape support the changes in behavioural function.

We have generated precise 3D geometric and surface reconstructions of MN5 at 4 critical developmental stages between larva and adult. The geometric reconstructions are used to generate multi-compartment models, whereas the surface reconstructions were used to extract a measure for synapse localization probability from 2<sup>nd</sup> channel confocal image data of immuno-labelled synapsin-I protein. With this in hand we address the consequences of neuronal shape and input synapse distribution on dendritic trees for the shaping of neuronal output in the following ways:

- how does the changing shape of the dendritic tree influence spiking capacity and frequency?
- how does the changing dendritic geometry influence the neurons responsiveness upon variable synaptic input synchrony?
- are computational properties different among different sub-trees of the same neuron?
- does stochastic synapse placement have different efficiency than synapse location and distribution as inferred from histology?

First results indicate on synaptic integration properties indicate that both, adult and larval dendritic tree architecture are well suited to subserve the different behavioural requirements at the different developmental stages.

*Supported by the DFG*

## **Satelite Symposia**

- [#Sat1](#)    The acoustics of emotions in nonhuman mammals and man  
Elke Zimmermann, Eckart Altenmüller and Sabine Schmidt, Hannover
  
- [#Sat2](#)    Functional brain proteomics  
Hans Gerd Nothwang and Marius Ueffing, Kaiserslautern and Oberschleißheim/  
Neuherberg
  
- [#Sat3](#)    Functional microdomains and embedded proteins  
Frank Lehmann-Horn and Albert Ludolph, Ulm
  
- [#Sat4](#)    Analysis of brain transcriptomes: principals, goals, achievements  
Gabriele Flügge, Nils Brose and Eleni Roussa, Göttingen
  
- [#Sat5](#)    Joint Symposium of the DFG Neuroscience Graduate Schools  
W. Paulus and G. Reifenberger, Göttingen und Düsseldorf

**Satellite Symposium #Sat1:**

**The acoustics of emotions in nonhuman mammals and man**  
**Elke Zimmermann, Eckart Altenmüller and Sabine Schmidt, Hannover**

**Introduction**

[#Sat1](#) Elke Zimmermann, Eckart Altenmüller and Sabine Schmidt, Hannover  
*The acoustics of emotions in nonhuman mammals and man*

**Slide**

[#Sat1-1](#) E. Zimmermann, Hannover  
*#Sat1: Opening Remarks*

[#Sat1-2](#) J. Burgdorf, Bowling Green, OH (USA)  
*Ultrasonic Vocalizations as Indices of Affective States in Rats*

[#Sat1-3](#) K-H. Esser, Hannover  
*Vocal expression of emotion in the lesser spear-nosed bat (*Phyllostomus discolor*)*

[#Sat1-4](#) S. Schmidt, Hannover  
*Effects of emotion on vocal communication in the Indian False Vampire bat, *Megaderma lyra**

[#Sat1-5](#) E. Zimmermann, Hannover  
*Vocal expression of emotions in archaic primates*

[#Sat1-6](#) U. Jürgens, Göttingen  
*How emotions are encoded in the acoustics of vocal communication in nonhuman primates and man*

[#Sat1-7](#) K. Wermke, Wuerzburg  
*The Expression of Emotions in Human Infants Crying*

[#Sat1-8](#) MJ. Owren, Ithaca, NY (USA)  
*Acoustics, perception, and function of human laughter*

[#Sat1-9](#) G. Ehret, Ulm  
*Communication-call perception and parental emotions in the brains of mice*

[#Sat1-10](#) K. Alter, Newcastle (UK)  
*Distinct fMRI responses to speech, laughter, and sounds*



- [#Sat1-11](#) K. Sander, Magdeburg  
*Neural correlates of laughter and crying in humans*
- [#Sat1-12](#) I. Peretz, N. Gosselin, S. Samson and R. Adolphs, Montreal (CDN), Paris (F) and Iowa (USA)  
*Impaired recognition of danger as expressed in music following lesions of the amygdala in humans*
- [#Sat1-13](#) EO. Altenmüller, K. Goydke, A. Eckstein and R. Kopiez, Hannover  
*Music as a model for acoustic communication of emotions in humans*
- [#Sat1-14](#) T. Fritz and S. Koelsch, Leipzig  
*Music as a tool to examine pleasantness and unpleasantness*
- [#Sat1-15](#) SA. Kotz, Leipzig  
*Linguistic and nonlinguistic expression and perception of emotions: acoustics and neural substrates*
- [#Sat1-16](#) C. Schröder and R. Dengler, Hannover  
*Expression and perception of emotional prosody in Parkinson`s disease*
- [#Sat1-17](#) E. Altenmüller, Hannover  
*#Sat1: Concluding remarks*

### Poster

- [#52A](#) M. Dietz and E. Zimmermann, Hannover  
*The effect of arousal on a social call of a nocturnal primate (*Microcebus murinus*)*
- [#53A](#) KN. Goydke, TP. Urbach, M. Kutas, E. Altenmüller and TF. Münte, Hannover, La Jolla, CA (USA) and Magdeburg  
*Combined perception of emotion from pictures and musical sounds*
- [#54A](#) O. Grewe, F. Nagel, E. Altenmüller and R. Kopiez, Hannover  
*Psychological and Physiological Correlates of Strong Emotions in Music*
- [#55A](#) E. Dujardin and U. Jürgens, Göttingen  
*Vocalization as an emotional indicator – neuroanatomical tracing of vocalization-related afferents to the midbrain periaqueductal grey in squirrel monkeys (*Saimiri sciureus*)*
- [#56A](#) D. Zaum and K. Alter, Leipzig and Newcastle (UK)  
*The encoding of emotion in human laughter*



## **Introductory Remarks to Sat. Symposium 1**

### **The acoustics of emotions in nonhuman mammals and man**

**Elke Zimmermann, Eckart Altenmüller and Sabine Schmidt, Hannover**

What are the biological roots of music and speech in man? To what extent do humans share mental capacities as well as coding and decoding strategies in acoustic communication with other animals with a highly developed auditory system? These are the central but yet unanswered questions in the evolutionary neurobiology of the acoustics of emotions.

A fundamental trait of the communication system of all mammals is to convey emotions. In the acoustic domain, emotions are transmitted by voice and music in man and by vocalisations of nonhuman mammals. For the first time, researchers working on different mammalian groups with highly developed auditory communication, including humans, will discuss cross-taxa information to give a critical synopsis on the current state of the art. We use an empirically and comparative approach to illuminate both shared and unique components important to reconstruct evolutionary pathways for emotion in the acoustic domain.

## Ultrasonic Vocalizations as Indices of Affective States in Rats

Jeffrey Burgdorf

Converging evidence from ethological, pharmacological, and brain stimulation studies indicate that rat ultrasonic vocalizations reflect discrete affective states. 55-kHz ultrasonic vocalizations appear to be a rat homolog of human laughter. These vocalizations are most robustly elicited by tickling, rough and tumble play, and mating. Euphorogenic / addictive drugs as well as rewarding brain stimulation also elevate 55-kHz calls. Conversely, rat 22-kHz calls reflect a negative affective state akin to anxiety or sadness. These calls are triggered by social defeat, presence of a predator, electrical foot shock. Pharmacologically, aversive drugs have been shown to increase levels of 22-kHz calls, while decreasing levels of positive affective 55-kHz calls. Recently, detailed analysis of both 55- and 22-kHz ultrasonic vocalizations have revealed multiple call subtypes. In sum, this work highlights the possibility that affective processes in laboratory animals can be monitored through a study of their emotional vocalizations.

## Vocal expression of emotion in the lesser spear-nosed bat (*Phyllostomus discolor*)

Karl – Heinz Esser

**Auditory Neuroethology & Neurobiology Lab, Institute of Zoology, School of Veterinary  
Medicine Hannover, Bünteweg 17, 30559 Hannover, Germany  
(kalle.esser@tiho-hannover.de)**

As stated by the organizers, a major goal of this symposium is to provide cross-taxa information of how emotions are transmitted in the acoustic domain, i.e., by voice and music in man and by vocalisations of nonhuman mammals.

The present report summarizes data from the Lesser spear-nosed bat (*Phyllostomus discolor*), a well-established animal model for *vocal learning* (for review see Esser 2003, Boughman & Moss 2003).

The species' vocal repertoire (Pistohl & Esser 1998) comprises at least 20 *structurally* well-defined call types: 4 types of infant isolation calls [behavioral context: pup detached from the mother's nipple or isolated], the maternal directive call [mother calling or searching for her own pup], 3 types of chirp calls [greeting, expression of a friendly mood], the contact call [roosting in physical contact], 2 types of agonistic signals [threat; attack] and a call uttered while playing. Other signals indicate superiority [termination of conflict], submissiveness, are associated with fear/selfdefense, facilitate entrance into a group, or are used predominantly for echolocation. For the remaining 3 (out of 20) types of calls, the context of emission remains to be determined.

In the present study, I used **Russell's** (see FIG. 1) **circumplex model of affect** (synonym = emotion) to interrelate vocal structure and the sender's (i.e., the calling animal's) emotional state in *P. discolor*. As evidenced in cognitive psychological studies, **valence** (ranging from unpleasantness over a neutral state to pleasantness) and **arousal** (ranging from deactivation over a neutral state to high activation) are orthogonal factors that capture the basic spectrum of emotions on a two-dimensional grid.

Pleasant activation (# 1 in FIG. 1) was found to be vocally reflected by solely downward frequency-modulated (= FM) signals and suppression of the fundamental. In contrast, quasi-constant frequency calls were indicative for a pleasant deactivation (# 2 in FIG. 2). A sinusoidal frequency modulation pattern or variations thereof (modulation frequency < 100 Hz) cooccurred with unpleasant deactivation

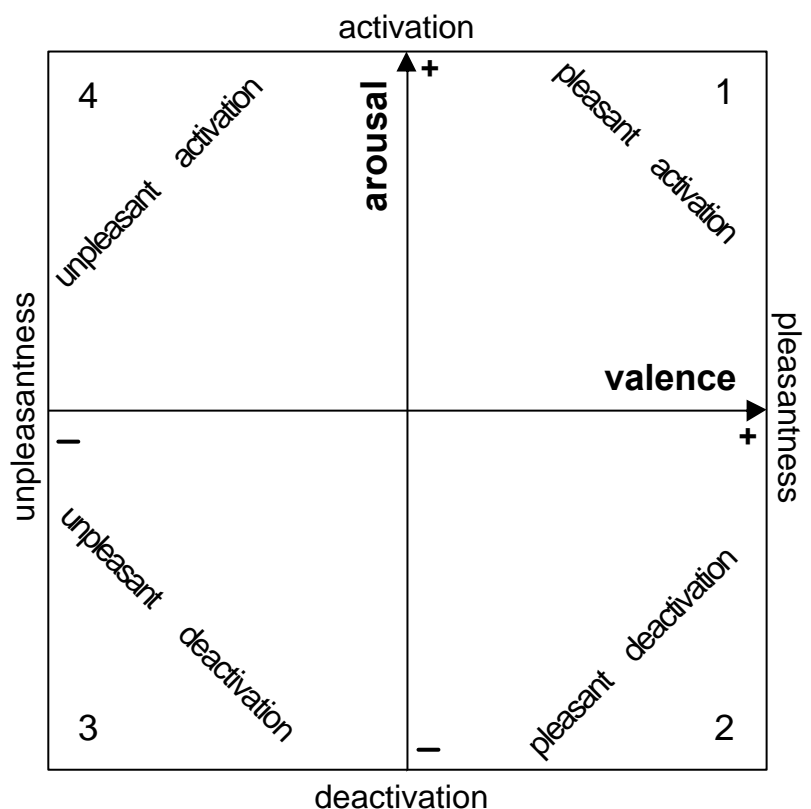


FIG. 1: Russell's circumplex model of affect [=emotion] (Russell 1980; adapted from Västfjäll & Gärling 2002).

tion (e.g. isolation). Unpleasant activation (e.g. threat, attack; # 4 in FIG. 1) was accompanied by noisy utterances with low-frequency (i.e., < 10 kHz) spectral components or by fast periodic FMs (modulation frequency > 110 Hz).

These results clearly indicate (i) an **interrelation between vocal structure and emotional state in a subprimate mammal** and (ii) the importance of further studies in this species of bat.

### References:

- Boughman JW, Moss CF (2003) Social sounds: vocal learning and development of mammal and bird calls. In: Simmons AM (ed.) Acoustic Communication. Springer, New York, 138-224. – Esser K-H (2003) Speech Communication 41, 179-188. – Pistohl D, Esser K-H (1998) The vocal repertoire of the lesser spear-nosed bat (*Phyllostomus discolor*) Zoology 101, Suppl. I, 84. – Russell JA (1980) J. Pers. Soc. Psych. 39, 1161-1178. – Västfjäll D, Gärling T (2002) Experimental Psychology. 49, 228-238.

## Effects of emotion on vocal communication in the Indian False Vampire bat, *Megaderma lyra*

Sabine Schmidt

Institute of Zoology, Tierärztliche Hochschule Hannover, Buenteweg 17, 30559 Hannover, Germany, sabisch@zoologie.tiho-hannover.de

Acoustic communication plays a prominent role in the social behaviour of bats. Consequently, rich communication call repertoires have been found in this archaic group, typically consisting of sequences of short syllables specifically combined in different social contexts. While call parameters mediating group-, gender- and individual-specific signatures have been described, the question of how bats transmit emotional states acoustically has not been addressed, so far. A review of bat communication literature revealed that emotions may be preferably coded in sequence parameters, e.g. the number of syllables, total call duration, and the overall frequency contour of a call. In order to investigate potential universals coding for emotion, I mapped the behaviour of the Indian False Vampire bat, *Megaderma lyra*, in a valence/arousal space, based on a two-dimensional model of emotion. Then, the vocalisations associated with behaviours in different sectors of the valence/arousal space were compared to extract structure rules. A first analysis suggested that clicks and multiharmonic syllables with contours comprising a broadband downward and upward frequency modulation were associated with negative valence situations, whereas multiharmonic, purely downward frequency modulated syllables and whistles were characteristic for positive valence situations. Moreover, syllable sequence frequency tended to increase with arousal. To test the latter rule, I investigated the structure of landing strophes of *M.lyra*, emitted by identified individuals in two situations representing different arousal states: when the bat landed without physical contact to others, or during landings resulting in direct body contact. Parameters tested were the median peak frequency of a strophe, the number of syllables in the strophe and the median intersyllable intervals. In this paradigm, the median peak frequency did not differ significantly in the two situations, and may convey individual- rather than emotion-specific information. In contrast, the number of syllables was increased and the median intersyllable intervals tended to decrease in situations with body contact. This provides a first experimental evidence for an effect of the emotional state of the caller on sequence parameters, thus confirming our hypothesis. Supported by the DFG FOR 499/SCHM879/6-1.

## **Vocal expression of emotions in archaic primates**

Elke Zimmermann

Institut für Zoologie, Tierärztliche Hochschule Hannover, Bünteweg 17, 30559 Hannover,  
Germany; (elke.zimmermann@tiho-hannover.de)

The expression and recognition of emotional states represent a prerequisite for the evolution of shared emotional experiences or empathy among socially living animals. Numerous studies indicate that facial expressions coding for distinct emotions such as anger, disgust or fear are homologous in human and nonhuman primates (e.g. Keltner & Ekman 2000) providing important insights into the origin and evolution of emotions in the visual domain as well as into the underlying processing mechanisms. Respective investigations for the acoustic domain are still in their infancy. Information for nocturnal, archaic primates is totally lacking.

We have studied vocal communication in mouse lemurs to examine the effect of emotional states on acoustic expressions. The nocturnal mouse lemurs are an excellent model for such an approach since they belong to the early primate stock and use a complex repertoire of vocal structures for the regulation of social interactions (Zimmermann 1995). We mapped the behavior of individuals confronted with particular situations in a two dimensional valence-arousal model and related vocalizations given during male-male and male-female interactions with individually known participants to the respective behaviors. This allowed us to extract coding rules governing the acoustic expression of emotions. Variations in valence seem to be expressed in frequency contours, variations in arousal in tempo. We tested this hypothesis in an infant separation paradigm in which we changed the valence dimension by particular manipulations and the arousal dimension by different degrees of need.

Our results revealed how emotions are expressed acoustically in a nocturnal archaic primate. They provide the basis for both subsequent experimental studies on emotional recognition in this primate group and a cross-taxa comparison of emotional communication across mammals including man.

Supported by the DFG (FOR 499).

### References:

- Keltner, D., Ekman, P. (2000): Facial expression of emotion. In: Handbook of emotion (eds. Lewis, Hariland-Jones), Guilford Press, pp. 236-249.
- Zimmermann, E. (1995): Acoustic communication in nocturnal prosimians. In *Creatures of the Dark* (eds. Alterman, Doyle, Izard), Plenum Press, pp. 311-330.

How emotions are encoded in the acoustics of vocal communication in nonhuman primates and man

Uwe Jürgens

Non-verbal emotional vocal utterances of humans, such as laughing, crying, moaning or jubilating, as well as the emotional intonations superimposed on the verbal component during affective speech have been found to show transcultural similarities, suggesting that the vocal expression of emotion is to some extent genetically determined. A similar conclusion can be drawn with respect to monkey calls: Kaspar-Hauser experiments in the squirrel monkey have shown that all call types of the species-specific vocal repertoire can be produced by animals which never had an opportunity to hear these calls from conspecifics. From this the question arises of whether there are common acoustic features used by humans as well as monkeys in the expression of specific emotional states. Such features would indicate common phylogenetic roots of human and non-human primate emotional vocal behaviour. In the present study, acoustic analyses of squirrel monkey calls and human emotional intonations were carried out with the aim to find out in which way aversive emotional states differ from non-aversive ones in their vocal expression. For this purpose, squirrel monkeys were tested in self-stimulation experiments with intracerebrally elicited vocalizations for the aversiveness of the emotional states accompanying specific call types. In humans, data were acquired by asking students of dramatic art to pronounce one and the same word in an aversive (rage, despair, disgust) or non-aversive (joyful surprise, voluptuous enjoyment, affection) mood. It turned out that in squirrel monkeys as well as humans, an increase in the aversiveness of the emotional state was accompanied by an increase in peak frequency (frequency of highest energy in the power spectrum), an increase in frequency range (difference between maximum and minimum frequency at a specific time) and an increase in the amount of non-harmonic time segments in relation to harmonic ones. As the evolutionary branches leading to squirrel monkeys on the one hand and modern humans on the other have separated already 45 million years ago, our findings point to deep-reaching phylogenetic roots in human emotional vocal behaviour.

## The Expression of Emotions in Human Infants' Crying

Kathleen Wermke

Center for Pre-Speech Development & Developmental Disorders, Dept. of Orthodontics,  
Julius-Maximilians-University Wuerzburg, Germany: wermke\_k@klinik.uni-wuerzburg.de

The traditional classification of the human infants' cries in birth cries, hunger cries, pain cries and pleasure cries implies both causes and acoustical design. Isolation, hunger, and fear are nearly universal causes of crying in all vocal mammalian species. However, human infants acquire new motives for crying as their intellectual grasp of the social world and their psychological needs for emotional interchange differentiate (Wolff 1969, 1985). So, we undoubtedly see in the graded signals of infant's crying at least the first roots of intentional affective expressions and emotions observable at later ages, when infants cry for additional reasons, like fear of strangers or frustration during playing (Panksepp et al. 1978). This demonstrates the linking of internal affective states to new experiences. However, there is another developmental trend, which is not directed to a linking mechanism of internal affective states, but an unlinking. This developmental trend is observable in the pre-speech development of human infants, starting from emotional expressions in form of the earliest cries or gooing utterances and exhibiting an increasing decoupling from strong affections during the babbling phase, ending up with the symbolic function of the first single words. The paper will provide evidence for this claim by presenting melody analysis of pre-speech sounds from different developmental stages and comparing cry features of pain cries from 30 healthy newborns with those of mitigated, spontaneous cries of the same infants.

The human infant cry is a graded signal, expressing an emotional continuum from reflex responses to strong pain to the use of different cry features to elicit attention, care as well as an intentional request to interact: It is well-known that the higher degree of noise-like elements or a higher fundamental frequency of infants' pain cries are more annoying to listeners. On the other hand, the infant is also able to utter mitigated cries, which typically exhibit an 'attracting/friendly' melodic sound pattern. They very often reminds one of simple musical melodies. These cries are produced with open eyes in the vicinity of the mother, sometimes even while looking at her face. There is no doubt that the emotions and feelings underlying these mitigated cries are different from those underlying e.g. hunger or pain cries, which are more similar to call types of non-human primates.

Mitigated cries of human infants go beyond primate calls in one important respect, the non-situation-specificity: There is a variety of well-substantiated studies describing e.g. alarm calls, food calls, isolation calls in non-human primates, but analogous substantiation of comparable situation-specific (what means also emotion-specific in this case) cry patterns in human infants could not be provided so far. In the contrary, the huge amount of variability documented for human infants' cry patterns points to their specificity and the human infant's aptitude for expressing graded emotional states. Hence, the above-mentioned traditional categories of cry types (birth cry, pain cry, hunger cry) may not longer be particularly useful as taxonomies for the characterisation of human infant's cries.

Mitigated cries become increasingly complex with greater coupling and tuning between their melody and their vocal tract resonance frequencies over the first months of life (e.g. Mende et al. 1990, Wermke et al. 2002, Wermke 2002, Wermke/Friederici 2004). The melodies have specific types with complex melodies generated by concatenations of these types. Moreover the melodies show evidence of being based on intervals used in musical scales. Thus, in the earliest development of vocal performance, elementary features of both music and language are present and reflect the bridging element – expression of emotions and feelings via melody.

Our longitudinal studies in singleton and twins demonstrate that melody complexification seems to be part of the pre-speech development and might even provide essential building bricks for the acquisition of prosodic features (Wermke/ Mende/ Friederici in preparation).

### References

- Mende, W. et al., *Early Child Development and Care* 65, 95 (1990).  
 Panksepp, J. Z., Herman, B.H., Conner, R., Bishop, P. & Scott, J.P., *Biological Psychiatry* 13, 607 (1978).  
 Wermke, K., PhD thesis, Humboldt-University Berlin, Germany (2002, available at <http://edoc.hu-berlin.de>).  
 Wermke, K. & Friederici, A.D., *Behav. Brain Sci.* 27 (4) in press.  
 Wermke, K. et al., Developmental aspects of infant's cry melody and formants. *Medical Engineering & Physics*, 24, 501 (2002).  
 Wolff, P.H., The natural history of crying and other vocalizations in early infancy, in Foss, B.M. (ed.) *Determinants of infant behavior* (Vol. 4), Methuen, London (1969).  
 Wolff, P.H., Epilogue, in Lester, B.M.; Boukydis, C.F. (eds.) *Infant Crying. Theoretical and Research Perspectives*, Plenum Press, New York (1985).

## Acoustics, Perception, and Function of Human Laughter

Michael J. Owren  
Cornell University  
mjo9@cornell.edu

Laughter plays a ubiquitous role in human social interaction, and is commonly understood to be a *representational* signal whose function is to provide listeners with information about the laugher's emotional state. Several kinds of empirical evidence are not obviously compatible with this approach. For instance, we have found laughter to be acoustically variable even when recorded from vocalizers in consistently positive states. Listeners hearing these sounds under controlled circumstances nonetheless differed in emotional response, depending on laugh acoustics. The major distinction that emerged was between voiced (phonated and vowel-like) and unvoiced (breathy and noisy) laughter, with listeners showing differentiated responses in both explicit and implicit response tasks. Listeners also responded more less positively to voiced laughter produced with the mouth open than with the mouth closed. Finally, we have found laughers to modify the amount and kind of laughter they produce when paired with a social partner, depending on the sex and familiarity of that individual. An alternative, *affect-induction* approach to understanding laughter may therefore provide a better account of this behavior than the representational perspective. In this interpretation, the function of laughter is not primarily to express vocalizer state, but to induce and accentuate positive affect in listeners as a strategy of nonconscious social influence.



## Communication-call perception and parental emotions in the brains of mice

Günter Ehret

Dept. of Neurobiology, University of Ulm, D-89069 Ulm, Germany

House mice (*Mus musculus*) produce eight acoustically different types of vocalizations. Four of these call types are emitted by mouse pups in situations of parental care (birth cry, wriggling calls, distress calls) or of loss of parental care (pure ultrasounds, USVs). Mothers and adult females and males show adequate instinctive response behaviors to the call types. This responsiveness can be used to test synthesized call models for acoustic properties important for perception (e.g. Ehret and Riecke 2002; Geissler and Ehret 2002). Call models can also be used as defined acoustic stimuli in studies characterizing spatial distributions of activation in the auditory and limbic systems of the brain via call-induced expression of immediate-early genes such as c-fos and the immunocytochemical documentation and quantification of Fos-positive cells.

Our studies on USV and wriggling call perception have shown that a discrimination of adequate from inadequate call models is expressed in a differential activation of primary and higher auditory cortices. Doing the discrimination or learning to associate a given call pattern with a response leads to higher activations in the second auditory cortical field. The same is true for perception under increased attention (induced by application of apomorphin, a dopamin agonist). Emotional components of responding to the calls are seen in a left-hemisphere advantage of activation both of the dorsoposterior field (higher-order field) of the auditory cortex and a, probably multimodal, field dorsal of the auditory cortex (dorsal field) (Fichtel and Ehret, 1999; Geissler and Ehret 2004).

Males listening to USVs show different numbers and distributions of Fos-positive cells in centers of their limbic system depending on their experience with the pups and their motivation to respond paternally to the USVs. The lateral septum, the medial preoptic area, and the piriform cortex are all significantly less activated (low numbers of Fos-positive cells) in non-paternal, naive males compared to pup-experienced fathers caring for their second litters. This shows that centers of the limbic system that are involved in the release of instinctive parental behaviors are differentially activated by the same acoustical stimulus depending on the emotional/motivational state of the animal while it perceives the sounds .

Together, the data support ethological concepts of instinctive behavioral control in the mouse brain saying that acoustical stimuli are filtered for information-bearing elements and parameters to create perceptions of basic meanings and of the “urgency of a response”. These perceptions are combined with state-dependent activities (attention, emotion, motivation) in the brain in order to control the release of an adequate, biologically significant response (Ehret, 2005).

Supported by the Deutsche Forschungsgemeinschaft, Eh 53/17 and 19.

Ehret G (2005) Common rules of communication sound perception. In Kanwal J, Ehret G (eds) Behaviour and Neurodynamics in Auditory Communication, Cambridge University Press, Cambridge  
 Ehret G, Riecke S (2002) Proc Natl Acad Sci USA 99: 479-482  
 Fichtel I, Ehret G (1999) NeuroReport 10: 2341-2345  
 Geissler DB, Ehret G (2002) Proc Natl Acad Sci USA 99: 9021-9025  
 Geissler DB, Ehret G (2004) Eur J Neurosci 19: 1027-1040

**Distinct fMRI responses to speech, laughter, and sounds****Kai Alter**

Newcastle University/UK  
School of Neurology, Neurobiology and Psychiatry  
Newcastle Auditory Group

In this study, we used event-related fMRI to examine the neural responses to speech, vocal (human laughter), and non-vocal sounds. We aimed to delineate distinct peri-auditory regions which preferentially respond to speech, laughter, and sounds.

Results show that (i) left inferior frontal as well as left and right superior temporal regions subserve the comprehension of spoken utterances, (ii) in particular left anterior and posterior lateral temporal regions can be associated with the processing of speech, (iii) bilateral areas in the medial portion of Heschl's gyrus and at the medial wall of the posterior Sylvian fissure (planum parietale and parietal operculum) mediate the processing of non-vocal sounds with the right hemisphere being more strongly recruited. (iv) Hearing human laughter more strongly involves secondary auditory and somatosensory fields also in the right rather than the left hemisphere, but (v) perceiving human laughter does not evoke responses in brain regions usually associated with emotions.

The data indicates that the perception of laughter does not activate regions which are associated with emotions but activates brain regions which control motor (larynx) functions. The latter observation speaks to the issue of a dense intertwining of expressive and receptive mechanisms functions in the auditory domain. Generally, the present study evidences a functional segregation of the temporo-parietal lobes and lend support to the notion of at least two separate pathways mediating speech and non-speech stimuli.

## Neural correlates of laughter and crying in humans

Kerstin Sander

Leibniz Institute for Neurobiology, Brennekestraße 6, 39118 Magdeburg, Germany  
sander@ifn-magdeburg.de

Non-speech vocalizations like laughing and crying not only activate the auditory cortex of the listener but also amygdala and insula, i.e. limbic and paralimbic brain structures which are involved in the processing of emotions (Sander & Scheich, 2001). But it is still unclear whether the known left auditory cortex specialization for speech includes any human vocalization. Here we investigated this question using low-noise functional magnetic resonance imaging (Sander & Scheich, 2004). Twenty volunteers listened to human laughing and crying presented either in original or in time-reversed manner while performing a pitch-shift detection task. From a point of view of stimulus properties the backward presentations served as a certain type of acoustical controls because the only difference between original and time-reversed stimuli was their short-term spectro-temporal dynamics, while their overall spectral contents were identical. Original laughing and crying activated auditory cortex and amygdala more strongly in the left hemisphere than the time-reversed laughing and crying. As a tendency, this was also observed in the left insula. Thus, processing these non-speech vocalizations involves, like speech, predominantly left auditory cortex capacities. This lateralization effect seems to be based more likely on acoustical similarities between speech and laughing or crying than on similar communicative functions. Both original and time-reversed laughing and crying activated the right insula more strongly than the left which is in line with its assumed function in emotional self-awareness (Craig, 2002).

In part supported by Deutsche Forschungsgemeinschaft (SFB 426).

### References

- Craig, A. D. (2002). How do you feel? Interoception: the sense of the physiological condition of the body. *Nature Reviews Neuroscience*, 3, 655-666.
- Sander, K., & Scheich, H. (2001). Auditory perception of laughing and crying activates human amygdala regardless of attentional state. *Brain Res Cogn Brain Res*, 12(2), 181-198.
- Sander, K., & Scheich, H. (2004). Left auditory cortex and amygdala, but right insula dominance for human laughing and crying. *submitted*.

Title: Impaired recognition of danger as expressed in music following lesions of the amygdala in humans

Authors: Isabelle Peretz<sup>1</sup>, Nathalie Gosselin<sup>1</sup>, Séverine Samson<sup>2</sup> & Ralph Adolphs<sup>3</sup>

Affiliations: <sup>1</sup>Psychology, University of Montreal; <sup>2</sup>La Salpêtrière Hospital, Paris; <sup>3</sup>University of Iowa College of Medicine

Music constitutes a choice means to evoke a sense of suspense in films. However, there has been minimal investigation into the underlying cerebral organization for fear perception via music. In comparison, the amygdala's role in recognition of fear in non-musical contexts has been well established. The present study sought to fill this gap in exploring how patients with amygdala resection recognize emotional expression in music. To this aim, we tested 16 patients with left and right medial temporal resection (including amygdala) for the relief of medically intractable seizures and 16 matched controls in an emotion recognition task involving instrumental music. The musical selections were purposely created to induce fear, peacefulness, happiness and sadness. Participants were asked to rate to what extent each music expressed these four emotions on 10-point scales. In order to check for the presence of an eventual perceptual problem, the same musical selections were presented to the participants in an error detection task. None of the patients were found to perform below controls in the perceptual task. In contrast, both LTR and RTR patients were found to be impaired in the recognition of danger. Recognition of happy and sad music was normal. These findings suggest that the anteromedial temporal lobe (including amygdala) plays a role in the recognition of danger in a musical context. The testing of a further case, SM, who suffers from a selective and complete atrophy of the amygdala confirms the role of this particular brain structure in mediating recognition of threat in general.

## **Music as a model for acoustic communication of emotions in humans**

**Eckart Altenmüller, Katja Goydke, Alexander Eckstein, Reinhard Kopiez**

Institute of Music Physiology and Musicians' Medicine

University of Music and Drama, Hannover, Hohenzollernstr. 47, D-30161 Hannover

Although music is generally acknowledged as a powerful tool for eliciting emotions, little is known concerning the neurobiological basis of these emotions. In a preliminary study, the neurobiological basis of emotional valence judgements while listening to complex auditory stimuli was investigated. Cortical DC-EEG-activation patterns were recorded from 16 right-handed students. Students listened to 160 short sequences taken from the repertoires of jazz, rock-pop, classical music and environmental sounds (each n=40). Emotional valences of the perceived stimuli were rated on a five-step scale after each sequence. Brain activation patterns while listening revealed widespread bilateral fronto-temporal activation, but showed a highly significant lateralisation effect: positive emotional attributions were accompanied by an increase in left-temporal activation, negative attributions by a more bilateral pattern with preponderance of the right fronto-temporal cortex. The results are in keeping with Davidson's "Hemisphere hypothesis", saying the valence judgements are processed in different hemispheres depending on whether positive or negative emotions are reported.

In a second experiment, we investigated the psychological and neurobiological basis of strong emotional responses to music (SEM), leading to shivers down the spine and changes in heart rate. From previous studies it is known that these SEMs are accompanied by the activation of a brain network that includes the ventral striatum, midbrain, amygdala, orbitofrontal cortex and ventral medial prefrontal cortex — areas that are thought to be involved in reward, emotion and motivation (Panksepp and Bernatzky 2002). Personality factors may influence intensity, frequency and nature of these physical responses. 40 subjects (22 female, 18 male) listened to 6 standard excerpts of classical music. Their physical reactions to the music were assessed by means of questionnaires. In addition, personality traits were recorded with the Affective Neuroscience Personality Scales (ANPS) and the Tellegen Absorption Scale (TAS). Overall, strong emotional responses were reported by 90% of the subjects. Emotional reactions were more frequent when pieces were familiar. Subjects scoring highly on the TAS, and thus revealing a greater ability to completely dedicate themselves to an object or a situation, were more likely to report physical reactions than others. Furthermore, higher scores on the SEEK scale of the ANPS (reflecting sensation seeking tendencies) paired with low FEAR scores was related to increased emotional reactivity.

These results demonstrate that strong emotional responses are not only related to the psychoacoustic properties of the respective pieces of music, but furthermore to biographical memories and personality traits.

Lit: Davidson RJ et al. *Brain Cogn.* 1987 ; 6: 403-11.

Panksepp J, Bernatzky G. *Behav Processes.* 2002; 60:133-155.

## Music as a tool to examine pleasantness and unpleasantness

T. Fritz, S. Koelsch

Max Planck Institute for Human Cognitive and Brain Sciences, Leipzig, Germany

fritz@cbs.mpg.de

Since the establishment of neuroimaging techniques in the early 90's, emotion research has had a renaissance. Yet, a number of factors complicate the search for neurophysiological correlates of emotion. (1) the term emotion is vaguely defined, (2) emotion is involved in a multitude of processes, (3) the same stimulus might be perceived as differently valenced by different individuals.

Thus it is advisable to approach the topic with a focus on aspects of emotion that are reasonably well defined. In this talk, I describe a research project that uses music as a tool to examine emotion with fMRI. In order to avoid effects of musical preference on how the participants perceive the valence of the music pieces, stimuli are used that vary along a well defined dimension of emotion: pleasantness/unpleasantness. 'Pleasant' stimuli were excerpts of joyful instrumental dance tunes from the last four centuries (all major-minor tonal music). 'Unpleasant' stimuli were electronically manipulated, cacophonous counterparts of the original tunes.

The investigation of positively valenced, 'pleasant' emotions is challenging, and the neurophysiology of positive emotion is still unclear. One reason for this is that positive emotions appear to be difficult to evoke in the laboratory setting of PET or fMRI. In the present study we used musical stimuli to induce emotion, because music has been shown to be capable of evoking strong emotions with both negative and positive emotional valence consistently across subjects (Krumhansl, 1997), even in a PET experiment setting (Blood&Zatorre,2001).

In a prior experiment, a block design was used to investigate the perception of 'pleasant' and 'unpleasant' musical stimuli with a long duration (approx. 1 min). Both categories of stimuli activated so-called limbic and paralimbic areas that are classically known to be involved in the processing of emotion: Unpleasant cacophonies activated the amygdala and the parahippocampal gyrus in both hemispheres. Pleasant music activated the left anterior insula, the left orbitofrontolateral cortex, and the ventral striatum in both hemispheres.

Another interesting finding is that the pleasant music activated the Rolandic operculum. This structure comprises the somatosensory representation of the larynx, i.e. of a vocal tract articulator that is crucially involved in vocalisation. The data thus indicates, that subjects coded vocal sound production (without subsequent actual movement) while they heard the pleasant versions of the musical signals that were composed and performed by other individuals. An analogue phenomenon (namely that the same motor-related brain regions are activated during perception and production) has been described for the auditory modality in monkeys: when listening to the sound of an action (like peanut breaking), neurons in the premotor cortex would discharge that do also fire when the animal performs the specific action (Kohler et al., 2002). This mechanism has also been extensively described in the visual domain, where in both monkeys and humans the observation of an action activates identical premotor areas in the brain as when executing that action (Decety et al., 1999; Buccino, 2001). It is argued, that when individuals visually perceive an object strongly associated with an action, an internal replica of that action is automatically generated in the PMC.

These results thus provide evidence for an auditory perception-action mediation that relies on vocalisation representations that are activated during listening to the pleasant musical input, even when this input is non-speech and non-linguistic.

In a recent experiment, a sparse temporal sampling design combined with oversampling was used to examine the initial brain response towards short music stimuli (3.5-10 s). This design has the advantage that auditory stimuli can be presented in the absence of scanner noise. Thus, stimuli are not masked by the scanner noise, and activations elicited by the scanner noise and experimental stimuli cannot interact.

Results reveal, that listening to short excerpts of 'pleasant' and 'unpleasant' musical stimuli activates a similar network of subcortical brain areas as when listening to the previously tested longer ones. No activity in the Rolandic operculum was elicited by the short 'pleasant' music excerpts, indicating that the supposed mechanism for auditory perception-action mediation is not activated as an initial response to music.

Linguistic and nonlinguistic expression and perception of emotions:  
acoustics and neural substrates

Sonja A. Kotz

MPI for Human Cognitive and Brain Sciences, Leipzig, Germany

kotz@cbs.mpg.de

Social interaction in daily life is strongly influenced by complex interactions of emotional communicative channels (e.g. prosody, content, face, gesture, body posture). However, brain damage or neurodegenerative disease may affect these channels individually or interactive. Here, ERP and fMRI investigations are presented that attempted to isolate the supporting brain networks as well as the time-courses of emotional prosody and emotional content. Recent ERP evidence shows that violations of emotional prosodic contour (neutral semantic context) elicit a positive component, while violations of combined emotional prosodic and emotional content elicit an N400-like negativity. Utilizing fMRI, a fronto-temporo-subcortical network was found for emotional speech perception and a bilateral-opercular-subcortical network for filtered emotional speech. Subsequent experiments revealed that men show a strongly lateralized pattern of a fronto-temporal network for the perception of emotional prosody and emotional content that can vary as a function of task demands. On the other hand, women show mainly bilateral activation in temporal and posterior brain regions for both emotional prosody and emotional content. The current data suggest that both task demands and sex modulate the activation pattern of emotional prosody and emotional content.

## Expression and perception of emotional prosody in Parkinson`s disease

C. Schröder, R. Dengler

The neurodegenerative disorder Parkinson`s disease (PD) is characterized by the progressive death of selected populations of neurons including the dopaminergic neurons of the pars compacta of the substantia nigra, thus causing a dopaminergic deficit in the persons affected. Even though the clinical course of PD is dominated by its impact on motor functions there is an increasing number of data showing that PD may also be associated with deficits in emotional processing. Expression and perception of emotional prosody plays a decisive role in every day social life. Nevertheless the relationship between PD and expression and perception of emotional speech is still not well understood. The results of behavioural studies in this field are contradicting (1,2).

The objective of our research is to learn about the influence of PD on the perception and expression of emotional prosody by means of behavioural data, event related potentials and functional magnetic resonance imaging.

In this talk we will present first results of our studies and will discuss them in terms of implications for our understanding of PD and its impact on the function of neuronal circuits underlying the expression and perception of emotional speech.

### Literature:

- (1) Breitenstein C, Daum I, Ackermann H. Emotional processing following cortical and subcortical brain damage: contribution of the fronto-striatal circuitry. *Behav Neurol* 1998; 11(1):29-42.
- (2) Blonder LX, Gur RE, Gur RC. The effects of right and left hemiparkinsonism on prosody. *Brain Lang* 1989; 36(2):193-207.

Supported by a grant of the Deutsche Forschungsgemeinschaft (FOR 499, KO 2267/ 1-1).



**The effect of arousal on a social call of a nocturnal primate (*Microcebus murinus*)**

Melanie Dietz, Elke Zimmermann

Institut für Zoologie, Tierärztliche Hochschule Hannover, Bünteweg 17, 30559 Hannover, Germany; (elke.zimmermann@tiho-hannover.de)

Arousal-based physiological changes are hypothesized to affect vocal production specifically. Studies on human speech indicated that tempo- and source-related features varied according to arousal (e.g. Scherer 1995). In nonhuman anthropoid primates, variation according to arousal condition was associated with variations in similar features (e.g. Hauser 2000). To date, there is no information on the relation between arousal and vocal morphology in nocturnal primates.

The grey mouse lemur (*Microcebus murinus*) produces a rich array of social calls during social interactions (Zimmermann 1995). We investigated the effect of arousal on call structure by focussing on the trill, a context-specific call, a male emits when paired with an unknown male. The level of arousal was determined by the behaviour of the males: interactions without aggression were classified as reflecting low arousal, those with aggression as reflecting high arousal. Trill calls given during the two different arousal states were analyzed in eight males and characterized by tempo- and source-related features, e.g. duration, inter-call interval, start/ peak/ end frequency of the fundamental, bandwidth. The comparison of trill calls between the two arousal states suggested specific differences in structure. Thus, high arousal was related to a prominent decrease in fundamental frequency and a significant increase in calling rate.

Our findings provide first evidence for arousal-related differences in the same call type for a nocturnal primate. Arousal-related changes in tempo within the agonistic context correspond to those found in anthropoid primates suggesting that universal principles govern the acoustic coding of arousal in primate vocal communication.

Supported by DFG (FOR 499).

References:

- Hauser, M.D. (2000): The sound and the fury: Primate vocalizations as reflections of emotions and thought. In: The Origins of Music (eds. Wallin, Merker, Brown), MIT Press, pp. 77-102.
- Scherer, K. (1995): Expression of emotion in voice and music. J. Voice 9, 235-248.
- Zimmermann, E. (1995): Acoustic communication in nocturnal prosimians. In Creatures of the Dark (eds. Alterman, Doyle, Izard), Plenum Press, pp. 311-330.

## Combined perception of emotion from pictures and musical sounds

Authors: Katja N. Goydke<sup>1</sup>, Thomas P. Urbach<sup>2</sup>, Marta Kutas<sup>2</sup>, Eckart Altenmüller<sup>1</sup>, Thomas F. Münte<sup>3</sup>

<sup>1</sup>Institute of Music Physiology and Musicians' Medicine  
University of Music and Drama, Hannover  
Hohenzollernstr. 47,  
D-30161 Hannover

<sup>2</sup>Department of Cognitive Science  
University of San Diego, California  
La Jolla, CA 90021-0515

<sup>3</sup>Department of Neuropsychology,  
University of Magdeburg,  
Universitätsplatz 2, Gebäude 24,  
D-39106 Magdeburg

Corresponding author: katja.goydke@hmt-hannover.de

Simultaneous perception of information in different sensory modalities results in multi-sensory percepts that are not always a mere summation of the inputs. In fact, it has been demonstrated that information from one modality can modulate information perceived in another to yield a completely new, illusionary percept (McGurk and MacDonald, 1976). Integration from different sensory modalities is typically required when judgment of the emotional content of a situation is needed. Here, vision and audition are the most prominent channels to provide information. The combined perception of affective auditory stimuli and complex visual stimuli as typical for movies, commercials or music videos, requires higher-order semantic processing because the affective meaning of a scene is less salient than e.g. a facial expression.

The aim of the present study was to examine if a cross-modal influence on the perceived affect can be found between abstractly related inputs such as affective pictures and music. To this end affectively sung notes (happy, neutral, sad) were combined with emotional pictures (happy, neutral, sad) taken from the IAPS (Lang et al., 1995). Picture-tone-pairs were either congruent or incongruent in emotional content. In two different tasks subjects were asked to attend either the voice or the picture and rate the expressed emotion on a 1-to-7-scale (sad to happy). Stimulus length ranged from 300 to 500 ms. The main objective of the study was to demonstrate an interaction between the affective content of the pictures and accompanying voice stimuli. To delineate the time-course, topography, and direction (visual → auditory, auditory → visual) of such interactive effects, if present, event-related-brain-potentials were recorded on 26 sites.

Participants' rating behavior for pictures was not influenced by the emotion expressed in the auditory stimulus. In contrast, ratings of vocal expression were partly influenced by the valence of the unattended picture: Happy and neutral voices were rated more positive when paired with a happy picture than when paired with a sad picture. Pairing of the attended pictures with voice stimuli of varying valences influenced the amplitudes of the early ERP components N1 and P2. In addition, clear effects of emotional congruency were found in P3 and the following sustained potential: Happy and sad pictures evoked larger (more positive) amplitudes when paired with voices of congruent valence than when paired with voices of incongruent valence. When voices were in the focus of attention (voice rating task), ERPs were less influenced by the valence of the pictures than ERPs to pictures were by the valence of the voice. Nevertheless, again, the P2 amplitude was affected. An effect of emotional congruency in the late sustained positivity was only present for sad voices.

The results indicate an interaction of affective information from auditory and visual modalities, even under circumstances in which one of the modalities is unattended and the information in the unattended modality is completely irrelevant for task performance. This suggests that affective information from different sensory channels is integrated in a more or less automatic fashion. The timing of the ERP effects related to the valence of the unattended modality stimuli suggests that this automatic integration is a comparatively early process (onset at 150 ms). The asymmetry between the observed effects indicates that the different channels do not influence each other to the same extent.

This work was supported by grants of the Gottlieb Daimler- and Karl Benz-Foundation and the GA-Lienert-Foundation to the first author.

Lit.: Lang, P. L., M. M. Bradley, et al. (1995). *International affective picture system (IAPS): Technical Manual and Affective Ratings*. Gainesville, FL, The Center for Research in Psychophysiology, University of Florida.  
McGurk, H. and J. MacDonald (1976). *Hearing lips and seeing voices*. *Nature*. **264**: 746-8.

## Psychological and Physiological Correlates of Strong Emotions in Music

Oliver Grewe (1), Frederik Nagel (1), Eckart Altenmüller (1), Reinhard Kopiez (2)

- (1) Institut für Musikphysiologie und Musikermmedizin, Hochschule für Musik und Theater Hannover, D-30161 Hannover. E-mail: [oliver.grewe@imail.de](mailto:oliver.grewe@imail.de)
- (2) Institut für Musikpädagogische Forschung, Hochschule für Musik und Theater Hannover, D-30161 Hannover.

Music can arouse extraordinarily strong emotional responses up to ecstatic “chill” experiences (Sloboda, 1991; Panksepp, 2001). Such strong psychological reactions are often accompanied by measurable bodily reactions such as goosepimples, shivers, heart racing etc.. Since emotional states may change in the course of every piece of music, it is necessary to measure psychological and bodily reactions continuously. In order to investigate distinct musical events related to chill reactions, we combined psychological, psychoacoustical and physiological methods in one experiment.

For a continuous rating of emotions on the dimensions 'valence' and 'arousal' the researcher-developed software 'EMuJoy' was used. By moving a cursor in a two dimensional space between the axes valence and arousal, emotions can be recorded continuously (Two Dimensional Emotion Space: Russell, 1980). Additionally, chill experiences could be indicated by pressing a mouse button.

35 subjects listened to different pieces of music and simultaneously rated their subjectively experienced emotions in the time course of each piece. Chills were defined as “goosepimples” and as “shivers down the spine”. A selection of 7 pieces from different musical styles was used for all subjects. Additionally, subjects were asked to bring 5-10 “personal” pieces of music with them, which regularly induced strong emotions. All kinds of musical styles were accepted. Subjects' mean age was 37,53 (SD = 16, 406) with a range between 11 and 72 years. Subjects had different musical experience and education.

During the experiment, skin conductance level (SCL), skin conductance reaction (SCR), heart rate, facial electromyography (EMG) and skin temperature of the test persons were measured, synchronized by the 'EMuJoy' software.

After each piece of music, subjects filled in a questionnaire regarding their knowledge about the piece, perceived bodily reactions (tears, lump in the throat, feeling in the stomach etc.) and recalls connected to the music.

After the experimental session, subjects answered further questionnaires concerning their musical tastes, experiences, and three standardized personality inventories (TCI, ANPS, SSS-V).

Psychoacoustical parameters of the stimuli were analyzed by use of the VIPER software.

### Preliminary results:

In spite of highly individual emotional reactions to music, constant inter-individual clusters of chill responses related to harmonic and dynamic changes could be found. Chills were much more frequent in previously known music and in familiar musical styles. Ratings of valence and arousal varied significantly between individuals: nonetheless, as a frequent pattern, distinct musical events could be identified, which caused strong dynamics in emotion rating within a narrow time gap.

According to our results, we hypothesize that chill experiences basically have two preconditions:

1. A general level of attention and sympathy for the music. This general emotional reaction depends on mostly individual parameters for each listener (musical style, listening situation, induced associations, knowledge of the piece etc.).
2. A striking event within the piece (strong contrasts, dynamics) that, by further focusing concentration (conscious perception) on both the music and the own emotional experience, stimulates the chill. Under the condition that a general level of attention and sympathy has been created (see 1), the characteristics of events that can induce a chill seem to be universal for most listeners.

This work was supported by the DFG (grant no. AL 269-6) and the *Center for Systemic Neurosciences Hannover*

### References:

- [1] Sloboda, John A. (1991): Music Structure And Emotional Response: Some Empirical Findings. *Psychology of Music* 19, 110-120.
- [2] Panksepp, Jaak; Bernatzky, Günther (2001): Emotional Sounds And The Brain: The Neuro-Affective Foundations Of Musical Appreciation. *Behavioural Processes* 60, 133-155.
- [3] Russell, J.A. (1980): A Circumflex Model Of Affect. *Journal of Personality and Social Psychology* 39, 1161-78

**Vocalization as an emotional indicator – neuroanatomical tracing  
of vocalization-related afferents to the midbrain  
periaqueductal grey in squirrel monkeys (*Saimiri sciureus*)**

**Eva Dujardin and Uwe Jürgens, German Primate Centre, Göttingen, Germany**

The midbrain periaqueductal grey (PAG) plays an essential role in the vocal expression of emotional states. Here, we investigated the afferent input to different vocalization-eliciting sites in the PAG of the squirrel monkey (*Saimiri sciureus*). Vocalization was elicited by injection of homocysteic acid into the PAG. Tracing of the afferent connections was carried out via wheat germ agglutinin-conjugated horseradish peroxidase (WGA-HRP), injected into the vocalization-eliciting sites. To find out, whether sites producing different call types receive different projections, we compared the retrogradely labeled brain areas of three groups. In one group, WGA-HRP was injected into sites yielding shriek calls which are normally uttered during defensive threat and express highly aversive emotional states. The second group was injected into sites yielding cackling which occurs usually during social mobbing accompanied by moderately aversive emotional states. The third group was injected into sites producing cluck calls, representing non-aversive close-distance contact calls. The results show a large overlap in the labeled structures of the three groups. Conspicuous common labeling was found in the prefrontal and middle temporal cortex, insula, basal forebrain, large parts of the hypothalamus, zona incerta, substantia nigra, locus coeruleus, paralemniscal and ventrolateral reticular formation and the solitary tract nucleus. In several structures, the amount of retrogradely labeled cells differ greatly between the groups, however. While some structures show the highest relative number of labeled cells in the cluck group (e.g. nucleus accumbens, medial preoptic region), others show the heaviest labeling in the shriek (e.g. posterior hypothalamus) or cackle group (e.g. anterior cingulate cortex). Some structures show virtually equal labeling intensity in all three groups (e.g. dorso- and ventromedial hypothalamus). These findings make clear, that PAG sites controlling different call types receive only partially segregated inputs. The fact that some structures show differences in labeling intensity between the groups indicates, that they participate in the production of individual call types to a different degree.

Supported by the Deutsche Forschungsgemeinschaft (Ju 181/14-1)

## The encoding of emotion in human laughter

Diana Zaum, Kai Alter

Within human communication the expression and perception of the emotional state is an important characteristic. In this aspect, it is essential in a social community to have the ability to assess the emotional content not only of verbal vocalisations but also of non-verbal expressions. But while the processing of spoken language requires knowledge of syntax and semantics, affective non-verbal vocalisations are processed without propositional content. Thus, the question arises, how different affective dimensions are encoded in nonverbal vocalisations.

In order to answer this question we examined human laughter, because it is an obvious and frequently used form of non-verbal vocalisation. Since laughing is advantageous for an individual in social communities it has an essential influence on human behaviour. Therefore it could be an optimal carrier of emotional content.

Our goal was to investigate the extent laughter can carry emotional content and the mechanisms of this. Furthermore, we will compare the human perception of human laughter to that of animal laughter.

In this framework we will present the first behavioural studies investigating different kinds of human laughter. We found that people are able to discriminate between different emotional settings in which the laughter has been produced. Furthermore, we will present three behavioural experiments which aimed at categorising laughter in terms of three emotional axes, which are valence, arousal, and dominance. Therefore, we showed that non-verbal vocalisation like laughter can carry emotional content.

Diana Zaum

Max Planck Institute for Human Cognitive and Brain Sciences  
Stephanstraße 1a  
D-04103 Leipzig  
Germany

Dr. habil. Kai Alter

School of Neurology, Neurobiology & Psychiatry (Neurobiology)  
The Medical School  
Framlington Place  
University of Newcastle  
Newcastle upon Tyne NE2 4HH  
UK

**Satellite Symposium #Sat2:  
Functional brain proteomics**  
**Hans Gerd Nothwang and Marius Ueffing, Kaiserslautern and  
Oberschleißheim/Neuherberg**

**Introduction**

[#Sat2](#) Hans Gerd Nothwang and Marius Ueffing, Kaiserslautern and Oberschleißheim/  
Neuherberg  
*Functional brain proteomics*

**Slide**

[#Sat2-1](#) HE. Meyer, Bochum  
*The HUPO Brain Proteome Project*

[#Sat2-2](#) HG. Nothwang, M. Becker, J. Schindler, I. Guillemin and E. Friauf, Kaiserslautern  
*Proteome analysis in the auditory brainstem*

[#Sat2-3](#) R. Jahn, Göttingen  
*Protein analysis of synaptic vesicles*

[#Sat2-4](#) M. Ueffing, MS. de Lange, H. Zischka and R. Braun, Munich  
*Neurogenetics through proteomics: analysing protein composition and interactions*

[#Sat2-5](#) E. Wanker, Berlin  
*Neuroproteomics: from interaction networks to protein function and disease mechanisms*

[#Sat2-6](#) C. Hopf, PO. Angrand, J. Gagneur, H. Ruffner, M. Stein, P. Volkel, B. Dimpelfeld, B.  
Kuster, G. Drewes, F. Wilson, B. Heffernan, R. Mangano, L. Pickard, E. O'Sullivan, S.  
Thomas, J. Choudhary and A. Rowley, Heidelberg  
*Proteomic Approaches to Drug Discovery in Alzheimer's Disease*

## **Introductory Remarks to Sat. Symposium 2**

### **Functional brain proteomics**

**Hans Gerd Nothwang and Marius Ueffing,  
Kaiserslautern and Oberschleißheim/Neuherberg**

To a large extent, the structure and function of any nervous system is defined by the specific set of its proteins, i.e. the respective proteome. Recently, novel techniques have been developed to study these proteomes on a so far unprecedented large-scale level. The goal of proteomics is to define the identities, quantities, dynamics, structures, interactions, and functions of all proteins and to dissect the metabolic, signaling and regulatory networks within a given biological system. Even though still in their infancy, the novel techniques have already provided us with astonishing insights into biological systems and physiological processes. It is therefore very likely that proteomics approaches will also have a major impact in the field of neurobiology. We think that it is time to present an overview of the current state of the art.

The suggested symposium attempts to present several facets of so-called proteomics approaches to CNS studies under both normal and pathological conditions. It includes various technical approaches, such as comparative 2-D gel electrophoresis, high-throughput mass spectrometry, and large-scale identification of protein interactions. Helmut Meyer, one of the leaders of the international Human Brain Proteome Project, will give a general introduction to this project, present the data obtained so far, and discuss their impact on neuroscience. Hans Gerd Nothwang will then present more detailed protein mapping data on the auditory brainstem and discuss current advantages and limitations of comparative proteomics compared to other large-scale gene expression profiling techniques. Reinhard Jahn will show results on the characterisation of synaptic vesicles. Proteomic approaches also deepen our knowledge on the underlying mechanisms leading to dysfunctional networks in diseases. Several strategies are available which will be illustrated and discussed by Marius Ueffing. The usefulness of proteomics for dissecting pathological pathways will be demonstrated by Erich Wanker and by Bernhard Kuester. Both speakers will illustrate the current states of different techniques to characterize protein interactions and protein complexes and their importance to better understand disorders such as polyglutamine diseases and Alzheimer.

## **The HUPO Brain Proteome Project**

Prof. Helmut E. Meyer, Medical Proteom-Center, Ruhr-University, Bochum, Germany  
Phone +49 234 32 22427, Fax: +49 234 32 14554, eMail: Helmut.E.Meyer@rub.de

The brain is the most complex tissue of higher organisms, differing from other organs due to its many different cell types, its structure at the cellular and tissue level, and by the fact that one of the most important cell type in the brain, the neuron, stops dividing in adult life. Elucidating the protein complement of the brain is therefore a significant challenge for current technologies in proteome analysis.

At the same time, the brain is of paramount interest to medical research and pharmaceutical industry because of the social impact of the more common neurological diseases such as Alzheimer, Parkinson, Multiple Sclerosis, Prion Diseases and Stroke. The prevalence of some of these diseases is increasingly high, e.g. every 5<sup>th</sup> person over 80 years in industrial countries is suffering from Alzheimer.

There is no strict relationship between the genome and the protein complement, as one gene can code for several proteins, protein expression levels are not predictable from mRNA expression level and proteins are often modified and processed after translation. In addition, it is to be shown if brain function is mediated largely by brain specific proteins or proteins common to different organs. Thus, the scientific problems of brain proteomics can not be solved with the resources of single laboratories or groups.

Therefore, the HUPO Brain Proteome Project (BPP, [www.hbpp.org](http://www.hbpp.org)) was established under the patronage of the Human Proteome Organisation (HUPO) in order to coordinate worldwide neuroproteomic efforts, as well as to reduce duplicate efforts. One aim of HBPP is the characterization of the human and mouse brain proteomes and the utilization of these data (identified proteins, mRNA profiles, protein/protein interactions, protein modifications and localization, validated targets) to elucidate human neurodegenerative diseases with the focus on Alzheimer's and Parkinson's Disease. Gained data, SOPs and new technologies obtained through these studies will be accessible to all active members of the HBPP. Two HUPO HBPP Workshops already took place at Castle Mickeln, Duesseldorf, Germany, and Paris, France. A pilot phase addressing the available methods of the participating groups has started (Feb/March 2004). Quantitative proteome analysis will be done to study aging processes (mice) and protein post mortem stability (human), leading to a reliable neuroproteome database. First results will be presented at the 3<sup>rd</sup> HUPO World Congress in Beijing (October 2004) as well as at the 3<sup>rd</sup> HUPO BPP Workshop in Rauischholzhausen (December 2004) and will lead to the start of the realization of the generated master plan.



## Proteome analysis in the auditory brainstem

Hans Gerd Nothwang, Michael Becker, Jens Schindler, Isabelle Guillemain, and Eckhard Friauf

Animal Physiology Group, Department of Biology, University of Kaiserslautern, POB 3049, D-67653 Kaiserslautern, Germany

The superior olivary complex (SOC) and the inferior colliculus (IC) are two conspicuous mammalian brainstem centers which play pivotal roles in processing auditory information. The SOC is important for sound localization by computing interaural time and intensity differences. The IC is an important integration center that obtains inputs from several auditory nuclei and is involved in the processing of complex signals and in reflex behavior.

To identify proteins that may be related to center-specific functions, we initiated proteome analyses using 2-D gel electrophoresis and mass spectrometry. Many of the identified cytoplasmic protein spots represented high-abundant housekeeping proteins and only few differences were detected between the two centers. The characterization of other cell compartments was precluded as they could not be separated by current fractionation protocols. Therefore, we established a protocol of subcellular fractionation by differential centrifugation that can be applied to small amounts of cultured cells and tissue. It yields a nuclear fraction, a cytoplasmic fraction, and a mixed membrane/organelle fraction. Immunoblot analysis and 2-D gel electrophoresis combined with tandem mass spectrometry revealed superior separation of these compartments compared to other protocols.

To enrich for the important class of integral membrane proteins, which are often low-abundant, the membrane/organelle fraction was washed with high salt and carbonate. Immunoblot analysis revealed reduction of the peripheral membrane marker protein actin and the enrichment of the integral membrane marker proteins KCC2 and Na<sup>+</sup>/K<sup>+</sup>-ATPase. Application of the novel subcellular fractionation protocol in a proteome analysis which compared between the IC and the cerebellum, a non-auditory brain structure, identified several differentially abundant proteins.

Since plasma membrane proteins are of particular interest in neurobiology, we additionally established an affinity partition protocol based on an aqueous two phase system to selectively enrich these proteins.

In summary, our analyses demonstrate the feasibility of proteome approaches in small brain structures. They furthermore illustrate that various approaches and techniques are required for their in-depth analysis.

## Neurogenetics through proteomics: analysing protein composition and interactions

Marius Ueffing, Magda Swiatek de Lange, Hans Zischka, Ralf Braun

Institute of Human Genetics, GSF-Research Center for Environment and Health, München and Technical University Munich, Klinikum Rechts der Isar

Interactions between genetic and environmental factors determine dynamics of normal neuronal function as well as the risk, penetrance, onset and progression of neurodegenerative diseases. Complementing the very successful classical gene discovery strategies that aim at elucidating the genetic contribution to disease, proteomic analysis can assist in understanding disease mechanisms.

Native separation and enrichment of protein complexes provide an opportunity to study proteins in relation to their functional and topological context. The conceptual principle is to reduce the complexity of proteomes to be analysed step by step without destroying their initial functional context by denaturation. When performed by methods that preserve nativity, this approach can greatly enhance analytical depth and in addition visualize functional relationships. Two examples will be presented:

1) Mitochondria are considered as effector sites or even cause for a variety of neurodegenerative disorders, their functional impairment due to mutation of a single mitochondrial protein alone can cause neurodegeneration. We have analysed yeast mitochondria from a normal yeast strain, as well as from corresponding cells impaired by a point mutation of *cdc48*, the yeast ortholog of Valosin-containing protein (VCP). VCP is a pathological effector for expanded polyglutamine-induced neurodegeneration and a disease-associated gene in frontotemporal dementia. Results will be presented on the molecular mechanisms underlying VCP-mediated apoptosis in yeast.

2) Genetically inherited blinding diseases are largely associated with mutations in genes coding for proteins expressed in photoreceptors. By separating and enriching multiprotein complexes in mammalian photoreceptor cells, we have identified several candidates as novel components of the phototransduction pathway, including small GTPases from Rho and Rab families, and established a preliminary protein interaction map for mammalian photoreceptors. We have identified protein interactions linked to the physiology of vision in mammalian photoreceptors. Protein interaction maps and analysis of their dynamics can be correlated to physiological states and will be used for a better understanding of vision processes and pathological mechanisms in retinal degenerative diseases causing blindness.

This work is supported by BMBF grants 031U108A/031U208A and –E, EU grants PRO-AGE-RET QLK6-CT-2001-00385 and INTERACTION PROTEOME LSHG-CT-2003-505520.

## Proteomic Approaches to Drug Discovery in Alzheimer's Disease.

**C. Hopf, P.O. Angrand, J. Gagneur, H. Ruffner, M. Stein, P. Volkel, B. Dümpelfeld, B. Kuster<sup>1</sup> & G. Drewes  
F. Wilson, B. Heffernan, R. Mangano, L. Pickard, E. O'Sullivan, S. Thomas, J. Choudhary & A. Rowley**

<sup>1</sup>Cellzome AG, Meyerhofstrasse 1, 69117 Heidelberg, Germany, [www.cellzome.com](http://www.cellzome.com)

A major challenge for drug discovery in Alzheimer's disease is the discovery of novel tractable targets that may provide alternatives to established secretase-directed approaches. To identify potential new targets, we have systematically analyzed multiprotein complexes associated with proteins currently implicated in beta-amyloid precursor protein (APP) processing as "baits", using a combination of dual epitope-tagging and viral transduction in human neuroblastoma cells, tandem-affinity purification (TAP), and protein identification by tandem mass spectrometry as well as bioinformatics network analysis. The current study represents the first successful adaptation of this strategy to membrane protein complexes.

Amongst the complexes we have analyzed are the beta-amyloid precursor protein itself and the secretases responsible for generation of Ab, the major component of senile plaques found in Alzheimer's disease brains. For example, using tagged presenilin or nicastrin, we find the mammalian orthologues of the *C. elegans* genes *Aph-1* and *Pen-2* as components of both high and low molecular weight gamma secretase complexes. Our experimental strategy recapitulates in one single approach the vast majority of all published components of the APP processing machinery, and provides many novel interacting proteins as candidates for target validation approaches. Our analysis demonstrates that the TAP-MS strategy provides a powerful means to identify novel components in human disease-related pathways.

The search for potential therapeutic molecules directed against gamma-secretase is focusing on compounds that modulate rather than inhibit the activity of this enzyme because the enzyme has multiple substrates in addition to APP which, in turn might almost certainly lead to undesired side effects. Using a chemical proteomics approach in which compounds that show an effect on Ab production are used as affinity reagents, we have identified the molecular target responsible for the observed effect. Using a quantitative mass spectrometry based immunoassay that monitors the changes in the production of all Ab species simultaneously, one can easily distinguish inhibitors from modulators and thus inform the prioritization of active compounds for lead optimization.

**Satellite Symposium #Sat3:**  
**Functional microdomains and embedded proteins**  
**Frank Lehmann-Horn and Albert Ludolph, Ulm**

**Introduction**

[#Sat3](#) Frank Lehmann-Horn and Albert Ludolph, Ulm  
*Functional microdomains and embedded proteins*

**Slide**

- [#Sat3-1](#) R. Schneggenburger, E. Neher, X. Lou, M. Wölfel and F. Felmy, Göttingen  
*The  $Ca^{2+}$ -microdomain signal at the site of vesicle fusion determines release probability at a CNS synapse*
- #Sat3-2 T. Böckers, Ulm  
*Dynamics of the synaptic membrane*
- #Sat3-3 C. Fahlke, Aachen  
*Molecular and cellular function of glutamate transporters*
- #Sat3-4 M. Langer, Ulm  
*Electrical activity due to cochlear hair cell movements*
- #Sat3-5 B. Qualmann and M. Kessels, Magdeburg  
*The role of cytoskeletal and cytomatrix components in the organization and function of synaptic specializations*
- #Sat3-6 U. Nienhaus and K. Jurkat-Rott, Ulm  
*Voltage sensor movements within the channel protein and surrounding membrane*

**Introductory Remarks to Sat. Symposium 3****Functional microdomains and embedded proteins****Frank Lehmann-Horn and Albert Ludolph, Ulm**

Microdomains are membrane areas rich in clustered proteins that permit cellular signaling and exo- and endocytosis. This symposium deals with microdomains of the surface membrane of excitable cells and their interaction with extra- and intracellular components. Essential elements of the excitable micro-domains will be discussed, e.g. receptor and ion channel proteins. The structure and function of these proteins is best characterized by use of fluorescence and various combined nanotechniques, e.g. force microscopy and patch clamping. Some of these techniques were originally applied to non-biological surfaces and are only recently being used for cell membranes and adjacent structures.

## **The $\text{Ca}^{2+}$ -microdomain signal at the site of vesicle fusion determines release probability at a CNS synapse**

Ralf Schneggenburger, Erwin Neher, Xuelin Lou, Markus Wölfel and Felix Felmy • Max-Planck Institute for Biophysical Chemistry, AG Synaptic Dynamics and Modulation & Dept. of Membrane Biophysics, 37077 Göttingen, Germany

The factors which determine transmitter release probability during short, and longer-lasting forms of synaptic plasticity are still under debate. Although it is generally accepted that vesicle fusion is triggered by elevations of the intracellular  $\text{Ca}^{2+}$  concentration ( $[\text{Ca}^{2+}]_i$ ), the amplitude, and the kinetics of the  $[\text{Ca}^{2+}]_i$  signal relevant for vesicle fusion have remained elusive. This is because the relevant  $[\text{Ca}^{2+}]_i$  signal is a microdomain signal created by  $\text{Ca}^{2+}$  channels co-localized in the immediate vicinity ( $< 0.3 \mu\text{m}$ ) of release-ready vesicles. Due to its spatial restriction and short ( $\sim 1 \text{ ms}$ ) duration, the  $\text{Ca}^{2+}$ -microdomain signal cannot be measured directly with current imaging methods. We have therefore used a "reverse" approach to gain insight into the amplitude, and the time-course of the  $\text{Ca}^{2+}$ -microdomain signal, using a giant glutamatergic brainstem synapse, the calyx of Held, which is accessible to direct pre- and postsynaptic whole-cell patch-clamp recording. The "reverse" approach involves (i) measuring transmitter release after global elevations of presynaptic  $[\text{Ca}^{2+}]_i$  produced by  $\text{Ca}^{2+}$  uncaging (ii) fitting the experimentally obtained relationship between transmitter release and  $[\text{Ca}^{2+}]_i$  with the simplest possible kinetic model, and (iii) finding a hypothetical  $\text{Ca}^{2+}$ -microdomain waveform that produces phasic transmitter release similar to the physiological release during a presynaptic action potential.

We found, first, that the relationship between release and presynaptic  $[\text{Ca}^{2+}]_i$  is highly non-linear (slope of 4 - 4.5 in a log-log plot between 2 - 8  $\mu\text{M}$   $[\text{Ca}^{2+}]_i$ ), requiring a kinetic model with cooperative binding of 5  $\text{Ca}^{2+}$  ions (Schneggenburger & Neher, 2000). We estimated that the physiological release is driven by a brief (half-width,  $\sim 0.5 \text{ ms}$ ) microdomain  $[\text{Ca}^{2+}]_i$  signal, with amplitude in the range of 15 - 25  $\mu\text{M}$ . During short-term facilitation, we showed that the intracellular  $\text{Ca}^{2+}$ -sensitivity of transmitter release was unchanged (Felmy et al., 2003). This implies that facilitation is caused by an enhanced  $\text{Ca}^{2+}$  microdomain signal for vesicle fusion; and thus, that the  $\text{Ca}^{2+}$  microdomain signal determines release probability. In contrast, longer-lasting potentiation of transmitter release by phorbol esters, which target presynaptic munc-13 / protein kinase C signaling pathways, led to a marked increase in the intracellular  $\text{Ca}^{2+}$  sensitivity of vesicle fusion, with a concomitant decrease in the apparent  $\text{Ca}^{2+}$  cooperativity. Thus, longer-lasting potentiation of transmitter release can act via increasing the intracellular  $\text{Ca}^{2+}$  sensitivity of synaptic vesicle fusion, but during short time intervals, changes in the microdomain  $\text{Ca}^{2+}$  signal produced by modulation of  $\text{Ca}^{2+}$  influx, summation of  $\text{Ca}^{2+}$  signals and saturation of  $\text{Ca}^{2+}$  buffers are the main determinants of release probability.

**Satellite Symposium #Sat4:**  
**Analysis of brain transcriptomes: principals, goals, achievements**  
**Gabriele Flügge, Nils Brose and Eleni Roussa, Göttingen**

**Introduction**

[#Sat4](#) Gabriele Flügge, Nils Brose and Eleni Roussa, Göttingen  
*Analysis of brain transcriptomes: principals, goals, achievements*

**Slide**

[#Sat4-1](#) N. Prakash, Munich  
*Dissection of the genetic pathway underlying dopaminergic neuron development*

[#Sat4-2](#) B. Liss, Marburg  
*Correlating function and gene-expression of individual dopaminergic neurons.*

[#Sat4-3](#) E. Vreugdenhil, Leiden (NL)  
*Corticosteroid-responsive genes in the rodent hippocampus: a genomics approach*

[#Sat4-4](#) A. Koehl, A. Rieger, N. Schmidt, E. Friauf and HG. Nothwang, Kaiserslautern  
*Transcriptome analysis in the rat auditory brainstem*

[#Sat4-5](#) K. Nieselt, Tübingen  
*Analysis of microarray brain expression data: computational and statistical challenges*

**Introductory Remarks to Sat. Symposium 4****Analysis of brain transcriptomes: principals, goals, achievements****Gabriele Flügge, Nils Brose and Eleni Roussa, Göttingen****organised by CMPB  
Centre for Molecular Physiology of the Brain  
University of Göttingen**

Analysis of gene transcripts via cDNA microarrays and related methods provide powerful tools to find new molecular components that underlie various processes of brain development, neuronal differentiation and central nervous disorders. Within the symposium, experts from different areas of neurobiology will describe latest results from their research on gene expression during differentiation of dopaminergic neurones, on expression of hippocampal and brain stem genes. Methodological aspects such as potentials, planing and interpretation of microarray experiments will also be addressed.



## Dissection of the genetic pathway underlying dopaminergic neuron development

Prakash, N.

GSF-National Research Center for Environment and Health, Technical University Munich, Institute of Developmental Genetics, 85764 Munich/Neuherberg, Germany, and Max-Planck-Institute of Psychiatry, 80804 Munich, Germany

Midbrain dopaminergic (mid-DA) neurons play a pivotal role in the control and modulation of different brain functions, including voluntary movement, rewarding and cognition. Their degeneration or dysfunction leads to severe neurological and psychiatric disorders, among them Parkinson's Disease (PD) as the most prominent one. Therapeutic strategies for PD include the replenishment of the degenerating by healthy mid-DA neurons that were generated either *in vitro* or by the stimulation of a putative mid-DA progenitor to proliferate and differentiate *in vivo*. Therefore, understanding the normal development of this cell population is also of high clinical interest.

Despite the importance of mid-DA neurons, the molecular mechanisms controlling their development are still poorly understood. During embryogenesis, midbrain dopaminergic neurons are specified rostral to the mid/hindbrain boundary (MHB), and another cell population, the hindbrain serotonergic neurons, is specified caudal to it. We have previously shown that the position of the MHB determines the location and size of the midbrain dopaminergic and hindbrain serotonergic cell populations *in vivo*. Furthermore, the secreted glycoprotein Wnt1 is expressed in close vicinity to developing mid-DA neurons in the mesencephalic flexure of the mouse embryo. It was shown before that Fgf8, a factor secreted from the rostral hindbrain at the MHB, and Shh, secreted from the ventral part of the neural tube (the floor plate), are necessary and sufficient for ectopic induction of mid-DA neurons (Ye et al, 1998). Now we provide evidence for the first time that, in addition to these two factors, Wnt1 is directly required for the generation of mid-DA neurons *in vivo*. We postulate that all three factors together act early in CNS development for induction of a mid-DA precursor which later will differentiate into a mature mid-DA neuron. Competence to respond to these signals is most likely provided by Otx2. However, on a time-scale of mid-DA neuron development during embryogenesis, it becomes clear that those factors involved in specification of the mid-DA neuronal fate are still largely unknown. We therefore performed a suppression-subtracted hybridization-based differential screen using our mutant mice to identify new genes involved in mid-DA neuron development. Preliminary data from these screens will be presented in this talk.

Correlating function and gene-expression of individual dopaminergic neurons.

Birgit Liss, Molecular Neurobiology, Institute for Physiology, Philipps University Marburg, Deutschhausstrasse 2, 35037 Marburg, Germany.

Dopaminergic (DA) midbrain neurons are involved in a variety of different brain functions, like cognition, emotion and control of voluntary movements. The selective and progressive degeneration of DA neurons is a pathophysiological hallmark of Parkinson's disease (PD). Strikingly, not all DA neurons are affected equally by the degenerative process. The molecular and functional mechanisms of this differential vulnerability of DA neurons found in PD and its related animal models are still unresolved. We propose that differences in vulnerability of DA neurons are closely related to cell-specific differences in function and gene-expression. More resistant DA neurons might either constitutively express a specific subset of genes that confer resistance to PD-inducing trigger factors, or they might be able to activate a neuroprotective response. We aim to define functional correlates of differential vulnerability of DA neurons - under control conditions as well as in response to PD-trigger factors (e.g. MPTP/rotenone). For this purpose, we study phenotype/genotype correlations of individual DA neurons by combining electrophysiological techniques (*in vitro* brain-slice patch-clamp) with gene-expression profiling approaches at the level of the individual neurons (single cell qualitative and quantitative real-time RT-PCR, DNA-array hybridization). In addition, we aim to apply laser-based microdissection-techniques to analyze related gene-expression profiles in human DA neurons from *post mortem* brain sections.

Keywords: transcriptome analysis, Parkinson, apoptosis and cell death

Corticosteroid-responsive genes in the rodent hippocampus: a genomics approach.

Erno Vreugdenhil,  
Medical Pharmacology/LACDR, University of Leiden.

The hippocampus, a brain structure with a crucial role in learning and memory, cognitive processes and stress regulation, is very sensitive to aberrant levels of corticosteroid stress hormones (B). We hypothesized that stress related brain disorders are the result of aberrant expression of specific B-responsive genes. In order to identify such genes, we have applied large scale screening techniques i.e. Serial Analysis of Gene Expression (SAGE) and DNA chips (Affymetrix) in rat and mice model systems. The expression of a total of approximately 40.000 hippocampal genes was analysed.

We have identified differential expression of over four hundred B-responsive genes in a mice model exhibiting features of HPA-axis dysregulation. In particular, a higher expression of hippocampal genes encoding components of the MAPK cascade, calcium binding proteins and several cytoskeleton-associated genes was detected. These findings were confirmed by in situ hybridization experiments.

Functional analysis of one of the novel corticosteroid-responsive genes, the doublecortin-like kinase (DCLK), shows that it exhibits structural resemblance with the family of CaMKs, in particular with that of CaMK-IV. The DCLK gene generates multiple mRNA by means of alternative splicing. One alternatively spliced DCLK mRNA encodes a peptide, which may be involved in adrenalectomy-induced apoptosis in the dentate gyrus. Another DCLK mRNA encodes a doublecortin-like protein, which is a microtubule-associated protein and polymerizes microtubules in mitotic spindles and may be involved in neurogenesis in the central nervous system. As such, the DCLK gene may fulfil a key role in B-affected neurogenesis and apoptosis.

## Transcriptome analysis in the rat auditory brainstem

Alexander Koehl, Anne Rieger, Nicole Schmidt, Eckhard Friauf and Hans Gerd Nothwang

*Animal Physiology Group, Department of Biology, University of Kaiserslautern, POB 3049, D-67653 Kaiserslautern, Germany*

As the first centre of binaural auditory processing, the superior olivary complex (SOC) plays an important role in computing acoustic information from both ears. An interesting feature of the SOC is the projection between the medial nucleus of the trapezoid body (MNTB) and the lateral superior olive (LSO), as it represents a model system to study inhibitory circuits. In order to unravel the neuronal mechanisms which underlie the auditory information processing on a molecular level and to identify the molecular anatomy of an inhibitory projection, we have performed serial analysis of gene expression (SAGE) in the SOC, the LSO, and the MNTB. SAGE is based on the position-specific generation of unique, 10- or 16-bp-long sequences, so-called tags, from the transcripts present in the tissue, which are sufficient for their identification.

To date, we have sequenced a total of 31,035 10-bp-long tags derived from the SOC of 60-day-old rats. These corresponded to 10,473 different transcripts. About 17 % of all tags were of mitochondrial origin, indicating a high energy requirement of the SOC. Sixty – six percent were assigned to genes or expressed sequence tags (ESTs), whereas 17 % could not be annotated. In parallel, we have generated a library of 16-bp-long tags derived from the LSO of 30-day-old rats. So far, 31,776 tags have been sequenced which represent 12,620 unique transcripts. Six percent of all tags mapped to the mitochondrial genome, 67 % can be assigned to distinct genes or at least ESTs and 27 % were not annotated at all. Furthermore, we have started to sequence a 16-bp-tag library from the MNTB aiming also at a tag number of >30 000. Comparison of SOC, LSO, MNTB and a publicly available library of rat hippocampus revealed significant differences in the transcript inventory between auditory and non-auditory brain regions and between auditory nuclei.

One interesting group of transcripts comprises membrane proteins, like plasma membrane receptors, transporters and channels. In this transcript category we identified several tags which exhibited significantly differential expression and thus serving as candidates for region-specific tasks. Another group of transcripts showing differential distribution is associated with energy metabolism. In this group, we have observed a significant upregulation of many transcripts in the SOC as compared to LSO and especially hippocampus, indicating a high energy expenditure in some nuclei of the SOC. *In-situ* hybridization and immunohistochemistry showed good correlation to the SAGE data. In addition, the advantage of using 16 instead of 10-bp-long tags will be discussed.

Supported by the German Research Foundation, Grant – No. DFG NO428/1-1 and 1-3.

## Analysis of microarray brain expression data: computational and statistical challenges

Dr. Kay Nieselt, Research Group Proteomics Algorithms and Simulation, Center for Bioinformatics Tübingen, Sand 14, 72076 Tübingen, Germany

DNA microarray experiments are now widely used for the simultaneous monitoring of expression levels of large numbers of genes. In my talk I will discuss the general problems of microarray data analysis, including basic design questions, how to adequately address the normalization question and some of the statistical challenges. Furthermore I will talk about the issue of visualizing and interactively exploring microarray data. A special emphasis will lie on the specific aspects of analysing brain transcriptomes. As an example I will present an analysis of a large-scale comparative microarray experiment of different brain regions of humans and chimpanzees.

**Satellite Symposium #Sat5:**  
**Joint Symposium of the DFG Neuroscience Graduate Schools**  
**W. Paulus and G. Reifenberger, Göttingen und Düsseldorf**

**Introduction**

[#Sat5](#) W. Paulus and G. Reifenberger, Göttingen und Düsseldorf  
*Joint Symposium of the DFG Neuroscience Graduate Schools*

**Slide**

- #Sat5-1 W. Paulus and G. Reifenberger, Göttingen und Düsseldorf  
*Welcome address and introduction to the symposium*
- #Sat5-2 M. Schachner, Hamburg  
*Recognition molecules and the rejuvenating nervous system*
- #Sat5-3  
*Oral presentations by doctoral students*
- #Sat5-4  
*Oral presentations by doctoral students*
- #Sat5-5 P. Bondre-Beil, Bonn  
*New features of DFG research training groups*

**Introductory Remarks to Sat. Symposium 5****Joint Symposium of the DFG Neuroscience Graduate Schools****W. Paulus, Göttingen & G. Reifenberger, Düsseldorf**

In addition to invited lectures by M. Schachner, Hamburg, and P. Bondre-Beil, Bonn, doctoral students of the German DFG Neuroscience Graduate Schools in Berlin, Bielefeld, Bochum, Bonn, Düsseldorf, Frankfurt/Main, Freiburg, Gießen/Marburg, Göttingen, Hamburg, Heidelberg, Magdeburg, Mainz, München, Potsdam and Tübingen are invited to contribute oral and poster presentations.

## Poster Subject Areas

- [#PSA1](#)      Mechanoreception and somatosensory systems
- [#PSA2](#)      Muscle, motor and sensorimotor systems
- [#PSA3](#)      Rhythmogenesis and motor pattern generation
- [#PSA4](#)      Audition, vibration and communication in invertebrates
- [#PSA5](#)      Audition and vocalization in lower vertebrates
- [#PSA6](#)      Audition and vocalization in birds and mammals: Periphery
- [#PSA7](#)      Audition and vocalization in birds and mammals: CNS and perception
- [#PSA8](#)      Lateral line systems; Vestibular systems
- [#PSA9](#)      Chemosensory and thermosensory systems
- [#PSA10](#)      Visual systems of invertebrates: Periphery
- [#PSA11](#)      Visual systems of invertebrates: Central areas and perception
- [#PSA12](#)      Visual systems of vertebrates: Periphery
- [#PSA13](#)      Visual systems of vertebrates: Central areas and perception
- [#PSA14](#)      Visual systems of vertebrates: Development and regeneration
- [#PSA15](#)      Cortex and Cerebellum
- [#PSA16](#)      Hippocampus and Limbic system
- [#PSA17](#)      Learning and Memory
- [#PSA18](#)      Neuroanatomical studies
- [#PSA19](#)      Neurohistochemical studies



<a href="#"><u>#PSA20</u></a>	Neurochemistry
<a href="#"><u>#PSA21</u></a>	Synapses and transmitters
<a href="#"><u>#PSA22</u></a>	Neuropeptides and neuromodulation
<a href="#"><u>#PSA23</u></a>	Ion channels and receptors
<a href="#"><u>#PSA24</u></a>	Neuropharmacology and -toxicology
<a href="#"><u>#PSA25</u></a>	Cell and tissue cultures
<a href="#"><u>#PSA26</u></a>	Glia cells; Myelin
<a href="#"><u>#PSA27</u></a>	Neuronal development
<a href="#"><u>#PSA28</u></a>	Regeneration and plasticity
<a href="#"><u>#PSA29</u></a>	Neurogenetics
<a href="#"><u>#PSA30</u></a>	Neuropathology
<a href="#"><u>#PSA31</u></a>	Neural-immune interactions
<a href="#"><u>#PSA32</u></a>	Neuroendocrinology
<a href="#"><u>#PSA33</u></a>	Neuropsychology and psychophysics
<a href="#"><u>#PSA34</u></a>	Neuronal networks theory and modeling
<a href="#"><u>#PSA35</u></a>	Methods and demonstrations

**Poster Subject Area #PSA1:  
Mechanoreception and somatosensory systems**

- [#60A](#) J. Hipp, W. Einhäuser and P. König, Zurich (CH) and Osnabrück  
*Activity driven emergence of texture representation in the vibrissa system*
- [#61A](#) B. Chagnaud and H. Bleckmann, Bonn  
*Responses of goldfish anterior lateral line afferents to a vibrating sphere stimulus in still- and running water*
- [#62A](#) HR. Dinse, D. Kraß, R. Maachaoui, I. van der Berg and P. Ragert, Bochum  
*Tactile 2-point discrimination and localization are differentially affected by synchronous and asynchronous coactivation*
- [#63A](#) A. Skorjanc and K. Draslar, Ljubljana (SLO)  
*Spontaneous activity and adaptation mechanisms of trichobothria in the bug *Pyrrhocoris apterus**
- [#64A](#) T. Kalisch, N. Kleibel, M. Tegenthoff and HR. Dinse, Bochum  
*Age-related loss of dominant hand superiority in fine motor performance*
- [#65A](#) T. Kalisch, M. Tegenthoff and HR. Dinse, Bochum  
*Improvement of right hand haptic skills following 3 hours of tactile coactivation of all fingers*
- [#60B](#) P. Ragert, T. Kalisch and HR. Dinse, Bochum  
*Perceptual changes in human tactile discrimination behavior induced by coactivation using LTP- and LTD-protocols*
- [#61B](#) P. Ragert, T. Kalisch and HR. Dinse, Bochum  
*Asymmetric learning transfer between hands of coactivation-induced changes in tactile discrimination thresholds*
- [#62B](#) P. Ragert, S. Franzkowiak, C. Heinisch, T. Kalisch, C. Wilimzig, G. Schöner and HR. Dinse, Bochum  
*End-effect suppression in a multiple choice reaction time task induced by tactile coactivation*
- [#63B](#) C. Wilimzig, P. Ragert, T. Kalisch, HR. Dinse and G. Schöner, Bochum  
*Dynamic Field Theory: The end effect and its learning-induced modulation explained by task information*
- [#64B](#) B. Curcic-Blake and SM. van Netten, Groningen (NL)  
*Rapid responses of the cupula in the lateral line of ruffe*

## Activity driven emergence of texture representation in the vibrissa system

Jörg Hipp<sup>1\*</sup>, Wolfgang Einhäuser<sup>1</sup>, Peter König<sup>2</sup>

<sup>1</sup>Institute of Neuroinformatics, University of Zurich & Swiss Federal Institute of Technology (ETH) Zurich

<sup>2</sup>Institute of Cognitive Science, Dept. Neurobiopsychology, University of Osnabrück

\*Correspondence: joerg@ini.phys.ethz.ch

In rodents the vibrissae (whisker) system is arguably the most important source of sensory information. Rats can discriminate textures solely on the basis of this modality. However, how cortical representations of texture stimuli emerge is unknown.

We here use a physical implementation of an artificial whisker system to collect whisker deflection signals. These signals serve as input to primary sensory neurons, which we model as band pass filters of various specificities for deflection angle and velocity. The output of these primary neurons is used as input for training secondary neurons to optimize various objective functions, which are based on general coding principles, such as sparseness or temporal coherence. To quantify the resulting representations, we compare the performance of secondary to primary neurons with respect to classifying textures with a simple linear classifier.

We find that - after training, secondary neurons form a representation that is better suited to classify textures than primary neurons, i.e. the former have a better signal to noise ratio than the latter. This shows that the same general coding principles, which have been studied extensively in the visual domain, are also useful in the somatosensory modality. Based on these findings we make predictions for the mechanisms of texture representation in the somatosensory cortex, which will be tested in electrophysiological experiments.

*Supported by the EU-AMOUSE project (JH, WE), Honda RI Europe (WE), SNF (PK, grant no. 31-61415.01)*

## Responses of goldfish anterior lateral line afferents to a vibrating sphere stimulus in still- and running water

Boris Chagnaud and Horst Bleckmann  
Institute for Zoology, Poppelsdorfer Schloss, Bonn, Germany  
[B.Chagnaud@uni-bonn.de](mailto:B.Chagnaud@uni-bonn.de)

The lateral line is a sensory system that responds to water motions such as those generated by a vibrating sphere (for review see Bleckmann 1994). The lateral line of fishes consists of superficial neuromasts (SN) and of canal neuromast (CN). Lateral line neuromasts are innervated by anterior (ALLN) or by posterior lateral line nerve (PLLN) fibers (Puzdrowski 1989). The PLLN of goldfish, *Carassius auratus*, contains flow sensitive (type I) and flow insensitive (type II) afferents (Engelmann et al. 2002). While the responses of type I PLLN-afferents to a vibrating sphere stimulus are masked in running water, type II PLLN-afferents respond equally well in still- and running water (Engelmann et al. 2002).

We investigated how ALLN-afferents of the goldfish respond to a vibrating sphere stimulus in both, still- and running water. Like PLLN-afferents (Engelmann et al. 2002), ALLN-afferents were either flow sensitive (type I, n = 37) or flow insensitive (type II, n = 21). The responses of type I ALLN-afferents to a dipole stimulus were masked under running water (8 cm/s) conditions. In contrast, type II ALLN-afferents responded equally well in still and running (8 cm/s) water. In type I afferents (n = 8) the degree of masking was positively correlated with the velocity (test range 2 – 15 cm/s) of unidirectional water flow.

### References

- Bleckmann H (1994) Reception of hydrodynamic stimuli in aquatic and semiaquatic animals. Fischer, Stuttgart  
Engelmann J, Hanke W, Bleckmann H (2002) J Comp Physiol A 188: 513-526.  
Puzdrowski R (1989) Brain Behav Evol 34:110-131

Supported by the DFG

## Tactile 2-point discrimination and localization are differentially affected by synchronous and asynchronous coactivation

Hubert R. Dinse, Dieter Kraß, Rizlan Maachaoui, Ingo van der Berg, Patrick Ragert

Institute for Neuroinformatics, Theoretical Biology, Ruhr-University, Bochum, Germany

[hubert.dinse@neuroinformatik.rub.de](mailto:hubert.dinse@neuroinformatik.rub.de)

Temporally correlated inputs play a key role in mediating plastic changes. To test directly the effects of timing on the induction of plastic changes, we used a stimulation protocol of tactile coactivation (refs). By manipulating the type of input statistics, this protocol allows to address the efficacy of correlated and uncorrelated inputs for the induction of perceptual learning. In the past we repeatedly showed that synchronous coactivation improves tactile 2-point discrimination parallel to cortical reorganization (1-4). Here we addressed the question of how both protocols effect not only tactile 2-point discrimination, but also tactile localization performance.

To apply coactivation, a small device consisting of two small independently driven stimulators separated by approximately 4 millimeter was taped to the tip of the right index finger (IF). Two sets of coactivation-stimuli were drawn from Poisson processes with interstimulus-intervals between 100 to 3000 ms (average stimulation frequency 1 Hz, pulse duration 10 ms). Duration of coactivation was 3 hours. For more details see (1-4). In the synchronous mode, both stimulators were driven with a single Poisson process resulting in simultaneous stimulation. In the asynchronous mode, both stimulators were driven with two independently generated processes leading to temporally uncorrelated trains of stimuli, with simultaneous events occurring by chance. Pulses were stored on tape or flashcards allowing full mobility of the subjects during the coactivation period. To assess the baseline pre condition performance, two-point discrimination was tested as described previously (1-4). After assessing absolute touch thresholds using von Frey-hairs, localization performance was measured within a 1 x 1 cm square on the tip of the IF subdivided into four quadrants. Then, the tip of the right IF was coactivated for a period of 3 hours to induce learning processes. Next, psychophysical measurements were repeated (post). To assess recovery, additional tests were performed 24 h later. As a control, the IF of the left hand was tested with an identical schedule, but without coactivation.

After synchronous coactivation using a single Poisson process, we found a lowering of 2-point discrimination thresholds on the coactivated IF, but not on the IF of the left hand, confirming previous findings (1-4). In contrast, asynchronous coactivation impaired discrimination performance by about the same amount, again with no effects on the left, not-coactivated IF. However, when localization was tested, the opposite behavior was found. Synchronous coactivation resulted in an impairment of localization performance, while asynchronous coactivation improved it. Absolute touch thresholds remained unaffected throughout all experiments.

The contrasting effects of coactivation on acuity and localization suggest a trade-off between discrimination and localization, and resemble similar findings reported for blind Braille readers (5). However, closer inspection of our data showed that changes in localization were correlated with changes in discrimination. Subjects that showed only little or no discrimination improvement were those with the largest localization impairment, while subjects that benefited most in discrimination showed only minor impairments, or even also improvements in localization.

The results indicate that manipulating the nature of correlated activity leads to complementary forms of perceptual learning, where different tactile tasks display opposite sensitivities to learning processes. The results confirm the view that because of the task-free nature of coactivation, the entire way of tactile processing is altered thereby shifting neural processing into new regimes, where a new balance between tasks is stabilized resulting in newly emerging haptic including sensorimotor capabilities.

1. Godde B, Stauffenberg B, Spengler F, Dinse HR (2000) *J Neurosci* 20: 1597
2. Pleger B, Dinse HR, Ragert P, Schwenkreis P, Malin JP, Tegenthoff M (2001) *Proc Natl Acad Sci USA* 98: 12255
3. Dinse HR, Ragert P, Pleger B, Schwenkreis P, Tegenthoff M (2003) *Science* 301: 91
4. Pleger B, Foerster AF, Ragert P, Dinse HR, Schwenkreis P, Nicolas V, Tegenthoff M (2003) *Neuron* 40: 643
5. Sterr A, Müller MM, Elbert T, Rockstroh B, Pantev C, Taub E (1998) *J Neurosci* 18: 4417

## Spontaneous activity and adaptation mechanisms of trichobothria in the bug *Pyrhocris apterus*

Ales Skorjanc and Kazimir Draslar

Department of Biology, Biotechnical faculty, University of Ljubljana, Vecna pot 111,  
SI-1000 Ljubljana, Slovenia

Abdominal trichobothria (filliform sensilla) in bugs (Heteroptera) are solitaire or arranged in clusters on the abdominal venter. Their position, type composition as well as the time of their emergence is very variable (Schaefer, 1975), which indicates a diversity in the combination of structural and functional characteristics. Our recent studies show that this may well be the case in *Pyrhocris apterus*. *Pyrhocris* has 28 trichobothria arranged in 7 clusters on 5 abdominal segments. We have classified them according to their functional and morphological properties into types T1, T2 and T3 (Draslar & Skorjanc, 2003). Our research was focused on trichobothria on the 5<sup>th</sup>, 6<sup>th</sup> and 7<sup>th</sup> abdominal segment. Their activity was estimated using extracellular recordings of spike potentials.

Trichobothria of type T1 have the longest cuticular hair (from 300 to 350  $\mu\text{m}$ ) and the highest level of spontaneous activity. It ranges from 3000 to 4000 spikes per minute at 20°C and is highly temperature dependent. The spontaneous activity is correlated to the length of the outer cuticular hair within the type, the trichobothria with longer hair having higher spontaneous activity. Since the mechanoreceptors with longer hair are more sensitive to low intensity stimuli it is reasonable to expect that uncontrolled air currents during the experiment could bias trichobothria with longer hair towards higher spontaneous activity. To test this assumption we shortened the hair either manually or by a laser beam. The spontaneous activity did not decrease, it even increased slightly in most cases. Interspike interval histogram (INTH) retained the shape of a Poisson distribution, but showed a small reduction in interval variability. This was probably the result of reduced influence of disturbances. The results were very consistent and independent of the procedure used or the extent of hair shortening. The destruction of the hair base reduced the spontaneous activity by half. The INTH was shifted from Poisson-like to normal distribution. Very uniform results indicate that two separate mechanisms determine the spontaneous activity of T1 type trichobothria. The only exception is one of T1 trichobothria on the 6<sup>th</sup> segment. Its hair is only 190  $\mu\text{m}$  long and its spontaneous activity is 1500 spikes per minute. We also could not get any consistent results when shortening its hair or destroying its base. It is interesting that this trichobothrium does not appear until the second larval stage, which is characteristic of T2 type. Type T2 trichobothria have a shorter hair (from 110 to 170  $\mu\text{m}$ ) and a lower spontaneous activity of 150 to 300 spikes per minute. The spontaneous activity is also in a positive correlation to the hair length. In contrast to T1 type shortening of the hair or destruction of its base always results in the cessation of spontaneous activity. Type T3 trichobothrium has an 80  $\mu\text{m}$  long hair. The spontaneous activity is limited to 40 spikes per minute and it has been registered in only 5% of all preparations.

In addition we tested the adaptation of the different trichobothria types to a ramp deflection of the hair. Both T1 and T2 type trichobothria have a phasic-tonic response. They encode the speed and the angle of the hair deflection. At the beginning of the hair deflection the spike rate almost instantaneously increases to the maximum value. After a few ms it starts to exponentially decrease although the hair is still deflecting. If we changed the temperature to 5°C, the adaptation became evidently slower. If the activity was proportional to the angle of deflection, it should have monotonously increased throughout the slow movement of the hair. When the hair stops in the new position, the activity quickly drops and settles after few ms on a level higher than before the stimulation. This level is proportional to the angle of deflection and does not adapt over a period of more than 15 minutes. With the return of the hair to resting position a silent period follows and then a gradual return to the spontaneous activity. T3 has a typically fast adapting phasic response. Its adaptation to hair movement is similar to T1 and T2 only slower. On the other hand it continues a few seconds after the hair movement has stopped, until the activity drops to zero. We do not know if passive mechanical or electrical properties of receptor cells could have produced such responses or whether there is an active mechanism. In any case there seem to be at least two different mechanisms of adaptation in trichobothria.

Schaefer, C. W. 1975. Int. J. Insect Morphol. & Embryol. 4(3): 193-264

Draslar and Skorjanc 2003. Proceedings of the 29<sup>th</sup> Goettingen Neurobiology Conference. 359

## Age-related loss of dominant hand superiority in fine motor performance

Tobias Kalisch<sup>1</sup>, Nadine Kleibel<sup>1</sup>, Martin Tegenthoff<sup>2</sup> and Hubert R. Dinse<sup>1</sup>

<sup>1</sup> Institute for Neuroinformatics, Ruhr-University Bochum, 44780 Bochum, Germany

<sup>2</sup> Department of Neurology, Ruhr-University Bochum, Buerkle-de-la-Camp-Platz 1

Tobias.Kalisch@neuroinformatik.rub.de

The biological basis of age-related changes in human fine motor movement is still poorly understood. Individual motor performance is influenced by many factors i.e. training, motivation, gender, handedness and especially age. However, there is controversy how aging affects asymmetries in lateralized behaviors, especially handedness.

In order to investigate age-related changes in fine motor performance and in the advantage of the dominant hand (handedness) we carried out a cross-sectional study. Participating subjects were classified as young adults (18-25 years), middle-aged adults (45-60 years), old adults (65-75 years) and very old adults (76-90 years).

Our test-battery for assessment of fine motor abilities (MLS) of upper extremities is an approved tool in neuropsychological diagnostics, especially for the early detection of movement disorders. It consists of several tests, all carried out with contact pencils on a work disk. Performance of left and right hand is measured separately to detect age-related changes in different parameters of arm-, hand- and finger movements: "Steadiness" describes the ability to obtain a prescribed arm-hand-position and to maintain it for a defined time. "Line tracing" describes the ability to fulfill precise, simultaneous arm- and hand movements. "Aiming" describes the ability to accomplish well-controlled arm-hand movements for small targets. "Tapping" describes the ability to perform fast repetitive wrist-finger movements. Recorded data were number of errors, error time and total time to fulfill a certain task. To discover possible changes in the extent of handedness, data of all practical tasks were used for the calculation of a laterality index  $(L-R)/(L+R)$  [L, R means left, right hand performance].

Hand dominance was also determined using the "Edinburgh Handedness Inventory", which classifies handedness on the basis of a short interview concerning hand preference in routine practical tasks. The evaluation of this questionnaire provides a handedness-score ranging from -100 for extreme left hand use, to +100 for extreme right hand use. All 60 subjects, who participated in our study, showed unambiguous right hand dominance ( $\geq +70$ ).

There was a striking side-specific age-related decline of fine motor performance in the practical tasks, which differed in magnitude according to the parameters tested. Our main finding was a shift of hand dominance in four tested movement-parameters that developed gradually over the three aged groups. As a rule, the right hand performance showed a stronger decline with age than the left hand. This asymmetrical age-influence on motor skills led to an equalization of manual dexterity. Interestingly, the age at which this equalization emerged differed for different motor tasks.

A major finding of our study was that aged subjects showed a significant inconsistency between the degree of handedness assessed by means of the questionnaire or by practical motor-tasks. While the self-assessment of handedness using rating scales did not change over age, practical performance did. Accordingly, subjects appear subjectively unaware of their altered motor performance consisting of a less inferior performance of their non-dominant hand.

Further experiments are needed to clarify whether the differential decline of hand motor performance is due to long-term training effects of the non-dominant hand, or to an enhanced sensitivity of the dominant hand to age-related changes.

## **Improvement of right hand haptic skills following 3 hours of tactile coactivation of all fingers**

Tobias Kalisch <sup>1</sup>, Martin Tegenthoff <sup>2</sup> and Hubert R. Dinse <sup>1</sup>

<sup>1</sup> Institute for Neuroinformatics, Ruhr-University Bochum, 44780 Bochum, Germany

<sup>2</sup> Department of Neurology, Ruhr-University Bochum, Buerkle-de-la-Camp-Platz 1

Temporally correlated inputs can induce transient plastic changes in the human cortex together with changes in perceptual and behavioral performance. To evoke cortical activity in primary somatosensory cortex we introduced a perceptual learning protocol consisting of paired tactile stimuli, the so-called coactivation (CA) (1-4). We have repeatedly shown that CA applied to a single digit improves tactile acuity (1-3). Here we used a modification where all fingers of the dominant hand were coactivated. The CA protocol was applied by means of small devices consisting of solenoids (diameter 8 mm), which were fixed on the tip of each finger of the right hand (d1-d5) to transmit the mechanical pulses to the skin. In this particular protocol, the aspect of coactivation is twofold: First, receptive fields in the skin portions underneath the solenoids are simultaneously stimulated and thus coactivated. Second, each finger receives stimulation leading to coactivation on all fingertips of the dominant hand. By means of this protocol we aimed at activating large portions of the cortical hand representation to induce large-scale perceptual and behavioral changes. In addition, this design allows to explore possible interactions between activated finger representations.

The average stimulation frequency was 1 Hz and the duration of a single pulse 10 ms as in the single digit CA experiments (1-4). Stimuli were drawn from a Poisson process with the interstimulus-intervals varying between 100 and 3000 ms. All five solenoids were triggered by digital pulse trains from a portable unit. The stimulation was applied for 3 hours. One group (10 subjects each) received a synchronous, and the other an asynchronous mode of coactivation on d1-d5 of the right hand.

To explore the behavioral consequences of the different protocols, subjects were tested in several haptic tasks: Static 2-point discrimination thresholds were determined using the method of constant stimuli. Using Von Frey-filaments, the absolute threshold of touch could be assessed. To evoke mislocalizations across the fingers we applied near-threshold tactile stimuli to the fingertips. To assess haptic object recognition performance, subjects had to identify small cubic objects solely by haptic impressions without viewing them. Here the required time and the number of classification errors were measured. All tests were performed before and after CA (immediate, after 24 h and after 96 h) to analyze the time course of reversibility and stability of induced changes.

We found a massive influence on haptic performance by the synchronous CA protocol. 2-point discrimination thresholds were reduced by about 20 % on all coactivated fingers. The distribution of mislocalizations showed significant changes consisting of a shift of the probability for localization errors towards more distant digits. Most remarkably, the number of errors and the time to fulfill the haptic object-classification task were significantly reduced after CA. No effects were found for touch-thresholds, in line with previous findings from single digit experiments (4).

In contrast, the asynchronous CA did not affect haptic performance in a comparable way. We observed a decline in tactile acuity after asynchronous CA for d1 and d3. This is a surprising effect, because the efficiency of our protocol on single digit performance is well documented: Former experiments showed that single-finger CA reduces 2-point discrimination threshold about 10-20 % (1-3). We speculate that interactions between the asynchronously activated finger representations might mask the CA-effects therefore leading to unchanged or even lowered tactile acuity after 5 finger CA.

In conclusion we demonstrate that synchronous tactile CA, including all fingers of the right hand, is a powerful tool to evoke not only changes such as tactile discrimination thresholds but also haptic object-classification skills. Because after asynchronous CA across all fingers there is no discrimination improvement, this activation pattern seems to generate interfering interactions between cortical finger representations.

1. Pleger B, Dinse HR, Ragert P, Schwenkreis P, Malin JP, Tegenthoff M (2001) *Proc Natl Acad Sci USA* 98: 12255
2. Dinse HR, Ragert P, Pleger B, Schwenkreis P, Tegenthoff M (2003) *Science* 301: 91
3. Pleger B, Foerster AF, Ragert P, Dinse HR, Schwenkreis P, Nicolas V, Tegenthoff M (2003) *Neuron* 40: 643
4. Dinse HR, Kraß D, Maachaoui R, van der Berg I, Ragert P (2005) this meeting



## **Perceptual changes in human tactile discrimination behavior induced by coactivation using LTP- and LTD-protocols**

Patrick Ragert<sup>1,2</sup>, Tobias Kalisch<sup>1</sup>, Hubert R. Dinse<sup>1</sup>

<sup>1</sup> Institute for Neuroinformatics, Theoretical Biology, Ruhr-University, Bochum, Germany

<sup>2</sup> International Graduate School of Neuroscience, Ruhr-University, Bochum, Germany

[patrick.ragert@rub.de](mailto:patrick.ragert@rub.de)

Cellular studies suggest that long-term potentiation (LTP) and long-term depression (LTD) of synaptic transmission are the leading candidates for the activity-dependent change in the strength of synaptic connections in the central nervous system. However, cellular studies alone do not allow to study perceptual or behavioral consequences of changes in synaptic efficacy. Hence, there is still little known about a causal link between synaptic plasticity and cortical map reorganization leading to behavioral changes in humans. Here we demonstrate, using a psychophysical 2-point discrimination task, that high-frequency (HFS) and low-frequency (LFS) stimulation protocols applied with a small solenoid on the tip of the index-finger (IF) evokes significant changes in tactile discrimination behavior.

HFS consisted of TTL-pulses that were applied on the tip of the right index-finger (IF) with a stimulation frequency of 20 Hz using a small solenoid with a diameter of 8 mm. Each train consisted of 20 single pulses of 20 Hz lasting 1s with an inter-train interval of 5s resulting in a total number of 4000 pulses. LFS was applied at 1 Hz with stimulus trains consisting of 1200 pulses. Duration of HFS and LFS was 20 min each. Pulses were stored on flashcards and played back via conventional MP3 player allowing full mobility of the subjects during the stimulation period.

Prior to HFS or LFS, subjects were tested in a 2-alternative forced-choice simultaneous spatial 2-point discrimination task (Dinse et al., 2003; Pleger et al., 2003) over 5 consecutive sessions on the right IF in order to obtain a stable baseline performance. After the 5<sup>th</sup> session, HFS or LFS was applied to the tip of the right IF for 20 min. Tactile performance of the right IF was re-tested starting about 15 min after the termination of stimulation. Furthermore, we investigated the recovery of HFS- and LFS-induced changes on the right IF 24 hrs after termination of both stimulation protocols. Additionally, the left non-stimulated IF was tested before and after the application of either HFS or LFS and served as control.

We found that 20 min of HFS induced a lowering of tactile discrimination thresholds, indicating improved tactile acuity, whereas LFS resulted in an impaired performance on the right, stimulated IF. Most interestingly, 24 hrs after HFS, we found that spatial 2-point discrimination thresholds were still lowered in comparison to baseline. In contrast, 24 hrs after LFS, discrimination thresholds recovered to baseline conditions.

The results indicate that brief stimulation protocols resembling those used in cellular LTP and LTD studies can induce meaningful and persistent alterations in tactile human discrimination behaviour.

### References

- Dinse HR, Ragert P, Pleger B, Schwenkreis P, Tegenthoff M (2003) Pharmacological modulation of perceptual learning and associated cortical reorganization. *Science* 301:91-94.
- Pleger B, Foerster AF, Ragert P, Dinse HR, Schwenkreis P, Malin JP, Nicolas V, Tegenthoff M (2003) Functional imaging of perceptual learning in human primary and secondary somatosensory cortex. *Neuron* 40:643-653.

## Asymmetric learning transfer between hands of coactivation-induced changes in tactile discrimination thresholds

Patrick Ragert<sup>1,2</sup>, Tobias Kalisch<sup>1</sup>, Hubert R. Dinse<sup>1</sup>

<sup>1</sup>Institute for Neuroinformatics, Theoretical Biology, Ruhr-University, Bochum, Germany

<sup>2</sup>International Graduate School of Neuroscience, Ruhr-University, Bochum, Germany

[patrick.ragert@rub.de](mailto:patrick.ragert@rub.de)

Numerous non-invasive human studies have demonstrated that passive stimulation protocols based on the Hebbian principle are capable to evoke perceptual learning that is paralleled by plastic reorganizational changes within the stimulated cortical area. In previous studies, we have repeatedly demonstrated that a few hours of coactivation resulted in fast and selective changes of tactile discrimination thresholds on the stimulated index-finger (IF), which were linearly correlated with cortical map changes within primary somatosensory cortex (Dinse et al., 2003; Pleger et al., 2003). However, we never observed changes in the IF of the contralateral, not coactivated left hand indicative for a limited transfer of learning to the non-dominant hand. Here we asked whether the other way round coactivation of the non-dominant left IF in right-handed subjects might influence tactile performance on the non-stimulated right IF of the dominant hand thereby demonstrating a different form of generalization.

Coactivation stimuli consisted of pulses of different interstimulus intervals from 100 to 3000 ms in pseudo randomized order; average frequency was 1 Hz (pulse duration 10 ms) and the duration of coactivation was 3 hrs. To apply coactivation, a small solenoid with a diameter of 8 mm was taped to the tip of the left IF and transmitted the tactile stimuli of the coactivation protocol simultaneously to the skin. Pulses were stored on flashcards and played back via MP3 player allowing full mobility of the subjects during the stimulation period.

Prior to coactivation, subjects were tested with the method of constant stimuli in a simultaneous spatial 2-point discrimination task (Dinse et al., 2003; Pleger et al., 2003) over 4 consecutive sessions on the left IF in order to obtain a stable baseline performance. According to the Edinburgh questionnaire all subjects were right-handed. After the 4<sup>th</sup> session, coactivation was applied to the tip of their non-preferred left IF. Tactile performance was re-tested starting about 15 min after the termination of stimulation. Furthermore, we investigated the recovery of coactivation-induced changes on the left IF 24 hrs after termination of coactivation. Additionally, the right non-stimulated IF was tested before and after the application of left-side coactivation and served as an indicator for transfer.

We found that 3 hrs of coactivation induced a lowering of tactile discrimination thresholds on the stimulated IF, indicating improved tactile acuity similar to the findings reported previously for the right IF after right IF coactivation (Dinse et al., 2003; Pleger et al., 2003). 24 hrs after coactivation, discrimination thresholds recovered to baseline conditions. Most interestingly, however, the right, non-stimulated IF showed a comparable and reversible lowering of tactile discrimination thresholds.

These results indicate that stimulating the left IF of right-handed subjects leads to changes in tactile acuity that transferred to the non-stimulated hand possible due to a functional asymmetry of the primary somatosensory cortex in humans.

### References

- Dinse HR, Ragert P, Pleger B, Schwenkreis P, Tegenthoff M (2003) Pharmacological modulation of perceptual learning and associated cortical reorganization. *Science* 301:91-94.
- Pleger B, Foerster AF, Ragert P, Dinse HR, Schwenkreis P, Malin JP, Nicolas V, Tegenthoff M (2003) Functional imaging of perceptual learning in human primary and secondary somatosensory cortex. *Neuron* 40:643-653.

## End-effect suppression in a multiple choice reaction time task induced by tactile coactivation

Patrick Ragert, Stephanie Franzkowiak, Christine Heinisch, Tobias Kalisch,  
Claudia Wilimzig, Gregor Schöner, Hubert R. Dinse

Institute for Neuroinformatics, Theoretical Biology, Ruhr-University, Bochum, Germany

Utilizing the knowledge about brain plasticity accumulated over the last years, we suggested to design specific stimulation protocols through which it is feasible to change purposefully brain organization and thus perception and behavior. We have therefore developed a so-called coactivation protocol that applies the idea of patterned “in-vitro” stimulation protocols to human subjects. Coactivation has been shown to improve tactile 2-point discrimination parallel to cortical reorganization (1-4). Coactivation follows closely the idea of Hebbian learning: Synchronous neural activity regarded instrumental to drive plastic changes is generated by the simultaneous tactile “co-stimulation”.

As coactivation is completely task-free, i.e. unrelated to a particular tactile task, we hypothesized that coactivation will alter the entire way of tactile processing. To test this assumption, we explored more systematically how coactivation alters tactile and haptic performance beyond 2-point discrimination (see also related abstracts of our group at this meeting). Here we report that coactivation leads to persistent changes of selection processes as revealed by multiple choice reaction time (RT) measurements during a finger selection task adopted according to (5).

An image of each hand was displayed on a monitor and a finger was selected by a visual marker. Subjects had to press the key corresponding to the selected finger on a hand-shaped 10-button keyboard. In addition, dual-choice RT measurements (left d5 vs. right d3, and left d3 vs. right d5) were performed to identify effects of the number of choices. To apply coactivation, a small device consisting of a small solenoid was taped to the tip of the right middle finger (right MF). Coactivation-stimuli were drawn from a Poisson process at interstimulus-intervals between 100 to 3000 ms (average stimulation frequency 1 Hz, pulse duration 10 ms). Duration of coactivation is 3 hours. For more details see (1-4). First, RT measurements were performed to obtain a stable baseline (pre). Then, the right MF was coactivated for a period of 3 hours to induce learning processes. Next, RT measurements were repeated (post). To assess stability and recovery, additional tests were performed 24 hours and 1 week later. For control, subjects were tested with an identical schedule, but without coactivation.

Our results revealed that RTs were longest for the MF (d3) of each hand, but shortest for d1 and d5 of each hand, indicative for a strong end-effect. The end-effect is typically attributed to classic cognitive paradigms, but has been shown for this paradigm before (5). After coactivation was applied to the right MF, we observed a slight speeding up of the RT of all fingers, most probably due to practice. However, RTs of the right MF showed a highly significant shorting of RT thereby almost eliminating the end-effect for the right, but not for the left hand. When subjects were tested in a dual-choice task, no effects of coactivation could be observed. Also, none of these effects could be observed in the control group except for a slight reduction in RTs comparable to the experimental group.

Analysis of the time course of effects revealed that the effects of end-effect elimination persisted even after 1 week after coactivation. This long-lasting efficacy of coactivation is in contrast to the typical effects observed in a 2-point discrimination task, where performance improvement recovered to baseline after 24 h (1-4). For a theoretical account of the end-effect see (6).

Our results demonstrate that learning processes induced by passive stimulation modify processing in early stages of somatosensory cortical areas that control selection processes. They further show that the end-effect is not restricted to higher cognitive processing, but emerges from lower level processing. In this view, the end-effect can be regarded as a task-dependent phenomenon resulting from basic forms of representations in both lower and higher brain areas. It should be noted that none of the classic cognitive approaches can account for the occurrence in early sensorimotor areas (see 6).

1. Godde B, Stauffenberg B, Spengler F, Dinse HR (2000) *J Neurosci* 20: 1597
2. Pleger B, Dinse HR, Ragert P, Schwenkreis P, Malin JP, Tegenthoff M (2001) *Proc Natl Acad Sci USA* 98: 12255
3. Dinse HR, Ragert P, Pleger B, Schwenkreis P, Tegenthoff M (2003) *Science* 301: 91
4. Pleger B, Foerster AF, Ragert P, Dinse HR, Schwenkreis P, Nicolas V, Tegenthoff M (2003) *Neuron* 40: 643
5. Alegria J; Bertelson P (1970) *Acta Psychologica* 33: 36
6. Wilimzig C, Ragert R, Kalisch T, Dinse HR, Schöner G (2005) this meeting

## **Dynamic Field Theory: The end effect and its learning-induced modulation explained by task information**

Claudia Wilimzig, Patrick Ragert, Tobias Kalisch, Hubert R. Dinse, Gregor Schöner

Institute for Neuroinformatics, Theoretical Biology, Ruhr-University Bochum, Germany

Dynamic field theory (DFT) is a neurophysiologically based framework of movement preparation (1) predicting reaction time in sensori-motor tasks by taking into account the metric structure of motor representation. In DFT task information provided by the task environment and prior activation gives an important if not dominant contribution to reaction time.

In a recent approach addressing categorical responses (2) it was shown that the end effect (i.e. responses located in the middle of a range being slower than responses at the end of ranges) arises when input of prior activation of possible responses and input of task environment ("task input") dominates the imperative sensory input specifying the appropriate response. Strong neuronal interaction with a locally excitatory interaction and a global inhibition component ("mexican-hat" interaction following well-known brain-like mechanisms) is crucial for the decision making process and response stabilization.

The end effect is typically seen as an effect arising in classical cognitive paradigms involving categorical responses to continuously varied stimuli. DFT can not only account for the occurrence of the end effect in the cognitive domain but also in a paradigm more closely related to sensori-motor surfaces. In this setting, the end effect arises as a consequence of the metric structure of the stimulus-response space inducing strong inhibitory interaction among possible responses (3).

Sequential analysis of individual RTs revealed a strong dependency of a single response from the previous one (for details of the experimental protocol, see 3). For both hands, when the middle finger had to respond consecutively, the second respond was significantly accelerated. In contrast, when a different finger, but from the same hand had to respond, the subsequent response was delayed as compared to the average response time of that finger. The strongest suppression was found when a finger of the left hand had to respond prior to the right finger. These results show strong ongoing interaction processes between fingers that are enhanced when neighbouring fingers are stronger activated due to the just executed response. It can be demonstrated by means of DFT how these strong interactions influence reaction times for each of the fingers leading to slower reactions for fingers receiving a high amount of inhibitory interaction (d3 of each hand).

Coactivation of d3 of the right hand resulted in a strong suppression of the end effect of the right hand due to a significantly shortening of the RT of d3 (3). After coactivation, sequential analysis revealed similar effects for the left hand as described above, but substantial changes for the coactivated hand. The suppression induced from fingers adjacent to right d3 was significantly reduced, while the accelerating effect of successive responses of d3 now resulted in an even stronger facilitation. These results indicate that coactivation modifies interaction processes between fingers. By means of DFT, we can demonstrate that coactivation results in changing the metric structure of the underlying representation, thus leading to altered interactions between fingers. These modified interactions in turn account for the changed sequential effects and lead to a disappearance of the end effect.

Our results suggest that the end effect emerges through the metric structure of the underlying representation regardless of modality. Specifically, by analysing previous trial effects we show that the end effect is really an effect of task structure and history of prior trial activation. Thus, given that coactivation alters neural representations in primary and secondary somatosensory representations (4), neuronal activation in early sensori-motor areas does not reflect purely stimulus-based information but is influenced and transformed by task-specific requirements.

1. Erlhagen W, Schöner G (2002) *Psych Rev* 109: 545
2. Wilimzig, C, Schöner, G. (2004) In preparation
3. Ragert R, Franzkowiak S, Heinisch C, Kalisch T, Wilimzig C, Schöner G, Dinse HR (2005) this meeting
4. Pleger B, Förster AF, Ragert P, Dinse HR, Schwenkreis P, Nicolas V, Tegenthoff M (2003) *Neuron* 40: 643

## Rapid responses of the cupula in the lateral line of ruffe

Branislava Ćurčić-Blake and Sietse M. van Netten

Neurobiophysics  
 University of Groningen  
 Nijenborgh 4  
 9747 AG, Groningen  
 Phone: +31503636891  
 Fax: +31503634741  
 Email: b.curcic@phys.rug.nl

Fish and amphibians use their lateral line organ to detect fluid motion with respect to their body. The lateral line consists of neuromasts – groups of hair cells of which hair bundles are coupled to the cupula. It has been shown that cupulae are displaced proportional to the velocity or acceleration of the surrounding fluid, depending on the frequency of the fluid motion (Denton and Gray 1983; van Netten and Kroese 1987; van Netten 1991; e.g. Kalmijn 1988).

We measured displacements of cupulae in the supraorbital lateral line canal in ruffe (*Gymnocephalus cernuus*) using laser interferometry and by applying transient as well as sinusoidal fluid stimuli in the lateral line canal. The measurements show that the cupula instantaneously follows the initial motion of a transient fluid stimulus. The cupular displacement in response to impulses of fluid velocity shows damped oscillations at approximately 120 Hz and a relaxation time-constant of 4 to 5 ms, commensurate with a quality factor of approximately 1.8. These values are shown to be in close agreement with the frequency characteristics determined via sinusoidal fluid stimuli. We also investigated the variation in cupular responses to a series of different stimulus amplitudes in order to evaluate the dynamics of the cupula, due to the nonlinear mechanics of the transducer channels. We found that these transducer non-linearities do not significantly affect the dynamic behaviour at the stimulus levels used, although differences were found in the detailed responses, which may relate to the nonlinear gating compliance of the hair bundles.

## Reference List

- Denton EJ, Gray J (1983) Mechanical factors in the excitation of clupeid lateral lines. *Proc R Soc Lond B Biol Sci* 218:1-26
- Kalmijn AJ (1988) Hydrodynamic and acoustic field detection. In: R.Atema, R.R.Fay, AN Popper, WN Tavalga (eds) *Sensory biology of aquatic animals*, Springer-Verlag, New York, pp. 83-130.
- van Netten SM (1991) Hydrodynamics of the excitation of the cupula in the fish canal lateral line. *J Acoust Soc Am* 89:310-319
- van Netten SM, Kroese AB (1987) Laser interferometric measurements on the dynamic behaviour of the cupula in the fish lateral line. *Hear Res* 29:55-61

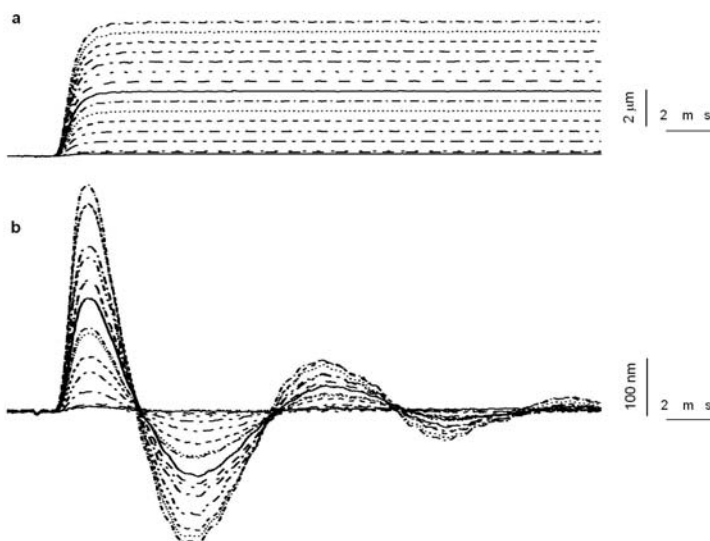


**Fig. 1** Experimental protocol for measurement of impulse responses. (a): Step stimulus with different amplitudes. The stimulus sphere displacement is proportional to input voltage. The input step voltage described with the function (X) was additionally filtered (cut-off at 950 Hz) and swept in steps from 0.05 V to 2.7 V. (b): Responses of the cupula for the series of steps.

**Poster Subject Area #PSA2:  
Muscle, motor and sensorimotor systems**

- [#66A](#) F-O. Lehmann, Ulm  
*Cyclic control of breathing during steady-state muscle performance in flying Drosophila*
- [#67A](#) D. Münch, H-J. Pflüger and SR. Ott, Berlin and Brighton (UK)  
*Nitric oxide in a wind-sensitive sensory system of the locust: possible role in gain control*
- [#68A](#) C. Guschlbauer, H. Scharstein and A. Büschges, Cologne  
*Contraction dynamics of the stick insect extensor tibiae muscle*
- [#69A](#) K. Dotzauer and H. Wolf, Ulm  
*Pre-adaptations for the evolution of jumping legs? Joint mechanics and muscle activity in the middle leg of a proscopiid grasshopper*
- [#70A](#) M. Wanischek and U. Rose, Ulm  
*Unusual tension receptors in an insect and how they compare to the Golgi tendon organ of mammals.*
- [#71A](#) M. Fischer and SS. Schäfer, Hannover  
*Effects of changes in pH on muscle spindle activity*
- [#72A](#) M. Mronz and F-O. Lehmann, Ulm  
*Free Flight Energetics in the Fruit Fly Drosophila melanogaster*
- [#73A](#) M. Nickmann, CR. Smarandache and W. Stein, Ulm  
*Temporal dynamics of facilitation at a crustacean neuromuscular junction*
- [#74A](#) AE-D. Sallam, ER. Horn and M. Schmäh, Ismailia (ET) and Ulm  
*A new approach for electrophysiological long-term experiments in desert scorpions*
- [#75A](#) M. Schmäh and ER. Horn, Ulm  
*Neurophysiological long-term studies in space: SCORPI-T and SCORPI*
- [#76A](#) AG. Fleischer, Hamburg  
*Motor schemas during trajectory formation*
- [#77A](#) CS. Konen, R. Kleiser, F. Bremmer and RJ. Seitz, Marburg and Düsseldorf  
*The cortical interaction of attention and intention*
- [#78A](#) R. Kleiser, CS. Konen, RJ. Seitz and F. Bremmer, Düsseldorf and Marburg  
*I know where you'll look: An FMRI study of Oculomotor intention and a change of motor plan*

- [#79A](#) K. Pipereit and O. Bock, Cologne  
*Learning visual and mechanical discordances: Effects of composition and decomposition*
- [#80A](#) D. Musella and S. Cardoso de Oliveira, Göttingen  
*Learning a nonlinear visuomotor rotation: generalization of learning and effects on kinematic parameters*
- [#81A](#) K. Haastert, C. Mauritz, C. Matthies and C. Grothe, Hannover  
*Adult Schwann cells over-expressing different isoforms of fibroblast growth factor-2 (FGF-2) – in vitro studies concerning therapeutic strategies in peripheral nerve repair*
- [#65B](#) V. Weiler, T. Mentel and A. Büschges, Cologne  
*Activity of modulatory neurons during leg movements in the stick insect*
- [#66B](#) J. Zakotnik, K. Page, T. Matheson and V. Dürri, Bielefeld, Cambridge (UK) and Leicester (UK)  
*Biomechanics and motor control of targeted limb movements in the locust*
- [#67B](#) M. Meseke, JF. Evers, S. Mapfumo and C. Duch, Berlin  
*Dendritic and synaptic remodelling during developmental changes in function of an identified insect motoneuron*
- [#68B](#) T. Seidl and R. Wehner, Zurich (CH)  
*Ant odometry: is locomotor activity a necessary prerequisite?*
- [#69B](#) T. Puschmann and C. Duch, Berlin  
*Downstream effects of ecdysteroids on motoneuron structure in Manduca cell culture*
- [#70B](#) SN. Fry, R. Sayaman and MH. Dickinson, Zürich (CH) and Pasadena (USA)  
*Instantaneous flight power in the fruit fly Drosophila*
- [#71B](#) C. Weigelt and O. Bock, Cologne  
*Unconscious motor adaptation in grasping: A function of task precision requirements?*
- [#72B](#) G. Schmitz, P. Vogt and O. Bock, Köln  
*Transfer of sensorimotor adaptation between sensory modalities*
- [#73B](#) S. Kreissl, M. Bernhardt, M. Schmäh, T. Mueller and W. Rathmayer, Konstanz  
*The dorsal extensor musculature of Idotea (Crustacea, Isopoda) based on single fiber analysis*
- [#74B](#) J. Strelau, A. Strzelczyk, O. von Bohlen und Halbach and K. Unsicker, Heidelberg  
*Neuron deficits in mice lacking Growth/differentiation factor-15*

- [#75B](#) J. Haß, JM. Herrmann and T. Geisel, Göttingen  
*Biomechanics and Low-Level Control of Bipedal Locomotion*
- [#76B](#) S. Göbel, O. Bock, M. Girgenrath, D. Sand and H. Pongratz, Köln  
*Isometric force production during hyper-G*
- [#77B](#) J. Henning, D. Koczan, A. Rolfs and U. Gimsa, Rostock  
*Deep brain stimulation of the subthalamic nucleus modulates gene expression and reverses limb use-asymmetry in rats with unilateral 6-hydroxydopamine lesions.*
- [#78B](#) G. Engler, CKE. Moll and AK. Engel, Hamburg  
*Coherent oscillatory activity along the cortico-striatal axis of the rat in relation to different brain-states.*
- [#79B](#) F-W. Zhou, U. Strauss, A. Wree, R. Benecke, A. Rolfs and U. Gimsa, Rostock  
*Influence of extracellular potassium on the behavior of subthalamic neurons from 6-OHDA lesioned and non-lesioned rats under deep brain stimulation*
- [#80B](#) D. Braun, A. Aertsen, S. Rotter and C. Mehring, Freiburg  
*Adaptive Optimal Control Methods Elucidate Sensorimotor Learning Phenomena*



**Cyclic control of breathing during steady-state muscle performance in flying *Drosophila***

F.-O. Lehmann

BioFuture Research Group, Department of Neurobiology, The University of Ulm, Albert-Einstein-Allee 11, 89069 Ulm, Germany, [fritz.lehmann@biologie.uni-ulm.de](mailto:fritz.lehmann@biologie.uni-ulm.de)

The respiratory system of insects must maximize the flux of respiratory gases through the spiracles of the tracheal system. During flight the supply of oxygen becomes crucial when locomotor activity is increased during maximum aerodynamic force production. In *Drosophila* most of the gas exchange is due to the 4 large thoracic spiracles that match their opening area to the metabolic need of the animal during flight. To estimate tracheal gas capacity in this insect and to understand the significance of spiracle opening behaviour for oxygen supply of flight muscles we have flown *Drosophila* in a flight simulator in which we measured carbon dioxide release and locomotor performance during visually controlled flight. By blocking various spiracle openings for gas exchange we varied oxygen supply and measured the changes in muscle mechanical power output delivered to each wing including muscle efficiency. Data show that a reduction of spiracle gas exchange area impairs maximum locomotor capacity that results in a decrease in stroke amplitude and aerodynamic force production. The release of carbon dioxide tends to be more cyclic under these experimental conditions suggesting that the insect might employ discontinuous breathing patterns even at elevated locomotor activity. Analytical modelling suggests that the cyclic oscillations might be an immanent feature of the neuromuscular control of all spiracles and do not require a CNS pace maker to elicit the measured behaviour.

## Nitric oxide in a wind-sensitive sensory system of the locust: possible role in gain control

Daniel Münch, Hans-Joachim Pflüger and Swidbert R. Ott\*

Institut für Biologie, Neurobiologie, FU-Berlin, Germany. email: danielmuench@gmx.de

\* current address: School of Life Sciences, University of Sussex, Brighton BN1 9QG, UK

A sensory system needs to encode stimuli over a wide range of intensities. In an animal that may in succession roost, jump, walk, and fly, a system that monitors the air flow around the body has to satisfy extremely different demands and may therefore benefit from activity-dependent modulation. We conducted experiments on a neuronal ensemble that is part of the locust (*Locusta migratoria*) flight steering network. About 150 wind-sensitive hair receptors on the prosternum synapse onto a single identified interneuron (A4II) whose response depends on the direction of the air flow (see Bucher & Pflüger 2000, *J Insect Physiol* 46:1545–56). Previous work suggests a role for the diffusible signaling molecule nitric oxide (NO) in mechanosensory processing (reviewed in Ott et al. 2001, *Amer Zool* 41:321–31). We therefore considered the possibility that NO might mediate sensory plasticity in this receptor – interneuron system.

Double-labelling experiments combining dye injection into A4II and NO synthase (NOS) immunostaining in the prothoracic ganglion revealed that the highest density of NOS immunoreactivity occurs in ventral areas (Fig. 1, low-power confocal volume reconstruction; green, NOS immunostaining; white, A4II), and thus in a region where distinct groups of hair receptors contact A4II. High-resolution confocal microscopy revealed NOS-immunoreactive profiles in immediate proximity to A4II-dendrites ( $<0.3 \mu\text{m}$ ; Fig. 2). Mapping these profiles onto 3D surface reconstructions of A4II showed very close juxtaposition in different areas of the dendritic tree.

These anatomical data suggest a role for NO in modulating the filiform hair afferent – A4II system. We therefore analyzed the effect of NO on information processing by recording the A4II response to wind puff stimulation of the prosternal filiform hairs in a reduced prosternum-ganglion preparation. First, we investigated the effects of direct NO-donor (DEA) application; stimuli were

carefully adjusted to not elicit habituation (300 ms puffs at 0.5 Hz). Low concentrations of DEA (10–30  $\mu\text{M}$ ) had either no effect, or slightly increased the spiking response of A4II, depending on the individual preparation in question. In contrast, higher DEA concentrations (100–300  $\mu\text{M}$ ) consistently caused a pronounced decrease in response. However, with the same concentrations, a slight rise of the interneuron's membrane potential was observed. This suggests that a shunting mechanism conveys the inhibitory effect of 100–300  $\mu\text{M}$  DEA on the spiking response. In some but not all preparations, however, this consistent reduction of the response was preceded by a transient increase, reminiscent of that observed occasionally with lower concentrations of DEA. These results suggest that NO has opposing effects on the synapse depending on concentration and — as evidenced by the inconsistent response to low concentration — on the internal state of the system.

We therefore investigated a possible role of NO in habituation, a form of non-associative learning that is induced by prolonged stimulation. In these experiments, the system was first driven continuously for 20 minutes with repetitive stimuli, which led to a decline to less than 50% of a single pulse response. We then measured the rate of habituation before and after blocking the NO – cyclic GMP pathway with ODQ, an inhibitor of the NO receptor soluble guanylyl cyclase. The rate of habituation increased when the NO pathway was blocked. Our interpretation of these results is that strong stimulation of hair receptors elevates the endogenous level of NO. An inhibitory effect of NO on habituation may counteract an otherwise declining spike response, which is unmasked when the NO – cyclic GMP pathway is blocked. We therefore propose that NO plays a key role in controlling the gain of the receptor – interneuron synapse, thus keeping the system sensitive even when strongly driven, for instance during flight.

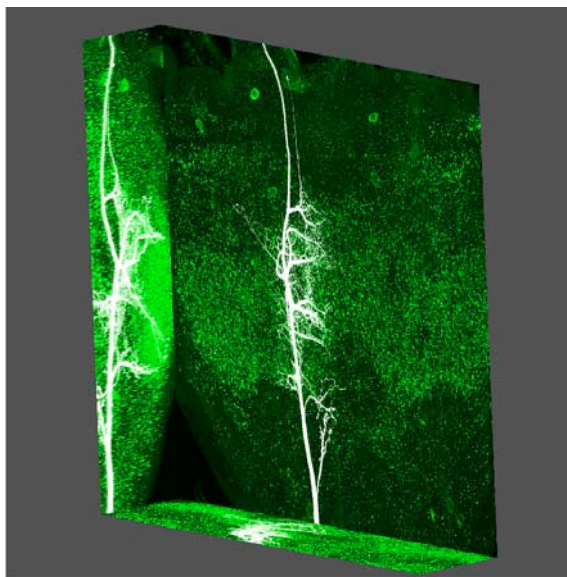


Figure 1.

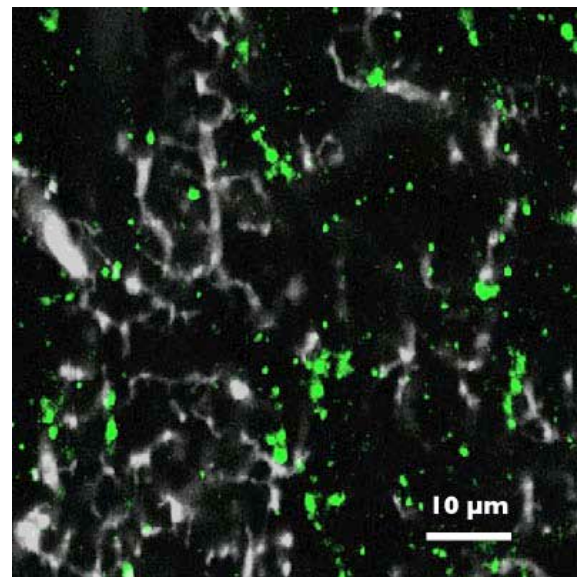


Figure 2.

† Supported by the DFG (Graduiertenkolleg GK 120, PhD Fellowship to D. Münch) and the DAAD (Senior Research Fellowship to S.R. Ott).

## CONTRACTION DYNAMICS OF THE STICK INSECT EXTENSOR TIBIAE MUSCLE

Christoph Guschlbauer, Hans Scharstein and Ansgar Büschges

Dept. Animal Physiology, Institute of Zoology, University of Cologne, 50923 Cologne, Germany

c.guschlbauer@uni-koeln.de

Limb posture and movement result from centrally generated trains of motoneuron action potentials. This information is translated into muscle activity according to the static and dynamic properties of the muscle-joint system. The stick insect extensor tibiae is an advantageous and relatively simple system in which to investigate muscle control during walking. We were in particular interested in how force, velocity, and stiffness correlate with each other with the goal of quantitatively describing the most important dynamic properties of the muscle. The force of the extensor tibiae muscle was therefore investigated both isometrically and isotonicly. The muscle's three motor units were simultaneously activated by electrical stimulation of their common nerve. Position and force clamp were achieved using a Aurora dual-mode lever system 300 B connected to the muscle tendon after it was cut at the Femur-Tibia (FT) joint.

Isometric and isotonic experiments show that both contraction force and velocity depend on the degree of muscle activation. The shape of the force-length and  $V_{\max}$ -length curves reflects the varying overlap of muscle thick and thin filaments as muscle length changes. For both curves force and  $V_{\max}$  first increase and then decrease as muscle length increases. However, the muscle lengths associated with the physiological range of FT joint angles ( $30^\circ$  to  $180^\circ$ ) are for both curves always on the ascending branch. The muscle generates maximal forces of 100-180 mN. Shortening and lengthening contraction velocities were determined by allowing the muscle to shorten, or by stretching it, while applying different load levels during steady state contractions. The force-velocity relationship (Hill characteristic) is approximately hyperbolic except there is a pronounced drop towards zero velocity in the high-force region ( $0.65-1 F/F_{\max}$ ). This drop depends on stimulation frequency and may be due to a catch-like effect in the attached cross-bridges. The force-velocity characteristic continues to negative velocities at high stimulation frequencies with a zero crossing with nearly horizontal slope. The muscle can contract with velocities up to 5 mm/s ( $\sim 3.5$  fibre lengths/s). The series elastic component can be calculated from the initial length change when tension is reduced during tetanus. It can be as great as 0.18 mm and is clearly nonlinear. Detailed analysis of one muscle shows that a simple parabola could fit all initial length changes at all load levels and stimulation frequencies. The higher the maximal isometric force, the more the quadratic spring will be stretched at tetanic force development.

The interaction of the hyperbolic Hill characteristic with the measured quadratic series elasticity is described by its differential equation and leads to a surprisingly good description of the time course of the force generation in the isometric force experiment.

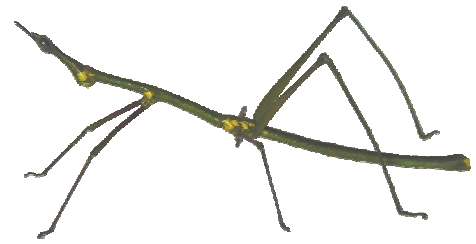
*Supported by the Boehringer Ingelheim Stiftung*

## Pre-adaptations for the evolution of jumping legs? Joint mechanics and muscle activity in the middle leg of a proscopiid grasshopper

Karin Dotzauer and Harald Wolf

Abteilung Neurobiologie, Universität Ulm, D-89069 Ulm,  
Germany

(correspondence to [harald.wolf@biologie.uni-ulm.de](mailto:harald.wolf@biologie.uni-ulm.de))



*Prosarthria teretirostris*, body length: 70mm

The hind leg of the locust is a highly specialised jumping leg (e.g. Heitler WJ & Burrows M 1977, J Exp Biol 66: 203-219 and 221-241). The hind leg of the proscopiid grasshopper *Prosarthria teretirostris*, by comparison, is a little specialised jumping leg (Burrows M & Wolf H 2002, J Exp Biol 205: 1519-1530) and appears to represent a relatively basic state. In the present study, we examined the *Prosarthria* **middle leg**, a normal walking leg, and used it as a model for the starting point of the evolution of the saltatorian jumping leg. A comparison between the *Prosarthria* walking leg, the little specialised *Prosarthria* jumping leg, and the specialised locust jumping leg should indicate the (evolutionary) changes that are required to construct a jumping leg from the plesiomorphic walking leg features, and to optimise it for the more compact and heavy locusts.

We examined the *Prosarthria* middle leg with regard to

(i) anatomical specialisations observed in the hind (or jumping) legs of saltatorians, (ii) the lever arms of flexor and extensor tibiae muscles at different angles of the femur-tibia joint, and (iii) the electromyographic pattern of muscle activity during the jump.

We observed

(i) none of the anatomical specialisations seen in saltatorian jumping legs, such as a ventral "lump" in the distal femur. This holds despite notable similarity in the general leg structure of middle and hind legs, including the presence of a semilunar process.

(ii) The flexor tibiae muscle gained an increasing lever advantage over the extensor muscle with more extended joint angles. This agrees with the predominant function of the middle leg in walking and climbing. And it contrasts with the lever ratio observed in the hind leg, which favours the extensor muscle at more extended joint angles and thus supports jumping performance.

(iii) During a jump, electromyographic activity of flexor and extensor tibiae muscles in the middle leg resembled that of the hind leg muscles. A co-contraction phase preceded triggering of the jump, which was characterised by abrupt shut-down of muscle activity. However, the critical timing of this shut-down – the flexor preceding the extensor by a few ms – was not recorded in the middle leg. This indicates that the middle legs do not deliver propulsive force during the jump but may rather play a role in steering.



In summary, the evolution of the saltatorian jumping leg required a number of important changes to the basic walking leg design, most notably inversion of the lever ratios between flexor and extensor tibiae muscles.

*Schistocerca gregaria*, body length: 70mm

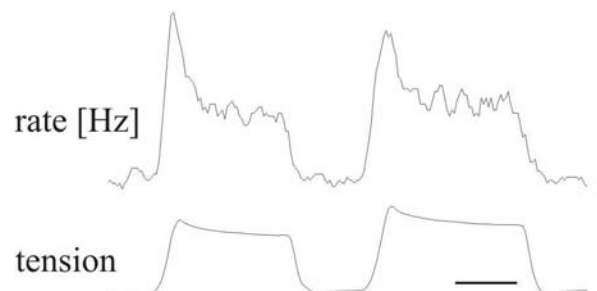
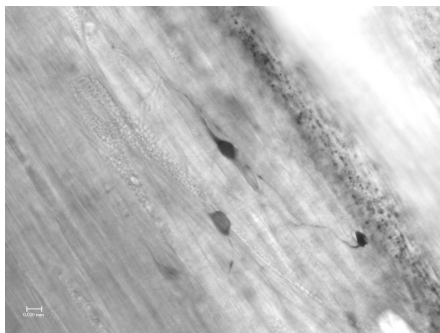
## Unusual tension receptors in an insect and how they compare to the Golgi tendon organ of mammals.

Mario Wanischek and Uwe Rose, Department of Neurobiology, University Ulm, Albert-Einstein-Alle 11, 89069 Ulm, Germany  
email: mario.wanischek@gmx.de, uwe.rose@biologie.uni-ulm.de

Force generated by muscles is usually monitored by specialised receptors. Mammals have Golgi tendon organs and crustaceans have receptors located on the apodemes of their muscles. In insects, receptors embedded in the cuticle (campaniform sensilla) monitor force produced by muscles when they distort the cuticle. Campaniform sensilla thus function as indirect receptors of muscle tension. Only individual receptor cells have so far been identified in the legs of insects which are embedded in the muscles themselves (flexor tibia muscle, coxa-trochanter MRO) and monitor the tension generated.

We have identified and characterised receptor cells on the ovipositor muscle of the locust *Locusta migratoria* which predominantly monitor muscle tension and not length. Approximately 250 to 300 of these receptor cells are found on the muscle at those sites where the muscle fibres blend with their tendons. Individual receptor cells are mono- or multipolar. Their afferent axons give off collaterals in the terminal ganglion, but branch more intensively in the seventh and sixth abdominal ganglion. The receptors respond best to force generated by active, isometric contractions of the ovipositor muscle. Their response characterises them as phasic-tonic receptors. Experimental activation of receptor cells leads to strong inhibition of motor activity and is thus comparable with the autogenic inhibition revealed for Golgi tendon organs.

The work presented here provides the first evidence of a tension receptor in insects with similar characteristics than the Golgi tendon organ in mammals.



## Effects of changes in pH on muscle spindle activity

M. Fischer and S.S. Schäfer

Department of Neurophysiology, Hannover Medical School, Carl-Neuberg-Str. 1  
D-30625 Hannover

Muscle spindle activity has been shown to decrease in the sustained isometric contracting muscle [Macefield et al., 1991]. It has been suggested that a reduced  $\gamma$ -activation is responsible for that gradually declining peripheral input from the fatigue muscle to the spinal motor nuclei. Since accumulation of metabolites including  $H^+$ , lactate and  $CO_2$  might also affect the muscle receptor, we investigated the influence of varying pH on the afferent activity of isolated muscle spindles from the cat tenuissimus muscle and from the rat gracilis muscle, thus excluding any effect on fusimotor activity, blood supply and extrafusal muscle fibers. Results were compared to pH effects on the nerve-muscle preparation of the rat gracilis muscle, where muscle spindles remained in their physiological environment.

Reduction in pH from 7.4 to 6.4 significantly decreased resting activity of primary (Ia) and secondary (II) endings of isolated muscle spindles (Fig. 1 and IA in Fig. 2). 30-40 % of the endings abruptly stopped firing in the acidic Ringer's solution, presumably caused by an increase in the threshold of firing at their encoder site. With alkalization from pH 7.4 to 8.4 resting discharge increased for both types of muscle spindle ending (Fig. 1). The effects of changes in pH on the basic discharge frequencies PD (peak dynamic discharge), MST (maximum static discharge) and FST (final static discharge) that were obtained under repeatedly applied ramp-and-hold stretches varied from one individual ending to the other. Fig. 2 displays a representative example of the effect of acidification on the basic discharge frequencies of a secondary muscle spindle ending. On average acidification increased the fast adaptive decay (FP) and the static index (SI) in primary endings and additionally the slow adaptive decay (SD) in secondary endings. Alkalization decreased FP, SD and SI in both types of ending. These results indicate that stretch sensitivity is increased at low pH and decreased at high pH. The initial burst that is often generated at the start of a stretch is also increased in the acidic and decreased in the alkaline milieu. Stiffness of intrafusal muscle fibers was slightly decreased in the acidic solution and slightly increased in the alkaline solution. Results obtained from non-isolated muscle spindles in the nerve-muscle preparation agree with the results obtained from the isolated receptor.

**Conclusion:** Muscle spindles are directly affected by changes in pH. We conclude that acidosis in the sustained contracting muscle reduces the input from muscle spindle afferents to spinal motor nuclei even in the absence of any fatiguing effect on  $\gamma$ -activation. An increased stretch sensitivity in the acidic milieu may increase the gain in the stretch reflex loop and may thus contribute to the well-known increase in the physiological tremor in fatigued muscles.

Fig. 1

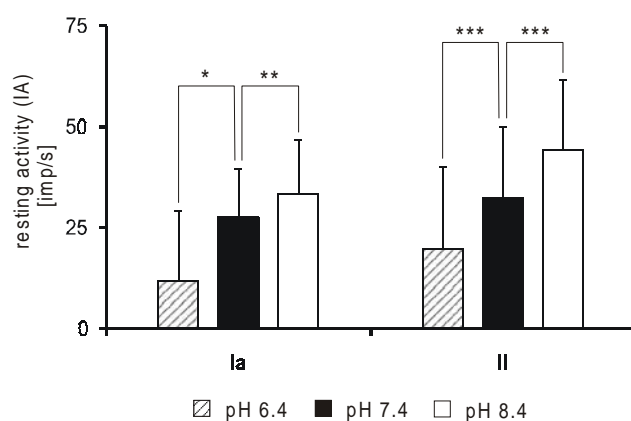
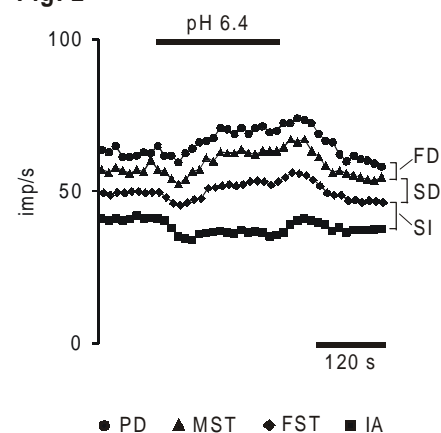


Fig. 2





## Free Flight Energetics in the Fruit Fly *Drosophila melanogaster*

Markus Mronz and Fritz-Olaf Lehmann  
BioFuture Research Group

Department of Neurobiology, University of Ulm, Albert-Einstein-Allee 11, 89081 Ulm, Germany

Flight is the energetically most demanding form of locomotion that has evolved in the animal kingdom. In a flying insect, total flight efficiency depends on two factors: the efficiency with which the asynchronous flight muscles turn metabolic energy into muscle mechanical power (muscle efficiency) and the efficiency with which the flapping wings produce aerodynamic lift (aerodynamic efficiency) to keep the animal airborne. In a behaving insect, muscle efficiency can be estimated by determining at least two of the following three factors: flight specific metabolic rate, metabolic heat production and muscle mechanical power output. Due to the small size of *Drosophila* heat production is difficult to measure and thus muscle efficiency has been typically estimated from the ratio between carbon dioxide release and mechanical power output produced by the muscle fibers. Previous studies have determined muscle efficiency in tethered flying *D. melanogaster* by simultaneously measuring stroke kinematics, locomotor performance and carbon dioxide release at minimum and maximum locomotor capacity of the animal. The results show that metabolic rate increases approximately linearly with increasing flight force production. While the fly varies locomotor performance, muscle efficiency is lowest (5.6%) when the animal produces minimum flight forces but increases up to a maximum of 23.5% during maximum force production. In contrast to muscle efficiency, aerodynamic efficiency appears to decrease with increasing force production. As a consequence of these two opposite trends mean total flight efficiency is small (2-4%) and stays relatively constant within a broad range of locomotor performance.

One concern in previous studies on tethered flying flies is that a tethered animal may produce aerodynamic forces and metabolic activity different from that produced during free flight. These differences might result from additional aerodynamic and energetic requirements to stabilize and manoeuvre the body of a freely flying fruit fly in space. To circumvent these problems, we developed an experimental procedure that allows us to measure simultaneously body position, stroke amplitude, stroke frequency and carbon dioxide release in a single freely flying fruit fly using laser-based imaging techniques and flow-through micro-respirometry. Two synchronised high speed video cameras capture the body position of the fly inside a respirometric chamber including the position of the wings at the ventral and dorsal stroke reversal. From the video images we calculate stroke amplitude in each stroke cycle and the position and orientation of the flying fly using imaging analysis software. The technique allows us to correlate metabolic rate with various types of flight manoeuvres in order to determine vital flight parameters such as aerodynamic and muscle efficiency during free flight conditions. Preliminary recordings suggest that metabolic rate during hovering flight force production might be lower than suggested by the tethered flight studies. This would run counter to theoretical predictions on energetic expenditures that suggest an increase in metabolic rate due to the additional energetic costs for flight stability and manoeuvrability in freely flying insects. In sum, the presented technique might provide a powerful tool to investigate and understand the details of flight energetics on a more elaborate level of investigation, and, moreover, allows us to evaluate previous results on flight energetics derived in tethered fruit flies *Drosophila* (Lehmann and Dickinson, *J. Exp. Biol.* **200**, 1133-1143).

The project is supported by a grant from the German Federal Ministry for Education and Research (BMBF, BioFuture 0311885, to F.-O. L.). E-mail address: markus.mronz@biologie.uni-ulm.de

## Temporal dynamics of facilitation at a crustacean neuromuscular junction

Melanie Nickmann, Carmen R. Smarandache & Wolfgang Stein

melanie@neurobiologie.de carmen@neurobiologie.de wstein@neurobiologie.de

Abteilung Neurobiologie, Universität Ulm

D-89069 Ulm, Germany

www.neurobiologie.de

We are studying the temporal dynamics of facilitation on the stomach musculature of the crab *Cancer pagurus*. The muscles of the crab stomach are driven by the rhythmic activity of the pyloric (filtering of food) and gastric mill (chewing of food) central pattern generators in the stomatogastric nervous system. The amplitude of the muscle contractions are given by the temporal pattern of motor neuron discharge. The motor pattern of the gastric mill rhythm, however, shows a great variability in firing frequency and temporal distribution of bursts of activity. In either case, the actual movements evoked by this motor pattern depend considerably on the temporal characteristics of the neuromuscular junction of the receiving muscle. Activity dependent facilitation and depression act presynaptically on the motor axon terminal and modulate the response of the muscle (Katz, Kirk, Govind, J Neurosci 13, 1993). Here, we are studying the temporal dynamics of facilitation at the neuromuscular junction of the gastric mill muscle gm6 (Maynard, Dando, Philos Trans R Soc Lond B Biol Sci 268, 1974) during a variety of gastric mill like stimulations. The gm6 muscle is innervated by a single motor neuron, the lateral gastric motoneuron LG.

The excitatory junction potentials (EJPs) recorded in gm6 are initially small but summate and facilitate strongly with repeated stimulation (Jorge-Rivera, Sen, Birmingham, Abbott, Marder, J Neurophysiol. 80, 1998). To extract the amplitudes of the EJP independently of temporal summation, the amplitudes were measured on a vertical line dropped from the peak of the EJP to the extrapolated exponential decay of the previous EJP.

Paired pulse stimulations revealed that facilitation acted on a short timescale with a time constant of decay of a few seconds. This was most obvious seen when single EJPs were preceded by a train of ten stimuli (Fig. 1, compare two arrows at left burst). Here, facilitation increased with stimulus frequency (5Hz, 10Hz, 20Hz).

During a gastric mill rhythm, bursts of motoneuron action potentials are followed by a rather long (4 - 15 seconds) lack of motoneuronal activity. To study the effects of such a temporal distribution of activity on the facilitation of EJPs, we stimulated with trains of spikes with various interspike intervals (5Hz, 10Hz, 20Hz) and various interburst intervals (2s, 4s, 8s, 16s, 32s). For measuring facilitation, every burst of activity was followed by a single test pulse. These experiments revealed that facilitation also increased on a longer timescale. With interburst intervals up to 16 seconds, EJPs amplitudes grew larger with every burst (Fig. 1, compare arrows at left and right burst; interburst: 4s, intraburst firing frequency 10Hz). Moreover, facilitation was also affected by the intraburst frequency in a way that higher firing frequencies caused a stronger facilitation. These results indicated that facilitation acted on two time scales, a short one in the range of seconds and a considerably longer one, in the range of tens of seconds. Stimulations with a previously recorded gastric mill rhythm showed that the slow facilitation also contributed to the muscle response to a realistic motoneuronal input.

Currently, we are testing whether this slow facilitation also affects the contraction properties of the muscle.

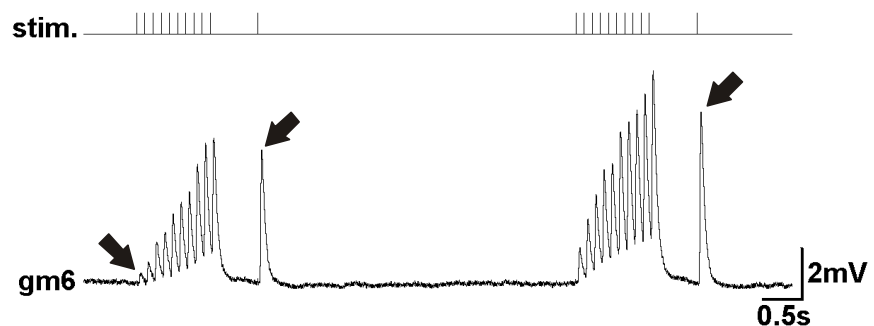


**Fig. 1:** gm6 muscle EJPs in response to two trains of 10Hz stimulations.

Supported by DFG STE 937/2-1.



# A New Approach for Electrophysiological Long-term Experiments in Desert Scorpions

Alaa El-Din Sallam<sup>1</sup>, Eberhard R. Horn<sup>2</sup>, Michael Schmäh<sup>2</sup>

<sup>1</sup>Zoology Department, Suez Canal University, Ismailia, Egypt; <sup>2</sup>Gravitational Physiology, University, Ulm, Germany  
alaadin60@hotmail.com; eberhard.horn@biologie.uni-ulm.de; michael.schmaeh@biologie.uni-ulm.de

Scorpions are known as “living fossils”. Since their first appearance as aquatic organisms in the Silurian (nearly 450 MYA), they have changed little. Nowadays about 1200 species are common in temperate, desert and tropical habitats of the world. The desert scorpions have the unique capacity to maintain physiological homeostasis and conserve metabolic energy, i.e. they are highly adapted to live under extreme xeric environments. Therefore, these species are excellent animal models to study neurophysiological and homeostatic adaptation to extreme living conditions. The aim of the present work was to develop an animal holder that optimizes the experimental conditions for an application of controlled environmental parameters on the animal in long-term observations.

The result of a long developmental and testing period was a design shown in Fig. 1A. A 3-point fixation with aluminum clamps restricts movements of the pedipalps and the metasoma. Although the animal maintains typical activity and resting postures under this type of restraint, the ability to feed is limited and wiring of electrodes is less protected. Two improved models have been developed (Fig. 1B, C1,2). For long-term studies, immobilization of the scorpion was replaced by a fixation of the animal at their coxae with surgery threads; this method increased the degree of pedipalp and leg movements, i.e. improved predation and motor activity. Electrodes became more protected by reforming the bridge at the hind part of the holder. Model B is designed for experiments under laboratory conditions; it offers a direct contact of the animal with its substratum sand and, consequently, optimizes its sensory niche. The prominent environmental parameters such as light, temperature and humidity can better be applied in a controlled manner. Model C was developed for space flight studies with scorpions. After slight modifications, these holders can also be used in other arthropods such as desert beetles.

More than ten electrodes can safely and permanently be implanted for long-term extracellular recordings. In fact, long-term simultaneous electrophysiological measurements lasting several months have been successfully performed in individual animals. The recording techniques included electroretinograms (ERG) evoked by brief light pulses to both median and lateral eyes, electromyograms (EMG) from leg muscles, electrocardiogram (ECG) and spontaneous electrical activity (SEA) of the supraesophageal ganglion using electrodes implanted near the median eyes.

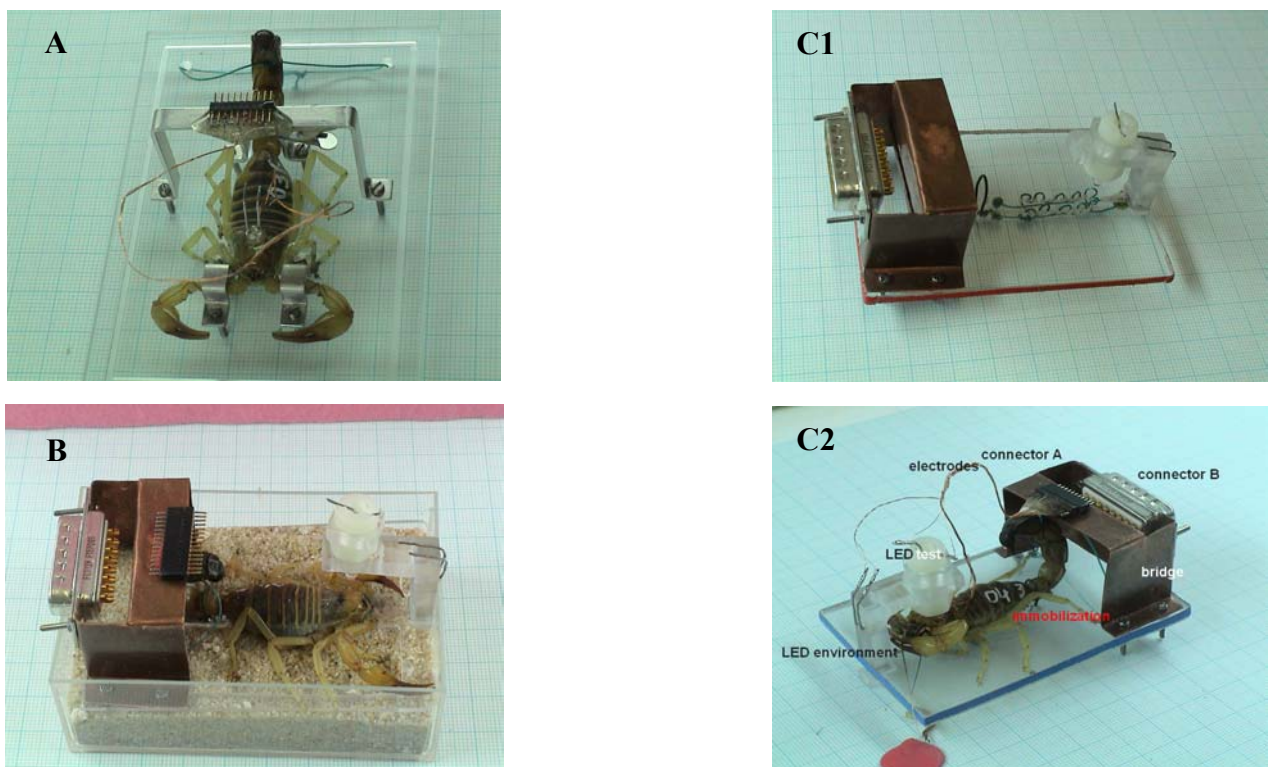


**Figure 1:** Animal holders for neurophysiological long-term observations in awake scorpions. – **A:** 3-point immobilization using aluminium clamps; the connector for the electrophysiological equipment is mounted on the small bridge. – **B:** Immobilization for ground-based studies. The scorpion is standing on a sand bed. – **C:** Immobilization technique for spaceflight experiments. C1 shows the green surgery threads which are attached to the coxae; C2 shows a scorpion feeding a cricket. These animal holders are also applicable for long-term observations of homeostatic mechanisms.

Model B offers several advantages for experiments under laboratory conditions including a minimum mounting stress, access to living food as well as optimum sensory niche under controlled environmental parameters, e.g. substrate texture, temperature, moisture and ambient photoperiod. These dominating features trigger all the animal physiological and behavioral adaptations in its natural environment. Moreover, controlling of the sensory niche which have informational value as a timing signal for the animal will undoubtedly help to analyze aspects of circadian regulation such as feed-back effects from sensory information of photoreceptors, tarsal, and pectine sensilla. Model C supports the advantage of the scorpion model to clarify several biological clock aspects in space research through long-term recording of different biological parameters simultaneously under microgravity.

## Neurophysiological Long-term Studies in Space: SCORPI-T and SCORPI

Michael Schmäh, Eberhard R. Horn

Gravitational Physiology, University, Ulm, Germany

michael.schmaeh@biologie.uni-ulm.de; eberhard.horn@biologie.uni-ulm.de

Life science research in space focused on two aspects, (1) the reduction of risks for men during long-term orbital flights, and (2) the particular role of gravity on living organisms. Experiments on spacecrafts such as biosatellites and space shuttles considered most areas of life sciences and contributed intensively to the understanding how the morphological and physiological stability and integrity of cells, micro-organisms, plants, animals and men depend on gravity. Methods used during the space flights were not limited if they were feasible with the spatial conditions in the spacecraft. The International Space Station ISS offers the opportunity to extend basic biological research to aspects concerning heredity, development from the fertilized egg to the adult organism and biological clocks or circadian rhythms. But because of the crew size (currently limited to 2 members) it also limits research to those methods that can run mainly automatically. Electrophysiology coupled with a space relevant question in systemic (integrative) biology using a suitable animal offers the best approach to use the resources of ISS in an optimal manner for biological research. Thus, an automatically running hardware for neurophysiological long-term studies in space is a promising technology. In 2000, the idea of a chronobiological experiment in scorpions was presented for the first time to the scientific community (PC Riewe and ER Horn: The scorpion. An ideal animal model to study long-term microgravity effects on circadian rhythms. In: *Space Technology and Applications International Forum*, edited by MS El-Gerk, American Institute of Physics, Melville, New York, pp383-388, 2000).

Circadian rhythms were chosen because their analysis demands a continuous data collection over a long time, which means the best use of ISS resources. The coordination of physiological mechanisms depends on the synchronization by external Zeitgebers such as the daily light-dark rhythm and on internal clocks. De-synchronization of these rhythmic events can cause physiological, behavioural and psychological disturbances. Some disturbances observed in crew members might arise from de-synchronization caused by the spatial environment and the altered physical periodicity. Scorpions were chosen because many species are adapted to arid environments which offer only temporarily food and water. Consequently, many of their physiological properties such as locomotion, eye responsiveness and cardiovascular activity reveal clear time patterns which make these species most suitable for basic research on the neurobiology of the biological clock system.

Currently, we prepare the space experiment SCORPI to find out whether vegetative and sensorimotor functions underlie different sensitivities to altered physical Zeitgeber rhythms in space. SCORPI was selected for a flight on the International Space Station ISS. It will be mounted in the European facility BIOLAB that was developed by the European Space Agency ESA for fundamental biological research in space. Besides microgravity, it offers an in-flight 1g-simulation. The automatically acting SCORPI hardware allows long-term recordings of the visual sensitivity (electroretinogram, ERG), muscular activity (electromyogram, EMG), arousal of the brain (spontaneous cerebral electrical activity, SEA) and heart beat frequency (electrocardiogram, ECG). The time schedule of the experiment includes a pre-flight observation period of at least one month, followed by a recording period of 3 to 4 months on ISS under microgravity and simulated 1g-conditions, and post-flight observations lasting 1 to 2 months in each selected scorpionaut. The physiological data will be recorded from the immobilized animals continuously for periods of synchronized and free-running activity.

The development of a breadboard (BB) was a mandatory step on the way to the final SCORPI flight hardware. The size of the BB had to be considerably smaller than that of the typical laboratory equipment because it had to consider the limited spatial conditions on ISS. On the other hand, it must have the same efficiency and has to offer the same recording quality as the laboratory set-up. Therefore, tests with both the BB and the laboratory equipment were done using the same animals. The aim was to adjust BB abilities to those of the earth-bound laboratory equipment. Space industry (EADS Space Transportation/Friedrichshafen; Kayser Italia/Livorno) delivered a BB which was tested successfully; despite of its significantly smaller size, the recordings of the ERG, the SEA and the EMG agreed (cf. Figure).

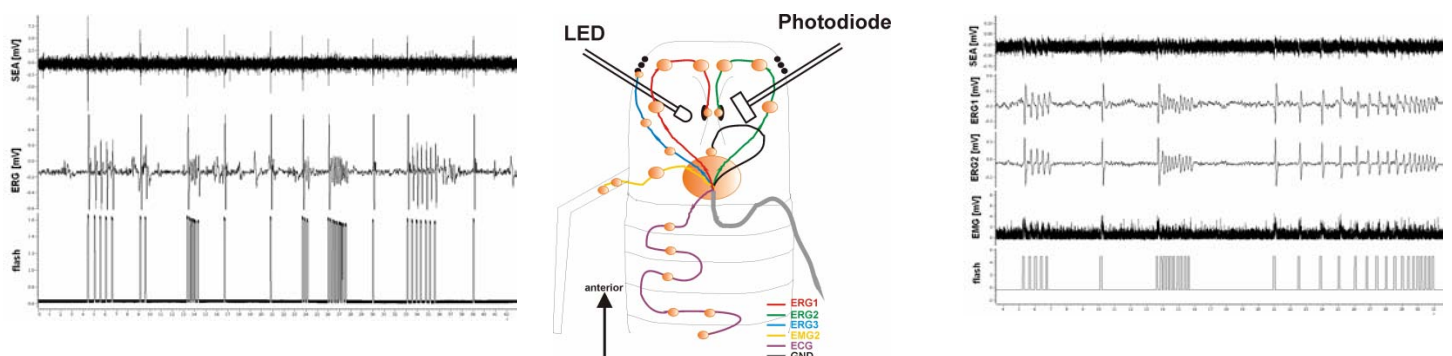


**Figure:** Typical observation from a test with the SCORPI breadboard (left) and the standard laboratory equipment (right). Both recordings were taken from one scorpion first in the laboratory, thereafter in the breadboard setup. The electrodes were implanted in the median eye and in the patella to record the electroretinogram and electromyogram, respectively (middle); the SEA was recorded via the ERG channel. A white LED light stimulus was applied to a median eye and recorded by a photodiode. For the flight version, additional electrodes will be implanted near the lateral eyes and within a tergite; this electrode is used to record the ECG. The development of the breadboard was financed by the European Space Agency; industry contract partners were EADS Space Transportation/Friedrichshafen and Kayser Italia/Livorno.

SCORPI has the precursor flight SCORPI-T on the Russian biosatellite FOTON-M2 in May/June 2005. The flight will last 2 weeks. The goal of SCORPI-T is to study critical aspects of the experiment SCORPI such as the quality of electrode implantation, the importance of movements (video observations are used) and stress to the animals caused by the microgravity environment and the restraint in the animal holder (cf. Sallam et al. at this conference), as well as the function of the electronic hardware.

Supported by the German Space Agency, grant 50WB0323 to Horn

## Motor schemas during trajectory formation

Andreas G. Fleischer

Biokybernetik, Department of Biology, University Hamburg,  
Vogt-Kölln-Str. 30, D-20146 Hamburg, Germany

Subjects have the capability to develop a motor schema to anticipate the path of a moving target and to compute an optimal course of interception. During the performance of perception-action-cycles such a schema may highly reduce the control load and thus the question arises, what are the optimization characteristics.

The task was to hit a moving target circle by means of a cursor. The position of the target and the cursor was displayed on a screen. The target moves along a circular path with a marked centre. Moving the cursor from this centre towards the target and exceeding a given distance from the centre made the target and the cursor disappear, respectively. This allows to analyse the effect of anticipating the target movement and the requirements of feedback.

The subjects were able to develop a stable and effective strategy on approaching the target even during early disappearing of target or cursor. During the start phase there is a highly significant lead of the hand with respect to the target position and during the final phase the hand movement lags behind. The anticipated course of the trajectories depends on target velocity. Therefore, one has to assume that the subjects develop a context-specific schema which is based on optimizing certain parameters of the pattern of the hand movement. To build the corresponding motor programs for different target locations and velocities long latencies of the hand movement, about 470 ms, are required. Obviously, programming a precise trajectory requires time.

In general the course of the anticipated movement trajectories is only partially sufficient to hit the target. Additionally feedback is required. Therefore, one has to assume there is a combination of preshaped trajectory and feedback. Clearly, the general course of the trajectory is modified by perception-action-cycles which leads to the behavioural structure described by the sample-data model. On the basis of asymmetric Hopfield nets the concept of context-dependent schemas was applied to obtain a differentiated structure of the trajectories. The associative net was enforced by latent learning. Additionally, the question was addressed, how to integrate feedback loops. Model considerations are based on a redundant dynamic arm model with 4 degrees of freedom, which were partially restricted by assuming specific ergonomic demands and by optimizing energy expenditure. A comparison between model and data is discussed.

## THE CORTICAL INTERACTION OF ATTENTION AND INTENTION

C.S. Konen<sup>1</sup>, R. Kleiser<sup>2</sup>, F. Bremmer<sup>1</sup>, R.J. Seitz<sup>2</sup><sup>1</sup>Department of Neurophysics, Philipps-University, Marburg, Germany;<sup>2</sup>Department of Neurology, Heinrich-Heine-University, Düsseldorf, Germany

Everyday life often necessitates a dissociation between our directed attention and the intention to direct our gaze. Accordingly, the differential role of visuomotor related areas in the one or the other process is an issue of an ongoing controversy debate. We used an event related fMRI study with concurrent eye tracking to elaborate a differentiation between attention and intention in these areas.

Thirteen subjects were asked to fixate a central target, while they directed attention to a colored cue in the left or right visual field. Regardless of its location, the color of the cue provided information about the direction of the upcoming saccade. The attention to the peripheral cue and the intention to perform the saccade were thus either directed to the same side or to opposite sides. The offset of the cue signaled the start of the memory saccade. Data analysis was performed with BrainVoyager QX and SPM2.

Strongest activation was found in MT, posterior parietal cortex, SEF, and FEF. BOLD signal change within area MT was dominated by the visual stimulus and direction of attention. A different response pattern emerged from the SEF and the posterior parietal cortex where the maximum of the fMRI signal change was found for the conditions when attention and intention were directed to the same side compared to attention and intention being directed to opposite sides. In contrast, the BOLD amplitude within FEF was strongest when attention and intention were spatially divergent.

Taken together, the visuomotor related areas split up regarding their involvement in attentional and intentional processes. Activation of area MT seems to result from visual and not intentional processes. Activation of the frontoparietal network, however, is correlated with both processes. The contrary time courses stress the prominent roles of the FEF in anti- and of the SEF as well as the posterior parietal cortex in pro-saccades and spatially congruent attention and intention.

## I KNOW WHERE YOU'LL LOOK: AN FMRI STUDY OF OCULOMOTOR INTENTION AND A CHANGE OF MOTOR PLAN

R. Kleiser<sup>2</sup>, C.S. Konen<sup>1</sup>, R.J. Seitz<sup>2</sup>, F. Bremmer<sup>1</sup><sup>1</sup>Department of Neurophysics, Philipps-University, Marburg, Germany;<sup>2</sup>Department of Neurology, Heinrich-Heine-University, Düsseldorf, Germany

Electrophysiological studies in monkeys showed that the intention to perform a saccade is reflected in the neural activation of the posterior parietal cortex (Bracewell et al. 1996). In such case, even the covert change in motor plan is indicated at the neuronal level. We asked whether such covert intentional oculomotor processes are detectable in humans as well.

We addressed this issue with an event related fMRI study and concurrent eye tracking. Thirteen subjects were instructed to fixate a central target, which changed its color in order to indicate the direction of the subsequent saccade. Without the advanced knowledge of the subjects, the color changed again in half of the trials to instruct a spatially opposite saccade. This allowed us to investigate the effect of covertly changing the motor plan without changing the direction of gaze and the spatial focus of attention. The offset of the fixation target signaled the start of the memory saccade. Data analysis was performed with Brain Voyager QX and SPM2.

Strongest activation was found in MT, posterior parietal cortex, SEF, and FEF. The group analysis revealed an enhanced and prolonged fMRI signal of both area MT and the posterior parietal cortex in case two cues were presented compared to a single cue. In contrast, an individual cue enhanced activation of the FEF. Even more interesting, the fMRI signal change of the posterior parietal cortex correlated with the change in motor plan, i.e. activation strongly decreased when the second cue instructed an ipsiversive saccade while it strongly increased when it instructed a contraversive saccade. In summary we show that the double-cue induced a synergistic effect of the BOLD signal in the posterior parietal cortex and area MT, whereas the reverse was true for the FEF. In addition, our data strongly imply that activation of the posterior parietal cortex indicates the intention to execute a contraversive saccade.

Learning visual and mechanical discordances:  
Effects of composition and decomposition

Katja Pipereit and Otmar Bock

Dept. of Physiology and Anatomy, German Sport University, Cologne, Germany

It is known that people who perform a manual motor learning task can adapt to visual as well as mechanical discordances. The current study addressed three questions: First, would subjects learn a visual discordance better or worse when simultaneously adapting to a mechanical one. Second, is it easier or harder to perform a visual discordance after having adapted to the mechanical one before. Third, how does performance change when adding the mechanical discordance to the learned visual one. We investigated the effects of composition (e.g., initial learning of one discordance and adding a second one thereafter) and decomposition (e.g., starting with both discordances simultaneously, followed by just one of the two) on subjects' performance using a visual (rotation) and a mechanical discordance (different effector resistance).

Using the index finger of their dominant hand, human subjects pointed at visual targets in the horizontal plane in a center-out task. Whereas rotation of the cursor by 60° about the workspace center served as visual disturbance, mechanical disturbance was achieved by introducing a flexible rod as effector. Due to a mirror, subjects were unable to see their hand. However, finger and rod position were registered by electromagnetic induction (Fastrack®), and their position as well as the target positions were displayed on a screen.

Subjects were randomly allocated to four groups: While two groups performed composition conditions where initial learning of either the visual or the mechanical discordance was followed by combined disturbance presentation, the other two completed decomposition conditions that were presented in reversed order. Baseline data collection preceded the introduction of the disturbances. Performance was assessed by the initial angular error.

Our results show that simultaneous learning of the two discordances had no effect on the initial angular error. In addition, neither previous adaptation to only the mechanical one nor adding the rod to the learned visual discordance had an effect on the error. Surprisingly, we had a significant effect of performing only the visual discordance after having adapted to both discordances before. We conclude that proprioception may have been enhanced by using the rod, and that removing it causes the subject to move less accurate.

## Learning a nonlinear visuomotor rotation: generalization of learning and effects on kinematic parameters

**Danilo Musella & Simone Cardoso de Oliveira**

German Primate Center, Kellnerweg 4, 37077 Göttingen, Germany (scardos@gwdg.de)

Previous studies investigating the learning of linear visuomotor rotations have proposed that learning is confined to the trained location and does not generalize to untrained locations, suggesting a basically local learning mechanism (1). Is this necessarily so, or is the degree of generalization dependent on the kind of visuomotor transformation? In order to investigate this question, we have designed a non-linear, space-dependent rotational transformation task that follows a principle more amenable to abstraction than those of previous studies. The transformation from arm space to visual space resembles the unfurling of a paper fan from partially open (90 degrees) to fully open (360 degrees). We tested how learning of such a transformation was affected by previous exposure to other versions of that same transformation that were rotated by 90 or 180 degrees. We found that performance in the second rotation was not dependent on the relation between the transformation angles at each target position, arguing against a local learning. Instead, people seemed to be able to generalize learning of the previous transformation to the 90 degrees rotated version. This result suggests that non-local generalization of visuomotor transformation learning is possible, and that it may rely on distilling an abstract transformation rule. However, subjects seemed to profit much less from this generalization in a 180 degrees rotated version. Applying the transformation rule to rotated versions of the same transformation may be constrained by a mental rotation procedure that depends on the rotation angle of the transformation rule.

Does learning of the visuomotor transformation only affect visuomotor mapping, or does it also influence kinematic parameters of motor control? Normal reaching movement have been shown to follow the so-called ‘two-third power law’ (2), describing the relation between angular velocity ( $\omega$ ) and curvature ( $C$ ) of the movement (equation 1),

$$\omega = k \bullet C^b \quad (\text{equation 1}),$$

with  $b$  typically being  $2/3$ .

This relation describes that, typically, movements slow down during curves, with an exponent of two-third. Does this relation still hold when the angular velocity of cursor movements is changed by our visuomotor transformation, i.e., is kinematic motor control influenced by the visual display of cursor movements? In order to answer this question, we fitted a power law to the transformed and non-transformed movements. We found differences between transformed and non-transformed movements, suggesting that indeed, the visual feedback does influence kinematic parameters of movement control.

This study was supported by the German Israeli Project Cooperation (DIP, funded by the BMBF) and the VW foundation.

1. Krakauer, J.W., Pine, Z.M., Ghilardi, M.-F., Ghez, C. Learning of visuomotor transformations for vectorial planning of reaching trajectories. *J. Neurosci.* 20, 8916-8924 (2000)

2. Flash T, Hogan N (1985) The coordination of arm movements: an experimentally confirmed mathematical model. *J Neurosci.* 5: 1688-703.



Adult Schwann cells over-expressing different isoforms of fibroblast growth factor-2 (FGF-2) – *in vitro* studies concerning therapeutic strategies in peripheral nerve repair

K. Haastert<sup>1,2</sup>, C. Mauritz<sup>1</sup>, C. Matthies<sup>3</sup> and C. Grothe<sup>1,2</sup>

<sup>1</sup>Dept. of Neuroanatomy, Hannover Medical School, 30623 Hannover, <sup>2</sup>Center for Systems Neuroscience (ZSN) Hannover, <sup>3</sup>Neurosurgical Clinic, Nordstadt Hospital, 30617 Hannover, Germany

We established enrichment and genetic modification of adult rat<sup>1</sup> and human Schwann cells (SC). Those cells are very interesting tools in a clinical context of autologous cell transplantation for peripheral nerve repair. SC are physiological sources of growth factors and cell surface molecules which are decisive in the regeneration process. The different isoforms of fibroblast growth factor-2 are independently injury-related up-regulated in SC *in vivo* and promote peripheral nerve regeneration either after exogenous application or due to over-expression by transplanted SC<sup>2</sup>. Our protocols will fit well into clinical proceedings as they are fast and not very expensive. Adult rat and human Schwann cells were highly enriched (> 90 %) and showed enhanced proliferation rates. Electroporation of both cell types resulted in 20 – 40 % genetically modified adult SC expressing the marker green fluorescent protein. Our electroporation protocol enables the genetic modification of adult human SC to over-express the different isoforms of FGF-2. Transfected adult SC expressed DsRed tagged FGF-2 isoforms and their proliferation rates and morphology after transfection and during over-expression of different FGF-2 isoforms is currently investigated *in vitro*.

<sup>1</sup>Mauritz C, Grothe C, Haastert K. 2004. Comparative study of cell culture and purification methods to obtain highly enriched cultures of proliferating adult rat Schwann cells. *J Neurosci Res* 77(3):453-461.

<sup>2</sup>Timmer M, Robben S, Muller-Ostermeyer F, Nikkhah G, Grothe C. 2003. Axonal regeneration across long gaps in silicone chambers filled with Schwann cells over-expressing high molecular weight FGF-2. *Cell Transplant* 12(3):265-277.

Supported by: Deutsche Forschungsgemeinschaft (CG), Kogge-Stiftung für veterinärmedizinische Forschung (KH)



## **Activity of modulatory neurons during leg movements in the stick insect**

Violetta Weiler, Tim Mentel and Ansgar Büschges

Institut of Zoology, University of Cologne, Weyertal 119, 50923 Cologne, Germany

Octopamine plays a major role in insect motor control. Octopamine has multiple effects in both the central nervous system and the periphery. For example, it influences the metabolic pathway in flight muscles (Mentel et al., 2003) and increases skeletal muscle relaxation rate and twitch contraction force (Evans & O'Shea, 1978; Evans & Siegler, 1982). In locusts and stick insects octopamine also increases sense organ responsiveness. To unravel the role these influences play in motor behavior several workers have recently begun to investigate the activity of neurones that release octopamine into the nervous system and the periphery during motor behaviors (Burrows & Pflüger, 1995; Duch & Pflüger, 1999; Bräunig & Pflüger, 2001). Despite the considerable knowledge about octopamine's effects, relatively little is known about octopamine release during any behavior. In most insects octopamine is released from dorsal unpaired median (DUM) neurones, a group of cells whose cell bodies lie on the dorsal midline of each ganglion and which bilaterally project to targets on both sides of the body. We were interested in whether these neurones are activated in the walking stick insect. We chose a preparation in which all legs were cut off except one middle-leg (Fischer et al., 2001). The remaining middle leg was stimulated to walk on a treadmill by brushing the abdomen with a paintbrush. DUM neurones were characterised by intracellular staining and named after their projections through the lateral nerves. A minimum of eight DUM neurone types were identified in the mesothoracic ganglion. Seven types were multimodal and received depolarising synaptic drive when the abdomen, antennae or different parts of the leg were mechanically stimulated. In no experiments was hyperpolarising synaptic drive observed. During walking these DUM neurones receive depolarising synaptic input during every stance phase of the step cycle. One type of DUM neurone, the DUMna neurone, exhibited spontaneous rhythmic activity, which was unaffected by different stimuli or walking movements.

## Biomechanics and motor control of targeted limb movements in the locust

Jure Zakotnik<sup>1</sup>, Keri Page<sup>2</sup>, Tom Matheson<sup>3</sup>, Volker Dürr<sup>1</sup>

<sup>1</sup>Dept. of Biol. Cybernetics, Univ. of Bielefeld, PO Box 10 01 31, 33501 Bielefeld, Germany

<sup>2</sup>Dept. of Zoology, Univ. of Cambridge, Downing Street, Cambridge CB2 3EJ, England

<sup>3</sup>Department of Biology, University of Leicester, University Road, Leicester LE1 7RH, England  
{jure.zakotnik, volker.duerr}@uni-bielefeld.de, kp231@cam.ac.uk, tm75@le.ac.uk

Biomechanics and muscle properties form the link between neural motor patterns and movements. A model behaviour for targeted limb movements is locust scratching, in which the animal aims its hind leg at a stimulus position on the wing. What role do muscles and mechanics play in the sensorimotor transformation of target position to movement generation? Locusts maintain targeting accuracy even if weights are applied to their legs [1]. How does the animal modulate its neural motor pattern to compensate for changed dynamics of the limb and its movement?

Scratching behaviour of the locust *Schistocerca gregaria* was studied in different loading conditions and for two distant stimulus sites on the wing. We performed 3-D-motion capture of the animal [2] and synchronously recorded electromyograms of femoral extensor and flexor muscles. Joint torque trajectories were calculated using inverse dynamics. The main objectives were ❶ to determine the torque range in which the animals can compensate for external loads, ❷ to analyse load-dependent changes of the underlying muscle activation and ❸ to obtain a forward model of the muscle transfer function.

❶ FT joint torques during unloaded scratching movements had a median value of  $1.08 \times 10^{-6}$  Nm (quartiles:  $0.63 \times 10^{-6}$ ,  $1.41 \times 10^{-6}$  Nm) and were larger for anterior than posterior stimulus sites. Animals fully compensated a load 8 times heavier than the tibia [1], although this increased median torque 14-fold and also the range of produced torques. Scratching movements were also observed for much heavier loads, with median torques up to 37-fold.

❷ FT joint movement is primarily driven by slow extensor tibiae (SETi) and slow flexor motoneurons. In loading conditions, mean SETi firing rate increased significantly with load. We also observed fast extensor tibiae (FETi) motoneuron activity in 19% of 318 trials, occurring in all loading conditions. So far, a simple dependency of FETi activity to load could not be determined.

❸ Simultaneous acquisition of both neural activity and limb dynamics enables us to estimate parameters of a Hill-type muscle model. Analysis of this model reveals how the neuromechanical system transforms the motor pattern into aimed scratching movements.

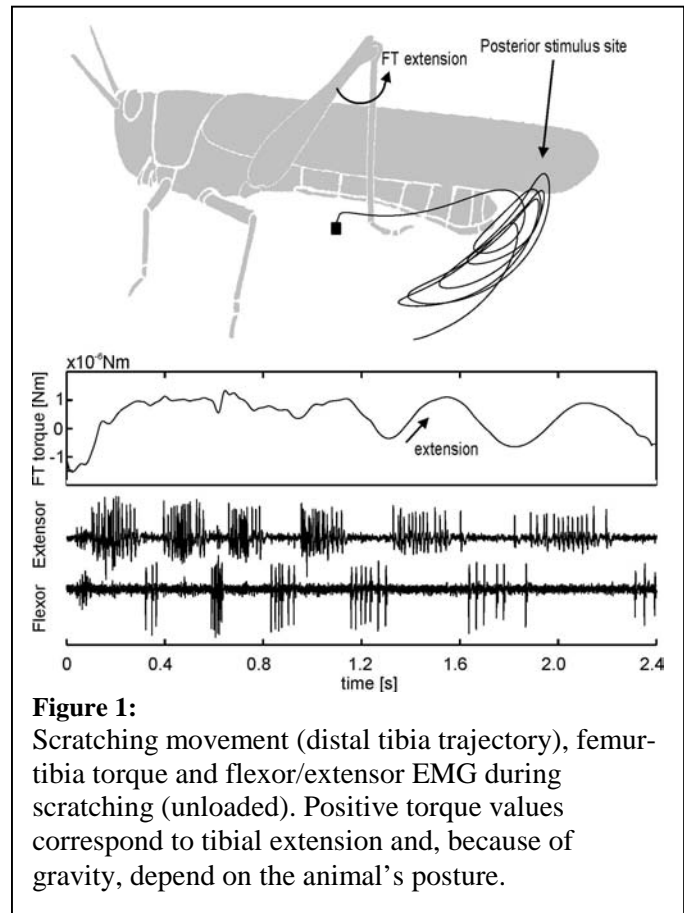


**Figure 1:**

Scratching movement (distal tibia trajectory), femur-tibia torque and flexor/extensor EMG during scratching (unloaded). Positive torque values correspond to tibial extension and, because of gravity, depend on the animal's posture.

## References

- [1] Matheson T, Dürr V (2003) Load compensation in targeted limb movements of an insect. *Journal of Experimental Biology*, 206/18, 3175-86
- [2] Zakotnik J, Matheson T, Dürr V (2004) A posture optimization algorithm for model-based motion capture of movement sequences. *Journal of Neuroscience Methods*, 135/1-2, pp 43-54

## **Dendritic and synaptic remodelling during developmental changes in function of an identified insect motoneuron**

**Maurice Meseke, Jan Felix Evers, Samanta Mapfumo, Carsten Duch**

Free University of Berlin, Institute of Neurobiology, 14195 Berlin

During metamorphosis of holometabolous insects, such as *Manduca sexta*, alterations in neuronal structure, membrane properties and synaptic connectivity of identified motoneurons subserve changing behavioural requirements. In the larval stage the identified motoneuron 5, MN5, is involved in larval-crawling behaviour. In contrast, in the adult it participates in flight. Therefore, metamorphosis leads to a respecification of the MN5 that facilitates adult behavioural tasks.

This study investigates the functions of changing dendritic architecture and altered distribution of GABAergic input synapses of MN5. Dendritic architecture is assessed by novel methods for highly precise 3-dimensional reconstructions from confocal image stacks. The distribution of putative GABAergic input synapses is addressed by calculating the correlation of Synapsin I and GABA immunolabeling within 300 nm distance from the dendritic surface of MN5. This method gives a good estimate of the distribution patterns of putative GABAergic input synapses on the entire dendritic tree.

In the larval stage, specific construction principles for the distribution of putative GABAergic inputs are found in a repeatable manner. Putative GABAergic inputs are found throughout the entire dendritic tree but not along the axon with this new method. At thin high order dendrites (radii below 0.3  $\mu\text{m}$ ) at the perimeter of the dendritic field putative GABAergic inputs are distributed randomly. But in contrast, at thicker, low order dendrites (radii above 0.5  $\mu\text{m}$ ) putative GABAergic inputs are predominantly located close to branch points, indicating that single inhibitory inputs might function as on/off switches for whole dendritic sub-trees. Imaging experiments will be conducted to test whether different dendritic sub-trees compute different input modalities.

During the loss of the larval function of MN5, dendritic regression is accompanied by a significant elimination of excitatory and inhibitory input synapses. Putative GABAergic inputs are lost to different extents in different branch orders, indicating a differential regulation of inhibitory synapse elimination within a single dendritic tree. Furthermore, the larval construction principle of putative GABAergic inputs located predominantly close to branch points is lost during synapse elimination. We currently test whether this construction principle might be rebuilt during re-gain of motor function during adult development.

Multi-compartment models are now used to get hints as to the function of the specific locations of putative GABAergic input synapses for synaptic integration. The long term goal is to integrate these results into a model system that explains the filtering and processing of incoming synaptic information within a complex dendritic tree of MN5 and to relate this to the different tasks of the different developmental stages.

*Supported by the DFG (GRK 837, SFB515)*

**Ant odometry: is locomotor activity a necessary prerequisite?**

Tobias Seidl and Rüdiger Wehner

Institute of Zoology, University of Zurich, Winterthurerstrasse 190,  
8057 Zurich, Switzerland

Previous experiments have shown that Saharan desert ants, *Cataglyphis fortis*, when trained to forage along an uphill-downhill array of channels and later tested within a horizontal (flat) channel, walked for a distance equivalent to the ground distance of the uphill-downhill array (Wohlgemuth, Ronacher, Wehner: Nature 411: pp. 795-798, 2001). This result implies that the ants have either performed path integration in the x-z plane (with the x-y plane being the horizontal desert floor) or have directly projected the length of each unit step on to the horizontal and then added up these horizontal increments. In either case the ants must have been able to assess the inclination of the channels relative to the horizontal.

In addressing this question we trained ants to walk on tilted surfaces that differed in their haptic fine structure, so that during walking the ants experienced different adhesive forces. First, the ants, *Cataglyphis fortis*, were trained to visit a feeder located at the end of a 9 m long flat channel. The horizontal surface, on which the ants walked, was covered with sand. In the tests, the homing ants were presented with a series of seven hills, in which the ascending and descending parts were of equal length (0.5 m) and inclined by 45° to the horizontal. Having passed this channel array the ants reached a flat test channel along which they continued their homebound runs, until they started to search for the nest, i.e. to zig-zag back and forth within the flat part of the test channel. The projection of the hill array on to the horizontal was 4.2 m (2.1 m for the ascending parts and 2.1 m for the descending parts of the tilted channels).

Having been trained in the flat channel the ants were presented with two test paradigms. In paradigm A both the ascending and the descending parts of the channels were provided with sand (glued to surface of the channel) allowing the ants to adopt their normal (tripod) walking gait, while in paradigm B the descending parts of the hills were covered with transparency foil, which caused the ants to slide or even tumble downhill. Hence, the slippery surface of the descending parts of the channel array prevented the ants from performing co-ordinated locomotor movements.

The non-sliding ants of test paradigm A searched at 10.5 m (median distance of the centre of search from the starting point; quartiles 9.1 m and 12.1 m), while the ants experiencing sliding descents in test paradigm B searched at 12.5 m (quartiles 10.5 m and 13.4 m). The difference between the centres of search in tests A and B is highly significant ( $p < 0.001$ ,  $N = 20$ ; Kruskal-Wallis). If the ant's odometer had disregarded the distances the ants had covered during their sliding downhill phase, in test paradigm B the ants' centres of search should be farther away from the starting point by 2.1 m than they were in test paradigm A. This is really what occurred.

In conclusion, the results of the experiments described here are in accord with the hypothesis that the ant's odometer depends on active locomotion for acquiring proper input signals.

Supported by the Swiss National Science Foundation, grant No. 31-61844.00.

## **Downstream effects of ecdysteroids on motoneuron structure in *Manduca* cell culture**

Till Puschmann and Carsten Duch

Free University of Berlin, Institute of Biology / Neurobiology, 14195 Berlin, Germany

The metamorphosis of holometabolous insects is governed by ecdysteroids, and thus, serves as a model for steroid actions in the control of neural development. In *Manduca sexta* the importance of ecdysteroid action for neuronal remodeling has been demonstrated by unraveling the expression of ecdysteroid receptor isoforms in the CNS (Fahrbach, 1992, J Exp Zool 261:245-53; Truman et al., 1994, Development 120:219-34), manipulating the hormonal environment of neurons in intact animals (reviewed in Weeks, 1999 Brain Behav Evol 54:51-60), and exposing cultured motoneurons to ecdysteroids (Levine and Weeks, 1996, Dev Neurosci 18:73-86). *In vitro* experiments on cultured motoneurons have shown that the steroid 20 hydroxyecdysone affects motoneurons in a stage specific manner, such as in some in induced programmed cell death, whereas in others it induces the formation of growth-cones and dendritic growth (Matheson and Levine, 1999, J Neurobiol 38:27-45). However, recent *in vivo* studies have shown that during the normal remodeling of motoneuron shape as occurring during metamorphosis to accommodate adult behavior, steroid effects act in concert with calcium- and activity dependent mechanisms (Duch and Mentel, 2003 Eur J Neurosci 17:945-62).

In this study, we use *Manduca* in primary cell culture to investigate motoneuron dendritic growth in two ways: First, mechanisms downstream of ecdysteroid action are analyzed by comparing motoneurons from the same ganglion in the presence and in the absence of ecdysteroids. At current we investigate the distribution of ion channels and of the calcium calmodulin dependent protein kinase II (CaM K II) by immunocytochemistry, as we know that ecdysteroids affect calcium membrane current amplitude and calcium current manipulations *in vivo* affect motoneuron dendritic structure. Preliminary results indicate significant differences in the sub-cellular localization of kinases upon ecdysteroid action.

In the second approach we investigate pathways which might translate changes in the intracellular calcium concentration into structural changes of the cytoskeleton? Good candidates for this mediation are the RHO GTPases Rac, RhoA, and Cdc42, as they are key players in shaping dendritic structure. We use the C3 transferase, an exoenzyme produced by *Clostridium botulinum*, which inactivates a rho-GTPase in mammalian neurons (Ayumu Tashiro et al., 2000, Cereb Cortex 10:927-38) by ADP-ribosylation. Preliminary results indicate that C3 toxin might also influence the neuronal growth of insect cells, such as the number of growth-cone filopodia are increased. However, further experiments and statistical analysis will have to be conducted to verify these results.

*Supported by the DFG*

# Instantaneous flight power in the fruit fly *Drosophila*

S.N. Fry<sup>1</sup>, R. Sayaman<sup>2</sup> and M.H. Dickinson<sup>2</sup>

<sup>1</sup>Institute of Neuroinformatics, ETH/University of Zürich; steven@ini.phys.ethz.ch

<sup>2</sup>Bioengineering, CalTech, Pasadena

The asynchronous power muscles of fruit flies allows them to flap their wings back and forth around 200 times per second, while generating the high power output required to hover in place. To move its wings, an animal must generate sufficient power to overcome both aerodynamic and inertial forces. The aerodynamic models developed by Ellington (1984) provide the theoretical framework for the estimation of flight power using basic descriptors of time-averaged kinematics and aerodynamic performance of insect wings. Using this approach, Lehmann and Dickinson (1997) estimated the mechanical power requirements of hovering at around  $60 \text{ W kg}^{-1}_M$  (power normalized to muscle mass). Using time-averaged input parameters is problematic, however, as it requires a number of simplifying assumptions to be made. Furthermore, previous analyses have been based on tethered fruit flies, whose behavior was subject to an unknown bias from the experimental procedures.

We have used a more direct approach to estimate flight power in tethered and freely flying fruit flies. Using 3D high speed videography (Fry et al., 2003), we measured the precise time course of 3D wing motion in free and tethered flying fruit flies (*D. melanogaster*). From these data, we then calculated the instantaneous specific inertial power,  $P^*_{Acc}$ , from the scalar product of wing velocity and the acceleration reaction force acting on the wings. We also measured instantaneous aerodynamic forces by playing the kinematics through a dynamically-scaled robotic wing and likewise calculated the instantaneous specific aerodynamic power,  $P^*_{Aero}$ .

In free flight,  $P^*_{Aero}$  peaks around the middle of each half stroke (red trace in Fig. 1A).  $P^*_{Acc}$  (blue trace) is of slightly lower magnitude and shows a sign reversal around the middle of each half stroke, when the wings begin to decelerate. The total mechanical power required to move the wings is calculated as  $P^*_{Mech} = P^*_{Aero} + P^*_{Acc}$  (black trace in Fig. 1A).  $P^*_{Mech}$  peaks at the onset of the down stroke (1), when both aerodynamic and inertial forces need to be overcome. As the wings begin to decelerate around mid-stroke (2),  $P^*_{Mech}$  gradually reduces to zero and becomes negative toward the end of the down stroke (3). Assuming that negative mechanical power dissipates as heat, we calculate a high estimate of mean muscle power from the integral of absolute mechanical power:  $P^*_{Mech, hi} = 126 \text{ W kg}^{-1}_M$ . Assuming perfect storage of negative mechanical power for the subsequent half stroke, we calculate a low estimate directly from the integral of mechanical power, which reduces muscle power by a mere 14% to  $P^*_{Mech, lo} = 108 \text{ W kg}^{-1}_M$ . The cost of wing acceleration is relatively minor and is further reduced by elastic storage (also see Dickinson and Lighton, 1995).

Our measurements of  $P^*_{Mech}$  are substantially higher than previous estimates that were in part based on unrealistic flight parameters. We also find that flight power in tethered flight differs substantially in time course and magnitude from that found in free flight (compare Fig. 1A and B), resulting in a reduction of  $P^*_{Mech}$  by about 40% to  $65\text{--}77 \text{ W kg}^{-1}_M$ . Taken together, the measurement of instantaneous wing motion and flight forces in free flight provides a more detailed and robust method to analyze the power requirements of insect flight. Comparative studies with other insect and vertebrate species, including hummingbirds, promise rewarding comparative studies in the future.

## References:

- Dickinson, M. H. and Lighton, J. R. B. (1995). *Science* 268, 87-90.  
 Ellington, C. (1984). *Phil. Trans. R. Soc. Lond. B* 305, 1-181.  
 Fry, S. N., Sayaman, R. and Dickinson, M. H. (2003). *Science* 300, 495-498.  
 Lehmann, F. O. and Dickinson, M. H. (1997). *J. Exp. Biol.* 200, 1133-1143.

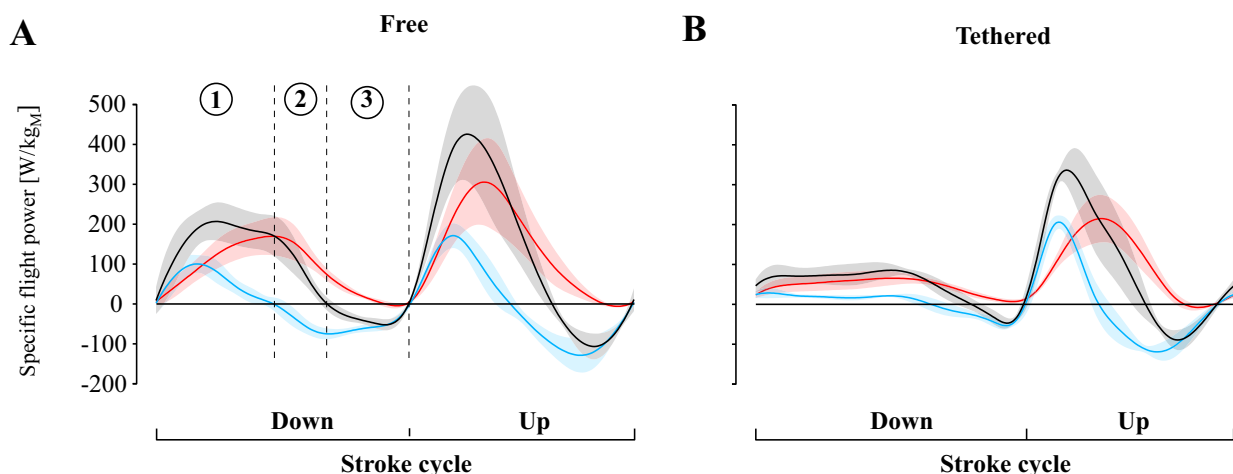


Fig. 1: Instantaneous aerodynamic ( $P^*_{Aero}$ , red), inertial ( $P^*_{Acc}$ , blue) and total power ( $P^*_{Mech}$ , black). **A:** Free flight power, averages were obtained from 67 stroke cycles (1539 frames, N=6 flies), shaded areas show standard deviation. **B:** Tethered flight power, from 59 stroke cycles (1550 frames, N=5 flies).

Unconscious motor adaptation in grasping:  
A function of task precision requirements?

Cornelia Weigelt & Otmar Bock

Department of Physiology & Anatomy, German Sport University, Cologne

When grasping an object, the maximal opening of the hand or fingers is scaled according to the visually perceived object size. So far, only two studies addressed the contribution of haptic information on prehensile movement control (Gentilucci et al '95; Säfström & Edin 2004). It is possible to investigate its influence by dissociating visual from haptic information about object size. This can be realised by presenting objects in front of a mirror (visual information), but letting participants grasp and lift objects (haptic information) located behind the mirror of either equal, increased or decreased size. While kinematic characteristics should show no change in the first condition, adaptation under the latter conditions would suggest that incongruent haptic information modifies previously established sensorimotor transformations. Using within-group designs, the published papers reported such an adaptation in the maximal grip aperture. Since participants had to grasp *and* lift the objects, it remains to be clarified whether the observed adaptation is due to felt size and/or felt weight. The current investigation focussed on the pre-contact phase in prehensile movements to objects that had to be touched only.

In Study I, using precision grips participants ( $n = 27$ ) had to touch wooden dowels (height: 3, 5 and 7 cm; depth: 4,4 cm; width: 1,8 cm), always presented at the same location. Subjects were randomly assigned to three groups. After baseline data collection (3 x 3 trials; grasping behind see-through glass), participants saw the dowels to-be-grasped in a mirror and grasped them behind it (3 x 18 = 54 trials; equal size). This condition was followed by 54 trials where the object size was kept the same, increased or decreased (equal size, ES; difference: +0,5 cm, IS; -0,5 cm, DS). The majority of participants were not aware of this experimental manipulation (23/27). In all conditions, maximal grip aperture was linearly scaled to object size. As expected, maximal grip aperture increased when introducing the mirror condition reflecting the impact of uncertainty commonly observed (e.g., safety margin). More important, after having introduced the experimental manipulation, maximal aperture significantly decreased in DS and increased in IS while no change was observed in the ES group. Interestingly, the adaptation occurred within the first 18 trials with no further significant changes towards the end of the experimental conditions. The results support the view of unconscious updating of sensorimotor transformations due to felt object size only.

A second study addressing the same question modified two points: First, the number of trials were reduced to 36 in each experimental condition. Second, the depth of the dowels were changed to 2 cm thus increasing the task precision requirements. The other dimensions were kept the same. Three groups ( $n = 8$ ) were tested under ES, IS and DS conditions, respectively. Preliminary data analysis showed again that baseline maximal grip aperture was significantly smaller than in behind-mirror grasping conditions. Also, the scaling of grip aperture was according to visually perceived object size. However, no adaptation of grip aperture was found although there was a trend in IS for greater apertures under the incongruent compared with the congruent mirror condition. These results may suggest that felt object size alone is not sufficient for motor adaptation when increasing task difficulty.

References:

- Gentilucci, M., Daprati, E., Toni, I., Chieffi, S. & Saetti, M.C. (1995). Unconscious updating of grasp motor program. *Experimental Brain Research*, 105, 291-303.
- Säfström, D. & Edin, B.B. (2004). Task requirements influence sensory integration during grasping in humans. *Learning & Memory*, 11(3), 356-363.

**Transfer of sensorimotor adaptation between sensory modalities.**

Gerd Schmitz, Patrick Vogt and Otmar Bock

Institute of Physiology and Anatomy, German Sport University, Köln, Germany

Keywords: spatial cognition, posture and movement control, learning and memory

When human subjects are exposed to a visual or mechanical distortion, their sensorimotor performance is initially degraded, but gradually normalizes with extended practice. This adaptive improvement typically shows transfer to the other, unpractised arm, suggesting that adaptive processes are located in the sensorimotor system *before* the divergence point for left and right arm control. The present study investigates whether these processes are located *before or after* the convergence point of different sensory modalities.

Human subjects pointed without hand vision at acoustic targets arranged along a semicircle about the starting point. Acoustic feedback about hand position (frequency ~ lateral error) was veridical during a baseline phase, and was then shifted laterally by 30 deg. Subjects adapted to this shift and adaptation transferred to the unpractised arm. Subjects then pointed without hand vision and without acoustic feedback at visual targets in the same locations, and exhibited adaptation transfer from the acoustic to the visual modality. A second experiment, using a complementary design, documented adaptation transfer from the visual to the acoustic modality.

We conclude that adaptive processes are located after the convergence point of sensory modalities, but before the divergence point for left and right arm control.



## The dorsal extensor musculature of *Idotea* (Crustacea, Isopoda) based on single fiber analysis

Sabine Kreissl, Marion Bernhardt, Michael Schmäh, Tobias Mueller and Werner Rathmayer<sup>‡</sup>

Department of Biology, University of Konstanz, D-78457 Konstanz, Germany

e-mail: s.kreissl@uni-konstanz.de

Members of the marine genus *Idotea* (23 species) are common and are distributed worldwide. The two species investigated in this study, *Idotea emarginata* and *I. baltica*, are abundant. They occur on floating seaweed, among algae and among or eelgrass in the sublittoral zone along the coasts of Europe down to depths of 80 m or have a circumpolar distribution down to depths of 300 m respectively. The largest males are twice as big as the females and may attain a length of 30 (*I. emarginata*) and 40 mm (*I. baltica*), with a width of 7 to 10 mm. The body consists of 21 segments, which are divided into four tagmata. In the course of analyzing the pre- and postsynaptic mechanisms, by which endogenous neuropeptides modulate neuromuscular parameters in crustaceans, we have developed a new muscle preparation with unique properties. The extensor muscle permits the preparation of single fibers, which allow the simultaneous analysis of membrane currents and isometric contractions and biochemical analysis of cellular mechanisms of peptidergic modulation (Erxleben et al. 1995; Kreissl et al. 1999; Brustle et al. 2001; Brustle et al, submitted; Rathmayer et al. 2002; Weiss et al. 2001; Weiss et al. 2002).

We describe the dorsal muscles of isopod crustaceans for a comparative anatomical analysis of trunk musculature in malacostracan crustaceans and provide a basis for ongoing physiological and biochemical work on single identifiable crustacean muscle fibers. The bilaterally symmetrical extensor muscles of *Idotea* consist of sets of five to eight fibers on each side, which are characteristic for a given segment and constant from animal to animal. Two layers of fibers are distinguished. The superficial layer is comprised of fiber 1, 2, 3 and 4, which are confined to single segments. The deep layer of fibers is comprised of fibers 5 and 6, which are two-segmental in most segments. The length of the one-segmental fibers in adult males range from about 0.4 mm in the pleon segments to 2.1 mm in the pereion segments. The two-segmental fibers are between 1.5 and 4.1 mm long.

In histochemical staining for myofibrillar ATPase and alkaline stability, two groups of fibers are clearly distinguished. Fibers 1, 2 and 4 stained lighter than the fibers 3, 5 and 6 when tested for their overall mATPase activity, but stained particularly dark after acidic pre-incubation. The fibers belonging to the two groups differ also in ultrastructural characteristics. In ultrathin sections of fibers with higher mATPase activity and shorter sarcomeres, the sarcomeres are interlaced, with the Z-lines of one fibril often aligned with H-bands of adjacent fibrils. In fibers with lower mATPase activity and longer sarcomeres, the fibers have irregular borders of A-bands and regularly aligned sarcomeres. T-tubules are small, but frequently interspersed among the fibrils at the ends of the A-band, where they form dyads with the sarcoplasmic reticulum.

The superficial and the deep fibers are innervated by separate nerve branches of the segmental nerve N3. All fibers receive polyneuronal innervation from at least two excitatory and one GABAergic common inhibitory axon.

Anatomical and histochemical characteristics suggest that the four one-segmental fibers are homologous to superficial extensor muscles and the two-segmental fibers are homologous to the deep extensor muscles in reptantian crustaceans.

<sup>‡</sup>The senior author deceased untimely in January 2003

This work was supported by grants of the DFG Ra 113/8-2, Ra 113/9-1

**Neuron deficits in mice lacking Growth/differentiation factor-15****Jens Strelau, Adam Strzelczyk, Oliver von Bohlen und Halbach, and Klaus Unsicker****Neuroanatomy and Interdisciplinary Center for Neurosciences (IZN), University of Heidelberg, Im Neuenheimer Feld 307, D-69120 Heidelberg, Germany****E-mail address: Jens.Strelau@urz.uni-heidelberg.de**

Growth/differentiation factor-15 (GDF-15), a novel member of the TGF-beta superfamily, is widely expressed in adult tissues including lung, liver, kidney, and skeletal muscle. In the CNS GDF-15 is detectable in the choroid plexus and the protein is present in the cerebrospinal fluid. Functional studies have demonstrated neurotrophic effects of the growth factor in vitro and in vivo. To further analyse the role of GDF-15 for the development and maintenance of neurons in the CNS we generated a GDF-15 deficient lacZ knockin mouse line. The exchange of the translated part in the GDF-15 encoding gene with the bacterial beta-galactosidase encoding lacZ gene allowed us to investigate lacZ expression under control of the GDF-15 specific promoter. Using in situ hybridization and X-Gal stainings we found lacZ expression and beta-galactosidase protein in the subventricular zone of the spinal cord of E 12 and E 14 mice. In parallel we started to quantify the numbers of dopaminergic neurons in the substantia nigra and in different brain stem nuclei. We compared 30-week-old wild-type and GDF-15 mutant mice on a C57Bl/6 background. Animals were perfused with 4% formaldehyde and serial cryosections of 25 µm were stained with cresyl violet. Neuron numbers were determined in every third section and corrected according to Abercrombie's formula. We found a significant reduction of 11% in the number of midbrain dopaminergic neurons. Notably, the number of facial motoneurons in GDF-15 <sup>-/-</sup> mice was 19% reduced. In contrast, hypoglossal motoneurons were not affected. Ongoing studies address the following three questions: i) Does GDF-15 also exert functions in the spinal cord? ii) When does the loss of neurons occur during development? iii) Is GDF-15 a target tissue derived factor? Preliminary results using real time PCR showed an up to 40 fold higher GDF-15 expression in peripheral nerves compared to the innervated muscles. We conclude that GDF-15 constitutes a novel candidate for a neuron survival factor.

This work was supported by Deutsche Forschungsgemeinschaft (Str 616/3-4)

## Biomechanics and Low-Level Control of Bipedal Locomotion

Joachim Haß, J. Michael Herrmann and Theo Geisel  
Georg-August-Universität Göttingen, Inst. für Nichtlineare Dynamik  
Bunsenstr. 10, 37073 Göttingen, Germany

In recent years, several walking robots have demonstrated that engineering and control problems arising in bipedal locomotion can be solved successfully. Human-like gaits have been produced, however, relying more on tracking control of presampled walking trajectories than on the underlying principles of biomechanics and neuro-control. On the other hand, it has been shown that under carefully chosen circumstances, a purely mechanical system can walk down a shallow slope without any actuation or control, powered only by gravity. This approach has become popular as 'passive dynamic walking' [1]. Although the size of viable parameter regions of such a walking model seems to be restrictive, it provides a good starting point to which control schemes can be added that are simple and efficient, for they exploit the intrinsic dynamics of the body. Their function can thus be reduced to be modulatory and error-correcting, while the applied forces stay small in many situations. Studying such a model provides a different perspective on human locomotion and can also be helpful in the design of an efficient leg prosthesis.

In the present work, we present a simulation study of a simple 2D pendulum-like walking model [1]. The physical parameters such as lengths, inertia, and centers of mass of all links have to be adjusted such that the system exhibits a periodic gait on a downhill slope. The identification of viable combinations of parameters forms a complex optimization task which is approached here by the NPOSA algorithm [2], a Monte Carlo method which combines the paradigms of simulated annealing and evolutionary algorithms. It maximizes a fitness function that evaluates periodicity, effectiveness and realism of the gait and identifies in this way a family of parameter combinations with high fitness values, which allows us to analyze the diversity of successful walkers.

When the slope angle is small, the gait of the walker is intrinsically stable. Most of the studies of passive walking have been performed under this condition. The gait cycle persists when the angle is increased, but it becomes sensitive to small perturbations at a certain point. Our simulations are run in this unstable regime to test how different control systems can interact with the mechanical system to induce stable locomotion. A standard reinforcement learning algorithm that relies on categorization of states and actions turns out to be successful, but its training phase seems to be prohibitively long considering the short time most animals need for learning to walk. An alternative algorithm based on the principle of homeokinesis [3] seems more promising to be of biological significance. The control forces are derived from an internal representation of how an optimal step should look like. This 'world model' can be of different complexity ranging from a mere recording of a sample trajectory to an adaptive neural network-based anticipation of which movements to use for the next step. The resulting system is still prone to environmental influences, but can now be described in terms of deviations from the internal representation, which obey a significantly simplified dynamics. These deviations are then adaptively suppressed by a homeokinetic controller.

In this control scheme, the trajectory of the legs is not predefined and enforced on the system, but any behavior is stabilized that minimizes the actual deviations from the model behavior. By inducing weak and noncritical perturbations, the controller is able to acquire information on the dynamics of the controlled system. Employing this dual control scheme, insights into human walking behavior are possible. Moreover, this work bears relevance for prosthetics, for the benefits of carefully adjusted mechanics and adaptive control can be combined in the design of a hybrid active/passive leg prosthesis. Here the target trajectory is provided by remaining nerve endings from the stump while the prosthetic leg stabilizes the most appropriate motion pattern in an autonomous manner. Thus different tasks in controlling the gait are separated to be performed in interacting sub-systems.

- [1] McGeer T (1993) Dynamics and control of bipedal locomotion, *J. Theor. Biol.* 163:277—314
- [2] Cho H-J, Oh S-Y, and Choi D-H (1998) A new population oriented simulated annealing based on local temperature concept, ICEC, *Proc. IEEE World Congress on Computational Intelligence*, 598—602
- [3] Der R, Steinmetz U, Pasemann F (1999) Homeokinesis - A new principle to back up evolution with learning. In: Mohammadian M (ed.) *Computational Intelligence for Modelling, Control, and Automation*. IOS Press, Concurrent Systems Engineering Series 55:43—47

## **Isometric force production during hyper-G**

S. Göbel<sup>1</sup>, O. Bock<sup>1</sup>, M. Girgenrath<sup>1</sup>, D. Sand<sup>1</sup>, H. Pongratz<sup>2</sup>

<sup>1</sup> Dept. Of Physiology and Anatomy, German Sport University, Germany

<sup>2</sup> Bundeswehr Aerospace Med. Flight Div., Air Force Office, Germany

### **Abstract**

In a previous study we have shown that subjects exposed to an increased gravitational load (hyper-G) produce exaggerated isometric forces (Sand et al. 2003). The present work expands these results to a three-dimensional workspace and examines the role of mechanical effects and of proprioceptive feedback.

Healthy volunteers were seated in a man-rated centrifuge and were exposed to resultant forces of 1.0 times (1G), 1.5 times (1.5G) and 3 times (3G) normal terrestrial gravity. Using an isometric joystick, subjects reproduced prescribed force vectors in one of eight directions and one of five magnitudes (5N to 25N). In two experiments, joystick orientation was such that forces were produced either orthogonally to (Sand et al. 2003), or in the plane of resultant acceleration.

Hyper-G had a significant effect on the magnitude of produced forces across all prescribed magnitudes and directions. In comparison to 1G, produced maximum forces were about 1.7N higher in 1.5G, and about 9.3N higher in 3G. This effect was not significantly higher for forces in vs. against the direction of hyper-G, and was already present 100 ms after response onset.

We conclude that excessive force production in hyper-G can not be explained by direct mechanical effects of hyper-G nor by faulty proprioceptive feedback, and is therefore most likely due to central mechanisms, e.g., to a contribution of descending vestibulospinal signals. The observed increased force production could affect the safe operation of high-performance aircraft.

This work was supported by the German Ministry of Defence, contract 1000-V-6703.

Responsibility for the contents rests with the authors.

**Deep brain stimulation of the subthalamic nucleus modulates gene expression and reverses limb use-asymmetry in rats with unilateral 6-hydroxydopamine lesions.**

Henning J.<sup>1</sup>, Koczan D.<sup>2</sup>, Rolfs A.<sup>1</sup>, Gimsa U.<sup>1</sup>

<sup>1</sup>Dept. of Neurology, <sup>2</sup>Inst. of Immunology, University of Rostock, Rostock, Germany

Deep brain stimulation (DBS) of the subthalamic nucleus (STN) is a powerful therapeutic strategy for basal ganglia diseases such as Parkinson's disease. Although widely used, little is known about the mechanisms at the molecular and cellular level. To elucidate those mechanisms, we investigated the effects of STN-DBS on gene expression and limb use-asymmetry in naive and 6-hydroxydopamine-lesioned (hemiparkinsonian) rats to analyze the specific transcripts after short-term stimulation. We implanted microelectrodes into the right STN of rats to analyze the gene expression and limb use-asymmetry after 3 hours (short term duration) of DBS (130 Hz, 60  $\mu$ s and 500 mA). Here we show that an *in vivo* stimulation of the rat STN for three hours induces the modulation of genes involved in several cellular functions (IGFBP2, IGF2, Sv2b, CaMK2a, TH and COMT) and the improvement of forelimb motor deficits. Thus, STN-DBS might be involved in dopamine metabolism, neuroprotection and calcium signal transduction. By extending the stimulation duration to 5 days, we are currently seeking information on putative reorganization processes in the basal ganglia of stimulated rats.

This work has been supported by the Bundesministerium für Bildung und Forschung (01 ZZ 0108).

## **Coherent oscillatory activity along the cortico-striatal axis of the rat in relation to different brain-states.**

Gerhard Engler, Christian KE Moll, Andreas K Engel

Institute of Neurophysiology and Pathophysiology, University Hospital Eppendorf,  
Martinistr. 52, 20246 Hamburg, Germany

Anatomically and physiologically, the cerebral cortex is tightly linked to the striatum, which is the head-end of cortico-basal ganglia circuits. However, the nature of cortico-striatal interactions is poorly understood. To assess the coupling between neuronal assemblies in the cerebral cortex and the striatum, we recorded single unit activity (SUA) and local field potentials (LFP) in healthy, halothane-anesthetized rats. To this end, we employed a bihemispherical multi-site approach with eight microelectrodes in the striatum together with simultaneous recordings of electro-corticographic activity (EcoG). EcoG served as the primary indicator of brain state. During halothane-anesthesia, cortical field potentials are generally dominated by oscillatory activity in the delta range (2-5 Hz). The fine structure of these delta-oscillations revealed an alternating pattern of two different activation states. Phases with a more irregular high-amplitude slow wave activity ("high-delta") were interrupted by episodes dominated by a regular, clockwork-like delta oscillation with low amplitude ("low-delta"). In addition to the spectral peak representing the slow wave activity, both cortical & striatal LFPs displayed a spectral peak in the upper gamma-frequency (range 45-75Hz). These high-frequency oscillations consistently showed a frequency-shift coinciding at the transition from high-delta to low-delta episodes. Spontaneous activity in cortex and striatum was significantly coherent in the delta-range during high-delta episodes, encompassing both hemispheres. Cortico-striatal coherence in the delta-frequency range was significantly lower during epochs of low- $\delta$ . Interestingly, beta-band-coherence (15-30 Hz) between cortex and striatum was low, while coherence in the upper gamma-band was significantly increased, irrespective of the prevailing cortical activation state. We found that during high-delta episodes, striatal single-unit-activity is synchronized even interhemispherically and shows a strong oscillatory modulation in the delta frequency range. In contrast to this, striatal spiking is desynchronized and tonical during low-delta epochs. Taken together, our results suggest that the cortex exerts a powerful influence on neuronal activity in the striatum. We propose that dynamical coupling and de-coupling of cortical and striatal neuronal assemblies is an important mechanism in the functional organization along the cortico-striatal axis.

### **Influence of extracellular potassium on the behavior of subthalamic neurons from 6-OHDA lesioned and non-lesioned rats under deep brain stimulation**

Fu-Wen Zhou<sup>1</sup>, Ulf Strauss<sup>1</sup>, Andreas Wree<sup>2</sup>, Reiner Benecke<sup>1</sup>, Arndt Rolfs<sup>1</sup>, Ulrike Gimsa<sup>1</sup>

<sup>1</sup> Neurobiological Laboratory, Dept. of Neurology; <sup>2</sup> Dept. of Anatomy, University of Rostock, Rostock, Germany

Increased output from the subthalamic nucleus (STN) is currently thought to play a critical role in the pathophysiology of Parkinson's disease. The firing behavior of rat STN neurons at different potassium ( $K^+$ ) concentrations was studied in *in vitro* slice preparations of adult Wistar rats with or without a unilateral 6-hydroxydopamine (6-OHDA) lesion of the median forebrain bundle. The majority of STN neurons of non-lesioned rats fired spontaneously in a regular or slightly irregular pattern. In lesioned rats, STN neurons from the ipsilateral hemisphere fired irregularly or even in bursts. No difference in the spike threshold was observed between lesioned and non-lesioned rats. In both lesioned and non-lesioned rats increased  $K^+$  concentrations led to an increase in the number of spontaneously firing neurons as well as in the action potential firing rates. This was associated with a decrease in the amplitude of fast AHP and both amplitude and duration of the slow AHP. A direct comparison of neurons from lesioned and non-lesioned rats revealed that in lesioned rats at 3.5, 5.0 and 12.5 mM extracellular  $K^+$  the number of spontaneously firing neurons and the firing rate ipsilateral to the lesion was increased. This was again associated with reduced fast and slow AHPs. No difference was observed in firing rates and among the groups at 1.5 mM extracellular  $K^+$ . Whether these findings are associated with an observed astrogliosis, remains to be elucidated. In summary, STN neuronal behavior ipsilateral to the lesion at physiological extracellular  $K^+$  and above resembles the effects of elevated  $K^+$  concentrations in non-lesioned rats. These data suggest that a disturbed potassium clearance from the extracellular space might contribute to an altered STN output. Deep brain stimulation (DBS) was performed *in vivo* for 3 hours using platinum/iridium electrodes before intracellular recording of STN neurons in slice preparations. DBS reversed lesion-associated STN hyperexcitability at all extracellular  $K^+$  concentrations.

This work has been supported by the Bundesministerium für Bildung und Forschung (01 ZZ 0108).

## Adaptive Optimal Control Methods Elucidate Sensorimotor Learning Phenomena

Daniel Braun<sup>1,2</sup>, Ad Aertsen<sup>2</sup>, Stefan Rotter<sup>2,3</sup>, Carsten Mehring<sup>1</sup>

<sup>1</sup> Neurobiology & Animal Physiology, Institute of Biology I, Albert-Ludwigs-University, Freiburg, Germany

<sup>2</sup> Neurobiology & Biophysics, Institute of Biology III, Albert-Ludwigs-University, Freiburg, Germany

<sup>3</sup> Theory & Data Analysis, Institute for Frontier Areas of Psychology and Mental Health, Freiburg, Germany  
correspondence: daniel.braun@biologie.uni-freiburg.de

Due to its explanatory power and theoretical perspicuity, optimal control theory has recently received vigorous attention in the field of biological motor control, as it allows to relate high-level goals of motor behaviour to limb mechanics and neural control [1][2]. One of the next steps is to use adaptive optimal control methods to explain motor learning phenomena as they occur in adaptation experiments. These have traditionally been interpreted in the context of the desired trajectory hypothesis.

Here we apply the optimal control framework to a sensorimotor adaptation experiment, where macaque monkeys had to learn a visuomotor rotation while neural signals were recorded from motor cortex area M1 [3]. When abruptly switching off the kinematic perturbation after the monkeys had adapted, Paz et al. found characteristic behavioural errors, termed *aftereffects*, that were interpreted as the consequence of the formation of an internal model.

Unfortunately, optimal control laws usually have to be computed backwards in time, which rules out a direct on-line performance. Under certain simplifying assumptions, however, a time-independent optimal policy can be iteratively approximated by employing reinforcement learning techniques, thus, allowing for on-line learning [4]. In an indirect reinforcement learning approach sensorimotor experience is used first to construct an internal model of the environment, which is subsequently exploited to improve the animal's policy. To this end, we introduced dual estimation methods that simultaneously estimate both states and model parameters, the latter being the weights of a biologically inspired radial basis function network that represents the presumptively learned internal model of the visuomotor transformation.

This adaptive optimal control model was able to reproduce the behavioural findings of the aforesaid study. Furthermore, as the aftereffect is a measure of spatial generalisation, the model allows predictions on the underlying basis function widths. These widths can be interpreted in terms of broadness of neural tuning curves and were fitted to match the generalisation function. However, the problem remained, that these tuning curves cannot be surely identified with tuning curves recorded in M1. Altogether, the conceptual generality of the approach should allow predictions for numerous motor learning paradigms, *inter alia* adaptation effects in force fields, and even permit statements on underlying neural phenomena by implementing appropriate biology oriented neural networks. One of the most interesting possible outcomes would be to anticipate an experimental design that could discern between optimal control and desired trajectory predictions.

## References

- [1] Todorov E, Jordan MI (2002) Optimal feedback control as a theory of motor coordination, *Nat. Neurosci.* 5:1226-1235
- [2] Scott SH (2004) Optimal feedback control and the neural basis of volitional motor control, *Nat. Neurosci.* 5:534-546
- [3] Paz R, Boraud T, Natan C, Bergman H, Vaadia E (2003) Preparatory activity in motor cortex reflects learning of local visuomotor skills, *Nat. Neurosci.* 6:882-890
- [4] Szita I, Lőrincz A (2004) Kalman filter control embedded into the reinforcement learning framework, *Neural Comp.* 16:491-499



**Poster Subject Area #PSA3:  
Rhythmogenesis and motor pattern generation**

- [#82A](#) W. Stein and CR. Smarandache, Ulm  
*Characterization of a sensory input that entrains a central pattern generator in the stomatogastric nervous system of the crab*
- [#83A](#) UBS. Hedrich, C. Eberle and W. Stein, Ulm  
*Nitric oxide indirectly controls the central pattern generators in the stomatogastric nervous system of the crab*
- [#84A](#) W-C. Li, SR. Soffe and A. Roberts, Bristol (UK)  
*The electrical properties of excitatory interneurons in a central pattern generator*
- [#85A](#) T. Bockemühl, V. Dürr and NF. Troje, Bielefeld and Ontario (CDN)  
*A small set of principal components can efficiently describe human arm movement*
- [#86A](#) T. Mentel, A. Krause and A. Büschges, Cologne  
*Generation of fin motoneuron activity during NMDA-induced fictive swimming in the isolated lamprey spinal cord*
- [#87A](#) JP. Gabriel and J. Schmidt, Cologne  
*Synaptic Drive to Leg Motoneurons During Walking Movements of the Stick Insect*
- [#81B](#) A. Borgmann, H. Scharstein and A. Büschges, Cologne  
*Intersegmental coordination of walking in the stick insect *Carausius morosus*: the influences of single walking legs on the motoneurons of the other hemisegments*
- [#82B](#) GBG. von Uckermann and A. Büschges, Cologne  
*NONSPIKING INTERNEURONS AND THE LOCAL CONTROL OF EXTENSOR TIBIAE MOTONEURON ACTIVITY DURING SINGLE LEG WALKING IN THE STICK INSECT*
- [#83B](#) S. Westmark, BC. Ludwar and J. Schmidt, Köln  
*Intersegmental Influence of Tonic and Phasic Modulation on Leg Motoneurons in Walking Stick Insects*
- [#84B](#) SM. Winter, J. Hirrlinger, F. Kirchhoff and S. Hülsmann, Göttingen  
*Regional differences of *Thy1.2* driven transgenic fluorescent protein expression in neurons of the medulla oblongata of mice*
- [#85B](#) M. Mörschel and M. Dutschmann, Göttingen  
*Influence of postnatal age on the expression of plasticity within the central pattern generator for breathing in rat.*

- [#86B](#) M. Mörschel, M. Kron, C. Gestreau and M. Dutschmann, Göttingen and Marseille (F)  
*Orexin B evoked modulation of respiratory activity in a in situ perfused brainstem preparation of rat*
- [#87B](#) S. Bar-Haim, N. Harries, A. Frank and J. Kaplanski, Zerifin (IL)  
*Dynamic Systems Perspectives in Treatment of Children with Cerebral Palsy*

## **Characterization of a sensory input that entrains a central pattern generator in the stomatogastric nervous system of the crab**

Wolfgang Stein & Carmen R. Smarandache

www.neurobiologie.de    wstein@neurobiologie.de    carmen@neurobiologie.de

Abteilung Neurobiologie, Universität Ulm

D-89069 Ulm, Germany

We are studying how sensory feedback selects distinct neural activity patterns from rhythmically active central pattern generators (CPGs). In the stomatogastric nervous system of the crab, *Cancer pagurus*, the CPGs of the pyloric (filtering food) and the gastric mill (chewing food) rhythms are strongly influenced by sensory feedback. The anterior gastric receptor (AGR; Combes, Meyrand, Simmers, J Neurosci 19, 1999) is a primary sensory neuron which responds to the power stroke of the gastric mill muscle gm1. We examined AGR *in vitro* with extra- and intracellular recordings to characterize its physiology and influence on both CPGs.

In all experiments, AGR was spontaneously active with low firing frequency (N=15). It showed postinhibitory rebound and a strong diminishment of spike amplitude with high firing frequencies. Independently of the firing frequency, we observed two classes of action potentials with different amplitudes. A comparison of intra- and extracellularly recorded spikes revealed that the action potentials of the two classes were generated at different spike initiation zones. In about 50% of our recordings, AGR spontaneously switched from tonic spiking to producing bursts of action potentials.

AGR activity affected both the gastric mill and the pyloric rhythm. For the latter, this was most obvious seen in the decrease of spike activity of several pyloric neurons. With an ongoing gastric mill rhythm, rhythmic AGR stimulation entrained this rhythm to faster or slower periods. The spike activities of the involved gastric mill neurons showed differences in their response to AGR stimulation: While the medial tooth protractor neurons GM fired stronger during AGR stimulation, the activity of the lateral tooth protractor neuron LG was weakened. The spike activity of the medial tooth retractor neuron DG was always terminated.

Most AGR actions were elicited indirectly via a change in the activity of descending projection neurons in the commissural ganglia: AGR activated the commissural projection neuron 2 (Norris, Coleman, Nusbaum, J Neurophysiol 72, 1994), which in turn monosynaptically excited the LG and GM neurons. Simultaneously, AGR inhibited the modulatory commissural neuron 1 (Nusbaum, Weimann, Golowasch, Marder, J Neurosci 12, 1992), which excites LG in a gastric mill rhythm. This reduction of excitation might explain the diminishment of LG spike activity during AGR stimulation. In addition, AGR weakly activated the modulatory commissural neuron 5 (Norris, Coleman, Nusbaum, J Neurophysiol 75, 1996), which inhibits those pyloric neurons that showed an attenuation of spike activity during AGR firing. When AGR's connection to the projection neurons was severed, it no longer affected the CPGs in the stomatogastric ganglion.

Currently, we are investigating the differential effects of AGR firing frequency on the activation and inhibition of projection neurons.

Supported by DFG STE 937/2-1.

## Nitric oxide indirectly controls the central pattern generators in the stomatogastric nervous system of the crab

Ulrike B. S. Hedrich, Christina C. Eberle & Wolfgang Stein

uli@neurobiologie.de tina@neurobiologie.de wstein@neurobiologie.de  
www.neurobiologie.de

Abteilung Neurobiologie, Universität Ulm  
D-89069 Ulm, Germany

The central pattern generators in the stomatogastric ganglion (STG) of the crab, *Cancer pagurus*, generate the rapid pyloric rhythm and the slow gastric mill rhythm. Neuromodulators released from descending projection neurons in the commissural ganglia (summary Nusbaum and Beenhakker, Nature 417, 2002) modulate the spontaneously active pyloric rhythm and activate the gastric mill rhythm. Both motor patterns are diminished or abolished when these descending inputs are blocked. In the present investigation, we studied the actions of the gaseous neurotransmitter nitric oxide (NO) on motor pattern generation and the activity of the descending projection neurons.

NO is used as a modulatory neurotransmitter which supports the partitioning of different, but related oscillatory networks (Scholz, de Vente, Truman, Graubard, J Neurosci 21, 2001). Here, we focused on the effects of NO on the pyloric and gastric mill rhythms and on its indirect effect on two projection neurons in the commissural ganglia, modulatory commissural neuron 1 (MCN1; Nusbaum, Weimann, Golowasch, Marder, J Neurosci 12, 1992) and commissural projection neuron 2 (CPN2; Norris, Coleman, Nusbaum, J Neurophysiol 72, 1994). We bath applied NO donors (L-Arginine, Hydroxylamine, SNP) and inhibitors of NO actions (L-Name, PTIO, ODQ) specifically to the STG, while all other parts of the stomatogastric nervous system were perfused with saline. Care was taken that no modulator was leaking from the STG perfusion well.

The spontaneously active **pyloric rhythm** sped up during bath application of the different NO donors. Surprisingly, bath application of the NO blockers also strengthened and sped up this rhythm.

While the pyloric rhythm was always spontaneously active (N=75 animals), the **gastric mill rhythm** was active in 44% (N=33) and inactive in 56% (N=42). In the latter case, NO donors usually elicited a gastric mill rhythm which was similar to the gastric mill rhythm that is elicited by the combined activity of the projection neurons MCN1 and CPN2. These neurons, however, are located in the commissural ganglia and thus had not been perfused with the donors. Nevertheless, the activity of MCN1 and CPN2 increased.

In preparations with a spontaneously active gastric mill rhythm, NO blockers always terminated this rhythm. The activity of both MCN1 and CPN2 mimicked the diminishment of gastric mill activity, indicating that also descending projection neurons in the commissural ganglia were affected.

Since only the STG was perfused with the NO reagents, an indirect ascending effect of NO on those projection neurons seemed likely. To test this hypothesis, we either elicited gastric mill rhythms with neuronal feedback from the STG to the projection neurons transected or we artificially sustained projection neuron activity while we bath applied NO blockers to the STG. In these experiments, blocking NO had either no or only a weak effect on the gastric mill rhythm, which indicates that the termination of the gastric mill rhythm had been caused by a diminishment of projection neuron activity.

Together, our results show that NO provides an ascending neuronal control of the descending projection neurons which in turn drive the gastric mill and pyloric central pattern generators. For the pyloric rhythm, this ascending feedback might explain the counterintuitive result that both, NO blockers and donors, sped up the rhythm. Direct and indirect NO effects seem to compete.

Currently, we are investigating the nature of the ascending neuronal pathway.

## The electrical properties of excitatory interneurons in a central pattern generator

W.-C. Li, S R Soffe and Alan Roberts

School of Biological Sciences, University of Bristol, Woodland Road, Bristol, BS8 1UG, U.K.

Wenchang.li@bristol.ac.uk

Intrinsic or conditional rhythmogenic properties of neurons may contribute to rhythm generation in many Central Pattern Generators in invertebrates and vertebrates. On the other hand, post-inhibitory rebound has also been proposed to be important when rhythm generation depends on network connections. The developing *Xenopus* tadpole spinal cord is capable of producing alternating motor activity underlying swimming. Two hypotheses based on the above mechanisms have been proposed to explain rhythm generation during swimming (Roberts and Tunstall, 1990; Dale, 1995). The critical difference between these hypotheses is whether CPG neurons can fire repetitively to sustained positive current injection.

We have recently identified interneurons with descending projecting axons (dINs) in the tadpole hindbrain and rostral spinal cord area that produce excitatory drive to the spinal swimming circuit. In this study, we used in situ whole-cell recording techniques in combination with neurobiotin labelling to measure the electrical properties of this group of interneurons. We concentrated on those neurons firing reliable spikes during fictive swimming which made excitatory connections to other CPG neurons in paired recordings. dINs had less negative resting membrane potentials than other spinal neurons ( $n=35$ ). Their responses to current injection were linear around the resting membrane potential. Input resistances measured from I-V curves were  $317 \pm 112 \text{ M}\Omega$  (range 208-612  $\text{M}\Omega$ ,  $n=19$ ). Firing thresholds of  $-27 \pm 3.9 \text{ mV}$  ( $n=16$ ) were estimated as the most positive response to current injection without firing. When the current injection reached firing threshold, most dINs only fired one spike ( $n=27/32$  neurons) at the onset of current injection even when the current was increased 1.3 - 6 times above the threshold ( $n=17$ ). dIN spikes were also wider than other types of CPG neurons in the tadpole spinal cord. dINs didn't fire rebound spikes after negative current injection when the membrane potential was at rest. However, when the membrane potential was depolarised above firing threshold, reliable rebound firing was observed ( $n=19$ ). The rebound spike heights increased with the amplitude of the negative current pulse, implying removal of inactivation of sodium channels.

Dale (1995) proposed that the shunt conductance introduced by sharp electrodes could make CPG neurons less excitable as all CPG neurons fired repetitively when recorded with whole-cell patch electrodes (Aiken et al., 2003). When dual electrode, simultaneous recordings were made from single CPG neurons in situ (Li et al., 2004) this was shown not to be the case. Here, we show that a type of interneuron which is critical to the tadpole swimming CPG typically fires only once to positive current injection but is capable of rebound firing. All the data point to post-inhibitory rebound playing an important role in rhythm generation during tadpole swimming.

Aiken SP, Kuenzi FM, Dale N (2003) *Xenopus* embryonic spinal neurons recorded in situ with patch-clamp electrodes--conditional oscillators after all? *Eur J Neurosci* 18:333-343.

Dale N (1995) Experimentally derived model for the locomotor pattern generator in the *Xenopus* embryo. *J Physiol* 489 (Pt2):489-510.

Li WC, Soffe SR, Roberts A (2004) A direct comparison of whole cell patch and sharp electrodes by simultaneous recording from single spinal neurons in frog tadpoles. *J Neurophysiol* 92:380-386.

Roberts A, Tunstall MJ (1990) Mutual Re-excitation with Post-Inhibitory Rebound: A Simulation Study on the Mechanisms for Locomotor Rhythm Generation in the Spinal Cord of *Xenopus* Embryos. *Eur J Neurosci* 2:11-23.

**A small set of principal components can efficiently describe human arm movement**

Till Bockemühl and Volker Dürr, Dept. of Biol. Cybernetics, Univ. of Bielefeld, PO Box 10 01 31, 33501 Bielefeld, Germany.

Nikolaus F. Troje, Department of Psychology, Queens University Kingston, Ontario, K7L 3N6, Canada

Email addresses: {till.bockemuehl,volker.duerr}@uni-bielefeld.de, niko@psyc.queensu.ca

One of the central questions in the study of motor control is how the central nervous systems (CNS) deals with redundant degrees of freedom (DOFs) inherent in musculoskeletal systems. The human upper limb, consisting of arm and hand, is a prime example for such a system. In everyday situations it exhibits a vast variety of motor behavior and plays a key role in almost every aspect of our lives while comprising more DOFs than would be necessary for successful reaching movements in three dimensional space. On the one hand these additional DOFs enhance the dexterity of the human arm. On the other hand they complicate the computations the CNS has to perform in order to move the arm, making additional constraints necessary.

In this study we analyzed the movement patterns performed by nine different subjects in a catching paradigm. Subjects were instructed to catch an approaching pinpong ball with their right arm starting from two different initial postures. Using a shooting device the ball was launched onto 16 different trajectories traversing the workspace of the arm. Subjects were free to catch the ball at a convenient point on its flight path. Only succesful catches were evaluated. This setup offers a series of advantages: The average subject can easily and intuitively execute the movements required for the task without the need for extensive training. Movements are very fast (between 400 and 1000 ms) thereby reducing the potential influence of deliberate control on the part of the subject. Futhermore the observed movements occur naturally, are unconstrained and cover a large portion of the arm's workspace.

Utilizing an optical motion capture system (VICON Systems) we recorded approximately 250 single movements per subject. Cartesian marker coordinates were transformed into time courses of 10 different joint angles by use of a kinematic model. Thus, we can describe every movement by a time series of postures which, in turn, can be unambiguously be formulated in terms of 10 dimensional vectors. In our analysis these vectors are the base for principal components analysis (PCA).

We applied PCA to average sets of angular time courses of each one of the 32 combinations of start posture and catching position. Though our kinematic model comprises 10 DOFs only 2 principal components (PCs) account mostly for more than 90% of the variance in the observed movements. This indicates a tight coupling between the joints involved in the movement. When we compared PCs belonging to movements leading to different catching positions, we found that PCs of nearby catching positions are more similar than those of catching positions farther apart. PCs thereby seem to vary smoothly across the workspace which might allow for easy transformation from one PC into another. When pooling all movements executed by a single subject, including only one start position, still only 3 PCs are required to capture 85 - 90% of the observed variance.

The basic joint angle space is 10 dimensional. PCA however indicates that the observed movements occupy a low dimensional subspace of the basic joint angle space. Based on this fact we used a reduced set of 3 PCs to reconstruct the time courses of all of the 10 joint angles for some representative movements. Most of the angular time courses were reconstructed with high accuracy. Those who lacked high accuracy still bore good resemblance to the original data and were always within physiological limits. Impossible postures never occurred.

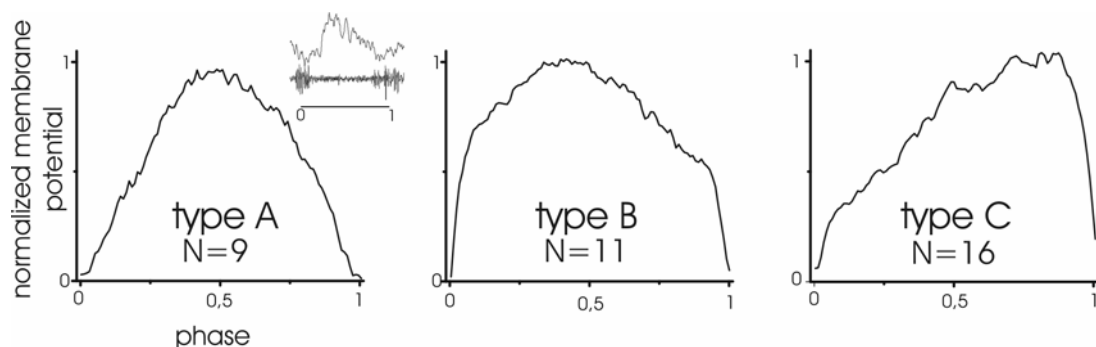
Based on these findings we hypothesize that flexible and variable behavior like multijointed human arm movement does not necessarily require complex neural algorithms. Instead we show that catching movements within the entire workspace can be generated efficiently by linear combinations of a small set of basic movements and simple task-dependent modulations thereof.

## Generation of fin motoneuron activity during NMDA-induced *fictive swimming* in the isolated lamprey spinal cord

Tim Mentel, Alexander Krause and Ansgar Büschges

Zoologisches Institut der Universität zu Köln, Weyertal 119, 50923 Cologne, Germany

Almost all forms of locomotion, including crawling, walking, swimming and flight, are rhythmic motor outputs generated in part by central pattern generator neural networks. These neuronal commands are executed by effector organs, in the case of a swimming lamprey by trunk muscles, that contract in an alternating fashion to produce undulating movement. The spinal cord of the lamprey, a lower vertebrate, contains in the region of the dorsal fins two different kinds of motoneurons. One group, the myotomal motoneurons, innervate the trunk muscles and the second group, the fin motoneurons (fMN), innervate a thin layer of muscle fibers at the basis of the dorsal fins. During “fictive swimming” evoked by perfusion of the isolated spinal cord with 150  $\mu$ M NMDA, all fin motoneurons are active in antiphase to the myotomal motoneurons of the ipsilateral hemicord. How are the activities of these two sets of motoneurons coordinated? We combined intracellular recordings and various spinal cord lesions in order to (i) analyze the activity pattern of fin MNs in detail and (ii) investigate the source of their synaptic inputs. During “fictive locomotion” fMNs exhibit three patterns of membrane potential oscillation. These are defined by the time course of the excitatory and inhibitory drive to these neurons compared to the myotomal burst cycle of the ipsilateral ventral root:



FMNs have two morphological types (Shupliakov et al. 1992 *J.Comp.Neurol.*321:112). The type A modulation is found only in type1 fMN which only branch ipsilaterally, whereas type 2 fMNs, which cross the midline of the spinal cord, show membrane potential oscillations of Type A and B. Preliminary data suggest that type C membrane potential oscillations correlate with a third fMN morphological type, which shows a sickle-like shape and whose dendrites sometimes cross the midline. Lesioning the spinal cord along the midline did not affect the basic rhythmic modulation of the membrane potential in the swimming cycle of any motoneuron type, but peak-to-peak amplitude in modulation significantly decreased by about 30%. The same result was observed when the lesion was extended one segment further caudally and rostrally, indicating that hemisegmental ipsilateral synaptic inputs are responsible for the different modulation patterns.

Supported by DFG grant Bu857/7.

## Synaptic Drive to Leg Motoneurons During Walking Movements of the Stick Insect

Gabriel, J.P.\* and Schmidt, J.

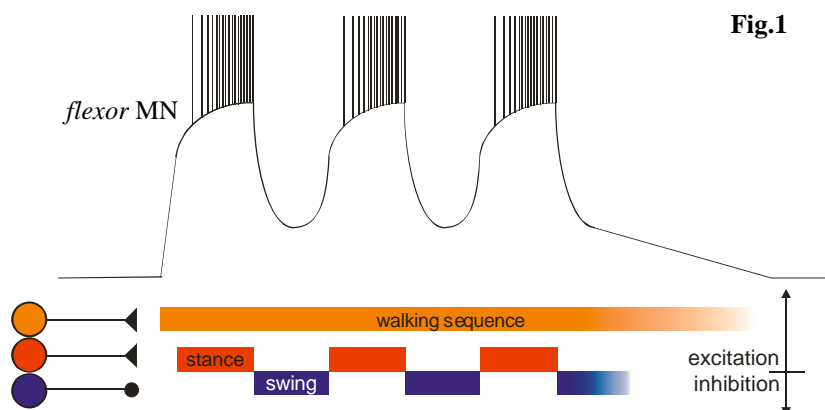
Institute of Zoology, University of Cologne, Weyertal 119, 50923 Köln, Germany

\*Jens.Gabriel@uni-koeln.de

The activity of motoneurons (MNs) during insect walking is determined by central pattern generator (CPG) networks, local sensory signals and coordinating signals from other segments. In stick insects, a number of preparations have been used in the past to investigate the nature of synaptic drive from these sources to leg MNs. In the single middle leg preparation that excludes influence from sense organs on the other legs (Fischer et al. 2001, *J Neurophys* **85**:341), evidence for alternating phasic depolarizing and hyperpolarizing inputs during the two different phases of the stepping cycle was found (Schmidt et al. 2001, *J Neurophys* **85**:354). During rhythmic activity of leg MNs in deafferented animals, a tonic depolarization paired with phasic hyperpolarization was observed (Büschges 1998, *Brain Res* **783**:262; Büschges et al. 2004, *Eur J Neurosci* **19**:1856). We used the single leg preparation (in which afferent input is present and the leg is performing walking movements on a treadmill) to analyze the role of the tonic depolarization and the synaptic drive from CPG networks and local sensory signals to leg MNs during walking movements.

Intracellular recordings of MNs of the major mesothoracic leg muscles (*pro-/retractor coxae*, *levator/depressor trochanteris* and *flexor/extensor tibiae*) revealed a tonic depolarization throughout the stepping cycle as well as an overlying phasic modulation related to the activity of the respective muscle and its antagonist. During injection of constant de- or hyperpolarizing current, the amplitude of the tonic depolarization de- and increased respectively while the amplitude of the phasic modulation remained rather constant. When the MN was hyperpolarized beyond the reversal potential of the inhibition, it reversed sign and could be observed as a depolarization. Together, our results imply a phasic excitation and inhibition during an underlying tonic depolarization (**Fig.1**). In case of the *flexor* MNs, the tonic excitation appears to be independent of local sensory signals (see poster by Westmark & Schmidt), while the phasic excitation correlates with stepping parameters such as treadmill friction and step velocity.

Also, mechanical stimulation of the load-sensitive femoral campaniform sensilla caused a depolarization of *flexor* MNs, suggesting that the phasic excitation derives from local sense organs. In contrast, the amplitude of the phasic inhibition is stereotypic and inert to variations in step parameters, which would be consistent with a centrally generated inhibition.





## Intersegmental coordination of walking in the stick insect *Carausius morosus*: the influences of single walking legs on the motoneurons of the other hemisegments

Anke Borgmann, Hans Scharstein, Ansgar Büschges; Institute of Zoology, University of Cologne, Weyertal 119, 50923 Cologne, Germany, aborgman@smail.uni-koeln.de

Proper leg coordination is required for functional locomotion. Presently, six behavioral rules are known that coordinate neighbouring legs of the stick insect (Cruse, 1990; Dürr et al., 2004) with all six rules being active between ipsilateral neighbours. Although detailed information is available on the action of those rules behaviorally, relatively little specific is known about the neural mechanisms and pathways underlying this coordination. This is partially due to the fact that there are few organisms in which the distinction between sender and receiver action of a particular segment with respect to coordination can be experimentally determined. In the stick insect *C. morosus* we can achieve this goal by analyzing the influences of one or two semi-intact walking legs on the activity of motoneuron pools in the neighboring hemisegments of the ipsilateral side under conditions in which sensory signals from the segment of interest are not present. We used a semi-intact preparation (cf. Fischer et al., 2001) with either one or two intact legs walking on one or two treadmills, respectively. All other legs were amputated at the mid-coxa level and the ganglion of the segment of interest was de-afferented. While the animal walked with either one or two intact legs on the treadmill, motoneurons innervating the protractor (ProMN) and the retractor (RetMN) coxae muscles were recorded extracellularly in that ipsilateral hemisegment.

- (i) *One single leg walking*: Single front leg walking was accompanied by alternating activity in ProMNs and RetMNs of the ipsilateral mesothoracic segment that was correlated to the stepping cycle of the front leg and was superimposed on a tonically increased activity in both MN pools. In ipsilateral metathoracic ProMNs and RetMNs stepping of the front leg induced only an uncorrelated increase of activity that outlasted the stepping sequence. Stepping activity of a single middle leg did not evoke an alternating activity pattern in ProMNs and RetMNs of either the pro- or the metathorax but instead only an uncorrelated increase of activity was observed. In contrast, when a single hind leg expressed backward walking, alternating activity in the ipsilateral ProMNs and RetMNs of the mesothoracic ganglion was observed in about 50% of the experiments, resembling the influence of the front leg on the mesothoracic segment in forward walking. These data suggest that only a functional "front leg" (i.e. defined relative to the direction of movement of the entire animal) provides a phasic influence on its functional posterior neighbour.
- (ii) *Two single legs walking*: Walking of both front and ipsilateral middle leg induced alternating activity in the ipsilateral ProMNs and ReMNs of the metathoracic ganglion. This was also true for the activity in ProMNs and ReMNs of the mesothoracic ganglion when both front and ipsilateral hind leg were stepping.

The present results indicate (i) that only the functional front leg has a phasic influence on MN activity in the neighboring ipsilateral segments and (ii) that walking of two legs on one side is required to elicit alternating activity in the MNs of the third ipsilateral hemisegment. We will now begin to investigate the influence of both middle and ipsilateral hind leg stepping on the activity of ipsilateral ProMNs and ReMNs of the prothoracic segment.

### References:

Dürr V., Schmitz J., Cruse H. (2004). Behaviour-based modelling of hexapod locomotion: linking biology and technical application *Athropod Structure and Development* 33: 287-300

Cruse, Holk (1990). What mechanisms coordinate leg movement in walking arthropods? *TINS* Vol. 13, No.1 S.15-21

Fischer H., Schmidt J., Haas R. und Büschges A. (2001). Pattern generation for walking and searching movements of a stick insect leg I. Coordination of motor activity *J. Neurophysiol.* 85: 341-353

Supported by DFG BÜ 857/6-3

## **NONSPIKING INTERNEURONS AND THE LOCAL CONTROL OF EXTENSOR TIBIAE MOTONEURON ACTIVITY DURING SINGLE LEG WALKING IN THE STICK INSECT**

Géraldine B. G. von Uckermann, Ansgar Büschges

Dept. of Animal Physiol., Zool. Inst., Univ. of Cologne, 50923 Cologne

gvuckerm@smail.uni-koeln.de

The motor output for walking of an insect leg results from an interaction of descending commands, intersegmental coordinating pathways and local premotor networks, with the latter ones encompassing sensori-motor pathways controlling the magnitude of motor output as well as central pattern generating networks driving the motoneuron pools of the leg joints (for review see Bässler & Büschges, 1998). A recent investigation has shown that tibial motoneuron activity during stepping is generated by a tonic depolarization on top of which phasic excitation and inhibition alternate (see poster by Gabriel and Schmidt). We were interested in how identified premotor nonspiking interneurons contribute to the synaptic drive onto tibial motoneurons during single-leg stepping of the stick insect middle leg.

To answer this question local premotor nonspiking interneurons (NSIs) in the mesothoracic ganglion were recorded in the *single-middle leg preparation* of the stick insect (Fischer et al., 2001). By amputation of all legs except one and reducing the walking system to an isolated single middle leg walking on a treadband the coordinating influence from the other legs were excluded. To monitor postsynaptic motoneuron activity the extensor tibiae motoneurons were recorded extracellularly in lateral nerve nl3.

All NSIs showed rhythmic membrane potential oscillations during middle leg stepping. In some interneurons (e.g. E4, E5/6, E8, I4) we observed a tonic shift in membrane potential indicating that these contribute to the tonic drive occurring in leg motoneurons during stepping. The phasic modulation of their membrane potential during walking showed a marked variability between different types of interneurons. Nearly all of them (e.g. E1, E5/6, E8, I1, I2, I4, I8) showed an inversion of polarisation from one half of the step cycle to the other. In relation to the activity of the tibial motoneurons the modulation in membrane potential during walking fell into two groups, with the one for which modulation in membrane potential corresponded to their drive onto motoneurons (e.g. E4, E8, I1, I2, I8) and a second for which it did not (e.g. E1, E2/3, E5/6, I4). Our results indicate that generation of locomotor activity in tibial motoneurons during single-leg stepping is organized in a distributed fashion, thereby closely resembling the situation in posture control (Büschges et al., 2000) and in six-legged walking (Wolf & Büschges, 1995).

Supported by DFG grant Bu857/8.

## Intersegmental Influence of Tonic and Phasic Modulation on Leg Motoneurons in Walking Stick Insects

S. Westmark\*, B. Ch. Ludwar, J. Schmidt

Institute of Zoology, University of Cologne, Weyertal 119, 50923 Köln, Germany

\*S.Westmark@uni-koeln.de

Locomotion of legged animals is based on the coordination of both, the joints of individual legs and the different legs. The movements of leg joints are based on the rhythmic activity of motoneurons (MNs) which is generated and coordinated by local neural networks. Physiological and morphological properties of the local networks are well known (e.g. Bässler & Büschges 1998, *Brain Res. Rev.* 27:65; Akay et al. 2004, *J. Neurophysiol.* 92:42), much less is known about the neural basis of inter-leg coordination. Intracellular recordings in semi-intact walking preparations showed a correlation of front leg walking and membrane potential modulation in ipsilateral mesothoracic MNs. Two modulation patterns have been found: a tonic shift of the membrane potential during a stepping sequence and a phasic pattern coupled to individual steps (Ludwar et al., *in prep.*). In this study we compare the activity pattern of mesothoracic flexor tibiae MNs that are ipsi- and contralateral to the single walking front leg.

A semi-intact preparation of the stick insect (*Cuniculina impigra*) was used in which all but a prothoracic leg were amputated at the level of mid-coxa. The front leg was walking on a treadmill while the activity of ipsi- or contralateral mesothoracic flexor tibiae MNs was recorded intracellularly from the deafferented ganglion.

The mean resting potential recorded in mesothoracic flexor tibiae MNs was  $-57 \pm 5$  mV. Starting from this potential, ipsilateral flexor tibiae MNs showed a tonic depolarization of about 5 mV ( $n=12$ ,  $N=5$ ) during a stepping sequence of the front leg. A similar tonic depolarization was also observed on the contralateral side, however, less pronounced ( $1.6 \pm 0.6$  mV;  $n=14$ ,  $N=11$ ). The tonic depolarization was accompanied by a decrease in input resistance by about 13 % for ipsilateral, and by 10 % for contralateral flexor tibiae MNs.

With regard to the phasic discharge pattern, ipsilateral flexor tibiae MNs depolarized 0.1 s before onset of front leg stance phase ( $N=5$ ) and reached a peak of up to 6 mV after the end of stance phase. For 39 % of contralateral flexor tibiae MNs ( $N=26$ ) a similar phasic discharge pattern could be observed. In 15 % of flexor tibiae MNs the phasic pattern showed a variable modulation of hyper- and depolarization. No phasic coupling was detected in 46 % of contralateral flexor tibiae MNs.

In conclusion, it appears that the tonic depolarization of mesothoracic flexor tibiae MNs during walking of a single front leg is indicative for arousal associated with motor activity. In contrast, the phasic modulation indicates a rather specific coupling of motoneuron activity to intersegmental signals (see also poster by Gabriel & Schmidt). The handling of these signals appears to be different in both mesothoracic hemi-segments.

Supported by the DFG Bu857/2, Schm1084/2-1

## **Regional differences of Thy1.2 driven transgenic fluorescent protein expression in neurons of the medulla oblongata of mice**

Stefan M. Winter<sup>1</sup>, J. Hirrlinger<sup>2,3</sup>, F. Kirchhoff<sup>2,3</sup>, S. Hülsmann<sup>1,3</sup>

<sup>1</sup>Abt. Neuro- und Sinnesphysiologie, Zentrum Physiologie und Pathophysiologie, Georg-August-Universität, Humboldtallee 23, 37073 Göttingen, Germany

<sup>2</sup>Dept. of Neurogenetics, Max Planck Institute of Experimental Medicine, Hermann-Rein-Str. 3, 37075 Göttingen, Germany

<sup>3</sup>DFG Research Center Molecular Physiology of the Brain, Göttingen, Germany

The medulla oblongata contains different neuron populations for the control of vital functions, which includes the cardiovascular center as well as the respiratory network. In addition, nuclei, which provide the control of central reflexes and sensory input, as well as cranial motor nuclei are located within this brainstem region. To visualize the complex organization and cellular heterogeneity in this vital part of the brain, we analyzed a series of transgenic mouse lines with cytoplasmic expression of modified fluorescent proteins from jellyfish or reef corals at postnatal day 15. Two mouse lines were analyzed in more detail. (1) In the first mouse line, neurons with strong Thy1.2 promotor-induced expression of the red fluorescent protein HcRed1 were identified in the lateral reticular nucleus, the spinal trigeminal tract and in the hypoglossal nucleus, while almost no neuron was labeled in the nucleus ambiguus and in the nuclei of the solitari tract. In the ventral respiratory group, we observed weakly labeled isolated neurons by epifluorescence and confocal laser-scanning microscopy. (2) Similar expression patterns were found in mice with Thy1.2 promoter-driven EYFP expression. In this line, however, considerably more neurons of the ventral respiratory group expressed EYFP although at a low level. Neurons with weak EYFP expression were also found in the nuclei of the solitari tract.

Taken together these transgenic mouse lines are an excellent tool to study both the structure as well as functional aspects of neurons in the medulla oblongata. By crossbreeding the TgN(Thy1.2-HcRed)-mice with mice, expressing the green fluorescent protein EGFP under the control of the human GFAP-promotor TgN(hGFAP-EGFP) we will be able to get insights into functional neuron-glia interaction.

This work was supported by the Deutsche Forschungsgemeinschaft through the DFG Research Center for Molecular Physiology of the Brain.

**Influence of postnatal age on the expression of plasticity within the central pattern generator for breathing in rat.** Mörschel M, Dutschmann M; *Dept. of Physiology, University of Göttingen, Humboldtallee 23, 37073 Göttingen*

The central respiratory pattern generator is permanently overwhelmed by afferent sensory information and commands from “higher” brain centres to adapt breathing to changes in behaviour or environment. For these short and long term adaptations of breathing the respiratory network has to be permissive for synaptic plasticity. Recent work from our group suggested that certain forms of plasticity (habituation sensitisation) in response to afferent stimulation is absent or suppressed in the neonatal respiratory network (*Dutschmann et al. 2004, Resp. Physiol. Neurobiol. in press*). In the present study we investigated the influence of postnatal age on the expression of two different forms of plasticity described for respiratory control.

For experiments we used the perfused brainstem preparation allowing for investigation of complex network function *in situ*. To study long term facilitation (LTF) of phrenic (PNA) and hypoglossal (XII) nerve activity following intermittent hypoxia, we injected NaCN (0.015%) via an external perfusor to the perfusion circuit to stimulate peripheral chemoreceptors. The duration of the injection ranged from 30s-1min and was repeated 3-5 times every 2min. During the NaCN injection we observed a stimulus dependent increase of PNA and XII amplitude and burst frequency which recovered 10-15 s after stimulus off-switch. 10-15 min after the repetitive stimulations we observed a stimulus independent augmentation of PNA and XII amplitude and burst frequency reflecting the phenomena of long term facilitation of both motor outputs. Analysis of 3 groups at different postnatal ages revealed that LTF of PNA and XII could be evoked in 6/8 (P5-9), 7/8 (P10-15) and in 6/6 preparation (P20-24), suggesting that this activity independent plasticity following intermittent hypoxia might be present at all maturational stages. In a second set of experiments we investigated plasticity related to fictive feedback from pulmonary stretch receptors (PSR). The PSR have a crucial role in the afferent evoked inspiratory off-switch (IOS) during the vital transition between inspiration and expiration. To evoke fictive feedback from PSR, we repetitively stimulated the cervical vagal nerve with stimulus trains (200-300ms, 20Hz, 0.5-2mA) applied at 1Hz for a minute at 2 min intervals. With the repetition of stimulus trails (n=10) the PNA entrained to the external rhythm. During early trails the entrainment was exclusively mediated via afferent termination of inspiratory phase. In later trails (e.g. trail 7-10) the IOS was mediated via an intrinsic network mechanism and the inspiratory phase was terminated before onset of the stimulus trains. We called this phenomenon network synchronisation reflecting a complex form of Hebbian learning. Studies on the influence of postnatal age (P5-8, n=, P10-15 n=, P20-24 n=) on this complex form of plasticity revealed that neonates never showed synchronisation of network activity to the vagal stimulation until P15.

We conclude that during postnatal development the respiratory network gets progressively permissive for activity dependent plasticity required for complex behavioural challenges. The late stage in maturation when the network becomes permissive for certain forms of plasticity potentially parallels the increasing repertoire of behavioural performance of rats. In contrast, at early postnatal stages the respiratory pattern generator is already permissive for compensatory and therefore vital forms of plasticity like long term adaptation of breathing to intermittent hypoxia. (*supported by DFG SFB 406/C12*)

**Orexin B evoked modulation of respiratory activity in a *in situ* perfused brainstem preparation of rat.** Mörschel M, Kron M, Gestreau C\*, Dutschmann M; *Dept. of Physiology, University of Göttingen, Humboldtallee 23, 37073 Göttingen, \*Physiologie Neurovegetative, Université Paul Cézanne, Aix-Marseille III, 13397 Marseille cedex 20.*

Orexin a neuropeptide selectively expressed in the lateral hypothalamus has implications in neuronal control of arousal (e.g. sleep-wake cycle) and nutrition. It was demonstrated that lack of orexin expression is associated with the clinical picture of narcolepsy. Beside severe disturbance of the arousal system narcoleptic patients are reported for a high prevalence of obstructive sleep apnoea, suggesting a potential role for orexin in respiratory control. However, the specific effects of orexin on respiratory activity and upper airway patency are still undefined. In the present study we investigated: (I) the distribution of orexin-receptor 2 (OX-R2) in the respiratory network of rat and (II) the effects on breathing following local microinjections of orexin B into selected brainstem nuclei.

Immunohistochemical analysis of the expression pattern of OX-R2 in ponto-medullary nuclei revealed potential targets for orexinergic modulation of respiratory functions. Dense punctiform labelling for OX-R2 was present in the ventrolateral aspect of the rostral medulla, a cluster of staining overlapped with the boundaries of the rostral ventral respiratory group, including the preBötzinger complex. Furthermore, we found heavy staining in pontine aspects of the respiratory network including the A5 and Kölliker-Fuse nucleus (KF). In the nucleus tractus solitarius (NTS) we could confirm the recently described labelling in medial, dorsomedial, interstitial, and ventrolateral subdivisions. Additionally less pronounced labelling was detected in the caudal respiratory group and in a central chemosensitive area (para pyramidal nucleus). Staining for OX-R2 was also found in several nuclei belonging to the brainstem arousal systems including the dorsal tegmental nuclei, dorsal parvocellular reticular formation, raphe nuclei and the sub-coeruleus region. Physiological experiments were performed in a *in situ* working heart brainstem preparation (WHBP). To monitor cardio-respiratory activity we recorded ECG and phrenic and hypoglossal nerve activity (PNA, XII). We could demonstrate effects of orexin B (10 $\mu$ M in ACSF) when microinjected (40-80nl) into the KF (n=7) or VRG (n=4) or NTS (n=7). Microinjections into the pontine KF area consistently increased frequency of phrenic and XII motor outputs (20 to 60%), but we never observed any cardiovascular response. In the VRG orexin B caused a mild increase in frequency of PNA and XII (20-30%). In 3 cases the respiratory response was associated with a sustained bradycardia (decrease in heart rate 40-70%). Injections into the NTS or more ventral hypoglossal motor nucleus did not consistently evoke respiratory responses.

We conclude that OX-R2 receptors are expressed within the central pattern generator for breathing (e.g. KF and VRG) as well as in the NTS. Orexin B appeared to have a general excitatory effect on respiratory frequency but not in particular on upper airway patency. *(supported by a research grant of the UKG)*

## Dynamic Systems Perspectives in Treatment of Children with Cerebral Palsy

S. Bar-Haim, N. Harries, A. Frank, J. Kaplanski

Faculty of Health Science, Ben-Gurion University of the Negev, Beer-Sheva, Israel

Motion Analysis Laboratory, Assaf-Harofeh Medical Center, Zerifin, Israel

Clinicians and basic researchers of movement disorders have recently begun to incorporate non-linear dynamics in this field. The dynamical systems perspectives have introduced new ways to address longstanding questions about the organization of motor functions in typical and atypical motor behaviors. The purpose of the study was to utilize and examine a novel approach in the treatment of children with Cerebral Palsy (CP). We used random stimuli (RS) as a control variable to break pathological motor patterns and force instability of the motor control system, thus enabling the motor controller to carry out new, more efficient motor functions. A theoretical framework of biomechanical functions has been used to analyze kinematic data observed in cycling in healthy and neurologically impaired individuals, with the conclusion that a similar motor control strategy might be operational in both walking and cycling.

The testing procedure incorporated active and passive cycling on a specialized device, and analysis of the data, based on recurrence plots. The cycling device and analyses were capable of discriminating the velocity features and variability of the cycling motor task among 23 normally developed (ND) children and 24 with CP. Ten children with CP received two one-month courses of intensive physiotherapy (one conventional and the second including RS) separated by a 10-month interval. The cycling motor performance of ND children was characterized by the ability to adapt to passive cycling at an early age. Kurtosis values of the distribution of angular velocities demonstrated both transient and stable phases in the improvement of active cycling in ND children. Initial lower velocity and high kurtosis values during active cycling in CP children indicated a tendency to recurrent behavior characterized by a stable attractor. Following RS treatment the CP group attained lower kurtosis values during active cycling and higher values during passive cycling that matched ND levels. Their overall motor functions, as expressed by the GMFM-66 improved significantly. RS treatment appeared to assist the children with CP to a transiently unstable stage, which is a necessary phase for improving motor function. The results can contribute to improved treatment and new diagnostic instruments for movement disorders.

**Poster Subject Area #PSA4:**  
**Audition, vibration and communication in invertebrates**

- [#88A](#) M. Hartbauer, S. Kratzer, K. Steiner and H. Römer, Graz (A)  
*The intrinsic calling rate as the major determinant for the leader role in a synchronous interaction between males of the bushcricket *Mecopoda elongata**
- [#89A](#) E. Ofner, H. Römer and J. Rheinlaender, Graz (A)  
*Spatial Orientation in a bushcricket (*Leptophyes punctatissima*): I. Phonotaxis on a walking compensator at different stimulus elevations*
- [#90A](#) K. Kostarakos, J. Rheinlaender and H. Römer, Graz (A)  
*Spatial Orientation in a bushcricket (*Leptophyes punctatissima*): II. Correlated binaural neuronal activity*
- [#91A](#) I. Fertschai, J. Stradner and H. Römer, Graz (A)  
*Female choice for leaders in synchronous song interactions of a bushcricket (*Mecopoda elongata*): why should followers call at all?*
- [#92A](#) A. Stumpner and R. Lakes-Harlan, Göttingen and Gießen  
*Carrier frequency discrimination in the parasitoid fly *Homotrixa alleni*.*
- [#93A](#) B. Hedwig and JFA. Poulet, Cambridge (UK)  
*Auditory Pattern Recognition Gates Steering Responses in Cricket Phonotaxis*
- [#94A](#) M. Weber, M. Kössl, W. Volknandt and E-A. Seyfarth, Frankfurt/Main  
*Acetylcholine is a transmitter candidate in sensory neurons of the bushcricket ear (*Mecopoda elongata*)*
- [#95A](#) A. Wolf, T. Gollisch, J. Benda and AVM. Herz, Berlin  
*Identification of mechanosensory transduction mechanisms in the Locust auditory system*
- [#88B](#) F. Creutzig, J. Benda and AVM. Herz, Berlin  
*Burst Encoding in the Metathoracic Ganglion of Grasshoppers*
- [#89B](#) D. Neuhofer, M. Stemmler and B. Ronacher, Berlin  
*The influence of noisy signal envelopes on song pattern recognition - a comparison between the behavioral and neuronal level*
- [#90B](#) S. Wohlgemuth and B. Ronacher, Berlin  
*Temporal resolution and processing capacities of auditory interneurons of the locust*
- [#91B](#) S. Glauser, M. Hennig, AVM. Herz and J. Benda, Berlin  
*Spike latency and the neural connectivity in the auditory pathway of locust*



- [#92B](#) L. Schwabe, K. Obermayer and M. Hennig, Berlin  
*Changes of the intensity-response curve of an auditory interneuron (AN2) in crickets induced by adapting sound stimuli*
- [#93B](#) L. Schwabe, A. Angelucci, P. Bressloff and K. Obermayer, Berlin and Salt Lake City (USA)  
*A recurrent network model of surround-suppression in the macaque striate cortex mediated by inter-areal and intra-areal interactions*
- [#94B](#) L. Schwabe and K. Obermayer, Berlin  
*Perceptual learning and attention explained as a dynamic re-calibration of the visual system at different time-scales*
- [#95B](#) KJ. Hildebrandt and RM. Hennig, Berlin  
*Neural Representation and Filtering of Simple Temporal Patterns in the Lower Auditory Pathway of Crickets*

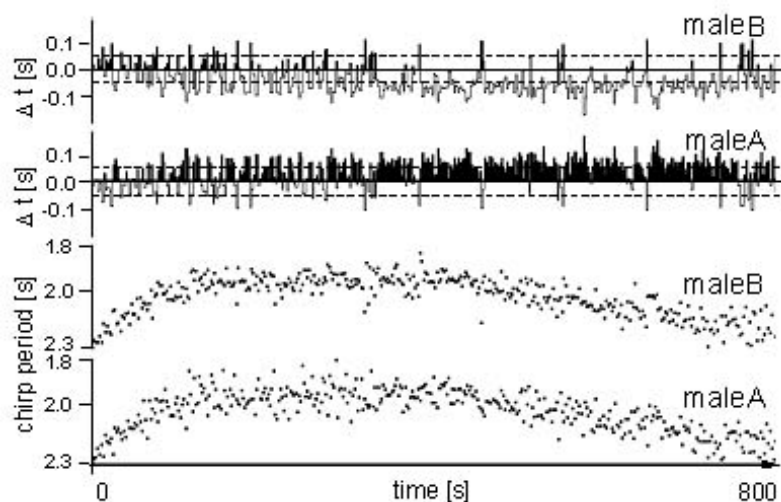
## The intrinsic calling rate as the major determinant for the leader role in a synchronous interaction between males of the bushcricket *Mecopoda elongata*

Hartbauer, M.<sup>1)</sup>, Kratzer, S., Steiner K. and Römer H.<sup>1)</sup>

<sup>1)</sup>Department for Neurobiology & Behaviour, Institute for Zoology, Karl-Franzens-University, Graz, Austria

Duetting males of the bushcricket *Mecopoda elongata* synchronize or alternate their chirps with neighbouring males in an aggregation. Since synchrony is imperfect, leader and follower chirps are established in song interactions; females prefer leader chirps in phonotactic trials. Using playback experiments with real males and computer simulations of song oscillator interactions we investigated the underlying mechanisms responsible for synchrony and alternation.

Results show that a major predictor for the leader role of a male is its intrinsic chirp period, which varies in a population from 1.6 to 2.3s. Faster singing males establish the leader role more often than males with longer chirp periods. Individual differences between song oscillators, characterised by their phase response curves obtained at 3 different stimulus intensities, will rather affect the type of acoustic interaction (synchrony or alternation) than chirp timing. Real male duets and simulation results have shown that as soon as the intrinsic chirp periods of two individuals differ by more than 150 ms the faster male will lead the chirps of his rival more often (see figure). The phase response curve of the song oscillators is different from other rhythmically calling or flashing insects, in that only the disturbed cycle is influenced in duration by a stimulus. This results in sustained leader- or follower chirps of one male, when the intrinsic chirp periods of two males differ by 150 ms or more. There seems to be no active mechanism which allows individual males to take over the leader role. The outcome of a male interaction is therefore mainly dependent on the difference between their intrinsic chirp periods.



Synchronous chirp timing in a song interaction between two males with differing intrinsic chirp periods (male B 1.98s; male A 2.17s). Male B was the leader more frequently with a  $\Delta t$  of more than 50 ms. Further, only 34 % of all chirps in the middle part of the interaction showed a  $\Delta t$  of less than  $\pm 50$  ms (dashed lines).

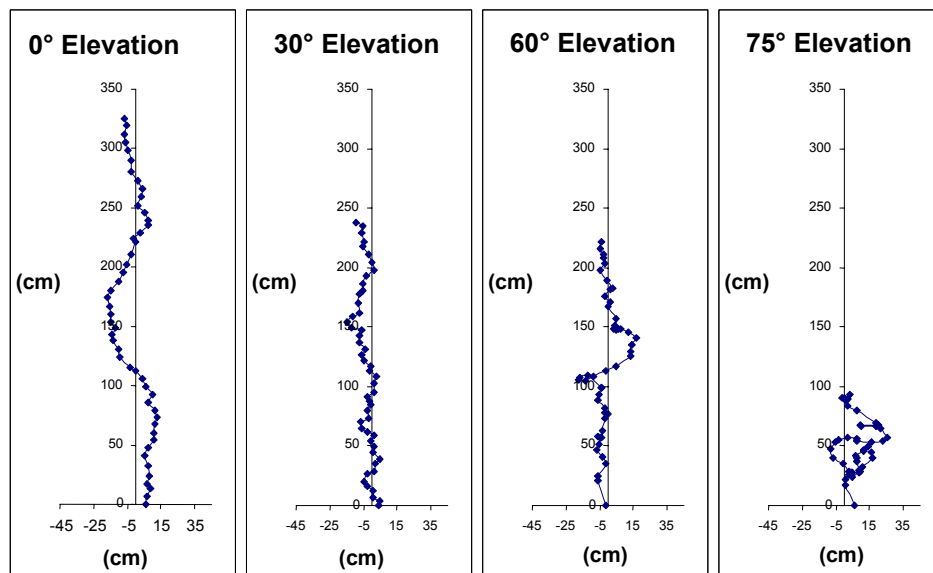
## Spatial Orientation in a bushcricket (*Leptophyes punctatissima*): I. Phonotaxis on a walking compensator at different stimulus elevations

Ofner, E.<sup>1)</sup>, Römer, H.<sup>1)</sup> and Rheinlaender J.

<sup>1)</sup>Department for Neurobiology, Institute for Zoology, Karl-Franzens-University, Graz, Austria

Directional hearing in insects has been studied in the horizontal plane to some extent, with respect to behaviour, neurophysiological mechanisms and biophysics. However, many insects live in a complex, three-dimensional habitat; hence for mate finding and orientation there is also a need for directional hearing in azimuth and elevation. Here we used the phonotactic behaviour of male bushcricket *Leptophyes punctatissima* (Phaneropterinae), who perform a duetting acoustic communication with females, to study three-dimensional hearing.

Male *L. punctatissima* were placed on a walking compensator, and after each call were offered a synthetic female reply (duration 1ms) from one of 5 frontal speakers placed at elevations of 0°, 30°, 60°, 75°, and 90°. In response to the female call males turn to the sound source, walk a few seconds and then chirp again. The phonotactic approaches of males were compensated with a walking compensator to keep them at the same distance to the speakers. With increasing elevation of the sound source (and thus decreasing directional cues) the males meandered more, the correlation between stimulus angle and turn angle decreased, and turns to the wrong side increased. Still most males performed phonotaxis with a high acuity up to 60° elevation. Individuals varied strongly in their performance especially at a sound elevation of 75°, where some were still very accurate in their approach whereas the acuity of others decreased rapidly (figure).



Phonotactic approach of a male *L. punctatissima* to synthetic female calls broadcast from elevated loudspeakers (line). Each dot indicates a male chirp and hence a synthetic female reply to which the male orients. The speakers are located in prolongation to the y-axis.

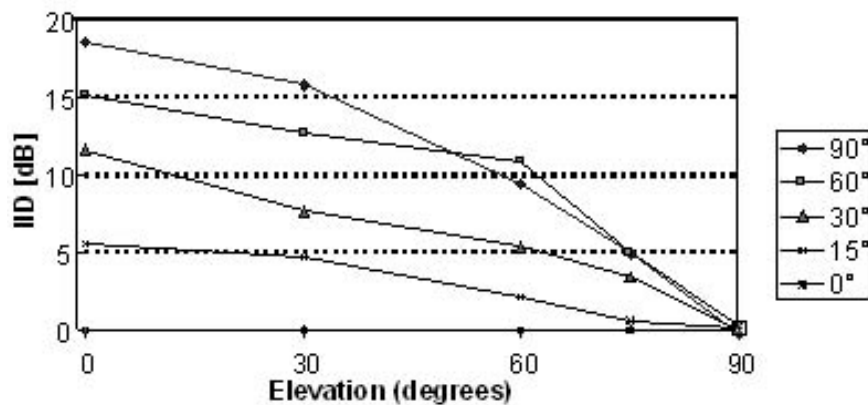
## Spatial Orientation in a bushcricket (*Leptophyes punctatissima*): II. Correlated binaural neuronal activity

Kostarakos K.<sup>1)</sup>, Rheinlaender, J. and Römer, H.<sup>1)</sup>

<sup>1)</sup>Department for Neurobiology & Behaviour, Institute for Zoology, Karl-Franzens-University, Graz, Austria

Male bushcricket *Leptophyes punctatissima* (Phaneropterinae) reliably approach duetting females phonotactically even in a complex three-dimensional space (Rheinlaender and Römer, unpublished), and on a walking belt the accuracy of phonotaxis decreases with more elevated sound sources. Here we examined the peripheral and central nervous mechanisms underlying the remarkable three-dimensional orientation.

First, we analysed the change in interaural intensity differences (IIDs) with variation of the sound source in azimuth and elevation, by using the variation in the threshold of an auditory interneuron (T-fibre) in a monaural preparation. At any position in the azimuth IIDs decrease systematically with increasing elevation of the sound source (figure). For example, with lateral stimulation at 90° IID decreases from 18 dB to 5 dB with source elevation from 0° to 75°, whereas with more frontal positions of 15° off the longitudinal axis IID decreases from about 5 to less than 1 dB. By recording the discharge of both T-fibres simultaneously in an intact preparation we also examined the resulting binaural discharge differences available for the insect at varying source elevations. Consistent with the peripheral data, such differences also decrease systematically with increasing source elevation. Also, some preparations exhibited asymmetrical binaural responses, in that the point of symmetrical discharge between left and right interneuron was shifted by 30° or more to one side.



Variation in interaural intensity differences (IIDs) with different elevations of the sound source in the bushcricket *L. punctatissima*.

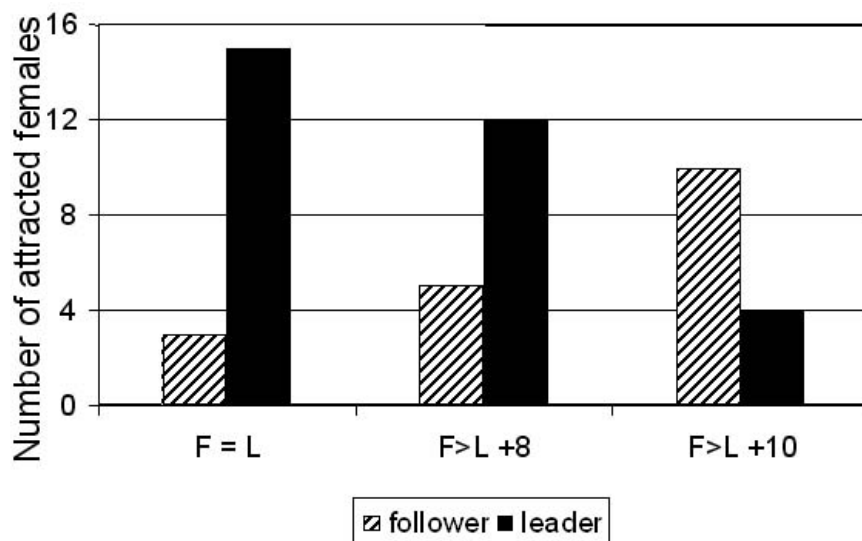
## Female choice for leaders in synchronous song interactions of a bushcricket (*Mecopoda elongata*): why should followers call at all?

Fertschai, I., Stradner, J. and Römer H.

Department for Neurobiology & Behaviour, Institute for Zoology, Karl-Franzens-University, Graz, Austria

Imperfect synchrony between male calls occurs widely in acoustically courting bushcrickets. In a choice situation female *Mecopoda elongata* prefer males with calls leading in time, and therefore it is unclear why males with follower calls should call at all. Nonetheless follower males interact acoustically with leaders for long periods of time. It has been suggested that at the proximate level female preference can be explained by the asymmetrical representation of leader and follower signals within the CNS of female receivers, which was confirmed in neurophysiological experiments (1). The results also predicted that a temporal advantage of the leader could be compensated by an increased loudness of the follower. In a series of neurophysiological time-intensity trading experiments we determined the excess intensity of the follower signal for a given time delay between both signals, necessary to achieve equal representation in female receivers. For example, an additional 9 dB was necessary for a time delay of 140 ms of the follower signal.

Subsequent behavioural female choice experiments strongly support these results (see figure). The preference for leading males within a choice situation was reduced, when the amplitude of the follower was increased by 8dB SPL, and turned into a preference for the follower with an increase in loudness of 10 dB, precisely corroborating the neurophysiological results. Thus, males producing follower signals may also attract females, if they manage to produce louder signals or call from sites in the habitat which provide an increased active space of the signal.



Preference of female *Mecopoda elongata* for leader and follower signals (time delay 140ms) at equal intensity, and with an intensity advantage of the follower of 8 and 10 dB.

(1) Römer et al. (2002) Eur. J. Neurosci. 15:1655-1662

## Carrier frequency discrimination in the parasitoid fly *Homotrixa alleni*.

Andreas Stumpner<sup>1</sup>, Reinhard Lakes-Harlan<sup>2</sup>

<sup>1</sup>Institut für Zoologie, Abt. Neurobiologie, Berliner Str. 28, D-37073 Göttingen

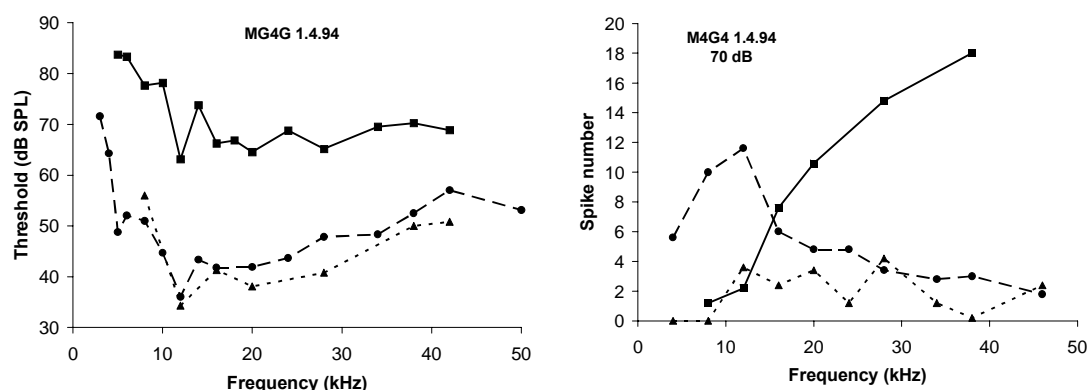
<sup>2</sup>Institut für Tierphysiologie, Wartweg 95, D-35392 Gießen

Within the tachinid flies some species have evolved a hearing organ at the prosternum of the thorax (D Robert et al., Science 258: 1135, 1992; R Lakes-Harlan, K-G Heller, Naturwiss. 79: 224, 1992). Females of these species use the ear to locate specific orthopteran hosts for their larvae. Here we investigate the ear of *Homotrixa alleni*, a parasitoid of some Australian orthopterans. Its main host is *Sciarasaga quadrata* which has an unusually low frequency spectrum peaking around 5kHz.

The ear is located ventrally at the prothorax. The scolopidial sensory organ consist of more than 200 sensory cells, which can be separated in two groups. The majority of cells is situated more peripherally, while a few large cells have scolopidia pointing apically. The sensory cells are characterised anatomically as single unit scolopidia and the axons project into the thoracic neuromeres. The ear is sexually dimorphic, with females having larger and more sensitive ears. The adaptation of the ear to its host's song spectrum has been investigated at first with a laser vibrometer. The tympanal membrane vibrates within a broad frequency spectrum, peaking from 8 to 20kHz, therefore not being specifically adapted to the 5 kHz peak of the host's calling song.

We furthermore performed anatomical and physiological studies of the central neuronal network. Ascending neurones, some of which were identified individually, show clear dependence of their responses to different frequencies, indicating the ability of frequency discrimination also in behaviour. Interestingly, the overall frequency tuning (threshold) was not very different between neurons, while differences in their response strength to different frequencies at stimuli above threshold were quite obvious. The neuron types included: (i) broadly tuned, sensitive neurons, with highest sensitivity between 10 and 15 kHz and a threshold below 40 dB SPL. Intensity dependences at different frequencies are similar. (ii) More or less broadly tuned neurones, which respond strongest to certain frequency ranges (see figures below): around 8 to 12 kHz, above 15 up to 50 kHz, above ca. 30 kHz. (iii) Broadly tuned, but relatively insensitive neurones with thresholds above 60 dB SPL.

These different neuron types were encountered in the same individual (as is shown in the figure). (iv) Some neurons show a strongest response at 5kHz (the peak frequency of the calling song of the host, therefore they may be "host detector neurones"). Responses to higher frequencies were much weaker.



Figures: Frequency tuning (left) and response at 70 dB SPL (right) of three neurons recorded in one female *Homotrixa alleni*. Note the a) similarity in tuning, b) differences in sensitivity and c) differences in response strength at a given intensity above threshold.

## **Auditory Pattern Recognition Gates Steering Responses in Cricket Phonotaxis**

***B. Hedwig & J.F.A. Poulet***

Department of Zoology / Cambridge CB2 3EJ / bh202@cam.ac.uk / jfap2@cam.ac.uk

Male crickets produce species-specific calling songs for mate attraction. Females use the acoustic cues and walk and orient towards singing males. To analyse the interaction of pattern recognition and steering, phonotaxis in *G. bimaculatus* was analysed with a fast and highly sensitive trackball system, which resolves walking at the level of the tripod stepping pattern (Nature 2004, 340:781-785).

Pattern recognition in *G. bimaculatus* is tuned to sound pulses of 15 ms duration repeated at intervals of 20 ms. However, even sound pulses/intervals of other durations evoke minute auditory steering responses when presented on their own. If these "non-effective" sound patterns are interspersed with the optimal test pattern, the animals change their behaviour. They now also steer strongly towards these "non-effective" patterns. Even when exposed to split-song paradigms with alternating representation of sound pulses from the left and right side, the animals will rapidly steer towards each sound pulse. This demonstrates that the auditory processing underlying steering is not selective for temporal patterns. Rather the recognition process gates the steering response. Gating is maximal 2 sec after song onset and decays within 5 sec after the end of a song. Thus once pattern recognition is activated, the complex acoustic orientation emerges from steering responses towards individual sound pulses. (Supported by BBSRC).

## ACETYLCHOLINE IS A TRANSMITTER CANDIDATE IN SENSORY NEURONS OF THE BUSHCRICKET EAR (*MECOPODA ELONGATA*)

Melanie Weber<sup>1</sup>, Manfred Kössl<sup>1</sup>, Walter Volknandt<sup>2</sup> and Ernst-August Seyfarth<sup>1</sup>

<sup>1</sup>Zoologisches Institut, Universität, Siesmayerstrasse 70, D-60054 Frankfurt am Main, Germany

<sup>2</sup>Biozentrum, Universität, Marie-Curie-Strasse 9, D-60439 Frankfurt am Main, Germany

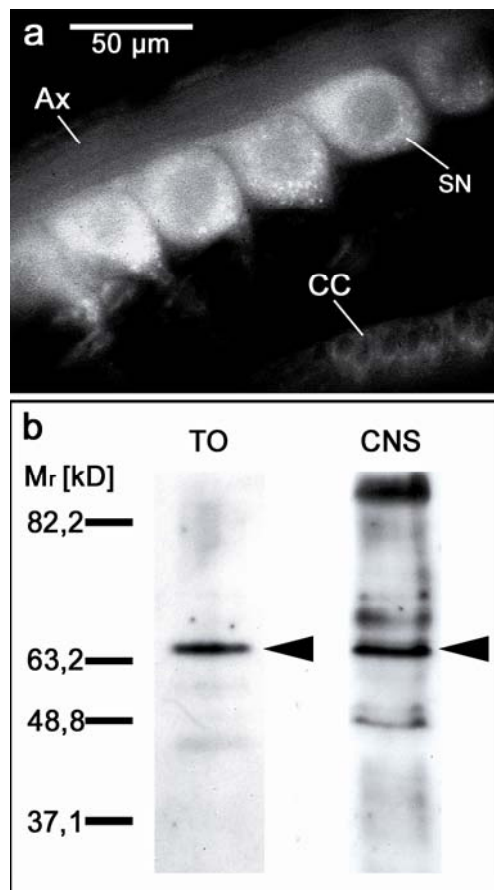
The neuroactive substances occurring in the auditory afferents of the tympanal organs of bushcrickets and locusts are unknown. Based on studies of other mechanoreceptors in insects and other arthropods (e.g., Lutz & Tyrer, J Comp Neurol 267, 1988; Fabian & Seyfarth, Cell Tissue Res 287, 1997) the most likely afferent transmitter candidate is acetylcholine (ACh). Here we have used histochemical and immunocytochemical techniques to search for neuroactive substances and transmitter candidates in identifiable sensory neurons of the tympanal organ of bushcrickets, *Mecopoda elongata* (Orthoptera, Phaneropterinae).

The auditory organ of *M. elongata* is part of a mechanosensory (chordotonal) organ complex situated in the tibia of each foreleg. It consists of ca. 45 bipolar sensory neurons (average soma diameter ranging from 22 to 33  $\mu$ m) that are linearly arranged in the form of a *crista acoustica*.

**1) VACHT:** A polyclonal antibody (Chemicon Inc.) against mammalian vesicular ACh-transporter protein (VACHT) strongly and uniformly labeled the sensory neurons (somata, dendrites and axons) in the crista acoustica, while accessory structures such as cap cells and scolopidia remained unstained (18 preparations; **Fig. 1**).

**2) AChE:** Histochemical staining for acetylcholine esterase (AChE) revealed enzyme activities that varied in the sensory neurons along the crista acoustica (19 preparations). These variations suggest a potential correlation between AChE-activities and a tonotopic organization of the auditory organ. Application of eserine (5 mM) blocked all AChE- activity.

**3) Peripheral synapses:** Immunolabeling with a monoclonal antibody against *Drosophila*-synapsin (SYNORF1; Klagges et al., J Neurosci 16, 1996) demonstrated single, fine varicose fibers (with putative synaptic terminals) in the vicinity of the chordotonal organ, but there was no evidence of peripheral contacts directly at the sensory neurons themselves.



The presence of VACHT and AChE implicates ACh as the primary afferent transmitter candidate in the sensory cells of the crista acoustica. Our results do not rule out the possibility that the sensory neurons contain additional (co-) transmitter substances such as histamine -- which has been found in mechanoreceptors of other arthropods (Buchner et al., Cell Tissue Res 273, 1993; Fabian & Seyfarth, Cell Tissue Res 287, 1997).

[We thank Heiner Römer and Reinhard Lakes-Harlan for advice and for providing us with bushcrickets.]

**Fig. 1.** (a) Immunofluorescent labeling of sensory neurons in the tympanal organ of *M. elongata* with an antibody against VACHT. Ax: axons SN: sensory neuron CC: cap cell. (b) VACHT-like immunolabeling in pooled samples from tympanal organs (TO) and from *Mecopoda*-CNS (CNS) as revealed by Western blot analysis. Note the labeled band at 65 kDa (arrowheads) corresponding to the molecular mass of *Drosophila*-VACHT (Kitamoto et al., J Biol Chem 273, 1998). Molecular size markers (Gibco) are shown on the left.



# Identification of mechanosensory transduction mechanisms in the Locust auditory system

*Alexander Wolf, Tim Gollisch, Jan Benda & Andreas V.M. Herz*

*Humboldt-Universität zu Berlin, FachInstitut Theoretische Biologie, 10115 Berlin, Germany*

In the Locust auditory system the transduction of an acoustic signal into the response of a receptor neuron consists of several distinct steps: at first, pressure fluctuations are translated into mechanical movement of a membrane (the tympanum), which is coupled via attachment cells to the ion-channels of the neuron. The flow of ions causes a change of the cell's potential, and eventually triggers an action potential.

Due to the fragility of auditory organs, it is very difficult to access the processing properties of the system directly. However, we recently showed that it is possible to extract detailed information about the transduction steps with microsecond resolution from the spikes recorded in the receptor's axon. We found that a LNLN-cascade, containing two linear (L) and two static nonlinear (N) steps, describes the transduction process. The oscillating membrane is modeled as a linear filter, whose vibrations are coupled nonlinearly via a mechano-sensory mechanism to ionic channels in the receptor membrane. These channels control the flow of ions that build up a membrane potential (the second linear filter), which then can lead to a generation of a spike (second nonlinearity).

The last nonlinear step of the cascade can be circumvented by using stimuli that evoke always the same response (Iso-Response-Method), measured as the receptor's firing rate or spike probability. The mechano-sensory nonlinearity was found to be quadratic which led to the conclusion that the energy of the signal is the decisive parameter for transduction (Gollisch *et al.*, 2002). Knowing the nonlinear steps of the cascade, it was then possible to derive the two linear filters. The properties of the filter describing the tympanum correspond well to the data acquired by measuring the oscillations of the tympanum directly. From the second filter we were able to determine the very fast integration time constant of the neuron (less than one millisecond), which reflects the auditory system's demand for high temporal resolution.

Here we examine the mechanosensory transduction in more detail: What possible mechanism gives rise to the quadratic nonlinearity, or is the square only an approximation of a more complicated process? From investigations of other animals, different mechano-sensory models have been suggested. For instance in mammalian ears, hair cells do not transmit the vibration of the ear drum symmetrically, but rather have a preferred direction. The probability for opening the ion channels follows a Boltzmann distribution (Hudspeth *et al.*, 2000).

In order to answer these questions, we simulated different nonlinear functions, implemented into the transduction chain. That way we investigated, how well different nonlinearities could be distinguished from one another within the framework of the Iso-Response-Method. We found that by means of the reconstructed filters, one can distinguish between a cascade that rectifies the signal as part of the first nonlinearity, and a cascade where the signal is transmitted symmetrically (simple square). However, this method is unable to tell apart two different symmetric nonlinearities.

## References:

- Gollisch, T., Schütze, H., Benda, J., and Herz, A. V. M. (2002). Energy Integration Describes Sound-Intensity coding in an Insect Auditory System. *J Neurosci.*, 22(23):10434-48. 85(4):1782-7.
- Hudspeth, A. J., Choe, Y., Mehta, A. D., and Martin, P. (2000). Putting ion channels to work: Mechano-electrical transduction, adaptation, and amplification by hair cells. *Proc Natl Acad Sci U S A*, 24;97(22):11765-72.

# Burst Encoding in the Metathoracic Ganglion of Grasshoppers

*Felix Creutzig, Jan Benda, Andreas V.M. Herz*

*Humboldt-Universität zu Berlin, FachInstitut Theoretische Biologie, 10115 Berlin, Germany*

The relevance of bursts for information transmission in sensory systems has been intensively discussed(1). In particular, bursts may increase the reliability of information transmission at synapses. Every burst may act as a „unit of information” (2) such that the response of the down-stream neuron is independent of the spike count within the burst. Bursts can also be involved in the detection of behaviorally relevant events. In weakly electric fish, for example, a stimulus can be recovered accurately from primary afferent spike trains. The performance of down-stream pyramidal neurons in encoding stimulus time courses is significantly worse than in receptor cells. However, these pyramidal cells are specialized in upstrokes, respectively downstrokes of electric field amplitudes and indicate these specific events by firing bursts(3). Grasshoppers of the group Acrididae rely on species-specific song recognition(4). These songs consist of alternating syllables and pauses. For positive behavioral response, the length of syllables and pauses may vary, but the ratio between both should be kept relatively constant. The metathoracic ganglion of the grasshopper pre-processes incoming information from the receptor cells and forwards the information content to the insect’s brain. One particular neuron - the so-called AN12 neuron - is known for marking the onset of syllables in mating songs with bursts(5) and thus takes an important part in rapid pattern processing.

We have investigated the role of bursting in AN12 in auditory information encoding. We find that the spike count within a burst characterizes naturally occurring mating songs: Each syllable evokes a burst with reproducible spike count. Hence, the sequence of consecutive spike counts within bursts is unique for each song and can be used to discriminate between different songs. This raises the question what feature of a syllable is encoded in the spike count per burst. Analysis of the burst triggered average, the average stimulus preceding each burst, reveals that the spike count corresponds both to the pause length between succeeding syllables and to a lower extent on the absolute sound amplitude at syllable onset. This suggests, first, that the spike count within bursts might be relevant for encoding: burst can be more than just a unit of information; second, that the spike count of bursts could be read out by downstream-neurons; third, the result is interesting as the encoding scheme of the pause length might be important for the behavioral response.

The dependence of spike count within bursts on both the amplitude of syllable onset and the preceding pause length indicates that adaptation in up-stream neurons and AN12 itself may be responsible for the phasic response. We check this hypothesis by simple integrate & fire models.

## References:

1. Krahe, R, Gabbiani, F (2004) Burst firing in sensory systems. *Nat. Rev. Neurosci.* 5, 13-24
2. Lisman, JE (1997) Burst as a unit of neural information: making unreliable synapses reliable. *Trends Neurosci.* 20, 38-43
3. Metzner, W, Koch, C, Wessel, R, Gabbiani, F (1998) Feature extraction by burst-like spike patterns in multiple sensory maps. *J. Neurosci.* 18, 2283-2300
4. Stumpner, A, von Helversen, D (2001) Evolution and function of auditory systems in insects. *Naturwissenschaften* 88, 159-170
5. Stumpner, A, Ronacher, B (1991) Auditory interneurons in the metathoracic ganglion of the grasshopper *Chorthippus biguttulus*. I. Morphological and physiological characterization. *J. Exp. Biol.* 158, 391-410

*Supported by Boehringer Ingelheim Fonds*

## **The influence of noisy signal envelopes on song pattern recognition –a comparison between the behavioral and neuronal level**

Daniela Neuhofer, Martin Stemmler, Bernhard Ronacher  
Institute of Biology, Humboldt University Berlin

In the grasshopper species *Chorthippus biguttulus*, it is the male that initiates mating by producing a species- and sex-specific song that consists of syllables alternating with noisy pauses. If a female recognizes this song and is inclined to mate, it produces a response song that allows the phonotactic approach of the male. The first step of this phonotaxis is a characteristic turning movement, which is shown exclusively and with high reliability to the female's signal. As such, the turning movement is a good indicator that the male has correctly identified a song as stemming from a conspecific female.

The recognition of species and sex is primarily based on the characteristic pattern of the song's amplitude modulations, also termed the signal envelope. The information needed for song recognition lies in the envelope shape in the time domain (von Helversen & von Helversen 1998, Biol Cybern 79: 467). In the field, classifying signals becomes more difficult as environmental noise acts on the signal during transmission from the sender to the receiver. We tested how stochastic modifications of the song envelope affect the recognition of the signals. As stimuli we used a female song model whose envelope was progressively degraded with broadband noise (3 different cut off frequencies of the modulating noise were used: 75 Hz, 200 Hz, 1000 Hz; noise levels were varied in 3 dB steps). The play-back experiments were performed (at 30°C) with *Chorthippus biguttulus* males in a sound attenuated room. A male was positioned on a cloth covered table. Whenever it started to sing it was answered by a computer-generated model song via a laterally situated loudspeaker. Signals with different levels of envelope noise were presented in pseudo-random order; we recorded the number of times the males made turns towards the loudspeaker as a function of the noise level. This procedure allowed us to determine the noise level at which recognition fails. The males' behaviour was fairly resistant to perturbation by noise, although the tests showed that the frequency bandwidth of the noise did have a profound effect on recognition. Low frequency noise (75Hz cut-off) had the least influence on song pattern recognition. Adding 200 Hz noise led to a 1.5-dB smaller noise tolerance, while the 1000-Hz noise most strongly interfered with recognition (a further reduction of 4.5 dB compared to the 200-Hz noise).

These behavioral data can now be compared to the results of the electrophysiological experiments performed on identified neurons within the metathoracic ganglion of locusts. Using the same stimuli as used in the behavioural experiments, we analyse the changes in the neuronal response that are caused by increasing levels of envelope noise. The differences between the spike trains in response to the original female song and to the spike trains from noisy songs are quantified by using the metric introduced by van Rossum (2001). This allows for a quantitative comparison of the noise levels tolerated by the nervous system as a whole (behaviour) and the changes in the spike responses of identified neurons induced by the same degraded stimuli (electrophysiology). We hope to derive an estimate of the precision with which the nervous system evaluates spike trains.

## Temporal resolution and processing capacities of auditory interneurons of the locust

Sandra Wohlgemuth, Bernhard Ronacher  
Institute of Biology, Humboldt-University Berlin, D 10099 Berlin

Many species of acridid grasshoppers use acoustic signals to identify and localize potential mates. The basic information for the recognition of the species-specific signal is conveyed in their characteristic pattern of amplitude modulations (von Helversen & von Helversen 1997; *J Comp Physiol A* 180: 373-386; Gerhardt & Huber: *Acoustic communication in insects and anurans*, Univ Chicago Press 2002). Hence, for the auditory pathway of these animals it is of prime importance to detect and process the amplitude fluctuations of sound signals, in order to be able to decide whether a signal stems from a potential mate – that is, a conspecific of the appropriate sex – from a heterospecific or even a predator.

Acoustic signals are generally characterized by fast changes in amplitudes, which poses great demands on the temporal processing capacities of the auditory pathway. We therefore investigated the temporal resolution and filter characteristics of second order and third order auditory interneurons in the metathoracic ganglion of the locust. The animals were stimulated with sinusoidally amplitude modulated noise stimuli of different frequencies and modulation depths while recording intracellularly from identified local or ascending interneurons. Modulations transfer functions were determined on the basis of the average spike rate (r-MTF) or on the basis of the vector strength of the spike locking to the stimulus envelope (t-MTF). From the t-MTF's high frequency cut-off the minimum integration times (MIT) could be calculated, which represent an upper limit for a neuron's temporal resolution (see Prinz & Ronacher 2002, *J Comp Physiol A* 188: 577-587). A total of 27 cells was investigated, belonging to 3 types of local interneurons, and 5 types of ascending neurons.

The t-MTFs of local neurons showed low-pass or band-pass characteristics, with cut-off frequencies of up to 200 Hz. Minimum integration times (MIT) were significantly smaller in these local neurons compared to the ascending third order neurons ( $1.04 \pm 0.29$  ms,  $N=11$  vs.  $2.49 \pm 0.96$  ms,  $N=16$ ). However, the MIT of local neurons were in the same range as those found in sensory neurons by Prinz & Ronacher 2002 ( $0.95 \pm 0.33$  ms). The t-MTFs of ascending neurons were also of the low-pass or band-pass type, their cut-off frequencies, however, were shifted to lower frequencies (mean value 73 Hz, maximum 127 Hz).

The r-MTFs of sensory neurons exhibited all-pass characteristics. All-pass behaviour was also found in some local neurons, while others showed a low-pass behaviour or transitions to a band-pass. Among ascending neurons low-pass and band-stop filter types were found.

This study yields data on how the auditory neurons of a grasshopper represent the pattern of amplitude modulations of acoustic signals in their spike responses, and on the upper limits of temporal resolution. These informations can now be compared with the specific features of the communication signals used by different grasshopper species.

## Spike latency and the neural connectivity in the auditory pathway of locusts

S. Glauser, R. M. Hennig, A. V. M. Herz, J. Benda

Institute for Theoretical Biology, Computational Neuroscience  
Group, Humboldt-Universität zu Berlin, Germany

In the auditory system of locusts, input from receptor cells is processed by local interneurons, and ascending neurons pass the information on to higher stages of processing. To understand how the neural circuitry extracts relevant acoustic information, it is of great importance to know the pattern the connectivity of this first stage of auditory signal analysis and computation. We stimulate the auditory nerve of locusts (*Locusta migratoria*) electrically to trigger synchronous spikes in the receptor cell axons. Simultaneously, we record intracellularly the evoked response in interneurons. By examining the latency between the stimulus onset and the response of a recorded interneuron, its position in the hierarchy of the auditory pathway of the locust can be inferred. Additionally, we compare the neural response, evoked by electrical stimulation of the auditory nerve with the response elicited by acoustic stimulation.

Supported by the Deutsche Forschungsgemeinschaft (GK 120 and SFB 618)

## Changes of the intensity-response curve of an auditory interneuron (AN2) in crickets induced by adapting sound stimuli

Lars Schwabe<sup>1\*</sup>, Klaus Obermayer<sup>1</sup>, and Matthias Hennig<sup>2</sup>

<sup>1</sup>Technische Universität Berlin, Fakultät IV, FR2-1, Franklinstrasse 28/29, 10587 Berlin, Germany

<sup>2</sup>Humboldt Universität zu Berlin, Institut für Biologie, Invalidenstrasse 43, 10115 Berlin, Germany

Local auditory interneurons in the lower auditory pathway of crickets and bushcrickets exhibit a strong hyperpolarization after prolonged firing induced by auditory stimulation with a time-scale of several seconds [1, 2]. The observed reduction of excitability has been suggested to be part of a gain-control mechanism that self-regulates the representation of the cricket's auditory world such that only the most intense out of multiple simultaneously presented sound signals is encoded [1, 2]. In the context of other sensory systems, however, it has been suggested, that adaptation of an input-response function is a consequence of an optimal coding principle [3, 4] and that the observed change in response properties serves the purpose of a reliable encoding of all input signals.

Motivated by above mentioned hypotheses we began to examine the consequences of adaptation to different ensembles of auditory stimuli for the AN2 interneuron in the lower auditory pathway of crickets. Action potentials of the AN2 were recorded by tungsten hook electrodes placed around the ascending connectives, and intensity response curves were determined by test stimuli for the following three adaptation protocols: (1) Amplitude modulated noise-like “adapting” stimuli (at 4.5 kHz or 16 kHz carrier frequency) with a unimodal intensity distribution of varying duration (75 ms - 5 s), followed by pauses of different durations (75 ms - 5 s). (2) Unimodal noise-like “adapting” stimuli (always 5 s duration) with the same mean intensity but different intensity variances. (3) Multimodal noise-like stimuli (two and three maxima, always 5 s duration) mimicking auditory scenes with multiple signals. The intensity response curves were determined by test stimuli (always pure tones of 1 s duration at 4.5 kHz or 16 kHz) following the respective adaptation stimulus.

For the unimodal “adapting” stimuli we found, that the threshold of the intensity response curve was always shifted to the mean intensity of the adapting stimulus and preliminary results indicate that both adaptation and recovery operated on a time-scale of seconds. For protocol 2 we did not find any changes of the slope of the intensity response curve caused by changing the variance of the “adapting” stimulus. Interestingly, protocol 3 (multimodal adapting stimuli) also induced a threshold shift only, and our results indicate that the threshold of the response curve is again shifted to the mean intensity of this adapting stimulus.

The shift of the threshold to the signal's mean intensity values as well as the constant slope speak against the optimal coding hypothesis. Likewise, a shift of the threshold to the mean value for multimodal stimuli would not be optimal for extracting the most intense signal out of a noise-like stimulus with, for example, three peaks. These first results indicate that neither of the two above mentioned hypotheses can fully account for the adaptation observed in the AN2 neuron – at least not when optimality is required. The consequences and implications of the simple adaptation rule we found – the adaptation to the signal's mean intensity - will be discussed.

[1] Römer and Krusch, *J Comp Physiol A*, 2000. [2] Pollack, *J Neurosci*, 1988. [3] Adorjan, Piepenbrock and Obermayer, *Rev Neurosci*, 1999. [4] Fairhall et al., *Nature*, 2001.

Sponsored by DFG (SFB 618)

\*Corresponding author: schwabe@cs.tu-berlin.de

## A recurrent network model of surround-suppression in the macaque striate cortex mediated by inter-areal and intra-areal interactions

Lars Schwabe<sup>1\*</sup>, Alessandra Angelucci<sup>2</sup>, Paul Bressloff<sup>3</sup>, and Klaus Obermayer<sup>1</sup>

<sup>1</sup>Fak IV - Electrical Engineering and Computer Science, FR2-1, TU Berlin, Franklinstr. 28/29, 10587 Berlin, Germany

<sup>2</sup>Department of Ophthalmology and Visual Science, Moran Eye Institute Univ of Utah, Salt Lake City, Utah 84132

<sup>3</sup>Department of Mathematics, Univ of Utah, Salt Lake City, Utah 84112

When both the center and the surround of the receptive field of a neuron in the macaque striate cortex (V1) are stimulated with oriented stimuli matching the neuron's preferred orientation, its response is suppressed compared to stimulation of the receptive field center alone. This suppression has long been thought of as being mediated by long-range lateral connections within area V1. However, recently it has been shown [1,2,3] that response suppression can be evoked by stimuli at locations in the visual field far beyond the monosynaptic range of the long-range lateral connections. Moreover, the relatively short temporal latency of suppression arising from the far surround cannot be accounted for by the slow conduction velocity of lateral connections. In contrast, the spatial scale [2] and fast conduction velocity [4] of feedback projections from extrastriate cortex to V1 are commensurate with these large-scale suppressive effects, suggesting that they could provide the associated anatomical substrate.

In order to pinpoint the concrete neuronal circuitry underlying suppressive contextual effects, we set up a recurrent neuronal network model whose architecture is constrained to fit with recent anatomical/physiological studies [2]. We consider two areas (striate cortex and an extrastriate area) of an idealized cortex with each area being composed of a one-dimensional line of cells. Cells in the striate cortex model receive excitatory inputs from four different sources (afferent inputs, local intra-cortical circuitry, long-range lateral projections, and feedback from the extrastriate area) as well as an inhibitory input from a local interneuron. Each interneuron is paired with an excitatory neuron, and receives purely excitatory inputs from the local circuitry, the lateral projections, and the feedback. The local circuitry is assumed to operate almost instantaneously, whereas transmission via the long-range lateral projections is slow (0.2 m/s) compared to the inter-areal feedback projections (1 m/s).

In this study, we show how our recurrent network model can account for a wide range of physiological data regarding the static and dynamic effects of surround suppression. This includes the variation of the degree of suppression with the size and contrast of the stimulus [2,3], transient and latency effects [3,5], and the reduction of suppression following elimination of feedback from extrastriate cortex [6].

[1] Levitt and Lund, *Vis Neurosci*, 2002. [2] Angelucci et al, *J Neurosci*, 2002. [3] Bair et al., *J Neurosci*, 2003. [4] Girard et al., *J Neurophysiol*, 2001. [5] Hupe et al, *J Neurophysiol*, 2001. [6] Hupe et al., *Nature*, 1998.

Sponsored by DFG (SFB 618)

\*Corresponding author: [schwabe@cs.tu-berlin.de](mailto:schwabe@cs.tu-berlin.de)

## Perceptual learning and attention explained as a dynamic re-calibration of the visual system at different time-scales

Lars Schwabe<sup>1\*</sup> and Klaus Obermayer<sup>1</sup>

<sup>1</sup>Technische Universität Berlin, Fakultät IV, FR2-1, Franklinstrasse 28/29, 10587 Berlin, Germany

The representation of orientation information in the adult visual cortex is plastic as exemplified by phenomena like perceptual learning and attention. However, neither their concrete functional interpretation nor the underlying neuronal mechanisms are clear. Previous theoretical studies focused on functional interpretations of observed tuning function changes for selected phenomena, but used only descriptive models. Hence, no predictions for the underlying neuronal mechanisms could be made. In this contribution we hypothesized that the observed tuning function changes, which are different for different phenomena, can be explained by a common principle, i. e. as an ongoing re-calibration of the neuronal codes used in the visual cortex.

We set up a generic recurrent network model of a cortical hypercolumn with a biophysical interpretation and asked for how to change concrete neuronal mechanisms (afferent and recurrent synapses, neuronal gains, and additive feedback inputs) in order to optimally encode the information about oriented visual stimuli. Depending on the plasticity mechanism which was operative in the model, the predicted changes of the tuning functions differed, but always the re-calibration resulted in a more accurate representation of the orientations which were selected to be represented more accurately, i. e. were currently more 'relevant'.

Specifically, for changes to the recurrent weights we found changes of the tuning functions like the ones reported experimentally after the perceptual learning of orientation discrimination tasks [1-3], including shifts of preferred orientations, sharpening of the tuning curves, and modulation of the response amplitude. In order to account for the experimental results reported for spatial attention [4] and attention to particular values of a continuous stimulus [5] we had to assume changes of the gains of single neurons as the mechanism being operative, because only in this case the experimentally observed approximately multiplicative modulation of the responses is predicted.

In summary, our results demonstrate that two apparently different phenomena (perceptual learning and attention) can both be explained as an attempt of the visual system to dynamically re-calibrate its representations in order to achieve a high-fidelity representation of currently relevant stimuli.

[1] Schoups et al., Nature, 1999.

[2] Ghose et al., J Neurophysiol, 2002.

[3] Yang et al, J Neurosci, 2004.

[4] McAdams et al., J Neurosci, 1999.

[5] Treue et al, Nature 1999.

Sponsored by DFG (SFB 618)

\*Corresponding author: [schwabe@cs.tu-berlin.de](mailto:schwabe@cs.tu-berlin.de)



## Neural Representation and Filtering of Simple Temporal Patterns in the Lower Auditory Pathway of Crickets

Hildebrandt KJ, Hennig RM

Behavioural Physiology, Department of Biology, Humboldt University Berlin

Receivers in many acoustic communication systems analyze the temporal structures of acoustic signals. Particularly cricket females rely mainly on temporal patterns in order to recognize the conspecific calling songs. Here, crickets were used as a model system to investigate how periodic pulse patterns are represented and processed in the lower auditory pathway. In crickets, two first-order auditory interneurons, AN1 and AN2, likely form a bottleneck for two respective frequency channels, a low frequency (3-6 kHz) and a high frequency (>12 kHz) processing pathway. These two interneurons were recorded extracellularly by tungsten hook electrodes placed around the ascending connectives of *Gryllus bimaculatus* females.

Usually, the coding capacities for temporal information by auditory neurons are investigated by measuring their transfer functions along a fixed duty cycle of 50%. In order to determine the coding characteristics of neural activity also for different duty cycles a wider stimulus array was used. In this array, pulse and pause duration were varied independently to construct periodical stimuli (range of periods: 10 ms to 200 ms). The goal was to examine, how the spike trains of AN1 and AN2 represent the temporal structure of the stimuli and how much filtering is already performed at this first stage of the auditory pathway.

Selectivity of neural excitation for certain temporal structures of the stimuli was quantified by mean and maximal instantaneous spike rate. For both neurons, the mean spike rate was only weakly dependent on the energy of the stimulus and did not show tuning to certain stimulus patterns. The maximal instantaneous spike rates did not reveal specific tuning to certain stimulus patterns either. Thus, these two measures for spike rate failed to reveal filtering at this first stage of auditory processing.

Neural representation of the temporal structures of the stimulus was quantified by the vector strength of the spike trains, a coefficient of synchrony and a simple form of cross-correlation between stimuli and neuronal response. These investigations revealed an accurate representation of pulse pause patterns over a broad range of period durations and duty cycles for AN1 and AN2. For both neurons, accuracy of representation decreased at short pulse and pause durations. Probably, the limited representation accuracy of both ascending interneurons already results in a "pre-filtering" of temporal patterns, while the final evaluation of the signals is done by filter processes in the cricket brain

**Poster Subject Area #PSA5:**  
**Audition and vocalization in lower vertebrates**

[#96A](#)

L. Dittrich and W. Walkowiak, Cologne

*Anatomical and Physiological Characterization of Auditory Neurons in the Medulla oblongata of the Chinese Fire Bellied Toad*

## Anatomical and physiological characterization of auditory neurons in the medulla oblongata of the Chinese Fire Bellied Toad

Lars Dittrich and Wolfgang Walkowiak  
Zoological Institute, University of Cologne, Germany

Anurans (frogs and toads) are well known to be able to localize sound very accurately and to use spectral and temporal parameters to identify sound. The two primary auditory nuclei are the dorsolateral nucleus (DLN) and the superior olivary nucleus (SON), both located in the medulla oblongata. Unlike in mammals, binaural cells are found in the DLN. This fact suggests that spatial information is at least partly analyzed already in the DLN. Neurons which are sensitive to temporal information like amplitude modulation frequency have been found in the medullary nuclei but occur mainly in higher auditory centres. The first two auditory nuclei therefore seem to process temporal information only to a certain extent but mainly convey it to higher centres.

Anuran auditory medullary neurons have been classified by anatomical as well as physiological aspects (Feng and Lin, 1996; Hall and Feng, 1990) but a combined structural-functional analysis is still lacking. Moreover, classification of auditory neurons is mainly based on data from the neobatrachian species. Comparison with archaeobatrachian species like *Bombina* is desirable to get more insight into the evolution and general organisation of the anuran auditory pathway.

In this study, isolated brain preparations of *Bombina orientalis* were used. The posterior branches of the eighth nerves (N.VIII) were stimulated electrically via suction electrodes to induce virtual sound-elicited activity. Using intracellular electrodes, cell responses to pulse train stimulation with different repetition rates were recorded. Moreover, binaural stimuli served to investigate the underlying neural mechanisms of sound localization. An evident advantage of isolated brain preparations is that strictly monaural stimulation is possible, while in intact animals slight excitation of the second ear can hardly be avoided.

Several neurons have been filled with neurobiotin after recording. Those cells have been stained with avidin-biotin-coupled HRP and diaminobenzidine to identify the morphology and to find possible correlations between physiology and anatomy. Additionally, the projection pattern of the auditory neurons to higher centres should be clarified.

In accordance with findings in neobatrachian species, most cells responded only to ipsilateral stimulation, some only to stimulation of the contralateral side, and some received binaural input. The most common response to pulse train stimulation was answering each pulse with a single action potential up to a neuron-specific cut-off frequency, thus performing a low pass filter characteristic. This feature was expected for most of the yet characterized celltypes (*Phasic*, *Pauser*, *Primary Like*). Some of the recorded cells responded to each stimulus with a burst of spikes, as it was expected for *Phasic Burst* and *Chopper* Cells. Behaviour of membrane potentials shows that intrinsic properties of cells could be responsible for their specific temporal discharge patterns.

---

### References:

- J.C.Hall and A.S.Feng, J. Neurophysiol. 64:1460-1473 (1990)  
A.S.Feng and W.-Y.Lin, J. Comp. Neurol. 366:320-334 (1996)

**Poster Subject Area #PSA6:**  
**Audition and vocalization in birds and mammals: Periphery**

- [#97A](#) M. v. Campenhausen and H. Wagner, Aachen  
*Influence of the facial ruff on the directionality of the barn owls ears*
- [#98A](#) M. Nowotny and AW. Gummer, Tübingen  
*Outer hair cell induced motion of the organ of Corti: Mechanisms of active amplification*
- [#99A](#) AA. Keller and G. Ehret, Ulm  
*Characterization and localization of rate-intensity functions in the inferior colliculus of the mouse*
- [#96B](#) U. Gröger and L. Wiegrebe, Planegg-Martinsried  
*Absolute hearing thresholds and their relationship to the hunting behaviour of the common vampire bat *Desmodus rotundus**
- [#97B](#) M. Müller, K. von Hünenbein, S. Hoidis and JWT. Smolders, Frankfurt/Main  
*Tonotopic frequency mapping on the basilar membrane of the CBA/J mouse measured by HRP labelling of auditory nerve fibres*
- [#98B](#) C. Köppl, Garching  
*An increased endocochlear potential in barn owls*

## Influence of the facial ruff on the directionality of the barn owls ears

Mark v.Campenhausen, Hermann Wagner  
Biologie II, RWTH Aachen, D-52056 Aachen

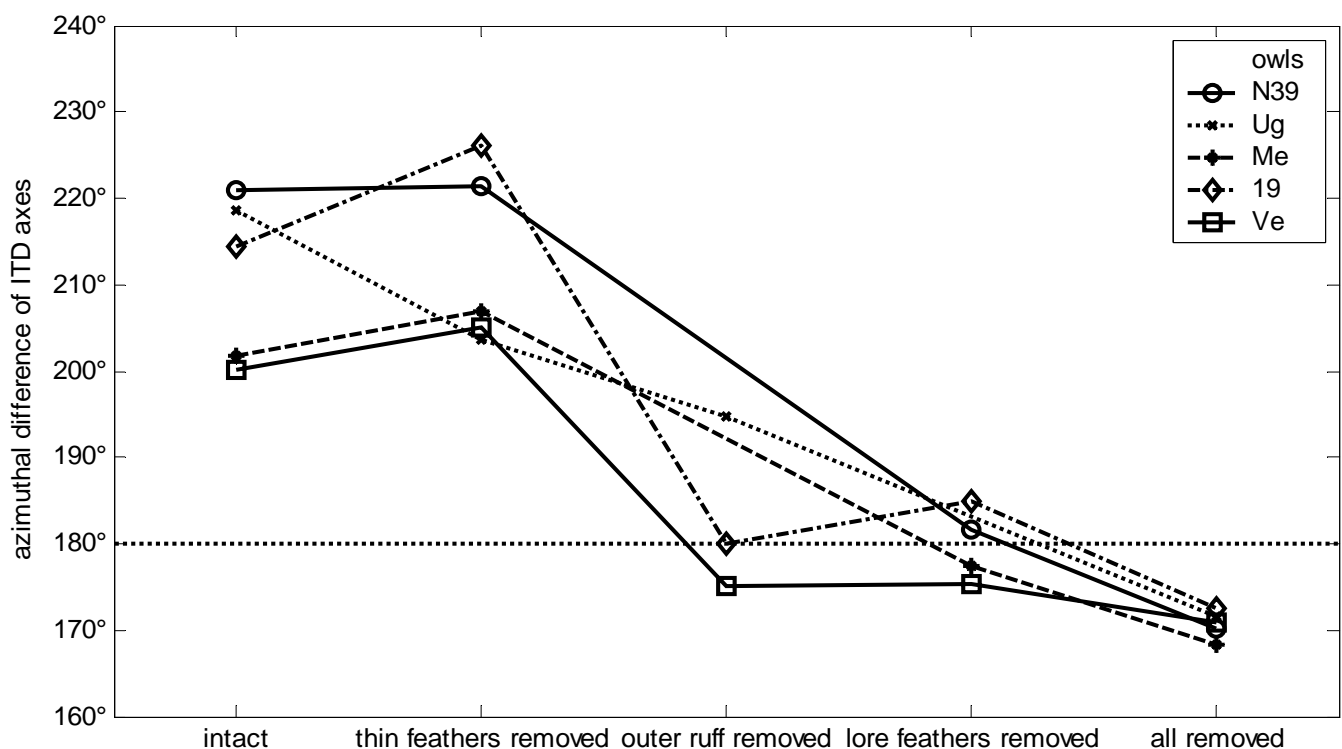
Barn owls are able to locate their prey on auditory cues only. Behavioural and electrophysiological studies show, that they use interaural timing difference (ITD) for localization in azimuth as most species do. But in contrast to other species, the interaural level differences are the major cue for localization in elevation.

Despite their symmetric outer appearance, barn owls have asymmetric outer ears. This is mainly due to the position of preaural earflaps, together with the position of the ear opening and the feathers around them, the elevational direction of highest sensitivity differs between the two ears.

Preliminary measurements indicated that the signal timing was affected by the outer ears, too. We wanted to find out, how much signal timing and the directionality of the ears is influenced by the feathers around the outer ear.

We measured the head related transfer functions of barn owls, using a moveable speaker and microphone tubes in the ear channels. After each measurement a fraction of the feathers was removed and the head related transfer function measured again. All feathers of the same anatomically kind were removed together. By this procedure we gained up to five measurements per animal: (1) untreated, (2) thin white feathers within the ruff removed, (3) additionally outer ruff removed, (4) additionally lore feathers (between the eyes) removed, (5) all feathers on the head removed.

Our main finding is that the feathers of the outer ruff (measurement 3) have the biggest influence on every calculated parameter (see figure). With the removal of these feathers the directionality and sensitivity of the ears change remarkably. At the same time the signal timing and spatial arrangement of interaural timing difference is affected. Our measurements show, that the position of the directions of maximal interaural timing difference in the untreated owl is shifted to the back on both sides, compared to the ear axes. This yields a larger range of physiological ITD values.



# Outer hair cell induced motion of the organ of Corti: Mechanisms of active amplification

**Manuela Nowotny, Anthony W. Gummer**

Section of Physiological Acoustics and Communication, Department of Otolaryngology,  
University of Tübingen, Tübingen, Germany

There is compelling evidence that somatic electromotility of the outer hair cells (OHC) amplifies the motion of the organ of Corti (OoC); see DALLOS and FAKLER (2002) for a review. This amplified motion is somehow coupled to the hair bundle of the inner hair cells (IHC). A number of coupling mechanisms have been proposed: 1) shearing motion between the reticular lamina (RL) and tectorial membrane (TM), induced by the travelling wave along the basilar membrane (BM) (TER KUILE, 1900; VON BÉKÉSY, 1960), 2) internal shearing motion inside the OoC also induced by BM motion (FRIEDBERGER et al., 2002) and 3) deformation of the subreticular space above the IHC, induced by OHC electromotility (NOWOTNY et al., 2003).

In a total of 81 guinea-pig cochleae (*Cavia procellus*), an electrical stimulus was applied to scala vestibuli and scala tympani (above and under the OoC). This stimulus lead to a movement of the OHCs which deformed the OoC. The stimulus was a multi-tone signal consisting of 81 frequencies, from 480 Hz to 70 kHz, with equal amplitude but random phase. The transversal vibration pattern of the OoC was measured throughout its depth, using a laser Doppler vibrometer (Polytec OFV 302), with a depth resolution of  $\pm 1.8 \mu\text{m}$  from the focus plane (at -10 dB). At three different places along the cochlea (basal: characteristic frequency (CF) 24 kHz, medial: CF 3 kHz and apical: CF 0.8 kHz), the transversal motions of the RL, upper and lower surfaces of the TM and of the BM were measured.

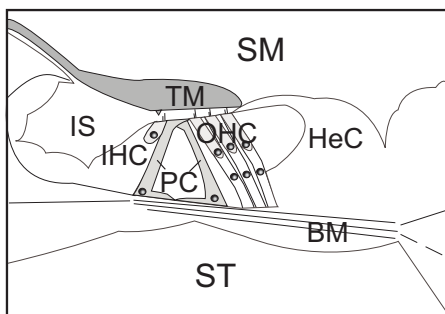


Figure 1. Schematic drawing of the organ of Corti in the basal turn of the guinea-pig cochlea. Abbreviations: basilar membrane (BM), region of Hensen's cells (HeC), inner hair cell (IHC), inner sulcus (IS), outer hair cells (OHC), pillar cells (PC), scala media (SM), scala tympani (ST) and the tectorial membrane (TM).

A complex vibration pattern of the RL was found. The RL did not move like a rigid plate: instead, two pivot points were uncovered - one at the pillar cells and the other at Hensen's cells (HeC). In contrast, TM motion was in-phase along its entire lower and upper surfaces.

This leads to counterphasic motion of the RL and TM above the IHCs. This peristaltic-like deformation of the subreticular space causes radial fluid motion inside this space, which is presumably capable of deflecting the IHC stereovilli. The vibration pattern of the BM, induced by OHC motion, exhibited at all radial and longitudinal positions (except under the HeC) a resonance between 11 – 21 kHz. At frequencies below this resonance, there was a local minimum in the amplitudes. At CF, the displacement was up to ten times smaller on the BM in the region of the OHCs compared with the RL. Between ISCs and HeCs there was a phase difference of  $90^\circ - 180^\circ$  in every turn; the phase response exhibited distinct phase shifts corresponding to the amplitude response.

The experiments, in comparing the measured vibration patterns of the RL, TM and BM under the influence of OHC electromotility, suggest that amplification of travelling wave motion on the BM is not the dominant result of OHC electromotility. Moreover, the inferred, OHC-induced fluid motion in the subreticular space will add (vectorially) to the shearing motion between RL and TM, and to shearing motion inside the OoC. Future experiments should be directed to the function of the inner sulcus as a fluid reservoir to pump the fluid inside the subreticular space.

BÉKÉSY, v.G. Experiments in Hearing. McGraw-Hill, New York, (1960).

DALLOS, P. and FAKLER, B. *Nat. Rec. Mol. Cell Biol.* **3**(2), 104-111, (2002).

FRIEDBERGER, A., BOUTET de MONVEL, J. and ULFENDAHL, M. *J. Neurosci.* **22**, 9850-9857, (2002).

NOWOTNY, M., ZENNER, H.P. and GUMMER, A.W. *Abstractband Proc. 29th Göttingen Neurobiology Conference*, (2003).

TER KUILE, E. *Arch. ges. Physiol.* **79**, 146-157, (1900).

*This work was supported by the Deutsche Forschungsgemeinschaft: SFB 430, Teilprojekt A4 and Gu 194/5-1,2.*

## Characterization and localization of rate-intensity functions in the inferior colliculus of the mouse

Agnes A. Keller & Günter Ehret  
agnes.keller@biologie.uni-ulm.de  
Dept. of Neurobiology, University Ulm

The inferior colliculus (IC) plays a central role in auditory sound processing, because of the multiple convergent inputs from lower brainstem and higher auditory centers. Various studies concerning neuronal response properties in the IC have shown a topographic representation of e.g. frequency (Stiebler & Ehret, 1985), tone response threshold (Stiebler, 1986) or latency (Schreiner & Langner, 1988). In contrast, very little is known about the representation of sound intensity in the IC.

We analyzed intensity coding by measuring rate-intensity functions of single units in the central IC (ICC) of female mice (outbred strain NMRI), anesthetized with Ketavet-Rompun. Our auditory signals were pure tone pulses with a duration of 80 ms, 5 ms rise and fall times and an intertone interval of 240 ms. The signals were presented contralaterally under free-field conditions. Excitatory receptive fields of neurons were mapped over 3 octaves relative to the characteristic frequency (CF) in 20 logarithmically spaced increments with intensity varying from 0 to 80 dB<sub>SPL</sub> in steps of 5 dB. This matrix of 340 frequency-intensity pairs was repeated 3 times randomly. So far, 143 neurons have been analyzed.

Among our results are the following. The rate-intensity functions at the CFs of the neurons could be distinguished in 5 classes on the basis of their shapes: Monotonic increase (MI), low-level constant (LLC), high-level constant (HLC), two stepped increase (TS) and peaked (P). Type MI occurred in neurons of all CFs tested (7-40 kHz). All other types were found mainly in certain CF ranges, i.e. type LLC from 7-20 kHz, type TS from 16-24 kHz, type P from 20-30 kHz, and type HLC from 28-40 kHz.

Our data indicate that the shapes of rate-intensity functions may depend on the CFs of the neurons. Since tone-intensity discrimination and loudness perception does not systematically depend on sound frequency, our results suggest that the shapes of rate-intensity functions of ICC neurons taken at their CFs are not directly related to the coding of sound intensity at the level of the auditory midbrain.

Schreiner CE & Langner G (1988) *J Neurophysiol* 60, 1823-1840

Stiebler I (1986) *Neurosci Lett* 65, 336-340

Stiebler I & Ehret G (1985) *J Comp Neurol* 238, 65-75

Absolute hearing thresholds and their relationship to the hunting behaviour of the common vampire bat *Desmodus rotundus*

U. Gröger and L. Wiegrebe

Department Biologie II, Ludwig-Maximilians-Universität, Großhaderner Strasse 2  
D-82152 Planegg-Martinsried

The common vampire bat *Desmodus rotundus* is able to hear far below the frequency range of its echolocation calls. Electrophysiological studies in the vampires' auditory midbrain have indicated high sensitivity to relative low-frequency breathing sounds (Schmidt et al., 1991). Here, absolute hearing thresholds were mapped using a psychoacoustical three-alternative, forced-choice paradigm.

Stimuli were pulse-trains of bandpass filtered noise with 500 ms signal duration and 500 ms gaps. Bandpass centre frequencies varied from 3 kHz to 80 kHz and were equally spaced on a log frequency axis. The stimuli were presented in free field. After a training time in which the threshold region was roughly estimated, signal level was varied randomly in 5-dB steps in a window of 35 dB around the absolute threshold. Absolute thresholds were derived by fitting a sigmoid curve to the psychometric functions.

Data was acquired from three male bats. In agreement with the physiological results, *D. rotundus* shows a threshold plot with highest sensitivity (-2 dB SPL) at about 10 to 15 kHz. Thresholds in the frequency region of the echolocation calls are about 25 dB higher.

Supported by physiological results, our hypothesis is that the high sensitivity at these relatively low frequencies is used by the bats to locate prey through their breathing noises. This led us to the question if *D. rotundus* is able to identify individual prey animals through their individual breathing noises. Preliminary data indicate that *D. rotundus* is well able to do so and that the breathing rate appears to be a critical parameter for breathing-sound identification.

Schmidt, U., Schlegel, P., Schweizer, H., and Neuweiler, G. (1991), "Audition in vampire bats, *Desmodus rotundus*," J. Comp Physiol [A] **168**, 45-51.

Supported by the DFG Graduiertenkolleg 'Sensomotorische Interaktion in biologischen und technischen' Systemen.



## **Tonotopic frequency mapping on the basilar membrane of the CBA/J mouse measured by HRP labelling of auditory nerve fibres**

**Marcus Müller, Karen von Hünenbein, Silvi Hoidis, Jean W.Th. Smolders**

J.W.Goethe-Universität, Institut für Physiologie II, Sinnes- und Neurophysiologie  
Theodor-Stern-Kai 7, D-60590 Frankfurt am Main, Germany  
E-mail: m.mueller@em.uni-frankfurt.de

Genetically manipulated mice have gained a prominent role in *in vivo* research on development and function of the auditory system. A prerequisite for the interpretation of normal and abnormal structural and functional features of the inner ear is the exact knowledge of the cochlear place-frequency map. Using a stereotaxic approach to the projection site of the auditory nerve fibres in the cochlear nucleus, we succeeded in labelling physiologically characterized auditory nerve afferents in normal hearing CBA/J mice and determined their peripheral innervation site in the cochlea.

All experiments were performed under anaesthesia. Glass micropipettes filled with 7.5% HRP in 0.5M KCl were inserted into the cochlear nucleus, while presenting noise bursts as an acoustic search stimulus. On the occurrence of stimulus-locked neural activity a frequency tuning curve in response to pure tone pips was determined, from which the neuronal characteristic frequency and threshold were derived. Then HRP was applied iontophoretically using a pulsed current of +2  $\mu$ A (800 ms) and -2  $\mu$ A (200 ms) for 15 minutes. After overnight survival and transcardial perfusion with fixative, serial frozen sections of brain and cochlea were made. The location of labelled spiral ganglion cells and their processes under the inner hair cells was determined from a computer aided 3-dimensional reconstruction of the cochlea coil.

From the neuronal characteristic frequency and the appertaining innervation site in the organ of Corti a place-frequency map was established for characteristic frequencies between 7.2 and 61.8 kHz, corresponding to locations between 90 and 10% basilar membrane length (base = 0%, apex = 100%, mean length of the basilar membrane measured under the inner hair cells 5.13 mm). The relation between normalized distance from the base (d) and characteristic frequency (f, kHz) can be described by a simple logarithmic function:  $d(\%) = 156.5 - 82.5 \cdot \log(f)$ . The slope of this function amounted to 1.25 mm/octave of frequency. So far this is the lowest value found among mammals (e.g. gerbil: 1.5 mm/octave; cat 3.5 mm/octave). The present map, recorded in normal hearing CBA/J mice under physiological conditions, differs from earlier maps in mice determined with different methods. The simple logarithmic place-frequency relation found in the mouse indicates that mice are acoustic generalists rather than specialists.

Supported by the DFG, SFB 269

## An increased endocochlear potential in barn owls

Christine Köppl

Lehrstuhl für Zoologie der Technischen Universität München, Lichtenbergstr. 4, 85747 Garching, Germany  
email: Christine.Koepl@wzw.tum.de

The vestibular and auditory system of vertebrates is housed within the inner-ear labyrinth. The auditory part of the labyrinth is subdivided into three principal fluid spaces: scala vestibuli, scala tympani and scala media. The sensory epithelium (basilar papilla or organ of Corti) forms part of the epithelial border separating scala vestibuli and scala media. In scala media, a very unusual ionic milieu is maintained, called endolymph, with high  $K^+$  and low  $Na^+$ -concentrations, otherwise typical for intracellular compartments only. In addition, a positive potential, called the endocochlear potential, is maintained in scala media relative to other extracellular spaces. Endolymph and endocochlear potential are generated by specialized tissues under considerable energetic cost. According to the accepted "battery theory" of hearing, the highly specialized milieu in scala media serves to increase the sensitivity of transduction and to lower the energy requirements at the level of the sensory hair cells.

While the endolymphatic ion composition is similar across vertebrates, the extent of the endocochlear potential varies widely. Lizards maintain only a few mV of endocochlear potential. In birds, it is about +15mV. In mammals, the endocochlear potential is typically about +90mV. There is no clear correlation between, e.g. sensitivity of hearing and the amplitude of the endocochlear potential, as would be expected if the battery theory is correct. However, too many other parameters differ between the hearing organs of different vertebrates to make a valid comparison across major groups. We therefore decided to investigate the endocochlear potential in the barn owl, a bird that is known for its exquisite hearing, and compare that to known values for the endocochlear potential in other bird species. To verify our recording setup and enable a direct comparison, measurements were also carried out in chickens (aged P26-P36).

Animals were anaesthetised with ketamine, xylazine and metamizol. In owls, an opening in the posterior skull provided a view of the columella (middle ear ossicle) and the oval and round windows of the inner ear. In chickens, the external ear canal was widened and the eardrum removed to achieve a similar view. The columella was clipped and the columellar footplate was carefully lifted from the oval window, opening scala tympani and exposing the tegmentum vasculosum. Glass electrodes filled with 3M KCl were advanced through the tegmentum into scala media and the electrode potential relative to a grounded reference electrode was continuously monitored. The endocochlear potential appeared as a sudden positive step in the recording which was reversible upon retreat. Control measurements under brief hypoxia or following a lethal dose of barbiturate confirmed the physiologically-vulnerable nature of this potential.

Measurements of the endocochlear potential were obtained from 3 ears of 3 chickens and from 7 ears of 4 barn owls. Values for the chicken ranged from 13.5 to 17.5 mV (median 13.8 mV), confirming previous measurements by other authors. Values for the barn owl ranged from 30.1 to 44.3 mV (median 33.8 mV).

Average values for the endocochlear potential in a range of bird species have been determined at between 9 and 20 mV. The barn owl thus maintains a clearly higher potential. All else being equal, this will result in a larger electromotive force for the hair-cell transduction current, which would increase both the sensitivity and the speed of transduction. High sensitivity and extreme temporal resolution are both hallmarks of barn owl auditory nerve fibres and distinguish it from other birds, especially at high frequencies. The higher endocochlear potential may be a crucial factor.

**Poster Subject Area #PSA7:**  
**Audition and vocalization in birds and mammals: CNS and perception**

- [#100A](#) P. Heil and H. Neubauer, Magdeburg  
*Temporal integration and hearing loss*
- [#101A](#) SC. Gaub and G. Ehret, Ulm  
*Influence of the gap duration on the perception of mouse pup calls*
- [#102A](#) SR. Hage and U. Jürgens, Ulm and Göttingen  
*Sensory-motor interaction at the pontine brainstem level during vocalization: A telemetric single-unit recording study in freely moving monkeys*
- [#103A](#) D. Isheim, B. Gaese and M. Kössl, Frankfurt/Main  
*Temporal processing of modulated acoustic stimuli in gerbil primary auditory cortex*
- [#104A](#) K. Vonderschen and H. Wagner, Aachen  
*Frequency integration in the auditory arcopallium of the barn owl (*Tyto alba*)*
- [#105A](#) I. Kollmar, P. Tripathi and B. Grothe, Munich, Neuherberg and Martinsried  
*Adult Plasticity of Interaural Time Difference Processing is Regulated by Glycinergic Inhibition*
- [#106A](#) M. Pecka and B. Grothe, Martinsried and Munich  
*Evidence for preceding inhibition in low-frequency E/E single cells in the gerbil auditory brainstem*
- [#107A](#) P. Bächerle and M. Kössl, Frankfurt/Main  
*Frequency organization of the medial geniculate body in the Mongolian gerbil*
- [#108A](#) P. Bremen, M. Singheiser, DTT. Plachta, RF. van der Willigen and H. Wagner, Aachen  
*Barn owls do not depend on high frequency auditory signals to approach a distant target.*
- [#109A](#) SC. Schmid-Fetzer and J. Ostwald, Tübingen  
*Simultaneous localization of multiple sound sources*
- [#110A](#) E. Budinger and H. Scheich, Magdeburg  
*Organization of the auditory corticofugal system in the Mongolian gerbil*
- [#111A](#) U. Firzlaff, B. Schwellnus, L. Wiegand and G. Schuller, Planegg-Martinsried  
*Basic properties of auditory cortex and processing of stimulus roughness in the bat *Phyllostomus discolor**

- [#112A](#) E. Foeller, E. Mora and M. Kössl, Frankfurt and Havana (C)  
*Topographic organization of the auditory cortex of the bat *Molossus molossus**
- [#113A](#) G. Schebesch and H-J. Leppelsack, München and Garching  
*Development-dependent Effects in the Auditory Field-L Complex of the Zebra Fish Brain*
- [#114A](#) O. Gleich, I. Hamann, MC. Kittel, GM. Klump and J. Strutz, Regensburg and Oldenburg  
*Psychometric functions for the detection of gaps in broad-band noise: the effect of age.*
- [#115A](#) AA. Alkhatib, D. Biedenkapp, UW. Biebel and JWT. Smolders, Frankfurt/Main  
*Inhibitory and excitatory response areas of neurons in the inferior colliculus in awake chinchillas*
- [#99B](#) D. Biedenkapp, AA. Khatib, UW. Biebel and JWT. Smolders, Frankfurt/Main  
*Effects of Carboplatin on ABR and local field potentials in neurons of the inferior colliculus of awake chinchillas*
- [#100B](#) S. Schörnich and L. Wiegerebe, Planegg-Martinsried  
*Discrimination of echo roughness in the fruit-eating bat *Phyllostomus discolor**
- [#101B](#) V. Weik, KB. Klink and GM. Klump, Oldenburg  
*Comodulation Masking Release in the house mouse (*Mus musculus*)*
- [#102B](#) A. Engelhorn, D. Ensberg, M. Deliano, H. Scheich and FW. Ohl, Magdeburg  
*A parametric study of electrically evoked activity in gerbil auditory cortex*
- [#103B](#) W. von der Behrens and B. Gaese, Frankfurt/Main  
*Investigating the influence of spatial attention on the processing of frequency-modulated tones in the rat*
- [#104B](#) E. Oshurkova, H. Scheich and M. Brosch, Magdeburg  
*Neural representations of temporally modulated sounds in the auditory cortex of macaque monkeys: effects of ketamine anesthesia.*
- [#105B](#) F. Nagel, O. Grewe, R. Kopiez and E. Altenmüller, Hannover  
*The relationship of psycho-physiological responses and self-reported emotions while listening to music*
- [#106B](#) M. Schuchmann, MM. Hübner and L. Wiegerebe, Planegg- Martinsried  
*Semantic meaning causes different strategies of echo suppression in echolocating bats*
- [#107B](#) A. Laszcz, E. Budinger, J. Goldschmidt, FW. Ohl, M. Schildt, W. Wetzel, W. Zusratter and H. Scheich, Magdeburg  
*Possible anatomical substrates of hemispheric lateralization in Mongolian gerbil auditory cortex*

- [#108B](#) B. Diekamp, JJ. Sartor, GF. Ball and ES. Fortune, Baltimore, MD (USA)  
*HORMONE-RELATED PLASTICITY OF SONG REPRESENTATION AND SELECTIVITY IN HVC OF MALE AND FEMALE CANARIES*
- [#109B](#) CB. Castelino, B. Diekamp and GF. Ball, Baltimore, MD (USA)  
*CATECHOLAMINERGIC PROJECTIONS TO THE VOCAL CONTROL NUCLEUS AREA X IN ZEBRA FINCHES (*Taeniopygia guttata*) AND THEIR SIGNIFICANCE FOR SOCIAL MODULATION OF IMMEDIATE-EARLY GENE EXPRESSION ASSOCIATED WITH SONG*
- [#110B](#) ES. Fortune, B. Diekamp, JJ. Sartor and GF. Ball, Baltimore, MD (USA)  
*MAINTENANCE OF HVC VOLUME IN DEVOCALIZED ZEBRA FINCHES BY NIGHT PLAYBACK OF THE BIRD'S OWN LEARNED SONG*
- [#111B](#) M. Hausmann, MC. Corballis, A. Paggi, M. Fabri and J. Lewald, Bochum, Auckland (NZ), Ancona (I) and Dortmund  
*Sound lateralization following hemispherectomy, callosotomy, or callosal agenesis*
- [#112B](#) CJW. Meulenberg, Groningen (NL)  
*Mechano-electrical transduction of mouse cochlear hair cells*
- [#113B](#) M. Becker, MFH. Müller, HG. Nothwang and E. Friauf, Kaiserslautern  
*Analysis of Protein Patterns in the rat auditory brainstem and cerebellum*
- [#114B](#) A. Koehl, A. Rieger, N. Schmidt, E. Friauf and HG. Nothwang, Kaiserslautern  
*Serial Analysis of Gene Expression (SAGE) in the rat auditory brainstem*
- [#115B](#) JD. Albrecht, B. Bogerts, H. Bielau, U. Mertens, K. Schiltz, S. Diekmann, H. Scheich and A. Brechmann, Magdeburg  
*Categorization of Frequency Modulated Tones in Schizophrenia*

## Temporal integration and hearing loss

**Peter Heil and Heinrich Neubauer**

Leibniz Institute for Neurobiology, Brennekestr. 6, D-39118 Magdeburg, Germany

For signal detection the auditory system needs to integrate sound over time. In fact, for every species examined, the sound pressure level needed to detect a sound decreases as sound duration increases. This trading relationship is frequently interpreted to indicate that the auditory system ultimately integrates sound intensity. And, it is often assumed that the integrator is located centrally. However, we have shown that absolute thresholds are much better specified as the temporal integral of the pressure envelope than of intensity, and have provided strong evidence that the integrator resides in the auditory pathway's first synapse [1, 2]. We proposed that thresholds are reached by summation of chance events where each of these events requires the interaction of about 4 statistically independent, or nearly independent, sub-events. We suggested that the events are exocytotic events at the inner hair cell to auditory-nerve fiber synapses and the sub-events the Ca-binding steps required for exocytosis. This physiologically plausible mechanism agreed well with the observed rate of temporal integration, i.e. the decrease of threshold sound pressure levels with increasing duration.

In listeners with sensori-neural hearing losses, that rate seems reduced, but it is not fully understood why. Here we propose that in such listeners there may be an elevation in the baseline above which sound pressure is effective in driving the system, in addition to a reduction in sensitivity. We test this simple model, using thresholds of cats to stimuli of differently shaped temporal envelopes and durations obtained before and after hearing loss. We show that thresholds, specified as the temporal integral of the effective pressure envelope, i.e. the envelope of the pressure exceeding the elevated baseline, behave almost exactly as the lower thresholds, specified as the temporal integral of the total pressure envelope before hearing loss. Thus, the mechanism of temporal integration is likely unchanged after hearing loss, but the effective portion of the stimulus is.

Our model constitutes a successful alternative to the model currently favoured to account for altered temporal integration in listeners with sensori-neural hearing losses, viz. reduced peripheral compression [3]. Our model does not seem to be at variance with physiological observations and also qualitatively accounts for a number of phenomena observed in such listeners with suprathreshold stimuli [4].

Supported by grants of the Deutsche Forschungsgemeinschaft to P. Heil

[1] Heil P, Neubauer H (2001) *J Neurosci* 21:7404-7415

[2] Heil P, Neubauer H (2003) *Proc Natl Acad Sci USA* 100:6151-6156

[3] Moore BCJ, Oxenham AJ (1998) *Psychol Review* 105:108-124

[4] Neubauer H, Heil P (2005) *J Assoc Research Otolaryngol* 5: in press

## **Influence of the gap duration on the perception of mouse pup calls**

Simone Christina Gaub and Günter Ehret

Dept. of Neurobiology, University of Ulm, 89069 Ulm, Germany

The gap duration between sequences of vocalizations plays an important role in the perception of human and animal sounds. For example, humans can discriminate phonemes in dependence of the gap duration between consonant and vowel, the so-called “voice-onset-time” [1]. This also applies to chinchillas and rhesus monkeys [2, 3]. Mouse pups (*Mus musculus*) in the nest produce so-called wriggling calls, mostly in series of several calls. While the mouse mother is in lactation position the wriggling calls release maternal care such as licking of pups, nest building and changing nursing position on the litter. Because the mother responds rarely to a single wriggling call, a sequence of wriggling calls is necessary to effectively release maternal behaviour. A synthesized call model consisting of three formants (3.8 kHz, 7.6 kHz and 11.4 kHz) and having a duration of 100 ms, resembles the natural wriggling call of young mice. Sequences of four synthesized call models with a gap duration of 200 ms are comparable with the pup calls in respect of releasing maternal care [4].

Here, we study the perception of sequences of four wriggling call models in dependence on the duration of the gaps between the single calls. We record both the maternal response behaviour to synthesized sequences of the call models with variable gap durations (50-500 ms) and the maternal responses to pup wriggling calls while the mother is nursing her litter (for detailed description of the behavioural tests see [4]).

The so far attained results show the following: the effectiveness of the call models with gap durations between 100 and 400 ms is not significantly different. The effectiveness of the call models decrease, when the gap becomes shorter than 100 ms or longer than 400 ms. Apparently mice can identify a series of wriggling calls as coherent or as one auditory stream, when the gap between the calls lasts 100 to 400 ms. Mice are sensitive to gap durations of 1-3 ms between two sounds [5]. We show that an interval time of less than 100 ms seems not to be enough for recognizing an auditory stream of wriggling calls. The relative low effectiveness of the call model with a gap duration of more than 400 ms suggests that mice perceive call series with this gap time as single sounds not as an auditory stream. Neurons in the primary and secondary auditory cortex of cats responding to sequences of five tones show a facilitation effect in the response to a tone, if the gap to the previous tone was 300 ms. There was no facilitation, if the gap was 900 ms [6]. These data are in accordance with our results and suggest that facilitation of neural responses in the time domain occurs over gap durations of about 100-400 ms.

Supported by the Deutsche Forschungsgemeinschaft, Eh 53/17

- [1] Lisker L, Abramson A (1964) *Word* 20: 384-422
- [2] Kuhl PK, Miller JD (1978) *J Acoust Soc Am* 63: 905-917
- [3] Waters RS, Wilson WA (1976) *Percept Psychophys* 19: 285-289
- [4] Ehret G, Riecke S (2002) *Proc Natl Acad Sci* 99: 479-482
- [5] Walton JP et al. (1997) *J Comp Physiol A* 181: 161-176
- [6] McKenna TM et al. (1989) *Brain Res* 481: 142-153

## **Sensory-motor interaction at the pontine brainstem level during vocalization**

A telemetric single-unit recording study in freely moving monkeys

**S.R. Hage<sup>1,2</sup> and U. Jürgens<sup>1</sup>**

<sup>1</sup>*German Primate Center, Department of Neurobiology, 37077 Göttingen, Germany*

<sup>2</sup>*University of Ulm, Department of Neurobiology, 89069 Ulm, Germany*

*shage@dpz.gwdg.de*

Up to now, little is known about vocal-motor control in the pontine brainstem and its role in audio-vocal interaction. Recent studies have shown that the ventrolateral pontine reticular formation has direct connections to all motoneuron pools involved in phonation and blocking of its excitatory neurotransmission eliminates vocalization elicitable from the periaqueductal gray<sup>1</sup>. It is still unclear whether audio-vocal interactions as they have been reported already for the peri-collicular area<sup>2</sup> and auditory cortex<sup>3</sup> take place also at pontine level.

Here, we use a miniature telemetric system, which allows simultaneous recording of single-unit activity and spontaneously uttered vocalizations in freely moving squirrel monkeys within their social group<sup>4</sup>. With this technique, we systematically explored the lateral pons, looking for neurons with vocalization- and/or acoustic stimuli-related activity.

First results show that, apart from the phonatory motoneuron pools, vocalization-correlated activity is found in an area dorsal to the motor trigeminal nucleus. These neurons show increased or decreased activity immediately before and during vocalization, but do not respond to external acoustic stimuli. Another group of neurons was found, lying dorsal to the superior olivary complex and in-between the medial and lateral nucleus of this complex, which changed their activity before and during vocalization as well as to auditory stimuli. These findings suggest that the ventrolateral pontine brainstem is involved in audio-vocal integration.

<sup>1</sup> Jürgens U (2000) J Acoust Soc Am 108, 1393-1396

<sup>2</sup> Tammer R, Ehrenreich L, Jürgens U (2004) Behav Brain Res 151, 331-336

<sup>3</sup> Eliades SJ, Wang X (2003) J Neurophysiol 89, 2194-2207

<sup>4</sup> Grohrock P, Häusler U, Jürgens U (1997) J Neurosci Methods 76, 7-13



## **Temporal processing of modulated acoustic stimuli in gerbil primary auditory cortex**

**Dagmar Isheim, Bernhard Gaese, Manfred Kössl**

**Zoological Institute, J.W. Goethe University, Frankfurt Main/ Germany**

Three prominent features of sound, namely: frequency, intensity and temporal pattern, are processed by the auditory system.

In the presented study we investigated how well the timing of neuronal firing rates in cortical neurons represent temporal features of acoustic stimuli. As high temporally structured stimuli we compared sinus amplitude modulated (SAM) signals to repetitive click and short pure tone stimuli.

Neurons of the primary auditory cortex react mostly in a low-pass manner. Slow repetition rates are well represented by the temporal pattern of the firing rate while the neuronal response at higher repetition rates is restricted to onset activity. Pharmacological manipulation with the GABA<sub>A</sub> antagonist Bicucullin reveals changes in the overall firing rate but has only minor effect on the synchronization of the firing rate to the stimuli.

The synchronization of neuronal firing rates also depends on sound intensity and the used stimuli types. Several neuronal classes can be distinguished with regard to their preferred repetitive stimulus type. Overall neurons either have a monotonic increase in synchronization of the firing rate with higher sound intensities or their synchronization is tuned to a specific sound intensity range.

## Frequency integration in the auditory arcopallium of the barn owl (*Tyto alba*)

**Katrin Vonderschen and Hermann Wagner**

Institut für Biologie II, RWTH Aachen, Kopernikusstr. 16, 52074 Aachen, Germany  
corresponding author: *katrin@bio2.rwth-aachen.de*

Auditory information processing in the barn owl can be divided into a midbrain pathway and a forebrain pathway. From the hair cells on, frequency information is processed in narrowband neurons which align in tonotopic maps up to the level of the ICCcore. In the ICC lateral shell and ICX single neurons integrate information over broad frequency ranges. This process may be characterized by two parameters: (1) neurons exhibit a characteristic delay (CD: the interaural delay (ITD) at which the neuron's relative response strength is independent of the frequency of a tonal stimulus) and (2) neurons show a characteristic phase (CP: the phase angle of the neuron's sinusoidal response to tonal ITD-stimuli that corresponds to the neuron's CD). In the forebrain pathway broadband neurons are first found in the auditory arcopallium (AAr), which receives its main inputs from narrowband neurons in Field L.

We determined general physiological properties and the frequency integration characteristics of neurons in the AAr and compared these with the known response properties of ICX neurons.

In total, we recorded extracellularly from 82 AAr neurons. From 46 neurons we obtained responses to varying ITDs with tonal stimuli for at least three different frequencies. Additionally, in 57 neurons, we utilized broadband noise to assess general tuning properties to binaural cues (interaural time and level differences), frequency tuning and monaural and binaural threshold levels. These characteristics helped to verify the location of recording and to compare the general properties with data from the literature (Cohen & Knudsen 1995). A preliminary analysis of our data indicates that ITD and ILD response functions of the neurons exhibited a lower general acuity than observed in ICX. AAr Neurons exhibited CDs and CPs. The distribution of CPs was not as tight as that observed in ICX (Takahashi & Konishi 1986), but reminiscent of observations in the mammalian auditory pathway (Yin & Kuwada 1983).

Our preliminary data indicate that AAr neurons employ diverse strategies to realize frequency integration at the single neuron level. Together with the low general acuity in tuning to binaural cues this points to a functional specialization of AAr that differs from the specialization of ICX to sound localization.

Cohen & Knudsen 1995, J. Neurosci. 15(7): 5152  
Takahashi & Konishi, J. Neurosci. 6(12): 3413 (1986)  
Yin & Kuwada, J. Neurophysiol. 50: 1020 (1983)

## Adult Plasticity of Interaural Time Difference Processing is Regulated by Glycinergic Inhibition

*Ida Kollmar<sup>1,2</sup>, Pratibha Tripathi<sup>2,3</sup> and Benedikt Grothe<sup>1,2</sup>*

<sup>1</sup>Biocenter of the Ludwig Maximilians University Munich, Dep. Biology II, Division of Neurobiology, Martinsried, Germany, <sup>2</sup>Max Planck Institute of Neurobiology, Martinsried, Germany, and <sup>3</sup>Stem Cell Institute (ISF), GSF – research center for health and environment, Neuherberg, Germany

Neuronal plasticity is an important mechanism for learning and adaptation to environmental changes. Plasticity in the auditory brainstem of mammals, however, has almost exclusively been investigated with invasive or damaging techniques. In the present study we investigate the plasticity of sound localization mechanism using a non-invasive approach. In mammals, interaural time differences (ITDs), a major cue for sound localization, are encoded in the medial superior olive (MSO) by a complex temporal interaction of binaural excitatory and inhibitory inputs. Earlier studies showed that the inhibitory inputs are crucial for adjusting the ITD-sensitivity to the behavior relative range, and that this adjustment depend on experience during a critical period of development (Kapfer et al. 2002). Here we tested if inhibition also plays a role in adult plasticity of ITD coding.

Using electrophysiological and molecular studies we compare three groups of adult gerbils. All animals were raised in a normal acoustic environment. The control group was never exposed to noise, the second group was exposed to noise for 14 days as adults and then tested within 7 days after exposure, and the third group exposed to noise but recovered for at least 14 days after exposure.

In the electrophysiological studies we measured the ITD-functions of 119 neurons of the dorsal nucleus of the lateral lemniscus (DNLL), which are directly excited by MSO neurons. Comparing the control and the second group we show that exposure to omnidirectional noise significantly shifts the average best ITD (cycles) to longer interaural delays (contralateral stimulus leading) and additionally increase the modulation depth in the physiological relevant range. The third group showed comparable ITD coding like the control group hence these changes were reversible.

Theoretically this plastic change of ITD tuning could be explained by increase of inhibitory input to the MSO (Brand et al. 2002). To confirm this hypothesis we started to measure expression levels of genes probably involved in ITD processing in the MSO by quantitative PCR. In contrast to the control animals the expression of glycine receptors (Gly $\alpha$ 1) of MSO neurons increases after noise exposure. Preliminary studies suggest that the Gly $\alpha$ 1 level in other binaural nuclei like the LSO getting the same input like the MSO are not affected by omnidirectional noise. As showed at the physiological level the induced change seems to be reversible at the molecular level. Further we would like to study whether excitatory inputs are also involved in this plastic mechanism.

The present study shows that omnidirectional noise induces reversible adult plasticity in sound localization mechanisms. Visible physiological changes could be linked to molecular expression levels confirming our hypothesis that ITD tuning is regulated by glycinergic inhibition not only during development but also in the adult auditory system.

## Evidence for preceding inhibition in low-frequency E/E single cells in the gerbil auditory brainstem

*Michael Pecka*<sup>1,2</sup> and *Benedikt Grothe*<sup>1,2</sup>

<sup>1</sup>Max-Planck-Institute of Neurobiology, Martinsried, Germany

<sup>2</sup>Biocenter of the Ludwig-Maximilians-University Munich, Department Biology II, Division of Neurobiology, Martinsried, Germany

Based on a computational model of interaural time difference (ITD) processing we recently proposed contralateral inhibition that precedes contralateral excitation as an essential component in the ITD detection circuitry in the medial superior olive (MSO) (Brand et al, Nature 417:543, 2002). Here we present indirect physiological evidence for such a preceding inhibition from extracellular recordings in the gerbil dorsal nucleus of the lateral lemniscus (DNLL).

DNLL neurons receive direct excitatory input from the ipsilateral MSO and to a large extent reflect the physiological properties of MSO projection neurons. In this study we only assessed neurons that responded to both monaural stimulation at the ipsilateral ear as well as to monaural stimulation at the contralateral ear. We tested 24 of these excitatory/excitatory (E/E) neurons using different combinations of ipsi- and contralaterally presented downward frequency modulated sweeps (FM↓) and adjusted stimulus amplitudes to elicit only one or two single action potentials in response to ipsilateral stimulation. Thus, the responses to each stimulus could be identified and analysed separately. Then the cell was tested for different interaural delays by starting with a contralateral delay of >1ms that was stepwise reduced.

Out of 24 cells 10 units showed no effect on the ipsilateral evoked response for any delay of the contralateral stimulus. In six ITD sensitive and 8 additional E/E neurons, however, the ipsilaterally evoked response was either strongly inhibited or showed significant changes in its latency at interaural delays at which the calculated (based on the monaural responses) coincidence of binaural excitation was not yet reached. The influence on the ipsi response arose for time-lags of the contralateral excitation of 0.3 to 0.8 ms.

Assuming that these effects are first generated at the level of the MSO and only mirrored by the neurons of the DNLL these findings may corroborate the hypothesis of contralateral inhibition preceding contralateral excitation in the MSO as proposed by Brand et al..

## **Frequency organization of the medial geniculate body in the Mongolian gerbil**

**Peter Bäuerle, Manfred Kössl**

**Zoological Institute, J.W. Goethe University, Frankfurt Main/ Germany**

A common organization pattern for the primary auditory pathway is the systematic variation of different frequencies along a spatial arrangement (tonotopic map). In the central part of the auditory pathway information is relayed from the inferior colliculus (IC) in the midbrain via the medial geniculate body (MGB) of the thalamus to the auditory cortex (AC). Based on cytoarchitectonics the MGB is classically divided in three main parts: the ventral, dorsal and medial part, while only the ventral part belongs to the primary auditory pathway. The aim of this study was to investigate the parcellation of auditory information processing and the appearance of a putative tonotopic organization in the vMGB in the Mongolian gerbil. We used extracellular single and multi-unit recordings techniques with white noise or randomly presented pure tones stimuli in varying intensities to map basic neuronal response properties. The recording sites were histologically verified.

We found according to the literature that neurons in the ventral part of the MGB are organized in a tonotopic fashion with a gradient in all three spatial directions. In medio-lateral direction low frequencies are located dorso-lateral, while high frequencies located ventro-medial. Additional we found a gradient in rostro-caudal direction with low frequencies represented dorso-rostral and high frequencies ventro-caudal. In this direction we could also observe a gradient in latencies with the occurrence of shorter latencies rostral and longer latencies caudal.

Supported by the Graduate Program "Neural plasticity: Molecules, Structures, Functions".

## **Barn owls do not depend on high frequency auditory signals to approach a distant target.**

**Peter Bremen, Martin Singheiser, Dennis T.T. Plachta, Rob F. van der Willigen, Hermann Wagner**

Institut für Biologie II, Kopernikusstr. 16, 52074 Aachen, Germany

Authors for correspondence: [peter.bremen@rwth-aachen.de](mailto:peter.bremen@rwth-aachen.de), [martin@bio2.rwth-aachen.de](mailto:martin@bio2.rwth-aachen.de)

Barn owls (*Tyto alba*) are able to catch prey in total darkness by using their auditory system, which is most sensitive in the frequency range from 0.5 to 10 kHz<sup>1</sup>. Payne claimed that owls would not strike targets producing sounds containing only frequencies below 5 kHz<sup>2</sup>. We are interested in the frequency range that is used by the owl for sound localization and, therefore, started an experimental series with free-flying barn owls. In a first step, we generated three noises, each containing a different frequency band by separation with a Biquad-filter (13 dB per octave). Noise 1 contained the frequency band from 1-10 kHz, noise 2 from 1-5 kHz, and noise 3 from 5-10 kHz.

A closed loop paradigm was used to train two owls to fly in a familiar anechoic chamber from a perch to a ramp (variable distance between 2.65 and 3.65 m), which contained 5 shielded loudspeakers at different azimuths (-18.4°, -9.2°, ±0°, +9°, +18.4° at 3.65 m, angle as seen from the perch). The speakers could be selected individually to emit a noise (23 dB SPL at 1 m distance from the speaker). A sound from the speaker initiated a lift off of the owl and an approach of the loudspeaker ("strike"). After striking, the owls had to wait before returning to their starting position until a LED, positioned above the perch, became switched on. Owls were rewarded after return for striking the target (correct performance: striking within a radius of 10 cm around the active loudspeaker). Target approach was monitored online using an infrared tracking system.

It took the owl 1 22 days and owl 2 13 days to learn the paradigm (75% correct performance). To avoid effects of learning concerning the positions of the speakers in the free flight chamber, we altered the distance between parts of the ramp including one or two speakers and the perch as well as the height of the perch itself.

In contrast to the finding mentioned above<sup>2</sup>, the owls did strike even if the stimulus contained only frequencies below 5 kHz.

As a next step on our experimental roadmap we will present more focused noise signals (in 1 kHz steps) and measure the flight path as a whole, as well as latencies and striking precision to be able to describe the frequency bands important for sound localization more precisely.

1. Masakazu Konishi: How the Owl Tracks Its Prey, 1973, American Scientist, Volume 61, 414-424

2. Roger S. Payne: Acoustic Location Of Prey By Barn Owls (*Tyto Alba*), 1971, J.Exp.Biol., 54, 535-5730

## **Simultaneous localization of multiple sound sources**

Sonja C. Schmid-Fetzer and Joachim Ostwald  
Tierphysiologie, Zoologisches Institut, Universität Tübingen,  
Auf der Morgenstelle 28, 72076 Tübingen, Germany

Echolocating animals like bats and dolphins receive multiple echoes from different reflecting surfaces for almost each of their echolocation calls. In order to represent their surroundings they have to simultaneously process the location of these different sound sources. In a psychophysical experiment we focused on the question whether human listeners are able to simultaneously process the direction of two concurrently presented acoustic stimuli and whether their ability depends on attention.

Subjects, all of them with normal hearing, had to solve a twofold 2-AFC localization task under open field conditions in a sound-attenuating, anechoic chamber. Two pairs of loudspeakers were arranged on a semicircle around the subject. In every trial, one loudspeaker of each pair, respectively, presented an independently generated white noise burst. Consequently, two similar non-coherent acoustic stimuli were presented simultaneously. The subject's task was to decide which of the two loudspeakers had been the sound source for each side, respectively, without any head movements.

To study the influence of attention we used stimuli of different durations. For long stimulus durations, such as 100 ms, subjects should be able to switch their attention from one pair of loudspeakers to the other, thus being able to process the stimuli successively. Short stimulus durations, such as 5 ms, on the other hand, should prevent this switching of attention, forcing the subjects to focus on one side only. We assume sound localization performance to be superior in attended pairs of loudspeakers, shortening stimulus duration should therefore reduce the rate of correct responses substantially.

Under certain conditions subjects were able to solve this twofold 2-AFC task. For a relatively simple task, featuring a within loudspeaker pair separation of  $24^\circ$ , all subjects were able to localize the sound source for both sides, even for stimulus durations as short as 2 ms. For a comparatively difficult task with a within pair separation of only  $8^\circ$ , the localization task could only be solved correctly for both sides for long but not for such short stimulus durations.

These results indicate the possibility of a simultaneous processing of concurrently presented stimuli for relatively simple tasks. For a stimulus duration of 2 ms, switching attention between the pairs can be ruled out and as all subjects still were able to localize the sound source almost as well as for long stimulus durations, the hypothesis of successive processing has to be rejected.

This is supported by the fact that subjects reported perceiving just one complex signal where the two stimuli had merged into one entity, instead of perceiving two distinct acoustic events. They based their decision on the perceived properties of this auditory scene. A series of experiments was designed to prevent a merged perception.

## Organization of the auditory corticofugal system in the Mongolian gerbil

Eike Budinger & Henning Scheich, Leibniz Institute for Neurobiology, Brennekestr. 6, 39118 Magdeburg, Germany

The auditory cortex is the centralmost processing stage of auditory information along the ascending auditory pathway. It is also the starting point of the descending auditory pathway which was hitherto thought to be organized mainly as a chain of discrete feedback loops with most prominent corticocollicular, colliculoolivary, and olivocochlear projections. Today, notably due to new and highly-sensitive tracing techniques, more direct descending connections between the structures of the auditory pathway are known, which bypass the local feedback loops. Here we like to show that even the auditory cortex directly projects to all major auditory subcortical structures, *viz.* to the medial geniculate body (MGB), inferior colliculus (IC), nuclei of the lateral lemniscus (NLL), nuclei of the superior olivary complex (SOC), and cochlear nuclei (CN). These corticofugal connections are largely field- and frequency-specific, *i.e.* the connectivity pattern vary for the different auditory fields and for different domains of high-frequency (hf) and low-frequency (lf) representations in these fields.

We investigated possible field-specific corticofugal projections by simultaneous injections of different fluorescent tracers (fluorescein-, tetramethylrhodamine-, cascade blue-labeled dextranamine) into the primary auditory field AI, anterior field AAF, dorsoposterior field DP, and ventroposterior field VP of the Mongolian gerbil (*Meriones unguiculatus*). A possible frequency-specificity in these projections was investigated by simultaneous injections of two different tracers (fluorescein-, and tetramethylrhodamine-labeled dextranamine) into the hf and lf representation area of AI.

A *field-specific* organization was observed in the corticothalamic and corticocollicular connections:

AI projected to all subdivisions of the MGB and IC with strongest projections to the principal ventral division of the MGB (MGv), the dorsal cortex of the IC (DCIC), and the external cortex of the IC (ECIC). There were only sparse projections to the central nucleus of the IC (CIC).

AAF also projected to all subdivisions of the MGB and IC but with strongest projections to the magnocellular medial division of the MGB (MGm), which is also related to other sensory modalities, and to the DCIC, where the projections terminated in more rostral aspects of the DCIC than the projections of AI and DP/VP.

DP and VP projected to all subdivisions of the MGB and IC but with strongest projections to the dorsal division of the MGB (MGd), which has also polymodal affiliations. Here, in its deep dorsal subnucleus (MGd/DD), projections from DP terminated in more medial parts of the MGd/DD than projections from VP, which terminated in more lateral parts of the MGd/DD. The axonal terminations of DP/VP in the DCIC were found in more caudal aspects than those of AI and AAF.

Field-specific corticolemniscal, corticoolivary, and corticocochlearnuclear connections were not observed.

A *frequency-specific* organization was observed in the corticothalamic, corticocollicular, and corticolemniscal connections of AI:

Hf projections of AI terminated in more medial parts of the laminated MGv (*pars lateralis*, Lv) than lf projections, which terminated in more lateral layers of the MGv/Lv. In addition, there was a slight caudoventral (hf) to rostradorsal (lf) gradient in the labeling pattern. In *pars ovoidea* (Ov) of the MGv, hf projections terminated in more peripheral layers than lf projections, which terminated in more central layers of the MGv/Ov. The projection patterns to MGv/Lv and MGv/Ov correspond to the known tonotopic organizations within these structures.

Within the DCIC, hf projections of AI mainly terminate in its outer layers, whereas lf projections mainly terminate in its inner layers. The sparse projections to the CIC are also topographically organized: endings of hf fibers can be found in the more ventromedially located fibrodendritic laminae of the CIC than the endings of lf fibers, which can be found in more dorsolateral laminae. Again, this projection pattern corresponds to the suggested tonotopic organization of the IC.

Within the NLL, the dorsal nucleus (DNLL) received frequency-specific input from AI. Hf projections of AI terminated in the more ventromedial aspects of this nucleus, whereas lf projections terminated in the more dorsolateral aspects of the DNLL, again matching the suggested tonotopic organization of the DNLL.

Frequency-specific corticofugal connections with the other nuclei of the lateral lemniscus, SOC, and CN were not observed but can not be excluded, since only a limited number of labeled terminations was seen in these structures.

Results show that the auditory cortical fields have common but also differentially organized direct corticofugal connections with the structures of the auditory pathway, bypassing the major local feedback loops. We suggest that AI is a major source for the corticofugal modulation of the lemniscal (tonotopic) pathway and acts on the subcortical auditory nuclei in a frequency-specific manner. AAF, DP, and VP seem to act particularly on neurons of the non-lemniscal (non-tonotopic, diffuse) pathway.



**Basic properties of auditory cortex and processing of stimulus roughness in the bat  
*Phyllostomus discolor***

U. Firzlaff, B. Schwellnus, L. Wiegrebe and G. Schuller  
Department Biologie II, Ludwig-Maximilians-Universität, Großhaderner Strasse 2  
D-82152 Planegg-Martinsried

The auditory cortex of the lesser spear-nosed bat *Phyllostomus discolor* was mapped with extracellular recording techniques in order to establish the extend and basic physiological properties of cortical fields. Pure tones with 20 ms duration were presented binaurally via earphones. Best frequencies of 62 single neurons recorded in two lightly anaesthetized bats were in a range between 18 to 85 kHz, with thresholds ranging from 20 to 70 dB sound pressure level. Two auditory cortical fields with mirror-imaged frequency gradients along the rostrocaudal axis and a common high frequency border could be distinguished. These fields probably represent the primary auditory field and the rostrally adjoining anterior auditory field, as found in a closely related bat species *Carollia perspicillata* (Esser and Eiermann, 1999) and other mammals.

In addition, the ability of cortical neurons to encode acoustic roughness was tested in a subset of 33 neurons. Stimuli consisted of echolocation calls convolved with impulse responses with different degrees of roughness. 21% of neurons responded significantly stronger to stimuli with higher roughness with the majority of selective neurons being located in anterior regions of auditory cortex. Echo roughness can be classified by *P. discolor* in behavioral experiments (Grunwald et al., 2004; cf. Abstract “Discrimination of echo roughness in the fruit-eating bat *Phyllostomus discolor*”) and might serve the classification of natural textures.

Esser, K.-H., Eiermann, A., Eur. J. Neurosci. 11, 1999.  
Grunwald, J.-E., Schörnich, S., Wiegrebe, L., PNAS 101 (15), 2004.

Supported by grants from the Deutsche Forschungsgemeinschaft (SCHU 390/6-5) and the Volkswagenstiftung (I/79782).

## Topographic organization of the auditory cortex of the bat *Molossus molossus*

Elisabeth Foeller<sup>1\*</sup>, Emanuel Mora<sup>2</sup>, Manfred Kössl<sup>1</sup>

<sup>1</sup> Zoologisches Institut J.W. Goethe Universität, Frankfurt

<sup>2</sup> Faculty of Biology, Havana University, Cuba

\*corresponding author: efoeller@zoology.uni-frankfurt.de

The bat *Molossus molossus* uses a large call repertoire with the highest level of plasticity in its echolocation system. While searching for prey, *M. molossus* emits pairs of narrow-band echolocation pulses that alternate in frequency (34.5 and 39.6 kHz). After the prey is detected, more broadband and frequency-modulated approach calls are emitted (frequency range: 42-52 kHz). In this study, we investigated auditory specializations complementing echolocation behavior in the auditory cortex. The cortical representation of call frequencies was measured and a frequency map of the auditory cortex was created.

Extracellular neuronal recordings were made at several penetration sites across the left cortical hemisphere in anaesthetized bats (cortical depths: 110-650 µm). Neuronal responses to pure tones (10ms duration) of various frequencies and intensities were measured. Peristimulus-time histograms were constructed and frequency tuning curves calculated. For each single or multi unit, we analyzed characteristic frequency, threshold, tuning sharpness and rate-level functions.

Auditory responses to pure tones could be elicited in a cortical area covering approximately 2 by 2 mm. Frequencies corresponding to search call frequencies were overrepresented and found mostly in the central part of the auditory cortex. Neurons with multi peaked tuning curves or separated response areas were often found in the dorsal part. Interestingly, several neurons were responsive to frequencies between 30-40 kHz and also 75-80 kHz suggesting neuronal sensitivity to a combination of the first and second harmonic of the search call.

Tuning sharpness was highest for neurons with characteristic frequencies between 30-50 kHz (maximum Q10dB: 48; maximum Q40dB: 32).

This study provides the basis for further investigating spectral and temporal processing of behaviorally relevant acoustic signals in *M. molossus*.

Supported by the DFG

## Development-dependent Effects in the Auditory Field-L Complex Of the Zebra Finch Brain

**Gabriele Schebesch (1), Hans - Joachim Leppelsack (2)**

(1) Dept. Neurobiologie, AG Grothe, Ludwig-Maximilians Universität, Muenchen, Germany

(2) Corresponding author, Fachgebiet Spezielle Zoologie, Techn. Univ. Muenchen, Garching, Germany

The field-L complex represents the highest processing centre of the auditory pathway in songbirds. In the zebra finch (*Taeniopygia guttata*) this complex can be subdivided in six functionally different areas due to their tonotopy and their response characteristics (Gehr et al., Neuroreport 10, 375, 1999; Gehr and Leppelsack, Europ. J. Neurophysiol. 12, 132, 2000).

The aim of this study was to investigate the development of the field-L complex in detail. Therefore, the functional characteristics of these regions in zebra finches from the age of 25 days after hatching to 60 days after hatching in comparison to an adult zebra finch were investigated. Multi-unit recordings were carried out in these auditory forebrain areas on seven awake male zebra finches. The stimulus sequence contained several pure tones, white noise and a part of a natural song.

The field-L complex showed a small increase in size over the examined development period, which has to be caused by new neurones outside the largest area NA-L, appearing and being activated during this time. These neurones belong to functional regions additional to NA-L. However, since these neurones started their distinct role in auditory processing the response behaviour of a region to presented stimuli was constant right from its appearance. Meaning that the tonotopy was completed and the spectral and amplitude composition of the answer to a stimulus was the same as in adult songbirds.

Some development effects were also observed in the response strength, and the spontaneous activity. The response strength increased during the investigated development period, whereas the spontaneous activity decreased. A possible explanation for the decrease of the spontaneous activity is an improvement of the energetic state of the neurones. The ambition is to achieve an efficient spontaneous discharge rate during the passive state. This gives the neurones the ability to fire with higher action potential rates, when they are stimulated by a stimulus. With higher firing rates the effects of inhibition gets clearer. In addition the ability of frequency discrimination improves with the development of the songbirds brain.

## Psychometric functions for the detection of gaps in broad-band noise: the effect of age.

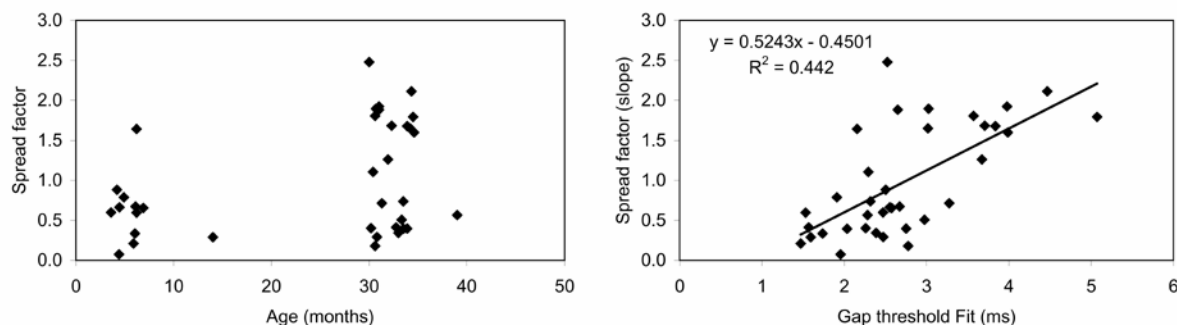
Otto Gleich<sup>1</sup>, Ingo Hamann<sup>1</sup>, Malte C. Kittel<sup>1</sup>, Georg M. Klump<sup>2</sup>, Jürgen Strutz<sup>1</sup>

<sup>1</sup> ENT-Department, University of Regensburg, FJS-Allee 11, 93042 Regensburg, Germany

<sup>2</sup> Fak. V, IBU, AG Zoophysiologie und Verhalten, Carl von Ossietzky Universität Oldenburg, Postfach 2503, 26111 Oldenburg, Germany

One measure to characterize temporal auditory resolution is to determine the minimal duration of a temporal gap in an ongoing sound or noise that can be detected by an individual (gap-detection threshold). It has been shown for humans (Snell and Frisina, 2000, JASA 107:1615-1626) and gerbils (Hamann et al., 2004, JARO 5:49-57) that the proportion of subjects with elevated gap-detection thresholds is higher in old as compared to young individuals. These studies also provide evidence that a peripheral high-frequency hearing loss is not a sufficient explanation for the observed impaired temporal resolution in some old subjects and rather suggest that processing deficits in the ascending auditory pathway are involved. According to signal detection theory, the slope of a psychometric function that relates response probability to signal level is affected by the internal noise (e.g. non-stimulus related neural activity) that interferes with the detection of the signal (Green and Swets, 1974, Signal detection theory and psychophysics. Krieger Publishing, Huntington New York; Penner, 1986, J Speech Hear Res 29:400-406). Consequently, the analysis of psychometric functions beyond simply determining a threshold but also considering the slope was attempted to further characterize potential age-dependent changes of auditory temporal processing.

A reanalysis of the psychometric functions for the detection of gaps in a broad-band noise that had been collected by Hamann et al. (2004 JARO 5:49-57) was performed. Adjusting the carrier level for each individual to 30 dB above the threshold for the detection of the noise pulse was intended to minimize the effects of any potential small peripheral hearing loss (Glasberg et al., 1987, JASA 81:1546-1556), although the individuals in the sample of animals tested showed no obvious sign of severe threshold elevation (threshold range for the broad-band noise: 2-18 dB SPL). To obtain a quantitative measure of the slope of the psychometric function, a best fit logistic function as suggested by Lam et al. (1996, JASA 99:3689-3693) was adapted to the raw data using "Excel solver". The parameters that were varied during the fitting procedure were the spread factor, that resembles a quantitative measure of the slope (where larger numbers characterize shallower slopes) and a threshold value that represents the midpoint of the psychometric function between the maximum-response rate and the response rate in the absence of a gap (shams).



The above figure summarizes the results. The left graph shows the spread factor as a function of age, and the statistical analysis revealed that the slopes of the psychometric functions in old animals were on average shallower as indicated by the larger spread factors (Mann Whitney U, 12 young, 24 old,  $p = 0.049$ ). The right graph shows the spread factor as a function of the gap-detection threshold and the correlation is highly significant ( $p < 0.001$ ). A separate analysis of mean  $d'$  (a quantitative measure of perceptibility) as a function of gap duration for animals with good ( $N = 23$ ) and animals with impaired ( $N = 13$ ) temporal resolution revealed that a doubling of the gap duration increased  $d'$  by approximately 1.0 and 0.7 respectively in the two groups.

These data show that the slopes of the psychometric functions in animals with impaired temporal resolution (predominantly old animals, Hamann et al., 2004 JARO 5:49-57) are shallower as compared to animals with good temporal resolution. In view of signal detection theory this finding indicates that the variability of the internal noise is higher in animals with impaired temporal resolution. One hypothesis to explain this observation is that an impaired function of the inhibitory, specifically of the GABAergic system (e.g. Caspary et al., 1995, Exp Gerontol 30:349-360) might contribute to elevated internal noise levels. This hypothesis is supported by our recent observation, that pharmacological intervention by increasing the availability of GABA can improve impaired temporal resolution (Gleich et al., 2003, Neuroreport 14:1877-1880).

Supported by the DFG Str275/4-3. We thank S. Kopetschek and C. Woegerbauer for help with animal care and assistance during the experiments.

## **Inhibitory and excitatory response areas of neurons in the inferior colliculus in awake chinchillas**

**Ala Al Khatib, Désirée Biedenkapp, Ulrich W. Biebel, Jean W. T. Smolders**

J.W.Goethe-Universität, Institut für Physiologie II, Sinnes- und Neurophysiologie, Theodor-Stern-Kai 7, Frankfurt am Main, Germany, E-mail: Ala\_Alkhatab@yahoo.de

The goal of the present study was to determine the frequency response area of neurons in the central nucleus of the inferior colliculus in awake unanesthetized chinchillas.

Chinchillas were implanted with a recording chamber and holder on the skull which allowed stereotactic microelectrode recordings from the inferior colliculus in awake restrained animals. Excitatory and inhibitory frequency response regions in the response area from over 250 neurons in the central nucleus of the chinchilla inferior colliculus (ICC) were measured by extracellular single- and multi-unit recordings. One-tone and two-tone stimuli were used to determine both response regions. In case of two-tone stimuli, one tone burst (65 ms duration) had a fixed frequency at the characteristic frequency (CF) of the neuron and a level of 10 dB above threshold at CF. The response area was determined as a function of the frequency and level of the second tone burst (70 ms duration), which was started 5 ms before, but ended with end of the the fixed tone burst.

Single-tone excitatory regions of the response area of ICC neurons from awake chinchillas could be classified as V-shaped asymmetrical (with steeper high-frequency slope), V-shaped symmetrical, or non-monotonous-complex. Single-tone inhibitory response regions were prominent mostly in units with high spontaneous firing rate. In general the single-tone and two-tone inhibitory regions of the same unit were markedly different.

With two-tone stimuli we observed different shapes of inhibition regions in neurons with similar excitatory response regions. Neural response areas were divided into 4 groups:

- (1) Areas with strong inhibitory response regions, which appeared to form the V-shaped excitatory response regions.
- (2) Areas with weak inhibitory regions which were not related to the shape of the excitatory response region.
- (3) Areas with inhibitory regions lying within the excitatory response region.
- (4) Areas which showed complex non-monotonic restricted or skewed excitatory regions.

The response areas neurons in group (4) were characterized by strong inhibitory regions, overlying most of the excitatory response region. These complex response areas were only observed at low frequencies ( $CF < 500$  Hz) in the dorsal part of the IC. Excitatory response regions were always similar in shapes at different depths of a dorso-ventral recording track. On the contrary, inhibitory response regions varied in shape with penetration depth.

The excitatory response types observed were similar to those reported in the anesthetized mouse (xylazine/ketamine, Egerova et al., 2001, Exp. Brain. Res. 140:145-161). However, inhibitory response regions in the ICC of awake chinchillas and their relation to the excitatory regions of the response area were more variable than reported in anesthetized mice. This may indicate that the relation of excitation and inhibition in the ICC in anesthetized and awake animals is different.

Supported by the DFG, SFB 269

## **Effects of Carboplatin on ABR and local field potentials in neurons of the inferior colliculus of awake chinchillas**

**Désirée Biedenkapp, Ala Al Khatib, Ulrich W. Biebel, Jean W.Th. Smolders**

J.W.Goethe-Universität, Institut für Physiologie II, Sinnes- und Neurophysiologie  
Theodor-Stern-Kai 7, Frankfurt am Main, Germany, E-mail: Desiree.Biedenkapp@web.de

Carboplatin preferentially damages inner hair cells and type I spiral ganglion neurons in the inner ear of the chinchilla. In order to understand the consequences of selective inner hair cell (IHC) loss, ABRs and local field potentials (LFP) in response to clicks were measured at different locations in the central nucleus of inferior colliculus (IC) in chronic operated unanaesthetized chinchillas.

Animals were implanted with a recording chamber and holder on the skull which allowed stereotactic microelectrode (1 MOhm) recordings from the IC. Sound stimuli were clicks presented at different sound pressure levels from a sound-source located 30 cm lateral to the contralateral ear. After control measurements the animals were given a total dose of 80 mg/kg Carboplatin in two doses of 40 mg/kg/24h each (day -1 and day 0) resulting in a partial loss of IHCs. ABRs and LFPs were recorded at regular intervals post Carboplatin over a period of at least 20 days. After the final recording session the animals were sacrificed and the brain and inner ear prepared for histological investigation of recording sites and verification of IHC loss respectively.

Starting at the first day after the second dose of Carboplatin (day 1) there was a progressive decline of amplitude of all ABR wave components. Peaks between 0-5 ms after click onset disappeared almost completely. ABR waveforms between 5-10 ms showed two to three peaks before medication but only one negative peak from day 7 on. Peaks with > 10 ms latency remained nearly unchanged in shape and amplitude. In addition the latencies of all peaks gradually increased after Carboplatin application. There was no conspicuous time period for the changes of the responses, rather the effects became progressively stronger with time after treatment.

The general waveform of the LFPs in the IC consisted of two positive peaks and two negative peaks in between. Peaks latencies ranged from 4 to 15 ms. Waveforms were similar in each dorso-ventral penetration track except for a shift in latencies corresponding to the tonotopic gradient. In some locations of the more ventral parts of the IC, the first positive waveform showed two peaks instead of one. From caudal to rostral and from lateral to medial locations in the IC, LFP waveforms differed considerably in amplitude and latency of the individual peaks. In the caudal IC, peak latencies were longer compared to the rostral part. Changes in LFPs were recorded over a period of 20 days after Carboplatin treatment from the same animals in one electrode track located centrally through the IC and one more peripheral track. The waveform of the LFPs from the peripherally located tracks gradually lost its complexity together with a decrease in amplitude over the observation interval. The centrally located tracks showed an almost unchanged waveform and much less amplitude reduction. In most tracks a transition period was observed around day 2. In this period the characteristic positive peaks remained but the negative ones in between disappeared. We did not observe an increase in amplitude of any component of the ABR or LFP waveform at any time after Carboplatin treatment, but the decrease in amplitude of the components > 5 ms was smaller than that of those with shorter latencies.

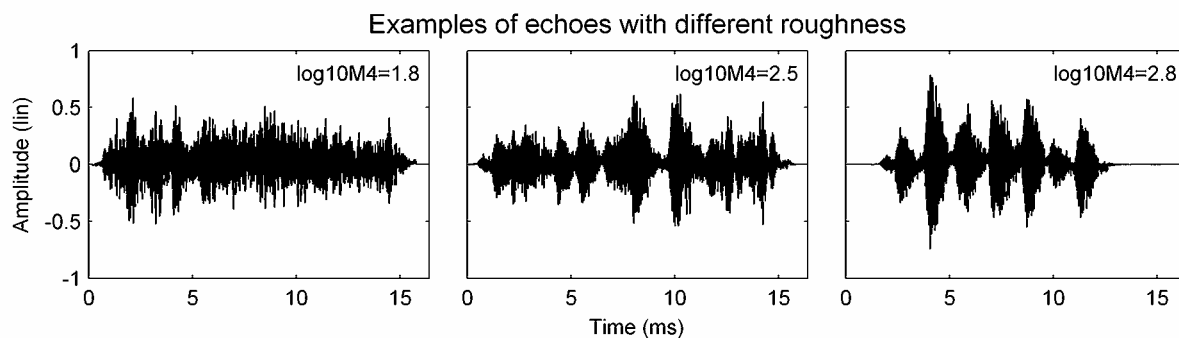
Supported by the DFG, SFB 269

## Discrimination of echo roughness in the fruit-eating bat *Phyllostomus discolor*

Sven Schörnich and Lutz Wiegrebe  
Department Biologie II, LMU Munich,  
Großhadernerstr. 2, D-82152 Planegg-Martinsried

Through echolocation, bats are not only able to detect an object in the darkness, but also to gather information about its structure. It has been shown that the fruit-eating bat *Phyllostomus discolor* is able to use the roughness (i.e. the amount of the envelope fluctuation) of a virtual object's impulse response as a parameter for the classification of complex natural objects like trees or bushes [1]. The roughness of an object's impulse response is quantified as the base-ten logarithm of its 4<sup>th</sup> Moment ( $\log_{10}M_4$ ).

In the current psychoacoustical playback experiment we investigate the ability of *P. discolor* to discriminate echoes generated with a fixed reference roughness from echoes with several higher test roughnesses. In a two-channel playback setup, the ultrasonic emissions of the bat are recorded with two microphones and convoluted both with an impulse response possessing the reference roughness and with an impulse response with a test roughness. The resulting echoes are played back over the two speakers, and the bats are trained to crawl towards the speaker delivering the echo with the reference roughness. The following figure shows examples of such convoluted echoes with different 4<sup>th</sup> Moments ( $M_4$ ).



Discrimination performance is assessed as a function of the test roughness.

When the reference roughness was 1.8, the test roughness had to be at least 2.5 for significant discrimination.

When the reference roughness was 2.5, the test roughness had to be at least 2.8.

Experiments with additional reference roughnesses are in progress.

These psychophysical results are compared with the performance of electrophysiologically recorded cells from the auditory cortex of *P. discolor*. (cf. Abstract "Basic properties of auditory cortex and processing of stimulus roughness in the bat *P. discolor*")

[1] Grunwald, J.-E.; Schörnich, S.; Wiegrebe, L.; *Classification of natural textures in echolocation*; PNAS 101 (15), 5670-5674, (2004)

Supported by the DFG (WI 1518/7)

## Comodulation Masking Release in the house mouse (*Mus musculus*)

**Verena N. Weik, Karin B. Klink, Georg M. Klump**

Zoophysiology and Behavior Group, Oldenburg University  
Carl-von-Ossietzky Str. 9-11, 26129 Oldenburg, Germany

The term "Comodulation Masking Release" (CMR) was used by Hall et al. (1984, J Acoust Soc Am 76: 50-56) to describe the improved detection of a signal in a band-limited noise masker that exhibits correlated amplitude fluctuations (i.e., comodulation) over a wide range of frequencies compared to the detection of the signal in an unmodulated masker of the same bandwidth. It has been suggested that the auditory system exploits two types of cues for improving detection in comodulated maskers: (1) within-channel cues that can be extracted from a single auditory filter centred on the signal frequency, and (2) across-channel cues that are computed by the auditory system comparing the excitation across separate auditory filters (Moore 1992, J Acoust Soc Jpn 13: 25-37). Using the psychoacoustic paradigm developed by Hall et al. (1984), we determined the amount of CMR in the house mouse, a species that has its best hearing at frequencies of 10 kHz and above and has relatively wide auditory filters (Ehret 1976, Biol Cybern 24: 35-42).

Four mice of the NMRI-strain and three mice of the strain C57BL/6 were trained to report the detection of a 10 kHz tone (total duration: 800ms, 10 ms Hanning ramps) centred in a continuous noise masker with a bandwidth of 0.1, 0.2, 0.4, 0.8, 1.6, 3.2, 6.4, 10, 12.8 or 20 kHz. Detection thresholds for the tone presented in modulated or unmodulated maskers were determined using a Go/NoGo-procedure with food rewards and the method of constant stimuli. The masking noise had a spectrum level of 40 dB SPL. The most salient signals were presented with a level of between 30 and 45 dB above the spectrum level of the background noise. Applying signal-detection theory, thresholds were calculated from a psychometric function summarizing data from two sessions with 50 trials each. Threshold criterion was a  $d'$  of 1.8.

The auditory filter bandwidth (critical band) can be determined from the relation between the detection threshold and the bandwidth of the unmodulated masking noise. At a frequency of 10 kHz, the auditory filter bandwidths of the NMRI mouse and the C57BL/6 mouse were 3.3 kHz and 5.1 kHz, respectively. Ehret (1976) observed an auditory filter bandwidth of 6.3 kHz in the NMRI mouse. In both mouse strains we found a considerable CMR that did not differ between the strains. For noise maskers that were larger than the auditory filter bandwidth (i.e., had a bandwidth of 6.4 kHz and more) the CMR ranged from 8.5 to 9.3 dB. A similarly large CMR was also observed for masking noise of a bandwidth ranging from 0.4 to 3.2 kHz, i.e., for masking noise with a relatively wide bandwidth that was smaller, however, than the auditory filter bandwidth. The CMR was reduced for maskers with a bandwidth of less than 0.4 kHz, and at a masker bandwidth of 0.1 kHz no significant difference was observed between the signal-detection threshold in comodulated and unmodulated noise indicating no masking release at the lowest bandwidth that was tested. The data suggest that within-channel cues are sufficient to explain CMR which is consistent with a model that was used to explain CMR in humans in this paradigm (Verhey et al. 1999, J Acoust Soc Am 106: 2733-2746). Further experiments applying an alternative paradigm (i.e., a flanking-band paradigm, see McFadden 1986, J Acoust Soc Am 80: 1658-1667) are needed to evaluate the contribution of across-channel cues to CMR in the mouse.

Supported by the Deutsche Forschungsgemeinschaft (SFB 517, FOR 306)



**A parametric study of electrically evoked activity in gerbil auditory cortex**

*Achim Engelhorn, Daniel Ensberg, Matthias Deliano, Henning Scheich, Frank W. Ohl*

Leibniz-Institut für Neurobiologie, Magdeburg

One of the main questions in neuroengineering is how to interface the brain for the exchange of information with artificial devices. Direct stimulation in the depth of cortex using brief electrical pulses produces characteristic changes in electrical potential at and near the stimulation site, comparable to sensory evoked potentials. In order to elucidate the mechanisms underlying the generation of electrically evoked responses and to investigate their suitability for exchanging information with artificial devices a proper understanding of their composition and dependency on stimulation parameters is required.

In this parametric study we stimulate the primary auditory cortex (AI) of the Mongolian gerbil (*Meriones unguiculatus*) and investigate the typical components of electrically evoked potentials (EEPs) and how they change according to variations in stimulus amplitude and pulse length duration. In a further experiment we compared EEPs with auditory evoked potentials (AEPs). Lastly, further inferences about the nature of the electrically and acoustically evoked neuronal populations, respectively, are drawn from collision-like experiments using combined electrical and acoustic stimulation.

Investigating the influence of spatial attention on the processing of frequency-modulated tones in the rat

Wolfger von der Behrens, Bernhard Gaese

Johann Wolfgang Goethe-Universität Frankfurt am Main, Zoologisches Institut

One important stimulus dimension in auditory perception is the frequency of a tone and its modulation. Besides its ecological meaning as a dominating part of species-specific signals in many mammalian species, including human speech, the feature of frequency-modulation is comparable with the perception of movements in the visual modality and has a significant neuronal correlate. Most neurons in the rat primary auditory cortex have a preference for either upward or downward modulated tones. This direction-preference is ordered in parallel to the characteristic frequency of the neurons in the primary auditory field.

Selective attention can be considered as an internal state of the brain which mediates the allocation of processing resources on certain aspects of the sensory environment. For spatial attention, as investigated in the present study, has been shown to facilitate selective listening in man in several cases. Its neuronal basis, however, remains unclear.

The behavioural paradigm used as a first approach combines the cued orienting of spatial attention with a 2AFC-discrimination task. The cue indicated the location of the following target with a predictability of 80%. The discrimination task demanded the distinction of upward modulated versus downward modulated tones (target stimulus). This paradigm has the advantage that the cueing and detection are fully separated. The cue did not convey any information regarding the discrimination task

We investigated neural correlates of the spatial orienting of attention at the level of the primary auditory cortex while the animal performed the behavioural task. Extracellular single unit activity was compared for the situations with or without attention being directed towards the location of the target stimulus. Recordings were performed in both hemispheres with 4 single channel electrodes and one tetrode. The tetrode allows for improved separation of multiple single units when performing spike separation based on the waveform of action potentials. This approach allows for the matching of defined behavioural situations with discrete neuronal conditions.

Rats were able to learn the task and perform with up to 500 decisions in one session (about 45 min.). The modulation rate of the exponentially frequency-modulated tones varied between 10 and 60 octaves/s. Discrimination between upward and downward modulation was a function of the modulation rate. Average hitrate (percent of correct discriminated tones) of 4 animals was best described by a psychometric function with its dynamic range between 20 and 50 octaves/s.

The behavioural data showed an attentional effect on the hit rate of the animals. Over the dynamic range there was a shift of the psychometric function towards slower modulation rates for stimuli without attention. Detection of stimuli with attention was only marginally effected. No effect was visible on the reaction times of the animals. Electrophysiological recording in the primary auditory cortex was very stable and showed clear responses noise bursts (being the cue). So far, however, only ambiguous effects of attention were visible.

# Neural representations of temporally modulated sounds in the auditory cortex of macaque monkeys: effects of ketamine anesthesia.

Elena Oshurkova, Henning Scheich, Michael Brosch

Leibniz Institute for Neurobiology, Department Auditory Learning & Speech, Magdeburg, Germany.

The results of recent studies showed that the functional properties of neurons distinguish between anesthetized and awake animals. The goal of the present study was to compare the effect of anesthesia for response properties of cortical neurons in the primary auditory cortex and caudomedial area of macaque monkeys (*Macaca fascicularis*).

With a multielectrode array we recorded at many sites the action potentials of small clusters of neurons in the left auditory cortex of four (two awake and two ketamine anesthetized) non-performing macaque monkeys. Acoustic stimuli were click trains of different rates, ranging from 0.5 to 300 clicks per second on a logarithmic scale, which were presented at different intensities (20 to 62 dB SPL). Individual trains had a duration of 2 sec (4 sec for the click rate of 1/s), followed by 4 sec of silence.

We calculated (1) the response strength, which was the total number of spikes that occurred during the train (excluding the first 200 ms of the train) and divided this number by the number of spikes during silence. (2) The number of spikes in the first 20 ms after each click (3) For define the degree of response synchronization we use the vector strength. (4) The latency of the first spike that occurred in response to the different click trains, which was the first significant bin in the post stimulus time histogram.

We found that the caudomedial area is more reacting to anesthesia than primary auditory cortex. In contrast to awake monkeys, in the most cases of anesthetized monkeys for rapid click rates encoding of stimuli are going at the expense of reduction number of spikes and saving synchronization neuronal discharge to the stimuli. The number of spikes in first 20 ms after click decrease and response latency strong increase in caudomedial area of anesthetized monkeys. Our results showed that neurons in the in primary and secondary auditory cortex of awake monkeys can encode higher temporal modulations of sounds than neurons in the anesthetized monkey in the same areas.

We observed two types of units. At low click rates (< 25 Hz) all units fired action potentials that were phase -locked to the individual clicks of the train. Beyond 25 Hz the first type of units exhibited increased firing without obvious phase-locking to the clicks (non-significant VS), whereas the second type of units did not respond to click trains at high rates (non-significant VS and response strength).

## Methods

**Recording:** Action potentials were recorded using tungsten microelectrodes advanced perpendicularly through the dura mater using a micromanipulator. We used a 7-electrode array and recorded at many sites of the auditory cortex the discharge of small clusters of neurons from left hemisphere of macaque monkeys (*Macaca fascicularis*), passively listening to the acoustic stimuli. Two adults males participated in experiment.

**Stimuli:** acoustic stimulus consisted of clicks sequences of different frequencies from 1 to 100 clicks per second. The loudness of clicks was from 20 to 62 dB SPL. The individual clicks were 50  $\mu$ s rectangular electric pulses. The stimulus was presented in two or four second long click trains every 5s in random order from a free-field loudspeaker, contralateral to the recording site. The speaker's output was measured using a sound pressure meter (Brueel & Kjaer 2233) placed above animal's head and facing the loudspeaker.

There is a dot displays with schematic representation of acoustic stimuli (a), and an example of temporal response pattern in the AC at different click rates (b). Clicks and responses are organized by rate. Horizontal axis shows time after onset of click train. Vertical axis indicates click rate in Hz. Each click train was repeated 13 times.

Data reported here were collected from 237 multiunits (130 from A1 and 107 from CM).

## Выводы:

Recent studies of cortex suggest that neurons in the in primary auditory cortex of awake monkeys can encode higher temporal modulations of sounds than neurons in the anesthetized monkey (Lu et al. 2001).

У него граница 20,4 58,8 мс, (кошки под наркозом Lu Wang 2000) у нас синхронизированный ответ идет на 100 и 300 Гц. Наши наркотизированные макаки до 50 Гц синхронизовались.

Our findings corroborate those of Lu et al., (Lu et al., 2001) that neurons in auditory cortex encode the temporally modulated sounds with their temporal discharge patterns or by non-phased-locked increases of the firing.

Phase-locking response on the click rates in the A1 and CM areas of auditory cortex of awake macaque monkeys occurred up to 300 Hz that support data of previously investigation (Steinschneider et al., 1998)

# The relationship of psycho-physiological responses and self-reported emotions while listening to music

Frederik Nagel<sup>a</sup>, Oliver Grewe<sup>a</sup>, Reinhard Kopiez<sup>b</sup>, Eckart Altenmüller<sup>a</sup>

<sup>a</sup>Institute for Music Physiology and Musicians' Medicine

<sup>b</sup>Institute for Research in Music Education

Hannover University of Music and Drama, Germany

Since Kate Hevner's [1] early investigations on perceived emotions while listening to music in 1936, there have been many different approaches to the measurement of emotions. For example, Gabrielsson and Lindström [2] investigated expression in speech while Schubert [3] tried to measure emotional expression by use of a continuous response method in a 2-dimensional emotion space (2DES).

Measurements of physiological responses while listening to music have been done by numerous researchers since the 1960s. They found that changes in skin conductivity response play a central role within the group of physiological parameters.

We investigated the emotions of 35 subjects induced by pre-selected standard musical pieces and by their favourite pieces. The aim was to reveal whether musical universals based on specific psychoacoustic cues exist, eliciting inter-individual comparable emotions. In particular we were interested in strong emotions such as chills, which commonly are described as shivers or goose-pimples.

We combined a continuous self report technique with psycho-physiological measures. The researcher-developed software "EMuJoy" was developed as an extension of Schubert's method, which enabled subjects to express their emotions "on-line" while listening to music. The dimensions used were valence (negative-positive) and arousal (high-low). Subjects controlled the software with a computer mouse. One of the mouse buttons was used to indicate chill experiences. As psycho-physiological measures, heart rate (HR), skin conductivity response (SCR) and level (SCL), skin temperature, breathing rate and an electromyogram of two facial muscles (the cygomaticus and the corrugator) were recorded.

In contrast to previous studies, subjects were instructed to express their own perceived emotions and not to rate the emotional expression intended by the composer. The experiment started with a learning phase during which subjects got accustomed to the continuous rating procedure. Handling the "EMuJoy" software was trained by rating perceived emotions while looking at ten pictures from the International Affective Picture System [4]. These pictures were selected according to the two-dimensional emotion space covering the edges and the center (arousing, calming, negative, positive valence,

The subjects listened to 7 selected pieces, 5 pieces were purely instrumental music and 2 included voice. After each piece, they had to fill in questionnaires concerning their associations related to the respective piece of music. At the end of the experimental session, information on musical expertise and personality factors was collected.

SCR and chills were positively correlated in all subjects. Additionally, there was a significant positive correlation between chills and increase in heart rate. We found no inter-individually consistent rules for the relationship between self report and physiological data. However, subject specific correlations between these parameters could be detected. Furthermore, there are smaller groups of subjects that show similarities in their reactions to music. As a common rule, strong changes in arousal or valence were linked to SCRs and increasing HR.

By coupling SCR and HR we had an improved procedure to distinguish between non-specific SCRs and autonomous reactions to music. Chill reports and changes in both parameters were correlated significantly. All subjects had more chills when listening to their own favourite music as compared to the pre-selected standard pieces.

According to the data, there is no simple stimulus-reaction pattern with respect to the relation between music and emotion. The emotional self monitoring as well as the physiological reactions are influenced by individual factors, such as musical expertise and experience, vigilance, etc. Although there are groups of individuals with similar reactions to music, only the self reported peak experiences are significantly correlated with the physiological data. This is probably due to the fact that the reported chills are based on sympathetic activations.

In a further step, we will attempt to identify distinct inner states of subjects while listening to music and relate these to specific physiological reactions. This relationship might be very individual. However, as has been demonstrated in speech recognition, these individual features can be used for mapping physiological reactions to emotional states.

As in speech recognition where the characteristics of speech can easily be correlated with words, the inner states can be correlated with physiological data (see [5]).

The work was supported by the DFG (Al 269-6) and the Center for Systemic Neurosciences Hannover

## References

- [1] K. Hevner. Experimental studies of the elements of expression in music. *American Journal of psychology*, 48:246–286, 1936.
- [2] A. Gabrielsson and S. Lindström Wik. Strong experiences related to music: A descriptive system. *Musicae Scientiae*, 7(2):157–217, 2003.
- [3] E. Schubert. Measuring temporal emotional response to music using the two dimensional emotion space. In *Proceedings of the 4th International Conference for Music Perception and Cognition*, pages 263–268, Montreal, Canada, 1996.
- [4] Cuthbert BN Lang PJ, Bradley MM. International affective picture system (iaps): technical manual and affective ratings. 1999.
- [5] R. W. Picard, E. Vyzas, and J. Healey. Toward machine emotional intelligence: Analysis of affective physiological state. *IEEE Transactions on Pattern Analysis and Machine Intelligence*, 2001.

## Semantic meaning causes different strategies of echo suppression in echolocating bats

Maike Schuchmann, Mathias M. Hübner and Lutz Wiegrebe  
Department Biologie II, Ludwig-Maximilians-Universität, Großhaderner Strasse 2  
D-82152 Planegg- Martinsried

Echoes are an essential part of the daily natural environment. They include misleading spatial information of a sound source and produce acoustic mirror images of objects.

Accurate sound localisation is enabled by the suppression of the misleading spatial information of echoes in reverberant environments. Only the directional information of the sound which reaches the ear first dominates the perceived position of a sound source. This dominance of the first sound for sound localisation is called 'localisation dominance'.

Until now, localisation dominance has never been examined in echolocating bats.

The present study investigates whether and to which extend the echolocating bat *Megaderma lyra* spontaneously suppresses the spatial information of echoes. It is assessed how localisation dominance is influenced by stimuli with different semantic meanings.

The stimuli were presented in an active as well as in two passive lead-lag-paradigms via two ultrasonic loudspeakers with a delay ranging from 0 to 12.8ms between the two speakers.

In the active paradigm the stimuli were reflections of the bats' sonar emission.

In the first passive paradigm the stimuli were impulses; in the second passive paradigm the stimuli were recordings of a *M. lyra* contact call. In these passive paradigms, stimulus presentation was independent of the bats' sonar emission.

In the active paradigm none of the tested individuals of *M. lyra* preferred the first of two reflections of their echolocation calls, independent of the delay between the first and the second reflection.

In the first passive paradigm, none of the tested individuals of *M. lyra* preferred the first of two impulses, independent from the delay between the first and the second impulse.

However, in the second passive paradigm, all tested individuals of *M. lyra* preferred the first of two contact calls when there was a delay of 0.2 to 0.8 ms between the contact calls emitted through the two speakers. Note that these calls include several echolocation calls which do not cause any echo suppression by themselves.

These data indicate that stimuli with different semantic meanings cause different strategies how bats deal with echoes.

Although bats are able to suppress the spatial information of echoes, this is not a mandatory auditory processing strategy and seems to depend on the semantic meaning of the echoes.

Supported by the DFG

## Possible anatomical substrates of hemispheric lateralization in Mongolian gerbil auditory cortex

Anna Laszcz, Eike Budinger, Jürgen Goldschmidt, Frank W. Ohl, Michael Schildt, Wolfram Wetzel, Werner Züschratter, and Henning Scheich.

Leibniz Institute for Neurobiology, Brennekestr. 6, 39118 Magdeburg, Germany.

Recent experimental data support the hypothesis of a functional lateralization in auditory cortex with respect to the processing of certain temporal and spectral aspects of sound. This is most evident in humans (*e.g.*, Nicholls *et al.*, Int. J. Psychophysiol. 44: 37-55, 2002) where various results show a clear trend of dichotomy in the way how temporal and spectral sound features are processed. Although similar studies in animals are relatively rare, results from lesion experiments in Mongolian gerbils are consistent with this trend, showing that the right auditory cortex is essential for the discrimination of the direction of frequency-modulated tones (Wetzel *et al.*, Neurosci. Letters 252: 115-118, 1998) and the left auditory cortex for the discrimination of tone sequences (Wetzel *et al.*, IBRO Abstr. 2196, 2003).

The incoming evidence, supporting a functional asymmetry of the auditory cortex, implicated investigations for a corresponding anatomical asymmetry. In humans such differences, even in gross anatomical features of the auditory cortex (mainly size of Heschl's gyrus and *Planum temporale*) and in cortical microcircuitry (*e.g.*, width and spacing of cortical cell columns), are well documented, as based on *post mortem* material and non-invasive imaging data obtained *in vivo*. In contrast, there are no comparable anatomical studies available in animals.

Here we investigated the anatomy of the left and right auditory cortex of the Mongolian gerbil on three respective levels: (1) general architecture (cyto-, fiber-, chemoarchitecture: *e.g.*, extent of koniocortex, degree of fiber myelinization, distribution of neurofilament and calcium-binding proteins); (2) micromodular structure (size and spacing of micromodules visualized by zinc-autometallography of excitatory corticocortical terminations in cortical layers I and II, *i.e.* TIMM staining); (3) morphology of single auditory neurons (juxtacellularly stained with biocytin) which were functionally characterized by means of electrophysiological recordings *in vivo* (*e.g.*, frequency tuning).

Inspection of general architecture did not reveal hemispheric asymmetries on a large scale, whereas TIMM staining did show a trend of hemispheric differences in the micromodular size and spacing in a range of approximately 10%. The diameter, surface area, perimeter, and averaged minimum distances of left hemisphere microcolumns tended to be smaller than those of the right hemisphere. Data on morphological asymmetries, *e.g.*, dendritic and axonal arborization and synapse distribution, of neurons from both hemispheres (mainly layer III pyramidal cells) with similar best frequencies, rostrocaudal, dorsoventral, and laminar location, will be discussed.

## HORMONE-RELATED PLASTICITY OF SONG REPRESENTATION AND SELECTIVITY IN HVC OF MALE AND FEMALE CANARIES

B. Diekamp, J.J. Sartor, G.F. Ball, E.S. Fortune

*Psychological and Brain Sciences, Johns Hopkins University, Baltimore, MD, USA*

Corresponding author: b.diekamp@jhu.edu

Canaries (*Serinus canaria*) and other temperate-zone birds show seasonal changes in song behavior, which are correlated with robust changes in brain morphology and chemistry of nuclei involved in song production and perception (1,2). These seasonal changes are mediated by changes in plasma testosterone (T) levels. Males exhibit concurrent seasonal changes in testosterone levels, song behavior and volume of nucleus HVC and females treated or not with exogenous testosterone exhibit similar variations (3, 4). HVC neurons are highly selective in their responses to song, most specifically to temporal features of the bird's own song (BOS) (5). Neuronal spiking activity in HVC in urethane-anesthetized birds, auditory responses to BOS during sleep, motor pattern during vocalization and spontaneous activity of HVC neurons have highly similar temporal patterns that closely match the temporal features of BOS (6, 7, 8). The representation of BOS in the pattern of HVC activity is the neural correlate of song learning and production. Recent data show differences in the response properties of HVC neurons between female and male canaries to conspecific songs under different photoperiods, i.e. seasonal, conditions (9). The functional relationship between the representation of song in HVC and sex differences and/or seasonal changes in HVC volume, mediated by circulating testosterone, are not understood.

In this study we investigated the auditory representation of species-specific song and BOS in HVC neurons of urethane-anesthetized female and male canaries with high and low plasma T levels. As HVC volume is correlated with T levels, this study directly addresses the question of whether structural morphological changes in HVC are directly related to the representation of song in HVC. Stimuli included several variants of each BOS, reversed BOS, and conspecific songs. Songs were recorded from males with exogenous T and held on long days. Another group of males will be castrated after recording their songs. Singing in females was elicited by application of exogenous T under long day conditions and the songs recorded. In half of the females the T implant was removed and these females were returned to a non-singing state before recording HVC activity. Plasma T-levels were determined at several stages throughout the experiment. Single unit recordings were made from male and female canaries under either high or low T concentrations.

In all birds HVC neurons exhibited a characteristic spontaneous "bursting" activity that differed from adjacent nidopallium. In males, HVC neurons exhibited a preference for BOS over other auditory stimuli. The responses to variants of the BOS differed dramatically. Nevertheless, the responses of the majority of neurons were temporally associated with specific BOS syllables or sequences of BOS syllables.

Auditory responses in T-treated singing females also showed a strong preference for BOS. However, the responses did not appear to be temporally associated with specific song elements. Rather, long bursts of activity resulted from song playback. Auditory responses in non-singing females were reduced and more variable. Some neurons were inhibited by BOS. These data suggest that song-related HVC activity is modulated as a function of variation in testosterone titers.

*Support Contributed By: NIH/NINDS R01 NS 35467 to GFB.*

### References

- 1) Ball GF (1999) The neuroendocrine basis of seasonal changes in vocal behavior among songbirds. In M. D. Hauser and M. Konishi (eds.) *The Design of Animal Communication*, pp. 213-253. Cambridge, MA: MIT Press.
- 2) Brenowitz EA (2004) Plasticity of the adult avian song control system. *Ann N Y Acad Sci.* 1016:560-585.
- 3) Nottebohm F (1980) Testosterone triggers growth of brain vocal control nuclei in adult female canaries. *Brain Res.* 189:429-436.
- 4) Nottebohm F, Nottebohm ME, Crane LA, Wingfield JC (1987) Seasonal changes in gonadal hormone levels of adult male canaries and their relation to song. *Behav Neural Biol.* 47:197-211.
- 5) Margoliash D (1983) Acoustic parameters underlying the responses of song-specific neurons in the white-crowned sparrow. *J Neurosci.* 3:1039-1057.
- 6) Dave AS, Yu AC, Margoliash D (1998) Behavioral state modulation of auditory activity in a vocal motor system. *Science* 282:2250-2254.
- 7) Dave AS, Margoliash D (2000) Song replay during sleep and computational rules for sensorimotor vocal learning. *Science* 290:812-816.
- 8) Rauske PL, Shea SD, Margoliash D (2003) State and neuronal class-dependent reconfiguration in the avian song system. *J Neurophysiol.* 89:1688-1701.
- 9) Del Negro C, Kreutzer M, Gahr M (2000) Sexually stimulating signals of canary (*Serinus canaria*) songs: evidence for a female-specific auditory representation in the HVC nucleus during the breeding season. *Behav Neurosci.* 114:526-542.

# CATECHOLAMINERGIC PROJECTIONS TO THE VOCAL CONTROL NUCLEUS AREA X IN ZEBRA FINCHES (*Taeniopygia guttata*) AND THEIR SIGNIFICANCE FOR SOCIAL MODULATION OF IMMEDIATE-EARLY GENE EXPRESSION ASSOCIATED WITH SONG

C.B. Castelino, B. Diekamp, G.F. Ball

*Psychological and Brain Sciences, Johns Hopkins University, Baltimore, MD, USA*

Corresponding author: ccasteli@jhu.edu; presenting author: b.diekamp@jhu.edu

Neurotransmitter systems like catecholamines that exhibit diffuse projections to forebrain regions are good candidates for regulation of context-dependent brain activity. In 1998, Jarvis and colleagues <sup>(1)</sup> discovered that singing to either males or females resulted in significantly lower levels of the immediate early gene ZENK in the song circuit as compared to that driven by solo song. The most remarkable difference was in area X of the song circuit.

Recent studies in our lab have uncovered a role for the noradrenergic (NA) system in modulating singing-induced context-dependent ZENK expression in area X of male zebra finches. We found that depleting the NA system systemically via a NA specific neurotoxin N-(2-Chloroethyl)-N-ethyl-2-bromobenzylamine hydrochloride (DSP-4) disrupts the context-dependent modulation of ZENK protein expression in area X. In the saline treated control males, ZENK expression resulting from directed song was significantly lower than that from undirected (solo) song. These findings were the same as Jarvis et al (1998) found using ZENK mRNA. However the DSP-4 treated male finches singing directed song had significantly higher levels of ZENK expression than the saline treated males singing directed song. Furthermore there was no significant difference between the ZENK expression that resulted from directed and undirected song <sup>(2)</sup>. Based on this we concluded that ascending NA projections to area X play a role in modulating context-dependent ZENK expression.

We know that area X in zebra finches contains receptors for alpha-adrenergic receptors <sup>(3)</sup>, variable amounts of the norepinephrine synthesizing enzyme dopamine beta hydroxylase <sup>(4)</sup> and significant amounts of the neurotransmitter norepinephrine <sup>(5)</sup> (~43% measured via high performance liquid chromatography). However a direct NA projection to area X has still not been demonstrated. Area X is considered a specialized sub-region of the medial striatum <sup>(6)</sup> and studies using a variety of anterograde and retrograde tracers in the medial striatum of chickens (*Gallus domesticus*) <sup>(7)</sup>, quail (*Coturnix japonica*) <sup>(8)</sup> and pigeon (*Columba livia*) <sup>(9)</sup> have revealed reciprocal connections between the medial striatum and the LC complex (and to different degrees the SC complex). An early attempt to uncover the catecholaminergic connections to area X using horseradish peroxidase in zebra finches revealed afferent projections from AVT and SN <sup>(10)</sup>.

In this experiment we attempted to locate a direct NA projection to the song nucleus area X using the tracer cholera toxin B (CTB) injected into area X of male zebra finches. We found retrogradely labeled CTB cells in song nuclei HVC, LMAN and DLM and catecholaminergic nuclei substantia nigra, locus coeruleus, and sub coeruleus. Our results fit well with what we know about projections to the medial striatum in other avian species and when combined with our earlier experiment, we now have information about the functional role of this NA projection to area X.

*Support Contributed By: NIH/NINDS R01 NS 35467 to GFB.*

## References

- 1) Jarvis ED, Scharff C, Grossman MR, Ramos JA, Nottebohm F (1998) For whom the bird sings: Context-dependent gene expression. *Neuron* 21:775-788.
- 2) Castelino CB, Ball GF (2003) Context dependent ZENK expression in male zebra finches is modulated by noradrenergic projections to the song circuit. *Society for Neuroscience*, No. 522.4.
- 3) Riters LV, Ball GF (2002) Sex differences in the densities of alpha 2-adrenergic receptors in the song control system, but not the medial preoptic nucleus in zebra finches. *J Chem Neuroanat.* 23:269-277.
- 4) Mello CV, Pinaud R, Ribeiro S (1998) Noradrenergic system of the zebra finch brain: Immunocytochemical study of dopamine-beta-hydroxylase. *J Comp Neurol.* 400:207-228.
- 5) Barclay SR, Harding CF, Waterman SA (1992) Correlations between catecholamine levels and sexual behavior in male zebra finches. *Pharmacol Biochem Behav.* 41:195-201.
- 6) Farries MA (2001) The oscine song system considered in the context of the avian brain: lessons learned from comparative neurobiology. *Brain Behav Evolution* 58:80-100.
- 7) Szekely AD, Boxer MI, Stewart MG, Csillag A (1994) Connectivity of the lobus parolfactorius of the domestic chicken (*Gallus domesticus*): an anterograde and retrograde pathway tracing study. *J Comp Neurol.* 348:374-393.
- 8) Bons N, Oliver J (1986) Origin of the afferent connections to the parolfactory lobe in quail shown by retrograde labelling with a fluorescent neuron tracer. *Exp Brain Res* 63:125-134.
- 9) Kitt CA, Brauth SE (1986) Telencephalic projections from midbrain and isthmal cell groups in the pigeon. I. Locus coeruleus and subcoeruleus. *J Comp Neurol.* 247:69-91.
- 10) Lewis JW, Ryan SM, Arnold AP, Butcher LL (1981) Evidence for catecholamine projection to area X in zebra finch. *J Comp Neurol.* 196:347-354.



## MAINTENANCE OF HVC VOLUME IN DEVOCALIZED ZEBRA FINCHES BY NIGHT PLAYBACK OF THE BIRD'S OWN LEARNED SONG

E.S. Fortune, B. Diekamp, J.J. Sartor, G.F. Ball

*Psychological and Brain Sciences, Johns Hopkins University, Baltimore, MD, USA*

Corresponding/presenting author: b.diekamp@jhu.edu

The learned, stereotyped songs of zebra finches (*Taeniopygia guttata*) are thought to be mediated by a central pattern generator in forebrain vocal control nuclei, particularly HVC (1). A correlate of this motor program is observed in the spontaneous spiking activity of neurons in the HVC of sleeping or lightly-anesthetized birds (2, 3). Similar activity patterns also occur during motor production and in auditory response to the bird's own song (BOS) (4, 5). This activity, therefore, "combines" sensory and motor aspects of this learned behavior.

Recent studies have shown that suppression of singing, either through disruption of airflow through the syrinx or by restriction of access to food at certain times of the day leads to a reduction in HVC volume (6, 7). HVC volumes in many species of temperate-zone songbirds are also known to vary dramatically. HVC volumes are modulated by seasonal changes in daylength. The mechanisms underlying these modulations may include modulations of spiking activity. At present the functional relation between song-related neuronal activity patterns and changes in volume of these nuclei is unclear. This experiment examines the relations between HVC activity and volume.

A reduction in presumed HVC activity was induced through devocalization and restricted food access. In experimental birds the reduction in motor-driven HVC activity resulting from the suppression of song behavior was replaced by auditory-driven activity by night playback of the bird's own song. Songs of isolated adult male zebra finches were recorded for up to 5 days. Birds were then devocalized by a bypass of airflow through the syrinx. After surgery, devocalized birds were housed individually and food access was restricted to 6 hr per day. Several song exemplars of one experimental bird were played at a rate of once per minute for 10 hours during the 12 hr night to a pair or group of birds. Thus, these birds experienced identical auditory stimulation at night, but one bird received its own song whereas others heard a conspecific song. Two to four weeks later, the birds were sacrificed, the brains collected, processed, and stained using cresyl violet. The volumes of HVC, RA, area X and control nuclei outside the song system were measured. A control group received no night song playback and others received a sham devocalization.

As expected, devocalized males that did not receive night playbacks of BOS had reduced HVC volumes. In contrast, birds that received BOS at night had significantly larger HVC volumes: the size for HVC in these birds are consistent with singing birds both in this study and in previously published reports. At present no statistically significant differences in volumes of RA or area X were found between groups. These data strongly suggest that spiking activity in HVC contributes to the maintenance of HVC volume.

*Support Contributed By: NIH/NINDS R01 NS 35467.*

### References

- 1) Margoliash D (1997) Functional organization of forebrain pathways for song production and perception. *J Neurobiol.* 33:671-693.
- 2) Dave AS, Margoliash D (2000) Song replay during sleep and computational rules for sensorimotor vocal learning. *Science* 290:812-816.
- 3) Rauske PL, Shea SD, Margoliash D (2003) State and neuronal class-dependent reconfiguration in the avian song system. *J Neurophysiol.* 89:1688-1701.
- 4) Yu AC, Margoliash D (1996) Temporal hierarchical control of singing in birds. *Science* 273:1871-1875.
- 5) Cardin JA, Schmidt MF (2003) Song system auditory responses are stable and highly tuned during sedation, rapidly modulated and unselective during wakefulness, and suppressed by arousal. *J Neurophysiol.* 90:2884-2899.
- 6) Sartor JJ, Charlier T, Pytte CL, Balthazart J, Ball GF (2002) Converging evidence that song performance modulates seasonal changes in the avian song control system. *Society for Neuroscience, 2002, Program No. 781.1.*
- 7) Jones C, Rashotte ME, Johnson F (2002). A songbird for all seasons: a 'winter-like' period of reduced song production is without effect on the fidelity of zebra finch vocal patterns. *Society for Neuroscience, 2002, Program No. 781.6.*

# Sound lateralization following hemispherectomy, callosotomy, or callosal agenesis

Markus Hausmann<sup>1</sup>, Michael C. Corballis<sup>2</sup>, Aldo Paggi<sup>3</sup>, Mara Fabri<sup>3</sup>, and Jörg Lewald<sup>1,4</sup>

<sup>1</sup> Institute for Cognitive Neuroscience, Faculty of Psychology, Ruhr University Bochum, D-44780 Bochum, Germany

<sup>2</sup> Department of Psychology, University of Auckland, Private Bag 92019, Auckland, New Zealand

<sup>3</sup> Department of Neuroscience, Section of Human Physiology, University of Ancona, 60020, Ancona, Italy

<sup>4</sup> Leibniz Research Centre for Working Environment and Human Factors, Ardeystr. 67, D-44139 Dortmund, Germany

Correspondence: joerg.lewald@rub.de

At present, still only little is known on the role of human cortical areas in sound localization. A particular topic of interest, that is discussed controversially, is the question of whether there is a functional asymmetry of the human cortical hemispheres in auditory spatial perception. Also, the potential role of interhemispheric transfer via callosal fibers in sound localization is still a matter of debate. Here we made an approach to these problems by investigating subjects with left (LHE) or right hemispherectomy (RHE), callosotomy (CT), or agenesis of the corpus callosum (CA). We used a simple task of sound lateralization, that did not involve any motor or higher-order cognitive functions.

Two subjects with LHE (one female and one male; age 43 and 36 yr, respectively), one male subject with RHE (47 yr), two subjects with CT (one female and one male; 44 and 40 yr), and one female subject with CA (37 yr) participated in the study. Twenty healthy subjects (ten females; mean age 41.4 yr), matched for age and gender, served as the control group. Hearing thresholds of the control group did not differ from those of the LHE, RHE, CT, and CA subjects. Dichotic pure-tone pulses (duration 20 ms; triangular envelope; frequency 1 kHz; sound-pressure level 80 dB), delivered via headphones, were used as auditory stimuli. Interaural time differences (ITDs) of the sound stimuli were varied between trials over a range from -362.8  $\mu$ s (sound leading at the left ear) to +362.8  $\mu$ s (leading at the right ear), in steps of 45.4  $\mu$ s. Subjects were instructed to decide whether the sound image appeared to the left or to the right of the median plane. The experimental session was composed of 136 trials (8 presentations of each ITD). The subjects' judgments were fitted to a sigmoidal function. Just noticeable differences (JNDs) and systematic shifts in sound lateralization were derived from the resulting equation.

Compared with the control group, the subjects with CT, CA, and RHE exhibited significantly enlarged JNDs, indicating reduced acuity of sound lateralization. The fit of the data of one subject with LHE to a sigmoidal function did not reach the level of statistical significance, thus indicating virtual inability of ITD perception. However, the results of the second subject with LHE did not differ from those of the control subjects in any respect. Systematic errors in sound lateralization were obtained in the subjects with CT, but not in subjects with CA, LHE, and RHE. These two CT subjects showed significant shifts of the auditory median plane (that ITD where the frequency of judgments "left" and "right" is 50%) by 81 and 145  $\mu$ s to the right, that is, ITDs around zero were consistently heard to the left of the median plane.

The most interesting finding of this study is the normal performance of a subject with LHE, which clearly shows that the integrity of the left cortical hemisphere is not essential for accurate sound lateralization. Obviously, the auditory system of this subject was able to fully compensate for the loss of the left hemisphere. On the other hand, the impairment of sound-lateralization acuity with CT and CA suggests that, in case both hemispheres are present, the transfer of auditory information between them via the corpus callosum may play a significant role in spatial hearing. Moreover, when one assumes a contralaterality of auditory cortical processing, as has been suggested by neuroimaging studies, the finding of a bias to the left following CT may be compatible with the view of a right-hemispheric dominance in auditory spatial functions.

## Mechano-electrical transduction of mouse cochlear hair cells

Dr Cécil J.W. Meulenberg  
Department of Neurobiophysics  
University of Groningen  
The Netherlands  
[c.j.w.meulenberg@phys.rug.nl](mailto:c.j.w.meulenberg@phys.rug.nl)

The modulating role of calcium in mechano-electrical transduction of mouse sensory hair cells was investigated. Cochlear hair cells were isolated from acutely dissected organs of Corti of mouse CD-1 pups (P2-P8) according to procedures that were adopted from the laboratory of Dr. Kros (Géléoc *et al.*, 1997). A piezo-electrically driven micro fluid-jet system was used to deflect hair bundles and whole-cell voltage clamp measurements were employed to record the simultaneously activated transducer currents. The sub-micrometer hair bundle displacement was measured using laser interferometric methods (Van Netten & Kros, 1997).

Géléoc, G.S.G., Lennan, G.W.T., Richardson, G.P. and Kros, C.J. (1997). A quantitative comparison of mechanoelectrical transduction in vestibular and auditory hair cells of neonatal mice. *Proc. R. Soc. Lond. B* 264, 611-621.

Van Netten, S.M. and Kros, C.J. (1997). Heterodyne laser interferometry of individual inner and outer hair cells in the neonatal mouse cochlea. *ARO abstracts*, 20, 73.

Supported by the Netherlands Organisation for Scientific Research (NWO).

## Analysis of Protein Patterns in the rat auditory brainstem and cerebellum

Michael Becker, Marcus F.H. Müller, Hans Gerd Nothwang, and Eckhard Friauf

Animal Physiology Group, Department of Biology, University of Kaiserslautern, POB 3049, D-67653 Kaiserslautern, Germany

Differential proteomic analysis is a powerful tool for the identification of developmentally regulated proteins and the elucidation of candidate molecules that grant functional specificity to a given cell or tissue. By comparing the proteome of two anatomically and functionally defined rat brain regions, namely the inferior colliculus (IC) as a higher order center of the auditory pathway and the cerebellum as a non-auditory structure, we attempt to identify molecular candidates that mediate the pronounced functional differences on a molecular level. To do so, we have established a protocol for subcellular fractionation of small tissue amounts by differential centrifugation. This protocol yields three fractions containing cytoplasmic, nuclear, or membrane/organellar proteins [Guillemin & Becker et al., in press].

Protein fractions obtained from the IC of the cerebellum were separated on two-dimensional gels. The comparison of the resulting spot patterns was performed with the Proteomweaver® software. To test the viability of this approach, numerous spot pairs, as indicated by the software, were identified by mass spectrometry (MS). Our results demonstrate the ability of Proteomweaver® to correlate spot patterns despite slight gel-to-gel differences.

To detect spots of varying abundance between IC and cerebellum, only such spots were considered which appeared on at least 2 of 3 replicate gels generated for each tissue. In the cytoplasmic fraction, from a total of 284 viable spots, 32 and 10 were up-regulated by a factor of 2 or more in the IC or cerebellum, respectively. Additionally, 19 spots were detected that appear exclusively in only one of the tissues analyzed.

The majority of differentially regulated protein spots are of overall low intensity. This complicates their identification by mass spectrometry. For proteins that we have identified thus far, such as glutamine synthetase and phosphoglycerate mutase (up-regulated 3.1-fold and 2.4-fold in the IC), the results are in line with the fact that the IC is one of the most active regions in the entire brain [Sokoloff, 1981].

Examination of the nuclear fraction is in progress and results will be presented on the poster. In addition to this study, which was performed on tissues harvested from an adult rat (P60), a similar analysis is being conducted for young (P4) rats. Taken together, the results from these studies will allow us to monitor developmentally related as well as region-specific differences in the proteome of auditory brain areas.

## Serial Analysis of Gene Expression (SAGE) in the rat auditory brainstem

Alexander Koehl, Anne Rieger, Nicole Schmidt, Eckhard Friauf, and Hans Gerd Nothwang

Animal Physiology Group, Department of Biology, University of Kaiserslautern, POB 3049, D-67653 Kaiserslautern, Germany

As the first center of binaural auditory processing, the superior olivary complex (SOC) plays an important role in computing acoustic information from both ears. It consists of several nuclei, like the lateral superior olive (LSO) and the medial nucleus of the trapezoid body (MNTB). In order to unravel the molecular mechanisms which underlie the auditory information processing, and in order to find specific patterns of gene expression, we have performed serial analysis of gene expression (SAGE). SAGE is based on the position-specific generation of unique, 10- or 16-bp-long sequences, so-called tags, from the transcripts present in the tissue. Such tags are sufficient for the identification of expressed genes and can be sequenced efficiently in an economical way after concatenation.

To date, we have sequenced a total of 31,035 10-bp-long tags derived from the SOC of 60-day-old rats. These corresponded to 10,473 different transcripts. About 17 % of all tags were of mitochondrial origin, indicating a high energy requirement of the SOC. Sixty-six percent were assigned to genes or expressed sequence tags (ESTs), whereas 17 % could not be annotated. In parallel, we have started sequencing a library of 16-bp-long tags derived from the LSO of 30-day-old rats. A total of 31,776 tags have been sequenced thus far, representing 12,620 unique transcripts. Six percent of all tags mapped to the mitochondrial genome, 67 % were assigned to distinct genes or ESTs and the remaining 27 % could not be annotated at all. The comparison between the libraries obtained from the SOC, the LSO and the rat hippocampus (Datson *et al.*, 2001; Hippocampus) revealed statistically significant differences in the transcript inventory between these 3 structures.

One interesting group of transcripts comprises membrane proteins, including plasma membrane receptors, transporters, and ion channels. Within this membrane protein group, several tags exhibited significantly different expression levels across the 3 structures and thus may be candidates for tissue-specific tasks. Another group of transcripts, which showed differential distribution, was associated with energy metabolism. In this group, we observed a significant over-expression of many genes in the SOC compared to the LSO and, especially, the hippocampus. Again this indicates a high energy expenditure of the SOC. Results obtained by *in-situ* hybridization and immunohistochemistry showed a good correlation to the SAGE data. Our aim is to expand these catalogues of expressed genes by another 30,000 tags from the LSO as well as 60,000 tags from the MNTB.

## **Categorization of Frequency Modulated Tones in Schizophrenia**

J.D. Albrecht<sup>1,2</sup>, B. Bogerts<sup>1</sup>, H. Biela<sup>1</sup>, U. Mertens<sup>1</sup>, K. Schiltz<sup>1</sup>,  
S. Diekmann<sup>1</sup>, H. Scheich<sup>2</sup>, A. Brechmann<sup>2</sup>

<sup>1</sup>Department of Psychiatry, University of Magdeburg, Germany

<sup>2</sup>Special Lab Non-Invasive Brain Imaging, Leibniz Institute of Neurobiology  
Brennekestr. 6, 39118 Magdeburg, Germany

The ability to discriminate fine nuances in human affective prosody is an important feature of human social functioning. In Schizophrenia, this aspect is thought to be disturbed. Some studies have addressed the recognition of affective prosody in Schizophrenia but without controlling for semantic aspects of language. Linear frequency modulations (FM) are a simplified model of human affective prosody, independent of semantic aspects of language. Several studies have shown that the right auditory cortex (AC) is predominantly involved in the categorization of affective prosody as well as categorization of FM-direction. To test the hypothesis that there are activation differences, while categorizing FM-direction, between patients with schizophrenia and matched healthy controls, we used a functional imaging paradigm. Participants and patients had to categorize upward vs. downward FM of 700ms duration. Two conditions were used. First, they had to listen passively to the FM, in the second condition they had to categorize upward vs. downward FM. In each scan 105 functional volumes were collected in a 3 Tesla scanner, using a low-noise gradient echo sequence (FLASH) (54dB(A)SPL). Data were corrected for movement artifacts. The results showed in comparison to healthy controls an opposite hemispheric distribution of AC activation in Schizophrenia. This suggests that the neural processing of prosody could be disturbed in Schizophrenia independent of semantic aspects of language. Moreover, this study strengthens the hypothesis of diminished hemispheric specialisation in Schizophrenia, importantly in this study a task, in which the right hemisphere is predominantly involved.

**Poster Subject Area #PSA8:**  
**Lateral line systems; Vestibular systems**

- [#116A](#) I. Nauroth and J. Mogdans, Bonn  
*Effects of running water on the detection of dipole stimuli by goldfish, Carassius auratus*
- [#117A](#) S. Fest, J. Engelmann, H. Bleckmann and J. Mogdans, Bonn  
*In Vivo Whole-Cell Recordings from Brainstem Lateral Line Neurons in Goldfish, Carassius auratus*
- [#118A](#) S. Geisen and J. Mogdans, Bonn  
*Responses to moving objects of primary afferent fibers in the anterior lateral line nerv of goldfish, Carassius auratus*
- [#119A](#) LA. Hurst, D. Meissner, RF. Sirbulescu and GKH. Zupanc, Bremen  
*Chirping in the weakly electric fish Apteronotus leptorhynchus: significance of conspecific's distance, angular orientation, and chirps*
- [#120A](#) J. Goulet and JL. van Hemmen, Garching  
*Hydrodynamic Analysis of the Fish Canal Lateral Line*
- [#116B](#) A. Elepfandt, S. Lebrecht, K. Schroedter and B. Brudermanns, Berlin  
*Discrimination of two simultaneous water surface waves in the clawed frog, Xenopus laevis laevis*
- [#117B](#) A. Elepfandt, B. Hellmann and F. Seifarth, Berlin  
*Sensory-motor transfer for turn responses to two non-visual stimuli in the clawed frog, Xenopus laevis laevis*
- [#118B](#) J. Benda, A. Longtin and L. Maler, Berlin and Ontario (CDN)  
*Two Coding Strategies for Communication Signals in a Population Rate Code*
- [#119B](#) J. Benda and RM. Hennig, Berlin  
*Spike-Frequency Adaptation in the Auditory Preprocessing Module of Crickets*

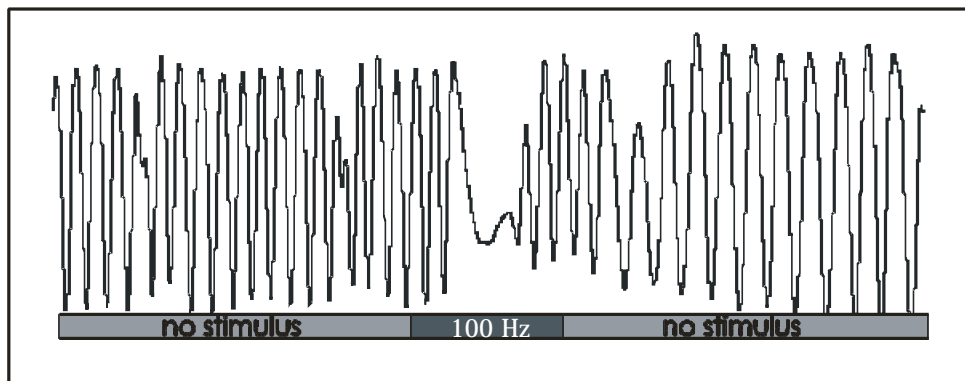
## Effects of running water on the detection of dipole stimuli by goldfish, *Carassius auratus*

Ines E. Nauroth and Joachim Mogdans

Institute for Zoology, University of Bonn, Germany ; inauroth@uni-bonn.de

Most previous studies on hydrodynamic stimulus detection by the fish lateral line were performed in still water. We wanted to know whether lateral line detection is impaired by running water.

Goldfish, *Carassius auratus*, were stimulated with sinusoidal (100 Hz) water motions generated by a dipole source (sphere with radius 5 mm) that was positioned just behind the right operculum at a distance of 10 mm to the fish. Stimulus duration was 6 s, displacements ranged from 14  $\mu\text{m}$  to 113  $\mu\text{m}$ , and the axis of vibration was parallel to the fish. Breathing activity was recorded with a piezo element at the left operculum and a change in breathing rate relative to the rate prior to stimulus presentation was used as an indicator for stimulus detection.



In still water, fish (N=4) responded to the greatest displacements applied with a 20-30 % change in breathing rate (see figure). With decreasing displacement, the breathing response decreased and reached values comparable to those obtained in blank trials (no stimulus) at displacements between 14 and 38  $\mu\text{m}$ . In running water (3,6 cm/s), changes in breathing rate were comparable to those obtained in still water for all displacements applied.

In three goldfish, canal neuromasts were selectively damaged by immersing the fish in Gentamycin (0,002% for 4 days). This treatment did not abolish dipole detection.

Impairment of the canal system with gentamycin and additional damage to the superficial neuromast system in one fish by scraping off the skin on head and opercula and by removing trunk scales also did not abolish dipole detection in still water, but apparently impaired dipole detection in running water

The data show that in goldfish, the detection of dipole stimuli is not impaired by running water. The fact that fish responded to the stimulus even after damaging the entire lateral line system suggests that the auditory system was involved in stimulus detection.

Supported by the DFG (Mo 718/3-1)



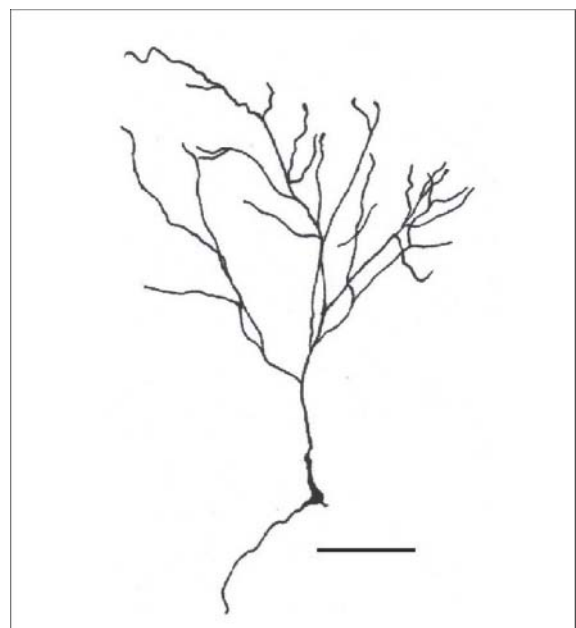
## **In Vivo Whole-Cell Recordings from Brainstem Lateral Line Neurons in Goldfish, *Carrasius auratus***

Silke Fest, Jacob Engelmann, Horst Bleckmann, Joachim Mogdans,  
Institute for Zoology, University of Bonn, Germany, sfest@uni-bonn.de

The medial octavolateralis nucleus (MON) is the first site of sensory processing in the ascending lateral line pathway of fish. We used the in-vivo whole-cell technique to investigate whether functionally different MON neurons can be distinguished based on their morphology. MON neurons (n=39) were recorded intracellularly with glass-microelectrodes filled with an iso-osmotic solution. The lateral line was stimulated with a laminar water flow ( $v=12$  cm/s) that was generated in a flow tank (dimensions) using a propeller (8 cm diameter). Neurons were defined as flow-sensitive if discharge rates in flow differed from those in still water. Neurons were defined as flow-insensitive if ongoing discharge rates were unaffected by flow. After physiological characterization, units were filled with biocytin and their morphology was reconstructed from histological sections using the DAB method.

Flow-sensitive neurons either increased (n=11) or decreased (n=15) discharge rates during flow (Mann-Whitney test,  $p<0.05$ ). In contrast, flow-insensitive neurons (n=13) did not alter their discharge rates during flow.

Twenty-eight neurons were injected with Biocytin. With one exception, somata were located in the crest cell layer of the MON. Most of the cells had wide apical dendritic trees that extended deep into the molecular layer, and five cells had additional basal dendrites. In 12 neurons an axon was identified that coursed ventrally or laterally in the MON. We obtained both morphological and physiological data from 19 neurons. Of these, 12 were flow-sensitive and 7 were flow-insensitive. A comparison of morphometric data, i.e., soma location, number of dendritic branchings, extent of apical dendritic tree and physiological results did not reveal systematic relationships between neuron structure and flow-sensitivity. Our study is the first in which the in-vivo whole-cell technique was applied in the lateral line system of fish. The data suggest that lateral line neurons in the goldfish MON have similar morphology despite differences in physiology. Supported by the DFG (BI 242/10-3)



Camera lucida drawing of a Goldfish MON neuron.  
Scale bar 100 $\mu$ m

## **Responses to moving objects of primary afferent fibers in the anterior lateral line nerve of goldfish, *Carassius auratus***

Susanne H. Geisen and Joachim Mogdans

Institute for Zoology, University of Bonn, Germany, susanne.geisen@gmx.de

From previous experiments<sup>1</sup> it was known that fibers in the posterior lateral line nerve (pllN) respond to a moving object with alternating periods of excitation and inhibition. Here, we present preliminary data from recordings of single fibers in the anterior lateral line nerve (allN), of goldfish to moving objects.

Experiments were performed with the same setup that was used previously to record from pllN fibers<sup>1</sup>. Fish were fixed with a holder in a 50x50x20 cm tank. Experiments were performed under still water conditions. Objects were moved with 15 cm/s on a circular orbit (radius 14 cm) from anterior to posterior (AP) or opposite (PA) along the side of the fish. We used different object sizes (bars, length 9.5 cm, square cross-sections of 0.5, 1.0, 1.5, 3.5 and 4.0 cm) and changed the lateral distance between object and fish (1, 3 and 6 cm).

Recordings were made from 31 allN fibers. Of these, 19 fibers responded to a moving object with a change in ongoing discharge rate and/or pattern. Response patterns were similar to those described for pllN fibers, i.e. they were characterized by alternating periods of excitation or inhibition. In response to a 1.0 cm object that passed the fish at a distance of 1 cm, most fibers (n=12) exhibited a biphasic pattern, which consisted of excitation followed by inhibition (E-I) or vice versa (I-E). Five fibers had triphasic responses, which consisted of excitation, inhibition and again excitation (E-I-E), or the inverse pattern (I-E-I). Two fibers responded with a single burst of excitation (E) to the moving object. In 13 fibers, the discharge pattern depended on object motion direction and was inverse when motion direction was reversed. In general, response rates increased with increasing object size and with decreasing lateral distance between object and fish.

In fishes, the pllN innervates neuromasts located on the trunk whereas the allN innervates head neuromasts. Trunk neuromasts are usually oriented with their axis of maximum sensitivity either parallel or perpendicular to the long axis of the fish whereas head neuromasts may have different orientations. The present data suggest, that despite differences in peripheral lateral line design on head and trunk, fibers in the goldfish allN and pllN respond to a moving object in a similar fashion.

## **Chirping in the weakly electric fish *Apteronotus leptorhynchus*: significance of conspecific's distance, angular orientation, and chirps**

LOUISE A. HURST, DANIELA MEISSNER, RUXANDRA F. SIRBULESCU, GÜNTHER K.H. ZUPANC

*School of Engineering and Science, International University Bremen, Germany*

The weakly electric fish *Apteronotus leptorhynchus* generates wave-like electric organ discharges distinguished by their enormous regularity. These self-generated discharges, as well as signals produced by other fish, are perceived by electroreceptors (thought to be derived from the lateral line system) in the periphery and further processed by specialized brain structures. Although the individual discharges are typically extremely constant in both frequency and waveform, modulations occur, particularly in the context of social interactions. A common form of such transient modulations consists of chirps, 20-200 ms long complex frequency and amplitude modulations. They are controlled by neurons of the central posterior/prepacemaker nucleus in the dorsal thalamus (cf. Abstract “Reciprocal Neural Connections between the Central Posterior/Prepacemaker Nucleus and Nucleus G in the Gymnotiform Fish, *Apteronotus leptorhynchus*” by G.K.H. Zupanc And S.A.L. Corrêa). Four types of chirps have been described, differing in duration and amount of amplitude and frequency change. Chirps, particularly of the type-2 variety, can be evoked by stimulation of a fish with the electric field of a neighboring conspecific, or mimics thereof. Stimulation of a male by presenting both males and females demonstrated that the range over which a conspecific can evoke chirps through its electric field is limited to approximately 10-15 cm, and thus is much shorter than previously assumed. Stimulation at such close distances is most effective if the two fish stay parallel to each other. By contrast, a perpendicular position reduces the number of chirps elicited dramatically. The latter angular orientation may be used by a conspecific to become electrically ‘invisible’ while approaching a territorial male. Analysis of the electric behaviour generated during the parallel stance revealed that, especially in the initial phase of aggressive encounters, the chirps produced by one fish follow the chirps of the other individual with a preferred latency of 500-1000 ms. We suggest to call this coordinated generation of alternating chirps ‘duetting’ and hypothesize that this behavior subserves a communicatory function.

# Hydrodynamic Analysis of the Fish Canal Lateral Line

Julie Goulet and J. Leo van Hemmen

Physik Department, TU München  
85747 Garching bei München, Germany

Fish use their lateral-line mechanoreceptive system to analyse water motion around their bodies. The functional unit of the fish lateral line is the neuromast. A neuromast is composed of a cupula, a gelatinous protuberance lying into the water that is deflected by local water flow. The deflection stimulates sensory hair cells at the base of the cupula and in this way generates spikes in the lateral-line nerves. Neuromasts are either free standing on the skin (superficial neuromasts, SN) or in a system of subepidermical canals (canal neuromasts, CN). It has been shown that CN are not sensitive to constant water flows whereas SN are. However, nobody has ever proposed a mathematical model to relate the water perturbation in the fish environment to the water motion in the canal, the neuromasts displacement, and the activity in the afferent nerves. That is what we propose to do here.

The CN system is composed of subepidermical water canals. These canals are open to the external environment by a system of pores. Between each pair of pores at the surface one could find, in the canal, one or more neuromasts. The pressure difference between the pores permits the water to move inside of the canals and hence to stimulate the neuromasts.

First, we demonstrate that the water flow around the fish is laminar. This assumption enables us to describe the water flow in terms of a velocity potential. We then solve the case of a small sphere oscillating near the body of the fish when the fish is swimming at a constant velocity. We show that the existence of the canals and their positions on the body enable the fish to filter out the constant velocity flow. We have also studied the influence of the perturbation on the stimuli due to geometry of the body. Finally, it is possible to relate the pressure difference between the pores of the canal lateral line system to the water motion in the canal, the neuromast displacement, the firing activity of the hair cells, and the spiking activity in the afferent nerves.

**Discrimination of two simultaneous water surface waves in the clawed frog,  
*Xenopus laevis laevis***

A. Elepfandt, S. Lebrecht, K. Schroedter, B. Brudermanns; Inst. Biology, Humboldt-Universität zu Berlin, Invalidenstr. 43, D-10115 Berlin, Germany; [Andreas.Elepfandt@rz.HU-Berlin.de](mailto:Andreas.Elepfandt@rz.HU-Berlin.de)

*Xenopus* is a fully aquatic frog that retains its lateral line system after metamorphosis. By means of this system, it can localize and distinguish several waves impinging simultaneously on its body. We examined by conditioning how good *Xenopus* can distinguish two synchronous waves. Waves 5 sec long with 0.5 sec rise and fall times were produced by rhythmically blowing small air puffs through pipettes onto the water surface. Discrimination conditioning started with large differences, and once the task had been learned the difference was reduced until the limen was attained.

In **frequency** discrimination, the discrimination limen for simultaneous waves was smaller than the limen for waves presented separately (except at very low frequencies). At its optimum, 17.5 Hz and 18 Hz could be distinguished, i.e., a beat of 2 sec duration was disentangled into its components. Since all lateral line organs in *Xenopus* possess identical tuning, the basis of this capability must be comparison of the different superposition patterns at various lateral line organs. This was tested in two ways. A. When wave source directions were approached to each other, thus reducing the superposition differences between organs, the discrimination limen increased, from 0.5 Hz at 90° interstimulus angle to 1.7 Hz at 40°. Smaller interstimulus angles could not be resolved. B. A conceivable alternative would be that, due to the animal's wave shadow, the organs perceive only the wave from the ipsilateral side and *Xenopus* perceives the difference between the left and right inputs. However, when specimens were tested where all lateral line organs had been destroyed except of four organs on the neck so that wave shadow did not play a role discrimination with undiminished accuracy was found.

**Distance** discrimination was examined by presenting two 18 Hz waves from different distance. *Xenopus* can localize two waves of equal frequency, that is, the stereo effect as in hearing does not occur in the lateral line system. Waves presented from 10 cm could be distinguished from waves originating at 11 cm distance. This means that *Xenopus* is capable of accurate distance discrimination. Since the waves were monofrequent and their frequency identical, the discrimination must be based on the difference in wave curvature. The result indicates that a 10% difference of wave curvature is detected in wave superposition.

Such an accuracy in the analysis of superimposed waves has been found so far only in electroreception. Since electroreception evolved from the mechanoreceptive lateral line, it seems conceivable that the high analytical capabilities for superimposed waves originated in the mechanoreceptive lateral line and then were passed on to electroreception.

**Sensory-motor transfer for turn responses to two non-visual stimuli in the clawed frog,  
*Xenopus laevis laevis***

A. Elepfandt, B. Hellmann, F. Seifarth, Inst. Biology, Humboldt-Universität zu Berlin, Invalidenstr. 43, D-10115 Berlin, Germany; [Andreas.Elepfandt@rz.HU-Berlin.de](mailto:Andreas.Elepfandt@rz.HU-Berlin.de)

Turning toward a stimulus involves two components: Sensory detection of the stimulus direction and transfer into a response turn with appropriate angle. While detection of stimulus direction has been investigated in a variety of sensory systems, the subsequent sensory-motor transfer has been studied only for responses to visual stimuli. They suggest that the neuronal organisation of visual sensory-motor transfer is largely equal in tetrapods, irrespective of the motor parts finally activated (eyes, neck, whole body). From the tectum, visual directional information is transferred into several tegmental nuclei, where the spatial axes for motion seem to be represented separately.

Those investigations did not elucidate whether the results refer only to the visual system or could reflect a general neuronal pattern for sensory-motor transfer. Therefore, we have investigated, in the fully aquatic clawed frog *Xenopus laevis*, sensory-motor transfer in response to water surface waves and to underwater sound, two non-visual stimuli that *Xenopus* can localize.

In the leopard frog, *Rana pipiens*, Grobstein and collaborators had shown that crossing tegmentospinal but not tectospinal fibres are involved in the turn response in visual prey capture (Masino & Grobstein 1989a,b). The involved fibres descend via the fasciculus longitudinalis medialis (flm). Studies of wave localisation in *Xenopus* after brain lesions that affected tegmental fibres had shown similar orientation deficits (Elepfandt 1988) as shown for the visual prey capture in *R.pipiens* after tegmental lesions. We therefore were interested whether the same descending tract is involved in turn responses in *X.laevis* as in *R.pipiens*.

Retrograde staining from the flm in *Xenopus* demonstrated a lack of tectospinal fibres. Instead the sensory projection area of the lateral line system is surrounded by many mesencephalospinal efferences. In addition, many descending fibres originated in the ventral tegmental nuclei.

Lesions of the flm at its entrance into the medulla resulted in the same type of localisation deficits for ipsilateral waves as had been described in *R.pipiens* for visual prey capture after flm lesions. Thus, the flm is involved in the turn response both in visual turns of *R.pipiens* and in wave response turns of *X.laevis*. Turns through all angles can be made by the animals, it is just the response angle to stimuli from some directions that is false after lesions of flm. The similarity of the deficits suggests that the flm might be involved generally in response turns toward stimuli irrespective of stimulus modality.

To test whether the response turn is organized in the flm through separate fibres for each sensory system or whether the same fibres are involved in the turn irrespective of sensory modality, we examined the turn response to both water waves and sound in specimens of *Xenopus*, in which the flm has been lesioned. In some specimens the localisation deficits were equal for both sensory modalities, indicating that at least some fibres of the flm are involved in response turns irrespective of the modality. Thus the intersensory convergence for response turns takes place at least partly in the midbrain.

References:

- Elepfandt, A. (1988) Brain Behav. Evol. 31: 358-368  
Masino, T, Grobstein, P, (1989a,b) Exp. Brain Res. 75: 227-244, 245-264

# Two Coding Strategies for Communication Signals in a Population Rate Code

Jan Benda<sup>1</sup>, André Longtin<sup>2</sup> & Len Maler<sup>3</sup>

<sup>1</sup>j.benda@biologie.hu-berlin.de, Institute for Theoretical Biology, Humboldt University, Berlin, Germany; <sup>2</sup>Dept. of Physics, <sup>3</sup>Dept. of Cellular and Molecular Medicine, University of Ottawa, Ontario, Canada

It is generally believed that encoding of stimuli in the firing rate of single neurons strongly limits a rapid readout by higher-order neurons. A rate code, however, that makes use of a whole population of neurons is much better suited for high speed processing. Here we present an example where different mechanisms are employed to encode two types of communication signals in a population rate depending on the time scale of the signal.

The weakly electric fish *Apteronotus leptorhynchus* generates a quasi sinusoidal electric field (EOD) of about 800 Hz that is used for both prey detection and communication. During male-male interaction the superposition of the EODs results in a beat of upto 60 Hz whereas during male-female interaction higher beat frequencies between 100 and 300 Hz occur. The fish produce two types of chirps, brief (15 – 25 ms) rises of their EOD frequency, for communication. We performed single unit, dual unit, and whole nerve recordings of P-unit electroreceptor afferents to investigate the encoding strategies that are used for the two types of chirps.

Small (type II) chirps that are emitted during antagonistic male-male interaction result in a phase shift of the beat by about 0.5 to 1.5 cycles. This generates short transients that interrupt the periodic beat pattern. Single unit recordings showed that the high-pass properties of the cells induced by spike-frequency adaptation strongly enhance the firing frequency response to the chirps compared to the response to low (less than 30 Hz) beat frequencies. We found the same response pattern in the summed activity of the whole population of P-units.

During large (type I) chirps that males emit in the presence of females, the high frequency beat is interrupted by a short period of essentially constant EOD amplitude. We found the spike response of the electroreceptors to be phase locked to the fast beat, and synchronized among each other. During the chirp, however, the response was desynchronized. The summed activity showed a strong oscillation evoked by the beat that is interrupted by a brief period of constant activity during the chirp.

In summary, two very different coding mechanisms result in a clear change in the population activity in response to the chirps. For the small chirps it is just the sum of an enhanced firing rate response that is already visible in a single cell. On the contrary, the encoding of the large chirps requires the whole population to translate the change from synchrony to asynchrony into an interruption of the oscillation of the population rate. How higher order neurons read out this code remains to be explored.

# Spike-Frequency Adaptation in the Auditory Preprocessing Module of Crickets

Jan Benda<sup>1</sup> & R. Matthias Hennig<sup>2</sup>

<sup>1</sup>j.benda@biologie.hu-berlin.de, Institute for Theoretical Biology, <sup>2</sup>Institute for Biology  
Humboldt University, Invalidenstr. 43, 10115 Berlin, Germany

Neural information processing of sensory information needs to adapt to changing environmental conditions on various time scales. By generating invariant object representations that are robust against different environmental conditions adaptation is important for reliable object recognition and classification. Here we analyze adaptation properties of two interneurons in the auditory system of crickets.

Female crickets recognize the song of a conspecific male from various distances. In the auditory system of crickets about 50 receptor neurons synapse onto two interneurons, the AN1 and the AN2, that ascend to the brain. The AN1 is excited by low frequency receptors only, that are tuned to the carrier frequency of the cricket's song. The AN2 receives input from both low and high frequency receptors, but is less sensitive than the AN1.

We performed extracellular recordings of the AN1 and AN2 in the neck connective of species from the genus *Gryllus* and *Teleogryllus*. For characterizing spike-frequency adaptation we measured the time course of the firing frequency evoked by low frequency (3–5 kHz) and high frequency (16 kHz) sound waves with constant amplitudes at intensities ranging from 30 to 90 dB SPL. By fitting a single exponential on the firing frequency we quantified the properties of adaptation (Benda & Herz, 2003) on a timescale up to 200 ms and determined the consequences for signal processing.

Adaptation shifted the neuron's intensity-response curve to higher stimulus intensities for both interneurons. In the AN1 this shift was accompanied by a substantial reduction of the maximum firing frequency. The AN1 can adapt its intensity-response curve to different stimulus intensities over a range of 35 dB. Therefore it transmits information about the temporal structure of a stimulus almost independently of the mean stimulus intensity. Although the adaptation properties of both the AN1 and AN2 in different species are qualitatively similar our preliminary data suggest some quantitative differences.

We conclude that spike-frequency adaptation in the AN1 and the AN2 plays a twofold role: It makes the spike response intensity invariant and by defining a steady-state firing frequency sets the temporal resolution.

## References

Benda, J. & Herz, A. V. M. (2003). A universal model for spike-frequency adaptation. *Neural Comput.*, 15, 2523–2564.



**Poster Subject Area #PSA9:  
Chemosensory and thermosensory systems**

- [#121A](#) T. Feistel, O. Levai, J. Strotmann and H. Breer, Stuttgart  
*Odorant receptor expressing cells in the vomeronasal organ*
- [#122A](#) R. Hoppe, Y. Zhang, H. Breer and J. Strotmann, Stuttgart  
*Olfactory receptor genes with clustered expression pattern: genomic organization, promotor elements and interacting transcription factors*
- [#123A](#) E. Grosse-Wilde, T. Gohl, H. Breer and J. Krieger, Stuttgart  
*Bombykol-responsive receptor of the silkworm *Bombyx mori**
- [#124A](#) J. Krieger, E. Grosse-Wilde, T. Gohl, YME. Dewer, K. Raming and H. Breer, Stuttgart and Monheim  
*Candidate pheromone receptors of the moth *Heliothis virescens**
- [#125A](#) T. Lambert, R. Hoppe, C. Rausch, J. Strotmann and H. Breer, Stuttgart and Tübingen  
*Evolution of the "OR37" subfamily of olfactory receptors: a cross-species comparison*
- [#126A](#) J. Strotmann, O. Levai, J. Fleischer, K. Schwarzenbacher and H. Breer, Stuttgart  
*Antibodies recognizing olfactory receptor subtypes*
- [#127A](#) O. Levai, JF. Kaluza, F. Gussing, S. Bohm, H. Breer and J. Strotmann, Stuttgart and Umeå (S)  
*Organization of the septal organ: olfactory receptor expression and nerve fiber projection*
- [#128A](#) M. Spehr, KR. Kelliher, T. Boehm, T. Leinders-Zufall and F. Zufall, Baltimore (USA) and Freiburg  
*Sensing genetic individuality: detection of MHC-related odor signals by the mouse main olfactory system*
- [#129A](#) J. Spehr, K. Ukhanov, F. Zufall and T. Leinders-Zufall, Baltimore (USA)  
*Calcium-activated channels in mammalian vomeronasal neurons*
- [#130A](#) T. Heinbockel, J. Zhao, S. Muralidharan, JPY. Kao and BE. Alger, Baltimore, MD (USA)  
*Lipid Messenger Signaling Dynamics Probed With Optical Tools: Endocannabinoid-Mediated Retrograde Signaling in the Hippocampus*
- [#131A](#) C. Faucher and M. de Bruyne, Berlin  
*Behavioral responses of *Drosophila melanogaster* to carbon dioxide*

- [#132A](#) AF. Silbering, R. Okada, K. Ito and CG. Galizia, Berlin, Tokyo (J) and Riverside, CA (USA)  
*PROCESSING OF ODOR IDENTITY AND CONCENTRATION IN THREE NEURAL POPULATIONS OF THE ANTENNAL LOBE OF DROSOPHILA*
- [#133A](#) P. Szyszka, M. Ditzen, A. Galkin, CG. Galizia and R. Menzel, Berlin and Riverside, CA (USA)  
*Transmission of Olfactory Information from Lower to Higher Brain Structures in the Brain of the Honey Bee*
- [#134A](#) P. Szyszka, A. Galkin, CG. Galizia and R. Menzel, Berlin and Riverside, CA (USA)  
*Imaging Odor Learning in the Mushroom Body of the Honey Bee*
- [#135A](#) A. Galkin, P. Szyszka, J. Rybak and R. Menzel, Berlin  
*Multi-compartment model of Kenyon Cells*
- [#136A](#) R. Dooley, G. Gisselmann, W. Zhang, K. Störtkuhl, H. Hatt and EM. Neuhaus, Bochum  
*Role of Odorant Receptor Heterodimerization in the Olfactory System of Drosophila*
- [#137A](#) A. Mashukova, W. Zhang, H. Hatt and EM. Neuhaus, Bochum  
*Investigation of odorant-induced olfactory receptor desensitization*
- [#138A](#) A. Husch, H. Demmer, I. Lauinger, H. Wratil and P. Kloppenburg, Köln  
*Voltage-Activated Calcium-Currents of Insect Olfactory Interneurons Recorded in Vitro and In Situ*
- [#139A](#) A. Pippow, A. Husch, H. Wratil and P. Kloppenburg, Köln  
*Calcium Buffering in Insect Olfactory Interneurons*
- [#140A](#) N. Lindemann, P. Hafner, C. Pouzat and P. Kloppenburg, Köln and Paris (F)  
*Modulation of Insect Olfactory Interneurons by Biogenic Amines*
- [#120B](#) MA. Carlsson and BS. Hansson, Alnarp (S)  
*Temporal sharpening of plant-odour representations in moth output neurons*
- [#121B](#) J. Barbour, B. Warscheid, K. Stühler, H. Meyer, D. Wolters, H. Hatt and E. Neuhaus, Bochum  
*Analysis of the mouse olfactory receptor associated micro-proteome*
- [#122B](#) N. Damann, B. Klupp, H. Hatt, TC. Mettenleiter and CH. Wetzel, Bochum and Insel Riems  
*Viral tracing of mouse primary afferent neurons allows functional analysis in cell culture*
- [#123B](#) JF. Dörner, H. Hatt and CH. Wetzel, Bochum  
*Modulation of ANKTM1 gating by intra- and extracellular Ca<sup>2+</sup>*

- [#124B](#) D. Brunert, P. Kleinbongard, M. Kelm, N. Damann, H. Hatt and CH. Wetzel, Bochum and Düsseldorf  
*Investigations on Presence and Function of Nitric Oxide in the Olfactory System of Mice*
- [#125B](#) J. Li, JA. Mack, M. Souren, S. Higashijima, G. Mandel, JR. Fetcho and RW. Friedrich, Heidelberg and Stony Brook, NY (USA)  
*Early functional development of chemotopy in the zebrafish olfactory bulb*
- [#126B](#) R. Tabor and RW. Friedrich, Heidelberg  
*Pharmacological investigation of mechanisms underlying temporal patterning of mitral cell responses in the zebrafish olfactory bulb*
- [#127B](#) A. Wertz, W. Rössler and U. Bickmeyer, Helgoland and Würzburg  
*Functional morphology of the rhinophore of Aplysia punctata*
- [#128B](#) C. Linster, S. Sachse and CG. Galizia, Ithaca (USA), New York (USA) and Riverside (USA)  
*Response properties rather than spatial position determine connectivity between olfactory glomeruli*
- [#129B](#) N. Haag and F. Weth, Jena  
*Single-cell transcriptional analysis of regenerating mouse olfactory sensory neurons*
- [#130B](#) C. Flecke, J. Schuckel, J. Seyfarth and M. Stengl, Marburg  
*The role of octopamine in the pheromone transduction of trichoid sensilla of Manduca sexta*
- [#131B](#) S. Krannich, P. Lucas and M. Stengl, Versailles (F) and Marburg  
*Diacylglycerol in moth olfactory transduction*
- [#132B](#) S. Sachse, A. Keller and LB. Vosshall, New York, NY (USA)  
*Experience-Dependent Plasticity in the Antennal Lobe of Drosophila melanogaster*
- [#133B](#) A. Keller and LB. Vosshall, New York, NY (USA)  
*Genetic Analysis of Odor-Evoked Behaviors in Drosophila*
- [#134B](#) H. Schuppe, M. Cuttle and PL. Newland, Southampton (UK)  
*Nitric Oxide Modulates Sodium Chloride Taste Sensitivity*
- [#135B](#) K. Schwarzenbacher, J. Fleischer, S. Conzelmann and H. Breer, Stuttgart  
*Expression of olfactory receptors in the cribriform mesenchyme during prenatal development*
- [#136B](#) C. Groh, B. Müller and W. Rössler, Würzburg  
*Ontogenetic plasticity of primary and secondary olfactory centers in the honeybee brain*

- [#137B](#) S. Kirschner, C. Zube, C.J. Kleinendam, B. Grünewald and W. Rössler, Würzburg and Berlin  
*Subsets of antennal-lobe glomeruli project via different output-tracts in the honeybee brain*
- [#138B](#) C.J. Kleineidam, M-L. Obermayer, W. Halbich and W. Rössler, Würzburg  
*Phenotypic plasticity of the antennal lobe and its behavioral significance in leaf-cutting ants*
- [#139B](#) C. Kelber, W. Rössler and C.J. Kleineidam, Würzburg  
*Functional organization of poreplate sensilla in the honeybee *Apis mellifera**
- [#140B](#) A. Weibel, C.J. Kleineidam and W. Rössler, Würzburg  
*Synaptic plasticity in olfactory centers of the adult ant brain*

## Odorant receptor expressing cells in the vomeronasal organ

Torben Feistel, Olga Levai, Jörg Strotmann and Heinz Breer

University of Hohenheim, Institute of Physiology, Garbenstrasse 30,  
70599 Stuttgart, Germany

In addition to the main olfactory system, most mammals comprise a well-developed vomeronasal system that is considered to be specialized for detecting pheromones, chemical cues which are emitted by other animals and convey specific information concerning gender and identity; they also induce innate behaviors, such as aggression and mating. Two populations of vomeronasal sensory neurons are distinguished; cells in the apical layer expressing V1R-receptors and  $G_i$ -protein, projecting to the anterior part of the accessory bulb and cells in the basal layer expressing V2R receptors and  $G_o$ -proteins projecting to the posterior part of the accessory bulb. *In situ* hybridization and analysis of transgenic mouse lines have provided evidence, that there is a third population of sensory neurons; these cells express odorant receptor subtypes. Only a limited number of OR-types was found to be expressed in the VNO, all of them are concomitantly expressed in the main olfactory epithelium. This observation raises the question if OR expressing cells in the VNO share the molecular transduction machinery as their counterparts in the MOE. Experiments towards a molecular phenotyping of these cells have indicated that the VNO-cells do not express adenylyl cyclase Typ III or  $G_{olf}$ , suggesting that at least some OR-subtypes appear to be promiscuous concerning G-protein coupling. Since olfactory neurons in the MOE which express a distinct receptor type all project to a common pair of glomeruli, it seems conceivable that cells in the VNO, which express the same OR-type may also project to the same glomeruli. Analysis of transgenic mice visualizing the OR-expressing cells and their axons revealed that the labeled nerve fibers from the VNO did not project to the main olfactory bulb but terminated in the anterior region of the accessory olfactory bulb, like the V1R-expressing cells. This characteristic wiring pattern of OR-expressing cells in the VNO and MOE suggest that certain odorants may act as both odors and pheromones. This work was supported by the Deutsche Forschungsgemeinschaft.

**Olfactory receptor genes with clustered expression pattern: genomic organization, promotor elements and interacting transcription factors**

Reiner Hoppe, Yongquan Zhang, Heinz Breer, Jörg Strotmann

University of Hohenheim, Institute of Physiology, Garbenstrasse 30,  
70599 Stuttgart, Germany

In the nasal epithelium of mammals, olfactory sensory neurons expressing a particular odorant receptor (OR) type are either restricted to one of several broad expression zones or, like the cells expressing a member of the *mOR262*-subfamily, are clustered within a small central region of the epithelium. Individual cells are likely to express only a single or at most a few receptors from the large OR gene superfamily. Very little is known about the molecular parameters and processes underlying the complex transcriptional regulation of olfactory receptor gene expression. Towards an understanding of the underlying mechanisms, the genomic sequences upstream from the receptor coding regions of clustered OR genes were studied in detail. 5'-RACE experiments and bioinformatic analyses revealed complex intron/exon structures and led to the identification of short DNA stretches of approximately 150 bp immediately upstream the transcription start sites. Comparative studies on the rat and human gene repertoires demonstrated the existence of similar sequence motifs across species border. To test whether these sequence motifs may indeed be part of the expression control machinery, a representative 5'-sequence was employed in gel-shift assays, demonstrating specific binding only of proteins from olfactory epithelium nuclear extracts. Yeast one-hybrid experiments identified distinct transcription factors expressed in the olfactory epithelium that interact with this region. In reporter gene assays, particular factors were capable to activate transcription. Altogether, these results suggest that the DNA-motifs present in the 5' non-coding regions of the clustered genes may indeed be important for expression control.

This work was supported by the Deutsche Forschungsgemeinschaft.

**Bombykol-responsive receptor of the silkmoth *Bombyx mori***

Ewald Grosse-Wilde, Thomas Gohl, Heinz Breer and Jürgen Krieger

University of Hohenheim, Institute of Physiology, Garbenstr. 30,  
70599 Stuttgart, Germany

The silkmoth *Bombyx mori* not only allowed to isolate the first pheromone (bombykol) but has also been an extremely valuable model for studying cellular and molecular mechanisms of pheromone signaling. Male *B. mori* recognize female released pheromone components with high specificity and selectivity. This is accomplished by means of specialized antennal neurons housed in sensillar hair structures. The dendrites of these cells respond to pheromonal compounds via intracellular reaction cascades elicited by G-protein coupled receptors. In spite of the progress in identification and characterization of insect olfactory receptors for general odorants, receptors for pheromone components are still elusive. Recently, we have discovered first candidate pheromone receptors of the pest insect *Heliothis virescens*. Using these sequences in screening an antennal cDNA library of the silkmoth and data mining the *B. mori* genome data base we have isolated five cDNAs which encode proteins with considerable sequence identity. RT-PCR-analysis revealed that all five subtypes were expressed in the antennae, with BR1 expression restricted to male moths. *In situ* hybridization studies showed that the receptor types BR1 and BR3 are expressed in neighboring cells beneath long trichoid hairs which contain pheromone responsive neurons. Moreover, two colour double *in situ*-hybridization approaches uncovered that each cell expressing one of these receptor types was surrounded by cells expressing pheromone binding proteins. To approach their ligand specificity BR1 and BR3 were heterologously expressed in HEK293 cells and the responsiveness to bombykol, bombykal and some odorants was assessed by  $\text{Ca}^{2+}$ -imaging of transfected cells. These experiments revealed that BR1 expressing HEK293 cells responded to bombykol but not to other compounds.

This work was supported by the Deutsche Forschungsgemeinschaft.

**Candidate pheromone receptors of the moth *Heliothis virescens***

Jürgen Krieger\*, Ewald Grosse-Wilde\*, Thomas Gohl\*, Youssef M.E. Dewer\*,  
Klaus Raming<sup>§</sup> and Heinz Breer\*

\*University of Hohenheim, Institute of Physiology, Garbenstrasse 30,  
70599 Stuttgart, Germany

<sup>§</sup>Bayer CropScience AG, Target Research, Alfred-Nobel-Strasse 50,  
40789 Monheim, Germany

Pheromones play a key role in initiating and controlling mating behavior of insects. The remarkable ability of male moths to recognize female released pheromones is based on the extremely sensitive and selective reaction of highly specialized sensory cells in the male antennae. These cells are supposed to be equipped with distinct, male-specific seven transmembrane domain receptor proteins for pheromonal compounds, which initiate intracellular reaction cascades. Due to their key role in the initial step of odor perception and their proposed potential in insect control, great efforts have been made over the past decade to identify olfactory receptors in moths; however, for many years their molecular identity remained elusive. Using a combination of genomic sequence analysis and cDNA library screening of the tobacco budworm *Heliothis virescens* led to the discovery of a divergent gene family encoding putative seven transmembrane domain proteins. Comparing the encoded amino acid sequences of all 21 candidate olfactory receptors emphasized their extreme diversity; however, a small family (identity > 40%) emerged, including the three receptor types HR14, HR15, HR16. RT-PCR-analysis revealed that all three subtypes were exclusively expressed in the antennae of male moths. More detailed *in situ* hybridization studies indicated that expression of these male-specific receptor types was confined to antennal cells located beneath sensillar hair structures which contain pheromone sensitive neurons. Moreover, two colour double *in situ*-hybridization approaches in combination with laserscanning microscopy uncovered that each cell expressing one of these receptor types was surrounded by cells expressing pheromone binding proteins. These findings suggest that the novel receptor types may render neurons in male antennae responsive to pheromones. This work was supported by the Deutsche Forschungsgemeinschaft.



**Evolution of the "OR37" subfamily of olfactory receptors: a cross-species comparison**

Thomas Lambert<sup>1</sup>, Reiner Hoppe<sup>1</sup>, Christian Rausch<sup>2</sup>, Jörg Strotmann<sup>1</sup> and  
Heinz Breer<sup>1</sup>

<sup>1</sup>University of Hohenheim, Institute of Physiology, Garbenstrasse 30,  
70599 Stuttgart, Germany

<sup>2</sup>Zentrum für Bioinformatik Tübingen, Lehrstuhl für Algorithmen der Bioinformatik, Sand 14,  
72076 Tübingen

Olfactory receptors (ORs) of the OR37 subfamily are characterized by several special properties, including an extended third extracellular loop and a clustered expression pattern in the olfactory epithelium. The human and mouse genome projects have allowed us to characterize the complete repertoire of OR37 receptor subtypes in these species. Uniquely among olfactory receptor subfamilies, genes encoding OR37 receptors are organized in 2 gene clusters. Cluster-I consists of 5 genes, which share a very high level of sequence homology (~ 90%). In line with the tendency of pseudogenisation for human OR-genes, the human cluster-I contains 4 pseudogenes; the mouse cluster-I: 1 pseudogene. Cluster-II comprises 3 genes in mouse and in human, surprisingly, 7 genes. The sequence similarity of cluster-II genes was only ~ 60%. To gain some insight into the origin and evolution of this special OR subfamily, we have cloned OR37-type receptors from animals which are considered as representative for different stages of mammalian evolution. From the Great Anteater, a member of insectivores, we have identified a total of 21 OR37 genes which are related to cluster-I and cluster-II genes, respectively; thus indicating that the arrangement of two OR37 gene clusters apparently existed prior to 130 million years ago. In the opossum, a representative of the marsupalia, five OR37-like receptors were identified which all seem to be cluster-II genes. All efforts to clone cluster-I-like genes from opossum failed; thus, one might speculate that cluster-II may be the original cluster and cluster-I appeared somewhere between 130 and 173 million years ago. Analyzing the egg-laying monotreme, Platypus, we were unable to identify any OR37 genes, however, a receptor type was identified, which is a member of the OR-family 262; interestingly, all OR37-receptors are members of the 262 family.

This work was supported by the Deutsche Forschungsgemeinschaft.

## **Antibodies recognizing olfactory receptor subtypes**

Jörg Strotmann, Olga Levai, Jörg Fleischer, Karin Schwarzenbacher and Heinz Breer

University of Hohenheim, Institute of Physiology, Garbenstrasse 30,  
70599 Stuttgart, Germany

Olfactory receptors are considered as multifunctional elements of olfactory sensory neurons; they are supposed to mediate the response to adequate odorants, to play an important role in target finding of the axons and may even contribute to a monoallelic expression of one receptor type per cell. Most of these views are based on studies performed on the level of the encoding nucleic acids, very little is known about the actual receptor proteins. Efforts to explore the features of distinct receptor subtypes have always been hampered by the fact that specific receptor antibodies were not readily available. In the present study, we have tried to generate subtype-specific antibodies. In a first approach, antibodies raised against a peptide, characteristic for the mouse OR37 receptors were assessed. Immunohistochemical analyses of nasal whole mount preparations revealed staining of individual cells; their clustered distribution matched that previously visualized by *in situ* hybridization. In tissue sections analysed by confocal microscopy, intense fluorescence was visualized in the cell body, dendrite and most notably the cilia of individual sensory neurons. In a second set of experiments, antibodies generated against mOR256-17 were assessed; this OR-subtype is expressed in the medial zone and *in situ* hybridization suggests it may also be expressed in cells within the cribriform mesenchyme during development. In fact, in distinct developmental stages, immunoreactive cells were visible in the cribriform mesenchyme, in particular the membrane of these cells was labeled. Moreover, the notion that receptor proteins may be present in the axons of olfactory neurons was confirmed; very distinct axon bundles and glomeruli were visualized by the antibodies. These results strongly suggest that the newly generated antibodies may represent useful tools for studying olfactory receptor proteins.

This work was supported by the Deutsche Forschungsgemeinschaft.

## Organization of the septal organ: olfactory receptor expression and nerve fiber projection

Olga Levai<sup>1</sup>, Jan F. Kaluza<sup>1</sup>, Fredrik Gussing<sup>2</sup>, Staffan Bohm<sup>2</sup>, Heinz Breer<sup>1</sup> and Jörg Strotmann<sup>1</sup>

<sup>1</sup> University of Hohenheim, Institute of Physiology, Garbenstrasse 30, 70599 Stuttgart, Germany

<sup>2</sup> Umeå University, Department of Molecular Biology, Umeå, Sweden

The septal organ (SO) is a small patch of olfactory epithelium located as an island in the respiratory epithelium on the nasal septum. Although discovered decades ago, its functional relevance remains enigmatic. Here, we have identified a repertoire of chemosensory receptors expressed in the SO. The results demonstrate that SO neurons express receptor genes belonging to class-II olfactory receptors that are also expressed in the main olfactory epithelium. In the SO, no topography analogous to the receptor expression zones of the main olfactory epithelium was evident. The majority of identified receptors corresponds to genes with restricted expression in the medial and lateral zones of the main olfactory epithelium. Most of the receptor types were found to be expressed in only few SO neurons, except for *mOR244-3* which was observed in a very high proportion of cells. Although a large fraction of SO neurons expressed *mOR244-3*, we found no evidence for the co-expression of different receptors in individual cells. Analyzing the projection pattern of SO neurons using the OMP-GFP transgenic mouse line revealed that axons navigate in highly variable fiber tracks across the main olfactory epithelium towards the main olfactory bulb. All SO axons cross through the cribriforme plate at a spatially defined site and terminate exclusively in the posterior, ventro-medial aspect of the bulb. Here, one portion of axons forms a dense network on the medial side where they apparently enter glomeruli which are mainly innervated by axons of olfactory sensory neurons from the main olfactory epithelium. Another significant portion of the axons targets a few glomeruli which appear to receive input exclusively from the septal organ neurons.

This work was supported by the Deutsche Forschungsgemeinschaft.

## Sensing genetic individuality: detection of MHC-related odor signals by the mouse main olfactory system

Marc Spehr<sup>1Φ</sup>, Kevin R. Kelliher<sup>1</sup>, Thomas Boehm<sup>2</sup>, Trese Leinders-Zufall<sup>1</sup>, and Frank Zufall<sup>1</sup>

<sup>1</sup> Dept. Anatomy and Neurobiology, University of Maryland School of Medicine, Baltimore, USA

<sup>2</sup> Max-Planck Institute of Immunobiology, Department of Developmental Immunology, Freiburg, Germany

In most non-primate mammals, information that is necessary for social recognition is encoded by olfactory or pheromonal signals. Aggression, sexual behavior, kin and individual recognition all depend on the detection and processing of specific chemosensory cues. In many cases, these behaviors are directly influenced by a unique set of odors that are associated with the genotype of an animal's major histocompatibility complex (MHC). The remarkably polymorphic loci of the MHC provide the immunological fingerprint of an individual, and MHC-derived body odors act as primary mediators of chemical individuality signaling.

We have begun to carry out a systematic analysis of the chemical identity of these MHC-associated cues including the cellular and molecular mechanisms underlying their detection. Here, we report that inbred mice are able to detect strain-specific MHC-related cues via their main olfactory system. Local field potential recordings demonstrate that MHC-related molecules are detected at remarkably low concentrations and evoke dose-dependent response patterns. Experiments using genetically altered mice provide first insight into the fundamental signaling mechanisms employed by the olfactory sensory neurons. These electrophysiological results are confirmed by behavioral studies. Habituation-dishabituation and odor preference assays show that mice can sense these MHC odors in a manner consistent with the physiological results.

We expect that these experiments will provide a cellular and molecular basis for the detection of social recognition cues by the mammalian olfactory system.

<sup>Φ</sup>This work is supported by the DFG Emmy Noether Programm (SP 724/1-1)

### **Calcium-activated channels in mammalian vomeronasal neurons**

Jennifer Spehr, Kyrill Ukhanov, Frank Zufall and Trese Leinders-Zufall

Department of Anatomy and Neurobiology, University of Maryland, Baltimore, MD, USA

The mammalian vomeronasal organ (VNO) is the chemoreceptive structure of the accessory olfactory system that plays an essential role in the detection of pheromones. Recent findings provided first insight into the basic mechanisms underlying vomeronasal signaling. Receptor activation in VNO neurons ultimately leads to generation of action potentials and an increase in intracellular  $\text{Ca}^{2+}$ , presumably via G-protein-mediated activation of phospholipase C and generation of the two second messenger molecules IP3 and DAG. We recently showed that DAG, in turn, activates a non-selective cation conductance that is critical for membrane depolarization and significantly impaired in mice lacking the TRPC2 ion channel (Lucas et al., 2003). However, potential roles of IP3 and / or TRPC2-dependent  $\text{Ca}^{2+}$  influx in vomeronasal signaling remain unresolved.

Hypothesizing a signaling-relevant function of cytosolically increased  $\text{Ca}^{2+}$ , we set out to characterize  $\text{Ca}^{2+}$ -activated ion channels in vomeronasal sensory neurons (VSNs). Whole-cell patch-clamp recordings from freshly dissociated mice VSNs and in vomeronasal slice preparations revealed a slowly increasing and persistent  $\text{Ca}^{2+}$ -activated current in the large majority of cells. Additional current clamp experiments showed a  $\text{Ca}^{2+}$ -induced depolarization with the same characteristics.

Pharmacological investigations showed an involvement of  $\text{Ca}^{2+}$ -activated potassium channels. Selective inhibition of these channels uncovers further  $\text{Ca}^{2+}$ -induced currents that could result from the activation of nonselective cation and / or chloride channels.

Our findings indicate the functional expression of several types of  $\text{Ca}^{2+}$ -activated channels in mouse VSNs. Studies are underway to dissect the functional roles of these channels during pheromone transduction.

Lucas P, Ukhanov K, Leinders-Zufall T, Zufall F (2003) Neuron 40, 551-561.

## **Presynaptic Inhibitory Modulation by Metabotropic Glutamate Receptors in Olfactory Bulb Glomeruli**

**Thomas Heinbockel<sup>1</sup> and Matthew Ennis<sup>2</sup>**

*<sup>1</sup>Dept. of Physiology and Program in Neuroscience, University of Maryland School of Medicine, Baltimore, MD 21201, USA, <sup>2</sup>Dept. of Anatomy and Neurobiology, University of Tennessee Health Science Center, Memphis, TN 38163, USA*

In the main olfactory bulb (MOB) various neuronal cell types express high levels of metabotropic glutamate receptors (mGluRs). Juxtaglomerular neurons (JGs) and mitral cells (MCs) express a Group I mGluR (mGluR1), whereas granule cells (GCs) express both Group I and II mGluRs (mGluR5, mGluR2). Synaptic transmission from olfactory sensory neurons (OSNs) to postsynaptic elements in the MOB is modulated by presynaptic inhibition. This inhibition is mediated through GABA<sub>B</sub> and dopamine (D2) receptors located on presynaptic axon terminals of OSNs in MOB glomeruli. JGs release both GABA and dopamine and presynaptically inhibit OSNs. Previously, we found that both JGs (Hayar et al., 2004, Chem Senses, in press) and MCs (Heinbockel et al., 2004, J Neurophysiol) are potently and directly activated by bath application of DHPG, a selective group I mGluR agonist. DHPG induces a strong depolarization and increased action potential firing in these neurons. Here, we explored the role of mGluRs in regulating afferent input to the MOB.

Electrical stimulation in the olfactory nerve layer reliably evokes short-latency postsynaptic responses in MCs (EPSCs or EPSPs with action potentials). In the presence of NMDA and GABA<sub>A</sub> receptor blockers application of DHPG reduces the response probability and amplitude of MCs to olfactory nerve stimulation. This effect persists in the presence of the D2 receptor blocker sulpiride but is abolished in the presence of the GABA<sub>B</sub> receptor blocker CGP 55845. The results suggest that the blockade of transmission from OSNs to MCs is mediated by activation of mGluRs on JGs, which in turn presynaptically inhibit OSNs through GABA<sub>B</sub> receptors. Therefore, mGluRs are potently involved in shaping synaptic input to glomeruli in the MOB.

*Supported in part by US PHS grants DC03195 and DC00347 and a University of Maryland School of Medicine Bressler Fund Award.*

**Behavioral responses of *Drosophila melanogaster* to carbon dioxide**

Cécile Faucher and Marien de Bruyne

Neurobiologie, Freie Universität Berlin, Koenigin-Luise-St. 28-30, 14195 Berlin, Germany

With their olfactory and gustatory systems insects are able to monitor their chemical environment. They selectively detect and respond to those molecules, which aid their orientation toward feeding sources, oviposition sites and mates. Detection of certain chemicals may also be essential to avoid toxins or other dangerous situations. CO<sub>2</sub> is a rather unspecific cue, constantly present at a relatively high level of 0.035% in the atmosphere. Nevertheless, it is perceived by many insect species and modulates their behaviours.

We are investigating the behavioural responses of *Drosophila melanogaster* to CO<sub>2</sub>. These flies feed on fermenting fruits, which produce large amounts of CO<sub>2</sub>. We have characterized a class of CO<sub>2</sub> specific receptor neurons in the antenna and discovered that the G-protein coupled receptor Gr21a is expressed exclusively in these cells. Flies in which we have genetically ablated Gr21a expressing cells do not respond to CO<sub>2</sub>.

In a choice situation with four converging airflows, individual flies are repelled by high CO<sub>2</sub> concentrations, above 0.1%. However, from physiological experiments we know that their receptor neurons can detect shifts in CO<sub>2</sub> concentrations of as little as 0.02%. In order to reveal behavioural responses close to sensory thresholds we tested 0.02% CO<sub>2</sub> on a background of an attractive odour mixture and found that females were repelled while males were not. This suggests that *Drosophila* avoids even minor increases of CO<sub>2</sub> and that this behaviour is sexually dimorphic.

In the same behavioural setting, larvae avoid CO<sub>2</sub> at a high concentration but are less sensitive than adults. The Gr21a receptor is also expressed in a single larval neuron, innervating the terminal organ. We therefore tested larvae that have the cell expressing Gr21a deleted. These results indicate that these larvae do not show repulsion to CO<sub>2</sub> and prove that the Gr21a receptor is expressed in CO<sub>2</sub> detecting cells of larvae as well.

We hypothesize that for flies an increased CO<sub>2</sub> concentration is an indication of toxic levels of fermentation products.

## PROCESSING OF ODOR IDENTITY AND CONCENTRATION IN THREE NEURAL POPULATIONS OF THE ANTENNAL LOBE OF *DROSOPHILA*

Silbering, Ana F.<sup>1</sup>; Okada, Ryuichi<sup>1</sup>; Ito, Kei<sup>2</sup> and Galizia, C. Giovanni<sup>3</sup>

<sup>1</sup>Institut für Neurobiologie, FU Berlin, Berlin, Germany; <sup>2</sup>Institute of Molecular and Cellular Biosciences, Centre of Bioinformatics, University of Tokyo, Tokyo, Japan; <sup>3</sup>Department of Entomology, UCR, Riverside, California, USA

### Abstract

The antennal lobes (ALs) are the first brain structures involved in odour processing in insects, and are the functional and structural analogues of the vertebrate olfactory bulb. In the ALs, olfactory sensory neurons (OSNs) converge in glomerular structures where they synapse with local inhibitory neurons (LNs) and projection neurons (PNs).

As a first approach to understand the coding mechanisms of the antennal lobe of *D. melanogaster* we have studied odour-elicited activity patterns in two populations of LNs and in the PNs using optical imaging methods. We expressed the genetically encoded calcium sensor *GCaMP* using the UAS-GAL4 system with two LN selective lines (Np2426 and Np1227, Kei Ito) and a PN selective line (GH146, Gertrud Heimbeck). The two LN enhancer trap lines represent two non-overlapping populations of local neurons that have different arborisation patterns (Okada, unpublished data). GH146 drives the expression of the calcium sensor in ~60% of the projection neurons.

In order to compare the functional properties and dynamic ranges of these three neuron populations, we analyzed their activity patterns when stimulating living flies with different odours at increasing concentrations. In all three lines we found that different odours induced responses in different areas of the antennal lobe. Furthermore, increasing stimulus concentrations resulted in stronger and spatially more extended response patterns.

*Supported by a grant of the VW Stiftung for CGG*



## Transmission of Olfactory Information from Lower to Higher Brain Structures in the Brain of the Honey Bee

Paul Szyszka, Mathias Ditzen, Alexander Galkin, Giovanni Galizia\* and Randolph Menzel

Institute für Biologie – Neurobiologie, Freie Universität Berlin, Berlin; \* Dept. of Entomology, University of California, Riverside

We analyzed the propagation and transformation of odor evoked neural activity in the brain of the honey bee *Apis mellifera*. In insects, the antennal lobe (AL) is the first olfactory relay station. Within the AL, neurons are grouped in one of 160 glomeruli. Uniglomerular projection neurons (PN) transmit olfactory information from the AL to the mushroom bodies (MB), which are higher order integration centers involved in odor learning. The intrinsic cells of the MBs (Kenyon cells, KC) receive olfactory input from PN boutons in the lip area of the calyx.

In order to reveal the contribution of pre- and postsynaptic mechanisms to the information transmission between the AL and the MB, we imaged odor evoked  $\text{Ca}^{2+}$  transients in the dendrites of PNs in the AL, in their presynaptic terminals (boutons) in the MB and in postsynaptic KCs. At all three processing stages odors activated specific combinatorial ensembles of units, but the activation patterns became less overlapping in the mushroom body. Odors evoked responses in a sparse population of KCs and the probability of a given KC to be activated by one of the tested odors was low ( $p=0.013$ ). In contrast PNs showed a higher response probability ( $p=0.2$ ) and were less odor selective. Moreover, Kenyon cells transformed temporally complex PN responses into brief phasic responses, by integrating inputs only within the first 200 ms after PN response onsets. Our results suggest that the sparsening of odor representations in the MB is the result of pre- and postsynaptic processing. The high odor specificity observed in KCs may be generated in part by local presynaptic inhibition of PN boutons. In contrast, the sharpening of the response dynamics is exclusively established at the postsynaptic KCs, since it is not visible in PN boutons.

## Imaging Odor Learning in the Mushroom Body of the Honey Bee

Paul Szyszka, Alexander Galkin, Giovanni Galizia\* and Randolph Menzel

Institut für Biologie – Neurobiologie, Freie Universität Berlin, Berlin; \* Dept. of Entomology, University of California, Riverside

In insects, neural plasticity underlying associative odor learning presumably takes place in the mushroom bodies (MB). MBs receive olfactory input from the first-order olfactory neuropil, the antennal lobe, via projection neurons (PN). In the MB of the honey bee PNs converge with an octopaminergic neuron ( $Vum_{mx1}$ ) which represents the rewarding function in associative olfactory learning. Thus, it has been suggested that the intrinsic cells of the MB (Kenyon cells, KC) act as coincidence detectors for the odor stimulus and the reward.

In order to understand the neural processes underlying associative odor learning in the MB, we combined  $Ca^{2+}$  imaging of KCs with learning experiments. MBs were imaged during differential conditioning, where bees learned to associate one odor (CS+) with a sucrose reward, while a second odor (CS-) was not rewarded. Before training both odors elicited brief  $Ca^{2+}$  transients in different KC populations. During training, the pairing of CS+ with sucrose did neither change the activation pattern, nor the initial odor response of KCs, but lead to a prolonged  $Ca^{2+}$  signal. 15 minutes after training the patterns of KCs activated by CS+ and CS- remained unchanged, however, the CS+ evoked stronger responses.

These results confirmed that KCs act as coincidence detectors for the CS and the reward and are associatively modulated. We present a model, which assumes that odor learning is based on sparse odor representations and associative plasticity in the MB. Odor learning presumably does not change the code of the odor identity, but strengthening KCs' odor responses might recruit MB output neurons which would then code the meaning of an odor.

## Multi-compartment model of Kenyon Cells

*A. Galkin, P. Szyszka, J. Rybak, R. Menzel**Institut fuer Neurobiologie, FU-Berlin, Germany.*

The mushroom bodies (MB) of insect brain is an important relay-station, where the information of many sensory modalities converge. Olfactory information is received by receptor cells on the antenna, whose axons convey the information to the antennal lobe (AL). The AL has a glomerular structure. Glomeruli include arborisation sites of second order neurons (projection neurons, PNs), which convey information via the medial and lateral antennocerebral tracts (m-ACT and l-ACT) to the MB. PNs project to the lip region of MB, where the olfactory input is further processed out by Kenyon cells (KC). We simulated how a subpopulation of KCs, the clawed KCs integrate input from l-ACT PNs. Clawed KCs are unipolar neurons, which consist of a soma, the primary dendrites with spines (the claw-like postsynaptic parts of synapses with the PNs and GABAergic inhibitory cells), and an axon which projects to the ventral part of alpha-lobe and the beta-lobe, the output regions of the MB. Optophysiological recordings showed that the probability for single l-ACT PN to fire in response to an odor stimulation is about 0.2, whereas clawed KC respond much sparser with  $p=0.013$ . From electrophysiological experiments we know, that PNs show spontaneous activity ( $3.6\pm 4.5$  Hz), whereas KC generate spikes only in response to stimulus.

In order to investigate the role of KC geometry and membrane properties on input read-out and processing, we implemented in Neuron (Hines & Carnevale, Yale University) a multi-compartment model of a single KC using the morphological and physiological data from our lab. The geometry of single Kenyon cell was simplified and presented as a model with only 15 compartments (soma, primary dendrite, main dendrite, axon, 10 spines). Using binomial distribution we deduced, that on average of 5.5 spines of one KC must be activated simultaneously for a KC to fire. Model A simulates the soma, primary dendrite and axon by Hodgkin-Huxley (HH) equations, whereas the secondary dendrite and spines are assumed to have only passive properties and are simulated using the cable equation. In this model the threshold of 0.00045 pS for single spine conductance was used to achieve the desired sparseness. This leads to a synaptic delay between stimulus on-set and axon firing of 2.8 msec and to the soma of 4.175 msec. This model is very stable against white noise (no spiking even at noise level of 10 mV). In model B we stimulated the whole KC as HH-model. In this case the threshold was 0.000125 pS for a single spine. The KC fires more rapidly, and the delay between stimulus on-set and spike maximum is 3.2 ms for both axon and soma. The model is as well very stable against white noise, but showed spontaneous spiking in response to Poisson's distributed single PN spikes. A third model (C) shows intermediate properties (slower on-set, more stable against Poisson's noise). Models A and C resist to Poisson noise input with a mean frequency 30 Hz. These data shows, that the robust response behavior of KCs observed in physiological measurements can be achieved with high spiking threshold, short integration time and that partially active membrane properties increase the robustness of the KC spiking threshold.

## Role of Odorant Receptor Heterodimerization in the Olfactory System of *Drosophila*

Ruth Dooley<sup>1</sup>, Günter Gisselmann<sup>1</sup>, Weiyi Zhang<sup>1</sup>, Klemens Störtkuhl<sup>2</sup>, Hanns Hatt<sup>1</sup> & Eva M. Neuhaus<sup>1</sup>

<sup>1</sup> Lehrstuhl für Zellphysiologie, <sup>2</sup>AG Molekulare Zellbiochemie, Ruhr-Universität Bochum, Universitätsstraße 150, 44780 Bochum, Germany

Despite increasing knowledge about dimerization of G-protein coupled receptors, nothing is known about the largest subfamily, odorant receptors. Odorant receptor (OR) genes that encode proteins with a putative seven-transmembrane domain structure have been identified in vertebrates and invertebrates, including different insects. A given OR gene is expressed only in a small fraction of olfactory receptor neurons (ORNs) and each ORN expresses a very small number of OR genes. However, in insects one extremely conserved member of the OR family is expressed in nearly all ORNs in addition to the conventional OR(s). The encoded proteins, DOR83b in *Drosophila melanogaster*, AgOr7 in *Anopheles gambiae*, HvirR2 in *Heliothis virescens* and AmelR2 in *Apis mellifera*, have between 64% and 88% sequence identity, a level not observed for any other insect OR gene. Antennal neurons in *D. melanogaster* that only express DOR83b do not respond to a large panel of odors, so it is unlikely that the receptor has ligand binding properties.

Using a combination of biochemical and electrophysiological approaches, we unambiguously demonstrate that insect odorant receptors can dimerize, and that heterodimerization improves functionality of the receptors. DOR83b forms heterodimeric complexes with other odorant receptor proteins, which strongly increase their functionality. Our results suggest that DOR83b functions as a co-receptor of conventional *D. melanogaster* ORs. DOR83b is expressed broadly in olfactory and gustatory tissues and may be of general importance to both modalities of chemosensation in insects.

## **Investigation of odorant-induced olfactory receptor desensitization**

Anastasia Mashukova, Weiyi Zhang, Hanns Hatt & Eva M. Neuhaus

Lehrstuhl für Zellphysiologie, Ruhr-Universität Bochum, Universitätsstrasse 150, D-44780 Bochum, Germany

Olfactory receptors comprise the largest single subfamily of the G-protein-coupled receptors (GPCRs) numbering nearly 1000 in many mammals. However, investigation of olfactory receptor (OR) trafficking steps have been severely impeded by poor OR expression in heterologous systems and by the lack of specific antibodies.

The main purpose of our studies is the investigation of olfactory receptor endocytosis after ligand exposure.

Endocytosis of GPCRs involves phosphorylation of the receptor by G-protein receptor kinases, PKA or PKC, followed by binding of arrestin and clathrin and accumulation of receptors in clathrin-coated pits. We showed beta-2-arrestin redistribution in response to activation of olfactory receptors in transiently transfected HEK293 and *odora* cells. This allows us to use a beta-arrestin-GFP translocation assay to follow olfactory receptor desensitization after ligand treatment. With this assay system, we investigate the role of olfactory receptor phosphorylation for the desensitization process by creating mutated receptor constructs, employing a pharmacological approach and using Ca-imaging technique.

## Voltage-Activated Calcium-Currents in Olfactory Interneurons of Insects Recorded in Vitro and in Situ

Andreas Husch, Heike Demmer, Ina Lauinger, Helmut Wratil and Peter Kloppenburg  
Zoologisches Institut, Universität zu Köln, Weyertal 119, D-50923 Köln, Germany

One of our long term goals is to analyse and better understand the cellular and biophysical mechanisms used by neuromodulators, especially biogenic amines, to control neuronal plasticity by modifying calcium handling in olfactory interneurons. The insect olfactory system has served very successfully as a general model to understand olfactory information processing and neuronal network function. We use whole-cell patch-clamp techniques *in vitro* and *in situ* to characterise voltage-activated calcium currents of olfactory interneurons from adult *Periplaneta americana*. The somata were voltage-clamped under conditions, in which other voltage gated currents ( $I_A$ ,  $I_{K(V)}$ ,  $I_{Na}$ ,  $I_H$ ) were pharmacologically blocked. Depolarising voltage steps from -60 mV generated voltage dependent inward currents. The currents consisted of a transient, fast inactivating component and a sustained, non inactivating component. Reduction of the extracellular calcium concentration reduced the currents reversibly. Cadmium at concentrations of 200  $\mu$ M blocked more than 90% of the current. When calcium was substituted with barium the currents were enhanced and the inactivation during a sustained voltage step was reduced, suggesting a calcium dependent inactivation of the current. *In vitro*,  $I_{Ca}$  started to activate above -35 mV to -30 mV, with a maximum around -5 mV. The inactivation of the calcium currents started with pre-pulse potentials above -50 mV to -45 mV. In the intact brain these parameters were shifted to more depolarised membrane potentials. *In situ*  $I_{Ca}$  began to activate above -30 mV to -25 mV, with a maximum around +20 mV. The inactivation in intact neurones of the antennal lobes started at pre-pulse levels above -35 mV to -30 mV. The shift of these parameters to more depolarised membrane potentials might have been caused by non perfect voltage control in the intact brain preparation, in which the neuronal arborizations were still intact, or by different voltage dependence of calcium channels that are localised in distal regions of the neurones.

Currently, experiments analysing the effects of potential neuromodulators on the calcium currents are on the way. Preliminary experiments demonstrated that somatic calcium currents were decreased by exogenous application of  $10^{-4}$  M 5-hydroxytryptamine.

## Calcium Buffering Properties in Insect Olfactory Interneurons

Andreas Pippow, Andreas Husch, Helmut Wratil and Peter Kloppenburg  
Zoologisches Institut, Universität Köln, Weyertal 119, D-50923 Köln, Germany

Calcium acts as a second messenger signal that controls many cellular functions, such as synaptic transmitter release, regulation of calcium dependent ion channels, activation of enzymes, gene expression, cell growth, cell death *via* apoptosis, and modification of synaptic strength or synaptic structure. Selective triggering of these functions is achieved by highly localised calcium signals. The dynamics of these intracellular signals are determined by cellular parameters, including the calcium source (localised influx or release from intracellular stores; see *Husch et al. at this conference*), the intracellular calcium buffering and the calcium extrusion from the cell. We used the 'added buffer approach' in combination with patch-clamp recordings and fast optical imaging techniques to analyse *in vitro* the voltage dependent  $\text{Ca}^{2+}$  influx, endogenous  $\text{Ca}^{2+}$  buffer capacity and effective extrusion rate in the somata of olfactory interneurons from the antennal lobes of adult *Periplaneta americana*.

The resting calcium level of cultured antennal lobe neurones ( $n = 12$ ) was  $170 \pm 140$  nM. Depolarising voltage steps from -60 mV to +5 mV (50 ms) generated a total calcium influx of  $18 \pm 13$  pC, which elevated in the cell volume of  $9.1 \pm 4$  pL the total intracellular calcium concentration by  $11.5 \pm 8.3$   $\mu\text{M}$ . The endogenous buffering capacity was 90, meaning that only ~1% of the total calcium influx remained free in the cytosol, whereas ~99% were buffered. Thus, the free intracellular calcium concentration increased by  $\sim 130 \pm 90$  nM. The total amount of calcium that had entered was moved out by a rate of  $27 \text{ s}^{-1}$ , meaning that the initial velocity of the reduction in calcium concentration was  $3.5 \mu\text{M s}^{-1}$ .  $\text{Ca}^{2+}$  signals decayed with a time constant of 3.3 s.

Analysing the calcium handling in the somata of antennal lobe neurones is an early step towards a better understanding of calcium handling in insect olfactory interneurons. To investigate a putative compartmentalisation of buffering capacities we have now started to study these parameters in intact neurones that are recorded in the living brain.

## Modulation of Insect Olfactory Interneurons by Biogenic Amines

Nicole Lindemann<sup>1</sup>, Patrick Hafner<sup>1</sup>, Christophe Pouzat<sup>2</sup> and Peter Kloppenburg<sup>1</sup>

<sup>1</sup>Zoologisches Institut, Universität zu Köln, Weyertal 119, D-50923 Köln, Germany

<sup>2</sup>Laboratoire de Physiologie Cerebrale, CNRS UMR 8118, 45, rue des Saints Peres, 75006 PARIS, France

Sensory systems have evolved a variety of mechanisms to adapt information processing to changes in the environment. These adaptations are often under modulatory control. In vertebrate and invertebrate sensory systems biogenic amines have been strongly implicated in such processes. Our research focuses on neuromodulation and the question of how plasticity of the olfactory system is regulated on the cellular and molecular level. We are especially interested in the biophysical mechanisms that determine neuronal excitability and synaptic plasticity. The aim of our studies is to understand how the modulation of intrinsic and synaptic properties of single neurones regulate the function of the olfactory system. To investigate the mechanisms of neuromodulation on the cellular and molecular level we use electrophysiological and optical recording techniques. We have shown that 5-hydroxytryptamine (5HT) increased the excitability of olfactory projection neurones by modulating at least 2 types of voltage-activated potassium currents. 5HT decreased the maximal conductance of a transient potassium current ( $I_A$ ) and shifted its voltage for half-maximal inactivation to more negative potentials without affecting the half-maximal voltage for activation. 5HT also decreased the maximal conductance of a sustained potassium current ( $I_{K(V)}$ ) without affecting its voltage dependence. We suggest that by controlling the responsiveness of antennal-lobe projection neurones to olfactory stimuli, 5HT has significant impact on the performance of odour-dependent behaviours.

To analyse the consequences of neuromodulation at the network level we have recently started to perform *in vivo* single- and multi-unit extracellular recordings. Multi-unit recordings are well suited to analyse aspects of neuronal information processing, such as neuronal synchronisation in sensory coding. Here, we present single-unit and population recordings from the first olfactory relay of insects that we use to analyse long lasting modulatory effects.



**Temporal sharpening of plant-odour representations in moth output neurons**

Mikael A Carlsson & Bill S Hansson

Division of Chemical Ecology, Department of Crop Science, SLU, P.O. Box 44, SE-230 53 Alnarp, Sweden. e-mail: [mikael.carlsson@vv.slu.se](mailto:mikael.carlsson@vv.slu.se)

We studied the  $\text{Ca}^{2+}$  dynamics of odour-evoked glomerular patterns in the antennal lobe (AL) of the moth *Spodoptera littoralis* using optical imaging. Here we selectively stained a large population of AL output neurons, projection neurons (PN), by retrograde filling with FURA-dextran from the inner antennocerebral tract in the protocerebrum. Different plant-associated odorants evoked distributed patterns of activated glomeruli that were odour-dependent and repeatable. These patterns were, however, not static during the period of odour exposure. Time courses differed across glomeruli, which caused a temporal change of patterns. In all glomeruli the peak of activity was reached at about 300 ms after stimulus onset. After that the response differed between stimuli and glomeruli. Some responses were phasic with a fast decay to baseline level, whereas other responses remained at a high level until the end of stimulation. Next we examined how the correlations between patterns evoked by different odorants changed over time. Within the period of odour exposure (from 300 ms to 900 ms after onset) we found a significant reduction in similarity of responses evoked by different odours. Our results suggest that olfactory information is contained in a code with both spatial and temporal components and that discrimination ability may improve over time.

Grant sponsor: EU-FET AMOTH IST-2001-33066.

## **Analysis of the mouse olfactory receptor associated micro-proteome.**

**Jon Barbour<sup>\*</sup>, Bettina Warscheid<sup>∞</sup>, Kai Stühler, Helmut Meyer<sup>∞</sup>, Dirk Wolters<sup>§</sup>, Hanns Hatt<sup>\*</sup> and Eva Neuhaus<sup>\*</sup>.**

<sup>\*</sup>Lst. Zellphysiologie, Ruhr-Universität Bochum, Universitätsstraße 150, 44780 Bochum, Germany

<sup>∞</sup>Medizinischen Proteom-Center, Ruhr-Universität Bochum, Universitätsstraße 150, 44780 Bochum, Germany

<sup>§</sup>Analytische Chemie, Ruhr-Universität Bochum, Universitätsstraße 150, 44780 Bochum, Germany

Olfactory receptors (OR) are G-protein-coupled membrane receptors that encode the largest vertebrate multigene family (~1,000 ORs in the mouse and rat, ~500–750 in human); they are expressed individually in the sensory neurons of the nose and have also been identified in human testis and sperm. OR signal transduction is facilitated via adenylyl cyclase upregulation of cAMP culminating in the opening of cyclic nucleotide-gated cation channels at the cell surface which elicits a graded receptor potential.

We examined short-term and long-term olfactory receptor plasticity using established biochemical techniques in conjunction with a relatively novel proteomic strategy. Firstly, the question of short-term plasticity (e.g. receptor desensitization) was addressed by identifying novel OR receptor-protein-protein interactions using tagged fusion peptides. Tagged peptides from the intracellular loop 3 (IC3) and carboxyl termini of various mouse OR were used as bait to pull-out binding partners from mouse olfactory epithelium (OE). Interaction partners were identified using LC-MS/MS. In order to determine how OR mediate odour perception and how they influence long-term neuronal responses a differential proteomic strategy was employed. Test mice were exposed to odorants and the olfactory epithelium was compared to the OE from control mice using Fluorescence 2-D Difference Gel Electrophoresis (DIGE). Statistically significant differences in protein expression and peptide fingerprinting were performed using DIGE and MALDI-TOF respectively. Both proteomic strategies afford a powerful means whereby novel protein-protein interactions can be elucidated and thereby provide greater insight into olfactory receptor plasticity.

### Viral tracing of mouse primary afferent neurons allows functional analysis in cell culture

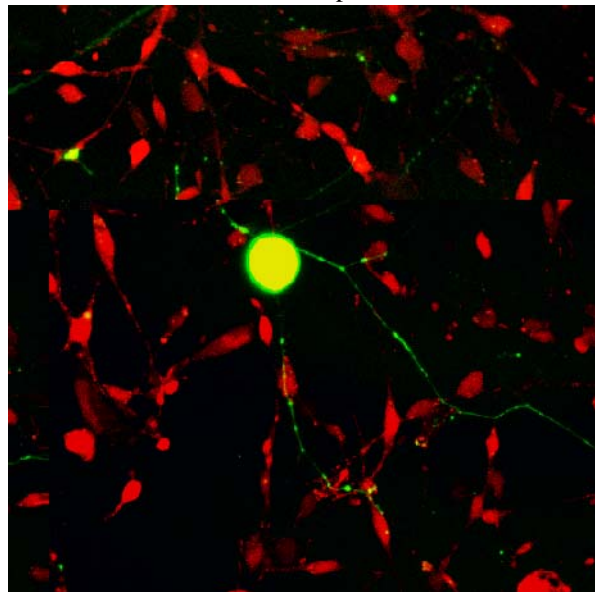
\*Damann N.<sup>1</sup>, Klupp B.<sup>2</sup>, Hatt H.<sup>1</sup>, Mettenleiter T.C.<sup>2</sup>, Wetzel C.H.<sup>1</sup>

<sup>1</sup>*Lehrstuhl für Zellphysiologie, Ruhr-Universität, Bochum, Germany;* <sup>2</sup>*Friedrich-Loeffler-Institute, Bundesforschungsanstalt für Viruskrankheiten der Tiere, Insel Riems, Germany*

[Nils.Damann@Ruhr-Uni-Bochum.de](mailto:Nils.Damann@Ruhr-Uni-Bochum.de)

Neurotrophic ( $\alpha$ -)herpes viruses including herpes simplex virus type-1 and pseudorabies virus (PrV) have emerged as powerful tools for labeling of whole chains of neurons functionally connected across synapses. After intracerebral (4, 1, 6) or peripheral (2, 3, 5) injection viral neurotropism was exploited to define the functional architecture of neural systems. However, cytopathic effects (7) and mRNA degradation (8) limit their use for tracing purposes and often lead to false negative immunohistochemical protein detection and loss of neuronal function making PrV ineligible for investigating living cells. Herein we describe a powerful life-cell tracing technique to perform fast labeling of trigeminal neurons (TGs) allowing subsequent electrophysiological and calcium imaging based analysis.

Tracing of nasal TGs was done with variants of the attenuated pseudorabies virus strain PrV-Bartha that has been widely used in tracing studies. PrV614 carries DNA for the fluorescent marker protein of a monomeric RFP (mRFP1) that is derived from a rapidly maturing DsRed derivative. The isogenic strain PrV-K61 $\Delta$ GCam comprises the gene sequence for the Yellow Cameleon 2.1 (YC2.1) construct and expresses a protein with a yellow shifted GFP emission spectrum. The calcium sensitive FRET effect which is described for YC2.1 by others could not be shown for PrV mediated expression neither in MDBK and PK15 cell lines, nor in TGs. In this study the role of YC2.1 was restricted to its fluorescent capacity for multiphoton laser scanning microscopy and tracing purposes. After intranasal inoculation of the described strains and incubation for 20 h fluorescent cells could be identified in whole mount preparations of the trigeminal ganglia. Also after dissociation and plating of the ganglionic tissue, traced cells could be detected allowing physiological measurements of this neuronal subpopulation in cell culture. Control experiments with patch clamp recordings and calcium imaging measurements one day after *in vitro* infection of cultured TGs revealed physiological features, close to uninfected cells.



Traced trigeminal neuron in cell culture expressing PrV mediated fluorescent marker protein. Glial cells have been counterstained with FuraRed.

PrV constitutes a powerful tool to perform rapid transneuronal tracing of the murine trigeminal system and affords the possibility to selectively label neurons innervating the nose. Electrophysiological and calcium imaging based characterization of these neurons concerning their specificity for selected chemical compounds shall be performed in future research. This technique may also be conferred to other mammalian primary afferent neurons and thus shall instance a viral tracing which is followed by physiological analysis.

#### Literature:

- 1 Ugolini G (1995) Transneuronal tracing with alpha-herpesviruses: a review of the methodology. In *Viral Vectors. Gene Therapy and Neuroscience Applications* (Kaplit, MG Loewy, AD eds.) pp293-317 Academic Press New York.
- 2 Horvath M, Ribari O, Repassy G, Toth IE, Boldogkoi Z, Palkovits M (2003) Intracochlear injection of pseudorabies virus labels descending auditory and monoaminergic projections to olivocochlear cells in guinea pig. *Eur J Neurosci* 18(6):1439-47.
- 3 Cano G, Sved AF, Rinaman L, Rabin BS, Card JP (2001) Characterization of the central nervous system innervation of the rat spleen using viral transneuronal tracing. *J Comp Neurol* 439(1):1-18.
- 4 Jasmin L, Burkey AR, Card JP, Basbaum AI (1997) Transneuronal Labeling of a Nociceptive Pathway, the Spino-(Trigemino-)Parabrachio-Amygdaloid, in the Rat. *J Neurosci* 17(10):3751-3765.
- 5 Kerman IA, Enquist LW, Watson SJ, Yates BJ (2003) Brainstem substrates of sympatho-motor circuitry identified using trans-synaptic tracing with pseudorabies virus recombinants. *J Neurosci* 23(11):4657-66.
- 6 Krout KE, Mettenleiter TC, Loewy AD (2003) Single CNS neurons link both central motor and cardiosympathetic systems: a double-virus tracing study. *Neuroscience* 118(3):853-66.
- 7 Serrano F, Enquist LW, Card JP (2002) Pseudorabies virus-induced expression of nitric oxide synthase isoforms. *Physiol Behav* 77(4-5):557-63.
- 8 Lin HW, Chang YY, Wong ML, Lin JW, Chang TJ (2004) Functional analysis of virion host shutoff protein of pseudorabies virus. *Virology* 324(2):412-8.

**Modulation of ANKTM1 gating by intra- and extracellular  $\text{Ca}^{2+}$** 

*Julia F. Dörner, Hanns Hatt, Christian H. Wetzel  
Lehrstuhl für Zellphysiologie, Ruhr-Universität Bochum,  
Universitätsstrasse 150, D-44780 Bochum, Germany*

ANKTM1 (TRPA1) is a member of the transient receptor potential (TRP) ion channel family and was initially reported to sense noxious cold temperatures ( $<17^{\circ}\text{C}$ ). It is found in a subset of nociceptive sensory neurons of the dorsal root (DRG) and trigeminal ganglia (TG), where the channel is co-expressed with the heat sensitive TRPV1/VR1. Among others, TRP channels located on free nerve endings of the sensory trigeminal nerve contribute to the common chemical sense and convey pain, touch, temperature, and chemosensory information. We studied the modulation of gating properties of the  $\text{Ca}^{2+}$ -permeable, cation channel ANKTM1 (human) transiently expressed in HEK 293 cells. At negative holding potentials, application of mustard oil (Allyl isothiocyanate,  $25\text{ }\mu\text{M}$ ) transiently activated an inward current through ANKTM1 in presence and absence of extracellular  $\text{Ca}^{2+}$ . Mustard oil-induced currents showed rapid desensitization or inactivation in presence of extracellular  $\text{Ca}^{2+}$  but did not desensitize in  $\text{Ca}^{2+}$ -free solution. During repeated application of agonist the current amplitudes declined in  $\text{Ca}^{2+}$ -containing solution. However, in absence of extracellular  $\text{Ca}^{2+}$ , the inducible currents increased until maximal amplitude was reached and then declined again. This effect was not dependent on intracellular  $\text{Ca}^{2+}$ , since infusion of the cell with  $5\text{ mM}$  BAPTA via the patch pipette was without effect on channel desensitization.

Interestingly, we found that the human ANKTM1 could be activated by intra- and extracellular  $\text{Ca}^{2+}$ . Julius and co-workers already suggested that intracellular calcium release is sufficient to activate ANKTM1. Our data show, that increasing the intracellular  $\text{Ca}^{2+}$  concentration to  $5\text{ mM}$   $\text{CaCl}_2$  via the patch pipette leads to a fast activation of ANKTM1 shortly after obtaining the whole-cell configuration. In addition, extracellular  $\text{Ca}^{2+}$  induced robust ANKTM1-mediated currents as well:  $\text{CaCl}_2$  in concentrations as low as  $2\text{ mM}$  (usually used for the extracellular solution) were sufficient to activate ANKTM1. Under those conditions, the elicited currents appeared after a period of time of 3 to 5 minutes and were blocked by the unspecific TRP channel inhibitor Ruthenium Red ( $1\text{ }\mu\text{M}$ ). Increasing the extracellular  $\text{Ca}^{2+}$  concentration up to  $10\text{ mM}$  leads to a faster activation of the channel. This activation was delayed upon chelating the intracellular  $\text{Ca}^{2+}$  with  $5\text{ mM}$  BAPTA.

Our findings show that ANKTM1 function is strongly dependent on intra- and extracellular  $\text{Ca}^{2+}$  concentration and favour the idea that ANKTM1 is a  $\text{Ca}^{2+}$  operated cation channel with a favoured Calcium permeability. Experiments will be conducted to clarify the mechanism underlying the  $\text{Ca}^{2+}$  dependency of the ANKTM1 channel.

**Investigations on Presence and Function of Nitric Oxide in the Olfactory System of Mice**

Daniela Brunert, Petra Kleinbongard<sup>†</sup>, Malte Kelm<sup>†</sup>, Nils Damann, Hanns Hatt,

Christian H. Wetzel

Ruhr-Universität Bochum, Department of Cellphysiology, 44780 Bochum, Germany

<sup>†</sup>Heinrich-Heine Universität Düsseldorf, Division of Cardiology, Pulmonary Diseases and Angiology, 40225 Düsseldorf, Germany

[daniela.brunert@rub.de](mailto:daniela.brunert@rub.de)

The gaseous signalling molecule nitric oxide (NO) is involved in many biological events including vascular smooth muscle relaxation, inhibition of platelet aggregation, immune regulation and neurotransmission. First evidence for its implication in olfactory neurotransmission was found in 1992, when Shepherd and Breer could show that an odour-induced elevation of cGMP-concentration in olfactory sensory neurons (OSN) can be prevented by the inhibition of nitric oxide synthase (NOS) or by NO-scavengers.

Nevertheless, existence and function of NO in the olfactory epithelium (OE) of adult rodents - except in OE regeneration - are still controversially discussed. In the present study we have begun to investigate the existence and function of NO as well as the expression of its synthesizing enzyme, NOS, in the OE of adult mice.

Using highly sensitive chemiluminescencedetection (CLD)-measurements, we were able to show an increase of NO concentration in in-vitro preparation of olfactory tissue after application of odorants or the adenylyl-cyclase-activator forskolin, respectively. No change in NO concentration was detected in eNOS deficient mice, indicating the contribution of the epithelial isoform of NOS (eNOS). Immunohistochemical investigations of paraffin embedded coronal sections of the adult mouse nose revealed eNOS-immunoreactivity in the olfactory sensory neuron layer of the OE. Loading of acutely dissociated OE with the highly sensitive NO-dye DAF-FM allowed detection of strong fluorescence in olfactory sensory neurons. Future studies will be performed to investigate the NO production at a cellular level. Our preliminary results show the presence and function of NOS in the adult mouse olfactory epithelium. NO production by eNOS is related to stimulation of the olfactory signal transduction pathway by odorants and adenylyl-cyclase activators. The physiological relevance of NO-signalling in olfactory perception remains to be elucidated.

## **EARLY FUNCTIONAL DEVELOPMENT OF CHEMOTOPY IN THE ZEBRAFISH OLFACTORY BULB**

**J. Li<sup>1</sup>, J. A. Mack<sup>1</sup>, M. Souren<sup>1</sup>, S. Higashijima<sup>2</sup>, G. Mandel<sup>2</sup>, J. R. Fetcho<sup>2</sup>, R. W. Friedrich<sup>1</sup>**

<sup>1</sup> **Max-Planck-Institute for Medical Research, Heidelberg, Germany**

<sup>2</sup> **SUNY, Stony Brook, NY, USA**

In the olfactory bulb (OB), axons of peripheral sensory neurons expressing the same odorant receptor converge onto distinct structures, the olfactory glomeruli. In adult zebrafish and other animals, glomeruli responding to odorants of the same class (e. g., amino acids or bile acids) tend to cluster and constitute a coarse chemotopic map of odor space. We examined the establishment of this coarse chemotopic map during development in zebrafish. We first analyzed the anatomical development of glomerular structures by presynaptic tracing with a lipophilic dye and postsynaptic GFP markers. At 2 - 3 days post fertilization (dpf), pre- and postsynaptic glomerular elements were organized in precursor structures, the protoglomeruli, that gradually differentiated into smaller glomerular structures during the following days. To assess the functional development of glomerular maps, odor-evoked activity patterns in the presumptive OB were measured by calcium imaging with transgenic and synthetic indicators. The transgenic calcium indicator, inverse pericam, was expressed under the control of the HuC promoter. In the olfactory bulb, expression levels were highest in the output neurons, the mitral cells. Odor-evoked activity patterns were then repeatedly measured in the same larvae between 2 dpf and 6 dpf. In addition, activity patterns were measured at high resolution with 2-photon microscopy after loading of neurons in the developing OB with AM-ester forms of conventional indicators. First odor responses were detected between 2 and 3 dpf. Already at this early protoglomerular stage, a coarse chemotopic organization similar to the adult was observed: responses to amino acids and bile acids were strongest in the lateral and medial olfactory bulb, respectively. The coarse chemotopy changed little between 2 and 6 dpf, even though the number of responding units increased substantially. Raising larvae in medium containing either amino acids or bile acids had little or no obvious effects on the establishment of the coarse chemotopy. A quantitative analysis of the development of chemotopy is in progress. We conclude that a chemotopic organization of the olfactory bulb is present already when the presumptive OB first responds to odorants and does not yet contain differentiated glomeruli. A second, finer level of chemotopy is likely to be established later during glomerular differentiation.

Supported: DFG (SFB 488, GK 791), Max-Planck-Society, Toyobo Biotechnology Foundation, Japan Society for the Promotion of Science, NINDS (NS-26539), HHMI.

## **Pharmacological investigation of mechanisms underlying temporal patterning of mitral cell responses in the zebrafish olfactory bulb**

Rico Tabor and Rainer W. Friedrich

Max Planck Institute for Medical Research Heidelberg, Jahnstrasse 29  
D-69120 Heidelberg

In the neuronal network of the adult olfactory bulb (OB), the processing of odor-evoked patterns of afferent activity across glomeruli results in an output activity pattern that is temporally modulated in a stimulus-dependent manner. In zebrafish it has been shown that the dynamics of OB output over time results in improved discriminability of activity patterns evoked by similar odors and permits the multiplexing of different information [1-3]. Here we investigate the underlying mechanisms by pharmacological manipulation of some important synaptic connections. Whole-cell and cell-attached patch-clamp recordings from mitral cells during odor stimulation were performed in an explant of the whole brain and nose. Bath-application of the GABA(B) receptor agonist baclofen and the GABA(B) receptor antagonist CGP54626 changed the spontaneous firing rate of mitral cells and the overall firing rate during odor responses. However, the effects were highly variable among several cells and not very strong. Moreover, temporal response patterns remained almost unchanged. GABA(B) receptor signalling is therefore unlikely to mediate the temporal patterning of mitral cell responses but may play a role in gain control. Antagonists of AMPA and NMDA receptors, in contrast, changed the temporal properties of mitral cell odor responses, especially during the early response phase after stimulus onset. Hence, synaptic connections mediated by glutamate receptors seem to be involved in the generation of odor-specific temporal patterning in the OB.

Supported by the Max-Planck-Society.

1. Friedrich RW, Laurent G (2001). *Science* 291:889-894.
2. Friedrich RW, Laurent G (2004). *J Neurophysiol* 91:2658-2669.
3. Friedrich RW, Habermann CJ, Laurent G (2004). *Nat Neurosci* 7:862-871.

## Functional morphology of the rhinophore of *Aplysia punctata*

Adrian Wertz <sup>a, b</sup>, Wolfgang Rössler <sup>b</sup>, Ulf Bickmeyer <sup>a</sup>

<sup>a</sup> Alfred-Wegener-Institut für Polar- und Meeresforschung in der Helmholtz-Gemeinschaft, Biologische Anstalt Helgoland, Kurpromenade, D-27498 Helgoland, Germany

<sup>b</sup> Lehrstuhl für Verhaltensphysiologie und Soziobiologie, Biozentrum, Universität Würzburg, Am Hubland, 97074 Würzburg, Germany

For marine snails, chemoreception is probably the most important sensory modality for perception at a distance as audition and optical information is limited. The posterior tentacle of *Aplysia*, the rhinophore, is a chemosensory organ [1] and several behavioral studies showed that the rhinophore can detect pheromones [2], initiate orientation and locomotion toward food [3]. We applied immunohistochemical and histological methods to describe the neuroanatomy of the rhinophore of the sea slug *Aplysia punctata*. For the functional approach we performed optical recordings representing the calcium response of neurons within the tentacle ganglion. As amino acids have been shown to be potent stimuli for aquatic animals [4], we used them to induce sensory responses of olfactory neurons in the rhinophore.

For neuroanatomical analyses, rhinophores of *Aplysia punctata* were stained with the fluorescent dyes propidium iodide, phalloidin, 5-HT antibody, DiA and Mallory's stain. Nuclear labeling with propidium iodide showed two layers of nuclei in the groove-epithelium. With the Mallory's stain single epithelial cell types could be compared with those found in other studies [5]. Olfactory glomeruli are embedded in a glial layer situated beneath the epithelium. The tentacle ganglion is located at the basis of the groove. The glomeruli and the tentacle ganglion are densely innervated by serotonergic fibers stained as shown by 5HT-immunoreactivity.

Ca<sup>2+</sup>- signals of neurons in the tentacle ganglion were measured using Fura-2 AM loading. Different amino acids were applied in concentrations ranging from 2μM to 20mM. The response of the neurons varies depending on the type of amino acid and the concentration. Our investigations on the function and neuroanatomy of the olfactory pathway in the rhinophore of *Aplysia punctata* are aimed to lead to a better understanding of neuronal processing of chemical cues and the chemical ecology of sea slugs.

[1] Audesirk TE and Audesirk GJ, 1976. Chemoreception in *Aplysia californica*. 2. Electrophysical evidence for detection of order of conspecifics. *Comp. Biochem. Physiol.* 56:267-270

[2] Levy M, Blumberg S, Susswein AJ, 1997. The rhinophore sense pheromones regulating multiple behaviors in *Aplysia fasciata*. *Neurosci. Lett.* 225:113-116

[3] Audesirk TE, 1975. Chemoreception in *Aplysia californica*. 1. Behavioral localization of distance chemoreceptors used in food-finding, *Behav. Biol.*, 15:45-55

[4] Caprio J and Bird RP, 1984. Electrophysiological evidence for acidic, basic, and neutral amino acid olfactory sites in the catfish. *J. Gen. Physiol.* 84,403-422

[5] Emery DG and Audesirk TE, 1977. Sensory cells in *Aplysia*. *J. Neurobiol.* 9:173-179.



**Response properties rather than spatial position determine connectivity between olfactory glomeruli****Christiane Linster<sup>1</sup>, Silke Sachse<sup>2</sup> & Giovanni Galizia<sup>3</sup>**<sup>1</sup>Cornell University<sup>2</sup>Rockefeller Institute<sup>3</sup>University of California Riverside

In recent years, research in olfaction has considerably increased our understanding of the representation of high dimensional olfactory space in essentially two-dimensional neural networks. While a number of researcher project's have shown the importance of inter-bulbar and inter-lobar inhibitory networks for the shaping and processing of olfactory information, it is not clear how exactly these inhibitory networks are organized in order to provide optimal filtering and contrast enhancement capabilities. Using a computational model of the honeybee antennal lobe, we here show that among other possibilities, a functionally inhibitory network, in which glomeruli inhibit each other proportionally to the similarity in their olfactory response profiles best reproduces the experimentally observed input-output function.

## **Single-cell transcriptional analysis of regenerating mouse olfactory sensory neurons**

Natja Haag and Franco Weth

Junior Research Group for Neurogenetics, University of Jena, Theoretikum, 07740 Jena, Germany

In the mammalian olfactory system, all olfactory sensory neurons (OSNs) that express the same odorant receptor (OR) project their axons to a single or very few precise locations (glomeruli) in the olfactory bulb. During differentiation, individual OSNs express only one out of ~1000 OR genes. The axons of OSNs of different specificities are segregated into distinct glomeruli in the bulb, thus generating a receptotopic map. The establishment of this map is partly based on the OR protein itself. Moreover, in contrast to other neuronal systems, OSNs extensively regenerate from stem cells throughout adult life. This continuous replacement requires olfactory neurons to be capable of executing their precise axon targeting program beyond embryonic development in order to maintain the highly discriminative capability of the olfactory system. Evidence suggests that, in addition to the OR, other molecules are required for axon guidance to the glomerular target. Their molecular identity, however, has remained elusive to date.

We are therefore analysing olfactory regeneration at the single-cell level by comparing the transcriptional profiles of mature vs. regenerating OSNs of identical specificity in order to identify differentially expressed genes involved in neuronal regeneration.

To this aim we pick individual mature OSNs obtained by enzymatic dissociation from dissected olfactory epithelium of OR37B-GFP transgenic mice (Strotmann et al., 2000) in which GFP (green fluorescent protein) is expressed from the locus encoding OR37B. Subsequent reverse transcription and PCR amplification (RT-PCR) of the whole-cell transcriptome is performed to generate single-cell cDNA libraries which are screened by differential hybridization. Hybridization probes are derived from single regenerating OSNs of the same specificity. Our first results indicate, that this technique provides a sensitive and unbiased tool for the comparison of single-cell transcriptomes. It should therefore be suited to yield genes upregulated in OSNs during the process of regeneration.

Supported by BMBF (NBL-3).

### **References**

Strotmann et al. (2000) J. Neurosci, 20(18):6927-6938

**The role of octopamine in the pheromone transduction of trichoid sensilla of *Manduca sexta***

C. Flecke\*, J. Schuckel, J. Seyfarth and M. Stengl

Biologie, Tierphysiologie, Philipps-Universität Marburg, 35032 Marburg, Germany

email: [flecke@staff.uni-marburg.de](mailto:flecke@staff.uni-marburg.de)

Octopamine, also known as the stress hormone of invertebrates, is a biogenic monoamine which acts as a neurotransmitter, neuromodulator and neurohormone (Roeder, 1999). It is also known to increase cAMP concentrations in different insect neurons. In wind tunnel experiments with various moth species, octopamine improved pheromone blend discrimination and orientation towards pheromone sources, possibly also via effects on antennal sensilla (Linn, 1997; Linn and Roelofs, 1986; Linn and Roelofs 1992, Linn et al., 1992; Linn et al., 1992; Linn et al., 1996). The injection of octopamine into the hemolymph increased the peak nerve impulse frequency of trichoid sensilla in response to pheromone in *Antheraea polyphemus* (Pophof, 2002) and also increased the peak nerve impulse frequency and sensillar potential amplitude in *Bombyx mori* (Pophof, 2002). In extracellular tip recordings of pheromone-stimulated antennal trichoid sensilla of male *Manduca sexta*, we investigated the effects of 8-bromo cAMP (8bcAMP) on pheromone transduction. When a bombykal (BAL) stimulus of 10 µg dose and 50 ms duration was applied every 5 min, the perfusion of the sensillar lumen with 10 mM 8bcAMP caused an increase of the sensillar potential amplitude. In addition, the day-time-dependent decrease in the action potential frequency at ZT 1 (beginning of the day) was counteracted with cAMP addition. In our recent studies we focus on the role of octopamine and its precursor tyramine in pheromone transduction of *Manduca sexta* and its possible circadian modulation of bombykal responses. Therefore, we test octopamine, tyramine and its antagonist serotonin in extracellular tip recordings of pheromone-stimulated trichoid sensilla. We applied stimuli with a dose of 1 µg BAL and 50 ms duration in intervals of 5 min. Since the calling behaviour and the release of pheromones of *M. sexta* females show a very distinct distribution with a maximum at the last 3 hours of the scotophase (Itagaki & Conner, 1988), we also started to investigate possible circadian changes in the sensitivity of pheromone-dependent trichoid sensilla of *M. sexta* to the main pheromone component BAL. Therefore, recordings were obtained at ZT 21 and ZT 8. Furthermore, to determine whether octopaminergic neurons project into the antenna we performed anti-tyramine and anti-octopamine immunocytochemistry on vibratome and cryostat sections of the antenna. In addition, we wanted to know whether the octopaminergic neurons contain circadian clock components such as the clock protein PERIOD.

Preliminary results showed that two tyramine- and octopamine-immunoreactive neurons project into the antenna. In addition, we found apparently PER-immunoreactive neuronal arborizations around pheromone-sensitive trichoid sensilla, hinting strong circadian control of pheromone-transduction. Also, preliminary evidence suggests an increase of the action potential frequency and of the sensillar potential amplitude under the influence of octopamine after bombykal stimulation in *M. sexta*. Thus, we hypothesize that two octopaminergic neurons project out into the antenna contacting pheromone-sensitive sensilla as well as axonal endings of possibly all sensory axons in the antenna via fine branches around the antennal nerve, controlling the sensitivity of different antennal sensilla in a circadian manner. [Supported by DFG grant STE531/13-1 and Human Science Frontier]

**Diacylglycerol in moth olfactory transduction**Krannich S.<sup>1,2\*</sup>, Lucas P.<sup>1</sup>, Stengl M.<sup>2</sup><sup>1</sup>INRA, Unité de Phytopharmacie et des Médiateurs Chimiques, Route de Saint Cyr, F-78026 Versailles Cedex, France; <sup>2</sup>Biology, Animal Physiology, Philipps-University of Marburg, Karl-von-Frisch Straße, D-35032 Marburg, Germany

\*Krannichs@students.uni-marburg.de

The molecular mechanisms that underlie olfactory transduction remain a central question in insects. The transduction cascade takes place in the outer dendrite of olfactory receptor neurons (ORNs) and is probably mediated by a G-protein-coupled receptor, which activates phospholipase C and leads to equimolar production of the second messengers inositol trisphosphate (IP<sub>3</sub>) and diacylglycerol (DAG). Based on biochemical<sup>1</sup> and electrophysiological<sup>2,3</sup> investigations IP<sub>3</sub> was proposed to be the first second messenger of the pheromone transduction cascade. Rapid increase of IP<sub>3</sub> after pheromone stimulation was observed in moth antennal homogenates<sup>1</sup>. The IP<sub>3</sub> rises trigger transient Ca<sup>2+</sup>-inward currents which gate Ca<sup>2+</sup>-dependent cation currents that share properties with the pheromone dependent current in ORNs of the moth *Manduca sexta*<sup>3</sup>. Also, *in vivo*<sup>4,5</sup> and *in vitro*<sup>6</sup> electrophysiological investigations suggest that DAG may gate ion channels in *Manduca sexta* as well as in other moth ORNs. In the silkmoths *Bombyx mori*<sup>4</sup> and *Antherea polyphemus*<sup>5</sup> DAG elicited nerve impulses in pheromone-sensitive ORNs. In pheromone-preincubated excised inside-out patches of the dendritic membrane of ORNs of *Antherea polyphemus* DAG activated a non specific cation channel, whereas IP<sub>3</sub> was ineffective<sup>6</sup>.

We compared the role of DAG in cultured ORNs of the male moths *Manduca sexta* and *Spodoptera littoralis*. In ORNs of *Manduca sexta* DAG activated ion channels via increase of the activity of protein kinase C (PKC), which activated cation currents<sup>2</sup>. In contrast, in ORNs of *Spodoptera littoralis* the activation of a cation current by DAG does not require PKC<sup>7</sup>. Thus, we started to examine whether DAG may also directly gate ion channels in *Manduca sexta* ORNs.

[Supported by Marie Curie Fellowship Association and DFG grants]

<sup>1</sup>Breer et al. 1990, Nature 345:65

<sup>2</sup>Stengl 1993, J Exp Biol 178:125

<sup>3</sup>Stengl 1994, J Comp Physiol A 174:187

<sup>4</sup>Pophof & van der Goes van Naters 2002, Chem Sens 27:435

<sup>5</sup>Maida et al. 2000, Neuroreport 11:1771

<sup>6</sup>Zufall & Hatt 1991, Proc Natl Acad Sci 88:8520

<sup>7</sup>Krannich et al. 2004, 7<sup>th</sup> ICN PO114

## **Experience-Dependent Plasticity in the Antennal Lobe of *Drosophila melanogaster***

**Silke Sachse, Andreas Keller, and Leslie B. Vosshall**

The Rockefeller University, Laboratory of Neurogenetics and Behavior,

New York, NY 10021, USA

email: sachses@mail.rockefeller.edu

The ability of the brain to adapt structurally and functionally in response to sensory stimuli is a striking property across animal phyla. Several studies have reported that continuous exposure to odors leads to global morphological effects in the first olfactory neuropil, the olfactory bulb of vertebrates or the insect antennal lobe. To investigate the specific effect of an odorant on the neuronal network it activates, we studied the plasticity in identified olfactory neurons with known odor response profiles in *Drosophila melanogaster*. Fruit flies are highly sensitive to CO<sub>2</sub>, which activates a population of approximately 25 olfactory sensory neurons that project to a single glomerulus in the antennal lobe (De Bruyne et al., 2003). Using the GAL4/UAS system to visualize the different olfactory neurons innervating this specific glomerulus, anatomical changes on separate processing levels due to long-term CO<sub>2</sub> exposure were investigated. The results showed an enlargement of the CO<sub>2</sub>-glomerulus in a concentration-dependent manner. This effect was stimulus- and glomerulus-specific. To determine whether these stimulus-evoked changes in olfactory circuitry produced behavioral consequences, we tested olfactory-evoked locomotor responses to CO<sub>2</sub> and other stimuli. Flies showed a reduced sensitivity to CO<sub>2</sub> after CO<sub>2</sub> pre-exposure, but showed normal responses to all other odors tested. The behavioral changes were stimulus-specific and concentration-dependent. Importantly, both anatomical and behavioral effects of CO<sub>2</sub> exposure were reversible. We are in the process of identifying the cellular and molecular basis of these experience-dependent changes.

Reference: De Bruyne et al. (2003). XXV. AChemS meeting, .no. 379.

Support contributed by: NIH/NIDCD (1R01DC005036-03), NSF (IBN-0092693), Beckman Foundation, McKnight Foundation, John Merck Fund.

## Genetic Analysis of Odor-Evoked Behaviors in *Drosophila*

A. Keller and L.B. Vosshall

Laboratory of Neurogenetics and Behavior, The Rockefeller University, 1230 York Avenue, New York, NY 10021 USA

Olfactory sensory systems detect structurally diverse odorants, identify them, measure their concentration and distinguish them. All four tasks are performed by a set of different types of olfactory sensory neurons (OSNs) that are sensitive to different but overlapping groups of odorants. The sensitivity of an OSN is determined by the odorant receptor (OR) gene it expresses. A large number of OR genes is encoded in the genome but only one or a few OR genes is expressed per OSN.

We used *Drosophila melanogaster* to study how the olfactory system performs these complex tasks. Behavioral experiments were carried out with intact flies and flies in which olfactory input is manipulated with microsurgical methods. We also used genetic manipulation to modulate the types of OSNs that are active in the fly, silencing the majority of OSN types or OSNs with known ligand sensitivity.

The sensitivity range of the *Drosophila* olfactory system as well as behaviorally determined detection thresholds and measurements of the resolution of the olfactory system will be presented and compared to olfactory systems of other species. The behavioral requirement for a given population of OSNs and the consequences of blocking subsets of OSNs will be discussed. The robustness and odor-specificity of detection, concentration measurement, and odor discrimination we observe in behavioral experiments is used to present a tentative model of how an olfactory system detects, measures, identifies, and distinguishes odorants.

## Nitric Oxide Modulates Sodium Chloride Taste Sensitivity

Hansjürgen Schuppe, Matthew Cuttle, Philip L Newland

School of Biological Sciences, University of Southampton, Bassett Crescent East,  
Southampton SO16 7PX, United Kingdom

Locusts require sodium chloride (NaCl) at low concentrations as part of their diet, and detect it with chemosensory sensilla scattered over the body surface, including the legs. When NaCl makes contact with a sensillum a volley of action potentials is elicited in 2-3 of its chemosensory neurons. Responses can be evoked by placing a blunt glass electrode, filled with 50 mM NaCl over a sensillum.

Perfusion of the leg with saline containing 2 mM of the nitric oxide (NO) donor PAPA NONOate, decreases the spike rate of responses to NaCl. On the other hand, perfusion with saline containing the nitric oxide scavenger PTIO (0.5 mM), or L-NAME (10 mM), an inhibitor of nitric oxide synthase, causes an increase in responses to NaCl. This suggests, that NO is endogenously generated and continuously attenuates the sensitivity of the chemosensory neurons to NaCl. Perfusion of the leg with saline containing the guanylate cyclase inhibitor ODQ (0.1 M) leads to a decrease in responses to NaCl, as does the application of the protein kinase inhibitor H-7 dihydrochloride (0.1 mM). Observations like these suggest, that NO exerts its effect via cGMP, which in turn targets protein kinases.

In the periphery, there are two potential sources of endogenous NO that could act on sensory neurons: from within the sensory cluster and support cells associated with basiconic sensilla, and from epithelial cells. Imaging studies in which the epidermis was loaded with the NO probe 4,5-diaminofluorescein diacetate (DAF-2 DA) indicate that epithelial cells close to the sensory clusters synthesise NO. In preparations that were pre-incubated in saline containing 10 mM L-NAME washout of the L-NAME after loading with 10 $\mu$ M DAF-2 DA caused increased cell-specific fluorescence due to endogenous NOS activity. Immunocytochemical studies using an universal NOS antibody, suggest that those epithelial cells that show DAF-2 fluorescence, express NOS. The question as to whether NO is also generated within the sensory cells is currently under investigation.

This work was supported by a project grant to P.L.N. from the BBSRC.

## **Expression of olfactory receptors in the cribriform mesenchyme during prenatal development**

Karin Schwarzenbacher, Jörg Fleischer, Sidonie Conzelmann and Heinz Breer

University of Hohenheim, Institute of Physiology, Garbenstrasse 30,  
70599 Stuttgart, Germany

Olfactory receptors are expressed in sensory neurons of the nasal epithelium, where they are supposed to be involved in the recognition of suitable odorous compounds and in the guidance of outgrowing axons towards the appropriate glomeruli in the olfactory bulb. During development, some olfactory receptor subtypes have also been found in non-sensory tissues, including the cribriform mesenchyme between the prospective olfactory epithelium and the developing telencephalon, but it is elusive if this is a typical phenomenon for olfactory receptors. Monitoring the onset and time course of expression for several receptor subtypes revealed that “extraepithelial” expression of olfactory receptors occurs very early and transiently, in particular between embryonic stages E10.25 and E14.0. In later stages, a progressive loss of receptor expressing cells was observed. *In situ* hybridization experiments showed that most investigated odorant receptor subtypes are only found in a rather small population of “extraepithelial” cells, however, receptor subtype mOR256-17 was found to be expressed in a significantly large portion of cells. Molecular phenotyping demonstrated that receptor expressing cells in the cribriform mesenchyme co-express key elements, including the G protein  $G_{\alpha_{olf}}$ , type III adenylyl cyclase (ACIII) and the olfactory marker protein (OMP), characteristic for olfactory neurons in the nasal epithelium. Immunohistochemical staining with a newly generated antibody specific for mOR256-17 revealed not only that the receptor protein seems to be located at the membrane of “extraepithelial” cells, but also in long protrusions originating from the cell somata. Studies on transgenic OMP/GFP-mice showed that “extraepithelial” OMP/GFP-positive cells are located in close vicinity to axon bundles projecting from the nasal epithelium to the presumptive olfactory bulb. Moreover, these cells are primarily located where axons fasciculate and change direction towards the anterior part of the forebrain.

This work was supported by the Deutsche Forschungsgemeinschaft.



## **Ontogenetic plasticity of primary and secondary olfactory centers in the honeybee brain**

**Claudia Groh\*, Britta Müller & Wolfgang Rössler**

*University of Würzburg, Biocenter, Zoology II, Am Hubland, D-97074 Würzburg, Germany*

*\*claudia.groh@biozentrum.uni-wuerzburg.de*

Olfaction plays an important role in a variety of behaviors throughout the life of social insects. The European honeybee represents a particularly promising model to examine mechanisms and consequences of environmentally mediated developmental plasticity within the olfactory pathway. In the present investigation we focused on differences between the queen and worker caste and influences of thermoregulation during pupal development. Queens develop from female eggs that are genetically not different from eggs that develop into workers. The developmental trajectory is mainly determined by nutritional factors during the larval period. During subsequent pupal metamorphosis, honey bee pupae are sealed in brood cells, and the rearing temperature is maintained actively and precisely around 34.5°C by thermoregulatory activity of adult workers. Behavior studies suggest that pupal rearing temperature affects olfactory learning in adult workers. In the present study we examined possible neuronal correlates for plasticity in olfactory behavior of queens and workers. We focused on the primary and secondary olfactory integration centers in the honeybee brain.

Synchronized sealed brood cells of worker and queen pupae were reared in incubators at temperatures between 29°C and 37°C. One day after emergence, brains were dissected, put into fixative solution and treated histochemically. To examine the primary olfactory centers, the antennal lobes (ALs), whole mount preparations were immunofluorescently labeled with an antibody against the synaptic-vesicle-associated protein synapsin (kindly provided by Dr. E. Buchner). Preparations were viewed with a laser-scanning confocal microscope and 3D reconstructions of whole ALs were processed and analyzed using AMIRA software. Individual olfactory glomeruli were identified according to size and location, and glomerular volumes were determined. Preliminary results show temperature and caste dependent changes in glomerular volumes and organization. Additionally, we focused on the olfactory input region of the mushroom-body (MB) calyx lip. Double-labeling with phalloidin and synapsin-immunoreactivity was used to quantify pre- and postsynaptic structures within characteristic synaptic complexes (microglomeruli). The results show that temperature differences as small as  $\pm 1^\circ\text{C}$  during pupal development affect the synaptic organization in the olfactory input region in the MB-calyx of the adult brain. Comparison with neighboring visual areas showed that these effects are region and modality specific. In addition, temperature effects were different in queens and workers. We conclude that environmentally induced postembryonic neuronal plasticity within the olfactory pathway may play an important role in regulating diversity of olfactory behavior, as it can be observed among different female castes and groups within the worker caste.

*Supported by DFG, GK 200 & SFB 554*

## **Subsets of antennal-lobe glomeruli project via different output-tracts in the honeybee brain**

**S. Kirschner<sup>1</sup>, C. Zube<sup>1</sup>, C.J. Kleineidam<sup>1</sup>, B. Grünewald<sup>2</sup> and W. Rössler<sup>1</sup>**

<sup>1</sup>*University of Würzburg, Biozentrum, Zoologie II, Am Hubland, D-97074 Würzburg, Germany*

<sup>2</sup>*Freie Universität Berlin, Neurobiology, Königin-Luise-Straße 28/30, D-14195 Berlin, Germany*

In the honey bee brain, the primary olfactory centers (the antennal lobes, ALs) contain about 165 olfactory glomeruli, spheroidal compartments of synaptic neuropil. Within the glomeruli, olfactory information is synaptically transmitted from axon terminals of olfactory receptor neurons, further processed by local interneurons and subsequently distributed to higher integration areas by antennal-lobe projection neurons (PNs). PN axons exit the AL via one of three antenno-cerebral tracts (lateral, medial or mediolateral - ACT) to the calyces of the mushroom bodies and to the lateral protocerebrum. In the present investigation we ask the question whether PNs of different ACTs have specific glomerular input regions within the AL.

We selectively labeled the medial and lateral ACT by application of different fluophore-conjugated dextrans using glass micropipettes or micro syringes. The resulting backfills showed PN somata and their dendritic arborisations within groups of olfactory glomeruli. In addition, individual PNs were labeled intracellularly using glass micropipettes and iontophoretic injection of Lucifer Yellow or Alexa Fluor Hydrazides. Whole brains with stained neurones were examined by confocal laser-scanning microscopy and 3D image processing using AMIRA software.

The results show that PNs leaving the AL via the medial and lateral ACT innervate two clearly separated subsets of olfactory glomeruli in the AL. PNs with axonal projections via the medial ACT have dendritic arborisations in a cluster of glomeruli in the ventral part of the AL. PNs with axonal projections via the lateral ACT innervate a cluster of glomeruli in the dorsal part of the AL. In addition, the somata of lACT- and mACT-PNs occupy specific positions within the main clusters of AL-neuron somata. These tract-specific PN innervation patterns and soma positions could be verified by individually stained PNs. The results indicate that olfactory information from subsets of glomeruli within topographically separated regions in the honeybee AL is transferred along different antenno-cerebral tracts.

## **Phenotypic plasticity of the antennal lobe and its behavioral significance in leaf-cutting ants**

Christoph J. Kleineidam, Malu Obermayer, Wolfgang Halbach, and Wolfgang Rössler  
*Universität Würzburg, Biozentrum, Zoologie II, Am Hubland, D-97074 Würzburg*  
kleineidam@biozentrum.uni-wuerzburg.de

Workers of leaf-cutting ants express an extraordinary size polymorphism up to a factor of 1000 in body mass. Foraging workers show less variation but still can be grouped in minor and media workers. We asked the question whether these workers differ in a) neuroanatomical organization within the first olfactory neuropil, the antennal lobe (AL), b) their receptor neuron response to trail pheromones c) their behavioral response to trail pheromones and. We found, for the first time in nonsexual individuals, a greatly enlarged glomerulus (macroglomerulus, MG) at the entrance of the AL. Comparison of two closely related species, *Atta sexdens* and *Atta vollenweideri*, using 3D-reconstructions of AL glomeruli revealed striking similarities as well as very distinct differences in the arrangement of MG among the two species. In both species, the size polymorphism is reflected in AL glomeruli. With a similar overall number of glomeruli, only medium workers possess a MG, and glomeruli at the entrance of the AL in minor workers are all of similar size. We tested the response of antennae in EAG recordings using two common and major components of the trail pheromone of leaf-cutting ants (4-Methylpyrrol-2-Carboxylat and 2-Ethyl-3,5/6-Dimethylpyrazine) and found that the relative responses to those two components differ significantly. If a larger glomerulus reflects a larger number of terminating receptor neurons, this result supports the idea that the MG is involved in trail detection. In behavior tests we found that trail following behavior is somewhat lower in minor workers than in *A. vollenweideri* medium workers. However, in a two choice experiment with gland extracts of nestmates compared with extracts of *A. sexdens* the minor workers outperformed the media workers.

*Supported by DFG, SFB 554 (A6)*

**Functional organization of poreplate sensilla in the honeybee *Apis mellifera*****Christina Kelber, Wolfgang Rössler and Christoph J. Kleineidam***University of Würzburg, Biozentrum, Zoologie II, Am Hubland,**D-97074 Würzburg, Germany**christina.kelber@biozentrum.uni-wuerzburg.de*

Poreplates (sensilla placodea) on the antennal flagellum of the worker honey bee *Apis mellifera* represent the most abundant type of sensilla. According to data in the literature each poreplate houses up to 35 olfactory receptor neurons (ORNs). Axons of these ORNs terminate in one of approximately 160 glomeruli in the antennal lobe (AL), the primary olfactory center. In other insect species, e.g. moths or flies, only few ORNs are located in the same morphological type of olfactory sensillum. Here, different functional sensilla are characterized by their subset of ORNs. It is not clear whether the sensilla placodea of honeybees or other hymenopteran species are equipped with characteristic subsets of ORNs or whether these subsets are arbitrary from the pool of all ORN types. Characteristic subsets could arise from developmental patterning and may well have a functional significance for odor reception since all ORNs are electrically coupled within the same receptor lymph cavity.

In the present investigation we asked the question whether different poreplates are equipped with characteristic subsets of ORNs. We labeled the ORNs of single poreplates and used their arborization pattern in the AL to draw conclusions about the equipment with ORNs in the sensillum. Selective labeling was obtained by perforation of pore plates with sharpened tungsten electrodes and subsequent application of biotin-dextran either with a glass electrode or a droplet onto the opened sensillum. After 24 hours their brains were dissected, and after fixation the brains were incubated with Alexa 568- or Alexa 488-conjugated streptavidin. The brains were examined using a laser scanning confocal microscope and the 3D software AMIRA 3.1. In order to confirm that only the ORNs of a single poreplate were labeled, the antennae were embedded in plastic, sliced and also investigated by confocal microscopy.

Our results show that the method is well suited to selectively label the ORNs of a single sensillum and to examine their arborization pattern in the corresponding and stained glomeruli in the AL. Between 12 and 23 glomeruli showed terminal arborizations from the ORNs of a single poreplate. The stained glomeruli were distributed across the entire antennal lobe rather than arranged in a single cluster of adjacent glomeruli. However, further analyses are needed to find out if glomeruli are arranged in several clusters or at least pairs of innervated glomeruli. Functional imaging of the AL showed that similar odors are represented in neighboring glomeruli (Sachse et al., 1999). Our results indicate that sensilla placodea are equipped with ORNs tuned to different odors rather than to similar odors.

Sachse S, Rappert A, Galizia CG (1999) The spatial representation of chemical structures in the antennal lobe of honeybees: step towards the olfactory code. *Eur J Neurosci* 11:3970 pp.

## Synaptic plasticity in olfactory centers of the adult ant brain

**Arnold Weibel, Christoph J. Kleineidam and Wolfgang Rössler**

*University of Würzburg, Biozentrum, Zoologie II, Am Hubland, D-97074 Würzburg, Germany  
roessler@biozentrum.uni-wuerzburg.de*

Chemosensory communication plays a key role in the organization of social behavior in ants. Ants use a variety of pheromones and recognition cues like caste-, life stage- and sex specific odors. The importance of the sense of smell is also reflected in elaborated olfactory sensilla (*sensilla trichodea curvata*) on their antennae, large olfactory centers in the brain and a rich diversity of olfactory mediated behaviors. Behavioral experiments indicate that especially responses to social odors like colony recognition cues change during early adulthood. In the present investigation we asked the question whether the early adult period is accompanied by synaptic changes in primary and/or secondary olfactory centers in the brain which may underlie the changes in behavior. In addition, unilateral removal of one antenna was used to investigate sensory influences on adult neuronal differentiation of the central olfactory pathway. Experiments were performed with the ant *Camponotus rufipes*. Small sub-colonies with workers only were separated from the main colony and maintained over several weeks together with manipulated individuals. All individuals including newly emerged ants were color marked for later identification. Brains of workers were removed and fixated after 1, 3, 5, 7, 10 and 15 days and compared with brains of older workers. Double labeling with phalloidin and an antibody to synapsin (kindly provided by Dr. E. Buchner) was used to analyze and quantify changes in pre- and postsynaptic structures in primary (antennal lobe, AL) and secondary olfactory centers (mushroom body, MB). The number and density of synaptic complexes (microglomeruli) in the olfactory input region of the MB calyx showed a significant increase (~30%) during the first two weeks of adult life, especially during the second week. Comparison with older workers revealed a total increase of up to 100%. Surprisingly, in manipulated workers no significant difference was found between synaptic changes in the MB calyx of the intact and deafferented sides, despite a marked decrease in the volume of olfactory glomeruli in the AL on the deafferented side. This suggests that degenerated receptor neurons cause a decrease in glomerular volumes but the AL network remains able to drive synaptic plasticity in the input region of the MB. Our results show that the ant's olfactory pathway has a remarkable synaptic plasticity, especially during the first weeks of adulthood. Resulting changes in the synaptic circuitry may support imprinting to social odors and changes in behavioral responses.

*Supported by DFG, SFB 554*

**Poster Subject Area #PSA10:  
Visual systems of invertebrates: Periphery**

- [#141A](#) JE. Niven and SB. Laughlin, Cambridge (UK)  
*The efficiency of information coding in the photoreceptors of *Drosophila virilis**
- [#142A](#) JE. Niven, SB. Laughlin, B. Wijnen and DG. Stavenga, Cambridge (UK) and Groningen (NL)  
*How does the size of an individual fly affect the efficiency of information coding in its photoreceptors?*
- [#143A](#) L. Zheng, GG. de Polavieja, V. Wolfram, MH. Asyali, RC. Hardie and M. Juusola, Cambridge (UK), Madrid (E) and Riyadh (KSA)  
*Adaptation and feedback regulation in the first visual synapse of in vivo *Drosophila**
- [#144A](#) MH. Hennig and F. Wörgötter, Stirling (UK)  
*The contribution of retinal ganglion cell nonlinearities to the perception of motion-induced illusions*
- [#145A](#) B. Greiner, WA. Ribi, TW. Cronin, WT. Wcislo and EJ. Warrant, Lund (S), Triesen (FL), Baltimore, MD (USA) and Balboa (PA)  
*POLARISATION VISION IN A NOCTURNAL BEE*
- [#146A](#) K. Draslar and U. Wolfrum, Ljubljana (SLO) and Mainz  
*Structures and mechanisms of light adaptation in the dorsal and the ventral eye of *Ascalaphus macaronius*.*
- [#147A](#) P. Stusek, G. Belusic, G. Zupancic and K. Draslar, Ljubljana (SLO)  
*The dynamical and spectral characteristics of pupillary response in the owl-fly *Ascalaphus macaronius**
- [#141B](#) O. Baumann and K. Führer, Golm  
*Rhabdomere twisting of the R1-R6 photoreceptors in the *Drosophila* eye depends on interaction with the R8 photoreceptor*
- [#142B](#) DG. Stavenga, Groningen (NL)  
*Sexual dichroism of pierid butterflies*
- [#143B](#) B. Wijnen, JE. Niven and DG. Stavenga, Groningen (NL) and Cambridge (UK)  
*Spatial resolution of the eyes of flies, bees and butterflies*
- [#144B](#) MA. Giraldo and DG. Stavenga, Groningen (NL)  
*Butterfly wing colouring by scattering, pigment absorption and multilayer reflection in pierids*

- [#145B](#) S. Kleinlogel and N.J. Marshall, St. Lucia (AUS)  
*The numerous spectral and polarization sensitivities within the tripartite eyes of gongodactyloid stomatopods (mantis shrimps)*
- [#146B](#) S. Bermudez i Badia and PFMJ. Verschure, Zürich (CH)  
*A model Of the Lobula Giant Movement Detector neuron of the Locust based on Reichardt Correlation*
- [#147B](#) M. Lehrer, Zürich (CH)  
*Honeybees generalize closed shapes among different types of contrast*

## The efficiency of information coding in the photoreceptors of *Drosophila virilis*

Jeremy E. Niven and Simon B. Laughlin

Department of Zoology, University of Cambridge, Cambridge CB2 3EJ, UK.

Insect photoreceptors must compress a vast spatiotemporal range of light intensities into voltage responses of limited amplitude and speed. This process requires energy, however, since insects have only a limited energy budget to expend, there is a trade-off between improving information coding and reducing energy expenditure. To understand how the interplay between energy and information coding varies between photoreceptors of different species we analysed the information coding in of photoreceptors from *Drosophila virilis*. By recording intracellularly from *Drosophila virilis* photoreceptors *in vivo* whilst presenting them with a dynamically modulated light stimulus it is possible to measure their information capacity (bits/sec). Electrical signalling dominates energy usage due to the large numbers of ions flowing across the membrane that must be pumped back to maintain concentration gradients. The activity of the pump can be estimated using a biophysical model from the currents recorded *in vivo*, enabling the metabolic cost of neural information to be calculated (ATP molecules/bit). *Drosophila virilis* R1-6 photoreceptors had consistently higher information capacities (up to 350 bits/sec) than those of *Drosophila melanogaster* over all background light intensities. The *Drosophila virilis* photoreceptors had significantly lower input resistances at each light intensity, thus, although they encoded more information, they had a much higher energy cost per bit than *Drosophila melanogaster*. Comparison of the cost per bit in *Drosophila virilis* photoreceptors with that of other fly photoreceptors (including *Calliphora vicina*, *Phormia regina*, *Sarcophaga canaria* and *Drosophila melanogaster*) showed that all the photoreceptors were most efficient whilst operating at high light intensities. Across all the species cost per bit was linked to the signalling capacity of the photoreceptors, larger photoreceptors being able to encode more information but at a higher energy cost per bit than their smaller counterparts. These relationships suggest that excess signalling capacity is penalized by increased energy costs and that neural structures should be reduced to minimize energy expenditure.



## How does the size of an individual fly affect the efficiency of information coding in its photoreceptors?

Jeremy E. Niven<sup>1</sup>, Simon B. Laughlin<sup>1</sup>, B. Wijnen<sup>2</sup>, Doekele G. Stavenga<sup>2</sup>

<sup>1</sup> Department of Zoology, University of Cambridge, Cambridge CB2 3EJ, UK.

<sup>2</sup> Department of Neurobiophysics, University of Groningen, Groningen, The Netherlands.

In insects, the precise spatiotemporal pattern of light intensities to which photoreceptors are exposed is determined by the interommatidial angle, the photoreceptor acceptance angle, self-generated movements and the environment in which these movements are made. Equivalent photoreceptors from individuals bred in captivity from the same species have broadly similar responses. This is due mainly to two factors; these insects are of similar sizes and have had similar experiences (e.g. light exposure, nutrition). In wild populations, however, there is considerable variation not only in the experiences of insects but also in their nutritional state during development and, hence, their size as adults. Large fluctuations in size between individuals of the same species are apparent in some fly species such as *Sarcophaga canaria*, the grey flesh fly. In this species individuals can vary in length between 6 and 16 mm depending upon the amount of food available during larval development. The compound eyes of smaller individuals have smaller facets, suggesting that the photoreceptors are also smaller. We examined the photoreceptors of small, medium and large individuals using transmission electron microscopy and found that photoreceptors of small individuals were, indeed, smaller. To examine the possible differences between photoreceptors of different sizes we recorded intracellularly from photoreceptors in small, medium and large individuals. Smaller individuals had higher input resistances than photoreceptors from larger individuals. Smaller individual photoreceptors also had lower information rates than larger individuals. Using a biophysical model of the photoreceptors we estimated the energetic cost of information coding and found that it was lower in smaller individuals than in larger individuals suggesting that they are saving energy. We conclude that the developmental history can have significant effects upon the efficiency of information coding in insect photoreceptors.

## Adaptation and feedback regulation in the first visual synapse of *in vivo* *Drosophila*

Lei Zheng<sup>1</sup>, Gonzalo G. de Polavieja<sup>1,2</sup>, Verena Wolfram<sup>1</sup>, Musa H. Asyali<sup>3</sup>, Roger C. Hardie<sup>4</sup> and Mikko Juusola<sup>1</sup>

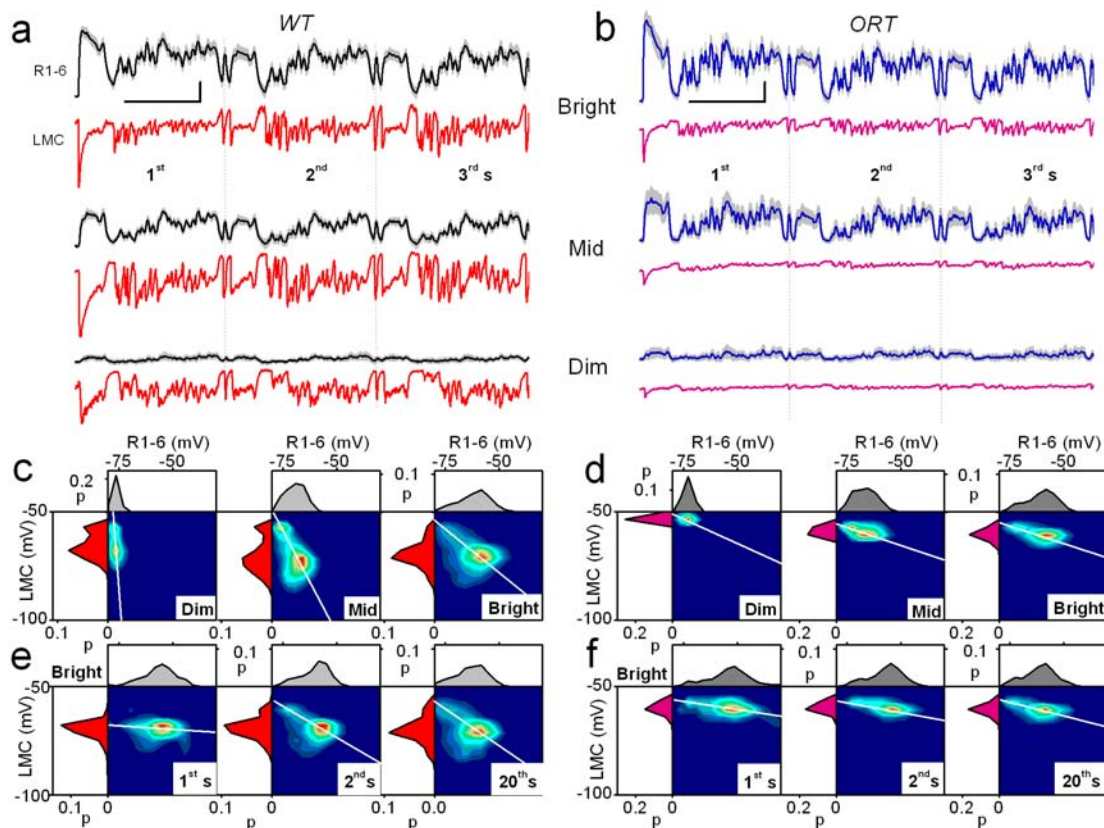
<sup>1</sup>Physiological Laboratory, University of Cambridge, CB2 3EG, UK

<sup>2</sup>Department of Theoretical Physics, Universidad Autónoma de Madrid, 28049 Spain

<sup>3</sup>Department of Biostatistics, Epidemiology and Scientific Computing, King Faisal Specialist Hospital and Research Centre, P.O. Box 3354, Riyadh, Saudi Arabia

<sup>4</sup>Department of Anatomy, University of Cambridge, CB2 3EG, UK

Information from the environment must be encoded within the size and speed range of responses that sensory neurones can produce. For maximum information transfer their responses should have low noise and match the statistics of stimuli encountered in nature so that more output range is dedicated to more frequent events. Hence, sensory neurones should 'learn' through their experience to prevent saturation and to accurately represent the stimuli they receive. Such optimisation requires *adaptable* intracellular reactions but also *feedback* from neurones downstream. By exploiting a defect in the first visual synapse in *ORT Drosophila* mutants that show limited throughput from photoreceptors to first visual interneurons (LMCs), we investigated the functional role of feedback synapses in regulating the signal transfer of this neural pathway. We show that in bright naturalistic conditions the feedback synapses can amplify and accelerate photoreceptor responses so that the synaptic information transfer rate in *ORT* LMCs reaches that of the wild-type neurones. These results identify that the feedback synapses can effectively reinstate the signal transfer across the graded potential synapse even when the primary neural pathway is malfunctioning. A physiological model that explains the findings is presented.



## The contribution of retinal ganglion cell nonlinearities to the perception of motion-induced illusions

Matthias H. Hennig\*, Florentin Wörgötter

Department of Psychology, University of Stirling, Stirling FK9 4LA, Scotland

E-mail: hennig,faw1@cn.stir.ac.uk.

The visual system of primates consists of two streams (magnocellular, MC, and parvocellular, PC) which have been associated mainly with motion- and form-analysis [1]. It is still controversial in how far this segregation has a direct influence on visual perception [2, 3]. In this study we will provide evidence that the retinal activity in the magnocellular (MC) pathway has direct influence on visual perception, while in specific cases the qualitatively different activity in the parvocellular (PC) system is bypassed. We quantified the activity of a MC- and PC-cell population in response to a star-shaped stimulus during fixation by means of detailed model of the primate retina [4], including fixational eye movements (slow drift and microtremor). In the simulated MC-cell population response, fixational eye movements lead to (1) a fading of the activity in sectors of the star-stimulus and (2) a splitting of the lines close to the fading sector into two. Both effects are temporally unstable and move circularly around the stimulus, equivalent to an apparent motion percept. They do not occur in PC-cells. The first effect can be attributed to fast adaptation of MC-ganglion cells, and is an expression of the aperture problem at the level of retinal ganglion cells. The second effect results from nonlinearities within the MC-cell receptive field, which also lead to frequency-doubled responses during contrast reversal of a fine grating [5].

These effects were confirmed by psychophysical experiments. The sectorial fading is observed by all of our subjects, splitting by 67%. The fading effect was additionally quantitatively assessed. Psychometric curves close to contrast detection threshold show that observers miss axially moving lines, while orthogonally moving lines remain well visible.

The effects that we find in the retinal activity are very similar to effects that have been described for a group of visual illusions which elicit apparent motion percepts and have even influenced the arts ("Op-Art") [6]. For these illusions, unstable flickering or apparent motion percepts are reported, which can affect the image as a whole or, more often, just parts of it. Current theories suggest that this perceptual unsteadiness is induced by the anisotropic stimulation of motion detectors by microsaccades [7, 8]. However, our model study suggests that the apparent motion effect observers report are solely a consequence of changing retinal activity patterns, which are caused by fixational eye movements rather than the properties of cortical motion detectors.

## References

- [1] Merigan, W. H. & Maunsell, J. H. How parallel are the primate visual pathways? *Annu Rev Neurosci* **16**, 369–402 (1993).
- [2] Schiller, P. H. & Logothetis, N. K. The color-opponent and broad-band channels of the primate visual system. *Trends Neurosci* **13**, 392–398 (1990).
- [3] Gegenfurtner, K. R. Cortical mechanisms of colour vision. *Nat Rev Neurosci* **4**, 563–572 (2003).
- [4] Hennig, M. H., Funke, K. & Wörgötter, F. The influence of different retinal subcircuits on the nonlinearity of ganglion cell behavior. *J Neurosci* **22**, 8726–8738 (2002).
- [5] Kaplan, E. & Shapley, R. M. X and Y cells in the lateral geniculate nucleus of macaque monkeys. *J Physiol* **330**, 125–143 (1982).
- [6] Wade, N. J. Movements in art: from Rosso to Riley. *Perception* **32**, 1029–1036 (2003). Biography.
- [7] Fermüller, C., Pless, R. & Aloimonos, Y. The Ouchi illusion as an artifact of biased flow estimation. *Vision Res* **40**, 77–96 (2000).
- [8] Zanker, J. M. Looking at Op Art from a computational viewpoint. *Spat Vis* **17**, 75–94 (2004).

## POLARISATION VISION IN A NOCTURNAL BEE

Birgit Greiner<sup>1</sup>, Willi A. Ribi<sup>2</sup>, Thomas W. Cronin<sup>3</sup>, William T. Wcislo<sup>4</sup> and Eric J. Warrant<sup>1</sup>

<sup>1</sup>Department of Cell and Organism Biology, Lund University, Helgonavägen 3, S-22362 Lund, Sweden.

<sup>2</sup>University of Human Sciences of the Principality of Liechtenstein, Dorfstrasse 24, FL-9495 Triesen, Principality of Liechtenstein. <sup>3</sup>Department of Biological Sciences, UMBC, 1000 Hilltop Circle, Baltimore, MD 21250, USA. <sup>4</sup>Smithsonian Tropical Research Institute, Apartado 2072, Balboa, Republic of Panama.

e-mail: birgit.greiner@cob.lu.se

During twilight light levels drop drastically making it extremely difficult for small animals to navigate visually. Nevertheless, the halictid bee *Megalopta genalis* is able to use landmark navigation to find its nest entrance at mere starlight intensities (Warrant et al. 2004, *Curr Biol* 14, 1309-1318). For long-distance foraging flights orientation is probably achieved using both landmarks and a compass.

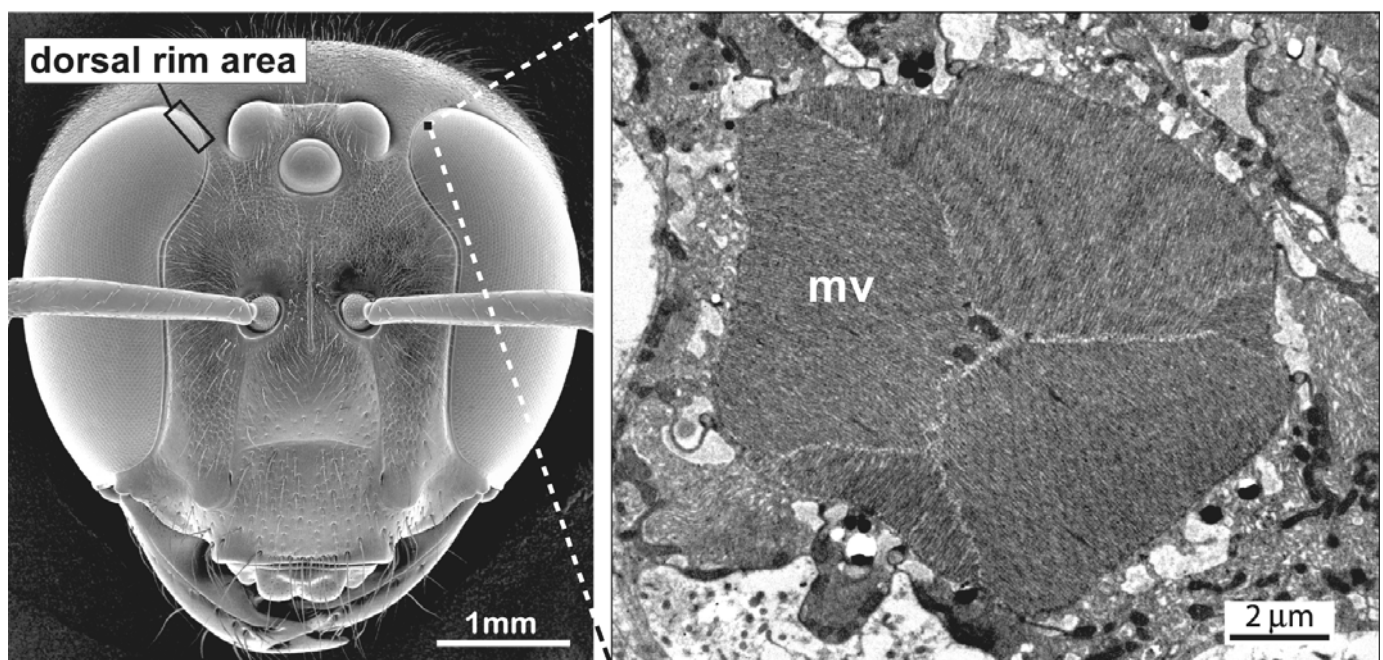
Polarisation patterns are used for compass navigation by many diurnal insects, including the worker honeybee *Apis mellifera*. During late twilight, when *Megalopta* is mostly active, simple, unidirectional polarisation patterns are present in the sky. Thus, we hypothesise that the nocturnal bees are able to use these polarised patterns for compass navigation.

Indeed, the anatomy of *Megalopta*'s apposition eyes reveals an area of specialised visual units (ommatidia) in its most dorsal region (*left figure*). This part of the compound

eye known as the dorsal rim area (DRA) has 4-5 rows of ommatidia with large odd-shaped rhabdoms (*right figure*). In these specialized ommatidia the microvilli (*mv*) of the rhabdom are straight and aligned parallel. These are necessary requirements for the detection of polarised light. Furthermore, to enhance polarisation contrast, the microvilli from the nine photoreceptors are arranged only in two orthogonal directions.

Electrophysiological recordings from different eye regions of the nocturnal bee confirm that photoreceptors within the DRA are highly sensitive to the e-vector orientation of polarised light ( $PS > 10$ ), whereas, cells outside the DRA have very low polarisation sensitivity values ( $PS < 2$ ). Spectral sensitivity recordings indicate that photoreceptors detecting polarised light are UV and UV-green sensitive.

We conclude that *Megalopta* is able to detect the e-vector orientation of light and probably uses polarised patterns for navigation at night.



**Structures and mechanisms of light adaptation in the dorsal and the ventral eye of *Ascalaphus macaronius*.**

Kazimir Drašlar and Uwe Wolfrum

Department of Biology, University of Ljubljana, Večna pot 111, 1000 Ljubljana, Slovenia; Institute of Zoology, University of Mainz, Muellerweg 6, D-55099 Mainz, Germany

The double compound eye of *Libelloides (Ascalaphus) macaronius* is a superposition eye of eucone type. The eye is divided into two parts, the larger dorso-frontal part consisting of approximately 5000 ommatidia and the smaller ventro-lateral part with a similar number of ommatidia.

Field experiments and observations of animal behaviour indicate that the dorsal eye is involved in regulation of flight and hunting activities in an environment with a high intensity of UV light accompanied by high temperature, whereas in the morning and evening, in the conditions of low light intensities and low environmental temperature when the animal is not able to escape by flight, the ventral eye provokes a behaviour consisting of turning around a grass stalk, thus exposing the smallest silhouette.

We suppose that the different strategies of eye functions are reflected in the structure and the mechanisms of light adaptation.

It is known that in the eye of *Ascalaphus* some kind of pupil mechanism is present regulating the light flux into the eye in changing light conditions (Nilsson et al. 1992, Stůšek and Hamdorf 1998, Stůšek et al, personal communication).

Based on our microscopical and molecular data about the ommatidia of dorso-frontal as well as of the ventro-lateral part of *Ascalaphus* eye we suppose a pupil mechanism located at the tip of crystalline cone. Our analyses of morphological data indicate that the pupil is formed as a functional unit, composed of the crystalline cone, the primary and the secondary pigment cells in conjunction with the most distal part of the seven retinula cells (cells 1-6 and cell 7). We gathered evidence that the closing mechanism of the functional diaphragm is operated mainly by the retinula cells. There is a very important difference between the two part of the eye, observed already by Ast (1920) and Schneider et al (1977) concerning the arrangement of retinula cells around the tip of the crystalline cone. In the dorso-frontal eye fibres, few microns in diameter combined of distal branches of retinula cells are attached to the tip of the crystalline cone, in the ventro-lateral eye a connection to the crystalline cone is made of the distal part of retinula cells forming a funnel like attachment.

In the dorso-frontal eye of *Ascalaphus*, during light adaptation, the most distal parts of retinula cells contract and in turn, the pigment cells move towards the tip of the crystalline cone. The expansion of the apical portion of the retinula cells should lead to reverse process and pupil opening. We have not detected massive pigment migrations in the secondary pigment cells toward the proximal part of ommatidium.

In the ventro-lateral eye of *Ascalaphus*, during light adaptation, the translocation of cellular elements around the tip of crystalline cone is more extensive. In light adapted eye, retinula cells and the pigment granules in the secondary pigment cells are shifted in the proximal direction. Thus, the retinula cells funnel contact a small part on the tip of the crystalline cone. The connection of retinula cells and the proximal part of crystalline cone is completely surrounded by a collar of the primary pigment cells. In the dark adapted eye, a shift in the opposite direction was observed. Whenever pigment granules in the secondary pigment cells migrate in distal direction, the pigment granules in the primary pigment cells also migrate in the same direction, leaving a thin layer of cells without pigment around the tip of the crystalline cone. The shift of the pigments is followed by an expansion of retinula cells in the distal direction where extensions of retinula cells enter into the space between the primary and the secondary pigment cells, surrounding the latter from the outside.

In the last set of experiments, we have analysed the presence and location of cytoskeletal elements as well regulatory proteins which presumably participate in these motile processes.

Ast, F. 1920 Zool. Jb. Anat.Ontog. Tiere 41.: 411-458

Nilsson, D.E. Hamdorf, K. Höglund, G. 1992 J.Comp. Physiol A 192 170: 217-226

Stůšek, P. Hamdorf, K. J.Comp. Physiol A 1999 184: 99 - 106

This study was supported as a part of the international *Ascalaphus* Summer School by the DAAD and the Universities of Ljubljana and Mainz

## The dynamical and spectral characteristics of pupillary response in the owl-fly *Ascalaphus macaronius*

Peter Stušek, Gregor Belušič, Gregor Zupančič, Kazimir Drašlar  
Department of biology, Večna pot 111, Ljubljana, Slovenia.

The owl-fly *Libelloides (Ascalaphus) macaronius* (Insecta: Neuroptera) has bipartite eyes composed of dorso-frontal (DF) part and ventro-lateral (VL) part. These are typical superposition eyes with an extensive clear zone and the screening pigments located in the primary and secondary pigment cells. These cells mediate a light adaptation mechanism which is not well suited for rapid fluctuations in environmental light intensities.

We investigated the dynamics of the pupillary action with reflectance measurements, electroretinography and microscopy. In the reflectance measurements, the amount of violet (405 nm), green (525 nm) and red (625 nm) measuring lights reflected from the tracheal tapetum in the proximal part of the eye was measured. The pupil response was elicited with 3 to 50 s flashes of intense UV and blue light (BG28). In the DF part, the decrease of the eye glow never exceeded more than 90 % in the violet band and was typically 60 % in the green band, and 20 % in the red band. With sufficiently strong adapting stimuli, the attenuation level reached saturation in the violet band and sometimes also in the green band but never in red. Not surprisingly, the amplitude of the ERG response followed the attenuation level of the eye glow in the violet band. The saturation effect and simultaneous ERG recordings suggest that a light filtering mechanism is present in this particular eye design, possibly in addition to the cone mechanism of diaphragm aperture regulation. The amplitudes of the changes in the eye glow correspond to the extinction characteristics of screening pigment in the primary pigment cells (Schneider et al 1978). On the basis of absorption characteristic of screening pigments and the decrease of eye glow we ascertained that the pupillary action in the DF part of the eye is due only to the primary pigment cells and that in contrast to previous reports (Stušek and Hamdorf 1999), the apparent double dynamic of the pupil response can be ascribed to the saturation effect of the extinction characteristics of primary pigment granules.

The effect of successive adapting stimuli is roughly inversely proportional to the amplitude of the eye glow. Therefore, we suggest that the location of the pupil trigger is proximal with respect to the primary pigment cells. In the VL part, the eye glow changes had similar time course, except that they could be elicited only with ten fold longer stimuli and their amplitude reached typically only 20 % attenuation in the violet band, 15% in the green band and 10% in the red band. The morphological data indicate a profound light dependent reshaping of the primary pigment cells in both DF and VL parts of the eye. However, the corresponding light dependent changes of the eye glow can be well discriminated only in the DF part of the eye.

By such light filtering mechanism, this type of the eye can not adjust the acceptance angle very sharply. This may not present a problem for an animal that catches prey against a considerably uniform UV background of the sky.

### References:

Feinstruktur und Schirmpigment - Eigenschaften der Ommatidien des Doppelauges von *Ascalaphus* (Insecta, Neuroptera) (1978). Schneider L, Gogala M, Drašlar K, Langer H, Schlecht P. Eur J Cell Biol 16:274-307

Properties of pupil mechanisms in owl-fly *Ascalaphus macaronius* (Neuroptera) (1999). Stušek P, Hamdorf K. J Comp Physiol A 184:99-106

## **Rhabdomere twisting of the R1-R6 photoreceptors in the *Drosophila* eye depends on interaction with the R8 photoreceptor**

Otto Baumann, Kathleen Führer

Institut für Biochemie und Biologie, Universität Potsdam, Karl-Liebknecht-Str. 24-26, D-14476  
Golm, Germany [E-mail: obaumann@rz.uni-potsdam.de]

Previous studies on various insects have shown that the microvilli within the rhabdomere are not arranged in parallel over the entire length of the visual cell; in other words, the rhabdomere is twisted along its length. Our ultrastructural analysis on *Drosophila* demonstrates that the microvilli of the visual cells R1-R6 within the *Drosophila* eye are also tilted in a characteristic manner with respect to the plane orthogonal to the apicobasal axis of the cell, and the tilt direction is different in the distal and proximal area of the cell. We show further that this morphological asymmetry is accompanied by a molecular polarization of the apical cell surface; antibodies against phosphotyrosine (PY) label a membrane domain next to the microvilli, and immunoreactivity resides always on the side the microvilli turn away of. Since the microvillar tilt direction and the anti-PY staining pattern changes midway along the ommatidia close to the R7/R8 junction, we examined whether absence of R7 effects these phenomena. In mutant eyes that lack R7 (*sev*<sup>D2</sup>, *sina*<sup>2</sup>/*sina*<sup>3</sup> and *boss*<sup>1</sup>), the microvillar incline and the anti-PY staining pattern also change halfway along the ommatidia, suggesting that these features are independent of R7. In these mutants, however, the position of R8 within the ommatidia is variable, and changes in R8 position are paralleled by changes in the microvillar tilt direction and in the anti-PY labelling pattern on the abutting visual cells. Our results suggest that (1) rhabdomere twisting is not the result of morphological constraints during retina morphogenesis, and (2) interaction with R8 plays a dominant role in the development of the rhabdomere twist on R1-R6.

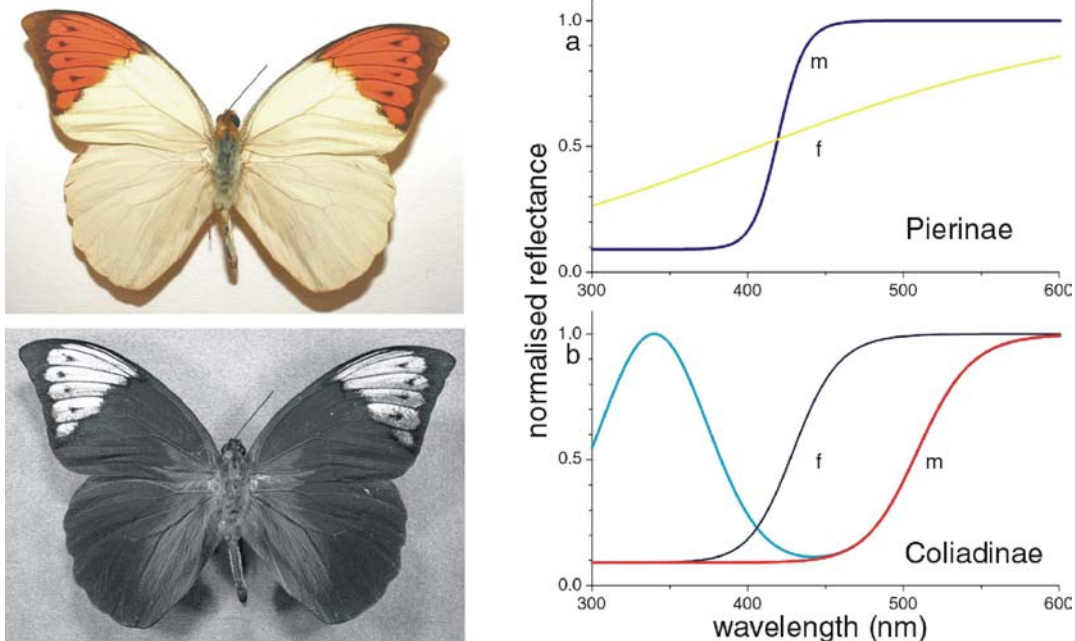


## Sexual dichroism of pierid butterflies

D.G. Stavenga

Department of Neurobiophysics, University of Groningen, the Netherlands

Butterflies are well-known for their display of striking, colourful patterns. The wing colouration of pierid butterflies seem to be comparatively rather inconspicuous, as the whites are rather white and the yellows are overall yellow. UV photography and reflectance spectrophotometry shows, however, that the reflectance at very short wavelengths is usually low, resulting in strong colour contrasts, invisible to the human eye. Wing colouration even is strongly dependent on sex. Two quite different methods of sexual dichroism appear to be developed among pierid butterflies. Female cabbage butterflies, *Pieris rapae*, have wings that are faintly yellow-white, i.e. the reflectance is rather uniform at all wavelengths. On the other hand, the wings of males have a low reflectance in the UV and a high reflectance at longer wavelengths (see figure, Pierinae). The wings of members of the other subfamily, Coliadinae, generally contain pigment that absorbs at short wavelengths, resulting in, for instance, orange wing tips of male *Hebomoia glaucippe*. In most coliadine species the pigmentation causes a yellow colouration. The females have the same pigmentation as the males, or they have pigment absorbing only at very short wavelengths. In many species the males have highly UV-reflecting wing areas, which causes a strong colour contrast compared with the females.



The dorsal wings of the male *Hebomoia glaucippe* have white scales that contain a UV absorbing pigment as demonstrated by UV photography. The scales at the orange wing tips contain a pigment that absorbs up to yellow wavelengths, but in addition they reflect in the UV, due to multilayer reflectors.

Many male Coliadinae (m) share the spectral organization of specific wing areas displaying strong reflectance in both the UV and at long wavelengths. The females (f) on the other hand have wing scales with pigment absorbing only at short wavelengths. The dichroism of many Pierinae species has a rather different spectral organization, namely the males (m) have scales that absorb strongly at short wavelengths and the females (f) have wings with lowly-pigmented scales.

Eisner T, Silberglied R, Aneshansley D, Carrell JE, Howland HC (1969) Ultraviolet video-viewing: the television camera as an insect eye. *Science* 166:1172-1174

Obara Y (1970) Studies on the mating behavior of the white cabbage butterfly, *Pieris rapae crucivora* Boisduval. III. Near-ultraviolet reflection as the signal of intraspecific communication. *Z Vergl Physiol* 69:99-116



## Spatial resolution of the eyes of flies, bees and butterflies

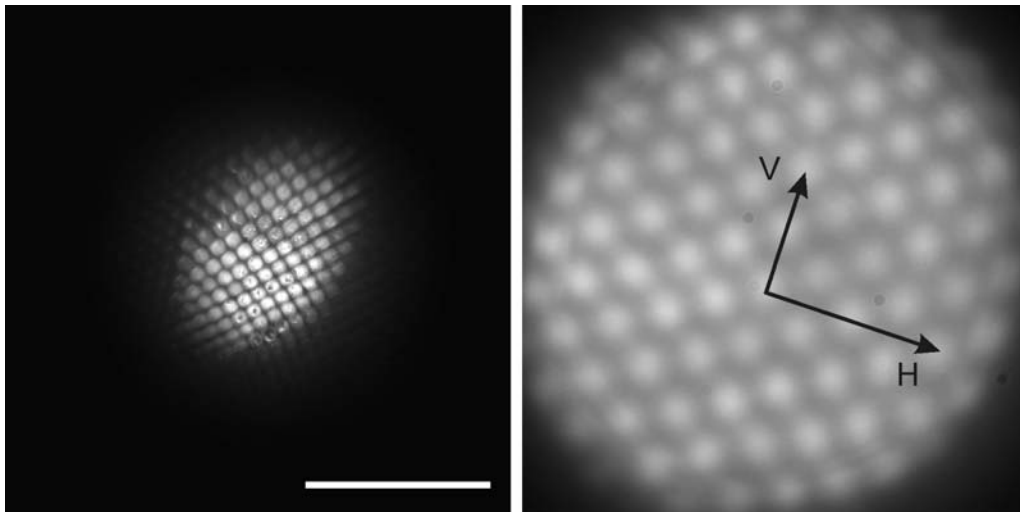
B. Wijnen<sup>a</sup>, J.E. Niven<sup>b</sup>, D.G. Stavenga<sup>a</sup>

<sup>a</sup>Department of Neurobiophysics, University of Groningen, the Netherlands

<sup>b</sup>Department of Zoology, University of Cambridge, UK.

The interommatidional angle, together with the acceptance angle of the photoreceptor cells, determines the spatial resolution of insect eyes. Quantitative values of these spatial characteristics are essential for proper understanding of insect vision. We have performed optical measurements of the spatial mapping of a number of insect species, specifically the fly *Sarcophaga carnaria*, the bee *Apis mellifica*, and the butterfly *Bicyclus anynana*, and compared the different optics.

The lattice of facet lenses in the cornea correlates with the shape of the cornea. Frontally in fly eyes, where the eye is more or less spherical, the facet lenses are packed in a so-called lying hexagonal lattice, but laterally, where the eye shape is very ovoid, the facet lenses are packed in a standing hexagonal lattice. In between, the facet lenses are square (see figure). Nevertheless, the visual axes, which determine the spatial resolution, are packed everywhere in an approximately lying hexagonal lattice, which is in fact dictated by the neural superposition organization of fly eyes. The spatial resolution of the fly eyes correlates with the body size.



Images obtained by antidromic illumination of the right ventral eye of the flesh fly *Sarcophaga carnaria*, photographed with a Franceschini-type setup equipped with a 5x, 0.15 NA objective. The left figure is taken at the corneal level and the right figure at a distance 1645  $\mu\text{m}$  distally from the cornea, yielding horizontal and vertical interommatidial angles of  $\Delta\phi_h = 1.52^\circ$  and  $\Delta\phi_v = 0.94^\circ$ , or  $\Delta\phi = 1.79^\circ$ ; the coordinate vectors H and V span  $4\Delta\phi_h$  and  $4\Delta\phi_v$ , respectively. The facet diameter locally is  $D_l = 22.1 \mu\text{m}$ . Bar 250  $\mu\text{m}$

Bees have quite ovoid eyes, with the facet lenses packed in a standing hexagonal lattice and the visual axes in a lying hexagonal lattice, as in the lateral regions of fly eyes. Butterflies have rather spherical eyes, with both facet lenses and visual axes in a lying hexagonal lattice, like in the frontal regions of fly eyes. The gradients in spatial resolution in butterfly eyes seem to be less severe than those in fly and bee eyes.

The two dimensional visual axes lattices can be described by a two coordinate system, H-V, with axes more or less perpendicular (Horizontal) and parallel (Vertical) to the insect body symmetry plane. The H-V-axes are approximately orthogonal, but deviations from orthogonality occur near the eye periphery.

Franceschini N (1975) Sampling of the visual environment by the compound eye of the fly: fundamentals and applications. In: Snyder AW, Menzel R (eds) Photoreceptor optics, pp. 98-125. Springer, Berlin, Heidelberg, New York

Stavenga DG (1979) Pseudopupils of compound eyes. In: Autrum H (ed) Handbook of Sensory Physiology, Vol VII/6A, pp. 357-439. Springer, Berlin-Heidelberg-New York

# **Butterfly wing colouring by scattering, pigment absorption and multilayer reflection in pierids**

*M.A. Giraldo, D.G. Stavenga*

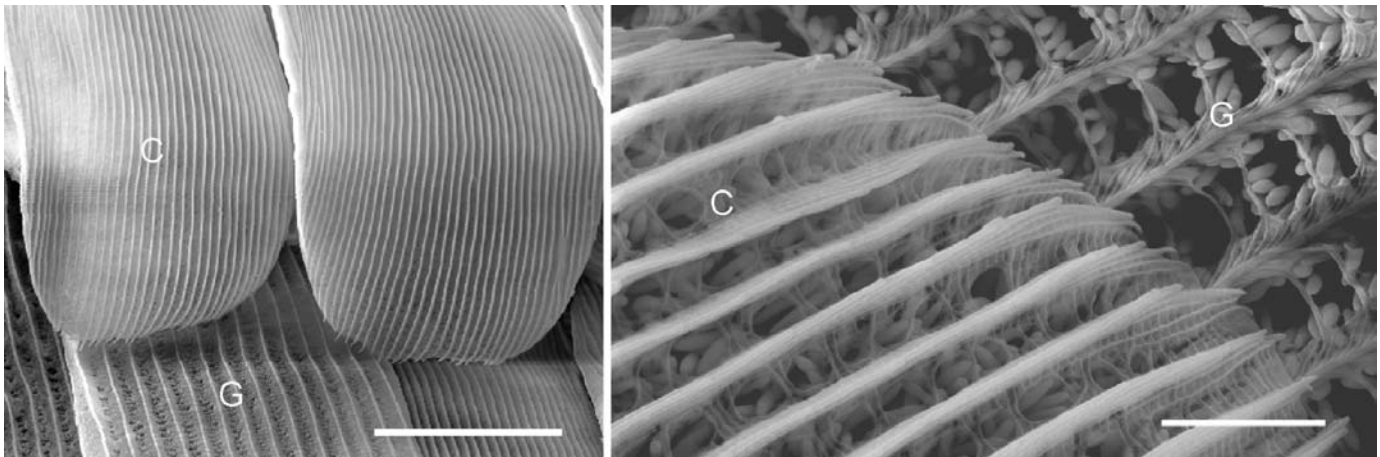
Department of Neurobiophysics, University of Groningen, the Netherlands.

e-mail: [giraldom@phys.rug.nl](mailto:giraldom@phys.rug.nl)

Butterfly wing colours originate from the cover of scales, which are arranged in a more or less regular pattern of rows. The scales have on the upper surface longitudinal ridges, consisting of overlapping lamellae, connected by crossribs. In pierid butterflies ridges and crossribs are adorned with beads that serve to enhance the light scattering by the scale structures. The white scales of the Pierinae (Whites) contain only a pigment absorbing in the UV, thus appearing unpigmented for the human eye. The yellow scales of the Coliadinae (Yellows, Sulphurs) contain pigment that absorbs UV, blue and green light. In the latter case, males of several species have scales reflecting strongly in the UV.

We have investigated the scales of the male brimstone, *Gonepteryx rhamni*. The dorsal forewings have two types of scales, cover and ground scales. Both scale types are yellow pigmented, but the cover scales reflect in the UV, due to a multilayer created by the lamellae of the longitudinal ridges. The distance between the ridges of the cover scales is much smaller than that of the ground scales (see figure). This organization appears to be similar to that of other Coliadinae.

Whereas the reflectance in the yellow is diffuse. The curvature of the cover scales broadens the spatial angle of the reflectance in the UV, resulting from the multilayer interference.



*The dorsal forewings of the male brimstone, *Gonepteryx rhamni*, have beaded scales, like most pierid butterflies. The longitudinal ridges of the cover scales (C) have in addition a UV-reflecting multilayer structure with width increasing from 80 nm at the top layer to ca 250 nm at the bottom layer; the layer distance is ca 50 nm. The distance of the ridges in the cover scales is 0.8  $\mu\text{m}$ , which is much smaller than the 1.8  $\mu\text{m}$  distance of the ridges in the ground scales (G). Bars 20 and 2  $\mu\text{m}$ , respectively*

Ghiradella H, Aneshansley D, Eisner T, Silberglied R, Hinton HE (1972) Ultraviolet reflection of a male butterfly: Interference color caused by thin-layer elaboration of wing scales. *Science* 178:1214-1217

Silberglied R, Taylor OR (1973) Ultraviolet differences between the sulphur butterflies, *Colias eurytheme* and *C. philodice*, and a possible isolating mechanism. *Science* 241:406-408

Stavenga DG, Stowe S, Siebke K, Zeil J, Arikawa K (2004) Butterfly wing colours: scale beads make white pierid wings brighter. *Proc R Soc Lond B* 271: 1577-1584 (2004)

## The numerous spectral and polarization sensitivities within the tripartite eyes of gonodactyloid stomatopods (mantis shrimps)

Sonja Kleinlogel (S.Kleinlogel@uq.edu.au) and N. Justin Marshall (justin.marshall@uq.edu.au)  
Vision Touch and Hearing Research Centre, School of Biomedical Sciences, University of Queensland,  
QLD 4072, Australia



The stalked apposition compound eyes of gonodactyloid stomatopods are regionally specialized and are subdivided into a dorsal and a ventral hemisphere bisected by an equatorial band of six distinct rows of enlarged ommatidia. This mid-band consists of four dorsal rows of anatomically specialized photoreceptors for colour vision (mid-band rows 1-4) and two ventral rows of anatomically specialized photoreceptors for polarization vision (mid-band rows 5 & 6). Each ommatidium consists of a distal 8<sup>th</sup> retinula cell (R8) and the main rhabdom formed by retinula cells 1-7 (R1-R7). Stomatopods exhibit a complex intra- and interspecific signalling network and display many polarized, coloured and fluorescent body markings. They use their mid-band photoreceptors to retrieve signal information displayed by conspecifics by sweeping the linear

array of specialized receptors forwards and backwards over the field of interest.

In this study we determined the spectral and polarization sensitivities of photoreceptors of all three eye regions in two gonodactyloid species by means of intracellular electrophysiology. We found that the stomatopod's hemispheric retinas, which are believed to be mainly involved in spatial and motion vision, contain two spectral sensitivities: a UV-sensitivity originating in the R8 cell and a broad green sensitivity lying in the R1-R7 cells, which could potentially form a dichromatic colour vision system. The R1-R7 cells show medium polarization sensitivity and may be involved in polarization vision. Mid-band rows 5 & 6 contain two narrow spectral sensitivities, one in the UV (R8) and one in the yellow spectral band (R1-R7). The R1-R7 cells possess very high polarization sensitivity and we therefore propose that they are specialized polarization receptors mainly used for signal recognition. This assumption is supported by the fact that the peak-absorbance of the R1-R7 cells matches the peak degree of polarization of polarized body-markings. We suggest that the stomatopod's mid-band rows 5 & 6 contain two 2-dimensional polarization vision systems, one receiving its inputs from the UV- cells and the other from the yellow-sensitive cells. From anatomical observations we speculate that the UV-sensitive R8 cells may act as  $\frac{1}{4}$ -wave retarders in the yellow spectral band to convert yellow, circularly polarized light into yellow, linearly polarized light so it can be analysed by the photoreceptors R1-R7 below. The colour vision system of mid-band rows 1-4 contains 12 narrowly tuned spectral sensitivities (4 of which are UV-sensitivities lying in the R8 cells) covering chromatic space continuously from 300 to 750 nm. The large number of narrow spectral sensitivities seems to be tuned to perceive coloured body signals (Osorio et al., 1997). Stomatopods are the only animals known to possess a hyperspectral retina which contains 16 spectral sensitivities!

We propose that the extraordinary retinal capabilities of gonodactyloid stomatopods serve the reliable and unambiguous recognition of intra- and interspecific communication signals at varying depth and light availability. Important body parts, which are displayed in encounters, possess in most cases VIS, UV, POL and sometimes even fluorescent reflection. Colour signals, for example, can be augmented by UV components in the bright and spectrally rich shallow waters, they can be replaced or augmented by polarized components in deeper water and replaced by fluorescence at even greater depth.

Cronin TW, Marshall NJ. 1989. *Nature* 339:137-140.  
Marshall NJ, Oberwinkler J. 1999. *Nature* 401:873-874.  
Osorio D, Marshall NJ, Cronin TW. 1997. *Vision Res* 37:3299-3309.

**A model of the Lobula Giant Movement Detector neuron of the Locust based on Reichardt Correlation.**

Sergi Bermúdez i Badia and Paul F.M.J. Verschure.

[sergi@ini.phys.eth.ch](mailto:sergi@ini.phys.eth.ch), [pfmjv@ini.phys.ethz.ch](mailto:pfmjv@ini.phys.ethz.ch)

Institute of Neuroinformatics, ETH Zürich, Winterthurerstr. 190, CH-8057 Zürich, Switzerland

In insects we can find very complex and compact neural structures that are task specific. These neural structures allow them to perform complex tasks such as visual navigation. One example of such a system is the neural circuitry supporting obstacle avoidance in the LGMD neuron of the Locust and its up- and downstream structures. These basic actions encoded by the insect visual system can be combined with more systems to make up more complex behaviors. Here we present a model of the Lobula Giant Movement Detector (LGMD) cell of the Locust, a wide-field visual neuron that responds to looming stimulus and it is supposed to trigger avoidance reactions whenever a collision is detected. Recent studies have suggested that the response of the LGMD cell can be explained as the result of a multiplication that includes the angular size ( $\theta$ ) and angular velocity ( $\theta'$ ) of the approaching object [1]. However, this implies that the previous layers of the locust visual system extract both angular size and velocity and convey this information reliably to the LGMD. Moreover, this model assumes that the LGMD subsequently performs a non-linear operation on this information. These are strong assumptions given our current understanding of this system. Hence, we present a new approach to the issue using a model based on the Reichardt correlation that prevents from calculating both angular size and velocity of the looming stimulus but still can give a response that fits the physiology of the LGMD and its theoretical interpretation with a high correlation ( $>0.9$ ). Thus, the putative non-linear behavior occurring at the level of the LGMD could be explained assuming only correlation detectors in its upstream structures. Our model also accounts for other factors like the non-linearity shown by the cell with respect to the speed of the approaching objects that not explained by the multiplicative hypothesis. The model presents a new approach to the issue of non-linear operations by neuronal structures and has been tested and successfully applied to the control of a flying robot.

[1] Fabrizio Gabbiani, Holger G. Krapp, Christof Koch and Gilles Laurent. Multiplicative computation in a visual neuron sensitive to looming. *Nature*, Vol 420, 2002.

This is a work supported by the AMOTH project, and was supported by the E.U. This research is supported by the European community and BBW (Grant "A Fleet of Artificial Chemosensing Moths for Distributed Environmental Monitoring (AMOTH)" to PFMJV, funded under the IST Future and Emerging Technologies Programme (IST-2001-33066, project website <http://www.amoth.org/>).

## **Honeybees generalize closed shapes among different types of contrast**

Miriam Lehrer

Dept. of Neurobiology, Institute of Zoology, University of Zurich  
Winterthurerstrasse 190, CH-8057 Zurich, Switzerland

In earlier studies we demonstrated that bees discriminate among closed (convex) shapes regardless of whether they produce luminance contrast or motion contrast against their background (Lehrer and Campan 2001, 28th Göttingen Neurobiol. Conf., 693), and that bees generalize specific shape features learned through motion contrast to unfamiliar shapes that contain those features (Campan and Lehrer 2003, 29th Göttingen Neurobiol. Conf., 635). Here we present some results obtained in experiments examining the bees' capacity to generalize a learned shape from one type of contrast to others.

Bees were trained using two shapes, one rewarding (positive), the other not (negative) and were then tested using shapes that produced different types of contrast than that used during the training. A measure for the bees' discrimination performance was the choice frequency CF, i.e. the percentage of landings on the positive shape. Only the first landing was recorded on every visit. Each CF is based on a total of at least 100 choices.

Experiment I. Bees trained with a blue square (positive) against a yellow square (negative), presented against a white background discriminated the training patterns very well (CF = 86.3%, average of five tests). When presented with a yellow square against a blue triangle, they preferred the blue triangle (CF = 77.4%), showing that the colour of the figure was more important than its shape. However, when a yellow square was tested against each of four different novel yellow figures (a disc, a diamond and two different triangles), bees always preferred the square (CF = 63.9%, average of the four tests). Similarly, with a black square tested against four different black figures, CF was 65.6%. Thus, bees have learned the shape in addition to colour, and use shape information when they cannot use colour.

Experiment II. A black diamond (positive) was trained against a black disc (negative), both on a white background. Discrimination was significant (CF = 69.4%), though, as expected, not as high as in the colour training. In further tests bees discriminated well between a yellow diamond and a yellow disc (CF = 77.6%) or a yellow square (CF = 67.3%), and also between a blue diamond and a blue disc (CF = 69.9%) or a blue square (CF = 65.0%). Moreover, discrimination was excellent (CF = 82.2%) when testing a black-and-white patterned diamond against a similarly patterned disc, presented 5cm in front of a patterned background. In this situation, bees can use neither luminance nor colour contrast. They can only perceive the shapes on the basis of motion contrast (i.e. relative motion between shape and background). Thus, bees transfer shape information extracted from luminance contrast to shapes that provide colour contrast, as well to such producing motion contrast.

Experiment III. Bees were trained using a patterned triangle and a patterned disc offered 5 cm in front of a similarly patterned background. Subsequent tests using homogenous shapes (black, blue or yellow disc against black, blue or yellow triangle, or against a black, blue or yellow square) rendered CF = 67.1% (average of all six tests), showing that bees transfer shape information extracted from motion contrast to luminance and colour contrast.

The generalization performance involved in extracting spatial information acquired using a particular type of contrast and applying this information to shapes that are perceived due to a different type of contrast might be considered to be a cognitive performance. It remains to search for the nature of the features that bees extract from the shape. There is much reason to believe that they are located at the circumference of the figure.

Correspondence: miriam.lehrer@ggaweb.ch

**Poster Subject Area #PSA11:**  
**Visual systems of invertebrates: Central areas and perception**

- [#148A](#) AM. Wertlen, N. Hempel de Ibarra, AA. Cocucci, A. Sersic, W. Kreisch and M. Ristow, Berlin, Córdoba (RA) and Potsdam  
*Sensory ecology of pollination: a survey of colour and nectar distribution in natural habitats*
- [#149A](#) J. Kalb, U. Beckers, M. Egelhaaf and R. Kurtz, Bielefeld  
*Characterization of synaptic transmission in the visual pathway of the blowfly using dual cell recording and laser ablation techniques*
- [#150A](#) K. Härtel and R. Hustert, Göttingen  
*Looming Sensitive Neurons in the Brain of the Locust. *Locusta migratoria*.*
- [#151A](#) M. Baldus and R. Hustert, Göttingen  
*Locust Landing Behaviour - a Tough but Safe Strategy*
- [#152A](#) J. Pahlberg, M. Jokela-Määttä, P. Ala-Laurila, M. Lindström and K. Donner, Helsinki (FIN), Bosten, MA (USA) and Hanko (FIN)  
*The photoactivation energy and absorbance spectra of the visual pigments in two populations of *Mysis relicta* sp. I (Mysidacea, Crustacea) from different light environments*
- [#153A](#) S. Greenberg and LY. Deouell, Jersualem (IL)  
*Crossmodal Visual-Auditory Interference in Object Recognition Process*
- [#154A](#) M. Wicklein and B. Lotto, London (UK)  
*Colour constant 'perception' and processing in Bumblebees*
- [#155A](#) K. Wyzisk and C. Neumeyer, Mainz  
*Experiments on form and size perception using illusory contours and visual illusions in goldfish (*Carassius auratus*)*
- [#148B](#) M-S. Mappes and U. Homberg, Marburg  
*Is the anterior optic tract essential for polarotactic flight behavior in the desert locust *Schistocerca gregaria*?*
- [#149B](#) T. Roeder, H. Marquardt and G. Schramm, Marburg  
*Analysis of the fruitfly retinal transcriptome*
- [#150B](#) K. Farrow, J. Haag and A. Borst, Martinsried  
*Inheriting Receptive Fields from Neighbours: How Lobula Plate Tangential Cells are tuned to Wide-Field Motion*

- [#151B](#) DF. Reiff, A. Ihring, J. Haag and A. Borst, Martinsried  
*Genetically encoded calcium probes in the visual system of Drosophila*
- [#152B](#) T. Hendel, A. Ihring, A. Borst and DF. Reiff, Martinsried  
*In vivo characterization of a GFP-based reporter molecule of neural activity by sequential epifluorescence- and 2P- imaging*
- [#153B](#) J. Stalleicken, M. Mukhida, T. Labhart, R. Wehner, B. Frost and H. Mouritsen,  
Oldenburg, Kingston (CDN) and Zurich (CH)  
*Do monarch butterflies use polarized skylight for migratory orientation?*
- [#154B](#) M. Sakura and T. Labhart, Zurich (CH)  
*Polarization-sensitive neurons in the central complex of the cricket, Gryllus bimaculatus*
- [#155B](#) MJ. Henze and T. Labhart, Zurich (CH)  
*Cricket polarization vision under difficult stimulus conditions*

## **Sensory ecology of pollination: a survey of colour and nectar distribution in natural habitats**

**Anna M Wertlen\*, Natalie Hempel de Ibarra\*, Andrea A Cocucci †,  
Alicia Sersic †, Werner Kreisch ‡, Michael Ristow ¥**

\*Institut für Biologie, Neurobiologie, Freie Universität Berlin, AMWertlen@gmx.net

† Facultad de Ciencias Exactas, Físicas y Naturales, Universidad Nacional de Córdoba, Argentina

‡ BGBM, Freie Universität Berlin ¥ Institut für Biochemie and Biologie, Universität Potsdam

Field observations suggest that blue-violet flowers may be highly rewarding to pollinators, in particular to bees. Therefore they would be visited more often. They could also be more attractive due to innate colour preferences as experimental data show. We approached this hypothesis by measuring colour properties and nectar reward of co-flowering plant species in several habitats. Bee-subjective colour properties were determined using the Receptor Noise Limited (RNL) Model of honeybee colour vision<sup>1</sup>. Maximum nectar volume, sugar concentration of the nectar, flower abundance and insect visitation rates were recorded in parallel over several days for 10-15 bee-pollinated and indicator plants at each of eight study sites (approx. 0.01 km<sup>2</sup>) in natural habitats in Europe and Argentina. Our results showed that highly rewarding and/or most abundant flowers are not strongly represented in the blue-violet part of the bee colour space. We further analysed other aspects of the floral display in relationship to the reward properties. Our findings are in agreement with the fact that bees, as well as other pollinators, can learn any colour as a food signal<sup>2</sup> and are able to adjust their foraging behaviour to the present food sources.

<sup>1</sup> Vorobyev et al. (2001) Vision Res 41: 639-653

<sup>2</sup> Menzel (1967) Z Vergl Physiol 56: 22-62



## Characterization of synaptic transmission in the visual pathway of the blowfly using dual cell recording and laser ablation techniques

Julia Kalb, Ulrich Beckers, Martin Egelhaaf and Rafael Kurtz

Neurobiologie, Fakultät Biologie, Universität Bielefeld, Postfach 100131, D-33501 Bielefeld, Germany

For neuronal network analysis it is of particular interest how the interaction between individual neurons produces behaviour. This critically depends on both the biophysical properties of single nerve cells as well as on how signals are transferred in neuronal ensembles. Synapses thus represent key elements to understand the computational capabilities of the nervous system.

In the visual system of the blowfly synaptic wiring and transfer properties appear to be highly specialized to process information in an efficient and fast manner in order to elicit rapidly appropriate behavioural responses to visual motion stimuli. In the fly brain, the cellular basis of neuronal computation can be studied *in vivo* and synaptic activity can be evoked by visual stimulation<sup>1</sup>. Synaptic operating range and temporal activity patterns can thus be held close to natural conditions. However, it is also possible to interfere with natural neuronal processing in a systematically controlled way, e.g. by voltage clamping or by laser ablation of selected neurons<sup>2-4</sup>.

Our studies are focused on a subset of identified neurons in the blowfly visual system, which are sensitive to vertical motion. This subset consists of a small ensemble of presynaptic neurons and a single postsynaptic neuron, which transmits the visual motion information gathered from its presynaptic elements to the contralateral brain hemisphere. The synapses under study combine properties of both graded and spike-mediated transmission, since the presynaptic cells encode visual motion information by graded potential shifts with superimposed spike-like depolarizations, which both influence frequency and timing of postsynaptic spiking activity. Up to now, these synaptic connections have been studied with respect to the gain and reliability of synaptic transmission during motion stimulation with either constant or dynamically fluctuating velocity<sup>5,6</sup>. Surprisingly linear transfer characteristics were observed over a large range of presynaptic activity levels and frequencies of voltage fluctuations.

However, with sensory stimulation alone, the presynaptic signal always contains both fast and slow components, which interplay in a complex way. Moreover, since their receptive fields overlap to some extent, visual stimulation always activates more than one presynaptic neuron. To overcome these problems we are currently using two complementary approaches:

First, the transfer of presynaptic voltage fluctuations of various frequencies is analyzed by controlling the membrane potential of one presynaptic neuron with single electrode voltage clamp during concomitant recording of the postsynaptic spike rate. Thus, synaptic gain and reliability during the transfer of signals with certain dynamics can be tested systematically. Second, by selective laser ablation of single presynaptic neurons we investigate in how far synaptic readout of motion information depends on the activity of the entire presynaptic ensemble. Thus it can also be assessed, which frequency range of synaptic transmission is affected most by the knock-out of a presynaptic element. Both approaches also allow to study whether individual synaptic connections of the ensemble differ in their characteristics.

Supported by the DFG grant KU 1520.

### References:

- 1 Egelhaaf M, Kern R, Krapp HG, Kretzberg J, Kurtz R, Warzecha A-K. Trends Neurosci, 25 (2002) 96-102.
- 2 Haag J, Theunissen F, Borst A. J Comput Neurosci, 4 (1997) 349-369.
- 3 Warzecha A-K, Egelhaaf M, Borst A. J Neurophysiol 69 (1993) 329-339.
- 4 Farrow K, Haag J, Borst A. J Neurosci 29 (2003) 9805-9811.
- 5 Kurtz R, Warzecha A-K, Egelhaaf M. J Neurosci, 21 (2001) 6957-6966.
- 6 Warzecha A-K, Kurtz R, Egelhaaf M. Neurosci, 119 (2003) 1103-1112.

## Looming Sensitive Neurons in the Brain of the Locust. *Locusta migratoria*.

Kai Härtel and Reinhold Hustert; Zoologie, Universität Göttingen

The detection of looming stimuli in the visual system is an important mechanism for a wide range of animals, since enlarging objects in the visual field often signal the approach of an potential predator or an harmful object.

Particularly for locusts spending most of their time on the ground, sitting e.g. on branches, leaves or grass, early perception of a predator enables them to react with escape or hiding responses that raise their chance of survival. Flying locust must also detect looming stimuli to recognise obstacles in their path or to avoid collisions with swarm mates. Their motor responses to looming stimuli require spatial localization of the expanding stimulus in the visual field for shaping an adequate motor output. This was studied in some detail for the hiding response of sitting locusts, where the turn angle of the movement depends on the position of the stimulus in the lateral visual field (HASSENSTEIN & HUSTERT, 1999).

Research on locust looming perception has focussed on the lobula giant movement detector (LGMD) and his postsynaptic partner the descending contralateral movement detector (DCMD, review by RIND, 2002). But these neurons respond to looming within a large field and cannot encode the position of the stimulus in the visual field. Only few position-coding looming sensitive neurons have been identified in insects (*L. migratoria*: GEWECKE & HOU, 1993; RIND, 1996; *M. sexta*: WICKLEIN & STRAUSSFELD, 2000).

We searched for interneurons in the brain of *Locusta migratoria*, which could contribute to the perception and location of looming stimuli in the lateral visual field. Our computer- generated stimuli depict all or only a part of the information of a looming object. That makes it possible to identify which optical parameter elicits a looming specific neuronal response. Representing the stimuli at different positions in the visual field enabled us to characterize the receptive field of the neurons.

Intracellular recordings in the lateral protocerebrum revealed a number of looming-sensitive neurons with different morphologies connecting the lobula with the protocerebrum and/or the deutocerebrum. Most of the neurons deal with a larger subset of all presented stimuli types. These are not just looming specific, but they could contribute to looming perception at a later stage of neuronal processing. In many cases the receptive fields covered the whole visual hemisphere but with a more or less focussed position-depending sensitivity for the looming stimuli. One neuron had subdivided antagonistic receptive fields where in one part the same stimulus type excited the cell while in the other part it inhibited. This neuron would fit the best in a neuronal network for the control of a target specific behaviour as the hiding response of the locust.

### References:

- Hassenstein, B. and Hustert, R. (1999). Hiding responses of locusts to approaching objects.  
J. Exp. Biol. 202: 1691-1700.
- Rind, F. C. (2002). Motion detectors in the locust visual system: From biology to robot sensors.  
Microsc. Res. Tech. 56: 256-269
- Rind, F. C. (1996). Intracellular characterization of neurons in the locust brain signaling impending collision.  
J. Neurophysiol. 75(3): 986 - 995.
- Wicklein, M. and Strausfeld, N. J. (2000). Organization and significance of neurons that detect change of visual depth in the hawk moth *Manduca sexta*.  
J. Comp. Neurol. 424: 356 - 376.

## Locust Landing Behaviour – a Tough but Safe Strategy

M. Baldus and R. Hustert, Zoologie, Universität Göttingen

Locusts can land after flight or jumps safely on difficult terrain and on exposed targets. For investigation of their strategy we recorded in 4<sup>th</sup>- 5<sup>th</sup> larval instars of *Schistocerca gregaria* by means of highspeed-video and electromyographic recordings.

Two main types of landing postures can be observed.

1) The first is a kind of “gliding”, at which all legs are spread laterally and somewhat dorsally in a fan-shaped manner while the tarsi of the two forelegs are held at a level above the head. The body tilt angle during approach towards the target's surface is relatively flat.

2) The second pre-landing posture (with a steeper tilt angle of the body on substrate approach) is derived from the typical aerodynamic flight position (Weis-Fogh 1956, Möhl 1989) where the hind- and middle legs are extended posterior and closer to the body and the forelegs are held next to the pronotum, with the tarsi pointing posterior. Just before the landing-contact the forelegs are extended and their tarsi become positioned above the head.

The most surprising result of frame by frame recording the sequence of landing is, that usually the locusts bump into the substrate with the ventral side of their head or thorax first. The forward thrust of an aimed jump onto a flat target is not absorbed at landing by means of leg muscle tension as we expected but mainly by the cuticle of the head and the body. Tarsal contacts of the forelegs and middle legs usually follow after a few milliseconds and are sometimes synchronous with the primary contact of head or thorax, but rarely earlier. Chronical electromyograms of the coxal depressor muscles and tarsal retractor muscles of the first two leg pairs show delayed activity of 1-3 milliseconds after the first landing contact. All tarsal claws hook immediately into the substrate after tarsal contact. Therefore, in landing of locusts leg function is not to absorb the impact of landing but rather to avoid bouncing off the substrate again.

Apparently, rebound from the substrate after the impact from landing represents more of a problem than the crash-landing itself. The myograms from leg muscles after substrate contact show higher relative muscle activity in the tarsal retractors than in the coxal depressors. This corresponds in the synchronous video frames with a clear retraction of the pretarsal claws and flexion of the tibiae of the first two legpairs that counteract the rebounding movement of the body. Rebound forces are high, due to the high approaching velocities (60-100 cm/s measured). Therefore, anchorage of the claws is essential for a safe landing, especially while landing on a flat vertical surface but that also holds for landing-behaviour on diagonal or horizontal surfaces.

When locust land on small objects and sticks the strategy seem to be more to aim a little lateral from the target and while the body misses the extended legs of one side get hold with any of the tarsal claws, which hook in the target automatically, while the rest of the body spins around this object until the other legs get hold automatically. This is better achieved with landing posture 1: spreading out legs laterally.

## **The photoactivation energy and absorbance spectra of the visual pigments in two populations of *Mysis relicta* sp. I (Mysidacea, Crustacea) from different light environments**

Johan Pahlberg<sup>1</sup>, Mirka Jokela-Määttä<sup>1</sup>, Petri Ala-Laurila<sup>2</sup>, Magnus Lindström<sup>3</sup>, & Kristian Donner<sup>1</sup>

<sup>1</sup> Department of Biological and Environmental Sciences, Division of Physiology, University of Helsinki, P.O. Box 65, FIN-00014 Helsinki, Finland

<sup>2</sup> Department of Physiology and Biophysics, Boston University School of Medicine, Boston, MA 02118, USA

<sup>3</sup> Tvärminne Zoological Station, University of Helsinki, FIN-10900 Hanko, Finland

We study the relation between the wavelength of maximum absorbance ( $\lambda_{\max}$ ) and minimum energy for photoactivation ( $E_a$ ) in the visual pigments of two populations of the same subspecies of opossum shrimp (*Mysis relicta* sp. I). The two populations have been separated for 9000 years, adapting to different light environments (the Baltic “Sea” and “Lake” Pääjärvi), with spectral sensitivities of the eye peaking at 550 nm (Sea) and 570 nm (Lake), in qualitative correlation with the difference in spectral transmission in the two bodies of water, which peak around 565-585 nm and 600-700 nm, respectively.

Spectral sensitivity was measured by electroretinogram recording (ERG) in the intact eye. This allows accurate determination of the long-wavelength limb of the spectrum, where the absorbance of the visual pigment has fallen below 1 % of maximum. From the temperature-dependence of spectral sensitivities in this range,  $E_a$  can be estimated according to theory originally proposed by Stiles<sup>1</sup>. Absorbance spectra of the visual pigment were recorded by single-cell microspectrophotometry (MSP) in single rhabdoms.

The wavelength of maximum absorbance for the Sea and Lake populations was 529 nm and 554 nm, respectively. The shapes of the absorbance spectra indicated that the pigments were pure A2 porphyropsins. The temperature effects on spectral sensitivity were qualitatively in accordance with theory, as relative sensitivity to long wavelengths increased with rising temperature. The estimates of the minimum energy needed for photoactivation from this effect were  $E_a = 47.8 \pm 1.8$  kcal/mol for the 529 nm (Sea) pigment and  $E_a = 41.5 \pm 0.7$  kcal/mol for the 554 nm (Lake) pigment.

Thus the relative red-shift of  $\lambda_{\max}$  in the Lake compared with the Sea population was associated with lower  $E_a$  and may carry a cost in terms of increased thermal noise. The chromophore was the same (A2) in both populations, so the difference must be due to differences in the amino acid sequence of the opsin. In itself the use of the A2 chromophore is an adaptation unusual in invertebrates.

<sup>1</sup> Stiles, W.S. (1948). In: Transactions of the Optical Convention of the Worshipful Company of Spectacle Makers, pp 97-107. London: Spectacle Makers' Co.

### Crossmodal Visual-Auditory Interference in Object Recognition Process

Shlomit Greenberg, Leon Y. Deouell

Hebrew University of Jerusalem, Department of Psychology

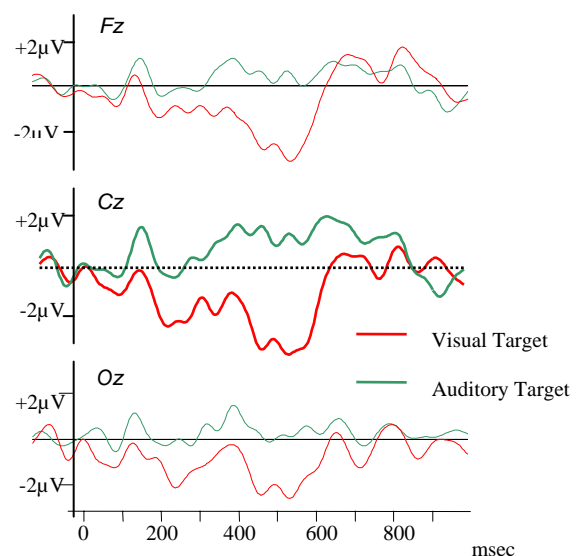
[Yuvalsh@pob.huji.ac.il](mailto:Yuvalsh@pob.huji.ac.il), [msleon@mscc.huji.ac.il](mailto:msleon@mscc.huji.ac.il)

Classical cognitive neuroscience normally views the visual and the auditory systems as separate mechanisms, which operate independently. In the past few years, the interaction between the different modalities has begun to receive more attention. Several studies have concentrated on resolution of spatial conflict between vision and audition ("ventriloquism"), and recently the temporal domain has been also addressed. Much less is known about auditory-visual interaction in object recognition. The present research addressed this issue.

The subjects were presented with bi-modal stimuli, composed of concurrently appearing pictures and voices of common and easy-to-identify animals (e.g., cow, rooster). The task was to identify either the picture ("visual condition") or the voice ("auditory condition") by answering a forced-choice question (e.g., "Rooster?") presented after the auditory-visual presentation. In one third of the trials the picture and the voice belonged to the same animal ('congruent' trials), in another third the picture and the voice belonged to different animals ('incongruent' trials). In the remaining trials, a neutral stimulus, not identified as an animal, was presented as the non-target stimulus. Reaction times and accuracy of responses were analyzed.

Performance on congruent trials was better than on incongruent trials, both in the visual and in the auditory conditions. This effect indicates that task-irrelevant objects of an unattended modality are processed and even recognized. An 'incongruity effect' was calculated as the difference between performance on incongruent trials and performance on congruent trials. This effect was significantly larger in the auditory condition than in the visual condition. In order to investigate whether this difference between the modalities originates in interference or enhancement, performance on neutral trials was used as bases for comparison. Significant interference effects were found in incongruent trials in both the auditory and the visual conditions, with no significant differences between the two conditions. This implicates a difficulty in suppressing object recognition processes of an unattended modality, despite its detrimental effect on performance. Another finding was the facilitation of object recognition in congruent trials of the auditory but not of the visual condition. That is, recognition of animal voices was facilitated by concurrent presentation of a congruent picture, whereas recognition of the pictures was unaffected by concurrent vocalization of the same animal. This finding tentatively suggests an asymmetry between the two modalities in the process of object-recognition. Because of the design of the task, this facilitation was probably not due to simple response (yes/no) selection, but to genuine recognition or naming processes.

Event related potentials were recorded in 14 subjects with a similar design. Results showed that incongruent trials elicited a more negative response than congruent trials in latencies of circa 200-650 ms post stimulus onset when the target was the auditory stimuli, reminiscent of an N400 effect. In contrast, no significant incongruity effect was found when the target was the visual stimulus. The figure shows this 'incongruity effect', calculated by subtracting the waveforms elicited during congruent trials from those elicited during incongruent trials. Looking at channel Cz, the difference-waves in the auditory condition showed a double peaked negativity, which had a fronto-central distribution. Both peaks were significantly different from zero in a random effect analysis across the 14 subjects. In contrast, none of the peaks in visual incongruity waveform was significantly different from zero.



Thus, visual information affects the process of auditory object recognition as early as 200-600 ms after stimulus onset, but the opposite interaction is much more tenuous. This is congruent with the behavioral results, and suggests that like the case of spatial conflict (e.g., the ventriloquism case), but unlike the case of temporal conflict, our cognitive system relies more on visual than on auditory information, in the case of conflict in object recognition.

# Colour constant 'perception' and processing in Bumblebees

Wicklein M and Lotto RB, University College London, London UK

[m.wicklein@ucl.ac.uk](mailto:m.wicklein@ucl.ac.uk), [lotto@ucl.ac.uk](mailto:lotto@ucl.ac.uk)

Recognizing a surface of particular reflectance under different conditions of illumination is fundamental for useful visually guided behaviour. Little, however, is known about how this is achieved in any natural system. We are addressing this question in bumblebees because they exhibit excellent colour vision, colour constant behaviour, and because we can completely control their spectral environment throughout their ontogenetic experience.



Behaviour experiments: Bees were trained to recognize a particular colour in an array of different colours under different illuminants, and then tested under a novel illuminant. Bees were presented with a vertical array of 64 artificial flowers (A), divided into 4 sectors (B) each of which could be illuminated by a different light (D). Within each sector, a pseudo random arrangement of 4 different colours of flowers were presented (C). Only one flower colour was rewarded (and is therefore designated as the 'target'; E, F show bees foraging on the rewarded flowers). After 10 to 20 training sessions, *individual* bees were tested for their foraging preferences under a novel illuminant. Bumblebees not only learned to recognize the target colour under different illuminants, but they also did so under the novel illuminant, demonstrating colour constancy under the experimental conditions used here.

Physiology: We performed multielectrode extracellular and single cell intracellular recordings in the optical lobes to probe the colour sensitivity and receptive field structure of colour sensitive neurons that may underlie bumblebee colour constancy. We use a "white noise" stimulus as well as fullfield and center surround stimuli presented on a LED screen containing blue, green and UV LEDs. The results contribute to our understanding of the neurocomputational foundations of colour vision.

Funded by a grant from the Wellcome Trust to RBL.

## Experiments on form and size perception using illusory contours and visual illusions in goldfish (*Carassius auratus*)

Katja Wyzisk and Christa Neumeyer

Institute of Zoology III (Neurobiology), Johannes Gutenberg-Universität, D-55099 Mainz

**Purpose:** It is known that many cyprinid fish possess the ability to discriminate visually different shapes. Shape discrimination seems to depend on differences at the base or top line of the figure or the position of the apex. The neuronal mechanisms for this perception are unknown.

In this study training experiments with a variety of illusory contours and visual illusions were performed to investigate these mechanisms.

Visual illusions are indicative of limitations of the visual system and can be used to create a theoretical model for the understanding of neuronal processing.

**Methods:** Four goldfish were kept separately in tanks (40 x 25 x 25 cm). Two openings (8 cm diameter) of a 'feeding plate' (25 x 23 cm) served as test fields, on which two figures were shown simultaneously using a TFT-display.

Tested stimuli in the experiments are the Kanizsa illusion, illusory contours defined by a line grating, the Müller-Lyer-illusion and the Ponzo-illusion.

In each test series the fish were trained by food reward to one training stimulus (for example a triangle). A second stimulus was given for comparison (for example a square). Transfer stimuli were generated which had an illusory similarity to either training or comparison stimulus (for example a Kanizsa-triangle and a Kanizsa-square) and were presented simultaneously during transfer tests. The fish choice behaviour was recorded manually.

**Results:** Goldfish are able to perceive the Kanizsa illusion.

Illusory contours defined by gaps in a line grating were also perceived. In contrast, square-shaped or triangle-shaped contours defined by phase-shifted gratings are not perceptible.

The results for the Müller-Lyer-illusion indicate that the goldfish are not able to perceive this illusion. Animals always preferred the test field with the larger vertical line. For identical line length the fish shows a choice frequency of 50 percent for both test fields independent of inward-facing or outward-facing wings.

The measurements for the Ponzo-illusion show that the animals can not perceive this illusion.

**Conclusion:** Visual illusions of size (Müller-Lyer and Ponzo illusion) were not perceived.

Goldfish are able to see illusory contours. This agrees with findings in other animals (for example monkeys and bees). This indicates that the detection of illusory contours is a fundamental visual capability.

In investigations on rhesus monkeys cells in V1 and V2 were found which equally respond to illusory contours and line drawings. Our results indicate that cells with similar properties may also exist in the goldfish brain.

### **Is the anterior optic tract essential for polarotactic flight behavior in the desert locust *Schistocerca gregaria*?**

Martina Mappes<sup>1</sup> and Uwe Homberg<sup>2</sup>, Philipps-University Marburg, Department of Biology, Animal Physiology, Karl-von-Frisch-Str., D-35043 Marburg, Germany  
<sup>1</sup>mappes@staff.uni-marburg.de, <sup>2</sup>homberg@staff.uni-marburg.de

Scattering of sunlight in the earth's upper atmosphere leads to a prominent polarization pattern in the blue sky. E-vectors of this pattern are oriented in concentric circles around the sun and provide insects and other animals with a unique and useful cue for celestial compass navigation. Desert locusts, *Schistocerca gregaria*, show specific behavioral responses to polarized light. In tethered flight, they perform periodic changes in yaw-torque under a slowly rotating polarizer. Photoreceptors of an eye region morphologically specialized for the detection of polarized light (dorsal rim area, DRA) were demonstrated to mediate this behavior (Mappes and Homberg 2004, J Comp Physiol A 90: 61-68). Further tests showed that one compound eye is sufficient to show the behavior. Polarotaxis in flights with both eyes free and with one eye covered was indistinguishable whereas painting both eyes black resulted in disappearance of polarotaxis.

The locusts' polarization vision pathway receives input from the DRA and continues through the dorsal rim of the lamina and the medulla of the optic lobe. Signals are further transferred via the anterior optic tract (AOT) to the anterior optic tubercle (AOTu) and the central complex of the brain (Homberg et al. 2003, J Comp Neurol 462: 415-430). The significance of the AOT for polarotactic behavior is still unknown. We, therefore, performed lesion experiments by cauterizing the AOT of one optic lobe to gain further insight into the locusts' polarization pathway.

After severance of the AOT we performed behavioral tests for polarotaxis under two conditions: (1) the eye of the intact brain hemisphere was covered; (2) both eyes were left free. Locusts with covered intact eye (test 1) showed loss of periodicity in yaw torque responses, while locusts with both eyes free showed polarotaxis. The experiments show that the AOT is an essential visual pathway governing polarotaxis in the locust and suggest that the AOTu and central complex which receive input from the AOT play a decisive role in sky navigation of the locust. Supported by DFG grant HO-950/13.



## Analysis of the fruitfly retinal transcriptome

Thomas Roeder, Helge Marquardt and Guido Schramm

Processing of sensory information is one of the major tasks of a nervous system. Among the different sensory modalities that are processed in different parts of the brain, visual information processing is presumably the most impressive one. This is not only true for man and most mammals, but also for most insects, especially for flying insects. The insect eye is a highly ordered structure with different cell types dedicated to specific tasks. Transduction of visual information occurs in the photoreceptor cells of the retina. Within the retina 8 different photoreceptor cells form a single ommatidium. The photoreceptors R1-R6 make synapses within the first visual neuropile of the optic lobe, the lamina with so-called lamina-monopolar cells. The axons of the photoreceptors R7 and R8 travel through the lamina to make synapses with yet unidentified neurons of the medulla. Information is further processed in the different neuropiles of the visual system, the lamina, the medulla, and the lobula. To identify the molecules that are transcribed in either the areas of interest, we used different methods to isolate specific parts of the visual pathway. The retina as well as the first neuropile of the optic lobes, the lamina was isolated using a modified freeze-drying method. In addition, we isolated the retinae as well as the laminae of flies devoid of the R7 photoreceptor (*sevenless*). The retinae of these flies are normal except the lack of this photoreceptor type. In addition, it could be assumed that these flies have deficiencies in the medulla, where these photoreceptors make synapses with yet unidentified first-order visual interneurons.

We isolated the RNA from the different tissues mentioned above and performed DNA-microarray analysis using a 12 k DNA-array. Differential hybridization revealed different features: The almost complete retinal transcriptome, the transcripts that are specific for the photoreceptor R7 and the transcripts of the different part of the neuropiles of the fruit flies optic lobe. Analysis of the complete set of transcription experiments should give us novel insights into the molecular organization of the visual pathway as well as into the differential transcription in the photoreceptor population.

This work was supported by the DFG (DFG Ro 1241).

## **Inheriting Receptive Fields from Neighbours: How Lobula Plate Tangential Cells are tuned to Wide-Field Motion**

Karl Farrow, Juergen Haag and Alexander Borst  
Max-Planck-Institute of Neurobiology, Martinsried, Germany

Self motion elicits characteristic flow-fields that are used to guide locomotion. In blowflies, such large field motion information is processed in the lobula plate where approximately 60 tangential neurons exist on each side of the brain. These lobula plate tangential cells (LPTCs) have large dendritic trees that receive local motion information from retinotopically arranged elementary motion detectors. Each cell integrates this local information motion across its dendrite to produce a directionally selective large-field motion response. We call this its primary receptive field. For each neuron, this primary receptive field is predicted from its dendritic geometry and the preferred direction of its local motion input. However, the receptive fields of many LPTCs are more complex than this basic circuitry implies. As a compelling example, tangential cells of the vertical system (VS-cells) respond to motion stimuli far outside their primary receptive field. Using dual intracellular recordings, a recent study (Haag and Borst, Nat Neurosci, 2004) found VS-cells to be electrically coupled to each other, most likely in a sequential order, such that each VS-cell is connected to its immediate left and right neighbour only. This coupling was suggested to form the basis of the broadening of the receptive field of VS-cells as compared to their primary field.

In this study, we tested this hypothesis directly by photo-ablating individual VS-cells and measuring the receptive field of remaining VS-cells before and after ablation. For example, we found that the receptive field width of VS4-cells narrowed after the ablation of either a VS2- or VS3-cell, which have more frontal but overlapping receptive fields'. Significantly, the narrowing only occurred in the most frontal divisions of the VS4-cell's receptive field, where the VS2/3-cells are most responsive, and not its lateral divisions. In summary, our experiments demonstrate that the extremely broad receptive fields of VS-cells are indeed the result of electrical coupling between neighbouring VS-cells.

Genetically encoded calcium probes in the visual system of *Drosophila*

Dierk F. Reiff, Alexandra Ihring, Juergen Haag, and Alexander Borst.

Max-Planck-Institute of Neurobiology, Dept. of Systems and Computational Neurobiology, Martinsried, Germany.

The directed expression of genetic probes of cellular activity provides a new tool for the functional analysis of neuronal assemblies and single neurons. We use this approach to visualize the activity of neurons in the fly visual system. We developed a preparation of *Drosophila* that allows optical imaging of visual interneurons while the fly is stimulated by visual motion. While the direction of motion is fundamental for the survival of the animal it cannot be retrieved directly from single photoreceptor signals. Instead it has to be computed from a comparison of neighboring photoreceptor signals. This process is well described in the "correlation type motion detector" model. The basic computational principles of this model seem conserved throughout the animal kingdom and, at the algorithmic level, are well understood. In contrast, very little is known about its neural implementation. Screening for specific Gal4-lines allows to direct genetic indicators to putative cells of this circuit and thereby to uncover the identities and relationships of neurons that participate in basic neuronal computations such as non-linear, multiplicative-like interactions and temporal filtering. We currently verify the response properties of directional selective lobula plate tangential cells (LPTCs) that are already well described in the blowfly *Calliphora vicina*. Building on these results we concentrate on the identification and analysis of presynaptic cells that constitute the input to LPTCs in order to provide a better understanding of visual motion detection at the cellular and biophysical level.

## ***In vivo* characterization of a GFP-based reporter molecule of neural activity by sequential epifluorescence- and 2P- imaging**

Thomas Hendel, Alexandra Ihring, Alexander Borst and Dierk F. Reiff

Max-Planck-Institute of Neurobiology, Dep of Systems and Computational Neurobiology, Martinsried, Germany

In the lobula plate of dipteran insects, large tangential cells (LPTCs) respond in a directionally selective manner to visual motion presented in their receptive fields. However, on the level of individual photoreceptors, this motion information is not explicitly encoded. Thus cells postsynaptic to the photoreceptors and presynaptic to the LPTCs are likely to provide the synaptic interactions that extract motion information from the visual input. In the 1950s Reichardt & Hassenstein proposed a model for motion detection based on arrays of local motion detectors. Each of these detectors is thought to compare the brightness values of neighboring photoreceptors at two time-points through a simple set of mathematical operations: temporal filtering, a nonlinear interaction such as a multiplication, and a subtraction. The importance of this model is further emphasized as there is some evidence for its fundamental mathematical principles being shared by a variety of species, from insects to higher vertebrates, including men. It is our aim to analyze where and how such a system is implemented in the fly-brain. So far this question could not be addressed as the physiological characterization of candidate cells failed due to their small size.

We are analyzing this problem in the fruit fly *Drosophila melanogaster* by taking advantage of genetically encoded calcium indicators (GECIs) and the GAL4-UAS system. This approach allows to target the expression of GECIs to defined populations of neurons within the optic lobes. This is currently done by using several strains that express Gal4 in different subsets of neurons in the fly visual system. We also generated a library of transgenic flies that carry different GECIs under UAS control. Two photon imaging may now allow to record from visual interneurons while the fly is looking at moving visual stimuli.

As a first step we use the larval neuromuscular junction preparation as a well characterized model system to analyze the function and response dynamics of different GECI molecules in neurons *in vivo*. We build a setup that allows to readily switch between two photon microscopy and traditional epifluorescence imaging. Thus we are able to compare the performance of different GECIs under both conditions. The acquired information will be an important prerequisite for the interpretation of optically monitored signals from neural networks such as the motion detection system in the fly brain.

## Do monarch butterflies use polarized skylight for migratory orientation?

Julia Stalleicken<sup>1</sup>, Maya Mukhida<sup>2</sup>, Thomas Labhart<sup>3</sup>, Rüdiger Wehner<sup>3</sup>, Barrie Frost<sup>2</sup> and Henrik Mouritsen<sup>1</sup>

<sup>1</sup>VW Nachwuchsgruppe “Animal Navigation“, Institute of Biology and Environmental Sciences, University of Oldenburg, 26111 Oldenburg, Germany; <sup>2</sup>Department of Psychology, Queen’s University, Kingston, Ont. K7L 3N6, Canada; <sup>3</sup>Zoological Institute, University of Zurich, Winterthurerstraße 190, 8057 Zurich, Switzerland

Monarch butterflies (*Danaus plexippus* L.) from eastern North America use a time-compensated sun compass during their annual autumn migration to orient in a south-westerly direction towards the population’s overwintering sites in Central Mexico [1,2]. What is unknown is whether the azimuthal position of the sun itself, or the pattern of polarized skylight, act as the main navigation cue and whether the butterflies exploit polarized skylight within a course control mechanism to fly straight. This question is of particular interest since recently a specialized dorsal rim area (DRA) was found in the monarchs’ complex eyes, strongly suggesting that the butterflies are able to perceive polarized light [3,4].

To investigate the monarchs’ use of polarized skylight for spatial orientation, migratory butterflies were tested in four Mouritsen-Frost flight simulators [1] that allowed the animals to orient freely in any geographical direction. An optical encoder recorded their instantaneous flight direction from which the mean flight direction and the directedness of each flight was calculated. As expected, the monarchs showed south-westerly orientation if they could see both the sun and the clear blue sky within a 120° visual field. However, if their visual field was restricted to 44° of clear zenithal sky that contained a high degree of polarized light, or a linear UV-transmitting polarizer, the butterflies oriented randomly. Thus we found no evidence that monarchs deduce their migratory direction from the polarization pattern of the sky in a time-compensated manner. Correcting each mean flight direction for the naturally occurring polarization angle in the zenith at the time of the experiment or for the orientation of the polarizer, revealed that the butterflies as a group did not show a line-up response towards linear polarized light. Nor did the monarchs respond to a 90° change in the orientation of the overhead polarizer. These results argue against the existence of a course control mechanism based on polarized skylight. If the DRA containing the polarization sensitive photoreceptors was painted out, the butterflies still exhibited clear south-westerly orientation to a 120° view of the sky including the sun.

Our study suggests that migratory monarch butterflies do not use polarized light for spatial orientation and that the sun plays the key role in the monarch’s time-compensated compass navigation.

### References:

1. Mouritsen, H. and Frost, B. J. (2002). Virtual migration in tethered flying monarch butterflies reveals their orientation mechanisms. P. Natl. Acad. Sci. USA 99, 10162-10166.
2. Froy, O., Gotter, A. L., Casselman, A. L. and Reppert, S. M. (2003). Illuminating the circadian clock in monarch butterfly migration. Science 300, 1303-1305.
3. Labhart, T. and Baumann, F. (2003). Evidence for a polarization compass in monarch butterflies. Proc. Neurobiol. Conf. Göttingen 29, 545.
4. Reppert, S. M., Zhu, H., and White, R. H. (2004). Polarized light helps monarch butterflies navigate. Curr. Biol. 14, 155-158.

## Polarization-sensitive neurons in the central complex of the cricket, *Gryllus bimaculatus*

Midori Sakura and Thomas Labhart

(E-mail: skr@zool.unizh.ch, labhart@zool.unizh.ch)

Department of Zoology, University of Zurich, Winterthurerstrasse 190,  
CH-8057 Zürich, Switzerland

Celestial compass navigation in insects, which relies on the polarization pattern of the sky, is a useful model to study the representation of space in an animal brain. Although the sensory mechanisms of polarization vision and navigation behavior have already been studied to some detail in several insect species, the central neural circuits that evaluate the sensory data and control motor output remain largely unknown. In crickets, sensory information on polarized light is integrated in the optic lobe by three types of polarization-sensitive neurons (POL-neurons) that are tuned to different e-vector orientations (Labhart and Meyer 2002, Curr Opin Neurobiol 12: 707-714). It is still unclear how the nervous system codes for actual e-vector orientation by using just three e-vector dependent signals. In a recent study, some neurons in the central complex of the locust brain showed polarization sensitivity. Based on these findings, it was suggested that the central complex plays a crucial role in polarization compass mediated navigation (Vitzthum et al. 2002, J Neurosci 22: 1114-1125). To clarify how e-vector orientation is coded in the insect brain, we studied the responses of polarization-sensitive neurons in the central complex of the cricket *Gryllus bimaculatus*.

Using intracellular recording and staining methods, we measured the activity of central complex neurons under a large-sized polarized stimulus ( $35^\circ$  in diameter) with slowly rotating e-vector (c.  $60^\circ/\text{s}$ ). The degree of polarization was either 99% or 58%, the latter being similar to strong natural polarization. We found that many neurons were polarization-sensitive, showing clear modulation of spike rate as a function of e-vector orientation (Fig. 1A).

Typically, these neurons had a cell body near the antennal lobe in the inferio-median protocerebrum and arborization areas in the lower part of the central body and in a brain area thought to be the lateral accessory lobe (Fig. 1B). Their shapes were quite similar to a certain type of polarization-sensitive tangential neurons in the central complex in locusts (Vitzthum et al. 2002, J Neurosci 22: 1114-1125).

Recent computational studies in our lab suggested the existence of a group of “compass neurons” in the insect brain, in which each neuron is tuned to a different e-vector orientation, i.e. each neuron represents a certain body orientation relative to the polarization pattern. Some of the central complex neurons showed indeed response properties that are expected for “compass neurons”, i.e. very low spontaneous spike activity, activation in a relatively narrow range of e-vector orientations, and sensory input from both eyes (Fig. 1). According to our hypothesis, the e-vector orientations producing maximal spike frequencies in compass neurons (tuning e-vector,  $\Phi_{\text{max}}$ ) should be equally distributed over the range of  $180^\circ$  to code exact e-vector orientation in the sky. So far,  $\Phi_{\text{max}}$ -values of the recorded neurons show a wide distribution from  $0^\circ$  to  $180^\circ$ , suggesting their possible function as compass neurons.

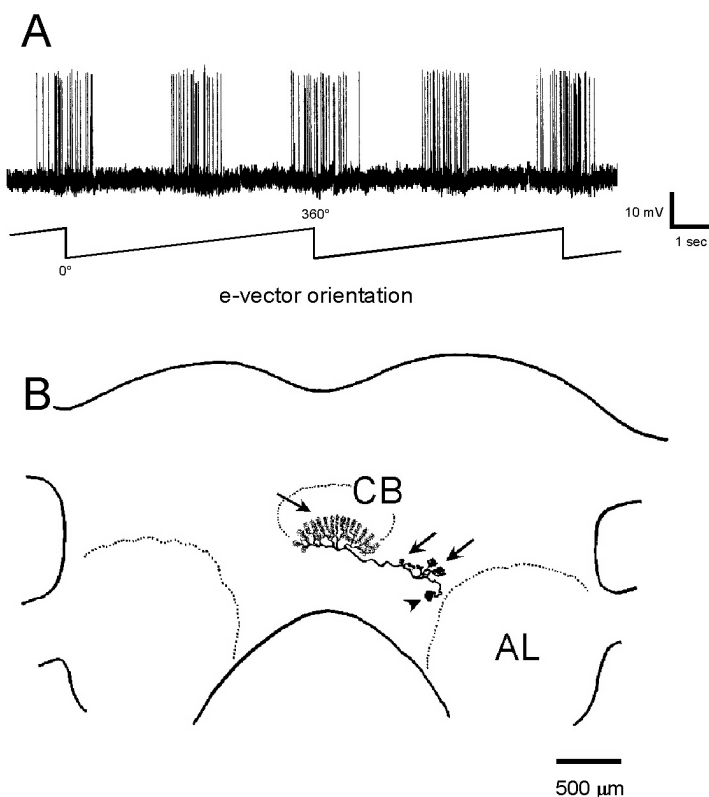


**Fig.1** Polarization-sensitive neuron in the central complex. (A) Intracellular recording under the 58% polarized light stimulus. The neuron shows spike activity in a relatively narrow range of e-vector orientations.  $0^\circ$  indicates e-vector parallel to the long axis of the head. (B) Morphology. The neuron was stained with Neurobiotin and traced using a camera lucida under the microscope. Arrowhead: cell body, Arrows: arborization areas, AL: antennal lobe, CB: central body of the central complex.

## Cricket polarization vision under difficult stimulus conditions

Miriam J. Henze and Thomas Labhart

(E-mail: miriam.henze@zool.unizh.ch, labhart@zool.unizh.ch)

Department of Zoology, University of Zürich, Winterthurerstr. 190, CH-8057 Zürich

Like several other arthropod species, field crickets (*Gryllus campestris*) have the sensory capability of polarization vision, which is believed to serve for navigation. Polarization vision in these insects can be tested by exploiting a spontaneous response: Tethered crickets treadmilling on an air-suspended ball adjust their turning tendency according to the *e*-vector orientation of a polarized light stimulus presented from above (Brunner D, Labhart T, *Physiol Entomol* 12:1-10, 1987).

In previous experiments an unnaturally high degree of polarization *d* (~ 100 %) was used to elicit this reaction. However, *d*-values observed in the sky do not exceed 75 % and are generally much lower (Horváth G, Wehner R, *J Comp Physiol A* 184:1-7, 1999). Consistent with the ecological circumstances, it was found that polarization-sensitive interneurons (POL-neurons) in the optic lobe of crickets can signal *e*-vector orientation at *d*-levels as low as 5 % (Labhart T, *J Exp Biol* 199:1467-1475, 1996). In the present study we are investigating the threshold for the behavioral response to polarized light in crickets. First results have shown that the reaction was independent of *d* down to a *d*-value of 20 % (Fig. 1 A, B). With further reduction of the polarization level, the response often became weaker. Nevertheless some individuals clearly responded to stimuli with *d*-values of only 6 % or even 4 % (Fig. 1 C). This high sensitivity might allow crickets to exploit polarized skylight even under unfavourable conditions such as haze or clouds.

In a second set of experiments we examine the procedure by which the nervous system extracts compass information from polarized skylight. Two alternatives were proposed in the literature (e.g. Wehner R, in: *Orientation and communication in arthropods*, Lehrer M (ed),

Birkhäuser 1997): (1) In the “sequential” procedure, the *e*-vector orientation is determined by comparing successive readings of POL-neurons while the insect rotates about its vertical body axis (scanning). Whenever a neuron exhibits maximal activity, this informs the animal that the *e*-vector of the stimulus is aligned with the *e*-vector tuning axis of the neuron. (2) In the “instantaneous” procedure, the simultaneously available signals of several POL-neurons with different tuning axes are compared. Detection of the *e*-vector is then possible at a glance, i.e. no body movements are required. Our results so far support the latter theory. This conclusion is based on the finding that crickets still responded to polarized light when they were rigidly fixed relative to the stimulus, thereby preventing them from performing any scanning movements. In future experiments we are also going to exclude scanning by presenting the stimulus as short flashes instead of continuously.

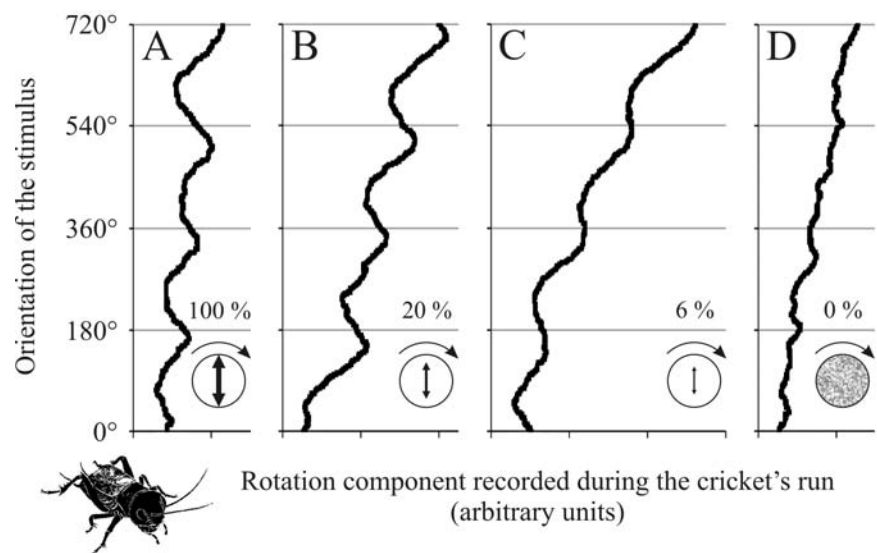


**Fig. 1 A-D:** Orientation response of a walking cricket to a visual stimulus presented from above. Exemplary results from one individual for different experimental conditions: (A) linearly polarized light from a rotating polarizer with degree of polarization *d* ~ 100 %, (B, C) as in A but *d*-value reduced to 20 % and 6 %, respectively, (D) unpolarized light from a rotating diffuser. In all diagrams the rotation component of the run is plotted as a function of the stimulus orientation. The animal's turning tendency modulates periodically with the orientation of the polarized stimulus even at the very low *d*-level of 6 %.

**Poster Subject Area #PSA12:**  
**Visual systems of vertebrates: Periphery**

- [#156A](#) ON. Dumitrescu and H. Wässle, Frankfurt/Main  
*Glutamate Receptor Expression in Amacrine Cells of Mouse Retina*
- [#157A](#) L. Heinze, SH. Haverkamp and H. Wässle, Frankfurt/Main  
*Differential Distribution of Glycine Receptor Subunits on Amacrine and Ganglion Cells in the Mouse Retina*
- [#158A](#) E. Ivanova and H. Wässle, Frankfurt/Main  
*Functional properties of glycine receptors in bipolar cells of the mouse retina.*
- [#159A](#) B. Müller and L. Peichl, Frankfurt/Main  
*Cone photoreceptors in the retinæ of microchiropteran bats.*
- [#160A](#) TW. Mühleisen and D. Schulte, Frankfurt/Main  
*The roles of cVax, Tbx5, and EphB receptor tyrosine kinases in axon fasciculation and intraretinal pathfinding*
- [#161A](#) H. Regus, S. tom Dieck, A. Fejtová, ED. Gundelfinger and JH. Brandstätter, Frankfurt/Main and Magdeburg  
*Molecular Dissection of the Early Postnatal Assembly of the Photoreceptor Ribbon Complex*
- [#162A](#) D. Brauner, J. Ammermüller, S. tom Dieck, ED. Gundelfinger and JH. Brandstätter, Frankfurt/Main, Oldenburg and Magdeburg  
*Plasticity in a Mutant Mouse Retina Lacking a Functional Bassoon Protein*
- [#163A](#) F. Schaeffel and C. Schmucker, Tuebingen  
*A battery of optical tests to measure visual function in mice*
- [#164A](#) H. Schmid and K. Kohler, Tuebingen  
*Immunohistochemical analysis of the porcine retina*
- [#165A](#) I. Chwalla, J. Fries, S. Bette and K. Kohler, Tuebingen  
*Localization of OPA1, the disease gene for autosomal dominant optic atrophy, in the retina of vertebrates*
- [#166A](#) J. Voss and H-J. Bischof, Bielefeld  
*Coordination of eye movements in the zebra finch*
- [#167A](#) M. Klar and K-P. Hoffmann, Bochum  
*Pretectal direction selective neurons in afoveate and foveate Teleost are important in the gain control of OKR and VOR*



- [#168A](#) B. Gürke and K-P. Hoffmann, Bochum  
*Projections originating from direction-selective neurons in the pretectum of the rainbow trout (Salmo gairdneri) to oculomotor structures*
- [#169A](#) GM. Zeck, Q. Xiao and RH. Masland, Boston (USA)  
*Functional diversity among ganglion cells in the rabbit retina*
- [#170A](#) A. Patrona and GN. Nöll, Giessen  
*Influence of Nitric Oxide on the recovery kinetics of flash responses of isolated frog rods*
- [#171A](#) V. Kozyrev and J. Kremers, Göttingen and Basel (CH)  
*Nonlinear lateral interactions in the visual perception and in the LGN neuronal responses*
- [#172A](#) G. Knop, F. Thiel, K. Hudl, M. Seeliger, UB. Kaupp and F. Müller, Jülich and Tübingen  
*Knock-out of HCN1 channels alters light-responses in the mammalian retina*
- [#173A](#) M. Wilms and R. Eckhorn, Marburg  
*Receptive fields of epiretinally recorded signals in cats: Spatial and temporal aspects*
- [#156B](#) J. Reiners, J. Harf, T. Märker, K. Jürgens and U. Wolfrum, Mainz  
*Expression and localization of the scaffold protein harmonin and its interaction partners at synapses*
- [#157B](#) P. Trojan, S. Rausch, A. Gießl, A. Pulvermüller, K-P. Hofmann and U. Wolfrum, Mainz and Berlin  
*Light-dependent phosphorylation of centrins in mammalian photoreceptor cells*
- [#158B](#) A. Gießl, A. Pulvermüller, P. Trojan, KP. Hofmann and U. Wolfrum, Mainz and Berlin  
*Differential expression and Ca<sup>2+</sup>-dependent interaction of the visual G-protein transducin with centrin isoforms in mammalian photoreceptor cells*
- [#159B](#) B. Reidel, A. Gießl, P. Trojan and U. Wolfrum, Mainz  
*Light-induced translocation of the signal transduction proteins transducin and arrestin analyzed in photoreceptor cells of organotypical retina culture*
- [#160B](#) T. Märker, J. Reiners, K. Jürgens, N. Overlack, T. Goldmann and U. Wolfrum, Mainz  
*The scaffold protein harmonin (USH1C) also integrates Usher syndrome 2 proteins into synaptic Usher protein complexes in retinal photoreceptor cells*
- [#161B](#) R-B. Schmidt-Hoffmann and C. Mora-Ferrer, Mainz  
*GLYCINE HAS NO EFFECT ON CONTRAST-SENSITIVITY OF GOLDFISH MEASURED WITH THE OPTOMOTOR RESPONSE*
- [#162B](#) C. Mora-Ferrer, C. Albrecht, B. Benkner, B. Lux, M. Gruber and K. Behrend, Mainz  
*EFFECTS OF GLUTAMATE ANTAGONISTS ON GOLDFISH TEMPORAL TRANSFER PROPERTIES MEASURED WITH THE ERG*

- [#163B](#) K. Dedek, S. Maxeiner, U. Janssen-Bienhold, J. Ammermüller, K. Willecke and R. Weiler, Oldenburg and Bonn  
*Connexin45 Deficiency in Retinal Neurons Leads to Impaired Visual Transmission*
- [#164B](#) T. Schubert, R. Weiler and A. Feigenpan, Oldenburg  
*Intracellular calcium is regulated by different pathways in horizontal cells of the mouse retina*
- [#165B](#) A. Thiel, M. Greschner and J. Ammermüller, Oldenburg  
*Retinal ganglion cell burst patterns are reproduced by a computational model of intraretinal processing*
- [#166B](#) L. van Ahrens, MT. Ahlers, M. Greschner, ED. Gundelfinger, JH. Brandstätter, D. Brauner and J. Ammermüller, Oldenburg, Magdeburg and Frankfurt/Main  
*Comparison of retinal ganglion cell responses from Bassoon deficient and wild type mice*
- [#167B](#) J. Shelley, K. Dedek, K. Schultz, P. Dirks, A. Schuldt, U. Janssen-Bienhold and R. Weiler, Oldenburg  
*Expression of Connexins in Horizontal Cells of the Mouse Retina*
- [#168B](#) L. Pérez de Sevilla and R. Weiler, Oldenburg  
*Displaced amacrine cells of the mouse retina*
- [#169B](#) U. Janssen-Bienhold, V. Gawlik, K. Schultz, P. Dirks and R. Weiler, Oldenburg  
*ZO-1 expression in the vertebrate retina and its co-localisation with connexin 43*
- [#170B](#) N. Jährling, K. Dedek, U. Janssen-Bienhold, S. Maxeiner, K. Willecke and R. Weiler, Oldenburg and Bonn  
*Immunohistochemical characterisation of connexin45 expressing bipolar cells in the mouse retina*
- [#171B](#) S. Bitzer, M. Goldbach, A. Bühlmann, S. Onat and P. König, Osnabrück and Zürich (CH)  
*Do stability and sparseness lead to binocular properties of simulated neurons comparable to physiology?*
- [#172B](#) M. Bongard and E. Fernandez, San Juan de Alicante (E)  
*Representation of optical illusions by retinal ganglion cell population*

**Glutamate receptor expression in amacrine cells of mouse retina*****Olivia N. Dumitrescu and Heinz Wässle****Max Planck Institute for Brain Research, Frankfurt am Main*

The mammalian retina contains over 20 morphological varieties of amacrine cell types. These interneurons receive excitatory glutamatergic input from bipolar cells and provide GABA- and glycinergic inhibition to other cells in the retina. Amacrine cells exhibit widely varying light evoked responses, in large part defined by their presynaptic partners. We wondered whether differential expression of glutamate receptors (GluRs) among amacrine cells might underlie some of this functional diversity.

In whole cell patch-clamp experiments on mouse retinal slices, we used selective agonists and antagonists to discriminate responses mediated by NMDA/ non-NMDA (NBQX) and AMPA/ KA receptors (GYKI 52446, cyclothiazide, SYM 2081). We sampled a large variety of individual cell types, which were classified by their dendritic field size into either wide field or narrow field cells after filling with LY or Neurobiotin.

All cells (n = 100) had good responses to non-NMDA agonists. AMPA R-specific responses could be obtained from almost all cells recorded (90% of the narrow field and 80% of the wide field cells), while KA R-selective drugs were also effective on the majority of the narrow field (85%) and wide field amacrine cells (80%). We could elicit small NMDA responses from most of the wide field cells tested (70%), whereas only a third (35%) of the narrow field amacrine cells reacted to NMDA.

Our data suggest that AMPA, KA and NMDA receptors (Rs) are differentially expressed among different types of amacrine cells rather than among populations with different dendritic coverage of the retina. Selective expression of kinetically different GluRs among amacrine types may be involved in generating transient and sustained inhibitory pathways in the retina. Since AMPA and KA Rs are not generally clustered at the same postsynaptic sites, a single amacrine cell expressing both AMPA and KA Rs may provide inhibition with different temporal characteristics to individual synaptic partners.

## Differential Distribution of Glycine Receptor Subunits on Amacrine and Ganglion Cells in the Mouse Retina

Liane Heinze, Silke Haverkamp, and Heinz Wässle

Department of Neuroanatomy  
Max-Planck-Institute for Brain Research  
Deutschordenstraße 46  
60528 Frankfurt

Glycine is a major inhibitory neurotransmitter of the mammalian retina, and glycine receptors (GlyRs) are expressed at synapses between amacrine, bipolar, and ganglion cells. GlyRs are ligand gated chloride channels, composed of ligand binding  $\alpha$  and structural  $\beta$  subunits. Molecular cloning has revealed 4 genes encoding  $\alpha$  subunits and one gene encoding the  $\beta$  subunit. In the retina, only three of the  $\alpha$  subunits ( $\alpha 1$ -3) are present. The properties of glycine receptors vary with their subunit composition, and therefore we addressed the question whether the various types of amacrine and ganglion cells accomplish their different functions by specifically expressing different GlyRs.

Shortly fixed (4% paraformaldehyde, 8 minutes) retinæ from thy1-GFP-transgenic mice (GFP-O line, Feng et. al. 2000) were processed for immunofluorescence double and triple labeling using specific antisera against the GlyR $\alpha 1$  (mAb2b, H. Betz, Frankfurt), GlyR $\alpha 2$  (goat, Santa Cruz) and GlyR $\alpha 3$  (rabbit, R. J. Harvey, London) subunit. The GFP-signal was enhanced immunocytochemically, and antibodies against Calretinin and Choline Acetyl Transferase (ChAT) were applied to define stratification levels within the IPL.

In every thy1-GFP retina, about 10 to 50 ganglion cells and a lower number of small-field amacrine cells were GFP-labeled. So far, 17 types of ganglion cells (classified according to Sun et. al. 2002) and about 10 types of amacrine cells have been identified. We found that GlyR $\alpha 1$  is expressed by the ganglion cell types A1, A2inner, A2outer and B1, whereas GlyR $\alpha 2$  is not expressed by these ganglion cell types. Instead, GlyR $\alpha 2$  preferentially co-localizes with the B3outer ganglion cell.

We found GlyR $\alpha 3$  to be distributed more widely, and it appears to be co-localized with several types of ganglion cells.

The amacrine cell types are currently under investigation but so far only a bistratified one (equivalent to the A8 amacrine cell in cat, Kolb et. al. 1981) has turned out to be colocalized with GlyR $\alpha 1$  and GlyR $\alpha 2$ .

Further work on the anatomical localization of GlyRs as well as electrophysiological experiments will shed light onto the specific role of the approximately 15 different glycinergic amacrine cell types and their postsynaptic partners in retinal function.

Supported by SFB 269/B4

## Functional properties of glycine receptors in bipolar cells of the mouse retina.

Elena Ivanova, Heinz Wässle

Department of Neuroanatomy  
Max-Planck Institute for Brain Research  
Deutschordenstraße 46  
60528 Frankfurt

Glycine receptors (GlyRs) are ligand-gated chloride channels. So far, four types of alpha and one type of beta subunits have been cloned. The channel isoforms exhibit functional differences and could be distinguished by electrophysiological methods. In the mammalian retina three types of alpha (alpha1, 2, 3) and one type of beta subunits were found immunocytochemically (Wässle et al., 1998; Haverkamp et al., 2003; Haverkamp et al., 2004) but little is known about the subunit composition and the functional properties of GlyRs in the subsets of the neurons.

GlyRs were studied in bipolar cells of the mouse retina using the patch-clamp technique. Functional properties of GlyRs were recorded in 200 voltage-clamped bipolar cells in retinal slice preparations. While recording, cells were filled with neurobiotin and Alexa488 dye, which allowed identification of bipolar cell types. On the basis of morphological criteria recorded and filled bipolar cells could be classified as 9 types of cone bipolar cells and one type of rod bipolar cell as previously described (Ghosh et al., 2003). In addition, a new method of prelabeling OFF-bipolar cells for patch-clamp recording was established.

By puffing glycine in different concentrations onto the inner plexiform layer we measured a dose-response curve and the maximal amplitude of glycine-evoked currents. Cone bipolar cells stratifying in the OFF-sublamina show large glycine-evoked currents. In the ON-sublamina, glycine-evoked currents were recorded in rod bipolar cells. ON-cone bipolar cells show small or no glycine-evoked currents, probably due to the low expression level of GlyRs.

Among all bipolar cell types, which express GlyRs, the affinity of GlyRs for glycine was similar. When glycine was coapplied with 50  $\mu$ M picrotoxinin (a blocker of homooligomeric GlyRs) the amplitude of glycine response was only slightly reduced suggesting that GlyRs in bipolar cells are heterooligomeric channels composed of alpha and beta subunits.

In order to further characterize the subunit composition of GlyRs, the inhibitory postsynaptic currents (IPSCs) were analyzed in different bipolar cell types. In the presence of GABA<sub>A</sub>R blocker bicuculline and GABA<sub>C</sub>R blocker TPMPA spontaneous glycinergic IPSCs were recorded in all OFF-bipolar cells. In rod bipolar cells glycinergic IPSCs could be induced by coapplication of high potassium concentrations with GABA receptor blockers. In all the cells recorded, glycinergic IPSCs could be blocked by 1  $\mu$ M strychnine. The amplitude and the decay time of IPSCs were analyzed in detail. The largest IPSCs were found in OFF-bipolar cells. Two groups of glycinergic IPSCs were detected in bipolar cells: fast  $\tau = 5$  ms and slow  $\tau = 10$  ms. The frequency of these two types of glycinergic IPSCs in bipolar cells was different and bipolar cell type specific. In Type 1, 2 and 4 cone bipolar cells the fast IPSCs were predominant. In Type 3 cone bipolar cells and in rod bipolar cells the slow IPSCs were encountered more frequently.

Further investigation of alpha3 knock-out mouse (Harvey et al., 2004) and alpha1 oscillator mouse (Buckwalter et al., 1994) will show the functional significance of glycine receptor isoforms in the retina.

Cone photoreceptors in the retinae of microchiropteran bats.

Brigitte Müller and Leo Peichl

Max Planck Institute for Brain Research

Deutschordenstr. 46, D-60528 Frankfurt am Main, Germany

Bats of the suborder Microchiroptera (microbats) are strongly nocturnal and most famous for their echolocation. Their eyes are commonly small and vision is considered a less important sense for them. Many older histological studies have described microbat retinae as pure rod retinae. On the other hand, an ERG study has reported a cone mechanism in four microbat species (Hope & Bhatnagar, 1979). For one vespertilionid microbat, a recent molecular genetic study has shown the presence of the typical two mammalian cone opsins: a middle-to-long-wave sensitive (L) opsin and a short-wave sensitive (S) opsin (Wang et al., 2004). For a better understanding of the photoreceptor complements in microbats, and of their prospects for cone-based vision (including colour vision) at dusk and dawn, we have started a comparative study across microbat superfamilies.

Here we report the results on eleven species from the superfamilies Emballonuridea, Rhinolopoidea and Vespertilionidea. Eyes were obtained from individuals sacrificed for taxonomic studies (kindly provided by S. M. Goodman, The Field Museum Chicago). In paraformaldehyde-fixed retinae, the spectral cone types were assessed using the antisera JH492 against the L-cone opsin and JH455 against the S-cone opsin (kindly provided by J. Nathans, Baltimore). These antisera are known to reliably label the respective cone types across mammals. Rod densities were assessed by conventional histology.

The retinae of all studied species are rod-dominated but possess significant cone populations. All eight vespertilionid and the one emballonurid species investigated have immunoreactive L-cones as well as S-cones. Depending on the species, L-cone densities are in the range of 5.000-10.000/mm<sup>2</sup> and S-cone densities in the range of 2.500-5.000/mm<sup>2</sup>. Hence the ratio of L-cones to S-cones is around 2:1. This would allow dichromatic colour vision, provided the necessary postreceptoral circuits for colour processing are present. In contrast, the two rhinolopoid species studied show only L-opsin immunoreactivity and no S-opsin-immunoreactivity, indicating L-cone monochromacy.

A preliminary assessment of rod densities at selected retinal locations yielded 215.000 rods/mm<sup>2</sup> in *Tadarida jugularis*, 235.000-330.000/mm<sup>2</sup> in *Myotis goudoti* (both Vespertilionidea), and 130.000-175.000/mm<sup>2</sup> in *Emballonura atrata* (Emballonuridea). With an overall cone density of 7.500-15.000/mm<sup>2</sup> in *E. atrata* this corresponds to a rod/cone ratio of roughly 13:1 (7% cones). If these data are representative, they indicate significantly lower rod densities and higher cone proportions than found in some other nocturnal mammals, e.g. in mouse (440.000 rods/mm<sup>2</sup> and 3% cones; Jeon et al., 1998) and in African giant rats (400.000-700.000 rods/mm<sup>2</sup> and 0.5% cones; Peichl & Moutairou, 1998). It appears that the eyes of microbats have adapted to somewhat higher light levels and may be useful for visual orientation at dusk and dawn. Ethological studies have shown the importance of vision for bats as an indispensable information channel in various behavioural activities.

## **The roles of cVax, Tbx5, and EphB receptor tyrosine kinases in axon fasciculation and intraretinal pathfinding**

Thomas W. Mühleisen and Dorothea Schulte  
Abteilung Neuroanatomie, Max-Planck-Institut für Hirnforschung,  
Deutschordenstr. 46, D-60528 Frankfurt/Main, Germany

During vertebrate eye development, gradually expressed molecules pattern the neural retina along three major axes, the temporal-nasal, the dorsal-ventral (D-V) and the central-peripheral. This axial polarity is reflected in the mapping preferences of retinal ganglion cell (RGC) axons while they project to their major midbrain target, the optic tectum of non-mammalian vertebrates or its mammalian homologue, the superior colliculus.

Early born RGCs are located in the central region of the retina, a short distance away from the optic disc. Later differentiated RGCs are added in progressively more peripheral retinal regions. Therefore, younger RGC axons growing towards the optic disc encounter the axons of older RGCs and fasciculate with these axons to form small bundles or fascicles. In the chick, but not the mouse, the thickness of axon fascicles differ remarkably between the dorsal and ventral retina: the ventral RGC axons exhibit a stronger fasciculation forming thicker bundles than their dorsal counterparts.

To study whether this difference depends on D-V axial polarity of the early retina, we ectopically expressed two key components of retinal D-V axis specification, the dorsal T-box transcription factor Tbx5, or the ventral homeodomain protein cVax (Schulte *et al.*, 1999; Kosiba-Takeuchi *et al.*, 2000). After retroviral misexpression of cVax, dorsal RGC axons consistently fasciculated stronger than dorsal RGC axons from wild type animals. Thus, ectopic cVax expression was sufficient to ventralize the fasciculation of dorsal RGC axons. Ventralization of dorsal RGC axons was also achieved by misexpression of a dominant-negative allele of Tbx5 (Tbx5 $\Delta$ EnR) comprising a fusion of the DNA-binding domain of Tbx5 and the engrailed repressor (EnR) domain (Rallis *et al.*, 2003). Ectopic expression of Tbx5, however, did not alter the fasciculation of ventral RGC axons. This suggests that Tbx5 and/or other dorsally expressed T-box factors also influence the strength of RGC axon fasciculation.

Ectopic expression of cVax or Tbx5 leads to expression changes of ventral EphB receptor tyrosine kinases and dorsal ephrin-B ligands as well as to severe defects in retinotectal map formation (Schulte *et al.*, 1999; Koshiba-Takeuchi *et al.*, 2000). To investigate whether the EphB / ephrin-B system is involved in the regulation of RGC axon fasciculation, we stimulated EphB receptors by misexpression of ephrin-B2. This resulted in defects in axons fasciculation and pathfinding within the ventral retina.

Taken together, our experiments show that cVax and Tbx5 not only contribute to retinotectal map formation but also to the regulation of intraretinal RGC axon fasciculation. In addition, our data indicate a novel function of EphB receptor tyrosine kinases in fasciculation of ventral RGC axons.

Koshiba-Takeuchi, K. *et al.* (2000). *Science* 287: 134-137.  
Rallis C *et al.* (2003). *Development* 130(12): 2741-2751.  
Schulte, D. *et al.* (1999). *Neuron* 24: 541-553.

## **Molecular Dissection of the Early Postnatal Assembly of the Photoreceptor Ribbon Complex**

Hanna Regus<sup>1</sup>, Susanne tom Dieck<sup>1,2</sup>, Anna Fejtová<sup>2</sup>, Eckart D. Gundelfinger<sup>2</sup>, Johann H. Brandstätter<sup>1</sup>

1) Department of Neuroanatomy, Max Planck Institute for Brain Research, Frankfurt, Germany, 2) Leibniz Institute for Neurobiology, Magdeburg, Germany

Bassoon and Piccolo, two giant proteins of the cytomatrix at the active zone (CAZ), play prominent roles at chemical synapses in the CNS. During synaptogenesis, they are the earliest proteins to appear at newly formed synaptic sites, where they are delivered on specialized transport vesicles. These "active zone precursor vesicles", which contain multiple active zone components, are suggested to lead to the rapid formation of new active zones on fusion with the presynaptic plasma membrane.

In an earlier study, we have shown that the mature photoreceptor ribbon complex consists of two separate molecular compartments: a ribbon-associated and an active zone compartment; both are composed of a set of CAZ proteins. Bassoon links the two compartments and is responsible for the physical integrity of the ribbon complex. In this study, we have examined the molecular assembly of the ribbon complex during photoreceptor synaptogenesis with immunocytochemistry and confocal laser-scanning microscopy and biochemistry.

Immunofluorescent aggregates of the ribbon-associated proteins Bassoon, Piccolo, RIBEYE and RIM1 are found in the neuroblast layer of the postnatally developing retina at the earliest time point examined, the day of birth. The proteins are transported together in a complex to the developing photoreceptor terminals, which form the outer plexiform layer at the end of the first postnatal week. As they seem much larger, the protein aggregates are presumably not identical to the 80 nm "active zone precursor vesicles" described in brain. In contrast to the ribbon-associated proteins, the active zone proteins Munc13-1, RIM2, ERC2/CAST1, a Ca<sup>2+</sup>-channel  $\alpha$ 1-subunit, and the kinesin motor protein KIF3A are detected earliest at P4, the time point when the first photoreceptor ribbon synapses form. As soon as the active zone proteins are detectable, they always colocalize with the ribbon-associated proteins.

From these data we conclude that the proteins of the ribbon-associated compartment are transported separately from the proteins of the active zone compartment to the future photoreceptor ribbon synaptic sites. The proteins of the active zone compartment become visible upon clustering at the developing ribbon synaptic sites in the photoreceptor terminals.

Supported by a DFG grant (SFB269/B4) to J. H. B.



## **Plasticity in a Mutant Mouse Retina Lacking a Functional Bassoon Protein**

Dana Brauner<sup>1</sup>, Josef Ammermüller<sup>2</sup>, Susanne tom Dieck<sup>1,3</sup>, Eckart D. Gundelfinger<sup>3</sup>, Johann H. Brandstätter<sup>1</sup>

1) Department of Neuroanatomy, Max Planck Institute for Brain Research, Frankfurt, Germany, 2) Institute for Zoology, Oldenburg, Germany, 3) Leibniz Institute for Neurobiology, Magdeburg, Germany

In a mutant mouse retina lacking a functional Bassoon protein, the photoreceptor ribbons are not anchored to the presynaptic membrane and photoreceptor synaptic transmission is greatly impaired. We studied the long time effects of the lack of Bassoon on the structure and function of the retina.

With immunocytochemistry and confocal laser-scanning microscopy, we examined the neurons and synapses in wild-type and mutant retinæ from postnatal week 1 up to 1-2 years postnatally. In a functional analysis, ERG recordings of wild-type and mutant retinæ were performed at different postnatal stages.

Up to 2 weeks postnatally, wild-type and mutant retinæ are indistinguishable by their structure. Between postnatal week 2 and 3 first few horizontal cell processes and bipolar cell dendrites in the mutant retina arborize in the outer nuclear layer. Here they contact ectopic synaptic sites which appear around the same time. Ectopic synapses are formed only by rods and not by cones. With increasing age, the number of ectopic synaptic sites, the number of sprouting processes and their branching density gradually increases. The structural and synaptic alterations in the outer retina of the mutant mouse are reflected in the ERG recordings. Mutant mice younger than 1 month show little to no b-wave and are practically blind. In older mutant mice it was possible to record a scotopic ERG. The b-wave, however, developed significantly slower, lasted longer and its amplitude was significantly smaller compared to wild-type littermates.

Loss of Bassoon prevents normal photoreceptor synaptic development and signaling. Strikingly, the mutant retina shows a yet unknown reactive plasticity with the genesis of ectopic photoreceptor synapses and the partial restoration of photoreceptor synaptic transmission. Only the rod system but not the cone system has this regenerative power. Supported by a DFG grant (SFB269/B4) to J.H.B and EU grant "CORTIVIS" to J.A.

## A battery of optical tests to measure visual function in mice

Frank Schaeffel, Christine Schmucker

Section of Neurobiology of the Eye, University Eye Hospital, Calwerstr. 7/1, 72076 Tübingen  
e-mail: frank.schaeffel@uni-tuebingen.de

**Introduction:** To study the mechanisms of myopia development, mice offer a number of advantages over the chicken model, including that knock-out models are available, that they can be easily bred, that their genome is extensively studied and that there is abundant information on their physiology. On the other hand, their eyes are small and vision is probably not their predominant sense. Also, there is a lack of techniques to study visual function and ocular biometry in vivo. Therefore, we have developed and tested a number of techniques to bridge this gap.

**Methods:** (1) Refractive state is measured in alert mice that are gently restrained by holding their tails, by automated infrared photoretinography at 25 Hertz sampling rate from 60 cm distance. This technique uses the light of infrared light emitting diodes to create a brightness gradient in the pupil of the mouse that is dependent on the refractive error relative to the camera. The brightness gradient is automatically quantified by digital video image processing. (2) The pupil response to light is recorded using the same video platform as in (1). A set of green light emitting diodes, which is attached to the camera, can be flashed from the key board. Pupil responses are recorded at standard video frequency (25 Hz). Further software automatically determines amplitudes and latencies of the pupil responses. (3) Ocular biometry in the mouse eye requires very high spatial resolution since one diopter of refractive error is equivalent to only about 4  $\mu\text{m}$  in axial length difference<sup>1</sup>. We have successfully applied low coherence laser interferometry, using a newly developed device, the Zeiss Meditec ACMaster (Carl Zeiss, Jena). This device was originally developed for high-resolution biometry in the anterior segment of human eyes, but can also resolve differences of only about 10  $\mu\text{m}$  in axial eye length in living mice. (4) To determine visual acuity in wildtype mice and mutants, an automated optomotor device was developed. Individual mice in the center of a large rotating optomotor drum, with stripe patterns of different spatial frequency, were tracked by a self-programmed video system and their bias to move in the direction of the moving stripes was automatically statistically analyzed.

**Results:** (1) Refractive errors can be determined with a resolution of less than 3 diopters. If the eyes were covered by frosted diffusers for 2 weeks, about 3 diopters of myopia could be induced<sup>2</sup>. (2) Among other findings, it could be observed that a single drop of 0.1% atropine blocks the pupil responses for almost 300 hours<sup>3</sup>. (3) It could be shown that covering the eye with a frosted diffuser produces axial elongation<sup>4</sup>, in line with the refractive findings in (1), and in other animal models. (4) In the optomotor set-up, the visual acuity of the mice was 0.3-0.4 cyc/deg. This was only achieved at an illuminance of 400 lux. Acuity declined severely with decreasing illuminance. Mutant mice lacking either rods or cones showed that the high acuity system in the mouse is apparently the rod system, not the cone system<sup>5</sup>.

**Conclusion:** Although the mouse is a demanding model of myopia research, the presented battery of techniques permits to study the typical questions.

Supported by the Fortune Program of the Medical Faculty of the University Tuebingen to CS.

References: 1. Schmucker & Schaeffel, Vision Res. 2004;44:1857-1867; 2. Schaeffel et al, Optom Vis Sci. 2004;8:99-110; 3. Schaeffel & Burkhardt, submitted; 4. Schmucker & Schaeffel, Vision Res. 2004;44:2445-2456; 5. Schmucker et al, submitted.

## **Immunohistochemical analysis of the porcine retina**

**Heiko Schmid, Konrad Kohler**

*Forschungsstelle für Experimentelle Ophthalmologie, Universitäts-Augenklinik Tübingen, Röntgenweg 11, 72076 Tübingen, Germany*

In recent years the pig has received growing importance as animal model in life science and as an alternative to the ethically problematic and costly use of non-human primates in this field. The pig's close similarity to humans in organ size and physiology have lead to its usage as a source for xenotransplants, in experimental surgery and even as a model for hereditary diseases. Research on visual diseases has put force on the development of a transgenic swine with a mutation in the rhodopsin gene; like patients with the same mutation, these swine manifest the symptoms of retinitis pigmentosa, a human retinal degeneration. In addition, pigs have been utilized to analyse function and biocompatibility of so called retinal prosthesis, microchips implanted into the eye to compensate the loss of photoreceptors and to restore vision. Due to the cone dominated structure of its retina and its human-like size the porcine eye clearly outplay the rodent models normally used in this research area.

To establish a basis for a direct comparison with the cell types present in other animal models used in retinal research and in the human retina we here describe the cellular organization of the porcine retina. For this task a series of 42 different antibodies were applied to cryo-sections of the porcine retina. The applied markers were categorized into the following groups: 1) antibodies against different types of photoreceptors, i.e. rhodopsin for rods, and JH 492/JH 455 for cones; 2) antibodies against calcium-modulating proteins, such as PKC, calbindin, recoverin, calbindin or parvalbumin; 3) antibodies against different neurotransmitter systems or neuromodulators such as GABA, glutamate, ChAT, biogenic amines, neuropeptides, neurotrophic factors; 4) antibodies that recognize receptors and ion-channels, e.g. NMDA and non-NMDA receptors, purinergic receptors; 5) antibody directed against intracellular structures such as PSD-95, SV-2, SNAP-25, synaptophysin, syntaxin 3, bassoon, kinesin II; 6) antibodies against glia-cells (GFAP, vimentin, glutamine synthetase); 7) antibodies correlated with human degenerative retinal diseases, e.g. autosomal dominant optic atrophy. Double-labeling was used to further sub-group cell populations of a uniform pattern. Most of the markers revealed a great similarity in their distribution when compared to other mammals. However, there were also differences in the staining pattern between porcine and rodent retinas, for instance in OPA1 expression, the protein involved in human optic atrophy.

## **Localization of OPA1, the disease gene for autosomal dominant optic atrophy, in the retina of vertebrates**

Ilona Chwalla<sup>1</sup>, Julia Fries<sup>1</sup>, Stefanie Bette<sup>2</sup>, Konrad Kohler<sup>1</sup>  
Experimentelle Ophthalmologie<sup>1</sup> und Molekulargenetisches Labor<sup>2</sup>, Universitäts-Augenklinik, Röntgenweg 11, 72076 Tübingen, Germany

Autosomal dominant optic atrophy is a hereditary disorder characterized by progressive loss of vision and caused by mutations in a dynamin-related gene, *OPA1*, which translates into a protein with a mitochondrial leader sequence. We report here on localization of the *OPA1* gene in the rodent retina and the OPA1 protein in different vertebrate species, including men. The expression pattern of *OPA1* was investigated by RNA *in situ* hybridization. A polyclonal OPA1 antiserum was used that recognizes the C-terminal domain of the OPA1 protein; this OPA1-sequence is highly conserved within the line of vertebrates (e.g. 100% between human, rodents, and salmon). The antibody was used for fluorescence and DAB immunocytochemistry on radial sections of the retina and on flat mounts. To further characterize the OPA1 positive neurons, retinal ganglion cells were retrogradely labeled by fluoro-gold in rats and double labeling with specific cell markers was performed in different species.

The *OPA1* gene was expressed in the ganglion cell layer (GCL), and in the innermost and outermost row of the inner nuclear layer (INL) in the rodent retina. This general pattern was confirmed with the OPA1 antibody for all species examined (Zebrafish, Xenopus, chicken, rat, mouse, pig, human). Double labeling revealed the presence of OPA1 in horizontal and amacrine cells, among these in starburst amacrine cells, both of which are involved in lateral signal processing within the retina. In the GCL, OPA1 was found in the ganglion cells themselves as well as in displaced amacrine cells as shown by retrograde labeling, cell counts, and a cell size criterion. Interestingly, only in pigs and men OPA1 was present in the nerve fiber layer (NFL), i.e. in the axons of the ganglion cells which form the optic nerve; in all other species neither the NFL nor the optic nerve itself was OPA1 positive. There was no expression in photoreceptors even though photoreceptors are the cells with the highest metabolic turnover and hence the highest density of mitochondria. This indicates a specific role for OPA1 in signal processing rather than in the requirement of mitochondrial energy supply in the retina.

Our data suggest an important and specific function of the OPA1 protein not only in the optic nerve forming ganglion cells but also in the intrinsic signal processing of the inner retina.

## Coordination of eye movements in the zebra finch

Joe Voss and Hans-Joachim Bischof

Department for Behavioral Research  
University of Bielefeld  
PO Box 100131  
33501 Bielefeld  
Germany  
Email: joe.voss@uni-bielefeld.de

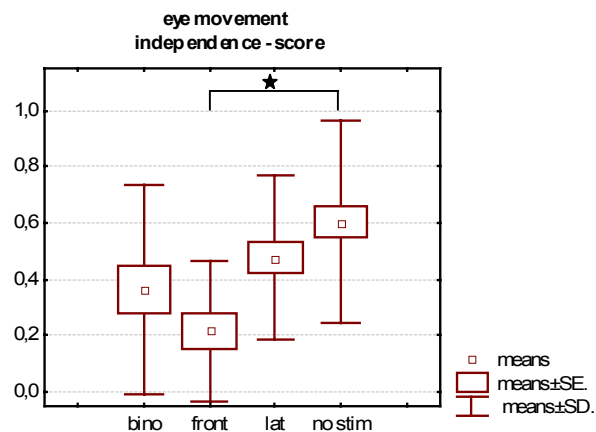
Zebra finches have laterally placed eyes with diverging foveal axes. The birds are looking into two largely separated visual hemifields with a small overlapping area at the frontal part. Compared with visual systems that use frontally directed eyes – like in humans - vision with lateral eyes needs an elementary different processing of visual information. The two images coming from the left and right hemifield contain different information, and it is still unknown whether the birds are integrating this to a single percept or whether they possess a neuronal mechanism that shifts the attention to either the right or the left eye.

One approach to obtain information about the interaction of the eyes is the monitoring of eye movements. We developed an **eyetracking system for laterally eyed birds**, which acquires movements of both eyes, simultaneously, under a variety of stimulus conditions.

In our first experiment we evaluated latencies between stimulus presentation and fixating eye movements. Stimuli were static and moving objects, presented with TFT screens in the frontal area (front), in one lateral visual field (lat) or simultaneously in both lateral fields (bino). In another condition no stimulus was presented (no stim). The experiment shows that the birds have at least two different viewing modes in which the eyes are moved either simultaneously or independently. After calculating an “independence score”, statistical analysis of the data showed significant differences in the occurrence of simultaneous and independent eye movements (ANOVA;  $N=110$ ;  $H=15,6$ ;  $p=0,0014$ ).

Comparison of the single groups revealed a significant difference in the occurrence of independent eye movements after a frontally presented stimulus and in a condition without any stimulus (Kruskal-Wallis;  $p=0,0017$ ).

In a further evaluation we will compare the trajectories of time correlated movements of the left and the right eye.



Supported by the Deutsche Forschungsgemeinschaft (BI 245/16)

## Pretectal direction selective neurons in afoveate and foveate Teleost are important in the gain control of OKR and VOR

M. Klar, K.-P. Hoffmann

Allg. Zoologie & Neurobiologie  
Ruhr-Universität Bochum  
D-44780 Bochum, Germany

Optokinetic stimulation displayed nearly symmetrical gain of the monocular horizontal optokinetic reflex (mhOKR) in the rainbow trout. We also showed in electrophysiological experiments the function and location of direction selective neurons in a subregion of the rainbow trout's pretectum. During optokinetic stimulation, these neurons exhibit comparable activation characteristics as neurons in the accessory optic system of other vertebrates. In contrast to other vertebrates, the neurons of the rainbow trout encode horizontal and vertical visual directions in one nucleus (Klar & Hoffmann, 2002). With lesion experiments in the rainbow trout's pretectum, we pointed out the involvement of pretectal direction selective neurons in the slow phase of the horizontal optokinetic eye movements (hOKN). After lesion the gain of the mhOKR dropped down. In this sequence of experiments in the rainbow trout it was not possible to elicit the vertical OKR (roll direction).

Our hypothesis is, that the vertical visual direction information of the rainbow trout's pretectal neurons is used to optimize the gain of the vertical vestibulocular reflex (VOR). Additionally, we found that the foveate fish species *Serranus cabrilla* is able to perform a vertical OKN. Thus, we tested the gain of horizontal and vertical OKN and VOR before and after lesion to analyze the influence of the pretectal direction selective neurons.

For visual stimulation we used a random dot pattern inside a cylinder (diameter = 20cm). The fish was centred positioned. The OKR in the horizontal and vertical plain, were tested monocularly in clock wise and counter clock wise direction (cw / ccw) at 4, 9, 18, 24°/s. Four different paradigms of sinuoidal stimulation were used in the horizontal and vertical VOR experiments. A : the fish is moved exactly with the random dot pattern. B : the fish is moved and the surrounding random dot pattern stands still. C: the fish is moved and the random dot pattern turns with the same velocity in the opposite direction. D: the fish is moved in darkness. Eye positions were recorded with the search coil technique.

The electrophysiological localization of the pretectal direction selective neurons, as tested with a random dot pattern inside a perimeter generated by a planetarium. Single unit recording were made with a tungsten mikroelectrode. Lesions are made with 20µA over 20 sec.

In the afoveat rainbow trout the gain in the different horizontal and vertical VOR paradigms was as follows: in A the gain is low (0.58 / 0.3) and no VOR cancellation was found. In B, the gain is higher (0.7 / 0.52). Highest gain can be seen in C (0.8 / 0.68). Stimulation in darkness showed the lowest gain (0.32 / 0.25). The gain of the horizontal VOR plain was always higher as in vertical plain. This results in the rainbow trout display clearly the visual influence to the VOR in both plain, the vertical and horizontal direction.

The experiments with the foveate *Serranus cabrilla* showed, that all tested fish have nearly a symmetric mhOKR in the horizontal stimulus directions. Additionally we could activate a vertical OKR and found asymmetries in the gain with a up to down preferred direction. The results in the VOR experiments was comparable with the rainbow trout.

After pretectal lesion we in *Serranus cabrilla* similar deficits were found in the gain of the OKR and VOR. The gain drops down in cw or ccw directions in the horizontal or vertical stimulus plain depending on the lesion sites in different fish.

The results suggest, that these pretectal direction selective neurons have an important influence on the gain control of the OKR and VOR in horizontal as well as vertical direction and that functional group for different direction are located in different parts of the area pretectalis (APT).

Acknowledgements: We thank all students of the excursion "Neurobiologie und Entwicklungsbiologie mariner Organismen" Banyuls-sur-mer 2004.

# Projections originating from direction-selective neurons in the pretectum of the rainbow trout (*Salmo gairdneri*) to oculomotor structures

B. Gürke, K.-P. Hoffmann

Allg. Zoologie & Neurobiologie  
Ruhr-Universität Bochum  
D-44780 Bochum, Germany

In this study we investigated the neuronal substrate for optokinetic eye movements in the rainbow trout. Recently, Klar & Hoffmann (2002) described the functional characteristics of direction selective neurons in the pretectum of the trout and compared them with neurons of the accessory optic system in other vertebrates. We hypothesised that these direction selective neurons in the pretectum are the neuronal substrate for optokinetic eye movements and provide visual input to modulate the VOR.

Intraocular tracer injections with tetramethylrhodamine-dextran (RD) revealed clearly labelled retinorecipient pretectal nuclei. One of these nuclei was the area praetectalis (APT). This area in the dorsal pretectum corresponds to the location of direction selective neurons described by Klar & Hoffmann (2002).

Iontophoretic RD applications were performed at the recording sites of direction selective neurons with a clear preferred direction. After iontophoretic RD-injection into the APT we found retrogradely labelled ganglion cells in regions with high ganglion cell density, namely the temporal area, the nasal area and the visual streak of the contralateral retina.

Anterograde tracer transport to the hindbrain originating from the APT clearly labelled the region of the nucleus oculomotorius, nucleus trochlearis and nucleus abducens, the oliva inferior and a medio-ventral region of the hindbrain which is thought to be the nucleus praepositus hypoglossi-equivalent of fish (Pastor et al., 1994; Aksay et al., 2000). Furthermore, we found a direct projection to the ipsilateral vestibulocerebellum. This projection was confirmed with retrograde tracing methods: after unilateral injections of Fluoro-Gold into the vestibulocerebellum retrogradely labelled neurons were found in the ipsilateral APT.

These results indicate that the pretectal direction selective neurons in the rainbow trout described by Klar & Hoffmann (2002) are situated in the APT and are part of the neuronal circuitry underlying the optokinetic reaction.

## References:

- Aksay, E., Baker, R., Seung, H. S. & Tank, D. W., 2000. Anatomy and discharge properties of premotor neurons in the goldfish medulla that have eye-position signals during fixation. *J. Neurophysiol.* 84, 1035-1049.
- Klar, M. & Hoffmann, K. P., 2002. Visual direction-selective neurons in the pretectum of the rainbow trout. *Brain Res. Bull.* 57, 431-433.
- Pastor, A. M., De La Cruz, R. R. & Baker, R., 1994. Eye position and eye velocity integrators reside in separate brainstem nuclei. *J. Neurophysiol.* 91, 807-811.

## Functional diversity among ganglion cells in the rabbit retina

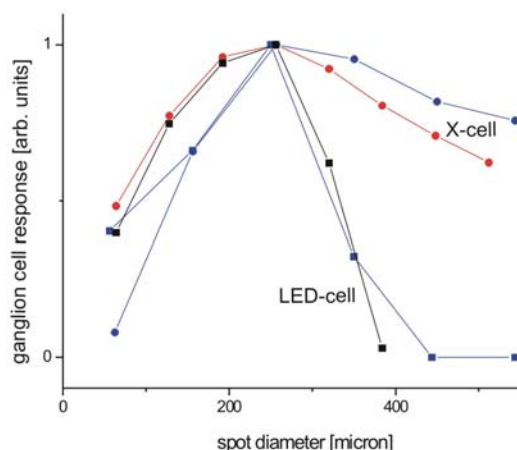
*Günther M. Zeck, Q. Xiao and Richard H. Masland*

*Massachusetts General Hospital and Harvard Medical School, Boston, U.S.A.*

How does the rabbit use its about a dozen different retinal ganglion cell types for vision ? In the present study we focused on the most numerous cell type, the “local edge detecting” (LED) cells [1] and compared their electrophysiological behavior with other cell classes.

The activity of ganglion cells in a small patch of the retina (500 x 500 micron) was recorded with multi-electrode arrays (MEA) with dense electrodes. Cells were stimulated with a battery of different visual stimuli centered on their receptive field. This enabled us to distinguish cell types.

Electrophysiological results together with morphological data [2] were combined to build a simple computational model of the rabbit retina. The model contains the five major retinal cell classes. Ganglion cell specificity is achieved by appropriate filter properties in the retina. The correspondence of the filters with retinal anatomy will be discussed.



Comparison of electrophysiological experiment and simulation for an area-response protocol in the rabbit retina. Ganglion cell response to centered spot stimuli is recorded with a multielectrode-array for a “local-edge detecting” cell and a X-cell in the same retinal patch. Data points in blue represent experimental results, in black simulation results for LED cells and in red for X-cells.

We compared simulated image computation for arrays of “local edge detecting” ganglion cells and arrays of classic luminance detectors - the X-like cells. Our results show that LED cells respond only to particular features in a natural scene. They recognize small, isolated objects but do not respond to high textured images. In contrast the output of the X-cell array resembles the initial image.

[1] Levick, W.R. (1967) *Journal of Physiology*, 188, 285-307

[2] Rockhill, R.L., Daly, F.J., MacNeil, M.A., Brown, S.P., & Masland, R.H. (2002) *Journal of Neuroscience*, 22, 3831-3843.

(G.M.Z. is supported by the Emmy Noether Program of the Deutsche Forschungsgemeinschaft)



## Influence of Nitric Oxide on the recovery kinetics of flash responses of isolated frog rods

Aikaterini Patrona, Gottfried N. Nöll

Physiologisches Institut, Justus-Liebig-Universität, Aulweg 129, 35392 Giessen, Federal Republic of Germany

**Abstract.** cGMP is a major second messenger in the visual transduction pathway. Flash response recovery of photoreceptors is the result of several biochemical reactions that end up with restoring the cGMP-concentration to preillumination levels. Substances affecting the cGMP-concentration in the photoreceptor outer segment could play a modulating role in the recovery process of the light response.

Nitric oxide is known to increase the formation of cyclic GMP in several tissues through the activation of soluble guanylate cyclases. Its endogenous synthesis was demonstrated in several cell types in the retina. Since rod outer segments are reported to contain guanylate cyclase activity in the cytosol, which is highly activated by nitroprusside, a nitric oxide generating agent, it was goal of this study to examine the influence of sodium nitroprusside on the kinetics of light responses of intact photoreceptors. We investigated the effect of extracellularly applied nitroprusside on the amplitude and recovery time of flash responses of isolated dark-adapted rods of the frog *Rana temporaria* using the pipette suction technique. The outer segments of single intact rods were drawn into a suction electrode, and the light induced changes in membrane current were amplified and recorded with a computer-controlled current-to-voltage converter system. The recorded signal was filtered and digitized for subsequent analysis at a sampling rate of 250 Hz. Light stimuli were unpolarized 30 ms monochromatic flashes of 550 nm wavelength, the flash intensities were defined by the voltage applied on the LED. The perfusing solution in the recording chamber was replaced with the nitroprusside containing solution during recording and identical light flashes on the rod as before solution changing were applied. The maximal amplitude and the time course of the recovery phase of the recorded signals in the standard and in the nitroprusside Ringer were compared with the Wilcoxon Signed-Rank Test. Nitroprusside induced a statistically significant ( $p < 0.01$ ) decrease of the amplitude and accelerated the recovery phase ( $p < 0.05$ ) of the light response on subsaturating flashes of a fixed low intensity. Increasing of light intensity of the applied flashes towards saturating levels attenuated both effects. The results suggest that sodium nitroprusside enhances termination of the rod response at non saturating low light intensities and reduces photosensitivity probably through early activation of cGMP synthesis; at high intensities there are no significant changes in both parameters, amplitude and time course, so that this effect is eventually neutralized by other mechanisms at increasing light level. We conclude that nitric oxide could act as an additional modulating factor in recovery under appropriate low light conditions.

## Nonlinear lateral interactions in the visual perception and in the LGN neuronal responses

Vladislav Kozyrev\* and Jan Kremers\*\*

*University of Tübingen Eye Hospital, Röntgenweg 11, 72076 Tübingen;*

*\* Cognitive Neuroscience Dept., German Primate Center, Kellnerweg 4, 37077 Göttingen;*

*\*\* Novartis Institutes for Biomedical Research, Disease Area Neuroscience, Basel*

The perception of flicker in a central stimulus can be altered by the presence of a simultaneously flickering surrounding annulus. We have worked on a model of a cortical detector to explain a significant influence of the relative phase of the surround modulation on the perceived flicker strength in the center [1]. The model assumes that the output of the detector is proportional to the maximal response amplitude difference in an array of LGN neurons responding to the stimulus [2]. The responses of cells in the array were described by a linear Difference-of-Gaussians model of the receptive field (RF) with a time delay in the surround. Our predictions were in good agreement with the psychophysical data at different temporal frequencies, but only if contrasts in the two subfields of the stimulus were same. The simulations did not though match so well the data obtained with different contrasts in the center and surround (Figure 1, dashed curve). To address this problem, we studied whether a linear model is sufficient to describe the RF structure of a neuron in the retino-geniculate pathway. Therefore, the responses of LGN cells in the common marmoset to stimuli that independently stimulated the RF centers and surrounds were measured. We have shown that linearity fails if the contributions of the RF center and surround responses to the combined stimulus are compared with responses to the selective center and surround stimuli [1]. We found that an increase of a response in the RF surround leads to a decrease of the center response amplitude. In its turn, the center response influences the surround response so that the RF surround phase lag relative to the center will be smaller when the contrast in the surround stimulus is lower. These nonlinearities are probably related to the change of firing modes in the thalamic neurons. Quantitative estimation of the contrast-dependent interactions between the LGN cell's RF center and surround allowed us to recalculate the RF parameters and consider them in the simulation of the cell array output. Then our model gives satisfactory predictions of the perceived flicker strength with any combination of contrasts in the combined stimulus.

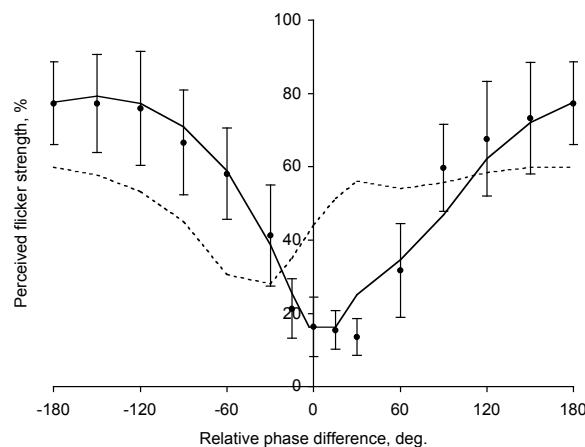


Figure 1. Perceived contrast in the center stimulus as a function of the surround relative phase at 4 Hz temporal frequency, 1° center size, contrasts in the center 25%, in the surround 50%. Averaged psychophysical data are depicted by close circles with error bars. Simulation of the cell array output using the RF parameters estimated from neuronal responses to stimuli with equal contrasts in the both subfields (dashed line) does not match the psychophysical data. Considering of a reduced RF center responsivity (approximately 1.6 times) when the surround contrast is increased from 25% to 50% provides a good prediction (solid line).

### References

1. Kremers, J., Kozyrev, V., Silveira, L. C. L., & Kilavik, B. E. (2004). Lateral interactions in the perception of flicker and in the physiology of the lateral geniculate nucleus. *Journal of Vision*, 4(7), 643-663, <http://journalofvision.org/4/7/10/>, doi:10.1167/4.7.10.
2. Kozyrev, V., Kremers J. (2004). Lateral interactions in the visual perception can be explained on the basis of LGN cell array output. *Perception (SUPPL)* 33: 177-177, 2004.

## Knock-out of HCN1 channels alters light-responses in the mammalian retina

Gabriel Knop<sup>1</sup>, Frank Thiel<sup>1</sup>, Kristiane Hudl<sup>2</sup>, Mathias Seeliger<sup>2</sup>, U. Benjamin Kaupp<sup>1</sup>, and Frank Müller<sup>1</sup>

<sup>1</sup> Institut für Biologische Informationsverarbeitung 1, Forschungszentrum Jülich, 52425 Jülich

<sup>2</sup> Abteilung für Pathophysiologie und Neuroophthalmologie, Universitätsaugenklinik Tübingen, 72076 Tübingen

Hyperpolarization-activated and cyclic nucleotide-gated channels (HCN channels) are widely expressed in the mammalian nervous system. Upon hyperpolarization, HCN channels conduct a depolarizing mixed  $K^+/Na^+$  current. HCN channels play an important role in the generation of rhythmic activity in neurons and in pace-maker cells of the heart. HCN channels codetermine the resting potential and membrane conductance and thereby influence the integrative behaviour of neurons and the sensitivity to synaptic input. The four HCN-isoforms HCN1 - 4 differ in their kinetics and in their sensitivity to modulation by cyclic nucleotides (for review: Kaupp and Seifert, *Ann Rev Physiol* 63, 235-257). Recently, we showed in a detailed immunohistochemical and electrophysiological study that HCN1 - 4 are differentially expressed in the mammalian retina (Müller et al., *Eur J Neurosci* 17, 2084-2096).

In the present study, we investigated the effect of the knockout of HCN1 on physiological responses in the mouse retina. Retinae of wild-type mice and of knock-out mice were studied using immunohistochemical and electrophysiological approaches. In wildtype mice, HCN1 immunoreactivity was prominent in rod and cone photoreceptors and in type 5 cone bipolar cells, but weaker in rod bipolar cells and in some amacrine and ganglion cells. This expression pattern was confirmed by electrophysiology. Cells in mouse retinal slices were recorded in the whole-cell mode of the patch-clamp technique and filled with fluorescent dyes to enable morphological classification of the cell (A, type5 bipolar cell). Upon hyperpolarization, rod photoreceptors, type 5 bipolar cells and rod bipolar cells showed slowly activating inward currents with time courses typical for HCN1 (B, type 5 bipolar cell). Time constants of activation ranged from  $\tau = 30$  ms in rods (average current amplitude -20 pA at -135 mV) to  $\tau = 110$  ms in type 5 bipolar cells (average current amplitude -40 pA at -135 mV).

In retinae of knock-out mice, neither HCN1 immunoreactivity nor HCN1 currents could be observed, indicating the complete loss of HCN1. Moreover, the deletion of HCN1 was not compensated by upregulation of other HCN channel isoforms (C, type 5 bipolar cell).

Physiological responses were recorded on the level of the electroretinogram as well as in single identified retinal cells in vitro. Functional implications of the HCN1 knock-out will be discussed.

**Acknowledgments:** HCN1 knock-out mice were kindly provided by Dr. Alexei Morozov and Dr. Eric R. Kandel, Center for Neurobiology and Behavior, Columbia University, USA.

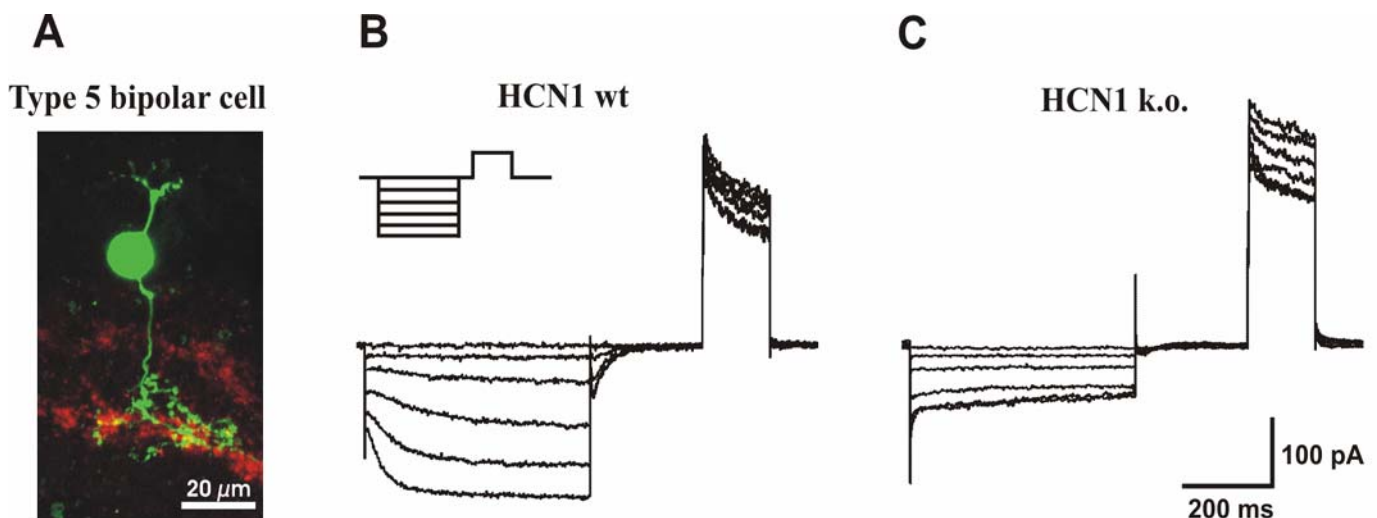


Fig.: A: Morphologically identified type 5 bipolar cell, labelled by dye injection. B: Recording from a type 5 bipolar cell in wild-type mouse; in voltage clamp hyperpolarizing steps from -60 to -135 mV evoked slowly developing HCN currents. C: Recording from a type 5 bipolar cell in HCN1 knock-out mouse; no HCN current was observed.

# Receptive fields of epiretinally recorded signals in cats: Spatial and temporal aspects

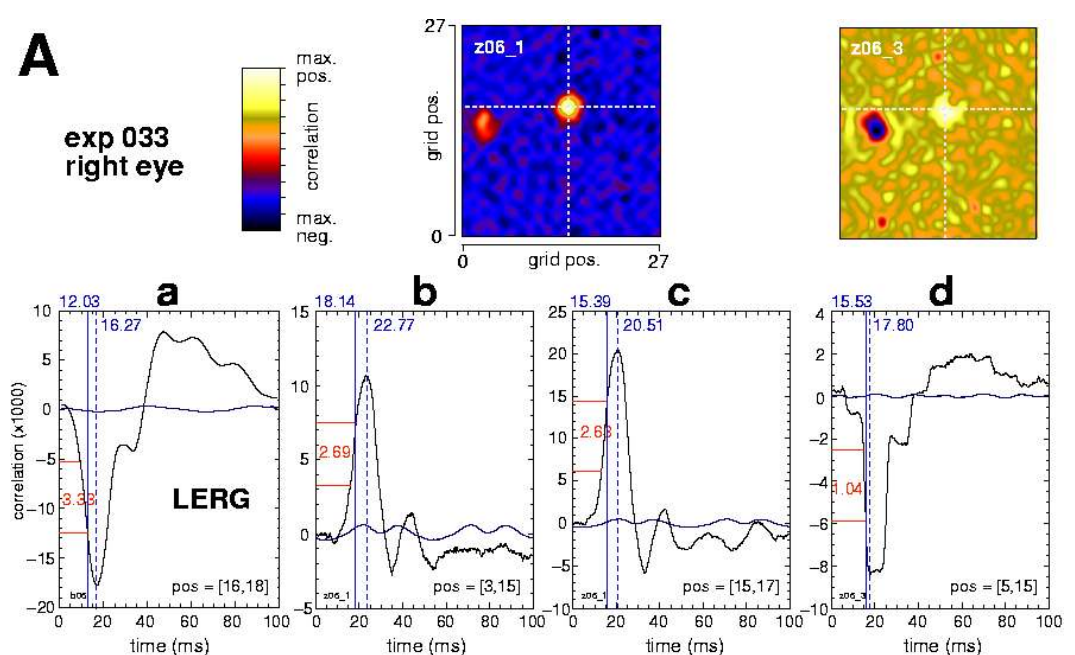
Marcus Wilms<sup>1,2</sup> and Reinhard Eckhorn<sup>1</sup>

<sup>1</sup> Institute of Neurophysics, Philipps-University Marburg, 35032 Marburg, Germany

<sup>2</sup> present address: Institute of Medicine, Research Center Jülich, 52425 Jülich, Germany

**Goal:** In the context of the development of a visual prosthesis, we ask whether epiretinal electrical stimulation can ensure a retinotopic mapping of visual information to a cortical representation that is meaningful to a blind patient. We do that by analyzing retinal visual receptive fields (RFs) of different epiretinally recorded signals assuming that about the same group of retinal neurons can be stimulated by as well as recorded from by an epiretinal microelectrode. **Methods:** Retinal broadband signals from multisite epiretinal microelectrode recordings in anesthetized cats are separated into local electroretinograms (LERG, 1-140 Hz) and single unit spike trains. We characterize the RFs of these signals using multifocal visual stimulation combined with stimulus-response cross-correlation. **Results:** We analyzed RFs of 44 recording positions in four cats. Retinal LERG exhibit spatially unimodal RFs that are always centered at the actual location of the retinal recording electrode (N=34). Retinal spikes from the same electrode have distinct RF center locations that are aligned along the fiber bundles at the recording location. We found an average of 1.8 spike-RFs per retinal recording position. Spike-RF positions are either congruent with LERG-RFs (*local RFs*, N=26/61) or shifted distally (*distal RFs*, N=35/61) but never proximally with respect to the optic disk. This indicates that displaced spike-RFs result from the recording of spikes that originate from more distal locations of the fibers passing the recording electrode *en route* to the optic disk. Comparisons of congruent *local* LERG-RFs and spike-RFs calculated from simultaneously recorded signals from the same electrode show that LERG-RFs temporally precede *local* spike-RFs by  $5.38 \text{ ms} \pm 3.64 \text{ ms}$ . Furthermore, the measured OFF-center spike latencies (time to 70% of peak amplitude) are shorter than ON-center spike latencies. We found congruent ON-center and OFF-center spike RFs in four recordings with OFF being  $2.40 \text{ ms} \pm 0.83 \text{ ms}$  faster than ON. **Discussion:** Our results indicate that epiretinal electrical stimuli might evoke phosphenes that are not confined to the electrode location but dispersed distally from the electrode position with respect to the optic disk and can therefore yield multiple visual percepts. Epiretinal implants should use precisely controlled stimulation strengths and the geometry of the stimulation fields such that erroneous phosphenes are kept subthreshold. E.g., small conical electrodes can bypass the fiber layer with their tips in the ganglion or bipolar cell layer. (Support by BMFT grant 01 IN 501 F and KP 0006 to R.E. greatly acknowledged.)

**Figure:** Two RF maps that were calculated from spike trains derived from the same broadband recording in a right cat eye. Note the ON- and OFF-center RFs that are shifted distally from the projected electrode position (crosshair). **a-d:** Time courses of the retinal responses to stimulation with the optimal stimulus (i.e., in the center of the particular RF): LERG (**a**), left RF of first spike train (**b**), right RF of first spike train (**c**), left RF of second spike train (**d**). Response rise times from 30%-70% of the peak amplitude (red), latency (blue), and peak time (dashed blue) are indicated. The baseline (dark blue) is calculated from the average correlation strength between the retinal signal and all pixel luminance time courses.



## **Expression and localization of the scaffold protein harmonin and its interaction partners at synapses**

Jan Reiners, Jürgen Harf, Tina Märker, Karin Jürgens, and Uwe Wolfrum  
Institute of Zoology, Johannes Gutenberg-University of Mainz, Germany.

Harmonin is encoded by the *USH1C* gene. Its defect results in a subtype of the human Usher syndrome (USH), the most common form of deaf-blindness. In addition, clinical reports on patients indicate USH defects may also effect brain function. Harmonin contains PDZ-motifs which are known from organizers of protein complexes.

RT-PCRs and Western blots revealed differential tissue expression of harmonin splice variants. Biochemical analyses of synaptosome preparations and tangential sections through retinas revealed the presence of harmonin in synapses. Immunocytochemistry of retinal and brain tissue showed that harmonin is localized in axons and synapses of neuron populations in the brain and at photoreceptor synapses. Complementary immunoelectron microscopy confirmed harmonin as a structural component of ribbon synapses. Double labeling in retinal sections demonstrated harmonin colocalization with other USH-proteins, namely myosin VIIa (USH1B), cadherin 23 (USH1D), protocadherin 15 (USH1F), SANS (USH1G), and NBC3 (USH2B) in specialized photoreceptor ribbon synapses. Furthermore, harmonin colocalizes with its interaction partners filamin A and  $\beta$ -catenin in retina and brain. Hence, harmonin provides a new link between cell adhesion molecules and the actin cytoskeleton.

USH molecules can assemble to harmonin organized supramolecular complexes at synapses. Such complexes may contribute to the cortical cytoskeletal matrices of the pre- and postsynaptic regions, which are thought to play a fundamental role in the organization of synaptic junctions. Dysfunction of any of the USH-complex partners may lead to synaptic dysfunction causing the clinical phenotype in the retina of USH patients.

Supports: FAUN-Stiftung; FcB - Initiative Usher Syndrom; DFG

## **Light-dependent phosphorylation of centrins in mammalian photoreceptor cells**

Philipp Trojan<sup>1</sup>, Sebastian Rausch<sup>2</sup>, Andreas Gießl<sup>1</sup>, Alexander Pulvermüller<sup>2</sup>,

Klaus Peter Hofmann<sup>2</sup>, Uwe Wolfrum<sup>1</sup>

Inst. Zoologie, Johannes Gutenberg-Univ. Mainz<sup>1</sup>

Inst. Med. Physik u. Biophysik, Humboldt-Univ. zu Berlin, Charité<sup>2</sup>, Germany

Centrins are members of the superfamily of  $\text{Ca}^{2+}$ -binding EF-hand proteins. In mammalian cells, up to 4 centrin isoforms are commonly associated with centrioles of centrosomes and spindle poles. Nevertheless, in ciliated cells, centrins are not only present in the centrioles of basal bodies but are also localized in the transition zone of cilia.

We have previously shown that centrins are prominent cytoskeletal components of the connecting cilium linking inner and outer segments of vertebrate photoreceptor cells. Furthermore, we provided evidence that centrins interact with the visual G-protein transducin in a  $\text{Ca}^{2+}$ -dependent way, a mechanism which may regulate the light-dependent translocation of transducin.

Here, we showed that in photoreceptor cells the function of centrin isoforms is not only regulated by  $\text{Ca}^{2+}$  but also by phosphorylation. *In vitro* and *ex vivo* phosphorylation assays indicated that centrins are phosphorylated in a light-dependent manner. Treatments with kinase inhibitors revealed the casein-kinase II (CKII) as a candidate for the light-dependent centrin phosphorylation. Furthermore, we analyzed the binding properties of CKII-phosphorylated centrins to transducin by GST pull-down and light scattering assays. The centrin phosphorylation alters the binding ability of centrins to transducin, as compared with the binding properties of  $\text{Ca}^{2+}$ -activated centrins.

Our results indicate for the first time that centrins are light-dependently regulated by CKII-mediated phosphorylation in visual cells. This phosphorylation may also be involved in the assembly of centrin-transducin protein-complex in mammalian photoreceptor cells.

Supports: DFG, FAUN-Stiftung

## Differential expression and $\text{Ca}^{2+}$ -dependent interaction of the visual G-protein transducin with centrin isoforms in mammalian photoreceptor cells

Andreas Gießl<sup>1</sup>, Alexander Pulvermüller<sup>2</sup>, Philipp Trojan<sup>1</sup>, Klaus Peter Hofmann<sup>2</sup>, Uwe Wolfrum<sup>1</sup>

Inst. Zoologie, Johannes Gutenberg-Univ. Mainz<sup>1</sup>

Inst. Med. Physik u. Biophysik, Humboldt-Univ. zu Berlin, Charité<sup>2</sup>, Germany

Centrins are members of the superfamily of  $\text{Ca}^{2+}$ -binding EF-hand proteins. In eukaryotic cells, up to 4 centrin isoforms are commonly associated with centrioles of centrosomes and spindle poles. Nevertheless, in ciliated cells, centrins are not only present in the centrioles of basal bodies but are also localized in the transition zone of cilia.

We have previously shown that centrins are prominent cytoskeletal components of the connecting cilium linking inner and outer segments of photoreceptor cells in the vertebrate retina. Here, we demonstrate that all 4 known centrin isoforms are expressed in the mammalian retina. Immunocytochemical analysis using isoform specific antibodies against the centrins reveals differential subcellular localizations of the centrin isoforms in the photoreceptors: **Centrin 1, 2 and 3 colocalize in the connecting cilium. In contrast, centrin 4 is exclusively found in the basal body, where it colocalizes with centrin 2 and 3.**

In the search for centrin interacting proteins, we identified the  $\beta$ -subunit of visual G-protein transducin as a binding partner to centrin 1. Recent analyses reveal that all 4 centrins interact with transducin in a  $\text{Ca}^{2+}$ -dependent way. Immunoelectron microscopy demonstrated that transducin colocalizes with centrin 1, 2 and 3 in the photoreceptor connecting cilium. Due to the fact that centrin 3 has much lower affinity to transducin than the other three centrin isoforms, centrin 1 and 2 remain as predominant candidates for the  $\text{Ca}^{2+}$ -dependent interaction with transducin. The binding of both centrin isoforms to transducin may regulate the previously described light-dependent movements through the photoreceptor cilium.

In general, the assembly of centrin-G-protein complexes are a novel aspect of the supply of signaling proteins in sensory cells, and potential links between molecular translocations and signal transduction.

Supports: DFG; FAUN-Stiftung

**Light-induced translocation of the signal transduction proteins transducin and arrestin  
analyzed in photoreceptor cells of organotypical retina culture**

Boris Reidel, Andreas Gießl, Philipp Trojan, Uwe Wolfrum

Institut für Zoologie, Johannes Gutenberg-Univ. Mainz

Vertebrate photoreceptor cells consist of morphological and functional distinct cellular compartments. They composed of the light sensitive outer segment and the synthetic active inner segment, linked by the connecting cilium which is the only intracellular bridge for intersegmental exchange. The visual G-protein transducin and arrestin - responsible for the “turn off” of activated rhodopsin - migrate between the inner and outer segment of the photoreceptor cell in a light dependent way. Upon illumination transducin moves from the outer to the inner segment of the photoreceptor cell and arrestin in the opposite direction. The transport mechanisms and regulation factors underlying this intracellular translocation of transducin and arrestin still remain elusive.

In the present project, we studied the movement of signaling proteins in the organotypic retina culture. Using this approach we are able to apply drugs, which differentially depolymerize cytoskeletal elements, to the retinal photoreceptor cells. The effects of the treatments on the translocation of arrestin and transducin provide new insights into the mechanisms of the intracellular movements of both proteins.

Our previous studies showed that the  $\text{Ca}^{2+}$ -binding centrin proteins interact with the  $\beta$ -subunit of transducin in the connecting cilium. Here, we also analyzed in a associated set of experiments the role of the centrin isoforms in the intersegmental exchange of transducin via the cilium in the retina culture. Our data strengthens the hypothesis that the exchange of transducin through the photoreceptor cilium is modulated by light-induced changes of the intracellular  $\text{Ca}^{2+}$ -concentration via the assembly of complexes between transducin and centrins. The assembly of the visual G-protein with centrins is a novel aspect of the supply of signaling proteins in photoreceptor cells, and a potential link between molecular translocations and signal transduction in general.

Support: FAUN-Stiftung; DFG; Pro-Retina e.V.



## **The scaffold protein harmonin (USH1C) also integrates Usher syndrome 2 proteins into synaptic Usher protein complexes in retinal photoreceptor cells**

Tina Märker, Jan Reiners, Karin Jürgens, Nora Overlack, Tobias Goldmann, Uwe Wolfrum

Institut fuer Zoologie, Johannes Gutenberg-Universitaet, Mainz

The Usher syndrome (USH) is the most common form of congenital combined deaf-blindness. The clinically and genetically heterogeneous USH is divided in 3 distinct types (USH1-USH3). USH1, the most severe form, is characterized by profound congenital deafness, constant vestibular dysfunction and prepubertal onset of retinitis pigmentosa. Whereas, USH2 is a mild form of USH with moderate to severe sensorineural hearing impairment at birth, normal vestibular responses and progressive retinitis pigmentosa. The 3 USH types in turn comprise 12 subtypes.

USH1C encodes for the protein harmonin, which contains PDZ-motifs known to organize protein complexes via protein-protein interactions. In previous studies, we and others have demonstrated that harmonin binds all 5 known USH1-proteins via its 3 PDZ domains. Their colocalization in photoreceptor synapses suggests that they may constitute the basis for a supramolecular USH1-complex in this subcellular synaptic compartment.

The aim of our present study was to validate the presence of the three USH2-proteins namely Usherin (USH2A), NBC3 (Na-Bicarbonate Co-transporter 3, USH2B) and the 7-transmembrane receptor VLGR1 (Very Large G-protein coupled Receptor 1, USH2C) in USH-protein-complexes. *In vitro* (GST-pull downs) and *in vivo* (yeast two hybrid system) assays of protein-protein interactions reveal that all three USH2-proteins also bind to the PDZ-domains of harmonin. Immunocytochemical analysis of cryosections of rat and mouse retinas further demonstrates additional colocalization of USH2-proteins with USH1-proteins in photoreceptor synapses. Our findings strongly suggest that ribbon synapses of photoreceptors bear supramolecular protein complexes composed of USH1- and USH2-proteins. Mutations of one of the components may cause dysfunction of the entire complex which probably leads to synaptic defects and in turn to retinal degeneration (retinitis pigmentosa), the phenotype observed in USH-patients.

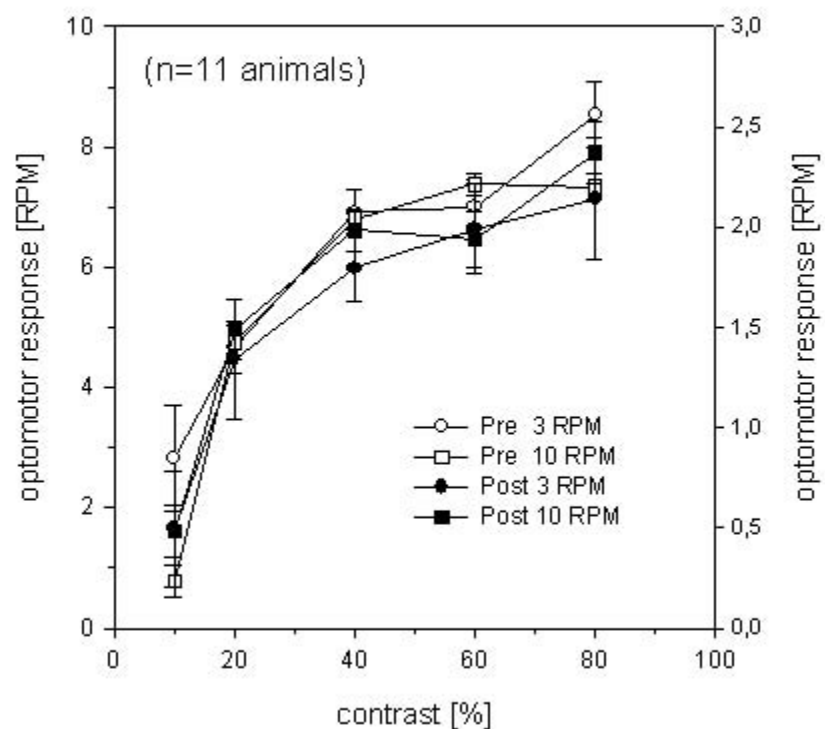
Supports: DFG, FAUN-Stiftung, FcB Initiative Usher Syndrom

## GLYCINE HAS NO EFFECT ON CONTRAST-SENSITIVITY OF GOLDFISH MEASURED WITH THE OPTOMOTOR RESPONSE

Ruth Schmidt-Hoffmann and Carlos Mora-Ferrer; Institut für Zoologie III, Johannes-Gutenberg-Universität, 55099 Mainz, Germany

**Purpose:** Different retinal transmitters are involved in retinal motion coding. Acetylcholine and GABA have both been shown to be essential for the coding of full-field motion in the retina. The contribution of glycine to retinal motion coding is unclear. Therefore, contrast-sensitivity of the optomotor response of goldfish was measured and the effect of the glycine-antagonist strychnine was investigated. **Method:** The photopic optomotor response to two stimulus velocities (3 and 10 rounds per minute [RPM]) was elicited utilizing paper cylinders (24 cm diameter) with sine-wave gratings (4 cm period) of differing contrasts (80, 60, 40, 20 and 10%). Contrasts were varied around the medium remission value of the paper pattern cylinders. Strychnine, a non-specific glycine antagonist, was injected into the vitreous of both eyes and used at intra-vitreous concentrations between 50 nM-5  $\mu$ M. **Results:** Results were similar for all Strychnine concentrations tested. For both pattern velocities the optomotor response decreased with contrast. The half-maximal response was elicited at about 25% contrast, irrespective of pattern velocity. Normalization of pre- and post-injection data for 3 and 10 RPM pattern velocity revealed nearly identical values for the optomotor response as a function of contrast. There is no significant difference between pre- and post-injection data. A slight difference could be observed between the contrast sensitivity functions at contrast 60% and 40% achieved with 3 and 10 RPM pattern velocity. **Conclusion:** The contrast sensitivity of the optomotor response is independent of pattern velocity. The half-maximal response is elicited by a contrast value of about 25%. This is similar to values obtained for guppy fish (Anstis et al., 1998). Glycine neither contributes to the neuronal processing underlying contrast coding nor to the directional-coding process.

Optomotor response as a function of contrast. Pre-/post injection data for 3 and 10 RPM pattern velocity (contrast=80 and 10%: n=5; c=60 and 20%: n=6; and c=40%: n=11). X-axis: contrast [%]; left Y-axis: optomotor response for 10 RPM pattern velocity, right Y-axis: optomotor response for 3 RPM pattern velocity.



# EFFECTS OF GLUTAMATE ANTAGONISTS ON GOLDFISH TEMPORAL TRANSFER PROPERTIES MEASURED WITH THE ERG

C.Mora-Ferrer, C.Albrecht, B.Benkner, B.Lux, M.Gruber & K.Behrend, Inst. Zoologie III (Neurobio.), Johannes Gutenberg Univ., 55099 Mainz, Germany

**Purpose:** Synaptic transmission from photoreceptors to bipolar cells, from bipolar cells to ganglion cells, and from bipolar cells to amacrine cells is mediated by glutamate. The different response properties, e.g. "ON" and "OFF", are generated through different glutamate receptor (Glu-R) types on "ON"- and "OFF"-bipolar cells, post-synaptic elements in the inner retina, their respective Glu-R and direct and indirect effects on bipolar cell output. Temporal transfer properties (TTP) at retinal level have been described to depend mainly upon the "OFF"-response and are characterized as a 3<sup>rd</sup> order filter with resonance (Mora-Ferrer & Behrend, 2004). The contribution of the "OFF"-response to the TTP was analyzed through the use of different Glu-R antagonists. **Method:** Photopic ERGs were recorded from the vitreous of anesthetized and immobilized goldfish. Both background and test light illumination was provided by a LED. Stimuli used were "ON"- and "OFF"-stimuli, i.e. light intensity increases and decreases of different durations, and periodic sine-wave flicker of different flicker frequencies. Drugs (calculated intraocular concentrations in microM, APB: 100, DNQX: 50, CNQX: 10, CGS-19755: 1.5) were injected, alone or in combination, intravitreally after recording pre-injection data and then measurements were repeated. **Results:** Responses to "ON-OFF"-stimuli post-injection of drugs blocking AMPA/Kainate-type Glu-R (DNQX) alone exhibit a drastic reduction of the "OFF"-response best seen in the DC-part interpreted as the balance between the sustained "ON"- and "OFF"-bipolar cell response. A similar result can be seen for the combination of DNQX-CNQX with CNQX also blocking the NMDA-Glu-R type. Blockade of NMDA-R alone (CGS-19755) increased the "OFF"-response amplitude. The combination of CGS 19755-DNQX resulted in a massively increased b-wave and a minute "OFF"-response to an "ON"-light stimulus. APB, a class III mGlu-R agonist, slightly lowered both the b-wave and "OFF"-response to an "ON"-stimulus and increased the response to an "OFF"-stimulus. Temporal filter characteristics are not changed, as seen in the "gain"-part of the bode-plot, post-injection of APB and CGS 19755 except for the corner frequency, at the -3 db point, which moved from ~23 Hz to ~14 Hz. Post-injection of all other drugs or combinations of them, the characteristics changed to pure low-pass with varying corner frequencies between ~4 (DNQX-CNQX), 7 (DNQX) and 11 (DNQX-CGS 19755) Hz. **Conclusions:** DNQX changed the course of the ERG to a pure "ON"-ERG, probably by effectively eliminating the "OFF"-component to an "ON"-stimulus, changing both the corner frequency and the filter characteristics. CGS 19755 enhanced both the "ON"- and "OFF"-ERG component to an "ON"-stimulus which is reflected by the gain-plot. The combination of CGS 19755-DNQX resulted in a increase of the corner frequency compared to DNQX alone, probably due to the CGS-enhanced "ON"- and "OFF"-component of the flash stimulus response. In contrast, CNQX-DNQX, resulted in a "ON"-flash response comparable to the one of DNQX alone, but the TTP changed even more to a pure 1<sup>st</sup> order low pass and the corner frequency shifted to ~4 Hz. In general, eliminating the "OFF"-component of the ERG results in the predicted effect, i.e. the TTP is dominated by the fast processing properties in the retinal "OFF"-pathway, mostly in the inner plexiform layer. Under photopic illumination conditions APB had little to no effect on the flash response as well as on the TTP.

## Connexin45 Deficiency in Retinal Neurons Leads to Impaired Visual Transmission

Karin Dedek<sup>1</sup>, Stephan Maxeiner<sup>2</sup>, Ulrike Janssen-Bienhold<sup>1</sup>, Josef Ammermüller<sup>1</sup>, Klaus Willecke<sup>2</sup>, and Reto Weiler<sup>1</sup>

<sup>1</sup> *Department of Neurobiology, University of Oldenburg, D-26111 Oldenburg, Germany*

<sup>2</sup> *Department of Molecular Genetics, University of Bonn, D-53117 Bonn, Germany*

Connexin45 (Cx45) is expressed in the retina but its functional analysis was hampered since general deletion of Cx45 resulted in early embryonic lethality at day 10.5 ED due to cardiovascular defects. We generated mice with neuron directed deletion of Cx45. Neuronal ablation of Cx45 was achieved after Cre-recombinase mediated deletion of exon3 of the Cx45 gene using Nestin-Cre mice which in turn led to activation of the enhanced green fluorescent protein (EGFP). EGFP labeling was observed in bipolar, amacrine and ganglion cell populations. To elucidate the morphology of EGFP-positive bipolar cells we performed tracer injections in vertical slices of the mouse retina. Cells were filled with Alexa594-hydrizide and subsequently stained with an antibody to calretinin. Confocal analysis of injected cells revealed that all four types of OFF bipolar cells were EGFP-positive and thus express Cx45. Rod ON bipolars were negative for EGFP, whereas type 5-7 ON cone bipolar cells were strongly labeled with EGFP.

The electroretinogram of Cx45 deficient mice showed a normal a-wave but a 40% reduction of the b-wave amplitude compared to wild-type animals. This retinal phenotype was very similar to the one found in Cx36 deficient animals, suggesting a possible defect in the rod pathway of visual transmission. The gap junctional coupling between AII amacrine cells and ON cone bipolar cells plays a crucial role in this pathway. AII amacrine cells employ Cx36 as the gap junctional protein whereas the connexin used by ON cone bipolar cells is currently unknown. To investigate whether the coupling between these two cell types is impaired in Cx45 deficient mice, we exploited the fact that glycine diffuses from the AII amacrine cells into the bipolar cells. Therefore, we analyzed the glycine content of bipolar cells using an antibody to glycine. Indeed, neurotransmitter coupling between AII amacrine cells and Cx45 expressing cone bipolar cells was disrupted in Cx45 deficient mice.

These data implicate that both, Cx45 and Cx36, participate in the formation of functional heterotypic electrical synapses between these two types of retinal neurons which form the major rod pathway.

This work was supported by grants from the Deutsche Forschungsgemeinschaft (SFB 517 to R.W., JA to U.J.-B. and SFB 400 to K.W.) and the European Community (CORTIVIS to J.A.).

# Intracellular calcium is regulated by different pathways in horizontal cells of the mouse retina

Timm Schubert, Reto Weiler and Andreas Feigenpan

*Neurobiology, University of Oldenburg, 26111 Oldenburg, Germany*

Activation of glutamate receptors (GluRs) and voltage activated calcium channels (VACCs) cause an elevation of the intracellular calcium concentration ( $[Ca^{2+}]_i$ ) in retinal neurons of the mouse retina. Although changes in ( $[Ca^{2+}]_i$ ) probably play an important role in feedback mechanisms, the underlying pathways are not yet clear. Therefore, we analyzed how ( $[Ca^{2+}]_i$ ) in horizontal cells is regulated by (i) VACCs, (ii) ionotropic and metabotropic GluRs, and (iii) internal  $Ca^{2+}$  stores.

Horizontal cells were enzymatically isolated from the retinæ of two-month-old C57BL/6 mice and identified according to their distinct morphology. Cells were incubated in Ringer solution (in mM: NaCl, 110; KCl, 3;  $CaCl_2$ , 2;  $MgCl_2$ , 3; glucose 10; Hepes, 10) additionally containing 15  $\mu M$  Fura-2 AM and 0.01% Pluronic F-127 for 40-50 min at 37°C. Free intracellular calcium concentration was monitored with a PTI calcium imaging system using the 340/380 nm ratio for excitation. Fluorescence images (515 nm) were obtained with an intensified CCD camera and analyzed off-line. The fluorescence intensity within a cell was normalized to its resting level and expressed as the ratio  $\Delta F/F(t) = [F(t) - F]/F$ , where  $F(t)$  is the intensity of the fluorescence at time  $t$ , and  $F$  is the averaged fluorescence intensity of a 60-s baseline period. We also performed experiments in the whole-cell mode of the patch-clamp technique to study the electrophysiological properties of VACCs. Calcium currents of isolated horizontal cells were activated by depolarizing voltage steps from a resting potential of -70 mV (Fig. 1).

All cells investigated exhibited non-inactivating calcium currents of various amplitudes in response to depolarization. Calcium currents were entirely blocked in the presence of extracellular  $Cd^{2+}$  or  $Co^{2+}$  (250  $\mu M$  each). Current amplitudes were partially blocked in the presence of the L-type channel blocker verapamil (100  $\mu M$ ), with an additional reduction induced by the N-type channel blocker  $\omega$ -conotoxin GVIA (1  $\mu M$ ). The specific GluR agonists AMPA (100  $\mu M$ ) or kainate (100  $\mu M$ ) evoked calcium signals in the presence of  $Cd^{2+}$  (250  $\mu M$ ). Application of caffeine (10 mM) lead to a massive increase of ( $[Ca^{2+}]_i$ ) indicating  $Ca^{2+}$  release from internal stores via ryanodine receptors. t-ACPD (200  $\mu M$ ) or quisqualate (100  $\mu M$ ) in combination with CNQX (10  $\mu M$ ), two agonists of mGluR1, had not effect on ( $[Ca^{2+}]_i$ ). These data show that different pathways caused an increase of ( $[Ca^{2+}]_i$ ) in horizontal cells of the mouse retina: (i) through L-type and N-type VACCs activated by depolarization, (ii) through ionotropic AMPA- and kainate-type GluRs, (iii) and by release from internal stores after activation of ryanodine receptors, but not by metabotropic GluR1-mediated release. Intracellular  $Ca^{2+}$  elevation during excitatory synaptic activity may thus serve as a feedback mechanism at the photoreceptor synapse.

Supported by DFG (SFB 517/A2).

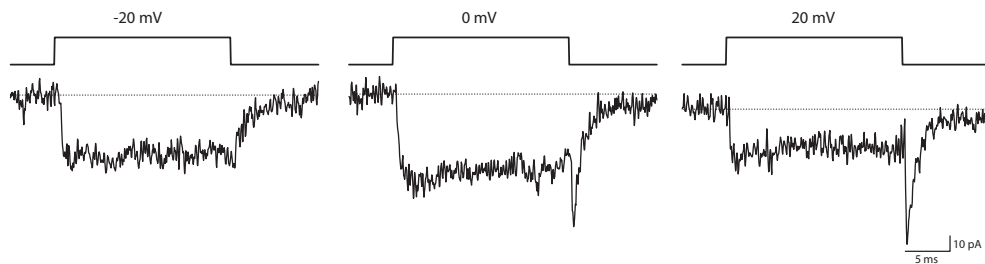


Figure 1: Depolarization-induced activation of HVA calcium currents.

# Retinal ganglion cell burst patterns are reproduced by a computational model of intraretinal processing

Andreas Thiel, Martin Greschner, and Josef Ammermüller  
Neurobiology, University of Oldenburg, D-26111 Oldenburg, Germany  
andreas.thiel@uni-oldenburg.de

When stimulated with a spatially homogenous full field light flash, many retinal ganglion cells (GC) respond with a series of action potentials grouped into bursts. In turtle, two to five bursts occur 50- 150 ms after the onset, and another two to five bursts 50- 300 ms after the offset of light stimulation. The latency of the first burst decreases with increasing light intensity, the subsequent bursts, however, show a more complex intensity dependence. When spike trains of single GC are arranged one above another with decreasing intensity, the bursts' varying latencies result in regular continuous patterns (Fig.1).

By varying flash duration and introducing consecutive flashes, we found the patterns are altered only slightly. Within a given adaptation range, patterns are highly distinct with respect to the applied intensity. Furthermore, in experiments with continuous stimulation consisting of a sequence of naturally occurring intensities, we found burst patterns similar to those observed with the single flash. This is also true for experiments with simulated eye movement, resulting in a smoother increase of intensity inside the GC receptive field. Here bursts depended on stimulus intensity as before, but also on the velocity of the simulated saccades.

To gain some insight into intraretinal processing leading to the complex bursts' latency patterns, we designed a computational retina model, consisting of all major cell classes. Due to the spatially homogeneous stimuli, a single retinal column was simulated. Photoreceptor (PR) and horizontal cell (HC) hyperpolarizations in response to light flashes were measured intracellularly, and the model PR and HC parameters were fit to the experimental data for all flash intensities. The model PR converts light intensity into membrane potential by a nonlinear transfer function and multiple temporal low pass stages, thereby already reproducing the correct latency of the initial hyperpolarization and repolarization after light off. PR signals are passed to four different types of sustained/transient and hyperpolarizing/depolarizing model bipolar cells (BC). Transient response characteristics in BCs are caused by delayed inhibition from sustained amacrine cells (AC). Another type of on-off ACs causes disinhibition of BCs for high intensities via attenuating the sustained ACs responses. This AC circuit is essential for generating the second burst and its typical intensity dependence, decreasing for low to intermediate intensities, and increasing latency from intermediate to high intensities. Since disinhibition of BCs is reported to be mediated by glycinergic ACs, the model predicts the second burst to disappear if the glycinergic on-off ACs are blocked. This prediction has been confirmed by experiments with the glycine antagonist strychnine. Further evidence for the involvement of ACs in the generation of the second burst comes from intracellular recordings of ACs that resemble the two different types proposed by the model. Finally, by passing BC signals to the model ganglion cell, the latency of the various bursts is correctly reproduced in the model (Fig.1).

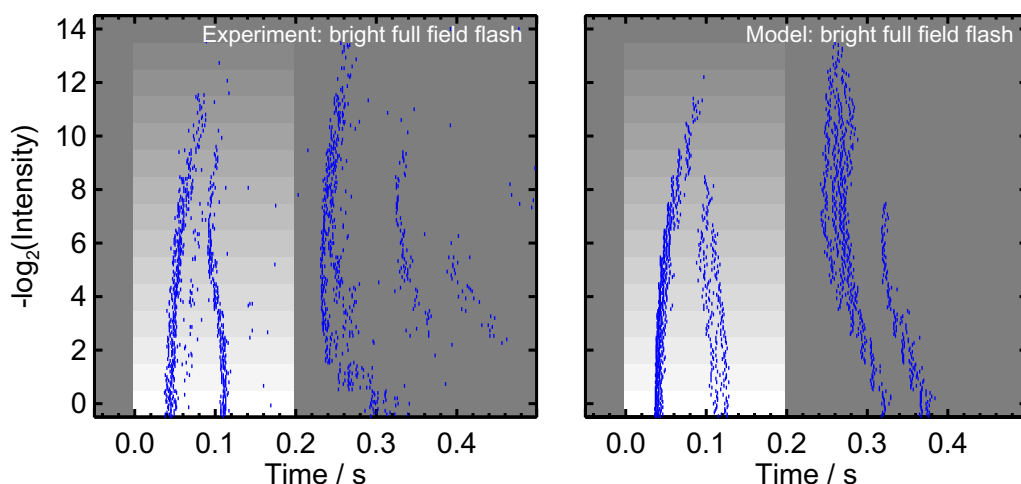


Fig.1: Ganglion cell response to full field stimulation of varying intensity. Flash duration was 0.2 s. Stimulus intensity is symbolized by the background.  
left panel: experimental data  
right panel: model simulation

## **Comparison of retinal ganglion cell responses from Bassoon deficient and wild type mice.**

**Lars van Ahrens<sup>1</sup>, Malte T. Ahlers<sup>1</sup>, Martin Greschner<sup>1</sup>, Eckart D. Gundelfinger<sup>2</sup>,  
Johann H. Brandstätter<sup>3</sup>, Dana Brauner<sup>3</sup> & Josef Ammermüller<sup>1</sup>**

<sup>1</sup>Neurobiology, Carl von Ossietzky University of Oldenburg, D-26111 Oldenburg, Germany

<sup>2</sup>Leibniz Institute for Neurobiology, D-39118 Magdeburg, Germany

<sup>3</sup>Dept. of Neuroanatomy, MPI for Brain research, D-60528 Frankfurt, Germany.

Bassoon is a large protein (420 kDa), localized at the presynaptic active zone of the photoreceptor ribbon synapse. It appears to be concentrated close to the ribbon base and is supposed to be involved in the formation and the function of photoreceptor ribbon synapses. From ERG recordings it was supposed that visual transmission is severely impaired in BSN deficient (BSN  $-/-$ ) mice, since their b-wave was largely reduced [1]. In this study we investigated possible differences at the retinal ganglion cell (GC) level.

Using a 10 x10 multielectrode array, extracellular recordings from GCs were performed in the isolated retinae of wild-type and BSN  $-/-$  mice at various ages. Full field light stimulation was applied to the retina using an LED. Stimuli were 20 ms (according to previously performed ERG studies) and 200 ms light flashes applied in darkness, and 300 ms dark periods applied during various constant background lights.

So far GC population responses of BSN  $-/-$  and the BSN  $+/+$  mice have been analyzed with respect to response rate and latency. Surprisingly, retinal ganglion cells of BSN  $-/-$  mice showed a similarly complex response pattern as it was produced by wild type mice. The response rates of the population responses did not differ significantly. Sensitivity seemed to be not affected at the GC level by the knockout of BSN. This was true for all studied ages (p15 – p178).

Consistent with an increase in b-wave implicit time in BSN  $-/-$  ERGs, their latency in the GC population response was significantly increased. At highest intensity (450 lx) the wild type responded  $17.5 \pm 1.8$  ms after stimulus onset compared to  $34.8 \pm 6.3$  ms for the BSN  $-/-$  mice.

Dark periods of 300ms duration applied upon the light adapted retina revealed a lack of the on-component in the population response of BSN  $-/-$  mice older than p23. This contrasts to a clear on-component in the dark adapted retina, as revealed by the 200 ms light flashes applied in the dark. The lack of the on-component in light adapted, older mutant mice may be due to the elimination of cone-input to the ganglion cells.

Supported by EU (CORTIVIS)

- [1] Dick O. et al. (2003) The presynaptic active zone protein bassoon is essential for photoreceptor ribbon synapse formation in the retina. *Neuron* 37:775-86.

## EXPRESSION OF CONNEXINS IN HORIZONTAL CELLS OF THE MOUSE RETINA

**Jennifer Shelley, Karin Dedek, Konrad Schultz, Petra Dirks, Angelika Schuldt, Ulrike Janssen-Bienhold, and Reto Weiler**

*Neurobiology, University of Oldenburg, 26111 Oldenburg, Germany*

Horizontal cells are laterally-oriented retinal interneurons which are electrically coupled, forming an extensive network that feeds back negatively onto the photoreceptors, generating the antagonistic surround of ganglion cell receptive fields. The mouse retina has a single type of horizontal cell, which has a large cell body, a long axon, and a branched axon terminal. The cell bodies and axon terminals form two separate coupled networks.

We have identified a connexin that forms gap junctions coupling the horizontal cells: Connexin 57 (Cx57) is expressed exclusively by horizontal cells. This was demonstrated in transgenic mice in which the Cx57 gene was knocked out and replaced with the reporter gene lacZ. In these mice, tracer coupling was reduced by 99% (Hombach et al., 2004). The remaining 1% suggests that Cx57 is not the only connexin expressed by these cells.

Here we confirm the expression of Cx57 using RT-PCR in isolated horizontal cells. In addition, we demonstrate expression of an additional connexin, Cx45, in horizontal cell bodies and axon terminals. We hypothesize that Cx57 is the main connexin that forms gap junctions coupling the cell bodies, while Cx45 may be involved in axon terminal coupling.

Loss of synaptic input has been shown to result in cell degeneration and/or neuronal reorganization. It is therefore likely that lack of input from neighboring horizontal cells via gap junctions causes morphological changes in the Cx57-deficient retina. Here we investigate this possibility by comparing histologically the development of the horizontal cell mosaic in Cx57-deficient animals with that in the wild type.

Retinas from wild type and Cx57 knockout mice were examined and compared on the confocal and electron microscopic levels. Organization of the outer plexiform layer was investigated in retinal cryosections using antibodies against calbindin and neurofilament. Horizontal cell mosaic regularity was investigated in the whole mount preparation using antibodies against calbindin. The influence of the Cx57 deletion on the development of cone pedicles and rod spherules was examined using electron microscopy.

The retina of the Cx57-deficient mouse was morphologically indistinguishable from that of the wild type mouse. Despite the lack of electrical coupling, we found no evidence of reorganization or degeneration. Although it is possible that coupling is not required for the development of the horizontal cell network, it is more likely that in the knockout mouse, the role of Cx57 is taken over by another connexin. A possible candidate for this backup connexin is Cx45.

Supported by the Deutsche Forschungsgemeinschaft (SFB 517/A2) and JA 854/1-1.

References: Hombach, S., Janssen-Bienhold, U., Söhl, G., Schubert, T., Büssow, H., Ott, T., Weiler, R., and Willecke, K. (2004) *European Journal of Neuroscience* **19**: 2633-2640.



## DISPLACED AMACRINE CELLS OF THE MOUSE RETINA

Luis Pérez de Sevilla Müller and Reto Weiler

*Neurobiology, University of Oldenburg, 26111 Oldenburg, Germany*

The ganglion cell layer (GCL) of the mammalian retina contains two types of neurons: ganglion cells and displaced amacrine cells (amacrine cell bodies within the ganglion cell layer). In the mouse retina 60% of the cells in the GCL are displaced amacrine cells. With the exception of starburst amacrine cells, which form about 40% of all displaced amacrine cells, the identity of displaced amacrine cells is largely unknown. Due to its transgenic potential, the mouse retina is becoming a preferred model system in retinal research, and knowing its cellular architecture is mandatory.

In this study we injected displaced amacrine cells in the GCL of the flat mounted wild type mouse retina. Electrodes were filled with 0.5% Lucifer Yellow and 4% Neurobiotin. Acridine orange (1  $\mu$ M, Sigma) was used to label retinal cells in the GCL, enabling the visualization of somata within the GCL for electrode penetration. After impaling the cell under a 40x water-immersion objective, Lucifer Yellow was iontophoresed with negative current pulses, and amacrine cells were evaluated by their dendritic morphology and the lack of an axon. The direction of the current was then reversed for 1-3 minutes in order to inject positively charged Neurobiotin molecules. Following the last injection, the retina remained for at least 30 min in the recording chamber, allowing diffusion of Neurobiotin. The retina whole-mount preparations were then fixed for 10 min in 4% paraformaldehyde in 0.1 M phosphate buffer (PB, pH 7.4) and washed several times. Intercellular spreading of Neurobiotin was visualized by incubation with streptavidin-indocarbocyanine solved in PB. In order to get an estimate of vertical distribution of processes within the inner plexiform layer, the two plexi of cholinergic starburst amacrine cells which characterize the somas the ON- and OFF-sublaminae were used as landmarks. To visualize these plexi, retinæ were incubated with antibodies against choline acetyltransferase and the corresponding FITC-labelled secondary antibodies. Subtypes of displaced amacrine cells were classified according to their horizontal and vertical stratification patterns, general morphology, dendritic field size and soma size. Analysis was done by confocal microscopy.

We found up to 9 different types of displaced amacrine cells which share many similarities with amacrine cells described in the rabbit retina. Based on their dendritic field size, three of these cells were characterized as small-field amacrine cells (150-300  $\mu$ m) and one as medium-field amacrine cells (300-500 $\mu$ m), most likely representing the starburst amacrine cells. Five amacrine cells subtypes were characterized as wide-field amacrine cells with dendritic fields over 500  $\mu$ m, and this group included one type of polyaxonal amacrine cell. Small-field amacrine cells were either mono- or bistratified, medium-field amacrine cells were monostratified, and wide-field amacrine cells comprised mono- and multistratified cells.

In addition to the nine displaced amacrine cells, we have also injected two yet unclassified amacrine cells which were included in the medium-field group, because their dendritic field were about 400  $\mu$ m. One of them has an oval shape dendritic field whereas the other type has a round dendritic field and their dendrites present many varicosities.

Supported by Deutsche Forschungsgemeinschaft (SFB 517/A2)

## **ZO-1 expression in the vertebrate retina and its co-localisation with connexin 43**

*Ulrike Janssen-Bienhold, Verena Gawlik, Konrad Schultz, Petra Dirks,  
and Reto Weiler*

Neurobiology, University of Oldenburg, 26111 Oldenburg, Germany

In the vertebrate retina neurons and glia cells form multiple networks by interacting via specialised membrane structures, including the synaptic complex and gap junctions. A common feature of these junctions is the assembly of highly organized multiprotein complexes that appear as electron-dense structures underneath the plasmamembrane. Within these submembranous complexes a number of PDZ (PSD95/SAP90, Dlg, ZO-1) domain-containing proteins coordinate the appropriate membrane-targeting of transmembrane proteins, their coupling to cytoskeletal elements and downstream cascades. Zonula Occludens-1 (ZO-1) is a multi-domain protein belonging to the membrane-associated guanylate kinase (MAGUK) family. ZO-1 was originally identified as a tight junctional protein expressed in epithelial and endothelial cells. PDZ-domains of ZO-1 interact with several members of the gap junction family (i.e. Connexin (Cx) 36, Cx43, Cx45, Cx50), and it is possible that ZO proteins play a general role in the assembly of gap junctions at particular membrane domains. Interestingly, recent findings provided evidence for the co-localisation and interaction between ZO-1 and connexins within neuronal tissue of different species. Since these studies are restricted to the association of ZO-1 and Cx36, we investigated the co-localisation of ZO-1 and Cx43 in the retina and pigment epithelium (PE) of mouse, rat and fish by means of RT-PCR, Westernblotting and immunohistochemistry.

ZO-1 mRNA expression in the fish retina was analysed by RT-PCR using degenerated primer. The deduced amino acid (aa) sequence of subcloned cDNA, which encodes for portions of the anti-ZO-1 binding epitope, revealed 90 % identities to the human orthologue. The specificity of the anti-ZO-1 antibody was tested by immunoblotting. Blots showed the presence of an appropriate 220 kDa-immunoreactive protein in retinal membrane samples prepared from mouse, rat and fish retina. The patterns of ZO-1-IR in mouse, rat and fish frozen eye cup sections revealed some similarities as well as some differences. In all animals a prominent line-like/membrane staining of the hexagonal array of PE-cells was found, which appeared to be in an almost complete overlap with the punctate Cx43-IR localised in the membrane of these cells. In addition, ZO-1- and Cx43-IR were co-localised in the distal processes of Müller cells, which form the outer limiting membrane. In mouse and rat retina substantial ZO-1-IR was also localised within the inner plexiform layer, in particular in layer 3, and in the outer plexiform layer (OPL). In both synaptic layers the staining appeared more punctate, which is characteristic for the patchy assemblies of proteins within junctional complexes. In contrast to this punctate staining was the eye-catching intense, but diffuse ZO-1-IR present in the rod photoreceptor terminals in the OPL of the fish retina. This might be indicative for a different function of ZO-1 within these neurons.

In summary, the present data indicate that ZO-1 is co-localised with Cx43 in junctional complexes formed between PE-cells and Müller cells within the outer limiting membrane. Both proteins might interact to regulate tight adhesion as well as metabolic coupling between these, the retinal function supporting, cells. Because the aa-sequence of carp Cx43 shows some variations to the mammalian orthologues, especially within its PDZ binding motif, an interaction between ZO-1 and carp Cx43 is currently under investigation.

Supported by the Deutsche Forschungsgemeinschaft (JA 854/1-1)

## **Immunohistochemical characterisation of connexin45 expressing bipolar cells in the mouse retina**

Nina Jährling, Karin Dedek, Ulrike Janssen-Bienhold, Stephan Maxeiner\*, Klaus Willecke\* and Reto Weiler

Neurobiology, University of Oldenburg, D-26111 Oldenburg, Germany

\*Inst. Molecular Genetics, University of Bonn, D-53117 Bonn, Germany

Bipolar cells play an important role in retinal circuits. They transmit signals from rod and cone photoreceptors to ganglion and amacrine cells in the inner retina. About 40% of the cells in the inner nuclear layer (INL) of the mouse retina are bipolar cells (Jeon et al., 1998). Based on physiological properties, bipolar cells are grouped into ON- and OFF-bipolar cells, which comprise several morphological subtypes. Some bipolar cells also form networks through gap junctional coupling involving connexins. One of the connexins involved in retinal networks is Cx45, and there is evidence for the expression of Cx45 in bipolar cells of the mouse retina. We were interested in identifying the subtypes of bipolar cells expressing Cx45 and used cytoplasmic markers and their axonal branching pattern. These characteristics have been used in a recent study (Ghosh et al., 2004) to classify bipolar cells in the mouse retina, revealing the presence of nine subtypes.

Retinal sections of transgenic mice, which express the enhanced green fluorescent protein (EGFP) instead of Cx45, were used together with antibodies directed against different cellular marker proteins (NK3R, CaB5, caldendrin, PKC) to identify Cx45-expressing bipolar cells. In addition antibodies against ChAT and calretinin which label distinct strata of the inner plexiform layer were used as landmarks for the characterisation of the axonal branching. Analysis was carried out by confocal laser scanning microscopy.

NK3R immunoreactivity was found in most Cx45-expressing bipolar cells, and only a few NK3R-stained bipolar cells were not Cx45 positive. A more detailed analysis revealed that anti-NK3R in particular labelled two OFF-bipolar cells which were identified as type 1 and 2 according to Ghosh et al. (2004). Anti-caldendrin appeared to label almost the whole population of Cx45-positive bipolar cells, including ON-cone bipolar cells. PKC labelled bipolar cells showed no co-localisation with Cx45-EGFP, indicating that rod bipolar cells do not express Cx45. Also anti-CaB5 labelled none of the Cx45-expressing bipolar cells.

In summary, the present immunohistochemical data strongly support our previous finding that Cx45 is expressed in ON- and OFF-bipolar cells but not in rod bipolars.

Supported by the Deutsche Forschungsgemeinschaft SFB 517/A2 and JA 854/1-1.

Ghosh, K. K. et al. (2004) *J. Comp. Neurol.* 469:70-82.

Jeon, C.-J. et al. (1998) *J. Neurosci.* 18(21):8936-8946.

## Do stability and sparseness lead to binocular properties of simulated neurons comparable to physiology?

Sebastian Bitzer<sup>1</sup>, Markus Goldbach<sup>1</sup>, Andres Bühlmann<sup>2</sup>, Selim Onat<sup>1</sup>, Peter König<sup>1,2</sup>

<sup>1</sup>Institute of Cognitive Science, University of Osnabrück, 49069 Osnabrück

<sup>2</sup>Institute of Neuroinformatics, University of Zürich/ETH Zürich, CH-8057 Zürich



Neurons in primary visual cortex are selective for many different features of visual stimuli (e.g. local contrast, orientation, spatial frequency, disparity, velocity ...; Hubel & Wiesel 1962, 1969). Recent studies show that the first 3 features of this list can be well understood by forming optimally stable or sparse representations of natural stimuli (Olshausen & Field 1996, Becker 1999, Körding et al. 2004). Here, we extend this line of work and investigate optimal representations of 3D natural videos and compare the resulting disparity selectivity to physiological results (Onat et al. 2004).

The simulations are based on a database of binocular cat-cam videos (see Onat et al. 2005, this conference). Receptive fields of simulated neurons are fitted with 2D-Gabor functions. The parameters of this fit are used to compute a number of statistical measures. These are compared to published data on cat and monkey primary visual cortex (Anzai et al. 1999, Prince et al. 2002).

As in primary visual cortex the simulated neurons respond selectively to the disparity of stimuli. Testing the simulated cells with random dot stereograms yields 100% of them being disparity selective. – Prince et al. (2002) found significant disparity tuning in 55% of simple and complex cells in primary visual cortex.

In primary visual cortex two mechanisms of encoding disparity, position and phase difference of right and left receptive fields, are uncorrelated ( $r=0.12$ , Anzai et al. 1999). – We observe a non-significant correlation between position and phase disparity as well ( $r=0.33$ , see Figure).

In the physiological data an anisotropy is reported with significantly lower variances of preferred phase differences for horizontal orientations as compared to vertical orientations (Ohzawa et al. 1996, Anzai et al. 1999). – In simulated neurons the distribution of preferred phase difference is independent of preferred orientation. Thus, the dependence of phase on orientation could not be confirmed in our simulation.

It is possible to define different types of disparity tuning (Poggio et al. 1988). However, scatter plots of phase and position difference of receptive fields of neurons in primary visual cortex do not indicate clustering into distinct groups (Prince et al. 2002). – Applying identical measures to the simulated cells we do not observe a clustering either.

Contrary to Prince et al. (2002) phases of neurons in our model cover a wider range of phase angle.

In primary visual cortex neurons with consistent inhibitory contribution from one eye are observed (Read & Cumming 2003). – In contrast, due to the limitation imposed by the energy model that is used in our study, this is not observed in any of the simulated neurons.

In summary, optimally stable or sparse simulated neurons match in several aspects of disparity coding their physiological counterparts. However, a number of measures give significantly deviating properties and modifications to the cell model and/or the objective functions have to be made to match all known biological properties.

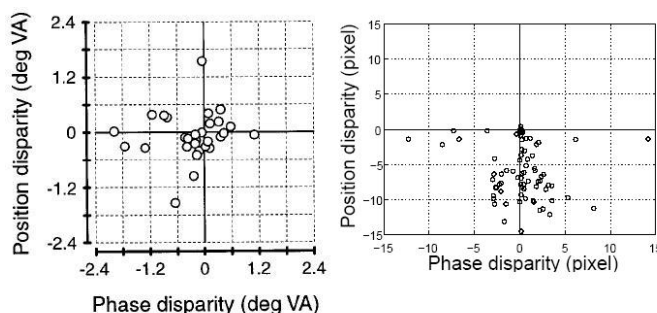


**Figure: Receptive field position disparity vs. phase disparity.** The left shows the simple cell data from Anzai et al. (1999), on the right we see the scatter plot for our sparseness data. In both data sets no significant correlation between the two RF properties was found ( $r_{\text{phys}} = 0.12$ ,  $r_{\text{sim}} = 0.33$ , respectively). Position disparities cover a smaller range than phase disparities (68% of phase range in Anzai et al. (1999) and 78% in our data, respectively).

## **Representation of optical illusions by retinal ganglion cell population**

**M. Bongard, E. Fernandez**

Universidad Miguel Hernandez, Institute of Bioengineering, Campus San Juan, Aptdo. correos 18, 03550 San Juan de Alicante, Spain

The complex structure of the visual system is sometimes exposed by illusions. We study the representation of selected optical illusions in the neuronal response pattern of retinal ganglion cell populations. The uncertainty of perceptual inference seems to be correctly represented even in this first stage of the visual processing path.

We are using a 3-dimensional sharpened tipped multi-electrode array to obtain extracellular recordings from random selected retinal ganglion cell populations with member sizes up to 400 identified neurons. Our experiments employed superfused, flattened preparations of intact rabbit and mouse retinas. Instead of looking on unitary spikes we are analyzing population responses and their representation of psychophysical effects and/or optical illusions. Stimuli cover a variety of optical illusions including e.g. Hermann grid illusions, "spinning wheel illusion" and contour completion.

Our results suggest that already retinal ganglion cell population represent perceptual contour completion and might be the starting locus for its computation via horizontal connections within different sub-ensembles of the population. A distributed activation which might be the neural correlate of perceptual changes and the resulting switches in the population response pattern can be shown for some cases of optical illusions even on the retina level.

**Poster Subject Area #PSA13:**  
**Visual systems of vertebrates: Central areas and perception**

- [#174A](#) K. Ohla, NA. Busch, MA. Dahlem and CS. Herrmann, Magdeburg  
*Perception of Glass patterns modulates early event-related potentials.*
- [#175A](#) KF. Schmidt, M. Kaschube, K. Kreikemeier, B. Godde, M. Schnabel, HR. Dinse, F. Wolf and S. Löwel, Magdeburg, Göttingen, Bochum and Tübingen  
*Adult plasticity: Long-term changes of orientation maps in cat visual cortex*
- [#176A](#) K. Kreikemeier, M. Kaschube, KF. Schmidt, B. Godde, M. Schnabel, F. Wolf, S. Löwel and HR. Dinse, Bochum, Göttingen, Magdeburg and Tübingen  
*Space-time characteristics of orientation preference map plasticity in visual cortex of adult cats*
- [#177A](#) N. Patzke, N. Freund, O. Güntürkün and M. Manns, Bochum  
*Lateralized organization of forebrain afferents to the optic tectum in pigeons*
- [#178A](#) R. Philipp, C. Distler and K-P. Hoffmann, Bochum  
*CHARACTERIZATION OF MOTION SPECIFIC AREAS IN FERRET VISUAL CORTEX*
- [#179A](#) HR. Dinse, C. Klaes, P. Ragert and M. Tegenthoff, Bochum  
*rTMS induced improvement of human visual orientation discrimination*
- [#180A](#) L. Jiménez-Ortega, O. Güntürkün and NF. Troje, Bochum and Ontario (CDN)  
*Interocular transfer in pigeons between the two yellow fields.*
- [#181A](#) WM. Blaszczyk, E. Neuhaus, C. Distler and K-P. Hoffmann, Bochum  
*Chloride cotransporter expression in the visual system of pigmented and albino rats*
- [#182A](#) D. Hupfeld and K-P. Hoffmann, Bochum  
*Visual motion perception in albinotic and pigmented ferrets (*Mustela putorius f. furo*)*
- [#183A](#) D. Hupfeld, K-P. Hoffmann and R. Heumann, Bochum  
*Behavioural phenotyping of synRAS-transgenic mice using a new first-step screening method: the M.O.U.S.E. test*
- [#184A](#) D. Jancke and A. Grinvald, Bochum and Rehovot (IL)  
*Cortical Representations of Motion Trajectories revealed by Voltage-Sensitive Dye Imaging in Early Visual Areas of the Cat*
- [#185A](#) M. Merkens and G. Westhoff, Bonn  
*Evidence for the processing of infrared stimuli within the dorsal Cortex of rattlesnakes*

- [#186A](#) A. Nagetusch, K-P. Hoffmann, C. Distler and D. Jancke, Bochum  
*Do albinotic animals lack selectivity for motion direction in the early visual cortex?*
- [#187A](#) G. Westhoff, M. Morsch and CW. Eurich, Bonn and Bremen  
*Infrared sensitive units and their response characteristics in the Tectum opticum of the rattlesnake Crotalus atrox*
- [#188A](#) WA. Freiwald, DY. Tsao, RBH. Tootell and MS. Livingstone, Bremen, Bosten, MA (USA) and Charlestown, MA (USA)  
*RECEPTIVE FIELD STRUCTURE AND SHAPE PROCESSING IN AREA V4*
- [#189A](#) D. Wegener, WA. Freiwald and AK. Kreiter, Bremen  
*Shifting attention is accompanied by a shift in the frequency components of monkey area MT neuronal responses*
- [#190A](#) A. Wannig, H. Stemmann and WA. Freiwald, Bremen and Bosten, MA (USA)  
*Neural correlates of non-space-based attention in macaque area MT: Top-down-control vs. bottom-up effects*
- [#191A](#) EL. Schulzke, H. Stemmann, WA. Freiwald and CW. Eurich, Bremen and Leipzig  
*Dynamic Stimuli and Dynamic Neurons: Encoding Properties of MT Cells in Awake Monkeys*
- [#192A](#) K. Taylor, S. Mandon and AK. Kreiter, Bremen  
*Attention Modulates Oscillatory Synchrony in Monkey Area V1 in a Shape Tracking Task*
- [#193A](#) V. Moliadze, D. Giannikopoulos, T. Kammer and K. Funke, Bochum and Ulm  
*Paired-pulse TMS effects on single unit activity in cat primary visual cortex*
- [#194A](#) K. Foltá, B. Diekamp, J. Kirsch and O. Güntürkün, Bochum and Baltimore, MD (USA)  
*Top-down innervation modulates visual activity of rotundal cells in pigeons*
- [#195A](#) H. Luksch, S. Scholz and R. Wessel, Aachen and Saint Louis, MO (USA)  
*Anatomy and electrophysiology of tecto-isthmic feedback loops in the chicken*
- [#196A](#) RF. van der Willigen, S. Vossen, W. Harmening and H. Wagner, Aachen  
*Shape from Stereo: a Comparative Approach*
- [#197A](#) S. Holtze and M. Vorobyev, Brisbane (AUS)  
*Chromatic and achromatic vision in zebra finches (taeniopygia guttata)*
- [#198A](#) S. Rubart and H-J. Bischof, Bielefeld  
*No Lateralization of Food Discrimination in Zebra Finches (Taeniopygia guttata castanotis)*

- [#199A](#) P. Wonderschütz, C. Lieshoff, J. Voss and H-J. Bischof, Bielefeld  
*The Distribution of Gamma-aminobutyric Acid in the Tectofugal System of White and Wild Type Zebra Finches (Taeniopygia guttata)*
- [#173B](#) PB. Forgacs, H. von Gizycki, H. Avitable and I. Bodis-Wollner, Brooklyn, NY (USA)  
*Does intrasaccadic gamma power increase reflect an internal mechanism of motor-sensory monitoring?*
- [#174B](#) G. Kovács, A. Antal and Z. Vidnyánszky, Budapest (H) and Göttingen  
*Event-related brain potential correlates of adaptation to faces and body parts*
- [#175B](#) J. Weiß and H. Wässle, Frankfurt/Main  
*Glycine receptors on amacrine cells in the mouse retina*
- [#176B](#) T. Schmidt, S. Niehaus and A. Nagel, Göttingen  
*The feedforward dynamics of action priming*
- [#177B](#) M. Schnabel, M. Kaschube, L. White, D. Coppola, S. Loewel and F. Wolf, Göttingen, Durham, NC (USA), Richmond, VA (USA) and Magdeburg  
*Signatures of Shift-Twist Symmetry in the Layout of Orientation Preference Maps*
- [#178B](#) F. Pieper, T. Peters and S. Treue, Göttingen  
*The influence of brief motion adaptation on direction perception*
- [#179B](#) M. Kaschube, M. Schnabel, K. Kreikemeier, HR. Dinse, B. Godde, KF. Schmidt, S. Löwel and F. Wolf, Göttingen, Bochum, Tübingen and Magdeburg  
*Orientation preference maps have sensitive spots*
- [#180B](#) B. Naundorf, M. Volgushev and F. Wolf, Göttingen and Bochum  
*Anomalous Spike Initiation in Cortical Neurons*
- [#181B](#) K. Maier, CR. Rau, MK. Storch, MB. Sättler, I. Demmer, R. Weissert, N. Taheri, AV. Kuhnert, M. Bähr and R. Diem, Göttingen  
*Ciliary neurotrophic factor protects retinal ganglion cells from secondary cell death during acute autoimmune optic neuritis in rats*
- [#182B](#) S. Bitzer, M. Goldbach, A. Bühlmann, S. Onat and P. König, Osnabrück and Zürich (CH)  
*Do stability and sparseness lead to binocular properties of simulated neurons comparable to physiology?*
- [#183B](#) M. Gehres and C. Neumeyer, Mainz  
*Perception of object-movement in goldfish (Carassius auratus)*
- [#184B](#) A. Gabriel, A. Gail and R. Eckhorn, Marburg  
*Traveling Gamma-Waves: Stimulus-dependent Signal Coupling in Monkey Primary Visual Cortex*



- [#185B](#) A. Kremper, A. Gail and R. Eckhorn, Marburg  
*Discrimination and prediction of perceptual states from multiple-electrode recordings in monkey striate cortex*
- [#186B](#) A. Kremper and R. Eckhorn, Marburg  
*Comparison of projection methods for dimension reduction and the determination of lower bounds for transmitted sensory information*
- [#187B](#) B. Al-Shaikhli and R. Eckhorn, Marburg  
*Unsupervised learning of cortical complex cell properties using spatio-temporally coherent visual stimuli and a recurrent network of spiking neurons*
- [#188B](#) T. Teichert, T. Wachtler, A. Gail, M. Wittenberg, F. Michler and R. Eckhorn, Marburg  
*Relations between spatial frequency preference and size of spatial-summation field in striate cortex of awake monkey*
- [#189B](#) SB. Hofer, T. Mrsic-Flogel, T. Bonhoeffer and M. Hübener, Martinsried  
*Extensive plasticity in adult mice after monocular deprivation revealed by optical imaging*
- [#190B](#) TD. Mrsic-Flogel, SB. Hofer, C. Creutzfeldt, T. Bonhoeffer and M. Hübener, Martinsried  
*Mapping retinotopy in mouse superior colliculus with optical imaging*
- [#191B](#) M. Liedvogel, U. Janssen-Bienhold, G. Feenders, J. Stalleicken, P. Dirks, R. Weiler and H. Mouritsen, Oldenburg  
*The mystery of magnetoreception in migratory songbirds*
- [#192B](#) H. Mouritsen, G. Feenders, M. Liedvogel and W. Kropp, Oldenburg  
*Migratory birds use head scans to detect the direction of the Earth's magnetic field*
- [#193B](#) G. Feenders, M. Liedvogel, K. Wada, ED. Jarvis and H. Mouritsen, Oldenburg and Durham, NC (USA)  
*Brain activity pattern during magnetic orientation tasks in night-migratory songbirds reveals a brain region involved in night-time vision*
- [#194B](#) S. Onat, C. Kayser and P. König, Osnabrück and Zurich (CH)  
*Stability of visual features and learning disparity selective complex cells*
- [#195B](#) S. Freyberg and UJ. Ilg, Tübingen  
*Smooth pursuit eye movements elicited by anticipation in humans and monkeys*
- [#196B](#) H. Fröhlich, B. Naundorf, M. Volgushev and F. Wolf, Tübingen, Göttingen and Bochum  
*What Membrane Potential Features Trigger a Neural Action Potential in Vivo?*
- [#197B](#) A. Nieder, Tübingen  
*Enumeration of Simultaneously and Sequentially Presented Visual Items by a Macaque Monkey*

[#198B](#)

K. Tichacek, S. Onat and P. König, Osnabrück

*Cross-modal integration in overt attention under natural conditions*

[#199B](#)

CF. Schmidt, P. Boesiger and A. Ishai, Zurich (CH)

*FACE PERCEPTION IS MEDIATED BY A DISTRIBUTED CORTICAL NETWORK*

**Perception of Glass patterns modulates early event-related potentials.**

Kathrin Ohla <sup>a\*</sup>, Niko A. Busch <sup>b</sup>, Markus A. Dahlem <sup>a</sup>, and Christoph S. Herrmann <sup>b</sup>

<sup>a</sup> *Clinic of Neurology II, Medical Faculty, Otto-von-Guericke University of Magdeburg, Germany*

<sup>b</sup> *Department of Biological Psychology, Otto-von-Guericke University of Magdeburg, Magdeburg, Germany*

\* Corresponding author. *E-mail adress:* kathrin.ohla@medizin.uni-magdeburg.de

**Abstract**

**Background:** Glass patterns are randomized dot patterns that generate the perception of a global structure. They consist of correlated dot pairs with direction, orientation, and arrangement that are described by geometric transformations.

**Methods:** The present study employed behavioral and event-related brain potentials (ERP) measures to characterize the neural processes underlying the perception of Glass patterns. Stimuli were circular, translational, and randomized Glass patterns presented in two isoluminant colors using a choice reaction paradigm. Subject (n=16) were instructed to differentiate between colors.

**Results:** The N170 component increased in amplitude for circular compared to translational and randomized patterns. This effect was most pronounced over occipito-temporal areas.

**Discussion:** The results suggest that the global form generated by Glass pattern perception occurs at an intermediate stage of visual processing and that the visual system is specialized in the perception of circular patterns.

### Adult plasticity: Long-term changes of orientation maps in cat visual cortex

Schmidt K. F. (1), Kaschube M. (2), Kreikemeier K. (3), Godde B. (4), Schnabel M. (2), Dinse H. R. (3), Wolf F. (2) & Löwel S. (1)

*(1) Leibniz-Institut für Neurobiologie, Magdeburg (2) MPI für Strömungsforschung, Göttingen (3) Institut für Neuroinformatik, Universität Bochum (4) Med. Psychol. & Behav. Neurobiol., Univ., Tübingen*

Recently, it was shown that even in adult visual cortex the layout of orientation preference (OR-) maps can be substantially reorganized by activity-dependent mechanisms: few hours of intracortical microstimulation (ICMS) led to an enlargement of the cortical representational zone at the ICMS site and to an extensive restructuring of the entire OR-map layout up to several millimeters away (1, 2). To assess whether such changes persist or recover under normal visual experience we performed long-term optical imaging experiments in area 18 of adult cats. We recorded 2 baseline OR-maps 0-4 days prior to applying ICMS, an OR-map immediately after and follow-up OR-maps 3 to 7 days after ICMS using optical imaging of intrinsic signals (3).

While baseline OR-maps remained essentially stable (correlation coefficient up to  $r = 0.86$ ), ICMS could cause long-ranging plasticity of OR-map layout as reported previously (1,2): In some cases, the changes were widespread, covering a range of several millimeters, while in other cases a cortical area of only 1 to 2 millimeters around the ICMS-site was altered. (1,2). As also reported for acute experiments (1,2), the recovery process showed considerable variation. In some cases, we could visualize OR-maps with a clearly modified layout compared to the pre-ICMS pattern even after many days of recovery in animals that were awake and had been living in a normal visual environment for the intermediate period of time. In other cases, we observed substantial ICMS-induced changes of OR-maps followed by largely complete restoration of the initial map layout after a prolonged recovery period.

A new and very interesting observation of the present experiments is that ICMS can induce strong changes in the orientation selectivity index (OSI) of the maps: OSI-values after ICMS were different from pre-ICMS-values, whereby values increased in the majority of cases.

Taken together, ICMS-induced plasticity is characterized by pronounced variability ranging from substantial reorganization persisting for several days under normal visual experience to largely complete recovery of the initial OR-maps from a strongly modified post ICMS state. Whether and how the observed variability in map plasticity depends on recovery time or on ICMS-location and whether there is a consistent relation between map plasticity and change in orientation selectivity is subject of current experiments.

(1) Godde et al. ('02) PNAS 99: 6352 (2) Kreikemeier et al. ('04) FENS Abstr. 2: A017.17.  
(3) Löwel et al. ('98) EJN 10: 2629

Supported by the Volkswagen Foundation (I/77 347, 348, 349)

## Space-time characteristics of orientation preference map plasticity in visual cortex of adult cats

Kreikemeier, K. <sup>(1)</sup>, Kaschube, M. <sup>(2)</sup>, Schmidt, K.-F. <sup>(3)</sup>, Godde, B. <sup>(5)</sup>, Schnabel, M. <sup>(2)</sup>, Wolf, F. <sup>(2)</sup>, Löwel, S. <sup>(3,4)</sup> and Dinse, H. R. <sup>(1)</sup>

<sup>(1)</sup> Institute for Neuroinformatics, Ruhr-University, Bochum, Germany,

<sup>(2)</sup> Max-Planck-Institut für Strömungsforschung, Göttingen, Germany,

<sup>(3)</sup> Leibniz-Institute for Neurobiology and <sup>(4)</sup> Otto-von-Guericke University, Magdeburg, Germany,

<sup>(5)</sup> Medical Psychology and Behavioral Neurobiology, Eberhard-Karls-University, Tübingen, Germany

In cat visual cortex, neurons that respond to similarly oriented stimuli are arranged in a two-dimensional pattern, giving rise to orientation preference maps (OPMs). Long-range tangential connections between cells of similar orientation preferences are assumed to shape and stabilize the spatial layout of OPMs. While a number of studies addressed the plastic reorganizational capacities of OPMs during development, little is known about OPM plasticity in adult visual cortex. Here we used ICMS to induce cortical reorganization on a short time scale by enforcing temporally synchronized neuronal activity <sup>(1)</sup>. Previous studies have shown that changes of in area 18 of adult cats induced by ICMS were not restricted to the ICMS site, but covered an observation window of approximately 3 x 2 mm <sup>(2)</sup>.

To clarify the spatial extent and the time course of ICMS-induced reorganizations we applied ICMS for 3 to 4 h and recorded pre and post ICMS single-condition maps (SCMs) using optical imaging of intrinsic signals for up to 40 hours after termination of ICMS. For recording SCMs, moving gratings of different orientations were used. Generally, ICMS-induced OPM plasticity varied in extent and magnitude. In about half of the cases studied we found an immediate onset of plastic changes, while in the remaining cases a delayed onset of plastic changes was observed. The “immediate” group showed a significant enlargement of the stimulated domain 1-3 hrs after termination of ICMS whereas in the “delayed” group a maximum of reorganization was reached only after 9-11 hrs.

The spatial extent of restructuring was also variable. In a number of experiments we found changes in the OPMs within the entire observation window of 9 x 5 mm window, while in other experiments changes were restricted to a few millimetre. Analysis of the area of orientation domains showed an enlargement of the domain representing the orientation at ICMS site at the expense of the oblique domains. Calculation of a similarity index describing global aspects of map similarity demonstrated that ICMS altered the layout of OPMs indicated by a decrease of similarity. Analysis of the time course of plastic changes revealed that remodeling could continue to develop up to several hours after termination of ICMS. While on average after 20 to 30 hrs the area of orientation domains recovered to baseline, the similarity index did not, which can be taken as evidence for the emergence of a new OPM with normal distributed domains but a new layout. Analysis of the temporal development of the distance dependence of a local similarity measure showed that ICMS effects were first present rather local around the ICMS site, but then spread out to over many millimetres. To analyse the time course of changes beyond our observation period of up to 40 h, chronic recordings over up to 10 days were used, see <sup>(3)</sup> for details. For theoretical predictions about plastic reorganizational processes in OPMs of adult visual cortex see <sup>(4)</sup> and <sup>(5)</sup>.

Our results indicate that ICMS, a local, presumably LTP/LTD-like stimulation, can remodel OPMs in adult visual cortex over 6 to 7 mm. ICMS-induced changes continue to develop even after termination of ICMS and show a limited capacity for recovery. Interestingly, both properties were found in rTMS experiments in humans, in which periods of high-frequency rTMS lead to improvement of orientation discrimination performance <sup>(6)</sup>. It is therefore conceivable that the observed ICMS-induced changes of OPMs in adult visual cortex might be related to associated changes in perception of orientation.

1) Recanzone et al. (1992) Cereb Cortex 2: 181; 2) Godde et al. (2002) PNAS 99: 6352 ;

3) Schmidt et al. (2005) this meeting ; 4) Kaschube et al. (2005) this meeting; 5) Schnabel et al.

(2005) this meeting ; 6) Klaes et al. (2005) this meeting

*supported by the Volkswagen Foundation (I/77 347, 348, 349)*

## **Lateralized organization of forebrain afferents to the optic tectum in pigeons**

**Nina Patzke, Nadja Freund, Onur Güntürkün and Martina Manns**

*Biopsychology, Institute of Cognitive Neuroscience, Faculty of Psychology, Ruhr-University Bochum, 44780 Bochum, Germany*

The visual system of pigeons is lateralized with a dominance of the right eye/ left hemisphere for detailed visual object analysis. In pigeons, this behavioural lateralization is accompanied by morphological left-right differences in the tectofugal pathway projecting from the retina via the optic tectum and nucleus rotundus to the entopallium in the forebrain. Apart from cell size asymmetries, the crossed portion of the tectorotundal projection is asymmetrically organized with more fibers traversing from the right tectum to the left rotundus than vice versa (Güntürkün, 2002). Recently, it has been shown that tectofugal processing is asymmetrically modulated by forebrain input whereby the descending activation after visual stimulation is guided entirely by the left forebrain and this influence presumably arises from the Wulst, the telencephalic target of the thalamofugal pathway (see Folta et al., 2004).

By means of a retrograde tracing study, we wanted to identify the morphological substrate for the lateralized forebrain control. The retrograde tracer cholera toxin subunit B (CtB; Sigma, Deisenhofen, Germany) was injected unilaterally into either the left or right optic tectum of adult pigeons (Hellmann and Güntürkün, 1999). After two days survival time, the animals were perfused and their brains were cryosectioned to perform an immunohistochemical detection of CtB-positive cells within the forebrain. The ipsi- and contralaterally located cells were counted and the size of the injection area was estimated. The percentage of ipsi- and contralateral cells relative to the size of the injection area served as an index for the laterality of the projection pattern.

Retrogradely labelled cells were located within the arcopallium, Area corticoidea dorsolateralis (CDC) and hyperpallium apicale (HA) of the Wulst. While the arcopallial and CDC tectopetal populations were completely confined to the ipsilateral hemisphere, HA gave also rise to a small contralateral population. The percentage of these contralaterally projecting cells was slightly higher in the left HA. However, in sum the number of cells projecting to the tectum was much smaller in the right than in the left HA. Thus, the higher number of tectopetal cells located in the left Wulst might be the morphological substrate for the fact that tectofugal forebrain control is completely subserved by the left hemisphere.

Hellmann B, Güntürkün O. 1999. *Eur J Neurosci* 11:2635-2650.

Güntürkün, O., 2002. In: *Brain Asymmetry*, 2<sup>nd</sup> Edition, Hugdahl, K. and Davidson, R.J. (Eds.), Cambridge, MA: MIT Press, 2002, pp. 3-36.

This research was supported by a grant from the SFB Neurovision of the Deutsche Forschungsgemeinschaft.

## CHARACTERIZATION OF MOTION SPECIFIC AREAS IN FERRET VISUAL CORTEX

Roland Philipp, Claudia Distler and Klaus-Peter Hoffmann  
General Zoology & Neurobiology, Ruhr-Universität Bochum,  
44780 Bochum, Germany

The ferret (*Mustela putorius furo*), a member of the canid lineage, became a very popular subject in visual research during the last years due to its early stage of neurogenesis at birth. Nevertheless we know very little about its motion processing system. Since there exist many similarities between cat and ferret visual cortex we turn our attention to a region posterior from ferrets suprasylvian sulcus (SSS) which was not specified up to now. The existence of motion analysing suprasylvian areas in cat (e.g. posteromedial lateral suprasylvian area, PMLS) gives reason for supposing that the motion analyzing areas should be in ferret suprasylvian cortex (SSC), too.

We have investigated the SSC of 5 pigmented and 2 albinotic ferrets, each of them in 3-5 sessions. The animals were initially anaesthetized with 20mg/kg ketamine and 2mg/kg thiazinhydrochloride, intubated through the mouth and placed into a stereotaxic frame. The craniotomy was performed under additional local anaesthesia with bupivacainhydrochloride. During electrical recordings they were anesthetized with halothan (0.2%-0.4% in air as needed) and positioned stereotaxically by means of an implanted head post into the experimental setup. The visual stimuli composed of a random dot-pattern could be moved in a circular pathway and as expanding or contracting radial motion simulating selfmotion (optic flow). Peri stimulus time histograms (PSTH) were generated online and stored in a PC for offline analysis.

Altogether 235 neurons were recorded in pigmented, 132 neurons in albino ferrets which were localized in a suprasylvian visual area just posterior from SSS. In 92% of the neurons in pigmented and in 72% of the neurons in albino ferrets stimulation in the preferred direction elicited at least twice as many spikes than stimulation in the non-preferred direction. Therefore, we tentatively call this motion sensitive area the posterior suprasylvian area (PSS).

Additionally, 192 neurons in pigmented and 116 neurons in albino ferrets were tested with the optic flow stimuli. In pigmented ferrets 35% of the neurons were classified as expansion cells and 13% as contraction cells. So expansion cells were significantly more frequent than contraction cells in pigmented ferret. This was not the case in albino ferrets where 20% of the neurons were classified as expansion and 12% as contraction cells.

Electrical stimulation experiments in the ipsiversiv nucleus of the optic tract and dorsal terminal nucleus (NOT-DTN) of the pigmented ferret have shown that PSS could be antidromically activated (21 cortical neurons out of 82 tested) and thus exhibits projections to the NOT-DTN.

All these data suggest that PSS may play an important role in motion and direction processing in ferret visual cortex and, by its direct projection to the NOT-DTN, in the optokinetic reaction (OKR). Recent behavioural studies after lesion of PSS (*Hupfeld et al., 2005*) support this hypothesis. Furthermore our data indicate a reduced direction selectivity in albino ferret PSS.

Supported by the DFG (SFB 509).

## rTMS induced improvement of human visual orientation discrimination

Hubert R. Dinse<sup>1</sup>, Christian Klaes<sup>1</sup>, Patrick Ragert<sup>1</sup>, Martin Tegenthoff<sup>2</sup>

<sup>1</sup>Institute for Neuroinformatics, Theoretical Biology, Ruhr-University, Bochum, Germany

<sup>2</sup>Department of Neurology Ruhr-University, BG-Kliniken Bergmannsheil, Bochum, Germany

[hubert.dinse@neuroinformatik.rub.de](mailto:hubert.dinse@neuroinformatik.rub.de)

At a cellular level, plastic changes of synaptic transmission can be evoked solely by patterned electrical stimulation lacking meaning, attention or task constraints. In an attempt to explore the efficacy of patterned, passive stimulation for perceptual learning in humans, we have recently demonstrated that 5 Hz repetitive transcranial magnetic stimulation (rTMS) applied over the hand representation of somatosensory cortex leads to improvement of tactile 2-point discrimination of the fingers (1). Here we demonstrate that 5 Hz rTMS applied over the foveal visual cortex representation is similarly effective in the visual domain by evoking persistent improvement of orientation discrimination performance.

Orientation discrimination was tested using the protocol introduced by Schoups et al. (2). The stimulus was a circular 2.5 deg diameter noise field positioned centrally, consisting of light and dark bars (0.075 to 0.31 deg, relative phases randomized). Intertrial interval was 1 s, stimulus exposure 300 ms. Subjects had to respond within 600 ms after stimulus onset. The reference orientation, which was never shown, was right oblique (45 deg); for control of generalization, a reference of -45 deg was also tested. The subjects had to decide whether the noise field was tilted clockwise or counterclockwise to the reference, auditory feedback was given for errors. An up-down staircase procedure was used converging on an just noticeable orientation differences (JND) corresponding to an 84 % criterion. Starting value was an orientation difference of  $\pm 7$  deg, step size was 20 %. Daily sessions consisted of 10 blocks of 100 trials each.

For details of the 5Hz rTMS application see (3,4). To position the coil over the foveal representation of primary visual cortex, we induced phosphenes within the central visual field using single pulse TMS. For rTMS, two sessions separated by 30 min through the tangentially oriented coil grip backwards were applied at an intensity 10 % below the phosphene induction threshold resulting in a total of 2500 pulses. First, orientation discrimination was tested over 10 sessions. In the 11<sup>th</sup> session rTMS was applied. About 15 min after termination, orientation discrimination was re-tested to study changes in discrimination performance. To assess the time course of recovery, additional tests were performed 24 hours and 1 week later. In the control group, subjects were tested with an identical schedule, but without rTMS application.

For each subject we found perceptual learning occurring over the first 5 to 6 sessions that was highly specific for the learned orientation with little transfer to an orientation 90 deg away confirming the data of (2). After reaching a stable plateau of discrimination in the remaining sessions, rTMS improved JND by about 10 % for both the learned and the non-learned orientation. Most notable, the improvement continued to develop resulting in an even higher gain of performance 24 h after rTMS. After 1 week, the improvement recovered, yet not reaching baseline performance. None of these effects could be observed in the control group.

The results provide further evidence that stimulation protocols resembling those used in LTP studies applied from outside directly to selected brain regions can induce persistent improvement of discrimination performance. While the improvement in the tactile domain lasted for about 2 h (1), the much longer persistence observed for orientation discrimination suggests a strong modality-specificity. Interestingly, plastic changes of cat orientation preference maps induced by intracortical microstimulation showed a similar pattern of stability (5,6).

1. Ragert P, Pleger B, Tegenthoff M, Dinse HR (2002) Soc Neurosci Abstr 28: 841.7

2. Schoups AA, Vogels R, Orban GA (1995) J Physiol 483,797

3. Ragert P, Dinse HR, Pleger B, Wilimzig C, Frombach E, Schwenkreis P, Tegenthoff M (2003) Neurosci Letters 348, 105

4. Ragert P, Becker M, Tegenthoff M, Pleger B, Dinse HR (2004) Neurosci Letters 356: 91

5. Kreikemeier K, Kaschube M, Schmidt KF, Godde B, Schnabel M, Wolf F, Löwel S, Dinse HR (2005) this meeting

6. Schmidt KF, Kaschube M, Kreikemeier K, Godde B, Schnabel M, Dinse HR, Wolf F, Löwel S (2005) this meeting



Interocular transfer in pigeons between the two yellow fields.

Laura Jiménez Ortega<sup>1</sup>(laura.jimenez-ortega@rub.de), Onur Güntürkün<sup>1</sup>, Nikolaus F. Troje<sup>1,2</sup>  
<sup>1</sup>Ruhr-Universität-Bochum, Germany, <sup>2</sup>Queen's University, Canada.

The pigeon's visual field is characterized by a small region of binocular overlap (red field) and a large area of monocular vision in each lateral visual field (yellow field). Previous research has shown the existence of interocular transfer in the binocular area of the visual field. Interocular transfer in the binocular region may be needed for building a coherent representation of the visual world and monitoring actions like pecking. In the current study, we tested whether unrestrained pigeons were capable of interocular transfer between the two lateral visual fields. For this purpose, we built an experimental arena and placed a feeder and two pecking keys on either side. For presenting the stimuli, two TFT screens were mounted on the sides of the chamber. Four pigeons were trained to walk between the distant feeders. The pigeons' task was to discriminate between two visual stimuli (a cross and a square) presented in one of the lateral visual fields by pecking on the keys situated near the feeders. Two pigeons were trained to solve the task in the left visual field and the other two in the right visual field. After the birds reached a criterion of 75% correct responses in three consecutive sessions, we presented catch trials in the non-trained lateral visual field. Three of the four pigeons were incapable of interocular transfer. After this test we trained these three pigeons in the naive hemisphere. One pigeon never learn the task. Two pigeons needed more than 3000 trials to learn it. A fourth pigeon was capable of binocular transfer and therefore did not need any training in the untrained hemisphere. These results suggest that interocular transfer in the lateral visual field is, most probably, not a common characteristic among pigeons. Frontal interocular transfer may be a condition for depth perception through binocular disparity. This is not the case for the lateral monocular fields that process unmatchable information.

## Chloride cotransporter expression in the visual system of pigmented and albino rats

W.M. Blaszczyk<sup>1,2</sup>, E. Neuhaus<sup>3</sup>, C. Distler<sup>2</sup> & K.-P. Hoffmann<sup>2</sup>

<sup>1</sup> International Graduate School of Neuroscience, <sup>2</sup> Lehrstuhl für Allgemeine Zoologie & Neurobiologie,  
<sup>3</sup> Lehrstuhl für Zellphysiologie, Ruhr-Universität Bochum, 44780 Bochum, Germany

In the central nervous system, cation-chloride co-transporters have been identified as important regulators of the neuronal chloride concentration. Especially the inwardly directed transporter NKCC1 as well as the outwardly directed transporter KCC2, that is exclusively expressed in neurons (Payne et al., 1996), are of special interest regarding neuronal chloride homeostasis. The expression balance between both transporters determines if a neuron responds with excitation or inhibition to GABA and glycine mediated signalling (Mercado et al., 2004).

NKCC1 and KCC2 are developmentally regulated and the expression varies with the developmental switch in GABA responses and the decrease in intracellular chloride concentration. In immature neurons, the intracellular chloride concentration is predominantly regulated by NKCC1 activity that leads to higher intracellular chloride levels than extracellularly (Plotkin et al., 1997; Delpire et al., 1999; Shimizu-Okabe et al., 2002). This accumulation of intracellular Cl<sup>-</sup> results in an outward Cl<sup>-</sup> current (depolarization) of the cell after GABA<sub>A</sub> receptor activation. Thereafter, such depolarizing GABA actions shift to more negative levels during development. A developmental upregulation of KCC2 and downregulation of NKCC1 expression correlates with the shift in intracellular chloride levels and may underlie the GABAergic functional switch from depolarisation to hyperpolarisation (Rivera et al., 1999; DeFazio et al., 2000).

Albinism is known to result in abnormalities of visual processing including the direction selective system (Hoffmann et al., 2004). Recent findings indicate an important role for GABA mediated signalling and chloride cotransporters in albino visual information processing: Biochemical changes of the retinal GABA concentration (Blaszczyk et al., 2004) as well as physiological differences in the mediation of inhibitory GABA<sub>A</sub> receptor currents in the visual cortex (Barmashenko et al., 2004) can be found in albino when compared to pigmented rats. These results imply alterations in the albino visual system on the molecular level.

In this study we examine the expression of NKCC1 and KCC2 in pigmented Long Evans and albino Wistar rats aged P28 at different levels of visual processing in order to monitor possible changes that could lead to alterations in excitability and neuronal communication.

*This work was supported by SFB 509/A11 and the International Graduate School of Neuroscience (IGSN).*

### References:

- Barmashenko G, Schmidt M & Hoffmann K-P 2004. Differences in cytosolic chloride [Cl<sup>-</sup>]<sub>i</sub> in neurons of the visual cortex in pigmented and albino rats. FENS Abstr., vol.2, A050.1
- Blaszczyk WM, Straub H & Distler C 2004. GABA content in the retina of pigmented and albino rats. Neuroreport 15(7):1141-4.
- DeFazio RA, Keros S, Quick MW & Hablitz JJ 2000. Potassium-coupled chloride cotransport controls intracellular chloride in rat neocortical pyramidal neurons. J Neurosci. 20(21):8069-76.
- Delpire E, Lu J, England R, Dull C & Thorne T 1999. Deafness and imbalance associated with inactivation of the secretory Na-K-2Cl co-transporter. Nat Genet. 22(2):192-5.
- Hoffmann K-P, Garipis N & Distler C 2004. Optokinetic deficits in albino ferrets (*Mustela putorius furo*): a behavioural and electrophysiological study. J Neurosci. 24(16):4061-9.
- Mercado A, Mount DB & Gamba G 2004. Electroneutral cation-chloride cotransporters in the central nervous system. Neurochem Res. 29(1):17-25.
- Payne JA, Stevenson TJ & Donaldson LF 1996. Molecular characterization of a putative K-Cl cotransporter in rat brain. A neuronal-specific isoform. J Biol Chem. 271(27):16245-52.
- Plotkin MD, Snyder EY, Hebert SC & Delpire E 1997. Expression of the Na-K-2Cl cotransporter is developmentally regulated in postnatal rat brains: a possible mechanism underlying GABA's excitatory role in immature brain. J Neurobiol. 33(6):781-95.
- Rivera C, Voipio J, Payne JA, Ruusuvuori E, Lahtinen H, Lamsa K, Pirvola U, Saarna M & Kaila K. 1999. The K<sup>+</sup>/Cl<sup>-</sup> co-transporter KCC2 renders GABA hyperpolarizing during neuronal maturation. Nature 397(6716):251-5.
- Shimizu-Okabe C, Yokokura M, Okabe A, Ikeda M, Sato K, Kilb W, Luhmann HJ & Fukuda A 2002. Layer-specific expression of Cl<sup>-</sup> transporters and differential [Cl<sup>-</sup>]<sub>i</sub> in newborn rat cortex. Neuroreport 20;13(18):2433-7.

## Visual motion perception in albinotic and pigmented ferrets (*Mustela putorius f. furo*)

Daniela Hupfeld<sup>°</sup>, Klaus-Peter Hoffmann

Allgemeine Zoologie & Neurobiologie, Ruhr-Universität Bochum  
Universitätsstrasse 150, 44780 Bochum

Oculocutaneous albinism causes remarkable changes in retinal differentiation and by this leads to various deficits in visual system development. One of the resulting impairments concerns the horizontal optokinetic nystagmus (hOKN), an oculomotor reflex which stabilises the image on the central retina (area centralis or fovea) during full field visual movement stimulation. In several species the gain of the monocular hOKN is reduced in albinotic individuals, whereas albino *ferrets* don't show such an oculomotor movement pattern at all, neither under binocular nor monocular conditions. They are thus referred to as "optokinetic blind". If they don't generate the reflectory movement which is usually elicited by a visual motion stimulus, may this be caused by a lack of perception of this stimulus? Are albino ferrets motion blind?

To test their perceptual ability for global motion 17 ferrets (4 wildtype pigmented males, 6 albino males, 3 wildtype females, 4 albino females) were trained on a 2AFC paradigm. The discriminative stimuli were moving random dot patterns with limited lifetime white dots on a black background. The rewarded stimulus was a random dot pattern with all dots moving coherently to the right, this had to be distinguished from a completely incoherent pattern with dots moving into oblique directions. To start the visual discrimination training a simple black-white discrimination task was used, this stimulus was modified in several steps to finally reach the coherence vs. noise discrimination.

The coherence detection was possible both for albinotic and pigmented ferrets of both genders. On the basis of this result a threshold for this visual ability was evaluated by using a set of different coherence values vs. a noise stimulus. Results showed that despite albinotic individuals are able to perceive global visual motion they are severely impaired in terms of the signal strength necessary for perception. The threshold values differ between albino and wildtype animals by a factor of two. A gender specific difference in performance on this task was observed, with females showing lower performance on all coherence values but not for the simple black-white discrimination task.

An electrophysiological study could identify a cortical area with a high percentage of directional selective cells located at the posterior bank of the suprasylvian sulcus, therefore referred to as the posterior suprasylvian area (PSS) (Philipp, Distler & Hoffmann 2004). Lesion studies on well trained ferrets were aimed to evaluate the role of area PSS in global motion perception of the ferret. Results indicate a nearly complete loss of coherence detection performance in PSS-lesioned ferrets as well as a reduced gain of both binocular and monocular optokinetic nystagmus in lesioned pigmented ferrets. Control lesions prove the specificity of this deficit to PSS lesions.

supported by SFB 509

<sup>°</sup>corresponding author: daniela.hupfeld@rub.de

## Behavioural phenotyping of synRAS-transgenic mice using a new first-step screening method: the M.O.U.S.E. test

D. Hupfeld<sup>°</sup>, K.-P. Hoffmann, R. Heumann\*

Allgemeine Zoologie & Neurobiologie, Ruhr-Universität Bochum

\*Molekulare Neurobiochemie, Ruhr-Universität Bochum

Universitätsstrasse 150, 44780 Bochum

The increasing amount of mouse strains, transgenic and knock-out models that have been, and are still, developed stresses the importance of valuable phenotyping methods. A detailed behavioural phenotyping needs a great number of experiments. The selection of necessary and useful tests at the beginning of the phenotyping process thus is an important step. Phenotyping protocols most often use a fixed set of tasks for basic behavioural elements (e.g. activity, anxiety, spatial learning) complemented by tests that specifically fit to the expected changes of behaviour. By this procedure it is not unlikely to miss unexpected influences of the breeding or manipulation. A new test abbreviated M.O.U.S.E. can be helpful for the first screening and the selection of further tests.

**Mouse Observation Using Spontaneous Exploration** is based on a setup that offers a complex environment for the spontaneously exploring individual. In contrast to observations of home cage activity, which is restricted to a plain and uniform environment under most standard housing conditions, this test environment enables a great variety of behavioural activities. Social contact to conspecifics of both sexes is one of the aspects tested by M.O.U.S.E. but seldom included in other standard phenotyping protocols. The M.O.U.S.E.-setup can be build from standard housing cages and a few additional materials, the test procedure is simple and behaviour can be recorded by a camera and analysed offline.



The M.O.U.S.E.-setup can be build from standard housing cages and a few additional materials, the test procedure is simple and behaviour can be recorded by a camera and analysed offline.

It has been used to start the behavioural phenotyping of synRAS mice, a transgenic mouse-line that has been developed to evaluate the function of the small G protein Ras for neuronal survival and plasticity within the central nervous system. A constitutively activated Val12-Ha-Ras has been combined with a specific promotor (synapsin) to ensure transgenic Ras expression only in postmitotic neurons. Albinotic NMRI mice have been chosen as background strain for this transgen.

M.O.U.S.E. showed results for locomotor activity, exploratory behaviour, anxiety and social contact. Remarkable differences have been found between the exploratory behaviour of the male but not the female heterozygot synRAS mice when compared with their wildtype (NMRI) counterparts. There is a gender specific deficit in social interaction which could be found by this test, with male transgenic mice showing reduced interest in both male and female conspecifics.

MOUSE proved to be a useful and effective tool for an initial behavioural screening, enabling the selection of further phenotyping tests on its basis.

<sup>°</sup> corresponding author: daniela.hupfeld@rub.de

# Cortical Representations of Motion Trajectories revealed by Voltage-Sensitive Dye Imaging in Early Visual Areas of the Cat

Dirk Jancke<sup>1,2</sup> & Amiram Grinvald<sup>2</sup>

<sup>1</sup>*Allgemeine Zoologie und Neurobiologie, Ruhr-Universität Bochum, 44801 Bochum, Germany*

<sup>2</sup>*Department of Neurobiology, Weizmann Institute of Science, 76100 Rehovot, Israel*

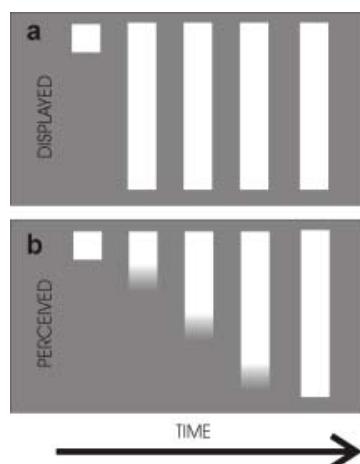
jancke@neurobiologie.ruhr-uni-bochum.de

Gestaltpsychologists Wertheimer (1921) and Kenkel (1913) made the surprising observation that even stationary stimuli evoke sensation of motion, the “gamma movement”. A briefly presented local stimulus is perceived as expanding or otherwise as contracting when it disappears from a homogenous background. Neurophysiologically it is still unclear how local stimuli are cortically represented in terms of spatio-temporal populations dynamics of both sub- and suprathreshold activity.

We used optical imaging of voltage-sensitive dyes in area 18 of the anaesthetized and paralyzed cat in order to visualize cortical representations of either briefly flashed or local moving stimuli. This technique measures changes in synaptic potentials of neural populations, thus monitoring patterns of evoked activity in real-time across the cortical surface.

We found that a flashed stimulus evoked far reaching subthreshold propagating activity that gradually slowed down as the response amplitude increased. Only at high (suprathreshold) levels activity stayed local, respectively motionless. We interpret these findings as the result of a synaptic process that transmits activity horizontally throughout the wide arborisation of neural dendrites. Deceleration of activity at higher amplitudes could arise from changes in the amount and time courses of synaptic transmission.

In the “line-motion” condition, in which two stationary stimuli were presented subsequently (see Figure) the subthreshold spread was rapidly enhanced by the second stimulus leading to a significant suprathreshold “wave front” of activity that moved at a constant speed away from the pre-cued location. Similar results were obtained for real moving stimuli. Signals of such expanding wave fronts may be fed into motion detectors at higher processing stages.



The “line-motion” illusion. a) A square of light (“pre-cue”) is presented just before a bar stimulus. b) Instead of sensing the bar at once, subjects report an illusory line drawing starting from the pre-cued location away from the dot.

Our results are in line with studies that referred to the phenomenon as motion induction by pre-attentive facilitation or as an apparent-motion process with no need of attention per se. Higher-level processes might modulate speed and shape of propagating activity to guide bottom-up attention in the behaving subject.

Supported by the Grodetsky Center, the Goldsmith and Korber and ISF Foundations (A.G.), the MINERVA Foundation, Germany and the BMBF (D.J.)

## **Evidence for the processing of infrared stimuli within the dorsal Cortex of rattlesnakes**

Malte Merkens and Guido Westhoff

Institute of Zoology, University of Bonn, Poppelsdorfer Schloss, 53115 Bonn, Germany, email: gwesthoff@uni-bonn.de

Pitvipers like rattlesnakes possess highly sensitive infrared detecting organs that are innervated by the trigeminal nerve. The pit organs enable the snake to detect minute thermal differences within their environment, which helps them to find their warm-blooded prey. Infrared stimuli are conducted via the trigeminal nerve and the rhombencephalon to the midbrains Tectum opticum. The processing of infrared stimuli is integrated with the processing of visual stimuli in the Tectum, the Nucleus rotundus and within the dorsal ventricular ridge of the forebrain (Berson and Hartline, 1988). A cortical representation of the visual system was shown in turtles but not in snakes. To date, nothing is known about the possible representation of the infrared sense within the dorsal Cortex of infrared sensitive snakes.

We mapped the dorsal Cortex of 14 rattlesnakes (*Crotalus atrox*) by means of electrophysiological recordings using tungsten electrodes. A red diode laser focussed into the contralateral pit organ served as a heat stimulus whereas a moving black paper square of 2x2cm was used to stimulate the visual system.

We found 30 units to respond upon visual stimuli, 8 of which were bimodal and also responded to the laser as a heat stimulus. In addition we found 5 units that responded unimodal on the heat stimulus with mean latencies of 433ms. These units were located in a small area of the rostral dorsal Cortex. Visual responding units were scattered over the entire dorsal Cortex. Although we only found very few infrared sensitive units our results suggest that the dorsal Cortex of rattlesnakes is involved in processing visual and infrared stimuli.

Berson DM, Hartline PH (1988). A Tecto-Rotundo-Telencephalic Pathway in the Rattlesnake: Evidence for a Forebrain Representation of the Infrared Sense." The Journal of Neuroscience **8(3)**: 1074-1088.

Supported by DFG

## **Do albinotic animals lack selectivity for motion direction in the early visual cortex?**

***Intrinsic optical imaging of parametric maps in ferrets (*Mustela putorius furo*)***

**Alexandra Nageusch, Klaus-Peter Hoffmann, Claudia Distler, Dirk Jancke**

Lehrstuhl für allgemeine Zoologie und Neurobiologie, Ruhr-Universität Bochum, D-44780 Bochum

nageusch@neurobiologie.rub.de

Albinism is going along with a number of functional deficits affecting the visual system. Previous psychophysical studies revealed that albinotic ferrets do not show the optokinetic reaction (OKR), a reflex that helps stabilizing gaze during motion across the retina. Moreover, albinotic animals revealed reduced detection thresholds for motion and reduced spatial resolution compared to normal animals.

We addressed the question whether albino ferrets may additionally lack direction selectivity in the primary visual cortex (Area 17) or may show an organization of orientation and directional maps that differs from that in normal pigmented animals. We also investigated how the contrast of the stimulus influences the strength of the cortical response and whether the threshold for the cortical maps differs between both phenotypes.

We used intrinsic optical imaging in order to derive functional maps of orientation and direction selectivity in Area 17. We stimulated with moving sinusoidal visual full-field gratings with a spatial frequency of 0.2 cycles/°, which were orientated in four angles (0°, 45°, 90° and 135°) and moved with a speed of 7.5 °/s in eight directions. The stimuli were presented to the contralateral eye.

Standard surgical methods were used. The animals were anaesthetized and artificially ventilated with a mixture of air and 0.6 % halothane. In order to exclude eye-movements we administered alcuronium chloride. Temperature, ECG, level of anesthetics and CO<sub>2</sub> were continuously monitored.

Preliminary results suggest the existence of direction and orientation selective cells in the primary visual cortex of the albinotic ferrets that are clustered in columns as it has been reported for pigmented animals (Weliky *et al.*, 1996).

The loss of OKR in the albinotic subjects may not be accompanied by cortical dysfunction of direction selectivity and might be therefore due to functional changes in subcortical structures.

Supported by the DFG (SFB 509 A11)  
and by the BMBF (D. J.)

### References:

Weliky M., Bosking W. H., Fitzpatrick D. (1996) A systematic map of direction preference in primary visual cortex  
Nature 379:725-728

## **Infrared sensitive units and their response characteristics in the Tectum opticum of the rattlesnake *Crotalus atrox***

Guido Westhoff <sup>1\*</sup>, Marco Morsch <sup>1</sup> and Christian W. Eurich <sup>2</sup>

<sup>1</sup>Institute of Zoology, University of Bonn, Poppelsdorfer Schloss, Germany

<sup>2</sup>Institute of Theoretical Physics, University of Bremen, Germany

\*Email: gwesthoff@uni-bonn.de

Pit vipers (Crotalinae) possess highly sensitive infrared reception that is mediated from the facial pit organs via the trigeminal nerve and the hindbrain into the midbrain and forebrain. The pit organs enable the snake to detect minute thermal differences within their environment, which helps them to find their warm-blooded prey. Infrared sensitive tectal neurons may receive additional visual input. We investigated the functional properties of infrared sensitive units by stimulating the pit organs with a red (650 nm) laser beam and recording with tungsten electrodes in the stratum griseum centrale of the contralateral Tectum opticum of anaesthetized western diamondback rattlesnakes (*Crotalus atrox*). The response latencies varied from 170 ms at threshold levels to 20 ms at higher stimulus intensities.

The latency of the first spike in the tectal neurons shows a systematic variation with the intensity of light falling on the pits membrane. The results indicate that infrared sensitive tectal neurons use the response latency to encode the stimulus intensity. Estimation-theoretical computations based on latency distributions obtained from repeated trials indeed suggest that response latencies may yield a population code for the intensity of incident light. The spike patterns favor the hypothesis for a binary code that may be used for spatial coding of objects within the infrared visual field.



**RECEPTIVE FIELD STRUCTURE AND SHAPE PROCESSING IN AREA V4**

Winrich A. Freiwald, Doris Y. Tsao, Roger B. H. Tootell, Margaret S. Livingstone

Department of Neurobiology, Harvard Medical School, Boston, MA, USA

Massachusetts General Hospital, Athinoula A. Martinos Center for Biomedical Imaging, Charlestown, MA, USA

Brain Research Institute and Center for Advanced Imaging, University of Bremen, Bremen, FR Germany

Shape processing along the ventral pathway critically depends on intermediate level steps within area V4. Receptive field structure of cells in early areas (V1 and V2) within this pathway can be characterized by reverse correlation techniques, while shape selectivity in higher areas (TEO and TE) has mainly been characterized by response profiles to sets of complex stimuli. To what extent can coding in V4 be understood within the same conceptual framework as that in early cortical areas? And can V4 responses to complex stimuli be explained by RF substructure?

We used a novel reverse correlation technique (Livingstone et al., 2001) to analyze RF substructure of neurons in cortical area V4d (whose correct location has been confirmed by structural MRI) in the macaque monkey. Cells were stimulated with a sparse noise stimulus consisting of pairs of small squares of same or opposite contrast flashed at 60 Hz at random positions over the RF. Reverse correlation of spikes to the absolute and relative position of the squares allowed the construction of first and second order RF maps, respectively. These experiments revealed complex and often dynamic receptive field organization beyond what has been reported for early cortical areas. Interaction maps provided evidence for a dependence on the integration and interaction of multiple stimulus orientations.

Extending the sparse stimulus protocol in a third set of experiments, we used pairs of randomly positioned and randomly oriented bars, thereby extending stimulus dimensionality from four to six. This specific choice of dimensions, motivated in part by considerations of input neuron selectivity, brings us one step closer to the study of shape selectivity. Results provided direct evidence for a spatially non-homogeneous orientation sampling within V4 receptive fields.

In a third experiment, cells were stimulated with random sequences of grating stimuli. Stimuli fell into one of five categories, Cartesian gratings, circular, radial, spiral or hyperbolic non-Cartesian gratings (Gallant et al., Science 259(1993):100-103), each described by three to four stimulus dimensions (orientation or center position, phase, spatial frequency, symmetry). We found a large proportion of category selective neurons, dominated by circular selective neurons. Even though this selectivity cannot be directly explained by second and first order maps, in case of cells with circular preference, a tight correlation with wreath-shaped second order maps (as determined in experiment 1) was observed.

Thus, sparse-noise-based and feature-space-based reverse correlation techniques provide new tools for characterizing RF substructure and shape selectivity of neurons at an intermediate-complexity level of the shape processing hierarchy.

*Support Contributed By: NIH, R01 MH67529 A01, R01 EB00790 A01, EY13135, SFB 517 (B7) and the Hanse Institute for Advanced Study (HWK)*

## Shifting attention is accompanied by a shift in the frequency components of monkey area MT neuronal responses

Detlef Wegener, Winrich A. Freiwald, Andreas K. Kreiter

*Center for Cognitive and Emotional Sciences, Brain Research Institute; Center for Advanced Imaging, University of Bremen, P.O. Box 33 04 40, D-28334 Bremen*

Selective visual attention has been found to strongly influence the temporal structure of neuronal responses. Recent studies in the temporal visual pathway demonstrated an attention-dependent increase of synchronization in the gamma band based on estimates of spike-field coherence and current source density [Fries et al., *Science* 291: 1560-1563, 2001; Taylor et al., *Soc Neurosci Abstr* 29: 385.11, 2003]. Here, we demonstrate that also the spectral composition of synchronized activity recorded from single neurons depends strongly on selective visual attention.

Multielectrode recordings of single neurons with overlapping receptive fields and similar direction preferences were obtained from macaque area MT. During recording, the animals were engaged in a motion tracking task, which required them to attend to one of two moving bars. One bar was located above the overlap of the receptive fields (RFs) of the recorded neurons, and the second bar was located either in the opposite visual hemifield (low spatial competition), or within the same hemifield close to, but still outside the RFs. Thus, the recorded cells were stimulated with a bar which either served as the behaviorally relevant target (the attended condition), or as the irrelevant distracter bar (the non-attended condition).

In both experiments (the low and the high spatial competition experiment), correlated responses to the attended stimulus were always found to have their strongest oscillatory modulation within the gamma band of the frequency range. In contrast, if cells were driven by the non-attended stimulus we found a shift of oscillatory power towards lower frequency components. In particular, with enhanced spatial competition between objects the most prominent oscillatory modulation of synchronized activity elicited by the distracter bar was found in the alpha range. Thus, the spectral analysis of crosscorrelated spike patterns not only revealed prominent gamma power in response to attended objects, but also demonstrated a frequency shift towards the alpha band for the non-attended condition. This result indicates that the attended and the non-attended stimuli are represented by neuronal assemblies which are distinguished by the different temporal structure of their synchronized neuronal activity.

*Supported by the DFG (SFB 517, Neurocognition)*

**Wannig A.<sup>1</sup>, Stemmann H.<sup>1</sup>, Freiwald W.A.<sup>1,2</sup>** Adresses: (1) *Inst. Brain Res., Bremen, Germany* ; (2) *Dept. Neurobiol., Harvard Med. School, Boston, MA, USA*

## **Neural correlates of non-space-based attention in macaque area MT: Top-down-control vs. bottom-up effects**

Attention can select spatial locations, feature dimensions and whole objects. While space-based mechanisms have been extensively studied, little is known about non-space based mechanisms of attention. Recently, an object-based paradigm has been introduced in psychophysical and event related potential studies, which precludes the use of space-based strategies (Valdes-Sosa et al., J. Cogn. NSci., 10:1:137151, 1999). Here we adapted this paradigm to assess top-down- and bottom-up-components of non-space-based attention in macaque monkeys. During fixation, two superimposed surfaces, segregated by different color and rotation direction, were presented within the neuron's receptive field. After a random interval either both or a single random-dot-surface underwent a translational movement in one of eight directions. Attention was directed to one of the surfaces either by an exogenous or an endogenous cue. In case of exogenous cueing, we used a short translation to direct attention to one of the surfaces. In this bottom-up-paradigm, fixation had to be maintained until the fixation spot disappeared. Neural responses to the second translation were analyzed, contrasting response rates due to cued vs. uncued translation. Endogenous cueing was realized through indicating the behaviorally relevant surface by color of the fixation spot (top-down-paradigm). Both surfaces underwent a translation period simultaneously. The monkey was required to report the translation direction of the cued surface by a saccade. Robust attention effects on neuronal firing rates was found with the top-down-paradigm, whereas the bottom-up-paradigm did not yield consistent effects. This suggests that the exogenous cue failed to capture attention in an object specific manner while the effects in the top-down-paradigm result from an endogenous controlled attention mechanism.

This work has been supported by the DFG through SFB 517 (B7) and the Hanse Institute for Advanced Study.

## Dynamic Stimuli and Dynamic Neurons: Encoding Properties of MT Cells in Awake Monkeys

E. L. Schulzke<sup>1</sup>, H. Stemmann<sup>2</sup>, W. A. Freiwald<sup>2</sup> and C. W. Eurich<sup>1,3</sup>

<sup>1</sup>Institute for Theoretical Neurophysics, University of Bremen, Germany

<sup>2</sup>Institute for Brain Research, University of Bremen, Germany

<sup>3</sup>Max-Planck-Institute for Mathematics in the Sciences, Leipzig, Germany

{schulzke,eurich}@neuro.uni-bremen.de, {stemmann,freiwald}@brain.uni-bremen.de

Visual stimuli in electrophysiological experiments are often chosen to be simple in order to characterize the statistics of neural responses. In particular, stimulus features such as the velocity or the movement direction of a grating or a cloud of random dots are held constant during a trial to determine the firing properties of cells. However, our visual environment is dynamic, due to the motion of objects in the visual field but also through body and eye movements. The use of dynamic stimuli poses new questions in the context of neural coding. For example, neurons are be-

lieved to have a finite integration time [1] which may limit the time scale of the dynamics of stimuli that are still processed by the visual system. An open question is the interference of the dynamics of MT neurons and the dynamics of visual stimuli that they process. Here we are especially interested in the influence of prior knowledge on dynamic stimulus representation.

Extracellular recordings were made in two awake monkeys (*Macaca mulatta*). Visual stimuli consisted of a random-dot surface (motion coherence 100%). Motion directions of the dots were discretized at 30° and were presented either for 20 ms or 50 ms during the whole stimulus sequence. Consecutive motion directions were chosen according to two different paradigms: first, a random walk in the direction domain (“continuous trajectory”) and second, a pseudorandomized order of directions (“discontinuous trajectory”).

Electrophysiological data were evaluated by reconstruction of the trajectories. Figure (a) shows an example of a continuous trajectory and a reconstruction based on 280 pooled trials from 23 neurons. The mean absolute error was 2.8°. Figure (b) compares a Bayesian reconstruction with a prior centered around the current direction estimate with a Maximum-Likelihood (ML) reconstruction. The analysis reveals that the response of a rather small neuron population is sufficient to obtain a ML estimate that is as good as the Bayesian estimate, thus limiting the necessity of prior information for an accurate perception of stimuli.

In addition, we found that reconstruction errors for trajectories composed of 20 ms presentations are larger than those for 50 ms presentations, even for large populations. This effect cannot exclusively be explained with a finite neural integration time: reconstructions from 50 ms trajectories that used only the first 20 ms of each movement directions turned out to be more accurate. A more detailed analysis showed that for short stimulus presentation times in discontinuous trajectories, neural estimates are biased toward the movement direction presented in the previous time step.

In summary, the encoding accuracy of MT neurons is determined by in interplay of neural dynamics (resulting in a finite stimulus integration time) and the dynamics of stimuli.

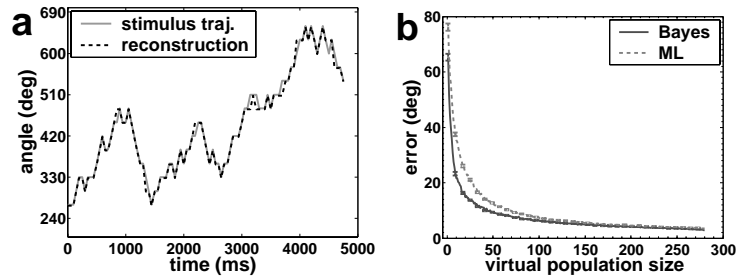


FIGURE 1: (a) Reconstruction of a continuous trajectory in the direction domain. A Bayesian two-step method was used [2], employing the responses of 23 MT neurons and pooled over trials which resulted in a virtual population of 280 neurons. (b) Comparison of Bayesian reconstruction and Maximum-Likelihood reconstruction. The absolute error is shown as a function of the virtual population size.

[1] L.C. Osborne, W. Bialek and S.G. Lisberger, J. Neurosci. **24** (2004) 3210–3222.

[2] K. Zhang, I. Ginzburg, B.L. McNaughton and T.J. Sejnowski, J. Neurophysiol. **79** (1998) 1017–1044.

## Attention Modulates Oscillatory Synchrony in Monkey Area V1 in a Shape Tracking Task

Katja Taylor, Sunita Mandon, and Andreas K. Kreiter

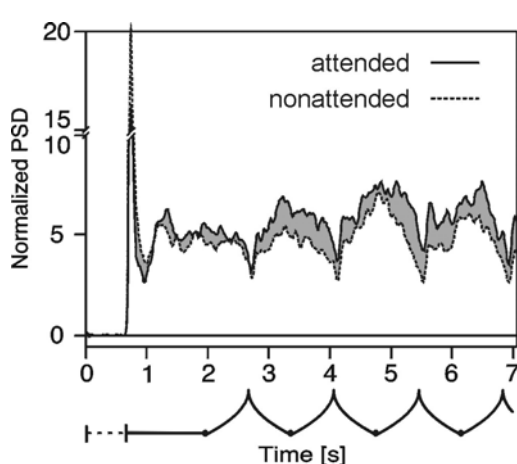
*Brain Research Institute, University of Bremen, D-28334 Bremen, Germany*

The influence of attention on responses in primary visual cortex is a source of ongoing controversy. Substantial attention-dependent modulation of neuronal activity in primary visual cortex (V1) has been demonstrated using fMRI (Gandhi, S.P. et. al. (1999) PNAS 96, 3314-9). In contrast, single-unit studies found for several classical attention paradigms only small or no effects of attention on firing rate in V1 (Marcus, D.S. and Van Essen, D.C. (2002) J Neurophysiol 88, 2648-58; McAdams, C.J. and Maunsell, J.H.R. (1999) J Neurosci 19, 431-41; Luck, S.J. et. al (1997) J Neurophysiol 77, 24-42) while for others larger effects were reported (Roelfsema, P.R. et. al. (1998) Nature 395, 376-81). An alternative neurophysiological mechanism, which has been proposed to underlie selective attention, is neuronal synchronization in the millisecond time range (Niebur, E. and Koch, C. (1994) J Comp Neurosci 1, 141-58). This mechanism may serve attentional stimulus selection as well as attention-dependent integration of different features into a coherent percept (Kreiter, A.K. (2001) Prog Brain Res 130, 111-40) as required in shape perception.

Here we study the role of oscillatory synchrony in V1 for selective attention using the previously introduced shape-tracking task (Taylor, K. (2003) Soc Neurosci Abstr. 29: 385.11), which requires sustained attention to one of two morphing shapes to identify the reoccurrence of the shape of a previously presented sample. As a measure of oscillatory synchrony we recorded field potentials (FPs) with an epidurally implanted electrode array covering parts of area V1. Analysis of recorded FPs in the frequency domain showed stimulus-induced increases of power spectral density (PSD) predominantly in the  $\gamma$ -range (55 – 110 Hz). Attention increased PSD by up to 50% in the same frequency range. This effect of attention is subject to additional modulation in time, depending on changing attentional demands during different parts of a trial. A control experiment showed that the modulation of PSD was not related to the memory aspects of the task. In addition to the major oscillatory component in the upper  $\gamma$ -band, another separable component, also subject to attentional modulation, could be observed between 20 and 40 Hz.

The attention-dependent enhancement of PSD observed specifically in the  $\gamma$ -band suggests an increase of oscillatory synchrony (Herculano-Houzel, S. (1999) J Neurosci 19, 3992-4010). This attention-dependent change of neuronal synchronization is well in line with the above-mentioned, attention-dependent changes in the fMRI's BOLD-response, which is thought to mainly reflect synchronized components of dendro-somatic potentials and subthreshold fluctuations (Kayser, C. et. al. (2004) Cereb Cortex 14, 881-91; Logothetis, N.K. et. al. (2001) Nature 412, 150-7). In summary our results indicate that in primary visual cortex oscillatory synchrony serves as a mechanism of selective attention.

*This work was supported by SFB 517 A7 and CAI*

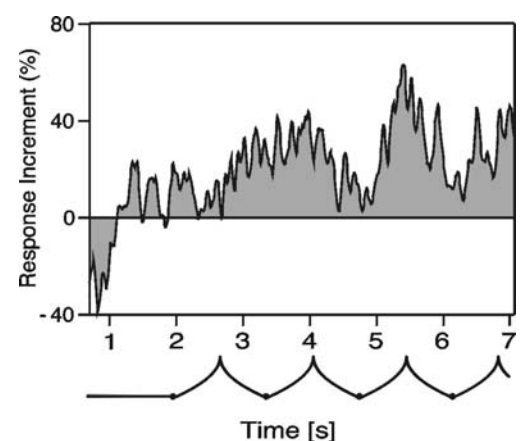


**Time course of  $\gamma$ -PSD during the shape-tracking task.**

**Left:** Solid and dotted lines show the time course of the peak normalized PSD in the  $\gamma$ -range for the attended and non-attended condition, respectively.

**Right:** Time course showing the increment of the  $\gamma$ PSD from the non-attended to the attended condition.

Beneath each plot a schematic time course of the task is shown



## Paired-pulse TMS effects on single unit activity in cat primary visual cortex

Moliadze V.<sup>1)</sup>, Giannikopoulos D.<sup>1)</sup>, Kammer T.<sup>2)</sup> and Funke K.<sup>1)</sup>

1) Department of Neurophysiology, Ruhr-University Bochum, D-44780 Bochum, Germany

2) Department of Psychiatry, University of Ulm, Leimgrubenweg 12-14, D-89075 Ulm, Germany

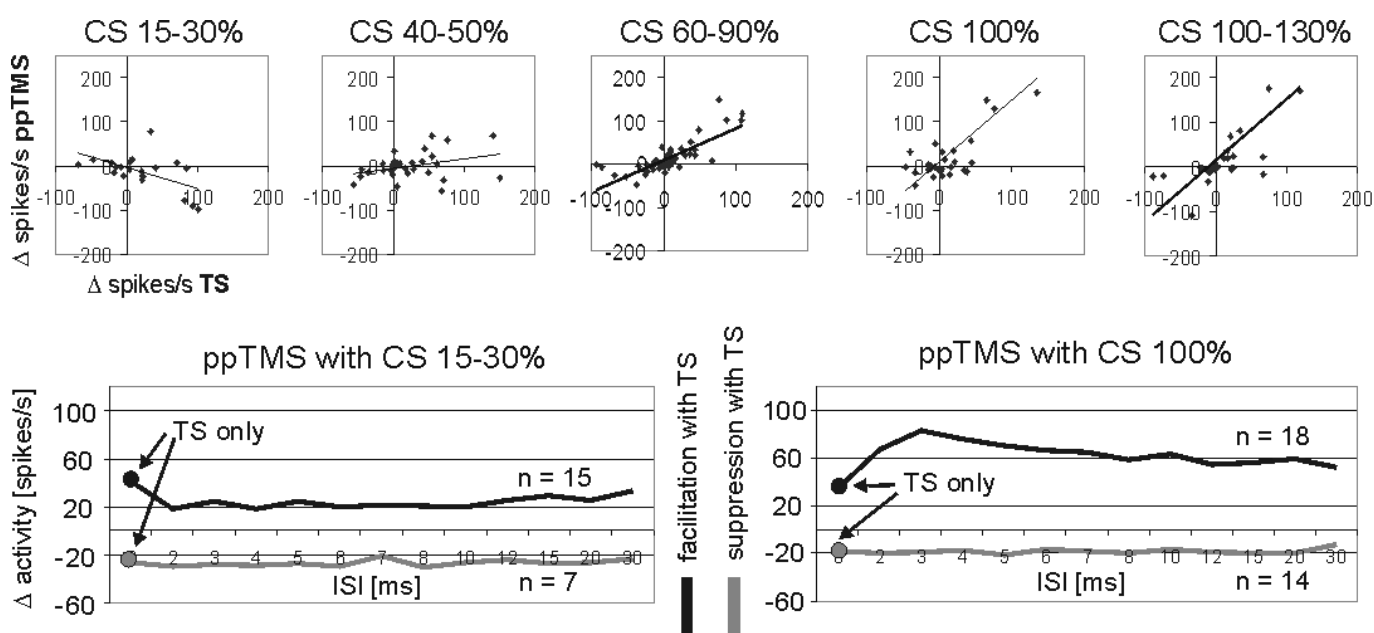
Paired-pulse transcranial magnetic stimulation (ppTMS) has become a tool for exploring the excitability of human cortical networks, especially in the motor system. Applying a subthreshold conditioning stimulus (CS) 2-5 ms prior to a suprathreshold test stimulus (TS) to human motor cortex has been found to weaken the motor evoked potential (MEP) triggered by the test stimulus, while an inter-stimulus interval (ISI) of 7-30 ms leads to a potentiation of the MEP (1,2). The effect observed with short ISIs has been interpreted as a strengthening of intracortical inhibition (ICI) while long ISIs favour intracortical facilitation (ICF). However, ICI evoked by short ISIs is only found with subthreshold CS. Increasing CS strength to that of TS, or a suprathreshold CS followed by a subthreshold TS leads to ICF also at short ISI (1,3,4).

In the present study, we tested the paired TMS paradigm for visually evoked single and multi-unit activity in cat primary visual cortex. Paired pulses were generated by 2 MagStim 200 units connected via a BiStim module (Micromed) and were applied via a 2x 70 mm figure-of-8 coil to area 17/18 of the anesthetized (N<sub>2</sub>O/O<sub>2</sub> [70/30%] + halothane [0,8%]) and paralyzed cat. Here, we defined the TS as being suprathreshold (100%) when it caused a significant increase or decrease in the visually evoked activity. By systematically varying the ISI between 2 and 30 ms and the strength of the CS within a range of 15-130% of TS, we found no dependence of ICI and ICF on ISI but a clear dependence of ppTMS effect on CS strength. By plotting the additional changes in visual activity achieved by ppTMS (ppTMS effect minus TS effect) versus the change evoked only with the single pulse TS (see upper row diagrams), we found a clear correlation between ppTMS and TS effect, but the correlation varied with CS strength. A significant negative correlation was found with weak CS strength in the range of 15-30%. Increasing the CS strength above 50% caused a flip to a clear positive correlation: within a CS range of 60-130% ppTMS resulted in a stronger facilitation if the TS caused facilitation of visual activity by itself and more suppression if the TS itself was suppressive. This correlation also indicates that the ppTMS effect scales with TS effect. Correlations shown are for an ISI of 3 ms between CS and TS. Correlations obtained with other ISI between 2 and 30 ms did not show significant differences.

The 2 lower diagrams of the figure show mean changes in activity achieved with different ISI between CS and TS in comparison with the change in activity resulting from TS alone (large dots at ISI 0). Cases in which TS had either a facilitatory (black curve) or a suppressive effect (gray curve) are averaged separately. The data with 15-30% CS strength show a reduced facilitation by TS, while the data with 100% CS strength show potentiation of the TS effect. Qualitatively identical effects were found for all tested ISI, but the strongest effects were found for ISI of 2 to 4 ms and declined for longer ISIs. Our results show that ppTMS effects on sensory activity evoked in the visual cortex (of cat) differ from ppTMS effects on artificially evoked efferent activity in human motor cortex.

(1) Kujirai et al. (1993) J. Physiol. 471, 501-519.  
(3) Ilic et al. (2002) J. Physiol. 545, 153-167.

(2) Ziemann et al. (1996) J. Physiol. 496, 873-881.  
(4) Ziemann et al. (1998) J. Physiol. 511, 181-190.



This study was supported by the "Deutsche Forschungs-Gemeinschaft" (DFG, 256/2-1) and by the Federal Ministry for Education and Science (BMBF), Competence Network Stroke (01GI9913).

## **Top-down innervation modulates visual activity of rotundal cells in pigeons**

**Kristian Folta<sup>\*1</sup>, Bettina Diekamp<sup>2</sup>, Janina Kirsch<sup>1</sup> and Onur Güntürkün<sup>1</sup>**

\* Corresponding author.

Tel.: +49-234-32-24032; fax: +49-234-32-14377.

E-mail address: kristian.folta@ruhr-uni-bochum.de

<sup>1</sup> Institute for Cognitive Neuroscience, Department of Biopsychology, Faculty of Psychology, Ruhr-University Bochum, D-44780 Bochum, Germany

<sup>2</sup> Department of Psychological and Brain Sciences, Johns Hopkins University, Baltimore, MD 21218, USA

### **Abstract**

In a previous study, we investigated visual responses of single units of the pigeons' n. rotundus and revealed neurons with both early and late response components. We argued that response components with short latencies very likely represent bottom-up components activated via the ascending retino-tecto-rotundal system. On the contrary, late response components were probably activated via a top-down telencephalo-tecto-rotundal system. In this study, we clarified the origin of top-down response components through reversible lidocaine inactivations of visual Wulst efferents of the left and right hemisphere. Before, during, and after the inactivation, we recorded from neurons of the left and right rotundus while visually stimulating the ipsilateral and/or contralateral eye. Lidocaine-injections evoked a temporal reduction or enhancement of exclusively late response components. Injections into the right visual Wulst produced no effects. This result pattern indicates that the left visual Wulst is a relevant telencephalic structure that exerts a top-down influence on rotundal cells and shapes tectofugal responses to visual stimuli.

## ANATOMY AND ELECTROPHYSIOLOGY OF TECTO-ISTHMIC FEEDBACK LOOPS IN THE CHICKEN

Harald Luksch<sup>1</sup>, Susanne Scholz<sup>1</sup>, and Ralf Wessel<sup>2</sup>

<sup>1</sup> Institut für Biologie II, RWTH Aachen, Germany

<sup>2</sup> Physics Department, Washington University at Saint Louis, MO, USA

email: [luksch@bio2.rwth-aachen.de](mailto:luksch@bio2.rwth-aachen.de)

The importance of feedback loops for neuronal responses even in early sensory areas has become widely acknowledged over the last years. Here, we present investigations on the effect of feedback loops in the optic tectum of birds. We have worked on a midbrain slice preparation that contains not only the tectal circuitry including the retinotopically organized retinal afferents, but also feedback loops with various elements of the nucleus isthmi ([1], Fig. 1). Both the parvocellular and the semilunar isthmic nucleus receive tectal input from radial neurons with small dendritic fields, and project back onto the same location with characteristic paintbrush endings. In contrast, the GABAergic neurons of the magnocellular isthmic nucleus project broadly upon both the tectum and the parvocellular as well as the semilunar isthmic nucleus. All elements are contained within a 500  $\mu\text{m}$  transversal slice and are accessible for stimulation and recording electrodes, as well as for pharmacological studies.

We have used whole-cell patch recordings and electrical stimulation with up to 8 bipolar electrodes at various positions in the nuclei to investigate the contribution of single neurons to the feedback network. First data indicate that even short electrical stimuli delivered to the tectal retinal afferents are sufficient to elicit long-lasting excitation in the network. Specifically, the tectal output neurons to the Ipc (shepherd's crook neurons) show a characteristic persistent activity upon short electrical stimulation of their input (Fig.2). After characterization of the response properties of all elements involved, we will investigate the system's influence on the computation of retinal input in tectal projection neurons (SGC neurons, Fig. 1).

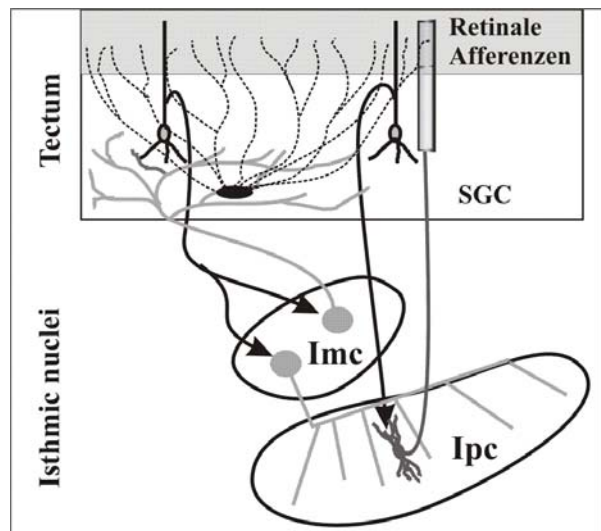


Fig 1: Elements of the tecto-isthmic loop. Imc = N. isthmi pars magnocellularis, Ipc = N. isthmi pars parvocellularis, SGC = Stratum griseum centrale

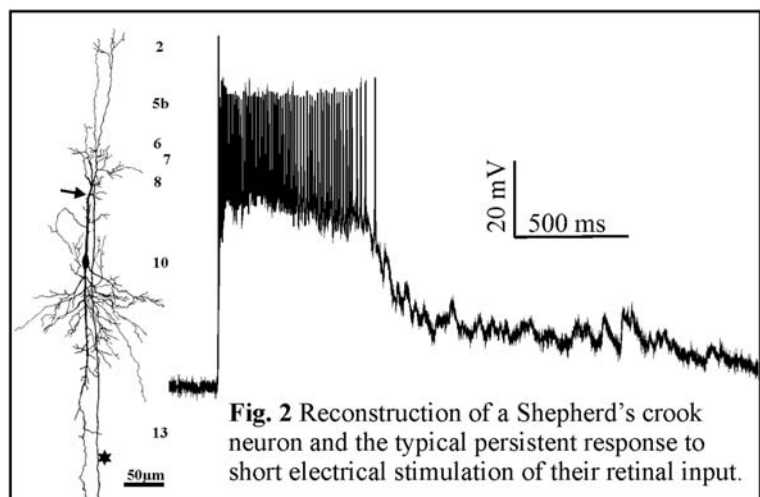


Fig. 2 Reconstruction of a Shepherd's crook neuron and the typical persistent response to short electrical stimulation of their retinal input.



### Shape from stereo: a comparative approach

R.F. van der Willigen, Sabine Vossen, Wolf Harmening and Hermann Wagner  
Institut für Biologie II, Rheinisch-Westfälische Technische Hochschule, D-52056 Aachen,  
Germany. E-mail: willigen@bio2.rwth-aachen.de

When humans view an object with their two eyes, the visual cortex compares the relative positions of the object's retinal images, called disparities, to infer its three-dimensional (3D) shape. The spatial resolution of this disparity-based stereo process is a key determinant of shape perception in everyday life. Spatial stereoresolution can be determined by presenting random-dot stereograms (RDSs) wherein disparity is a periodically modulated function of position. In humans, such corrugated-RDSs produce gratings in depth, which provide a way of relating sensitivity for perceiving depth corrugations to their corrugation frequencies. This relationship defines the disparity-contrast sensitivity function (DSF), which is characteristically inverted U-shaped, implying that spatial stereoresolution is the highest at some intermediate frequency. It is unclear why such a bandwidth limitation occurs. If bandwidth limitation is an essential characteristic of shape-from-stereo processing in the sense that it minimizes the amount of binocular interaction in the brain, then all vertebrates known to use disparity as a depth cue should conform to an inverted U-shaped DFS. Yet, no behavioural data exists to define spatial stereoresolution in non-primate animals. We report on a series of psychophysical tests determining the DSFs in two barn owls (*Tyto alba*) and two human subjects. DFSs were measured over a ~5 octave range (0.04-1.49 cycles/°) from corrugated-RDSs. In both the owl and man, the bandwidths of spatial stereoresolution spanned 3-4 octaves. The owls' maximal sensitivity, however, was shifted toward the low spatial frequency end (owl: 0.09-0.17 cycles/°; man: 0.35-0.57 cycles/°). Our discovery that both the owl and the human visual system are more effective in processing intermediate disparity modulation frequencies establishes a functional equivalence for the processing of shape-from-stereo in these two species.

## **Chromatic and Achromatic Vision in Zebra Finches (*Taeniopygia guttata*)**

Susanne Holtze, Dr. Misha Vorobyev

Vision, Touch and Hearing Research Centre (VTHRC), The University of Queensland  
Brisbane QLD 4072 Australia.

In many animals, vision has both chromatic and achromatic aspects. Chromatic vision is sensitive to the spectral composition of a light stimulus but insensitive to absolute changes in light intensity. Achromatic vision is sensitive to changes in light intensities, but less sensitive to the spectral distribution of light stimuli. We hypothesized that in birds, pattern-recognition tasks are mediated by achromatic vision, while chromatic cues are mainly used to distinguish objects. Typically, birds possess four single cone types and one type of double cone. We assumed that chromatic vision in birds is mediated by single cones, while achromatic vision is mediated by double cones alone. Adult zebra finches (*Taeniopygia guttata guttata*) were trained to distinguish between different stimuli (coloured food containers). One set of tests was conducted with uniformly coloured stimuli; in the other set of tests, birds were trained to distinguish patterns (stripes vs. checkerboard), composed of two different colours. The same two sets of colours were used in all tests: one set differing only in brightness and one differing only in chromatic properties. In the tests with uniformly coloured containers, birds learned to distinguish between the stimuli differing in chromatic cues faster than between the ones differing in achromatic cues. In training to patterns, birds learned to distinguish between patterns with achromatic contrast faster than between patterns with chromatic contrast. Repeating the same experiment with another set of colours and one additional test in each set of experiments (chromatic patterns and plain stimuli with an additional small brightness contrast the previous results could be confirmed and a quantitative influence of brightness contrast was found. The study is based on approximately 25,000 recorded individual choices. These results suggest that achromatic vision is used mainly for high-resolution vision (pattern recognition), while chromatic cues are used for low resolution vision (discrimination of objects).

## **No Lateralization of Food Discrimination in Zebra Finches (*Taeniopygia guttata castanotis*)**

**Stefanie Rubart and Hans-Joachim Bischof**

Department for Behavioral Research  
University of Bielefeld  
PO Box 100131  
33501 Bielefeld / Germany  
Email: [srubart@gmx.de](mailto:srubart@gmx.de)

Lateralization of brain function, which was solely attributed to humans for a long time, has now been demonstrated also in a variety of other vertebrates. Especially in birds, there is a large body of evidence for lateralization of visually guided feeding. However, most experiments were as yet done in the pigeon. Generalization of the findings to other avian species is at present only possible on a very narrow data base. To this end, we performed a visually guided feeding experiment with the zebra finch, a small Australian songbird. We used the so called pebble floor experiment because it has been used also in pigeons (Güntürkün and Kesch, 1987).

The experiment was divided into three main conditions: the binocular one, where the birds could see with both eyes, and two monocular experiments, where either left or right eye was occluded by a plastic cap. The birds were deprived of food for at least 10 hours prior to the start of experiment. Two groups of birds (14 wild types and 9 white birds) were tested in all three conditions. White zebra finches were examined because its visual system is physiologically different from the wild type thus we were interested whether these differences affect foraging ability and probably lateralization. Both groups were tested in an experimental cage which contained a fixed amount of grain on a pebble floor with the pebbles glued to the floor. While foraging, the birds had to discriminate between grit and grains. We then compared the proportion of successful and unsuccessful pecks of birds in each condition and between the morphs.

Our experiments did not reveal an influence of eye coverage on discrimination success of the birds, meaning that there is no significant lateralization for food discrimination tasks. There is just a slight tendency towards being more successful when using the left eye.

There was, however, a difference in performance between wild type and white birds. Wild type birds generally had a higher frequency of food pecking under binocular conditions than the white ones. In contrast the white birds made less mistakes when both eyes could be used. Under monocular conditions, the normally coloured finches had the same frequency of food pecking compared to binocular conditions. In contrast, white birds did not differ in pecking frequency under monocular and binocular conditions, and their performance was worse.

Our results thus support previous findings that white zebra finches have a deviating visual system. They do not support, however, the idea that lateralization of the visual system is a common feature in all avian species.

Supported by the Deutsche Forschungsgemeinschaft (BI 245/15)

# The Distribution of $\gamma$ -aminobutyric Acid in the Tectofugal System of White and Wild Type Zebra Finches (*Taeniopygia guttata*)

Patrizia Wonderschütz, Carsten Lieshoff, Joe Voss  
and Hans-Joachim Bischof

Department for Behavioral Research  
University of Bielefeld  
PO Box 100131  
33501 Bielefeld  
Germany  
Email: Patrizia24@web.de

Compared to normally coloured (wild type) zebra finches white leucistic mutants of this species show a decreased performance in avoiding obstacles during flight.

A probable cause for this phenomenon could be found in anatomical differences in brain structures between the coloured and the white morph. Birds have two parallel visual pathways, the thalamofugal and the tectofugal one. In birds with laterally placed eyes, like zebra finches, the tectofugal pathway is more prominent.

Within the tectofugal pathway, white zebra finches have a more prominent projection from the tectum opticum to the contralateral nucleus rotundus and an additional connection between the nuclei rotundi of both hemispheres [Leminski and Bischof, 1996].

Accordingly, Breidenkötter et al. [1996] showed enhanced responses to ipsilateral stimuli in the tectofugal pathway of white birds. Their experiments, however, suggested that a lack of inhibition in visual processing areas causes these enhanced responses.

We therefore compared the number of the GABAergic neurons in several areas of the tectofugal system of wild type and white zebra finches. The birds were perfused, the brains sectioned and treated with GABA antibodies and visualized using DAB (3'3 Diaminobenzidine). We counted GABAergic neurons in nuclei which could be of importance for interhemispheric processing of visual information, such as SP/IPS, nucleus rotundus and entopallium.

Our results indicate that the number of inhibitory neurons is decreased in some areas of the tectofugal system of the white morph. While there were no significant differences between the wild type and white birds in the thalamic areas SP/IPS and nucleus rotundus, the number of GABAergic neurons in the entopallial core and belt region of white zebra finches were decreased. It is still not known how the flight performance in white birds is affected by the lack of inhibition within the entopallium. Probably, the lack of suppression of ipsilateral visual information leads to problems in integration of information coming from the left and the right eye in an appropriate way. This could prevent fast decision making and thus lead to problems in obstacle avoidance.

Supported by the Deutsche Forschungsgemeinschaft (Bi 245/16)

## Does intrasaccadic gamma power increase reflect an internal mechanism of motor-sensory monitoring?

Forgacs PB<sup>1</sup>, von Gizycki H<sup>3</sup>, Avitable H<sup>3</sup> and Bodis-Wollner I<sup>1,2</sup>

Department of <sup>1</sup>Neurology and <sup>2</sup>Ophthalmology and <sup>3</sup>Center for Scientific Computing,  
SUNY Downstate Medical Center, 450 Clarkson Ave., Brooklyn, New York, USA,  
11203

**Purpose:** To evaluate if an inverted U-shaped function of gamma power represents gamma power increase during saccades or reflects pre- and postsaccadic gamma power suppression.

**Background:** We have shown that gamma power increases during saccades, even in the total absence of visual input, over posterior cortical (occipital-temporal-parietal) recording sites. One plausible explanation is that gamma power increase represents a mechanism involved in the preparation for new fixation. Alternatively, it is possible that the observed gamma power increase is not real: that it actually reflects a return to baseline gamma, between gamma power suppression preceding and following the saccade. Premotor gamma power decrease would be consistent with a role of gamma in motor preparation.

**Method:** 19 subjects were studied. 12 EEG channels over the posterior cortex and horizontal EOG were recorded. Saccades were executed between two markers 20-20° from midline. Perisaccadic EEG was analyzed in four time windows (pre-, 2 intra- and postsaccade). Gamma power (38.4 Hz) was estimated applying Continuous Wavelet Transform followed by Hilbert transform. General linear model for ANOVA was used for statistical analysis.

**Results:** Gamma power remained at the same level in the 300 msec time window preceding each saccade and descended toward baseline level following each saccade.

**Conclusion:** Intrasaccadic gamma power increase is not reflecting baseline gamma power, unless presaccadic gamma suppression starts more than 300 msec before the initiation of the movement. Intrasaccadic gamma is not a motor preparatory signal. While this conclusion is consistent with the general understanding of the role of gamma in reflecting neuronal connectivity changes, the results also raise the possibility that intrasaccadic gamma reflects neuronal mechanisms associated with monitoring and predicting sensory outcome of initiated action.

**Key Words:** voluntary saccades, gamma, motor-sensory interaction, internal monitoring, cognition, visuospatial orientation

## Event-related brain potential correlates of adaptation to faces and body parts

Gyula Kovács Department of Cognitive Sciences, Budapest Univ. Technology and Economics, Budapest, Hungary

Andrea Antal Dept. of Clinical Neurophysiology Georg August University of Göttingen, Göttingen Germany

Zoltán Vidnyánszky Neurobiology Research Group, Hungarian Academy of Sciences, Hungary

Prolonged exposure to an individual face or an image of a body part leads to adaptation and will bias the perception of subsequently presented test faces or body part images. The goal of the present study was to uncover the mechanisms of neural plasticity underlying such high level figural adaptation using ERP. As our stimuli, we used computationally derived morphs of female and male faces as well as morphed female and male hands. Behavioural effects of a 5 second adaptation with either a specific face or hand stimulus (or as a control condition with their Fourier randomised version) were measured using face or hand gender discrimination task. In our ERP experiments we measured the effect of face and hand adaptation on the N170 component of the ERP (recorded from 23 channels, positioned according to the 10-20 system).

Our behavioural results showed a strong category-specific adaptation to both faces and hands. We found no cross-category adaptation effects; i.e. adapting with a face did not affect hand gender discrimination just as adapting with a hand image was not affecting face gender discrimination. Our ERP measurements revealed that both adaptation to faces and hands significantly increases the latency and decreases the amplitude of the N170 component (compared to the adaptation with the Fourier randomised images) in the case of when the test and the adaptor are from the same category but not when they are from different categories. There were no category-specific adaptation effects on the P100 components of the ERP responses. To conclude, we suggest that high level configural adaptation is reflected in the N170 components of the ERP responses..

This work was supported by DAAD-MÖB and NKFP 5/0079/2 to G.K. and NKFP 2/035 to Z.V.

## Glycine receptors on amacrine cells in the mouse retina

**Jan Weiß and Heinz Wässle**

*Dept. Neuroanatomy, Max Planck Institute for Brain Research,  
Deutschordenstrasse 46, D-60528 Frankfurt am Main, Germany*

There are more than 30 morphologically different amacrine cell types in the mammalian retina. About 50 % of these amacrine cells have glycine as a neurotransmitter and provide inhibitory input to amacrine, bipolar and ganglion cells. Immunocytochemical studies revealed that 3 of the 4 known  $\alpha$ -subunits and the one  $\beta$ -subunit are expressed in the mouse retina. To investigate the functional characteristics of glycine receptors (GlyRs) in amacrine cells, we examined the kinetics of glycinergic IPSCs (inhibitory postsynaptic currents).

In whole-cell patch-clamp experiments on mouse retinal slices, we recorded spontaneous or potassium-induced synaptic activity. To isolate the glycinergic from GABAergic IPSCs, we applied the GABA receptor antagonists TPMPA and bicuculline onto the inner plexiform layer (IPL). Strychnine, which is a selective antagonist of the GlyR, could block the glycinergic IPSCs.

The kinetics of glycinergic IPSCs were characterized by their decay times ( $\tau_w$ ). Considerable variation with both monoexponentially and biexponentially decaying events were found. Though the average  $\tau_w$  was  $22.1 \pm 5.8$  ms (n=9), values between 5 ms and 50 ms were recorded. The average amplitude of the IPSCs was about 50 pA.

Most amacrine cells responded to the application of glycine with large currents, though their affinity for glycine differed. Glycine dose-response-curves for different amacrine cell types were measured and the cells were identified by Alexa 488 dye injection. Type AII-amacrine cells had an  $EC_{50}$  value of approximately 130 mM glycine (n=6), while that of type A17-amacrine cells was around 240 mM glycine (n=6).

These data suggest that the various kinetic properties of the GlyR observed might be dependent on their subunit combination and different amacrine cell types express different subunits. Thus the molecular composition of GlyR may modulate the inhibition on light signals passing through the retina.

### **The feedforward dynamics of action priming**

Thomas Schmidt, Silja Niehaus & Annabel Nagel

*Georg Elias Müller Institute of Psychology, University of Göttingen, Gosslerstr. 14, D-37073 Göttingen, Germany*

Visual stimuli elicit a wave of early brain activation that reaches most cortical areas within 120 ms (Lamme & Roelfsema, 2000). Because typical cells can fire only once in the interval before activity is passed on to the next area, it has been proposed that this *feedforward sweep* must be largely free from intracortical feedback, whereas conscious perception is supposed to be possible only with recurrent processing. However, extremely fast feedback mechanisms have been demonstrated in early visual areas, and it is not clear yet whether feedforward waves can proceed to the level of overt behaviour uncompromised by forthcoming waves. By measuring pointing responses to colour targets preceded by colour stimuli priming either the same or opposite response as the targets, we found that early pointing kinematics depended mainly on properties of the primes and were largely independent of motor and perceptual effects of the actual targets provided that the prime-target SOA (stimulus onset asynchrony) was long enough (about 70 ms). With shorter intervals, even the earliest phases of the pointing response were influenced by properties of the mask. We propose that the pointing movements are under continuous control of successive feedforward waves of prime and target; these waves have an effective duration well exceeding the first few spikes of the wavefront and have substantial overlap if the prime-target SOA is as short as 33 ms. We show that the feedforward dynamics of pointing actions can be traced quantitatively in the early phases of overt human pointing responses, providing a missing link between single-cell studies of feedforward processing and psychophysical studies of recurrent effects on visual awareness.

#### References:

Lamme, V. A. F. & Roelfsema, P. R. (2000). The distinct modes of vision offered by feedforward and recurrent processing. *Trends in Neurosciences* 23, 571-579.

*Supported by the German Science Foundation.*



# SIGNATURES OF SHIFT-TWIST SYMMETRY IN THE LAYOUT OF ORIENTATION PREFERENCE MAPS

M.SCHNABEL<sup>1</sup>, M.KASCHUBE<sup>1</sup>, L.WHITE<sup>2</sup>, D.COPPOLA<sup>3</sup>, S.LOEWE<sup>4</sup>, F.WOLF<sup>1</sup>

1. MPI f. Strömungsforschung, Göttingen, Germany, 2. Duke Univ. Med. Ctr., Durham, NC, USA,  
3. Randolph-Macon College & Medical College of Virginia, Richmond, VA, USA, 4. IFN, Magdeburg, Germany

Experimental and theoretical evidence suggests that the development of orientation preference maps (OPMs) constitutes an activity-dependent self-organization process. The formation of OPMs in the visual cortex can be modeled by dynamic field equations [1,2]. Key features of such models crucially depend on the symmetries of the dynamics [2].

Previously [3] we presented a new class of Gaussian random maps which allows us to study the consequences of shift-twist symmetry (STS), a fundamental symmetry of visual cortical circuitry, on the layout of orientation maps. This symmetry mathematically describes that the position of stimuli in the visual field and the preferred orientation of visual cortical neurons ought to be represented in a common coordinate system. Here we use this approach to identify signatures of this new symmetry which are accessible to experimental testing. We find that STS predicts a locking of the layout of the OPM to the retinotopic map.

First, we show that as a consequence of STS saddle points of the OPMs get locked to the retinotopic map: Saddle points are characterized by their preferred orientation and two principal axes along which the preferred orientation stays constant. In the presence of STS there is a tendency for those principal axes to align either parallel or orthogonal to the retinotopic projection of the preferred orientation. Second, we calculate the joint probability density of the relative orientation preference of separate columns, as a function of their relative distance and direction. We find that this distribution exhibits a characteristic cloverleaf-like shape. The theoretical predictions are compared to OPMs obtained from primate and carnivore primary visual cortex.

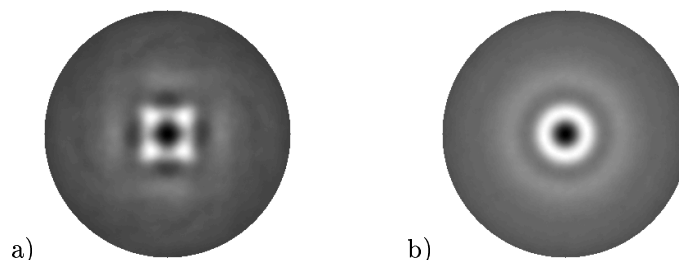


FIGURE 1. Probability density of finding columns of  $90^\circ$  OP in the vicinity of a column with  $0^\circ$  OP located in the center. Theoretical Prediction **a)** in the presence and **b)** in the absence of shift-twist symmetry.

- [1] Swindale, N.V. Network, **7**:161 (1996)
- [2] Wolf & Geisel, Nature (1998) **395**:73
- [3] Timme, Schnabel, Kaschube, Lowel, Geisel and Wolf, Society of Neuroscience Abstracts (2003)
- [4] Bressloff, Cowan, Golubitsky, Thomas, Wiener, Phil.Trans.R.Soc.London.B (2001) **356**:299

*Support Contributed by: HFSP (RGP63/2003), MPG, and WGL and EY11488, Whitehall Foundation*

Florian Pieper, Tina Peters & Stefan Treue

Cognitive Neuroscience Laboratory,  
German Primate Center, Germany

Corresponding author: fpieper@gwdg.de

### **The influence of brief motion adaptation on direction perception**

Motion adaptation (MA) induced by extensive (tens of seconds or more) viewing of a constant motion pattern (adaptor) elicits the motion after-effect (MAE) and direction after-effects (DAE). The MAE is the illusory motion of a static pattern in the opposite direction of the adaptor whereas the DAE is the misperception of the direction of motion of a subsequent test-stimulus of up to 10°.

These misperceptions are thought to be the expression of a calibration of the cortical motion network to the statistics of the visual input. This optimizes the system for the detection of changes in the input rather than for the representation of absolute values. A continuous calibration and optimization on a short timescale appears beneficial because of the frequent changes in the retinal image due to eye-movements and changes in the visual scene. We therefore hypothesize that motion adaptation should already occur at much shorter time scales than previously investigated.

In a psychophysical experiment we systematically varied the duration of motion adaptors and determined the amount of the DAE as an objective indicator for the strength of the adaptation. Adaptor and test stimuli were coherently moving random dot patterns (RDP), presented successively at 8° eccentricity of a fixation point. Subjects had to judge the perceived direction of motion of the adaptor (presented for 250 ms). The perceived direction of the test stimulus was determined as a function of the angle between the adaptor and the test stimulus. The adaptor's duration and direction varied from trial to trial. Trials were separated by 1.5-2 seconds.

We found a substantial and systematic misjudgment of the test patterns' direction of motion even for adaptation durations of less than 3 secs. This supports our hypothesis that the visual system is continuously adapting to the ever-changing visual input statistics on a short time-scale.

This study was supported by the German Primate Center and the Volkswagen Stiftung.

## Orientation preference maps have sensitive spots

Kaschube, M (1), Schnabel, M (1), Kreikemeier, K (2), Dinse, H R (2),

Godde B. (3), Schmidt, K F (4), Löwel, S (4,5) and Wolf, F (1)

(1) MPI Strömungsforschung, Göttingen (2) Inst. Neuroinformatics, Univ.  
Bochum (3) Med. Psychol. & Behav. Neurobiol., Univ., Tübingen (4)  
Leibniz-Inst. Neurobiol., Magdeburg (5) Univ. Magdeburg, Germany

Recently, experiments by Godde et al. [1] demonstrated that in the visual cortex of adult cats substantial reorganization of orientation maps can be induced by local intracortical microstimulation (ICMS). In these experiments the degree of map reorganization varied strongly between experiments. This variability might in principle reflect a systematic dependence of susceptibility to ICMS on the precise location of stimulation in orientation maps. It is therefore an important question how the induced changes depend on the location of the ICMS site within the orientation map, e.g. whether ICMS is applied in pinwheel centers or in iso-orientation domains. We explored this question in a phenomenological model for the dynamics of visual cortical orientation maps. The model is based on biologically plausible symmetry assumptions and includes local and non-local intracortical interactions [2]. Effects of ICMS were mimicked by including a local stimulation term in the dynamics. In good agreement with experimental findings [3,4] ICMS induced strong changes in the map layout ranging over several hypercolumns and continuing to develop after the end of ICMS. In some cases the initial state fully recovered, whereas in other cases, remarkably, it was replaced by a new columnar layout. Furthermore, the model predicts a systematic dependence of the effect on the ICMS location in the orientation map: Strongest susceptibility occurred at pinwheel centers, weakest influence resulted at iso orientation domains. The observed effects of ICMS are interpreted within this theoretical framework as a switching between different equilibrium states of a cortical learning dynamics. VW(I/77 347-9). (1) Godde et al., PNAS 99 (2002) (2) Wolf and Geisel, Soc.Neurosc.Abs (2000) (3) Schmidt et al. (2005) this meeting (4) Kreikemeier et al., Soc.Neurosc.Abs (2004) .

# Anomalous Spike Initiation in Cortical Neurons

Björn Naundorf<sup>1</sup>, Maxim Volgushev<sup>2</sup>, Fred Wolf<sup>1</sup>

<sup>1</sup>Dept. of Nonlinear Dynamics, Max-Planck Institut für Strömungsforschung, Göttingen, Germany

<sup>2</sup>Abteilung Neurophysiologie, Ruhr-Universität Bochum, Germany

Action potential (AP) initiation in cortical neurons is fundamental for all higher computational processes in the brain. In most neurons this process is mediated by fast sodium channels, which activate and inactivate in a voltage-dependent fashion. Here we describe features of the dynamics of AP initiation which differ qualitatively from the predictions of the classical Hodgkin-Huxley theory of AP initiation. We show that APs from neocortical neurons recorded *in vivo* and *in vitro* initiate much more rapidly than predicted by the steady state sodium activation curve, while at the same time APs are emitted in a large voltage range. We then demonstrate that the two effects are mutually exclusive in conductance based models, i.e. a sharp AP upstroke leads to small range of AP onset voltages, a large range of AP onset voltages can only be achieved by a slow AP onset. We show that the anomalies in the AP onset dynamics lead to dramatic discrepancies in the description of the information processing capabilities of neocortical neurons [1].

Taken together our results indicate that the initiation of APs in cortical neurons can not be adequately understood in the framework of Hodgkin-Huxley type conductance-based models. The elucidation of the biophysical mechanisms of AP initiation thus remains an open challenge.

This study is supported by the Max-Planck Society, the HFSP and the DPG.

[1] B. Naundorf, F. Wolf, T. Geisel, submitted, (2004)

[2] X.J. Wang, Y. Liu, M.V. Sanches-Vives, D.A. McCormick, *J Neurophysiol* 89, 3279 (2003)

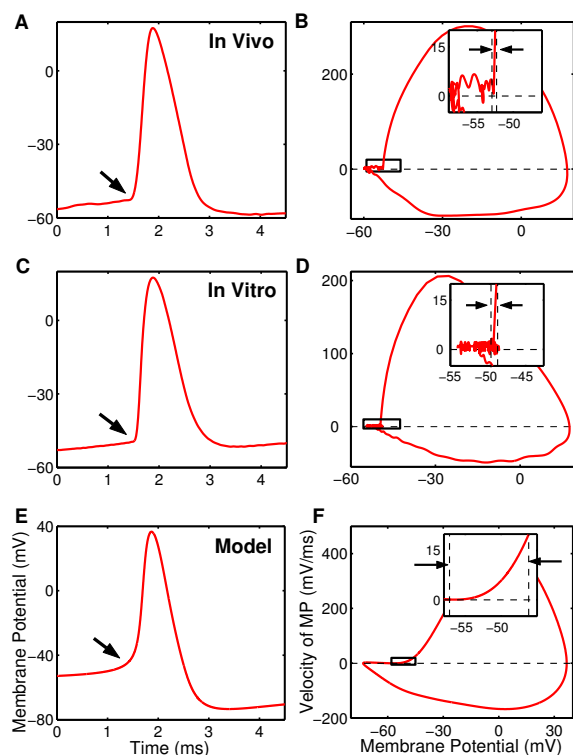


FIGURE 1: AP initiation *in vivo*, *in vitro* and in a conductance based neuron model. (A,B) AP recorded *in vivo* in cat visual cortex. (C,D) AP recorded *in vitro*, in a slice of rat visual cortex, at room temperature. (E,F) Typical shape of an AP simulated using a recently proposed conductance based model [2]. (A,C,E) Plots of one AP at high temporal resolution. While the APs in real neurons exhibit a sharp upstroke, the AP in the conductance based model starts very smoothly (arrows). (B,D,F) Phase space plots of the APs from (A,C,E). In each plot the loop corresponds to an AP. Insets show the initial phase of each AP (black boxes). In (B) and (D) the AP start very abruptly, while in (F) the AP builds up very slowly over a large voltage range.

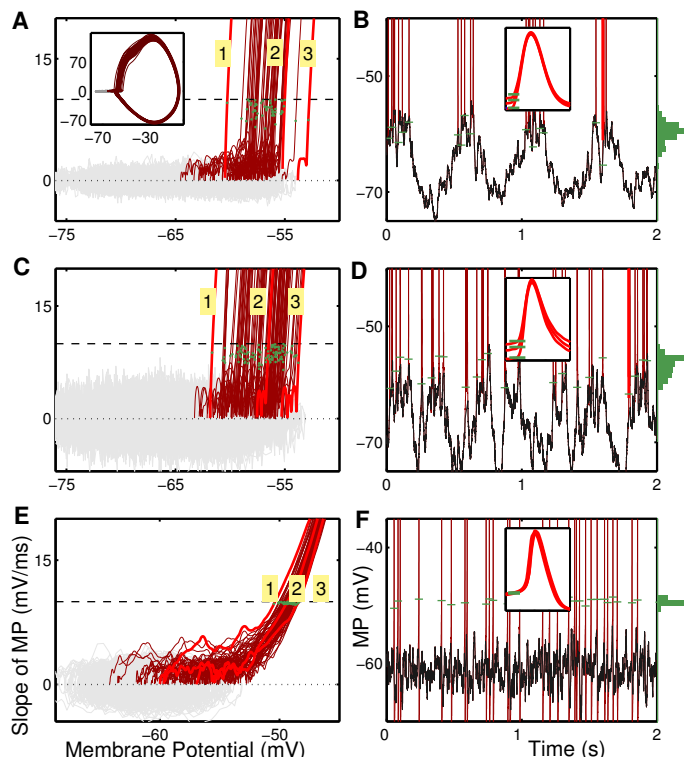


FIGURE 2: AP initiation in neurons from visual cortex recorded *in vivo* and in a conductance based model of a neocortical neuron. (A,B) Response of a neuron with a simple receptive field to a moving grating. (C,D) Response of a neuron with a complex receptive field to a moving grating. (E,F) Simulation result using a conductance based model [2] of a neocortical neuron subject to a fluctuating synaptic input. (A,C,E) Phase space plot of the APs. Only the AP initial phases and the subthreshold fluctuations are shown. (B,D,F) Part of membrane potential traces. Insets: Three sample APs labeled in (A,C,E). The green histograms show the distribution of the AP onsets. In (A-F), APs are shown in dark red, their onsets with green dots or bars. Note the much steeper upstroke and the larger variability of the onset potentials of the recorded APs, as compared to the simulations of the conductance neuron model.

Ciliary neurotrophic factor protects retinal ganglion cells from secondary cell death during acute autoimmune optic neuritis in rats

Katharina Maier, Christian R. Rau, Maria K. Storch, Muriel B. Sättler, Iris Demmer, Robert Weissert, Naimeh Taheri, Antje V. Kuhnert, Mathias Bähr and Ricarda Diem

Multiple Sclerosis (MS) is a chronic inflammatory disease of the CNS which leads to demyelination, axonal destruction and neuronal loss in the early stages. Available therapies mainly target the inflammatory component of the disease but fail to prevent neurodegeneration. To investigate the effect of ciliary neurotrophic factor (CNTF) on the survival of retinal ganglion cells (RGCs), the neurons that form the axons of the optic nerve, we used a rat model of myelin oligodendrocyte glycoprotein-induced experimental autoimmune encephalomyelitis. Optic neuritis in this model was diagnosed by recording visual evoked potentials, and RGC function was monitored by measuring electroretinograms. This study demonstrates that CNTF has a neuroprotective effect on affected RGCs during acute optic neuritis. Furthermore, we demonstrate that CNTF exerts its neuroprotective effect through activation of the Janus kinase/signal transducer and activator of transcription pathway, mitogen activated protein kinases and a shift in the Bcl-2 family of proteins towards the anti-apoptotic side. In summary, our results demonstrate that CNTF can serve as an effective neuroprotective treatment in a rat model of MS that especially reflects the neurodegenerative aspects of this disease.

## Do stability and sparseness lead to binocular properties of simulated neurons comparable to physiology?

Sebastian Bitzer<sup>1</sup>, Markus Goldbach<sup>1</sup>, Andres Bühlmann<sup>2</sup>, Selim Onat<sup>1</sup>, Peter König<sup>1,2</sup>

<sup>1</sup>Institute of Cognitive Science, University of Osnabrück, 49069 Osnabrück

<sup>2</sup>Institute of Neuroinformatics, University of Zürich/ETH Zürich, CH-8057 Zürich



Neurons in primary visual cortex are selective for many different features of visual stimuli (e.g. local contrast, orientation, spatial frequency, disparity, velocity ...; Hubel & Wiesel 1962, 1969). Recent studies show that the first 3 features of this list can be well understood by forming optimally stable or sparse representations of natural stimuli (Olshausen & Field 1996, Becker 1999, Körding et al. 2004). Here, we extend this line of work and investigate optimal representations of 3D natural videos and compare the resulting disparity selectivity to physiological results (Onat et al. 2004).

The simulations are based on a database of binocular cat-cam videos (see Onat et al. 2005, this conference). Receptive fields of simulated neurons are fitted with 2D-Gabor functions. The parameters of this fit are used to compute a number of statistical measures. These are compared to published data on cat and monkey primary visual cortex (Anzai et al. 1999, Prince et al. 2002).

As in primary visual cortex the simulated neurons respond selectively to the disparity of stimuli. Testing the simulated cells with random dot stereograms yields 100% of them being disparity selective. – Prince et al. (2002) found significant disparity tuning in 55% of simple and complex cells in primary visual cortex.

In primary visual cortex two mechanisms of encoding disparity, position and phase difference of right and left receptive fields, are uncorrelated ( $r=0.12$ , Anzai et al. 1999). – We observe a non-significant correlation between position and phase disparity as well ( $r=0.33$ , see Figure).

In the physiological data an anisotropy is reported with significantly lower variances of preferred phase differences for horizontal orientations as compared to vertical orientations (Ohzawa et al. 1996, Anzai et al. 1999). – In simulated neurons the distribution of preferred phase difference is independent of preferred orientation. Thus, the dependence of phase on orientation could not be confirmed in our simulation.

It is possible to define different types of disparity tuning (Poggio et al. 1988). However, scatterplots of phase and position difference of receptive fields of neurons in primary visual cortex do not indicate clustering into distinct groups (Prince et al. 2002). – Applying identical measures to the simulated cells we do not observe a clustering either.

Contrary to Prince et al. (2002) phases of neurons in our model cover a wider range of phase angle.

In primary visual cortex neurons with consistent inhibitory contribution from one eye are observed (Read & Cumming 2003). – In contrast, due to the limitation imposed by the energy model that is used in our study, this is not observed in any of the simulated neurons.

In summary, optimally stable or sparse simulated neurons match in several aspects of disparity coding their physiological counterparts. However, a number of measures give significantly deviating properties and modifications to the cell model and/or the objective functions have to be made to match all known biological properties.

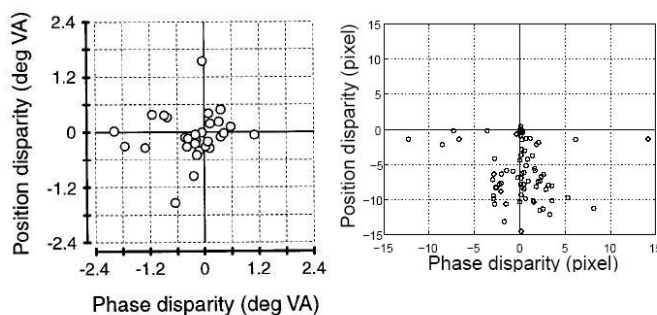


**Figure: Receptive field position disparity vs. phase disparity.** The left shows the simple cell data from Anzai et al. (1999), on the right we see the scatter plot for our sparseness data. In both data sets no significant correlation between the two RF properties was found ( $r_{\text{phys}} = 0.12$ ,  $r_{\text{sim}} = 0.33$ , respectively). Position disparities cover a smaller range than phase disparities (68% of phase range in Anzai et al. (1999) and 78% in our data, respectively).

## Perception of object-movement in goldfish (*Carassius auratus*)

Martin Gehres and Christa Neumeyer

Institut für Zoologie III, Johannes-Gutenberg-Universität, D-55099 Mainz

**Purpose:** Motion perception is a basic property of the visual system. Usually the optomotor response, a standard method for full field motion vision, is used to investigate the ability of motion detection. In goldfish motion vision measured with the optomotor response is colour-blind and dominated by the L-cone type (Schaerer & Neumeyer, 1996). Object motion as a movement of an object in front of a stationary background can also be perceived by animals. The two different kinds of motion seem to be processed by two distinct mechanisms (Egelhaaf et al. 1989; Frost et al. 1990; Born 1992). To investigate the properties of object-movement perception we trained goldfish to discriminate moving objects from non-moving objects.

**Methods:** Four goldfish were kept separately in tanks (50 x 30 x 30 cm). Two quadratic openings (5 x 5 cm, 5cm apart) in a 'feeding plate' served as test fields, on which two scenes were shown using a Liquid Crystal Display. Food reward was given at the training stimulus.

### First experiment:

Animals were trained on a moving black dot ( $\varnothing$  1 cm) on a white background vs. a uniform white background. Object movement vision was tested in transfer experiments: a moving dot was tested against a stationary dot, a moving black square against a stationary square, a stationary square against a stationary dot and a moving dot against a stationary dot with some unmoving dots in the background, in both cases.

### Second experiment:

The fish were trained to detect a group of 20 moving dots (each dot  $\varnothing$  1 mm) within a background dot pattern vs. a stationary dot pattern.

**Results:** All goldfish were able to discriminate the black moving dot from the white field. However, only one fish seems to have distinguished between a moving and stationary object independent of the object's shape in the transfer experiments. The others just showed a reaction to a black dot. They did not make a distinction between a black moving dot and a black stationary one. Also they did not react to a black square neither moving nor stationary. In the transfer test 'stationary square vs. stationary dot' they chose the stationary dot. In the second experiment all goldfish were able to distinguish between a moving and a stationary object..

**Conclusion:** The random dot pattern is the appropriate method to test the perception of object-movement of goldfish. The fish were always able to detect the object motion, irrespective of one does not have to know whether the fish learned the shape of the moving object or the motion itself. Using this methods do not need to know which aspect of the training situation was associated with food reward. We are not able to say, whether the fish have a concept of 'moving vs. stationary' or not. This method is independent of such a concept, because the fish can see the object only in the moving scene. Now we can analyse further parameters of the perception of object-movement in goldfish such as contrast, speed and colour.

## Traveling Gamma-Waves: Stimulus-dependent Signal Coupling in Monkey Primary Visual Cortex

Andreas Gabriel, Alexander Gail, Reinhard Eckhorn

Philipps-Univ., Deptm. Physics, NeuroPhysics Group, D-35032 Marburg, Germany

**Introduction and Goal.** The phenomenon of traveling waves in excitable neural structures is well known for a long time but its functional role in cortical sensory processing is still unclear. During visual stimulation we found traveling plane waves in multiple-channel recordings from monkey striate cortex in the gamma-frequency range (30–90 Hz). Synchronized gamma-activity gained interest in recent years due to their proposed role in associative processing, including perceptual binding of object representations. However, gamma-synchrony in cat and monkey primary visual cortex (area V1) is restricted to few millimeters of cortical surface, challenging the synchronization hypothesis for larger cortical object representations (e.g. [1, 2]).

**Methods.** We developed a spatio-temporal correlation method capable of detecting and quantifying traveling waves from multiple-site recordings [3]. In the present investigation we analyzed multiple-channel local field potential (LFP) recordings from the striate cortex of awake monkeys during visual stimulation with grating textures, forming figure (object) and back-ground.

**Results.** By applying this method, we demonstrate (1) that the spatial restriction of gamma-synchrony is due to the fact that the underlying gamma-signals are waves traveling in random directions across the representation of the visual object in V1; (2) that neural representations coding similar local features of the object surface are strongly coupled by gamma-waves (here: similar orientation preferences among the recording sites); (3) that the coupling dynamics of gamma-waves depend strongly on the continuity of the object's surface. This means that phase continuity of gamma-waves exists either inside or outside of the cortical representation of an object, but does not cross its boundaries.

**Conclusions.** From these and previous results [4] we suggest that the phase-continuity of gamma-waves can support the coding of object continuity and that the hypothesis of object representation by gamma-synchronization should be extended to more general forms of signal coupling and associative processing.

[1] Eckhorn, R. (1994). Oscillatory and non -oscillatory synchronizations in the visual cortex of cat and monkey. In Pantev, C., Elbert, T., and Lütkenhöner, B. (ed.), *Oscillatory Event-Related Brain Dynamics*, pp. 115–134. New York, London: Plenum Press.

[2] Fien, A. and Eckhorn, R. (2000). Functional coupling shows stronger stimulus dependency for fast oscillations than for low-frequency components in striate cortex of awake monkey. *Eur J Neurosci*, 12:1466–1478.

[3] Gabriel, A. and Eckhorn, R. (2003). A multi-channel correlation method detects traveling gamma-waves in monkey visual cortex. *J Neurosci Meth*, 131:171–184.

[4] Gail, A., Brinksmeyer, H.-J., and Eckhorn, R. (2004). *Cereb Cortex*, 14(3):300–314.

Supported by Deutsche Forschungsgemeinschaft DFG (FOR 254) to R.E.



## Discrimination and prediction of perceptual states from multiple-electrode recordings in monkey striate cortex

Alexander Kremper, Alexander Gail, Reinhard Eckhorn

Philipps-University, Physics Department, NeuroPhysics Group, 35032 Marburg, Germany

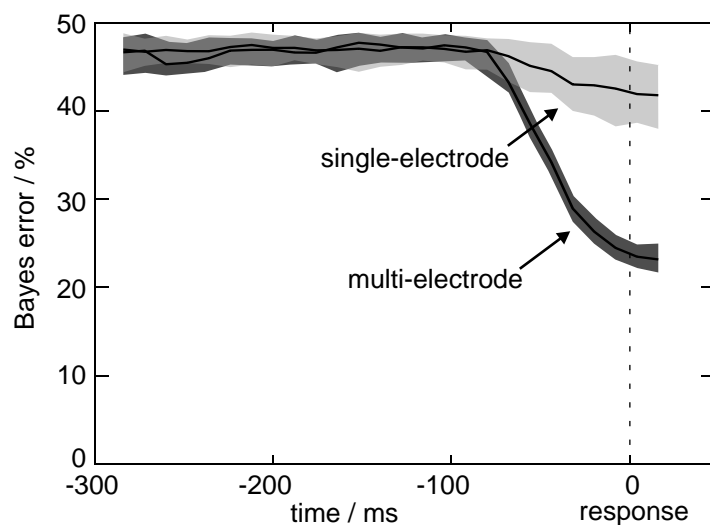
**Goal.** Can we predict different perceptual states, evoked by ambiguous visual stimulation, from neural signals as early as in striate cortex?

**Methods.** We investigated this by using our recently developed non-linear classifier, which takes into account the spatio-temporal statistical dependencies of multiple simultaneously recorded channels [1]. Our method is based on dimension reduction by radial basis functions with a multi-quadric kernel, where the weights are determined by supervised learning in combination with repeated k-fold cross-validation. This method is relatively insensitive to outliers and especially successful in high-dimensional small sample cases, as often encountered with neural recordings. Our approach is not restricted in dimensionality and can be applied to other signal types, including multiple-channel EEG and MEG. Here we demonstrate its potential by analyzing population signals (local field potentials and multi-unit activity) from multi-channel micro-electrode recordings in striate cortex of awake monkeys [2]. Stimuli consisted of perpendicularly oriented gratings, presented dichoptically, resulting in rivaling percepts. In contrast to previous prediction studies, which used disjoint subsets of the same data for learning and discrimination, we also combine different sets of data, in which responses to congruent stimuli (identical in both eyes) were used for training of our algorithm but testing was done with responses to incongruent (rivalrous) stimuli.

**Results.** Based on simultaneous recordings from, e.g., 11 channels trained on local field potentials in the congruent condition and tested by the rivalrous condition, the average Bayes error decreases in the data, prior to one monkey's response to 23 %. In contrast, with single-channel analysis of the same data, prediction is near chance (see Figure below). This means that about 77 % will be correct classified by the multi-channel approach.

### Figure.

Comparison of the time-resolved discrimination of local field potentials recorded in monkey primary visual cortex (sliding window width 48 ms)  
gray: analyzing each electrode signal separately  
black: using signals from all electrodes simultaneously  
(shaded: 90 % confidence interval)



**Conclusions.** Our multi-channel approach enabled a better discrimination or at least the same discrimination compared to single-electrode approaches. Its high sensitivity can be explained by the fact that it takes into account the spatio-temporal statistical dependencies of all recorded channels simultaneously.

### References.

- [1] Kremper A, Schanze T, Eckhorn R (2002) Classification of neural signals by a generalized correlation classifier based on radial basis functions. *Journal of Neuroscience Methods* 116(2):179-187.
- [2] Gail A, Brinksmeyer H-J, Eckhorn R (2004) Perception-related modulations of local field potential power and coherence in primary visual cortex of awake monkey during binocular rivalry. *Cerebral Cortex* 14:300-313.

Supported by Konrad Adenauer Stiftung to AK and Deutsche Forschungsgemeinschaft (FOR 254) to RE.

## Comparison of projection methods for dimension reduction and the determination of lower bounds for transmitted sensory information

Alexander Kremper, Reinhard Eckhorn

Philipps-University, Physics Department, NeuroPhysics Group, 35032 Marburg, Germany

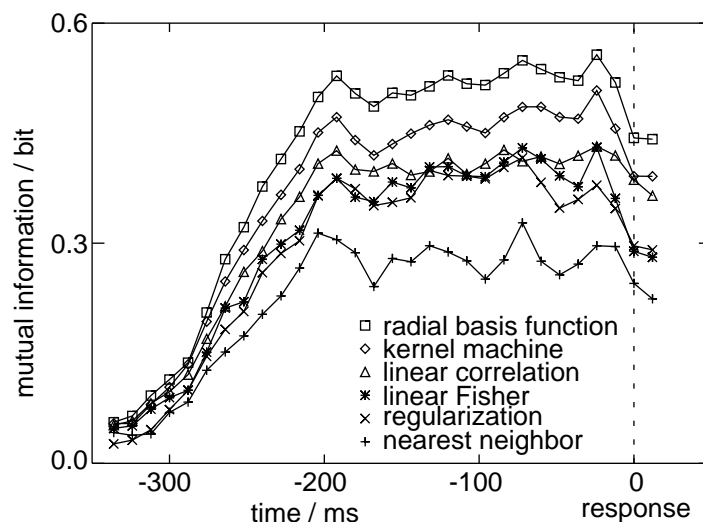
**Introduction.** Estimating the transmitted sensory information from neural signals is often made difficult by the low number of stimulus-response pairs obtained during an experiment with awake animals or humans and the high dimensionality of the measured stimulus-response space.

**Methods.** Instead of estimating the underlying probability density functions of stimuli and response signals, we compared different projection methods generating simpler, lower-dimensional representations of the data. In addition to two common linear approaches, we investigated methods based on regularization, kernel machines, nearest neighbors and radial basis functions. Each approach requires at most the solution of a linear system of equations. To quantify the reduction of the mutual information after dimension reduction, we estimated the information loss by cross-validation in combination with Monte-Carlo sampling for various sets of artificial data. Emphasis was placed on the relationship between training size and dimensionality. Performance for more realistic data was examined by discriminating signals from small simulated neural networks during different states and recordings from monkey primary visual cortex during a match-to-sample experiment [1].

**Results.** As expected, increasing the number of irrelevant signal components has a negative effect on the transmitted information for all methods. From the neural network simulations we found a monotone increasing dependence of the transmitted information on the signal-to-noise ratio. In general, the performance of the various methods was related to the type of data, in particular to their signal correlations. As expected, none of the methods performed optimally under all conditions, e.g., in special situations, linear prediction is quite accurate. With respect to the analysis of multiple-channel population recordings from monkey visual cortex [1], radial basis functions revealed the most reliable and robust results in the typical high-dimensional small sample case of electrophysiological recording experiments (see Figure below and Abstract Kremper et al, this Vol)). In contrast to classical approaches our method enables to quantify the information increase with increasing numbers of recording channels without any assumptions about statistical dependencies.

### Figure:

Estimates of time-resolved mutual information for six projection methods from multiple-channels of multiple unit spike activity (MUA) recorded in monkey primary visual cortex. Sliding window width: 48 ms with 12 ms time shifts. Standard deviation varies by about 0.04. The method with radial basis functions outperforms all other methods significantly ( $p < 0.01$ ).



**Conclusions.** We propose to use kernel methods for estimating transmission of sensory information from multiple-site population recordings, particularly if predictions based on single-trial responses are required. One reason why kernel methods perform so well might be their adapted regularization properties, in combination with optimized generalization. If computational time plays a critical role radial basis functions should be preferred to other highly sophisticated methods.

### References.

[1] Gail A, Brinksmeyer H-J, Eckhorn R (2004) Cerebral Cortex 14:300-313.

Supported by Konrad Adenauer Stiftung to AK and Deutsche Forschungsgemeinschaft (FOR 254) to RE.

## Unsupervised learning of cortical complex cell properties using spatio-temporally coherent visual stimuli and a recurrent network of spiking neurons

Basim Al-Shaikhli, Reinhard Eckhorn

Philipps-University, Physics Department, NeuroPhysics Group, 35032 Marburg, Germany

**Introduction and Goal.** Neurons in primary visual cortex are commonly classified as simple and complex cells. While simple cells are selective for the position of a visual stimulus in their classical receptive field (cRF), complex cells respond independently of stimulus position within their cRF (resembling local position invariance). In contrast to the model of Hubel and Wiesel [1], which proposes the emergence of complex cell properties through feed-forward convergence of simple cells, it was recently argued that simple and complex cells can emerge as low- and high-gain limits of the same recurrent cortical circuit [2, 3]. We aim to show in a basic model of the primary visual cortex that such circuits can arise through unsupervised learning with spatio-temporally coherently moving stimuli.

**Methods.** Our network model of the visual cortex consists of several simplified cortical hypercolumns of spiking neurons. Each excitatory neuron receives feed-forward input whose strength resembles the selectivity of a cortical simple cell to a visual stimulus. Feed-forward synaptic connections are modelled with short-term depression. Within one hypercolumn, these neurons interact through mutually recurrent excitatory connections, which are initially weak. They excite a common inhibitory neuron feeding back to them. The lateral connection strengths are updated according to a spike-timing dependent learning rule similar to the empirical model proposed by Nelson et al. [4]. Importantly, LTD is independent of the post-synaptic firing rate while LTP is scaled according to it. Only nearest-neighbour pre- and post-synaptic spikes take part in learning events and if a postsynaptic spike takes part in causing LTP it is ineffective in triggering further LTD. Therefore, with low postsynaptic firing rates LTP- and LTD-influences depend strongly on the sign of the temporal difference of pre- and postsynaptic spikes while for high firing rates weights are strengthened independently of the sign of the temporal difference. Thus, with high firing rates this rule acts similar to the *'trace rule'* proposed by Földiák [5] by which invariance properties can be learned. Feed-forward and recurrent connection strengths are conjointly normalized. Consequently, strengthening of recurrent connections causes weakening of feed-forward connections.

**Results.** With stimuli moving coherently in space and time the recurrent connections become strengthened, changing the cRF-properties to those of complex-cells. This learning effect is much weaker with stimuli presented at random locations. Our results did not emerge by using a spike-timing dependent learning rule with a balanced, asymmetric learning window.

**Discussion and Conclusions.** While other authors investigated learning of complex-cell cRF properties with feed-forward networks, we show that these properties can also emerge with recurrent excitatory connections through unsupervised learning, particularly with spatio-temporally coherently moving stimuli. Further work has to show whether the principles applied in this work, namely strong recurrent connections and a learning rule which depends both on spike timing and firing rate, can be applied to the learning of other invariant representations of visual features in higher cortical areas.

[1] Hubel DH, Wiesel TN (1962) *J Physiol* 160:106-154. [2] Chance et al. (1999) *Nature Neurosci* 2:277-282 [3] Tao et al. (2004) *PNAS* 101:366-371 [4] Nelson et al. (2002) *Phil Trans Roy Soc Lond B* 357:1851-1857 [5] Földiák P (1991) *Neural Comput* 3:194-200

This work was supported by Friedrich-Ebert-Stiftung to BA and Deutsche Forschungsgemeinschaft (FOR 254) to RE.

## Relations between spatial frequency preference and size of spatial-summation field in striate cortex of awake monkey

Tobias Teichert, Thomas Wachtler, Alexander Gail, Markus Wittenberg, Frank Michler,  
Reinhard Eckhorn

Philipps-University, Department of Physics, NeuroPhysics Group, 35032 Marburg, Germany

**Introduction.** Our visual system is selective for spatial frequencies (SF), which are a measure of spatial resolution. Psychophysical evidence suggests the existence of SF-channels, primarily based on adaptation to grating stimuli. Models of visual perception often use a set of localized SF-filters, typically based on oriented Gabor-wavelets that are scaled in spatial size inversely proportional with their optimal SF. This results in identical relative SF-tuning widths. In striate cortex (V1), already within a narrow representation of the visual field, neurons show SF-tuning with best frequencies over a range of 3 to 4 octaves [1]. If these *neural SF-filters* represent a Gabor- or other wavelet basis, the sizes of their receptive fields are expected to increase inversely proportional to their optimal SF (or proportionally to their spatial wavelength).

**Methods.** We recorded in macaques multi-unit activity in the upper layers of striate cortex. Classical receptive fields (cRFs) were first mapped using small (10') bright spots, flashed randomly for 50 ms at one of 16x16 positions within a 2.5° field. cRF sizes were measured by determining the spatial contour at 70% of the maximal response. Subsequently, the size of the spatial-summation field was determined from recordings of responses to Gabor patches of different sizes (0.1-5.0°) and spatial frequencies (0.7-8.0 cycles/°), centered on the previously determined cRF centers. Summation field size was determined by interpolating the patch size that evoked the strongest responses.

**Results.** Spatial-summation fields were several times larger than cRF sizes, consistent with previous comparisons of these methods [2]. At eccentricities between 4° and 6°, average summation field size was  $1.0^\circ \pm 0.7^\circ$ . SF preferences covered the expected range, with best frequencies spreading over more than 3 octaves. Response latency increased with SF and decreased with patch size, also consistent with previous findings [3]. However, we did not find positive correlations between summation field size and inverse of best SF, as would be expected under the assumption of a wavelet-like basis of neural SF-filters in V1. On the contrary, our preliminary data, from one hemisphere of one monkey, show a weak negative correlation ( $r^2=0.33$ ) between these parameters.

**Discussion and Conclusions.** The results suggest that the spatial-summation fields in V1 do not constitute a wavelet-like basis. The independence of summation field size and SF-preference can be explained by different models of connectivities of geniculate and cortical neurons.

- [1] De Valois RL, Albrecht DG, Thorell LG (1982) Spatial frequency selectivity of cells in macaque visual cortex. *Vision Research* 22:545-559
- [2] Angelucci A, Levitt JB, Walton EJS, Hupe JM, Bullier J, Lund JS (2002) Circuits for local and global signal integration in primary visual cortex. *J. Neurosci.* 22:8633-8646
- [3] Brinkmeyer H, Michler F, Gail A, Eckhorn R (2002) Properties of spatial frequency channels and their modulation by stimulus distance in striate cortex of awake monkey. *Soc. Neurosci. Abs.* 457.3

Supported by DFG (to RE) and DFG GK NeuroAct (to TT)

## **Extensive plasticity in adult mice after monocular deprivation revealed by optical imaging**

**Hofer SB, Mrcic-Flogel TD, Bonhoeffer T, Hübener M**

Max-Planck-Institute of Neurobiology, Martinsried, Germany

Deprivation of one eye reduces the responsiveness of visual cortex neurons to stimulation of that eye, while responses to stimulation of the non-deprived eye are enhanced. This type of experience-dependent plasticity is assumed to be mostly restricted to a phase early in life, the so-called critical period. Here we present a reliable method for assessing monocular deprivation (MD) induced plasticity in juvenile and adult mice by optical imaging of intrinsic signals. This relatively non-invasive approach, which allows repeated measurements in the same animal, revealed substantial visual cortex plasticity long after the critical period.

In order to compare the effect of MD in juvenile and adult mice, one eyelid was sutured shut either around postnatal day (P) 26, or between P60 and P90. The visual cortex contralateral to the deprived eye was imaged through the intact skull after 2-10 days of deprivation in halothane-anaesthetized mice. Small, moving gratings presented to either eye in the upper central visual field evoked restricted activation patches in the visual cortex. The strength of responses elicited by stimuli in the binocular visual field was compared for the two eyes.

In non-deprived animals, the responses to the contralateral eye were invariably stronger than those to the ipsilateral eye. The ratio of contralateral to ipsilateral eye response strength (CI ratio) was  $2.5 \pm 0.3$  (mean  $\pm$  s.d.) in juvenile mice, and slightly lower in adult mice (CI ratio =  $2.0 \pm 0.2$ ). During the critical period, MD led to a significant reduction in the CI ratio. Four days of deprivation were sufficient to induce a saturating effect (CI ratio =  $0.8 \pm 0.2$ ). The shift in ocular dominance resulted mostly from a large decline in deprived-eye responsiveness, while only a small but significant strengthening of responses to the non-deprived eye was detectable. In adult mice (P60-90), MD also resulted in a significant but somewhat slower shift in ocular dominance (4 days: CI ratio =  $1.3 \pm 0.2$ ; 6 days: CI ratio =  $1.0 \pm 0.2$ ). In contrast to the findings in juvenile mice, this shift was primarily due to an enhancement of responses to the non-deprived eye.

Our results are consistent with studies using field potential recordings in showing extensive capability for plasticity in adult mouse visual cortex which seems to arise from mechanisms different to the processes apparent earlier in life. Studying the differential effects of MD with optical imaging in genetically-modified mice of different ages will provide insight into the underlying cellular and molecular mechanisms.

Supported by the Max Planck Society and the Humboldt Foundation

## Mapping retinotopy in mouse superior colliculus with optical imaging

T.D. Mrsic-Flogel, S.B. Hofer, C. Creutzfeldt, T. Bonhoeffer, M. Hübener  
Max-Planck-Institute of Neurobiology, Martinsried, Germany

Optical imaging of intrinsic signals has been proven to be very useful for high resolution mapping of response properties in a variety of cortical areas as well as the olfactory bulb. Here we show that this technique can be readily used to visualize a topographic map in another part of the brain, the superior colliculus (SC).

Mice were anesthetized with halothane or with a mixture of urethane and ketamine, and the cortex overlaying the SC was removed by suction. Small, square-shaped grating stimuli were presented at different locations in the contralateral visual field, while images were taken of the surface of the left SC. Stimuli at a given position evoked clear, sharp-edged patches of activity in the SC. In many experiments the signal-to-noise ratio was excellent, such that clear intrinsic signal responses could be obtained with a single stimulus presentation, without averaging. The position of the activity patches varied systematically with changes in stimulus location, thus revealing the retinotopic map in the SC. Within experiments, these retinotopic maps were highly reproducible. Consistent with previous electrophysiological and anatomical studies, the magnification factor varied only little across the surface of the SC.

A comparison with maps obtained from mouse visual cortex revealed that patches evoked by neighboring stimuli overlapped substantially less in the SC than in the visual cortex. We are currently investigating with single cell recordings whether this difference is due to differences in receptive field size, a larger scatter of receptive field positions in the visual cortex, or differences in the lateral spread of the intrinsic signal.

Our results show that optical imaging allows rapid visualization of the retinotopic map in the SC, thus making this technique ideally suited for the fast screening of mice mutants lacking molecules involved in the development of topographic maps. In addition, as the SC also contains maps for other stimulus modalities, e.g. auditory and tactile space, this method opens up the possibility to study cross-modal interactions at the level of topographic maps.

Supported by the Max Planck Society and the Alexander von Humboldt Foundation.

## The mystery of magnetoreception in migratory songbirds

Miriam Liedvogel<sup>\*</sup>, Ulrike Janssen-Bienhold<sup>†</sup>, Gesa Feenders<sup>\*</sup>, Julia Stalleicken<sup>\*</sup>, Petra Dirks<sup>†</sup>, Reto Weiler<sup>†</sup> & Henrik Mouritsen<sup>\*,‡</sup>

<sup>\*</sup>Volkswagen Nachwuchsgruppe "Animal Navigation",

<sup>†</sup>Neurobiology, Institute of Biology, University of Oldenburg, D-26111 Oldenburg, Germany.

<sup>‡</sup>To whom correspondence should be addressed. [henrik.mouritsen@uni-oldenburg.de](mailto:henrik.mouritsen@uni-oldenburg.de).

Migratory birds can use a magnetic compass for orientation during their migratory journeys covering thousands of kilometers. But how do they sense the reference direction provided by the Earth's magnetic field?

Two types of potential magnetoreception mechanisms have been suggested over the past decades, one based on magnetite particles and one based on photoreceptors forming radical pair intermediates by photo excitation. Behavioral evidence and theoretical considerations suggest that birds perceive the direction of the magnetic field by specialised retinal photo pigments, requiring light from the blue-green part of the spectrum. Radical-pair processes in differently oriented, light sensitive molecules of the retina could potentially enable migratory birds to perceive the magnetic field as visual patterns.

The cryptochromes (CRY) with an absorption spectrum of 300-500nm have been suggested as the most likely candidate class of molecules. But do cryptochromes exist in the retina of migratory birds?

Here, we show that at least one member of the cryptochrome family exists in the retina of migratory garden warblers (*Sylvia borin*). We also found that gwCRY1 is concentrated in specific cells, particularly in ganglion cells and in large displaced ganglion cells, which also showed high levels of neuronal activity at night when our garden warblers performed magnetic orientation. In addition, there seem to be striking differences in CRY1 expression between migratory and non-migratory songbirds at night.

To further characterise the candidate class of primary receptor molecules, we used retinal cDNA of garden warblers as template for amplification of cryptochromes expressed in the eyes of night-migrating songbirds. We identified and sequenced independent PCR products of this multigene family.

# Migratory birds use head scans to detect the direction of the Earth's magnetic field

Henrik Mouritsen\*, Gesa Feenders, Miriam Liedvogel & Wiebke Kropp

Volkswagen Nachwuchsgruppe "Animal Navigation", Institute of Biology, University of Oldenburg, D-26111 Oldenburg, Germany.

\*To whom correspondence should be addressed. [henrik.mouritsen@uni-oldenburg.de](mailto:henrik.mouritsen@uni-oldenburg.de),

Night-migratory songbirds are known to use a magnetic compass [1-3], but how do they detect the reference-direction provided by the geomagnetic field and where is the sensory organ located? The most prominent characteristic of geomagnetic sensory input, whether based on visual patterns [4-6] or magnetite-mediated forces [7, 8], is the predicted symmetry around the north-south or east-west magnetic axis. Recently, we discovered that caged migratory garden warblers perform head scanning behaviour well-suited to detect this magnetic symmetry plane. In the natural geomagnetic field, birds move towards their migratory direction after head scanning. In a zero magnetic field [9] where no symmetry plane exists, the birds almost triple their head scanning frequency and the movement direction following a head scan becomes random. Thus, the magnetic sensory organ is located in the birds' head and head scans are used to locate the reference direction provided by the geomagnetic field.

1. Wiltschko, W., and Wiltschko, R. (1972). Magnetic Compass of European Robins. *Science* 176, 62-64.
2. Wiltschko, W., and Wiltschko, R. (1996). Magnetic orientation in birds. *J. Exp. Biol.* 199, 29-38.
3. Cochran, B., Mouritsen, H., and Wikelski, M. (2004). Migrating songbirds recalibrate their magnetic compass daily from twilight cues. *Science* 304, 405-408.
4. Wiltschko, W., Munro, U., Ford, H., and Wiltschko, R. (1993). Red light disrupts magnetic orientation of migratory birds *Nature* 364, 525-527.
5. Ritz, T., Adem, S., and Schulten, K. (2000). A model for photoreceptor-based magnetoreception in birds. *Biophysical Journal* 78, 707-718.
6. Ritz, T., Thalau, P., Phillips, J. B., Wiltschko, R., and Wiltschko, W. (2004). Resonance effects indicate a radical-pair mechanism for avian magnetic compass. *Nature* 429, 177-180.
7. Walker, M. M., Diebel, C. E., Haugh, C., Pankhurst, P. M., Montgomery, J. C., and Green, C. R. (1997). Structure and function of the vertebrate magnetic sense. *Nature* 390, 371-376.
8. Fleissner, G., Holtkamp-Rotzler, E., Hanzlik, M., Winklhofer, M., Fleissner, G., Petersen, N., and Wiltschko, W. (2003). Ultrastructural analysis of a putative magnetoreceptor in the beak of homing pigeons. *J. Comp. Neurol.* 458, 350-360.
9. Mouritsen, H. (1998). Redstarts, *Phoenicurus phoenicurus*, can orient in a true-zero magnetic field. *Anim. Behav.* 55, 1311-1324.



## **Brain activity pattern during magnetic orientation tasks in night-migratory songbirds reveals a brain region involved in night-time vision**

Gesa Feenders<sup>a</sup>, Miriam Liedvogel<sup>a</sup>, Kazuhiro Wada<sup>b</sup>, Erich D. Jarvis<sup>b</sup> and Henrik Mouritsen<sup>a</sup>

<sup>a</sup> VW Nachwuchsgruppe Animal Navigation, University of Oldenburg, Germany; <sup>b</sup> Duke University Medical Center, Department of Neurobiology, Durham, North Carolina, USA

Studies of migratory orientation in songbirds have, until now, mainly focused on behavioural analysis. This has led to a broad understanding of how migratory birds find their way back and forth between their breeding and wintering regions thousands of kilometres apart. It was shown that they can use a variety of cues: mainly the sun, the stars and the magnetic field. Nevertheless, the neuronal mechanisms underlying these abilities remain unclear. Here, we used behavioural molecular mapping to examine the brain activation patterns in night-migratory Garden Warblers and European Robins performing magnetic orientation behaviour. Our aim was to locate possible brain areas involved in processing orientation-relevant information.

We used the well-known migratory restlessness behaviour: caged migratory songbirds are so eager to migrate that they try to jump/fly in the direction corresponding to the migratory direction of their free-flying conspecifics. If a bird is placed in an altered magnetic field, the direction will shift according to the artificial magnetic north whereas the bird is disoriented in a compensated zero magnetic field. Taking brain samples from birds tested under these different conditions we compared brain activity patterns by visualizing the activity-dependent immediate-early gene ZENK. This revealed a distinct region in the telencephalon showing very pronounced gene expression. We also analysed additional brains from birds during day-time and from non-migratory Zebra Finches at day and night. The day-time group as well as the non-migratory birds didn't show this increase in gene expression in the specific brain region we named "Cluster N". Thus, Cluster N is specific for night-migratory birds at night-time.

To test whether visual input affects the gene expression in Cluster N, we examined brains of birds that had their eyes occluded by light-tight eye-caps. This resulted in almost complete disappearance of neuronal activity in Cluster N. These data show that Cluster N is a region involved in some kind of night-vision, which is specialized in at least the two tested species of night-migratory songbirds. The results are in line with current theoretical, behavioural and molecular studies suggesting that magnetic field perception in birds is vision-dependant. According to this hypothesis, the magnetic field is sensed through modulations of a primary visual signal. Since this (unmodulated) visual signal will be sent to the brain whenever there is light-input to the eyes, this visual signal may induce Cluster N expression regardless of the conditions of the magnetic field.

## Stability of visual features and learning disparity selective complex cells

Selim Onat<sup>1,2</sup>, Christoph Kayser<sup>2</sup>, Peter König<sup>1,2</sup>

<sup>1</sup> Institute of Cognitive Science, University of Osnabrück, 49069 Osnabrück Germany

<sup>2</sup> Institute of Neuroinformatics, University of Zurich/ETH Zürich, Winterthurerstr. 190, 8057-CH



Recent neuroscience research emphasizes the relationship of receptive fields properties and statistics of natural images. For example, forming optimally stable representation of natural visual stimuli leads to receptive fields similar to complex cells found in the primary visual cortex (Körding et al., 2004). This suggests that as a general principle neurons extract local stable features. In the present study, we analyze temporal properties of a number of different visual features and, subsequently, extracted stable features from a database of natural stimuli.

We have used two microcameras carried on the head of a freely moving cat in a natural environment. The binocular parallax of the cameras was set to zero at infinity and the interocular distance to 4.8 cm. With this setup we have been able to record stereoscopic natural movies for about 10 minutes. On these movies we extracted color, contrast, orientation, disparity, mean luminance information and evaluate how fast they are changing over time. For disparity, the goodness of the value is also evaluated by a confidence measure. As an upper limit we computed the stability of pixel values. As a next step, we adopted the inverse approach and using a neural network (Körding et al., 2004) to obtain an optimally stable representation of the stereoscopic movies.

Analyzing temporal properties of these movies with respect to visual features, we find that disparity is the slowest of all. This is followed by color, contrast and orientation (Figure 1). This is taken as an indication that optimizing stability of visual representations should lead to disparity selective cells.

Building optimally stable representations of these movies, by implementing a disparity energy model (Adelson & Bergen 1985, Ohzawa et al. 1990), we obtained receptive fields that encode disparity information similar to simple and complex cell in the primary visual cortex (Figure 2). Different subunits being in a quadrature phase relationship this endowed the neurons to be translation invariant at a given disparity. The same kind of disparity coding has been described for complex cells in the primary visual cortex (Anzai et al. 1999). This shows that in addition to the monocular properties of complex cells, the stability criterion when applied to stereoscopic images can lead to disparity selective complex cells showing the validity of this approach for binocular input.

For this line of research it is important to compare more extensively the properties of the simulated receptive fields to physiological results (Bitzer et al, 2005, this conference) in order to gain more insights about the principles of sensory coding.

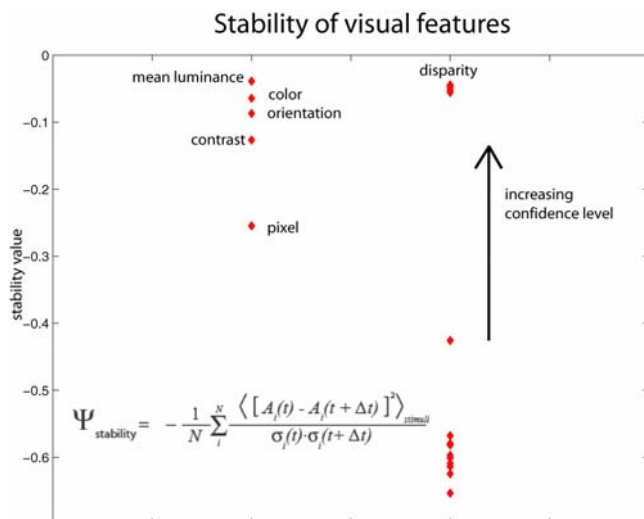


**Figure 1. Stability of visual features.** Stability is measured by normalizing the squared temporal derivative of a given feature's value by its variance. Stability of disparity increases with increasing confidence level of the fit and stabilizes at a maximum. The low values of stability at low confidence levels are due to the bad matches of left and right camera image. As an upper limit, the stability of a pixel value is computed.

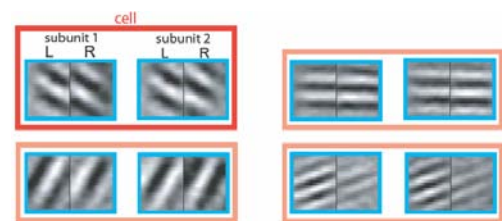


**Figure 2: Optimally stable binocular receptive fields learnt from natural stereoscopic images.** A complex cell (red rectangles) receives input from two subunits (blue rectangles), each having left and right receptive fields. The receptive fields of subunits are similar to simple cells: they are localized, orientation, spatial frequency and disparity selective. Some are binocularly unbalanced as in the primary visual cortex. Different subunits of a given complex cells are in quadrature phase relationship. This leads to complex cells that are translation invariant for their preferred stimulus at a given depth.

## Smooth pursuit eye movements elicited by anticipation in humans and monkeys

Sylvana Freyberg and Uwe J. Ilg

Department Cognitive Neurology, Hertie-Institute of Clinical Brain Research  
Otto-Friedrich-Müller-Straße 27, 72076 Tübingen, Germany  
sylvana.freyberg@uni-tuebingen.de

In the total absence of a moving target, neither humans nor monkeys can generate smooth pursuit eye movements (SPEM). Back in 1967, it was reported that humans, but not monkeys, were able to generate anticipatory eye movements (Fuchs 1967). Here, we tried to develop a paradigm in which humans as well as rhesus monkeys generate SPEM in the expectation of the presentation of a moving target.

In order to do so, we used a ramp-like stimulus movement with constant speed (5, 10 or 15 °/s, respectively) and constant direction (always rightward). In 50% of the *predict-gap* trials, the target moved initially for 500 ms invisible and, subsequently, became visible. In these trials, the disappearance of the fixation target indicated the onset of the invisible target movement. As a control (*random-gap* trials), we used ramps randomized to the left and right with 5, 10 and 15 °/s, respectively. We determined the mean SPEM velocity in the time window 100 ms before the appearance of the moving target ( $V_{400}$ ). Trials with saccades in that time interval were excluded from further analysis. In the control trials with a visible target, the identical time interval was used to average eye velocity. The horizontal eye movements from the human subjects were recorded via an infrared eye tracker and from the monkey via the search coil system. All data processing was performed using Matlab.

Although the moving target was initially absent for 500 ms, all of our human subjects and the monkey were consistently able to generate SPEM during that epoch in every trial (Fig. 1). We performed a 1-way ANOVA to determine the influence of the expected *target velocity* on the executed eye velocity.

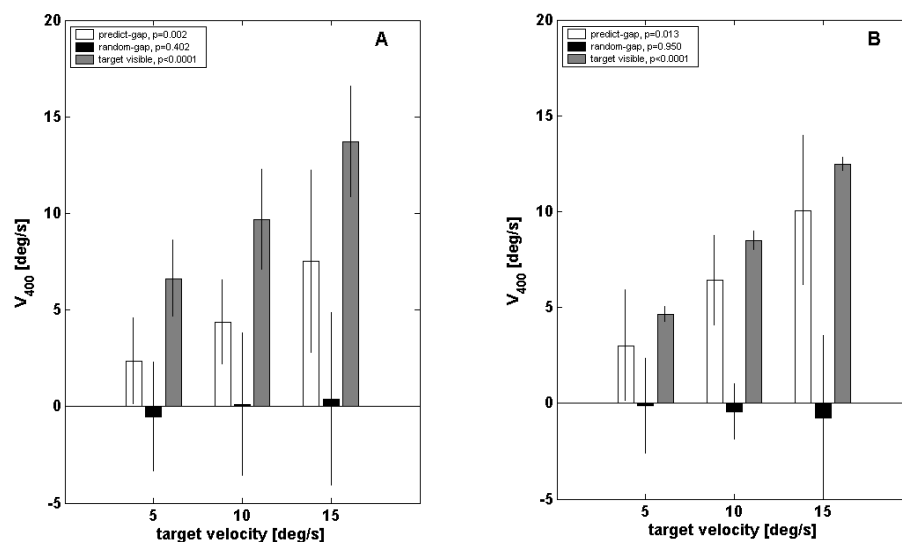


**Fig. 1.** Mean and standard error of smooth pursuit eye movement velocity in the time window 100 ms before the reappearance of the moving target ( $V_{400}$ ) for three target velocities. *P*-values obtained by 1-way ANOVA comparing the eye velocity across the three target velocities. Results received from 12 humans (A) and 5 sessions of a monkey (B).

The expected target velocity influenced the anticipatory eye velocity significantly in humans ( $p=0.002$ ) and monkeys ( $p=0.013$ ). In the control condition (*random-gap*) no significant influence was observed (human  $p=0.402$ ; monkey  $p=0.950$ ). Our findings demonstrate that with the appropriate training, rhesus monkeys can produce anticipatory smooth pursuit eye movement in the appearance of a moving target. The contradiction to the study by Fuchs (1967) most likely consists in different training procedures: we especially trained the monkey to perform anticipatory eye movements.

### References

Fuchs AF (1967) Periodic eye tracking in the monkey. *J. Physiol* **193**: 161-171

## What Membrane Potential Features Trigger a Neural Action Potential *in Vivo*?

Holger Fröhlich<sup>1</sup>, Björn Naundorf<sup>2</sup>, Maxim Volgushev<sup>3</sup>, Fred Wolf<sup>2</sup>

<sup>1</sup>Eberhard-Karls University Tübingen, Center for Bioinformatics Tübingen (ZBIT), Sand 1, 72076 Tübingen, Germany

<sup>2</sup>Dept. of Nonlinear Dynamics, Max-Planck Institut für Strömungsforschung, Göttingen, Germany

<sup>3</sup>Abteilung Neurophysiologie, Ruhr-Universität Bochum, Germany

We study the initiation of action potentials (APs) in neocortical neurons from cat visual cortex *in vivo*. Recently, it was shown that cortical neurons are not simple threshold devices, emitting an AP each time a fixed voltage threshold is reached, but that the emission of an AP partly depends on the rate of change of the membrane potential preceding an AP [1]. Here we assess systematically, which features of the membrane potential lead to an AP using the concept of a Support Vector Machine (SVM), which is a recently developed powerful Machine Learning approach [2].

To train the SVM we defined two sets of membrane potential trajectories, where each trajectory is of length  $T$ . As the first set we take all membrane potential trajectories  $\tau$  milliseconds prior the AP maxima in a given recording (positive examples). The second set consists of membrane potential trajectories which have the same membrane potential distribution at their endpoints as the trajectories in the first set, however do not lead to an AP within the next 10ms (negative examples).

We show that using higher order features, APs can be predicted much more reliably compared to a discrimination based on simple linear regression between the membrane potential and its rate of change prior an AP. Moreover our approach provides a general classification framework which allows to incorporate higher order multidimensional features and provides a major step to uncover the computation accomplished by cortical neurons.

[1] R. Azouz and C.M. Gray, Dynamic Spike Threshold Reveals a Mechanism for Synaptic Coincidence Detection in Cortical Neurons *in Vivo*, PNAS **97** (2000)

[2] B. Schölkopf and A. Smola, Learning with Kernels, MIT Press (2002)

This work was supported by the Max-Planck Society.

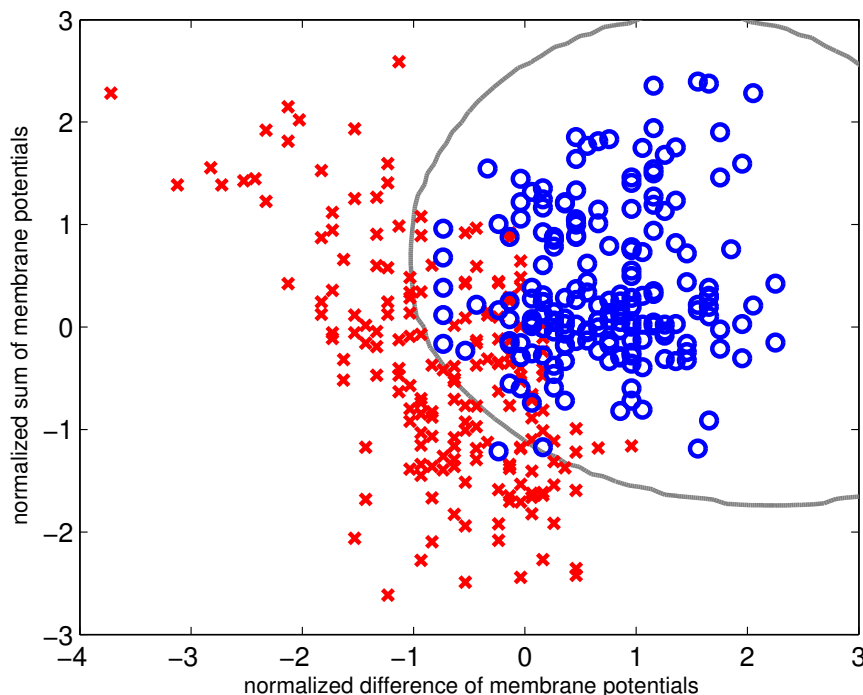


FIGURE 1: Sample result of the training of the Support Vector classification algorithm. The algorithm tries to distinguish the set of membrane potential trajectories which lead to an AP in a given time  $\tau$  (red crosses) from the set of membrane potential trajectories, which do not lead to an AP. The second set (blue circles) is chosen such that it can not be distinguished based just on its membrane potential distribution at the endpoints of the trajectories.

## **Enumeration of Simultaneously and Sequentially Presented Visual Items by a Macaque Monkey**

Andreas Nieder

*Primate NeuroCognition Laboratory, Dept. of Cognitive Neurology, Hertie-Institute for Clinical Brain Research, University of Tübingen, Otfried-Müller-Strasse 27, 72076 Tübingen, Germany*

Language-based numerical competence does not emerge *de novo* in evolution but arises from biological predispositions. This hypothesis is supported by studies on pre-linguistic representations of numerosity in human infants and non-verbal numerical competence in animals.

Most of the evidence for numerical skills in animals comes from procedures in which visual items were presented simultaneously in a given array. Techniques involving the simultaneous presentation of visual stimuli may allow an animal to assess numerosity in a direct, perceptual-like way. Sequential enumeration, however, requires a more complex assessment of numerical information involving multiple encoding, storage and integration stages of temporally delayed events. In addition, the most complex and precise form of numerical cognition, namely counting in adult humans, is a sequential process. The aim of this study, thus, is to compare simultaneous and sequential enumeration processes in non-human primates.

A monkey was trained in a visual delayed match-to-numerosity (DMN) task to decide whether the stimulus presented in the test phase contains the same number of objects/events as the previously displayed sample stimulus. The monkey first learned to match simultaneously presented sample numerosities (random-dot patterns showing 1 to 4 items) with simultaneously presented test numerosities. In a second step, the dot pattern in the sample period was replaced by consecutively flashed single dots. To prevent the monkey from solving the task by memorizing purely sensory cues rather than discriminating numerosity, non-numerical parameters that may co-vary with an increase of numerosity were controlled. For sequential visual stimuli, this included the control for overall stimulus rhythm, single flash duration, inter-flash intervals and total flash train duration. For the simultaneous-numerosity displays, items were placed pseudo-randomly on a matrix, and controls for total area, circumference, dot density and arrangements were included.

The monkey was able to discriminate small numerosities that were sequentially or simultaneously presented, respectively. Even more, it was able to match sequential events onto the set size of dot displays, indicating a most abstract representation of the number of items independent of their temporal relationship. Future electrophysiological investigations may help to elucidate similarities and differences in the neural processing of simultaneously and sequentially processed numerical information.

## Cross-modal integration in overt attention under natural conditions

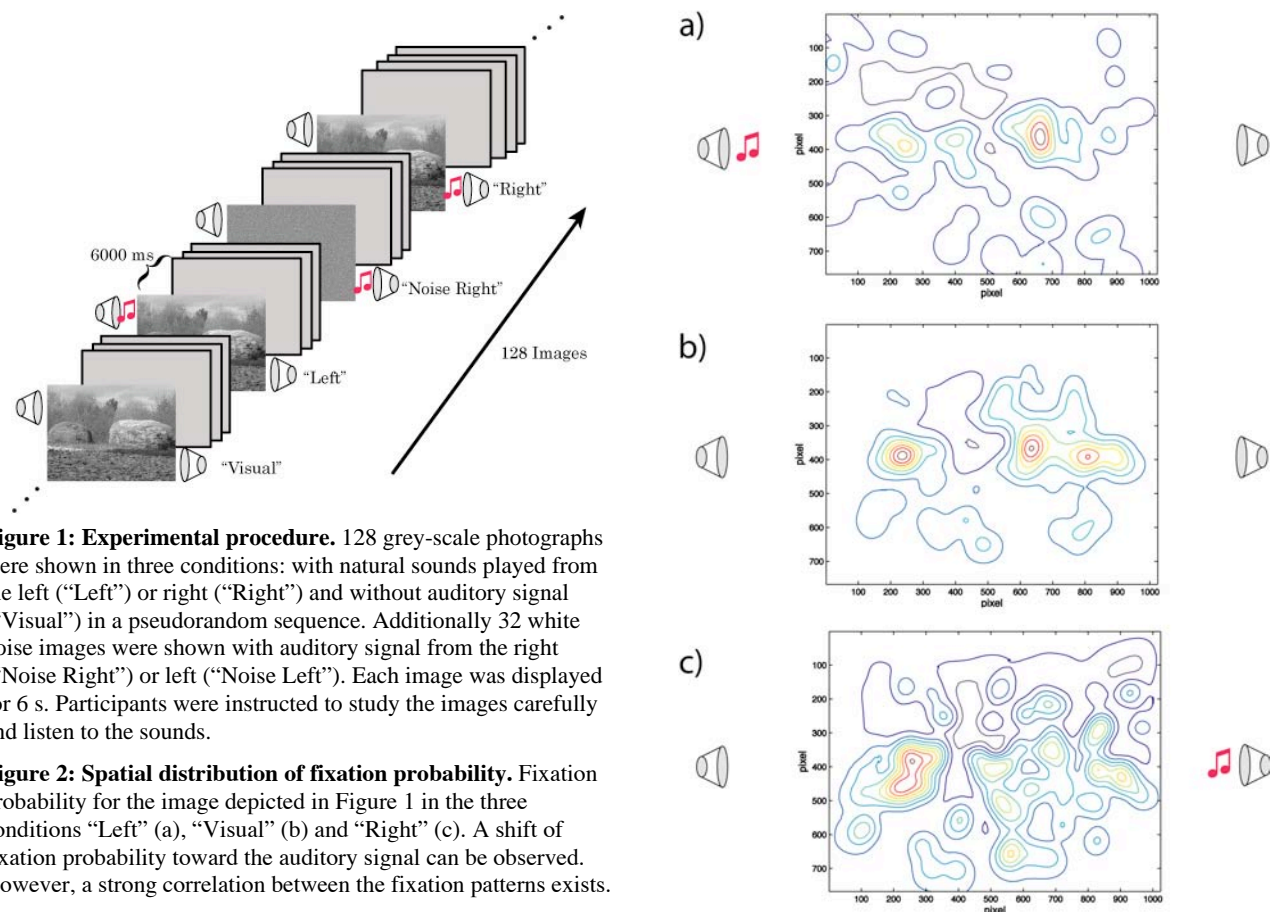
Klaus Tichacek, Selim Onat, Peter König  
Institute of Cognitive Science, University of Osnabrück, 49069 Osnabrück

An important function of attention is to direct our sensory organs towards objects of interest. Recent studies elucidate the relation between selected fixation points and statistical properties of the visual stimulus (Reinagel & Zador 1999, Parkhurst et al. 2002, Einhäuser & König 2003). The underlying mechanisms are well described by the concept of saliency maps (Itti & Koch, 2000). Remarkably, other modalities are equally effective in directing overt visual attention. Here, we study the integration of simultaneously presented auditory and visual cues for the selection of fixation points.

Eye traces of participants were recorded by a high precision optically based system (EyeLink II). Pictures of natural landscapes and bird sounds were used as visual and auditory stimuli in different combinations (Figure 1).

Lateralized auditory stimuli attract overt visual attention and lead to increased fixation probability towards the side of stimulation. This effect decays over a time course of 4.5s. Upon combined presentation of auditory and visual cues the spatial distribution of fixation points displays a strong bias to the side of the auditory cue and, simultaneously, is spatially structured as determined by the visual stimulus (Figure 2). Factorizing the effect of the auditory cue leads to a high correlation of the distribution of fixation points in visual stimuli presented on their own and in combination with the auditory stimuli ( $r = 0.45$ ). This implies that 20% of the variance in the distribution of fixation points can be understood by adding the effect of the auditory cue to a visually determined saliency map.

In summary, the interaction of cues from different modalities in overt attention under natural conditions is an integrative process that maintains structured information of the visual modality when adding auditory information.



## FACE PERCEPTION IS MEDIATED BY A DISTRIBUTED CORTICAL NETWORK

Conny F. Schmidt<sup>1</sup>, Peter Boesiger<sup>1</sup>, Alomit Ishai<sup>2</sup>

<sup>1</sup>Institute for Biomedical Engineering, University of Zurich, and Swiss Federal Institute of Technology Zurich <sup>2</sup>Institute of Neuroradiology, University of Zurich, Switzerland.

We investigated the neural system associated with face perception in the human brain, using functional Magnetic Resonance Imaging (fMRI). Face stimuli (black and white line drawings and gray-scale photographs of unfamiliar, famous, and emotional faces), and their phase scrambled versions were presented in a block design. Thirteen subjects were instructed to view the faces attentively while T2\*-weighted images were collected using a SENSE-EPI sequence on a 3T Philips Intera scanner. Statistical analysis was performed in SPM2. We identified a network of face-responsive regions that included the inferior occipital gyrus, fusiform gyrus, superior temporal sulcus, hippocampus, amygdala, and the inferior frontal gyrus. Although we found bilateral activation in all regions, the response in the right hemisphere was stronger, in terms of both the spatial extent of the activation and the amplitude of the fMRI signal. We then performed a region-of-interest (ROI) analysis to reveal the differential response to the various stimulus formats. While all faces evoked significant activation within all regions, famous and emotional faces evoked stronger activation in extrastriate cortex and in the limbic system, consistent with previous reports of 'valence enhancement' (e.g., Ishai et al., 2004). Our results indicate that a simple task, namely attentive viewing, is sufficient to localize activation within the distributed cortical network that mediates the visual analysis of facial identity and expression.

**Poster Subject Area #PSA14:**  
**Visual systems of vertebrates: Development and regeneration**

- [#200A](#) M. Manns and O. Güntürkün, Bochum  
*Posthatch retinal BDNF-injections affect visual lateralization in pigeons*
- [#201A](#) A. Klausmeyer, J. Garwood and A. Faissner, Bochum and Strasbourg (F)  
*Differential Expression of Phosphacan Isoforms in the Developing Mouse Visual System*
- [#202A](#) S. Siddiqui, A. Horvat-Bröcker and A. Faissner, Bochum  
*Tenascin-C and its Alternatively Spliced FNIII Domains: a Possible Role as Modulators of Axonal Outgrowth in the Developing Rat Visual System*
- [#203A](#) A. Horvat-Bröcker, T. Paech, A. Zaremba and A. Faissner, Bochum  
*Expression of Protein Tyrosine Phosphatases in the Developing Mouse Retinocollicular System*
- [#204A](#) J. Grabert, S. Patz and P. Wahle, Bochum  
*Dopamine and serotonin differentially affect Parvalbumin expression in rat visual cortex*
- [#205A](#) M. Wirth and P. Wahle, Bochum  
*Axonal transport of neurotrophin-4 and transcellular induction of neuropeptide Y expression*
- [#200B](#) M. Ader, A. Palfi, A-S. Kiang, P. Humphries and J. Farrar, Dublin (IRL)  
*RNAi-Mediated Suppression of RDS/Peripherin and Rhodopsin in Photoreceptor Cells*
- [#201B](#) MB. Hoffmann, B. Lorenz and P. Seufert, Magdeburg, Regensburg and Freiburg  
*Spotting abnormal visual pathways in humans with multifocal visual evoked potentials*
- [#202B](#) C. Gebhardt and F. Weth, Jena  
*A novel computational model for the development of topographic neural maps based on properties of the retinotectal projection*
- [#203B](#) GF. Volk, K. Rose, U. Schroer and S. Thanos, Münster  
*Velocity plots of neuronal regeneration of monkey and rat retinal ganglion cell axons in organ culture*
- [#204B](#) MA. Giese and DA. Leopold, Tübingen and Bethesda, MA (USA)  
*PHYSIOLOGICALLY INSPIRED MODEL FOR THE PROTOTYPE-REFERENCED ENCODING OF FACE SPACES*



## **Posthatch retinal BDNF-injections affect visual lateralization in pigeons**

**Martina Manns, and Onur Güntürkün**

*Biopsychology, Institute of Cognitive Neuroscience, Faculty of Psychology, Ruhr-University Bochum, 44780 Bochum, Germany*

The visual system of birds serves as a model to examine how a skewed sensory input leads to the development of functional and morphological asymmetries in the brain. Lateralization is triggered by asymmetric light exposure of the embryo in the egg resulting from an asymmetrical head turning of avian embryos. This asymmetric stimulation presumably affects activity-dependent differentiation processes culminating in the functional dominance of the stronger stimulated right eye/ left hemisphere for detailed visual object analysis. In pigeons, this behavioral lateralization is accompanied by left-right differences in tectal cell size. Different aspects of light-dependent neuronal differentiation are known to be mediated by the anterograde transport of the neurotrophic factor BDNF (Brain-derived Neurotrophic Factor). Since BDNF is present in the developing visual system of pigeons, it is conceivable that lateralized retinal influences are mediated by BDNF. To test the role of BDNF in asymmetry formation, we incubated pigeon embryos into complete darkness what is known to prevent the development of visual lateralization. After hatching, 50 ng BDNF dissolved in 5 µl saline or 5 µl saline for control were injected one or three times into the right eye of pigeon hatchlings. As adults, the birds were tested in a grit-grain discrimination task to estimate the degree and direction of visual lateralization. After behavioral testing, the animals were perfused to perform a morphometric analysis of immunohistochemically identified tectal cells.

The grit grain discrimination task demonstrated that single intraocular BDNF-injections induced a dominance of the BDNF-enriched left hemisphere. In contrast, triple BDNF-injections decreased the performance conveyed by the BDNF-treated hemisphere hence leading to the functional dominance of the ipsilateral right hemisphere. The morphometric analysis evinced differential effects onto distinct tectal cell types. Compared to saline controls, calbindin-positive cells in the BDNF-enriched left tectum were enlarged within the retinorecipient layer 5, the main target layer of retinal fibers while calbindin-positive cells in the efferent layer 13 were not affected. Moreover, the body sizes of parvalbumin-positive nonGABAergic cells in all layers expressing parvalbumin were reduced in both tectal hemispheres after triple BDNF-injections.

Thus, intraocular BDNF-injections modulate the differentiation of tectal circuitries and ultimately affect lateralized visuomotor processing in a dose-dependent manner. While a single BDNF-injection promotes development of the BDNF-enriched brain side, an excess supply of BDNF exerts the opposite effect presumably because this treatment prevents activity-dependent pruning of exuberant fibers. In this respect, the decreased performance of the BDNF-enriched hemisphere represents reduced fine-tuning of visual circuits. However, BDNF- effects are not confined to the injected brain side. The final asymmetry pattern results from a modulation of differentiation processes in both hemispheres. Comprising, the present results further substantiate that it is the retinal input which is the critical factor for the development of visual lateralization in pigeons modulating the balance of visuomotor processing between the left and right brain half.

This research was supported by a grant from the SFB Neurovision of the Deutsche Forschungsgemeinschaft.

## Differential Expression of Phosphacan Isoforms in the Developing Mouse Visual System

Alice Klausmeyer<sup>1)</sup>; Jeremy Garwood<sup>2)</sup>; Andreas Faissner<sup>1)</sup>

1) Cellmorphology and molecular Neurobiology, Ruhr-University Bochum, Germany

2) Centre de Neurochimie de CNRS, Strasbourg, France

Correspondence: Andreas.Faissner@rub.de

The chondroitin sulfate proteoglycan (CSPG) DSD-1-PG/phosphacan represents one of four splice variant of receptor protein tyrosine phosphatase (RPTP) beta/zeta. This receptor is expressed by glial cells and occurs in two isoforms named RPTP-beta (long) and RPTP-beta (short) [1]. Phosphacan and phosphacan-short-isoform (PSI) [1;2] bind to extracellular matrix and adhesion molecules and could mediate astroglial effects on neuronal differentiation. The RPTP- $\beta$  isoforms might function as glial transmembrane receptors of these glycoproteins in this context. The CSPG phosphacan and the long receptor carry the DSD-1-epitope, a glycosaminoglycan modification which is specifically recognized by mAb 473HD [3] and is by itself sufficient to stimulate neurite outgrowth. Functionally, phosphacan inhibits neurite outgrowth of embryonic cortical neurons in the presence of laminin, but not in a polycationic environment [4]. In light of these functional properties, we have examined the expression patterns of the DSD-1-epitope and phosphacan isoforms in the developing mouse visual system.

During retinal development the DSD-1-epitope appears around embryonic day 13 when retinal precursor cells begin to differentiate, peaks around postnatal day 5 and is progressively down-regulated from P8 to adolescence. By comparison, the phosphacan core protein is first detectable at E12, reaches maximal levels around P14 and subsequently persists, although at lower levels, to adulthood. The DSD-1-epitope is restricted to the nerve fibre and the inner plexiform layers, where it might design a boundary for retinal ganglion cells. In contrast, the phosphacan core protein immunoreactivity extends from the nerve fibre layer to the outer plexiform layer, with pronounced expression in the inner plexiform layer.

In order to answer the question whether the downregulation of the DSD-1-epitope is parallel by differential isoforms, Western blots were carried out on retinal and collicular tissue using antibodies against different parts of the protein core.

The level of expression of the phosphacan/RPTP- $\beta$  gene was investigated by RT-PCR performed on retinal and collicular mRNA Samples. These experiments suggest that there is a shift in the expression patterns of the different phosphacan/RPTP- $\beta$  isoforms during late embryonic and early postnatal development. In situ hybridization experiments support the conclusion that at least one of the phosphacan/RPTP- $\beta$  isoforms in the retina is expressed by neurons.

Taken together, these results show that there is a change in the occurrence and the pattern of glycosylation of the different phosphacan/RPTP- $\beta$  isoforms during the development of the retina and superior colliculus which may represent an important mechanism for the maturation of the visual system. Currently, functional studies are carried out to investigate the effect of phosphacan/RPTP- $\beta$  isoforms on retinal cells and transplants *in vitro* (Supported by DFG, SFB 509).

- [1] J. Garwood, O. Schnäbelbach, A. Clement, K. Schütte, A. Bach, A. Faissner (1999): DSD-1-Proteoglycan is the Mouse Homolog of Phosphacan, and Displays Opposing Effects on Neurite Outgrowth Dependent on Neural Lineage. *J. Neuroscience* 19(10), 3888-3899
- [2] J. Garwood, N. Heck, F. Reichardt, A. Faissner (2003): Phosphacan Short Isoform, a Novel Non-proteoglycan Variant of Phosphacan RPTP $\beta$ , Interacting with Neuronal Receptors and Promotes Neurite Outgrowth. *J. Biological Chemistry* 278(27); 24164-24173
- [3] A. Faissner, A. Clement, A. Lochter, A. Streit, C. Mandl, M. Schachner (1994): Isolation of a Neural Chondroitin Sulfate Proteoglycan with Neurite Outgrowth Promoting Properties, *J. Cell Biology* 126(3), 783-799
- [4] A. Dobbertin, K.E. Rhodes, J. Garwood, F. Properzi, N. Heck, J.H. Rogers, J.W. Fawcett, A. Faissner (2003): Regulation of RPTP $\beta$  Phosphacan Expression and Glycosaminoglycan Epitopes in Injured Brain and Cytokine-treated Glia. *Mol. Cell. Neuroscience* 24, 951-971

## Tenascin-C and its Alternatively Spliced FNIII Domains: a Possible Role as Modulators of Axonal Outgrowth in the Developing Rat Visual System

Sonia Siddiqui\*, Andrea Horvat-Bröcker\* and Andreas Faissner\*

<sup>1</sup>International Graduate School of Neuroscience (IGSN) at Ruhr-University, <sup>\*</sup>Department of Cell Morphology and Molecular Neurobiology, Ruhr University Bochum, 44801 Bochum, Germany  
Correspondence: andreas.faissner@ruhr-uni-bochum.de

The glial-derived extracellular matrix (ECM) glycoprotein Tenascin-C (TN-C) is a multifunctional molecule that could either promote or inhibit neurite outgrowth depending upon the neuronal cell types. These diverse functions have been localized to alternatively spliced fibronectin type III (FNIII) domains of TN-C (1, 2). However, the knowledge about effects of TN-C and its domains in the retinal neuronal network is still limited. To elucidate potential roles of TN-C and different FNIII domains for neurite outgrowth in the visual system we performed *in vitro* experiments using rat retinal stripes from embryonic stage E18. The retinal stripes were cut and plated on PDL/TN-C (25 µg/ml) or the FNIII domains A1A2, A1D, BD, CD, 78 and D6 (25 and 50 µg/ml). As a control, the retinal stripes were plated on PDL. The Morphometric analysis of neurite lengths was performed with Image Tools Software by measuring 10 longest neurites of the retina. The present study shows that TN-C significantly reduces neurite outgrowth at a concentration of 25 µg/ml. D6 domains also exert inhibitory effects on retinal axonal outgrowth at 25 and 50 µg/ml. The lower concentration (25 µg/ml) of CD and A1A2 domains inhibits, whereas the higher concentration (50 µg/ml) stimulates neurite outgrowth. In contrast, A1D domains show stimulatory effect on neurite outgrowth at both concentrations, whereas 78 domains remain neutral at 50 µg/ml. These results suggest that in the rat visual system the distinct sites of TN-C have different effects on retinal axon outgrowth.

Purified proteins are not equivalent with the biological environment encountered by neurites. Previous studies have shown that glial cells produce ECM molecules that regulate axonal outgrowth. For example, the astrocytic cell line Neu7, which acts as a non-permissive cell line towards neurite outgrowth, expresses laminin (LN) and fibronectin in lower but the chondroitin sulphate proteoglycan (CSPG) NG2 and TN-C in higher concentrations. In contrast, the astrocytic cell line A7 expresses LN and fibronectin at higher concentrations as compared to TN-C and is permissive for axon extension (3, 4). In order to assay for outgrowth on complete ECM, we plated the retinal explants on ECM prepared by water lysis of glial cell lines (A7, Neu7) and Müller glia. When matrix deposited by glia or glial cell lines was assessed for axon-outgrowth promoting activity, the length and the number of neurites were found to be higher on matrix from Müller glial and A7 than on Neu7 cells. Since these cell lines express to differing degrees both axon-growth promoting and axon-growth inhibiting molecules, whether or not a cell is capable of supporting axon growth may ultimately be dependent on the result of their respective interactions. These results suggest that the functional differences between permissive (A7, Müller glia) and inhibitory (Neu7) astrocytic cell lines reside largely with the ECM (Supported by DFG, SFB 509 and IGSN).

1. Götz B, Scholze A, Clement A, Joester A, Schütte K, Wigger F, Frank R, Spiess E, Ekblom P, Faissner A. (1996) Tenascin-C contains distinct adhesive, anti-adhesive, and neurite outgrowth promoting sites for neurons. *J Cell Biol* 132: 681-699
2. Götz M, Bolz J, Joester A, Faissner A. (1997) Tenascin-C synthesis and influence on axonal growth during rat cortical development. *Eur J Neurosci* 9: 496-506
3. Fok-Seang J, Smith-Thomas LC, Meiners S, Muir E, Housden E, Johnson AR, Faissner A, Geller HM, Keynes RJ, Rogers JH, Fawcett JW. (1995) An analysis of astrocytic cell lines with different abilities to promote axon growth. *Brain Research* 689: 207-223
4. Fidler PS, Schuette K, Asher RA, Dobberty A, Thornton SR, Calle-Patino Y, Muri E, Levine JM, Geller HM, Rogers JH, Faissner A, Fawcett JW. (1999) Comparing astrocytic cell lines that are inhibitory or permissive for axon growth: the major axon-inhibitory proteoglycan is NG2. *J Neurosci* 19: 8778-8788

## Expression of Protein Tyrosine Phosphatases in the Developing Mouse Retinocollicular System

Andrea Horvat-Bröcker, Tina Paech, Angelika Zaremba, Andreas Faissner

*Department of Cell Morphology and Molecular Neurobiology, Ruhr University Bochum, 44801 Bochum, Germany*

*Correspondence: andreas.faissner@ruhr-uni-bochum.de*

The vertebrate retinocollicular system provides an excellent model to explore the molecular and cellular mechanisms of axonal growth and topographic mapping (1). These processes rely on the recognition by growth cones of environmental cues including ephrins and their eph receptors, netrins, semaphorins as well as cell adhesion molecules (CAMs) (2). One important component in axonal growth signalling through many of these molecules is the regulation of tyrosine phosphorylation. The level of phosphotyrosine on intracellular substrate proteins is controlled by the balance between the activities of protein tyrosine kinases and protein tyrosine phosphatases (PTPs) (3, 4).

In this study we wanted to investigate a potential role of PTPs that regulate tyrosine phosphorylation and contribute to axonal outgrowth and signalling in the retinocollicular system. Using a degenerate primer-based RT-PCR approach we isolated cDNAs of different PTPs from mouse retina and superior colliculus at embryonic stage E15. This developmental stage encompasses the period of retinal axonogenesis and axonal growth, the first contact with the superior colliculus target, and the period of initial map formation in the superior colliculus. Both types of tissue, retina and superior colliculus, exhibited overlapping pattern of PTPs expression: 10 known receptor PTPs and 6 known cytoplasmic PTPs. Currently, using in situ hybridisation and real-time PCR, 9 of the RT-PCR-amplified PTPs are being analysed for spatiotemporal expression in the developing mouse retinocollicular system (Supported by DFG, SFB 509).

1. Thanos S, Mey J (2001) Development of the visual system of the chick. II. Mechanisms of axonal guidance. *Brain Res Brain Res Rev* 35:205-245
2. Dickson BJ (2002) Molecular mechanisms of axon guidance. *Science* 298:1959-64
3. Walsh FS, Doherty P (1996) Cell adhesion molecules and neuronal regeneration. *Curr Opin Cell Biol* 8:707-713
4. Desai CJ, Sun Q, Zinn K (1997) Tyrosine phosphorylation and axon guidance: of mice and flies. *Curr Opin Neurobiol* 7:70-74

## **Dopamine and serotonin differentially affect Parvalbumin expression in rat visual cortex**

Jochen Grabert, Silke Patz and Petra Wahle

AG Entwicklungsneurobiologie ND 6/72, Ruhr-Universität, 44780 Bochum, Germany

Differentiation of cortical interneurons is controlled by environmental factors. For instance, in organotypic monocultures (OTC) of visual cortex parvalbumin (PARV) expression has been shown to depend on neuronal activity and TrkB ligands during the first three weeks; both appear to prime PARV expression already before its developmental onset (Patz et al., 2004). However, PARV expression is delayed compared to in vivo. In frontal cortex, PARV expression is dramatically accelerated by dopamine (Porter et al., 1999). In schizophrenia, frontal cortical interneurons display PARV deficits which might be caused by the presumed imbalance in aminergic transmission. In fact, the DA innervation is particularly strong in frontal, but little in visual cortex, which is much denser innervated by serotonin (5-HT). Yet, OTC become deprived of both, the DA and the 5HT innervation. We therefore analysed the effect of both transmitters on PARV mRNA expression in OTC in different time windows.

Indeed, at 10 and 20 DIV, DA increased PARV mRNA expression. The action was D2-independent at 10 DIV, but D2-dependent at 20 DIV. Thus, despite the minor innervation, DA in visual cortex serves the same function as in frontal cortex. By contrast, 5-HT delayed PARV expression via 5-HT<sub>1</sub> and 5-HT<sub>3</sub> receptors during the first 10 DIV, but expression normalized until 20 DIV despite the presence of 5-HT. Further, DA and 5-HT failed to influence PARV expression in activity-deprived cultures indicating that only active neurons respond to the transmitters, and that neuronal activity is a master regulator of PARV expression.

The delayed upregulation of PARV in visual cortex OTC allowed to test the role of DA in older cultures. Unexpectedly, DA application from 30 to 50 DIV prevented the late upregulation of PARV, and rather reduced the expression. This suggested that the PARV-promoting action of DA is limited to an early period of molecular plasticity and reverses with age.

Since TrkB ligands early postnatally accelerate PARV mRNA expression, it appears possible that aminergic transmitters and neurotrophins cooperate in shaping the PARV phenotype. To this end, we asked whether DA or 5-HT regulate BDNF and NT4 mRNA expression in OTC. At 10 DIV, DA slightly increased NT4 mRNA (and promoted PARV) while BDNF mRNA was unaffected. At 20 DIV, DA reduced NT4 and BDNF mRNA (although PARV was still promoted). 5-HT increased BDNF mRNA at 10 DIV (although PARV was concurrently reduced). At 20 DIV, BDNF mRNA was decreased, and NT4 mRNA was increased by 5HT (with no concurrent action on PARV). Although this suggests independent actions, we shall try a coapplication of NT4 and DA during the first 10 DIV to test whether the two factors together are able to evoke at 20 DIV the PARV expression levels typically seen in age-matched visual cortex in vivo.

The results suggest a differential influence of DA and 5-HT on PARV mRNA expression in visual cortex. In particular, DA accelerates PARV expression, but with age switches to inhibit PARV expression.

Supported by SFB 509 "Neurovision" and Graduiertenkolleg 736.

Patz et al., (2004) *Cereb Cortex.*, 14: 342-51; Porter et al. (1999) *J Neurosci* 19 :8990-9003.

## **Axonal transport of neurotrophin-4 and transcellular induction of neuropeptide Y expression**

**Marcus J. Wirth and Petra Wahle**

AG Entwicklungsneurobiologie, Fakultät für Biologie, ND 6/72, Ruhr-Universität,  
44780 Bochum, Germany

Many studies address the effect of neurotrophins on neuropeptide expression in mammalian cortex, but less is known about the routes of delivery and transcellular signaling of neurotrophins. Further, the role of bioelectric activity and calcium-influx for an upregulation of neuropeptide expression by neurotrophins needs to be analyzed in more detail. We transfected organotypic cocultures of cortex, cortex and thalamus and cortex and superior colliculus with expression plasmids for BDNF and NT4 using a gene gun. GFP was chosen as a reporter. Neuropeptide Y in situ hybridization was used to quantify changes in NPY mRNA expression.

We show that a small number of NT4 overexpressing neurons in the cortical explant in aged thalamocortical cocultures rapidly (within 16 h) evoked an upregulation of NPY mRNA in interneurons in a Trk receptor-dependent manner. In contrast to BDNF, the action of NT4 was not depending on calcium influx. NPY neurons outnumbered the neurotrophin overexpressers by an order of magnitude arguing for a delivery of the factors to interneurons rather than autocrine pathways. Further, NT4 transfection of one explant of wired corticocortical cocultures evoked high numbers of NPY neurons in both explants. Delivery was not by diffusion via the medium which was checked by application of "conditioned" medium collected from NT4 overexpressing cultures to non-transfected cocultures. Moreover, cortical NPY neuron numbers increased in the cortical explant after NT4 transfection of a cocultured superior colliculus innervated selectively by cortical layer V pyramidal neurons indicating a transcellular action. These results suggest a source-to-sink model for axonal transport: a retrograde import of NT4 from tectal cells via the layer V pyramidal cell axons is followed by a local cortical redistribution either by anterograde or retrograde delivery to interneurons competent for NPY expression.

## **RNAi-Mediated Suppression of RDS/Peripherin and Rhodopsin in Photoreceptor Cells**

Marius Ader\*, Arpad Palfi\*, Anna-Sophie Kiang, Peter Humphries, Jane Farrar

*Ocular Genetics Unit, Department of Genetics, Trinity College Dublin, Dublin 2, Ireland*

RNAi is a promising technology to silence the expression of genes of interest in specific tissues and may also be applied to suppress disease genes in human gene therapy approaches. To test the feasibility of RNAi in photoreceptor cells, small hairpin RNAs (shRNAs) were used to knock-down mouse *rds*/peripherin (*rds*) and rhodopsin (*rho*) expression. *Rds* and *rho* are photoreceptor-specific genes in which a cumulative number of some 150 (mostly single base-) mutations have been described to be responsible for various forms of retinitis pigmentosa (RP), a hereditary and progressive retinal degeneration in humans.

Potential shRNA sequences targeting *rds* or *rho* were tested and selected in COS7 cells in previous studies. The most efficient sequences targeting each *rds* or *rho*, as well as a non-targeting construct as a negative control (transcribed from the human H1 promoter) were tagged with an enhanced green fluorescent protein (EGFP) expression cassette (using the CMV promoter). Whole retinal explants isolated from newborn mice were electroporated with the shRNA vectors and subsequently the EGFP marker was used to detect successful transfection.

*In vitro* electroporation of retinal explants is a highly efficient way to introduce foreign genes, as up to 20% of cells in retinal explants were EGFP-positive after transfection. Transfected retinal explants were dissociated after 14 days *in vitro* and EGFP-labeled cells separated by fluorescence-activated cell sorting (FACS). Quantitative analysis of mRNA levels was carried out by real time RT-PCR in RNA samples from sorted (transfected) cells. Our results indicate that the endogenously expressed shRNAs targeting *rds* or *rho* decreased the level of their corresponding mRNAs by 85% or 80%, respectively, when compared to the non-targeting control shRNA. Furthermore, immunocytochemical analysis of *rho*-targeted photoreceptor cells revealed a strong decrease in the number of rhodopsin expressing cells at protein level.

Thus, RNAi technology can significantly silence mouse *rds* and *rho* expression in photoreceptor cells and might therefore be a promising tool (i) to study development and function of photoreceptor cells, and (ii) for the development of therapeutic approaches targeting inherited diseases involving these cells. RNAi might be especially useful to knock-down mutant disease genes with dominant negative effects in a mutation-independent suppression and replacement strategy.

\* *these authors contributed equally to this work*

## Spotting abnormal visual pathways in humans with multifocal visual evoked potentials

<sup>1</sup>Hoffmann MB, <sup>2</sup>Lorenz B, <sup>1,3</sup>Seufert P

<sup>1</sup>Visual Processing Lab, Universitäts-Augenklinik Magdeburg

<sup>2</sup>Abtl. für Kinderophthalmologie, Strabismologie und Ophthalmogenetik, Universitäts-Klinikum Regensburg

<sup>3</sup>Sektion für funktionelle Sehforschung, Universitäts-Augenklinik Freiburg

**Purpose:** Visual evoked potentials (VEPs) are a routine tool to detect the partial abnormal projection of the temporal retina to the contralateral hemisphere, which is typical for human albinism [1]. Multifocal VEPs (mfVEPs) open the possibility to screen a large number of distinct visual field locations for such abnormal cortical representations.

**Methods:** Using VERIS 4.8 (EDI) we recorded from 4 patients with albinism and from 4 controls pattern-reversal mfVEPs during monocular stimulation of each eye to 60 locations comprising a visual field of 44° diameter. The differences of the VEPs recorded over opposing hemispheres were calculated to assess the lateralisation of the responses [1]. An SNR-measure was used to eliminate ‘silent’ visual field locations from further analysis. The difference traces obtained for each eye were correlated with each other, which allows the differentiation between a normal and an abnormal projection of the optic nerves: Correlated traces indicate that both eyes project to the same cortical regions, while anti-correlated traces indicate that both eyes project to opposing hemispheres.

**Results:** Sizable mfVEPs were only obtained if patients with albinism had negligible nystagmus. In these two patients anti-correlated VEPs were prominent especially at visual field locations along the vertical meridian. In the control subjects VEPs for the vast majority of visual field locations were correlated.

**Conclusion:** The projection abnormality typical for patients with albinism can be detected with mfVEPs in patients with negligible nystagmus. Visual field locations along the vertical meridian are affected by misrouted optic nerves, which is in close correspondence to a recent fMRI report [2].

[1] Apkarian et al. (1983) *Electroenceph Clin Neurophysiol*; [2] Hoffmann et al. (2003) *J Neurosci* 23:8921-8930



## A novel computational model for the development of topographic neural maps based on properties of the retinotectal projection

Christoph Gebhardt and Franco Weth

Klinikum der Friedrich-Schiller-Universität Jena, Theoretikum, D-07740 Jena, Germany

A commonly seen feature of the genetically determined wiring of the brain during embryonic development is the establishment of topographic maps. In topographic projections neighbouring neurons in the projecting brain structure send their axons to neighbouring points in the target region. Although there are many examples for topographic projections in the vertebrate brain, the best studied model system is the retinotectal (eye to midbrain) projection of lower vertebrates (*e.g.* chickens). The discovery of gradients of repulsive ephrin ligands along the anterior/posterior axis of the tectum and of their corresponding receptors (Eph) in the retina has corroborated the gradient matching model originally proposed by Roger Sperry (Sperry, 1963) and quantitatively elaborated by Alfred Gierer (Gierer, 1981). Although in principle explaining the self-organization of topography, gradient matching models fail to reproduce major results of diverse *in vivo* and *in vitro* manipulations of retinotectal development. Therefore it seems indispensable to us to refine existing models to incorporate more of the experimental evidence in order to understand the actual mechanisms of topographic mapping more thoroughly.

Based on a contemporary version of the gradient matching model (Honda, 1998; Loschinger et al., 2000) we tried to incorporate several experimental results not generally considered to date. In particular we implemented the observation of a ligand countergradient in the retina in addition to the well-known receptor gradient, thus providing the basis for direct fibre-fibre interactions that are strongly suggested by results of recent genetic manipulations. Moreover we include a receptor countergradient observed in the tectum in addition to the canonical ligand gradient. Beyond that it seems reasonable to us to consider the possibility of random fluctuations of ligand and receptor expression levels to render the model robust against changes of gradient shape. The lack of robustness is in fact one of the major drawbacks of strict gradient matching models.

We are currently trying to implement experimental evidence on growth cone adaptation towards guidance cues that is particularly challenging to gradient matching models. Additionally, we try to validate key predictions of our theoretical model by *in vitro* experiments. Hopefully this work will contribute to a more comprehensive understanding of the mechanisms underlying the generation of topographic maps during brain development.

---

Sperry, R.W. (1963). Chemoaffinity in the orderly growth of nerve fiber patterns and connections. *Proc. Natl. Acad. Sci. USA* 50, 703–710.

Gierer, A. (1981). Development of projections between areas of the nervous system. *Biol Cybern.* 42(1), 69-78.

Honda, H. (1998). Topographic mapping in the retinotectal projection by means of complementary ligand and receptor gradients: a computer simulation study. *J Theor Biol.* 192(2), 235-46.

Löschinger J., Weth F., Bonhoeffer F. (2000). Reading of concentration gradients by axonal growth cones. *Philos. Trans. R. Soc. Lond. B. Biol. Sci.* 355(1399), 971-82.

## Velocity plots of neuronal regeneration of monkey and rat retinal ganglion cell axons in organ culture

Gerd Fabian Volk, Karin Rose, Uwe Schroer, and Solon Thanos

Department of Experimental Ophthalmology, University Eye Hospital Münster, Domagkstr. 15, 48149 Münster, Germany

The retina serves as a model to study axonal regeneration during postnatal maturation and in adulthood. The present study concentrated on quantifying the in vitro age- and species-specific rate of regeneration of Retinal Ganglion Cells (RGC) from rats and monkeys.

The method consisted of explanting retinal tissue from Sprague-Dawley rats and *Callithrix jacchus* monkeys of different ages. The youngest retinas were from newborn rats and monkeys (P0), the oldest from adults (6 month old rats and 4 year old monkeys). After explantation, axon outgrowth of the RGCs was monitored by computer-assisted direct microscopy over 100 hours in culture (Fig. 1.). A velocity plot was drawn by measuring the advancing axonal growth cones during several three hour periods.

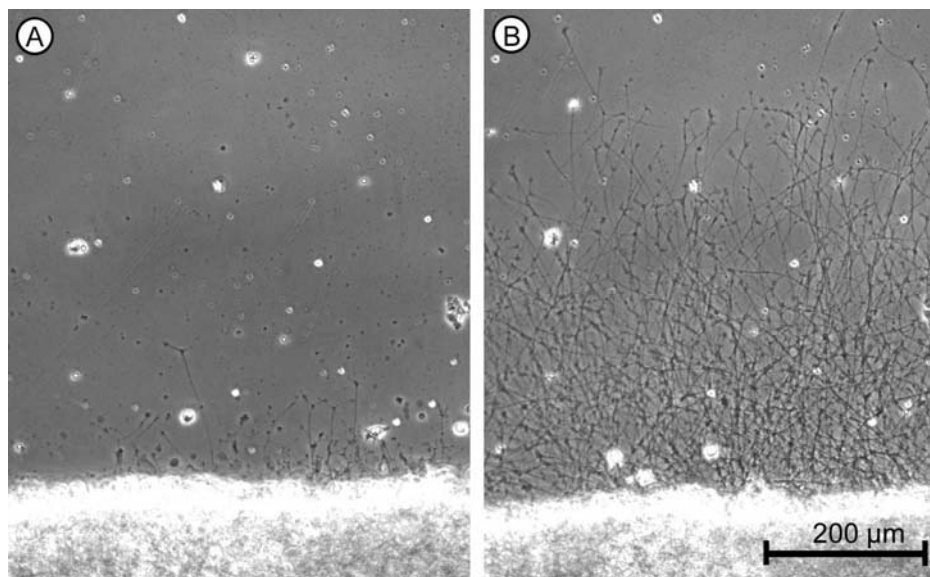


**Figure 1.**

Advancement of monkey retinal axons in culture. The same explant at 30 hours (A) and 45 hours (B) in culture.

The velocity plots show increasing mean values during the time in culture. RGCs from P0 monkeys began to regenerate after 24 hours at a rate of 30  $\mu\text{m}$  per hour. During the next days of monitoring, the rate of growth increased to around 50  $\mu\text{m}$  per hour. In contrast, RGCs from adult monkeys first started to regenerate after 70 hours in culture. They also had a lower starting velocity (20  $\mu\text{m}$  per hour) and a lower maximum velocity after 100 hours in culture (35  $\mu\text{m}$  per hour). There was an age-dependent decline in the rate of growth of the monkey RGCs (Fig. 2.).

Unlike the monkey cells, the rat RGCs did not grow out in culture during the first postnatal week. Consequently, the rate of growth can first be calculated for P12 axons, when these retinas regain the ability of axonal growth in culture. But even then, the rate of growth is comparable to the monkey retinas.

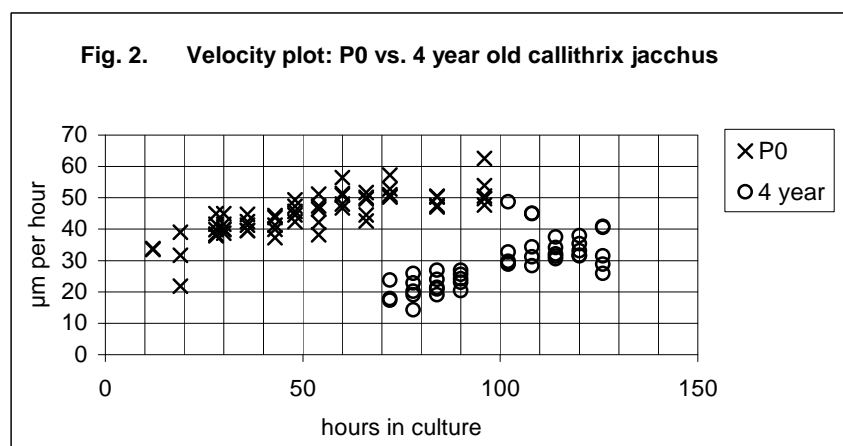


**Figure 2.**

The rates of growth of the five fastest axons, measured over three hour periods, show a variable onset. One can clearly differentiate the group of P0 axons from those of the four year old callithrix jacchus.

The initial data prove that this experimental setup is suitable to determine both age- and species-specific characteristics in the regenerative abilities of neuronal cells. Furthermore, this setup could be used for quantifying the effects of pharmacological treatments or molecular biological trials.

## PHYSIOLOGICALLY INSPIRED MODEL FOR THE PROTOTYPE-REFERENCED ENCODING OF FACE SPACES

M.A. Giese\*, D.A. Leopold<sup>†</sup>

\*ARL, Department for Cognitive Neurology, Hertie Institute for Clinical Brain Research, University Clinic Tübingen, Germany

<sup>†</sup>National Institute of Health, Bethesda, MD, USA

Several psychological models for face recognition assume that faces are encoded as vectors in abstract spaces relative to an average face, or face prototype [e.g. T Valentine, Q J Exp Psychol A. 43, 161 (1991)]. The neural basis of such a prototype-referenced encoding has been largely unclear. Recent electrophysiological data seems to support the relevance of this type of encoding for monkey *inferotemporal* cortex. Neurons in area IT, after training with human faces, show monotonic tuning with respect to the caricature level of face stimuli [D Leopold et al., Soc. of Neurosci., Poster 590.7 (2003)].

We present two neural models for the encoding of face spaces that realize different neural encoding strategies. One model is based on a prototype-based encoding by radial basis function units that represent randomly chosen training faces. The second model realizes norm-referenced encoding. Faces are represented by neural units whose tuning is determined by the difference between the feature vector that represents the stimulus and an average vector, which is computed by averaging the stimulus history over many previous training stimuli. Both models work on gray-level images and consist of a hierarchy of layers with neural detectors that approximate properties of cortical neurons in the ventral visual pathway. The different levels of the hierarchy extract form features of different levels of complexity. The highest hierarchy level of the models consists of face-tuned neural units whose properties can be compared to the electrophysiological data.

The models were tested using photorealistic face stimuli that were generated with a morphable 3D face model [V Blanz, T Vetter, SIGGRAPH '99, pp. 187-194 (1999)] that approximates pictures of faces by linear combinations of laser scans of human heads. Matching the stimuli in the electrophysiological experiment, we tested normal and lateral caricatures of four example faces from a representative data basis of human faces.

After optimization of the parameters of the models the simulation results were compared with the original data. The model with norm-referenced encoding shows better quantitative agreement with the experimental results. In particular, opposed to the prototype-based encoding model, it reproduces the property that most face-selective units show a monotonic increase of their activity with the identity level for normal caricatures. Also the percentages of intermediate extrema of the tuning curves with respect to the facial identity level seem to match better for the norm-referenced encoding model. Both models match correctly the behavior of IT real neurons for lateral caricature stimuli.

We conclude that the encoding of face stimuli in monkey visual cortex might be based on a norm-referenced encoding strategy, where the response of the neurons represents the deviation from the expected stimulus, which corresponds to the average face.

Supported by the Deutsche Volkswagenstiftung, Hermann and Lilly Schilling Foundation, and the Max Planck Society.

**Poster Subject Area #PSA15:  
Cortex and Cerebellum**

- [#206A](#) R. Cohen-Kadosh, A. Henik, O. Rubinsten, H. Mohr, H. Dori, Vvd. Ven, M. Zorzi, T. Hendler, R. Goebel and DEJ. Linden, Beer-Sheva (IL), Frankfurt/Main, Maastricht (NL), Padua (I), Tel-Aviv (IL) and Bangor (UK)  
*Are Numbers Special? The Comparison Systems of the Human Brain Investigated by fMRI*
- [#207A](#) M. Bajbouj, P. Neu, A. Neuhaus, J. Rentzsch, J. Vesper and I. Heuser, Berlin  
*Increased cortical inhibition in patients with major depression after longterm vagus nerve stimulation*
- [#208A](#) A. Neuhaus, J. Rentzsch and M. Bajbouj, Berlin  
*Early sensory information processing after left vagal stimulation in patients with major depressive disorder*
- [#209A](#) AN. Garratt, L. Li, S. Britsch and C. Birchmeier, Berlin  
*Mutation of the Type II isoform of Neuregulin-1 leads to a rostro-medial cerebellar defect*
- [#210A](#) M. Denker, M. Timme and S. Grün, Berlin and Göttingen  
*Detecting Transient Phase Synchronization between Spiking Activity and Local Field Potentials*
- [#211A](#) T. Berger, S. Lefort, H-R. Lüscher and CCH. Petersen, Bern (CH)  
*COMBINED IMAGING OF MEMBRANE VOLTAGE AND INTRACELLULAR CALCIUM IN THE SOMATOSENSORY CORTEX*
- [#212A](#) M. Volgushev, M. Mukovski, S. Chauvette, S. Boucetta and I. Timofeev, Bochum and Quebec (CDN)  
*THE ONSETS OF ACTIVE STATES IN NEOCOTRICAL NEURONS: HOW SYNCHRONEOUS ARE THEY?*
- [#213A](#) J. Pilli and KA. Wiese, Hamburg  
*Recurrency in cortical pyramidal cells and role in cortical processing compared to a recurrent circuit of identified function in an arthropod experimental system*
- [#205B](#) A. Morrison, J. Hake, S. Straube, HE. Plesser and M. Diesmann, Freiburg and As (N)  
*Precise spike timing with exact subthreshold integration in discrete time network simulations*
- [#206B](#) T. Tetzlaff, TTA. Morrison, M. Timme and M. Diesmann, Freiburg and Göttingen  
*Heterogeneity breaks global synchrony in large networks*
- [#207B](#) T. Tetzlaff, A. Aertsen and M. Diesmann, Freiburg  
*Time-scale dependence of inter-neuronal spike correlations*

- [#208B](#) D. Schöner, T. Tetzlaff, A. Aertsen and M. Diesmann, Freiburg  
*Dynamics of rate and correlation in balanced random networks*
- [#209B](#) C. Perez-Cruz, U. Heilbronner, J. Müller-Keuker, G. Flügge and E. Fuchs, Göttingen  
*Boundary definition and neuronal morphology of sub areas of the rat prefrontal cortex*
- [#210B](#) S. Goedeke, T. Geisel and M. Diesmann, Göttingen and Freiburg  
*On neuronal mechanisms determining synchronization dynamics in cortical feed-forward networks*
- [#211B](#) U. Reich, N. Marquardt, M-N. Klingberg, G. Paasche, M. Lenarz, T. Lenarz and G. Reuter, Hannover  
*FREQUENCY-SPECIFIC ACTIVITY OF THE AUDITORY PATHWAY WITH AUDITORY MIDBRAIN IMPLANTS*
- [#212B](#) M. Deliano, A. Engelhorn, D. Ensberg, H. Scheich and FW. Ohl, Magdeburg  
*Spatiotemporal patterns in auditory cortical activity after discrimination learning of auditory stimuli and of intracortically applied electrical stimuli*
- [#213B](#) M-L. Lee, H-P. Thier and V. Gauck, Tübingen  
*Serotonergic modulation of intrinsic properties and its effect on the signal processing in deep cerebellar nucleus neurons.*

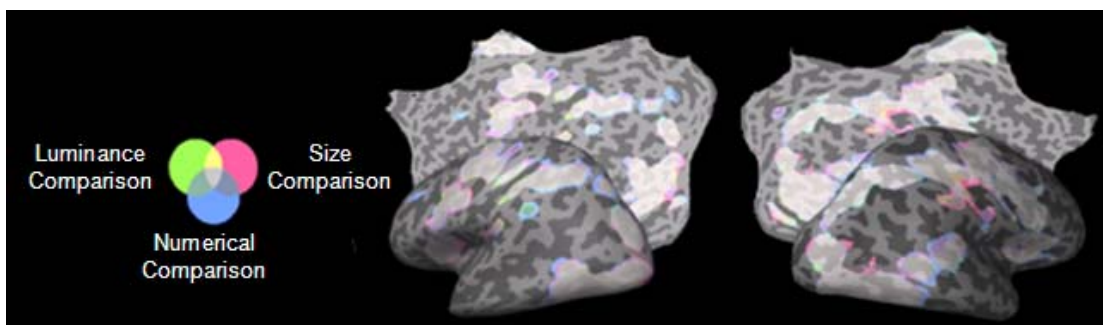
## Are Numbers Special? The Comparison Systems of the Human Brain Investigated by fMRI

Roi Cohen-Kadosh<sup>a</sup>, Avishai Henik<sup>a</sup>, Orly Rubinsten<sup>a</sup>, Harald Mohr<sup>b</sup>, Halit Dori<sup>a</sup>, Vincent van de Ven<sup>b,c</sup>, Marco Zorzi<sup>d</sup>, Talma Hendler<sup>e</sup>, Rainer Goebel<sup>c</sup>, David E. J. Linden<sup>b,f,g</sup>

<sup>a</sup> Department of Behavioral Sciences and Zlotowski Center for Neuroscience, Ben-Gurion University of the Negev, Beer-Sheva, Israel, <sup>b</sup> Laboratory for Neuroimaging and Neurophysiology, Department of Psychiatry, Goethe University, Frankfurt am Main, Germany, <sup>c</sup> Department of Psychology, Neurocognition, University of Maastricht, Maastricht, The Netherlands, <sup>d</sup> Department of Psychology, Padua University, Padua, Italy, <sup>e</sup> Tel-Aviv Sourasky Medical Center and Tel-Aviv University, Tel-Aviv, Israel, <sup>f</sup> Max Planck Institute for Brain Research, Frankfurt, Germany, <sup>g</sup> School of Psychology, University of Wales, Bangor, Wales, U.K.

### Abstract

Neuropsychological studies have suggested that the intraparietal sulcus (IPS), particularly in the dominant hemisphere, is crucially involved in numerical comparisons. However, by using imaging techniques a bilateral IPS activation has been found to be involved in numerical comparison and other tasks that require spatial processing or visuospatial attention as well. We used fMRI to investigate three different magnitude comparisons in an event-related-block design: a) Which digit is larger in numerical value (e.g., 2 5)? b) Which digit is brighter (e.g., 3 3)? c) Which digit is physically larger (e.g., 3 3)? Results indicate a widespread cortical network including a bilateral activation of the intraparietal sulci for all different comparisons. However, by computing contrasts of brain activation between the respective comparison conditions and applying a cortical distance effect as an additional criterion, we revealed number-specific activation in left IPS. These results indicate that there are both commonalities and differences in the spatial layout of the brain systems for numerical and physical comparisons and that especially the left IPS, while involved in magnitude comparison in general, plays a special role in number comparison.



This work was partly supported by grants to Roi Cohen-Kadosh from the German Academic Exchange Service (DAAD) and Minerva "Seed Grant".

## Increased cortical inhibition in patients with major depression after long-term vagus nerve stimulation

**Malek Bajbouj, Peter Neu, Andres Neuhaus, Johannes Rentzsch, Jan Vesper\*, Isabella Heuser**

Department of Psychiatry  
Charité – University Medicine Berlin  
Campus Benjamin Franklin  
Eschenallee 3  
14050 Berlin  
Germany

and

\* Department of Neurosurgery

**INTRODUCTION:** Vagus nerve stimulation (VNS) is an approved treatment for epilepsy and has been investigated in several clinical trials of depression. Little is known about the effect of vagus nerve stimulation on inhibitory brain function. Using transcranial magnetic stimulation (TMS), we tested whether one year of VNS would produce an increased in cortical inhibitory pathways.

**METHODS:** Six adult patients with major depression, treated with VNS, underwent two sessions of diagnostic magnetic stimulation at baseline and after one year of VNS treatment. By means of transcranial magnetic stimulation the silent period, intracortical inhibition and facilitation were assessed.

**RESULTS:** As compared to baseline, patients showed after one year of VNS an increase in intracortical inhibition, whereas intracortical facilitation and silent period remained unchanged.

**CONCLUSIONS:** The data confirm the hypothesis that longterm treatment of vagus nerve stimulation has an effect on some inhibitory brain circuits. These data support the hypothesis of an anticonvulsive mode of action. These data suggest that diagnostic magnetic stimulation may produce important variables in evaluating VNS effects.

## Early sensory information processing after left vagal stimulation in patients with major depressive disorder

Neuhaus AH, Rentzsch J, Bajbouj M

Department of Psychiatry, Charité – University Medicine Berlin, Benjamin Franklin Campus,  
Eschenallee 3, 14050 Berlin, Germany

**Background:** Vagus nerve stimulation (VNS) is a new therapy option for the treatment of therapy-resistant major depressive disorder, yet the mechanism of central nervous anti-depressive action is largely unknown. Electrophysiological studies are of particular interest since peripheral current application to afferent fibers may well exert certain effects on central electrical activity. In an exploratory study design we investigated effects of VNS on sensory information processing by recording auditory evoked potentials (AEP) in the electroencephalogram (EEG).

**Methods:** Seven patients receiving VNS for therapy of a major depressive disorder were investigated prior to implantation and 10 weeks after stimulation onset with the pulse generator turned off 1h prior to investigation. Event-related potentials were elicited using an auditory oddball paradigm recorded with 29-channel EEG.

**Results:** After VNS, the auditory evoked potential showed a significant increase in amplitude of an early positive component peaking approximately 30ms after the target stimulus onset (P30) at electrode positions Fz and Cz ( $p < .05$ ).

**Conclusion:** Auditory evoked potentials are a useful tool for investigating VNS-induced changes in early sensory information processing. The modification of the P30 component is supposed to reflect long-term effects of VNS and might indicate altered perceptive functions in the course of the therapy. This result may be a relevant finding for the understanding of the neurophysiological mechanism of action of VNS and for the pathophysiology of depression.



**Mutation of the Type II isoform of *Neuregulin-1* leads to a rostro-medial cerebellar defect**

Alistair N. Garratt\*, Li Li, Stefan Britsch and Carmen Birchmeier

Max-Delbrück-Centre for Molecular Medicine (MDC), Robert-Rössle-Str. 10, Postfach 740238, 13092 Berlin, Germany

The *Neuregulin-1* (*NRG1*) gene encodes an EGF-like growth factor which binds to receptors of the ErbB family of receptor tyrosine kinases. Three major types of NRG1 isoforms can be distinguished by their specific N-terminal domains. Type I NRG1 has essential functions in the early migration of neural crest cells (signaling through ErbB2/ErbB3 heteromers), is released by muscle sensory spindle afferent neurons and necessary for the induction of differentiation of the muscle spindle (most likely through the ErbB2/ErbB3 heteromer) and is important in the development of the heart and of the mammary gland (both mediated by the ErbB2/ErbB4 heteromer). Type III NRG1, signaling through the ErbB2/ErbB3 heteromer, is a crucial axonal signal required for the migration of early Schwann cell precursors, the regulation of Schwann cell numbers along peripheral nerve tracts, and for correct peripheral nerve myelination. Here, we show that the Type II NRG1 isoform (also known as glial growth factor, or GGF) is important in cerebellar development. The vermis (medial region of the cerebellum) of mutant mice is reduced in size, and has fewer folia. Furthermore, Bergmann glial fibers appear disorganized and Purkinje cell neurons are found ectopically in the granule cell layer and white matter.

# Detecting Transient Phase Synchronization between Spiking Activity and Local Field Potentials

Michael Denker<sup>1,2</sup>, Marc Timme<sup>2</sup>, and Sonja Grün<sup>1</sup>

<sup>1</sup>Neuroinformatics, AG Neurobiology, Free University, Berlin, Germany

<sup>2</sup>Dept. of Nonlinear Dynamics, MPI für Strömungsforschung, Göttingen, Germany

mdenker@chaos.gwdg.de

Spiking activity is often recorded in parallel to the local field potential (LFP, the low-pass filtered electrode signal), that typically exhibits oscillatory behavior. It is proposed that these LFP oscillations may be related to increased synchronous synaptic activity of neurons in a large volume near the electrode. In consequence, it is hypothesized that spikes occur preferably within a distinguished range of phases during an LFP oscillation period. In particular, it has been argued that this relationship between instantaneous LFP phases and spikes may be involved in the representation of information in networks (see, e.g., [1]). However, the detailed relationship between the LFP and spikes is not well understood.

Established methods to detect dependencies between LFP oscillations and spikes are the spike triggered average (STA), and its normalized power spectrum (spike field coherence, [2]). These are based on averaging the LFP segments surrounding individual spikes, thus pronouncing frequency components that spikes are locked to. However, the averaging inherent in these measures may cause difficulties in detecting phase relationships, in particular when dealing with weak locking of spikes, LFPs that exhibit a high degree of temporal variability in their dominant frequency, and coexistence of locked and unlocked spikes. Recently, various methods have been proposed to quantify the phase-locked dynamics between simultaneously recorded physiological time series, e.g. EEG signals [3]. First studies have extended this idea to include data characterized by discrete points in time [4]. In contrast to the STA, these approaches are based upon instantaneous phases that are obtained from the original signals. Nevertheless, it remains difficult to detect transient synchronization if phase-locking occurs during short periods of pronounced LFP activity and for few spikes only (e.g., spindles [5]).

Here, we present first steps towards developing such an approach for the analysis of experimental spike and LFP data with a focus on transient locking. We demonstrate how to analyze time-resolved phase measures obtained from phases extracted for each spike time from the broad-band LFP signal. Using surrogate data and tools of circular statistics, the significance of observed locking in small data samples are assessed. In particular, we develop methods that allow us to detect and quantify transient, weakly phase-locked activity. Our approach is calibrated on simulated data sets and applications to experimental data are illustrated.

[1] Friedrich, Habermann, and Laurent, *Nat Neurosci* 7: 862 (2004).

[2] Fries, Schröder, Roelfsema, Singer, and Engel, *J Neurosci* 22: 3739 (2002).

[3] Varela, Lachaux, Rodriguez, and Martinerie, *Nat Rev Neurosci* 2: 229 (2001).

[4] Schäfer, Rosenblum, Abel, and Kurths, *Phys Rev E* 60: 857 (1999).

Harris, Henze, Hirase, Leinekugel, Dragol, Czurkó, and Buzsáki, *Nature* 417: 738 (2002).

[5] Eckhorn, and Obermüller, *Exp Brain Res* 95: 177 (1993).

Acknowledgments: Partial funding by the Volkswagen Foundation and the Stifterverband für die Deutsche Wissenschaft.

## COMBINED IMAGING OF MEMBRANE VOLTAGE AND INTRACELLULAR CALCIUM IN THE SOMATOSENSORY CORTEX

**Berger Th.<sup>1,2</sup>, Lefort S.<sup>1</sup>, Lüscher H.-R.<sup>2</sup> and Petersen C.C.H.<sup>1</sup>**

<sup>1</sup>LSENS, EPFL, Lausanne, Switzerland; <sup>2</sup>Institute of Physiology, University of Bern, Switzerland

Information flow within networks of interconnected cells is difficult to study with sufficient spatial and temporal resolution. In order to record and to analyze the activity in a multitude of spatially dispersed neurons with a sufficient time resolution, either multi-electrode arrays (MEAs) or imaging techniques can be used. Both technical approaches have their advantages and disadvantages. MEA recordings result in an acceptable time and a bad spatial resolution. Imaging of membrane voltage with fast voltage-sensitive dyes is characterized by a bad spatial resolution while subthreshold voltage changes can be detected. Calcium imaging, on the other hand, seems to allow primarily the detection of action potential activity, while subthreshold activity is not detected.

In order to combine the advantages from these different imaging techniques we have imaged both membrane potential and intracellular calcium concentration together on the same preparation. In acute mouse brain slices (P15-P24), columns within the barrel somatosensory cortex were identified in a brightfield view. 500  $\mu$ M of the acetoxymethyl (AM) ester form of the calcium-sensitive dye Oregon Green 488 BAPTA-1 (OGB-1 AM; Molecular Probes, Eugene, OR) were expelled from an application pipette in a dispersed and controlled way (tip diameter  $\sim$ 25  $\mu$ m). OGB-1 AM entered the cells within these columns subsequently being cleaved by internal esterases. In an alternative loading approach, mice were anesthetized with urethane and a small craniotomy ( $\sim$ 0.2 mm<sup>2</sup>) was performed above the barrel cortex. A pipette was inserted into the cortex and OGB-1 AM was expelled from the pipette in a depth between 100  $\mu$ m and 700  $\mu$ m within a cortical column using positive pressure. After 30 min the animal was decapitated and slices of the somatosensory cortex were prepared. The resting fluorescence of the internalized and cleaved OGB-1 was detected. With *in vivo* application, staining was found primarily in layers 2 to 4. Multiple injections of dye directly into slices resulted in a homogeneous loading. Independent on the application approach, a thin layer of brightly fluorescent cells was always situated at the surface of the slices – cells which seemed to be dead when inspected with DIC optics. Below this layer, a homogeneous low level of fluorescence was found with epifluorescence optics. It was difficult to identify single cell bodies within the slice, presumably due to the low fluorescence of the high affinity dye OGB-1 in these healthy cells and due to the staining of non-somatic elements. Following OGB-1 AM loading, 1.6 mM of the voltage sensitive dye RH1691 (Optical Imaging, Rehovot) was applied to the slice surface. This led to a homogeneous staining of the slice. A CCD camera (Redshirt NeuroCCD, Fairfield, CT) with a full frame rate of 2 kHz and a high well depth was used to image the changes in intracellular calcium concentration and membrane potential. In a first set of experiments, no clear differences were seen between these signals with regard to spatial and temporal distribution following extracellular stimulation in the slice. The signal to noise ratio, however, was much better for OGB-1 in comparison to RH1691.

Supported by Swiss National Foundation (Grants 3100-061335.00, 3100-066651.01 and 3100-103832/1), the Silva Casa Foundation and the Leenaards Foundation.

## THE ONSETS OF ACTIVE STATES IN NEOCORTICAL NEURONS: HOW SYNCHRONEOUS ARE THEY?

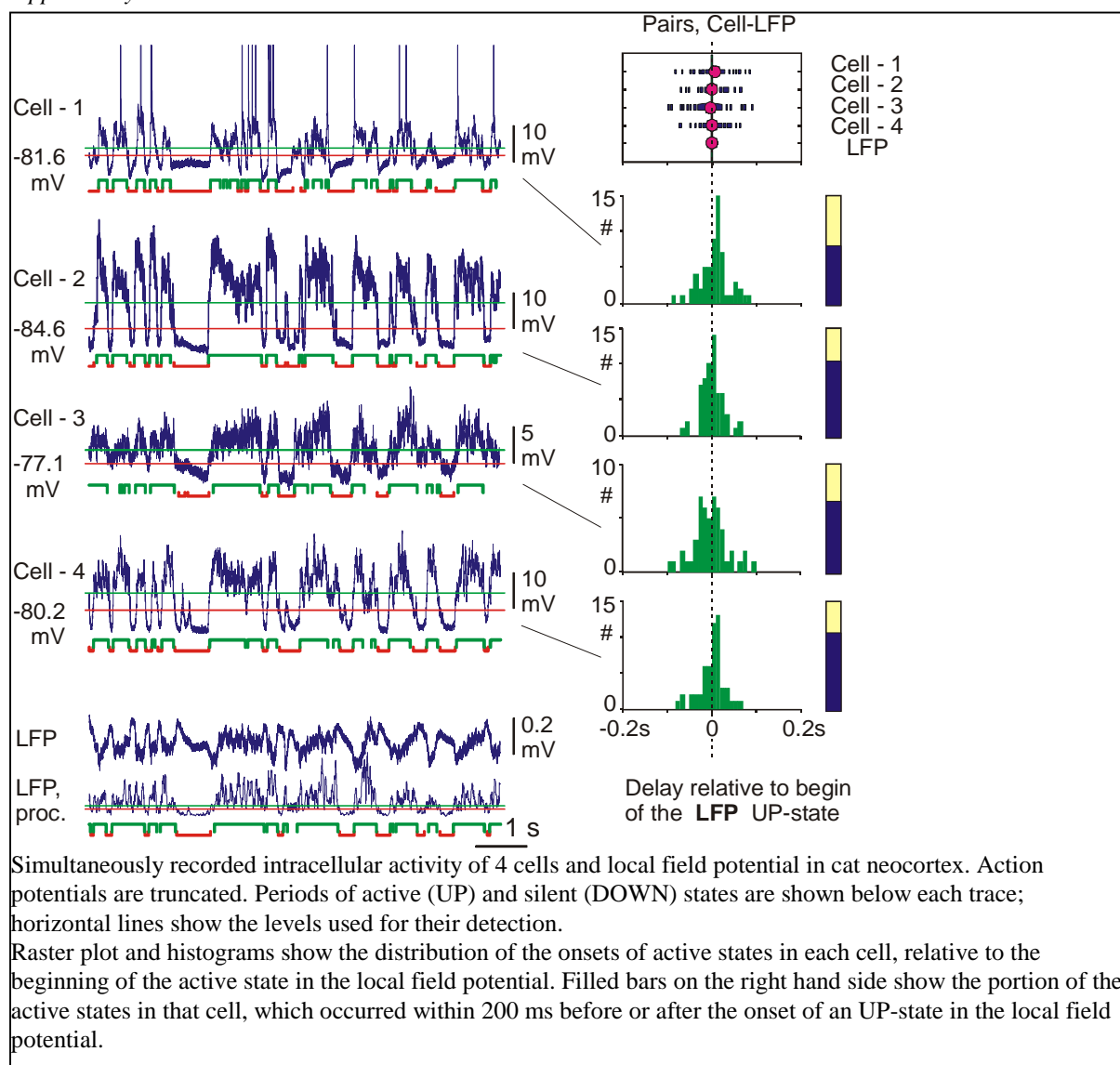
*M Volgushev, M Mukovski, S Chauvette, S Boucetta, I Timofeev*

*Dept. Neurophysiology, Ruhr-University Bochum, Germany*

*Dept. Anatomy and Physiology, Laval University, Quebec, Canada*

Rhythmic activity is a fundamental property of neural networks. During slow-wave sleep the thalamocortical network displays slow oscillation that is characterized by alternating silent and active states. During silent states the membrane potential of cortical neurons is hyperpolarized and cells are silent, during active states the membrane potential is depolarized and fluctuates rapidly, leading to cell discharges. The mechanisms of switching between the silent and active states remain unclear. One possibility is initiation of activity in a specific local focus, or in a certain group of cells, with sequential lateral propagation. Alternatively, activity may originate occasionally at any cortical location, whereby the number of simultaneously active sites and the strength of activity at each site determine, which portion of the whole network would engage into an active state. To estimate which of the two scenarios is valid, we recorded simultaneously intracellular activity of 2-4 neurons and local field potentials in the cat neocortex (area 5, 7, 21, 18). The recorded neurons were separated by >4 mm. Although the onsets of the active states in distantly located cells were clearly correlated, on the fine time-scale the synchronization was only loose. The difference in the mean onset times within a group of simultaneously recorded cells varied from 6.1 to 88.6 ms (23 groups of 3-4 cells). The standard deviation of the timing of the state onset in one cell relative to the group mean varied from 21.2 to 85 ms (mean 45.2 ms). Furthermore, the order of involvement of cells in the active state was variable. A cell, which was the first during one cycle, may become the last in the next episode. Taken together, our data are consistent with the hypothesis that an active state could be initiated at multiple loci, with following rapid involvement of entire neocortical network.

*Supported by the CIHR and the DGF.*

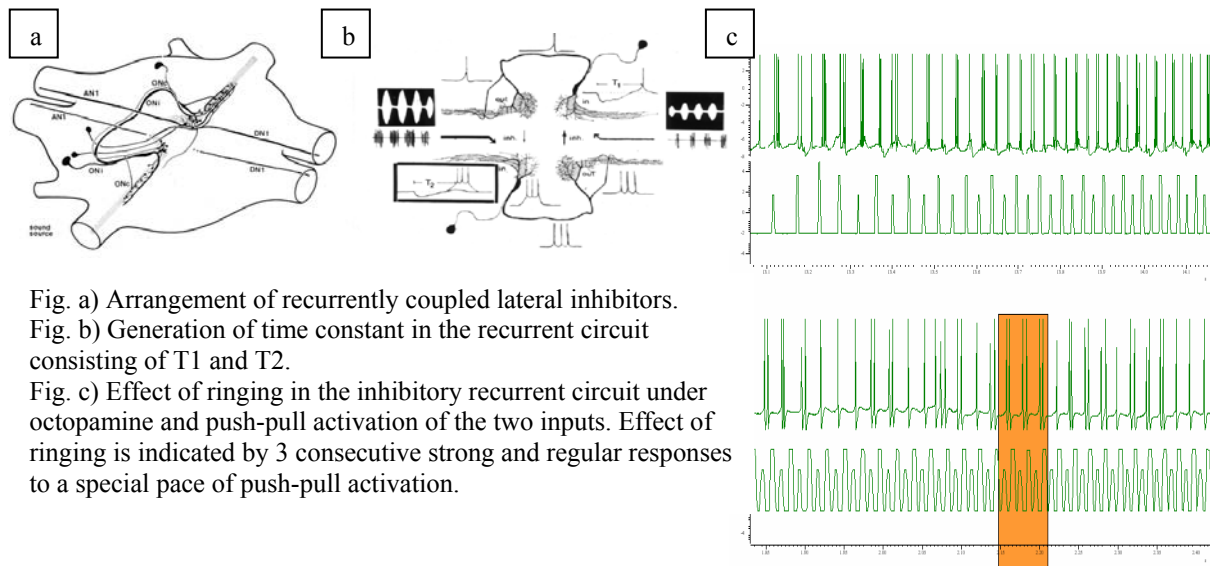


## Recurrency in cortical pyramidal cells and role in cortical processing compared to a recurrent circuit of identified function in an arthropod experimental system.

Pilli, J., Wiese, K.

Zoologisches Institut und Zoologisches Museum der Universität, Martin Luther King Platz 3,  
20146 HAMBURG, FRG      kwiese@zoologie.uni-hamburg.de

The recurrent excitatory coupling of cortical pyramidal cells of layer IV and VI represent core building blocks in vertebrate and human brains which, in line with sensory and synchronizing inputs and focused modulation, shift from non existing recurrency to effective recurrency and back. A suitable experimental system to study neural recurrent circuits is the recurrent lateral inhibitory circuit from the auditory pathway in the CNS of the cricket. The recurrency in this circuit becomes active under modulation by octopamine. Only then the circuit expresses the expected time constant and a maximum in lateral inhibition in response to the frequency of modulation in the vocalization of conspecific crickets.



In the experimental system the dendrite of each of the recurrently coupled cells shows integration of inputs from estimated 40 sensory axons, perhaps comparable to the integration observed at the dendrite of the pyramidal cell. The experimental system convincingly shows, that the modulator increases  $R_m$ , that is the transmembrane resistance in neuronal dendrites, thereby improves conduction and spatial summation of graded potentials from subsynaptic sites to the spike initiating zone. The positive feedback system among pyramidal cells is formed into an alternating oscillation between coupled cells by a GABA-ergic cell distributing asymmetric inhibition. In the inhibitory recurrent system in cricket audition, representing a passive filter, this is not required. Cricket song is a dynamic stimulus per se (Fig.c).

Dynamic stimulation or repetitive activation of a recurrent circuit is required to test the match or mismatch between inherent time constant and stimulus pattern. Hence oscillations in cortex observed by EEG likely reflect activity of cortical recurrent oscillators and are a prerequisite of cortical processing using recurrent circuits throughout. We assume that the modulation involved to start recurrency in both systems is under command of a prefilter which detects subjectively interesting actual sensory activity. Equipment provided by DFG

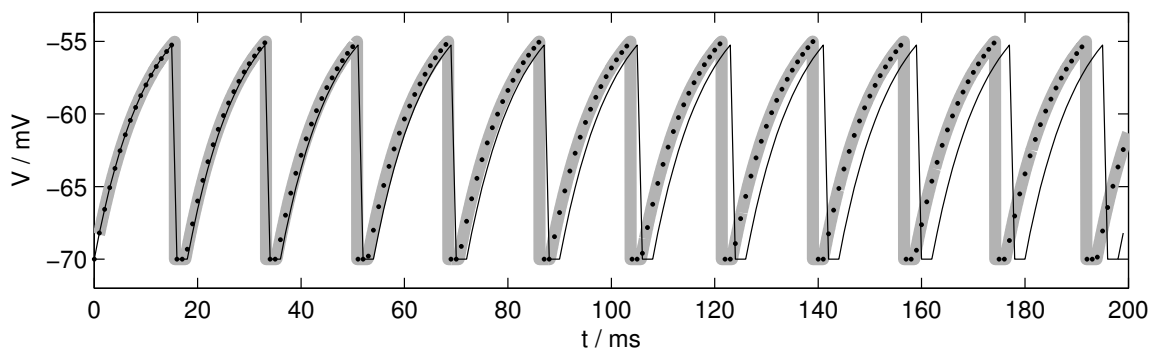
## Precise spike timing with exact subthreshold integration in discrete time network simulations

Abigail Morrison<sup>1,\*</sup>, Johan Hake<sup>2,‡</sup>, Sirko Straube<sup>1</sup>,  
Hans Ekkehard Plesser<sup>2</sup> and Markus Diesmann<sup>1</sup>

<sup>1</sup>Neurobiology & Biophysics, Inst. of Biology III, Albert-Ludwigs-University, Freiburg

<sup>2</sup>Dept. of Mathematical Sciences & Technology, Agricultural University of Norway, Ås

The subthreshold dynamics of a wide class of integrate-and-fire type neuron models can be integrated exactly [1]. It has previously been shown that even very large networks of spiking neurons can be simulated efficiently under the constraint that spike times are bound to an equidistant time grid [2]. This simulation scheme has two drawbacks: Firstly, it introduces artificial synchronisation by forcing all threshold crossings occurring in the integration interval  $(t - h, t]$  to the point  $t$  on the time grid, potentially distorting the synchronisation dynamics of a network model. Secondly, restricting spikes to the time grid introduces an integration error which declines only linearly with the resolution  $h$ . Several authors have discussed the advantages of interpolating spike times within the grid based simulation of neural networks [3,4]. Based on an implementation in our simulation tool NEST [5], we demonstrate that the exact integration scheme can be naturally combined with off-grid spike events found by interpolation. This facilitates the precise simulation of large networks for which event-driven simulation schemes are inherently inefficient.



The figure shows the exact solution for the membrane potential of an integrate-and-fire neuron driven by a supra-threshold DC current (grey curve). Using exact integration with a resolution of  $h = 1\text{ms}$  incurs a progressive error (black curve). Combining exact integration with interpolated spike timing essentially eliminates the progressive error (dotted curve).

We evaluate the new scheme in a relevant scenario of a neuron receiving input from a large network. A cost/benefit analysis of the integration error is provided parameterised by the resolution and the interpolation order. Cross-correlation analysis is used to characterise the error in spike train structure. The advantages and limitations of the approach are discussed.

This research is part of our long term project to provide the technology for neural systems simulations. Partially funded by DAAD/NFR 313-PPP-N4-Ik, BMBF-DIP F1.2, GIF, and Honda Research Institute.

- [1] Rotter S, & Diesmann M (1999) *Biol Cybern* **81**:381–402.
- [2] Morrison A, Mehring C, Geisel T, Aertsen A, & Diesmann M (2004) submitted.
- [3] Hansel D, Mato G, Meunier C, Neltner L (1998) *Neural Comput* **10**:467–483.
- [4] Shelley MJ, & Tao L (2001) *J Comp Neurosci* **11**:111–119.
- [5] [www.nest-initiative.org](http://www.nest-initiative.org).

\* [abigail@biologie.uni-freiburg.de](mailto:abigail@biologie.uni-freiburg.de). ‡ Present address: Dept. of Physiology, University of Oslo.

## Heterogeneity breaks global synchrony in large networks

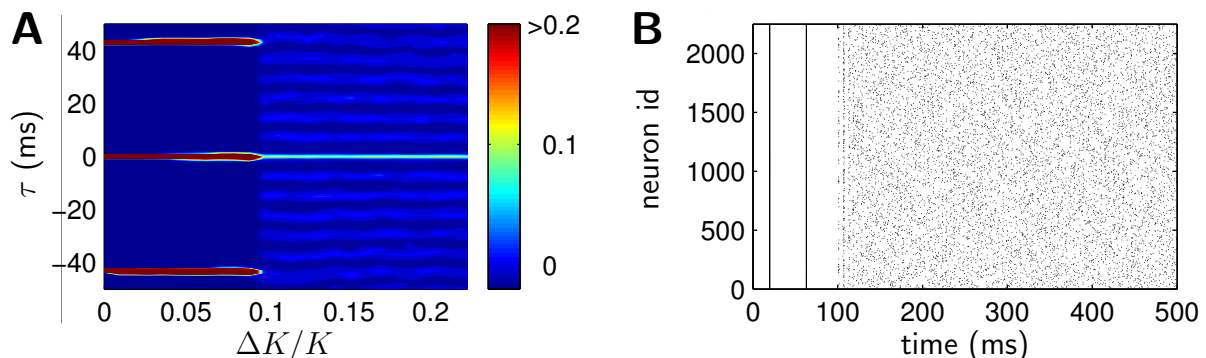
Tom Tetzlaff<sup>1,\*</sup>, Abigail Morrison<sup>1</sup>, Marc Timme<sup>2</sup>, & Markus Diesmann<sup>1</sup>

<sup>1</sup>Neurobiology & Biophysics, Inst. of Biology III, Albert-Ludwigs-University, Freiburg

<sup>2</sup>Dept. of Nonlinear Dynamics, Max-Planck-Institute for Fluid Dynamics, Göttingen

Balanced random networks have been proposed as models of the local cortical volume ( $1 \text{ mm}^3$ ,  $\sim 10^5$  neurons, connectivity  $\sim 0.1$ ). Many aspects of these systems have been thoroughly investigated [1,2,3]. They are attractive as the irregularity of individual spike trains and the large membrane potential fluctuations are consistent with in vivo data. However, a similarly realistic wide distribution of spike rates is only easily obtainable in small networks and with large post-synaptic potentials [1]; in large binomial random networks the narrow distribution  $\rho(K)$  of the number of synapses per neuron  $K$  and the averaging of a neuron's input over thousands of synaptic weights results in very low variability in the spike rates. Furthermore, although the individual spike trains are irregular, global oscillations can be observed which are not substantiated by experimental data.

Here, we investigate whether network parameters not subject to synaptic averaging can account for the rate variability and global activity statistics. It turns out that the width  $\Delta K$  of  $\rho(K)$  effectively controls the distribution of spike rates. Fig. A illustrates that  $\Delta K$  is a parameter which also abruptly destroys the slow global oscillations (cf. [4]), but not the distinct fast oscillatory (FO) states, which in inhibitory networks coexist with the slow oscillatory states for small  $\Delta K$  [5]. A distribution of spike thresholds shows a similar phenomenology. The FOs are controlled by synaptic delays and rise times [2,3]. We verified that even in the absence of external noise an appropriate distribution of delays removes the FOs and, as suggested by [4], the slow oscillations too. Thus, an asynchronous irregular state free of oscillations emerges (Fig. B) that can exhibit the desired variability of rates.



**A** Averaged cross-correlations  $c(\tau)$  (color coded) for different  $\Delta K/K$  and a fixed synaptic delay.

**B** Asynchronous spiking activity for  $\Delta K = 0$  and distributed synaptic delays.

The FOs are difficult to observe because raster displays of hundreds of neurons or averaging over many cross-correlations is required to detect them. However, FOs are relevant in the context of studies concerned with common input correlations, for example the embedding of feed-forward subnetworks [6] and spike time dependent plasticity [7].

Partially funded by BMBF-DIP F1.2 and GIF.

- [1] van Vreeswijk C & Sompolinsky H (1996) *Science* **274**:1724–1726.
- [2] Brunel N (2000) *J Comput Neurosci* **8**(3):183–208.
- [3] Brunel N & Hakim V (1999) *Neural Comput* **11**(7):1621–1671.
- [4] Denker M et al (2004) *Phys Rev Lett* **92**(7):074103.
- [5] Timme M et al (2002) *Phys Rev Lett* **89**(25):258701.
- [6] Tetzlaff T et al (2003) *Neurocomputing* **58–60**:117–121.
- [7] Morrison A et al (2004) In *The Monte Verita Workshop on STDP*, Ascona.

\* [tom@biologie.uni-freiburg.de](mailto:tom@biologie.uni-freiburg.de)



## Time-scale dependence of inter-neuronal spike correlations

Tom Tetzlaff\*, Ad Aertsen, Markus Diesmann

Neurobiology & Biophysics, Inst. of Biology III, Albert-Ludwigs-University, Freiburg

Reports on interneuronal spike-correlations are widely spread in the neuroscientific literature. A common way of quantifying the interdependence between two neurons is the estimation of the cross-correlation function  $c(\tau)$  describing the probability of seeing a spike from one neuron at time  $t + \tau$  given that the other neuron fired at time  $t$ . Depending on the underlying question usually two extreme cases are considered: spike time correlation and spike count correlation. The first approach is typically applied when the central peak of the cross-correlogram covers a range of only few milliseconds. The area of the peak is then used to quantify the strength of the spike time correlation. By contrast, spike count correlation is measured by the correlation coefficient of the numbers of spikes obtained from broad time intervals  $h$  ( $\sim$  seconds). Spike correlations can arise on both short and large time scales simultaneously [1,2]. The relationship between the two measures, however, is not yet clear.

Here, we address this issue by systematically varying the bin width  $h$  of the correlation analysis from very narrow ( $\sim$  spike time correlation) to very broad ( $\sim$  spike count correlation). We show with the help of artificial spike data that the interpretation of measured correlations is in general difficult. First, the cross-correlation strongly depends on the details of the mechanism generating the interdependence between the spike trains. Moreover, only for Poisson processes does the cross-correlation function purely reflect the interdependence between both spike trains.

For other processes, the temporal structure of the individual processes shapes the correlation function as well. Fig.1 illustrates that the correlation coefficient for spike trains modeled by gamma processes [3] depends on the width of the counting interval  $h$  and on the temporal structure parameterised here by the  $\gamma$ -order. The data were generated by randomly copying spikes from a Poissonian mother process with a given probability  $\epsilon$  [4]. Gamma statistics were obtained by thinning the two child processes, keeping only every  $\gamma$ -th event [5]. The example shows that quantitative measures of spike correlation should be interpreted with care.

For the specific class of correlations arising between random subsets drawn from a joint mother process with arbitrary auto-correlation we present a consistent normalisation of the cross-correlation function which eliminates the effects of the auto-correlation. The extension of this result to other correlation models is the subject of current investigation.

We acknowledge constructive discussions with Stefan Rotter.  
Partially funded by GIF and BMBF-DIP F1.2.

- [1] Vaadia E et al (1995) *Nature* **373**(6514):515–518.
- [2] Bair W et al (2001) *J Neurosci* **21**(5):1676–1697.
- [3] Cox DR (1967) *Renewal theory* Chapman and Hall London.
- [4] Kuhn A et al (2003) *Neural Comput* **15**(1):67–101.
- [5] Baker SN & Gerstein GL (2000) *Neural Comput* **12**:2597–2620.

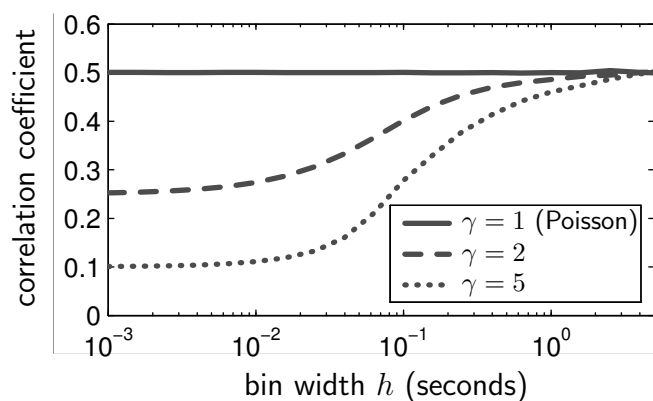


**Fig.1:** Correlation coefficients for different  $\gamma$ -orders (legend) as a function of the length of the counting interval  $h$ . The 'injected' correlation is  $\epsilon = 0.5$ .

\* [tom@biologie.uni-freiburg.de](mailto:tom@biologie.uni-freiburg.de)



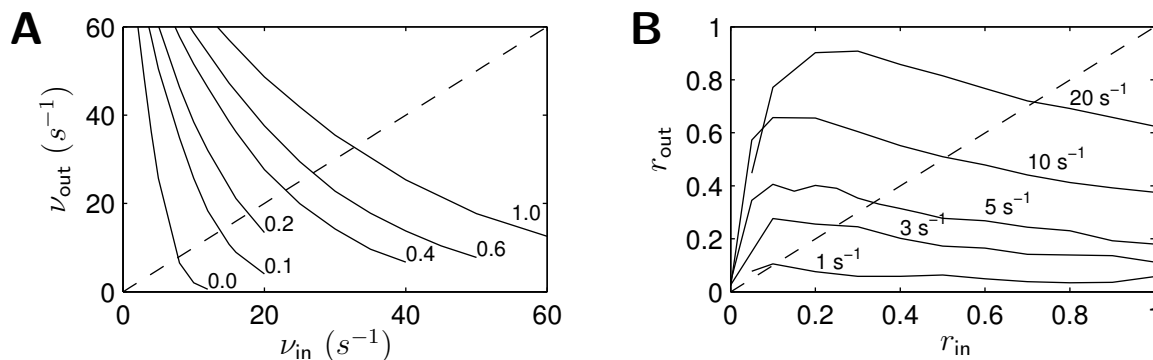
# Dynamics of rate and correlation in balanced random networks

Daniel Schöner\*, Tom Tetzlaff, Ad Aertsen, Markus Diesmann

Neurobiology & Biophysics, Inst. of Biology III, Albert-Ludwigs-University, Freiburg

*In vivo* recordings of cortical neurons show irregular asynchronous spiking activity at low firing rates (e.g. [1]). Networks of randomly connected populations of excitatory and inhibitory neurons have been suggested as simple models for a local cortex volume exhibiting this type of activity [2]. Several experimental studies report the existence of correlated firing occurring in relation to internal or external events (e.g. [3]). It is not yet clear, to what extent these observations can be explained on the basis of a balanced random network.

Since neurons in a finite network share parts of their synaptic inputs inter-neuronal correlations naturally do exist. Indeed, network simulations reveal pairwise correlations even in stationary states. With the help of a simplified model we investigate how the synaptic input structure of two arbitrarily selected neurons causes correlated firing. In a consistent two-neuron description pairwise correlations  $r_{in}$  among the neurons constituting the two partially overlapping input populations have to be considered. However, this cannot be done without simultaneously generating higher-order dependencies. In order to be in control over these higher-order interactions, we use a specific input model [4] parameterised by only two quantities: the rate of each individual channel  $\nu_{in}$  and the pairwise correlation  $r_{in}$ . As shown in previous studies [5, 6, 7] both output rates  $\nu_{out}$  and output correlations  $r_{out}$  are modulated by  $\nu_{in}$  and  $r_{in}$ . In a mean-field approach the resulting two-dimensional transmission characteristic  $(\nu_{in}, r_{in}) \mapsto (\nu_{out}, r_{out})$  (Fig. A,B) is utilised to determine self-consistent rates and correlations (cf. [8]).



**A** Rate transmission functions for different  $r_{in}$ , **B** Correlation transmission functions for given  $\nu_{in}$ .

The fixed-point analysis reveals a solution at a high correlation and an intermediate rate, inconsistent with corresponding network simulations and experimental data. The input model overestimates the impact of higher-order interactions, thus leading to a large correlation gain. Current work focuses on a parameterisation of higher-order statistics more adapted to the activity observed in recurrent networks.

We acknowledge helpful discussions with Stefan Rotter. Partially funded by GIF and BMBF-DIP F1.2.

- [1] Softky WR & Koch C (1993) J Neurosci **13**(1):334–350.
- [2] Brunel N (2000) J Comp Neurosci **8**(3):183–208.
- [3] Riehle A et al (1997) Science **278**:1950–1953.
- [4] Kuhn A et al (2003) Neural Comput **15**:67–101.
- [5] Shadlen M & Newsome W T (1998) J Neurosci **18**(10):2870–3896.
- [6] Stroeve S & Gielen S (2001) Neural Comput **13**(9):2005–2029.
- [7] Tetzlaff T et al (2003) Neurocomputing **52–54**:949–954.
- [8] Amit D & Brunel N (1997) Cereb Cortex **7**:237–252.

\* [schoener@biologie.uni-freiburg.de](mailto:schoener@biologie.uni-freiburg.de)

## **Boundary definition and neuronal morphology of sub areas of the rat prefrontal cortex**

**Perez- Cruz C., Heilbronner U., Müller-Keuker J., Flügge G. and Fuchs E.**

Clinical Neurobiology Laboratory, German Primate Center, Kellnerweg 4, Göttingen 37077, Germany

The rat prefrontal cortex (PFC) can be considered to be analogous to the human PFC regarding neuronal connections with medial thalamic nuclei and other sub cortical areas. Nowadays, there is still some controversy with respect to rat PFC boundaries and inclusion of different areas. Therefore, we performed an immunocytochemical study to define specific PFC sub areas. The criterion for PFC boundaries definition was to observe same sub area delineation after staining with different antibodies, parvalbumin (1:2000), SMI-32 (1:1000), Neu-N (1:500), calbindin (1:500), calretinin (1:500) and after Nissl staining.

Our results show clear boundaries between sub areas of the rat PFC. The pattern of staining was similar among all subjects and showed three defined PFC sub-areas: Infralimbic, prelimbic and anterior cingulate cortex.

In a second experiment we have combined whole-cell recordings with neurobiotin labeling to examine the morphological properties of pyramidal neurons from the above-mentioned PFC sub areas. Adult male Sprague-Dawley rats ( $n=10$ ) were used for these experiments. Thick slices (400  $\mu\text{m}$ ) were produced from fresh brains and neurons were filled via a patch-pipette with neurobiotin (2 mg/ ml). At least two neurons from each PFC sub region (restricted to layers III-V) were examined in each rat. After filling, slices were transferred to a fixative for neurobiotin staining using immunocytochemical techniques. Neurons were then visualized with a light microscope and were three-dimensionally reconstructed using the neuron tracing system Neurolucida. Dendritic morphology such as apical dendritic length and branch points, secondary dendritic branches and axon length were analyzed. So far, our results show different dendritic characteristics depending on the PFC sub area.

Partially supported by CONACyT (Mexican National Counseling for Sciences and Technology).

## On neuronal mechanisms determining synchronization dynamics in cortical feed-forward networks

Sven Goedeke<sup>1,\*</sup>, Theo Geisel<sup>1</sup>, & Markus Diesmann<sup>2</sup>

<sup>1</sup>Dept. of Nonlinear Dynamics, MPI for Fluid Dynamics, Göttingen

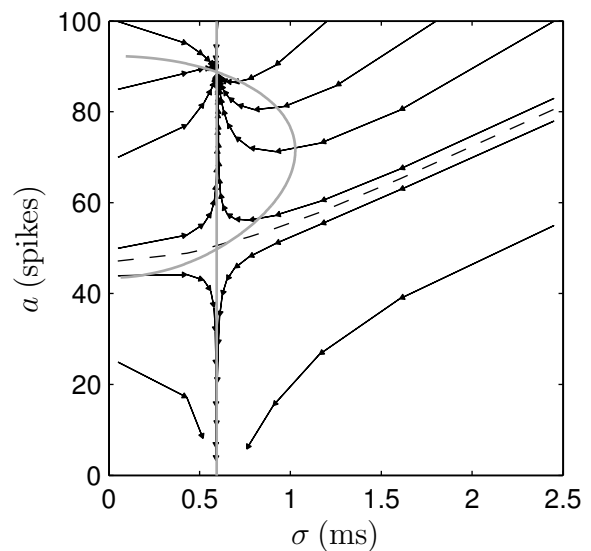
<sup>2</sup>Neurobiology & Biophysics, Inst. of Biology III, Albert-Ludwigs-University, Freiburg

A possible explanation of precise spike patterns observed in the cortex are network structures consisting of groups of neurons connected in an excitatory divergent/convergent feed-forward manner [1]. Simulations demonstrated that synchronous spiking can stably propagate in these networks. The synchronization dynamics is reducible to an iterative mapping of two variables: the number of spikes  $a$  and the standard deviation of the spike time distribution  $\sigma$ . A transmission function describing the single neuron response to synchronous input is obtainable from simulations. This function suffices to construct the iterative mapping [2].

However, the mechanisms shaping the transmission function are not well understood. A suitable theoretical framework is provided by stochastic neuron models based on an instantaneous firing probability  $f$ . Often  $f$  is assumed to be a function of the membrane potential  $V$  alone. Applying  $f(V)$ -models it was reported that neuronal refractoriness is necessary and sufficient for stable synchronization [3,4]. In a previous contribution [5] we showed that  $f(V)$  is inconsistent with the integrate-and-fire neuron model when exposed to synchronized input in addition to fluctuating background activity. The inconsistency is removed by considering  $f(V, \dot{V})$  and a simple argument explains the factorization of  $f$  into a  $V$  dependent term and a term depending on the slope  $\dot{V}$ . The importance of  $\dot{V}$  in the synchronization dynamics was already pointed out by Abeles [1].

Here, we remove the tightening effect of refractoriness on the transmission function obtained from simulations of an integrate-and-fire neuron. This enables us to disentangle the influence of the instantaneous firing probability  $f$  and the refractory mechanism in cortical feed-forward networks. We find that the behavior of the system remains unchanged when removing refractoriness. This suggests that the synchronization dynamics is governed by the  $\dot{V}$ -dependence of  $f$ . Refractoriness limits the number of response spikes.

In a second step we consider a minimal model of  $f$  which is linear in  $V$  and  $\dot{V}$ . The figure shows the resulting  $(a, \sigma)$ -dynamics in a feed-forward network with 100 neurons per group. Essential features observed in network simulations of integrate-and-fire neurons are reproduced: an attractor for synchronous spiking at high temporal precision, coexistence of a domain where initial activity decays, and the shape of the separatrix (dashed curve). Equipped with this minimal model we gain analytical insight into the origin of the isoclines (gray curves) and the bifurcation creating the attractor.



[1] Abeles M *Corticonics* Cambridge University Press, Cambridge, 1991.

[2] Diesmann M et al (1999) *Nature* **402**:529–533.

[3] Gewaltig M-O *Evolution of Synchronous Spike Volleys in Cortical Networks* Shaker, Aachen, 2000

[4] Kistler W & Gerstner W (2002) *Neural Comput* **14**(5):987–997.

[5] Diesmann M et al (2003) In *Proc 29th Göttingen Neurobiol Conf*, p 660, Thieme, Stuttgart.

\*sven@chaos.gwdg.de

# FREQUENCY-SPECIFIC ACTIVITY OF THE AUDITORY PATHWAY WITH AUDITORY MIDBRAIN IMPLANTS

U. Reich, N. Marquardt, M.-N. Klingberg, G. Paasche, M. Lenarz, T. Lenarz, G. Reuter

Department of Otolaryngology, Medical University of Hannover, Germany

## Introduction:

Auditory brainstem implants with electrodes positioned in the cochlear nucleus are now used for the auditory rehabilitation of patients with neural deafness [1]. Alternative concepts for targeted tonotopic stimulation of the higher auditory areas, such as colliculus inferior (IC), are currently under investigation [2,3]. Electrical stimulation along the auditory pathway must be such that more central areas are activated physiologically, i.e. comparable to acoustic stimulation. With penetrating electrode in inferior colliculus acoustic evoked signals are detectable. The same electrode was also used for electrical stimulation in the IC to activate the more central auditory areas. Electrically evoked potentials can be registered at the auditory cortex using surface and/or deep insertion electrodes and compared with acoustically induced cortical signals. This experiments will be continued in chronic implanted animals for safety studies.

## Material and Methods:

In collaboration with Cochlear Ltd. (Sydney), a 4 mm 20-channel rod electrode was developed, electrode contacts being arranged in a circle on a rod at 200  $\mu\text{m}$  intervals. This electrode inserted in IC allowed measuring acoustically evoked potentials and also electrical stimulation of IC. Acoustical stimulation was performed in a range of 1-16 kHz. Electrical stimulation was performed using single bipolar square pulses of various duration (60-200  $\mu\text{s}$  per phase) and intensity (50-600  $\mu\text{A}$ ), ten pulses per second. For cortical measurements on the auditory cortex we used a surface electrode with 21 round electrodes. The use of several electrodes allowed stimulation and multi channel measurement on several sites along the auditory pathway up to the auditory cortex.

## Results and Discussion:

Electrode insertion in IC proved to be easy and reproducible. Tissue damage is limited to the insertion channel. The potentials evoked by acoustic stimulation can be recorded in the IC. The electrode showed various frequency-specific signal amplitudes and latency at the individual electrode contacts. It is also possible to record acoustically evoked signals in the IC and on the auditory cortex. These help to determine the ideal angle of insertion and showed frequency-specific responses on cortex. Electrically in the IC evoked potentials were measured with multi channel set up on the auditory cortex. They offered a input-output characteristic. Short pulses showed higher thresholds then longer pulses. Long-term studies carried out in order to investigate the safety and feasibility of this approach. Animals implanted with this electrode in IC showed no noticeable neurological and motoric diseases. First experiments with electrical stimulation in IC a little above hearing threshold evoked no avoidance reaction.

## Perspective:

The acute experiments have been carried out in order to investigate the activity of the central auditory pathway following selective electrical stimulation in the individual IC layers. Consequently, multi channel recording in the deeper layers of the auditory cortex could provide a more specific responses. The overall aim is to evoke frequency-specific signals using a penetrating electrode to achieve tonotopic activation.

More long-term animal studies with and without stimulation will be the next step. The goal is auditory rehabilitation in patients suffering from neural deafness more efficiently than surface electrodes places on the cochlear nucleus.

## References:

- [1] Lenarz, M.; Matthies, C.; Lesinski-Schiedat, A.; Frohne, C.; Rost, U.; Illg, A.; Battmer, R. D.; Samii, M; Lenarz, T. (2002): Auditory Brainstem Implant Part II: Subjective Assessment of Functional Outcome. *Otology & Neurotology*. 23.(5):.694-697
- [2] Lenarz, M; Reuter, G.; Patrick, J.; Lenarz, T. (2004): Auditory Midbrain Implant-Design an Evaluation. ARO Midwinter Meeting, Daytona Beach, USA, Abstracts of 27th. Midwinter Research Meeting of the Association for Research in Otolaryngology (ISSN 0742-3152), 54
- [3] Lim, H. H.; Anderson, D. J. (2004): Effects of Electrical stimulation of the Inferior Colliculus on Tonotopic Projections to the Auditory Cortex in Light of a Midbrain Auditory Prosthesis. ARO Midwinter Meeting, Daytona Beach, USA, Abstracts of 27th. Midwinter Research Meeting of the Association for Research in Otolaryngology (ISSN 0742-3152), 53

# **Spatiotemporal patterns in auditory cortical activity after discrimination learning of auditory stimuli and of intracortically applied electrical stimuli**

**Matthias Deliano, Achim Engelhorn, Daniel Ensberg, Henning Scheich and Frank W. Ohl**

Leibniz Institute for Neurobiology, Brenneckestraße 6, D-39118 Magdeburg, Germany

The critical step for the development of a cortical neuroprosthesis is the generation of meaningful structured perception on the basis of patterned multi-site electrical stimulation, which can guide the actions of blind or deaf subjects in their everyday life. Currently it is not known whether this is possible. Previous attempts in the development of sensory cortex prostheses focusing on the encoding of environmental stimuli into patterns of intracortical microstimulation (ICMS) have been largely unsuccessful (Brindley & Lewin 1968, Schmidt et al. 1996). The problem is that even in the simple case of the discrimination of phosphenes or audenes electrically evoked at single cortical sites, the generation of meaningful discriminable percepts is poorly understood. In the present work it is therefore proposed that successful patterned multi-site electrical stimulation will rely on a better understanding of cortical processes already involved in the generation of meaningful perception induced by single-site stimulation.

We have recently shown that with discrimination and categorization learning of acoustic stimuli, spatial patterns emerge in the ongoing cortical activity of the auditory cortex of the Mongolian gerbil, which were related to the meaning of the stimuli to the animal rather than to their physical properties (Ohl et al., 2001; Ohl et al., 2002; Ohl et al., 2003). These patterns could be identified in the  $\beta$ - and  $\gamma$ -band of the ECoG at unpredicted points in time after the stimulus. These patterns lasted for only a few tens of milliseconds, and displayed a distributed, "holographic" spatial organization. ICMS applied to the cortex is likely to interfere with the (endogenous) cortical dynamics from which activity patterns emerge that are related to the meaning of the stimuli. In the present study we therefore compared the cortical activity patterns found with the discrimination learning of acoustic stimuli with the patterns induced by the discrimination learning of intracortical electrical stimuli.

We applied ICMS to the auditory cortex of the Mongolian gerbil via a simple unidirectionally operating cortical implant (Scheich & Breindl 2002). In parallel we recorded an epidural multichannel electrocorticogram. Animals were trained in a GO/(NO-GO)-paradigm to discriminate stimulation sites in the low and high frequency region of the tonotopic map of the primary auditory cortex (Deliano et al. 2003). We analyzed patterns of ongoing cortical activity in relation to ICMS and its behavioral interpretation.

Cortical activity patterns emerging during discrimination learning of electrical stimuli were spatially more focal than in the case of using acoustic stimuli. This indicates principle differences in the modes how cortical dynamics is recruited to form discernable percepts when using acoustic or electrical stimuli. To restore the mode of cortical operation seen with acoustic stimulation, a proper timing of the electrical stimuli in reference to changing cortical states might be crucial. Therefore we are aiming at the development of an interactive cortical neuroprosthesis that guarantees for the proper timing and shaping of the electrical stimuli conditional on the momentary cortical state, and by this improve the perceptual interpretation of stimuli delivered by the neuroprosthetic device.

Brindley, G.S. & Lewin, W.S. (1968) *J. Physiol.* 196: 479-493.

Deliano M. et al. (2003) *Proc. Int. Conf. Auditory Cortex*, Magdeburg, Abstr. No. 57.

Ohl, F.W. et al. (2001) *Nature* 412: 733-736.

Ohl, F.W. et al. (2002) *Biological Cybernetics* 88: 374-379, 2003.

Ohl, F.W. et al. (2003) *Rev. Neurosci.* 14: 35-42, 2003.

Scheich, H. and Breindl, A. (2002) *Audiol. Neurotol.* 7: 191-194.

Schmidt, E.M. et al. (1996) *Brain* 119: 507-522.

**Serotonergic modulation of intrinsic properties and its effect on the signal processing in deep cerebellar nucleus neurons.**

M.-L. Lee, H.-P. Thier, and V. Gauck

Dept. Cognitive Neurol., Hertie-Institut for Clinical Brain Research, Univ. Tübingen, D-72076 Tübingen, Germany.

Corresponding author: [volker.gauck@uni-tuebingen.de](mailto:volker.gauck@uni-tuebingen.de)

The widespread serotonergic innervation of the cerebellum from the brainstem areas suggests that it has an important role in the modulation of cerebellar function. In the present study we performed patch clamp recordings in rat cerebellar slices to investigate the effect of serotonin on the intrinsic properties of deep cerebellar nucleus (DCN) neurons and the resulting consequences for the signal processing performed by these neurons. A depolarization and an increased spike rate were found in current clamp experiments. The voltage clamp experiments that we performed indicate that serotonin increased the net inward current altering the activity of more than one persistent ionic current. The reduction of a tonic potassium current and the increase of a tonic depolarizing cationic current are likely to be involved. Under dynamic current clamp conditions the effect of serotonin on the spike rate of DCN neurons depended on their pre-drug activity level. A reduction was found for high pre-drug DCN frequencies, while an increase or no change was found for low DCN pre-drug frequencies. The pre-drug frequency of DCN neurons in turn was determined by the activity level of the simulated synaptic input elements. Our analysis revealed the synaptic shunting as one major mechanism mediating this effect. Overall our results indicate that the synaptic background activity is modulating the effect that serotonin has on its target neurons.

**Poster Subject Area #PSA16:  
Hippocampus and Limbic system**

- [#214A](#) CJ. Behrens, Berlin  
*Induction of sharp wave ripple-complexes (SPW-R) in hippocampus by tetanic stimulation –*
- [#215A](#) M. Njunting, S. Gabriel, K. Schulze, K. Jandova, U. Heinemann and T-N. Lehmann, Berlin  
*RELATION OF CELL LOSS AND SEIZURE FREQUENCY IN THE ENTORHINAL CORTEX AND HIPPOCAMPUS IN THE PILOCARPINE MODEL OF TEMPORAL LOBE EPILEPSY*
- [#216A](#) M. Moisel, K. Gebert, C. Leibold, A. Gundlfinger, D. Schmitz and R. Kempter, Berlin  
*Principal Component Analysis of Hippocampal Mossy Fiber fEPSPs and Modeling of Short-Term Synaptic Plasticity*
- [#217A](#) C. Kehrer, D. Schmitz, U. Heinemann and T. Gloveli, Berlin  
*Pretreatment with MK-801 affects the properties of kainate-induced gamma oscillations in area CA1 of the hippocampus*
- [#218A](#) E. Kipiani, T. Dugladze, H. Monyer, U. Heinemann and T. Gloveli, Berlin and Heidelberg  
*Differential involvement of perisomatic targeting interneurons in hippocampal network oscillations in vitro*
- [#219A](#) H-J. Bischof, C. Lieshoff and S. Watanabe, Bielefeld and Tokyo (J)  
*Spatial Learning Leads to Expression of the Immediate Early Genes C-Fos and Zenk in the Zebra Finch Hippocampus*
- [#220A](#) B. Wolynski, P. Erhard and M. Meier, Bremen  
*Applying the dissociated spatial attention task (DSAT) to humans during fMRI-scans.*
- [#221A](#) C. Heinrich, A. Depaulis, M. Frotscher and CA. Haas, Freiburg and Grenoble (F)  
*Regulation of reelin but not neurogenesis is critical for granule cell dispersion: evidence from a mouse model of temporal lobe epilepsy*
- [#222A](#) U. Häussler, U. Egert and A. Depaulis, Freiburg and St Martin d'Hères (F)  
*The role of the contralateral hippocampus in the generation of seizure activity in a model of focal temporal lobe epilepsy in mice*
- [#223A](#) C. Koester-Patzlaff, M. Hosseini and B. Reuss, Göttingen  
*Expression of Connexin 36 and Connexin 43 in the Hippocampus of Borna Disease Virus infected rats*

- [#224A](#) JIH. Müller-Keuker, JN. Keijser, C. Nyakas, PGM. Luiten and E. Fuchs, Göttingen, Groningen (NL) and Budapest (H)  
*REDUCTION OF SEROTONERGIC INNERVATION IN THE AGING TREE SHREW HIPPOCAMPUS*
- [#225A](#) P. Tovote, I. Misane, A. Ronnenberg, SO. Ögren, M. Meyer, J. Spiess and O. Stiedl, Göttingen, Saskatoon (CDN), Stockholm (S) and Amsterdam (NL)  
*INVOLVEMENT OF THE DORSAL HIPPOCAMPUS IN TRACE FEAR CONDITIONING IN MICE: A TIME-DEPENDENT PROCESS*
- [#226A](#) B. Cooper, E. Rüther and G. Flügge, Göttingen  
*Expression of central nervous genes related to chronic stress in the rat*
- [#227A](#) L. Fester, Cv. Schassen, V. Ribeiro-Gouveia, M. Böttner and GM. Rune, Hamburg and Göttingen  
*Endogenous estradiol synthesis regulates proliferation, apoptosis and neurite outgrowth in rat hippocampus.*
- [#228A](#) O. von Bohlen und Halbach, D. Medina, L. Minichiello and K. Unsicker, Heidelberg and Monterotondo (I)  
*TrkB receptors are involved in the structural remodeling of hippocampal spines*
- [#229A](#) T. Fritz and S. Koelsch, Leipzig  
*Music as a tool to examine pleasantness and unpleasantness: An fMRI-study*
- [#230A](#) A. Guanella, R. Wyss and PFMJ. Verschure, Zürich  
*The use of place cells in locale navigation: a model of rodent spatial learning applied to mobile robots*
- [#214B](#) MF. Geiger, T. Seidenbecher and H-C. Pape, Magdeburg  
*Seizure-related influences on fear behavior and theta synchronization in a mouse model of temporal lobe epilepsy*
- [#215B](#) RT. Narayanan, T. Seidenbecher, O. Stork and H-C. Pape, Magdeburg  
*Patterns of theta synchronisation in amygdalo-hippocampal-prefrontal cortical circuits during consolidation of fear memory and extinction*
- [#216B](#) S. Kostenko, JU. Frey and S. Frey, Magdeburg  
*LTP and reinforcement of early-LTP by stimulation of ventral tegmental area in freely moving rats in vivo.*
- [#217B](#) C. Stoppel, O. Stork and H-C. Pape, Magdeburg  
*Involvement of somatostatin in formation of contextual fear memory*
- [#218B](#) C. Kluge, C. Szinyei and H-C. Pape, Magdeburg  
*Contribution of somatostatin to long term potentiation in the mouse hippocampus*



- [#219B](#) L. Sosulina, S. Meis and H-C. Pape, Magdeburg  
*Molecular and physiological diversity of neurones in the rat lateral amygdala revealed by electrophysiological, single-cell RT PCR and cluster analysis*
- [#220B](#) M. Fendt, T. Endres, V. Hambrecht and B. Steininger, Tübingen  
*The neural basis of fox odor-induced fear behavior*
- [#221B](#) T. Endres, R. Apfelbach and M. Fendt, Tübingen  
*THE INFLUENCE OF FOX ODOR ON THE BEHAVIOR OF NAIVE RATS*
- [#222B](#) K. Becker, C. Helmeke and K. Braun, Magdeburg  
*QUANTITATIVE CHANGES OF PARVALBUMIN-, CALBINDIN-D28K- AND CRF-IMMUNOREACTIVE NEURONS IN THE HIPPOCAMPUS AND AMYGDALA OF OCTODON DEGUS AFTER EARLY LIFE STRESS*
- [#223B](#) S. Zehle, J. Bock and K. Braun, Magdeburg  
*EFFECTS OF EARLY DEPRIVATION AND METHYLPHENIDATE TREATMENT ON BEHAVIOR, BRAIN ACTIVITY AND SPINE MORPHOLOGY IN JUVENILE RODENTS (OCTODON DEGUS):*
- [#224B](#) D. Yilmazer-Hanke, R. Fritz, T. Roskoden, H. Schwegler and R. Linke, Magdeburg  
*Divergent projections of the central nucleus of the amygdala to the substantia innominata and the magnocellular pontine nucleus of the rat*
- [#225B](#) O. Levai and ME. Calhoun, Tübingen  
*Localization of activity-related cytoskeletal protein in dendrites of hippocampal neurons activated by behavioral tasks*
- [#226B](#) G. Casteller, M. Laconi, M. Fraile, P. Melonari, M. Olguin, L. Llano, S. Taley, MF. Tarrazó, A. Landa, RJ. Cabrera and PA. Gargiulo, Mendoza (RA)  
*EFFECTS OF ALOPREGNANOLONE INJECTED INTO THE MEDIAL PRE-FRONTAL CORTEX IN THE PLUS MAZE TEST IN RATS*
- [#227B](#) P. Melonari, M. Olguin, M. Fraile, L. Llano, S. Taley, MF. Tarrazó, G. Casteller, A. Landa and PA. Gargiulo, Mendoza (RA)  
*EFFECTS OF METOPROLOL INJECTED INTO THE NUCLEUS ACCUMBENS SEPTI IN THE PLUS MAZE TEST IN RATS*
- [#228B](#) M. Hutzler and P. Fromherz, Martinsried  
*Silicon chip with capacitors and transistors for interfacing organotypic brain slice of rat hippocampus*
- [#229B](#) U. Kaupert and Y. Winter, Munich and Seewiesen  
*Hippocampal enlargement in nectar-feeding mammals*
- [#230B](#) C. Stangl and P. Fromherz, Martinsried  
*Field potentials of acute brain slices recorded with field effect transistor array*

## **Induction of sharp wave ripple-complexes (SPW-R) in hippocampus by tetanic stimulation –**

### **Abstract**

Hippocampal sharp-wave ripple complexes (SPW-R) occur during slow wave sleep and behavioral immobility and are thought to represent stored information that is transferred to the cortex in a process of memory consolidation. Here we show for the first time that stimuli which induce long-term potentiation, a neurophysiological correlate of learning and memory, led to generation of SPW-R that were identical to those observed spontaneously. Induction of SPW-R was dependent on activation of NMDA receptors and involved time-dependent changes in interactions between clusters of neurons in the associational network of hippocampal area CA3.

## RELATION OF CELL LOSS AND SEIZURE FREQUENCY IN THE ENTORHINAL CORTEX AND HIPPOCAMPUS IN THE PILOCARPINE MODEL OF TEMPORAL LOBE EPILEPSY

Marleisje Njunting, Siegrun Gabriel, Katrin Schulze, Katerina Jandova, Uwe Heinemann and Thomas-Nicolas Lehmann\*

Johannes Müller Institute of Physiology, \*Departments of Neurosurgery, Charité - Universitätsmedizin Berlin

Mesial temporal lobe epilepsy (mTLE) is frequently associated with cell loss. Whether the degree of cell loss has any impact upon expression of seizure frequency is not clear. In this study we employed the rat post-pilocarpine status model of mTLE in order to compare morphological alterations in the hippocampal formation of less frequently and frequently seizing animals. Sections/horizontal slices from 13 chronic epileptic and four control animals were prepared 4 month after status epilepticus/sham treatment and stained with cresylviolet in order to count neurons and to determine granule cell dispersion, fluorescent dextran-amine to grade dendritic alteration in area CA1 and Neo-Timm to assess mossy fiber sprouting. Seizure frequency was evaluated by video monitoring. Neuron loss was most pronounced in the hilus (81%) and in the medial entorhinal cortex layer III (48%). It was also evident in fields CA3 and CA1 of the hippocampus and in other layers of the medial and lateral entorhinal cortex (MEC and LEC). Animals displaying >3 seizures have larger neuron loss comparing to animals displaying <1.5 seizures per day: in the MEC layer III and hippocampal area CA3 (59 vs. 38% and 53 vs. 34%), but also in area CA1 and the hilus (49 vs. 41% and 86 vs. 77%). In contrast, widening of the dentate granule cell layer and the Timm staining score were similar in the two groups. The findings suggest indirect relations between defects of the entorhinal-hippocampal network and expression of seizure frequency.

*Supported by a grant of the DFG and SFB-TR 3 to TNL*

Keywords: cell loss, pilocarpine model, seizure frequency, temporal lobe epilepsy

# Principal Component Analysis of Hippocampal Mossy Fiber fEPSPs and Modeling of Short-Term Synaptic Plasticity

M. Moisel<sup>1</sup>, K. Gebert<sup>1</sup>, C. Leibold<sup>1</sup>, A. Gundlfinger<sup>2</sup>, D. Schmitz<sup>2</sup>, R. Kempter<sup>1,2</sup>

<sup>1</sup>Institute for Theoretical Biology, Humboldt-Universität, Invalidenstr. 43, 10115 Berlin

<sup>2</sup>Neuroscience Research Center, Charité, Universitätsmedizin, Schumannstr. 20/21, 10117 Berlin

Synapses exhibit different forms of plasticity over a wide range of time scales. The mossy fiber synapse plays a decisive role in information transmission in the hippocampus, since it holds a bottleneck position by providing the main feedforward input into the CA3-region. Earlier studies on the mossy fiber synapse have shown its specific properties such as a large mean unitary postsynaptic potential size and pronounced frequency facilitation.

Extracellular postsynaptic field potentials (fEPSPs) were recorded from mouse hippocampal slices. These field potential recordings exhibit a good signal-to-noise ratio because they provide an average over many mossy fiber synapses. A disadvantage of extracellularly recorded data is that responses of mossy fibers are superimposed by other processes, such as fiber excitability, activation of associational/commissural synapses and action potential generation of CA3 pyramidal cells.

We have analyzed fEPSPs by means of Principal Component Analysis (PCA) in order to separate pure mossy fiber signals from underlying processes. PCA indicates the presence of at least two different processes which could not be separated due to their interdependence. Spikes of CA3 pyramidal cells for instance occur only when synapses are strongly facilitated and evoke large fEPSP amplitudes.

Application of PCA to simulated fEPSPs that consisted of mossy fiber EPSPs and CA3 pyramidal cell spikes leads to similar results as PCA applied to neurophysiological data. Analysis of data subsets leads to the identification of the two dependent processes. We conclude that in experiments the mossy fiber contribution to fEPSP amplitudes is overestimated due to action potentials of CA3 pyramidal cells. Intracellular patch clamp recordings, which do not contain superimposed spikes, support this hypothesis.

Based on the fEPSP amplitudes in response to irregular stimulus trains (Figure 1) we have developed a computational model that captures essential features of the short-term plasticity of mossy fiber synapses. The model allows for an efficient estimate of synaptic parameters such as the time constant and the amount of facilitation. A fit of model parameters to experimentally obtained data is sufficient to predict the response to other stimulus trains. Our results show that experimental responses are described best by two facilitation terms, a stronger one that decays on a time scale of several hundred milliseconds and a weaker one that decays on a time scale of ten seconds. Synaptic depression is less prominent.

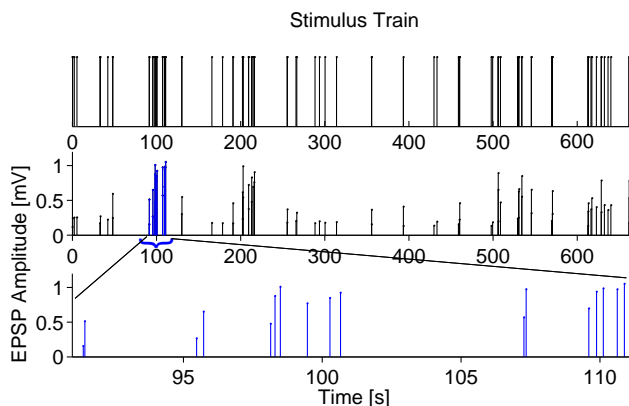


**Figure 1:** Irregular stimulus trains were adopted to optimally scan the dynamical range of fEPSP amplitudes. The top panel shows an example of a stimulus train with a distribution of interstimulus intervals (ISI) proportional to  $1/\text{ISI}$ . The two bottom panels illustrate the large dynamical range of resulting fEPSP amplitudes.

Supported by the DFG, Ke 788/1-2,3, R.K.

SFB 618 "Theoretical Biology", DFG Schm 1383/3-3, D.S.

Berliner Programm zur Förderung von Frauen in Wissenschaft und Lehre, M.M.

**Pretreatment with MK-801 affects the properties of kainate-induced gamma oscillations in area CA1 of the hippocampus**

Colin Kehrer<sup>1</sup>, Dietmar Schmitz<sup>2</sup>, Uwe Heinemann<sup>1</sup> and Tengis Gloveli<sup>1</sup>

<sup>1</sup>Johannes-Müller-Institute of Physiology at the Charité, Berlin, Tucholskystr. 2, 10117 Berlin, <sup>2</sup>Neuroscience Research Center of the Charité, Berlin, Schumannstr. 20/21, 10117 Berlin

The phencyclidine compound MK-801 is a non-competitive antagonist of the NMDA-receptor and induces symptoms which closely resemble those observed in schizophrenia. Increases in power of gamma frequency oscillations, have been proposed to underlie positive schizophrenic symptoms. Using simultaneous field potential and intracellular recordings we studied the effects of systemic administration of MK-801 on the properties of gamma frequency oscillations in area CA1 of the hippocampus. Bath application of kainate (100-200  $\mu$ M) in animals exposed to MK-801 induced field gamma activity (30-45 Hz) with significantly higher power than those in control condition. This effect is not transient as it persists at least seven days after a single administration of MK-801. In order to establish the underlying mechanism we further studied the intrinsic and synaptic properties of principal cells in area CA1 using intracellular recordings. Intrinsic membrane properties, such as membrane input resistance, time constant as well as amplitude and kinetic of monosynaptically evoked GABA-A-receptor mediated IPSPs at similar membrane potentials were not significantly different. In contrast, IPSP amplitudes recorded at rest were about twice the size in MK-801 treated animals ( $7.8 \pm 0.9$  mV vs.  $4.1 \pm 0.4$  mV). This effect is likely to be caused by significant differences in the resting membrane potential, which was more depolarized ( $-55.0 \pm 1.0$  mV) in MK-801 pretreated mice than in control animals ( $-63.4 \pm 1.8$  mV). The larger IPSPs received by CA1 pyramidal cells at rest can account for the increases in power of gamma frequency oscillations observed in MK-801 pretreated animals.

**Differential involvement of perisomatic targeting interneurons in hippocampal network oscillations *in vitro***

Ekaterine Kipiani<sup>1</sup>, Tamar Dugladze<sup>1</sup>, Hannah Monyer<sup>2</sup>, Uwe Heinemann<sup>1</sup>, Tengis Gloveli<sup>1</sup>

<sup>1</sup>Johannes-Müller-Institute of Physiology at the Charité, Berlin, Tucholskystr. 2, 10117 Berlin, <sup>2</sup>Univ. Hospital Neurol., Dept. Clin. Neurobiol. Im Neuenheimerfeld 364, D-69120 Heidelberg

Hippocampal interneurons have a pivotal role in driving inhibition-based rhythms, such as gamma and theta frequency network oscillations. Using whole-cell patch-clamp recordings in conjunction with posthoc anatomy, we investigated the physiological properties of hippocampal parvalbumin-positive perisomatic targeting inhibitory interneurons following kainate-induced transient epochs of gamma frequency oscillations. Horizontal combined entorhinal cortex-hippocampal slices (450  $\mu$ m thickness) were prepared from C57 mice (P 18-25). Perisomatic interneurons (basket and axo-axonic cells) were studied using transgenic mice that expressed enhanced fluorescent protein under the control of the parvalbumin promoter. Field potential and patch-clamp recordings as well as pressure application of kainate (1 mM) were done in area CA3. In the active network, these two types of interneurons showed clear differences in their output patterns. While basket cells discharged on every gamma cycle and phase-locked to the field, axo-axonic cells (AACs) showed very high frequency ( $\sim$ 110 Hz) AP-firing during field gamma. Thus, within a locally excited network, basket cells are involved in the generation of locally synchronous gamma band oscillations, whereas AACs cells are likely to provide a high frequency patterned output to axon initial segments of principal cells. We further investigated the functional relevance of a high frequency firing of the AACs. Direct electrical activation of the monosynaptic inhibitory input to the pyramidal cells with different frequencies (10-300 Hz) demonstrate the strongest suppression of antidromically-evoked field potentials in stratum pyramidale in the frequency range between 100-150 Hz. Similar frequency preference was also mimicked by direct intrasomatic activation of AACs. These results demonstrate the important role of AACs in suppressing AP-propagation from the distal part of the axon to the somato-dendritic region of principal cells during physiologically relevant network activity, such as gamma frequency oscillation.

## **Spatial Learning Leads to Expression of the Immediate Early Genes C-Fos and Zenk in the Zebra Finch Hippocampus**

Hans-Joachim Bischof<sup>1</sup>, Carsten Lieshoff<sup>1</sup> and Shigeru Watanabe<sup>2</sup>

<sup>1</sup>Bielefeld University, Neuroethology ([lieshoff@uni-bielefeld.de](mailto:lieshoff@uni-bielefeld.de), [bischof@uni-bielefeld.de](mailto:bischof@uni-bielefeld.de) )

<sup>2</sup>Keio University, Tokyo, Japan ( [swat@flet.keio.ac.jp](mailto:swat@flet.keio.ac.jp) )

We have recently shown that the zebra finch, a small Australian songbird, is able to solve spatial tasks (Watanabe and Bischof 2002), and that hippocampal lesions affect learning as well as retention of these tasks (Watanabe and Bischof in press). Zebra Finches with hippocampal lesions developed alternative strategies not based on spatial cues to solve the spatial task. Here we show that the hippocampus expresses the immediate early gene products fos and zenk during spatial learning, indicating a temporary activation and probably plastic changes of this structure.

Ten male zebra finches were trained in a “dry version” of the Morris water maze which is used for mice and rats (Watanabe and Bischof 2002). They had to enter a central cage (180x180x180 cm) from four different positions in the side walls to get food from four symmetrically arranged food trays on the ground. Spatial orientation was possible by extramaze cues like a poster at one wall of the experimental room, a door on another wall, and differing structure of the wall covers. From the starting points, the birds were not able to see whether a food tray was baited or not. After the birds had learnt this task, all but one of the trays were closed by tape so that the birds had to learn the position of the one open food tray to get food.

Zebra finch males are able to learn this task in two to three sessions with 4 trials each, that is after about 6 to 10 trials. To monitor IEG activity at the peak of the learning process, we processed the 5 experimental birds for fos and zenk immunohistochemistry after 8 trials. The control birds had to enter the cage and to feed without learning a food try position also 8 times.

Control birds did not express any zenk or fos protein within hippocampus. In contrast, experimental birds showed patches of immunoreactive neurons at different hippocampal locations. Size, number and distribution of these patches varied substantially.

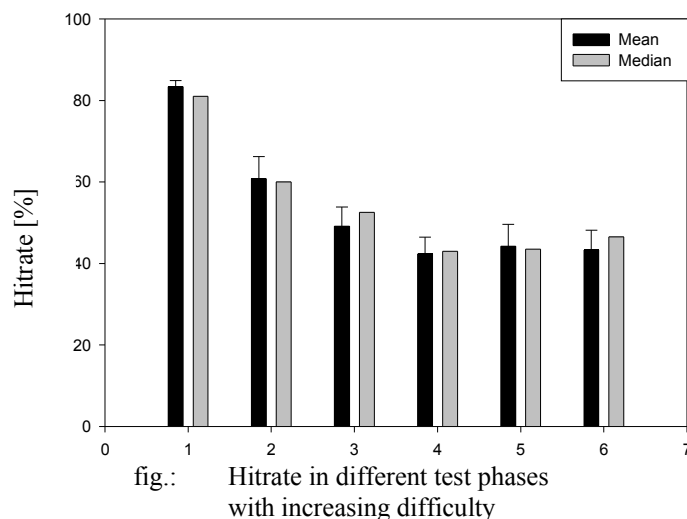
We propose that the big variation in the amount of immunoreactive neurons is related to the stage of learning at the time of sacrificing the bird. In early and late stages, reaction is limited to small patches, while at the apex of the learning curve , activity includes a bigger proportion of the hippocampal formation.

## Applying the dissociated spatial attention task (DSAT) to humans during fMRI-scans.

B. Wolynski.<sup>1</sup>, P. Erhard<sup>2</sup>, M. Meier<sup>1</sup>

<sup>1</sup>Brain Research Institute, <sup>2</sup>Center for Advanced Imaging,  
University of Bremen, FB2, POBox 330440, D-28334 Bremen

Inactivating one hippocampus specifically impairs the ability of rats to distinguish between two sets of continuously dissociated spatial cues (Vlček et al. 2002). This suggests that the hippocampus may also be crucial for organizing dissociated attention. In a computer-based test for humans (DSAT) to determine whether unilateral hippocampal lesions impair the ability to organize attention when spatial cues are dissociated, performance was compared between subjects that have received unilateral medial temporal lobe stereotaxic thermal lesions for intractable epilepsy and matched controls. The results suggest that the hippocampus plays a role in organizing attention among dynamic objects in humans as well. The DSAT tests the ability for dissociated attention of two separate spatial tasks. The subjects' tasks are to remember the position of a target, and locate it afterwards, and at the same time to avoid collision of the cursor with two interfering objects. This scenario takes place within a computerized game arena.



A group of 34 volunteers performed this behavioral test in our lab. An exclusively right handed subset of this group volunteered to repeat an adapted version of this test in a 3T MRI-scanner (Siemens Allegra) while BOLD images were acquired continuously. In some preliminary examinations we compared the performances of a) subjects in the scanner and b) subjects in the normal DSAT situation.

We found that DSAT is suitable for fMRI scanning and we will present our findings of brain activation patterns during the different test phases.

K. JEZEK, M. WESIERSKA, A. A. FENTON, *Physiol. Res.* 51 (Suppl 1): S35-S47, 2002

Vlček K. and Fenton A.A. Laboratory of Neurophysiology of Memory, Institute of Physiology, Academy of Sciences of the Czech Republic, Prag, personal communication

Supported by DFG SFB-517, TP-A8



Regulation of reelin but not neurogenesis is critical for granule cell dispersion: evidence from a mouse model of temporal lobe epilepsy

C. Heinrich<sup>1,3</sup>, A. Depaulis<sup>3</sup>, M. Frotscher<sup>1</sup>, C.A. Haas<sup>1,2</sup>

<sup>1</sup>Inst. of Anatomy and Cell Biology, <sup>2</sup>Dept. of Neurosurgery, University of Freiburg, Freiburg, Germany, <sup>3</sup>JE2413, University of Grenoble, France

Temporal lobe epilepsy (TLE) is one of the most common neurological disorders in humans, which is often accompanied by Ammon's horn sclerosis. This pathology is characterized by a selective neuronal loss in the hippocampal subfields CA1 and CA3 and in the hilus of the dentate gyrus. In addition, there is often an enlargement of the granule cell layer, termed granule cell dispersion (GCD) which has been suggested to be a local migration defect. Interestingly, mice with mutations in the reelin signal transduction pathway show a disturbed lamination pattern of granule cells in the dentate gyrus indicating that this signalling pathway is critical for the correct positioning of granule cells. We have recently shown that the extent of granule cell dispersion correlates with a local reelin deficiency in the dentate gyrus of TLE patients, indicating a role for reelin in the development of GCD (Haas et al, J. of Neurosci. 22, 2002). In order to further investigate this issue we used a mouse model of experimentally induced epilepsy which mimics the histopathological and electrophysiological features of TLE including recurrent focal seizures, cell death and GCD. Following intrahippocampal kainate injection, ipsilateral GCD started to develop within two weeks and was accompanied by the appearance of a radial glial network in the area of dispersion as demonstrated by double immunolabeling for NeuN and GFAP. The development of this radial glial scaffold appeared to coincide with an increase of reelin synthesis, as evidenced by quantitative Western blot analysis. At later time points, however, when GCD developed further, reelin mRNA expression was strongly reduced in the ipsilateral dentate gyrus as monitored by *in situ* hybridization indicating a local reelin deficiency. In order to clarify, whether GCD may result from a mal-positioning of newborn granule cells we investigated neurogenesis in the kainate-injected dentate gyrus by systemic BrdU injection and immunocytochemistry for doublecortin. Both approaches revealed that there is no increased neurogenesis in this model of TLE. Taken together, these results suggest that GCD may be caused by a reelin-mediated mal-positioning of adult granule cells and that neurogenesis does not contribute to the development of GCD. (Supported by the DFG: TR-3).

## The role of the contralateral hippocampus in the generation of seizure activity in a model of focal temporal lobe epilepsy in mice

Ute Häussler<sup>1,2</sup>, Ulrich Eger<sup>1</sup>, Antoine Depaulis<sup>2</sup>

<sup>1</sup>*Neurobiology and Biophysics, Institute of Biology III, Albert-Ludwigs-Universität, Schänzlestr. 1, 79104 Freiburg Germany*

<sup>2</sup>*JE2413 'Contrôle des réseaux synchrones épileptiques', Université Joseph-Fourier de Grenoble, 2280 rue de la Piscine, 38400 St Martin d'Hères, France*

Mesial temporal Lobe Epilepsy (MTLE) in humans is associated with histological changes in the hippocampus including granule cell dispersion, cell losses in the CA1 and CA3 areas and hilus of the dentate gyrus and mossy fiber sprouting. These pathological changes can be mimicked by the unilateral injection of kainate in the dorsal hippocampus of adult mice, thus offering a validated model for the investigation of MTLE<sup>1</sup>. After an initial status epilepticus, kainate-injected mice undergo a phase of epileptogenesis during the three weeks post-injection. During this period EEG activity changes from sporadic hippocampal spikes and short discharges to recurrent hippocampal seizures with a frequency of about one seizure/minute. It is currently unknown, which areas of the injected hippocampus are involved in epileptogenesis and act as the generator of seizures and if additional brain areas are involved in these processes. Because of the important interconnectivity between both hippocampi, the role of the contralateral, non-injected hippocampus in the generation, maintenance or propagation of seizures was examined in this study.

We injected 4 adult C57/Bl6 mice with 1 nmol (in 50 nl) of kainate in the right dorsal hippocampus and implanted bipolar electrodes in the ipsi- and contralateral hippocampus and monopolar electrodes in the right and left cortex. Freely moving mice were recorded at least twice a week for 90 min with a digital EEG acquisition system (Deltamed).

All injected mice were verified to show granular cell dispersion and cell loss on the injected side. During the 3 weeks postinjection, a progressive change from single spikes to organized discharges of spikes, polyspikes and spike-and-wave was recorded in the injected hippocampus. Spike amplitudes were continuously increasing along with these changes. Recordings in the contralateral hippocampus revealed a similar pattern changing from single spikes to organized discharges during these 3 weeks. These discharges were generally concomitant and synchronized with those recorded in the injected side. However, their amplitude remained stable during the 3 weeks. In contrast to the injected side, no granular cell dispersion or cell loss could be observed on the contralateral side.

These preliminary results indicate that seizures do not remain focal in the injected hippocampus, in contrast with previous observations. Whether the contralateral hippocampus participates in the generation of seizures or constitutes a mirror-focus as can be often observed as a complication of MTLE treatment in humans remains to be determined.

Ute Häussler is supported by a DAAD scholarship.

---

<sup>1</sup>Riban et al., (2002), Neuroscience 112, 101-111

## **Expression of Connexin 36 and Connexin 43 in the Hippocampus of Borna Disease Virus infected rats**

Koester-Patzlaff C. , Hosseini M. and Reuss B.

Georg-August-University Goettingen, Center for Anatomy/Neuroanatomy, Neurovirology group

**Introduction:** Borna disease virus (BDV) is a neurotropic, noncytolytic, nonsegmented negative stranded RNA virus, and neonatal BDV infection is suggested as a model system for a putative infectious etiology of neuropsychiatric disorders like schizophrenia, bipolar disorder and autism. The infection results in morphological alterations of dentate gyrus and cerebellar cortex as well as mild behavioural deficits. Cellular mechanisms generating BDV dependent changes in postnatal brain development are still unknown. A mechanism known to regulate brain development is gap junctional intracellular communication (GJIC). „Abnormal“ cell coupling via gap junctions is causally involved in the pathogenesis of different human disorders like heart failure (connexin43), Charcot-Marie-Tooth-Disease (connexin32) or hereditary non-syndromic sensorineural deafness (Cx 26, Cx30 and Cx31). Here we show that BDV dependent malformations and functional deficits are accompanied by clear changes in expression of neuronal and astroglial gap junction connexins Cx36 and Cx43 respectively.

**Methods:** Newborn Lewis rats were injected intracranially with 30 µl of a 10% w/v brain homogenate in PBS from BDV infected or control animals. Rats were killed 4 or 8 weeks post infection by oxygen deprivation with nitrogen. Brains were taken out and dissected. First, BDV infection was verified by immunohistochemistry and RT-PCR analysis. RNA's were used for PCR with primers specific for Cx36 and Cx43. For immunohistochemistry (IHC), Lewis rat brains were fixed in 4 % buffered paraformaldehyde, embedded in paraffin and cut with a rotation-microtome in serial frontal sections of 5 µm. Morphological alterations were investigated by Hematoxylin and Eosin (HE) staining. For the detection of gap junctions, slides were incubated with monoclonal mouse anti-connexin 36 and monoclonal mouse anti-connexin 43 antibodies. Counterstaining was done with DAPI. Expression profiling was performed by hybridising labeled cRNA, derived from pools of the total hippocampal and cerebellar RNA from six animals, to the Affymetrix Rat 230 DNA microarray.

**Results:** Compared to our control-treated animals our results demonstrate a distinct increase in numbers and staining intensity of Cx43 gap junction plaques in the dentate gyrus at 4 weeks post infection (p.i.). At 8 weeks p.i. the dentate gyrus was nearly dissolved. However, the remaining cells in this area show a distinct increase in number and staining intensity of Cx43 gap junction plaques, whereas in the CA3 region less positive staining as compared to control sections could be observed. With respect to the neuronal gap junction protein Cx36 we have seen a slight decrease in number and staining intensity at 4 weeks p.i. in the area CA3 of the BDV infected hippocampus and a strong decrease in the dentate gyrus. At 8 weeks p.i. we have found almost no positive staining of Cx36 in the remaining cells of the dentate gyrus in BDV infected animals and only a weak staining in the area CA3 with both areas demonstrating a decrease as compared to mock-treated controls. We couldn't detect any visible difference in RNA expression with PCR analysis for both Cx36 and Cx43. However Micro Chip analysis demonstrated a 1.5 fold increase in hippocampal Cx43 expression. In addition several genes known to regulate connexin function and expression like pp60(src) (+ 1.7 fold) and GAS 5 (+ 1.8 fold) were increased.

**Conclusions:** With the present study we have demonstrated for the first time that BDV dependent dentate gyrus degeneration is accompanied by spatial and temporal changes in the expression of astroglial and neuronal gap junction proteins. Whereas the changes in expression of Cx36 seem to originate in the dentate gyrus, spreading later to the CA3 region, for Cx43 the inverse pattern can be observed. However, more detailed analysis of the time course of these changes will be necessary. Our findings suggest that BDV infection might lead to changes in neuronal and astroglial intercellular communication likely contributing to the functional and morphological deficits observed in these animals.

## REDUCTION OF SEROTONERGIC INNERVATION IN THE AGING TREE SHREW HIPPOCAMPUS

J.I.H. Müller-Keuker <sup>1</sup>; J.N. Keijser <sup>2</sup>; C. Nyakas <sup>2,3</sup>; P.G.M. Luiten <sup>2</sup>; E. Fuchs <sup>1</sup>

1. Clinical Neurobiology Laboratory, German Primate Center, Göttingen, Germany
2. Department of Molecular Neurobiology, University of Groningen, The Netherlands
3. Brain Physiology Research Group, Hungarian Academy of Sciences, Semmelweis University, Budapest, Hungary

The serotonergic and cholinergic neurotransmitter systems interact during processes of learning and memory. Although the effects of aging on cholinergic innervation has been extensively investigated, it is not clear how the serotonergic innervation is altered during aging. The hippocampal formation, a target area of both cholinergic and serotonergic fibers, is a crucial structure for learning and memory processes. In this study, we used immunocytochemistry against serotonin to assess serotonergic fiber densities in the various hippocampal subfields of 6 young (approximately 1 year) and 5 aged (4-9 years) tree shrews (*Tupaia belangeri*). Our results revealed a negative correlation of serotonergic fiber density with age in the stratum radiatum of CA1 and CA3, and in the stratum oriens of CA3.

Still, it remains to be investigated whether the decrease in fiber densities coincides with a loss of serotonergic neurons in the raphe nuclei. Further research could clarify how the fiber distribution could be preserved by pharmacological interventions.

# INVOLVEMENT OF THE DORSAL HIPPOCAMPUS IN TRACE FEAR CONDITIONING IN MICE: A TIME-DEPENDENT PROCESS

Philip Tovote<sup>1</sup>, Ilga Misane<sup>1,2\*</sup>, Anja Ronnenberg<sup>1</sup>, Sven Ove Ögren<sup>3</sup>, Michael Meyer<sup>4</sup>, Joachim Spiess<sup>1</sup>, Oliver Stiedl<sup>1,3,5</sup>

<sup>1</sup>Dept. of Molecular Neuroendocrinology, Max Planck Institute for Experimental Medicine, Göttingen; <sup>2</sup>Dept. of Psychiatry, University of Saskatchewan, Saskatoon, Canada; <sup>3</sup>Dept. of Neuroscience, Karolinska Institutet, Stockholm, Sweden; <sup>4</sup>Fractal Physiology Group, Max Planck Institute for Experimental Medicine, Göttingen; <sup>5</sup>CNCR, Free University Amsterdam, The Netherlands.

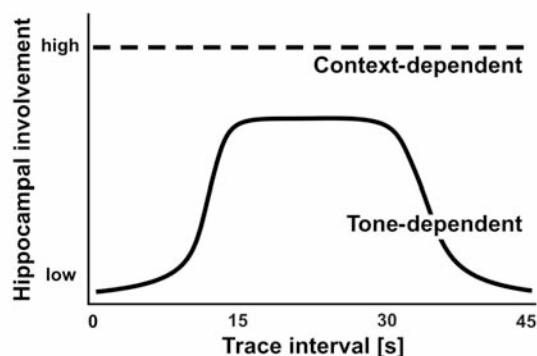
Pavlovian fear conditioning (FC) involves neuroplasticity in the hippocampus and amygdala nuclei. In trace FC, conditioned and unconditioned stimuli are timely separated. The hippocampus has been implicated in this paradigm, but a systematic investigation of the hippocampal involvement as a function of the trace interval has not been performed yet. We investigated the time-dependent involvement of the dorsal hippocampus (DH) in one-trial auditory trace FC in male C57BL/6J mice by selectively inactivating NMDA receptors in this brain area. The NMDA receptor antagonist APV (3.2  $\mu$ g/mouse) was injected 15 min before the conditioning process (training) via intracerebral cannulae terminating bilaterally in the DH. Mice injected with artificial cerebrospinal fluid (aCSF) served as controls. Mice were exposed during training to tone (conditioned stimulus: CS) and foot shock (unconditioned stimulus: US) in the conditioning context without delay (0 s) or with CS-US (trace) intervals ranging from 1 to 45 s. Conditioned auditory fear was determined by the assessment of the freezing behavior and computerized evaluation of inactivity during re-exposure of the mice to the CS in a new context 24 hrs after training. Conditioned context-dependent fear (memory) was tested 2 hrs later in the conditioning context.

Significantly lower freezing scores and inactivity values in APV- than in aCSF-injected mice indicated that injection of APV impaired conditioned auditory fear at longer trace intervals of 15 s and 30 s. At trace intervals of 5 and 10 s, lower inactivity values of APV-treated mice suggested mildly attenuated conditioned fear. No significant freezing or inactivity differences were observed at trace intervals shorter than 5 s. Prolongation of the trace interval to 45 s prevented the aversive CS-US association

(conditioned fear) as indicated by low freezing and inactivity values. Contextual memory was impaired by APV in all mice independent of the trace interval.

It is concluded that NMDA receptors in the DH are required for auditory FC, especially at extended trace intervals of 15-30 s. In contrast, dorsal hippocampal NMDA receptors are involved in contextual FC irrespective of the trace interval. These results confirm a time-dependent role of the dorsal hippocampus in encoding of non-contingent explicit stimuli. The processing of the long CS-US contingencies in the hippocampus appears to be essential for the final processing and execution of fear memories through amygdala circuits.

*(Supported by the Max Planck Society)*



Simplified model of the time-dependent involvement of the dorsal hippocampus in tone- and context-dependent fear conditioning as a function of the trace (tone-shock) interval.

## Expression of central nervous genes related to chronic stress in the rat

Cooper B.<sup>1</sup>, Rütther E.<sup>2</sup>, Flügge G.<sup>1</sup>

<sup>1</sup> Clinical Neurobiology Laboratory, German Primate Centre, 37077 Göttingen

<sup>2</sup> Department of Psychiatry and Psychotherapy, Medical School, University of Göttingen, 37075 Göttingen

Morphological CNS changes are implicated in the pathogenesis of depression and are thought to reflect aberrant adaptive neuroplasticity presumably initiated by an altered programme of gene expression in response to stressful or aversive stimuli. Membrane glycoprotein M6a was previously reported to be downregulated by chronic psychosocial stress in the hippocampus of male tree shrews (*Tupaia belangeri*), but restored to normal levels following treatment with the tricyclic antidepressant clomipramine (Alfonso *et al.* 2004). Although the function of M6a remains to be determined, the developmental pattern of M6a expression, its predominantly synaptic location, and its responsiveness to growth factors suggest it may be involved in neuroplastic synaptic events. In the present study M6a expression was investigated in normal rat brain using *in situ* hybridization and immunocytochemistry to analyse M6a transcript and protein expression, respectively. The main objective was to optimise these techniques for future analysis of M6a expression in a chronic stress model of depression with a particular focus on the prefrontal cortex. Rat M6a was cloned and <sup>33</sup>P-labeled probes were synthesised for *in situ* hybridization. In prefrontal cortex hybridization signals were interspersed among relatively large neurons with no apparent laminar preference, whereas strong hybridization signals were detected in specific subregions of the hippocampal formation (including granule neurons of the dentate gyrus and pyramidal neurons of the CA regions). Immunocytochemical detection of M6a with a monoclonal antibody revealed strong staining in the hilus and apical dendritic fields of CA3, 2, and 1 pyramidal neurons, but not in the granule cell layer of the dentate gyrus. Staining in the prefrontal cortex exhibited a granular appearance with no obvious difference in intensity with respect to cortical laminae. In the near future these data will be compared with M6a mRNA and protein expression in the CNS of chronically stressed rats.

Funded by Deutsche Forschungsgemeinschaft through the DFG-Research Centre for Molecular Physiology of the Brain (CMPB).

Cooper B. is a Christophorus-Lichtenberg stipend fellow.

### Reference:

Alfonso J, Pollevick GD, Van Der Hart MG, Flügge G, Fuchs E, Frasch AC (2004) Identification of genes regulated by chronic psychosocial stress and antidepressant treatment in the hippocampus. **Eur J Neurosci.** 2004 Feb;19(3):659-66.

**Endogenous estradiol synthesis regulates proliferation, apoptosis and neurite outgrowth in rat hippocampus.**

Lars Fester<sup>1</sup>, Christian von Schassen<sup>1</sup>, Veronika Ribeiro-Gouveia<sup>1</sup>, Martina Böttner<sup>2</sup>, Gabriele M. Rune<sup>1</sup>

<sup>1</sup> Institute of Anatomy I: Cellular Neurobiology, Universitätsklinikum Hamburg-Eppendorf, Martinistr. 52, D-20246 Hamburg, Germany; <sup>2</sup> Department of Clinical and Experimental Endocrinology, University of Göttingen, Robert-Koch-Str. 40, D-37075 Göttingen

Neuroprotective effects of exogenous estrogen on cell survival and regeneration have been frequently shown. Here we ask for the role of brain-derived, endogenous estrogen synthesis on proliferation, apoptosis and neurite outgrowth in rat hippocampus. To this end we cultivated dissociated hippocampal cells under serum- and steroid-free condition and treated the cultures with various doses of letrozole, an aromatase inhibitor. At a dose of  $10^{-7}$  M letrozole, estradiol release into the medium was maximally reduced. We determined the number of proliferate cells, using the Ki67 antibody and the TUNEL staining for counting apoptotic cells. Double labeling experiments of Ki67 with microtubule associated protein (MAP-2), glia fibrillaric acid protein (GFAP), or calbindin identified proliferative cells as granule cells. Letrozole led to a dose-dependent decrease of Ki67-positive granule cells. A significant increase in TUNEL-positive cells was only found at a dose of  $10^{-7}$  M letrozole. Surprisingly, application of estradiol to the medium had no effect on proliferation and apoptosis. Neurite outgrowth was judged by quantitative immunohistochemistry of growth associated protein (GAP-43) and by measurement of neurite length after defined time intervals. After 3-7 days of treatment GAP-43 expression was significantly downregulated and neurite length significantly reduced in response to letrozole. After application of estradiol to the medium opposite effects on neurite outgrowth were not found before 5 days of treatment. Our results suggest that only endogenous estradiol synthesis regulates proliferation and apoptosis whereas both, exogenous and endogenous estradiol induce neurite outgrowth in the hippocampus.

**TrkB receptors are involved in the structural remodeling of hippocampal spines**

von Bohlen und Halbach, O.<sup>1</sup>, Medina, D.<sup>2</sup>, Minichiello, L.<sup>2</sup>, Unsicker, K.<sup>1</sup>

<sup>1</sup> Interdisciplinary Center for Neurosciences (IZN), Department of Neuroanatomy,  
University of Heidelberg, Im Neuenheimer Feld 307, 69120 Heidelberg, Germany

<sup>2</sup> European Molecular Biology Laboratory (EMBL), via Ramarini 32, 00016 Monterotondo, Italy

Spines are small postsynaptic structures that protrude from the surface of dendrites of many neurons. Dendritic spines are major sites of excitatory synaptic transmission and the majority of neurotransmitter receptors are located on spines. Specifically, dendritic spines have been shown to be the predominant site of excitatory synapses on CA1 pyramidal neurons in the rat hippocampus [1]. Dendritic spines can undergo morphological plastic changes, leading to structural remodeling of synapses and formation of new synaptic contacts. Thus, some forms of learning have been shown to increase the number of dendritic spines [2]. Brain-derived neurotrophic factor (BDNF), via its receptor trkB, is critically involved in hippocampal LTP [3] and hippocampus-dependent learning, and mice with a forebrain-specific conditional knockout of the trkB gene display impaired learning as well as LTP [4]. To examine whether there is a link between impaired hippocampal synaptic plasticity, altered spines and trkB receptors, we investigated spine densities and spine length in the hippocampal area CA1 and in the dentate gyrus in forebrain-specific trkB mice knockout mice (trkB<sup>lox/null</sup>;CaMKII-CRE mice). Fifteen weeks old conditional knockout mice showed an area specific reduction in spine densities of apical and basal dendrites in area CA1, which was accompanied by a significant increase in spine-length. These data indicate that trkB has an essential function in structural remodeling of hippocampal dendritic spines, which in turn may affect synaptic transmission and plasticity.

Supported by SFB 636/A5.

**References**

- [1] Megias M, Emri Z, Freund TF, Gulyas AI. Total number and distribution of inhibitory and excitatory synapses on hippocampal CA1 pyramidal cells. *Neuroscience* 2001; 102: 527-540.
- [2] Yuste R, Bonhoeffer T. Morphological changes in dendritic spines associated with long-term synaptic plasticity. *Annu.Rev.Neurosci.* 2001; 24: 1071-1089.
- [3] Figurov A, Pozzo-Miller LD, Olafsson P, Wang T, Lu B. Regulation of synaptic responses to high-frequency stimulation and LTP by neurotrophins in the hippocampus. *Nature* 1996; 381: 706-709.
- [4] Minichiello L, Korte M, Wolfer D, Kuhn R, Unsicker K, Cestari V, Rossi-Arnaud C, Lipp HP, Bonhoeffer T, Klein R. Essential role for TrkB receptors in hippocampus-mediated learning. *Neuron* 1999; 24: 401-414.



**Music as a tool to examine pleasantness and unpleasantness: An fMRI-study**

T.Fritz, S.Koelsch

Max Planck Institute for Human Cognitive and Brain Sciences, Leipzig, germany  
fritz@cbs.mpg.de

The present study uses pleasant/unpleasant music as a tool to induce emotion and examine perception-action mediation in the auditory domain. Functional magnet resonance imaging (fMRI) is used to determine the underlying neural correlates. Contrasting unmanipulated tunes that have been rated as 'pleasant' versus their manipulated cacophonous counterparts showed activations in the larynx representation in the rolandic operculum. The larynx is the source of vocal sound, and involved in the production of melody, rhythm, and emotional modulation of the vocal timbre during vocalization. The activation of the larynx is reminiscent of the activation of premotor areas during the observation of movements and might indicate that a system for the perception-action mediation which has been reported for the visual and auditory domain is activated when listening to 'pleasant' music.

# The use of place cells in locale navigation: a model of rodent spatial learning applied to mobile robots

Alexis Guanella, Reto Wyss, Paul F.M.J. Verschure

Institute of Neuroinformatics  
University - ETH Zürich  
190 Winterthurerstrasse  
8057 Zürich, Switzerland  
guanella@ini.phys.ethz.ch

## Abstract

The presence of place cells in CA1, CA3 and DG proves the existence of an allocentric representation of space in the rat hippocampal formation. However, little is known about how this allocentric spatial information can be supported in navigation.

In earlier work, we have shown that a visual encoding scheme applied to a mobile robot can learn place cells (PCs) with realistic physiological properties. Here we present a locale navigational system that can exploit this acquired allocentric information for goal directed navigation. Concrete navigational tasks as homing in open field environments and the Morris water maze are investigated to validate the performance of the system. Our results show that PCs can be integrated successfully into a real-world navigational system relying on only simple cues.

**Keywords:** navigation and orientation, spatial cognition, neural networks.

## **Seizure-related influences on fear behavior and theta synchronization in a mouse model of temporal lobe epilepsy**

*Matthias F. Geiger, Thomas Seidenbecher, Hans-Christian Pape*

Institut für Physiologie, Medizinische Fakultät, Otto-von-Guericke-Universität Magdeburg,  
Leipziger Str. 44, D-39120 Magdeburg, Germany

Interactions between the amygdala and the hippocampus are importantly involved in the emotional modulation of long-term memory formation. Both areas also play a major role in temporal lobe epilepsy (TLE). In human TLE, the most commonly observed affect is fear (1). In our study we analyzed seizure-induced effects on the expression of fear in a pilocarpine mouse model of TLE, using the light-dark-avoidance-test (LD-test) and the elevated-plus-maze-test (EPM-test), respectively. Pilocarpine-treated animals which had developed *status epilepticus* (S.E.) displayed an increase in basic anxiety level, in that they spent 43% of the recording time in the light compartment in the LD-test (compared with 79% in saline-treated controls), stayed 5.9% on the open arms in the EPM-test (16.5% in controls). In order to characterize neurophysiological correlates of epilepsy-related modulations in fear behaviour, we made use of theta rhythm synchronization indicating fear memory consolidation in amygdalo-hippocampal pathways (2). Following Pavlovian fear conditioning, behavioral states (e.g. risk-assessment, freezing) and electrical activity from the lateral amygdala (LA) and the CA1 region of the hippocampus were recorded in pilocarpine treated epileptic animals and non-epileptic controls. In comparison to controls, epileptic animals displayed an increased duration and expression of conditioned fear behaviour (freezing), that was paralleled by an increase in the degree of freezing-related theta-synchronization in amygdalo-hippocampal pathways

In conclusion, the basic level of anxiety and acquired fear responses are altered in the mouse pilocarpine model of TLE. The aggravation of conditioned fear responses in TLE seems to be reflected by an increase in theta rhythm synchronisation in amygdalo-hippocampal pathways, indicating a possible neurophysiological correlate of epilepsy-related fear in these pathways.

- (1) Biraben A., Taussig D., Thomas P., Even C., Vignal J.P., Scarabin J.M., Chauvel P. (2001) Fear as the main feature of epileptic seizures. *J Neurol Neurosurg Psychiatry*.70:186-91
- (2) Seidenbecher T., Laxmi T.R., Stork O., Pape H.-C. (2003) Amygdalar and hippocampal theta rhythm synchronization during fear memory retrieval. *Science*. 301:846-50

Supported by Deutsche Forschungsgemeinschaft (SFB-TR3, TP B7)

## Patterns of theta synchronisation in amygdalo-hippocampal-prefrontal cortical circuits during consolidation of fear memory and extinction

*Rajeevan T. Narayanan, Thomas Seidenbecher, Oliver Stork, Hans-Christian Pape*

Institut für Physiologie, Medizinische Fakultät, Otto-von-Guericke Universität Magdeburg,  
Leipziger Str. 44, D-39120 Magdeburg, Germany

Pavlovian fear conditioning has been used for studying long-term memory in animals, in which the conditioned stimulus (CS) such as a tone, is paired with an aversive unconditioned stimulus (US), such as foot shock (1). After several pairings the animals show conditioned fear responses like freezing when the CS is presented alone. This conditioned fear response rapidly extinguishes when the CS is repeatedly presented in the absence of a foot shock, a phenomenon known as extinction. The prefrontal cortex (PFC) has gathered much attention in recent years because of its role in extinction of fear memories (2). One line of evidence indicates that PFC has a direct influence on the amygdala, and also on the hippocampus, two of the key structures of fear memory consolidation and expression. Another line of evidence indicates that amygdalo-hippocampal interactions are important in terms of theta activity during fear memory retrieval (3). In particular, activity in both brain structures synchronises in the theta frequency range (4-8 Hz) during conditioned fear responses. In our present study electrical activity was recorded in the lateral amygdala (LA), PFC and CA1 area of the hippocampus in freely behaving fear-conditioned mice during retrieval and extinction trials. We found that theta synchronisation upon CS presentation was prominent between all three areas (LA-PFC-CA1) during the first retrieval session, remained stable between LA-PFC and PFC-CA1 during the extinction trials, whereas CA1-LA synchronisation vanished. Theta synchronisation was strictly associated with conditioned fear responses in CA1-LA, and with a broader range of defensive behaviour in LA-PFC and PFC-CA1. With consolidated extinction and also during re-instatement of the fear memory, synchronisation remained low between all three areas under study.

In conclusion, consolidation of fear memory and extinction of fear memory seems to be associated with a balance of theta synchronisation in the tripartite circuit LA-PFC-CA1, with the PFC exerting an executive control function.

(1) LeDoux JE (2000) Emotion circuits in the brain. *Annu Rev Neurosci* 23:155-84.: 155-184.

(2) Milad MR, Quirk GJ (2002) Neurons in medial prefrontal cortex signal memory for fear extinction. *Nature* 420: 70-74.

(3) Seidenbecher T, Laxmi TR, Stork O, Pape HC (2003) Amygdalar and hippocampal theta rhythm synchronization during fear memory retrieval. *Science* 301: 846-850.

## LTP and reinforcement of early-LTP by stimulation of ventral tegmental area in freely moving rats *in vivo*.

Sergiy Kostenko, Julietta U. Frey and Sabine Frey

Dept. Neurophysiology, Leibniz-Institute for Neurobiology, Brenneckestr. 6,  
39118 Magdeburg, Germany

It has been shown that the prolonged maintenance of hippocampal long-term potentiation (LTP) requires heterosynaptic events during its induction. In recent studies was shown that stimulation of modulating brain structures within a distinct time window can reinforce a transient early-LTP into a long-lasting late-LTP in the dentate gyrus in freely moving rats. This reinforcement was dependent on  $\beta$ -adrenergic and/or muscarinergic receptor activation and protein synthesis. The question arose as to whether also similar mechanisms can be described for forms of LTP in the hippocampal CA1 area. Experiments *in vitro* revealed that here, other modulatory inputs such as the dopaminergic system maybe required than those important for the dentate gyrus. The ventral tegmental area (VTA) is a heterogeneous group of dopaminergic cells and a major component of the mesolimbic dopamine system. Neurons of the VTA are involved in the regulation of motor and motivational aspects of behaviour and reveal high neuronal plasticity. The VTA is the major dopaminergic input to the CA1 region of the hippocampus. Thus, we have studied the effect of VTA-stimulation of CA1-LTP in freely moving animals. First, we have solved technical problems with respect to reliable recordings of the population spike and field-EPSPs in freely moving animals. Thus, we stimulate the contralateral CA3 and record ipsilaterally from CA1 principal cells. This allowed us to induce different forms of LTP in the CA1-region *in vivo* in a very reliably manner. We now present first data studying the effect of VTA-stimulation on early-LTP in CA1. Stimulation of the mesolimbic input to the hippocampus resulted in the reinforcement of this early-LTP into the long-lasting late-form of LTP.

## **Involvement of somatostatin in formation of contextual fear memory**

*Christian Stoppel, Oliver Stork, Hans-Christian Pape*

Institut für Physiologie, Medizinische Fakultät, Otto-von-Guericke Universität Magdeburg,  
Leipziger Str. 44, D-39120 Magdeburg, Germany

Somatostatin (SOM) has been shown to be involved in aversive learning and other memory tasks. However, the role of SOM in fear conditioning has not been elucidated so far. In this study we investigated the effects of genetically and pharmacological induced SOM deficiency onto cued and contextual fear conditioning in mice. After conditioning to an auditory cue (CS+) SOM null mutants (SOM  $-/-$  mice) were scored for freezing behaviour onto background context, the CS+ and an unconditioned tone (CS-; previously presented during adaptation). SOM  $-/-$  mice displayed selectively decreased freezing to the background context, while no differences in response to CS+ and CS- could be observed compared to their heterozygous and wild-type controls. To further investigate the involvement of SOM in different aspects of fear memory formation, foreground contextual fear conditioning was performed. As in the cued fear conditioning paradigm freezing behaviour to the context was reduced in SOM  $-/-$  mice. To test whether the observations in SOM  $-/-$  mice are due to an acute involvement of SOM in fear memory formation rather than to developmental deficits, pharmacological depletion of SOM was performed by intraperitoneal infusion of cysteamine (50 or 150 mg/kg). On one hand, application 4h pre-training led to a specific decrease in freezing to background context, thus phenocopying the null mutant phenotype. This cysteamine effect was not observed upon injection to SOM  $-/-$  mice. On the other hand, cysteamine infusion 10min post-training led to a more generalised fear-response to all stimuli presented (context, CS+, CS-). Together, our results indicate that SOM plays a critical role in memorising contextual information interconnected with a threatening experience. This further suggests that hippocampal SOM may be relevant in acute contextual fear memory formation, as integration of complex contextual information crucially depends on processing in the hippocampal formation.

Supported by the Deutsche Forschungsgemeinschaft (SFB 426 TP B7; Leibniz-Programm) and the Studienstiftung des Deutschen Volkes.

## Contribution of somatostatin to long term potentiation in the mouse hippocampus

*Christian Kluge, Csaba Szinyei and Hans-Christian Pape*

Institut für Physiologie, Medizinische Fakultät, Otto-von-Guericke-Universität Magdeburg,  
D- 391020 Magdeburg, Germany

The neuropeptide somatostatin (SST) is released from hippocampal interneurons during high frequency discharges. Although a number of effects of SST have been described at the cellular and subcellular level (**for review see: Møller LN et al., 2002**), little is known about its effects on the properties of the hippocampal synaptic network. Here we show a contribution of SST to synaptic long term potentiation (LTP) in the CA1 region of the rat hippocampus elicited by high frequency stimulation of the Schaffer-collateral – pathway in slice preparations *in vitro*. Recordings were obtained as field potentials in the *stratum radiatum*. Mice with a knock-out of the SST gene (SST<sup>-/-</sup>) showed a significant reduction of LTP (as compared to SST<sup>+/+</sup> litter mates) with respect to the immediate post-tetanic potentiation and the overall magnitude up to one hour following tetanic stimulation. Baseline synaptic transmission as measured by an input/output relationship and paired-pulse ratio as determined by varying the interpulse interval stepwise from 50 to 300ms were not different in wild type compared with knock-out animals. Furthermore, the effect of the SST gene knock-out on hippocampal LTP could be mimicked by somatostatin depletion in wild type animals, achieved by intraperitoneal injection of cysteamine (50 mg/kg) four hours prior to slice preparation. The time course and magnitude of LTP after cysteamine injection closely resembled that in SST<sup>-/-</sup> mice, whereas a saline injected control group showed no alterations. To control for effects of cysteamine other than depletion of SST, we injected SST<sup>-/-</sup> mice with the compound. An effect of cysteamine on LTP was not observed. In conclusion, our results show that SST contributes to synaptic plasticity in the hippocampus and thereby provides one possible explanation of the effects of SST depletion on fear-learning and memory formation (**Stoppel C et al., 2005, German Neuroscience Society meeting - Abstract**).

Supported by Deutsche Forschungsgemeinschaft (SFB426, TPB7)

## **Molecular and physiological diversity of neurones in the rat lateral amygdala revealed by electrophysiological, single-cell RT PCR and cluster analysis**

*Ludmila Sosulina, Susanne Meis, Hans-Christian Pape*

Institute of Physiology, Medical School, Otto-von-Guericke-University,  
D-39120 Magdeburg, Germany

The amygdala has long been known to critically contribute to the emotional components of behavior and memory, and to clinically relevant alterations like stress and anxiety disorders. One major obstacle in our understanding of the molecular and cellular basis of these important functions relate to the large diversity of neuronal cell types in the amygdala. Therefore we have attempted to classify neurons in amygdala using unsupervised cluster analysis based on the comparison of electrophysiological and molecular characteristics, which were obtained through whole-cell patch-clamp recordings combined with single-cell multiplex reverse transcription PCR in slices of the rat lateral amygdala (LA) *in vitro*. A total of 74 LA neurons were analyzed. Electrophysiological parameters included membrane resting potential, input resistance, and the form of action potentials generated upon injection of depolarizing current steps. A multiplex reverse transcription-PCR protocol was designed to detect simultaneously the expression of vesicular glutamate transporter I (VGLuT1), GAD67, calbindin, parvalbumin, calretinin, neuropeptide Y, vasoactive intestinal peptide (VIP), somatostatin (SOM), and cholecystikinin (CCK). The morphological characteristics were analyzed in a subpopulation of neurons after biocytin injection.

At least four groups of neurons with distinctive features could be determined by the cluster analysis. The majority of neurons (n=43) fell into one class, characterized by relatively broad action potentials (mean duration at half maximal amplitude: 2.5 ms), low firing rates (range 5-20 Hz) and frequency adaptation in response to depolarizing stimuli. Concerning molecular markers, these neurones were characterised by high expression of VGLuT1 (86%), expression of NPY (23 %), low expression of GAD67 and calcium binding proteins. These characteristics, and the existence of spiny dendrites in these neurons, are indicative of projection neurons in the LA. The second type of neurones (class II, n=6) displayed high frequent activity (up to 70 Hz) of fast spikes (half-width 1.2 ms) with little frequency adaptation, that was often initiated by burst-like discharges. These cells expressed GAD67 (50%), VIP (66%) and calbindin (33.3 %). The third type of neurones (class III, n=10) resembled those of class II in major electrophysiological terms, low expression level of VGLuT1 (20%), and high GAD67 expression (50%). Different from class II neurons, cells of the third class displayed significant SOM expression (70%), but not calbindin nor VIP. The membrane input resistance of class II (605 M $\Omega$ ) and III neurons (430 M $\Omega$ ) was significantly higher than that in projection cells (class I, 320 M $\Omega$ ). Finally, class IV neurones (n=7) possessed a molecular profile similar to that of projection neurones (class I), but distinctive electrophysiological properties, such as a high input resistance (900 M $\Omega$ ) and more depolarised resting membrane potential (-59 mV, compared with -71 mV). The remainder of the cells (n=8) was heterogeneous in terms of electrophysiological and molecular properties and did not fall in any of the four categories defined above.

In conclusion, at least four types of neurones with a distinctive molecular and electrophysiological profile seem to exist in the rat LA, comprising one class of projection neurones and at least two classes of GABAergic neurones. A minimum combination of markers (VGLuT1, GAD67, calbindin, VIP, SOM) is required to reliably distinguish between the neuronal classes.

Supported by Deutsche Forschungsgemeinschaft (SFB426, TPB8; SFBTR3, TPC3).



# The neural basis of fox odor-induced fear behavior

**Fendt M, Endres T, Hambrecht V & Steiniger B**

Tierphysiologie, Zoologisches Institut, Universität Tübingen,  
Auf der Morgenstelle 28, D-72076 Tübingen, Germany

Trimethylthiazoline (TMT), a component of the anal gland secretions of the red fox (*Vulpes vulpes*), is able to induce fear behavior in naive rats (immobility, startle potentiation, etc. - see also Endres et al. on this meeting) and mice (Hebb et al., 2003). We think that TMT-induced immobility might be a useful animal model to investigate the behavioral, pharmacological, and neuro-anatomical characteristics of unlearned fear. Here, we present first data to the neural basis of TMT-induced fear behavior.

Temporary inactivation of the bed nucleus of the stria terminalis (BNST) by local injections of the GABA agonist muscimol blocks TMT-induced immobility (Fendt et al., 2003). This effect was also observed after inactivation of the medial parts of the amygdala which receive the olfactory input to the amygdala. Against that, temporary inactivation of the lateral and basolateral nuclei of the amygdala did not affect TMT-induced immobility.

Microdialysis studies to the neurochemical basis of TMT-induced fear showed that noradrenaline release within the BNST is increased during TMT exposure. This noradrenaline increase can be blocked by local administration of the alpha-2 receptor blocker clonidine into the BNST. Furthermore, microinjections of clonidine into the ventral part but not into the dorsal part of the BNST totally block TMT-induced immobility. Immunohistochemical data further demonstrate that the ventral part of the BNST receives intense noradrenergic input.

Taken together, these results demonstrate that the ventral part of the BNST and the neurotransmitter noradrenaline are important parts of the neural pathway mediating TMT-induced fear behavior. The basolateral amygdala, which plays a crucial role in the learning of conditioned fear, is not important for TMT-induced fear, whereas the medial part of the amygdala which receives prominent olfactory input is involved.

## Literature:

Fendt M, Endres T, Apfelbach R (2003) Temporary inactivation of the bed nucleus of the stria terminalis but not of the amygdala blocks freezing induced by trimethylthiazoline, a component of fox feces. *J Neurosci* 23: 23-27.

Hebb AL, Zacharko RM, Gauthier M, Drolet G (2003) Exposure of mice to a predator odor increases acoustic startle but does not disrupt the rewarding properties of VTA intracranial self-stimulation. *Brain Res* 982: 195-210.

*Supported by the German Science Foundation (SFB550/C8).*

## THE INFLUENCE OF FOX ODOR ON THE BEHAVIOR OF NAIVE RATS

**Thomas Endres, Raimund Apfelbach and Markus Fendt**

Tierphysiologie, Zoologisches Institut, Universität Tübingen

Auf der Morgenstelle 28, D-72076 Tübingen, Germany

In the past forty years, a lot of studies investigated the influence of predator odors on the behavior of rats. Most of these experiments were done with odor of cat fur or skin. One conspicuous behavior that was observed during exposure to cat odor was freezing. Freezing is a prominent behavioral sign for anxiety and fear in rats.

Vernet-Maury (1984) showed that trimethylthiazoline (TMT) is the most effective component of the fox feces in inducing behavioral signs of anxiety in rats. Recent studies showed that TMT reliably elicit freezing in naive rats (Wallace and Rosen, 2000; Fendt et al., 2003). In the present study, we characterize the influence of TMT on the behavior of the naive rat with the following experiments:

We measured that the lowest concentration of TMT that can be detected by rats is  $2.5 \times 10^{-9}$  % Vol. (olfactory threshold). II: We found that  $1 \times 10^{-3}$  % Vol. is the lowest dose of TMT that initiate freezing behavior in naive rats (behavioral threshold). III: We showed that there is no between-session habituation after one week with daily TMT exposure. IV: Furthermore, we demonstrated that the acoustic startle response, which is potentiated by anxiety and fear, is increased during TMT exposure. V: In a last experiment we showed that there is a potentiation of anxiety-like behavior in the elevated plus-maze until three days after TMT exposure.

### References

Fendt M, Endres T, Apfelbach R (2003) Temporary inactivation of the bed nucleus of the stria terminalis but not of the amygdala blocks freezing induced by trimethylthiazoline, a component of fox feces. *J Neurosci* 23: 23-28.

Vernet-Maury E, Polak EH, Demael A (1984) Structure-activity relationship of stress-inducing odorants in the rat. *Journal of Chemical Ecology* 10: 1007-1018.

Wallace KJ, Rosen JB (2000) Predator odor as an unconditioned fear stimulus in rats: elicitation of freezing by trimethylthiazoline, a component of fox feces. *Behav Neurosci* 114: 912-922.

*This study is supported by the SFB 550/C8*

**QUANTITATIVE CHANGES OF PARVALBUMIN-, CALBINDIN-D28K- AND CRF-  
IMMUNOREACTIVE NEURONS IN THE HIPPOCAMPUS AND AMYGDALA OF *OCTODON*  
*DEGUS* AFTER EARLY LIFE STRESS**

**K. Becker, C. Helmeke & K. Braun**

*Dept. Zoology/Developmental Neurobiology, Otto von Guericke University, 39118 Magdeburg,  
Germany. e-mail: Katja.Becker@ifn-magdeburg.de*

Early adverse experience results in both physical and psychological alterations. Previous results in the trumpet-tailed rat (*Octodon degus*) pointed out, that early life stress leads to a variety of morphological changes including monoaminergic fiber systems and synaptic densities in cortical and subcortical structures of the limbic system. These experiments showed distinct, region-specific changes of spine densities in the dentate gyrus and in the medial subdivision of the lateral amygdaloid nucleus in early-stressed trumpet-tailed rats (*Octodon degus*). Are these changes of excitatory input accompanied or compensated, respectively, by altered GABAergic modulation and CRF expression in these regions? To test this hypothesis, we determined the impact of early life stress, induced by repeated separation from the parents during the first three postnatal weeks, on the development of inhibitory GABAergic and stress-related CRF-containing neurons (CRF acts as an extra-hypothalamic neuromodulator) in the rodent hippocampus and amygdala. Interneurons were characterized by their content of either calcium-binding protein Parvalbumin or Calbindin-D28k. in 21 day old early stressed and control animals.

**GABAergic interneurons:** The early stressed animals showed significantly lower densities of Parvalbumin-immunoreactive interneurons (down to 85%) in the dentate gyrus and particularly in the molecular layer (down to 59%). Also a reduction of Calbindin-D28k-positive neurons, labeling not exclusively inhibitory local circuit neurons but also granule cells, in this hippocampal subregion was detectable (down to 74%). Accordingly, the decreased excitatory input (lower spine densities) in the dentate granule cells of early stressed animals appears to be compensated by decreased numbers of inhibitory interneurons. In the CA1 region, the increased excitatory input (enhanced spine densities) appears neither to be compensated nor amplified by altered numbers of GABAergic interneurons, since no changes of GABAergic interneurons were detected in this area. Thus, for this hippocampal subregion an overall enhanced neuronal excitability in the early stressed animals could be predicted. The stress-induced neuronal adaptation in the lateral amygdala again differs from that observed in the hippocampal formation. Increased cell densities of Parvalbumin- (up to 395%) and Calbindin-D28k- (up to 327%) immunoreactive neurons were detectable in the basolateral amygdala of early stressed *degus*, where they represent inhibitory local circuit neurons. In contrast, in the central amygdaloid nucleus, where similar to the striatum the labeled neurons represent GABAergic projection neurons, no differences in GABAergic neuron numbers were found between the two animal groups. Accordingly, the decreased excitatory input (decreased spine densities) which was reported for the lateral amygdala appears to be even more downregulated by increased numbers of GABAergic interneurons, from which an overall dampening of neuronal excitability could be expected.

**CRF-containing neurons:** In the hippocampus no differences in CRF-immunoreactive cell densities were detectable in both analyzed subregions. In the basolateral amygdala the number of CRF-immunoreactive neurons was increased (up to 292%), whereas in the central amygdaloid nucleus, which was characterized by dense CRF-positive fibers and terminals, a pronounced decrease of CRF-immunopositive terminal clusters (down to 40%) was observed in the early stressed animals.

Our results provide the first evidence that juvenile emotional experiences induce region- and cell-specific changes of interneurons in the hippocampal formation and the amygdala.

*Supported by a doctoral fellowship to K. Becker and a grant from the state of Saxony-Anhalt*

## EFFECTS OF EARLY DEPRIVATION AND METHYLPHENIDATE TREATMENT ON BEHAVIOR, BRAIN ACTIVITY AND SPINE MORPHOLOGY IN JUVENILE RODENTS (*OCTODON DEGUS*):

S. Zehle, J. Bock & K. Braun

Dept. Zoology/Developmental Neurobiology,  
Otto von Guericke University, 39118 Magdeburg, Germany

e-mail: katharina.braun@nat.uni-magdeburg.de

We have previously shown that early stressful experience can induce behavioral changes such as increased locomotor activity and reduced responses to familiar conspecific vocalizations. These behavioral changes are paralleled by reduced dopaminergic innervation and increased densities of presumptive excitatory spine synapses in prefrontal cortex. Since these changes might resemble hyperactivity and attention deficit syndrome, we performed a pharmacological study in which we applied methylphenidate and tested its effects on behavior, brain activity and brain morphology.

Stressful experience was applied by one hour separation of *Octodon degus* pups from their parents once daily from postnatal day (PND) 1 until 21. Open field tests on PND 22 confirmed the development of increased locomotor activity (running, rearing, jumping) in stressed animals, as well as an increase in the distance moved in the center of the arena and a higher amount of defecation. Methylphenidate (MP) (doses 1, 5, 10mg/kg) treatment lead to a dose dependent increase of locomotor activity in both groups. In parallel experiments brain activity patterns during MP treatment were measured using the  $^{14}\text{C}$ -2-fluoro-2-deoxyglucose (2-FDG) autoradiography on PND 22. These studies revealed an increased metabolic activity in distinct cortical and subcortical brain areas, such as the prefrontal cortex, striatum and nucleus accumbens. Parallel analysis of experience and pharmacologically induced changes of spine density and morphology are currently performed for the anterior cingulate cortex.

The presented data demonstrate that the observed behavioral effects of an acute MP-treatment are paralleled by alterations of brain activity in relevant brain areas.

Supported by DFG/SFB426 & doctoral fellowship from the OvG-Uni. to S.Z.

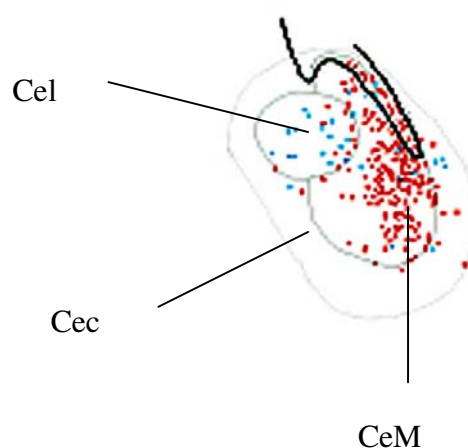
### **Divergent projections of the central nucleus of the amygdala to the substantia innominata and the magnocellular pontine nucleus of the rat**

D.M. Yilmazer-Hanke, R. Fritz, T. Roskoden, H. Schwegler, R. Linke  
 Institut für Anatomie, Otto-von-Guericke Universität, D-39120 Magdeburg  
 e-mail: deniz.yilmazer-hanke@medizin.uni-magdeburg.de

The central nucleus of the amygdala (CeA) is generally regarded as a control nucleus of subcortical target systems. Due to its widespread projections to different brain areas it is able to modulate the emotional behavior of the organism. Among the target areas of the CeA, the substantia innominata (SI) mediates arousal reactions, whereas the caudal pontine reticular nucleus (PNC) receives nociceptive spinal afferents and modulates the somatomotor output including postural changes and the startle response. However, it is still not clear whether single neurons of the CeA project to different areas or to one target area. In the present study, injections of the retrograde tracers Fluorogold and True Blue into the target areas of the CeA, the SI and PNC of the Wistar rat, revealed overlapping but otherwise distinct neuronal populations mainly within the medial division of the CeA. Moreover, topographically distinct injections of True Blue into the PNC resulted in a different retrograde labeling pattern in the medial division of the CeA. Injections into the lateral PNC medioventral to the trigeminal motor nucleus and dorsal to the superior olive gave rise to much less retrogradely labeled neurons in the CeA as compared to more caudal and medial injections. The non-collateralization of axons terminating in the SI and PNC is in marked contrast to extensive double labeling of CeA projection neurons following injections into some other target regions of the CeA, i.e. the dorsal motor nucleus of vagus (DMV) and PNC. From our study we conclude that the SI and PNC receive input from separate subsets of amygdala neurons, and therefore the CeA may be able to separately activate the SI and PNC.

This study was supported by the DFG SFB 426, TP B4.

### **Distribution of Retrogradely Labeled Neurons in the Central Nucleus of Amygdala**



blue spots	=	Fluorogold injection into the substantia innominata
red spots	=	True Blue injection into the caudal pontine reticular nucleus

**Localization of activity-related cytoskeletal protein in dendrites of hippocampal neurons activated by behavioral tasks.**

Olga Levai and Michael E. Calhoun

Department of Cellular Neurology, Hertie-Institute for Clinical Brain Research, University of Tübingen, Otfried-Müller-Str. 27, D-72076 Tübingen, Germany

Synaptic activity at individual dendritic spines results in a wide array of structural and biochemical changes, thus forming the basis for long-term memory as originally postulated by Hebb. Studies inducing changes in synaptic strength through electrical or pharmacological stimulation have provided valuable information about molecular mechanisms, new synapse formation, and morphological changes within existing pre- and post-synaptic elements. However research on dendritic plasticity *in-vivo* has been limited by the lack of activity-related markers to localize plastic zones within the complex dendritic structure of individual neurons. We have, with colleagues, been able to demonstrate that activity-related cytoskeletal protein (Arc) is specifically localized to recently-activated dendritic spines in the dentate gyrus following perforant-path stimulation. Together with techniques to non-invasively visualize dendritic structure and plasticity-related gene expression, we here demonstrate *in-vivo* localization of Arc protein in the dendritic tree of hippocampal neurons specifically activated by behavioral tasks. Following activation, individual neurons rapidly express Arc, and both the mRNA and protein show a distinct time-course and localization within dendritic compartments. These results indicate that immunostaining for Arc protein can be used to identify recently-activated spines, with broad implications for study of neural computation and the parallel structural and molecular changes underlying learning and memory.

## **EFFECTS OF ALOPREGNANOLONE INJECTED INTO THE MEDIAL PRE-FRONTAL CORTEX IN THE PLUS MAZE TEST IN RATS**

Casteller, G.<sup>1,2</sup>; Laconi, M.<sup>2</sup>; Fraile, M.<sup>1</sup>; Melonari, P.<sup>1</sup>; Olguin, M.<sup>1</sup>; Llano, L.<sup>1</sup>; Taley, S.<sup>1</sup>; Tarrazó, M.F.<sup>1</sup>; Landa, A.<sup>1</sup>; Cabrera, R.J.<sup>2</sup>; Gargiulo, P.A.<sup>1</sup>

1. Lab. Neuroc. Psicol. Exp. (IMBECU-CONICET). Dep. Patol. F.C.M. U.N. de Cuyo. Cát. Psicopatol. FHCE. U. Católica Argentina. C.C. 7, 5500. Mendoza. Argentina.
2. Lab. Invest. Neuroq. Comport. Neuroendocr. (LINCE-IMBECU-CONICET). F.C.M. U.N. de Cuyo.

The medial Pre-Frontal Cortex (mPFC) projects to the Nucleus Accumbens Septi (Acc), and these projections has been implicated in emotional driving. In previous reports, we have communicated that glutamatergic transmission within Acc modulates anxiety. Additionally, we have previously reported the action of intracerebroventricular administration of Allopregnanolone (ALL) induces an anxiolytic like effect in rats in the plus maze test. The aim of the present work is to study the behavioral action of ALL in male rats bilaterally cannulated into the mPFC in the plus maze test. Rats were divided in three groups (n=8-13). They received either 1 µl injections of Krebs solution or ALL (0.06 or 0.06 mM). Time spent into the open arm and the time spent in the distal extreme of the open arm were significantly increased by both doses ( $p<0.001$ ) when compared with controls. Open arm entries were increased by the lower ( $p<0.001$ ) and the higher ( $p<0.05$ ) doses. Closed arm entries were increased only by the lower dose ( $p<0.05$ ). No differences were seen in the quotient time spent in the open arm / number of entries to the open arm. All these results show that ALL has an anxiolytic-like effect, and a disinhibitory action when injected into the mPFC. We conclude that present results show a new modulatory action of ALL in mPFC mediating anxiety levels in male rats, and also an important evidence about the role of forebrain structures in the mediation of anxiety.

Supported by Grants of Volkswagen Foundation (Germany) and Secretary of Science and Technology, National University of Cuyo (Argentina).

## **EFFECTS OF METOPROLOL INJECTED INTO THE NUCLEUS ACCUMBENS SEPTI IN THE PLUS MAZE TEST IN RATS**

Melonari, P.; Olguin, M.; Fraile, M.; Llano, L.; Taley, S.; Tarrazó, M.F.; Casteller, G.; Landa, A.; Gargiulo, P.A.

Lab. Neuroc. Psicol. Exp. (IMBECU-CONICET). Dep. Patol. F.C.M. U.N. de Cuyo. Cát. Psicopatol. FHCE. U. Católica Argentina. C.C. 7, 5500. Mendoza. Argentina.

The Nucleus Accumbens Septi (Acc) has been extensively studied because of its role in several behavioral processes, like locomotion, stereotypies, reward and cognitive functions, such as learning, memory and visual discrimination. In previous reports we have communicated that glutamatergic transmission within Acc modulates anxiety. The aim of the present work is to study the behavioral action of  $\beta$ -adrenergic antagonist metoprolol in male rats bilaterally cannulated into the Acc using the plus maze test. The rats were divided in three groups (n=15) that received either 1  $\mu$ l injections of saline or metoprolol (0.5 and 1.0  $\mu$ g). Time spent into the open arm was significantly increased by the lower ( $p<0.05$ ) and the higher ( $p<0.001$ ) doses when compared with saline controls. A dose-response curve was observed, with significant difference between 0.5 and 1.0  $\mu$ g ( $p<0.001$ ). These results suggests a specific action on the behavioral display. Open arm entries and closed arm entries were not modified by the treatment. The quotient time spent in the open arm / number of entries to the open arm was significantly increased by the higher dose ( $p<0.05$ ). Presents results show that metoprolol has an anxiolytic-like effect when injected into the Acc. We conclude that present results show a new and important evidence about the role of  $\beta$ -adrenergic mediation of anxiety levels in the Acc.

Supported by Grants of Volkswagen Foundation (Germany) and Secretary of Science and Technology, National University of Cuyo (Argentina).



## **Silicon chip with capacitors and transistors for interfacing organotypic brain slice of rat hippocampus**

M. HUTZLER, P. FROMHERZ

Max Planck Institute of Biochemistry, Martinsried, Germany

In the past, field potentials of cultured hippocampal slices evoked by tungsten electrode stimulation could be recorded by electrolyte-oxide-silicon field effect transistors. We developed a new silicon chip with a  $\text{TiO}_2$ -coated surface, containing capacitor arrays for eliciting as well as transistor arrays for detecting neuronal activity. After cultivating the brain slices on the silicon chips for one week, we were able to capacitively stimulate the slices in CA3 by application of defined voltage pulses. The resulting field potential in CA1 could be recorded with the transistors and its amplitude described by a mathematical sheet conductor model. By combining a row of capacitors with a row of transistors we determined a simple transfer matrix from CA3 to CA1. Preliminary experiments indicate that induction of Long Term Potentiation and Depression is also possible with the chip. This novel type of purely capacitive interfacing allows a mechanically noninvasive and electrically minimally interfering contact compared to traditional electrophysiological methods.

# **Hippocampal enlargement in nectar-feeding mammals**

**Ursula Kaupert and York Winter**

University of Munich, Department of Biology and Max-Planck Institute for Ornithology,  
Seewiesen

The evolution of behavioural competences is constrained by the possibilities, limitations and trade-offs between neural mechanisms and brain design. We examined the phylogenetic pattern of brain evolution in an ecologically unique group of mammals: tropical bats feeding on the nectar of flowers. This involves the hippocampus, which in mammals has a central function in the processing of spatial and episodic-like memory content. The analysis of phylogenetically corrected brain measurements and trophic niche data revealed that flower-visiting species in the Neotropical bat family Phyllostomidae from three different subfamilies exceeded by 50% up to a 100% in relative hippocampal size the carnivorous/insectivorous members of the same taxonomic group. This hippocampal hypertrophy surpasses values reported for any other group of closely related mammals. It suggests a specialized cognitive adaptation to a trophic niche where spatio-temporal dynamics maintain resources (flower nectar) in continuous but tractable change and where behavioural optimisation should depend on rapid spatial learning and memory. The specific behavioural competences gained from hippocampal enlargement and the trade-offs involved, however, remain open questions.

## Field potentials of acute brain slices recorded with field effect transistor array

Christian Stangl, Peter Fromherz

*Max-Planck-Institut für Biochemie, Abteilung Membran- und Neurophysik, Am Klopferspitz 18, D-82152 Martinsried. (email: stangl@biochem.mpg.de)*

Electrical coupling of acute brain slices with field effect transistor arrays afford a novel approach in investigating the brain. Whereas in [1] *cultured* slices has been used, the innovation of this study is the successfully coupling of *acute* slices of rats and mice with transistor chips.

Dead cell layers at the surface of the slices caused by cutting procedure complicate basically the coupling with transistors. This effect was investigated by a computer based simulation, which examines the distribution of evoked field potentials within the slice. The calculated profiles of neural field potentials could be confirmed by measurements with conventional extracellular microelectrodes.

The electrical coupling of acute hippocampus slices with field effect transistor chips admitted successful experimentations on acute hippocampus slices. Anticipated distributions of field potentials could be verified as well as projections from CA3 to CA1 via Schaffer collateral. This non-invasive novel technique also permitted studying the plasticity of the hippocampus slices by LTP experiments.

[1] Besl B., Fromherz P. Transistor array with an organotypic brain slice: field potential records and synaptic currents. Eur. J. Neurosci. 15, 2002, pp. 999-1005

**Poster Subject Area #PSA17:  
Learning and Memory**

- [#231A](#) O. Wiegert, M. Joëls and HJ. Krugers, Amsterdam (NL)  
*Corticosterone both facilitates and hampers NMDA-receptor-dependent synaptic plasticity*
- [#232A](#) F. Locatelli, G. Bundrock and U. Müller, Berlin and Saarbrücken  
*Functional role of the neurotransmitter glutamate in CNS of *Apis mellifera**
- [#233A](#) F. Hutzler, J. Bergmann, M. Conrad, M. Kronbichler, P. Stenneken and AM. Jacobs, Berlin and Salzburg (A)  
*Electrophysiological correlates of reading: Item based analysis of ERP data*
- [#234A](#) I. Plekhanova and U. Müller, Berlin and Saarbrücken  
*FUNCTION OF THE MAPK p44/42 AND MAPK p38 IN LONG-TERM MEMORY FORMATION*
- [#235A](#) A. Froese, N. Stollhoff and D. Eisenhardt, Berlin  
*AmCREB in memory consolidation of the honeybee (*Apis mellifera*)*
- [#236A](#) B. Komischke, M. Strube and J-C. Sandoz, Berlin and Toulouse (F)  
*Honeybees (*Apis mellifera*) build configurations between olfactory stimuli and the perceiving antennae*
- [#237A](#) G. Grah, D. Heß, R. Wehner and B. Ronacher, Berlin and Zürich (CH)  
*How do desert ants locate the position of a food source in 3-D?*
- [#238A](#) C. Huchzermeyer, P. Husemann, C. Lieshoff and H-J. Bischof, Bielefeld  
*Zenk and Fos Expression in Adult Zebra Finch Males After Presenting Learned and Non-learned Stimuli*
- [#239A](#) Y. Freund, D. Hupfeld and KP. Hoffmann, Bochum  
*The differences in horizontal optokinetic nystagmus between albino wistar and pigmented Long Evans rats are not correlated with their ability of movement detection*
- [#240A](#) T. Kirschstein, J. Chen, AJ. Becker and H. Beck, Bonn  
*Loss of metabotropic glutamate receptor-dependent LTD via downregulation of mGluR5 following status epilepticus*
- [#241A](#) S. Klein, K. Schwabe and M. Koch, Bremen  
*Neonatal lesions of the rat medial prefrontal cortex together with pubertal phencyclidine treatment affect spatial behaviour but not sensorimotor gating*

- [#242A](#) SR. Ott, A. Philippides, MR. Elphick and M. O'Shea, Brighton (UK) and London (UK)  
*Model of nonsynaptic integration by spatially segregated nitric oxide sources and targets in the locust mushroom body*
- [#243A](#) F. Kreul and R. Schmidt, Gießen  
*Functional redistribution of ependymin cell adhesion molecules after learning of an active shock avoidance task in fish*
- [#244A](#) S. Schneider and R. Schmidt, Gießen  
*Detection of mammalian ependymin-related protein (MERP) transcripts in mouse brain and investigation of a possible involvement in memory formation*
- [#245A](#) E. Ofek and H. Pratt, Haifa (IL)  
*Distracting effect of emotionally significant stimuli on cognitive brain activity: Electrophysiological functional brain imaging*
- [#246A](#) A. Dityatev, O. Bukalo, AYW. Lee, B. Salem, JWS. Law, M. Schweizer and M. Schachner, Hamburg  
*Impaired synaptic plasticity in mice conditionally deficient in neural cell adhesion molecule NCAM is restored by elevation of extracellular Ca<sup>2+</sup> concentration*
- [#247A](#) T. Celikel, V. Marx and R. Sprengel, Heidelberg  
*Phosphorylation of GluR-A containing neocortical AMPA receptors is required for intact object recognition*
- [#248A](#) AV. Egorov, K. Unsicker and O. von Bohlen und Halbach, Heidelberg  
*Persistent activity in basolateral amygdala neurons*
- [#249A](#) S. Laudenklos, T. Celikel and P. Osten, Heidelberg  
*The role of excitatory neurons in supragranular layers for the acquisition of a whisker dependent learning task*
- [#250A](#) G. Schmitz, P. Vogt and O. Bock, Köln  
*Transfer of sensorimotor adaptation between sensory modalities.*
- [#251A](#) M. Girgenrath and O. Bock, Köln  
*CORRELATION BETWEEN PERFORMANCE IN A SENSORIMOTOR ADAPTATION TASK AND FRONTAL-EXECUTIVE CONTROL IN ELDERLY*
- [#252A](#) L. Marshall, M. Mölle, K. Laske, S. Gais and J. Born, Lübeck  
*Transcranial direct current stimulation improves a visual discrimination skill*
- [#253A](#) D. Domenger, Z. Dincheva and RKW. Schwarting, Marburg  
*Analysis of instrumental sequential behavior in the rat*

- [#254A](#) M. Wöhr, A. Borta and RKW. Schwarting, Marburg  
*Sounds in silence I: Rat ultrasound vocalization during fear conditioning - a dose/response study*
- [#255A](#) A. Borta, M. Wöhr and RKW. Schwarting, Marburg  
*Sounds in silence II: Individual differences in ultrasound vocalization and freezing during fear conditioning*
- [#256A](#) K. Neuser, J. Husse, P. Stock and B. Gerber, Würzburg  
*Appetitive olfactory learning in Drosophila larvae: Testing for effects of training amount, reinforcer intensity, age, gender, assay type, and memory span*
- [#257A](#) B. Michels, S. Diegelmann, H. Tanimoto, I. Schwenkert, E. Buchner and B. Gerber, Würzburg  
*A ROLE FOR SYNAPSIN IN ASSOCIATIVE LEARNING: THE DROSOPHILA LARVA AS A STUDY CASE*
- [#258A](#) T. Riemensperger, E. Buchner and A. Fiala, Würzburg  
*Neuronal activity of dopaminergic cells in the Drosophila brain analyzed by optical calcium imaging*
- [#259A](#) M. Boyer and R. Wehner, Zurich (CH)  
*Ant navigation: can landmark-based routes be reversed?*
- [#260A](#) F. Loertscher and R. Wehner, Zurich (CH)  
*Landmark-based route memories in desert ants, Melophorus bagoti : can sequentially acquired landmark memories be retrieved at any point of the sequence?*
- [#231B](#) S. Uzakov, JU. Frey and V. Korz, Magdeburg  
*Cognitive reinforcement of rat hippocampal LTP*
- [#232B](#) S. Navakkode, S. Sajikumar and JU. Frey, Magdeburg  
*The effect of rolipram, a type IV-specific phosphodiesterase inhibitor, on distinct forms of long-term depression and 'synaptic tagging'*
- [#233B](#) S. Sajikumar, S. Navakkode and JU. Frey, Magdeburg  
*In search for the specificity of 'synaptic tags' during LTP and LTD*
- [#234B](#) A. Albrecht, J. Bergado, H-C. Pape and O. Stork, Magdeburg  
*Generalisation of conditioned fear in mice deficient for the neural cell adhesion molecule NCAM*
- [#235B](#) T. Ahmed and JU. Frey, Magdeburg  
*Compartmentalized modulation of PDE4B isotypes and cAMP-levels during long-term potentiation in rat hippocampal slices in vitro*

- [#236B](#) W. Wetzel and D. Balschun, Magdeburg  
*Enhancement of spatial memory retention following posttraining allosteric potentiation of the metabotropic glutamate receptor subtype 5 (mGluR5)*
- [#237B](#) S. Schäble, G. Poeegel, K. Braun and M. Gruss, Magdeburg and Leipzig  
*The impact of juvenile stress exposure and pre-experience on shuttle box learning in adult rats: involvement of the dopaminergic system.*
- [#238B](#) C. Roth-Alpermann, RGM. Morris, T. Bonhoeffer and M. Korte, Martinsried and Edinburgh (UK)  
*Fast homeostatic control of synaptic potentiation in the adult hippocampus*
- [#239B](#) Y. Winter, J. Ludwig, U. Kaupert and H-U. Kleindienst, Munich and Seewiesen  
*Rodent cognition in virtual reality: time dynamics of place and spatial response learning by mice on a servosphere virtual maze*
- [#240B](#) KP. Stich and Y. Winter, München and Seewiesen  
*Foraging in a complex naturalistic environment: Capacity of spatial working memory in flower visiting bats*
- [#241B](#) Y. Winter, S. von Merten and H-U. Kleindienst, München and Seewiesen  
*Visual landmark orientation by flying bats at a large-scale touch and walk screen for bats, birds and rodents*
- [#242B](#) A. Oppelt, D. Tafur, KP. Stich and Y. Winter, München  
*Echoacoustic object generalization and spatial dependence of two-alternative forced-choice (2AFC) learning set acquisition in bats*
- [#243B](#) A. Siegmund and CT. Wotjak, Munich  
*Sensitisation of C57BL/6N mice: a proposed mouse model of PTSD*
- [#244B](#) H. Adelsberger, JZ. Tsien and A. Konnerth, München and Boston, MA (USA)  
*Superior spatial learning abilities of NR2B transgenic mice in a new labyrinth task*
- [#245B](#) K. Holthoff, Y. Kovalchuk, R. Yuste and A. Konnerth, München and New York, NY (USA)  
*Single-shock synaptic plasticity induced by local dendritic spikes*
- [#246B](#) A. Kaiser, Planegg-Martinsried  
*Adult neurogenesis is present in the rostral migratory stream but not in the dentate gyrus of the nectar-feeding bat *Glossophaga soricina**
- [#247B](#) R. Gagné and S. Gagné, Quebec (CDN)  
*Creating Mental Representations using the Spatial Dimension of Dendrite Trees*

- [#248B](#) H. Aonuma, M. Iwasaki, C. Katagiri and A. Delago, Sapporo (J)  
*Role of NO/cGMP signaling during formation of social hierarchy in the cricket*
- [#249B](#) J. Thiele and Y. Winter, München and Seewiesen  
*Knowledge base for complex behaviours in Nature: Spatial memory based foraging of nectar-feeding bats on a computer simulated artificial flower field in the rain forest*
- [#250B](#) M. Tamosiunaite, B. Porr and F. Wörgötter, Glasgow (UK) and Stirling (UK)  
*How learning influences itself: The recurrent dependence of membrane potential shapes and synaptic plasticity*
- [#251B](#) J. Schweimer and W. Hauber, Stuttgart  
*Involvement of the Rat Anterior Cingulate Cortex in Control of Instrumental Responses Guided by Reward Expectancy*
- [#252B](#) N. Neumann, AM. Dubischar-Krivec, C. Braun, S. Bölte, F. Poustka and N. Birbaumer, Tübingen, Frankfurt/Main and Trento (I)  
*Recognition memory in autistic savants: an MEG study*
- [#253B](#) CF. Plappert, S. Kuhn, H-U. Schnitzler and PKD. Pilz, Tübingen  
*Prepulse Inhibition of the Acoustic Startle Response increases during repetitive testing*
- [#254B](#) S. Schmid and M. Weber, Tübingen and Würzburg  
*Altered short-term plasticity is responsible for the depression of burst responses in the startle mediating neurons of the rat pontine reticular formation*
- [#255B](#) C. Schlumberger, PKD. Pilz, K. Becker, C-M. Becker, H-U. Schnitzler and CF. Plappert, Tübingen and Erlangen  
*Sensory and Behavioral Changes in Glycine-Receptor deficient spa Mice*
- [#256B](#) Y. Jin, S. Gillner and HA. Mallot, Tübingen  
*How are eye movements involved in landmark recognition?*
- [#257B](#) N. Becker, H. van der Putten, H-U. Schnitzler and S. Schmid, Tübingen and Basel (CH)  
*The role of mGluR8 in synaptic plasticity in the lateral amygdala*
- [#258B](#) A. Schnee, H. Dahmen, C. Hölscher and HA. Mallot, Tübingen and Coleraine (UK)  
*Investigating rat spatial behavior in virtual environments*
- [#259B](#) P. Lohmann, C. Lange-Asschenfeldt and MW. Riepe, Ulm  
*Induced hippocampal long-term potentiation correlates with early spatial learning performance in male CD-1 mice*



**Corticosterone both facilitates and hampers NMDA-receptor-dependent synaptic plasticity**

O Wiegert, M. Joëls, H. J. Krugers

Swammerdam Institute for Life Sciences, Universiteit van Amsterdam.

Secretion of the adrenal hormone corticosterone (CORT) is enhanced during and after exposure to stressful situations. Corticosteroid-hormones modulate brain function via the local mineralo- and glucocorticoid receptors (MR and GR respectively). These receptors differ o.a in affinity for corticosterone (i.e the GR has a 10-fold lower affinity for corticosterone than the MR).

Corticosterone has been reported both to facilitate and impair learning and memory processes. The context and timing of corticosterone appears to be relevant for these positive and negative effects. Using a reductionistic approach we addressed this issue at the cellular level, and examined how timing of corticosterone application affects synaptic plasticity. Therefore mouse hippocampal slices were treated with corticosterone (100 nM) or vehicle and synaptic plasticity was examined during corticosterone application or 1-4 hrs later. Our results reveal that NMDA-receptor-dependent synaptic plasticity is hampered 1-4 hours after corticosterone application, but facilitated when corticosterone is applied during high frequency stimulation. Current studies address the question which corticosteroid receptors are involved.

Olof Wiegert

owiegert@science.uva.nl

**Functional role of the neurotransmitter glutamate in CNS of *Apis mellifera***

Fernando Locatelli<sup>1</sup>, Gesine Bundrock<sup>1</sup> & Uli Müller<sup>1,2</sup>

<sup>1</sup> Institut für Neurobiologie, Freie Universität, Berlin

<sup>2</sup> Zoologie-Physiologie, Universität des Saarlandes, Saarbrücken

Previous works aimed at studying the role of the neurotransmitter glutamate in learning and memory in *Apis mellifera* were based on interfering glutamate recycling. These works lead to controversial interpretations of glutamate function, since different drugs that are expected to block glutamate recycling demonstrated somehow opposite effects on memory, either amnesic or facilitatory.

In order to find an explanation for this controversy, we tested the effectiveness of the drugs to modulate glutamate levels. Given also the quite opposite effects of some of these drugs in memory and the tight relation between glutamate and GABA metabolisms, effect of the drugs on both neurotransmitters were tested.

Glutamate and GABA levels were measured in CNS after injection of drugs reported to induce the amnesic and the facilitatory effects: a) inhibitors of plasma-membrane glutamate transporters, which are directly involved in removing glutamate from the synaptic cleft; b) inhibitors of the enzyme glutamine-synthetase, which converts glutamate into glutamine in glial cells and constitutes a critical step in glutamate re-uptake. Results demonstrate that while drugs reduce glutamate levels in the insect brain, both kinds of drugs induce opposite changes in GABA levels, probably explaining the reported differential modulation of learning processes.

In order to gain specificity, temporal and spatial resolution, we designed an alternative pharmacological approach based in the photo-release of glutamate at specific brain sites. The role of glutamate was evaluated in a non associative form of learning, the habituation of proboscis extension reflex by repetitive sucrose-stimulation of the antennae. Animals were injected systemically either vehicle or caged-Glutamate and neurotransmitter release was induced by light-flashes directed either to the mushroom bodies, or antennal lobes (AL). Glutamate release was assessed at different times respect to the stimulation protocol in order to evaluate a role of the neurotransmitter in habituation and dishabituation processes. Results showed that glutamate release into the contra-lateral AL respect to the stimulated antennae enhances the dishabituating effect of sucrose stimulation of the contra-lateral antennae.

This result constitutes the first direct evidence of a functional role of glutamate in CNS in *Apis mellifera* and suggests a role of this neurotransmitter in the sucrose signaling pathway. The observation that the effects were observed only after stimulation of specific brain sites and in precise temporal relation with the stimuli, argues in favor of the photo-release of glutamate as an effective and precise tool to further study the functional role of glutamate in CNS of insects.

*Supported by DAAD, Fundacion Antorchas and SFB-515(DFG).*

Keywords: Glutamate, GABA, honeybee, learning, photo-release

## Electrophysiological correlates of reading: Item based analysis of ERP data

Florian Hutzler<sup>1</sup>, Jürgen Bergmann<sup>2</sup>, Markus Conrad<sup>1</sup>, Martin Kronbichler<sup>2</sup>, Prisca Stenneken<sup>1</sup>, Arthur Jacobs<sup>1</sup>

<sup>1</sup>Freie Universität Berlin

<sup>2</sup>University of Salzburg

**Corresponding author:** Florian Hutzler, Allgemeine Psychologie, Fachbereich Erziehungswissenschaft und Psychologie, Freie Universität Berlin, Habelschwerdter Allee 45, 14195 Berlin, [fhutzler@zedat.fu-berlin.de](mailto:fhutzler@zedat.fu-berlin.de)

In an event-related potential (ERP) experiment the time course of the behaviourally well-documented [1, 2, 3, 6, 7, 8, 9, 10] inhibitory effect of first syllable-frequency during lexical access was examined by means of a novel, item based analysis. During a lexical decision paradigm, response times to words with high-frequency first syllables were longer than those to words with low-frequency first syllables and resulted in more negative ERPs in an early time window from 190-280 ms and in the N400 component. Of theoretical relevance is that the observed effect of first syllable-frequency was prior to onset of the effect of lexicality (i.e., the first reliable differentiation in ERP waveforms in response to words and pseudowords, a potential marker of lexical access). The present study's results do not only support Barber et al.'s [5] notion of the prelexical nature of the first syllable frequency effect by providing evidence for electrophysiological correlates of first syllable-frequency in another, non-Romance orthography (i.e., German) but also strengthens this pattern of results by additionally introducing a novel, item based analysis of ERP data. Whereas the item-based approach is commonly used in the analysis of response times, to our knowledge, item-based analysis of ERP data was not reported before. Implications of the prelexical nature of the inhibitory first syllable-frequency effect for computational models of reading, specifically for Ans et al.'s [4] multiple-trace memory (MTM) model of reading are discussed.

- [1] Álvarez, C.J., Carreiras, M. and de Vega, M., Syllable-frequency effect in visual word recognition: Evidence of sequential-type processing, *Psicológica*, 21 (2000) 341-374.
- [2] Álvarez, C.J., Carreiras M. and Taft M., Syllables and morphemes: Contrasting frequency effects in Spanish, *J. Exp. Psychol. Learn.*, 27 (2001) 545-555.
- [3] Álvarez, C.J., de Vega M. and Carreiras M., The syllable as an activational unit in reading trisyllabic words, *Psicothema*, 10 (1998) 371-386.
- [4] Ans, B., Carbonnel, S. and Valdois, S., A connectionist multiple-trace memory model for polysyllabic word reading, *Psychol. Rev.*, 105 (1998) 678-723.
- [5] Barber, H., Vergara, M. and Carreiras, M., Syllable-frequency effects in visual word recognition: evidence from ERPs, *Neuroreport*, 15 (2004) 545-548.
- [6] Carreiras, M., Alvarez, C.J. and de Vega, M., Syllable frequency and visual word recognition in Spanish, *J. Mem. Lang.*, 32 (1993) 766-780.
- [7] Conrad, M. and Jacobs, A.M., Replicating syllable-frequency effects in Spanish in German: One more challenge to computational models of visual word recognition, *Lang. Cognitive Proc.*, (in press).
- [8] Perea, M. and Carreiras, M., The effects of syllable frequency in identification tasks, *Psicológica*, 16 (1995) 483-496.
- [9] Perea, M. and Carreiras, M., The effects of syllabic frequency and orthographic neighborhood on the pronunciation of words and pseudo words, *Psicológica*, 17 (1996) 425-440.
- [10] Perea, M. and Carreiras, M., Effects of syllable frequency and syllable neighborhood frequency in visual word recognition, *J. Exp. Psychol. Hum. Percept. Perform.*, 24 (1998) 134-144.

## FUNCTION OF THE MAPK p44/42 AND MAPK p38 IN LONG-TERM MEMORY FORMATION

Irina Plekhanova<sup>1</sup> and Uli Müller<sup>2</sup>

<sup>1</sup>Dept. of Neurobiology, Freie Universität Berlin, Germany

<sup>2</sup>Dept. 8.3 - Biosciences Zoology, Saarland University, Saarbrücken, Germany

Mitogen-activated protein kinases (MAPKs), or extracellularly-regulated kinases (ERKs), are components of cascades mediating growth, proliferation, apoptosis and differentiation but also stress in mammalian cells. The cascades are organized hierarchically into three modules that are activated by distinct stimuli and signal inputs. External signals activate the MAPKs via kinases that activate each other. A module that mediates inputs from growth factors, cytokines and stress factors such as ultraviolet radiation and heat shock is the Ras/Raf/MEK/ERK cascade.

In rats and mice it has been demonstrated that MAPK activity is required for induction of long-term potentiation (LTP) in the hippocampus and also required for formation of long-term memory (LTM) in fear conditioning tasks. Studies in *Aplysia* show that activation of MAPK is important for long-term facilitation but not necessary for short-term facilitation.

The goal of this work is to investigate the role of the MAPK-cascade in honeybee associative learning and hence in LTM formation. In a first step we tested whether mammalian antibodies against different members of the MAPK family can be used to identify the corresponding members in the honeybee brain.

In a behavioral assay we tested whether blocking MEK interferes with learning and memory formation. Our results show that inhibition of MEK activity during and shortly after learning impairs long-term memory formation but does not affect learning, short- and mid-term memory. A significant increase in the relative phosphorylation of the MAPK in the mushroom bodies 40 minutes after training was observed only in forward-conditioned animals (measured by ELISA).

These findings suggest that MAPK, localized in mushroom bodies, may play a crucial role in LTM formation.

*Supported by DFG-GK 120-3*

Keywords: MAPK, ERK, learning and memory

## **AmCREB in memory consolidation of the honeybee (*Apis mellifera*)**

Anja Froese, Nicola Stollhoff & Dorothea Eisenhardt

Freie Universität Berlin, FB Biologie/Chemie/Pharmazie. Institut für Biologie,  
Neurobiologie, Königin-Luise-Straße 28/30, 14195 Berlin,

The transcription factor CREB (cAMP response element binding protein) is required for the switch from short-term to long-term synaptic plasticity and from short-term to long-term memory. It is believed to mediate this switch by inducing gene expression that underlies the formation of long-term synaptic plasticity and long-term memory. CREB is phosphorylated by several kinases, like PKA, PKC, CaMKIV and MAPK at a conserved consensus phosphorylation site (Ser 133) in the kinase inducible domain (=KID domain) of the protein. This phosphorylation is necessary for its activation and the expression of its target genes.

We want to analyze the role of CREB in memory consolidation of the honeybee. Hence we identified several CREB homologs, AmCREB 1-8, from the honeybee central brain. We characterized commercially available CREB-antibodies. Three antibodies detect different epitopes in the AmCREB proteins and are used to identify different AmCREB proteins in the honeybee brain. One antibody detects AmCREB phosphorylation in the KID-domain of the AmCREB variants. Using this antibody we are examining AmCREB activation at different time points after learning.

Supported by the Deutsche Forschungsgemeinschaft and the VW Stiftung

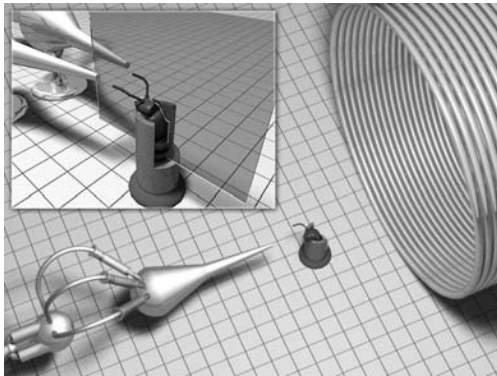
## Honeybees (*Apis mellifera*) build configurations between olfactory stimuli and the perceiving antennae

Bernhard Komischke (1), Martin Strube (1) & Jean-Christophe Sandoz (2)

(1) AG Neurobiologie, FU Berlin

(2) Centre de Recherches sur la Cognition Animale, Université Paul Sabatier Toulouse

Foraging honeybees orientate on olfactory cues produced by flowers as coevolutionary partners. This kind of orientation might depend only on the perception of one antenna as it does in Lepidoptera, because the animal is moving in an olfactory space. Another possibility could be a building of a configuration between the perceived olfactory cues of both antennae in a given time point. Therefore the animal has to compare odors between both antennae.

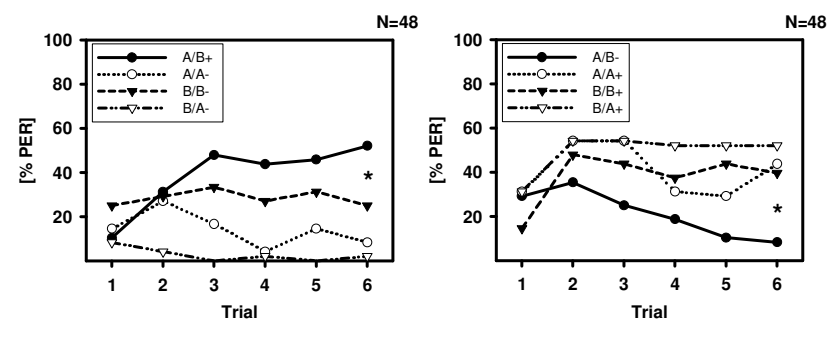


To investigate this hypothesis bees have been trained with different odors on both antennae simultaneously in a proboscis extension reflex (PER) conditioning (see figure 1). The antennae were separated by use of a little plastic foil, fixed with low temperature melting wax on the bees' heads (fig. 1). To be sure that the bees use olfactory information of both head sides, they had to discriminate a combination of odor A given to the left antenna and odor B given simultaneously to the right antenna (A/B) from B/A and from A/A and B/B.

Bees are indeed able to fulfil such a task (see figure 2).

They distinguish the combination A/B from the other stimuli if it is reinforced as well as it is non-reinforced (fig. 2). Therefore bees have to be able to build a configuration between different odors given simultaneously to both antennae. Our data show for the first time a configuration of stimuli within the olfactory modality which has to be established on the level of the mushroom bodies of the honeybee brain, because olfactory information coming from different antennae does not converge on a lower proceeding level of the bee brain.

Experiment 1: A/B vs. B/A, A/A & B/B



In the next step we tried to show, that bees are able to learn such a configuration also during an operant conditioning using free flying bees. In this experimental setup, animals have to walk through little tubes in which they are confronted with two different odors, one is given to the right antenna, the other to the left antenna simultaneously. In a first experiment using this experimental setup, bees had to discriminate A left / B right from B left / A right. Nearly half of the animals are able to learn to chose the right olfactory combination by entering the tube offering the reinforced combination (A/B) and therefore avoiding another tube offering the non-reinforced combination (B/A).

Further investigations will follow, which combine operant conditioning with the classical PER conditioning as a test to ensure, that bees learn about both olfactory stimuli also during free flight in an operant conditioning.

## How do desert ants locate the position of a food source in 3-D?

Gunnar Grah<sup>1</sup>, Doreen Heß<sup>1</sup>, Rüdiger Wehner<sup>2</sup>, Bernhard Ronacher<sup>1</sup>

<sup>1</sup> Department of Biology, Humboldt University Berlin, D10099 Berlin, Germany

<sup>2</sup> Department of Zoology, University of Zürich, CH8057 Zürich, Switzerland

Desert ants (*Cataglyphis fortis*) perform foraging excursions and homing in a two-dimensional environment by means of path integration. They determine a global vector by combining directional information from the sky's polarization pattern and distance information derived from an odometer. If the ants walk on upward or downward slopes, their vector calculation is based on ground distances covered, not on the actual walking distances (Wohlgemuth et al. 2001, Nature 411:795). In the present study, we investigated how movements in the vertical direction during outward runs are incorporated into the ants' vector navigation, by training ants either to an elevated feeder or to a feeder located at ground level. These experiments aimed at the question of whether desert ants do reduce the 3-D path integration problem to a 2-D problem that can be solved in the horizontal plane, or to what extent they acquire and store information about the vertical position of a food source.

A group of ants was trained to forage in an aluminium channel at a feeder situated on level ground at a distance of 10.5 m from the nest (TR flat). A second group of ants was trained to an elevated feeder (1.8m height) at the same ground distance (TR ramp). This feeder could be reached via a 6-m piece of flat channel, followed by a steep 2-m ascent (70 deg inclination) which led into a horizontal channel until the feeder at 10.5m. Ants that had visited the feeder several times were tested on one of their next outbound runs by leading them via a switch into a test channel, laid out in parallel to the training channel. Both training groups completed two tests: (i) In distance control experiments, single ants entered a 15.5m horizontal test channel and their first U-turns, indicative of an ants' searching behaviour at the end of a vector run, were recorded. (ii) In ramp choice experiments, 6 ramps of 150 cm length and inclination of 70 deg were set up in the test channel at 3 / 4.5 / 6 / 7.5 / 9, and 10.5 m distance. Access to the ramps was made possible by small "gateways", whose sides led up the ramp, while an opening in the centre allowed the ants to pass through underneath the ramp. Climbing frequencies, climbing heights and choice of the ramp in first ascents were recorded.

In the distance control many of the ants (17 out of 38) that were trained on the elevated feeder made their first U-turns around 6 to 8 m, i.e. shortly after the distance where the ramp was located in training. In contrast, after TR flat only few ants performed so early first U-turns (8 out of 42; difference between conditions  $p < 0.02$ ). In ramp choice tests, ramp-trained animals climbed more frequently on one of the ramps than animals trained on the ground level (63% vs. 41%,  $p = 0.015$ ). In particular, the height of ascents differed considerably between the two training conditions; after ramp training more than 90% of the animals entering a ramp climbed immediately and with high speed to the end of the ramp (median climbing heights ramp vs. flat: 150 cm vs. 25 cm,  $p < 0.0001$ ).

These results show that ants that were trained to an elevated feeder have a notion of its elevated location and try possible ascents to reach this food source. Although ants trained on level ground also showed an unexpectedly large proportion of ascents, the much smaller ascent heights after this training indicate that this was rather expression of an exploration behaviour, in contrast to the fast and direct ascents of ants that had been trained to the elevated feeder. At present, however, it cannot be decided whether the ants had acquired a global 3-D vector, or whether they had learnt the way to the feeder in a procedural way, searching for a possibility to ascend after having covered a certain distance from the nest. The differences found between trainings in the distance control tests may hint at the second possibility.

## **Zenk and Fos Expression in Adult Zebra Finch Males After Presenting Learned and Non-learned Stimuli**

**Christine Huchzermeyer, Pamela Husemann, Carsten Lieshoff  
Hans-Joachim Bischof**

Department for Behavioral Research  
University of Bielefeld  
PO Box 100131  
33501 Bielefeld  
Germany

Sexual imprinting is an early learning process by which young birds acquire the features of a potential sexual partner. For example, rearing zebra finches by Bengalese finches results in a preference for this species. It was shown that sexual imprinting in zebra finches consists of two phases. In the first stage, the acquisition, the young zebra finch males learn features of its social environment. In the second stage, the consolidation, the young zebra finch males that court a female for the first time develop a stable preference for this female. Earlier studies showed that the two forebrain areas LNH (lateral neo-and hyperstriatum) and MNH (medial neo-and hyperstriatum) are important for the storage of information acquired during consolidation. To examine whether the imprinted information can be recalled in adult birds, we investigated the expression of immediate early genes (IEG), zenk and fos (reaction products), in sexually imprinted adult zebra finch males after exposure to imprinted and to non-imprinted stimuli. The first group of our experiment were zebra finch males normally reared by their own parents. One half of them were exposed to the imprinted stimulus, a zebra finch female, for one hour, and the other half to a not imprinted stimulus, a Bengalese finch female. The birds of the second group were reared by Bengalese finches and were exposed for one week to a zebra finch female in the consolidation phase. Later they were exposed to a zebra finch female for one hour as the first group. Following their exposure, the birds were prepared for immunocytochemistry. We then counted the density of zenk ir-cells and fos ir-cells in the two forebrain areas LNH and MNH.

In group 1, the expression of both, zenk and fos, was higher when the unlearned stimulus was presented. The birds of group 2, according to rearing conditions, developed differing preferences for zebra finches or Bengalese finches. Compared to group 1, there was a higher expression of both IEG's in MNH and LNH of the birds of group 2. While the expression pattern of fos within group 2 cannot be interpreted as yet, the zenk expression seems to be low when the presented stimulus is the learned and already stored one. In contrast, there is a high expression when the stored information does not correspond with the presented stimulus.

Supported by the Deutsche Forschungsgemeinschaft (Bi 245/17)



## **The differences in horizontal optokinetic nystagmus between albino wistar and pigmented Long Evans rats are not correlated with their ability of movement detection**

Y. Freund<sup>ca</sup>, D. Hupfeld, K.P. Hoffmann  
Department of general zoology and neurobiology  
Ruhr Universität Bochum/Germany

ca: [yvonnefreund@freenet.de](mailto:yvonnefreund@freenet.de)

### **Abstract:**

The genetic disorder albinism is linked with many deficits of which the white colour and the therefore missing camouflage is the most obvious. Albinos have also many changes in their nervous system. The visual system is mostly affected. Albinotic individuals in all animal groups (including human) have a delayed retinal development, different retinal ganglion axon crossing at the optic chiasm and abnormal projection to higher visual centres like the CGL or the visual cortex V1.

Due to this it is not surprising that behaviour of albinos is also affected by these changes. Like many other albinotic specimen wistar rats lack a functional hOKN or show at least only a reduced hOKN under certain circumstances. Considering whether a decreased ability of movement detection because of the misrouted pathways in the albino brain is the reason for this, we developed a behavioural test to prove this hypothesis. 20 rats (*rattus norvegicus*) were tested in two visual discrimination experiments on global motion perception.

We used male and female adult wistar (n=6,6) and Long Evans (n=4,4) rats and tested them in a modified Lashley jumping stand. The rats were food deprived and meant to distinguish a coherent from an incoherent moving pattern in this forced choice two alternative procedure. For choosing the incoherent stimulus (S+) the rats were reinforced with single food items.

At the beginning of the test the rats' age was between 4-6 months and at the end of the tests about 12 month. In the first experiment n=4,4 pretrained wistar rats were examined. In the second experiment naive wistar (n=2,2) and Long Evans (n=4,4) were used. The testing ended when the motion detection threshold had been determined.

During both experiments no differences could be detected between the motion detection ability of pigmented and albino rats. The results of both genders in each phenotype were pooled. Two different motion detection thresholds were found for wistar (30%) and Long Evans (12, 5%) ( $p < 0,001$  (t-test)).

These results lead us to the question what is the reason for this differences. Although the different thresholds are surely based on different perception, differences in learning and memory might also play an important role. In many studies performances in autoshaping, spatial learning and openfield of albinos vs. pigmented rats were investigated and show a decreased learning ability and changed explorative behaviour in many albino rat strains. This is equal to our own observations during the experiments. We therefore developed a phenotyping experiment based on a skinner box and a forced two choice paradigm and a reversal learning to evaluate the cognitive abilities of wistar and Long Evans rats and of backcrossed (wistar x Long Evans) F2 phenotypes.

Supported by DFG grant SFB 509-A11

## **Loss of metabotropic glutamate receptor-dependent LTD via downregulation of mGluR5 following status epilepticus**

Timo Kirschstein<sup>1</sup>, Jian Chen<sup>1</sup>, Albert J. Becker<sup>2</sup>, and Heinz Beck<sup>1</sup>

Departments of Epileptology<sup>1</sup>, and Neuropathology<sup>2</sup>, University of Bonn

Sigmund-Freud-Strasse 25, D-53105 Bonn, Germany

The hippocampal Schaffer collateral-CA1 synapses express a metabotropic glutamate receptor-dependent form of long-term depression (mGluR-LTD). This LTD is readily induced by brief application of the specific group I mGluR agonist (R,S)-3,5-dihydroxyphenylglycine (DHPG) acting at both mGluR1 and mGluR5. In this study, we tested whether DHPG-induced LTD is affected by the prior history of intense synaptic activity in vivo using the pilocarpine-induced status epilepticus. After the occurrence of spontaneous limbic seizures hippocampal slices were prepared, and conventional extracellular field potential recordings in the CA1 region were obtained. In controls, brief application of DHPG (100  $\mu$ M, 5 min) induced an acute inhibition of field potentials as well as a persistent depression of Schaffer collateral-CA1 synapses after 60 min of washout (DHPG-induced LTD). In pilocarpine-treated rats, however, both the acute depression and LTD were significantly reduced. When the specific mGluR5 antagonist 2-methyl-6-(phenylethynyl)-pyridine (10  $\mu$ M) was pre-applied, both acute and long-lasting depression were no longer different between control and pilocarpine-treated rats. Moreover, mGluR-dependent LTD induced by paired-pulse low-frequency stimulation was also significantly reduced in pilocarpine-treated rats as compared to controls. Using real-time PCR, mGluR1- and mGluR5-encoding mRNA in the CA1 region was determined, and revealed a specific downregulation of mGluR5. We conclude that the reduction of DHPG-induced LTD after pilocarpine-induced status epilepticus is due to a subtype-specific downregulation of mGluR5 in the CA1 region.

**Neonatal lesions of the rat medial prefrontal cortex together with pubertal phencyclidine treatment affect spatial behaviour but not sensorimotor gating**

Steffen Klein, Kerstin Schwabe and Michael Koch  
*Brain Research Institute, University of Bremen, PO Box 33 04 40,  
28334 Bremen, Germany*

According to the „Two-Hit-Model“ of schizophrenia early brain damage, particularly within frontal cortex regions, renders the brain vulnerable to adverse events in puberty. Additionally, patients with schizophrenia show symptom exacerbation in response to N-methyl-D-aspartate (NMDA) receptor antagonists. Aim of this study was to test whether neonatal excitotoxic lesions of the rat medial prefrontal cortex (mPFC) lead to enhanced vulnerability to chronic pubertal treatment with NMDA receptor antagonists, resulting either in behavioural deficits of adult rats and/or enhanced vulnerability to acute drug challenge. Memory processes were assessed in a spatial radial arm maze task. Additionally, sensorimotor gating processes, measured as prepulse inhibition (PPI) of the acoustic startle reflex (ASR), were tested with and without acute drug challenge.

Neonatal (postnatal day 7) lesions were induced by bilateral microinjection of ibotenate (0.2µg in 0.3 µl PBS) into the mPFC of anesthetized male Wistar rats. Sham lesioned rats microinjected with vehicle only and naive rats served as controls. From day 42 to 49 rats were chronically injected with either the NMDA receptor antagonist phencyclidine (PCP) (5mg/kg, twice daily) or the vehicle saline. Behavioural testing started from postnatal day 70 on. Spatial memory was tested in a 4-arm baited 8-arm radial maze task. During training, working memory errors (WME) and reference memory errors (RME) were assessed. After initial training, reversal learning started with the previously unbaited arms now baited. Subsequently, all groups were tested for PPI, without injection as well as after systemic challenge with PCP (2 and 5 mg/kg) and the dopamine receptor agonist apomorphine (2 mg/kg). Finally the brains of all rats were histologically processed for Nissl-staining.

Neonatal ibotenate-injection produced thinning and altered cytoarchitecture of the mPFC. In the radial arm maze task rats with neonatal lesions together with chronic pubertal PCP treatment showed increased RME during initial training and increased WME during reversal learning. Neonatal lesions or chronic PCP treatment alone had no effect. Baseline PPI was not affected by neonatal lesions or pubertal PCP treatment. However, acute PCP challenge failed to disrupt PPI in neonatal lesioned rats while the PPI-disruptive effect of apomorphine was not affected. Chronic pubertal treatment with PCP had no effect.

Early damage of the mPFC together with pubertal PCP challenge lead to deficits in spatial memory in line with the “Two-Hit-Model” of schizophrenia but does not affect sensorimotor gating. However, the mPFC is important for NMDA receptor antagonist induced PPI-deficits, a function that is not compensated after neonatal lesions.

Supported by the DFG (SFB 517, TP A11)

## Model of nonsynaptic integration by spatially segregated nitric oxide sources and targets in the locust mushroom body

Swidbert R. Ott,<sup>1</sup> Andrew Philippides,<sup>1</sup> Maurice R. Elphick<sup>2</sup> and Michael O'Shea<sup>1</sup>

S.R.Ott@cantab.net

<sup>1</sup>. School of Life Sciences, University of Sussex, Brighton, United Kingdom

<sup>2</sup>. School of Biological Sciences, Queen Mary, University of London, London, United Kingdom

The gaseous messenger molecule nitric oxide (NO) is implicated in several forms of synaptic plasticity, including associative olfactory learning and memory. In line with this notion, NO synthase (NOS) is highly expressed in the mushroom bodies (MBs), centres for higher level olfactory processing and associative memory in the insect brain.<sup>1–3</sup> However, the cellular architecture of NO signalling in the MB and its role at the network level are poorly understood. NO can bypass the conventional point-to-point route of synaptic transmission and act over considerable distances. As a consequence, the NO signal has no address and is inherently ambiguous in that a given NO concentration at the receptor can represent many different numbers and combinations of active sources (*number-of-senders ambiguity* and *identity-of-senders ambiguity*).

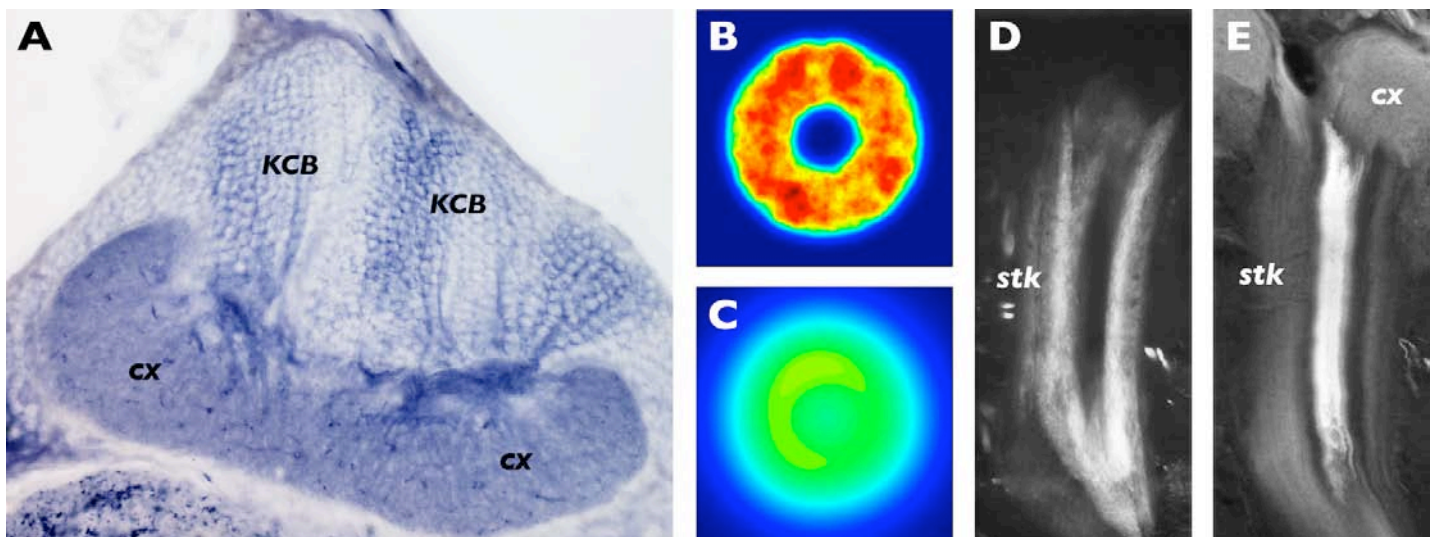
Here we combine precise analysis of the signalling architecture with computer models of the spatiotemporal dynamics of NO diffusion to elucidate the significance of NO signals in the MB of the locust. In the MB stalk and lobes, NOS is expressed at very high levels and in an intriguing compartmentalized fashion.<sup>1,3</sup> Densely NOS-positive zones form the walls of a tubular structure, enclosing a core region that does not express NOS. The presence of NOS in the MB has in the past been attributed to unidentified extrinsic neurones.<sup>1–3</sup> Using more sensitive detection techniques<sup>4</sup> we show that it arises in fact from the expression of NOS in many thousands of the MB intrinsic neurones or Kenyon cells (KCs; Fig. A). The axons of these KCs run in curved (i.e., hemicylindrical) strata in the two frontal columns of the stalk and thus together give rise to a tube. Within each NOS-positive KC, NOS shows very high expression specifically in the axonal compartment in the stalk and the lobes of the MB. In the cell bodies and dendrites in the calyx expression levels are in comparison exceedingly low. NO is therefore unlikely to play a major role in the transformation of the olfactory code that takes place in the KC dendrites.<sup>5</sup> Downstream of the calyx, odors are thought to be represented by synchronised sparse firing among small percentages of the KC population. We therefore propose that the release of NO in the MB is coupled to the odour-induced firing of individual KCs.

Modelling NO release from individual slender fibres (KC axon diameter: ~0.5  $\mu$ m) shows that they have only a limited capacity for generating an NO signal. However, upon release from only a small percentage of KC axons, NO reaches concentrations many times greater than those reached by an individual axon. NO first

accumulates in the wall of the tube (Fig. B), but with a slight delay NO also rises in the centre. After the end of synthesis, the concentration peak shifts from the wall into the centre (Fig. C), where NO remains elevated for several hundreds of ms. This raises the question of whether the NO target cells reside in the wall (where proximity to some of the sources would be greatest) or in the centre. Improved immunohistochemical detection of NO-donor-induced cGMP confirms the earlier finding that KCs can respond to NO by elevating cCMP.<sup>6</sup> Crucially, however, strongly NO-responsive KC axons occurred specifically in the tube centre. KCs therefore fall into NO-producing (NOP) and NO-responsive (NOR) subpopulations whose axons are segregated in a centre-surround arrangement (Fig. E,F). An immediate conclusion is that NO is used for communication between KC axons that are not physically connected. Moreover, the concentric segregation minimizes the total population variance in distance between NOP- and NOR-axons. This in turn equalizes the contribution of each single active NOP-KC to the NO concentration in the central target region.

Our modelling data suggest that this segregated arrangement confers advantages over a situation where NOP- and NOR-axons are randomly mixed in a salt-and-pepper fashion. Firstly, it provides a noise-filter by ensuring that concentrations at the targets are minimally affected by uncoordinated background activity among the NOP-axons. Secondly, the NO concentrations at the targets are much more accurate predictors of the number of NOP-KCs that have been activated by a stimulus. Concentric segregation of NOP- and NOR-axons thus minimizes the number-of-senders ambiguity, albeit at the cost of maximum identity-of-sender ambiguity. The architecture thus appears to be designed for maximizing the reliability of the NO signal as a nonsynaptic measure of integrated activity in NOP-KCs. In combination, our anatomical and theoretical data add significantly to understanding at the network level the role of NO in the insect MB. Moreover, they suggest that the properties of NO signals have shaped the structure of animal brains.

1. Bicker G & Hähnel I, *Neuroreport* 6:325–328 (1995)
2. Müller U. *Prog Neurobiol* 51:363–381 (1997)
3. O'Shea M et al., *Neuroreport* 9:333–336 (1998)
4. Ott SR & Elphick MR, *J Comp Neurol* 448:165–185 (2002)
5. Perez-Orive J et al., *Science* 297:359–365 (2002)
6. Bicker G et al., *Eur J Neurosci* 8:2635–2643 (1996)



**A**, Presence of NOS in subpopulations of KC cell bodies (KCB); NADPH diaphorase histochemistry after methanol/formalin-fixation, see Ref. 4. **B,C**, Predicted NO distribution in a cross-section through the MB stalk following a brief burst of synthesis (5 ms) in 20% of the KC axons at the end of synthesis (**B**) and 50 ms later (**C**). **D,E**, Longitudinal sections through the stalk of the MB, stained for NADPH diaphorase (**D**) and NO-induced cGMP immunoreactivity (**E**). The complementary pattern is due to expression of NOS and cGMP in separate and concentrically segregated populations of KC axons. cx, calyx, and stk, stalk of the MB.

## **Functional redistribution of ependymin cell adhesion molecules after learning of an active shock avoidance task in fish**

Florian Kreul and Rupert Schmidt

Zentrale Biotechnische Betriebseinheit der Justus-Liebig-Universität Gießen  
Leihgesterner Weg 217  
D-35392 Gießen

Fish ependymins are brain specific glycoproteins that are highly enriched in the extracellular brain matrix after learning. Ependymins comprise the HNK-1 carbohydrate epitope characteristic of many cell adhesion molecules, and they support outgrowth of ganglion cell axons from explanted goldfish retinæ *in vitro*.

Goldfish were trained on a shuttle-box to avoid electric shocks administered after a conditioning light signal. In situ hybridisations revealed a marked increase in the level of ependymin mRNA in the goldfish and zebrafish leptomeninx three hours after learning of the active avoidance response.

Here, we report on light- and electron-microscopic studies on the localisation of ependymin immunoreactivity. Immunogold particles were observed at the rough endoplasmic reticulum of leptomeningeal fibroblasts confirming the leptomeninx as major, or possibly the exclusive, site of ependymin biosynthesis in the teleostean brain. By immunofluorescence and immunogold labelling of cryofixed brain sections ependymin was found to be distributed throughout the extracellular brain fluid and to reach all cell layers of the optic tectum.

When the goldfish brain was perfused with buffer solution prior to fixation with Duboscq-Brasil's fixative, immunofluorescence in the optic tectum was seen to be most prominent at the somata and apical dendrites of type I neurones in the superficial grey and plexiform layer. These neurones obtain their major synaptic input from myelinated retinal ganglion cell axons forming synapses on the shaft of the apical dendrites. Furthermore, type I neurones are innervated on dendritic spines of their apical dendrites by unmyelinated marginal fibres from the longitudinal torus. Both types of synapses were stained by anti-ependymin immunolabelling. The immunoreactivity in the optic tectum, and in particular at synapses on type I neurones, appeared to increase after avoidance learning.

Intracerebroventricular injections of anti-ependymin antibodies interfere with memory consolidation during a defined time-frame after avoidance learning that corresponds to the time-course of ependymin synthesis and secretion. Anti-ependymin antibodies, however, neither affect learning nor memory retrieval.

In conclusion, the labelling in the immediate proximity of postsynaptic densities of type I neurones suggests that ependymin molecules are redistributed after secretion and are bound to synapses, activated during the preceding learning-event, that have to be modified in order to improve their efficacy for future use.

## Detection of mammalian ependymin-related protein (MERP) transcripts in mouse brain and investigation of a possible involvement in memory formation

Sandra Schneider and Rupert Schmidt

Zentrale Biotechnische Betriebseinheit der Justus-Liebig-Universität Gießen  
Leihgesterner Weg 217  
D-35392 Gießen

Fish ependymins are brain specific glycoproteins synthesized by leptomeningeal fibroblasts and secreted into the cerebrospinal fluid. They represent major components of the cerebrospinal fluid in many teleosts and are known to be involved in a variety of cellular functions related to neuronal regeneration, long-term memory formation and acclimation to cold-stress (1).

Mammalian homologues of fish ependymins named “mammalian ependymin-related proteins” or “MERPs” were first identified by reverse transcription differential display analyses (2). Human *MERP1* was characterized by its sequence homology to fish ependymins and to calcium-dependent cell adhesion molecules of the protocadherin family. It is found in various tissues including brain, heart and skeletal muscle and adrenal gland. The level of transcription of human *MERP1* was reported to be increased in several hematopoietic cell lines and in malignant tissues. Further sequencing analyses identified two putative murine ependymin-related proteins, named *MERP1* and *MERP2*, with sequence homologies to piscine ependymins (3).

Earlier experiments described immunological cross-reactivity of cultured embryonic rat hippocampal neurones with goldfish brain ependymins (4). Recently, we analysed expression of murine *MERP1* and *MERP2* mRNAs in mice by reverse transcription polymerase chain reaction. Our experiments revealed that murine *MERPs* are already expressed in mouse brain by postnatal day 1, whereas human *MERP1* is not expressed in fetal brain.

In order to test for a possible involvement of murine *MERP* proteins in biochemical mechanisms of learning and memory formation, we used the Morris water maze to train adult male mice on a spatial memory task. In this learning paradigm the mouse is placed into a water tank, where it has to find a platform, invisible to the animal, to rest from swimming. Two hours after acquisition of the task, mice were decapitated and whole brains were analyzed for expression levels of murine *MERP* mRNA by means of semi-quantitative RT-PCR, using  $\beta$  actin as a control. Preliminary results obtained with 5 brains from learning mice indicate that murine *MERP2* mRNA was increased as compared with untreated litter mates. Based on the apparent over-expression of *MERP2* mRNA two hours after water maze learning, it is tempting to expect a functional involvement of mammalian ependymin-related proteins in memory consolidation analogous to the role of fish ependymins, despite the differences in the regional expression of the mammalian and piscine messages.

- 1) Shashoua and Schmidt: Ependymins: adhesion proteins of the extracellular matrix. In: *Encyclopedia of Neuroscience*, eds: Adelman and Smith; Elsevier, 3<sup>rd</sup> ed., 2004
- 2) Nimrich et al., *Cancer Lett.* **165** (2001) 71-79
- 3) Gregorio-King et al., *Gene* **286** (2002) 249-257
- 4) Schmidt et al., *Brain Res.* **386** (1986) 245-257

**Distracting effect of emotionally significant stimuli on cognitive brain activity:  
Electrophysiological functional brain imaging**

Einat Ofek and Hillel Pratt

Evoked Potentials Laboratory, Technion –Israel Institute of Technology,

e-mail: einato@tx.technion.ac.il

*Objective:* To study the distracting effect of emotionally significant stimuli on unrelated cognitive brain activity. Brain activity related to emotional and cognitive processing has been typically traced with fMRI's temporal resolution of seconds. In this study, the time course of activation in the brain areas involved was traced with millisecond temporal resolution.

*Methods:* Electrical brain activity (event related potentials) was recorded from 12 normal subjects while they performed an auditory (tones) cued attention task, in which cues, in most cases accurate, provided information on the appropriate response to the subsequent target stimulus. In one third of the trials, verbal distracters were administered at different times between the cue and the target. Subjective affective valence of verbal distracters was determined separately for each subject after the experiment, using a structured interview based on a validated questionnaire. Evoked potentials to the targets were averaged according to the preceding cue's validity and the affective valence of the distracter. Potentials were averaged across different onset times of distracters, so that brain activity was locked in time to the targets but not to the distracters, and the indirect effect of the distracters on cognitive brain activity to the targets could be assessed.

*Results:* Brain response to targets was enhanced when administered after verbal distracters and was modulated by the affective valence of the distracters. Brain sources involved in the processing of targets in auditory cued attention task included secondary auditory cortex and insula. Additional brain areas were involved if verbal distracters preceded the target. These areas included language- (Broca's and Wernicke's areas) and emotion (medial PFC and anterior cingulate gyrus) related areas. Emotion related brain areas were involved only following emotionally significant verbal distracters, while only language related brain areas were shown to be involved following neutral verbal distracters. Time course of activation within those areas was characterized.

*Conclusions:* The processing of auditory stimuli is modulated by unrelated preceding distracters, involving different brain sources, depending on the subjective significance of the distracters.

*Significance:* These results demonstrate how emotionally significant stimuli affect cognitive brain activity. The close interaction between cognitive processes (evaluation of cue validity) and emotional processes indicates the unity of brain processing.

**Impaired synaptic plasticity in mice conditionally deficient in neural cell adhesion molecule NCAM is restored by elevation of extracellular  $\text{Ca}^{2+}$  concentration**

*Alexander Dityatev (dityatev@zmnh.uni-hamburg.de),  
Olena Bukalo, Alan Y. W. Lee, Benedikt Salmen, Janice W. S. Law,  
Michaela Schweizer and Melitta Schachner*  
Zentrum für Molekulare Neurobiologie, Universität Hamburg,  
Martinistr. 52, D-20246 Hamburg, Germany

NCAM, a neural cell adhesion molecule of the immunoglobulin superfamily, is involved in neuronal migration and differentiation, axon outgrowth and fasciculation, and synaptic plasticity. To dissociate the functional roles of NCAM in the adult brain from developmental abnormalities, we have generated a mutant in which the NCAM gene is inactivated by cre-recombinase under the control of the  $\text{Ca}^{2+}$ /calmodulin-dependent kinase II promoter, resulting in reduction of NCAM expression predominantly in the hippocampus after cessation of major developmental events. This mutant (NCAM<sup>ff</sup>+) did not show the overt morphological abnormalities, such as a reduced olfactory bulb, previously observed in constitutive NCAM deficient (NCAM<sup>-/-</sup>) mice. LTP in the CA3 region was also normal, consistent with normal mossy fiber lamination in NCAM<sup>ff</sup>+/+ as opposed to abnormal lamination in NCAM<sup>-/-</sup> mice. However, similar to the NCAM<sup>-/-</sup> mouse, a reduction in long-term potentiation (LTP) in the CA1 region of the hippocampus was revealed. Long-term depression was also abolished in NCAM<sup>ff</sup>+/+ mice. The deficits in LTP in NCAM<sup>ff</sup>+/+ and NCAM<sup>-/-</sup> mice could be rescued by elevation of extracellular  $\text{Ca}^{2+}$  concentrations from 1.5 or 2.0 mM to 2.5 mM, suggesting an involvement of NCAM in regulation of  $\text{Ca}^{2+}$ -dependent signaling during LTP. Thus, mice conditionally deficient in hippocampal NCAM expression in the adult share certain abnormalities characteristic of NCAM<sup>-/-</sup> mice, highlighting the role of NCAM in the regulation of synaptic plasticity in the CA1 region.



## Phosphorylation of GluR-A containing neocortical AMPA receptors is required for intact object recognition

Tansu Celikel<sup>1</sup>, Verena Marx<sup>2</sup> and Rolf Sprengel<sup>2</sup>

(1) Abteilung Zellphysiologie und (2) Abteilung Molekulare Neurobiologie, Max-Planck Institut fuer Medizinische Forschung, Heidelberg-Germany

Fast excitatory synaptic transmission in the central nervous system is mediated by AMPA receptors. It's been shown in those animals with no GluR-A containing neocortical AMPA receptors (GluR-A<sup>-/-</sup>) that these receptors take a role in spatial working (Reisel et al, 2002) and nonassociative spatial memory (Celikel et al, submitted) but not in associative spatial memory (Zamanillo et al, 1999) and object recognition (Celikel et al, submitted). The molecular basis of such AMPA receptor functions are speculated to rely on activity induced AMPA receptor phosphorylation that (a) increases the conductance of AMPA receptor and (b) leads to a change in the number of AMPA receptor in individual synapses. We studied GluR-A<sup>-/-</sup> mice that express N-terminal GFP-tagged GluR-A phosphorylation mutants (GluR-A-SA) at the PKA (S845A) and  $\alpha$ CaMKII/PKC phosphorylation sites (Ser831A) in the forebrain of adult mice and compared the effect of lack of phosphorylation with deletion of the GluR-A subunit of neocortical AMPA receptors (GluR-A<sup>-/-</sup>) in nonassociative spatial memory and object recognition tasks. GluR-A-SA (n=5), GluR-A<sup>-/-</sup> (n=6) and wild type (WT, n=7) mice received 7 sessions (intersession interval= $\sim$ 4 min) of training with or without novel objects in an open field measuring 60x60x40(h) cm. The three groups did not show different amount of motor activity as measured during the first session in the open field without any objects (Figure 1a). To study nonassociative spatial memory, we first habituated animals to 5 novel objects and to their spatial locations for three sessions (Sessions 2-4), then repositioned two of them in novel spatial locations (Session 5) and measured the amount of exploration onto displaced (DO) and nondisplaced (NDO) objects to calculate the spatial novelty discrimination index (DO-exploration/(DO-exploration+ NDO-exploration)). Results (Figure 1b) showed that WT mice preferred to explore objects in novel locations although GluR-A-SA and GluR-A<sup>-/-</sup> mice did not ( $p<0.05$ ). After habituating the mice to the new spatial locations for another session, we replaced one of the previously nondisplaced objects with a novel object (Session 7) to quantify object novelty discrimination index. All three groups explored the novel object more than chance level however GluR-A-SA mice had impaired novel object exploration compared to WT and GluR-A<sup>-/-</sup> ( $p<0.05$ ), which didn't statistically differ from each other (Figure 1c). These results suggest that phosphorylation of GluR-A containing receptors is required for intact object recognition however lack of receptor phosphorylation after deletion of GluR-A subunits can be compensated behaviorally.

**Supported by** DFG:SFB636-A4 and Alexander von Humboldt Foundation.

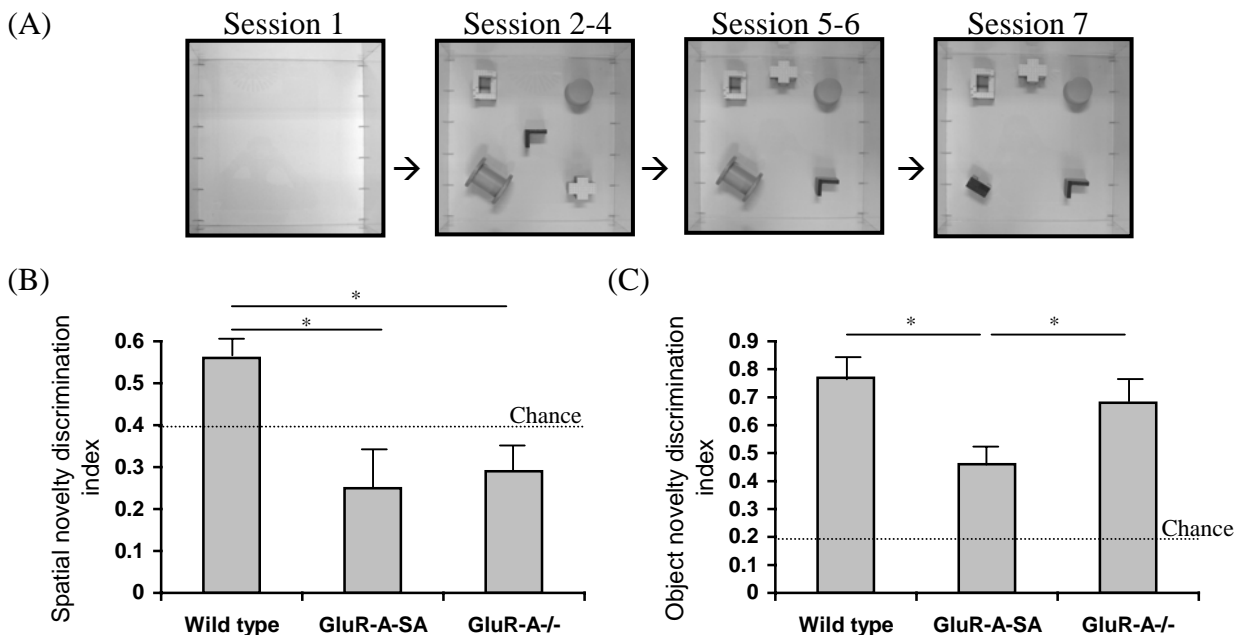


**Figure 1.** Experimental design and principal results. (A) Seven sessions of exposure to novel and habituated environments. Spatial novelty was induced by repositioning previously explored objects (Sessions 5-6). Object novelty was due to novel objects in the environment (Sessions 2 and 7) (B) Non-associative spatial learning is impaired in GluR-A-SA and GluR-A<sup>-/-</sup> animals. Spatial novelty discrimination index shows that WT preferred displaced object exploration more than did GluR-A-SA and GluR-A<sup>-/-</sup> mice. (C) Object recognition is impaired in GluR-A-SA mice although WT and GluR-A<sup>-/-</sup> mice do have statistically indistinguishable object recognition.

## Persistent activity in basolateral amygdala neurons

Alexei V. Egorov\*†, Klaus Unsicker\* and Oliver von Bohlen und Halbach\*

\* *Interdisciplinary Center for Neuroscience (IZN), Department of Neuroanatomy, University of Heidelberg, Heidelberg, Germany* † *Institute of Higher Nervous Activity and Neurophysiology, Russian Academy of Science, Moscow, Russia*

Design of long-term memory traces requests participation of working memory, i.e. the process by which brain systems may hold externally or internally driven information for relatively short period of time. Persistent neuronal activity is the elementary process underlying working memory. It has long been known that emotionally affecting experiences tend to be well remembered. According to the modulation hypothesis, the positive effect of emotion on memory is due to modulatory influences of the basolateral amygdala (BLA) on encoding and consolidation processes occurring in medial temporal lobe memory structures, including the hippocampus and associated parahippocampal regions (i.e., entorhinal-, perirhinal-, and parahippocampal cortices). However, the cellular basis of this modulation remains unknown. Recent fMRI studies have also identified anterior parahippocampal regions, particularly the entorhinal cortex (EC), as brain sites sensitive to amygdalar modulatory influences (Dolcos et al., 2004). Principal neurons from layer V of the EC can generate oscillatory "persistent" activity that can maintain multiple levels of stable firing rate in the absence of synaptic reverberations (Egorov et al., 2002). This firing behavior is linked to cholinergic muscarinic receptor activation, and relies on activity-dependent changes of a  $\text{Ca}^{2+}$ -sensitive non-specific cation current. Such an intrinsic neuronal ability to generate graded persistent activity constitutes an most elemental form of working memory.

Here we investigate the opportunity for generation of oscillatory "persistent" activity in BLA neurons using sharp microelectrodes recordings in mouse brain slices. We found that under activation of cholinergic receptors (CCh,  $10\mu\text{M}$ ) BLA neurons could respond to a short stimulus with delayed firing at a constant frequency and for an apparently indefinite period of time. In similarity to EC layer V cells, plateau-potential of BLA neurons that sustained persistent firing displayed pronounced activity- and voltage-dependence and could be induced equally well during pharmacological blockade of glutamatergic and ionotropic GABAergic receptors. A sustained level of firing frequency could be either increased or decreased in a step-like fashion and in an input specific manner. This plateau potential relied on the activation of muscarinic receptors since its induction was completely blocked by atropine. Electrical stimulation of deep layer of medial EC could elicited antidromic action potentials in the majority of BLA neurons, thus indicating axonal projections to EC.

We conclude that graded persistent activity are a common intrinsic behavior of EC and BLA neurons. We propose that the internal ability of BLA neurons to generate graded oscillatory "persistent" activity could be essential in the acquisition and consolidation of lasting memories of emotional experiences.

Dolcos F., LaBar K.S., and Cabeza R. (2004) Interaction between the Amygdala and the Medial Temporal Lobe Memory System Predicts Better Memory for Emotional Events. *Neuron* 42, 855-863.

Egorov A.V., Hamam B.N., Fransén E., Hasselmo M.E. and Alonso A.A. (2002) Graded persistent activity in entorhinal cortex neurons. *Nature* 420, 173-178.

Supported by SFB 636/A5

## The role of excitatory neurons in supragranular layers for the acquisition of a whisker dependent learning task

Sabrina A. Laudenklos<sup>1</sup>, Tansu Celikel<sup>2</sup>, and Pavel Osten<sup>1</sup>

(1) Abteilung Molekulare Neurobiologie und (2) Abteilung Zellphysiologie, Max-Planck Institut fuer Medizinische Forschung, Heidelberg-Germany

The barrel cortex, a subregion of the primary somatosensory cortex representing facial vibrissae of rodents, consists of six layers. Earlier studies revealed that cortical layers are functionally as well as anatomically nonuniform, and that the time course and expression of plasticity in the cortex are layer-specific. Based on the findings that supragranular and infragranular layers show plasticity earlier and to a larger extent than the cells of the granular layer, it has been postulated that the majority of the synaptic plasticity induced during learning and altered sensory experience takes place within the cortex. In order to test this hypothesis, we designed an experiment to examine the role of excitatory neurons in supragranular layers in a single-whisker dependent learning task. First, using a lentivirus-based gene delivery, we manipulate the excitability of supragranular principal neurons in identified columns of the barrel cortex. The genetic manipulations include expression of a modified ATP-dependent RFP-tagged Kir6.2 ( $\Delta N30$ ,  $\Delta C36$ , K185Q) (Reimann *et al.* 1999) or GFP-tagged Kir2.1 (Burrone *et al.* 2002). The Kir6.2 is a weak rectifier that was modified to limit its dependence on endogenous ATP and to enhance its surface expression (Liss and Roeper, 2001). Lentivirus-based expression of either RFP-Kir6.2mut or GFP-Kir2.1 is expected to reduce the firing rate of infected neurons. These constructs are currently being tested by patch clamp recordings in acute cortical slices. Second, after establishing that the expression of the constructs reduces cortical cell excitability, animals with the viral delivery targeted to a single column's supragranular layer will be tested in an one whisker-based gap-crossing task. Animals are trained to find a target platform, using a single whisker after depriving (trimming) all other whiskers. This task was shown to be whisker- and barrel cortex-dependent and, moreover, the plasticity induced by gap-cross training is restricted almost exclusively to the trained whisker's cortical column and the ones immediately surrounding it. Four groups of animals are planned to be included in the experiment: animals with injections of the lentiviral vector to express the Kir channels (i.e. Figure 1a), and animals injected with a lentiviral vector expressing EGFP or RFP (i.e. Figure 1b) or injected with phosphate buffer only (the later three groups serving as a control for specificity of the Kir-based effects). An initial series of experiments performed with EGFP-expressing and mock-injected animals indicated that these two groups perform the task equally well. Final results of this study will be discussed in terms of necessity of supragranular excitatory cells' activity for acquisition of whisker dependent learning.

**Supported by** Alexander von Humboldt foundation.

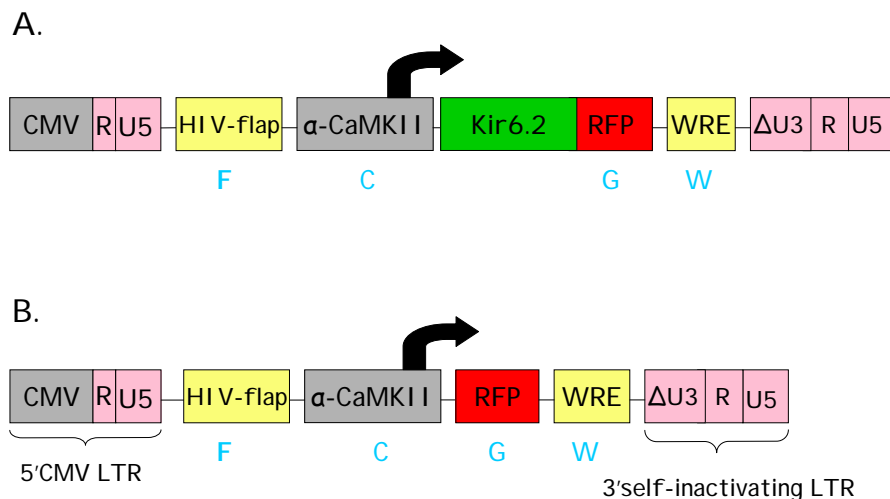


**Figure 1. Lentiviral expression system.** The expression vector carries the target gene expression under the control of the  $\alpha$ CaMKII promoter. The LTR flanking sequences are responsible for integrating the reverse transcribed DNA into the host genome. The deletion of the U3 viral promoter and enhancer prevents uncontrolled viral transcription of the integrated DNA. The HIV1-flap sequence is required for the transport of the dsDNA into the nucleus whereas the WRE enhances the transfer of mRNA transcribed from the  $\alpha$ CaMKII promoter from the nucleus to the cytoplasm. (A) RFP-Kir6.2mut fusion construct. (B) RFP construct.

## **Transfer of sensorimotor adaptation between sensory modalities.**

G. Schmitz, P. Vogt, and O. Bock

Inst. of Physiology and Anatomy, German Sport Univ., Köln, Germany

When human subjects are exposed to a visual or mechanical distortion, their sensorimotor performance is initially degraded, but gradually normalizes with extended practice. This adaptive improvement typically shows transfer to the other, unpractised arm, suggesting that adaptive processes are located in the sensorimotor system *before* the divergence point for left and right arm control. The present study investigates whether these processes are located *before or after* the convergence point of different sensory modalities.

Human subjects pointed in complete darkness (i.e., without target or hand vision) at acoustic targets arranged along a semicircle about the starting point. Acoustic feedback about hand position was provided as a sound the frequency of which coded finger lateral error. This feedback was veridical during a baseline phase, and was then rotated by 30 deg to the left during the subsequent adaptation phase. Intersensory transfer was tested by asking subjects to point at visual targets without visual or acoustic feedback.

Subjects baseline performance was reasonably accurate, and they subsequently adapted to the acoustic rotation. Responses remained adapted when subjects used their untrained arm or pointed at visual targets, i.e., subjects exhibited intermanual and intersensory transfer. A second experiment, using a complementary design, documented an intersensory transfer from the visual to the acoustic modality.

We conclude that adaptive processes are located downstream from the convergence point of sensory modalities, but upstream from the divergence point for left and right arm control.

Supported by DFG and BMBF. Responsibility for the contents rests with the authors.

## CORRELATION BETWEEN PERFORMANCE IN A SENSORIMOTOR ADAPTATION TASK AND FRONTAL-EXECUTIVE CONTROL IN ELDERLY

M. Girgenrath, O. Bock

Dept. of Physiology and Anatomy, German Sport University, 50933 Köln, Germany

When exposing elderly subjects to a complex motor task such as the sensorimotor adaptation to visuomotor rotation, behavioural results are contradictory and characterized by a high amount of interindividual variance, which cannot be solely explained by the factor biological age. Furthermore, it is well known that higher-order cognitive functions deteriorate with ageing, due to cell decline in the frontal lobes, with dorsolateral prefrontal areas being more affected than ventromedial areas. Since frontal lobe function is also essential for sensorimotor adaptation, its functional state might be a stronger indicator for the level of adaptation than the biological age. In order to explain the high variance in performance, we combined a complex sensorimotor adaptation task with several reaction time (RT) tasks, involving mainly either the ventral or dorsal prefrontal cortex (PFC).

In the sensorimotor adaptation task subjects performed a classical center-out pointing task with a pen on a digitizing tablet (SummaSketch III®). Subjects' task was to move the pen as quickly and accurately as possible in a straight trajectory to the target. After a training block with a veridical relationship between pen and cursor position, subjects were exposed to a visual distortion with a 60 deg rotation between pen and cursor coordinates. Initial error was taken to assess performance. In addition, several RT tasks were carried out, consisting of a single RT task, a four-choice RT task, a four-choice RT task with a 180° rotation, a delayed sequence task (ventral PFC), a four-choice RT task with a shift between 0° and 180° rotation, and a delayed sequence task with 180° rotation (dorsal PFC).

In general we found a strong correlation between the level of sensorimotor adaptation and the performance in the RT tasks, which was even stronger with increased complexity of the RT tasks. We also observed a tendency of a higher relationship when dorsolateral PFC was mainly involved.

Due to our findings, we propose a strong association between the ability to adapt to distortions and the functional level of frontal-executive control. This fact should be taken into account when conducting studies with elderly and might explain interindividual variance in a better way than the factor biological age.

## **Transcranial direct current stimulation improves a visual discrimination skill**

Marshall L, Mölle M, Laske K, Gais S, Born J

Institute of Neuroendocrinology, H23a, University of Lübeck, Germany

email: marshall@kfg.uni-luebeck.de

Application of transcranial direct current stimulation (tDCS) to the cortex has been shown to shift the resting membrane potential of superficial neurons in a de- or hyperpolarizing direction, and to modulate spontaneous neuronal activity as well as the processing of afferent signals. In humans, tDCS has been shown to modulate excitability measures of the motor and visual cortex. Here we show that tDCS can modify performance on a basic visual texture discrimination task<sup>1</sup>. The performance improvement for a basic texture discrimination task takes place in the earliest cortical visual processing area in primates. Substantial improvement in perceptual performance of this task does not occur until several hours after it has ended. In particular the occurrence of sleep, rather than the simple passage of time, leads to consolidation and improvement on this task. We applied anodal, cathodal or sham tDCS during the task to the scalp over V1 for 8 min in 11 young healthy humans. As expected, tDCS had no immediate effect on discrimination performance or on attention. When tested 24 h later the performance of subjects who had received cathodal tDCS was significantly improved as compared to sham stimulated subjects. The same effect, but weaker was found for anodal tDCS. These results show that tDCS effects on cortical plasticity can be long-lasting. It extends and complements studies revealing long-lasting effects of tDCS on cortical activity and neurochemical transmission.

<sup>1</sup>Karni A, Sagi D (1991) PNAS 88:4966-70.

*Supported by the DFG (FOR457)*

## Analysis of instrumental sequential behavior in the rat

Domenger D, Dincheva Z, Schwarting RKW

Experimental and Physiological Psychology, Philipps-University of Marburg, Marburg, Germany

Sequential learning, a type of procedural learning, has intensively been investigated in humans. This work has mainly been done using so-called serial reaction time tasks. In such tasks, subjects have to respond rapidly to simple visual stimuli appearing at one of four locations by pressing a corresponding response key. Unknown to the subjects, these stimuli can follow a specific repeating sequence. Learning of such a sequence is typically inferred from faster reaction times to sequence as compared to random blocks. Unlike humans, the analysis of sequential behavior has not received considerable attention in rodents; however, the implementation of a comparable sequential paradigm in rodents would be highly desirable, since it would allow detailed analyses of the underlying brain mechanisms, especially of cortico-striatal networks. Here, we describe the development and application of an instrumental task in rats which is designed similar to the human one. Operant testing chambers were used, which contained four nose-poke holes with cue lights arranged in a square fashion with a pellet receptacle in the center. The rats had to respond within a limited time period to a visual stimulus, namely the illumination of one of the four holes, by poking into it in order to obtain food-reward. The visual stimulus varied permanently in location. We varied these changes either in a random or a sequential fashion. Data from experiments with different schedules of reinforcement (fixed ratio; FR2, 6, or 12), with different presentation orders of random and sequential blocks (daily session presentation of the random or sequential condition, within session presentation of the two conditions, systematical or non-systematical order of alternation of the presentation of these two conditions), and with different types of sequence presentation (fixed-sequence, shifted-sequence) will be presented. These data show how rat performance during serial responding differs under random or sequential conditions, indicating that this kind of instrumental task might be useful to analyse sequential learning, memory, and their underlying brain mechanisms in the rat.

Supported by the DFG (research group: „dynamics of cognitive representations”)

## Sounds in silence I: Rat ultrasound vocalization during fear conditioning - a dose/response study

Wöhr M, Borta A, Schwarting RKW

Experimental and Physiological Psychology, Philipps-University of Marburg, Germany

Rats are known to emit distinct types of ultrasound vocalization, which differ dependent on animal age, and physical, or psychological demands of the environment. Adult rats, for example, emit 22-kHz vocalizations when exposed to predators, pain, or during intermale aggression, whereas 50-kHz vocalization occurs during juvenile play, copulation, or exploratory activity (for review see Knutson et al. 2002).

Given these context- and state-dependencies, one can assume that ultrasound vocalizations may serve as helpful and additional variables when studying emotional and motivational mechanisms in such animal subjects. We therefore started a series of behavioural experiments where we performed detailed analyses of rat ultrasound vocalizations during experimental situations where behaviour is determined by aversive motivation.

Specifically, we choose a conventional paradigm of fear conditioning, where freezing behavior is classically conditioned to an auditory cue (CS) predicting electric footshocks (UCS). Adult male Wistar rats were tested as follows: On day 1, they were habituated to the testing environment without tone or shock. On day 2, six 3 kHz tones of 20sec duration were administered, each of which was ended by a 0.5sec electric footshock. Shock intensity was systematically varied in five separate groups of rats (0, 0.2, 0.5, 0.8, 1.1mA). On day 3, the six tones were again administered, but not followed by shock. Ten days later, the procedure of day 3 was repeated (re-test). On all days, behaviour (freezing, locomotion, rearing etc.) and ultrasound vocalization were measured. For ultrasound vocalization, an Avisoft system (UltrasoundGate 116 with recorder 2.7), and an Emkay FG series ultrasound microphone were used.

The results show that rats did not vocalize when simply exposed to the novel apparatus (day 1), or when confronted with tones not ended by shock (day 2). Furthermore, not only freezing, but also ultrasound vocalization in shock-exposed rats was dependent on shock intensity, since, for example, the percentage of rats which vocalized increased with shock intensity. In those rats, the patterns of vocalization were dose-dependent regarding call frequency and overall duration, frequency modulation, or amplitude. During the test on day 3, where tones but not shocks were given, conditioned ultrasound vocalizations were observed in about half of the animals which had experienced the higher shock intensities (0.5-1.1mA) on the day before. A similar pattern was observed during the re-test performed ten days later.

The results show that the analysis of ultrasound vocalization can substantially extend the spectrum of dependent behavioural variables in biopsychological analyses of aversively motivated behaviour in the rat. Such an analysis not only adds to overt behavioural indices (like freezing, avoidance behaviour etc.), but can also indicate behavioural states which may not be measurable with the latter.

### References:

- Knutson B, Burgdorf J, Panksepp J. Ultrasonic vocalizations as indices of affective states in rats. *Psychological Bulletin*, 128 (2002), 961-977.



## Sounds in silence II: Individual differences in ultrasound vocalization and freezing during fear conditioning

Borta A, Wöhr M, Schwarting RKW

Adult Wistar rats identical in sex, age and housing conditions, can differ systematically in their behavioral response to the elevated plus maze (EPM; Schwarting & Pawlak 2004). There, they can be identified as so-called “high anxiety” (HA) or “low anxiety” (LA) rats based on the time spent in the open arms. Such HA and LA rats behave differently in specific other tasks, especially when aversive stimuli are used. For example, HA rats were more anxious in an object burying test and showed slower acquisition of active avoidance than LA rats (Ho et al. 2002), whereas they did not differ in an inhibitory avoidance task (Borta & Schwarting, in preparation). Furthermore, we found that HA and LA rats can already be distinguished at an early postnatal period: When examining ultrasound vocalization of male rat pups during a brief isolation phase from their dam, we found a correlation of pup vocalization to adult EPM behavior, since pups that vocalized more during isolation behaved less anxious when tested in the EPM as adults (Schwarting and Pawlak, 2004). Since ultrasound vocalization can also be elicited in adult rats, like when exposed to aversive stimuli, we now asked whether adult rats might also differ in such vocalization.

To test this issue, we screened adult rats in the EPM, defined them as HA or LA rats ( $n=10$  each), and tested them in a standard fear conditioning paradigm for possible differences in freezing and ultrasound vocalization. As a CS we used a 3kHz sine wave tone (approximately 70dB; 20sec duration) immediately followed by an unescapable footshock (UCS; 0.5mA, 0.5sec). Rats were tested on 3 consecutive days (11 minutes per day). On day 1, baseline activity in the fear conditioning apparatus was scored without tone or shock. On day 2, the rats received 6 tone/shock pairings with an interstimulus interval of 60s. After 24 hours (day 3) the rats were again placed into the test apparatus and 6 tones were administered without shocks. On each day, freezing behavior was recorded by video analysis. Furthermore, ultrasound vocalization was recorded and analysed via the Avisoft system (UltrasoundGate 116 with recorder 2.7).

During baseline testing, freezing behavior of HA and LA animals did not differ, and none of them emitted ultrasound vocalization. On day 2, all HA and 7 LA rats vocalized when confronted with tone/shock pairings. HA rats tended to vocalize more often than LA rats ( $p=.071$ ), and showed higher frequency components ( $p<.05$ ). Furthermore, freezing behavior increased over time ( $p<.001$ ) in all animals, but HA rats showed more freezing during tones than LA rats ( $p=.053$ ). On the third day, where only tones were presented, 6 HA and 3 LA rats vocalized. No significant differences in vocalization could be observed in those animals. Again, HA rats showed more freezing behavior than LA ( $p<.05$ ).

These findings add to previous evidence in showing that HA and LA rats differ behaviourally, especially when confronted with aversive stimuli, or when learning is determined by such stimuli (here classical conditioning). The data also show that differences are not only observable at the level of overt behavior (like freezing), but also in ultrasound vocalization. The analysis of ultrasound vocalization can therefore substantially extend the spectrum of methodological variables for the study of motivation, emotion and learning in rats.

### References:

- Ho Y-J, Eichendorff J and Schwarting RKW. (2002) Individual profiles of male Wistar rats in animal models of anxiety and depression. *Behavioural Brain Research*, 136: 1-12.
- Schwarting RKW and Pawlak CR. (2004) Behavioral neuroscience in the rat: taking the individual into account. *Methods and Findings in Experimental and Clinical Pharmacology*, 26: 17-22.

## **Appetitive olfactory learning in *Drosophila* larvae: Testing for effects of training amount, reinforcer intensity, age, gender, assay type, and memory span**

KIRSA NEUSER, JANA HUSSE, PATRICK STOCK, & BERTRAM GERBER

University of Würzburg, Germany

bertram.gerber@biozentrum.uni-wuerzburg.de

Associative plasticity is a basic characteristic of behaviour. We chose larval *Drosophila* as a study case and provide a parametric analysis of associative olfactory learning in this animal. We use a reciprocal conditioning assay: one group of animals is rewarded with fructose in the presence of odour A but not in the presence of odour B (A+/ B). The companion group receives reciprocal training (A/ B+). During test, animals are given a choice between A and B; animals which had received A+/ B training show a higher preference for A than reciprocally trained animals. As all other parameters are equal between groups, this difference is exclusively due to associative learning. We find that: (I) learning reaches asymptote after as few as three training trials; (II) 2.0 mol/ l fructose concentration yields asymptotic learning; (III) learning is not modulated by larval age between 4, 5, and 6 days after egg laying; (IV) learning is not modulated by gender; (V) *en masse* assays are feasible as well, and confirm the lack of gender differences; (VI) memory is fully stable for at least 30 min. These experiments provide a basis for future queries into the cellular and molecular underpinnings of appetitive olfactory learning in larval *Drosophila*.

## A ROLE FOR SYNAPSIN IN ASSOCIATIVE LEARNING: THE *DROSOPHILA* LARVA AS A STUDY CASE

Birgit Michels, Sören Diegelmann, Hiromu Tanimoto, Isabell Schwenkert, Erich Buchner & Bertram Gerber

University of Würzburg

bertram.gerber@biozentrum.uni-wuerzburg.de

Synapsin is an evolutionarily conserved, highly abundant vesicular phosphoprotein in presynaptic terminals. It is thought to regulate the recruitment of synaptic vesicles from the reserve pool to the ready-releasable pool, in particular when vesicle release is to be maintained at high spiking rates. As regulation of transmitter release is a prerequisite for synaptic plasticity, we ask whether synapsin has a role in behavioural plasticity as well. We tackle this question for associative olfactory learning in *Drosophila* larvae by using the deletion mutant *Syn<sup>97</sup><sup>CS</sup>*, which had been backcrossed to the Canton-S wild type strain (CS) for thirteen generations to yield an essentially identical genetic background for the mutant and the wild type control. We first provide a molecular account of the genomic status of *Syn<sup>97</sup><sup>CS</sup>* by PCR and then prove the complete absence of gene product in the larva by using an anti-synapsin monoclonal antibody on western blots and nerve-muscle preparations. Interestingly, we find on the behavioural level that olfactory associative learning in *Syn<sup>97</sup><sup>CS</sup>* larvae is reduced to appr. 50 % of wild type CS level; in contrast, responsiveness to the to-be-associated stimuli and motor performance are normal in *Syn<sup>97</sup><sup>CS</sup>*. Our results thus suggest that larval *Drosophila* can be used as a case study for a role of synapsin in associative learning.

# Neuronal activity of dopaminergic cells in the *Drosophila* brain analyzed by optical calcium imaging

Riemensperger Thomas, Buchner Erich, Fiala André

Theodor-Boveri-Institut, Lehrstuhl für Genetik und Neurobiologie,  
Julius-Maximilians-Universität Würzburg,  
Biozentrum am Hubland  
97074 Würzburg, Germany

## Abstract:

Olfactory learning and memory formation in *Drosophila melanogaster* is studied extensively using an odour stimulus paired with an electro shock as an aversive reinforcer. Whereas appetitive olfactory learning is dependent on octopamine, the dopaminergic system is necessary for aversive olfactory memory formation. This suggests that dopaminergic neurons might mediate the negative reinforcer during aversive training. We test this hypothesis by employing the fluorescent calcium sensor cameleon to optically record neuronal activity in vivo (1). The sensor is driven selectively in dopaminergic neurons using the Gal4-line TH-Gal4(2) that expresses Gal4 under the control of the regulatory sequence of the gene for tyrosine hydroxylase, an enzyme of the dopamine synthesis pathway. We confirm the high specificity of the TH-Gal4 line by combining imaging of cameleon driven by the Gal4 line and anti-tyrosine hydroxylase or anti-dopamine immunohistochemistry. We show that several parts of the mushroom bodies, brain centres involved in olfactory memory formation, are densely innervated by dopaminergic neurons. We observe that dopaminergic neurons projecting into the mushroom body's alpha-, beta-, and gamma-lobes respond to electric shock stimulation by an increase in intracellular free calcium. Current experiments address the question whether all dopaminergic neurons or only a subset are involved in the shock response and whether pairing of odorants with electric shocks modifies the response of those neurons. First results will be presented.

## References:

- 1) Fiala et al (2002). Genetically expressed cameleon in *Drosophila melanogaster* is used to visualize olfactory information in projection neurons. *Curr Biol*.12: 1877-84.
- 2) Friggi-Grelín et al (2003) Targeted gene expression in *Drosophila* dopaminergic cells using regulatory sequences from tyrosine hydroxylase. *J Neurobiol*. 54: 618-627.

**Ant navigation: can landmark-based routes be reversed?**

Martin Boyer and Rüdiger Wehner

Institute of Zoology, University of Zurich, Winterthurerstrasse 190,  
8057 Zurich, Switzerland

Path integration provides foraging desert ants with a continually updated global vector that guides the animal directly back to its starting point, the nest, and later allows it to return to the former feeding site. Extensive experiments have shown that the inbound state of the global vector is always the inverse, i.e. the 180° reversal, of the outbound state of the global vector (review Wehner and Srinivasan, in Jefferey, K. J., ed., *The Neurobiology of Spatial Behavior*, pp. 9-30, 2003). Hence, within the ant's navigational machinery, vectors can be reversed. Does the same ability hold true for the use of landmark-based routes, which the ants have acquired during, say, their outbound journeys?

Australian desert ants, *Melophorus bagoti*, have been shown to acquire and use fixed routes when foraging within cluttered environments. These routes differ idiosyncratically between one ant and another as well as between the outbound (foraging) and inbound (homing) paths of the same ant (Kohler and Wehner: *Neurobiol. Learn. Mem.*, in press). Inbound ants recognize their former inbound routes even if their path integrator is at zero state, i.e. if the ants have already returned to the nest before they are tested.

Here we ask whether an inbound ant can also recognize its outbound route and follow it, in a reversed way, back to the nest. In particular, we used a barrier device to deflect the outbound ants just after having left the nest entrance as well as the inbound ants just after having left the feeder (located at a 11-m distance from the nest). This device resulted in the ants acquiring completely different inbound and outbound routes within the maze-like array of grass tussocks covering the Australian desert near Alice Springs.

In the critical tests homebound ants, which had run off 50 per cent of their home vector and hence had still to continue for the remaining 50 per cent (semi-vector ants), or which had already run off their entire home vector (zero-vector ants), were displaced to their individual outbound routes and released there at a location midway between the nest and the feeder. Ants of neither group recognized their outbound corridors. The semi-vector ants ran off their home vector (which according to the training paradigm pointed away from the outbound landmark route), and the zero-vector ants started their systematic search for the nest.

In conclusion, homebound ants tested in the natural landmark settings are not able to use the sequence of landmarks acquired during their outbound runs, in a reversed order, for returning to the nest. As judged from the visual cues experienced by an ant moving within a cluttered environment, it will indeed be extremely difficult to predict the way in from the sequence of landmark images experienced on the way out.

Supported by the Swiss National Science Foundation, grant No. 31-61844.00.

# Landmark-based route memories in desert ants, *Melophorus bagoti* : can sequentially acquired landmark memories be retrieved at any point of the sequence?

Florian Loertscher and Rüdiger Wehner

Institute of Zoology, University of Zurich, Winterthurerstrasse 190,  
8057 Zurich, Switzerland

Besides path integration (vector navigation) landmark-based route navigation is one of the most powerful tools used in long-distance navigation of desert ants. This has been demonstrated most comprehensively in North African and Australian desert ants belonging to the genera *Cataglyphis* and *Melophorus*, respectively (Wehner, Michel, Antonsen: J. Exp. Biol. 199: 129-140, 1996, Kohler and Wehner: Neurobiol. Learn. Mem., in press). Moreover, in the ant's navigational toolkit route fidelity is exhibited independently of the state of the ant's path integrator. For example, full-vector and zero-vector ants released at the feeder follow their idiosyncratic inbound routes with the same high accuracy (lit. cit.).

Here we address the question whether landmark images acquired sequentially along the inbound or outbound routes have to be retrieved in the sequence experienced during learning. In particular, we ask whether a zero-vector ant, which outside the route has to rely exclusively on its search routine, can recognize its route at any point it happens to hit it.

Within the grass-tussock semi-desert of central Australia we trained individually marked ants to follow separate inbound and outbound routes. After the trajectories of at least three inbound paths had been recorded in any particular ant, zero-vector ants (i.e. ants, which had already returned to the nest and had been captured there just prior to entering the colony) were displaced to various locations to the left and right of their idiosyncratic inbound routes. Amazingly, the ants instantly channelled into their proper routes wherever they hit them, be this close to the feeder, close to the nest, or anywhere in between. No search movements or any other obvious orientation movements occurred after the ants had arrived at their proper routes. They immediately turned in the right (homeward) direction and followed the route as accurately as in the former training runs.

In conclusion individual ants can recognize their idiosyncratic landmark-based routes at any particular place at which they happen to enter them arbitrarily.

Supported by the Swiss National Science Foundation, grant No. 31-61844.00.

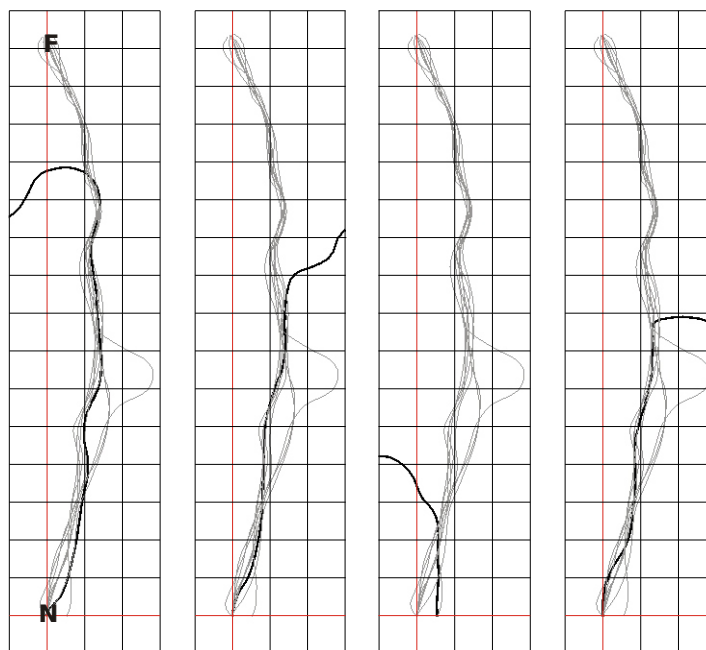


**Fig. 1 :** Four homebound runs (bold black trajectories) of the same ant tested at 0-vector state. The ant was released to the left (1<sup>st</sup> and 3<sup>rd</sup> panel) or to the right (2<sup>nd</sup> and 4<sup>th</sup> panel) of its habitual route. The latter indicated by eight control inbound runs (grey trajectories). F (feeder), N (nest).

## Cognitive reinforcement of rat hippocampal LTP

Shukhrat Uzakov, Julietta U. Frey and Volker Korz

Dept. Neurophysiology, Leibniz-Institute for Neurobiology, Brennekestr. 6, 39118 Magdeburg, Germany

Hippocampal long-term potentiation (LTP) can be dissociated by inhibitors of protein synthesis into two separate phases: early-LTP lasting about 4 h and late-LTP with a duration beyond 4 h, the latter of which requiring the synthesis of new macromolecules. Several studies have documented that early hippocampal long-term potentiation can be reinforced into late-LTP by novel, behavioral arousing stimuli and stress. Here we show (1) a cognitive reinforcement of LTP induced by complex learning using a holeboard paradigm and (2) its dependency on protein synthesis as it was the case for memory consolidation. Four groups of animals received a spatial training on a fixed pattern of baited holes of five, seven, eight and ten trials, respectively. The last trial was performed 15 min after weak tetanization, i.e. a stimulation pattern which would induce only early-LTP if not combined with reinforcing stimuli. Four additional groups served as controls: animals that remained untreated, holeboard procedure naïve animals (novelty control), animals that received only food in the holeboard and pseudotrained animals. Errors of long-term reference memory during the last trial were significantly decreased only in the eighth and tenth trial experimental groups compared to pseudotrained animals. Correlating to this learning effect we found a reinforcement of early-DG-LTP only in the eighth and ten trial experimental animals and no reinforcement in controls. The data suggest that plasticity proteins required for spatial memory formation are the same as those contributing to LTP maintenance in the hippocampal dentate gyrus.

## **The effect of rolipram, a type IV-specific phosphodiesterase inhibitor, on distinct forms of long-term depression and 'synaptic tagging'**

Sheeja Navakkode, Sreedharan Sajikumar and Julietta U. Frey

### **Abstract**

Our earlier experiments investigating the action of rolipram, a type IV-specific phosphodiesterase inhibitor, revealed that a transient early-form of LTP could be reinforced to a late, protein synthesis-dependent long-lasting form. Furthermore, we have shown that the reinforcement of early- into late-LTP followed the rules of 'synaptic tagging'. These data support our assumption that phosphodiesterases (PDE) may represent one of the plasticity-related proteins (PRPs) required for the establishment of long-lasting plastic changes to occur (Ahmed and Frey, 2003 and 2004; Navakkode et al., 2004). Here we investigated the effect of rolipram on early-LTD and synaptic tagging during LTD in CA1 of rat hippocampal slices in vitro. Application of rolipram during the induction of early-LTD (the protein synthesis-independent form with a duration of up to 2-3 h) converted the early- form into a long-lasting one, with a duration of at least 6 h. This rolipram-reinforced LTD (RLTD), was blocked by a NMDA-receptor antagonist, AP5 or the reversible protein synthesis inhibitor, anisomycin, respectively, thus proving that RLTD is NMDA-receptor- and protein synthesis- dependent. We have then more subtly characterized the specific cellular action of rolipram. RLTD was blocked by the MEK inhibitor, U0126 showing that the induction of RLTD by rolipram involves the activation of MAP kinases. In a further series of experiments we studied whether rolipram can interact with processes of 'synaptic tagging' as it was the case for RLTP (see Navakkode et al. 2004). Inhibition of PDEs by rolipram and thus, reinforcement of early-LTD into late-LTD in one synaptic input S1 was able to influence early-LTD in second independent input S2. Early-LTD in S2 was transformed into late-LTD by RLTD in S1. Furthermore, we could also show that PDE-inhibition by rolipram, RLTD as well as RLTD-induced synaptic tagging were dependent on the activation of the dopaminergic D1/D5-receptor. This result is in contrast to our data observed during RLTP (Navakkode et al.2004). We will discuss this discrepancy in more detail.

### *References*

Ahmed T, Frey JU. *Neuroscience*. 2003;117(3):627-38.

Ahmed T, Frey S, Frey JU. *Neuroscience*. 2004;124(4):857-67.

Navakkode S, Sajikumar S, Frey JU. *J Neurosci*. 2004 Sep 1;24(35):7740-4.



## **In search for the specificity of 'synaptic tags' during LTP and LTD**

Sreedharan Sajikumar, Sheeja Navakkode & Julietta Uta Frey

Department for Neurophysiology, Leibniz-Institute for Neurobiology,  
Brennekestr. 6, D-39118, Magdeburg, Germany.

Individual synapses or a group of synapses are capable of being modified independently according to the stimulus which they receive. A weak tetanus can induce an early form LTP (early-LTP) lasting 2-3 h, while a strong tetanus can induce a late form of LTP (late-LTP) lasting 6-8 h, the latter of which being dependent on translation and transcription for its persistence. The logical problem arises of how mRNAs or proteins can selectively target synapses that have undergone early-LTP and convert the transient early-LTP to a long lasting late-LTP. The 'synaptic tagging' hypothesis (Frey & Morris, 1997) has been put forward as a way to address this problem. According to this hypothesis the persistence of LTP is mediated by the intersection of two dissociable events. The first event involves the generation of a transient local 'synaptic tag' at specific synapses in association with the induction of early-LTP. The second involves the production and diffused distribution of 'plasticity related -proteins' (PRPs) that are captured and utilised only at those synapses possessing a tag. Recently we have also reported 'synaptic tagging' during LTD and have shown a positive associative phenomenon of LTP and LTD which we named 'cross-tagging' (Sajikumar.S & Frey.J.U, 2004). Here, process-specific tags can capture process-unspecific PRPs. We also reported that the local 'tags' can be reset by depotentiation in a time-dependent manner. (Sajikumar.S& Frey .J.U, 2004). However, the identity of the 'synaptic tag' and its specificity for LTP or LTD remained still elusive even though it was speculated to be either a role of spine morphological changes, or of the involvement of PKC-isotype: PKM $\zeta$ , or the role of other kinases. Here we present data identifying candidate molecules which make the tags specific for either LTP or LTD.

## **Generalisation of conditioned fear in mice deficient for the neural cell adhesion molecule NCAM**

Anne Albrecht, Jorge Bergado, Hans-Christian Pape and Oliver Stork

Institut für Physiologie, Medizinische Fakultät, Otto-von-Guericke Universität Magdeburg,  
Leipziger Str. 44, D-39120 Magdeburg, Germany

In classical fear conditioning animals learn quickly to associate a previously neutral sensory stimulus (CS+) like a tone with an aversive stimulus (US) such as foot shock. Although a commonly used instrument for studying processes of emotional memories, little is known about mechanisms underlying fear memory specificity and generalisation in this paradigm. Generalisation, describing a transfer of the conditioned response to neutral test stimuli (CS-) or the training environment (context) without presence of the CS+, is known to occur after intensive training with highly stressful US (overtraining). In this study we began to investigate, with an auditory fear conditioning paradigm, molecular aspects of such fear memory generalisation in mice deficient for the neural cell adhesion molecule (NCAM<sup>-/-</sup> mice) and their wild type (NCAM<sup>+/+</sup>) littermates. NCAM is a glycoprotein of the immunoglobulin superfamily which plays important roles in both development and synaptic plasticity of the central nervous system. NCAM<sup>-/-</sup> mice display deficits in emotional behaviour (increased aggression and anxiety) and memory formation in amygdala- and hippocampus dependent tasks. We could show that moderate pre-exposure to context and CS- could overcome previously observed deficits in cued and contextual fear conditioning in the NCAM<sup>-/-</sup> mice. Moreover, we found a comparable increase of defensive behaviour (risk assessment and freezing) and generalisation towards the neutral CS- in overtrained NCAM<sup>-/-</sup> and NCAM<sup>+/+</sup> animals. However, while overtrained NCAM<sup>+/+</sup> mice also increased their defensive response to the conditioning context, their NCAM<sup>-/-</sup> littermates showed no such generalisation. Previous studies have shown that changes of NCAM expression in the amygdala and hippocampus of fear conditioned animals are dependent on stress level. Our data now suggest that NCAM-mediated cellular processes are critically involved in the stress-dependent modulation of emotional memory, in particular, its generalisation to contextual background information. This deficit was correlated with changes of synchronised network activities in the amygdalo-hippocampal pathway of fear conditioned NCAM<sup>-/-</sup> mice.

Supported by Deutsche Forschungsgemeinschaft (SFB 426 TP B7; Leibniz-Programm)

**Compartmentalized modulation of PDE4B isotypes and cAMP-levels during long-term potentiation in rat hippocampal slices *in vitro*.**

**T. Ahmed and J. U. Frey**

Leibniz-Institute for Neurobiology, Department of Neurophysiology, Brennekestrasse 6, D 39118 Magdeburg, Germany.

Molecular events associated with mnemonic processes and neuronal plasticity are postulated to result in functional changes in synaptic structure. One possible site is the post-synaptic density, where activity-dependent changes modulate signal transduction cascades. In this report we detail spatial-temporal changes for phosphodiesterase 4B (PDE4B) proteins and their substrate cAMP within three neuronal compartments during early- and late- long-term potentiation (LTP). The cAMP-dependent protein kinase A cascade - which can be regulated by distinct PDE4B activity - is required for mnemonic processes as well as mechanisms of neuronal plasticity, such as those during the maintenance or late-LTP.. Fluorescence *in situ* hybridisation studies (FISH) identified no translocation of *PDE4B3* from the soma after late-LTP induction indicating a subtle, local control of PDE4B activity. Protein changes were detected within the PSD-enriched fraction. From these results we conclude that either the changes in PDE4B are due to modulation of pre-existing mRNA, or that the protein is specifically translocated to activated synaptic structures. Furthermore, we report late changes in cAMP levels in the somato-dendritic fraction and discuss this result with the increased PDE4B3 in the PSD-enriched fraction

## **Enhancement of spatial memory retention following posttraining allosteric potentiation of the metabotropic glutamate receptor subtype 5 (mGluR5)**

Wolfram Wetzels and Detlef Balschun

Leibniz Institute for Neurobiology (IfN), Brenneckestr. 6,  
39118 Magdeburg, Germany

Metabotropic glutamate receptors (mGluRs) are suggested to play an important role in synaptic plasticity and learning and memory. Previously, we found different effects of group I mGluR agonists (trans-azetidine-2,4-dicarboxylic acid, tADA; S-3,5-dihydroxyphenylglycine, DHPG; RS-2-chloro-5-hydroxyphenylglycine, CHPG; S-3-hydroxyphenylglycine, 3HPG) and antagonists (RS- $\alpha$ -methyl-4-carboxyphenylglycine, MCPG; S-4-carboxyphenylglycine, 4CPG; 2-methyl-6-phenylethynyl-pyridine, MPEP) on spatial learning in rats (1-5). In posttraining application experiments, most of these substances had either no effects (MPEP, 4CPG, 3HPG) or displayed a tendency to decreased (MCPG, DHPG) or increased retention values (tADA). Posttraining injection of the mGluR5 agonist CHPG, however, resulted in a significant increase of memory retention, i.e. the mean percent-savings in the CHPG group were twice as large as in the NaCl control group. These data led us to hypothesize that a selective activation of mGluR5 receptors, but not mGluR1 receptors, after learning improves retention of spatial memory in rats.

Recently, a family of highly selective allosteric modulators of the mGluR subtype 5 was identified (6). In the present study we used the allosteric potentiator 3,3'-difluorobenzaldazine (DFB) to test the effect of an enhanced posttraining activation of mGluR5 on memory retention. Male Wistar rats were chronically implanted with microcannulas in the right lateral ventricle. DFB (49  $\mu$ g, dissolved in 5  $\mu$ l 1% DMSO) was injected intracerebroventricularly (icv.) immediately after training of a 40-trial footshock-motivated spatial alternation reaction tested in a Y-maze as described previously (7). Furthermore, the open-field behaviour was observed 30 min following icv. injection. In DFB treated animals, we found a highly significant improvement of memory retention tested 24 hours after training. On the other hand, open-field behaviour was not influenced by DFB.

Our results demonstrate that posttraining activation of mGluR5 (CHPG; DFB) but not mGluR1 (3HPG) has beneficial effects on spatial memory retention in rats qualifying mGluR5 as a promising target for the treatment of cognitive deficits in humans (8).

(1) Balschun and Wetzels: *Neurosci. Lett.* 249, 41-44, 1998; (2) Balschun et al.: *Learning & Memory* 6, 138-52, 1999; (3) Wetzels and Balschun: *Behav. Pharmacol.* 12 (Suppl.1), 109, 2001; (4) Balschun and Wetzels: *Pharmacol. Biochem. Behav.* 73, 375-80, 2002; (5) Wetzels and Balschun: *FENS Abstr. Vol.1*, 107.30, 2002; (6) O'Brien et al.: *Mol. Pharmacol.* 64, 731-40, 2003; (7) Riedel et al.: *Neuroreport* 5, 2061-2064, 1994; (8) Moghaddam: *Psychopharmacology* 174, 39-44, 2004.

## **The impact of juvenile stress exposure and pre-experience on shuttle box learning in adult rats: involvement of the dopaminergic system.**

S.Schäble\*<sup>#</sup>, G.Poeggel\*, K.Braun<sup>#</sup>, M. Gruss<sup>#</sup>

\*University of Leipzig, Department of Human Biology, Leipzig; <sup>#</sup> Otto von Guericke University, Institute of Biology, Magdeburg, Germany

The present study was carried out to test the hypothesis that juvenile stress exposure and pre-experience as well as the treatment with a D2 receptor antagonist (haloperidol) during pre-experience has an impact on the performance of adult *female* rats in a two-way active avoidance paradigm (shuttle box). Therefore, between postnatal day (PND) 1 and PND 16 female rat pups were *socially reared* (reared undisturbed with their mother/ siblings) or *repeatedly separated* (separated from their mother/ siblings for 3 hours per day = juvenile stress exposure). Starting at PND 17, pups were trained (= pre-experience) on 5 consecutive days with 50 trials per day in a shuttle box with a 2.4 kHz tone (CS) and electric footshocks (0.6 mA, UCS). In a parallel pharmacological approach we tested the role of the dopaminergic system during pre-experience. Each day, 30 minutes before pre-experience pups received either injection (i.p.) of vehicle or injections of 0.5, 0.1, or 0.01 mg/kg haloperidol. At adulthood all rats were tested with the same parameters as used during pre-experience as adults (starting at PND 80).

The learning tests in adult rats revealed that: 1.) in tendency, after juvenile stress an improved performance was observed compared to unstressed animals, and 2) pre-experience enhanced learning performance compared to animals without pre-experience. This effect was independent of juvenile stress exposure. Furthermore, 3.) D2 receptor blockade by haloperidol suppressed the improvement in learning performance in pre-experienced animals in a dose-dependent manner in socially reared as well as repeatedly separated animals.

These results support our hypothesis, that juvenile stress exposure as well as juvenile, D2 mediated pre-experience improves learning performance in adult female rats. These data underline the importance of early experience for adult learning and the role of dopamine during pre-experience and may help to improve our knowledge of the neurobiological basis underlying learning deficits.

*Supported in part by SFB 426*

**Fast homeostatic control of synaptic potentiation in the adult hippocampus**

Claudia Roth-Alpermann<sup>1</sup>, Richard G. M. Morris<sup>2</sup>, Tobias Bonhoeffer<sup>1</sup>, Martin Korte<sup>1</sup>

<sup>1</sup>Max-Planck-Institute of Neurobiology, Martinsried, Germany

<sup>2</sup>The University of Edinburgh, Edinburgh, Scotland, UK

It has been shown that in developing neuronal circuits, homeostatic regulation of global synaptic strength can operate over a timeframe of several days (Turrigiano et al., 1998). However, also in the adult nervous system, protection against runaway synaptic strengthening might be necessary, especially in highly plastic brain structures such as the hippocampus. If too many synapses of a single neuron are potentiated, a neuron might be at risk of overexcitation; and in addition, this might reduce the information-storage capacity of the respective neuronal circuits (Moser et al., 1998). We therefore hypothesized that some fast-acting homeostatic mechanism might be in place that, after a certain threshold of overall potentiation is reached, limits further synaptic strengthening at heterosynaptic sites. To test this hypothesis we performed long-lasting extracellular and intracellular electrophysiological recordings in acute hippocampal slices of rats using the classical NMDA-receptor dependent CA3-CA1 LTP.

In a first series of experiments we observed, that one hour after saturating LTP through multiple tetanization of one Schaffer collateral pathway, hippocampal CA1 neurons still exhibited additional potentiation at heterosynaptic sites in response to a LTP stimulus in a second independent pathway. Neither the amount nor the persistence of this LTP differed from the LTP induced in naïve control slices that had not sustained saturating LTP induction. These findings argued against homeostatic protection against LTP saturation, but were not conclusive as it is possible that the number of synapses activated by the first stimulus was too low to trigger a homeostatic down regulation of the remaining synapses' ability to undergo LTP.

In an attempt to overcome this threshold, we have now performed experiments using chemical potentiation to induce very widespread synaptic strengthening throughout the slice. Initial experiments confirmed that chemical LTP was NMDA-receptor dependent and previous chemical potentiation occluded later tetanic LTP induction, indicating that both forms of potentiation share intracellular signaling pathways. We used a local superfusion technique to selectively spare a small number of synapses from being chemically potentiated. Pharmacological blockade of synaptic transmission outside the superfusion spot allowed to electrophysiologically isolate the inside-spot synapses. We then tested whether these superfused and hence unpotentiated synapses inside the spot were still capable of exhibiting LTP. Our data show, that under these conditions the inside-spot synapses do not exhibit potentiation. Control experiments established that LTP can be induced at inside-spot synapses if prior chemical potentiation did not occur. These findings point towards a homeostatic mechanism in circumstances in which a sufficient proportion of a neuron's synapses have previously undergone LTP.

**Rodent cognition in virtual reality:  
time dynamics of place and spatial response learning by mice  
on a servosphere virtual maze**

York Winter, Jens Ludwig, Ursula Kaupert and Hans-Ulrich Kleindienst  
University of Munich, Department of Biology and Max-Planck-Institute for Ornithology,  
Seewiesen

Spatial relationships provide the context for most adaptive behaviours, as well as the framework in which episodic or episodic-like memories are encoded. The evolution of neural mechanisms underlying an animal's ability to orient in space has been driven by the principle of fitness maximization and adapted to an animal's use of space within its natural habitat. Any systems approach based on the analysis of neurophysiological correlates of mental processes should eventually explain the full extent of quantifiable behavioural competences under naturalistic conditions. Cognition may be defined by the complexity of behavioural competences that are supported. The planning of foraging routes may be the most common use of the cognitive map. While inherently "cognitive" in nature, this type of higher level information processing has yet to be incorporated into experimental designs of research on spatial cognition by animals. The information processing required by animals planning multi-destination foraging routes clearly surpasses the requirement for establishing mere landmark-place associations. We developed the *virtual sphere maze* as an immersible virtual reality (VR) experimental paradigm for rodents. It simulates spatially extensive naturalistic artificial environments with multiple-destinations and food reward schedules following natural dynamics. It allows the comprehensive examination of higher order cognitive demands on rodents using space during the foraging for food. Here, we present results showing that mice show true spatial orientation behaviour within the VR of the servosphere virtual maze during a simulated T- and cross-maze food finding orientation task. As has been demonstrated previously for real mazes, the behavioural mechanisms applied to solve a T-maze orientation task changes from allothetic orientation based on external landmarks during an early stage to a mostly idiothetically driven routine behaviour during the later stage of the spatial learning process. We found this same behavioural sequence of orientation mechanisms used by mice confronted with a food-finding task on the virtual sphere maze simulating a VR T-maze.

## **Foraging in a complex naturalistic environment: Capacity of spatial working memory in flower visiting bats**

**Kai Petra Stich and York Winter**

Biozentrum der Universität München and Max-Planck Institut für Ornithologie, Seewiesen

Memory systems have evolved under selection pressures including the need to remember the locations of resources and past events within spatiotemporally dynamic, natural environments. The full repertoire of complex behaviours exhibited by animals in dynamic surroundings are, however, difficult to elicit within simply structured laboratory environments. We developed a computer controlled naturalistic environment with an array of feeders for simulating dynamic patterns of water or food resource availability (depletion and replenishment) within the laboratory. It is based on a computer controlled six-cage and 76-feeder system for automated exchange of experimental animals, behavioural data collection and event control. In the present study we investigated spatial working memory capacity of nectar-feeding bats (*Glossophaga soricina*, Phyllostomidae) collecting food from a 64-feeder array. The experimental schedule of food availability from the feeder array required the experimental animals to use a win-shift strategy in order to feed efficiently and therefore the need to remember past feeding actions. The results indicate that these bats can hold more than 40 behaviour actions (feeder visits) in spatial working memory without indication of decay. Such a capacity of spatial working memory surpasses previous findings for other vertebrate taxa.



## **Visual landmark orientation by flying bats at a large-scale touch and walk screen for bats, birds and rodents**

**York Winter, Sophie von Merten & Hans-Ulrich Kleindienst**

Biozentrum der Universität München and Max-Planck Institut für Ornithologie, Seewiesen

Orientation depends on multi-modal information about the locally perceptible environment ('local view') in many situations. We developed a behavioural paradigm for investigating visual orientation of flying bats based on a large-scale touch-screen (1.2 x 1.8 m). It functions by a grid of rows and columns of infra-red beams just in front of a screen with back-projected visual stimuli. Approaching animals interrupt the beams and thus permit automatic recording of the time and place of an animal's locational choice. We used it as a vertical touch surface. Installed as a horizontal walk surface, it may also serve as a more natural 'firm ground', circular arena analogue to the 'Morris water maze' for investigating orientation behaviour and spatial cognition from rodents to birds while offering automatic real-time recording of paths, times and latencies with enhanced possibilities to score details of motor behaviour and to control stimuli interactively.

Bats offer a unique possibility to investigate the use of both echo-acoustic and visual information processing pathways for the process of self-localization and orientation. In our first experiment, a bat was presented with five identical targets, one central and four peripheral and had to choose the central target. After task acquisition, the array was shifted by the distance between targets, so that a formerly peripheral landmark was now in the absolute location of the formerly central target. At small intertarget distances, the bat 'went with' the array, and chose the new central target (at a new absolute location). With 30 cm or more of intertarget distance (60 cm across the landmark configuration), however, the bat went with absolute location, and chose a peripheral target. In Expt. 2, the bat was presented with two landmarks 30 cm apart and an unmarked target located at midline beneath them. On tests, the landmarks either maintained training distance or were expanded to 50 cm apart. On such expansion tests, the bat chose most the location at the correct vector from the right landmark. This showed that the bat first identified a single landmark by the configuration and then applied a previously learnt vector (angle and distance) to locate the target. *Glossophaga* did not orient by pure angular geometry between landmarks and target.

## **Echoacoustic object generalization and spatial dependence of two-alternative forced-choice (2AFC) learning set acquisition in bats**

**Angelika Oppelt, Denisse Tafur, Kai Petra Stich & York Winter**

Discrimination (the ability to distinguish) and generalization (the ability to group) are cognitive abilities of importance for foraging, predator avoidance, partner choice and many other tasks within the daily lives of animals. The extent to which an animal should distinguish between two stimuli or generalize and thus group them should be context dependent. We performed a series of experiments to investigate the ability for echo-acoustic object generalization in nectar-feeding bats (*Glossophaga soricina*). As these bats exploit flowers by night for nectar we expected them to readily develop search images for the echo-acoustic signals of specific floral shapes experienced with sugar water rewards. Experiments were conducted with multiple pairs of two-alternative forced choice feeders. Within each pair of feeders a pair of a positive and a negative echoacoustically distinct object could be exchanged automatically. Bats were first operantly conditioned to the positive object at a training location and afterwards confronted with the same pairing of positive and negative objects simultaneously at ten other locations within a 120 sqm experimental room. Our first results indicated, rather unexpectedly, that bats did not transfer or generalize the positive object reward association to new locations presenting the same 2AFC task. Rather, the identity in slopes of the learning curves indicated that the echoacoustic object reward associations were learnt independently for each spatial location within the experimental room. Such a result would be expected if spatial location had been learnt in conjunction with the other characteristics defining an echoacoustic object's representation. From the results of a series of further experiments we learnt the following. Acquiring 2AFC echoacoustic object discrimination constituted two independent learning tasks for the bats. Bats first had to learn the 'learning set' of the two-alternative forced-choice paradigm. This required them to overcome their inherent and very strong spatial preference for locations experienced previously with reward and instead make a locational choice dependent on presented stimuli. This learning set acquisition had a very strong component of spatial location. At each new spatial location where bats were confronted with the 2AFC paradigm their performance always began at random choice level. However, 2AFC task acquisition at new locations occurred increasingly faster the more experience a bat had had with this paradigm. On the other hand, once bats had acquired the 2AFC paradigm for all our experimental spatial locations the ability for echoacoustic object generalization was evident: bats reliably discriminated positive echoacoustic objects conditioned to previously at other spatial locations. Beyond this ability, our results indicate that multiple learning mechanisms can be involved in a simple 2AFC object discrimination task. The consideration of an animal's natural behaviour is relevant for realistically judging aspects of cognitive competence.

**Sensitisation of C57BL/6N mice: a proposed mouse model of PTSD**

A. Siegmund &amp; C.T. Wotjak

Max-Planck-Institute of Psychiatry, Munich

Animal models of psychiatric disorders are employed to understand pathomechanisms of the respective illness and to find new therapeutic strategies, e.g. by screening new substances for their psychopharmacological potential. So far no widely accepted animal model has been established for Posttraumatic Stress Disorder (PTSD). Backing the symptoms of human PTSD, an animal model of this disturbance should present (1) persisting fear with (2) delayed onset, (3) elicited through a single short aversive encounter, (4) as a function of stimulus intensity and (5) genetic background. PTSD related symptoms should consist of both (6) hyperarousal and signs of emotional blunting (Yehuda, 1993, extended).

To this end we analysed the fear behaviour of the two genetically similar inbred mouse strains, C57BL/6JOlaHsd (B6JOla) and C57BL/6N (B6N), in a variety of fear conditioning and sensitisation tasks, using a single electric footshock as aversive encounter. Following the traumatic incident, B6JOla mice recovered from their initial fear reaction on (i) recall of the aversive memory and (ii) their sensitised defensive behaviour elicited by a neutral tone, both acutely and on repeated stimulus exposure. B6N mice, in contrast, showed sustained fear. Freezing behaviour proved to be dependent on footshock intensity and incubation time after the aversive stimulation. B6N mice exhibited increasing depression like symptoms (floating in the forced swimming test) and decreasing interaction time with a juvenile CD1 mouse in an incubation-time dependent manner.

Currently we are investigating (i) epigenetical influences on the respective phenotypes through prenatal cross-fostering, (ii) the hormonal stress axis and the central CRH system, (iii) vegetative PTSD-related symptoms by means of telemetry and (iv) potential of antidepressants in prevention and therapy of PTSD-related symptoms in B6N mice.

We consider shock sensitisation of B6N an appropriate mouse model of PTSD, following Yehuda's criteria. The most compelling potential of this animal model lies in the exclusiveness of the behavioural difference in the adaptation to an aversive encounter of the two genetically similar mice strains B6JOla and B6N. This model will enable us to investigate cellular and molecular mechanisms that underlie adaptive and maladaptive processing of aversive memories, with the goal to forward new therapeutic strategies in the treatment of PTSD.

## Superior spatial learning abilities of NR2B transgenic mice in a new labyrinth task

Helmuth Adelsberger, Joe Z. Tsien\*, Arthur Konnerth

Physiologisches Institut, Universität München, Pettenkoferstr. 12, 80336 München

\*Center for systems neurobiology, Department of Pharmacology, Boston University School of Medicine

Learning and memory is associated with changes in the strength of synaptic transmission as well as with the presumed formation of new synaptic connections between the participating neurons. One of the key molecules involved in these processes is the NMDA-type glutamate receptor subunit NR2B. It had been previously reported that transgenic mice overexpressing NR2B in the hippocampus exhibit an enhanced memory performance in different behavioral tasks, like novel-object recognition, fear conditioning and water maze (Tang Y. et al., *Nature* 1999; 401:63-69). However, the improved spatial learning ability of the transgenic mice in the water maze task was only significant on the third day of the test as compared to the control group. At the end of the test, the wildtype mice reached the same performance level.

We developed a new test for spatial learning that allows a better differentiation between the individual learning steps and provides a better quantification of the results. The task consists the repeated walk through a newly designed labyrinth made of acrylic glass tubes with a length of 50 cm each (the inner diameter of the tubes is 5 cm). The test is primarily based on the positive motivation of the animals and largely avoids the fear associated with the classical water maze tests. The crossing points of the labyrinth consist of vertically oriented acrylic glass tubes. The bottoms of these vertical tubes were filled with water (1 cm high) to prevent the animals from resting there. The number of crossing points was varied in a task-specific manner up to 9 times. In an initial training phase, the mice were placed for three times in one end of a single acrylic glass tube and were allowed to walk through the tube in order to reach the familiar home box on the other end. For the present analysis, control and transgenic NR2B mice walked through a labyrinth with 9 crossings. After each single trial, six horizontal tubes were changed randomly to avoid the influence of olfactory cues. The standard test consisted of 1 trial/day on 6 consecutive days. The first trial was an inspection trial in which the animals from both groups became familiar the new environment and finally found their home cage by chance after about 20 min. Starting with the second trial, both groups showed a marked learning, as indicated by a decrease in both the time and the total walking distance needed to reach the home box. While the total walking time was not significantly different for the two groups, NR2B overexpressing mice needed a significantly shorter walking distance (= travel number through the different tubes). In contrast to the water maze, this difference persisted throughout all further trials and, remarkably, the control animals never reached the level of performance of the transgenic mice. An additional trial was performed two weeks after the first series to test for the long term memory performance. In this test, both groups kept their level of performance, however, the significant difference in skills persisted.

Taken together our results demonstrate that the new labyrinth task is well suited to resolve impairments in spatial learning abilities. Moreover, it allowed to detect subtle changes that are not prominent in the classical tasks, like the water maze test. Our results confirm and extend the notion that NR2B overexpressing transgenic mice are superior spatial learners. Furthermore, our results provide for the first time evidence that NR2B contributes to long term memory.

## Single-shock synaptic plasticity induced by local dendritic spikes

K.Holthoff<sup>1,2</sup>, Y. Kovalchuk<sup>1</sup>, R. Yuste<sup>2</sup> and A. Konnerth<sup>1</sup>

<sup>1</sup> Physiologisches Institut, LMU München, Germany

<sup>2</sup> Dept. of Biological Science, Columbia University, New York, USA

Mammalian dendrites are active structures capable of regenerative electrical activity. Besides sodium-based action potentials, which can propagate throughout the dendritic tree, neocortical pyramidal neurons can also sustain dendritic spikes that are spatially localized. The function of these dendritic spikes is still unclear, but could underlie the computational properties of neurons.

Using two-photon and fast confocal imaging we have investigated the characteristics and function of local dendritic spikes in layer 5 pyramidal neurons from mouse visual cortex. To obtain a quantitative estimation of the changes in intracellular  $\text{Ca}^{2+}$  concentration, the low affinity dye Oregon Green BAPTA-6F was calibrated in a two-step *in vitro* and *in vivo* procedure. We find that these dendritic spikes initiate a fast calcium transient of high amplitude in a small spine-dendritic compartment. We should note that in our experiments synaptic inhibition was intact, so dendritic inhibition may have contributed to the restriction of the dendritic spikes to relatively small dendritic segments. The dendritic spike-associated  $\text{Ca}^{2+}$  transients had a mean peak value of  $3.9 \pm 0.8 \mu\text{M}$  ( $n=11$ ) and a mean decay time constant of  $75 \pm 7 \text{ ms}$  ( $n=11$ ). Furthermore, these local dendritic spikes, which require activation of N-methyl-D-aspartate receptors, induce long-term synaptic depression (LTD). Different from Hebbian synaptic plasticity like STDP this depression does not require somatic spiking. This form of LTD is input specific, since it does not affect distant inputs. Moreover, a *single* stimulus, evoking a dendritic spike and brief local dendritic calcium transient, is sufficient for the full induction of LTD. Preliminary experiments indicate that dendritic spike-producing repetitive stimulation may evoke long-term synaptic potentiation (LTP).

We would highlight that current protocols to elicit long-term plasticity in central synapses always require many fold repetitions of pairing protocols that may not be entirely physiological. The rapidity of the induction of the synaptic change we observe could be due to the high calcium concentrations reached during the dendritic spike. This instantaneous and massive change in synaptic transmission could be used to implement rapid circuit plasticity or circuit accommodation. Therefore, this new form of single-shock synaptic plasticity represents a model of on-line learning in the mammalian brain.

Supported by DFG and HFSP.

## **Adult neurogenesis is present in the rostral migratory stream but not in the dentate gyrus of the nectar-feeding bat *Glossophaga soricina***

**Alexander Kaiser**

Ökologische Neurobiologie, Department Biologie II, Biozentrum der Ludwig-Maximilians-Universität München, 82152 Planegg-Martinsried

While in non-mammalian vertebrates adult neurogenesis is present in many areas of the brain, in mammals the incorporation of newly-generated neurons into neuronal networks is restricted to the olfactory bulb and the dentate gyrus of the hippocampal formation. The neurons of the dentate gyrus originate from astrocyte-like cells within the dentate gyrus and those destined for the olfactory bulb descend from cells in the subventricular zone and migrate in the so-called “rostral migratory stream” to their final location. In several studies it has been shown that adult neurogenesis is present in various mammalian species including mice, voles, rats, tupaia, old-world (Macaque) monkeys, new-world monkeys (*Callithrix*) and man. The functional significance of newly-generated neurons in adult mammals is still unclear, but there is strong evidence for a role in the plasticity of the neuronal networks of the olfactory and memory system, respectively (Gould, Beylin et al., 1999; Rochefort, Gheusi et al., 2002). Behavioural studies of the nectar-feeding bat, *Glossophaga soricina*, have shown that these animals have a highly-accurate spatial memory (Stich and Winter, unpublished). Furthermore, the volumetric brain analysis in these bats revealed a hypertrophic hippocampal formation when compared to other mammalian species (Kaupert and Winter, unpublished). In our study we investigated the adult neurogenesis in *Glossophaga soricina* with immunohistochemical methods using anti-BrDu (5-Bromo-2'-deoxyuridine) and anti-DCX (doublecortin) as markers for newly-proliferated cells.

With both of these markers IR-positive cells were present in the rostral migratory stream of these bats. In the dentate gyrus of the hippocampal formation, however, we could not detect IR-positive cells with both of the above markers. We therefore suggest that in the dentate gyrus of *Glossophaga soricina* adult neurogenesis is absent and not necessary for the plasticity in spatial memory of this species.

### References:

Gould E, Beylin A, Tanapat P, Reeves A, and Shors TJ. 1999. Learning enhances adult neurogenesis in the hippocampal formation. *Nat Neurosci* 2:260-265.

Rochefort C, Gheusi G, Vincent JD, and Lledo PM. 2002. Enriched odor exposure increases the number of newborn neurons in the adult olfactory bulb and improves odor memory. *J Neurosci* 22:2679-2689.

# Creating Mental Representations using the Spatial Dimension of Dendrite Trees

Richard Gagné and Simon Gagné<sup>a</sup>

<sup>a</sup>Université Laval, Quebec, Canada

This work introduces a novel hypothesis that the brain uses the spatial dimension of its fractal dendrites to create long term representations of mental activity, where “dimension” describes how the dendrite fills space. The developing brain is characterized by dynamic periods of growth and subsequent regression of its axons and dendrites. It is assumed the brain uses these periods to create three dimensional representations of mental activity using synaptic connection strengths. In their adult form, neurons are thought to be stable and learning consists of adjusting their connection strengths. However, recent images of spines show that their actin cytoskeleton are not stable but fluctuating structures.

This apparent instability of spines and recent experimental results which show that dendrites can be structurally rearranged to mirror afferent activity, have led several authors to propose moving the burden of representation from the synapse to the dendrite. A neuron responds to synaptic activity by changing its membrane potential and when the potential at its soma reaches a threshold, the neuron generates an action potential. Therefore, to test the dimension proposal, the random membrane potential fluctuations at the neuron’s soma due to massive synaptic activity were investigated. This was done using biologically plausible model neurons with various spatial dimensions.

A simple method was developed to determine the mean, variance, and covariance functions of the resulting fluctuations. Using this method, it was possible to show a direct relationship between the inter-spike interval average of the neuron and the spatial dimension of its passive dendrite tree. It was also demonstrated that dendrite atrophy did not affect the neurons response. The model fractal dendrite tree also required exuberant growth of its branches before the neurons response stabilized. Once the neurons response stabilized, the distal branches could be removed without changing the response.

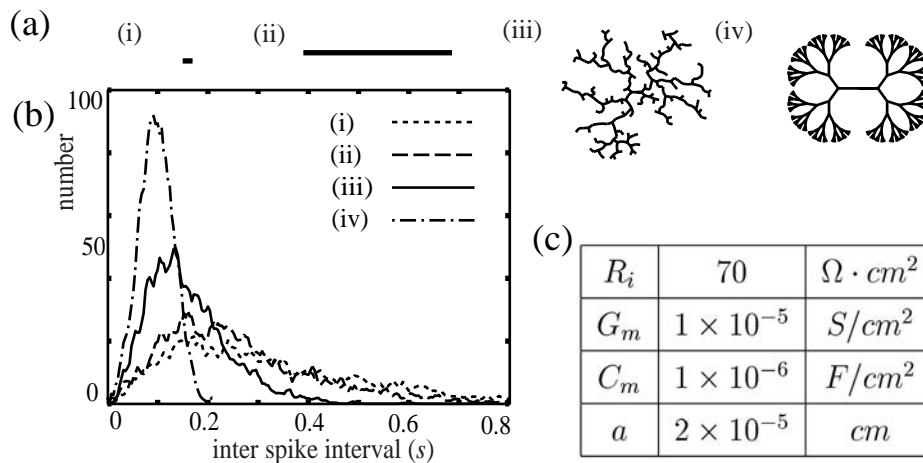


**Figure 1.** (a) Schematic diagrams of the four linear cable dendrite trees whose volumes increase as a: (i) zero (ii) one, (iii) fractal and (iv) two dimensional object. (b) Their respective inter-spike interval histograms (IIH) and (c) summary of cable parameters.

These results hint at a possible way the brain creates its mental representation. Instead of varying its synaptic strengths, a neuron may use its dendrite tree to learn about local activity and translate this information into variations of the dendrite’s local dimension. If this model is valid, these experiments show that the dimension of the dendrite tree as a storage site is remarkably robust.

## Role of NO/cGMP signaling during formation of social hierarchy in the cricket

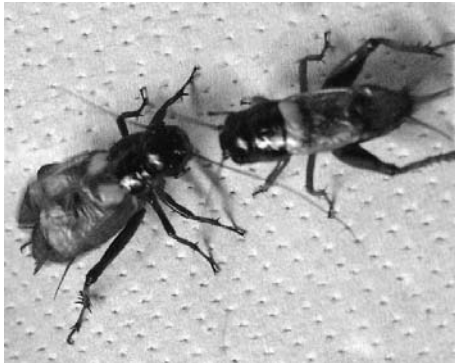
Hitoshi Aonuma<sup>1</sup>, Masazumi Iwasaki<sup>1</sup>, Chihiro Katagiri<sup>2</sup>, Antonia Delago<sup>1</sup>

Email: [aon@ncp8.es.hokudai.ac.jp](mailto:aon@ncp8.es.hokudai.ac.jp)

<sup>1</sup>Research Institute for Electronic Science, Hokkaido Univ., Sapporo 060-0812 JAPAN.

<sup>2</sup>Institute of Low Temperature Science, Hokkaido Univ., Sapporo 060-0819, JAPAN.

Many of pheromone behaviors in insects seem to be hard-wired but we know some of them can be modified after their experiences. Crickets recognize cuticular pheromones on the surface of other crickets and express hierarchical behaviors. One of the most famous behaviors of male crickets is fighting behavior. When male crickets contact other male crickets, they start fighting and one of them will be beaten. The winner crickets (dominant) started aggressive song and drove the loser (indominant) crickets away. The indominant crickets on the other hand had aversion to fight again against the dominant crickets. Aggressive interactions between male crickets are pheromone behavior and can be good model system to investigate the neuronal mechanisms of formation of social hierarchy.



At first we tried to identify the components of cuticular pheromones on the surface of cricket body using gas-liquid chromatography and thin layer chromatography and found that cuticular pheromones contained unsaturated hydrocarbons, saturated hydrocarbons. Behavioral observation revealed that courtship behavior was evoked in male crickets by saturated hydrocarbons from both sexes and avoidance by unsaturated hydrocarbons, but aggressive behavior was not evoked by the hydrocarbons although fresh male pheromone introduced aggressive behavior. We then tried to collect airborne volatile substances using

Porapak-Q. These volatile substances were found to elicit aggressive behavior in male crickets.

Nitric oxide (NO) is signaling molecule that is produced by NO synthetase (NOS) and activates soluble guanylate cyclase (SGC) to elevate second messenger cGMP in target cells. NO/cGMP signaling is implicated in mechanisms of neural plasticity underlying learning and memory. We then investigated how NO/cGMP signaling regulates learning behavior and memories to formation of social hierarchy in the crickets. The beaten experience was retained as a short term memory in the cricket because if the interval of twice sequential fighting was more than 1hr, the beaten crickets showed the aggressive again but most indominant crickets would not fight again if the interval was less than 30 min. We then examined the effects of NO/cGMP signaling on the avoidance behavior of indominant crickets by head-injection of 1μl NOS inhibitor L-NAME at 1mM or 1μl SGC inhibitor ODQ at 100μM. The agents were head-injected 15min before the initial fighting. The indominant animals that were injected L-NAME or ODQ did not show avoidance behavior at the reengagement but aggressive again. For control D-NAME at 100μM and normal cricket saline were injected onto the brain and avoidance behaviors were introduced in the indominant crickets. Furthermore, co-injection of L-NAME and NO-donor NOR3 at 100μM and co-injection of ODQ and 8-br-cGMP at 200μM rescued the effects of L-NAME and ODQ respectively.

These results suggested that NO/cGMP signaling regulated cuticular pheromone learning and short-term memory, which might be important factor in the neuronal mechanism during formation of social hierarchy.



## **Knowledge base for complex behaviours in Nature: Spatial memory based foraging of nectar-feeding bats on a computer simulated artificial flower field in the rain forest**

**Johannes Thiele & York Winter**

Biozentrum der Universität München and Max-Planck Institut für Ornithologie, Seewiesen

Foraging for food is an ecologically relevant behavior that requires from the forager spatial movements following context-dependent decisions on where to move. The true complexity of behavioural competences of spatial memory and navigational abilities involved can only be revealed within the natural context. Tropical nectar-feeding bats forage on flowers that are stationary by nature and are visited repeatedly due to continuous nectar secretion throughout the night. They thus provide one of the few mammalian systems where a quantitative experimental approach to investigate the use of space during foraging is possible within the natural setting. Our experiments were conducted in Costa Rica with free-ranging individuals of *Glossophaga commissarisi* bats feeding on up to 50 artificial flowers distributed over a 1 ha experimental area within the open forest. Artificial flowers were under real-time computer control, each equipped with a photoelectric sensor to detect visits, a transponder reading device to identify visiting bats individually and a nectar reservoir with an electronic valve to pay out sugar water rewards. Prior to experiments conducted over a period of 18 months, 46 bats had been captured and marked individually with transponder tags. During experiments, several individuals were active on the flower field simultaneously. Computer control of nectar refilling rates of each single flower allowed the simulation of spatially and individually heterogeneous resource distributions within the flower field. The animals' preferences for distinct spatial flower positions correlated with flower quality when animals were confronted with a spatially heterogeneous flower quality distribution. However, individuals went through a learning process lasting several days and several hundred flower visits before the discrimination between high and low quality locations reached a steady state. On the other hand, animals were able to change their spatial behaviour quickly (within hours), when the quality of an individual flower decreased. Learning processes involved thus followed different temporal scales. The organization of spatial behaviour was not characterized by simple or stereotypic route following (or "trap lining" behaviour). Instead, animals followed foraging trajectories that could be highly variable between different foraging bouts. Thus bats appeared to have independent representations of each single feeder location and were able to combine them into visit sequences with great flexibility. It is not clear yet, to which extent bats are able to take the time component of the spatio-temporal dynamics of a continually but predictably changing nectar-resource distribution into account for their planning of foraging trajectories.

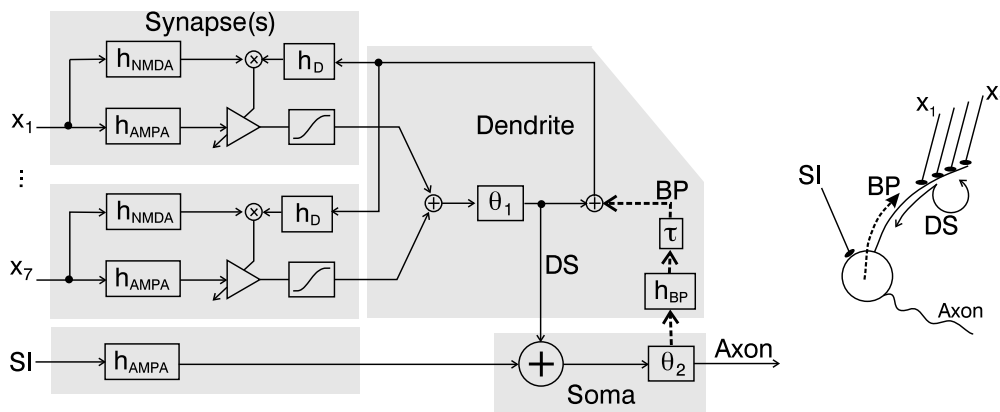
## How learning influences itself: The recurrent dependence of membrane potential shapes and synaptic plasticity

M. Tamosiunaite<sup>1,3</sup>, B. Porr<sup>2</sup>, F. Wörgötter<sup>3</sup>

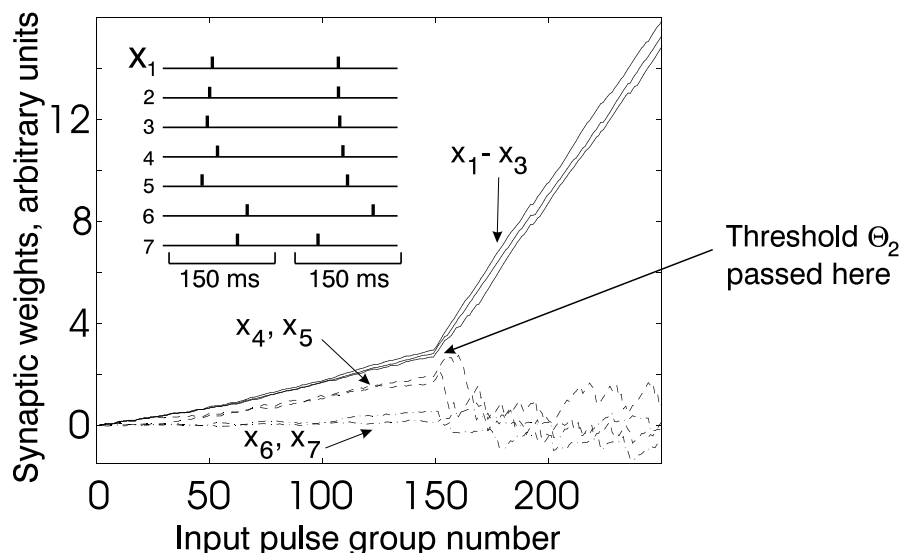
<sup>1</sup>Department of Informatics, Vytautas Magnus University, <sup>2</sup>Department of Electrical Engineering, University of Glasgow,

<sup>3</sup>Department of Psychology, University of Stirling, [worgott@cn.stir.ac.uk](mailto:worgott@cn.stir.ac.uk)

Recently it has been shown that spike timing dependent plasticity (STDP) may be similar to standard Hebbian learning (LTP only) if the postsynaptic depolarization rises shallow, while LTP and LTD are observed if it is steep. Hence, it was hypothesized that weight growth can have a different characteristic at different synaptic sites or at different times during development (Saudargiene *et al*, Neural Computation 16, 595-625). In the current computer modeling study we investigate possible functional consequences of synaptic plasticity whose characteristic is defined by the shape of the post-synaptic depolarization: first coming from a dendritic spike and later from a dendritic spike complemented by a back-propagating (BP) spike. The model includes a cluster of remote dendritic synapses trained by a differential Hebbian learning rule, and a relatively strong, unchanging synapse delivering an additional input close to the soma. The remote synapses initiate a dendritic spike (DS) if sufficient synaptic input arrives within a small time window. It is assumed that dendritic spikes drive synaptic learning only locally. Furthermore we assume that neither the DS nor the additional somatic input (SI) will be able to drive the cell on their own. Yet they drive the cell when acting in a correlated manner, which produces a BP spike that will also influence learning. Learning experiments were based on the circuit in the figure below. Initially, weights are too small to drive the cell (together with SI) at the soma but after some learning this will occur, eliciting a BP spike. The synaptic transfer characteristics were modeled by filters:  $h_{\text{AMPA}}$  imitating a  $\sim 5$  ms pulse of AMPA receptor activation, and  $h_{\text{NMDA}}$  giving a  $\sim 100$  ms pulse of the NMDA receptor activation. The threshold  $\theta_1$  was included to capture the time moment when there is enough input activity for initiation of a dendritic spike. BP- and dendritic-spikes (duration 20, 200 ms; resp.) were shaped by another set of filters  $h_D$  and  $h_{\text{BP}}$ .



Seven input lines were included into the model. The lines were divided into three groups corresponding to the input correlation within each group (see inset in Fig.2). Inputs to the lines  $x_1-x_3$  were strongly correlated (distributed uniformly over an interval of 6 ms width),  $x_4, x_5$  were more dispersed (distributed over an interval of 35 ms width), and  $x_6, x_7$  were uncorrelated (interval width 150 ms). The seven pulses  $x_1 \dots x_7$  were set to arrive in groups separated in time, such that two seven-pulse groups did not interfere with each other. SI would follow the pulse group  $x_1-x_3$  by approx. 10 ms. The resulting learning curves are depicted in the graph below, where a BP spike occurs after 150 pulse groups when the soma passes threshold  $\theta_2$ . When the learning is driven only by a dendritic spike the weights of the two groups of all better correlated-input synapses grow ( $x_1-x_5$ , solid and dashed lines), while the ones at the least correlated inputs ( $x_6-x_7$ , dash-dotted lines) remain close to zero. After learning is complemented by the BP spike, only the most strongly correlated synapses ( $x_1-x_3$ , solid lines) remain growing, while all the less correlated ones shrink. In summary: When the post-synaptic depolarization changes during learning, we find that different learning characteristics are obtained, which in this case allow for the separation and selection of inputs. We believe that such mechanisms can also be used in artificial neural networks for input structuring.



## **Involvement of the Rat Anterior Cingulate Cortex in Control of Instrumental Responses Guided by Reward Expectancy**

**Judith Schweimer and Wolfgang Hauber**

Dept. Animal Physiology, Institute of Biology, University of Stuttgart  
Pfaffenwaldring 57 D-70550 Stuttgart, Germany

The prefrontal cortex is a heterogeneous region which includes the prelimbic, the anterior cingulate, the agranular insular and the orbitofrontal areas. The anterior cingulate cortex (ACC) plays a critical role in appetitive stimulus-reinforcement learning. For instance, neuronal activity within the primate ACC is related to the degree of reward expectancy [1] and primates with ACC lesions are impaired with reward-guided selection of actions [2]. Furthermore, ACC lesions in rats interfered with acquisition of stimulus-reward associations in autoshaping, a selective test of Pavlovian conditioning [3] and altered effort-related decisions in a cost-benefit task [4].

Here we conducted a series of experiments in rats to elucidate the role of the ACC in control of instrumental responses guided by reward-predictive stimuli as well as instrumental behaviour involving decision-making. Different groups of rats received either sham lesions or quinolinic acid lesions of the ACC. In the first experiment, acquisition and reversal learning of an instrumental task demanding conditioned lever release was investigated; the upcoming reward magnitude (5 vs. 1 food pellet) was signalled in advance by discriminative stimuli. Results reveal that rats with ACC lesions were able to discriminate the significance of cues predictive of different reward magnitudes and to adapt instrumental behaviour to reversed stimulus-reward contingencies in the same manner as sham animals. Thus, the ACC appears not to be required to discriminate reward magnitude-predictive cues in a simple discrimination task as used here and to use the learned significance of the predictive cues to guide instrumental behaviour.

In a second experiment, rats were trained on a cost-benefit T-maze task in which they could either choose to climb a barrier (25 cm) to obtain a high reward (4 pellets) in one arm or could obtain a low reward (2 pellets) in the other with no barrier present. In line with previous studies [4] our data demonstrate that the ACC plays a role in evaluating how much effort to expend for reward. Rats with ACC lesions select the response involving less work and smaller reward when faced with a choice between a high reward arm with barrier and a low reward arm without barrier. This is not caused by a reduced motivation to work for food reward as performance under a progressive ratio schedule was not impaired in rats with ACC lesions.

A third experiment involved effort-based decision-making in a lever-press task, where the animals had the choice between pressing a lever to receive preferred food, or free feeding on a less preferred food. Performance of ACC-lesioned and sham-lesioned animals was similar if they had a choice between pressing a lever to obtain a more preferred food on a progressive ratio schedule and free feeding on less-preferred food. Thus, it seems that the ACC is not necessary in all situations requiring an assessment of costs and benefits.

Collectively, our results support a role of the ACC in evaluating some effort-related decisions underlying instrumental behaviour.

Supported by the DFG (Ha 2340/5-1)

[1] Shidara, M. and B.J. Richmond, *Science*, 2002. **296**(5573): p. 1709-11.

[2] Hadland, K.A., et al., *J Neurophysiol*, 2003. **89**(2): p. 1161-4.

[3] Cardinal, R.N., et al., *Behav Neurosci*, 2003. **117**(3): p. 566-87.

[4] Walton, M.E., et al., *J Neurosci*, 2003. **23**(16): p. 6475-9.

## Recognition memory in autistic "savants": an MEG study

Nicola Neumann<sup>1\*</sup>, Anna M. Dubischar-Krivec<sup>1</sup>, Christoph Braun<sup>1</sup>, Sven Bölte<sup>2</sup>, Fritz Poustka<sup>2</sup>, Niels Birbaumer<sup>1,3</sup>

1 Institute of Medical Psychology and Behavioral Neurobiology, University of Tübingen, Tübingen, Germany

2 Department of Child and Adolescent Psychiatry, Johann Wolfgang Goethe-University, Frankfurt/M, Germany

3 Center for Cognitive Neuroscience, University of Trento, Trento, Italy

\*Corresponding author: [Nicola.Neumann@uni-tuebingen.de](mailto:Nicola.Neumann@uni-tuebingen.de)

Savant syndrome is a rare condition in which persons with various developmental disorders, including autistic disorder, have astonishing islands of ability that stand in contrast to their overall limitations. Savant skills are usually combined with a prodigious memory. The aim of this study was to investigate memory encoding in autistic individuals with reported extraordinary memory skills. In a continuous old-new-paradigm six autistic and six healthy participants were presented with 300 pseudowords and 300 meaningless shapes that were either shown for the first ("new") or for the second time ("old"). Autistic and healthy participants did not differ in sex (all male), age (mean aut: 19; ctrl: 25 years), intelligence (mean aut: 113; ctrl: 121), or handedness (all right-handed). Participants were required to indicate by button press whether an item was new or old, while their brain activity was recorded with 151-channel whole-head magnetencephalography. Behavioral data indicated that the groups did not differ in recognition performance of shapes, but there was a trend that the group of healthy participants outperformed autistic participants in the recognition of pseudowords. Memory encoding has been assessed by comparing event-related magnetic fields to newly presented and later correctly recognized stimuli with newly presented and later not recognized stimuli (DM effect). Global field power indicated a main DM effect in two time windows from 185-240 and 400-500 ms. Autistic and healthy participants differed significantly in the first time window during the encoding of shapes with global field power being higher in autistic participants. Healthy individuals showed a stronger activation in the second time window, when pseudowords were presented. There was a trend that autistic individuals showed more activation than healthy individuals in the first time window left centro-parietally. Generally there was a stronger activation for pseudowords than for shapes left frontally. In sum there is evidence that autistic savants show more activation in earlier stages of information processing, as suggested by a recent hypothesis <sup>1</sup>.

---

<sup>1</sup> Birbaumer, N., Rain man's revelations, *Nature*, 399 (1999) 211-212.

## **Prepulse Inhibition of the Acoustic Startle Response increases during repetitive testing**

***C. F. Plappert, S. Kuhn, H.-U. Schnitzler, and P.K.D. Pilz***

*Universität Tübingen, Zoolog. Institut, Morgenstelle 28, D-72076 Tübingen*

The acoustic startle response (ASR) is a general coordinated muscle contraction elicited by loud acoustic stimuli. A non-startling acoustic prepulse administered before the startle-eliciting stimulus elicits two opposite and independent processes: either an ASR decrease (prepulse inhibition, PPI) or an ASR increase (prepulse facilitation, PPF). The respective strengths of PPI and PPF mainly depend on the interpulse interval (IPI) between prepulse and startle-eliciting stimulus. In mice, PPI overbalances PPF at an IPI of 50 ms leading to an overall ASR inhibition. This inhibition increases when it is repetitively elicited over several days. The reason for this may be either an increase in PPI or a decrease in PPF.

Here we show that the PPI increase over days is not caused by a PPF decrease. In C3H mice, PPI increased over days while PPF remained constant. In C57 mice almost no PPF occurred (which we believe to be typical for this strain), while PPI increased.

We further show that the full amount of the PPI increase over days is only produced if the prepulse and the startle-eliciting stimulus are presented in a contingent manner. We trained 5 different groups of C57 mice on 4 days: In 1 group the two stimuli were presented contingently, while in 4 control groups only (i) the startle-eliciting stimulus, (ii) the prepulse, (iii) the experimental context were presented or (iv) startle stimulus and prepulse were given in a non-contingent manner. The amount of PPI was then compared between the groups on days 5-8, on which all groups got contingent pairs of prepulses and startle stimuli. In the 4 control groups PPI increased, but this increase was in all groups only about half of the amount of the PPI-increase of the contingent group. From this we conclude that the PPI increase during repetitive testing is due to a learning process of the association between prepulse and startle stimulus, and that this process is facilitated by previous presentation of context or stimuli.

*(Supported by DFG, Schn 23/1-4).*

## **Altered short-term plasticity is responsible for the depression of burst responses in the startle mediating neurons of the rat pontine reticular formation**

Susanne Schmid<sup>1</sup> and Maruschka Weber<sup>1,2</sup>

<sup>1</sup>*Tierphysiologie, Zoologisches Institut, Universität Tübingen;* <sup>2</sup>*Physiologie, Universität Würzburg; susanne.schmid@uni-tuebingen.de*

Giant neurons in the caudal pontine reticular formation (PnC) form the sensorimotor interface of the startle response in rats and mice. Homosynaptic depression of PnC responses to bursts of action potential in the afferent sensory input neurons has been suggested to be the neuronal correlate for short-term habituation of the startle response.

We examined the dynamic properties of the sensory synapses on PnC giant neurons in more detail by patch-clamp recordings in brain slices. Homosynaptic depression was induced by 100 applications of extracellular bursts of 4 pulses within 12 ms, applied at 1 or 0.1 Hz to presynaptic fibres, mimicking the *in vivo* activity of presynaptic auditory neurons. The amplitude of the compound EPSC (cEPSC) in PnC giant neurons were depressed to about 60% of its initial value by this protocol. Our analysis revealed selectively responses to late stimuli within a burst were depressed, whereas the response to the first pulse within a burst was unchanged. Correspondingly, paired-pulse facilitation was reduced during synaptic depression from  $EPSC2/EPSC1 = 1.83 \pm 0.16$  (n=17) to  $EPSC2/EPSC1 = 1.36 \pm 0.08$  (n=17, paired t-test: p=0.004), while the amplitude of EPSC1 was unchanged ( $-116.59 \pm 28.33$  pA before and  $-122.71 \pm 33.14$  pA during depression, n=17). In further experiments we combined electrical stimulation with brief local uncaging of glutamate and thus circumventing the presynaptic terminal. 100 applications of glutamate yielded postsynaptic responses comparable to burst evoked cEPSCs that did not decrease in amplitude during the protocol. Subsequent burst responses, however, were depressed by 100 glutamate applications, supporting previous results that the activation of metabotropic glutamate receptors (mGluRs) plays an important role in the depression of burst responses. The constant amplitude of glutamate responses locate the mGluRs to the presynaptic site. The selective depression of late responses within a burst further indicate, that activation of presynaptic mGluRs does not generally depress transmitter release, but depresses release from separate releasing sites that are selectively accessed by later stimuli. A similar mechanism has been reported in *Aplysia* sensory synapses by Jiang and Abrams (J. Neurosci. 1998).

In conclusion our data indicate that the depression of responses in PnC giant neurons to presynaptic bursts of action potentials is due to alterations in presynaptic short-term plasticity and not to a general depression of synaptic transmission.

*This work was supported by the DFG (SFB 430, C7 and Schm 1710/-1)*

# Sensory and Behavioral Changes in Glycine-Receptor deficient *spa* Mice

Chantal Schlumberger<sup>1</sup>, Peter K.D. Pilz<sup>1</sup>, Kristina Becker<sup>2</sup>,  
Cord-Michael Becker<sup>2</sup>, Hans-Ulrich Schnitzler<sup>1</sup>, Claudia F. Plappert<sup>1</sup>

<sup>1</sup>Universität Tübingen, Zoolog. Institut, Morgenstelle 28, 72076 Tübingen, Germany,

<sup>2</sup>Universität Erlangen-Nürnberg, Institut für Biochemie, Fahrstr. 17, 91054 Erlangen, Germany

Mice with the mutation “spastic” (“*spa*”) have a strongly reduced density of glycine receptors. They show an extremely high startle reaction to loud acoustic stimuli and sometimes a pronounced shaking with spasms. The genetic defect of *spa* mice is identical to the defect of humans affected by the hereditary disease hyperexplexia (also called startle disease). The phenotype of *spa* mice is similar to that of spasmodic (“*spd*”) mutants who have a reduced affinity of the glycine receptors (Becker, The Neuroscientist, 1995). In homozygous *spd* mice the startle threshold is lowered (Plappert et al., Behav. Brain Res., 2000), whereas in *spa* mutants this seems not to be the case (Koch, Kling & Becker, Neuro Report, 1996). We wanted to test in detail the threshold of *spa* mice, and clarify whether eventual changes in threshold are due to a general change in auditory perception.

The acoustic startle response (ASR) was elicited by noise stimuli and measured by a movement sensible platform.

1) *Spa* mice exhibited strongly increased ASR amplitudes during the presentation of 200 stimuli (105 dB SPL) in contrast to the wildtype (and heterozygous) littermates

2) Startle threshold was strongly lowered in some of the *spa* mutants (preliminary experiments indicated this may depend on the genetic background of the deficient mice).

3) Weak, sub-threshold stimuli (“prepulses”) presented shortly before the startle stimuli change the ASR. Our first results indicate that in *spa* mutants the effect of these prepulses is stronger as in the wildtype littermates. This would point towards a change in the sensory input (i.e. stronger perception of acoustic stimuli).

4) *Spa* mice did not habituate during the presentation of 200 startle stimuli (105 dB SPL) in contrast to the healthy littermates. According to the Dual Process Theory of Groves and Thompson (Psychol. Rev. 1970), this indicates strong sensitization by the acoustic stimuli counteracting habituation.

5) Only if the SPL of the startle stimuli was lowered (55-90 dB SPL), i.e. acoustic sensitization was reduced, footshocks were able to induce additional sensitization in each of the *spa* mice.

Our results suggest that the acoustic stimuli are more effective in *spa* mice which is reflected in increased ASR, mean lowered startle threshold, increased effect of prepulses and increased acoustic sensitization. This could be the result of a missing glycinergic inhibition of the auditory input. To further investigate the sensory changes in the *spa* mice we will expand our experiments to visual and tactile stimuli.

Supported by the DFG (Schn23/1-4)

## How are eye movements involved in landmark recognition?

Yu Jin, Sabine Gillner and Hanspeter A. Mallot

Dept. of Cognitive Neuroscience, University Tübingen, Germany

yu.jin@uni-tuebingen.de

To better understand the concept of landmarks, it is necessary to understand not only how agents use them in navigation, but also how they are identified in the scene. Landmarks are often noticed or memorized because they are capable of attracting attention. Landmark saliency may accrue by a unique visual property of an object, but also depends on the functional content of this object: how an agent uses it in a navigation task. In our experiment we used landmarks and distractors with matched visual properties. Unlike landmarks, distractors are identical in the whole environment and contain no spatial information. Eye gaze patterns were analyzed while subjects performed a navigation task in a virtual reality environment. Subjects were trained to learn a route in the virtual environment and perform tests using landmarks. We examined the gaze fixation with respect to landmarks and distractors in the environment. Our results showed that there are more gaze fixations on landmarks than on distractors. Also, the fixation duration on landmarks is longer than on distractors. Interestingly, an object elicits longer fixation when it acts as landmark in the environment than as distractor. This suggests that gaze fixation selectively focuses on landmarks, rather than random free-viewing. Additionally, the distribution of eye-gaze is strongly relative to the focus of expansion, but biased by the position of landmarks in the scene. Our experiment demonstrates the highly task-specific nature of our vision system: information is actively extracted from the fixation point for certain task demands. Here, subjects actively search for landmark information for the purpose of performing navigation task.



Figure 1: *Bird-eye view of virtual reality environment with landmarks and distractors*



## The role of mGluR8 in synaptic plasticity in the lateral amygdala

Nadine Becker<sup>1</sup>, Hermann van der Putten<sup>2</sup>, Hans-Ulrich Schnitzler<sup>1</sup>, Susanne Schmid<sup>1</sup>

<sup>1</sup> Tierphysiologie, Zoologisches Institut Universität Tübingen, Germany

<sup>2</sup> Novartis Pharma AG, Basel, Switzerland

The lateral amygdala (LA) has been associated with cellular mechanisms underlying Pavlovian fear conditioning, suggesting long-term potentiation (LTP) as a cellular learning correlate for fear conditioning. LTP is an extremely well studied phenomenon of synaptic plasticity in the hippocampus. Yet, the underlying mechanisms in the LA seem to deviate from the ones found in the hippocampus. However, LTP in both brain regions occurs at glutamatergic synapses, allowing an influence on LTP through metabotropic glutamate receptors.

The mGluR8 subtype belongs to the mGluR III group. This group is implicated in the modulation of neuronal plasticity during learning processes like LTP. Although *in situ* hybridisation does not show high concentrations of mGluR8 mRNA in the LA, the specific mGluR8 agonist (S)-3,4-dicarboxyphenylglycine (DCPG) has a striking effect on EPSP amplitudes in amygdaloid principal neurons. Neurotransmitter release at glutamatergic and GABAergic synapses is depressed by mGluR8 action, presumably via presynaptic inhibition of voltage-gated calcium channels. On glutamatergic synapses, mGluR8 serves as an autoreceptor mediating negative-feedback inhibition on glutamate release.

A previous study of our group has shown that DCPG injected into the LA inhibits the expression and acquisition of conditioned fear in rats *in vivo*. Correspondingly, it depresses synaptic responses in the rat LA *in vitro*. These findings presumably result from the negative feedback inhibition exerted on glutamatergic synapses via mGluR8. However, an effect on LTP in the presence of DCPG was not detected.

In this study, we examined the effects of mGluR8 on LTP and paired-pulse ratio (PPR). We made whole-cell patch clamp recordings in principle neurons in the LA of wild-type and mGluR8 knockout (KO) mice (host strain C57/Bl6). LTP was induced *in vitro* by stimulation of thalamic and cortical afferents, with the EPSPs elicited by thalamic stimulation paired 45 times with strong postsynaptic depolarisation. Preliminary results revealed that wild-type (WT) littermates (n=5) of the mGluR8 knockout mice and the C57/Bl6 (n=7) showed increased EPSP amplitudes of 111 % and 130 %, respectively, after LTP induction, whereas the homozygous KO mice (n=2) showed a slight decrease (7 %) of EPSP amplitudes compared to baseline amplitudes. We also tested whether PPR was altered through LTP induction or mGluR8 deficit. Applying the stimulation protocol as described, the C57/Bl6 showed paired-pulse depression (PPD, 0,85, n=5), which did not change after the application of the pairing protocol (0,85). The mGluR8 WT mice showed a PPR of 1,03 and 0,93 (n=5) before and after pairing, respectively, neither showing an effect on PPR by LTP induction. The mGluR8 KO mice showed a PPR of 0,93 (n=2) before application of the pairing protocol, but interestingly, they showed an effect on PPR after application of the pairing protocol, increasing the PPR to 1,10.

Our findings indicate that mGluR8 plays an important role in long-term potentiation in the LA, and suggest a presynaptic participation of mGluR8 in the induction of LTP in the LA.

## Investigating rat spatial behavior in virtual environments

Alexander Schnee<sup>1</sup>, Hansjürgen Dahmen<sup>1</sup>, Christian Hölscher<sup>2</sup>, Hanspeter A. Mallot<sup>1</sup>.

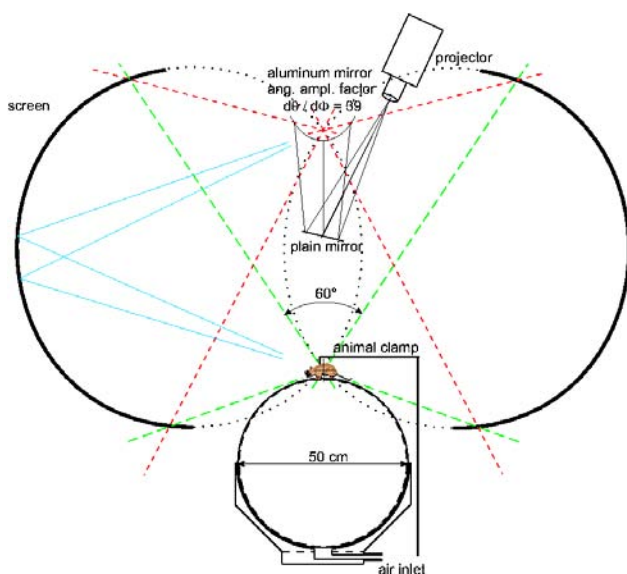
<sup>1</sup>LS Kognitive Neurowissenschaft, Universität Tübingen, 72076 Tübingen,

<sup>2</sup>School of Biomedical Sciences, University of Ulster, Coleraine

The use of virtual reality technology is meanwhile quite common in research on human spatial cognition. In rats, however, all previous attempts have failed to develop VR systems that are interpreted as spatial environments by the animals. We designed a VR system for rats that covers most of their visual field (360° of azimuth, -20 – +60 elevation). Our set-up consists of a projection system that displays a virtual environment via a mirror system onto a torus-shaped screen that completely surrounds the rat. The animal is stationarily running on top of an air cushioned polystyrene ball of 50 cm diameter. In its mount, the rat is free to rotate about the vertical axis, but its translational movements are transferred to the ball. Motion detectors register the ball's movement and relay it to a computer system which produces the virtual environment and updates the projected view in relation to the current position of the rat. This novel set-up allows to present large environments with the advantage to quickly change and continuously control those environments.

In a first experiment we presented an infinite environment with vertically striped, black and white cylinders of 50 cm diameter suspended from the ceiling (1m height). The cylinders were arranged on a squared grid of 2m side length and the animals were rewarded with sugar water when they approached the area below any cylinder. After 10 days of training the rats showed a significant increase of performance, reflected by the amount of hits, walking distance and time interval between hits. In a continuously following experiment we enlarged the distance between these cylinders to 10 m and the animals still improved their performance to navigate towards these targets.

In a second experiment the animals had to learn a discrimination task. For this purpose we introduced a virtual environment which also consisted of cylinders of 50 cm diameter suspended from the ceiling. Twelve of these cylinders, where six cylinders colored in dark grey and six cylinders colored in light grey were arranged alternately along a circle with a starting point in the centre. Only one type of those cylinders was rewarded. The animals were instantly able to discriminate between the two types of cylinders, but they also showed a strong preference to the light grey cylinders which were rewarded in the first part of the experiment. To retrain the animals to prefer the dark grey cylinders in the second part of the experiment, more than a month of training was required.



A:



B:

A: Schematic and, B: photo image of the set-up with the projection screen lowered onto the ball.

## Induced hippocampal long-term potentiation correlates with early spatial learning performance in male CD-1 mice

Lohmann P\*, Lange-Asschenfeldt C\*, Riepe MW

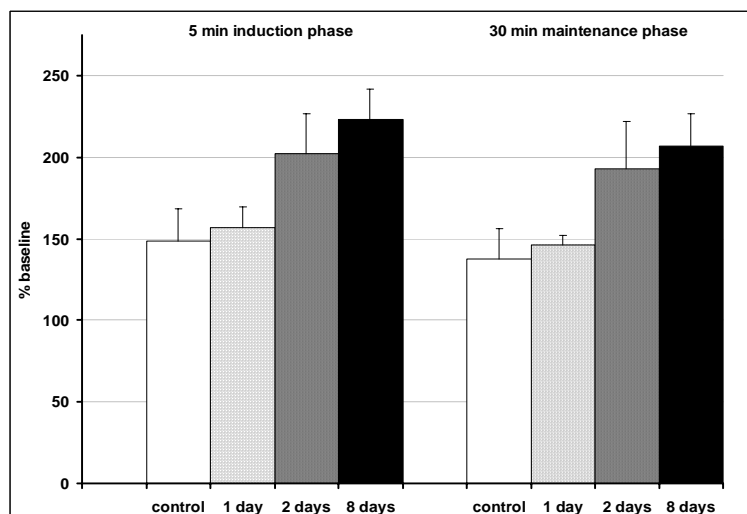
For the understanding of learning at the cellular level long-term potentiation (LTP) is one of the most promising method. We tried to find out whether spatial learning performance of mice correlates with LTP in the hippocampal CA1 region in vitro.

For behavioral experiments we used a complex maze comprising a starting-place, several crossings, t-crossings, blind alleys and a goal zone. Mice had to perform the maze 5 times a day. One group of mice was exposed to the maze for only one day, another group for two days and a third group had to perform the maze for a period of eight days. A control group did not perform the maze. One day after the last maze trial extracellular field excitatory postsynaptic potentials (fEPSPs) were evoked from the CA1 region of acute hippocampal slices and LTP was induced by using a single train stimulus protocol. Potentiation of the response was measured in the induction phase after 5 min and in the maintenance phase after 30 min. LTP was expressed as percent of fEPSP baseline slope.

After eight days of training there is a significant increase of LTP both in the induction phase (control:  $148 \pm 20$  %,  $n = 7$ ; 8 days:  $223 \pm 19$  %,  $n = 9$ ;  $p < 0.05$ ) and in the maintenance phase (control:  $138 \pm 18$  %,  $n = 7$ ; 8 days:  $207 \pm 20$  %,  $n = 9$ ;  $p < 0.05$ ). Time mice need to perform the complex maze decreased from  $122.1 \pm 27.7$  s on first day to  $29.8 \pm 15.8$  s on eighth day ( $p < 0.05$ ). The LTP effect after two days of training showed a remarkable increase (induction phase :  $202 \pm 25$  %, maintenance phase:  $193 \pm 29$  %,  $n = 5$  each) but is not significant to control. On first day mice need  $81.4 \pm 30.8$  s to solve the maze and time decreased to  $51.9 \pm 11.7$  s on second day, also not significant. LTP after one day in the maze only tend to increase (induction phase:  $157 \pm 13$  %, maintenance phase:  $146 \pm 6$  %) and mice need  $107.7 \pm 24.0$  s to find the goal zone of the complex maze.

Increase of hippocampal CA1-LTP in its induction and maintenance phase reflects behavioral performance in a complex maze.

\*CLA and PL contributed equally to this study



**Poster Subject Area #PSA18:  
Neuroanatomical studies**

- [#261A](#) P. Bräunig, Aachen  
*A direct line from the appendages to the brain in insects?*
- [#262A](#) R. Loesel, NJ. Strausfeld, E-A. Seyfarth and H-J. Agricola, Aachen, Tucson (USA), Frankfurt/Main and Jena  
*A 450 Million Year Leitmotif for a Locomotor Control Center in the Brain: Conserved Neuroarchitecture of the Central Complex of Chelicerates and Hexapods*
- [#263A](#) I. Frambach, F-W. Schürmann and H. Gras, Göttingen  
*Differential Distribution of Filamentous Actin and Globular Beta-Actin in Intrinsic Mushroom Body Kenyon Cells of an Insect Brain*
- [#264A](#) T. Reischig, Göttingen  
*Comparative anatomy of the accessory medulla, a circadian pacemaker centre in insects, by pigment-dispersing factor (PDF) immunohistology*
- [#265A](#) T. Reischig, Göttingen  
*Search for the neurotransmitters and transmitter receptors in the pigment-dispersing factor (PDF) immunoreactive neurons of the cockroach *Leucophaea maderae**
- [#266A](#) GKH. Zupanc and SAL. Correa, Bremen and Manchester (UK)  
*Reciprocal Neural Connections between the Central Posterior/Prepacemaker Nucleus and Nucleus G in the Gymnotiform Fish, *Apteronotus leptorhynchus**
- [#260B](#) M. Hollmann and G. von der Emde, Bonn  
*Two electrical foveae at the skin of the weakly electric fish, *Gnathonemus petersii**
- [#261B](#) S. Zechel, H. Kulaksiz, K. Unsicker and O. von Bohlen und Halbach, Heidelberg  
*Distribution of the iron-binding protein hepcidin in the CNS*
- [#262B](#) J. Jarosik, B. Legutko, K. Unsicker and O. von Bohlen und Halbach, Heidelberg  
*Olfactory bulbectomy induces neurodegeneration in the amygdala*
- [#263B](#) H. Endepols, K. Roden and W. Walkowiak, Köln  
*The septum of anuran amphibians: Subnuclei and connections*
- [#264B](#) AE. Kurylas, J. Schachtner and U. Homberg, Marburg  
*3-D reconstruction of the central complex in the brain of the locust *Schistocerca gregaria**
- [#265B](#) A. Jenett, J. Schindelin and M. Heisenberg, Würzburg  
*The Standard Protocol: Towards a genetic atlas of the *Drosophila* brain*

## A direct line from the appendages to the brain in insects?

Peter Bräunig  
Institut Biologie II, RWTH Aachen

Filling specific branches of the leg nerves in migratory locusts with neurobiotin revealed small-diameter afferent fibers that project without ramifications through thoracic and suboesophageal ganglia to the brain. Here they terminate in a defined neuropile that is located ventrally and medially, close to the border between deutocerebrum and protocerebrum. Filling the circumoesophageal connectives in adults and older larvae (4th and 5th instar hoppers) revealed fibers entering the leg nerves of all three thoracic ganglia. The source of these projections remained obscure in older larvae and adults. Filling the circumoesophageal connectives in younger instars and embryos showed that the source of these fibers are single neurons in specific locations: One neuron is located in the proximal tibial region, and two cells in the tarsus. The cells are reminiscent of multipolar sensilla, but they exhibit only one stout dendrite with very short branches. The cells appear to be located within peripheral nerve branches. Together with previous results these findings indicate that a few specialized afferent neurons within insect appendages directly convey sensory information to the brain. Their sensory modality remains presently unknown.

# A 450 Million Year Leitmotif for a Locomotor Control Center in the Brain: Conserved Neuroarchitecture of the Central Complex of Chelicerates and Hexapods

Rudi Loesel<sup>1</sup>, Nicholas J. Strausfeld<sup>2</sup>, Ernst-August Seyfarth<sup>3</sup> and Hans-Jürgen Agricola<sup>4</sup>

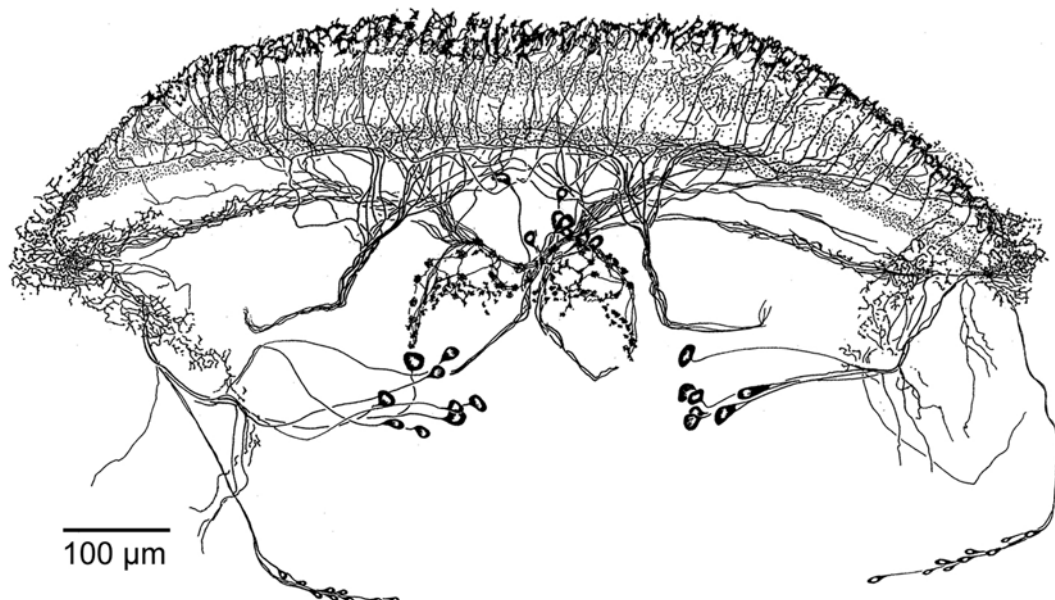
<sup>1</sup>Institut für Biologie II, RWTH Aachen, D-52056 Aachen, Germany, email: [loesel@bio2.rwth-aachen.de](mailto:loesel@bio2.rwth-aachen.de);

<sup>2</sup>Division of Neurobiology, University of Arizona, Tucson, AZ 85721, USA;

<sup>3</sup>Zoologisches Institut, Universität, D-60054 Frankfurt am Main, Germany;

<sup>4</sup>Institut für Allgemeine Zoologie und Tierphysiologie, Universität D-07743 Jena, Germany

Hexapods and malacostracan crustaceans possess an assemblage of midline neuropils in their protocerebrum called the central complex. Several lines of evidence from behavioral and comparative studies suggest that the central complex serves as a motor control center that is involved in orchestrating limb actions. Based on the anatomical architecture, the central complex of various arthropod groups is characterized by several distinct features: (i) It is the only unpaired midline neuropil structure in the central nervous system, (ii) it comprises tangential neurons in distinct layers, and (iii) it is innervated by columnar fibers which in part cross the midline of the brain before they enter the central body; this presumably to facilitate interhemispherical information processing. Furthermore, antibodies directed against certain neuroactive substances label putative homologous subunits of the central complex in different arthropod groups. (For a comprehensive list of relevant literature see Loesel et al. 2002, *Arth. Struc. & Dev.* 31, 77-91)



Proctolin immunopositive neurons and their projections in the central body of the spider *Cupienius salei* (Ctenidae, Araneomorphae), reconstruction from frontal vibratome sections.

Here we present detailed anatomical data on the neuroarchitecture of the central midline neuropil of chelicerates based on immunohistochemical stainings and on Bodian silver impregnations. As is the case in the hexapod-malacostracan clade, the central body (CB) of chelicerates comprises distinct layers and interweaving columnar fibers. The same set of antibodies (e.g. anti-allatostatin, anti-proctolin) used at identical concentrations stains subsets of CB-neurons in spiders that are comparable to those found in insects. Bodian silver stainings reveal that a CB is present not only the Araneomorphae but also in basal chelicerate species such as *Heptathela kimurai* (Mesothelae) and in horseshoe crabs and scorpions.

Our data suggests that the neuroanatomical Leitmotif of the CB has been highly conserved during arthropod evolution and evolved at least 450 million years ago, when the first terrestrial hexapods emerged. In fact, the basic neuroarchitecture of this locomotor control center might even be more ancient than the phylum Arthropoda itself. It is now tempting to ask whether the central complex Leitmotif is as ancient as the origin of bilaterian brains and whether locomotor control centers in chordates might share a common ancestor with those of non-chordates.

We thank Angelika Schmidt and Rosemarie Meißner for excellent technical help. Supported by BMBF-project 0316919.

## **Differential Distribution of Filamentous Actin and Globular $\beta$ -Actin in Intrinsic Mushroom Body Kenyon Cells of an Insect Brain**

**Ina Frambach, Friedrich-Wilhelm Schürmann und Heribert Gras**

Institute of Zoology, Anthropology and Developmental Biology,  
University of Göttingen, Berliner Str. 28, 37073 Göttingen

Actin is an essential molecule involved in motility and growth processes. It is highly concentrated at chemical synapses where it mediates structural and functional dynamics (Matus; 2000, Science 290: 754-758). We investigated the distribution of the  $\beta$ -actin isoform in the mushroom body neuropil of the cricket *Gryllus bimaculatus* using a monoclonal antibody binding filamentous (F-actin) and globular  $\beta$ -actin in comparison to F-actin labeled with fluorescent phalloidin. Mushroom bodies are a prominent neuropil in the central insect brain considered to be crucially involved in learning and memory functions (Heisenberg; 1998, Lern Mem 5: 1-14). In crickets newly generated intrinsic mushroom body neurons - the so called Kenyon cells - are continuously added to the neuropil throughout the animal's lifetime.

We found both F-actin and  $\beta$ -actin highly concentrated in sprouting Kenyon cells as well as in the dendritic arborizations of mature Kenyon cells within the calyces, the main input area of the mushroom bodies. Here both actin forms were concentrated at postsynaptic tips contacted by presynaptic cholinergic boutons of deutocerebral projection neurons. In double stainings with F-actin and  $\beta$ -actin previous antibody binding prevented F-actin detection with phalloidin. Thus postsynaptic F-actin should at least be partly made up from the  $\beta$ -actin isoform. In dendritic processes of intrinsic mushroom body neurons distant from synapses only the  $\beta$ -isoform but no F-actin was detected. Axons of different Kenyon cell types showed a varied equipment with F-actin and  $\beta$ -actin. Strikingly high amounts of  $\beta$ -actin compared to very low F-actin levels were found in Kenyon cell axons of a large Kenyon cell type. Hence Kenyon cell axons prove to be a reservoir of the globular transport form of the protein.

In vertebrate nerve tissue  $\beta$ -actin is concentrated in structures having a high capacity for remodelling (Micheva et al.; 1998, Eur J Neurosci 10: 3785-3798). The high level of F-actin in Kenyon cell dendritic tips as well as the large amount of globular  $\beta$ -actin found in Kenyon cell axonal and dendritic fibers may point to a high structural and functional plasticity of these intrinsic mushroom body cells. This is in accordance with a postulated role of the mushroom bodies in view of their reactivity to environmental influences, behavioral changes and of learning and memory functions.

Supported by DFG, Graduiertenkolleg 723 „Neuronal Signalling and Cellular Biophysics“.



# Comparative anatomy of the accessory medulla, a circadian pacemaker centre in insects, by pigment-dispersing factor (PDF) immunohistology

Thomas Reischig

Institute of Zoology and Anthropology, Dept. of Neurobiology, Georg August University, Berliner Str. 28, 37073 Göttingen, Germany. Email: neurobio@reischig.de

**Introduction:** The accessory medulla (AMe) is a small but conspicuous neuropil situated adjacent to the medulla of the optic lobes in insects, and is supposed to be a circadian pacemaker (Reischig and Stengl 2003, J Exp Biol 206:1877; reviewed by Homberg et al. 2003, Chronobiol Int 20:577). The well-characterised AMe of the cockroach *Leucophaea maderae* is not organised in columns and layers as the large optic neuropils (i.e., no retinotopic organisation), but consists of dense nodular neuropil that is interwoven by and surrounded with coarse neuropil (Reischig and Stengl 2003, Cell Tissue Res 314:421). The pigment-dispersing factor-immunoreactive (PDF)-neurons, which are presumptive circadian pacemaker neurons, arborise differentially in the subcompartments of the AMe.

The AMe was first discovered in plant-lice, which have special larval eyes (stemmata), and later in holometabolous insects that retain their larval stemmata in the imaginal stage (e.g., Trichoptera; Ehnbohm 1948, Opusc Entomol Suppl VIII, Konstanz, Germany). Since then the AMe was, together with the accessory lamina, regarded as a specialised visual centre in the larvae of holometabolous insects.

The discovery of a prominent AMe-like structure in orthopteromorph insects, which do not have larval stemmata, raises the question whether this structure is in fact homologous to the AMe of holometabolous insects. To elucidate the evolution of the AMe throughout insect phylogeny, comparative morphological and immunohistochemical studies of the AMe and its adjacent PDF-neurons were performed in representative species of various insect orders (springtail *Folsomia candida*, silverfish *Lepisma saccharina*, damselfly *Coenagrion puella*, cricket *Gryllus bimaculatus*, locust *Schistocerca gregaria*, firebug *Pyrrhocoris apterus*, honeybee *Apis mellifera*, moth *Manduca sexta*, flies *Musca domestica* and *Drosophila melanogaster*).

**Results and Conclusions:** All insects investigated herein, except the entognath *F. candida*, possess a more or less conspicuous AMe, which is innervated by PDF-neurons. The PDF-neurons of the springtail may have been secondarily lost due to reduction of the optic lobe, since PDF-neurons are common in the optic lobes of the sistergroup of insects, the crustacea.

In most hemimetabolous as well as holometabolous insects (*G. bimaculatus*, *S. gregaria*, *M. sexta*, *A. mellifera*, *M. domestica*, *D. melanogaster*) the AMe shares common features. These are

- the presence of a non-retinotopic, nodular neuropil at the frontomedial border of the medulla,
- PDF-neurons innervating the AMe, which appear in at least two size classes with different staining intensities,
- a group of interneurons with conspicuous large somata in vicinity to the AMe. Neurons corresponding to this type are GABA-immunopositive in *L. maderae* and the butterfly *Papilio xuthus* (Petri et al. J Exp Biol 205:1459, Ichikawa 1994, J Comp Neurol 340:185),
- a conspicuous group of (probably local) interneurons with small somata and dark staining nucleus in vicinity to the AMe.

In the silverfish *L. saccharina*, a PDF-immunoreactive, AMe-like structure occupies the whole distalmost layer of the medulla (Fig. 1A). In this insect, the position of the medulla is closer to the basal situation with its layers perpendicular to the main visual axis. I assume that the AMe of higher insects developed after a rotation of the medulla around the vertical axis, and by condensation of parts of the first layer neuropil into the nodular neuropil of the AMe lying at the frontomedial medulla.

The AMe of the orthopterid insects (*G. bimaculatus*, *S. gregaria*; Fig. 1B) are very similar to that of *L. maderae* in respect to the separation into coarse anterior and dense nodular neuropil (most prominent in *S. gregaria*), and the assembly of AMe-associated neurons. However, obvious compartmentalisation of the nodular neuropil as in *L. maderae* is less conspicuous or does not occur at all.

In *Apis mellifera* and the dipterans (Fig. 1C), the neuropil of the AMe is largely reduced independently from each other. I suppose that in bees and flies the AMe changed its function and/or lost its importance as an integration centre for timing information owing to changes in the assembly of the circadian system.

**Due to the common features shared by most AMe in the insect groups investigated so far, the AMe comply with primary criteria for homology, i.e. criteria of similar position and specific quality. Hence, the AMe of hemimetabolous as well as holometabolous insects appears to be derived from a common ancestral structure at least in dicondylian insects.** It remains an interesting question, how the AMe developed into a primary visual centre in the larvae of holometabolous insects.

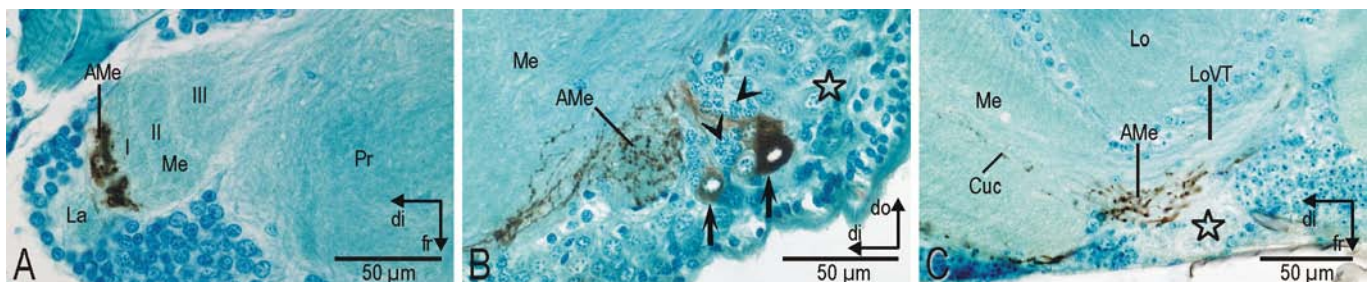


**Fig. 1 A:** Optic lobe with accessory medulla (AMe) of the silverfish *L. saccharina*. I-III: layers I-III of the medulla (Me). **B:** AMe of the locust *S. gregaria*. Arrows: PDF-immunoreactive somata. Arrowheads: small interneurons. Asterisk: large

interneurons. **C:** Optic lobe with AMe of the housefly *M. domestica*. Asterisk: large interneurons. Cuc Cucatt bundle. La lamina; Lo lobula; LoVT lobula valley tract; Pr protocerebrum. Coordinates: di distal, do dorsal, fr frontal.



# Search for the neurotransmitters and transmitter receptors in the pigment-dispersing factor (PDF) immunoreactive neurons of the cockroach *Leucophaea maderae*

Thomas Reischig

Institute of Zoology and Anthropology, Dept. of Neurobiology, Georg August University, Berliner Str. 28,  
37073 Göttingen, Germany. Email: neurobio@reischig.de

**Introduction:** The pacemaker driving circadian locomotor activity of the cockroach *Leucophaea maderae* is located in its optic lobes (Page 1982, Science 216:73). Transplantation studies (Reischig and Stengl 2003, J Exp Biol 206:1886), as well as comparison with the circadian clock of the fruitfly *Drosophila melanogaster* (reviewed by Stanewsky 2002, Cell Tissue Res 309:11), point to the pigment-dispersing factor (PDF) immunoreactive (-ir) medulla neurons (PDFMe) as circadian pacemaker neurons of the cockroach. Their somata lie in two groups in the pacemaker region at the anterior (aPDFMe, n=12) or posterior (pPDFMe, n=4) proximal medulla. Two other groups of PDF-ir neurons with numerous somata are situated at the dorsal and ventral lamina, respectively (PDFLa).

The PDFMe neurons densely innervate a small neuropil at the anterior ventroproximal edge of the medulla, the accessory medulla (AMe). The AMe is supposed to be an integration centre for timing information in the cockroach, which couples the ipsi- and contralateral pacemaker neurons, processes light information for clock synchronisation (entrainment), and mediates output of timing information to central brain areas (reviewed by Homberg et al. 2003, Chronobiol Int 20:577). The aPDFMe neurons, which are subdivided into three morphological distinguishable groups, arborise differentially in the subcompartments of the AMe (Reischig and Stengl 2003, Cell Tissue Res 314:421). Although the PDFMe neurons are known to form synapses in the AMe, their transmitters and the identity of pre- and postsynaptic neurons are unknown so far.

The nodular neuropil of the AMe is largely composed by  $\gamma$ -aminobutyric acid (GABA)-ir neurons, which are supposed to be at least partly involved in the photic entrainment pathway (Petri et al. 2002, J Exp Biol 205:1459). However, since GABA-ir neurons are also present in the ventral neurons of the AMe that contain the majority of the aPDFMe neurons, some PDFMe neurons might employ GABA as neurotransmitter. To elucidate the neuronal network of the AMe, I therefore started the search for the transmitters of the PDF-ir neurons with GABA.

**Methods:** For general histology, cockroach brains were embedded in Steerman's wax and sectioned at 10  $\mu$ m. Polyclonal anti-GABA-antiserum was applied at 1:2000 (Chemicon, Temecula, Canada), and detected with the peroxidase-antiperoxidase method. For double labelling on 40  $\mu$ m vibratome sections, polyclonal anti-PDF antiserum (Dirksen et al. 1987, Cell Tissue Res 250:377) and anti-GABA were used. Since both antisera were raised in rabbits, a method for antibody labelling was applied that involves covering of the first primary antibody with Fab fragments. Cy2 and Cy5 fluorescence was detected with a Leica TCS SP2 confocal laserscan microscope.

**Results and outlook:** The anti-GABA-antiserum stained intrinsic neurons of the AMe as was shown by Petri et al. 2002. Moreover, these neurons could now be mapped to the identified neuron soma groups of the AMe. GABA-ir fibres were additionally found in the anterior neuropil of the AMe, which is the main innervation site of PDF-ir fibres in the AMe. However, in no case colocalisation of PDF and GABA immunoreactivity could be observed, neither in any of the PDFMe neurons (Fig. 1A, B), nor in the PDFLa neurons (Fig. 1C). Obviously, no PDF-ir neuron employs GABA as neurotransmitter. However, not only in the AMe, but also in the distal layer and medial layers of the medulla GABA-ir fibres overlap with PDF-ir fibres (Fig. 1C). For this reason it is likely that PDF-ir neurons are postsynaptic to GABA-ir neurons, since they lie more downstream in the entrainment pathway. This hypothesis is currently be tested with double labelling with anti-PDF and antisera against insect GABA receptors.

Also serotonin (5HT) could have been a good candidate for a transmitter of the PDF-ir neurons, since 5HT-ir arborisations overlap with PDF-ir arborisations in the AMe (Petri et al. 1995, Cell Tissue Res 282:3), but colocalisation in PDFMe neurons was not found by the authors. Therefore, and because of physiological similarities in the action of 5HT and PDF in cockroaches (discussed in Reischig and Stengl 2003, Cell Tissue Res 314:421) it is possible, that PDF-ir neurons are postsynaptic to 5HT-ir neurons, what is now be tested in ongoing studies. The search for the transmitter(s) of the PDFMe neurons continues with immunocytochemical staining for dopamine, octopamine, acetylcholine, and amino acid transmitters.

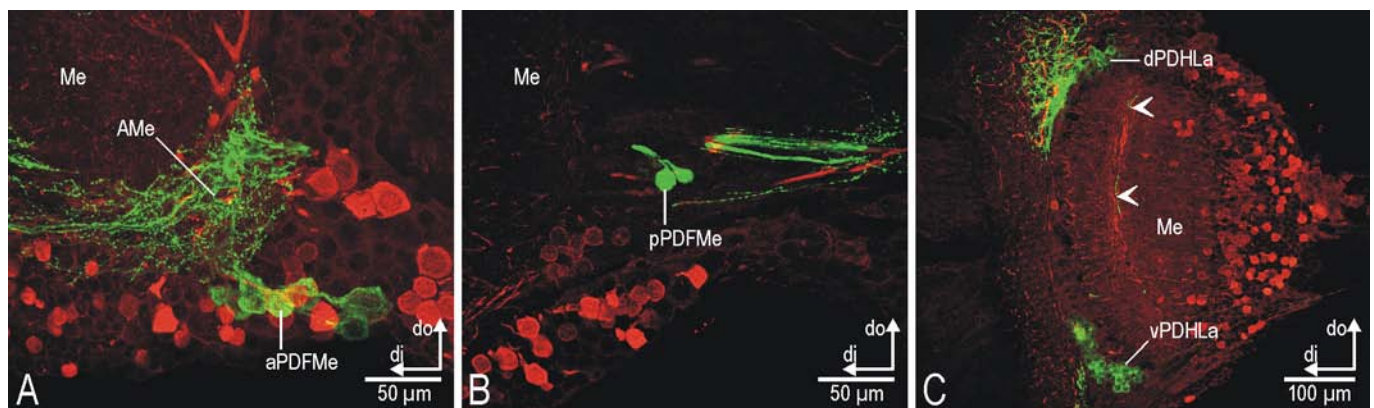


**Fig. 1:** Double labelling with anti-PDF (green) and anti-GABA (red) in the optic lobe of *L. maderae*. **A, B:** Neither in the somata of the anterior PDF-ir medulla neurons (aPDFMe), nor in posterior PDFMe (pPDFMe), nor in fibres of the accessory medulla (AMe) colocalised staining is detectable. **C:** Also the

dorsal and ventral PDF-ir lamina neurons (dPDFLa, vPDFLa) do not show GABA immunoreactivity. PDF-ir fibres in middle layers of the medulla (Me, arrowheads) are closely associated with GABA-ir fibres. Coordinates: di distal, do dorsal.

# **Reciprocal Neural Connections between the Central Posterior/Prepacemaker Nucleus and Nucleus G in the Gymnotiform Fish, *Apteronotus leptorhynchus***

GÜNTHER K.H. ZUPANC<sup>1,2</sup> SÔNIA A.L. CORRÊA<sup>2</sup>

<sup>1</sup>*School of Engineering and Science, International University Bremen, Bremen, Germany;*

<sup>2</sup>*School of Biological Sciences, University of Manchester, Manchester, UK*

The central posterior nucleus of teleost fish is a cluster of neurons in the dorsal thalamus that plays an important role in controlling social behaviors. In the weakly electric gymnotiform fish, *Apteronotus leptorhynchus*, this nucleus forms a larger complex together with the pacemaker nucleus, hence called central posterior/prepacemaker nucleus (CP/PPn). This complex is crucially involved in neural control of transient modulations of the electric organ discharge, which occur both spontaneously and in the context of social interactions. This control function is intimately linked to its pattern of connectivity with other brain regions. By employing an in vitro neuronal tract-tracing technique, we have, in the present study, identified a novel reciprocal connection between the CP/PPn and a cell group situated in the region between the ventral thalamus and the inferior lobe. Despite the previous interpretation by other authors of this cell group as the glomerular nucleus, the lack of a projection of this nucleus to the hypothalamus, as also demonstrated in the present investigation, makes such a homology unlikely. We, therefore, interpret this nucleus as a brain structure of unknown homology in other teleosts and suggest ‘nucleus G’ to identify it.

## Two 'electrical foveae' at the skin of the weakly electric fish, *Gnathonemus petersii*

Michael Hollmann & Gerhard von der Emde

Institute of Zoology, Dept. Neuroethology / Sensory Ecology, University of Bonn  
Endenicher Allee 11-13, 53115 Bonn, Germany  
Emails: mhollmann@uni-bonn.de, vonderemde@uni-bonn.de

The visual fovea of many vertebrates is a particular region of the retina, which is characterized by a high density of specialized photoreceptors. Animals with foveal eyes often show behavioural adaptations which include fixation of an object under investigation with the fovea, and saccadic eye (fovea) movements. In analogy to the visual fovea we suggest that the African electric fish *Gnathonemus petersii* has two specialized electroreceptive foveae used during active electrolocation of objects at night. These foveae may consist of electroreceptive skin regions with a high density of specialized receptor organs. The electrical foveae of electric fish may be specialized for different sensory functions comparable to those of the bifoveal eyes of some birds (e.g. pigeons) which possess two visual foveae used for different tasks.

We identified two regions of the skin of *G. petersii* as potential electroreceptive foveae, both of which appear to be essential for foraging. One of these regions is the chin appendix ('Schnauzenorgan'), the other one is the 'nasal region' just above the mouth (Fig. 1). We suggest that the Schnauzenorgan is used for prey analysis, i.e. it focuses on close-by (prey) objects, while the nasal region simultaneously focuses on more distant objects and therefore might be used for the detection and avoidance of obstacles.

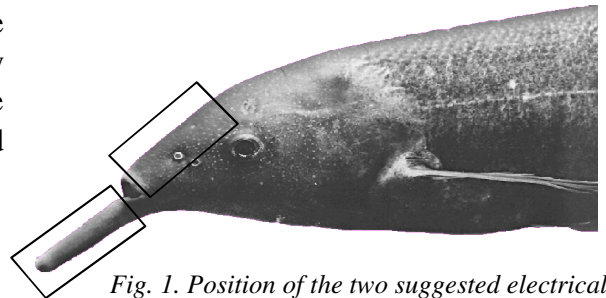


Fig. 1. Position of the two suggested electrical foveae on the head of a *G. petersii*.

To test our hypothesis we determined electroreceptor-organ densities in different skin areas. In addition, semi-thin sections from the presumed foveal regions and from a reference region on the fish's back were prepared and analysed with regard to the size of the receptor organ channel, its cavity and the receptor cells. Finally, we conducted behavioural experiments, during which we determined the positioning of different skin areas towards electrolocation targets while the fish was foraging. We measured the dynamics and the angles of the lateral movements of the Schnauzenorgan in order to identify saccadic movements.

The densities of 'mormyromast' receptor organs (which are utilised exclusively for active electrolocation) on the Schnauzenorgan and in the nasal region were found to be significantly higher than in other skin areas. Our results also show morphological differences of mormyromast organs occurring in different skin regions. Mormyromasts on the Schnauzenorgan are smaller than those in the nasal region, which in turn are smaller than organs in all other areas. In addition, the dimensions of some inner parts of the organs differ from region to region.

Our behavioural experiments showed that *G. petersii* positions its two foveae in a certain way towards prey and obstacles during foraging. The nasal region is held at a constant angle relative to the ground, pointing in front and slightly upwards. The Schnauzenorgan, in contrast, is constantly moved laterally left and right with the tip almost touching the ground. When a possible food item is encountered, Schnauzenorgan movements focus around this object. While scanning the ground for food, the movement of the Schnauzenorgan is comparable to saccadic eye movements of other animals during visually scanning their surroundings. Our results indicate that during food search the Schnauzenorgan is used for food detection and analysis at a close range, while the nasal region is simultaneously used to detect obstacles and other objects located in front at a greater distance.

## Distribution of the iron-binding protein hepcidin in the CNS

Zechel S.<sup>a</sup>; Kulaksiz, H.<sup>b</sup>; Unsicker, K.<sup>a</sup>; von Bohlen und Halbach, O.<sup>a</sup>

<sup>a</sup> IZN-Interdisciplinary Center for Neurosciences, Neuroanatomy, University of Heidelberg, Germany

<sup>b</sup> Department of Internal Medicine, Division of Gastroenterology, University of Heidelberg, Germany

Iron is an essential element for all body tissues including the CNS. Iron binding proteins, such as transferrin, ferritin and ferroportin are important to balance body iron requests. Regulation of iron levels is crucial, because excessive uptake can be toxic to the CNS and iron deficiency can induce myelination deficits in the developing brain. Recently, a new iron-binding peptide, hepcidin, was identified in blood and urine of humans. Mutation of the hepcidin gene causes severe juvenile hemochromatosis in humans and excessive iron overload in mice <sup>1</sup>. Overexpression of hepcidin in transgenic mice causes a severe anemia <sup>2</sup>. In addition, upregulation of hepcidin-mRNA was shown in response to iron overload ( $\beta$ -microglobulin-knockout-mice). Hepcidin-mRNA decreases dose-dependently if hepcidin mice were fed on a low iron diet <sup>1</sup>. Thus, it has been suggested that hepcidin has a key role in down-regulating intestinal iron absorption and placental transport of iron and the release of iron by macrophages <sup>3</sup>. Expression of hepcidin-mRNA occurs mainly in the liver, where the protein is synthesized and released, but also in other tissues. We have investigated the distribution of prohepcidin/hepcidin-protein in the mouse brain and spinal cord by immunohistochemistry using recently published antibodies <sup>4</sup>. Intense prohepcidin/hepcidin-protein-like immunoreactivity was mapped to different brain areas, as e.g. motor-, sensory- and piriform cortex, amygdala (anterior cortical, basolateral nuclei), hypothalamic nuclei (supraoptic nucleus, arcuate nucleus, mamillary nuclei) and thalamic nuclei of the midline and ventral complex. In addition, some mesencephalic and pontine nuclei were immunoreactive, especially the raphe magnus nucleus and motor nuclei of the cranial nerves (facial-, trigeminal-, hypoglossal-, abducens-, and trochlear nucleus). In the mesencephalon expression of hepcidin was mainly found in the red nucleus. The substantia nigra and the hippocampus exhibited only moderate staining, confined to a few distributed cells. In the cerebellum hepcidin-immunoreactivity was observed in Purkinje cells. Also, motoneurons of the ventral, ventrolateral and dorsal column of the spinal cord were stained. Since prohepcidin/hepcidin immunoreactivity was found in Neu-N-positive cells, protein expression is restricted to neurons. This distribution pattern suggests that hepcidin is involved in the regulation of iron uptake in neurons. Furthermore, hepcidin may play an important role in neurodegenerative diseases, in which intracellular iron accumulation occurs.

References: <sup>1</sup> Pigeon et al., J. Biol.Chem. 2001; 276 (11):7811-7819

<sup>2</sup> Nicolas G. et al., PNAS 2002; 99 (7): 4596-4601

<sup>3</sup> Ganz T., Blood 2003; 102(3): 783-788

<sup>4</sup> Kulaksiz H. et al., Gut 2004; 53:735-743

Supported by the Deutsche Forschungsgemeinschaft (SFB 636/A5)

## ***Olfactory bulbectomy induces neurodegeneration in the amygdala***

Jarosik, J.<sup>1</sup>, Legutko, B.<sup>2</sup>, Unsicker, K.<sup>1</sup>, von Bohlen und Halbach, O.<sup>1</sup>

<sup>1</sup> IZN – Interdisciplinary Center for Neurosciences, Neuroanatomy, Im Neuenheimer Feld 307

69120 Heidelberg, Germany

<sup>2</sup> Institute of Pharmacology, Polish Academy of Sciences, Smetna 12, 31-343 Krakow, Poland

Olfactory bulbectomy is considered as a model of depression [1]. Like in human major depression, bulbectomy induces behavioural alterations that can be ameliorated by chronic antidepressant treatment. Neurons of the olfactory bulb project to the amygdala, the hippocampus and the piriform cortex. In humans, these brain areas are known to be involved in major depression. By magnetic resonance imaging (MRI) it has been shown that depressed human subjects have smaller hippocampal and amygdalar volumes [2].

We performed bulbectomy and by using Nissl-stained sections we estimated neuronal densities in the amygdala (olfactory-, medial-, basolateral- and central amygdaloid areas). Moreover, we used Fluoro-Jade stained sections to quantify degenerated neurons in these areas. We found that about 8% of the neurons located in the posterolateral cortical amygdaloid nucleus were degenerated in bulbectomized mice. In addition, 2-5% of the neurons located in the medial amygdaloid nucleus, central amygdaloid nucleus, lateral amygdaloid nucleus, basolateral amygdaloid nucleus, and anterior cortical amygdaloid nucleus showed also signs of neurodegeneration. These data indicate that bulbectomy induces neuronal degeneration in the amygdala, which may cause reductions in neuronal densities. Indeed, we found that neuronal densities were decreased by ~15% in the olfactory amygdala, by ~10% in the central amygdala and by ~2% in the basolateral amygdala of bulbectomized animals. Our recent data show that neurodegeneration induced by bulbectomy is not restricted to the piriform cortex, as it has been described in the literature. It remains to clarify whether antidepressant treatment will reduce bulbectomy-induced neurodegeneration.

*Supported by the BMBF, Germany and KBN, Poland*

[1] Kelly et al 1997: *Pharmacol. Ther.* 74: 299-316

[2] Hastings et al 2004: *Neuropsychopharmacology*, 29: 952-959.

## The septum of anuran amphibians: Subnuclei and connections

Heike Endepols, Katja Roden, and Wolfgang Walkowiak

Institute of Zoology, University of Cologne, Weyertal 119, 50923 Köln, Germany

On the basis of Nissl stained sections, we subdivided the septum of the Gray treefrog *Hyla versicolor* in the lateral (dorsolateral and ventrolateral septal nuclei), central (dorsal and central septal nuclei), and medial septal complex (medial septal nucleus and nucleus of the diagonal band of Broca). The afferent and efferent projections of the septal nuclei were studied by combined retrograde and anterograde tracing with biotin ethyldiamine ("Neurobiotin").

The central and medial septal complex receive direct input from regions of the olfactory bulb and from all other limbic structures of the telencephalon (e.g. amygdalar regions, nucleus accumbens), while projections to the lateral septal complex are absent or less extensive. The medial pallium projects to all septal nuclei. In the diencephalon, the anterior thalamic nucleus provides the main ascending input to all subnuclei of the anuran septum, which can be interpreted as a limbic/associative pathway. The ventromedial thalamic nucleus projects to the medial and lateral septal complex, and may thereby transmit multisensory information to the limbic system. Anterior preoptic nucleus, suprachiasmatic nucleus, and hypothalamic nuclei innervate the central and lateral septal complex. Only the nuclei of the central septal complex receive input from the brainstem. Noteworthy is the relatively strong projection from the nucleus raphe to the central septal complex, but not to the other septal nuclei. The lateral septal complex projects mainly to the medial pallium, limbic regions (e.g. amygdala and nucleus accumbens) and hypothalamic areas, but also to specific sensory nuclei in diencephalon and midbrain. The central septal complex strongly innervates the medial pallium, limbic, and hypothalamic areas, but also specific sensory (including olfactory) regions. The medial septal complex sends major projections to all olfactory nuclei, and a weaker projection to the hypothalamus.

Our results indicate that all septal nuclei may modify the animal's internal state via efferents to limbic and hypothalamic areas. Via projections to the medial pallium, lateral and central septal complexes may be involved in learning processes as well. Because of their connections to specific sensory regions, all septal areas are in a position to influence sensory processing. Furthermore, our data suggest that both postolfactory eminence and bed nucleus of the pallial commissure are not part of the septal complex. Rather, the postolfactory eminence seems to be comparable to the mammalian primary olfactory cortex, while the bed nucleus may be analogous to the mammalian subfornical organ.

Supported by the Deutsche Forschungsgemeinschaft (Wa 446/4, En 439/1).

### **3-D reconstruction of the central complex in the brain of the locust**

#### ***Schistocerca gregaria***

Angela E. Kurylas, Joachim Schachtner, and Uwe Homberg

Department of Biology, Animal Physiology, Philipps-University Marburg, 35032 Marburg,  
Germany, kurylas@staff.uni-marburg.de

The central complex is one of the most prominent structures of the insect brain. The central complex spans the brain midline and consists of four interconnected neuropils, the protocerebral bridge, the upper and lower divisions of the central body, and a pair of noduli. A topographically highly ordered arrangement of columns, layers and chiasmal fiber crossings between layers characterizes the central complex in all investigated insects (Williams, 1975, J Zool 76:67; Hanesch et al., 1989, Cell Tissue Res 257:343; Müller et al., 1997, Cell Tissue Res 288:159). Principal neuronal cell types of the central complex can be distinguished by their arborization patterns and include tangential, columnar, and pontine neurons.

Recent evidence, particularly from work on the fly *Drosophila melanogaster* and the locust *Schistocerca gregaria* suggest that the central complex serves a role in motor control and visual integration, particularly in spatial navigation and sky-compass orientation (Strauss, 2002, Curr Opin Neurobiol 12:633; Homberg, 2004, Naturwissenschaften 91:199). Especially at the neuronal level, our understanding of the functional organization and significance of this brain structure is still highly incomplete. We, therefore, initiated a three-dimensional reconstruction of the anatomical organization of the central complex to serve as a basis for the analysis of its internal neural circuitries and connections to other brain areas.

In this study we established a three-dimensional (3D) reconstruction of the central complex of the locust *Schistocerca gregaria*. To visualize the subdivisions of the central complex, thick vibratome sections (150-250 µm) were stained with markers revealing the distribution of f-actin and the synaptic proteins synapsin and synaptotagmin. Optical sections obtained with a confocal laser scan microscope were evaluated using the 3D software Amira 3.1 (Indeed-Visual Concepts, Berlin, Germany).

Supported by DFG grant HO 950/14



# The Standard Protocol: Towards a genetic atlas of the *Drosophila* brain

Arnim Jenett, Johannes Schindelin, Martin Heisenberg

Lehrstuhl für Genetik und Neurobiologie, Bayerische Julius-Maximilians Universität Würzburg, Am Hubland, 97074 Würzburg

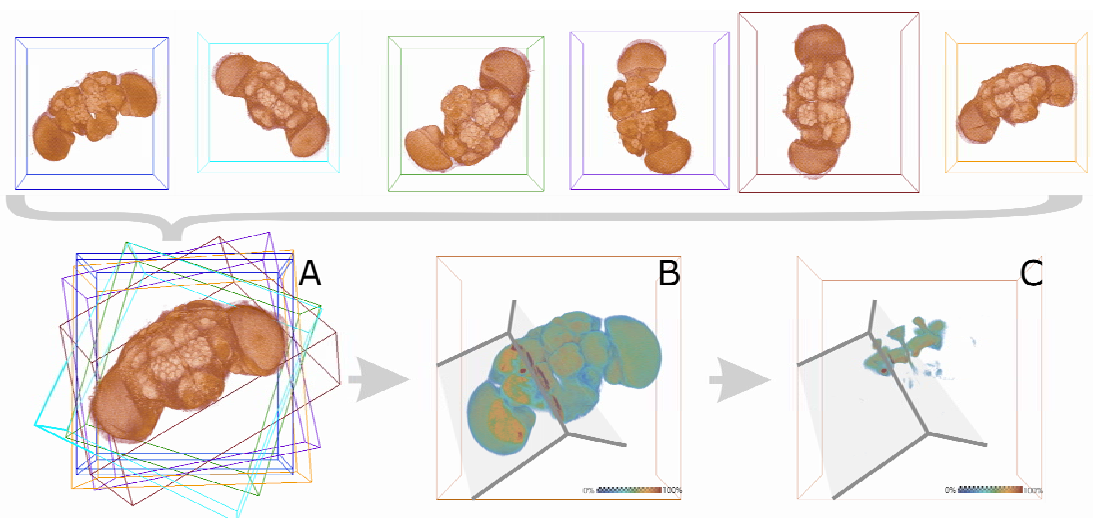
[arnim.jenett@biozentrum.uni-wuerzburg.de](mailto:arnim.jenett@biozentrum.uni-wuerzburg.de)

In *Drosophila melanogaster* genetic intervention can support the analysis of brain function using cell- and tissue-specific transcriptional control in the 2-component Gal4 system developed by Brand and Perrimon (Development 118: 401-415; 1993). This approach requires a precise knowledge of the gene expression patterns in the brain. Traditionally, these are assessed looking at small numbers of preparations. To cope with the biological (and experimental) variability of gene expression patterns a statistical analysis is needed.

Gene expression patterns in wholemount fly brains are visualised driving GFP or an immunohistochemical marker by the GAL4 transgene, and scanning with the confocal microscope. These datasets can now be compared and evaluated as aligned standard brains using the Virtual Insect Brain (VIB) protocol (Standard Protocol). The computation reveals and quantifies interindividual variability of the expression patterns. Typically, crosses of Gal4 driver and UAS reporter are standardised and compared to expression patterns of other crosses. A databank has been developed to collect and host the standardised expression patterns for usage via the www (<http://www.neurofly.de>).

In the Gal4 system tissue specificity is thought to be provided by the expression pattern of Gal4 in the driver line whereas the reporter construct is usually assumed to have no influence on the pattern. We have made use of the Standard Protocol to compare the expression patterns of Gal4 driver/UAS reporter combinations differing only in the genomic location of the reporter insert. Contrary to belief, expression patterns are highly dependent on the genomic positions of the reporter construct. Using Gal4 enhancer trap strains as well as promoter strains we found substantial differences in the visualised patterns. While the patterns agreed in several basic features they differed in many details which could not be explained assuming only differences in general expression levels. Variability among flies of the same genotype was much smaller. Our results suggest that the GAL4/UAS<sub>GAL4</sub> control is not entirely independent of *Drosophila* transcriptional regulators.

Scheme of the creation of a standard brain.  
Upper row: individual wholemount brain scans (nc82-stained).  
Lower row:  
A: aligned brains with their individual data volumes.  
B: Standard brain in common data volume (nc82).  
C: Standardised Gal4 expression pattern (201y).



B+C: The frontal part of the left hemisphere is taken away to provide insight into deeper brain regions. The percentage of identity in between the standardised brains is colour coded as shown in the graphics.



**Poster Subject Area #PSA19:  
Neurohistochemical studies**

- [#267A](#) R. Necker, J. Schweer and O. Leske, Bochum  
*Choline acetyltransferase (ChAT) and NO synthase (NOS) in the developing spinal cord of pigeons and chickens*
- [#268A](#) V. Bader, X. Zhu, C. Stichel and H. Lübbert, Bochum and Leverkusen  
*Spatial expression of DJ-1, a gene associated with Parkinson's disease*
- [#269A](#) A. Ray, G. Zoidl, S. Weickert, P. Wahle and R. Dermietzel, Bochum  
*Site specific and developmental expression of Pannexins in the CNS*
- [#270A](#) G. Schlaf, T. Manzke, T. Demberg and DW. Richter, Göttingen  
*Production of specific monoclonal antibodies directed against the serotonin 7 receptor using hamster-mouse hetero-hybridoma cells*
- [#271A](#) B. Orłowski, E. Roussa and M. Rickmann, Göttingen  
*Localisation of electrogenic sodium bicarbonate cotransporter NBC1 in mouse central nervous system*
- [#272A](#) I. Bendikov, VN. Foltyn, E. Dumin, P. Li, MD. Toney and H. Wolosker, Haifa (IL) and Davis, CA (USA)  
*Serine racemase modulates intracellular D-serine levels through an alpha,beta-elimination activity*
- [#273A](#) P. Blaesse, S. Ehrhardt, E. Friauf and HG. Nothwang, Kaiserslautern  
*Developmental pattern of three vesicular glutamate transporters (VGLUTs) in the rat superior olivary complex*
- [#266B](#) SR. Ott, H. Aonuma, PL. Newland and MR. Elphick, Brighton (UK), Sapporo (J), Southampton (UK) and London (UK)  
*Analysis of nitric oxide synthase expression in the thoracic nerve cord of crayfish*
- [#267B](#) A. Karpova and T. Behnisch, Magdeburg  
*Involvement of mTOR-p70S6K signalling pathway in LTP-expression in acute rat hippocampal slices*
- [#268B](#) W. Hütteroth and J. Schachtner, Marburg  
*Standardized 3D glomeruli of the Manduca sexta antennal lobe as a tool to study the influence of nitric oxide-stimulated cGMP on neuropilar development*
- [#269B](#) S. Utz, R. Predel, C. Wegener, J. Kahnt and J. Schachtner, Marburg and Jena  
*Distribution, steroid regulation, and identification of A-type allatostatins during development of the antennal lobe of the sphinx moth Manduca sexta*

- [#270B](#) M. Gräbner, C. Groh, W. Rössler and J. Schachtner, Marburg and Würzburg  
*Development of allatostatin-A immunoreactivity in antennal lobe neurons of the honeybee*
- [#271B](#) F. Kuperstein, E. Yakubov, R. Eilam, A. Brand, N. Salem jr and E. Yavin, Rehovot (IL) and Rockville, MD (USA)  
*Alterations in Dopamine receptors gene expression after n3 fatty acid deprivation in the perinatal brain*
- [#272B](#) C. Marin, J. Sales, C. Botella, I. Aranda, R. McDermott, R. Norman and E. Fernández, San Juan (E) and Salt Lake City (USA)  
*Cellular response to implantation of penetrating intracortical microelectrode arrays into cerebral cortex*

## **Choline acetyltransferase (ChAT) and NO synthase (NOS) in the developing spinal cord of pigeons and chickens**

*Reinhold Necker, Jennifer Schweer and Oliver Leske*

*Lehrstuhl für Tierphysiologie, Ruhr-Universität Bochum, D-44780 Bochum, Germany*

Acetylcholine is a well known transmitter of somatic and autonomic motor systems in the spinal cord. There are, however, in addition cholinergic neurons which are most probably local propriospinal interneurons with a modulatory function. Such a modulatory function has been ascribed also to nitric oxide (NO) which is synthesized by NOS, an NADPH diaphorase. The distribution of the acetylcholine synthesizing enzyme ChAT and of NOS has been described recently for the adult pigeon.<sup>1</sup> As to the modulatory function of both systems which may also serve learning it was of interest to look for the embryonic development and its presence at the time of hatching. Whereas chickens are precocial feeding by themselves immediately after hatching pigeons are less well developed (semiprecocial) staying in the nest and being fed for about 3 weeks post hatching. Eggs were incubated in a commercial breeder and embryos of different periods of incubation (embryonic days, E) were studied (pigeon: E12, E14, E16, E18 = day of hatching; chicken: E14, E16, E20 = one day before hatching). Cervical, thoracic and lumbosacral spinal segments were removed and fixed in paraformaldehyde (4% in PBS) which was replaced by PBS after a couple of days. After cryoprotection by sucrose (30% in PBS) spinal segments were cut at 50 µm by a cryostat. The distribution of both enzymes was studied immunocytochemically using the ABC-method. Antibodies were rabbit anti ChAT (Chemicon AB144P) and rabbit anti NOS (Sigma N7280). In addition a standard histochemical technique was used to show the location of NADPH diaphorase (NADPH-d).

In adult birds ChAT occurs mainly in motoneurons, in preganglionic neurons of the autonomic nervous system (in birds column of Terni) and in a dense band of small neurons and processes in lamina III of the dorsal horn. In the pigeon and in the chicken ChAT-positive motoneurons and preganglionic neurons are present in the earliest embryonic day studied. However, the adult-like labeling of lamina III appears only at E18 in the pigeon and at E20 in the chicken, i.e. at the time of hatching. In adults NADPH-d- and NOS-containing neurons are scattered throughout the spinal gray. In the dorsal horn labeling consists of a dense band of neurons and processes in lamina II. Labeling of lamina II appears first at E14 in the pigeon and at E16 in the chicken and is well developed at the time of hatching.

Altogether both ChAT and NOS are well expressed at the time of hatching in both avian species. In mammalian species most developmental studies have been done in the rat, which is at birth clearly less well developed than pigeons or chickens. In the rat a similar distribution of both enzymes is found in the adult dorsal horn but the ChAT-labeling of lamina III appears only about 2 weeks and NOS-labeling of lamina II only about one week after birth. The earlier appearance of NOS in the dorsal horn seems to be similar in both classes of vertebrates. Altogether ChAT and NOS in the spinal dorsal horn appear rather late during development which supports the view of a modulatory function of these propriospinal systems.

---

<sup>1</sup> Necker, R.: Distribution of choline acetyltransferase and NADPH-diaphorase in the spinal cord of the pigeon. *Anat Embryol* 208:169-181 (2004)

**Spatial expression of DJ-1, a gene associated with Parkinson`s disease**

Verian Bader<sup>1</sup>, Xinran Zhu<sup>1</sup>, Christine Stichel<sup>2</sup>, Hermann Lübbert<sup>1,2</sup>

<sup>1</sup>Department of Animal Physiology, Ruhr-University of Bochum, D-44780 Bochum;

<sup>2</sup>Biofrontera Pharmaceuticals AG, D-51377 Leverkusen, Germany

Mutations in DJ-1, a protein of unknown function, were recently identified as cause for an autosomal recessive, early onset form of Parkinson`s disease (PD). Since no data is available regarding the distribution pattern of the DJ-1 mRNA and protein in the mouse brain, we performed in-situ hybridisation using an RNA-probe generated from full length cDNA, and immunohistochemistry. For the latter we overexpressed mouse DJ-1 in *E. coli* and generated a polyclonal antibody against the fusion protein.

We analysed the expression of DJ-1 in the entire brain, taking into special account crucial structures involved in PD. Our data indicated that DJ-1 mRNA is mainly expressed in neurons, with strong signals in the substantia nigra pars compacta, hippocampus, cerebellum (Purkinje cells) and certain brainstem nuclei (e.g. facial nucleus). Beside neurons, glial cells in the corpus callosum and other brain regions were also stained, although signals were weaker than in neurons. Using an mRNA probe generated from the sense DNA, no signal could be detected.

These results were confirmed by immunohistochemistry showing a similar distribution of the protein with the same prominent neuronal staining. Specificity of the antibody was confirmed by blocking experiments and Western blots.

**Site specific and developmental expression of Pannexins in the CNS**

Arundhati Ray<sup>1</sup>, Georg Zoidl<sup>1,3</sup>, Svenja Weickert<sup>1</sup>, Petra Wahle<sup>2</sup> and Rolf Dermietzel<sup>1</sup>

<sup>1</sup> Neuroanatomy and Molecular Brain Research, <sup>2</sup> Dept. of Developmental Neurobiology, Ruhr-University Bochum, Germany, <sup>3</sup> Presenting Author.

Gap junctions constitute the structural equivalent of electrical synapses in the CNS. Traditionally, connexin genes have been considered as the structural protein units of Gap junctions in vertebrates. This view was challenged, when Panchin et al. (Curr Biol, 2000) reported of three genes (Pannx1-3) in vertebrates homologous to the invertebrate Gap junction family of innexin proteins. Since recent studies have shown the expression of Pannx1 and Pannx2 in the CNS and their ability to form communicating channels (Bruzzone et al, PNAS, 2003, Baranova et al, Genomics, 2004) pannexins are likely to represent a second class of Gap junction forming proteins. This finding is particularly intriguing as the extent of connexin expression does not entirely overlap with regions of electrical coupling. Since pannexins could serve as candidate molecules responsible for electrical coupling in those areas of the brain lacking connexin mediated coupling or having low level connexin expression only, we analyzed the developmental and tissue expression of Pannx 1 in the CNS. Real time PCR results showed that Pannx1 is developmentally regulated in the brain and eye. *In situ* hybridization combined with immunohistochemistry confirmed abundant and widespread expression in brain and retina and aided in identification of neuronal subtypes expressing Pannx1. Pannx1 expression in the hippocampus and retina was further confirmed by RT-PCR combined with laser capture microdissection. Our data demonstrate that Pannx1 is a major component of neuronal subpopulations known to be electrically coupled. Furthermore, the identification of expression sites not previously recognized for coupling raise speculations whether pannexins might fulfill other functions aside of electrical coupling.

Supported by SFB509, GRK 736 and IGSN-Bochum

## **Production of specific monoclonal antibodies directed against the serotonin 7 receptor using hamster-mouse hetero-hybridoma cells**

Gerald Schlaf<sup>2\*</sup>, Till Manzke<sup>1\*</sup>, Thorsten Demberg<sup>2</sup> and Diethelm W. Richter<sup>1</sup>

<sup>1</sup>Dept. of Neuro-and Sensory Physiology, University of Göttingen, Humboldtallee 23, 37073 Göttingen and <sup>2</sup>Dept. of Immunology, Kreuzberggring 57, 37073 Göttingen; \*these authors are equally contributed to the work

The 5-HT<sub>7</sub> receptor has been identified recently as a member of the G-protein coupled serotonin receptor superfamily that is involved in the regulation of the circadian rhythm as well as in sensory and limbic processing. So far, there were only polyclonal antibodies available all of which were lacking specificity. The aim of this project therefore was to generate specific monoclonal antibodies (mAb) to be used in different assays.

The high homology of the 5-HT<sub>7</sub> receptor between mouse and rat (98% on the level of amino acids) prompted us to immunise Syrian hamsters with a polypeptide (FPRVQPESVISLNG) derived from the third intracellular domain (the putative G-protein binding site). As expected, the hyperimmunisation of Syrian hamsters led to peptide-specific serum titres of more than 1 : 500,000 in contrast to several mice in which a titre of only 1 : 1000 was reached using an ELISA assay with the solid phase-coated peptide. Hybridoma cells producing antibodies were subcloned twice. Selected IgG antibody secreting hybridoma clones were expanded and the mAb of their supernatants were purified by protein-A chromatography ('high salt' method). In FACS-analyses both the wildtype rat basophilic leucocyte cell line (RBL) and the human neuroblastoma cell line (NBT) were recognised by the 5-HT<sub>7</sub> specific mAb SY18 demonstrating cross-reactivity of the anti-rat 5-HT<sub>7</sub>R mAb with the human 5-HT<sub>7</sub> receptor. NBT cells transiently transfected with Green Fluorescent Protein- (GFP-) conjugated mouse 5-HT<sub>7</sub> receptor clearly demonstrated co-localisation with the mAb SY18 (with a secondary Alexa 647-conjugated antibody).

Immunohistochemical stainings of various areas of the rat brain (e.g. purkinje cells in the cerebellum, pyramidal cells in the cortex) were highly congruent with signals obtained using in-situ hybridisation. Taken together, all of the performed control experiments provide evidence that in the present study the first specific and reliable monoclonal antibody for the detection of 5-HT<sub>7</sub> receptor in man and rat have been generated.

## **Localisation of electrogenic sodium bicarbonate cotransporter NBC1 in mouse central nervous system**

**B. Orlowski, E. Roussa, M. Rickmann**

**Zentrum Anatomie, Dept. Neuroanatomy, University of Göttingen, Germany**

Sodium bicarbonate cotransporters (NBC) are transmembrane proteins that mediate electrogenic or electroneutral transport of  $\text{Na}^+$  and  $\text{HCO}_3^-$ . In situ hybridisation has shown that the electrogenic sodium bicarbonate cotransporter NBC1 is present in brain. However, exact cellular localization remains to be determined. Data from the running project has shown the distribution of electrogenic  $\text{Na}^+\text{HCO}_3^-$  cotransporters in adult mouse brain. Immunofluorescence, light microscopy and pre-embedding staining electron microscopy was applied. Rabbit polyclonal antibodies directed against specific N-terminal regions of pNBC1 splice variant and kNBC1 variant were used.

In cerebellum, Purkinje cell bodies with dendrites and some cell bodies in granular layer were labeled by anti-kNBC1. Anti-pNBC1 showed weak staining in Purkinje cells and of Bergman glial processes. In olfactory bulb, periglomerular cells were strongly labeled by anti-kNBC1 antibody and only weakly stained with anti-pNBC1. Large neurons in the external plexiform layer and mitral cells showed strong labeling by anti-kNBC1. In hippocampus proper, apical pyramidal cell dendrites were stained with anti-pNBC1. Both antibodies strongly reacted with non-pyramidal neurons. In dentate gyrus, some neurons lying basal to the granular layer were intensely stained with anti-kNBC1.

In cerebral cortex, there was strong labeling of non pyramidal cell bodies with anti-kNBC1. Pyramidal cell bodies were less intensely stained by both antibodies. There were surprisingly few stained astroglial perikarya. In all cortical regions, both antibodies showed punctuate structures in the neuropil. Electron microscopical examination showed labeled astroglial lamellae (anti-kNBC1: 70% of all labeled structures, anti-pNBC1: 58%), presynaptic (anti-kNBC1: 10%, anti-pNBC1: 17%), small postsynaptic elements (anti-kNBC1: 2%, anti-pNBC1: 9%), and relatively few neuronal processes.

The results show a widespread and differential neuronal expression of kNBC1 and pNBC1 whereas astrocytes expressed both NBC1 variants preferentially in smaller processes and lamellae. These data indicate that neuron subpopulations are differentially equipped with NBC1 variants, suggesting distinct functions of pancreatic and kidney NBC1 variants in the nervous system. The presence of pNBC1 and kNBC1 in astrocytes suggest an involvement of these transporters in regulation of intracellular pH and/or bicarbonate transport.

## Serine racemase modulates intracellular D-serine levels through an $\alpha,\beta$ -elimination activity.

Inna Bendikov<sup>1</sup>, Veronika N. Foltyn<sup>1</sup>, Elena Dumin<sup>1</sup>, Pu Li<sup>2</sup>, Michael D. Toney<sup>2</sup>, and Herman Wolosker<sup>1</sup>

<sup>1</sup> Dept of Biochemistry, Technion-Israel Institute of Technology, The B. Rappaport Fac. of Medicine, Haifa 31096, Israel and <sup>2</sup>Dept of Chemistry, U. California-Davis, CA 95616, U.S.A.

Mammalian brain contains high levels of D-serine, an endogenous coagonist of N-methyl D-aspartate type of glutamate receptors. The presence of D-serine in the brain challenges the idea that only L-amino acids will be present or play a role in mammals. We now sought to understanding the mechanism of biosynthesis and degradation of brain D-serine, which will shed light on several aspects of D-serine disposition and neurobiology. D-Serine is synthesized by serine racemase, a brain enriched enzyme converting L- to D-serine. Degradation of D-serine is achieved by D-amino acid oxidase, but this enzyme is not present in forebrain areas that are highly enriched in D-serine. We now report that serine racemase catalyzes the degradation of cellular D-serine itself, through the  $\alpha,\beta$ -elimination of water. The enzyme also catalyzes water elimination with L-serine and L-threonine and elimination of these substrates is observed both *in vitro* and *in vivo*. In order to further investigate the role of elimination in regulating cellular D-serine, we generated a serine racemase mutant displaying selective impairment of elimination activity (Q155D). Levels of D-serine synthesized by the Q155D mutant are several fold higher than the wild-type both *in vitro* and *in vivo*. This suggests that elimination reaction limits the achievable D-serine concentration *in vivo*. Additional mutants in vicinal residues (H152S, P153S and N154F) similarly altered the partition between the  $\alpha,\beta$ -elimination and racemization reactions. Elimination also competes with the reverse serine racemase reaction *in vivo*. While the formation of L- from D-serine is readily detected in Q155D mutant-expressing cells incubated with physiological D-serine concentrations, reversal with wild-type serine racemase-expressing cells required much higher D-serine concentration. We propose that elimination provides a novel mechanism for regulating intracellular D-serine levels, especially in brain areas that do not possess D-amino acid oxidase activity. Extracellular D-serine is more stable toward elimination, likely due to physical separation from serine racemase and its elimination activity.



## Developmental pattern of three vesicular glutamate transporters (VGLUTs) in the rat superior olivary complex

Blaesse P, Ehrhardt S, Friauf E, and Nothwang HG

Animal Physiology Group, Department of Biology, University of Kaiserslautern, POB 3049, D-67653 Kaiserslautern, Germany

Glutamatergic neurotransmission is of crucial importance for processing acoustic information. The molecular composition of glutamatergic synapses undergoes dynamic changes during development, e.g. age-dependent expression of glutamate receptors. Here, we have investigated the distribution and the developmental expression of the three known vesicular glutamate transporters (VGLUTs), which mediate the packaging of glutamate into synaptic release vesicles. Immunoreactivity for VGLUT1-3 was analyzed in 6 nuclei of the superior olivary complex (SOC), the medial nucleus of the trapezoid body, the ventral nucleus of the trapezoid body, the lateral nucleus of the trapezoid body, the lateral superior olive, the medial superior olive, and the superior paraolivary nucleus. Furthermore, we differentiated between 4 developmental stages between birth and adulthood (postnatal days 0, 4, 12, and 60). Confocal microscopy was applied to provide information about the cellular distribution of the VGLUTs.

Our results demonstrate that all three VGLUTs are present in the neonatal and adult SOC. In most nuclei, more than one VGLUT isoform is expressed. This is in contrast to other brain regions where a complementary pattern was described. VGLUT2-immunoreactivity is present at all ages and within all SOC nuclei, providing evidence for a basic function of this isoform within the auditory brainstem. Interestingly, there are several changes concerning the intensity and cellular distribution of VGLUT1- and VGLUT3-immunoreactivity during development. Some nuclei show VGLUT3 immunoreactivity at a high level during development, whereas only weak VGLUT3 labeling occurs throughout the SOC in adulthood. Another developmental change is a transient, perisomatic VGLUT1 and VGLUT3 staining in several SOC nuclei, implying profound synaptic reorganization. Such considerable changes in the spatio-temporal distribution of VGLUTs suggest differential roles of the transporters during maturation and in adulthood.

*Supported by the Graduate Research School "Molecular, physiological and pharmacological analysis of cellular membrane transport", DFG GRK 845/1.*

# Analysis of nitric oxide synthase expression in the thoracic nerve cord of crayfish

Swidbert R. Ott,<sup>1</sup> Hitoshi Aonuma,<sup>2</sup> Philip L. Newland<sup>3</sup> and Maurice R. Elphick<sup>4</sup>

S.R.Ott@cantab.net

<sup>1</sup> Life Sciences, University of Sussex, Brighton BN1 9QG, UK

<sup>2</sup> Laboratory of Neuro-Cybernetics, RIES, Hokkaido University, Sapporo, Japan

<sup>3</sup> Biological Sciences, Division of Cell Sciences, University of Southampton, Southampton SO16 7PX, UK

<sup>4</sup> Biological Sciences, Queen Mary, University of London E1 4NS, UK

In insects, strong expression of nitric oxide synthase (NOS) is frequently associated with primary sensory neuropiles. In the segmental thoracic ganglia of orthopterans and cockroaches, the highest density of NOS occurs in exteroceptive (mixed tactile and gustatory) neuropiles, suggesting a role for NO in early stages of sensory processing.<sup>1,2</sup> It is unknown whether this also applies in malacostracans, the putative sister group of hexapods within the pancrustacean clade.<sup>3,4</sup> Here we exploit recent advances in NADPH diaphorase (NADPHd) histochemistry<sup>2,5</sup> to study the expression of NOS in the thoracic nerve cords of two species of crayfish, *Pacifastacus leniusculus* and *Procambarus clarkii*. Specificity of the staining was validated by NOS immunohistochemistry.

All five thoracic ganglia (T1–T5) contain NADPHd-positive cell bodies (~75 pairs in T2). Most intensely stained are a single pair of very large cells (diam. ~80 µm; arrows) in the ventral medial group, segmentally repeated in T2, T3 and T4 but missing in T1 and T5. They belong to intersegmental interneurons with contralaterally ascending axons that are part of the VN fibre system (see below).

The fibre architecture is highly intersegmental (~80 axons in each T2–T3 connective) and includes exceedingly complex projections. The neuropilar fibre distributions are at first approximation identical in T2 and T3, but T1 and particularly T4 and T5 are strikingly different. These differences, which most likely reflect functional specializations of the thoracic appendages, are to a large extent the result of a differential development of three distinct fibre systems. Two prominent systems of neurites run superficially in the thin ventral shell of the lateral lobe (LL). The *anterior shell system* (ass) emanates from stout dorsoventral neurites of uncertain origin that curve around the anterior edge of the neuropile and fan out into a loose mesh of fibres. It is present in all thoracic ganglia. The *posterior shell system* (pss) comprises 1–4 giant neurites that run medio-

laterally along the ventral face of the neuropile and derive from small medial cell bodies. Their fine primary neurites expand dramatically in diameter and arborize into several thick main branches. These continue around the lateral and posterior edges of the neuropile and eventually produce coarsely beaded arborizations in dorsal neuropile. The pss is present only in T1–T3. The *ventral neuropile system* (vns) consists of medial intersegmental axons and their segmentally arranged collaterals that innervate exclusively the ventral neuropile (VN) of the LL, a sensory centre homologous to the exteroceptive ventral association centre (VAC) of insects. This nitrergic innervation of the VN is extremely prominent in T2 and T3, where it gives rise to the highest densities of staining in the entire thoracic cord. It is somewhat less conspicuous in T1, greatly reduced in T4 and virtually absent (but still recognizable) in T5. Neither the ass nor the pss contribute to the staining in the VN.

The thoracic neuroarchitecture of NOS in T1–T3 thus shows conserved or convergent features in malacostracans and hemimetabolous insects that indicate similar roles for NO in sensory processing in both taxa. First, homologous exteroceptive neuropiles (VAC and VN) receive exceedingly dense NOS-positive innervation. Second, this innervation comes from intersegmental interneurons that do not contribute to the looser meshworks in the mixed premotor/motor neuropiles. In the light of these remarkable parallels across the two taxa, the near-complete reduction of the VN system in T4 and T5 is noteworthy and calls for an explanation.

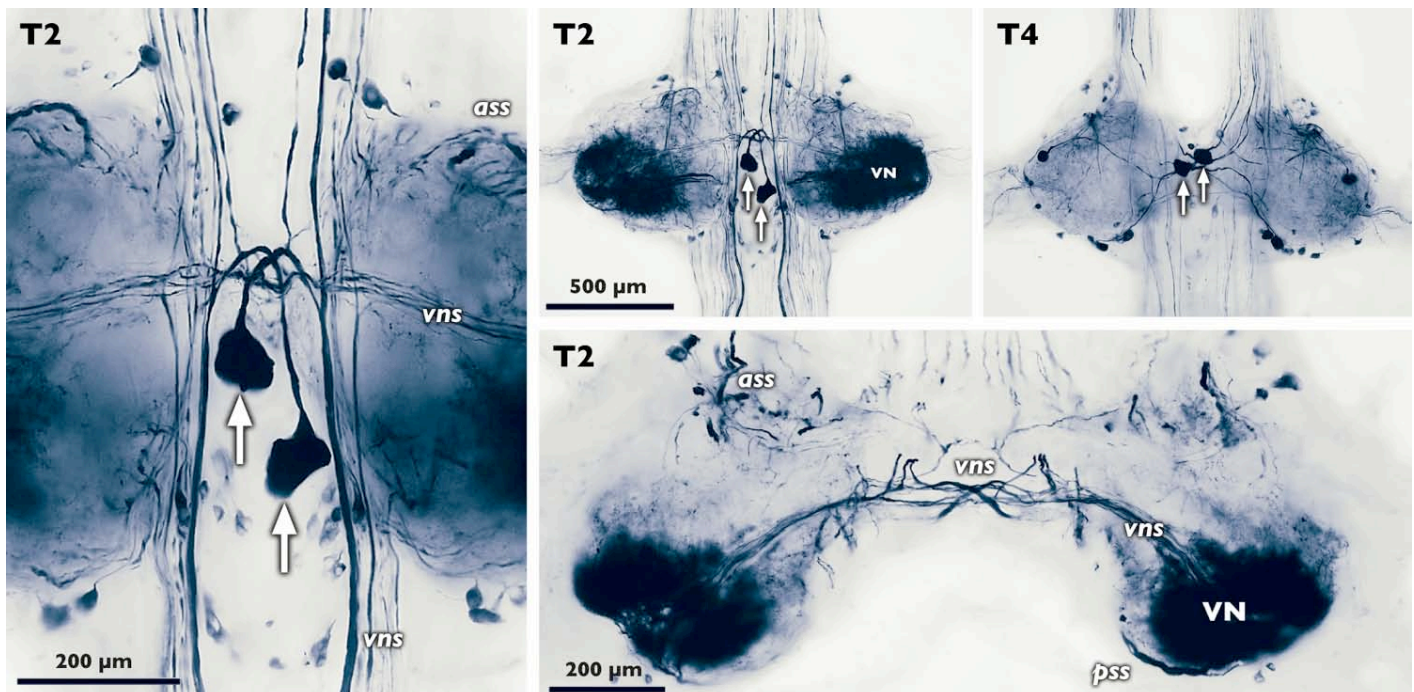
1. Ott SR & Burrows M, *J Comp Neurol* 395:217–230 (1998)

2. Ott SR & Elphick MR, *J Comp Neurol* 448:165–185 (2002)

3. Strausfeld NJ, *Brain Behav Evol* 52:186–206 (1998)

4. Wilson K, Cahill V, Ballment E & Benzie J, *Mol Biol Evol* 17:863–874 (2000)

5. Ott SR & Elphick MR, *J Histochem Cytochem* 51:523–532 (2003)



All images from whole-mount preparations except bottom right, transverse vibratome section. For explanation of symbols see main text.

## Involvement of mTOR-p70S6K signalling pathway in LTP-expression in acute rat hippocampal slices

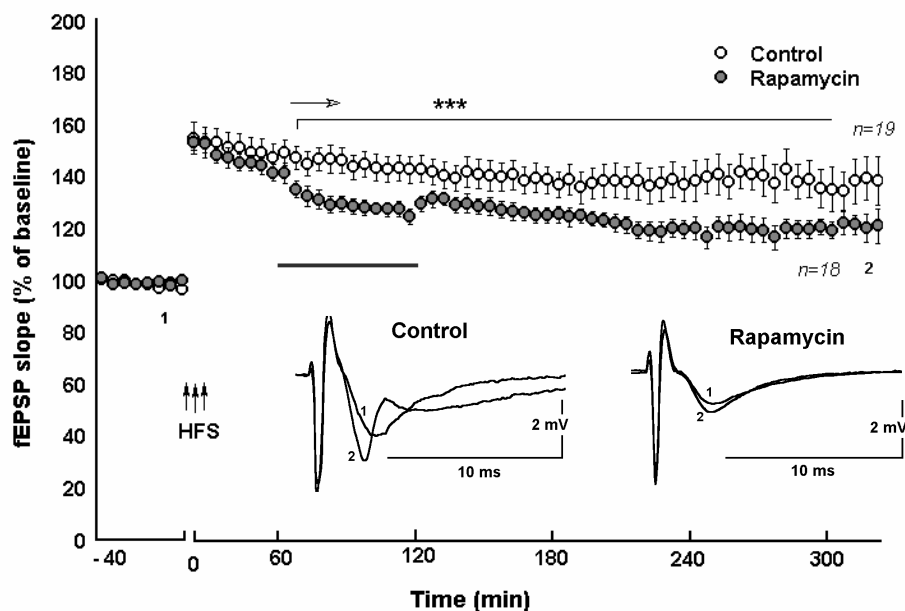
**Anna Karpova and Thomas Behnisch**

Leibniz Institute for Neurobiology, Brennecke Str. 6, 39118, Magdeburg, Germany

[Anna.Karpova@ifn-magdeburg.de](mailto:Anna.Karpova@ifn-magdeburg.de); [Behnisch@ifn-magdeburg.de](mailto:Behnisch@ifn-magdeburg.de)

Recently it has been reported that hippocampal long-term potentiation (LTP) is sensitive to application of an mRNA translation inhibitor rapamycin (Cammallery M., et al., JNS, 2003). It is known that rapamycin inhibits protein synthesis by suppressing mTOR activity and the subsequent p70S6 kinase phosphorylation in Thr389. Protein synthesis takes place also in dendrites, so that it might be the case that steady state dendritic protein synthesis plays a role in LTP-expression. To investigate this particular question we induced late-LTP by 3 trains 100 Hz 1 sec every 10 minutes and after one hour rapamycin (200 nM) was applied and continued the next hour. The stratum radiatum signals were evoked and tested every one minute by standard field potential recording procedures.

Our experiments show that rapamycin application resulted in a rapid decrease in the fEPSP slope of about 6% that recovers slightly after washout.



Then it further declines and remains significant different from control measurements up to the end of the experiment. The control (open circle) and experimental (filled circle) data are presented as mean $\pm$ sem in the diagram where the arrows indicate the time point of tetanization; the dark bar represents the drug application moment and the bracket is the significant interval of  $p < 0.05$ .

Additional immunohistological investigations show that between 2 and 4 hrs after LTP induction Thr389 phosphorylated p70S6 kinase is localized uniformly at the cell bodies, nucleus and in apical dendrites ( $n=4$ ). In contrast, directly after rapamycin application the immunosignal was very weak and only detectable in a few cell bodies in the CA1 neurons ( $n=4$ ) of the stratum pyramidale. After one hour washout the level of the phospho-p70S6K immunosignal was increased and after two hours the signal was not distinguishable from the LTP control cases for the same time point. This immunohistological investigation indicates that rapamycin effectively inhibits the p70S6 kinase phosphorylation leading to a decline of synaptic potentiation and this phosphorylation recovers when rapamycin is washed out without recovery of field potential potentiation.

We conclude that rapamycin sensitive translation processes are involved weakly but significantly in LTP-expression and that a permanent p70S6 kinase phosphorylation is maintained.

## Standardized 3D glomeruli of the *Manduca sexta* antennal lobe as a tool to study the influence of nitric oxide-stimulated cGMP on neuropilar development

Wolf Hütteroth\* and Joachim Schachtner

Dept. Biology, Animal Physiology, Philipps-University Marburg, Karl-von-Frisch-Str., 35032 Marburg, Germany, \*corresponding author: [huetteroth@staff.uni-marburg.de](mailto:huetteroth@staff.uni-marburg.de)

The antennal lobe (AL) is the first brain center in insects where olfactory signals are processed. The neuropil of the antennal lobe of the sphinx moth *Manduca sexta* is organized into about 63 so-called glomeruli which are arranged around a core of coarse neuropil. Glomeruli are sphere-like structures, which are also found to organize the neuropil in the olfactory bulb of vertebrates and thus seem to be a universal feature for odor recognition [1]. Olfactory receptor neurons receive the odor signals in the antennae and converge in the AL into specific glomeruli, where this information is integrated and processed by local interneurons and sent to the calyces of the mushroom body and the lateral protocerebrum via projection neurons [2].

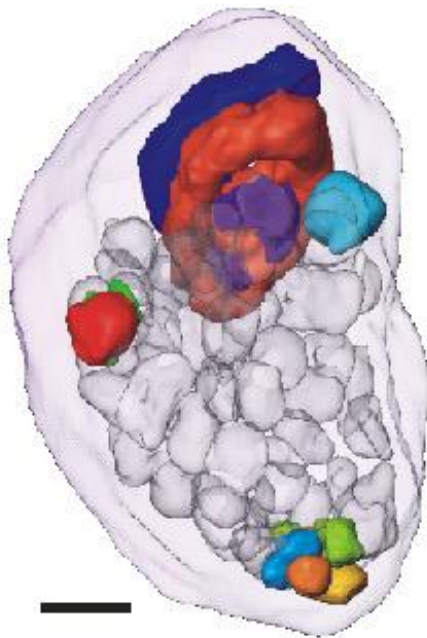


Figure 1:  
Reconstruction of a right pupal antennal lobe (P13, medial view, anterior left, dorsal up) from a *Manduca sexta* male. Outlines of the AL are transparent, colors label the ten identified glomeruli, other glomeruli are also displayed transparently.

Scale bar = 100  $\mu$ m

The AL of *M. sexta* is formed during 21 days of pupal development (P0 – P20). AL development can be subdivided in three main phases: in phase I (P0 – P7/8) all cells comprising the AL are born and glomerular templates are laid out, during phase II (P7/8 – P12) the main wave of synaptogenesis occurs in the AL and glomeruli are formed, and finally in phase III (P12 – adult eclosion) the established synaptic network matures and undergoes further refinement [3].

We are interested in the establishment of synaptic connections made during phase II, especially in the involvement of the nitric oxide / cGMP-pathway during glomerulus formation. Therefore we produced 3D standards of ten identified glomeruli from *M. sexta* males at P12/13 regarding location, shape and volume (Figure 1). Based on these data we are currently examining the volumes of the same ten glomeruli from males which were injected at the beginning of phase II with the soluble guanylyl cyclase inhibitor 1H-[1,2,4] oxadiazolo [4,3-a] quinoxalin-1-one (ODQ) and prepared at P13.

Volume measurements were based on immunostainings with a monoclonal antibody against the ubiquitous synaptic vesicle protein synaptotagmin which reliably labels glomeruli during development [3]. Wholemounts of ALs were scanned on a confocal laserscan microscope (Leica TCS SP2), and structures were reconstructed with AMIRA 2.3 (TGS, San Diego, USA).

Supported by a DFG grant SCHA 678/3-3

[1] Eisthen HL (2002) Why are olfactory systems of different animals so similar? *Brain Behav Evol* 59:273-293

[2] Tolbert LP, Oland LA, Tucker ES, Gibson NJ, Higgins MR, Lipscomb BW (2004) Bidirectional influences between neurons and glial cells in the developing olfactory system. *Prog Neurobiol* 73:73-105

[3] Dubuque SH, Schachtner J, Nighorn AJ, Menon KP, Zinn K, Tolbert LP (2001) Immunolocalization of synaptotagmin for the study of synapses in the developing antennal lobe of *Manduca sexta*. *J Comp Neurol* 441:277-287

## **Distribution, steroid regulation, and identification of A-type allatostatins during development of the antennal lobe of the sphinx moth *Manduca sexta***

**Sandra Utz<sup>1</sup>, Reinhard Predel<sup>2</sup>, Christian Wegener<sup>1</sup>, Jörg Kahnt<sup>3</sup> and Joachim Schachtner<sup>1</sup>**

<sup>1</sup>Dept. Biology, Animal Physiology, Philipps-University, 35032 Marburg, Germany;

<sup>2</sup>Sächsische Akademie der Wissenschaften, Research Group Jena, 07743 Jena, Germany.

<sup>3</sup>Dept. Biochemistry, MPI For Terrestrial Microbiology, 35043 Marburg, Germany

The antennal lobe is the primary integration unit for odor information in the insect brain and compares to the olfactory bulb of vertebrates (Eisthen, 2002, Brain Behav Biol 59:273). Antennal lobe and olfactory bulb not only share their principal morphological organization into so called olfactory glomeruli, but also a number of basic physiological properties with respect to information processing (Hildebrand and Shepherd, 1997, Annu Rev Neurosci 20:595). Olfactory glomeruli represent the basic functional units for odor processing and contain thousands of synapses between olfactory receptor neurons and neurons of the antennal lobe or the olfactory bulb.

The aim of our studies is to reveal mechanisms underlying the formation of the olfactory glomeruli during development. The system we are using to study this task is the particularly well established antennal lobe of the sphinx moth *Manduca sexta*.

The antennal lobe of adult *M. sexta* contains many peptidergic neurons. Formation of the antennal lobe occurs during the defined period of metamorphosis (Tolbert et al., 2004, Prog Neurobiol 73:73). To find out whether neuropeptides are suited to play a role during antennal lobe development we studied neuropeptides of the A-type allatostatin (AST-A) family. To determine time of occurrence and cellular location of AST-As during AL development we used an antiserum recognizing all members of the AST-A neuropeptide family. To specify which family members are expressed at a certain time of development we used MALDI-TOF mass spectrometry.

Based on morphology and developmental appearance we distinguished four types of AST-A-immunoreactive cell types. The majority of the cells were local interneurons of the lateral cell group of the antennal lobe (type Ia) which acquired AST-A immunostaining in a complex pattern consisting of three rising (RI-RIII) and two declining phases (DI, DII). Type Ib neurons consisted of two local neurons with large cell bodies not appearing before 7 to 8 days after pupal ecdysis (P7/8). Type II and III neurons accounted for single centrifugal neurons, with type II neurons present in the larva and disappearing in the early pupa. The type III neuron appeared not before P7/8.

RI and RII coincide with rises of the ecdysteroid hemolymph titer. Artificially shifting the pupal 20-hydroxyecdysone (20E) peak to an earlier developmental time point resulted in the precocious appearance of AST-A immunostaining in type Ia, b and III neurons. This result supports the hypothesis that the pupal rise in 20E plays a role for AST-A expression during antennal lobe development.

MALDI-TOF analysis of the lateral cell group of the antennal lobe revealed at least three A-type allatostatins. Only cydiastatin 1 was present in mass spectra of early pupa, whereas cydiastatins 3 and 4 did not occur before P6/7.

Supported by DFG grant SCHA 678/3-3 to JS



## Development of allatostatin-A immunoreactivity in antennal lobe neurons of the honeybee

Maria Gräbner<sup>1</sup>, Claudia Groh<sup>2</sup>, Wolfgang Rössler<sup>2</sup>, and Joachim Schachtner<sup>1</sup>

<sup>1</sup>Dept. Biology, Animal Physiology, Philipps-University, 35032 Marburg, Germany

<sup>2</sup>Dept. Behav. Physiol. and Sociobiol., University of Würzburg, 97074, Würzburg, Germany

Formation of the antennal lobe of the honey bee *Apis mellifera* occurs during the defined period of metamorphosis, which includes 9 pupal stages, each lasting proximately one day (P1-P9; Schröter and Malun, 2000, J Comp Neurol 422:229). To find out whether neuropeptides may play a role during AL development, we studied neuropeptides of the A-type allatostatin (AST-A) family (Y/FXFGLamides). To determine time of occurrence and cellular localization of AST-A during AL development, we used an antiserum which is thought to recognize all members of the AST-A neuropeptide family (Vitzthum et al., 1996, J Comp Neurol 369:419).

Based on morphology and localization we distinguished four types of AST-A-immunoreactive (ir) cell types located in three different cell groups of the AL. With one exception, all cell types started to gain AST-A immunoreactivity between pupal stage 1 and 2 (P1/2).

In a ventral anterior cell group about five cells gained AST-A immunostaining between P1/2 and P7 (VC, Fig. 1C). Similarly, in a large lateral cell group cell numbers increased from P1/2 to P7 to about 7 AST-A-ir cells (LC, Fig. 1A). According to their morphology, both cell types seem to belong to the group of local interneurons with cell body diameters of about 20 µm. In the lateral cell group one cell with a cell body diameter of about 40 µm and large diameter neurite stained from P4 with the AST-A antiserum (LLC, Fig. 1B). In a median posterior cell group numbers of small diameter (about 10 µm) AST-A-ir cells increased from P1/2 to P4/5 to about 35 cells (MC, Fig. 1B). Diffuse AST-A immunostaining was seen in the area of the developing AL-neuropil from P1 to P2/3 (Fig. 1A). AST-A-ir arborisations seem to enter the forming glomeruli from P4/5. This appears to coincide with the beginning of synaptogenesis in the forming glomeruli, as indicated by synapsin immunostaining.

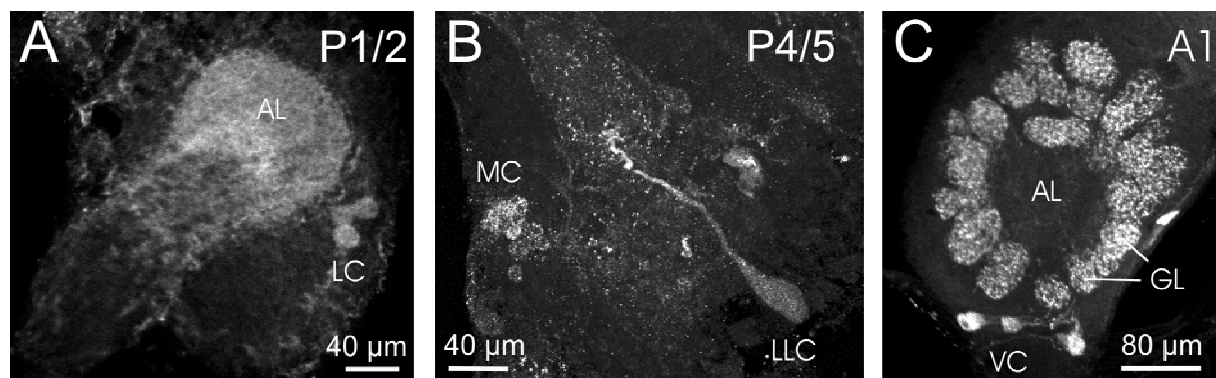


**Abb. 1.** Confocal images of 40 µm Vibratom sections labeled with the AST-A antiserum. **A.** frontal section through a P1/2 AL. **B.** Oblique section through a P4/5 AL. **C.** Frontal section through an adult AL at the day of eclosion (A1). GL, glomeruli; LC, lateral cells; LLC, large lateral cell; MC, median cells; VC, ventral cells.

## **Alterations in Dopamine receptors gene expression after $n^3$ fatty acid deprivation in the perinatal brain**

F Kuperstein<sup>\*1</sup>, E Yakubov<sup>1</sup>, R Eilam<sup>1</sup>, A Brand<sup>1</sup>, N Salem Jr<sup>2</sup>, E Yavin<sup>1</sup>

<sup>1</sup>*Department of Neurobiology, Weizmann Institute of Science, Israel, <sup>2</sup>LMBB, NIAAA, NIH, Rockville MD.*

[Faina.Kuperstein@weizmann.ac.il](mailto:Faina.Kuperstein@weizmann.ac.il)

$n^3$ docosahexaenoic acid ( $n^3$ DHA) is a most ubiquitous polyunsaturated fatty acid (FA) compound in brain. Experimental studies with animals have demonstrated that depriving the  $n^3$  FA precursor linolenic acid ( $n^3$  LNA) from the diet, reduces markedly the DHA content of cerebral membrane lipids, a process that is accompanied by impairment in behavior, learning ability, sensory motor activity, motivational processes and vision.  $n^3$  LNA deficiency induces abnormal functioning of the mesolimbic and mesocortical dopaminergic pathways by reducing levels of the available dopamine in the synaptic cleft. To evaluate possible molecular mechanisms responsible for altering these brain functions we have examined gene profiles that may be associated with these biochemical and functional changes. Cross subtracted libraries prepared from total RNA extracts of hippocampus and cortex regions from two-weeks old rats subjected to an intrauterine and early postnatal  $n^3$  FA dietary deficiency were used for identification and profiling of specific genes. A commercial array was used and hybridization of the labeled cDNAs probes revealed approximately 46 known up-regulated genes. The results were verified by both relative and quantitative RT-PCR. Among the over-expressed genes, a group of neurotransmitter receptors of the dopaminergic (DA) system were most prominent. In addition several receptors for the excitatory neurotransmitters molecules acetylcholine and glutamate and the inhibitory GABA-ergic and serotonergic receptors, were elevated. Immunohistochemical visualization using a specific antibody for the dopamine 2 (DA2) receptor was applied to determine the relative levels the receptors in discrete sections of the postnatal brain. An enrichment of DA2 receptors was found in brain structures innervated by dopaminergic neurons, particularly of the limbic system. The expression was sustained. Emerging experimental evidence suggest that the overall increase in receptor gene expression levels may constitute an adaptive mechanism induced by  $n^3$  FA deprivation to possibly cope with a decrease in the neurotransmitter levels in the synaptic cleft. Additional elements of the dopamine regulatory circuit are currently under extensive study. These include expression and subcellular localization of tyrosine hydroxylase, dopamine transporters and monoamine oxidase in order to elucidate the metabolic state of the DA system under these environmental stress conditions.

*Supported by a grant from the Gulton Foundation, NY.*

## **Cellular response to implantation of penetrating intracortical microelectrode arrays into cerebral cortex**

Cristina Marin<sup>1</sup>, Juan Sales<sup>2</sup>, Carlos Botella<sup>2</sup>, Ignacio Aranda<sup>2</sup>,  
Ryan McDermott<sup>3</sup>, Richard Norman<sup>3</sup>, Eduardo Fernández<sup>1</sup>

<sup>1</sup>Institute of Bioengineering, Univ. Miguel Hernandez, San Juan (Alicante), Spain.

<sup>2</sup>Hospital General Universitario de Alicante, Spain.

<sup>3</sup>John Moran Laboratories, Univ. of Utah, Salt Lake City, USA .

Many nervous system disorders, long considered to be unapproachable with conventional surgical or pharmacological interventions, may be partially relieved through neuroprosthetic devices. Until a few decades ago, these neural interfaces were relatively large and incapable of providing highly selective communication with large numbers of individual neurons. However, recent work has resulted in the development of microelectrode arrays with feature dimensions that are of the same order of magnitude as the neurons they are intended to interact. These new generation of intracortical microelectrode devices must be implanted into the nervous system and remain fully functional for periods that will eventually extend to many decades. Thus one of the major prerequisites for its clinical application is long-term viability and biocompatibility.

This study was designed to investigate the reactive responses of neurons and glial cells in response to the implantation of intracortical microelectrode arrays in order to provide a baseline for future studies. We used arrays of 100 or 25 penetrating silicon electrodes (Utah Electrode Array) designed to focally stimulate or record cortical neurons located in a single layer up to 1.5 mm beneath the surface of the cerebral cortex. After several time intervals (ranging from 1 hour to 6 months) the animals (cats, rabbits and rats) were sacrificed. The microelectrode arrays were explanted and the implant site and surrounding tissue removed and processed using histopathological, immunocytochemical and biochemical techniques.

The most typical findings in acute experiments were some interstitial microhemorrhages emanating from the electrode tracks. Aside from a few mechanically-distorted and somewhat hyperchromic neurons, the neurons near all tracks appeared normal. Astrocytes, blood-derived cells and microglia proliferated rapidly and developed a sheath around microelectrode tracks. The sheath was labelled with antibodies to glial fibrillary acidic protein (GFAP), CD68 and microglia (lectinas). The absence of haemorrhages in chronic experiments indicates that injury to the blood vessels occurs early and that it is usually limited. It was concluded that reactive gliosis is an important part of the process forming the cellular sheath and should be better understood. Further, the continuous presence of the microelectrodes appears to result in a sustained response, at least partially composed of reactive glia, that maintains a compact sheath which isolates the microelectrodes from the brain.

Supported by EC, specific RTD programme “Quality of Life and Management of Living Resource “, QLK6-CT-2001-00279



**Poster Subject Area #PSA20:  
Neurochemistry**

- [#274A](#) M. Brackmann, R. Anand and K-H. Braunewell, Berlin and New Orleans (USA)  
*NEURONAL CALCIUM SENSOR (NCS) PROTEIN VILIP-1 MODULATES CYCLIC GMP SIGNALLING BY REGULATING RECEPTOR GUANYLYL CYCLASE B CELL SURFACE EXPRESSION AND ACTIVITY IN NEURAL CELLS AND HIPPOCAMPAL NEURONS*
- [#275A](#) A. Richter, K. Barlow, R. Raymond and JN. Nobrega, Berlin and Toronto (CDN)  
*Changes in adenosine A1 and A2A receptor binding in an animal model of inborn dyskinesia*
- [#276A](#) MC. Jockers-Scherübl, H. Danker-Hopf, F. Selig, R. Mahlberg, UE. Lang, J. Rentzsch, F. Schürer and R. Hellweg, Berlin  
*Cannabis increases serum concentrations of the neurotrophins NGF and BDNF in drug-naïve schizophrenic patients and precipitates disease-onset*
- [#273B](#) C. Herold, B. Diekamp, D. Karakuyu and O. Güntürkün, Bochum and Baltimore, MD (USA)  
*Stimulation of D1 Dopamine Receptors in the Pigeons Prefrontal Cortex Improves Working Memory Performance in a Delay- Matching- To- Sample Task*
- [#274B](#) M. Hörner and R. Heblich, Göttingen  
*OCTOPAMINE ENHANCES SYNAPTIC EFFICACY IN THE CRICKET GIANT FIBER PATHWAY*
- [#275B](#) A. Inciute, B. Qualmann, TM. Boeckers, ED. Gundelfinger and MM. Kessels, Magdeburg and Ulm  
*Abp1 links the actin cytoskeleton with the postsynaptic density via direct interactions with the ProSAP/Shank family and modulates the morphology of spines*
- [#276B](#) R. Dahlhaus, MM. Kessels and B. Qualmann, Magdeburg  
*SynbAPE1, a novel interaction partner of Syndapins, modulates spine morphology upon overexpression*

# NEURONAL CALCIUM SENSOR (NCS) PROTEIN VILIP-1 MODULATES CYCLIC GMP SIGNALLING BY REGULATING RECEPTOR GUANYLYL CYCLASE B CELL SURFACE EXPRESSION AND ACTIVITY IN NEURAL CELLS AND HIPPOCAMPAL NEURONS

M. Brackmann<sup>1</sup>, R. Anand<sup>2</sup> and K.-H. Braunewell<sup>1</sup>

<sup>1</sup>Signaltransduction Research Group, Neuroscience Research Center, Charité, Berlin, Germany,

<sup>2</sup>Neuroscience Center of Excellence, Louisiana State University, New Orleans, Louisiana, USA

The family of neuronal calcium sensor (NCS) proteins, including NCS-1, VILIP-1 and Hippocalcin, have multiple key roles in controlling neuronal function. The dynamic regulation of membrane signalling via NCS proteins has recently started to be elucidated by examining their activity-dependent membrane association via the mechanism of the "calcium-myristoyl switch". In hippocampal neurons VILIP-1 shows a fast, stimulus-dependent and reversible translocation to Golgi and cell surface membranes and some dendritic specializations (1). The calcium-myristoyl switch of VILIP-1 may provide a fast signalling mechanism to shuttle cellular signals to cellular compartments and/or to influence membrane-associated signalling effectors. In line with this notion, VILIP-1 has been implicated in a variety of calcium-dependent signal transduction processes. We have observed effects on membrane-localized signalling systems including nicotinic acetylcholine receptors and receptor guanylyl cyclases. Interaction with these receptors have previously been shown by yeast two hybrid interaction and surface resonance plasmon (SRP) studies, respectively. The functional influence of VILIP-1 on acetylcholine and guanylyl cyclase receptor signalling have been examined in transfected cell lines and oocytes (2, 3). Here we report for the first time the effect of VILIP-1 on guanylyl cyclase activity in hippocampal neurons, where the proteins co-localize as shown by immunofluorescence microscopy. The overexpression of VILIP-1 in hippocampal neurons increases cGMP accumulation following stimulation of GC-B with the agonist C-type natriuretic peptide (CNP). In order to investigate the underlying molecular mechanisms, we examined the influence of VILIP-1 on receptor phosphorylation and cell surface expression, which are known mechanisms for receptor regulation. VILIP-1 modulates phosphorylation of the receptor in neural cells and hippocampal neurons following stimulation of GC-B. In addition, in ligand binding assays VILIP-1 influences the surface expression of GC-B in neural cells and hippocampal neurons.

In summary, the NCS protein VILIP-1 is a calcium-dependent modulator of important membrane-localized neuronal signalling cascades in hippocampal neurons. Therefore, the protein is likely to play a novel physiological and pathological role in hippocampal function.

1. Spilker, C., Dresbach, T. and Braunewell, K.-H. (2002) Reversible translocation and activity-dependent localization of the calcium-myristoyl switch protein VILIP-1 to different membrane compartments in living hippocampal neurons. *J. Neurosci.* 22, 7331-7339.
2. Lin, L., Jeanclos, E.M., Treuil, M., Braunewell, K.H., Gundelfinger, E.D. and R. Anand (2002) The Calcium Sensor Protein Visinin-like Protein-1 Modulates the Surface Expression and Agonist-Sensitivity of the  $\alpha 4\beta 2$  Nicotinic Acetylcholine Receptor. *J. Biol. Chem.* 277, 41872-41878.
3. Braunewell, K.-H., Brackmann, M., Schaupp, M., Spilker, C. Anand, R., and Gundelfinger, E. D. (2001) Intracellular neuronal calcium sensor (NCS) protein VILIP-1 modulates cGMP signalling pathways in transfected neural cells and cerebellar granule neurones. *J. Neurochem.* 78, 1277-1286.

## Changes in adenosine A<sub>1</sub> and A<sub>2A</sub> receptor binding in an animal model of inborn dyskinesia

A. Richter<sup>1</sup>, K. Barlow<sup>2</sup>, R. Raymond<sup>2</sup>, J.N. Nobrega<sup>2</sup>

<sup>1</sup>Department of Pharmacology and Toxicology, School of Veterinary Medicine, FU Berlin, Berlin, Germany; email: richtera@zedat.fu-berlin.de

<sup>2</sup>Neuroimaging Research Section, Centre for Addiction and Mental Health, Toronto, Ontario, Canada

In patients with paroxysmal non-kinesigenic dyskinesias, episodes of dystonia can be provoked by stress and also by methylxanthines (e.g., caffeine), which inhibit adenosine A<sub>1</sub>/A<sub>2A</sub> receptors. In the *dt<sup>sz</sup>* mutant hamster, a model of this movement disorder, adenosine A<sub>1</sub> receptor antagonists were previously found to worsen dystonia, while adenosine A<sub>1</sub> and A<sub>2A</sub> receptor agonists exerted pronounced beneficial effects. Therefore, in the present study, adenosine receptor A<sub>1</sub> and A<sub>2A</sub> binding was determined by autoradiographic analyses in *dt<sup>sz</sup>* hamsters under basal conditions, i.e., in the absence of dystonia, and in a group of mutant hamsters which exhibited severe stress-induced dystonic attacks immediately prior to sacrifice. In comparison with non-dystonic control hamsters, [<sup>3</sup>H]CPCPX (8-cyclopentyl-1,3-dipropylxanthine) binding to adenosine A<sub>1</sub> receptors and [<sup>3</sup>H]CGS 21680 (2p-(2carboxyethylphen-ethylamino-5'-N-ethylcarboxamindoadenosine) binding to adenosine A<sub>2A</sub> receptors were significantly lower throughout the brain of dystonic animals. Under normal resting condition, mutant hamsters showed significant decreases in adenosine A<sub>1</sub> (-12 to -42%) and in A<sub>2A</sub> (-19 to -34%) receptor binding compared to non-dystonic controls. Stressful stimulation increased adenosine A<sub>1</sub> and A<sub>2A</sub> receptor binding in almost all brain regions in both control and dystonic hamsters. The stress-induced increase was more marked in mutant hamsters, leading to a disappearance of changes in most regions, except the striatum. With regard to previous findings of striking beneficial effects of adenosine A<sub>1</sub> and A<sub>2A</sub> receptor agonists and of striatal dysfunctions in the *dt<sup>sz</sup>* mutant, the reduced adenosine receptor binding may be an important factor in the pathogenesis of paroxysmal dystonia (Supported by: DFG Ri 845).

**Cannabis increases serum concentrations of the neurotrophins NGF and BDNF in drug-naïve schizophrenic patients and precipitates disease-onset**

MC Jockers-Scherübl, H Danker-Hopfe, F Selig, R Mahlberg, UE Lang, J Rentzsch, F Schürer, R Hellweg

Department of Psychiatry and Psychotherapy, Charité-University Medicine Berlin, Campus Benjamin Franklin, Eschenallee 3, 14050 Berlin, Germany, e-mail:maria.jockers@charite.de

Neurotrophic factors are known to play a crucial role in growth, differentiation and maintenance of function in neurons during development and during adult life. Neurodevelopment is reported to be impaired in schizophrenia and vulnerable schizophrenic brains may be more sensitive to toxic influences. Thus, cannabis as a neurotoxin may be more harmful to schizophrenic brains than to non-schizophrenic brains with chronic use. Such neurotoxic events may promote disease-onset and lead to exaggerated release of neurotrophins.

We investigated 109 drug-naïve first-episode schizophrenic patients and found no difference in NGF serum concentrations compared to healthy controls (n=61) when no substance abuse prevailed. However, NGF was significantly raised with former chronic cannabis or multiple substance abuse. This may represent an endogenous repair mechanism of damaged neurons in vulnerable brains (1). Likewise we examined 157 sera of drug-naïve schizophrenic patients for BDNF and again found significant differences between the groups (2). BDNF serum concentrations were elevated by up to 34% in patients with long-term cannabis abuse or multiple substance abuse prior to disease onset. Drug-naïve schizophrenic patients without cannabis consumption showed similar results to normal controls and cannabis controls without schizophrenia. Thus, raised BDNF serum levels are not related to schizophrenia and/or cannabis abuse itself but reflect a cannabis-related idiosyncratic damage of schizophrenic brain. In line with this hypothesis, disease-onset was 5.2 years earlier in the cannabis-consuming group ( $p<0.001$ ). We thus concluded that neurotrophins may play a role in the origin and outcome of schizophrenia at least with respect to drug intake.

1. Jockers-Scherübl MC, Matthies U, Danker-Hopfe H, Mahlberg R, Lang UE, Hellweg R: J Psychopharmacology 2003. 17: 439-445.
2. Jockers-Scherübl MC, Danker-Hopfe H, Mahlberg R, Selig F, Rentzsch J, Schürer F, Lang UE, Hellweg R: Neurosci Lett, in press.

Dr. Maria C. Jockers-Scherübl  
Department of Psychiatry and Psychotherapy  
Charité- University Medicine Berlin  
Campus Benjamin Franklin  
Eschenallee 3  
14050 Berlin  
e-mail: maria.jockers@charite.de  
Tel.: 030-8445-8707/5

## **Stimulation of D1 Dopamine Receptors in the Pigeons 'Prefrontal Cortex' Improves Working Memory Performance in a Delay- Matching- To-Sample Task**

Chr. Herold<sup>\*1</sup>, B.Diekamp<sup>2</sup>, D. Karakuyu<sup>3</sup> and O. Güntürkün<sup>1</sup>

\*Corresponding author.

Tel: 0049-0234-3224032 Mail to: tina@heroldweb.de

<sup>1</sup>Institute for Cognitive Neuroscience, Department of Biopsychology, Faculty of Psychology, Ruhr- Universität Bochum, D- 44780 Bochum, Germany

<sup>2</sup>Department of Psychological and Brain Sciences, John Hopkins University, Baltimore, MD 21218, USA

<sup>3</sup>Institute for Physiology, Department of Neurophysiology, Faculty of Medicine, Ruhr- Universität Bochum, D- 44780 Bochum, Germany

### **Abstract**

Several studies have shown that Dopamine (DA) D<sub>1</sub> receptors are involved in cognitive processes of the prefrontal cortex (PFC) of mammals, especially in working memory functions. In these studies supranormal stimulation as well as inhibition with fully agonists or antagonists for D<sub>1</sub> receptors led to an impairment in working memory performance while slightly stimulation with an fully agonist improved performance. To test the hypothesis of an involvement of DA D<sub>1</sub> receptors in the pigeons Nidopallium caudolaterale (NCL), the avian 'prefrontal cortex', we used a 10µM solution of the fully Antagonist SCH23390 and the fully Agonist SKF81297, in an in vivo microdialysis study. We chose this concentration because of the electrophysiological effects on neurons from PFC. While we applied the drugs into the NCL, the pigeons performed a delay- matching- to- sample- task (DMTS- task), as a paradigm for working memory. Like the PFC, the NCL is characterized by a dopaminergic input, a high number of D<sub>1</sub> receptors and lesions in both areas cause deficits in working memory performance. What we have found out is that SKF81297 significantly improved the performance of working memory, while SCH23390 did not lead to an impairment in the DMTS- task in relation to our control. But pigeons showed a significantly decreased performance in the task under SCH23390 treatment in relation to a the treatment with SKF81297. Both drugs had no effects on reaction times or the total time in which the pigeons performed one session, as a measurement for motivational aspects. So this study role out that DA D<sub>1</sub> receptor mechanisms are involved generally in working memory functions of pigeons NCL like in mammals PFC and suggest a possibility to improve the efficiency of cognitive functions in a healthy system.

## OCTOPAMINE ENHANCES SYNAPTIC EFFICACY IN THE CRICKET GIANT FIBER PATHWAY

Michael Hörner and Rolf Heblich

Institute of Zoology, Anthropology and Developmental Biology, Dept. Cell Biology,  
University of Göttingen, Berliner Str. 28, 37073 Göttingen, Germany

Triggering of vital escape behavior in many insect species is directly controlled by the spike activity of the sensory-to-motor giant interneuron (GIN) pathway. This identified neuronal network is activated by mechano-sensory afferents coupled to the abdominal cercal sense organs. Thus, the sensitivity of this network is one crucial factor for the decision making process in the CNS. Electrophysiological, pharmacological and behavioral studies in crickets (*Gryllus bimaculatus*) show that biogenic amines such as octopamine (OA), dopamine or serotonin may affect synaptic transmission, sensory sensitivity and activation thresholds [Goldstein, Camhi *J Comp Physiol A* 168,103,1991; Hörner et al. *Verh Dtsch Zool Ges*: 90,10,1997; Stevenson et al. *J Neurobiol* 43,107,2000; Heblich, Hörner *Proc. 29<sup>th</sup> Göttingen Neurobiol Conf* 133,148,2003]. Immunocytochemistry revealed endings from amine-containing neurons in the region of monosynaptic connections between wind-sensitive afferents and post-synaptic giant interneurons in the terminal ganglion [Spörhase-Eichmann et al. *Cell Tiss Res* 268,287,1992; Hörner et al. *ibid.* 280,563,1995]. The present study focuses on octopamine-induced changes of electrical properties in pre-/postsynaptic neurons and describes how modulation of cellular and network characteristics may influence behavioral choice.

Electrophysiological recordings were made from identified postsynaptic GINs, presynaptic afferents and other elements of the pathway both *in-vivo* and *in-vitro*. The effects of bath-applied aminergic drugs were tested during spontaneous and/or stimulus-evoked activity.

*In-vivo* recordings from GINs demonstrate that OA, the analogue of norepinephrin in invertebrates, slightly depolarizes the resting potential, increases the membrane resistance and the frequency and amplitude of spontaneous PSPs, which eventually leads to spontaneous spiking normally never occurring in GINs without stimulation. Furthermore, OA enhances the GINs' spike response to synaptic activation after electrical stimulation of the cercal nerve by lowering their spike threshold. However, despite this enhanced excitability of GINs, the stimulus response of sensory neurons (i.e. the number of spikes/stimulus) remains unchanged. These findings suggest that OA either acts on interneurons presynaptic to GINs or affects postsynaptic GINs directly. The finding that OA induces 'spike-broadening' in postsynaptic GINs supports the latter hypothesis. Both, the delayed repolarization phase of action potentials and the increased membrane resistance point to direct OA-induced changes of potassium conductances in GINs. *In-vitro* recordings from isolated GIN cell bodies, which show reduced 'delayed-rectifier' potassium currents upon OA application, provide further evidence for this. However, OA effects on other neuron types have also been found. OA effects can be blocked by epinastine, an antagonist of the neuronal OA<sub>3</sub> receptor.

The described OA-induced changes of membrane properties and stimulus response levels suggest direct postsynaptic OA actions on GINs. Thus, an OA-induced modulation of potassium currents found in GINs could be one mechanism generating an increased excitability level with lowered spike thresholds, which may contribute to a more sensitive escape reaction with lowered behavioral thresholds observed upon OA application.

## **Abp1 links the actin cytoskeleton with the postsynaptic density via direct interactions with the ProSAP/Shank family and modulates the morphology of spines**

Akvile Inciute<sup>1</sup>, Britta Qualmann<sup>1</sup>, Tobias M. Boeckers<sup>2</sup>, Eckart D. Gundelfinger<sup>1</sup> and Michel M. Kessels<sup>1</sup>

<sup>1</sup>Department of Neurochemistry and Molecular Biology, Leibniz Institute for Neurobiology, Magdeburg, Germany

<sup>2</sup>Department of Anatomy and Cell Biology, University of Ulm, Germany

### **Abstract**

Synaptic contacts contain elaborate cytomatrices on both sides of the synaptic cleft, which are believed to organize and link the different synaptic functions in time and space and can respond to different inner and outer cues with massive structural reorganizations. At the postsynaptic density (PSD), activity-dependent reorganizations of the cortical actin cytoskeleton are hypothesized to play a role in synaptic plasticity required for learning and memory. While the main PSD scaffolding proteins may be known by now, the current challenge is to unravel the molecular interconnections of these proteins to the machineries for synaptic signal transduction, receptor endocytosis and the actin cytoskeleton. Here, we report on interaction of Abp1, which we identified and characterized as a novel, signal-responsive F-actin binding protein with members of the ProSAP/Shank family. ProSAP/Shanks are multidomain scaffolding PSD proteins that interconnect glutamate receptors with other synaptic components. Affinity purifications demonstrate that the interactions are mediated by the Abp1 SH3 domain associating with a proline-rich motif that is conserved within the C-terminal parts of ProSAP1/Shank2 and ProSAP2/Shank3. The distribution of Abp1, ProSAP1/Shank2 and ProSAP2/Shank3 overlaps within the brain, all three proteins are part of the PSD and show enrichments especially in the cortex and hippocampus. Coimmuno-precipitation of endogenous Abp1 and ProSAP2 and colocalization studies of Abp1 ProSAP/Shanks in hippocampal neurons indicate the *in vivo* relevance of the interactions. Intriguingly, *in vivo* recruitment assays demonstrate that Abp1 can bind to dynamic F-actin structures and ProSAP/Shanks simultaneously suggesting that Abp1 might link different organizing elements in the PSD. Importantly, we discovered a redistribution of Abp1 into ProSAP/Shank-positive spines upon synaptic stimulation in culture. In line with Abp1's cytoskeletal functions we observed a increase in postsynaptic spine length upon Abp1 overexpression. We were able to clearly assign the effect to the functions of the two independently working F-actin binding modules of Abp1, which when overexpressed alone also caused a significant increase in the frequency of thin spines and filopodial structures. Overexpression of the ProSAP/Shank –binding SH3 domain had a negative impact on mushroom spine morphology, both the percentage of mushroom spines as well as their density was significantly reduced. While the same was observed upon overexpression of the actin binding modules of Abp1, an excess of full length Abp1 led to a significant increase in density and relative frequency of mushroom spines. We would like to suggest that ProSAP/Shanks may thereby act as attachment points for the dynamic postsynaptic cortical actin cytoskeleton and create a functional connection between synaptic stimulation and cytoskeletal rearrangements brought about by the actin binding domains of Abp1 and their functions in actin dynamics.

## SynbAPE1, a novel interaction partner of Syndapins, modulates spine morphology upon overexpression

Regina Dahlhaus, Michael M. Kessels, B. Qualmann

Leibniz Institute for Neurobiology, Dept. of Neurochemistry and Molecular Biology, Research group Membrane Trafficking & Cytoskeleton

Syndapins are a family of SH3 domain containing proteins that are involved in endocytotic processes via their binding to the large GTPase dynamin and furthermore modulate the actin cytoskeleton by an interaction with N-WASP, a potent activator of the Arp2/3 complex actin polymerisation machinery. Consistently, Syndapin I and II overexpression was demonstrated to induce filopodia formation in HeLa cells. By utilizing the Yeast-Two-Hybrid System, we identified further potential interaction partners of Syndapin. Among others, one so far unknown protein was found and is currently named SynbAPE1. Western-Blott analysis of homogenates from different rat tissues revealed SynbAPE1 is exclusively expressed in brain and testis. SynbAPE1 binds specifically to the SH3 domain of Syndapin I, an isoform that is restricted to the brain, as well as to those of the more ubiquitous expressed isoforms II-long and II-short as demonstrated by coprecipitation assays. Coimmunoprecipitation analysis and Colocalisation studies in primary hippocampal cultures support an interaction of syndapins and SynbAPE1 in vivo. Moreover, SynbAPE1 is found to localize to very different cell compartments, such as spines or nuclei. Since the spines of SynbAPE1 overexpressing neurons are significantly altered in shape, SynbAPE1 interactions seem to be involved in spine morphology control.

SynbAPE1 = Syndapin binding and purimic endonuclease



**Poster Subject Area #PSA21:  
Synapses and transmitters**

- [#277A](#) A. Gundlfinger, J. Breustedt, M. Torvinen and D. Schmitz, Berlin  
*The role of adenosine at hippocampal mossy fiber synapses*
- [#278A](#) J. Breustedt and D. Schmitz, Berlin  
*Assessing the role of GLUK5 and GLUK6 at hippocampal mossy fiber synapses*
- [#279A](#) O. Beck, M. Chistiakova, K. Obermayer and M. Volgushev, Berlin and Bochum  
*Adaptation of synaptic properties of intracortical connections to layer 2/3 pyramidal cells in the rat*
- [#280A](#) T. Koehler, J. Grabert, E. Weiler, P. Wahle, V. Lessmann, UT. Eysel and T. Mittmann, Bochum and Mainz  
*Stimulation dependent impairment of LTP in heterozygous BDNF knock-out mice*
- [#281A](#) K. Jüngling and K. Gottmann, Düsseldorf  
*Role of N-cadherin in selective stabilisation of glutamatergic synapses*
- [#282A](#) C. Walz, V. Lessmann and K. Gottmann, Düsseldorf and Mainz  
*Presynaptic long-term induction of immature glutamatergic synapses in cultured neocortical neurons*
- [#283A](#) A. Boehlen and K. Gottmann, Düsseldorf  
*Insulin-like growth factor-1 (IGF-1)-induced long-term plasticity in thalamo-cortical synapses in vitro*
- [#284A](#) J. Burré, M. Morciano, T. Beckhaus, M. Karas, W. Volkandt and H. Zimmermann, Frankfurt/Main  
*Synaptic vesicle proteins under conditions of rest and activation: A proteomic approach using differential in gel electrophoresis*
- [#285A](#) M. Morciano, J. Burré, T. Beckhaus, M. Karas, H. Zimmermann and W. Volkandt, Frankfurt/Main  
*Analysis of the proteome of synaptic vesicles docked to the plasma membrane under conditions of rest and activation*
- [#286A](#) P. Jedlicka and KH. Backus, Frankfurt/Main  
*Postsynaptic depolarizations mediated by GABAA receptors: a computational study*
- [#287A](#) K. Heupel and K. Krieglstein, Göttingen  
*Absence of Transforming Growth Factor-beta2 (TGF-beta2) causes changes in acetylcholine receptor clustering at the mouse neuromuscular junction*

- [#288A](#) A. Lacmann and K. Krieglstein, Göttingen  
*Activity-dependent Release of Transforming Growth Factor-beta (TGF-beta) in Neuronal Networks in vitro*
- [#289A](#) VJ. Mueller and J. Klingauf, Göttingen  
*An early fast phase of endocytosis sorts synaptic vesicles less efficiently back into the recycling pool*
- [#290A](#) O. Kochubey, RF. Toonen, M. Verhage and J. Klingauf, Goettingen and Amsterdam (NL)  
*Munc-18-1 is a positive regulator for secretory granule docking in chromaffin cells as visualized by evanescent wave microscopy*
- [#291A](#) D. Khimich, P. Pirih, F. Wolf and T. Moser, Göttingen  
*Analysis of Non-stationary Fluctuations of Exocytotic Capacitance Changes in Mouse Inner Hair Cells*
- [#292A](#) M. Wienisch and J. Klingauf, Göttingen  
*SYNAPTIC VESICLES LOOSE THEIR PROTEIN COMPLEMENT DURING EXO-ENDOCYTIC CYCLING*
- [#293A](#) C. Heck and R. Heinrich, Göttingen  
*Converging signaling pathways in the grasshopper brain and the control of context-specific behavior – an in vitro approach*
- [#294A](#) U. Heilbronner, M. Kole and G. Flügge, Göttingen  
*Alpha-Methyl-Noradrenaline Stimulates Alpha-1 and Alpha-2 Adrenoceptors in the Paraventricular Thalamic Nucleus of the Rat*
- [#295A](#) G. Aramuni, F. Varoqueaux, V. Sargsyan, N. Brose and W. Zhang, Göttingen  
*NEUROLIGINS ARE ESSENTIAL FOR NEURONAL NETWORK FUNCTION IN THE RESPIRATORY NETWORK OF MICE*
- [#296A](#) K. Szöke, J. Hirrlinger, M. Handschuh, C. Neusch, F. Kirchhoff and S. Hülsmann, Göttingen  
*Glial cells in the respiratory network express functional transporters and receptors for glycine*
- [#297A](#) I. Dudanova and M. Missler, Göttingen  
*Structural alterations in the brains of adult alpha-neurexin double knockout mice may be a long-term consequence of impaired synaptic transmission*
- [#298A](#) T. Roeder and M. Seifert, Marburg  
*Control of behavior and metabolism through the adrenergic system in the nematode C. elegans*

- [#277B](#) T. Heinbockel and M. Ennis, Baltimore, MD (USA) and Memphis, TN (USA)  
*Presynaptic inhibitory modulation by metabotropic glutamate receptors in olfactory bulb glomeruli*
- [#278B](#) EE. Voronezhskaya, MY. Khabarova and LP. Nezlin, Moscow (RUS), Tula (RUS) and Göttingen  
*Serotonin overproduction induces exogastrulation in both invertebrate and vertebrate embryos*
- [#279B](#) K. Piechotta, V. Beglopoulos, M. Montag-Sallaz, D. Montag and M. Missler, Göttingen, Boston, MA (USA) and Magdeburg  
*RESTRICTED EXPRESSION OF NEUREXOPHILIN 3 AND SPECIFIC BEHAVIORAL DEFICITS IN KNOCKOUT MICE FAVOR A MODULATING ROLE IN SYNAPTIC TRANSMISSION*
- [#280B](#) X. Lou and R. Schneggenburger, Göttingen  
*Allosteric modulation of presynaptic vesicle fusion explains potentiation of transmitter release by phorbol esters*
- [#281B](#) N. Korogod and R. Schneggenburger, Göttingen  
*Post-tetanic potentiation and its presynaptic Ca<sup>2+</sup> dependence at the calyx of Held*
- [#282B](#) D. Khimich, R. Nouvian, R. Pujol, S. tom Dieck, M. Eybalin, E. Gundelfinger and T. Moser, Goettingen, Montpellier (F) and Magdeburg  
*Synaptic Ribbons are essential for synchronous auditory signaling*
- [#283B](#) C. Wichmann, LE. Swan, R. Kittel, M. Schmidt, D. Wenzel, M. Heckmann and SJ. Sigrist, Göttingen and Freiburg  
*Drosophila Glutamate Receptor Interacting Protein acts in the presynaptic endocytic pathway*
- [#284B](#) LE. Swan and SJ. Sigrist, Göttingen  
*A Structure-function characterization of the Glutamate Receptor-Interacting Protein Grip.*
- [#285B](#) E. Kartvelishvily, L. Balan, M. Schleper and H. Wolosker, Haifa (IL)  
*Neuronal Synthesis and Release of D-Serine to Activate NMDA Receptors*
- [#286B](#) M. Naujock and G. Bicker, Hannover  
*Evidence for acetylcholinesterase as a moonlighting protein during grasshopper development*
- [#287B](#) A. Groh and T. Kuner, Heidelberg  
*Optical Measurements of Transmitter Release at the Calyx of Held*

- [#288B](#) F. Zheng, T. Seeger, J. Gomez, J. Wess and C. Alzheimer, Kiel, Munich and Bethesda, MD (USA)  
*Disinhibition of GABAergic synapses might contribute to impaired hippocampal plasticity in M2 muscarinic acetylcholine receptor knockout mice*
- [#289B](#) V. Nimmrich, A. Möller, G. Gross and K. Wicke, Ludwigshafen  
*Activation of calpains is not a prerequisite of long-term potentiation (LTP)*
- [#290B](#) WD. Altmann, A. Fejtova, S. tom Dieck, B. Qualmann, MM. Kessels, SH. Gerber, CC. Garner, TC. Südhof, JH. Brandstätter and ED. Gundelfinger, Magdeburg, Frankfurt/Main, Heidelberg, Dallas (USA) and Palo Alto (USA)  
*Bassoon and Piccolo interact with members of the CtBP protein family*
- [#291B](#) UV. Nägerl, G. Köstinger, JC. Anderson, KAC. Martin and T. Bonhoeffer, Martinsried and Zürich (CH)  
*Activity-dependent spinogenesis: (When) do new spines carry functional synapses?*
- [#292B](#) N. Tobisch, UV. Nägerl, T. Bonhoeffer and S. Cambridge, Martinsried  
*Immunohistochemical characterization of activity-dependent spinogenesis in hippocampal neurons*
- [#293B](#) UV. Nägerl, N. Tobisch, S. Cambridge and T. Bonhoeffer, Martinsried  
*Bidirectional activity-dependent morphological plasticity in hippocampal neurons*
- [#294B](#) J. Kretzberg, A. Marin-Burgin and WB. Kristan, Oldenburg and La Jolla, CA (USA)  
*Characterization of a central synapse in the local bend circuit of the leech*
- [#295B](#) O. Yizhar, U. Matti, U. Becherer, J. Rettig and U. Ashery, Tel Aviv (IL) and Homburg  
*Illuminating vesicle priming with live-cell TIRF microscopy*
- [#296B](#) A. Mezer, E. Nachliel, M. Gutman and U. Ashery, Tel Aviv (IL)  
*A NEW PLATFORM TO STUDY THE MOLECULAR MECHANISMS OF EXOCYTOSIS*
- [#297B](#) D. Wagh, T. Rasse, A. Hofbauer, I. Schwenkert, H. Dürrbeck, S. Buchner, M-C. Dabauvalle, S. Sigrist and E. Buchner, Würzburg  
*The Drosophila nc82 antigen: gene structure, expression analysis, and localization at presynaptic active zones*

## **The role of adenosine at hippocampal mossy fiber synapses**

Anja Gundlfinger, Jörg Breustedt, Maria Torvinen, Dietmar Schmitz

Neurowissenschaftliches Forschungszentrum (NWFZ)

Charité, Universitätsmedizin Berlin

AG Dietmar Schmitz

Schumannstr. 20/21, 10117 Berlin

email: anja.gundlfinger@charite.de

The hippocampus has extensively been studied in the last decades and is presumed to play an important role in memory formation and learning tasks. In this context, the mossy fiber (mf) synapses, connecting dentate gyrus granule cells with CA3 pyramidal cells, are of special interest, as they serve as the main input structure for the hippocampal trisynaptic circuit. The mf synapse exhibits unusual physiological properties, including special forms of short- and long-term synaptic plasticity, with a large dynamical range of synaptic response. This requires the existence of a very low basal release probability of the mossy fibers, which we recently found to be due to a tonic activation of presynaptic  $G_{i/o}$ -protein by adenosine ( $A_1$ ) receptors (Moore et al., PNAS 2003).

This project is now aimed at determining the responsible intracellular pathways leading to an altered synaptic response under adenosine receptor activation. Herefore, we use whole-cell, field potential recordings and  $Ca^{2+}$ -imaging techniques of the hippocampal CA3 region.

In pharmacological experiments, we could show that application of adenosine reversibly depresses mossy fiber EPSPs in a concentration dependent manner. This effect is mimicked by application of the specific  $A_1$ -receptor agonist CPA and blocked by DPCPX, an  $A_1$ -receptor-specific antagonist. In order to determine the locus of action of adenosine-mediated changes, we performed short-term plasticity experiments, failure rate and  $1/CV^2$  analyses, which all gave evidence of a presynaptic mechanism. It has previously been shown that presynaptic  $G_{i/o}$ -proteins couple to adenylyl-cyclase and therefore interfere with the 2<sup>nd</sup> messenger cascade involving cAMP and PKA. We now found that the  $A_1$ -specific inhibition of synaptic efficacy is independent of this intracellular pathway. Preliminary  $Ca^{2+}$ -imaging results rather point at a decreased  $Ca^{2+}$ -influx through voltage-dependent  $Ca^{2+}$ -channels (VDCCs) as the source of the adenosine effect.

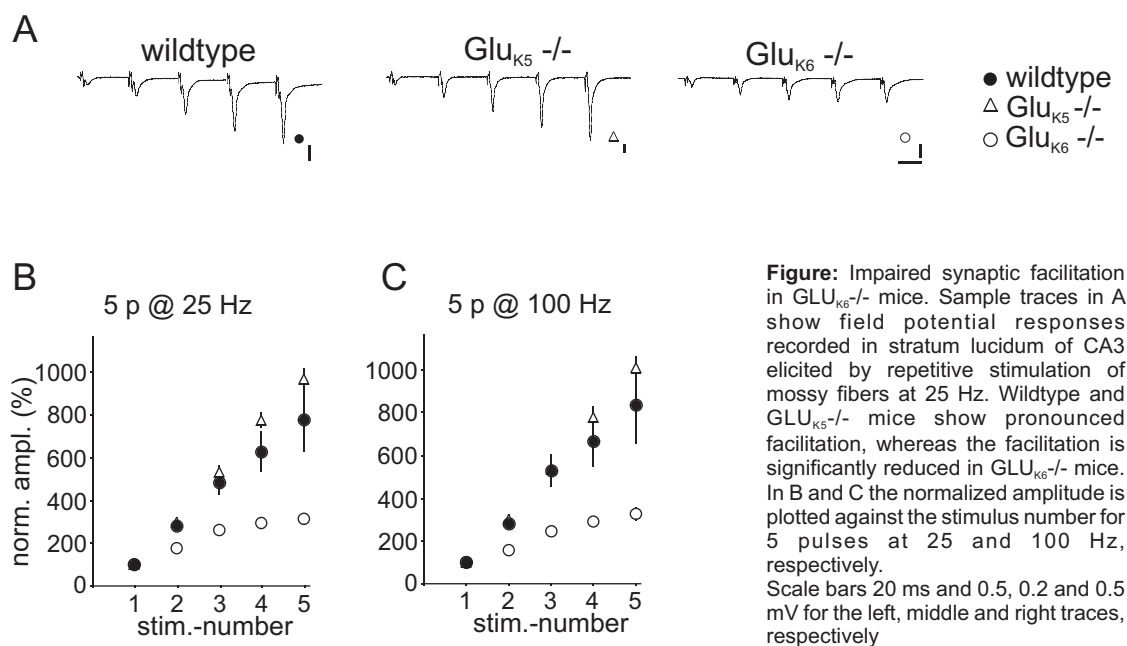
In future experiments it still has to be clarified, whether the effect of adenosine on mossy fiber synaptic transmission is solely mediated by a modulated presynaptic  $Ca^{2+}$ -influx or there is still a remaining mechanism to be found.

# Assessing the role of $GLU_{K5}$ and $GLU_{K6}$ at hippocampal mossy fiber synapses.

J. Breustedt and D. Schmitz\*

Neuroscience Research Center at the Charité, Berlin, Schumannstr. 20/21, 10117 Berlin, Germany

Recently, it has been suggested that presynaptic kainate receptors (KAR) are involved in short term and long term synaptic plasticity at hippocampal mossy fiber synapses. Using genetic deletion and pharmacology we here assess the role of  $GLU_{K5}$  and  $GLU_{K6}$  in synaptic plasticity at hippocampal mossy fiber synapses. We found that the kainate-induced facilitation was completely abolished in the  $GLU_{K6}^{-/-}$  mice, while it was unaffected in the  $GLU_{K5}^{-/-}$ . Consistent with this finding, synaptic facilitation was reduced in the  $GLU_{K6}^{-/-}$  and normal in the  $GLU_{K5}^{-/-}$  (see Figure).



In agreement with these results and ruling out any compensatory effects in the genetic deletion models, application of the  $GLU_{K5}$ -specific antagonist LY382884 did not affect short term and long term synaptic plasticity at the hippocampal mossy fiber synapses. Moreover, we did not find any evidence for the involvement of calcium induced calcium release in mossy fiber synaptic plasticity. We therefore conclude, that the facilitatory effects of kainate on mossy fiber synaptic transmission are mediated by  $GLU_{K6}$ -containing KARs.

## Adaptation of synaptic properties of intracortical connections to layer 2/3 pyramidal cells in the rat

O. Beck<sup>1</sup>, M. Chistiakova<sup>1,2</sup>, K. Obermayer<sup>1</sup> & M. Volgushev<sup>2</sup>

<sup>1</sup>Neuronale Informationsverarbeitung, Fakultät für Informatik und Elektrotechnik, Technische Universität Berlin, 10587 Berlin, Germany

<sup>2</sup>Abteilung für Neurophysiologie, Medizinische Fakultät, Ruhr-Universität Bochum, 44801 Bochum, Germany

Neocortical synapses express differential dynamic properties. When activated at high frequencies, the amplitudes of the subsequent postsynaptic responses may increase or decrease, depending on the stimulation frequency and on the properties of that particular synapse. These changes in the synaptic dynamics can dramatically affect the communication between nerve cells. Motivated by the question whether changes of dynamic properties of synapses may contribute to mechanisms of neural adaptation [1], we made intracellular recordings from layer 2/3 pyramidal cells in slices of rat visual cortex. Synaptic responses were evoked by electric pulses applied through stimulation electrodes, positioned below and/or aside the recorded cell. Test stimuli consisted of trains of 10 pulses at different frequencies (5-40 Hz). Test stimulation was performed either without any adaptation (control) or 2s after an adaptation, which consisted of 4s stimulation of the same synapses at 10, 25 or 40 Hz. Stimuli with or without adaptation were applied intermingled, every 40-60 seconds.

The data were then fitted with a three-parameter model of synaptic dynamics [2]. Our estimates of the synaptic parameters without adaptation are broadly consistent with previous studies [3]. After applying the adaptation protocol, we found a statistically significant reduction in release probability after weak adaptation (Fig. 1) as well as a decrease in the recovery time constant after strong adaptation (Fig. 2). Finally, we found a significant drop in the first response to test stimuli after adaptation that correlates with the drop in release probability for weak (Fig. 3) but not for strong adaptation. To account for this latter finding we introduce an extended model, which includes an interaction between a ready to release and a reserve pool of synaptic vesicles.

[1] Adorjan et al., Rev. Neurosci. 1999, pp. 181-200

[2] Tsodyks et al., PNAS 1997, pp. 719-723

[3] Markram et al., PNAS 1998, pp. 5323-5328

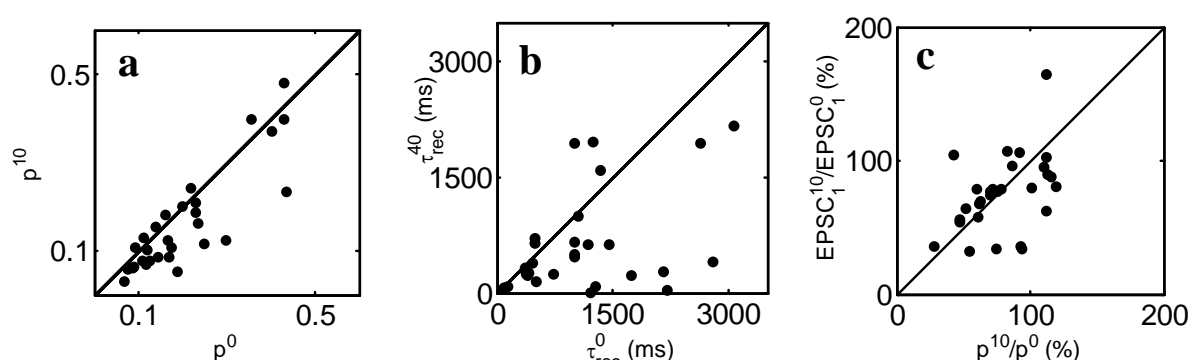


**Fig. a:** Estimated synaptic release probability in control (without adaptation,  $p^0$ ) and after 10Hz adaptation ( $p^{10}$ ). **Fig. b:** Estimated recovery time constant in control ( $\tau_{rec}^0$ ) and after 40Hz adaptation ( $\tau_{rec}^{40}$ ). **Fig. c:** Change of the amplitude of the first EPSC versus change of release probability after 10 Hz adaptation relative to control. In a-c each point shows data from one synaptic connection.

Supported by the DFG (SFB 618 and SFB 509)

**Stimulation dependent impairment of LTP in heterozygous BDNF knock-out mice**

<sup>2</sup>T Koehler, <sup>1</sup>J Grabert, <sup>2</sup>E Weiler, <sup>1</sup>P Wahle, <sup>3</sup>V Lessmann, <sup>2</sup>UT Eysel, <sup>2</sup>T Mittmann,

<sup>1</sup>Dept. Neurobiology and <sup>2</sup>Dept. Neurophysiology, Ruhr-Univ. Bochum, Germany

<sup>3</sup>Physiology & Pathophysiology, Univ-Mainz, Germany

BDNF is known to have numerous effects on synaptic plasticity and neuronal development in the mammalian brain. It is discussed as a factor for neuronal survival in cell cultures, and application of BDNF *in vivo* has been shown to preserve the function of central neurons following injury. The actions of BDNF include a facilitation of synaptic transmission at hippocampal and cortical excitatory synapses. The present study investigated effects of BDNF deprivation on synaptic plasticity by using an animal model of heterozygous BDNF knock-out-mice.

We recorded extracellular field potentials (FPs) in slices of the hippocampus and the visual cortex in wildtype (wt, n=18) and in heterozygous BDNF knock-out (BDNF(+/-), n=16) mice at the age of 35-40 days. Afferent fibers in area CA3 of the hippocampus were electrically stimulated to evoke FPs in area CA1. The visual cortex was stimulated in layer IV and the resulting FPs were recorded in cortical layer II. The input specificity of FPs was controlled in the visual cortex by evoking a second FP with an additional stimulation electrode that was located lateral to the recording site in layer II. The basal synaptic transmission was not different between the 2 experimental groups as shown for the FP shape ( $p > 0.2$  in all parameters, n=26) and for the input-output curves ( $p > 0.4$ , n=26). Theta-burst stimulation (TBS) evoked a reliable LTP ( $190\% \pm 13\%$ , n=6) of FPs in the hippocampus of wt animals, whereas the level of LTP was markedly reduced in slices of BDNF(+/-) mice ( $130\% \pm 11\%$ , n=6). However, the same stimulation protocol failed to show any differences in the strength of LTP between slices of wt (n=12) and BDNF(+/-) (n=14) mice in the visual cortex. Since it is known that BDNF shifts the strength of LTP in the visual cortex in a frequency-dependent manner, we repeated the LTP experiments with a 20 Hz tetanic stimulation protocol. Here we observed a significantly reduced LTP in the BDNF(+/-) mice ( $104\% \pm 4\%$ , n=14) compared to controls ( $119 \pm 3\%$ , n=13,  $p < 0.05$ ). To verify the level of expression for neurotrophins in the hippocampus and visual cortex of heterozygous BDNF knock-out mice, we performed semiquantitative PCR experiments. The mRNA for BDNF was reduced by 20% in visual cortex, but by 30% in the hippocampus at the age of p35-p40 ( $p < 0.01$ , n>25 PCRs each from cDNA of 10 WT and 9 BDNF(+/-) mice). Compensatory effects of other neurotrophins as NT3, NT4 and NGF could be ruled out, since the level of these neurotrophins were not increased in heterozygous knock-out mice. The expression of m-RNA for NT4 and NGF was even decreased ( $p < 0.05$ ) at P35.

These data indicate that tetanic stimulation at 20 Hz is a more sensitive protocol than TBS to unmask the deficient synaptic plasticity in the visual cortex of BDNF(+/-) mice. The reduction of BDNF in the visual cortex is not as pronounced as in the hippocampus and could explain the differences in LTP expression between the two brain areas.

Supported by the Deutsche Forschungsgemeinschaft (DFG, GK 736 & SFB 509)



**Role of N-cadherin in selective stabilisation of glutamatergic synapses.**

Kay Jüngling and Kurt Gottmann

Institut für Neuro- und Sinnesphysiologie, Heinrich Heine-Universität Düsseldorf

Synaptic adhesion molecules of the cadherin superfamily, consisting of classical cadherins and protocadherins, have been proposed to control selective synapse formation. Classical cadherins, e.g. neural (N-) cadherin, mediate homophilic cell-cell adhesion in a  $\text{Ca}^{2+}$ -dependent manner and are found in the perisynaptic region, bordering the active zone and the postsynaptic density. We are analysing the role of N-cadherin in synapse formation, function and plasticity using embryonic stem (ES) cells from N-cadherin knock-out mice (Radice *et al.*, 1997).

Because of the early embryonic lethality of N-cadherin knock-out mice, we established *in vitro* differentiation and immunoisolation of ES cell-derived neurons (Jüngling *et al.*, 2003) genetically null for N-cadherin. Glutamatergic synapses were studied in microisland cultures of these cells after 10-14 days *in vitro* by ultrastructural, immunocytochemical and electrophysiological methods. Previously we have shown that axon outgrowth, dendrite morphology and the number and ultrastructure of synapses are not altered in homogenous cultures of N-cadherin knock-out neurons. However, we found a clear-cut defect in the activity-induced recruitment of synaptic vesicles to the active zone (Jüngling *et al.*, submitted).

To further investigate the possible importance of N-cadherin as target recognition molecule in competitive synapse formation, we studied chimeric co-cultures consisting of N-cadherin-expressing and N-cadherin-deficient neurons. Preliminary results indicate that glutamatergic synapses formed by a presynaptic N-cadherin expressing neuron and a postsynaptic N-cadherin deficient neuron show a similar defect in vesicle recruitment as described above. Intriguingly, glutamatergic synapses formed by a presynaptic N-cad<sup>-/-</sup> neuron and a postsynaptic N-cad<sup>+/+</sup> neuron were almost undetectable. This indicates an additional role of N-cadherin in selective synapse stabilisation that deserves further investigation.

1. Radice, G.L. *et al.*, 1997. *Dev. Biol.* 181 : 64-78.
2. Jüngling, K. *et al.*, 2003. *FASEB J.* Nov 17(14):2100-2.
3. Jüngling, K., Eulenburg, V., Moore, R., Kemler, R., Lessmann, V. and Gottmann, K., 2004. submitted.

## **Presynaptic long-term induction of immature glutamatergic synapses in cultured neocortical neurons**

C. Walz<sup>1</sup>, V. Lessmann<sup>2</sup> and K. Gottmann<sup>1</sup>

<sup>1</sup> Institut für Neuro- und Sinnesphysiologie, Heinrich Heine-Universität Düsseldorf; <sup>2</sup> Institut für Physiologie und Pathophysiologie, Johannes Gutenberg-Universität Mainz

In the immature neocortex excitatory glutamatergic synapses are formed initially as functionally inactive (“silent”) synapses and are thought to be activated in an activity-dependent manner during postnatal development. Postsynaptically silent synapses lack AMPA receptors, which are acquired during NMDA receptor-dependent induction of these silent synapses. Presynaptically silent synapses that are ultrastructurally normal but lack actively recycling vesicles have been proposed recently. However, a direct demonstration of this type of silent synapses is still missing. To study the dynamics of individual synapses, EGFP-expressing cortical neurons were stained with the styryl dye FM 4-64 to visualize presynaptic terminals. Staining was done with K<sup>+</sup> depolarization and destaining was elicited by tetanic extracellular stimulation. After a resting period of 1.5 hrs staining/destaining was repeated and again a difference image from the same dendrite was obtained.

In these experiments the vast majority of release sites showed an increase in staining intensity suggesting an increase in the number of actively recycling synaptic vesicles. In addition the emergence of new functional release sites was repeatedly observed. No changes in the kinetics of synaptic vesicle exocytosis (destaining) were found. Parallel patch clamp recordings revealed a significant increase in the frequency of AMPA receptor-mediated miniature PSCs suggesting that the vast majority of dendritic release sites imaged were glutamatergic. Intriguingly, these dynamic changes at the level of individual release sites were blocked by addition of the NMDA receptor antagonist D-AP5 suggesting that the activity-dependent activation of NMDA receptors is necessary to induce this form of long-term synaptic plasticity. *De novo* formation of synapses appeared not to contribute to the observed emergence of new functional release sites because this phenomenon was also blocked by D-AP5. Therefore we hypothesize that presynaptically silent synapses lacking active vesicles are formed initially. During maturation some vesicles acquire the ability to fuse and recycle leading to functional induction of presynaptically silent synapses.

## **Insulin-like growth factor-1 (IGF-1)-induced long-term plasticity in thalamo-cortical synapses *in vitro***

A. Boehlen and K. Gottmann

Institut für Neuro- und Sinnesphysiologie, Heinrich-Heine Universität Düsseldorf,  
Universitätsstrasse 1, 40225 Düsseldorf, Germany

A variety of neurotrophic factors has been identified that control neuronal growth and survival. Moreover, long-term synaptic plasticity has been demonstrated to be strongly influenced by the neurotrophin BDNF. However, whether other classes of neurotrophic factors have similar effects on functional synaptic transmission has remained unclear. IGF-1 is one of the most interesting neurotrophic factors in the brain and its genetic inactivation leads to dramatic effects on neuronal survival. We now addressed a potential role of IGF-1 in regulating synapse formation, function and long-term synaptic plasticity at glutamatergic synapses in mouse thalamo-cortical co-cultures.

Thalamic explants obtained from E17 mouse fetuses were co-cultured with dissociated neocortical neurons. Massive thalamic innervation of neocortical target neurons occurred during the first week in culture. Addition of IGF-1 (100ng/ml) was done either at 5 days *in vitro* (DIV) or at 9 DIV. To study functional glutamatergic synapses we performed whole-cell patch-clamp recordings from neocortical target neurons at 8/9 DIV or at 12/13 DIV. Spontaneous miniature excitatory postsynaptic currents (mEPSCs) were pharmacologically isolated by addition of TTX and picrotoxin. AMPA receptor-mediated mEPSCs were completely blocked by addition of the AMPA/kainate receptor antagonist DNQX.

Strikingly, chronic addition of IGF-1 led to a significant increase in both frequency and amplitude of AMPA mEPSCs at 8/9 DIV. The mean frequency in 5 mM K<sup>+</sup>-containing extracellular solution increased 4fold from 0.4 Hz to 1.8 Hz. The mean amplitude increased by 32% from 10.6 pA to 14.0 pA. Intriguingly, the effects of chronic IGF-1 addition were less pronounced at a later stage in culture. At 12/13 DIV the mean amplitude increased only by 23% from 13.5 pA to 16.6 pA. No increase in the mean frequency was detected. This result suggests that IGF-1 induces an accelerated maturation of glutamatergic synapses *in vitro*. Both pre- and postsynaptic actions of IGF-1 on the number of release sites, the release probability and the membrane incorporation of AMPA receptors are conceivable.

## **Synaptic vesicle proteins under conditions of rest and activation: A proteomic approach using differential in gel electrophoresis**

Jacqueline Burré, Marco Morciano, Tobias Beckhaus, Michael Karas, Walter Volkhardt and Herbert Zimmermann

Department of Neurochemistry, Biocenter, JW Goethe-University, Frankfurt/Main

Within the past two decades, converging work from several laboratories resulted in the molecular and functional description of a considerable variety of synaptic vesicle proteins that govern the docking and fusion process during exocytosis. Synaptic vesicle proteins are involved in essential tasks such as storage, release and reuptake of neurotransmitter. In order to analyze presumptive modifications of the synaptic vesicle proteome during cycles of exo- and endocytosis we combined two dimensional differential in gel electrophoresis and mass spectrometric analysis. This includes the evaluation of modification changes of both, membrane integral and membrane-associated proteins.

Rat brains were perfused either by high potassium concentrations to chemically induce exocytosis or to block exocytosis by a perfusate containing the membrane permeable calcium chelator BAPTA-AM. Synaptic vesicles are isolated from rat brain synaptosomes by hypoosmotic shock and subcellular fractionation techniques as well as by immunoaffinity methods for organelle isolation. Synaptic vesicle proteins obtained under conditions of rest or activation were labeled by different fluorescent dyes, combined and concomitantly separated by 16-BAC polyacrylamide gel electrophoresis in the first and SDS-PAGE in the second dimension. The polypeptide pattern was analyzed and spots revealing differences were excised from the gels and subjected to analysis by matrix assisted laser desorption/ionization – time of flight - mass spectrometry (MALDI-TOF-MS). The sequence data obtained were employed to identify the respective proteins. This information provides the basis for additional investigations including the functional analysis of the synaptic vesicle proteins identified.

## **Analysis of the proteome of synaptic vesicles docked to the plasma membrane under conditions of rest and activation**

Marco Morciano, Jacqueline Burré, Tobias Beckhaus, Michael Karas, Herbert Zimmermann and Walter Volkandt

Department of Neurochemistry, Biocenter, JW Goethe-University, Frankfurt/Main

Converging work from several laboratories within the past two decades, resulted in the molecular and functional description of a considerable variety of synaptic vesicle proteins and of proteins of the target presynaptic plasma membrane that govern the docking and fusion process during exocytosis. Synaptic vesicle proteins are key players in these processes and involved in essential tasks such as storage, release and reuptake of neurotransmitter. A subpopulation of vesicles ready for release are docked to the presynaptic plasma membrane via complex protein interactions. The proteome of this docked vesicle compartment is expected to undergo dynamic changes during induced transmitter release. In order to analyze presumptive modifications of proteins of docked synaptic vesicle during cycles of exo- and endocytosis we combined two dimensional differential in gel electrophoresis and mass spectrometric analysis. This includes the evaluation of modificational changes of both, membrane integral and membrane-associated proteins.

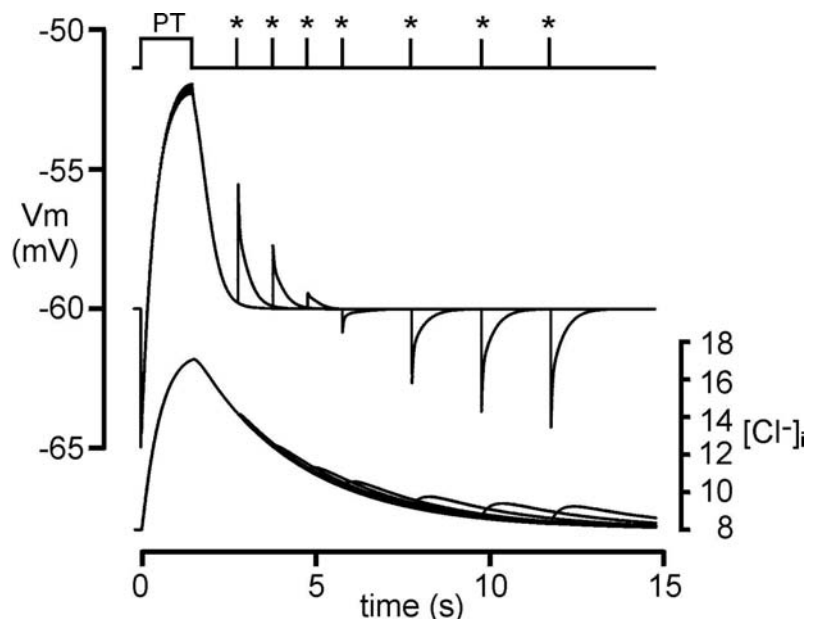
Rat brains were perfused either by high potassium concentrations to chemically induce exocytosis or to block exocytosis by a perfusate containing the membrane permeable calcium chelator BAPTA-AM. The compartment of docked vesicles including the presynaptic plasma membrane was then isolated from rat brain synaptosomes by hypoosmotic shock and subcellular fractionation techniques as well as by immunoaffinity methods for organelle isolation. Docked synaptic vesicle proteins obtained under conditions of rest or activation were labeled by different fluorescent dyes, combined and are concomitantly separated by 16-BAC acrylamide gel electrophoresis in the first and SDS-PAGE in the second dimension. The polypeptide pattern was analyzed and spots revealing differences were excised from the gels and subjected to analysis by matrix assisted laser desorption/ionization - time of flight - mass spectrometry (MALDI-TOF-MS). The sequence data obtained were employed to identify the respective proteins. This information provides the basis for additional investigations including the functional analysis of the docked synaptic vesicle proteins identified.

## Postsynaptic depolarizations mediated by GABA<sub>A</sub> receptors: a computational study

**P. Jedlička and K.H. Backus, Institute of Physiology II, Cellular Neurophysiology, J.W. Goethe-University Frankfurt, Theodor-Stern-Kai 7, D-60590 Frankfurt/Main, Germany**

GABA<sub>A</sub> receptors (GABA<sub>A</sub>Rs) are ligand-gated ion channels that regulate a Cl<sup>-</sup>/HCO<sub>3</sub><sup>-</sup> conductance through neural membranes. The direction of the net anion flux through these receptors is determined by the relative permeability of HCO<sub>3</sub><sup>-</sup> and Cl<sup>-</sup> and their electrochemical gradients. Brief activation of GABA<sub>A</sub>Rs commonly results in hyperpolarization of adult neurons. In postnatal neurons, depolarizing or biphasic response have been frequently observed. In the adult brain, prolonged or repetitive activation of GABA<sub>A</sub>Rs also evoked biphasic responses consisting of an initial hyperpolarization followed by a depolarization (Thomson, Neurosci 1988, 25:503). A possible mechanism underlying the GABA-induced depolarizing postsynaptic potential (GDPSP) is attributable to an acute Cl<sup>-</sup> accumulation that results in a shift of the GABA<sub>A</sub> reversal potential ( $E_{\text{GABA}}$ ; Staley et al., 1995, Science 269:977; Kaila et al., 1997, J Neurosci. 17: 7662; Dallwig et al., 1999, Pflügers Arch. 437:289). We have developed a computational model of the GABAergic synapse to study the effects of monosynaptic GABA<sub>A</sub>R-mediated Cl<sup>-</sup> accumulation and its role for depolarization. An equivalent circuit model of the dendritic compartment was implemented in the simulation environment NEURON (www.neuron.yale.edu). To incorporate the GABA-induced gating of postsynaptic receptors, an established kinetic model of GABA<sub>A</sub>R was used (Jones & Westbrook, 1995, Neuron 15:181). In physiological conditions, our simulations indicated that the activation of GABA<sub>A</sub>Rs increased the intracellular Cl<sup>-</sup> concentration ( $[\text{Cl}^-]_i$ ) and shifted  $E_{\text{GABA}}$  to more positive values. By using different stimulation frequencies, we could show that the GDPSP amplitude was frequency-dependent and correlated with intracellular Cl<sup>-</sup> accumulation. We also investigated the effects of changes in the kinetics of Cl<sup>-</sup> regulation by varying the Cl<sup>-</sup> extrusion rate and found that higher Cl<sup>-</sup> extrusion rates decreased GDPSPs. However, when using a physiological Cl<sup>-</sup> extrusion rate ( $\tau=3\text{s}$ ; Wagner et al., J Physiol. 537:853), the GABA-induced Cl<sup>-</sup> accumulation evoked by stimulation frequencies  $\geq 10\text{ Hz}$  persisted several seconds on a level, sufficient to induce GDPSPs. Thus, single pulse stimulations following a transient pulse train induced GDPSPs with amplitudes that depended on the frequency of the conditioning train and their delay (Fig. 1).

Fig. 1: Superimposed traces evoked by single pulse stimulations (asterisks) were applied at different time points following high frequency stimulation (PT; 40 Hz). The responses remained depolarizing up to several seconds. Lower traces show the corresponding changes in  $[\text{Cl}^-]_i$ .



In addition, we found that presynaptic depression could attenuate acute Cl<sup>-</sup> accumulation, but did not block GDPSPs in most conditions tested.

Our study shows that GABA<sub>A</sub>R-mediated  $[\text{Cl}^-]_i$  increase is sufficient to generate GDPSPs. The activity-dependent acute switch of GABA<sub>A</sub>-mediated hyperpolarization to depolarization could modulate interneuronal  $\gamma\beta$ -oscillations and may contribute to some epileptic conditions. Thus, our model may bring insights into the synaptic and ionic mechanisms of GABA-induced oscillations and seizure-like discharges. (Supported by the Graduiertenkolleg „Neuronale Plastizität: Moleküle, Strukturen, Funktionen“ and SFB 269 „Molekulare und zelluläre Grundlagen neuronaler Organisationsprozesse“; Teilprojekt B6).

## Absence of Transforming Growth Factor- $\beta$ 2 (TGF- $\beta$ 2) causes changes in acetylcholine receptor clustering at the mouse neuromuscular junction

Katharina Heupel and Kerstin Krieglstein

Center of Anatomy/Department of Neuroanatomy, University of Goettingen, Kreuzberggring 36, 37075 Goettingen, Germany

Formation of synapses requires the exact apposition of pre- and postsynaptic elements. To a certain degree development of either side is independent from the other, but there is also the need for signals that orchestrate the process. Transforming Growth Factor- $\beta$ s (TGF- $\beta$ s) are cytokines known for their various functions in development including differentiation and apoptosis. Several studies on drosophila mutants of different molecules of the TGF- $\beta$  signaling pathway pointed out its significance for synapse development and underlined TGF- $\beta$ 's role as a retrograde signal in synapse formation.

We focus on the ligand TGF- $\beta$ 2 and explore its role in the development of synapses in vertebrates and examine different synapses of the peripheral nervous system. In a first experiment we investigated how the lack of TGF- $\beta$  influences the formation of the neuromuscular junction of the diaphragm of TGF- $\beta$ 2-/- knockout mice compared to their wild type littermates. In order to clarify whether TGF- $\beta$  is important for initial axon path finding and sprouting, clustering of postsynaptic acetylcholine receptors (AChRs) and/or dispersion of aneural AChR clusters, we examined the innervation pattern of the phrenic nerve by using an antibody to neurofilament 150 kD and visualize the clustering of the AChRs by alpha-bungarotoxin.

Preliminary results showed a reduced number of AChR clusters in E 18.5 ko mice and malformation of the skeletal muscle of the diaphragm, but no gross alteration in branching and arborization of the nerve.

This work is funded by the European Graduate School (DFG) 632 "Neuroplasticity: From molecules to systems" and SFB 406.

## **Activity-dependent Release of Transforming Growth Factor-beta (TGF- $\beta$ ) in Neuronal Networks *in vitro***

Anke Lacmann and Kerstin Krieglstein

Department for Neuroanatomy, Center of Anatomy,  
Georg-August-University Göttingen,  
Kreuzberggring 36, 37075 Göttingen, Germany

Besides the well known functions of neurotrophic factors on neurons concerning the regulation of survival and differentiation during development and the maintenance of characteristic properties in the adult brain, some studies revealed new aspects giving hints that these factors can modulate the activity-dependent neuronal plasticity. The documented activity-dependent regulation of synthesis and release of neurotrophic factors, together with the observation that the secretion of neurotransmitters is initiated by these factors, leads to the hypothesis that they might act as retrograde modulators enhancing the efficacy and stabilization of synapses. This is suggested for neurotrophins and also for members of the TGF $\beta$ -family. In the present study we addressed this aspect with experiments on the release of TGF- $\beta$  *in vitro* from primary hippocampal neurons of mice at embryonic stage E16.5. Experiments were performed with cultures at day 12 *in vitro*, following a differentiation protocol by Dotti et al. (1988) forming a dense neuronal network. To quantify the amount of TGF- $\beta$  released into the culture medium we used a well established assay quantifying TGF- $\beta$  activity. We tested for an activity-dependent component of the release of TGF- $\beta$  by using different agonists stimulating neuronal activity (e.g. KCl, Veratridine) and characterized it by application of appropriate antagonists e.g. TTX for the dependence on sodium and e.g. BAPTA for the influence of extracellular calcium. In our experiments we found a clear increased amount of TGF- $\beta$  in culture supernatant following a stimulation for example with 55 mM KCl or 10  $\mu$ M Veratridin, suggesting a correlation between neuronal activity and TGF- $\beta$  release from these neurons. The amount of TGF- $\beta$  detected after stimulation with the two agonists mentioned above was reduced when the neurons were pretreated with 1.5  $\mu$ M TTX, indicating a dependence on sodium for the activity-dependent release. Additionally an influence of extracellular calcium was obvious due to a decreased amount of released TGF- $\beta$  when 10  $\mu$ M BAPTA was applied prior to stimulation of the cultured neurons. Taken together, the results suggest an activity-dependent release of TGF- $\beta$  from cultured primary hippocampal neurons *in vitro* influenced by different cations in the surrounding milieu like sodium and calcium.

Funded by the Deutsche Forschungsgemeinschaft, SFB406.



## **An early fast phase of endocytosis sorts synaptic vesicles less efficiently back into the recycling pool**

Veronika J. Mueller and Jurgen Klingauf

Department of Membrane Biophysics, Max-Planck Institute for Biophysical Chemistry, 37077 Goettingen, Germany

For maintaining neuronal communication recycling of synaptic vesicles is essential. The mechanisms underlying this process remain unclear and various modes of vesicle recycling have been proposed for central nervous synapses: a fast ‘kiss-and-run’ mechanism, where the vesicle connects only briefly to the plasma membrane without full collapse, a slow pathway via large infoldings of membrane and/or endosomes, and the recovery of vesicle membrane by clathrin-coated pit formation.

We used a fusion construct of enhanced green fluorescent protein (EGFP) and clathrin light chain  $\alpha$  (LC $\alpha$ 1) to study clathrin redistribution during clathrin-mediated endocytosis as well as the styryl dye FM 1-43 to measure overall endocytotic activity in hippocampal synapses. We investigated the fate of vesicles retrieved at distinct phases of endocytosis by applying FM 1-43 for 10 second pulses at different times during and after stimulation.

We show that the time course of clathrin redistribution for stimuli above 200 action potentials (APs) at 20 Hz did not depend on AP number. A significant delay between stimulus onset and increase of fluorescence intensity of EGFP-LC $\alpha$ 1, due to clathrin recruitment to sites of endocytosis, indicated that endocytosis during the first few seconds of 20 Hz stimulation cannot be mediated by newly formed clathrin-coated pits. During this early phase the rate of endocytosis measured with FM 1-43, however, was at least 2.5 fold faster than at later times. These findings suggested that during this early wave fast endocytosis is either supported by preassembled clathrin-lattices, not requiring clathrin redistribution, or by a clathrin-independent, presumably ‘kiss-and-run’ mechanism. In addition, this phase of endocytosis led to different sorting of retrieved vesicles back into the recycling pool indicated by their lower re-availability after an 8 minute washing period. Since the number of vesicles labeled within the first 10 sec’s of prolonged stimulation is independent of stimulation length (up to 30 sec’s), vesicles endocytosed during this fast phase were apparently not rapidly reused. Vesicles retrieved after stimulus cessation (post stimulus endocytosis), however, seemed to be preferentially reused, as revealed by more efficient destaining during a test pulse 8 min later as well as faster destaining kinetics. Thus, dependent on stimulus duration and the time (and maybe the mode) of endocytosis vesicles are recycled differentially.

## **Munc-18-1 is a positive regulator for secretory granule docking in chromaffin cells as visualized by evanescent wave microscopy**

O Kochubey<sup>1</sup>, RF Toonen<sup>2</sup>, M Verhage<sup>2</sup>, J Klingauf<sup>1</sup>

<sup>1</sup>Dept. of Membrane Biophysics, MPI for Biophysical Chemistry, Am Fassberg 11, 37077 Goettingen, Germany

<sup>2</sup>Dept. of Functional Genomics, Free University of Amsterdam, De Boelelaan 1087, 1081 HV Amsterdam, the Netherlands

Munc-18-1 is thought to be a key element of the molecular machinery at early steps of synaptic vesicle exocytosis. Its null mutation impairs morphological and functional membrane docking of large dense-core vesicles (LDCVs) in adrenal chromaffin cells while at the central synapses it completely abolishes synaptic transmission. Evanescent wave microscopy (or TIRFM) is a powerful technique for visualization of fluorescent objects within ~200 nm distance from the cover glass which makes it suitable to investigate the movement of single vesicles in the vicinity to the cell membrane. We applied the TIRFM to study single LDCVs dynamics in chromaffin cells from munc-18-1 KO and WT mice at the age E18. The average density of LDCVs fluorescently labeled with NPY-Venus at the membrane was about two times smaller in KO than in WT cells or cells rescued by viral expression of munc-18-1 in line with known electron microscopic data. By three-dimensional tracking of docked LDCV in x, y, and z we found parameters of diffusion such as excursions from central positions, point-to-point velocities and mean square displacement plots to be similar for KO and WT cells. However, the velocity autocorrelation function (VACF) calculated for LDCV movement along z axis revealed a distinct negative component at small correlation times  $\tau \sim 0.5\text{-}1$  s for WT cells which was not observed in KO cells. This feature, being more prominent for LDCVs located closer to the membrane, was rescued in KO cells by munc-18-1 overexpression and partially recovered after introduction of a mutated munc-18-1 with low affinity to syntaxin1A. Also, application of the phorbol ester PMA rescued this feature in the KO completely. The negative component of the VACF indicates repetitive changes in movement direction along the z axis and thus a deviation from simple free diffusion. Simulations of diffusion show that these repeated movement direction changes are caused either by restricted diffusion (when the LDCV is 'encaged' near the membrane) or by tethering forces acting on the LDCV. Since the 'cage' could be provided by the cytoskeleton, we tested the first possibility by disrupting the actin network using latrunculin A. This treatment, however, did not change the VACF in both WT and KO. Furthermore, in WT cells LDCV 3D-trajectories showed a tendency of having several 'centers of mass', probably reflecting multiple docking sites. This feature could also be rescued. In summary our data indicate that munc-18-1 is an essential positive regulator during docking, which promotes it by strengthening tethering forces probably requiring interaction with the t-SNARE syntaxin.

Supported: GRK 723, Goettingen

# Analysis of Non-stationary Fluctuations of Exocytotic Capacitance Changes in Mouse Inner Hair Cells

**Darina Khimich<sup>1</sup>, Primoz Pirih<sup>1</sup>, Fred Wolf<sup>2</sup> & Tobias Moser<sup>1,3</sup>**

<sup>1</sup> InnerEarLab, HNO University Clinic Goettingen,  
Robert-Koch-Strasse 40, D-37075 Göttingen, Germany

<sup>2</sup> Nonlinear Dynamics Group, MPI für Strömungsforschung,  
Bunsenstrasse 10, D-37073 Göttingen, Germany

<sup>3</sup> tmoser@gwdg.de

Ribbon synapses are specialized structures, found in neurons driven by graded potentials (e.g. retinal photoreceptors, bipolar cells and the hair cells). It has been proposed that ribbons act as attractors or reservoirs for the synaptic vesicles, thus enabling multivesicular release and rendering these synapses able of transmitting information over a broad dynamic range of stimuli with short latency.

Recently, an exponential-like distribution of release event sizes has been measured on the postsynaptic side of immature mouse inner hair cells. This EPSC distribution can not be explained with the usual Poisson/binomial model of synaptic transmission, developed for the neuro-muscular junction and some central synapses. This unusual finding might reflect the existence of differently sized vesicles (compound fusion) or statistical dependence of individual vesicles (concerted release).

In analogy to the current noise analysis revealing the single channel conductance, the non-stationary fluctuation analysis of the evoked exocytic capacitance steps can reveal the apparent quantal vesicle size and thus give insight into the statistical properties of the fusion mechanism.

We have measured the cell capacitance in perforated patch clamp recordings using a software lock-in amplifier. In order to reliably measure the fluctuations of exocytic capacitance changes out from the noisy signal, we have developed some enhancements of the non-stationary fluctuation analysis (e.g. demixing of crosstalk between the lock-in channels, trend-correction procedures, bootstrapping randomization for the estimation of the apparent quantal size confidence interval).

Preliminary results have shown that the apparent quantal vesicle sizes, estimated with this method, are similar to the real size of a single vesicle, suggesting statistical independence of individual vesicles in the mature mouse inner hair cells.

**SYNAPTIC VESICLES LOOSE THEIR PROTEIN COMPLEMENT DURING EXO-ENDOCYTIC CYCLING**

M Wienisch, J Klingauf

Max-Planck Institute for Biophysical Chemistry, Microscopy of Synaptic Transmission, Dept. Membrane Biophysics, Am Faßberg 11, 37077 Göttingen, Germany

Overall endocytic activity can be measured with synapto-pHluorin (spH), a fusion construct of the vesicle protein VAMP and a pH-sensitive form of GFP. The GFP-moiety resides in the acidic vesicle lumen, rendering it a good indicator for exo-endocytosis, since the fluophore is unquenched upon exocytosis and reacidification of endocytosed vesicles is accomplished within seconds. A fraction of up to 30% of spH has been shown to be present on the external axonal membrane of transfected hippocampal neurons.

To test whether synaptic vesicles maintain their identity with respect to their protein composition during exo-endocytic cycling we introduced a TEV-protease cleavage site between the VAMP and GFP moieties accessible only by external enzyme if TEV-spH is in the plasma membrane. Uncleaved TEV-spH behaved identical to the original fusion protein and fluorescence transients evoked by 200 action potentials (APs) at 20 Hz usually decayed fully with a similar time course as previously published. After digestion of the plasma membrane TEV-spH pool for 25 min, a challenge with 200 APs lead to a fluorescence increase of similar amplitude, but with only little (~ 50 %) recovery having the same kinetics. This indicates that mostly digested molecules have been recycled during compensatory endocytosis, i.e. VAMP molecules deposited on the plasma membrane prior to digestion. In line with this, full recovery with identical kinetics was observed again in the same boutons after equilibrating both pools by low frequency stimulation at 5 Hz for 160 s. The same results were obtained, when selectively bleaching the membrane spH pool by repeated laser scanning instead of cutting off the fluorophore by digestion, showing that neither the protease treatment nor the presence of the large GFP moiety affect VAMP recycling or rates of endocytosis.

We conclude that under these stimulus conditions most recycling synaptic vesicles loose their protein complement during exocytosis and, since the rate of endocytosis post bleach/digest did not increase, only a minor contribution of 'kiss and run' can be assumed.

*Support contributed by the Boehringer Ingelheim Fonds.*

## **Converging signaling pathways in the grasshopper brain and the control of context-specific behavior – an *in vitro* approach**

**Christian Heck and Ralf Heinrich**

**Dept. of Neurobiology, Berliner Str. 28, 37073 Göttingen, Germany**

Acridid grasshoppers communicate with specific song patterns in the context of attracting partners for reproduction, courting and agonistic behavior. When to sing and which song pattern to perform is determined by the brain, particularly by the central body complex and a distinct neuropil that contains the dendrites of command neurons, each of which controls the performance of a particular stridulatory pattern. Sensory information related to acoustic communication behavior is first analyzed by specific neural circuits and then relayed to the central body to generate arousal that promotes the production of specific sound patterns.

Various sensory systems relay information to the central nervous system, about whether it appears appropriate to stridulate with a particular pattern or not. Accordingly, multiple signaling pathways (excitatory transmitters/second messengers: ACh, proctolin/cAMP, IP<sub>3</sub>/DAG; inhibitory transmitters/second messengers: GABA, glycine, NO/cGMP) have been demonstrated to converge in the central body and to contribute to the control of stridulation by mediating both fast ionotropic and prolonged metabotropic excitatory and inhibitory effects respectively.

In order to identify central body neurons that integrate signals associated with sensory stimuli relevant for stridulation and mediate the decision about when to produce which sound pattern, we followed an *in vitro* approach. Initially, intact grasshopper were placed in an experimental setup suitable for pressure injections of small volumes of dissolved drugs into the brain. At particular locations within the protocerebrum, where either specific singing behavior could be pharmacologically stimulated or pharmacologically stimulated stridulation could be suppressed by interfering with a particular signaling pathway, small fluorescent dextrans were co-injected as vital tracers. The dextrans were incorporated by intact neurons via their postsynaptic sites, thereby labeling those neurons that potentially were directly affected by the stimulating or inhibiting drug. After taking whole grasshopper brains into dissociated cell culture, these neurons could be recognized by their dextran-related fluorescence and their responses to the particular neuroactive drug used in the preceding physiological experiment.

During electrophysiological recordings, the cultured neurons were subjected to drugs, known to interfere with the generation of excitation during song control in the central body neuropil. Various combinations of transmitters and membrane permeable drugs known to interfere with specific intracellular signaling pathways were applied to each recorded neuron, to generate a pharmacological profile. The physiological data were complemented by subsequent immunocytochemical detection of transmitters and other cellular components indicative for the functional presence of specific signal transduction mechanisms. According to their characteristics, the cultured neurons were classified and their potential contribution to the control of stridulation by the central body was estimated on the basis of the existing knowledge from previous behavioral and pharmacological studies.

The studies were supported by *Deutsche Forschungsgemeinschaft* and *SFB 406: Synaptische Interaktionen in Neuronalen Zellverbänden*.

## Alpha-Methyl-Noradrenaline Stimulates Alpha-1 and Alpha-2 Adrenoceptors in the Paraventricular Thalamic Nucleus of the Rat

Heilbronner, U., Kole, M.<sup>\*</sup>, and Flügge, G.

Clinical Neurobiology Laboratory, German Primate Center (DPZ),  
Kellnerweg 4, 37077 Göttingen

<sup>\*</sup> Present Address: Neuron Signaling Laboratory, Division of Neuroscience John Curtis School of Medical Research, The Australian National University, Canberra, ACT 0200 Australia

We have previously shown an increase in expression of the alpha-2 adrenoceptor (AR) subtype B in the tree shrew paraventricular thalamic nucleus (PVT) after chronic psychosocial stress (1). However, the function of alpha-2 ARs in the PVT remains unknown. We have therefore investigated the effects of the alpha-2 agonist alpha-methyl-noradrenaline (alpha-m-NE) on PVT cells in male Wistar rats using whole-cell voltage recordings. The PVT cells under study were routinely filled with the tracer neurobiotin during recording and afterwards visualized for morphological identification. When alpha-m-NE (1-25  $\mu$ M) was applied to the bath, it induced two opposite responses which were both reversible and dose-dependent:

- (1) A subset of PVT cells (14 of 72) were **hyperpolarised** which was accompanied by a reduction in the membrane resistance. This effect was mediated by alpha-2 ARs because it was reversibly blocked by the specific alpha-2 antagonist yohimbine (1  $\mu$ M).
- (2) Other cells (21 of 72) slowly **depolarised** with a concomitant increase in membrane resistance. This effect was mediated by alpha-1 ARs because it was blocked by pre-application of the alpha-1 antagonist prazosin (0.075  $\mu$ M) and mimicked by the alpha-1 agonist phenylephrine (5  $\mu$ M).

Furthermore, our results show that cells stimulated with alpha-m-NE (5  $\mu$ M) exhibit either hyperpolarisation or a depolarisation but rarely both. We currently perform morphological analysis of these cells to evaluate whether these distinct and opposite effects are dependent on morphological identity of the heterogeneous PVT cell population.

In conclusion, our data show that alpha-2 ARs in the PVT mediate membrane hyperpolarisation and decrease membrane resistance. Also, the data show alpha-m-NE to be an agonist at both alpha-2 and alpha-1 ARs in the PVT.

(1) Heilbronner, U, van Kampen, M, Flügge, G (2004) The alpha-2B adrenoceptor in the paraventricular thalamic nucleus is persistently upregulated by chronic psychosocial stress. **Cell Mol Neurobio**, *in press*.

*Supported by the German Science Foundation SFB 406*

## **NEUROLIGINS ARE ESSENTIAL FOR NEURONAL NETWORK FUNCTION IN THE RESPIRATORY NETWORK OF MICE**

G. Aramuni<sup>1</sup>, F. Varoqueaux<sup>2</sup>, V. Sargsyan<sup>1</sup>, N. Brose<sup>2</sup> and W. Zhang<sup>1</sup>

<sup>1</sup>Center of Physiology, University of Göttingen; <sup>2</sup>Max-Planck-Institute for Experimental Medicine, Göttingen

Neuroligins constitute a family of brain-specific cell adhesion proteins, which are encoded by three genes. They are localized postsynaptically and interact with presynaptic cell adhesion proteins of the  $\beta$ -neurexin family to form heterotypic intercellular junctions. Although the interaction of neuroligins with other proteins has been proposed to be important for synaptic function, their exact physiological role has remained elusive. We have used a combined molecular biological and electrophysiological approach to investigate the function of neuroligins in the brain. All three neuroligin genes were deleted by conventional knockout strategies, and all possible combinations of double (DKOs) and triple mutant mice (TKOs) were generated. Mutant mice lacking all three neuroligin genes (TKOs) die within a few hours after birth, demonstrating that neuroligins are essential for postnatal development. In newborn mutant neuroligin TKO mice, ventilation as measured by whole body plethysmography is severely impaired in a neuroligin gene dosage dependent manner. Patch-clamp recordings of neurons in the respiratory rhythm-generating network (pre-Bötzinger complex; PBC) located in the ventral medulla revealed a severe reduction of spontaneous GABAergic and glycinergic inhibitory postsynaptic transmission in TKO mice to less than 10% of wild type values. On the other hand, evoked glutamatergic excitatory postsynaptic responses of hypoglossal motor neurons were less affected in TKOs. Thus, our results strongly support the hypothesis that neuroligins play a key role in regulating synaptic function. (supported by CMPB Göttingen)

Glial cells in the respiratory network express functional transporters and receptors for glycine

Katalin Szöke<sup>1</sup>, Johannes Hirrlinger<sup>2,4</sup>, Melanie Handschuh<sup>3</sup>, Clemens Neusch<sup>3</sup>, Frank Kirchoff<sup>2,4</sup>, and Swen Hülsmann<sup>1,4</sup>

<sup>1</sup> University of Göttingen, Department of Neuro- and Sensory Physiology

<sup>2</sup> Max Planck Institute for Experimental Medicine, Department of Neurogenetics

<sup>3</sup> University of Göttingen, Department of Neurology

<sup>4</sup> DFG Research Center Molecular Physiology of the Brain, Göttingen, Germany

Inhibitory synaptic transmission within the respiratory network plays a key role in the generation and modulation of the neuronal rhythm for breathing. To understand how astrocytes and oligodendrocytes are involved in glycinergic neurotransmission of the respiratory network, we used a combined approach of immunohistochemistry, electrophysiology and single-cell RT-PCR analysis to determine the expression of glycine transporter 1 (GlyT1) and glycine receptors (GlyR) in the ventral respiratory group of the medulla. Immunohistochemistry against GlyT1 and GlyR was performed in brainstem slices from transgenic mice, in which astrocytes (TgN(hGFAP-EGFP)) and oligodendrocytes (TgN(PLP-DsRed)) were fluorescently labeled. In the ventral respiratory group, GlyT1 was expressed preferentially by astrocytes with bright EGFP-fluorescence. In this type of astrocytes, GlyT1 expression overlapped with glycine receptor expression. To determine the functional expression of glycine transporters and –receptors, whole-cell currents were recorded in voltage-clamp experiments from identified astrocytes and oligodendrocytes using acutely isolated brainstem slices. Astrocytes with bright EGFP-fluorescence that showed linear steady-state IV-curves expressed both receptor- and transporter-mediated currents in response to glycine. In contrast, in an additional population of cells with weak EGFP-expression and outwardly rectifying IV relationship, we were not able to detect glycine-induced currents. Oligodendrocytes responded with both receptor- and transporter mediated glycine currents. As expected, mRNA of GlyT1 was detected by single-cell RT-PCR in astrocytes with linear IV relationship and in oligodendrocytes but also in a subset of outwardly rectifying astrocytes. These data suggests that in the respiratory network both astrocytes and oligodendrocytes may interfere with glycinergic synaptic transmission and thereby modulate respiratory rhythm generation. (supported by the DFG, SFB 406 TP C10)



**Structural alterations in the brains of adult  $\alpha$ -neurexin double knockout mice may be a long-term consequence of impaired synaptic transmission**

Irina Dudanova and Markus Missler

Zentrum für Physiologie, Georg-August Universität Göttingen 37073

Neurexins are neuron-specific cell-surface proteins that are essential for synaptic transmission by regulating the function of high-voltage activated  $\text{Ca}^{2+}$  channels. Mutant mice lacking all three  $\alpha$ -neurexin genes (neurexin 1 $\alpha$ , 2 $\alpha$ , and 3 $\alpha$ ) die shortly after birth because of severely reduced neurotransmitter release, and only few of the  $\alpha$ -neurexin double knockout animals reach adulthood. In newborn mutants, no major morphological defects were observed. We now investigated the brains of surviving neurexin 1 $\alpha$ /2 $\alpha$  and neurexin 2 $\alpha$ /3 $\alpha$  double knockout mice to study the long-term effects of impaired synaptic function on brain structure. Neurexin 2 $\alpha$  single knockout mice were used as genetically matching littermate controls. Consistent with the previous analysis of newborn mutants, no gross abnormalities were found in the general brain architecture of double knockouts (e.g., intact layering and projections, no signs of apoptosis). However, in serial sections we observed a significant reduction of the neuropil fraction (= the tissue compartment containing axons, dendrites and glial processes) that was most prominent in the upper layers of neocortical areas, the caudate-putamen and the olfactory bulb. The morphological changes amounted to about 20% but did not differ significantly between the two types of double knockouts. The reduction of neuropil was independently validated by a defect in the dendritic architecture of Golgi-impregnated neocortical pyramidal neurons. The distal branches of apical and basal dendrites were  $\approx$ 30-50% shorter in double knockouts than in single knockouts, with a corresponding loss of dendritic spines on the periphery of dendritic arbors. An ongoing electron microscopic study of neocortex will clarify whether synapse density and ultrastructure are changed in  $\alpha$ -neurexin double knockout mice. The structural deficits in adult  $\alpha$ -neurexin mutants suggest that chronically depressed neurotransmission may result in reduced dendritic arbors and possibly elimination of synapses.

Control of behavior and metabolism through the adrenergic system in the nematode  
*C. elegans*

Thomas Roeder and Mark Seifert

The importance of adrenergic signaling mediated through adrenaline and noradrenaline in vertebrates and through their invertebrate equivalents octopamine and tyramine has been assigned through specific drugs and numerous pharmacological studies. However, the analysis of conventional knockout mice has not been very conclusive because amine-synthesizing enzymes or a constellation of receptors are still functional after targeting a single gene, thus masking the expected phenotypes.

Here we report the analysis of behavioral and metabolic changes after impairment of tyraminerpic/octopaminergic neurotransmission in the soil nematode *Caenorhabditis elegans*. These animals showed an increased egg-laying rate, reduced activity, prolonged defecation cycles, and they store large amounts of fat although they do not enter the dauer stage. Behavioral and metabolic effects are controlled through two different branches in the intracellular signaling cascade downstream of the PLC-enzyme, the  $\text{Ca}^{2+}$ -phosphoinositide cascade (behavior) and tubby-pathway (metabolism). This tyraminerpic/octopaminergic system is an equivalent of the vertebrate adrenergic system controlling the animals' response to starvation and other stressful stimuli. Worms impaired either pre- or postsynaptically in tyraminerpic/octopaminergic signaling represent ideal models to study the pharmacology and molecular events underlying the most prevalent type of obesity, the diet induced obesity.

## **Lipid Messenger Signaling Dynamics Probed With Optical Tools: Endocannabinoid-Mediated Retrograde Signaling in the Hippocampus**

**Thomas Heinbockel<sup>1,2</sup>, Jun Zhao<sup>3</sup>, Sukumaran Muralidharan<sup>3</sup>,  
Joseph P.Y. Kao<sup>1,2,3</sup>, Bradley E. Alger<sup>1,2</sup>**

*<sup>1</sup>Dept. of Physiology, <sup>2</sup>Program in Neuroscience, University of Maryland School of Medicine, Baltimore, MD 21201, USA <sup>3</sup>Medical Biotechnology Center, University of Maryland Biotechnology Institute, Baltimore, MD, 21201, USA*

In the hippocampus, retrograde signaling can be initiated by briefly depolarizing CA1 pyramidal cells and is expressed as a reduction in GABA release from presynaptic interneurons (depolarization-induced suppression of inhibition, DSI). The retrograde messenger for DSI is an endocannabinoid (eCB) that targets presynaptic cannabinoid receptors (CB1R). Endocannabinoids can also be released by activation of group I mGluRs on the pyramidal cells. We have used the hippocampal endocannabinoid system as a model to address general questions about lipid signaling dynamics. We have applied whole-cell patch clamping,  $\text{Ca}^{2+}$  imaging (intracellular Fluo-3), and photolytic uncaging of photoprobes (caged glutamate and newly developed caged eCB, anandamide), to study retrograde signaling in rat organotypic hippocampal slice cultures. Anandamide is an endogenous ligand for CB1R. Real time release of eCBs was tested on spontaneous (s) IPSCs recorded from CA1 pyramidal cells.

Three different aspects of eCB signaling were explored: (1) Release of eCBs evoked by activation of mGluRs on CA1 pyramidal cells through photorelease of caged glutamate, (2) initiation of DSI by depolarization of the recorded pyramidal cell, and (3) direct activation of presynaptic CB1R through photorelease of caged anandamide. Under all three conditions, we observed a distinct reduction in sIPSC frequency. A sharp calcium transient accompanied the step depolarization, but not mGluR activation of the pyramidal cell. A specific CB1R antagonist, AM 251, blocked the anandamide effect establishing that uncaged anandamide did activate CB1Rs. The sIPSC reduction started in less than 1 sec after receptor activation or depolarization, and there was no pronounced temporal difference between the three means of activating CB1R. This suggests that synthesis and release of CBs from pyramidal cells is very fast, and a substantial delay in endocannabinoid signaling occurs downstream from CB1R activation.

*Supported by: PHS grants NS30219, DA14625 to B.E.A., GM56481 to J.P.Y.K., and University of Maryland School of Medicine Bressler Fund Award to T.H.*

## **Serotonin overproduction induces exogastrulation in both invertebrate and vertebrate embryos.**

Elena E. Voronezhskaya<sup>1</sup>, Marina Yu. Khabarova<sup>2</sup> and Leonid P. Nezlin<sup>1,3</sup>

<sup>1</sup>Institute of Developmental Biology, Rus. Ac. Sci., Moscow, Russia (lena\_vor@mail.ru);

<sup>2</sup>Tula State Pedagogical University, Tula, Russia;

<sup>3</sup>Department of Molecular Neurophysiology, University of Göttingen, Germany.

Serotonin (5-HT) is a major neurotransmitter in both vertebrate and invertebrate species which is involved in a wide variety of physiological and morphogenetic processes. 5-HT and 5-HT receptors have been demonstrated to exist in embryos starting from the one cell stage, and suggested to regulate cell cleavage, adhesiveness, migration, etc. Hypofunction of the 5-HT system is known to underlie many physiological, behavioral and developmental disorders, thus a drug induced 5-HT increase is a commonly used way of treatment in medicine. However, the developmental roles of 5-HT overproduction are not yet known.

We report that pharmacologically induced overproduction of 5-HT at the early stages of embryonic development results in exogastrulation in both freshwater snail *Lymnaea stagnalis* and cleaved frog *Xenopus laevis*. In both species, incubation of developing eggs in the solution of biochemical precursor of 5-HT, 5-hydroxy-L-tryptophan (5-HTP) in a defined time window between the one cell and early blastula stage induced the formation of exogastrula. Incubation in 5-HTP at the stages later than early blastula never resulted in exogastrulation. Development of experimental embryos was normal until the stage of late gastrula. At the time when control embryos became early trochophores, the 5-HTP treated embryos underwent exogastrulation. The effect was concentration dependent: 0% exogastrulae appeared in 0.1 mM and 100% in 1 mM 5-HTP (30% in *Xenopus*). In all cases, embryos that did not undergo exogastrulation developed and hatched normally.

Exogastrulae of *Lymnaea* had normal pattern of ectodermal ciliated areas, and survived for four days more. In contrast to exogastrulae induced by lithium (a widely accepted drug to induce exogastrulation in numerous organisms), 5-HTP induced exogastrulae exhibited normal development of ectoderm and no reduction of animal differentiation. Immunocytochemical analysis revealed overexpression of 5-HT in a specific set of blastomeres belonging to the molluscan cross in the animal hemisphere.

Pharmacological analysis showed that (i) the acting substance involved in this developmental malformation is 5-HT itself, and (ii) the effect is carried out via activation of intracellular 5-HT<sub>2</sub>-like receptors at certain pre-gastrulation stages. Thus, 5-HTP-induced exogastrulation was mimicked by amides of arachidonic acid with 5-HT (but not 5-HT itself), and 5-HT<sub>2</sub> receptor agonist, DOI. The effect of 5-HTP was blocked by the inhibitor of monoamine synthesis, 3-hydroxybenzylhydrazine (NSD-1015), and 5-HT receptor antagonists, mianserin, cyproheptadine and sulpiride.

Our data suggest that abnormal activation of intracellular 5-HT<sub>2</sub>-like receptors by elevated endogenous 5-HT at the early developmental stages triggers yet unknown mechanisms that later will disrupt adhesion of cellular layers at the late gastrula stage.

## RESTRICTED EXPRESSION OF NEUREXOPHILIN 3 AND SPECIFIC BEHAVIORAL DEFICITS IN KNOCKOUT MICE FAVOR A MODULATING ROLE IN SYNAPTIC TRANSMISSION

Piechotta, K.<sup>1</sup>, Beglopoulos, V.<sup>1,2</sup>, Montag-Sallaz, M.<sup>3</sup>, Montag, D.<sup>3</sup>, and Missler, M.<sup>1</sup>

<sup>1</sup>Center for Physiology, Georg-August-University, 37073 Göttingen, Germany

<sup>2</sup>Brigham and Women's Hospital, Harvard Medical School, Boston, MA, USA

<sup>3</sup>Neurogenetics Research Group, Leibniz Institute for Neurobiology, Magdeburg, Germany

Neurexophilins are neuropeptide-like glycoproteins that are only present in vertebrates. In mice, Nxph 1 & 3 have been identified as specific extracellular binding partners of  $\alpha$ -neurexins, synaptic cell-adhesion proteins involved in regulating neurotransmitter release. Here, we studied the Nxph3 distribution by analyzing its expression pattern in epitope-tagged knockin mice, and investigated their putative functional role in knockout animals. In Nxph3 knockin mice, a lacZ reporter gene fused to a nuclear localization signal is co-expressed with Nxph3 via a bicistronic entry site. In addition, the marker and selection cassettes together with exon2 are flanked by LoxP sites to allow conversion to the Nxph3 knockout in the presence of Cre recombinase.  $\beta$ -galactosidase staining in knockin mice revealed that Nxph3 expression is surprisingly restricted: Prominent labeling was mostly found in the deep cortical layers (especially layer 6b) and in cerebellar lobules 9 & 10. Additionally, transient Nxph3 expression was detected in Cajal-Retzius cells of the cortex and hippocampus during ontogenesis. Consistent with this limited expression, Nxph3 knockout mice are viable and fertile, and display no gross-anatomical changes of their brain structure: Quantifications of the thickness of neocortical layers, and analysis of the cell density in sublayer VIb on Nissl stained serial sections showed no significant structural differences between the genotypes. Similarly, immunohistochemistry revealed no differences using a variety of antibodies against synaptic markers, calcium-binding proteins and neuropeptides. Systematic behavioral analysis, however, demonstrated a specific deficiency in tests related to sensorimotor gating (reduced paired-pulse inhibition) and motor coordination (impaired rotarod performance), reflecting the very areas where Nxph3 is normally present. The highly restricted expression pattern together with a functional knockout phenotype but apparent lack of structural defects in absence of Nxph3 suggest a modulating role for Nxph3 in synaptic transmission, possibly mediated via their  $\alpha$ -neurexin receptors. - Supported by the SFB406 (DFG).

## **Allosteric modulation of presynaptic vesicle fusion explains potentiation of transmitter release by phorbol esters**

Xuelin Lou, Ralf Schneggenburger

AG Synaptic Dynamics & Modulation, Dept. of Membrane Biophysics, Max-Planck Institute for Biophysical Chemistry, 37077 Göttingen

Phorbol esters potentiate synaptic transmission by activating protein kinase C and/or the presynaptic vesicle priming factor, munc-13. This presynaptic signaling pathway is probably targeted during short-term enhancement of transmitter release, and by activation of presynaptic G-protein coupled receptors or neurotrophin receptors. We investigated the  $\text{Ca}^{2+}$ -dependent step(s) in transmitter release which are subject to potentiation by phorbol esters, using the calyx of Held as a model synapse.

Bath application of 1  $\mu\text{M}$  Phorbol-ester (PDBu) strongly potentiated EPSCs evoked by fiber stimulation ( $227 \pm 14$  % of baseline) and miniature EPSC frequency (from  $1.2 \pm 0.3$  to  $5.1 \pm 2.1$  Hz,  $n = 4$ ). In simultaneous pre- and postsynaptic recordings, small EPSCs ( $< 5$  nA) induced by short presynaptic voltage-clamp steps (1-2 ms to 0 mV) were strongly potentiated by PDBu ( $378 \pm 110$  %;  $n = 10$ ), whereas large EPSCs induced by prolonged presynaptic depolarization (30 ms to 0 mV) were potentiated to only  $135 \pm 9$  % of control. This indicates that PDBu increased the release probability without a strong increase in the size of the readily-releasable vesicle pool (RRP). Similarly, when transmitter release was induced by presynaptic  $\text{Ca}^{2+}$  uncaging, the EPSC responses to weak  $\text{Ca}^{2+}$  uncaging ( $[\text{Ca}^{2+}]_i$  steps of 2.5 - 5  $\mu\text{M}$ ) were strongly potentiated by PDBu ( $395 \pm 39$  %), whereas the potentiation was smaller ( $122 \pm 24$  %) for higher  $[\text{Ca}^{2+}]_i$  steps (9.5 - 12.5  $\mu\text{M}$ ). Thus, PDBu increased the apparent  $\text{Ca}^{2+}$  sensitivity of vesicle fusion concomitant with a reduction in the apparent cooperativity of  $\text{Ca}^{2+}$ .

We next asked how PDBu modulates the frequency of mEPSCs at low presynaptic  $[\text{Ca}^{2+}]_i$ . To do so, presynaptic calyces were perfused with strongly buffered  $\text{Ca}^{2+}$  solutions, with free  $[\text{Ca}^{2+}]$  in the range of 30 nM - 700 nM. The plot of transmitter release rate (obtained from mEPSC frequency) as a function of  $[\text{Ca}^{2+}]_i$  revealed that the  $\text{Ca}^{2+}$  cooperativity was strongly reduced close to the resting  $[\text{Ca}^{2+}]_i$  ( $\sim 1$ ), as compared to the classical high value ( $\sim 4$ ) found in the range of 2 - 8  $\mu\text{M}$   $[\text{Ca}^{2+}]_i$ . PDBu increased the frequency of mEPSCs at constant, low (30 - 700 nM) presynaptic  $[\text{Ca}^{2+}]_i$ . The strongly reduced  $\text{Ca}^{2+}$  cooperativity at low  $\text{Ca}^{2+}$  can be accounted for by a novel, allosteric model of  $\text{Ca}^{2+}$ -activation of vesicle fusion, in which low rates of vesicle fusion occur without bound  $\text{Ca}^{2+}$ , and in which increased occupancy of the  $\text{Ca}^{2+}$  sensor for vesicle fusion leads to enhanced vesicle fusion rates. PDBu acts by increasing the "willingness" of vesicle fusion, which explains the effects of PDBu on both spontaneous vesicle fusion, and on the apparent reduction in  $\text{Ca}^{2+}$  cooperativity. This identifies a novel mechanism, linking the rate of spontaneous vesicle fusion to its apparent  $\text{Ca}^{2+}$  sensitivity during presynaptic plasticity.

## Post-tetanic potentiation and its presynaptic $\text{Ca}^{2+}$ dependence at the calyx of Held

Natalya Korogod, Ralf Schneggenburger

MPI für biophysikalische Chemie, AG Synaptische Dynamik und Modulation, Göttingen

The calyx of Held is a glutamatergic excitatory synapse in the auditory brainstem pathway which reliably induces postsynaptic spikes in response to presynaptic firing frequencies up to a few hundred Hz. Here we show that brief trains of afferent high frequency stimulation (100 Hz for 1-8 s) induce post-tetanic potentiation of EPSCs at the calyx of Held synapse, in addition to the well-known depression of synaptic transmission during high frequency trains. During the peak of PTP, synaptic strength was increased about two-fold, and the decay of PTP proceeded over 10s of seconds to more than 1 minute, depending on the length of the induction train. PTP was accompanied by a decrease in paired-pulse ratio (EPSC2 / EPSC1). The frequency of spontaneous mEPSCs was increased more than 20-fold in a 10 s period following the induction train, but the mEPSC amplitude was unchanged. These findings indicate that PTP was presynaptic in origin. PTP was induced more easily in synapses from young rats (postnatal days, P4 - P7) as compared to an older age group (P8 - P10), suggesting that PTP is developmentally regulated, and might play a role during the developmental maturation of the calyx of Held.

To investigate the presynaptic  $\text{Ca}^{2+}$  requirements of PTP, we initially imaged presynaptic  $[\text{Ca}^{2+}]_i$  with fura-4F (100  $\mu\text{M}$ ) in paired pre- and postsynaptic recordings under presynaptic current clamp conditions. Surprisingly, PTP was absent under these conditions, but PTP recovered when the presynaptic patch pipette was retracted ( $n = 7$  cells). Thus, whole-cell recording of the presynaptic terminal reversibly suppressed PTP, either by leading to a reversible loss of a diffusable intracellular messenger, or by preventing the build-up of an intracellular messenger necessary for PTP. For imaging presynaptic  $[\text{Ca}^{2+}]_i$  during PTP, we pre-loaded calyces with 80 - 100  $\mu\text{M}$  fura-4F during a brief presynaptic whole-cell recording episode (60 - 90 s). After removal of the presynaptic pipette, PTP was reliably induced. We found that during 2 - 4 s trains at 100 Hz, the spatially averaged  $[\text{Ca}^{2+}]_i$  increased to 3 - 8  $\mu\text{M}$ . Following the train,  $[\text{Ca}^{2+}]_i$  decayed in two clearly distinct phases, with a fast decay component ( $\sim 200$  ms) followed by a much slower decay ( $\tau = 81 \pm 60$  s) of a residual  $[\text{Ca}^{2+}]_i$  with initial amplitude of  $\sim 200$  nM. Over different trials, the decay time constant of PTP correlated well with the decay of the slow phase of residual  $[\text{Ca}^{2+}]_i$  ( $n = 19$  trials, 5 cells). At the peak of PTP, the residual  $[\text{Ca}^{2+}]_i$  signal had an amplitude of only 60 nM over baseline  $[\text{Ca}^{2+}]_i$ . The surprisingly high efficacy of a small residual  $[\text{Ca}^{2+}]_i$  signal during PTP, and the sensitivity of PTP to presynaptic whole-cell recording suggest that other presynaptic intracellular messengers besides  $\text{Ca}^{2+}$  are involved in PTP. It will be interesting to test whether the cAMP/protein kinase A -pathway, or the protein kinase C / munc-13 pathway, which are both known to potentiate transmitter release, are involved in PTP.

## **Synaptic Ribbons are essential for synchronous auditory signaling**

**Darina Khimich,<sup>1</sup> Regis Nouvian,<sup>1</sup> Remy Pujol,<sup>2</sup> Susanne tom Dieck,<sup>3</sup> Michel Eybalin<sup>4</sup>,**

**Eckart Gundelfinger<sup>3</sup> and Tobias Moser<sup>1</sup>**

<sup>1</sup>Department of Otolaryngology, University of Goettingen, 37075 Goettingen, Germany

<sup>2</sup>Centre Régional d'Imagerie Cellulaire, Institut Universitaire de Recherche Clinique, 34093 Montpellier cedex 5, FRANCE

<sup>3</sup>Dept. of Neurochemistry and Molecular Biology, Leibniz Institute for Neurobiology, 39118 Magdeburg, Germany

<sup>4</sup>Institut des Neurosciences de Montpellier - INSERM U583, 34091 Montpellier cedex 5, FRANCE

Hearing relies on faithful synaptic transmission at the ribbon synapse of cochlear inner hair cells (IHCs). Here we investigated the role of synaptic ribbons in hearing by analyzing mouse mutants for the presynaptic protein Bassoon. Their IHCs lacked functional ribbons, showed halved  $\text{Ca}^{2+}$  current and defective fast exocytosis but robust sustained release. Large membrane profiles populated the mutant active zones, suggesting a defect of vesicle recycling from endosomes. The synaptic defect caused hearing impairment despite intact cochlear amplification. We conclude that the ribbon maintains the readily releasable pool of vesicles at the IHC active zone, which is essential for normal hearing.



*Drosophila* Glutamate Receptor Interacting Protein acts in the presynaptic endocytic pathway

Carolin Wichmann<sup>1</sup>, Laura E. Swan<sup>1</sup>, Robert Kittel<sup>1</sup>, Manuela Schmidt<sup>1</sup>, Dirk Wenzel<sup>2</sup>, Manfred Heckmann<sup>3</sup> and Stephan J. Sigrist<sup>1,#</sup>

1) European Neuroscience Institute, Max-Planck-Society, Waldweg 33, 37073 Göttingen (Germany)

2) Max-Planck-Institute for Biophysical Chemistry, Am Faßberg 11, 37077 Göttingen (Germany)

3) Physiologisches Institut, Albert-Ludwigs-Universität Freiburg, Hermann-Herder-Str. 7, 79104 Freiburg (Germany)

# corresponding author: ssigrist@gwdg.de

The Glutamate Receptor Interacting Protein (GRIP) has been suggested to participate in the synaptic trafficking of postsynaptic AMPA receptors using cell culture models. However, GRIP is widely expressed outside postsynaptic structures and in non-neuronal tissues as well, suggesting a generalized requirement for the protein. In fact, our recent genetic analysis demonstrated that *Drosophila* GRIP (Grip) acts as a key component of proper muscle guidance (Swan et al., 2004). Here, we provide evidence for Grip being functionally active within the presynaptic endocytic pathway of glutamatergic synapses. After genetic elimination of Grip, increased release probability was observed using two-electrode voltage clamp recordings. Simultaneously, atypical vesicles (70 to 250 nm diameter), suggestive of disturbed intracellular membrane trafficking, were observed within the presynaptic terminals using electron microscopy. In contrast, the readily-releasable pool of synaptic vesicles appeared unchanged after reducing Grip function. Consistent with a role of Grip in endosomal trafficking, FYVE-GFP and Rab5-GFP, both markers of early endosomes, are consistently up-regulated within the presynaptic terminal. We are now combining biochemical, cell biological and genetic analyses to mechanistically address the role of Grip within endosomal trafficking of synaptic vesicles and its connection to the regulation of synaptic vesicle release probability.

- Swan, LE, Wichmann, C, Prange, U, Schmid, A, Schmidt, M, Schwarz, T, Ponimaskin, E, Madeo, F, Vorbrüggen, G and Sigrist, SJ. A Glutamate Receptor-Interacting Protein Homolog organizes muscle guidance in *Drosophila*. *Genes & Development* 18(2), 223-237 (2004).

## ABSTRACT:

Laura E. Swan and Stephan J. Sigrist  
Neuroplasticity Group, European Neuroscience Institute,  
Max-Planck Society, Waldweg 33, 37073 Göttingen Germany

A Structure-function characterization of the Glutamate Receptor-Interacting Protein Grip.

The glutamate receptor-interacting protein GRIP is involved in many protein complexes and has functions in several different tissues over development, ranging from glutamate receptor trafficking [1, 2] to cell adhesion [3]. However, a coordinated understanding of the many potential interactions of the Grip molecule and their effect on Grip function has been lacking. We used the robust *Grip*<sup>-</sup> phenotype in *Drosophila* muscle guidance [4] as a basis to identify functional and regulatory domains in the Grip protein. DGrip, as many PDZ domain proteins, contains multiple PDZ domains arranged in tandem clusters. Yet far from being independent protein-protein interaction domains as was originally thought, interactions over PDZ domains have lately been demonstrated to be critically dependent on cooperative interactions from neighbouring PDZ domains [5]. Here, we identify regions necessary to mediate Grip-dependant muscle guidance. Furthermore, we identify a dominant active form of DGrip and characterize the molecular logic underlying Grip's function, indicating that Grip is a self-regulating molecule.

1. Dong, H., et al., *GRIP: a synaptic PDZ domain-containing protein that interacts with AMPA receptors*. Nature, 1997. **386**: p. 279-284.
2. Osten, P., et al., *Mutagenesis reveals a role for ABP/GRIP binding to GluR2 in synaptic surface accumulation of the AMPA receptor*. Neuron, 2000. **27**: p. 315-325.
3. Takamiya, K., et al., *A direct functional link between the multi-PDZ domain protein GRIP1 and the Fraser syndrome protein Fras1*. Nature Genetics, 2004. **36**: p. 172 - 177.
4. Swan, L.E., et al., *A glutamate receptor-interacting protein homolog organizes muscle guidance in Drosophila*. Genes Dev, 2004. **18**(2): p. 223-37.
5. Long, J., F., et al., *Supramodular structure and synergistic target binding of the N-terminal tandem PDZ domains of PSD-95*. J Mol Biol., 2003. **327**(1): p. 203-14.

## Neuronal Synthesis and Release of D-Serine to Activate NMDA Receptors

Elena Kartvelishvily, Livia Balan, Maria Schleper and Herman Wolosker

Dept of Biochemistry, B. Rappaport Faculty of Medicine, Technion-Israel Inst of Technology, Haifa 31096, Israel

High concentrations of D-serine occur in central nervous system where it may play an important role in excitatory neurotransmission. D-Serine levels in the brain are a third those of L-serine and it appears to be an endogenous co-agonist of a subtype of glutamate receptor referred to as NMDA receptor. D-serine is synthesized from L-serine by the serine racemase, an enzyme previously shown to be enriched in glia. We now investigated possible localization and synthesis of D-serine in neuronal cells using new antibodies for both serine racemase and D-serine. We observed significant synthesis of D-serine and expression of serine racemase in purified neuronal cultures of cortex, hippocampus, striatum and cerebellum. Levels of D-serine and serine racemase were comparable or higher to those in purified astrocyte cultures and the synthesis of D-serine required the presence of L-serine in culture media. Immunohistochemistry experiments confirmed the expression of serine racemase in neurons in rat cerebral cortex and hippocampus. D-serine immunoreactivity was also detected in neurons of rat brain, indicating that neuronal cells play a role in synthesizing D-serine *in vivo*. We found the release of D-Serine from cultured neurons to be elicited by agonists of several glutamate receptor subtypes. Depletion of endogenous D-serine in cortical cultures by the enzyme D-serine dehydratase was neuroprotective against NMDA-elicited cell death. Our data indicate that regulated release of endogenous neuronal D-serine plays a role in NMDA receptor activation, with implications for the regulation of glutamatergic neurotransmission.

## **Evidence for acetylcholinesterase as a moonlighting protein during grasshopper development**

Mario Naujock and Gerd Bicker

Physiologisches Institut, Abt. Zellbiologie, Tierärztliche Hochschule Hannover

Bischofsholer Damm 15/102, D-30173 Hannover

We examined the cellular expression of acetylcholinesterase (AChE) in the nervous system and in epidermal body structures during the complete embryonic development of the locust. The histochemical labelling was blocked by the enzyme inhibitors eserine and BW284c51, but not by iso-OMPA, showing that the staining reflects true AChE activity. The majority of the staining was localized on the cell surface, but in many cell bodies granular intracellular staining was also visible. Initially, mainly epidermal tissue structures are stained on the various body appendages. Then, the labelling appeared in outgrowing neurons of the central nervous system and in the nerves innervating the limbs and dorsal body wall. The latter staining was transient and originated in motoneurons of the ventral nerve cord. In a third phase, the somata of certain identified mechanosensory neurons start to express AChE activity, reflecting presumably cholinergic differentiation. Primary cultures of the ventral nerve cord at different stages revealed an increase of up to 83% AChE-positive somata at the end of embryogenesis. The histochemical study shows a developmental appearance of AChE in the CNS that largely precedes synaptogenesis suggesting other developmental functions.

Research on morphogenetic properties of vertebrate AChE has taken advantage of peptides, that have been isolated from snake venom and that bind to the peripheral anionic site of AChE. We are currently using the ligand fasciculin I to investigate effects on neurite outgrowth in cultured grasshopper neurons. A reduction in neurite growth and branching indicates that AChE is also involved in morphogenetic interactions during the development of an insect nervous system.

## Optical Measurements of Transmitter Release at the Calyx of Held

Alexander Groh and Thomas Kuner

The calyx of Held giant presynaptic terminal and its postsynaptic neuron, the principal cell of the medial nucleus of the trapezoid body (MNTB), serve as a model for central mammalian synapses. Simultaneous pre- and postsynaptic electrophysiological recordings provide access to the biophysics of synaptic transmission, however, the rate of neurotransmitter release needs to be inferred indirectly from the recorded excitatory postsynaptic currents (EPSCs). As yet, the only direct experimental readout of synaptic vesicle fusion in the calyx has been achieved with capacitance recordings, but these are sometimes difficult to interpret. Here, we employ a genetically encoded indicator of synaptic vesicle fusion to perform optical, non-invasive, direct recordings of transmitter release from the calyx terminal. SynaptopHluorin, a fusion protein of synaptobrevin with pHluorin (a pH-dependent variant of GFP), is quenched by intravesicular protons and increases fluorescence as the intravesicular pH equilibrates with the extracellular pH upon membrane fusion and neurotransmitter release. This highly sensitive method allows detection of single vesicle fusion events. Targeted expression of proteins in the calyx of Held is possible with viral gene transfer into projection neurons of the ventral cochlear nucleus (VCN) by stereotaxic delivery of recombinant SFV or Sindbis virions. Expressing synaptobrevin-EGFP in cells of the VCN revealed that, unexpectedly, this fusion protein did not get transported to the calyx but rather produced strong perinuclear fluorescence signals, possibly arising from synaptobrevin-EGFP accumulating in the endoplasmic reticulum or Golgi apparatus. However, other GFP fusions of synaptic vesicle proteins are trafficked to the calyx terminals efficiently. Hence, we used pHluorin fused to synaptotagmin (syntagpHluorin, construct provided by T. Ryan) and expressed it together with a fluorescent marker (mRFP1) to facilitate detection of infected neurons giving rise to calyx terminals. In hippocampal neurons, coexpression of syntagpHluorin and mRFP1, driven by two separate subgenomic promoters, was found in more than 70% of the neurons. However, in the MNTB only a minority of calyces contained both proteins. Application of high potassium solution resulted in an increase of calyceal syntagpHluorin-fluorescence, consistent with neurotransmitter release. In summary, we provide proof of principle that pHluorin is applicable as a sensor of neurotransmitter release in the calyx of Held. Further improvements will be necessary to harness the full potential of this approach in examining synaptic vesicle fusion at the calyx of Held.

## Disinhibition of GABAergic synapses might contribute to impaired hippocampal plasticity in M<sub>2</sub> muscarinic acetylcholine receptor knockout mice

Fang Zheng<sup>1</sup>, Thomas Seeger<sup>2</sup>, Jesus Gomeza<sup>3</sup>, Jürgen Wess<sup>3</sup>, Christian Alzheimer<sup>1</sup>

<sup>1</sup>*Dept. of Physiology, University of Kiel, 24098 Kiel, Germany,* <sup>2</sup>*Bundeswehr Institute of Pharmacology and Toxicology, Munich, Germany,* <sup>3</sup>*Laboratory of Bioorganic Chemistry, NIDDK, NIH, Bethesda, MD, USA.*

Muscarinic acetylcholine receptors are critically involved in the proper functioning of cognitive processes. In particular, muscarinic receptors located in the hippocampus are known to play a central role in promoting learning and memory. Long-term potentiation (LTP) at excitatory synapses of the hippocampus is a likely neurobiological substrate of learning and memory at the cellular level. Elucidating the principles of muscarinic modulation of LTP should thus offer insights into the neuronal mechanisms underlying the cholinergic facilitation of learning and memory processes. So far, however, the lack of specific agonists and antagonists for the five muscarinic receptor subtypes (M<sub>1</sub> - M<sub>5</sub>) expressed in hippocampus precluded a clear understanding of which of these receptors play a role in cholinergic modulation of LTP. In order to unravel the contribution of individual muscarinic receptor subtypes to hippocampal synaptic plasticity, we performed field potential and whole-cell recordings in the CA1 region of hippocampal slices prepared from wild-type (M<sub>2</sub><sup>+/+</sup>) and from M<sub>2</sub> receptor-deficient mice (M<sub>2</sub><sup>-/-</sup>).

Field-EPSP recordings from CA1 stratum radiatum demonstrated that synaptic plasticity induced by theta burst stimulation (TBS) differed profoundly between M<sub>2</sub><sup>+/+</sup> and M<sub>2</sub><sup>-/-</sup> hippocampi. In M<sub>2</sub><sup>+/+</sup> preparations, TBS produced reliably the characteristic sequence of the initial, partially declining short-term potentiation (STP) followed by stable LTP. In M<sub>2</sub><sup>-/-</sup> hippocampi, however, TBS failed to induce STP and produced significantly weaker LTP. Because the M<sub>2</sub> receptor-preferring antagonist, gallamine (20 µM), abrogated STP and significantly impaired LTP in M<sub>2</sub><sup>+/+</sup> hippocampi, we conclude that TBS induces STP and robust LTP only if M<sub>2</sub> receptors are concomitantly activated by endogenously released acetylcholine. Interestingly, the GABA<sub>A</sub> receptor antagonist, bicuculline, restored STP and significantly increased LTP in M<sub>2</sub><sup>-/-</sup> hippocampi. This suggested that M<sub>2</sub> receptors, presumably located on the terminals of GABAergic interneurons, promote synaptic plasticity by controlling the strength of GABAergic inhibition.

This concept was corroborated by whole-cell recordings of pharmacologically isolated IPSCs of CA1 pyramidal cells. The following observations indicated that M<sub>2</sub> receptor activation exerts a powerful inhibitory control over GABAergic synapses. (1) The genetic disruption of the M<sub>2</sub> receptor dramatically impaired the cholinergic suppression of IPSCs. (2) In M<sub>2</sub><sup>-/-</sup> hippocampi, paired-pulse inhibition of IPSCs was significantly reduced. (3) The strong depression of IPSCs during trains of stimuli was significantly alleviated in M<sub>2</sub><sup>-/-</sup> hippocampi. We hence propose that the impaired synaptic plasticity of M<sub>2</sub><sup>-/-</sup> hippocampi results, at least partially, from a disinhibition of GABA release, keeping the depolarization of pyramidal cells below the critical range for short- and long-term changes in synaptic efficacy.

*Supported by the SFB 391 (TP A9) and the BMVg.*

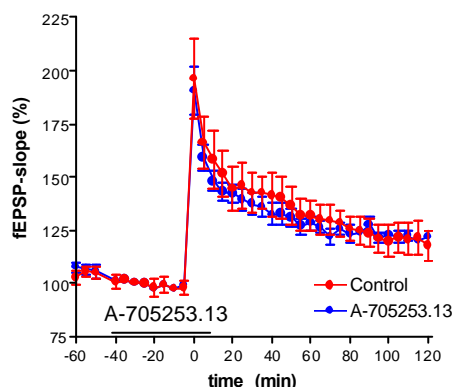
## Activation of calpains is not a prerequisite of long-term potentiation (LTP)

Volker Nimmrich, Achim Möller, Gerhard Gross, Karsten Wicke  
Neuroscience Discovery Research, Abbott, Ludwigshafen, Germany

LTP is considered to play a crucial role in mechanisms of learning and memory. It has been shown that different types of LTP, including theta burst-induced forms, were blocked by inhibition of calpain, a calcium-dependent cysteine protease<sup>1,2</sup>. Furthermore, calpain serves to cleave proteins of the LTP cascade such as protein kinase C $\zeta$  or the NMDA receptor. These and other data lead to the generally accepted assumption that activation of calpain is necessary for LTP formation<sup>3</sup>.

We have recently described a highly specific inhibitor of calpain, A-705253<sup>4</sup>, which does not affect the multifunctional proteasome complex. This inhibitor is effective at concentrations as low as 10 nM in myocardial tissue<sup>5</sup>. Here we show that even under ten-fold higher concentrations (100 nM) theta burst-induced long-term potentiation in hippocampal slices is not impaired. We also did not detect any effect of the inhibitor on baseline synaptic transmission and short-time potentiation.

In light of these data, we suggest that the calpain hypothesis of LTP needs to be reconsidered. We conclude that inhibitors used in previous studies might have impaired LTP by affecting mechanisms other than calpain. Alternatively, the calpain cascade may only be activated during certain forms of LTP.



<sup>1</sup> del Cerro et al. (1990), Brain Res, 530:91-95

<sup>2</sup> Denny et al. (1990), Brain Res, 534:317-320

<sup>3</sup> Tomimatsu et al. (2002), Life Sci, 72:355-361

<sup>4</sup> Lubisch et al. (2003), J Med Chem, 46:2404-2412

<sup>5</sup> Neuhof et al. (2003), Biol Chem, 384:1597-1603

## Bassoon and Piccolo interact with members of the CtBP protein family

Wilko D. Altmann<sup>1</sup>, Anna Fejtova<sup>1</sup>, Susanne tom Dieck<sup>2</sup>, Britta Qualmann<sup>1</sup>,  
Michael M. Kessels<sup>1</sup>, Stefan H. Gerber<sup>3</sup>, Craig C. Garner<sup>4</sup>, Thomas C. Südhof<sup>5</sup>,  
Johann H. Brandstätter<sup>2</sup>, Eckart D. Gundelfinger<sup>1</sup>

<sup>1</sup>Leibniz Institute for Neurobiology, D-39118 Magdeburg, Germany

<sup>2</sup>Max Planck Institute for Brain Research, D-60528 Frankfurt/Main, Germany

<sup>3</sup>Heidelberg University Medical Center, D-69115 Heidelberg, Germany

<sup>4</sup>The Center for Basic Neuroscience, University of Texas Southwestern Medical Center, Dallas, TX 75390, USA

<sup>5</sup>Department of Psychiatry and Behavioral Science, Stanford University, Palo Alto, CA 94305-5485, USA

Signalling at chemical synapses is mediated by regulated neurotransmitter release from presynaptic nerve terminals. This regulated release is restricted to a specific region of the presynaptic plasma membrane, the so called active zone. Core components of the cytomatrix assembled at the active zone (CAZ) are thought to define and organize this site. Among these components are Bassoon and Piccolo, two 420 kDa and 560 kDa-large scaffolding proteins of the CAZ. They are related proteins specifically localized at the active zone of excitatory and inhibitory synapses. To date only one protein could be identified as an interacting protein for Bassoon. Therefore a yeast two-hybrid screen was initiated to identify other potential binding partners for this protein.

Using a fragment encoding the second and third coiled-coil domain of Bassoon we could identify the C-terminal binding protein 1/Brefeldin A-ADP-ribosylation substrate of 50 kDa (CtBP1/ BARS-50) as a potential binding partner. CtBP1/BARS-50 was independently identified as a nuclear transcriptional co-repressor with the ability to bind to several transcription factors, and in addition as a cytoplasmic, Golgi-associated protein involved in the Golgi structure maintenance. Another member of the CtBP protein family is the nuclear transcriptional co-repressor CtBP2, which synaptically localized retina specific isoform RIBEYE is thought to be the core component of ribbon structures of ribbon synapses. We could show by yeast two-hybrid that CtBP2/RIBEYE interacts with Bassoon as well. Using various deletion constructs we were able to pinpoint the interacting site of CtBPs to a region C-terminal of the second coiled-coil domain of Bassoon. Piccolo is able to interact with the CtBP members via a corresponding region, which shares high homology with Bassoon. The interaction could be confirmed by coimmunoprecipitation and MitoTargeting assays. Furthermore we have assessed the subcellular distribution of CtBP1/BARS-50 in rat primary hippocampal neurons using immunofluorescence analysis. These experiments revealed that a fraction of CtBP1/BARS-50 co-localizes at synaptic contact sites with Piccolo. To answer the question, whether this synaptic localization is Bassoon and/or Piccolo dependent, we used cultured primary hippocampal neurons of *Bsn* mutant, *Pclo* mutant and *Bsn-Pclo* double mutant mice for a detailed immunofluorescence analysis. As expected from the yeast two-hybrid data the synaptic staining of CtBP1/BARS-50 remains undisturbed in single mutants, but is completely vanished in double mutants suggesting that the presence of at least one of the two large CAZ proteins is essential for transportation and/or anchoring of CtBP1/BARS-50 to the synapse.

This work was supported by the DFG to EDG, BQ and MMK. AF was supported by a fellowship from the Swiss National Foundation



**Activity-dependent spinogenesis:  
(When) do new spines carry functional synapses?**

Nägerl UV<sup>\*</sup>, Koestinger G<sup>†</sup>, Anderson JC<sup>†</sup>, Martin KAC<sup>†</sup>, Bonhoeffer T<sup>\*</sup>

<sup>\*</sup>Max-Planck-Institute of Neurobiology, Martinsried, Germany

<sup>†</sup>Institute for Neuroinformatics, University of Zürich and ETH Zürich,  
Switzerland

The demonstration in the past of growing spines and filopodia on CA1 hippocampal neurons after LTP-inducing electrical stimulation has raised the intriguing possibility that a synaptic network may acutely and selectively build new synapses in response to plasticity inducing synaptic stimulation. However, while the connection between activity-dependent spinogenesis and synaptogenesis has been postulated, the experimental proof of this hypothesis has been notably absent.

We set out to address this issue by imaging living neurons in hippocampal slice cultures with time-lapse 2-photon microscopy and correlating these images with electron microscopic (EM)-based reconstructions of the newly born spines and filopodia. To this end neurons were briefly co-filled via a patch pipette with calcein for 2-photon fluorescence imaging and with biocytin to produce an electron-dense label. Growth of new processes from CA1 dendrites was induced by local theta-burst electrical stimulation. Images were acquired every 30 min to backdate the age of the new spines relative to the timepoint of fixation. In the end slices were fixed and processed for EM. Correlated light and serial reconstructions were made.

We could readily induce the growth of new spines. None of the ten spines examined and completely reconstructed showed any of the structures associated with functional synapses such as a post-synaptic density, a synaptic cleft or a bouton associated with a synaptic specialization. Interestingly, however, the majority of new spines were in contact with boutons, which formed synapses with other, unlabeled targets. Our analysis has so far focused on young spines (typically 1 to 8 hours old) and it may well be that the maturation process to a full-blown synapse requires more time. We are therefore currently extending the duration of the experiments which will enable us to analyze also older spines.

## **Immunohistochemical characterization of activity-dependent spinogenesis in hippocampal neurons**

Tobisch N, Nägerl UV, Bonhoeffer T, Cambridge S  
Max-Planck-Institute of Neurobiology, Martinsried, Germany

Previous experiments demonstrated that induction of LTP leads to the formation of new spines. However, an open question is if and when the newly grown spines are contacted by a presynaptic terminal and form a functional synapse. To address this, we used antibody staining for synapsin, a marker of mature presynaptic terminals to look for evidence that newly born spines are functionally innervated. Using two-photon time-lapse microscopy, we imaged dendritic spines of CA1 pyramidal GFP-positive neurons in organotypic slice cultures of Thy1-GFP mice. Selective growth of dendritic spines was induced by extracellular local stimulation with a theta-burst protocol. We acquired high-resolution image stacks of dendritic stretches within the vicinity of the stimulating electrode every 30 min for up to six hours. This allowed us to narrowly confine the age of the newly born spines prior to fixation. Subsequently, the slices were processed for immunohistochemistry. Our results show 80 -85 % of all mature spines colocalize with distinct synapsin puncta, indicating that this approach can be used to mark presynaptic terminals in three-dimensional tissue cultures. So far, about a dozen of newly grown spines could be reidentified in the fixed and antibody stained preparation. A considerable fraction of these spines colocalizes with synapsin staining. This indicates that newly generated spines are often in the immediate vicinity of presynaptic terminals. Further analysis will allow us to establish a close link between activity-dependent spinogenesis and synaptogenesis, thereby elucidating their temporal relationship.

## **Bidirectional activity-dependent morphological plasticity in hippocampal neurons**

Nägerl UV, Tobisch N, Cambridge S, Bonhoeffer T  
Max-Planck-Institute of Neurobiology, Martinsried, Germany

Dendritic spines on pyramidal neurons receive the vast majority of excitatory input and are considered electro-biochemical processing units, integrating and compartmentalizing synaptic input. Following synaptic plasticity, spines can undergo morphological plasticity, which possibly forms the structural basis for long-term changes in neuronal circuitry. Here, we demonstrate that spines on CA1 pyramidal neurons from organotypic slice cultures show bidirectional activity-dependent morphological plasticity. Using two-photon time-lapse microscopy, we observed that low-frequency stimulation induced NMDA receptor-dependent spine retractions, whereas theta-burst stimulation led to the formation of new spines. Moreover, without stimulation the number of spine retractions was on the same order of magnitude as the stimulus-induced spine gain or loss. Finally, we found that the ability of neurons to eliminate spines in an activity-dependent manner depended on developmental age. Taken together, our data show that hippocampal neurons can undergo bidirectional morphological plasticity; spines are formed and eliminated in an activity-dependent way.

## Characterization of a central synapse in the local bend circuit of the leech

Jutta Kretzberg<sup>1,2</sup>, Antonia Marin-Burgin<sup>1</sup>, William B. Kristan<sup>1</sup>

<sup>1</sup>: UCSD, Neurobiology, 9500 Gilman Dr., La Jolla, CA 92093, USA

<sup>2</sup>: Universität Oldenburg, Institut für Biologie und Umweltwissenschaften,  
Postfach 2503, 26111 Oldenburg, Germany

email: jutta.kretzberg@uni-oldenburg.de

When a leech is touched locally it responds by bending its body away from the stimulus. This behavior is carried out by a network consisting of only 4 sensory cells,  $\approx 20$  interneurons and  $\approx 16$  motoneurons. All of these neurons have been individually characterized and can be found in every midbody ganglion of any individual. The simplicity and identifiability of this network makes the local bend of the leech a very suitable system to study questions of neuroethology and coding.

We have characterized the synapse between the interneuron 115 (green in fig) and motoneuron 4 (red in fig) which is a ventral excitor of the longitudinal muscles. Both of these neurons are part of the circuits for the local bend and for swimming. They are connected with a relatively weak inhibitory chemical synapse. If the presynaptic cell is depolarized  $\approx 20$  mV by current injection, the postsynaptic cell hyperpolarizes  $\approx 1$  mV. The synaptic strength depends on the preceding activity of the presynaptic interneuron: after strong presynaptic stimulation the subsequent postsynaptic responses are reduced.

When recorded in the soma, both neurons have small spike amplitudes ( $< 5$  mV). Presumably because there are few voltage-sensitive channels in the soma and the spike initiation zone is distant from the soma. As in other invertebrate nervous systems, generating spikes distant from the soma is a common property of leech neurons. Because of this, synaptic transmission is often at least partly independent of spikes. For instance, chemical synapses between motoneurons of the local bend circuit show graded synaptic transmission in the absence of spikes [Granzow et al., J. Neurosci., 1985].

In contrast, we found that the inhibitory synapse between interneuron 115 and motoneuron 4 depends exclusively on spikes, even though there are no IPSPs visible in response to individual presynaptic spikes. We showed this by replacing normal saline with  $\text{Na}^+$ -free solution. In this condition, the resting potentials of the cells hyperpolarize and firing stops. In contrast to the connection between motoneurons, there is no synaptic transmission between the interneuron and the motoneuron when no spikes are generated (fig, right). The effect is reversible by washing with normal saline. Hence, information transmission between interneurons and motoneurons works qualitatively different than in connections between motoneurons, because it depends exclusively on spikes.

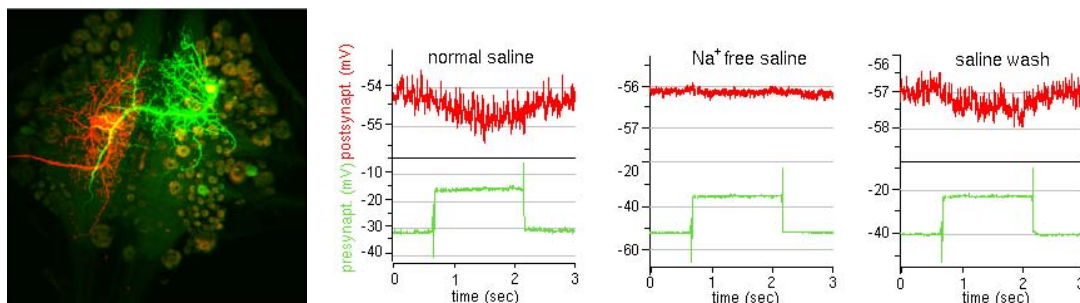


Figure 1: **Left:** Cell fills of postsynaptic motoneuron 4 (red – Rhodamine Dextran) and presynaptic interneuron 115 (green – Alexa Fluor 488). **Right:** Postsynaptic response (red) to presynaptic current injection (green) in normal saline and  $\text{Na}^+$ -free saline which blocks spikes.

## **Illuminating Vesicle Priming with live-cell TIRF microscopy**

*Yizhar O.<sup>1</sup>, Matti U.<sup>2</sup>, Becherer U.<sup>2</sup>, Rettig J.<sup>2</sup> and Ashery U.<sup>1</sup>*

*<sup>1</sup>Department of Neurobiochemistry, Tel Aviv University, Israel; <sup>2</sup> Physiologisches Institut, Saarland University, Homburg, Germany.*

Vesicles in neurons and neurosecretory cells undergo multiple steps of maturation in order to become fusion competent and eventually undergo exocytosis when intracellular calcium is elevated. The first requirement for fusion-competence is morphological docking of the vesicle at the plasma membrane. A docked vesicle is then primed for exocytosis by a series of molecular steps. A key step in vesicle priming is the formation of the SNARE complex from monomers of Syntaxin and SNAP25 on the plasma membrane and VAMP (Synaptobrevin) on the vesicle membrane. Formation of this complex has been shown to be a crucial step in neurotransmitter release and as such it is regulated by numerous protein-protein interactions. Previous studies have used biochemical and electrophysiological methods to investigate the effect of SNARE interactions on exocytosis. It was suggested that the degree of “release-readiness” of different vesicle populations is defined by the molecular machinery that regulates docking and priming. We have used total internal reflection fluorescence microscopy (TIRF) to track single large dense-core vesicles (LDCV's) inside living chromaffin cells and analyze their mobility. Using a custom-written software we have obtained trajectories of individual vesicles within control cells and cells overexpressing the inhibitory protein Tomosyn. Tomosyn was shown to form SNARE complexes with Syntaxin and SNAP25 and inhibit the association of Synaptobrevin with these two proteins. We have previously shown that Tomosyn dramatically reduces the amount of fusion-competent vesicles in chromaffin cells but does not affect the amount of docked vesicles. In the present study we examined whether the inhibition of priming is correlated with changes in vesicle mobility. We observe that in control cells, 50% of the vesicles detected near the plasma membrane are virtually immobile. However, when tomosyn is overexpressed, the size of this pool is reduced by 50% and overall vesicle mobility is increased. This is the first evidence for a correlation between vesicle priming and mobility. Using the TIRF system, we will be able to better understand the molecular mechanisms underlying vesicle docking, priming and fusion.

## A NEW PLATFORM TO STUDY THE MOLECULAR MECHANISMS OF EXOCYTOSIS

Aviv Mezer<sup>\*,§</sup>, Esther Nachliel<sup>\*</sup>, Menachem Gutman<sup>\*</sup> and Uri Ashery<sup>#,§</sup>

<sup>\*</sup>The Laser Laboratory for Fast Reactions in Biology, Department of Biochemistry. The George S Wise Faculty of Life Sciences, Tel Aviv University, Tel Aviv, Israel.

<sup>#</sup>Department of Neurobiochemistry, The George S Wise Faculty of Life Sciences, Tel Aviv University, Tel Aviv, Israel.

§ Correspondence should be addressed to A.V ([aviv@hemi.tau.ac.il](mailto:aviv@hemi.tau.ac.il)) or U.A. ([uria@post.tau.ac.il](mailto:uria@post.tau.ac.il)).

### ABSTRACT

The exocytotic process in neurons and neuroendocrine cells consists of a sequence of reactions between well-defined proteins. In the present study, we have created for the first time a comprehensive kinetic model describing the dynamics of interactions between key synaptic proteins that are associated with exocytosis. The interactions between the synaptic proteins were transformed into differential rate equations that, upon their integration over time, reconstructed the experimental signal. This model can perfectly reconstruct the kinetics of exocytosis, the calcium-dependent priming and fusion processes and the effects of genetic manipulation of synaptic proteins. The model suggests that fusion occurs from two parallel pathways and assigns precise, non-identical, synaptic protein complexes to the two pathways. In addition, it provides a unique opportunity to study the dynamics of intermediate protein-complexes during the fusion process, a possibility that is hidden in most experimental systems. We thus developed a novel approach that allows detailed characterization of the temporal relationship between synaptic protein complexes. This model provides an excellent platform for prediction and quantification of the effects of protein manipulations on exocytosis and opens new avenues for experimental investigation of exocytosis.

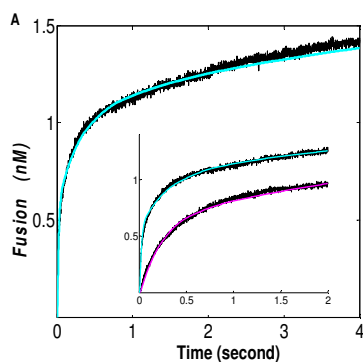


**Figure: Reconstruction of the secretion dynamics from WT and synaptotagmin-I knock-out (SytIKO) chromaffin cells.** The main frame presents the measured capacitance of a chromaffin cell following a flash photolysis experiment (black line) and their reconstruction by the model (cyan line). The inset depicts the experimental results (black lines) and simulations (WT cells cyan and SytIKO cells Magenta lines) at a higher time resolution.

The *Drosophila* nc82 antigen: gene structure, expression analysis, and localization at presynaptic active zones

Dhananjay Wagh, Tobias Rasse, Alois Hofbauer, Isabell Schwenkert, Heike Dürrbeck, Sigrid Buchner, Marie-Christine Dabauvalle, Stefan Sigrist and Erich Buchner

The monoclonal antibody (MAB) nc82 was identified in the screen of a large hybridoma library against *Drosophila* head homogenate for antibodies binding selectively to synaptic neuropil of the brain. Confocal immunohistochemistry localizes the protein at the active zones of presumably all synaptic terminals. The fact that in each synaptic terminal only the small spots of the active zones are labeled makes this antibody especially useful for confocal immunofluorescence microscopy of *Drosophila* brain wholemounts because the resulting neuropil stacks are more transparent compared to stainings with antibodies that bind e.g. to synaptic vesicles. On Western blots MAB nc82 recognizes two protein isoforms of about 190 and 180 kDa. We have identified the gene coding for this active zone protein employing 2D-gel electrophoresis and MALDI-TOF mass spectrometry. RT-PCR sequencing using RNA from larvae and adults in comparison with cDNA fragments and genomic DNA from *Drosophila melanogaster*, *D. pseudoobscura*, and *Anopheles*, identifies at least two alternatively spliced transcripts and reveals a complex gene structure. Northern Blots of head mRNA identifies transcripts at 10, 6, and 4 kb. In-situ hybridization and antibody staining reveal expression of the gene in presumably all neurons of late embryonic, larval and adult stages. Homologies with vertebrate proteins and mutational strategies to reveal the function of the encoded proteins will be discussed.

**Poster Subject Area #PSA22:  
Neuropeptides and neuromodulation**

- [#299A](#) S. Berger and B. Grünewald, Berlin  
*Octopamine induces Ca<sup>2+</sup>-signals in cultured antennal lobe neurons of the honeybee*
- [#300A](#) I. Abidin, E. Weiler, UT. Eysel and T. Mittmann, Bochum  
*Excitatory neurotransmitter release at synapses in the visual cortex of BDNF heterozygote mice*
- [#301A](#) D. Gocht and R. Heinrich, Göttingen  
*Postactivation inhibition of spontaneously active serotonin-releasing neurosecretory cells in the medicinal leech*
- [#302A](#) M. Kron, M. Mörschel, W. Zhang and M. Dutschmann, Göttingen  
*Developmental changes of brain derived neurotrophic factor (BDNF) evoked modulation of synaptic activity within the Kölliker-Fuse Nucleus (KF)*
- [#303A](#) M. Kron, T. Manzke and M. Dutschmann, Göttingen  
*Changes in the expression pattern of BDNF and tyrosine kinase receptor B (trkB) during postnatal maturation of brainstem respiratory nuclei.*
- [#304A](#) M. Dutschmann, T. Manzke, M. Mörschel, U. Günther and DW. Richter, Göttingen  
*Systemic activation of 5-HT<sub>1A</sub> receptors compensates opioid induced respiratory depression.*
- [#305A](#) T. Manzke, M. Dutschmann and DW. Richter, Göttingen  
*Effects of 5-HT<sub>2A</sub> and 5-HT<sub>2B</sub> receptor isoform activation on spontaneous breathing of anaesthetised rat*
- [#306A](#) T. Manzke, M. Kron, M. Dutschmann and DW. Richter, Göttingen  
*Expression patterns of 5-HT<sub>1A</sub>, 2A, 2B, 4(a) and 7 receptor isoforms in the ponto-medullary respiratory network of rat*
- [#307A](#) S. Titz, A. Lewen and U. Misgeld, Heidelberg  
*Acid shifts in response to NH<sub>4</sub><sup>+</sup> application provide a measure for KCC2 activity in single neurons*
- [#308A](#) N. Rogalla and S. Kreissl, Konstanz  
*G-proteins mediating DF2 and Proctolin induced enhancement of muscle contracture in *Idotea emarginata**
- [#298B](#) S. Schöneich, PA. Stevenson and K. Schildberger, Leipzig  
*Differential octopaminergic modulation of giant descending antennal mechanosensory interneurons in the cricket brain*



- [#299B](#) D. Fritsche, N. Rogalla, B. Philipp and S. Kreissl, Konstanz  
*The myotropic neuropeptide allatostatin elevates cGMP-concentration via an inhibition of the phosphodiesterase in the extensor muscle fibres of the isopod Idotea emarginata*
- [#300B](#) E. Buhl, P.A. Stevenson, J. Rillich and K. Schildberger, Leipzig  
*Cholinergic activation of flight motor activity in the locust, Schistocerca gregaria*
- [#301B](#) T. Brigadski, R. Kolarow, M. Hartmann and V. Lessmann, Mainz  
*Synaptic targeting and time course of secretion of neurotrophins from hippocampal neurons.*
- [#302B](#) S. Hofer and U. Homberg, Marburg  
*Evidence for a role of orcokinin-related peptides in the circadian clock of the cockroach Leucophaea maderae*
- [#303B](#) S. Soehler, S. Neupert, R. Predel, H. Agricola, S. Meola, R. Nichols and M. Stengl, Marburg, Jena, College Station (USA) and Michigan (USA)  
*Are FMRFamide-related peptides involved in the circadian coupling pathway of the cockroach Leucophaea maderae?*
- [#304B](#) N-L. Schneider and M. Stengl, Marburg  
*Pigment-dispersing factor and GABA synchronize insect circadian clock cells*
- [#305B](#) C. Talke, H. Schneider, H.A. Braun and K. Voigt, Marburg  
*Noradrenergic alpha-1 receptor mediated modulation of thermo-sensitive neurons in the rat hypothalamic paraventricular and supraoptic nuclei*
- [#306B](#) S. Klein, A. Jurkevich and R. Grossmann, Neustadt and Vilnius (LT)  
*Co-localization of arginine vasotocin and galanin immunoreactivity in the chicken brain*
- [#307B](#) S. Karg, L. Torner, J. Winkler, G. Kuhn and ID. Neumann, Regensburg and Göteborg (S)  
*Chronic stress effects on hippocampal neurogenesis are prevented by Prolactin administration*
- [#308B](#) M. Feldkaemper, R. Schippert and F. Schaeffel, Tübingen  
*Visual control of gene expression in retina and sclera in chick eyes with intact or sectioned optic nerves.*

## Octopamine induces $\text{Ca}^{2+}$ -signals in cultured antennal lobe neurons of the honeybee

S. Berger and B. Grünewald

Neurobiologie, Freie Universität Berlin, Institut für Biologie, Königin-Luise-Str. 28/30,  
14195 Berlin, Germany  
email: sandberge@web.de

The primary olfactory neuropil in insects are the antennal lobes. In the honeybee *apis mellifera* the antennal lobes and the mushroom bodies are involved in the formation of an olfactory memory.

From *in vivo* experiments it is known, that octopamine is released by neurons as a primary transmitter that mediates the rewarding function of the unconditioned stimulus during classical olf. conditioning.

Octopamine as other biogenic amines acts as a neuromodulator, it induces synaptic plasticity by activating second messenger pathways.

Intracellular  $\text{Ca}^{2+}$ -signals are one important second messenger pathway that may be induced by biogenic amine receptor activation in insects.

In order to understand the cellular physiological consequences of octopamine-induced  $\text{Ca}^{2+}$ -signals in cultured antennal lobe neurons from the honeybee brain, pupal antennal lobe cells are taken in primary neuron cultures.

24h after dissociation, cells were loaded with Fura-2-AM (6.5 $\mu\text{M}$ ) for 1 hr and fluorescence was measured at excitation wavelengths of 340 and 380 nm. At a frequency of 60 frames per minute  $\text{Ca}^{2+}$ -signals were recorded stable for at least 2-3 hr.

Pressure applications of octopamine (concentration 100nM to 100 $\mu\text{M}$ , pulse duration 20s) induced a transient elevation of the intracellular  $\text{Ca}^{2+}$ -concentration. That increase differs from cell to cell reaching its maximum within 5s. It remains at that level for as long as octopamine is applied. After ceasing to apply octopamine the concentration decreases but does not reach its original value within 60s.

If the cell is perfused with  $\text{Ca}^{2+}$ -free extracellular solution a rise of the concentration of  $\text{Ca}^{2+}$  is induced, which leads to the assumption, that  $\text{Ca}^{2+}$  is released out of intracellular stores. These  $\text{Ca}^{2+}$ -signals are blocked by bath application of the octopamine antagonist mianserine (500  $\mu\text{M}$ ).

In some cells the mianserine block was reversible.

At present we examine the dependency of the octopamine-induced  $\text{Ca}^{2+}$ -signals to the concentration of octopamine.

Preliminary results indicate the existence of two different octopamine receptors on antennal lobe neurons.

This study showed for the first time that octopamine induces  $\text{Ca}^{2+}$ -signals in native insect neurons. Thus  $\text{Ca}^{2+}$ -dependent pathways probably participate during the neuromodulatory actions of octopamine. *Supported by the DFG SFB515/C5.*

## **Excitatory neurotransmitter release at synapses in the visual cortex of BDNF heterozygote mice**

Abidin I<sup>\*#</sup>, Weiler E<sup>\*</sup>, Eysel UT<sup>\*</sup>, Mittmann T<sup>\*</sup>

<sup>\*</sup>Department of Neurophysiology, Faculty of Medicine, Ruhr-University Bochum, D-44780 Bochum, Germany

<sup>#</sup>International Graduate School of Neuroscience (IGSN), Ruhr-University Bochum, D-44780 Bochum, Germany

[abidin@neurop.ruhr-uni-bochum.de](mailto:abidin@neurop.ruhr-uni-bochum.de)

Brain derived neurotrophic factor (BDNF) is expressed in the developing and mature mammalian central nervous system. It binds to TrkB receptors and triggers a signaling pathway, which leads to activation of Phospholipase C (PLC), Mitogen Activated Kinase (MAPK) and phosphatidylinositol-3-OH kinase (PI3K). BDNF is involved in axonal and dendritic growth and synapse formation. BDNF is also reported to mediate fast synaptic transmission and plasticity. The effects of BDNF are specific for each brain area and synapse type. In the present study we characterized the glutamatergic neurotransmission in the visual cortex of BDNF heterozygote mice, and we investigated the functional contribution of the pre- or postsynaptic site to the observed effects.

We used 21-27 days old mice, which partially lack the BDNF coding gene (heterozygous mice, HT, n=19). Age matched wild type littermates served as controls (n=20). First we showed that the expression of BDNF is nearly %50 percent reduced in the heterozygous mice by using ELISA technique. Postsynaptic currents were recorded from layer II/III pyramidal neurons of the visual cortex by using the whole-cell patch clamp method. We analyzed miniature excitatory postsynaptic currents (mEPSCs). Furthermore, paired pulse modulation (PPM) and repetitive stimulation of afferent fibers in cortical layer IV was recorded to analyze evoked EPSC signals in the transgenic cortex. The frequency of mEPSCs was decreased ( $p=0.019$ ) in the visual cortex of HT mice (n=9) when compared to wild type tissue (n=9), whereas the amplitude of mEPSCs did not differ the two experimental groups. The ratio of paired pulse stimulations was significantly higher at inter stimulus intervals of 20 ms, 35 ms and 50 ms in HT animals (n=13) compared to wild type controls (n=8) ( $p=0.037$ ,  $p=0.03$  and  $p<0.001$  for 20, 35 and 50 ms respectively). In HT animals synaptic fatigue was significantly stronger expressed. However, rise time and decay tau values of eEPSCs were similar between the two groups.

These findings indicate that a reduced level of BDNF modulates the excitatory neurotransmission in the neocortex. Furthermore, these differences can be mainly attributed to functional changes of the presynapse.

This study was supported by the IGSN and DFG (SBF 509, C4)

## **“Postactivation inhibition” of spontaneously active serotonin-releasing neurosecretory cells in the medicinal leech.**

**Daniela Gocht and Ralf Heinrich**

**Dept. of Neurobiology, Berliner Str. 28, 37073 Göttingen, Germany**

Levels of biogenic amines and the activity of neurosecretory neurons releasing them have been correlated with behavioral states like wakefulness, arousal, depression and social status.

Serotonin has been demonstrated to initiate and orchestrate feeding behaviors of the medicinal leech, *Hirudo medicinalis* by simultaneously acting on both central nervous control circuits and peripheral tissues like muscles and glands. Each ganglion of the ventral nerve cord contains a pair of large Retzius cells whose axons enter the lateral roots, branch repeatedly and project to various peripheral organs. The Retzius cells contain about half of the total ganglionic serotonin and store even larger quantities in their peripheral endings. Their serotonin content correlates with the state of satiation and is thought to be causative for the initiation of feeding-related behaviors. The Retzius cells of leeches share a number of physiological characteristics with neurosecretory neurons from both other invertebrates (e.g. serotonergic, octopaminergic and CCH-containing cells in crustaceans) and vertebrates (e.g. serotonergic neurons of midline raphe nuclei, dopaminergic neurons in the retina and substantia nigra). They spontaneously fire at slow rates, generate large overshooting action potentials with prominent afterhyperpolarizations and respond to periods of high-frequency firing with a “postactivation inhibition” during which no action potentials are generated and synaptic input is selectively altered. This activity-dependent inhibition could be caused by autoreceptors for the amine released by the neuron or may alternatively rely on intrinsic mechanisms independent of synaptic release.

Leech Retzius cells were stained with neutral red and recorded from in isolated ventral nerve cords. Spontaneous firing frequencies under these conditions ranged from 0.2 to 4.0 Hz. Current injections into spontaneously active Retzius cells increase their rates of firing to up to 20 Hz depending on the amount of current injected. This activation is followed by a pronounced afterhyperpolarization and a period of up to 18 sec in duration during which no action potentials are generated. The duration of the period of suppressed spike generation is directly related to both the magnitude and the duration of current injection during the activation period and may thus depend on the number of spikes generated. This, together with the observation that bath application of serotonin inhibits spontaneous firing of Retzius cells, pointed suggested a mechanism for the “postactivation inhibition” mediated by the synaptic release of serotonin during periods of high activity. However, “postactivation inhibition” persisted under conditions that prevent the synaptic release of serotonin (e.g. in  $\text{Ca}^{2+}$ -free saline, and in serotonin-depleted nerve cords), indicating that its mechanism may be independent of transmitter release. In addition, the duration of the “postactivation inhibition” period was found to be inversely related to the spontaneous firing frequency of a particular Retzius cell, allowing more active cells to resume firing after shorter periods of inhibition. Initial studies suggest that a  $\text{Na}^+/\text{K}^+$ -ATPase may contribute to this mechanism.

Although it is presently not clear whether and how the Retzius cells’ intrinsic firing frequencies and their differential responses to periods of high activity may be connected to a particular behavioral state of the leech, the mechanism underlying “postactivation inhibition” may be common to neurosecretory neurons in general, since it has also been demonstrated in other species.

**Developmental changes of brain derived neurotrophic factor (BDNF) evoked modulation of synaptic activity within the Kölliker-Fuse Nucleus (KF).** Kron M, Mörschel M, Zhang W, Dutschmann M. *Dept. of Physiology, University of Göttingen, Humboldtallee 23, 37073 Göttingen*

BDNF was attributed a role as neurotrophine involved in regulating neuronal cell proliferation and survival. Meanwhile there is growing evidence that BDNF might have additional functions as neuromodulator mediating short time effects on neuronal excitability and plasticity. The role of BDNF acting via tyrosine kinase receptor B (trkB) in respiratory control is yet not well understood. Recent publications showed that BDNF k.o. mice die due to severe breathing disorders after birth, implicating an essential role for the development and function of the central pattern generator of breathing. Furthermore it could be revealed that BDNF-signalling might be involved in the mediation of long term facilitation of phrenic motor outputs following intermitted hypoxia in mature rats. These two results are reflecting the changing view regarding the role of BDNF in central nervous system. In the present study we investigated a putative function of BDNF as neuromodulator during postnatal development of the KF, a key area of the respiratory pattern generator.

On the cellular level we investigated the effects of direct application of BDNF (picospritzer) on neurones recorded in the whole cell patch configuration (voltage clamp  $-70$  mV) in transversal slice preparations of the pons containing the KF. Local application of BDNF yield heterogeneous results in neonatal slice preparations (P8-13). In 11 of 20 cells recorded in the KF area we detected no obvious effects on frequency and amplitude of spontaneous postsynaptic currents (PSCs) following application of BDNF. In 7 cells we observed a mild increase in frequency of PSCs and only 2 cells showed a short latency (2-3s) volley of PSCs after local BDNF application. In contrast, at later developmental stages (P18-20) we have seen pronounced short latency volleys of PSCs in neurones recorded. At the functional network level, microinjections of BDNF (40nl, 200ng/ml) into the KF of a *in situ* perfused brainstem preparation of juvenile rat (P20-28, n=10) caused dependent on the injection site: transient apnoea (n=5), tachypnoea (n=3) or apneusis (-> pathological prolongation of the inspiratory phase, n=2). Injections of glutamate at the same loci evoked the same modulations of respiratory activity, while vehicle injections showed no effect. The same experimental approach showed that BDNF injection into the neonatal KF (P5-8) never evoked respiratory modulation, but glutamate injections were effective (n=5). At later postnatal stages (P12-15) BDNF injection partially evoked respiratory modulation, but the strength of the modulation was never comparable to glutamate evoked effects at the same loci (n=4).

We suggest that BDNF might have dual functions during the postnatal maturation of KF neurones. During the early stages of postnatal development BDNF might act as neurotrophine, but has no direct effect on membrane conductance. In contrast, at later stages BDNF exerts functions as neuromodulator with obvious effects on neuronal excitability.

*founded by DFG (SFB 406/C12)*

**Changes in the expression pattern of BDNF and tyrosine kinase receptor B (trkB) during postnatal maturation of brainstem respiratory nuclei.** Miriam Kron, Till Manzke, Mathias Dutschmann; *Dept. of Physiology, University of Göttingen, Humboldtallee 23, 37073 Göttingen*

BDNF (brain derived neurotrophic factor) is implicated in cell survival and maturation of neuronal networks by acting on trk (tyrosine kinase) receptors. The importance of BDNF for stabilizing respiratory function becomes apparent in knock out models which suffer from severe respiratory dysfunctions and die shortly after birth. The expression pattern of BDNF and trkB during postnatal maturation in the respiratory network has not been analysed. Thus, we employed immunohistochemical methods to investigate the expression patterns of BDNF and trkB during different postnatal stages (P0, P6, P11, P23) with a special reference to brainstem nuclei important for respiratory control. This included the preBöttinger complex (PBC) and the pontine Kölliker Fuse nucleus (KF) as key regions of the central pattern generator for breathing and the nucleus of the solitary tract (NTS), the main termination field of viscerosensory afferents of the airways.

We could demonstrate that BDNF and trkB had an ubiquitous expression pattern in the respiratory

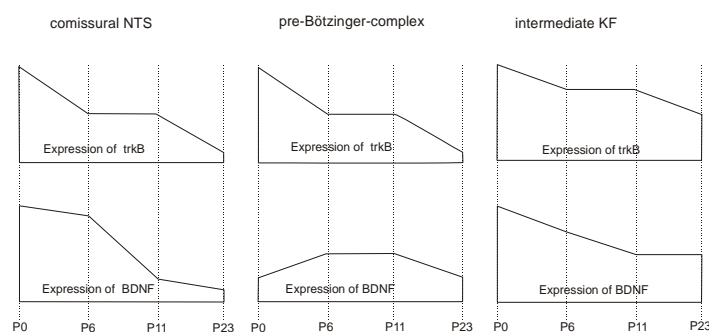


**Fig. 1:** Illustrates the relative changes in the strength and density in the expression of BDNF and trkB in selected nuclei of the autonomic brainstem during different stages of postnatal maturation.

network during early postnatal stages. Later during development the expression significantly decreased. Nevertheless, developmental changes in the expression pattern had specific features for some of the autonomic brainstem nuclei. The NTS showed a continuous decrease in both BDNF- and trkB-expression over postnatal development (see Fig. 1). In contrast, the PBC showed a remarkably low expression of BDNF at P0,

compared to other brain areas (see Fig.1). Later the expression increased and plateaued at P6 and P11 and decreased again at P23. In contrast, expression of trkB was high at P0 and progressively decreased during the postnatal maturation. In the KF we observed a parallel decrease of BDNF- and trkB-expression. Interestingly, at P23 the KF maintained the highest expression levels for both BDNF and trkB in comparison to other autonomic brain areas (see Fig.1), implicating a potential function of BDNF-signalling after maturation. Together with electrophysiological data (see abstract Kron et al. same session) the developmental changes in the expression pattern suggest a potential switch in the physiological role of BDNF. During early postnatal stages BDNF might serve as "classic" neurotrophine controlling neuronal survival and differentiation. In the mature brainstem and in particular in the KF, BDNF might exert a role as neuromodulator mediating direct effects on the excitability of synapses.

*founded by DFG (SFB 406/C12)*

**Systemic activation of 5-HT<sub>1A</sub> receptors compensates opioid induced respiratory depression.** Dutschmann M, Manzke T, Mörschel M, Günther U, Richter DW. Dept. of Physiology, University of Göttingen, Humboldtallee 23, 37073 Göttingen

We have demonstrated that opioid evoked depression can be reliably compensated by stimulating the 5-HT<sub>4(a)</sub> receptor (Manzke *et al.* 2003). The proposed mechanism is convergent 5-HT<sub>4(a)</sub> receptor induced compensatory activation of adenylate cyclase after negative signaling of by  $\mu$ -opioid ( $\mu$ -OR) receptors. (see Fig.1). However, opioid induced depression of respiration can also be treated with 5-HT<sub>1A</sub> receptor activation (Sahibzada N. *et al.* 2000), which exerts a negative effect on adenylate cyclase. However, 8-OH-DPAT the standard agonist for 5-HT<sub>1A</sub> receptors is also a partial agonist for

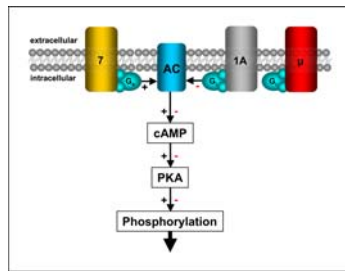


**Fig. 1** illustrates the signalling pathways of the 5-HT-1A and 7 receptor isoforms and their convergence onto the  $\mu$ -OR.

5-HT<sub>7</sub> receptor. The purpose of the study was to separate the putative actions of 8-OH-DPAT on both receptor types.

Systemic application (i.v., n=5) of 8-OH-DPAT (100 $\mu$ g/kg) increased respiratory minute volume (RMV) from 58.2  $\pm$  8.4 to 109.3 $\pm$ 9.2 ml ( $p \leq 0.01$ ), which could be blocked again by a subsequent injection of the 5-HT<sub>1A</sub> receptor antagonist WAY-100635 (1mg/kg, n=3). In the untreated animal, injection of WAY did not have any significant effect on baseline breathing, although a subsequent injection of 8-OH-DPAT did no longer exert stimulatory effects (RMV: 75.1 $\pm$ 7.0

vs. 65.0 $\pm$ 6.5 ml, n.s.). In contrast, after injection of 5-HT<sub>7</sub> antagonist SB 269970 systemic application of 8-OH-DPAT still increased RMV from 62.9 $\pm$ 17.0 to 97.3 $\pm$ 24.5 ( $p \leq 0.05$ ). Our results suggest that the pharmacological effects of 8-OH-DPAT are mediated via 5-HT<sub>1A</sub> receptors. Due to its excitatory effects on breathing activity, we furthermore tested if 8-OH-DPAT recovers opioid evoked depression also in vivo. In our experimental set up (n=6), we subsequently applied fentanyl ( $\mu$ -OR agonist, 10 $\mu$ g/kg) and 8-OH DPAT. Injection of fentanyl led to apnoea (RMV: 68.2 $\pm$ 6.3 vs. 0.0 $\pm$ 0.0 ml,  $p < 0.001$ ), but 2-3 min. after i.v. application of 8-OH-DPAT breathing recovered (RMV: 21.2 $\pm$ 4.1ml,  $p < 0.001$ ). Later RMV returned almost to baseline (RMV 59.7 $\pm$ 2.5ml,  $p < 0.001$ ).

In conclusion, we confirmed that activation of 5HT-1A receptors is a powerful tool to prevent opioid induced respiratory depression. This effect does not seem to result from 8-OH-DPAT mediated effects on Gs coupled 5-HT<sub>7</sub> receptors. As 5-HT<sub>1A</sub> receptors utilise the same signaling cascade as  $\mu$ -OR and inhibit the adenylate cyclase, the rescue phenomena is hardly to be explained by a simple molecular mechanism. We believe that a network analysis is required to investigate if there is a specific subpopulation of inhibitory respiratory interneurons that is inhibited by 8-OH DPAT potentially leading to a disinhibition and/or reconfiguration of the neuronal circuits controlling breathing. Preliminary experiments revealed that local application of either 8-OH-DPAT or fentanyl reduced the firing frequency (-16.4 and -23.1% respectively) of respiratory neurons (n=28), but co-application of both drugs did not exert any inhibitory effects on neuronal discharge.

**Literature:** Sahibzada N. *et al.*: J. Pharmacol. 292, 704-13, 2000  
Manzke T, *et al.* (Science 301. 226-229, 2003)

**Effects of 5-HT<sub>2A</sub> and 5-HT<sub>2B</sub> receptor isoform activation on spontaneous breathing of anaesthetised rat.** Till Manzke, Mathias Dutschmann, Diethelm W. Richter; *Dept. of Physiology, University of Göttingen, Humboldtallee 23, 37073 Göttingen*

Immunohistochemical studies and RT-PCR analyses demonstrated that 5-HT<sub>2A</sub> and 2B receptor isoforms are expressed in neurones of the ponto-medullary respiratory network (*see abstract Manzke et al. – same session*). Both receptor isoforms utilise a Gq mediated signalling cascade leading to activation of phospholipase C and IP<sub>3</sub>/DAG pathways. This signal pathway predicts an excitatory action of 5-HT<sub>2A</sub>, 2B agonists on respiration (*see Fig. 1*) as previously verified on the cellular level (Lalley et al. 1995). Our question was whether the effects can be utilised to treat opioid-induced depression of breathing when agonists are given systemically.

In the present study, we investigated the effects of i.v. application of agonists and antagonists for the 5-HT<sub>2A</sub> ( $\alpha$ -methyl-5-HT, Ketanserin) and 5-HT<sub>2B</sub> (BW 723C86, LY 272015) receptors on spontaneous breathing activity in anaesthetised rats (pentobarbital, 60 mg/kg). Then we tested if these agonists are suitable to also recover opioid-induced respiratory depression.

Systemic application of  $\alpha$ -methyl-5HT (100  $\mu$ g/kg) initially caused a transient respiratory depression as seen by a decrease in respiratory minute volume (RMV) from  $80.8 \pm 9.2$  to  $18.4 \pm 8.4$  ml ( $p < 0.01$ ).

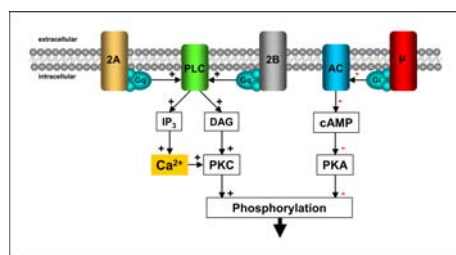


**Fig.1** illustrates the signalling transduction pathways of the 5HT-2A and 2B receptor isoforms. and their potential secondary convergence on the  $\mu$ -OR pathways

This depression was accompanied by a pronounced increase in mean arterial pressure (MAP:  $76.7 \pm 3.9$  vs.  $110.3 \pm 10.3$  mmHg,  $p < 0.05$ ). Approximately two min after injection, RMV was still suppressed ( $44.4 \pm 19.7$  ml), while MAP slowly returned to baseline values ( $78.3 \pm 8.3$  mmHg). Later on, RMV recovered ( $75.2 \pm 13.6$  ml), while MAP remained depressed ( $54.3 \pm 4.7$  mmHg,  $p < 0.05$ ) and a hypotonia persisted. Injection of Ketanserin (1 mg/kg) caused only an insignificant transient respiratory depression and there was

also only a mild decrease in MAP ( $83.3 \pm 7.6$  vs.  $68.0 \pm 11.5$  mmHg). Injection of the 5-HT<sub>2B</sub> agonist BW 723C86 (1 mg/kg) together with the antagonist LY 272015 (1 mg/kg) caused neither transient nor longer lasting changes of breathing and MAP. As control for the transient effect, we injected saline which caused no effect. In addition we tested if 5-HT<sub>2A</sub> and 2B receptor agonists recover opioid-induced respiratory depression. However, i.v. injection of  $\alpha$ -methyl-5-HT or BW 723C86 had no effects.

We suggest that systemic activation of 5-HT<sub>2A</sub> or 2B receptors does not exert an excitatory effect on breathing. The transient depressive effects after systemic drug application were most likely associated with the pressor responses known to have strong inhibitory influence on respiration.

**Literature:** Lalley PM, Bischoff AM, Schwarzacher SW, Richter DW. (1995) 5-HT<sub>2</sub> receptor-controlled modulation of medullary respiratory neurones in the cat. *J Physiol* 487(3). 653-61



**Expression patterns of 5-HT1A, 2A, 2B, 4(a) and 7 receptor isoforms in the ponto-medullary respiratory network of rat.**

Manzke T, Kron M, Dutschmann M, Richter DW; Dept. of Neuro- and Sensory Physiology, University of Göttingen, Humboldtallee 23, 37073 Göttingen

Experimental data demonstrated that systemic application of agonists for the 5-HT<sub>4</sub>(a) (see Manzke et al. 2003) and 1A (see abstract Dutschmann et al. same session) receptor isoforms stimulated breathing activity and recovered opioid-induced respiratory depression. In contrast, activation of 5-HT<sub>2A</sub>, 2B, and 7 receptor isoforms had no significant effect on breathing and failed to recover pharmacologically evoked respiratory depressions (see abstract Manzke et al. same session). The heterogeneous results yield after manipulation of specific 5-HT-receptor isoforms in physiological experiments, might be due to spatially distinct distributions of 5-HT receptor isoforms. In the present study we analysed the specific expression patterns within the ponto-medullary respiratory network.

We performed immunohistochemistry on brainstem transversal slices (40 µm, cervical cord – midbrain level superior colliculus) with antibodies directed against 5-HT<sub>1A</sub> (Chemicon), 2A (Santa Cruz), 2B, 4(a) and 7 (all custom made) receptor isoforms. The distribution of labelled cells within the ponto-medullary respiratory network was plotted using a neuroLucida system and documented on photomicrographs.

Analysis revealed that all 5-HT receptor isoforms are expressed in the respiratory column comprising the medullary ventral respiratory group (VRG), including the preBötzinger complex (preBöt), the retrofacial nucleus (RTN), as well as the pontine A5 cell group and Kölliker-Fuse nucleus (KF). Comparative analysis of the expression pattern yield a particular strong labelling for 5-HT<sub>1A</sub>, 2A, and 7 receptor isoforms in essential parts of the respiratory network like the preBöt and KF. The remaining serotonin receptor isoforms 4(a) and 2B in comparison showed a less dense expression in these area.

We suggest that although specific 5-HT receptor isoforms potentially have more physiological relevance compared to others this is not simply reflected by distinct features of their expression pattern in the respiratory network. To receive more detailed information multiple labelling experiments for additional receptor types (e.g. µ-OR, GABA, Glycine) are required to assign the 5-HT receptor expression to specific neuronal populations of the respiratory network (supported by the DFG, SFB 406/C2).

**Literature:** Manzke T, et al., Science 301, 226-229, 2003

**Acid shifts in response to  $\text{NH}_4^+$  application provide a measure for KCC2 activity**  
**in single neurons**

S. Titz, A. Lewen, U. Misgeld

Institut für Physiologie und Pathophysiologie und Interdisziplinäres Zentrum für Neurowissenschaften, Universität  
Heidelberg, Im Neuenheimer Feld 326, 69120 Heidelberg, Germany

We have shown previously that the  $\text{Cl}^-$  extruding neuron-specific  $\text{K}^+$ - $\text{Cl}^-$  co-transporter KCC2 which establishes hyperpolarizing inhibition, mediates  $\text{NH}_4^+$  uptake through binding of the ion at the  $\text{K}^+$  site (Liu et al. 2003).  $\text{NH}_4^+$  applied to a cell initially induces an increase in  $\text{pH}_i$  since  $\text{NH}_3$  permeates rapidly the membrane until  $[\text{NH}_3]_i$  rises to equal  $[\text{NH}_3]_o$ . Provided there is a pathway,  $\text{NH}_4^+$  will subsequently enter the cell and dissociate into  $\text{NH}_3 + \text{H}^+$ . The amplitude of the resulting acid shift can be used to evaluate  $\text{NH}_4^+$  flux across the membrane (Marcaggi and Coles, 2000) and, hence, to evaluate cation-chloride co-transport provided other pathways for  $\text{NH}_4^+$  to enter the cell are excluded.

Here we show now that  $\text{NH}_4^+$  uptake induced acid shifts can be used to detect KCC2 activity in single neurons. Application of  $\text{NH}_4^+$  (5 mM, 30 s) to hippocampal neurons cultured for 42 d induced a strong acidosis ( $0.59 \pm 0.05$ ,  $n = 29$ ). Bumetanide, in a concentration (1  $\mu\text{M}$ ) sufficient to block the  $[\text{Cl}^-]_i$  accumulating  $\text{Na}^+$ - $\text{K}^+$ - $2\text{Cl}^-$  co-transporter NKCC1 (Russell, 2000), did not alter the  $\text{NH}_4^+$  induced acidosis ( $107 \pm 3\%$  of control  $\Delta\text{pH}_i$ ,  $n = 10$ ). A high concentration of bumetanide (100  $\mu\text{M}$ ), which also inhibits KCC, reduced the  $\text{NH}_4^+$  induced acidosis (to  $57 \pm 5\%$  of control  $\Delta\text{pH}_i$ ,  $n = 96$ ). Inhibition of cation-chloride co-transport by 100  $\mu\text{M}$  furosemide reduced the  $\text{NH}_4^+$  induced acidosis more strongly (to  $33 \pm 2\%$  of control  $\Delta\text{pH}_i$ ,  $n = 125$ ).  $\text{NH}_4^+$  uptake could be blocked competitively by  $\text{K}^+$  with an apparent inhibitory constant,  $K'_i$  of 3 mM.  $\text{Ba}^{2+}$ -sensitive, inwardly rectifying  $\text{K}^+$  channels did not provide a pathway for  $\text{NH}_4^+$  entry (1 mM  $\text{Ba}^{2+}$ ,  $85 \pm 2\%$  of  $\Delta\text{pH}_i$  control,  $n = 29$ ).

This pharmacological and biophysical profile indicates that  $\text{NH}_4^+$  transport in cultured hippocampal neurons is achieved by KCC2. The advantage of this assay is that it can be used to determine KCC2 co-transport rate in single neurons and is independent from the actual driving force of the transporter.

*Supported by the SFB 488 / D-9*

## **G-proteins mediating DF<sub>2</sub> and Proctolin induced enhancement of muscle contracture in *Idotea emarginata***

**Nicole Rogalla and Sabine Kreissl**

Department of Biology, University of Konstanz, D-78457 Konstanz, Germany

e-mail: nicole.brenscheidt@uni-konstanz.de

The neuropeptide proctolin and the FMRFamide DF<sub>2</sub> are present in the nervous system of the marine isopode *Idotea emarginata*. They augment muscle contractions of extensor muscles through pre- and postsynaptic mechanisms. Proctolin increases the inward current through L-type-Ca<sup>2+</sup> channels and closes voltage-independent K<sup>+</sup> channels (Rathmayer et al., 2002) and DF<sub>2</sub> augments postsynaptic inward currents in voltage-clamped fibres (Weiss et al., 2003). Consequently, application of proctolin or DF<sub>2</sub>, respectively should depolarise the membrane potential of muscle fibres. In simultaneous recordings of membrane potential and contracture in single fibre preparations proctolin (10<sup>-6</sup> M) increases contractures without increasing depolarisations induced by high (30 mM) K<sup>+</sup>, whereas DF<sub>2</sub> (10<sup>-7</sup> M) induces a depolarisation of these fibres. This suggests that proctolin activates additional outward currents. Blocking Ca<sup>2+</sup>-activated K<sup>+</sup> channels (K<sub>Ca</sub>) with the specific blocker iberiotoxin (10<sup>-7</sup> M) increases membrane resistance after applying proctolin but not in controls suggesting that K<sub>Ca</sub> channels are recruited by proctolin. However, DF<sub>2</sub> had no effect on these channels.

Blocking of G<sub>s</sub>-proteins with the specific blocker NF449 (10<sup>-4</sup> M) prevented the potentiation of K<sup>+</sup>-induced contractures by DF<sub>2</sub>. We thus conclude that DF<sub>2</sub> binds to a G<sub>s</sub>-protein coupled receptor and therefore might directly activate sarcolemmal Ca<sup>2+</sup> channels without an activation of Ca<sup>2+</sup>-dependent K<sup>+</sup> channels.

The augmentation of contractions by proctolin is mediated by the activation of PKC because applying the cell permeable specific PKC-inhibitor BIM-1 (10<sup>-8</sup> M) prevented the augmentation of contractures elicited by high (30 mM) K<sup>+</sup> and activation of PKC by the specific PKC-activator PMA mimics the effect on muscle contractions by proctolin (Phillipp et al., 2004). Likewise the recruitment of iberiotoxin sensitive K<sub>Ca</sub> channels could be prevented by the PKC-inhibitor. The specific G<sub>i</sub>-protein-blocker GP Antagonist-2A (10<sup>-5</sup> M) prevented the increasing effect on K<sup>+</sup>-induced contractures. Therefore we assume that proctolin activates PKC via a G-protein-coupled receptor with a q<sub>i</sub>-subunit. The resulting enhancement of calcium influx is counteracted by the recruitment of iberiotoxin sensitive K<sub>Ca</sub> channels, which maintains contractions graded.

(supported by DFG, grants Ra 113/8-4, Ra 113/9-2)

Philipp, B., Rogalla, N. and Kreissl, S1 (submitted)

Rathmayer, W., Erxleben, C., Djokaj, S., Gaydukov, A., Kreissl, S., und Weiss, T. (2002)

In: The Crustacean Nervous System / Konrad Wiese (ed.), 2-19 Springer Verlag: Berlin, Heidelberg, New York

Weiss, T., Kreissl, S., und Rathmayer, W. (2003) Eur.J.Neurosci., 17, 239-248

# Differential octopaminergic modulation of giant descending antennal mechanosensory interneurons in the cricket brain

Stefan Schöneich, Paul A. Stevenson & Klaus Schildberger

Institut für Zoologie, Universität Leipzig, Liebigstraße 18, 04103 Leipzig, Germany

We are investigating the neurochemical control of descending brain interneurons in the cricket (*Gryllus bimaculatus* De Geer). We show that two of these interneurons receive suprathreshold, monosynaptic, inputs from antennal mechanoreceptors. Both branch extensively in antennal mechanosensory neuropil of the brain, and each has a contralaterally descending axon that conducts action potentials at 4-5 m/s as far as the metathoracic ganglion. They differ mainly in that one (**A**) has arborization on only one side of the metathoracic ganglion, whereas the other (**B**) has bilateral projections (Fig.1). The responsiveness of neuron **A** to mechanical antennal stimulation is considerably enhanced in a dose dependent (5-100 mM) and reversible fashion by the tissue-permeable octopamine agonist chlordimeform (CDM). Contrasting this, CDM has either no effect (10 mM) or reversibly abolishes (50 mM) the response of interneuron **B** (Fig.2). We speculate that such differential modulation of physiologically and anatomically related cells could form the basis of experience-dependent octopaminergic modulation of the behavioural response to sensory commands.

Fig.1

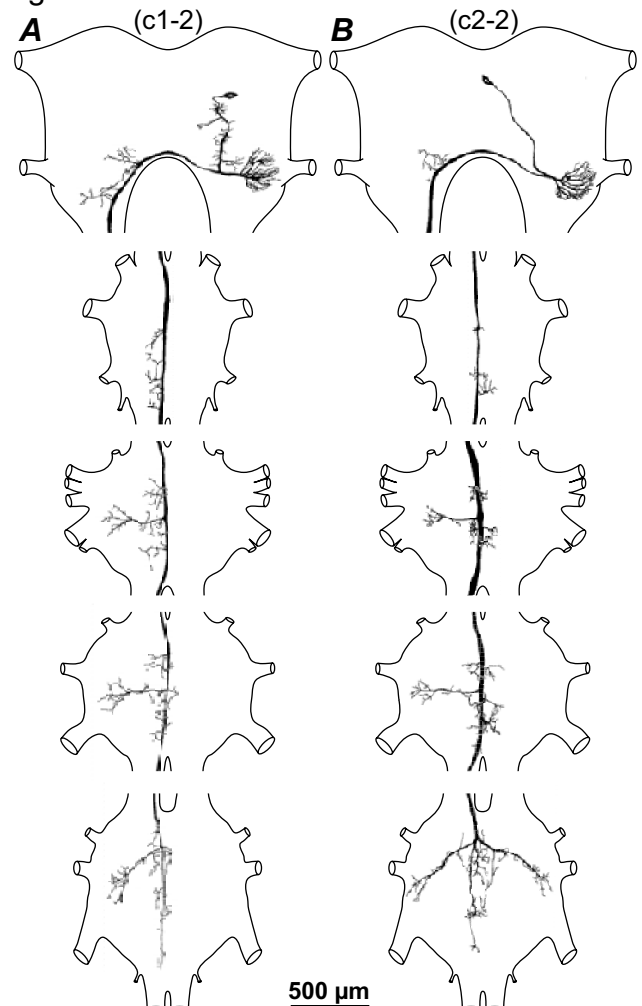
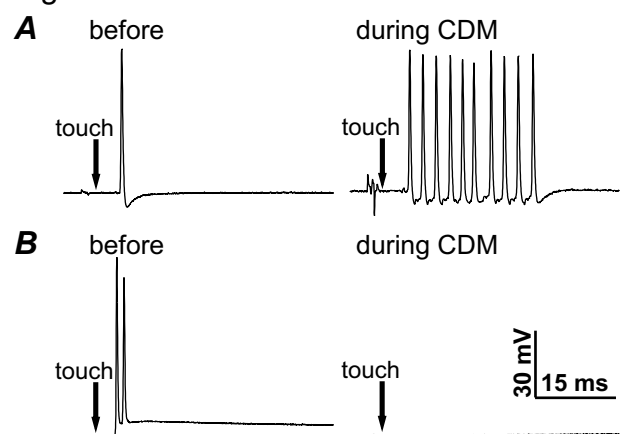


Fig.2



**The myotropic neuropeptide allatostatin elevates cGMP-concentration via an inhibition of the phosphodiesterase in the extensor muscle fibres of the isopod *Idotea emarginata***

**Daniel Fritsche, Nicole Rogalla, Berit Philipp and Sabine Kreissl**

Department of Biology, University of Konstanz, D-78457 Konstanz, Germany

e-mail: Daniel.fritsche@uni-konstanz.de

The neuropeptide allatostatin (Dip-AST 7), present in the nervous system of the marine isopode *Idotea emarginata*, modulates skeletal muscle contractions through pre and postsynaptic mechanisms. It reduces transmitter release from the presynaptic motoneuron and decreases muscle tension elicited by direct depolarisations in current clamped fibres (Kreissl et al., 1999).

In an effort to identify the postsynaptic signal transduction mechanism associated with the reduction of muscle tensions by this neuropeptide, levels of the cyclic nucleotides 3'-5'-cyclic adenosine monophosphate (cAMP) and 3'-5'-cyclic guanosine monophosphate (cGMP) were measured in the extensor muscle fibres of the isopod *Idotea emarginata*.

Allatostatin ( $10^{-6}$  M) did not change the intracellular cAMP-concentration of the muscle fibres. The intracellular cGMP-concentration was significantly elevated by allatostatin. 8-Bromo-cGMP, a membrane permeable cGMP-analogue, mimics the effect of allatostatin by reducing the contractures significantly, compared to control.

To further investigate if the allatostatin-induced effect on muscle contracture and on the intracellular cGMP-concentration is either mediated by the activation of a cGMP-specific guanylate cyclase or by an inhibition of a phosphodiesterase, we used the blockers ODQ and IBMX, respectively. The allatostatin-induced reduction of high (30 mM) potassium-induced muscle contracture was not prevented by inhibition of the guanylate cyclase with the specific inhibitor ODQ ( $10^{-5}$  M). This findings exclude that allatostatin activates the guanylate cyclase. Application of the phosphodiesterase-inhibitor IBMX ( $5 \times 10^{-7}$  M) prevented the allatostatin-induced elevation of cGMP.

Additionally we show that the reducing effect on potassium-induced muscle contracture by allatostatin is induced via a  $G_i$ -protein, because the specific  $G_i$ -protein-blocker pertussis toxin ( $1 \mu\text{g ml}^{-1}$ ) prevents the effect of allatostatin.

Taken together our data indicate, that allatostatin elevates the intracellular cGMP-concentration by inhibition of a phosphodiesterase in the extensor muscle fibres of *Idotea emarginata*.

(supported by DFG, grants Ra 113/8-4)

Kreissl, S., Weiss, T., Djokaj, S., Balezina, O., und Rathmayer, W. (1999) Eur.J.Neurosci., **11**, 2519-2523

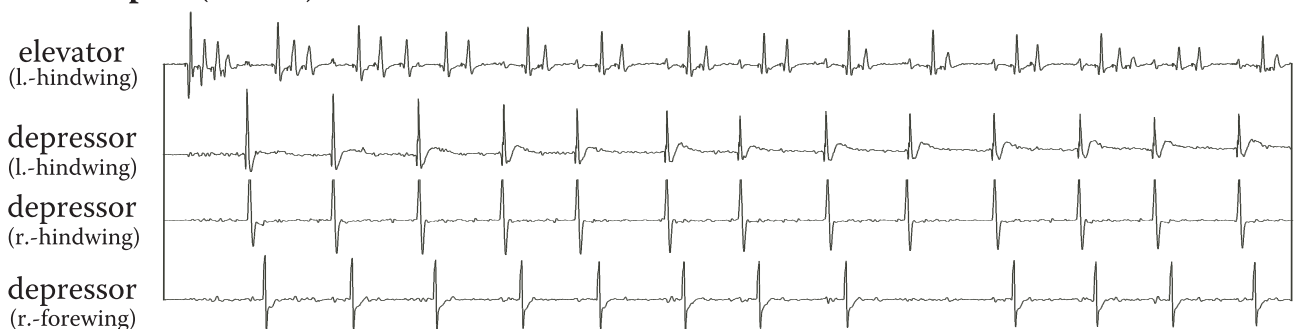
## Cholinergic activation of flight motor activity in the locust, *Schistocerca gregaria*

Edgar Buhl, Paul A. Stevenson, Jan Rillich & Klaus Schildberger

Institute of Zoology, University of Leipzig, Liebigstrasse 18, 04103 Leipzig, Germany

Injectations of octopamine into the locust central nervous system can initiate flight motor activity (e.g. Stevenson and Kutsch, 1987 J. Comp. Physiol. A. 161:115-129), possibly by inducing bursting properties in flight interneurons (Ramirez and Pearson, 1991 Brain Res. 549:332-337). The critical question is, however, whether this mechanism is important for the natural release of flight? Our data suggest that endogenous octopamine is not essential for flight initiation, and that a cholinergic mechanism may underlie the natural activation of the flight central pattern generator. Locusts treated with reserpine, which effectively depletes octopamine, dopamine and serotonin from the central nervous system, still produce flight motor activity in response to natural releasing stimuli (e.g. an air-stream directed to the head hairs) (Fig. A). Furthermore, none of the known flight-initiating interneurons label with an antiserum that detects octopamine. Interestingly, however, we found that both acetylcholine and the muscarinic agonist pilocarpine readily evoke flight motor activity. This cholinergic activation of flight is equally effective in reserpinised locusts (Fig. B), suggesting that the response is not dependent on endogenous amines. We are currently testing our hypothesis that flight initiation depends on the activation of cholinergic neurones, and that this process may be modulated by octopamine.

### A - reserpine (+ wind)



### B - pilocarpine (+ reserpine)



100 ms

## Synaptic targeting and time course of secretion of neurotrophins from hippocampal neurons.

Tanja Brigadski, Richard Kolarow, Matthias Hartmann, Volkmar Lessmann

*Johannes Gutenberg-Universität Mainz, Institut für Physiologie, Duesbergweg 6, 55128 Mainz*

The neurotrophins (BDNF, NT-3, NT-4/5 and NGF) modulate the survival, differentiation and synaptic plasticity in the central nervous system (CNS). These homodimeric proteins are secreted from innervated target tissue and neurons, or from the axon terminals of projecting neurons and mediate their biological effects via activation of specific tyrosine kinase receptors (Trks) and the p75 neurotrophin receptor, respectively (Patapoutian and Reichardt, 2001). In spite of the wealth of knowledge regarding the biological downstream targets of neurotrophin action there is relatively little information about the sites and mechanisms of neurotrophin secretion (Lessmann et al., 2003). BDNF is secreted upon intense synaptic stimulation of CNS neurons (Hartmann et al., 2001), thus mediating changes in synaptic efficacy (Lu, 2003). However, the signaling mechanisms regulating synaptic release of neurotrophins are far from being understood.

In order to enable a direct comparison, we overexpressed GFP-tagged versions of NGF, BDNF, NT-3 and NT-4 in hippocampal neurons, and explored quantitatively the vesicular targeting and the synaptic release of these NTs. Hippocampal neurons were chosen, because all NTs have been described to be expressed endogenously in this brain area (Murer et al., 2001).

Cultured rat hippocampal neurons were transfected at 8 DIV with the GFP fusion constructs, and investigated at 9-11 DIV. NT secretion was monitored by time lapse video microscopy as a decrease in intracellular fluorescence intensity.

BDNF and NT-3 were targeted more efficiently to secretogranin II positive, dendritic secretory granules (BDNF: in 98% of cells; NT-3: 85%) than NGF (45%) and NT-4 (25%). Fusing the BDNF pre-pro sequence to NT-4 redirected NT-4 to the regulated pathway of secretion, suggesting the existence of targeting signals in the pre-pro domain of BDNF.

All neurotrophins were detected near synapsin I positive presynaptic terminals and colocalized with PSD95-DsRed, suggesting postsynaptic targeting of the neurotrophins to glutamatergic synapses. Depolarization induced (50 mM K<sup>+</sup> or high frequency electrical stimulation) release of all neurotrophins from synaptic secretory granules was slow (delay in onset: 10-30 s,  $\tau$ : 120-307 s) compared to transmitter release kinetics monitored with FM 4-64 destaining (onset: <5 s,  $\tau$ : 13  $\pm$  2 s). Among the neurotrophins, NT-4 secretion was most rapid but still proceeded seven times more slowly than transmitter secretion. Preincubation of neurons with monensin (neutralising intragranular pH thus solubilising the peptide core) increased the speed of secretion of BDNF, NGF and NT-3 to the value of NT-4. These data suggest that synaptic secretion of the four mammalian NTs proceeds substantially more slowly than release of conventional transmitters, and is determined by the speed of peptide core dissolution in secretory granules.

*Supported by the DFG (SFB 509; SFB 553)*

### References:

- Hartmann M, Heumann R, Lessmann V (2001) Synaptic secretion of BDNF after high-frequency stimulation of glutamatergic synapses. *EMBO J* 20: 5887-5897.
- Lessmann V, Gottmann K, Malsangio M (2003) Neurotrophin secretion: current facts and future prospects. *Prog Neurobiol* 69: 341-374.
- Lu B (2003) BDNF and activity-dependent synaptic modulation. *Learn Mem* 10: 86-98.
- Murer MG, Yan Q, Raisman-Vozari R (2001) Brain-derived neurotrophic factor in the control human brain, and in Alzheimer's disease and Parkinson's disease. *Prog Neurobiol* 63: 71-124.
- Patapoutian A, Reichardt LF (2001) Trk receptors: mediators of neurotrophin action. *Curr Opin Neurobiol* 11: 272-280.

**Evidence for a role of orcokinin-related peptides in the circadian clock of the cockroach  
*Leucophaea maderae***

Sabine Hofer and Uwe Homberg

Fachbereich Biologie, Tierphysiologie, Philipps Universität Marburg, 35032 Marburg  
sabihofer@yahoo.de

Orcokinins are a family of highly conserved crustacean neuropeptides that have mytotropic effects and apparently also act as neuromodulators in the nervous system (Bungart et al. 1995, Peptides 16:67-72; Dircksen et al. 2000, J Exp Biol 203:2807-2818). Recent biochemical characterization and immunostaining suggest that orcokinins are also present in the nervous systems of various insect species (Hofer et al. 2004 J Comp Neurol, submitted). In the brain of the cockroach *Leucophaea maderae*, we found prominent orcokinin immunoreactivity in the accessory medulla (AMe), a small neuropil in the optic lobe associated with circadian pacemaker functions. To investigate whether orcokinin-related peptides play a role in the circadian timing system of the cockroach, we analyzed the morphology of the immunostained neurons of the AMe in detail and studied the effects of orcokinin injections on circadian locomotor activity.

In total, about 30 somata in five of the six established cell groups of the AMe showed orcokinin immunostaining, including staining in three ventromedian neurons. The neurons have arborizations in the internodular neuropil of the AMe and in a median layer of the medulla and send axonal fibers via the posterior optic commissure to the contralateral AMe and medulla. Double labeling experiments showed colocalization of orcokinin immunostaining with immunoreactivity for pigment dispersing hormone and FMRFamide in the ventral neurons of the AMe but not in the anterior and posterior optic commissure. By means of tracer injections into one AMe combined with orcokinin immunostaining, we show that one orcokinin-immunoreactive ventral neuron and three ventromedian neurons directly connect both AMae via the posterior- and, probably, via the anterior optic commissure.

To determine a possible circadian function of orcokinin in the cockroach, we injected 150 fmol Asn<sup>13</sup>-orcokinin into the vicinity of the AMe at different circadian times. Orcokinin injections revealed significant phase delays in circadian locomotor activity of the cockroach at the early subjective night and phase advances during the middle of the subjective night, similar to the effect of light pulses applied at these times. Together with the anatomical data, the results suggest that orcokinin-related peptides play an important role in light entrainment pathways to the circadian clock via the contralateral compound eye and/or coupling of the bilateral clocks. This study, furthermore, provides the first evidence for a physiological role of an orcokinin-related peptide in insects.

Supported by DFG grant HO/950-9



## Are FMRFamide-related peptides involved in the circadian coupling pathway of the cockroach *Leucophaea maderae*?

<sup>1</sup>S. Söhler, <sup>2</sup>S. Neupert, <sup>2</sup>R. Predel, <sup>2</sup>H. Agricola, <sup>3</sup>S. Meola, <sup>4</sup>R. Nichols and <sup>1</sup>M. Stengl

<sup>1</sup>Philipps University Marburg, Department of Biology, Animal Physiology, Karl v. Frisch Str. D-35032 Marburg, E-mail: [ssoehler@web.de](mailto:ssoehler@web.de), [stengl@staff.uni-marburg.de](mailto:stengl@staff.uni-marburg.de)

<sup>2</sup>Saxonian Academy of Sciences, Research Group Jena, Ebertstr. 1, D-07743 Jena. <sup>3</sup>Areawide Pest Management Research Unit, Department of Agriculture-Agricultural Research Service, College Station, Texas. <sup>4</sup>University of Michigan, Medical School, Department of Biological Chemistry, Michigan.

Locomotor activity rhythms of the cockroach *Leucophaea maderae* are orchestrated by two bilaterally paired circadian pacemakers, the so called accessory medullae (AMae), located in the optic lobes. The accessory medulla (AMe) is innervated by about 12 pigment-dispersing-factor-immunoreactive (PDF-ir) neurons. Synchronization of the bilaterally symmetric circadian pacemakers is achieved by direct neuronal coupling pathways. A group of four neurons [three of them (PDF-ir)] arborize in the accessory medulla and connect both optic lobes via the anterior and posterior optic commissures (Reischig & Stengl, 2002, J Comp Neurol 18:443). Computer models of coupled PERIOD/TIMELESS feedback loops predicted that the phase delaying PDF cannot be the only coupling synchronizing signal. It needs at least one more factor to achieve the coupling properties, which can be observed experimentally (Petri & Stengl, 2001, J Biol Rhythms 16:125). Petri et al. (1995, Cell Tissue Res, 282) postulated that FMRFamide-immunoreactive (FMRFamide-ir) neurons are possible coupling candidates because next to the AMe reside also about 30 FMRFamide-ir somata. Up to six of these neurons show colocalising PDF- and FMRFamide-immunoreactivity. And there is FMRFamide immunoreactivity in the posterior optic commissure. FMRFamide-immunoreactivity suggests the presence of either a sulfakinin, a FMRFamide, a FLRFamide or a RFamide. We used immunocytochemistry and MALDI-TOF to determine which members of the FMRFamide related peptides (FaRPs) are located in the AMe. Stainings with antibodies against perisulfakinin [e.g. Perisulfakinin I: EQFDDY(SO<sub>3</sub>)GHMRFamide], head peptide (*Periplaneta Americana* head peptide: ANRSPSLRLRFamide) and FMRFamide showed up to 40 immunoreactive AMe neurons. MALDI-TOF experiments of excised AMae with associated neurons suggested the presence of at least eight different FaRPs, one FIRLamide, one FVRamide, leucomyosuppressin, four FIRFamides, and head peptide. With injections of leucomyosuppressin no phase shifts of locomotor activity onset were obtained in running-wheel assays. Injections of FMRFamide caused variable phase delays at CT 9 and statistically significant phase-delays at CT 18. Since we injected only the last 4 amino acids possibly the 4 amino acids bind to different FaRP receptors. Thus, we assume that this PRC results from interactions of different FaRPs. As MALDI-TOF experiments identified four different FIRFamides in the AMe (three of them with the C-terminus DNFIRamide) we injected DRSDNFIRamide which resulted in phase delays at CT 9 but not at CT 18. Therefore, this latter PRC differs from the FMRFamide-dependent PRC. Thus, apparently FaRPs, which are colocalized with PDF in about 1-6 cells also phase-delay the onset of the locomotor activity. Currently, with injections of texas red-conjugated dextran in the AMe as neuronal tracer combined with FMRFamid immunocytochemistry we examine whether FMRFamid-ir neurons directly connect both AMae. The so far accomplished dextran injections suggest that there is one dextran/FMRFamide colocalized neuron. [Supported by DFG STE531/12-1]

**Pigment-dispersing factor and GABA synchronize insect circadian clock cells****Nils-Lasse Schneider and Monika Stengl****Philipps-University of Marburg, Biology, Animal Physiology, Germany**

The temporal organization of physiological and behavioral states is controlled by circadian clocks in apparently all eukaryotic organisms. In the cockroach *Leucophaea maderae* transplantation studies (Reischig and Stengl 2003, J. Exp. Biol. submitted) located the circadian pacemaker in the accessory medulla (AMe). The AMe is densely innervated by GABA-immunoreactive and peptidergic neurons, among them the pigment-dispersing hormone-immunoreactive (PDH-ir) neurons. These neurons are circadian pacemaker candidates controlling circadian locomotor activity rhythms in the fruitfly *Drosophila melanogaster* as well as in the cockroach *Leucophaea maderae*. Three of about 12 PDF-ir circadian pacemaker candidates in the cockroach directly connect the bilaterally symmetric circadian clocks and appear to form a synchronizing coupling pathway. Thus, we tested whether the peptide PDF and the neurotransmitter GABA are circadian coupling signals for clock cells. In extracellular recordings of the excised AMe we examined the effect of PDF and GABA on circadian clock cells during the day. Autocorrelation analysis of long-term recordings revealed ultradian action potential oscillations in the AMe. Injections of PDF and GABA transiently synchronized these ultradian oscillators via inhibition of electrical activity. To examine whether the regular (ultradian oscillatory) action potential activity of AMe neurons is a property of the single cell or whether it is caused by synaptic synchronization of irregularly spiking neurons, we superfused the AMe with  $\text{Ca}^{2+}$ -free saline to inhibit neurotransmitter release. Without synaptic communication cells remained synchronized ultradian oscillators, with constant phase relationships. Therefore, we are currently testing whether gap junction mediated communication is responsible for clock cell synchronization. [Supported by DFG STE531/12-1, and Human Science Frontier]

# Noradrenergic $\alpha_1$ – receptor mediated modulation of thermo-sensitive neurons in the rat hypothalamic paraventricular and supraoptic nuclei

**C. Talke, H. Schneider, H. A. Braun, K. Voigt**

**Institut für Normale und Pathologische Physiologie, Philipps – Universität, Marburg**

The paraventricular nucleus (PVN) and the supraoptic nucleus (SON) are the major sites of neuronal control for many homeostatic functions, such as the osmoregulation, the adjustment of the body temperature and others. Accordingly, these neurons have to integrate a manifold of multi-modal signals. For example, the neuronal activity is modulated by osmotic stimuli, including the osmotic signal substance Angiotensin II, as well as by temperature changes. Moreover, the neurons receive direct input via noradrenergic afferents, the cell bodies of which originate primarily in the A2 and A6 cell groups of the medulla oblongata and locus coeruleus.

In the presented study we have examined the effects of the  $\alpha_1$  noradrenergic agonist phenylephrine (2-10  $\mu\text{M}$ ) on the firing rate of the neurons in Slices of the PVN and SON. Additionally we have examined the neuromodulatory effects with phenylephrine application during slow sinusoidal temperature changes ( $37 \pm 3^\circ\text{C}$ ,  $f=0.01\text{Hz}$ ).

Application of phenylephrine generally increased the firing rate up to 200% depending on the concentration. The threshold of recognizable effects varied between 2 and 5  $\mu\text{M}$ . Remarkable effects could be observed when phenylephrine was applied in combination with temperature stimuli.

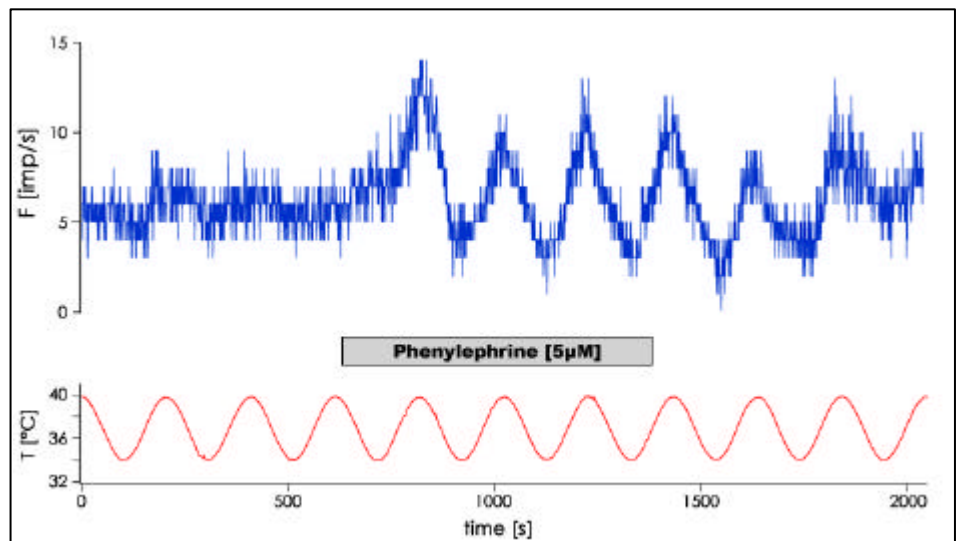


Fig.: Phenylephrine (5 $\mu\text{M}$ ) induced a profound increase of temperature sensitivity in a single SON neuron.

Bath application of phenylephrine resulted in most of the investigated thermo-sensitive neurons to a profound and reversible increase in thermo-sensitivity (see Fig.).

These findings indicate nonlinear neuronal signal integration which can become of functional relevance whenever the neurons are simultaneously subjected to different types of stimuli, which probably is the case in most physiological situations.

**Co-localization of arginine vasotocin and galanin immunoreactivity in the chicken brain**

Sabine Klein, Aleksandr Jurkevich<sup>1</sup>, Roland Grossmann,

Dept. of Functional Genomics and Bioregulation, Institute for Animal Science Mariensee,  
Federal Agricultural Research Center (FAL), 31535 Neustadt, Höltystr. 10, Germany

<sup>1</sup> Institute of Ecology, Vilnius LT-2600, Lithuania

The arginine vasotocin (AVT) system in the avian brain includes sexually dimorphic nuclei in addition to the hypothalamic magnocellular AVT neurons projecting to the neurohypophysis. For the magnocellular AVT system including the paraventricular (PVN) and supraoptic nucleus (SON) the antidiuretic function of AVT is well documented. We have previously shown that the Bed nucleus of the stria terminalis (BnST) is involved in regulation of male sexual behaviour in chickens and that estrogens perform permanent organizational effect during neurogenesis on AVT synthesis. In this study, galanin as potent modulator of neuroendocrine and behavioral regulation was investigated by immunocytochemistry in the sexual dimorphic BnST as well as in SON and PVN. Comparative confocal imaging of AVT and galanin clearly demonstrates high degree of co-localization of both peptides in sexually dimorphic AVT regions with intense immunoreactivity (ir) in BnST and lateral septum (LS) in males only. Injection of estradiol benzoate (EB) in male and fadrozole (F) in female embryos at incubation day 8 (E8) proved to perform organizational effects on galanin- and AVT-ir in BnST of adult chickens. In EB treated cocks, the galanin-ir was abolished in BnST neurons and severely reduced in fibers of BnST region. In hens, treated with F at E8, galanin and AVT ir neurons were detected as in normal cocks. In the magnocellular neurons of female SON, the extremely intense ir of AVT was accompanied by co-localizing galanin-ir. SON neurons in male chicken that have lower AVT-ir than females do not show co-localization with galanin. In contrast, the periventricular part of PVN does not provide any indication of sexual dimorphic galanin synthesis in the area of AVT synthesis. No co-localization of AVT and galanin was found in this region.

Thus, the structural interaction with galanin in sexual dimorphic AVT nuclei in chickens could be an indication for the involvement of galanin in the sex specific regulation of AVT synthesis.

**Keywords:** co-localisation, endocrine control and development, limbic system

## Chronic stress effects on hippocampal neurogenesis are prevented by Prolactin administration

**Sandra Karg \* (1), Luz Torner \* (1), Jürgen Winkler (2), Georg Kuhn (2/3) and Inga D. Neumann (1)**

(1) *Institute of Zoology, University of Regensburg, 93053 Regensburg, Germany*

(2) *University of Göteborg, Sweden*

(3) *Department of Neurology, University of Regensburg, 93053 Regensburg, Germany*

*\* authors contributed equally to the study*

Adult neurogenesis is regulated by endocrine, neuronal and environmental factors. One of these factors is stress. Chronic stress can lead to a downregulation of adult neurogenesis. The neuropeptide Prolactin (PRL) is known to inhibit the HPA response to stress and recently, PRL was shown to increase neurogenesis in the olfactory bulb. Here we studied whether the stress induced downregulation in neurogenesis in the dentate gyrus could be prevented by PRL. C57BL/6 mice were either chronically stressed by immobilization or left undisturbed. To examine cell survival, the mice were injected with BrdU (50mg/kg) during the first seven days. To study the influence of PRL, the mice received a daily dose of 8µg PRL (subcutan), or vehicle (VEH), over a period of 14 days starting at the beginning of the experiment. On day 22 the mice were killed by perfusion. Stress-VEH mice showed significantly ( $p<0.01$ ) less surviving cells compared to control-VEH mice. Surprisingly, stressed mice treated with PRL showed significantly ( $p<0.05$ ) more surviving cells in the dentate gyrus compared to stressed mice receiving vehicle. Furthermore no differences in cell survival were found between stressed and control animals receiving PRL. Stereological estimation of the Volume of the examined area showed no significant differences between experimental groups. However, significant differences in cell density were observed between Stress-VEH and Stress-PRL groups ( $p<0.05$ ) and between Control-VEH and Stress-VEH groups ( $p<0.01$ ). The adrenal weights were significantly increased in both stressed groups compared to unstressed groups. Also thymus weights were significantly reduced in the stress groups compared to controls. No differences in adrenal and thymus weights were found between the stress-PRL and stress-VEH groups.

Our results clearly show that PRL prevents the decrease in neurogenesis in the dentate gyrus of chronically stressed C57BL/6 mice and suggest that PRL could have neuroprotective effects. Since no differences were found in adrenal and thymus weights between the groups we speculate that PRL's effect on neurogenesis at the dentate gyrus is not necessarily due to inhibiting effects of PRL on the HPA-Axis.

## Visual control of gene expression in retina and sclera in chick eyes with intact or sectioned optic nerves.

Marita Feldkaemper, Ruth Schippert, Frank Schaeffel

Section of Neurobiology of the Eye, University Eye Hospital, Calwerstr. 7/1, 72076 Tübingen  
e-mail: marita.feldkaemper@uni-tuebingen.de

**Introduction:** In animal models, it has been shown that development of myopia and hyperopia can be artificially induced by placing the image either behind (negative lenses) or in front of (positive lenses) the retina. The retina is able to detect the sign of imposed defocus and neither accommodation nor image processing in the brain is necessary. Recently, changes in gene expression were detected in different fundal layers during changes in eye growth. It was found that expression of the transcription factor ZENK in glucagon amacrine cells is enhanced after treatment with positive lenses and decreased after treatment with negative lenses. ZENK may therefore have an important role in emmetropization<sup>1</sup>. Surprisingly, if only one eye was treated with a lens, similar changes occurred in the contralateral control eyes, despite that the final changes in eye growth were confined to the treated eye. The pathways connecting both eyes remain obscure. Therefore, we tested if the contralateral effect was still present after optic nerve sectioning. Moreover, we measured gene expression changes in the sclera, in which the altered growth takes place, and investigated if a contralateral eye effect could be seen in this tissue, too.

**Methods:** Male White Leghorn chickens were raised under a 12 hr light / 12 hr dark cycle. Optic nerve section (ONS) surgeries were performed on 1 day-old chicks. All surgeries were monocular. After a recovery period of 10-12 days, the lesioned eyes were subsequently fitted with -5 D lenses for different periods of time (30 minutes, 2 hours). Different control groups were included. They either received the same lens treatments but did not undergo any surgery, or the optic nerve was cut and no lens attached or they were completely untreated. Each group consisted of 5 animals. Moreover, chicks were unilaterally treated with -7 D and +7 D lenses for different periods of time (4 hours, 1 day, 3 days). Gene expression levels in retina and sclera were measured semi-quantitatively using real-time PCR. The used primers for measurements of 18S-rRNA, beta-actin, and ZENK were already described in detail<sup>2,3</sup>. Additionally, MMP-2, TIMP-2 and TGF- $\beta$ 2 expression levels were measured in the cartilaginous and fibrous layer of the chick sclera.

**Results:** ZENK expression was significantly down-regulated after 2 hours of minus lens treatment in both, ONS eyes and eyes that did not undergo any surgery. Moreover, ZENK expression in the contralateral eyes of the 2 hours minus lens treated groups was decreased in comparison to the no lens group, but this effect did not reach significance. There was no sign of defocus dependent regulation of MMP-2 and TIMP-2 in both, the fibrous and cartilaginous scleral layer, whereas TGF- $\beta$ 2 mRNA expression in the cartilaginous layer was significantly up-regulated after 1 day of plus lens treatment and down-regulated after 1 day of minus lens treatment. In the contralateral eye, no co-regulation of TGF- $\beta$ 2 expression was observed.

**Conclusion:** Imposed defocus triggers transcriptional changes of ZENK expression in the retina, and of TGF $\beta$ -2 in the cartilaginous sclera. Changes in retina were rapid and were not influenced by former optic nerve sections. No contralateral effect on TGF $\beta$ -2 mRNA expression was found in the cartilaginous sclera of chicks.

References: 1. Bitzer, M.; Schaeffel, F. (2004). *Optom Vis Sci* 81: 127-136. 2. Simon, P.; Feldkaemper, M.; Bitzer, M.; Ohngemach, S.; Schaeffel, F. (2004) *Molecular Vision* 10:588-597. 3. Buck, C.; Schaeffel, F.; Simon, P.; Feldkaemper, M. (2004). *Invest Ophthalmol.Vis.Sci.* 45: 402-409.

**Poster Subject Area #PSA23:  
Ion channels and receptors**

- [#309A](#) F. Döring, H. Scholz, RP. Kühnlein, A. Karschin and E. Wischmeyer, Würzburg and Göttingen  
*Novel Drosophila TASK channels: evidence for change of function following heteromerization*
- [#310A](#) U. Rose, Ulm  
*Hyperpolarisation activated chlorid current in larval body wall muscle of drosophila*
- [#311A](#) U. Rose and C. Zint, Ulm  
*Cellular changes of locust body wall muscle during reproductive development*
- [#312A](#) S. Maljevic, K. Krampfl, J. Rebstock, N. Tilgen, YG. Weber, P. Cossette, GA. Rouleau, J. Bufler, A. Heils and H. Lerche, Ulm, Hannover, Bonn and Montreal (CDN)  
*A de novo mutation in GABRA1, encoding the GABAA receptor  $\alpha 1$ -subunit, in a sporadic case of childhood absence epilepsy*
- [#313A](#) I. Schön and P. Fromherz, Martinsried  
*Capacitive opening of recombinant voltage-gated Na<sup>+</sup> channels on silicon chips*
- [#314A](#) M. Schmidtner and P. Fromherz, Martinsried  
*Functional Sodium Channels in Cell Adhesion Probed by Transistor Recording*
- [#315A](#) SG. Meuth, H. Wiendl, S. Krause, T. Kanyshkova, P. Meuth, T. Broicher, T. Budde and R. Weissert, Magdeburg and Tübingen  
*EXPRESSION AND ROLE OF TASK CHANNELS IN EXPERIMENTAL AUTOIMMUNE ENCEPHALOMYELITIS*
- [#316A](#) P. Meuth, SG. Meuth, T. Kanyshkova, T. Broicher, H-C. Pape and T. Budde, Magdeburg  
*ROLE OF I(TASK) and I(h) CHANNELS IN A SINGLE THALAMOCORTICAL RELAY NEURON: A MODELLING APPROACH*
- [#317A](#) MC. Göpfert, ADL. Humphris, JT. Albert, D. Robert and O. Hendrich, Cologne and Bristol (UK)  
*Pushing the swing: Mechanical energy contributed by neurons in the ear of the fly*
- [#318A](#) JT. Albert and MC. Göpfert, Cologne  
*Pulling the spring: Mechanical signatures of transducer adaptation in the ear of the fly*
- [#319A](#) D. Bosch, H-U. Schnitzler and S. Schmid, Tübingen  
*Inhibition of PnC giant neurons mediated by G-protein coupled receptors*

- [#320A](#) S. Hirsch, H. Lüddens and W. Hevers, Mainz  
*Pharmacological Properties of GABA-A Receptors in Acutely Dissociated Murine Hippocampal Neurons*
- [#321A](#) DG. Weiss, W. Baumann, E. Schreiber, G. Krause, A. Podßun, M. Lehmann, I. Freund, S. Stüwe, A. Gramowski, K. Jügelt, O. Schröder and R. Ehret, Rostock, Freiburg and Borsdorf  
*CMOS Neurochip for Long-Term Recording from Neuronal Networks*
- [#322A](#) D. Wicher and C. Derst, Jena  
*The TRPgamma channel in the cockroach *Periplaneta americana* is regulated by cAMP and occurs in neurosecretory pacemaker neurons*
- [#323A](#) M. Gruhn, J. Guckenheimer, B. Land and RM. Harris-Warrick, Ithaca, NY (USA)  
*Modulation of delayed rectifier-type potassium currents in cells of the lobster stomatogastric ganglion by dopamine*
- [#324A](#) P. Punnakal and G. Köhr, Heidelberg  
*The NR2A C-terminus controls peak open probability in hippocampal synapses*
- [#325A](#) B. Callsen, D. Isbrandt, K. Sauter, O. Pongs and R. Bähring, Hamburg  
*Mutational analysis of N- and C-terminal Kv4.2 domains required for the binding and functional interaction of Kv Channel Interacting Proteins (KChIPs)*
- [#326A](#) J. Schlenstedt, A. Baumann and W. Blenau, Potsdam and Jülich  
*HONEYBEE SEROTONIN RECEPTORS: CLONING, CHARACTERIZATION AND TISSUE DISTRIBUTION*
- [#309B](#) T. Zannat, R. Menzel and G. Lebouille, Berlin  
*Localisation of the NMDA-R1 mRNA in the brain of *Apis mellifera**
- [#310B](#) S. Ryglewski, E. Heidel and H-J. Pflüger, Berlin  
*GABA receptor activation and induced ion currents of locust metathoracic DUM neurons*
- [#311B](#) E. Heidel and H-J. Pflüger, Berlin  
*Hyperpolarization activated cation channels increase excitability in locust efferent octopaminergic DUM neurons*
- [#312B](#) G. Gisselmann, H. Pusch and H. Hatt, Bochum  
*GABA-gated cation channels and ion-channel gating by multiple neurotransmitters in invertebrates*
- [#313B](#) A. Saras, G. Gisselmann, CH. Wetzel, H. Pusch and H. Hatt, Bochum  
*Identification of a Novel Branch of Invertebrate Ionotropic Acetylcholine Receptors in *C. elegans**



- [#314B](#) I. Joshi, M. Werner, A. Smith, T. Grunwald, K. Gottmann and M. Hollmann, Bochum, Edinburgh (UK) and Duesseldorf  
*Developmental expression pattern of ionotropic glutamate receptors in differentiating embryonic stem cells.*
- [#315B](#) P. Coulon, PW. Dierkes, P. Hochstrate and W-R. Schlue, Duesseldorf  
*Swelling-Activated Chloride Current in Leech Retzius Neurones*
- [#316B](#) G. Klees, PW. Dierkes, P. Hochstrate and W-R. Schlue, Düsseldorf  
*Sodium-dependent potassium channels in leech P neurons*
- [#317B](#) R. Almedom, T. Schedletsky, A. Kruse, S. Anderson, J. Yates, B. Schafer and A. Gottschalk, Frankfurt and San Diego (USA)  
*Functional proteomics of nicotinic acetylcholine receptors and associated proteins in Caenorhabditis elegans*
- [#318B](#) T. Chandra, W. Maier, T. Schüler, A. Chandra and B. Laube, Frankfurt  
*Molecular interactions of the HIV-1 Tat protein with NMDA receptor subunits*
- [#319B](#) C. Keipert and KH. Backus, Frankfurt/Main  
*The activation of muscarinic acetylcholine receptors modulates the intracellular cAMP level in the developing rat inferior colliculus*
- [#320B](#) S. Majumdar and SK. Sikdar, Bangalore (IND) and Frankfurt/Main  
*Induction of pseudo-periodic oscillation in voltage gated sodium channel properties by prior depolarization.*
- [#321B](#) K. Lindemeyer, J. Leemhuis, S. Löffler and DK. Meyer, Freiburg  
*Metabotropic glutamate receptors modulate the ionotropic receptors in the regulation of gene expression*
- [#322B](#) H. Thurm, B. Fakler and D. Oliver, Freiburg  
*Calcium dependence of BK channels in auditory inner hair cells*
- [#323B](#) A. Al-Sabi, D. Lennartz, M. Ferber, J. Gulyas, JEF. Rivier, BM. Olivera, T. Carlomagno and H. Terlau, Göttingen, La Jolla (USA) and Salt Lake City (USA)  
*The interaction of kappaM-Conotoxin RIIK with voltage activated K<sup>+</sup> Channels*
- [#324B](#) V. Sargsyan, G. Aramuni and W. Zhang, Göttingen  
*THE ROLE OF PROTEIN-INTERACTION IN MUTUAL REGULATION OF THE FUNCTION OF GABAA AND GABAB RECEPTORS DURING POSTNATAL DEVELOPMENT*
- [#325B](#) E. Tantalaki, G. Aramuni and W. Zhang, Göttingen  
*GABAB-RECEPTOR-MEDIATED SIGNALING CHANGES DURING EARLY POSTNATAL DEVELOPMENT IN BRAINSTEM OF MOUSE*

[#326B](#)

S. Hepp, F. Gerich and M. Müller, Göttingen

*SULFHYDRYL OXIDATION REDUCES HIPPOCAMPAL SUSCEPTIBILITY TO  
HYPOXIA-INDUCED SPREADING DEPRESSION BY ACTIVATING BK-CHANNELS*

## Novel *Drosophila* TASK channels: evidence for change of function following heteromerization

Frank Döring<sup>1</sup>, Henrike Scholz<sup>2</sup>, Ronald P. Kühnlein<sup>3</sup>, Andreas Karschin<sup>1</sup>  
& Erhard Wischmeyer<sup>1</sup>

<sup>1</sup>Institute of Physiology, <sup>2</sup>Department of Genetics and Neurobiology, University of Würzburg, 97070 Würzburg,

<sup>3</sup>Molecular Developmental Biology, Max-Planck-Institute for biophysical Chemistry, 37070 Göttingen, Germany

In mammals tandem pore domain (2P) K<sup>+</sup> channels are grouped into functionally diverse subfamilies: (i) weak inward rectifiers (TWIK); (ii) acid-sensitive outward rectifiers (TASK); (iii) lipid-sensitive, mechano-gated TREK and TRAAK channels; (iv) halothane-inhibited THIK channels; (v) alkaline-activated TALK channels; (vi) TRESK channels. They are regulated by several physical and chemical stimuli and likely represent the molecular correlate of background (leak) K<sup>+</sup> conductances.

In *Drosophila* only one homologue (dORK1) of mammalian 2P K<sup>+</sup> channels had been found so far. Screening the *Drosophila* genome database ten additional genes were identified. Of these, two deduced protein sequences displayed substantial amino acid similarity to mammalian TASK channels (39% - 46%), whereas all others were <22% similar to any mammalian homologue. In the present study we characterize two *Drosophila* TASK channels (dTASK I and dTASK II) cloned by RT PCR from RNA of adult fruit flies. In Northern blots dTASK transcripts were found predominantly in the head fraction of adult flies and whole mount brain *in situ* hybridizations show strongly overlapping expression patterns of both dTASK isoforms.

When expressed in *Drosophila* S2 cells dTASK I gave rise to rapidly activating ( $\tau_{on} = 3.62 \pm 2.24$  ms,  $V_h = 30$  mV) K<sup>+</sup>-selective currents ( $7.41$  nA  $\pm 4.05$ ; n=16) that steeply depend on extracellular pH with an EC<sub>50</sub> of pH 6.8. In mammalian TASK channels a single extracellular histidine adjacent to the GYG selectivity filter is critical for acid sensitivity. The equivalent residue in dTASK I, however, is not involved in sensing protons.

As revealed by mutational analysis functional expression of dTASK II was prevented by two nonconserved amino acids (ala91-met92) in the pore domain. With these two residues replaced by conserved thr91-thr92 typical K<sup>+</sup>-selective leak currents were generated that were insensitive to changes in external pH. Surprisingly, nonfunctional wildtype dTASK II channels appeared to form heteromeric assemblies with dTASK I. Following cotransfection of dTASK I and wt dTASK II (or when engineered as concatemers) K<sup>+</sup> currents were observed that were smaller in amplitude ( $2.32$  nA  $\pm 1.29$ ) and harbored slower activation kinetics ( $\tau_{on} = 24.66 \pm 3.03$  ms,  $V_h = 30$  mV) as compared to dTASK I.

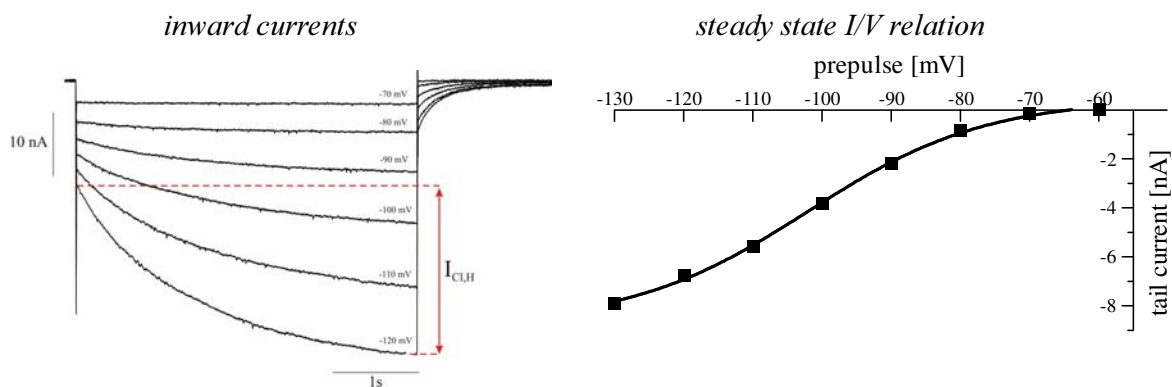
Thus, colocalized dTASK I and dTASK II subunits in *Drosophila* neurons may generate functionally different acid-sensitive leak K<sup>+</sup> currents *in vivo*.

## Hyperpolarisation activated chlorid current in larval body wall muscle of *Drosophila*

Uwe Rose, University Ulm, Department of Neurobiology, Albert Einstein Allee 11  
89069 Ulm, Germany  
email: uwe.rose@biologie.uni-ulm.de

In the last decades *Drosophila* has become a powerful model system for neurobiologists. The genetic malleability and amenability to electrophysiological methods make *Drosophila* an attractive model to study the structure, function and plasticity of ion channels. A fundamental characteristic of the nervous system and associated tissue is their ability to compensate for changes (homeostatic plasticity) that would otherwise compromise nervous system function and eventually lead to impaired or inadequate behaviour. The cellular mechanisms and pathways responsible for this ability are not well understood.

I have started to work on *Drosophila* body wall muscles which are especially well suited to study regulation of muscle cell excitability and ion channel function. In a first step of my work, I identified an inward current that was slowly activated by hyperpolarisation to values negative to -65 mV and slowly deactivated by stepping back to -60 mV. Once activated, the current showed no inactivation. Application of millimolar concentrations of barium or zink failed to block the current. Inward current reversal potential was around -40 mV. Lowering the extracellular chlorid concentration increased currents and shifted their reversal potential to more positive values, as predicted by the Nernst equation. Lowering or raising the potassium concentration had no effect on inward current and did not shift the reversal potential. Besides the already identified potassium and calcium currents of larval body wall muscles, I have characterised an additional current that is mainly carried by chlorid ions. Similar chlorid currents exist in many tissues of invertebrate and vertebrates. They are involved in the regulation of cell volume and act against hyperpolarisation.



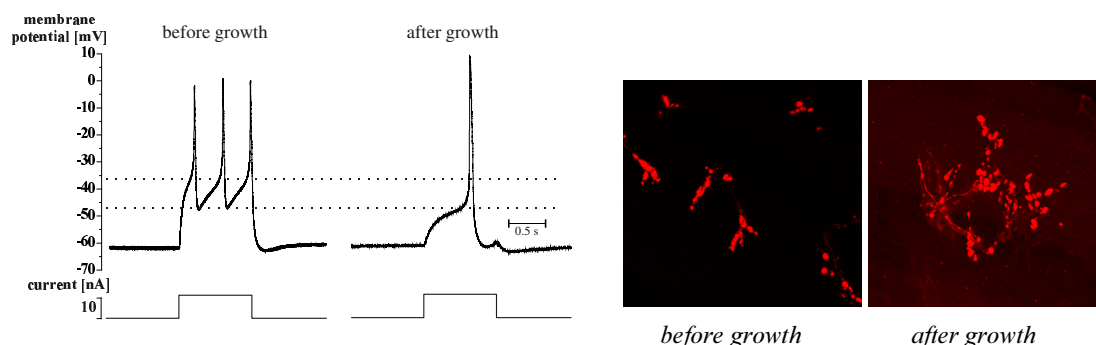
## Cellular changes of locust body wall muscles during reproductive development.

Uwe Rose and Caroline Zint, University Ulm, Department of Neurobiology, Albert-Einstein-Allee 11  
89069 Ulm, Germany  
email: uwe.rose@biologie.uni-ulm.de

During development animals undergo considerable growth of their muscle fibres. To maintain functional integrity and excitability, growth is usually accompanied by various structural and functional changes on the muscle fibres itself or their nervous innervation. In the female locust *Locusta migratoria* considerable growth of body wall muscles is regulated by juvenile hormone (JH). Growth is restricted to those segments involved in oviposition behaviour. As a consequence, muscle fibre growth usually lead to increased membrane surface area and resting conductance and hence to decreased excitability. Thus, we were interested in determining the passive membrane properties of muscle fibres and their excitability both before and after JH regulated growth. Possible structural and functional changes of muscle fibres and their synapses were revealed by measuring muscular voltage activated calcium currents with the two-electrode voltage clamp technique and labelling of neuromuscular synapses.

The resting membrane potential of single muscle fibres did not change during growth, whereas membrane capacity increased 6-fold and membrane conductance 2-fold. Miniature endplate potentials recorded in current clamp mode were considerably decreased after growth and thus suggest lowered excitability of muscle fibres. Before growth of muscle fibres (young females) neuromuscular synapses are evenly distributed over the muscle fibres, and synaptic clusters containing up to ten buttons could be identified. In contrast, synaptic clusters of muscle fibres from mature females occurred less frequently but contained more than twice the number of buttons found on muscle fibres of young females. Furthermore, these muscle fibres express large voltage dependent calcium currents that activate at membrane potentials 10 mV more negative than young females.

These results suggest that lowered excitability of muscle fibres after growth is compensated by additional synaptic release sites and altered characteristics of voltage activated calcium currents.



**A de novo mutation in *GABRA1*, encoding the GABA<sub>A</sub> receptor  $\alpha_1$ -subunit, in a sporadic case of childhood absence epilepsy**

Snezana Maljevic<sup>1</sup>, Klaus Krampfl<sup>2</sup>, Johannes Rebstock<sup>3</sup>, Nikola Tilgen<sup>3</sup>, Yvonne G. Weber<sup>1</sup>, Patrick Cossette<sup>4</sup>, Guy A. Rouleau<sup>4</sup>, Johannes Bufler<sup>2</sup>, Armin Heils<sup>3</sup>, Holger Lerche<sup>1</sup>

<sup>1</sup> Depts. of Neurology and Applied Physiology, University of Ulm, D-89081 Ulm, Germany

<sup>2</sup> Dept. of Neurology, Medizinische Hochschule Hannover, Germany

<sup>3</sup> Clinic of Epileptology and Institute of Human Genetics, University of Bonn, Germany

<sup>4</sup> McGill University, Montreal, Canada

Following the recent discovery of mutations in GABA<sub>A</sub> receptor encoding genes (*GABRG2*, *GABRA1*) in a few families with dominantly inherited generalized epilepsy, we investigated the frequency of *GABRA1* mutations in 98 patients with common forms of idiopathic generalized epilepsy (IGE), 38 of which were sporadic, 60 were familial cases, by sequencing all coding exons and adjacent splice-sites. A single base pair deletion (975delC) was detected in a sporadic patient with childhood absence epilepsy (CAE) predicting a frameshift and premature stop-codon of the GABA<sub>A</sub> receptor  $\alpha_1$ -subunit (S326fs328X), whereas the unaffected parents and one unaffected brother carried two wild type (WT) alleles. Patch clamping of HEK293 cells transfected with WT or mutant  $\alpha_1$ - together with  $\beta_2$ - and  $\gamma_2$ -subunits revealed normal GABA-evoked currents of WT receptors, and no detectable currents in cells transfected with the mutant receptor. To estimate the subcellular fate of the mutant receptor, we used fusion proteins of GABA<sub>A</sub> receptor subunits with the green fluorescent protein, and performed confocal imaging and immunoblot analyses. Our results suggested that mutant receptors were degraded and not integrated in the cell surface membrane in contrast to the WT. We conclude that (i) this second mutation identified in *GABRA1* in humans causes CAE by a loss-of-function and haploinsufficiency of the GABA<sub>A</sub> receptor  $\alpha_1$ -subunit reducing GABA-ergic synaptic inhibition, and that (ii) *GABRA1* mutations are a rare cause of IGE but can be responsible for this disease in sporadic cases.

**Capacitive opening of recombinant voltage-gated Na<sup>+</sup> channels on silicon chips**

Ingmar Schön and Peter Fromherz

Membrane- and Neurophysics, Max Planck Institute for Biochemistry,  
Am Klopferspitz 18a, 82152 Martinsried, Germany

To understand and optimize non-invasive capacitive excitation of neurons from silicon microstructures, it is important to study the response of defined voltage-gated sodium channels to voltage transients applied to the chip.

We focus on a simple model system consisting of the voltage gated sodium channel from rat skeletal muscle (rNav1.4) stably expressed in human embryonic kidney cells (HEK293). The cells are cultured on a silicon chip which carries a thin layer of hafnium oxide and which was coated with fibronectin. In the experiment itself the intracellular potential of the cell is kept constant by a patch clamp amplifier in voltage clamp mode. By applying a voltage transient to the bulk silicon a capacitive current flows over the oxide and through the narrow extracellular space between cell and chip which leads to a voltage drop therein. The chip voltage was chosen such that a stationary, negative voltage developed in the cleft. Sensing this depolarization the sodium channels in the adherent membrane open and the ionic current through them is monitored by the patch clamp amplifier.

We succeeded in capacitive gating of rNav1.4 channels by means of negative extracellular voltages elicited from silicon. Extracellular voltage-clamp with sufficient amplitude and sufficient duration, however, requires an enhanced time constant of cell-chip coupling that was achieved by using a bath electrolyte with reduced conductance.

# Functional Sodium Channels in Cell Adhesion Probed by Transistor Recording

**Markus Schmidtner, Peter Fromherz**

*Department of Membrane- and Neurophysics, MPI for Biochemistry, Martinsried;  
email: schmidt@biochem.mpg.de*

To understand the coupling of neuronal excitation and transistors it is necessary to study the behaviour of a simple and defined system.

Therefore HEK293 cells were stably transfected with the rat skeletal sodium channel  $rNa_v1.4$  ( $\mu 1$ ) and were cultivated on the gate of a field effect transistor. We controlled the potential of the cell interior with a patch clamp amplifier in voltage clamp mode after establishing the whole cell configuration. When applying voltage steps, both the current, measured with the patch clamp amplifier, and the signal of the field effect transistor were recorded.

To explain the signal of the field effect transistor we used the point contact model. In this model the gap between cell and transistor gate is represented by a single resistance. If the channels in the adhesion region open, a current of sodium ions flows from the bath through the gap resistance into the cell and causes a voltage drop on the gate oxide. This voltage drop modulates the source drain current of the transistor.



## EXPRESSION AND ROLE OF TASK CHANNELS IN EXPERIMENTAL AUTOIMMUNE ENCEPHALOMYELITIS

Sven G.Meuth<sup>1</sup>, Heinz Wiendl<sup>2</sup>, Stephanie Krause<sup>1</sup>, Tatyana Kanyshkova<sup>1</sup>, Patrick Meuth<sup>1</sup>, Tilman Broicher<sup>1</sup>  
Thomas Budde<sup>1</sup> and Robert Weissert<sup>2</sup>

<sup>1</sup>Institute of Physiology, Otto-von-Guericke University, Magdeburg, Germany

<sup>2</sup>Department of General Neurology, Hertie-Institute for Clinical Brain Research, University of Tübingen, Germany

Inflammation and demyelination both contribute to the neurological deficits characteristic of multiple sclerosis (MS) and experimental autoimmune encephalomyelitis (EAE). Clinical observations in laboratory models and MS patients, however, indicate that other factors may also contribute to the waxing and waning symptoms of MS. The role of  $\text{Ca}^{2+}$  and  $\text{Na}^{+}$  channels has recently been characterized in EAE as well as in multiple sclerosis lesions in the central nervous system (CNS). TASK channels that encode two-pore domain potassium channels generating background or leak  $\text{K}^{+}$  currents ( $I_{\text{Kl}}$ ) have been identified in various cells of the CNS. Physiologically, most TASK channels give rise to time- and voltage-independent  $\text{K}^{+}$  background currents. Various stimuli (e.g., pH, temperature, anesthetics, phospholipids) are regulating the channel activity in a complex manner, while some family members are further inhibited by G-protein-mediated signalling cascades.

By combining electrophysiological, molecular biological and modelling strategies we assessed the involvement of TASK channels in the pathogenesis of EAE induced with myelin-oligodendrocyte-glycoprotein (MOG) in DA rats. Quantitative PCR displayed a massive reduction of TASK-channel expression in the optic nerve, spinal cord and the dorsal lateral geniculate nucleus (LGNd) of rats with MOG-EAE in comparison to controls. The functional consequence of this loss was assessed by whole-cell patch-clamp experiments of thalamocortical relay (TC) neurons and computer modelling. From hyperpolarized membrane potentials, TC neurons revealed typical burst responses with 2-5 action potentials riding on top of a low threshold  $\text{Ca}^{2+}$  spike. Addition of TASK-channel inhibitors (e.g. lowering extracellular pH from 7.2 to 6.4) mimicked TASK channel loss and resulted in a depolarization of the membrane to  $-42 \pm 3$  mV accompanied by a change in firing mode from burst to tonic generation of action potentials. We confirmed these results by a computational single compartmental model of a thalamic cell where a significant proportion of  $I_{\text{Kl}}$  was modelled as a pH-sensitive TASK current ( $\sim 50\%$ ). Our results suggest a disease-dependent regulation of TASK channels in the course of MOG-induced EAE and possibly MS. The functional role of two-pore domain  $\text{K}^{+}$  channels in the pathogenesis of EAE and MS so far remains elusive.

(Supported by DFG BU 1019/5-1/5-2)

**ROLE OF I(TASK) and I(h) CHANNELS IN A SINGLE THALAMOCORTICAL RELAY NEURON: A MODELLING APPROACH**

Patrick Meuth, Sven G. Meuth, Tatyana Kanyshkova, Tilman Broicher, Hans-Christian Pape and  
Thomas Budde

*Institute of Physiology, Otto-von-Guericke University, Magdeburg, Germany*

Thalamocortical relay (TC) neurons display rhythmic burst firing during slow-wave sleep and tonic generation of action potentials during wakefulness. In a series of computer simulations, a previously described single-compartmental model of a thalamic relay neuron was adapted to NEURON®. The original model was based on the mathematical description of the currents  $I_A$ ,  $I_{K2}$ ,  $I_C$ ,  $I_L$ ,  $I_T$ ,  $I_{Na}$  persistent, and  $I_h$  and displayed both firing modes. Here we extended the model by incorporating Hodgkin-Huxley formalisms of the inward rectifying current  $I_{KIR}$  and the leak potassium current  $I_{TASK}$ .

In brain slices a drop in extracellular pH decreased both the current through hyperpolarizing TASK channels ( $I_{TASK}$ ) and depolarizing HCN channels ( $I_h$ ) thereby limiting the effect on the resting membrane potential of TC neurons. The modified TC neuron model was used to assess the relative contribution of HCN and TASK channels to the resting membrane potential and simulate the effect of extracellular acidification. Therefore the outwardly rectifying TASK current component was set to make up 49% of the total  $K^+$  leak current. Under these conditions the resting membrane potential of the model cell could be determined at -72 mV. From this potential a step depolarization evoked a low-threshold  $Ca^{2+}$  spike and a burst of action potentials. In one set of simulations, the modulation of TASK and HCN channels by extracellular and subsequent intracellular acidification was simulated by the reduction of the availability of HCN and TASK channels by 25% and 90%, respectively. As a result the membrane potential of the model cell depolarized to -68 mV. In a second set of simulations, the block of HCN channels by ZD7288 was simulated by completely removing  $I_h$  from the computer model, resulting in membrane hyperpolarization to -82 mV. Using DC current injection the membrane potential of the model cell was reset to -72 mV and a subsequent step depolarization elicited a burst response. Extracellular acidification was simulated by removing 90 % of the TASK channels, thereby leading to a depolarization of the membrane potential to -58 mV accompanied by a change of firing mode.

These simulations closely reproduce electrophysiological recordings obtained from TC neurons in brain slices and indicate a counterbalancing stabilization of the resting membrane potential of these cells by TASK and HCN channels.

(Supported by DFG BU 1019/5-1/5-2)

## Pushing the swing: Mechanical energy contributed by neurons in the ear of the fly

M. C. Göpfert<sup>1</sup>, A. D. L. Humphris<sup>2</sup>, J. T. Albert<sup>1</sup>, D. Robert<sup>3</sup> & O. Hendrich<sup>1</sup>

<sup>1</sup>Volkswagen-Foundation Research Group, Institute of Zoology, University of Cologne, Weyertal 119, 50 923 Cologne, Germany; <sup>2</sup>H. H. Wills Physics Laboratory, University of Bristol, Tyndall Avenue, Bristol BS8 1TL, UK; <sup>3</sup>School of Biological Sciences, University of Bristol, Woodland Road, Bristol BS8 1UG, UK .E.mail: m.gopfert@uni-koeln.de

The cochlear amplifier is the dominant unifying concept of how vertebrate hearing works (Robles & Ruggero 2001, *Phys. Rev.* 81:1304). The concept assumes that the cochlea is endowed with a biological energy source that feeds back mechanical energy into the vibrations inside the ear, thus amplifying the ear's mechanical input (Hudspeth 1997, *Curr. Opin. Neurobiol.* 7:480). Motile hair cells provide an energy source, yet the question of whether and how much energy these cells contribute within intact auditory systems has remained uncertain (Robles & Ruggero 2001). We have quantified this energy contribution for the motile mechanosensory neurons in the auditory system of *Drosophila melanogaster* by analyzing the mechanics of the antennal sound receiver to which these neurons connect (Göpfert & Robert 2003, *PNAS* 100:5514). Using dead flies and live mechanosensory mutants (*tilB*<sup>2</sup>, *btv*<sup>5P1</sup>, *nompA*<sup>2</sup>) with defective neurons as a background, we show that the intact, motile neurons exhibit power gain. In WT-flies, this gain amounts to a mean total energy of 19 zJ (19x10<sup>-21</sup> Joules), corresponding to 4.6 times the thermal energy the neurons add to the receiver's Brownian motion. Larger energy contributions (200 zJ) associate with self-sustained oscillations, suggesting that the neurons adjust their energy expenditure to maintain the ear on the verge of an oscillatory instability, thus maximizing its sensitivity to sound. These findings validate the concept of the cochlear amplifier for the ear of the fly and show that –in the fly– the amplifier resides in motile mechanosensory cells.

Supported by the Volkswagen-Foundation (I/79 147) and the German Science Foundation (HBFG –1111-582).

## Pulling the spring: Mechanical signatures of transducer adaptation in the ear of the fly

J. T. Albert & M. C. Göpfert

<sup>1</sup>*Volkswagen-Foundation Research Group, Institute of Zoology, University of Cologne, Weyertal 119, 50 923 Cologne, Germany; E-mail: joerg.albert@uni-koeln.de*

Adaptation is a vital feature of sensation, preserving high incremental sensitivity for the relevant stimuli in different stimulus environments. Vertebrate hair cells display an unconventional form of sensory adaptation that is based on a chain of micromechanical events. The gating spring model (Howard & Hudspeth 1988, Neuron 1:189) of hair cell transduction provides a mechanistic concept of how this adaptation works. The model assumes that the pull of a gating spring opens the mechanotransduction channels. Adaptation then actively adjusts the tension of this spring in two ways: by a rapid, calcium-dependent reclosure of the transducer channels (fast adaptation) and by a slower, myosin-dependent displacement of the spring-channel complex itself (slow adaptation) (Holt & Corey 2000, *PNAS* 97:11730). We have identified the mechanical key signatures of hair cell adaptation in the antennal hearing organ of the fruit fly *Drosophila melanogaster*. Mechanical step responses of the antennal sound receiver closely resemble those of hair cells. Mutant analysis shows that mechanical adaptation depends on i) the physiological condition of the animal, ii) the integrity of the neurons, iii) the proper function of the transduction machinery, including the transduction channels, and iv) intracellular calcium dynamics. These findings put forward *Drosophila* for the study of hair cell adaptation and suggest the gating spring model as a general concept in mechanosensation.

Supported by the Volkswagen-Foundation (I/79 147) and the German Science Foundation (HBFG –1111-582).

## Inhibition of PnC giant neurons mediated by G-protein coupled receptors

Daniel Bosch, Hans-Ulrich Schnitzler and Susanne Schmid

Tierphysiologie, Zool. Inst., Universität Tübingen, Auf der Morgenstelle 28, 72076 Tübingen

The nucleus reticularis pontis caudalis (PnC) receives inhibitory GABAergic input from the substantia nigra and inhibitory cholinergic input from the pedunculo pontine tegmental nucleus (PPTg), mediated via G-protein coupled receptors. This inhibitory projection was supposed to mediate prepulse inhibition (PPI) of the startle response. Here, we examined how PnC giant neurons, which represent the sensorimotor interface of the startle pathway, are influenced by the activation of G-protein-coupled receptors for GABA and ACh. Presynaptic stimulation was combined with whole cell patch clamp recordings of PnC giant neurons in rat brain slices in order to investigate the cellular mechanisms underlying the inhibitory effect of GABA<sub>B</sub> and mACh receptors.

The GABA<sub>B</sub> agonist baclofen (20µm) and the mACh agonist oxotremorine (10µm) were added to the bath solution to examine the effect on the presynaptically evoked EPSCs. Both baclofen and oxotremorine significantly reduced the auditory and trigeminally evoked EPSC-amplitudes (e.g. for auditory stimulation to  $42,7\% \pm 14,6$  SEM (n=10) and  $58,9\% \pm 10,3$  SEM (n=8), respectively). The effect of baclofen was partially reversible. We further analyzed the influence of the agonists on paired pulse facilitation (ppf) and on postsynaptic membrane resistance to gain information about the pre- or postsynaptic localization of the inhibitory receptors. Oxotremorine significantly increased ppf, whereas baclofen had no significant effect on ppf. Instead, baclofen significantly reduced membrane resistance. This indicates a presynaptic localization of the mACh receptors and a postsynaptic effect of GABA<sub>B</sub> receptors.

Our results show that the startle mediating PnC giant neurons are substantially inhibited by the action of GABA<sub>B</sub> and mACh receptors. Further experiments will examine whether this inhibition is part of the PPI pathway.

*Pharmacological Properties of GABA<sub>A</sub> Receptors in Acutely Dissociated  
Murine Hippocampal Neurons*

*Silke Hirsch\*, Hartmut Lüddens & Wulf Hevers*

*Laboratory of Molecular Biology at the Department of Psychiatry, University of Mainz, Untere Zahlbacher  
Str.8, 55131 Mainz, hevers@uni-manz.de*

The most abundant inhibitory neurotransmitter in the mammalian central nervous system,  $\gamma$ -aminobutyric acid (GABA), mediates its fast actions solely by the ionotropic GABA type A receptors (GABA<sub>A</sub>Rs). They assemble as heteropentamers composed of 19 different subunits, which determine the mode of action of GABAergic drugs. The modulation of cell responses is therefore indicative of the cell's GABA<sub>A</sub>R repertoire.

Here we recorded acutely dissociated hippocampal neurons in the whole-cell patch-clamp configuration. Voltage-gated currents were routinely recorded from each cell to identify principal neurons. GABAergic drugs were focally applied with a rapid Y-tube application system. Besides the neurotransmitter itself, we employed the benzodiazepine diazepam, which modulates the GABA mediated current of  $\alpha\beta\gamma 2$  ( $i = 1-3, 5$ ) receptors with identical potency; loreclezole, which selectively acts on GABA<sub>A</sub>R containing  $\beta 2/3$  subunits; zolpidem, a ligand with high, moderate and no affinity to  $\alpha 1$ -,  $\alpha 2/3$ - and  $\alpha 5$ -containing receptors, respectively; the  $\alpha 4/6$  specific diuretic furosemide and lanthanum, that is presumed to preferentially act on  $\delta$ -containing receptors. Positive modulators of GABA<sub>A</sub>Rs were applied together with GABA at a concentration eliciting appr. 30% of the maximal current of the respective cell ( $EC_{30}$ ). For negative modulators the coapplied GABA represented the  $EC_{70}$ . Based on their morphology, the neurons were divided into groups resembling CA1- and CA3 pyramidal cells, dentate granule cells and stellate cells from the subiculum.

All currents were blocked by the GABA<sub>A</sub>R competitive antagonist bicuculline (20  $\mu$ M) and the Cl<sup>-</sup>-channel blocker picrotoxinin (100  $\mu$ M), indicating that they were GABA<sub>A</sub>R mediated. GABA dose-response relationships were recorded using a concentration range from 10 nM to 3 mM GABA and were fitted to a logistic function. Few cells showed sensitivities with  $EC_{50}$  values below 1  $\mu$ M (4 % of cells) or above 100  $\mu$ M (12 %). In the majority of cells the  $EC_{50}$  values were between 3 and 40  $\mu$ M. Here, multiple Gaussian fits indicated clusters with  $EC_{50}$  at 8  $\mu$ M, 16  $\mu$ M and 38  $\mu$ M GABA.

Diazepam (1  $\mu$ M) and loreclezole (10  $\mu$ M) enhanced the GABA<sub>A</sub>R function in 97 % of all tested cells, indicating the presence of  $\gamma 2$  and  $\beta 2/3$  subunits in these neurons. Zolpidem at low concentrations (100 nM) enhanced GABA<sub>A</sub>R currents in 47 % of the cells, suggesting the existence of the high affinity  $\alpha 1$ -containing GABA<sub>A</sub>Rs. 53 % of the cells showed lower sensitivities, being potentiated only at higher concentrations of zolpidem, indicating the predominance of  $\alpha 2$ - or  $\alpha 3$ -containing receptors. Only a small fraction of cells was completely zolpidem-insensitive, perhaps due to a large  $\alpha 5$  subunit containing receptor population. Low millimolar concentrations of ethanol potentiated the currents in 73 % of cells.

The loop diuretic furosemide reduced currents in all cells at high micromolar concentrations but only in 70 % at low concentrations (30  $\mu$ M), suggesting a major contribution of  $\alpha 4$  subunit containing receptors. As lanthanum (1 mM) did not inhibit any current, the presence of  $\delta$  subunits could not be verified.

The diverse pharmacological properties of acutely dissociated hippocampal neurons reveal the presence of several functional GABA<sub>A</sub>R subtypes differing in their GABA sensitivity, their pharmacological profile and thus in their putative physiological role.

\* present address: Dept. of Physiology, University of Mainz, Duesbergweg 6, 55128 Mainz, Germany

## CMOS Neurochip for Long-Term Recording from Neuronal Networks

Dieter G. Weiss<sup>1</sup>, Werner Baumann<sup>2</sup>, Erik Schreiber<sup>2</sup>, Guido Krause<sup>2</sup>, Angela Podßun<sup>2</sup>, Mirko Lehmann<sup>3</sup>, Ingo Freund<sup>3</sup>, Simone Stüwe<sup>1</sup>, Alexandra Gramowski<sup>1</sup>, Konstantin Jügelt<sup>1</sup>, Olaf Schröder<sup>4</sup>, Ralf Ehret<sup>5</sup>

Institute of Cell Biology and Biosystems Technology, Departments of <sup>1</sup>Animal Physiology and of <sup>2</sup>Biophysics, University of Rostock, 18051 Rostock, <sup>3</sup>Micronas GmbH, Hans-Bunte-Str. 19, 79108 Freiburg, <sup>4</sup>Pattern Expert GmbH, 04451 Borsdorf, <sup>5</sup>Bionas GmbH, Friedrich-Barnewitz-Str.3, 18119 Rostock, Germany

e-mail: [dieter.weiss@biologie.uni-rostock.de](mailto:dieter.weiss@biologie.uni-rostock.de), fon: +49 (0)381/498-6300

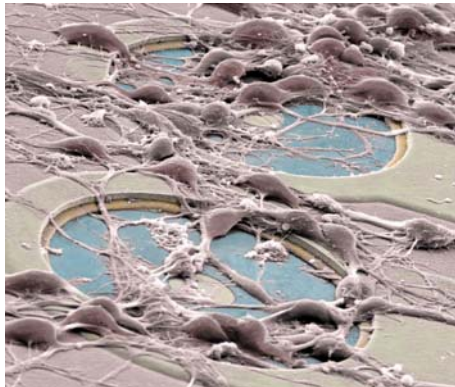


Fig. 1: Nerve cells on Si-neurochip electrodes

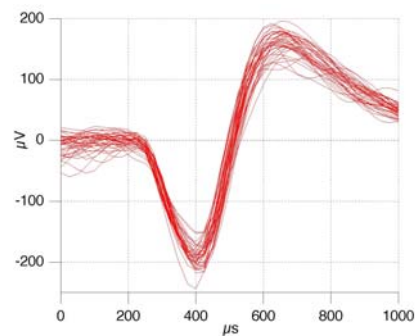


Fig. 2: Action potentials recorded from electrode

Neuronal tissue and a suitable recording/stimulating electronic system form a functional bio-electronic hybrid system (fig. 1). This system provides a platform for pharmaceutical drug development, for high-content drug screening, and for safety pharmacology as well as for diagnostics of human diseases.

We culture electrically active neuronal networks from embryonic mouse spinal cord or brain directly on glass/ITO- or silicon-based multi-electrode arrays with stable cell-electrode coupling for several months. This allows the monitoring of the onset of electrical activity, of bursting activity stabilization and of the development of histiotypic native or drug-modified electrical activity patterns. The glass neurochip sensor system [1] was extensively used over the last years to monitor states of toxic or metabolic impairment of neurons accompanied by characteristic electrical activity changes. Network activity is classified and characterized at the level of spike and burst patterns using more than 40 different activity-describing variables to quantify the effects of defined network activity states. Results will be reported from studies on the effects on the electrical activity of neurotoxins, ammonia and other putative encephalopathy-causing compounds, neurosteroids, benzodiazepines, anaesthetics and anticonvulsive drugs as well as studies on detecting neuronal side-effects of compounds.

A new standard CMOS technology-based silicon chip with unique features has recently been introduced (fig. 1) [2]. Besides the recording electrodes for action potentials (fig. 2), temperature diodes and ion sensitive field effect transistors (ISFET) were integrated to measure temperature and pH changes of the cultures and their metabolic activity at the silicon chip. Sensor prototypes for oxygen and ammonia are also integrated on the chip surface. A flow through system allows integration of additional sensors and control of physiological conditions. Based on our results and experience, a ready to apply system will soon be offered commercially.

1. Gramowski, A., K. Jügelt, D.G. Weiss, G.W. Gross (2004) Substance identification by quantitative characterization of oscillatory activity in cultured murine spinal cord networks on microelectrode arrays. *Eur. J. Neurosci.* 19 2815-2825.
2. Baumann, W., Schreiber, E., Krause, G., Stüwe, S., Podssun, A., Homma, S., Anlauf, H., Freund, I. and Lehmann, M. (2002) Multiparametric neurosensor microchip: *Proceedings Eurosensors XVI*, Prague, Sept. 2002, 1169-1172

Supported by Landesforschungsschwerpunkt Mecklenburg-Vorpommern "Innovationsnetzwerk Biosystemtechnik" and European Community (EFRE).

**The TRP $\gamma$  channel in the cockroach *Periplaneta americana* is regulated by cAMP and occurs in neurosecretory pacemaker neurons**

D. Wicher and C. Derst

Saxon Academy of Sciences, Dept. Neurohormones, Erbertstr. 1, 07743 Jena, Germany

By searching for orthologs of *Drosophila* TRP channels in *Periplaneta* we identified pTRP $\gamma$ , the counterpart to dTRP $\gamma$ . This channel has 1194 amino acids and shows 63% identity to the *Drosophila* channel. Expression of pTRP $\gamma$  in HEK293 cells produced a constitutive conductance permeable to monovalent and divalent cations including calcium. LOE908, a blocker of non-selective cation channels, strongly attenuated the pTRP $\gamma$  currents in HEK293 cells. Similarly, application of 8-bromo-cAMP, a membrane-permeable analog of cAMP, reduced these currents.

Dorsal unpaired median (DUM) neurons are neurosecretory cells in the insect central nervous system which release the biogenic amine octopamine into the periphery thereby modulating target structures such as visceral muscles, skeletal muscles and the heart. The somata of DUM neurons are spontaneously active, i.e. there are endogeneous pacemaker conductances. Previous investigations have shown that a calcium background current contributes to pacemaking (Heine and Wicher, Neuroreport 9 (1998) 3309). Up-regulation of this current by the adipokinetic peptide hormone neurohormone D (NHD) accelerates spiking of DUM neurons (Wicher et al., J. Comp. Physiol. 174 (1994) 507). On the other hand, down-regulation, e.g. by a FMRFamide-related peptide, attenuates the spike frequency of these neurons (Predel et al., Eur. J. Neurosci. (2004) in press).

The calcium background current was shown to be sensitive to LOE908 (Wicher et al., J. Biol. Chem. (2004) in press). Furthermore, the final step of the NHD-initiated signal transduction process leading to potentiation of the calcium background current is the reduction of cAMP concentration by up-regulation of phosphodiesterase 2 activity.

The similar biophysical and pharmacological properties of pTRP $\gamma$  currents in the heterologous expression system and the calcium background current in DUM neurons suggest that pTRP $\gamma$  may be involved in forming the DUM cell calcium background channel. In line with this, single cell PCR-analysis demonstrated the occurrence of pTRP $\gamma$  cDNA in DUM neurons.

This work was supported by the DFG (1422/2-5).



## Modulation of delayed rectifier-type potassium currents in cells of the lobster stomatogastric ganglion by dopamine

Matthias Gruhn<sup>1</sup>, John Guckenheimer<sup>2</sup>, Bruce Land<sup>1</sup>, and Ronald M. Harris-Warrick<sup>1</sup>  
Cornell University, Departments of Neurobiology and Behavior<sup>1</sup>, and Mathematics<sup>2</sup>, Ithaca, NY, 14853

Delayed rectifier potassium currents ( $I_{K(V)}$ ) generate sustained, non-inactivating outward currents with characteristic fast rates of activation and deactivation and play important roles in shaping spike frequency. The pyloric motor network in the stomatogastric ganglion (STG) of the spiny lobster, *Panulirus interruptus*, is made up of one interneuron and 13 motor neurons of five different classes. Dopamine (DA) increases the firing frequencies of the AB, PY, LP and IC neurons and decreases the firing frequencies of PD and VD. In all 6 types of pyloric neurons,  $I_{K(V)}$  is a small current with a high threshold of activation, and is made up of at least two components that are differentially blocked to varying degrees by 4AP and Quinidine. We report the modulation of  $I_{K(V)}$  in the different pyloric neurons by DA, studied under two-electrode voltage clamp. A subset of PY neurons show a marked depolarization with DA; the steady state  $I_{K(V)}$  shows a pronounced reversible increase in the conductance at maximal depolarization of up to 30%. Based on the conductance-voltage relationship, we have separated the two currents mathematically, and show that DA significantly increases both components in the PY neurons studied. The AB neuron also shows a reversible increase in the steady state  $I_{K(V)}$  of approximately 20%. In both cases the increase affects the second, high-threshold component more than the low-threshold component of the current. DA had no effect on  $I_{K(V)}$  in PD, VD and IC neurons. DA also reversibly eliminated a very slow and partial inactivation of  $I_{K(V)}$  in PY neurons and increased the time constant of deactivation in both PY and AB neurons. An increase in conductance during DA application could support the increase in firing frequency in the actively cycling neurons. Supported by NIH grant NS 17323 (RMH-W)

**The NR2A C-terminus controls peak open probability in hippocampal synapses**

P. Punnakal, G. Köhr

Max-Planck-Institute for Med. Research, Heidelberg, Germany.

The peak open probability of NMDARs potentially affects the temporal dynamics of NMDAR signaling during synaptic transmission and plasticity. Former experiments in HEK293 cells expressing recombinant NMDARs and using the open channel blocker MK-801 showed that NMDARs containing NR1 and C-terminally truncated NR2A (NR1/NR2A $\Delta$ C) compared to NR1/NR2A receptors have a 2-3fold lower peak open probability (peak  $p_o$ ,  $0.11 \pm 0.02$  (n=6) vs.  $0.26 \pm 0.03$  (n=8)). Here, we investigated the peak  $p_o$  of the NMDARs in hippocampal synapses of two week old wild type and mice lacking the NR2A C-terminus (NR2A $\Delta$ C/ $\Delta$ C). Synaptic EPSCs were evoked by stimulating the Schaffer collaterals in normal Ringer solution at  $-40$  mV in the presence of the GABA<sub>A</sub> receptor antagonist bicuculline ( $5 \mu$ M) and the AMPA receptor antagonist NBQX ( $5 \mu$ M). After achieving a stable baseline, the NR1/NR2B subtype specific antagonist CP-101,606 ( $10 \mu$ M) was applied for 10 to 15 min, which reduced the peak amplitude by 60% in both genotypes. After blocking the NR1/NR2B type receptors, the stimulation was stopped and the NMDAR open channel blocker MK-801 ( $40 \mu$ M) was added to the bathing medium for 10 min. When the stimulation was resumed in the presence of MK-801, the NMDAR mediated EPSCs progressively decreased in amplitude with each stimulus event (Huang and Stevens, 1997). The peak  $p_o$  calculated for NMDARs in wild type vs. NR2A $\Delta$ C/ $\Delta$ C mice was  $0.036 \pm 0.019$  (n=5) and  $0.014 \pm 0.005$  (n=6), respectively. Thus, the peak  $p_o$  of NR2A type NMDARs is about 7 fold reduced in hippocampal synapses compared to HEK cells. Furthermore, C-terminal truncation of NR2A reduces the peak  $p_o$  of the NR2A type NMDARs 2-3 fold in HEK cells and in hippocampal synapses. Thus we conclude that the C-terminus of the NR2A subunit plays an important role in the peak  $p_o$  of synaptic NMDARs.

## **Mutational analysis of N- and C-terminal Kv4.2 domains required for the binding and functional interaction of Kv Channel Interacting Proteins (KChIPs)**

Britta Callsen, Dirk Isbrandt, Kathrin Sauter, Olaf Pongs and Robert Bähring\*

Institut für Neurale Signalverarbeitung, Zentrum für Molekulare Neurobiologie Hamburg,  
Martinistrasse 52, 20246 Hamburg, Germany

Kv4.2 channels represent the molecular substrate of the somatodendritic subthreshold A-type current ( $I_{SA}$ ) in many pyramidal neurons. Kv4.2  $\alpha$ -subunits associate with cytoplasmic Kv channel interacting proteins (KChIPs), which causes a modulation of channel inactivation gating and an increase in channel surface expression in heterologous expression systems. Unexpectedly, we find that Kv1, Kv2 and HERG channels can be coimmunoprecipitated with KChIP2 isoforms when transiently coexpressed in Chinese hamster ovary (CHO) cells. However, rapidly inactivating Kv1.5(4.2N40) chimeras, which contain the Kv4.2 proximal N-terminus, bind KChIP2 but show no change in inactivation behaviour when coexpressed with KChIP2. The goal of this study was to identify, and to characterize both biochemically and functionally, interaction domains for KChIPs on the Kv4.2  $\alpha$ -subunit. For this purpose we coexpressed wild-type and mutant Kv4.2 channels with KChIP2 isoforms in mammalian cell-lines. Binding of KChIP2 isoforms to Kv4.2 channels was tested with coimmunoprecipitation experiments. Functional interaction was defined by an effect of KChIP2 coexpression on the kinetics of fast inactivation, the kinetics of recovery from inactivation and/or peak current densities. These parameters were studied with the whole-cell patch-clamp technique. Different cytoplasmic portions of the Kv4.2  $\alpha$ -subunit were examined regarding their role in binding and functional interaction of KChIP2: Mutational analysis of the cytoplasmic Kv4.2 N-terminus included partial deletions of its proximal 40 amino-acid portion and a lysine-scanning mutagenesis between amino-acid residues 8 and 30. Furthermore, point mutations were introduced in the Kv4.2 T1-domain at exposed sites, likely to be accessible from the cytoplasm. Mutational analysis of the cytoplasmic Kv4.2 C-terminus consisted in partial deletions distal from S6. Our results underscore the central role of the proximal Kv4.2 N-terminus in binding and functional interaction of KChIPs. They further indicate an interaction of KChIPs with laterally exposed regions of the Kv4.2 T1-domain, and finally, they show that both N- and C-terminal domains of the Kv4.2  $\alpha$ -subunit are involved in binding and functional interaction of KChIPs.

\* Corresponding author: baehring@zmnh.uni-hamburg.de

## HONEYBEE SEROTONIN RECEPTORS: CLONING, CHARACTERIZATION AND TISSUE DISTRIBUTION

J. Schlenstedt<sup>1</sup>, A. Baumann<sup>2</sup> & W. Blenau<sup>1</sup>

<sup>1</sup>Universität Potsdam, Institut für Biochemie und Biologie, -Zoophysiologie-, Karl-Liebknecht-Straße 24-26, D-14476 Potsdam, <sup>2</sup>Forschungszentrum Jülich, IBI-1, Postfach 1913, D-52425 Jülich

The indolalkylamine serotonin (5-hydroxytryptamine, 5-HT) acts as a neurotransmitter, neuromodulator, and even as a circulating neurohormone in invertebrates. Serotonin affects a wide range of physiological and behavioural functions by activating G protein-coupled receptors. Using a homology based screening approach on a brain-specific cDNA library of the honeybee *Apis mellifera*, we have cloned a gene encoding a putative serotonin receptor. The longest open reading frame codes for a protein of 503 amino acid residues. Hydrophobicity analysis of this sequence reveals seven hydrophobic domains, a characteristic feature of G protein-coupled receptors. The deduced amino acid sequence of the honeybee receptor shows the greatest sequence homology to 5-HT<sub>7</sub> receptors from *Drosophila melanogaster* and *Aedes aegyptii*. We have studied the distribution of this 5-HT<sub>7</sub> receptor in several tissues of the honeybee by RT-PCR. Using *in situ*-hybridization we detected the 5-HT<sub>7</sub> mRNA in slices of honeybee brain. Currently, we are generating a cell line stably expressing the receptor protein in order to investigate its intracellular signalling pathways and its pharmacological properties. Using the information available from the honeybee genome project, we have amplified partial cDNAs of two additional serotonin receptor candidates from *Apis mellifera* (Am5-HT1 and Am5-HT2). The amino acid sequences of these receptors are most closely related to the 5-HT<sub>1</sub> receptor of *Panulirus interruptus* and the 5-HT<sub>2</sub> receptor of *Drosophila melanogaster*, respectively. So far, we have investigated the tissue distribution of these two receptors by RT-PCR, and for Am5-HT2 by *in situ*-hybridization.

This work was supported by grants from the German Research Foundation (Ba 1541/4; Bl 469/4).

## Localisation of the NMDA-R1 mRNA in the brain of *Apis mellifera*

Thangima Zannat, Randolph Menzel and Gérard Leboulle

Freie Universität Berlin, Neurobiologie, Königin-Luise-Straße 28/30, D-14195 Berlin

Glutamate is an important excitatory neurotransmitter in the mammalian brain. Its role in the mechanisms of memory formation and LTP has been mostly studied by focusing on the different types of glutamate receptors (AMPA, Kainate, NMDA, and metabotropic receptors).

In insects, glutamate has been described as a neurotransmitter at the neuromuscular junction. In addition, glutamate and glutamate receptors have been identified in the central nervous system, but their role in neuronal plasticity has not yet been seriously addressed. The study of glutamate receptor in invertebrate models appears as being a difficult task because of different pharmacological profiles of the receptor channels compared to vertebrates.

In this study, the NMDA-R1 sub-unit mRNA, whose protein is composing each NMDA receptor, have been identified in the honeybee *Apis mellifera*. The properties of the corresponding protein are discussed. In addition, the expression sites of the NMDA-R1 gene were localised in the brain. These results will be confirmed by studying the corresponding proteins by immunohistochemistry. Then, the RNA interference technique will be used to study the implications of this protein in the mechanisms of learning and memory.

## **GABA receptor activation and induced ion currents of locust metathoracic DUM neurons**

Stefanie Ryglewski, Einar Heidel, Hans-Joachim Pflüger  
Institute of Biology, Neurobiology, Free University Berlin, Königin-Luise-Str. 28-30,  
14195 Berlin, [einar@zedat.fu-berlin.de](mailto:einar@zedat.fu-berlin.de)

As key players of a neuromodulatory system, the efferent dorsal unpaired median (DUM-) neurons of the locust metathoracic ganglion are activated specifically during motor behaviors and affect e.g. muscle function by the release of octopamine. Their neuronal activity is controlled by a differential synaptic input. Inhibitory postsynaptic potentials (IPSPs) and hyperpolarizing responses are thought to be caused by GABAergic innervation. Therefore, we analyzed the responsivity to  $\gamma$ -aminobutyric acid (GABA) and relevant GABA receptor agonists in isolated thoracic DUM neuron somata using the patch clamp technique in the whole-cell configuration. In all DUM neurons held at negative holding potentials (HP -90mV), pressure applied GABA (100  $\mu$ M) induced a large inward current which showed hardly any desensitization even during prolonged applications (> 2 s). Whereas cadmium chloride (500  $\mu$ M) that effectively blocks  $\text{Ca}^{2+}$  currents in this preparation, showed no significant effect on GABA induced currents, these were strongly sensitive to the chloride channel blocker picrotoxin (PTX, 100  $\mu$ M). Moreover, changes of internal or external  $\text{Cl}^-$  concentrations shifted the reversal potential of the GABA induced current towards the calculated chloride equilibrium potential.

Similar results were obtained by application of the (vertebrate)  $\text{GABA}_A$  and  $\text{GABA}_C$  receptor agonists, 4,5,6,7-tetrahydroisoxazolo[5,4-c]pyridin-3-ol (THIP, 1 mM) and cis-4-aminocrotonic acid (CACA, 1 mM), respectively. Both induced a  $\text{Cl}^-$  conductance which could be completely blocked by PTX. In contrast, responses to baclofen (1 mM), a potent agonist on vertebrate  $\text{GABA}_B$  receptors, were insensitive to PTX, but also not affected by the  $\text{GABA}_B$  receptor antagonists CGP 52432 (100  $\mu$ M) and phaclofen (300  $\mu$ M). The baclofen induced current showed a reversal potential deviating strongly from the calculated  $\text{Cl}^-$  equilibrium potential.

We conclude that the somata of locust efferent DUM neurons mainly contain GABA receptors which are linked to chloride channels. An additional GABA receptor subtype, probably a metabotropic  $\text{GABA}_B$ -like receptor, was suggested because of the shown sensitivity to baclofen. (With support by the DFG)

## Hyperpolarization activated cation channels increase excitability in locust efferent octopaminergic DUM neurons

Einar Heidel & Hans-Joachim Pflüger

Institute of Biology, Neurobiology, Free University Berlin, Königin-Luise-Str. 28-30,  
14195 Berlin, [einar@zedat.fu-berlin.de](mailto:einar@zedat.fu-berlin.de)

In locusts, thoracic octopaminergic dorsal unpaired median (DUM) neurons modulate the innervation and function of peripheral target tissues. Some of them are easily excitable and show rebound excitation after strong hyperpolarizations. A lot of different voltage dependent ion channels was found in DUM neuron somata which determine the celltype specific excitability. Nothing is known so far about the existence of hyperpolarization activated cation channels in locust DUM neurons which generally could determine specific firing properties e.g. by counterbalancing transient potassium currents. In this study, we characterized a hyperpolarization induced cation current by means of whole-cell patch clamp recordings on isolated somata of DUM neurons.

In current clamp, membrane hyperpolarizations to potentials more negative than -80 mV induced inward rectification in form of slow depolarizing voltage sags (Fig. 1). Hyperpolarizations were followed by a prolonged (~ 2 s) rebound depolarization of the resting membrane potential that caused somatic spike activity. The depolarizing sag and rebound responses were suppressed in solutions with a low external  $\text{Na}^+$  concentration and eliminated by  $\text{Cs}^+$  (2 mM) or ZD7288 (100  $\mu\text{M}$ ), a selective h-current blocker. Both substances also induced a slight hyperpolarization of the resting membrane potential. Voltage clamp studies revealed a slowly activating inward current that was evoked by potentials more negative than -70 mV (Fig. 2). The maximum current amplitude and the time for exponential activation showed steep voltage dependence (e.g.  $\tau = 500$  ms at -130 mV). Similar to its activation, a slow deactivation was found at resting potentials. The hyperpolarization induced inward current was strongly dependent on a high external  $\text{Na}^+$  ion concentration and could be selectively blocked by  $\text{Cs}^+$  or ZD7288. Potassium channel blockers like 4-Aminopyridine (4-AP, 2 mM), barium (5 mM) or tetraethylammonium ( $\text{TEA}^+$ , 20 mM) had no effect on the hyperpolarization activated current.

We conclude that at least some of the locust neuromodulatory DUM neurons are equipped with hyperpolarization activated  $I_{\text{H}}$  channels which could help setting a more depolarized resting membrane potential, limit inhibitory inputs and cause a higher excitability by fast rebound excitation. (With support by the DFG)

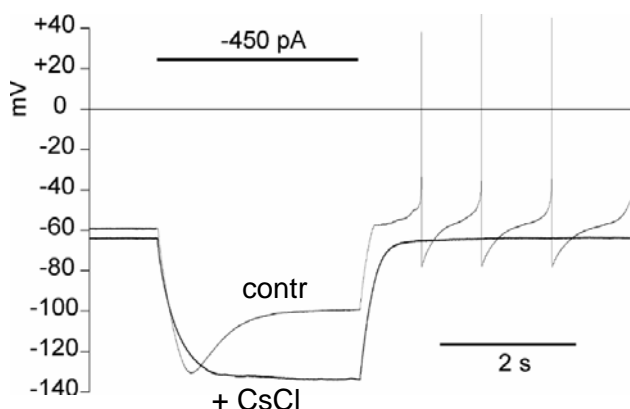


Figure 1: Negative current injection induced hyperpolarization that showed a depolarizing sag and was followed by rebound activity. Both was blocked by external application of cesium chloride ( $\text{CsCl}$ ).

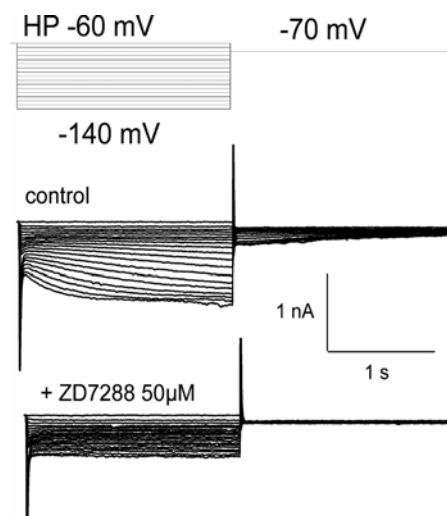


Figure 2: Hyperpolarizing voltage steps induced slowly activating inward currents which were sensitive to the h-current blocker ZD7288.

## **GABA-gated cation channels and ion-channel gating by multiple neurotransmitters in invertebrates**

**G. Gisselmann, H. Pusch and H. Hatt**

Lehrstuhl für Zellphysiologie, Ruhr-Universität Bochum,

Universitätsstraße 150, 44780 Bochum, Germany

Ligand gated ion channels mediate the fast responses of neuronal and muscle cells to neurotransmitters. They form a large family of cation channels that can be activated by acetylcholine, serotonin and anion channels that are opened by gamma-amino-butyric-acid (GABA) and glycine. In addition glutamate, histamine and serotonin gated anion channels exist which can only be found in invertebrates. Recently there was considerable progress in the characterization of ligand-gated chloride channels in invertebrates due to the cloning of histamine and serotonin gated channels from *Drosophila* and *C. elegans*, but the molecular basis of several other types of ion channels known from electrophysiological studies, like ACh- and multitransmitter-gated anion channels is unknown.

The wealth of accumulating information from the *D. melanogaster* genome sequencing project has given us the possibility to describe all members of the superfamily of ligand gated ion channels used by an individual species. A systematic analysis reveals that this superfamily consists of 23 genes. The corresponding cDNAs cloned by RT-PCR, were expressed in *Xenopus oocytes* and the function was investigated by two-electrode voltage clamp. We identified the first insect GABA-gated cation channel genes and give further evidence of the existence of ion channels gated by multiple neurotransmitters. The pharmacological properties of the recombinant heteromeric GABA-gated cation channel match those of native channels found in different invertebrates. Therefore such channels are probably the molecular basis for the excitatory action of GABA in insects.



## Identification of a Novel Branch of Invertebrate Ionotropic Acetylcholine Receptors in *C. elegans*

Arunesh Saras, Günter Gisselmann, C.H. Wetzel, Hermann Pusch & Hanns Hatt

Lehrstuhl für Zellphysiologie, Ruhr-Universität Bochum, Universitätsstraße 150, 44780 Bochum, Germany

### **Abstract**

The wealth of the complete *C. elegans* genome sequence has given us the possibility to describe all members of the superfamily of ligand gated ion channels used by an individual species. Homology analysis of candidate genes for ligand gated cation channels revealed that the previously described ACR-22 defines a new subfamily consisting of 14 putative ligand-gated ion channel subunits with weak sequence homology to nicotinic acetylcholine receptors. In ACR-22 subfamily, all characteristic sequence features of ligand gated ion channels are present like the general topology at four membrane spanning domains but there are distinct differences in the vital conserved regions typical to acetylcholine gated cation channels. Especially the two adjacent cysteines are absent that are present in nearly all ligand binding acetylcholine receptor  $\alpha$ -subunits. The M2-region shows an untypical charge distribution. ACR-22<sub>A</sub> and R13A5.4, both of them are newly defined members, able to build functional homomultimeric ion channels activated by acetylcholine when expressed in *Xenopus* oocytes (ACR-22<sub>A</sub>: EC<sub>50</sub> = 15  $\mu$ M, R13A5.4: EC<sub>50</sub> = 95  $\mu$ M). ACR-22<sub>A</sub> is permeable for monovalent cations and calcium. At ACR-22<sub>A</sub>, carbachol and choline are agonists, but nicotine failed to activate ACR-22<sub>A</sub>. d-Tubocurarine, levamisole and strychnine blocked the channel. Our electrophysiological and molecular biological data suggest that ACR-22<sub>A</sub> and R13A5.4 define a novel branch of acetylcholine receptors in *C. elegans*.

**Developmental expression pattern of ionotropic glutamate receptors in differentiating embryonic stem cells.**

Joshi I. <sup>\*‡</sup>, Werner M. <sup>\*</sup>, Smith A. <sup>°°</sup>, Grunwald T <sup>°</sup>, Gottmann K. <sup>†‡</sup>, and Hollmann M. <sup>\*‡</sup>

*\*Department of Biochemistry, Receptor Biochemistry and <sup>‡</sup>Graduate School- Development and Plasticity of Nervous System, Ruhr University, Bochum, Germany.*

*†Department of Neurophysiology, Heinrich-Heine-University, Duesseldorf, Germany.*

*°° Institute of Stem Cell Research, University of Edinburgh, Edinburgh, UK*

*° Grunwald T, Department of Virology, Bochum, Germany.*

Ionotropic glutamate receptors play an essential role in neuronal development and are expressed in neural precursor cells. Some studies have demonstrated the critical role of glutamate in early development of the ventral telencephalon, particularly in promoting the proliferation of cortical progenitors via an NMDA receptor-dependent mechanism while the proliferation of cortical progenitors derived from dorsal telencephalon is regulated by activation of AMPA/KA receptors. The developing mammalian CNS has an extremely wide array of progenitor cells that are heterogenous in their lineage specification and proliferation potential even within the same brain regions. Therefore we study the developmental expression pattern of ionotropic glutamate receptors in well defined neural precursors derived from embryonic stem cells. We analyse a wide range of ionotropic glutamate receptor subunits and their splice variants at the cellular level. Techniques used are RT-PCR, real time PCR, and immunocytochemistry. For analysis, the 46C mouse embryonic stem cell line is used. 46C ES cells were generated by gene targeting in E14Tg2a.IV ES cells (Ying et. al.; 2003). The open reading frame of the Sox1 gene was replaced with *GFPiresPac*. The transcription factor Sox1 is the earliest and most specific marker for mammalian neural progenitors. We obtained neural stem cells from ES cells by adherent monoculture method (Ying et. al.; 2003). We were able to get around 40% Sox1-positive cells which are retrieved by FACS sorting. We are looking at three cellular stages for expression of glutamate receptor subunits: undifferentiated ES cells, neural stem cells and terminally differentiated neurons. Our preliminary results are based on real time RT-PCR analysis where the specificity of the band amplified is determined by size analysis. So far we showed that GluR7, KA1 and KA2 are present in undifferentiated embryonic stem cells. Receptor subunits present in neural stem cells are GluR3, GluR4flip, GluR5, GluR6, GluR7, KA1 and KA2. Detailed analysis of other subunits at these two cell stages and analysis of terminally differentiated neurons and glial cells is on-going.

## SWELLING-ACTIVATED CHLORIDE CURRENT IN LEECH RETZIUS NEURONES

Philippe Coulon, Paul Wilhelm Dierkes, Peter Hochstrate, Wolf-Ruediger Schlue  
E-mail: coulou@uni-duesseldorf.de

Institut fuer Neurobiologie, Heinrich-Heine-Universitaet Duesseldorf,  
Universitaetsstr. 1, 40225 Duesseldorf, Germany

Most animal cells cannot sustain osmotic gradients across their cell membrane, and therefore, changes of the extracellular osmolarity will lead to changes in cell volume which in turn can disturb normal cell functions. In general, cell volume changes are counteracted by specific cellular mechanisms, either causing a regulatory volume decrease (RVD) – in response to cell swelling – or a regulatory volume increase (RVI) – in response to cell shrinkage. Leech Retzius neurones typically do not show these forms of regulation. Nevertheless volume changes upon alteration of the extracellular osmolarity are distinctly smaller than calculated for an ideal osmometer, suggesting that osmotically induced volume changes and volume regulation occur more or less in parallel (Dierkes et al. 2002a). Current clamp experiments showed that raising the extracellular osmolarity causes an increase in the input resistance of the cells as well as a membrane depolarisation. Vice versa, reducing the extracellular osmolarity evokes a decrease in the input resistance and a membrane hyperpolarisation. While the cellular mechanisms mediating the effects of raising extracellular osmolarity are unknown, the effects of reducing extracellular osmolarity are most probably due to a swelling-activated chloride current: 1. Voltage-clamp experiments revealed the activation of a current with a reversal potential of  $-58 \pm 11$  mV ( $n = 32$ ), which is close to the chloride equilibrium potential in these cells ( $-60.1$  mV, Munsch and Schlue 1993). 2. This current was largely suppressed in the presence of the chloride channel blocker DIDS as well as in chloride-free solution. The swelling-activated chloride current could contribute to an electroneutral efflux of KCl, thereby reducing cytosolic osmolarity and hence cell volume. Under resting conditions the

cytosolic chloride concentration is low (10 mM, Dierkes et al. 2002b), and thus the effect of KCl efflux on cell volume would be small. However, after high neuronal activity both cell volume and cytosolic chloride concentration are increased. Under these conditions, the volume-regulatory effect of the swelling-activated chloride current should be substantially increased.

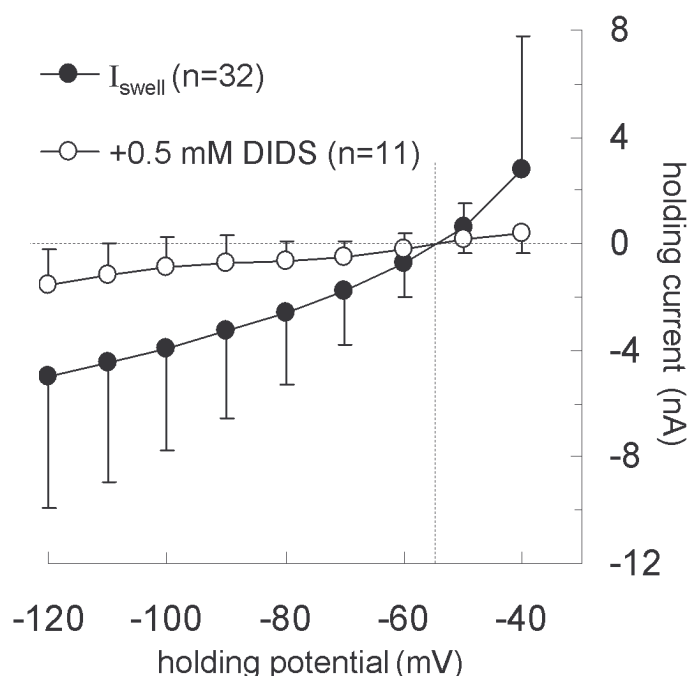


Fig. 1: Swelling-activated chloride current under control conditions (filled circles) and in the presence of 0.5 mM DIDS (open circles).

Dierkes et al. (2002a) In: Electrochemical Microsystem Technologies. Taylor & Francis Group, Ch. 21, 526-40

Dierkes et al. (2002b) Anal Bioanal Chem 373: 762-6

Munsch & Schlue (1993) Eur J Neurosci 5: 1551-7

**Sodium-dependent potassium channels in leech P neurons**

Guido Klees, Paul W. Dierkes, Peter Hochstrate, Wolf-R. Schlue

Institut für Neurobiologie, Heinrich-Heine-Universität Düsseldorf, Germany

The inhibition of the  $\text{Na}^+\text{-K}^+$  pump by ouabain or removal of extracellular  $\text{K}^+$  causes the breakdown of the electrochemical gradients for  $\text{Na}^+$  and  $\text{K}^+$ , which is usually accompanied by a depolarization of the plasma membrane. In leech P neurons, however, upon ouabain application the membrane potential remained virtually unaffected for a prolonged period, and after omitting  $\text{K}^+$  from the bath solution the cells even hyperpolarized, although in both cases the electrochemical gradients for  $\text{Na}^+$  and  $\text{K}^+$  were substantially attenuated. As shown previously, the temporary stabilization of the membrane potential after inhibition of the  $\text{Na}^+\text{-K}^+$  pump is due to the activation of  $\text{K}^+$  channels which strongly enhance the  $\text{K}^+$  selectivity of the plasma membrane and hence shift the membrane potential close to the  $\text{K}^+$  equilibrium potential (Schlue & Deitmer 1984, Schlue 1991). The following results indicate that these  $\text{K}^+$  channels are activated by the increase in the cytosolic  $\text{Na}^+$  concentration: 1) In the absence of extracellular  $\text{Na}^+$  the inhibition of the  $\text{Na}^+\text{-K}^+$  pump had only a minor effect on the  $\text{K}^+$  conductance of the plasma membrane (see Schlue 1991). 2) Shortly after the impalement of a P neuron by a  $\text{Na}^+$ -sensitive microelectrode the cytosolic  $\text{Na}^+$  concentration was often high and the input resistance low, while the membrane potential was close to its normal value. Subsequently, both  $\text{Na}^+$  concentration and input resistance slowly approached their resting values in parallel. 3) Very similar effects were observed after the application of 5-HT, which activates unselective cation channels mediating a strong  $\text{Na}^+$  influx and hence increase in the cytosolic  $\text{Na}^+$  concentration (see Dierkes & Schlue 2004). 4) The iontophoretic injection of  $\text{Na}^+$  evoked a decrease in the input resistance, while the injection of other alkali ions had no effect. Furthermore, the cells repolarized during the  $\text{Na}^+$  injection, and after its cessation they hyperpolarized temporarily. In contrast, during the injection of other alkali ions the cells were constantly depolarized and afterwards the membrane potential immediately returned to its resting value (compare Jansen & Nicholls 1973). It is noted that  $\text{Na}^+$  injection into leech Retzius neurons had no comparable effects, suggesting that in these cells  $\text{Na}^+$ -dependent  $\text{K}^+$  channels are absent.

The activation of the  $\text{Na}^+$ -dependent  $\text{K}^+$  channels in leech P neurons became detectable at a cytosolic  $\text{Na}^+$  concentration of about 10 mM. With increasing  $\text{Na}^+$  concentration channel activation was progressively enhanced, and the maximum activity was reached at concentrations near 60 mM. The physiological significance of the  $\text{Na}^+$ -dependent  $\text{K}^+$  channels seems to be substantial, since at high cytosolic  $\text{Na}^+$  concentrations the input resistance of the cells was reduced to less than 10% of the resting value. The  $\text{Na}^+$ -dependent  $\text{K}^+$  channels may effectively control the excitability of leech P neurons in that they progressively impede the generation of action potentials upon repetitive excitation.

*References*

Dierkes & Schlue (2004) *J Neurobiol* (in press), Jansen & Nicholls (1973) *J Physiol* 229: 635-655, Schlue (1991) *J Neurophysiol* 65: 736-746, Schlue & Deitmer (1984) *J Neurophysiol* 51: 689-704

Functional proteomics of nicotinic acetylcholine receptors and associated proteins in *Caenorhabditis elegans*

Ruta Almedom 1, Thorsten Schedletzky 1, Anja Kruse 1, Scott Anderson 2, John Yates 2, Bill Schafer 3 and Alexander Gottschalk<sup>1</sup>

1 Goethe-University Frankfurt, Institute for Biochemistry, Biocenter N210, Marie-Curie-Str. 9, D-60439 Frankfurt, Germany

2 The Scripps Research Institute, San Diego, USA

3 University of California, San Diego, San Diego, USA

Little is known about factors modulating nicotinic acetylcholine receptor (nAChR) function and governing their expression. To identify such proteins, we have purified the *Caenorhabditis elegans* levamisole-sensitive nAChR (levamisole receptor) using the tandem affinity purification (TAP). Proteins that co-purified with TAP-tagged levamisole receptor subunits were identified by mass spectrometry.

In addition to levamisole receptor subunits, many other proteins were found in the eluate. We depleted each of them by RNAi and assayed *in vivo* nicotine responses of the animals. Where possible, phenotypes were confirmed in genomic mutants. We could thus identify 11 proteins whose depletion caused resistance to nicotine-induced paralysis, and 45 proteins that caused hypersensitivity to nicotine.

Among the proteins causing resistance was SOC-1, which is involved in the *egl-15* fibroblast growth factor receptor (FGFR) pathway and believed to link the activated receptor tyrosine kinase with its targets. Mutation of several positive regulators of the EGL-15 pathway caused resistance to nicotine. In contrast, mutation of *clr-1*, encoding a protein tyrosine phosphatase that antagonizes signalling through activated EGL-15, caused hypersensitivity to nicotine. Thus, the *egl-15* pathway could affect nicotine sensitivity by regulating the expression levels of the levamisole receptor. Total expression of GFP-tagged LEV-1, one of the subunits of the levamisole receptor, was not significantly altered in these mutant backgrounds. However, when we analyzed surface expression and clustering of levamisole receptors on muscles (and neurons) in these mutants, we found that in *soc-1*, *egl-15*, *sos-1*, *sem-5* and *soc-2* mutants, fewer levamisole receptors were expressed on the cell surface. In addition, mutation of a second receptor tyrosine kinase, CAM-1, also reduced synaptic levamisole receptor expression. We are currently testing the possibility that SOC-1 also interacts with CAM-1.

Another protein whose absence causes nicotine resistance is a member of the class of copines. These proteins contain C2 domains, that bind to phospholipids in a  $\text{Ca}^{2+}$ -dependent manner, and a protein/protein interaction module. Copines may thus recruit other proteins to the (plasma-) membrane in an activity-dependent manner. A deletion mutant of this protein shows nicotine resistance, and expression of levamisole receptor subunits at synaptic sites is significantly reduced in animals lacking the copine. A GFP-fusion of this protein localizes to the plasma membrane of neurons and muscles, consistent with a functional interaction with nicotinic receptors. We are currently investigating the function of individual domains of this protein in synaptic expression of nAChRs.

Analysis of deletion mutants of other proteins that were co-purified with the levamisole receptor are underway, and results will be presented at the meeting.

**Molecular interactions of the HIV-1 Tat protein with NMDA receptor subunits**

Tamir Chandra,<sup>1</sup> Wolfgang Maier,<sup>1</sup> Thomas Schüler,<sup>1</sup> Angelika Chandra,<sup>2</sup> and Bodo Laube<sup>1</sup>

<sup>1</sup>Abteilung Neurochemie, Max-Planck-Institut für Hirnforschung, Deutschordenstr. 46, 60528 Frankfurt; <sup>2</sup>Institut für medizinische Virologie und Institut für Immunhämatologie des Klinikums der Universität Frankfurt, 60590 Frankfurt.

We investigated the effect of the human immunodeficiency virus type 1 (HIV-1) regulatory protein Tat on NMDA receptors expressed in *Xenopus laevis* oocytes by voltage-clamp recording and its role in NMDA-mediated neurotoxicity using cultured rat hippocampal neurons. Recombinant HIV-1 Tat potentiated NMDA-induced inward currents of heterologously expressed NR1/NR2B NMDA receptors. However, in the presence of inhibitory  $Zn^{2+}$  concentrations, the potentiating effect of Tat was much more pronounced, indicating a  $Zn^{2+}$ -related effect of Tat on the NMDA receptor. Consistent with this idea, Tat potentiated NMDA-induced inward currents of the particularly  $Zn^{2+}$ -sensitive NR1/NR2A NMDA receptor combination with a higher efficacy, whereas currents recorded from cells expressing a  $Zn^{2+}$ -insensitive mutant were only marginally augmented by HIV-1 Tat. In addition, Tat-toxoid, whose functional site responsible for metal binding is chemically modified, did not reverse  $Zn^{2+}$ -mediated inhibition of the NMDA responses, demonstrating that HIV-1 Tat disinhibits NMDA receptors from  $Zn^{2+}$ -mediated antagonism by complexation of the divalent cation. We therefore investigated the interplay of HIV-1 Tat and  $Zn^{2+}$  in NMDA-mediated neurotoxicity using long-term cultures of rat hippocampal neurons.  $Zn^{2+}$  (1  $\mu$ M) exhibited a prominent rescuing effect when added together with the excitotoxicant NMDA, which could be reverted by adding the specific  $Zn^{2+}$ -chelator tricine. Similar to tricine, HIV-1 Tat enhanced NMDA-mediated neurotoxicity in the presence of neuroprotective  $Zn^{2+}$  concentrations. We therefore propose that release of  $Zn^{2+}$ -mediated inhibition of postsynaptic NMDA receptors by HIV-1 Tat increases the neurotoxic effect of glutamate and may participate in the complex pathogenesis of AIDS-associated dementia.

## The activation of muscarinic acetylcholine receptors modulates the intracellular cAMP level in the developing rat inferior colliculus

C. Keipert and K.H. Backus, Institute of Physiology II, Cellular Neurophysiology, University of Frankfurt/M. Theodor-Stern-Kai 7, D-60590 Frankfurt/M., Germany

GABA<sub>A</sub> receptors play an important role in signal processing in the inferior colliculus (IC), a major relay station of the mammalian auditory pathway. We have recently shown that the activation of muscarinic acetylcholine receptors (mAChRs) expressed in IC neurons modulated the GABAergic transmission in the developing IC. Using the patch-clamp technique, we recorded bicuculline-sensitive, thus GABAergic, spontaneous postsynaptic currents (sPSC) in neurons of acutely isolated rat (P4 – P14) IC slices. In the presence of kynurenate (1 mM) and strychnine (0.5  $\mu$ M), muscarine (10  $\mu$ M) potentiated the frequency of GABAergic PSCs to 618% compared to the control (n=38). The pharmacological profile indicated that the muscarinic modulation of the GABAergic transmission in the IC is primarily mediated by mAChRs of the M3-subtype (Yigit et al. 2003, *Neuropharmacol* 45: 504). In order to unravel the underlying mechanism, we investigated the possible involvement of several intracellular signaling pathways. Thereby, we found that the activation of PLC, NO-synthase, NO, guanylatcyclase and cGMP-activated CNG-channels were not contributing to the muscarine-mediated modulation of the GABAergic transmission in the IC. However, the presence of H7, a blocker of PKA and PKC, resulted in a complete inhibition of the muscarine-evoked effect. Since a PKC blocker (chelerythrine, 5  $\mu$ M) showed no effect, these findings suggested that PKA could be involved in the mechanism activated by M3 receptors in the IC. We further investigated the contribution of cAMP with an cAMP enzymeimmunoassay. Therefore, we applied 10  $\mu$ M muscarine to freshly isolated rat ICs (obtained at P0, P4, P8 and P12) for 1, 2, 5 or 10 min in the absence and presence of IBMX, a non-specific phosphodiesterase inhibitor. Both, in the absence and presence of IBMX (200  $\mu$ M), muscarine evoked a significant increase in [cAMP]<sub>i</sub> compared to the control. This muscarine-evoked effect on [cAMP]<sub>i</sub> increased with the duration of the application and with increasing age, reaching a maximum at P12 (Fig. 1).

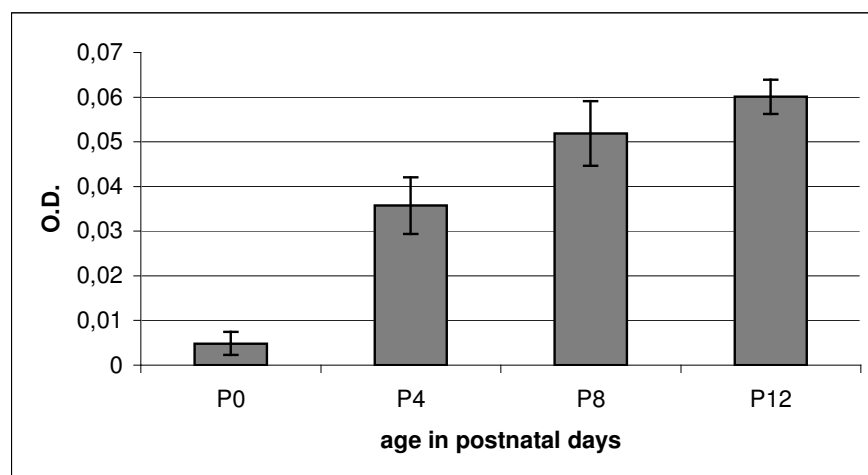


**Fig. 1.** In the absence of IBMX, muscarine was applied for 10 min to acutely isolated IC samples obtained at different postnatal days as indicated. Muscarine potentiated the O.D. indicating an increase of [cAMP]<sub>i</sub>.

Our findings suggest that the activation of M3 mAChRs increases the intracellular cAMP level in IC neurons. Thus, the PKA/cAMP pathway may be involved in the muscarinic enhancement of the GABAergic transmission in the developing IC.

### **Induction of pseudo-periodic oscillation in voltage gated sodium channel properties by prior depolarization.**

Sriparna Majumdar<sup>1,2</sup> and S.K. Sikdar<sup>1</sup>

1. Molecular Biophysics Unit, Indian Institute of Science, Bangalore-560012.
2. Present address: Department of Neuroanatomy, Max Planck Institute of Brain Research, Deutschordenstrasse 46, D-60528, Frankfurt/Main, Germany.

Voltage gated sodium channels regulate the excitable properties of neurons and consist of a single pore forming (226 kDa)  $\alpha$  subunit, and auxiliary  $\beta$  subunits. In response to a voltage pulse the channel shows activation followed by inactivation.

We have examined the relationship between the duration of prior depolarization on the kinetic properties of rNa<sub>v</sub>1.2a voltage gated sodium channel  $\alpha$  subunit expressed in Chinese Hamster Ovary (CHO) cells using a combination of whole cell patch-clamp, Wavelet analysis and single neuron simulation. Effects of both longer (1-160 s) and shorter (10 – 1000 ms) pulse durations were studied. The duration and amplitude of prolonged depolarization altered the steady state and kinetic parameters in a pseudo-oscillatory fashion with time-variable period and amplitude, often superimposed on a linear trend. The pseudo-periodicity was confirmed using weighted wavelet (WWZ) analysis. The slow time periods of oscillation for most parameters, determined by WWZ analysis, lie close to 30 s, suggesting consistent oscillation in the channel that couples activation, fast and slow inactivation. A similar search for pseudo-periodic changes in the channel was made with short depolarizing prepulses whose duration varied between 10-1000 ms. The steady-state activation and inactivation parameters as well as time constant of recovery from fast inactivation depended on the shorter prepulse duration range and amplitude in a pseudo-oscillatory manner. Most of the parameters showed a time period of oscillation close to 225 ms. While co-expression of  $\beta$ 1 subunit decreased the periods of oscillation (close to 22 s for  $\alpha$ + $\beta$ 1) in steady state activation parameters in the prolonged depolarisation range, a suppression of the oscillatory component in the steady state inactivation parameters was observed in the shorter depolarisation range. When sodium channel activation and fast inactivation parameters, subject to variable prepulse duration, in both longer and shorter duration ranges were incorporated in a single neuron simulation using the Hodgkin-Huxley model, subthreshold oscillation and periodic burst and silence activity in action potential firing, similar to epileptic seizure was observed. This history dependence mechanism of sodium channel may offer a complex molecular memory mechanism intrinsic to the neuron, independent of synaptic activity.

*(Supported by the Department of Science & Technology, India)*



**Metabotropic glutamate receptors modulate the ionotropic receptors  
in the regulation of gene expression**

K. Lindemeyer, J. Leemhuis, S. Löffler, and D.K. Meyer

Department of Experimental and Clinical Pharmacology and Toxicology, Albert-Ludwigs-University  
Freiburg, Germany

The postsynaptic density of excitatory synapses contains ionotropic NMDA and AMPA receptors as well as group I metabotropic glutamate receptors (mGluRs). The receptors are linked to multiprotein complexes, which transmit signals to the nucleus and also regulate the densities and activities of the receptors. In rat neocortical neurons, stimulation of NMDA as well as AMPA receptors increases the expression of the proenkephalin gene. In the present study, we used high density cultures of neocortical neurons, to investigate how the simultaneous activation by endogenous glutamate of mGluRs and ionotropic glutamate receptors affects the gene expression. For this purpose, we analyzed the phosphorylation of the transcription factor CREB and the expression of the proenkephalin gene. The group I mGluR antagonists LY367385 and MPEP decreased the enhancement of CREB phosphorylation and gene expression induced by NMDA but increased that caused by AMPA. Stimulation of the mGluRs was due to neuronal activity and could be blocked by tetrodotoxin. Also in organotypic cultures of neocortex, mGluRs modulated the gene expression induced by NMDA or AMPA receptor stimulation. To analyze the effects of mGluRs on the density of cell surface receptors, we used receptor immunolabelling and biotinylation followed by Western blotting. AMPA applied for 24 h reduced the density of AMPA receptors at the cell surface, and the mGluR antagonists diminished this effect. In contrast, the density of NMDA receptors at the cell surface was not influenced by mGluR antagonists. Our results suggest that mGluRs play a physiologically relevant role by regulating the glutamate-induced gene expression.

**Keywords:** endogenous glutamate, metabotropic receptors, CREB, gene expression

## Calcium dependence of BK channels in auditory inner hair cells

**Henrike Thurm, Bernd Fakler, Dominik Oliver**

Physiologisches Institut II, Universität Freiburg

Large conductance  $\text{Ca}^{2+}$  dependent potassium channels (BK or *slo* channels) are involved in the modulation of neurotransmitter release, smooth muscle contraction and in shaping the receptor potential in auditory inner hair cells. Being activated by voltage as well as by intracellular  $\text{Ca}^{2+}$ , BK channels operate as an integrator of these two cellular signals.

BK channels in different tissues share a rather shallow voltage dependence (18 mV for an e-fold change in activation) but differ in their activation voltage range in the nominal (buffered) absence of intracellular  $\text{Ca}^{2+}$  (voltage of half-maximal activation  $V_h$  is typically between +50 to +150mV). This diversity may depend on the various local  $\text{Ca}^{2+}$  sources (i.e. extracellular  $\text{Ca}^{2+}$ , SR, ER), BK subunit composition and post-translational modification.

Contrasting with this general pattern, BK currents measured in the intact IHC show a steep voltage dependence (8 mV) and a very negative  $V_h$  (−45mV). To understand the unique BK channel activation properties, we determined **(i)** the  $\text{Ca}^{2+}$  dependence of BK gating, evaluated **(ii)** the role of voltage gated  $\text{Ca}^{2+}$  channels ( $\text{Ca}_v$ ) as  $\text{Ca}^{2+}$  sources and **(iii)** the role of the BK subunit composition. Experiments were done in excised patch as well as whole-cell voltage-clamp conditions with pharmacologically isolated IHCs from acutely excised mouse and rat cochleae.

**(i)** In excised patches,  $V_h$  was +11.7 (inside-out) and −14.1mV (outside-out) in the absence of  $\text{Ca}^{2+}_i$  and was shifted to hyperpolarised potentials with micromolar  $\text{Ca}^{2+}_i$ . Similarly, elevation of  $\text{Ca}^{2+}_i$  in the whole-cell mode by blocking the plasma membrane  $\text{Ca}^{2+}$ -ATPase (50  $\mu\text{M}$  eosin) led to hyperpolarisation of  $V_h$ .

**(ii)** The whole-cell BK activation curve was not changed by either withdrawal of extracellular  $\text{Ca}^{2+}$  or blockage of  $\text{Ca}^{2+}$ -channels (10 $\mu\text{M}$  isradipine; intracellular  $\text{Ca}^{2+}$  buffered with 5mM EGTA). Replacing extracellular  $\text{Ca}^{2+}$  with  $\text{Sr}^{2+}$ , which is equally permeable through the IHCs  $\text{Ca}_v$ -channels but less potent in activating BK, also did not substantially change  $V_h$ .

**(iii)** In IHCs, the  $\beta_1$ -subunit is known to be the main BK  $\beta$ -subunit. However in IHCs of BK- $\beta_1$  knockout mice,  $\text{Ca}^{2+}$ -sensitivity of BK in patches was only slightly reduced, but the BK whole cell characteristics were not affected.

These results indicate that while BK channels in IHCs are perfectly  $\text{Ca}^{2+}$ -sensitive with an exceptional negative activation in  $\text{Ca}^{2+}$  free medium, their gating in the intact IHC does not rely on voltage-dependent  $\text{Ca}^{2+}$  influx, nor on the channel's subunit composition. In general, these results suggest that BK channels may be gated exclusively by membrane potential in the physiological range even without the prerequisite of elevation of intracellular calcium.

## The interaction of $\square$ M-Conotoxin RIIK with voltage activated K<sup>+</sup> Channels

Ahmed Al-Sabi<sup>1</sup>, Dirk Lennartz<sup>2</sup>, Michael Ferber<sup>1</sup>, Jozsef Gulyas<sup>2</sup>, Jean E. F. Rivier<sup>3</sup>, Baldomero M. Olivera<sup>4</sup>, Teresa Carlomagno<sup>2</sup>, and Heinrich Terlau<sup>1</sup>

<sup>1</sup>Molecular and Cellular Neuropharmacology Group, Max Planck Institute for Experimental Medicine, Hermann-Rein-Strasse 3, D-37075 Göttingen, Germany, <sup>2</sup>Department of NMR Based Structural Biology, Max Planck Institute for Biophysical Chemistry, Am Fassberg 11, D-37077 Göttingen, Germany, <sup>3</sup>The Clayton Foundation Laboratories for Peptide Biology, The Salk Institute, La Jolla, California 92037, and <sup>4</sup>Department of Biology, University of Utah, Salt Lake City, Utah 84112

Venomous organisms have evolved an amazing variety of polypeptide neurotoxins interacting with different potassium (K<sup>+</sup>) channels. Despite the structural divergence of the peptides interacting with the voltage-gated K<sub>v</sub>1 subfamily of K<sup>+</sup> channels (such as the *Shaker* channel from *Drosophila*), a convergent functional feature has been identified. All these peptides seem to share a dyad motif composed of a lysine and a hydrophobic amino acid residue, usually a phenylalanine or a tyrosine. Peptidic neurotoxins from the venomous cone snails (“conotoxins”) are well-known, highly subtype-selective ligands that interact with a variety of different voltage-gated and ligand-gated ion channel targets. Recently, we described a novel *Conus* peptide ligand,  $\square$ M-conotoxin RIIK ( $\square$ M-RIIK), which blocks the *Shaker* K<sup>+</sup> channel in a state-dependent manner. The teleost homologue of *Shaker*, the trout *TShal* K<sup>+</sup> channel, is the highest-affinity target of  $\square$ M-RIIK yet identified. Interestingly, the 24-amino acid sequence of  $\square$ M-RIIK contains three positively charged residues but no aromatic side chain. Here we report on an extensive mutational analysis with the aim to identify the functionally important residues of the toxin. Analogues of  $\square$ M-RIIK containing alanine substitutions at each amino acid position except for the cysteine’s were used. The affinity of the alanine isoforms was functionally assayed by two-electrode voltage clamp measurements using *Xenopus* oocytes expressing *TShal* K<sup>+</sup> channel. It is shown that several mutations affect the binding affinity and kinetics of  $\square$ M-RIIK. The mutational analysis indicated that four amino acids (Leu1, Arg10, Lys18, and Arg19) are essential for K<sup>+</sup> channel binding and forming the pharmacophore of the toxin. Following the hypothesis that Leu1, the major hydrophobic amino acid determinant for binding, serves as the hydrophobic partner of a dyad motif, we investigated the effect of several mutations of Leu1 on the biological function of  $\square$ M-RIIK. Surprisingly, both the structural and mutational analysis results are clearly indicating that  $\square$ M-RIIK lacks the dyad motif found in the other K<sup>+</sup> channel-targeted polypeptide antagonists characterized to date. A mutant cycle analysis was performed to obtain further information on how  $\square$ M-RIIK binds to the channel. For this analysis the functional effects of mutations of amino acids on the toxin and on the channel protein are used to calculate the distance between those residues. Our results indicate that  $\square$ M-RIIK may block the channel by covering the pore as a lid. This pharmacophore model represents a novel mechanism of K<sup>+</sup> channel block by conotoxins.

## THE ROLE OF PROTEIN-INTERACTION IN MUTUAL REGULATION OF THE FUNCTION OF GABA<sub>A</sub> AND GABA<sub>B</sub> RECEPTORS DURING POSTNATAL DEVELOPMENT

Vardanush Sargsyan, Gayane Aramuni & Weiqi Zhang  
Center of Physiology, University of Göttingen, Humboldtalle 23, 37073 Göttingen

GABA is the main inhibitory neurotransmitter in the mammalian central nervous system. It exerts its action mainly through two different receptor subtypes: GABA<sub>A</sub> and GABA<sub>B</sub>. GABA<sub>A</sub> receptors are pentameric ligand-gated ion channels mediating fast inhibitory action, whereas GABA<sub>B</sub> receptors belong to the family of heptahelical G-protein coupled receptors mediating slow inhibitory action. In neonatal respiratory network of mice, GABAergic inhibition has been shown to be functional and is exclusively mediated by GABA<sub>B</sub> receptors at the first postnatal day. Within the first postnatal week GABA<sub>A</sub>-receptor-mediated inhibition becomes operational in parallel with postnatal appearance of Cl<sup>-</sup>-mediated hyperpolarization. Recently, evidence has been shown that GABA<sub>A</sub>-receptor can form complexes with other proteins *in vitro*. Although the functional consequences of the interactions is not fully understood, the formation of GABA<sub>A</sub>/protein complexes has been suggested to be important for regulating the function and trafficking of GABA<sub>A</sub>-receptor. In the present study we use a combined neurobiological approach to demonstrate functional relevance of protein-protein interaction between GABA<sub>A</sub> and GABA<sub>B</sub> receptors. Our results show that GABA<sub>A</sub>R- and GABA<sub>B</sub>R-immunoreactivity (IR) was present from the first postnatal day (P0) on and they were colocalized in most regions of the brain in all tested ages. We further demonstrate that the receptor GABA<sub>A</sub>R interact directly with the GABA<sub>B</sub>R in different regions of the neonatal mouse brain, suggesting a direct link between intracellular domains of GABA<sub>A</sub> and GABA<sub>B</sub> receptors. Co-immunoprecipitation analysis also reveal that the interaction efficiency between GABA<sub>A</sub>- and GABA<sub>B</sub>-receptors markedly changed during postnatal development in the mouse brain. Taken together our results suggest a novel mechanism at which GABA<sub>A</sub>- and GABA<sub>B</sub>-receptors mutually regulate their trafficking and function through intracellular protein-protein-interaction during postnatal development. (supported by CMPB Göttingen)

## **GABA<sub>B</sub>-RECEPTOR-MEDIATED SIGNALING CHANGES DURING EARLY POSTNATAL DEVELOPMENT IN BRAINSTEM OF MOUSE**

Evangelia Tantalaki, Gayane Aramuni & Weiqi Zhang

Center of Physiology, University of Göttingen, Humboldtallee 23, 37073 Göttingen

In brain stem respiratory network of mouse, GABA<sub>B</sub>-receptor play a crucial role in rhythmic modulation from the first postnatal day. In adult animals, activation of GABA<sub>B</sub>-receptors causes inhibition of adenylate cyclase via G<sub>i</sub> subunits and liberation of G<sub>q</sub> subunits, leading to modulation of LVA- and HVA Ca<sup>2+</sup>-currents as well as K<sup>+</sup>-currents in different types of neurones. So far little is known about changes of GABA<sub>B</sub>-receptor-mediated signaling during postnatal maturation. In the present study, the effect of GABA<sub>B</sub>-receptor-mediated modulation of Ca<sup>2+</sup>-currents and the involving intracellular signaling pathway was investigated in brain stem slices of neonatal mice (P0-P15) using a combined electrophysiological, biochemical and immunohistochemical approach. In neurons of pre-Bötzinger-complex (PBC), activation of GABA<sub>B</sub>-receptor enhanced the low voltage activated Ca<sup>2+</sup>-currents (LVA) in P0-P3 mice, while it decreased the LVA-Ca<sup>2+</sup>-currents later (P7-P15). During the same postnatal stage the expression of different G<sub>i/o</sub>- and G<sub>s</sub>-protein subtypes altered in brain stem respiratory network. In addition coupling of GABA<sub>B</sub>-receptor to different G-protein subtypes changed dramatically coinciding with the changing effect of GABA<sub>B</sub>-receptors. Our results suggest that changes of GABA<sub>B</sub>-receptor-mediated cellular effect might be caused by changes in involving second-messenger pathways in brain stem respiratory network of neonatal mouse. (supported by CMPB Göttingen)

## **SULFHYDRYL OXIDATION REDUCES HIPPOCAMPAL SUSCEPTIBILITY TO HYPOXIA-INDUCED SPREADING DEPRESSION BY ACTIVATING BK-CHANNELS**

Sebastian Hepp, Florian Gerich and Michael Müller

Zentrum Physiologie und Pathophysiologie, Georg-August-Universität Göttingen,  
Humboldtallee 23, D-37073 Göttingen, Germany

[mike@neuro-physiol.med.uni-goettingen.de](mailto:mike@neuro-physiol.med.uni-goettingen.de)

The cytosolic redox status modulates various cellular proteins such as ion channels and receptors by oxidizing/reducing their sulfhydryl groups, thereby critically affecting neuronal excitability. We therefore asked, whether sulfhydryl modulation also affects the susceptibility of nerve tissue to hypoxia. In rat hippocampal slices, severe hypoxia caused within 2-4 min a massive depolarization of CA1 neurons accompanied by a negative shift of the extracellular DC potential, termed hypoxia-induced spreading depression (HSD). Oxidizing sulfhydryl groups by DTNB (5,5'-dithiobis[2-nitrobenzoic acid], 2 mM) postponed HSD by 30%, while their reduction by DTT (1,4-dithio-DL-threitol, 2 mM) hastened HSD onset. The DTNB-induced postponement of HSD was not affected by tolbutamide (200  $\mu$ M), DL-AP5 (150  $\mu$ M) or CNQX (25  $\mu$ M). It was abolished, however, by  $\text{Ni}^{2+}$  (2 mM), withdrawal of extracellular  $\text{Ca}^{2+}$ , charybdotoxin (25 nM), and iberiotoxin (50 nM), clearly indicating an involvement of voltage-gated  $\text{Ca}^{2+}$  influx and BK-type  $\text{K}^{+}$  channels. In single CA1 neurons DTNB induced a moderate hyperpolarization, decreased spontaneous spike discharges and postponed the massive hypoxic depolarization. In contrast, DTT induced burst firing, blocked the initial hyperpolarization and hastened the massive hypoxic depolarization. Schaffer-collateral/CA1 synapses were blocked by DTT, but were almost not affected by DTNB. Axonal conduction remained intact. Mitochondrial membrane potential, probed in cultured hippocampal neurons, did not markedly respond to DTNB or DTT. The finding that DTNB postpones HSD is promising, since the tolerance of hippocampal tissue against hypoxia was clearly increased. The postponement of HSD is mediated by the activation of BK channels in a  $\text{Ca}^{2+}$ -sensitive manner. Accordingly, the loss of membrane potential and ionic disregulation occur later and might even be prevented during short-term insults. Therefore, well-directed oxidation of SH-groups could mediate neuroprotection during metabolic insults.

*Supported by the Deutsche Forschungsgemeinschaft (SFB 406 C14)*

**Poster Subject Area #PSA24:  
Neuropharmacology and -toxicology**

- [#327A](#) K. Krüger, M. Ahnefeld, V. Schulze, C. Wackerbeck, M. Madeja, N. Binding and U. Musshoff, Münster  
*BLOCKADE OF GLUTAMATERGIC AND GABAERGIC RECEPTOR CHANNELS BY TRIMETHYLTIN CHLORIDE (TMT)*
- [#328A](#) A. Rex and H. Fink, Berlin  
*Dose-dependent effects of 8-OH-DPAT on mitochondrial activity in the ventral hippocampus in vivo*
- [#329A](#) B. Bert, LF. Felicio, H. Fink and AG. Nasello, Berlin and São Paulo (BR)  
*The use of sudden darkness in mice: A behavioural and pharmacological approach*
- [#330A](#) C. Reinhard and J. Wolffgramm, Tübingen  
*VOLUNTARY ORAL SELF-ADMINISTRATION OF MDMA AND THC IN THE RAT*
- [#331A](#) M. Hadamitzky, S. Schmadel, M. Koch and K. Schwabe, Bremen  
*Deficient prepulse inhibition induced by selective breeding of rats can be restored by antipsychotics*
- [#332A](#) S. Röskam and M. Koch, Bremen  
*Differential effects of chronic intermittent ethanol treatment during adolescence on sensorimotor gating and motor activity in rats postnatally exposed to ethanol*
- [#333A](#) T. Enkel and M. Koch, Bremen  
*Neonatal cortical lesions and chronic pubertal stress: Effects on locomotor activity*
- [#334A](#) B. Schmelting, M. Simon and E. Fuchs, Göttingen  
*The antidepressant agomelatine counteracts stress-induced sleep EEG perturbations*
- [#335A](#) P. Hülper, B. Erdlenbruch, W. Kugler, H. Eibl and M. Lakomek, Göttingen  
*Alkylglycerol-mediated opening of the blood-brain barrier for enhanced drug delivery to the brain and to brain tumors in rats.*
- [#336A](#) W. Wendt, B. Sontag, H. Lübbert and CC. Stichel, Bochum, Heidelberg and Leverkusen  
*In vitro analysis of the neuroprotective potencies of natural compound derivatives*
- [#337A](#) PW. Dierkes, G. Klees, HJ. Wüsten, A. Müller, P. Hochstrate and W-R. Schlue, Düsseldorf  
*The ouabain-induced cell swelling of leech Retzius neurons is due to NaCl uptake*

- [#338A](#) T. Hassenklöver, S. Predehl, J. Pili, M. Assmann and U. Bickmeyer, Hamburg, Bremerhaven and Helgoland  
*Bromophenols, present both in marine organisms and in industrial flame retardants, disturb cellular calcium signaling in neuroendocrine cells (PC12)*
- [#339A](#) B. Legutko, P. Brański, A. Palucha, B. Szewczyk, J. Wierońska, G. Nowak and A. Pilc, Krakow (PL)  
*Antidepressant-like effects of group I mGluRs antagonists are associated with the changes in BDNF gene expression*
- [#327B](#) I. Antonow-Schlorke, T. Müller, M. Loehle, CE. Wood, H. Schubert, OW. Witte and M. Schwab, Jena and Gainesville, FL (USA)  
*GLUCOCORTICOID MEDIATED DECREASE OF THE INCIDENCE OF INTRAVENTRICULAR HEMORRHAGE IS PROBABLY DUE TO MATURATIONAL EFFECTS ON CEREBRAL AUTOREGULATION AT THE EXPENSE OF INCREASED NEURONAL DAMAGE IN VULNERABLE BRAIN REGIONS*
- [#328B](#) M. Brodhun, I. Antonow-Schlorke, T. Coksaygan, T. Müller, H. Schubert, PW. Nathanielsz, OW. Witte and M. Schwab, Jena and New York, NY (USA)  
*TIME COURSE OF CELL BIRTH AND DEATH DURING INTRAUTERINE BRAIN DEVELOPMENT - EFFECTS OF GLUCOCORTICOIDS*
- [#329B](#) A. Klettner, S. Eminel, L. Roemer, V. Waetzig and T. Herdegen, Kiel  
*JNK2 translocates to the mitochondria and mediates cytochrome c release in PC12 cells following 6- hydroxydopamine*
- [#330B](#) S. Eminel and T. Herdegen, Kiel  
*JNK mediate death and sprouting of primary hippocampal neurons*
- [#331B](#) B. Seidel, M. Bigl, H. Franke, H. Kittner, P. Illes, W. Kiess and U. Krügel, Leipzig  
*EXPRESSION OF PURINERGIC RECEPTORS IN THE HYPOTHALAMUS OF THE RAT IS MODIFIED BY REDUCED FOOD AVAILABILITY*
- [#332B](#) K. Wicke and G. Gross, Ludwigshafen  
*Serotonin 5-HT<sub>1A</sub> and 5-HT<sub>1B</sub> antagonists exhibit antidepressant-like activity in the guinea pig forced swim test*
- [#333B](#) M. Weber, C. Boeddinghaus, H. Buschbacher, S. Butty, G. Gross and K. Wicke, Ludwigshafen  
*Antidepressants inhibit wheel running activity in NMRI mice*
- [#334B](#) E. Schuetz, AL. Jongen-Rêlo, K. Drescher, U. Ebert, G. Gross and H. Schoemaker, Ludwigshafen  
*Behavioral sensitization to quinpirole in rats: no change of striatal density of dopamine D<sub>1</sub>, D<sub>2</sub> receptors and the dopamine transporter*



- [#335B](#) BT. Wollweber, H. Schneider, K. Voigt and HA. Braun, Marburg  
*Alcohol Effects on Firing Rate and Temperature-Sensitivity of Hypothalamic Neurons in Rat Brain Slices*
- [#336B](#) G. Vollmer, K. Schwabe, M. Koch and C. Richter-Landsberg, Oldenburg and Bremen  
*Effect of Antisense Oligonucleotides on Reelin Translation and Synaptic/Dendritic Protein Expression in the Rat Brain*
- [#337B](#) S. Stüwe, A. Gramowski and DG. Weiss, Rostock  
*Comparison of acute effects of the antiepileptic drugs valproate and topiramate on electrical activity patterns of primary frontal cortex networks on microelectrode arrays*
- [#338B](#) A. Gramowski, S. Stüwe and DG. Weiss, Rostock  
*NEURONAL TISSUE SPECIFICITY IN VITRO: A MULTI-PARAMETRIC COMPARISON OF MURINE SPINAL CORD AND FRONTAL CORTEX NETWORK ACTIVITY -NEUROTRANSMITTER RECEPTOR RESPONSES AND CULTURING CONDITIONS*

## BLOCKADE OF GLUTAMATERGIC AND GABAERGIC RECEPTOR CHANNELS BY TRIMETHYLTIN CHLORIDE (TMT)

K. Krüger<sup>1</sup>, M. Ahnefeld<sup>1</sup>, V. Schulze<sup>1</sup>, C. Wackerbeck<sup>1</sup>, M. Madeja<sup>1</sup>, N. Binding<sup>2</sup>, U. Musshoff<sup>1</sup>

<sup>1</sup>Institute of Physiology I, <sup>2</sup>Institute of Occupational Medicine, University of Münster, 48149 Münster, Germany

[katharina.krueger@uni-muenster.de](mailto:katharina.krueger@uni-muenster.de)

Organotin compounds such as trimethyltin (TMT) found in the environment are known to be among the most toxic of the organometallics and to be especially neurotoxic. As their main toxicity target is the central nervous system, the aim of the present study was to investigate the effects of TMT on receptor channels involved in miscellaneous processes of synaptic transmission.

The *Xenopus* oocyte system was chosen for direct assessment of TMT effects on voltage-operated potassium channels and glutamatergic and GABAergic receptors heterologously expressed from rat brain. Membrane currents of ion channels were measured by conventional two-electrode voltage-clamp techniques. TMT was applied in concentrations of 0.1 to 100  $\mu\text{mol/l}$ . To verify our results and to analyze TMT effects on identified synaptic sites, we extended our investigations to an established neuronal in vitro system, the hippocampal slice model.

Voltage-operated ion channels: TMT was found to be ineffective against several potassium-operated ion channel (Kv1.1, Kv1.2, Kv2.1 or Kv3.1) functions.

Ligand-operated ion channels: 100  $\mu\text{mol/l}$  TMT induced mean ion currents of 4 nA without co-application of any transmitter. These currents were considered in the calculation of the effects of TMT on glutamate and GABA receptors by subtraction. The functions of the ionotropic glutamate and the GABA<sub>A</sub> receptor channels were affected by TMT in an inhibitory manner by micromolar concentrations of TMT. Thus, at a maximum concentration of 100  $\mu\text{mol/l}$  around 20-30% of the AMPA and GABA<sub>A</sub> receptor-mediated ion currents and 35% of the NMDA receptor-mediated ion currents were blocked. TMT was found to be ineffective against the metabotropic glutamate receptor.

Hippocampal slice model: the depressing effects of TMT were surprisingly much stronger than expected from the ion channel level. Bath application of TMT significantly reduced the amplitudes of evoked fEPSPs in a concentration-dependent and non-reversible manner. As expected from the blocking effects on the NMDA receptors, 1  $\mu\text{mol/l}$  TMT reduced the high frequency stimulus-evoked potentiation to approximately 50% of the control value and fEPSP was almost completely blocked after a 60 min application of 10  $\mu\text{mol/l}$  TMT.

Similar inhibitory effects of TMT occurred after LTP at the Schaffer collateral/CA1 synapse, which is mainly conditioned by NMDA receptors. The induction of LTP, recorded from the CA1 dendritic region, was affected by TMT and failed completely at a concentration of 10  $\mu\text{mol/l}$ .

The principal finding of this study is that some of the neurotoxic effects of TMT are probably provoked by functional impairments of ligand-operated ion channels, in particular glutamatergic and GABAergic receptor channels. Since TMT inhibits glutamatergic and GABAergic-operated ion channels, we propose that this organotin compound affects the neural transmission at the Schaffer collateral-CA1 synapse.

(Supported by Deutsche Forschungsgemeinschaft)

## **Dose-dependent effects of 8-OH-DPAT on mitochondrial activity in the ventral hippocampus *in vivo***

A. Rex and H. Fink

Institute of Pharmacology and Toxicology, School of Veterinary Medicine, Freie Universität Berlin, Koserstr. 20, 14195 Berlin, Germany, email: andrerex@zedat.fu-berlin.de

Serotonin (5-HT) produces its effects through a variety of receptors in the central nervous system. 5-HT<sub>1A</sub> receptors, distributed largely throughout the CNS, have been implicated in the aetiology of numerous disease states, including depression, anxiety-disorders and eating disorders. Presynaptic 5-HT<sub>1A</sub> receptors located in the raphé nuclei are somatodendritic and act as autoreceptors to inhibit cell firing; whereas postsynaptic 5-HT<sub>1A</sub> receptors are present in a number of limbic structures, particularly the hippocampus.

Systemic administration of the 5-HT<sub>1A</sub> receptor agonist 8-OH-DPAT modifies 5-HT neuronal transmission via stimulation of presynaptic and postsynaptic receptors. Compared to the effects of presynaptic receptor-stimulation, there are less data on the effects of postsynaptic 5-HT<sub>1A</sub> receptors and the net effects of a stimulation of both, pre- and postsynaptic, 5-HT<sub>1A</sub> receptors available. We measured the neuronal activity in the hippocampus of anaesthetised Wistar rats following systemic treatment with 8-OH-DPAT in doses (30 – 300 µg/kg) known to reduce 5-HT release and anxiety-like behaviour in rodents. Neuronal activity was assessed by laser-induced fluorescence spectroscopy determining changes in nicotinamide adenine dinucleotide (NADH) fluorescence in the ventral hippocampus *in vivo*. NADH, a co-substrate for energy transfer in the respiratory chain, mirrors mitochondrial activity. Increased NADH fluorescence signals indicate a lower consumption of NADH caused by neuronal inhibition.

8-OH-DPAT at a dose of 300 µg/kg increased NADH fluorescence by maximal 27.0±3.5%, suggesting a decreased neuronal activity in the ventral hippocampus. 8-OH-DPAT at a dose of 100 µg/kg had no effect, whereas the lowest dose of 30 µg/kg decreased, but not significantly, NADH fluorescence.

The results show that systemic administration of the 5-HT<sub>1A</sub> agonist 8-OH-DPAT dose-dependently affects neuronal activity in the ventral hippocampus. The dose of 300 µg/kg seemingly activates presynaptic and postsynaptic receptors with dominating inhibitory postsynaptic effects.

## **The use of sudden darkness in mice:**

### **A behavioural and pharmacological approach**

Bettina Bert<sup>1\*</sup>, Luciano F. Felicio<sup>2</sup>, Heidrun Fink<sup>1</sup> and Antonia G. Nasello<sup>3</sup>

<sup>1</sup>*Institute of Pharmacology and Toxicology, School of Veterinary Medicine, Freie Universität Berlin, Koserstrasse 20, 14195 Berlin, Germany - \*bertb@zedat.fu-berlin.de*

<sup>2</sup>*Departamento de Patologia, Faculdade de Medicina Veterinária e Zootecnia, Universidade de São Paulo, Av. Orlando Marques Paiva 87, 05508-900, São Paulo, SP, Brazil*

<sup>3</sup>*Departamento de Ciências Fisiológicas da Faculdade de Ciências Médicas da Santa Casa de São Paulo, R. Dr. Cesário Motta Jr. 61, 11 andar, 01221-090, São Paulo, SP, Brazil*

Sudden darkness is a non-invasive tool in behavioural analysis to increase motor activity and decrease anxiety in rats. Previous studies have shown that in rats dark test conditions can also modify behavioural responses to drugs acting at the dopaminergic system. The increasing amount of transgenic mice in behavioural research has raised interest in new tests for phenotyping. Hence, the aim of the present study was to adapt the sudden darkness paradigm for mice. In the first part of this study, effects of sudden darkness on the performance of mice in the elevated plus maze test were evaluated. Both genders of two mouse strains (Swiss and Balb/c) were either tested under bright illumination or were exposed to sudden darkness. In the second part, responses to the 5-HT<sub>1A</sub> receptor agonist 8-OH-DPAT (0.5 and 1.0 mg/kg) and 5-HT<sub>2C</sub> receptor agonist mCPP (1.0 and 2.0 mg/kg) were investigated in male Swiss mice. Sudden darkness induced a clear anxiolytic effect in male and female Swiss mice. In Balb/c mice, anxiety-related behaviour was only decreased in females, whereas in males the anxiety state remained unchanged. An increase in motor activity was just observed in male Swiss mice; in the other groups, sudden darkness did not affect locomotion. Depending on light condition the behavioural response to substances was more evident: The anxiety state was only significantly decreased if 8-OH-DPAT (1.0 mg/kg) was tested under bright illumination, whereas the anxiogenic effect of mCPP (1.0 and 2.0 mg/kg) was only visible in the dark. Hence, sudden darkness is also in mice a useful tool to modulate the anxiety level without administering drugs. Depending on the mouse strain, equivalent effects on anxiety and motor activity were observed as it was shown for rats. Therefore, sudden darkness can also serve in mice as an experimental paradigm to analyse the behavioural effects of substances in more detail.

*This work was supported by DFG grant FI 491/2-3, by FAPESP grant 02/07331-8, CNPq grant 300833/03-2 as well as by the DAAD and CAPES.*

## VOLUNTARY ORAL SELF-ADMINISTRATION OF MDMA AND THC IN THE RAT

Reinhard, C.\*; Wolffgramm, J.

Section of Addiction Research, University Hospital of Psychiatry, University of Tübingen,  
Oslanderstr. 24, 72076 Tübingen

We have established an animal model for the long-term free-choice intake of MDMA (3,4-methylenedioxymethamphetamine, “ecstasy”) as well as THC (the main psychoactive component of cannabis) in a single and a polydrug paradigm, respectively.

Rats were given free-choice between water and solutions of MDMA and THC over a period of nearly one year. Housing conditions were changed regularly and comprised single housing, contact housing (two animals in one cage, subdivided by a wire mesh), group housing (four animals) and housing in groups of eight animals in a seminatural colony.

We found that the animals adapted their MDMA as well as THC consumption to external factors (change of housing conditions) and that the amount of drugs consumed was predictable for each individual. Therefore, the animals developed controlled consumption. Animals ceased MDMA intake after several months. Although the underlying reasons for this are not clear, this is in agreement with findings in human MDMA consumers.

After a period of abstinence, a retest was performed. All drug-containing solutions were adulterated with bitter tasting quinine. Under these conditions all animals stopped drug-consumption, which leads to the conclusion that no animal has lost control over intake.

## Deficient prepulse inhibition induced by selective breeding of rats can be restored by antipsychotics

Martin Hadamitzky, Silke Schmadel, Michael Koch and Kerstin Schwabe  
Brain Research Institute, University of Bremen, PO Box 33 04 40,  
28334 Bremen, Germany

A deficit of sensorimotor gating reflects disturbed information processing in several neuropsychiatric disorders, such as schizophrenia. Prepulse inhibition (PPI) of the acoustic startle response (ASR) is a cross species model to measure sensorimotor gating processes. Thus, an experimentally induced PPI-deficit serves as an animal model or endophenotype for schizophrenia. The level of PPI varies among rats of an outbred population but shows high test-retest reliability for individual rats. Since rats selectively bred for a high or low level of a given phenotype are an interesting approach to study pathophysiological mechanisms underlying certain disorders, the aim of this study was to selectively breed two separate rat lines with either high or low level of PPI. In case of successful breeding we wanted to test, if the “PPI-deficit” of the line with low PPI-level can be antagonized by typical or atypical antipsychotics.

Ten male and female Wistar rats were repeatedly (three times) tested for their PPI performance. Two females and males with the highest and the lowest expression of PPI respectively, were chosen for selective breeding of two lines with either high or low level of PPI. Offspring of these rats (F1 generation) was repeatedly tested for PPI as adults. Again, rats with the highest and lowest PPI-level were selected for subsequent breeding procedure, now using brother and sister pairing. This breeding procedure resulted in two separate lines of rats that differ in their PPI, one line with high level (*High PPI*) and one line with low level of PPI (*Low PPI*). The F1 generation already differed in their level of PPI ( $p < 0.001$ ), an effect that was further enhanced in the F2 generation ( $p = < 0.001$ ).

In order to test, whether the “PPI-deficit” of the *Low PPI* would be restored by antipsychotic drugs, male rats of the F2 generation were tested for PPI after injection of either the dopamine antagonist haloperidol, a typical antipsychotic compound, (0.1mg/kg in saline,  $n = 14$ ) or the atypical antipsychotic compound clozapine (2 mg/kg in saline,  $n = 14$ ). Compared to vehicle injection, haloperidol restored the “PPI-deficit” of the *Low PPI* to a level similar to that of the *High PPI* ( $p = 0.005$ ) while clozapine treatment tended to reverse the PPI-deficit ( $p = 0.082$ ).

These results indicate that disturbed sensorimotor gating in rats can be achieved by selective breeding. The “PPI-deficit” of the *Low PPI* can be restored by the typical antipsychotic haloperidol, indicating a disturbed dopamine system in these rats. Therefore, rats with low expression of PPI may be a valid model to study pathophysiological mechanisms underlying disorders like schizophrenia.

Supported by the DFG (SFB 517, TP A11)

Differential effects of chronic intermittent ethanol treatment during adolescence on sensorimotor gating and motor activity in rats postnatally exposed to ethanol

Stephan Röskam and Michael Koch

Department of Neuropharmacology, Brain Research Institute, University of Bremen, P.O. Box 330440, 28334 Bremen, Germany

Early postnatal exposure to ethanol during the 1-2 weeks of age can lead to a variety of cognitive and behavioural deficits in rats. In addition, recent studies showed that adolescence (including puberty) represents another period of sensitivity to the effects of ethanol. However, little is known about the effects of both postnatal and adolescent ethanol administration on subsequent adult behaviour in rats. Therefore, the objective of this study was to evaluate whether rats postnatally treated with ethanol exhibit an enhanced vulnerability to repeated ethanol exposure during puberty.

Rats received 5 g/kg of ethanol or vehicle on pd 7 in two separate treatments, 2 hours apart, each treatment delivering 2.5 g/kg ethanol intraperitoneally (ip). Chronic treatment of ethanol (1 g/kg) or vehicle lasted 3 weeks from pd 40 to pd 65 (rats puberty). In this period, the rats received 20 i.p. injections, which were not delivered regularly. After chronic ethanol treatment there was a rest period of 10 days before adult behavioural testing was started.

Spontaneous motor activity and prepulse inhibition (PPI) of the acoustic startle response (ASR), an operational measure of sensorimotor gating, were assessed on pd 35 (juvenile stage) and pd 75 (adult stage).

PPI in juvenile rats was significantly reduced by early postnatal ethanol exposure. Furthermore, locomotor activity was not disrupted by postnatal ethanol administration. Chronic ethanol treatment during adolescence in the same rats significantly reduced locomotion, number of rearings and total activity on pd 75, whereas PPI in adult rats was not affected by repeated ethanol exposure.

These data suggest that postnatal and chronic intermittent ethanol exposure during adolescence have a lasting impact on subsequent adult motor behaviour, but not on PPI. Since PPI is disrupted only by early postnatal ethanol exposure, it might be that at different stages of postnatal development the neural circuits underlying motor behaviour and sensorimotor gating show different sensitivity to the effects of ethanol. Moreover, the systems responsible for locomotor activity seem to be more vulnerable to the effects of combined postnatal and pubertal ethanol exposure compared to the systems responsible for PPI of the ASR.

This work was supported by DFG (SFB 517, TP A11)

## Neonatal cortical lesions and chronic pubertal stress: Effects on locomotor activity.

T. Enkel and M. Koch

Department of Neuropharmacology, Brain Research Institute, University of Bremen, P.O. Box 330440,  
28334 Bremen, Germany

Neurodevelopmental deficits are thought to underlie the psychopathology of a number of psychiatric disorders, like schizophrenia. Accordingly, neonatal brain lesions are a widely used animal model. On the other hand it is known that the experience of chronic stress or stressful life events precipitate or exacerbate psychotic symptoms and stress is a major factor in influencing the course and outcome of the disease. Impairments in prefrontal cortical functions cause various cognitive deficits similar to those observed in patients suffering from neuropsychiatric diseases and, moreover, the prefrontal cortex is also involved in mediating and modulating the stress response. In this study we therefore combined a neonatal lesion of the medial prefrontal cortex (mPFC) with a chronic pharmacological stress challenge during puberty, being a life span in which the brain undergoes various differentiation and reorganization processes and in which it is particularly vulnerable to stress. Since the manifestation of psychiatric symptoms occurs mainly at early adulthood the treatment effects on locomotor activity were assessed in rats at a juvenile and at an adult stage.

A mPFC lesion was induced on postnatal day 7 (pd7) by injecting male Wistar rats bilaterally with ibotenic acid (0,2µg/0,3µl/hemisphere). Control groups received either 0,3µl tris-buffered saline/hemisphere or were left untreated. Animals were then subjected to a mild chronic stress regimen in which a low dose of the stress hormone corticosterone (5mg/day) was applied via the tap water for 20 days in an irregular manner between pd35 and pd63. Locomotor activity was assessed by placing the animals in an open field arena for 30 min on pd35 (juvenile stage) and on pd70 (adult stage) and measuring the number of rearings and distance covered.

While we found no effect of the neonatal lesion on locomotor activity in juvenile rats, the same animals showed an increased number of rearings compared to control groups when tested on pd70. The chronic pubertal corticosterone treatment led to an increased locomotor activity regarding covered distance and number of rearings, the latter being most pronounced in lesioned animals. Analysis of the time courses revealed that the observed increase in locomotor activity resulted from a slower adaptation to the novel environment of the open field arena rather than from hyperactivity.

The effect observed resembles symptoms seen in patients suffering from psychiatric disorders, since an impaired ability to adopt to novel situations is found in schizophrenic patients. Our results show that a neonatal mPFC lesion can induce a behavioural abnormality that does not manifest until early adulthood. Furthermore, chronic pubertal stress per se can lead to an adaptation deficit and additionally worsens already existing lesion-induced symptoms. Thus, the psychopathological mechanism underlying psychiatric diseases like schizophrenia may possibly be a combination of an early developmental insult and a second stressful experience later in life.

This work was supported by the DFG (SFB 517, A 11).



**The antidepressant agomelatine counteracts stress-induced sleep EEG perturbations**

Schmelting B., Simon M. and Fuchs E.

Clinical Neurobiology Laboratory, German Primate Center, 37077 Göttingen, Germany

Stress can alter the sleep pattern in humans and animals. Agomelatine, an antidepressant with potent melatonin receptor agonist and 5HT<sub>2C</sub> receptor antagonist properties, has a restorative effect on sleep disturbances following acute stressful situations in laboratory rodents. However, it is unclear, how agomelatine acts in animals exposed to chronic stress. In the present study we investigated the nocturnal sleep pattern of psychosocially stressed male tree shrews – a valid animal model for depression - and the effect of agomelatine on the quantity and quality of sleep during chronic stress. In contrast to laboratory rodents, tree shrews are day active and show a monophasic night sleep. For registration of EEG and EMG activity animals received radiotelemetric implants (Datascience Int., St. Paul, USA). One control week was followed by a seven day period of psychosocial stress before the onset of daily oral administration of agomelatine (40 mg/kg), with stress continued throughout the 28-day treatment period. Night sleep was analyzed as wakefulness, NREM, REM sleep or movement for each 15 sec. epoch by visually scoring the EEG and EMG data imported to SleepSign® (Kissei Comtec, Irvine, USA). During the first stress week, the total amount of REM sleep showed a substantial increase whereas the average length of each REM period was reduced, the sleep pattern became fragmented. Despite the stress exposure continued, agomelatine led to a reduction of the total amount of REM sleep and created a less fragmented sleep pattern. Although no alteration in REM sleep latency was observed, agomelatine treatment seems to normalize the disturbed sleep pattern of stressed animals. Hence, our preliminary results suggest that sleep disturbances induced by chronic psychosocial stress might be treated successfully by agomelatine.

Supported in part by Institut De Recherches Internationales Servier, Courbevoie, France.

**Alkylglycerol-mediated opening of the blood-brain barrier for enhanced drug delivery to the brain and to brain tumors in rats.**

Hülper P<sup>1</sup>, Erdlenbruch B<sup>1</sup>, Kugler W<sup>1</sup>, Eibl H<sup>2</sup>, Lakomek M<sup>1</sup>

<sup>1</sup>Department of Pediatrics I, University of Göttingen, Robert-Koch-Str. 40, 37075 Göttingen, Germany

<sup>2</sup>Max-Planck-Institute for Biophysical Chemistry, Göttingen, Germany

Successful treatment of many brain disorders like neurodegenerative diseases or malignant brain tumors is impeded due to ineffective penetration of active drugs across the blood-brain barrier (BBB). Intracarotid bolus administration of the alkylglycerols 1-O-pentylglycerol (PG) or 2-O-hexyldiglycerol (HG) has been described as a potent method to increase the transfer of various drugs to the brain in the ipsilateral hemisphere, whereas the contralateral hemisphere remains largely unattached.

To visualize the differential permeability of the BBB, we have investigated the penetration of fluorescein sodium as well as of albumin- and gamma-globulin-coupled fluorescent dyes into the brain of normal and RG2-glioma bearing rats. The fluorescent markers were administered into the internal carotid artery in the presence and absence of PG and HG. Microscopic evaluation showed a marked ipsilateral extravasation of the fluorescent markers in PG- and HG-treated animals. The intensity of tissue fluorescence depended on the molecular weight (MW) of the respective marker. Fluorescein sodium (MW 376) showed a strong and homogeneous staining of the tissue. The large molecules rhodamine B200-albumin (MW 66.000), Alexa-Fluor488- and rhodamine B200-gamma-globulin (MW 150.000) resulted in a more patchy penetration into brain tissue. Tissue fluorescence was semiquantitatively analyzed using digital imaging and the strongest alkylglycerol-mediated increase in fluorescence was observed with the small fluorescein sodium. In glioma bearing rats, the presence of PG and HG was followed by enhanced tissue fluorescence in both, tumor and surrounding normal brain. The results were in agreement with those obtained using intracarotid methotrexate (MTX) in the absence or presence of alkylglycerols. Treatment with HG (100 mM) resulted in 10-fold higher concentrations of MTX in the tumor and 7-fold higher concentrations in surrounding ipsilateral brain as compared to controls without alkylglycerols. To evaluate the antitumor effects of an intraarterial chemotherapy in conjunction with alkylglycerols, the single and the repetitive administration of carboplatin with either PG or HG is under current investigation.

In conclusion, intracarotid alkylglycerols like PG or HG enhance the delivery of drugs of low and high molecular weight to the brain, and offer new options for the treatment of malignant brain tumors and other CNS-diseases.

Supported by Deutsche Krebshilfe (10- 1995-Er 3).

## **In vitro analysis of the neuroprotective potencies of natural compound derivatives**

**Wendt W.<sup>1</sup>, Sontag B.<sup>2</sup>, Lübbert H.<sup>1, 2, 3</sup> & Stichel C. C.<sup>3</sup>**

<sup>1</sup>*Department of Animal Physiology, Ruhr-University of Bochum, D-44780 Bochum;*

<sup>2</sup>*Biofrontera Discovery GmbH, D-69123 Heidelberg, Germany;*

<sup>3</sup>*Biofrontera Pharmaceuticals GmbH, D-51377 Leverkusen, Germany;*

Natural products of microorganisms are a source of cure for many CNS diseases. Some of the products have been identified as neuroprotective and may be beneficial in the treatment of neurodegenerative diseases such as M. Parkinson and M. Alzheimer. We aimed to identify new chemical derivatives of natural compounds with improved neurotrophic efficacy.

Therefore, we established several in vitro screening models that reflect major pathological processes of neurodegeneration. In detail, we treated different neuronal cell lines with either (i) staurosporine, an unspecific protein kinase inhibitor, (ii) thapsigargin or (iii) tunicamycin, two endoplasmic reticulum-stress inducing toxins. Moreover, we established a (iv) coculture model, composed of a neuronal cell line intoxicated with the supernatant of LPS-stimulated microglial cells. Cell death was analysed in the presence or absence of test compounds by MTS- and LDH-tests as well as immunohistochemical and histological stainings for degenerating cells.

In the present study we concentrate on derivatives of cyclosporin A, which is produced by a wide range of fungal strains. Cyclosporin A possesses immunosuppressive and neurotrophic activities and has been shown to reduce neuronal cell death in neurodegenerative diseases. We will compare the neuroprotective activities of different derivatives and discuss their therapeutic potential.

### **The ouabain-induced cell swelling of leech *Retzius* neurons is due to NaCl uptake**

Paul W. Dierkes, Guido Klees, Joachim Wüsten, Anja Müller, Peter Hochstrate, Wolf-R. Schlue  
Institut für Neurobiologie, Heinrich-Heine-Universität Düsseldorf, Germany

The electrochemical gradients for  $\text{Na}^+$  and  $\text{K}^+$  built up by the  $\text{Na}^+$ - $\text{K}^+$  pump are the prerequisite for the excitability of sensory, nerve, and muscle cells. Moreover, in virtually all cells the free energy of these gradients is used for the active transport of various ions and organic compounds. Therefore, the inhibition of the  $\text{Na}^+$ - $\text{K}^+$  pump will not only cause the breakdown of the gradients for  $\text{Na}^+$  and  $\text{K}^+$  but also trigger a complex chain of cellular events. One global parameter that might change upon pump inhibition is the total amount of osmolytes within the cytosol, which determines the water content of the cell and hence its volume. By using electrophysiological and microfluorometric methods we found that leech *Retzius* neurons swell after inhibition of the  $\text{Na}^+$ - $\text{K}^+$  pump by the cardiac glycoside ouabain. To explore the mechanism of this swelling we measured the effect of ouabain on the cytosolic concentrations of  $\text{Na}^+$ ,  $\text{K}^+$ , and  $\text{Cl}^-$  ( $[\text{Na}^+]_i$ ,  $[\text{K}^+]_i$ ,  $[\text{Cl}^-]_i$ ), as well as on the membrane potential by applying triple-barrelled ion-sensitive microelectrodes. As shown previously, ouabain induced a marked increase in  $[\text{Na}^+]_i$ , a corresponding drop in  $[\text{K}^+]_i$ , and a membrane depolarization (Deitmer & Schlue 1983, Kilb & Schlue 1999). In addition, we found that ouabain evoked a substantial increase in  $[\text{Cl}^-]_i$ . All these changes proceeded in several phases, which may be explained by the suppression of the electrogenic pump current and the subsequent activation of ion channels, in particular persistently active voltage-dependent  $\text{Na}^+$  channels ( $I_{\text{NaP}}$ , Angstadt 1999). The quantitative analysis of the data showed that the ouabain-induced inhibition of the  $\text{Na}^+$ - $\text{K}^+$  pump causes a net uptake of NaCl, which is responsible for the ouabain-induced cell swelling: 1) The increase in the intracellular osmolyte content due to NaCl uptake closely matches the volume increase. 2) In the absence of extracellular  $\text{Na}^+$  or  $\text{Cl}^-$  the cell volume remained unaffected by ouabain.

Surprisingly, a cell swelling did not occur upon inhibition of the  $\text{Na}^+$ - $\text{K}^+$  pump by removing  $\text{K}^+$  from the bath solution. In  $\text{K}^+$ -free solution,  $[\text{Na}^+]_i$  increased and  $[\text{K}^+]_i$  dropped, but  $[\text{Cl}^-]_i$  and the intracellular osmolyte content remained virtually unchanged. The changes in  $[\text{Na}^+]_i$  and  $[\text{K}^+]_i$  proceeded more slowly than upon ouabain application, which suggests that pump inhibition was less efficient, probably because  $\text{K}^+$  could not be washed out completely from the extracellular space (Schlue & Deitmer 1980). However, the main reason for the different effects of ouabain and the removal of bath  $\text{K}^+$  is that  $\text{K}^+$  removal induced only an initial, slight depolarization which turned to a long-lasting hyperpolarization, possibly due to the temporary increase of the electrochemical  $\text{K}^+$  gradient. It is concluded that the prerequisite for the ouabain-induced NaCl uptake or, respectively, cell swelling is the depolarization of the plasma membrane, which generates an inwardly directed electrochemical  $\text{Cl}^-$  gradient (see Armstrong 2003).

#### *References*

Angstadt (1999) *J Comp Physiol A* 184: 49-61, Armstrong (2003) *PNAS* 100: 6257-6262, Deitmer & Schlue (1983) *Pflügers Arch* 397: 195-201, Kilb & Schlue (1999) *Brain Res* 824: 168-182, Schlue & Deitmer (1980) *J exp Biol* 87: 23-43

Supported by the DFG (Graduiertenkolleg 320 "Pathophysiologische Prozesse des Nervensystems")

**Bromophenols, present both in marine organisms and in industrial flame retardants,  
disturb cellular calcium signaling in neuroendocrine cells (PC12)**

Thomas Hassenklöver<sup>1\*\*</sup>, Sabine Predehl<sup>1\*\*</sup>, Jyotsna Pili<sup>1\*\*</sup>, Michael Assmann<sup>2 (\*)</sup>,  
Ulf Bickmeyer<sup>3\*</sup>

<sup>1\*\*</sup> Students of Biology/Zoology at the University of Hamburg, Germany

<sup>2</sup> Alfred-Wegener-Institut für Polar- und Meeresforschung in der Helmholtz-GemeinschaftAWI, Am Handelshafen 12, 27570 Bremerhaven, Germany

<sup>3 \*</sup> Alfred-Wegener-Institut (AWI) für Polar- und Meeresforschung in der Helmholtz-Gemeinschaft, Biologische Anstalt Helgoland, Kurpromenade, 27498 Helgoland, Germany

Bromophenols are present in marine polychaetes as well as in algae like e.g. the brown macroalgae *Sargassum siliquastrum* and *Padina arborescens*, containing high concentrations up to 7000 ng/g. They are thought to cause the typical sea-like taste and flavour (Chung *et al.*, 2003).

The ecological role of brominated phenols is not clear, they may play a role in chemical defence and deterrence (Kicklighter *et al.*, 2004). Some brominated phenols are commercially used as industrial flame retardants as 2,4,6-tribromophenol and are suspected to disrupt the humoral system by binding to the estrogen receptor (Legler & Brouwer, 2003). We found that some of the compounds we tested, especially 2,4-dibromophenol and 2,4,6-tribromophenol show a disturbance of calcium homeostasis in endocrine cells (PC12) at concentrations in the  $\mu\text{M}$  range. The reduction of depolarization induced calcium elevations by 2,4-dibromophenol and 2,4,6-tribromophenol and the increase of intracellular calcium levels by both substances at higher concentrations may suggest a link to the disrupting effect of endocrine systems by brominated phenols. 2,4-Dibromophenol was the most potent substance we tested, reducing voltage dependent calcium currents as revealed in whole cell patch clamp experiments. In respect to a related experimental approach using brominated pyrrole alkaloids from marine *Agelas* sponges (Bickmeyer *et al.*, 2004), brominated marine phenol and pyrrole metabolites seem to disturb cellular calcium signaling with differential efficacy.

Bickmeyer U., Drechsler C., Köck M., Assmann M., (2004). Brominated pyrrole alkaloids from marine *Agelas* sponges reduce depolarization-induced cellular calcium elevation. *Toxicon.*, **44**,. 45-51. 2004

Chung H. Y., Ma W. C. J., Ang P. O., Kim J. S., Chen F., (2003). Seasonal variations of bromophenols Bromophenols in brown algae (*Padina arborescens*, *Sargassum siliquastrum* and *Lobophora variegata*) collected in Hong Kong. *J. Agric. Food Chem.*, **51**,. 6752-6760. 2003

Kicklighter C. E., Kubanek J., Hay M. E., (2004). Do brominated natural products defend marine worms from consumers? Some do, most don't. *Limnol. Oceanogr.*, **49**,. 430-441. 2004

Legler I., Brouwer A., (2003). Are brominated flame retardants endocrine disruptors? *Environ. Int.*, **29**,. 879-885. 2003

## Antidepressant-like effects of group I mGluRs antagonists are associated with the changes in BDNF gene expression

Beata Legutko<sup>1</sup>, Piotr Brański<sup>2</sup>, Agnieszka Pałucha<sup>2</sup>, Bernadeta Szewczyk<sup>2</sup>, Joanna M. Wierońska<sup>2</sup>, Gabriel Nowak<sup>2,3</sup>, Andrzej Pilc<sup>2,3</sup>

<sup>1</sup>Department of Pharmacology, <sup>2</sup>Department of Neurobiology, Institute of Pharmacology, Polish Academy of Sciences, Krakow, Poland; <sup>3</sup>Collegium Medicum, Jagiellonian University, Krakow, Poland.

Glutamate, the major excitatory neurotransmitter in the brain, acts by stimulation of two distinct groups of receptors: ionotropic glutamate receptors (iGluR; including NMDA, AMPA and kainate receptors), which are coupled to ion channels, and metabotropic glutamate receptors (mGluR), a family of G-protein-coupled receptors. The mGluR are classified into three groups according to their sequence homology, effector coupling and agonist selectivity. Group I mGluR (mGlu1 and mGlu5) are coupled to phosphatidylinositol hydrolysis/ $\text{Ca}^{2+}$  signal transduction pathway, while group II (mGluR2 and mGluR3) and group III mGluR (mGluR4, mGluR6, mGluR7 and mGluR8) are both coupled in an inhibitory manner to adenylyl cyclase signal transduction pathway.

The studies concerning implications of glutamate in affective disorders, including depression, have been intensified in recent years. Since functional NMDA receptor antagonists have been shown to exhibit antidepressant-like effects in animal tests and models of depression, it became clear that NMDA receptor may be one of promising targets of a novel antidepressant therapy. Unfortunately, potential clinical use of NMDA antagonists is limited due to the fact that these drugs produce several adverse effects. Discovery of selective ago/antagonists, which activate/inhibit central nervous system function via mGluRs, provides a novel target for development of therapeutic agents. In the last few years, attention has focused on antagonists of group I mGluRs, which are known to inhibit glutamatergic neurotransmission.

According to the recently proposed hypotheses, the brain-derived neurotrophic factor (BDNF) is involved in the mechanism of antidepressant action as one of the main targets of antidepressants. Antidepressant drugs of different types were shown to induce an increase in hippocampal and/or cortical BDNF mRNA level.

The present study was carried out to investigate whether prolonged (14 days) treatment with group I mGluRs antagonists (MPEP, MTEP,  $\text{Zn}^{2+}$ ) induces changes in BDNF mRNA level in rat cerebral cortex and hippocampus. Moreover, potential antidepressant-like effects of MPEP and MTEP (potent and highly selective mGluR5 antagonists) were evaluated using the forced swimming test in rats, the tail suspension test in mice and the olfactory bulbectomy (OB) model of depression in rats. All the experiments were performed on male Wistar rats and male C57BL/6J mice.

The results of the Northern blot analysis showed, that chronic treatment with  $\text{Zn}^{2+}$  (11 mg/kg) induced an increase in cortical but not hippocampal level of BDNF mRNA. On the other hand, repeated administration of MPEP (10 mg/kg) induced an increase in BDNF mRNA level in hippocampus, without affecting it in the cerebral cortex.

The results of behavioural studies showed, that both MPEP (1 – 20 mg/kg) and MTEP (0.3 – 3 mg/kg) produced a significant dose-dependent decrease in the immobility time of mice in the tail suspension test, without affecting the locomotor activity, however, they did not influence the behaviour of rats in the forced swimming test and in the locomotor activity test in rats. Moreover, repeated administration of both mGluR5 antagonists, used at doses of 10 mg/kg (MPEP) and 1 mg/kg (MTEP), attenuated the OB-related behavioural changes in the manner similar to that seen following chronic (but not acute) treatment with a variety of typical and atypical antidepressants.

In conclusion, the results of our experiments show that group I mGluRs antagonists induce increases in BDNF gene expression, which is the effect shared by most of clinically effective antidepressants; moreover, they possess potential antidepressant-like activity. Thus, the results of our studies strongly suggest, that group I mGluRs antagonists may play a role in the therapy of depression.

*Support Contributed By: Grant No K058/P05/2003 to BL*

## GLUCOCORTICOID MEDIATED DECREASE OF THE INCIDENCE OF INTRAVENTRICULAR HEMORRHAGE IS PROBABLY DUE TO MATURATIONAL EFFECTS ON CEREBRAL AUTOREGULATION AT THE EXPENSE OF INCREASED NEURONAL DAMAGE IN VULNERABLE BRAIN REGIONS

I Antonow-Schlorke<sup>1</sup>, T Müller<sup>2</sup>, M Loehle<sup>1</sup>, CE Wood<sup>3</sup>, H Schubert<sup>2</sup>, OW Witte<sup>1</sup>, M Schwab<sup>1</sup>

<sup>1</sup>Dept. Neurology, <sup>2</sup>Inst. Lab Animal Science, Friedrich Schiller University, Jena, Germany;

<sup>3</sup>Dept. Physiology Functional Genomics, University of Florida, Gainesville, FL

**Objective:** Antenatal glucocorticoids (GC) administered to accelerate fetal lung maturation in women threaten premature labor prevent intraventricular hemorrhage (IVH). Clinical studies examining the incidence of periventricular leukomalacia and the neurological outcome after GC treatment showed inconclusive results. The same applies to experimental studies showing neuroprotective effects in juvenile and neurotoxic effects in adult rats after cerebral hypoxia or ischemia. Maintenance of glycolytic flux were assumed to be the cause of the former and inhibition of neuronal glucose uptake of the latter effect. We hypothesized direct vascular GC effects are rather critically in perinatal asphyxia than metabolic effects based on our previous findings that antenatal GC increase cerebral vascular resistance (CVR).

**Methods:** Our studies were performed in utero in chronically instrumented fetal sheep the species in which antenatal GC therapy has been developed. We examined GC effects on cerebral autoregulation using laser Doppler flowmetry during fetal blood pressure (FBP) changes induced by phenylephrine and sodium nitroprusside 24h after the start of fetal infusion of 3 µg/kg/h betamethasone (BM) at 0.8 gestation. At the time, brain damage was induced by repetitive umbilical cord occlusion (UCO) for 4x4min 30min apart in a second set of animals. Perfusion fixed brain tissue slices were stained with HE and immunostained with polyclonal antibodies against the glucose transporter GLUT1, the rate limiting transporter in the brain blood barrier, and GLUT3, occurring in neuronal membranes.

**Results:** The GC induced CVR increase shifted the upper limit of cerebral autoregulation from 50±2 to >80 mmHg within 24h. Such a shift occurs usually slowly during late gestation when the cardiovascular system matures. This shift is probably responsible for preventing rupture of small vessels during post-asphyxia hyperperfusion and, thus, preventing IVH. Due to the CVR increase the lower limit of cerebral autoregulation shifted from 35±1 to 43±2 mmHg and may endanger the brain during hypotension. Consistently, GC led to an increase of neuronal damage in the parasagittal cortex and hippocampus after UCO (p<0.05). Post-asphyxia increase of GLUT1 was enhanced and GLUT3 was not affected by BM (p<0.05). Hence, inhibition of glucose transport seems not to be the mechanism of GC mediated neuronal endangerment.

**Conclusions:** The increase of CVR and the concomitant shift of the upper limit of cerebral autoregulation seems to be crucial for the protective effect of antenatal GC against IVL. This protection is paid for by an endangerment to more subtle brain lesions that may contribute to the disturbances in neuronal function after perinatal asphyxia.

## TIME COURSE OF CELL BIRTH AND DEATH DURING INTRAUTERINE BRAIN DEVELOPMENT - EFFECTS OF GLUCOCORTICOIDS

M Brodhun<sup>1</sup>, I Antonow-Schlorke<sup>2</sup>, T Coksaygan<sup>4</sup>, T Müller<sup>3</sup>, H Schubert<sup>3</sup>, PW Nathanielsz<sup>4</sup>, OW Witte<sup>2</sup>, M Schwab<sup>2</sup>

<sup>1</sup>Inst. Pathology, <sup>2</sup>Dept. Neurology, <sup>3</sup>Inst. Lab Animal Science, Friedrich Schiller University, Jena, Germany; <sup>4</sup>Dept. Obstetrics Gynecology, New York University School of Medicine, NY, USA.

**Objective:** Knowledge of the time-course of cell proliferation and its association to programmed cell death (PCD) during fetal brain development is sparse and not systematically explored. PCD plays a regulatory role in the developing rat and chicken embryo brain. Glucocorticoids (GC) are necessary for cell proliferation in the rat hippocampus. On the other hand, selective occupation of type II glucocorticoid receptors (GR) induces apoptosis and synthetic GC inhibit growth of the developing brain. We examined the developmental profile of cell proliferation and PCD in the gyrencephalic fetal sheep brain that develops mainly prenatally. In addition, we evaluated the effects of antenatal GC at the dose used clinically to accelerate fetal lung maturation in babies threaten premature labor.

**Methods:** Cell proliferation and PCD was estimated at 0.27 (n=7), 0.40 (n=7), 0.55 (n=7), 0.75 (n=11), 0.85 gestation (n=10) and at the 1<sup>st</sup> (n=5) and 6<sup>th</sup> (n=5) postnatal day with NCL-Ki-67-MM1 antibodies, Caspase-3 and the TUNEL method. The dose of 2x12 mg betamethasone (BM) i.m. 24 h apart that is used clinically to accelerate fetal lung maturation was injected before expression of GR at 0.27 gestation (n=4). The equivalent dose of 3 µg/kg/h BM was infused to the fetus over 48h before (0.75 gestation, n=5) and during (0.85 gestation, n=5) prepartum maturation of the HPA axis. GR were stained using using a monoclonal antibody against GR (Clone BuGR2, Affinity Bioreagents Inc).

**Results:** Cell proliferation was highest between 0.27 and 0.4 gestation in the subventricular zone and started to decrease at 0.55 gestation (p<0.05). PCD, however, was constantly low from 0.27 to 0.55 gestation and reached a maximum of  $17 \pm 3\%$  at 0.75 gestation. This may reflect higher rates of odd cells produced at the end of the high-proliferation period. Number of proliferating cells in the other brain regions showed no clear peak but ceased also towards the end of gestation. Here, PCD showed temporal and regional differences, typically a peak, and no close association to cell proliferation suggesting target related cell death. PCD peaked first in the brainstem at 0.27 gestation and last in the hippocampus at 0.75 gestation (p<0.05). At 0.27 gestation when no GR are expressed, BM did not affect cell proliferation or PCD. At 0.75 gestation when GR are expressed, BM tended to increase cell proliferation accompanied by an increase in PCD in the subcortical white matter and thalamus (p<0.05). During maturation of HPA axis when endogenous cortisol levels rise, cell birth and death were not affected by BM.

**Conclusions:** The fetal sheep brain was proliferative most active around 0.4 gestation. Proliferation is associated to less than 5% proliferative cell death. Proliferation and migration continues until after birth at a low level. PCD in the brain regions where the cells migrate to reflects mainly target related cell death. Synthetic GC increase PCD in the brain when GR are expressed but endogenous cortisol level is still low. This effect is probably secondary to increased cell proliferation.



## **JNK2 translocates to the mitochondria and mediates cytochrome c release in PC12 cells following 6-hydroxydopamine**

A. Klettner, S. Eminel, L. Roemer, V. Waetzig, T. Herdegen

Institute of Pharmacology, Hospitalstrasse 4, Klinikum Schleswig-Holstein, Campus Kiel, 24105 Kiel, Germany

### **Mailing addresses**

A. Klettner: Soenke.Klettner@t-online.de

S. Eminel: eminel@pharmakologie.uni-kiel.de

L. Roemer: lutz.roemer@pharmakologie.uni-kiel.de

T. Herdegen: t.herdegen@pharmakologie.uni-kiel.de

V. Waetzig: vicki.waetzig@pharmakologie.uni-kiel.de

6-hydroxydopamine (6-OHDA) causes death of dopaminergic neurons by mitochondrial dysfunction with c-Jun N-terminal kinases (JNKs) as central mediators. Here, we provide novel insights into specific actions of JNK isoforms in 6-OHDA-induced death of PC12 cells. Twenty-five  $\mu\text{M}$  6-OHDA enhanced total JNK activity in the cytoplasm, nucleus and at the mitochondria. Inhibition of JNKs by 2  $\mu\text{M}$  SP600125 and transfection with dominant-negative JNK2 (dnJNK2) rescued more than 60% of the otherwise dying PC12 after 24 h, while transfection with dominant-negative JNK1 (dnJNK1) had no protective effects. In contrast to constitutively present JNK1, JNK2 increased in the nucleus and at the mitochondria. JNK-inhibition by SP600125 or transfection of dnJNK2 reduced the pool of active JNKs in the nucleus and the release of cytochrome c. In consequence, dnJNK2 also attenuated the transcription of *bim* between 18 and 24 h following 6-OHDA. Moreover, dnJNK2 abrogated the activation of MKK4 at the mitochondria, but did not affect its presence. Transfection with dnJNK1, however, had no effects on the translocation of JNKs to the mitochondria, the release of cytochrome c or the phosphorylation of MKK4.

Our data provide novel details on the pathological role of individual JNK isoforms, the signalosome at the mitochondria and the mode of JNK-induced release of cytochrome c.

**JNK mediate death and sprouting of primary hippocampal neurons.****Sevgi Eminel and Thomas Herdegen**

Glutamate plays a crucial role in synaptic plasticity and excitotoxic cell death. In this study, mixed neuronal cultures from new born rat pups (0-24 h) were stimulated with 250  $\mu$ M glutamate for 24 hours. Cell death was accompanied by a marked decrease of MAP-2 immunoreactivity and DAPI staining accompanied by the death of 35% of the neurons examined. Surviving neurons displayed morphological signs of stress with shortened dendrites and vacuolated cytoplasm. Staining of neurons with DAPI also showed morphological features of apoptotic cell death (nuclear condensation) after 24 h glutamate stimulation while glutamate had no effect on astrocytes. Inhibition of JNKs by 2  $\mu$ M SP600125 rescued more than 75% of dying neurons.

Caspase-3-activation is also considered to play a vital role in the execution of apoptosis. To determine whether caspase-3 activation was involved in glutamate-induced cell death, Western blot analysis was performed using a cleaved-caspase-3 specific antibody that recognizes the p17 subunit of activated caspase-3. Glutamate stimulation for 24 h induced caspase-3 activation which was inhibited after 2  $\mu$ M SP600125.

Finally, we wanted to know whether JNKs are essential for the formation and elongation of neuritis as shown in PC12 cells. Mixed hippocampal cultures were exposed to 2  $\mu$ M SP600125 on the 2<sup>nd</sup>, 3<sup>rd</sup> and 5<sup>th</sup> day *in vitro*. At early stages of culture, inhibition of JNKs (at DIV 2 and DIV 3) prevented neurite elongation while at DIV 5 inhibition of JNKs had no or little effects on neurite elongation.

Our data provide evidence that JNKs have apoptotic effects after an excitotoxic stimulus but in contrast to their apoptotic effects they have also physiological functions on neurite formation and elongation *in vitro* at early stages of development.

# EXPRESSION OF PURINERGIC RECEPTORS IN THE HYPOTHALAMUS OF THE RAT IS MODIFIED BY REDUCED FOOD AVAILABILITY

B. Seidel<sup>\*</sup>, M. Bigl<sup>#</sup>, H. Franke, H. Kittner, P. Illes, W. Kiess<sup>\*</sup>, U. Krügel

The receptors for ATP and its metabolite adenosine are probably of functional relevance in the process of reward and reinforcement, e.g. in feeding behavior. It was shown recently that purinergic receptors play a role in the response to reduced food availability in the nucleus accumbens<sup>1</sup>.

The present study investigates how a restricted feeding regimen affects the purinergic transmission at the level of ADP/ATP - sensitive P2Y<sub>1</sub> receptor mRNA expression in the rat hypothalamus. Expression levels were examined after three days (in the situation of acute restriction) and after ten days (when adaptive changes in response to the restriction could be expected). In order to characterize the actual state of nutrition, plasma levels of the anorectic peptide leptin as well as the expression of leptin receptor mRNA (OB-RL, long form) were recorded.

Leptin levels were decreased within three days of feeding restriction, and the expression of OB-RL mRNA was augmented at day ten of food restriction by approximately 20 %.

With respect to the P2Y<sub>1</sub> receptor, the specific mRNA expression was elevated on day three by 38% and on day ten by 29 %. These data were confirmed by Western Blotting experiments where the P2Y<sub>1</sub> protein amount was increased by 35% and 65%, respectively, and by immunohistochemical analysis on rat brain slices at the level of the lateral and dorsomedial hypothalamus.

In summary, this outcome suggests that, during food restriction, peripheral signals such as the plasma leptin level trigger regulatory mechanisms in the hypothalamus. It also indicates that purinergic receptors of the P2Y<sub>1</sub>-subtype, which are important for the reinforcement of neuronal transmission, participate in these mechanisms.

<sup>1</sup> Krügel, et al., 2003, Drug Dev. Res. 59, 95-103

<sup>\*</sup>Children's Hospital, <sup>#</sup>Institute of Biochemistry and Rudolf-Boehm-Institute of Pharmacology and Toxicology, University of Leipzig, D-04107 Leipzig, Germany

## **Serotonin 5-HT1A and 5-HT1B antagonists exhibit antidepressant-like activity in the guinea pig forced swim test**

K.M. Wicke, G. Gross

Neuroscience Discovery Research, Abbott, Ludwigshafen, Germany

The behavioral despair paradigm has high predictive value for antidepressant activity. So far, such models were limited to rats and mice. Drug targets, like neurotransmitter transporters and receptors, however, often show species differences and a pharmacology, which differs between murids and humans. In many cases guinea pig receptors display higher homology with their human counterparts as compared to the murid receptor: e.g. the serotonin 5-HT1B receptor. Recently, we reported, that guinea pigs can be used in the forced swim test as a model of behavioral despair<sup>1</sup>. The objective of the present study was to validate this model for its ability to detect antidepressant-like activity. For this purpose we used a variety of established antidepressants, like the tricyclic antidepressants desipramine (0.3-30 mg/kg) and amitriptyline (1-30 mg/kg), the MAO inhibitor tranylcypromine (1-10 mg/kg), and the selective serotonin reuptake inhibitors (SSRI) fluoxetine (5-20 mg/kg) and paroxetine (0.1-3 mg/kg). We also investigated the effects of the selective 5-HT1A receptor antagonist WAY 100635 (0.003-1 mg/kg) and the 5-HT1B/D receptor antagonists GR127935 (3-10 mg/kg) alone and in combination for potential antidepressant-like properties.

Male guinea pigs were habituated to the swimming procedure 24 h before the experiment: for five minutes, they were transferred to a glass cylinder filled with water of 30°C. On the following day, swimming and climbing activity were measured for 5 min. Animals received i.p. injections of either saline or test compounds 24, 4 and 0.5 h before the test procedure.

Both tricyclic antidepressants, desipramine ( $\geq 3$ mg/kg) and amitriptyline ( $> 10$ mg/kg), reduced the immobility time by 60% ( $p < 0.05$ ). Tranylcypromine (10mg/kg) as well as the SSRIs paroxetine ( $> 0.3$ mg/kg) and fluoxetine ( $> 10$  mg/kg) reduced immobility significantly, but only by 25-40%. WAY 100635 dose-dependently and significantly reduced the immobility by 25% at 0.03mg/kg and 85% at 1mg/kg. GR 127935 also leads to a significant decrease of 20% at 10mg/kg. The combination of low doses WAY 100635 (0.003mg/kg) and GR 127935 (3mg/kg) was not superior to the effect of either compound alone.

Our study demonstrates that (i) the forced swim test can be adapted to the guinea pig to predict antidepressant activity: reference compounds are similarly effective as in rats and mice. (ii) The forced swim test in guinea pigs seems to be suited to characterize 5-HT1A antagonists in vivo, since WAY 100635 decreases immobility at low doses. In other behavioral models, effects of HT1A antagonists are hardly detectable. (iii) The 5-HT1B/D receptor antagonist GR127935 has antidepressant-like effects in this model, which cannot be enhanced by 5-HT1A antagonism.

<sup>1</sup> Wicke and Gross (2004) Soc Neurosci Abstr 30: The guinea pig forced swim test: a new model for behavioral despair

**Antidepressants inhibit wheel running activity in NMRI mice**

Martin Weber\*, Christine Boeddinghaus, Helga Buschbacher, Sonja Butty, Gerhard Gross and Karsten Wicke

Neuroscience Discovery Research, Abbott, Ludwigshafen, Germany

The central nervous serotonin system controls motor behavior by acting on different regions of the brain and the spinal cord<sup>1</sup>. Serotonergic brainstem neurons mediating such effects display distinct changes of activity pattern across the sleep-wake-arousal cycle<sup>1,2</sup>. Virtually all classes of antidepressant drugs are assumed to enhance the serotonergic tone by inhibiting the neuronal serotonin transporter, blocking the metabolism of serotonin, or indirectly via enhancing noradrenergic mechanisms. In the present study, we used NMRI mice to investigate drugs representing different antidepressant classes for their effects on running-wheel activity (RWA), a model, which reflects both, motor output and circadian function.

Running wheel activity was measured as rotations over a period of 24 h. Test compounds or vehicle were administered i.p. 2 h prior to the onset of the activity period ( $n \geq 6/\text{group}$ ). As expected, the neuroleptic haloperidol in doses known to depress motor activity (0.5 and 25 mg/kg) reduced running-wheel activity to 16 % and 13 % of control, respectively, whereas the psychostimulant methamphetamine (3 mg/kg) was found to increase running-wheel activity to 154 % of controls. The selective serotonin reuptake inhibitor (SSRI) fluoxetine (10 and 20 mg/kg) dose-dependently reduced RWA to 69 % and 35 % of control, respectively. Other antidepressants were also found to suppress RWA in a similar manner: paroxetine, another SSRI, (30 mg/kg; 7 % of control), the monoamine oxidase inhibitor tranylcypromine (3 mg/kg; 76 % of control), and the tricyclic antidepressant imipramine (30 mg/kg; 75 % of control). All effects were significant ( $p < 0.05$ ). Desipramine (30 mg/kg), a predominant noradrenaline reuptake inhibitor, failed to produce a significant reduction (91 % of control;  $p = 0.126$ ).

These results demonstrate that antidepressants with a predominant serotonergic component decrease RWA. The decreased activity in RWA is in contrast to enhanced locomotor activity found for acutely administered SSRIs in NMRI mice in a novel environment<sup>3</sup>. It remains to be investigated, if effects of antidepressants on the sleep-wake-arousal cycle might explain the decreased RWA. Compared to behavioral despair models, RWA seems to discriminate better between antidepressants and psychostimulants and can thus be useful for the characterization of antidepressants.

<sup>1</sup> Jacobs and Fornal (1997), Handbook Exp Pharmacol 129: 91-116

<sup>2</sup> Morin (1999), Ann Med 31, 12-33

<sup>3</sup> Brocco et al. (2002), Pharmacol Biochem Behav 71: 667-680

\* corresponding author

**Behavioral sensitization to quinpirole in rats: no change of striatal density of dopamine D<sub>1</sub>, D<sub>2</sub> receptors and the dopamine transporter**

Erik Schuetz, Ana Lucia Jongen-Rêlo, Karla Drescher, Ulrich Ebert, Gerhard Gross, Hans Schoemaker

Neuroscience Discovery Research, Abbott, Ludwigshafen, Germany

Behavioral sensitization is a mechanism supposed to contribute to psychopathologic states like drug abuse and psychosis. In this study we analyzed, if sensitized responses to quinpirole, a mixed D<sub>2</sub>/D<sub>3</sub> agonist, can be attributed to changes in the density of dopamine receptors and the dopamine transporter.

Adult Sprague-Dawley rats (n = 8-10 per group) received eight s.c. injections (every second day) of either quinpirole (0.25 mg/kg) or vehicle. One week after completion of this regimen, the quinpirole-treated animals were challenged with quinpirole (Q/Q) or vehicle (Q/V). Likewise, vehicle-pretreated subjects were given either quinpirole (V/Q) or vehicle (V/V). The horizontal motor activity was registered in separate motility cages. Striatal brain slices covering a rostro-caudal distance of about 1400 µm were taken after the challenge injections. [<sup>3</sup>H]Sch 23390, [<sup>3</sup>H]raclopride, and [<sup>3</sup>H]mazindol were used to visualize dopamine D<sub>1</sub>, and D<sub>2</sub> receptors and the dopamine transporter, respectively, by receptor autoradiography (n = 4-5 per group). Changes of expression were determined densitometrically.

Repetitive administration of quinpirole resulted in a gradual increase of the locomotor response. When challenged with quinpirole one week later, chronically treated animals (Q/Q) showed a significantly stronger locomotor response to quinpirole (+72%, p < 0.001) than vehicle-pretreated animals (V/Q). The activity of the withdrawn animals (Q/V) was not different from that of controls (V/V). No changes of the expression of D<sub>2</sub> receptors and the dopamine transporter were discernable in the investigated brain areas in the different experimental groups. Only D<sub>1</sub> receptors displayed a significantly increased density (p < 0.05) in the ventral striatum and the olfactory system in both, rats acutely ([V/Q], +32% and +27% vs. controls [V/V], respectively) and chronically ([Q/Q], +29% and +33% vs. controls, respectively) treated with quinpirole.

The results suggest that environmental cues do not contribute significantly to the development of behavioral sensitization to quinpirole, since quinpirole-pretreated animals display only basal locomotor activity in the withdrawal state when reexposed to the environment of previous drug experience. Quinpirole-induced sensitization cannot be explained by altered density of D<sub>2</sub> receptors and dopamine transporters. Quinpirole seems to acutely rather than chronically influence the number of D<sub>1</sub> receptors. Other mechanisms, for instance the D<sub>3</sub> receptor, must be assumed to account for sensitized behavioral responses.

## Alcohol Effects on Firing Rate and Temperature-Sensitivity of Hypothalamic Neurons in Rat Brain Slices

Bastian T Wollweber, Horst Schneider, Karlheinz Voigt, Hans A Braun  
Institut für Normale und Pathologische Physiologie, Philipps-Universität, Marburg

We have used electrophysiological experiments with extracellular impulse recording from rat hypothalamic slices to examine the neuromodulatory effects of alcohol. Specifically, we wanted to examine to what extent alcohol contributes to firing rate changes when substances are applied which, like PGE<sub>2</sub>, are diluted in alcohol. Moreover, we wanted to evaluate the neuronal correlates of systemic alcohol effects on autonomous functions like neurosecretion and temperature regulation.

We have addressed these questions with extracellular impulse recordings from single neurons (n=59) in different hypothalamic nuclei mainly in the PVN, SON and ARC. Alcohol induced changes of the firing rate have been examined during application of ethanol (EtOH, 17-137mM in ACSF according to 0.1-0.8%). Moreover, we have examined the neuromodulatory alcohol effects with application of ethanol during ongoing sinusoidal temperature changes (37°C±2°C, f=0.01Hz).

EtOH induced firing rate changes showed a remarkable time course. There was an immediate but only transient increase of the firing rate which after 1-5 min decreased, often down to zero (for 2-20 min), before it spontaneously recovered, during ongoing EtOH application, to a constant firing rate which was sometimes even higher than under control conditions. When EtOH application was stopped the firing rate gradually approached almost the same level as before. Such triphasic frequency changes could be seen in more than 50% of the neurons, preferably at higher EtOH concentrations.

The triphasic time-course still could be recognized when EtOH was applied during sinusoidal temperature changes (see Fig.). Superimposed on the temperature induced frequency changes, there is a transient frequency increase (phase 1) which is followed by an inhibition (phase 2). Remarkably, the spontaneous recovery (phase 3) was generally associated with a drastic increase of the neurons thermosensitivity which mainly results from stronger inhibition during cooling. In contrast, the firing rate at the temperature maxima, rather seem to be increased.

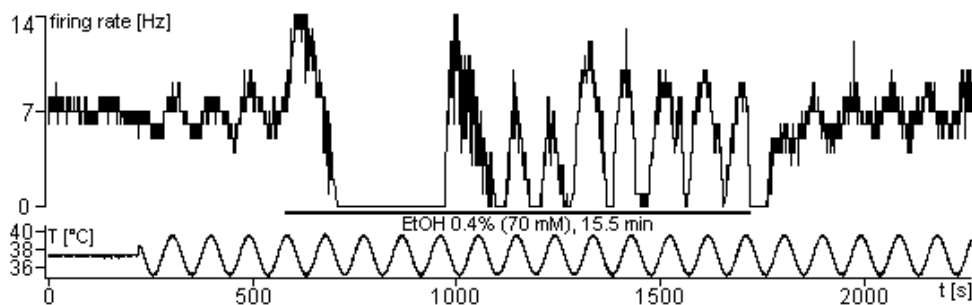


Fig.:  
EtOH effects on  
the firing rate of a  
hypothalamic  
neuron during  
sinusoidal  
temperature  
changes.

In conclusion, these electrophysiological data elucidated complex EtOH effects on firing rate and temperature sensitivity which suggest multiple sites of action of EtOH (e.g. different ion channels and membrane fluidity) with different time delays and thresholds. Although, these electrophysiological data do not seem to fit easily to the current concepts of alcohol effects, at least in case of neurosecretion, it is known that lower concentrations of EtOH inhibit the vasopressin release whereas higher concentrations can potentize the release of vasopressin (Brinton 1986 Neurosci Lett 67:213-217). In a more general sense, these findings indicate strong nonlinear interactions between different types of stimuli in neuronal encoding which are of relevance for systemic functions and which cannot be predicted from the knowledge about the individual stimulus responses.

Supported by the "Medizinstiftung" of the University of Marburg and INTAS grant 01-2061.

## Effect of Antisense Oligonucleotides on Reelin Translation and Synaptic/Dendritic Protein Expression in the Rat Brain

Grit Vollmer<sup>+</sup>, Kerstin Schwabe\*, Michael Koch\*, Christiane Richter-Landsberg<sup>+</sup>

<sup>+</sup> Department of Biology, Molecular Neurobiology,  
University of Oldenburg, POB 2503, 26111 Oldenburg, Germany

\* Brain Research Institute,  
University of Bremen, POB 330440, 28334 Bremen, Germany

Reelin, a protein of the extracellular matrix (ECM), is downregulated in the prefrontal cortex (PFC) and subcortical brain regions of schizophrenic patients. During development, reelin regulates cortical and cerebellar lamination. Furthermore, in adult subjects reelin seems to play a role in synaptogenesis. In heterozygous reeler mutant mice, that express only 50% of the normal amount of reelin, the number of synaptic contacts is reduced, as seen as a decrease of neuropil and dendritic spine expression. A lack of reelin also seems to affect glial differentiation, as shown in reeler mice. In the neonatal cortex reelin is secreted by Cajal-Retzius cells as well as GABAergic interneurons, in the adult brain only by GABAergic interneurons. After secretion in the ECM it binds to cell surface receptors of Purkinje cells or pyramidal neurons triggering a tyrosine kinase cascade.

In this study, we tested whether application of antisense oligonucleotides (ODN) reduces reelin mRNA translation in rats *in vitro* in neuronal cell cultures as well as *in vivo* by local injection in neonatal or adult rat brains. Additionally, we tested the effects of reelin-ODN on expression of synaptic or dendritic proteins after local injection into neonatal and adult rat brains.

*In vitro* experiments were performed in primary cultures of rat brain neurons (timed pregnant dams, embryonic day 17). After 4 days *in vitro* cells were treated with 6 or 8  $\mu$ M reelin-antisense or a scrambled oligonucleotide sequence as control. After 48 hours ODNs were added again and cells were incubated for another 48h. Culture medium was collected and cells were scraped off in sample buffer. Proteins in the media were concentrated and compared to cellular extracts by immunoblotting. For *in vivo* experiments anesthetized rats, either postnatal day 7 or adults, were microinjected with reelin-ODN (0.2 nM or 2 nM in 1  $\mu$ l) or a scrambled oligonucleotide sequence as control by direct injection in the PFC of one hemisphere. The other hemisphere served as control. Twelve hours after microinjection animals were decapitated and the PFC of both hemispheres homogenized in sample buffer and subjected to immunoblotting. Samples were analyzed with antibodies against reelin, microtubule associated protein (MAP2), synaptophysin and myelin basic protein (MBP).

A suppression of reelin protein could be obtained in neuronal cell cultures as well as in PFCs of neonatal and adult rats. This effect was more obvious with higher concentrations of ODNs. In adult rats suppression of reelin was accompanied by a decrease in MBP, synaptophysin and MAP2.

Our results indicate that a downregulation of reelin can be achieved by local injection of reelin ODNs into the rat brain that is accompanied by the downregulation of certain synaptic and dendritic proteins, an effect also seen in the pathology of schizophrenia.

Supported by the DFG (SFB 517, TP A11) and Tönjes Vagt-Stiftung



**Comparison of acute effects of the antiepileptic drugs valproate and topiramate on electrical activity patterns of primary frontal cortex networks on microelectrode arrays**

Simone Stüwe, Alexandra Gramowski and Dieter G. Weiss

Institute of Cell Biology and Biosystems Technology, University of Rostock, 18051 Rostock, Germany

Antiepileptic properties of valproate and topiramate are known to depend on several different mechanisms of action, i.e. effects on ion channels, amino acidergic neurotransmission, brain metabolism and direct effects on excitable membranes.

We compared the influence of valproate and topiramate on the electrical activity patterns in primary cultures of murine frontal cortex. Mature networks (valproate:  $n=16$ , topiramate:  $n=12$ ) grown on 64-microelectrode arrays were acutely exposed (30 min stable phase per step) to increasing concentrations (10 steps) of valproate (100 nM – 20 mM) or topiramate (100 nM – 1 mM). Multielectrode extracellular recordings of network activity revealed a concentration-dependent decrease of activity for both substances, beginning at 10  $\mu$ M ( $p=0.05$ ) with cessation of activity between 10 and 20 mM for valproate vs. decrease at 1  $\mu$ M and cessation at 500  $\mu$ M to 1 mM for topiramate.

During valproate exposure the network patterns remained stable over a wide concentration range, activity synchronization and regularity were finally lost at 5 mM. At 10 mM valproate 26 of the 30 evaluated activity features had changed significantly compared to native activity with an EC<sub>50</sub> of 2.2 mM for spike and burst rate. The effects were reversible by medium changes. Blockage of the GABA-A receptor by 40  $\mu$ M bicuculline prior to valproate exposure shifted the EC<sub>50</sub> to 4.2 mM ( $n=5$ ).

Besides an activity decrease (EC<sub>50</sub>: 200  $\mu$ M), topiramate caused a loss of pattern synchronicity beginning already at 100 nM, reflected by increased coefficients of variation over the network (CV<sub>net</sub>) for the features burst rate, burst period and interburst interval. After bicuculline pre-treatment topiramate up to 100  $\mu$ M decreased burst duration and interspike intervals and removed the epileptiform high frequency firing by reducing the peak frequencies in bursts.

This confirms reports that the clinical efficacy of valproate and topiramate are partially related to their ability to influence GABAergic neurotransmission by different mechanisms and to various extent and demonstrates that highly detailed studies on neuroactive drug effects can be performed with neuronal network-multielectrode array hybrid biosensors.

Supported by Landesforschungsschwerpunkt Mecklenburg-Vorpommern Biosystemtechnik and European Community (ERDF)

**NEURONAL TISSUE SPECIFICITY *IN VITRO*: A MULTI-PARAMETRIC COMPARISON OF MURINE SPINAL CORD AND FRONTAL CORTEX NETWORK ACTIVITY - NEUROTRANSMITTER RECEPTOR RESPONSES AND CULTURING CONDITIONS**

Alexandra Gramowski, Simone Stüwe, Dieter G. Weiss

Institute of Cell Biology and Biosystems Technology, University of Rostock, 18051 Rostock, Germany

Spontaneously active neuronal networks on microelectrode arrays have been proposed as sensitive and efficient model systems for the study of toxic properties of neuroactive compounds.

To demonstrate *in vitro* networks as pharmacologically histiotypic representations of their parent tissues, we investigated the spiking and bursting activity of murine spinal cord and frontal cortex networks. We selected antagonists for the relevant neurotransmitter receptors of GABA<sub>A</sub> glycine, dopamine, serotonin, muscarinic and nicotinic acetylcholine, AMPA, NMDA, as well as blockers for the electrical synapses to study the influence of these receptors and gap junctions on the composition of the electrical activity. We used 30 spike and burst features to characterize the electrical activity patterns.

For both tissue types the blockage of inhibitory circuits with bicuculline and/or strychnine elicited rhythmic and synchronized activity. There were definite differences between the two network types: the activity resulting from blockage of the glycine receptor with strychnine and the GABA<sub>A</sub> receptor with bicuculline revealed a 5-8 fold higher inhibition in spinal cord than in frontal cortex networks. Similar to *in vivo* data, the results showed that inhibition in spinal cord is mainly mediated through glycine receptors, whereas in frontal cortex the GABA<sub>A</sub> receptors cause the main part of the inhibition. Co-application of the NMDA and AMPA receptor antagonists MK801 and NBQX to both tissue types eliminated all bursting. These results demonstrate that rhythmic activity in both tissues originates from an activation of the excitatory glutamate receptors. The gap junction blockers 1-octanol, sodium propionate and carbenoxolone showed substance and tissue specific differences in their activity pattern responses.

In conclusion, this study demonstrates that neuronal networks cultured under our conditions remain tissue-specific and maintain differences in a set of parameters. This greatly improves the value of such neuronal network biosensor systems as they can be used for *in vitro* screening of drugs designed for different regions of the CNS.

Supported by the Landesforschungsschwerpunkt Mecklenburg-Vorpommern „Innovationsnetzwerk Biosystemtechnik“ and the European Community (ERDF).

**Poster Subject Area #PSA25:  
Cell and tissue cultures**

- [#340A](#) B. Mönig, S. Scholz and H. Luksch, Aachen  
*Physiological development of different neuronal subtypes from the chick optic tectum in cell culture*
- [#341A](#) N. Lautemann, P. Bräuning and S. Weigel, Aachen and Jülich  
*Primary Culture of identified Neurons of the CNS of Locusta migratoria*
- [#342A](#) F. Hofmann, F.J.L. Arnold, P. Bengtson, M. Wittmann, P. Vanhoutte and H. Bading, Heidelberg and Cambridge (UK)  
*Input-induced sustained recurrent activity in hippocampal networks*
- [#343A](#) B. Buschle and H. Bading, Heidelberg  
*FAST CALCIUM SIGNALING TO THE NUCLEUS: ACTIVATION OF IMMEDIATE EARLY GENE TRANSCRIPTION WITHIN SECONDS AFTER ELECTRICAL ACTIVATION OF HIPPOCAMPAL NEURONS*
- [#344A](#) J-M. Weislogel and H. Bading, Heidelberg  
*Imaging of distinct spatial calcium signals using recombinant Ca<sup>2+</sup> probes in vitro model systems*
- [#345A](#) G. Grossrau, R. Konang and O. Brüstle, Bonn  
*Embryonic stem cell-derived peripheral neurons - a potential donor source for peripheral nervous system repair*
- [#346A](#) S. Greschat, C. Rosenbaum, MA. de Souza-Silva, J. Bender, G. Koegler, P. Wernet and HW. Müller, Düsseldorf  
*Human umbilical cord blood stem cells: analysis in vitro and after implantation into the intact adult rat brain*
- [#347A](#) M. Timmer, K. Krampfl, J. Großkreutz, F. Schlesinger, M. Wesemann, L. Just, J. Bufler and C. Grothe, Hannover and Tübingen  
*Proliferated and Differentiated Neural Precursors express functional Calcium-permeable AMPA Receptors, Develop into Functional Dopaminergic Neurons and Improve Behaviour after Grafting*
- [#348A](#) S. Kreis, V. Senner, K. Rose, S. Püttmann and S. Thanos, Münster  
*Glioma cell migration along axons as in vitro model for glioma invasion*
- [#339B](#) L. Tönges, P. Lingor, G. Dietz and M. Bähr, Göttingen  
*Stearylated octaarginine for siRNA-transfection into rat primary neurons*

- [#340B](#) S. Siedenberg, CP. Dohm, J. Liman, JC. Reed, M. Bähr and P. Kermer, Göttingen and La Jolla, CA (USA)  
*BII mediated neuroprotection*
- [#341B](#) J. Liman, CP. Dohm, S. Krajewski, JC. Reed, S. Ganesan, FS. Wouters, M. Bähr and P. Kermer, Göttingen and La Jolla, CA (USA)  
*BAG1 neuroprotectivity is mediated by HSP70 binding*
- [#342B](#) P. Schulte, S. Weigel, S. Böcker-Meffert and A. Offenhäusser, Jülich  
*Cricket neurons of terminal ganglion forming functional networks in vitro*
- [#343B](#) T. Decker, S. Schäfer, S. Schaal, S. Böcker-Meffert and A. Offenhäusser, Jülich  
*Aligned Two-step Microcontact Printing for the Construction of Defined Neuronal Networks*
- [#344B](#) S. Weigel, P. Schulte, S. Böcker-Meffert, P. Bräunig and A. Offenhäusser, Jülich and Aachen  
*Cell culture of locust neurons regaining functional networks*
- [#345B](#) S. Weigel, P. Schulte, S. Böcker-Meffert, G. Wrobel, S. Ingebrandt and A. Offenhäusser, Jülich  
*Extracellular signals recorded from locust neurons using field-effect transistors*
- [#346B](#) R. Müller, Ludwigshafen  
*The human neuroblastoma cell line SH-SY5Y: a model system to study caspase 3/7 and caspase 9 activity in apoptosis*
- [#347B](#) RS. Yamidanov, JV. Vakhitova, MG. Mikhaylova and SB. Seredenin, Moscow (RUS) and Magdeburg  
*GENE EXPRESSION PATTERNS ASSOCIATED WITH PSYHOSTIMULATING DRUG LADASTEN ACTION IN RAT BRAIN*

## **Physiological development of different neuronal subtypes from the chick optic tectum in cell culture**

**Benedikt Mönig, Susanne Scholz, Harald Luksch**

Institut für Biologie II, RWTH, Kopernikusstr. 16, 52074 Aachen, Germany

*e-mail: moenig@bio2.rwth-aachen.de*

The optic tectum is a prominent structure in the avian midbrain with a highly laminated architecture. Retinal axons innervate layers 2-5 and 7 of the optic tectum, while the majority of tectal efferents arises in layer 13 (Stratum griseum centrale, SGC) and projects to the thalamic nucleus rotundus. Within the optic tectum several neural circuits have been identified that form the computational basis of its function of multisensory integration [1]. Since most of the tectal layers consist of only one specific cell type, this structure constitutes an ideal model system to study cellular physiology and computation.

To analyse the contribution of single cell properties to the computational output of distinct tectal circuits in vivo we prepared single cell cultures of chick optic tectum [2] and identified optimal parameters for their cultivation. We isolated E6-9 embryonic tectal cells and cultivated them for up to two weeks in serum-free medium (DMEM/B27 supplement). Cells showed morphological differentiation, generated extensive neurites and formed synapses within complex neural networks in vitro. These were first characterized immunohistochemically: Cultures contained differentiated neurons (MAP2+/NF200+/GFAP-), astroglial-like cells (MAP2-/GFAP+) and other non-neuronal cells. Based on immunoreactivity against vimentin, calbindin, calretinin, parvalbumin, cellular retinoic acid binding protein-I, N-cadherin, synapsin-I and GABA, we observed the development of various neuronal cell types known from the in-vivo situation. In order to cultivate distinct neuronal subpopulation separately, we are now isolating neuronal subtypes with antibodies coupled to magneto-beads (MACS®, Miltenyi Biotech).

For functional investigation of the tectal culture, cultivated neurons were analysed with whole-cell patch recordings. Among neuronal physiological characteristics, we detected responses to somatic current injections that are characteristic for specific tectal neurons ( $I_H$ -current of SGC neurons).

These results demonstrate that different subtypes of avian tectal neurons develop their specific characteristics in primary cell culture. This approach offers the opportunity to study mechanisms of neuronal differentiation and computation in vitro.

*Supported by the Deutsche Forschungsgemeinschaft, LU622 3-1.*

[1] Luksch, H. Cytoarchitecture of the avian optic tectum: neuronal substrate for cellular computation. *Rev. Neurosci.* 14, 85-106 (2003). [2] Moenig, B. & Luksch, H. Primary Culture of Cells from the optic Tectum of the Chick: establishment and characterisation. *Proc. Of the 29<sup>th</sup> Göttingen Neurobiology Conference* (2003)

## Primary Culture of identified Neurons of the CNS of *Locusta migratoria*

Nico Lautemann<sup>1</sup>, Peter Bräunig<sup>1</sup>, Stefan Weigel<sup>2</sup>

<sup>1</sup>Institute for Biology II, RWTH Aachen, Kopernikusstr. 16, D-52056 Aachen

<sup>2</sup>Institute of Thin Films and Interfaces (ISG), Bio Signal Processes (ISG2-BE),  
Forschungszentrum Jülich GmbH, D-52425 Jülich.

In order to construct biohybrid networks of neurons grown on semiconductors we established culture conditions for specific, identified neurons of migratory locusts. Our long-term aim is to establish simple networks from identified neurons.

Because there are still difficulties in effective coupling small neurons (10-20  $\mu\text{m}$  soma diameter) with the field effect transistors (FETs) that subserve the function of recording electrodes in the semiconductor circuits, our first goal was the cultivation of larger (40-80  $\mu\text{m}$ ) arthropod cells. In a first step we tried to optimize culturing conditions such as composition of media, variations of substrate coating, as well as different preparation methods for identified neurons.

Along with this we tested various techniques for marking, subsequent isolation, and transfer of cells from ganglia into the culture dishes. One question we tried to answer is whether cells synaptically connected *in vivo* are more likely to form synaptic contacts in culture in comparison to cells that have no connection prior to isolation.

## Input-induced sustained recurrent activity in hippocampal networks

Frank Hofmann <sup>2\*</sup>, Fiona J.L. Arnold <sup>1,2\*</sup>, Peter Bengtson <sup>2</sup>, Malte Wittmann <sup>2</sup>,  
Peter Vanhoutte <sup>1,2</sup>, Hilmar Bading <sup>1,2</sup>

\* These authors contributed equally to the study

<sup>1</sup> MRC Laboratory of Molecular Biology, Cambridge, England

<sup>2</sup> Department of Neurobiology, Interdisciplinary Center for Neurosciences (IZN)  
University of Heidelberg, Heidelberg, Germany

The ability of the brain to retain information is thought to involve input-induced changes in the collective behaviour of neuronal assemblies that is sustained in the absence of external stimuli. Thus, the induction of stable periods of slow rhythm, recurrent neural activity in cortical circuits may be important for memory. However, the molecular mechanisms and intracellular signalling pathways through which synaptic inputs can switch on and switch off particular firing patterns are unknown. The aim of our study was to investigate biochemical mechanisms underlying the induction and maintenance of stimulus-induced persistent activity states.

We used hippocampal neurons that, after a culturing period of 10 to 14 days, form an elaborate and highly interconnected network consisting of about 90 % excitatory neurons and about 10 % inhibitory interneurons. A brief exposure of hippocampal cultures to the GABA<sub>A</sub> antagonist bicuculline resulted in a change in network behaviour. Repeated multi-site electrical recordings on Microelectrode Arrays (MEA) revealed that, after stimulation, the initial random spike pattern is replaced by rhythmic spike bursts. Recurrent activity was synchronous, self-sustaining and could persist for several days after washout of bicuculline. We could show that this recurrent activity was induced by calcium flux through synaptic NMDA receptors while activation of L-type Ca<sup>2+</sup>-channels was not necessary. The long time maintenance of recurrent synchronous bursting appears to require activation of MAP kinases (ERK1/2) and was readily switched off after temporary blockade of glutamatergic synaptic transmission. The late phase (> 4 hours) of this form of network plasticity was also dependent on gene transcription taking place in a critical period of 120 minutes following induction.

Thus, this study established a novel, very simple and experimentally accessible system for studying activity-induced changes in network behavior. The results obtained illustrate that both local, near-NMDA receptor signaling (activating ERK1/2) and the dialogue between the synapse and the nucleus are important to induce and uphold a particular activity pattern. Non-invasive multi-site recordings will facilitate in particular studies of the transcription-dependency of certain network behaviour and may prove useful for testing the hypothesis that nuclear calcium-regulated gene expression is important for late phase synaptic plasticity.

# FAST CALCIUM SIGNALING TO THE NUCLEUS: ACTIVATION OF IMMEDIATE EARLY GENE TRANSCRIPTION WITHIN SECONDS AFTER ELECTRICAL ACTIVATION OF HIPPOCAMPAL NEURONS.

Bettina Buschle and Hilmar Bading

Department of Neurobiology, Interdisciplinary Center for Neurosciences, University of Heidelberg, Germany

Corresponding author: Bettina.Buschle@urz.uni-heidelberg.de

Electrical activity-induced calcium signals can activate gene transcription in neuron. Synapse-to-nucleus communication takes place either via calcium-regulated protein kinase cascades (such as the ERK-MAP kinase pathway triggered in the vicinity of the calcium entry channel) or via calcium itself that can invade the cell nucleus (1). Signaling to the nucleus via protein kinase cascades is expected to be slower than signal propagation by calcium that is detected in the nucleus within a second after electrical activation. The speed of the activation of genomic responses may therefore provide information on the mode of calcium signal propagation used. Using the cellular compartment analysis of temporal activity by fluorescence in situ hybridization (catfish) (2) the temporal profile of transcription of immediate early genes (IEG) were assessed in rat hippocampal neurons after depolarization with 50mM extracellular KCl. Individual IEG intranuclear foci are already apparent just 30sec after KCl treatment. These intranuclear foci (INF) are the genomic sites of IEG transcription. Particularly at later time points, IEG RNA can also be seen in a characteristic cytoplasmic localization pattern outside of the nucleus. IEG intranuclear foci represent the accumulation of primary transcripts at genomic alleles, indicating the initiation of IEG transcription which occurs within seconds. This time scale would be too rapid to involve the translocation of signal molecules from dendrites to the nucleus. Pharmacological experiments were done to examine the contribution of the ERK-MAP kinase pathway to KCl-induced IEG transcription.

Supported by the Alexander von Humboldt Foundation

## Literature cited:

- (1) Bading, H. (2000) Transcription-dependent neuronal plasticity: the nuclear calcium hypothesis. *Eur. J. Biochem.* 267, 5280-5283.
- (2) Worley PF, Bhat RV, Baraban JM, Erickson CA, McNaughton BL, Barnes CA. (1993) Thresholds for synaptic activation of transcription factors in hippocampus: correlation with long-term enhancement. *Neurosci. Nov*;13(11):4776-86.
- (3) Guzowski J, Worley PF (2001) *Current protocols in neuroscience*.

## Keywords :

Calcium signaling, gene transcription, immediate early gene, in situ hybridization





## Imaging of distinct spatial calcium signals using recombinant $\text{Ca}^{2+}$ probes in vitro model systems

Jan- Marek Weislogel and Hilmar Bading

**Department of Neurobiology, Interdisciplinary Center for Neurosciences, University of Heidelberg, Germany**

Changes in the intracellular calcium concentration following synaptic activity is a fundamental property of neurons that controls many neuronal processes. Calcium is required for regulation of gene expression that affect synaptic connectivity, promote survival, or cause cell death. For synapse-to-nucleus communication, neurons exploit the spatial and temporal diversity of calcium transients associated with electrical activation. The nucleus integrates the distinct calcium signals induced by neural firing patterns and specifies the transcriptional outputs. Dendritic calcium signals, activating the ERK-MAP kinase signaling cascade, stimulate gene expression mediated by the serum response element. Increases in the nuclear calcium concentration are critical for the activation of gene expression mediated by the transcription factor CRE-binding protein (CREB) and the coactivator CREB-binding protein (CBP) (1). The CREB/CBP complex has been implicated in gene expression- dependent plasticity and neuronal survival. Our central hypothesis is that increases in the nuclear calcium concentration, evoked by synaptic activity, are key regulators of transcription–dependent neuronal adaptation.

To develop calcium indicators that allow us to monitor calcium signals, we have been using the recombinant  $\text{Ca}^{2+}$  probes Inverse Pericam (2) and G-CaMP (3). Either calcium probe allowed the detection of global calcium transients evoked by KCl- induced membrane depolarization in primary rat hippocampal neurons. G-CaMP was also suitable for monitoring slow calcium oscillations triggered by recurrent burst activity in a hippocampal network. To monitor calcium signals in distinct subcellular compartments, particularly in the cell nucleus, we fused localization signals to the amino terminus of G-CaMP. A nuclear localization signal added to G-CaMP visualized exclusively nuclear calcium signals whereas the nuclear export signal completely prevented nuclear calcium staining. The results obtained with the NLS G-CaMP and NES G-CaMP will be discussed.

### References :

- (1) Hardingham GE, Arnold FJ, Bading H (2001) Nuclear calcium signalling controls CREB-mediated gene expression triggered by synaptic activity. *Nat Neurosci.* 4: 261-267
- (2) Nagai T, Sawano A, Park ES, Miyawaki A (2001) Circularly permuted green fluorescent proteins engineered to sense  $\text{Ca}^{2+}$ . *Proc Natl Acad Sci USA* 98:3197-3202
- (3) Nakai J, Ohkura M, Imoto K (2001) A high signal-to-noise  $\text{Ca}^{2+}$  probe composed of a single green fluorescent protein. *Nat Biotechnol* 19:137-141.

**Keywords:** nuclear calcium signals, localisation of recombinant calcium probes

Embryonic stem cell-derived peripheral neurons – a potential donor source for peripheral nervous system repair

Gudrun Gossrau, Rachel Konang, Oliver Brüstle

Institute of Reconstructive Neurobiology, University of Bonn Medical Center

Embryonic stem cell-derived neural precursors (ESNPs) have been shown to differentiate into various neuronal and glial phenotypes. We set out to explore the applicability of ESNPs in the treatment of peripheral nervous system (PNS) disorders

such as Morbus Hirschsprung, a common childhood disorder caused by focal lack of ganglion cells in the gut wall. To promote a neural crest fate, FGF2-dependent ESNPs were treated with BMP2 (10ng/ml) for 4 days. This resulted in a significant increase in peripherin-positive neurons expressing choline acetyl transferase and Mash1. Other neural crest-associated markers induced by BMP2 included Snail, Sox10, dHand, c-ret and Msx1. Interestingly, Brn3.0-positive putative peripheral sensory neurons were negatively regulated by BMP2. Transplantation studies in organotypic cultures derived from embryonic mouse gut indicate that purified BMP2-treated ES cell-derived neurons survive and incorporate seamlessly with endogenous neurons of the intestinal wall. Thus, ESNPs may represent an attractive donor source for neuronal replacement in Hirschsprung's disease.

Supported by DFG (Go-1066/1-1) and the Hertie Foundation.

## Human umbilical cord blood stem cells: analysis *in vitro* and after implantation into the intact adult rat brain

**Greschat S<sup>1</sup>, Rosenbaum C<sup>1</sup>, de Souza-Silva MA<sup>2</sup>, Bender J<sup>3</sup>, Koegler G<sup>4</sup>, Wernet P<sup>4</sup> and Müller HW<sup>1</sup>.**

<sup>1</sup>Molecular Neurobiology, Dept. of Neurology, University Clinic Düsseldorf; <sup>2</sup>Dept. of Physiological Psychology, University of Düsseldorf, <sup>3</sup>Kourion Therapeutics, Langenfeld; <sup>4</sup>ITZ, University Clinic, Düsseldorf, Germany

Human umbilical cord blood represents an easily available source of unrestricted somatic stem cells (USSC) which can give rise to neural and other cell types. USSC represent the neonatal stage of multipotent human umbilical cord blood stem cells. These cells are defined and characterized as a CD34- and CD45-negative, non-haematopoietic, stem cell compartment, which can be easily expanded in cell culture up to at least 16 passages. We have developed a protocol to differentiate USSC into the neural direction followed by lineage selection of neuronal cells *in vitro*. The differentiation of USSC was monitored by immunocytochemical detection of neural antigens, different neurotransmitters and transmitter synthesizing enzymes. These findings enabled us to discriminate between neuronal subtypes, like GABAergic, and dopaminergic cells. Additional treatment with a dopamine containing medium led to a massive increase of tyrosine-hydroxylase immunoreactivity. In order to test whether immunocytochemical data correlate with functionality we currently analyse the cellular release of neurotransmitters (dopamine, serotonin) by HPLC. To investigate the potential of the USSC with regard to cell replacement therapies, we carried out transplantation experiments. Different batches of PKH26 pre-labelled and unlabelled USSC were stereotactically and unilaterally implanted into intact adult rat brains. In these experiments PKH26 labelled USSC showed detectable persistence for at least three months after implantation. Currently, immunohistochemistry with human specific antibodies is carried out to confirm these data. Human Tau-protein positive cells could be found distributed in different regions of the rat brain three months after implantation, e.g., in cortex, hippocampus and the striatum. Human Tau immune-positive cells could not only be found ipsilateral to the implantation but also in the contralateral hemisphere. In addition to these findings we have, thus far, obtained no evidence for tumour formation within the USSC implanted brains.

**Proliferated and Differentiated Neural Precursors express functional Calcium-permeable AMPA Receptors, Develop into Functional Dopaminergic Neurons and Improve Behaviour after Grafting**

M.Timmer<sup>\*</sup>, K.Krampf<sup>1\*</sup>, J.Großkreutz<sup>1\*</sup>, F.Schlesinger<sup>1\*</sup>, M.Wesemann<sup>\*</sup>, L.Just<sup>3</sup>, J.Bufler<sup>1\*</sup>, C.Grothe<sup>\*</sup>

Medical School Hannover, Dept. of Neuroanatomy & <sup>1</sup>Neurology, Carl-Neuberg-Str. 1, 30625 Hannover, Germany; <sup>3</sup>University of Tübingen, Anatomical Institute, Exp. Embryology, Section Tissue Engineering, Österbergstr. 3, 72076 Tübingen, Germany. <sup>\*</sup>and Center for Systems Neurosciences Hannover (ZSN).

Generation of dopaminergic neurons from pluripotent embryonic progenitors represents a promising therapeutical strategy for Parkinson's disease. In the present study, we have investigated ventral mesencephalic (VM) precursors from embryonic day (E)12 under different proliferation and differentiation conditions, respectively. The precursors were at first expanded for 5-6 days, and afterwards differentiated for 2-7 days. The cells were characterized with immunocytochemistry, cell ELISA, patch clamp and calcium-imaging and transplanted into postnatal and adult 6-OHDA lesioned rats. We demonstrate that CNS precursors expanded *in vitro* can efficiently differentiate into dopaminergic (DA) neurons and survive intrastriatal transplantation into hemiparkinsonian rats. After 4-5 days in differentiation medium, more than 70% of the neurons were TH+, whereas after shorter respectively longer differentiation intervals only 50-60% of the neurons were TH+. The survival rate after transplantation was comparable to results after direct grafting of E14 VM, when the precursors were differentiated for 2 to 4 days. DA progenitors express AMPA and GABA receptor subunits *in vitro*. Calcium-imaging revealed, that these AMPA receptors are calcium permeable and are therefore capable to contribute in many developmental processes including dendritic differentiation. The 6-OHDA lesioned animals recovered significantly after treatment with differentiated VM progenitor cells. Thus, DA progenitors generate functionally active neurons which are integrated into the host striatum. Overall, our results suggest that the numerical expansion of primary CNS precursor cells is an approach that could improve both the ethical and the technical outlook for the use of fetal tissue in clinical transplantation.

## Glioma cell migration along axons as in vitro model for glioma invasion

Stefan Kreis, Volker Senner<sup>1</sup>, Karin Rose, Sylvia Püttmann<sup>1</sup> and Solon Thanos

Department of Experimental Ophthalmology, University Eye Hospital Münster, Domagkstr. 15, 48149 Münster, Germany

<sup>1</sup>Institute of Neuropathology, Domagkstr. 19, 48149 Münster, Germany

Glioma cell migration along intracerebral pathways serves as model to understand the mechanisms of glioblastoma invasion within the brain. Critical to these mechanisms are interactions between the migrating cells and axons which express cell adhesion molecules. Glioma cells may recognize both axonal adhesion molecules and extracellular matrix components in order to assemble proper signaling cascades with migratory outcome.

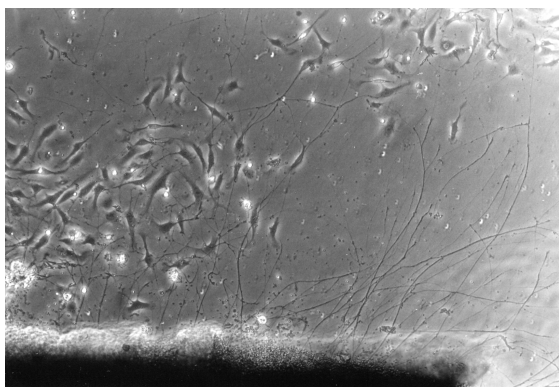
We established a co-culture model of adult axons and C6-glioma cells which enables to monitor the cell behaviour along axons using time-lapse cinematography. The method consists of explanting retinal tissue from Sprague-Dawley rats. After explantation it takes at least 2 days to get a sufficient axon outgrowth of the retinal ganglion cells.

C6 glioma cells from the rat are adapted to the conditions of axon cultures. By the use of special glass cylinders these cells are placed next to the axons and co-cultured with them. The microscopy is recorded over 48 hours in culture by a timelapse method. This recording allows to qualify the interactions and the behaviour of the cells afterwards.

Glioma cells encountering axons showed typical responses which could be categorized into the following groups:

- a) migration of the cell along the axon in an anterograde or retrograde directory
- b) cell crosses the axon or retracts
- c) habituation
- d) incoping of an axon by a C6 cell
- e) neuroptosis
- f) adhesion time

These groups can be used as parameters to quantify and to qualify the interactions and to get an insight into the behaviour of migration.



Interactions between C6 cells and axons

The results showed that quantification and categorization of the cell responses may help interfering with these responses by either changing axonal surface or the cell motility. Initial attempts to interfere comprised experiments with antibodies to either neural cell adhesion molecule (NCAM) or cytoskeleton (GFAP).

**Stearylized octaarginine for siRNA-transfection into rat primary neurons**

Lars Tönges, Paul Lingor, Gunnar Dietz, and Mathias Bähr

Dept. of Neurology, University of Göttingen, Waldweg 33, 37073 Göttingen, Germany

RNA interference (RNAi) is a powerful experimental tool for sequence-specific gene silencing allowing for efficient analysis of gene function. RNAi has been shown to work in a multitude of cell types, including cultured mammalian neurons. However, its application is limited by low efficiency and high toxicity of conventional transfection methods in primary neuron cultures.

Recently, peptide-mediated transfection has been used for transfecting DNA into cell lines. We have evaluated a peptide-mediated cellular delivery method for fluorescein-labeled siRNAs into rat primary neurons using stearylized octaarginine (Stearyl-R<sub>8</sub>), and have compared the results to transfections of the neuronal SH-SY5Y cell-line.

Our results show that Stearyl-R<sub>8</sub> mediates siRNA-transfection into primary hippocampal neurons and SH-SY5Y cells as efficient as conventional cationic liposomes. Application of Stearyl-R<sub>8</sub> complexes resulted in an intracellular siRNA pattern in both SH-SY5Y cells and hippocampal neurons with a clear endosomal localization, as verified by confocal microscopy. Cytotoxicity was comparable with cationic liposomes and was Stearyl-R<sub>8</sub> dose-dependent. While being efficient for siRNA transfection, Stearyl-R<sub>8</sub> yielded only low numbers of DNA-transfected cells.

We conclude that this novel approach yields performances comparable with cationic liposome-mediated transfection for siRNA, while not being superior for DNA-transfection. Stearylized octaarginine may therefore represent a novel and more cost-efficient alternative to conventional siRNA-transfection reagents.

Funded by Deutsche Forschungsgemeinschaft through the DFG-Research Center for Molecular Physiology of the Brain.

## **BI1 mediated neuroprotection**

**Sandra Siedenberg, Christoph P. Dohm, Jan Liman, John C. Reed<sup>1</sup>, Mathias Bähr, and Pawel Kermer**

Dept. Neurology, Medical School Univ. Göttingen, Robert-Koch-Str. 40, 37075 Göttingen, Germany

<sup>1</sup>The Burnham Institute, 10901 N. Torrey Pines Rd., 92037 La Jolla, Calif., USA

BI-1 (Bax inhibitor-1) has been characterized as inhibitor of Bax-induced cell death in plants and various mammalian cell systems. To explore the function of BI1 in neurons we over-expressed BI-1 in rat nigral CSM14.1 and human SH-SY5Y neuroblastoma cells. Surprisingly, transient transfection assays resulting in an overload with BI-1 rather caused decreased cell survival. In contrast, stable BI1-expression on a moderate level proved to have a mild neuroprotective effect against various death stimuli. Examination of the subcellular distribution revealed that BI-1 mostly locates to the ER and nuclear envelope but not mitochondria or other cell organella.

Taken together, moderate BI-1 expression in the ER is protective in neurons. Since BI1 has been discussed to be involved in calcium homeostasis, future experiments are aiming at the mechanisms underlying BI1 neuroprotectivity.

## **BAG1 neuroprotectivity is mediated by HSP70 binding**

J. Liman, C. P. Dohm, S. Krajewski<sup>1</sup>, J. C. Reed<sup>1</sup>, S. Ganesan<sup>2</sup>, F.S. Wouters<sup>2</sup>, M. Bähr, and P. Kermer

Dept. of Neurology, Univ. of Göttingen, Robert-Koch-Str. 40, 37075 Göttingen, Germany

<sup>1</sup>The Burnham Institute, Program on Apoptosis and Cell Death Research, 10901 N. Torrey Pines Rd., La Jolla, CA 92037, USA

<sup>2</sup>Cell Biophysics Group, European Neuroscience Institute, Waldweg 33, 37073 Göttingen, Germany

Recently, we have shown that BAG1 (Bcl-2 associated athanogene-1) is a regulator and marker of neuronal differentiation. Moreover, BAG1 proved to be neuroprotective when stably over-expressed in immortalized neuronal CSM 14.1 cells. Since there seems to be an equilibrium within a cell between BAG1 binding to heat-shock protein-70 (Hsp70) and BAG1 binding to Raf-1 kinase, we hypothesized that changing BAG1 binding characteristics might significantly alter BAG1 function. Hence, we stably over-expressed a BAG1-mutant (BAG1 $\Delta$ C) no longer binding to Hsp70 in CSM cells and compared their phenotype to such over-expressing full-length BAG1 or Bcl-2. Interestingly, in contrast to full-length BAG1, where we observed a shift from mostly nuclear to exclusively cytosolic during differentiation, BAG1 $\Delta$ C was expressed exclusively in the cytosol already under control conditions. Similar to cells over-expressing full-length BAG1, these cells presented an accelerated neuronal differentiation assessed by morphology, expression of differentiation markers, axon-growth and generation time. On the other hand, cells over-expressing BAG1 $\Delta$ C were no longer protected against apoptotic stimuli like staurosporine and serum-deprivation. In addition, the upregulation of chaperone activity in cells over-expressing full-length BAG1, but not BAG1 $\Delta$ C, was shown using a novel chaperone-dependent folding mutant of the yellow fluorescent protein. Taken together these results suggest that BAG1 binding to Hsp70 is important and may mediate BAG1 neuroprotectivity while shifting BAG1 binding to Raf-1 kinase modulates neuronal differentiation in vitro.

supported by a starter grant of the University of Göttingen (P.K.)



**Cricket neurons of terminal ganglion forming functional networks *in vitro***

SCHULTE P., WEIGEL, S., BÖCKER-MEFFERT S. & OFFENHÄUSSER A.

Forschungszentrum Jülich, Institute of Thin Films and Interfaces, Bio and Chemo Sensors, D-52425 Jülich

Escape orientation of crickets is a highly stereotypic, quick and precise behaviour. It is based on a proper recognition of air flow detected by mechanosensory hairs followed by complex neuronal information processing in the terminal ganglion. To analyze synaptogenesis, development and neuronal processing of these networks *in vitro* we want to reproduce the *in vivo* situation of neuronal processing during escape reaction on arrays of non metallized field-effect transistors (FET's). Due to the large size of cell bodies in combination with the opportunity to identify individual cells by fluorescence staining techniques the CNS of crickets provides a capable model for the examination of simple neuronal networks on planar sensor arrays.

Cell culture conditions reobtaining morphological differentiation and electrophysiological properties for neurons of *Gryllus bimaculatus* were established. The terminal ganglion was excised and dissociated by enzymatic treatment (collagenase, dispase). Isolated neurons were plated on pre-coated coverslips placed in petri-dishes and cultured in modified Leibowitz (L-15) medium at 29°C and 95 % humidity. The soma diameter of isolated cells varied between 10 µm and 90 µm. The primary neurons from adult *Gryllus bimaculatus* showed regrowth of neurites and survived for up to 3 weeks under our culture conditions.

With respect to network formation, we tested different pre-coatings (laminin, poly-(D)-lysine, concanavaline A, extracellular matrix-gel (ECM-gel), silicone, poly(ethylene glycol) (PEG)) and found that silicone was toxic to the cells, while ECM-gel and PEG were cell-repulsive.

Whole cell patch clamp recordings were performed on cells grown on laminin and concanavaline A after 4 – 12 days in cell culture. Voltage clamp stimulation from a holding voltage of -70 mV to a stimulating voltage of 0 mV yielded large inward and outward directed currents with amplitudes up to 12 nA suggesting expression of several types of voltage-activated ion channels. During current clamp configuration a resting potential between -30 mV and -60 mV was observed and action potentials were evoked by a stimulation current of 50 pA – 100 pA. Simultaneous recordings from morphologically connected cell pairs (double patch clamp) delivered graduated postsynaptic potentials when presynaptic cell was stimulated. Reversal signal propagation was impossible indicating chemical synapses between these neurons.

In future the *in vitro*-networks with identified neurons will be reproduced on sensor arrays, since we are able to control the formation of synaptically connected neurons of crickets with optimized cell culture conditions.

Aligned Two-step Microcontact Printing for the Construction of Defined Neuronal Networks

Tanja Decker, Susanne Schäfer, Stephan Schaal, Simone Böcker-Meffert and Andreas Offenhäusser

*Institute for Thin Films and Interfaces, Bio- and Chemosensors (ISG-2), Forschungszentrum Jülich, 52425 Jülich, Germany*

Control over cell position and connectivity provides an important tool for studying fundamental principles of neuronal signal processing. Microcontact printing is a commonly used technique to create patterns of biomolecules. Cortical neurons grown on these patterns differentiate morphologically and form functional synapses. Moreover, the long-term electrophysiological studies of neuronal networks require a non-invasive stimulation and recording technique. The method of choice is the cultivation of rat neuronal cells on cell culture dishes and microdevices (Vogt et al. 2003, Lauer et al. 2001).

The aim of our study is to construct the networks of neurons with defined polarity on culture dishes and subsequently on microdevices. The two-step microcontact printing technique (2-step  $\mu$ CP) enables us to print two different biomolecules with different characteristics as guiding cues in a grid pattern.

We have established 2-step  $\mu$ CP to print various neuronal guiding cues. Netrin-1 (Kubota et al. 2004), laminin (Matsuzawa et al. 1998) and ECM-gel were tested as axon guiding cues, poly-D-lysine as dendritic guiding cue (Oliva et al. 2003). We printed poly-D-lysine (25  $\mu$ g/ml) in combination with netrin-1 (5  $\mu$ g/ml), laminin (25  $\mu$ g/ml), ECM-gel (1%) on different substrates. For stamping these aqueous proteins on microdevices we used small hybrid stamps made of glass and polydimethylsiloxane in combination with a Fineplacer (Lauer et al. 2001). The stamps were pretreated with 10% SDS, incubated in the protein solution and dried with nitrogen. In the first step we printed poly-D-lysine-lines (2 $\mu$ m) with nodes (10 $\mu$ m and 20  $\mu$ m diameter) as dendritic guiding biomolecule. The poly-D-lysine-nodes were aligned to the gates of the microdevice by using a Fineplacer under visual control of the superimposed images from stamp and microdevice surface. In the second step lines of the proposed axon-guiding biomolecule (netrin-1, laminin or ECM-gel) were aligned in a 90° angle to the printed polylysine-nodes. By printing these lines in grids, patterns with axon guiding- and dendritic guiding potential were formed.

Cortical neurons from embryonic rats were cultivated on these patterns. After 8-15 days in culture the network of neurons were analyzed morphologically by phase contrast and raster electron microscopy. In parallel experiments the effect of defined guiding cues on neuronal polarity were investigated by double patch-clamp recordings.

1. Kubota, Chikara, Nagano, Takashi, Baba, Hisatoshi & Sato, Makoto. (2004) *Journal of Neurochemistry*, **89**, 1547-1554.
2. Lauer, Ingebrandt, Scholl, Offenhäusser. (2001) *IEEE Trans Biomed Eng.*; **48**, 838-42.
3. Matsuzawa, Tokumitsu, Knoll, Liesi. (1998) *J Neurosci Res.*; **53**, 114-24.
4. Oliva, James, Kingman, Craighead, Banker. (2003) *Neurochem Res.*; **28**, 1639-48.
5. Vogt, Lauer, Knoll, Offenhäusser. (2003) *Biotechnol. Prog.*; **19**, 1562 –1568

## Cell culture of locust neurons regaining functional networks

Stefan Weigel<sup>1</sup>, Petra Schulte<sup>1</sup>, Simone Böcker-Meffert<sup>1</sup>, Peter Bräunig<sup>2</sup> and Andreas Offenhäusser<sup>1</sup>

<sup>1</sup> Forschungszentrum Jülich, Institute of Thin Films and Interfaces (ISG 2), Bio- and Chemosensors, D-52425 Jülich, Germany

<sup>2</sup> RWTH Aachen, Department of Zoology and Animal Physiology, Institute of Biologie II, D-52074 Aachen, Germany

To decipher the neural code we want to reconstruct simplified networks of neurons *in vitro* which mimic the *in vivo* situation of neuronal processing as closely as possible. These network-forming neurons are coupled to planar sensor arrays of field-effect transistors to study the neural information processing in detail (see also the poster “Extracellular signals recorded from locust neurons using field-effect transistors”).

The insect CNS provides an interesting model for the investigation of signal processing in networks of a small number of neurons. For instance the neuronal circuit mediating the jump of *Locusta migratoria* is well documented. Because of its less complicated composition and the possibility to identify the involved neurons by backfill staining it is an ideal neuronal network for our study.

Cell culture conditions were established for locust neurons to regain their morphological differentiation and electrical activity. The meta- and mesothoracic ganglia of adult locusts were excised, followed by dissociating the neurons mechanically and by enzymatic treatment (dispase). The neurons were plated on petri dishes coated with different substrates (laminin, poly-D-lysine, concanavalin A) and cultured in modified Leibowitz medium (L-15). Cultures were maintained in 95% relative humidity, at 29°C. The neurons were controlled with respect to cell viability and neurite outgrowth. At these culture conditions primary neurons showed regrowth of their neurites and survived for up to 4 weeks.

Electrophysiological properties of morphologically differentiated neurons were examined by patch-clamp recordings in the whole-cell configuration. We observed three different neuron types concerning their responses at voltage-clamp stimulation to different voltage steps (from -90 mV to +100 mV): 1. neurons without or with masked inward currents; 2. neurons with transient inward currents followed by sustained outward currents; 3. neurons with a series of short-term inward and outward currents. In current-clamp configuration action potentials could be observed from neurons showing response type 2 or 3.

Additionally we performed double patch-clamp experiments on *in vitro* connected neurons: current-clamp stimulation of a neuron led to unidirectional, delayed graduated potentials in the other neuron. On the base of this signal processing we demonstrated that primary neurons from adult locust develop chemical synapses *in vitro*.

With this culture protocol we obtain electrophysiologically active neurons which build up networks with chemical synapses. We established a basis for the study of constructed simple networks mimicking *in vivo* neuronal circuits.

## Extracellular signals recorded from locust neurons using field-effect transistors

Stefan Weigel, Petra Schulte, Simone Böcker-Meffert, Günter Wrobel, Sven Ingebrandt and Andreas Offenhäusser

Forschungszentrum Jülich, Institute of Thin Films and Interfaces (ISG 2), Bio- and Chemosensors, D-52425 Jülich, Germany

Extracellular recording techniques with planar, non-metallized field-effect transistors (FETs) or multi electrode arrays (MEAs) are alternatively used for investigation of neuronal signals instead of common recording techniques like patch-clamp or sharp electrode recordings.

In our study we want to analyse networks of neurons, which are involved in the neuronal control of locusts jump. The large size of these neurons and the possibility to identify individual neurons of this circuit by backfill staining facilitates the reconstruction of the *in vivo* situation on the FETs. Thus we want to investigate the signal processing without interference of any other neuronal projection to the circuit of interest.

Isolated thoracic neurons were seeded on arrays of 4x4 FETs coated with 100µg/ml cellulose nitrite. The cells were cultured in modified Leibowitz (L-15) at 29°C. Cell culture conditions are described in detail on the poster “Cell culture of locust neurons regaining functional networks”.

The electrical activity of neurons attached to the FET gate was recorded at 2-6 *DIV* with the FET device and the patch-clamp pipette (whole-cell mode) simultaneously. We measured action potentials in the current-clamp configuration as well as membrane currents in the voltage-clamp configuration. The resulting ion flux over the membrane leads to voltage changes in the small cleft between the cell membrane and the FET gate, which are monitored by the FET. These signals were analysed and compared to the corresponding patch-clamp signal.

The recording of neuronal activity with FET devices in comparison to classical electrophysiological methods shows great promise for non-invasive long-term recordings and recordings of many neurons simultaneously. In the future, we want to use this powerful tool to investigate the synaptogenesis, the development and the signal processing of reconstructed neuronal networks *in vitro*.

## **The human neuroblastoma cell line SH-SY5Y: a model system to study caspase 3/7 and caspase 9 activity in apoptosis**

Reinhold Müller

Neuroscience Discovery Research, Abbott, Ludwigshafen, Germany

The cysteine proteases of the caspase family are central mediators in the process of apoptosis. Two well-defined pathways of apoptosis induction, both converging on the main executor caspases 3 and 7, are known: the extrinsic pathway acts by a receptor-mediated activation of caspase 8 whereas the intrinsic pathway is mediated by caspase 9/Apaf-1 interaction. The intrinsic pathway is activated by cytochrome c release from mitochondria, e.g. after DNA damage or chemical stress. Four cell lines, PC12, HEK293, SK-N-MC, and SH-SY5Y, were investigated to find a cellular system well suited to study the process of apoptosis.

For that purpose, first the nuclear morphology was investigated after staining with the DNA-intercalating dye Hoechst 33252. Basal apoptosis was low in all cell lines. Apoptosis was induced by UV irradiation or treatment with the protein kinase C inhibitor staurosporine. HEK293 cells were very resistant to induction of apoptosis, PC12 cells were moderately sensitive, whereas SH-SY5Y and SK-N-MC showed a high sensitivity towards UV irradiation and staurosporine treatment. Especially the human neuroblastoma cell line SH-SY5Y displayed clear apoptotic body formation and was selected for further studies. The process of apoptosis was further investigated by measuring the activities of caspase 3/7 and caspase 9, respectively. In addition to the stimuli used above, apoptosis was also induced by treatment with  $\alpha$ -(trichloromethyl)-4-pyridineethanol (PETCM), which activates the intrinsic pathway due to the interference with the apoptosis inhibitory protein prothymosin  $\alpha$ . Caspase 3/7 activity was dose-dependently increased by all treatments. It reached a maximum 24h after treatment of cells with PETCM and UV irradiation and 4-5h after treatment with staurosporine, respectively. To measure the activation of the intrinsic pathway, an assay was developed to monitor caspase 9 activity without the involvement of a cell lysis step. This assay omits the detergents typically present in caspase assay buffers and uses the tetrapeptide caspase 9 substrate Ac-LEHD-AFC for a sensitive fluorescence readout after 1h of incubation. Caspase 9 activity was dose-dependently induced by all three different treatments. Activity was completely suppressed by the addition of 15 $\mu$ M of the irreversible cell permeable inhibitor z-LE(OMe)HD(OMe)-fmk. Using 600nM staurosporine, which robustly induces caspase 9 activity within 4-5h, IC<sub>50</sub> values for this as well as for other peptidic caspase inhibitors were determined.

In conclusion, these data are in agreement with the stimulation of a complete apoptotic cascade via the intrinsic pathway: all three treatments increased caspase 9 and caspase 3/7 activity, typical for apoptosis initiation and execution, respectively, and resulted in the fragmentation of the nucleus into apoptotic bodies, the hallmark of the terminal stage of apoptosis. Therefore, the human neuroblastoma cell line SH-SY5Y seems to be particularly well suited as a tool for the study of different aspects of the intrinsic pathway in apoptosis.

## GENE EXPRESSION PATTERNS ASSOCIATED WITH PSYHOSTIMULATING DRUG LADASTEN ACTION IN RAT BRAIN

Yamidanov R.S.<sup>1</sup>, Vakhitova J.V.<sup>1</sup>, Mikhaylova M.G.<sup>1,3</sup>, Seredenin S.B.<sup>2</sup>

<sup>1</sup>Institute of Biochemistry and Genetics, Ufa, Russia

<sup>2</sup>Institute of Pharmacology Russian Academy of Medical Sciences, Moscow, Russia

<sup>3</sup>Leibniz Institute for Neurobiology, Magdeburg, Germany

Microarrays are a powerful high throughput tool that allows the simultaneous analysis of the expression profile in a variety of genes. We have used the Rat Atlas cDNA Array (BD Bioscience) to assess changes in mRNA expression of 1176 genes in rat brain after acute treatment of original derivative of 2-aminoadamantane - Ladasten, which exhibits the psychostimulating, anxiolytic and immunomodulating actions. It's also known that the substance has a positive influence on mnemonic process. It accelerates the formation of memory traces, improving their consolidation and facilitating the extraction of the stored information.

**Methods:** Whole brains from adult male Wistar rats were quickly removed and homogenized one and half hour after intraperitoneal Ladasten (50 mg/kg) or saline for control treatment. Total RNA was isolated using Trizol reagent and dissolved in water. Rat Atlas cDNA Array was used according to the protocol. <sup>32</sup>P-labeled cDNA probes were generated from total RNA samples through reverse transcription using MMLV reverse transcriptase and primers specific for the gene sequences of the cDNA array. Generated probes were hybridized to individual array membranes and after washing the blots were visualized by phosphorimaging. The results were subsequently corroborated by real-time RT-PCR.

**Results and discussion:** Our data show that twenty-two genes are differentially expressed. In addition the differential expression of eleven genes was confirmed by quantitative real-time RT-PCR. The GABA transporter and carboxypeptidase E, H genes should be considered as primary pharmacologically significant targets and the changes of their functional conditions allow to explain the distinct mechanisms of the anxiolytic properties of the drug. One part of Ladasten-responsive genes APC, Rb, calmodulin, PKC inhibitor protein is involved in a different of signaling pathways. Whereas other effected genes encode the cytoskeletal (tubulin, actin), cell adhesion (NCAM, insulin-like growth factor binding protein) and vesicular proteins (synapsins 1A&1B, PLP). It is necessary to note that exact functions of most genes found in the central nervous system are still unknown. It is possible to assume that proteins encoded by the given genes participate separately, or as parts of cascades in the compensatory and/or neuroplastic adaptation by Ladasten.

Supported by the RFBR grant 02-04-97904.

**Poster Subject Area #PSA26:  
Glia cells; Myelin**

- [#349A](#) T. Pannicke, JE. Fries, I. Goczalik, M. Francke, TH. Wheeler-Schilling, K. Kohler, S. Wolf, P. Wiedemann, A. Bringmann and A. Reichenbach, Leipzig and Tübingen  
*Identification of P2Y receptor subtypes in human Müller glial cells*
- [#350A](#) O. Uckermann, A. Wolf, P. Wiedemann, A. Reichenbach and A. Bringmann, Leipzig  
*Neuropeptide Y-mediated inhibition of retinal glial cell swelling*
- [#351A](#) E. Ulbricht, M. Goczalik, M. Raap, M. Weick, A. Reichenbach and M. Francke, Leipzig  
*Glial cells from Human Retinas produce IL-8 and express CXCR1 and CXCR2 Receptors*
- [#352A](#) C. Röhl, Kiel  
*Astrogliosis is downregulated by lipopolysaccharide-activated microglia in astroglial cell cultures*
- [#353A](#) G. Ponath, V. Arolt, C. August and M. Rothermundt, Münster  
*Intracellular S100B regulates astrocytic intermediate filament assembly and neurite outgrowth in vitro*
- [#354A](#) NG. Bauer and C. Richter-Landsberg, Oldenburg  
*Inclusion body formation in oligodendroglial cells depends on the dynamic instability of the microtubule network*
- [#355A](#) S. Zierler and H. Kerschbaum, Salzburg (A)  
*PMA – induced ramification in the microglia cell line, BV-2, does not depend on PKC*
- [#348B](#) M. Schmitz, S. Klopffleisch, S. Klöppner and HH. Althaus, Goettingen  
*Effect of Oligodendroglial Microdomain Components on NGF Signaling*
- [#349B](#) M. Handschuh, K. Szöke, S. Hülsmann, F. Kirchhoff, M. Bähr and C. Neusch, Göttingen  
*Differential cellular expression of aquaporin 4 and 8 in mouse spinal cord cultures and coenrichment with the Kir4.1 channel subunit*
- [#350B](#) N. Papadopoulos, C. Neusch, I. Maletzki, M. Handschuh, F. Kirchhoff and S. Hülsmann, Göttingen  
*Inactivation of the Kir4.1 channel subunit abolishes K<sup>+</sup> siphoning properties in astrocytes of the respiratory network*
- [#351B](#) GV. Michailov, MH. Schwab, BG. Brinkmann, C. Humml, C. Birchmeier, MW. Sereda and K-A. Nave, Goettingen and Berlin  
*A THRESHOLD LEVEL OF NEUREGULIN-1 INDUCES MYELINATION*

- [#352B](#) AS. Dhaunchak and K-A. Nave, Göttingen  
*An essential role of disulfide bridges in myelin proteolipid protein (PLP): implications for protein misfolding in Pelizaeus-Merzbacher disease*
- [#353B](#) CR. Malz, J. Gralla, P. Riederer and ME. Götz, Göttingen, Bern (CH), Würzburg and Kiel  
*Antioxidant defense in sockeye salmon brain during aging*
- [#354B](#) AE. Rünker, I. Kobsar, T. Fink, T. Tilling, G. Loers, P. Putthoff, C. Wessig, R. Martini and M. Schachner, Hamburg and Würzburg  
*A MOUSE MODEL OF HUMAN CHARCOT-MARIE-TOOTH TYPE 1B (CMT1B) DISORDER*
- [#355B](#) S. Maysami, S. Heine and M. Stangel, Hannover  
*Characterization of oligodendrocytes responses towards chemokines CCL11 and CXCL2*



## Identification of P2Y receptor subtypes in human Müller glial cells

Thomas Pannicke<sup>1</sup>, Julia E. Fries<sup>2</sup>, Iwona Goczałik<sup>1</sup>, Mike Francke<sup>1</sup>, Thomas H. Wheeler-Schilling<sup>2</sup>, Konrad Kohler<sup>2</sup>, Sebastian Wolf<sup>3</sup>, Peter Wiedemann<sup>3</sup>, Andreas Bringmann<sup>3</sup>, Andreas Reichenbach<sup>1</sup>

<sup>1</sup>*Paul-Flechsig-Institut für Hirnforschung, Universität Leipzig, Jahnallee 59, D-04109 Leipzig, Germany*

<sup>2</sup>*Forschungsstelle für Experimentelle Ophthalmologie, Universitätsaugenklinik, Universität Tübingen, Röntgenweg 11, D-72076 Tübingen, Germany*

<sup>3</sup>*Klinik und Poliklinik für Augenheilkunde, Universität Leipzig, Liebigstr. 10/14, D-04103 Leipzig, Germany*

ATP and other nucleotides have been demonstrated to act as signaling molecules by activation of P2 receptors, which are divided into two groups: the ionotropic P2X receptors and the metabotropic P2Y receptors which belong to the superfamily of G protein-coupled receptors. Activation of P2Y receptors results in the release of  $\text{Ca}^{2+}$  from intracellular stores and, thus, in an increase of the intracellular  $\text{Ca}^{2+}$  concentration ( $[\text{Ca}^{2+}]_i$ ), which may modify different cellular functions. Nine different subtypes of P2Y receptors have been identified in mammals: P2Y<sub>1</sub>, P2Y<sub>2</sub>, P2Y<sub>4</sub>, P2Y<sub>6</sub>, P2Y<sub>11</sub>, P2Y<sub>12</sub>, P2Y<sub>13</sub>, P2Y<sub>14</sub>, and P2Y<sub>15</sub>. Several P2Y receptor subtypes have been described in the rat retina and in individual retinal cells (Fries et al., Mol Brain Res, in press; IOVS, in press) and in Müller glial cells from the salamander retina using pharmacological means (Reifel Saltzberg et al., Glia 42:149-59, 2003). The identification of P2Y receptor subtypes expressed in the retina may improve the understanding of retinal physiology. Because the expression of receptors may differ among species (as has been shown for the P2X<sub>7</sub> receptor), we decided to investigate the expression of P2Y receptors in Müller cells from the human retina. Since the access to human retinal tissue is limited, we confined our study to the subtypes P2Y<sub>1</sub>, P2Y<sub>2</sub>, P2Y<sub>4</sub>, and P2Y<sub>6</sub>. These subtypes are widely accepted as functional receptors in mammals and their structure is well characterized. The use of human material was approved by the ethics committee of the University of Leipzig Medical School. Retinal tissue from patients with proliferative vitreoretinopathy (PVR) was obtained during vitreoretinal surgery (samples from 15 patients). Müller cells were enzymatically isolated from retinal pieces. Because these cells express  $\text{Ca}^{2+}$ -dependent  $\text{K}^+$  (BK) channels, an increase in  $[\text{Ca}^{2+}]_i$  mediated by the activation of P2Y receptors could be recorded in the whole-cell configuration of the patch-clamp technique. Application of different P2Y agonists (ATP, 2MeSATP, 2MeSADP, ADP $\beta$ S, UTP, UDP) resulted in increases of BK current amplitudes, pointing to the existence of different receptor subtypes in Müller cells. Subsequently to the current recording, the cytoplasm of the recorded cell was harvested into the recording electrode and expelled into a PCR tube. After reverse transcription, the cDNA from a single cell was split into two samples and separately used for a PCR reaction with P2Y<sub>1</sub>- and P2Y<sub>2</sub>-specific primers. In 12 of 30 cells (40%) a PCR product of the predicted size for P2Y<sub>1</sub> and in 7 of 32 cells (23%) the PCR product for P2Y<sub>2</sub> were found. To increase efficiency of the experiments, a second suction pipette was used for harvesting the complete cell. Cells harvested by two pipettes were used for P2Y<sub>1</sub>/P2Y<sub>2</sub>-PCR (n=14) and for P2Y<sub>4</sub>/P2Y<sub>6</sub>-PCR (n=17) as described. The number of cells positive for the respective PCR product was n=9 for P2Y<sub>1</sub> (64%), n=3 for P2Y<sub>2</sub> (21%), n=13 for P2Y<sub>4</sub> (76%), and n=14 for P2Y<sub>6</sub> (82%). Thus, whereas the mRNA for all investigated P2Y receptor types was expressed in human Müller cells, the incidence of P2Y<sub>2</sub> receptors was significantly lower than that of the other subtypes. In addition, we used human retinal tissue to demonstrate the existence of the respective P2Y receptor subtypes immunohistochemically.

**Neuropeptide Y-mediated inhibition of retinal glial cell swelling**

O. Uckermann<sup>1,2</sup>, A. Wolf,<sup>1</sup> P. Wiedemann,<sup>2</sup> A. Reichenbach,<sup>1</sup> A. Bringmann,<sup>2</sup>

<sup>1</sup>Paul Flechsig Institute of Brain Research, University of Leipzig, 04109 Leipzig, Germany

<sup>2</sup>Department of Ophthalmology and Eye Clinic, Liebigstrasse 10-14, University of Leipzig, 04103 Leipzig, Germany

Various different ocular diseases are accompanied by the development of retinal edema which has been implicated in photoreceptor cell death after ischemia or trauma. Retinal edema is thought to be caused by both opening of blood-retinal barriers (extracellular edema) and glial cell swelling (cytotoxic edema). While the regulation of blood-retinal barriers is a focus of research since many years, almost nothing is known about the mechanisms of retinal glial cell swelling and its modulation by neurotransmitters. Recently, we suggested a  $K^+$  channel- and aquaporin-dependent mechanism which may be involved in retinal glial cell swelling in postischemic rat retinas (Pannicke et al., 2004, Mol. Cell. Neurosci, 26 (4): 493). Since neuropeptide Y (NPY) is the most abundant neuropeptide in the brain, and is also released in the retina in response to light, we investigated the effect of this peptide on the retinal glial (Müller) cell swelling evoked by hypotonic stress (a situation resembling hypoxia-induced cytotoxic edema in the brain).

Acutely isolated slices of the rat retina were exposed to hypotonic solution (60 % of control ionic strength) plus  $Ba^{2+}$  (1 mM) which has been shown to induce somatic swelling of Müller cells in control rat retinas (Pannicke et al., 2004). NPY dose-dependently inhibited the glial cell swelling evoked by hypotonic challenge, with a half-maximal effect at ~ 2.6 nM. The effect of NPY was mimicked by a selective  $Y_1$  receptor agonist, while selective agonists of  $Y_2$  and  $Y_5$  receptors were without effect. In addition, NPY did not have an effect in the presence of a selective  $Y_1$  receptor antagonist (BIBP 3226). Preincubation with a membrane-permeable  $Ca^{2+}$  chelator (BAPTA/AM) as well as incubation with an inhibitor of the PKC (Gö 6976) reversed the effect of NPY.

The data suggest that NPY inhibits hypotonic glial cell swelling by activation of  $Y_1$  receptors; this effect is mediated by intracellular  $Ca^{2+}$  increase and subsequent activation of PKC. The results may have impact for the understanding of light-induced cell volume regulation in the retina, as well as for the development of new therapeutic strategies for inhibition of postischemic and posttraumatic glial cell swelling.

Supported by the Interdisziplinäres Zentrum für Klinische Forschung (IZKF) Leipzig, Faculty of Medicine, University of Leipzig, project C21

## **Glial cells from Human Retinas produce IL-8 and express CXCR1 and CXCR2 Receptors**

E. Ulbricht, I. M. Goczalik, M. Raap, M. Weick, A. Reichenbach and M. Francke

Paul-Flechsig-Institute for Brain Research, Neurophysiology, University of Leipzig,  
Jahnalle 59, 04109 Leipzig, Germany

Interleukin-8 (IL-8) belongs to the group of pro-inflammatory chemokines. Several diseases of the eye (e.g. uveitis, PVR) are associated with increased levels of IL-8 in the vitreous. Various cell types are potential sources for the secreted IL-8. The aim of our study was to evaluate whether retinal glial cells are able to produce IL-8 and/or to express IL-8 receptors. We examined an immortalized human Müller cell line (MIO-M1) as well as primary cultures of isolated glial cells and tissue from human donor retinas. The cultured cells and the retinal tissues were prepared for immunohistochemistry (IHC), Western blotting and RT-PCR. Ca<sup>2+</sup> imaging was performed to test the activation of IL-8 receptors.

IL-8 immunoreactivity was accompanied by GFAP immunoreactivity and was co-localized with other glial specific markers. IL-8 mRNA could be detected in human Müller cell cultures. Immunoreactivity for CXCR1 and CXCR2 was observed in human primary cultures and in the Müller glial cell line. Western blot analysis revealed proteins with about 40 kDa. The RT-PCR method confirmed the expression of CXCR1 and CXCR2 receptors in the human Müller cell line. Application of recombinant IL-8 protein caused an increase in intracellular Ca<sup>2+</sup> levels in subpopulations of Müller cells. It is concluded that Müller cells may participate in the inflammatory response of pathologically altered or injured eyes. Surprisingly, we also detected the expression of CXCR1 and CXCR2 in healthy retinas from human donors by means of IHC, RT-PCR and Western blotting. The receptors were localized in the glial cells around blood vessels therefore an involvement of these receptors in controlling the vascularization is suggested.

## **Astrogliosis is downregulated by lipopolysaccharide-activated microglia in astroglial cell cultures**

C. RÖHL

*Department of Anatomy, University of Kiel, Olshausenstr. 40, D-24098 Kiel, Germany*

*(c.roehl@anat.uni-kiel.de)*

Astrogliosis, characterized by a cellular increase of the structural protein GFAP (glial fibrillary acidic protein) in astrocytes, is a common phenomenon seen in many neurological diseases. The relevance of astrogliosis, especially with respect to its beneficial or detrimental role in CNS recovery, remains controversial. Nevertheless, considerable efforts have been made to understand the etiology of astrogliosis. One popular standpoint is, that proinflammatory cytokines released from activated microglia are responsible for the onset of astrogliosis, because microgliosis precedes or accompanies astrogliosis in many pathological changes of the nervous system. At the same time increasing evidences exist, that enhanced expression of proinflammatory compounds are not directly related to the induction of astrogliosis (*Little and O'Callaghan, 2001*).

The present study was undertaken to examine the role of activated microglia in the etiology of astrogliosis. Therefore, we used an in vitro model of astrogliosis, which takes advantage of the physiological increasing cellular GFAP levels in younger astroglial cell cultures and of the existing high levels in older ones (*Röhl et al., 2003*).

Purified cortical astrocytes from neonatal Wistar rats were cultivated over a period of 9 and 32 days. Then, astrocytes were incubated for further two weeks with either unconditioned medium with or without LPS (lipopolysaccharides) or with conditioned medium from LPS-activated or native microglial cells from neonatal Wistar rats. Nitric oxide (NO) has been taken as parameter for the determination of microglial activation. After two weeks of incubation total protein, cell number and amounts of GFAP were determined in culture.

Whereas, compared to all controls, the total protein content of astroglial cultures treated with conditioned medium from LPS-activated microglia was unchanged, the cell number increased about 30 % and GFAP levels were about 50 % lower in younger cultures and about 30 % in older ones. Cellular GFAP contents even were about 60 % and 50 % lower in 23-day-old and 46-day-old cultures, respectively, than those of controls. Thus, conditioned medium from LPS-activated microglia inhibits the increase of glial fibrillary acidic protein (GFAP) in younger astroglial cell cultures as well as it decreases the cellular GFAP content in older cultures.

These findings support the hypothesis, that proinflammatory substances released from activated microglia are not necessarily involved in the induction of astrogliosis and that, furthermore, soluble factors of LPS-activated microglia might even reduce astrogliosis. Taken together, activated microglia is possibly not etiological responsible for the astrogliotic processes in many neurological diseases and maybe even delay glial scar formation.

*Little, A. R.; O'Callaghan, J. P. (2001): Astrogliosis in the adult and developing CNS: Is there a role for proinflammatory cytokines? Neurotoxicology (22), 607-618.*

*Röhl, C.; Held-Feindt, J. and Sievers, J. (2003): Developmental changes of parameters for astrogliosis during cultivation of purified cerebral astrocytes from newborn rat. Developmental Brain Research (144), 191-199.*

## **Intracellular S100B regulates astrocytic intermediate filament assembly and neurite outgrowth in vitro**

Gerald Ponath<sup>1</sup>, Volker Arolt<sup>1</sup>, Christian August<sup>2</sup>, Matthias Rothermundt<sup>1</sup>

University of Münster, <sup>1</sup>Department of Psychiatry, Molecular Psychiatry Division and

<sup>2</sup>Gerhard-Domagk Institute of Pathology

### **OBJECTIVE**

In several neurodegenerative diseases the secretion of the astrocytic protein S100B is upregulated. Its role in the pathogenesis of these disorders, however, remains to be characterized. Under certain circumstances such as ischemic conditions upregulated extracellular S100B is accompanied by low intracellular S100B content. In protein binding assays it was shown that S100B inhibits intermediate filament assembly of GFAP and vimentin by inhibition of protein kinase C mediated phosphorylation. Here we show that in primary cultured astrocytes from wildtype and S100B<sup>-/-</sup> mice S100B regulates GFAP, vimentin and nestin intermediate filament assembly influencing neurite outgrowth and neuronal survival.

### **METHODS AND RESULTS**

Intermediate filament density was increased in S100B<sup>-/-</sup> cortical astrocytes in situ identified by electron microscopy. Knockout-proven S100B immunoreactivity was co-localized with the filamentous structures of GFAP in cultured astrocytes. In S100B<sup>-/-</sup> astrocytes GFAP and Vimentin were upregulated whereas nestin immunoreactivity was reduced compared to wildtype astrocytes. As a consequence, laminin expression was downregulated on S100B<sup>-/-</sup> astrocytes leading to a reduced neurite outgrowth and neuronal survival after 4 days of co-culture with S100B<sup>-/-</sup> astrocytes shown by  $\beta$ -Tubulin III immunoreactivity. This was caused by intracellular S100B since recombinant S100B protein added to the wildtype or S100B<sup>-/-</sup> astrocyte culture medium had no effect on intermediate filament protein expression.

### **CONCLUSION**

Intracellular S100B content regulates the intermediate filament protein assembly in astrocytes. Downregulation of intracellular S100B leads to lower production of laminin by astrocytes and inhibition of neurite outgrowth. Our data indicate a pathway how S100B might be involved in the pathogenesis of neurodegenerative diseases.

## **Inclusion body formation in oligodendroglial cells depends on the dynamic instability of the microtubule network**

Nina G. Bauer and Christiane Richter-Landsberg

Department of Biology, Molecular Neurobiology, University of Oldenburg  
Oldenburg, Germany

Tau-positive inclusions in oligodendrocytes, containing ubiquitin and the small heat shock protein  $\alpha$ B-crystallin, are consistent neuropathological features of corticobasal degeneration, progressive supranuclear palsy, and frontotemporal dementia with Parkinsonism linked to chromosome 17 (FTDP-17). The occurrence of protein accumulations or inclusion bodies in these diseases have been implicated in cellular degeneration. Furthermore, proteasome impairment and altered proteasomal function have been linked to their pathogenesis, and might contribute to protein aggregate formation. In a number of cell culture models, including OLN-t40 cells, an oligodendroglial cell line stably transfected to express the MT-associated protein tau, proteasome inhibitors like MG-132 induce the formation of protein aggregates termed aggresomes, which are assembled near the microtubule (MT)-organizing center (MTOC). MTs and dynein-based retrograde transport along the MTs have been suggested to play a role in the assembly of aggresomes. Using indirect immunofluorescence, we have shown previously that aggresomes in OLN-t40 cells contain tau, ubiquitin, and  $\alpha$ B-crystallin, a stress-inducible chaperone which modulates cytoskeletal functions.

Here, we demonstrate that treatment with MG-132 (0.5  $\mu$ M, 6-18h), led to the disorganization of the MT-network and its retraction from the cell periphery. Concomitantly, MTs assembled around the nucleus and aggresome. MT-binding assay further revealed that  $\alpha$ B-crystallin and ubiquitin were bound to the MTs. Analysis of tau-immunoprecipitates showed that  $\alpha$ B-crystallin and ubiquitin were associated with tau after proteasomal inhibition.

The role of MTs was further investigated by pretreating the cells with the MT-disrupting drug nocodazole (1  $\mu$ M, 18-24h) or with the MT-stabilizing drug taxol (0.5  $\mu$ M, 18-24h), followed by MG-132. Both compounds resulted in the inhibition of aggresome formation. Instead, small punctuate  $\alpha$ B-crystallin positive deposits were observed, which remained in the cytoplasm and did not assemble near the MTOC.

Since not only nocodazole-induced MT disassembly, but also MT stabilization by taxol, which leads to an inhibition of MT depolymerization and possibly to a disturbance of transport processes, prevents the assembly of large protein aggregates, it might be suggested that the dynamic instability of the MT network is required for aggresome formation.

## **PMA – induced ramification in the microglia cell line, BV – 2, does not depend on PKC**

Susanna Zierler and Hubert Kerschbaum

Division of Animal Physiology, Department of Cellular Biology, University of Salzburg,  
Hellbrunnerstr. 34, 5020 Salzburg, Austria

Microglia cells, bone marrow - derived macrophages of the brain, are dimorphic. Activated cells are amoeboid, whereas resting cells have a ramified phenotype. Several lines of evidence indicate that kinases play important roles in the transition from an amoeboid to a ramified phenotype. In the present study, we examined the role of phorbol 12 – myristate 13 – acetate (PMA), a widely used activator of  $\text{Ca}^{2+}$  / phospholipids – dependent protein kinase [protein kinase C (PKC)], on the phenotype of BV – 2 cells.

BV – 2 cells were incubated for 12 hours with 10 nM PMA before we evaluated the frequency distribution of distinct phenotypes of BV – 2 cells. In all experiments examining the effect of inhibiting PKC activity, PKC inhibitors (calphostin C, chelerythrine, and bisindolylmaleimide II) were applied 30 minutes before application of PMA. An additional 12 hour incubation period with PMA and PKC inhibitors was used before we evaluated the frequency distribution of cell phenotypes. The significance of the frequency distribution of BV – 2 cell phenotypes in the presence or absence of PMA or PMA and PKC inhibitors was quantified using a  $\chi^2$  test statistic. Cell phenotypes were visualized using labeling of actin in BV – 2 cells with Alexa - coupled phalloidin.

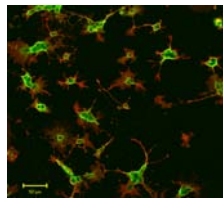
Four groups of cells were examined in parallel. One group did neither contain PMA nor PKC inhibitors, a second group contained 10 nM PMA, a third group was incubated with 10 nM PMA and PKC inhibitors, and a fourth group was exposed to PKC inhibitors. Exposure of BV – 2 cells to PMA decreased the number of amoeboid phenotypes, increased the number of tripolar and multipolar phenotypes, but did not affect the number of bipolar phenotypes ( $\chi^2 = 169.66$ ). The treatment of BV 2 cells with calphostin C (30 nM), chelerythrine (30 nM, 300 nM), or bisindolylmaleimide II (300 nM) in the presence of 10 nM PMA was similar to that of PMA alone ( $\chi^2$  is between 3.08 and 13.44;  $\alpha = 0.001$ ). Moreover, incubation of BV – 2 cells with PKC inhibitors alone did not affect the frequency distribution of cell phenotypes ( $\chi^2$  is between 0.23 and 1.52;  $\alpha = 0.001$ ). Thus, our results indicate that PKC isoforms are not involved in PMA – dependent ramification in BV – 2 cells.

## Effect of Oligodendroglial Microdomain Components on NGF Signaling

Schmitz M; Klopffleisch S; Klöppner S; Althaus HH

MPI for Experimental Medicine, D-37075 Goettingen, H-Reinstr.3

Recent results indicate that the integrity of the myelin sheath is compromised with age (1), and that myelin destruction could be a precipitating event in age-related disorders (2). Furthermore, oligodendrocytes (OL), which furnish the CNS myelin, do not support remyelination in older animals to the same extent as in younger animals. An increased process formation reflects an OL response to NGF, however, differentially depending on age of the donor (3). We were interested to know as to whether NGF signaling is modulated by microdomain components such as caveolin and cholesterol, which might undergo age-related



changes. Immunocytochemistry of cultured pig OL revealed the co-expression of caveolin-1 and the 140 kDa NGF receptor TrkA. Caveolin-containing microdomains were isolated via previously published buoyant density centrifugation methods (+/- Triton X-100) and by using MACS technology. Western blotting showed a co-labeling of the caveolar protein, flotillin-1, in addition to TrkA, which is enriched in the Triton X-100 insoluble fraction, p75 NTR, and p21 Ras. Preliminary results indicate that oligodendroglial caveolin and cholesterol are up-regulated from 8 DIV to 16 DIV, a period of extensive oligodendroglial process regeneration. Afterwards, both components remained on this level up to 30 DIV, the time of investigation. At this time, MAPK activity was less inducible by NGF than at 8 DIV, when compared with controls. Cells exposed to PEG-cholesterol increased their process formation; PEG-cholesterol plus NGF accelerated the NGF response; under both conditions, an in-gel-kinase assay demonstrated an increased MAPK activity, a step of the downstream TrkA signaling. On the other hand, exposure to cyclodextrin (1.2mM), which disrupts caveolar microdomains by removing cholesterol from the plasma membrane, resulted in a less effective NGF response. The results at present indicate that NGF signaling is modulated by cholesterol; the effect of caveolin-1 siRNA is under investigation.

1. Peters A et al.(2000): J Comp Neurol 419, 364-376
2. Bartzokis G (2004) : Neurobiol of Aging 25, 5-18
3. Althaus HH et al. (2001): MRT 52, 689-699



## **Differential cellular expression of aquaporin 4 and 8 in mouse spinal cord cultures and coenrichment with the Kir4.1 channel subunit**

Melanie Handschuh<sup>1</sup>, Katalin Szőke<sup>2</sup>, Swen Hülsmann<sup>2</sup>, Frank Kirchhoff<sup>3</sup>, Mathias Bähr<sup>1</sup>, and Clemens Neusch<sup>1</sup>

<sup>1</sup>Department of Neurology, Georg-August-University Göttingen, 37099 Göttingen, Germany

<sup>2</sup>Department of Neuro- and Sensory Physiology, Georg-August-University Göttingen, 37075 Göttingen

<sup>3</sup>Department of Neurogenetics, Max-Planck-Institute of Experimental Medicine, 37075 Göttingen

Aquaporin (AQP) water channels represent a large family of integral membrane proteins that mediate the entry and release of water. Heteromeric complexes of AQP4 channels with the Kir4.1 channel subunit represent putative structural correlates of K<sup>+</sup> driven water flux in astrocytes. Expression of Kir4.1 channels in the spinal cord suggests a similar important role in extracellular K<sup>+</sup> and water homeostasis not only for astrocytes, but also for oligodendrocytes. We investigated the expression of two glial aquaporins, AQP4 and AQP8 in spinal cord cultures and correlated it with the expression of the Kir4.1 potassium channel subunit. AQP8, but not AQP4, was detected on oligodendrocytes by immunocytochemistry. AQP8 immunolabeling was colocalized with the Kir4.1 channel on cell bodies and along oligodendrocytic branches. Cultured spinal cord astrocytes, however, expressed predominantly AQP4. Astroglial AQP4 expression could be further substantiated in transgenic mice that express the fluorochrome EGFP under the GFAP promoter. Here, immunostaining revealed a strong expression of AQP4 on astroglial endfeet enwrapping small capillaries. Codetection of Kir4.1 at these sites suggests the formation of both proteins as a complex in situ. Developmental regulation of AQP4 and AQP8 protein expression was detected in spinal cord lysates by Western blot analysis. While AQP8 was upregulated during the second postnatal week, AQP4 levels did not change postnatally suggesting a pre- or perinatal expression. Furthermore, AQP4 protein levels did not change significantly when investigated in Kir4.1 null mice up to P17.

We suggest that AQP8 represents a major AQP channel in spinal cord oligodendrocytes and forms specialized membrane domains with Kir4.1. AQP8 may thus mediate oligodendrocytic water transport associated with K<sup>+</sup> siphoning or edema in pathological conditions, e. g. spinal cord injury, inflammatory spinal cord diseases or ischemia. Furthermore, colocalization of AQP4 with Kir4.1 at distinct subcellular compartments surrounding microvessels in the spinal cord provides evidence that Kir4.1/AQP4 complexes mediate water flux associated with astrocytic K<sup>+</sup> siphoning. However, our results using a Kir4.1 null mouse suggests that formation of a astrocytic Kir4.1/AQP4 complex at the cell membrane does not require Kir4.1 expression in the spinal cord.

## **Inactivation of the Kir4.1 channel subunit abolishes K<sup>+</sup> siphoning properties in astrocytes of the respiratory network**

Nestoras Papadopoulos<sup>1</sup>, Clemens Neusch<sup>2</sup>, Iris Maletzki<sup>2</sup>, Melanie Handschuh<sup>2</sup>, Frank Kirchhoff<sup>3</sup>, and Swen Hülsmann<sup>1</sup>

<sup>1</sup>Department of Neuro- and Sensory Physiology, Georg-August-University Göttingen, 37073 Göttingen,

<sup>2</sup>Department of Neurology, Georg-August-University Göttingen, 37099 Göttingen

<sup>3</sup>Department of Neurogenetics, Max-Planck-Institute of Experimental Medicine, 37075 Göttingen

The vital neuronal activity in the ventral respiratory group (VRG) of the brainstem involves rapid exchange of extracellular ions by astrocytes. The neuronal rhythmic activity is thought to require glial K<sup>+</sup> selective channels that buffer K<sup>+</sup> fluctuations in order to maintain ionic balance. To understand the functions of K<sup>+</sup> channels in astrocytes, we have studied the expression and function of the weakly inwardly rectifying K<sup>+</sup> channel subunit Kir4.1 (KCNJ10) in the mouse respiratory network. Immunolabeling for the Kir4.1 subunit from postnatal day 7-17 reveals that Kir4.1 protein expression is upregulated on astrocytes of the ventral respiratory group (VRG). Kir4.1 is expressed along fine processes and surrounds blood capillaries of the brainstem. To understand the physiological role of Kir4.1, we studied mice with a null mutation in the weakly inwardly rectifying K<sup>+</sup> channel subunit Kir4.1 (KCNJ10). Prior to experiments, these mice have been interbred with transgenic mice expressing EGFP under the control of the human GFAP promoter to visualize astrocytes. Kir4.1<sup>-/-</sup> astrocytes of the VRG that are located in proximity to respiratory neurons show strongly depolarized membrane potentials, a reduced K<sup>+</sup> conductance and profoundly reduced Kir currents.

We conclude that the Kir4.1 channel subunit (i) is expressed abundantly on astroglial processes and capillaries in the VRG, (ii) regulates the resting membrane potential of GFAP-positive astrocytes and (iii) forms the major K<sup>+</sup> conductance of brainstem astrocytes and therefore supports K<sup>+</sup> siphoning in such vital areas as the VRG.

(Supported by the DFG).

**A THRESHOLD LEVEL OF NEUREGULIN-1 INDUCES MYELINATION**

[G.V.Michailov<sup>1</sup>](#); [M.H.Schwab<sup>1</sup>](#); [B.G.Brinkmann<sup>1</sup>](#); [C.Humml<sup>1</sup>](#); [C.Birchmeier<sup>2</sup>](#); [M.W.Sereda<sup>1</sup>](#); [K.A.Nave<sup>1</sup>](#)

*1. Dept Neurogenet, Max-Planck-Inst. of Exptl. Med., Goettingen, Germany*

*2. Max Delbrueck Ctr. for Mol. Med., Berlin, Germany*

Myelination of axonal fibers in the vertebrate nervous system allows rapid and accurate impulse conduction. We have previously shown that in the peripheral nervous system the precise relation between axon diameter and myelin sheath thickness is regulated by an axonal growth factor, Neuregulin-1 (Nrg1) type III. Reduced gene dosage in Nrg1 heterozygous mutants causes abnormally thin myelin. Correspondingly, transgenic Nrg1 type III overexpression in neurons results in thicker than normal myelin. Thus, Nrg1 type III signals information about axon size to Schwann cells.

During early postnatal development Schwann cells in the sciatic nerve associate with axonal fibers, and myelinate axons that are typically larger than 1  $\mu\text{m}$  in diameter. How myelination is initiated and restricted to larger-diameter axons is not well understood.

Here we show, that a reduction of Nrg1 gene dosage causes a delay of sciatic nerve myelination, as determined by an increased number of unmyelinated fibers at postnatal day 10 which is not observed in the adult nerve. Moreover, in transgenic mice, overexpressing Nrg1 type III under control of the Thy1.2 promoter, we observe numerous myelinated fibers smaller than 1  $\mu\text{m}$  in diameter. This finding is supported by an increased number of myelinated fibers that express peripherin, a marker of unmyelinated sensory C-fibers in wild-type mice.

Taken together, these observations suggest that a threshold level of axonal Nrg1 type III serves as a signal for Schwann cells to initiate myelination and only enwrap fibers larger than 1  $\mu\text{m}$  in caliber.

**An essential role of disulfide bridges in myelin proteolipid protein (PLP): implications for protein misfolding in Pelizaeus-Merzbacher disease**

**A.-S. Dhaunchak, K.-A. Nave**

**Dept. Neurogenetics, Max-Planck-Institute of Experimental Medicine, Göttingen**

In humans, point mutations of the X-linked PLP gene (*Plp*) cause a severe dysmyelinating phenotype and define *Pelizaeus-Merzbacher Disease* (PMD). The encoded *Proteolipid Protein* is highly abundant, comprising about approximately 50% of myelin protein in the central nervous system. At the molecular level, PLP is a 30kDa polytopic membrane protein with four transmembrane domains (tetraspan), and one intracellular and two extracellular loop regions. Both N- and C-termini of PLP protrude into the cytosol. PLP point mutations that map into the second extracellular loop region (EC2) have a particular severe phenotype *in vivo*, but their effect on protein structure and function are poorly understood. PLP has two disulfide bridges, involving 4 cysteine residues in EC2. Here we asked whether the ability of PLP to form these disulfides is required for the normal tetraspan conformation and for the normal intracellular trafficking. Moreover, we investigated whether unpaired cysteines contribute to the retention of mutant PLP in the endoplasmic reticulum. For transfection with cDNA expression constructs, encoding PLP lacking 1-4 cysteine residues (Cys->Ser), we used an oligodendroglial cell line (Oli-neu; kindly provided by J. Trotter) and primary mouse oligodendrocytes. By laser confocal microscopy, we determined that bridge C1C4, but not C2C3, is required for intracellular sorting and surface expression of PLP. Moreover, some PMD point mutations that map into EC2, may act by exposing cysteines C1 and C4, that remain unpaired and are recognized by luminal chaperones.

## Antioxidant defense in sockeye salmon brain during aging

Cordula R. Malz<sup>1</sup>, Jan Gralla<sup>2</sup>, Peter Riederer<sup>3</sup> and Mario E. Götz<sup>4</sup><sup>1</sup>Department of Anatomy and Embryology, Center of Anatomy, University of Göttingen, Germany<sup>2</sup>Department of Neuroradiology, Inselspital Bern, University of Bern, Switzerland<sup>3</sup>Department of Psychiatry, Division of Clinical Neurochemistry, University of Würzburg, Germany<sup>4</sup>Department of Pharmacology, University of Kiel, Germany

The antioxidant glutathione (GSH) is essential for cellular detoxification of reactive oxygen species in brain cells. Recent data demonstrate that besides intracellular functions GSH has also important extracellular functions. In this respect glial cells appear to play a key role in the GSH metabolism of the brain, since astroglial GSH export is essential for providing GSH precursors to neurons. In vitro, astrocytes release substantial amounts of GSH and efficiently export glutathione disulfide (GSSG) during oxidative stress.

A higher need for detoxification of superoxide and hydrogen peroxide up to an age of 4 years is suggested by a marked increase in activities of CuZnSOD and catalase from 22 months to 49 months old sockeye salmon (*Oncorhynchus nerka*). As activation of GSH-dependent peroxidases yields GSSG as a product which indicates peroxide turnover, we analysed the GSH-GSSG redox couple in five distinct age groups (8-60 months) representing different life stages of *Oncorhynchus nerka* (juvenile, early mature, late mature, sexually mature female spawning and dying ones). We studied the biochemical parameters GSH and GSSG, reflecting stress response and the glial marker GFAP in the optic tectum, to identify possible cellular targets of biological reactive intermediates in the aging salmon brain.

We detected a gradual decrease of salmon brain GSH content at all stages, which can be correlated with the reduced distribution of GFAP in the radial glial cells of the optic tectum. Lower GSSG values occurred in the 15-months-old sea water adapted and in the dying salmon. However molar GS-redox ratios, i.e.  $\frac{[GSH]}{[GSH]+2[GSSG]}$ , remain rather constant over a salmon's lifetime. Here, decreased GSH levels could indicate oxidative stress or decreased activities of glutathione synthesizing enzymes.

A tendency towards increased GSSG levels, and a significant decrease of the molar GS redox ratio was detected in 49-month-old and spawning sockeye salmon as compared to 22-month-old fish. Redox ratios are only marginally affected by these alterations since GSH levels are by far higher than GSSG values. Although compromised in the old female salmon brains studied, GSH levels are considered to be still high enough to maintain cell survival, we wonder if further investigations of biomarkers of oxidative stress in the old male salmon brain will offer similar results.

## **A MOUSE MODEL OF HUMAN CHARCOT-MARIE-TOOTH TYPE 1B (CMT1B) DISORDER**

Annette E. Rünker (1) <sup>\*,+</sup>, Igor Kobsar (2) <sup>\*</sup>, Torsten Fink (1) , Thomas Tilling (1)§ ,  
Gabriele Loers (1) , Peggy Putthoff (1) , Carsten Wessig (2) , Rudolf Martini (2) <sup>\*\*</sup>,  
and Melitta Schachner (1) <sup>\*\*</sup>

(1) University of Hamburg, Center for Molecular Neurobiology (ZMNH), Hamburg, Germany; (2) University of Würzburg, Department of Neurology, Developmental Neurobiology, Würzburg, Germany; <sup>\*</sup> equal contribution; <sup>\*\*</sup> equal contribution; <sup>+</sup> Annette E. Rünker's present address: Developmental Neurobiology, Smurfit Institute, Department of Genetics, Trinity College Dublin, Dublin, Ireland  
§ presenting author (thomas.tilling@zmnh.uni-hamburg.de)

The peripheral myelin protein zero (P0) is a member of the immunoglobulin-like superfamily of cell recognition molecules. Mutations in the corresponding gene give rise to several peripheral neuropathies, among them Charcot-Marie-Tooth type 1B disease (CMT1B). To investigate the pathomechanisms of a specific point mutation in the *P0* gene, we generated two independent transgenic mouse lines expressing the pathogenic CMT1B missense mutation Ile106Leu (P0sub) under the control of the P0 promoter on a wild-type background. Patients carrying the respective mutation are clinically severely affected and exhibit the formation of characteristic folded myelin profiles, termed tomacula. Both P0sub-transgenic mouse lines showed the same myelin abnormalities. In addition to these features, retarded myelination, onion bulb formation and dysmyelination was seen, as well as shivering. Functionally, the mutation leads to dispersed compound muscle action potentials and severely reduced conduction velocities. Our observations support the view that the Ile106Leu mutation acts by a dominant-negative gain of function and that the P0sub-transgenic mouse represents an animal model for a severe, tomaculous form of CMT1B in humans.

Supported by the Deutsche Forschungsgemeinschaft (SFB 581, Priority Program „Microglia” MA1053/3, to R.M.) and by the Gemeinnützige Hertie-Stiftung (to M.S. and R.M.).

## Characterization of oligodendrocytes responses towards chemokines CCL11 and CXCL2

Samaneh Maysami (MD, MSc.), Sandra Heine (Vet), Martin Stangel (MD, BMedSci.)

[maysami.samaneh@mh-hannover.de](mailto:maysami.samaneh@mh-hannover.de)

Dept. of Neurology

Medical School of Hannover - OE 7210

Carl-Neuberg Str. 1, 30625, Hannover, Germany

### Introduction

The neuropathological hallmark of demyelinating diseases of the central nervous system (CNS) including multiple sclerosis (MS) is the loss of myelin. In the CNS, oligodendrocytes are small process-bearing cells, which are responsible to manufacture myelin sheaths around axons. The Chemokine GRO $\alpha$  (CXCL1) as well as many other factors has recently been shown to influence oligodendroglial functions. Previous studies showed that oligodendrocytes are expressing chemokine-receptors including CXCR2 and CCR3. The aim of this study was to evaluate the effect of the ligands eotaxin (EOT, CCL11) and macrophage inflammatory protein-2 (MIP-2, CXCL2) on proliferation and migration of oligodendrocyte progenitor cells (OPCs) in vitro.

### Methods

Cell Proliferation was measured by BrdU incorporation and immunocytochemistry in primary rat OPCs. Migration of OPCs was measured using a boyden chemotaxis chamber. EOT, ligand of CCR3, and MIP-2, ligand of CXCR2, were used at concentrations ranging from 0 to 25 ng/ml. Migration and proliferation of OPCs were measured in two different media B104 conditioned medium (B104-CM) and N2B3 medium. B104-CM contains neuroblastoma (B104) conditioned medium in eagle medium (EM) plus substances which are necessary for oligodendrocytes' survival, including insulin, transferrin, biotin, putrescine, and progesterone. Moreover, OPCs remain mainly in a proliferative precursor state in B104-CM. N2B3 medium consists of EM plus insulin, transferrin, biotin, putrescine, progesterone, T3 and T4. OPCs are differentiating in N2B3 medium. Student's t test or Mann-Whitney non-parametric test was used for statistical analysis, data values are expressed as mean  $\pm$  S.E., and statistical significance was defined as a *p* value of 0.05 or less.

### Results

OPCs migrated less towards EOT at 0.5 ng/ml in N2B3 medium, and at 0.1, 0.5, and 1 ng/ml in B104-CM. This result was statistically significant. Proliferation of OPCs in presence of EOT showed some changes in both media, but these were not statistically significant.

OPCs migrated less towards MIP-2 in both B104-CM and N2B3 medium at concentrations 0.1 and 0.5 ng/ml, respectively. Using MIP-2, OPCs showed a reduction in proliferation at 10 ng/ml in B104-CM, which was statistically significant. Migration and proliferation of OPCs showed some changes in presence of other concentrations of MIP-2 in both media which were not statistically significant.

### Conclusion

These data show that chemokines can modulate the migration and proliferation of OPCs. In accordance to published data of another CXCR2 ligand, GRO $\alpha$ , MIP-2 can inhibit the migration and proliferation of OPCs. Activation of other chemokine receptors such as CCR3 has a similar effect. Thus, chemokines seem to play an important role in OPC regulation, which may have implications for physiological myelination as well as remyelination in demyelinating diseases including MS.

**Poster Subject Area #PSA27:  
Neuronal development**

- [#356A](#) K. Frebel, E. Nichiporuk, M. Sendtner and S. Wiese, Wuerzburg  
*Overexpression of Bag-1 in differentiated PC12 cells leads to reduced neurite outgrowth*
- [#357A](#) A. Yarali, M. Kiebler and P. Macchi, Wuerzburg and Tuebingen  
*Investigating the Role of Barentsz in Zebrafish Development*
- [#358A](#) T. Künzel, B. Claaßen, B. Mönig, H. Wagner, J. Mey and H. Luksch, Aachen  
*Development of avian embryonic auditory brainstem neurons in vitro*
- [#359A](#) P. Burkert and C. Duch, Berlin  
*Changes in CaM kinase II activity and localization during postembryonic CNS remodeling in Manduca sexta*
- [#360A](#) S. Sirko, A. von Holst and A. Faissner, Bochum  
*DSD-1-PG/Phosphacan is Expressed by a Subset of Multipotent Embryonic Neural Stem Cells*
- [#361A](#) MI. Holst, B. Pintea, CH. Juengen, K. Woellner, K. Duffe, J. Lind and SL. Baader, Bonn  
*Tetraspanin-5 expression parallels neuronal maturation in the cerebellum of normal and L7En-2 transgenic mice*
- [#362A](#) T. Goschzik, R. Quade, V. Kominek, C. Laurini, P. Maness, B. Schmitz and S. Diestel, Bonn and Chapel Hill, NC (USA)  
*THE ROLE OF PHOSPHORYLATION OF THREONINE-781 OF HUMAN NCAM IN ENDOCYTOSIS AND NEURITE OUTGROWTH*
- [#363A](#) O. Ganeshina and R. Menzel, Brisbane (AUS) and Berlin  
*Development of synaptic neuropile in the mushroom bodies of honeybee during metamorphosis*
- [#364A](#) LE. Paraoanu and PG. Layer, Darmstadt  
*Binding of acetylcholinesterase to the extracellular matrix component laminin-1 implies a role in heterophilic adhesion.*
- [#365A](#) AE. Rünker, G. Little, J. Dolan and KJ. Mitchell, Dublin (IRL)  
*Bi-Directional Signaling By Sema6A And PlexinA2 Interaction?*
- [#366A](#) D. Del Turco, C. Gebhardt, GJ. Burbach, SJ. Pleasure, DH. Lowenstein and T. Deller, Frankfurt/Main and San Francisco (USA)  
*Laminar organization of the dentate gyrus in BETA2/NeuroD null mice.*



- [#367A](#) SK. Mishra, N. Braun, C. Schomerus, H-W. Korf, J. Sévigny, SC. Robson and H. Zimmermann, Frankfurt/Main, Québec (CDN) and Boston (USA)  
*Neurogenesis in the adult subventricular zone: a functional role for extracellular nucleotides*
- [#368A](#) S. Brinker, S. Klöß and KH. Backus, Frankfurt/Main  
*Nicotinic modulation of GABAA receptor subunit expression in the developing rat inferior colliculus*
- [#369A](#) V. Shukla, N. Braun, J. Sévigny, SC. Robson, S. Raab and H. Zimmermann, Frankfurt/Main, Québec (CDN) and Boston (USA)  
*Association of the ecto-ATPase NTPDase2 with transient cell populations of the neurogenic pathway in the adult dentate gyrus*
- [#370A](#) T. Bass, M. Ebert and M. Frank, Freiburg  
*Clustered Protocadherin Genes Expressed in the Zebrafish Nervous System*
- [#371A](#) D. Junghans, V. Taylor, I. Hack, M. Frotscher and R. Kemler, Freiburg  
*beta-catenin mediates cell adhesion in the early neuroepithelium*
- [#372A](#) M. Ebert, R. Kemler and M. Frank, Freiburg  
*Disruption of the Protocadherin-Gamma Cluster in Gene-trap Mice Leads to Neuronal Degeneration and Perinatal Lethality*
- [#373A](#) F. Seidl and M. Gebhardt, Garching  
*Development of antennal mechanosensory neurons in crickets*
- [#374A](#) H. Heuer, MK. Maier, S. Iden, J. Mittag, E. Friesema, TJ. Visser and K. Bauer, Hannover and Rotterdam (NL)  
*The monocarboxylate transporter 8 (MCT8) linked to human psychomotor retardation is highly expressed in thyroid hormone-sensitive neurons*
- [#375A](#) C. Peuckert, R. Niehage, S. Barchmann, F. Weth and J. Bolz, Jena  
*Eph/ephrin expression patterns in the developing cortex*
- [#376A](#) M. Schwab, K. Schwab, M. Kott and HH. Szeto, Jena and New York, NY (USA)  
*INTRAUTERINE DEVELOPMENT OF SLEEP STATES*
- [#377A](#) M. Schwab, C. Menz, T. Bludau, KJ. Gerhardt and RM. Abrams, Jena and Gainesville, FL (USA)  
*Fetal Cerebral Processing of External Vibroacoustic Stimuli*
- [#378A](#) M. Oberhofer, E. Friauf and S. Löhrke, Kaiserslautern  
*Differential regulation of intracellular chloride concentration in various nuclei of the developing rat superior olivary complex*

- [#356B](#) GKH. Zupanc, UM. Wellbrock, K. Hinsch, D. Meissner and FH. Gage, Bremen, Manchester (UK) and La Jolla (USA)  
*Proliferation, Migration, Neuronal Differentiation, and Long-Term Survival of New Cells in the Adult Zebrafish Brain*
- [#357B](#) M. Wiehle, O. Oehlke, E. Roussa and K. Krieglstein, Göttingen  
*Role of TGF-beta, Shh and FGF8 in differentiation of ventral mesencephalic neurospheres in vitro*
- [#358B](#) M. Behrendt, K. Krieglstein and Z. Wang, Göttingen  
*Tiegl and Tiegl3 in the developing nervous system of mouse*
- [#359B](#) O. Oehlke, E. Roussa and K. Krieglstein, Göttingen  
*The role of Ptx3 in the development and differentiation of mouse mesencephalic dopaminergic neurons in vitro.*
- [#360B](#) E. Roussa, M. Wiehle, O. Oehlke and K. Krieglstein, Göttingen  
*Characterization of neurospheres derived from ventral and dorsal mouse mesencephalon.*
- [#361B](#) S. Schemmel, K. Krieglstein and M. Rickmann, Göttingen  
*Neuronal cell death during postnatal development of superior cervical ganglion of mouse*
- [#362B](#) MM. Brzozka, T. Wolfram, K-A. Nave and MJ. Rossner, Göttingen  
*Characterization of ME2 as the obligate E-protein interaction partner for the adult expressed neuronal bHLH proteins and regulated overexpression of dominant-negative versions of ME2 in transgenic mice*
- [#363B](#) P. Alifragis, O. Britanova and V. Tarabykin, London (UK) and Göttingen  
*THE EFFECT OF REELIN IN THE MIGRATION OF CORTICAL SVZ NEURONS*
- [#364B](#) E. Fischer and H. Taschenberger, Göttingen  
*The role of presynaptic activity during functional maturation of a fast glutamatergic CNS synapse*
- [#365B](#) D. Hess, E. Ponimaskin and D. Richter, Göttingen  
*Modulation of neuronal outgrowth by selective 5-HT receptors activating the G12/13 signaling pathways in hippocampal neurons*
- [#366B](#) S. Hou and E. Pera, Göttingen  
*A secreted serine protease with IGF binding motif involved in anterior-posterior patterning of Xenopus embryos*
- [#367B](#) A. Miquelajauregui and V. Tarabykin, Göttingen  
*Functional characterization of Smad-interacting protein 1 (SIP1) in the neocortex and hippocampus by conditional gene inactivation*

- [#368B](#) M. Jose, D. Nair, T. Dresbach, K. Kemnitz, M. Kreutz, ED. Gundelfinger and W. Zusratter, Magdeburg, Heidelberg and Berlin  
*Visualisation of Interactions in Living Hippocampal Neurons at Ultra-Low Excitation Levels Using the Calcium Indicator Cameleon*
- [#369B](#) D. Nair, M. Jose, T. Kuner, R. Hartig, C. Reissner, K. Kemnitz, M. Kreutz, ED. Gundelfinger and W. Zusratter, Magdeburg, Heidelberg and Berlin  
*Imaging Interactions in Living Hippocampal Neurons at Minimal Invasive Conditions Using the Chloride Indicator Clomeleon*
- [#370B](#) S. Heck, IL. Hanganu and HJ. Luhmann, Mainz  
*Effects of in vitro ischemia on synaptic activity of subplate neurons in the neonatal rat cerebral cortex*
- [#371B](#) M. Hartmann, T. Brigadski, KS. Erdmann, B. Holtmann, M. Sendtner, F. Narz and V. Lessmann, Mainz, Bochum and Würzburg  
*Truncated TrkB receptor induced outgrowth of dendritic filopodia involves the p75 neurotrophin receptor*
- [#372B](#) W. Kilb, P. Dierkes, Y. Yanytska and HJ. Luhmann, Mainz and Duesseldorf  
*Inhibitory role of GABA on epileptiform activity in hippocampal slices of the immature rat*
- [#373B](#) S. Lang, T. Bonhoeffer and C. Lohmann, Martinsried-München  
*Endogenous BDNF-mediated spontaneous Ca<sup>2+</sup>-signaling in developing hippocampal pyramidal cells*
- [#374B](#) M. Güntner and G. Boyan, Martinsried-Planegg  
*Embryonic development of the sensory innervation of the antenna in the grasshopper Schistocerca gregaria : molecular expression domains and stepping stone pattern of pioneering confirm its appendicular nature*
- [#375B](#) JC. Schwamborn and AW. Püschel, Münster  
*THE SEQUENTIAL ACTIVITY OF THE GTPASES RAP1B AND CDC42 DETERMINES NEURONAL POLARITY*
- [#376B](#) K. Vilpoux and S. Harzsch, Ulm  
*Comparison of neurogenesis and neuronal engrailed expression in embryos of a parthenogenetic crayfish, the Marmorkrebs (marbled crayfish), and the grasshopper*
- [#377B](#) M. Philipp and ET. Stoeckli, Zurich (CH)  
*RAB GDI CONTROLS AXON GUIDANCE BY REGULATING ROBO LOCALIZATION*

## **Overexpression of Bag-1 in differentiated PC12 cells leads to reduced neurite outgrowth**

Karin Frebel, Ekaterina Nichiporuk, Michael Sendtner, Stefan Wiese

Institute for Clinical Neurobiology, University of Würzburg, Josef Schneider Str. 11,  
D-97080 Würzburg, Germany

### **Abstract**

Bag-1 is a co-chaperone for Hsp70 which also interacts with B-Raf, C-Raf and Akt in a complex. Bag-1 together with Hsp70 also participates in a complex with glucocorticoid receptors and thus inhibits glucocorticoid receptor initiated transcriptional activation. In the developing nervous system of mice *Bag-1* is expressed in at least two isoforms. The L-form (Bag-1L) contains a nuclear localisation signal and the s-form (Bag-1s) has been described exclusively in the cytoplasm. Former studies of our group have shown the specific role of B-Raf in neurotrophine-mediated survival signalling in motor- and sensory neurons. In the absence of B-Raf, cultured motoneurons and sensory neurons from E12.5 mice were not able to survive or grow out neurites. Upon NGF treatment proliferating rat pheochromocytoma cells (PC12) become postmitotic and grow out neurites. Thus PC12 cells can be used to study mechanisms of neurite outgrowth in vitro. Here we show that Bag-1s interferes with differentiation of PC12 cells. In contrast Bag-1L does not disturb neurite outgrowth and differentiation. Taken together these experiments suggest that Bag-1 interacts in a complex together with B-Raf Hsp70 and Akt to act as a signaling complex for the growth of neuritic processes.

## Investigating the Role of *Barentsz* in Zebrafish Development

Ayşe Yaralı<sup>1</sup>, Michael Kiebler<sup>2</sup> and Paolo Macchi<sup>2</sup>,

1. Department of Genetics and Neurobiology, Biocentre Am Hubland, University of Würzburg, Würzburg, Germany.

[ayse.yarali@student.uni-tuebingen.de](mailto:ayse.yarali@student.uni-tuebingen.de)

2. Max-Planck-Institute for Developmental Biology, Tübingen, Germany

Asymmetric subcellular localization and subsequent local translation of defined mRNAs contributes to the establishment of cell polarity in a variety of cell types as well as to complex phenomena such as synaptic plasticity in neurons. One common identified component of the mRNA localization machinery in *Drosophila* oocytes and mammalian neurons is the *Barentsz* (*Btz*) protein.

We started by investigating the intracellular localization of zebrafish *Btz* (*zfbtz*). The *ZfbtzGFP* fusion protein has a cytoplasmic localization in transfected cultured cells. *Zfbtz*, similar to its mammalian homologues, contains both nuclear localization (NLS) and export (NES) signals, suggesting that it might behave as a nucleocytoplasmic shuttling protein. Unlike its mammalian homologues, however, *zfbtz* does not accumulate in the nucleus upon treatment with Leptomycin B, an inhibitor of the CRM1-dependent export pathway.

We then analyzed the spatio-temporal expression pattern of *zfbtz* mRNA during the embryonic development. Using real time RT-PCR and wholemount *in situ* hybridization, we showed that a ubiquitous *zfbtz* mRNA expression starts as early as 4 hours post fertilization (hpf), which gets concentrated in the head at around 2 days post fertilization (dpf). At 4 dpf, the expression is significantly decreased. To exclude a possible *btz* gene duplication, we performed radiation hybrid mapping of *btz* and detected one single *btz* gene in the zebrafish genome, which is located on the 3rd chromosome.

In order to get a first insight into the function of *zfbtz*, we knocked down its expression in zebrafish embryos using antisense morpholino oligonucleotides. Different concentrations of two antisense morpholino oligonucleotides were injected into the yolk of 1-2 cell stage embryos. Amounts that are acceptable for most other morpholino oligonucleotides were lethal in our case, suggesting an essential pleiotropic role for *Btz* in early development. When lower amounts of morpholinos were injected, concentration-dependent abnormalities in the head and/or tail region were observed. The general character of abnormalities also speak for a pleiotropic essential role of early *zfbtz* expression. A more detailed investigation using tissue-specific markers shall yield a better understanding of the role *Btz* plays during development. Since interfering with the early ubiquitous *Btz* expression results in either death or severe morphological problems, the function of the later head-restricted *Btz* expression remains unclear. Therefore, we plan future experiments to investigate this role by knocking down *zfbtz* at later developmental stages which might result in a central nervous system-specific phenotype.

## Development of avian embryonic auditory brainstem neurons in vitro

**Thomas Künzel, Björn Claßen, Benedikt Mönig, Hermann Wagner, Jörg Mey, Harald Luksch**

Institut für Biologie II, RWTH Aachen, Kopernikusstr. 16, 52074 Aachen, Germany.

*kuenzel@bio2.rwth-aachen.de*

In birds, the brainstem nuclei *N. magnocellularis* (NM) and *N. laminaris* (NL) contain the second and third order neurons of the auditory pathway. They form a relatively simple and well studied circuit that fulfills a complex task, the calculation of azimuth of a perceived auditory stimulus. This calculation is based on delay lines (varying lengths of NM axons) and detection of coincidence in NL neurons, consistent with a modification of a model suggested by Jeffress in 1948. Our goal is to establish a model of this circuit in a biohybrid system, which will allow us to address basic questions about the development of neuronal circuits and the physiological function of neuronal coincidence detectors. First, we are addressing the question, whether cellular specialisations of the NM-NL connection develop in vitro.

We have established a primary cell culture system of auditory brainstem neurons. Microsurgical preparation is performed at embryonal stage HH29, when NM and NL neurons have just reached their prospective positions in the brainstem. Cultivation in serum free medium (DMEM:F12 with B27 supplement) is possible for up to 14 days. We have identified auditory hindbrain neurons in vitro by immunocytochemical staining against calretinin, which serves as a characteristic marker for the hindbrain auditory pathway. The morphological, molecular and electrophysiological properties of these neurons are being characterized. Positive immunoreactivity for synapsin suggests that NM/NL neurons form synaptic contacts in vitro. As demonstrated with whole-cell patch recording, neurons that were cultivated for 7 DIV, are able to fire action-potentials after current injection. Our data show, that embryonic NM/NL neurons seem to develop towards a more mature state in vitro.

*Supported by the Helmholtz Gesellschaft (Virtuelles Institut Bioelektrische Hybridschaltkreise).*

## Changes in CaM kinase II activity and localization during postembryonic CNS remodeling in *Manduca sexta*

Peter Burkert and Carsten Duch

Freie Universität Berlin; Fachbereich Biologie, Chemie, Pharmazie; Institut für Biologie,  
Königin-Luise-Straße 28-30, 14195 Berlin, Germany

Developmental changes in intracellular calcium concentrations are critical for structural development of neuronal processes. Calcium-dependent enzymes like Calcineurin and CaM kinase II can translate activity-dependent calcium influx into structural changes in the CNS. The role of CaM K II for the development of neuronal architecture has been demonstrated in several cell culture systems. However, despite in the *Xenopus* optical tectum, little is known about the role of CaM K II for neuronal architecture development. We address this question by using precisely staged alterations in the neuronal morphology during the metamorphosis of *Manduca sexta*. Metamorphosis is characterized by axonal and dendritic regression during the dismantling of larval circuits followed by outgrowth of new adult processes (Libersat and Duch, 2004, *Mol Neurobiol* 29:303-20). Furthermore, specific phases of dendritic growth correlate in time with changes in calcium and potassium membrane currents, which in turn strongly affect the dendritic calcium levels upon spiking activity (Duch and Levine, 2000, *J Neurosci* 20:6950-61; 2002, *J Neurophysiol* 87:1415-25).

To address the role of CaM kinase II for structural remodeling we investigated its localization (immunohistochemistry) and activity (substrate phosphorylation-assays) during metamorphosis. In phosphorylation-assays of thoracic ganglia homogenate, we measured the intrinsic activity, which occurs naturally in the respective stage in comparison to the total amount of potential activity by activating with  $\text{Ca}^{2+}$ . Intrinsic CaM kinase II activity increased continuously as the amplitude of motoneuron calcium membrane currents increased significantly between the larval stage (L5) and pupal stage 8 (P8), but remained rather constant thereafter (P8 to adult). Developmental changes in the intrinsic activity of other kinases, such as PKA, followed a different time course. Furthermore, blocking calcium membrane currents *in vivo* during normal development by systemic verapamil injections blocked developmental increases in CaM K II activity. These data suggested that CaM K II activity was specifically regulated during *Manduca* metamorphosis and may represent a precise readout for activity-dependent calcium influx.

Substrate phosphorylation assays were conducted with whole ganglion homogenate. CaM K II immunohistochemistry was conducted to test which neuron populations, or which neuronal compartments were the carrier for developmental changes in CaM K II activity. CaM K II expression changed drastically during metamorphosis. In the larval stages CaM K II was predominantly localized in axons and in some cell bodies, but not that much in the thoracic neuropile regions. Somata expression ceased during early pupal life. In parallel, immunostaining in the neuropile increased continuously during pupal life. Investigation of the intracellular dispersion of CaM K II revealed striking changes between pre- and postsynaptic localization during metamorphosis. During late larval life and during the onset of metamorphosis, CaM K II was localized predominantly presynaptically in association with synaptic vesicles, where it may affect neurotransmitter release. At later pupal stages, the main expression had changed to postsynaptic structures, where it remained until adulthood. This developmental translocation suggested that CaM K II might have different functions in pre- and in postsynaptic neurons during different stages of *Manduca* postembryonic development. Preliminary results indicate that pharmacological inhibition of CaM kinase II affects motoneuron dendritic shape during *Manduca* metamorphosis. Blockade of Calcium membrane currents during critical stages revealed similar results.

*Supported by the Deutsche Forschungsgemeinschaft (DU331-2/4)*

**DSD-1-PG/Phosphacan is Expressed by a Subset of Multipotent Embryonic Neural Stem Cells****Swetlana Sirko, Alexander von Holst, Andreas Faissner***Department for Cell morphology & molecular Neurobiology; Ruhr-University Bochum; Germany**Correspondence: Andreas.Faissner@ruhr.uni-bochum.de*

The ventricular zone of the early embryonic cerebral cortex contains stem cells whose development is driven by the combination of intrinsic temporal programmes and extracellular signals from the ECM. The molecule DSD-1-PG/Phosphacan is a chondroitin sulfate proteoglycan (CSPG) that represents a splice variant of the receptor protein tyrosine phosphatase (RPTP)-beta gene and is thought to be involved in the regulation of many developmental events<sup>1-6</sup>. In this study we used the monoclonal antibody 473HD, which detects a cell surface-associated antigen containing the CS-D motif of glycosaminoglycan chains present on DSD-1-PG/RPTP- $\beta$ <sup>1-3</sup>.

A developmental immunohistochemical analysis of 473HD expression during corticogenesis was performed. In the neurogenic phase a prominent expression of DSD-1-PG/RPTP- $\beta$  on nestin-positive cells in the ventricular zone, with radial processes extending towards the pial surface was detected. After the neurogenic period, the expression of the 473HD-epitope shifted to wards, the secondary germinal area, the subventricular zone. When the number of 473HD-positive cells was determined on freshly isolated cortical tissue, we observed that they persisted throughout neurogenesis and decreased during gliogenesis. Thus, the localization and the developmental decline of 473HD-positive cells suggests that they might be multipotent neural stem cells which give first rise to neurons, followed by the generation of glia. Using the mAb 473HD for immunopanning DSD-1-PG/RPTP- $\beta$  expressing cells were selectively isolated from acutely dissociated embryonic forebrain tissue. The immunocytochemical analysis of the selected 473HD-positive cell population demonstrated that almost all cells are mitotically active, co-express nestin as well as the radial glia markers RC2 and BLBP, identifying them as radial glia cells<sup>7-10</sup>. The majority of 473HD-selective cells isolated at E13.5 differentiated into neurons after 2 days in vitro, consistent with the observation that radial glia cells generate neurons at this developmental stage in vivo. When grown under neurosphere-forming conditions, 20% of the 473HD-positive cells generated multicellular neurospheres, which contained multipotent cells and can be differentiated to neurons, astrocytes and oligodendrocytes. This represents a six fold increase in comparison to the non-selected cell population. To extend these findings, similar experiments were performed on neurospheres generated from cortical and striatal neural stem cells. Immunohistochemical staining of neurosphere sections demonstrated the localization of the 473HD-epitope on the mitotically active, nestin-positive cells in the outer cell layers of the neurospheres. The analysis of the 473HD-positive cells after immunopanning confirmed that most of the selectively isolated cells are BrdU-positive precursor cells. As expected, many of the selected cells were found to express the radial glia cell markers RC2 and GLAST. Nearly all of the 473HD-positive cells isolated from neurospheres were BLBP positive and differentiated into neurons. However, when grown under neurosphere-forming conditions almost 40% of the 473HD-positive cells generated neurospheres.

These observations demonstrate a strong correlation in two independent experimental settings that allow for the enrichment of neural stem cells through the 473HD-epitope. Taken together, the study describes a significant aspect of the biology of embryonic neural stem cells – a subset of early multipotent neural progenitor/stem cells express the DSD-1-PG/RPTP- $\beta$ , which aids their identification and enrichment. (Supported by DFG, SFB 509 and SPP 1109)

<sup>1</sup> Faissner A, Clement A, Locher A, Streit A, Mandl C, Schachner M (1994) Isolation of a neuronal chondroitin sulfate proteoglycan with neurite outgrowth promoting properties. *J Cell Biol* **126**:783-799

<sup>2</sup> Garwood J, Schnadelbach O, Clement A, Schutte K, Bach A and Faissner A (1999) DSD-1-proteoglycan is the mouse homolog of Phosphacan and displays opposing effects on neurite outgrowth dependent on neuronal lineage. *J Neurosci*, **19**, 3888-3899

<sup>3</sup> Clement A, Nakanaka K, Masayama K, Mandl C, Sugahara K and Faissner A, (1998) The DSD-1 carbohydrate epitope depends on sulfation, correlates with chondroitin sulfate D motifs, and is sufficient to promote neurite outgrowth. *J Biol Chem* **273**, 28444-28453

<sup>4</sup> Lander A.D (1993) Proteoglycans in the nervous system. *Curr Opin Neurobiol*, **3**, 716-723

<sup>5</sup> Bandtlow CE and Zimmermann DR (2000) Proteoglycans in the developing brain: new conceptual insights for old proteins. *Phys Rev* **80**:1267-1290

<sup>6</sup> Maeda N and Noda M (1998) Involvement of receptor-like protein tyrosine phosphatase zeta/RPTPbeta and its ligand pleiotrophin/heparin-binding growth-associated molecule (HB-GAM) in neuronal migration. *J Cell Biol* **142**:203-216

<sup>7</sup> Hartfuss E, Galli R, Heins N, Götz M (2000) Characterisation of CNS precursor subtypes and radial glia. *Dev Biol* **229**, 15-30

<sup>8</sup> Malatesta P, Hartfuss E, Götz M (2000) Isolation of radial glia cells by FACS reveals a neuronal lineage. *Develop* **127**, 5253-5263

<sup>9</sup> Noctor S, Flint A, Weissman T, Dammerman RS and Kriegstein AR (2001) Neurons derived from radial glial cells establish radial units in neocortex. *Nature* **409**:714-720

<sup>10</sup> Noctor S, Flint A, Weissman T, Wong WS, Clinton BK and Kriegstein AR (2001) Dividing precursor cells of embryonic cortical ventricular zone have morphological and molecular characteristics of radial glia. *J Neurosci* **22**:3161-3173



### **Tetraspanin-5 expression parallels neuronal maturation in the cerebellum of normal and L7En-2 transgenic mice**

Holst M.I., Pintea B., Juenger C.H., Woellner K., Duffe K., Lind J., Baader S.L.

Department of Anatomy, University of Bonn, Nussallee 10, D-53115 Bonn, Germany

Tetraspanins are cell surface membrane proteins involved in functions such as cell motility, metastasis and fertilization. Tetraspanin-5 was recently shown to be strongly expressed within the central nervous system. Its function, however, remained unknown. In order to address tetraspanin-5 function during nervous system development we performed a detailed expression analysis in the postnatal mouse cerebellum using in situ hybridizations and immunohistochemistry. In cerebellar Purkinje cells, tetraspanin-5 was expressed at very low levels at the day of birth (P0). After P7, tetraspanin-5 expression strongly increased reaching a high level in all Purkinje cells at P11. This expression level persisted into adulthood. Thus, low expression was found in postmitotic neurons prior to settling, higher expression could be shown in settled and strongest expression in mature PCs. In consistency, expression of tetraspanin-5 was specifically reduced in PCs of L7En-2 animals which display a characteristic delay in PC maturation postnatally. For cerebellar granule cells (GCs), a similar relation could be found. Postmitotic, premigratory GCs expressed low levels of tetraspanin-5 whereas high levels could be found in settled and differentiated GCs. Molecular homologies between tetraspanin-5 and other tetraspanins support a function of tetraspanin-5 in cell-cell and/or cell-matrix adhesion. Cell culture experiments proving this hypothesis are in progress.

## THE ROLE OF PHOSPHORYLATION OF THREONINE-781 OF HUMAN NCAM IN ENDOCYTOSIS AND NEURITE OUTGROWTH

T. Goschzik, R. Quade, V. Kominek, C. Laurini, P. Maness\*, B. Schmitz, S. Diestel  
Institute of Physiology, Biochemistry and Animal Health, University of Bonn,  
Katzenburgweg 9a, 53115 Bonn

\*Dep. Biochemistry, School of Medicine, University of North Carolina, Chapel Hill, NC/USA  
email: [tobiasgoschzik@web.de](mailto:tobiasgoschzik@web.de)

The neural cell adhesion molecule NCAM is a member of the immunoglobulin superfamily and has important functions during the development of the nervous system, in regeneration and synaptic processes in the adult nervous system. NCAM has multiple, yet unknown potential phosphorylation sites in its cytoplasmic tail most of which are not yet characterized with respect to their function(s).

Since the PEST sequence of apCAM - a homologue of NCAM in *Aplysia* - has been shown to be important for endocytosis we investigated whether the PEST sequence of human NCAM and within the PEST sequence particularly threonine-781 plays a role in NCAM's internalization. B35 were, therefore, transfected with cDNA constructs of human NCAM with threonine-781 mutated to either alanine or aspartate. Antibody induced endocytosis was studied by confocal laser microscopy and neurite outgrowth analysed on poly-L-lysine as substrate or on NCAM transfected COS cells.

We here show that the mutations strongly influence endocytosis of NCAM as well as the cell autonomous and NCAM stimulated neurite outgrowth on pLL and NCAM expressing COS cells, respectively, suggesting that phosphorylation of this threonine is implicated in the regulation of these processes.

## Development of synaptic neuropile in the mushroom bodies of honeybee during metamorphosis.

Olga Ganeshina<sup>1,2</sup> and Randolph Menzel<sup>2</sup>

<sup>1</sup>Vision, Touch and Hearing Research Centre, School of Biomedical Sciences, Brain Institute, University of Queensland, Brisbane, QLD 4072, Australia  
[o.ganeshina@uq.edu.au](mailto:o.ganeshina@uq.edu.au)

<sup>2</sup>Institute of Neurobiology, Free University of Berlin, Germany

Insect mushroom bodies are central brain neuropiles involved in the control of complex behaviour. The intrinsic mushroom body interneurons – Kenyon cells – receive synaptic inputs from olfactory, visual and other primary sensory centres, integrate multimodal sensory information and transmit signals to other associative and premotor brain centres. The mushroom body input neuropiles, calyces, are characterised by regular microglomerular structure. Within each microglomerulus, large presynaptic terminal, or bouton, which belongs to sensory or other extrinsic mushroom body interneurons, is surrounded by small postsynaptic spines, belonging mainly to the Kenyon cells. Previously we have demonstrated that complex synaptic microcircuits are formed by extrinsic and intrinsic mushroom body neurons within the microglomeruli (Ganeshina and Menzel, 2001).

Here we show by means of electron microscopy how the fine structure of the neuropile, as well as its synaptic contacts, are established in the mushroom body calyces during postembryonic development of honeybee workers. We focused our study on the lip region, which represents olfactory input area of the mushroom bodies. At early pupal stages (P1-P3), calycal neuropile is composed by sparsely distributed neural processes and does not exhibit regular microglomerular structure. At stage P3, profiles containing small clear vesicles are observed among the neural processes, which may reflect early accumulation of a neurotransmitter in presynaptic neurons. During subsequent stages (P4-P5), the neuropile acquires a more regular pattern, and by stage P5, it is composed by islands of small, tightly packed spines surrounded by neural fibres, running in different directions. At the same stage, large boutons appear in the neuropile. These boutons are found predominantly at the periphery of the lip region. Clusters of small vesicles occasionally are observed near the surface of the boutons. The accumulation of vesicles at the cell membrane probably reflects an initial step of synaptogenesis. By stage P6, the microglomerular structure of the neuropile is established: large presynaptic boutons appear within the compact islands of the small postsynaptic profiles. Output synapses from the presynaptic boutons into the surrounding small profiles are found at this stage. The immature state of these synapses is reflected by absence of both presynaptic tuft and postsynaptic density. Maturation of the synaptic contacts occurs at late pupal stages (P8-P9). However, by the end of pupal development, the synaptic microcircuits, characteristic for adults, are not yet established.

Ganeshina, O. and Menzel, R. (2001) GABA-immunoreactive neurons in the mushroom bodies of the honeybee: an electron microscopic study. *J Comp Neurol* 437:335-349

Binding of acetylcholinesterase to the extracellular matrix component laminin-1 implies a role in heterophilic adhesion. **L.E. Paraoanu, P.G. Layer.** Darmstadt University of Technology, Devel. Biology & Neurogenetics, D-64287 Darmstadt, Germany

Acetylcholinesterase (AChE) is not just the enzyme that hydrolyses the neurotransmitter acetylcholine at the cholinergic synapses, but also a protein with multiple other functions, related to processes of embryonic development and diseases. However, the mechanisms supporting the developmental functions of AChE are not understood. A yeast two-hybrid screen was initiated aimed at identifying novel proteins that interact directly with AChE. One of the interaction partners was the chain beta of laminin-1, an extracellular matrix protein involved in neuronal differentiation and adhesion. The yeast two-hybrid results were confirmed by co-immunoprecipitation experiments with antibodies against mouse AChE and laminin-1. To verify that this binding is likely to occur *in vivo*, the expression pattern of both AChE and laminin-1 was analyzed in the CNS system. Neurons and glial cells co-expressed both AChE and laminin-1. This led to the model in which AChE is binding to laminin-1 during early developmental stages. The AChE-laminin-1 complex will then use the laminin-1 signaling pathways to send signals into the cell modulating intracellular cascades. Taken together, the results of this present study suggest a role for AChE in heterophilic adhesion. Understanding this role will bring a major progress in the field of non-classical functions of AChE.

## Bi-Directional Signaling By Sema6A And PlexinA2 Interaction?

Annette E. Rünker, Graham Little, Jackie Dolan, and Kevin Mitchell  
Department of Genetics, Trinity College Dublin, Dublin 2, Ireland  
runkera@tcd.ie

Despite the fact that several semaphorins are known to function as guidance signals, increasing evidence suggests a novel role of transmembranous Sema6A as a guidance receptor. Thus, Sema6A comprises a long cytoplasmic tail that binds to intracellular Evl. Additional hints came from Sema6A null mice, obtained by isolation of a gene trap insertion into the *Sema6A* gene, which abolishes *Sema6A* transcripts and simultaneously labels neurons that normally express Sema6A by  $\beta$ -gal in cell bodies and axonally by PLAP (Mitchell et al., 2001; Leighton et al., 2001). These mice show an aberrant projection of PLAP-stained thalamocortical axons (TCAs) and an impaired migration of cerebellar granule cells that normally express Sema6A. The fact that Sema6A is expressed in the malfunctioning neurons suggests that Sema6A acts cell-autonomously as a receptor.

We studied the nervous system of *Sema6A*-deficient mice extensively throughout development and in adulthood for other abnormalities. Diverse morphological defects were found, which indicate impaired axon guidance and/or cell migration of the posterior arm of the anterior commissure (pAC), the corticospinal tract (CST), the lateral olfactory tract, and the spinal trigeminal nucleus and tract. Importantly, at least axons that form the pAC showed strong PLAP-staining, underlining a possible function of Sema6A as a receptor.

Interestingly, recent findings indicate PlexinA2 as an interacting partner of Sema6A. Therefore, we are analysing whether *PlexinA2*- and *Sema6A*-deficient mice have overlapping phenotypes. Indeed, Dil tracing experiments using newborn mice revealed the same misrouting defect for pAC axons also in *PlexinA2*-deficient mice. In contrast, TCAs of *PlexinA2*-deficient mice showed no abnormalities. These data indicate that, while an interaction between Sema6A and PlexinA2 is important for axon guidance in specific brain areas, PlexinA2 is not the exclusive binding partner of Sema6A. Future work includes further analysis of axon guidance defects that involve Sema6A and PlexinA2 interaction and the question of the direction of signaling following this interaction, i.e. whether Sema6A acts as a receptor, ligand, or even both.

## Laminar organization of the dentate gyrus in BETA2/NeuroD null mice.

Domenico Del Turco<sup>1</sup>, Carl Gebhardt<sup>1</sup>, Guido J. Burbach<sup>1</sup>, Samuel J. Pleasure<sup>2</sup>, Daniel H. Lowenstein<sup>2</sup>, and T. Deller<sup>1</sup>.

<sup>1</sup>Department of Clinical Neuroanatomy, J.W. Goethe University, D-60590 Frankfurt/Main, Germany; <sup>2</sup>Department of Neurology, University of California, San Francisco, CA 94143-0114, USA.

The dentate gyrus of rodents is characterized by a highly laminar organization: above a compact granule cell layer, commissural/associational (C/A) fibers terminate on proximal granule cell dendrites and entorhinal fibers terminate on distal granule cell dendrites in a non-overlapping fashion. To gain insights into mechanisms that underlie the formation of this laminar structure, we studied mice deficient for BETA2/NeuroD, a basic helix-loop-helix transcription factor essential for granule cell differentiation. Anterograde tracing was employed to label C/A and entorhinal fibers and combined with confocal double-immunofluorescence for calbindin, calretinin, parvalbumin, and reelin to visualize putative target cells. The dentate gyrus of mutant mice contained only few granule cells which formed a cap-like structure adjacent to area CA3. In spite of the severe hypoplasia of the dentate gyrus, the remaining BETA2/NeuroD-deficient granule cells expressed mature markers, extended dendrites into the molecular layer, and extended mossy fibers into area CA3. Entorhinal and C/A fibers terminated in a non-overlapping fashion in the dendritic field overlying the rudiment. Entorhinal fibers terminated in the outermost portion of the dentate gyrus where they surrounded reelin-positive Cajal-Retzius cells, and C/A fibers terminated above and within the dentate rudiment. The laminar termination of C/A fibers was closest to normal in zones of the rudiment in which granule cells were densely packed. These data indicate that granule cells are able to differentiate in the absence of BETA2/NeuroD and suggest that the signals underlying the laminar anatomy of the dentate gyrus are present in the absence of most target cells.

Supporting grants: DFG (SFB 269; SFB TR-3) to TD; NIH grant NS39950 to DHL.

## Neurogenesis in the adult subventricular zone: a functional role for extracellular nucleotides

S.K. Mishra<sup>1\*</sup>, N. Braun<sup>1</sup>, C. Schomerus<sup>2</sup>, H.-W. Korf<sup>2</sup>, J. Sévigny<sup>3</sup>, S.C. Robson<sup>4</sup>, H. Zimmermann<sup>1</sup>

<sup>1</sup>Frankfurt University, Biocenter; <sup>2</sup>Frankfurt University, Medical School, Germany; <sup>3</sup>Sainte-Foy, Québec, Canada; <sup>4</sup>Harvard Medical School, Boston, USA  
s.mishra@zoology.uni-frankfurt.de

Studies in particular of the last decade showed that active neurogenesis continuously takes place in the subventricular zone (SVZ) of the lateral ventricles of the adult rodent brain. Neurogenesis in the SVZ leads to migration of neuroblasts within the rostral migratory stream (RMS) and neuron formation mainly in the olfactory bulb (OB). According to present understanding, glial cells with astrocytic properties represent the actual adult neural stem cells. The cell types representing the various cellular transition states leading to the formation of mature neurons as well as the mechanisms controlling adult neurogenesis and neuroblast migration are poorly understood. We show that the ATP-hydrolyzing enzyme nucleoside triphosphate diphosphohydrolase 2 (NTPDase2) is associated with type B cells, the presumptive neural stem cells. NTPDase2 is a protein of the plasma membrane with its catalytic site facing the extracellular space. It hydrolyzes extracellular nucleoside triphosphates to their respective nucleoside diphosphates. This raises the possibility that the signaling pathway via extracellular nucleotides is involved in the control of adult neurogenesis. Neurons as well as glial cells express several subtypes of receptors that are responsive to the nucleotides ATP, ADP, UTP, or UDP (P2 receptors). P2X receptors are ion channels, P2Y receptors are coupled to trimeric G-proteins. In order to probe for a functional role nucleotides we referred to an *in vitro* system for analyzing stem cell properties. Neurospheres produced from isolates of the mouse SVZ and cultured in the presence of EGF and FGF-2 express NTPDase2 as well as tissue non-specific alkaline phosphatase. Accordingly, neurospheres hydrolyze extracellular ATP to adenosine. Since these ecto-nucleotidases control the availability of extracellular nucleotide agonists we studied the potential expression and functional role of nucleotide receptors in isolated neurospheres. Neurospheres respond to extracellular nucleotides with a rise in  $Ca^{2+}_i$  (ATP = ADP > UTP). The P2Y<sub>1</sub> antagonist MRS 2179 strongly reduces the ATP- or ADP-induced increase in  $Ca^{2+}_i$ , suggesting the involvement of a P2Y<sub>1</sub> receptor. The agonistic activity of UTP and the lack of response to UDP imply the additional presence of a P2Y<sub>2</sub> and/or a P2Y<sub>4</sub> receptor. The P2Y<sub>1</sub> antagonist MRS 2179 also reduces neurosphere proliferation. Taken together with previous observations of a synergistic effect on cell proliferation of ATP and growth factors, our results suggest that P2Y-mediated nucleotidergic signaling is involved in neurosphere function and possibly also in adult neurogenesis *in situ*.

## Nicotinic modulation of GABA<sub>A</sub> receptor subunit expression in the developing rat inferior colliculus

S. Brinker, S. Klöß and K.H. Backus. Institute of Physiology II, Cellular Neurophysiology, University of Frankfurt/M. Theodor-Stern-Kai 7, D-60590 Frankfurt/M., Germany

In the inferior colliculus (IC) the activation of nicotinic acetylcholine receptors (nAChRs) potentiates the GABA release. Since many developing IC neurons depolarize in response to GABA and show an increased  $[Ca^{2+}]_i$ , this may contribute to the development of GABAergic synapses. To investigate whether the activation of  $\alpha 7$  nAChRs could modulate the expression of GABA<sub>A</sub> receptors (GABA<sub>A</sub>Rs), we prepared IC slice cultures (at P5). A part of the cultures was incubated for 24h prior to and during the experiments with the  $\alpha 7$  nAChR-selective antagonist  $\alpha$ -Bungarotoxin ( $\alpha$ BgTx, 10nM). We monitored the effect of  $\alpha 7$  nAChR inhibition on the GABAergic transmission by recording spontaneous GABAergic postsynaptic currents (PSCs) using the whole-cell patch-clamp configuration. Recordings were performed at a  $V_h$  of  $-60$ mV in the presence of MCPG (200  $\mu$ M), CNQX (10  $\mu$ M), D-APV (10  $\mu$ M), DH $\beta$ E (1  $\mu$ M) and atropine (1  $\mu$ M) to block the contribution of glutamate receptors, non- $\alpha 7$  nAChRs and muscarinic AChRs, respectively. IC neurons grown in  $\alpha$ BgTx-treated cultures showed a significant reduction in the frequency of spontaneous GABAergic PSCs from 0.91 Hz (control:  $n=7$ ) to 0.03 Hz ( $\alpha$ BgTx:  $n=11$ ;  $p<0.01$ ; Figure A). We found no effect on the mean peak amplitude of GABAergic PSCs (9.63 pA vs. 9.88 pA, in the absence (9.6 pA) and presence of  $\alpha$ BgTx (9.9 pA;  $p=0.869$ ), respectively. These data suggest that the inhibition of  $\alpha 7$  nAChRs affects the development of GABAergic synapses in the IC. Furthermore, we investigated the expression of GABA<sub>A</sub>R subunits with immunocytochemistry and RT-PCR. We found that the postnatal expression pattern of GABA<sub>A</sub>R subunits exhibited a unique temporal developmental profile (Figure B). Accordingly, an enhanced expression of the  $\alpha 3$  and  $\alpha 5$  GABA<sub>A</sub>R subunits was present from P4 to P12. However, a delayed expression of the  $\alpha 2$  GABA<sub>A</sub>R subunit was observed at P12. Furthermore, we showed a significant increase of  $\alpha 1$  GABA<sub>A</sub>R subunits at P4 followed by a maximal expression rate between P12 and P16. In cultures grown in the presence of  $\alpha$ BgTx, the  $\alpha 1$  and  $\alpha 5$  subunits were significantly downregulated ( $n=6$ ) compared to control cultures. These findings were confirmed by RT-PCR analyses that showed a significant decrease of the  $\alpha 1$  and  $\alpha 5$  mRNA levels in neurons from  $\alpha$ BgTx-treated cultures, while the mRNAs for the  $\alpha 7$  nAChR and the  $\alpha 3$  and  $\alpha 5$  GABA<sub>A</sub>R subunits were not significantly affected. We conclude that the activation of  $\alpha 7$  nAChRs modulates the expression pattern of GABA<sub>A</sub>R subunits in the developing IC.

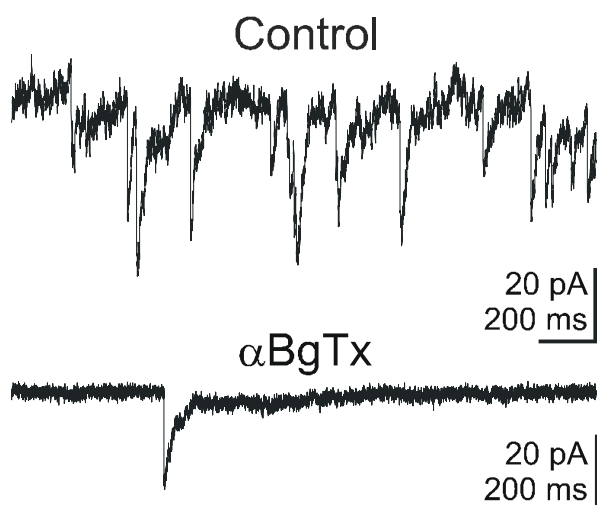


**Figure A:** Spontaneous GABAergic PSCs in control and  $\alpha$ BgTx-treated cultures.

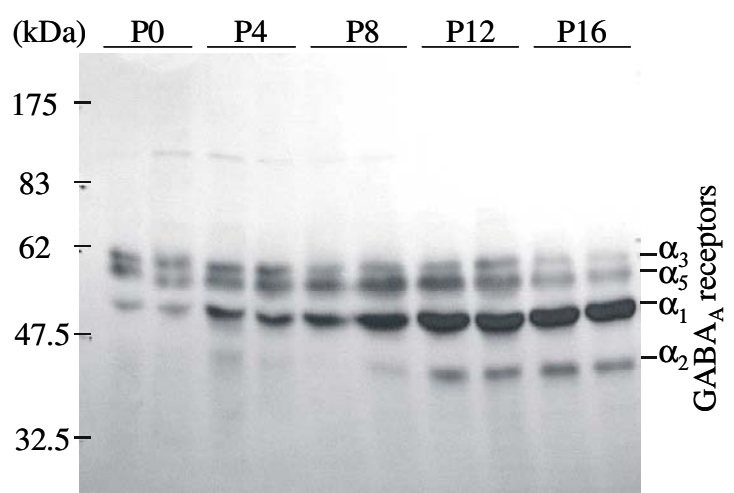


**Figure B:** Expression pattern of GABA<sub>A</sub>R subunits in the developing IC.



Association of the ecto-ATPase NTPDase2 with transient cell populations of the neurogenic pathway in the adult dentate gyrus

V. Shukla<sup>1\*</sup>, N. Braun<sup>1</sup>, J. Sévigny<sup>2</sup>, S.C. Robson<sup>3</sup>, S. Raab<sup>4</sup>, H. Zimmermann<sup>1</sup>

<sup>1</sup>Biocenter, Frankfurt University, Germany; <sup>2</sup>Sainte-Foy, Québec, Canada; <sup>3</sup>Harvard Medical School, Boston, USA; <sup>4</sup>Neurological Institute, Frankfurt University, Germany  
varsha@zoology.uni-frankfurt.de

Active neurogenesis continuously takes place in the dentate gyrus of the adult mammalian brain. The dentate gyrus of the adult rodent hippocampus contains an astrocyte-like cell population that is regarded as residual radial glia. These cells reside with their cell bodies in the subgranular layer. Radial processes traverse the granule cell layer and form bushy ramifications in the inner molecular layer. The residual radial glial cells apparently represent neuronal progenitor cells that can give rise to functionally integrated granule cells. To date the cellular and molecular events driving a subpopulation of these cells into neurogenesis as well as the cellular transition states are poorly understood. We show that in the mouse dentate gyrus this cell type selectively expresses surface-located ATP-hydrolyzing activity and is immunopositive for nucleoside triphosphate diphosphohydrolase 2 (NTPDase2). NTPDase2 is a protein of the plasma membrane with its catalytic site facing the extracellular space. It hydrolyzes extracellular nucleoside triphosphates such as ATP or UTP to their respective nucleoside diphosphates. The enzyme becomes expressed in the hippocampus during late embryogenesis from E17 onwards, and is thus not involved in early brain development. Its embryonic pattern of expression mirrors dentate migration of neuroblasts and the formation of the primary and finally the tertiary dentate matrix. NTPDase2 is also expressed by a transient population of cortical radial glia from late embryonic development until postnatal day 5. NTPDase2 can be employed as a novel marker for defining cellular transition states along the neurogenic pathway. It is associated with subpopulations of GFAP- and nestin-positive cells. These intermediate filaments are typically expressed by the progenitor cells of the dentate gyrus. In addition there is a considerable overlap with doublecortin-positive cells. Expression of the microtubule-associated protein doublecortin is indicative of a transition of progenitors to a neural phenotype or an immature form of granule cell. NTPDase2 is no longer associated with mature granule cells as indicated by the lack of double-immunostaining for NeuN. Furthermore S100-positive astrocytes do not express NTPDase2. Experiments with the S-phase marker bromodeoxyuridine (BrdU) demonstrate that NTPDase2-positive cells proliferate. Postmitotic BrdU-labeled cells preferentially acquire an NTPDase2-positive phenotype. Our results suggest that NTPDase2 is associated with cell types of varying maturation states but not with mature neurons. They suggest that the signaling pathway via extracellular nucleotides and nucleotide receptors may play a role in the control of hippocampal neurogenesis.

## **Clustered Protocadherin Genes Expressed in the Zebrafish Nervous System**

Thilo Bass, Matthias Ebert and Marcus Frank

Department of Molecular Embryology, Max-Planck Institute of Immunobiology, Stübeweg 51, D-79108 Freiburg (e-mail: frank@immunbio.mpg.de)

More than 50 protocadherin genes are present in the mammalian genome in three sequentially arrayed clusters termed protocadherins (Pcdhs) -alpha,-beta- and -gamma. In the mouse, these Pcdhs are highly expressed in the nervous system. Unlike other cadherins, the clusters are absent in sequenced invertebrate genomes, suggesting a rather recent evolutionary origin. To explore this issue, we have analyzed these protocadherin clusters in the zebrafish as a non-mammalian model organism.

Interestingly, two independent sets of clustered protocadherin genes are present in the zebrafish, each containing arrayed Pcdh-alpha and Pcdh-gamma genes, but apparently no Pcdh-beta genes. In total, more than 90 protocadherins are predicted from these four clusters. Using RT-PCR on the cluster-specific “constant” region sequences, we have shown that Pcdh transcripts are expressed from all four clusters in zebrafish embryos. Highest expression is found in embryos 48 hours post fertilization, correlating with the progress of neuronal differentiation, similar to our observations in the mouse. In situ hybridization localized the transcripts of the two zebrafish Pcdh-gamma clusters to the nervous system, revealing largely overlapping, yet cluster-specific differential expression patterns. Immunocytochemistry supports the idea of Pcdh-gamma proteins being expressed in a subset of neuronal cells. Further insight into protocadherin functions during neuronal differentiation may be gained from in vivo analysis of the zebrafish model system.

**beta-catenin mediates cell adhesion in the early neuroepithelium**Dirk Junghans<sup>1</sup>, Verdon Taylor<sup>1</sup>, Iris Hack<sup>2</sup>, Michael Frotscher<sup>2</sup>, Rolf Kemler<sup>1</sup><sup>1</sup>*Max-Planck Institute of Immunobiology, Dept. Molecular Embryology, Germany*<sup>2</sup>*University of Freiburg, Department of Anatomy and Cell Biology, Germany*

Forming a complex structure such as the murine brain requires the interplay between different signalling cascades during early embryonic development.  $\beta$ -Catenin is known to play pivotal roles in mediating Wnt-signalling and N-Cadherin mediated cell adhesion. We show that in the developing telencephalic neuroepithelium  $\beta$ -catenin is highly enriched at the apical endfeet of the neural precursors and is co-localised with N-cadherin at adherens junctions. A TCF/LEF/ $\beta$ -catenin reporter mouse shows no lacZ-activity in the early telencephalon indicating, together with a lack of nuclear  $\beta$ -catenin staining, that the canonical Wnt-pathway is not crucial in this structure. To elucidate the function of  $\beta$ -catenin during early telencephalon development, we used the Cre/*loxP* system to ablate  $\beta$ -Catenin from this region of the embryonic mouse brain. The ablation of  $\beta$ -catenin in the telencephalon using the FoxG1-Cre line leads to a disruption of apical adherens junctions and a breakdown of neuroepithelial structures resulting in apoptosis.  $\beta$ -catenin mutant embryos lack forebrain and anterior facial structures. In summary, we demonstrate that  $\beta$ -Catenin is necessary for maintaining the integrity of the neuroepithelium and the developing brain.

## **Disruption of the Protocadherin-Gamma Cluster in Gene-trap Mice Leads to Neuronal Degeneration and Perinatal Lethality**

Matthias Ebert, Rolf Kemler and Marcus Frank

Department of Molecular Embryology, Max-Planck Institute of Immunobiology, Stübeweg 51, D-79108 Freiburg (e-mail: frank@immunbio.mpg.de)

Within the cadherin superfamily of cell adhesion molecules, the clustered protocadherins (Pcdhs) comprise more than 50 genes in man and mouse. Many of these are strongly expressed in neurons and especially in synapses of the developing and adult nervous system, suggesting functions of clustered Pcdhs during neuronal differentiation and in synaptogenesis. The Pcdh-gamma cluster contains 22 arrayed Pcdh genes (termed “variable exons”), which are spliced to three separate exons (termed “constant exons”) together coding for a family-specific cytoplasmic domain.

Mouse embryonic stem cells (ES cells) harboring a gene-trap insertion following Pcdh-gamma constant exon 2 were obtained from the German Gene Trap Consortium (<http://genetrap.gsf.de/>). Generation of chimeric mice by injection of the ES cells into blastocysts allowed subsequent germline transmission of the protocadherin trap allele.

Heterozygous offspring were phenotypically normal and viable, but breeding to homozygosity resulted in a strong neurological phenotype and perinatal lethality. Homozygous mice displayed a strong general rigor and tremor of the fore- and hindlimbs. They had difficulties in breathing, did not feed, and died a few hours after birth. Histological examination of the mutants showed a strong decrease in the size of the spinal cord. Also, abnormal protrusion of the gut was evident. This phenotype is closely reminiscent of mice in which the entire Pcdh- $\gamma$  cluster has been deleted (Wang et al., 2002, *Neuron* 36, 843-854.) Indeed, further analysis showed that wild-type Pcdh-gamma proteins are largely absent in the homozygous trap mice and are reduced in the heterozygous littermates. Staining for enzymatic activity of beta-galactosidase expressed as a fusion transcript from the trapped locus revealed staining of the nervous system and of other organs, e.g. heart and lung, similar to our previous observations of Pcdh-gamma transcript and protein expression. We conclude that the trap allele disrupts the proper generation of wild-type Pcdhs-gamma and thus represents a functional knock-out allele. Detailed examination of the phenotype caused by the lack of protocadherins will help to elucidate their vital functions in neural and tissue development.

Supported by the Max-Planck Society and a grant of the Deutsche Forschungsgemeinschaft (SFB 592) to R.K.

## Development of antennal mechanosensory neurons in crickets

Fatime Seidl and Michael Gebhardt  
Lehrstuhl für Zoologie, TU München  
Lichtenbergstr. 4, 85748 Garching, Germany.

The antennae of insects are actively moveable, multimodal sensors which participate in a broad range of behaviours, e.g. the antennal tracking behaviour of crickets ([1]). Antennal tracking depends on proprioceptors located at the two basal segments of the antenna, the scape and the pedicel. A backfill study of the pedicel of adult crickets ([2]) has demonstrated hair plates, campaniform sensillae, two chordotonal organs, a presumptive Johnston's organ, and a receptor organ of hitherto unknown type. The high number of the different sensory neurons and their dense packing in the pedicel so far prevented to further characterise these sensory neurons. Studying the embryonic development of the basal antennal mechanosensory neurons can assist to accomplish this task.

The investigation of the temporal developmental pattern of the sensory neurons in the antenna requires accurate staging of the embryos. By means of quantitative morphometric and external morphological features, the age of embryos can be determined with an accuracy of approximately 2.5% of the total developmental time. The absolute length of an antenna proved to be the most accurate parameter to predict the age of an embryo between 30% and 100% of embryogenesis.

The spatio-temporal developmental pattern of the antennal mechanosensory neurons was examined using neuron-specific immunocytochemistry with antisera directed against horse radish peroxidase ([3]). The sensory nervous system of the cricket antenna is pioneered by two pairs of cells at the tip of the embryonic antenna flagellum ([4, 5]). These pioneer neurons form the first neuronal pathway between the embryonic antenna and the central nervous system. At 36% of embryogenesis, the first sensory neurons appear at the tip and in the middle of the antenna flagellum and close to the antennal base. The development of the sensory neurons between 36% and 45% of embryogenesis seems to be restricted to these three zones. From 45% of embryogenesis onward sensory neurons form proliferating zones in each segment of the antenna. Similarly, at 45% of embryogenesis, large neuronal somata with dendrites become visible in the pedicel. At about 48% of embryogenesis, sensory neurons show up in the scape. These neurons probably belong to the scapal chordotonal organ. This pattern closely resembles the pattern found in locust embryos ([5]).

Intracellular injections of Lucifer Yellow or neurobiotin are currently being carried out to reveal the central nervous projections of pedicellar proprioceptors.

### References:

- [1] Honegger H.-W. (1981), J. Comp. Physiol. A 142, 419-421.
- [2] Yildiz, F. and Gebhardt, M. (2003), Proc. 29<sup>th</sup> Göttingen Neurobiol. Conf., abstract 238.
- [3] Jan, L. Y. and Jan, Y. N. (1982), Proc Natl Acad Sci USA; 79 (8), 2700-4.
- [4] Bate, C.-M. (1976), Nature 260, 54-55.
- [5] Boyan, G.S. and Williams J.L.D. (2004), Arthropod Structure & Development, article in press.

This work is supported by the DFG Graduiertenkolleg 267.

## **The monocarboxylate transporter 8 (MCT8) linked to human psychomotor retardation is highly expressed in thyroid hormone-sensitive neurons**

Heike Heuer, Michael K. Maier, Sandra Iden, Jens Mittag, Edith Friesema\*, Theo J. Visser\*, and Karl Bauer

Max-Planck Institute f. Exp. Endocrinology, Hannover;

\*Erasmus University, Rotterdam, The Netherlands

Absence of thyroid hormones (TH) during brain development leads to severe neurological manifestations known as cretinism. As one putative mechanism causing this syndrome, an impaired TH transport across cell membranes that prevents intracellular TH action has been proposed. Recently, a form of X-linked mental retardation combined with elevated serum T3 levels was diagnosed in several human patients. Genetically, this condition could be linked to mutations in the monocarboxylate transporter 8 (MCT8) gene. Since MCT8 has been shown to be an active and specific TH transporter, it might fulfill a unique function in providing TH access to the brain.

Here, we studied the expression pattern of MCT8 in the murine CNS by in situ hybridization histochemistry (ISH). In addition to the choroid plexus, highest transcript levels were found in neo- and allocortical regions (namely in the olfactory bulb, cerebral cortex, hippocampus, and the amygdala). Moderate signal intensities were observed in the striatum and in the cerebellum, whereas low levels were detected in a few neuroendocrine hypothalamic nuclei. The transcript levels were not altered in athyroid Pax8<sup>-/-</sup> mice as analysed by ISH suggesting that MCT8 expression is not affected by the thyroid status. Comparison of deiodinase type II (D2) and MCT8 localization revealed a rather complementary expression pattern, an observation that argues against a role of MCT8 as a carrier for the prohormone T4 into astrocytes but favors a function as an important transporter for T3 into its neuronal target cell.

**Eph/ephrin expression patterns in the developing cortex**

*Christiane Peuckert<sup>1</sup>, Ronny Niehage<sup>2</sup>, Sandra Barchmann<sup>1</sup>, Franco Weth<sup>2</sup>, Jürgen Bolz<sup>1</sup>*

<sup>1</sup>Friedrich-Schiller Universität Jena, Institut für allgemeine Zoologie und Tierphysiologie,  
Erbertstr.1, 07743 Jena, Germany

<sup>2</sup>Klinikum der Friedrich-Schiller Universität Jena, Nachwuchsgruppe Neurogenetik

The Eph receptor tyrosine kinases and their ligands constitute a large family of putative signaling molecules. Almost all of these molecules are expressed in the developing nervous system and the expression of several receptors and ligands persists during adulthood. Eph receptors and ligands appear to play many different roles during brain development. In the cortex, for example, they have been implicated as a guidance signal for thalamocortical projections and the formation of local cortical circuits. These effects are achieved in part by repulsive effects on growth cones and migrating cells, but there are also attractive effects on specific populations of neurons. The Eph/ephrin family is divided in A and B subclasses, and there is a binding preference within each subclass. However, recent studies demonstrated cross-binding between A-receptor and B-ligand and vice versa. Moreover, there is also evidence that at least some receptor-bound ephrin ligands can trigger signalling cascades. Given this complexity of possible interactions in the Eph/ephrin system we were interested in the expression patterns of these molecules in the developing thalamocortical system. We therefore performed *in situ* hybridizations at different embryonic and postnatal stages of all members of the Eph/ephrin family. Our results revealed distinct temporal and spatial labelling of ligands and receptors in the frontal and somatosensory cortex and corresponding thalamic divisions. There was a transient expression of Eph/ephrins in specific thalamic nuclei and cortical areas. Within a cortical area, subsets of Eph receptors and ephrin ligands were often confined to individual cortical layers. We also found specific expression patterns in the ventral telencephalon, which at specific stages of embryonic development allowed distinguishing the regions which give rise to cortical interneurons, their pathway to the cortex and their arrival in their cortical target. Taken together these results lead to several predictions about possible roles of specific Eph/ephrins for the formation of thalamocortical projections and for directing tangentially migrating neurons from the ganglionic eminences to their targets, which can now be tested with functional assays and with transgenic models.

## INTRAUTERINE DEVELOPMENT OF SLEEP STATES

M. Schwab<sup>1</sup>, K. Schwab<sup>2</sup>, M. Kott<sup>1</sup> and H.H. Szeto<sup>3</sup>

<sup>1</sup>Dept. of Neurology, <sup>2</sup>Institute for Medical Statistics and Computer Science, Friedrich Schiller University, Jena, Germany, <sup>3</sup>Dept. of Pharmacology, Cornell University Medical School New York, NY

**Objective:** Most knowledge of the development of sleep states comes from the postnatal rat brain. The gyrencephalic fetal sheep brain develops mainly prenatally. The sequence of sleep states and its development reflects closer the human situation. We aimed to investigate the intrauterine functional brain maturation in regard to the development of sleep states.

**Methods:** Five fetal sheep were chronically instrumented via Caesarean section at 100 days gestation (dGA, term 150 dGA). EOG, nuchal EMG and biparietal and bifrontal electrocorticogram (ECoG) electrodes were implanted. After recovery ECoG was recorded *in utero* from the un-anesthetized healthy fetuses between 105 and 139 dGA. Three to five artifact-free 10 min ECoG-epochs from NREM and REM sleep, respectively, were analyzed every third day using linear (power spectral analysis) and nonlinear methods because the ECoG is a highly complex signal that does not fit the criteria of "linearity". For nonlinear analysis we used an algorithm based on the Wolf-Algorithm (calculation of the leading Lyapunov Exponent) which calculates a point prediction error (PE) regarding to the course of the time series in the phase space. A high PE stands for a low predictability or causality and vice versa.

**Results:** The sheep fetus developed distinct sleep states from approximately 115-120 dGA conventionally defined by ECoG, EOG and EMG measures alternating between REM and NREM sleep. This age corresponds to the first occurrence of fetal behavior states at 28 to 30 weeks of gestation in human pregnancy. The PE of the REM sleep ECoG was higher than in NREM sleep revealing the higher complexity of brain activity during REM sleep and the occurrence of coordinated thalamocortical rhythms on a regular base during NREM sleep. We did not find phases of wakefulness. At 106 dGA, ECoG showed a predominantly premature REM sleep pattern defined by a relatively high PE that did not reach values of mature REM sleep. This pattern was interrupted by short phases with a lower PE suggesting the occurrence of a premature NREM sleep. This phases were not detectable with power spectral analysis. The PE decreased continuously between 106 and 139 dGA in the (premature) NREM sleep that become longer and more stable suggesting maturation of the ECoG synchronization mediating thalamic pacemaker circuits. Development of complex neuronal interactions reflected by a PE increase during premature REM sleep could not be proven before 124 dGA, i.e. after emergence of distinct sleep states between 115 and 120 dGA.

**Conclusions:** Maturation of thalamic pacemaker circuits leads to the occurrence of organized sleep states and precedes maturation of complex cortical neuronal interactions. PE changes after transition to cyclic electrocortical activity reflect continued functional brain development during REM and NREM sleep.



## Fetal Cerebral Processing of External Vibroacoustic Stimuli

M. Schwab<sup>1</sup>, C. Menz<sup>1</sup>, T. Bludau<sup>1</sup>, K.J. Gerhardt<sup>2</sup>, R.M. Abrams<sup>3</sup>

<sup>1</sup>Dept. of Neurology, <sup>2</sup>Institute for Medical Statistics and Computer Science, Friedrich Schiller University, Jena, Germany, <sup>2</sup>Dept. of Communication Sciences and Disorders, <sup>3</sup>Dept. of ObGyn, University of Florida, Gainesville, FL, USA

**Objective:** The human and the sheep fetus, the most important animal model of human pregnancy, respond to external stimuli as vibrations or noises with behavior state changes from 0.8 gestation onwards. It is not clear yet (1) if the behavior state changes that represent a „subcortical“ arousal are accompanied by a „cortical“ arousal as a condition of conscious experience of the stimuli; (2) to what extent the perception of the stimuli depends on the behavior state and (3) on the quality of the stimulus; and (4) whether the proprioceptive system is important for perception of the vibratory component of the signal.

**Methods:** At 0.8 gestation, sheep fetuses were chronically instrumented via Cesarean section with ECoG (electrocorticogram) electrodes as well as EOG, EMG and EKG electrodes to define fetal behavior states. After a recovery period of five days, stimuli were presented from the abdominal wall of the ewe during periods of NREM and REM sleep. We tested pure vibratory (30 min) and acoustic (broad band noise over 5 h) stimuli as well as a dynamic amplitude and frequency modulated and two static vibroacoustic stimuli (VAS) produced by an electronic artificial larynx (EAL) and a laboratory shaker. All stimuli produced intrauterine sound pressure levels at least 20 dB above the background noises. ECoG changes were analyzed using linear (power spectral analysis) and nonlinear methods. For nonlinear analysis we used an algorithm based on the Wolf-Algorithm (calculation of the leading Lyapunov Exponent) which calculates a point prediction error (PE) regarding to the course of the time series in the phase space. A high PE stands for a low predictability or causality and vice versa. The PE of the REM sleep ECoG is higher than in NREM sleep revealing the higher complexity of brain activity during REM sleep.

**Results:** The pure vibratory and acoustic stimuli did not induce a cortical arousal. The VAS produced a cortical arousal with similar effectiveness during NREM and REM sleep within 32 ms. Processes of cortical activation and deactivation during spontaneous sleep state changes and VAS were similar in their time-course. The dynamic stimulus induced 100%, the EAL 70% and the laboratory shaker 40-50 % responses. Although the ECoG power spectrum changes differed between VAS in NREM (decrease of delta activity) and REM-sleep (beta activation), the PE showed that the cortical activation pattern did not depend on the sleep state and the stimulus. The cortical arousal was reflected by an increase of the PE in NREM sleep (cortical activation stops the thalamo-cortical pacemaker circuits) and a decrease of the PE during REM sleep (“undirected” cortical activity of REM sleep is stopped by “directed” cortical processing of the stimulus). The cortical arousal was regressive at the end of stimulation. Processes of cortical activation and deactivation during spontaneous sleep state changes and VAS were similar in their time-course. Cochlea ablation prevented from arousal suggesting stimuli were detected through the auditory rather than the proprioceptive system.

**Conclusions:** The results show that external VAS induce a cortical arousal during the last trimester depending on the stimulus. The time-course of cortical activation within 32 ms suggests an arousal via the ascending activating reticular system rather than via specific fiber systems.

## Differential regulation of intracellular chloride concentration in various nuclei of the developing rat superior olivary complex

Martin Oberhofer, Eckhard Friauf, Stefan Löhcke

Animal Physiology Group, Department of Biology, University of Kaiserslautern, POB 3049, D-67653 Kaiserslautern, Germany

The developmental regulation of intracellular chloride concentration ( $[Cl^-]_i$ ) in the lateral superior olive (LSO), a prominent nucleus in the superior olivary complex (SOC) of the auditory brainstem, has been well investigated (Kandler and Friauf, 1995, J Neurosci 15:6890-6904; Ehrlich et al., 1999, J Physiol 520:121-137; Balakrishnan et al., 2003, J Neurosci 23:4134-4145). In LSO neurons, high  $[Cl^-]_i$ , responsible for glycine/GABA depolarizations, shifts to low  $[Cl^-]_i$ , responsible for glycine/GABA hyperpolarizations, between postnatal day (P) 5 and P7. Whether other nuclei of the SOC also show a developmental shift of  $[Cl^-]_i$  and whether it appears at the same time as in the LSO is not known so far.

Here, we investigated the presence and time of shift in  $[Cl^-]_i$  in three SOC nuclei, namely the medial superior olive (MSO), the superior paraolivary nucleus (SPN) and the medial nucleus of the trapezoid body (MNTB) between embryonic day (E) 18 and P9. We measured glycine-induced chloride currents and their reversal potential ( $E_{Cl}$ ) using gramicidin perforated-patch recordings, which provide electrical access to the neurons without disturbing the native  $[Cl^-]_i$ .

In the MSO, we found an age-dependent decrease in  $E_{Cl}$ , equivalent to a decrease in  $[Cl^-]_i$ , that resulted in a shift in glycine action from depolarization to hyperpolarization at P6. Thus, the development of  $[Cl^-]_i$  regulation in MSO neurons is similar to that in LSO neurons. As in the LSO and MSO,  $[Cl^-]_i$  of SPN neurons decreased during the first postnatal days. However, the time of shift occurred much earlier, i.e., between E18 and E20. In the MNTB, we found only a non-significant reduction in  $[Cl^-]_i$  during the age range tested (P0-9). Accordingly, no shift in glycine action occurred, i.e., almost every tested MNTB neuron (22 out of 25) showed a depolarization in response to glycine applications.

In order to assess the capacity of  $Cl^-$  transporter activity, we applied a protocol for cellular  $Cl^-$  loading or  $Cl^-$  depletion and thus for the manipulation of  $[Cl^-]_i$ . By measuring the time course of chloride back regulation, this protocol enables the characterization of  $Cl^-$  transporter activity. Examples of inward and outward  $Cl^-$  transport activity will be presented.

In summary, our results show a shift in glycine action from depolarization to hyperpolarization in the MSO and SPN, but not in the MNTB. Interestingly, the shift occurred at different ages, with a difference of more than one week (P6 vs. E18-20), illustrating a differential timing in  $[Cl^-]_i$  regulation in functionally related nuclei.

# **Proliferation, Migration, Neuronal Differentiation, and Long-Term Survival of New Cells in the Adult Zebrafish Brain**

<sup>1,2,3</sup>GÜNTHER K.H. ZUPANC, <sup>1</sup>URSULA M. WELLBROCK, <sup>1</sup>KAREN HINSCH, <sup>1</sup>DANIELA MEISSNER, <sup>2</sup>FRED H. GAGE

<sup>1</sup>*School of Engineering and Science, International University Bremen, D-28725 Bremen, Federal Republic of Germany*

<sup>2</sup>*Laboratory of Genetics, Salk Institute for Biological Studies, La Jolla, California 92037, USA*

<sup>3</sup>*School of Biological Sciences, University of Manchester, Manchester M13 9PT, UK*

In contrast to mammals, fish exhibit an enormous potential to produce new cells in the adult brain. By labeling mitotically dividing cells with 5-bromo-2'-deoxyuridine (BrdU), we have characterized the generation and further development of these cells in the zebrafish (*Danio rerio*). Proliferation zones were located in specific regions of the olfactory bulb, dorsal telencephalon (including a region presumably homologous to the mammalian hippocampus), preoptic area, dorsal zone of the periventricular hypothalamus, optic tectum, torus longitudinalis, vagal lobe, parenchyma near the rhombencephalic ventricle, and in a region of the medulla oblongata lateral to the vagal motor nucleus, as well as in all three subdivisions of the cerebellum — the valvula cerebelli partes lateralis and medialis, the corpus cerebelli, and the lobus caudalis cerebelli. In the two divisions of the valvula cerebelli and in the corpus cerebelli, the young cells migrated from their site of origin in the respective molecular layers to the corresponding granule cell layers. By contrast, in the lobus caudalis cerebelli and optic tectum, no indication of migration of the newly generated cells over wider distances could be obtained. In the cerebellum, approximately 20% of the newly generated cells remained alive for at least several months, and probably for the rest of the fish's life. The combination of BrdU immunohistochemistry with immunolabeling against the neural marker protein Hu revealed that a large number of the young cells developed into neurons. Taken together, these results demonstrate continuous neurogenesis in the adult brain of zebrafish.

## Role of TGF-beta, Shh and FGF8 in differentiation of ventral mesencephalic neurospheres *in vitro*

Michael Wiehle, Oliver Oehlke, Eleni Roussa and Kerstin Krieglstein  
Department of Neuroanatomy, University of Goettingen, Kreuzberggring 36  
D-37075 Goettingen, Germany

The mesencephalic dopaminergic system is known to regulate a variety of brain functions, including behavior and movement control. Degeneration of mesencephalic dopaminergic neurons is associated with Parkinson's disease. Therefore, the molecules and mechanisms involved in the differentiation process of progenitor cells into dopaminergic neurons are of major interest.

In the present study we investigated in detail differentiation potential of precursor cells cultured as neurospheres derived from mouse ventral mesencephalon at embryonic day 12 (E12) and focused on the influence of Transforming Growth Factor-beta (TGF-beta), Sonic hedgehog (Shh) and Fibroblast Growth Factor 8 (FGF8).

Progenitor cells from primary ventral mesencephalic tissue of mouse E12 were isolated and cultivated in suspension with the mitogen FGF2 until neurosphere formation occurred. Spheres were dissociated, plated on polyornithin-laminin coated coverslips and treated with Shh, FGF8 and TGF-beta alone or added together. Endogenous expression of individual factor was neutralized using function blocking antibodies.

RT-PCR analysis showed that mouse primary ventral mesencephalic tissue expressed Nestin, Nurr1, Ptx3, beta III-tubulin and tyrosine hydroxylase (TH). Ventral neurospheres also expressed Nestin, Nurr1, Ptx3, beta III-tubulin and TH. However, Nestin, Nurr1 and Ptx3 expression in neurospheres was found increased compared to primary tissue. In contrast, beta III-tubulin and TH expression was decreased in neurospheres, compared to primary tissue. In addition, endogenous expression of TGF-beta, Shh and FGF-8 was also detected in primary tissue.

Neurosphere treatment with TGF-beta resulted in an increase of Nurr1 and TH immunoreactive cells, in comparison to controls. Application of all factors together even increased the number of Nurr1 and TH positive cells, compared to TGF-beta treated cells. Neutralization of endogenous TGF-beta, Shh or FGF8 resulted in a dramatical decrease of Nurr1 and TH immunoreactive cells compared to controls. Taken these results together we conclude that TGF-beta, Shh and FGF8 play an essential role in differentiation process of dopaminergic neurons. However, it appears that TGF-beta, Shh and FGF8 need each other to exert their differentiation promoting effect on dopaminergic neurons.

## *Tieg1* and *Tieg3* in the developing nervous system of mouse

Maik Behrendt, Ziyuan Wang and Kerstin Krieglstein  
Center of Anatomy, University of Goettingen, Kreuzberggring 36, D-37075 Goettingen,  
Germany

Transforming growth factor ( $\text{TGF-}\beta$ )-inducible early gene (*Tieg*) plays a critical role in regulation of cell proliferation, differentiation and apoptosis. Two isoforms, *Tieg1* and *Tieg3*, are identified as the only members of the Sp1-like mediated function of transcription factors in the mouse genome. However, little is known about the cellular distribution of the *Tiegs* in the developing central and peripheral nervous system.

In this study we have investigated *Tieg1* and *Tieg3* expression in mouse embryos at embryonic day (E) E7, E11, E15 to E17, using Northern blot analysis. Cellular distribution of *Tieg1* and *Tieg3* transcript and protein were further determined by *in situ* hybridization and immunohistochemistry (E10 to E16), using specific probes and antibodies, respectively. The results show that at E10, *Tieg1* and *Tieg3* are expressed in neuroepithelial cells of the cortex and optic vesicle as well as in neural crest-derived components. At E12 to E14 *Tieg* expression was found in the inner neural layer of retina, in the marginal, intermediate and the ventricular zone of neopallial cortex and most prominently in peripheral ganglia. At E16, *Tiegs* were present in neurons of the sensory dorsal root and cranial ganglia as well as in differentiated retinal ganglion cells. Our results document *Tieg1* and *Tieg3* expression in the developing nervous system and suggest an involvement in cell migration and neuronal differentiation.

The role of Ptx3 in the development and differentiation of mouse mesencephalic dopaminergic neurons *in vitro*.

Oehlke O, Roussa E and Krieglstein K

Center of Anatomy, Department of Neuroanatomy, University of Goettingen, Kreuzberggring 36, D-37075 Goettingen

Mesencephalic dopaminergic (MesDA) neurons play a pre-eminent role in the control of voluntary movement. Degeneration of these cells results in Parkinson's disease. Although a number of genes have been identified in participating in patterning and development of mesencephalon, specific factors involved in the induction of mesDA remain substantially unacquainted. Transcription factors, such as Nurr1, Ptx3 and Lmx1b, are eligible candidates to play essential roles in induction, development, differentiation and survival of mesDA. In this study, protein expression pattern of Ptx3 at different developmental stages, as well as the role of SHH, FGF8 and TGF- $\beta$  in the expression of Ptx3 *in vitro* was examined.

To track these aims, distribution of Ptx3 immunoreactivity (Ptx3-IR) in mouse embryonic day 12 (E12) and E14, in brains of newborn (P0) mice, as well as in cultures derived from mouse E12 ventral mesencephalon were investigated by immunohistochemistry and immunocytochemistry, respectively. Briefly, for immunohistochemistry tissue was fixed in 4% PF and tissue sections were incubated with a Ptx3-specific polyclonal antibody at 4°C overnight. The following day sections were incubated with a goat-anti-rabbit-horseradish peroxidase-conjugated secondary antibody. Ptx3-IR was visualized by diaminobenzidine and H<sub>2</sub>O<sub>2</sub>. For cell culture experiments, progenitor cells were isolated from mouse E12 ventral mesencephalon, and cultured in suspension in the presence of FGF2. Neurospheres were formed and plated onto PORN/laminin coated coverslips. At day in vitro (DIV) 1, cells were treated with SHH, FGF8, TGF- $\beta$ , anti-SHH, FGF-R3 $\alpha$  or anti-TGF- $\beta$ . At DIV3, the cells were fixed in 4 % PF, permeabilized and processed for immunocytochemistry.

Our results show that at E12, Ptx3-IR was present in mouse ventral mesencephalon. At E14, Ptx3 was additionally detected in the myenteric plexus. In brains of P0 mice, Ptx3 was expressed in the cerebellum and hippocampus.

Treatment of plated neurospheres with SHH, FGF8 and TGF- $\beta$  showed that these factors differentially influenced Ptx3 expression. Application of TGF- $\beta$  displayed no significant increase in the number of Ptx3 immunoreactive cells compared to untreated controls. In addition, the combined application of SHH, FGF8 and TGF- $\beta$  also evinced no significant change in the number of Ptx3 immunoreactive cells compared to controls. Interestingly, neutralizing endogenous SHH, FGF8 or TGF- $\beta$  using function blocking antibodies against individual factors, lead to a decreased number of Ptx3 immureactive cells compared to controls, in such a way as to likely enable these factors to maintain Ptx3 expression.

The results suggest that Ptx3 might participate in additional developmental processes in the developing brain as previously believed as well as in maintainance of neuronal populations in the adult mouse brain.

Characterization of neurospheres derived from ventral and dorsal mouse mesencephalon.

Roussa E, Wiehle M, Oehlke O, Krieglstein K.

Center of Anatomy, Department of Neuroanatomy, University of Goettingen, Kreuzberggring 36, D-37075 Goettingen, Germany

Neural stem cells have attracted a great deal of research interest as model system for understanding brain development and for their therapeutic potential in several human neurodegenerative diseases. Among neurological disorders, Parkinson's disease is associated with degeneration or functional impairment of the mesencephalic dopaminergic system. However, the molecular mechanisms underlying generation of mesencephalic dopaminergic neurons from stem cells and the extrinsic and intrinsic determinants that control their induction and differentiation are not fully understood.

In the present study, we have investigated stem cell characteristics, cellular composition and differentiation potential of neurospheres derived from mouse E12 ventral and dorsal mesencephalon by RT-PCR and immunocytochemistry.

To that end, ventral and dorsal mesencephalon from mouse at embryonic day (E) 12 was isolated, and dissociated. Cells in suspension were plated in non-coated culture dishes and cultured in the presence of fibroblast growth factor (FGF2). Cells were allowed to expand for 7 days before the neurospheres were plated onto polyornithin and laminin coated cover slips.

The results showed that the majority of ventral and dorsal mesencephalon neurosphere cells expressed nestin and were able to generate secondary neurospheres. Moreover, immunocytochemistry with specific antibodies revealed that plated mesencephalic ventral and dorsal neurospheres were able to differentiate into neurons, glia or oligodendrocytes. However, cellular composition analysis of ventral and dorsal neurospheres revealed distinct cell subpopulations within the spheres. Additionally to nestin, ventral neurospheres expressed Nurr1, Ptx3, beta-III tubulin and tyrosine hydroxylase (TH). In contrast, dorsal neurospheres expressed beta-III-tubulin, but were devoid of Nurr1, Ptx3 and TH immunoreactivity. In addition, differential expression of signaling molecules, such as transforming growth factor (TGF) beta, Sonic hedgehog (Shh) and FGF8 was observed in ventral and dorsal mesencephalic neurospheres.

These data demonstrate that the main properties of stem cells, by means of self renewal capacity and multilineage differentiation, are conserved between ventral and dorsal mesencephalon. In addition, it appears that these different stem cells express molecular markers of regional identity *in vitro*.

## Neuronal cell death during postnatal development of superior cervical ganglion of mouse.

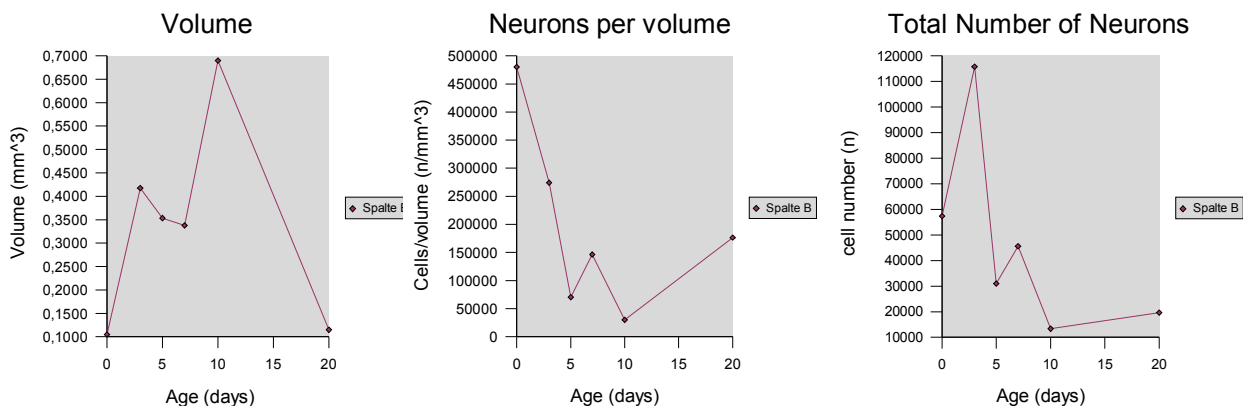
S. Schemmel, K. Krieglstein, M. Rickmann

Zentrum Anatomie, Dept. Neuroanatomy, University of Göttingen, Germany

The development of cell numbers and volume of the superior cervical ganglion (SCG) has been explored in detail in rats and other species. But for mouse there is no study which shows when the natural neuronal cell death in SCG actually takes place. This, however is prerequisite for studies which try to identify molecules involved in the apoptosis in SCG neurons. Therefore, we have performed a morphometric study to determine the absolute numbers of neurons in the SCG.

We examined NMRI mice at the postnatal days 0, 3, 5, 7, 10 and 20. Complete SCG's were dissected from perfusion fixed animals and embedded for semithin sectioning. The volume was calculated from cross section areas. The density of neurons was determined using a physical disector method.

The measured parameters changed a great deal. The volume of the ganglia increased until day 10 and thereafter declined until day 20. This was due to increases in neuronal size and of non-neuronal cell number. Neuron density showed a minimum at postnatal day 10. The total number of neurons increased early postnatally and showed a steep decline after day 3.



It is apparent that most changes occur around postnatal day 3. This was confirmed by a high density of pycnotic cell nuclei which indicated neuronal apoptosis. Currently we are performing a DNA microarray analysis comparing between SCG's at day 3 and 20. We will focus on apoptosis related genes.

Funded by Deutsche Forschungsgemeinschaft



**Characterization of ME2 as the obligate E-protein interaction partner for the adult expressed neuronal bHLH proteins and regulated overexpression of dominant-negative versions of ME2 in transgenic mice**

M.M. Brzozka\*, T. Wolfram, K.-A. Nave and M.J. Rossner.

Department of Neurogenetics, Max Planck Institute for Experimental Medicine, Göttingen, Germany.

There is growing evidence available that a complex network of bHLH proteins controls early neuronal development, but the role of these and related bHLH proteins in postnatal development and in the adult CNS are not well understood. The sustained expression of the bHLH neurogenic differentiation factors (NDFs) NeuroD, NEX/NeuroD6 and NDRF/NeuroD2 in the hippocampus and neocortex suggests a function of these proteins also in adult nervous system plasticity. Furthermore, the genetic analysis of adult-expressed bHLH proteins has been hampered by the high degree of functional redundancy that is observed in corresponding single-gene mouse mutants. NeuroD, NEX/NeuroD6 and NDRF/NeuroD2 belong to the cell-type specific 'class B' bHLH proteins and their function is dependent on the heterodimerization with ubiquitously expressed 'class A' or E-proteins. Using biochemical and reporter gene based assays we have previously shown that all NDFs interact with ME2 in COS7 and PC12 cells. With northern blotting and in-situ hybridization, we can show that ME2 is the only E-protein expressed in the postnatal hippocampus and cortex and is therefore the obligate dimerization partner for the NDFs. Performing co-immune precipitations with antibodies directed against native ME2, we proved the in vivo relevance of this hypothesis. Reporter gene assays show that ME2 is required for E-Box dependent transcriptional activation of a downstream luciferase gene. The analysis of a series of deletion constructs reveals that the ME2 moiety dominates the overall transcriptional activity of NDF-ME2 heterodimeric complexes. In order to generate mouse models better suited for the analysis of the postulated function of the NDFs in adult nervous system plasticity, we have decided to generate transgenic mice expressing a dominant-negative version of ME2 (dnME2) in the brain. To circumvent any developmental interference, we have used the Tet-system to control the level of overexpression by adding doxycyclin to the drinking water. So far, we have been able to establish two mouse lines with a forebrain restricted overexpression of dnME2. The analysis is in progress.

## THE EFFECT OF REELIN IN THE MIGRATION OF CORTICAL SVZ NEURONS

Alifragis Pavlos<sup>1,2</sup>, Britanova Olga<sup>2</sup>, Tarabykin Victor<sup>2</sup>

1 MRC, CSC Imperial College London, 2 Max-Planck Institute of Exp. Med. Goettingen

A unique feature of brain development is that newborn neurons migrate away from their site of birth in the proliferative zones towards their final destinations. Neuronal migration in the cerebral cortex begins when the first post-mitotic neurons leave the germinal ventricular zone (VZ) and form a transient structure called the preplate. Subsequent generations of post mitotic neurons split the preplate into the superficial layer I or marginal zone (MZ) and the deeper layer VI or subplate (SP) forming the cortical plate (CP). [<sup>3</sup>H]-Thymidine incorporation studies have shown that layers II-VI of the cerebral cortex are generated in an inside-out sequence, such that neurons that are generated early on reside in deeper layers, whereas later born cells migrate past the existing ones and form more superficial layers. There has been a great interest in how neurons migrate towards their final destination and in the mechanisms that make this journey possible. The migration of cortical neurons is a well orchestrated procedure, and defects in their migration lead to neurological disorders. A key molecule in the migration is Reeler. *Reeler* encodes for a large extracellular matrix protein secreted by Cajal Redzious cells in the MZ. The spontaneous *reelin*-gene deficient mouse has been used to investigate the mechanisms of neuronal layering over the past years. Reeler mice show severe abnormalities of the neuronal positioning in the central nervous system. Labeling experiments with [3H] thymidine have shown an overall inversion of neuronal positioning within the cortical plate ("outside-in" pattern). Cortical neurons that migrate radially to the cortical plate are thought to do so through two distinct modes of migration: translocation and locomotion. In addition, a third mode of migration has been described for neurons born in the cortical SVZ: multipolar or branched migration. In our poster we will present data on how Reeler affects the migration of cortical neurons that are generated in the SVZ.

## **The role of presynaptic activity during functional maturation of a fast glutamatergic CNS synapse.**

Emilio Fischer, Holger Taschenberger

Dept. of Membrane Biophysics, Max-Planck Institute for Biophysical Chemistry,  
37077 Göttingen

During early postnatal development the calyx of Held synapse of the mammalian auditory brainstem undergoes a multiplicity of morphological and functional modifications, which eventually transform this synapse into an ultra fast and highly reliable relay (Joshi and Wang, 2002). Relatively little is known about the role of sensory input during this maturation process. To address this question, we compared the functional properties of control synapses with those of calyces developing in the absence of sensory input in mice lacking the voltage-gated Ca channel subunit  $\text{Ca}_v1.3$ . This latter subunit is expressed in cochlear hair cells where it governs Ca-dependent glutamate release. Since  $\text{Ca}_v1.3^{-/-}$  mice are deaf (Platzter et al., 2000), we were thus able to investigate how afferent activity driven by sensory input shapes the developmental maturation of calyx of Held synapses.

We studied functional properties of calyx of Held synapses at two developmental stages: shortly before (postnatal day [P] 8-11) and after (P14-17) the onset of hearing (approx. P12-13) in wt and  $\text{Ca}_v1.3^{-/-}$  mice using standard patch-clamp techniques. From P8 to P17, the kinetics of AMPAR-mediated mEPSCs and eEPSCs evoked by afferent fiber stimulation showed a similar acceleration in both wt and  $\text{Ca}_v1.3^{-/-}$  animals, but eEPSC peak amplitudes reached significantly higher values at P14-17 in  $\text{Ca}_v1.3^{-/-}$  (mean 17.6 nA,  $n = 27$ ) compared to wt (9.80 nA,  $n = 19$ ) mice. Occasionally, AMPA EPSCs of  $>30$  nA were measured in  $\text{Ca}_v1.3^{-/-}$  MNTB neurons. In contrast, mEPSC amplitudes in wt and  $\text{Ca}_v1.3^{-/-}$  mice were comparable.

Peak amplitudes of NMDAR-mediated EPSCs continued to decline from P8-11 (6.9 nA,  $n = 11$ ) to P14-17 (2.5 nA,  $n = 7$ ) in wt synapses. This down regulation of synaptic NMDARs was, however, strongly delayed in  $\text{Ca}_v1.3^{-/-}$  mice. In fact, a small increase from 6.2 nA ( $n = 8$ ) to 6.8 nA ( $n = 11$ ) was observed. During repetitive stimulation at high frequencies,  $\text{Ca}_v1.3^{-/-}$  mice exhibited significantly stronger depression (89.5 %;  $n = 18$ ) compared to wt mice (76.3 %;  $n = 12$ ) while the rates of recovery from depression were comparable ( $\tau$  recovery = 4.29 s;  $n = 8$ , for wt; vs. 3.34 s;  $n = 10$ , for  $\text{Ca}_v1.3^{-/-}$  mice).

Our results suggest that the developmental acceleration of the time course of AMPAR EPSCs occurs unchanged in congenital deaf compared with wt mice. However, in the absence of presynaptic activity, down regulation of synaptic NMDARs appears to be delayed. In addition, our data is consistent with an elevated vesicular release probability in deaf mice which leads to larger AMPAR EPSC amplitudes and more pronounced synaptic depression during trains. This suggests that presynaptic activity plays a differential role during the development of the calyx of Held synapse.

Joshi I, Wang LY (2002) Developmental profiles of glutamate receptors and synaptic transmission at a single synapse in the mouse auditory brainstem. *J Physiol* 540: 861-873.  
Platzter J et al. (2000) Congenital deafness and sinoatrial node dysfunction in mice lacking class D L-type  $\text{Ca}^{2+}$  channels. *Cell* 102: 89-97.

**Modulation of neuronal outgrowth by selective 5-HT receptors activating the G<sub>12/13</sub> signaling pathways in hippocampal neurons**

*Hess, D., Ponimaskin, E. and Richter, D.*

During development and maturation, the direction and velocity of neurite outgrowth is influenced by multiple factors. In this process, G-protein coupled receptors activating small GTPases of the Rho family play an important role.

Recently we identified the G<sub>13</sub> protein as a novel interaction partner of the 5-HT<sub>4</sub> receptor. Activation of this signaling pathway results in RhoA-mediated modulation of gene transcription and reorganization of the actin cytoskeleton. We also demonstrated that the serotonin receptor 5-HT<sub>7</sub> can activate the heterotrimeric G<sub>12</sub> protein leading to a selective activation of the small GTPases RhoA and Cdc42. Agonist-dependent activation of the 5-HT<sub>7</sub> receptor induced pronounced filopodia formation via a Cdc42-mediated pathway which occurs in parallel to RhoA-dependent cell rounding.

Here, we show that activation of endogenous 5-HT<sub>7</sub> receptors induces a significant increase in neurite growth of mouse hippocampal neurons, whereas stimulation of the endogenous 5-HT<sub>4</sub> receptors induced a pronounced decrease of the length and number of neurites. In addition, we used periodic pressure application of receptor agonists through a micropipette that was positioned at a defined distance and angle to the growth cone. Periodic applications generated transient and locally restricted concentration gradients of agonists to analyse specific outgrowing neurites and identify the basic parameters determining their navigation.

**A secreted serine protease with IGF binding motif involved in anterior-posterior patterning of *Xenopus* embryos**

Shirui Hou and Edgar Pera

Department of Developmental Biochemistry, Georg August University Göttingen,  
Justus von Liebig Weg 11, 37077 Göttingen, Germany

We present a novel serine protease with IGF binding motif (SPIB) involved in anterior-posterior patterning of the *Xenopus* embryo. SPIB was isolated in a screen for secreted proteins from a gastrula stage cDNA library. Microinjection of *SPIB* mRNA resulted in loss of head tissue and induction of ectopic tail-like structures. At the onset of gastrulation, *SPIB* mRNA blocked the expression of the anterior brain marker *Otx2* and expanded the mesodermal markers *Xbra* and *Xwnt8* into the animal hemisphere, indicating a conversion of ectoderm into mesoderm. *SPIB* mRNA also enlarged the neural plate at the expense of neural crest and epidermis and induced ectopic neurons. A mutant *SPIB* construct, in which the catalytic serine residue was replaced by alanine, failed to induce anencephaly and ectopic tails, indicating a crucial role of the proteolytic domain for the activity of *SPIB*. In loss-of-function experiments, an antisense morpholino oligonucleotide that blocks SPIB protein synthesis (*SPIB-MO*) enlarged head structures and reduced tail development. *SPIB* mRNA interfered with the ability of young dorsal marginal zone explants to induce ectopic heads, and caused induction of trunk and tail structures instead. In contrast, *SPIB-MO* impaired with ectopic tail induction by advanced dorsal marginal zone grafts. These results suggest that *SPIB* is both sufficient and required for tail induction and acts as a posteriorizing factor in *Xenopus* embryos.

## **Functional characterization of Smad-interacting protein 1 (SIP1) in the neocortex and hippocampus by conditional gene inactivation**

Amaya Miquelajáuregui

Supervisor: Victor Tarabykin

Smad- interacting protein 1 (SIP1) is a two-handed zinc finger/homeodomain transcription factor presumably involved in the TGF- $\beta$ /BMP signaling. It has been shown in epithelial cells that SIP1 downregulates the transcription of E-cadherin and induces cell invasion. Additionally, mutations of *sip1* have been directly associated with the etiology of the Mowat-Wilson syndrome, characterized by severe cerebral anomalies such as agenesis of the corpus callosum, cerebral atrophy and poor hippocampal formation.

We have identified *sip1* in a screen designed to isolate genes involved in the development of the mouse cerebral cortex. In the neocortex, SIP1 mRNA can be detected starting from the embryonic day until adulthood and is predominantly expressed in the cortical plate.

We have analyzed the *in vivo* role of SIP1 in the cerebral cortex by conditional gene inactivation. We produced a mouse strain where exon 7 of *sip1* is flanked by loxP sites. When crossing this line with a cortex-specific Cre line, the exon of *sip1* that contains both the homeodomain and the smad-binding domain is removed by the Cre recombinase. This recombination event causes a frameshift that eventually leads to a truncated, non-functional protein in all cortical cells including progenitors.

We observed a remarkable phenotype both in the neocortex and the hippocampus. By mid-gestation, the hippocampus and dentate gyrus of conditional knock-out mice are missing or represented by a tiny population of residual cells. Further data on the function of SIP1 in the mouse telencephalon will be presented.

## Visualisation of Interactions in Living Hippocampal Neurons at Ultra-Low Excitation Levels Using the Calcium Indicator Cameleon

Mini Jose<sup>1</sup>, Deepak Nair<sup>1</sup>, Thomas Dresbach<sup>3</sup>, Klaus Kemnitz<sup>2</sup>, Michael Kreutz<sup>1</sup>,  
E. D. Gundelfinger<sup>1</sup> and Werner Zuschratter<sup>1</sup>

<sup>1</sup>Leibniz Institute for Neurobiology Magdeburg, Germany, (<http://www.ifn-magdeburg.de>)

<sup>2</sup>EuroPhoton GmbH, Berlin, Germany (<http://www.europhoton.de>)

<sup>3</sup>Institute for Anatomy and Cell Biology, Heidelberg, Germany

Most of the visualisation techniques like CLSM or 2-Photon that have been developed so far to study the dynamic events taking place inside living cells, use high illumination intensities that cause considerable photo-dynamic reactions and therefore, do not allow a non-distorted continuous observation of dynamic processes for a longer period. In this situation, we take advantage of the high sensitivity of the novel ultra-sensitive delay-line (DL) and non-scanning imaging detectors (QA = quadrant anode), based on Time- and Space-Correlated Single Photon Counting (TSCSPC) for studying interactions in living cells under minimal invasive conditions ( $<100\text{mW}/\text{cm}^2$ ). In order to study interactions in the nanometer scale with the light microscope, we have utilised the technique of Förster's Resonance Energy Transfer (FRET). Fluorescence Lifetime Imaging Microscopy (FLIM) allows the lifetimes of one or more fluorophores to be spatially resolved and can be used to provide information about the state of the fluorescent species and their immediate molecular environment. By combining FRET and FLIM, we overcome the difficulty of the concentration dependence of energy transfer, which cannot be determined in living cells. We observe the contribution of different artefacts like autofluorescence which is unavoidable in living cells and completely contaminates the measured data, giving a different impression of the dynamics. In the present work, we present the importance of Decay Associated Spectra (DAS), which give the relative contribution of the different lifetimes at different wavelength channels, in biophysical experiments and how they can be used for discriminating FRET from artefacts. Apart from their complicated photo physics, ECFP and EYFP are used as a common FRET pair to study protein - protein interactions in cells by fusing to the respective protein of interest and in development of FRET based fluorescent protein biosensors like cameleon, clomeleon etc. In the present study, we have monitored FRET in the biological calcium sensor, cameleon (YC2.3) at different developmental stages of hippocampal neuronal cell cultures (DIV 7, 11 and 15) which may have a physiological relevance in revealing the intracellular dynamics taking place inside these cells. Neuronal development is characterized by changes in intracellular ionic concentrations among which  $\text{Ca}^{2+}$  is very important. The biochemical  $\text{Ca}^{2+}$  sensors called 'cameleons' consist of tandem fusions of cyan emitting GFP, the calcium sensing protein calmodulin, the calmodulin binding peptide M13 and an enhanced yellow emitting GFP. Binding of  $\text{Ca}^{2+}$  to the YC2.3 protein makes calmodulin wrap around the M13 domain, thereby increasing the efficiency of energy transfer between the flanking GFPs. Analysis of fluorescence emission in DIV 7 and 11 revealed a quenching of ECFP and simultaneous enhancement of Citrine (YFP), indicating the presence of a  $\text{Ca}^{2+}$  mediated energy transfer. Analysis of DAS corroborated the presence of an energy transfer with a rise in the decay and a negative pre-exponential factor corresponding to the lifetimes participating in the transfer. On addition of EDTA, which is a well known powerful calcium chelator, a strong influence on the fluorescence spectra as well as decay was observed, with the DAS showing only positive values indicating the absence of any energy transfer. Neuronal development is marked by reduction in intracellular  $\text{Ca}^{++}$  concentration. Consequently in mature cameleon transfected neurons (DIV 15), no energy transfer could be observed, indicating the lowering of intracellular  $\text{Ca}^{2+}$  concentration with maturation. Analysis of DAS at this age also gave consistent results, with the pre exponential factors corresponding to all lifetimes showing only positive values. A spatial variability of energy transfer at different regions of neurons was also observed, as evident from acceptor mapping which may correspond to the different ionic concentrations in different intracellular compartments of cells. A detailed analysis of such studies could in fact throw some light on the calcium signalling pathways taking place inside living cells. In conclusion, Fluorescence Lifetime Imaging microspectroscopy with DL and QA detectors form an excellent tool in analysing the dynamic interactions in living hippocampal neurons at minimal-invasive conditions.

## Imaging Interactions in Living Hippocampal Neurons at Minimal Invasive Conditions Using the Chloride Indicator Clomeleon

Deepak Nair<sup>1</sup>, Mini Jose<sup>1</sup> Thomas Kuner<sup>3</sup>, Roland Hartig<sup>4</sup>, Carsten Reissner<sup>1</sup>, Klaus Kemnitz<sup>2</sup>, Michael Kreutz<sup>1</sup>, E. D. Gundelfinger<sup>1</sup> and Werner Zuschratter<sup>1</sup>

<sup>1</sup>Leibniz Institute for Neurobiology Magdeburg, Germany, (<http://www.ifn-magdeburg.de>)

<sup>2</sup>EuroPhoton GmbH, Berlin, Germany (<http://www.europhoton.de>)

<sup>3</sup>Max-Planck-Institut for Biomedical Research, Heidelberg, Germany

<sup>4</sup>Institute for Immunology, Otto von Guericke Univ., Magdeburg, Germany

A number of techniques have been developed so far to study the dynamic events taking place inside living cells. The drastic fall in FRET efficiency with distance ( $\propto 1/R^6$ ) makes it a powerful tool for studying interactions in living cells. FLIM monitors localised changes in the probe fluorescent lifetime, which is concentration independent. In other FRET techniques like acceptor bleaching where fluorescence emission is alone monitored, concentration of fluorophores play a critical role. The conventional methods for observing FRET utilises very high laser illumination intensities, which induces photo toxicity and photo damage in cells, thereby completely altering the microenvironment within living cells. Thus the use of high intensity techniques does not allow a non distorted observation of dynamic events in cells for a longer period of time. In the present work, we have combined FRET and FLIM techniques to study the dynamics inside living hippocampal cells by monitoring their lifetimes. We have tried to maintain the natural state of the cells throughout the measurement by using very low excitation levels ( $<100 \text{ mW/cm}^2$ ). To get a good S/N ratio, we have taken advantage of the sensitivity of the DL/point (Delay line) and QA/imaging (Quadrant Anode) detectors, based on Time and Space Correlated Single Photon Counting (TSCSPC). Apart from the conventional way of monitoring the donor lifetimes alone, we have observed the donor and acceptor lifetimes simultaneously. Moreover, we have also studied the Decay Associated Spectra (DAS), which give an account of the contribution of the different lifetimes along the different wavelength channels and have shown the changes in the pre exponential factors as a proof of FRET. We have analysed DAS in all measurements using the Global Analysis software, by which we could distinctly prove whether there is an energy transfer taking place or not, even in the presence of different artefacts inside a living cell. Chloride ions play a major role in many physiological functions. Developmental regulation of intracellular  $\text{Cl}^-$  concentration determines whether GABAergic synapses excite or inhibit their post synaptic target. Making use of the high sensitivity of YFP on the ionic concentrations, a novel optical indicator called 'Clomeleon' for studying the intracellular  $\text{Cl}^-$  concentrations was developed by Kuner et al. In Clomeleon, a chloride sensitive variant of YFP called Topaz was linked with a relatively chloride insensitive CFP by using a 24 amino acid linker to form a ratiometric chloride indicator. In the present work, we have studied the fluorescence dynamics of Clomeleon in neurons of hippocampal cell cultures at three different stages of maturation (DIV 7, 11 and 15). In young hippocampal cells (DIV 7), we found a quenching of the YFP moiety of Clomeleon in majority of neurons, indicating the absence of energy transfer which might be due to the high intracellular  $\text{Cl}^-$  concentration present. Since the intracellular chloride concentration drops down dramatically with development from E18 to P14, a drastic change in the YFP/CFP ratio as well as kinetics was observed from DIV 7 to 15, with the cells from DIV 15 expressing the highest efficiency of energy transfer. This was observed as a change in the pre-exponential values from positive to negative corresponding to the lifetimes which participate in the transfer. The Clomeleon constructs with different linkers namely, 8aa, 16aa, 24aa between ECFP and Topaz were also measured and a difference in FRET efficiency was observed between the constructs corresponding to the distance between the fluorophores. A topographical analysis of the measured neurons revealed various lifetimes within different ROIs indicating a variability in FRET. This might be explained by the different  $\text{Cl}^-$  concentrations present in the different intracellular compartments of these cells. Thus, by a combination of FRET and FLIM and using ultrasensitive DL and QA detectors, we were capable of monitoring the differences in energy transfer at different developmental stages of hippocampal neurons as well as at different intra neuronal compartments, which could in fact give an idea of the different dynamic events taking place in the cells.



## Effects of *in vitro* ischemia on synaptic activity of subplate neurons in the neonatal rat cerebral cortex

Sebastian Heck, Ileana L. Hanganu, Heiko J. Luhmann

Institute of Physiology & Pathophysiology, Johannes Gutenberg-University, Mainz, Germany

The acute and long-term consequences of pathophysiological activity pattern on early cortical development are poorly understood. During cortical development, the correct formation of synaptic circuits requires the presence of a transiently expressed neuronal population [1], the subplate neurons (SPn), which are able to integrate and process information from cortical and subcortical sources. SPn show spontaneous synaptic activity mediated by AMPA, NMDA, and GABA<sub>A</sub> receptors [2]. They receive glutamatergic synaptic inputs from the thalamus and cortical plate, as well as GABAergic inputs from neighbouring SPn [3]. SPn seem to be actively involved in ischemia-induced disorders of cortical development, since transient ischemic episodes induce profound dysfunctions in SPn [4]. In order to address the question how SPn respond to ischemia, the effects of *in vitro* ischemia (hypoxia: 95% N<sub>2</sub>-5% CO<sub>2</sub> and aglycaemia) on spontaneous and stimulus-evoked synaptic activity were assessed by performing whole-cell patch-clamp recordings from SPn in somatosensory cortex of newborn rats. All SPn (n=23) responded to ischemia with an initial ischemic hyperpolarization (IH), generally accompanied by a decrease in the frequency of AMPA, NMDA and GABA<sub>A</sub> receptor-mediated spontaneous postsynaptic currents (sPSCs) (n=16). In addition, synaptic inputs from the thalamus, elicited by electrical stimulation of thalamocortical afferents, were significantly ( $p < 0.05$ ) reduced in amplitude from  $31.9 \pm 18.6$  pA to  $10.2 \pm 6.3$  pA, and the failure rate increased significantly ( $p < 0.05$ ) from 21% during control to 57% during IH (n=12). The synaptic inputs from other SPn, elicited by stimulation of the subplate, were also reduced during IH. The IH was followed by an ischemic depolarization (ID). All investigated SPn showed a highly significant ( $p < 0.01$ ) increase in the frequency of glutamatergic sPSCs (control:  $0.12 \pm 0.08$  Hz, ID:  $0.34 \pm 0.2$  Hz) due to the ischemia-induced increase in glutamate release. In the majority of the investigated SPn, the stimulus evoked synaptic inputs from thalamus and other SPn were almost abolished. These data indicate that ischemia-induced changes in synaptic activity during early development may influence the pathfinding of thalamocortical and corticofugal projections, thereby contributing to early neurological defects associated with ischemia.

- [1] Kostovic and Rakic, 1980
- [2] Hanganu et al., 2001
- [3] Hanganu et al., 2002
- [4] Albrecht et al., submitted

## Truncated TrkB receptor induced outgrowth of dendritic filopodia involves the p75 neurotrophin receptor

M. Hartmann<sup>1,2</sup>, T. Brigadski<sup>1</sup>, K.S. Erdmann<sup>2</sup>, B. Holtmann<sup>3</sup>, M. Sendtner<sup>3</sup>, F. Narz<sup>2</sup>, V. Lessmann<sup>1</sup>

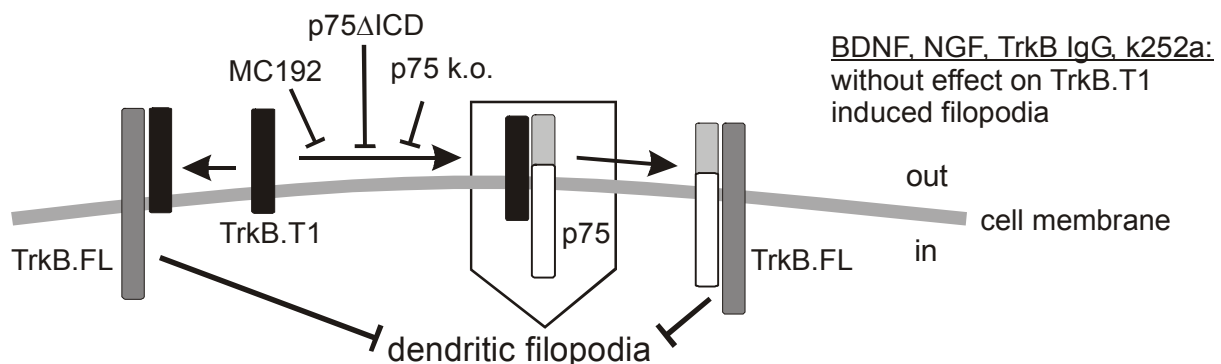
1) Inst. of Physiology, Johannes Gutenberg-University Mainz, Germany; 2) Biochemistry II, Ruhr-University Bochum; 3) Inst. Clin. Neurobiology, University Würzburg

The Trk family of mammalian receptor tyrosine kinases is known to mediate the effects of neurotrophins (NGF, BDNF, NT-3 and NT-4/5) on the survival, differentiation and several forms of synaptic plasticity in CNS neurons. In addition, all neurotrophins bind with equal specificity to the p75 neurotrophin receptor (p75<sup>NTR</sup>). Whereas Trks activate a tyrosine kinase signalling cascade, the p75<sup>NTR</sup> modulates Trk signalling and can even initiate cellular responses independent from Trk signaling. Thus, activation of p75<sup>NTR</sup> leads to the production of ceramide which mediates the growth of processes in hippocampal neurons (Brann et al., 1999). The rat TrkB receptor for BDNF and NT-4/5 (TrkB.FL) can also exist as alternatively spliced truncated receptor isoforms TrkB.T1 and TrkB.T2, which lack the intracellular kinase domain. Although the TrkB.T1 receptor is the dominant TrkB isoform in the adult rodent CNS, the physiological function of the truncated receptors are still not well established. Intriguingly, overexpression of TrkB.T1 in cortical neurons can initiate dendritic branching (Yacoubian and Lo, 2000). However, the underlying signaling mechanism of this effect remained elusive.

Here we investigate the role of truncated TrkB receptors (TrkB.T1, TrkB.T2) in the formation of dendritic filopodia, which are the known precursors of synaptic spines. GFP-tagged TrkB.T1 or TrkB.T2 were overexpressed in postnatal (P0-P2) rat hippocampal neurons at 8-9 DIV, and the number of filopodial dendritic protrusions (1-10  $\mu\text{m}$  in length) were analyzed 1-2 days after transfection. TrkB.T1 induced the formation of  $6.8 \pm 0.9$  filopodia per 40  $\mu\text{m}$  dendritic length compared to  $2.9 \pm 0.6$  in GFP expressing controls ( $p < 10^{-5}$ ). This effect was independent of neurotrophin binding and was also seen with a mutant TrkB.T1 that lacked the cytoplasmic tail. Coexpression of TrkB.FL had a dominant negative effect on TrkB.T1 induced filopodial growth. Incubation with a function blocking, monoclonal antibody against the p75<sup>NTR</sup> extracellular epitope (MC192, 8  $\mu\text{g/ml}$ ) indicated that the TrkB.T1 effect was mediated by the p75<sup>NTR</sup>. The TrkB.T1 induced growth of dendritic filopodia was significantly reduced in neurons derived from exon III p75<sup>NTR</sup> k.o. mice, and was inhibited by coexpression of a dominant negative p75<sup>NTR</sup> (p75 $\Delta\text{ICD}$ ) which lacks the cytoplasmic domain. Intriguingly, expression of this dominant negative p75 $\Delta\text{ICD}$  in hippocampal neurons also inhibited basal growth of dendritic filopodia, thus supporting the physiological significance of p75<sup>NTR</sup> signaling in the growth of dendritic filopodia.

These data add a new facet to the functions of NT receptor signaling, suggesting an activation of certain aspects of p75<sup>NTR</sup> signaling by interaction with non-liganded truncated TrkB receptors (see Fig.). This interaction could play a role in promoting synapse formation via dendritic filopodia.

*Supported by the DFG (SFB 509, 553, 452, 487)*



**References:** Brann et al. 1999, *J. Neurosci.*, **19**, 8199-8206.; Yacoubian and Lo 2000, *Nat. Neurosci.*, **3**, 342-349.

## Inhibitory role of GABA on epileptiform activity in hippocampal slices of the immature rat

W. Kilb<sup>1</sup>, P. Dierkes<sup>2</sup>, Y. Yanytska<sup>1</sup> and H.J. Luhmann<sup>1</sup>

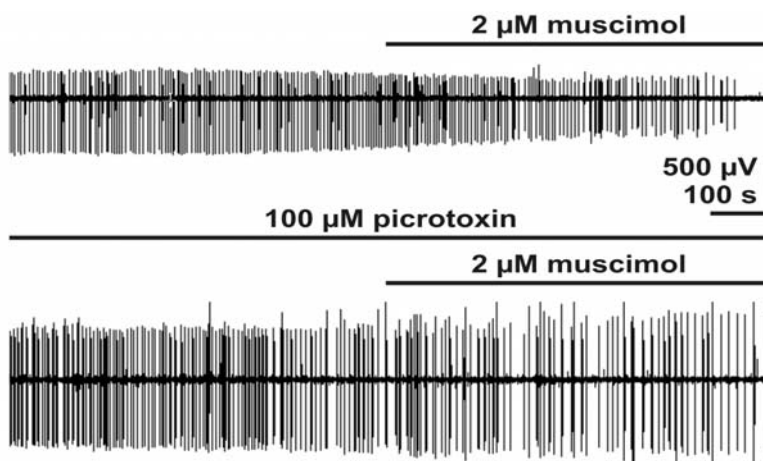
<sup>1</sup>*Institute of Physiol. and Pathophysiol., Johannes Gutenberg-University, Mainz, Germany*

<sup>2</sup>*Institute of Neurobiology, Heinrich Heine-University, Duesseldorf, Germany*

Activation of GABA<sub>A</sub> receptors elicits depolarizing membrane responses in immature neurons. However, it is controversial whether this membrane depolarization induces inhibitory or excitatory actions. To clarify the role of GABA<sub>A</sub> receptor-mediated depolarizing membrane responses in the modulation of epileptiform activity, we analyzed the effects of GABAergic agonists and antagonists on epileptiform activity in hippocampal slices of immature (P4-7) rats. For this purpose field potentials were recorded with tungsten electrodes (4-5 MΩ) in the stratum radiatum of the CA3 area.

In nominally Mg<sup>2+</sup>-free solution epileptiform activity was only very rarely observed. In Mg<sup>2+</sup>-free solution containing 10-100 μM 4-AP epileptiform activity with a late recurrent discharge (LRD) pattern was induced in 48 out of 54 slices. These LRDs were completely blocked by the GABA<sub>A</sub> agonist muscimol (2 μM). While application of the GABA<sub>A</sub> antagonist picrotoxin (100 μM) had only minor effects on the LRDs, the blocking effect of muscimol was nearly completely prevented in the presence of 100 μM picrotoxin. On the other hand, application of 100 μM picrotoxin to Mg<sup>2+</sup>-free solution without 4-AP induced epileptiform activity in 5 out of 9 slices. GABA (1 mM) had no effect on epileptiform activity (n=7), unless the GABA uptake blocker tiagabine was added to the extracellular solution. In the presence of 30 μM tiagabine epileptiform activity was attenuated by 1 mM GABA (n=8). Tiagabine itself had only small effects on epileptiform activity.

In summary, these results suggest that GABA<sub>A</sub> receptors have an inhibitory influence on epileptiform activity in immature hippocampal slices. However, since a block of GABA<sub>A</sub> receptors or GABA uptake mechanisms had only small effects on epileptiform activity, intrinsic GABA release may contribute only marginally to inhibition.



Field-potential recording in CA3 Str. radiatum of a P6 rat. Application of 2 μM muscimol blocked LRD activity completely (top trace). In the presence of 100 μM picrotoxin application of 2 μM muscimol had only a small effect on LRDs (bottom trace).

Supported by DFG grants Lu 375/4-1 and Ki 835/2-1



# Endogenous BDNF-mediated spontaneous $\text{Ca}^{2+}$ -signaling in developing hippocampal pyramidal cells



Susanne Lang, Tobias Bonhoeffer, and Christian Lohmann

MPI für Neurobiologie, Am Klopferspitz 18,  
82152 Martinsried-München, Germany

The neurotrophin brain-derived nerve growth factor (BDNF) plays an important role during neuronal development and it is involved in structural plasticity as well as in modifications of synaptic strength. It is thought that many of these effects are mediated by  $\text{Ca}^{2+}$  acting downstream of BDNF as an important signal transduction element. While it has been shown that the application of exogenous BDNF modulates the intracellular calcium concentration of neurons (Berninger et al. 1993, Neuroreport 4, p.1303; Canossa et al. 1994, PNAS 94, p.13279; Kovalchuk et al. 2002, Science 295, p.1729), the role of endogenous BDNF in spontaneous calcium signaling is not clear. Recently, it has been demonstrated that spontaneous calcium events are critical factors for neuronal plasticity and dendritic outgrowth (Lohmann et al. 2002, Nature 418, p. 177; Lohmann et al. in preparation). We were wondering how many of these calcium events were actually triggered by BDNF and therefore started to investigate the role of endogenous BDNF for spontaneous  $\text{Ca}^{2+}$ -signaling.

We used organotypic rat hippocampal slices (P0-2, DIV 3-4) and loaded single pyramidal cells with the  $\text{Ca}^{2+}$ -indicator Oregon Green BAPTA-1 by single cell electroporation. Images were acquired using a Zeiss Axioplan-2 microscope and a cooled CCD camera.

Calcium imaging of labeled neurons confirmed the existence of two types of spontaneous  $\text{Ca}^{2+}$ -events: global transients, which occurred in the soma, dendrites and axons as well as spatially restricted local  $\text{Ca}^{2+}$ -transients in dendrites. To test whether BDNF is involved in the generation of these  $\text{Ca}^{2+}$ -transients, we used function blocking antibodies against BDNF in the medium to scavenge endogenous BDNF. In the presence of these antibodies, we observed a reversible reduction of the frequency of local  $\text{Ca}^{2+}$ -signals compared to baseline level (-34%  $\pm$  6%,  $n=10$ ,  $p<0.05$ ). We also applied K252a, a reversible blocker of intracellular phosphorylation of the tyrosine residues of Trk receptors. We found a very similar reduction in the frequency of local  $\text{Ca}^{2+}$ -signals after bath application of K252a (-27%  $\pm$  9%,  $n=10$ ,  $p<0.05$ ). Together, this indicates that endogenous BDNF influences intracellular  $\text{Ca}^{2+}$ -signals via activation of TrkB receptors.

To show more directly whether BDNF can trigger local  $\text{Ca}^{2+}$ -transients in dendrites of pyramidal cells, we applied exogenous BDNF (200ng/ml) by pressure pulses through a micropipette. This spatially (10 $\mu\text{m}$ ) and temporally (40ms) restricted BDNF pulse evoked rapid and transient rises (duration of 1-2s) in local  $\text{Ca}^{2+}$ -concentration. These  $\text{Ca}^{2+}$ -rises could be elicited repetitively while application of control solution did not induce any change in the intracellular  $\text{Ca}^{2+}$ -concentration.

Taken together, these results indicate that endogenous BDNF may directly induce dendritic  $\text{Ca}^{2+}$ -transients. Currently, we are interested in the mechanisms underlying BDNF-mediated calcium signaling. In the future, we will start to investigate whether BDNF can regulate dendritic and synaptic plasticity via  $\text{Ca}^{2+}$ -signaling.

## Embryonic development of the sensory innervation of the antenna in the grasshopper *Schistocerca gregaria* : molecular expression domains and stepping stone pattern of pioneering confirm its appendicular nature

Michaela Güntner, George Boyan

Developmental Neurobiology Group, Department Biology II; Ludwig-Maximilians-Universität Munich, Grosshadernerstrasse 2, 82152 Martinsried-Planegg

The antenna is fundamentally involved in many insect behaviours and therefore possesses a large array of mechano-, thermo-, chemo- and hygroreceptors. These direct axons into the deutocerebrum of the brain, from which the antennal base also receives a motor innervation. Although the form of the antenna varies considerably according to the lifestyle of the insect, its basic organization remains sufficiently conserved for homeotic mutations to demonstrate clear equivalences with other appendages such as the leg.

The antenna of the grasshopper *Schistocerca gregaria* has proven to be a valuable model system for studying the development of a peripheral innervation. The grasshopper follows a hemimetabolous developmental pattern so that the innervation established during embryogenesis is maintained throughout subsequent postembryonic stages. Our interest focussed on the early embryonic development of the sensory nervous system of the grasshopper antenna, and we interpret our findings with respect to the appendicular nature of this structure.

The sensory nervous system of the antenna was originally proposed to be pioneered by two pairs of cells from the ventral and dorsal epithelial surfaces at the tip of the antenna<sup>1,2</sup>. These cells delaminate into the mesodermal lumen and direct growth cones along the epithelial border towards the antennal base<sup>3</sup>. Furthermore there is a so-called base pioneer cell which fasciculates with the ventral pioneers and then with the motor pioneers from the brain. Previous studies have all proposed that the pioneer cells from the tip pioneer the entire nervous system of the antenna. If so, then this pattern is at odds with that shown for putatively homologous appendages such as the legs and mouthparts where pioneers arise in each segment.

We re-analysed the pioneering of the antennal sensory system using a range of molecular markers. Early in embryogenesis (29%), expression of the glial homeobox gene *repo* is restricted to a pair of cells at the antennal base. This identical pattern is present concomitantly in each appendage of the insect. Subsequently *repo* expression is localized at the epithelial-mesodermal border midpoint along the antenna, and again at the tip. These expression domains we term A1, A2 and A3 are the sites of restricted expression of other molecular markers and the differentiation of pioneer neurons.

Bromodeoxyuridine incorporation reveals that these regions are the sites of intense cell differentiation. Using antibodies against horseradish peroxidase and the GPI-linked lipocalin Lazarillo, both of which are expressed by pioneer neurons throughout the nervous system, we showed that the A1, A2 and A3 domains are also the sites where pioneer cells differentiate. We identified a range of pioneer cells which differentiate at specific sites along the entire antennal epithelium. Their axons project towards the antenna base and fasciculate with one another to establish two parallel nerve tracts: a ventral tract and a dorsal tract. En route their filipodia contact guidepost cells which in some cases generate bipolar axon processes.

We conclude that the antenna is not pioneered by the pioneers at its tip, but in a stepwise manner by cells from several zones as might be expected from a segmented appendage. The pattern strongly resembles that previously described for other appendages such as mouthparts and legs<sup>2,4,5,6</sup> and supports the homologous appendage hypothesis.

### Literature cited

- 1 Bate (1976): Nature **260**, 54-56
- 2 Ho and Goodman (1982): Nature **297**, 404-406
- 3 Berlot and Goodman (1984): Science **223**, 493-496
- 4 Bentley and Keshishian (1982): Science **218**, 1082-1088
- 5 Meier and Reichert (1991): J Comp Neurol **305**, 201-214
- 6 Boyan et al. (2003): Arthropod Structure and Development **32**, 289-302

## THE SEQUENTIAL ACTIVITY OF THE GTPASES RAP1B AND CDC42 DETERMINES NEURONAL POLARITY

Jens C. Schwamborn and Andreas W. Püschel

Abteilung Molekularbiologie, Institut für Allgemeine Zoologie und Genetik, Westfälische Wilhelms-Universität Münster, Schloßplatz 5, D-48149 Münster, Germany.

The establishment of a polarized morphology is an essential step in the differentiation of neurons with a single axon and multiple dendrites. In hippocampal neurons, one of several initially indistinguishable neurites is selected to become the axon. Both PI(3,4,5)P<sub>3</sub> production and the evolutionarily conserved Par3/Par6/aPKC (Par) complex are required for axon specification. However, the initial signals that establish cellular asymmetry and the pathways that subsequently translate it into structural changes remain to be elucidated. To investigate the initial events that determine which neurite becomes the axon and restrict the Par complex to a single neurite, we investigated the role of the GTPases Rap1B and Cdc42 in the establishment of neuronal polarity. Here we show that localization of Rap1B to the tip of a single neurite place before the axon becomes morphologically distinguishable is the decisive step in determining which neurite becomes the axon. Subsequently Rap1B recruits Cdc42 to the growth cone of the axon. Rap1B and Cdc42 are necessary and sufficient to initiate the development of axons. Overexpression of active Rap1B or Cdc42 results in the development of multiple axons, while knock-down by RNA interference results in a complete loss of polarity. Rap1B acts downstream of PI3K and upstream of Cdc42 and the Par complex.



# Comparison of neurogenesis and neuronal *engrailed* expression in embryos of a parthenogenetic crayfish, the Marmorkrebs (marbled crayfish), and the grasshopper.

Kathia Vilpoux<sup>1</sup>, Steffen Harzsch<sup>1,2</sup>

<sup>1</sup> Abteilung Neurobiologie und <sup>2</sup> Sektion Biosystematische Dokumentation, Universität Ulm, D-89069 Ulm.  
kathia.vilpoux@biologie.uni-ulm.de, steffen.harzsch@biologie.uni-ulm.de

## The Marmorkrebs – a new model organism

The Marmorkrebs or marbled crayfish (Decapoda, Astacida, Cambaridae) is a yet unidentified crayfish of uncertain geographical origin that was introduced into the German aquarium trade in the mid-1990s (Scholtz et al. 2003. Nature 421:806). Under laboratory conditions, females repeatedly lay eggs in the absence of males and there is convincing evidence now that the marbled crayfish provides the first example for parthenogenesis within the decapod crustaceans (Vogt et al. 2004. J. Morphol. 261: 286-311). Due to its rapid reproduction, high fertility, and fast growth the marbled crayfish is an interesting organism for developmental studies. In order to perform ontogenetic studies, we established a staging scheme of the embryonic development by photographing embryos at two-day intervals and charting externally visible ontogenetic events. Furthermore, we stained dissected embryos with a nuclear dye to examine their morphology. In order to explore if certain aspects of nervous-system formation in this parthenogenetic species correspond to those examined in other decapod crustaceans we performed histochemical and immunohistochemical experiments to analyse the arrangement of the developing commissures and connectives, the location of serotonergic neurons, the proliferation of neuronal stem cells and the neuronal expression of *engrailed*. Our results show that these processes are similar in marbled crayfish embryos and those of other Decapoda so that this animal may be taken as a representative valid model organism for future developmental studies on Crustacea.

cells, the neuroblasts. These repeatedly undergo unequal divisions to produce ganglion mother cells, which later divide again to give birth to ganglion cells (neurons). Neuroblasts emerge in the early germ band and are singled out by cell-to-cell interactions within the neuroectoderm. Neuroblasts with similar proliferative characteristics are also present in malacostracan Crustacea. However, contrary to Hexapoda, malacostracan neuroblasts originate from ectotoblasts by an invariant lineage. The pivotal question whether crustacean and hexapodan neuroblasts represent a homologous class of neuronal stem cells has been discussed controversially (Harzsch 2003. Arthropod. Struct. Dev. 32:17). Duman-Scheel and Patel (1999; Development 126: 2327) have analysed the neuronal *engrailed* expression in various arthropods and have suggested similar patterns of *engrailed* positive neuroblasts to be present in grasshopper and crayfish ventral nerve cords. This claim has been strongly contradicted by Whittington (2004; In "Evolutionary Developmental Biology of Crustacea" Crustacean issues Vol.15. ed. G. Scholtz. A.A. Balkema, Lisse, Netherlands. pp.135ff) who suggested that the *engrailed* positive cells which Duman-Scheel and Patel (1999) reported to be neuroblasts are instead ectodermal cells. In order to determine whether similar patterns of neuronal development are present in Malacostracan crustaceans and Hexapoda, we have re-examined this issue by comparing neurogenesis in the grasshopper and marbled crayfish by *in vivo* incorporation of the mitosis marker bromodeoxyuridine (BrdU), by immunohistochemistry against the proliferating cell nuclear antigen (PCNA) and against *engrailed*.

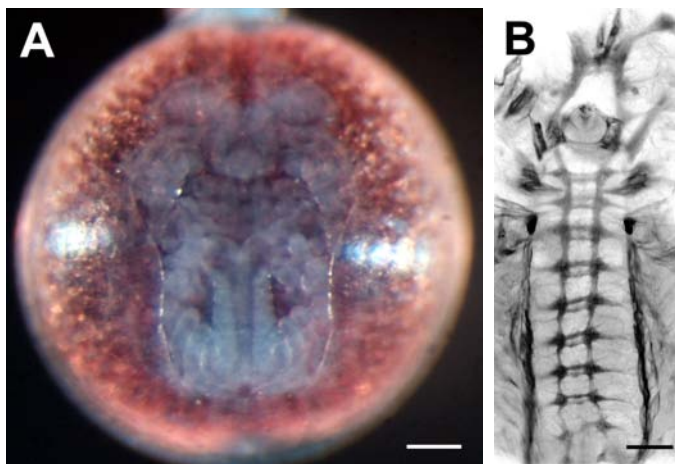


**Fig. 1.** Embryos of the Marmorkrebs (marbled crayfish) at 52% of embryonic development (E 52%). **A.** Scale bar 200 µm. **B.** Dissected embryo stained with Phalloidin denotes the developing ventral nerve cord. Scale bar 100 µm.

## Neurogenesis in Hexapoda and Crustacea

In Hexapoda, neuronal precursor cells (the ganglion mother cells) are generated by the mitotic activity of neuronal stem

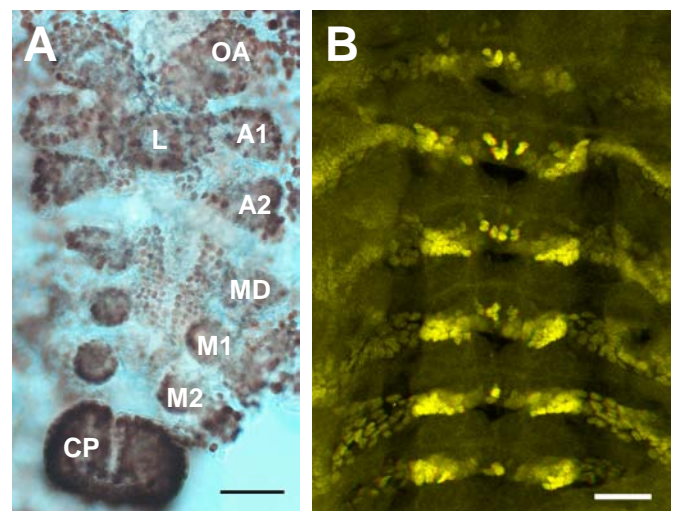


**Fig. 2. A.** BrdU labeling in a dissected embryo at E38% showing a high level of mitotic activity; A1, A2: antenna one and two, CP: caudal papilla, L: labrum, M1, M2: maxilla one and two, MD: mandible, OA: optic anlagen. Scale bar 60 µm. **B.** Anti-*engrailed* immunoreactivity in the embryonic ventral nerve cord at E52% showing segmentally repeated clusters of engrailed-positive cells. Scale bar 50 µm.

## **RAB GDI CONTROLS AXON GUIDANCE BY REGULATING ROBO LOCALIZATION**

Melanie Philipp and Esther T. Stoeckli

Institute of Zoology, University of Zurich, 8057 Zurich, Switzerland

Rab GDI (Rab GTPase guanine nucleotide dissociation inhibitor) is an important component of the intracellular trafficking and vesicle fusion machinery. So far, three isoforms have been characterized, but only one could be found in chicken. The Rab GDI knockout mouse shows a relatively mild impairment of spatial memory, whereas mutations in human Rab GDI have been associated with X-linked mental retardation. In the context of a screen for guidance cues for commissural axons we found Rab GDI to be upregulated in commissural axons of the chicken spinal cord, when they cross the midline and turn into the longitudinal axis. By Northern Blot analysis of different neuronal and non-neuronal tissues we found widespread expression of Rab GDI with highest levels in the central nervous system. Functional analysis of Rab GDI during development of the CNS using in ovo RNAi demonstrated the requirement for Rab GDI for commissural axons to cross the midline of the embryonic chicken spinal cord. In its absence, axons stalled and failed to reach the contralateral border of the floor plate. At least two different explanations could account for this observed phenotype. First, axons could simply be unable to extend any further due to the lack of protein and lipid delivery to their tip in the absence of vesicle fusion. Second, axons could lack the stimulus driving them across and out of the floor plate. This hypothesis is based on the observation of the midline crossing behavior of commissural axons in many different species. It predicts that the behavior of axons at the midline is determined by a balance between positive and negative signals arising from molecular interactions between the growth cone and the floor-plate surface. Initially, commissural axons are attracted toward the midline. Upon contact with the floor-plate commissural growth cones change the composition of their surface receptors. This in turn induces a shift in the balance between positive and negative signals resulting in the expulsion of axons from the floor plate. One of the candidate receptors for inducing the predicted shift in the balance could be Robo1. In cell culture experiments we could show that Rab GDI can indeed regulate the surface expression of Robo1 by modulating its membrane insertion.



**Poster Subject Area #PSA28:  
Regeneration and plasticity**

- [#379A](#) J. Mey, D. Morasutti, K. Schrage and P. McCaffery, Aachen and Waltham, MA (USA)  
*Upregulation of retinoic acid synthesis following acute spinal cord injury*
- [#380A](#) E. Kampmann, N. Rombach and J. Mey, Aachen  
*Effect of retinoic acid on BDNF-dependent axonal regeneration and neurotrophin receptor expression of retinal ganglion cells*
- [#381A](#) N. Zhelyaznik and J. Mey, Aachen  
*Expression of retinoic acid receptors and retinoid X receptors after sciatic nerve injury*
- [#382A](#) M. Höltje, A. Hoffmann, F. Hofmann, G. Große, I. Just and G. Ahnert-Hilger, Berlin, Göttingen and Hannover  
*Clostridium botulinum C3 proteins exert Rho-dependent and -independent effects on neuronal and astrocytic process outgrowth*
- [#383A](#) B. Picker, EMJ. Peters, R. Nitsch and S. Müller-Röver, Berlin  
*First steps towards a characterization of cutaneous reinnervation after skin nerve lesion (SNL) in mice*
- [#384A](#) S. Patz and P. Wahle, Bochum  
*Neurotrophins induce short-term changes and long-term potentiation of cortical neurotrophin expression*
- [#385A](#) C. Theiss, A. Schröder, K. Meller, K-P. Steuhl and D. Meller, Bochum and Essen  
*Promotion or inhibition: amniotic membrane displays a diversity of effects on axonal growth in neuronal cell cultures*
- [#386A](#) T. Sobik, A. Horvat-Bröcker, G. Zoidl, R. Dermietzel and A. Faissner, Bochum  
*Identification of Intracellular Interacting Partners of the Receptor Protein Tyrosine Phosphatase beta/zeta using a Bacterial two-hybrid System*
- [#387A](#) E. Weiler, A. Benali and UT. Eysel, Bochum  
*Loss and renewal of neurons within few hours? A potential pitfall of the neuronal marker NeuN*
- [#388A](#) R. van de Wal, J. Rustemeyer and U. Dicke, Bremen  
*Functional recovery and immunological response after allograft transplantation of rat sciatic nerve*
- [#389A](#) RM. Cooke, S. Bevan and D. Parker, Cambridge (UK)  
*Adaptive Plasticity after Disruption of the Lamprey Locomotor Network*

- [#390A](#) F. Bosse, K. Hasenpusch-Theil, U. Pippirs and HW. Müller, Düsseldorf  
*Gene Expression in distal fragments of adult rat sciatic nerves: do regeneration recapitulate postnatal development?*
- [#391A](#) N. Abumaria, R. Rygula, E. Rütther, U. Havemann-Reinecke and G. Flügge, Göttingen  
*Upregulation of transcripts for synaptic and synaptic vesicle proteins in the dorsal raphe nucleus of male Wistar rats after chronic social stress*
- [#392A](#) MB. Sättler, D. Merkler, K. Maier, C. Stadelmann, H. Ehrenreich, M. Bähr and R. Diem, Göttingen  
*Neuroprotective effects and intracellular signaling pathways of erythropoietin in a rat model of multiple sclerosis*
- [#393A](#) B. Czéh, C. Heckmann, J. Schindehütte, B. Schmelting, A. Mansouri, G. Flügge and E. Fuchs, Göttingen  
*Establishing a Parkinson Disease model in marmoset monkeys with unilateral 6-OHDA lesion of the nigrostriatal pathway*
- [#394A](#) SC. Tauber, C. Stadelmann, A. Spreer, R. Nau and J. Gerber, Göttingen  
*Increased Expression of BDNF and Proliferation of Dentate Granule Cells after Bacterial Meningitis*
- [#395A](#) J. Schlachetzki, G. Rohde, M. Bähr, A. Schneider and JH. Weishaupt, Göttingen and Heidelberg  
*G-CSF: neuroprotective effect and signal transduction in the optic nerve transection model*
- [#378B](#) A. Reisch and R-B. Illing, Freiburg  
*Electrical intracochlear stimulation induces c-Fos expression in specific neuronal populations of the cochlear nucleus*
- [#379B](#) D. Löttrich, C. Bernreuther, A. Papazoglou, A. Klein, M. Schachner and G. Nikkhah, Freiburg and Hamburg  
*L1 over-expressing mouse embryonic stem cells xenografted in a rat model of Parkinson's disease*
- [#380B](#) A. Papazoglou, C. Hackl and G. Nikkhah, Freiburg  
*Neonatal rat brain transplantation: a tool to study restoration and reinnervation of the striatum*
- [#381B](#) C. Hackl, A. Papazoglou, A. Klein and G. Nikkhah, Freiburg  
*Effects of double-grafting on the survival of embryonal (E14) mesencephalic dopaminergic neurons transplanted in a rat model of Parkinson's disease*
- [#382B](#) A. Klein, GA. Metz, J. Wessolleck, A. Papazoglou, M. Knieling, M. Timmer and G. Nikkhah, Freiburg, Lethbridge (CDN) and Jena  
*Remodelling of the damaged brain by fetal transplants? - Implications from studies in a rat model of Parkinson's disease*

- [#383B](#) J. Maciaczyk, D. Maciaczyk and G. Nikkhah, Freiburg  
*Transplantation of long-term expanded human fetal neural precursor cells – evidence of distant migration and multi-lineage differentiation*
- [#384B](#) MA. Meidinger and R-B. Illing, Freiburg  
*Ultrastructural analysis of plasticity in the cochlear nucleus of the rat induced through deafening*
- [#385B](#) Y. Avramovich-Tirosh, T. Amit and MBH. Youdim, Haifa (IL)  
*Molecular mechanisms of a novel iron chelator/ propargylamine bifunctional drug: neurorescue, differentiation and regulation of amyloid precursor protein/ amyloid –beta peptide processing.*
- [#386B](#) C. Haupt, O. Waitz, OW. Witte and C. Frahm, Jena  
*Connexin 43 mRNA and protein are upregulated in the vicinity of the photothrombotic lesion in rat brain*
- [#387B](#) S. Schmidt, A. Divanach, C. Bruehl and OW. Witte, Jena  
*Age-dependent alterations of functional inhibition in a rat model of cortical lesion*
- [#388B](#) J. Ruediger, A. Aschoff, RA. Hut, EA. Van der Zee and S. Daan, Jena and Groningen (NL)  
*Synaptic plasticity in the frontal cortex of the European ground squirrel (*Spermophilus citellus*) in the course of torpor-arousal cycles*
- [#389B](#) ME. Spira and G. Malkinson, Jersualem (IL)  
*Real-time imaging of Golgi derived vesicle exocytosis during the formation of growth cone lamellipodium after axotomy of cultured *Aplysia* neurons*
- [#390B](#) D. Kamber and ME. Spira, Jersualem (IL)  
*DISTRIBUTION AND ACTIVITY OF PROTEASOME IN REGENERATING NEURONS*
- [#391B](#) W. Luo, Y. Wang and G. Reiser, Magdeburg  
*Two types of protease-activated receptors (PAR-1 and PAR-2) mediate calcium signaling in rat retinal ganglion (RGC-5) cells*
- [#392B](#) VV. Loginov, VB. Dorokhov, GN. Fesenko and VM. Kovalzon, Moscow (RUS)  
*CEREBRAL ISCHEMIA AND PARADOXICAL SLEEP*
- [#393B](#) SJ-P. Haas, S. Beckmann, O. Schmitt, S. Petrov and A. Wree, Rostock  
*Transplantation of CSM14.1-cells in the neonatal dopaminergic deafferented striatum leads to a therapeutic improvement and dopaminergic reinnervation*
- [#394B](#) D. Fischer, V. Petkova, S. Thanos and L. Benowitz, Ulm, Boston (USA) and Münster  
*Switching mature retinal ganglion cells to a robust growth state in vivo: gene expression and synergy with RhoA inactivation*

## Upregulation of retinoic acid synthesis following acute spinal cord injury

Jörg Mey<sup>1</sup>, Dante Morasutti<sup>2</sup>, Kirsten Schrage<sup>1</sup> and Peter McCaffery<sup>2</sup>

1 Institut für Biologie II, RWTH Aachen, Kopernikusstr. 16, 52074 Aachen, Germany

2 UMMS/E.K. Shriver Center, 200 Trapelo Road, Waltham, MA 02452, USA

e-mail: mey@bio2.rwth-aachen.de

Retinoic acid (RA) promotes growth and differentiation in many developing tissues, and recent data indicate that peripheral nerve injury induces RA signaling [1], but little is known about its influence on regeneration in the CNS. In this study we investigated the possible involvement of RA in spinal cord injury (SCI). The New York University (NYU) impactor was used to cause mild or moderate spinal cord contusion injury. Changes in RA at the lesion site were determined by measuring the activity of the enzymes for its synthesis, the retinaldehyde dehydrogenases (RALDHs). A marked increase in enzyme activity occurred by day 4 and peaked at day 8-14 following the injuries. By day 21 the activity returned to baseline in the mildly injured animals while in the moderately injured animals RA activity at the site of the injury remained 2-3 times greater than the baseline level. A zymography bioassay determined that RALDH2 was the only detectable RALDH present in the control or injured spinal cord. The cellular localization of RALDH2 was identified by immunostaining at the time of peak enzyme activity in the injured spinal cord. In the non-injured spinal cord, RALDH2 was detected in RIP- and CNPase-positive oligodendroglia, corroborating previous experiments with oligodendrocyte cell culture experiments [2]. Expression was also intense in the arachnoid membrane surrounding the spinal cord. After spinal cord injury the increase in RALDH2 was independent of the RIP/CNPase-positive cells, which were severely depleted. Instead, RALDH2 was present in an NG-2 expressing cell type negative for markers of astrocytes (GFAP, vimentin), oligodendroglia (RIP, CNPase), microglia (OX42, ED-1), neurons (MAP-2), Schwann cells (p75) and immature lymphocytes (Thy1.1). We postulate that the RALDH2/NG-2 positive cells migrate into the injured sites from the adjacent arachnoid membrane, where the RALDH2 positive cells proliferate substantially following spinal cord injury. These findings indicate that close correlations exist between RA synthesis and spinal cord injury and that RA may play a role in the secondary events that follow acute SCI.

*Supported by NIH grant HD05515 to P.M. and the Deutsche Forschungsgemeinschaft, SFB542, Teilprojekt A6 to J.M.*

[1] Zhelyaznik et al., *Eur. J. Neurosci.* 18 (2003): 1033-1040. [2] Mey and Hammelmann, *Cell Tiss. Res.* 302 (2000): 49-58.

## Effect of retinoic acid on BDNF-dependent axonal regeneration and neurotrophin receptor expression of retinal ganglion cells

Eric Kampmann, Nanette Rombach and Jörg Mey

Institut für Biologie II, RWTH Aachen, Kopernikusstr. 16, 52074 Aachen, Germany  
e-mail: mey@bio2.rwth-aachen.de

Retinoic acid (RA) has been reported to support axonal regeneration of various populations of developing and differentiated neurons [1-3]. Since RA enhances the NGF-dependent survival of chick sympathetic ganglia neurons [4] and regulates trkA and trkC expression in mouse sympathetic neuroblasts [5], we are investigating the transcriptional regulation of neurotrophin receptors by RA as a possible mechanism of its neuritogenic activity. Using chick retinal explant cultures we measured the effect of RA on BDNF-dependent axonal outgrowth and on gene expression of the neurotrophin receptors trkA, trkB, trkC and p75.

To administer RA, stage E17 chick embryos were exposed *in ovo*, and 5 µl of 0.1 M all-*trans* RA (in DMSO) were dropped onto the chorio-allantoic membrane. Injections of 5 µl DMSO were used as controls. After a survival period of 24 hrs the retinas were prepared, explanted on poly-lysine/laminin-coated petridishes and cultivated at 37 °C in DMEM/10% FCS containing 20 ng/ml BDNF for another 24 hrs, when the extent of axonal regeneration was examined under an inverted microscope. Alternatively, we isolated the total RNA, reverse transcribed mRNA to cDNA and quantified the expression of neurotrophin receptors by RT-PCR using the Light Cycler system (SYBR-green format™). The mRNA levels of target genes were analyzed in relation to the expression of GAPDH, used as a control gene.

At the time shortly before hatching, when the chick retina is fully differentiated, we found that RA enhanced the BDNF-dependent regeneration of retinal ganglion cells. The dose-dependent and highly significant effect (U-Test,  $p < 0,001$ ) was observed after application of RA *in ovo* and subsequent use of the neurotrophin. Treatment with RA alone or as a supplement to the medium produced no increase in fiber numbers. Quantitative RT-PCR revealed gene expression of neurotrophin receptors trkA, trkB, trkC and p75 in the E18 chick retina. Of these receptors, the trkA and p75 genes were not regulated by RA. Quantification analyses of trkB and trkC are in progress.

*Supported by the Deutsche Forschungsgemeinschaft, SFB 542/Teilprojekt A6.*

[1] Corcoran and Maden. *Nat. Neurosci.* 2 (1999): 307-308. [2] Mey and Rombach. *Neuroreport* 10 (1999): 3573-3577. [3] Corcoran et al., *J. Cell Sci.* 115 (2002): 3779-8786. [4] v.Holst et al. *Mol. Cell. Neurosci.* 6 (1995):185-198. [5] Wyatt et al. *J. Neurosci.* 19 (1999):1062-1071.

## **Expression of retinoic acid receptors and retinoid X receptors after sciatic nerve injury.**

**Nina Zhelyaznik and Jörg Mey**

Institut für Biologie II, RWTH Aachen, Kopernikusstr. 16, 52074 Aachen, Germany  
*e-mail: nina@bio2.rwth-aachen.de*

It was recently discovered that the retinoic acid (RA) signaling system is activated after peripheral nerve injury. All necessary components of RA signaling pathway are detectable in rat sciatic nerves, and the expression and protein levels of cellular retinoid binding proteins CRBP-I and CRABP-II are strongly upregulated by the lesion [1]. Since the effect of RA is mediated via retinoic acid receptors (RAR) and retinoid X receptors (RXR), which act as ligand-activated transcription factors, the levels of these were measured in the present study with RT-PCR and immunoblotting. Seven days after sciatic nerve crush, elevated levels of gene expression of RAR $\alpha$ , RAR $\beta$  and RXR $\alpha$  were detected (ANOVA,  $p < 0.05$ ). These results were corroborated on the protein level ( $p < 0.05$ ).

Thus, indicating a possible influence of sciatic nerve injury on the expression of RARs/RXRs in the peripheral nervous system, our results confirm the suggested biological function of retinoic acid signaling after peripheral nerve injury. Since the RAR $\beta$  gene contains RA-responsive elements, the upregulation of RARs may constitute a positive feedback mechanism.

*Supported by the Deutsche Forschungsgemeinschaft, SFB542, Teilprojekt A6.*

[1] Zhelyaznik et al, *Eur. J. Neurosci.*, 18 (2003): 1033-40

## ***Clostridium botulinum* C3 proteins exert Rho-dependent and -independent effects on neuronal and astrocytic process outgrowth**

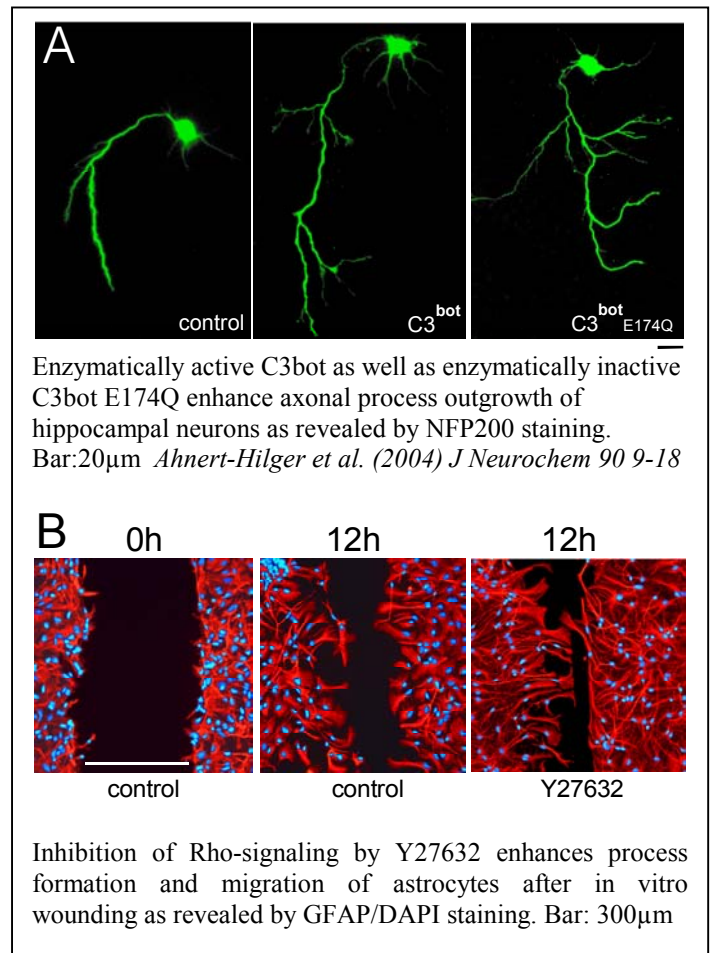
M. Hölte<sup>1</sup>, A. Hoffmann<sup>2</sup>, F. Hofmann<sup>3</sup>, G. Grosse<sup>1</sup>, I. Just<sup>3</sup> and G. Ahnert-Hilger<sup>1</sup>

<sup>1</sup> Centrum für Anatomie, AG Funktionelle Zellbiologie, Charité-Hochschulmedizin Berlin, Germany

<sup>2</sup> Institut für Neuropathologie, Universitätsklinikum, Göttingen, Germany

<sup>3</sup> Institut für Toxikologie der Medizinischen Hochschule Hannover, Germany

Small GTPases of the Rho family are key regulators of the cytoskeleton in virtually all eukaryotic cells, including neurons and astrocytes. Accordingly, Rho function mediates morphological changes as well as locomotory activity. C3 proteins are well established tools to study Rho effects. Apart from its enzymatic activity, C3 derived from *Clostridium botulinum* (C3bot) is considered to selectively promote axonal outgrowth. By generating peptide fragments derived from C3bot we aimed to identify the C3bot domain responsible for the observed neurotrophic effect. Since neuronal regeneration depends on a balanced activity of neurons and glial cells the effects of C3 protein on glial cells like astrocytes have to be carefully considered. By using astrocyte cultures established from neonatal mice we investigated the role of Rho in process formation during astrocyte stellation. Additionally, we examined the impact of Rho on astrocytic wound healing in a scratch-wound model. Impairment of Rho signaling with low nanomolar concentrations of C3 proteins added to serum-free medium significantly promoted glial process outgrowth that was accompanied with an increased process branching. Wound healing was accelerated in scratch-wounded astrocyte cultures incubated with C3bot. By inhibiting the Rho downstream-effector ROCK with the selective inhibitor Y27632 we were able to demonstrate that the accelerated wound closure was both due to an enhanced polarized process formation and an increased migratory activity of astrocytes into the site of lesion. Taken together, these results suggest that C3 proteins utilize both Rho-dependent and -independent pathways. Furthermore, they reveal that Rho is differentially involved in the regulation of neuronal and astrocytic process growth. Whereas axonal growth may benefit from Rho-activity, inactivation of Rho by nanomolar concentrations of C3bot rather promotes astrocytic migratory responses and process formation.



**First steps towards a characterization of cutaneous reinnervation after skin nerve lesion (SNL) in mice**

Björn Picker<sup>1</sup>, Eva M. J. Peters<sup>2</sup>, Robert Nitsch<sup>1</sup>, Sven Müller-Röver<sup>1</sup>

<sup>1</sup>Center for Anatomy, Institute of Cell Biology and Neurobiology, Charité University Hospital, Berlin, Germany

<sup>2</sup>Dept. of Dermatology and Allergy, Charité University Hospital, Berlin, Germany

In order to investigate the influence of T cells and mast cells on peripheral neuroregeneration and reinnervation, we have established and analysed a novel skin nerve lesion (SNL) model. We used female B10.PL mice in the telogen stage of the hair cycle (6–9 weeks old) to study the effect of unilateral surgical denervation of dorsal cutaneous nerves (DCNs) in the T3–T12 dermatomes. A 3-cm midline incision was made in the dorsal skin under anaesthesia. The DCNs were exposed under a dissection microscope and DCNs T3–12 on the right side were removed from near their exit point from the back muscles to their entry into the skin. The skin was closed with 9-mm steel wound clips and the completeness of denervation was verified by testing the appropriate skin region for pinch sensitivity. We analysed the immunoreactivity patterns of PGP9.5 (pan-neuronal marker), CD3 (T cell marker) and CD8 (cytotoxic T cell marker). At days 7 and 14 after lesion, immunoreactivity for PGP9.5 was fully absent from the epidermis. Single fibers in the epidermis were found at day 21 after lesion, indicating the start of reinnervation. At day 56 after lesion, the mean epidermal fiber density increased to 30 fibers/microscopic field. Interestingly, the contralateral, non-denervated side also displayed a decreasing fiber density between days 7 and 14 after lesion. No substantial changes in mast cell numbers were detected. Increased numbers of CD3+ and CD8+ T cells were present in the denervated area at days 7 and 14 after lesion.

The skin nerve lesion model offers an attractive tool for analysing the spatio-temporal distribution patterns of nerve fibers and immune cells during reinnervation of murine back skin.

\*corresponding author: sven.mueller-roever@charite.de

*Supported by a grant from the Deutsche Forschungsgemeinschaft to RN (SFB507 B11).*



## **Neurotrophins induce short-term changes and long-term potentiation of cortical neurotrophin expression**

**Silke Patz and Petra Wahle**

AG Entwicklungsneurobiologie, Fakultät für Biologie, ND 6/72, Ruhr-Universität,  
44780 Bochum, Germany

### **Abstract**

Exogenous neurotrophins promote structural, neurochemical, and physiological differentiation of neurons in vitro and in vivo. Yet, it is completely unknown whether and how the endogenous neurotrophin expression responds to exogenous neurotrophins. Here we investigate the mRNA expression level of BDNF, NT-4, NT-3 and NGF as well as the trkB and trkC receptor in response to BDNF, NT-4, NT-3 and NGF pulses in organotypic cultures of postnatal rat visual cortex. A single neurotrophin pulse already evoked a dramatic up- or downregulation of specific neurotrophin mRNAs within 3-24 hr indicating an immediate impact on the neurotrophin transcription. Most strikingly, neurotrophin pulses during the first 10 DIV potentiated the expression of specific neurotrophin mRNAs at 20 DIV suggesting that early trophic factor experience influences the expression levels seen later in development.

The NT-3 mRNA expression, for example, was highly dynamic. In all experimental conditions NGF and BDNF consistently promoted the NT-3 mRNA expression suggesting that these two factors help to maintain the low level of NT-3 found in adult cortex. Rapid bidirectional changes characterized the NT-4 mRNA expression and as a consistent action, NT-4 enhances its own expression. Already a single NT-4 pulse transiently increases, whereas BDNF transiently reduces NT-4 transcription which then normalizes within 24 h. Surprisingly, NGF strongly potentiated BDNF and in particular NT-4. In contrast, TrkB mRNA represented a perfect internal control, since it remained constant at ages or time points where some of the other mRNAs amplified in the very same cDNA libraries revealed dramatic increases or decreases. Our study suggests the existence of a regulatory neurotrophin network controlling the expression of other neurotrophins with an unexpected complexity.

Supported by DFG SFB 509 „Neurovision“ and DFG GRK 736.

## Promotion or inhibition: amniotic membrane displays a diversity of effects on axonal growth in neuronal cell cultures.

Carsten Theiss<sup>1</sup>, Alice Schröder<sup>1</sup>, Karl Meller<sup>1</sup>, Klaus-Peter Steuhl<sup>2</sup>, Daniel Meller<sup>2</sup>

<sup>1</sup>Institute of Anatomy, Department of Cytology, Ruhr-University Bochum, Bochum

<sup>2</sup>Dept. of Ophthalmology, University Hospital Essen, Essen

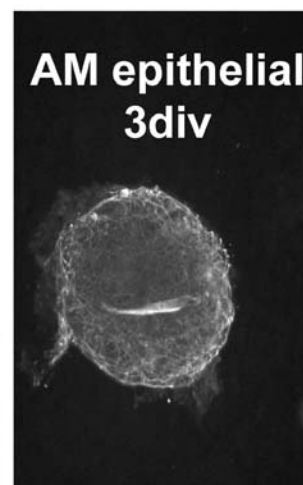
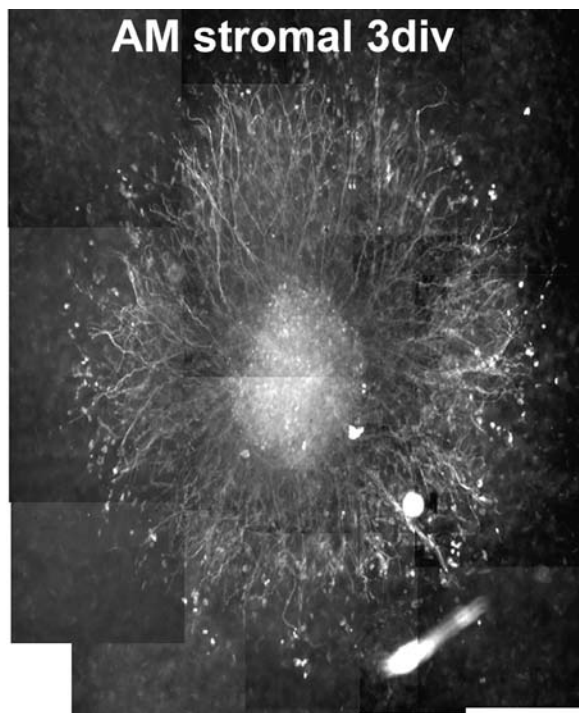
e-mail: carsten.theiss@ruhr-uni-bochum.de

Transplantation of amniotic membrane (AMT) has been successfully applied to promote corneal wound healing in neurotrophic ulcers with different aetiologies. In this line, healing of corneal surface after AMT correlated clinically with a partial recovery of corneal sensitivity. Moreover, AMT compared to conventional treatment strategies accelerated axonal sprouting in an experimental animal model of keratitis induced by Herpes virus. In this study, we investigated potentially underlying neurotrophic action mechanisms of AM.

Organ-typical cell cultures of dorsal root ganglion (DRG) neurons were gained from 10-day-old chick embryos and cultured with MEM on the stromal or epithelial side of intact amniotic membrane (AM) for 3 to 5 days. In an additional group AM was pretreated with Dispase for 15 min at 37°C in order to remove the amniotic epithelium. Afterwards, DRG neurons were cultured in the same manner on the exposed basement membrane side of AM. Sprouting of neuronal axons was screened with monoclonal antibodies against cytoskeletal proteins such as neurofilament (NF-M) and tubulin (Tub). Finally, the specimens were morphometrically analyzed.

DRG neurons cultured on the stromal or basement membrane side of AM exhibit within few days the formation of numerous NF-M and Tub-positive axonal neurites. These typically run a radial fashion and are arranged partially in nerve bundles. However, axonal sprouting of DRG neurons is drastically inhibited when cultured directly on the amniotic epithelium of AM.

In vitro the basement membrane and the stromal side of AM extensively promote the outgrowth of axonal neurites. However, a substantial inhibition of axonal sprouting is induced by the amniotic epithelium. If soluble, neurotrophic growth factors and/or adhesion-molecules mediated mechanisms are enrolled in these events and thereby potentially promote wound healing in neurotrophic keratopathy, will be analyzed in further studies.



## Identification of Intracellular Interacting Partners of the Receptor Protein Tyrosine Phosphatase beta/zeta using a Bacterial two-hybrid System

Thomas Sobik<sup>§</sup>, Andrea Horvat-Bröcker<sup>§</sup>, Georg Zoidl\*, Rolf Dermietzel\*, Andreas Faissner<sup>§</sup>

<sup>§</sup>*Department of Cell Morphology and Molecular Neurobiology, Ruhr University Bochum, 44780 Bochum, Germany*

<sup>\*</sup>*Department of Neuroanatomy and Molecular Brain Research, Ruhr University Bochum, 44780 Bochum, Germany*

*Correspondence: andreas.faissner@ruhr-uni-bochum.de*

Receptor protein tyrosine phosphatase (RPTP) beta/zeta is a distinct member of the group of transmembrane tyrosine phosphatases. RPTP beta/zeta is mainly expressed in the central nervous system and involved in cell-cell and cell-matrix interactions. Structurally, RPTP beta/zeta is characterized by the presence of an aminoterminal carbonic-anhydrase-like (CAH) and a fibronectin type III (FNIII) domain in the extracellular part (1). Four isoforms of RPTP beta/zeta are known, two of which are secreted into the extracellular matrix whereas the other two represent transmembrane receptors (2). Although several ligands of RPTP beta/zeta have been identified, e.g. Tenascin-C, Pleiotrophin and F3/contactin, little is known about the intracellular signal transduction pathways regulated by this tyrosine phosphatase (3, 4, 5).

In order to investigate potential intracellular interacting partners, a two-hybrid screen using the complete cytoplasmatic part of RPTP beta/zeta was carried out. A **bacterial two-hybrid system** (BacterioMatchII™, Stratagene®) was chosen for this approach and the intracellular segment of RPTP beta/zeta was cloned into the pBT-Plasmid as a bait. The screen was performed with a rat brain cDNA library which contained 3.05 x 10<sup>6</sup> target plasmids (40 pooled brains, 7-10 weeks old), according to the manufacturers description.

In the course of the first screens, 96 clones were selected and sequenced. According to preliminary database search we identified intracellular ligand candidates which pertain to several protein families, including cytoskeletal and scaffolding components, and proteins that are involved in signal transduction pathways or vesicular traffic. In future experiments, the interactions will be investigated further with immunohistochemical and biochemical methods (Supported by DFG, SFB 509).

1. Levy JB, Canoll PD, Silvennoinen O, Barnea G, Morse B, Honegger AM, Huang JT, Cannizzaro LA, Park SH, Druck T, et al. (1993) The cloning of a receptor-type protein tyrosine phosphatase expressed in the central nervous system. *J Biol Chem* 268:10573-10581
2. Garwood J, Heck N, Reichardt F, Faissner A. (2003) Phosphacan short isoform, a novel non-proteoglycan variant of phosphacan/receptor protein tyrosine phosphatase-beta, interacts with neuronal receptors and promotes neurite outgrowth. *J Biol Chem* 278:24164-24173
3. Barnea G, Grumet M, Milev P, Silvennoinen O, Levy JB, Sap J, Schlessinger J. (1994) Receptor tyrosine phosphatase beta is expressed in the form of proteoglycan and binds to the extracellular matrix protein tenascin. *J Biol Chem* 269:14349-14352
4. Maeda N, Nishiwaki T, Shintani T, Hamanaka H, Noda M. (1996) 6B4 proteoglycan/phosphacan, an extracellular variant of receptor-like protein-tyrosine phosphatase zeta/RPTPbeta, binds pleiotrophin/heparin-binding growth-associated molecule (HB-GAM). *J Biol Chem* 271:21446-21452
5. Peles E, Nativ M, Campbell PL, Sakurai T, Martinez R, Lev S, Clary DO, Schilling J, Barnea G, Plowman GD, et al. (1995) The carbonic anhydrase domain of receptor tyrosine phosphatase beta is a functional ligand for the axonal cell recognition molecule contactin. *Cell* 82: 251-260

**“Loss and renewal” of neurons within few hours?  
A potential pitfall of the neuronal marker NeuN**

Elke Weiler, Alia Benali and Ulf T. Eysel

Dept. Neurophysiology, Ruhr-University Bochum, Universitätsstr. 150, 44801  
Bochum, Germany. email: weiler@neurop.rub.de

Neurons are commonly identified by neuronal markers such as NeuN, a neuronal specific nuclear protein. Dependent on the immunoreactivity, a cell will be considered to be a neuron or not. Loss of neurons, especially following lesions, are thus revealed by the reduction in the number of NeuN positive cells. Reversely, an increase in the number of NeuN positive cells is interpreted as neurogenesis.

We report here that a decrease and increase in the number of NeuN positive cells can occur within few hours when cells were activated by electrical stimulation, a temporal pattern impossibly due to the processes of cell death and induced cell proliferation. Using immunohistochemical and cell counting techniques, we demonstrate that the number of NeuN positive cells decreased by 13% in the cortex of rats following activation of the neurons by intracortical electrical stimulation. This “loss” of neurons could not be confirmed by either TUNEL staining, which did not reveal any apoptotic cell death nor by Nissl-staining, which showed no reduction in the total number of cells. Already five hours post-stimulation, the number of NeuN positive cells increased again to nearly pre-stimulatory values. This time course cannot be due to proliferation and differentiation of neurons. The proliferation markers, Ki-67 and MIB1, did not confirm birth of new neurons during this time.

The activation of the neurons induces expression of activity markers, such as cFOS. However, the staining for cFOS at the stimulation site revealed a metabolic exhaustion of the neurons. Optical density measures of the intensity of the RNA showed a decrease in the values indicating and supporting the idea of a metabolic exhaustion following increased activation of the neurons. Thus, the neuronal marker NeuN might either be not expressed or more likely the expressed protein might be changed due to the cellular pH and other metabolic changes during exhaustion (metabolic stress) and therefore temporarily not be detected by the antibody.

In conclusion, the loss of NeuN immunoreactivity does not necessarily imply loss of neurons. More than one neuronal marker should therefore be used to identify neurons and investigate neuronal cell death and neurogenesis. The neuronal marker NeuN might be used as an indicator for the physiological state of a neuron.

Supported by the DFG, SFB 509 C4.

## Functional recovery and immunological response after allograft transplantation of rat sciatic nerve

Remske van de Wal, Jan Rustemeyer\*, Ursula Dicke

Brain Research Institute, University of Bremen, 28834 Bremen

\*Klinik für Mund-, Kiefer- und Gesichtschirurgie, Zentralkrankenhaus St.Jürgen Str., 28205 Bremen

**Purpose:** The aim of the present study was to investigate the structural and immunological responses during nerve regeneration and to correlate them with walking track analysis over a longer period of regeneration (20 weeks).

**Methods:** DA and Lew rats (n=8 for each strain) were grafted a 1 cm segment of the sciatic nerve, and were treated with FK 506 during regeneration. The functional recovery was assessed bi-weekly over 20 weeks postoperative. The sciatic functional index (SFI) and the ankle stance angle (ASA) was analyzed in the midstance phase of locomotion. Immunohistochemistry was performed on transverse sections of transplanted and control nerves 10 days, 5, 9, 13 and 20 weeks after allograft transplantation. Antibodies against basic myelin protein (Anti-BMP), activated macrophages (Anti-ED1), and endothelial cells (Anti-Reca1) were used; the degree of myelination, and the number of macrophages and blood vessels was determined.

**Results:** The functional recovery of SFI and ASA (Fig.1; averaged data of 7 animals), develops in a decrease of values after 10 weeks, and data then gradually approximate that of the control side. Myelination and number of endothelial cells of the transplanted nerve (Fig. 2; averaged data of 4 animals) increase steadily until five weeks, remain at that level for some weeks, and highest values are obtained after 20 weeks. The number of activated macrophages peaked at five weeks postop.; a small number was still present after 20 weeks.

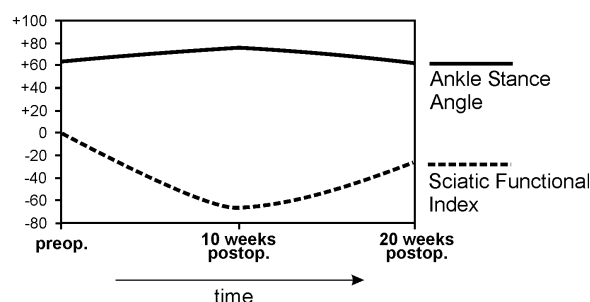


Fig.1 Sciatic functional index (SFI): 0% = normal function (control side); -100% = total degeneration. Ankle stance angle (ASA): +100% = Control side.

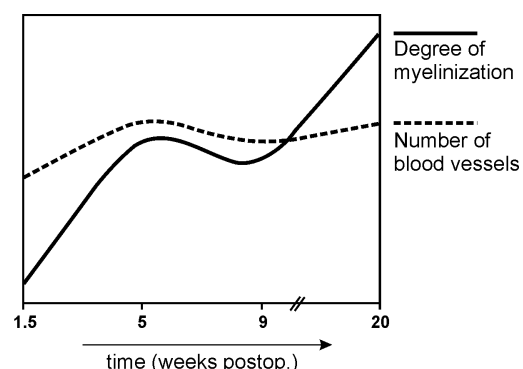


Fig.2 Myelination and number of endothelial cells of transplanted nerves over regeneration time.

**Conclusion:** Preliminary results suggest that the functional recovery indicated by SFI and ASA parallels an increase in myelination and neovascularization of the transplanted sciatic nerve in rats. The immunological responses over time were comparable to those after regeneration following nerve crush as reported in other studies, and suggest that the pro-regenerative effects of FK 506 does not exclusively depend on the type of injury.

Supported by Fujisawa GmbH München

## **Adaptive Plasticity after Disruption of the Lamprey Locomotor Network**

Ria Mishaal Cooke\*, Sarah Bevan, David Parker

Department of Zoology, University of Cambridge, Downing Street, Cambridge, CB2 3EJ

\*Corresponding author. *Email address:* rmc41@cam.ac.uk (Ria Mishaal Cooke)

Neural networks in the spinal cord generate basic locomotor outputs. These networks are activated and modulated by descending inputs from the brain. Spinal cord injury disrupts these descending inputs, resulting in paralysis. Locomotor networks are preserved below lesion sites, but the absence of the descending drive prevents their activation.

The lamprey is a lower vertebrate model system for studying locomotor network function. In addition, it has been used as a model system to examine the effects of spinal lesions. The lamprey recovers locomotor function after being paralysed by complete spinal lesions that remove the descending inputs from the brain. This is of obvious general importance. As in mammalian systems, the analysis of functional recovery in the lamprey has focused on the regrowth of ascending and descending axons across lesion sites. However, there is evidence that regrowth alone cannot account for functional recovery in the lamprey. Regrowth lags behind functional recovery. Where regrowth occurs, it is limited in its extent, recovery can occur without any regeneration, and even where regeneration occurs locomotor activity can still be dysfunctional.

A complementary approach to regeneration after spinal injury is to utilise the plasticity of spinal networks to alter network properties, and thus try to optimise network function below lesion sites. This plasticity could be evoked extrinsically as a result of neuromodulator or activity-dependent effects on network cellular or synaptic properties. Alternatively, plasticity could be evoked through intrinsic changes in network properties (i.e. adaptive or homeostatic plasticity that attempts to compensate for the injury-induced changes in network properties to restore function to within the normal operating range). Thus, while it is important to understand which inputs regenerate and which are sufficient and necessary for restoring the descending drive to spinal central pattern generators, it is also essential to understand the mechanisms operating caudal to the lesion site.

As an initial stage in the analysis of homeostatic plasticity, the role of adaptive plastic changes has been examined by disrupting network function. Larval, transformer, and adult spinal cords were incubated in tetrodotoxin (TTX) for 20 hours to abolish all action potential-evoked synaptic transmission in the network, and thus significantly disrupt network function. Several electrophysiological parameters were examined to identify potential changes in presynaptic and postsynaptic properties, including the resting membrane potential, input resistance, and the amplitude and frequency of spontaneous miniature EPSPs and IPSPs. In addition, transmission electron microscopy was used to measure TTX-induced changes in synaptic ultrastructure.

The results suggest that disrupting network activity can evoke adaptive plasticity. This indicates that spinal networks can be altered in response to extreme functional changes, and provides a basis for examining the presence of adaptive changes in animals that have recovered locomotor function after complete spinal lesions.

Supported by a studentship from the UK Medical Research Council and the Royal Society.

**Gene Expression in distal fragments of adult rat sciatic nerves: do  
regeneration recapitulate postnatal development?**

Frank Bosse\*, Kerstin Hasenpusch-Theil, Ulrich Pippirs and Hans Werner Müller

Molecular Neurobiology Laboratory, Department of Neurology, Heinrich-Heine-  
University Düsseldorf, Germany

One of the most striking features of the mature peripheral nervous system (PNS) is the ability to survive and to regenerate following axonal injury. The lesioned PNS undergoes a stereotypical reaction to injury characterized by Wallerian degeneration in the distal portion of the nerve and a sprouting process at the proximal site. At the molecular level, there is an evidence for a coordinated neural gene program involved in the repair process. Previous research has identified a few components of this molecular genetic switch from a mature transmitting mode to a regeneration-specific growth mode. These distinct alterations in gene expression within the lesioned distal nerve stump were hypothesized to be a recapitulation of developmental processes.

Differential gene expression in the rat after sciatic nerve crush and during postnatal sciatic nerve development was analyzed using membrane-based cDNA arrays. The analyses were carried out to study the genetic basis of peripheral nerve regeneration and to compare gene regulation of (i) the regenerating distal nerve stump (5-8h – 28d) and (ii) the developing sciatic nerve (P0 – P90).

When comparing the unlesioned control nerve to injured nerves 192 out of 2361 genes (~8%) exhibited significant regulation from baseline. Most of these genes show biphasic expression profiles suggesting initial de-differentiation followed by re-differentiation. During postnatal development (P0 – P90) 233 regulated genes (~10%) could be identified. Interestingly, the genes showing significant differential regulation during regeneration or development represented all aspects of cellular processes. Furthermore, 93 genes (48% of the regeneration associated genes (RAGs)) were significantly regulated in both study groups, obviously suggesting that regeneration in part recapitulates development. However, further analysis revealed contradictory data. Significant differences in identified genes of e.g. signal transduction processes and/or the transcription regulation make evident that in the adult sciatic nerve regeneration-specific reactions exist. These reactions may reflect adult gene regulation rather than developmentally controlled expression and are partly imposed by the different environment of adult vs. developing axons of the peripheral nerve.

**Upregulation of transcripts for synaptic and synaptic vesicle proteins  
in the dorsal raphe nucleus of male Wistar rats  
after chronic social stress**

Abumaria N.<sup>1</sup>, Rygula R.<sup>2</sup>, Rütther E.<sup>2</sup>, Havemann-Reinecke U.<sup>2</sup>, Flügge G.<sup>1</sup>

*1 Clinical Neurobiology Laboratory, German Primate Center, 37077 Göttingen*

*2 Department of Psychiatry and Psychotherapy, Medical School, University of Göttingen, 37075 Göttingen*

Stress effects on the brain are of particular interest because stress may lead to central nervous disorders such as depression. Candidate genes that may contribute to stress-mediated neuropathologies can be identified through the analysis of differentially expressed genes. Therefore we analysed effects of chronic social stress on gene expression in the dorsal raphe nucleus of rats. Animals were stressed using a resident-intruder-paradigm (see Koolhaas *et al.*, 1997). Male Wistar rats were subjected to daily social defeat by a dominant male for 5 weeks. Two subtractive cDNA libraries (approx. 500 clones) were generated from the dorsal raphe nucleus and we identified sequences representing approx. 50 genes whose expression differs between stress and control animals. Real time PCR data confirmed the upregulation of two genes, a synaptic protein and a synaptic-vesicle protein. Investigations are in progress to confirm up and/or downregulation of the other candidate genes identified by subtractive cDNA hybridization. Behavioural studies are performed in parallel. Our findings suggest that a new pattern of gene expression potentially related to synaptic plasticity is induced in the dorsal raphe nucleus by chronic social stress.

Funded by Deutsche Forschungsgemeinschaft through the DFG-Research Center for Molecular Physiology of the Brain (CMPB).

Abumaria N. is a Christophorus-Lichtenberg stipend fellow.

Reference:

Koolhaas JM, De Boer SF, De Rutter AJ, Meerlo P, Sgoifo A (1997) *Social stress in rats and mice. Acta Physiol Scand Suppl.* 640: 69-72.



**Neuroprotective effects and intracellular signaling pathways  
of erythropoietin in a rat model of multiple sclerosis**

Muriel B. Sättler<sup>1</sup>, Doron Merkler<sup>2</sup>, Katharina Maier<sup>1</sup>, Christine Stadelmann<sup>2</sup>, Hannelore Ehrenreich<sup>3</sup>, Mathias Bähr<sup>1</sup>, and Ricarda Diem<sup>1</sup>

<sup>1</sup> Neurologische Universitätsklinik, Göttingen, Germany

<sup>2</sup> Institut für Neuropathologie, Universitätsklinik Göttingen, Germany

<sup>3</sup> Max-Planck-Institut für Experimentelle Medizin, Göttingen, Germany

In multiple sclerosis (MS) long-term disability is primarily caused by axonal and neuronal damage. We demonstrated in a previous study that neuronal apoptosis occurs early during experimental autoimmune encephalomyelitis (EAE), a common animal model of MS. In the present study we show that in rats suffering from myelin oligodendrocyte glycoprotein (MOG)-induced optic neuritis, systemic application of erythropoietin (Epo) significantly increased survival and function of retinal ganglion cells (RGCs), the neurons that form the axons of the optic nerve. We identified three independent intracellular signaling pathways involved in Epo-induced neuroprotection *in vivo*: Protein levels of phospho-Akt, phospho-MAPK 1 and 2, and Bcl-2 were increased under Epo application. Using a combined treatment of Epo together with a selective inhibitor of phosphatidylinositol 3-kinase (PI3-K) prevented up-regulation of phospho-Akt and consecutive RGC rescue. We conclude that in MOG-EAE the PI3-K/Akt pathway has an important influence on RGC survival under systemic treatment with Epo.

## **Establishing a Parkinson Disease model in marmoset monkeys with unilateral 6-OHDA lesion of the nigrostriatal pathway**

**Czéh B.<sup>1</sup>, Heckmann C.<sup>1</sup>, Schindehütte J.<sup>2</sup>, Schmelting B.<sup>1</sup>, Mansouri A.<sup>2</sup>, Flügge G.<sup>1</sup>, Fuchs E.<sup>1</sup>**

<sup>1</sup>Clinical Neurobiology Laboratory, German Primate Center, Göttingen, Germany

<sup>2</sup>Max-Planck-Institute for Biophysical Chemistry, Göttingen, Germany

Experimental lesions of the ventral tegmental area resulted in Parkinson-like symptoms in rats. This and a number of other studies led to the discovery of the degeneration of the dopaminergic nigrostriatal system as the primary cause for Parkinson's disease (PD). Most experimental studies on PD have been performed in rodents. These studies are useful and important but they have a limited value as predictors of the therapeutic outcome in humans. Phylogenetically and behaviorally, non-human primates are substantially closer to humans than rodents and the complexity of their central motor regulation (the system whose function is destroyed by the loss of dopaminergic neurons) resembles that of humans. Thus, the investigation of non-human primate models is a prerequisite before new therapeutic strategies for neuroprotection and neuroregeneration can be applied in patients.

In a first step we established the unilateral 6-hydroxydopamine (6-OHDA) lesion model in marmoset monkeys (*Callithrix jacchus*) as a model for PD. This model has been recently validated and shown to be suitable for assessing dopaminergic graft function (Annett L.E. et al., Exp. Neurol. 125: 228-246, 1994). Compared to bilateral lesions, the unilateral approach offers the advantage that the intact and the lesioned side of the nigrostriatal system can be compared in one individual by observing the resulting asymmetry in motor behavior. Spontaneous recovery processes after lesioning the dopaminergic system represent a practical problem for all animal studies. This is particularly true for experiments investigating the effects of neurotransplants into the dopamine-depleted striatum since the transplant may take weeks or even months to become functionally integrated in the host brain.

Four marmoset monkeys were subjected to a unilateral 6-OHDA lesion of the nigrostriatal bundle and a series of behavioral tests was used to assess skilled forelimb reaching of the monkeys prior to surgery and following the 6-OHDA lesion at regular intervals for 24 months. All animals showed significant unilateral impairment in all behavioral tasks, and during these two years of postoperative observation period no spontaneous behavioral recovery occurred.

Furthermore, two non-lesioned animals were grafted with PKH26-labeled human embryonic stem cells at multiple striatal sites in the caudate nucleus and the putamen. The animals were perfused after five weeks of survival time, during which they received immunosuppressive treatment. Currently we are investigating the fate of the transplanted cells by histological means.

Supported by the BMBF (01GNNO104) and the DFG-Forschungszentrum Molecular Physiology of the Brain (CMPB)

## **Increased Expression of BDNF and Proliferation of Dentate Granule Cells after Bacterial Meningitis**

Simone C. Tauber<sup>1</sup>, Christine Stadelmann<sup>2</sup>, Annette Spreer<sup>1</sup>, Roland Nau<sup>1</sup>, Joachim Gerber<sup>1</sup>

<sup>1</sup> Department of Neurology, Georg-August-University, Göttingen, Germany

<sup>2</sup> Department of Neuropathology, Georg-August-University, Göttingen, Germany

Proliferation and differentiation of neural progenitor cells is increased after bacterial meningitis. In order to identify endogenous factors involved in neurogenesis, expression of BDNF, NGF and GDNF was investigated in a mouse model of pneumococcal meningitis. Male C57BL/6 mice were infected by injection of  $10^4$  CFU of *S. pneumoniae* into the right forebrain. Control animals received saline only. Mice were killed 30h later (each group n = 19) or treated with CRO (100mg/kg twice daily) and sacrificed 4 days after infection (each group n = 19). Four days after infection, hippocampal BDNF mRNA levels were increased 2.4-fold ( $p = 0.026$ ). Similarly, BDNF protein levels in the hippocampal formation were higher in infected mice compared to control animals ( $p = 0.0003$ ). This was accompanied by an elevated proliferation of dentate granule cells as indicated by BrdU-incorporation ( $p = 0.0002$ ). Conversely, NGF mRNA levels at 30 hours after infection were reduced by approximately 50% ( $p = 0.004$ ). No significant changes in GDNF expression were observed. BDNF protein was located predominantly in the hippocampal CA3/4 area and the hilus. The density of dentate granule cells expressing the BDNF receptor TrkB was increased 4 days after infection ( $p = 0.027$ ). In conclusion, increased synthesis of BDNF and TrkB suggests a contribution of this neurotrophic factor to neurogenesis after bacterial meningitis.

## **G-CSF: neuroprotective effect and signal transduction in the optic nerve transection model**

J. Schlachetzki<sup>1</sup>, G. Rohde<sup>1</sup>, M. Bähr<sup>1</sup>, A. Schneider<sup>2</sup>, J. H. Weishaupt<sup>1</sup>

<sup>1</sup>Neurologische Universitätsklinik, Waldweg 33, D-37073 Göttingen, Germany

<sup>2</sup>Axaron Biosciences AG, Im Neuenheimer Feld 515, 69120 Heidelberg, Germany

It has been recently demonstrated that the hematopoietic factor Granulocyte Colony Stimulating Factor (G-CSF), which reduces apoptosis and promotes differentiation of granulocyte precursors, protects against neuronal cell death in a rodent model of acute cerebral ischemia. In addition, G-CSF receptor (G-CSFR) protein has surprisingly been demonstrated on neurons in many areas of the CNS.

By immunohistochemistry, we demonstrate that G-CSF receptor protein is also expressed by rat retinal ganglion cells (RGCs), suggesting that G-CSF may also have a protective function for these neurons. *In vitro*, G-CSF protected immunopurified cultured RGCs from apoptosis after neurotrophic factor deprivation. Thus, we investigated G-CSF neuroprotection against delayed apoptosis after optic nerve transection, i.e. axotomy, of RGCs *in vivo*. Daily systemic as well as direct intraocular administration of G-CSF led to a dose-dependent increase of RGCs surviving axotomy.

Moreover, by immunohistochemistry and Western blot analysis as well as real-time PCR, we delineated anti-apoptotic signalling cascades mediating G-CSF neuroprotection in retinal ganglion cells.

In summary, our data suggest that G-CSF, which is in routine clinical use for the treatment, may be a suitable candidate molecule for the treatment of chronic neurodegenerative diseases like Parkinson's disease or glaucoma. In addition, we provide the first *in vivo* data about G-CSF-mediated anti-apoptotic signalling in neurons.

## Electrical intracochlear stimulation induces c-Fos expression in specific neuronal populations of the cochlear nucleus

Adrian Reisch and Robert-Benjamin Illing

*Neurobiological Research Laboratory, Dept. of Otorhinolaryngology, University of Freiburg  
Kilianstr. 5, 79106 Freiburg, Germany  
[reisch@hno.ukl.uni-freiburg.de](mailto:reisch@hno.ukl.uni-freiburg.de)*

Neuronal activity in sensory organs not only invokes fast electrical responses but may also trigger molecular changes via complex signaling cascades in central neurons. Unilateral changes of sensory activation in the auditory system by electrical intracochlear stimulation (EIS) leads to morphological and molecular changes in the adult auditory brainstem of the rat.

Changes in the expression of the immediate early gene c-fos were observed in a tonotopically precise pattern in central auditory neurons after electrical stimulation for 2h with a cochlear implant under urethane anesthesia. C-Fos was expressed only in the anteroventral cochlear nucleus ipsilateral to the stimulation but not contralaterally [Fig. 1]. Such a stimulation-dependent modulation of the transcription factor c-Fos in the ascending auditory system suggests modifications in electrochemical and structural properties of the affected cells. Here we raised the question if neurons of the cochlear nucleus are indiscriminately affected by EIS, or if only subsets of neurons respond to stimulation with the expression of c-Fos. Fluorescence double-stainings were performed to characterize c-Fos positive cells by the neurotransmitter they contain [Fig. 2]. We found that 40% of c-Fos positive nuclei belonged to glutamatergic neurons and about 60% to glycinergic neurons. Remarkably, GABAergic cells seem not to respond to the stimulation with the expression of c-Fos. We therefore conclude that only a distinct subpopulation of neurons responds to EIS with modulated expression of the transcription factor c-Fos, suggesting that these cells preferentially undergo structural plasticity upon changes in afferent activity. Supported by DFG, Graduiertenkolleg 843.

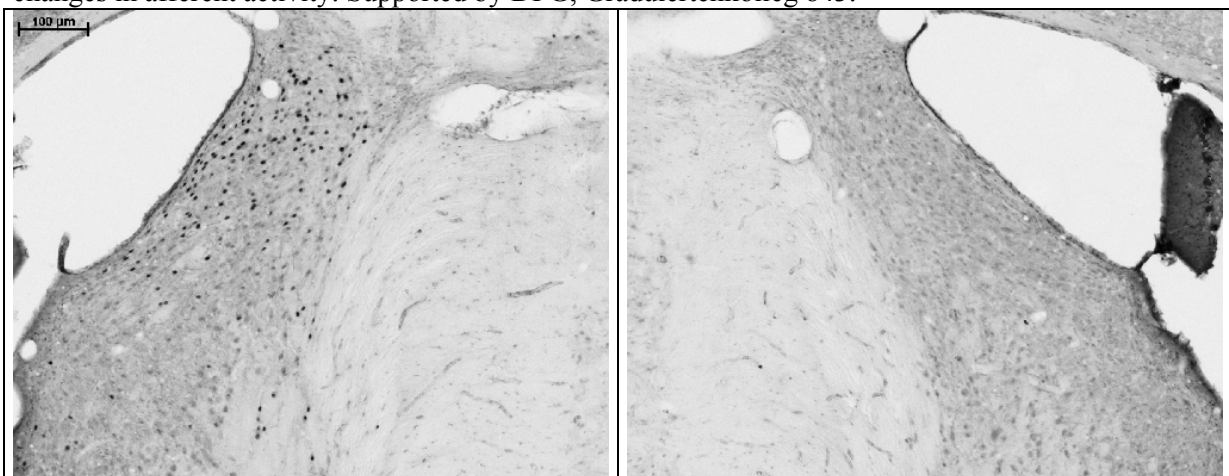


**Fig. 1:** Tonotopically localized c-Fos expression in the ipsilateral AVCN [left] after 2 hours of basal EIS. No expression in the contralateral AVCN [right].

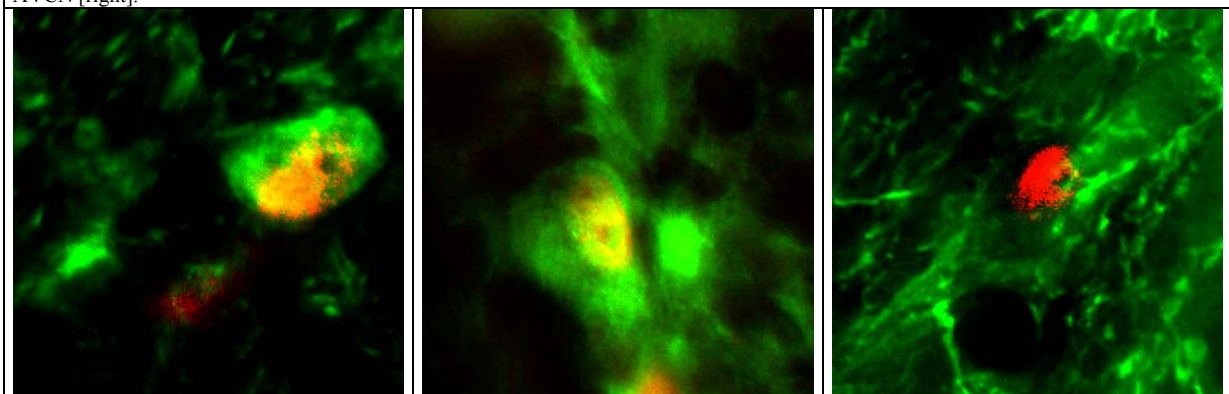


**Fig. 2:** Characterization of c-Fos expressing cells in the AVCN. High power images of neurons expressing c-Fos (red) in the nucleus, doublestained with antibodies against neurotransmitters (green). C-Fos is expressed in glutamatergic (left) and glycinergic (middle) but not in GABAergic cells (right).

## **L1 over-expressing mouse embryonic stem cells xenografted in a rat model of Parkinson's disease**

Loettrich, D., Bernreuther, C.\*, Papazoglou, A., Klein A., Schachner, M.\*, Nikkhah, G.

Lab of Molecular Neurosurgery, Dept. Stereotactic Neurosurgery, University Hospital Freiburg - Neurocentre, Germany

\*Centre for Molecular Neurobiology, Institute for the Biosynthesis of Neural Structures, University Hamburg, Germany

The cell adhesion molecule L1 which is present in most of the differentiated neurons has been demonstrated to promote dopaminergic (DAergic) differentiation and cell survival *in vitro*. The main purpose of the present study was to examine the potential of L1 in a rat model of Parkinson's disease. L1 over-expressing mouse embryonic stem cells were transplanted into the striatum of hemiparkinsonian rats. We focused on functional integration, cell survival and differentiation *in vivo*. The cells were derived from the inner mass of mouse blastocyte and were transfected with the L1 gene which was co-expressed with the green fluorescent protein (GFP) sequence. The L1 over-expressing mouse embryonic stem cells (L1 ES cells) were proliferated in DMEM/F12, L-Glutamine, B27-Supplement, Penicilline/Streptomycine and FGF2 and pre-differentiated for three days under withdrawal of mitogens. Fifty Sprague-Dawley rats received a unilateral 6-hydroxydopamine (6-OHDA) lesion of the medial forebrain bundle (MFB). Seventeen of the lesioned rats were transplanted with the L1 ES cells and another seventeen were grafted with the GFP+ wild type cells (L1 negative). Sixteen animals received only sham surgery and eight animals served as healthy controls. Lesion and transplantation effects were evaluated by apomorphine and amphetamine rotation and paw reaching tests before and after transplantation. The morphological analysis revealed teratoma-like tumour formation in a high percentage within the L1 ES cells grafted group (70%). Inside these tumours Tyrosinhydroxylase (TH) positive neurons were present in the range from dozens up to several hundreds. In contrast, there was no tumour formation observed in the wild type group but concomitant TH expression (further details will be presented at the conference). In none of the experimental groups a graft-induced effect could be observed for rotational behaviour and paw reaching analysis. In conclusion, a possible coherence between L1 over-expression, tumour formation and TH expression was found. Despite promising results in other neurodegenerative disease models (Huntington) and *in vitro* data the cell adhesion molecule L1 may act differently in a xenograft environment and further investigations to better understand the role of L1 on DA development and functional integration needed.

**Neonatal rat brain transplantation: a tool to study restoration and reinnervation of the striatum**

Papazoglou A., Hackl C., and Nikkhah G.

Lab of Molecular Neurosurgery, Dept. of Stereotactic Neurosurgery, Univ. Hospital Freiburg, Germany

Grafts of the ventral mesencephalon (VM) of E14 rat embryos, implanted into the striatum of an adult rat 6-hydroxydopamine (6-OHDA) model of Parkinson's disease, can restore dopamine (DA) neurotransmission in the transplanted area and reverse the phenotype induced by the neurotoxin. However, these DA-rich grafts are unable to completely restore the motor deficits since striatal DA levels are restored only up to 30% of normal. Furthermore, when the same cells are transplanted into the adult substantia nigra (SN) they fail to outgrow fibers to reach and reinnervate the DA denervated striatum. In contrast, in the neonatal brain graft derived fiber and outgrowth can be observed until postnatal day (P) 10 when fetal VM cell suspension is transplanted into lesion brain. Here we use the neonatal rat brain as a model to study firstly, the reinnervation potential of fetal VM grafts in relation to the host age and secondly, the fate of adult human neural stem cells (hNSC) grafted into the developing rat brain. Neonatal rats were lesioned bilaterally by intraventricular injection of 6-OHDA at P1 and received VM grafts at P10, P11, P12, P13, P15 and P18 into the right SN. Within six months from surgery the animals underwent drug-induced rotations and finally immunohistochemistry will be performed. Furthermore, the correlation between Nogo A expression pattern and axonal extension is currently in progress.

hNSC were successfully obtained from surgical samples taken during of partial temporal lobotomy for epilepsy. These hNSC are proliferating as neurospheres and can be spontaneously differentiate into  $\beta$ -tubulin and nestin positive cells. In order to differentiate and characterize these cells *in vivo*, we transplanted them into the right SN of P5 neonatal rats with or without 6-OHDA lesions. Further results from these ongoing studies will be provided. Taken together, the neonatal model is a highly useful tool for restorative approaches based on NSC.

## **Effects of double-grafting on the survival of embryonal (E14) mesencephalic dopaminergic neurons transplanted in a rat model of Parkinson's disease**

Hackl C, Papazoglou A, Klein A, Nikkhah G

Laboratory of Molecular Neurosurgery, Department of Stereotactic Neurosurgery, Breisacher Str. 64, University Hospital Freiburg, 79106 Freiburg, Germany

Rat models of Parkinson's disease are based on unilateral injections of 6-hydroxydopamine (6-OHDA) into the mid forebrain bundle (MFB) of the rat, resulting in a complete loss of nigral dopaminergic neurons and leading to a depletion of dopamine within the relevant striatum. Six weeks after the lesion, primary cell suspensions rich in dopaminergic neurons, derived from dissociated ventral mesencephalon of E14 rat embryos, are transplanted into the lesioned striatum. According to the standard transplantation protocol, 400,000 cells per animal are grafted, equally divided into 4 deposits.

A significant positive outcome of the graft can be observed two weeks after transplantation, although 90-95% of the grafted cells degenerate within several days after transplantation. Furthermore, only 8-10% of cells in the grafted cell suspension will become dopaminergic afterwards. However, recent publications have shown that the neonatal brain exhibits a higher plasticity, survival and functional integration of grafts compared to the adult brain.

In this study, in order to improve the survival and functional integration of the grafted cells, we established a new protocol based on two transplantation time points. During transplantation, the lesioned rats received half of the standard amount of embryonal mesencephalic cell suspension (200,000 cells – four deposits). At defined time points of 3, 5, 7 or 9 days after the first transplantations, the animals received a second graft, placed in the middle of the first graft (200,000 – 2 deposits). In principle, our first graft should simulate the embryonal microenvironment within the lesioned striatum for a better integration of the second graft. The total amount of transplanted cells per animal is equal to the standard transplantation protocol. To distinguish between the two grafts, the cells used for the transplantations were labelled either with PKH26 (red) or PKH67 (green) lipophilic fluorescent dyes. In vitro studies showed that the cell labelling protocol did not influence viability or survival of dopaminergic cells.

Lesion and transplantation effects were evaluated by apomorphine and amphetamine induced rotation, performed 6 weeks after lesion and 2, 5, 9 and 14 weeks after the first grafting. Statistical analysis showed a significant improvement between the rotational data before and after transplantation in all groups. A significant difference was observed in the two weeks amphetamine induced rotation among the groups of 3 and 7 days; 5 and 7 days; 3 and 9 days difference between the grafting. Morphological and stereological analysis showed a significant higher cellnumber in the group of 5 days compared to the groups of 7 and 9 days as well as compared to the standard transplantation protocol. The graft-volume in the group of 5 days difference is significantly higher then in the group of 7 days difference and also shows a strong tendency to be higher then in the group of 9 days difference. Taken together, the double-grafting strategy offers an interesting model to study graft-host-interactions in Parkinson's disease.



## **Remodelling of the damaged brain by fetal transplants? - Implications from studies in a rat model of Parkinson's disease**

*Klein A, \*Metz GA, Wessolleck J, Papazoglou A, \*\*Knieling M, Timmer M, and Nikkhah G*

Lab of Molecular Neurosurgery, Dept. of Stereotactic Neurosurgery, Univ. Hospital Freiburg, Germany

\* CCBN, Univ. of Lethbridge, Lethbridge, Alberta, Canada

\*\* Univ. Hospital Jena, Dept. of Neurology, Jena, Germany

Unilateral injections of 6-OHDA into the medial forebrain bundle lead to permanent impairments of skilled limb movements (SLM), especially in forelimb reaching tasks and gait performance. Fetal dopaminergic (DAergic) grafts promote an improvement of sensorimotor behaviour, however, the mechanisms and the qualitative aspects of graft-induced recovery are still unclear. The aim of this study was to determine whether transplantation of fetal DAergic neurons mediates recovery in SLM and gait performance by rewiring neural motor patterns for reaching movements and limb coordination, or whether transplants support compensation of motor deficits. The rats were trained in skilled reaching tasks (single pellet grasping task for qualitative and quantitative evaluation, staircase test for quantitative evaluation). Gait analysis (rung walking task and footprint analysis) was performed to test skilled walking and forelimb/hindlimb coordination. After 6-OHDA lesion and transplantation of E14 VM neurons rotational behaviour was assessed. After transplantation grafted rats showed overcompensation under amphetamine administration and a reduction of apomorphine-induced rotation. This indicates a significant graft survival and graft effect on simple motor behaviour. Morphological and stereological analyses demonstrated substantial graft survival and reinnervation. For gait performance an incomplete but significant improvement after transplantation could be observed. The quantitative evaluation of SLM demonstrated significant enhancement whereas the qualitative analysis revealed no improving graft effect. We conclude that in hemiparkinsonian rats graft-induced recovery in SLM is due to graft-induced compensatory mechanisms. Supported by DFG and AHFMR.

**Transplantation of long-term expanded human fetal neural precursor cells – evidence of distant migration and multi-lineage differentiation**

Maciaczyk J., Maciaczyk D., and Nikkhah G.

Laboratory of Molecular Neurosurgery, Dept. of Stereotactic and Functional Neurosurgery, University of Freiburg – Neurocenter, Freiburg, Germany

Cell replacement therapy, based on human fetal cell transplantation, proved to be beneficial under experimental conditions and in clinical trials. The ethical concerns and limited availability of the aborted tissue make it difficult to become a routine clinical strategy. One way to overcome these obstacles is the in vitro expansion of human fetal-derived neural precursor cells, their characterization and differentiation into the desired phenotype for further clinical applications.

Cortex (CTX), ventricular eminence (STR), ventral midbrain (VM) and spinal cord (SC) were obtained from elective abortions up to 12<sup>th</sup> week post conception and expanded as free floating aggregates (neurospheres) for prolonged period of time in medium supplemented with basic fibroblast growth factor (bFGF) and epidermal growth factor (EGF).

Adult female immunosuppressed Sprague-Dawley rats were grafted stereotactically into right striatum or hippocampus with long term expanded human fetal neural precursors derived from CTX, STR, VM and SC. 9 weeks post grafting the animals were sacrificed and the transplanted cells were identified using anti-human nuclei antibody following characterization with lineage specific (type III  $\beta$ -tubuline (TuJ1), microtubule associated protein 2 (MAP-2), glial fibrillary acid protein (GFAP), nestin) and phenotype specific (neurogranin, GABA, tyrosine hydroxylase (TH), doublecortin (DCX) calbindin, parvalbumin) markers. Proliferative activity of the transplanted cells was monitored with anti-Ki67 immunostaining.

Survival and migration pattern was correlated with the source of grafted tissue and placement of the transplant. Intrastratial grafts migrated radially in the parenchyma infiltrating even distant parts of caudate-putamen unit (CPU) and after entering white matter tracts like corpus callosum or bundles of internal capsule they reached distant locations from forceps minor of the corpus callosum in most frontal aspect to cerebral peduncle of the brain stem. Small proportions of intrastratially transplanted cells migrated along the nigro-striatal pathway to reticular part of substantia nigra (SNr). The migratory potential declined with the most caudal origin of the grafted tissue. All intrahippocampal transplants were confined within the structure and migration was directed preferentially towards dentate gyrus. The migratory phenotype was typical for immature cells expressing markers for neuroepithelial precursors (nestin) or young neuroblasts (DCX).

Although the majority of the grafted cells remained non-fully committed more mature phenotypes were also observed, mainly within the core of the transplant and its proximity.

The present study demonstrates successful proliferation of human fetal-derived neural precursors as well as their good survival, extensive migration and multi-lineage differentiation after transplantation into adult recipients. Therefore in vitro proliferation of human fetal neural precursor cells might be an alternative cell source for experimental and clinical research directed towards neural restorative strategies.

## Ultrastructural analysis of plasticity in the cochlear nucleus of the rat induced through deafening

Markus A. Meidinger and Robert-Benjamin Illing

Neurobiological Research Laboratory, Department of Otorhinolaryngology,  
University of Freiburg, Killianstraße 5, 79106 Freiburg, Germany  
[meidinger@hno1.ukl.uni-freiburg.de](mailto:meidinger@hno1.ukl.uni-freiburg.de)

Alterations of the sensory input to the brain cause modifications at the molecular and the structural level. A well established molecular plasticity marker is the growth-associated protein 43 (GAP-43). GAP-43 is strongly expressed in the developing nervous system and is associated with neurite outgrowth and synaptogenesis. With maturation its expression is down-regulated in most neurons. Unilateral deafening disturbs the balance of the auditory input between left and right side and leads to a re-expression of GAP-43 and other plastic events in the mature rat brain (Illing et al., 1997). GAP-43 was originally considered as an exclusive neuronal molecule. The situation changed after the demonstration that GAP-43 may also be expressed in glia precursors in the developing nervous system and is inducible through lesioning in mature glia cells (Sensenbrenner et al., 1997).

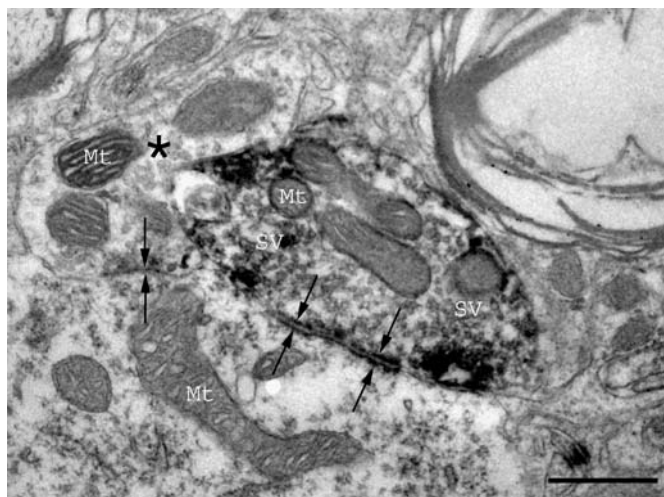
Now, in order to identify the structures containing GAP-43, we began to study its re-expression and the occurrence of plastic modifications induced through cochlear ablation at the ultrastructural level. Adult wistar rats aged 6 weeks or older were unilaterally cochleotomized to survive for 7 to 8 days. Following fixation, the brains were cut in the frontal plane on a vibratome in 50- $\mu$ m-thick sections. To label the binding sites of the antibody against GAP-43 the indirect avidin-biotin technique using diaminobenzidine as chromogen was applied. Sections were postfixated in osmium tetroxide and potassium ferricyanide, dehydrated and flatembedded. After hardening, sections were studied under the light microscope and photographed. Selected sections were re-embedded and ultra-thin sections were cut for ultrastructural studies.

In the VCN ipsilateral to the lesion, we detected presynaptic terminals, fibers and growth cone-like structures immunopositive for GAP-43. Presynaptic terminals (see figure) were identified based on the following criteria: a synaptic cleft between the pre- and postsynaptic membrane, membrane-associated densities (synaptic junctions), and the presence of synaptic vesicles.

The growth cone-like structures were considered as neuronal in origin if they contained neuronal features like synaptic vesicles or had an uninterrupted connection to an identified neuronal structure such as a synapse. On the contrary, the classification of structures as glial profiles rested upon the occurrence of characteristic glial filaments (glial fibrillary acidic protein, GFAP) or an uninterrupted connection to a glia cell body. Both neuronal and glial elements were found to be GAP-43 positive.

In summary, unilateral cochlear lesioning led to a re-expression of GAP-43 in presynaptic terminals as well as in glial profiles in the VCN of adult rats ipsilateral to cochleotomy. This is evidence for a plastic response of the central auditory system to the unilateral loss of afferent activity at the level of interneuronal connectivity.

Supported by DFG, Grant IL 18/12-1



A presynaptic terminal positive for GAP-43 located in the ipsilateral ventral cochlear nucleus of a unilaterally deafened rat. The immunocytochemical stain using diaminobenzidine as chromogen resulted in a black precipitate. Next to the immunopositive presynaptic terminus on the left side is an unstained one (\*). The arrows point to synaptic junctions. SV = synaptic vesicles, Mt = mitochondrion. Scale bar = 500 nm.

**Molecular mechanisms of a novel iron chelator/ propargylamine bifunctional drug: neurorescue, differentiation and regulation of amyloid precursor protein/ amyloid –beta peptide processing.**

**Yael Avramovich-Tirosh, Tamar Amit and Moussa BH Youdim.**

*Eve Topf and NPF Centers of Excellence for Neurodegenerative Diseases Research and Department of Pharmacology, Technion-Faculty of Medicine, Haifa.*

Massive evidence suggests that iron plays an important role in the etiology of various neurodegenerative diseases, such as Parkinson's disease (PD) and Alzheimer's disease (AD). Indeed, iron has been shown to accumulate, in association with oxidative stress, at sites where neurons degenerate. Recently, we have demonstrated that the brain permeable iron chelator, VK28, as well as the propargylamine moiety of rasagiline (an anti- PD/ MAO-B inhibitor drug), exert neuroprotective activities against a variety of insults. Therefore, we developed, a novel bifunctional drug, M30, from the prototype neuroprotective iron chelator VK-28 possessing a propargylamine moiety, which is expected to have a greater ability in preventing neuronal death.

Here we report, for the first time, that M30 (1-10  $\mu$ M) decreased apoptosis of SH-SY5Y neuroblastoma (NB) cells in a neurorescue, serum deprivation model, via multiple protection mechanisms, including: reduction of the pro- apoptotic Bad and Bax; reduction of apoptosis-associated Ser139 phosphorylated H2A.X; induction of the anti- apoptotic Bcl2; inhibition of the cleavage and activation of caspase3.

Moreover, M30 promoted some noticeable morphological changes inducing axonal growth- associated protein- 43 (GAP-43) implicating neuronal differentiation. However, VK28 did not show any significant effect on cell differentiation.

M30 markedly regulated the processing of the holo- amyloid precursor protein (APP). Thus, holo- APP expression was extensively reduced, in a dose dependent manner after M30 treatment both in NB cells and in Chinese Hamster Ovary (CHO) cells stably transfected with APP "Swedish" mutation. These findings are well coordinated with the presence of an iron-responsive element (IRE) in the 5'- untranslated region (5'UTR) of the APP and the iron chelator properties of the drug. Importantly, the amyloidogenic A $\beta$  peptide in cell media, was distinctly reduced, following M30 treatment. In correlation the C-terminal fragment (CTF) - $\beta$  levels, were also reduced. In addition, the non- amyloidogenic soluble APP $\alpha$  levels were elevated as well the levels of CTF- $\alpha$  in cell lysate.

This study implies that the bifunctional drug, M30 possessing properties of neurorescue and regulation of APP processing, resulting in a substantial reduction in A $\beta$  levels, might be a leading drug in AD.

## Connexin 43 mRNA and protein are upregulated in the vicinity of the photothrombotic lesion in rat brain

Corinna Haupt, Oliver Waitz, Otto W. Witte, Christiane Frahm  
Dept. of Neurology, Friedrich-Schiller-University, Jena, Germany

Intercellular coupling via gap junction channels is vitally for astrocytic function. The role of gap junctional communication under ischemic conditions is still discussed controversially. Concerning the outcome of an ischemic insult studies in connexin 43 knock out animals yielded contrary results to rats with blocked gap junctional coupling. In our model of focal cerebral ischemia, we studied the expression of connexin 43, one of the major gap junction proteins in astrocytes. Seven days after the infarction connexin 43 mRNA is elevated in cells surrounding the lesion site, which was shown by RNA/RNA *in situ* hybridization. The hybridization signal in pericarya around the lesion was much higher than in the remaining cortical areas. The strong staining of cells encompassing the lesion accounts for high cellular levels of the appropriate mRNA. Immunohistochemical staining for connexin 43 showed an increased signal in the cortical tissue flanking the infarcted area 7 days after photothrombosis. In contrast the tissue delineating the lesion from the corpus callosum showed very low staining, indicating that not all cells which elevate their mRNA level for connexin 43 concomitantly synthesize larger amounts of the protein. The role of this differentiated upregulation of connexin 43 mRNA and protein around the lesion is unclear. With the implicit understanding that the additionally synthesized protein is functional, an elevated coupling between cells could be beneficial in areas demarcating the uninjured cortex but unfavorable at the borderline to the corpus callosum. Nevertheless, connexin 43 mRNA as well as protein are upregulated after photothrombosis.

Supported by BMBF 01GZ0306, 0311578 and 01GI9905

## **Age-dependent alterations of functional inhibition in a rat model of cortical lesion.**

S. Schmidt; A. Divanach; C. Bruehl and O.W. Witte *Clinic of Neurology, Friedrich Schiller-University, Jena, Germany*

Cortical lesions in the rat brain induce changes in neuronal activity like reduced functional inhibition. Here we investigated post-lesional effects of focal lesion on cortical field-potentials in young, middle aged and old rats.

Focal cortical lesions were induced at the border of parietal and occipital areas by injection of the photosensitive dye rose bengal and illumination of the skull. The surgery was performed on 3, 12 and 24 month old rats. Cortical field potentials were recorded 7 days after lesion induction on coronal brain slices using the paired pulse protocol. A bipolar stimulation electrode was placed in layer VI and field potentials recorded in layer II/III. GABA-ergic paired-pulse inhibition was investigated through the application of double pulses of 50 $\mu$ s duration with 20ms inter-stimulus interval.

In young rats with a photothrombotic lesion the ratio of the second versus the first evoked EPSP was significantly increased over wide regions of the neocortex, both in the ipsilateral and contralateral hemispheres. This pattern of alterations between sham operated and lesioned animals was not observed in older rats. Furthermore, we found significant age-dependent alteration in the functional inhibition mainly of the parietal cortex. The mean ratio throughout the ipsilateral and contralateral cortex are  $0.57 \pm 0.02$  in 3 month old sham operated rats. This mean ratios are  $0.71 \pm 0.02$  in 12 month and  $0.76 \pm 0.02$  in 24 month old sham operated rats.

These results suggest that neocortical infarcts induce different changes in inhibition, depending on the animal age. This supports the hypothesis of differential plasticity and functional reorganization in juvenile versus aging brains.

**Synaptic plasticity in the frontal cortex of the European ground squirrel  
(*Spermophilus citellus*) in the course of torpor-arousal cycles**

J. Ruediger<sup>1</sup>, A. Aschoff<sup>1</sup>, R.A. Hut<sup>2</sup>, E.A. Van der Zee<sup>2</sup> and S. Daan<sup>2</sup>

<sup>1</sup>Institute of Anatomy, Teichgraben 7, Friedrich-Schiller-University, Jena, Germany

<sup>2</sup>Zoological Laboratory, University of Groningen, Groningen, The Netherlands

**Summary.**

Synapses of cortical pyramidal neurons from European ground squirrels (*Spermophilus citellus*) were counted, and their dimensions measured in euthermy-torpor cycles during hibernation. Morphometric data (active zone length, post synaptic density (PSD) dimensions, apposition length) from synapses during torpor bouts and in the euthermy phases were compared with synaptic dimensions in normal euthermy. 5 groups of animals (n=6) were compared. Euthermic animals (EU), animals during entrance into torpor (TS), animals in deep torpor (TL), animals at the beginning of arousal (AL), and animals in the middle of arousal (AL). The results show during torpor and at the beginning of arousal the length of the PSD, length active zone or the size of the synapse is significantly increased when compared to synapses in during arousal and in summer. However the thickness and surface area of the PSD is decreased in the torpor phases. At the beginning of arousal the thickness of the PSD increases and becomes maximum values in euthermy and during summer. We believe, that this result reflects synaptic loss during torpor bouts and synaptogenesis during arousal, whereby during synaptic loss only large and stable synapses remain whereas the small synapses, dependent on ongoing activation disappear. During arousal new, mobile and smaller synapses are formed in abundance and due to continuous activation thickness of the PSD increases.

Real-time imaging of Golgi derived vesicle exocytosis during the formation of growth cone lamellipodium after axotomy of cultured *Aplysia* neurons

Micha E. Spira and Guy Malkinson

Life Sciences Institute, The Hebrew University of Jerusalem.

THE TRANSFORMATION OF A STABLE AXONAL SEGMENT INTO A MOTILE GROWTH CONE IS A CRITICAL STEP IN THE REGENERATION OF AMPUTATED AXONS. AXOTOMY OF CULTURED *APLYSIA* NEURONS IS FOLLOWED BY RAPID EXTENSION OF A GROWTH CONES (GC) LAMELLIPODIUM. CALCULATIONS REVEALED THAT TO ACCOUNT FOR THIS RATE OF GROWTH, 80-180 VESICLES/SEC FUSE WITH THE PLASMALEMMA.

HERE WE BEGAN TO EXPLORE WHERE, WHEN AND HOW GOLGI DERIVED VESICLES FUSE WITH THE PLASMA MEMBRANE IN SUPPORT OF THE GROWTH PROCESS. TO THAT END, WE EXPRESSED THE PH-SENSITIVE GFP FUSED TO THE LUMINAL DOMAIN OF VAMP - SYNAPTO-PHLUORIN (A GIFT FROM J. E. ROTHMAN, MEMORIAL SLOAN-KETTERING CANCER CENTER, NY) IN CULTURED NEURONS. DETECTION OF VESICLES DISTRIBUTION BEFORE, DURING AND AFTER AXOTOMY AS WELL AS THROUGHOUT THE PROCESS OF GC EXTENSION WAS DONE BY CONFOCAL IMAGING USING EXCITATION WAVELENGTH OF 488 NM TO IMAGE THE PROBE DURING OR AFTER FUSION OF THE LABELED VESICLES, AND BY IMAGING OF THE TOTAL POPULATION OF SYNAPTO-PHLUORIN LABELED VESICLES WITH EXCITATION WAVELENGTH OF 405NM. CALCIUM WAS IMAGED BY INTRACELLULAR INJECTION OF FLUO-4 OR RHOD -2. A FRACTION OF THESE INDICATORS IS TAKEN UP BY THE VESICLES AND REVEALS RELATIVELY HIGH INTRAVESICULAR CALCIUM LEVELS.

WE FOUND THAT AXOTOMY LEADS TO: (A) FUSION OF ANTEROGRADLY TRANSPORTED VESICLES WITH THE PLASMA MEMBRANE AT THE TIP OF THE AXON WHERE THE  $[Ca^{2+}]_i$  IS ELEVATED TO  $> 1\text{mM}$ . (B) AFTER THE RECOVERY OF THE  $[Ca^{2+}]_i$  TO CONTROL, SYNAPTO-PHLUORIN LABELED VESICLES ACCUMULATE AT THE FORMING GC'S CENTER. (C) THESE VESICLES FUSE WITH THE GC'S PLASMA MEMBRANE IN THE VICINITY OF THE GC CENTER. THE FUSION PROCESS PROCEEDS IN THE ABSENCE OF ANY DETECTABLE FLUCTUATIONS IN THE  $[Ca^{2+}]_i$ .

IN CONCLUSION, THE ADDITION OF NEW MEMBRANE TO AXOTOMYZED AXON IS EXCLUSIVELY LOCALIZED TO THE GC CENTER. WE PROPOSE THAT THE PREFERENTIAL FUSION OF VESICLES AT THE GC CENTER IS FACILITATED BY RELEASE OF CALCIUM FROM THE VESICLES THEMSELVES AND THEIR LOCAL CONCENTRATION.

SUPPORTED BY: THE ISF AND THE BSF



## **DISTRIBUTION AND ACTIVITY OF PROTEASOME IN REGENERATING NEURONS**

Dotan Kamber and Micha E. Spira, *Dept. of Neurobiology, Life Science Institute, The Hebrew University of Jerusalem.*

Recent studies indicate that proteasomes play central roles in different forms of neuroplasticity including turning and retraction of growth cones (GC) in response to signaling molecules (Douglas & Holt, 2001, Neuron 32) and in establishment of short and long term synaptic plasticity (Zhao et al., 2003, Curr. Biol. 13). These reports as well as earlier findings by our laboratory (Gitler & Spira, 1998, Neuron 20) raise the possibility that proteasomes participate in other forms of neuroplasticity such as neuronal regeneration after trauma.

In the present study we use cultured *Aplysia* neurons and on line confocal imaging to examine the distribution and activity of proteasomes in the transformation of a differentiated axon into a GC after axotomy.

To image proteasome activity we used the membrane-permeable proteasome substrate succinyl-Leu-Leu-Val-Tyr-7-amido-4-trifluoromethyl coumarin (suc-LLVY-AFC). Unlike suc-LLVY-AFC its cleavage product AFC is highly fluorescent. Baseline proteolytic activity was imaged in intact neurons, and was found to reach a steady state (SS) level ~40 min after addition of the indicator to the bathing solution. Axonal transection leads to elevation of the product's fluorescence in the most distal zone (DZ) of the transected axon, reaching a new SS level that remains high for hours.

Immunolabeling with anti prosomes p25K (ICN Pharmaceuticals, Inc) revealed that axotomy leads to proteasomes accumulation at the DZ and to its translocation to the membrane and submembrane domains of the GC's lamellipodium. Thus the distribution of the proteasome and the proteolytic product colocalizes within the GC.

To examine whether proteasomes activity play any role in the transformation of an axon into a GC, we bathed the intact neuron in 10 $\mu$ M clasto-Lactacystin  $\beta$ -lactone, a membrane-permeable proteasome inhibitor. Under these conditions the proteolysis of Suc-LLVY-AFC and the formation of a GC's lamellipodium after axotomy were greatly inhibited.

Supported by the BSF

## **Two types of protease-activated receptors (PAR-1 and PAR-2) mediate calcium signaling in rat retinal ganglion (RGC-5) cells**

**Weibo Luo, Yingfei Wang, Georg Reiser**

Institut für Neurobiochemie, Medizinische Fakultät, Otto-von-Guericke-Universität  
Magdeburg, Leipziger Straße 44, 39120 Magdeburg, Germany.  
Weibo.luo@medizin.uni-magdeburg.de

Protease-activated receptors (PARs), the unique G protein-coupled receptors, are widely expressed in various tissues, where they participate in many physiological and pathological processes, such as hemostasis, proliferation, tissue repair and inflammation. There are four members of this family: PAR-1, PAR-3, and PAR-4, which are activated by thrombin; and PAR-2, which is activated by trypsin. PARs activation could result in calcium mobilization. Calcium, an important second messenger, plays an important role in neurons. Increasing calcium activates various signal pathways that lead to the expression of genes that are essential for dendritic development, neuronal survival and synaptic plasticity. In the present study, we used RGC-5 cells, a rat transformed retinal ganglion cell line, as a cell model *in vitro* to study PAR-mediated calcium signaling. Using reverse transcription-polymerase chain reaction (RT-PCR), we demonstrate that RGC-5 cells mainly express PAR-1 and PAR-2, which was confirmed by indirect immunofluorescence. Short-term stimulation of RGC-5 cells with thrombin (0.001-1 U/ml) and trypsin (1-100 nM) dose-dependently induced a transient increase in intracellular calcium concentration ( $[Ca^{2+}]_i$ ). An increase in  $[Ca^{2+}]_i$  was also induced by both TRag (PAR-1 activating peptide, Ala-pFluoro-Phe-Arg-Cha-HomoArg-Tyr-NH<sub>2</sub>) and PAR-2 activating peptide (PAR-2 AP; SLIGRL, Ser-Leu-Ile-Gly-Arg-Leu). The EC<sub>50</sub> values were 0.3 nM for thrombin, 12.0 nM for trypsin, 1.3  $\mu$ M for TRag and 1.6  $\mu$ M for PAR-2 AP, respectively. Desensitization studies showed that a second addition of thrombin after pre-pulse challenge with thrombin or TRag significantly reduced the calcium response, but the preceding stimulation with PAR-2 AP did not decrease the amplitude caused by thrombin as a second challenge. A second addition of trypsin after a pre-pulse challenge with trypsin, TRag or PAR-2 AP also significantly reduced the calcium response. These results suggest that thrombin could activate PAR-1, but not PAR-2. Trypsin, however, could activate PAR-1, as well as PAR-2 in RGC-5 cells. Calcium source studies showed that PAR-induced calcium mobilization mainly comes from intracellular calcium stores in RGC-5 cells. This result was quite different from that of astrocytes and OLN-93 oligodendrocytes, where PAR-mediated calcium mobilization comes from both intracellular stores and extracellular space. Intracellular calcium overload via calcium influx could lead to neuronal degeneration. The role of calcium release from intracellular stores in neurons, however, is not clear till now. Some studies showed that PARs were involved in neuronal degeneration. Therefore, it will be interesting to investigate the effect of calcium from intracellular stores induced by PAR on neuronal degeneration in RGC-5 cells.

## CEREBRAL ISCHEMIA AND PARADOXICAL SLEEP

V.V.Loginov<sup>1</sup>, V.B.Dorokhov<sup>1</sup>, G.N.Fesenko<sup>2</sup> and V.M.Kovalzon<sup>2</sup><sup>1</sup>Institute Higher Nervous Activity/Neurophysiology, and <sup>2</sup>Severtsov Institute Ecology/Evolution, Russian Academy of Sciences, Moscow <[kovalzon@sevin.ru](mailto:kovalzon@sevin.ru)>

Classical morphological studies of the cerebral ischemia and hypoxia revealed not degenerative only but also restorative processes in the brain tissue, including stem cells proliferation [2]. On the other hand, classical early somnological studies of Ian Oswald clearly demonstrated an important role of the natural sleep in tissue restoration [5]. While studying sleep structure changes in healthy humans and patients after such influences as physical and mental exercises during the day, starvation, sleep deprivation and acute intoxication by psychotropic drugs, Oswald *et al.* came to the conclusion that general anabolic processes in the brain and body cells are realized mostly during slow wave sleep (SWS) periods, though specific synthetic processes into the central nervous system took place during fast (paradoxical) sleep (PS) phase. In accordance to the above-mentioned hypothesis, objective qualitative changes of sleep structure should be anticipated in survived post-ischemic rats related to initial sharp decrease in cerebral energetic and synthetic capacities which are followed by activation of intrinsic reparative functions of the brain [4].

To check up the hypothesis, young male Wistar rats (180-200 g body weight) were implanted under pentobarbital anesthesia (40 mg/kg b.w., i.p.) with electrodes for the cerebral cortex and hippocampal EEG, and the EMG of neck muscles; then one or both common carotid arteries were completely and permanently ligated. Each day of the following period at the same time (09-12AM), free-moving animals survived were subjected to polygraphic recording until the 40<sup>th</sup> day since operation. From the total amount of more than 100 rats, only 30 animals have been survived, that is, about 30%. Survival level was the same after unilateral and bi-lateral occlusion. EEG scoring revealed a tremendous increase in PS percentage which reached almost 20% of the recording time (RT), or 30% of total sleep time (TST) at the 1<sup>st</sup>-2<sup>nd</sup> day since occlusion, then gradually decreased day by day and finally reached the control value of 2.5% of RT (6% of TST) by the end of the observation period (40<sup>th</sup> day). SWS percentage showed lesser though significant changes within the 1<sup>st</sup> day of the observation period. Unilateral and bilateral occlusion resulted in the same PS increase.

Figure 1

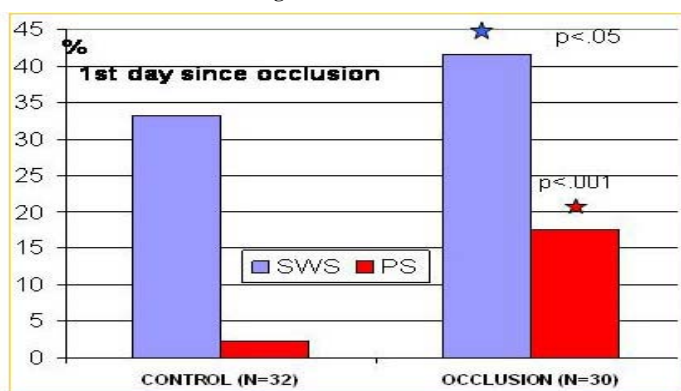


Fig. 1 Changes in SWS and PS percentage from 3-hr total recording time in the rat 24 hr since occlusion of one or both common carotid arteries.

Figure 2

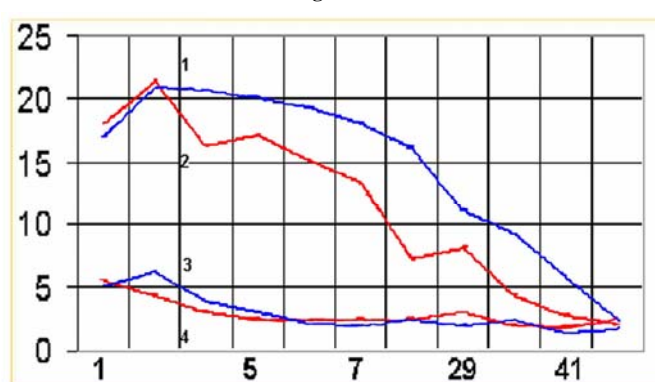


Fig. 2. Time-course of paradoxical sleep percentage from 3-hr total recording time (Y-axis) in the rat survived after uni- (line 1) or bi-lateral (line 2) occlusion. Line 3 and 4 – control groups. X-axis, day since operation.

Figure 3

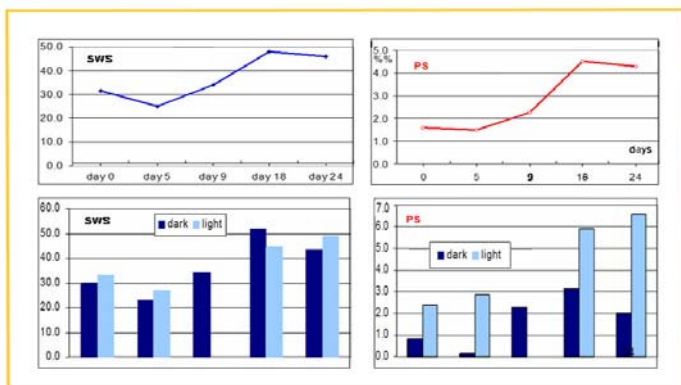


Figure 3. 24 hr continuous digital polygraphic recording in the rabbit after uni-lateral carotid occlusion; 0 – day before occlusion

The same procedure has been performed in aged male chinchilla rabbits (2-2.5 years old, 4-5 kg b.w.) preliminarily implanted (under local procain anesthesia) with the same electrodes for polygraphic recording. Several weeks later when the animals were completely rehabilitated and fully adapted to experimental chambers, they were subjected to uni-lateral complete and permanent carotid occlusion under chloral-hydrate anesthesia (0.5 g/kg b.w., i.p.). As in a case of the rats, survival level was about 25-30%. The survived free-moving animals were subjected to continuous 24-hr (12/12 LD) digital paperless polygraphic recording on the 5<sup>th</sup>, 9<sup>th</sup>, 18<sup>th</sup> and 24<sup>th</sup> day since the operation as well as before it (zero day). Preliminary results confirmed an important gradual increase in PS following occlusion: from 1.6% of RT on the control day 0 (0.8% during the dark and 2.4% during the light period) up to 4.5% on the 18<sup>th</sup> day (3.1 and 5.9%, consequently). SWS also increased from 31.5% of RT on day 0 to 48% on the 18<sup>th</sup> day. On the 24<sup>th</sup> day both parameters began to decrease (46% of SWS and 4.3% of PS).

The results strongly support a hypothesis of the paramount role of PS in cerebral tissue restoration. Minor discrepancies between two experimental series could be attributed to species and age differences as well as experimental conditions. It is known from both clinical and experimental studies that cerebral stroke is followed by a general shift of the brain activity down to a predominance of phylogenetically old mechanisms, that is in a good concordance to an idea of evolutionary ancient origin of PS mechanisms [3]. Thus the present results could be used in clinical studies for estimation of a stroke itself and time-course of its restoration [1].

The study is supported by the Russian Foundation for Humanitarian Science (04-06-00242a).

## References

1. Gasanov R.I., Gitlevich T.R., Levine I.I., Lesnyak V.N. The dynamics of sleep structure in patients with stroke//Modern problems of somnology (abstracts). Moscow, 1998. P. 29. (In Russian)
2. Kositsyn N.S., Ionkina E.G., Serdyuchenko E.G. Reaction of the cortical pyramidal neurons apical dendrites on experimental ischemia// Dokl.Biol.Sci. (Moscow). 1988. V.298. №1. P.247-250.
3. Kovalzon V.M. Origin of sleep//Neurobiology of Sleep-Wakefulness Cycle. 2002. V.2. N1. P.33-36 (<http://www.sleepcycle.org>).
4. Loginov V.V., Dorokhov V.B. Increase in paradoxical sleep time after carotid occlusion in rats//Pav.J.High.Nerv.Activ. (Moscow). 2003. V.53. №6. P.677-680. (In Russian, English summary).
5. Oswald I. Sleep. Penguin:Baltimore, 1966.

## **Transplantation of CSM14.1-cells in the neonatal dopaminergic deafferented striatum leads to a therapeutic improvement and dopaminergic reinnervation**

Stefan Jean-Pierre Haas, Stephan Beckmann, Oliver Schmitt, Stanislav Petrov and Andreas Wree

Institute of Anatomy, Medical Faculty, University of Rostock, Gertrudenstr. 9, 18055 Rostock, Germany

Cell replacement strategies for the treatment of Parkinson's disease are promising, but still discussed controversially. Immortalized progenitor cells could be of further therapeutic interest, because they have several advantages (ethical, availability and handling) compared to primary cells or ES-cells. We therefore investigated the effect of an immortalized progenitor cell line (CSM14.1), which has the capability to differentiate into a dopaminergic fate *in vitro* (Haas and Wree, 2002, J Anat, 201: 61-69), after transplantation into the dopaminergic deafferented neonatal rat striatum. On postnatal day one, 23 rats were bilaterally lesioned by a stereotactic intraventricular 6-OHDA-injection (2 x 1µl, containing 12µg 6-OHDA, coordinates according to bregma: AP -0.6; L ±0.8; V (dura) -2.1). On P3, 6 lesioned animals received a unilateral graft consisting of 100.000 PKH26-labelled CSM14.1-cells into the right Caudate-Putamen (CPu, coordinates: AP +0.7; L -1.8; V -2.9). Five weeks after transplantation, forelimb preference was evaluated with the cylinder test in age matched intact controls (n = 10), bilaterally lesioned (n = 17) and unilaterally transplanted (after lesion) animals (n = 6). Six weeks after birth, animals were perfused and brain sections of the different animals were processed equally for immunohistochemistry to detect changes in tyrosine hydroxylase (TH) by densitometric measurements of optical densities (OD). Moreover, parallel brain sections were treated as described earlier to investigate the differentiation of the PKH26-labelled transplanted cells by immunohistochemistry (Haas et al., 2000, Acta Histochem, 102: 273-280). No paw preference (right : left) was observed in intact (ratio 15 : 15 ±1.76) and bilaterally lesioned (ratio 14.8 : 15.2 ±2.1) animals, whereas lesioned animals, which received a unilateral cell graft in the right CPu showed a significant preference for the left paw (ratio 12.8 : 17.2 ±1.72, p = 0.042, U-test). This kind of lesion leads to a nearly complete bilateral striatal dopaminergic deafferentiation, whereas transplanted animals had strong graft-derived TH-immunoreactivity (ir) in the right CPu with many TH-ir cell bodies. For the densitometric measurements of TH-ir in the various striata we obtained the following results: Intact controls (n = 7) had a mean OD of 11.11 (±2.73) and lesioned animals (n = 7) had a significantly lower OD of 2.08 (±0.39, p = 0.02). Lesioned and subsequently transplanted animals (n = 6) had an OD of 14.45 (±1.84) and were significantly different from lesioned animals (p = 0.03), whereas they did not differ significantly from intact controls (p = 0.116). Due to the PKH26-labelling we were also able to show that grafted cells migrated 1200µm into the host parenchyma and confocal laser scanning microscopy confirmed their differentiation into TH- and NeuN-ir neurons or astrocytes containing GFAP or S100β.

We conclude that the preferential forelimb use could be due to the dopaminergic reinnervation by the grafted cells and that trophic factors in the neonatal brain parenchyma supported the differentiation of the transplanted undifferentiated CSM14.1-cells into a dopaminergic fate.

## **Switching mature retinal ganglion cells to a robust growth state *in vivo*: gene expression and synergy with RhoA inactivation**

Dietmar Fischer<sup>1,2,3</sup>, Victoria Petkova<sup>4</sup>, Solon Thanos<sup>5</sup> and Larry I. Benowitz<sup>1,2,6</sup>

<sup>1</sup>Laboratories for Neuroscience Research in Neurosurgery, Children's Hospital, Boston MA 02115; <sup>2</sup>Department of Surgery and <sup>6</sup>Program in Neuroscience, Harvard Medical School, Boston; <sup>3</sup>Department of Experimental Neurology, University of Ulm, Germany; <sup>4</sup>Harvard Institutes of Medicine, Beth Israel-Deaconess Hospital, Boston; <sup>5</sup>Experimental Ophthalmology, Westfälische Wilhelms-University, Münster, Germany

The inability of mature CNS neurons to regenerate injured axons has been attributed to a loss of inherent growth potential and to inhibitory signals associated with myelin and the glial scar. The present study investigated two complementary issues: (i) whether mature CNS neurons can be stimulated to alter their gene expression profile and switch into a strong growth state; and (ii) whether inactivating RhoA, a convergence point for multiple inhibitory signals, is sufficient to produce strong regeneration, or whether activation of the neuron's growth state is still required. In the mature rat, retinal ganglion cells (RGCs) normally fail to regenerate axons through the injured optic nerve, but can be stimulated to do so by activating macrophages in the eye, e.g., by lens injury. To investigate underlying changes in gene expression, we retrogradely labeled RGCs with a fluorescent dye, performed optic nerve surgery with or without lens injury, and 4 days later, dissociated retinas, isolated RGCs by fluorescence-activated cell sorting, and examined their profiles of gene expression using microarrays. To investigate the effects of inactivating RhoA, we transfected RGCs with adeno-associated viruses carrying a gene for C3 ribosyltransferase. Our results show that, with appropriate stimulation, mature CNS neurons are capable of undergoing dramatic changes in gene expression comparable to those seen in regenerating neurons of the PNS; and that RhoA inactivation by itself results in moderate regeneration, but greatly potentiates the regeneration obtained by activating neurons' growth state *in vivo*.

**Poster Subject Area #PSA29:  
Neurogenetics**

- [#396A](#) H. Lahat, H. Wolf, A. Aharonov, L. Gabis and E. Pras, Tel-Hashomer (IL)  
*Chromosome X studies on multiplex Ashkenazi Jewish families with Autism*
- [#397A](#) U. Geisler, G. Flügge, E. Fuchs and L. Walter, Göttingen  
*Analysis of major histocompatibility complex class I gene expression in the primate brain*
- [#398A](#) R. Schulz, D. Boinska and K. Krieglstein, Göttingen  
*Identification and Characterisation of TGF-beta-induced pro-apoptotic BH3-only proteins*
- [#399A](#) B. Rahhal, S. Heermann, N. Dünker and K. Krieglstein, Göttingen  
*TGF-beta/GDNF Synergism in the Brain Development in vivo and in vitro*
- [#400A](#) B. Spittau, M. Leischke, Z. Wang, D. Boinska and K. Krieglstein, Göttingen  
*Analysis of the regulatory abilities and interacting partners of Tieg3, a new member of the Sp1-like Transcription Factor Family*
- [#401A](#) JA. Reinecke, A. Schneider, K-A. Nave and MJ. Rossner, Göttingen and Heidelberg  
*The transcriptional repressors SHARP-1 and -2 are potential antagonists of HIF-1 activity and may be involved in hypoxia induced transcriptional responses*
- [#402A](#) T. Rasse, W. Fouquet, A. Schmid, A. Guzman, RJ. Kittel, CB. Sigrist, M. Richter, M. Heckmann and S. Sigrist, Göttingen and Freiburg  
*Postsynaptic densities at the Drosophila NMJ do not split but assemble de novo*
- [#403A](#) P. Chapouton, B. Adolf and L. Bally-Cuif, Munich and Neuherberg  
*Characterization of a new neurogenic zone in the adult zebrafish brain*
- [#404A](#) S. Haupt, L. Nolden, H. Siemen, T. Wunderlich, F. Edenhofer and O. Brüstle, Bonn and Cologne  
*Cre protein transduction in human and murine ES cells and their neural progeny*
- [#395B](#) S. Knapinski, J. Ustinova, M. Hennig, H. Saumweber and B. Ronacher, Berlin and Erlangen  
*The expression of behavioural genes in the CNS of crickets.*
- [#396B](#) S. Lehmann, S. Moritz, A. von Holst and A. Faissner, Bochum  
*An Induction Gene Trap Screen for Chondroitin Sulphate Proteoglycan Target Genes in Neural Stem Cells*
- [#397B](#) S. Moritz, S. Lehmann, A. Faissner and A. von Holst, Bochum  
*An Induction Gene Trap Screen for Tenascin-C Target Genes in Neural Stem Cells*

- [#398B](#) P. Claus, A-F. Bruns, J. van Bergeijk, K. Haastert and C. Grothe, Hannover  
*Functional domain mapping of the survival of motoneuron (SMN) protein: effects on axonal growth*
- [#399B](#) C. Hohoff, JM. McDonald, BT. Baune, EH. Cook, J. Deckert and H. de Wit, Muenster and Chicago, IL (USA)  
*Relevance of Exonic Adenosine A2A Receptor Gene Polymorphisms for Amphetamine induced Mood States*
- [#400B](#) A. Jung, C. Hohoff, C. Freitag, S. Brady, G. Ponath, P. Krakowitzky, J. Fritze, P. Franke, B. Bandelow, R. Fimmers, MM. Nöthen, J. Flint and J. Deckert, Münster, Saarland, Oxford (UK), Frankfurt, Bonn and Göttingen  
*Polymorphisms of the RGS 2-gene: Relevance for the development of panic disorder?*
- [#401B](#) C. Hohoff, N. Tidow, M. Stoll, S. Rust, R. Lencer, S. Purmann, E. Schwinger, B. Brandt, J. Deckert and V. Arolt, Muenster and Luebeck  
*Schizophrenia Families Characterized for the Endophenotype Eye Tracking Dysfunction : Analysis of Polymorphisms in the Tumor Necrosis Factor alpha gene*
- [#402B](#) MO. Popa, K. Hallmann, J. Rebstock, N. Tilgen, S. Maljevic, A. Heils and H. Lerche, Ulm and Bonn  
*A novel mutation associated with childhood absence epilepsy affects G-protein modulation of P/Q type calcium channels*
- [#403B](#) A. Schmitt, S. Fritzen, E. Claes, P. Gass, K-P. Lesch and A. Reif, Wuerzburg and Mannheim  
*Neuronal nitric oxide synthase knockout impacts on the survival of neural stem cells and growth factor expression*
- [#404B](#) S. Fritzen, A. Schmitt, A. Strobel, CP. Jacob, S. Chourbaji, P. Gass, K-P. Lesch and A. Reif, Wuerzburg, Dresden and Mannheim  
*Converging lines of evidence argue for a role of endothelial nitric oxide synthase (NOS-III) in affective disorders*

## **Chromosome X studies on multiplex Ashkenazi Jewish families with Autism**

Hadas Lahat<sup>1</sup>, Haike Wolf<sup>1</sup>, Ala Aharonov<sup>1</sup>, Lidia Gabis<sup>2</sup>, Elon Pras<sup>1</sup>

1. Institute of Human Genetics, Sheba Medical Center, Tel-Hashomer, Israel

2. Pediatric Neurology Department, Sheba Medical Center, Tel-Hashomer, Israel

corresponding author : epras@post.tau.ac.il

**Background:** Involvement of the X chromosome in autism is especially appealing given the 4:1 male to female ratio. Recently, mutations in two X linked genes, NLGN3 and NLGN4 were reported in siblings with autism-spectrum disorders. These mutations affect cell-adhesion molecules localized at the synapse and suggest that a defect of synaptogenesis may predispose to autism. **Ashkenazi Jews** are a small and homogenous population that has been genetically isolated for many generations and has originated from a small number of founders. Since genetic heterogeneity may be considerably smaller in this population, we will investigate the possibility that in the Ashkenazi Jewish population, there is/are subgroup/s in which a common major gene(s) on the X chromosome may have a major effect on the occurrence of autism. Skewed x inactivation is a well established phenomena in x linked mental retardation and other x linked disorders, but has not been diligently studied in autism. Recently, a trend for X chromosome skewing was detected in mothers of autistic children. Such skewing may indicate that x linked genes are involved in the pathogenesis of this disorder in their children.

**Aim:** To perform intensive studies on the X chromosome in Ashkenazi families that might fit to X linked inheritance. The study may help to determine the part (if any) of chromosome X in the genetics of the Ashkenazi population.

**Preliminary results:** A unique DNA pool of 22 Ashkenazi families with at least 2 sibs (male brothers – not twins) diagnosed with autism was created. The families were analyzed with polymorphic markers very close to NLGN3 and NLGN4. Families who showed evidence for a segregation, were analyzed for mutations by direct sequencing of NLGN3 (n=5) and/or NLGN4 (n=4). We have not found mutation or uncommon polymorphism in these families.

**Future studies** : **X-inactivation** studies will be performed on mothers from these families. We will use the androgen receptor gene, as a marker for X chromosome skewing. Finding skewed x inactivation in a subset of the families, will enhance further studies as to the involvement of the X chromosome in these families. We also intend to perform **Fine Mapping** of chromosome X, using an additional large set of polymorphic markers located every 2 Mb.

**Conclusion and significance:** Our results indicate that in the Ashkenazi Jewish population the part of NLGN3 and NLGN4 in multiplex autistic families is minor if any.



## Analysis of major histocompatibility complex class I gene expression in the primate brain

Ulrike Geisler (1,2), Gabriele Flügge (1), Eberhard Fuchs (1), Lutz Walter (2)

(1) Clinical Neurobiology, German Primate Center, 37077 Göttingen, Germany

(2) Primate Genetics, German Primate Center, 37077 Göttingen, Germany

Neurons of the central nervous system are usually regarded not to express major histocompatibility complex (MHC) class I genes. However, recent in vivo studies in rodents and cat revealed important functions of class I molecules in neuronal plasticity in both the developing and the adult brain (Corriveau et al., 1998; Lindå et al., 1999; Huh et al., 2000). In the present study we examined MHC class I gene and protein expression in neurons of a non-human primate, the common marmoset monkey (*Callithrix jacchus*).

For the expression analysis on the cellular level, we performed in situ hybridisation. Reverse transcription PCR from marmoset hippocampal and cerebellar RNA identified transcripts of MHC class I loci *Caja-G* and *Caja-E*. In situ hybridisation revealed distinct patterns of *Caja-G* expression in certain areas of the brain, i.e. hippocampus, substantia nigra, areas of the nucleus ruber and area ventral to the third ventricle. In contrast, expression pattern of *Caja-E* was substantially lower.

To answer the question whether expression of MHC class I genes extends also to the protein level, immunohistochemistry was carried out using monoclonal mouse anti-human MHC class I antibody Tü 149 (detects all HLA-B, HLA-C, and some HLA-A molecules) and the monoclonal mouse anti-rat MHC class I antibody MRC Ox-18 (detects most rat MHC class I molecules). Both antibodies cross-react with marmoset MHC class I molecules according to flow cytometry analysis. The fluorescence signals analysed so far revealed corresponding MHC class I protein and mRNA expression.

This is the first description of MHC class I expression in the primate brain. Further studies are needed to clarify the function of these MHC molecules in the brain.

Supported by the DFG-GRK 289 'Perspectives in Primatology'.

## References

- Corriveau, R.A., Huh, G.S., Shatz, C.J. (1998) Regulation of class I MHC gene expression in the developing and mature CNS by neuronal activity. *Neuron*, **21**, 505-520.
- Lindå, H., Hammarberg, H., Piehl, F., Khademi, M., Olsson, T. (1999) Expression of MHC class I heavy chain and  $\beta$ 2-microglobulin in rat brainstem motoneurons and nigral dopaminergic neurons. *Journal of Neuroimmunology*, **101**, 76-86.
- Huh, G.S., Boulanger, L.M., Du, H., Riquelme, P.A., Brotz, T.M., Shatz, C.J. (2000) Functional requirement for class I MHC in CNS development and plasticity. *Science*, **290**, 2155-2159.

## Identification and Characterisation of TGF- $\beta$ -induced pro-apoptotic BH3-only proteins

Ramona Schulz, Dagmara Boinska and Kerstin Krieglstein

Center of Anatomy, Department of Neuroanatomy, University of Goettingen, Germany

Transforming growth factor-beta (TGF- $\beta$ ) is a multifunctional cytokine which regulates numerous cell activities like cell-cycle control, early development, differentiation, hematopoiesis and the induction of apoptosis (programmed cell death). Specifically, lack of TGF- $\beta$  prevents death of neurons during ontogenetic cell death periods.

Jointly responsible for the apoptotic effect of TGF- $\beta$  are the Bcl-2 family members which are induced by the mitochondrial 'death' pathway by TGF- $\beta$  besides many other death stimuli. The Bcl-2 family includes both pro- as well as anti-apoptotic proteins whereas the ratio between these two subsets determine the apoptotic event to induce the caspase cascade by forming pores in the outer mitochondrial membrane to release cytochrome c. The characteristic to form pores is generated by the pro-apoptotic BH3-only proteins by neutralization of anti-apoptotic proteins or by heterodimerization of pro-apoptotic proteins.

The importance of TGF- $\beta$ -mediated apoptosis can be seen in its restriction to certain cell types, to a certain state of differentiation and to other growth factors which was shown in several in vitro and in vivo models. Further it was shown that the TGF- $\beta$ -induced caspase activation associates with the downregulation of the anti-apoptotic Bcl-2 family members.

To investigate the mechanism of TGF- $\beta$ -induced programmed cell death we will characterize pro-apoptotic BH3-only proteins. Therefore we will perform GST-Pulldown experiments with a Neuroblastoma cell-line to identify interactions between anti- and pro-apoptotic Bcl-2 family members. Further we will screen new BH3-only proteins via a yeast Two-Hybrid System.

***TGF- $\beta$ /GDNF Synergism in the Brain Development in vivo and in vitro***

**\*Belal Rahhal, \*Stephan Heermann, Nicole Dünker and Kerstin Krieglstein**

Center of Anatomy/Department of Neuroanatomy, University of Göttingen,  
Kreuzberggring 36, 37075 Goettingen, Germany

A major area of investigations in neurobiology is directed at understanding factors that participate in neuronal survival versus death. A number of neurotrophic growth factors have been identified that promote neuronal survival, death and differentiation. Therefore they are good candidates to be responsible for different developmental and neurodegenerative diseases such as Alzheimer, Amyotrophic lateral sclerosis and Parkinson's disease. The TGF-beta family consists of three isoforms for mammalian tissue, TGF beta 1,2,3. Their spectrum of function is very broad and contains control of cell proliferation and differentiation, production of extracellular matrix components, chemotaxis, immunosuppression and regulation of cell survival and death. Glial cell line-derived neurotrophic factor (GDNF) itself is distantly related to TGF- $\beta$ . It maintains survival of various neuronal populations such as midbrain dopaminergic neurons. Several evidences suggest that GDNF may require cofactors for acting as neurotrophic factor. GDNF does not support the survival of most peripheral neurons in low-density dissociated cultures and defined media. Neutralization of endogenous TGF- $\beta$  using antibodies against the three TGF- $\beta$  isoforms abolishes the neurotrophic effect of GDNF in vivo. Current work aims at elucidation of TGF- $\beta$  and GDNF synergism in vivo and in vitro. Heterozygous animals of TGF- $\beta$ 2 and GDNF are crossed in order to receive mice lacking both TGF- $\beta$ 2 and GDNF. The analysis focuses on the ventral aminergic neurons such as midbrain dopaminergic neurons and 5-HT positive neurons in dorsal raphe, medial raphe and raphe magnus nucleus. In vitro, TGF $\beta$ /GDNF synergism is analysed by identification and characterisation of transcription factors mediating the common response. Tha data suggest that GDNF and TGF- $\beta$  serve important function in brain development.

Funded by DFG Forschungszentrum CMPB.

# **Analysis of the regulatory abilities and interacting partners of Tieg3, a new member of the Sp1-like Transcription Factor Family**

Björn Spittau, Mandy Leischke, Ziyuan Wang, Dagmara Boinska, Kerstin Kriegelstein  
*University of Göttingen, Center of Anatomy, Department of Neuroanatomy*

TGF- $\beta$  is a multifunctional cytokine playing important roles during nervous system development and maintenance. Transcriptional regulation of TGF- $\beta$  target genes is mediated by TGF- $\beta$  early response genes (Tiegs) Tieg1 and Tieg 3. Tieg3 belongs to the growing family of Sp1-like zinc finger transcription factors characterized by three highly homologous c-terminal zinc finger motifs that bind GC-rich sequences. These sequences are present in the promoters of more than thousand different gene products indicating a fundamental role of Sp1-like transcription factors in the regulation of cell growth and differentiation. Recent studies have shown the ability of Tieg proteins to inhibit epithelial cell growth (1) and to induce apoptosis in different cell lines (2,3). These inhibitory effects are mediated by three transcriptional repressor domains which are conserved within the Tieg family (4). The presence of these domains suggests that, in contrast to other Sp1-like proteins, the Tiegs evolved to silence gene expression in mammalian cells. In fact, up to now no activation of gene expression mediated by members of the Tieg family has been shown.

In this study, we use the Yeast Two-Hybrid System to identify potential target proteins of Tieg3. By utilizing a bait construct containing full-length Tieg3 we are screening a BD Matchmaker cDNA BALB/c mouse brain (ages 9-12 weeks) library. For more detailed investigations we will apply a construct containing the N-terminal regulatory domain of Tieg3 exclusively. This region differs among the SP1-like family and is supposed to mediate specific interactions with other regulatory proteins.

On the other hand we applied the Gal4-dependent luciferase reporter assay system to analyse the regulatory abilities of definite parts of Tieg3 protein on gene expression. This approach has been previously used to characterize the transcriptional regulatory activity of several members of the Sp1-like family of proteins. We focused on the zinc finger motif, representing the DNA binding domain of the Tieg proteins. Interestingly, we elucidated that the three zinc fingers have partially opposite regulatory effects. Cook et al. (4) have shown that the c-terminus of the human Tieg2 has no effect on gene expression. In contrast, we demonstrated that the c-terminus of murine Tieg3 has the ability to activate the expression of genes. Taken together these results suggest that the function of Tieg3 is not only restricted to silence gene expression. This feature represents a totally new aspect of this zinc finger transcription factor and augments the functional prospects of Tieg3.

## References:

- (1) Cook et al. 2000, *Am J Physiol Gastrointest Liver Physiol.* 278(4):G513-21
- (2) Tachibana et al. 1997, *J Clin Invest.* 99(10):2365-74
- (3) Chalaux et al. 1999, *FEBS Lett.* 457(3):478-82
- (4) Cook et al. 1999, *J Biol Chem.* 274(41):29500-4

**The transcriptional repressors SHARP-1 and -2 are potential antagonists of HIF-1 activity and may be involved in hypoxia induced transcriptional responses**

J. A. Reinecke<sup>1\*</sup>, A. Schneider<sup>2</sup>, K.-A. Nave<sup>1</sup>, M. J. Rossner<sup>1</sup>

<sup>1</sup>MPI for Experimental Medicine, Goettingen, Germany, <sup>2</sup>Axaron Bioscience AG, Heidelberg, Germany

SHARP-1 and -2 (enhancer-of-Split and *Hairy Related Proteins*) are transcription factors belonging to the basic helix-loop-helix (bHLH) protein family. Both are transcriptional repressors and their mRNA expression in cultured cells is regulated by various stimuli, such as cAMP, retinoic acid and hypoxia. In addition, it was shown that the rapid SHARP-1 and -2 protein turnover is controlled by ubiquitination. In the brain, the mRNA expression of SHARP-2 is induced by neuronal activity. Furthermore, reporter gene assays showed that SHARP-1 and -2 may be direct HIF-1 $\alpha$  (Hypoxia Inducible Factor 1 alpha) target genes. HIF-1 $\alpha$  belongs to the bHLH-PAS family of transcription factors and is the major effector of oxygen dependent transcriptional responses. Analyzing the respective SHARP null-mutant mice, we could currently show that SHARP-1 and -2 are likely to be antagonists of the circadian control genes CLOCK and NPAS2, which are also members of the bHLH-PAS family.

To further investigate the potential role of SHARP-2 in oxygen dependent transcriptional processes in vivo, we generated transgenic mice where the mRNA coding for a FLAG-tagged SHARP-2 full-length protein can be overexpressed. We used the 'Tet-system' to control for the level of expression in time and in space simply by adding doxycyclin to the drinking water. So far, we could establish two independent and functional reporter mouse lines. The SHARP-2 overexpression in the developing forebrain leads in one mouse line to an embryonal lethal phenotype, pups of the second mouse line die 8-10 days after birth. Preliminary results reveal heavily magnified ventricles in the brains of the transgenic mice. This 'hydrocephalus like' phenotype resembles the observation that was made with mice carrying brain specific HIF-1 $\alpha$  null alleles. Published results as well as our preliminary mouse data strengthen our hypothesis that SHARP-2 may fulfil HIF-1 $\alpha$  antagonistic roles in vivo. To complement the mouse analysis, we are currently studying the potential protein-protein interactions between SHARP-1 and -2 and the HIF bHLH-PAS family members. In addition, we are investigating the potential role of SHARP-1 and -2 in HIF-dependent gene expression using reporter gene assays.

**Postsynaptic densities at the *Drosophila* NMJ do not splitt but assemble *de novo***

Tobias Rasse<sup>1</sup>, Wernher Fouquet<sup>1</sup>, Andreas Schmid<sup>1</sup>, Asja Guzman<sup>1</sup>, Robert J. Kittel<sup>1</sup>, Carola B. Sigris<sup>1</sup>, Miriam Richter<sup>1</sup>, Manfred Heckmann<sup>2</sup> and Stephan Sigris<sup>1</sup>

(1) European Neuroscience Institute Göttingen, Max-Planck-Society, Waldweg 33, D-37073 Göttingen (Germany)

(2) Physiologisches Institut, Hermann-Herder-Str. 7, D-79104 Freiburg

**Splitting of postsynaptic densities (PSDs) at glutamatergic synapses was suggested to contribute to synapse formation relevant for learning and memory. Here, PSDs were visualized during the formation of new glutamatergic synapses in living *Drosophila*. We find that additional small PSDs form distant from existing synapses and then grow to a mature size. *In vivo* labeling of glutamate receptors showed that newly forming PSDs grow by local entry of glutamate receptors from diffuse extra-synaptic pools. In contrast, receptors from pre-existing synapses seemingly do not contribute to PSD growth. Our data show that PSDs assemble *de novo* during the formation of glutamatergic synapses. We further apply this assay to explore the molecular dynamics of postsynaptic assembly. We can show that the PSD component pak has a much faster turnover when compared to glutamate receptors. Our work implies that glutamate receptor availability directly controls PSD and thus synapses formation. The new assay developed will allow us to further study the dynamics of synaptic proteins at the level of individual synapses in the context of an intact organism.**

## Characterization of a new neurogenic zone in the adult zebrafish brain

Prisca Chapouton, Birgit Adolf and Laure Bally-Cuif

Zebrafish Neurogenetics Junior Research Group, Institute of Virology, Technical University-Munich, Trogerstrasse 4b, D-81675 Munich, Germany and GSF-National Research Center, Institute of Developmental Genetics, Ingolstaedter Landstrasse 1, D-85764 Neuherberg, Germany

In the past few years, an increasing number of studies have described zones of proliferation and neurogenesis in the adult mammalian telencephalon: the subventricular zone and the dentate gyrus. In teleost adult brain, a zone of proliferation located in the midbrain, at the posterior border of the optic tectum (tectal proliferation zone), has also been discovered (Nguyen et al., 1999). We describe here in the adult zebrafish a new midbrain proliferation zone that we call isthmic proliferation zone, at the boundary region between dorsal midbrain, ventral midbrain and hindbrain. This region incorporates the thymidine analogon BrdU and expresses the neurogenic genes *ngn1* and *zash1a*. It also expresses two genes encoding for transcription factors of the Hairy/E(s) family, *her5* and our newly isolated *her10* gene. We are currently studying the anatomical and lineage relationship between the different populations expressing *her5*, *her10*, *notch1a* and *neurogenin1* in the tectal and isthmic proliferation zone. Using BrdU incorporation followed by long survival times as well as transplantation experiments in slice culture, we are also analyzing the fate of cells born in the isthmic and tectal proliferation zone. Our preliminary data indicate that cells from the isthmic proliferation zone enter the neurogenic pathway, suggesting that they are true neuronal progenitors.

**Cre protein transduction in human and murine ES cells and their neural progeny**

Simone Haupt\*, Lars Nolden\*, Henrike Siemen, Thomas Wunderlich<sup>#</sup>, Frank Edenhofer\* & Oliver Brüstle

\*Stem Cell Engineering Group, Institute of Reconstructive Neurobiology, University of Bonn Medical Center, Bonn

<sup>#</sup>Institute for Genetics, University of Cologne, Cologne

Inducible site-specific recombination is a powerful tool for the controlled genetic modification of mammalian cells both *in vitro* and *in vivo*. While efficient in mouse transgenics, *in vitro* stem cell engineering and clinical applications of human ES cells would greatly benefit from a system that bypasses an additional step involving Cre expression. We have developed a Cre protein transduction system that permits the direct delivery of biologically active Cre protein to mammalian cells. Recently, we successfully applied this system during neural differentiation of murine ES cells. Cre protein transfer was achieved in undifferentiated murine ES cells with an efficiency of more than 95%. Now we demonstrate efficient Cre protein transduction into ES cell-derived pan-neural and glial precursors. Transduction efficiency was analyzed using the Z/EG ES cell reporter line which displays green fluorescence upon Cre-mediated recombination. Double labeling with antibodies to neural marker antigens demonstrated that neuronal and glial differentiation of Cre-treated precursors was unaffected. Moreover, Cre protein transduction into terminally differentiated post-mitotic neurons was achieved. We next adapted the Cre protein transduction technology to human ES cells. As a first step, we established a human reporter ES cell line which displays a Cre-mediated switch from red to green fluorescent color. Based on this read-out system, we obtained recombination efficiencies in undifferentiated human ES cells of up to 90%. Analysis of Oct-4 and alkaline phosphatase expression revealed that Cre-transduced human ES cells maintain their pluripotency. Current studies focus on the translation of Cre protein transduction to human ES cell-derived neural precursors and their differentiated progeny. We expect this technology to provide an efficient strategy for stage-specific transgene regulation in differentiating human ES cells.



## The expression of “behavioural genes” in the CNS of crickets.

Sven Knapinski <sup>1</sup>, Jana Ustinova <sup>2</sup>, Matthias Hennig <sup>1</sup>, Harald Saumweber <sup>3</sup> and Bernhard Ronacher <sup>1</sup>

<sup>1</sup> Behavioural Physiology, Humboldt University Berlin, Invalidenstr. 43, 10115 Berlin

<sup>2</sup> Institute of Zoology 2, Friedrich-Alexander-University, Staudstr. 5, 91058 Erlangen

<sup>3</sup> Cytogenetics, Humboldt University Berlin, Chausseestr. 117, 10115 Berlin

A characteristic feature of many insects is their ample repertoire on innate species-specific behaviours. Such behavioural sequences depend on central pattern generators that must be genetically predefined. In other words, the expression of genes initiates a developmental programme that in turn leads to the assembly of a neural network exhibiting the appropriate functions. In this context, however, one has to remember that the requirements on the behavioural traits will also change during an individual's ontogeny. While a major goal of a juvenile is to grow until sexual maturity (and to escape predators at the same time), reproduction becomes a major incentive once an animal has reached adulthood.

Adult male crickets produce a species-specific stereotypical song pattern to attract mates, whereas juveniles are not able to produce such acoustic signals due to the lack of appropriate wing structures. In contrast to holometabolic insects, where the animal is almost completely reassembled during the pupal stage, hemimetabolic insects (like crickets) develop gradually. While the ability to chirp is obtained after the last ecdysis, at least parts of the neural network responsible for the acoustic communication probably already exist in late juvenile stages.

We try to identify genes responsible for species-specific song traits in crickets and to knock them down via RNAi, in order to learn about their respective function. For this purpose it is important to know how these genes are expressed in different parts of the CNS during the development and in adult animals. To find these “song genes” we created a cDNA library of *Gryllus bimaculatus* and screened for genes homologous to “song genes” already known in *Drosophila*. Until now we found three genes, which show a considerable amount of homology to *Drosophila* “song genes” and therefore may play a role in acoustic communication in crickets as well. We prepared expression profiles of these genes, covering all developmental stages as well as the adult stage.

## An Induction Gene Trap Screen for Chondroitin Sulphate Proteoglycan Target Genes in Neural Stem Cells

**Stefanie Lehmann, Sören Moritz, Alexander von Holst & Andreas Faissner**

Department for Cell Morphology & Molecular Neurobiology, Ruhr-University Bochum, Universitätsstraße 150, D-44780 Bochum; [Andreas.Faissner@ruhr.uni-bochum.de](mailto:Andreas.Faissner@ruhr.uni-bochum.de); supported by DFG SPP 1109 and IGSN, Bochum

The differentiation and proliferation potential of neural stem cells (NSCs) are controlled by environmental factors, including extracellular matrix (ECM) molecules. We are investigating the role of chondroitin sulphate proteoglycans (CS-PGs) which are defined components of the extracellular matrix present in the germinative layers of the embryonic CNS and in the adult neural stem cell niche<sup>1</sup>, where neural progenitors and/or NSC reside. The functional properties of the chondroitin sulphate proteoglycans are often associated with the glycosaminoglycan (GAG) sugar chains attached to the core protein. The CS-GAGs are essential for several developmental processes<sup>2,3,4</sup> and play also a role in the regenerative context<sup>5</sup>. For instance, the enzymatic removal of CS-GAGs by chondroitinase ABC (Chase ABC) *in vivo* after injury results in neurite growth promoting effects<sup>6</sup>. However, the molecular mechanisms and the downstream signalling events after treatment with Chase ABC are entirely unknown. To obtain information about the molecular cascades which are affected by CS-GAG removal, the induction gene trap technology<sup>7</sup> has been adapted for use in NSCs cultivated as free-floating neurospheres<sup>8</sup>. After dissociation neurosphere-derived cells are electroporated with different gene trap vectors via the nucleofection technology. The gene trap vectors consist of a splice acceptor in front of the open reading frame of a *lacZ* reporter gene and a *neo*<sup>R</sup> selection marker. The integration of the gene trap vectors into the genome occurs at random<sup>7</sup>. Thus, upon integration into an active locus a fusion transcript is generated which consists of the upstream regulatory sequences and a reporter gene through mRNA splicing. The resistant gene trap clones are tested for  $\beta$ -galactosidase activity, which reflects the expression level of the trapped gene. In the screening procedure individual clones are tested for  $\beta$ -galactosidase activity in the presence or absence of Chase ABC. We have so far generated > 500 independent gene trap clones. More than 200 of them have been screened for regulation by Chase ABC treatment. We have found 5 induced and 0 repressed gene trap vector integrations as a result of CS-GAG removal. These candidates will be analysed further by 5'RACE and will, hopefully, allow further insight into the function of CS-GAGs in neural stem cells.

<sup>1</sup> GATES M.A., THOMAS C.B., HOWARD E.M., LAYWELL E.D., SAJIN B., FAISSNER A., GOTZ B., SILVER J., STEINDLER D.A.: Cell and molecule analysis of the developing and adult mouse subventricular zone of the cerebral hemispheres, *J Comp. Neurology* **361** 249-266 (1995).

<sup>2</sup> MIZUGUCHI S., UYAMA T., KITAGAWA H., NOMURA K.H., DEJIMA K., GENGYO-ANDO K., MITANI S., SUGAHARA K., NOMURA K.: Chondroitin proteoglycans are involved in cell division of *Caenorhabditis elegans*, *Nature* **423** 443-448 (2003).

<sup>3</sup> HÄCKER U., LIN X., PERRIMON N.: The *Drosophila* sugarless gene modulates Wingless signalling and encodes an enzyme involved in polysaccharide biosynthesis, *Development* **124** 3565-3573 (1997).

<sup>4</sup> HWANG H.-Y., OLSON S.K., ESKO J.D. & HORVITZ H.R.: *Caenorhabditis elegans* early embryogenesis and vulval morphogenesis require chondroitin biosynthesis, *Nature* **423**, 439-443 (2003).

<sup>5</sup> RHODES K.E., FAWCETT J.W.: Chondroitin sulphate proteoglycans: preventing plasticity or protecting the CNS?, *J. Anat.* **204**, 33-48 (2004).

<sup>6</sup> BRADBURY E.J., MOON L.D.F., POPAT R.J., KING V.R., BENNETT G.S., PATEL P.N., FAWCETT J.W. & MCMAHON S.B.: Chondroitinase ABC promotes functional recovery after spinal cord injury, *Nature* **416**, 636-640 (2002).

<sup>7</sup> FLOSS T., WURST W.: Functional genomics by gene-trapping in embryonic stem cells, *Meth. in Mol. Biol.* **184**, 347-379 (2002).

<sup>8</sup> REYNOLDS B.A., WEISS S.: Clonal and Population Analyses Demonstrate That an EGF-Responsive Mammalian Embryonic CNS Precursor Is a Stem Cell, *Developmental Biology* **175** 1-13 (1996).

## An Induction Gene Trap Screen for Tenascin-C Target Genes in Neural Stem Cells

Sören Moritz, Stefanie Lehmann, Andreas Faissner & Alexander von Holst; Department for Cell Morphology & Molecular Neurobiology,  
Ruhr-Universität-Bochum

Correspondence: andreas.faissner@ruhr-uni-bochum.de

We are interested in the functions of environmental factors that control the self-renewal and differentiation potential of neural stem cells (NSCs). The modular extracellular matrix (ECM) glycoprotein Tenascin-C (Tn-C) is expressed in the ventricular and subventricular zone during embryonic forebrain development where neural progenitors and/or NSCs reside. Postnatally, expression persists in the neural stem cell niche of the adult CNS<sup>1</sup>. For Tn-C several interaction partners (e.g. phosphacan, neurocan) and some cell surface receptors have been described (e.g. integrin  $\alpha 3$ , RPTP- , F3/Contactin). Also several inhibitory and stimulatory functions regarding cell adhesion/migration and axon growth/guidance have been attributed to Tn-C and mapped to specific Tn-C modules, but in most cases neither signalling pathways nor Tn-C regulated target genes are known<sup>2</sup>. Recently, it has been shown that Tn-C regulates the NSC pool during embryonic development by modulating growth factor responses of NSCs. It increases the sensitivity of NSCs to FGF2 and interferes with the BMP4 signalling pathway which results in the correct temporal EGFR expression during development<sup>3</sup>. It is, however, incompletely understood how Tn-C regulates self-renewal and differentiation of NSCs. Therefore, the molecular basis of Tn-C signaling was investigated further.

To analyse this question, NSCs grown as free-floating neurospheres<sup>4</sup> were used, which serve as a widespread model system for NSCs maintenance and neural differentiation. Their stem cell character is documented by two major features: namely self renewal and the capability to differentiate into the three major neural cell types of the CNS (neurons, astrocytes and oligodendrocytes).

In order to gain insight into the molecular events which are influenced by Tn-C, an induction gene trap method in NSCs has been established. A gene trap vector consisting of a splice acceptor site fused to the lacZ reporter gene and a neomycin selector was electroporated into cells derived from 3<sup>rd</sup> passage neurospheres. These cells were transfected with 56±9% efficiency as determined 1 d after electroporation. Upon integration into the genome, transfected neural stem cells were selected with G 418 (neomycin) giving rise to clonal neurospheres. Each clone, containing the lacZ reporter is driven by the endogenous promoter of the trapped gene and was tested in parallel for  $\beta$ -galactosidase activity in the absence or presence of Tn-C (or Tn-C-derived fragments). So far >500 clonal lines were generated which will independently be screened for gene trap vector integrations that show a Tn-C-dependent regulation of  $\beta$ -galactosidase activity. Using 5'-RACE the trapped genes will be identified. Furthermore, the clones thus obtained can be stored in and retrieved from liquid nitrogen, constituting a growing gene trap library in NSCs.

(supported by DFG, SPP 1109)

<sup>1</sup> Gates M.A., Thomas C.B., Howard E.M., Laywell E.D., Sajin B., Faissner A., Gotz B., Silver J., Steindler D.A.: Cell and molecule analysis of the developing and adult mouse subventricular zone of the cerebral hemispheres, *J Comp. Neurology* **361** 249-266 (1995).

<sup>2</sup> Garwood J, Rigato F, Heck N, Faissner A.: Tenascin glycoproteins and the complementary ligand DSD-1-PG/ phosphacan--structuring the neural extracellular matrix during development and repair. *Restor Neurol Neurosci.* **19** 51-64. Review. (2001)

<sup>3</sup> Garcion E, Halilagic A, Faissner A, French-Constant C.: Generation of an environmental niche for neural stem cell development by the extracellular matrix molecule tenascin C. *Development* **131** 3423-32 (2004)

<sup>4</sup> Reynolds B.A., Weiss S.: Clonal and Population Analyses Demonstrate That an EGF-Responsive Mammalian Embryonic CNS Precursor Is a Stem Cell, *Developmental Biology* **175** 1-13 (1996).

## Functional domain mapping of the survival of motoneuron (SMN) protein: effects on axonal growth

Peter Claus<sup>1,2,\*</sup>, Alexander-Francisco Bruns<sup>1</sup>, Jeroen van Bergeijk<sup>1</sup>, Kirsten Haastert<sup>1,2</sup>, Claudia Grothe<sup>1,2</sup>

<sup>1</sup>Department of Neuroanatomy, Hannover Medical School, and <sup>2</sup>Center for Systems Neuroscience (ZSN) Hannover, OE 4140, Carl-Neuberg-Str.1, 30625 Hannover, Germany

\*e-mail address of the corresponding author: claus.peter@mh-hannover.de

Spinal muscular atrophy (SMA) is a neurodegenerative disease affecting motoneurons in the spinal cord. SMA is caused by mutations or a deletion of the survival of motoneuron (SMN) gene 1. In most cases of SMA the C-terminus of the SMN protein is missing. SMN has a functional role as an assembly protein for small nuclear ribonucleoprotein particles (snRNP) in the cytoplasm. After assembly of Sm-proteins on catalytic small nuclear RNA molecules the complex is transported into the nucleus. SMN dissociates from snRNPs in the nucleus and localizes to certain nuclear bodies called Cajal bodies and nuclear gems. Patients with SMA display significantly less or missing nuclear gems. We have recently shown a direct interaction of the neurotrophic and nuclear fibroblast growth factor – 2 (FGF-2) with SMN (Claus et al., 2003; Claus et al., 2004; Gringel et al., 2004). In this study, we performed a functional domain mapping of the SMN protein with respect to differential nuclear localization and effects on neurite outgrowth in PC12 cells. SMN deletions were fused to green fluorescent protein (EGFP) and localization analyzed in living Schwann cells. A mutant without the C-terminus lost the ability to form nuclear gems and located instead diffusely to the nucleoplasm. In the neurite outgrowth assay in PC12 cells, full-length SMN enhanced neurite outgrowth after nerve growth factor treatment. Interestingly, the C-terminal deletion mutant demonstrated the same effect, whereas its ability to assemble snRNPs was impaired. These data argue for a splicing-independent contribution of the C-terminal SMN-domain to neurite growth.

Supported by: This work was supported by the following grants to P.C.: Deutsche Gesellschaft für Muskelkranke (DGM e.V.) and Fritz Thyssen Stiftung, Köln, Germany.

### References:

Claus P., Döring F., Gringel S., Müller-Ostermeyer F., Fuhlrott J., Kraft T., Grothe C. (2003) Differential Intranuclear Localization of Fibroblast Growth Factor - 2 (FGF-2) Isoforms and Specific Interaction with the Survival of Motoneuron Protein. *J. Biol. Chem.*, 278:479-485.

Claus P., Bruns AF, Grothe C. (2004): Fibroblast growth factor-223 is binding directly to the survival of motoneuron protein and is associated with small nuclear RNAs. *Biochem J.*, in press.

Gringel S., van Bergeijk J., Haastert K., Grothe C., Claus P. (2004): Nuclear Fibroblast Growth Factor - 2 Interacts Specifically with the Splicing Factor SF3a66. *Biol. Chem.*, in press.

## **Relevance of Exonic Adenosine A<sub>2A</sub> Receptor Gene Polymorphisms for Amphetamine induced Mood States**

C Hohoff<sup>1,\*</sup>, JM McDonald<sup>2</sup>, BT Baune<sup>1</sup>, EH Cook<sup>2</sup>, J Deckert<sup>1</sup>, H de Wit<sup>2</sup>

<sup>1</sup>Department of Psychiatry, University of Muenster, Germany; \*hohoffch@uni-muenster.de

<sup>2</sup>Department of Psychiatry, The University of Chicago, IL, USA

Amphetamine is a psychostimulant drug that increases feelings of energy, well-being and alertness. Some individuals report increased anxiety or nervousness after amphetamine. These effects are assumed to be mainly mediated by the dopamine neurotransmitter system. Dopamine D<sub>2</sub> and adenosine A<sub>2A</sub> receptors form a functional heterodimer complex in cell membranes. In the present study we studied the relevance of the three presently confirmed exonic adenosine A<sub>2A</sub> receptor gene polymorphisms for the interindividual variability in subjective responses to amphetamine.

A group of 99 healthy young volunteers received placebo or d-amphetamine (10 mg or 20 mg, respectively) double-blind, in randomised order and under standardised conditions. Self-report questionnaires on subjective mood states using the Profile of Mood States (POMS) were obtained. The exonic A<sub>2A</sub> polymorphisms 263C/T, 1976C/T (formerly known as 1083C/T) and 2592C/T<sub>ins</sub> were genotyped by means of PCR-based restriction fragment length polymorphism (RFLP)-assays or single strand conformation polymorphism (SSCP)-analysis.

All polymorphisms were in Hardy-Weinberg equilibrium and the 1976C/T and 2592C/T<sub>ins</sub> polymorphisms were in nearly complete linkage disequilibrium. The 263C/T polymorphism was associated to increases in vigor (at 10 mg), the 1976C/T and 2592C/T<sub>ins</sub> polymorphisms to increases in anxiety (at both doses) and arousal (at 10 mg). In contrast, no significant association could be detected for the other moods. No difference in the demographic measures age, gender, race/ethnicity, BMI, education and current drug use was observed between the genotypic groups.

These findings are consistent with observations indicating a role for A<sub>2A</sub> receptor gene polymorphisms in panic disorder (Deckert et al. 1998) and variability in anxiety after acute caffeine administration (Alsene et al. 2003). The non-coding polymorphisms might influence transcription efficiency or mRNA stability. Alternatively, they may reflect linkage disequilibrium with other functionally relevant variants. Replication studies in independent samples and functional characterisation of the three investigated exonic polymorphisms are necessary.

Deckert J, Nöthen MM, Franke P, Delmo C, Fritze J, Knapp M, Maier W, Beckmann H, Propping P. Systematic mutation screening and association study of the A<sub>1</sub> and A<sub>2A</sub> adenosine receptor genes in panic disorder suggest a contribution of the A<sub>2A</sub> gene to the development of disease. *Molecular Psychiatry* 3, 81-85, 1998

Alsene K, Deckert J, Sand PG, de Wit H, Association between A<sub>2A</sub> receptor gene polymorphisms and caffeine-induced anxiety, *Neuropsychopharmacology* 28, 1694-1702, 2003

## Polymorphisms of the RGS 2-gene: Relevance for the development of panic disorder?

A. Jung<sup>1</sup>, C. Hohoff<sup>1</sup>, C. Freitag<sup>2</sup>, S. Brady<sup>6</sup>, G. Ponath<sup>1</sup>, P. Krakowitzky<sup>1</sup>, J. Fritze<sup>4</sup>, P. Franke<sup>3</sup>, B. Bandelow<sup>5</sup>, R. Fimmers<sup>3</sup>, M.M. Nöthen<sup>3</sup>, J. Flint<sup>6</sup>, J. Deckert<sup>1</sup>

<sup>1</sup>Psychiatrie and Psychotherapy and Institut of Transfusion-Medicin, Univ. Münster, <sup>2</sup>Children- and Youthpsychiatry, Univ. of Saarland, <sup>3</sup>Psychiatry and Psychotherapy, Medical Biometrie and Human Genetics, Univ. Bonn, <sup>4</sup>Psychiatry and Psychotherapy, Univ. Frankfurt, <sup>5</sup>Psychiatry and Psychotherapy, Univ. Göttingen, <sup>6</sup>Wellcome Trust Centre for Human Genetics, Univ. Oxford

RGS 2 (regulator of G-protein 2) reduces G protein activity via its GTPase function. Hence a lack of function is combined with increased GTP mediated neurotransmission. Accordingly, RGS 2-knock-out-mice show increased excitability in hippocampal CA1 neurons. RGS 2, however, also plays a role in emotional behaviour as RGS 2 knock-out-mice are more anxious than their wild-type counterparts (Oliveira-dos-Santos et al. 2000). Human panic disorder is characterized by sudden, unexpected attacks of intense fear, often associated with agoraphobia. We therefore hypothesized that functionally relevant variations in the RGS 2 gene may influence the development of human panic disorder.

We genotyped 173 patients with panic disorder and 173 gender-, age- and ethnicity-matched controls for four non-coding RGS 2 gene single nucleotide polymorphisms (SNP 1, 2, 3, 4) using PCR-based RFLP-assays. Statistical analysis at the genotype level revealed significance for all four SNPs (SNP 1:  $p=0.045$ , SNP 2:  $p=0.023$ , SNP 3:  $p=0.049$ , SNP 4:  $p=0.023$ ), and at the allele level for SNP 2:  $p=0.033$  and SNP 4:  $p=0.03$ . These significances are mainly due the subgroup of men with agoraphobia (significance at the genotype level: SNP 1:  $p=0.037$ , SNP 2:  $p=0.0517$ , SNP 3:  $p=0.0279$ , SNP 4:  $p=0.0408$ ). Interestingly we found the strongest association with haplotype SNP 3 - SNP 4 in the subgroups men ( $p\text{-value}=0.0119$ ) and men with agoraphobia ( $p\text{-value}=0.0303$ ).

Polymorphisms of the RGS 2 gene may thus raise the vulnerability to human panic disorder. Our results are consistent with the animal-model with regard to the influence of RGS 2 gene variation on emotions and behaviour. Replication studies in independent panic disorder samples as well as functional analyses of the investigated RGS 2 gene polymorphisms are now necessary.

### Reference:

Oliveira-dos-santos AJ, Matsumoto G, Snow BE, Bai D, Houston FP, Whishaw IQ, Mariathasan S, Sasaki T, Wakeham A, Ohashi PS, Roder JC, Barnes CA, Siderovski DP, Penninger JM (2000) Regulation of T cell activation, anxiety, and male aggression by RGS 2. PNAS 97: 12272-12277

## **Schizophrenia Families Characterized for the Endophenotype Eye Tracking Dysfunction : Analysis of Polymorphisms in the Tumor Necrosis Factor alpha gene**

C. Hohoff<sup>1</sup>, N. Tidow<sup>2</sup>, M. Stoll<sup>3</sup>, S. Rust<sup>3</sup>, R. Lencer<sup>4</sup>, S. Purmann<sup>5</sup>, E. Schwinger<sup>5</sup>, B. Brandt<sup>2</sup>, J. Deckert<sup>1</sup>, V. Arolt<sup>1</sup>

<sup>1</sup>Department of Psychiatry, <sup>2</sup>Institute of Clinical Chemistry and Laboratory Medicine and <sup>3</sup>Institute of Arteriosclerosis Research, University of Muenster, Germany; <sup>4</sup>Department of Psychiatry and <sup>5</sup>Institute of Human Genetics, University of Luebeck School of Medicine, Luebeck, Germany

Genetic studies aimed at identifying susceptibility genes or gene regions for schizophrenia often produce inconsistent results. This may be partly due to the difficulties in defining the relevant clinical phenotype. The use of well-defined endophenotypes, which are assumed to be more closely related to the underlying neurobiological pathology of schizophrenia, is a promising way to facilitate genetic analyses. Such endophenotypes may be obtained by neuropsychological, neurophysiological or neuroimaging paradigms. Applying this approach we reported positive linkage for both the neurophysiological parameter eye tracking dysfunction (ETD) and schizophrenia to the chromosomal region 6p22-p21 (Arolt et al. 1996). One positional candidate gene on 6p22-p21 is the gene tumor necrosis factor (TNF) alpha. Association of the functionally relevant -308G/A TNFalpha gene polymorphism with schizophrenia has been proposed on the basis of large case-control samples.

We therefore investigated twelve German schizophrenia multiplex families characterised for the endophenotype ETD with 100 members (35 schizophrenic and 44 ETD-positive members), diagnosed on the basis of DSM-IV (SADS/L, SCID-II and SIS). Family members were genotyped for the functionally relevant -308G/A polymorphism and additional five polymorphisms by 5' nuclease assays for amplifying and detecting specific SNP alleles on an ABI Prism 7900. Linkage and association were calculated by Genehunter (version 2.1).

Most SNP markers were in complete linkage disequilibrium. TDT analyses with both schizophrenia and ETD as the relevant phenotype were negative for single point as well as haplotype analyses in the investigated families. No linkage or association of any of the investigated polymorphisms could thus be detected. Our results, thus, fail to provide support for a major contribution of polymorphisms in the gene of the cytokine TNF alpha for schizophrenia susceptibility in this particular German family sample.

Arolt V, Lencer R, Nolte A, Müller-Myhsok B, Purmann S, Schürmann M, Leutelt J, Pinnow M, Schwinger E. Eye tracking dysfunction is a putative phenotypic susceptibility marker of schizophrenia and maps to a locus on chromosome 6p in families with multiple occurrence of the disease. *Am J Med Genet* 67:564-579, 1996.

## **A novel mutation associated with childhood absence epilepsy affects G-protein modulation of P/Q type calcium channels**

M.O. Popa<sup>1</sup>, K. Hallmann<sup>2</sup>, J. Rebstock<sup>2</sup>, N. Tilgen<sup>2</sup>, S. Maljevic<sup>1</sup>, A. Heils<sup>2</sup>, H. Lerche<sup>1</sup>

<sup>1</sup> Depts. of Neurology and Applied Physiology, University of Ulm, D-89081 Ulm, Germany

<sup>2</sup> Clinic of Epileptology and Institute of Human Genetics, University of Bonn, Germany

Childhood absence epilepsy (CAE) is a type of idiopathic generalized epilepsy observed in 2-10% of epileptic children. We identified a novel mutation in a highly conserved region of the CACNA1A gene cosegregating in a small family (affected father and three children) with CAE. We introduced the newly identified C-terminal mutation into the human  $\alpha_{1A-2}$  subunit of the P/Q type Ca channel (Ca<sub>v</sub>2.1) and compared the electrophysiological behaviour of mutant and wild type (WT) channels using the patch clamp technique. Coexpression of  $\alpha_{1A-2}$  with the modulatory subunits  $\alpha_2\delta$  and  $\beta_{2e}$  (1:1:1) resulted in functional mutant channels with identical gating characteristics as the WT. However, the P/Q type Ca channels are colocalized with synaptic vesicles and subject to modulation by G-proteins activated upon binding of neurotransmitters or hormones to a G-protein coupled receptor. Their inhibition by G-protein  $\beta\gamma$  subunits is considered a key mechanism for regulating presynaptic calcium levels. To investigate if the G-protein  $\beta\gamma$  subunits differentially modulate mutant and WT channels, we used GTP $\gamma$ S, a non hydrolysable GTP analog to activate the G-proteins within the cells transiently cotransfected with  $\alpha_{1A-2}$ ,  $\alpha_2\delta$  and  $\beta_{2e}$ . Our investigations show that the novel mutation affects the kinetics of G-protein dissociation from the channel occurring faster than for the WT (at 0 mV,  $\tau = 57 \pm 12$  ms for the mutant compared with  $118 \pm 10$  ms for the WT). As shown by Bertram et al. (J Neurophysiol 2003;90:1643-53), G-protein modulation of Ca channels acts as a high-pass filter on presynaptic impulse trains whose threshold is most effectively changed through variation of the G-protein dissociation rate. The faster dissociation rate of the mutant channel should decrease the filter threshold, so that lower frequency presynaptic stimuli will produce postsynaptic impulses. Our results are thus consistent with a facilitation of synaptic transmission due to a faster recovery from G-protein mediated inhibition of the mutant P/Q type channel which can well explain the occurrence of epileptic seizures.



## **Neuronal nitric oxide synthase knockout impacts on the survival of neural stem cells and growth factor expression**

Angelika Schmitt<sup>1</sup>, Sabrina Fritzen<sup>1</sup>, Ellen Claes<sup>1</sup>, Peter Gass<sup>2</sup>, Klaus-Peter Lesch<sup>1</sup> and Andreas Reif<sup>1</sup>

From the <sup>1</sup>Molecular and Clinical Psychobiology, Department of Psychiatry and Psychotherapy, Julius-Maximilians-University Wuerzburg, Fuechslinstr. 15, 97080 Wuerzburg, Germany, and the <sup>2</sup>Central Institute of Mental Health, J5, Mannheim, Germany.

Attention-deficit/hyperactivity disorder (ADHD) is a heterogeneous, neurobiological disorder. The most noticeable symptoms include inattention, impulsivity, hyperactivity (in males) and dreaminess (in females). Mainly dopaminergic and noradrenergic transmitter pathways have been implicated in its pathogenesis, yet other messenger cascades have barely been investigated. Nitric oxide (NO) acts as an atypical, gaseous second and third messenger in both the central and peripheral nervous systems. The physiological functions of NO in the central nervous system are manifold; behavioral domains which are known to be influenced by NO include emotionality, memory and learning. Mice with targeted disruption of the neuronal isoform of nitric oxide synthase (NOS-I) display an highly aggressive and impulsive phenotype. Thus, NOS-I knockout mice might serve as an animal model of ADHD. To examine the molecular basis of the behavioral phenotype, which also includes an increase in activity and impaired spatial learning, we investigated whether NOS-I knockout mice display altered levels of adult neurogenesis and neural growth factors. While stem cell proliferation was unaltered in NOS-I knockout animals, the survival of newly formed neurons was significantly and substantially increased in NOS-I-deficient mice. Quantitative real-time PCR revealed neither NOS-III upregulation nor changes in Vascular endothelial growth factor levels, as found in NOS-III deficient animals, but subtle yet significant changes in the expression of Brain derived neurotrophic factor. These abnormalities in adult neurogenesis, a process which has been implicated in memory formation, might underlie the cognitive abnormalities of NOS-I knockout animals. Additionally planned behavioral studies on mice will further reveal the possible correlation between NOS-I and human ADHD.

## **Converging lines of evidence argue for a role of endothelial nitric oxide synthase (NOS-III) in affective disorders**

<sup>1</sup>\*S. Fritzen, <sup>1</sup>A. Schmitt, <sup>2</sup>A. Strobel, <sup>1</sup>C.P. Jacob, <sup>3</sup>S. Chourbaji, <sup>3</sup>P. Gass, <sup>1</sup>K.-P. Lesch and <sup>1</sup>A. Reif

<sup>1</sup>Clinical and Molecular Psychobiology, Department of Psychiatry and Psychotherapy, University of Würzburg, Germany

<sup>2</sup>Institute of Psychology II, Dresden University of Technology, Dresden, Germany

<sup>3</sup>Central Institute of Mental Health, J5, D-68159, Mannheim, Germany

\*corresponding author

e-mail to: Fritzen\_S@klinik.uni-wuerzburg.de

The gaseous messenger molecule nitric oxide (NO) has been implicated in a variety of higher CNS functions, as it is involved in learning and memory formation as well as in emotionality. In the mammalian brain, NO is formed by three different NO synthase isoforms: neuronal (NOS-I), inducible (NOS-II) and endothelial (NOS-III). We recently demonstrated that NOS-III knockout mice display reduced adult neurogenesis. As it has been postulated that adult neurogenesis plays a role in the pathophysiology of depression, we reasoned that NOS-III knockout mice might display behavioral traits related to depression. Therefore, besides behavioral tests aiming at activity and anxiety, we subjected 10 male NOS-III knockout- and 10 male wildtype mice to a Learned Helplessness test, which is an animal-based model of depression. Whereas NOS-III knockout animals did not display abnormalities in the Open Field, Light-Dark-Box, Novel Cage and Forced Swim Tests, they were significantly less helpless in the Learned Helplessness paradigm. These results indicate that NOS-III knockout mice display an anti-depressant phenotype. To investigate a possible association of NOS-III genotype with affective disorders in men, we examined a functional 3-marker haplotype in patients suffering from bipolar affective disorder (Bip) or unipolar depression (MD). We found a significant global haplotype association with bipolar disorder, but not unipolar depression, due to the underrepresentation of two low-activity haplotypes. This suggests that the NOS-III genotype may convey a modest genetic risk to develop bipolar disorder. In conclusion, two different yet converging lines of evidence argue for a role of NOS-III in the pathogenesis of affective disorders.

**Poster Subject Area #PSA30:  
Neuropathology**

- [#405A](#) M. Hamann, R. Raymond, S. Varughesi, JN. Nobrega and A. Richter, Berlin and Toronto (CDN)  
*Cholinergic interneuron density and acetylcholine receptor binding are unaltered in a genetic animal model of primary paroxysmal dystonia*
- [#406A](#) F. Yildirim, C. Harms, A. Meisel, J. Bösel and M. Endres, Berlin  
*MECHANISMS OF NEUROPROTECTION BY TRICHOSTATIN A*
- [#407A](#) K. Hasenpusch-Theil and HW. Müller, Duesseldorf  
*Analysis of the early CMT1A pathogenesis in the murine model PMP22tgC61*
- [#408A](#) S. Fabian, F. Blaes and A. Scholz, Gießen  
*IgG antibodies from patients with polyneuropathies effects currents in thin slices of rat dorsal root ganglia*
- [#409A](#) S. Balakrishnan, F. Von Lewinsky and BU. Keller, Göttingen  
*Mitochondria differentially regulate  $[Ca^{2+}]_i$  in brain stem motoneurons that are selectively vulnerable or resistant in ALS-related motoneuron disease*
- [#410A](#) R. Diem, MB. Sättler, D. Merkler, I. Demmer, K. Maier, C. Stadelmann, H. Ehrenreich and M. Bähr, Göttingen  
*Combined therapy with methylprednisolone and erythropoietin in a model of multiple sclerosis*
- [#411A](#) K. Meuer, M. Bähr and JH. Weishaupt, Göttingen  
*Regulation and role of mitochondrial network dynamics during apoptosis of dopaminergic neurons*
- [#412A](#) L. Tal, S. Mandel and MBH. Youdim, Haifa (IL)  
*The Role of Bad in the Neuroprotective Action of the Major Green Tea Polyphenol, (-)-Epigallocatechin 3-Gallate (EGCG)*
- [#413A](#) T. Herdegen, M. Götz, S. Brecht, J. Wessig, A. Chromik, T. Nicolaus, M. Willesen and G. Raivich, Kiel  
*Specific pathophysiological functions of JNK isoforms in the brain following neuronal injuries*
- [#414A](#) M. Belokopytov, G. Dubinsky, Y. Epstein, M. Belkin and M. Rosner, Tel Hashomer (IL)  
*COPAXONE VACCINATION FOR RETINAL NEUROPROTECTION*

- [#415A](#) T. Claudepierre, I. Buard, K. Nieweg, M. Simonutti and F. Pfrieder, Strasbourg (F) and Paris (F)  
*Changes in retinal architecture and neurotransmission after perturbation of cholesterol synthesis and transport.*
- [#416A](#) NA. Gorenkova and AV. Volkov, Moscow (RUS)  
*GENDER DIFFERENCES OF ALBINO RATS IN RECOVERY FROM CEREBRAL ISCHEMIA INDUCED BY 12-MIN CARDIAC ARREST*
- [#405B](#) M. Holzer, M. Craxton, R. Jakes, T. Arendt and M. Goedert, Leipzig and Cambridge (UK)  
*Tau gene (MAPT) analysis in non-human primates*
- [#406B](#) S. Garcia de Arriba, F. Wegner, K. Grüner, H. Sobottka, A. Wagner, K. Wohlfahrt and C. Allgaier, Leipzig  
*Ischemic cell death in human NT2 neurons is prevented by NMDA receptor antagonists but not by antagonists at the glycine binding site*
- [#407B](#) V. Ogunlade, R. Schober, S. Grimm and C. Allgaier, Leipzig  
*Immunohistochemical localization of N-methyl-D-aspartate receptor NR1, NR2A, NR2B and NR2C/D subunits in human and Bennett rat dorsal root ganglia*
- [#408B](#) U. Gärtner, A. Alpar, G. Seeger, R. Heumann and T. Arendt, Leipzig, Budapest (H) and Bochum  
*Enhanced neuronal Ras activity triggers spine formation*
- [#409B](#) S. Schmetsdorf, U. Gärtner and T. Arendt, Leipzig  
*Putative relation between neuronal cell cycle proteins and neuroplasticity*
- [#410B](#) K. Schmidt, U. Ueberham, U. Gärtner, E. Ueberham and T. Arendt, Leipzig  
*Activation of cell cycle proteins after excitotoxic brain lesion with NMDA, Kainate and 3-Nitropropionic acid*
- [#411B](#) B. Moscha, D. Lenz, A. Tarnok and T. Arendt, Leipzig  
*LSC as powerful tool for the analysis of DNA content in neurons*
- [#412B](#) M. Morawski, T. Reinert, G. Brückner, P. Riederer, FE. Wagner, W. Meyer-Klaucke, T. Butz and T. Arendt, Leipzig, Würzburg, Garching and Hamburg  
*Iron binding properties of perineuronal nets in the rat brain*
- [#413B](#) E. Ramminger, T. Arendt and M. Holzer, Leipzig  
*Searching for microtubule-associated protein tau-interacting proteins*
- [#414B](#) T. Bullmann, W. Härtig, N. Sergeant, M. Holzer, R. De Silva and T. Arendt, Leipzig, Lille (F) and London (UK)  
*Tau mRNA Splicing and Protein Isoform Expression during Development in vivo and in vitro.*

[#415B](#)

H. Wolburg, M. Mittelbronn, B. Erdlenbruch and A. Warth, Tübingen and Göttingen  
*Organizing the blood-brain barrier: Interplay between astroglia, the extracellular matrix  
and the endothelial cells*

### **Cholinergic interneuron density and acetylcholine receptor binding are unaltered in a genetic animal model of primary paroxysmal dystonia**

M. Hamann<sup>1</sup>, R. Raymond<sup>2</sup>, S. Varughesi<sup>2</sup>, J. N. Nobrega<sup>2</sup>, A. Richter<sup>1</sup>

<sup>1</sup>Dept. of Pharmacology and Toxicology, Freie Universität Berlin, Faculty of Veterinary Medicine, Koserstr. 20, 14195 Berlin, Germany; <sup>2</sup>Neuroimaging Research Section, Centre for Addiction and Mental Health, Toronto, Canada

The underlying pathophysiological mechanisms of hereditary types of paroxysmal dyskinesias are still unknown, but basal ganglia dysfunctions seem to play a critical role. In fact, numerous pharmacological, neurochemical, immunohistochemical and electrophysiological investigations in the *dt<sup>sz</sup>* hamsters, a unique rodent model of a type of age-dependent primary paroxysmal dystonia, revealed alterations within the basal ganglia, particularly of the GABAergic and dopaminergic neurotransmitter system. A deficit in several types of striatal GABAergic interneurons in *dt<sup>sz</sup>* mutant hamsters seems to play a crucial pathophysiological role, but deficits in other types of striatal interneurons cannot be excluded by previous studies. In view of ameliorating effects of anticholinergic drugs in dystonic patients, we therefore investigated the density of striatal cholinergic interneurons in the present study. These interneurons were marked specifically by the enzyme choline acetyltransferase and counted by using a stereological counting method in a blinded fashion. Additionally, acetylcholine receptor binding was determined in mutant and non-dystonic control hamsters by autoradiographic analyses with the non selective muscarinic ligand [<sup>3</sup>H]-quinuclidinyl benzilate (QNB) in 11 brain (sub)regions.

There were no significant differences in the density of striatal cholinergic interneurons between *dt<sup>sz</sup>* mutant hamsters ( $789 \pm 39$  interneurons/mm<sup>3</sup>) and non-dystonic controls ( $807 \pm 36$  interneurons/mm<sup>3</sup>). The [<sup>3</sup>H]-QNB binding was also comparable between mutant and control hamsters.

These results are in line with previous pharmacological investigations showing that anticholinergic drugs were not able to reduce the severity of dystonia in *dt<sup>sz</sup>* hamsters. The lack of changes within the cholinergic neurotransmitter system further underlines the pathophysiological importance of alterations within the GABAergic and dopaminergic neurotransmitter systems found in mutant hamsters.

Supported by grants from the *Deutsche Forschungsgemeinschaft* (Ri 845).

## MECHANISMS OF NEUROPROTECTION BY TRICHOSTATIN A

F. Yildirim, C. Harms, A. Meisel, J. Bösel, M. Endres

Department of Experimental Neurology, Charite Medical Faculty, Humboldt University, Berlin, Germany

Trichostatin A (TSA), a streptomyces metabolite, inhibits histone deacetylase (HDAC) at nanomolar concentrations. However, neither the significance of this function nor the possible genes which might be affected as a consequence of this inhibition have not been fully revealed yet. Here we demonstrate that TSA is neuroprotective against an experimental model of cerebral ischemia: Pretreatment with TSA, in a dose-dependent manner (300nM), protected cortical neurons against combined Oxygen-Glucose Deprivation (OGD) (assessed by LDH release into the medium). To explore a possible mechanism behind this neuroprotection, we identified gelsolin, an anti-excitotoxic and anti-apoptotic protein, which has been shown to be upregulated by TSA in non-neuronal cells. Since TSA, by inhibiting HDACs, would be expected to cause a more acetylated status of histones, we explored whether TSA induces a change in the acetylation status of histones close to gelsolin gene expression regulatory sequences. By using chromatin immunoprecipitation technique(ChIP), we showed more than 90-fold increase in acetylation of histone H4 at gelsolin promoter region. To characterize possible consequences of this epigenetic event regarding gelsolin expression, we used (real-time) RT-PCR and Western Blotting and observed an upregulation of gelsolin both at transcriptional and protein level, following treatment of cortical cultures with TSA. The neuroprotective effects of TSA were attenuated in cortical neurons lacking gelsolin gene, which demonstrates that gelsolin – at least in part - mediates the neuroprotective effects of TSA. Together, we identify gelsolin as a candidate gene contributing to neuroprotection through gene-specific changes in histone acetylation patterns induced by trichostatin A treatment.

Keywords: trichostatin A, gelsolin, cortical neurons, oxygen-glucose deprivation.

## Analysis of the early CMT1A pathogenesis in the murine model PMP22<sup>tg</sup>C61

**K. Hasenpusch-Theil<sup>1,2</sup> and H.W. Müller<sup>1</sup>**

<sup>1</sup>Molecular Neurobiology Laboratory, Department of Neurology, University of Duesseldorf, Duesseldorf (Germany)

<sup>2</sup>email: Kerstin.Hasenpusch-Theil@uni-duesseldorf.de

Hereditary neuropathies are a diverse group of human neurological disorders and are caused by mutations in at least 26 different disease genes. Gene duplication / deletion or mutations in the myelin gene PMP22 result in Charcot-Marie-Tooth 1A (CMT1A), hereditary neuropathy with liability to pressure palsies (HNPP) or Dejerine-Sottas syndrome (DSS). To study the pathomechanism of CMT1A, several animal models have been established showing different clinical and pathological phenotypes based on different expression levels of the PMP22 transgene. The transgenic mouse strain C61 which carries 4 copies of a human YAC-clone encompassing the complete huPMP22 gene (Huxley et al., Hum. Mol. Genet. 7, 1998, 449-458) shows a doubling of PMP22 expression level and closely mimics the human disease. This includes mild demyelination and abundant appearance of myelin-phagocytosing macrophages in the peripheral nerves.

We first tested if doubling of PMP22 expression leads to changes in gene expression detectable by DNA array technology. Using Atlas cDNA-Expression Arrays and RT-PCR with RNA from wild-type and mutant sciatic nerves, we could identify 12 abnormally expressed genes. Most of these genes are known to be involved in cell communication and immunological processes. Abnormal expression of four of these genes was previously observed in suralis nerve biopsies from CMT1A patients (LNGFR p75, GFAP and S100; Hanemann et. al., Brain 119, 1461-1469, 1996) as well as in the sciatic nerve of a CMT1A rat model (cyclin D1; Atanasoski et al., J Neurosci Res 67, 443-449, 2002). In addition, the small inducible cytokine MCP1 was identified as differentially expressed. In CMT1A the latter cytokine may activate resident or hematogenous macrophages in the peripheral nerve in a similar way as hypothesised for two other models of hereditary neuropathies with macrophage-mediated demyelination (Carenini et al., J. Cell Biol. 152, 301-308, 2001; Kobsar et al., Brain 126, 804-813, 2003). Our results based on DNA array analyses clearly demonstrate that enhanced PMP22 gene dosage is followed by the abnormal regulation of specific, possibly pathogenesis-relevant, genes in peripheral nerve of PMP22 overexpressing mice.



## **IgG antibodies from patients with polyneuropathies effects currents in thin slices of rat dorsal root ganglia**

S Fabian, F Blaes\*, A Scholz

Physiologisches Institut, Universität Gießen,

\*Neurologische Klinik Universitätsklinikum Gießen

There are different kinds of inflammatory polyneuropathies. Chronic inflammatory demyelinating polyneuropathy (CIDP) is a chronic and Guillain Barré Syndrome (GBS) is an acute inflammatory and demyelinating neuropathy that can affect motor, sensory and autonomic nerves. A large number of data indicates that anti-glycolipid antibodies are present in the acute phase sera of a proportion of patients with GBS (Willison & Yuki, 2002). Clinically it is defined by weakness, loss of sensory function, areflexia and elevated protein levels in the cerebrospinal fluid. In clinical and electrophysiological studies it has been shown that symptoms can be reduced by plasma exchange (Hughes *et al.*, 2003). However the underlying mechanisms are still open to be fully explained.

In Lambert Eaton Myasthenic Syndrome (LEMS) are autoantibodies present against the P/Q type voltage-gated calcium-channels which are expressed on the presynaptic motor nerve terminals, autonomic nerve terminal, and cerebellar Purkinje cells. Functional loss of this channel leads to a reduced calcium influx into the nerve terminal and insufficient ACh is released to elevate the end plate potential above that required for sodium channel activation (for review see Lang & Vincent, 2003). Patients suffering from LEMS have difficulties in walking, generally because of proximal leg weakness but also because of ataxia. They also suffer from a variety of autonomic symptoms such as constipation, dry mouth.

We examined small diameter superficial neurons in a thin slice preparation of dorsal root ganglia (DRG) of young rats by means of the patch-clamp technique (Scholz *et al.*, 1998) to test the acute effect of IgG antibodies. The IgG fraction from patients which underwent plasmapheresis was eluted similar to methods as already described (Buchwald *et al.*, 1998; Schäfer *et al.*, 2000) and finally dialysed against HEPES buffered solution. This system was tested with the known "channel disease" LEMS.

Interestingly the IgG sera of LEMS patients (0.5 g/l) induced a reduction of about 15% of the outward currents in small sensory neurons within 3-8 min. In IgG sera of patients with acute forms of inflammatory GBS no changes of outward currents were found in small DRG neurons.

IgG sera of chronic inflammatory forms of GBS revealed about 14% outward current reduction within 3-5 minutes.

However the control of the system with IgG from patients suffering from LEMS revealed a possible K<sup>+</sup> current blockade, indicating that not only a calcium channel block underly this myasthenic syndrome. The effects of application of IgG sera of acute GBS patients could not explain the observed clinical neuropathy.

Buchwald B, Weishaupt A, Toyka KV & Dudel J (1998). *Eur J Neurosci* **10**, 281-290.

Hughes RA, Wijdicks EF, Barohn R, Benson E, Cornblath DR, Hahn AF, Meythaler JM,

Miller RG, Sladky JT, Stevens JC (2003) *Neurology* **61**, 736-740.

Schäfer KH, Klotz M, Mergner D, Mestres P, Schimrigk K & Blaes F. (2000) *J Autoimmun.* **15**, 479-484.

Scholz A, Gruß M & Vogel W (1998). *J Physiol* **513**, 55-69.

Willison HJ & Yuki N. (2002) *Brain* **125**, 2591-2625

The study was supported by DFG and Volkswagenstiftung.

**Mitochondria differentially regulate  $[Ca^{2+}]_i$  in brain stem motoneurons that are selectively vulnerable or resistant in ALS-related motoneuron disease**

**Saju Balakrishnan, Göttingen Germany; Friederike Von Lewinsky, Göttingen Germany; Bernhard U Keller, Göttingen Germany**

Defined motoneuron populations in the brain stem and spinal cord are selectively damaged during pathophysiological conditions like hypoxia and amyotrophic lateral sclerosis (ALS), which has been linked to their low calcium buffering capacity and an exceptional vulnerability to mitochondrial disturbances. To elucidate underlying events, we performed patch clamp recordings and CCD imaging in selectively vulnerable and resistant motoneuron types in slice preparations from mouse brain stem. In vulnerable hypoglossal motoneurons (HMNs), disruption of the mitochondrial electrochemical potential by bath application of the mitochondrial “uncoupler” FCCP provoked a significant retardation of cytosolic calcium clearance rates and substantial  $Ca^{2+}$  release events from mitochondria-controlled stores in somatic and dendritic compartments. Application of the SERCA inhibitor CPA (Cyclopiazonic acid) in the presence of FCCP was associated with *secondary*  $Ca^{2+}$  release, indicating that ER stores operated independently from mitochondria. Corresponding experiments on vulnerable facial motoneurons (FMNs) revealed a set of results that were similar to those found in HMNs. These observations were significantly different from those obtained in selectively resistant dorsal vagal (DVN) and oculomotor neurons (OMN) under identical experimental conditions. Both DVN and OMN displayed only minor  $Ca^{2+}$  release events after FCCP application, where peak amplitudes were ~4 fold smaller compared to those in HMNs. Moreover, FCCP did not significantly affect cytosolic  $Ca^{2+}$  clearance rates in DVN and OMNs. Taken together, these observations suggest that selective motoneuron vulnerability results from a characteristic specialisation of cytosolic  $Ca^{2+}$  signaling, where low concentrations of cytosolic calcium buffers enhance the role of mitochondria as dominant regulators of  $[Ca^{2+}]_i$ . Under physiological conditions, this arrangement provides an energy-efficient coupling between electrical activity,  $[Ca^{2+}]_i$  and mitochondrial metabolism. During pathophysiological states like those found during hypoxia and ALS, it facilitates a vicious circle where initial mitochondrial disturbances increase electrical excitability and  $[Ca^{2+}]_i$ , and the resulting augmentation in neuronal energy demand potentiates neuronal damage.

**Combined therapy with methylprednisolone and erythropoietin in a model of multiple sclerosis**

R. Diem<sup>a</sup>, M.B. Sättler<sup>a</sup>, D. Merkler<sup>b</sup>, I. Demmer<sup>a</sup>, K. Maier<sup>a</sup>, C. Stadelmann<sup>b</sup>, H. Ehrenreich<sup>c</sup> & M. Bähr<sup>a</sup>

<sup>a</sup>Neurologische Universitätsklinik, Göttingen, Germany, <sup>b</sup>Institut für Neuropathologie, Göttingen, Germany, <sup>c</sup>Max-Planck-Institut für Experimentelle Medizin, Göttingen, Germany

**Background:** Neurodegenerative processes determine the clinical disease course of multiple sclerosis (MS). None of the established MS therapies has been shown to clearly reduce neurodegeneration. In a rat model of experimental autoimmune encephalomyelitis (EAE), we recently demonstrated even increased neuronal apoptosis under methylprednisolone (MPred) therapy although CNS inflammation was effectively controlled.

**Objectives:** The aim of the study was to therapeutically target inflammatory as well as neurodegenerative aspects of EAE. We investigated effects of combined treatment with MPred and erythropoietin (Epo) on survival and function of retinal ganglion cells (RGCs), the neurons that form the axons of the optic nerve (ON), in rats suffering from severe optic neuritis. To induce optic nerve inflammation, we used a model of myelin oligodendrocyte glycoprotein (MOG)-induced EAE.

**Methods:** After immunization, brown Norway rats were randomly assigned into six treatment groups receiving different combinations of Epo and MPred, or respective monotherapies. After MOG-induced EAE became manifest, optic neuritis was monitored by recording visual evoked potentials. The function of RGCs was measured by electroretinograms. Survival of RGCs as well as the extent of axonal damage within the ONs was assessed by immunostaining and histopathological methods. Signal transduction in RGCs was investigated by Western blot analysis.

**Results:** Whereas the day of disease manifestation as well as the severity of symptoms at this time did not differ between the groups, further clinical disease course in rats which were treated with combinations of Epo and Mpred significantly improved. Functional and histopathological data of RGCs and ONs revealed that neuron and axon protection was most effective when Epo treatment started at immunization was combined with high-dosage MPred therapy given from days 1 – 3 of MOG-EAE. In contrast, isolated neuronal or axonal protection without clinical benefit was achieved under monotherapy with Epo or MPred, respectively. Western blot analysis showed that Mpred and Epo antagonistically regulate phosphorylation of mitogen-activated protein kinases in RGCs and thereby influence neuronal survival.

**Conclusions:** We provide evidence for beneficial effects of combined anti-inflammatory and neuroprotective treatment in EAE.

**Fundings:** Medical Faculty of the University of Göttingen, Gemeinnützige Hertie Stiftung

## **Regulation and role of mitochondrial network dynamics during apoptosis of dopaminergic neurons**

K. Meuer, M. Bähr and J. H. Weishaupt

Department of Neurology, Georg-August-University Göttingen, Robert-Koch-Str. 40  
37075 Göttingen, Germany

Mitochondria are essential for maintaining cellular viability, and have been shown to be involved in most neuronal cell death pathways. They are semi-autonomous organelles that change in number and morphology within a cell during development, cell cycle or when challenged by toxic conditions. Mitochondria are continuously redistributed within mammalian cells, and mitochondrial morphology is regulated by controlled action and fusion events, often forming branched tubular networks extending throughout the cell. Mammalian proteins have been identified that actively regulate mitochondrial morphology, e.g. dynamin-related protein 1 (Drp1) or Fis1. The extend of the mitochondrial network determines size and dynamics of mitochondrial calcium pools and allows energy transmission between different cellular regions.

Recent reports have described dramatic alterations in mitochondrial morphology during early stages of apoptotic cell death of mammalian, non-neuronal cells. The mitochondrial network becomes fragmented and the mobility of mitochondria is reduced during apoptosis. In this study we examined mitochondrial movement and morphology during apoptosis of dopaminergic midbrain neurons using a mitochondrially targeted enhanced red fluorescent protein (mt-RFP).

For data acquisition time-lapse microscopy was used. Morphology of mitochondria was quantified and mitochondrial motility was analysed. Our preliminary data show that application of the neurotoxin MPP<sup>+</sup> or treatment with a calcium ionophore results in rapid reduction of mitochondrial movement, and fragmentation of the mitochondrial network, preceding caspase activation. Moreover, a dominant negative mutant of Drp1 decreased mitochondrial fragmentation induced by MPP<sup>+</sup>. In a search for molecular upstream mechanisms regulating mitochondrial morphology, we investigated the role of cyclin-dependent kinase 5 (CDK5), which, in contrast to other members of the CDK family, is not involved in cell cycle control. Inhibition of CDK5, which induces neuronal apoptosis in models for Parkinson's disease and was shown to act upstream of mitochondrial dysfunction, reduced mitochondrial fragmentation.

Thus, we present evidence supporting the hypothesis that mitochondrial fragmentation might be an upstream and causal event during apoptosis of dopaminergic neurons.

**The Role of Bad in the Neuroprotective Action of the  
Major Green Tea Polyphenol, (-)-Epigallocatechin 3-Gallate (EGCG)**

*Eve Topf and National Parkinson Foundation Centers of Excellence, Technion-  
Faculty of Medicine, Haifa, Israel*

Limor Tal, Silvia Mandel and Moussa B.H. Youdim

The intense investigation on the mechanism by which neurons die has led to the therapeutic use of antioxidants in aging and neurodegenerative diseases. The beneficial effects ascribed to tea drinking are believed to rely on the pharmacological actions of catechins and their derivatives components. They act as radical scavengers and exert indirect antioxidant effect through activation of transcription factors and antioxidant enzymes. EGCG have also been reported to exert potent neuroprotection in both in vivo and in vitro models of neurodegeneration. Studies from our and more recently another laboratory have demonstrated that the neuroprotective action of the major green tea polyphenol, (-)-epigallocatechin-3-gallate (EGCG) is mediated by activation of protein kinase C (PKC). The aim of this study was to further determine the potential cell signaling pathways, downstream of PKC, involved in EGCG neuroprotective effect. EGCG promoted a biphasic effect on the pro-apoptotic Bad protein: an immediate (30 min) down-regulation of about 35% of its protein levels, returning to control values 2h later and a long-term (24h), more pronounced reduction of about 55%. The expression of Bax was not affected during the first 24h exposure to EGCG. The acute Bad reduction was accompanied by a 1.65 fold increase in phosphorylated PKC alpha isoform. By contrast, pretreatment with a general PKC inhibitor GF 109203X, abolished EGCG-induced Bad decline. This result indicates that PKC is a tight regulator of Bad protein expression levels, being essential for its degradation or synthesis. In view of this finding, the potential involvement of the Ubiquitin Proteasome System (UPS) in EGCG-induced Bad degradation was examined. Pre-incubation with MG-132, a reversible proteasome inhibitor, blocked the degradation of Bad by EGCG. The present study reveals a novel pathway in the neuroprotective mechanism of action of EGCG, which involves a rapid PKC-dependent degradation of Bad protein by the UPS. This may result in inhibition of the apoptotic machinery, thereby modulating mitochondrial responses to oxidative insults.

## Specific pathophysiological functions of JNK isoforms in the brain following neuronal injuries

Thomas Herdegen, Mario Götz, Stephan Brecht, Jan Wessig, Ansgar Chromik, Thomas Nicolaus, Mette Willesen and Genadij Raivich

We have investigated the effect of JNK1 ko, JNK2 ko, JNK3 ko, JNK2+3 ko and c-JunAA mutation on neuronal survival in adult transgenic mice following ischemia, neurotoxicity, axotomy and excitotoxicity. Deletion of JNK isoforms indicated the compartment-specific expression of JNK isoforms with 46 kD JNK1 as the main phosphorylated JNK isoform. Permanent occlusion of the MCA significantly enlarged the infarct area in JNK1 ko which showed an increased expression of JNK3 in the penumbra. Survival of dopaminergic neurons in the substantia nigra compacta (SNc) following intrastriatal injection of 6-hydroxydopamine was transiently improved in JNK3 ko and c-JunAA mice after 7 d, but not 60 d. JNK3 ko conferred *persisting* neuroprotection, however, of axotomized SNc neurons following transection of the medial forebrain bundle. None of the JNK ko and c-JunAA mutation affected the survival of facial motoneurons following peripheral axotomy when investigated after 90 d. Finally, we determined the impact of JNK ko on the survival of animals and the degeneration of hippocampal neurons following kainic acid (KA). JNK3 ko mice were substantially resistant against and survived KA induced seizures. JNK3 ko and JNK1 ko showed a non-significant tendency for decreased or increased death of hippocampal neurons, respectively; significance was not reached due to the high intra-animal and inter-animal variability of degenerating neurons within one group.

This comprehensive study provides novel insights into the context-dependent physiological and pathological functions of JNK isoforms.

## COPAXONE VACCINATION FOR RETINAL NEUROPROTECTION

**M.Belokopytov, G.Dubinsky, Y.Epstein, M.Belkin, M.Rosner.**

**Goldschleger Eye Research Institute, Sackler Faculty of Medicine, Tel Aviv University,  
Sheba Medical Center, Tel Hashomer, Israel.**

As is the case with other diseases and injuries of the nervous system, retinal damage induced by laser photocoagulation is much increased by secondary degeneration processes whereby tissues adjacent to the primary lesion are destroyed. We attempted to demonstrate whether the newly developed modality of neuroprotective vaccination with the multiple sclerosis drug, Glatiramer acetate (Copolymer-1, Cop-1, trade name Copaxone) is effective in reducing the extent of secondary degeneration in the retina, a tissue devoid of myelinated axons.

**Aim:** To assess the neuroprotective effect of immunization by Cop-1 on the retina against laser-induced damage.

**Methods:** Standard lesions were created by argon laser (514 & 544 nm, 200 mm, 0.1 W, 0.05 second) in 114 DA pigmented rats. The animals were divided into five groups of 18 animals each. Three groups received a single treatment of Cop-1 at different times: 7 days before, immediately after, or 24 hours after the laser injury. Treatments were given by administering 200 µg Cop-1 emulsified with an equal volume of complete Freund's adjuvant (CFA) (0.2 ml in volume) into the rats' two footpads. One group was treated twice: 7 days before and 20 days after the laser irradiation. The rest of animals were divided into three control groups: one treated by 200 µgm of saline seven days before the injury; another treated by 0.2 ml of CFA 7 days before the injury, and the third group, treated by intraperitoneal injection of 1 mg/kg MK-801 immediately after the laser session, served for positive control (1).

The effect of treatment in all groups was evaluated morphometrically at three time points: 3, 20, and 60 days after the primary injury (six animals for each time point).

**Results:** The histological and morphological evaluation of the lesions 3, 20, and 60 days after the injury revealed significant reduction in photoreceptor loss in the pre-immunized animals at all time points as measured over the central zone of the lesion. The same protective effect was observed 3 and 20 days after lasing as measured over the whole damaged area. Significant reduction in lesion diameter after pretreatment with Cop-1 was seen only 60 days after laser injury. Cop-1 given immediately after the laser damage reduced cell loss 20 and 60 days after the laser damage, when measured in the whole lesion and 20 days after the laser irradiation, when measured in the center of lesion. The immediate treatment had no effect on lesion diameter. Treatment by Cop-1 24 hours after the laser session had no effect on cell density, but reduced the lesion diameter at all time points. Repeating the treatment once, 20 days after the injury, led to enhancement of the neuroprotective effect, decreasing the cell loss in the center of lesion and reducing the diameter of lesion.

**Conclusions:** The results show that immunization with Cop-1 is neuroprotective against laser-induced retinal injuries, repeating the treatment enhances this effect, and immune neuroprotection is possible in a tissue with non-myelinated neurons, not only in tissues containing myelinated nerve fibers (2,3). The putative mechanisms for the successful neuroprotective action of autoimmunization are the inhibition of the neurotoxic mediators of the secondary degeneration and release of neurotrophic factors. The higher effectiveness of the immunological neuroprotection, when compared to pharmacological neuroprotective agents may be due to its complex multiple specific actions that are local to the lesion site and presumably of appropriate quantity and duration. If proven to be effective, the neuroprotective vaccination may possibly be used for prevention and treatment of various neurological and ophthalmic diseases.

1. Solberg Y, Rosner M, Turetz J, Belkin M. MK-801 has neuroprotective and antiproliferative effects in retinal laser injury. *Invest Ophthalmol Vis Sci.* 1997;38:1380-1389.
2. Yoles E, Schwartz M. Degeneration of spared axons following partial white matter lesion: implications for optic nerve neuropathies. *Exp Neurol.* 1998;153:1-7.
3. Schori H, Kipnis J, Yoles E, WoldeMussie E, Ruiz G, Wheeler LA, and Schwartz M. Vaccination for protection of retinal ganglion cells against death from glutamate cytotoxicity and ocular hypertension: Implications for glaucoma. *Proc Natl Acad Sci USA.* 2001;98:3398-3403.

## **Changes in retinal architecture and neurotransmission after perturbation of cholesterol synthesis and transport.**

**Claudepierre T<sup>1</sup>, Buard I<sup>1</sup>, Nieweg K<sup>1</sup>, Simonutti M<sup>2</sup>, Pfrieger F<sup>1</sup>**

**<sup>1</sup>Atip CNRS/Max Planck, CNRS UPR2356  
5, rue Blaise Pascal 67084 Strasbourg Cedex France**

**<sup>2</sup>Inserm 592 Hôpital St Antoine  
27, rue de Chaligny 755571 Paris Cedex 12**

**[Claudepierre@neurochem.u-strasbg.fr](mailto:Claudepierre@neurochem.u-strasbg.fr)**

Neuron/glia interactions are crucial for CNS development and glia-derived cholesterol has been shown to promote synaptogenesis in rat retinal ganglion cells in vitro (Mauch et al., 2001). Here we aim to define the role of glia-derived cholesterol in retinal development and function. Following our hypothesis that neurons reduce the synthesis of cholesterol after birth and import it from an external source (glia), we analysed how inhibition of cholesterol synthesis and transport affect neurons survival and function in the retina.

First, we tested the effect of an inhibitor of cholesterol synthesis (zaragozic acid) on retinal development using organotypic cultures of retinae from postnatal mice. We analyzed the global retinal architecture using specific markers and on cell survival. In a second part, effects of a defect in intracellular cholesterol transport were studied in mice deficient for NPC1, a protein that is involved in the endosomal shuttle of endocytosed cholesterol and absent in Niemann-Pick disease type C (NPC). NPC is a lysosomal storage disorder characterized by severe neurodegenerative processes. We performed an immunohistological and biochemical analysis of retinae from postnatal wild type and NPC1 mutant mice of different ages. The functional integrity of retinae was determined by electroretinogram.

After two weeks of treatment of retinal organotypic cultures with zaragozic acid, cholesterol synthesis was blocked as revealed by thin-layer chromatography. Surprisingly, the expression and the localization of synaptic proteins remained unaffected. Synaptophysin, a cholesterol binding protein was the only synaptic marker that was reduced in plexiform layers. The cellular composition of the retina was modified as shown by the reduced number of parvalbumin- and calbindin-positive neurons in the treated explants. Retinae from NPC1-deficient mice exhibit several developmental abnormalities. Cone outer segments were reduced and disorganized and RGCs appeared less numerous. At the biochemical level RGC (parvalbumin, calbindin) and dendritic markers (MAP2) were clearly reduced. Neurotransmission was impaired: scotopic ERG revealed a reduction of both a and b wave amplitudes. The oscillatory potentials were perturbed and there was almost no detectable cone response as seen by photopic ERG and flicker experiments. In summary, our results suggest that subtypes of retinal neurons are highly vulnerable to cholesterol homeostasis.

Supported by Ara Parseghian Medical Research Foundation, Retina France, Fondation pour la Recherche Médicale, Fondation de France, DFG.



## **GENDER DIFFERENCES OF ALBINO RATS IN RECOVERY FROM CEREBRAL ISCHEMIA INDUCED BY 12-MIN CARDIAC ARREST**

Gorenkova N.A., Volkov A.V.

Research Institute of General Reanimathology, Russian Academy of Medical Sciences  
Petrovka Str.25, Building 2, 103031 Moscow, Russia

### **Introduction**

Earlier, it has been found that a single applications of sex hormones progesterone, testosterone or 17-beta-estradiol after 15-min of ischemia significantly decrease mortality in animals. This suggests importance of sex hormones and of sex differences in compensatory mechanisms of survival. Therefore, we aimed to study more in detail gender differences in recovery from cerebral ischemia caused by 12-min cardiac arrest type in albino rats.

### **Methods**

37 adult albino rats, 19 females and 18 males were used in our study. Rats were exposed to global cerebral ischemia induced by 12-min cardiac arrest, which has been performed under anaesthesia. Cardiovascular and respiratory parameters were monitored throughout the procedure. Examination of neurological parameters was performed daily during a time period of 2 weeks. This analysis included measurement of parameters of visual and acoustic systems, locomotor abilities, sensitivity and responsiveness to pain, eating and drinking behavior.

### **Results**

In females, parameters of cardiovascular activity were found to be recovered within 1,17 min after termination of 12-min cardiac arrest; in males, cardiovascular activity recovered in 1,24 min after induction of ischemia. Recovery of parameters of respiration was registered 7,74 min after termination of cardiac arrest in female rats and 7,08 min in male animals. Both cardiovascular and respiratory parameters did not differ significantly between genders. There was a significant difference between two groups in reinstatement of corneal reflex: in males the latency of reinstatement was found to be significantly longer (30,67 min) than in females (24,95 min;  $p < 0.05$ ). Females showed faster recovery of locomotor activity that has been observed in 68 % of female population within a time period of 2 h after termination of cardiac arrest, whereas only 33 % of males showed the same restoration of locomotion during this time period.

There was a significant difference between females and males in time course of recovery from neurological deficits. In 53 % of females, complete recovery of neurological functions was observed on the 4<sup>th</sup> day in 89,5% of population, while majority of males showed neurological recovery on the 6<sup>th</sup> day after termination of cardiac arrest. This difference was significant ( $p < 0.05$ ). Moreover, during all time period of observation, female rats showed lower scores in neurological deficit, induced by ischemia, in comparison to their male counterparts (day 1: 12,1 and 14,7; day 2: 6,8 and 8,7; day 3: 4,0 and 6,1; day 4: 1,4 and 3,7; day 5: 0,3 and 1,6, correspondingly;  $p < 0.05$ ).

### **Conclusion**

The obtained data suggest that female albino rats show less profound effects of termination of 12-min cardiac arrest and faster recovery from its neurological consequences in comparison to their male counterparts. There were no significant differences found in recovery of cardiovascular and respiratory functions. One of the possible explanations for found differences could be sex hormones. Our results emphasize a role of gender in choosing more proper therapeutical methods in humans, taking into account sex differences.

**Tau gene (MAPT) analysis in non-human primates****Max Holzer**<sup>1</sup>, Molly Craxton<sup>2</sup>, Ross Jakes<sup>2</sup>, Thomas Arendt<sup>1</sup>, Michel Goedert<sup>2</sup><sup>1</sup>Paul Flechsig Institut for Brain Research, Leipzig<sup>2</sup>MRC LMB, Cambridge

Tau protein is an axonally localized microtubule-associated protein and occurs as six splice variants in the adult human brain. Hyperphosphorylated tau protein is implicated in a variety of neurodegenerative disorders, where it is the main constituent of intracellular fibrillar deposits in neurons and glial cells. These neurodegenerative disorders include pure tauopathies like Progressive Supranuclear Palsy (PSP), Corticobasal Degeneration (CBD), Pick's Disease (PiD) and Frontotemporal Dementia and Parkinsonism linked to chromosome 17 (FTDP-17) and mixed tauopathies like Alzheimer's disease.

Mutations in the tau gene have been identified in FTDP-17. In addition, polymorphisms in the tau gene have been associated with PSP, CBD and Parkinson's disease. Most polymorphisms are in linkage disequilibrium with haplotypes H1 and H2. Knowledge of the evolution of the tau gene in the non-human primates may yield insights in the mechanism of disease initiation and progression.

We have sequenced tau exons 1-13, including intronic flanking regions and a region in intron 9 containing a proposed nested gene, saitohein, in two chimpanzees, one gorilla, two gibbons and partially in one macaque and a cell line derived from green monkey.

We found no non-synonymous base substitutions in constitutively spliced exons 1,4,5,7,9,11,12 and 13 in the chimpanzees, when compared to the human tau haplotype H1 or H2. Alternatively spliced exon 10 was conserved in all species analyzed. Other exons, which are not constitutively spliced such as exons 2, 3, 4a, 6 and 8, showed an increased rate of synonymous and non-synonymous base substitutions. Nucleotides in MAPT in humans close to or in exons 1, 3, 9, 11 and 13 used to define haplotypes H1 and H2 were conserved from gibbon to chimpanzee and can be assigned to the human haplotype H2. Analysis of the saitohein gene in intron 9 revealed that its open reading frame is absent in rodents, is interrupted in gibbon and macaque but present in gorilla and chimpanzee.

Keywords : Alzheimer, aging, cytoskeleton

## **Ischemic cell death in human NT2 neurons is prevented by NMDA receptor antagonists but not by antagonists at the glycine<sub>B</sub> binding site**

Garcia de Arriba S, Wegner F, Grüner K, Sobottka H, Wagner A, Wohlfarth K, Allgaier C

Rudolf-Boehm-Institut für Pharmakologie und Toxikologie, Klinik und  
Poliklinik für Neurologie, Leipzig, Germany

Human NT2 neurons (NT2-neurons) obtained from embryonic teratocarcinoma (NT2) cells by treatment with retinoic acid were established as in-vitro model to investigate the mechanisms associated with hypoxia/ischemia-induced neuronal injury. NT2-neurons exhibit the properties of central neurons and express both NMDA and GABA<sub>A</sub> receptors. In particular, expression of NMDA receptor subunits depended on the stage of neuronal differentiation. In differentiated 11 week-old neurons, the expression of various NMDA receptor and GABA<sub>A</sub> receptor subunits was demonstrated immunocytochemically. In patch-clamp recordings (whole-cell mode), NMDA (plus 10 glycine, each) and GABA induced inward currents with an EC<sub>50</sub> of approximately 40 and 20  $\mu$ M, respectively. The NMDA responses were antagonized by memantine, a blocker of the NMDA receptor associated channels and required the presence of glycine as co-agonist.

To study the effect of hypoxia/ischemia on neuronal survival, NT2 neurons were exposed to reduced oxygen concentration (1%) and/or glucose deprivation for 3 hours. Necrotic cell death was assessed by using propidium iodide as marker for plasma membrane integrity and analysed with flow cytometry. Necrosis was higher upon ischemia (percentage of necrotic cells: 36.6 $\pm$ 1.6%) than after either aglycemia (26.5 $\pm$ 3.0%) or hypoxia (31.7 $\pm$ 1.6%). In addition, necrosis continued during subsequent reoxygenation over a period of 22 h. Memantine and CGS19755 (a competitive NMDA receptor antagonist) significantly reduced ischemia-induced cell death (19.7 $\pm$ 1.6%; 22.9 $\pm$ 3.7%). In contrast, 5,7-dichlorokynurenic acid (DKCA), an antagonist at the glycine binding site of the NMDA receptor did not reveal any significant neuroprotective effect (32.6 $\pm$ 2.7%). Changes in mitochondrial membrane potential were assessed by using the fluorescent probe JC-1. Ischemic conditions for 3 h were associated with a decrease of 31% in the relative green/red fluorescent intensity, indicating a reduction in mitochondrial membrane potential and, hence, mitochondrial dysfunction. The present study verifies cultured NT2 neurons as human *in vitro* model for studying the molecular mechanisms associated with ischemic injury. Interestingly, neuroprotection could be achieved with NMDA receptor antagonists but not with an antagonist at the glycine<sub>B</sub> binding site of the NMDA receptor.

The present study was supported by the Interdisziplinäre Zentrum für Klinische Forschung (IZKF) Leipzig at the Faculty of Medicine of the Universität Leipzig (Project C20)

## **Immunohistochemical localization of *N*-methyl-D-aspartate receptor NR1, NR2A, NR2B and NR2C/D subunits in human and *Bennett* rat dorsal root ganglia**

Vera Ogunlade<sup>1,2</sup>, Ralf Schober<sup>1</sup>, Stefan Grimm<sup>1,2</sup>, Clemens Allgaier<sup>2</sup>

<sup>1</sup>Abt. Neuropathologie, Institut für Pathologie · <sup>2</sup>Rudolf-Boehm-Institut für Pharmakologie und Toxikologie, Universität Leipzig, Germany

Ionotropic glutamate receptors play an important role in the transmission of pain signals from the periphery to the central nervous system via the dorsal root ganglion (DRG). In particular, NMDA receptor activation potentiates transmission through the dorsal horn and contributes to the development of neuropathic pain. The subunit composition of the NMDA receptors (NR1, NR2A-D) largely affects their pharmacological and physiological properties. Therefore, information about the distribution of the NMDA receptor subunits in human DRG and spinal cord may help to better understand the importance of the NMDA receptors in pathophysiological processes related to chronic pain.

The present work investigated the distribution of NR1 and NR2 subunits in the human DRG by immunohistochemistry. Moreover, using the *Bennett* rat model for peripheral mononeuropathy, we studied the possible changes in subunit expression of NMDA receptors in DRG. The *Bennett* rat model consists in four loose ligatures placed unilaterally around the common sciatic nerve. Sham-operated animals were used as control. The post mortem human material was obtained from 17 patients (both sexes, aged 22 to 88) suffering or not from neuropathic pain. Autopsies were carried out within 24–72 h after death and lumbar human DRGs were removed and fixed with 4% formaldehyde (pH 7.4) for at least 2 weeks. DRGs from *Bennett* rats (3 and 5 weeks after ligation) were fixed by perfusion and removed. Thereafter, tissue was dissected in blocks and embedded in paraffin wax. H&E stainings were used for histological analysis. Mayer's Hemalum counterstaining was used for immunohistochemical procedures using polyclonal anti-NMDA receptor subunit-specific antibodies (Santa Cruz). NMDA receptor immunoreactivity in the human DRG was found for all investigated subunits in neuronal cell bodies (localized in the cytoplasm) as well as in their axons, but also in some satellite cells as well as in the Schwann cells of the DRG. However, the expression pattern was found largely different among individual patients regarding the number of positive neurons as well as the immunoreactivity intensity. Mainly, the small neurons, which are supposed to be involved in nociception, were more intensively stained than the large neurons transmitting other sensory inputs. Similar staining patterns were found in rat DRG although in neurons located in the ipsilateral (ligated) DRG of *Bennett* rats, the immunoreactivity for NR2A and NR2B subunits was significantly increased as compared to the contralateral side. This finding was not observed in sham-operated animals. The immunoreactivity for NR2C and NR2D subunits did not change markedly after ligation. The described alterations on NMDA receptor expression were found in the small neurons but also in the large ones. In conclusion, the present study demonstrates changes of functional significance in the expression of NMDA receptor subunits in the DRG presumably implicated in the development of neuropathic pain.

**Enhanced neuronal Ras activity triggers spine formation**

Ulrich Gärtner<sup>1</sup>, Alán Alpár<sup>1,2</sup>, Gudrun Seeger<sup>1</sup>, Rolf Heumann<sup>3</sup>, Thomas Arendt<sup>1</sup>

<sup>1</sup>Department of Neuroanatomy, Paul Flechsig Institute for Brain Research, University of Leipzig, D-04109 Leipzig, Germany; <sup>2</sup>Department of Anatomy, Histology and Embryology, Semmelweis University Medical School, Tűzoltó u. 58, H-1450, Budapest, Hungary; <sup>3</sup>Molecular Neurobiochemistry, Ruhr-University, D-44780 Bochum, Germany

Spines represent specific dendritic membrane protrusions mainly on principal neurons where they function as the primary postsynaptic compartments for excitatory input. Although spines are distinctive anatomical features, their structural dynamics is considerable even in the adult neocortex. The integrative capacity of the neuron seems to be greatly depending upon spine density, which can be remarkably enhanced and restored by neuronal activity and the action of neurotrophins. Both stimuli result in various cellular responses via small GTPases. Recent interest has been focused on members of the Rho family GTPases that are involved in the regulation of spine formation. However, also the small G-protein Ras has been implicated in neuronal spinogenesis.

In the present study, the effect of enhanced Ras activity upon dendritic spine formation has been investigated on pyramidal cells in the adult neocortex of synRas mice overexpressing Val12-Ha-Ras specifically in postmitotic neurons [2]. For quantitative analysis, commissural neurons of layers II/III were retrogradely labelled with biotinylated dextran amine. In synRas mice, spine frequency on several orders of basal dendrites and apical oblique branches was significantly increased. Whereas density on basal dendrites was overall augmented, on apical dendrites, distal regions were most affected. The proportions of different morphological types of spines remained unchanged.

Ras is critically involved in neurotrophic signal transduction downstream of Trk receptors and is therefore in a perfect position to mimic effects of neurotrophins on spine morphology and density. Recently, long-term exposure to BDNF has been shown to increase dendritic spine density on hippocampal neurons in a MAPK dependent manner [1]. Consistently, Ras has been implicated to participate in the activity-dependent spine morphogenesis *in vitro* by activating the MAPK pathway [3].

It is concluded that Ras dependent mechanisms are involved in the regulation of dendritic spine number in the adult brain *in vivo*. The results confirm the critical morphoregulatory role of Ras in the central nervous system.

1. Alonso M, Medina JH, Pozzo-Miller L. ERK1/2 activation is necessary for BDNF to increase dendritic spine density in hippocampal CA1 pyramidal neurons. *Learn Mem* 2004; 11:172-178.
2. Heumann R, Goemans Ch, Bartsch D, Lingenhöhl K, Waldmeier PC, et al. Constitutive activation of Ras in neurons promotes hypertrophy and protects from lesion-induced degeneration. *J Cell Biol* 2000; 151:1537-1548.
3. Wu GY, Deisseroth K, Tsien RW. Spaced stimuli stabilize MAPK pathway activation and its effects on dendritic morphology. *Nature Neurosci* 2001; 4:151-158.

**Putative relation between neuronal cell cycle proteins and neuroplasticity**

Stefanie Schmetsdorf, Ulrich Gärtner, Thomas Arendt

Paul-Flechsig-Institut für Hirnforschung, Neuroanatomy, University of Leipzig, 04109 Leipzig, Germany

Developmental structuring of brain is the result of a strictly coordinated process that involves controlled cell division, neuronal migration and terminal differentiation. Neurogenesis occurs generally during the embryonic and early postnatal stages and will be finished in the mature brain. Once differentiated, neurons are incapable of further division but retain the capability of structural and functional plasticity. In general, the cell cycle progression is regulated by the sequential expression and activation of regulatory proteins like cyclins, cyclin dependent kinases (cdk) or cdk inhibitors (cdki). In postmitotic and terminally differentiated neurons cell cycle activity is arrested by enrichment of cdkis. Proliferative phase is followed by neuronal migration, differentiation and the establishment of neuronal networks. The morphological correlates of interneuronal connectivity are synapses. During the development as well as during the whole lifespan synapses undergo a high degree of turnover which is characterised by structural and functional changes. This plastic process is accompanied by dynamic rearrangements of the cytoskeleton, i. g. neurofilament and microtubule-associated proteins.

In the present study we have examined the expression of cell cycle regulatory proteins in layer V pyramidal neurons of murine neocortex (P11, adult) using immunohistochemical methods. As expected, the expression of cdkis was detectable both in immature and adult neocortex. However, several cyclins and cdks could be localised not only in immature neurons, but in adult neurons as well. Staining was prominent both in neuronal perikarya and dendrites. In parallel to immunohistochemical studies, expression of cell cycle proteins was verified by Western blotting. Additionally, we demonstrate a physical interaction of cdk5 both with cyclin D and p27<sup>KIP1</sup>. Cdk5 is known to be expressed in the adult brain and to control cytoskeletal functions in postmitotic neurons. Furthermore, we demonstrated by Western blot analyses that cdk1, 2, 4, and cyclins E, D do interact with MAP-tau. Findings suggest, that in mammalian brain, the expression of cell cycle markers in postnatal and adult pyramidal neurons of neocortex is likely associated with additional physiological functions beyond cell cycle regulation. Thus, they might be involved in processes of neuronal and synaptic plasticity.

## Activation of cell cycle proteins after excitotoxic brain lesion with NMDA, Kainate and 3-Nitropropionic acid

Kristin Schmidt<sup>1</sup>, U. Ueberham<sup>1</sup>, U. Gärtner<sup>1</sup>, E. Ueberham<sup>2</sup>, Th. Arendt<sup>1</sup>

- 1) Department of Neuroanatomy, University of Leipzig, Paul Flechsig Institute of Brain Research, Jahnallee 59, 04109 Leipzig, Germany
- 2) Institute of Biochemistry, University of Leipzig, Liebigstraße 16, Germany

### **Abstract:**

In human brain, the expression of cell cycle proteins in neurons is assumed to be associated with aging and degeneration. In contrast, different cell cycle proteins are expressed in neurons during the ontogenesis of the normal mouse brain and in the adult animal. The underlying function of these proteins in terminally differentiated cells and their role during pathogenetic processes are discussed controversially and not yet clarified until now. They seem to be involved in the neuronal homeostasis, in maintaining the differentiation status as well as in an apoptotic fate of neurons. To identify critical regulators of cell cycle protein expression in differentiated neurons we disturbed the neuronal homeostasis using different excitotoxic substances. The expression of cyclins, cyclin-dependent-kinases and their inhibitors in the brain was analyzed after intrahippocampal or intraperitoneal administration of NMDA, Kainate and 3-Nitropropionic acid. We monitored the neuronal lesion in hippocampus, cortex and striatum by fluorojade staining. Using immunohistochemical analysis we could demonstrate that in the lesion site different cyclins (Cyclin E, Cyclin A, Cyclin C), cdks (cdk 2, cdk 4) and cdks (p16, p27, p21) were elevated and/or translocated from cytoplasm to the nucleus. Compared to results obtained previously our data suggest an active attempt of affected neurons to prevent apoptosis.

**Keywords:** Alzheimer, neurotoxicity, animal models for diseases

## **LSC as powerful tool for the analysis of DNA content in neurons**

Birgit Mosch<sup>a</sup>, Dominik Lenz<sup>b</sup>, Attila Tarnok<sup>b</sup> and Thomas Arendt<sup>a</sup>

<sup>a</sup> Paul Flechsig Institute of Brain Research, Department of Neuroanatomy, University of Leipzig, Germany

<sup>b</sup> Pediatric Cardiology, Cardiac Center, University of Leipzig, Germany

Neurons as terminally differentiated cells are permanently withdrawn from the cell cycle and are diploid as most somatic cells. However there are some exceptions.

Studies from the 70's and early 80's using Feulgen stained brain slices and cytophotometry indicate that neurons, namely purkinje cells and hippocampal pyramidal cells, seem to be polyploid in rodents and also in humans. The functional background of this polyploidy remained obscure, and contrary results were obtained with the same technique so that, as a result of methodological deficiencies, studies were no longer enforced.

Nearly two decades later, two papers were published where a new technique, fluorescence in situ hybridisation (FISH) was applied for analysing the DNA content of neurons in human brain in schizophrenia and Alzheimer's disease (AD). Yang et al. (2001) demonstrated that a significant fraction of hippocampal pyramidal and basal forebrain neurons in AD have fully or partially replicated four separate genetic loci on three different chromosomes. This was the first study suggesting a "genuine" cell cycle with DNA replication in AD neurons.

The aim of our study was to quantify neuronal DNA content in a high number of cells to ascertain if neurons are able to replicate their genome. With Laser Scanning Cytometry (LSC), measuring of DNA content is well established but mostly accomplished by means of cell suspensions. To obtain the tissue architecture and to distinguish between neurons and glial cells, we transferred the LSC technique to slices of AD patients and control brains. Thus, we were able to measure many cells in a relative short time, depict diverse cell types, morphological details and analyse the ploidy status of different cell populations.

First results reveal that DNA replication might occur at least in some neurons in AD and to a minor degree also in control brains.

Keywords : Alzheimer, aging



## Iron binding properties of perineuronal nets in the rat brain

M. Morawski<sup>a</sup>, T. Reinert<sup>b</sup>, G. Brückner<sup>a</sup>, P. Riederer<sup>c</sup>, F. E. Wagner<sup>d</sup>, W. Meyer-Klaucke<sup>e</sup>,  
T. Butz<sup>b</sup> and T. Arendt<sup>a</sup>

<sup>a</sup>Paul Flechsig Institute for Brain Research, University of Leipzig, Jahnallee 59, D-04109, Leipzig

<sup>b</sup>Faculty of Physics and Geosciences, University of Leipzig, Linnestraße 5, D-04103, Leipzig

<sup>c</sup>Clinical Neurochemistry, University of Würzburg, Fücksleinstrasse 15, D-97080, Würzburg

<sup>d</sup>Physics-Department E15, University of Munich, J-Franck-Straße, D-85748 Garching

<sup>e</sup>EMBL Hamburg, Building 25A, DESY, Notkestraße 85, D-22603 Hamburg

A specialized form of extracellular matrix termed perineuronal nets (PN's) consisting of large aggregating chondroitin-sulfate proteoglycans, with hyaluronan and aggrecan as main components, surrounds subpopulations of neurons. The relevance of the perineuronal nets of the extracellular matrix as a possible protection against metal ion-induced oxidative stress is an actually discussed theory. Due to their glycosaminoglycan components, these PN form highly charged structures in the direct microenvironment of neurons and might, thus, be involved in local ion homeostasis. Through their polyanionic character, PN's might also potentially be able to scavenge and bind redox-active iron ions, and reduce the local oxidative potential in the neuronal microenvironment, thus providing a certain level of neuroprotection to net-associated neurons. The characteristics of iron-charged PN's of the extracellular matrix in the rat cortex and the red nucleus were measured using the powerful combination of Particle-Induced X-ray Emission (PIXE), Extended X-ray Absorption Fine Structure (EXAFS) and Mössbauer spectroscopy (MS). PIXE was used to localize and quantify the iron stoichiometry. The binding affinity-constant ( $K_D$ ) was calculated from a *Michaelis-Menten* fit to measured values. EXAFS and MS were performed to obtain information on the chemical state, valence and coordination sphere of the PN-bound iron as well as on the chemical surrounding of the iron.

The results show that the PN-ensheathed neurons accumulate up to 4.6 times more iron than any other ECM structures depending on the applied Fe concentration in the investigated brain areas with local concentration maxima of 480 mmol/l Fe at PNs. The affinity-constants  $K_D$  are in the range from 2,2 mmol/l to 3,3 mmol/l in the different analysed brain areas.

The present results suggest a neuroprotective function of perineuronal nets against iron induced oxidative stress, potentially involved in neurodegeneration.

Keywords : Alzheimer, membrane composition and cell-surface macromolecules, oxidants

**Searching for microtubule-associated protein tau-interacting proteins**

Ellen Ramminger, Thomas Arendt, Max Holzer

University of Leipzig, Faculty of Medicine

Paul-Flechsig-Institute of Brain Research, Dept. Neuroanatomy

Jahnallee 59, 04109 Leipzig

The main characteristic of neurodegeneration in Alzheimers disease (AD) is progredient neuronal death within brain regions of high plasticity caused by intraneuronal neurofibrillary tangles (NFTs) and extracellular  $\beta$ -amyloid plaques. NFTs consist of abnormally phosphorylated tau protein, which is polymerized into paired helical filaments or straight filaments.

The role of tau protein in neurodegeneration is emphasized by pathological tau fibrils occurring separately, without  $\beta$ -amyloid-depositions in several neurodegenerative diseases, summarized as tauopathies. The identity of factors facilitating tau aggregation remains elusive. One approach to identify such factors is to screen for proteins that interact with human microtubule associated protein tau (MAP-tau).

FE65 was identified to be a potential MAP-tau-interacting protein by screening a human brain cDNA-library using the Cyto-Trap-Yeast-two-hybrid system. Co-localisation of FE65 and tau-proteins within intracellular tangles and ultrastructural observations has been observed (Delatour et al., 2001).

Our aim was to investigate if the proteins FE65 and a related protein Mint3 interact with human MAP-tau and to define the interacting domains by means of Yeast-two-hybrid system and co-immunoprecipitation.

Surprisingly no interaction of MAP-tau with FE65 or with Mint3 was observed using Duplex-Yeast-two-hybrid system and co-immunoprecipitation. This might indicate a transiently occurring interaction not detectable by these methods, or may point to an absence of interaction.

Keywords : Alzheimer, protein interaction, cytoskeleton

**Tau mRNA Splicing and Protein Isoform Expression during Development in vivo and in vitro.**

Torsten Bullmann<sup>1</sup>, Wolfgang Härtig<sup>1</sup>, Nicolas Sergeant<sup>2</sup>, Max Holzer<sup>1</sup>, Rohan De Silva<sup>3</sup>, and Thomas Arendt<sup>1</sup>

<sup>1</sup> University of Leipzig, Paul-Flechsig Institute for Brain Research, Department of Neuroanatomy, Jahnallee 59, 04019 Leipzig

<sup>2</sup> INSERM U422, 1 Place de Verdun, 59045 Lille Cedex, France.

<sup>3</sup> Reta Lila Weston Institute of Neurological Studies and UCL Monoclonal Antibody Unit Department of Immunology & Molecular Pathology, University College London, London, UK

A major constituent of neurofibrillary tangles in Alzheimer's disease is the microtubule associated protein tau. Alternative splicing of three exons leads to four or six isoforms in rodents or humans, respectively.

We studied tau mRNA splicing and protein isoform expression in different regions of rat brain. RT-PCR and western blotting showed that for all regions studied exon 10 splicing switched around postnatal day 14 whereas exon 2 and 3 splicing differed between regions. Single cell RT-PCR was further used to study tau mRNA splicing in granule and pyramidal cell layer of the hippocampus in combination with molecular markers.

Primary cell culture of hippocampus and cerebellum maintained up to 5 weeks showed characteristic developmental course of exon splicing although the adult isoform pattern was not fully achieved.

Immunohistochemistry using exon specific tau antibodies showed developmental expression of tau isoforms in rat brain. We could show that the juvenile isoform of tau devoid of exon 10 is expressed in some small cells beneath the stratum granulosum of hippocampus. Furthermore in the layer III of the cingulate and piriform cortex a few small cell bodies and dendrites were labeled, whereas the caudate putamen showed numerous large labeled cell bodies. This labeling showed a remarkable change with increasing age with only the large cells in the caudate putamen remaining in brain of rats older than 1 year.

Keywords : Alzheimer, aging, cytoskeleton

## Organizing the blood-brain barrier: Interplay between astroglia, the extracellular matrix and the endothelial cells.

Hartwig Wolburg<sup>1</sup>, Michel Mittelbronn<sup>2</sup>, Bernhard Erdlenbruch<sup>3</sup>, Arne Warth<sup>1</sup>

<sup>1</sup>Institute of Pathology, University of Tübingen, Liebermeisterstr. 8, D-72076 Tübingen,

<sup>2</sup>Institute of Brain Research, University of Tübingen, Calwer Str. 3, D-72076 Tübingen,

<sup>3</sup>Children's Hospital, University of Göttingen, Robert Koch-Str. 40, D-37075 Göttingen

The blood-brain barrier (BBB) regulation is characterized by an interplay between endothelial tight junctions, perivascular basal laminae and astrocytic cells. Glial cells are highly polarized by the differentiation of astroglial membrane domains: where the glial membrane contacts the endothelial basal lamina, orthogonal arrays of particles (OAPs; Fig. 1) are highly concentrated; glial membranes show an abrupt decrease of the OAP density where this contact is lost. In cultured astrocytes as well as in reactive or neoplastic glial cells, this polarity is clearly reduced, and this reduction is consistently associated with a compromised BBB.

In the last years, the OAPs were identified to contain the water channel protein aquaporin-4 (AQP4). It has been shown recently that  $\alpha$ -syntrophin contains a PDZ-domain binding to the C-terminus of AQP4. Syntrophin is a member of the dystrophin-dystroglycan complex (DDC; Fig.2) which is well investigated in muscle cells, but present in astrocytes as well. Alpha-dystroglycan, a further DDC member, is a linker molecule between the transmembrane protein  $\beta$ -dystroglycan and the extracellular matrix components laminin and agrin. Agrin, a heparan sulfate proteoglycan, has been suggested to be important for the maintenance of the BBB. In vessels of human glioblastoma, agrin was partly absent from the perivascular basal lamina, and where this was the case, tight junction molecules such as occludin, claudin-3 and claudin-5 were lacking in the endothelial cells (Rascher et al. [2002] *Acta Neuropathol* 104:85). Moreover, where agrin was lacking, AQP4 was both upregulated and redistributed across the whole surface of the glioma cell (Warth, Kröger and Wolburg [2004] *Acta Neuropathol* 107:311). But since under glioma conditions the OAPs were reduced, this contradiction can only be resolved by the suggestion that AQP4 can dissociate from the arrays. Thus, since agrin seems to be able to cluster AQP4 and OAPs at the glial endfoot membrane, but binds to  $\alpha$ -dystroglycan rather than to AQP4, the OAPs may contain more molecules than AQP4. Moreover, we found in human gliomas that the weakly inwardly rectifying  $K^+$  channel Kir4.1 redistributed across the whole cell (Warth et al., submitted). Kir4.1 is bound to the PDZ-domain of  $\alpha$ -syntrophin as AQP4 (Connors et al. [2004] *JBC* 279:28387) and is normally colocalized together with the DDC and AQP4 suggesting that Kir4.1 may contribute to the OAPs, too (Fig.2). The normally polarized distribution of Kir4.1 is believed to be essentially involved in the important physiological role of astrocytes to perform spatial buffering of extracellular  $K^+$ . Because water fluxes are osmotically driven by ion fluxes, it was hypothesized that  $K^+$ -clearance is coupled to water flux.

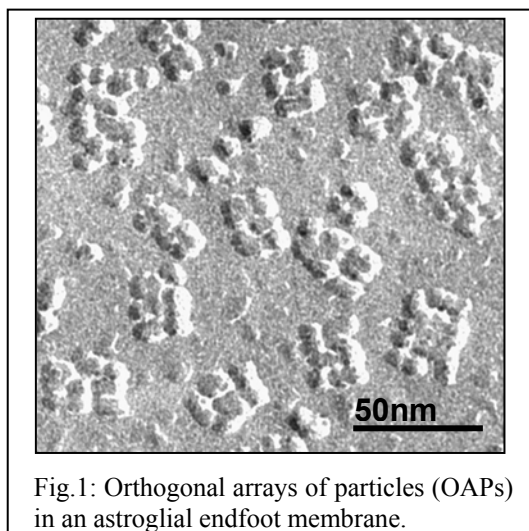


Fig. 1: Orthogonal arrays of particles (OAPs) in an astroglial endfoot membrane.

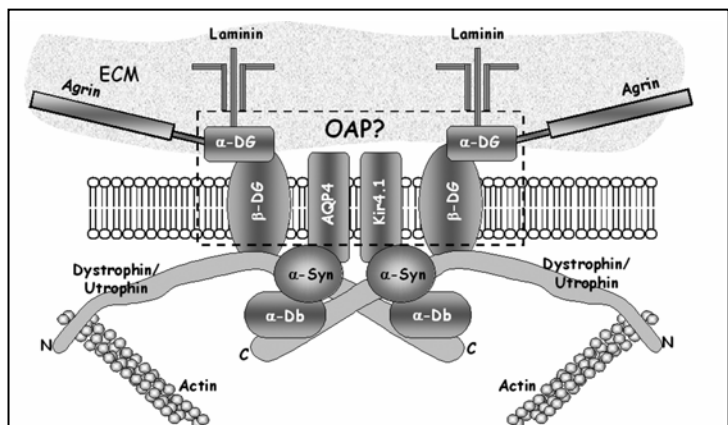


Fig. 2: Hypothetical view of the DDC: AQP4 aquaporin-4,  $\alpha$ -DB  $\alpha$ -dystrobrevin,  $\alpha$ -DG  $\alpha$ -dystroglycan,  $\alpha$ -Syn  $\alpha$ -syntrophin,  $\beta$ -DG  $\beta$ -dystroglycan, Kir4.1 inward rectifying  $K^+$ -channel 4.1

Redistribution of Kir4.1 may compromise the spatial buffering capacity, and, as a consequence, intracellular  $K^+$  concentration increases and consecutive water flux is causative for the observed cell swelling (cytotoxic edema). In addition, the dissociation of the molecular complex consisting of Kir4.1 and AQP4 would lead to cell swelling due to a failure to release water at the endfoot membrane. Interestingly, in low-grade astrocytoma, Kir4.1 is redistributed across the whole surface of the cell, whereas AQP4 is maintained at the endfeet membranes. In high grade astrocytomas, both molecules are redistributed. In the RG2 rat glioma we found swollen astrocytic endfeet with many OAPs. Assuming a redistribution of Kir4.1 in this system (work in preparation) this would suggest that the dissociation of Kir4.1 from the putative Kir4.1/AQP4/DDC-complex must not necessarily lead to the disappearance of OAPs. However, only the dissociation of AQP4 from the complex (in high-grade gliomas or in the AQP4-knockout) leads to disappearance of OAPs.

Thus, better understanding the complicated network of factors managing the BBB may also explain the formation of brain edema.

**Poster Subject Area #PSA31:  
Neural-immune interactions**

- [#417A](#) N. Benaroya-Milshtein, N. Hollander, T. Kukulansky, N. Raz, A. Apter, I. Yaniv, Y. Haberman, H. Halpert and CG. Pick, Tel Aviv (IL)  
*ENRICHED ENVIRONMENT PROLONGS SURVIVAL OF LYMPHOMA- BEARING IDIOTYPE-VACCINATED MICE*
- [#418A](#) E. de Jong, IM. Dijkstra, N. Brouwer, M. van Amerongen, R. Liem, HWGM. Boddeke and K. Biber, Groningen (NL)  
*EXPRESSION, TRANSPORT AND RELEASE OF CCL21 IN APOPTOTIC CORTICAL NEURONS*
- [#419A](#) V. Waetzig, K. Czeloth, U. Hidding, K. Mielke, M. Kanzow, S. Brecht, M. Götz, R. Lucius, U-K. Hanisch and T. Herdegen, Kiel, Hannover and Goettingen  
*c-Jun N-terminal kinases (JNKs) mediate pro-inflammatory actions of microglia*
- [#420A](#) CR. Pawlak, A. Bauhofer and RKW. Schwarting, Marburg  
*Anxiety-like behaviour in the rat is related to levels of interleukin-2 mRNA in the brain*
- [#416B](#) AV. Kuhnert, N. Taheri, MB. Sättler, D. Merkler, K. Maier, C. Stadelmann, M. Bähr and R. Diem, Göttingen  
*Effects of glatiramer acetate on neuronal and axonal damage in a rat model of multiple sclerosis*
- [#417B](#) K. Takahashi, CD. Rochford and H. Neumann, Göttingen  
*Clearance of apoptotic neurons without inflammation by microglial TREM2*
- [#418B](#) M. Stagi, N. Frank, P. Gorlovoi and H. Neumann, Göttingen  
*Effect of inflammatory mediators on axonal transport of synaptic vesicle proteins and mitochondria*
- [#419B](#) S. Gaupp, F. Lühder, N. Beyersdorf, J. Schmidt, G. Köllner, T. Kerkau, T. Hünig and R. Gold, Göttingen  
*Experimental autoimmune encephalomyelitis (EAE) is ameliorated by superagonistic anti-CD28 treatment via the induction of protective CD4+CD25+ T cells*

# ENRICHED ENVIRONMENT PROLONGS SURVIVAL OF LYMPHOMA-BEARING IDIOTYPE-VACCINATED MICE

Benaroya-Milshtein N.<sup>1</sup>, Hollander N.<sup>2</sup>, Kukulansky T.<sup>2</sup>, Raz N.<sup>2</sup>, Apter A.<sup>3</sup>, Yaniv I.<sup>4</sup>, Haberman Y.<sup>1</sup>, Halpert H.<sup>1</sup>, Pick C.G.<sup>1</sup>

Departments of <sup>1</sup>Anatomy, <sup>2</sup>Human Microbiology, Sackler Faculty of Medicine, Tel Aviv University, Israel, and Departments of <sup>3</sup>Psychiatry and <sup>4</sup>Hemato-Oncology, Schneider Children's Medical Center of Israel.

**Background:** The importance of the environment in the regulation of brain, behavior and physiology has long been recognized in the biological, social and medical sciences. Animals maintained under enriched conditions clearly have better learning abilities than animals maintained under standard conditions. However, the effects of environmental enrichment on immune responses and cancer prognosis are less documented and remain questionable.

**Objective:** To investigate the effect of enriched environment on immune responsiveness, tumor development and survival of lymphoma bearing mice treated by idiotypic-vaccination.

**Methods:** C3H male mice were maintained under enriched or standard conditions for 6 weeks. The mice were vaccinated twice with the immunoglobulin of the B-cell lymphoma 38C-13. Following vaccination, mice were inoculated with tumor cells and monitored for tumor development and survival. Anti-idiotypic antibodies in sera of immunized mice were determined by ELISA.

**Results:** Vaccinated mice in the enriched environment produced higher levels of anti-idiotypic antibodies compared to vaccinated mice in the standard environment. Moreover, tumor development in enriched vaccinated mice was slower than in standard vaccinated mice, with 40% long-term survival in the enriched mice compared to 0% survival in the standard mice ( $p < 0.001$ ).

**Conclusions:** The synergistic effect of enriched environment and vaccination on tumor rejection may be of utmost importance for cancer treatment. Further investigation is required in order to determine the mechanisms involved in this synergistic effect.

## EXPRESSION, TRANSPORT AND RELEASE OF CCL21 IN APOPTOTIC CORTICAL NEURONS

E. de Jong\*, I.M. Dijkstra\*, N. Brouwer\*, M. van Amerongen\*, R. Liem<sup>#</sup>, H.W.G.M. Boddeke\*, and K.Biber\*.

\*Department of Medical Physiology, University of Groningen, The Netherlands

<sup>#</sup>Department of Cellular Biology, University of Groningen, The Netherlands

Whenever neurons in the CNS are injured microglia are the first cells that become activated. In addition to local activation, also microglia remote from the primary lesion site are stimulated. Since this so called secondary activation of microglia is instrumental for long-term changes after neuronal injury it is important to understand how microglia activity is controlled. The remote activation of microglia implies that the activating signals are transported along neuronal projections. However, the identity of these signals has not yet been identified.

We have recently provided evidence that CCL21 (formerly known as SLC, TCA4, Exodus-2 or 6CKine) mRNA expression is upregulated in damaged cortical neurons in a stroke model. Cultured microglia responded to CCL21 stimulation with intracellular calcium transients, chemotaxis and a rapid chloride conductance the via chemokine receptor CXCR3. Moreover it was observed that CXCR3 deficient microglia do not get activated in response to entorhinal cortex lesion, showing the importance of CCL21-CXCR3 signaling for microglial activation *in vivo*.

Here it is shown that endangered pre-apoptotic neurons rapidly express and release the chemokine CCL21. We further provide evidence that neuronal CCL21 is packed in vesicles and transported throughout neuronal processes to reach pre-synaptic structures. Chemotaxis assays show that functional CCL21 is released from endangered neurons and activate microglia via the chemokine receptor CXCR3. Based on these findings we suggest that neuronal CCL21 is important in directed neuron-microglia signaling, and that this communication could account for the remote activation of microglia, far distant from a primary lesion.

**c-Jun N-terminal kinases (JNKs) mediate pro-inflammatory actions of microglia**

Vicki Waetzig (1), Karen Czeloth (1), Ute Hidding (1), Kirsten Mielke (1,2), Moritz Kanzow (1), Stephan Brecht (1), Mario Götz (1), Ralph Lucius (3), Uwe-Karsten Hanisch (4), Thomas Herdegen (1)

(1) Institute of Pharmacology, University of Kiel, Hospitalstrasse 4, 24105 Kiel, Germany

(2) Institute of Biochemistry, Medical University, 30419 Hannover, Germany

(3) Institute of Anatomy and Cell Biology, University of Kiel, Olshausenstrasse 40, 24098 Kiel, Germany

(4) Institute of Neuropathology, University of Goettingen, Robert-Koch-Strasse 40, 37075 Goettingen, Germany

**Abstract**

The activation and function of c-Jun N-terminal kinases (JNKs) were investigated in primary microglia cultures from neonatal rat brain which express all three JNK isoforms. Lipopolysaccharide (LPS), tumor necrosis factor alpha (TNF $\alpha$ ) and thrombin preparations induced in the cytoplasm a rapid and lasting activation of JNKs, which were not activated in resting microglia. In the nucleus, however, the activation patterns were rather complex. In untreated microglia, the small pool of nuclear JNKs was strongly activated but without phosphorylation of the constitutively high-affinity substrate c-Jun. Stimulation with LPS increased the total amount of nuclear JNKs and the phosphorylation of c-Jun transcription factor. The pool of activated JNKs in the nucleus, however, rapidly decreased. Analysis of nuclear JNK isoforms revealed that the amount of JNK1 declined, while JNK2 increased, and the weakly expressed JNK3 did not vary. This observation suggests that JNK2 is mainly responsible for the activation of transcription factors. Upstream of JNKs, LPS induced a lasting activation of the constitutively present MKK4. The function of JNKs in LPS-triggered cellular reactions was investigated by the use of SP600125 (1-5  $\mu$ M), a direct inhibitor of JNKs. Inhibition of JNKs significantly attenuated the LPS-induced (i) cellular enlargement, (ii) metabolic activity, and (iii) expression of the AP-1 target genes *Cox-2*, *TNF $\alpha$* , *MCP-1* and *IL-6*. Summarizing, JNKs are essential mediators of relevant pro-inflammatory functions in microglia with different contribution of the JNK isoforms.



**Anxiety-like behaviour in the rat is related to levels of interleukin-2 mRNA in the brain**

Cornelius R. Pawlak\*, Artur Bauhofer<sup>#</sup>, Rainer K.W. Schwarting\*  
pawlak@staff.uni-marburg.de

\* Physiological Psychology, Philipps-University of Marburg, Germany

<sup>#</sup> Theoretical Surgery, Philipps-University of Marburg, Germany

There is evidence that interleukin (IL)-2 in the brain may be related to anxiety-like behaviour in the elevated plus-maze (EPM), and that IL-2 interacts with the striatal serotonergic system. Our previous experiments have shown that adult male Wistar rats can differ systematically in EPM behaviour, which was related to the neurotransmitter serotonin in the ventral striatum. Recently, we have also shown that rats with high anxiety-like behaviour in the EPM had higher striatal levels of IL-2 mRNA compared to those with low anxiety-like behaviour, but did not differ significantly in expression of other striatal cytokine mRNA (Pawlak et al. 2003, *Neurosci Lett*, 341, 205-208). Here, we investigated whether these expression effects are anatomically specific to the striatum. Therefore, we studied brain regions which play a role for anxiety, namely the amygdala, hippocampus, and prefrontal cortex. In this double-blind study we asked whether EPM behaviour may also be related to endogenous levels of cytokine mRNA in these tissues. As peripheral control tissues, adrenal glands and the spleen were also analysed. Based on open arm time in the EPM, male Wistar rats were divided into sub-groups with either low or high anxiety-like behaviour. Then, IL-1 $\beta$ , IL-2, IL-6, and tumor necrosis factor (TNF)- $\alpha$  cDNA levels were measured post mortem using semi-quantitative, competitive, reverse transcription polymerase chain reaction. Rats with low anxiety-like compared to high anxiety-like behaviour in the EPM showed higher IL-2 mRNA levels in the prefrontal cortex. There were no differences between the two sub-groups in IL-1 $\beta$ , IL-6, and TNF- $\alpha$  mRNA in any of the tissues analysed. Additional analyses in comparison with our recent data (Pawlak et al. 2003) revealed also a negative correlation between prefrontal cortex and striatum for IL-2 mRNA. These results provide new evidence indicating that specific cytokine mRNA patterns in the brain, particularly prefrontal cortex and striatum, are associated with anxiety-like behaviour in the EPM in rats.

Supported by grant Schw 559/4-3 from the Deutsche Forschungsgemeinschaft

## **Effects of glatiramer acetate on neuronal and axonal damage in a rat model of multiple sclerosis**

AV Kuhnert, N Taheri, MB Sättler, D Merkler, K Maier, C Stadelmann, M Bähr, R Diem

Multiple sclerosis (MS) is a chronic autoimmune disease of the central nervous system which induces persistent neurological deficits in young adults. Inflammatory infiltration, demyelination and axonal loss are its histopathological characteristics. The occurrence of acute axonal damage seems to be depending on ongoing inflammatory reactions and is the main reason for the progressive disability in this disease. Glatiramer acetate (GA), a copolymer of four different amino acids, is one of the standard therapies of MS. The immunomodulatory activity of this drug is mediated by immunological cross reactions between myelin proteins and GA.

In our present study, we investigated the effects of GA on axonal and neuronal damage in a rat model of MS. In myelin oligodendrocyte glycoprotein-induced experimental autoimmune encephalomyelitis, we observed an increased survival of retinal ganglion cells, the neurons that form the axons within the optic nerve (ON), if GA treatment was started at early stages during the disease course. Additionally, the numbers of APP-positive axons and CD45-positive inflammatory cells were decreased within the ONs. We conclude that, in parallel with reducing the autoimmune inflammation, GA can prevent ongoing axonal and neuronal damage.

## Clearance of apoptotic neurons without inflammation by microglial TREM2

Kazuya Takahashi, Christian DP Rochford and Harald Neumann

Neuroimmunology, European Neuroscience Institute Göttingen  
Waldweg 33, 37073, Göttingen

### Abstract

*Background.* Elimination of apoptotic neurons without inflammation is crucial for brain tissue homeostasis, but the molecular mechanism has not been firmly established. Triggering receptor expressed on myeloid cells-2 (TREM2) is a recently identified innate immune receptor. Mutations in TREM2 and DAP12 have been described in polycystic lipomembranous osteodysplasia with sclerosing leukoencephalopathy (PLOS)/ Nasu-Hakola disease patients. We now analyzed microglial function in response to TREM2 stimulation or after knock down of TREM2.

*Methods.* Cultured microglia were transduced with Flag-tagged TREM2, GFP, short hairpin TREM2 for RNA interference, short hairpin control, wild type TREM2 for over-expression, or its control GFP lentiviral vector. Function in response to TREM2 stimulation or after knock down of TREM2 was analyzed by flow cytometry, RT-PCR, and immunohistochemistry.

*Results.* TREM2 stimulation of microglia neither induced transcription of inflammatory mediators nor up-regulated immunoreceptors involved in antigen presentation. However, TREM2 stimulation increased phagocytic activity of microglia. Furthermore, TREM2 knock down microglia showed impaired clearance of apoptotic neurons and increased gene transcription of tumor necrosis factor- $\alpha$  (TNF $\alpha$ ), interleukin-1 $\beta$  (IL-1 $\beta$ ) and nitric oxide synthase-2 (NOS2). TREM2 over-expression resulted in increased phagocytosis of apoptotic neurons and decreased gene transcription of inflammatory cytokines.

*Conclusion.* TREM2 signaling participates in clearance of apoptotic neurons and down-regulation of inflammation to maintain the local immunosuppressive microenvironment in the CNS. Lack of TREM2 signaling in microglia results in impaired clearance of apoptotic neurons and inflammation.

## **Effect of inflammatory mediators on axonal transport of synaptic vesicle proteins and mitochondria.**

**Massimiliano Stagi, Nadjia Frank, Philippe Gorlovoi and Harald Neumann**

**Neuroimmunology Unit, European Neuroscience Institute Goettingen, Germany**

Axonal transport disturbance is an early sign of most inflammatory brain diseases, but the molecular mechanism of this dysfunction remains elusive. Activated microglial cells are found to be in close proximity to dystrophic neurites and release nitric oxide (NO) and inflammatory cytokines such as tumor necrosis factor-alpha (TNF- alpha).

Confocal microscopy of fluorescence recovery after photobleaching (FRAP) was performed to analyze the axonal transport of the synaptic vesicle precursor protein synaptophysin tagged with green fluorescent protein (synaptophysin-EGFP) in transfected cultured hippocampal neurons.

In addition, we used a specific marker for mitochondria (SP-YFP), with which we directly measured the velocity of axonal transport. This marker allowed us visualise transport in both anterograde and retrograde direction

Microglia, pre-stimulated by inflammatory cytokines to produce NO and TNF-alpha, focally suppressed the axonal motility of synaptophysin-EGFP at the contact point. Direct application of TNF- alpha or short-term NO donor to cultured hippocampal neurons inhibited axonal motility of synaptophysin-EGFP within 10 minutes. Inhibition of axonal transport by this inflammatory mediator significantly increased the immobile fraction of synaptophysin-EGFP and was dependent on phosphorylation of c-jun NH(2)-terminal kinase (JNK). In particular, TNF- alpha stimulated phosphorylation of JNK in axons. Reduced motility of synaptophysin-EGFP after TNF- alpha treatment was dependent on phosphorylation of JNK as determined by the JNK inhibitor SP600125.

Thus, overt production of TNF- alpha and reactive NO by activated microglial cells blocks the motility of synaptic vesicle precursor via phosphorylation of JNK and may cause axonal and synaptic dysfunction in inflammatory and degenerative brain diseases.

## **Experimental autoimmune encephalomyelitis (EAE) is ameliorated by superagonistic anti-CD28 treatment via the induction of protective CD4+CD25+ T cells**

Stefanie Gaupp<sup>1</sup>, Fred Lühder<sup>3\*</sup>, Niklas Beyersdorf<sup>2</sup>, Jens Schmidt<sup>1</sup>, Gabriele Köllner<sup>1</sup>, Thomas Kerkau<sup>2</sup>, Thomas Hünig<sup>2</sup> and Ralf Gold<sup>1,3</sup>

<sup>1</sup>Dep. of Neurology and <sup>2</sup>Virology and Immunobiology, University of Würzburg, Germany; <sup>3</sup>Institute for MS research, University of Göttingen, Germany

\* presenting author

CD28 is the critical costimulatory molecule for the activation of naïve CD4+ T cells, although normally a separated CD28 signal mediated by monoclonal antibodies (mAB) or the natural ligands is inert. Recently, superagonistic CD28 specific antibodies have been described which allow T cell activation and differentiation without any additional TCR signal. The epitope which is recognized by these antibodies has been mapped to the C''-D loop of the CD28 molecule. EAE as a widely accepted animal model for human MS can be actively induced in rodents by immunization with MBP or MOG (active EAE) or by adoptive i.v. transfer of MBP-specific T cells (AT-EAE). Here we focused on the therapeutic efficacy of the superagonistic CD28 specific mAB JJ316 on monophasic EAE in Lewis rats and relapsing EAE in DA rats.

In the monophasic EAE model in Lewis rats, JJ316 showed preventive (given at the induction of EAE) or therapeutical (given at the maximum of disease) effects. However, the modulatory capacity of JJ316 was most evident in Lewis or DA rats treated on at both time points (day 0 and 12). In these rats the disease was characterized by a delayed onset, milder disease course and lack of relapses. JJ316 was also effective in AT-EAE of Lewis rats. Immunohistochemical analysis revealed a significantly reduced number of T-cells ( $p<0.001$ ) and macrophages ( $p<0.01$ ) in lumbar spinal cord cross sections of treated as compared to control rats.

After JJ316 treatment the proportion of CD4+CD25+ lymph node cells increased by fivefold. By transferring CD4+CD25+ lymph node cells, but not CD4+CD25- lymph node cells from JJ316 treated rats into littermates both active and AT-EAE could be significantly ameliorated.

Our results show that the superagonistic CD28 antibody JJ316 has a preventive and therapeutic effect on monophasic and relapsing EAE. The mechanism seems to include the generation of CD4+CD25+ regulatory T cells (Treg) that protect against the immune attack and additionally are able to transfer protection in vivo.

**Poster Subject Area #PSA32:  
Neuroendocrinology**

- [#421A](#) E. Frank, T. Horn, R. Landgraf and A. Wigger, Munich and Magdeburg  
*Anxiety/depression-related behavior and social recognition: a key role of hypothalamic AVP*
- [#422A](#) MS. Keßler, J. Rafael and R. Landgraf, Munich  
*Mice bred for anxiety/depression: once again vasopressin*
- [#423A](#) M. Bunck, M. Schmidt, N. Singewald, R. Landgraf and A. Wigger, Munich and Innsbruck (A)  
*Neuropeptides and neuronal activity in the PVN of HAB and LAB mice*
- [#424A](#) L. Czibere, MS. Keßler, M. Panhuysen, B. Pütz and R. Landgraf, Munich  
*Behind behaviour: a comparison of gene expression between two mouse lines bred for either high or low anxiety-related behaviour*
- [#425A](#) E. van den Burg, J. Metz, M. Huising and G. Flik, Nijmegen (NL)  
*Neuroendocrine communication in vertebrates: CRH and CRH-BP in the teleostean hypothalamo-pituitary complex*
- [#420B](#) T. Rose and M. Rupnik, Göttingen  
*Ca<sup>2+</sup>-secretion coupling in beta-cells of healthy and diabetic rats in pancreatic tissue slices*
- [#421B](#) S. Speier and M. Rupnik, Göttingen  
*Gap junction coupling confines the electrical excitability of beta-cells*
- [#422B](#) K. Tessmar-Raible, J. Colombelli, S. Klaus, G. Balavoine, J. Wittbrodt, H. Stelzer, M. Hassel and D. Arendt, Heidelberg, Gif-Sur-Yvette (F) and Marburg  
*Ancestral cell types in modern brains*
- [#423B](#) H. Schäfer, Bauer, C. Hornstein, H. Sauer, Z. Herbert and GF. Jirikowski, Jena and Wiesloch  
*Altered Expression of oxytocin receptor and sex hormone binding globulin in the olfactory bulb of schizophrenics*
- [#424B](#) H. Dirksen, F. Elghazali, E. Kravitz and D. Soye, Stockholm (S), Boston, MA (USA) and Paris (F)  
*Crustacean hyperglycemic hormones (CHH)- and ion transport peptides (ITP) in central and peripheral neurones of arthropods*

## **Anxiety/depression-related behavior and social recognition: a key role of hypothalamic AVP**

Elisabeth Frank<sup>1</sup>, Thomas Horn<sup>2</sup>, Rainer Landgraf<sup>1</sup> and Alexandra Wigger<sup>1</sup>

<sup>1</sup> Behavioral Neuroendocrinology, Max Planck Institute of Psychiatry, Kraepelinstr. 2, 80804 Munich, Germany

<sup>2</sup> Institute of Medical Neurobiology, Otto-von-Guericke-University Magdeburg, Universitätsplatz 2, 39106 Magdeburg, Germany

The paraventricular nucleus (PVN) plays a major role in the anxiety/depression-related response to stressors as the lateral septum does, which additionally is involved in social recognition/memory processes. Both structures are richly provided with arginine vasopressin (AVP) neurons/projections. To assess the critical involvement of AVP in anxiety/depression-related behavior on the one hand and social recognition/memory on the other, we studied the effect of antisense oligodeoxynucleotides (AS) directed against AVP mRNA. AS was injected into the PVN or the bed nucleus of the stria terminalis (BNST), containing AVP neurons projecting to the lateral septum. Rats genetically predisposed to high (HAB) or low (LAB) anxiety-related behavior, with HABs over-expressing AVP in the PVN, were treated for 3 days with AS or with scrambled sequence oligodeoxynucleotides or vehicle as controls. As efficiency control, FITC-labeled AS were similarly injected into both the PVN and BNST, and diffusion distance as well as cellular uptake were illustrated via fluorescence microscopy. While AS given into the PVN decreased the hyper-anxiety and depression state of HABs in both the anxiety-related elevated plus-maze test (EPM) and the depression-indicating forced swim test, scrambled sequence and vehicle had no effect. Injected into the BNST, AS significantly decreased the ability of recognition/memorization in both HABs and LABs in a social discrimination task compared to controls. Further, the anxiety-related behavior on the EPM was slightly decreased in HAB but not LAB animals treated with AS compared to scrambled sequence and vehicle.

These findings confirm a key role of AVP in both anxiety/depression-related behavior as well as social memory/recognition mediated via the PVN and the BNST, respectively.

**Mice bred for anxiety/depression: once again vasopressin**

Melanie Sabine Keßler, Johannes Rafael, Rainer Landgraf

Behavioural Neuroendocrinology, Max Planck Institut of Psychiatry, Kreapelinstr. 2, 80804 Munich, Germany

To investigate neurobiological correlates of trait anxiety, two lines of mice, differing extremely in their anxiety-related behaviour, were bred from CD1 mice purchased from Charles River, named high anxiety-related behaviour mice (HAB-M) and low anxiety-related behaviour mice (LAB-M). Selection criterion was anxiety-related behaviour as assessed on the elevated plus-maze (EPM) at an age of 7 weeks. Most anxious HAB-M and least anxious LAB-M, respectively, were used for selective, bidirectional breeding.

At present, mice are in their 18<sup>th</sup> generation, and the two lines show distinct and robust differences in their behaviour, with time on open arms averaging 13.2% in HAB male mice and 11.3% in HAB female mice and 55.1% in LAB male and 54.5% in LAB female mice ( $p < 0.01$  vs. HAB-M each).

Additionally, we tested the mice in two depression paradigms, the forced swim test and the tail suspension test (TST), with HAB mice exhibiting a depression-like passive coping strategy and LAB mice behaving more active. Thus, though not being the primary selection criterion, depression-like indices are clearly associated with trait anxiety, suggesting comorbidity typical of psychiatric patients.

In situ hybridisation and immunohistochemistry for AVP mRNA and AVP, respectively, revealed higher levels in the PVN of HAB animals in comparison to LAB mice, correlating with their anxiety- and depression-related behaviour.

The releasable pool of AVP was studied via intra-PVN microdialysis under basal conditions and after hypertonic stimulation in freely moving mice. Under basal conditions, we detected no differences, whereas hypertonic stimulation led to a significant difference, with an increased release in HAB mice compared to LAB mice. Therefore, we tried to manipulate anxiety-related and depression-like behaviour in HAB mice by AVP antisense treatment and in LAB animals by AVP overexpression via an adeno-associated vector (AAV). For further investigation, we additionally blocked the  $V1_{a/b}$  receptors by an antagonist administered via icv injection in HABs, resulting in a reduced anxiety-like behaviour in the EPM and a significantly decreased depression-like behaviour in the TST.

The elevated expression and release of AVP within the PVN of HABs together with the behavioural effects of the  $V1_{a/b}$  receptors antagonist suggest a critical involvement of this neuropeptide in behavioural and neuroendocrine phenomena associated with trait anxiety and depression.



**Neuropeptides and neuronal activity in the PVN of HAB and LAB mice**

Mirjam Bunck<sup>1</sup>, Mathias Schmidt<sup>1</sup>, Nicolas Singewald<sup>2</sup>, Rainer Landgraf<sup>1</sup> and Alexandra Wigger<sup>1</sup>

<sup>1</sup>Behavioural Neuroendocrinology, Max Planck Institute of Psychiatry  
Kraepelinstr.2, 80804 Munich, Germany

<sup>2</sup>Department of Pharmacology and Toxicology, University of Innsbruck,  
Peter-Mayr-Str.1, Innsbruck, Austria

To get further insight into the pathology of anxiety/depression, CD1 mice were bred for either high (HAB) or low (LAB) anxiety-related behaviour as measured on the elevated plus-maze (EPM). The inbred behavioural extremes were confirmed by a variety of additional tests, including some reflecting depression-like behaviour. Interestingly, HAB and LAB mice also differ in their stress-coping strategies, with HAB animals being more passive and immobile indicating depression-like behaviour.

Here, we tested central mRNA expression of neuropeptides thought to be critically involved in the regulation of both anxiety-related behaviour and the hypothalamo-pituitary-adrenal (HPA) axis. Thus, arginine-8-vasopressin (AVP), oxytocin (OXT) and corticotropin-releasing hormone (CRH) mRNAs were studied under basal conditions by in-situ hybridisation in the paraventricular nucleus (PVN) of HAB, LAB and normal anxiety-related behaviour (NAB) mice as controls. Furthermore, we measured the basal AVP amount and Fos-positive cells after open arm exposure (OA) on the EPM as a marker for neuronal activity after a mild stressor in the PVN of HAB and LAB animals by immunohistochemistry.

Compared to LABs, the PVN of HAB mice contained more AVP mRNA, AVP and CRH mRNA. OXT mRNA which is highly homologous to AVP mRNA, did not exhibit any difference between the lines.

HAB animals showed an increased number and time of explorative head movements as well as a higher defaecation rate on the OA indicating their hyper-emotionality. Additionally, the number of Fos-positive neurons was significantly increased in the PVN of HAB animals, indicative of elevated neuronal activity.

Overall, the increased stress-induced neuronal activity, the elevated expression of AVP and CRH together with a larger releasable pool of AVP suggest a critical involvement of these neuropeptides in behavioural and neuroendocrine phenomena typical of high anxiety- and depression-related behaviour and psychopathology, including HPA axis hyperactivity.

**Behind behaviour: a comparison of gene expression between two mouse lines bred for either high or low anxiety-related behaviour**

Ludwig Czibere<sup>1</sup>, Melanie Sabine Keßler<sup>1</sup>, Markus Panhuysen<sup>2</sup>, Benno Pütz<sup>3</sup>, Rainer Landgraf<sup>1</sup>

<sup>1</sup>Behavioural Neuroendocrinology, <sup>2</sup>Molecular Neurogenetics, <sup>3</sup>Computational Genetics  
Max Planck Institute of Psychiatry, Kraepelinstr. 2, 80804 Munich, Germany

Two mouse lines, derived from normal CD1 mice, were bred to create an animal model of trait anxiety and depression. Selective breeding for high (HAB) and low (LAB) anxiety-related behaviour resulted in very robust phenotypic differences between these two lines, with the offsprings showing the respective behaviour in several anxiety and depression tests. This animal model gives the opportunity to study the basics of behavioural differences at the level of gene expression in distinct brain areas.

Arginine vasopressin (AVP) and corticotropin releasing hormone (CRH) are coexpressed in the hypothalamic paraventricular nucleus (PVN) and control the hypothalamo-pituitary-adrenal (HPA) axis. As shown in previous studies, the quantity of AVP mRNA in the PVN differs between HAB and LAB mice. Therefore, the hypothalamic area was chosen as a start point for a more comprehensive gene expression screening.

HAB and LAB animals were selected based on the breeding criteria, followed by a light/dark box test. To assure genetic consistency, the animals were genotyped for a single nucleotide polymorphism (SNP) in the signal peptide coding region of the vasopressin-neurophysin II-copeptin gene, that differs between these two lines. With total RNA extracted from the PVN, a microarray assay was put up with pooled samples from 6 animals of each line.

Using the MPI 24K Microarray, the expression of genes corresponding to about 14370 unique unigene clusters can be measured in a single experiment.

Evaluation of these expression profiles as well as further studies in additional brain regions on the candidate genes and proteins will contribute to understand how complex traits such as anxiety-related and depression-like behaviours are regulated at the molecular level, highlighting new targets for pharmacological treatment.

Neuroendocrine communication in vertebrates: CRH and CRH-BP in the teleostean hypothalamo-pituitary complex

Erwin van den Burg, Juriaan Metz, Mark Huising, Gert Flik

Department of Organismal Animal Physiology, Faculty of Science, Radboud University Nijmegen, Toernooiveld 1, 6525 ED Nijmegen, The Netherlands

The vertebrate brain integrates information and governs the body via neural and endocrine communication systems. Because these systems should not convey conflicting messages, they must communicate with each other. The pituitary gland holds a key position in this integration, as it converts neural and neuroendocrine signals from the brain into endocrine signals. In this way, it controls a multitude of physiological processes, in which the stress response is pivotal. Malfunctions in the stress response communication hierarchy are involved in several diseases. To understand neuroendocrine integration, it is necessary to identify signal origins and targets. At the level of the pituitary gland, such communication can conveniently be studied in fish, because, in contrast to mammals, the pituitary gland in fish is directly innervated by hypothalamic neurons. We have now set up a research project to map structural and functional relations between brain and pituitary cells in the stress response and to determine at what levels in the communication hierarchy signals are modulated to alter pituitary responses. The project combines neuroanatomical and electrophysiological studies in common carp. Currently, the input, internal organisation, and output of the hypothalamic nucleus preopticus (NPO) are under investigation, with emphasis on the stress hormone corticotropic-releasing hormone (CRH). Preliminary results reveal CRH-positive cells in both the magnocellular and parvocellular subdivision of the NPO, which project to the pituitary gland. CRH-binding protein (CRH-BP) does not colocalise with CRH, and its expression is limited to the periphery of the NPO. However, the mixed nerve fibres to the pituitary gland contain CRH as well as CRH-BP. We conclude that the release of pituitary stress hormones is under control of both CRH and CRH-BP. Other studies that are nearing completion include the distribution of CRH and other neuropeptides related to stress in the carp brain (AVT, ACTH), and glutamatergic and GABAergic innervation of the NPO.

## Ca<sup>2+</sup>-secretion coupling in $\beta$ -cells of healthy and diabetic rats in pancreatic tissue slices

Tobias Rose and Marjan Rupnik

European Neuroscience Institute Göttingen (ENI-G), Neuroendocrinology Group,  
Waldweg 33, 37085 Göttingen

**Background:** The Goto Kakizaki (GK) rat is a well established animal model for non-obese type 2 diabetes. The molecular mechanisms governing glucose-dependent insulin release from  $\beta$ -cells of GK rats are significantly impaired. Former studies failed to identify a defect in late steps of stimulus-secretion coupling in  $\beta$ -cells of this model, suggesting faulty glucose metabolism rather than impaired secretory machinery since non-nutrient secretagogues trigger release similar to that in wild type  $\beta$ -cells (1). Still, independent studies showed reduced expression of exocytotic proteins ( $\alpha$ -SNAP, SNAP-25, syntaxin-1, Munc13-1, Munc18-1, NSF and synaptotagmin III) in  $\beta$ -cells of GK rats, allowing for a lesion close to the release site (2, 3). The aim of this study was to use fresh tissue slices of rat pancreas (4) to elucidate the kinetics of stimulus-secretion coupling in healthy and diabetic rats.

**Methods:** We studied  $\beta$ -cells in pancreatic slices of adult male Wistar and GK rats. We recorded electrophysiological parameters like membrane potential, currents and cell capacitance ( $C_m$ ) by standard whole-cell patch-clamp technique. To monitor secretory activity changes in  $C_m$  in response to trains of depolarizing pulses were measured. We acquired data with a SWAM II lock-in amplifier (Celica, Slovenia; 1.6 kHz lock-in frequency) and WinWcp 3.4.9 software (John Dempster, University of Strathclyde, UK). We measured cytosolic Ca<sup>2+</sup>-concentration ([Ca<sup>2+</sup>]<sub>i</sub>) with ratiometric imaging of Fura-PE3 (50  $\mu$ M) excited at 340 and 380 nm and recorded the fluorescence signal at 50 Hz with a cooled electron multiplying CCD camera (Ixon887FI, Andor Technology, Japan). To elicit spatially uniform increases in [Ca<sup>2+</sup>]<sub>i</sub> we performed slow photolysis of the caged Ca<sup>2+</sup>-compound nitrophenyl-EGTA (NP-EGTA) by continuous UV illumination.

**Results:**  $\beta$ -cells of the stable hyperglycemic (14.5 $\pm$ 1.93 vs. 6.6 $\pm$ 0.22 mM plasma glucose) and hyperinsulinemic GK rats had a significantly bigger peak of HVA current compared to cells from Wistar rats (-221.9 $\pm$ 27.62 vs. -45.8 $\pm$ 7.94 pA). Considering the larger cell size of GK  $\beta$ -cells (11.7 $\pm$ 0.62 vs. 6.1 $\pm$ 0.23 pF), Ca<sup>2+</sup> current density was more than doubled as compared to control (16.2 $\pm$ 3.6 vs. 7.5 $\pm$ 1.33 pA/pF). Measurements of [Ca<sup>2+</sup>]<sub>i</sub> during a depolarization train also showed a roughly doubled Ca<sup>2+</sup> increase (507 $\pm$ 33 vs. 194 nM). The total cumulative change in  $C_m$  ( $\Delta C_m$ ) in response to a train of depolarizing pulses was slightly higher in GK  $\beta$ -cells than in control (277.8 $\pm$ 60.03 vs. 194.6 $\pm$ 34.74 fF) at respective current densities. However, when the charge entry in controls was augmented to similar levels as in GK rats (by elevation of [Ca<sup>2+</sup>]<sub>o</sub> from 2 to 7 mM), Wistar  $\beta$ -cells showed significantly larger secretory responses (579.9 $\pm$ 205.73 fF). Under this condition, the initial rate of release in GK rats was lower compared to control (454.5 $\pm$ 78.1 fF/s,  $\sim$ 150 vesicles/s vs. 1082.5 $\pm$ 305 fF/s,  $\sim$ 360 vesicles/s). Whereas the release rate in control stayed high during the first 1.5 s of stimulation, GK  $\beta$ -cells showed a rapid initial decline in secretion speed followed by a secondary acceleration peaking at 1.7 s with 287.6 $\pm$ 60.28 fF/s. The data thus suggests apparently lower Ca<sup>2+</sup> sensitivity of exocytosis and different pool depletion kinetics in  $\beta$ -cells of GK rats. In accordance to previous reports on wild type  $\beta$ -cells subsequent application of a depolarization train resulted in the reduction of secretory competence in controls by 47 % ( $\Delta C_m$ =103.9 $\pm$ 18.29 fF), suggesting depletion of release ready pools and limited priming. Contrarywise, the same stimulation in GK  $\beta$ -cells augmented the secretory competence by 32 % ( $\Delta C_m$ =367 $\pm$ 67.97 fF), suggesting an increased priming rate in the diabetic  $\beta$ -cells.

**Conclusion:** We conclude that Ca<sup>2+</sup>-secretion coupling in  $\beta$ -cells of GK rats is impaired in addition to ineffective glucose metabolism. A decreased Ca<sup>2+</sup> sensitivity of late exocytotic steps is paradoxically accompanied by enhanced granule mobilization. Further experiments allowing more precise control of [Ca<sup>2+</sup>]<sub>i</sub> are underway to pinpoint the exact lesion site.

### Literature:

1. Hughes, S. J., Faehling, M., Thorneley, C. W., Proks, P., Ashcroft, F. M. & Smith, P. A. (1998) *Diabetes* **47**, 73-81.
2. Zhang, W., Khan, A., Ostenson, C. G., Berggren, P. O., Efendic, S. & Meister, B. (2002) *Biochem Biophys Res Commun* **291**, 1038-44.
3. Sheu, L., Pasyk, E. A., Ji, J., Huang, X., Gao, X., Varoqueaux, F., Brose, N. & Gaisano, H. Y. (2003) *J Biol Chem* **278**, 27556-63.
4. Speier, S. & Rupnik, M. (2003) *Pflugers Arch* **446**, 553-8.

## Gap junction coupling confines the electrical excitability of $\beta$ -cells

Stephan Speier and Marjan Rupnik

Neuroendocrinology Group, European Neuroscience Institute Göttingen,  
Waldweg 33, 37073 Göttingen, Germany

### Background and Aims:

Electrical activity of  $\beta$ -cells is induced by metabolism-dependent  $K_{ATP}$  channel closure leading to an increased cytosolic  $Ca^{2+}$  concentration ( $[Ca^{2+}]_i$ ) and insulin release. In intact islets of Langerhans synchronous  $[Ca^{2+}]_i$  oscillations throughout  $\beta$ -cells of the whole islet were reported. The favored mechanism underlying this phenomenon is the coupling of  $\beta$ -cells via gap junctions. The aim of the present study was to reveal the influence of gap junctions on excitability of  $\beta$ -cells, using a transgenic animal model.

### Materials and Methods:

In this study  $\beta$ -cells in the pancreatic tissue slice preparation of mouse were investigated (Speier and Rupnik, 2003). To measure electrophysiological parameters of the  $\beta$ -cells we applied the standard whole-cell patch-clamp technique (EPC9, Heka, Germany). We recorded electrical activity in response to extracellular applied glucose or tolbutamide and different ATP concentrations in the pipette solution.  $K_{ATP}$  channel conductance was measured as a slope of the current response to a voltage-ramp protocol. Experiments were performed on transgenic connexin36 (Cx36) knock-out mice. Controls were heterozygous and homozygous littermates.

### Results:

The residual conductance measured after application of 100  $\mu$ M tolbutamide and 5 mM ATP in  $\beta$ -cells of Cx36 (+/+), (+/-) and (-/-), which is primarily due to gap junctions, was  $1.4 \pm 0.1$ ,  $1.3 \pm 0.1$  and  $0.2 \pm 0.07$  nS, respectively. In each of the three littermates dialysis of 5 mM ATP was able to lower conductance to a similar value indicating the closure of most  $K_{ATP}$  channels. However, in Cx36 (+/+) and (+/-) mice the electrical excitability depended on additional application of extracellular glucose or tolbutamide. The electrical activity was induced by current injections from coupled neighboring cells as shown by voltage-clamp recordings. In contrast, all tested  $\beta$ -cells in Cx36 (-/-) mice dialyzed with 5 mM ATP fired action potentials without interference from neighboring cells.

### Conclusion:

As a result of electrical coupling closure of  $K_{ATP}$  channels in a single  $\beta$ -cell is not enough to induce electrical activity as long as neighboring cells are hyperpolarized. By this mechanism heterogeneity in excitability of single  $\beta$ -cells is reduced. The physiological consequence is a synchronization of the secretion response and an increase in the threshold glucose concentration that induces insulin release.

Speier, S., and Rupnik, M. (2003). A novel approach to in situ characterization of pancreatic beta-cells. *Pflugers Arch* 446, 553-558.

## Ancestral cell types in modern brains

Kristin Tessmar-Raible (1), Julien Colombelli (1), Sebastian Klaus (1)\*, Guillaume Balavoine (2), Joachim Wittbrodt (1), Horst Stelzer (1), Monika Hassel (3) and Detlev Arendt (1)

(1) European Molecular Biology Laboratory, Meyerhofstr. 1, D-69117 Heidelberg, Germany

(2) CNRS-CGM, Avenue de la Terrasse - Bât. 26, 91198 Gif-Sur-Yvette Cedex, France

(3) Fachbereich Biologie, Philipps-Universität Marburg, Karl-von-Frisch-Straße 8, D-35032 Marburg, Germany

\*present address: University of Bayreuth, Faculty of Biology, D-95440 Bayreuth, Germany

The main neurosecretory structures in the forebrain of vertebrates are known as the preoptic area (POA) and the hypothalamus. The neurons located in these structures control major body functions, from weight regulation and metabolism to reproduction. Despite their importance, the majority of cell types contained in these structures have been assumed to be specific for the chordate/vertebrate lineage, because many of the relevant developmental control genes and functional molecules (e.g. receptors and neuropeptides) are absent from the "classical" invertebrate model organisms *Drosophila melanogaster* and *C.elegans*. However, recent molecular studies strongly indicate that the failure to detect cell type homologies between *Drosophila*/ *C.elegans* and vertebrates may reflect the strong molecular derivation of the current protostomian model organisms rather than being indicative of the absence of 'vertebrate-specific' cell types or structures from the common bilaterian ancestor (reviewed in 1, 2). Therefore, we chose to investigate the cell types of the brain of the protostomian polychaete annelid *Platynereis dumerili* and compare them to the cell types of the vertebrate brain.

In the *Platynereis* larval brain, ciliary photoreceptors (PRCs) and the cells of the apical organ (APO) are conspicuous structures with a distinct morphology. Furthermore, the APO is a highly conserved neurosecretory structure in primary ciliated larvae of bilateral symmetric animals (Bilateria) in both the protostome and deuterostome branch of the phylogenetic tree (3, 4). Our analysis revealed striking molecular parallels between the median brain region including the cells of the APO and cPRCs of the *Platynereis* larval brain and the vertebrate POA and hypothalamus. Cells of the APO in *Platynereis* contain the neuropeptide RFamide and serotonin, both co-expressed with the transcription factor *nk2.1*. In vertebrates, *nk2.1* is exclusively confined to – and in mouse essential for – the development of the median forebrain (hypothalamus and POA) (5) that also harbor serotonergic and RFamide containing central-spinal-fluid (CSF)-contacting neurons in lower vertebrates (6). Furthermore, the *Platynereis* APO and surrounding median cells express the transcription factor *vax* and the guidance molecule *netrin*, and are tightly associated with the developing median axon tracts around the APO in space and time. Notably, a *vax* expressing cell population that directs the growth of ventral axons via *netrin* expression is exclusively confined to the ventral forebrain of vertebrates, including the POA (7). Another highly restricted subpopulation of the *Platynereis* APO and median brain cells expresses the *orthopedia* gene. In the vertebrate brain, this gene is almost exclusively present in the hypothalamus and POA, regulating the development of specific neuropeptidergic cell types (8, 9). The neuropeptides present in the *Platynereis* otp-positive cells are under current investigation.

Morphologically, two photoreceptor cell (PRC) types have been described in Bilateria. The rhabdomeric type, storing the Opsin pigment in microvilli, is the PRC-type commonly used in the eyes of invertebrates. The ciliary type, storing the Opsin pigment in membrane extensions of cilia, is the PRC-type commonly used in the eyes and pineal of vertebrates (see e.g.(10)). In addition to the eye, ciliary PRCs closely related to the ciliary PRCs of the pineal organ and eye exist in the vertebrate hypothalamus (11). In *Platynereis*, the median brain ciliary photoreceptors (cPRCs) express an Opsin molecule closest related to the vertebrate Opsin found in the ciliary PRCs of the eye, pineal and hypothalamus, but distinct from the Opsin present in the rhabdomeric PRCs of the invertebrate eyes and the vertebrate retinal ganglion cells, further supporting the comparability of the ventral forebrain in vertebrates and the *Platynereis* median larval episphere.

Besides the striking resemblance of cell types in the *Platynereis* median larval brain and in the vertebrate POA and hypothalamus, it is highly remarkable that (where analyzed) these cell types exhibit a strikingly similar localisation in the primary ciliated larvae and early developmental stages in lower deuterostomes, and thus exhibit a remarkable conservation across Bilateria (12-14). Our comparative studies allow us to hypothesize that, in contrast to the common assumptions, Urbilateria (the last common ancestor of all bilateral symmetric animals) already possessed an elaborated set of neurosecretory and sensory cell types that probably were concentrated in a median area of the ancestral brain. During the evolution of chordates/vertebrates these cell types multiplied and diversified, giving rise to major cell types in the recent vertebrate hypothalamus and preoptic area. We also infer that some of the diversified cells started to migrate, and joined with other cell types to form new composite structures. An example for this likely occurred during the evolution of the vertebrate eye. In this case a subset of ciliary PRCs joined together with rhabdomeric PRCs.

Finally, we started to investigate how the development of the *Platynereis* median larval brain is influenced by the underlying tissue.

1. F. Raible, D. Arendt, *Curr Biol* **14**, R106 (Feb. 3, 2004).
2. K. Tessmar-Raible, D. Arendt, *Curr. Opin. Genet. Dev.* **13**, 331 (2003).
3. P. Ax, *Microfauna Marina*. W. a. H. Westheide, C.O., Ed. (Gustav Fischer Verlag, Mainz, 1988), pp.
4. C. Nielsen, *Animal Evolution: Interrelationships of the Living Phyla*. (Oxford University Press, Oxford, 1995), pp.
5. K. Nakamura *et al.*, *Brain Res Dev Brain Res* **130**, 159 (2001).
6. B. Vigh, I. Vigh-Teichmann, *Microsc Res Tech* **41**, 57 (1998).
7. S. Bertuzzi, R. Hindges, S. H. Mui, D. D. O'Leary, G. Lemke, *Genes & Development* **13**, 3092 (1999).
8. D. Acampora *et al.*, *Genes Dev* **13**, 2787 (1999).
9. W. Wang, T. Lufkin, *Dev Biol* **227**, 432 (2000).
10. D. Arendt, *Int. J. Dev. Biol.* **47**, 563 (2003).
11. B. Vigh *et al.*, *Histol Histopathol* **17**, 555 (2002).
12. C. M. Takacs, V. N. Moy, K. J. Peterson, *Evol Dev* **4**, 405 (2002).
13. C. J. Lowe *et al.*, *Cell* **113**, 853 (2003).
14. C. M. Takacs *et al.*, *Dev Biol* **269**, 152 (May 1, 2004).

**Altered Expression of oxytocin receptor and sex hormone binding globulin in the olfactory bulb of schizophrenics**

Schäfer H.<sup>1</sup>, Bauer<sup>3</sup>, Hornstein C.<sup>3</sup>, Sauer H.<sup>2</sup>, Herbert Z.<sup>1</sup>, Jirikowski G.F.<sup>1</sup>

1. Dept of Anatomy II FSU Jena,
2. Dept. of Psychiatry, FSU Jena,
3. Psychiatrisches Zentrum Nordbaden, Wiesloch.

Schizophrenia is linked to dysfunctions of olfactory perception and cognition. While schizophrenia is certainly a multifactorial ailment, degeneration of the olfactory bulbs and related limbic structures is thought to be part of the causes that trigger the onset of the psychosis. Altered levels of hypothalamic and CSF oxytocin (OT), paralleled by changing levels of gonadal steroids are known to occur in schizophrenics. In the present study we examined immunocytochemically and biochemically olfactory bulbs of diseased schizophrenic patients and of matched controls for oxytocin receptor (OTR) and sex hormone binding globulin (SHBG). OTR immunoreactivity was observed in a portion of the Mitral cells and in Tufted cells. OTR was much more abundant in schizophrenics than in controls. Most of the OTR positive neurons stained with the antibody to SHBG as visualized in consecutive semithin sections. With Western blots and SELDI TOF mass spectrometry, we confirmed the presence of both proteins in tissue homogenates of olfactory bulbs. The increased OTR expression may be a consequence of the reduced OT levels in schizophrenics. Our findings indicate that a portion of the neurons in the human olfactory bulb is capable of producing SHBG. Since synthesis and secretion of OT is modulated by estradiol, it is likely that an intrinsic expression of the binding globulin may enhance the bioavailability of the steroid in the brain. It has been shown that estradiol treatment improves symptoms in acute state of schizophrenia. Our findings may explain some of the underlying cellular mechanisms.

Crustacean hyperglycemic hormones (CHH)- and ion transport peptides (ITP) in central and peripheral neurones of arthropods.

Dircksen H., Elghazali F., Kravitz E.\*, Soyez D.\*\*

Dept. Zoology, Stockholm University, Sweden,

\*Dept. Neurobiology, Harvard Medical School, Boston, USA

\*\*UMR CNRS 7079, Universite P&M Curie, Paris, France

The distribution and structures of closely related peptides of the family of crustacean CHHs and insect ITPs have been studied in lobsters (*Homarus gammarus*, *H. americanus*), crayfish (*Orconectes limosus*), locusts (*Locusta migratoria*), and a fly (*Drosophila melanogaster*). Immunocytochemistry with cross-reacting antisera against crayfish CHH revealed in all crustaceans X-organ-sinus gland (XOSG) neurons in the eyestalk and bipolar to multipolar thoracic root neurons projecting to pericardial organs (POs). In locusts (L5, adults) and flies (L3, adults), ITP-like neurons project from frontal lateral neurosecretory cells to the corpora cardiaca and corpora allata (CC-CA), and occur as peripheral neurosecretory cells, associated with perisymphathetic organs in locusts and aorta in flies. These distribution patterns suggest homologous central and peripheral neurones containing similar neuropeptides. As shown previously in crabs (Dircksen et al., Biochem J 356:159, 2001), SGCHH and POCHH peptides (72-73aa long), are identical in the first 40aa but are different in the rest of the amino acid sequence. A similar situation is found in the lobsters and the insects. In *Drosophila*, there are three peptides which have been deduced from genome-based bioinformatics and molecular cloning. Peptide mass spectrometry (MALDI-TOF) revealed in lobsters and flies similar situations for neuropeptides identified as identical in the first 40aa. The peptides, however, differed in the last aa and were differentially located in central and peripheral neurons, which suggests similar cell type specific alternative splicing processes in crustaceans and insects.



**Poster Subject Area #PSA33:  
Neuropsychology and psychophysics**

- [#426A](#) P. Stenneken, L. van Eimeren, AM. Jacobs, I. Keller and G. Kerkhoff, Berlin, Bad Aibling and München  
*Visual Word Processing in Patients with Unilateral Spatial Neglect*
- [#427A](#) J. Rentzsch, A. Neuhaus, MC. Jockers-Scheruebl, M. Dettling and M. Bajbouj, Berlin  
*P50 sensory gating in schizophrenic patients and healthy controls at two different interpair intervalls*
- [#428A](#) W. Backhaus, Berlin  
*A Graphical Model of Neuronal Color Coding and Elementary Color Sensations in Man*
- [#429A](#) Z. Galoch and H-J. Bischof, Bielefeld  
*Communication Signals In Courtship Behaviour Of Birds – Can Zebra Finches Recognize Conspecifics On Video ?*
- [#430A](#) A. Horstmann and KP. Hoffmann, Bochum  
*Characteristics of Target Selection in Eye-Hand Coordination*
- [#431A](#) B. Affeldt, J. Weiler, J. Peters and K-P. Hoffmann, Bochum  
*Investigation of Corollary Discharge during Anti-Saccades in a Double-Step Paradigm*
- [#432A](#) M. Metzen, J. Bacelo, J. Engelmann, K. Grant and G. von der Ende, Bonn and Gif-sur-Yvette (F)  
*Receptive field organisation of electrosensory neurons in the ELL of the weakly electric fish, Gnathonemus petersii (Teleostei)*
- [#433A](#) DN. Markowski, FO. Galashan, D. Wegener and AK. Kreiter, Bremen  
*Effects of selective attention on the detection of changes in the velocity of moving objects by human observers*
- [#434A](#) S. Mandon, UA. Ernst, S. Neitzel, N. Schinkel, KR. Pawelzik and AK. Kreiter, Bremen  
*Neuronal Mechanisms of Contour Integration Investigated by Combining Psychophysical Experiments with Probabilistic Modelling*
- [#435A](#) P. Guardiera, O. Bock and H. Allmer, Cologne  
*Effects of psychomotor training on motor functions and cognition in the elderly*
- [#436A](#) I. Mutschler, A. Schulze-Bonhage, U. Halsband, S. Gräf, R. Martmüller, S. Rummeler and T. Ball, Freiburg  
*Listening to melodies related to newly learned piano movement sequences: changes in corticospinal excitability investigated using TMS*

- [#437A](#) R. Rygula, N. Abumaria, E. Ruether, G. Flügge and U. Havemann-Reinecke, Göttingen  
*Behavioural effects of chronic psychosocial stress in rats*
- [#438A](#) R. Niebergall, T. Womelsdorf, T. Tzvetanov and S. Treue, Goettingen  
*The spatial distribution of attentional facilitation/inhibition of contrast sensitivity depends on task context*
- [#439A](#) K. Jordan, T. Wüstenberg, J. Schadow, A. Fellbrich and N. von Steinbüchel, Göttingen and Magdeburg  
*Neuronal correlates of spatial cognition - cognitive and differential aspects*
- [#440A](#) A. Rokem and M. Ahissar, Jerusalem (IL)  
*Interactions Between Sensory and Cognitive Abilities in Early Blind Individuals*
- [#441A](#) MM. Shovman and M. Ahissar, Jerusalem (IL)  
*Isolating the Role of Visual Perception in Dyslexia*
- [#442A](#) M. Nahum, A. Rokem, I. Nelken and M. Ahissar, Jerusalem (IL)  
*Speech Intelligibility & Binaural Interactions: Effects of Stimulus Familiarity, Stimulus Similarity & Set Size*
- [#425B](#) M. Walter, YA. Dahlem and G. Northoff, Magdeburg  
*Sexual and emotional processing in the brain: an fMRI study*
- [#426B](#) LT. Boenke, FW. Ohl, AR. Nikolaev, T. Lachmann and C. van Leeuwen, Magdeburg, Wako-shi (J), Moscow (RUS), Leipzig and Sunderland (UK)  
*Interaction of features of visual stimuli within-trials (Stroop interference) and between-trials (Garner interference). A human reaction time and ERP study.*
- [#427B](#) A. Kaminiarz, M. Rohe and F. Bremmer, Marburg  
*Localization of visual targets during optokinetic eye movements*
- [#428B](#) S. Klingenhoefer and F. Bremmer, Marburg  
*Perisaccadic localization of auditory targets*
- [#429B](#) T. Wachtler and R. Hertel, Marburg and Freiburg  
*Color categories of dichromats*
- [#430B](#) S. Engmann, K. Tichacek, W. Einhäuser and P. König, Osnabrück and Zürich (CH)  
*Integration of luminance- and colour contrast of natural visual stimuli in overt attention*
- [#431B](#) N. Nortmann, W. Einhäuser and P. König, Osnabrück and Zürich (CH)  
*On the complexity of natural visual stimuli at trajectories of fixation points*

- [#432B](#) S. Schall, K. Tichacek, S. Engmann, S. Onat and P. König, Osnabrück  
*The Influence 2nd order and higher-order correlations in natural visual stimuli on human overt attention*
- [#433B](#) H-P. Frey, P. König and W. Einhäuser, Osnabrück and Zürich (CH)  
*Natural colour images and overt visual attention*
- [#434B](#) P. König, A. Acik, BC. Bernhardt, C. Carl, T. Dierkes, I. Dombrowe, S. Gelez, C. Honey, L. Jansen, C. Kabisch, T. Kringe, LM. Kurzen, C. Lörken, R. Maertin, SK. Nagel, KH. Park, H. Saal, M. Stefaner, C. Stöbel and V. Willenbockel, Osnabrück  
*feelSpace – report of a study group*
- [#435B](#) SP. Heinrich and K. Grill-Spector, Stanford, CA (USA)  
*The time course of item-specific and category-specific visual object processing*
- [#436B](#) AA. Karim, A. Schueler, E. Friedel, Y. Li Hegner and B. Godde, Tuebingen  
*Effects of Transcranial Magnetic Stimulation (TMS) on tactile perceptual learning*
- [#437B](#) M. Lotze, R. Veit and N. Birbaumer, Tübingen  
*Brain activity during social role reversal of offender and victim*
- [#438B](#) O. Tudusciuc and A. Nieder, Tübingen  
*Subliminal Priming in a Numerosity Judgment Task*
- [#439B](#) SW. Bock, PW. Dicke and P. Thier, Tübingen  
*How precise is gaze following in humans?*
- [#440B](#) K. Gust, U. Bitz, M. Kiefer, K. Hille and M. Spitzer, Ulm  
*Different mismatch negativity (MMN) in dyslexic children with phonological deficit compared to non-impaired-readers*
- [#441B](#) U. Bitz, K. Gust, M. Kiefer, K. Hille and M. Spitzer, Ulm  
*Phonological Deficit in 6 - 7 years Old Children: An EEG-Study*
- [#442B](#) W. Einhäuser, KAC. Martin and P. König, Zurich (CH) and Osnabrück  
*Are changes in the perception of the Necker cube related to eye-position?*

## Visual Word Processing in Patients with Unilateral Spatial Neglect

Stenneken, Prisca<sup>1</sup>, Van Eimeren, Lucia<sup>1</sup>, Jacobs, Arthur M.<sup>1</sup>, Keller, Ingo<sup>2</sup> & Kerkhoff, Georg<sup>3</sup>

<sup>1</sup> Allgemeine Psychologie, Freie Universität Berlin

<sup>2</sup> Abteilung für Neuropsychologie, Neurologische Klinik Bad Aibling

<sup>3</sup> Entwicklungsgruppe Klinische Neuropsychologie, Abteilung Neuropsychologie Städtisches Krankenhaus München Bogenhausen

### Corresponding Author

Dr. Prisca Stenneken, Freie Universität Berlin, [PStenn@zedat.fu-berlin.de](mailto:PStenn@zedat.fu-berlin.de)

### Abstract

Patients with unilateral spatial neglect fail to orient towards or to respond to stimuli in the contralesional side of the space (left visual field for patients with right hemisphere damage). Research has shown that hemi spatial neglect is a fragmentary syndrome that includes many complex symptoms, which often involve impaired reading performance (neglect dyslexia). The ability to process single words in neglect patients has been reported to be task-specific: Recent studies with Italian patients with left-sided neglect indicated that word naming tends to be relatively more impaired than lexical or semantic decision, i.e. indicating whether a displayed letter string is a real word or not or indicating the semantic category (e.g., Arduino, Burani & Vallar, 2003; Ladavas, Umiltà & Mapelli, 1997).

The present study compared a word naming task and a lexical decision task in a group of German-speaking neglect patients, using a computerized version of the two tasks with identical stimulus material and procedures. By manipulating the presentation duration of the stimuli, error rates were kept constant in all participants and both tasks.

The results confirm the previously reported task-specific performance in visual word processing. Dissociations between word naming and lexical decision are reflected by linguistic factors (i.e., word frequency, neighborhood size) as well as spatial factors (i.e., viewing position). Implications for current theories of neglect dyslexia and models of (unimpaired) visual word processing are discussed.

### Literature cited

Arduino, L.S., Burani, C. & Vallar, G. (2003). Reading aloud and lexical decision in neglect dyslexia patients: A dissociation. *Neuropsychologia*, 41, 877-885.

Ladavas, E., Umiltà, C., & Mapelli, D. (1997). Lexical and semantic processing in the absence of word reading: Evidence from neglect dyslexia. *Neuropsychologia*, 35(8), 1075-1085.

## **P50 sensory gating in schizophrenic patients and healthy controls at two different interpair intervalls**

**Johannes Rentzsch, Andres Neuhaus, Maria Jockers-Scheruebl, Michael Dettling,  
Malek Bajbouj**

Department of Psychiatry  
Charité – University Medicine Berlin  
Campus Benjamin Franklin  
Eschenallee 3  
14050 Berlin  
Germany

**INTRODUCTION:** Sensory gating deficits of auditory evoked P50 potential in schizophrenia are thought to be an endophenotypic marker of the illness. In common, it is measured in a paired stimuli paradigm with an interstimulus-intervall (ISI) of 500 ms and an interpair-intervall (IPI) of 8 s. The long IPI is thought to be necessary for a full recovery of the potential. It is not known whether shorter IPIs have an influence on these evoked potentials. To our knowledge, studies with IPIs shorter than 8 s have not been performed so far.

**METHODS:** To address this question, we examined 10 clinically stable schizophrenic patients on atypical medication and 10 healthy controls in a classical paired stimuli paradigm (100dB, ISI=500ms) with two different IPI (4 s and 8 s). A Wilcoxon-test was performed to analyse differences in latencies, amplitudes, gating-ratios and gating-differences for the two IPI, separately for the patient and control group. To clarify gating and latency deficits in schizophrenia compared to controls a Mann-Whitney-U test was performed.

**RESULTS:** The results show no differences in the control group for the P50 parameter at both IPI. However, in the patient group there was a significantly smaller P50 amplitude in the 8s-IPI-group as compared to the 4s-IPI-group. Compared to the control group, patients showed a lower P50 amplitude to the first stimuli and a smaller P50 gating-difference.

**CONCLUSION:** Our findings indicate that patients with schizophrenia have a lower sensory gating as compared to the healthy control group. However, there were no differences for the gating-ratio at both IPI levels which may be a consequence of the atypical antipsychotic medication. Further implications are discussed.

# A Graphical Model of Neuronal Color Coding and Elementary Color Sensations in Man

Werner Backhaus

Theoretical and Experimental Biology, Bioinformatics, Technical University and Freie University Berlin

The color vision system in man consists of an unconscious neuronal color coding part and conscious color sensations as the phenomenological part. Neuronal color coding is well described by the model of neuronal color coding (Backhaus, 2001, 2004), describing two types of color opponent coding (COC) neurons (**Red/Green**, **Blue/Yellow**), and a **Black/White** coding (BWC) neuron type. The physiological model explains and describes precisely the results of color discrimination and color similarity experiments (wavelength discrimination-, and  $V(\lambda)$ -functions). Color discrimination and color similarity judgments are exclusively related to the unconscious electrical excitations of the three types of color coding (CC) neurons. Thus, this type of judgment does not say anything about structural or qualitative properties of our conscious color sensations (colors) *per se*. Color content analytical judgments, on the other hand, actually allow determining the relative amounts of the six elementary color sensations which constitute our color sensations.

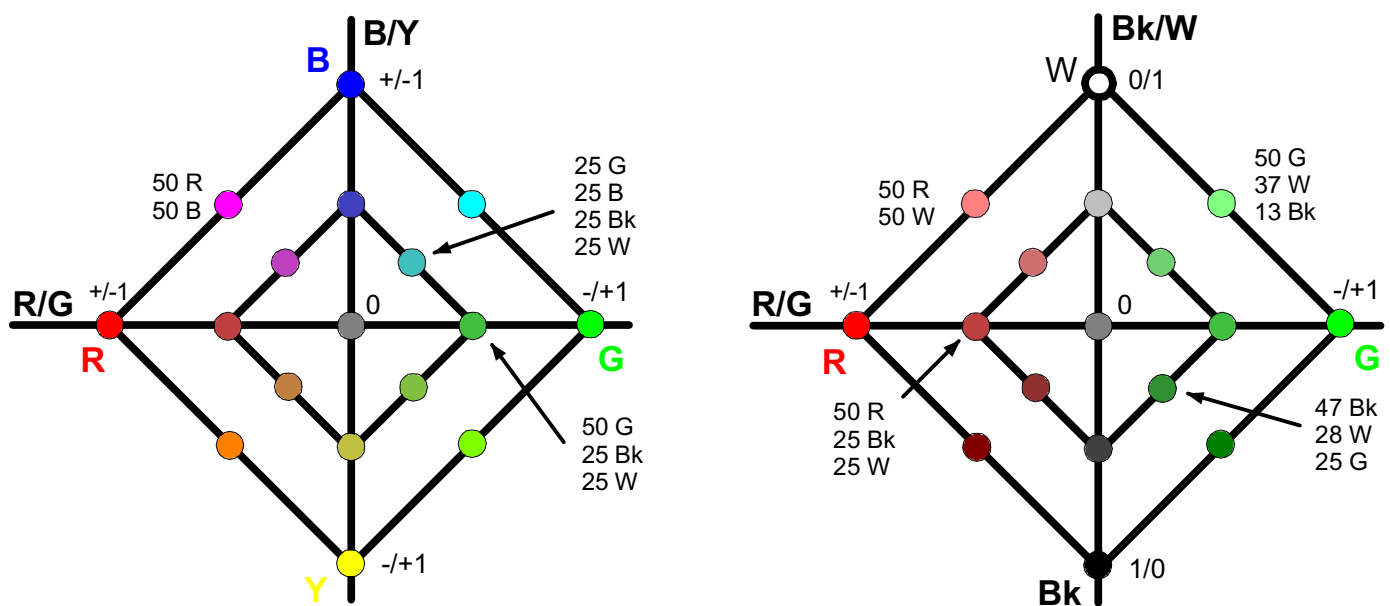


**Fig. 1** Graphical representation of the relationship between the electrical excitations of the three types of color coding (CC) neurons and the amounts of the six elementary colors. The model reasonably assumes piecemeal linear relations (Backhaus, 1998). **Left:** The axes give the normalized spike frequencies (lowest: +/-1, rest: 0, highest: -/+1) of the COC neuron types R/G and B/Y (accounting for "mirrored" subtypes) for the case that the third, BWC neuron type (perpendicular to the plane) has a constant medium excitation (center: medium grey). **Right:** The same R/G-axis is combined with the Bk/W-axis (lowest and highest spike frequencies normalized to 0/1 and 1/0, respectively) coding for Bk and W simultaneously (relative amounts Bk + W = const.). The combination of the excitations of the three CC neuron types determines the relative amounts of the elementary colors which constitute the color sensations (colors). The numbers denote the relative amounts of the elementary colors in %, adding up to 100%. Pure elementary colors (edges of the diagrams) have the maximum amount of 100%.

Now, the "Graphical Model of Neuronal Coding and Elementary Colors in Man" straightforward relates the phenomenology of elementary colors to the excitations of the three types of CC neurons (**Fig. 1**). The combination of both the models allows 1) the determination of the electrical excitations of the CC neurons from the spectral intensity distributions of the color stimuli and 2) the prediction of the relative amounts of the elementary colors of the respective color sensations. The predicted amounts can be directly compared to the amounts measured in color content analytical experiments. First results will be presented and discussed. The graphical model will be developed further to a psychophysiological model of color vision in man.

Backhaus, W., 1998. Physiological and psychophysical simulations of color vision in humans and animals. In: Color Vision – Perspectives from Different Disciplines, eds. W. Backhaus et al., pp. 45-77. De Gruyter, Berlin.

Backhaus, W., 2001. Measurement and simulation of color sensations. In: Neuronal Coding of Perceptual Systems, ed. W. Backhaus. World Scientific, London, pp. 445-474.

Backhaus, W., 2004. A physiological model of human color discrimination. In: Proceedings of the 4<sup>th</sup> Forum of European Neuroscience (FENS), July 10 – 14, 2004, Lisbon, Portugal, Abstracts, Vol. 2, A, p. 194.5. FENS, Lisbon.

**Communication Signals In Courtship Behaviour Of Birds –  
Can Zebra Finches Recognize Conspecifics On Video ?**

**Zdzislaw Galoch and Hans-Joachim Bischof**

Department for Behavioural Research  
University Bielefeld  
PO Box 100131  
33501 Bielefeld  
Germany

e-mail: [zdzislaw.galoch@uni-bielefeld.de](mailto:zdzislaw.galoch@uni-bielefeld.de)

Communication between animals is performed by sending and receiving signals, with a certain meaning for both, the sender and the receiver. The problem for a human observer of animal behaviour is the lack of knowledge about the code which is used: which signal elicits which response. Analysis of natural behaviour shows a big variation in the stimulus response relation. This may be due to intrinsic variation, but may be also based on the fact that each observed behavioural bout is unique and not directly comparable in the sequence of both, signals and reactions.

The development of video techniques provides new excellent tools for analysing stimulus-response relationships. It allows the standardisation of the stimuli used and could therefore help to analyze more exactly which stimulus elicits which behaviour. However, it is not entirely clear whether birds react to video screens. TV screens have low repetition rates and are not ideal for birds with flicker fusion frequencies above 100 Hz. We therefore used TFT screens and videos stored on a computer. To test whether zebra finch males react to videos and whether they can also extract contextual information from the videos, we prepared movies with a zebra finch female in three different situations. First, the female on video did not have any visual or acoustic contact to other birds. Second, the female (not the male observing the video) saw and heard a male in another cage. Third, it saw and heard a female in another cage. In addition, a video of an empty cage and one showing different birds from a bird park were presented. The behaviour of the observing male was recorded on video tape during presentation of the different videos and thereafter analysed from these videos. First results show that zebra finch males can recognize a sexual partner on videos. They show different behaviours like song or beak wiping if a zebra finch female is shown on the video, but not the empty cage and to the other birds. At present we cannot decide from our data whether contextual information is also perceived.

*Supported by DFG (Graduiertenkolleg Verhaltensstrategien & Verhaltensoptimierung Universität Bielefeld).*

## Characteristics of Target Selection in Eye-Hand Coordination

Annette Horstmann & Klaus-Peter Hoffmann

Dept. General Zoology & Neurobiology, Ruhr-University, D-44780 Bochum

*Contact: horstmann@neurobiologie.ruhr-uni-bochum.de*

During a goal-directed movement of the hand to a visual target the controlling nervous system depends on information provided by the visual system. This implies that a coupling between these two systems is necessary. We asked whether the manual system employs the visual system for coordinated movements of eyes and hand or vice versa.

Therefore we examined the preference of human subjects to select a leftward or rightward target depending on the performed action (eye, arm or combined movement) and the horizontal position of the target. Two targets were presented at the same distance to the left and right of a fixation point and the stimulus onset asynchrony (SOA) was adjusted until both targets were selected equally often. This balanced SOA is then a quantitative measure of selection preference. We compared these preferences at three horizontal positions for the different movement types (eye, arm, both).

At the peripheral positions the subjects showed a preference for the target that was more central with respect to the head, regardless of the movement type. At the central position they showed on average a bias to select the right target.

Comparing the preferences for the different movement types the data for the 'arm' and 'combined' movement types were correlated. The target preference of the arm movement seems to outweigh the preference for the saccadic system in the combined movement. These findings provide evidence that the control of gaze is in this case a means to an end, namely a tool to conduct the arm movement properly.



## **Investigation of Corollary Discharge during Anti-Saccades in a Double-Step Paradigm**

**B. Affeldt, J. Weiler, J. Peters, K.-P. Hoffmann**  
**General Zoology & Neurobiology, Ruhr-Universität Bochum**

For the investigation of corollary discharge information during anti-saccades in healthy human subjects we introduced anti-saccades into the classical double-step paradigm. Subjects had to make first a horizontal and second a vertical saccade. Anti-saccades could come first or second. Previous studies have shown that corollary discharge information about pro-saccades contributes to the correct execution of second saccades (Sommer & Wurtz, 2004). If corollary discharge information about the first saccade is not incorporated into the second saccade, the trajectory of the second saccade should be impaired. We investigated, if this is also the case for anti-saccades. Since we found no significant differences in direction deviation between experimental and control condition, we conclude that corollary discharge information of anti-saccades is included in the planning of second saccades in the double-step paradigm. Inaccuracies in amplitudes and directions in the pro-anti and anti-anti task could be explained by general precision deficits in anti-saccades. We found that second saccade amplitudes were reduced for anti-saccades, regardless of the type of the first saccade in the double-step paradigm but only with brief target presentations.

Furthermore, we confirmed longer latencies and decreased performance for anti-saccades compared to pro-saccades.

In our experiment, second saccades were all vertical, so we cannot say in which hemisphere they were programmed. Further experiments with a horizontal double-step paradigm, in which the location of saccadic programming is known, have to verify a possible lateralisation of corollary discharge.

## Receptive field organisation of electrosensory neurons in the ELL of the weakly electric fish, *Gnathonemus petersii* (Teleostei)

M. Metzen<sup>1</sup>, J. Bacelo<sup>2</sup>, J. Engelmann<sup>2</sup>, K. Grant<sup>2</sup> and G. von der Emde<sup>1</sup>

<sup>1</sup>Institut für Zoologie, Universität Bonn, Endenicher Allee 11-13, 53115 Bonn, Germany

<sup>2</sup>Unité de Neurosciences Intégratives et Computationnelles, C.N.R.S., 91190 Gif-sur-Yvette, France

Email: michael.metzen@uni-bonn.de

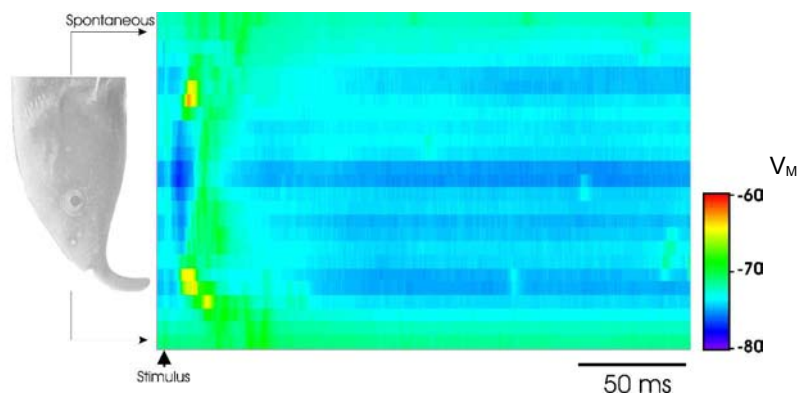
The weakly electric fish *Gnathonemus petersii* perceives its environment through its electrosensory system. An electric organ in the tail produces short electrical pulses which are perceived by epidermal electroreceptors distributed over much of the body. Objects are detected by their alteration of the electric field, sensed by mormyromast electroreceptors which project to the brainstem electrosensory lateral line lobe (ELL) to form several somatotopic maps.

Previous studies have shown that the responses of ELL neurons to sensory input can be used to distinguish two main categories: those which are excited (E-cells) and those which are inhibited (I-cells) by a threshold intensity stimulus at the centre of their receptive field. We have measured the spatial structure of the receptive fields (RF) of individual E- and I-cells in the medial zone of ELL, in fish in which the EOD was blocked by curare, using artificial local stimuli delivered at the time at which the EOD would normally occur.

RF measurements were performed by moving the artificial stimulus vertically and horizontally along the rostro-caudal axis of the fish, passing through the centre of the RF. In the excitatory centre of E-cells, we observed a local increase in discharge rate, decreasing when the stimulus was moved to either side. Determined in most cases from extracellular records, these RFs appeared asymmetrical, the horizontal axis being greater than the vertical axis. Intracellular recordings and extracellular spike data from Large Fusiform (LF) efferent neurons and some inhibitory interneurons (MG-cells) revealed an excitatory RF centre flanked by an inhibitory surround. An inhibitory surround was not found for the second most frequently encountered type of interneuron, the medium fusiform cells.

I-cells were most strongly inhibited in the centre of their receptive fields, with inhibition decreasing towards the field periphery. Most I-cells had a small excitatory area surrounding the inhibitory centre, again revealing a centre-surround organization. Intracellular recordings from a second subpopulation of MG inhibitory interneurons (see figure) and from Large Ganglionic layer (LG) efferent neurons, showed this type of inhibitory-centre/excitatory-surround structure.

For both I and E cells, first spike latencies were minimal at the centre of the receptive fields and increased towards the periphery; the latency of the first spike in the sensory response was correlated with the inter-spike interval. No differences were found in the sizes of the RFs of E- and I-cells, or between different cell types when RFs were measured at equal intensities relative to spiking threshold determined in the RF centre. However, RFs were smaller in skin regions with higher receptor densities, such as at the 'Schnauzenorgan' or in the 'nasal region' above the mouth.



Example of the subthreshold membrane potential ( $V_M$ ) changes over the RF of an MG-cell with an inhibitory RF centre (I-cell). Stimulus position (vertical axis) is indicated relative to the fish's head on the left: the stimulating electrode was moved in 2mm steps. 25 responses were averaged for each position.  $V_M$  (horizontal axis) is colour coded, showing a complex IPSP-EPSP-IPSP response at the centre of the receptive field. Note that the I-centre is flanked by a small E-surround.  $V_M$  in the absence of sensory stimulation is shown in the top and bottom rows of the plot.

## Effects of selective attention on the detection of changes in the velocity of moving objects by human observers

Dominique N. Markowski<sup>1</sup>, F. Orlando Galashan<sup>1</sup>, Detlef Wegener<sup>1,2</sup>, Andreas K. Kreiter<sup>1,2</sup>

<sup>1</sup>*Center for Cognitive and Emotional Sciences, Brain Research Institute;* <sup>2</sup>*Center for Advanced Imaging, University of Bremen, P.O. Box 33 04 40, D-28334 Bremen*

Recent neurophysiological evidence demonstrated that selective visual attention modulates direction selectivity of neurons in macaque area MT [Wegener et al., J Neurosci. 24: 6106-6114, 2004]. In these experiments, monkeys had to attend one of two moving bars and to indicate a small acceleration of a target bar, whereas velocity changes of the competing distracter bar had to be ignored. Analysis of neuronal responses prior to acceleration revealed a strong decrease of the direction selectivity of MT neurons in response to non-attended bars, especially for prolonged periods of attentional engagement.

Previously, neuronal signals in area MT have been directly linked to perceptual judgments of moving stimuli [Salzman et al., Nature 346: 174-177, 1990]. Therefore, the reduced ability of MT neurons to represent the direction of motion under non-attention conditions predicts deficits for the detection of changes in direction and velocity of moving objects presented outside the focus of attention on the perceptual level.

In order to test the relation between attentional effects on neuronal responses and perceptual accuracy we carried out a number of experiments that tested the benefits of attention on motion perception in human subjects.

Participants were asked to detect a change in the direction or velocity of one out of two, or more, simultaneously presented moving bars. The spatial position of the object which would undergo this change was cued prior to object presentation. In 75% of all cases the spatial cue indicated the correct position of the target, but in the remaining cases the cue misdirected attention. The preliminary analysis of the experimental results demonstrates a strong influence of attention on the ability of human observers to detect a change in motion direction or velocity. As expected by the degraded neuronal representation of non-attended motion, objects outside the focus of attention suffer from a reduced ability to be explicitly perceived.

*Supported by the DFG (SFB 517, Neurocognition)*

## Neuronal Mechanisms of Contour Integration Investigated by Combining Psychophysical Experiments with Probabilistic Modelling

Sunita Mandon<sup>1</sup>, Udo A. Ernst<sup>2</sup>, Simon Neitzel<sup>1</sup>, Nadja Schinkel<sup>2</sup>, Klaus R. Pawelzik<sup>2</sup>, and Andreas K. Kreiter<sup>1</sup>

<sup>1</sup> Institute for Brain Research, University of Bremen, D - 28334 Bremen, Germany

<sup>2</sup> Institute for Theoretical Physics, University of Bremen, D - 28334 Bremen, Germany

Contour integration is a dynamical process which links oriented, local elements into the percept of a coherent contour. Detailed psychophysical studies have described the basic properties of this process. In particular, studies on a contour-detection paradigm where subjects have to find a continuous path of Gabor elements embedded in a background of randomly orientated Gabor elements have demonstrated the impact of several stimulus parameters on contour integration. For example, element distance, alignment of the elements relative to the contour path, or curvature of the contour path itself influence the saliency of a contour [1].

While these geometrical factors of contour integration have been thoroughly investigated, their impact on processing time is still largely unknown. In addition, time constraints turn out to be even more interesting because a psychophysical study with monkeys has demonstrated that contour integration can be performed much faster than previously assumed [2], thus challenging standard neuronal models of contour integration.

Motivated by these observations, we investigate the following questions in a study combining human psychophysical and modeling studies: First, in which way do temporal constraints on the contour-integration process interact with geometrical parameters like the distance and number of edge elements in a contour, or the jitter on the contour path? Second, which neuronal mechanisms can explain the noise tolerance of human observers in our contour integration experiments? And third, how can suitable contour integration algorithms be implemented in a neurophysiologically plausible model, meeting both the temporal demands and being at the same time compatible with the anatomical substrate found in primary visual cortex?

Using a backward masking paradigm, we characterize the temporal constraints of contour integration while several parameters of the contour elements are varied. These experiments confirm the high speed of contour integration found in the monkey psychophysical study [2]. However, the time required for contour integration grows with distance between elements and with increasing deviation of alignment between contour elements and the contour's path. For investigating the neuronal mechanisms underlying contour integration we combined psychophysical experiments with probabilistic modeling [3]. The theoretical framework allows defining an ideal observer for a contour detection task. This ideal observer can be subjected to various neurophysiologically plausible boundary conditions, yielding the maximum performance achievable for a given contour ensemble under the given constraints. We show that the structure of horizontal projections in cortical area V1, connecting neurons of similar orientation preference, is not sufficient to explain the performance of human observers. The probabilistic framework provides also an approximation for an iterative contour detection algorithm. We are now investigating how this algorithm can be implemented in neuronal hardware with stochastically firing neurons. Preliminary results show that few spikes per input neuron are sufficient to achieve a detection performance which is comparable to the experimental results. Currently, we study whether nonlinearities like NMDA synapses are prerequisites for achieving high detection performance with a low number of spikes.

[1] Hess RF & Field DJ. (1999). Integration of contours: new insights. *TICS* 3, 480-486.

[2] Mandon S, Kreiter AK (2004). Rapid contour integration in macaque monkeys. *Vision Res.* in the press

[3] Williams LR, Thornber KK (2001). *Neur. Comp.* 13, 1683-1711.

*Supported by Volkswagen-Stiftung and SFB 517*

## Effects of psychomotor training on motor functions and cognition in the elderly

P. Guardiera<sup>1</sup>, O. Bock<sup>1</sup>, H. Allmer<sup>2</sup>

<sup>1</sup>Department of Physiology and Anatomy, <sup>2</sup>Department of Psychology, German Sport University

**Introduction:** Postural stability during standing and walking is often degraded in old age and might lead to severe accidents such as falls. According to recent literature, apart from cardiovascular, muscular and vestibular deficits also cognition seems to be a limiting factor to the control of body posture. In consequence of preceding experiments, which indicated increased dual-task costs in the elderly when performing complex tasks, we investigated the influence of regular physical activity involving cognitive processing on dual-task performance. In an **explorative** study (Exp. A) we first examined walking velocity and the cognitive demands of walking in young versus exercised and non-exercised elderly subjects using a dual-task design.

**Experiment A:** 12 young sports students, 17 non-exercised elderly and 12 exercised elderly, who had attended a psychomotor training in a neighbor town for about 4 years, participated in the experiment. Subjects had to walk a distance of 25 m and to simultaneously perform a motor task ((un-)button an experimental jacket with 9 buttons of different forms and shapes) or alternatively a cognitive task (memorize a sequence of ten geometric symbols).

**Results:** Non-exercised elderly walked significantly more slowly in single- and dual-task conditions than young and exercised elderly, there was no difference between the two latter groups. Buttoning performance was significantly lower in single- and dual-task in non-exercised elderly compared to young and exercised elderly. Again, there was no difference between the young and the exercised elderly. In the memory task non-exercised elderly did significantly worse in single- and dual-task than young subjects, exercised elderly performed on a mid-level. Although there were no differences in dual-task costs between groups, exercised elderly did not show any single task deficits as compared to their non-exercised counterparts.

**Experiment B:** In order to control the effects of a training program properly, in a following Experiment (Exp. B) we carried out our own psychomotor training. In a twelve weeks' intervention we investigated a group of non-exercised elderly in order to check, whether results found in Exp. A were due to an effect of regular exercise rather than subject-related preconditions.

13 elderly subjects attending a twelve weeks' psychomotor training and 10 elderly subjects attending a control group participated in Exp. B. Prior to and at the end of the training program walking velocity and the cognitive demands of walking in both experimental groups were examined using the dual-task design described in Exp. A. The training program took place for 60 min once a week, the control group only attended pre- and post-testing.

**Results:** Concerning walking velocity, the interaction showed a significant difference after the training when two motor tasks (walking + (un-)buttoning) had to be performed simultaneously. In the training group walking velocity had increased significantly after a training period of three months, whereas walking velocity in the control group showed exactly the opposite. There were no differences between groups in the walking + memorizing condition. Concerning additional tasks, the motor task did not show any single- or dual-task differences between groups, either. However, the analysis of the cognitive task yielded clear group differences in both single- and dual-task conditions: whereas the control group performed worse after a three months' period, memory performance in the training group had clearly increased. Dual-task costs slightly decreased in both dual-task conditions in the training group, whereas costs increased in the control group.

**Conclusion:** As indicated in Exp. A, regular exercise in Exp. B seems to ameliorate the performance of complex daily tasks in old age. According to Whipple and Wolfson (1989) individuals with a walking velocity less than 0.45 m/s might be classified as fallers, as their gait pattern often shows an increased step variability, hesitancy and lack of commitment in stepping and arm swing. In Exp. B the training group walked with about 0.9 m/s in the pre-test, but showed a significant improvement of about 6% already after a short intervention period. Therefore we suppose that regular exercise might help retain postural control also in old age and consequently reduce the risk of falling. We posit that besides motor functions also cognitive processing improved due to the psychomotor training, as memory performance improved as well. Subjects possibly needed to allocate fewer resources to motor functions than prior to the training and consequently might have performed more successfully in the dual task conditions, because a greater amount of cognitive resources could have been spent on the additional tasks.

The present study was supported by an internal grant of the German Sport University.

***Listening to melodies related to newly learned piano movement sequences: changes in corticospinal excitability investigated using TMS***

Isabella Mutschler<sup>1</sup>, Andreas Schulze-Bonhage<sup>2</sup>, Ulrike Halsband<sup>1</sup>, Susanne Gräf<sup>1</sup>,  
Ruth Martmüller<sup>1</sup>, Stephanie Rummeler<sup>1</sup>, Tonio Ball<sup>2</sup>

<sup>1</sup>*Department of Psychology, Neuropsychology, Albert-Ludwigs-University Freiburg, Germany*

<sup>2</sup>*Epilepsy Center, University Clinics, Albert-Ludwigs-University Freiburg, Germany*

Audiovisual mirror neurons are a class of neurons originally described in macaque premotor cortex that responds to the active performance of an action as well as to visually observing the action and to hearing the sound related to the action (Kohler et al., 2002). In humans, evidence for a similar auditory mirror (or “echo”) system (Rizzolatti & Craighero 2004) has recently been reported based on results from a transcranial magnetic stimulation (TMS) study: the mean amplitude of motor evoked potentials (MEPs) in hand muscles was found to be significantly larger when subjects listened to everyday manual action sounds as opposed to e. g. sounds related to leg movement (Aziz-Zadeh *et al.* 2004). However, it is unclear whether also sounds related to newly learned movements can modulate the excitability of the human cortical motor system. To investigate this question, eight non-musicians were instructed to learn simple melodies on a piano using their right hand. Single pulse induced MEPs obtained by stimulation above the left hemisphere were recorded from the first dorsal interosseus muscle of the right hand prior to this learning procedure and afterwards, and while subjects passively listened to the learned melodies, unknown melodies, and white noise, respectively. Motor corticospinal excitability was assessed by comparing the normalized relative MEP-amplitudes during these conditions.

We found a trend towards greater amplitudes of MEPs during the exposure to learned melodies than during exposure to novel melodies or noise. Thus, our results suggest that functions of the human auditory “echo” system may be modulated by learning on short time scales. Currently, we investigate the reproducibility of these findings in a larger group of subjects.

References:

Aziz-Zadeh *et al.*, (2004). *European Journal of Neuroscience* 19: 2609 - 2612

Kohler *et al.*, (2002). *Science* 297: 846 - 848

Rizzolatti & Craighero, (2004). *Annual Review Neuroscience* 27: 169 - 192

## Behavioural effects of chronic psychosocial stress in rats

R. Rygula<sup>1</sup>, N. Abumaria<sup>2</sup>, E. Ruether<sup>1</sup>, G. Flügge<sup>2</sup>, U. Havemann-Reinecke<sup>1</sup>

<sup>1</sup>Department of Psychiatry and Psychotherapy, University of Goettingen, 37075 Goettingen; Germany, <sup>2</sup>German Primate Centre, 37077 Goettingen, Germany

**Objectives:** Stress, especially encountered chronically, is one of the most important factors responsible for precipitation affective disorders in humans. Animal models commonly used for investigation of stress effects are basing mainly on strong physical stressors which in the most cases are irrelevant to situations of human beings and may be encountered in every-day life. In our study an animal model of chronic psychosocial stress was developed in rats applying a resident-intruder paradigm. This paradigm is considered as a model of loss of social status (social defeat) and subordination and therefore may mimic situations observed in humans. Rats were subjected to chronic psychosocial stress for period of 5 weeks and in parallel checked in battery of behavioural tests which should reveal changes evoked by social defeat.

**MATERIALS AND METHODS:** Social Defeat: The social defeat procedure (Koolhaas et al., 1990) consisted of daily resident intruder sessions lasting for 1 hour on 35 consecutive days. The experimental male *Wistar* rat was introduced to resident's cage (wild type rat). In less than one minute, the animal was attacked by the resident, after which it adopted the freezing response and submissive posture. Measuring of Motility and Exploratory Activity: Changes in locomotor activity as well as diminished exploratory activity are often associated with stress related psychomotor symptoms. Therefore motility measurements were performed by use of Opto-Varimex-3 activity monitor from Columbus Instruments, Columbus, Ohio, USA. Animals were tested at the beginning of each experiment (baseline), after one week of stress and after five weeks of stress. The recording periods lasted for 10 min each. During the recordings animals were observed and elements of exploratory activity scored. Sucrose Preference Test: Sucrose test is a widely known procedure for measuring changes in sensitivity to rewards in rodents. Since normal, healthy animals always prefer to drink sweet sucrose solution, decrease in this preference is considered as indication of decreased sensitivity to rewards (anhedonia). Rats were exposed for 24 hrs to 2 bottles, one containing water, second 0.8% sucrose solution. Tests were performed in one week intervals along the entire experiment. Intake of each fluid was measured by weighing the bottles before and after the test. Forced Swim Test: According to the method described by Porsolt et al. (1978) the animals were placed individually in transparent glass cylinders (40 cm height; 18 cm diameter) containing 18 cm of water at 23 °C, and 15 min later they were moved to a 30 °C drying environment for 30 min (pre-test). The animals were placed again in the cylinder 24 h later for 5 min (test) and were recorded by a video camera allowing to measure the immobility time as test parameter. Body Weight: Body weight was measured in one week intervals along the entire experiment. Organs: Up-regulation of HPA axis activity as well as changes in immune system are well known indication of chronic stress. Thus, weights of stress-related organs such as adrenal glands, testes, thymus and spleen were measured. At the end of the experiment animals were sacrificed, organs dissected, weighed and calculated as a percentage of body weight.

**RESULTS:** Chronically stressed rats showed a broad spectrum of behavioural changes including decreased motility and exploratory activity, decreased body weight gain, reduced preference to sweet sucrose solution and increased immobility time in Forced Swim Test. Locomotor Activity: Psychosocially stressed animals showed aslight decrease in horizontal locomotor activity after one week of stress and significant ( $P<0.05$ ) decrease after 5 weeks of stress. Exploratory Activity: One week of stress significantly decreased climbing ( $P<0.05$ ) and sniffing head-up ( $P<0.05$ ). Five weeks of stress evoked robust decrease in climbing ( $P<0.05$ ), rearing ( $P<0.05$ ), sniffing head-up ( $P<0.01$ ) and sniffing head down ( $P<0.05$ ). Sucrose Test: Psychosocial stress caused decrease in preference to sweet sucrose solution with significant ( $P<0.01$ ) change after 3 weeks. Reduced preference was observed till the end of the experiment. Forced Swim Test: Chronically stressed animals showed significant ( $P<0.001$ ) elongation of immobility time during five minutes test. Body Weight: Stressed animals have shown decreased body weight gain ( $P<0.01$ ) since week 2 of stress, along the entire following stress period. Organs: Weight of adrenal glands was significantly increased ( $P<0.05$ ) in stressed animals compared to controls. Surprisingly, also an increase ( $P<0.05$ ) in the weight of the testes was observed. Other stress-related organs (thymus, spleen) did not show any significant differences.

**CONCLUSION:** Diminished sucrose preference indicates desensitisation of brain reward systems (anhedonia). Increased immobility time in Forced Swim Test represents behavioural despair characteristic for depressive disorder. Since anhedonia is also one of the core symptoms of depression our findings may support the model presented as an animal model of depressive disorder.

*Funded by Deutsche Forschungsgemeinschaft through the DFG-Research Centre for Molecular Physiology of the Brain*

## **The spatial distribution of attentional facilitation/inhibition of contrast sensitivity depends on task context**

**Robert Niebergall, Thilo Womelsdorf, Tzvetomir Tzvetanov & Stefan Treue**  
Cognitive Neuroscience Laboratory, German Primate Center, Kellnerweg 4, Goettingen D 37077

Spatial attention enhances the efficiency of visual processing as is evident in higher accuracy, faster response time and enhanced contrast sensitivity. The distribution of these facilitatory effects is frequently reported to be spatially restricted and followed by a suppression of visual processing in the surround of the attentional focus, which either gradually rises or levels off at larger distances. In most previous studies attentional suppression was strongest for visual stimuli presented in the immediate neighborhood of an attended location specified by either an exogenous precue, or automatic and transient capture by abrupt-onset or feature-singletons. We therefore set up an experiment to test the extent and distribution of attentional facilitation and suppression in various task contexts involving endogenously, rather than exogenously, cued spatial attention.

We probed perception at 18 locations in a circular arrangement with four alternative forced choice luminance detection tasks, in the following three conditions:

Dual task condition: A valid endogenous cue was used to direct the subjects' attention to a particular location on the circle for a direction discrimination. At the same time they had to report at which of four possible locations a contrast target (stationary dot pattern) appeared. We systematically varied the distance between the direction target and the contrast target. Using the staircase method we measured contrast thresholds as a function of target distance.

Single task condition: The cue and the direction stimulus were presented but irrelevant. Subjects only had to localize the contrast target.

No cue condition: As the single task condition but without the cue presentation.

The results show distance dependent effects of attention. In the single task condition we find reduced contrast sensitivity near the direction stimulus location. In the dual task condition this reduction is less distinctive. For a spatially restricted area around the direction target, contrast thresholds were lower compared to those in the single task condition. In both conditions the effect of reduced sensitivity declines at farther distances. Indeed, contrast thresholds were lowest when presented diametrically opposite on the circle. In the no cue condition contrast sensitivity was dramatically reduced regardless of the distances between the two stimuli.

In agreement with other studies we conclude that attending to a particular location reduces sensitivity for stimuli near it. In addition, with spatial certainty about the location of the relevant or the irrelevant position, we observe two task dependent effects.

First, at irrelevantly cued positions in the single task condition we find a decrease in contrast sensitivity. This could be due to an attentional inhibition of this irrelevant location.

Secondly, we find enhanced contrast sensitivity within a region of about  $6^\circ$  around the direction stimulus in the dual task condition. Additionally, we observed a spatially unspecific lowering of contrast sensitivity in the no cue condition.

Together our results demonstrate a spatial distribution of attentional influences on the detection of low-contrast stimuli that is dependent on the exact task conditions.



# Neuronal correlates of spatial cognition - cognitive and differential aspects

Kirsten Jordan<sup>1</sup>, Torsten Wüstenberg<sup>1</sup>, Jeanette Schadow<sup>2</sup>, Anja Fellbrich<sup>2</sup>, Nicole von Steinbüchel<sup>1</sup>

<sup>1</sup>Department of Medical Psychology, Georg-August-University Göttingen,

<sup>2</sup>Department of Biological Psychology, Institute of Psychology, Otto-von-Guericke-University Magdeburg

## Introduction:

Contemporary research has demonstrated, that spatial ability is not a global skill, but should be divided into subfactors (McGee, 1979; Linn & Petersen, 1985; Quaiser-Pohl et al., 2004). Two of these subfactors are mental rotation and spatial orientation. Mental rotation has been defined as the ability to mentally rotate a two or three-dimensional figure rapidly and accurately. Spatial orientation has been defined as the ability to identify spatial configurations from a different perspective (Quaiser-Pohl et al. 2004). Along with one theoretical model mental rotation is considered as a small-scale spatial task where the observer can see the whole space of interest from its point of view, whereas spatial orientation is a large-scale spatial tasks where the observer is part of the environment and cannot see the whole space of interest at once (i.e. Quaiser-Pohl et al. 2004). Spatial abilities are one of the most prominent cognitive abilities which are known for large sex differences (Linn & Petersen, 1985; Voyer et al., 1995; Voyer & Saunders, 2004).

## Objective:

The core regions of mental rotation and spatial orientation and possible common ones were investigated in different fMRI-studies. Differential aspects were assessed like sex differences, experience and strategies.

## Methods and Results:

In the first study three different mental rotation stimuli were presented in a classical block-design (letters, abstract figures, three-dimensional figures). Nine healthy volunteers (students of psychology, one male, 21+/- 1.2 years) took part in this study. The results revealed bilateral core regions in the superior and inferior parietal cortex (centered on the intraparietal sulcus), which were similarly activated in all three mental rotation conditions. The mental rotation of three-dimensional figures evoked the strongest hemodynamic responses in these areas, likely corresponding to the poorest performance in this task (Jordan et al., 2001). During a second study twenty-four subjects (10 men, students of psychology) solved the same three mental rotation tasks as in the first study. Men and Women did not differ in the overall level of performance in the three tasks. Besides the common network in mental rotation (bilateral superior and inferior parietal lobule, premotor cortex) in both groups, women showed additional activation in the inferior temporal gyrus, likely corresponding to a different strategy in women than in men. According to known sex differences in mental rotation strategies we assumed a more analytic strategy in women than in men (Fig.1) (Jordan et al., 2002). After two weeks of training both groups (men and women) showed a decrease in cortical activation or no changes, whereas the control groups revealed stronger hemodynamic responses. In a third study 10 women and 10 men (students of computer-visualistics) solved a mental rotation and a spatial orientation task. The fMRI-results revealed a common network for mental rotation and spatial orientation comprising the bilateral superior and inferior parietal areas, premotor cortices and higher visual regions. For the orientation task a stronger activation of frontal areas in women than in men and stronger activation of visual areas in men than in women were observed. In the behavioural data no differences between men and women were seen. The analysis of individual strategies of subjects and hemodynamic responses revealed interesting positive correlations between the so-called survey-strategy (to see the maze from a birds-view) and activation of the precuneus only in men (Fig.2). Additionally a positive correlation was seen between the route-strategy (to count the left and right turns) and the activation of the cerebellum for the whole group.

## Conclusions:

Generally we suggest, that mental rotation and spatial orientation evoke similar cortical networks in men and in women. Furthermore according to the different nature of both spatial components also different regions were activated (for ex. in spatial orientation task the precuneus and frontal areas). Additionally we assume that factors like individual strategies, training and professional experience have a significant influence as well as on the behavioural performance and on cortical networks.

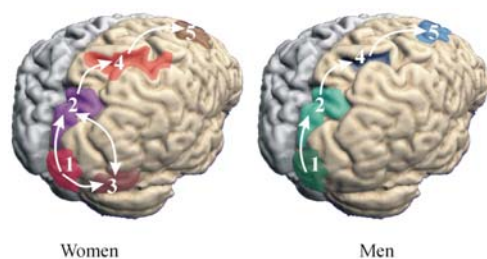


Fig.1: Hypothetical pathways for solving mental rotation tasks in women and men: (1) primary visual area, (2) extrastriate cortex, (3) inferior temporal/inferior occipital regions, (4) parietal regions (intraparietal sulcus), (5) premotor cortex.

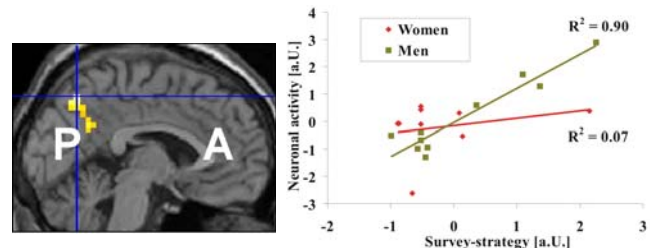


Fig. 2: Correlation of individual factor-values in the "survey-strategy" in the spatial orientation task and hemodynamic responses in the precuneus

## Reference List

- Jordan, K., Heinze, H. J., Lutz, K., Kanowski, M., & Jancke, L. (2001). Cortical activations during the mental rotation of different visual objects. *NeuroImage*, 13, 143-152.
- Jordan, K., Wüstenberg, T., Heinze, H. J., Peters, M., & Jancke, L. (2002). Women and men exhibit different cortical activation patterns during mental rotation tasks. *Neuropsychologia*, 40, 2397-2408.
- Linn, M. C. & Petersen, A. C. (1985). Emergence and characterization of sex differences in spatial ability: a meta-analysis. *Child Development*, 56, 1479-1498.
- McGee, M. G. (1979). Human spatial abilities: psychometric studies and environmental, genetic, hormonal, and neurological influences. *Psychological Bulletin*, 86, 889-918.
- Quaiser-Pohl, C., Lehmann, W., & Eid, M. (2004). The relationship between spatial abilities and representations of Large-Scale Space - A structural-equation-modelling analysis. *Personality and Individual Differences*, 36, 95-107.
- Voyer, D. & Saunders, K. A. (2004). Gender differences on the mental rotations test: a factor analysis. *Acta Psychologica (Amst)*, 117, 79-94.
- Voyer, D., Voyer, S., & Bryden, M. P. (1995). Magnitude of sex differences in spatial abilities: a meta-analysis and consideration of critical variables. *Psychological Bulletin*, 117, 250-270.

## **Interactions Between Sensory and Cognitive Abilities in Early Blind Individuals**

**Ariel Rokem & Merav Ahissar**

*The department of Psychology, the Hebrew University, Jerusalem*

*e-mail: arokem@pob.huji.ac.il*

Several studies reported superior auditory perception and superior memory in blind individuals. Yet findings are mixed, particularly regarding cognitive abilities. In this study, we show that the cognitive advantages may rely on the sensory advantage.

We examined the perceptual-cognitive profile of early blind individuals and compared their performance to that of sighted controls. We replicated findings that blind individuals show advantage in auditory tasks of frequency discrimination and in verbal short-term memory spans (e.g. their average span is 8 rather than 7 digits). However, when blind individuals were tested with working memory tasks requiring manipulation of input elements (e.g. repeating a series of digits backwards) they did not show an advantage over sighted individuals. This result suggests that when the bottleneck for performance is cognitive rather than sensory, blind individuals do no better than sighted individuals.

To assess whether their memory has a greater capacity in terms of element number, or their superior spans stem from superior perception, we tested their threshold intensity (80% correct repetition) for speech perception (pseudo-words) in quiet and in noise, and assessed their span under “perceptual clamp” conditions (speech intensity presented for each participant at his/her threshold level). Thresholds for perception measure 2 aspects of internal noise: general, additive (revealed in quiet), and selective, multiplicative (in noise).

Blind individuals had significantly lower threshold levels in quiet, but no difference was found under noisy conditions. This suggests that their general speech perception system is less noisy, but in a manner which does not stem from better tuned speech detectors.

Surprisingly, when memory spans are measured under “perceptual clamp” no significant advantage was found for blind individuals, indicating that they have no superior memory per se.

Taken together, these results suggest that blind individuals’ advantage in cognitive tasks stems from superior sensory abilities. These, in turn, stem from a quieter auditory system for speech perception, and not from finer tuned speech detectors.

### Isolating the Role of Visual Perception in Dyslexia

*Mark M. Shovman (1), Merav Ahissar (2, 3)*

*1: Department of Cognitive Sciences, Hebrew University, Jerusalem; 2: Department of Psychology, Hebrew University, Jerusalem; 3: Israeli Center for Neural Computation*

Despite the current prevalence of phonological theory of dyslexia, there are several theories (e.g. the magnocellular hypothesis) that attribute an important role to visual deficits as a basis for dyslexia. These theories stem from introspective reports of many dyslexics of visual discomfort while reading and are further supported by findings of various visual deficits in dyslexic subjects. However, these findings were argued against and largely explained as resulting from impaired perceptual memory rather than poor immediate perception.

To assess the role of (possibly impaired) visual perception in dyslexics' reading, we composed a task that was as similar as possible to normal reading in all its visual characteristics, but lacked all the other aspects of reading (phonological, morphological, semantic etc.), and compared performance of dyslexics and controls on it under several paradigms.

The task was to identify a letter of an alphabet unknown to subjects, but similar to Hebrew and English in all graphical details (11 most similar to each other Georgian letters). Eight different conditions were assessed, measuring threshold duration of presentation (SOA) and threshold contrast levels for identification of small and large letters, with and without flanker letters, with and without white noise.

Twenty adult native-Hebrew speaking dyslexics, mainly students, and 20 controls, matched for gender, age, and general cognitive abilities, participated in this study.

We found all the predicted effects in both groups. Namely, adding flankers and decreasing letter size increased threshold SOAs, and adding white noise increased contrast thresholds. However, there was no difference between the experiment group and the controls, neither in single-set comparison, nor in effect magnitude, nor in an all-inclusive analysis of variance (MANOVA  $d=0$ ;  $p>0.9$ ).

We conclude that the visual processing deficits found among dyslexic individuals by other researchers do not affect reading performance, and that therefore, the cause of their reading deficit resides elsewhere.

## **Speech Intelligibility & Binaural Interactions: Effects of Stimulus Familiarity, Stimulus Similarity & Set Size**

Mor Nahum<sup>1</sup>, Ariel Rokem<sup>2</sup>, Israel Nelken<sup>1,3</sup> & Merav Ahissar<sup>1,2</sup>

<sup>1</sup> *Interdisciplinary Center for Neural Computation, Hebrew University, Jerusalem 91904, Israel*

<sup>2</sup> *Department of Psychology, Hebrew University, Jerusalem 91905, Israel*

<sup>3</sup> *Department of Neurobiology, Hebrew University, Jerusalem 91904, Israel*

The magnitude of the contribution of binaural interactions to speech intelligibility, as measured by the Binaural Intelligibility Level Difference (BILD), is not well understood, and, in contrast to speech detection, has even been estimated as marginal (e.g. Yost, 1997). We reasoned that the magnitude of BILD may depend on stimulus characteristics and asked whether factors such as stimulus familiarity, inter-stimulus similarity and set size affect identification thresholds of speech in noise, under diotic vs. dichotic conditions.

We tested 25 subjects under 8 different identification conditions that manipulated familiarity of the stimulus set (digits versus pseudo-words), similarity (changes in a single phoneme or in all phonemes) and set size (2 or 10 words). We applied an adaptive procedure (manipulating stimulus intensity) to measure thresholds for 80% correct identification when noise was in-phase in the two ears, and stimulus was either in-phase (N0S0) or anti-phase (N0S $\pi$ ), in an interleaved manner. BILD is the difference between these thresholds.

In general, identification thresholds depended significantly on all tested factors. Thus, highest thresholds were found for largest set, minimal familiarity, and maximal similarity (10 pseudo-words). The dominant factor for lowering of the threshold was similarity, and set size (2 versus 10) was the weakest factor.

On the other hand, the magnitude of binaural configuration depended only on inter-set stimulus similarity, with no effect to set size (up to 10) or familiarity (using pseudo-words with feedback). Very small BILDs were found when stimuli were perceptually similar (~3dB), whereas up to 9dB were found when word pairs were very different (e.g. /dilen/ versus /talug/).

Taken together, our results show that all three factors examined are beneficial for absolute identification thresholds of speech in noise. On the other hand, the benefit of binaural cues may be rather small, as previously documented in the literature, depending on the structure of the stimulus set. Surprisingly, however, quite large binaural effects were found when stimulus set consisted of perceptually different words.

## **Sexual and emotional processing in the brain: an fMRI study**

Martin Walter, Yuliya A. Dahlem and Georg Northoff

Clinic for Psychiatry, Psychotherapy and Psychosomatic medicine,  
Otto-von-Guericke University Magdeburg

The study is focused on the neurobiological bases of sexual arousal in healthy subjects. Sexual arousal includes emotional, motivational, cognitive and autonomic components. Though distinct brain regions are supposed to be related to these components, their exact determination in sexual arousal remains to be established.

Our study was designed to reveal the emotional and cognitive component of sexual processing in the brain using fMRI. Ten healthy subjects (age range: 21-36, all male) with no history of neurological or psychiatric illness participated in the experiment. Standardized photographs taken from the International Affective Picture System were used to induce sexual and emotional arousal. Cognitive stimulation was achieved by a sexual or emotional expectancy period preceding sexual and emotional pictures respectively.

Preliminary results show that sexual arousal induced signal changes in a widespread limbic-cortical network. Emotional stimulation involved predominantly ventromedial cortex and anterior cingulate. Cognitive modulation leads to signal changes in lateral prefrontal and parietal cortex.

We conclude that anterior medial prefrontal regions seem to be involved in the emotional component of sexual arousal, whereas the cognitive component might rather be accounted for by neural activity in lateral prefrontal and posterior association cortex.

## Interaction of features of visual stimuli within-trials (Stroop interference) and between-trials (Garner interference). A human reaction time and ERP study.

Lars T. Boenke<sup>a, b</sup>, Frank W. Ohl<sup>a</sup>, Andrey R. Nikolaev<sup>b, c</sup>,  
Thomas Lachmann<sup>b, d</sup> & Cees van Leeuwen<sup>b, e</sup>

<sup>a</sup> *Leibniz Institut für Neurobiologie, Magdeburg, Germany*

<sup>b</sup> *Laboratory for Perceptual Dynamics, RIKEN BSI, Wako-shi, Japan*

<sup>c</sup> *Institute of Higher Nervous Activity, Moscow, Russia*

<sup>d</sup> *Universitaet Leipzig, Leipzig, Germany*

<sup>e</sup> *University of Sunderland, UK*

In visual perception, features interact to form an integral representation of an object. When one feature is the target of a classification task, and the other is irrelevant, the latter sometimes interferes with the former. This interference can be used as a measure of perceptual integration. We distinguish between within-trial and between-trial interference. Within-trial interference results from incongruence between the relevant and the irrelevant feature ("Stroop effect"). Between-trial interference results from variation of the irrelevant feature across trials as opposed to a condition with the irrelevant feature held constant across trials ("Garner effect"). Several studies have dissociated these effects; and it was proposed that within-trial interference occurs earlier in the perceptual process than between-trial interference (van Leeuwen & Bakker, 1995). This was assumed on the basis of the notion that dynamic self-organization of brain activity proceeds from narrow to broad context domains. To test this assumption we used an approach similar to the behavioral study by van Leeuwen and Bakker (1995), with a slightly modified design and a simplified set of stimuli, in combination with scalp EEG recording in 16 human participants. Four geometrical objects were successively presented on a screen consisting of an inner shape (the target feature) and an outer shape (the irrelevant feature), both of which could be either a triangle or a rectangle. Participants were asked to classify the target dimension as either rectangle or triangle in a speeded classification task. Within-trial interference was obtained by comparing trials invoking *congruent* (target and irrelevant feature belonging to the same class) and *incongruent* (target and irrelevant feature belonging to different classes) compound stimuli. Between-trial interference was obtained by comparing trials invoking compound stimuli with the irrelevant feature held constant (*baseline condition*) with those trials invoking stimuli in which the irrelevant feature was randomly varied (*filtering condition*).

Reaction time data showed strong effects of within-trial and between-trial interference. While within-trial interference occurred in all conditions, between-trial interference was obtained only with incongruent stimuli. Between-trial interference but not within-trial interference, moreover, declined over subsequent sessions. Both results support the view that within-trial interference and between-trial interference do not share the same neuronal origin. In our presentation we will report the data from our electrocortical observations which are currently being analyzed.

## Reference

van Leeuwen, C., & Bakker, L. (1995). Stroop can occur without Garner interference: Strategic and mandatory influences in multidimensional stimuli. *Perception & Psychophysics* **57**: 379-392.

## Localization of visual targets during optokinetic eye movements

Andre Kaminiarz, Marc Rohe & Frank Bremmer

Dept. Neurophysics, Philipps-University Marburg, Germany

When the eyes move, the image of a static object shifts across the retina, while, perceptually, the visual world remains stable. It has been suggested that the CNS achieves this stability by integrating the current direction of gaze with the object's retinal location (e.g. von Helmholtz. Treatise on physiological optics, Opt. Soc. America, 3, 1925). Such an integration would be based on a vector addition of the point at which the gaze is directed and the object's location on the retina. This process requires, however, that retinal signals be integrated with gaze signals relating to the same moment in time. Since retinal signals and oculomotor efferent signals have very different latencies, temporal matching of these signals creates a computational problem for the CNS. Any temporal mismatch between the signals would produce localization errors. Accordingly, as one would expect, vision during eye movements is not veridical: by presenting brief visual stimuli previous psychophysical studies have demonstrated a perceptual distortion of space during smooth pursuit and saccadic eye movements. Both types of eye movements have in common that they are voluntarily controlled. To our best knowledge, localization has yet not been tested for reflexive eye movements. In our present study we therefore asked how accurately human subjects can localize briefly presented visual targets during optokinetic eye movements, which can be considered an alternating pattern of smooth and fast, saccade-like resetting eye movements.

Four human subjects with normal or corrected to normal vision participated in the experiments, which were performed in a light tight chamber. The subjects' head was supported by a chin rest. Eye movements were sampled at 500 Hz with an EyeLink2 eye tracker (SR Research Inc.). Visual stimuli were presented at 100 Hz within a circular aperture of 25° diameter on a computer monitor placed 57 cm in front of the subjects' head. In blocks of trials subjects performed either control or eye movement tasks. In control trials subjects freely viewed a homogeneous gray monitor for 4000 ms. After 3500 ms a visual target (white circle, 0.35 degree in diameter) was flashed for 10 ms at one of five possible locations. In the eye movement condition a random dot pattern was moving horizontally for 6000 ms in pseudorandomized order either to the left or to the right eliciting reliably an optokinetic nystagmus (OKN) in all subjects. After 5500 ms the same visual target as in the control condition was presented with the same spatial and temporal properties. After the end of a trial (control or eye movement condition) subjects had to indicate the perceived horizontal location of the target with respect to a ruler.

Localization during free viewing (Base line condition) was not veridical but rather biased towards a location centered on the vertical meridian in head centered space. Localization during OKN, corrected for the bias obtained in the base line condition, was shifted into the direction of the slow eye movement. Our results therefore clearly indicate that localization of visual targets is influenced not only during voluntarily controlled but rather also during reflexive eye movements.

## Perisaccadic localization of auditory targets

Steffen Klingenhoefer & Frank Bremmer

Dept. Neurophysics  
Philipps-University Marburg  
35032 Marburg, Germany

[steffen.klingenhoefer@physik.uni-marburg.de](mailto:steffen.klingenhoefer@physik.uni-marburg.de), [frank.bremmer@physik.uni-marburg.de](mailto:frank.bremmer@physik.uni-marburg.de)

Recent psychophysical studies have demonstrated visual mislocalization effects at the time of saccades: In case spatial visual references are available immediately after the saccade, perceived target locations are shifted towards and compressed around the endpoint of the saccade. In total darkness targets appear to be shifted in the direction of an impending saccade. In both cases mislocalization starts about 100 ms before a saccade and reaches a peak at the time of saccade onset. The goal of our present study was to investigate whether also auditory spatial perception is influenced by saccadic eye movements and, if this was the case, whether it would show the same spatial and temporal properties as in the visual domain. In our experiments, we asked subjects to localize brief sound bursts that were presented at the time of saccades and compared the results to different auditory and visual control trials.

Human subjects were seated in a light tight and sound attenuated chamber performing blocks of either visual saccades or control tasks with steady fixation at either 7.5° left (F1) or 7.5° right (F2) from straight ahead. In half of the trials with fixation at F1 the second fixation point F2 was presented during the trial acting as a visual distractor. In all tasks target stimuli were presented at one of 4 possible positions symmetrically located around F2. Target stimuli in auditory localization tasks were bursts of white noise (duration: 5ms) presented via a moveable loudspeaker. In visual control trials bars (0.5 x 5 degree) were flashed for 10 ms. Saccades were directed from F1 to F2 with the target stimuli being presented within +/-200ms relative to saccade onset.

In visual control trials all perceived target positions were shifted perisaccadically in the direction of the saccade, i.e. due to missing visual references we did not observe a compression effect in the visual domain. In auditory localization tasks subjects reliably discriminated different speaker locations in all tasks, yet during fixation trials localization was strongly influenced by the current eye position. In saccade and distractor trials perceived locations were shifted (compressed) towards F2. In saccade trials this effect was significantly more pronounced (Wilcoxon Rank test,  $p < 0.05$ ). Perisaccadic mislocalization was stationary, i.e. it did not reveal the dynamics observed in the visual domain.

As these crossmodal results differ from the pure visual control data (dynamics; compression vs. shift) we conclude that the effect of perisaccadic mislocalization of auditory targets is an independent phenomenon. In other words: the spatial and temporal properties of perisaccadic localization of visual targets do not generalize across senses.



## Color categories of dichromats

Thomas Wachtler<sup>1</sup>, Rainer Hertel<sup>2</sup>

<sup>1</sup>Neurophysics Group, Department of Physics, Philipps University, 35032 Marburg, Germany

<sup>2</sup>Institut of Biology III, Albert-Ludwigs-University, 79104 Freiburg, Germany

thomas.wachtler@physik.uni-marburg.de, rainer.hertel@biologie.uni-freiburg.de

Protanopes and deuteranopes, despite lacking a chromatic dimension at the receptor level, use the color terms “red” and “green”, together with “blue” and “yellow”, to describe their color percepts elicited by monochromatic stimuli of different wavelengths [1,2]. A plausible multi-stage model of color processing could explain these findings [2].

To investigate color percepts of dichromats for more general stimuli, we performed hue scaling experiments with broadband spectra, generated on a CRT screen. Subjects were dichromats with only a single X-chromosomal opsin gene, as determined by molecular genetic analysis, and color-normal trichromats. Stimuli were 0.5 or 1 degree square patches with chromaticities regularly spaced along the azimuth of cone-opponent color space [3,4] and with elevations corresponding to between  $\pm 50\%$  luminance contrast with respect to the neutral background. In each trial, the stimulus was presented for 500 ms. After the presentation, the subject had to describe the perceived color by indicating the relative proportions of basic colors.

For stimuli brighter than the background, “blue” and “yellow” dominated the dichromats’ responses in different azimuth ranges, with only low percentages of “red” and “green”. However, at the transitions between the “blue” and “yellow” regions, “green” was reported with proportions up to 60%, consistent with the results obtained using monochromatic stimuli. Around isoluminance, the hue proportions reported showed an elevated trial-by-trial variability, and the color category regions were less distinct. For stimuli darker than the background, the category regions were different than for bright stimuli. In particular, regions dominated by “red”, with hue proportion up to 90%, were found. Additional experiments revealed evidence for a contribution of rods when larger stimuli were used. In contrast to the results of dichromats, the hue scaling results of color-normal trichromats showed only weak dependence on luminance.

We extended our earlier model to account for luminance increments as well as decrements by explicitly considering parallel On- and Off- pathways, originating from the two types of cones of dichromats. We assume multiple, neurophysiologically plausible stages, including antagonistic center-surround mechanisms and mutual inhibition between pathways. In addition, the model includes some rod input to parvocellular receptive fields. The model explains the color categories of dichromats as determined in our hue scaling experiments, including the dependence on luminance.

The results suggest that color categories may be traced back to low-level mechanisms of color processing. Even when one cone type is missing, as in dichromats, the visual system is able to map the signals from the reduced receptor color space onto color categories comparable to those in trichromats.

- [1] Boynton RM, Scheibner H (1967) On the perception of red by “red-blind” observers. *Acta Chromatica* 1:205–220
- [2] Wachtler T, Dohrmann U, Hertel R (2004) Modeling color percepts of dichromats. *Vision Research* 44:2843–2855
- [3] MacLeod DIA, Boynton RM (1979) Chromaticity diagram showing cone excitation by stimuli of equal luminance. *J. Opt. Soc. Am.* 69:1183–1186
- [4] Derrington AM, Krauskopf J, Lennie P (1984) Chromatic mechanisms in lateral geniculate nucleus of macaque. *J. Physiol.* 357:241–266

## Integration of luminance- and colour contrast of natural visual stimuli in overt attention

Sonja Engmann<sup>1</sup>, Klaus Tichacek<sup>1</sup>, Wolfgang Einhäuser<sup>2</sup>, Peter König<sup>1</sup>

<sup>1</sup>Institute of Cognitive Science, University of Osnabrück, 49069 Osnabrück

<sup>2</sup>Institute of Neuroinformatics, University of Zürich/ETH Zürich, CH-8057 Zürich



When viewing complex natural scenes humans select information for detailed processing by selection of fixation points. The control of this so-called “overt” attention is classically described by a saliency map (Koch & Ullman, 1985; Itti & Koch, 2000). It implements a bottom-up stimulus-driven guidance for selection of fixation points. It combines the contrast of different features, such as luminance, orientation, colour and texture contrast, in a single saliency map. Here we investigate the relative contribution of luminance and colour contrast on human fixation behaviour and their interaction in the absence of local changes of other features.

We use a high precision optical, head-mounted system (Eye-Link II) to measure eye-movements of human subjects while viewing natural images. Images are shown in pseudorandom sequence in their original form, and with colour- and/or luminance contrast decreasing horizontally or vertically down to zero contrast. Thus, we are working a range where luminance and colour contrast unquestionably have an

effect on fixation probability (Reinagel & Zador 1999, Parkhurst et al. 2002, Einhäuser & König 2003).

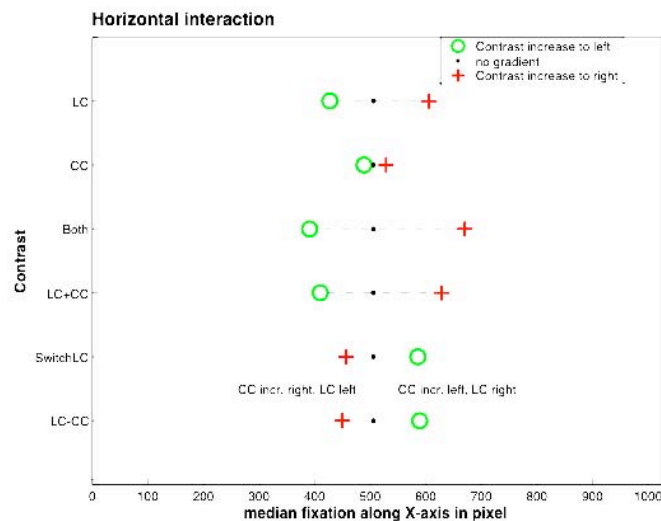


**Figure: Interaction of contrast gradients in the horizontal direction.** The median horizontal position of fixation points measured in pixel on the screen, is shown for different conditions: only luminance contrast gradient (LC), only colour contrast gradient (CC), both gradients parallel (Both), and gradients anti-parallel (SwitchLC). Gradients increase to the left (green circle), to the right (red plus), or no gradient (black dot). For comparison, the sum (LC+CC) and difference (LC-CC) of distance from the control in conditions LC and CC is shown. This simulates the prediction of additive interaction of contrast gradients in conditions Both and SwitchLC.

In summary, in this paradigm the combined effect of high luminance and colour contrasts is additive. The findings of this study are consistent with the classical saliency map model, which assumes independence and linear interaction of features.

We find that:

- (1) Both, strong luminance- and colour contrasts, show an effect on selection of fixation points. Fixation points are biased in the direction of high contrasts. Luminance contrast has a stronger influence on the selection of fixation points than colour contrast (Figure).
- (2) The qualitative effect of feature contrast is consistent across subjects, but its strength varies strongly among individuals.
- (3) When luminance and colour contrast both have parallel gradients the joint effect equals the sum of the effects of individual gradients.
- (4) When gradients are anti-parallel the joint effect equals the difference of the individual effects.
- (5) When both features vary in orthogonal directions the influence of each contrast gradient on subject's fixation patterns in one direction does not depend on the presence of the other contrast gradient.

## On the complexity of natural visual stimuli at trajectories of fixation points

Nora Nortmann<sup>1</sup>, Wolfgang Einhäuser<sup>2</sup>, Peter König<sup>1</sup>

<sup>1</sup>Institute of Cognitive Science, University of Osnabrück, 49069 Osnabrück

<sup>2</sup>Institute of Neuroinformatics, University of Zürich/ETH Zürich, CH-8057 Zürich



Analysing natural visual scenes humans direct their gaze in sequence to a number of fixation points. Recent studies revealed that contrast at fixation points is systematically increased (Reinagel and Zador 1999). However, little is known about the rules governing a sequence of fixation points. Here, we investigate image content at whole trajectories of fixation points with information theoretical measures.

Eye tracking data from greyscale images of natural scenes were used for analysis (Einhäuser & König 2003). The analysis is based on probability distributions of amplitudes of a wavelet decomposition. To measure the entropy, these amplitudes are mapped onto 100 evenly spaced bins. To measure mutual information (MI) the amplitudes are mapped onto 8 bins, which are adjusted such that all bins are chosen with equal probability. To measure complexity the amplitudes of fixation points of a trajectory are mapped onto 3 bins.

We find that at individual fixation points, compared to control locations, average entropy is higher. Similarly, the amplitudes of local coefficients at actual fixation locations tend to be higher as well. This result is in agreement with previous studies of bottom-up control of selective attention (Itti & Koch, 2002).

We measure the relation between successive fixation points by the means of mutual information. For horizontal orientation and at a spatial frequency of 1 cycle/degree visual angle the mutual information between two successive fixation points on the actual image (condition 1) is 0.063 bit. As a control, we compute the mutual information between succeeding fixation points applied to a different image (condition 2), which is not significantly different from condition 1 (0.071 bit,  $p=0.38$ , t-test). Furthermore, averaging over 7 spatial frequencies and 4 orientations, achieving a sensitivity of 0.003 bit, we do not find a significant difference between condition 1 and 2. In contrast, constructing pairs of randomly selected fixation points (condition 3), we obtain a mutual information of 0.047 bit. This is significantly lower than in condition 1 and 2 ( $p < 0.001$ ). Mutual information between image regions at fixation points on different stimuli is very low at 0.015 bit (condition 4). We interpret this as the noise due to the limited data points compared to the number of bins used by our procedure. Thus, the mutual information between successive fixation points is completely explained by the general spatial correlations within natural stimuli (condition 2 vs. condition 4) and the general statistical properties of trajectories (condition 2 vs. condition 3) and does not require a selection mechanism that is specific for the stimulus viewed (condition 1 vs. condition 2).

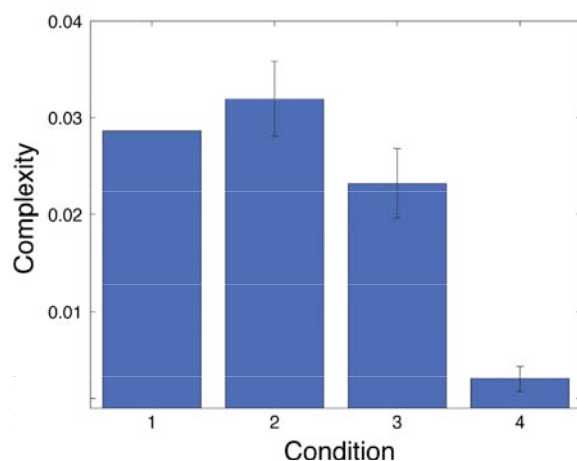


**Figure: Example of complexity of at trajectories of fixation points on natural visual stimuli.** Explanation of conditions see text.

Statistical dependencies of image content within trajectories were investigated using the measure of neuronal complexity (Tononi et al. 1994). This definition of complexity contrasts the mutual information in the complete set of fixation points and the mutual information between subsets. Consistent with the aforementioned results, we observe a high complexity in conditions 1 and 2, a reduced complexity condition 3, and the lowest complexity in condition 4 (Figure). These differences are largely explained by the mutual information within the complete trajectories.

In summary, we find at entropy at fixation points to be systematically increased, but find no indication of a maximization of mutual information at fixation points within a trajectory.

## The Influence 2<sup>nd</sup> order and higher-order correlations in natural visual stimuli on human overt attention

Sonja Schall, Klaus Tichacek, Sonja Engmann, Selim Onat, Peter König  
Institute of Cognitive Science, University of Osnabrück, 49069 Osnabrück



When viewing natural scenes selection of fixation points is influenced by various stimulus-driven factors. These include second order statistics as well as higher order structures. The former includes the precisely defined luminance contrast, the latter relate to the semantic content and are poorly understood. Moreover, feature contrast and higher order structure are correlated, making a dissection of their effects on overt attention difficult (Reinagel & Zador 1999, Parkhurst et al. 2002; Einhäuser & König 2003). Here we investigate the contribution of different features to human overt attention by disturbing the correlation between 2<sup>nd</sup> and higher order structures in natural visual stimuli.

Eye traces are recorded by a high precision optically based system (EyeLink II). Visual stimuli are pictures of natural scenes, and superimpositions of 2, 4, 8, or 16 of such images. The data analysis is based on a comparison of luminance contrast at fixation points of the actual stimuli and control fixations.

When viewing natural scenes we find in accordance with previous studies that at fixation points luminance contrast at medium spatial frequencies is systematically increased. In superimpositions of natural scenes, however, this effect is diminished (see Figure). In 2-superimposed images the effect is reduced by the factor of 0.57. The difference between actual and control fixations tends to decrease with the number of images used for the superimposition. At superimpositions of 8 and 16 natural stimuli contributing to the superimposition this difference is reduced to below 20% and not significantly different from 0 anymore.

These findings are compatible with the hypothesis that in natural visual stimuli luminance contrast is correlated with higher order structures, but does not by itself play a crucial role on selection of fixation points in natural scenes.

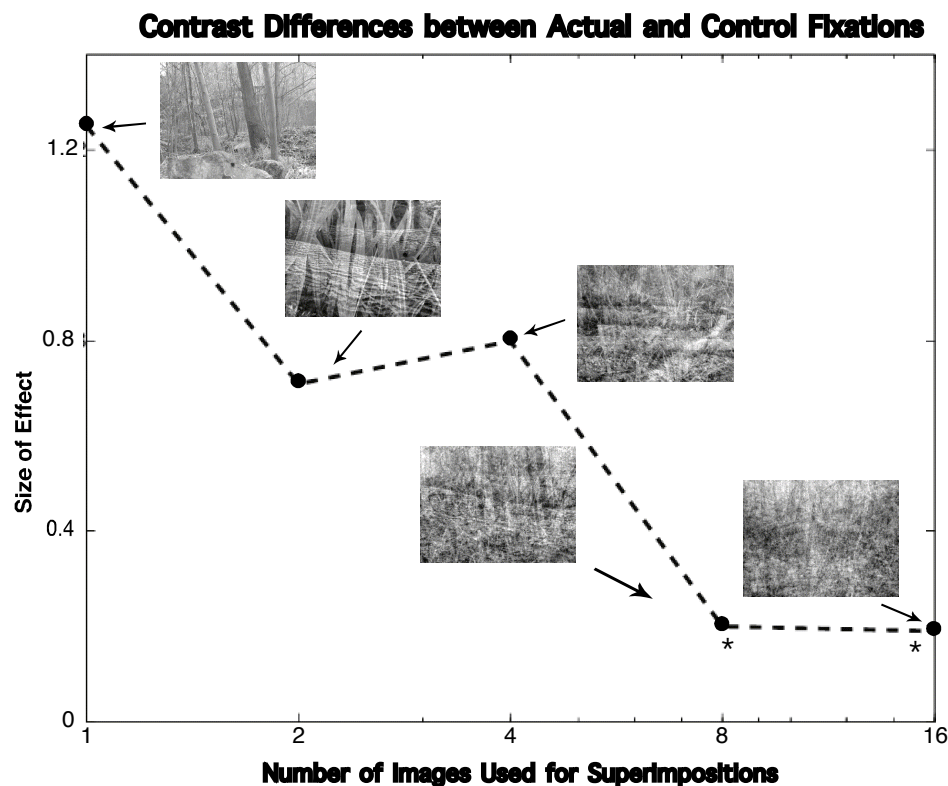


**Figure: Correlation of 2<sup>nd</sup> order statistics (luminance contrast) and fixation points.** Difference of mean contrast at fixation points and controls is plotted for different stimuli: unmodified images (1) and each category of superimposition (2, 4, 8, 16). A correlation between the size of effect and numbers of images contributing to the superimposition can be observed. The effect is not significant for 8- and 16- superimpositions.

## Natural colour images and overt visual attention

Hans-Peter Frey<sup>1,2\*</sup>, Peter König<sup>1</sup>, Wolfgang Einhäuser<sup>2</sup>

<sup>1</sup>Institute of Cognitive Science, Dept. Neurobiopsychology, University of Osnabrück

<sup>2</sup>Institute of Neuroinformatics, University of Zurich & Swiss Federal Institute of Technology (ETH) Zurich

\*Correspondence: [hans@ini.phys.ethz.ch](mailto:hans@ini.phys.ethz.ch)

When viewing natural scenes, humans direct their attention to a subset of the stimulus for further detailed processing. Shifts of gaze towards the attended locations form a measurable correlate of these shifts of attention. It is widely assumed that this so-called “overt” visual attention is influenced by higher cognitive mechanisms as well as by stimulus features. We investigate to what extent low level stimulus features influence overt visual attention in different types of visual stimuli.

We recorded eye-movements of human subjects while they were looking at photographs of natural scenes as well as modified versions thereof. These stimuli were presented in four different conditions (Figure 1):

- (i) as they were taken (“naturally coloured”),
- (ii) devoid of any colour-information, but with the same luminance content as in the “naturally coloured” condition (“greyscale”) and
- (iii) in two colour-modified conditions, in which luminance and saturation were as in the “naturally coloured” condition, but the hue (azimuth) of the colour was changed at each pixel according to rotations of  $\pm 90^\circ$  in Derrington-Krauskopf-Lennie (DKL) colour space (“clockwise” and “counter-clockwise” condition).

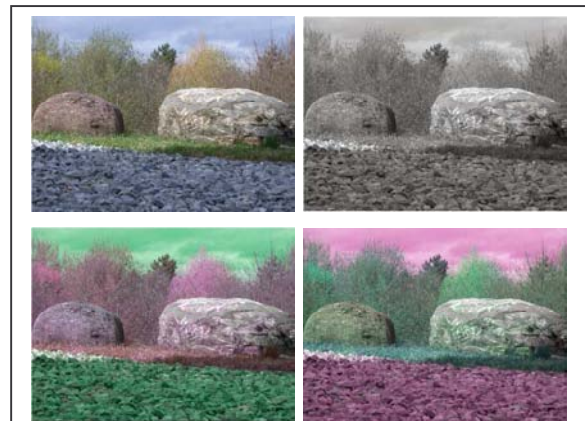


**Figure 1** Four stimulus conditions of one natural stimulus. Top left: “naturally coloured” top right: “greyscale”, bottom left: “colour-rotated  $90^\circ$  counter-clockwise”, bottom right: “colour-rotated  $90^\circ$  clockwise”.

In each condition we compare the occurrence of certain stimulus features, such as luminance, saturation and hue at fixation locations to randomly chosen locations. A feature attracts attention, i.e. is salient, if increased likelihood to fixate correlates to increased values of these features. In addition we directly compare the occurrence of these features at fixation locations across conditions.

First we investigate the effect of luminance contrast. In accordance with previous results (Reinagel & Zador, 1999) it is significantly higher at fixation locations compared to control locations in greyscale images. Surprisingly, at fixation locations in natural colour images luminance contrast is significantly smaller than in greyscale images and even smaller than at control locations. In colour rotated images luminance contrast at fixation locations is not significantly different from luminance contrast at control locations. Hence luminance contrast is not a salient feature in naturally coloured images.

The feature of colour is characterized by colour contrast and by saturation (variance along cardinal axes and mean amplitude in the DKL space respectively). Viewing naturally coloured images, saturation and colour contrast are not different at fixation points as compared to control locations. The same holds for viewing greyscale images and analysing the colour distribution in the respective originals. Only in colour rotated images we do observe a systematic influence of colour contrast on the selection of fixation points. Thus, in the naturally looking stimuli (naturally coloured or greyscale) saturation and colour contrast are not salient.

Our results imply, that low-level features like saturation, luminance- and colour contrast are most relevant in images devoid or with manipulated colour content. Their relevance for natural visual stimuli is strictly limited.

*Supported by Swiss National Science Foundation (PK, grant no. 31-61415.01), Honda RI Europe (WE) and the EU-AMOUSE project (WE).*



## feelSpace – report of a study group

Peter König, Alper Acik, Boris C. Bernhardt, Christine Carl, Torsten Dierkes, Isabel Dombrowe, Susan Gelez, Christian Honey, Lina Jansen, Christiane Kabisch, Tobias Kringe, Lena M. Kurzen, Christopher Lörken, Robert Maertin, Saskia K. Nagel, Kyoung Ho Park, Hannes Saal, Moritz Stefaner, Christian Stöbel, Verena Willenbockel  
Institute of Cognitive Science, University of Osnabrück, 49069 Osnabrück

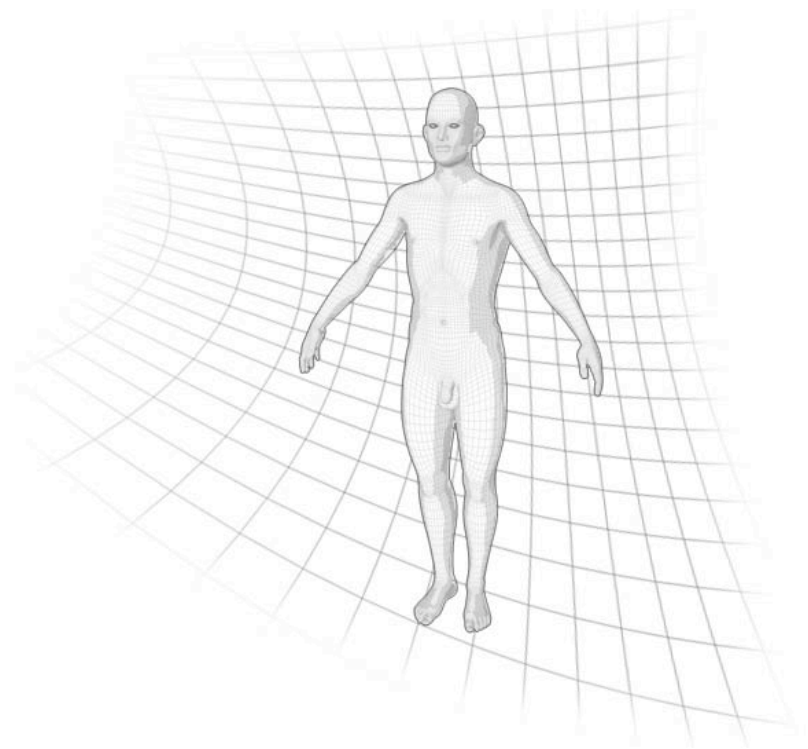


Humans enjoy a unified perception of their environment. In view of different sensory modalities contributing to the global percept, the process of binding different pieces of information has received considerable attention in philosophical, psychological and, in more recent times, physiological research. Notwithstanding such a concentrated effort, proposed solutions range from localized convergence zones in cortex, neural correlates of conscious perception in specific cortical lamina, binding distributed representation by synchronization of neuronal activity to claims that it is a non-problem. Here we follow an experimental approach and concentrate on the perception of space.

We combine psychological questionnaires, psychophysical measures of performance, specific and unspecific stimulation with physiological recordings. Information about space is given by visual, auditory and tactile stimulation. The experiments are conducted partly in a natural environment, partly under controlled laboratory conditions.

- In a standardized questionnaire we evaluate the quality of perception of space of 4 experimental subjects over a time span of several weeks. Its dependence on the experience, the immediate history and actions of the subject are documented.
- The subjects perform several different navigation tasks of increasing complexity. We compare performance w/out visual, auditory and tactile information available. Furthermore, we supply misleading cues in one modality and, thus, investigate the interaction between different modalities.
- Performance in navigation tasks is related to the active behaviour of subjects. In controlled laboratory settings we record eye movements during performance of equivalent tasks in a virtual environment. Finally we conduct physiological recordings of EEG in different phases of a navigation task. In particular we compare coupling of distant cortical areas when information from different sensory modalities is available.

In this approach we address the quality of perception using the example of perception of space. We can demonstrate that information from different sensory modalities is combined and that the perception of space is a plastic process.



## The time course of item-specific and category-specific visual object processing

*Sven P. Heinrich & Kalanit Grill-Spector*

Dept. of Psychology, Stanford University, Stanford, CA 94305, USA

sven.heinrich@stanford.edu

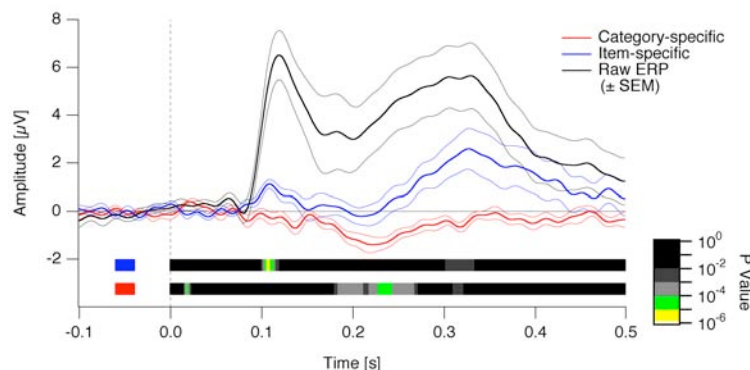
Objects can be recognized by the visual system both as a specific item and as representing a certain category. In the present study we assess the timing of these two processes using repetition effects in event-related potentials (ERPs).

Eleven subjects participated in high-density ERP experiments in which we recorded data from 61 electrodes. Subjects viewed pictures of animals (cats or dogs) or scrambled animals, which were presented in alternating blocks. Each stimulus block contained 15 images of one category, and 1–3 images from the other category. In 36 of the 72 blocks with non-scrambled images, all 15 stimuli of the majority category were identical (“repeated”). In the other 36 blocks, all images were different (“non-repeated”). Each image was displayed for 1 s, followed by a blank period of 400 ms. Subjects were asked to categorize images to “cat” or dog while fixating. Trials were averaged according to condition (repeated/non-repeated) and whether they had occurred in the first (early) or second part of the block (late). We computed category effects as “early non-repeated” minus “late non-repeated” and item-specific effects as “late non-repeated” minus “late repeated”.

Item-specific repetition revealed a reduction in the amplitude of the P1 peak around 100 ms in occipital and occipito-temporal electrodes. Starting around 250 ms, a second item-specific effect was evident as a reduced signal, mainly at occipito-temporal and frontal electrodes. A category repetition effect (a smaller negativity for late vs. early non-repeated items from the same category) occurred occipito-temporally around 200 ms.

Item-specific and category-specific repetition effects have different time courses. The amplitude reduction around 100 ms for item repetition might be attributed to low-level adaptation processes. This should hardly affect higher processing stages, though, such as those giving rise to the effect around 250 ms. The category effect cannot be explained by low-level effects since non-repeating stimuli were used. The results therefore suggest distinct item-specific and category-specific neural mechanisms acting at different stages of stimulus processing.

Supported by DFG (HE 3504/2-1) and NSF (345920).



Difference traces showing category-specific (red) and item-specific (blue) effects as recorded at the occipital pole. For reference, one of the original ERP curves (early non-repeated) is also shown. The bars underneath the curves represent color-coded time-resolved  $P$  values.

## Effects of Transcranial Magnetic Stimulation (TMS) on tactile perceptual learning

Ahmed A. Karim<sup>1,2</sup>, Anne Schueler<sup>1</sup>, Eva Friedel<sup>1</sup>, Yiwen Li Hegner<sup>1</sup>, Ben Godde<sup>1</sup>,

<sup>1</sup> Institute of Medical Psychology and Behavioral Neurobiology, University of Tuebingen, Gartenstrasse 29,  
D-72072 Tuebingen, Germany

<sup>2</sup> International Max Planck Research School of Neural & Behavioral Sciences, Tuebingen, Germany

Repetitive transcranial magnetic stimulation (rTMS) is a tool to modify cortical processes non-invasively and almost pain free (Hallett, 2000). Depending on the applied frequency, rTMS results in either cortical facilitation or inhibition leading to changes in sensory or motor thresholds and even to modulation of higher cognitive functions (Karim et al., 2003; Walsh & Cowey, 2000). To test the hypothesis that TMS is also able to facilitate perceptual learning processes we combined a tactile discrimination training procedure with a protocol of high-frequency rTMS.

16 subjects were actively trained under auditory feedback in a spatial and a temporal tactile discrimination task with their left ring finger. During training 15 Hz rTMS was applied over the contralateral primary somatosensory cortex. Discrimination thresholds during training were compared to performance in pre and post training sessions without TMS and feedback.

As compared to control subjects receiving sham rTMS (as placebo control) and the same tactile training, the combination of training and rTMS led to stronger training effects in the spatial discrimination task. Significant improved performance was found in the post training session only for the test but not for the control group. Therefore, for the first time we are able to show that high-frequency rTMS is able to facilitate active perceptual learning.

On the other hand, no differences between the experimental groups were seen for the frequency discrimination task. Both groups improved during training and in the post session, therefore we argue that other cortical areas are predominantly involved in tactile frequency than spatial discrimination.

Therapeutic potentials of the application of rTMS in the neuropsychological rehabilitation of functional deficits after lesions of the somatosensory cortex are discussed.

*Supported by the Volkswagenstiftung*

### References:

Hallett (2000). Transcranial magnetic stimulation and the human brain. **Nature**, 406: 147-50.

Karim et al. (2003). Effects of repetitive transcranial magnetic stimulation (rTMS) on slow cortical potentials (SCP). **Clin. Neurophysiology**, 56:331-37

Walsh, V. & Cowey, A. (2000). Transcranial magnetic stimulation and cognitive neuroscience. **Nature Review Neuroscience**, 1:73-9.



**Brain activity during social role reversal of offender and victim****M. Lotze<sup>1</sup>, R. Veit<sup>1</sup>, N. Birbaumer<sup>1</sup>***<sup>1</sup>Institute of Medical Psychology and Behavioral Neurobiology, University of Tübingen, Germany*

Imaging studies of the cerebral areas active during social interaction related to aggressive behavior are absent. In a competitive reaction time task subjects can easily be provoked to react aggressive if repetitively painfully punished. With this task an investigation of the victim and the offender role within the same subject is possible also during functional imaging. Here we demonstrate that human brain activation assessed with fMRI during the victim role is characterized by activation of fear and pain related areas. In contrast the offenders role results in an increase of anterior medial prefrontal cortex (aPFC) activation during adjustment of an increasing amount of punishment. An increase of aPFC-activity during punishment was significantly larger in those subjects who showed lower psychopathy scores and no decrease of empathy for their opponent during the experiment. The aPFC might therefore play an important role in empathy and compassion towards the opponent.

Imaging studies of the cerebral areas active during social interaction related to aggressive behavior are absent. In a competitive reaction time task subjects can easily be provoked to react aggressive if repetitively painfully punished. With this task an investigation of the victim and the offender role within the same subject is possible also during functional imaging. Here we demonstrate that human brain activation assessed with fMRI during the victim role is characterized by activation of fear and pain related areas. In contrast the offenders role results in an increase of anterior medial prefrontal cortex (aPFC) activation during adjustment of an increasing amount of punishment. An increase of aPFC-activity during punishment was significantly larger in those subjects who showed lower psychopathy scores and no decrease of empathy for their opponent during the experiment. The aPFC might therefore play an important role in empathy and compassion towards the opponent.

## Subliminal Priming in a Numerosity Judgment Task

Oana Tudusciuc and Andreas Nieder

*Primate NeuroCognition Laboratory, Dept. of Cognitive Neurology, Hertie-Institute for Clinical Brain Research, University of Tübingen, Otfried-Müller-Strasse 27, 72076 Tübingen, Germany*

Numerous studies have shown that stimuli that are too brief to be consciously detected or recognized may nevertheless affect observers' behavior. This phenomenon has been called subliminal priming. For instance, exposure to a visually presented word (a 'prime') fully prevented from reaching consciousness by preceding and following 'masking' stimuli makes the processing of the next visible word (a 'test stimulus') faster and more accurate if the two words are in the same semantic category. Priming effects have been observed in many stages of cognitive processing, ranging from visual object identification to semantic word processing.

In number processing, it has been shown that the subliminally presented prime enhances the accuracy (as illustrated by lower error rates) and the speed (as reflected in shorter mean reaction times) of numerical smaller/larger judgments if the prime falls into the same category as the test stimulus. This effect has been revealed so far for primes and targets represented by Arabic numerals and by number words, both of which are symbols for discrete quantities in human language. Whether subliminal priming is also present for non-symbolic discrete quantities (the number of items in a set, or 'numerosity') remained unknown.

We have tested human subjects on a numerosity comparison task, using the priming method. Both primes and targets were random dot patterns, ranging from 1 to 9 dots. In a two-alternative forced choice task, subjects were asked to judge whether the number of dots they saw (in the target) was smaller or larger than five, by pressing one of two alternative keys. Shortly before the target presentation, and unknown to the subjects, they also saw a briefly presented masked prime, which could be either congruent with the target (on the same side of five), or incongruent with it. The primes were flashed on the screen for 33 ms, and they were preceded by a 300 ms long forward mask and followed by a 33 ms long backward mask. Gratings consisting of an array of partly overlapping dots served as masks. Masking, prime and target stimuli were pseudo-randomly generated and randomly presented across trials.

Subjects were significantly faster in categorizing the targets in the congruent trials than in the incongruent ones; the average reaction time difference between congruent and incongruent trials was in the range of 20 ms. A similar priming effect has been described for symbolic numerical notations. Preliminary data also indicate priming interactions between numerals, number words and numerosities. This suggests that non-symbolic and symbolic numerical formats may have access to a generic neural substrate encoding numerical information as notation-independent magnitude.

## How precise is gaze following in humans ?

Simon W. Bock\*, Peter W. Dicke, Peter Thier

Hertie-Institute for Clinical Brain Research, Department of Cognitive Neurology  
 Otfried-Müller-Str. 27, 72076 Tübingen, Germany  
 \*sbock@uni-tuebingen.de

Joint attention can be thought of as the basis of understanding other individuals as intentional beings, whose attention to outside objects may be shared, followed into, and directed in various ways. Gaze following, a prerequisite of joint visual attention may be paraphrased as “looking where someone else is looking“. Many studies have tested this ability in human and nonhuman primates, but as yet no quantitative measure of gaze following judgements has been obtained. However, knowledge of the precision of gaze following is indispensable for the understanding of the underlying neural circuitry.

In the present study we therefore investigated the capability of adult human ‘receivers’ to direct their gaze to the position of one out of many objects, which was defined by the gaze of an adult human ‘sender’. Sender and receiver faced each other at 100 cm distance, looking at the opponent through a ring of 90 pinhead objects (Fig. 1 B, object size  $0.44^\circ$ , object spacing  $1.03^\circ$  at  $15^\circ$  visual angle eccentricity, 50cm distance). The sender looked at object positions following a given pseudo-randomized order and the receiver reported the perceived target of the sender’s gaze. Receivers’ performance was tested under different conditions (e.g. binocular and monocular vision).

In order to assess gaze following precision, we studied pooled responses of seven receivers. The histogram of their deviations from the target indicated by three senders (Fig. 1 A) shows normal distribution and surprisingly high precision (standard deviation  $2.66^\circ$  visual angle). Assessment of responses based on target object location suggests that the deviations may be anisotropically distributed (Fig. 1 B). Preliminary experiments comparing monocular vision of two receivers (std. dev.  $2.3^\circ$  in 240 trials) with binocular vision of four receivers (std. dev.  $2.6^\circ$  in 600 trials) did not reveal statistically significant differences. The finding that binocular disparity does not seem to contribute significantly to the precision implies that 2D photographs of the sender may be sufficient in studies of gaze following.

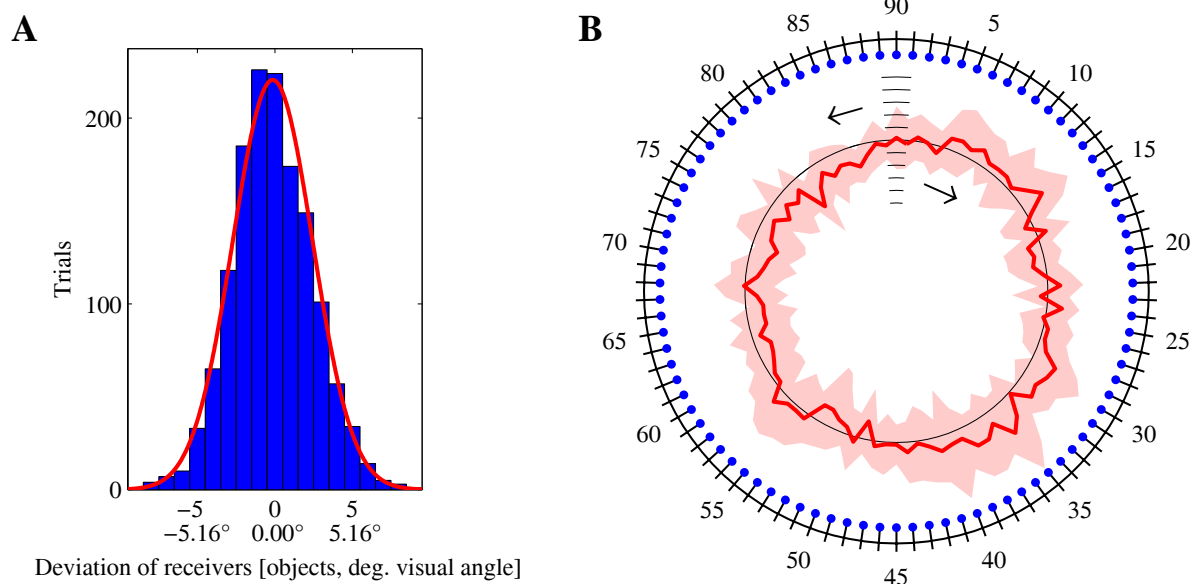


**Fig. 1.** Pooled performance of seven receivers interacting with three senders. Receivers’ deviations from the senders’ targets are given in multiples of objects, corresponding to steps of  $1.03^\circ$  visual angle.

**A** Histogram of receivers’ deviations from the target position, 1411 trials, mean  $-0.15^\circ$ , std. dev.  $2.66^\circ$  visual angle, fit to normal distribution  $r^2=0.994$ . Positive values represent counterclockwise deviation.

**B** Outer ring: Objects (pinheads) of the experimental setup as seen from the receivers’ side. Inner ring: Mean deviation (thick red line) of the reported object from the target (black circle representing zero eccentricity). Clockwise deviation is displayed as lower eccentricity, counterclockwise deviation as higher eccentricity. Eccentricities are scaled as plotted below ‘90’ in steps of  $1.03^\circ$  visual angle.

## **Different mismatch negativity (MMN) in dyslexic children with phonological deficit compared to non-impaired-readers**

K. Gust<sup>1</sup>, U. Bitz<sup>1</sup>, M. Kiefer<sup>2</sup>, K. Hille<sup>1</sup>, M. Spitzer<sup>1,2</sup>

<sup>1</sup>University of Ulm, Transfercenter for Neuroscience and Learning (ZNL), Germany

<sup>2</sup>University of Ulm, Department of Psychiatry III, Germany

kilian.gust@znl-ulm.de

### **Abstract**

Developmental dyslexia affects reading performance - often in combination with a reduced ability in writing - despite normal intelligence and average to good results in other school subjects. Different deficits in the auditory, visual and somatosensory system have been shown in studies using different diagnostic methods such as fMRI, MEG, and EEG.

The aim of this EEG-study is to specify the auditory deficit in dyslexic children with a diagnosed deficit in their phonological awareness (PR <25 in the BAKO 1-4).

The test battery included an IQ-Test, a reading and writing test, and the detection of the subjects' performance in phonological skills using the BAKO 1-4 ("Basic competences for reading and writing") including tasks like segmentation of nonwords, vowel substitution or word reversal.

Subjects were selected out of 276 right-handed boys (8;0 to 10;2 [years; months]) attending grade three in 24 different German schools. 37 boys were tested using EEG: 22 dyslexics and 15 non-reading-impaired controls.

Naturally spoken 250ms phonemes /ba/ vs. /da/, /da/ vs. /ta/ and synthetic 75ms pure tones of 500 and 750 Hz with an offset-onset-interval of 600ms were used as acoustic stimuli. Stimuli were presented via headphones during the EEG session.

The study demonstrates smaller mismatch negativity (MMN) for the speech stimuli in the dyslexic group compared to the children with normal reading performance. Both groups show similar responses to pure tones.

# Phonological Deficit in 6 - 7 years Old Children: An EEG-Study

Ulrich Bitz<sup>1</sup>, Kilian Gust<sup>1</sup>, Markus Kiefer<sup>2</sup>, K. Hille<sup>1</sup>, Manfred Spitzer<sup>1,2</sup>

<sup>1</sup>Transfercenter for Neuroscience and Learning, University of Ulm, Germany

<sup>2</sup>Department of Psychiatry III, University of Ulm, Germany

ulrich.bitz@znl-ulm.de

## Abstract

Developmental dyslexia (specific reading disability) represents the failure to acquire readings skills, despite adequate intelligence, education, and social background. The disorder is widespread, with prevalence estimates ranging from 4% to 9% of the age matched population.

Several theories have been proposed for the causation of dyslexia. The most unifying hypothesis suggests that dyslexic children have specific impairments in representing, storing, and retrieving phonological information (phonological deficit hypothesis). Speech perception was found to be a prerequisite condition for phonological processing.

The Mismatch Negativity (MMN) is a neurophysiological paradigm to examine pre-attentive and automatic central auditory processing. The MMN, a change-specific component of the auditory event-related potential (ERP), is elicited by any noticeable change in auditory stimulation irrespective of the subjects' attention and behavioral task.

We conducted a study of 248 male German first grade children (6 - 7 years old) at elementary schools, who were just beginning to learn to read and to write. We investigated their phonological skills after testing for non-verbal IQ. A group of children with a phonological deficit was identified using the Differenzierungsprobe II by Breuer/Weuffen. In this group as well as in a control group of 15 children without this deficit, we measured the MMN by presenting tone stimuli (500 Hz vs. 750 Hz) and speech stimuli (/ga/ vs. /ka/).

The relevant electrodes for our study were F3, FC3, C3, F4, FC4, C4, Fz, FCz and Cz. Analyzing the tone stimuli we found no significant differences between the groups. However, when looking at the speech stimuli, we found a significant difference. Furthermore dyslexic children showed a reduced asymmetry when looking at the differences of the MMN on both hemispheres.

## Are changes in the perception of the Necker cube related to eye-position?

Wolfgang Einhäuser<sup>1\*</sup>, Kevan AC Martin<sup>1</sup>, Peter König<sup>2</sup>

<sup>1</sup>Institute of Neuroinformatics, University of Zurich & Swiss Federal Institute of Technology (ETH) Zurich

<sup>2</sup>Institute of Cognitive Science, Dept. Neurobiopsychology, University of Osnabrück

\*Correspondence: weinhaeu@ini.phys.ethz.ch

The issue of the relation of eye-movements and perceptual reversals of the ‘Necker cube’ dates back as early as Necker’s original article in 1832. Despite the interest of many distinguished psychophysicists since then, the question, whether perceptual switching is a cause or a consequence of associated eye-movements, has remained a matter of debate.

Here we overcome the methodological problems that bedevilled previous studies:

- (i) a precise non-invasive eye-tracking technique is used;
- (ii) any instruction that could interfere with a subject’s rate of perceptual switching or with the cues it uses is avoided
- (iii) each subject’s eye-position bias associated with either Necker cube percept is objectively determined by using unambiguous (‘biased’) versions of the cube.

We show that under these free viewing conditions there is a close link between the perception of the Necker cube and the following changes in eye-position: Most subjects’ average eye-position is at an extreme value at about the time when the subject’s perception switches (Figure 1). From the biased cube trials we can infer that the polarity of the extreme corresponds to the percept the subject had *before* the switch. These data indicate a bi-directional coupling between eye-position and perceptual switching, so that *after* a subject’s perceptual state changes, their eye-position shifts to view the newly established percept. When the eye-position approaches the corresponding extreme, the percept becomes in turn more and more likely to switch. Our data may reconcile seemingly conflicting previous results, by suggesting a negative feedback mechanism of eye-position on perception.

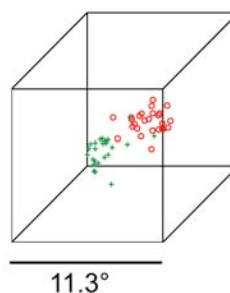


**Figure 1** Red: Eye-positions of an individual subject 300ms after perceptual switching from percept I (lower face in front) to percept II (upper face in front); green: eye-positions 300ms after switching from percept II to percept I. Note the clear separation of eye-position depending on switch polarity.

**Poster Subject Area #PSA34:  
Neuronal networks theory and modeling**

- [#443A](#) C. Leibold, K. Thurley and R. Kempter, Berlin  
*A Computer Model of Sequence Learning through Phase Precession in the Hippocampal CA3 Region: Compression, Storage and Fast Replay*
- [#444A](#) P. Wiesing, L. Schwabe, O. Beck, J. Mariño, J. Schummers, DC. Lyon, M. Sur and K. Obermayer, Berlin and Cambridge, MA (USA)  
*Invariant computations in local cortical networks with balanced excitation and inhibition*
- [#445A](#) D. Rotermund, U. Ernst and K. Pawelzik, Bremen  
*Processing Natural Images with Single Spikes*
- [#446A](#) T. Kromer, Zwiefalten  
*Scanning Patterns in Fractal Neural Nets*
- [#447A](#) T. Kromer, Zwiefalten  
*Learning not by Changing Synapses but by generating Memory-Molecules*
- [#448A](#) P. Jedlicka and KH. Backus, Frankfurt/Main  
*Postsynaptic depolarizations mediated by GABAA receptors: a computational study*
- [#449A](#) C. Klisch, S. Mahr and H. Meissl, Frankfurt/Main  
*Activity rhythms of individual neurons of the rodent suprachiasmatic nucleus cultured on microelectrode arrays*
- [#450A](#) N. Voges, A. Aertsen and S. Rotter, Freiburg  
*Statistical Analysis and Modeling of Cortical Network Architecture based on Neuroanatomical Data*
- [#451A](#) A. Kumar, J. Kremkow, S. Rotter and A. Aertsen, Freiburg  
*Redistribution of synaptic input leads to gain modulation in layer V pyramidal neurons*
- [#452A](#) S. Schrader, A. Kumar, S. Rotter and A. Aertsen, Freiburg  
*Self- sustained asynchronous activity in large- scale random networks of spiking neurons*
- [#453A](#) B. Kriener, A. Morrison, A. Aertsen and S. Rotter, Freiburg  
*How the Structure of Cortex Relates to Its Function*
- [#443B](#) P. Friedel and JL. van Hemmen, Garching  
*Prey localisation by sand swimmer snakes using a population vector model*

- [#444B](#) B. Porr and F. Wörgötter, Glasgow (UK) and Stirling (UK)  
*Non-hebbian synaptic plasticity allows for the stable implementation of one-shot predictive learning*
- [#445B](#) T. Tzvetanov, T. Womelsdorf and S. Treue, Göttingen  
*Model for attentional shift of the receptive field*
- [#446B](#) MT. Wiechert, B. Judkewitz and RW. Friedrich, Heidelberg  
*Dynamic computations in network models of the olfactory bulb*
- [#447B](#) E. Olbrich and P. Achermann, Leipzig and Zurich (CH)  
*Sleep stage and cycle specific properties of oscillatory events in the human sleep EEG*
- [#448B](#) A. Schierwagen, A. Schubert, A. Alpár, U. Gärtner and T. Arendt, Leipzig  
*Scaling properties of dendrites of pyramidal neurons in wildtype and p21H-rasVal12 transgenic mice*
- [#449B](#) J. Tusch and MA. Dahlem, Magdeburg  
*Retino-cortical magnification on naturally curved human cortical surfaces*
- [#450B](#) D. Bibitchkov, B. Blumenfeld, S. Naaman, A. Grinvald and M. Tsodyks, Rehovot (IL)  
*Attractor model of the primary visual cortex based on its functional properties*
- [#451B](#) O. Straub, N. Daur, J. Ausborn, W. Mader and W. Stein, Ulm  
*How to switch from standing to walking*
- [#452B](#) J. Ausborn, W. Mader, H. Neumann and H. Wolf, Ulm  
*Interaction of sensory feedback and central network in the locust flight control system: a modeling study*



# A Computer Model of Sequence Learning through Phase Precession in the Hippocampal CA3 Region: Compression, Storage and Fast Replay

Christian Leibold, Kay Thurley, Richard Kempter

Institute for Theoretical Biology, Humboldt University Berlin

Invalidenstr. 43, 10115 Berlin, Germany

The hippocampus is known to play a crucial role in learning the temporal order of sequences of events. Events can be odors, spatial locations and many other kinds of sensory incidences. Recent experiments suggest that the recurrent network in the CA3 subregion of the hippocampus is essential for sequence learning (Brun et al. (2002) *Science* **296**). We present a network of conduction-based integrate-and-fire elements as a systems model of the CA3 region. Our simulations explain how local synaptic learning rules at recurrent associative CA3 connections allow the storage of sequences of input events, while the network is in an oscillatory ‘theta’ state of about 10 Hz. In order to stabilize synaptic growth during repetitive sequence learning, we propose a solution to the emerging stability-plasticity dilemma in that we confine recurrent connectivity in a self-organized manner by a local synaptic learning rule that is controlled by the postsynaptic firing rate.

Storage of sequences requires their temporal compression from the behaviourally relevant time scale of a few seconds to a few milliseconds, the time scale on which spike-timing dependent synaptic plasticity is induced. Compression is implemented by means of phase precession in CA3 (O’Keefe & Recce ML, (1993) *Hippocampus* **3**). Our model comprises a new mechanism that explains phase precession as a result of the interplay of short-term synaptic plasticity and subthreshold theta oscillations of the membrane potential of pyramidal cells. In agreement with experiments (Skaggs et al. (1996) *Hippocampus*, **6**), the phase vs. position plots generated by our model exhibit a non-linear precession of spike phases over a range of up to 360 degrees; see figure. Our model also accounts for other features of in-vivo data like a bimodal distribution of spike phases (Yamaguchi et al. (2002) *J Neurophysiol* **87**) and the absence of recession of the mean spike phase. On the level of a single pyramidal cell, the proposed mechanism of phase precession is independent of NMDA receptors as has been found by Ekstrom et al. (2001) *Neuron* **31**.

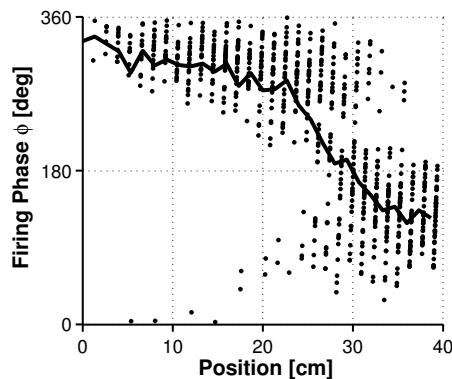


Figure 1: Phase vs. position plots generated by our model for a theta oscillation at a frequency of 10 Hz. The mean phase (solid line) of pyramidal cell action potentials decreases (precesses) non-linearly as the hypothetical animal runs through a place field of the simulated cell with a constant speed of 13.3 cm/s. We observe two almost separated clusters of spike phases (dots), a bimodality which is an inherent feature of the proposed mechanism.

The stored sequences can be ‘recalled’ during a non-oscillatory ‘sharp wave/ripple’ network state, where the activity is governed by the recurrent connections (Lee & Wilson (2002) *Neuron* **36**). A stable and fast replay of the stored sequences requires a network of inhibitory interneurons whose activity accounts for a sharp-wave like behaviour. During fast replay, pyramidal cell activity exhibits a ripple-like (200 Hz) temporal structure. Finally, we assess our model’s storage capacity for sequential memory in dependence on the parameters governing the stabilization of the synaptic dynamics.

## Invariant computations in local cortical networks with balanced excitation and inhibition

Peter Wiesing<sup>2</sup>, Lars Schwabe<sup>2</sup>, Oliver Beck<sup>2</sup>, Jorge Mariño<sup>1,3</sup>, James Schummers<sup>1</sup>, David C. Lyon<sup>1,3</sup>, Mriganka Sur<sup>1</sup> & Klaus Obermayer<sup>2</sup>

<sup>1</sup>Department of Brain and Cognitive Sciences and Picower Center for Learning and Memory, Massachusetts Institute of Technology, Cambridge, MA 02139, USA.

<sup>2</sup>Department of Computer Science and Electrical Engineering, Berlin University of Technology, FR2-1, Franklinstrasse 28/29, 10587, Berlin, Germany.

<sup>3</sup>Present addresses: Department of Medicine, Neuroscience and Motor Control Group (Neurocom), Univ. A Coruña, Fac. CC. da Saúde, Campus de Oza, 15006, A Coruña, Spain (JM); The Salk Institute, SNL-C, 10010 North Torrey Pines Road, La Jolla, CA 92037, USA (DCL).

Intracellular recordings from orientation selective neurons in the area 17 of the cat revealed that the tuning of the spike response remained sharp and independent of the position in the orientation map [1], while the orientation tuning of the total excitatory and inhibitory conductances differed significantly between pinwheel and domain regions [2]. A subsequent double labelling study showed that the area of origin of inhibitory as well as excitatory inputs to cells at a given cortical location is always roughly circular, ignoring the differences in the distribution of orientation preferences for different locations in the map, and is roughly equal in size for excitation and inhibition [3]. While this anatomical finding can potentially explain, why tuning curves of total excitatory and inhibitory conductances vary with the location in the orientation map, the question arises, how different inputs and neuronal properties interact to – finally – generate a normalized spike response.

To investigate this question we first set up a Hodgkin-Huxley type single neuron model (cf. [4]) that receives effective excitatory and inhibitory inputs. By convolving the experimentally obtained excitatory spatial interaction profiles from our anatomical measurements [3] with experimentally obtained maps, we calculated the tuning of the excitatory conductance for every location – averaged over locations with similar orientation selectivity index (OSI). Then, given the calculated excitation tuning curves, we determined the tuning curve of the inhibitory conductances which would be necessary to cause a sharp and location invariant spike tuning for each local input. By construction, the difference between pinwheel locations and orientation domains is reflected in the tuning curves of the total excitatory conductance, but due to the appropriate inhibitory balance, not in the spike responses. The deduced tuning curves of the inhibitory conductances, however, are in quantitative agreement with the measured data indicating that a proper balance between excitation and inhibition is a likely cause of the location independent tuning of the spike response. But how can it happen that excitation and inhibition are always properly balanced – given the heterogeneity of an orientation map?

In order to address these questions we set up a large-scale network of 128x128 recurrently connected excitatory and inhibitory Hodgkin-Huxley-type point neurons receiving orientationally tuned afferent input. Optically imaged orientation maps, as well as artificial orientation maps, were used for assigning orientation preferences to cortical locations. Recurrent input to the neurons was provided via two different recurrent excitatory (fast, AMPA-, and slow, NMDA-mediated, components) and inhibitory (GABA-A mediated) connections. Again we find that the tuning of the total inhibitory and excitatory conductances clearly depends on the local input OSI. If the network – however – operates in a regime, where the recurrent inputs dominate the afferent ones, the equal sampling area of excitation and inhibition leads to a neat balance between excitatory and inhibitory conductances and causes the spike tuning to remain location independent. Furthermore, a quantitative analysis shows a close match between model predictions and experimental measurements. When the model is reparameterized to operate in a regime, where recurrent excitation is weak, inhibition dominates and the neurons are mainly driven by feedforward inputs, excitation and inhibition do not co-vary, and the spike tuning becomes dependent on map location as had been predicted, e.g. in [3].

These results show that a simple rule of spatial integration is sufficient to explain, why orientation tuning remains invariant of map location, although the underlying computations are carried out by networks which can vary widely within a cortical area. A necessary ingredient is the fact that the network operates in a recurrent rather than in an afferent mode. One may speculate that a similar mechanism may account for the tuning of other functional properties in the visual areas, and may be a general mechanism for generating and preserving response selectivity in sensory cortex.

[1] Neuron 2002: Schummers et al.: Synaptic integration by V1 neurons depends on location of the orientation map

[2] SfN 2003: Marino et al.: Input conductance at different locations within V1 orientation map.

[3] SfN 2003: Lyon et al.: Distribution of inhibitory and excitatory inputs to pinwheel centers and orientation domains.

[4] Neuroscience 2001: Destexhe et al.: Fluctuating synaptic conductances recreate in-vivo-like activity in neocortical neurons.

This work was funded by the DFG (SFB 618)

# Processing Natural Images with Single Spikes

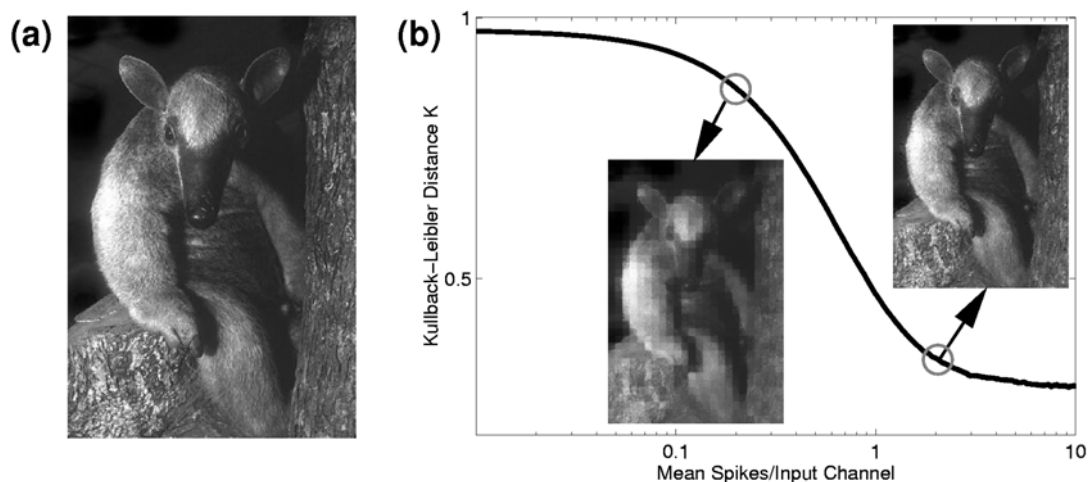
D. Rotermund, U. Ernst, and K. Pawelzik

Institute for Theoretical Physics, University of Bremen, Otto-Hahn-Allee 1, 28334 Bremen  
 {pawelzik, udo, davrot}@neuro.uni-bremen.de

Generative models compute the likelihoods of hidden states given the data. The resulting representations can then be used for optimal processing like estimation of single features, classification and control. Since the times of Helmholtz it has been suggested that such a process might underly perception, especially because the brain often approaches the performance of an ideal observer [1, see also Poster of Mandon et al.]. If taken as a framework for cortical computation, however, realistic generative models need to take into account biological constraints like the irregularity of single action potentials, the unreliability of synaptic transmission, and the limited amount of time available for processing stimuli in a dynamic environment. For example, it has been estimated that despite the stochasticity of spikes, few action potentials per neuron and processing step are sufficient to achieve nearly perfect classification of complex scenes [2].

Here we present a framework for generative models which incorporates some important biological prerequisites [3]. Our spike-by-spike model iteratively generates nearly optimal representations from each stochastic action potential, without relying on a strict rank ordering of the incoming spikes [2]. For a rapid reconstruction of natural images, we derive an update rule for the activities in the neurons representing the hidden states, which connects the evidence for the presence of a specific object in a scene to the actual stimulus in a multiplicative way. Furthermore, we devise an on-line learning rule which updates the connection weights of the generative network with each incoming spike. The learning rule includes a Hebbian term and a saturation term, and it is capable of learning ensembles of typical features which underly natural visual stimuli.

When applied to natural image patches we obtain classical receptive field properties in about 35% of the neurons, while the remaining 65% represent more complex image features and therefore can not be observed by using simple bar stimuli. These receptive fields allow for a nearly perfect image reconstruction within 1-2 spikes per input channel, measured as the Kullback-Leibler distance between the original image and the reconstructed image as shown in graph (b). The insets in (b) show the reconstructed image after 0.2 and 2.0 mean spikes per input channel in comparison to the original image (a). When stimulated with isolated, oriented bars instead of natural image patches, 1/3 of the neurons exhibit a pronounced orientation preference with tuning curves having a half-width of about 30 degrees. We are currently investigating a modified version of our network aiming at extracting higher correlations in natural images, and we are extending our framework for the analysis and representation of natural image sequences for fast reconstruction of movies.



**This work has been supported by the DFG (SFB 517 'Neurocognition') and by the BMBF (DIP/MetaComp).**

- [1] M.O. Ernst und M.S. Banks, *Humans integrate visual and haptic information in a statistically optimal fashion*, Nature **415**, 429-433 (2002); K.P. Körding und D.M. Wolpert, *Bayesian integration in sensorimotor learning*, Nature **427**, 244-247 (2004).
- [2] S.J. Thorpe, D. Fize und C. Marlot, *Speed of processing in the human visual system*. Nature **381**, 520-522 (1996); S.J. Thorpe, A. Delorme and R. van Rullen, *Spike-based strategies for rapid processing*, Neural Networks **14**, 715-725 (2001).
- [3] U. Ernst, D. Rotermund, and K. Pawelzik, *An algorithm for fast pattern recognition with random spikes*, in: Lecture Notes in Computer Science **3175**, eds. C.E. Rasmussen et al., Springer-Verlag, 399-406 (2004).

## Scanning Patterns in Fractal Neural Nets

Thomas Kromer, Muensterklinik Zwiefalten

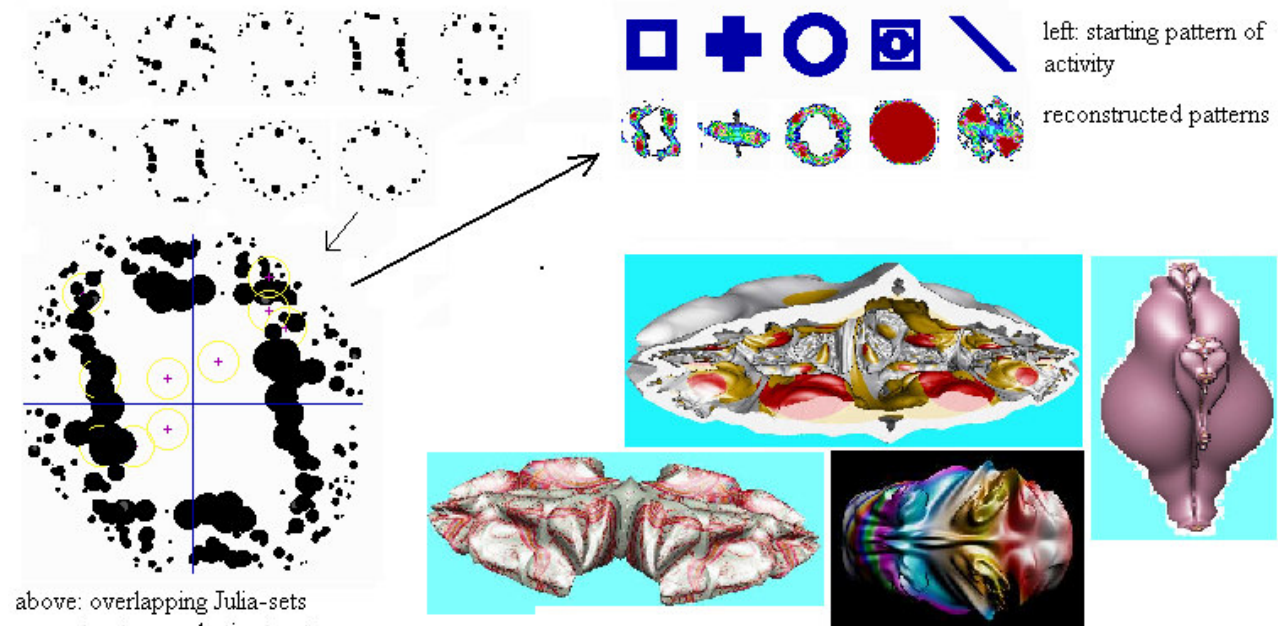
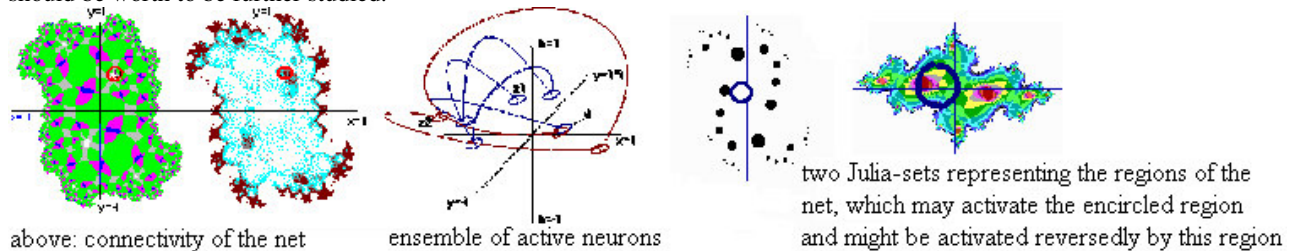
[Thomas.Kromer@t-online.de](mailto:Thomas.Kromer@t-online.de)

Fractal functions define how to project the complex plane to itself. As shown earlier(1), neural nets may reflect those functions directly. (Neurons will project their activity to neurons, which are determined by the fractal function. In this model, neurons replace complex numbers, their axones follow the course of the corresponding trajectories through the complex plane). Like in fractals, in fractal neural nets, a neural activity will be projected to another place within the neural net. Thus we get a topographic(“somatotopic”) projection of the net to itself. By iterating the projecting procedure, a remarkable connectivity between the neurons of the net will be established. A neuron at any place of the net might be activated by neurons at a very distance. Assuming, (as it is the case in most biological neural systems), recurrent connections between neural columns, any neuron might, by its dendritic tree, get activity from a wider part of the net. In reverse, activation spreading out from this neural column may activate these parts of the net again. These regions represent in fractal neural nets parts of Julia-sets. The neurons, respectively neural columns, of these Julia-sets are not directly, but functionally, connected with each other. Using these connections, they might be able to synchronize their activity, to form ensembles of synchronous active neural columns, which might be an important feature to represent complex concepts.

Starting with any specific pattern, the course of the iteration will lead to a degree of activity at each neural column, which is completely specific for this pattern. The starting pattern might thus be stored by a specific distribution of activity at each neural column (and within the net). The starting pattern might be reconstructed by the reversed activation of the corresponding Julia-sets. Each Julia-set will be quite different in shape to the starting pattern, but the overlapping action of the Julia-sets may reconstruct the starting pattern successfully. (This might be a good model for thinking in complex patterns).

It may be allowed to emphasize, that there are multiple options to use the specific sequences of activity occurring at each neuron of the net. Each starting pattern will cause a specific sequence of activity at each neural column, depending on the localization within the neural net, the constant vector, which is determining the course of the axons within the net and the radius of the dendritic tree. Assuming (hypothetically), neurons might be able to store the degree of the incoming activity in form of a molecular chain (f.e. a nucleic acid)(2), this memory-“string” could be used to activate the net reversedly to reconstruct the original pattern within the net. These intracellular strings might be used to compare patterns to reproduce associative sensible “answers” of the net to any presented pattern(2).

All these mechanisms could not only occur in two-dimensional fractal neural nets, but as well in three-dimensional fractal nets, which reflect corresponding three-dimensional fractals. Some figures might illustrate these concepts and demonstrate, that they should be worth to be further studied.



## References:

- (1) Kromer T, Spatial neural networks based on fractal algorithms. B. REUSCH (ed.) lecture notes in computer science; Vol. **1625** (1999) pp. 603-614. 3)
- (2) Kromer T, Tomography in fractal neural networks. B. REUSCH (ed.), lecture notes in computer science; Vol. **2206** (2001) pp. 917-923.



# Learning not by Changing Synapses but by generating Memory-Molecules

Thomas Kromer, Muensterklinik Zwiefalten

[Thomas.Kromer@t-online.de](mailto:Thomas.Kromer@t-online.de)

Although the theory of changing synaptical weights has brought an enormous progress in understanding mechanisms of learning and memorizing patterns in artificial and biological neural nets, there are still some doubts remaining, whether these mechanisms are indeed the main procedures, on which biological neural systems will work. Because the structure of the neural net is changed by learning patterns, the capacity of the net is principally limited, even in nets with very sophisticated connectionism.

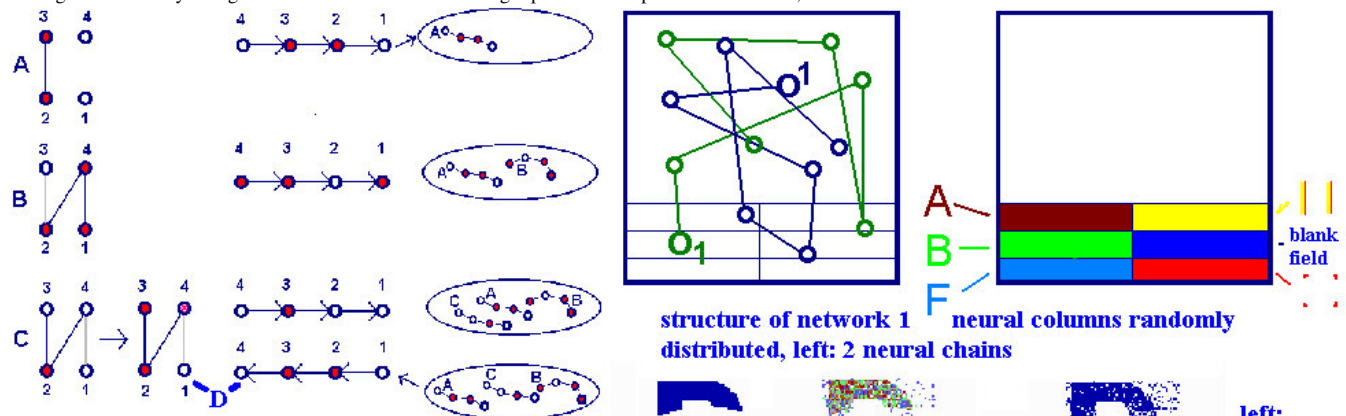
In this paper, another paradigm, how neural nets might work, shall be presented. Edelman reports anecdotically about a poor physicist, who, in the 1940's, hypothetically stated, that brains will produce protein-molecules, specific for the state of activity of the brain at each moment and use these molecules, to compare and reproduce the according patterns by mechanisms analogue immunological antibodies, recognizing specific antigens. Leo Szilard, being present then, would laugh at him and quit the room, saying: "Maybe, Your brain works like this". - The poor physicist felt embarrassed and never propagated his idea furthermore.

-He lacked a clear idea, **how** a brain might produce specific molecules according to its state of activity and reproduce these states of activity, using such molecules.

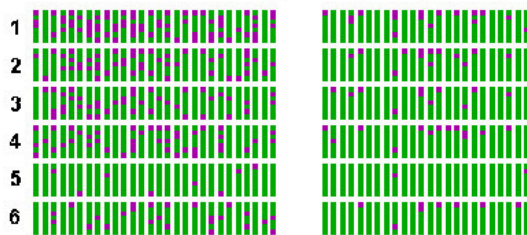
But maybe, poor physicist was not very far from goal:

In biological neural systems, neurons are projecting their activity to another neuron (or neural column), which belongs to the same net. In a more abstract sense, this is equivalent to a (topographic) projection of a map to itself. At each neuron, each starting distribution of activity, will cause a specific sequence of activity, coming in. Assuming, the neurons will record these sequences in form of a molecular chain, we will get intracellularly records of each pattern. These chainlike "molecules", which might be in biological systems chains of nucleic acids or according protein-molecules, might enable the net, to reproduce the according specific pattern within the net, by activating the net in reversed direction (according a principle shown by Fink(1)). For this, the connections between the neural columns have to be recurrent, as they are in most cases in biological neural systems.

To demonstrate the efficiency of this paradigm, the function of two networks, based on this principle shall be demonstrated: First a neural net of 4600 chains, each of 7 randomly distributed neurons and a second net of about 5000 chains, again each containing 7 neurons, distributed on the net according to a fractal function(2). The figures might show some of the aspects of the way, these nets work. (To produce an associative answer to a given pattern, the memory-strings will be compared, and the string with the most homologous sequence will be used to reproduce a sensible pattern in the net. The neurons of the different neural chains are overlapping at neural columns, thus, the answer of a chain might influence the answer of the others. Training might be done by multiplying sensible memory-strings, so, these might have a better chance to be used for pattern-reproduction. Each memory-string might get an valuing attachment to favorize sensible memory-strings. The concept of storing those memory-strings in form of f.e. nucleic acids might provide an explanation of inborn, instinctive behaviour.



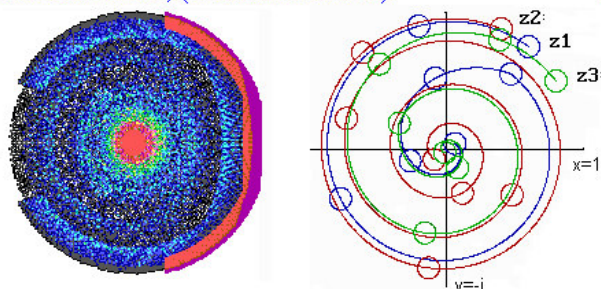
Comparing the different principles of function:  
left: conventional net, strengthening synapses between synchron. active neurons  
right: forming specific memory-strings intracellularly repr. pattern A, B and C  
last line: associative answer of the nets, presented pattern C, answer: pattern D



Above: memory-strings

left: intact network right: lesioned network

below: network 2, (fractal neural net)



distribution of neurons

3 neural chains

Starting pattern, picture after 1,

above: pattern reproduction, intact and lesioned network  
"paraphasia" in case of network lesion (grey region)



pattern incompletely presented

pattern reproduction

References: 1. Fink M (1996) Time reversal in acoustics, Contemporary Physics 37, 2: 95 - 109

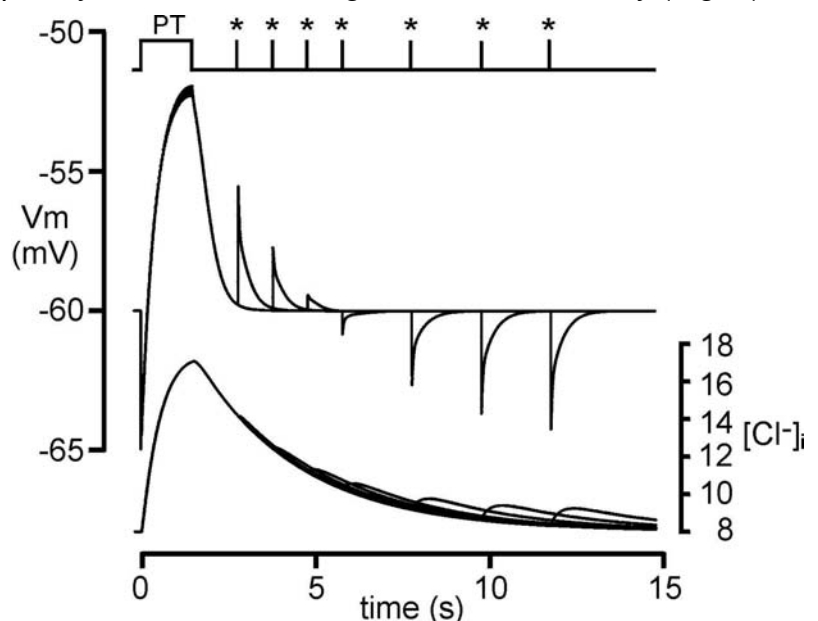
2. Kromer T, 'Biomorph Neural Networks Based on Fractal Algorithms', B. Reusch (ed.), Springer 1999, (lecture notes in computer science; Vol. 1625, pp 603 -614 )

## Postsynaptic depolarizations mediated by GABA<sub>A</sub> receptors: a computational study

**P. Jedlička and K.H. Backus, Institute of Physiology II, Cellular Neurophysiology, J.W. Goethe-University Frankfurt, Theodor-Stern-Kai 7, D-60590 Frankfurt/Main, Germany**

GABA<sub>A</sub> receptors (GABA<sub>A</sub>Rs) are ligand-gated ion channels that regulate a Cl<sup>-</sup>/HCO<sub>3</sub><sup>-</sup> conductance through neural membranes. The direction of the net anion flux through these receptors is determined by the relative permeability of HCO<sub>3</sub><sup>-</sup> and Cl<sup>-</sup> and their electrochemical gradients. Brief activation of GABA<sub>A</sub>Rs commonly results in hyperpolarization of adult neurons. In postnatal neurons, depolarizing or biphasic response have been frequently observed. In the adult brain, prolonged or repetitive activation of GABA<sub>A</sub>Rs also evoked biphasic responses consisting of an initial hyperpolarization followed by a depolarization (Thomson, *Neurosci* 1988, 25:503). A possible mechanism underlying the GABA-induced depolarizing postsynaptic potential (GDPSP) is attributable to an acute Cl<sup>-</sup> accumulation that results in a shift of the GABA<sub>A</sub> reversal potential ( $E_{\text{GABA}}$ ; Staley et al., 1995, *Science* 269:977; Kaila et al., 1997, *J Neurosci.* 17: 7662; Dallwig et al., 1999, *Pflügers Arch.* 437:289). We have developed a computational model of the GABAergic synapse to study the effects of monosynaptic GABA<sub>A</sub>R-mediated Cl<sup>-</sup> accumulation and its role for depolarization. An equivalent circuit model of the dendritic compartment was implemented in the simulation environment NEURON ([www.neuron.yale.edu](http://www.neuron.yale.edu)). To incorporate the GABA-induced gating of postsynaptic receptors, an established kinetic model of GABA<sub>A</sub>R was used (Jones & Westbrook, 1995, *Neuron* 15:181). In physiological conditions, our simulations indicated that the activation of GABA<sub>A</sub>Rs increased the intracellular Cl<sup>-</sup> concentration ( $[\text{Cl}^-]_i$ ) and shifted  $E_{\text{GABA}}$  to more positive values. By using different stimulation frequencies, we could show that the GDPSP amplitude was frequency-dependent and correlated with intracellular Cl<sup>-</sup> accumulation. We also investigated the effects of changes in the kinetics of Cl<sup>-</sup> regulation by varying the Cl<sup>-</sup> extrusion rate and found that higher Cl<sup>-</sup> extrusion rates decreased GDPSPs. However, when using a physiological Cl<sup>-</sup> extrusion rate ( $\tau=3\text{s}$ ; Wagner et al., *J Physiol.* 537:853), the GABA-induced Cl<sup>-</sup> accumulation evoked by stimulation frequencies  $\geq 10$  Hz persisted several seconds on a level, sufficient to induce GDPSPs. Thus, single pulse stimulations following a transient pulse train induced GDPSPs with amplitudes that depended on the frequency of the conditioning train and their delay (Fig. 1).

Fig. 1: Superimposed traces evoked by single pulse stimulations (asterisks) were applied at different time points following high frequency stimulation (PT; 40 Hz). The responses remained depolarizing up to several seconds. Lower traces show the corresponding changes in  $[\text{Cl}^-]_i$ .



In addition, we found that presynaptic depression could attenuate acute Cl<sup>-</sup> accumulation, but did not block GDPSPs in most conditions tested.

Our study shows that GABA<sub>A</sub>R-mediated  $[\text{Cl}^-]_i$  increase is sufficient to generate GDPSPs. The activity-dependent acute switch of GABA<sub>A</sub>-mediated hyperpolarization to depolarization could modulate interneuronal  $\gamma\beta$ -oscillations and may contribute to some epileptic conditions. Thus, our model may bring insights into the synaptic and ionic mechanisms of GABA-induced oscillations and seizure-like discharges. (Supported by the Graduiertenkolleg „Neuronale Plastizität: Moleküle, Strukturen, Funktionen“ and SFB 269 „Molekulare und zelluläre Grundlagen neuronaler Organisationsprozesse“; Teilprojekt B6).

Activity rhythms of individual neurons of the rodent suprachiasmatic nucleus cultured on microelectrode arrays

Christopher Klisch, Sabine Mahr and Hilmar Meissl

Max Planck Institute for Brain Research, Neuroanatomical Department, Deutschordenstr. 46, 60528 Frankfurt/Main, Germany

The circadian clock is an endogenous biological oscillator that generates daily patterns of neuronal and neuroendocrine activity rhythms and regulates the temporal organisation of many physiological, behavioural and endocrine functions. In mammals, the principal oscillator is located in the suprachiasmatic nucleus (SCN) of the hypothalamus, a paired neuronal structure just above the optic chiasm (Klein et al., 1991). The endogenous rhythmicity in the SCN is synchronized with the external light/dark cycle by photic information transmitted from the retina to the SCN via the retinohypothalamic tract. In the absence of external time cues, the SCN generates endogenous circadian periods *in vivo* as well as after isolation of the tissue under *in vitro* conditions, i.e. in brain slices or in individual dissociated cells, which are not synchronised with the external environment. In the present study, we examined the behaviour of individual SCN neurons from 1- to 3-day-old rats or mice (CD1) cultured on multi-microelectrode arrays (MEAs). Cells were dissociated from cylindrical punches of the SCN region from 500  $\mu\text{m}$  sections of the hypothalamus using Papain. Neurons were cultured on MEAs at a density of approximately 3000 cells/ $\text{mm}^2$  according to the procedure of Kopp et al. (1999) for periods of up to 9 months without losing their neuronal excitability. Cells were identified as SCN neurons by immunolabeling for the neuropeptides arginine-vasopressin (AVP) and vasoactive intestinal polypeptide (VIP). SCN neurons had compact cell bodies, were round or spindle-shaped with long processes. Neurons usually rested on a dense layer of astrocytes as identified by immunolabeling for glial fibrillary acidic protein (GFAP). However, the astrocyte layer did not prevent the recording of extracellular action potentials from our cultures. Spontaneous action potentials in individual SCN neurons were observed as early as five days after dissociation and plating the cells on the MEAs. In some experiments, spontaneously active cells, expressing a circadian rhythm, were recorded after 9 months in culture. Circadian rhythms of clock cells could be usually followed for two or three consecutive days, only in some cases for up to 6 days. An analysis of the firing pattern showed frequently regular ultradian rhythms. In many cases, neurons at adjacent electrodes exhibited synchronized spontaneous spike discharges with intercellular spike intervals between 0.7 and 1.5 ms. In other neuron pairs neuronal firing was suppressed for more than 70 ms indicating an inhibitory synaptic communication. These data show that SCN cells in long-term cultures form functioning networks on multi-microelectrode arrays. The development of culture techniques of SCN neurons on multi-microelectrode arrays is a first step for analyzing the clock-work mechanism, especially the interaction of clock cells in the SCN and the question how these neurons communicate with each other.

Klein, D.C., Moore, R.Y., Reppert, S.M. (1991) Suprachiasmatic Nucleus. Oxford University Press, New York, Oxford.

Kopp, M.D.; Schomerus, C.; Dehghani, F.; Korf, H.W.; Meissl, H. (1999) *J. Neurosci.* 19: 206-219.

# Statistical Analysis and Modeling of Cortical Network Architecture based on Neuroanatomical Data

Nicole Voges<sup>1,2</sup>, Ad Aertsen<sup>1</sup>, Stefan Rotter<sup>1,2</sup>

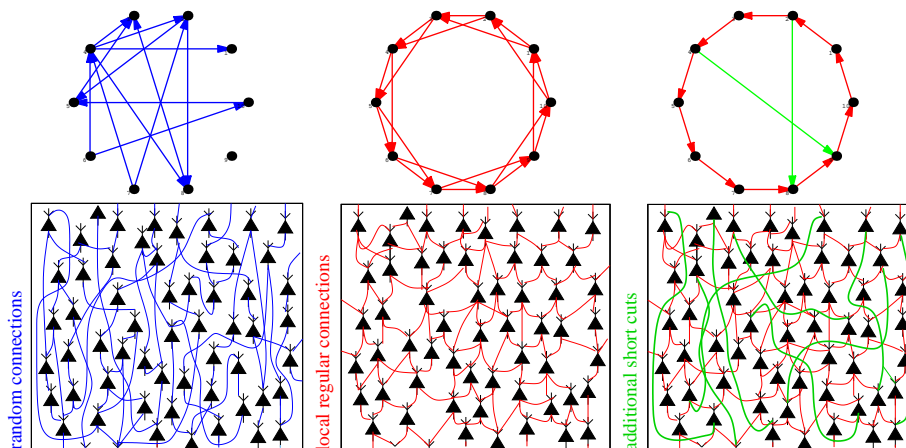
<sup>1</sup>*Neurobiology and Biophysics, Institute of Biology III, Albert-Ludwigs-University, Schänzlestr. 1, 79104 Freiburg, Germany*

<sup>2</sup>*Theory and Data Analysis, Institute for Frontier Areas in Psychology and Mental Health, Wilhelmstr. 3a, 79098 Freiburg, Germany*

Most current studies of functional network dynamics are based on completely random wiring. Such models are chosen for mathematical convenience rather than biological grounds. However, there is only little knowledge about the impact of specific architectural features in biological cortical networks. Our aim in this project is to design and analyze more realistic, but still tractable parametric models of the cortical neuronal network. These models are based on neuroanatomical data, and stochastic graph theory will be used to describe and investigate their structure.

First, we statistically analyze the spatial organization and the resulting connectivity of cortical cells. The combination of known quantitative and qualitative aspects of both neuronal geometry and connectivity allows us to better capture essential structural features of the cortical network. Then, we will attempt to analyze the resulting network topology by means of generalized random graphs. This field has recently seen exciting progress that is crucial for the analysis of all sorts of complex networks<sup>1</sup>. We will investigate to which extent the cortical neuronal network exhibits biologically and/or functionally relevant properties that have been described e.g. for *scale-free* or *small-world* networks.

Here we present the starting point of our model: the neuroanatomical data basis used, several quantitative assumptions derived in collaboration with A. Schüz<sup>2</sup>, and some open issues. Distinguishing between local connections with distance-dependent connectivity<sup>3</sup> and long-range *patchy* pyramidal cell projections<sup>4</sup>, we explain our approach of combining topology and geometry, see figure. Finally, we present a list of important network properties to investigate, and results from the study of a preliminary probabilistic network model with distance-dependent connectivity.



Bottom, three 2D-sections of a cortex model composed of pyramidal cells with three different connectivity patterns. Top, corresponding network topologies: random, regular and small-world, respectively.

Supported by the Institute for Frontier Areas in Psychology. We acknowledge stimulating discussions with A. Schüz.

<sup>1</sup>Albert R., Barabasi A.-L. (2002), Reviews of Modern Physics 74, 48-94

<sup>2</sup>Schüz A., Braitenberg V. (1998), Springer, Berlin-Heidelberg

<sup>3</sup>Hellwig B. (2000), Biol. Cybern. 82, 111-121

<sup>4</sup>Amir Y., Harel M., Malach R. (1993), J. of Comparative Neurobiology 334, 19-46



## Redistribution of synaptic input leads to gain modulation in layer V pyramidal neurons

Arvind Kumar<sup>1\*</sup>, Jens Kremkow<sup>1\*</sup>, Stefan Rotter<sup>1,2</sup>, Ad Aertsen<sup>1</sup>

<sup>1</sup>Neurobiology and Biophysics, Institute of Biology III, Albert-Ludwigs-University, Freiburg, Germany.

<sup>2</sup>Theory and Data Analysis, Institute for Frontier Areas in Psychology and Mental Health, Wilhelmstr. 3a D-79098 Freiburg, Germany.

E-mail: [kumar@biologie.uni-freiburg.de](mailto:kumar@biologie.uni-freiburg.de)

Recently it was proposed<sup>1</sup> that layer 5 pyramidal neurons, having three distinct functional parts (soma, apical dendrite, tuft), can be considered as a 3-compartment structure. Here we present a new method of reducing the detailed morphology of an L5 pyramidal neuron to a 3-compartment model. The soma is modeled as a leaky-integrate&fire compartment, while the apical dendrite and tuft are modeled as leaky integrators without spiking. Model parameters are derived from morphological reconstructions of L5 pyramidal neurons. Previously we have shown that this model presents an attractive description of a pyramidal neuron.

The separation into three distinct compartments enables us to distribute synaptic input (modeled as conductance changes) across compartments. Here, we determined the neuron's input/output rate transfer function for three cases: (A) The synapses were distributed over the compartments according to anatomical data. In addition, we studied the effect of redistributing synaptic input, while keeping the total excitation and inhibition as in A, by either shifting the balance towards (B) more excitation or (C) more inhibition on the soma.

We found that in A, the transfer function at balance of excitation and inhibition shows a monotonic behavior<sup>3</sup>, unlike reported for point neuron models with conductance-based synapses. The effective membrane time constant,  $\tau^{\text{eff}}$  is in the order of 10ms. Thus, the model response is in between that of a point neuron with current-based synapses and one with conductance-based synapses. Redistribution of synaptic input resulted in gain modulation. An increase of excitatory synapses on the somatic compartment (B) leads to a smaller rate gain compared to A, while the mean membrane potential becomes already supra-threshold at lower input rates. By contrast, when inhibition on the soma is increased (C), the rate gain increases, but the neuron needs higher input rates to become supra-threshold.

Overall, the model is computationally inexpensive, while it preserves key aspects of the neuron morphology, making it suitable for simulation of large cortical networks.

\*Both authors contributed equally to this work

Funded by GIF and DFG-GraKo, further information at [www.brainworks.uni-freiburg.de](http://www.brainworks.uni-freiburg.de).

<sup>1</sup>Larkum et al. (2001) JPhysiol 533(2): 447- 466

<sup>2</sup>Kumar et al. (2004) FENS Abstr, Vol 2: A014.27

<sup>3</sup>Kuhn et al. (2004) JNeurosci 24(10): 2345- 2356

## Self-sustained asynchronous activity in large-scale random networks of spiking neurons

Sven Schrader<sup>1\*</sup>, Arvind Kumar<sup>1\*</sup>, Stefan Rotter<sup>1,2</sup>, Ad Aertsen<sup>1</sup>

<sup>1</sup>*Neurobiology & Biophysics, Inst Biology III, Albert-Ludwigs-University, Freiburg, Germany*

<sup>2</sup>*Theory and Data Analysis, IGPP, Freiburg, Germany*

E-mail: [{schrader,kumar}@biologie.uni-freiburg.de](mailto:{schrader,kumar}@biologie.uni-freiburg.de)

We investigated the dynamics in large, sparsely connected random networks of excitatory and inhibitory spiking neurons, interconnected by conductance-based synapses. Global population activity, single neuron firing rates and irregularity of spike timing were studied as a function of external input and relative strength of inhibition. The network was able to exhibit asynchronous population activity while individual neurons fired in an irregular manner at low rates (AI state) for weak external input in the inhibition-dominated regime. Increasing the input and/or excessive inhibition lead to synchronous activity and individual neurons spiking more regularly (SR state).

We then studied a single-neuron approximation of the activity in the large network. We found that the single-neuron model provided an excellent approximation of the network in the AI state. Small deviations between the predicted firing rate using the single-neuron approximation and the observed network rates presumably reflected correlations in the network activity due to shared connectivity.

Based on the single-neuron approximation, we predicted that the random network of spiking neurons should be able to show self-sustained asynchronous irregular spiking activity at low firing rates, in the absence of any external input. We tested this prediction in large (~10<sup>3</sup> neurons) network simulations. In contrast to reports from a previous study we found that, indeed, the network could show self-sustained AI type activity for intervals lasting up to a second, in the absence of any external drive. The self-sustained network rate deviated slightly from the firing rate predicted by the single-neuron model. A systematic study of this deviation revealed that the deviation was partially consistent with small differences in the slope of the transfer function at the fixed point rate and a slight increase in pairwise correlations in the network activity which were, however, not significant for such short epochs of activity.

\*Both authors contributed equally to this work

Funded by GIF and DFG-GraKo, further information at [www.brainworks.uni-freiburg.de](http://www.brainworks.uni-freiburg.de).

<sup>1</sup>Kumar et al (2003) Proc 29th Goettingen Neurobiology Conf. p 1035- 1036. Thieme: Stuttgart

<sup>2</sup>Brunel N (2000) JComput Neurosci 8: 183- 208

<sup>3</sup>Latham et al (2000) JNeurophysiol. 83: 808- 827

## How the Structure of Cortex Relates to Its Function

Birgit Kriener<sup>1</sup>, Abigail Morrison<sup>1</sup>, Ad Aertsen<sup>1</sup>, & Stefan Rotter<sup>1,2</sup>

<sup>1</sup>Neurobiology & Biophysics, Inst. of Biology III, Albert-Ludwigs-University, Freiburg

<sup>2</sup>Theory & Data Analysis, Inst. for Frontier Areas of Psychology and Mental Health, Freiburg

Complex real-world networks such as the internet have recently become subject of intense research. In that context Watts and Strogatz [1] revived the idea of employing stochastic graph theory to describe the connectivity in complex high-dimensional networks by only few characteristic structural parameters (for recent reviews, see [2,3]).

Our project bases on exploiting this approach to describe and understand activity dynamics in sub-systems of the brain by treating them as networks, with neurons as nodes and synaptic couplings as directed edges. The two basic features of our study are, thus, the individual dynamics of each neuron and the underlying topology determining their synaptic interactions.

To this end we study and compare different types of neuron models, either spiking or based on firing rates, either deterministic or stochastic, depending on which parameters are assumed to describe the dynamics of the biological system.

To explore the impact of structure on network dynamics we first investigated different statistically defined interaction topologies, including randomly connected networks, regular networks with a fixed number of neighbors per node, and so-called 'small world' and 'scale-free' networks, that take a position in between the two extremes mentioned first.

Our main aim, however, is the examination of networks with structural parameters as obtained by neuroanatomical methods, to find out how they deviate from the more abstractly defined substrates, and what the functional implications of these deviations are.

Most of the present results were obtained by simulations of networks of a size ranging from 1,000 neurons up to the order of  $10^5$  neurons to identify the interesting regions in state space.

To quantify the characteristic features of network dynamics we investigate the stationary states of the dynamics in terms of the spectra of the relevant dynamical operators (e.g. the covariance matrix or the Jacobian) and how much these mirror the respective features of the spectra of the so-called adjacency matrix  $\mathcal{A}$ , which stores whether any two neurons are interconnected ( $\mathcal{A}_{ij} = 1$ ) or not ( $\mathcal{A}_{ij} = 0$ ).

We expect that the application of this emerging mathematical apparatus will shed new light on structural determinants of brain activity dynamics as observed in physiological experiments at different levels (e.g. single-neuron spike trains, local field potentials, electroencephalogram).

Partial funding by GIF is acknowledged.

[1] Watts DJ, Strogatz SH (1998) *Nature* **393**: 440–442

[2] Albert R, Barabasi A (2002) *Rev Mod Phys* **74**: 47–97

[3] Newman MEJ (2003) *Siam Rev* **45**(2): 167–256

## **Prey localisation by sand swimmer snakes using a population vector model**

Paul Friedel & J. Leo van Hemmen  
pfriedel@ph.tum.de  
Physik Department, TU München  
85748 Garching, Germany

For a long time, it was widely believed that snakes are deaf and cannot respond to sounds. Contrary to this believe, snakes are now known to be able to respond to sound and to vibrations.

Snakes can receive air-borne sounds, as well as ground-borne vibrations, which are transmitted to the inner ear via the lower jaw. Since the right and the left half of the lower jaw are not rigidly connected to allow swallowing of large prey, the hearing of stereo sound is possible. A rigid prove, however, that sound is indeed a biologically relevant stimulus for snakes has not been established until quite recently.

One of the most interesting experimental results is that snakes use vibrations for prey localization during hunting. In fact, sand swimmer snakes, which move and hunt below the surface of their desert habitat, are known to feed on sand swimmer lizards, which in turn feed on arthropods living under the sand surface, a technological war of submarines chasing each other.

To receive the sound waves generated by the prey, the snake not only uses its ears (through its jaws) but also a set of specialised vibration receptors, distributed over the face of the snake. Several thousands of receptors are present, which are clustered in small groups.

Comparing the arrival time of the sound signal at both ears directly gives the prey angle but it is of course impossible to compare the input signals from the enormous amount of vibration receptors one by one. Instead, we propose a population vector model.

This model consist of adding the directional contributions of all receptors, weighted by their firing rate, and finding the direction of the resulting vector, pointing to the prey. This simple procedure turns out to be enough for the snake to determine the striking angle with sufficient precision. A large advantage is that very simple neuronal processing suffices to achieve the biologically required degree of accuracy, which makes the estimate very robust.

We presume that the inner ear and the facial vibration receptors are used simultaneously to discern the precise location of the prey. Thus, with their inner ear and the specialised facial receptors, snakes have all the hardware they need to hunt their prey below the surface of the sand, where ordinary sensory systems are bound to fail.

# Non-hebbian synaptic plasticity allows for the stable implementation of one-shot predictive learning

Bernd Porr<sup>1</sup>, Florentin Wörgötter<sup>2</sup>

<sup>1</sup>Department of Electronics and Electrical Engineering, University of Glasgow, B.Porr@elec.gla.ac.uk

<sup>2</sup>Department of Psychology, University of Stirling, worgott@cn.stir.ac.uk

The central assumption of probably all biologically plausible learning algorithms is that the modification of synaptic weight follows the correlation between a pre-synaptic input signal with the post-synaptic output signal of a neuron (Hebb, 1949; Sutton and Barto, 1987; Porr and Wörgötter, 2003). In this study we show that learning can also be performed by correlating only pre-synaptic input signals with each other. In fact, we argue that such non-Hebbian learning is more stable and much faster than the traditional Hebbian learning, because even learning rates towards one are in principle permissive. We will first present the new learning rule and then show an application which demonstrates that it can be used in a behavioural task.

We take a summation unit which receives signals from two inputs  $x_0(t)$  and  $x_1(t)$  filtered by low pass filters  $h$  (see Fig. 1a):  $v = u_0(t) + \rho_1 u_1(t)$ ,  $u_{0,1}(t) = x_{0,1}(t) * h_{0,1}(t)$ . For simplicity, we consider only one synaptic weight  $\rho_1$ . In general, the summation needs not to be linear. We only require that the filter functions  $h$  must have a low pass characteristic. Furthermore, the derivative of  $u_0$  must be calculated to implement the learning rule as:  $\frac{d}{dt}\rho_1 = \mu u_1 u'_0$ , where  $\mu$  is the learning rate. Fig 1b shows the weight change depending on different temporal differences between  $x_0$  and  $x_1$ . Note that weight change is completely independent of the output signal  $v$  and, hence, independent of the actual weight  $\rho_1$ . Thus, the destabilising positive feedback effect of weight growth onto itself, which is common for Hebbian learning does not exist in our case. For Hebbian learning this leads to the fact that the learning rate  $\mu$  must be chosen small. Accordingly learning is slow. Here, on the other hand, we can choose large values for  $\mu$ , which leads to very fast learning. In an open loop situation, however, the weights will continuously grow. This is not the case in a closed loop setup. To demonstrate this we have simulated a simple behavioural task, where the behaviour leads to a negative feedback onto the inputs of the system, finally eliminating  $x_0$ . As a consequence, at reaching  $x_0 = 0$ , the weight  $\rho_1$  will no longer change. The task is to smoothly steer towards a bright spot from a distance (Fig. 1c, see (Porr and Wörgötter, 2003) for a similar setup). Initially the simulated agent will turn abruptly inwards on laterally touching the bright centre of the spot. A lateral touch of the spot corresponds to a signal  $x_0 \neq 0$  (right:  $x_0 > 0$ , left  $x_0 < 0$ ). During learning this reflex reaction will be superseded by a smooth turning reaction on encompassing the graded outer "sound" field which surrounds the spot (indicated by the gray shading). When this behaviour is successfully learned the spot will be touched centrally,  $x_0$  becomes zero and weight change stops. The results are shown in Fig. 1d. The graph shows the weight development during the experiment. It can clearly be seen that the weight  $\rho_1$  stabilises. Because we could use a high learning rate, the actual behaviour was correct after one trial and the weight finally stabilised after five trials. This approaches a one-shot learning condition and is in strict contrast to other learning schemes (Porr and Wörgötter, 2003; Sutton and Barto, 1987). A control performed on the same system with a more traditional differential Hebbian learning rule needed more than 30 trials (Porr and Wörgötter, 2003).

It is conceivable that such mechanisms for synaptic plasticity could be found in neurophysiology, both, at the neuronal and the dendritic level. On the neuronal level such plasticity can take place presynaptically with the help of neuromodulators, e.g.; dopamine (Ikeda et al., 2003). In this case the modulator takes the role of  $u'_0$  which facilitates a plastic synapse by increasing its gain until it has increased its own efficacy. At the level of a dendrite such interaction could in principle take place between closely adjacent structures, e.g. at spines or other specific synaptic structure (e.g.; triades in the thalamus, etc.)

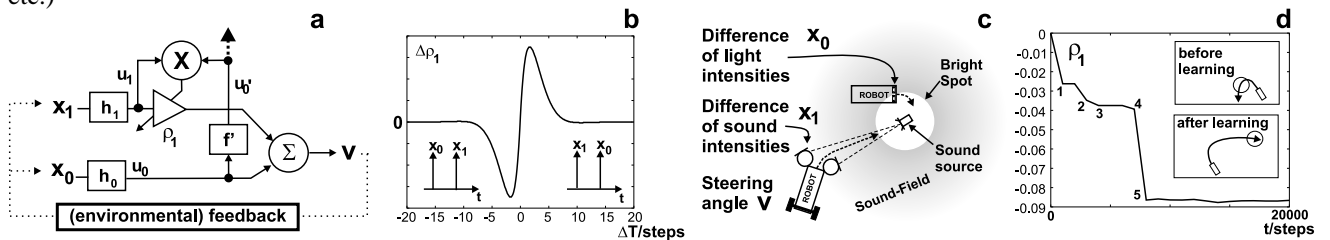


Figure 1: a) Circuit diagram of the learning scheme:  $h_0$  and  $h_1$  are low pass filters.  $\times$  is a multiplier,  $\rho_1$  a synaptic weight,  $f'$  the derivative, and  $\Sigma$  is a summation unit. b) Weight change curve depending on the temporal difference  $\Delta T$  between events at  $x_0$  and  $x_1$ . Low pass filters are 2nd order ( $Q = 0.51$ ,  $f = 0.1$ ). c) Simulated agent: Sound and light is emitted from a spot placed randomly in the simulated area.  $x_0$  = difference of the two light sensors.  $x_1$  = difference of the two sound sensors.  $v$  = steering angle.  $\mu = 0.004$ . Low pass filters as before. d) Weight development  $\rho_1$  during the experiment. The numbers are learning events. The full simulation can be seen at <http://www.cn.stir.ac.uk/predictor/forwardLearning/>.

# Model for attentional shift of the receptive field

T.Tzvetanov, T.Womelsdorf & S.Treue

Cognitive Neuroscience Laboratory,  
German Primate Center, Kellnerweg 4, 37077 Göttingen

Spatial attention to a region in the visual field overlapping the receptive fields (RFs) of sensory neurons typically enhances their response magnitude. This modulation has frequently been reported as a gain change, i.e. a multiplicative influence on sensory responses. Alternatively, attentional modulation has been described to bias competition of neuronal responses by mutual inhibitory interactions causing receptive fields to contract around attended visual stimuli.

We previously reported that attention shifts neuronal RFs in area MT of macaque monkey visual cortex towards the attended location without a systematic shrinkage of the RFs. Here we present a simple two-layer feedforward model that reproduces the observed RF shift and predicts attentional shift of RF center with size shrinkage dependence on attentional spread, based only on multiplicative interactions between sensory representations and attentional influences.

**Model** The model consists of two layers connected with a simple feedforward mechanism represented by a Gaussian connectivity profile (continuous curve in figure 1) with attention acting multiplicatively on the feedforward input connections. The model assumes a Gaussian shaped attentional influence (dotted curve). The response of layer 2 neuron with an initial RF center and size is modified, and the new parameters of the RF of the neuron computed. Moreover, we can redefine the attentional spread relative to the RF size ( $\sigma_{Att} = k\sigma_R$ ). This allows us to compute the new RF parameters, i.e. its new center, size and amplitude, as a function of only two parameters,  $k$  and the distance between the original RF center and the attentional center.

**Results** The model explains the neurophysiologically observed RF shift. Furthermore, it estimates the spread of the attentional focus given the observed attentionally modulated RF parameters. In our neurophysiological experiments we observed an average RF shift of 28% of the RF distance to the attentional focus. The average RF radius was  $7.4^\circ$ . With this data, the parameter  $k$  of the model is 1.6, indicating a radius of the attentional spotlight of about  $12^\circ$ , well in line with psychophysical estimates. Moreover, the model predicts changes in RF size with attention, i.e. a RF shrinkage but only when the spread of the attentional focus is smaller than twice the size of the RF of the neuron.

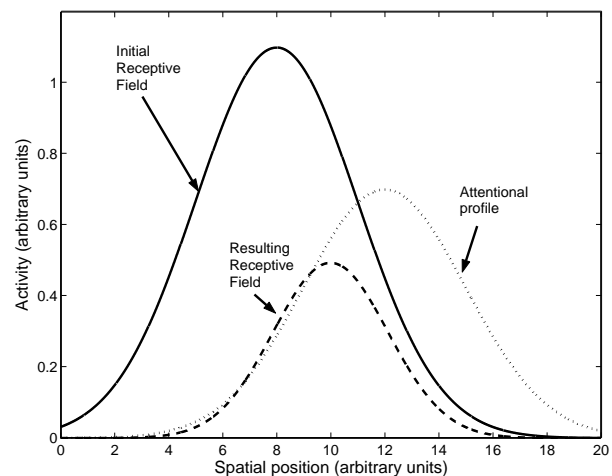


Figure 1: Example of theoretical RF profile (continuous curve), modulated by a Gaussian shaped attention (dotted line), and the new RF (dashed curve).

## Dynamic computations in network models of the olfactory bulb

Martin T. Wiechert, Benjamin Judkewitz, Rainer W. Friedrich

*Max Planck Institute for Medical Research, Jahnstr. 29, D-69120 Heidelberg*

Mitral cells (MCs) in the olfactory bulb (OB) receive input from sensory neurons and form a complex network together with inhibitory interneurons (mainly granule cells; GCs). Odor-evoked activity patterns across MCs are temporally structured on at least two time scales: (1) during the first few hundred milliseconds, the firing pattern across the MC population changes profoundly. (2) Odor-specific subsets of MCs transiently synchronize their action potentials with millisecond precision and phase-lock to an oscillation in the local field potential (LFP). The dynamics of MC activity patterns results in at least two computations: (1) a decorrelation of initially similar activity patterns evoked by related odors<sup>1,2</sup>, and (2) synchrony-based multiplexing of information, i. e., patterns of asynchronous and synchronized MC spikes simultaneously convey information about different stimulus features (identity and category, respectively)<sup>3</sup>. Here we used mathematical models and biophysical simulations, constrained by physiological and anatomical data, to explore network interactions underlying these computations.

First, a purely rate-based model consisting of analog neurons with piecewise linear gain function was constructed. Two reciprocally interacting cell populations, namely excitatory MCs and inhibitory GCs were considered. This model does not describe neuronal activity on fast (millisecond) time scales and, thus, does not take into account neuronal synchronization. Nevertheless, it reproduces the temporal decorrelation of input activity patterns as well as other properties of odor responses in the OB.

Second, we constructed a more detailed, conductance-based simulation. Each neuron was modeled as single compartment containing standard Hodgkin-Huxley conductances, and only conventional synaptic currents were used. Network topology and stimulus patterns were as in the first model. For a certain parameter range, this simulation could reproduce both the decorrelation of slow temporal activity patterns and synchrony-based multiplexing. These results

- suggest mechanisms by which neuronal circuits in the OB achieve a contrast enhancement between representations of similar odors,
- show that seemingly complex activity patterns can arise from synaptic interactions in a network without assuming complex physiological properties of individual neurons,
- demonstrate that rate-based and spike timing-based coding can coexist in relatively simple neuronal networks, and
- suggest that spatial patterning of glomerular input activity may be important for computations in the OB.

Supported by DFG (SFB 488) and Max-Planck-Society.

<sup>1</sup> Friedrich RW, Laurent G (2001) Science 291:889-894.

<sup>2</sup> Friedrich RW, Laurent G (2004) J Neurophysiol 91:2658-2669.

<sup>3</sup> Friedrich RW, Habermann CJ, Laurent G (2004) Nat Neurosci 7:862-871.

# Sleep stage and cycle specific properties of oscillatory events in the human sleep EEG

E. Olbrich<sup>1</sup> and P. Achermann<sup>2</sup>

<sup>1</sup>Max Planck Institute for Mathematics in the Sciences, Leipzig, Germany

<sup>2</sup>Institute of Pharmacology and Toxicology, University of Zurich, Zurich, Switzerland

The different brain states during sleep are characterized by the occurrence of distinct oscillatory patterns such as spindles or delta waves. We studied the change of their properties in the course of the night.

Sleep EEG data of 8 healthy young males were analyzed (4 nights lasting 8 h, C3-A2 derivation, sampling rate 128 Hz). By estimating autoregressive (AR) models on 1-s EEG segments, the EEG may be described as a superposition of stochastically driven harmonic oscillators with damping and frequency varying in time. Oscillatory events were detected, whenever the damping of one or more frequencies was below a predefined threshold.

Oscillatory events in the human sleep occurred essentially in three frequency bands: sigma (11.5-16 Hz), alpha (8-11.5 Hz) and delta (0.75-4.5 Hz). Their incidence showed only small intra- but large inter-individual differences (Fig. 1). Visual inspection of selected events revealed that the events in the sigma band corresponded basically to sleep spindles, while the events in the delta band were fast ( $> 2$  Hz) delta waves, K-complexes or slow delta oscillations (0.5-2 Hz). Regarding events in the alpha frequency band subjects could be divided into two groups: One showing large amount of oscillatory events in the alpha frequency band (subjects 05,06,15 - high alpha group) and one showing a few or almost no alpha events (low alpha group).

As expected, the highest incidence of sleep spindles was observed in sleep stage 2 while delta events occurred most frequently in sleep stage 4. The alpha event density in the high alpha group was maximal in deep sleep. The mean frequencies of delta events and spindles decreased with the deepening of sleep (Fig. 2). The density of delta events was highest in the first NREM sleep episode and lowest in the third one while the density of sleep spindles increased monotonically in the course of the night. If the analysis was restricted to sleep stage 2 the mean frequency of both delta oscillations and sleep spindles was highest in the first cycle and lowest in the second one, while increasing again in the later cycles.

These results indicate a connection between delta oscillations and sleep spindles beyond the complementary relationship (the more delta waves the less spindles) described in earlier studies.

*Research supported by the Swiss National Science Foundation, the Wolfermann-Nägeli Foundation and the Max Planck Society.*

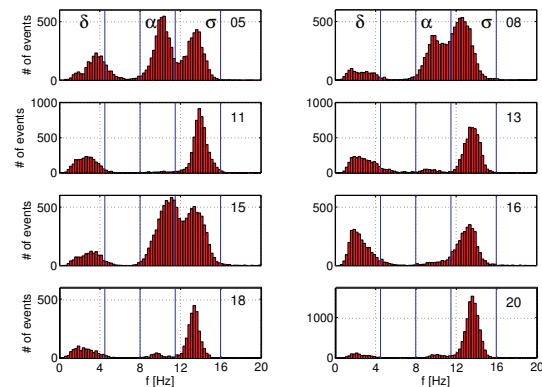


Figure 1: Distributions of the frequency of the detected events of the 8 subjects. Numbers are subject identifier.

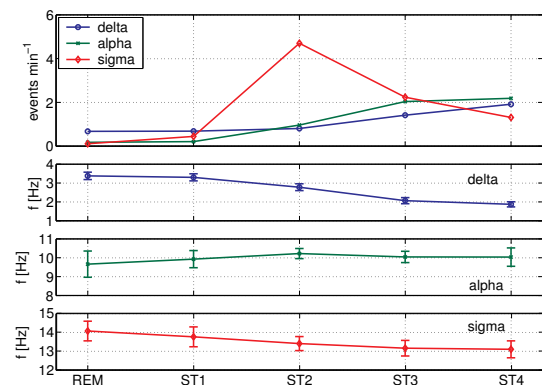


Figure 2: Event density (top) and mean event frequency as function of sleep stage. REM ... REM sleep, ST1-ST4 ... NREM sleep stages 1-4.



## Scaling properties of dendrites of pyramidal neurons in wildtype and p21H-ras<sup>Val12</sup> transgenic mice

<sup>1</sup>Andreas Schierwagen, <sup>1</sup>Alexander Schubert, <sup>2</sup>Alán Alpár, <sup>2</sup>Ulrich Gärtner, <sup>2</sup>Thomas Arendt

<sup>1</sup>Institute for Computer Science, University of Leipzig, D-04109 Leipzig, Germany

<sup>2</sup>Department of Neuroanatomy, Paul Flechsig Institut for Brain Research, University of Leipzig, D-04109 Leipzig, Germany;

Recent studies have documented the effect of postmitotic expression of constitutively active p21Ras on the adult neocortex in p21H-Ras<sup>Val12</sup> transgenic mice. If compared with the wildtype, the volume of cerebral cortex is increased in these animals by approximately 20%, due to the enlargement of pyramidal cells [1]. Pyramidal neurons in layer II/III are characterised by a significant somal and dendritic growth and establish a more ramified, complex dendritic tree [2].

Dendritic morphology is the structural correlate for receiving and processing inputs to a neuron. An interesting question then is what the design principles and the functional consequences of enlarged dendritic trees might be. As yet, only a few studies have examined the effects of neuron size changes. Two theoretical scaling modes have been analyzed, conservative (isoelectrotonic) scaling (preserves the passive and active response properties), and isometric scaling (steps up low pass-filtering of inputs). Both scaling modes were verified in neuroanatomical studies [3]. They are only two among many patterns of growth in which the diameters of dendritic segments change according to a functional relationship to their increase in length.

In the present study we used multicompartmental modeling to explore the scaling mode realized by the larger and more complex dendritic trees of transgenic mice pyramids. Two sets of pyramidal neurons (28 cells from wildtype and 26 cells from p21H-ras<sup>Val12</sup> transgenic mice) were reconstructed and digitized using Neurolucida<sup>TM</sup>, as described elsewhere [2]. The morphology files created were edited and converted with CVAPP, a free Java application [4], into the file format necessary for using them as cell description files in the simulation package NEURON.

The simulations were used to calculate the morphoelectrotonic transform (MET) of each neuron. The MET maps the neuron from anatomical space into electrotonic space, using the logarithm of voltage attenuation as the distance metric. Since attenuation depends on signal frequency and propagation direction, we calculated METs at several different frequencies and for somatopetal and somatofugal inputs, respectively.

The statistical analysis of the sample METs computed with NEURON showed partly significant differences, mainly of the properties related to branching orders higher than five of both basal and apical dendrites. The results partly depend on input frequency and direction of signal spread. In conclusion, our results suggest a differentiated impact of p21Ras on the dendritic growth pattern and integrative function, with little changes of the inner part of the MET.

### References

- [1] R. Heumann et al., J. Cell. Biol. 151 (2000) 1537–1548.
- [2] A. Alpár et al., J. Comp. Neurol. 467 (2003) 119–133.
- [3] O.H. Olsen et al., J. Neurophysiol. 76 (1996) 1850–1857.
- [4] R.C. Cannon, (2000). <http://www.compneuro.org/CDROM/nmorph/usage.html>

Supported by Deutsche Forschungsgemeinschaft (grant GA 716/1-1), Hirnliga e. V., and Interdisciplinary Center for Clinical Research at the University of Leipzig (IZKF-C1).

# Retino-cortical magnification on naturally curved human cortical surfaces

Jan Tusch and Markus A. Dahlem

Department for Neurology II, Otto-von-Guericke University Magdeburg and  
Leibniz-Institute for Neurobiology, Magdeburg.  
{jan.tusch,dahlem}@ifn-magdeburg.de

A retinotopic map in primary visual cortex (V1) is usually specified by local linear cortical magnification factors that indicate the relationship between small displacements in retinal eccentricity and azimuthal coordinates and the corresponding displacements in cortical coordinates. The map is completely specified if the Jacobian matrix, a  $2 \times 2$  matrix of first-order partial derivatives, is known at each point. Experiments usually characterize only one or two derivatives, or may only provide an areal magnification factor defined by the Jacobian determinant. To compensate these deficits maps are assumed to be conformal, i.e. locally isotropic, and sometimes even meridionally symmetric. Another simplification of the retino-cortical map is introduced by measuring cortical displacements on flattened cortex.

We apply Kohonen's self-organizing feature map algorithm to obtain retino-cortical maps. The training set is chosen such that its density function meets the requirements usually imposed on simplified retino-cortical maps (inverse-linear magnification, isotropy, etc.). The set is learned on a curved Kohonen-layer reconstructed from MRI data representing the human cortical surface. The delineation of V1 on the cortical surface was estimated assuming two-thirds of V1 within the calcarine sulcus beginning near the occipital pole and extending half way along the calcarine fundus. Overall size of about  $2400 \text{ mm}^2$  was used as cross-check.

The naturally curved Kohonen-layer learns to preserve the topology of the training set. Without external supervision fovea and horizontal meridian are represented close to their natural position on the cortical surface. Isotropy or meridional symmetry are not preserved, because the curved cortical surface can not correctly represent the training set without distortions. It remains to be seen whether the observed deviations from conformal mapping due to anatomical landmarks are in agreement with individual retinotopic maps obtained from fMRI.

**Attractor model of the primary visual cortex based on its  
functional properties**

**Dmitri Bibitchkov, Barak Blumenfeld, Shmuel Naaman,  
Amiram Grinvald and Misha Tsodyks**

*Department of Neurobiology, Weizmann Institute of Science,  
76100 Rehovot, Israel*

Voltage-sensitive dye imaging of area 17/18 in the anesthetized cat reveals that primary visual cortex is able to generate patchy patterns of neural activity both in response to visual stimulation and spontaneously [Kenet *et. al.*, 2003]. In particular, some of the spontaneously emerging patterns are similar to those evoked by moving gratings of various orientations. We suggest that these patterns can be generated by an intracortical network which has intrinsic preferred states correlated with functional maps. We derive possible connections in such a network from a set of single condition orientation maps. We assume that the maps are attractors of a recurrent neural network and use a modified version of the pseudo-inverse rule of the Hopfield network to model its connectivity [Personnaz *et al.*, 1985]. The resulting long-range connections depend mainly on the selectivity properties of the interacting columns. The coupling strength depends on the difference between the preferred orientations of the connected neurons and strongly correlates with the product of their tuning strengths. This connectivity pattern can be approximated by a simple rule which incorporates both dependencies. The network with this connectivity rule can be treated analytically, and expressions for the attractors and conditions for their stability can be calculated. The full pseudo-inverse model also suggests the dependence of connectivity on a distance between neurons in the form of a Mexican-hat function. The dependence of the obtained synaptic weights on the distance correlates with the pattern of correlations in the recorded spontaneous activity, suggesting that intrinsic connectivity in neuronal networks in this area of the brain underlies the activity in both spontaneous and evoked regimes. Supported by Israeli Science Foundation, Heineman Foundation and Minerva Foundation.

## How to switch from standing to walking

Oliver Straub, Nelly Daur, Jessica Ausborn, Wolfgang Mader & Wolfgang Stein

wolfgang.mader@biologie.uni-ulm.de

www.neurobio.de/MadSim

Abteilung Neurobiologie, Universität Ulm

D-89069 Ulm, Germany

All animal behavior is characterized by the movement of the body and by its response to sensory stimuli. The nervous system shows a great plasticity in the processing of sensory information and thus also in its response to such information. Here, we tried to combine the physical structure of the nervous system with the activity of nerve cells and the required computation within the nervous system. We used an insect model system, the femur-tibia joint control system of the stick insect, for the investigation of how the nervous system can switch between two different motor outputs, walking and standing. For this task, the nervous system has to toggle from a static joint control during standing (resistance reflex, Fig. 1 top) to movement control of the limbs (reflex reversal, Fig. 1 bottom) when the animal starts to walk although it receives the same sensory input.

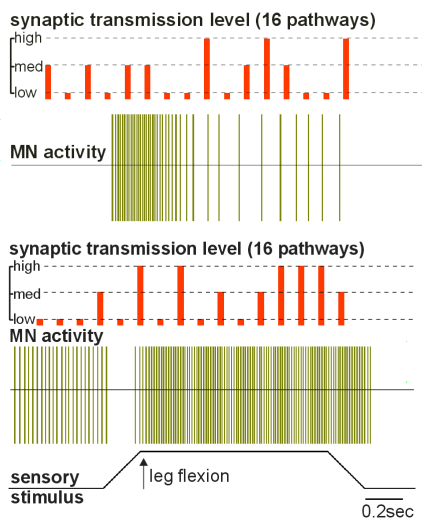


**Fig. 1:** Different motor outputs. MN: Motoneuron. Red bars indicate synaptic transmission levels of interneuron pathways.

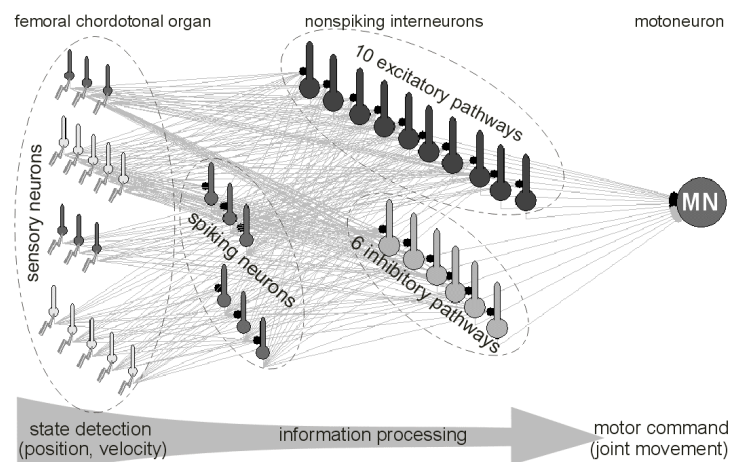


**Fig. 2:** Simulated femur-tibia joint control system with information flow. Small arrows: Current injections.

We used a computer simulation based on the known network structure (Fig. 2, an extension of Sauer, Driesang, Büschges, Bässler, *J comput Neurosci* 3, 1996) to permute the strength of specific identified nonspiking interneuronal pathways (Büschges, *J exp Biol* 151, 1990; Stein, Sauer, *J comp Physiol A* 183, 1998) which process velocity and position information from leg proprioceptors. Two independent analysis of the resulting database of more than 43 million network outputs showed that the same neural network can produce the two different behaviors by specifically altering the weighting of interneuronal pathways. We obtained specific combinations of pathway transmission levels for each behavior (Fig. 1, red bars on top of motoneuron activity). This means, that solely changing the pathway transmission strengths is sufficient to switch between different behaviors, like from standing to walking. In our model this was achieved by activating or deactivating additional network parts. During walking, the transition between stance and swing phase of the leg is likely to be produced by these components, for example by a relaxation oscillator (Driesang, Büschges, *J comp Physiol A* 179, 1996). In a reduced model in which the femur-tibia control system was provided with such an oscillator circuit, the network only generated the appropriate output when position, but not velocity information was fed into this circuit. This was achieved by either applying a negative velocity signal to the oscillator (Bässler, Koch, *Biol Cybern* 62, 1989) or by providing the oscillator with a strong position dependent switch that rapidly attenuated velocity information. The latter circuit predicted a dependence of the transition between stance and swing phase on the velocity of the leg movement. We are currently testing this prediction with measurements of the leg movement in a walking animal.

In conclusion, our results show that the same neuronal network can produce two different behaviors (standing and walking in the stick insect) despite having the same sensory information. The transition between both behaviors can be produced by specific changes in the weighting of parallel information pathways to the motoneuron. Those changes seem to be implemented by a relaxation oscillator circuit that resides presynaptically to the known interneuronal pathways.

## Interaction of sensory feedback and central network in the locust flight control system: a modeling study

Jessica Ausborn, Wolfgang Mader, \*Heiko Neumann & Harald Wolf

Abteilung Neurobiologie & \*Abteilung Neuroinformatik  
Universität Ulm  
D-89069 Ulm, Germany  
jessica.ausborn@biologie.uni-ulm.de  
www.neurobio.de/madsim

Networks that control motor behavior are often well understood with regard to their cybernetic properties and the cellular functions of involved neurons. By contrast, the functional consequences of the underlying network structure often remain unclear. The goal of the present study is to examine possible relationships between network structure and network function in the locust flight control circuit.

Previous simulations employing simpler models were able to demonstrate basic features such as robustness resulting from network redundancy (Grimm & Sauer 1995, Biol. Cybern. 72). However, they could not reproduce more subtle features such as graded transmitter release or dynamic spike frequency ranges up to 300Hz, which may well prove relevant for network function.

To investigate structure - function relationships in the central pattern generator of locust flight, we used the simulation environment *madSim* (Mader et al. 2003, Proc. Goettingen Neurobiology Conf. 29: 1055). Multi-compartment neurons with Hodgkin-Huxley-like currents (Hodgkin & Huxley 1952, J. Physiol 117) were used to model the neural network (see Fig.) based on the known connectivity of the interneurons in the flight central pattern generator.

The locust flight control circuit is electrophysiologically well-studied and at the same time sufficiently complex (e.g. Robertson & Pearson 1984, J. Insect Physiol. 30) to show emergent network properties.

In our studies, particular emphasis is on the functional relevance of (i) interconnected neuron circles with recurrent inhibition, (ii) structural redundancy and functional robustness and (iii) integration of sensory feedback into central network function.

The latter aspect is the present focus of our work. Two sets of wing receptors are of particular importance for flight pattern generation. These are the wing stretch receptors and the tegulae (Wolf & Pearson 1988, J. Neurophysiol. 59). They signal upper and lower stroke reversals, respectively, and the tegula effectively resets the wing stroke. Connectivity with flight interneurons is well-known for the tegula, however, the functional relevance of these connections (and their relative synaptic strengths) in comparison to external reflex pathways is not understood. We are currently investigating these aspects.

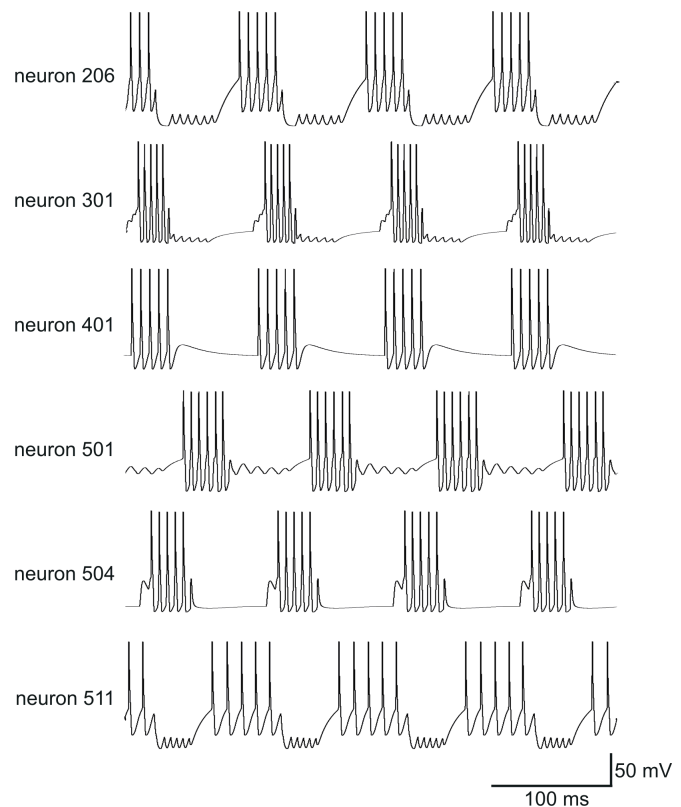


**Fig.:** Oscillations in simulated interneurons of the flight control circuit (nomenclature from Robertson and Pearson 1983, J. Comp. Neurol. 215).

## Poster Subject Area #PSA35: Methods and demonstrations

- [#460A](#) A. Pazienti and S. Grün, Berlin  
*Influence of Spike Sorting Errors on Unitary Event Statistics*
- [#461A](#) R. Vollgraf, M. Munk and K. Obermayer, Berlin and Frankfurt/Main  
*Spike Sorting of Multi-Site Electrode Recordings Based on Amplitude Ratios*
- [#462A](#) R. Ritz, T. Förster and A.V. Herz, Berlin  
*NIPClassifier: Contributing to an evolvable neuroinformatics ontology*
- [#463A](#) M.A. Gaudnek, A. Hess, K. Obermayer, L. Budinsky, K. Brune and M. Sibila, Berlin and Erlangen/Nürnberg  
*Geometric reconstruction of the vascular system imaged by MRA, supporting the spatially confined analysis of fMRI Bold signals with respect to the vascular system.*
- [#464A](#) K. Meller and C. Theiss, Bochum  
*A synergy of technologies: combining confocal laser scanning microscopy and atomic force microscopy to study the cytoskeleton*
- [#465A](#) F. Bussmann and A. Hess, Erlangen/Nürnberg  
*Robust vital monitoring support for neurophysiologic experiments in animals even inside MRI scanners*
- [#466A](#) R. Meier, A. Schulze-Bonhage, A. Cichocki and A. Aertsen, Freiburg and Wako-shi (J)  
*Artifact removal from the EEG – Blind source separation and complex artifacts*
- [#467A](#) M.C. Wehr, R. Laage, K.-A. Nave and M.J. Rossner, Göttingen and Heidelberg  
*Measuring and Visualizing Protein-Protein-Interactions in Living Cells Using a Protease-based Complementation System*
- [#468A](#) R. Tammer, L. Ehrenreich, S. Boretius, J. Frahm and T. Michaelis, Göttingen  
*3D MRI visualisation of microelectrodes in the brainstem of the squirrel monkey*
- [#469A](#) P.S. Salonikidis, F.S. Wouters and D.W. Richter, Göttingen  
*Using a combination of FRET/FLIM and electrophysiology to study GPCR-signalling pathways*
- [#470A](#) M.W. Nolte, W. Loscher and M. Gernert, Hannover  
*High frequency stimulation of the subthalamic nucleus – Investigations in the kindling model of epilepsy*

- [#471A](#) J. Reidel, D. Omer-Backlash, A. Grinvald, J. Starke and H. Spors, Heidelberg and Rehovot (IL)  
*Identifying neuronal ensembles in the olfactory and visual systems using independent component analysis (ICA)*
- [#460B](#) T. Strekalova, O. Dolkov, N. Gorenkova and D. Bartsch, Mannheim  
*Distinct behavioral and cognitive correlates of hedonic deficit and chronic stress in a new model of stress-induced anhedonia in mice*
- [#461B](#) T. Strekalova, O. Dolgov, N. Gorenkova and D. Bartsch, Mannheim  
*Distinct behavioral and cognitive correlates of hedonic deficit and chronic stress in a new model of stress-induced anhedonia in mice*
- [#462B](#) HA. Braun, H. Schneider, B. Wollweber, N. Anthes and K. Voigt, Marburg  
*Virtual Neurophysiology Labs for Students Practical Courses: cLabs-Neuron and cLabs-SkinSenses.*
- [#463B](#) SB. Cambridge, B. Cürten and T. Bonhoeffer, Munich/Martinsried  
*A Caged Doxycycline Analog for Photoactivated Gene Expression with High Spatiotemporal Resolution*
- [#464B](#) R. Blum, GM. Durand, N. Marandi, S. Herberger and A. Konnerth, München  
*Quantitative single cell RT-PCR and calcium imaging in acute brain slices*
- [#465B](#) A. Santoso, A. Kaiser and Y. Winter, Planegg/Martinsried  
*Stress-free oral administration of drugs in group-living mice through a transponder-controlled water dispenser*
- [#466B](#) MS. Dittmar, NP. Fehm, B. Vatankhah, G. Schuierer and M. Horn, Regensburg  
*Ischemic etiology of masticatory lesions in the MCAO filament model is questionable*
- [#467B](#) O. Schmitt, S. Wirtz, J. Modersitzki, B. Fischer, S. Heldmann and A. Wree, Rostock, Lübeck and Atlanta, GA (USA)  
*Direct access to all cells of a mouse brain*
- [#468B](#) MP. Bonomini, JM. Ferrandez and E. Fernandez, Elche (E) and Cartagena (E)  
*Datase1: an open source tool for the classification of multielectrode data*
- [#469B](#) W. Hanke, Stuttgart  
*Using the Retinal Spreading Depression for neuropharmacological studies*
- [#470B](#) BA. Müller, H. Scheich and J. Goldschmidt, Ulm and Magdeburg  
*Patterns of neuronal activity in cerebral cortex of anaesthetized mice - a thallium uptake study*

# Influence of Spike Sorting Errors on Unitary Event Statistics

Antonio Pazienti and Sonja Grün

Neuroinformatics, AG Neurobiology, Free University, Berlin, Germany

{antonio.pazienti}{gruen}@neurobiologie.fu-berlin.de

The aim of spike sorting is to reconstruct single unit signals from multi-unit recordings. Failure in the identification of a spike or assignment of a spike to a wrong unit are typical examples of sorting errors. We refer to them as false negative errors (FN) and false positive errors (FP), respectively. Sources of such errors may be e.g. noise classified as spiking activity, waveforms distorted by sampling or overlapping spikes, changes of spike shapes during the experiment, etc and any combinations of those. Harris et al. [1] estimated experimentally spike sorting error rates by comparing extracellular and intracellular measurements and found average error rates of 6.2 % for FP and 15.9 % for FN.

Earlier studies [2, 3] focused on the influence of unresolved multi-neuron recordings, e.g. multi-unit activity, on the cross-correlation measure. They found that synchronization between unresolved spike recordings may lead to an overestimation of the correlation between two spike trains. We are interested to estimate the influence of spike sorting errors onto the evaluation of spike synchronization by the Unitary Event analysis (UE) [4]. UE analysis detects the presence of conspicuous spike coincidences in multiple parallel spike recordings and evaluates their statistical significance. The method enabled us to study the relation of spike synchronization to behavioral events [5, 6]. Here we study if spike sorting errors (FN and FP) may lead to an under- or overestimation of the significance of spike synchronization as compared to the original data, and concentrate for now on the case of  $N = 2$  neurons.

In the UE analysis, the empirically found number of coincidences  $n_{emp}$  is compared to the number of coincidences expected by chance given the rates of the neurons ( $n_{pred}$ ). In the case of stationary Poissonian processes the latter can be estimated by the product of the firing rates. The significance of the deviation is evaluated by the joint-surprise measure  $S(n_{emp}, n_{pred})$  [4]. All of these measures are influenced by spike sorting errors. Assuming uniformly distributed errors over the data, we are able to compute the empirical number of coincidences  $n_{emp}^\sigma$ , the expected number  $n_{pred}^\sigma$  and the significance as a function of the error rates  $\sigma^+$  for FP and  $\sigma^-$  for FN. Trivially, sorting errors influence the rate estimate: FP enhance and FN reduce the rate estimate proportional to the error rates:  $p^\sigma = p \cdot (1 + \sigma^+ - \sigma^-)$ . Since  $n_{pred}^\sigma$  is estimated based on the product of the firing rate estimates  $p^\sigma$ , it is affected quadratically. The relationship between  $n_{emp}^\sigma$  and  $n_{emp}$  is obtained analytically as well as on the basis of simulations. These measures enable us to obtain the relation between the experimental significance and the original one. Interestingly, even for the case of no false negatives but only false positives the significance of synchronized activity is reduced. Additional presence of FN further decreases the significance.

In future work we will study also cases with  $N > 2$  neurons. In addition we will relax the assumption of uniformly distributed errors and include more specific assumptions e.g. about overlapping spikes.

- [1] K.D. Harris, D.A. Henze, J. Csicsvari, H. Hirase and G. Buzsàki (2000) J Neurophysiol 84(1): 401–414.
- [2] P. Bedenbaugh and G.L. Gerstein (1997) Neural Computation 9: 1265–1275.
- [3] G. L. Gerstein (2000) J Neurosci Meth 100(1–2): 41–51.
- [4] S. Grün, M. Diesmann and A. Aertsen (2002) Neural Computation 14: 43–80.
- [5] A. Riehle, S. Grün, M. Diesmann, and A. Aertsen (1997) Science 278: 1950–1953.
- [6] A. Riehle, F. Grammont, M. Diesmann and S. Grün (2000) J Physiol (Paris) 94(5–6): 569–582.

Acknowledgments: Partial funding by the Volkswagen Foundation and the Stifterverband für die Deutsche Wissenschaft.



# Spike Sorting of Multi-Site Electrode Recordings Based on Amplitude Ratios

Roland Vollgraf<sup>1</sup>, Matthias Munk<sup>2</sup> and Klaus Obermayer<sup>1</sup>

<sup>1</sup> Berlin University of Technology, Sekr. FR 2-1, Franklinstr. 28/29, 10587 Berlin

<sup>2</sup> Max-Planck-Institut für Hirnforschung, Deutschordenstraße 46, 60528 Frankfurt am Main

We present a method for spike detection and spike sorting of extra-cellular multi trode recordings. The method is based only on the amplitude ratios of the action potentials, and hence is appropriate for data where wave forms vary only slightly between the recorded units and the recorded channels. In order to reduce the distortion of the amplitudes for overlapping spikes, a linear filter is applied, which is optimal in the sense that it responds to the wave form with the narrowest possible impulse. Overlapping action potentials are thus transformed into overlapping narrow impulses, which can be resolved, if the temporal distance between them is larger than the impulse width.

If the wave form is known, the objective for the optimal filter can be formulated as the squared sum over the response to this wave form. This objective has to be minimized under the constraint of unit amplitude at the center of the response. This leads to a quadratic optimization problem with a linear constraint, which can be solved in closed form. For noise corrupted inputs the complexity of the filter has to be limited in order to achieve a reasonable SNR in the output. Note that also the background neural activity contributes to the (colored) noise. We introduce a regularization term into the cost function, which controls the tradeoff between sharpness of the response and noise suppression.

We then show that the optimal filter can also be estimated blindly from the raw recordings, i.e. without prior knowledge of the wave form. Therefore we assume as a data generating model that the recorded spike trains are binary spike trains with low firing rate, which are convolved with the wave form and corrupted by colored noise. Under this assumption we can show that solving above mentioned optimization problem is equivalent to maximizing the skewness of the filtered recordings. We derive an iterative learning algorithm, similar to *FastICA*, which yields the optimal filter without knowledge of the wave form in advance. The wave form can then be expressed as a function of the optimal filter in closed form. Fig. 1 shows an example of a filter, the corresponding wave form and its response that have been derived from tetrode recordings from cat visual cortex.

Once the optimal filter has been learned, the amplitudes of the impulses in the filtered recordings can be taken as estimates of the amplitudes of the action potentials. They are more reliable estimates than the peaks of the actual wave form, in particular, if spikes overlap (cf. Fig. 2). Events are detected using the Mahalanobis distance w.r.t. the covariance of the background noise as a distance measure, and the event amplitudes are clustered in order to assign events to individual units. Although any clustering algorithm would perform well, we applied a Gaussian mixture model, because it allows the assignment of class probabilities.

The new method is fast and robust, and we demonstrate its performance by applying it to real tetrode recordings of spontaneous activity in the visual cortex of an anesthetized cat.

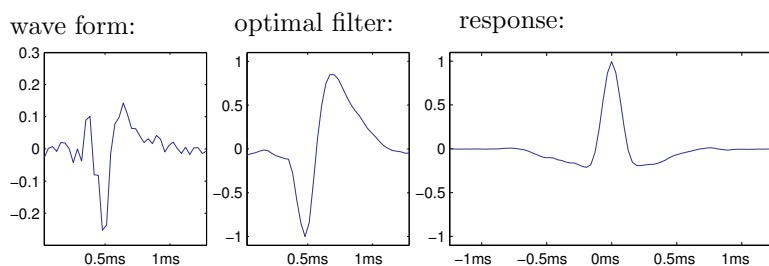


Figure 1: *Left:* Optimal linear filter achieved through skewness maximization on real tetrode recordings of the visual cortex of an anesthetized cat. *Center:* Wave form derived from the filter. *Right:* Response of the filter to the wave form. The response is narrow and the undershoots are greatly reduced.

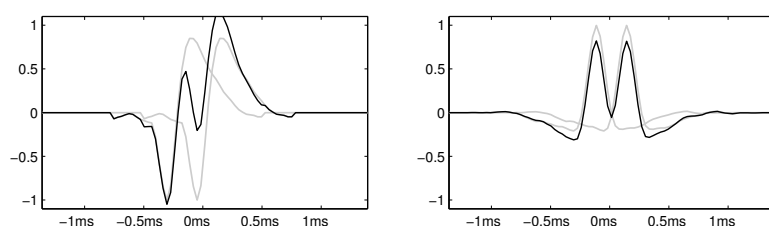


Figure 2: *Left:* Two overlapping wave forms with 0.25ms delay (gray lines) and their sum (black line). The individual peaks cannot be resolved in the summed signal. *Right:* After filtering, both spikes are separable (cf. Fig. 1, right, for the filter response).

## NIPClassifier: Contributing to an evolvable neuroinformatics ontology

Raphael Ritz, Thomas Förster, and Andreas VM Herz

Institute for Theoretical Biology, Humboldt–University Berlin, Invalidenstr. 43, D–10 115 Berlin, Germany

The Neuroinformatics Portal Pilot (NIP; <http://www.neuroinf.de>) is part of a larger effort to promote the exchange of neuroscience data, data-analysis tools, and modeling software [1, 2]. We develop the basic infrastructure needed for an optimal utilization of the many available resources on the web. Conceptual and technical problems have to be solved before the Portal can serve the community in a most efficient way. In this contribution, we describe the design and planned usage of NIP’s classification system.

At NIP any content can be classified by relating it to an arbitrary number of existing keywords. In addition, every user can propose new keywords together with a brief description defining the meaning of the new term as well as its relationships to the already existing terms. Keyword submissions are then treated just like any other content submission and in case of acceptance the new term will be generally available to all (including its relations to other terms). This will make it possible to build up and maintain an up-to-date keyword base to classify any content of interest to the community.

*User Interface:* The approach sketched above will lead to a substantial amount of terms (on the order of thousands and above) which will make it hard for the user to directly interact with it via the web. It is just impracticable to put such an amount of terms in a selection box to choose from. Therefore specifying keywords (for classifying content as well as for formulating searches) is usually a two step process: First you enter the term that you expect to be a keyword, then in a second step this term is looked up in the keyword base. If there is an exact match then this term is taken literally; otherwise the system tries to infer related terms and it will ask you to select from those. Currently this inference is based on syntactic similarity (using the algorithm by Ratcliff and Obershelp) but more powerful inference engines are to be included as NIP further develops.

*Establishing Relationships Between Keywords:* Since keywords themselves are treated as content items it is also possible to establish arbitrary relationships between different keywords. Examples are *is parent of/is child of* to establish tree structures or *is synonym of* to allow several terms to be used for the same concept (think of abbreviations or different languages). It is even possible to have the same term referring to different concepts, e.g., *neuron* can be used to generally specify a nerve cell or the simulation software package of that name. To the latter end, there are two keyword items with the same name but different identifiers, descriptions etc. related via *not the same*. Just as with the keywords themselves, every user of the portal can propose to add such a relationship between keywords. Based on this approach, it will become feasible to incorporate an increasing amount of knowledge into the system.

*Inference:* The advantages of this approach become obvious when considering questions like *What’s related?* starting from an individual content item. Most often one would also like to know *...and why?* or *...how closely?* something else is considered related. To this end, NIP’s classification system allows for introspection (answering *why*) as well as ranking of relationships (answering *how close*). The ranking is established by assigning appropriate weights to the relationships between keywords (e.g., 0.5 for *is parent of* or 1 for *is synonym of* or 0 for *not the same*) and then multiplying all weights along the shortest possible path from one content item to the other based on their classification. How to best choose the weights and even let the user manipulate these weights for certain tasks is an open question and the matter of ongoing research in the field of machine learning and artificial intelligence.

*Outlook:* As NIP’s classification system described here is currently a pilot project, further developments are to be expected. You are invited to browse the site and to join the portal community to actively contribute content, keywords, relationships, and therefore knowledge. The more you do so, the more useful the portal will be to the whole community.

Supported by BMBF

- [1] R. Ritz, R. Förster and A.V.M. Herz, Facilitating data and software sharing in the neurosciences – a neuroinformatics portal, in: R. Kötter, ed., *Neuroscience Databases: A Practical Guide* (Kluwer, Norwell, MA, 2003) 293–306.
- [2] R. Ritz, R. Förster and A.V.M. Herz, Internetplattform Neuroinformatik: A Pilot Study for the OECD Neuroinformatics Portal, *Neurocomputing*, 52–54 (2003) 335–340.

## **Geometric reconstruction of the vascular system imaged by MRA, supporting the spatially confined analysis of fMRI Bold signals with respect to the vascular system.**

M. A. Gaudnek<sup>1</sup>, A. Hess<sup>2</sup>, K. Obermayer<sup>1</sup>, L. Budinsky<sup>2,3</sup>, K. Brune<sup>3</sup>, M. Sibila<sup>1</sup>

1 Neural Information Processing, Faculty IV, Technical University Berlin

2 Institute for Pharmacology and Toxicology, FAU-Erlangen Nürnberg

3 Doerenkamp Professor for Innovations in Animal and Consumer Protection

Functional Magnetic Resonance Imaging (MRI) based on hemodynamic signals, e.g. the commonly used BOLD signal, strongly depends on the underlying anatomy of the vascular system (Hess et al, JNS, 2001). Hereby two parameters are of special importance in their relation to the functional domain: i) size distribution of the vessel diameters, ii) spatial relation of the distribution of arteries and veins.

As one advantage the non invasive MRI method is capable of measuring the vascular anatomy by Magnetic Resonance Angiography (MRA) besides measuring fMRI signals in the very same experiment. Common methods for MRA are the so called inflow methods.

They measure the inflow of pre-saturated blood in a vessel orthogonal to the image plane. Usually axial images are taken, because in rodent brains the predominant direction of the blood flow is from anterior to posterior. This leads to a systematic underestimation regarding vessels parallel or oblique to this axial image plane. In this study we try to overcome this problem by reconstructing a more complete view of the vascular system by merging the vessels obtained at different imaging planes (axial, sagittal, horizontal) by warping. As a second bias source, the inflow methods tend to image vessels with high flow velocities which are normally arteries. We address this problem by incorporating vessels with smaller flow velocities by applying a contrast agent. Today angiographies are evaluated by visual inspection only and usually no quantification of the (whole) vessel system is performed. This is so, because automatic quantification of the geometry of the vascular system needs highly sophisticated image segmentation and reconstruction procedures which. Exactly for this purpose of automatic vessel segmentation in MRA we present here new developed algorithms.

The imaging is performed on a 4.7 T BRUKER Biospec 47/40 equipped with an actively RF-decoupled coil system. A whole-body birdcage resonator enables homogenous excitation, and a 3 cm surface coil, located directly above the head to maximize the signal-to-noise-ratio, is used as a receiver coil. The angiographs are acquired after a shimming to the imaging volume with a 3D Gradient Echo sequence with a field of view 25 x 25 x 25 mm, matrix 256 x 256 x 128 cm, TR = 30 ms, TE<sub>eff</sub> = 3.5 ms, flip angle = 45 degree, NEX 4). Complete 3D datasets are obtained sequentially at three different orientations. Next, a contrast agent (Endorem 1.2 ml / kg) is applied intravenously and again MRA datasets are recorded.

The reconstruction process of the vascular system consists of the following basic steps: i) recording MRA datasets from three orthogonal spatial directions. ii) semiautomatic extraction of a geometric model of the inspected vascular system by means of a self developed reconstruction method using locally adapting snakes (Schmitt et. al., NeuroImage, in press) iii) defining corresponding landmarks in all datasets iv) merging the single reconstructions by means of graph matching techniques and landmark based warping schemes. Thereby local distortions introduced either by unavoidable inhomogeneities during the initial imaging process or during the extraction of the single blood vessel models are eliminated.

The resulting reconstruction is free of artifacts caused by the imaging process (nonlinearities of the field resp. resulting geometry), maintaining greatest possible detail by incorporating three different scanning directions at once.

In conclusion, based on these algorithms we are able to automatically segment, quantify (especially vessel diameters) and model the vessel systems in MRAs. Moreover, the algorithms allow us to address both bias sources mentioned above. First by fusing the vessel systems obtained at different imaging directions a much more complete vessel system is reconstructed. Second, by comparing the vessel system before and after contrast agent application we can separate arterial from venous parts of the vessel system. By applying these analyses of the vascular system to the fMRI BOLD signals derived on top of the vessels in the future will allow for a much better description.

Supported by the BMBF (0311559, 0311557/UP2, CCN Berlin 10025304), the Doerenkamp Professorship in Innovations in Animal and Consumer Protection and the IZKF Erlangen.

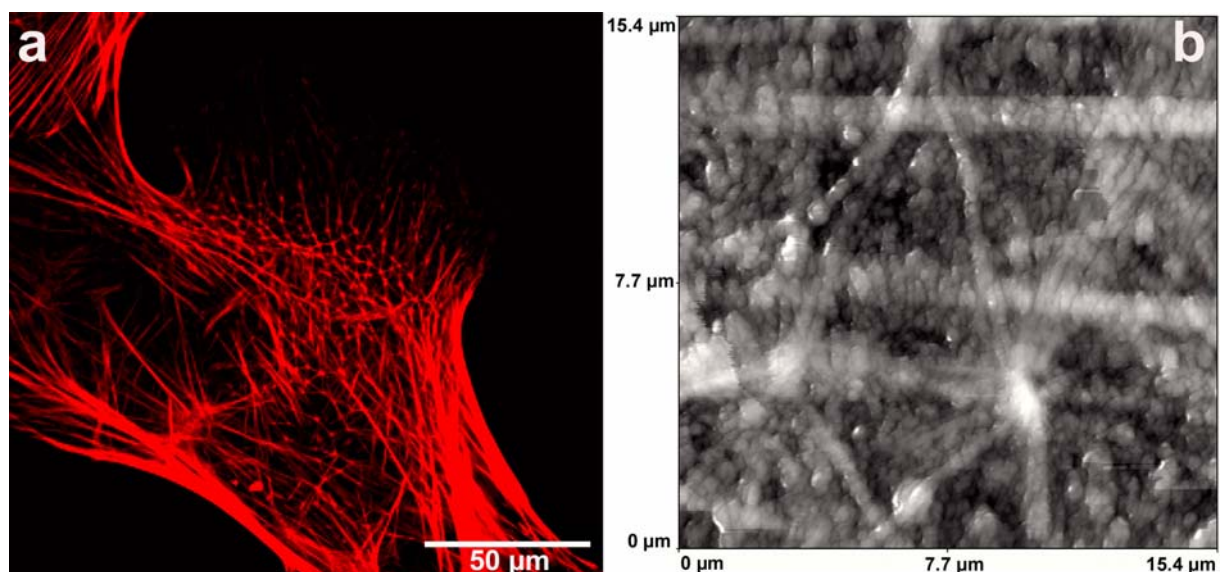
## **A synergy of technologies: combining confocal laser scanning microscopy and atomic force microscopy to study the cytoskeleton**

Karl Meller and Carsten Theiss

Institute of Anatomy, Department of Cytology, Ruhr-University Bochum, Bochum

e-mail: [karl.meller@ruhr-uni-bochum.de](mailto:karl.meller@ruhr-uni-bochum.de)

This poster describes a new method to combine confocal laser scanning microscopy and atomic force microscopy (AFM) to study the cytoskeleton in cultured cells. Whereas confocal laser scanning microscopy is useful for the identification of certain proteins subsequent labeling with specific markers or antibodies, atomic force microscopy allows the observation of macromolecular structures on fixed or living cells. Here, we illustrate a protocol focusing specially onto the actin cytoskeleton in cultured lens epithelial cells using both techniques on the same specimen. First, cells were permeabilized and fixed, followed by staining of the actin cytoskeleton with phalloidin-rhodamine, and studied using confocal laser scanning microscopy (Fig. a). Thereafter cells were embedded in Durcupan water-soluble resin, followed by UV-polymerization of resin. Subsequent this preparation procedure actin filaments were investigate by aid of AFM on the same probe, to get complementary information, which can easily be correlated from an optical to an ultra-structural level (Fig. b).



**Robust vital monitoring support for neurophysiologic experiments in animals even inside MRI scanners**F. Bussmann<sup>1</sup> and A. Hess<sup>1</sup><sup>1</sup> Institute for Pharmacology and Toxicology, FAU-Erlangen Nürnberg

Email: andreas.hess@pharmacologie.uni-erlangen.de

Meaningful neurophysiologic experiments in living animals such as mice and rats put great demands on an optimized animal monitoring device. This is particular the case in the high sophisticated experiments nowadays e.g. MRI scanners. MR scanners at first glance disturb any electrically recorded signal due to the RF and gradient pulses applied for imaging. Since in most experiments the animals are anesthetized an optimal device should at least monitor heating and body temperature, respiration rate, ECG, and arterial blood pressure for the vital functions of the animal. Additional measurement of the EEG provides analysis of the depth of anesthesia as routinely performed for humans (e.g. BIS index). Moreover, in many experimental setups, like optical recording or fMRI, a flexible trigger derived from certain combinations of vital functions should be provided in order to trigger the neurophysiologic recording system and by doing so reduce artifacts due to respiratory, heart motion, or anesthesia. Recording of all these vital signals should be realized within one device easy to use and mount on the animal. Moreover the device should compensate for changes in the signals e.g. amplitude reduction of the respiration or ECG signal in long term recording sessions by flexible amplification and filtering without the need of remounting the vital sensors.

From the electronic design point of view at least two important prerequisites have to be met: I) The strong disturbances from the RF and gradient pulses have to be eliminated. II) The electronic filtering has to take into account the fast heartbeats in small animals (50 to 500 beats/min).

Today no device is available which fulfills all the mentioned demands. Therefore, we have developed a new animal vital function monitor based modern electronic SMD circuits realized as an optical isolated bidirectional transmitter-receiver system. The transmitter can preprocess and digitize up to 8 different analog channels. This transmitter is housed in a shielded aluminium box and therefore can be used even inside an MRI scanner. The different channels can be conditioned for a certain physiological signal (respiration, ECG, EEG etc.) by a first stage amplification circuit (headstage) followed by a specially designed filtering system. This multistage analog filtering system is specially designed for rejecting any artifacts from the RF and gradient pulses of the MR scanner. One important feature here is that the filter frequencies can be fine tuned at the receiver outside of the MR scanner. This guarantees that the analog signals especially for ECK and EEG are low pass filtered “just enough” and not smeared by too much low-pass filtering as in some other ECG only systems. Additionally, a second stage amplifier can be adjusted from outside e.g. to compensate for changing or drifting signals during long recording sessions. In the receiver all vital functions are displayed, additional filtering and amplification can be performed as well as flexible generation (automatic - manual) and settings of trigger conditions (single or combinations) as well as alarm thresholds for the different vital signals.

In conclusion our system combines monitoring different vital functions into one device which is designed to provide a stable but tunable vital monitoring of temperatures, respiration, ECG, arterial blood pressure, and EEG/LFP even inside an MR scanner.

## Artifact removal from the EEG – Blind source separation and complex artifacts

Ralph Meier<sup>1,2</sup>, Andreas Schulze-Bonhage<sup>2</sup>, Andrzej Cichocki<sup>3</sup>, Ad Aertsen<sup>1</sup>

<sup>1</sup>Neurobiology & Biophysics, Inst. Biology III, Albert-Ludwigs-University, Freiburg

<sup>2</sup>Center for Epilepsy, Dept. Neurosurgery, University Clinics, Freiburg

<sup>3</sup>Brain Science Institute, RIKEN, Wako-shi, Japan

Email: [meier@biologie.uni-freiburg.de](mailto:meier@biologie.uni-freiburg.de)

The goal of Blind Source Separation (BSS) is to recover independent sources from sensor observations that are unknown linear mixtures of the unobserved independent source signals. In contrast to correlation-based transformations (e.g. PCA) BSS not only de-correlates the signals (2nd-order statistics), but also reduces higher-order statistical dependencies, attempting to make the signals statistically as independent as possible. After performing blind separation of signals, unnecessary (or undesirable) components that were hitherto hidden in the mixture (e.g. by superimposed or overlapping data) can then be removed.

Here, we tested the capability of two different BSS algorithms to remove different types of artifacts from EEG recordings of healthy subjects. Specifically, we compared the algorithms *AMUSE* (Cichocki and Amari 2003), based on second order statistics, and *ThinICA* (Cruces and Cichocki 2003), based on joint maximization of several cumulants and/or second order time-delayed covariance matrices. We analyzed EEG recordings from 2 subjects that produced different types of artifact signals in a well controlled manner. In total, 10 different artifacts were produced 10 times per subject with precise timing, using visual and sound cues. Amongst them were eye-related artifacts (eye blinks, eye movements), movement artifacts (changes of posture, head movements) and tongue/jaw generated artifacts (e.g. speech, chewing, swallowing).

Generally, most activity of eye-related artifacts was revealed on only few components. Therefore, these artifacts could easily be removed. Complex artifacts, either having a large spread over EEG channels and/or containing multiple components (i.e. signals from several muscular groups) resulted in artifact-related activity on most of the extracted independent components. Complete removal of these artifacts, therefore, appears very difficult. Nevertheless, specific aspects of the artifacts (e.g. the most prominent low-frequency components) could be removed in most generated artifacts. The two different BSS algorithms exhibited similar problems with complex artifacts, both resulted in a comparable spread of the artifact-related activity in component space. Preliminary results of a similar approach to clean peri-ictal EEG to improve automated seizure detection (Meier et al. 2004) appear promising.

Work supported by the Committee for Research, University Clinics, Freiburg and RIKEN Summer Program 2004. Further information at [www.brainworks.uni-freiburg.de](http://www.brainworks.uni-freiburg.de).

Cichocki A, Amari S-I (2003) *Adaptive Blind Signal and Image Processing* (Revised Edition). John Wiley, Chichester, UK

Cruces S, Cichocki A (2003) Combining blind source extraction with joint approximate diagonalization. In: *Thin Algorithms for ICA. Proc. 4th Symp Independent Component Analysis and Blind Signal Separation*, Japan, pp. 463-469

Meier R, Dittrich H, Schulze-Bonhage A, Aertsen A (2004) Automatische Detektion verschiedener Anfallsmorphologien im Oberflächen-EEG ohne Verwendung von Vorinformation. *Z Epileptol* 17: 182

## Measuring and Visualizing Protein-Protein-Interactions in Living Cells Using a Protease-based Complementation System

M.C. Wehr<sup>1</sup>, R. Laage<sup>2</sup>, K.A. Nave<sup>1</sup>, M.J. Rossner<sup>1</sup>.

<sup>1</sup>MPI for Experimental Medicine, Goettingen, Germany, <sup>2</sup>Axaron Bioscience AG, Heidelberg, Germany

Cellular functions are coordinated by a tremendous network of protein-protein-interactions, e.g. determining specific regulatory responses to different extracellular signals. To date, the methods used to detect protein-protein-interactions (PPIs) in living cells are limited. Here we describe a novel approach which enables us to transfer transient and inducible PPIs into a stable and simple readout *in vivo*. The technique is based on the complementation of two fragments of the NIa (nuclear inclusion protein a) proteinase of the tobacco-etch-virus (TEV protease) which are fused to potential interacting proteins. With respect to the interacting partners, the TEV fragments can be fused either N-terminal or C-terminal. An active protease is only formed when the proteins of interest interact with each other. TEV-dependent reporter systems which are either based on visualization or are luciferase-coupled allow quantitative readouts. The specific interaction between proteins is demonstrated with homodimerizing GCN4-zipper proteins and heterodimerizing GABA-B receptor coiled-coil domains. The novel technique is also verified for the well characterized rapamycin-inducible interaction between FKBP12 (FK506-binding protein of 12 kDa) and FRB (binding domain of the FKBP12-rapamycin-associated protein). So far, PPIs occurring at the membrane and in the cytosol can be analyzed. Here, we present the measurement of PPIs in the cytosol with novel reporters which are based on a TEV cleavage. Basically, a fluorescently inactive protein becomes fluorescently active upon TEV cleavage. The fluorescent signal strength can be correlated with the intensity of the PPI. Analogously, an enzymatically inactive luciferase can be activated allowing rapid and easy quantitative measurements. A TEV-mediated reporter system to detect interactions in the nucleus is currently in development. Although designed in particular to detect PPIs of transcription factors, this system will not be influenced by secondary effects on the basal transcription machinery, a common problem of classical two-hybrid based approaches. In the future, various reporters designed for different subcellular locations might allow the distinct determination of PPIs in time and space in living cells.



### 3D MRI visualisation of microelectrodes in the brainstem of the squirrel monkey

R. Tammer<sup>1</sup>, L. Ehrenreich<sup>1</sup>, S. Boretius<sup>2</sup>, J. Frahm<sup>2</sup>, T. Michaelis<sup>2</sup>

<sup>1</sup>Neurobiologie, Deutsches Primatenzentrum GmbH, Göttingen, Lower Saxony, Germany, <sup>2</sup>Biomedizinische NMR Forschungs GmbH am MPI für biophysikalische Chemie, Göttingen, Lower Saxony, Germany

#### Introduction

The exact placing of long-term implanted electrodes is essential for efficient telemetric electrophysiological exploration of very small mesencephalic brainstem areas of the squirrel monkey (*Saimiri sciureus*). The purpose of this study was (i) to evaluate the MRI compatibility of the self-made electrode and microdrive equipment, and (ii) to determine the exact position of the electrode tip relative to the neuronal target structure.

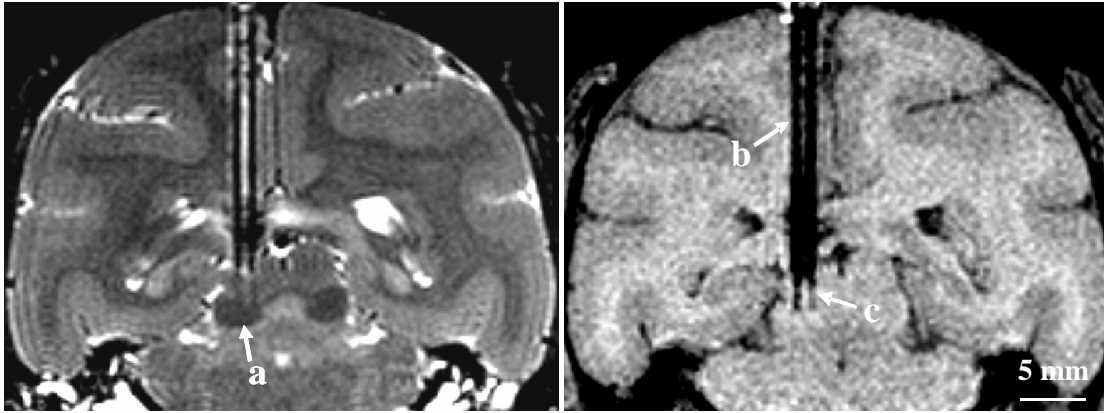


Figure 1: T2-weighted (left) and T1-weighted image (right) of a squirrel monkey brain with two implanted electrodes. (a) inferior colliculus, (b) glass tubes with metal core, (c) advanced microelectrode.

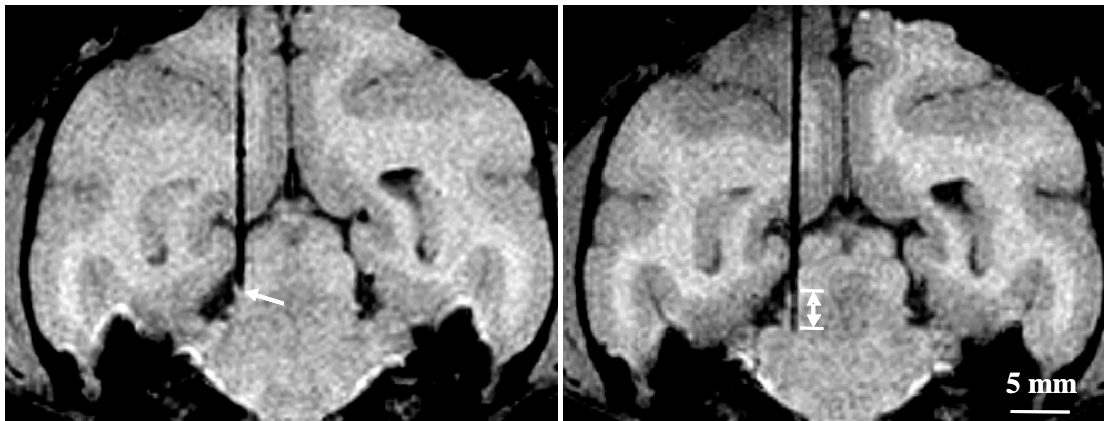


Figure 2: T1-weighted images showing two different positions of the electrode tip: 0.4 mm (left) and 2.9 mm (right) distance to the glass tube end.

#### Methods

A quartz glass insulated platinum-tungsten microelectrode (metal core 25µm, o.d. 80µm) was inserted into a boro-silicate glass stabilizing tube (i.d. 84µm, o.d. 250µm). Both slid within a glass guiding tube (i.d. 300µm, o.d. 400µm). The electrode with its protecting glass tubes was attached to a manually operated microdrive. After electrode implantation via a vertically moving stereo-tactical manipulator, the micro-drive was affixed to a synthetic platform chronically implanted onto the head of the animal. The telemetric device and ground electrode made of steel were removed before MRI. Monkeys (n=4) were anesthetized using pentobarbital and fixed with a head holder in a prone position. T1-weighted (3D FLASH, TR/TE = 22.3/10.1 ms, isotropic resolution: 330 µm) and T2-weighted (3D FSE, TR/TE = 3000/127.3 ms, 16 echos, inter-echo-spacing = 16.1 ms, isotropic resolution: 469 µm) 3D MRI was performed, both before and after implantation at 2.35 T (Bruker Biospin) using a 10 cm Helmholtz coil.

#### Results

Figure 1 demonstrates that platform, microdrive, glass capillaries, and microelectrodes are well delineated without generating distortions in MRI. While T2-weighted images reveal better grey/white matter contrast, T1-weighted images more clearly differentiate between the glass tubes and the microelectrode. As shown in Fig. 2 T1-weighted images are therefore particularly useful for monitoring the positions of the electrode tip at different stages during electrophysiological exploration of the same animal.

#### Conclusions

MRI-compatibility of all necessary components could be ensured. T1-weighted 3D MRI allowed for a non-invasive verification of the positioning of microelectrodes relative to the targeted neuronal structure at multiple times during exploration of an individual animal.



Using a combination of FRET/FLIM and electrophysiology to study GPCR-signalling pathways.

Salonikidis P.S., Wouters F.S., Richter D.W.

Center for Physiology and Pathophysiology, Department of Neuro- and Sensory Physiology

Serotonin (5-HT) is an ubiquitous neuromodulator that interacts with different G-protein coupled receptor (GPCR) isoforms to activate or inhibit various signal pathways. 5-HT activates GPCRs of the 1A, 4 and 7 type 5-HT receptors regulating the cAMP pathway and thereby various voltage-regulated ion channels: e.g. inward rectifying  $K_{ir}$ -channels, hyperpolarization-activated  $I_h$ -channels and LVA- or HVA- $Ca^{2+}$  channels.

In order to analyse the effects on those signalling pathways and their target-channels, we combined the FRET-technology with Patch-Clamp-method. "Fluorescence resonance energy transfer" (FRET) allows to visualize protein-protein-interactions and to test for their functional significance. To study fast interactions between oligomerization-partners of 5HT-receptors or fast activations of G-proteins by GPCRs, we used measurements of the "fluorescence lifetime" (FLIM) to detect FRET-effects, which allows a much more accurate and in orders of magnitude faster measurement than intensity-analysis. We analysed FRET-signals of single living cells by focussing the excitation-laser-beam directly on one cell of a neuroblastoma-N1E-culture. We correlated these measurements with the electrophysiological responses of pathway-targeted channels.

We also performed experiments to study oligomerization of 5HT<sub>1a</sub>-receptors. For this we expressed 5HT<sub>1a</sub>-receptors labelled with CFP and/or YFP to express them individually or together in N1E-cells. We found significant differences in the fluorescence phase-shifts when we excited cells with sinusoidal modulated light-intensity, which suggests that there is a homo-dimerization of 5HT<sub>1a</sub>-receptors. This is in accordance with experiments of E. Ponimaskin *et al.*, who performed the same experiments with intensity-FRET-analysis. We will also present effects of agonist and changes of the membrane potential on such GPCRs-homo-dimerizations.

Acknowledgement: Financed by the DFG Research Centre Molecular Physiology of the Brain (CMPB)

**High frequency stimulation of the subthalamic nucleus – Investigations in the kindling model of epilepsy**

*Nolte MW, Loscher W & Gernert M*

Dept. of Pharmacology, Toxicology, and Pharmacy, University of Veterinary Medicine Hannover, Germany

High frequency electrical stimulation (HFS) of brain structures has become an interesting tool in the therapy of several neurological disorders and is clinically established most notably as a treatment for Parkinson's disease (PD). In epilepsy, however, the correct parameters and location for stimulation have yet to be determined. Pharmacological inhibition of the subthalamo-nigral network has been shown to be anticonvulsant in experimental epilepsy. HFS of the subthalamic nucleus (STN) was suggested to have a net inhibitory effect on the target structures and is of potential interest as an adjunctive treatment option for intractable epilepsy.

In our study, we investigated the effects of bilateral HFS (biphasic, bipolar, 130 Hz, 60  $\mu$ s stimulus width, individual currents) of the STN on the seizure threshold in the amygdala kindling model of epilepsy. We compared the effects of continuous versus intermittent (30 sec every 5 min or 5 sec every 5 min) STN-HFS, as well as different times of HFS preceding the amygdala-stimulation (2 and 5 sec, 1 and 24 hrs).

Preliminary data did not reveal robust anticonvulsant effects. However, we observed that continuous STN-HFS and preceding times of 2 sec or 24 hrs seem to be potentially effective in increasing seizure thresholds in kindled rats.

We conclude that anticonvulsant effects of bilateral HFS of the STN are highly dependent on the stimulation parameters used. Further studies are needed to decide, which stimulation parameters need to be chosen or whether STN-HFS in epilepsy is not as promising as in PD.

## Identifying neuronal ensembles in the olfactory and visual systems using independent component analysis (ICA).

Jürgen Reidel<sup>1,2</sup>, David Omer-Backlash<sup>3</sup>, Amiram Grinvald<sup>3</sup>, Jens Starke<sup>1,2</sup>, and Hartwig Spors<sup>1,4</sup>

<sup>1</sup> WIN Research Group on Olfactory Dynamics, Heidelberg Academy of Science, <sup>2</sup> Institute of Applied Mathematics, University of Heidelberg, INF 294, 69120 Heidelberg, <sup>3</sup> Dept. of Neurobiology, Weizmann Institute of Science, 76100 Rehovot, Israel, <sup>4</sup> Abteilung Zellphysiologie, MPI für medizinische Forschung, Jahnstrasse 29, 69120 Heidelberg

External stimuli are processed by different populations of neurons. Neuronal populations with similar receptive fields are clustered in modules or columns in the neocortex, or by glomeruli in the olfactory bulb. Stimulus specific spatio-temporal patterns of evoked responses can be measured *in vivo* with a variety of optical imaging methods like, intrinsic signal voltage sensitive dyes, or calcium sensitive dyes. However, the optimal analysis of such rich data sets poses a challenge. Blind source separation, e.g. independent component analysis (ICA), works without assumptions of the data structure in the frequency domain, therefore both spatial and temporal response characteristics can be obtained. Here we demonstrate that ICA can not only extract mapping signals, but also can identify different neuronal ensembles based on their stimulus specific time courses of activation.

Modern imaging methods provide data sets with high dimensionality. To reduce the dimensionality in a first step principal component analysis in time was used to describe the data set. Between 80 and 90 % of the variance in the original data could be retained while reducing the size of the data set by more than a factor of 20. When combining measurements with and without stimulation in one data set, more of the stimulus related variance was retained compared to the variance not related to the stimulus.

As a second step functionally independent signal components were separated by ICA. Using our data sets consisting of calcium sensitive dye, voltage sensitive dye and intrinsic signal measurements of odor evoked activity in the mouse olfactory bulb the ICA in space proved to be superior to ICA in time. Individual glomeruli and groups of glomeruli could be identified and separated. Two or more groups of glomeruli could be identified after stimulation with odors (e.g. ethylbutyrate). We compared responses measured on the input level to the olfactory bulb using a calcium sensitive axon tracer (CaGreenDetran) and on the network level using the voltage sensitive dye (RH 1838). The location of the fast and phasic glomeruli group and the slower and tonic group of glomeruli corresponded well. Whereas the time courses of the separated functional units correlated well with stimulus onset, the time course of the identified “artifact” (e.g. heartbeat pulsation) and noise components (e.g. camera pattern noise) was significantly different: e.g. the heartbeat artifact was correlated with the ECG recording.

As a third step we compared different independent component analysis (ICA) algorithms. The results of different ICA algorithms were comparable in terms of separation of the resulting patterns. Considering speed and ease of use the JadeR algorithms worked best in our hands.

To test if ICA can also be used for other brain areas and stimulation paradigms we analyzed voltage sensitive dye recordings from behaving monkeys by the above described analysis. Heartbeat artifacts and visually evoked responses were well separated. The resulting spatial patterns had a high correlation with the traditional differential and even single condition maps, without the need to specify the respective stimulus type during the analysis.

Thus ICA allows reduction of dimensionality, removal of artifacts and noise sources, and separation of different functional neuronal groups in different brain areas using different methods of *in vivo* imaging.

Support by BMBF, MPG, Heidelberg Academy of Science

## **Distinct behavioral and cognitive correlates of hedonic deficit and chronic stress in a new model of stress-induced anhedonia in mice**

Strekalova T, Dolgov O, Gorenkova N, Bartsch D  
Zentralinstitut für Seelische Gesundheit, Mannheim  
J5 68159 Mannheim, Germany

Anhedonia, a decreased ability to experience pleasures, is a core symptom of human depression that can also be induced in animals, including mice. One of the most established methods to evoke anhedonia in rodents is chronic stress. However, besides anhedonia, chronic stress is known to alter a number of physiological and behavioral variables. Thus, behavioral correlates of the anhedonic status are currently not well characterized. To address this question, we have established a new chronic stress procedure in mice that induces anhedonia only in a subgroup of stressed animals, while the rest of stressed animals does not show hedonic deficits and can serve as an internal control for the stress effects not associated with anhedonia.

We subjected male C57BL/6 mice to a 4-week long chronic stress procedure, comprising of a rat exposure and restrained stress. This procedure resulted in a strong decrease of sucrose preference, a measure of anhedonia in rodents. Interestingly, vulnerability to stress-induced anhedonia was associated with subdominant behavior, as shown by a resident-intruder test. Most animals with dominant behavior did not show a decrease of sucrose preference. All stressed animals without decrease of sucrose preference were regarded as resistant to stress-induced anhedonia and were used as an internal control for the effects of chronic stress alone. Behavioral analysis performed after terminating the stress procedure demonstrated that anhedonia is associated with key analogues of depressive symptoms, such as increased floating in forced swimming, decreased exploration activity and increased immobilization time in tail suspension test. In contrast, in new object exploration paradigm, novel cage, forced swim and tail suspension tests, mice resistant to stress-induced anhedonia showed behavior, similar to that of non-stressed control group. Anhedonic and resistant mice showed different abilities in acquisition of fear conditioning and step down avoidance tests. Contrary, both stressed mice with and without anhedonia showed similarly increased parameters of anxiety in elevated O-maze and dark/light box, hyperlocomotion in the open field test and increased aggressive behavior. Thus, behavioral correlates of stress-induced anhedonia and that of chronic stress can be separated in proposed model of depression.

## **Distinct behavioral and cognitive correlates of hedonic deficit and chronic stress in a new model of stress-induced anhedonia in mice**

Strekalova T, Dolgov O, Gorenkova N, Bartsch D  
Zentralinstitut für Seelische Gesundheit, Mannheim  
J5 68159 Mannheim, Germany

Anhedonia, a decreased ability to experience pleasures, is a core symptom of human depression that can also be induced in animals, including mice. One of the most established methods to evoke anhedonia in rodents is chronic stress. However, besides anhedonia, chronic stress is known to alter a number of physiological and behavioral variables. Thus, behavioral correlates of the anhedonic status are currently not well characterized. To address this question, we have established a new chronic stress procedure in mice that induces anhedonia only in a subgroup of stressed animals, while the rest of stressed animals does not show hedonic deficits and can serve as an internal control for the stress effects not associated with anhedonia.

We subjected male C57BL/6 mice to a 4-week long chronic stress procedure, comprising of a rat exposure and restrained stress. This procedure resulted in a strong decrease of sucrose preference, a measure of anhedonia in rodents. Interestingly, vulnerability to stress-induced anhedonia was associated with subdominant behavior, as shown by a resident-intruder test. Most animals with dominant behavior did not show a decrease of sucrose preference. All stressed animals without decrease of sucrose preference were regarded as resistant to stress-induced anhedonia and were used as an internal control for the effects of chronic stress alone. Behavioral analysis performed after terminating the stress procedure demonstrated that anhedonia is associated with key analogues of depressive symptoms, such as increased floating in forced swimming, decreased exploration activity and increased immobilization time in tail suspension test. In contrast, in new object exploration paradigm, novel cage, forced swim and tail suspension tests, mice resistant to stress-induced anhedonia showed behavior, similar to that of non-stressed control group. Anhedonic and resistant mice showed different abilities in acquisition of fear conditioning and step down avoidance tests. Contrary, both stressed mice with and without anhedonia showed similarly increased parameters of anxiety in elevated O-maze and dark/light box, hyperlocomotion in the open field test and increased aggressive behavior. Thus, behavioral correlates of stress-induced anhedonia and that of chronic stress can be separated in proposed model of depression.

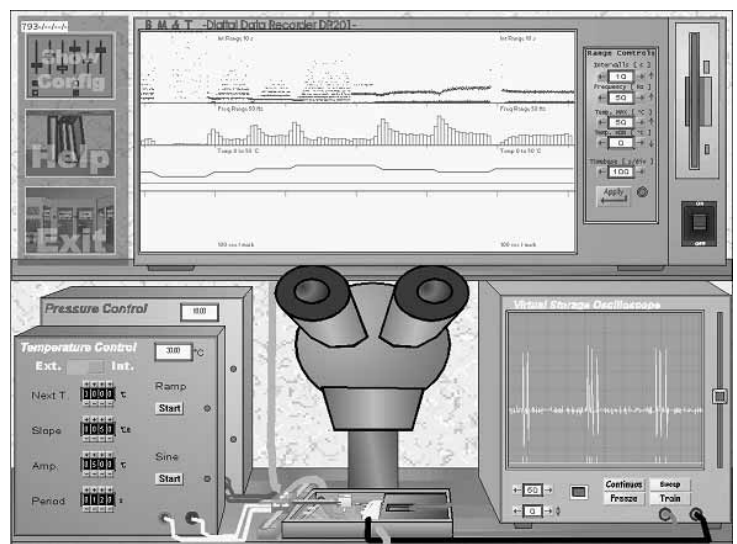
## Virtual Neurophysiology Labs for Students' Practical Courses: cLabs-Neuron and cLabs-SkinSenses.

**Hans A. Braun, Horst Schneider, Bastian Wollweber, Norman Anthes, Karlheinz Voigt**  
Neurodynamics Group at the Institute of Physiology, University of Marburg, D-35037 Marburg, Germany  
([www.uni-marburg.de/physiology/braun](http://www.uni-marburg.de/physiology/braun) and [www.clabs.de](http://www.clabs.de))

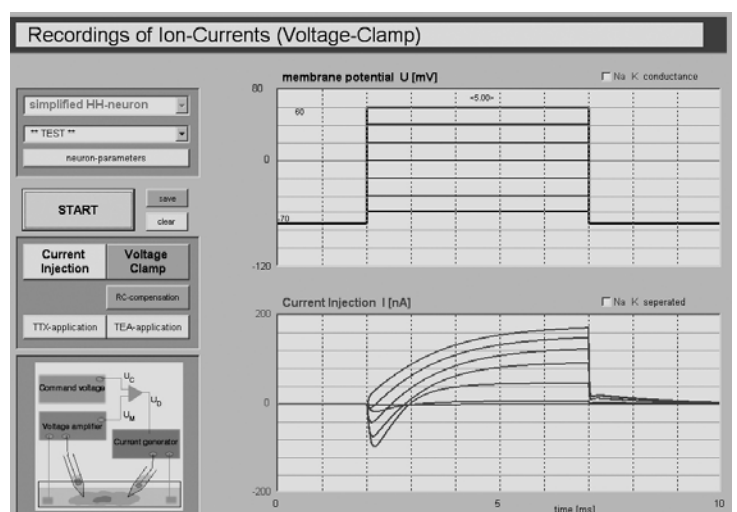
Since several years, teaching programs of the "Virtual Physiology" series (SimNerv, SimPatch, SimMuscle, etc.) are successfully used in practical physiology courses in hundreds of medical, biological and related faculties all over the world. It is the tutors impression that the students find it interesting and stimulating to work with these programs and that the virtual experiments can essentially help to attain a better understanding of physiological functions. These impressions were additionally confirmed by an evaluation of "SimNerv" which simulates recordings of compound action potentials according to the classical experiments with the frog's sciatic nerve.

Such positive evaluation results together with numerous enthusiastic replies from other users have stimulated us to develop an advanced series of virtual computer labs ("cLabs") which also includes experiments which would be too difficult to be physically carried out within the context of a student's coursework, but are realizable in silico. This is the situation, for example, for single fibre recordings from sensory afferents and for intracellular current/voltage-clamp recordings which have been realized as virtual computer laboratories called "cLabs-SkinSenses" and "cLabs-Neuron", respectively.

"cLabs-SkinSenses" is made in the tradition of the "Virtual Physiology" programs. It provides a virtual lab where the students can record the neuronal impulse activity of single-fibre preparations from different types of mechano- and thermosensitive skin receptors. It is the students' task to identify the unknown, randomly distributed receptors on the basis if their impulse patterns in response to ramp-shaped or sinusoidal thermal and mechanical stimuli of pre-selectable amplitude, slope or frequency. The action potentials are displayed on a virtual oscilloscope. Interspike-intervals and peri-stimulus-time-histograms (PSTH) are plotted together with the stimuli on a virtual chart recorder (see figure) and can be stored for subsequent data analysis. Additional modules offer the possibility to look at real data (published, for example, in Braun et al., Nature 367: 270-273, 1994) or to run computer programs which have been developed for scientific aims, i.e. for a better understanding of the dynamical interactions of possible ionic mechanisms of the transduction processes (e.g. Braun et al., Biosystems 71: 39-50, 2003).



Another program, "cLabs-Neuron", offers virtual laboratories for single-channel and whole-cell voltage- and current-clamp experiments - also under application of specific ion channel blockers like TTX or TEA. Compared to "SimPatch", which is a very realistic representation of a voltage-clamp lab, "cLabs-Neuron" has an easy to overlook screen design (see figure) which makes experimentation also possible for technically inexperienced students. The programs come along with detailed tutorials and manuals for practical exercises including protocol forms. The neurons are simulated with simplified Hodgkin-Huxley-type algorithms and a "Neuron-Editor" allows the teacher to generate neurons with different properties. "cLabs-Neuron" also includes computer animations and simulations to teach basic Neurophysiology, e.g. the gating of voltage-dependent ion-channels. "cLabs-Neuron" can be used for practical exercises as well as for lectures and seminars and its modular structure with detailed tutorials makes them well suited for home-studies, too. Part of the animations and simulations are available for experimentation at the cLabs homepage [www.clabs.de](http://www.clabs.de).



**A Caged Doxycycline Analog for Photoactivated Gene Expression  
with High Spatiotemporal Resolution**

Sidney B. Cambridge, Beate Cürten, Tobias Bonhoeffer  
Max-Planck-Institute of Neurobiology, 82152 Munich-Martinsried, Germany

We have established a system that allows induction of transgene expression in a defined set of cells by irradiation with UV light. To this end, we developed a photoactivatable version of the inducible tetracycline (tet) system (Tet-on) pioneered by Bujard and coworkers. A more potent analog of tetracycline, doxycycline was reversibly inactivated or “caged” to be used for photoactivated gene expression. Upon irradiation with UV light, doxycycline is released in its unmodified and biologically active form. By confining irradiation to a small area, gene expression can be induced with unprecedented spatial resolution, possibly in single cells.

Caged doxycycline was synthesized and purified to homogeneity as determined by HPLC analysis. The transcriptional activity of caged versus photoactivated doxycycline was compared in three different model systems. These included CHO cells with tet-dependent EGFP expression, transgenic tobacco leaves with tet-dependent expression of a GUS reporter gene, and mouse brain organotypic hippocampal Müller cultures with a tet-dependent EGFP construct. In all cases, following administration of caged doxycycline and subsequent photoactivation, transgene expression was detected in irradiated areas but not in the unirradiated control. Importantly, doses of UV light necessary for uncaging appeared to be non-toxic as cells in irradiated areas did not show signs of necrosis. Furthermore, spatially restricted irradiation of organotypic cultures produced local EGFP expression in restricted areas.

Our results clearly demonstrate, that caged doxycycline can be used to induce transgene expression in defined cells making it a powerful tool for biomedical research.

## Quantitative single cell RT-PCR and calcium imaging in acute brain slices

Robert Blum, Guylaine M. Durand, Nima Marandi, Simone Herberger and Arthur Konnerth

We established a reversed transcriptase (RT) polymerase chain reaction (PCR) approach that allows a rapid and quantitative analysis of RNA transcript levels in individual cells of living brain slice preparations. The procedure consists of the aspiration of visually-identified neurons through a patch pipette, the reverse transcription reaction, purification and the use of a 'real-time' PCR device. Quantification is achieved by constructing *in vitro* cDNA standard curves of the gene of interest. An important advance of our technique is that it can be readily used in combination with  $\text{Ca}^{2+}$  imaging, opening the possibility of a systematic analysis of functional parameters in relation to cell-specific mRNA levels. The viability of the method was tested, in parallel, in a particularly small and in a very large type of neuron, in cerebellar granule and Purkinje cells, respectively. The analysis of the well-known developmental switch of NMDA receptor subunits during early postnatal development revealed the single cell subunit NR2B as well as the subunit NR2C transcript levels that determine this switch. The glutamate receptor expression profiles in cerebellar granule and Purkinje cells were related to the NMDA-evoked  $\text{Ca}^{2+}$  signaling patterns, by means of two-photon imaging recordings performed just prior to the RT-PCR analysis, in the same cells. The new procedure is highly reproducible and capable of quantifying even low numbers of cDNA copies from individual, small cells. In conclusion, our results demonstrate that the combined RT-PCR/imaging approach is efficient and robust, suited for combined molecular-functional analyses with a relatively high throughput.



## **Stress-free oral administration of drugs in group-living mice through a transponder-controlled water dispenser**

**Ariane Santoso, Alexander Kaiser & York Winter**

Ökologische Neurobiologie, Department Biologie II, Biozentrum der Ludwig-Maximilians-Universität München, 82152 Planegg-Martinsried

In adult mammals newly-generated neurons are either incorporated in the neuronal networks of the olfactory bulb or the dentate gyrus of the hippocampal formation. The rate of proliferation and survival of these neurons has shown to be influenced by different factors, i.e. behavioural context, species, age, sexual hormones and also stress (for review see Gould et al., 1999). The thymidine analog 5-Bromo-2'-deoxyuridine (BrDu) is a widely-used reliable marker for the study of proliferating cells. The method of choice for application of BrDu in a great number of studies is by intraperitoneal injection, which, however, could evoke stress in animals due to handling and disturbance. In order to avoid such stress in studies of neurogenesis in mice we established a method for computer-controlled oral administration of BrDu via the drinking water. Our system is built on a computer-controlled valve and a feeder incorporating transponder identification (RFID) technology. On entering the feeder opening, a transponder-marked individual is identified and a small calibrated quantity of liquid is released to the animal. The total amount of the drug incorporated by each individual is controlled via the settings of the volume and the number of permitted successive visits to the water feeder.

In our experiments we compared adult neurogenesis in two groups of mice which received BrDu solution via an i.p. injection or through the computer-controlled water dispenser, respectively. The daily dosage for both groups was 100 µg BrDu/g body mass and was given on 4 consecutive days. The maximum time required for consuming the daily dosage for the "dispenser group" was 3h. Following a survival time of 28 days the animals were deeply anesthetized with pentobarbital and perfused transcardially with 4 % PFA. The brains were cut at 40-µm thickness in the coronal plane using a cryostat and processed for immunohistochemistry using BrDu-antiserum (anti-mouse, Roche), avidin/biotin complex (Vector) and DAB reaction. Sections were analyzed using a Zeiss Axioskop with a digital camera (SpotCam) and Metamorph software package. The quantitative analysis of cells in the dentate gyrus in both groups of mice revealed no statistically significant difference in total number of BrDu-positive cells. Thus, the computer-controlled delivery of substances like BrDu or other water-soluble drugs is a promising application method for animals without disturbing their natural behaviour. Furthermore, the combination of a computer-controlled water dispenser and transponder technology allows precise drug application for individuals even in group-living animals.

### Reference:

Gould E, Tanapat P, Hastings NB, and Shors TJ. 1999. Neurogenesis in adulthood: a possible role in learning. Trends Cogn Sci 3:186-192.



## Ischemic etiology of masticatory lesions in the MCAO filament model is questionable



Dittmar MS <sup>a</sup>, Fehm NP <sup>b</sup>, Vatankhah B <sup>b</sup>, Schuierer G <sup>c</sup>, Horn M <sup>b</sup>

<sup>a</sup> Department of Anesthesiology, <sup>b</sup> Department of Neurology, University of Regensburg

<sup>c</sup> Institute of Neuroradiology, Regensburg District Medical Center

Address for correspondence: Michael S. Dittmar, Klinik für Anästhesiologie, Klinikum der Universität Regensburg, D – 93042 Regensburg, Germany. E-mail: m.dittmar@gmx.de.

**Objective:** The intraluminal filament model of middle cerebral artery occlusion (MCAO) is a widely used model of experimental stroke. Recently, the complication of necrosis of the ipsilateral mastication musculature has been reported which was associated with impaired functional recovery [1]. These lesions were interpreted as ischemia of the external carotid artery (ECA) territory due to ECA transection for filament introduction.

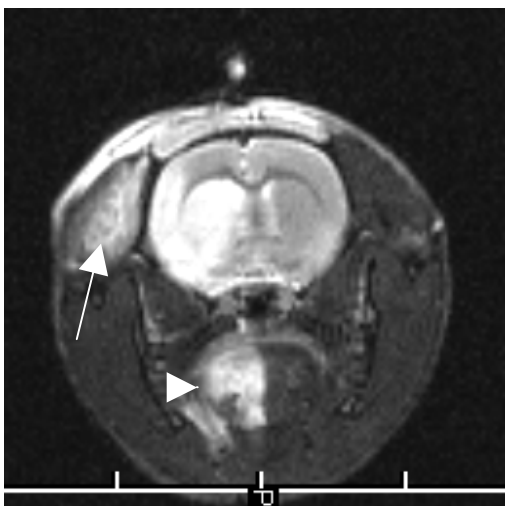
**Methods:** To verify the ischemic etiology of the masticatory lesions we developed a modification of the filament model with preservation of the ECA in male Wistar rats (MCAO n = 10, sham n = 7). The filament was introduced via an incision in the common carotid artery (CCA) which was surgically closed after MCAO. In addition, we examined whether transection of the ECA alone (n = 6), in combination with ligation of the pterygopalatine artery (PA) (n = 7), or transection of ECA + PA ligation + CCA ligation (n = 3) was sufficient to provoke ECA ischemia. Integrity of masticatory tissue was assessed by magnetic resonance imaging 24 – 48 hours after surgery.

**Results:** Despite ECA conservation, masticatory lesions were observed in 24 % of all cases (figure) compared to 48 % in the historical collective of animals with ECA transection [1] (not significant). Transection or ligation of cervical arteries without MCAO did not lead to conspicuity of extracranial tissue in any case.

**Discussion:** Since neither the conservation of the ECA during surgery for MCAO did prevent masticatory lesions nor a disturbance in blood supply to the masticatory system was eligible to provoke lesions, an ischemic etiology is unlikely. Therefore, other etiologies like congestion due to disturbance of venous efflux have to be taken into account as a damaging factor.

### References:

1. Dittmar M, Spruss T, Schuierer G, Horn M. External carotid artery territory ischemia impairs outcome in the endovascular filament model of middle cerebral artery occlusion. *Stroke* 2003; 34: 2252-2257.



Hyperintense signal changes in ipsilateral mastication (arrow) and swallowing system (arrow head) 24 hours after surgery for MCAO.

## Direct access to all cells of a mouse brain

Schmitt O<sup>1</sup>, Wirtz S<sup>2</sup>, Modersitzki J<sup>3</sup>, Fischer B<sup>2</sup>, Heldmann S<sup>2</sup>, Wree A<sup>1</sup>

<sup>1</sup>Institute of Anatomy, University Rostock, Gertrudenstr. 9, D-18055 Rostock, <sup>2</sup>Institute of Mathematics, University of Lübeck, Wallstraße 40, D-23560 Lübeck, <sup>3</sup>Mathematics & Science Center Suite W401, 400 Dowman Drive, Emory University, 30322 Atlanta, GA, USA.

Biological geno-phenotyping projects demands for high quality and high spatial resolution data to understand genetic and morphologic relationships from the microscale up to the macroscale. To obtain accurate spatial information of cellular elements of the CNS histologic images deformed by the processing steps need to be spatially corrected. A prerequisite for recognizing cells of the CNS is a resolution smaller than 12  $\mu\text{m}$  in the x and y direction and a section thickness of less than 40  $\mu\text{m}$ . A mouse brain was embedded in paraffin wax and cut into 20  $\mu\text{m}$  thick sections that were stained by a modification of the Gallyas method. All sections were scanned by a high resolution transparent flat bed scanner (x: 5  $\mu\text{m}$ , y: 5  $\mu\text{m}$ ) equipped with an autofocus function. The 587 sections have a size between 0.073  $\text{mm}^2$ , resp. 0.02 MB, and 40.22  $\text{mm}^2$ , resp. 7.1 MB. The size of all 8-Bit gray scale images is 743 MB.

The images were preprocessed, preregistered by a rigid and an affine linear transformation and finally nonlinear aligned. Finally, they were reconstructed for surface visualizations and virtual sections through the 3D-object (Fig. 1). Segmentations of subregions of the brain were performed for volume measurements of nuclei and visualization of cell populations (Fig. 2). Especially, the spatial extension of the substantia nigra (pars compacta, pars reticulata), the ventral tegmental area, the subthalamic nucleus and the nucleus accumbens are represented in transparent views. Furthermore, the volumes of these regions were calculated. The approach we introduced here provides promising results w.r.t. high resolution spatial analysis of further functional relevant cellular features like immuno-histochemically visualized neurotransmitters, neuromodulators, receptors, axons and dendrites.



**Fig. 1:** 3D-reconstruction of 500 images exhibiting an internal xy-transversal resolution of 5  $\mu\text{m}$  x 5  $\mu\text{m}$ .

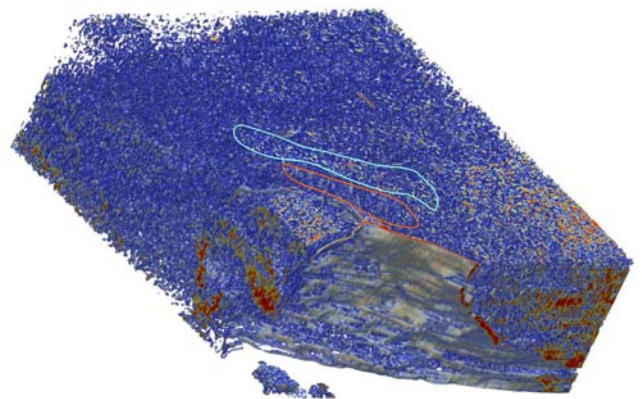


**Fig. 2:** Cell clusters and large cells were segmented by a global threshold and visualized by a spectral LUT. The substantia nigra pars compacta (blue) and reticularis (red) can be recognized.

## **Dataset: an open source tool for the classification of multielectrode data**

**Maria Paula Bonomini<sup>1</sup>, José Manuel Ferrandez<sup>2</sup>, Eduardo Fernandez<sup>1</sup>**

<sup>1</sup> Instituto de Bioingeniería, Universidad Miguel Hernández, Elche, Spain

<sup>2</sup> Dept. Electrónica y Tecnología de Computadores, Univ. Politécnica de Cartagena.

The number of laboratories using methods for simultaneously recording extracellular activity of several single neurons is growing more and more each day. This technique allows new approaches in the study of large neuronal networks dynamics by means of multielectrode arrays (MEA). This paradigm, however, led to a new technical challenge: the huge amount of data generated per experiment, which can end up in quite an useless mountain of data if an appropriate management is not carried on. Moreover, the data exchange between laboratories using different MEA acquisition systems is hindered by the commercial constraints such as exclusive file structures, many times considered to be intellectual property, high priced licences and hard policies on intellectual rights imposed by the companies of this field.

We introduce here, a free open-source application for the management of data based on a general purpose philosophy aimed to the effective data exchange between laboratories. It allows the user to retrieve and quickly identify data from different hardware systems by means of a consistent set of routines for visualization and analysis. These routines enable the user to classify and filter units according to their responses to simple control stimulus presentations. In addition, a component for the easy incorporation of new algorithms is integrated. Classification can be accomplished by automatic clustering of a matrix of processed units calculated from a certain processing stage or simply by removing them by hand from the dataset. Also, a method for data reduction based on temporal windows is implemented. The output of the program is file-structured so that exporting the results to other packages is possible. Finally, the source code is freely available for extension or adaptation.

## Using the Retinal Spreading Depression for neuropharmacological studies

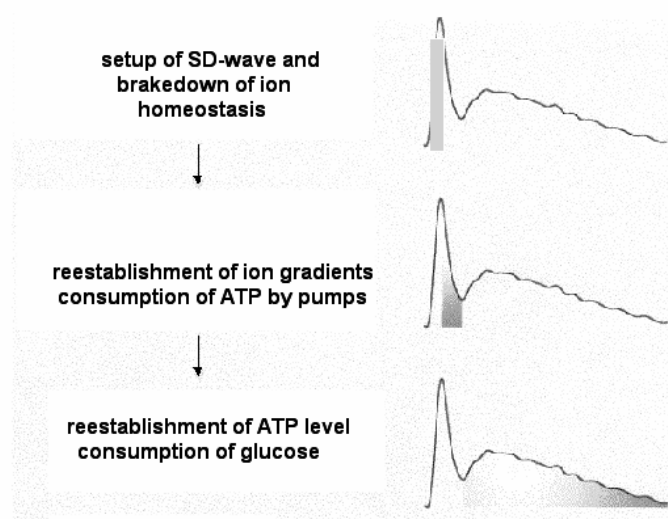
Wolfgang Hanke

*Universität Hohenheim, Institut für Physiologie-230, Garbenstrasse 30, 70599 Stuttgart*

The retinal spreading depression (rSD), an excitation-depression wave in neuronal tissue, has been verified to be a very useful tool to study the systemic action of neuropharmacologically active substances. The SD itself is related to a variety of functional syndromes of the CNS such as migraine, transient global amnesia and certain forms of epilepsy.

In the SD-system a variety of parameters are given delivering information about the action of drugs. Mainly electrophysiological and optical methods have been applied to investigate SD, but for systematic studies of drug action optical techniques are by far more adequate. From the study of the intrinsic optical signal (IOS) of the retinal SD the propagation velocity of waves, the latency of waves which is related to the tissue excitability, information about metabolic processes, about neuroprotectivity and others can be obtained.

Comparing the molecular, electrophysiological, immuno-histochemical and biochemical data available for different drugs with the data from the rSD for the first time allows to understand the action of drugs on the system level of neuronal tissue. From our data possibly basic information about the pharmacological treatment of some CNS diseases can be withdrawn.



Profile of an IOS of retinal SD and correlation of the different phases to metabolic processes. Changes of the IOS in a defined small area of the retina were plotted over the time

## **Patterns of neuronal activity in cerebral cortex of anaesthetized mice - a thallium uptake study**

Birgit A. Müller, Henning Scheich\* and Jürgen Goldschmidt\*

Abt. Neurobiologie/Bio IV, Universität Ulm, Albert-Einstein-Allee 11,  
D-89081 Ulm, Germany

\*Leibniz-Institut für Neurobiologie, Brennekestrasse 6,  
D-39118 Magdeburg, Germany

Large numbers of neurobiological studies that analyze neuronal in vivo activity are performed in anaesthetized animals. But the knowledge about how the different anaesthetics that are in use affect the patterns of neuronal activity in the mammalian brain is limited.

We used thallium autometallography (TI-AMG), a novel method for mapping neuronal activity (Goldschmidt et al., NeuroImage, in press), to study the effects of anaesthetics on neuronal network activity in mouse cerebral cortex. This method is based on the fact that in neurons Na, K-ATPase activity and the rate of potassium ( $K^+$ ) uptake increase with increasing activity. The  $K^+$ -analogue thallium ( $Tl^+$ ) is used as a tracer for mapping these activity-dependent changes in neuronal  $K^+$ -uptake. The distribution of this tracer in the brain can be mapped non-radioactively at high spatial resolution by means of an autometallographic method (a modified Timm-technique for the detection of heavy metals in the brain).

The patterns of  $Tl^+$ -uptake in the cerebral cortex of anesthetized mice differ markedly from the uptake patterns in the normal awake state.  $Tl^+$ -uptake in the awake state is high in large multipolar inhibitory neurons in cortical layer IV and in large pyramidal cells in layer Vb. In the anaesthetized animals, in contrast,  $Tl^+$ -uptake is highest in the neuropil and in neurons in superficial cortical layers I–III but comparably low in neurons in layer IV. Slight differences exist between different anaesthetics: with Ketamin  $Tl^+$ -uptake is highest in layer I, with Equitesin  $Tl^+$ -uptake is highest in layers II/III.

Our finding of a reduced  $Tl^+$ -uptake in layer IV during anaesthesia argues for a reduced activity in specific – topographically ordered - thalamic afferents that terminate in this layer.

Conversely, activity in non-specific thalamocortical projections that terminate in superficial cortical layers may be enhanced – relative to the activity of the specific projections - and could mediate or contribute to the comparably high activity in layers I–III.

[A](#) • [B](#) • [C](#) • [D](#) • [E](#) • [D](#) • [E](#) • [F](#) • [G](#) • [H](#) • [I](#) • [J](#) • [K](#) • [L](#) • [M](#) • [N](#) • [O](#) • [P](#) • [Q](#) • [R](#) • [S](#) • [T](#) • [U](#) • [V](#) • [W](#) • [X](#) • [Y](#) • [Z](#)

- Abankwa, D [S17-2](#)
- Abidin, I [300A](#)
- Abrahamczyk, C [S1-5](#)
- Abramowski, D [5A](#)
- Abrams, RM [377A](#)
- Abumaria, N [391A](#), [437A](#)
- Achermann, P [447B](#)
- Acik, A [434B](#)
- Addicks, K [S15-1](#)
- Adelsberger, H [S13-1](#), [244B](#)
- Ader, M [200B](#)
- Adolf, B [47A](#), [403A](#)
- Adolphs, R [Sat1-12](#)
- Aertsen, A [29B](#), [30B](#), [31B](#), [32B](#), [80B](#), [207B](#), [208B](#), [450A](#), [451A](#), [452A](#), [453A](#), [466A](#)
- Affeldt, B [431A](#)
- Agricola, H-J [262A](#), [303B](#)
- Aguzzi, A [S2-2](#)
- Aharonov, A [396A](#)
- Ahissar, M [440A](#), [441A](#), [442A](#)
- Ahlers, MT [166B](#)
- Ahmed, T [235B](#)
- Ahnefeld, M [327A](#)
- Ahnert-Hilger, G [382A](#)
- Akopov, S [50A](#)
- Al-Sabi, A [323B](#)
- Al-Shaikhli, B [187B](#)
- Ala-Laurila, P [152A](#)
- Albert, JT [317A](#), [318A](#)
- Albrecht, A [234B](#)
- Albrecht, C [162B](#)
- Albrecht, JD [115B](#)
- Aldenhoff, JB [S23-5](#)
- Alfaro-Sáez, A [37B](#)
- Alger, BE [277B](#)
- Alifragis, P [363B](#)
- Alkhatib, AA [115A](#)
- Allebrandt, KV [49A](#)
- Allgaier, C [406B](#), [407B](#)
- Allmer, H [435A](#)
- Almedom, R [317B](#)
- Alpar, A [408B](#), [448B](#)
- Altenmüller, EO [Sat1](#), [Sat1-13](#), Sat1-17, [53A](#), [54A](#), [105B](#)
- Alter, K [Sat1-10](#), [56A](#)
- Althaus, HH [4A](#), [348B](#)
- Altrock, WD [290B](#)
- Alzheimer, C [288B](#)
- Ambrée, O [2A](#)
- Amit, T [385B](#)
- Ammermüller, J [162A](#), [163B](#), [165B](#), [166B](#)
- Amstrong, N [S17-1](#)
- Anand, R [274A](#)
- Anderer, P [S23-1](#)
- Anderson, JC [291B](#)
- Anderson, S [317B](#)
- Angelucci, A [93B](#)
- Angrand, PO [Sat2-6](#)
- Annies, M [52B](#)
- Antal, A [174B](#)
- Anthes, N [462B](#)
- Antonow-Schlorke, I [327B](#), [328B](#)
- Aonuma, H [248B](#), [266B](#)
- Apfelbach, R [221B](#)

[A](#) • [B](#) • [C](#) • [D](#) • [E](#) • [D](#) • [E](#) • [F](#) • [G](#) • [H](#) • [I](#) • [J](#) • [K](#) • [L](#) • [M](#) • [N](#) • [O](#) • [P](#) • [Q](#) • [R](#) • [S](#) • [T](#) • [U](#) • [V](#) • [W](#) • [X](#) • [Y](#) • [Z](#)

Apter, A [417A](#)

Aramuni, G [295A](#), [324B](#), [325B](#)

Aranda, I [272B](#)

Arenas, E [S12-4](#)

Arendt, D [422B](#)

Arendt, T [405B](#), [408B](#), [409B](#), [410B](#), [411B](#), [412B](#), [413B](#), [414B](#), [448B](#)

Arnhold, S [S15-1](#)

Arnold, FJL [342A](#)

Arolt, V [353A](#), [401B](#)

Aschoff, A [388B](#)

Ashery, U [295B](#), [296B](#)

Assmann, M [338A](#)

Asyali, MH [143A](#)

Aszódi, A [29A](#)

Attardo, A [S12-1](#)

Attems, J [45B](#)

August, C [353A](#)

Ausborn, J [451B](#), [452B](#)

Avargues, A [14A](#)

Avitable, H [173B](#)

Avramovich-Tirosh, Y [385B](#)



[A](#) • [B](#) • [C](#) • [D](#) • [E](#) • [D](#) • [E](#) • [F](#) • [G](#) • [H](#) • [I](#) • [J](#) • [K](#) • [L](#) • [M](#) • [N](#) • [O](#) • [P](#) • [Q](#) • [R](#) • [S](#) • [T](#) • [U](#) • [V](#) • [W](#) • [X](#) • [Y](#) • [Z](#)

- Baader, SL [361A](#)
- Bacelo, J [30A](#), [432A](#)
- Backhaus, W [428A](#)
- Backus, KH [286A](#), [319B](#), [368A](#), [448A](#)
- Bader, V [268A](#)
- Bading, H [342A](#), [343A](#), [344A](#)
- Bähr, M [S20](#), [S20-4](#), [49B](#), [181B](#), [339B](#), [340B](#), [341B](#), [349B](#), [392A](#), [395A](#), [410A](#), [411A](#), [416B](#)
- Bähring, R [325A](#)
- Bäuerle, P [107A](#)
- Bagnard, D [23A](#)
- Baines, RA [S24-1](#)
- Bajbouj, M [207A](#), [208A](#), [427A](#)
- Balakrishnan, S [41B](#), [409A](#)
- Balakrishnan, V [S24-5](#)
- Balan, L [285B](#)
- Balavoine, G [422B](#)
- Baldus, M [151A](#)
- Ball, GF [108B](#), [109B](#), [110B](#)
- Ball, T [29B](#), [30B](#), [31B](#), [436A](#)
- Bally-Cuif, L [403A](#)
- Balschun, D [236B](#)
- Bandelow, B [400B](#)
- Bar-Haim, S [87B](#)
- Barbour, J [44B](#), [121B](#)
- Barchmann, S [375A](#)
- Bareyre, FM [S17-4](#)
- Barlow, K [275A](#)
- Bartoszek, I [3A](#)
- Bartsch, D [460B](#), [461B](#)
- Bass, T [370A](#)
- Bauer, [423B](#)
- Bauer, CK [S1-3](#)
- Bauer, K [374A](#)
- Bauer, NG [354A](#)
- Bauhofer, A [420A](#)
- Baumann, A [326A](#)
- Baumann, O [141B](#)
- Baumann, W [321A](#)
- Baune, BT [399B](#)
- Bayer, TA [S2-4](#)
- Becherer, U [295B](#)
- Beck, H [240A](#)
- Beck, O [279A](#), [444A](#)
- Beck, T [S7](#)
- Becker, AJ [240A](#)
- Becker, C-M [255B](#)
- Becker, CG [S7](#), [S7-1](#)
- Becker, K [222B](#), [255B](#)
- Becker, M [Sat2-2](#), [113B](#)
- Becker, N [257B](#)
- Becker, T [S7-1](#)
- Becker, TS [47A](#)
- Beckers, U [149A](#)
- Beckhaus, T [284A](#), [285A](#)
- Beckmann, S [393B](#)
- Beglopoulos, V [279B](#)
- Behnisch, T [267B](#)
- Behrend, K [162B](#)
- Behrendt, M [358B](#)
- Behrens, CJ [214A](#)
- Belkin, M [414A](#)
- Bell, CC [S8-4](#)
- Bell, SM [S12-3](#)

[A](#) • [B](#) • [C](#) • [D](#) • [E](#) • [D](#) • [E](#) • [F](#) • [G](#) • [H](#) • [I](#) • [J](#) • [K](#) • [L](#) • [M](#) • [N](#) • [O](#) • [P](#) • [Q](#) • [R](#) • [S](#) • [T](#) • [U](#) • [V](#) • [W](#) • [X](#) • [Y](#) • [Z](#)

- Belokopytov, M [414A](#)
- Belusic, G [16B](#), [147A](#)
- Benali, A [387A](#)
- Benard, J [14A](#)
- Benaroya-Milshtein, N [417A](#)
- Benda, J [95A](#), [88B](#), [91B](#), [118B](#), [119B](#)
- Bender, J [346A](#)
- Bendikov, I [272A](#)
- Benecke, R [79B](#)
- Bengtson, P [342A](#)
- Benkner, B [162B](#)
- Benoit, P [S2-4](#)
- Benowitz, L [394B](#)
- Berbaum, K [S14-4](#)
- Bergado, J [234B](#)
- Berger, S [299A](#)
- Berger, T [211A](#)
- Bergmann, J [233A](#)
- Bermudez i Badia, S [146B](#)
- Bernhardt, BC [434B](#)
- Bernhardt, M [73B](#)
- Berninger, B [S12-2](#)
- Bernreuther, C [379B](#)
- Bert, B [329A](#)
- Bette, S [165A](#)
- Bettencourt Relvas, J [S12-5](#)
- Bevan, S [389A](#)
- Beyersdorf, N [419B](#)
- Beyreuther, K [S2-5](#)
- Bezzi, P [S11](#), [S11-3](#), [S11-5](#)
- Biber, K [418A](#)
- Bibitchkov, D [450B](#)
- Bicker, G [S15](#), [S15-2](#), [286B](#)
- Bickmeyer, U [127B](#), [338A](#)
- Biebel, UW [115A](#), [99B](#)
- Biedenkapp, D [115A](#), [99B](#)
- Bielau, H [115B](#)
- Bigl, M [331B](#)
- Binding, N [327A](#)
- Birbaumer, N [S18-4](#), [252B](#), [437B](#)
- Birchmeier, C [S5-4](#), [209A](#), [351B](#)
- Bischof, H-J [166A](#), [198A](#), [199A](#), [219A](#), [238A](#), [429A](#)
- Bitz, U [440B](#), [441B](#)
- Bitzer, S [171B](#), [182B](#)
- Blaes, F [408A](#)
- Blaesse, P [273A](#)
- Blanchard, V [S2-4](#)
- Blankertz, B [S18-1](#)
- Blaszczyk, WM [181A](#)
- Bleckmann, H [61A](#), [117A](#)
- Blenau, W [326A](#)
- Blottner, D [S15-5](#)
- Bludau, T [377A](#)
- Blum, R [464B](#)
- Blumenfeld, B [450B](#)
- Bock, J [223B](#)
- Bock, O [79A](#), [71B](#), [72B](#), [76B](#), [250A](#), [251A](#), [435A](#)
- Bock, SW [439B](#)
- Bockemühl, T [85A](#)
- Boddeke, HWGM [418A](#)
- Bodis-Wollner, I [173B](#)
- Böcker-Meffert, S [342B](#), [343B](#), [344B](#), [345B](#)

[A](#) • [B](#) • [C](#) • [D](#) • [E](#) • [D](#) • [E](#) • [F](#) • [G](#) • [H](#) • [I](#) • [J](#) • [K](#) • [L](#) • [M](#) • [N](#) • [O](#) • [P](#) • [Q](#) • [R](#) • [S](#) • [T](#) • [U](#) • [V](#) • [W](#) • [X](#) • [Y](#) • [Z](#)

- |  |  |
|--|--|
| Boeckers, TM <a href="#">275B</a>  | Borta, A <a href="#">254A</a> , <a href="#">255A</a>   |
| Böckers, T <a href="#">Sat3-2</a>  | Bosch, D <a href="#">319A</a>  |
| Boeddeker, N <a href="#">15B</a> , <a href="#">22B</a>   | Bosse, F <a href="#">S17-2</a> , <a href="#">390A</a>  |
| Böddeker, N <a href="#">19B</a>  | Botella, C <a href="#">272B</a>  |
| Boeddinghaus, C <a href="#">333B</a>   | Bottenberg, W <a href="#">S24-2</a>  |
| Boehlen, A <a href="#">283A</a>  | Boucetta, S <a href="#">212A</a>   |
| Boehm, C <a href="#">27B</a>   | Boucsein, C <a href="#">32B</a>  |
| Boehm, T <a href="#">128A</a>  | Boyan, G <a href="#">374B</a>  |
| Boekhoorn, K <a href="#">24A</a>   | Boyer, M <a href="#">259A</a>  |
| Boelmans, K <a href="#">35B</a>  | Brackmann, M <a href="#">274A</a>  |
| Bölte, S <a href="#">252B</a>  | Bradke, F <a href="#">S17-3</a>  |
| Boenke, LT <a href="#">426B</a>  | Brady, S <a href="#">400B</a>  |
| Bösel, J <a href="#">406A</a>  | Bräuer, AU <a href="#">26A</a>   |
| Boesiger, P <a href="#">199B</a>   | Bräunig, P <a href="#">261A</a> , <a href="#">344B</a>   |
| Böttner, M <a href="#">227A</a>  | Bräuning, P <a href="#">341A</a>   |
| Bogdan, S <a href="#">S5-5</a>   | Braig, C <a href="#">S3-4</a> , <a href="#">S3-6</a> , <a href="#">6A</a> , <a href="#">9A</a>             |
| Bogerts, B <a href="#">115B</a>  | Brakebusch, C <a href="#">S12-5</a>  |
| Bohm, S <a href="#">127A</a>   | Brand, A <a href="#">271B</a>  |
| Boinska, D <a href="#">398A</a> , <a href="#">400A</a>   | Brand, M <a href="#">S5-3</a>  |
| Bolmont, T <a href="#">S2-1</a>  | Brandstätter, JH <a href="#">161A</a> , <a href="#">162A</a> , <a href="#">166B</a> , <a href="#">290B</a> |
| Bolz, J <a href="#">23A</a> , <a href="#">375A</a>   | Brandt, A <a href="#">S3-3</a>   |
| Bondre-Beil, P <a href="#">Sat5-5</a>  | Brandt, B <a href="#">401B</a>   |
| Bongard, M <a href="#">37B</a> , <a href="#">172B</a>  | Brandt, C <a href="#">1B</a>   |
| Bonhoeffer, T <a href="#">189B</a> , <a href="#">190B</a> , <a href="#">238B</a> , <a href="#">291B</a> ,<br><a href="#">292B</a> , <a href="#">293B</a> , <a href="#">373B</a> , <a href="#">463B</a> | Branski, P <a href="#">339A</a>  |
| Bonomini, MP <a href="#">468B</a>  | Braun, C <a href="#">43A</a> , <a href="#">44A</a> , <a href="#">252B</a>                                  |
| Boonman, A <a href="#">37A</a>   | Braun, D <a href="#">80B</a>   |
| Boretius, S <a href="#">468A</a>   | Braun, HA <a href="#">305B</a> , <a href="#">335B</a> , <a href="#">462B</a>                               |
| Borghgraef, P <a href="#">24A</a>  | Braun, K <a href="#">222B</a> , <a href="#">223B</a> , <a href="#">237B</a>                                |
| Borgmann, A <a href="#">81B</a>  | Braun, N <a href="#">367A</a> , <a href="#">369A</a>   |
| Born, J <a href="#">S23</a> , <a href="#">S23-7</a> , <a href="#">252A</a>   | Braun, R <a href="#">Sat2-4</a>  |
| Borst, A <a href="#">S16-2</a> , <a href="#">150B</a> , <a href="#">151B</a> , <a href="#">152B</a>  | Brauner, D <a href="#">162A</a> , <a href="#">166B</a>   |
|  | Braunewell, K-H <a href="#">274A</a>   |

[A](#) • [B](#) • [C](#) • [D](#) • [E](#) • [D](#) • [E](#) • [F](#) • [G](#) • [H](#) • [I](#) • [J](#) • [K](#) • [L](#) • [M](#) • [N](#) • [O](#) • [P](#) • [Q](#) • [R](#) • [S](#) • [T](#) • [U](#) • [V](#) • [W](#) • [X](#) • [Y](#) • [Z](#)

Brechmann, A [115B](#)

Brecht, S [413A](#), [419A](#)

Breer, H [S21-2](#), [121A](#), [122A](#), [123A](#), [124A](#),  
[125A](#), [126A](#), [127A](#), [135B](#)

Bremen, P [108A](#)

Bremmer, F [77A](#), [78A](#), [427B](#), [428B](#)

Bressloff, P [93B](#)

Breustedt, J [277A](#), [278A](#)

Brigadski, T [301B](#), [371B](#)

Bringmann, A [349A](#), [350A](#)

Brinker, S [368A](#)

Brinkmann, BG [351B](#)

Britanova, O [50A](#), [363B](#)

Britsch, S [209A](#)

Brodhun, M [328B](#)

Broicher, T [315A](#), [316A](#)

Brosch, M [104B](#)

Brose, N [Sat4](#), [295A](#)

Brouwer, N [418A](#)

Brown, DA [S1-2](#)

Brudermanns, B [116B](#)

Brück, W [S14](#)

Brückner, G [S7-3](#), [412B](#)

Bruehl, C [387B](#)

Brüstle, O [345A](#), [404A](#)

Brune, K [463A](#)

Brunert, D [124B](#)

Bruns, A-F [398B](#)

Brzozka, MM [362B](#)

Buard, I [42A](#), [415A](#)

Buchner, E [257A](#), [258A](#), [297B](#)

Buchner, S [297B](#)

Budde, T [S1-5](#), [315A](#), [316A](#)

Budinger, E [110A](#), [107B](#)

Budinsky, L [463A](#)

Bühlmann, A [171B](#), [182B](#)

Büschges, A [68A](#), [65B](#), [86A](#), [81B](#), [82B](#)

Bufler, J [312A](#), [347A](#)

Buhl, E [300B](#)

Bukalo, O [S7-5](#), [246A](#)

Bullmann, T [414B](#)

Bumsted o'Brien, KM [51A](#)

Bunck, M [423A](#)

Bundrock, G [232A](#)

Burbach, GJ [5A](#), [27A](#), [366A](#)

Burgdorf, J [Sat1-2](#)

Burkert, P [359A](#)

Burré, J [284A](#), [285A](#)

Busch, NA [174A](#)

Buschbacher, H [333B](#)

Buschle, B [343A](#)

Bussmann, F [465A](#)

Butty, S [333B](#)

Butz, T [412B](#)

[A](#) • [B](#) • [C](#) • [D](#) • [E](#) • [D](#) • [E](#) • [F](#) • [G](#) • [H](#) • [I](#) • [J](#) • [K](#) • [L](#) • [M](#) • [N](#) • [O](#) • [P](#) • [Q](#) • [R](#) • [S](#) • [T](#) • [U](#) • [V](#) • [W](#) • [X](#) • [Y](#) • [Z](#)

Cabrera, RJ [226B](#)

Calegari, F [S12-1](#)

Calhoun, ME [225B](#)

Callsen, B [325A](#)

Cambridge, SB [292B](#), [293B](#), [463B](#)

Campbell, K [S12-3](#)

Campos, L [S12-5](#)

Caputi, L [S1-5](#)

Cardoso de Oliveira, S [80A](#)

Carl, C [434B](#)

Carlomagno, T [323B](#)

Carlsson, MA [47B](#), [120B](#)

Carmignoto, G [S11-2](#)

Casas, C [S2-4](#)

Castelino, CB [109B](#)

Casteller, G [226B](#), [227B](#)

Celikel, T [247A](#), [249A](#)

Chagnaud, B [61A](#)

Chandra, A [318B](#)

Chandra, T [318B](#)

Chapouton, P [403A](#)

Chauvette, S [212A](#)

Chelazzi, L [S19-5](#)

Chen, H-C [33B](#)

Chen, J [240A](#)

Chen, S-W [33B](#)

Chistiakova, M [279A](#)

Chourbaji, S [404B](#)

Chowdhury, J [5B](#)

Chromik, A [413A](#)

Chwalla, I [165A](#)

Cichocki, A [466A](#)

Cimerman, J [S3-6](#), [9A](#)

Claaßen, B [358A](#)

Claes, E [403B](#)

Claudepierre, T [42A](#), [415A](#)

Claus, P [398B](#)

Clemens, Z [51B](#)

Clement, A [S20-2](#)

Climent, R [37B](#)

Cocucci, AA [148A](#)

Cohen, LG [P2](#)

Cohen-Kadosh, R [206A](#)

Coksaygan, T [328B](#)

Collett, TS [S4-1](#)

Colombelli, J [422B](#)

Concepción, L [37B](#)

Conrad, M [233A](#)

Conzelmann, S [S21-2](#), [135B](#)

Cook, EH [399B](#)

Cooke, RM [389A](#)

Coomaraswamy, J [S2-1](#)

Cooper, B [226A](#)

Coppola, D [177B](#)

Corballis, MC [111B](#)

Correa, SAL [266A](#)

Cossette, P [312A](#)

Coulon, P [315B](#)

Craxton, M [405B](#)

Creutzfeldt, C [190B](#)

Creutzig, F [88B](#)

Cronin, TW [145A](#)

Cürten, B [463B](#)

Curcic-Blake, B [64B](#)

[A](#) • [B](#) • [C](#) • [D](#) • [E](#) • [D](#) • [E](#) • [F](#) • [G](#) • [H](#) • [I](#) • [J](#) • [K](#) • [L](#) • [M](#) • [N](#) • [O](#) • [P](#) • [Q](#) • [R](#) • [S](#) • [T](#) • [U](#) • [V](#) • [W](#) • [X](#) • [Y](#) • [Z](#)

Curio, G [S9-6](#), [S18-1](#)

Cuttle, M [134B](#)

Czéh, B [S6-4](#), [393A](#)

Czeloth, K [419A](#)

Czibere, L [424A](#)

Czub, S [6B](#)

[A](#) • [B](#) • [C](#) • [D](#) • [E](#) • [D](#) • [E](#) • [F](#) • [G](#) • [H](#) • [I](#) • [J](#) • [K](#) • [L](#) • [M](#) • [N](#) • [O](#) • [P](#) • [Q](#) • [R](#) • [S](#) • [T](#) • [U](#) • [V](#) • [W](#) • [X](#) • [Y](#) • [Z](#)

- Daan, S [388B](#)
- Dabauvalle, M-C [297B](#)
- Dahlem, MA [174A](#), [449B](#)
- Dahlem, YA [425B](#)
- Dahlhaus, R [276B](#)
- Dahmen, H [258B](#)
- Dalton, PD [25A](#)
- Damann, N [122B](#), [124B](#)
- Danker-Hopfe, H [53B](#), [276A](#)
- Dauner, M [9B](#)
- Daur, N [451B](#)
- de Bruyne, M [131A](#)
- de Jong, E [418A](#)
- de Lange, MS [Sat2-4](#)
- De Pietri Tonelli, D [S12-1](#)
- de Polavieja, GG [33A](#), [143A](#)
- De Silva, R [414B](#)
- de Souza-Silva, MA [346A](#)
- de Wit, H [399B](#)
- Decker, T [343B](#)
- Deckert, J [399B](#), [400B](#), [401B](#)
- Dedek, K [163B](#), [167B](#), [170B](#)
- Deicke, U [5A](#)
- Deisig, N [19A](#)
- Del Turco, D [5A](#), [366A](#)
- Delago, A [248B](#)
- Deliano, M [102B](#), [212B](#)
- Deller, T [5A](#), [27A](#), [366A](#)
- Delorme, A [S9-5](#)
- Demberg, T [270A](#)
- Demmer, H [138A](#)
- Demmer, I [181B](#), [410A](#)
- Demuth, L [S19-3](#)
- Dengler, R [S20-7](#), [Sat1-16](#)
- Denker, M [210A](#)
- Deouell, LY [153A](#)
- Depaulis, A [221A](#), [222A](#)
- Dermietzel, R [269A](#), [386A](#)
- Derst, C [322A](#)
- Dettling, M [427A](#)
- Dewer, YME [124A](#)
- Dhaunchak, AS [352B](#)
- Dicke, PW [439B](#)
- Dicke, U [388A](#)
- Dickinson, MH [70B](#)
- Dickson, B P1
- Diegelmann, S [257A](#)
- Diekamp, B [108B](#), [109B](#), [110B](#), [194A](#), [273B](#)
- Diekmann, S [115B](#)
- Diem, R [181B](#), [392A](#), [410A](#), [416B](#)
- Dierkes, PW [315B](#), [316B](#), [337A](#), [372B](#)
- Dierkes, T [434B](#)
- Diesmann, M [205B](#), [206B](#), [207B](#), [208B](#), [210B](#)
- Diestel, S [362A](#)
- Dietz, GPH [49B](#), [339B](#)
- Dietz, M [52A](#)
- Dijkstra, IM [418A](#)
- Dimou, L [S17-4](#), [26B](#)
- Dincheva, Z [253A](#)
- Dinse, HR [62A](#), [64A](#), [65A](#), [60B](#), [61B](#), [62B](#), [63B](#), [175A](#), [176A](#), [179A](#), [179B](#)
- Dircksen, H [424B](#)
- Dirks, P [167B](#), [169B](#), [191B](#)
- Distler, C [178A](#), [181A](#), [186A](#)

[A](#) • [B](#) • [C](#) • [D](#) • [E](#) • [D](#) • [E](#) • [F](#) • [G](#) • [H](#) • [I](#) • [J](#) • [K](#) • [L](#) • [M](#) • [N](#) • [O](#) • [P](#) • [Q](#) • [R](#) • [S](#) • [T](#) • [U](#) • [V](#) • [W](#) • [X](#) • [Y](#) • [Z](#)

Dittmar, L <a href="#">19B</a>	Dünker, N <a href="#">399A</a>
Dittmar, MS <a href="#">466B</a>	Dürr, V <a href="#">66B</a> , <a href="#">85A</a>
Dittrich, L <a href="#">96A</a>	Dürrbeck, H <a href="#">297B</a>
Dityatev, A <a href="#">S7</a> , <a href="#">S7-5</a> , <a href="#">29A</a> , <a href="#">48A</a> , <a href="#">246A</a>	Duffe, K <a href="#">361A</a>
Dityateva, G <a href="#">29A</a>	Dugladze, T <a href="#">218A</a>
Ditzen, M <a href="#">133A</a>	Dujardin, E <a href="#">55A</a>
Divanach, A <a href="#">387B</a>	Dumin, E <a href="#">272A</a>
Döring, F <a href="#">309A</a>	Dumitrescu, ON <a href="#">156A</a>
Dörner, JF <a href="#">123B</a>	Durand, GM <a href="#">464B</a>
Dohm, CP <a href="#">340B</a> , <a href="#">341B</a>	Dutschmann, M <a href="#">85B</a> , <a href="#">86B</a> , <a href="#">302A</a> , <a href="#">303A</a> , <a href="#">304A</a> , <a href="#">305A</a> , <a href="#">306A</a>
Dolan, J <a href="#">365A</a>	Dvorak, F <a href="#">11B</a>
Dolgov, O <a href="#">461B</a>	
Dolkov, O <a href="#">460B</a>	
Dombrowe, I <a href="#">434B</a>	
Domenger, D <a href="#">253A</a>	
Donner, K <a href="#">152A</a>	
Dooley, R <a href="#">136A</a>	
Dori, H <a href="#">206A</a>	
Dorokhov, VB <a href="#">392B</a>	
Dotzauer, K <a href="#">69A</a>	
Draslar, K <a href="#">63A</a> , <a href="#">146A</a> , <a href="#">147A</a>	
Dreesmann, L <a href="#">9B</a>	
Dresbach, T <a href="#">368B</a>	
Drescher, K <a href="#">334B</a>	
Drewes, G <a href="#">Sat2-6</a>	
Dubinsky, G <a href="#">414A</a>	
Dubischar-Krivec, AM <a href="#">252B</a>	
Dubreuil, V <a href="#">S12-1</a>	
Duch, C <a href="#">S24</a> , <a href="#">S24-4</a> , <a href="#">55B</a> , <a href="#">67B</a> , <a href="#">69B</a> , <a href="#">359A</a>	
Ducray, A <a href="#">50B</a>	
Dudanova, I <a href="#">297A</a>	
Dümpelfeld, B <a href="#">Sat2-6</a>	



[A](#) • [B](#) • [C](#) • [D](#) • [E](#) • [D](#) • [E](#) • [F](#) • [G](#) • [H](#) • [I](#) • [J](#) • [K](#) • [L](#) • [M](#) • [N](#) • [O](#) • [P](#) • [Q](#) • [R](#) • [S](#) • [T](#) • [U](#) • [V](#) • [W](#) • [X](#) • [Y](#) • [Z](#)

- Eberle, C [83A](#)
- Ebert, M [370A](#), [372A](#)
- Ebert, U [334B](#)
- Eckhorn, R [38B](#), [39B](#), [173A](#), [184B](#), [185B](#),  
[186B](#), [187B](#), [188B](#)
- Eckstein, A [Sat1-13](#)
- Edeline, J-M [S10-1](#)
- Edenfeld, G [S5-5](#)
- Edenhofer, F [404A](#)
- Edlund, T [S5-1](#)
- Egelhaaf, M [15B](#), [17B](#), [18B](#), [19B](#), [20B](#), [22B](#),  
[23B](#), [24B](#), [149A](#)
- Egert, U [222A](#)
- Egorov, AV [248A](#)
- Ehrenreich, H [392A](#), [410A](#)
- Ehrenreich, L [468A](#)
- Ehret, G [S10-2](#), [Sat1-9](#), [99A](#), [101A](#)
- Ehret, R [321A](#)
- Ehrhardt, S [273A](#)
- Ehrlich, I [S24-5](#)
- Eibl, H [335A](#)
- Eichhammer, P [38A](#)
- Eiffert, H [8B](#)
- Eilam, R [271B](#)
- Einhäuser, W [60A](#), [430B](#), [431B](#), [433B](#), [442B](#)
- Eisenhardt, D [235A](#)
- Eisenhardt, G [27B](#)
- Elepfandt, A [116B](#), [117B](#)
- Elger, C [S18-4](#), [S23-2](#)
- Elghazali, F [424B](#)
- Elhilali, M [S10-5](#)
- Ellingsen, S [47A](#)
- Elphick, MR [242A](#), [266B](#)
- Eminel, S [329B](#), [330B](#)
- Endepols, H [263B](#)
- Endres, M [406A](#)
- Endres, T [220B](#), [221B](#)
- Engel, AK [36B](#), [78B](#)
- Engel, J [S3](#), [S3-4](#), [6A](#)
- Engelhorn, A [102B](#), [212B](#)
- Engelmann, J [117A](#)
- Engelmann, JP [30A](#), [432A](#)
- Engler, G [78B](#)
- Engmann, S [430B](#), [432B](#)
- Enkel, T [333A](#)
- Ennis, M [130A](#)
- Ensberg, D [102B](#), [212B](#)
- Epstein, Y [414A](#)
- Erdlenbruch, B [335A](#), [415B](#)
- Erdmann, KS [371B](#)
- Erhard, P [220A](#)
- Ernst, UA [434A](#), [445A](#)
- Esser, K-H [Sat1-3](#)
- Eurich, CW [187A](#), [191A](#)
- Evers, JF [S24-4](#), [55B](#), [67B](#)
- Eybalin, M [282B](#)
- Eysel, UT [280A](#), [300A](#), [387A](#)

[A](#) • [B](#) • [C](#) • [D](#) • [E](#) • [D](#) • [E](#) • [F](#) • [G](#) • [H](#) • [I](#) • [J](#) • [K](#) • [L](#) • [M](#) • [N](#) • [O](#) • [P](#) • [Q](#) • [R](#) • [S](#) • [T](#) • [U](#) • [V](#) • [W](#) • [X](#) • [Y](#) • [Z](#)

Fabian, S [408A](#)

Fabó, D [51B](#)

Fabri, M [111B](#)

Fässler, R [S12-5](#)

Fahlke, C [Sat3-3](#)

Faissner, A [S12-5](#), [S12-6](#), [201A](#), [202A](#), [203A](#),  
[360A](#), [386A](#), [396B](#), [397B](#)

Fakler, B [322B](#)

Farkas, L [S12-1](#)

Farrar, J [200B](#)

Farrow, K [150B](#)

Fassbender, K [S2](#), [S2-3](#)

Faucher, C [131A](#)

Fawcett, JW [S7-2](#)

Feenders, G [191B](#), [192B](#), [193B](#)

Fehm, NP [466B](#)

Feigenpan, A [164B](#)

Feil, R [S15-3](#)

Feinstein, P [S21-1](#)

Feistel, T [121A](#)

Fejtová, A [161A](#), [290B](#)

Feldkaemper, M [308B](#)

Felicio, LF [329A](#)

Fell, J [S23-2](#)

Fellbrich, A [439A](#)

Felmy, F [Sat3-1](#)

Fendt, M [220B](#), [221B](#)

Ferber, M [323B](#)

Fernández, E [37B](#), [172B](#), [272B](#), [468B](#)

Fernández, G [S23-2](#)

Ferrandez, JM [468B](#)

Fertschai, I [91A](#)

Fesenko, GN [392B](#)

Fest, S [117A](#)

Fester, L [227A](#)

Fetcho, JR [125B](#)

ffrench-Constant, C [S12-5](#)

Fiala, A [258A](#)

Fimmers, R [400B](#)

Fink, H [328A](#), [329A](#)

Fink, S [8A](#)

Fink, T [354B](#)

Firzlaff, U [111A](#)

Fischer, B [467B](#)

Fischer, D [394B](#)

Fischer, E [364B](#)

Fischer, M [71A](#)

Fish, J [S12-1](#)

Flecke, C [130B](#)

Fleischer, AG [76A](#)

Fleischer, J [S21-2](#), [126A](#), [135B](#)

Flik, G [425A](#)

Flint, J [400B](#)

Flügge, G [Sat4](#), [209B](#), [226A](#), [294A](#), [391A](#),  
[393A](#), [397A](#), [437A](#)

Foeller, E [112A](#)

Förster, T [462A](#)

Folta, K [194A](#)

Foltyn, VN [272A](#)

Forgacs, PB [173B](#)

Fortune, ES [108B](#), [110B](#)

Fouquet, W [402A](#)

Frahm, C [386B](#)

Frahm, J [468A](#)

[A](#) • [B](#) • [C](#) • [D](#) • [E](#) • [D](#) • [E](#) • [F](#) • [G](#) • [H](#) • [I](#) • [J](#) • [K](#) • [L](#) • [M](#) • [N](#) • [O](#) • [P](#) • [Q](#) • [R](#) • [S](#) • [T](#) • [U](#) • [V](#) • [W](#) • [X](#) • [Y](#) • [Z](#)

Fraile, M [226B](#), [227B](#)

Frambach, I [263A](#)

Francke, M [349A](#), [351A](#)

Frank, A [87B](#)

Frank, E [421A](#)

Frank, M [370A](#), [372A](#)

Frank, N [S14-3](#), [418B](#)

Franke, H [331B](#)

Franke, P [400B](#)

Franzkowiak, S [62B](#)

Frebel, K [356A](#)

Freitag, C [400B](#)

Freiwald, WA [188A](#), [189A](#), [190A](#), [191A](#)

Freudenstein, D [S18-4](#)

Freund, I [321A](#)

Freund, N [177A](#)

Freund, Y [239A](#)

Frey, H-P [433B](#)

Frey, JU [216B](#), [231B](#), [232B](#), [233B](#), [235B](#)

Frey, S [216B](#)

Freyberg, S [195B](#)

Friauf, E [S24-5](#), [Sat2-2](#), [Sat4-4](#), [113B](#), [114B](#),  
[273A](#), [378A](#)

Friedel, E [436B](#)

Friedel, P [443B](#)

Friedrich, RW [125B](#), [126B](#), [446B](#)

Fries, JE [165A](#), [349A](#)

Friesema, E [374A](#)

Fritsche, D [299B](#)

Fritz, JB [S10-5](#)

Fritz, R [224B](#)

Fritz, T [Sat1-14](#), [229A](#)

Fritze, J [400B](#)

Fritzen, S [403B](#), [404B](#)

Fröhlich, H [196B](#)

Froese, A [235A](#)

Fromherz, P [228B](#), [230B](#), [313A](#), [314A](#)

Frost, B [153B](#)

Frotscher, M [221A](#), [371A](#)

Fry, SN [70B](#)

Fuchs, E [S6](#), S6-1, [S6-4](#), [209B](#), [224A](#), [334A](#),  
[393A](#), [397A](#)

Führer, K [141B](#)

Funke, K [193A](#)

[A](#) • [B](#) • [C](#) • [D](#) • [E](#) • [D](#) • [E](#) • [F](#) • [G](#) • [H](#) • [I](#) • [J](#) • [K](#) • [L](#) • [M](#) • [N](#) • [O](#) • [P](#) • [Q](#) • [R](#) • [S](#) • [T](#) • [U](#) • [V](#) • [W](#) • [X](#) • [Y](#) • [Z](#)

- |   |  |
|---|--|
| Gabis, L <a href="#">396A</a>   | Gebert, K <a href="#">216A</a>   |
| Gabriel, A <a href="#">184B</a>   | Gebhardt, C <a href="#">202B</a> , <a href="#">366A</a>  |
| Gabriel, JP <a href="#">87A</a>   | Gebhardt, M <a href="#">373A</a>   |
| Gabriel, S <a href="#">215A</a>   | Gehres, M <a href="#">183B</a>   |
| Gärtner, U <a href="#">408B</a> , <a href="#">409B</a> , <a href="#">410B</a> , <a href="#">448B</a>                          | Geiger, MF <a href="#">214B</a>  |
| Gaese, B <a href="#">103A</a> , <a href="#">103B</a>  | Geisel, T <a href="#">1A</a> , <a href="#">75B</a> , <a href="#">210B</a>  |
| Gage, FH <a href="#">356B</a>   | Geisen, S <a href="#">118A</a>   |
| Gagné, R <a href="#">247B</a>   | Geisler, U <a href="#">397A</a>  |
| Gagné, S <a href="#">247B</a>   | Geissler, H-S <a href="#">9A</a>   |
| Gagneur, J <a href="#">Sat2-6</a>   | Gelez, S <a href="#">434B</a>  |
| Gail, A <a href="#">184B</a> , <a href="#">185B</a> , <a href="#">188B</a>  | Gerber, B <a href="#">256A</a> , <a href="#">257A</a>  |
| Gais, S <a href="#">S23</a> , <a href="#">S23-7</a> , <a href="#">252A</a>  | Gerber, J <a href="#">8B</a> , <a href="#">394A</a>  |
| Galashan, FO <a href="#">433A</a>   | Gerber, SH <a href="#">290B</a>  |
| Galizia, CG <a href="#">S21-3</a> , <a href="#">132A</a> , <a href="#">133A</a> , <a href="#">134A</a> , <a href="#">128B</a> | Gerhardt, KJ <a href="#">377A</a>  |
| Galkin, A <a href="#">133A</a> , <a href="#">134A</a> , <a href="#">135A</a>  | Gerich, F <a href="#">326B</a>   |
| Galle, PR <a href="#">11B</a>   | Gernert, M <a href="#">470A</a>  |
| Galoch, Z <a href="#">429A</a>  | Gestreau, C <a href="#">86B</a>  |
| Ganesan, S <a href="#">341B</a>   | Ghislain, J <a href="#">47A</a>  |
| Ganeshina, O <a href="#">363A</a>   | Giannikopoulos, D <a href="#">193A</a>   |
| Garaschuk, O <a href="#">S13-1</a>  | Giehl, KM <a href="#">S22-1</a>  |
| Garcia de Arriba, S <a href="#">406B</a>  | Giese, MA <a href="#">204B</a>   |
| Garcion, E <a href="#">S12-5</a>  | Gießl, A <a href="#">157B</a> , <a href="#">158B</a> , <a href="#">159B</a>  |
| Gargiulo, PA <a href="#">226B</a> , <a href="#">227B</a>  | Gillner, S <a href="#">256B</a>  |
| Garner, CC <a href="#">290B</a>   | Gimsa, U <a href="#">77B</a> , <a href="#">79B</a>   |
| Garratt, AN <a href="#">209A</a>  | Giraldo, MA <a href="#">144B</a>   |
| Garwood, J <a href="#">201A</a>   | Girgenrath, M <a href="#">76B</a> , <a href="#">251A</a>   |
| Gass, P <a href="#">403B</a> , <a href="#">404B</a>   | Gisselmann, G <a href="#">136A</a> , <a href="#">312B</a> , <a href="#">313B</a>   |
| Gaub, SC <a href="#">101A</a>   | Giurfa, M <a href="#">S4</a> , <a href="#">S4-5</a> , <a href="#">14A</a> , <a href="#">15A</a> , <a href="#">16A</a> , <a href="#">17A</a> ,<br><a href="#">18A</a> , <a href="#">19A</a> |
| Gauck, V <a href="#">213B</a>   | Glauser, S <a href="#">91B</a>   |
| Gaudnek, MA <a href="#">463A</a>  | Gleich, O <a href="#">114A</a>   |
| Gaupp, S <a href="#">419B</a>   | Gloveli, T <a href="#">217A</a> , <a href="#">218A</a>   |
| Gawlik, V <a href="#">169B</a>  |  |

[A](#) • [B](#) • [C](#) • [D](#) • [E](#) • [D](#) • [E](#) • [F](#) • [G](#) • [H](#) • [I](#) • [J](#) • [K](#) • [L](#) • [M](#) • [N](#) • [O](#) • [P](#) • [Q](#) • [R](#) • [S](#) • [T](#) • [U](#) • [V](#) • [W](#) • [X](#) • [Y](#) • [Z](#)

- |   |  |
|---|--|
| Gocht, D <a href="#">301A</a>   | Grabert, J <a href="#">204A</a> , <a href="#">280A</a>   |
| Goczalik, I <a href="#">349A</a>  | Gräbner, M <a href="#">270B</a>  |
| Goczalik, M <a href="#">351A</a>  | Gräf, S <a href="#">436A</a>   |
| Godde, B <a href="#">175A</a> , <a href="#">176A</a> , <a href="#">179B</a> , <a href="#">436B</a>    | Graefe, A <a href="#">46A</a>  |
| Goebel, R <a href="#">206A</a>  | Grah, G <a href="#">237A</a>   |
| Göbel, S <a href="#">76B</a>  | Graham, PR <a href="#">S4-1</a>  |
| Goedeke, S <a href="#">210B</a>   | Gralla, J <a href="#">353B</a>   |
| Goedert, M <a href="#">405B</a>   | Gramowski, A <a href="#">321A</a> , <a href="#">337B</a> , <a href="#">338B</a>                    |
| Goelz, G <a href="#">1B</a>   | Grandgirard, D <a href="#">10B</a>   |
| Göpfert, MC <a href="#">317A</a> , <a href="#">318A</a>   | Grant, K <a href="#">30A</a> , <a href="#">432A</a>  |
| Göritz, C <a href="#">41A</a>   | Gras, H <a href="#">263A</a>   |
| Görtz, N <a href="#">2A</a>   | Grauvogel, F <a href="#">8A</a>  |
| Götz, M <a href="#">S12-2</a>   | Grebenshchikova, S <a href="#">5B</a>  |
| Götz, ME <a href="#">353B</a> , <a href="#">413A</a> , <a href="#">419A</a>                           | Greenberg, S <a href="#">153A</a>  |
| Gohl, T <a href="#">123A</a> , <a href="#">124A</a>   | Greenlee, MW <a href="#">S19-1</a>   |
| Gold, R <a href="#">419B</a>  | Greenspan, RJ <a href="#">S4-3</a>   |
| Goldbach, M <a href="#">171B</a> , <a href="#">182B</a>   | Greggers, U <a href="#">S4-2</a>   |
| Goldmann, T <a href="#">160B</a>  | Greiner, B <a href="#">145A</a>  |
| Goldschmidt, J <a href="#">107B</a> , <a href="#">470B</a>  | Greschat, S <a href="#">346A</a>   |
| Gollisch, T <a href="#">95A</a>   | Greschner, M <a href="#">165B</a> , <a href="#">166B</a>   |
| Golz, S <a href="#">20A</a>   | Grewe, J <a href="#">24B</a>   |
| Gomeza, J <a href="#">288B</a>  | Grewe, O <a href="#">54A</a> , <a href="#">105B</a>  |
| Gorenkova, N <a href="#">460B</a> , <a href="#">461B</a>  | Grill-Spector, K <a href="#">435B</a>  |
| Gorenkova, NA <a href="#">416A</a>  | Grimm, S <a href="#">407B</a>  |
| Gorlovoy, P <a href="#">S14-3</a> , <a href="#">3A</a> , <a href="#">418B</a>                         | Grinvald, A <a href="#">184A</a> , <a href="#">450B</a> , <a href="#">471A</a>                     |
| Goschzik, T <a href="#">362A</a>  | Gröger, U <a href="#">96B</a>  |
| Gosselin, N <a href="#">Sat1-12</a>   | Groh, A <a href="#">287B</a>   |
| Gosztonyi, G <a href="#">6B</a>   | Groh, C <a href="#">136B</a> , <a href="#">270B</a>  |
| Gottmann, K <a href="#">281A</a> , <a href="#">282A</a> , <a href="#">283A</a> , <a href="#">314B</a> | Gross, G <a href="#">289B</a> , <a href="#">332B</a> , <a href="#">333B</a> , <a href="#">334B</a> |
| Gottschalk, A <a href="#">317B</a>  | Große, G <a href="#">382A</a>  |
| Goulet, J <a href="#">120A</a>  | Grosse-Wilde, E <a href="#">123A</a> , <a href="#">124A</a>  |
| Goydke, KN <a href="#">Sat1-13</a> , <a href="#">53A</a>  | Großkreutz, J <a href="#">347A</a>   |

[A](#) • [B](#) • [C](#) • [D](#) • [E](#) • [D](#) • [E](#) • [F](#) • [G](#) • [H](#) • [I](#) • [J](#) • [K](#) • [L](#) • [M](#) • [N](#) • [O](#) • [P](#) • [Q](#) • [R](#) • [S](#) • [T](#) • [U](#) • [V](#) • [W](#) • [X](#) • [Y](#) • [Z](#)

Grossmann, R [306B](#)

Grossrau, G [345A](#)

Grothe, B [S10-4](#), [105A](#), [106A](#)

Grothe, C [81A](#), [347A](#), [398B](#)

Gruber, M [162B](#)

Grün, P [S10-2](#)

Grün, S [210A](#), [460A](#)

Grünblatt, E [6B](#)

Grüner, K [406B](#)

Grünewald, B [137B](#), [299A](#)

Gruhn, M [323A](#)

Grunwald, T [314B](#)

Gruss, M [237B](#)

Gruss, P [50A](#)

Grzyb, A [S12-1](#)

Gu, N [S1-4](#)

Guanella, A [230A](#)

Guardiera, P [435A](#)

Guckenheimer, J [323A](#)

Guddat, SS [S1-3](#)

Günther, U [304A](#)

Güntner, M [374B](#)

Güntürkün, O [177A](#), [180A](#), [194A](#), [200A](#), [273B](#)

Gürke, B [168A](#)

Guillemin, I [Sat2-2](#)

Gullo, M [26B](#)

Gulyas, J [323B](#)

Gummer, AW [7A](#), [98A](#)

Gundelfinger, ED [28A](#), [161A](#), [162A](#), [166B](#),

[275B](#), [282B](#), [290B](#), [368B](#), [369B](#)

Gundersen, V [S11-3](#), [S11-5](#)

Gundlfinger, A [216A](#), [277A](#)

Guschlbauer, C [68A](#)

Gussing, F [127A](#)

Gust, K [440B](#), [441B](#)

Gutman, M [296B](#)

Guzman, A [402A](#)

[A](#) • [B](#) • [C](#) • [D](#) • [E](#) • [D](#) • [E](#) • [F](#) • [G](#) • [H](#) • [I](#) • [J](#) • [K](#) • [L](#) • [M](#) • [N](#) • [O](#) • [P](#) • [Q](#) • [R](#) • [S](#) • [T](#) • [U](#) • [V](#) • [W](#) • [X](#) • [Y](#) • [Z](#)

Haag, J [S16-2](#), [150B](#), [151B](#)

Haag, N [129B](#)

Haas, B [S11-4](#)

Haas, CA [5A](#), [27A](#), [221A](#)

Haas, SJ-P [393B](#)

Haase, A [S15-2](#)

Haastert, K [81A](#), [398B](#)

Haberman, Y [417A](#)

Hack, I [371A](#)

Hack, M [S12-2](#)

Hackl, C [380B](#), [381B](#)

Hadamitzky, M [331A](#)

Härtel, K [150A](#)

Härtig, W [414B](#)

Haessler, U [S24-2](#)

Häussler, U [222A](#)

Haffner, Ch [S12-1](#)

Hafner, P [140A](#)

Hage, SR [102A](#)

Hahnloser, R [S9-2](#)

Hajak, G [38A](#)

Hake, J [205B](#)

Halász, P [51B](#)

Halbich, W [138B](#)

Halilagic, A [S12-5](#)

Haller, S [34B](#)

Hallmann, K [402B](#)

Halpert, H [417A](#)

Halsband, U [436A](#)

Hamann, I [114A](#)

Hamann, M [12B](#), [405A](#)

Hambrecht, V [220B](#)

Handschuh, M [296A](#), [349B](#), [350B](#)

Hanganu, IL [370B](#)

Hanisch, U-K [3B](#), [419A](#)

Hanke, W [469B](#)

Hanssen, M [8B](#)

Hansson, BS [47B](#), [120B](#)

Harasztosi, C [7A](#)

Hardie, RC [143A](#)

Harf, J [156B](#)

Harmening, W [196A](#)

Harms, C [406A](#)

Harries, N [87B](#)

Harris-Warrick, RM [323A](#)

Harsch, A [33A](#)

Hartbauer, M [88A](#)

Hartig, R [369B](#)

Hartmann, K [16B](#)

Hartmann, M [301B](#), [371B](#)

Harzsch, S [12A](#), [376B](#)

Hasenpusch-Theil, K [390A](#), [407A](#)

Haß, J [75B](#)

Hassel, M [422B](#)

Hassenklöver, T [338A](#)

Hatt, H [S21-6](#), [44B](#), [136A](#), [137A](#), [121B](#), [122B](#), [123B](#), [124B](#), [312B](#), [313B](#)

Hauber, W [251B](#)

Haupt, C [386B](#)

Haupt, S [404A](#)

Hausmann, M [111B](#)

Havemann-Reinecke, U [391A](#), [437A](#)

Haverkamp, SH [157A](#)

Heblich, R [274B](#)

[A](#) • [B](#) • [C](#) • [D](#) • [E](#) • [D](#) • [E](#) • [F](#) • [G](#) • [H](#) • [I](#) • [J](#) • [K](#) • [L](#) • [M](#) • [N](#) • [O](#) • [P](#) • [Q](#) • [R](#) • [S](#) • [T](#) • [U](#) • [V](#) • [W](#) • [X](#) • [Y](#) • [Z](#)

- |  |  |
|--|--|
| Heck, C <a href="#">293A</a>   | Hempel de Ibarra, N <a href="#">148A</a>   |
| Heck, S <a href="#">370B</a>   | Hendel, T <a href="#">152B</a>   |
| Heckmann, C <a href="#">393A</a>   | Hendler, T <a href="#">206A</a>  |
| Heckmann, M <a href="#">283B</a> , <a href="#">402A</a>                            | Hendrich, O <a href="#">317A</a>   |
| Hedrich, UBS <a href="#">83A</a>   | Heneka, MT <a href="#">43B</a>   |
| Hedwig, B <a href="#">S8</a> , S8-1, <a href="#">S8-2</a> , <a href="#">93A</a>    | Henik, A <a href="#">206A</a>  |
| Heermann, S <a href="#">399A</a>   | Henn, FA <a href="#">S6-3</a>  |
| Heffernan, B <a href="#">Sat2-6</a>  | Hennig, MH <a href="#">144A</a>  |
| Heidel, E <a href="#">310B</a> , <a href="#">311B</a>                              | Hennig, RM <a href="#">S9</a> , <a href="#">S9-3</a> , <a href="#">91B</a> , <a href="#">92B</a> , <a href="#">95B</a> , <a href="#">119B</a> , <a href="#">395B</a> |
| Heikenwälder, M <a href="#">S2-2</a>   | Henning, J <a href="#">77B</a>   |
| Heil, P <a href="#">100A</a>   | Henning, M <a href="#">S15-3</a>   |
| Heilbronner, U <a href="#">209B</a> , <a href="#">294A</a>                         | Henningfeld, KA <a href="#">21A</a> , <a href="#">22A</a>  |
| Heils, A <a href="#">312A</a> , <a href="#">402B</a>                               | Henze, MJ <a href="#">155B</a>   |
| Heinbockel, T <a href="#">130A</a> , <a href="#">277B</a>                          | Hepp, S <a href="#">326B</a>   |
| Heine, P <a href="#">51A</a>   | Heppenstall, PA <a href="#">S15-3</a>  |
| Heine, S <a href="#">355B</a>  | Herberger, S <a href="#">464B</a>  |
| Heine, VM <a href="#">S6-4</a>   | Herbert, Z <a href="#">423B</a>  |
| Heinemann, U <a href="#">215A</a> , <a href="#">217A</a> , <a href="#">218A</a>    | Herdegen, T <a href="#">329B</a> , <a href="#">330B</a> , <a href="#">413A</a> , <a href="#">419A</a>  |
| Heinisch, C <a href="#">62B</a>  | Herold, C <a href="#">273B</a>   |
| Heinrich, C <a href="#">221A</a>   | Herrmann, CS <a href="#">174A</a>  |
| Heinrich, R <a href="#">293A</a> , <a href="#">301A</a>                            | Herrmann, JM <a href="#">75B</a>   |
| Heinrich, SP <a href="#">435B</a>  | Hertel, R <a href="#">429B</a>   |
| Heinze, H-J <a href="#">35B</a>  | Herz, AVM <a href="#">32A</a> , <a href="#">95A</a> , <a href="#">88B</a> , <a href="#">91B</a> , <a href="#">462A</a>   |
| Heinze, L <a href="#">157A</a>   | Herzig, M <a href="#">S2-1</a>   |
| Heisenberg, M <a href="#">S16-1</a> , <a href="#">S16-6</a> , <a href="#">265B</a> | Hess, A <a href="#">463A</a> , <a href="#">465A</a>  |
| Heitwerth, J <a href="#">17B</a>   | Heß, D <a href="#">237A</a>  |
| Heldmann, S <a href="#">467B</a>   | Hess, D <a href="#">365B</a>   |
| Hellmann, B <a href="#">117B</a>   | Heuer, H <a href="#">374A</a>  |
| Hellweg, R <a href="#">5A</a> , <a href="#">276A</a>                               | Heumann, R <a href="#">183A</a> , <a href="#">408B</a>   |
| Helmchen, F <a href="#">S13-3</a>  | Heupel, K <a href="#">287A</a>   |
| Helmeke, C <a href="#">222B</a>  | Heuser, I <a href="#">53B</a> , <a href="#">207A</a>   |
| Helmstaedter, C <a href="#">S23-2</a>  |  |



[A](#) • [B](#) • [C](#) • [D](#) • [E](#) • [D](#) • [E](#) • [F](#) • [G](#) • [H](#) • [I](#) • [J](#) • [K](#) • [L](#) • [M](#) • [N](#) • [O](#) • [P](#) • [Q](#) • [R](#) • [S](#) • [T](#) • [U](#) • [V](#) • [W](#) • [X](#) • [Y](#) • [Z](#)

Hevers, W [320A](#)

Hidding, U [419A](#)

Hiemisch, H [27B](#)

Higashijima, S [125B](#)

Hildebrandt, KJ [95B](#)

Hille, K [440B](#), [441B](#)

Hinsch, K [356B](#)

Hinterberger, T [S18-4](#)

Hipp, J [60A](#)

Hirdes, W [S1-3](#)

Hirrlinger, J [43A](#), [44A](#), [84B](#), [296A](#)

Hirsch, S [320A](#)

Hoch, T [34A](#)

Hochstrate, P [315B](#), [316B](#), [337A](#)

Hölscher, C [258B](#)

Höltje, M [382A](#)

Hörner, M [274B](#)

Hofbauer, A [297B](#)

Hofer, S [302B](#)

Hofer, SB [189B](#), [190B](#)

Hoffmann, A [382A](#)

Hoffmann, K-P [167A](#), [168A](#), [178A](#), [181A](#),  
[182A](#), [183A](#), [186A](#), [239A](#), [430A](#), [431A](#)

Hoffmann, MB [201B](#)

Hofmann, F [S15-3](#), [342A](#), [382A](#)

Hofmann, KP [157B](#), [158B](#)

Hohoff, C [399B](#), [400B](#), [401B](#)

Hoidis, S [97B](#)

Hollander, N [417A](#)

Hollmann, M [260B](#), [314B](#)

Holst, MI [361A](#)

Holthoff, K [245B](#)

Holtmann, B [371B](#)

Holtze, S [197A](#)

Holzer, M [405B](#), [413B](#), [414B](#)

Homberg, U [S16-5](#), [21B](#), [148B](#), [264B](#), [302B](#)

Honey, C [434B](#)

Hopf, C [Sat2-6](#)

Hopf, J-M [35B](#)

Hoppe, R [122A](#), [125A](#)

Horn, ER [74A](#), [75A](#)

Horn, M [466B](#)

Horn, T [421A](#)

Hornstein, C [423B](#)

Hornung, OP [53B](#)

Horstmann, A [430A](#)

Horvat-Bröcker, A [202A](#), [203A](#), [386A](#)

Hosseini, M [5B](#), [223A](#)

Hou, S [S5-2](#), [366B](#)

Hu, H [S1-1](#), [S1-4](#)

Huber, A [S14-4](#), [16B](#)

Huchzermeyer, C [238A](#)

Hudl, K [172A](#)

Hübener, M [189B](#), [190B](#)

Hübner, MM [106B](#)

Hülper, P [335A](#)

Hülsmann, S [43A](#), [84B](#), [296A](#), [349B](#), [350B](#)

Hünig, T [419B](#)

Hütteroth, W [268B](#)

Huising, M [425A](#)

Humml, C [351B](#)

Humphries, P [200B](#)

Humphris, ADL [317A](#)

Hupfeld, D [182A](#), [183A](#), [239A](#)

[A](#) • [B](#) • [C](#) • [D](#) • [E](#) • [D](#) • [E](#) • [F](#) • [G](#) • [H](#) • [I](#) • [J](#) • [K](#) • [L](#) • [M](#) • [N](#) • [O](#) • [P](#) • [Q](#) • [R](#) • [S](#) • [T](#) • [U](#) • [V](#) • [W](#) • [X](#) • [Y](#) • [Z](#)

Hurst, LA [119A](#)

Husch, A [138A](#), [139A](#)

Husemann, P [238A](#)

Husse, J [256A](#)

Hustert, R [150A](#), [151A](#)

Huston, SJ [S16-3](#)

Hut, RA [388B](#)

Huttner, WB [S12-1](#)

Hutzler, F [233A](#)

Hutzler, M [228B](#)

[A](#) • [B](#) • [C](#) • [D](#) • [E](#) • [D](#) • [E](#) • [F](#) • [G](#) • [H](#) • [I](#) • [J](#) • [K](#) • [L](#) • [M](#) • [N](#) • [O](#) • [P](#) • [Q](#) • [R](#) • [S](#) • [T](#) • [U](#) • [V](#) • [W](#) • [X](#) • [Y](#) • [Z](#)

Iden, S [374A](#)

Ihring, A [151B](#), [152B](#)

Ilg, UJ [195B](#)

Illes, P [331B](#)

Illing, R-B [378B](#), [384B](#)

Inciute, A [275B](#)

Ingebrandt, S [345B](#)

Isbrandt, D [S1-1](#), [325A](#)

Ishai, A [S19-2](#), [199B](#)

Isheim, D [103A](#)

Ito, K [S16-1](#), [132A](#)

Ivanova, E [158A](#)

Iwasaki, M [248B](#)

[A](#) • [B](#) • [C](#) • [D](#) • [E](#) • [D](#) • [E](#) • [F](#) • [G](#) • [H](#) • [I](#) • [J](#) • [K](#) • [L](#) • [M](#) • [N](#) • [O](#) • [P](#) • [Q](#) • [R](#) • [S](#) • [T](#) • [U](#) • [V](#) • [W](#) • [X](#) • [Y](#) • [Z](#)

Jacob, AM [28B](#)

Jacob, CP [404B](#)

Jacobs, AM [233A](#), [426A](#)

Jährling, N [170B](#)

Jahn, R Sat2-3

Jaiswal, MK [41B](#)

Jakes, R [405B](#)

Jancke, D [184A](#), [186A](#)

Jandova, K [215A](#)

Jansen, L [434B](#)

Janssen-Bienhold, U [163B](#), [167B](#), [169B](#),  
[170B](#), [191B](#)

Jarosik, J [262B](#)

Jarvis, ED [193B](#)

Jedlicka, P [286A](#), [448A](#)

Jellinger, KA [45B](#)

Jenett, A [265B](#)

Jensen, CH [50B](#)

Jentsch, TJ [S3-7](#)

Jimenez, CR [S17-1](#)

Jiménez-Ortega, L [180A](#)

Jin, Y [256B](#)

Jirikowski, GF [423B](#)

Jockers-Scherübl, MC [276A](#), [427A](#)

Joels, M [S6-4](#), [24A](#)

Joëls, M [231A](#)

John, N [28A](#)

Johnson, SL [S3-2](#)

Jokela-Määttä, M [152A](#)

Jongen-Rêlo, AL [334B](#)

Jordan, K [439A](#)

Jose, M [368B](#), [369B](#)

Joshi, I [314B](#)

Jovanovic, S [4B](#)

Jucker, M [S2-1](#), [5A](#)

Judkewitz, B [446B](#)

Jügel, K [321A](#)

Juengen, CH [361A](#)

Jüngling, K [281A](#)

Jürgens, K [21A](#), [156B](#), [160B](#)

Jürgens, U [Sat1-6](#), [55A](#), [102A](#)

Jung, A [400B](#)

Junghans, D [371A](#)

Jurkat-Rott, K Sat3-6

Jurkevich, A [306B](#)

Just, I [382A](#)

Just, L [347A](#)

Juusola, M [33A](#), [143A](#)

[A](#) • [B](#) • [C](#) • [D](#) • [E](#) • [D](#) • [E](#) • [F](#) • [G](#) • [H](#) • [I](#) • [J](#) • [K](#) • [L](#) • [M](#) • [N](#) • [O](#) • [P](#) • [Q](#) • [R](#) • [S](#) • [T](#) • [U](#) • [V](#) • [W](#) • [X](#) • [Y](#) • [Z](#)

Kabisch, C [434B](#)

Käser, S [S2-1](#)

Kahnt, J [269B](#)

Kaila, K [S22-1](#)

Kaiser, A [246B](#), [465B](#)

Kalb, J [149A](#)

Kalisch, T [64A](#), [65A](#), [60B](#), [61B](#), [62B](#), [63B](#)

Kallerhoff, P [34A](#)

Kaluza, JF [127A](#)

Kamber, D [390B](#)

Kaminiaz, A [427B](#)

Kammann, SE [12B](#)

Kammer, T [193A](#)

Kampmann, E [380A](#)

Kaneko, T [7A](#)

Kanyshkova, T [S1-5](#), [315A](#), [316A](#)

Kanzow, M [419A](#)

Kao, JPY [277B](#)

Kaplanski, J [87B](#)

Karakuyu, D [273B](#)

Karas, M [284A](#), [285A](#)

Karg, S [307B](#)

Karim, AA [436B](#)

Karmeier, K [23B](#)

Karpova, A [267B](#)

Karschin, A [309A](#)

Kartvelishvily, E [285B](#)

Kaschube, M [175A](#), [176A](#), [177B](#), [179B](#)

Katagiri, C [248B](#)

Kaupert, U [229B](#), [239B](#)

Kaup, UB [172A](#)

Kayser, C [194B](#)

Kehrer, C [217A](#)

Keijser, JN [224A](#)

Keipert, C [319B](#)

Kelber, C [139B](#)

Keller, A [132B](#), [133B](#)

Keller, AA [99A](#)

Keller, BU [S20](#), [S20-3](#), [40B](#), [41B](#), [42B](#), [409A](#)

Keller, I [426A](#)

Kelliher, KR [128A](#)

Kelm, M [124B](#)

Kemler, R [371A](#), [372A](#)

Kemnitz, K [368B](#), [369B](#)

Kempermann, G [S6](#), [S6-2](#)

Kempter, R [36A](#), [216A](#), [443A](#)

Kerkau, T [419B](#)

Kerkhoff, G [426A](#)

Kermer, P [340B](#), [341B](#)

Kern, J [25A](#)

Kern, R [15B](#), [19B](#), [20B](#)

Kerschbaum, H [355A](#)

Kessels, MM [Sat3-5](#), [275B](#), [276B](#), [290B](#)

Keßler, MS [422A](#), [424A](#)

Kettenmann, H [S11-4](#)

Keyvani, K [2A](#)

Khabarova, MY [278B](#)

Khatib, AA [99B](#)

Khimich, D [291A](#), [282B](#)

Kiang, A-S [200B](#)

Kiebler, M [357A](#)

Kiefer, M [440B](#), [441B](#)

Kiess, W [331B](#)

Kikuta, H [47A](#)

[A](#) • [B](#) • [C](#) • [D](#) • [E](#) • [D](#) • [E](#) • [F](#) • [G](#) • [H](#) • [I](#) • [J](#) • [K](#) • [L](#) • [M](#) • [N](#) • [O](#) • [P](#) • [Q](#) • [R](#) • [S](#) • [T](#) • [U](#) • [V](#) • [W](#) • [X](#) • [Y](#) • [Z](#)

- Kilb, W [372B](#)
- Kilian, SB [10A](#)
- Kimmig, H [34B](#)
- Kinoshita, M [21B](#)
- Kipiani, E [218A](#)
- Kirchhoff, F [43A](#), [44A](#), [45A](#), [84B](#), [296A](#),  
[349B](#), [350B](#)
- Kirsch, J [194A](#)
- Kirschner, S [137B](#)
- Kirschstein, T [240A](#)
- Kittel, MC [114A](#)
- Kittel, RJ [283B](#), [402A](#)
- Kittner, H [331B](#)
- Klämbt, C [S5-5](#)
- Klaes, C [179A](#)
- Klapka, N [S17-2](#), [25B](#)
- Klar, M [167A](#)
- Klaus, S [422B](#)
- Klausmeyer, A [201A](#)
- Klees, G [316B](#), [337A](#)
- Kleibel, N [64A](#)
- Klein, A [379B](#), [381B](#), [382B](#)
- Klein, S [241A](#), [306B](#)
- Kleinbongard, P [124B](#)
- Kleindienst, H-U [239B](#), [241B](#)
- Kleineidam, CJ [138B](#), [139B](#), [140B](#)
- Kleinendam, CJ [137B](#)
- Kleinjung, T [38A](#)
- Kleinlogel, S [145B](#)
- Kleiser, R [77A](#), [78A](#)
- Kleppe, I [33A](#)
- Klettner, A [329B](#)
- Klimesch, W [S23-1](#)
- Klingauf, J [289A](#), [290A](#), [292A](#)
- Klingberg, M-N [211B](#)
- Klingenhoefer, S [428B](#)
- Klink, KB [101B](#)
- Klisch, C [449A](#)
- Klisch, TJ [21A](#)
- Klöppner, S [4A](#), [348B](#)
- Klöß, S [368A](#)
- Klopfleisch, S [4A](#), [348B](#)
- Kloppenburg, P [138A](#), [139A](#), [140A](#)
- Kluge, C [218B](#)
- Klump, GM [S10-6](#), [114A](#), [101B](#)
- Klupp, B [122B](#)
- Knapinski, S [395B](#)
- Knieling, M [382B](#)
- Knipper, M [S3](#), [S3-1](#), [S3-4](#), [S3-6](#), [6A](#), [9A](#), [10A](#)
- Knirsch, M [S3-4](#), [6A](#)
- Knop, G [172A](#)
- Knüsel, P [47B](#)
- Knust, E [S5-6](#)
- Kobsar, I [354B](#)
- Koch, M [241A](#), [331A](#), [332A](#), [333A](#), [336B](#)
- Kochubey, O [290A](#)
- Koczan, D [77B](#)
- Koegler, G [346A](#)
- Koehl, A [Sat4-4](#), [114B](#)
- Koehler, T [280A](#)
- Köhling, R [39A](#)
- Köhr, G [324A](#)
- Köllner, G [419B](#)

[A](#) • [B](#) • [C](#) • [D](#) • [E](#) • [D](#) • [E](#) • [F](#) • [G](#) • [H](#) • [I](#) • [J](#) • [K](#) • [L](#) • [M](#) • [N](#) • [O](#) • [P](#) • [Q](#) • [R](#) • [S](#) • [T](#) • [U](#) • [V](#) • [W](#) • [X](#) • [Y](#) • [Z](#)

- |   |  |
|---|--|
| Koelsch, S <a href="#">Sat1-14</a> , <a href="#">229A</a>   | Kovalzon, VM <a href="#">392B</a>  |
| König, P <a href="#">36B</a> , <a href="#">60A</a> , <a href="#">171B</a> , <a href="#">182B</a> , <a href="#">194B</a> , <a href="#">198B</a> ,<br><a href="#">430B</a> , <a href="#">431B</a> , <a href="#">432B</a> , <a href="#">433B</a> , <a href="#">434B</a> , <a href="#">442B</a> | Kozyrev, V <a href="#">171A</a>  |
| Köppl, C <a href="#">98B</a>  | Krahe, R <a href="#">S9-1</a>  |
| Köpschall, I <a href="#">6A</a>   | Krajewski, S <a href="#">341B</a>  |
| Kössl, M <a href="#">94A</a> , <a href="#">103A</a> , <a href="#">107A</a> , <a href="#">112A</a>   | Krakowitzky, P <a href="#">400B</a>  |
| Koester-Patzlaff, C <a href="#">5B</a> , <a href="#">223A</a>   | Krampf, K <a href="#">312A</a> , <a href="#">347A</a>  |
| Köstinger, G <a href="#">291B</a>   | Krannich, S <a href="#">131B</a>   |
| Kohler, K <a href="#">164A</a> , <a href="#">165A</a> , <a href="#">349A</a>  | Krapp, HG <a href="#">S16-3</a> , <a href="#">23B</a>  |
| Koitschev, A <a href="#">8A</a>   | Kraß, D <a href="#">62A</a>  |
| Kolarow, R <a href="#">301B</a>   | Kratzer, S <a href="#">88A</a>   |
| Kole, M <a href="#">294A</a>  | Krause, A <a href="#">86A</a>  |
| Kollmar, I <a href="#">S10-4</a> , <a href="#">105A</a>   | Krause, G <a href="#">321A</a>   |
| Kominek, V <a href="#">362A</a>   | Krause, S <a href="#">315A</a>   |
| Komisarczuk, AZ <a href="#">47A</a>   | Kravitz, E <a href="#">424B</a>  |
| Komischke, B <a href="#">236A</a>   | Kreikemeier, K <a href="#">175A</a> , <a href="#">176A</a> , <a href="#">179B</a>  |
| Konang, R <a href="#">345A</a>  | Kreis, S <a href="#">348A</a>  |
| Konen, CS <a href="#">77A</a> , <a href="#">78A</a>   | Kreisch, W <a href="#">148A</a>  |
| Konnerth, A <a href="#">S13-1</a> , <a href="#">244B</a> , <a href="#">245B</a> , <a href="#">464B</a>  | Kreissl, S <a href="#">73B</a> , <a href="#">308A</a> , <a href="#">299B</a>   |
| Kopiez, R <a href="#">Sat1-13</a> , <a href="#">54A</a> , <a href="#">105B</a>  | Kreiter, AK <a href="#">189A</a> , <a href="#">192A</a> , <a href="#">433A</a> , <a href="#">434A</a>  |
| Korf, H-W <a href="#">367A</a>  | Kremers, J <a href="#">171A</a>  |
| Korogod, N <a href="#">281B</a>   | Kremkow, J <a href="#">451A</a>  |
| Korte, M <a href="#">238B</a>   | Kremper, A <a href="#">185B</a> , <a href="#">186B</a>   |
| Korz, V <a href="#">231B</a>  | Kretzberg, J <a href="#">294B</a>  |
| Kosodo, Y <a href="#">S12-1</a>   | Kreul, F <a href="#">243A</a>  |
| Kostarakos, K <a href="#">90A</a>   | Kreutz, MR <a href="#">28A</a> , <a href="#">368B</a> , <a href="#">369B</a>   |
| Kostenko, S <a href="#">216B</a>  | Krieger, J <a href="#">123A</a> , <a href="#">124A</a>   |
| Kott, M <a href="#">376A</a>  | Kriegelstein, K <a href="#">287A</a> , <a href="#">288A</a> , <a href="#">357B</a> , <a href="#">358B</a> ,<br><a href="#">359B</a> , <a href="#">360B</a> , <a href="#">361B</a> , <a href="#">398A</a> , <a href="#">399A</a> , <a href="#">400A</a> |
| Kotz, SA <a href="#">Sat1-15</a>  | Kriener, B <a href="#">453A</a>  |
| Koutsilieri, E <a href="#">6B</a>   | Kringe, T <a href="#">434B</a>   |
| Kovács, G <a href="#">174B</a>  | Kristan, WB <a href="#">294B</a>   |
| Kovalchuk, Y <a href="#">245B</a>   | Kröger, S <a href="#">52B</a>  |

[A](#) • [B](#) • [C](#) • [D](#) • [E](#) • [D](#) • [E](#) • [F](#) • [G](#) • [H](#) • [I](#) • [J](#) • [K](#) • [L](#) • [M](#) • [N](#) • [O](#) • [P](#) • [Q](#) • [R](#) • [S](#) • [T](#) • [U](#) • [V](#) • [W](#) • [X](#) • [Y](#) • [Z](#)

Kromer, T [446A](#), [447A](#)

Kron, M [86B](#), [302A](#), [303A](#), [306A](#)

Kronbichler, M [233A](#)

Kropp, W [192B](#)

Kros, CJ [S3-2](#)

Krügel, U [331B](#)

Krüger, K [327A](#)

Krugers, H [24A](#)

Krugers, HJ [231A](#)

Kruse, A [317B](#)

Kruse, F [S17-2](#)

Kühbandner, S [S15-3](#)

Kühnlein, RP [309A](#)

Kuenzel, T [25A](#)

Künzel, T [358A](#)

Küppers-Munther, B [S24-2](#)

Küry, P [S17-2](#)

Kugler, W [335A](#)

Kuhn, G [307B](#)

Kuhn, S [253B](#)

Kuhnert, AV [181B](#), [416B](#)

Kukulansky, T [417A](#)

Kulaksiz, H [261B](#)

Kumar, A [451A](#), [452A](#)

Kuner, T [287B](#), [369B](#)

Kuperstein, F [271B](#)

Kurtz, R [S13](#), [S13-5](#), [149A](#)

Kurylas, AE [264B](#)

Kurzen, LM [434B](#)

Kuster, B [Sat2-6](#)

Kutas, M [53A](#)

Kvachnina, L [48A](#)



[A](#) • [B](#) • [C](#) • [D](#) • [E](#) • [D](#) • [E](#) • [F](#) • [G](#) • [H](#) • [I](#) • [J](#) • [K](#) • [L](#) • [M](#) • [N](#) • [O](#) • [P](#) • [Q](#) • [R](#) • [S](#) • [T](#) • [U](#) • [V](#) • [W](#) • [X](#) • [Y](#) • [Z](#)

- Laage, R [467A](#)
- Labhart, T [153B](#), [154B](#), [155B](#)
- Lachmann, T [426B](#)
- Lacmann, A [288A](#)
- Laconi, M [226B](#)
- Lahat, H [396A](#)
- Lakes-Harlan, R [92A](#)
- Lakomek, M [335A](#)
- Lal, TN [S18-4](#)
- Lambert, T [125A](#)
- Land, B [323A](#)
- Landa, A [226B](#), [227B](#)
- Landgraf, R [421A](#), [422A](#), [423A](#), [424A](#)
- Landgrebe, J [40B](#)
- Landreth, GE [43B](#)
- Lang, S [373B](#)
- Lang, T [S11-6](#)
- Lang, UE [276A](#)
- Lange, P [8B](#)
- Lange-Asschenfeldt, C [259B](#)
- Langenfeld, K [S12-1](#)
- Langer, M [Sat3-4](#), [8A](#)
- Langguth, B [38A](#)
- Laplante, MA [47A](#)
- Laske, K [252A](#)
- Lasrado, R [24A](#)
- Laszcz, A [107B](#)
- Laube, B [318B](#)
- Laudenklos, S [249A](#)
- Laughlin, SB [141A](#), [142A](#)
- Lauinger, I [138A](#)
- Laurini, C [362A](#)
- Lautemann, N [341A](#)
- Lavrnja, I [4B](#)
- Law, JWS [246A](#)
- Layer, PG [49A](#), [364A](#)
- Leboulle, G [309B](#)
- Lebrecht, S [116B](#)
- Leclerc, C [18A](#)
- Lee, AYW [246A](#)
- Lee, M-L [213B](#)
- Leemhuis, J [321B](#)
- Lefort, S [211A](#)
- Legutko, B [262B](#), [339A](#)
- Lehmann, F-O [66A](#), [72A](#)
- Lehmann, M [321A](#)
- Lehmann, S [396B](#), [397B](#)
- Lehmann, T-N [215A](#)
- Lehmann-Horn, F [Sat3](#)
- Lehrer, M [147B](#)
- Leib, SL [10B](#)
- Leibold, C [216A](#), [443A](#)
- Leinders-Zufall, T [128A](#), [129A](#)
- Leiner, B [S22-1](#)
- Leischke, M [400A](#)
- Lelong, J [S23-4](#)
- Lenarz, M [211B](#)
- Lenarz, T [211B](#)
- Lencer, R [401B](#)
- Lennartz, D [323B](#)
- Lenz, D [411B](#)
- Leone, DP [S12-5](#)
- Leopold, DA [204B](#)
- Leppelsack, H-J [113A](#)

[A](#) • [B](#) • [C](#) • [D](#) • [E](#) • [D](#) • [E](#) • [F](#) • [G](#) • [H](#) • [I](#) • [J](#) • [K](#) • [L](#) • [M](#) • [N](#) • [O](#) • [P](#) • [Q](#) • [R](#) • [S](#) • [T](#) • [U](#) • [V](#) • [W](#) • [X](#) • [Y](#) • [Z](#)

Lerche, H [312A](#), [402B](#)

Lesch, K-P [403B](#), [404B](#)

Leske, O [267A](#)

Lesslauer, A [47A](#)

Lessmann, V [280A](#), [282A](#), [301B](#), [371B](#)

Letiembre, M [S2-3](#)

Levai, O [S21-2](#), [121A](#), [126A](#), [127A](#), [225B](#)

Lewald, J [111B](#)

Lewen, A [307A](#)

Lewin, GR [S15-3](#)

Li, J [125B](#)

Li, KW [25B](#)

Li, L [209A](#)

Li, P [272A](#)

Li, W-C [S8-3](#), [84A](#)

Li Hegner, Y [436B](#)

Liebscher, T [26B](#)

Liedvogel, M [191B](#), [192B](#), [193B](#)

Liem, R [418A](#)

Lieshoff, C [199A](#), [219A](#), [238A](#)

Lietz, M [9B](#)

Liman, J [340B](#), [341B](#)

Lind, J [361A](#)

Lindemann, JP [18B](#), [22B](#)

Lindemann, N [140A](#)

Lindemeyer, K [321B](#)

Linden, DEJ [206A](#)

Lindström, M [152A](#)

Lingor, P [339B](#)

Linke, R [224B](#)

Linster, C [128B](#)

Liss, B [Sat4-2](#)

Little, G [365A](#)

Liu, G [48A](#)

Liu, Y [S2-3](#)

Livingstone, MS [188A](#)

Llano, L [226B](#), [227B](#)

Locatelli, F [232A](#)

Löffler, K [8A](#)

Löffler, S [321B](#)

Loehle, M [327B](#)

Löhr, R [S24-2](#)

Löhrke, S [S24-5](#), [378A](#)

Lörken, C [434B](#)

Loers, G [354B](#)

Loertscher, F [260A](#)

Löschinger, J [52B](#)

Loesel, R [262A](#)

Löttrich, D [379B](#)

Loewel, S [177B](#)

Löwel, S [175A](#), [176A](#), [179B](#)

Loginov, VV [392B](#)

Lohmann, C [S24-3](#), [373B](#)

Lohmann, P [259B](#)

Lohr, C [S24](#), [S24-6](#)

Longtin, A [118B](#)

Lorenz, B [201B](#)

Loscher, W [470A](#)

Lotto, B [154A](#)

Lotze, M [437B](#)

Lou, X [Sat3-1](#), [280B](#)

Lowenstein, DH [366A](#)

Lucas, P [131B](#)

Lucassen, PJ [S6-4](#), [24A](#)

[A](#) • [B](#) • [C](#) • [D](#) • [E](#) • [D](#) • [E](#) • [F](#) • [G](#) • [H](#) • [I](#) • [J](#) • [K](#) • [L](#) • [M](#) • [N](#) • [O](#) • [P](#) • [Q](#) • [R](#) • [S](#) • [T](#) • [U](#) • [V](#) • [W](#) • [X](#) • [Y](#) • [Z](#)

Lucius, R [419A](#)

Luck, SJ [35B](#)

Ludolph, AC [Sat3](#), [S20-6](#)

Ludwar, BC [83B](#)

Ludwig, J [239B](#)

Lübbert, H [268A](#), [336A](#)

Lüddens, H [320A](#)

Lühder, F [419B](#)

Lüscher, H-R [211A](#)

Luhmann, HJ [370B](#), [372B](#)

Luiten, PGM [224A](#)

Luksch, H [25A](#), [195A](#), [340A](#), [358A](#)

Lukyanov, S [50A](#)

Luo, W [40A](#), [391B](#)

Lux, B [162B](#)

Lyon, DC [444A](#)

[A](#) • [B](#) • [C](#) • [D](#) • [E](#) • [D](#) • [E](#) • [F](#) • [G](#) • [H](#) • [I](#) • [J](#) • [K](#) • [L](#) • [M](#) • [N](#) • [O](#) • [P](#) • [Q](#) • [R](#) • [S](#) • [T](#) • [U](#) • [V](#) • [W](#) • [X](#) • [Y](#) • [Z](#)

- Maachaoui, R [62A](#)
- Macchi, P [357A](#)
- Maciaczyk, D [383B](#)
- Maciaczyk, J [383B](#)
- Mack, JA [125B](#)
- Madeja, M [327A](#)
- Mader, W [451B](#), [452B](#)
- Märker, T [156B](#), [160B](#)
- Maertin, R [434B](#)
- Mahlberg, R [276A](#)
- Mahr, S [449A](#)
- Maier, K [181B](#), [392A](#), [410A](#), [416B](#)
- Maier, MK [374A](#)
- Maier, W [318B](#)
- Majumdar, S [320B](#)
- Maler, L [118B](#)
- Maletzki, I [350B](#)
- Malin, D [29A](#)
- Maljevic, S [312A](#), [402B](#)
- Malkinson, G [389B](#)
- Mallot, HA [256B](#), [258B](#)
- Malz, CR [353B](#)
- Mandel, G [125B](#)
- Mandel, S [412A](#)
- Mandon, S [192A](#), [434A](#)
- Maness, P [362A](#)
- Mangano, R [Sat2-6](#)
- Manns, M [177A](#), [200A](#)
- Mansouri, A [393A](#)
- Manzini, I [S21](#), [S21-4](#)
- Manzke, T [270A](#), [303A](#), [304A](#), [305A](#), [306A](#)
- Mapfumo, S [67B](#)
- Mappes, M-S [148B](#)
- Marandi, N [464B](#)
- Marcotti, W [S3-2](#)
- Marienhagen, J [38A](#)
- Marin, C [272B](#)
- Marin-Burgin, A [294B](#)
- Mariño, J [444A](#)
- Markowski, DN [433A](#)
- Marquardt, H [149B](#)
- Marquardt, N [211B](#)
- Marshall, L [252A](#)
- Marshall, NJ [145B](#)
- Martin, KAC [291B](#), [442B](#)
- Martini, R [354B](#)
- Martmüller, R [436A](#)
- Marx, V [247A](#)
- Marzesco, A-M [S12-1](#)
- Mashukova, A [44B](#), [137A](#)
- Masland, RH [169A](#)
- Massou, I [18A](#)
- Mathalon, DH [S8-6](#)
- Matheson, T [66B](#)
- Matos, N [24B](#)
- Matthies, C [81A](#)
- Matti, U [295B](#)
- Maurer, M [1B](#)
- Mauritz, C [81A](#)
- Maxeiner, S [163B](#), [170B](#)
- Maye, A [36B](#), [55B](#)
- Maysami, S [355B](#)
- McCaffery, P [379A](#)
- McDermott, R [272B](#)

[A](#) • [B](#) • [C](#) • [D](#) • [E](#) • [D](#) • [E](#) • [F](#) • [G](#) • [H](#) • [I](#) • [J](#) • [K](#) • [L](#) • [M](#) • [N](#) • [O](#) • [P](#) • [Q](#) • [R](#) • [S](#) • [T](#) • [U](#) • [V](#) • [W](#) • [X](#) • [Y](#) • [Z](#)

McDonald, JM [399B](#)

Medina, D [228A](#)

Mee, CJ [S24-1](#)

Mehring, C [29B](#), [30B](#), [31B](#), [32B](#), [80B](#)

Meidinger, MA [384B](#)

Meier, M [220A](#)

Meier, R [466A](#)

Meis, S [219B](#)

Meisel, A [406A](#)

Meissl, H [449A](#)

Meissner, D [119A](#), [356B](#)

Meli, DN [10B](#)

Meller, D [385A](#)

Meller, K [385A](#), [464A](#)

Melonari, P [226B](#), [227B](#)

Mentel, T [65B](#), [86A](#)

Menz, C [377A](#)

Menzel, R [S4-2](#), [133A](#), [134A](#), [135A](#), [309B](#),  
[363A](#)

Meola, S [303B](#)

Merkens, M [185A](#)

Merkler, D [392A](#), [410A](#), [416B](#)

Mertens, U [115B](#)

Meseke, M [67B](#)

Mestres, P [S22-1](#)

Mettenleiter, TC [122B](#)

Metz, GA [382B](#)

Metz, J [425A](#)

Metzen, M [432A](#)

Meuer, K [S20-4](#), [49B](#), [411A](#)

Meulenberg, CJW [112B](#)

Meuth, P [315A](#), [316A](#)

Meuth, SG [315A](#), [316A](#)

Mey, J [20A](#), [25A](#), [358A](#), [379A](#), [380A](#), [381A](#)

Meyding-Lamade, U [10B](#), [11B](#)

Meyer, DK [321B](#)

Meyer, HE [Sat2-1](#), [121B](#)

Meyer, M [S22-1](#), [50B](#), [225A](#)

Meyer, T [S20-6](#)

Meyer-Klaucke, W [412B](#)

Meyer-Lühmann, M [S2-1](#)

Mezer, A [296B](#)

Michaelis, T [468A](#)

Michailov, GV [351B](#)

Michal, A-S [2B](#)

Michalak, S [7B](#)

Michels, B [257A](#)

Michler, F [38B](#), [188B](#)

Michna, M [S3-4](#)

Mielke, K [419A](#)

Mikhaylova, MG [347B](#)

Miller, C [P4](#)

Minichiello, L [228A](#)

Miquelajauregui, A [367B](#)

Misane, I [225A](#)

Misgeld, U [307A](#)

Mishra, SK [367A](#)

Missler, M [297A](#), [279B](#)

Mitchell, KJ [365A](#)

Mitchell, TJ [S14-1](#)

Mittag, J [374A](#)

Mittelbronn, M [415B](#)

Mittmann, T [280A](#), [300A](#)

Modersitzki, J [467B](#)

[A](#) • [B](#) • [C](#) • [D](#) • [E](#) • [D](#) • [E](#) • [F](#) • [G](#) • [H](#) • [I](#) • [J](#) • [K](#) • [L](#) • [M](#) • [N](#) • [O](#) • [P](#) • [Q](#) • [R](#) • [S](#) • [T](#) • [U](#) • [V](#) • [W](#) • [X](#) • [Y](#) • [Z](#)

Möller, M [252A](#)  
Möller, A [289B](#)  
Möller, T [3B](#)  
Mönig, B [340A](#), [358A](#)  
Mörschel, M [85B](#), [86B](#), [302A](#), [304A](#)  
Moffat, KG [S24-1](#)  
Mogdans, J [116A](#), [117A](#), [118A](#)  
Mohr, H [206A](#)  
Moisel, M [216A](#)  
Moliadze, V [193A](#)  
Moll, CKE [78B](#)  
Mombaerts, P [S21-1](#)  
Montag, D [279B](#)  
Montag-Sallaz, M [279B](#)  
Montani, L [S17-4](#)  
Monyer, H [P9](#), [218A](#)  
Mora, E [112A](#)  
Mora-Ferrer, C [161B](#), [162B](#)  
Morasutti, D [379A](#)  
Morawski, M [412B](#)  
Morciano, M [284A](#), [285A](#)  
Moré, MI [S15-3](#)  
Moreau, M [18A](#)  
Mori, T [S12-2](#)  
Moritz, S [396B](#), [397B](#)  
Morris, RGM [238B](#)  
Morrison, TTA [205B](#), [206B](#), [453A](#)  
Morsch, M [187A](#)  
Moscha, B [411B](#)  
Moser, T [S3-3](#), [291A](#), [282B](#)  
Mostarica-Stojkovic, M [4B](#)  
Mouritsen, H [153B](#), [191B](#), [192B](#), [193B](#)

Mourrain, P [47A](#)  
Mronz, M [S16-4](#), [72A](#)  
Mrsic-Flogel, TD [189B](#), [190B](#)  
Mühleisen, TW [160A](#)  
Mueller, T [73B](#)  
Mueller, VJ [289A](#)  
Müller, A [337A](#)  
Müller, B [7A](#), [136B](#), [159A](#)  
Müller, BA [470B](#)  
Müller, CHG [12A](#)  
Müller, F [172A](#)  
Müller, HW [S17](#), [S17-2](#), [25B](#), [346A](#), [390A](#),  
[407A](#)  
Müller, K-R [S18-1](#)  
Müller, M [97B](#), [326B](#)  
Müller, MFH [113B](#)  
Müller, R [346B](#)  
Müller, T [S5-4](#), [327B](#), [328B](#)  
Müller, U [232A](#), [234A](#)  
Müller-Keuker, JIH [209B](#), [224A](#)  
Müller-Röver, S [1B](#), [383A](#)  
Münch, D [67A](#)  
Münch, G [S14-4](#)  
Münkner, S [S3-4](#)  
Münste, TF [53A](#)  
Mukhida, M [153B](#)  
Mukovski, M [212A](#)  
Multhaup, G [S2-4](#)  
Munk, M [461A](#)  
Munsch, T [S1-5](#)  
Muralidharan, S [277B](#)  
Musella, D [80A](#)

[A](#) • [B](#) • [C](#) • [D](#) • [E](#) • [D](#) • [E](#) • [F](#) • [G](#) • [H](#) • [I](#) • [J](#) • [K](#) • [L](#) • [M](#) • [N](#) • [O](#) • [P](#) • [Q](#) • [R](#) • [S](#) • [T](#) • [U](#) • [V](#) • [W](#) • [X](#) • [Y](#) • [Z](#)

Musshoff, U [327A](#)

Mutschler, I [436A](#)

[A](#) • [B](#) • [C](#) • [D](#) • [E](#) • [D](#) • [E](#) • [F](#) • [G](#) • [H](#) • [I](#) • [J](#) • [K](#) • [L](#) • [M](#) • [N](#) • [O](#) • [P](#) • [Q](#) • [R](#) • [S](#) • [T](#) • [U](#) • [V](#) • [W](#) • [X](#) • [Y](#) • [Z](#)

- Naaman, S [450B](#)
- Nachliel, E [296B](#)
- Nägerl, UV [291B](#), [292B](#), [293B](#)
- Naegler, K [42A](#)
- Nagel, A [176B](#)
- Nagel, F [54A](#), [105B](#)
- Nagel, SK [434B](#)
- Nagetusch, A [186A](#)
- Nahum, M [442A](#)
- Nair, D [368B](#), [369B](#)
- Narayanan, RT [215B](#)
- Narz, F [371B](#)
- Nasello, AG [329A](#)
- Nathanielsz, PW [328B](#)
- Nau, R [S14](#), [S14-6](#), [8B](#), [394A](#)
- Naujock, M [286B](#)
- Naundorf, B [1A](#), [180B](#), [196B](#)
- Nauroth, I [116A](#)
- Navakkode, S [232B](#), [233B](#)
- Nave, K-A [27B](#), [351B](#), [352B](#), [362B](#), [401A](#), [467A](#)
- Nawrot, MP [29B](#), [30B](#), [31B](#), [32B](#)
- Necker, R [267A](#)
- Nedeljkovic, N [4B](#)
- Neher, E [Sat3-1](#)
- Neitzel, S [434A](#)
- Nelken, I [442A](#)
- Neu, P [207A](#)
- Neubauer, H [100A](#)
- Neuhaus, A [207A](#), [208A](#), [427A](#)
- Neuhaus, EM [44B](#), [136A](#), [137A](#), [121B](#), [181A](#)
- Neuhofer, D [89B](#)
- Neumann, H [S14-3](#), [3A](#), [417B](#), [418B](#), [452B](#)
- Neumann, ID [307B](#)
- Neumann, N [252B](#)
- Neumeyer, C [155A](#), [183B](#)
- Neupert, S [303B](#)
- Neusch, C [296A](#), [349B](#), [350B](#)
- Neuser, K [256A](#)
- Newland, PL [134B](#), [266B](#)
- Newrzella, D [27B](#)
- Newsome, WT [P6](#)
- Nezlin, LP [46B](#), [278B](#)
- Nichiporuk, E [356A](#)
- Nichols, R [303B](#)
- Nickmann, M [73A](#)
- Niclou, SP [25B](#)
- Nicolaus, T [413A](#)
- Nicolelis, MAL [P3](#)
- Niebergall, R [438A](#)
- Nieder, A [197B](#), [438B](#)
- Niehage, R [375A](#)
- Niehaus, S [176B](#)
- Nienhaus, U [Sat3-6](#)
- Nieselt, K [Sat4-5](#)
- Nieweg, K [41A](#), [415A](#)
- Nikkhah, G [379B](#), [380B](#), [381B](#), [382B](#), [383B](#)
- Nikolaev, AR [426B](#)
- Nikonenko, O [S7-5](#)
- Nimmrich, V [289B](#)
- Nitsch, R [26A](#), [46A](#), [1B](#), [383A](#)
- Niven, JE [141A](#), [142A](#), [143B](#)
- Njunting, M [215A](#)
- Nobrega, JN [275A](#), [405A](#)



[A](#) • [B](#) • [C](#) • [D](#) • [E](#) • [D](#) • [E](#) • [F](#) • [G](#) • [H](#) • [I](#) • [J](#) • [K](#) • [L](#) • [M](#) • [N](#) • [O](#) • [P](#) • [Q](#) • [R](#) • [S](#) • [T](#) • [U](#) • [V](#) • [W](#) • [X](#) • [Y](#) • [Z](#)

Nöll, GN [170A](#)

Nöthen, MM [400B](#)

Nolden, L [404A](#)

Nolte, MW [470A](#)

Norman, R [272B](#)

Northoff, G [425B](#)

Nortmann, N [431B](#)

Nothwang, HG [Sat2](#), [Sat2-2](#), [Sat4-4](#), [113B](#), [114B](#), [273A](#)

Nouvian, R [282B](#)

Nowak, G [339A](#)

Nowotny, M [98A](#)

Nyakas, C [224A](#)

[A](#) • [B](#) • [C](#) • [D](#) • [E](#) • [D](#) • [E](#) • [F](#) • [G](#) • [H](#) • [I](#) • [J](#) • [K](#) • [L](#) • [M](#) • [N](#) • [O](#) • [P](#) • [Q](#) • [R](#) • [S](#) • [T](#) • [U](#) • [V](#) • [W](#) • [X](#) • [Y](#) • [Z](#)

Oberhofer, M [378A](#)

Overlack, N [160B](#)

Oberhoffner, S [9B](#)

Owren, MJ [Sat1-8](#)

Obermayer, K [34A](#), [92B](#), [93B](#), [94B](#), [279A](#),  
[444A](#), [461A](#), [463A](#)

Obermayer, M-L [138B](#)

Ögren, SO [225A](#)

Oehlke, O [357B](#), [359B](#), [360B](#)

Oertner, TG [S13-2](#)

Ofek, E [245A](#)

Offenhäusser, A [342B](#), [343B](#), [344B](#), [345B](#)

Ofner, E [89A](#)

Ogunlade, V [407B](#)

Ohl, FW [S10](#), [S10-3](#), [102B](#), [107B](#), [212B](#), [426B](#)

Ohla, K [174A](#)

Ohlendorf, S [34B](#)

Okada, R [132A](#)

Olbrich, E [447B](#)

Olguin, M [226B](#), [227B](#)

Oliver, D [S3-5](#), [322B](#)

Olivera, BM [323B](#)

Omer-Backlash, D [471A](#)

Onat, S [171B](#), [182B](#), [194B](#), [198B](#), [432B](#)

Oppelt, A [242B](#)

Oren, T [2B](#)

Orit, G [2B](#)

Orlowski, B [271A](#)

O'Shea, M [242A](#)

Oshurkova, E [104B](#)

Osten, P [249A](#)

Ostwald, J [109A](#)

O'Sullivan, E [Sat2-6](#)

Ott, SR [67A](#), [242A](#), [266B](#)

[A](#) • [B](#) • [C](#) • [D](#) • [E](#) • [D](#) • [E](#) • [F](#) • [G](#) • [H](#) • [I](#) • [J](#) • [K](#) • [L](#) • [M](#) • [N](#) • [O](#) • [P](#) • [Q](#) • [R](#) • [S](#) • [T](#) • [U](#) • [V](#) • [W](#) • [X](#) • [Y](#) • [Z](#)

- |  |  |
|--|--|
| Paasche, G <a href="#">211B</a>  | Pera, E <a href="#">S5</a> , <a href="#">S5-2</a> , <a href="#">366B</a>       |
| Pachnis, V <a href="#">S22-2</a>   | Peretz, I <a href="#">Sat1-12</a>  |
| Paech, T <a href="#">203A</a>  | Pérez de Sevilla, L <a href="#">168B</a>                                       |
| Page, K <a href="#">66B</a>  | Perez-Cruz, C <a href="#">209B</a>   |
| Paggi, A <a href="#">111B</a>  | Perry, VH <a href="#">S14-5</a>  |
| Pahlberg, J <a href="#">152A</a>   | Peters, EMJ <a href="#">383A</a>   |
| Palfi, A <a href="#">200B</a>  | Peters, HC <a href="#">S1-1</a>  |
| Palme, R <a href="#">2A</a>  | Peters, J <a href="#">431A</a>   |
| Palmer, TD <a href="#">S6-6</a>  | Peters, T <a href="#">178B</a>   |
| Palucha, A <a href="#">339A</a>  | Petersen, CCH <a href="#">211A</a>   |
| Panhuysen, M <a href="#">424A</a>  | Peterziel, H <a href="#">S22</a> , <a href="#">S22-3</a>                       |
| Pannicke, T <a href="#">349A</a>   | Petkova, V <a href="#">394B</a>  |
| Papadopoulos, N <a href="#">350B</a>   | Petrov, S <a href="#">393B</a>   |
| Papazoglou, A <a href="#">379B</a> , <a href="#">380B</a> , <a href="#">381B</a> , <a href="#">382B</a>  | Peuckert, C <a href="#">375A</a>   |
| Pape, H-C <a href="#">S1-5</a> , <a href="#">214B</a> , <a href="#">215B</a> , <a href="#">217B</a> , <a href="#">218B</a> ,<br><a href="#">219B</a> , <a href="#">234B</a> , <a href="#">316A</a> | Pezeron, G <a href="#">47A</a>   |
| Paraoanu, LE <a href="#">364A</a>  | Pfeiffer, K <a href="#">S16-5</a> , <a href="#">21B</a>                        |
| Parker, D <a href="#">389A</a>   | Pflüger, H-J <a href="#">67A</a> , <a href="#">310B</a> , <a href="#">311B</a> |
| Patrona, A <a href="#">170A</a>  | Pfriege, FW <a href="#">41A</a> , <a href="#">42A</a> , <a href="#">415A</a>   |
| Patz, S <a href="#">204A</a> , <a href="#">384A</a>  | Pfurtscheller, G <a href="#">S18-3</a>   |
| Patzke, N <a href="#">177A</a>   | Philipp, B <a href="#">299B</a>  |
| Paulsen, R <a href="#">16B</a>   | Philipp, M <a href="#">377B</a>  |
| Paulus, W <a href="#">Sat5</a> , Sat5-1, <a href="#">2A</a>  | Philipp, R <a href="#">178A</a>  |
| Pawelzik, KR <a href="#">434A</a> , <a href="#">445A</a>   | Philippides, A <a href="#">242A</a>  |
| Pawlak, CR <a href="#">420A</a>  | Pick, CG <a href="#">417A</a>  |
| Pawlowski, PG <a href="#">43A</a> , <a href="#">44A</a> , <a href="#">45A</a>  | Pickard, L <a href="#">Sat2-6</a>  |
| Pazienti, A <a href="#">460A</a>   | Picker, B <a href="#">383A</a>   |
| Pecka, M <a href="#">106A</a>  | Piechotta, K <a href="#">279B</a>  |
| Peichl, L <a href="#">159A</a>   | Pieler, T <a href="#">S5</a> , <a href="#">21A</a> , <a href="#">22A</a>       |
| Peigneux, P <a href="#">S23-3</a>  | Pieper, F <a href="#">178B</a>   |
| Pekovic, S <a href="#">4B</a>  | Pilati, E <a href="#">S11-3</a>  |
| Pelz, D <a href="#">S21-3</a>  | Pilc, A <a href="#">339A</a>   |
|  | Pili, J <a href="#">338A</a>   |

[A](#) • [B](#) • [C](#) • [D](#) • [E](#) • [D](#) • [E](#) • [F](#) • [G](#) • [H](#) • [I](#) • [J](#) • [K](#) • [L](#) • [M](#) • [N](#) • [O](#) • [P](#) • [Q](#) • [R](#) • [S](#) • [T](#) • [U](#) • [V](#) • [W](#) • [X](#) • [Y](#) • [Z](#)

Pilli, J [213A](#)  
 Pilz, PKD [253B](#), [255B](#)  
 Pintea, B [361A](#)  
 Pipereit, K [79A](#)  
 Pippirs, U [390A](#)  
 Pippow, A [139A](#)  
 Pirih, P [291A](#)  
 Plachta, DTT [108A](#)  
 Plappert, CF [253B](#), [255B](#)  
 Pleasure, SJ [366A](#)  
 Plekhanova, I [234A](#)  
 Plessner, HE [205B](#)  
 Podzun, A [321A](#)  
 Poeggel, G [237B](#)  
 Ponath, G [353A](#), [400B](#)  
 Pongratz, H [76B](#)  
 Pongs, O [S1-1](#), [325A](#)  
 Ponimaskin, EG [48A](#), [365B](#)  
 Popa, MO [402B](#)  
 Porr, B [250B](#), [444B](#)  
 Portelli, G [14A](#)  
 Potter, SS [S12-3](#)  
 Poulet, JFA [S8](#), [S8-2](#), [31A](#), [93A](#)  
 Poustka, F [252B](#)  
 Pouzat, C [140A](#)  
 Pradier, L [S2-4](#)  
 Prakash, N [Sat4-1](#)  
 Pras, E [396A](#)  
 Pratt, H [245A](#)  
 Predehl, S [338A](#)  
 Predel, R [269B](#), [303B](#)  
 Prokop, A [S24-2](#)

Püschel, AW [375B](#)  
 Püttmann, S [348A](#)  
 Pütz, B [424A](#)  
 Pujol, R [282B](#)  
 Pulvermüller, A [157B](#), [158B](#)  
 Punnakkal, P [324A](#)  
 Purmann, S [401B](#)  
 Pusch, H [312B](#), [313B](#)  
 Puschmann, T [69B](#)  
 Putthoff, P [354B](#)  
 Pym, ECG [S24-1](#)

[A](#) • [B](#) • [C](#) • [D](#) • [E](#) • [D](#) • [E](#) • [F](#) • [G](#) • [H](#) • [I](#) • [J](#) • [K](#) • [L](#) • [M](#) • [N](#) • [O](#) • [P](#) • [Q](#) • [R](#) • [S](#) • [T](#) • [U](#) • [V](#) • [W](#) • [X](#) • [Y](#) • [Z](#)

Quade, R [362A](#)

Qualmann, B Sat3-5, [275B](#), [276B](#), [290B](#)

- Raab, S [369A](#)  
 Raap, M [351A](#)  
 Radde, R [S2-1](#)  
 Rafael, J [422A](#)  
 Ragert, P [62A](#), [60B](#), [61B](#), [62B](#), [63B](#), [179A](#)  
 Rahhal, B [399A](#)  
 Rainer, G [S19](#), [S19-6](#)  
 Raivich, G [413A](#)  
 Rakic, Lj [4B](#)  
 Ram, R [2B](#)  
 Raming, K [124A](#)  
 Ramminger, E [413B](#)  
 Ramseger, R [52B](#)  
 Rasch, B [S23-7](#)  
 Rasse, T [297B](#), [402A](#)  
 Rathjen, FG [S15-3](#), [13B](#)  
 Rathmayer, W [73B](#)  
 Rau, CR [181B](#)  
 Rausch, C [125A](#)  
 Rausch, S [157B](#)  
 Rauvala, H [S7-4](#)  
 Ray, A [269A](#)  
 Raymond, R [275A](#), [405A](#)  
 Raz, N [417A](#)  
 Rebstock, J [312A](#), [402B](#)  
 Reed, JC [340B](#), [341B](#)  
 Regen, F [53B](#)  
 Regus, H [161A](#)  
 Rehder, V [S15](#), [S15-4](#)  
 Reich, U [211B](#)  
 Reichenbach, A [349A](#), [350A](#), [351A](#)  
 Reidel, B [159B](#)  
 Reidel, J [471A](#)  
 Reif, A [403B](#), [404B](#)  
 Reifenberger, G [Sat5](#), Sat5-1  
 Reiff, DF [151B](#), [152B](#)  
 Reinecke, JA [401A](#)  
 Reiners, J [156B](#), [160B](#)  
 Reinert, T [412B](#)  
 Reinhard, C [330A](#)  
 Reisch, A [378B](#)  
 Reischig, T [264A](#), [265A](#)  
 Reiser, G [40A](#), [391B](#)  
 Reissner, C [369B](#)  
 Rentzsch, J [207A](#), [208A](#), [276A](#), [427A](#)  
 Rettig, J [295B](#)  
 Reuss, B [5B](#), [223A](#)  
 Reuter, G [211B](#)  
 Rex, A [328A](#)  
 Rheinlaender, J [89A](#), [90A](#)  
 Ribeiro-Gouveia, V [227A](#)  
 Ribi, WA [145A](#)  
 Richter, A [12B](#), [275A](#), [405A](#)  
 Richter, DW [48A](#), [270A](#), [304A](#), [305A](#), [306A](#),  
[365B](#), [469A](#)  
 Richter, M [402A](#)  
 Richter-Landsberg, C [336B](#), [354A](#)  
 Rickmann, M [271A](#), [361B](#)  
 Riederer, P [6B](#), [353B](#), [412B](#)  
 Rieger, A [Sat4-4](#), [114B](#)  
 Riemensperger, T [258A](#)  
 Riepe, MW [259B](#)  
 Riethmacher, D [29A](#)  
 Rillich, J [14B](#), [300B](#)

- Rister, J [S16-1](#)
- Ristow, M [148A](#)
- Ritz, R [462A](#)
- Rivera, C [S22-1](#)
- Rivier, JEF [323B](#)
- Robert, D [317A](#)
- Roberts, A [S8-3](#), [84A](#)
- Robinson, R [33A](#)
- Robson, SC [367A](#), [369A](#)
- Rochford, CD [417B](#)
- Roden, K [263B](#)
- Roeder, T [149B](#), [298A](#)
- Röder, B [S19-3](#)
- Röhl, C [352A](#)
- Roemer, L [329B](#)
- Römer, H [88A](#), [89A](#), [90A](#), [91A](#)
- Röper, J [S1-6](#)
- Röskam, S [332A](#)
- Rösler, F [S19-3](#)
- Rössler, W [127B](#), [136B](#), [137B](#), [138B](#), [139B](#), [140B](#), [270B](#)
- Rogalla, N [308A](#), [299B](#)
- Rohbock, K [6A](#)
- Rohde, G [S20-4](#), [395A](#)
- Rohe, M [427B](#)
- Rokem, A [440A](#), [442A](#)
- Rolfs, A [77B](#), [79B](#)
- Rombach, N [380A](#)
- Ronacher, B [S9](#), [S9-3](#), [89B](#), [90B](#), [237A](#), [395B](#)
- Ronnenberg, A [225A](#)
- Rose, CR [S11-1](#)
- Rose, K [203B](#), [348A](#)
- Rose, T [420B](#)
- Rose, U [70A](#), [310A](#), [311A](#)
- Rosenbaum, C [346A](#)
- Roskoden, T [224B](#)
- Rosner, M [414A](#)
- Rossner, M [27B](#), [362B](#), [401A](#), [467A](#)
- Rotermund, D [445A](#)
- Roth-Alpermann, C [238B](#)
- Rothermundt, M [353A](#)
- Rothstein, JD [S20-5](#)
- Rotter, S [35A](#), [32B](#), [80B](#), [450A](#), [451A](#), [452A](#), [453A](#)
- Rouleau, GA [312A](#)
- Roussa, E [Sat4](#), [271A](#), [357B](#), [359B](#), [360B](#)
- Rubart, S [198A](#)
- Rubinsten, O [206A](#)
- Ruediger, J [388B](#)
- Ruediger, T [23A](#)
- Rünker, AE [354B](#), [365A](#)
- Ruether, E [437A](#)
- Rüther, E [226A](#), [391A](#)
- Rüttiger, L [10A](#)
- Ruffner, H [Sat2-6](#)
- Rummler, S [436A](#)
- Rune, GM [227A](#)
- Rupnik, M [420B](#), [421B](#)
- Rust, B [22A](#)
- Rust, S [401B](#)
- Rustemeyer, J [388A](#)
- Rybak, J [135A](#)
- Ryglewski, S [310B](#)
- Rygula, R [391A](#), [437A](#)

[A](#) • [B](#) • [C](#) • [D](#) • [E](#) • [D](#) • [E](#) • [F](#) • [G](#) • [H](#) • [I](#) • [J](#) • [K](#) • [L](#) • [M](#) • [N](#) • [O](#) • [P](#) • [Q](#) • [R](#) • [S](#) • [T](#) • [U](#) • [V](#) • [W](#) • [X](#) • [Y](#) • [Z](#)

- |   |  |
|---|--|
| Saarma, M <a href="#">S22-1</a> , <a href="#">S22-4</a>   | Schachtner, J <a href="#">S15-6</a> , <a href="#">264B</a> , <a href="#">268B</a> , <a href="#">269B</a> , <a href="#">270B</a>  |
| Sachse, S <a href="#">128B</a> , <a href="#">132B</a>   | Schadow, J <a href="#">439A</a>  |
| Sachser, N <a href="#">2A</a>   | Schäble, S <a href="#">237B</a>  |
| Sättler, MB <a href="#">181B</a> , <a href="#">392A</a> , <a href="#">410A</a> , <a href="#">416B</a>   | Schäfer, H <a href="#">423B</a>  |
| Sajikumar, S <a href="#">232B</a> , <a href="#">233B</a>  | Schäfer, K-H <a href="#">S22</a> , <a href="#">S22-5</a>   |
| Sakura, M <a href="#">154B</a>  | Schäfer, S <a href="#">343B</a>  |
| Salem, B <a href="#">246A</a>   | Schäfer, SS <a href="#">71A</a>  |
| Salem jr, N <a href="#">271B</a>  | Schaeffel, F <a href="#">163A</a> , <a href="#">308B</a>   |
| Sales, J <a href="#">272B</a>   | Schäffer, S <a href="#">S15-3</a> , <a href="#">13B</a>  |
| Saletu, B <a href="#">S23-1</a>   | Schaette, R <a href="#">36A</a>  |
| Sallach, S <a href="#">1B</a>   | Schafer, B <a href="#">317B</a>  |
| Sallam, AE-D <a href="#">74A</a>  | Schall, S <a href="#">432B</a>   |
| Salonikidis, PS <a href="#">469A</a>  | Scharstein, H <a href="#">68A</a> , <a href="#">81B</a>  |
| Samengo, I <a href="#">32A</a>  | Schassen, Cv <a href="#">227A</a>  |
| Samson, S <a href="#">Sat1-12</a>   | Schebesch, G <a href="#">113A</a>  |
| Sanchez-Soriano, N <a href="#">S24-2</a>  | Schedletzky, T <a href="#">317B</a>  |
| Sand, D <a href="#">76B</a>   | Scheich, H <a href="#">110A</a> , <a href="#">102B</a> , <a href="#">104B</a> , <a href="#">107B</a> , <a href="#">115B</a> ,<br><a href="#">212B</a> , <a href="#">470B</a> |
| Sander, K <a href="#">Sat1-11</a>   | Scheller, C <a href="#">6B</a>   |
| Sandoz, J-C <a href="#">15A</a> , <a href="#">17A</a> , <a href="#">18A</a> , <a href="#">19A</a> , <a href="#">236A</a>  | Schemmel, S <a href="#">361B</a>   |
| Santoso, A <a href="#">465B</a>   | Schierwagen, A <a href="#">448B</a>  |
| Sara, SJ <a href="#">S23-4</a> , <a href="#">54B</a>  | Schiffelholz, T <a href="#">S23-5</a>  |
| Saras, A <a href="#">313B</a>   | Schild, D <a href="#">S21-4</a> , <a href="#">46B</a>  |
| Sargsyan, V <a href="#">295A</a> , <a href="#">324B</a>   | Schildberger, K <a href="#">14B</a> , <a href="#">298B</a> , <a href="#">300B</a>  |
| Sartor, JJ <a href="#">108B</a> , <a href="#">110B</a>  | Schildt, M <a href="#">107B</a>  |
| Sauer, H <a href="#">423B</a>   | Schillo, S <a href="#">16B</a>   |
| Saumweber, H <a href="#">395B</a>   | Schiltz, K <a href="#">115B</a>  |
| Sauter, K <a href="#">325A</a>  | Schindehütte, J <a href="#">393A</a>   |
| Savaskan, NE <a href="#">26A</a>  | Schindelin, J <a href="#">265B</a>   |
| Sayaman, R <a href="#">70B</a>  | Schindler, J <a href="#">Sat2-2</a>  |
| Schaal, S <a href="#">343B</a>  | Schinkel, N <a href="#">434A</a>   |
| Schachner, M <a href="#">S7-1</a> , <a href="#">S7-5</a> , <a href="#">Sat5-2</a> , <a href="#">48A</a> , <a href="#">246A</a> ,<br><a href="#">354B</a> , <a href="#">379B</a> | Schipke, C <a href="#">S11</a>   |



[A](#) • [B](#) • [C](#) • [D](#) • [E](#) • [D](#) • [E](#) • [F](#) • [G](#) • [H](#) • [I](#) • [J](#) • [K](#) • [L](#) • [M](#) • [N](#) • [O](#) • [P](#) • [Q](#) • [R](#) • [S](#) • [T](#) • [U](#) • [V](#) • [W](#) • [X](#) • [Y](#) • [Z](#)

Schipke, CG [S11-4](#)

Schippert, R [308B](#)

Schlachetzki, J [395A](#)

Schlaf, G [270A](#)

Schlenstedt, J [326A](#)

Schleper, M [285B](#)

Schlesinger, F [347A](#)

Schlosshauer, B [9B](#)

Schlue, W-R [315B](#), [316B](#), [337A](#)

Schlumberger, C [255B](#)

Schmadel, S [331A](#)

Schmäh, M [74A](#), [75A](#), [73B](#)

Schmelting, B [334A](#), [393A](#)

Schmetsdorf, S [409B](#)

Schmid, A [402A](#)

Schmid, H [164A](#)

Schmid, S [254B](#), [257B](#), [319A](#)

Schmid-Fetzer, SC [109A](#)

Schmidt, CF [199B](#)

Schmidt, H [S15-3](#), [13B](#)

Schmidt, J [87A](#), [83B](#), [419B](#)

Schmidt, K [410B](#)

Schmidt, KF [175A](#), [176A](#), [179B](#)

Schmidt, M [283B](#), [423A](#)

Schmidt, N [Sat4-4](#), [114B](#)

Schmidt, R [243A](#), [244A](#)

Schmidt, S [Sat1](#), [Sat1-4](#), [387B](#)

Schmidt, T [176B](#)

Schmidt-Hoffmann, R-B [161B](#)

Schmidtner, M [314A](#)

Schmitt, A [403B](#), [404B](#)

Schmitt, O [393B](#), [467B](#)

Schmitz, B [362A](#)

Schmitz, C [S2-4](#)

Schmitz, D [P8](#), [216A](#), [217A](#), [277A](#), [278A](#)

Schmitz, G [72B](#), [250A](#)

Schmitz, M [4A](#), [348B](#)

Schmucker, C [163A](#)

Schmuker, M [48B](#)

Schnabel, M [175A](#), [176A](#), [177B](#), [179B](#)

Schnee, A [258B](#)

Schneeggenburger, R [Sat3-1](#), [280B](#), [281B](#)

Schneider, A [395A](#), [401A](#)

Schneider, G [48B](#)

Schneider, H [305B](#), [335B](#), [462B](#)

Schneider, N-L [304B](#)

Schneider, R [26B](#)

Schneider, S [244A](#)

Schnell, L [26B](#)

Schnitzler, H-U [253B](#), [255B](#), [257B](#), [319A](#)

Schnürch, H [S10-4](#)

Schober, R [407B](#)

Schoch, K [14B](#)

Schoelkopf, B [S18-4](#)

Schoemaker, H [334B](#)

Schön, I [313A](#)

Schöneich, S [298B](#)

Schöner, D [208B](#)

Schöner, G [62B](#), [63B](#)

Schönknecht, S [55B](#)

Schörnich, S [100B](#)

Scholpp, S [S5-3](#)

Scholz, A [408A](#)

Scholz, H [309A](#)

[A](#) • [B](#) • [C](#) • [D](#) • [E](#) • [D](#) • [E](#) • [F](#) • [G](#) • [H](#) • [I](#) • [J](#) • [K](#) • [L](#) • [M](#) • [N](#) • [O](#) • [P](#) • [Q](#) • [R](#) • [S](#) • [T](#) • [U](#) • [V](#) • [W](#) • [X](#) • [Y](#) • [Z](#)

Scholz, S [195A](#), [340A](#)

Schomburg, ED [42B](#)

Schomerus, C [367A](#)

Schrader, S [452A](#)

Schrage, K [379A](#)

Schramm, G [149B](#)

Schredl, M [53B](#)

Schreiber, E [321A](#)

Schreiber, S [32A](#)

Schröder, A [385A](#)

Schröder, C [Sat1-16](#)

Schröder, M [S18-4](#)

Schröder, O [321A](#)

Schroedter, K [116B](#)

Schroer, U [203B](#)

Schubert, A [448B](#)

Schubert, H [327B](#), [328B](#)

Schubert, M [15A](#)

Schubert, T [164B](#)

Schuchardt, A [44A](#), [45A](#)

Schuchmann, M [106B](#)

Schuckel, J [130B](#)

Schueler, A [436B](#)

Schüler, T [318B](#)

Schürer, F [276A](#)

Schürmann, F-W [263A](#)

Schuetz, E [334B](#)

Schütz, B [43B](#)

Schuierrer, G [466B](#)

Schuldt, A [167B](#)

Schuller, G [111A](#)

Schulte, D [51A](#), [160A](#)

Schulte, P [342B](#), [344B](#), [345B](#)

Schultz, K [167B](#), [169B](#)

Schulz, R [398A](#)

Schulze, H [S10](#), [S10-7](#)

Schulze, K [215A](#)

Schulze, V [327A](#)

Schulze-Bonhage, A [29B](#), [30B](#), [31B](#), [436A](#),  
[466A](#)

Schulzke, EL [191A](#)

Schummers, J [444A](#)

Schuppe, H [134B](#)

Schuricht, KS [S1-3](#)

Schwab, K [376A](#)

Schwab, M [327B](#), [328B](#), [376A](#), [377A](#)

Schwab, ME [P5](#), [S17-4](#), [26B](#)

Schwab, MH [351B](#)

Schwabe, K [241A](#), [331A](#), [336B](#)

Schwabe, L [92B](#), [93B](#), [94B](#), [444A](#)

Schwamborn, JC [375B](#)

Schwarting, RKW [253A](#), [254A](#), [255A](#), [420A](#)

Schwarz, JR [S1](#), [S1-3](#)

Schwarzacher, SW [27A](#)

Schwarzenbacher, K [S21-2](#), [126A](#), [135B](#)

Schweer, J [267A](#)

Schwegler, H [224B](#)

Schweimer, J [251B](#)

Schweitzer, J [S7-1](#)

Schweizer, M [S1-3](#), [246A](#)

Schwellnus, B [111A](#)

Schwenkert, I [257A](#), [297B](#)

Schwerdtfeger, G [19B](#), [20B](#)

Schwinger, E [401B](#)

[A](#) • [B](#) • [C](#) • [D](#) • [E](#) • [D](#) • [E](#) • [F](#) • [G](#) • [H](#) • [I](#) • [J](#) • [K](#) • [L](#) • [M](#) • [N](#) • [O](#) • [P](#) • [Q](#) • [R](#) • [S](#) • [T](#) • [U](#) • [V](#) • [W](#) • [X](#) • [Y](#) • [Z](#)

Scott, WJ [S12-3](#)

Seamari, Y [32B](#)

Seeger, G [408B](#)

Seeger, T [288B](#)

Seeliger, M [172A](#)

Seidel, B [331B](#)

Seidenbecher, CI [28A](#)

Seidenbecher, T [214B](#), [215B](#)

Seidl, A [S10-4](#)

Seidl, F [373A](#)

Seidl, T [68B](#)

Seifarth, F [117B](#)

Seifert, M [298A](#)

Seitz, RJ [77A](#), [78A](#)

Selig, F [276A](#)

Sellner, J [10B](#), [11B](#)

Sendtner, M [S20-1](#), [356A](#), [371B](#)

Senner, V [348A](#)

Sereda, MW [351B](#)

Seredenin, SB [347B](#)

Sergeant, N [414B](#)

Sersic, A [148A](#)

Seufert, P [201B](#)

Sévigny, J [367A](#), [369A](#)

Seyfarth, E-A [94A](#), [262A](#)

Seyfarth, J [130B](#)

Shafir, S [S4-4](#)

Shamma, S [S10-5](#)

Shelley, J [167B](#)

Shors, T [S6-5](#)

Shovman, MM [441A](#)

Shukla, V [369A](#)

Sibila, M [55B](#), [463A](#)

Siddiqui, S [202A](#)

Siebenhaar, F [1B](#)

Siedenberg, S [340B](#)

Siegmund, A [243B](#)

Siemen, H [404A](#)

Sigl, T [S22-1](#)

Sigrist, CB [402A](#)

Sigrist, S [297B](#)

Sigrist, SJ [283B](#), [284B](#), [402A](#)

Sikdar, SK [320B](#)

Silbering, AF [S21-3](#), [132A](#)

Simon, M [334A](#)

Simonen, M [26B](#)

Simonutti, M [415A](#)

Sinakevitch, I [S16-1](#)

Singewald, N [423A](#)

Singheiser, M [108A](#)

Sirbulescu, RF [119A](#)

Sirko, S [S12-6](#), [360A](#)

Skorjanc, A [63A](#)

Sloviter, RS [27A](#)

Smalla, K-H [28A](#)

Smarandache, CR [73A](#), [82A](#)

Smirnova, L [46A](#)

Smit, AB [S17-1](#), [25B](#)

Smith, A [S4-2](#), [314B](#)

Smith, B [S4](#), S4-5

Smolders, JWT [97B](#), [115A](#), [99B](#)

Sobik, T [386A](#)

Sobottka, H [406B](#)

Söhl, G [S11-4](#), [39A](#)

[A](#) • [B](#) • [C](#) • [D](#) • [E](#) • [D](#) • [E](#) • [F](#) • [G](#) • [H](#) • [I](#) • [J](#) • [K](#) • [L](#) • [M](#) • [N](#) • [O](#) • [P](#) • [Q](#) • [R](#) • [S](#) • [T](#) • [U](#) • [V](#) • [W](#) • [X](#) • [Y](#) • [Z](#)

- |   |  |
|---|--|
| Soehler, S <a href="#">303B</a>   | Staufenbiel, M <a href="#">5A</a>  |
| Soffe, SR <a href="#">S8-3</a> , <a href="#">84A</a>  | Stavenga, DG <a href="#">142A</a> , <a href="#">142B</a> , <a href="#">143B</a> , <a href="#">144B</a> |
| Sommer, MA <a href="#">S8-5</a>   | Steffens, H <a href="#">42B</a>  |
| Sontag, B <a href="#">336A</a>  | Stein, M <a href="#">Sat2-6</a>  |
| Sopper, S <a href="#">6B</a>  | Stein, W <a href="#">73A</a> , <a href="#">82A</a> , <a href="#">83A</a> , <a href="#">451B</a>        |
| Sosulina, L <a href="#">219B</a>  | Steiner, K <a href="#">88A</a>   |
| Souopgui, J <a href="#">21A</a>   | Steinhäuser, C <a href="#">39A</a>   |
| Souren, M <a href="#">125B</a>  | Steininger, B <a href="#">220B</a>   |
| Soyez, D <a href="#">424B</a>   | Steinmetz, CC <a href="#">42A</a>  |
| Speck, O <a href="#">34B</a>  | Stelzer, H <a href="#">422B</a>  |
| Spehr, J <a href="#">129A</a>   | Stemmann, H <a href="#">190A</a> , <a href="#">191A</a>  |
| Spehr, M <a href="#">128A</a>   | Stemmler, M <a href="#">89B</a>  |
| Speier, S <a href="#">421B</a>  | Stengl, M <a href="#">130B</a> , <a href="#">131B</a> , <a href="#">303B</a> , <a href="#">304B</a>    |
| Spence, C <a href="#">S19-3</a>   | Stenneken, P <a href="#">233A</a> , <a href="#">426A</a>   |
| Spielbauer, B <a href="#">40B</a>   | Steuhl, K-P <a href="#">385A</a>   |
| Spiess, J <a href="#">225A</a>  | Stevenson, PA <a href="#">14B</a> , <a href="#">298B</a> , <a href="#">300B</a>                        |
| Spira, M <a href="#">389B</a> , <a href="#">390B</a>  | Stich, KP <a href="#">240B</a> , <a href="#">242B</a>  |
| Spittau, B <a href="#">400A</a>   | Stichel, CC <a href="#">268A</a> , <a href="#">336A</a>  |
| Spitzer, M <a href="#">440B</a> , <a href="#">441B</a>  | Stiedl, O <a href="#">225A</a>   |
| Spors, H <a href="#">471A</a>   | Stock, P <a href="#">256A</a>  |
| Spreer, A <a href="#">8B</a> , <a href="#">394A</a>   | Stoeckli, ET <a href="#">377B</a>  |
| Sprengel, R <a href="#">247A</a>  | Störtkuhl, K <a href="#">136A</a>  |
| Srinivasan, G <a href="#">S24-5</a>   | Stojiljkovic, M <a href="#">4B</a>   |
| Staak, R <a href="#">S1-5</a>   | Stojkov, D <a href="#">4B</a>  |
| Stach, S <a href="#">16A</a>  | Stoll, M <a href="#">401B</a>  |
| Stadelmann, C <a href="#">392A</a> , <a href="#">394A</a> , <a href="#">410A</a> , <a href="#">416B</a> | Stollhoff, N <a href="#">235A</a>  |
| Stagi, M <a href="#">S14-3</a> , <a href="#">3A</a> , <a href="#">418B</a>                              | Stoppel, C <a href="#">217B</a>  |
| Stalleicken, J <a href="#">153B</a> , <a href="#">191B</a>  | Storch, MK <a href="#">181B</a>  |
| Stam, FJ <a href="#">S17-1</a>  | Storch-Hagenlocher, B <a href="#">10B</a>  |
| Stangel, M <a href="#">355B</a>   | Stork, O <a href="#">215B</a> , <a href="#">217B</a> , <a href="#">234B</a>                            |
| Stangl, C <a href="#">230B</a>  | Stork, T <a href="#">S5-5</a>  |
| Starke, J <a href="#">471A</a>  | Storm, JF <a href="#">S1-1</a> , <a href="#">S1-4</a>  |

[A](#) • [B](#) • [C](#) • [D](#) • [E](#) • [D](#) • [E](#) • [F](#) • [G](#) • [H](#) • [I](#) • [J](#) • [K](#) • [L](#) • [M](#) • [N](#) • [O](#) • [P](#) • [Q](#) • [R](#) • [S](#) • [T](#) • [U](#) • [V](#) • [W](#) • [X](#) • [Y](#) • [Z](#)

Stosic-Grujicic, S [4B](#)

Szewczyk, B [339A](#)

Stradner, J [91A](#)

Szinyei, C [218B](#)

Strand, S [11B](#)

Szöke, K [296A](#), [349B](#)

Straub, O [451B](#)

Szyszk, P [133A](#), [134A](#), [135A](#)

Straube, S [205B](#)

Strausfeld, NJ [S16-1](#), [262A](#)

Strauss, R [S16](#), [S16-4](#)

Strauss, U [79B](#)

Strehl, U [S18](#)

Strekalova, T [460B](#), [461B](#)

Strelau, J [74B](#)

Stricker, R [40A](#)

Strobel, A [404B](#)

Strotmann, J [S21-2](#), [121A](#), [122A](#), [125A](#),  
[126A](#), [127A](#)

Strube, M [236A](#)

Strutz, J [114A](#)

Strzelczyk, A [74B](#)

Stubbe, H [S11-3](#)

Stuchbury, G [S14-4](#)

Stühler, K [121B](#)

Stuenkel, C [27B](#)

Stüwe, S [321A](#), [337B](#), [338B](#)

Stumpner, A [92A](#)

Stusek, P [147A](#)

Subasic, S [4B](#)

Südhof, TC [290B](#)

Sugawara, Y [30A](#)

Sur, M [444A](#)

Suter, U [S12-5](#)

Swan, LE [283B](#), [284B](#)

Szeto, HH [376A](#)

[A](#) • [B](#) • [C](#) • [D](#) • [E](#) • [D](#) • [E](#) • [F](#) • [G](#) • [H](#) • [I](#) • [J](#) • [K](#) • [L](#) • [M](#) • [N](#) • [O](#) • [P](#) • [Q](#) • [R](#) • [S](#) • [T](#) • [U](#) • [V](#) • [W](#) • [X](#) • [Y](#) • [Z](#)

- |  |  |
|--|--|
| Tabor, R <a href="#">126B</a>  | Thiel, F <a href="#">172A</a>  |
| Tafur, D <a href="#">242B</a>  | Thiele, J <a href="#">249B</a>   |
| Taheri, N <a href="#">181B</a> , <a href="#">416B</a>                          | Thier, H-P <a href="#">213B</a>  |
| Takahashi, K <a href="#">417B</a>  | Thier, P <a href="#">439B</a>  |
| Tal, L <a href="#">412A</a>  | Thomas, S <a href="#">Sat2-6</a>   |
| Taley, S <a href="#">226B</a> , <a href="#">227B</a>                           | Thomas-Crusells, J <a href="#">S22-1</a>   |
| Talke, C <a href="#">305B</a>  | Thurley, K <a href="#">443A</a>  |
| Tammer, R <a href="#">468A</a>   | Thurm, H <a href="#">322B</a>  |
| Tamosiunaite, M <a href="#">250B</a>   | Tichacek, K <a href="#">198B</a> , <a href="#">430B</a> , <a href="#">432B</a>                         |
| Tanimoto, H <a href="#">257A</a>   | Tidow, N <a href="#">401B</a>  |
| Tantalaki, E <a href="#">325B</a>  | Tilgen, N <a href="#">312A</a> , <a href="#">402B</a>  |
| Tarabykin, V <a href="#">50A</a> , <a href="#">363B</a> , <a href="#">367B</a> | Tilling, T <a href="#">354B</a>  |
| Tarnok, A <a href="#">411B</a>   | Timme, M <a href="#">210A</a> , <a href="#">206B</a>   |
| Tarrazó, MF <a href="#">226B</a> , <a href="#">227B</a>                        | Timmer, M <a href="#">347A</a> , <a href="#">382B</a>  |
| Taschenberger, H <a href="#">364B</a>  | Timofeev, I <a href="#">212A</a>   |
| Tatagiba, M <a href="#">S18-4</a>  | Titz, S <a href="#">307A</a>   |
| Tauber, SC <a href="#">394A</a>  | Tobisch, N <a href="#">292B</a> , <a href="#">293B</a>   |
| Taylor, K <a href="#">192A</a>   | Tönges, L <a href="#">339B</a>   |
| Taylor, V <a href="#">371A</a>   | tom Dieck, S <a href="#">161A</a> , <a href="#">162A</a> , <a href="#">282B</a> , <a href="#">290B</a> |
| Tegenthoff, M <a href="#">64A</a> , <a href="#">65A</a> , <a href="#">179A</a> | Toney, MD <a href="#">272A</a>   |
| Teichert, T <a href="#">188B</a>   | Toonen, RF <a href="#">290A</a>  |
| Teisner, B <a href="#">50B</a>   | Tootell, RBH <a href="#">188A</a>  |
| ter Meulen, V <a href="#">6B</a>   | Torner, L <a href="#">307B</a>   |
| Terlau, H <a href="#">323B</a>   | Torvinen, M <a href="#">277A</a>   |
| Terwel, D <a href="#">24A</a>  | Touma, C <a href="#">2A</a>  |
| Tessmar-Raible, K <a href="#">422B</a>   | Tovote, P <a href="#">225A</a>   |
| Tetzlaff, T <a href="#">206B</a> , <a href="#">207B</a> , <a href="#">208B</a> | Treier, M <a href="#">S5-4</a>   |
| Tetzlaff, W <a href="#">S22-1</a>  | Tremp, G <a href="#">S2-4</a>  |
| Thanos, S <a href="#">203B</a> , <a href="#">348A</a> , <a href="#">394B</a>   | Treue, S <a href="#">178B</a> , <a href="#">438A</a> , <a href="#">445B</a>                            |
| Theis, M <a href="#">P7</a>  | Tripathi, P <a href="#">S10-4</a> , <a href="#">105A</a>   |
| Theiss, C <a href="#">385A</a> , <a href="#">464A</a>                          | Trischler, C <a href="#">15B</a>   |
| Thiel, A <a href="#">165B</a>  | Trojan, P <a href="#">157B</a> , <a href="#">158B</a> , <a href="#">159B</a>                           |

[A](#)•[B](#)•[C](#)•[D](#)•[E](#)•[D](#)•[E](#)•[F](#)•[G](#)•[H](#)•[I](#)•[J](#)•[K](#)•[L](#)•[M](#)•[N](#)•[O](#)•[P](#)•[Q](#)•[R](#)•[S](#)•[T](#)•[U](#)•[V](#)•[W](#)•[X](#)•[Y](#)•[Z](#)

Troje, NF [85A](#), [180A](#)

Tsao, DY [188A](#)

Tsien, JZ [244B](#)

Tsodyks, M [450B](#)

Tudusciuc, O [438B](#)

Turck, CW [28B](#)

Tusch, J [449B](#)

Tzvetanov, T [438A](#), [445B](#)

[A](#) • [B](#) • [C](#) • [D](#) • [E](#) • [D](#) • [E](#) • [F](#) • [G](#) • [H](#) • [I](#) • [J](#) • [K](#) • [L](#) • [M](#) • [N](#) • [O](#) • [P](#) • [Q](#) • [R](#) • [S](#) • [T](#) • [U](#) • [V](#) • [W](#) • [X](#) • [Y](#) • [Z](#)

Uckermann, O [350A](#)

Ueberham, E [410B](#)

Ueberham, U [410B](#)

Ueffing, M [Sat2](#), [Sat2-4](#)

Ukhanov, K [129A](#)

Ulbricht, E [351A](#)

Ullrich, A [9B](#)

Unsicker, K [S22](#), [74B](#), [228A](#), [248A](#), [261B](#), [262B](#)

Urbach, TP [53A](#)

Ustinova, J [395B](#)

Utz, S [269B](#)

Uzakov, S [231B](#)



[A](#) • [B](#) • [C](#) • [D](#) • [E](#) • [D](#) • [E](#) • [F](#) • [G](#) • [H](#) • [I](#) • [J](#) • [K](#) • [L](#) • [M](#) • [N](#) • [O](#) • [P](#) • [Q](#) • [R](#) • [S](#) • [T](#) • [U](#) • [V](#) • [W](#) • [X](#) • [Y](#) • [Z](#)

v. Campenhausen, M [97A](#)

Vakhitova, JV [347B](#)

Valbuena, PC [49B](#)

van Ahrens, L [166B](#)

van Amerongen, M [418A](#)

van Bergeijk, J [398B](#)

van de Wal, R [388A](#)

van den Burg, E [30A](#), [425A](#)

van der Berg, I [62A](#)

van der Putten, H [257B](#)

van der Schors, RC [25B](#)

van der Willigen, RF [108A](#), [196A](#)

Van der Zee, EA [388B](#)

van Eimeren, L [426A](#)

van Hateren, JH [20B](#)

van Hemmen, JL [120A](#), [443B](#)

van Leeuwen, C [426B](#)

Van Leuven, F [24A](#)

van Netten, SM [64B](#)

van Swinderen, B [S4-3](#)

Vanhoutte, P [342A](#)

Varoqueaux, F [295A](#)

Varughesi, S [405A](#)

Vatankhah, B [466B](#)

Veit, R [437B](#)

Ven, Vvd [206A](#)

Vergoz, V [17A](#)

Verhaagen, J [S17](#), [S17-1](#), [25B](#)

Verhage, M [290A](#)

Verschure, PFMJ [47B](#), [146B](#), [230A](#)

Vervaeke, K [S1-4](#)

Vesper, J [207A](#)

Vidnyánszky, Z [174B](#)

Vilanova, H [37B](#)

Vilpoux, K [376B](#)

Visser, TJ [374A](#)

Vogel, A [S9-3](#)

Vogels, R [S19-4](#)

Voges, N [450A](#)

Vogt, P [72B](#), [250A](#)

Voigt, K [305B](#), [335B](#), [462B](#)

Volgushev, M [180B](#), [196B](#), [212A](#), [279A](#)

Volk, GF [203B](#)

Volkel, P [Sat2-6](#)

Volkmandt, W [94A](#), [284A](#), [285A](#)

Volkov, AV [416A](#)

Vollgraf, R [461A](#)

Vollmer, G [336B](#)

Volterra, A [S11-3](#), [S11-5](#)

von Ahsen, O [27B](#)

von Bohlen und Halbach, O [74B](#), [228A](#), [248A](#),  
[261B](#), [262B](#)

von der Behrens, W [103B](#)

von der Emde, G [260B](#)

von der Ende, G [432A](#)

von Gizycki, H [173B](#)

von Holst, A [S12](#), [S12-5](#), [S12-6](#), [360A](#), [396B](#),  
[397B](#)

von Hünerbein, K [97B](#)

Von Lewinsky, F [409A](#)

von Merten, S [241B](#)

von Steinbüchel, N [439A](#)

von Uckermann, GBG [82B](#)

Vonderschen, K [104A](#)

[A](#) • [B](#) • [C](#) • [D](#) • [E](#) • [D](#) • [E](#) • [F](#) • [G](#) • [H](#) • [I](#) • [J](#) • [K](#) • [L](#) • [M](#) • [N](#) • [O](#) • [P](#) • [Q](#) • [R](#) • [S](#) • [T](#) • [U](#) • [V](#) • [W](#) • [X](#) • [Y](#) • [Z](#)

Vorobyev, M [197A](#)

Voronezhskaya, EE [278B](#)

Voss, J [166A](#), [199A](#)

Vossen, S [196A](#)

Vosshall, LB [132B](#), [133B](#)

Voyno-Yasenetskaya, T [48A](#)

Vreugdenhil, E [Sat4-3](#)

Vuksic, M [27A](#)

[A](#) • [B](#) • [C](#) • [D](#) • [E](#) • [D](#) • [E](#) • [F](#) • [G](#) • [H](#) • [I](#) • [J](#) • [K](#) • [L](#) • [M](#) • [N](#) • [O](#) • [P](#) • [Q](#) • [R](#) • [S](#) • [T](#) • [U](#) • [V](#) • [W](#) • [X](#) • [Y](#) • [Z](#)

Wachtler, T [188B](#), [429B](#)

Wackerbeck, C [327A](#)

Waclaw, RR [S12-3](#)

Wada, K [193B](#)

Wässle, H [156A](#), [157A](#), [158A](#), [175B](#)

Waetzig, V [329B](#), [419A](#)

Wagener, R [29A](#)

Wagh, D [297B](#)

Wagner, A [406B](#)

Wagner, FE [412B](#)

Wagner, H [97A](#), [104A](#), [108A](#), [196A](#), [358A](#)

Wahle, P [204A](#), [205A](#), [269A](#), [280A](#), [384A](#)

Waitz, O [386B](#)

Waka, N [S3-4](#)

Walkowiak, W [96A](#), [263B](#)

Wallraff, A [39A](#)

Walter, L [397A](#)

Walter, M [425B](#)

Walter, S [S2-3](#)

Walz, C [282A](#)

Wang, Y [40A](#), [391B](#)

Wang, Z [358B](#), [400A](#)

Wanischeck, M [70A](#)

Wanker, E Sat2-5

Wannig, A [190A](#)

Warnke, K [1B](#)

Warrant, EJ [145A](#)

Warscheid, B [121B](#)

Warth, A [415B](#)

Warzecha, A-K [S9-4](#), [24B](#)

Watanabe, S [219A](#)

Waters, J [S13](#), [S13-4](#)

Wcislo, WT [145A](#)

Weber, F [28B](#)

Weber, JR [S14-2](#)

Weber, M [94A](#), [254B](#), [333B](#)

Weber, YG [312A](#)

Webster, J [S14-4](#)

Wegener, C [269B](#)

Wegener, D [189A](#), [433A](#)

Wegner, F [406B](#)

Wehner, R [11A](#), [13A](#), [68B](#), [153B](#), [237A](#),  
[259A](#), [260A](#)

Wehr, MC [467A](#)

Weibel, A [140B](#)

Weick, M [351A](#)

Weickert, S [269A](#)

Weigel, S [341A](#), [342B](#), [344B](#), [345B](#)

Weigelt, C [71B](#)

Weik, V [101B](#)

Weiler, E [280A](#), [300A](#), [387A](#)

Weiler, J [431A](#)

Weiler, R [163B](#), [164B](#), [167B](#), [168B](#), [169B](#),  
[170B](#), [191B](#)

Weiler, V [65B](#)

Weishaupt, JH [S20](#), [S20-4](#), [49B](#), [395A](#), [411A](#)

Weislogel, J-M [344A](#)

Weiss, DG [321A](#), [337B](#), [338B](#)

Weiss, H [18B](#)

Weiß, J [175B](#)

Weissert, R [181B](#), [315A](#)

Welcher, AA [S22-1](#)

Wellbrock, UM [356B](#)

Wendt, W [336A](#)

[A](#) • [B](#) • [C](#) • [D](#) • [E](#) • [D](#) • [E](#) • [F](#) • [G](#) • [H](#) • [I](#) • [J](#) • [K](#) • [L](#) • [M](#) • [N](#) • [O](#) • [P](#) • [Q](#) • [R](#) • [S](#) • [T](#) • [U](#) • [V](#) • [W](#) • [X](#) • [Y](#) • [Z](#)

- Wenning, G [34A](#)  
 Wenzel, D [283B](#)  
 Wermke, K [Sat1-7](#)  
 Werner, M [S15-3](#), [314B](#)  
 Wernet, P [346A](#)  
 Werning, M [36B](#)  
 Wertlen, AM [148A](#)  
 Wertz, A [127B](#)  
 Wesemann, M [347A](#)  
 Wess, J [288B](#)  
 Wessel, R [195A](#)  
 Wessig, C [354B](#)  
 Wessig, J [413A](#)  
 Wessolleck, J [382B](#)  
 Westhoff, G [185A](#), [187A](#)  
 Westmark, S [83B](#)  
 Weth, F [129B](#), [202B](#), [375A](#)  
 Wetzel, CH [S21-6](#), [122B](#), [123B](#), [124B](#), [313B](#)  
 Wetzel, W [107B](#), [236B](#)  
 Wheeler-Schilling, TH [349A](#)  
 White, L [177B](#)  
 Wicher, D [322A](#)  
 Wichmann, C [283B](#)  
 Wicke, K [289B](#), [332B](#), [333B](#)  
 Wicklein, M [154A](#)  
 Widmann, G [S18-4](#)  
 Widmer, H [50B](#)  
 Wiechert, MT [446B](#)  
 Wiedemann, P [349A](#), [350A](#)  
 Wiegert, O [24A](#), [231A](#)  
 Wiegrebe, L [96B](#), [111A](#), [100B](#), [106B](#)  
 Wiehle, M [357B](#), [360B](#)  
 Wiendl, H [315A](#)  
 Wienisch, M [292A](#)  
 Wieronska, J [339A](#)  
 Wiese, KA [213A](#)  
 Wiese, S [356A](#)  
 Wiesing, P [444A](#)  
 Wigger, A [421A](#), [423A](#)  
 Wijnen, B [142A](#), [143B](#)  
 Wildner, H [S5-4](#)  
 Wilimzig, C [62B](#), [63B](#)  
 Willecke, K [S11-4](#), [39A](#), [163B](#), [170B](#)  
 Willesen, M [413A](#)  
 Wilms, M [173A](#)  
 Wilson, F [Sat2-6](#)  
 Wilson, MA [S23-6](#)  
 Winkler, J [307B](#)  
 Winter, H [S3-6](#), [6A](#), [9A](#)  
 Winter, SM [84B](#)  
 Winter, Y [229B](#), [239B](#), [240B](#), [241B](#), [242B](#),  
[249B](#), [465B](#)  
 Wirth, M [205A](#)  
 Wirths, O [S2-4](#)  
 Wirtz, S [467B](#)  
 Wischmeyer, E [309A](#)  
 Wittbrodt, J [422B](#)  
 Witte, OW [327B](#), [328B](#), [386B](#), [387B](#)  
 Wittenberg, M [188B](#)  
 Wittlinger, M [13A](#)  
 Wittmann, M [342A](#)  
 Wöhr, M [254A](#), [255A](#)  
 Wölfel, M [Sat3-1](#)  
 Wöll, S [52B](#)

[A](#) • [B](#) • [C](#) • [D](#) • [E](#) • [D](#) • [E](#) • [F](#) • [G](#) • [H](#) • [I](#) • [J](#) • [K](#) • [L](#) • [M](#) • [N](#) • [O](#) • [P](#) • [Q](#) • [R](#) • [S](#) • [T](#) • [U](#) • [V](#) • [W](#) • [X](#) • [Y](#) • [Z](#)

Woellner, K [361A](#)

Wulfsen, I [S1-3](#)

Wörgötter, F [144A](#), [250B](#), [444B](#)

Wunderlich, T [404A](#)

Wohlfahrt, K [406B](#)

Wyss, R [230A](#)

Wohlgemuth, S [90B](#)

Wyzisk, K [155A](#)

Wolburg, H [415B](#)

Wolf, A [95A](#), [350A](#)

Wolf, F [1A](#), [175A](#), [176A](#), [177B](#), [179B](#), [180B](#),  
[196B](#), [291A](#)

Wolf, H [11A](#), [12A](#), [13A](#), [69A](#), [396A](#), [452B](#)

Wolf, R [S16](#), [S16-6](#)

Wolf, S [349A](#)

Wolffgramm, J [330A](#)

Wolfram, T [362B](#)

Wolfram, V [143A](#)

Wolfrum, U [146A](#), [156B](#), [157B](#), [158B](#), [159B](#),  
[160B](#)

Wollweber, BT [335B](#), [462B](#)

Wolosker, H [272A](#), [285B](#)

Wolpow, JR [S18-2](#)

Wolters, D [121B](#)

Wolynski, B [220A](#)

Womelsdorf, T [438A](#), [445B](#)

Wonderschütz, P [199A](#)

Wood, CE [327B](#)

Wotjak, CT [243B](#)

Wouters, FS [341B](#), [469A](#)

Wratil, H [138A](#), [139A](#)

Wree, A [79B](#), [393B](#), [467B](#)

Wrobel, G [345B](#)

Wüsten, HJ [337A](#)

Wüstenberg, T [439A](#)

Wulczyn, FG [46A](#)

[A](#)•[B](#)•[C](#)•[D](#)•[E](#)•[D](#)•[E](#)•[F](#)•[G](#)•[H](#)•[I](#)•[J](#)•[K](#)•[L](#)•[M](#)•[N](#)•[O](#)•[P](#)•[Q](#)•[R](#)•[S](#)•[T](#)•[U](#)•[V](#)•[W](#)•[X](#)•[Y](#)•[Z](#)

Xiao, Q [169A](#)

[A](#) • [B](#) • [C](#) • [D](#) • [E](#) • [D](#) • [E](#) • [F](#) • [G](#) • [H](#) • [I](#) • [J](#) • [K](#) • [L](#) • [M](#) • [N](#) • [O](#) • [P](#) • [Q](#) • [R](#) • [S](#) • [T](#) • [U](#) • [V](#) • [W](#) • [X](#) • [Y](#) • [Z](#)

Yakubov, E [271B](#)

Yamidanov, RS [347B](#)

Yan, J [S10-2](#)

Yan, Q [S22-1](#)

Yaniv, I [417A](#)

Yanytska, Y [372B](#)

Yarali, A [357A](#)

Yates, J [317B](#)

Yavin, E [271B](#)

Yeshenko, O [S23-4](#), [54B](#)

Yildirim, F [406A](#)

Yilmazer-Hanke, D [224B](#)

Yizhar, O [295B](#)

Youdim, MBH [385B](#), [412A](#)

Yuste, R [245B](#)

[A](#) • [B](#) • [C](#) • [D](#) • [E](#) • [D](#) • [E](#) • [F](#) • [G](#) • [H](#) • [I](#) • [J](#) • [K](#) • [L](#) • [M](#) • [N](#) • [O](#) • [P](#) • [Q](#) • [R](#) • [S](#) • [T](#) • [U](#) • [V](#) • [W](#) • [X](#) • [Y](#) • [Z](#)

Zahng, Y-P [S13-2](#)

Zakotnik, J [66B](#)

Zannat, T [309B](#)

Zaremba, A [203A](#)

Zaum, D [56A](#)

Zechel, S [261B](#)

Zechner, D [S5-4](#)

Zeck, GM [169A](#)

Zehle, S [223B](#)

Zeil, J [22B](#)

Zeitlhofer, J [S23-1](#)

Zhang, W [44B](#), [136A](#), [137A](#), [295A](#), [302A](#),  
[324B](#), [325B](#)

Zhang, Y [S17-1](#), [122A](#)

Zhao, J [277B](#)

Zhelyaznik, N [381A](#)

Zheng, F [288B](#)

Zheng, L [143A](#)

Zhou, F-W [79B](#)

Zhou, Y [11B](#)

Zhu, M [S5-5](#)

Zhu, X [268A](#)

Ziemssen, T [28B](#)

Zierler, S [355A](#)

Zimmer, A [43B](#)

Zimmermann, E [Sat1](#), [Sat1-1](#), [Sat1-5](#), [52A](#)

Zimmermann, H [284A](#), [285A](#), [367A](#), [369A](#)

Zimmermann, U [S3-6](#), [6A](#), [9A](#)

Zint, C [311A](#)

Zischka, H [Sat2-4](#)

Zoidl, G [269A](#), [386A](#)

Zorzi, M [206A](#)

Zube, C [137B](#)

Zufall, F [S21](#), [S21-5](#), [128A](#), [129A](#)

Zupanc, GKH [119A](#), [266A](#), [356B](#)

Zupancic, G [147A](#)

Zuschratter, W [107B](#), [368B](#), [369B](#)

Zwickel, T [39B](#)